physics abstracts

U. of ILL. LIBRARY
JUN 9 1971
CHICAGO CIRCLE

An INSPEC Publication
The Institution of
Electrical Engineers

Molecular beams continued

IF7, polar distortions 0-55318

IP-, polar distortions 0-5518 In monohalide, comp., mass spectrometric study 0-39392 Li atom reactions with Cl₂, ICl, Br₂, SnCl₄, PCl₃ and NO₂ 0-77989 N₂, electron scattering, meas. of total differential cross section at 40 keV, correlation, and binding effects and Bethe corrections 0-74290 N₃, emission spectrum and radiative lifetime of metastable $E^3\Sigma_z^+$ state 0-61120

0-61120
N₃, interaction with solid N₂ surface 0-65567
NH₃ and ND₃, photoelectron spectra 0-58186
NaBr, r.f. Stark spectra, elec. reson. method 0-39392
NaCl, r.f. spectra by electric resonance 0-61126
NaCl, r.f. Stark spectra, elec. reson. method 0-39392
RbBr, rotational state distrib. of molecular beam 0-77835
ReF₃, polar distortions 0-55318

Molecular orbitals see Molecules/electronic structure; Orbital calculation

Molecular relaxation see Molecules/relaxation

Molecular spectra see Spectra/inorganic molecules; Spectra/molecules; Spectra/organic molecules and substances

Molecular structure see Molecules/configuration and dimensions

Molecular weight
carbon black suspension, HAF, from Zimm plots 0-50274
polybutadienes, critical molecular weight from viscosity measurements -55386 polymer systems, distribution, effect on shear dependence of viscosity

polymers, electron microscopic determ. 0–55385 water, anomalous, cryoscopic method 0–64863 He-Ar mixture with He-driver, role on formation of contact surfaces He-Ar mixture with He-driver, role on formation of contact surfaces 0–39663
Ni, Pd and Pt complexes, Ni(PF₃)₄, Pd(PF₃)₄ and Pt(PF₃)₄, determ. 0–55309

Molecular weight determination

chromatography, concentration of each component 0-59514

Molecules

see also Kinetic theory; Spectra

absolutely inequivalent pure interchange symmetry 0-70857 asymmetric rotor type, determ, of higher rotational terms by extrapolation 0 - 43060

atomic and molecular physics, advances, collection of articles in book 0-74081

biological, iron containing, Mossbauer effect 0-69094

bound state, new type, resulting from corrections to Born-Oppenheimer approximation 0–64312 Brillouin scattering, stimulated, rel. to interaction of light with sound 0–53000

chain type with random force constant defects, distrib. of eigenvalues and

eigenvectors 0-77976 charge transfer complexes, dielectric properties as function of temperature 0-65763

O-70832

Debye-Ehrenfest model of X-ray and electron diffr. 0—43071

depolarization study by odd-parity Raman effect and Racah's algebra
0-70836

diamagnetic, positronium quenching 0–53314 diamagnetic mean props., estimate 0–44486 diamagnetic theory of Faraday effect 0–64358 diamagnetism, uncoupled cales. for two centre systs.

diamagnetic theory of Faraday effect 0–64358 diamagnetism, uncoupled cales, for two centre systs. 0–61047 diatomic, inelastic electron scatt, cross-sections 0–64371 diatomic, nonreactive collision with atom, energy transfer 0–74437 diatomic, photoelectron spectroscopy, theory of angular distrib. 0–64327 diatomic, potential curves in second approxim. of generalized WKB method 0–49839 diatomic optical properties calc, by time-dependent coupled Hartree-Fock method 0–67603 diffusion coeff. meas. by quasi-elastic light scattering, small molecules 0–64884

0-64884

U-04884
donor, fluorescence quenching by acceptor 0-64313
dynamics, cold neutron spectra, cyclic hydrocarbons 0-47511
Eckart conditions considered geometrically, separation of motions for normal molecules 0-53006
electron moving in field of many stationary nuclei, suggestive approximate dynamical symmetry 0-73915
electron scattering, elastic partial wave method and zero-range approx.

0-74195
electron scattering, spin polarization meas, and collision description by independent-atom model 0-73460
estimation of nuclear magnetic shielding constants in atoms, extension of procedure to molecules 0-39259
Faraday effect for diamagnetic molecules, theory 0-64358
gas-solid molecular complex, props. by cell model calc. 0-78712
glyoxal, torsional vibration effect on molecular structure 0-70847
hamiltonian, for translating, rotating, vibrating mol. in presence of constant external e.m. field 0-64318
internal coordinate space, symmetry props. deriv. from its G matrix 0-77755
interstellar, formation and radio radiation from 0-66510

interstellar, formation and radio radiation from 0–66510 ions, negative, in alkali halide cryst., alignment and reorientation 0–53529 libration in polar liquid dielectric, statistical model, noise spectrum 0–46935

0-46935
[lower-bound calcs., by overlap integrals 0-74194
model of strong shock wave structure in gas of point center molecular repulsion 0-39662
molecular crystal Hall effect study in triangular model 0-78864
neutron scattering from rigid rotor, sum rule 0-46441
Nitrobenzene, torsional vibration effect on molecular structure 0-70847
nitromethane, liquid or solution, magnitude of opposing potential barrier
0-67809

0-07699 optically active, props., rel. to cholesteric phase helical structure 0-39733 orientation in rhombic cryst., by computation 0-65184 overlap between true and approx. wavefunctions, upper and lower bounds 0-64197

polar, thermal electron scatt. cross sections 0-70834 polyatomic, Herzberg-Teller theory of vibronic intensity borrowing, examination 0-74203

polyatomic, multiple scattering model using Johnson's Hartree-Fock SCF approach 0-64309

polyatomic, temp. depend. of photoionization cross section 0-43073

Molecules continued

polymers, n.m.r. studies of mol. motion 0-64569

polymers, n.m.r. studies of mol. motion 0—64569 pressure virial coeffs. for nonspherical hard-core molecules 0—43037 protonic spectra similar to electronic spectra 0—70835 quantum mechanics, use of multiple constraints and Hellman-Feynman theorem 0—43066 SCF LCAO MO calculations with added contracted H 2p orbitals, polarizabilities of hydrocarbons 0—55354 saturation and Stark effect in optical freq. fields 0—64310 spin states, in space media 0—76533 structural group anal. and spectral correls., symbolic logic methods 0—58134 symmetry, groups for linear mole, classification of routbronic states.

symmetry groups for linear mols., classification of rovibronic states 0-67703

tetrahedral harmonics for arbitrary J 0-43036

thioformaldehyde, migrowave detection 0–71035 torsional vibration effect on molecular structure 0–70847 two-photon absorption of tumbling molecules, polarization depend. 0–55267

0–55267
water, motions in dilute aqueous soln. of tertiary butyl alcohol, neutron scattering study of hydrophobic hydration 0–71314
B complexes, solid, molecular motion by n.m.r. study 0–45009
Br, molecule formed by atomic combination, comparison of ground and excited states 0–46460
CO electron scatt. cross sections calc. 0–70886
CO₂ dissociation, kinetics of 0–71046
CO₃ electron scatt., cross sections calc. 0–70886
CO₃—polarizability determ. from crystal birefringence 0–49859
Cl, molecule formed by atomic combination, comparison of ground and excited states 0–46460
H, dipole polarizability single-centre calc. 0–70903

excited states 0-46460
H₂, dipole polarizability, single-centre calc. 0-70903
1₃, molecule formed by atomic combination, comparison of ground and excited states 0-46460
Mo VII, vacuum spark u.v. spectra, term anal. of 4p-nd and 4p-ns transitions 0-55238
N₂-, shape resonances, local potential 0-77818
NH₃+ radical ion hyperfine coupling const., UHF calc. 0-70930
NO₂- polarizability determ. from crystal birefringence 0-49859
N₃O electron scatt., cross sections calc. 0-70886
SF, vertical electron affinities for neutral and charged species 0-74304
SeF, vertical electron affinities for neutral and charged species 0-74304
Xe-Hg(P₂) complex emission band obs. during irradiation of Xe-Hg gas mixture rate constant for reaction determ. 0-74274

configuration and dimensions

configuration and dimensions

see also Chemical structure; Crystal structure, atomic acconitring. Noxide, symmetric top structure, microwave determ. 0–74325 bond angles, relation with photoelectron spectra in neutral molecules

0-64409

bond length prediction by ab initio SCF LCAO MO calc, using STO 2G expansions 0-61060 book 0-58610

book 0–58610 book 0–58610 bridged structure M-L-M, angular correlation of symmetric and antisymmetric frequencies 0–67698 C₃r, symmetry molecules in excited state v_t=2, rotational spectrum 0–43055

0-43055
Cartesian coordinates from internal coordinates, second and higher derivatives 0-70852
centrifugal stretching consts., eqns. for determination 0-49841
conference, structure and spectroscopy, Columbus, USA (1969) 0-61044
conformational anal. by u.s. relaxation 0-74364
conformations in various electronic states, review 0-58156
electron diffr. intensities precise meas. unit 0-64362
energetics of conformational changes, conference 0-74218
energetics of conformational changes 0-74219
energy levels, lower, of asymmetric rotor molecule 0-43060
equilibrium geometries, ab initio self-consistent MO calc. 0-39358
inertia tensor derivatives with respect to normal coordinates, eqns. for
determination 0-49841
internal coordinate space, symmetry props. deriv. from its G matrix
0-77755
methyl nitrate, molecular structure 0-64521

methyl nitrate, molecular structure 0-64521

models, miniature, construction 0–59858
Mossbauer spectra, determination, native of bonding 0–69096
non-rigid molecules in crystal 70 K, singlet and triplet state differences 0–52998 optical active, synthesis of racemates 0-49829

polyatomic, inner shell correlation energy, invariance with geometry changes 0-43072 polyatomic, stable geometric configurations using symmetry arguments 0-77757

polyatomic, stable geometric configurations using symmetry arguments 0-77757

polyatomic, symmetry arguments as basis of stable geometric configurations 0-70861

configurations 0–70861 shape functions method, totally localized functions approx. 0–55280 solvent induced conformational kinetics, study by e.s.r. 0–55281 spherical top, Raman band contours, computer programme 0–46418 symmetry groups of non-rigid molecules as semi-direct products 0–74220 torsional vibration effect on molecular structure 0–70847 C-H distance variations rel. to C hybridization 0–53008 H-O struct. and props. 0–71307 N-O;²⁻², cis configuration, C;h point group, root mean square amplitude determ. 0–74287 NO-SO;F structure from i.r. and Raman spectra 0–70925 NO-(SO;);F structure from i.r. and Raman spectra 0–70925 Ni complex, ethylenebisbiguanide=Ni(II) chloride monohydrate 0–65267 PH; in nematic solvent, from p reson spectrum 0–64445 configuration and dimensions, inorganic

PH₃ in nematic solvent, from p reson, spectrum 0-04445 configuration and dimensions, inorganic carboranes, CNDO/2 calc. 0-74246 cobalt complex, cobalt (III) isothiocyanato-dinitro-(ethylenediamino)-ammine, cryst. struct. 0-78465 hydrides, diatomic, relationship between internuclear distance and vibrational frequency 0-74229 lanthanide complexes, metal-ligand spacing from spectral bands positions 0-70915

0-/0915 silyl halides, from microwave spectra 0-64454 tetravinyl-lead 0-77847 tetravinylgermanium 0-77847 tetravinylsilicon 0-77847

S 1110 SUBJECT INDEX

Molecules continued configuration and dimensions, inorganic continued

tetravinyltin 0-77847

uranyl salts, distance determ, for U-O bond 0–46516 water, assignment of i.r. abs. band at 2130 cm⁻¹ 0–50230 [Co(NO)(NH₃)₃]Cl₂ 0–78466 (Agpy₃)²⁺ complex ion, e.s.r., wavefunctions and ring angle determ. 0–46447

0-46447
AlBr₃, n.q.r. of ⁷⁹Br, Zeeman effect rel. to bond nature and molecular structure 0-45043
B-Ce₄, B-F₄, from matrix-isolated i.r. spectra 0-70876
B-H₂Br, structural parameters from microwave spectrum 0-70875
BaF₃, in solid Kr matrix, from i.r. spectra shifts on isotopic substitution 0-77779
BaF₃, in solid Kr matrix, from i.r. spectra and vibr. mode shift 0-54095
BeB₂H₈, from i.r. spectra 0-67717
CO₂, geometrical parameters determination by electron diffraction 0-64385
CO₃, ab initio calc. 0-70881

0-64385

CO₃, ab initio calc. 0-70881

C₃O₅, CCC bending potential function 0-74245

C₃O₅, high temp. phase 0-78458

CaF₃, apex angles from i.r. spectra shifts on isotopic substitution 0-77779

CaF₃, in solid Kr matrix, from i.r. spectra and vibr. mode shift 0-54095

[CeMo₅, O₄;]-⁸ anion, X-ray obs. 0-43095

ClN₃, from microwave spectra 0-70892

ClN₃, 4750 A band syst., rot. anal., force field and intensity calc. 0-64392

Co complex, bisacetatobis (ethylenethiourea)Co(II) 0-68300

Co complex, chlorotetraethylenepentamine cobalt(III), αα isomer, conformation 0-78464

Co isonitrile complexes, structural study from Raman and i.r. spectra 0-61085

Cr complex, [N,N-bis(2-diphenylphosphinoethyl)ethylamineltricarbonylch-

Cr complex, [N,N-bis(2-diphenylphosphinoethyl)ethylamine]tricarbonylch-romium, X-ray diffraction 0-40075 Cr(III) complexes, fluorides, assignments of configurations from i.r. spec-tra 0-49862

Cu complex, bis(N-cyclohexylthiopicolinamido) copper (II) 0–49863 Cu complex, β -hydroxy- α -naphthaldehyde-[β -hydroxy- α -naphthyl-methylimid] X-ray structure study 0–71587

Cu complex, di- μ -chlorotris(trans-cyclooctene)dicopper (I), X-ray study 0-65230

Cu complex, dr.4-chlorotris(trans-cyclooctene)dicopper (I), X-ray study 0-65230

Cu complex, with triethanolamine, i.r. spectra and structure 0-64397

Cu(II) complex, dichloro (1.7,10,16-tetraoxa-4, 13-diazacyclooctadecane) copper II 0-67730

D₂Co(CN)₆, bond lengths, neutron diffraction study 0-68301

D₂O, study at 20°K in solid N₂ matrix 0-70911

F₃NO, study of electron-diffraction 0-77785

F₃SNF₃, electron diffr. obs. 0-65234

GaH₄, planar geometry indicated by NEMO calc. 0-46469

H bonded water, resonance stabilization 0-64412

H₂+, equilibrium bond length 0-61090

H₂+, ground state energies at various internuclear separations 0-58170

HCO² geometry of protonated CO species 0-64384

HDO, study at 20°K in solid N₂ matrix 0-70911

HF dimer, SCF MO LCGO studies of H bond 0-74258

HF₃-, bond lengths, LCAO MO SCF calc. 0-43106

H₂-NO, ab initio calc. of geometry 0-61088

H₃-O, study at 20°K in solid N₂ matrix 0-70911

HO polymers, MO calc. 0-53033

H₂-O₂ in on in perchloric acid crysts. 0-41195

(H₂-OH) of the properties of the policy of the policy in symmetric H bond 0-58168

0-38108
NF3, polar distortions 0-55318
NF3, harmonic freqs., potential function, Coriolis coupling consts., centrifugal stretching consts. 0-43128
NH4, inner shell correlation energy, invariance with geometry changes
0-43072

0-43072
N:H+ geometry of N: protonated species 0-64384
N:H+, theoretical predictions of structures 0-53044
(NO);, i.r. 0-58187
Ni complex, [Et₄N] [Ni(H:dma)], bond length data 0-53512
Ni complex, asymmetric 1,2-dimethyl-1,2- dicarbollide racemic, crystal struct. mol. config. 0-47198
Ni complex, bis-(3)-1,7-dicarbollylnickelate (III) dianion, crystal and molecular structure 0-43640
Ni complex, bis(4)-1,7-dicarbollylnickelate (III) dianion, crystal and molecular structure 0-43640
Ni complex, bis(4)-thutyl isocyanide) (tetracyanoethylene)nickel(0) 0-78490

0 - 78490

Ni complex, cyclopentadienyl Ni nitrosyl, bond lengths and angles from microwave spectra 0–49883 Ni complex, ethylenediaminetetraacetate Ni(II), struct. in aq. soln. from ¹³C and ¹⁷O n.m.r. 0–78309

and ¹⁷O n.m.r. 0–78309

Ni complex, pentacyanonickelate ion, structure Raman spectrum, CN stretching frequencies 0–46501

Ni(PCl)₃, symmetry of T_d point group confirmed by solid and liquid state spectrum. 0–64443

P, red i.r. and Raman spectra, structure 0–49886

P₃-I₄ normal coordinate analysis using F-G matrix method, P-P and P-I stretching freqs. 0–58195

PNCl₃, electron diffr. obs. 0–64446

PbCl₃, dissociation energy of ground state, from A-X band system study 0–46507

0 - 46507

0-46507

Pt complex, (histidine): i.r. spectra confirming trans structure 0-64447

ReF₈, electron diffr. exam. heavy atom corrections 0-70945

ReF₇, pland distortions 0-55318

S₈(AsF₆):, S₂²⁺ obs. 0-7838

SO₃, bond angle, interpretation using results of extended basis SCFMO calculation 0-67753

SO₃, and i.r. spectrum, obs. 0-43134

SbCl₃, Raman spectra, low frequencies, temp. changes 0-49888

Se-O bonds linear relationship between force constants and bond lengths 0-46513

0 - 46513

0-46513
SeO₂, equil. struct. parameters from microwave spectrum, 8000-36000
MHz 0-64453
Si₂BF₂, determ. by electron diffraction 0-67751
Si₂BF₂, electron diffr. obs. 0-64455
(SiF₃)₂O molecular structure determined by electron diffraction 0-53056
(SiH₃)₂CH₂ and (SiD₂)₂CH₂ 0-77845
SiH₃Ni(CH₃)₃ 0-77843
SnO₂ Sn₂O₃, Sn₃O₃, Sn₄O₄ 0-61138

Molecules continued

configuration and dimensions, inorganic continued SrF₂, apex angles from i.r. spectra shifts on isotopic substitution 0-77779

SrF2, in solid Kr matrix, from i.r. spectra and vibr. mode shift 0-54095

UF₆, force consts. calcs. 0–43138 VF₅ relation of features of Raman spectra and force constants to intramole-cular shifting of 3 fold symmetry axis 0–70871

PA 1970 - Part II (July-Dec.)

XeO₄, electron diffr. obs. 0–64460 Zn(II) complex, μ , μ' , μ'' , μ''' , oxo-hexakis(1,3-diphenyltriazenido) tetrazinc(II) molecular structure 0–55328

configuration and dimensions, macromolecules

configuration and dimensions, macromolecules amine-cured epoxy polymmer relation between network structure and dynamic mechanical properties 0—55945 copolymer (dAT), helix-coil transition determ, by light scatt. 0—54180 enzymes, and catalytic mechanics 0—46612 excluded volume effect on helix-to-coil transitions in n-stranded mols, 0—64564 haemoglobin, e.p.r., mag. susceptibility fluctuation 0—43199 light scattering, small-angle with molecules expansion allowance for dimensions determination 0—77972 mucopolysaccharides, heparin, chondroitins, structure and composition from p.m.r. 0—77978 network chain, analysis of acting forces, force Balance eqn, for tetrafunctional networks 0—58259 polarizability calc., elastic uniform fluctuating thread model 0—39465 polyarylenes-cyanoethenylenes mol. strict. rel. to optical props. and photo-

polyarylenes-cyanoethenylenes mol. strict. rel. to optical props. and photo-cond. 0–49949 poly-y-benzyl-L-glutamate, helix-coil transition press. depend., model 0–39473

polybutadienes, microstructure 0–55386 poly- ϵ -carbonbenzoxy-L-lysine, helix-coil transition press, depend., model 0–39473

0-394/3
polyethylene, melt rheological props., low-shear behaviour, molecular structure dependence 0-46853
polyethylene, mixed crystal i.r. study of chain segregation 0-58261
polyethylene melt viscosity, effect of molecular structure variables
0-46854

polyethylene terephthalate, reorientation, and deform, optical meas, on deform band 0-41110

polyethylenes, linear and branched, flow instability 0–53290 polyisobutylene, in decahydronaphthalene soln., shear depend of intrinsic viscosity and ion formation 0–58468

poly-L-lysine, helix-coil transition press, depend., model 0–39473 polymer, crystalline, melting, lattice theory 0–39870 polymer, reorientation, and deform., optical meas, on deform, band 0–41110

polymer, reorientation, and deform, refractive indices calc. 0–41109 polymers, effect of chain length and helical conformation on optical properties 0–74424

ttes 0—/4424 polypeptide chains, conformations 0—39466 polypeptide chains, conformation, chain folding, fibril struct. 0—61498 polysaccharides, conformation, chain folding, fibril struct. 0—47211 polytetrafluoroethylene, phase transitions 0—41244 polyvinyl fluoride, structure i.r. spectra 0—46623 polyvinylformal, steric struct., p.m.r. and i.r. spectra 0—67833 polywater structural model proposed 0—46867 statistical zigzag model for conformational characts, of optically active mols. 0—58257 stiff chains, particle scatt, factor, for wormlike and discrete chain models.

stiff chains, particle scatt. factor for wormlike and discrete chain models 0-58258

β-D-1,3-xylan, helical struct. 0-46614

configuration and dimensions, organic absolute determ. by anomalous scattering of X-rays from oxygen 0-61139

acetic and perdeuteroacetic anhydrides, conformation 0-53059

acetylene, linear and bent, trans and cis isomers found for most low-lying excited states 0–74324 alicyclic compounds, structure and conformation determination using intramolecular nuclear Overhauser effect 0–67758 alicyclic hydrocarbons, conformational anal. by MINDO/2 method 0–77915

0-77915
alkanes, consistent force field calc. 0-58608
alkanes, liquid, branching rel. to viscosity-pressure relationship 0-61504
alkyl chlorides, dependence of C-Cl stretching frequency on molecular
structure 0-77862
alkyltriphenylarsonium compounds, neighbouring group effect from i.r. and
u.v. spectra 0-64475
amildes, secondary, MO calc. of configuration 0-77864
aniline derivatives, ortho disubstituted, degree of nonplanarity of amino
group 0-55334
aromatic compounds, structure and conformation determination using
intramolecular nuclear Overhauser effect 0-67758
aromatic cpds., nuclear conformation correl. with fluoresc. and absorpt.
spectra 0-77868
aromatic cpds., structure and conformation determination using
intramolecular nuclear conformation correl. with fluoresc. and absorpt.
spectra 0-77868
aromatic cpds., strained, bridged 0-77869
aryliodonium and related compounds, u.v. and i.r. spectral study of symmetry 0-53061
azaporphyrines, distrib, of mol. oscillators 0-67767

metry 0-33061
azaporphyrines, distrib, of mol. oscillators 0-67767
azomethane, electron diffraction determ. 0-77870
benzenes, substituted, rotational constants of 1st singlet excited state, interpretation 0-55340
benzil, in various solid-state environments 0-64483

benzil, in various solid-state environments 0–64483 benzoporphyrins, azo-substituted 0–43151 benzothiacyclene derivatives, stereochemistry 0–46543 N-benzyl oxo-2 piperazines, magnetic inequivalence of protons and introduction of asymmetry in positions 3 or 6 0–70977 bicyclo [1.1.1.] pentane, struct, by electron diffr., vapour phase 0–53064 bicyclo [2.1.0] pentane, bond lengths, electron diffraction determ. 0–67774 bicyclo [2.2.2] octane system, conformation 0–64488 bicyclo [2.2.2] octane system, conformation products, structure and n.m.r. 0–64489 biphenyl, geometry in excited electronic states 0–59434 bis(trifluoromethyl) nitroxide, SCF cales, using INDO approximation 0–70979 5.5°-bis-isoxazole, non-bonded interaction and PPP cales. 0–49911 5.5°-bis-isoxazole, trans planar structure from i.r. and Raman spectra 0–49910 0-49910

2-bromoethanol, microwave spectral study 0-43155

configuration and dimensions, organic continued

bromovinylcyclopropanes, n.m.r. spectra, structure of isomers proposed 0-43152

bullvalene, oriented in liquid cryst. solvent 0-77882 cis-2-butene microwave spectrum, conformation 0-46546

cannabinoids, conformational anal. 0-77886

cellobiose, absolute determ, from anomalous X-ray scatt, 0-64495

2-chloroethanol, microwave spectral study 0-43155

2-chloroethyl radical conformation, unsymmetrical bridged structure 0-53066

3-chloropropene, cis and skew 0-77889

conjugated, molecules, N and O containing, bond lengths, LCAO SCF MO treatment 0-46565

copolymers, sequence distribution determ., methods 0-71055

copolymers, sequence distribution determ., methods 0—71055 corannulene, phosphorescent in first triplet state 0—46551 cyclobutane, puckering structure, ir. spectra 0—49914 cyclobutane, struct. determ. from proton n.m.r. in nematic solvent 0—39420 cyclohexane derivatives, absolute configs. 0—78514 cyclohexanels and derivatives, conformational effects on ¹³C carbinyl carbon shielding 0—39432 cyclohexyl iodide, conformational isomerism, i.r. spectra 0—55347 cyclohexyl iodide, conformational isomerism, i.r. spectra 0—55347

caroon shieding 0—39432 cyclohexyl iodide, conformational isomerism, i.r. spectra 0—55347 cyclopentane, structure, equilibrium conformation, pseudorotation, electron diffraction determ. 0—77890 cyclopentanol, out-of-phase ring deforms. 0—67785 cyclopentene, bond lengths and angles electron diffraction 0—49916 cyclopentylamine, out-of-phase ring deforms. 0—67785 cyclopropyl-allyl ring opening modes, mechanism 0—49917 dibenzhiepin derivatives, assignments of configuration by nuclear Overhauser effects 0—43156 closo-2, 3-dicarbahexaborane (6), skeletal molecular structure from microwave spectra 0—64500 2.6-dichlorobenzylfluoride, long-range spin-spin coupling consts. conformational depend. 0—39423 4.4'-dichlorobiphenyl, configuration in cryst, and soln. 0—79324 1.4-bis(dicyanomethylene)cyclohexane, and crystal structure 0—40112 dicyclopentadienylnickel 0—61158 cisoid-dienes, effect on proton coupling constants, n.m.r. spectra 0—70987 4-diethylcarbamoyl-1-cyclohexene-5-carboxylic acid, solid-state conformation 0—78516 N. difluoroboryl disilazane, e diffr. determ. 0—64507 dihaloacetyl chlorides, rotational isomerism, i.r. and Raman spectra/0—74363 2.3-dihydrofuran, skeleton struct, study from vibr. spectra 0—64534

0-74363

2,3-dihydrofuran, skeleton struct, study from vibr, spectra 0-64534

1,2-dihydronaphthalene, effect on proton coupling constants, n.m.r. spectra 0-70987
dihydrothymine cryst. p-irrad., e.p.r. study of radical form. 0-77970
dimethylacetylene, symmetry from i.r. and Raman spectra 0-49920
dimethylsulphoninime, by e diffr. at gas 0-64520
diphenyl-1,2-pentanedione-1,4-n.m., spectra and conformation 0-77900

2,3-diphenylpropanoic acids and esters, diastereomeric 3-substituted, configuration assignment from n.m.r. data 0-67813
dye, aggregates, quantum-mech. calc. 0-58159
enantiomorphism rel. to H* diffusion in cryst. on pulsed photolysis 0-48202

0-48202

enantiomorphism rel. to H* diffusion in cryst. on pulsed photolysis 0–48202 epihalohydrins, structural correlations of coupling constants 0–64503 epoxides, isomerisation in bicyclic heptic series, in the presence of zinc bromide 0–70995 esters and diesters, conformational anal. by u.s. relaxation 0–74364 ethylene, geometric approx. to two-particle Green function 0–58220 ethylene copolymers, n.m.r. study of structure 0–46621 fluorobenzene, first excited state π*-π, dipole moment correlation with structure 0–46561 furan, bond angles by minimizing molecular energies 0–55353 germylcyclopentane 0–58222 glycine, i.r. spectra study 0–74372 glycoxal, torsional vibration effect on molecular structure 0–70847 glyoxylic acid, symmetry and conform. 0–61164 H·C= group containing, HCH angle correlation with CH₂ stretch freqs. separation 0–46527 heavy-atom analysis, automatic 0–50558 heptafulvalene, molecular symmetry groups for cations and anions 0–64510

0 - 64510

N heterocyclic compounds, X-ray diffraction study 0-40113 heterocyclic cpds., ring inversion 0-74373 hexafluoroacetone, gaseous, electron diffraction structure determination

0–61165 hexafluoroazomethane, electron diffraction determ. 0–77870

hexafluoroisobutene, gaseous, electron diffraction structure determination 0-61165

hexafluoropropylimine, gaseous, electron diffraction structure determination 0-61165

tion 0–61165 hydrocarbons, conjugated, using LCAO SCF MO method 0–46564 hydrocarbons, saturated isomerization energies calc., shape functions method applic. 0–55280 hydrocarbons, simple, equilibrium bond lengths and angles, NDDO and CNDO productons 0–49928 imidazole, bond angles by minimizing molecular energies 0–55353 isohalfordin structure from n.m.r. solvent shift in methoxyl groups 0–49930

0 - 49930

0-49900 (2.3' isopropylidene- 3.5' cycloguanosine, nuclear Overhauser effect and molecular geometry 0-7854 ketones, cyclic, angular strain influence on carbonyl stretching vibration 0-53074

0-3074
lactic acid derivatives 0-65303
lithium naphthalenide anion, e.s.r. study 0-39433
macromolecules, branched Gauss chains, size of whole and branch from X-ray scattering analysis 0-64562
membrane, biological cell, molecular adlineation, charge-fluctuation forces 0-58448

metalloporphyrins, ring geometry effects on triplet and singlet energies $0\!-\!74382$

0–74382 methane ion, CH₄*, open shell CNDO/2 calcs. 0–71008 methane ion, CH₅*, near Hartree-Fock calculations for different geometries equilibrium bond lengths and angles 0–43173 methane ions, CH₅* and CH₇s, STO calculations, electron pair interpretation of stabilities of structure 0–58232

Molecules continued configuration and dimensions, organic continued

configuration and uninessons, organic continued α -methoxyphenylacetic acid, alkali acid salt complexes, structure studies, i.r. spectra 0-46578 methyl acetylene, mol. consts. from anal. of vibr.-rot. bands 0-71020

metryl acetylene, mol. consts. from anal. of vibr-rot. bands 0–/1020 methyl and other radicals, rel. to electronegativity 0–39434 methyl silyl ether, e diffr. determ. 0–64518 3-methyl-4- bromo-5-carboxamide-pyrazole, hydrogen bonding system 0–78519

3-methyl-4- bromo-5-carboxamide pyrazole, hydrogen bonding system 0–78519 methyl- bromodiazirine 0–67804 methylcyclopentane, out-of-phase ring deforms. 0–67785 trans-methyldimide, consistent with rot. consts. 0–74387 methylene, nonlinearity of triplet ground state 0–77920 methylene fluoride, microwave spectrum, centrifugal distortion and molecular structure 0–46577 methylene-ground state 0–77920 methylene-ground state 0–77920 methylene-ground state 0–77920 methylene-ground state 0–73077 methylene-ground state 0–73077 mirror equality in entiomorphism 0–48202 monocarboxylic cyclobutane acid, dimer forms and config. 0–74388 monomethin cyanine dye, stearyl substituted and long chain hydrocarbon, 1:1 mixture, Scheibe aggregate formation 0–64499 narcissidine, struct. 0–53523 nitrophenylhydrazone α-carbonyls, n.m.r. study 0–71024 nitrotehane, model calculated from microwave spectral features 0–77938 nitrophenylhydrazone α-carbonyls, n.m.r. study 0–71024 nitroxide radicals, fluoro-substituted, angular dependence of β-fluorine e.s.r. hyperfine coupling 0–55367 optically active origin and development on primordial Earth 0–41476 oxalyl chloride 0–58234 oxazole, bond angles by minimizing molecular energies 0–55353 2-oxazoline, skeleton struct. study from vibr. spectra 0–64534 pentafulvalene, molecular symmetry groups for cations and anions 0–64510 perchorol4|radialene 0–77943 perfluorocyclobutanone ketyl, angular dependence of β-fluorine splitting 0–55366 phenol, in vapour, liq. and solid 0–39443 4-ohenyl. 3-oxy. 1,2-benzofluorenone, in polar and non-polar solvents.

pendiotocycloutatione ketyl, angular dependence of p-huorine splitting 0–55366 phenol, in vapour, liq. and solid 0–39443 4-phenyl, 3-oxy. 1,2-benzofluorenone, in polar and non-polar solvents, structure from electronic absorption spectra 0–67814 phenyl derivatives of group Vb elements in solid state 0–76117 4-phenylazo-1 naphthols 0–64537 phenylphosphine d., C.P-D angle, liq. cryst. soln. 0–53082 phosphine, H-P-H angle, liq. cryst. soln. 0–53082 phosphine, H-P-H bond angle, liq. cryst. soln. 0–53082 photorearrangement products of phenethylamine derivatives, phase determination, X-ray diffir. 0–66202 piperazines, n.m.r. spectral parameters and ring interconversion 0–74401 polyamides, structural transitions, i.r. spectroscopic studies 0–67835 polyvinyl chloride, struct. of branching, new macromol. model 0–64560 polyvinylidenefluoride, conformation rel. to polymerization conditions 0–71439 1-pyrazoline, out-of-phase ring deforms. 0–67785

0–71439

1-pyrazoline, out-of-phase ring deforms. 0–67785

1-pyrazoline 0–58240

pyrrole, bond angles by minimizing molecular energies 0–55353

pyrrolid-2-ones, optically active crysts. 0–75116

pyrrolidine, out-of-phase ring deforms. 0–67785

rotation about single bonds, chemical reactivity 0–43142

selenacyclopentane, symmetry and ring skeleton struct, from vibr. spectra anal. 0–64544

self-consistent conformational analysis of conjugated and aromatic mols. with steric hindrance 0–58201

sparteine and stereoisomers, monocation struct, from i.r. spectra 0–64545

steric compression effect on proton-proton and spin-spin coupling consts. 0–74318

structure study by dielectric relax, times in liquid state 0–53366

0—74318 structure study by dielectric relax, times in liquid state 0—53366 succinimide, struct, initial component study leg infrared meas. 0—58243 sulphonylamines, halogen-substituted struct. 0—53085 1.2,3.4-tetrachloro-5.6-diphenylcalicene, struct. 0—55867 tetramethylammonium bichloride, linear bichloride ion config. 0—78522

2-p-toluidinyl-0-77955 6-naphthalenesulphonate, rel. to fluorescence props 0—77955
triafulvalene, molecular symmetry groups for cations and anions 0—64510
1,11-trifluoroazomethane, electron diffraction determ. 0—77870
trifluoromethylarsenic tetramer 0—78523
trimethyl phosphine borane, from microwave spectrum 0—71042
trimethyl phosphine-(pentahaptocyclopentadienyl)copper(1), crystal and molecular structure 0—61929
vinyltrifluorosilane 0—77952
CH₄*ion 0—55359
CH₂NO radical, geometry from MO calc. 0—77911
Cd[H₄]O₆].6H₂O₇ by X-ray diffr. methods 0—61879
Fe allyl complexes, from n.m.r. spectra 0—67760
Mg(OH₂)₆.H₃O₆, by X-ray diffr. methods 0—61879
Ru allyl complexes, from n.m.r. spectra 0—67760
dissociation

dissociation

dissociation

see also Heat of dissociation
cross section for slow collision in emitted state 0–53091
cyanic acid, photodissociation in vacuum u.v., NCO A²Σ and NH(A³πc³)
production 0–74419
cyclohexane, excited, photon irradiated 0–79457
diatomic, predissociation 0–77961
diatomic, predissociation 0–77961
diatomic, two-photon dissoc. 0–49943
diatomic gas, vibration vibration coupling 0–77960
ethanothiol, photodissociation, energy disposal 0–48203
gases, 5-45 keV He atom induced 0–43342
halogens, photodissoc. translational spectroscopy 0–77963
hydrocarbon ions, collisional dissoc. 0–74415
hydrocarbon molecules, doubly ionized, auger spectra rel. to dissociation
0–77926
in recombination rate, temp. dependence 0–78162

in recombination rate, temp. dependence 0–78162 ion recombination, temp. dependence 0–78161 methane, bromine substituted, doubly ionized, auger spectra rel. to dissociation 0–77926

methane, photodissociation 0–53092 methane, photodissociation at 1236 Å 0–77969 photodissociation, dynamics 0–43191 photodissociation, two-photon diatomic heteronuclear, green function

photodissociation in reactive gas, wave propagation 0-76278

dissociation continued

polyatomic, predissociation 0-77961
predissociation, isotope effects 0-77962
predissociation in elec. field 0-43190
predissociation in induced by mag. field 0-39452
predissociation linewidths from scattering theory 0-43187
recombination rate, dissociative, temp. depend. 0-53090
transition entropy for diat. mols. 0-64555
two-photon dissoc. of diatomic mols. 0-49943
unimolecular reactions, vibrational relaxation and dissociation 0-46607
by van der Waals interaction, fluorescence quenching cross-section theory 0-64556
BCI., by CO₂ laser radiation 0-39664

BCl₃, by CO₂ laser radiation 0-39664 BCl₃, vibrational spectra, recombination radiation, CO₂ laser excited 0-46604

0–46604
Br, electronic energy transfer by $O_2^{-1}\Sigma_g^{+}$, $1\Delta_g^{-}$ 0–58161
Br₃ study by two photon spectroscopy 0–61183
CD, predissociation in $C^{-2}\Sigma^{+}$ state 0–71045
CH, predissociation in $C^{-2}\Sigma^{+}$ state 0–71045
CH, predissociation or $C^{-2}\Sigma^{+}$ state 0–71045
CN molecules, decomposition reaction chain following shock wave 0–48182
CO, production of O_2^{-} and C_2^{-} by dissociative attachment of electrons

0-4882
CO, production of O⁻ and C⁻ by dissociative attachment of electrons 0-74605
CO⁺, by collisions with He, velocity distributions of fragments 0-77967
CO₂, and adsorption on Ti film 0-43572
CO₃, elec. dissoc. 0-58254
CO₂ dissociative electron attachment cross-sections, 300° to 1000°K

0-64559

CO₂, elec. dissoc. 0–58254
CO₃, elec. dissociative electron attachment cross-sections, 300° to 1000°K
0–64559
CO₂ kinetics of dissociation processes 0–71046
CO²⁺, metastable dissociation 0–55381
Cl₃=Cl₄-Cl₄-Cl₄, high- and low-temperature data, comparison 0–79431
D₂, metastable 2⁵S_{1/2} production, measurement 0–77965
D₃, predissociation in elec. field 0–43190
H₃, discrete absorption and photodissociation 0–46608
H₄, predissociation in elec. field 0–43190
H₅, atte at hot W surface 0–67826
H₇ obs. in discharges 0–43188
H₇ photodissoc, near threshold energies 0–39455
H₇, dissociation and ionization by electron impact 0–43113
H₇+, dissociation and ionization by electron impact 0–43114
H₇+, diving collisions with He and Ar 0–74417
H₇+ vibrational, angular distribution of protons 0–43189
(HeH)⁺, nons, to proton and neutral helium atom 0–71048
L₈, study by two photon spectroscopy 0–61183
ICN, photodissociation, quasidiatomic model 0–43191
ICN dynamics of dissociation, quasidiatomic model 0–43191
ICN dynamics of dissociation following direct photon absorption using theory of scattering by 2 potentials 0–58255
N₇, overall recombination and dissociation rate coefficients, phase space theory calculation 0–76259
N₇, simultaneous ionization and dissociation rate coefficients, phase space theory calculation with He, velocity vector distributions 0–46603
N₇-dissociative electron attachment cross-sections 0–64558
N₇-dissociative electron attachment cross-sections 0–64588
N₇-dissociative electron attachment cross-sections 0–64558
N₇-ton, collision with He, velocity vector distributions 0 fragments 0–77967
N₇-ton, collision with He, velocity vector distributions 0–46603
N₇-0-70-100, collision with He, velocity vector distributions 0–76658
N₇-0-100, collision with He, velocity vector distributions 0–46603
N₇-0-100, collision with He, velocity vector distributions 0–46603
N₇-0-100, collision with He, velocity vector distributions 0–46603
O₇-0-100, collision with H

O dissociative electron attachment cross-sections, 300° to 1000°K 0-64559

O₂ predissociation lifetimes of $B^3\Sigma_u$ -state, determ. 0–77830 O₂+, collision-induced at low kinetic energies, effects of internal ionic excita-

tion 0–67827 O.3+, collision-induced reactions at low kinetic energies 0–77966 O.3+, by collisions with He, velocity distributions of fragments 0–77967 O.3+, ion, collision with He, velocity vector distributions 0–46603 OH $A^3\Sigma^+$ state, radiative and predissociation probabilities 0–61129 SD, probable predissociation between V!=0 and 1 0–74306 SH, probable predissociation between V!=0 and 1 0–74306 W- halogen lamps, dissoc. and reaction phenomena 0–54928

dissociation energies
alkaline-earth chlorides, mass spectrometric studies 0-46449
diatomic, from vibrational spacings of higher levels and long-range potential 0-39453

estimation method, and application to correlation of core-electron binding energies from X-ray photoelectron spectra 0-77959 inert gas mols. and ions, diatomic 0-43082 intra-bond interference energy correlation 0-43186 rare-earth monoselenides, gaseous, mass spectrometric determ. 0-61180 rare-earth monoselenides, gaseous, mass spectrometric determ. 0-61180

rare-earth monosclendes, gaseous, mass spectrometric determ. 0–61180 rare-earth monosclendes, gaseous, mass spectrometric determ. 0–61180 transition metal borides, mass spectrometric determ. 0–61181 transition metal silicides, mass spectrometric determ. 0–61181 AgGa, expt. determ. 0–73923

Ar., ground state 0–67714

AuBe, bond strength 0–70874

CeB 0–61185

F. 0–61182

H. binding energy using integral Hellmann Feynman formula 0, 30454

17. 0–01102. Ht, binding energy using integral Hellmann-Feynman formula 0–39454 Ht, using long-range forces 0–64557 HBr $^+$, of A $^2\Sigma^+$ and X $^2\Pi$, states, from predissociation data of A $^2\Sigma^+$ state 0–71047

0-71047

1, ground state, and spectroscopic reassignment 0-53039

LiH, binding energy using integral Hellmann-Feynman formula 0-39454

NS and NS 0-39456

NS on NS 0-39456

NO, gas, from condensed Na O 0-77968

NO, of ground state 0-74292

SiCN, by mass spectroscopy 0-66177

TiN 0-46605

UB; and UB 0-61185

Molecules continued dissociation energies continued YC2 and YC4 0-53406

electronic structure see also Bonds

3d orbitals, minimum Gaussian lobe representation 0-70831 π electron systems, spin-extended SCF calcs., technique 0-42922

 π -electron systems, stability conditions of Hartree-Fock solns. 0-60891 π-electrons, rapid convergence in open-shell SCF calcs. 0-53007

all valence electron, configuration interaction, self-consistent field study, parameter selection 0-39353

antibonding mol. orbitals, kinetic and pot. energy 0–46431 atomic and bond charges, calc. from electronegativity 0–64311 benzenes, substituted, excited state, and props. 0–64482 binding energies for inner-shell electrons, theory 0–64364 book 0–58610

book 0–58610
book on orbitals and symmetry for undergraduates 0–60890
Born-Oppenheimer method, new method of transforming Hamiltonian to body-fixed coordinates 0–58138
bound state energies for molecular interactions 0–79427
bound-state calc, of electron scatt, resonance energies 0–42997
complex molecules as harmonic oscillators with damping 0–61053
complex molecules as harmonic oscillators with damping 0–61053
complex molecules as harmonic oscillators with damping 0–61053
complexes, classification of electronic transitions on basis of crystal field and M.O. theory 0–53319
corre-level binding energy shifts, compared with theory 0–39354
correlation function approach to radiationless transitions 0–74205
correlation of electron relaxation and molec, vibrations 0–39361
coupled systems with loosely connected fragments, transition energies, oscillator forces 0–53009
density matrices from one-centre wavefunctions 0–64353
diatomic, neutral, Thomas-Fermi equations, variational principle 0–43038
diatomic, used to determ, temp. of a gas 0–60089

0-430.8 diatomic, used to determ, temp. of a gas 0-60089 diatomic ion, one-dimensional model solution, mol. orbital calc. 0-49845 diatomic molecule, effect of breakdown of Born-Oppenheimer approximation on determ. of B_e and ω_e 0-70859 diatomic molecules, new calc. method 0-53028 diatomic simplified method for evaluating potential energy curves 0-67705

dimensions of excited states computed by intermol, pot, and matrix shifts $0\!-\!71064$ dissolved molecules observed under different crystallization conditions $0\!-\!64319$

0–64319
electron deficient molecules, maximum overlap MOs 0–77762
electron diffr. exam. 0–74116
electron population calc. in large mols. 0–64363
electron spectroscopy determ. 0–55276
electron-energy formula, relativistic corrections 0–39350
electronic energy transfer, multi-author book 0–58139
electronic wavefunctions of linear molecules, correlation coefficients 0–42933
energy levels, using electron expectages and control of the control

energy levels, using electron spectrometer, excitation cross sections $0\!-\!58157$

excited states, variational principle, exact formulation 0–58077 excited states of neutral molec, fragments, from appearance potentials 0–53011

0–53011
excited-state variational calc, with orthogonality constraint 0–58152
fluorinated methane, carbon 1s electrons, ionisation potential, chemical substitution depend. 0–39435
Franck-Condon principle, extension to nuclear spins 0–58133
Gaussian-type functions for polyatomic systems 0–58149
HF energies, second order, upper bounds for calculation 0–39356
Hamiltonian matrix elements from symmetric wave function 0–77734
Hartree-Fock orbitals, derivation of necessary conditions 0–58080
Hartree-Fock theory, virtual orbitals 0–49748
Hill-Van Vleck eqn. for diatomic mols, with spin-orbital coupling, particular solns. 0–49842
integral transform function for calc, for atomic and molecular calcular calcular integral transform function for calc, for atomic and molecular calcular calcular integral transform function for calc, for atomic and molecular calcular calc

integral transform function for calc. for atomic and molecular calc 0-74102

interaction parameters, correlation effects 0-49847 intermolecular interactions effects, vibrational spectral intensities obs.

inversion, natural system in discharges, broadband gain 0–39339 isoelectronic mols., first- and second-order physical props. 0–64351 K-shell electron binding energy chemical shifts, interpretation 0–39357 least-energy minimal atomic orbitals 0–61058 level dependence on rotational effects on spin-orbit coupling in diatomics 0–49843

linear Raman scattering, role of intermediate electronic states 0–43043 MC SCF wavefunctions, expectation values of one-electron operators, error 0–42918

macromolecule, polarizability calc., elastic uniform fluctuating thread model 0–39465
maser quantum mechanical model, exact analysis 0–42244
method of moments for determ. of molec. props. 0–61059
model, continuous charged spheres 0–39355
model, description, use in dielect props. of line multi-component syst.

model description, use in dielec. props. of liq. multi-component syst. 0 - 49834

Morse function adjustment to represent electronic state accurately 0-46413

nonradiative decay of large mols., multiphonon processes 0–53010 octahedral hybrid orbitals, d²sp³ shape 0–67697 open-shell, photoelectron spectra, band intensities 0–77735 orbital interpretation of low energy satellite lines in X-ray emission spectra

0-56573 orbital theory, neighbour atom effects calc.

orbitals, approx., energy localization 0—39349 orbitals, orthogonalized best hybrid, according to maximum overlap principle 0—43065 oscillator strength, MO formulations in one dimension using double well potentials 0—43052

oscillator strengths, reasons for failure of π electron M.O. methods 0-46566

parameter selection for all valence electron, configuration interaction, self-consistent field study 0–39353 photoelectron spectra, number of bands observed, relation to number of occupied energy levels 0–64322

electronic structure continued

polyatomic, inner shell correlation energy, invariance with geometry changes 0-43072

prolate asymmetric ton molecules, band contours in electronic spectra

radiationless processes, role of mol. stationary states 0-77738

radical, alternant, split-orbital method 0-64554

rate consts. of processes involving lowest triplet state at low temp. 0-58158

relativistic effects in diatomic mols., evaluation of one-electron integrals 0-64352

resonance charge exchange, diatomic molecule and molecular ion 0-74441

or-vibronic states of linear mols., symmetry classification 0–67703 SCF LCAO MO theory, approx., INDO scheme realization on LOAO basis 0–43064

SCF π electron theory, optimum parametrization 0-46439 Slater-type atomic orbitals in calc. of first- and second-order props. 0-58153

spin-orbit coupling, rel. to photochemical decomposition 0-43070 steepest-descent method for energy-level densities, extension to higher orders 0-46434 symmetric tops, rotational ΔK =3 transitions 0-64346

symmetry-adapted wave functions, dual-space-operator technique, for mols, with Abelian symmetry group 0—70842 vibronically induced electronic transitions, theoretical band shapes 0—58141

wave function zero in some region of space, justification 0–70841 wavefunctions calc, for excited states of polyatomic mols. 0–58150 wavefunctions containing first- and second-row atoms, simple basis set 0–58151

V-ray diffraction method of determ. electron population parameters 0-46440

HF-Ne, many-body perturbation theory based on united atom model 0-61092

0-61092
H.S ground and excited states 0-46472
many-body perturbation theory based on united atom model 0-61092
Pr(III) complexes, interelectronic repulsion, spin-orbit interaction and bonding 0-43132

electronic structure, inorganic alkali hydrides, modified form of Rittner's potential function 0-53017 antibonding mol. orbitals, kinetic and pot. energy 0-46431 AsH₃, exact minimum Slater basic sets yielding LCAO MO SCF wavefunc-tions 0-46469

tions 0–46469 carboranes, CNDO/2 calc. 0–74246 DFIBr¹, DFIBr¹ rotational analysis of 0-0, 0-1, 0-2, 0-3 bands 0–58200 group IV tetrahalides, ionization potential rel. to MO description of electron structure 0–64369 halides, groups III, IV, V and VI, orbital structure interpretation of photoelectron spectra 0–64368 inert gas mols, and ions, diatomic, potential curves 0–43082 phosphites, i.r. and Raman spectra, electronic structure 0–70906 propyine, elec. polarizability anisotropies from microwave spectroscopy 0–70923

second-row-element mols., self-consistent-field electron distributions -53014

second-row-element mols., self-consistent-field electron distributions 0–53014 transition metal ion complexes, spin-orbit coupling and Slater parameters, covalency effect 0–70956 triatomic systems of first-row elements, electron relax. and molec. vibr. 0–39361 AlO, A²Σ-X²Σ system, oscillator strength determ. 0–74234 Ar-N gas mixture, thermal equilibrium calc. at 1 atmos. and between 5000-3500°K 0–53269 Ar₃. P₃ metastable state, collision induced emission in vac. u.v. 0–58176 As₃ configuration of excited states, rotational analysis 0–43083 AsF band systems obs. in microwave discharge 0–77766 B cpds., X-ray diffr. studies 0–40063 B; calc. of Σ_ω state 0–64379 BH, wavefunctions using SOGI method 0–39366 BH₃, BH-F, BHF₃ and BF₃, ab initio studies 0–53018 B-H₄, comparison of electronic structure with ethylene 0–77904 B-H₆, electron deficient molecule, maximum overlap MOs 0–77762 B₃H₁₁ in n.m.r., anomalous hydrogen 0–777767 BN free radical, ground state obs. in rare gas matrix 0–46451 BaF, Franck-Condon factors for A-X, B-X and D'-X bands, intensity 0–70878 B-H-1, LCAO-MO-SCF clac. using Gaussian basis functions 0–61075

BeH-, LCAO-MO-SCF clac. using Gaussian basis functions 0–61075 BeH₂, ground state valence-bond calcs. 0–74240 Bi₂, 3 new band systems revealed by emission spectrum of vapour

Berti, ground state valence-bond cales. 0-14240 Bis, 3 new band systems revealed by emission spectrum of vapour 0-14242 BiCl molecule, A'-X band system obs. and classification modified 0-74241

0–74241
Bry Morse function adjustment, P.E. curve for B³Π⁺_{cut} state 0–46413
CF B-X, band system studied, potential curves discussed 0–46458
CH, LCAO-MO-SCF calc. 0–61077
CN electron configuration of electronic states 0–43085
CN Morse function adjustment, P.E. curve for A²Π_{3/2} state 0–46413
CN⁻ ion, LCAO-MO-SCF calc. with double-zeta basis set of Slater functions 0–77775

CO, radiative lifetime of $b^3\Sigma^+$ state 0-67727 CO, vibrational energy levels determ. in CO-He laser 0-74247

CO ground state, improved molecular constants determ, using laser data 0-74248

0—12.48
CO hydrocarbons, molecular orbital interpretation of X-ray emission spectra 0—46567
CO₂ and CO₃₊ calc. method 0—53073
CO₂ e diffr. exam. 0—74116
CO₂ hydrocarbons, molecular orbital interpretation of X-ray emission spectra 0—46567

tra 0–46567 (C_4O_4)²⁻, calc. by two MO methods 0–67722 (C_4O_4)²⁻ ion by improved LCAO method 0–58163 (C_5O_2)²⁻, calc. by two MO methods 0–67722 (C_5O_2)²⁻ ion by improved LCAO method 0–58163 (C_6O_6)²⁻, calc. by two MO methods 0–67722 (C_6O_6)²⁻ ion by improved LCAO method 0–58163 (C_6O_6)²⁻, ion by improved LCAO method 0–58163 (C_6O_6)²⁻, polarizability anisotropies from microwave spectroscopy 0–70923

Molecules continued

electronic structure, inorganic continued

CP, potential energy curves constructed by Rydberg-Klein-Rees method 0–67736

CaO, electronic struct, and low-lying triplet states 0-43094 Cl₂, high precision valence bond potential curve 0-39372

CaV, electronic struct, and low-lying triplet states 0–43094
Cls, high precision valence bond potential curve 0–39372
Cls, new calc, method 0–53028
ClNs, from microwave spectra 0–70892
Co complex, bis(dithioacetylacetonato)Co(II) planar molecule 0–39375
Co complex, bis(dithioacetylacetonato)Co(II) 0–68300
CrF6, construction of molecular orbitals, transition energies 0–53023
CrO6-construction of molecular orbitals, transition energies 0–53023
CrO6, construction of molecular orbitals, transition, energy level ordering and population 0–64396
Cu(II) dialkylselenocarbamate 0–41323
D-, autoionization and predissociation, vibrationally induced, by perturbed-stationary-state theory 0–39379
DBr electronic spectrum and structure of b ³II_I and C ¹II states 0–46475
DCl b ³II_I and C ¹II states from absorption spectra 0–39377
DI, analyses of ¹B ²+X and C +X transitions 0–46476
F-, new calc. method 0–53028
F-CS, ³A state 0–77772
F-, S, molecule, ¹A₃-1³A, transition, spectra analyzed 0–74255
Fe complex, Fe(II) phthalocyanine, paramagnetic anisotropy study 0–64399
Fe complex, monochloro-bis(diethyldithiocarbamato)Fe(III), ligand field

0-64399 Fe complex, monochloro-bis(diethyldithiocarbamato)Fe(III), ligand field models 0-64401 Fe(III) complex with 2,2'-bipiridyl and 1,10-phenanthroline, σ , π delocalization 0-58166 GaF, exact minimum Slater basic sets yielding LCAO MO SCF wavefunctions 0-46469

tions 0–46469
GaH₃, exact minimum Slater basic sets yielding LCAO MO SCF wavefunctions 0–46469
GeBr band system for A²Σ-X²Π transition, vibrational analysis 0–49868
GeH₄, exact minimum Slater basic sets yielding LCAO MO SCF wavefunctions 0–46469
H₃, autoionization and predissociation, vibrationally induced, by perturbed-stationary-state theory 0–39379
H₃, calc. using ellipsoidal Gaussian wavefunctions 0–61087
H₃, diabatic coupling processes in highly excited states, general formalism 0–39378

0-39.78
H₂, Lyman and Werner systems, isotope effects 0-64407
H₂, many-body perturbation theory 0-58173
H₃, quantum defect theory of 1 uncoupling, channel-interaction treatment 0-64411

0–64411 H₂, radiative lifetimes for $2p\pi^3\Pi_{\mu}$ 0–77793 H₃, SCF-MO-CI calc. using Gaussian basis sets 0–53036 H₃ ground and first excited state, DCSCF energies and orbitals 0–70907 h₂+, one-centre Slater orbitals, modification 0–39381 H₃+, prediction of discrete transition $2p\pi_{\mu}$ 3d σ_{π} 0–77791 H₃+ δ function model changes 0–74263 H₃+ ground state energy, equilibrium distances and vibration frequencies 0–74259

0=14259 H₂+ ground state energy calc. using Laplace transform-type wave function 0=70905

H₂+ ground state energy calc. using Laplace transform-type wave function 0−70905
H₂+, calc. using ellipsoidal Gaussian wavefunctions 0−61087
H₃+, integral transform Gaussian wavefunctions 0−64405
H₃+, SCF-MO-CI calc. using Gaussian basis sets 0−53036
H₃+ ground state, single-centre configuration-interaction calcs. 0−74265
H₃2+, integral transform Gaussian wavefunctions 0−64405
H₃2+, integral transform Gaussian wavefunctions 0−64405
H₄2+, integral transform Gaussian wavefunctions 0−64405
HCN, calc. method 0−53073
HCI b³H₁ and C³H states from absorption spectra 0−39377
HCI ground state SCF wave functions and molecular properties 0−77842
HD, autoionization and predissociation, vibrationally induced, by perturbed-stationary-state theory 0−39379
HF, bond behaviour in elec. field 0−61093
HF dimer, orbital calculations 0−43105
HF₂-, LCAO MO SCF study 0−43106
HH₃-, LCAO MO SCF study 0−43106
HN₃- orbitals from which electrons ejected in photoelectron spectra identification 0−64409
HNCS orbitals from which electrons ejected in photoelectron spectra identification 0−64409
HNCS orbitals from which electrons ejected in photoelectron spectra identification 0−64409
HNCS orbitals from which electrons ejected in photoelectron spectra identification 0−64409
HNCS orbitals from which electrons ejected in photoelectron spectra identification 0−64409
HNF, absorpt. spectrum of A²A'-X̄²A' system 0−77796
HNF, absorpt. spectrum of A²A'-X̄²A' system 0−77796

HNCS orbitals from which electrons ejected in photoelectron spectra identification 0–64409
HNF, absorpt, spectrum of \$\bar{A}^2A'.\bar{X}^2A''\$ system 0–77796
H-NO, hyperfine splittings, ab initio calc. 0–61088
H-O.H*-Li- syst, bond behaviour in elec. field 0–64414
H-O-HF dimer, orbital calcs. 0–43105
H-O, lowest singlet and triplet potential surfaces 0–70904
H-O, minimum basis wavefunctions 0–64182
H-O, proton magnetic shielding consts. 0–58171
H-O, spin-generalized SCF wavefunctions using GF method 0–67732
H-O, strongly orthogonal geminals, transferability to H-O; 0–43107
H-O, variational-perturbation calc. of ground-state energy 0–43101
H-O bond behaviour in elec. field 0–64414
H-O one-electron props. experimental data and ab initio calc. 0–74260
H-O polymers, MO calc. 0–53033
H-O structure, simplified model 0–64856
H-O-S, strongly orthogonal geminals, transferability to H-O 0–43107
H₃O⁺ bond behaviour in elec. field 0–64414
H₃PO₃, it., and Raman spectra, electronic structure 0–70906
H-S, 3 vibrationally resolved bands from photoelectric spectrum 0–53031
H-S, vibr. fine struct. from photoelec. spectra 0–61121
H-S ground state SCF wave functions and molecular properties 0–77842
H-SS, ground state SCF wave functions and molecular properties 0–77842
H-SN, exact minimum Slater basic sets yielding LCAO MO SCF wavefunctions 0–46469
He, N gas mixture, thermal equilibrium calc. at 1 atmos and between

tions 0–46469
Hd, Lyman system 0–53034
He-N gas mixture, thermal equilibrium calc. at 1 atmos, and between 5000-35000°K 0–53269
HeF₂, LCAO MO SCF study 0–43106
HeFF⁴; antibonding mol. orbitals, kinetic and pot. energy 0–46431

1999HgD magnetic hyperfine structure obs. 0–77802

1991gT magnetic hyperfine structure obs. 0–77802

1, from u.v. spectrum in vacuum 0–46480

electronic structure, inorganic continued

I2 spectroscopic reassignments 0-53039

 ${\rm trBre}^{2-}$, electronic transitions assignment from magnetic circular dichroism and absorption spectra 0-74276

and absorption spectra 0–74276

K₃, radiative lifetime of B¹H_u state 0–74277

KCl, SCF calc. on molec. props. 0–58180

LaO, potential energy curves constructed by Rydberg-Klein-Rees method 0–67736

Li-NH₃ complexes, ab initio SCF MO calc. 0–43120

Li₅ bond behaviour in elec. field 0–64414

LiBr, SCF calc. on molec. props. 0–58180

Li+, hyperfine coupling constants for Na and H for various bond lengths 0–49854

LiH(X¹Z⁺), pot. energy curve and mol. consts., calc. 0–49876

MgH, theoretical calc. of props. 0–39384

Min cmplex, Mn(II) phthalocyanine, magnetic anisotropy determ. 0–64427

MnO₄- electronic transitions in near i.r., vibrational fine structure of bands

 $MnO_{4^{\circ}}$ electronic transitions in near i.r., vibrational fine structure of bands $0{-}58182$

0-58182
MnO₄²- electronic transitions in near i.r., vjbrational fine structure of bands 0-58182
MnO₄²-, construction of molecular orbitals, transition energies 0-53023
N₃, emission cross-sections in vac. u.v. by electron impact 0-61114
N₃, identification of two low-lying non-Rydberg states 0-61111
N₃, lifetimes of rotational and vibrational levels of electronic states 0-55303 0-55303

N₃, Morse function adjustment, P.E. curve for $X^1\Sigma^+_{\epsilon}$ state 0–46413 N₂, oscillator strengths of Hopfield absorption series 0–61116 N₂e diffr. exam. 0–74116 electron scatt., molecular-orbital calc. of 2 eV shape resonance

0 - 46493NCO radical, calc. method 0-53073

NCO radical, rot. transitions, from microwave spectrum 0-64429 ND, A ${}^3\Pi_I \cdot X$ ${}^3\Sigma^-$ (0,0) band, rot. anal. 0-64432 NF₃, electronic structure calculations 0-70920 NF¹ Σ^+ radiative lifetime and rate constant for electronic query $VF^1\Sigma^+$ radiative lifetime and rate constant for electronic quenching 0–74281

NH, potential energy curves and spectra, natural-orbital VCI studies 0-46490

NH⁺, LCAO-MO-SCF calc. 0–61077 NH₃, ab initio MO calc. 0–39388 NH₃, Franck-Condon factors for A–X transition 0–61112

 NH_3 , inner shell correlation energy, invariance with geometry changes 0-43072

0–43072
NH₃, proton magnetic shielding consts. 0–58171
NH₃, thermally excited, inversion- rotation spectrum, 60-200 cm⁻¹, freq. assignments 0–64433
NH₃, vibr. fine struct. from photoelect spectra 0–61121
NH₃ and ND₃, from photoelectron spectra 0–58186
N-H₂, theoretical predictions of structures 0–53044
NMe₃, electronic structure calculations 0–70920
NO₂, from photoelectron and vac. u.v. spectra 0–61110
N-O, elec. polarizability anisotropies from microwave spectroscopy 0–70923
N-O, rot. transitions, from microwave spectrum 0–64430

0–70923
N₂O, rot. transitions, from microwave spectrum 0–64430
N₂O, rot. transitions, from microwave spectrum 0–64430
N₃O e diffr. exam. 0–74116
NS Franck-Condon factors for B²π-x²π transitions 0–58185
NSe Franck-Condon factors for S²y-X²π_{3/2} transitions 0–58185
¹⁸N¹⁶O, ¹⁴N¹⁶O, spectra, vibrational isotope effect 0–39385
¹⁵NH₃, frequency of (v₂=1, J=1, K=0)–(v₂=0, J=0, K=0) transition meas. by CO₂ laser spectroscopy 0–61122
N₂1PG band system, relative intensities in normal and type-B aurora 0–76426 0 - 76426

Na₃, laser-induced fluorescence at 632.8 and 640.1 nm 0–58189
Na₂, laser-induced fluorescence at 632.8 and 640.1 nm 0–58189
NaCl, theoretical study of ¹Σ+, ³Σ+, ³Π, ¹Π states 0–43129
NaH+, hyperfine coupling constants for Na and H for various bond lengths 0–49854
NaLi+, ²Σ+ state, theoretical study 0–43129
Nd³⁺β-diketonates, spectual intensities 0–58489
Nd³⁺β-diketonates, spectual intensities 0–58489
Nd³⁺β-diketonates, spectual intensities 0–58489
Ni (II) complex of 1-amidino-2-thiourea, correlation with K-absorption spectrum 0–61127
Ni complex of 1-amidino-2-thiourea, correlation with K-absorption spectrum 0–61127
Ni complex of 1-amidino-2-thiourea, correlation with K-absorption spectrum 0–61127
Ni complex of 1-amidino-2-thiourea, correlation with K-absorption spectrum 0–61127
Ni complex of 1-amidino-2-thiourea, correlation with K-absorption spectrum 0–61127
Ni complex of 1-amidino-2-thiourea, correlation with K-absorption spectrum 0–61127
Ni complex of 1-amidino-2-thiourea, correlation with K-absorption spectrum 0–61127
Ni complex of 1-amidino-2-thiourea, correlation with K-absorption spectrum 0–61127
Ni complex of 1-amidino-2-thiourea, correlation with K-absorption spectrum 0–61127
Ni complex of 1-amidino-2-thiourea, correlation with K-absorption spectrum 0–61127
Ni complex of 1-amidino-2-thiourea, correlation with K-absorption spectrum 0–61127
Ni complex of 1-amidino-2-thiourea, correlation with K-absorption spectrum 0–61127
Ni complex of 1-amidino-2-thiourea, correlation with K-absorption spectrum 0–61127
Ni complex of 1-amidino-2-thiourea, correlation with K-absorption spectrum 0–61127
Ni complex of 1-amidino-2-thiourea, correlation with K-absorption spectrum 0–61127
Ni complex of 1-amidino-2-thiourea, correlation with K-absorption spectrum 0–61127
Ni complex of 1-amidino-2-thiourea, correlation with K-absorption spectrum 0–61127
Ni complex of 1-amidino-2-thiourea, correlation with K-absorption spectrum 0–61127
Ni complex of 1-amidino-2-thiourea, correlation with K-absorption spectrum

self-consistent-field calculations 0–70935
0₂, 1_{Δp}, by high resolution on vac. u.v. photoelectron spectroscopy
0–77824
0₃, A²Π_u state, obs. in photoelectron spectrum 0–55312
0₃, groundstate, effects of electron correlation on fine-structure constants and spin-spin interaction 0–58193
0₃ 1_{2p} t, 1_{Δp} energy transfer to dissociated bromine 0–58161
0₃ trapped in solid matrices, vibl. terms of B³Σ_u ← X³Σ_g transition
0–55311

 O_2^+ , ING band system, relative intensities in normal and type-B aurora 0-76426

0—76426

OD+, electronic transitions ${}^{3}\Pi_{-}{}^{3}\Sigma^{-}$, rotational anal. 0—70938

OH, spin-generalized SCF wavefunctions using GF method 0—6773

OH ${}^{4}\Sigma^{+}$ state, radiative and predissociation probabilities 0—61129

OH+ ${}^{3}\Pi_{-}{}^{3}\Sigma^{-}$ transition 0—77827

OH+electronic transitions ${}^{3}\Pi_{-}{}^{3}\Sigma^{-}$, rotational anal. 0—70938

OH₃+, oxygen electric field gradient 0—61128

ONF₃, electronic structure calculations 0—70920

ONMe₃, electronic structure calculations 0—70920

ONMe₃, validity of Franck-Condon factor for photoionizing transit

 $O_3(^3\Sigma_g^{-})$, validity of Franck-Condon factor for photoionizing transitions 0-74297

0–74297 Os(III) complex with 2.2′-bipiridyl and 1,10-phenanthroline, σ , π delocalization 0–58166 OsO4, study from absorpt. spectrum 0–70941 P compounds, 2p electron binding energies, correlation with extended Huckel charges 0–46504 PF₃, i.r. spectra. p_1 band recorded 0–74300 PF₃O, ab initio SCF MO calcs., rel. to ligand props. of PF₃ 0–70942 PH₃ ground state SCF wave functions and molecular properties 0–77842 PO, new bands in the visible and their rotational analysis 0–58194 PO, rotational analysis of bands in 4800-3800 Å region, lower and upper level constants 0–74299

Molecules continued

electronic structure, inorganic continued

PO radical, rotational anal. of new visible electronic band system 0-55315

PO radical, rotational study and spectroscopic data 0-55314 Pd complex, dithioacetylacetone Pd(II), electronic spectra, MO calc. Pd(II) tetraamine complexes, square-planar, from polarized u.v. reflection

spectra 0-70944 Pt complex, dithioacetylacetone Pt(II), electronic spectra, MO calc. 0-67748

Pt(II) tetraamine complexes, square-planar, from polarized u.v. reflection spectra 0-70944

Ru(III) complex with 2.2′-bipiridyl and 1,10-phenanthroline, σ , π delocalization 0–58166

RuO₄, study from absorpt. spectrum 0–70941 S₈, MO calc. 0–77837 S₈, orbitals and charge-carrier transport 0–75492

S₈, S₈⁻, S₈⁺, rel. to carrier mobility in liquid and solid 0–56149 SF Hartree-Fock binding energy of ground state and of positive and negative ions 0–74304

ive ions 0–74304

SF4 gaseous, exam. by soft X-ray spectroscopy 0–46511

SF6, LCAO, MO SCF wave functions 0–74305

SF6 gaseous, exam. by soft X-ray spectroscopy 0–46511

SO radical, microwave obs. of first electronically excited state 0–70962

SO₂, ¹A₁ ground state, self-consistent field wavefunctions 0–74233

SO₃, theoretical study using SCFMO calculations on both minimal and extended basis 0–67753

SO₃, vibr, fine struct. from photoelec, spectra 0–61121

SbCl₃, Raman spectra, low frequencies, temp. changes 0–49888

SbF, rotational anal., of C₁ system 0–64451

SeD h.f.s., A-doubling from e.s.r. obs. 0–49892

SeF Hartree-Fock binding energy of ground state and of positive and negative ions 0–74304

SeH h.f.s., A-doubling from e.s.r. obs. 0–49892

SeO₂ matrix violated, evidence for slow internal conversion between excited states 0–46512

SeO₂ matrix violated, evidence for slow internal conversion between excited states 0–46512 Si₂ new band systems discovered, rotational and vibrational constants 0–77844 Si₁Si₂ nature of excited state and transition involved during emission spectrum of SiF₄ vapour 0–46514 SiH₄ ground state SCF wave functions and molecular properties 0–77842 SiO₃S₂-3/II transition found 0–61136

SiO 32-3II transition found 0-61136
TiBr vibrational analysis of electronic states 0-49895
TiF(H₂O)₅²⁺, from e.p.r. meas. 0-70955
VO, potential energy curves constructed by Rydberg-Klein-Rees method 0-67736
Xe-N gas mixture, thermal equilibrium calc. at 1 atmos. and between 5000-35000°K 0-53269
Xe-X, Ye-t, potential curves, estimates 0-43082
XeFa, magnetic shielding of ¹⁹F 0-53052

electronic structure, organic

 π -electron system, many-body methods applic. rel. to theoret. superconduction 0–75598

σ-bonded mols. containing N and/or O, extension of MINDO/2 method

σ-bonded mols. containing N and/or O, extension of MINDO/2 method 0–77855 acetone, triplet energy transfer to π-bonded mols. 0–77871 acetylene, linear and bent, trans and cis isomers found for most low-lying excited states 0–74324 acetylene d, electric field gradients near deuteron calculated by floating spherical gaussian orbital method 0–64524 acrolein. π*κ-n singlet transition, application of contour analysis, a-component of excited state electric moment 0–49899 active centres, similar to linear oxonium ions, rel. to cationic polymerization of vinyl ethers and cyclic acetals 0–70960 alicvolic hydrocarbons, conformational anal, by MINDO/2 method

alicyclic hydrocarbons, conformational anal, by MINDO/2 method $0\!-\!77915$ aliphatic saturated, C 1s energies meas, by ESCA, binding energy shift 0-74335

alkane, linear, ionization potentials, equivalent orbital calc. 0–39408 n-alkanes. MO theory predictions of mass spectra 0–77861 alkanes, atomic and bond charges, calc. from electronegativity 0–64311 N-alkyl-N-nitrosoanilines 0–77860 alkyltri-p-tolyl arsonium compounds, i.r. spectra, band assignment 0–74328

alloxazine, lowest triplet and singlet state from polarized phosphoresc, spec tra 0-72448

aminoanthracenes, excited states, electron density distrib. 0–49903 aminopyridines and their deuterated analogues, band analysis of i.r. spectra 0–77865

1.4- and lowest n, π^* state energy 0-53068 anthracene e.p.r. studies of optical spin polarization in triplet state anthracene e.p.r. studies of optical spin polarization in triplet state 0–74333 anthracene ion, use of FEMO theory to calc, transition energies 0–74392 anthracyl radical, ground states 0–6765 aromatic carbonyl cpds., T₁-S₀ transitions rel. to vibronic interaction between nr* and rr* states 0–70969 aromatic compounds, C Is energies meas, by ESCA, binding energy shift 0–74335

aromatic hydrocarbons, intersystem crossing mechanism, effect of deuteration on rate 0-64467 aromatic mols. in excited state, magnetic anisotropy 0-46536 aromatic vapours, triplet states, obs. following inter-system crossing 0-58202

aromatics, nitrogen containing zero-field splitting parameters of phosphorescent triplet states 0-46537 azulene, electron attachement in field of ground and excited electronic states 0-46538

azulene, electronic states calc. by CNDO/2 CI 0–61145 azulene, plasma effects of π electrons 0–43149 3- benzanthrone, in hydrocarbon solutions 0–49905 benzanthrone, in hydrocarbon solutions 0–49905 benzane, Franck-Condon overlap factors between vibronic levels benzene, 0-61148

benzene, distortions of lowest triplet state in solvents 0-72446 benzene, effect of fluorosubstitution on π -electron energy levels 0-49926 benzene, exact soln, of one-band π -electron theory 0-39413 benzene, influence of substituents on $^{1}B_{2u}$ state 0-64487

electronic structure, organic continued

benzene, intersystem crossing mechanism, effect of deuteration on rate 0-64467

benzene, lowest singlet-triplet separation, ab initio AMD calc. 0-39414 benzene, substituted, SCF calcs., charge distrib., chemical shift 0-39415 benzene, triplet energy transfer to π -bonded mols. 0-77871 benzene, vibr. relax. and competition with radiationless transitions in $^{1}B_{24}$ state 0-55337 benzene, vibrational structure use in identification of degenerate and non-degenerate orbitals 0-53062 benzene ring cpds., low-energy collective electron excitation obs. 0-50238 benzenes, homo-substituted, semi-empirical PPP-SCF-MO-CI calcs. by π electron approx. 0-46540 benzenes, substituted, excited state props., SCF-MO calc. 0-77875 benzofuran, $\pi \rightarrow \pi^{*}$ transition, hybrid character and rotational structure 0-74411 benzoporphyrins, azo-substitution, splitting of degenerate states. 0.42161benzene, lowest singlet-triplet separation, ab initio AMD calc. 0-39414

0-4441 benzoporphyrins, azo-substitution, splitting of degenerate states 0-43151 p-benzoquinone, in mixed cryst., T-Spimission, n, τ^* states 0-64485 para-benzoquinone CNDO-CI calculations, and charge distributions 0-61147

0–61147
benzoselenophene, applic. of Huckel's method 0–55339
benzyl, and naphthalenic and azulenic homologues, LCAO SCF CI calculations 0–67772
benzyl radical, non-empirical calc., unrestricted SCF method 0–55383
biacetyl, triplet energy transfer to π-bonded mols. 0–77871
bicyclic hydrocarbon radicals, e.s.r. structure study 0–74344
biphenyl, geometry in excited electronic states 0–59434
biphenyl and analogues, identification of lowest excited singlet state 0–46545

0-46545 biphenyl and biphenylene, electronic spectra 0-39442 bond separation, MO theory 0-77851 butadiene, spatial wavefunctions 0-61151 carbonyl compounds, C 1s energies meas, by ESCA, binding energy shift 0-74335

0-74335
charge distribution studies using minimal Slater-type basis 0-61140
chlorobenzene, 2699Å electronic band system 0-49906
cyanuric acid, electron population parameters by X-ray diffraction
0-46440
cyclic 0-46522

0–46440 cyclic 0–46522 cyclic 0–46522 cyclic 0–46522 cyclic polyenes, Hartree-Fock solutions instabilities rel. to spin and charge density fluctuations 0–74402 transcyclo-octene, excited-state transitions 0–58213 cyclobutadiene and derivatives, LCAO study, π and σ energies 0–67784 cyclopentane, vibrational structure in first electronic band 0–55346 cytosine, polarization of electronic transition 0–79370 DNA, energy band structure by SCF-LCAO-CO method 0–46609 diazines, magnetic evidence for delocalization of lone pairs 0–58217 diazomethane, electron relax, and molec, vibr. 0–39361 p-dichlorobenzene, electronic spectra, band assignment 0–70990 2.3- dichloroquinoxaline in durene, polarization of mag. zero-field transitions 0–54117 dicyanodiacetylene, linear $^{12}E_{g}^{+}$ ground state and linear excited state $^{12}E_{g}^{+}$, $^{12}E_{g}^{-}$ rel. to abs. spectra 0–43158 p-dihalobenzene, cryst. T-S emission, n, π * states 0–64485 2.4-dimethylphenol vapour, u.v. spectrum band analysis in terms of excited and ground states 0–46558 dye-polymer complexes, exciton theory of electronic states 0–61187 electron donor-acceptor complexes, symmetry classification and selection rules 0–78511 electron spectroscopy determ, of O-C and S-C links 0–55276

rules 0–78511 electron spectroscopy determ, of O-C and S-C links 0–55276 electronic energy levels and optical properties of doped, mixed molecular crystals, Green function method 0–40653 ethane and other mols., MO explanation for barrier to internal rotation 0–77902 ethylene, T and V states, interpretation of open-shell SCF calcs. 0–64504 ethylene, or and π electronic structures in ground, triplet, and ionic states 0–77903

ethylene, comparison of electronic structure with diborane 0–77904 ethylene, higher-order RPA to system of two π electrons in double bond 0–77852

0-1/03/2 ethylene and its cation, isomerization processes, energy barrier calcs., semiempirical quantum chemical method 0-39428 ethylene-d, electric field gradients near deuteron calculated by floating spherical gaussian orbital method 0-64524

spherical gaussian orbital intention 0—04324 excited state polarizabilities symmetries and energies studied by means of induced birefringence 0—74196 external heavy atom effect on S=T transitions 0—41276 ferricenium cation, from e.s.r. meas. of cations of ferrocene derivatives

0 - 71001

0–71001
o-fluoroanisole, from emission spectra, 2765-3000 Å 0–64508
fluoromethanes, from photoelectron spectra 0–71009
m-fluorophenol, vibrations in ground and excited states 0–53072
m-fluorophenol from emission spectra, 2765-3000 Å 0–64508
formaldehyde, calc. method 0–53073
formaldehyde, low-lying states, calc. by combined SCF and CI method 0–61163
formaldehyde beam, Autler-Townes effect 0–61162
formaldehyde-water system, CNDO study on ground and lowest excited state 0–74370
glyoxal, band assignment of laser induced emission 0–58224
haemoglobin, modifications of Fe(II) electronic struct., Mossbauer determ.
0–61186

0 - 61186

N-heterocyclic benzene analogues, calc. using approximate MO theory

heterocyclic molecules, configuration mixing and double perturbation treat-

neterocyclic molecules, cominguration imaging and observed the ment including doubly excited configurations 0–43164 hexahydro-1, 3, 5-trinitro-s-triazine (RDX), MO calc. 0–67799 hydrocarbons, MO theory of internal rotation using minimal Slater-type basis 0–77916 hydrocarbons, alternant, oscillator strengths 0–46566 hydrocarbons, molecular orbital interpretation of X-ray emission spectra

hydrocarbons, molecular orbital interpretation of X-ray emission spectra 0-46567 hydrocarbons, p and β bands calc. in accordance with HMO-SCF theory with configuration interaction 0-77917 hydrocarbons, photochemical decomposition into radicals, triplet states 0-43141

instabilities, configuration interaction approach 0-74315 instabilities, mixing and consistency conditions 0-74316

Molecules continued

electronic structure, organic continued ketene, electron relax. and molec. vibr. 0-39361

magnesium phthalocyanine negative ions, LCAO-SCF-CI cales. 0-71023 metalloporphyrins, ring geometry effects on triplet and singlet energies 0-74382

0–74382 methane, e diffr. exam. 0–74116 methane, orbitals, integrals by Gaussian transform method 0–39429 methane, proton magnetic shielding consts. 0–58171 methane ions, CH*3 and CH*3, STO calculations, electron pair interpretation of stabilities of structure 0–58232 methane through Ne isoelectronic sequence, config. interaction calcs. 0–39437

0–39437 methane-d, electric field gradients near deuteron calculated by floating spherical gaussian orbital-method 0–64524 methanes, substituted, self-consistent group calc. 0–58231 3-methoxy-substituted benzanthrones, in hydrocarbon solutions 0–49905 methyl and other radicals, rel. to electronegativity 0–39434 methyl chloride, bond behaviour in elec. field 0–64519 methyl chloride + Cl⁻ gas phase reaction, potential energy surfaces 0–69204

0-09204
methyl fluoride, proton magnetic shielding consts. 0-58171
methyl in pyramidal configuration, temperature dependence of hyperfine
splitting 0-46575

splitting 0-40/15 methyl negative ion, density matrices 0-64353 methyl radical, electron relax, and molec, vibr. 0-39361 methyl rotor, torsional ground state model using single particle wavefunctions 0-64523

tions 0-04523 methylallylbenzenes, Huckel approx. calc. 0-46581 methylallylbenzenes, Huckel approx. calc. 0-46581 methylazabenzyl radicals, excited electronic states 0-46576 1- methylcyclopentane, vibrational structure in first electronic band 0-55346

methylene, CH2, e.p.r. of triplet state 0-61169

methylene, CH3, e.p.f. of triplet state 0–01109 methylene, collision-induced singlet-striplet intersystem crossing 0–72558 methylene, nonlinearity of triplet ground state 0–77920 3- methylsydnone, all-valence electron study by CNDO method 0–58244 naphthalene, electronic states calc. by CNDO/2 CI 0–61145 naphthalene, improved calc. of charge transfer integrals 0–59149 naphthalene, intersystem crossing mechanism, effect of deuteration on rate 0.64467.

naphthalene, intersystem crossing mechanism, effect of deuteration on rate 0–64467 naphthalene adsorbed on zeolite, from fluorescence and abs. spectra at 77°K 0–46583 naphthalene ion, use of FEMO theory to calc, transition energies 0–74392 naphthalene-d₈, electronic transitions and polarizability 0–74196 naphthalenes, fluorinated, cation radicals, e.s.r. study of spin-density splitting and 0 parameters 0–74393 naphthyl radical, ground states 0–67765 nitro-compounds, photochromic absorpt, bands 0–53079 nucleotide base pairs, energy levels and wavefunctions, SCF calcs. 0–46610 cetalkylnorphins, O. B. N. and M. bands found in vapour absorption spec-

octalkylporphins, Q, B, N, and M bands found in vapour absorption spectra 0-74396

a-oxalic acid dihydrate, electron population parameters by X-ray diffraction 0-46440

peptide groups, account of polar states 0–55384 permethylcyclopolysilanes anion-radicals, electron delocalization 0–74408

permethylcyclopolysilanes anion-radicals, electron delocalization 0—74408 phenyl radical, ground states 0—67765 phenyl ring in ligands of paramagnetic complexes, 'anomalous' spin density distribution 0—58238 polarization of mag. zero-field transitions, optical detection 0—54117 polyenes, linear, correlation effects on $\pi\pi^*$ transition energies 0—46619 polyenes, linear, correlation effects on $\pi\pi^*$ transition energies 0—46619 polyenes, linear, correlation effects on $\pi\pi^*$ transition energies 0—58260 polymers. linear, CNDO/2 approximation, Hartree-Fock procedure formulation and application 0—64572 polymers with conjugated systems, rel. to semiconduction 0—75695 polynucleotides, optical activity of $n\pi^*$ transitions 0—74423 polypeptides, H-bonded, charge distribs. 0—64574 polypeptides, exciton states and hypochromism 0—74431 polyribonucleotides, u.v. absorpt, spectra 0—39467 potential energy surfaces for Walden inversion reaction 0—69204 propylene, CNDO-INDO calc. 0—77944 pyrazine, relationship with spin-state ordering 0—76118 pyrenyl radical, ground states 0—67765 pyridiviphosphine derivatives, 5-spin energy level diagrams assigned 0—49936 pyrrole, all-electron SCF-LCAO-MO wavefunction 0—39451

0—4936 pyrrole, all-electron SCF-LCAO-MO wavefunction 0—39451 quinones, ortho and para, by improved LCAO method 0—58242 quinoxaline, intersystem crossing quantum yield, evidence for high yield of internal conversion of first excited singlet state to ground state 0—74407

quinoxaline, intersystem crossing quantum yield, evidence for high yield of internal conversion of first excited singlet state to ground state 0—74407 review 0—58206 riboflavin, lowest triplet and singlet state from polarized phosphoresc, spectra 0—72448 rel. to superconduction possibility 0—75599 sydnone, all-valence electron study by CNDO method 0—58244 tetracene use of FEMO theory to calc, transition energies 0—74392 thiobanzophenone, 6500 Å transition 0—61175 thionaphthene, n→n* transition, hybrid character and rotational structure 0—74411 thiopehno-(4,5-c) and thiopheno(4,5-b) tropones 0—64549 thiophene and thiepine derivatives, SCF MO treatment 0—53088 thiophosgene, rotational structure in n*-n transition 0—58245 three-membered ring molecules, LCAO SCF MO calculations for ground state 0—43143 thymine 0—553375 2-p-toluidinyl-6-naphthalenesulphonate, rel. to fluorescence props. 0—77955 triplet-singlet energy transfer in fluid soln. 0—78282

triplet-singlet energy transfer in fluid soln. 0-78282 triplet-state molecules, energy levels and eigenstates, approximations

triplet-state molecules, energy levels and eigenstates, approximations 0-64468 urazole, all-electron SCF-LCAO-MO wavefunction 0-39451 urazole radicals, cation and anion, all-electron SCF-LCAO-MO wavefunctions 0-39451 vinyl fluoride 0-77957 vinyl fluoride 0-77957 CH $_2^{+}$ ion, charge distribution 0-55359 CH $_2^{+}$, electron deficient molecule, maximum overlap MOs 0-77762 CO $_2^{+}$, cross sections for formation of $A^2\Pi$, $B^2\Sigma^+$ and $X^2\Sigma^+$ by 0.05-5 keV electrons 0-77777

electronic structure, organic continued

NH₃, density matrices 0-64353

OF($^2\Pi$), Hartree-Fock wavefunction, binding energy, ionization potential, electron affinity, moments 0-70936

S compounds, correlation of electron binding energy with structure 0-77752

SiF molecule, matrix element of dipole moment of A^2 – X^2 electron transition 0–53050

alcohols, self-associated, double excitation in i.r. spectra 0-53060 alkali halide beam, degree of internal excitation rel. to sensitivity of surface ionization detector 0-39363

aromatic photoexcited molecules, e.s.r. spectra 0–55336 aromatics, singlet levels, energy transfer to fluorescent solutions 0–79360 benzene, and 'd₈ vapour excited to single vibronic levels, fluorescence lifetime 0–74342

time 0-74342
benzene, deuteration eff. on triplet state lifetimes 0-74198
benzene, induced non-radiative transitions 0-64484
benzene, induced non-radiative transitions 0-64484
benzene, inexcited singlet state, fluoresc, and nonradiative transitions from
single vibr. levels 0-77877
benzene ring cpds., low-energy collective electron excitation obs. 0-50238
benzenes, substituted, electronic structure and props. 0-64482
benzimidazole, determ, of dipole moment of excited state 0-64514
2-benzylaminopyridine, fluorescence 0-77899
biscarbazolyl propane intramol. excimers, kinetics 0-64326
Born-Oppenheimer state decay, study from Heitlers theory 0-74193
bromobenzene, excited state rotational constants 0-53065
carbon dispublide, pure rotational Raman scatt, from vibrational levels,

carbon disulphide, pure rotational Raman scatt. from vibrational levels, obs. 0-61083

complex organic, light generation in allowed transitions, effect of nonlinear photochemical transformations 0–46520 cross section from zero to more than 10 eV above threshold of excitation 0–58157

DNA base pair, hydrogen-bonded, absorpt., luminescence 0-74422 diatomic, by atom collision, vibr. relax. rel. to anisotropic intermol. potential 0-53096

diatomic mol. collisions, rotational excitation 0–53100 diatomic molecular scatt. of low energy electrons 0–61065 2-(N,N-dimethylamino)pyridine, fluorescence 0–77899 dimethylether transition probability at 3.508 μ He-Xe laser line 0–55363 dinaphthylalkanes, fluorescence quenching and excimer formation 0–79371

dinaphthylalkanes, fluorescence quenching and excimer formation 0–79371 aphenyl propane intramol. excimers, kinetics 0–64326 electron scatt., fixed-dipole and free-dipole models, relationship 0–61048 electronic structure and props. 0–64482 energy transfer in molecular systems, theory 0–55279 ethylene, intravalence character of V excited state 0–70998 excimers intramol., formation and deactivation kinetics 0–64326 ferrocene, vapour, from inelastic scatt. of 30 keV electrons 0–58250 fluorescent mol., rot. relax, by light pulse method 0–70840 p-fluoroaniline, struct. changes, from rot. analysis 0–53071 fluorobenzene, first excited state π^* – π , dipole moment correlation with structure 0–46561 formaldehyde, interstellar, rot. 0–66514 formaldehyde temps., in interstellar H clouds 0–66513 heterocyclic molecules, configuration mixing and double perturbation treatment including doubly excited configurations 0–43164 high current hollow cathode, excitation mechanism 0–71211 hydrocarbons, aromatic, temp. and matrix eff. on fluoresc. 0–74319 hydrocarbons, polycyclic conjugated, LCAO MO calculations for energies

0–43141, hydrocarbons, polycyclic conjugated, LCAO MO calculations for energies of singlet and triplet transitions 0–64464 indazole, determ, of dipole moment of excited state 0–64514 indole, determ, of dipole moment of excited state 0–64514 indole, determ, of dipole moment of excited state 0–64514 indole, determ, of dipole moment of excited state 0–64514 indole, determ, of dipole moment of excited state 0–64514 indole, determ, of dipole moment of excited state 0–64514 indole, determ, of dipole moment of excited state 0–64514 indole, determ, of dipole moment of excited state of 0–64514 inversion, natural system in discharges, broadband gain 0–39339 life-times, breakdown of relationship to integral absorption 0–67689 lifetime determ, by universal correlation method 0–67688 lifetime determ, by universal correlation method 0–67688 lifetime determ, by universal correlation method 0–67684 luminescence lifetime variation near interface between differently polarizable dielectrics 0–77742. Lyman- α radiation from electron collisions with H-containing mols. 0–64329 metastable, formed by electron bombardment, velocity and angle distrib, effect of recoil 0–70865 methoxy benzaldehyde, m- and p-, vapour, n- Π * electronic emission spectra 0–74380 molecular beam, e bombarder, high current 20 V 0–73173

tra 0–74380
molecular beam, e bombarder, high current 20 V 0–73173
molecular ions, collisional excitation 0–53102
naphthalene, deuteration eff. on triplet state lifetimes 0–74198
naphthalene, fluorescence as function of vibrational level and excitation energy 0–77932
non-radiative transitions, radiative theory 0–43051
nonradiative decay of large mols., multiphonon processes 0–53010
organic, review of production methods 0–58206
perylene vapour, from inelastic scatt. of 30 keV electrons 0–58250
2-(N-phenylamino)pyridine, fluorescence 0–77899
photon irrad. homogeneous system, photon and electron energy spectra
0–55266
predissociation induced by mag field 0–39452

0–55266
predissociation induced by mag. field 0–39452
quasi-bound state energies for molecular interactions 0–79427
quenching of excited singlets by nucleophiles 0–77732
rare earthions, deuteration eff. on triplet state lifetimes 0–74198
resonance energy transfer, exchange-induced 0–58203
rhodamine 62h stimulated radiation due to single and two-photon excitation cross section 0–68121
rotational, during ion-molecule collisions 0–61198
rotational, exponential Born approx. computational studies 0–74435

rotational, exponential Born approx., computational studies 0–74435 rotational, in inelastic collision statistics 0–61194 rotational, statistical anal. of matrices in strong coupling 0–55389 rotational, compound state resonances formed in atom-diatom collisions 0 - 53097

rotational excit. in collisions, strong coupling approx. 0-58132

Molecules continued excitation continued

rotational and vibrational, of polar mols. by low-energy electron collision

shock wave induced, review 0-58104

singlet-singlet resonance energy transfer, exchange-induced 0-58203

singlet-singlet resonance energy transfer, exchange-induced 0–58203 state wavefunctions, calc. by variational method 0–58078 tetraphenylporphin, halo derivatives, spin-orbital, fluorescence yield with increase of halogen atomic number 0–67820 transitional rates from sound absorption and dispersion curves, relaxation processes, analysis 0–53004 trioxane, I type doublets in degenerate excited vibr. states 0–61178 triphenylene, vapour, from inelastic scatt. 0–58250 triplet mols. in two-quantum photoionization 0–72551 triplet state lifetimes, eff. of deuteration 0–74198 two-level, by ultrashort crossed optical pulses 0–61054 two-level syst., effect of pulse of coherent light 0–77748 v.h.f. pulse discharge source, spectra 0–74532 vibrational, in atom-diatom and diatom-diatom collinear collisions 0–53099

0 - 53099

vibrational energy transfer from highly excited mols. 0-55393 vibrational-rotational, in collisions with atoms and molecules, modified Born approximation 0-67839 Ag₈₇In₁₃, optical absorption and photoelectron energy distribution for electronic structure 0-65577

As₂ nature of excited states, rotational analysis, electronic configuration 0-43083

0–43083 BCl₃, dissociation, recombination radiation, vibrational spectra, CO₂ laser induced 0–46604 Bil values of various constants for excited states 0–64381 Br₂, dissociated, electronic energy transfer by O₂ $^{1}\Sigma_{z}^{+}$, $^{1}\Delta_{z}$ 0–58161 CO, radiation emission in u.v. by electron impact 0–46456 CO, slow electron collision, differential cross section 0–39370 CO, vibrationally excited produced when CS₂ is mixed in laser cavity with oxygen atoms continuous-wave emissions 0–58162 CO chemiluminescent emission of 4th positive band in N/O/reactive carbon compound systems 0–76257 CO⁺, anomalous vibrational, on CO-R⁺ collisions (R=inert gas atom) 0–67728 CO+, anomalous vibrational, on CO-R+ collisions (R=inert gas atom) 0-67728

0–67728 (CO₂, amplification coeff. in ν_1 - ν_1 laser transition 0–74244 (CO₃, pure rotational Raman scatt. from vibrational levels, obs. 0–61083 (CO₂ laser, energy resonances between mol. species present 0–49046 (CO₂ zero angle electron scattering with vibrational excitation 0–43123 (CO₂·(A· Π_x -X· Π_y) transitions, kinetics of emissions and absorptions by pulsed radiolysis 0–64386 (Co rel. to flames, extra-equilibrium excitation and electron temperatures 0.6.60206

0-69209

0–9209 Co. rel. to flames, extra-equilibrium excitation and electron temperatures 0–69209 CsCl molecules on Ir, surface ionization, influence of adsorption of O₂, H₂, CO, meas. 0–53444

Ctu₃Ge₆, optical absorption and photoelectron energy distribution for electronic structure 0-65577
D₂, by 34 keV electrons, Lyman and Werner total vib. band intensities 0-64423

D₃, excited by 0 to 500 eV electrons, extreme u.v. emission obs. 0-64441

D₂ rotational excitation by low energy electrons 0-77786 D₂ scatt. of He atoms, effects of rotational excitation 0-77987

Fe(III) complex, simultaneous pair electronic excitations, from u.v. abs. spectrum 0–58165
H₂, by 34 keV electrons, Lyman and Werner total vib. band intensities 0–64423

H2, diabatic coupling processes in highly excited states, general formalism 0 - 39378

H₂, effect of strong optical field, multiphoton ionization 0-39380 1₂, electron impact excitation, resonances, trapped electron method obs 0-43099

H₂, excited by 0 to 500 eV electrons, extreme u.v. emission obs. 0–64441 H₂, excited states, abs. lifetimes 0–74271 H₃, of individual vibl. states in collisions with Li⁺ 0–71059 H₂, resonance scattering of electrons, differential excitation functions

0-61099

0–61099
H₂, rotational excitation by low energy electrons 0–77786
H₃, simultaneous rot.-vib., by slow electron impact 0–64421
H₃, simultaneous vib. and rot., by slow electrons 0–64418
H₃, simultaneous vib. and rot., by slow electrons 0–64418
H₃, vibrational, by electron scatt., quantum-mech. theory 0–43102
H₃, vibrational, by electron scatt. 0–43103
H₃, X¹ $\Sigma_{\rm F}$ electron scatt. at 10 eV, calc. and expt. 0–64422
H₃ electron impact, $c^{3}\Pi_{\rm H}$ state, resonance 0–61067
H₃ electron scatt., differential elastic and vibrational cross-sections 0–61098

0-61098
H. electron scatt., resonances, 11 to 13 eV 0-61097
H. electronic transfer between atom and molecule 0-74168
H. scatt of He atoms, effects of rotational excitation 0-77987
H. simultaneous electronic and rot., by electron impact 0-64419
H. compound state formation effect on vacuum u.v. excitation 0-64424
H. cotation, cross sections, adiabatic approx. 0-53037
H. excited states pot. energy surfaces 0-77794
H.CO, interstellar, initial excitation temp. 0-51705
HCl, vibr. excited, scatt. and accommodation coeffs. determ. 0-77787
HD, by 34 keV electrons, Lyman and Werner total vib. band intensities 0-64423

HD, rot. excitation by low-energy electron collision 0–49875 HD scatt. of He atoms, effects of rotational excitation 0–77987 HD+, non-symmetry of cross section of collision induced excitation to $2p\sigma_u$ state 0–43100

H₂+He collisions, vibrational excitation cross sections, impact parameter dependence 0-61191
He, by fast protons, energy dependence of singlet excitation cross sections 0-77799

He2, luminescence in positive column of discharge 0-43118

1s, by singlet molecular oxygen 0-58178 K_s, radiative lifetime of B¹ Π_u state 0-74277 LiCl molecular ionization from Re absorbed layer, chemical eqbm. investigation 0-53443

N2-NO collisional ionization cross section rel. to internal excitation energy N_2 , α -irrad., radiative and non-radiative de-excitate rates 0-53043

Molecules continued excitation continued

N₂, B² Σ_{κ} vibr. and rot. levels lifetimes, obs. 0-46485

N, by 50 to 5000 eV electrons, radiation emission obs. 0-64440

N₃, by protons and H atoms in aurora, 1 to 25 keV 0-41518

N₂, C³ π_u and B³ π_g vibr. and rot. levels lifetimes, obs. 0–46485 N₃, e bombardment 0.65-1.6 MeV obs. absolute fluoresence of first negative (0,0) band 0–46494

N₂, efficiencies for excitaion of first and second positive bands 0-67739

N₃, electron impact, secondary effects 0–64439
N₃, emission cross-sections in vac. u.v. by electron impact 0–61114
N₃, emission cross-sections of 1st negative band system produced by proton impact 0–70929
N₃, excitation and relaxation of triplet states by metastable Ar atoms

N₃, excitation and relaxation of triplet states by metastable Ar atoms 0-64609
N₃, excited by 0 to 500 eV electrons, extreme u.v. emission obs. 0-64441
N₃, intercombination transition and intensity distributions, elimination of discrepancy between experimental and theoretical results 0-64434
N₃, second positive emission system by electrons of energies near 10keV 0-46486

No, threshold excitation spectrum 6-13 eV, excitation of triplet states

0-61118

0-61118
N; ultraviolet-induced first negative system 0-70959
N; by electron bombardment, theoretical, exptl. study 0-53045
N; electron scatt., resonances, 11 to 12 eV 0-61097
N; first positive and Meinel bands, electron excit. cross-sections. 0 to 700 eV 0-64438

ev 0-044.8 N-low energy collisons with He, unitarized Born approximation for rotational excitation 0-55302 N-rel, to flames, extra-equilibrium excitation and electron temperatures 0-69209

 $N_{\rm F}$ rotational, electron collision frequency, G-factor and electron energy loss rate parameter 0-69310 $N_{\rm F}$ electron scatt., molecular-orbital calc. of 2 eV shape resonance

0-46493

0—46493 N₂*, bands in first negative system, by 21.3S and 21.3P He atoms 0—58188 N₂*, effective cross section of (0-0) band at 3914 Å in first negative system resulting from collisions between fast electrons and N₂ molecules 0—46492

resulting from collisions between fast electrons and N₂ molecules 0–46492 N.*, efficiencies for excitation of 3914Å first negative band 0–67739 N.*($B^3\Sigma_u^*-\lambda\Sigma_g^*$) transitions, kinetics of emissions and absorptions by pulsed radiolysis 0–64386 N.*($B^3\Sigma_u^*$), populations of vibrational levels v'=0 to 7, electron temperature, electron concentration measurements in a He-N discharge 0–64435 NO*, collisional excitation 0–53102 NO., lifetime meas, by dye laser excitation 0–77811 N.O., scatt. and de-excitation coeffs. Calc. 0–61106 N.O., vibr. relax. 0–39386 N.O zero angle electron scattering with vibrational excitation 0–43123 O., electron impact cross sections 0–77825 O., vibr. absorpt., 1850 to 2245 Å 0–74416 O. emission bands obs. at 4784, 5165, 5788 Å in afterglow, assignments to $^1\Delta_g$, $^1\Sigma_g$ states 0–74294 O. predissociation lifetimes of $B^3\Sigma_u$ - state, determ. 0–77830 O. rotational, electron collision frequency, G-factor and electron energy loss rate parameter 0–69310 O. to b $^1\Sigma_g^*$ state in energy transfer reaction with metastable atomic oxygen 0–39398 O.*, collisional excitation 0–53102

Ox*, collisional excitation 0-53102 Ox*, vibrationally excited, production by solar u.v., effect of autoionizaon 0-77826 beams, vibrational excitation in collisions with neutral mols.

O,* beams, vibrational excitation in collisions with neutral mols. 0-53103 O.* first negative bands excitation by electron impact on O.* 0-43131 O.* $(^{1}\Delta_{e})$, collisional quenching by gases in atmosphere 0-39396 O.* $(^{1}\Delta_{e})$, emission in airglow, production and loss mechanism, O₃-distrib. study 0-54265 PO, B²H_I-X²H_I, transition established 0-74299 SD chemical, of A²E*-XII system 0-74306 SH, chemical, of A²E*-XII system 0-74306 SO radical, microwave obs. of first electronically excited state 0-70962 SO₃, vibrational, in i.r. fluorescence 0-61134 TiPs hand spectrum excited in emission in radio-frequency discharge.

TiBr band spectrum excited in emission in radio-frequency discharge 0-43137

intermolecular mechanics
see also Association; Collision processes/molecules; Kinetic
theory/gases; Liquids/structure; Liquids/theory; Solids/theory
acetone in various solns., width of polarized Raman lines as function of
conc. 0–50234

anharmonic ososilator, classical, collisional excitation by refined impulse approx. 0-43203

aniline derivatives, ortho disubstituted, intramolecular proton exchange 0-55334

0-55334
anisotropic pseudo- potential for nematic liquid crystals 0-67845
anthracene-gas pair interac. from second cross virial coeffs. 0-43432
aromatic compounds, relative intensities of intramolecular and lattice vibrations in Raman spectra 0-51327
asymmetric molecules, pairwise nonadditive dispersion potential 0-43207
beam scatt. data inversion for intermolecular potential determ. 0-64594
benzene-halogen weak complexes, intermolec, interactions 0-58268
cell model, single occupancy, variation treatment extension 0-64621
charge overlap effects, dependence on nature of interaction 0-64587
chloro-alkanes, secondary, liquid spectra and intermolec, vibr. 0-39808
chloroform, liquid, Raman spectra, effect of intermolecular interactions
0-43460 0-43460

0-43460
combining rule for intermolec, distances in potential functions 0-58265
crystal, forces, rel. to equilib. form 0-61700
crystals, forces, review 0-43841
cyclic hydrocarbons, dynamics, cold neutron spectra 0-47511
cyclopropane-Ar mixture, translational and vibrational energies exchange
efficiencies, velocity dispersion analyses 0-53098
diatomic mols. effect of nuclear motion 0-46630
dipole-octupole interactions contrib. to pot. energy
dipole-quadrupole dispersion forces associated with metastable atoms
0-67657
dve molecules in aggregates, extended dipole model for calculation of inte-

0-0/657
dye molecules in aggregates, extended dipole model for calculation of interaction integrals 0-64578
energy transfer, electronic, review 0-58264
energy transfer meas, using picosecond light pulses 0-64576
exchange energy dependence on orbital overlap 0-64588

Molecules continued

intermolecular mechanics continued excited atoms and molecules, intermol. potential from matrix shifts $0\!-\!71064$

flow field density profile over flat plate, molecular mean free path concept applic. 0-43385

hard nonspherical molecules, virial expansion 0-64618

hexamethylenetetramine, dynamics, neutron scattering investigation

hexamethylenetetramine, dynamics, neutron scattering investigation 0–71069
inert gas, exp-6 cell model calc., triple-dipole term effect on thermodynamic props. 0–47497
inert gas atom interaction in region of small overlap, comparison of HF and LCAO-MO solns. 0–64583
inert gas crystals 0–39898
inert gas solids, exp-6 cell model calc., characterization of pair potential parameters 0–47496
interaction energies of non-bonded H in A-H...H-B systs. 0–74440
interactions, bound and quasi-bound state energies 0–79427
interactions on air table, apparatus for demonstrations 0–77980
intermolecular forces, origin, teaching 0–74439
ion-molecule interaction in acetonitrile solution 0–67846
ion-molecule reactions 0–61199
Lennard-Jones 3, 9 pair potential study 0–67840
Lennard-Jones fluid, molecular dynamics investigation of coherent scattering function 0–77990
Lennard-Jones fluid, molecular dynamics investigation of coherent scattering function 0–77990
liquid, force constants rel. to Gruneisen coeff. 0–64853
liquid structure factor S(k) and velocity autocorrelation function $\psi(t)$ computation, Monte Carlo and molecular dynamics technique 0–50196
liquids and solns., fluctuation processes, broadening of i.r. abs. bands 0–43047
membrane, biological cell, molecular adlineation, charge-fluctuation forces

membrane, biological cell, molecular adlineation, charge-fluctuation forces

0—58448 methane, gaseous, interaction effect in neutron scattering 0—67854 methane, viscosity 293 to 1050°K and inteermol, forces 0—74686 mobility macromolecular polymers, in solns, study by polarized luminesc. 0—67830

Morse parameters, general eqns. 0–77979
multicomponent solns., intermolecular interactions and spectra, composition of solvate sheath 0–58266
multilayer syst., Lifshitz theory of van der Waals interactions 0–74449
naphthalene adsorbed on zeolite, Van der Waals forces rel. to abs. and fluorescence spectra 0–46583

nuorescence spectra 0-46583 naphthalene in foluene, solns., triplet-triplet annihilation prod. by mol. interact. 0-68118 nitrobenzene-n-anisidine (diphenylamine, diphenyl methane), interactions, u.v. spectra and optical density investig. 0-49951 non-polar molecules in liquids. ¹H chemical shifts, intermolecular effects 0-49849

0—49649
optically active, pair-wise interaction, formulation for dispersion and resonance forces 0—64579
organic, inter- and intramol, forces study by dielec, relax times in liq, state
0—5336

organic, ultrafast intermolecular electronic energy transfer using picosecond light pulses 0-64576

Pade approximants for two- and three-body dipole dispersion interactions 0-5392 pair potential of polyatomic mols., nonadditivity 0-61195 pairwise nonadditive dispersion potential for asymmetric molecules 0-43207

Percus-Yevick hard sphere radial distribution function, analytical representation 0-55397

representation 0-5597 picoline. Raman spectra, intermolecular interactions for picoline dissoved in water, ethanol and methanol 0-64926 polar, potential function and second virial coeffs. 0-64580 polar-quadrupolar gas mixtures 0-39681 polymer coil expansion in solvent, interfacial free-energy effects 0-39743

potential, mol. beam scatt. obs., thermal to ~ leV, and theory 0-46625 potential energy, elec. dipole-octupole interactions contrib. 0-43204 potential energy consts. using order-disorder phenomenon of melting 0-46624

potentials and width of pressure broadened spectral lines 0-61089 potentials determ. from crossed beam differential elastic scatt. meas. 0-67844

0-67844
pyridine, matrix isolated, pair assoc. obs. 0-71027
relativistic long-range interactions 0-43004
retarded van der Waals potential, arc-tangent approximation 0-64246
scattering, anisotropy effects in potential 0-46629
site factors in n.m.r. solvent effects 0-55284
small molecular interactions calc. by differences of separate total energies
0-64589

solution, multi-component, molecular spectra 0–49834 solvent effects on molecular electronic spectra 0–58140 spectral intensities, vibrational effects 0–46920

structured mols., coupling between linear and ang. momentum 0–43202 thermodynamic excess functions for mixtures of nearly spherical mols 0–53312

0-3312 trichlorofluoromethane, liquid, Raman spectra, effect of intermolecular interactions 0-43460 triplet-triplet energy transfer, orientation, for donor-acceptor pairs 0-76277

0-76277
two subsystems in states with given spins, interact., calc. via coordinate wave functions 0-46631
uniqueness of intermolec, potential determ, from differential cross-section extrema 0-55390
van der Waals coefficients from quantum mechanical oscillator strength sum 0-71070
Van der Waals consts. determ, from total cross sections 0-61204
van der Waals forces on function of distances 0-61205
van der Waals forces on function of distances 0-61205

combination rules 0-74448 van der Waals forces as function of distance 0-61205 van der Waals interaction between anisotropic macroscopic objects 0-74447 van der Waals interactions in multilayer syst. Lifshitz theory 0-74449 van der Waals interactions optimal choice for aromatic mols. with steric hindrance 0-58201

Van der Waals pot. for He adsorbed on glass 0–71497 vanadyl acetylacetonate nematic liquid crystal, anisotropic pseudo-potential 0–67845

velocity dependence of total cross-section 0-61196

intermolecular mechanics continued

vibrational energy transfer and storage, multiauthor book 0-58144 virial eqn. of state, book 0-55560

Ar He intermol. pot., from supersonic beam scatt, obs. 0-39365 Ar, intermolecular potentials from differential cross section meas.

Ar, rainbow scattering and intermolecular potential 0-77981
Ar, repulsive potential, from gas viscosity data 0-77986
CO₂-N₂ inter- and intra molecular vibrational energy transfer, shock technique 0-43096

CO₃, energy transfer and vibr. relax., gas laser obs. 0–49954 CeO₃ adsorbed on synthetic zeolites, hindered motion obs. from e.p.r. 0–70922

0-70922 Cft viscosity 293 to 873°K and intermol. forces 0-74686 D₃, quantum corrections for noncentral intermolec, forces to second virial coeff. 0-61439 H₂-He nuclear relaxation, multistate, potential fit up to 300K 0-49955

Hydre nuclear retaxation, multistate, potential fit up to 300K 0-49955. H halides, i.r. vibrational spectra, effect of intermolecular forces 0-43112. Hy, chart range interaction with H atom, energy calculation 0-71071. Hy, orientation dependent van der Waals coeffs, for various interacting species 0-61201. Hy intermolecular potential from inelastic collision processes. 0-74442.

Hs intermolecular potential from inelastic collision processes 0–74442 HCl, intermolec. potentials and width of pressure-broadened lines 0–61089

0-61089
HF, solid, intermol. binding 0-59078
HF, solid, intermol. binding 0-59078
HO, in ionic solns., low freq. motions, neutron scattering spectra 0-61483
H-O polymers 0-53033
He-H-1 nuclear relaxation, multistate, potential fit up to 300K 0-49955
He a two parameter intermolecular potential which fits the temperature range, 1-2000K 0-46808
Hg(\$P_0\$) Xe complex emission band obs. during irradiation of Xe-Hg gas mixture rate constant for reaction determ. 0-74274
Li-HF interaction potential 0-46633
Li-HF interaction potential, analytical expression 0-64608
Li*+H₂, interaction potential, rotational excitation region 0-64601
NO₂ adsorbed on synthetic zeolites, hindered motion obs. from e.p.r.

 NO_2 adsorbed on synthetic zeolites, hindered motion obs. from e.p.r. 0-70922

Ne-Ar (Kr,Xe) crossed beam differential elastic scatt., potentials determ. 0-67844

Ne, intermolecular potentials from differential cross-section meas. 0-64599

D₂ trapped in solid matrices. Lennard-Jones potential for $E^3I_{u^2}$ state 0.55311

OH groups, weak interactions, i.r. study of phenol and diisopropyl phenol 0-55395

SF₄ viscosity 293 to 873°K and intermol. forces 0–74686 Xe G mixtures (G=other gas), ¹²⁹Xe chem. shift density depend. 0–71068

internal mechanics

internal mechanics A_0 determ. by resonance interactions with v_S 0-61167
chlorophyll, mol. energy 0-67779
coupling consts. of directly bonded nuclei 0-46444
cyclopropyl-allyl ring opening modes 0-49917
p dimethoxybenzene attached to spirocyclopropane- norbornane frame, energy transfer 0-77856
distortion constants, fourth-order centrifugal, XY; type mols. 0-49844
ethane, bi- and tri-halogen derivatives, isomers, $I_0I_0I_0$ products of principal inertia moments 0-43161

ethylene, excited and cation, isomerization processes, energy barrier calcs, semiempirical quantum chemical method 0–39428 ethylene, secondary dispersion due to motion of chain branches 0–47327

fluorotoluene, torsion-vibration interaction, microwave spectral obs

halogens, perturbations in long range interactions, second order effects 0-64426

isopropyl alcohol, internal rotation and microwave spectrum 0-43169 long-range Born-Oppenheimer interatomic potentials, adiabatic corrections 0-39307

tions 0–39307
methyliodide, A₀ determ, by resonance interactions with v_5 0–61167
phenanthrene attached to spirocyclopropane norbornane frame, energy transfer 0–77856
5-phenyl 2 pentene, intramolecular energy transfer 0–72552
polyatomic, inertia defect formula, derivation 0–46427
polymer, chain, excluded volume effect 0–74426
polymers, molecular motion, halogen effects 0–49946
porphyrin, mol, energy 0–67779
potential energy curves, diat, mols. 0–64406
propane, clathrate hydrate, p.m.r. study of motion 0–64540
quinolines, hydrated, internal interactions on the basis of absorption spec-

propane, clathrate nydrate, p.m.r. study of motion 0-04540 quinolines, hydrated, internal interactions on the basis of absorption spectra 0-53084 triglycine sulphate, y-irrad., e.p.r., internal motion of H and glycine (I) activation energy 0-62768 united-atom model for XH_n molecules 0-49828 vibrational-rot, interactions in polyat, mols., algebraic struct. 0-46421 XY₂ type, mean internucl. distances, Coriolis interaction influence 0-55282 0-5282
XY:-type, fourth-order centrifugal distortion consts. 0-49844
AuBe, potential energy curves 0-70874
C: pot. energy curves 0-64406
C: pot. energy curves 0-64406
H:, many-body perturbation theory 0-58173
H: pot. energy curves 0-64406
He:, \(\frac{12}{2}\tilde{x}\) potential calc. at intermediate and large separations 0-74273

He₂, 'D₂* potential calc. at intermediate and large separations 0–74273 He₂, potential-energy curves 0–43117 He₂ pair correlation energy calc. 0–77798 He₁, ground-state energy 0–58177 Hezh₂²⁴, potential energy surfaces 0–53038 I₂ pot. energy curves 0–64406 ICl, perturbations in long range interactions, second order effects 0–64426 KCl, SCF calc. on molec. props. 0–58180 LiBr, SCF calc. on molec. props. 0–58180 MgH, theoretical calc. of props. 0–39384 N₂ pot. energy curves 0–64406 O₃, pot. energy curves 0–64406 O₃, pot. energy curves 0–64406 O₅, pot. energy curves 0–64406 O₅, pot. energy curves 0–64406 VCS, second-order force consts. and F-matrix soln. 0–53047 SO₃, Coriolis couplings consts. i.r. obs. 0–43134 WF₅Cl, molec. consts. 0–74311

Molecules continued

moments

acetonitrile N-oxide, dipole moment from Stark effect 0-74325 acetylacetone and deuterioacetylacetone molecules, dipole moments of indi-

vidual bands 0-64472

alkyl mesityl ketones and aliphatic and phenyl analogs, dipole moments 0-49901

0-49901
anilines in cyclohexane at infinite dilution, dipole moments 0-64479
aryltricyanoethylenes, dipole moments 0-61144
benzimidazole, determ, of dipole moment in excited state 0-64514
bicyclol2.1.0lpent-2-ene, dipole and quadrupole 0-77873
cis-2-butene, dipole moment from Stark effect 0-46546
carboranes. CNDO/2 calc. 0-74246
chloroform, dipole moment from microwave spectra 0-61179
condensed predium e m. dipole interaction, quantum electrodynamics

condensed medium, e.m. dipole interaction, quantum electrodynamics treatment 0-47009

diamagnetic susceptibility of infinite bands, II electron ring currents, quantum mechanical calculations 0–53058 difluoroethylene, dipole moment derivs., appl. to i.r. itensity interpretation 0–74362

1,1-difluoro-3-methylbutadiene dipole moment from microwave spectra 0-46557

dimethyl ether, mag. susceptibility anisotropy and quadrupole moments

0-43160

0–43160 dimethyl sulphide, mag. susceptibility anisotropy and quadrupole moments 0–43160 dipole, binding of an electron by critical dipole moments 0–49830 dipole, binding of an electron by critical dipole moments 0–49830 dipole-quadrupole polarization correlation in photo-selection 0–46438 electric dipole moments and relaxation times, abs. of microwave radiation by solutions 0–39822 electric moment, dependence of average reaction field of arbitrary charge distribution in ellipsoidal cavity 0–49846 electric-dipole transition moments calc. 0–74217 electron, critical binding to non-stationary electric dipole epihalohydrins, dipole moments 0–64503 ethane, bi- and tri-halogen derivatives, isomers, I₄I₄I₆, products of principal inertia moments 0–43161.

ethane, chemical polarization of protons, n.m.r. meas. 0–71007 fluoroacetylene, mag, susceptibility anisotropy and mol. Zeeman effect 0–77910

p-fluoroaniline, dipole moment of lowest singlet $\pi^*\leftarrow \pi$ state 0–71002 fluorobenzene, first excited state $\pi^*\leftarrow \pi$, dipole moment correlation with structure 0–46561 p-fluorophenol, dipole moment of lowest singlet $\pi^*\leftarrow \pi$ state 0–71002 formaldehyde, electric dipole moment in 3A_2 excited state, Stark effect 0–43162

0-43162
glycolaldehyde, dipole moment determ, from Stark effect meas. 0-58223
group IV/VI compounds, electric dipole for ground vibrational state
0-70866
HCl, dipole moment functions from i.r. line intensities 0-70888
N-heterocyclic benzene analogues, dipole, calc. using approximate MO
theory 0-39441
hydrocarbons, aromatic, polarizability in ground and first excited state
0-43068
hydrocarbons, polarizabilities, bond additive property 0-55354

hydrocarbons, polarizabilities, bond additive property 0-55354 hydrocarbons, simple, dipole moments, NDDO and CNDO predictions 0-49928 impulse distrib., wave functions on Gaussian function base 0-49766

impulse distrib., wave functions on Gaussian function base 0–49766 indazole, determ. of dipole moment in excited state 0–64514 indole, determ. of dipole moment in excited state 0–64514 ketones, diamagnetic susceptibility meas. 0–53356 measurement of dipole moments in solutions 0–74767 methane. Zeeman splitting obs. in vibration- rotation spectra of ¹Σ, rotational magnetic moment determ. 0–77924 methane, chemical polarization of protons, n.m.r. meas. 0–71007 methane ion, CH₅*, dipole moments for different possible geometries 0–43173

methane polarizability tensor components, CNDO/II calculations 0-64355 methane-d₁, elec. dipole moment from elec. resonance spectra 0-71022

methyl and methylene fluorides CH stretching deviations due to hybridization dipole moment of methyl group 0–53057

2-methyl thiophene, microwave spectrum, internal rotation and dipole moment 0–64525
methylacetylene, mag. susceptibility anisotropy and mol. Zeeman effect 0–77910 microwave spectrum, internal rotation and dipole

methyldiacetylene, mag. susceptibility anisotropy and mol. Zeeman effect 0-77910

methylene halides, intensity of v_5 band, connection with induced dipole moment 0-49933 methylenecyclopropane, dipole moment 0-53077

methylenecyclopropane, dipole moment 0-53077
2-methylfurane, dipole moment 0-46572
nitroaromatics, contribution of dipole moment of ground and lowest triplet state to polarization of phosphorescence 0-64533
nitroethane, dipole moment components 0-77938
organic molecules, diamagnetic susceptibility calculation 0-58204
perturbed mols., quadrupolar moments determ, method using n.m.r.
0-43075

phenanthrene, excited state dipole moments by Stark modulation spectroscopy 0-58237

4-phenylazo-1-naphthols, in benzene and dioxane soln., dipole moments 0-64537

polarizabilities of excited molecules from second-order perturbation theory $0\!-\!43068$

0-43008
polarizability and hyperpolarizability components, finite perturbation SCF valence shell calculations 0-58155
polarizability tensor components, CNDO/II calculations, axially symmetric molecules 0-64355
polarization, induced dynamic nuclear spin, and contact hyperfine interac-

tion 0-64356 polymethacrylic esthers, dipole moments meas, in dilute solns., 10-120°C 0-58262

polypeptides, H-bonded, dipole moments 0-64574

polypeptides, H-bonded, dipole moments 0–64574 polypeptides, molecular wavefunctions of monomeric amides study, to account for polarization 0–64573 propyl alcohol, microwave spectrum 0–53083 pyridine, magnetic susceptibility and quadrupole moment 0–46586 pyrimidine, dipole moment, from microwave spectra 0–77949 quadrupole, study ret, to mol, Zeeman effect 0–77828 quadrupole moments and g-values of eight ring compounds 0–77892

Molecules continued moments continued

noments continued
quinones, ortho and para, dipole moment calculation 0–58242
second harmonic generation in a 2 level system 0–42917
stimulated electric polarization, photon echoes 0–64360
symmetric top molecule, nuclear electronic quadrupole interaction energy
0–74216

trichloromethyl fluoride, dipole moment from microwave spectra 0-61179 trimethylene oxide magnetic susceptibilities and quadrupole moments 0-46595

trimethylene sulphide magnetic susceptibilities and quadrupole moments 0-46595

0-46595
trioxane, solid state dipole moment determ. 0-61930
vinyl isocyanide, dipole, in ground state 0-55378
Beß Hs, dipole 0-67715
CF₃SF₃, dipole, from dielec, relaxation of vapour 0-64390
CO, dipole moment functions from i.r. line intensities 0-70888

CO₂ compressed, quadrupole moment from absorption coefficient 0-43086

CO, dipole moment functions from i.r. line intensities 0–70888
CO: compressed, quadrupole moment from absorption coefficient 0–43086
CS, Al TI state, dipole moment 0–46455
CS, dipole moments for rot. levels J=3 through 9, by optical-r.f. double reson. expts. 0–70891
CISFs. dipole, from dielec. relaxation of vapour 0–64390
D. quadrupole 0–61439
D³5Cl. dipole moment from molecular-beam electronic resonance spectra 0–67731
GaF elec. dipole moment 0–46470
GeTe elec. dipole moment 0–46470
GeTe elec. dipole moment 0–46470
H.; electric dipole polarizabilities calc. by geometric approx.. magnetic susceptibility 0–74097
H.; electric dipole moment by investigation of Stark effect 0–46473
HCN, calculated dipole-moments and i.r. intensities 0–64403
HCl dipole moment matrix elements of vibration-rotation bands 0–77790
H³5Cl. dipole moment from molecular-beam electronic resonance spectra 0–67731
HD and HD*, electric-dipole transitions 0–74266
HI electric dipole moment play investigation of Stark effect 0–46473
HO, quadrupole moment and sign of elec. dipole moment 0–70912
H-O polarizability tensor components. CNDO/II calculations 0–64355
InF elec. dipole moment, from microwave absorpt. spectra 0–67713
NCO radical, dipole moment, from microwave absorpt. spectra 0–67713
NS and NS*, dipole moment and i.r. intensities 0–64403
NS and NS*, dipole moment and i.r. intensities 0–64403
NS and NS*, dipole moment from microwave spectrum 0–67429
ACI, dipole, from r.f. spectra 0–61126
ACI, dipole, from r.f. spectra 0–61126
ACI, dipole moment calc. from millimeter wave spectrum 0–77829
O. dipole moment calc. from millimeter wave spectrum 0–77829
O. dipole moment calc. from millimeter wave spectrum line-width calc. 0–77823
OCS, elec. dipole and mag. moments, by molecular-beam electric-reson. spectroscopy 0–77822

0-7823
OCS, elec. dipole and mag. moments, by molecular-beam electric-reson. spectroscopy 0-77822
OCS, elec. dipole moment and mol. quadrupole moment 0-70940

OCSe, magnetic susceptibility anisotropy and quadrupole moment 0–74295

0—74295
OF(²II), dipole and quadrupole 0—70936
OH, 79-ym electric dipole moment meas, by magnetic resonance absorption method 0—61130

tion method 0-61130
PbSe elec. dipole moment 0-46470
PbTe elec. dipole moment 0-46470
SF, dipole and quadrupole, for neutral and charged species 0-74304
SO₂, dipole-dipole interaction, microwave spectral line-width calc. 0-77823

0-77823
SO₂, dipole mom i.r. spectra obs. 0-55320
SO₃, dipole moment correlation for SCFMO calculations on both minimal and extended basis 0-67753
SO₃, elec, dipole moment in ³B, state 0-79317
SO₃, SCF calculations 0-74233
SeD, dipole, e.s.r. determ. 0-49892
SeF, dipole and quadrupole, for neutral and charged species 0-74304
SeH, dipole, e.s.r. determ. 0-49892
SeF, dipole set of the special control of the special species of the special species of the special speci

nuclear coupling actonities N-oxide, 14N quadrupole coupling constant 0-43139 actonities N-oxide, 14N quadrupole coupling constant 0-74325 acetylenes, halogen substituted, J_{eb} couplings 0-43146 acid fluorides, vicinal proton-fluorine coupling constant, obs. of change of sign with dihedral angle 0-67793 acyclic phosphates, P-H spin-spin coupling consts. 0-77858 aldehydopyridines, monosubstituted, long range coupling consts. 0-77922

0-1922 allenic ketones, solvent effects on spin-spin coupling constants 0-43170 allenic phosphines, solvent dependence of \$\foat{3}(P-H)\$ and \$\foat{4}(P+H)\$ 0-67761 amino acids, \$\foat{18}N-H\$ coupling as source of proton resonance line broadening 0-74330 aniline derivatives, ortho disubstituted, long-range proton coupling 0-55334

0-35334 anisotropy of indirect nuclear spin spin coupling constant, treatment by finite perturbation method 0-74222 anthracene, spin-orbit coupling and radiative triplet lifetimes 0-67807 azines, neutral and protonated, H-H and C-H coupling constants azines, ne 0-67766

benzenes, substituted, SCF-MO theory of proton-proton coupling 0-74338

0–74338
benzenethiol-d, deuterium quadrupole consts. 0–53082
benzocycloalkenes and benzocycloalkenediones, proton-proton spin-spin consts..rel. to strain 0–53063
benzotrifluoride, nuclear spin-internal rotation coupling 0–77876
N-benzyl-2-methylpiperidines, para- and meta-substituted, substituent effects on geminal proton-proton coupling constants 0–67768
bicycle compounds, fluoro-substituted, vicinal H-F coupling, combined substituent and angular effects 0–49909
bicyclic hydrocarbon radicals, e.s.r. study 0–74344
bicyclo[2.2,2]octane derivatives, n.m.r. obs. 0–39416
bromovinylcyclopropanes n.m.r. spectra, coupling constants interpreted 0–43152

0-68153

Molecules continued

nuclear coupling continued

0–43059 cyclopropanes, monosubstituted 0–74353 dibromomethane, nuclear quadrupole coupling tensor 0–46555 2.3-dibromopropene, using double irradiation for assignment of very small coupling const. 0–77894 2.6-dichlorobenzaldoxime, long-range spin spin couplings signs, nonplanarity degree 0–39424 2.6-dichlorobenzylduoride, long-range spin-spin coupling consts. conformational depend. 0–39423 dichlorodifluoromethane, liq., from ¹⁹F relax. times, temp. and field depend. 0–74792 1.2-dichlorofluoroethylenes, solvent depend. of coupling constants 0–77897

tert-butyl radical, e.s.r. study of effect of temp. on hyperfine coupling 0-74409 2-chloroethyl and related radicals, hyperfine coupling constants 0-53066 3-chlorogrophene, 3-Cl nuclear quadrupole coupling constants 0-53066 skew, cis forms 0-77889

conjugated molecules, long distance coupling, dependence on environment and delocalization of π electrons 0–43077 coordinated solvents, electric field effects of highly charged cations

Coriolis interac. consts., for vibr. problem of tetrahedral mols. of XY4 type

0—77897
dichlorotetrafluorocyclopropanes, F-F coupling constants 0—67777
1,2-difluoroethane, vicinal coupling constants 0—67792
diffurylmercury isomers. ¹⁹³Hg ¹H long-range coupling constants 0—74361
2,5 dihydrobenzoquinone, long range coupling, spatial factor associated with π electrons 0—43077

with π electrons. U-43077 (2.6-dinitrobenzaldehyde, spin spin coupling between aldehydic and ring protons, hyperconjugative contrib. 0-39422 directly bonded nuclei, coupling consts. 0-46444 directly bonded nuclei, systematic trends in coupling consts. 0-61061 dithienylmercury isomers, ¹⁹⁹Hg-¹H long-range coupling constants 0-74361

durosemiquinone triplet-ions (DQ-, 2Na+), sodium coupling constant 0-59477 0-34417 epichlorohydrin, signs of long-range spin-spin coupling constants 0-64502

0-0402 epihalohydrins, coupling constants 0-64503 ethanes, substituted, SCF-MO theory of vicinal proton-proton coupling 0-74366

ethanes, substituted, depend. of vicinal H-H coupling on internal rotation 0-39427

0—39427
ethanes, substituted, medium effects on coupling constants 0—74367
N-ethyl -4-chloro-2- nitroaniline, signs of long-range amino proton-ring proton coupling constants 0—58219
ethylenes, substituted, SCF-MO theory of vicinal proton-proton coupling 0—74366

6-17900 fluorinated small ring systems, effect of substituents on coupling constants 0-67797

fluorobenzaldehyde radical anions, e.s.r., hyperfine coupling constants

fluorobenzyl radicals e.s.r., hyperfine coupling constants 0–49944 fluoropyridines, (N, F) coupling constants, temperature and medium effects 0–49925

gaseous systems, spin-spin coupling constants, temp. dependence 0-67710

0–67710
hexafluorobutyne-2, nuclear spin-internal rotation coupling 0–77876
hexafluorobutyne-2, nuclear spin-internal rotation coupling 0–77876
hydrocarbons, aromatic, effect of spin-orbit coupling on radiative and nonradiative transitions 0–77853
N-methyl 2-carbomethoxy- 4.6-dinitroaniline, long range spin-spin established by p.m.r. 0–5361
methyl fluoride, anisotropy of indirect nuclear spin spin coupling constant,
treatment by finite perturbation method 0–74222
methylammonium ion, small correlation coupling effect 0–62693
methylbromodiazirine, Br quadrupole coupling consts. 0–67804
methylchlorodiazirine, Cl quadrupole coupling consts. 0–77958
methylfluoride, in liq. cryst., vibr. corrections on dipole dipole interactions
0–77919
methylpryridines monosubstituted long range coupling consts. 0–77022

morpholine, quadrupole coupling consts. from microwave spectrum 0-77930 0–77930 n.m.r. linewidths homogeneous broadening due to intermolecular relaxation 0–46442 naphthalene, spin-orbit coupling and radiative triplet lifetimes 0–67807 nitrobenzenes, deuterium quadrupole coupling consts. 0–53080 nitroxide radicals, fluoro-substituted, angular dependence of β -fluorine e.s.r. hyperfine coupling 0–55367 orbital contribution to spin coupling tensor, and screening tensors 0–67707

organophosphorous and organoselenium cpds., ¹K_{pc} signs 0–39445 oxetane n.m.r. analysis of coupling constants 0–49940 penta- and hexadienes, coupling consts. involving methyl protons 0–77889.

0—/1883 perfluoroalkyl-fluoroaromatic compounds, F-F coupling constants from ¹⁹F nmr spectra 0—64536 perfluorocyclobutanone ketyl, long range fluorine coupling 0—55366 phenanthrene, spin-orbit coupling and radiative triplet lifetimes 0—67807 phenyl ring protons in ligands of paramagnetic complexes, σ-contribution to hyperfine coupling constants, 'anomalous' spin density distribution 0—58238

phenyphosphine-d₃, deuterium quadrupole consts. 0–53082 phenysilane-d₃, deuterium quadrupole consts. 0–53082 propylene oxide, coupling constants 0–64503 proton hyperfine coupling consts. in radicals, effect of orbital overlap 0–64361

purine, subst. derivatives, spin-orbit coupling induced by S atoms 0-77946

0-/1946
2-pyridones proton coupling constants from p.m.r. spectra 0-55370
2-pyridylphosphine derivatives. 'H-31P coupling constants | 0-49936
pyrimidine, subst. dervatives, spin-orbit coupling induced by S atoms 0-77946

quadrupole, nuclear volume effect 0–74215 quadrupole coupling consts., semiempirical calc. 0–43076 radicals, proton hyperfine coupling consts. and effect of orbital overlap 0–64361

SCF MO theory, geminal proton-proton coupling consts. 0-74317

nuclear coupling continued

nuclear coupling continued

SCF-MO theory of nuclear spin coupling 0-74338

SCF-MO theory of nuclear spin coupling 0-74338

SCF-MO theory of nuclear spin coupling 0-74368

spin relaxation in presence of internal rotation 0-77876

spin-spin coupling constants, calculation, investigation of average energy and other approximation methods 0-64365

steric compression effect on proton-proton and spin-spin coupling consts. 0-74318

2,3.5.6-tetrafluoroaniline, n.m.r., aromatic H-F and F-F coupling constants, relative signs 0-46443

1,1.2.2-tetrafluoroethane, solvent dependence of coupling constants 0-49438

0-49938 1,1,2.2 tetrafluoroethane, vicinal couplings constants 0-67792 thietane, n.m.r. analysis of coupling constants 0-49940 2-thioalky/pyridines proton coupling constants from p.m.r. spectra 0-55370

transition metal complexes, P-P coupling constants 0-67711 transition metal fluorides and cyanides, hyperfine coupling to ligands 0-64372

11-3-12 spin coupling constants 0-67822 tri-3-thienylphosphine, and derivatives, 1H ^{31}P spin coupling constants 0-67822

0-67822 tricyclopropyllorane, n.m.r. spectrum, correlation between coupling constants and substituent electronegativities 0-43184 3,3.3-trifluoropropyl tin cpds., Sn coupling consts. 0-67823 tri-(5-methyl-2furyl)phosphine derivatives. ¹H-³¹P spin-spin coupling constants 0-74384 vicinal coupling constants, in X.CH-CH-.Y fragments, effect of substituents 0-67755

vinyl compounds, substituent effects on J_{c^-h} Coupling constants 0–58253 xylene derivatives, intermethyl proton spin-spin coupling constants signs

(CH)PF₄, P-H and P-F coupling consts. from mag. double reson.

0–46506
CH:NO radical, hyperfine coupling consts. from MO calc. 0–77911
CICN, ¹⁴N quadrupole coupling const. in liquid phase 0–53376
CINs, from microwave spectra 0–70892
C(IN), from microwave spectra 0–70892
C(II), complex, dichlorobis(picoline)cobalt(II), in CDCl₃, paramagnetic shift evaluation of proton-electron hyperfine coupling 0–49861
CrO(III) complex, dithiophosphenes, hyperfine interaction of ³¹P 0–70898
Cu(II) complex, dithiophosphenes, hyperfine interaction of ³¹P 0–70898
GaF elec, quadrupole const, from microwave absorpt, spectra 0–67713
H, indirect spin spin coupling by truncated matrix sum method 0–55297 GaF elec. quadrupole const. from microwave absorpt. spectra 0–67713 H · indirect spin spin coupling by truncated matrix sum method 0–55297 HF and DF. h.f.s. constants 0–53035 HPFs., P-H and P-F coupling consts. from mag. double reson. 0–46506 'H-3'P coupling constants in organophosphorus compounds determ. from 'H-n.m.r. obs. 0–39450 'H-3'P spin coupling constant in 2-pyridylphosphine 0–49936 'H quadrupole coupling constant anomaly explained 0–74261 'H quadrupole coupling consts., semiempirical calc. 0–43076 InF elec. quadrupole coupling 0–43121 LiH-, hyperfine coupling 0–43121 LiH-, hyperfine coupling constants for Na and H for various bond lengths 0–49854

MoO(III) complex, dithiophosphenes, hyperfine interaction of ³¹P

Notify complex, diminiprospienes, hyperfine interaction of ³⁴P 0-70898 N₂(A³Σ_a+), metastable, r.f. spectrum, mag, hyperfine and elec. quadrupole constants 0-70921 NH₂ radical, calculated hyperfine coupling constants 0-67742 NH₂CONHO radical, relative signs of principal elements of α-proton hyperfine coupling insor 0-79421 NH₂ quadrupole coupling consts, semiempirical calc. 0-43076 NH₂-Hefect of solvent interactions and H bonding 0-78313 NaCl and NaBr, hyperfine interaction consts., for vibr. states 0-39392 NaH⁴, hyperfine coupling constants for Na and H for various bond lengths 0-49854 ScF₆³ anion in aqueous soln., Sc-F coupling const. 0-78310 SiH₃SeFeH₃, long-range H-H coupling 0-70950 SiH₃SeFeH₃, long-range H-H coupling 0-70950 VO(II) complex, dithiophosphenes, hyperfine interaction of ³¹P 0-70898 WO(III) complex, dithiophosphenes, hyperfine interaction of ³¹P 0-70898 NO(III) complex, dithiophosphenes, hyperfine interaction of ³¹P 0-70898 NO(III) complex, dithiophosphenes, hyperfine interaction of ³¹P 0-70898 NO(IIII) complex, dithiophosphenes, hyperfine interaction of ³¹P 0-70898 NO(IIIII) complex, dithiophosphenes, hyperfine interaction of ³¹P 0-70898 NO(IIII) complex, dithiophosphenes, hyperfine interaction of ³¹P 0-70898 NO(I

see also Acoustic wave propagation; Dielectric phenomena; Liquids/theory; Nuclear magnetic resonance and relaxation; Paramagnetic resonance and relaxation aldehydes, aromatic, T₁-S₀ radiationless transition 0–46570 anisotropic relaxation time, average, for orientation of molecules, statistically calc. 0–64387

anthracene and derivatives, non-radiative transitions 0-77867 aromatic vapours, vibr. relaxation following inter-system crossing 0-58202

0–58202
benzene, radiative and nonradiative decay from 3 vibronic levels in $^{1}B_{2u}$ state. absolute rates 0–70970
benzene, vibr. relax. and competition with radiationless transitions in $^{1}B_{2u}$ state 0–55337
benzene, vibr. relax. in S₁ state 0–77878
chain model, free jointly of random coil polymer 0–46616
correlation function approach to radiationless transitions 0–74205
cyclic hydrocarbons, dynamics, cold neutron spectra 0–47511
deuterobenzenes, radiationless transitions, at 77°K 0–77893
diatomic nonpolar gases, rot. relax. 0–49956
electronic, due to breakdown of Born- Oppenheimer approx., theory 0–77749
fluorescent mol., rot. relax, by light pulse method 0–70840

0-77749
fluorescent mol., rot. relax. by light pulse method 0-70840
in gas, acoustic meas. method 0-58145
gas of diatomic molecules, relaxation, improvement to Montroll-Shuter
eqn. 0-55277
gases, polar, rot. collision numbers 0-49952
gases, rel. to classical absorption, precautions in applic. 0-70833
glass- forming systems of rigid molecules, secondary relax. 0-71366
hexafluoroacetone, vibrational relaxation and radiationless processes in gas
phase 0-46513.

phase 0-64513

Molecules continued relaxation continued

hydrocarbons, aromatic, effect of spin-orbit coupling 0–77853 ketones, aromatic, T₁+S₀ radiationless transition 0–46570 in liquids, processes and meas, methods, review 0–58148 liquids Kneser, binary mixtures of, sound absorpt, obs. 0–64900 long chain systems relaxation rates as evidence for twisting 0–61188 measurement using pulsed Kerr effect method, limitations 0–64333 molecular ion, vibrational state population, rel. to pulse discharge aftergroup melecular, time count, determine 0–6504

grow 0-40420 monomolecular, time const. determ. 0-55264 n.m.r. line broadening due to intramolec. dipolar relax. 0-53012 n.m.r. linewidths homogeneous broadening due to intermolecular relaxation 0-46442

naphthalene. fluorescence as function of vibrational level and excitation energy 0-77932 naphthalene. vibr. relax. in S₁ state 0-77878

non-radiative decay, line broadening and interference effects, novel mechanism 0-70846

ism 0-70846
non-radiative life-time, effect of successive light pulses 0-77748
non-radiative processes in photochemistry 0-79454
non-radiative transitions, conference 0-77737
non-radiative transitions from photoelectron spectra 0-77739
non-radiative transitions due to electronic energy transfer by donor in triplet state 0-77741
polar gases, rotational relaxation 0-61437
polyamides, i.r. spectroscopic studies 0-67835
polyatomic mols., large, non-radiative decay of fluorescing state, deuteration effect 0-39333
polymers 0-57688
polyurethanes, motion study by nmr and dielectric methods 0-67837
radiationless decay from phosphorescent triplets by zero-field spectro-scopy 0-77740
radiationless decay in large molecules, optical selection studies 0-70845

radiationless decay from phosphorescent triplets by zero-field spectro scopy 0-77740 radiationless decay in large molecules, optical selection studies 0-70845 radiationless processes, role of mol. stationary states 0-77738 rotational, fluctuation barrier model 0-64350 rotational relax times meas, from gas thermal transpiration obs. 0-39346 rotational relax times from thermal conductivity in gases 0-43396 toluene, vibr. relax, in S. state 0-77878 transition rates obtained from sound absorption and dispersion curves 0-64328

0–64328 unimolecular reactions, vibrational relaxation and dissociation 0–46607 vibration, relaxation rate shock tube meas, review 0–58147 vibration, relaxation rate shock tube meas, review 0–58147 vibrational, anharmonic oscillators with vibration-vibration and translation vibration energy exchanges 0–77744 vibrational, relaxation time absorption and dispersion curves for obtaining transitional rates, analysis 0–53004 vibrational relaxation of an optically excited gas 0–49856 vibronic levels in large molecules, nornadiative decay 0–70853 CH+, metastable decomposition rel. to predissociation mechanisms 0–77964 CO₂/D-S mixtures and pure D-S, sound absorpt, meas. 0–64398 CO₂-D-S sound absorption meas, at 300°K, 400°K, vibrational-relaxation time analysis, exptl. results 0–53026 CO rotational relaxation numbers determ, from u.s. absorption 0–77776 CO vibrational relaxation of an optically excited gas 0–49856

CO vibrational relaxation meas, in shock-tube expansion wave 0–71057 CO vibrational relaxation of an optically excited gas 0–49856 CO+, non-radiative transitions, theory and expt. 0–77773 CO, compressed, vibr.-translation transition probability, temp. effect 0–55291

 $(O_3, of asymmetric v_3)$ vibration, meas. by optic-acoustic method $(O_3, of asymmetric v_3)$

 CO_3 , pure and in gas mixtures, vibrational relaxation, shock tube study 0-53021

 $\rm CO_{2},$ shock heated, vibrational relaxation studies of $10^{\rm o}0$ and $02^{\rm o}0$ states $0{-}70885$

O-70885

O-70886

O-70886

O-70887

O-70773

O-70887

O-80797

O-8 N., rot. relax. 0-49956 N., vibr., rates meas., behind shock waves 0-77814 N., vibrational, rel. to absorption of sound in air 0-53277

N₂, vibrational, rel. to absorption of sound in air 0–53277
N₃, vibrational relaxation in collisions with metal atoms 0–74446
N₃ rotational relaxation numbers determ. from u.s. absorption 0–77776
N₃O₂ excited, vibr. relax. 0–39386
N₃O₄ vibr. Napier relax. time. -H₁₅ -D₂ collisions effects, 32 and 52°C 0–39390
N₃O⁴, non-radiative transitions, theory and expt. 0–77773
O₃, rot. relax. 0–49956
O₃, vibr., rates meas., behind shock waves 0–77814
SCO⁴, non-radiative transitions, theory and expt. 0–77773
SF₆, i.r. double resonance study 0–46510
SF₆, i.r. double resonance study 0–46510
SF₆, b₃ vibr. mode fluoresc. lifetime 0–53048
rotation

rotation acetone, rotational Brownian motion from the width of vibrational band contours in molecular spectra 0-61143 p·X-acetophenone anion radicals, hindered rot, of acetyl group 0-64471 acrolein, excited state rotational constant, line width of rotational line from π^* -n singlet transition 0-49899 aminophosphines, P·N rotational barriers 0-49902 analysis of i.r. torsional data 0-74208 aromatic, rot, correl, times by proton spin-lattice relax. 0-61556 asymmetric rotor, i.r. spectrum, intensity perturbations and selection rule breakdown 0-70848 asymmetrical top mol., centrifugal distortion effects, Kivelson-Wilson theory applic. 0-61064

Molecules continued rotation continued

barriers to internal rotation, determination method 0-55273

benzene adsorbed on graphite, hindered rotation 0-39970

benzenes, substituted, rotational constants of 1st singlet excited state, interpretation in terms of molecular geometry 0–55340 benzofuran, rotl. analysis of 0-0 bands 0–74411

benzotrifluoride, nuclear spin-internal rotation coupling 0-77876

bromobenzene, rotational band contour analysis in 2700 Å system

butadiene-1,3, evi bands 0-74346 evidence for Cariolis coupling from vibration-rotation

butadiene-2,3 nitrile, microwave spectrum 0-49912

cis-2-butene microwave spectrum, internal rotation 0-46546

calculation of line strength factors for doublet transitions 0–67700 centrifugal distortion theory, matrix formulations 0–77751 chloro- and fluoro-substituted ethanes, barriers to internal rotation 0–74348

chlorobenzene, rotational Brownian motion from the width of vibrational band contours in molecular spectra 0-61143

3-chloropropene molecule, rotational constants of ground state isomers 0-77889

0-/1889
chloropropenes, rotational isomerism 0-67778
clathrate hydrates 0-62161
compound state resonances formed in subthreshold atom-diatom collisions 0-53097

corannulene, phosphorescent, e.s.r. studies, of pseudorotation and configuration 0-46551

configuration 0—46551 transcrotononitrile, microwave spectrum, rotational constants 0—39419 cyanogen, vibr.-rot. bands obs. 0—61156 cyclic hydrocarbons, dynamics, cold neutron spectra 0—47511 Cyclohexane, plastic crystal phase, rate of rotation of individual molecules 0—70850

cyclohexanol, liquid, mol. motions, quasi-elastic incoherent cold neutron scatt. obs. 0-78262

cyclopentane, pseudorotation, electron diffraction determ. 0–77890 diatomic, rot-vibr, energies, systematic procedure for perturbation calcs. 0–64340

0-04340 diatomic, used to determ, temp, of a gas 0-60089 diatomic molecule adsorbed on plane uniform surface, hindered rotation, eigenvalues and eigenstates 0-55275 diatomic nonpolar gases, rot. relax. 0-49956 p-dichlorobenzene, rotational band contour analysis in 2800 Å system

dichlorodifluoromethane, vibr.-rot. transitions, saturated absorpt. spectra 0-70844 p difluorobenzene, rotational band contour analysis in 2710 Å system

0-39423 1.1-difluoro-3-methylbutadiene, height of barrier hindering internal rotation of methyl group 0-46557 difluorophosphine borane, rot. consts. from microwave spectrum

0-10992
 dihalobenzenes, ortho- and meta-, far infrared absorption spectra explained by rotational transitions 0-46925
 N. N-dimethyl acetamide, n.m.r. studies, solvent effects on N-methyl reso-

N, N-dimethyl acetamide, n.m.r. studies, solvent effects on N-methyl resonance shifts and activation parameters 0-67806 dimethylcyclopropylcarbinyl cation, rotation barrier 0-67787 N, Ndimethylformamide, n.m.r. studies, solvent effects on N-methyl resonance shifts and activation parameters 0-67806 dissolved complexes, correlation times from rotational tracers 0-58256 with double-minimum potentials, constants of successive levels showing staggering 0-70860 e.p.r. line shape in viscous media 0-74788 energy operator of effective non-rigid asymmetrical rotor 0-64331 energy transfer from translational to rotational degree of freedom in atom-diatomic molecule collisions 0-74437 ethane and other mols., MO explanation for barrier to internal rotation 0-77902 ethanes, substituted, depend of vicinal H-H countries.

0-77902 ethanes, substituted, depend. of vicinal H·H coupling on internal rotation 0-39427 ethanes, substituted, internal rotation determ. by u.s. relaxation 0-74368 ethanes, substituted, n.m.r. study of rotational isomerism and barriers internal rotation 0-67791 ethylene, vibr.-rot. lines, saturated absorpt, spectra 0-70844 ethylene sulfone, constants from microwave spectrum in 8-26 GHz region 0-71000

ethyleneimine-type, rot.-inversion problem, exactly soluble model 0-77906

0-77906
excitation, exponential Born approx., computational studies 0-74435
excitation, exponential Born approx., computational studies 0-74435
excitation, statistical anal. of matrices in strong coupling 0-55389
excitation during ion-molecule collisions 0-61198
excitation in inclusitic collisions, strong coupling approx. 0-88132
excitation in inelastic collisions, statistics 0-61194
far i.r. spectroscopy, interferometers 0-49147
fluorescent mol., rot. relax. by light pulse method 0-70840
p-fluoroaniline, electronic bands analysis 0-53071
fluorobenzene, analysis of 0-0 band of 2644 Å system 0-55351
2-fluoroethyl radical, internal rotation 0-33066
o-fluorotoluene, internal rotation barrier, microwave spectral obs.
0-71037
formaldehyde, l₁₁₋₁-1₁₀ trapsition, in interstellar absorption details and other statistics. formaldehyde, 111-110 transition, in interstellar absorpt., in dark nebulae

0-66513

0-6513 formaldehyde, interstellar, 1₁₁-1₁₀ transition 0-66511 formaldehyde, interstellar, excitation 0-66514 formaldehyde, rotational spectra study by submillimeter microwave spectroscopy, rotational and centrifugal constants 0-64509 formaldehyde (H; ¹³Cl⁶O), interstellar, L₁₂-L₁₀ rotational transition, obs. at 4593 MHz 0-59729 globular type, barriers to internal rot. of methyl groups 0-64491 glycine, internal rotation from low temp, heat capacity data 0-62214 glycolaidehyde, constants from microwave spectrum 0-77913 glyoxal-d₃, structure of 4540 Å band system 0-77912 hamiltonian, for translating, rotating, vibrating mol. in presence of constant external e.m. field 0-64318 hamiltonian, vibrationa rotation, of linear molecules 0-64334

hamiltonian, vibrationa-rotation, of linear molecules 0–64334 heteroaromatic, rot. correl. times by proton spin-lattice relax. 0–61556 hexafluorobutyne-2, nuclear spin-internal rotation coupling 0–77876

Molecules continued rotation continued

> higher rot, terms of asymmetric rotor type mol., determ, by extrapolation 0-43060

0-43000 Hill-Van Vleck eqn. for diatomic mols, with spin-orbital coupling, particular solns. 0-49842

solutions. 0-45042 hindered rotation, polar molecules, in capture collisions with ions 0-64577

hydrocarbon, simple, rotl, barriers, NDDO and CNDO predictions

hydrocarbon, simple, rotl. barriers, NDDO and CNDO predictions 0-49928 hydrocarbon flame bands, struct. 0-49929 hydrocarbons, MO theory of internal rotation using minimal Slater-type basis 0-77916 indene, O-O band of 2800 Å transition, hybrid character and rotational

undene, O-O band of 2800 Å transition, hybrid character and rotations structure 0-46568 ion-dipole collisions, rot.-translational motion 0-64597 ion-dipole collisions, time histories plotted by computer 0-64598 ions, charge exchange with Ar* and Kr*, rot. and vib. populations obs. 0-61379

0-61379
isobutane, potential barrier from i.r spectra 0-46584
isopropyl alcohol, internal rotation and microwave spectrum 0-43169
isopropyl alcohol in the trans conformation, rotational constants 0-64516
laser, molecular, chemically pumped, vibr.-rot. transitions, simultaneous
inversion 0-73206
laser transitions, far-i.r. using Q-switching, resonator proposal 0-52268 level dependence on rotational effects on spin-orbit coupling in diatomics 0-49843

linear molecules, vibration-rotation hamiltonian 0–64334 in liquids, Frenkel model and the anisotropic component of Rayleigh scatt. 0–43449

methane_d, rot. struct. of v_6 band, 1161cm⁻¹ 0-55357 methane. 2947.906 cm⁻¹ line. appl. to frequency stabilisation of He-Ne laser 0-73226

methane, deuterated, fund. v_4 band interpret. .0-74374

metnane, deuterated, fund. p_1 band interpret. .0—74374 methane, dissolved in inert solvents, of i.r. bands 0—70910 methane, solid, near melting pt. 0—59092 methanethiol, 3 μ vib. rot. spectra, hindered internal rot. 0—39438 methanol, anal. from spectrum in region 550 to 900 cm⁻¹ 0—64528 methanol, torsion-rotation spectrum 0—64527 methyl alcohols, partially deuterated, α depend, of vibr. zero-point energy 0—58230

methyl chloride, vibr.-rot, band, 2080 cm⁻¹ 0-61166

methyl iodide, rot, constant A₀, direct spectroscopic obs. 0–71011 methyl rotor, torsional ground state model 0–64523

methyl frotor, torsional ground state model 0-64523 2-methyl thiophene, microwave spectrum, internal rotation and dipole moment 0-64525 methyl three-top mols. barriers to internal rotation 0-55358 2-methyl-1-buten-3-yne, methyl group barriers to internal rot. 0-77928 methyl-phosphorus compounds, torsional barriers, obs. from vibr. spectra 0-64530

0-64530 methylamine, internal rot, and amino-wagging vibr. 0-61171 methylarsine, barrier to internal rot, of methyl group 0-71015 methylbromodiazirine, barrier to internal rotation 0-67804 methylcyclopropyl ketone 0-77929 trans-methyldiimide, consts. from microwave spectrum 0-74387

methylene chloride, rotational diffusion in liquid, from i.r. spectrum 0-61510

methylenecyclopropane.rot. consts. 0-53077 microwave meas, using high-precision mm-wave spectroscopy and Lamb dip 0-61052

microwave spectra study of internal rotation 0–74209 microwave spectroscopy, calculation of nuclear quadrupole splittings 0–39347 morpholine, constants of ground vibr. state 0-77930

morpholine, constants of ground vibr, state 0—7/30 aphthalene in biphenyl cryst. hindered rot, in vibronic spectra 0—72379 neopentane, potential barrier from i.r. spectra 0—46584 nitroethane, rotational constants 0—77938 nitroethylene, constants of forsionally excited states 0—77941 organic, broad bands in microwave spectra, interpretation 0—70961 organic, configurational changes, about single bonds, chemical reactivity 0—43142

organometallic molecules, broad bands in microwave spectra, intepreta-

organometatic molecules, oroac bands in microwave spectra, interpretation 0-70961 orthorhombic moles, struct. of singlet transitions 0-77750 ozone, band origin of vs fundamental 0-39395 ozone, energy levels, comparison with rigid rotor 0-64331 1,3-pentadiene, trans and cis, methyl group barriers to internal rot. 0-77928

0-1726 phenanthridinium compounds, restricted rotation and magnetic non-equivalence 0-67812 9-phenyl thiaxanthyl radical, evidence of restricted rotation from e.s.r. spectra 0-67811

polar gases, rotational relaxation 0–61437 polar liquids, for infrared absorption spectra explained by rotational transitions 0–46925

polar molecules in condensed phases, microdynamics studied by dielectidispersion and vib.-rot. spectra 0-43054 polyatomic, vibr.-rot. interaction terms, algebraic struct. for high order 0-64341

0-64341
polyethylene oxide chains, rotational state populations, for bonds, effect of 'OH' end groups and temp, variations 0-55387
polymethacrylic esthers, internal rotation of side chains discovered by method of dipole moments 0-58262
polypeptides, H-bonded, int. rot. energies 0-64574
pressure shift in microwave region 0-68005
propane, potential barrier from i.r spectra 0-46584
propanes, substituted, n.m.r. study of rotational isomerism and barriers to internal rotation 0-67791
propyl alcohol, microwave spectrum 0-53083
propylene, deuterated, rot. spectra, internal rot. of asymmetric top 0-64541
propylene, internal rotation, CNDO-INDO calc. 0-77944

propylene, internal rotation, CNDO-INDO calc. 0-77944

pyridine, rotational Brownian motion from the width of vibrational band contours in molecular spectra 0-61143

contours in molecular spectra 0–6114.3 pyrimidine, consts., determ. from microwave spectrum 0–77949 pyrrole, rot. fine struct. of NH stretching band 0–77948 quantum rot. numbers limiting values determ.. diat. 0–55272 quasi-linear, curvilinear versus rectilinear kinetic energy operators for vibr.-rot. eigenvalues 0–64342 Raman scattering, depolarization ratios for rotating molecule 0–58137

Molecules continued rotation continued

relaxation process, fluctuation-barrier model 0-64350

resonance freq. shift due to non-resonant microwave pumping 0-53003 regid linear top rotor, Stark perturbed rotational energy levels 0-46414 rotation vibration energies of polyatomic mols... numerical determ. 0-64343

Totation vipration energies of polyatomic inois, numerical determ, 0–64343 rotational relax times meas, from gas thermal transpiration obs. 0–39346 rotational relaxation and broadening rates, equivalence in MRR spectroscopy 0–70854 rotational and vibrational excitation of polar mols, by low-energy electron collision 0–64349 rovibrational bands in i.r. spectra, 1-resonance perturbations 0–64316 silyl halides, consts, from microwave spectra 0–64454 spherical, rotational diffusion in liquid and solid states 0–70850 structure study by odd-parity Raman effect and Racah's algebra 0–70856 symmetric top molecules, degenerate vibration-rotation bands, computer program calc. 0–74204 symmetric top mols. ΔK=3 transitions in C₃- mols. 0–64346 symmetric top mols in liquids, rotational diffusion, n.m.r. 0–61551 symmetric tops, intensity distrib. within rotational struct, vibrational of bands 0–74213 symmetric- and spherical-top mols., rot. struct. of novel Raman effect 0–46423 1.1,2,2-tetrabromoethane, internal rotation 0–77953

1,1,2.2 tetrabromoethane, internal rotation 0–77953 tetrahedral mols., vibr.-rot. Hamiltonian, tensorial expression 0–43053 tetramethylammonium bromide, reorientation, 100-400°K, p.m.r. obs. 0–49931

0-4951 tetramethylammonium chloride, reorientation, 100-400°K, p.m.r. obs. 0-49931 tetramethylgermane, barrier to rotation of methyl groups 0-43513 thoraphthene, excited state consts. from absorpt, spectrum of 0-0 band 0-71036

0–71036
thionaphthene, rotl. analysis of 0-0 bands 0–74411
thiophosgene, rotational structure in π*—n transition 0–58245
time correl. Functions for internal, anisotropic rot. motion 0–43063
triatomic, Hamiltonian deriv, for K-type rot. and large amp. bending 0–64347
triatomic, linear, mag. Renner effect, direct orbital and spin interaction with vibrational rotation 0–70849
triatomic molecule, vibration-rotation Hamiltonian allowing for large amplitude bending vibration 0–43056
1,1,1-trifluoroethane, barrier to internal rotation 0–71041
trimethylene selenide, consts. for 7 vibrational states of ring bending mode 0–74413.

0 - 74413

trioxane, rotational spectrum, ground and several excited vibrational states

trioxane, rotational spectrum, ground and several excited vibrational states study 0-46596 two-top molecules, general theory of internal rotation 0-55274 vibrational-rot, interactions in polyat, mols., algebraic struct. 0-46421 vinyl bromide, pure rotational spectrum of fundamental vibration state. 8-59 GHz 0-46601 vinyl bromide, pure rotn. spectra of type a rat mm. wavelengths 0-46600 vinyl isocyanide, rot. spectra 0-55378 vinylcyclopropanes, rotational isomerism, n.m.r. spectroscopic studies 0-67825 wavefunctions for vibr. rotation states of diatomic mols, using Dunham

vinylcyclopropanes, rotational isomerism, n.m.r. spectroscopic studies 0–67825
wavefunctions for vibr. rotation states of diatomic mols. using Dunham potential 0–58142
X-y linear molecules, rotational distortion constants 0–46415
Zeeman eff. in rot. spectra of mols. with internal rot. 0–64338
Zeeman effect theory in rot. spectra 0–39345
zero point rot. consts. estimation of equilib. structs. after isotopic substitution 0–70855
AlF rot. consts. from microwave absorpt. spectra 0–67713
AlF 0–39364
AlF oct. consts. from microwave absorpt. spectra 0–67713
AlF 0–39364
AlF oz. consts. from microwave absorpt. spectra 0–67713
AlF vibracy system, rotational constants 0–46450
Ass., viii - X-V Σ + ysytem, rotational constants 0 – 46450
Ass., viii - X-V Σ + ysytem, rotational constants 0 – 70872
AsN., viii - X-V Σ + ysytem, rotational constants 0 – 70872
AsO-, rotational analysis of far u.v. 0 – 61071
B-H₂Br., rotl. constants from microwave spectra 0–70875
Bel analysis of viisible A-X system 0 – 64380
Br., anal. of four abs. bands of weak A ³ III (1u) – x ¹Σ_g + syst. 0 – 67718
BrCN. vibr.-rot. spectrum 0 – 53019
^{**}Br³Cl., Pational all analysis of absorption bands 0 – 67719
CF, anal. of bands in A and B states of absorpt. spectrum 0 – 70890
CF, solid, vibr.-rot. lines of ν₀₋₁ band 0 – 49858

CH₁F molecules optically pumped, laser action study at 452, 496, 541 µm 0–61153
CO, compressed, vibr.-rot. lines of v_{0-1} band 0–49858
CO, compressed by N₃ and HCl, vibr.-rot. lines of v_{0-3} band 0–49857
CO, fund, band linewidths 0–74243
CO, perturbed by Ar, v_{0-3} band vibr-rot. lines 0–39368
CO rotational relaxation numbers determ. from u.s. absorption 0–77776
CO₂ calc. of high-temp, steradiancy for vibr.-rotation bands 0–43088
COS isotopic species, vibr.-rot. consts. 0–49887
"C¹⁸CO, Angstrom bands, rotationless vibr. levels rot. perturbations 0–46454

0-46454

**O-40 Angstrom bands, rotationies vibr. levels for. perturbations 0-46454

**O-18 O Angstrom system, vibr. and rot. consts., perturbation shifts, electronic shifts, determ. 0-77781

**PC-18 O, B¹Σ* state consts. 0-43084

Cl., accurate data for high rotational levels obtained 0-39371

ClCN gas phase i.r. rotational constants 0-46461

ClN3, from microwave spectra 0-70892

ClO1, rot. anal. of 4750 Å band syst. 0-64392

**S*ClO2, rotational constants for (0.0,1) band determ. by band contour analysis 0-74251

Cr(II) paramagnetic complexes, p.m.r., hindered methyl rotation 0-46465

D- heat capacities and entropies of different nuclear spin species as free and hindered rotators 0-55296

D- rotational excitation by low energy electrons 0-77786

D- scatt. of He atoms, effects of rotational excitation 0-77987

D**Br*+, D**Br*+ rotational analysis 0-58200

DCN, transitions and consts. determ. by submm. mol. beam maser spectroscopy 0-74269

DCN, vibration-rotation Hamiltonian allowing for large-amplitude bending vibration 0-43056

vibration 0–43056

DCI, dissolved in inert solvents, of i.r. bands

DCI dissolved in liquid SF₆, far i.r. spectrum

0–39803

D-O. rot. spectra. microwave

0–53030

Molecules continued rotation continued

D'-O, rotational levels of ground vibrational state, microwave spectrum $0\!-\!74254$

GaF rot. consts. from microwave absorpt. spectra 0-67713

H halide molecules in collision, vibration rotation energy transfer probability 0–74443

ity 0–74443
H₂, interstellar obs., from vibr.-rot, emission lines 0–45304
H₃, rotational excitation by low energy electrons 0–77786
H₃, simultaneous rot.-vib. excitation by slow electron impact 0–64421
H₃, simultaneous vib. and rot. excitation by slow electrons 0–64418
H₂ collision cross-section dependence on rotational state 0–74442
H₃ electron impact excitation 0–64417
H₄ heat capacities and entropies of different nuclear spin species as free and hindered rotators 0–55296
H₃ rot, quantum numbers limiting values determ. 0–55272
H₃ simultaneous electronic and rot, excitation by electron impact 0–64419

0-64419

H,+, excitation cross sections, adiabatic approx. 0-53037

0-04419

H-*, excitation cross sections, adiabatic approx. 0-53037

HBr, dissolved in inert solvents, of i.r. bands 0-70910

HBr, effect of matrix environment 0-49870

HCN, rot. Zeeman effects of l-type transitions 0-43116

HCN, transitions consts. determ. by submm. mol. beam maser spectroscopy 0-74269

HCN, vibration-rotation Hamiltonian allowing for large-amplitude bending vibration 0-43056

HCl. dissolved in inert solvents, of i.r. bands 0-70910

HCl. effect of matrix environment 0-49870

HCl. rot. vibr. consts. calc. 0-43110

HCl compressed gas, vibr.-rot. spectrum, intensities and widths in ν₀-band 0-43109

HCl dissolved in liquid SF₆, far i.r. spectrum 0-39803

HD, rot. excitation by low-energy electron collision 0-49875

HD scatt, of He atoms. effects of rotational excitation 0-77987

HF, vibrational-rotational transitions, generation in 2.8 μm range 0-46479

H, effect of matrix environment 0-49870

0-46479

H. effect of matrix environment 0-49870

H-O. line intensity, 6.3 µm band 0-53032

H-O in potassium oxalate monohydrate, hindered rotation 0-66157

H-O vapour, and isotopic species, vibr. rot. bands 0-64415

H-O. and D₂O₃, barriers to internal rotation, determ, by new method 0-55273

Hcl, rot. lines press, broadening and shift 0-43098

HgH rotational constants of levels 0-77802

I., excited, vibrational and rotational energy transfer efficiencies 0-77803

I., quantum number J rel. to absorpt, linewidths in B ³Π₀₁-X ¹Σ_g⁺ system 0-70914

15. quantum number J ref. to absorpt. Intewloths in B $^{3}H_{0}$ 1. A $^{2}\Sigma_{g}^{*}$ system 0 $^{-}$ 0 $^{-}$ 00914
L₂ overlapping vibr. rot. lines near 6330 Å, rel. to He-Ne laser freq. stabilization 0 $^{-}$ 58179
InF rot. consts. from microwave absorpt. spectra 0 $^{-}$ 67713
LiBH₄ and LiBD₃, n.m.r. obs. of hindered rot. 0 $^{-}$ 75975
Mg₂, rot. struct. of abs. bands, consts. eval. 0 $^{-}$ 46484
N. lifetimes of rotational levels of electronic states 0 $^{-}$ 55303
N. rot. relax. 0 $^{-}$ 49956
N. glow discharge positive column, temp. 0 $^{-}$ 67978
N. low energy collisons with He, unitarized Born approximation for rotational excitation 0 $^{-}$ 55302
N. rotational relaxation numbers determ. from u.s. absorption 0 $^{-}$ 77776
NCO radical, rot. transitions, from microwave spectrum 0 $^{-}$ 64429
ND mol. A $^{3}H_{1}$ X $^{3}\Sigma^{-}$ (0.0) band, rot. anal. 0 $^{-}$ 64432
NH₃, PF₃ and AsF₃, rot.-vibr. interaction consts. 0 $^{-}$ 55305
NH₄, collision-induced transitions between rotational levels, microwave studies 0 $^{-}$ 7810
NH₃, hyperfine structure on inversion transition for various rotl. states

 NH_3 , hyperfine structure on inversion transition for various rotl. states 0-43126

0–43126
NH₂Cl, vibr.-rot. lines, saturated absorpt, spectra 0–70844
NH₂D₁, rotational-vibrational spectroscopy, transitions of v band 0–74282
NO, fluoresc., Hanle effect and level obs. 0–61105
NO beta band system, RKR Franck-Condon factors, rotational contribution 0–74283
NO₂, consts., from (3.0.1) band anal. 0–64431
NO₃, in inert matrices 0–61115
N₂O, rot. transitions, from microwave spectrum 0–64430
N₂O₃, barrier to internal rot, study from i.r. spectra of iio. 0–74288

N₂O₂ rot. transitions, from microwave spectrum 0-64430 N₂O₃ barrier to internal rot. study from i.r. spectra of liq. 0-74288 NSe, rot. struct. of bands of A-X system 0-49879 NSe, vibr. bands obs. 0-61107 NSe rot. anal. of 0.5 and 0.6 bands for ⁵/₂-X²Π_{3/2} syst. 0-67738 NSe structure of several bands 0-61108 Na₂, laser-induced 0-58189 Ni complex, cyclopentadienyl nickel nitrosyl rotational transitions 0-7821

0–77821

No, struct. of pair of ${}^2\Delta$ ${}^2\Pi$ bands in emission spectrum 0–67746

O.; rot. relax. 0–49956

OCS, rot. Zeeman effect of 1-type transitions 0–43116

OH($\Delta^2\Sigma^2$), rotation-vibration energy transfer in collisions with Ar and N-0–64614

PF₃, vibr.-rot. lines, saturated absorpt. spectra 0–70844

PH₃, rotational analysis of V-1 bands 0–77832

PO, new bands in the visible and their rotational analysis 0–58194

PO radical, rot. obs. of Rydberg- Rydberg transition 0–49884

PO radical, rotational anal. of new visible electronic band system 0–55315

0-55315

PO radical, rotational study and spectroscopic data 0-55314

PO radical, spectra analysis, new state obs. 0-49885

PO rotational analysis of degenerate band at 4672.09 Å 0-77831

RbBr, rotational state distrib. of molecular beam 0-77835

ReFr, pseudorotation, electron diffr, exam. 0-70946

S containing isotope replacement effects on vibr. rot. consts. 0-49887

SF6, rotational vibrational transitions, narrow reson, within Doppler line during absorpt, saturated absorpt, setzer 0-70844

SO radical, microwave obs. of first electronically excited state 0-70962

SO₃, rot. consts. from i.r. spectrum obs. 0-43134

SbF, anal. of C₃ system 0-67750

SbF, rot. anal. of C₃ system 0-64451

ScCl. electronic-vibr. rot. spectrum, 2200-9000 Å 0-49891

SeD, e.s.r. determ, of const. 0-49892

SeH, e.s.r. determ, of const. 0-49892

rotation continued Si₂ new band systems discovered, rotational and vibrational constants 0.-77844

0-77844
SiCl, analysis of bands of B-X system 0-61137
SiO ³Σ⁻³Π transitions, rotational constants determ. 0-61136
SrS, ¹Σ⁺⁻¹Σ⁺ syst. rot. anal. 0-70953
TiN. rotational analysis of the red electronic emission system 0-53051
TIF rot. consts. from microwave absorpt. spectra 0-67713

vibration - 0-77807

acetane, valence force field calc. using vibrational frequencies of isotopic species 0-67759

species 0–67759 acetic acid dimers, H-bond vibrations 0–46529 acetic acid dimers, H-bond vibrations 0–46529 acetic acid monomers, matrix-isolated, assignment of i.r. spectra 0–64470 acetic and perdeuteroacetic anhydrides, vibr. assignment 0–53059 acetonitrile, CC stretching vibr., i.r. band, effect of gas soln, phase transition 0–43147 acetonitrile, C≡N, C-C, C-H and CH₃ stretch vibrations produced by dissolved salts 0–67846

C-H and CH3 stretch vibrations produced by

dissolved salts U-67846 % acetonitrile hydrogen fluoride complexes i.r. spectrum 0-43144 N-acetonyl quinolinium iodide, assignment of bands in i.r. spectrum to different modes of vibration 0-58208 acetylacetone, enol form, study of nonplanar vibrations 0-64472 acetylene ¹²C.HD bands in region 6-10 μ , vibrational energy levels 0-46532

o-4032 acridine in n-alkane matrices at 4°K, vibrational analysis 0-77866 alcohols, self-associated, double excitation in i.r. spectra 0-53060 alkali metal chlorates, bromates and iodates, powders, i.r. absorpt. spectra 0 - 53016

alkali metal oxides, matrix isolated, i.r. spectra and force consts. 0-66033 alkyl chlorides, dependence of C-Cl stretching frequency on molecular structure 0-77862

amplitudes, mean, calc., charact. vib. method 0-77754 analysis of i.r. torsional data 0-74208

anharmonic oscillators, quantum mechanics by numerical integration 0-59908

0-59908
anharmonic oscillators with vibration-vibration and translation-vibration energy exchanges, relaxation 0-77744
anharmonicity consts. of symmetric top mols., from band contours with hotbands 0-46416
aniline, far-ir. absorpt. spectrum 0-55335
anions MX₆** force consts, and mean amplitudes 0-55295
anthracene and deuterated derivative in n-alkane matrices at 4°K, vibrational analyses 0-77866
9.10-anthraquinone single crystal layers, vibrational bands assignment, of i.r. spectra 0-51295
antimonates, rutile struct., i.r. absorpt. spectra, freqs. determ. 0-39393
aromatic cyds., interaction between nr* and rr* states 0-70969
aromatic sulphines, stretching vibrs, and i.r. absorpt. bands 0-74320
aromatic vapours, vibra relaxation following inter- system crossing 0-58202
ascharite, OH- obs., i.r. spectrum 0-41214

0–58202
ascharite, OH⁻ obs., i.r. spectrum 0–41214
azaporphyrines, oscillatory model 0–67767
aziridines, substituted, $v_{0-1}(NH)$ and $v_{0-2}(NH)$ freqs. variation in various solvents 0–39410
band contours, effect of temp. 0–64344
benzaldehydes, substituted, torsional barriers 0–77874
benzene, Franck-Condon overlap factors between vibronic levels 0–61148

0–61148 benzene, exciton band profile for entire Brillouin zone 0–70978 benzene, inexcited singlet state, fluoresc, and nonradiative transitions from single vibr. levels 0–77877 benzene, vibr, relax, and competition with radiationless transitions in ¹B_{2u} state 0–55337

benzene, vibr. relax. in S₁ state 0—77878 benzene derivatives, m-disubstituted 0—70973 benzene derivatives, p-disubstituted 0—70971

benzene derivatives, p-disubstituted 0-70971
benzene-halogen charge transfer complexes, Raman scatt, 77K 0-74337
benzenes, o-disubstituted 0-77849
benzodioxanes-1.4, substituted, i.r. spectra 0-55338
p-benzoquinone, chloro-derivatives, increase in C=O stretching frequency
on chloro substitution 0-64486
p-benzoquinone, force field calculation pot, energy of fundamental vibrations 0-64466
benzoyl chloride, in liq, and gas phase, i.r. abs. spectra, freq. assignment
0-46541

benzyl benzoate, spectra 0-58210 biphenyl 0-59434

biphenyls, symmetrically deuterated, in-plane fundamental frequencies 0-77880

50–7780 bis(trifluoromethyl) nitroxide, rel. to temp, dependence of e.p.r. spectrum 0–70979
5.5'-bis-isoxazole, complete assignment of fundamentals 0–49910 book 0–58610 book of review articles on energy transfer and storage 0–58144 branched polymers, normal modes of ring and star shaped mols. 0–64566 bridged polymuclear metal atom complexes, alternate force fields in normal coord, anal. 0–74232 bridged structure M-L-M, angular correlation of symmetric and antisymmetric frequencies 0–67698 bromoacetylene, electronic spectrum 2500 to 900Å 0–74322 bromobenzaldehydes; o, m and p. freq. from Raman spectra 0–70980 bromoethynyl benzene and chloroethynyl benzene, vibr. spectra 0–55342 butadiene-1,3, evidence for Cariolis coupling from vibration-rotation bands 0–74346 butadiene-2,3 nitrile, microwave spectrum 0–49912 carbon dissulphide, pure rotational Raman scatt, from excited levels, obs. 0–61083

0 - 61083

carbonyl stretching bands, integrated intensities, acetonitrile solution 0-46521

0-46521
chains, disordered, modes in next nearest neighbour interaction 0-71818
4-chloro- and 4 bromo-phenylmethylsulphide 0-70972
chloro-alkanes, secondary, liquid spectra and intermolec. vibr. 0-39808
2-chloroacryjonitrile 0-74349
chlorobenzene, i.r. and Raman bands, solvent and temp. effect 0-43080

chlorobenzene, planar ground state fundamentals 0—55344 chlorobenzene in-planar ground state fundamentals 0—55344 chlorobenzene in-plane vibration modes in excited states 0—49906 l-chloro-2-fluoroethylenes, cis and trans and deuterated modifications vibrational assignments of i.r. and Raman spectra 0—64497

Molecules continued vibration continued

> chloroform, i.r. and Raman bands, solvent and temp. effect 0-43080 chloroform, liquid, Raman spectra, effect of intermolecular interactions

> chloroform and deuterochloroform, vibr. spectra and force consts.

α-chloronaphthalene, assignment of frequencies in i.r. region 0-74351 cobaltammine skeleton, of monodentate selenato complexes 0-55324 complex. Einstein coefficients for vibronic transitions 0-46428

complex branched polymers, normal modes 0-64567 Coriolis coupling in symmetric top molecules, computer program calc. 0-74204

0—14.204 correlation of electron relaxation and molec, vibrations 0—39361 crystal, point defects, vibrational self-entropy 0—47219 2-cyanoethanol, ground state assignment of trans isomer from microwave spectrum 0—70986 cyanogen, vibr.-rot. bands obs. 0—61156

cyclobutanone, ¹A₂ state, oxygen wagging vibr, levels from u.v. spectrum 0-61157

cyclohexane and related oxanes, vibr. spectra and potential functions 0-58215

0-3213 cyclohexanol, liquid, mol. motions, quasi-elastic incoherent cold neutron scatt, obs. 0-78262 cyclopentadiene, deform. vibr. freqs., solvent influence 0-61155 cyclopentanone, deuterated isomers, assignments from vibr. spectra

evelopentanone, ring-puckering pot, functions from i.r. absorpt, spectra

0-74356 0-74336 cyclopentene oxide, ring-puckering pot, functions from i.r. absorpt, spectra 0-74356

0-14-330 eyclopropane-Ar mixture, translational and vibrational energies exchange efficiencies, velocity dispersion analyses 0-53098

ethciencies, velocity dispersion analyses 0–53098
Darling-Dennison rule for calc. of anharmonicity corrections to frequencies
of isotopic molecules 0–43058
N-deuterated N-methylpropionamide, i.r. and Raman obs. 0–53075
deuterobromoacetylene, electronic spectrum 2500 to 900Å 0–74322
diatomic, correl, effects, force consts, determ. 0–39341
diatomic, homologous, relationship between reduced mass and vibration

diatomic, homologous, relationship between reduced mass and vibration freq. 0–52999 diatomic, homonuclear mols, three-dimensional model of collision-induced vibr. transitions 0–77747 diatomic, rot.-vibr. energies, systematic procedure for perturbation calcs. 0–64340

diatomic, used to determ, temp. of a gas 0–60089 diatomic gases, de-excitation rate 0–77745 diatomic mol., Schrodinger eqn. resolution 0–77743 diatomic molecule in atomic collision, relaxation 0–53096

diatomic-diatomic molecule collisions, quantum vibrational transition probabilities 0-67843

bablintes — 17943 2.3-diazanaphthalene, vibronic perturbations and phosphorescence 0-71025

0-71025
diazomethane, wagging and rocking force consts. w.r.t. ethylene. electron relax. effect 0-71005
diazomethane free radical, vibr. spectrum, obs. 0-46571
2.2-dichloro and 2,2-dibromopropane, vibr. spectra 0-55349
dichlorodifluoromethane, vibr. rot. transitions, saturated absorpt. spectra
0-70844
dichlorofluoroamine, force field, mean square amplitudes and Coriolis coupling coefficients 0-61160
2.3-dichlorophenol, C, point group modes of vibration of fundamental
0-40942

0 -49942

2,5-dichlorophenol C₅ point group modes of vibration of fundamental 0 -49942 2.4-dichlorophenol C₅ point group modes of vibration of fundamental

0-49942
2.5-dichlorotoluene, in liq. phase, Raman and i.r. spectra, freq. assignment to diff. modes 0-49919 dicyanodiazomethane, vibr. spectrum, obs. 0-46571 cisoid-dienes, proton coupling constants rel. to mol. config. n.m.r. spectra 0-70987

0-10967 diethylether complexes with metallic halides, sensitivity of skeletal and CH frequencies of CH, to complexation 0-70991 diethylthiocarbaminate ion and Se analogur, frequencies and vibration forms 0-67790

difluorodiazirine, force constants and Coriolis coupling constants

0–58218
difluoromethyl radical in solid Ar, force and pot. consts. from i.r. absorpt. spectra 0–66061
dihaloacetylenes 0–70989
dihalofumaronitriles 0–77896
1.2-dihydronaphthalene, proton coupling constants rel. to mol. config., n.m.r. spectra 0–70987
ß diketones, triketones, enolized spectroscopic examination of stretch vibrations 0–53069
dimethylethers, i.r. spectra obs. 0–70988
dimethyl-da amine, vibr. assignments and barrier to inversion 0–70993
dimethylamine, vibr. assignments and barrier to inversion 0–70993
dimethylnitrosamine, fundamental modes from Raman and i.r. spectra 0–71010
dimethylthiocarbaminate ion and Se analogue, frequencies and vibration dimethylthiocarbaminate ion and Se analogue, frequencies and vibration

forms 0–67790
diphenyl ether, vibr. selection rules 0–53089
direct effects of electron relaxation 0–71005
dissociation energy of diatomic mols. from vibr. spacings of higher levels

0 - 39453

dissociation of diatomic gas, vibration-vibration coupling 0-77960 electronic transitions, vibronically induced, theoretical band shapes electronic transitions. 0-58141

energy transfer, multiple transition probabilities 0–61193 energy transfer, vibrational-translational, preferential orientations 0–71060

0—71060 energy transfer during impacts, fluorometric anal. 0—49831 energy transfer from highly excited mols. 0—55393 energy transfer from translational to vibrational degree of freedom in atom-diatomic molecule collisions 0—74437 ethane, torsional oscill, in solid and liq. states 0—70996 ethylene, force consts., semiempirical ASMO SCF calc. 0—61161

Molecules continued vibration continued

ethylene, influence of solvents out-of-plane deformation frequency ν_7 $_{\rm 0.4} \pm 0.5$

ethylene, vibr.-rot. transitions, saturated absorpt. spectra 0-70844

ethylene and deuterated derivative, vibrational structure associated with transitions leading to ionisation potentials 0-64436 ethylene oxide, force consts. and mean square amplitudes 0-77905

ethylene sulphide, force consts. and mean square amplitudes 0-77905 ethylenes, halogenated, ionization potential and vibrational structure from photoelectron spectra 0-49923

ethylenes, perhalogenated, mean amplitudes 0-49921

ethylenimine, i.r. absorpt, spectra comparison in solid Ar and N- matrices 0 49922

exchange kinetics, radiation amplification in hydrogen halides by elec. or chem. pumping 0-74211 Fermi resonance, triple involving two fundamental vibrations of a mole cule 0-64335

fine structure analysis of photoelectron spectra 0-64322
4 fluoro and 4 bromo benzenethiol 0-70972
o fluorotoluene, torsion-vibration interaction, microwave spectral obs.

o fluoro tolluene, torsion-vibration interaction, microwave spectral obs. 0.71037
1. fluoro 2,4,5 trichlorobenzene, vibr. spectrum assignment 0-55352
force, const. calc. from vib. freqs., iterative method 0-77753
force constant computation extremal force constant relationships in general secular equations 0-74202
force constants, quadrature, cubic and quartic of diatomic molecule, from electron density by inspection 0-77746
force consts., continuous charged spheres model 0-39355
force consts., extremal, bent XY, pyramidal XY, tetrahedral XY, Coriolis coeffs. 0-39344
force consts., for strongly coupled vibrs. 0-53001
force consts., for strongly coupled vibrs. 0-53001
force consts., determ. of diat. mol., correl. effects 0-39341
frequencies of periodic mols, of finite length, allowance for interac. of non neighbouring units 0-43061
gas of diatomic molecules, relaxation, improvement to Montroll Shuter cqn. 0-55277
germylacetylene, force consts. and Coriolis coupling const. 0-74323

germylacetylene, force consts. and Coriolis coupling const. 0—74323 germylacetylene, barrier to pseudorotation 0—58222 globular, torsional vibrs, and barriers to internal rot. of methyl groups 0.64491

glyoxal, CO stretching, C C stretching, CCO bending 0–43163 glyoxal d., constants for 4540 Å band system 0–77912 glyoxime in soln., fund, freqs. symmetry and assignment 0–78281 glyoxylic acid, vibr. spectra and free mol. symmetry 0–61164 group IV/VI compounds, electric dipole for ground vibrational state 170866

10,70866
guanine:cytosine helices, interbase coupling 0-39472
hamiltonian, for translating, rotating, vibrating mol. in presence of constant
external c.m. field 0-64318
hamiltonian, vibrationa rotation, of linear molecules 0-64334
harmonic force constants, ab initio cales, by different methods 0-74207
harmonic oscillator representation, general soln. 0-46424
harmonic oscillator representation in two dimensions, matrix elements
0-46425
Herzberg Teller theory of vibronic intensity borrowing, examination
0-74203
hexachlorobenzene, high field Zeeman effects of vibronic transitions in

0. 74203 hexachlorobenzene, high field Zeeman effects of vibronic transitions in lowest triplet states 0–64511 hexafluorides, metal, Coriolis coupling constants 0–46468 hexafluorides, metal, force constants from extremal properties, mean amplitudes of vibration 0–46468 hexafluoroacetone, vibrational relaxation and radiationless processes in gas phase 0–64513 hexafluoroanions of IVA and VA group elements, shrinkages at various temperatures 0–46467 hexafluoroanions of IVA and VA group elements and internuclear distance 0–74229 hydrocarbon, conjugated, absorption spectra, determination of vibrational

harder 0-14229 hydrocarbon, conjugated, absorption spectra, determination of vibrational structure 0-67800 hydrocarbon, simple, force constants, NDDO and CNDO predictions 0-49928

0.49928 induced i.r. absorption of symmetric triatomic mols, in soln. 0–39362 induced i.r. absorption of symmetric triatomic mols, in soln. 0–74757 intramolecular pot, functions, from vibr, analysis. 0–39397 invariant substances, constr. to symmetry coordinates. 0–43039 ions, charge exchange with Ar⁺ and Kr⁺, rot, and vib. populations obs. 0.61379

0 61379 oions, tetrahedral, orbital valence force field for force const. calcs. 0–46422 isoquinoline, vibrational spectra and assignments 0–43180 ketene, wagging and rocking force consts. w.r.t. ethylene, electron relax, effects 0–71005 ketones, cyclic, carbonyl stretching vibration 0–53074 laser, molecular, chemically pumped, vibr. rot. transitions, simultaneous inversion 0–73206 linear molecules, vibration-rotation hamiltonian 0–64334 metal halides (II A) absorption spectra, stretching vibrations 0–49860 methane, 2947-906 cm⁻¹ line, appl. to frequency stabilisation of He Ne laser 0–73226 methane. Zegman solitting obs. in vibration, rotation spectra of ½ rotal metals and control of the control of t

laser 0–73226 methane. Zeeman splitting obs. in vibration rotation spectra of ${}^{1}\Sigma$, rotational magnetic moment determ. 0–77924 methane. deuterated. fund. ν_a band interpret. 0–74374 methanethiol, 3μ vib. rot. spectra, hindered internal rot. 0–39438 methanol.1.f. modes study 0–64527 methyl alcohols, partially deuterated, α depend. of vibr. zero-point energy 0–58230 methyl boron diffuoride and deuterated derivative, complete assignment in basis of molecular model 0–64526 methyl chloride, vibr. rot. band. 2080 cm $^{-1}$ 0–61166 methyl group, vibrational resonances involving E modes 0–74377 methyl halide, method of hypermatrices commutable in pairs 0–49932 methyl halide, positive ions, vibrational frequencies and vibronic interaction 0–55360 methyl halides, deuterated, determ. of A_0 0–71017

methyl halides, deuterated, determ. of A₀ 0-71017

methyl iodide, anal. of p_s from i.r. spectrum 0—77927 methyl ketene and isotopic molecules including D, 13 C and 18 O substitutions, amplitudes 0—55362

Molecules continued vibration continued

N- methyl phosphoramidodichloridothioate and deuterium analogues, assignment of vibrational spectra 0-46579

methyl three-top mols., torsional modes 0-55358

2-methyl 4,5-dihydrofuran, ring-puckering pot. functions from i.r. absorpt. spectra 0–74356

spectra 0–74356
methyl-phosphorus compounds, l.f. vibrs. and torsional barriers 0–64530
methylacetylene, force consts. and Coriolis coupling const. 0–74323
methylamine, amino wagging vibr. and rotational struct. 0–61171
methylarsenic halides 0–71006
methylchlorosilanes, integral intensities of vibrational bands in i.r. obs.
bands 0–43181
methyldiboranes 0–74376
methyldithiocarbaminate ion and Se analogue, frequencies and vibration
forms 0–67790
methylene fluoride, microwave spectrum, centrifugal distortion and molecular structure 0–46577
methylene halides, intensity of v₅ band appearing in liquid and solution
0–49933
methylenecyclobutane, ring puckering pot, function from mid-i.r. combinamethylenecyclobutane, ring puckering pot, function from mid-i.r. combina-

methylenecyclobutane, ring puckering pot. function from mid-i.r. combination bands 0--71014 methylenecyclobutane, ring-puckering potential function from mid-i.r. combination bands 0-43174 3-methylenecyctane, ring bending vibr., from microwave spectrum 0--46574

methylfluoride, in liq. cryst., vibr. corrections on dipole-dipole interactions 0-77919

methylfluoride, in liq. cryst., vibr. corrections on dipole-dipole interactions 0–77919
methyliodide, A_o determ. by resonance interactions with ν_S 0–61167
β-methylioridines assignment of frequencies in i.r. region 0–74351
N-methylpropionamide. i.r. and Raman obs. 0–53075
methylpyridines and their n oxides, C-H out-of-plane vibrations, normal coordinate treatment 0–74383
methylthioethyne, force field 0–77921
molecular ion, relaxation process of state population rel. to pulse discharge afterglow 0–46426
molecular solids, vibrational spectra review 0–76062
monobutyl naphthalenes, i.r. spectra 0–39439
monochloromethyl radical, C CI force constant and assignment of absorptions in i.r. to various modes 0–74389
monohalogenodiacetylenes, molecular constants 0–55364
naphthalene, fluorescence as function of vibrational level and excitation energy 0–77932
naphthalene-d_R, vibrational assignment 0–77931
naphthalene-d_R, vibrational assignment 0–77931
naphthol, assignment of frequencies in i.r. region 0–74351
α naphthol, assignment of frequencies in i.r. region 0–74351
1.4 naphthoquinone single crystal layers, vibrational bands assignment 0–51295
niobates, rutile struct, i.r. absorpt, spectra, freqs, determ. 0–39393

0-31295
nitrobenzenes, monosubstituted 0-77937
nitrophenols. N group vibrations with intramolecular H bond in proton acceptor solvents 0-61172
non-radiative transitions, radiative theory 0-43051
non-rigid, normal modes, classification method 0-53089

nonequilibrium vibr. distrib. functions in i.r. active anharmonic oscillators 0 -39476

nonradiative decay of individual vibronic levels in large molecules 0 -70853

0 - 70853
O alkyl phosphorodichloridothioates, vibr. spectra 0-55350
organic, containing H-C= group, CH- stretch freqs. separation, correlation with HCH angle 0-46527
oxalic acid, spectra, freqs. assignment 0-49935
oxalyl chlorate, mean square amplitude of vibration and Coriolis coupling constants 0-58235
oxalyl chloride 0-58234
oxalyl chloride o-58234
oxalyl fluoride mean square amplitude of vibration and Coriolis coupling constants 0-58235
paraddchyde, effects of low energy, vibrations in microwave spectrum

constants 0-58235 paradichydde, effects of low energy vibrations in microwave spectrum 0-61173 pentadeuterotetraphenylgermane, low wavenumber vibrations, i.r. and Raman spectra 0-46592 pentaerythritol single crystal, polarized ATR spectra, assignment of vibrations 0-48054 perdeuterodimethyl amine, vibr. assignments and barrier to inversion 0-70993

phenol mixed with cyclic ketones shift of hydroxyl group vibration band 0 -64538

phenylarsenic halides 0-71006 phosphorous oxyhalides and derivatives. Urey Bradley force consts.

0 /0943 phthalocyanine, metal derivatives, metal-ligand vibrations 0-74397 polar molecules in condensed phases, microdynamics studied by dielec, dispersion and vib. rot. spectra 0-43054 poly -L. alanine, alpha-helix, analysis of normal modes and their dispersion 0-64571

polyalanine, planar zig and helical chains vibr. spectra calc. 0–39470 polyatomic, radiationless transitions 0–74210 polyatomic, vibr.-rot. interaction terms, algebraic struct. for high order 0 64341

polyatomic mols., potential, two parameter study for second order case 0-39342

polyethylene and deuteroderivatives, spectra 0-39471

polyglycine chain, frequency distribution functions 0–71051 polyisoprenes, deuterated 0–77977 polypeptide chains 0–39466 polyterafilturorethylene, valence force field calc. by damped least-squares method 0–53094

polyvinyl chloride, containing mass defects, spectra 0-39471 porphyrins, vibr. struct. of electronic spectra, using quasi-linear spectral method 0--67815

method 0-67815 potential energy, computer program for calc, distribution 0-53002 potential energy of diatomic mols., construction of true curves 0-39343 predissociation, isotope effects as function vibr, quantum no. 0-77962 propane, methyl libration meas, by neutron inelastic scatt. 0-43178 propargyl mercaptan, vibrational transitions of torsion mode 0-64542 1-pyrazoline, ring puckering 0-58240 pyrene, transferability of simplified valence force field 0-74404 pyridine, deform, vibr, freqs., solvent influence 0-61155 pyrimidine, substituted derivatives 0-74405

vibration continued pyrrole, rot, fine struct, of NH stretching band 0-77948

quadratic force consts. ab initio self- consistent MO calc. 0-39358

quasi-linear, curvilinear versus rectilinear kinetic energy operators for vibr.-rot. eigenvalues 0–64342 quinoline, vibrational spectra and assignments 0–43180

range of definition of vibrational coordinates, separation of motions 0-53006

relaxation of an optically excited gas 0–49856 relaxation of polyatomic molecules, kinetics 0–64330 relaxation rates, shock tube meas, review 0–58147

Renner effect, pot, curves for bending vibrs. 0-61055

review of calculation methods 0–58146 ring bending modes, potential function 0–58215 rotation coupled vibrs., and second-order vibronic interaction calc. 0–39429

rotation-vibration energies of polyatomic mols... numerical determ. 0-64343 rotational and vibrational excitation of polar mols, by low-energy electron

collision 0-64349
rovibrational bands in i.r. spectra, l-resonance perturbations 0-64316

roviorational dands in i.r. spectra, i-resonance perturbations 0-4316 salicylaldazinate metal chelates, i.r. spectroscopic studies 0-71030 selenate ion, in monodentate selenato complexes 0-55324 selenium dialkylamino compounds, i.r. and Raman spectra force constants 0-46588

o-46590 vibrational spectra, normal coordinate analyses

0-46590 silacycylopent-2-ene, ring-puckering pot. from far i.r. spectrum 0-71032 silico-organic cpds., [(CH₂);Sil₂El¹⁶ (El¹⁴=C. Si, Ge, Sn), vibrational spectra and force constants 0-46589 silyacetylene, force consts. and Coriolis coupling const. 0-74323 silya and trimethylsilyl compounds of group 5 elements, force constants 0-46511

0–46591 spectral intensities, intermolecular interactions effects 0–46920 stretching frequencies C-H and M-CH₂ correlation with effective electronegativity 0–53057 succinic acid in saturated aqueous soln., Raman spectrum obs. 0–39447 sulphonylamines, halogen-substituted, force consts. 0–53085 sulphur dialkylamino compounds, i.r. and Raman spectra force constants 0–46588

0-46588 symmetric top molecules, degenerate vibration-rotation bands, computer program calc. 0-74204 symmetric top mols., calc. of anharmonicity consts. from band contours with hotbands 0-46416

with hotbands 0–46416 symmetric tops, intensity distrib, within rotational struct, vibrational of bands 0–74213 symmetry, by appl. of kinetic energy matrix 0–74206 symmetry coords, for vibs. of six-at mols. 0–43062 tantalates, rutile struct., ir. absorpt. spectra, freqs. determ. 0–39393 tertiary butyl acetylenes, vib. spectra and force consts. 0–77859 tetra cyano ethylene (TCNE), molecular constants 0–55331 tetrahedral, orbital valence force field for force const. calcs. 0–46422 tetrahedral Tyl-4 molecules, energy levels and the ν - band 0–49837 tetrahedral mols., vibr-rot. Hamiltonian, tensorial expression 0–43053 tetrahedral mols. of XY₁ type, use of Coriolis interaction consts. 0–39448 tetramethylsilane, integral intensities of vibrational bands in i.r. abs. bands 0–43181 tetramethyltitanium 0–71033

0-43161 tetramethyltitanium 0-71033 tetraphenylgermane, low wavenumber vibrations, i.r. and Raman spectra 0-46592

theory, hypermatrices with blocks commutable in pairs 0-49932 theory, relationship between nonlinear and linear internal coordinates 0-49840

0—49840 1.3.4-thiadiazoles, absorption spectra in near i.r. 0—58249 2.4-thiazoleidindione, i.r. spectra, calc., normal frequencies 0—39449 thiazolidine, i.r. spectra of 2- and 4-thioderavitives, deformation and vibra-tions 0—61176

tions 0–61176 thiohydantoin, i.r. absorpt, spectra, frequencies, calc. 0–46593 thiophene derivatives, C-H out of-plane, from force constants 0–46594 thiophenes, 2-substituted 0–74410 three-membered ring mols, normal coordinate anals. 0–67701 toluene, vibr. relax. in S. state 0–77878 toluene, vibr. selection rules 0–53089 torsional vibration effect on molecular structure 0–70847 transformations to symmetry co-ordinates, direct method of constr. 0–43039

0 - 43039

0-43039
transition metal complexes, octahedral, containing halogen bridges, M-Hal stretching modes in far i.r. spectra 0-49853
transition metal complexes, trioxalate, vibr. spectra 0-55327
transition metal complexes with bis-dimethylglyoximates 0-77784
1.3,5- triamino -2.4,6- trinitrobenzene, neutron spectra and vibrational assignments 0-64551
triatomic, CO-, CS-, Parr-Brown anharmonic potential function 0-70883
triatomic, effective pot. curves for degenerate vibrs. in Jahn-Teller effect
0-70843

0-70843 triatomic, linear, mag. Renner effect, direct orbital and spin interaction with vibrational rotation 0-70849 triatomic molecule, vibration-rotation Hamiltonian allowing for large-amplitude bending vibration 0-43056 trichlorofluoromethane, liquid, Raman spectra, effect of intermolecular interactions 0-43460 1.1,1-trifluoro-2-butyne, normal coordinate analysis and Coriolis coupling 0-77956

1.1.1-trifluoroethane, torsional mode, direct obs. by neutron scatt. 0 - 71041

trigonal bipyramidal mols, anisotropic thermal motion rel. to temp. 0-67702 1,1,1-trihaloethanes and deuterium derivatives, vibrational assignments

1.1.1-trihalocthanes and deuterium derivatives, vibrational assignments from Raman spectra 0—43182 trimethylene selenide, rotational consts, for 7 vibrational states of ring bending mode 0—74413 trimethylsilyl cyanide and isocyanide, vibr. spectra 0—55377 trioxane. I type doublets in degenerate excited vibr. states 0—61178 triphenylene and triphenylene and triphenylene and triphenylene and solution, normal coordinate calculations 0—43183 rangle site force consts. for II-Q bond 0—46516

nate calculations 0-43183 uranyl salts, force consts. for U-O bond 0-46516

Molecules continued vibration continued

 v_{i} =2 excited state in molecules with C_{3r} symmetry, rotational spectrum 0-43055

valence force field, frequency-coupled, limiting case 0-64339 y-valerolactone, fundamental vibl. assignment from i.r. and Raman spec tra 0-46599

vibrational-rot, interactions in polyat, mols., algebraic struct. 0-46421

vinyl isocyanide, vibr. spectra 0-55378 vinyltrifluorosilane 0-77952

vinyttriliuorositane 0=77952
water, H-bonded in crysts., librational modes, n scatt, obs. 0-40533
water in crysts., vibrational freqs., nonlinear H-bond model 0-39992
wavefunctions for vibr-rotation states of diatomic mols, using Dunham
potential 0-58142

linear molecules, force constants and amplitudes of vibration 0-46415

0-40415
zinc uranyl acetate, ground state levels 0-46602
O₃₊H₋OH^{*(lot}-O₅, distribution of vibrational population in OH radicals for the H+O-atomic flame 0-61132
AgBi absorpt, band system in visible 0-61068
AgBo(OH)₆, i.r. absorpt, spectra obs. 0-61125
AlBr₁ 0-74235

AIBr₄ 0-742: AIF 0-39364

AIF 0-39364

AI-O, gaseous, bending freq. in i.r. absorpt. 0--64376

Ar-, levels in ground state 0-67714

AsF, vibrational analysis, assignments 0-77766

AsFs, force constants and normal modes, in terms of orbital-valency-force-field model 0-70871

AsH3, harmonic freqs, calc, from anharmonic ones, and AsD3 0-77816

B-Ce, B-F4, from matrix-isolated i.r. and liq, Raman spectra 0-70876

BCl3, dissociation, spectra, recombination radiation, CO- laser excited 0-46604

BF4 (CH-)-CO-isotopically substituted coordination compounds, 0-77770

0–4604
BF₁-(CH₁)-CO isotopically substituted coordination compounds
0–77770
BF₁-(CH₁)-SO isotopically substituted coordination compounds
0–74238
BF₁-(CH₁)-SO isotopically substituted coordination compounds
0–74238
BF₁-(through the coordination compounds
0–74237
B₁-(through the coordination compounds)
0–74238
BX₁-trihalides, kinematical evaluation of force constants
0–46437
B₂-(through the coordination constants modified 0–67716
B₃-(through the coordination constants coordination compounds coordination compounds coordination compounds 0–74238
BT₂-(1-1)-(1-1

Bi-vrihalides, intramolecular force fields 0—70949
Bi-vapour, vibrational analysis of 3 new bands and A-X system 0—74242
Bi₂(OH)₁,6+ complexes, alternate force fields in normal coord. anal. 0—74232

0-74232

"BiCl vibrational scheme proposed, isotope shifts meas. 0-74241

Br-, numbering of A ³ H(1_m) state 0-67718

Br-, numbering of A ³ H(1_m) state 0-67718

Br-, in solid. Raman obs. 0-48089

Br-, polycrystalline, laser-excited Raman spectra, molecular modes assigned 0-72387

BrCN, vibr.-rot. spectrum 0-53019

BrCN, vibr.-rot. spectrum 0-53019

BrCN bending force constants from gas phase frequencies and I type doubling constant 0-49864

C-H i.r. stretching freq. of H-bond formation variations rel. to C hybridization 0-53008

Phillips system new vibrational and equilib. consts. 0-53022

CH i.r. stretching freq. of H-bond formation variations rel. to C hybridization 0–53008
C, Phillips system, new vibrational and equilib. consts. 0–53022
CCI- free radical revised estimate of force constants 0–76279
CCI₄, Fermi resonance of Raman spectra in gas. liquid phases 0–43091
CH stretch, influence of nitrogen, lone pair of electrons 0–49838
CH₂CH-SH vapor and solid state, vibrational fundamentals 0–39426
CH₂CH-St vapor and solid state, vibrational fundamentals 0–39426
CH₂CH-F vapor and solid state, vibrational fundamentals 0–39426
CH₂CH-F vapor and solid state, vibrational fundamentals 0–39426
CH₂CH-SH vapor and solid state, vibrational fundamentals 0–39426
CH₂CH-I vapor and solid state, vibrational in solid 0–62647
CN- force field measurements 0–43087
CO-D-S sound absorption meas. at 300°K, 400°K, vibrational- relaxation time analysis, exptl. results 0–53026
CO-He lasers, vibrational energy transfer 0–39477
CO-N-HO (or He) supersonic expansion, population inversion 0–74666
CO-N-syst., vibrational distrib. of populations 0–70880

0–74666 (O-N-syst., vibrational distrib. of populations 0–70880 (O-N-syst., vibrational distrib. of populations 0–70880 (O-N-syst., vibrational distrib. of populations 0–70880 (O-N-syst., vibrational energy transfer, shock technique 0–43096 (O-compressed by N-sand HCl, vibr.-rot. lines of v_0) band 0–49857 (O-compressed by N-sand HCl, vibr.-rot. lines of v_0) band 0–49857 (O-compressed by N-sand HCl, vibr.-rot. lines of v_0) band 0–49857 (O-compressed by N-sand HCl, vibr.-rot. lines 0–39368 (O-compressed by N-sand vibr-rot. lines 0–39368 (O-compressed by Ar. v_0) band vibr-rot. lines 0–39368 (O-compressed by Ar. v_0) band vibr-rot. lines 0–39368 (O-compressed by Ar. v_0) band vibr-rot. lines 0–39368 (O-compressed by N-sand Vibr

CO₂, nonequilibrium population distribs, of vibr, energy levels in CO₂ flames 0-67726 CO, pure and in gas mixtures, vibrational relaxation, shock tube study 0-53021

CO₂, pure rotational Raman scatt, from excited levels, obs. 0–61083 CO₂, R- and P-branch absorpt, functions, 2260-2450 cm⁻¹, calc. 0–39369

O-39369

Oo. relative populations of vibr. energy levels from i.r. emission spectra 0-67725

Oo. shock heated, vibrational relaxation studies of 10°0 and 02°0 states 0-70885

Oo. calc. of high-temp, steradiancy for vibr. rotation bands 0-43088

Co. relaxation time of asymmetric \(\nu_2\) vibration, meas, by optic-acoustic method 0-43092

Co. vibrational energy transfer to N-O, rate constant calc. 0-70887

Co. zero angle electron scattering with vibrational excitation 0-43123

COS isotopic species, vibr. rot. consts. 0-49887

CS., Fermi resonance of Raman spectra in gas, liquid phases 0-43091

CS-, \(\nu_3\) intensity, solvent effects 0-39802

CS-, self-focusing effect on stimulated Raman scatt., due to vibr. states 0-44861

Molecules continued vibration continued

 $^{12}C^{16}O,\ Angstrom$ bands, rotationless vibr, levels rot, perturbations 0-46454

12C18O Angstrom system, vibr, and rot, consts., perturbation shifts, electronic shifts, determ. 0–77781

C-O, band parameters and profiles of valence vibr. as function of conc.

C -O valence vibr. of ketones, band parameters and profiles, (-)30-70°C 0-64493

CaBr, consts. from u.v. emission spectrum 0-46459

CdBr, vibrational analysis of bands in u.v. spectrum 0-46549

CeCl₆, force constant, mean amplitude, Bastiansen Morino shrinkage

CI- centrifugal stretching constants, vibrational levels meas, at 670 K $0\!-\!39371$

Cl. in solid. Raman obs. 0-48089

Cl polycrystalline, laser-excited Raman spectra, molecular modes assigned 0-72387

assigned 0–72387
Ch', valence force field consts. from Raman spectra 0–70893
Cl'CN bending force constants from gas phase frequencies and l-type doubling constant 0–49864
ClCN Fermi doublet in gas phase i.r., wibrational energies, rotational constants 0–46461
ClF-*, valence force field consts. from Raman spectra 0–70893
Cl-F-*, Valence force field consts. from Raman spectra 0–70893
ClO, force field and intensity calc., rot, anal. of 4750 Å band syst.

ClO₂, force field and intensity calc., rot, anal. of 4750 A band syst. 0–64392
Co complex, nitrosyltricarbonylcobalt and monosubst, derivatives, C=O and N=O stretching 0–64394
Co₂, CS₂, Parr-Boron anharmonic potential function 0–70883
Co₃(CO₃) and derivatives substituted by PF₃, P(MeO)₃ and P(Me)₃, force constants 0 58191
Co₃(CO₃) and derivatives substituted by PF₃, P(MeO)₃ and P(Me)₃, force constants 0 58191
Co₃(CO₃) and derivatives substituted by PF₃, P(MeO)₃ and P(Me)₃, force constants of electronic spectra 0–64395
Cr(III) ammine complexes, metal-ligand vibrations 0–70897
Cr₃(Sr₃Mr₂F₆, force const., from i.r. and Raman spectra 0–64373
Cs₃[ReF₆] and Cs₃-[TcF₆] force consts. on basic of D₄_h symm. 0–39402
D₃, shift in vibr. frequencies caused by gas soln, phase transition 0–43111
D⁴ vibrational constants of ground state from photoelectron spectra 0–58169
D⁵Br₇, D⁷Br⁺ vibrational constants from rotational analysis 0–58200
DCN, vibration-rotation Hamiltonian allowing for large-amplitude bending vibration 0 43056
DCI, intensities of fundamental bands, solvent effects 0–39802
D-O, rotational levels of ground vibrational state, microwave spectrum 0–742.54
D-S sound absorption meas, at 300°K, 400°K, vibrational-relaxation time

0–74254
D-S sound absorption meas, at 300°K, 400°K, vibrational-relaxation time analysis, exptl. results 0–53026
PCN bending force constants from gas phase frequencies and 1-type doubling constant 0–49864
F-CS, ³A state 0–77772
Fe(CO)₂⁴ and derivatives substituted by PF₃, P(MeO)₃ and P(Me)₃, force constants 0–58191
FeCl system I assignments 0–49865
GdO 0–64402
Ge compounds mol force fields 0–58167

Ge compounds, mol. force fields 0-58167 GeBr. vibrational analysis of band system for $A^2\Sigma$ - $X^2\Pi$ transition GeBr. vibrational analysis of band system for $A^2\Sigma \cdot X^2\Pi$ transition 0–49868 GeCl₂. Ge-Cl stretching freqs. and force constants from i.r. spectra

0–49868
GeCl. Ge-Cl stretching freqs. and force constants from i.r. spectra 0–49866
GeCl., normal coordinate analysis using four-constant valence potential function 0–66200
GeCl., normal coordinate analysis using four-constant valence potential function 0–66200
GeH₂CN, and -d₃, constants 0–46523
H halide molecules in collision, vibration rotation energy transfer probability 0–74443
H₂, 0–2 vibr. transition from abs. spectra in liq, Ar and N = 0–43457
H₃, discrete absorption and photodissociation 0–49872
H₄, excitation by electron scatt., quantum-mech, theory 0–43102
H₄, excitation by electron scatt., quantum-mech, theory 0–43102
H₅, excitation of individual vibl. states in collisions with Li⁺ 0–71059
H₅, interstellar obs., from vibr. rot. emission lines 0–45304
H₇, shift in vibr. frequencies caused by gas soin, phase transition 0–43111
H₇, simultaneous rot. vib. excitation by slow electron impact 0–64421
H₇, simultaneous vib. and rot. excitation by slow electrons 0–64418
H₇, vibronic coupling, general formulation 0–39378
H₄ assignment of levels near dissociation in B¹Σ_u⁻⁷ state 0–64557
H₇ electron impact excitation 0–64417
H₇ electron impact excitation 0–64417
H₈ electron impact excitation 0–64417

1*, proton angular distribution from vibrational dissociation 0–43189 1* ground state energy, equilibrium distances and vibration frequencies 0–74259

 $4.^{+}$ vibrational constants of ground state from photoelectron spectra 0-58169

HBr, coupling consts. from hyperfine struct. of submm. spectrum 0-70913

HBr, coupling consts. from hyperfine struct, of submm. spectrum 0-70913
HBr (ν"=1), relaxation by HCl at 300 °K 0-64408
H-CCl radical, C-Cl stretching force constant 0-76279
HCN, calculated dipole-moments and i.r. intensities 0-64403
HCN, vibr, and ro-vibr, consts. from absorpt, and laser meas. 0-61094
HCN, vibration rotation Hamiltonian allowing for large-amplitude bending vibration 0-43056
HCN vibrational transitions in emission spectrum 0-74262
HCl, anharmonicity in polar and nonpolar solvents of varying dielectric constants 0-43108
HCl, condensed phases. Raman obs. 0-72357
HCl, intensities of fundamental bands, solvent effects 0-39802
HCl, rot. vibr. consts., calc. 0-43110
HCl, vibr. excited, scatt. and accommodation coeffs. determ. 0-77787
HCl compressed gas, vibr,-rot. spectrum, intensities and widths in ν₀-band 0-43109
HCl dipole moment matrix elements of vibration-rotation bands 0-77790

HCl dipole moment matrix elements of vibration-rotation bands 0-77790 HD¹ vibrational constants of ground state from photoelectron spectra 0-58169

Molecules continued vibration continued

HDO in C:Cl₂F₁-CS- mixtures, valence vibrs, contact complexes obs. 0-49873

HF. vibra 0-46479 vibrational rotational transitions, generation in 2.8 um range

HF-, potential function, LCAO MO SCF calc. 0-43106

H · O, in hydrates, intramol, stretch stretch force consts. 0–77795 H · O, in ionic solns.. low freq. motions, neutron scattering spectra 0–61483 H · O, line intensity, 6.3 μm band 0–53032 H · O in C·Cl₃F₃-CS- mixtures, valence vibrs.. contact complexes obs. 0–49873

0-496.75 H. O librational modes in single cryst. hydrates 0-43851 H. O vapour, and isotopic species, vibr.- rot, bands 0-64415 H. O force constants of Bu class vibrations comparison with H_5O^{-1} 0-58175

H₂O₂³ force constants of Bu class vibrations comparison with H3O+ -5817

0–58175
H-X+D-X=2HDX, (X-O, S, or Se), anharmonicity correction to zeropoint energy 0–76254
H-+D-→2HD, nonequilibrium vibrational excitation mechanism 0–66170
H-+He collisions, vibrational excitation cross sections, impact parameter
dependence 0–61191
H-++He→H++H+He, specific vibrational states of H-+, 0 to 10 eV

H;++He→HeH++H, specific vibrational states of H;+, 0 to 10 eV

0 - 64603He-1, exact calculation of force const. 0-64404

He-1, exact calculation of force const. 0—64404
1., excited, vibrational and rotational energy transfer efficiencies 0—77803
1., excited, vibrational energy-transfer cross sections for B state 0—77804
1., overlapping vibr., rot. lines near 6330 Å, rel. to He-Ne laser freq. stabilization 0—58179
1CN bending force constants from gas phase frequencies and 1-type doubling constant 0—49864
1Fs. IOF-s and IF1 molec, force field 0—77805
1nCl₈, force constant, mean amplitude, Bastiansen-Morino shrinkage 0—55299
1CM p.E. force const. from in and Raman spectra. 0—64373

InCls. force constant, mean amplitude, Bastiansen-Morino shrinkage 0–55299
K·MnF₆, force const., from i.r. and Raman spectra 0–64373
K·ReF₆| and K2|TcF₆| force consts., on basis of D₁₆, symm. 0–39402
LaO, emission spectrum, u.v., vibr. struct. 0–61101
La¹⁸O vibrational ahalysis of green- yellow system, band spectrum 0–43119
LiCN,LiNC, vibr. freqs. when matrix isolated 0–69122
LiO·, vibr. potential and force constants 0–70916
Me₁₀X; absorption spectra, stretching vibrations 0–49860
Mg·, consts. from abs. bands 0–46484
MgBr· and Mg1· diethyl ether complexes 0–74278
MgO. Franck-Condon factors and r-centroids for D¹Δ-A¹Π and C¹1Σ-A¹Π systems 0–49877
Mg6O₁₀A·5H·O·, i.r. spectra, vibrations of B·O·, Mg·O bonds 0–53040
Mn·(CO)₁₀. i.r. and Raman obs. 0–39391
N·, ifetimes of vibrational levels of electronic states 0–55303
N·, relax. rates meas., behind shock waves 0–77814
N·, vibrational relaxation in collisions with metal atoms 0–74446
N·glow discharge positive column, temp. 0–67978
NF·, mean-square amplitudes 0–43128
NF·, FF·; and AsF·; anharmonic consts. and rot, vibr. interaction consts. 0–55305
NF·, and deuterated derivative vibrational structure associated with transities collections to a second constant of the constraint of the constant of the

0–55305
NH₃, and deuterated derivative vibrational structure associated with transitions leading to ionization potentials _0–64436
NH₃. Franck-Condon factors for A←X transition 0–61112
NH₄. harmonic freqs. calc. from anharmonic ones. and ND₃ 0–77816
NH₄. inversion barrier, ab initio MO calc. 0–39388
NH₃, u.v. absorption bands, intensities of vibrational components 0–70928
NH₃ and ND₃, from photoelectron spectra 0–58186
NH₄Cl. vibr.-rot. transitions, saturated absorpt. spectra 0–70844
NH₂D, rotational-vibrational spectroscopy, transitions of v- band 0–74282

NH-D, rotational-vibrational spectroscopy, transitions of *v*-band 0–74282
NH-NH-1, antisymmetric wagging band 0–77813
NO, absolute oscillator strength of (0,0) band of *v* system 0–61119
NO, fluoresc., Hanle effect and level obs. 0–61105
NO-ion isolated in Ar matrix 0–41215
NO-, photoelectron spectrum, high resolution, and electron impact energy loss spectrum 0–67741
NO-, vib. rot. interac. consts., from (3,0,1) band anal. 0–64431
N-O, calculated dipole-moments and i.r. intensities 0–64403
N-O, excited, vibr. relax. 0–39386
N-O, Napier relax. time. -H., -D. collisions effects, 32 and 52°C 0–39390
N-O, scatt. and de-excitation coeffs. Calc. 0–61106
N-O vibrational spectrum, potential constants 0–43127
N-O zero angle electron scattering with vibrational excitation 0–43123
N-O-3-, isotopic species, spectroscopic study of root-mean-square amplitudes 0–74287
NSE, vibrational analysis of subsystems 0–77809
NSE, vibrational analysis of subsystems 0–77809
NSE, vibrational analysis of -61107
¹⁵N¹⁶O, ¹⁶N¹⁶O, electronic spectrum, isotope effect 0–39385
¹⁵N¹³, v-band. Stark spectra by 10 *u* lasers 0–61113
Na., laser-induced 0–58189
NaCl, from r.f. spectra 0–61126
NaCl, quadrupole coupling consts. from r.f. spectrum 0–70933
Na-Cr-(CO)₁₀, i.r. and Raman obs. 0–39391
NaHCr-(CO)₁₀, i.r. and Raman obs. 0–39391
NaHCr-(CO)₁₀, i.r. and Raman spectra, force constants of complex ion 0–46497
NaSO(OH)₈, i.r. absorpt. spectra obs. 0–61125
Ni, Pd and Pt complexes, Ni(PF₃)₄, Pd(PF₃)₄ and Pt(PF₃)₄, vibr. spectra 0–53309
Ni complex, Ni(CO)_{4-n} (PA₃)_n, force constants, symmetry coords, and G and F matrices 0–49880

0-53:09

Ni complex, Ni(CO)₄₋₁, (PA₂)_m, force constants, symmetry coords, and G and F matrices 0-49880

Ni complex, Ni(CO)_{4-m}(PA₂)_m (A=F, OCH₃,CH₃), fundamental vibration freqs. 0-49881

Ni complex, Ni(C)_{4-m}(PA₂)_m (A=F, OCH₃, CH₃), force constant calc. 0-49882

Ni complex, nitrosyl microwave spectrum in an E_1 vibrational state 0-77821

vibration continued

Ni complex, pentacyanonickelate ion, structure Raman spectrum, CN stretching frequencies 0-46501

Ni complexes, phosphines, metal isotope effect on metal-ligand vibrations

Ni(CO)₄ and derivatives substituted by PF₂, P(MeO)₃ and P(Me)₃, force constants 0-58191

constants 0–58191 Ni(PCI), force constants 0–64443 O., excited, absorpt., 1850 to 2245 Å 0–74416 O., relax, rates meas, behind shock waves 0–77814 O., relaxinon time, temp. dependence 0–61131 O. Schumann Runge bands photographed, vibrational and rotational constants 0–74296 O. trapped in solid matrices, vibl. terms of $B^3\Sigma_{\mu}$ + $X^3\Sigma_g$ transition 0–55311

0-55311
O-vibrational populations and synthetic spectra of Herzberg bands in night airglow 0-41515
O-thy vibrationally excited, production by solar u.v., effect of autoionization 0-77826
O-the autoionized reson, states, rel. to photo e spectra, obs. 0-46502
O-the beams, vibrational excitation in collisions with neutral mols. 0-53103
O-mil* complexes formed in O-+O-m* reactions, weak mode vibrational frequencies 0-72529
OCS, rel. to second-order force consts. determ. 0-53047
O-F, 0-43130

O:F. 0–43130
OsOa vapour, force constants Raman spectra 0–46503
P complex, diphosphorus tetrafluoride sign and temp. depend. of coupling constants 0–46505
P complex, methyl-aminobis (difluorophospine sign and temp. depend of coupling constants 0–46505
P complex, u-thio-bis(difluorophosphine sign and temp. depend. of coupling constants 0–46505
PCL₂F₃, molecular constants from spectroscopic data 0–55313
PCl₃F₄, molecular constants from spectroscopic data 0–55313
PCl₃F₄, molecular constants from spectroscopic data 0–55313
PCl₃F₄, molecular constants from spectroscopic data 0–56313
PCl₃F₄, molecular constants from spectroscopic data 0–57844

held model 0-708/1 PFs, vibr.-rot. transitions, saturated absorpt, spectra 0-70844 PHs, harmonic freqs, calc. from anharmonic ones, and PD 0-77816 POc3-, general valence force field force constants 0-55316 PbCls, Pb-Cl stretching freqs, and force constants from i.r., spectra

Polls, Poll stretching freqs, and force constants from i.r. spectra 0-49866
Pb₄(OH)₄⁺⁺ complexes, alternate force fields in normal coord, anal. 0-74232

Pd complexes, phosphines, metal isotope effect on metal-ligand vibrations 0-77763

0-77763
Pfs, E' force field 0-61133
ReFr, anharmonic coupling, electron diffr, exam. 0-70946
S containing isotope replacement effects on vibr.-rot. consts. 0-49887
SFs, force constants 0-53049
SFs, force constants 0-53049
SFs, torce constants 0-70947
SFs, torce rot. rensitional transitions, narrow reson. within Doppler line during absorpt, saturation 0-70947
SFs, vibr.-rot. transitions, saturated absorpt, spectra 0-70844
SFs, v) and v) mode fluoresc. lifetime 0-53048
SO, v) and v) modes, solvent effects 0-39802
SO adsorbed, vibrational frequencies 0-74303
SO), i.r. spectrum assignements, obs. 0-43134
SOCl₁, v) intensity, solvent effects 0-39802
Sb (III) halide complexes with DMSO, i.r. and Raman assignments 0-49890

0-49890
Sb trihalides, intramolecular force fields 0-70949
Sb trihalides, sensitivity of normal vibrations to their parameters 0-64452
SbCl3, Raman spectra, low frequencies, temp. changes 0-49888
SbF, new band system in 4050-5450 Å region 0-49889
SbH3, harmonic freqs. calc. from anharmonic ones, and SbD3 0-77816
ScCl. electronic-vibr-rot. spectrum, 2200-9000 Å 0-49891
Se-O bonds linear relationship between force constants and bond lengths 0-46513

ScCl, electronic-vibr.rot. spectrum, 2200-9000 Å 0-49891
Se-O bonds linear relationship between force constants and bond lengths 0-46513
Se hexahalide ions, mol. force fields 0-43136
SeO. force constants, by microwave spectroscopy 0-64453
SeOF-, molecular force field, Se-F stretching force constant 0-49893
SeO-F-, molecular force field, Se-F stretching force constant 0-49893
Si- new band systems discovered, rotational and vibrational constants 0-77844
SiCl, analysis of bands of B-X system 0-61137
Si-Cl₆. Si-Br₆ and Si₂l₆, force consts. and vibr. spectrum 0-55325
SiH₃/sAH₃ and SiD₂/sA₂D₂ 0-74307
SiH₃/sC₁/s₂ and (SiD₂)-CH₁ 0-77845
SiHCl₁ and SiD₂/s₂C₁ force constants 0-70951
SiH₃/sC₁ frequencies 0-77846
SiH₃PH- and SiD₂PD- 0-74307
SiH₃/s₂ (Frequencies 0-77846
SiD₃ (Frequencies 0-77846
SiD₃ (Frequencies 0-77846
SiD₃ (Frequencies 0-77847
SiCl₄ (SiH₃)-CH₃ (SiD₃)-CH₃ 0-74307
SiH₃ (SiD₃ (SiD₃)-CH₃ 0-74307
SiH₃ (SiD₃)-CH₃ (Si

0–49895 TiF₄ diadducts with 4-subst, quinoline 1-oxides, l.f. i.r. spectra, ν_{n-o} and ν_{m-o} stretching freqs. 0–49894 Tl₄(OEt)₄ complexes, alternate force fields in normal coord. anal. 0–74232 UF₄ force constants on basis of tetrahedral symmetry 0–64459 VF₅, Force constants and normal modes, in terms of orbital-valency-force field model 0–70871 (VF₆)²-, vibrational structure of electronic spectra 0–64395 V(IV) complexes, VF₄ para-substituted pyridine-N-oxides, N-O stretching mode, obs. 0–39403 WCl₆, force constants and mean amplitudes of vibration, normal coordinate analysis 0–43139 WCl₆ mean amplitude of vibration from spectroscopic data 0–43139

analysis 0-43139 WCl₈ mean amplitude of vibration from spectroscopic data 0-43139 WCl₈ shrinkage effect from spectroscopic data 0-43139 XY₂-type, graphical analytical method for determining force field 0-43057

XY₆ type, force constants, mean amplitudes, Bastiansen-Morino shrin-kages 0-55288

Molecules continued vibration continued

XYn type, bond charge model for symmetric stretching vibrs.

XYn type, bond charge model for symmetric stretching vibrs. 0–64345 XeO₁ vapour and solid force constants, Raman spectra 0–46503 Zn(II) complex, Zn(NH₃); Cl₂, classification, by factor and site group analysis 0–55329 Zn(II) halide complexes, of NH₃ and imidazole. Zn-N and Zn-halogen stretching force consts. 0–55329

Molecules, mesic and muonic

nuclear spin precession 0-55388

Mollier diagrams see Thermodynamic properties

Molybdenum

Jybdenum

2-81 permalloy powder cores, heat treatment 0—65452
addition in V alloy, interactions with interstitial impurities, effect on tensile properties, meas, at 77 to 673°K 0—50722
adsorption of Ba, on (110) face, struct, LEED obs. 0—71495
adsorption of Hafnium 0—43574
b.c.c., irradiated at low-temp, internal friction 0—68411
carrier mean free path, 4.2K, 3.2 Me/s, plane parallel plates 0—44060
cathode, potential drop rel. to press, for inert gases 0—39627
cathodes for thermoemission converters, optimal Electrical power, interelect trode separation fin. Cs pressure 0—38453
chemisorption of 0-, N-, H-, CO, on Mo(112), LEED obs. 0—56698
cold-worked, stage III recovery conc. depend. 0—58966
crystals single, thermal cycling influence of substructure, migration of sub-boundaries, method 0—47241
cvclotron resonance, effective mass determ. 0 −78858

sub-boundaries, method 0—47241 cyclotron resonance, effective mass determ. 0 -78858 deep drawing 0—43808 defect concentration after 4 MeV electron irrad., 77K, dose and impurity depend. 0—50566 density of states, electronic, calculation from energy band structures 0—65582

0-65582 desorption of H. O. and H.O by electron impacts 0-39973 diffusion of nitrogen 0-65342 ductile-brittle transition temp., annealing temp. effect 0-58895 effect on V-Ta-C and Nb-Ta-C system, equilibrium at high temperature investigation 0-50821

investigation 0–50821 elastic constant, second and third order, Morse pot. calc. 0–78596 electrical resististivity, thermal enff, lattice parameter, neutron irrad, and annealing depend. 0–40725 electron emission, secondary 0–47890 electronic structure, photoemission and reflectance studies 0–65596 film, optical absorpt., 3130-7500Å 0–51306 film, partial diffusion masks in m.o.s. processing 0–79027 film, prepared by low pressure triode sputtering, stress analysis 0–50674 film produced by laser volatilisation, resistivity and struct. 0–71959 films, electrical properties and superconductivity 0–71944 films, monocrystalline, negative surface ionization of 1, temp. depend. 0–40917

nims, monocrystatine, negative surface tonization of 1, temp. depend. 0–40917
heat capacity, elec. resistivity and thermal rad. props. in range 1900 to 2800°K. 0–47546
heat-softening, single crystals, effect of previous work hardening and mechanism 0–78657
internal friction and interstitial impurities on grain boundary. 0–50733
internal friction in low-temp. irradiated b.c.c. samples. 0–68411
internal friction peaks associated with dislocations. rel. to cold-work, 77700K, 5-50 kHz. 0–68410
internal friction peaks due to dislocs. rel. to stress-deform. curve. 0–65368
ions in molten LiCl-KCl eutectic, equilib. with solution. 0–59496
Kossel line X-ray exam. of local lattice distortions. 0–68348
mechanical behaviour and twinning, polycrystalline. 0–40353
microyielding and failure in ductile and brittle polycrysts. 0–75256
monocrystals, Rb¹ and Cs² ions scattering, energy spectra rel. to angular functions. 0–57501
Mossbauer fraction of ⁵⁷Fe, force const. changes obs. 0–40531
neutron irradiated, microstructural defects, temp. depend., 50-800°C
0–61966
neutron-irradiated, defect recovery, isochronal resistivity obs. 0–47221

0–61966
neutron-irradiated, defect recovery, isochronal resistivity obs. 0–47221
photoelectric work function 0–75859
plastic flow, strain rate and temp. effect 0–40307
plastic stress relaxation, interaction of moving dislocations with interstitial impurities 0–50575
powder, hot pressing, 1400 1600°C 0–65451
proton irradiated, emitted Lyman a radiation, Doppler shift 0–40620
scattering of atomic and mol. ions, energy distribs. of emitted particles 0–40912
slip behaviour of deformed cryst., stress-strain characts. 0–78643
solutions, photochromatic, optical props. depend. on composition, conc. and u.v. irrad, strength 0–61520
spin-orbit coupling, large, and Fermi surface 0–53760
sputtering and electron emission under Hg ion bombardment, 15-100 keV 0–71883
surface oxidation obs. by secondary ion mass spectroscopy 0–72539

0—71883 surface oxidation obs. by secondary ion mass spectroscopy 0—72539 thermionic converter, cylindrical Mo/Mo, low temp. performance 0—76999 work hardening of single crystals, effect on subsequent heat-softening, mechanism 0—78657 mechanism 0—78657 cl and Br — bombardment, electron emission, ions scattering 0—59292 Mo/UN cermet fabrication using mixed powders or coated particles 0—40407

0-40470

Mo-Au film for Si contact technology, vacuum depositions 0–56306 Mo-UO cermet fuels, determination of postirradiation disposition of ⁸⁵Kr 0–77623

Mo VI, spectrum 6800-2200 A in Penning type arc discharge, 4 new levels

Mo VI. spectrum 6800-2200 A in Penning type arc discharge, 4 new levels determ. 0-42974
Mo VIII. term analysis of the 4p 4d and 4p-5s transitions 0-60937
Mo³⁺ in K-Zn-phosphate glass, e.p.r. spectra 0-54156
Ni-Al-Nb Mo solid soln, y and y' phases, investig. 0-47459
in Ni, additive effect on high temp. Elinvar prop. 0-58855
Sn film growth on (100) face, thin film of Sn, growth study using Auger-LEED technique 0-47121
Ti/Mo, substrate ion secondary emission kinetics during initial stage film deposition 0-50391

Molybdenum compounds

alloy, deep drawing 0-43808 alloys, carbide-strengthened, dynamic strain ageing 0-47446 dichlorotetrafluoroethane-MoF₆ binary mixture liquid-vapour equilibrium at 2600 torr 0-64984

Molybdenum compounds continued

quid-vapour equilibrium, dew and boiling curves 0-64981

Mo-Au composites, thin strips, current induced mass transport obs., by scanning electron microscope 0–47648 molybdates, Yb³⁺ Er³⁺ doped, i.r. pumped visible emission, controlling factors 0–62720

molybdates, spectra, 2000 to 40 cm⁻¹, and structs. 0-55323 permalloy, 4-79 Mo, permeability, annealing environment depend. permalloy, 0-41025

permalloy-Mo, linear magnetostriction, magnetization, permeability 0-51210

0-31210
Permalloy-Mo, mag. props., sulphur impurity depend. 0-44580
Al-Mo alloy, supersaturated solid soln., expansion coeff., temp. depend. 0-78783
Co-27Cr-7Mo alloys, ductility effect of C 0-53642
Cr-Mo, alloys, effect of Neel transition on thermal and elec. cond. 0-65623

Cr-Mo alloy, hydrostatic pressure effect on Neel point, elec. resistivity meas. 0-41053
38 CrMoV 21.14 steel, incomplete solutions of C. metallographic examina-

tion and contact thermal e.m.f. meas. 0–40458 Fe-Mo. diffusion of Cu. 707-870°C 0–50622 Fe-Mo alloy, Fe-rich variable freq. n.m.r. meas. rel. to hyperfine field distrib. 0–56682

Fe-Ni-Co-Mo alloy, preprecip, and reversion 0–59023 Fe-Ni-Mo (-Co) alloys with ageing martensite, recovery 0–50770 Fe-Ni-Mo alloy, ageing of martensite, 450-500°C, kinetics and mechanism 0–78675

Per-Ni-Mo alloys, ageing of martensite, 450-500°C, kinetics and mechanism 0-78675
Fe: Ni Ti-Mo alloys, austenite obs. 0-61865
HfMo: alloy, lattice parameters, supercond. 0-59177
Mo-Cu interaction, by explosive heating 0-75302
Mo-Fe dil, alloys, Mossbauer obs. 0-72336
Mo-N solid soln., low temp. recovery behaviour 0-53634
Mo-Re alloy, plastic deformation, 78 425 K 0-43745
Mo-Ra alloys, elastic and plastic props., -190°C to +100°C 0-43711
Mo-Ta alloys, interdiffusion parameters determ. 0-40198
Mo(CO)₆, vacuum u.v. spectra 0-70867
MoF₆, negative ion formation 0-64763
MoF₆, Raman spectrum in vapour state 0-58183
MoO₁:Cr¹⁺, e.s.r. 0-44990
MoO₂:SiV(⁹Nb). e.s.r., electron hole centre interactions. 0-48149
MoO₃ interaction with graphite, mechanism 0-72547
MoO₃ (CN)₄*, complex anion, geometry 0-55845
MoO(III) complex, ditholphosphenes, hyperfine interaction of ³¹P
0-70898

0—/08/98
MOO.2H-O, cryst. struct. and bonds 0—61886
MoS . anode catalyst for fuel cells with acid electrolyte 0—63541
MoS . layered, lattice mode degeneracy 0—65519
MoS . optical absorpt. spectra, photocond. excitons 0—47875
MoS . test as anode catalyst for H oxidation in acid electrolytes 0—67009

MoS-, test as anode catalyst for H oxidation in acid electrolytes 0–67009 MoS- single crystals optical anisotropy from obs. of electron energy loss spectra 0–44747 MoS- solid film for lubrication 0–53429 MoSe, photocond., optical absorpt, spectra, excitons 0–47875 M Mo₃Se₄, where M=Fe, Co, Ni, synthesis and X-ray diffraction patterns 0–58740 Mo₅Si₂/Ta(W)₂Si₃, Ta/Mo and W/Mo interdiffusion kinetics 0–71647 MoSi₂-film on Mo, stress meas, using X-ray method 0–75246 MoTe₃, photocond., optical absorpt, spectra, excitons 0–47875 Mo—Ti-C, creep, tensile properties, 1800 to 3200°F, dynamic strain ageing 0–40331

Mo—Ti – C, creep, tensile properties, 1800 to 3200°F, dynamic strain ageing 0–40331
Nb-Mo Au system, supercond. 0–40743
Nb-Mo-N alloys in air and H-, int. friction and mech. props. 0–55955
Nb-Mo N solid solution. N solubility 0–58982
Nb-Mo alloy, mech. behaviour and twinning 0–40353
Nb-Ti-Mo alloy, b.e.c., superconducting transition temp., critical field. current carrying capacity 0–40744
Nb_xMo_{1-x}. Solute alloy, with 0≤x≤0.4. n.m.r., local moment formation 0–45028
Ni-Fe-Cu-Mo, magnetic, high permeability, sintering process resist varia.

Ni-Fe-Cu-Mo. magnetic, high permeability, sintering process, resist, variation 0-62089

Ni-Fe-Mo, thin film, anisotropic field var. with thickness, temp., and Mo conc. 0-79185

Ni-Pe-Mo, thin him. anisotropic field var. with thickness, temp., and Mo conc. 0–79185

Ni-Fe-Mo films, magnetiz., low temp. 0–65944

Ni-Mn-Mo, Nimalloy, permeability, comp. depend. 0–75935

Ni-(23at.%)Mo, alloy, Ni atom electrotransport 0–47649

Ni-Mo, alloy electrotransport of Mo, 1100 1300°C, donor-acceptor interaction 0–50987

Ni-Mo alloy, surface layer, mag. props. adsorbed anions depend. 0–59324

Ni-Mo alloy, compressive strength, tengle deformation, temp. decend.

Ni-Mo alloy, compressive strength, tensile deformation, temp. depend.

0-47377

Ni-Mo alloys, thermomag, effect temp. depend. 0-62534

Ni-Mo phase diagrams 1200-2100°C 0-71408

Ni-(20at.%)Mo alloys, electrotransport, 950-1300°C, donor acceptor interactions 62306 0-62306

Ni Nb-Mo, isothermal section at 1400°C 0-71408

NisMo alloys, structural changes during isothermal annealing after quenching 0-65269

Pd-Mo:Co solid solution, mag, susceptibility, elec. resist., temp. and comp. depend. 0-62309

Ta-Mo-C alloy, effect of Re and Al, phase equilibrium investigation 0-50822

0–50822
Ta-Mo, b.c.c. alloy, short range order, X-ray diffr. 0–40101
β-Ti:(Mo,Nb,V) isomorphous alloy, phase transformations 0–53663
Ti-Mo-Zr-Sn alloy, β-III, as-quenched, stability 0–71807
Ti-Mo alloy, cermet, production and corrosion props. 0–78686
Ti-Mo dil, alloy, microstruct, influence on supercond. 0–71986
Ti-Mo phase boundaries determ. 0–53665

11 Mo phase boundaries determ. 0—33053 Ti-Mo wire, grain-boundary, matrix- crystalline fracture, scanning electron microscopy 0—61908 Ti-Mo wires, crystalline and polycrystalline, fractography, scanning elec-tron microscopy 0—68494 Ti_xMo_{1-x}²⁹Co dilute alloy, with 0≤x≤0.4, n.m.r., local moment formation 0.45038

0-45028 U-(1.5~wt.%)Mo alloys, continuous and discontinuous precip. reactions 0--68561

U-Mo alloys, shear transform, from y-phase 0-62137 U-Mo alloys, stress corrosion props. 0-55998

U-Mo alloys, stress corrosion props. 0–55998 y-U-Mo fuel alloy, thermal cycling and irrad, stability 0–40467

Molybdenum compounds continued

W-Ir Mo alloy anode for X ray tube, patent 0–59851
W-Mo Ag based powder metallurgy, pseudo- alloy production for elec. contact making 0–68544
50%W-50%Mo, creep in low-pressure O-, correlation with sublimation rate 0–78636
Zr-(1.0 wt.%)Cu- (1.5 wt.%)Mo alloy, cracking in oxide films 0–40419
β-Zr-Mo alloy, quenched, Al influence on stability 0–50826
Zr-Mo alloy, lattice parameters, supercond. 0–59177

Monitoring see Radiation monitoring

Monochromators

see also Filters, optical; Light sources; X-ray monochromators alignment, geometrically exact, grating and collimating mirrors using laser and spectral lamp 0–73351 concave system, normal incidence, for far u.v. 0–60433 Ebert, double pass, pseudo-half orders 0–57587 electron, anomalous energy spread 0–60165 graphite, singly bent, for neutron crystal spectrometer setups 0–75072 i.r., diffraction grating, spectral characts, of filters for first order isolation 0 60434 incidence, grazing, constant during a content during a content

0 60434 incidence, grazing, constant deviation, 2m, efficiency, use with synchrot-ron 0-73347 instrumental function determ. 0-63722 rel.to luminescence spectra meas. 0-54943 multiple dispersion, optical techniques 0-52388 neutron, focusing, Fe-Si use 0-61807 ring-slit for light sources of small radiation density 0-52389 for scintillator obs., at entrance slit light output and decay time vs. λ 0-60664

for scintillator obs., at entrance shringht output and detay 0-60664 seemingly Doppler-shifted radiation prod. by time- and space-dependent sources 0-70080 spectral scanning of i.r., u.v., visible regions, tech. 0-65998 vacuum, cylindrical chopper analysis of useful properties 0-67182 Zeiss MM12, transmission and reflection meas, on small crystalline samples 0-62606 by crystal for neutron beam, integrated reflection and reflectivity rel. to mosaic spread and thickness 0-47169

Monolayers see Adsorbed layers

Monomers see Molecules

Monomolecular layers see Adsorbed layers Monte Carlo method see Statistical analysis

'afterglow', post sunset horizon 0–69434
acoustic energy localisation, Apollo 12 obs. 0–66576
age, from "9Ar/3"Ar dating of rock samples 0–48491
age, from Rb-Sr, U and Th-Pb dating of samples 0–48492
age, from Rb Sr chronology and chemistry of igneous rock samples
0–48493

age, from Rb-Sr isotopic data and elemental and isotopic abundances of trace elements 0-45338

age, from Rb-Sr isotopic data and elemental and isotopic abundances of trace elements 0—45338
age, from Rb-Sr relations in Tranquillity Base samples 0—45337
age, from U-Th-Pb isotope relations in samples 0—45334
age, isotopic study of U-Th-Pb systematics of samples 0—45334
age determ, and isotopic abundance meas, on samples 0—45339
age of Mare Tranquillitatis crystallisation from rare gas analysis 0—45362
age of Mare Tranquillitatis surface material, Pb and Tl isotopes 0—48494
age of formation of Sea of Tranquillity from rock samples 0—45335
age of samples from radioactivity determ. 0—48510
albedo of rocks, pulverization effects 0—48550
anorthosites, relation with those in early crust of Earth 0—51492
Apollo 11 mission, probes analysis 0—41772
Apollo 11 sample analysis, zodiacal light models 0—66620
Apollo 12 lunar module impact, lab, simulation and possible downrange ballisfic effects 0—79722
Apollo passive seismic experiment 0—76626
atmosphere creation by breaking crust and releasing gases 0—59764
atmospheric pressure 10 m above lunar surface from Surveyor-VII twilight photography 0—48554
backscattering, radar echo studies at 6, 7.5, 12 meter wavelengths

backscattering, radar echo studies at 6, 7.5, 12 meter wavelengths 0-51743basins, circular distributions and relations, Lunar Orbiter data obs. review 0-76623

0—76623
bench mark network, systematic and accidental differences 0—57089
bibliography (third quarter of 1969) 0—76630
bio-organic compounds and glassy microparticles in samples 0—48550
carbon compounds in Apollo 11 samples, discussion of origin 0—41770
cathodoluminescence props, of rock samples 0—48529
chemical analysis of surface, rel. to Surveyor program 0—59751
chemical composition of surface in Sinus Medii 0—51737
compressibility and sound velocity for samples 0—45395
compressibility of crystalline rock, microbreccia and fines to 40 kilobars 0—45304

0-45394 conference on Apollo 11 samples 0-45332 cosmic ray production of rare gas radioactivities and tritium in samples 0-48504

crater Aristarchus, obs. of red spot due to CN molecules crater formation controversy before Apollo 11 0-41760

cratered surfaces, distrib. and covariance function of elevations, derivation 0-48562

0–48562
cratering, volcanic hyphothesis 0–41778
cratering rates over last 3.9 aeons 0–54429
cratering, rates over last 3.9 aeons 0–54429
craters, large, maria, absolute ages 0–48558
craters, small, in southern highlands, counts 0–76621
craters sharp to fast, erosion, incremental diameter-freq, relations, Orbiter 5
photographs 0–51742
Delaunay's reduced Hamiltonian checked against new theory based on his
transforms 0–69439
distance, laser ranging retro-reflector, meas, and expected results 0–48490
distance, from earth measurement, laser reflector array 0–41779
drainage craters, terrestrial analogs 0–41766
drift scans, (differential) low-resolution, at 22 u temperature distribution of
cold-limb 0–76624
dust, glassy spherules 0–72762
e.p.r. of samples 0–48541
Earth-to-Moon trajectories, periodic obits asymptotic solution 0–48488
eclipses, 1921-1968, photometric analysis of peripheric umbra 0–63086

Moon continued

elastic energy propag., anomalous, represented as diffusive process 0-51747

elastic wave velocities in samples, at high press., geophysical implications 0-45393

electroiet intensity modulation 0-48314

elemental abundances in rocks, soil and core samples 0–45349 elemental composition of surface material 0–45348 ephemeris, analytical, response to Brouwers' suggestion 0–66573

ephemeris, analytical, response to Brouwers' suggestion 0–66573 ephemeris construction revealing systematic longit, difference 0–51748 FK4 catalogue's orientation from meridian obs., orbital elements, discussion 0–72760 fines, glassy particles in, morphology optical properties 0–79719 formation conditions, implications from trace elements and radioactivity meas, in samples 0–45341 garnet in lunar rocks 0–79725 glass spherules in samples, morphology and related chemistry 0–48523 glasses and micro-breccias in samples, props. and origin 0–48525 grain size distribution and mineralogy al constituents in soil 0–45380 gravimetry and mascons 0–76619 gravitational field 0–48593 gravitational field influence on location of sun-earth exterior libration point 0–66571

gravitational harmonics, from secular and long period effects of satellites

0-66585

O-66385
gravity features estimation, using mass density model Q-59759
gravity field from long-arc anal. of Lunar orbiters 0-41764
gravity over large craters from Apollo 12 tracking data 0-59763
gypsometric map of the visible side, construction 0-45411
heat flow from interior measurements during Apollo 13 0-57098
heights, relative, meas. series 0-41773
i.r., radio and radar obs., surface evolution, symposium, Woods Hole
(1969) 0-59765

(1969) 0-99/65 i.r. emission spectra, enhancement of diagnostic features 0-79724 i.r. emission spectra, enhancement of diagnostic features 0-89754 Impact-theory interpretation of surface distrib. of maria 0-41765 inerior, nature rel. to petrogenesis of basalts 0-45372 inert gases in samples, distribution and variations, microprobe study 0-45364

0-45364 interaction with solar wind 0-56862 interior, nature rel. to petrology of samples 0-45371 internal strain and fissions due to tidal force, calc. using Kelvin theory 0-66575

ionosphere detector expt. using Mass Analyser and Total Ion Detector

10-10028 isotope abundances in lunar samples, rare gases 0-45361 isotope abundances in samples, H/D, ¹³C/¹²C and ¹⁸O/¹⁶O ratios 0-45358

isotope abundances in samples, O, Si, H and C ratios 0–45356 isotope abundances in samples, O isotope fractionation between minerals rel. to formation temp. 0–45357 isotope abundances in samples, S¹³C and δ^{34} S determ. 0–45359

isotope abundances in samples, rare gases, rel. to irradiation history 0–48502

0-48502 isotope abundances in samples, rare gases 0-48505 isotope abundances in samples, rare gases 0-48503 isotope abundances in samples, trapped solar wind inert gases 0-48506 isotopic abundances in samples, H, N and rare gases 0-45360 laser ranging retro-reflector, measurements from McDonald observatory 0-51736

0-31/30
laser-range-retroreflector experiment 0-72765
lavas, viscosity, Earth experiment extension 0-59761
libration, physical, in longitude, appl. of computing techniques to its study 0-48561

0-48561 libration regions, photometric obs., libration clouds brightness, upper limit determ. 0-51749 libration tables 0-41767 light scattering function, spatial for continental regions of the moon 0-51738

0–51738 limb, solar wind shock wave, conducting islands 0–48560 limb correction data from Watts' charts, refinement using stellar grazing and total occultations 0–66572 local areas optical reflectance, photoelectric meas., analysis 0–69430 luminescence, study during Apollo mission 0–48486 luminescence and neutral particles, spectral distrib., dependence on bombarding ions energy and dose 0–51744 luminescence and thermoluminescence induced by 159 MeV proton bombardment in samples 0–45399 luminescence «f samples, proton and u.v. excitation, irradiation and vitrification effects 0–45391 luminescence of samples, under u.v. excitation 0–45390 luminescence of samples 0–48541 luminescence of samples 0–48541 luminescence of samples 0–48541 luminescence of samples 0–48540 luminescence of samplescence of samplescence of samplescence of samplescence of samplescence of samplescence of samplesc

lunar surface photography colour, stereo close-up Apollo 11 and 12 0-76622

lunar surface photography colour, stereo close-up Apollo 11 and 12 0-76622 lunar tide phase in ionospheric D-region absorption near mag. equator, sunspot variations 0-45189 magnetic monopoles, search 0-59746 magnetic monopoles, search for in samples 0-48537 magnetic properties of dust and rock samples 0-48534 magnetic properties of samples. NRM and susceptibility 0-48536 magnetic properties of samples. O-45387 magnetic properties of samples 0-45387 magnetic properties of samples 0-45385 magnetic properties of samples 0-48535 magnetic properties of samples 0-48531 magnetic resonance properties of samples 0-48487 magnetic resonance properties of samples 0-48539 major elements in samples, O. Si and Al abundance by 14 MeV neutron activation 0-45353 major elements in samples, analytical data 0-45352 major elements in samples, chemical analyses of there samples 0-45355 major elements in samples, chemical and emission spectrographic analyses 0-45354 major elements in samples, high Ti content determ. 0-48501

major elements in samples, high Ti content determ. 0-48501 major elements in samples, rock compositions and interpretations 0-48500

major elements in samples, semimicro chemical and X-ray fluorescence analysis 0–48498 manned landings, preliminary assessment 0–72763 Mare Marginis and Mare Orientalis, large mascons absence, obs. 0–41777

Moon continued

Mare Orientale gravity anomaly, further outer rings 0-66578 marginal zone, Watts' charts limb profiles orientation 0-57095 maria, absolute ages 0-48558

maria, absolute ages 0–48558
maria, evolution and structure rel. to 50 km thick crustal layer 0–41775
maria distributions and relations, Lunar Orbiter data obs. review 0–76623
maria spreading and continental migration 0–41768
maria surface distrib., satellite impact interpretation 0–41765
mascons, appl. to detection of gravitational waves from pulsars 0–48480
mascons, creation as structural relief 0–45331
mascons, discussion using results of mineralogy of anothosites 0–45370
mascons, existence explained rel. to petrogenesis of basalts 0–45372
mascons, origin and nature 0–59760
mascons beneath circular basins, rel. to dynamical asymmetries 0–41774
mass, earth/moon ratio rel. to Martian mass, obs. of Mariners 6 and 7
0–51751
mass ratio to earth, three hody crebtary 0–23264

0–51751
mass ratio to earth, three body problem 0–72766
mechanical properties of soil 0–45397
methane and ethane indigenous in lunar samples 0–51746
micromorphology and surface characts. of dust and breccia samples
0–48552

0—48532 micropaleontological study of samples 0—45410 micropaleontological study of samples 0—45408 mineralogy, petrography and crystallography of samples, rel. to petrologic history 0—45366 mineralogy, petrography and crystallography of samples, rel. to petrologic history 0–45366 mineralogy, petrology, and surface features of samples 0–45383 mineralogy, petrology and chem. of rock samples 0–59743 mineralogy and composition of fines and rocks 0–48530 mineralogy and deformation in samples 0–48513 mineralogy and petrography of samples 0–48511 mineralogy and petrology of samples 0–48511 mineralogy and petrology of samples 0–48512 mineralogy of genous-type rocks and spherules 0–45369 mineralogy of sample, igneous rocks, high indicated crystallization temps. 0–48522

mineralogy of samples, Fe-Ti oxides and olivine 0-48514 mineralogy of samples, X-ray diffraction and Mossbauer study of minerals 0-48518

rais 0-46316
mineralogy of samples, anorthositic rocks 0-45370
mineralogy of samples, clinopyroxenes, chemical composition, structural
state and texture 0-48519

mineralogy of samples, clinopyroxenes, chemical composition, structural state and texture 0–48519 mineralogy of samples, coarse particulate material, mineralogy 0–45381 mineralogy of samples, coarse particulate material, mineralogy 0–45381 mineralogy of samples, coarse particulate material, mineralogy 0–45381 mineralogy of samples, crystallisation of mafic magmas and generation of rhyolitic liquid 0–45373 mineralogy of samples, electron microprobe analysis 0–45367 mineralogy of samples, internal substructure determ. by h.v. transmission electron microscopy 0–45377 mineralogy of samples, melt inclusions rel. to silicate liquid immiscibility in magmas 0–45378 mineralogy of samples, opaque minerals, microscope study and electron microprobe analysis 0–48517 mineralogy of samples, opaque minerals in dust and rock 0–45374 mineralogy of samples, opaque phases, quantitative optical and electron-probe studies 0–48516 mineralogy of samples, proxenes, compositional zoning and it significance 0–45376 mineralogy of samples, rocks and fines, search for magnetite 0–48515 mineralogy of samples, troilite crystals, three-dimensional counter intensity data 0–45375 mineralogy of samples 0–45368 mineralogy of samples 0–45368 mineralogy of samples 0–45368 mineralogy of samples 0–45368 moments of inertia and density distribution 0–76625 Mossbauer effect study of minerals 0–48518 Mossbauer effect study of minerals 0–48518 Mossbauer effect study of minerals 0–48532

0-48531
Mossbauer effect study of minerals 0-48518
Mossbauer spectroscopy of samples 0-48532
Mossbauer study of samples, of ⁵³Fe 0-45386
motion, translational-rotational, under attraction by the Earth 0-45412
neutron radiation due to interaction of surface with cosmic rays 0-51739
new, centre, quiet sun, brightness temp., and brightness temp. ratio at 3.3
and 5.7-mm \(\lambda \) 0-76671
new moons, computed list for 319 B.C. to 316 B.C. from Babylon
0-54427

obscuration associated with transient phenom., rel. to glow discharge in escaping gas 0-41769 occultation measurements, interpretation of traces with special reference to limb effects 0-54357 occultation measurements, photoelectric, review of methods and applications 0-54355

occultation measurements at McDonald University, instrumentation 0-54356

occultations of galactic center region in 21-cm neutral H--line obs. 0-59742

0-59742
coculations of stars, anal. of 1950-1968 obs. 0-51750
optical and h.f. electrical props. of samples 0-48540
optical properties, nature and evolution of surface inferences 0-59758
optical properties of samples 0-48541
orbital evolution under radiation press. influence, secular effects investigation 0-57102
orbital science 0-79716
organic compounds in samples, analysis 0-45409
organic compounds in samples, carbon detection by pyrolysis-hydrogen flame ionization 0-45405
organic compounds in samples, mass spectrometric analysis 0-45404
organic compounds in samples, search and characterization 0-45401
organic compounds in samples, search for 0-48548
organic compounds in samples, search for 0-48548
organic compounds in samples, search for by mass spectrometry

organic compounds in samples, search for by mass spectrometry 0-45403

organic compounds in samples, search for porphyrins 0-48549 organic compounds in samples, search for porphyrins by fluorescence activation 0-45402

organic compounds in samples 0-48551

Moon continued

organogenic elements and compounds in samples 0-45406

Orientale region, structure geological interpretations 0-41761

origin, composition of Apollo 11 basaltic rock samples, rel. to precipitation hypothesis 0-45416

origin, composition of Apollo 11 basaltic rock samples, rel. to precipitation hypothesis 0–45416
origin, rel. to petrogenesis of basalts 0–45372
petrography and meneralogy of samples 0–45382
petrologic history, rel. to mineralogy, petrography and crystallography of samples 0–45366
petrology mineralogy and surface features of samples 0–45383
petrology and mineralogy of samples 0–48512
petrology and mineralogy of samples 0–48512
petrology of samples, coarse particate material 0–45381
petrology of samples, coarse particate material 0–4831
petrology of samples rel. to nature of mascons, seas and interior 0–45371
petrology of samples rel. to shock effects 0–45379
phases in samples, electron-microprobe analyses 0–45351
photography, star calibrated, technique 0–41763
photography, wide angle lens 0–60446
planetary production at surface 0–54434
radar echoes studies high delay resolution at 6, 7.5, 12 meter wavelengths 0–51743
radar obs, at wavelength 70 cm. maps interpretation 0–59756
radiation history of samples, solid state studies 0–45363
radiation meas, in 1.2 mm wavelength range, surface roughness effect 0–51745
radioactivities of samples, tritium and argon 0–48507
radioactivities of samples, tritium and argon 0–88507
radioactivities of samples, tritium and argon 0–88507

0-51745 radioactivities of samples, tritium and argon 0-48507 radioactivity in samples rel. to meteorite infall, solar-wind flux and formation conditions 0-45341 radioactivity of surface at Surveyor 5, 6 and 7 sites 0-59762 radioemission, at 1 42 mm 0-69431 radionactioles in samples, bombardment-produced 0-48509 radionuclides in samples, cosmogenic and primoridal, p-ray spectrometry 0-4536

0-43365
radionuclides in samples by p-ray spectrometry 0-48510
Ranger photographs, topographic and geologic obs. 0-59747
receiver bandwidth effect on occultation obs. 0-66584
reference points, revision, for high accuracy selenodetic obs. 0-79718
reflectance of samples, irradiation and vitrification effects 0-45391
reflecting layer, upper, structure radiowave reflection factor spectrum anal
ysis 0-72761

renecting layer, upper, structure radiowave renection factor spectrum analysis 0–72761 regolith meas, by Surveyor, photometric and polarimetric properties determination 0–59749 regolith physical characteristics, determination from Surveyor television obs. 0–59748 regolith solid substrate covered by broken up debris, depth 0–66577 relief, correlation functions determ, by stochastic differential equations 0–57091

remote probing, by i.r. and microwave emission and by radar 0-59753

remote probing, by i.r. and microwave emission and by radar 0–59753 rocks, Igneous, metal grains in Apollo 12 expt. 0–76620 rocks, Isotope analysis 0–63087 rocks, sustope analysis 0–63087 rocks, sustance transmission electron microscopy obs. 0–59745 rocks, substruct., transmission electron microscopy obs. 0–59745 rocks, type analysis, use of mass-spectrometric method 0–57092 roughness, intermediate scale 0–48557 sample findings 0–63088 samples. ³³Mn determ, by neutron activation 0–45399 samples, ³⁷Fe Mossbauer spectroscopy 0–48532 samples, C and S concentration and isotopic composition 0–45359 samples, Ga. Ge. In and Ir concentrations 0–45345 samples, Ho, H, D, C, ¹³C and ¹⁸O content 0–45358 samples, K, Sr, Ba and rare earth concentrations in rocks and separated phases 0–45342 samples, Mare Tranquillitatis surface material, Pb and Tl isotopes samples, 1 0-48494 Mare Tranquillitatis surface material, Pb and Tl isotopes

0-48494
samples, Mossbauer effect and h.v. electron microscppy of pyroxenes 0-48531
samples, Mossbauer spectromety, of \$^7Fe 0-45386
samples, Rb-Sr, U and Th-Pb dating 0-48492
samples, Rb-Sr age and elemental and isotopic abundances of trace elements 0-45338
samples, U-Th-Pb isotope relations 0-45336
samples, U-Th-Pb isotope relations 0-45336
samples, abundance of alkali metals, alkaline and rare earths, and \$^7Sr/^86Sr
ratios 0-48495
samples, abundance of rare-earth elements 0-45340

samples, abundance of rare-earth elements 0-45340 samples, abundances of 30 elements in rocks, soil and core samples 0-45349

samples, abundances of O, Si and Al by 14 MeV neutron activation 0-45353 samples, actinide elements, isotopic abundances 0–48496 samples, age determ, and isotopic abundance meas. 0–45339 samples, alkanes of 15 to 30 C atom length, search for 0–48547 samples, alpha-particle activity 0–45350 samples, analysis for organic compounds 0–45409 samples, anorthositic rocks 0–45370 samples, health participated to integral continuity.

samples, anorthostic rocks 0–45370 samples, basalts, petrogenesis rel. to internal constitution and origin of moon 0–45372 samples, bio-organic compounds and glassy micro particles 0–48550 samples, bombardment-produced radionuclides, in rock and soil 0–48509 samples, cathodoluminescence props. of rocks 0–48529 samples, chemical and emission spectrographic analyses 0–45354 samples chemical and emission spectrographic analyses 0–45354

samples, clinopyroxenes, chemical composition, structural state and texture 0-48519

samples, coarse particulate material, mineralogy and petrology 0–45381 samples, compressibility of crystalline rock, microbreccia and fines to 40 kilobars 0–45394

samples, c 0-45334 concentrations of U, Th and Pb rel. to age determination

samples, cosmic ray production of rare gas radioactivities and tritium 0-48504

samples, cosmogenic and primordial radionuclides, by nondestructive y-ray spectrometry 0–45365 samples, crystalline and vesicular rock and dust, chemical analyses 0–45355

samples, crystalline rock, ⁴⁰Ar/₃₉Ar dating 0–48491 samples, crystallisation of mafic magmas and generation of rhyolitic liquid 0–45373

samples, density and adhesive characts. 0-45397

samples, dielectric properties, comparison with earth materials 0–69440 samples, drive tube core, physical analysis of surface sediment 0–45396

Moon continued

samples, dust and rock, magnetic props. 0-48534

samples, dust and rock, opaque minerals 0-45374 samples, e.p.r. and n.m.r. spectra 0-48539

samples, e.p.r. and p.m.r. studies 0–48487 samples, elastic wave velocities at high press., geophysical implications 0–45393

samples, electron-microprobe analyses of phases 0-45351 samples, elemental composition of surface material 0-45348 samples, elemental compositions and ages by γ -ray spectrometry 0-48510

0-48510
samples, fine grained igneous rock, petrology 0-48521
samples, fines and rocks, mineralogy and composition 0-48530
samples, lines and rocks, mineralogy and composition 0-48525
samples, igneous rocks, Rb-Sr chronology and chemistry 0-48525
samples, igneous rocks, Rb-Sr chronology and chemistry 0-48493
samples, igneous rocks, high indicated crystallization temps. 0-48522
samples, impact metamorphism 0-48528
samples, instrumental neutron activation analyses 0-48505
samples, internal substructure determ. by h.v. transmission electron microscopy 0-45377
samples, isotopic composition of rare gases 0-48503
samples, luminescence, e.p.r. and optical properties 0-48541
samples, luminescence and reflectance, irradiation and vitrification effects
0-45391
samples, luminescence and thermoluminescence induced by 159 MeV pro-

0 - 45391
samples, luminescence and thermoluminescence induced by 159 MeV proton bombardment 0-45389
samples, luminescence under u.v. excitation 0-45390
samples, magnetic properties, NRM and susceptibility 0-48536
samples, magnetic properties 0-48535
samples, magnetic properties 0-48533
samples, magnetic properties 0-45387
samples, magnetic properties 0-45387
samples, magnetic properties of crystalline rock and fines 0-48538
samples, magnetic properties of crystalline rock and fines 0-48538
samples, magnetic properties of crystalline rock and fines 0-48538

samples, major and trace elements and cosmic-ray produced radioisotopes 0-45352

samples, melt inclusions rel. to silicate liquid immiscibility in magmas 0-45378

samples, micromorphology and surface characts, of dust and breccia 0-48552

samples, micropaleontological study 0-45410 o-45408

samples, micropaleontological study 0-45410 samples, micropaleontological study 0-45408 samples, mineral chemistry 0-45368 samples, mineralogical and petrological investigations 0-48512 samples, mineralogy, Pe-Ti oxides and olivine 0-48514 samples, mineralogy, petrolgoy and surfaces features 0-45383 samples, mineralogy and deformation 0-48513 samples, mineralogy and petrology 0-45312 samples, mineralogy and petrology 0-48511 samples, minerals, grant of the surface of

samples, opaque minerals, microscope study and electron microprobe analysis 0–48517 samples, opaque phases, qualitative optical and electron probe studies 0–48516

0 46316 samples, optical and h.f. electrical props. 0—48540 samples, organic analysis 0—45404 samples, organic carbon detection by pyrolysis-hydrogen flame ionization 0—45405

samples, organic compounds, search and characterization 0–45401 samples, organic compounds 0–48551 samples, organogenic elements and compounds 0–45406

samples, oxygen isotope fractionation between minerals rel. to formation temp. 0-45357

samples, particle track, X-ray, thermal and mass spectrometric studies 0-48508

0—48508
samples, petrography, mineralogy and crystallography, rel. to petrologic history 0—45366
samples, petrology of unshocked rocks 0—45379
samples, petrology rel. to nature of mascons, seas and interior 0—45371
samples, phase chemistry, structure and radiation effects 0—48524
samples, phase chemistry, structure and radiation effects 0—48524
samples, plagioclases, crystallography 0—48520
samples, pyroxenes, compositional zoning and its significance 0—45402
samples, quantitative chemical analysis 0—48501
samples, radiation history, solid state studies 0—45363
samples, rare gas analysis 0—45362
samples, rare gas distribution and variations, microprobe study 0—45364
samples, rare gases, H and N concentrations and isotopic composition 0—45360
samples, rare gases, isotopic analysis from stepwise heating of fines and

samples, rare gases, H and N concentrations and isotopic composition 0—45360
samples, rare gases, isotopic analysis from stepwise heating of fines and rocks 0—45361
samples, rock compositions and interpretations 0—48500
samples, rocks and fines, search for magnetite 0—48515
samples, rocks and sinerals, O, Si, H and C isotope ratios 0—45366
samples, rocks and soils, neutron activation analysis of multigram quantities 0—45347
samples, rocks and spherules, petrographic, mineralogic and x-ray fluorescence analysis 0—45369
samples, search for organic compound 0—48548
samples, search for organic material by mass spectrometry 0—45403
samples, search for organic material by mass spectrometry 0—45403
samples, search for organic material by mass spectrometry 0—48498
samples, search for oremical and X-ray fluorescence analysis 0—48498
samples, shock effects in rocks and minerals 0—45379
samples, shock metamorphism, evidence and implications 0—48348
samples, shock wave damage in minerals 0—45385
samples, silicates, deformation evidence 0—48526
samples, size distribution and mineralogical constituents 0—45380
samples, small glassy spherules and related objects, interferometric examination 0—48545
samples, small particles, morphology and related chemistry 0—48523
samples, small particles, morphology and related chemistry 0—48523
samples, small particles, morphology and related chemistry 0—48525
samples, small particles, morphology and related chemistry 0—48525

samples, small particles, morphology and related chemistry 0_48523 samples, soils and rocks, X-ray diffraction and Mossbauer study of mine-

samples, solis and rocks, X-ray diffraction and Mossbauer study of minerals 0.48518 samples, solar radiation effects 0-45398 samples, solar wind gases, cosmic ray spallation products and irradiation history 0-48502

```
Moon continued
```

samples, sound velocity and compressibility, rocks and glass spheres 0-45395

samples, specific heats, 90·350 K 0–45400 samples, spectral reflectivity 0–48544 samples, surface properties 0–48546 samples, thermal diffusivity and conductivity 0–48543

samples, thermal diffusivity and conductivity 0–48543 samples, thermal radiation props, and thermal conductivity 0–45392 samples, thermoluminescence 0–45388 samples, total C and N abundances 0–45343 samples, trace elements, emission spectrographic determ. 0–48499 samples, trace elements and accessory minerals 0–48497 samples, trace elements and radioactivity, rel. to meteorite infall, solar-wind flux and formation conditions 0–45341 samples, trapped solar wind inert gases. ⁸¹Kr/Kr exposure ages and K/Ar ages 0–48506 samples, tritium and Ar radioactivities. 0–48507

ages 0-46500 samples, tritium and Ar radioactivities 0-48507 samples, troilite crystals, three-dimensional counter intensity data 0-45375

0-45375
samples from Apollo 11, conference 0-45332
samples from Apollo 12, prelim. examination 0-54430
samples from Sea of Tranquillity, ages, irradiation history and chemical composition 0-45335
samples from Tranquillity Base, Rb-Sr relations 0-45337

satellite motion around moon, theory and semianalytical soln. 0-41562 saturation and equilibrium conditions for impact cratering, criteria and implications 0–59757 scattering of solar X-rays, Rayleigh and Compton fluxes and K fluoresc. flux 0–57135

seas, nature rel. to petrology of samples 0–45371 secular accel. 0–41780 secular acceleration indicated from stellar occultation measurements since advent of Atomic Time 0–54428

advent of Atomic Time 0-54428 secular changes, in four elements of lunar orbit, FK4 equinox location and obliquity of ecliptic 0-57100 sessimic energy coupling using untamped surface charge 0-48556 seismogram and anelasticity from Apollo 12 LP, Q-regolith layer model, diffusion eqn. 0-51741 seismogram of regolith layer, Apollo-12 expt., anelastic parameters values, analysis 0-51740

analysis 0–51740 seismology, power law model for anelastic behaviour of sedimentary earth rocks applic. 0–51740 seismometer operation at Tranquillity Base 0–48489 shock metamorphism in samples, evidence and implications 0–45384 shock metamorphism in samples 0–48527 shock-wave damage in minerals of rocks 0–45385 sinuous rilles, similarity with terrestrial desert stream channels 0–41771 sinuous rilles, similarity with terrestrial desert stream channels 0–41771 soil, analysis rel. to structure and history 0–66582 soil, feasibility and advantages of mass spectrometric anal. 0–57093 soil and rock samples from Apollo 11, isotopic composition of Gd. Ba determination 0–45414 so ar radiation effects in samples 0–45398 solar wind flow past moon, hydromagnetic aspects 0–48555

solar wind flow past moon, hydromagnetic aspects 0-48555 solar wind inert gases, 81Kr/Kr exposure ages and K/Ar ages in samples 0-48506

0-48306 solar wind interactions, findings since 1966, review 0-79755 sound velocity and compressibility for samples 0-45395 specific heats of samples, 90-350 K 0-45400 spectra, 1 to 4 micron 0-66468 spectral reflectivity, implications for remote mineralogical analysis 0-79723

spectral reflectivity, implications for remote mineralogical analysis 0–79723 spectral reflectivity of samples 0–48544 structure controversy, conclusions 0–69435 structure to depths of at least 10 to 20 km, difference from earth by comparison of seismic signals 0–57099 sunlit surface, steady state electrostatic potential distrib. 0–57101 surface, evolution, monographic study with mechanical and statistical analysis of impacts 0–72764 surface in the surface distribution of the surface model for small impact erosion 0–69436 surface, physical condition 0–69433 surface, physical condition 0–69433 surface, physical condition 0–69433 surface, physical condition of the surface demical composition, in terra region, derivation from α-particles scattering data 0–69437 surface composition from neutron radiation due to cosmic ray interaction with surface 0–51739 surface composition from neutron radiation due to cosmic ray interaction with surface composition obs., balloon-borne meas, in mid-i.r. region 0–59755 surface craters, correlation with dynamic properties of impacting meteoroids 0–54431 surface elements, X-ray emission, non-dispersive analyt, system on Apollo supposed the composition of the surface elements, X-ray emission, non-dispersive analyt, system on Apollo supposed the surface of the default.

surface elements. X-ray emission, non-dispersive analyt, system on Apollo spacecraft 0–69441

surface features, controversy 0-66574 surface features, infrared emissivity (7.0-13.5 μ), balloon borne obs.

0-69442 surface fines and rock. Apollo II samples, morphological obs., scanning electron microscopy 0-68291 surface layer comparison with strength-density relations in terrestrial particulate silicates 0-41776 surface mapping, physical, principles 0-57087 surface mapping from photometric data 0-57088 surface material, chemical composition, mechanical properties and small-scale structure, direct obs. by spacecraft 0-59752 surface material mech, props. 0-47304 surface material chemical composition determination, comparison of radioastronomical technique with analysis by Surveyor 0-66579 surface mechanical properties, interpretation from Surveyor results 0-59750 surface properties of samples 0-48546

0-39/30 surface properties of samples 0-48546 surface rock composition at Tranquility Base, evidence of differentiation 0-57097

surface samples 10019, 10046 from Apollo 11, impact crater phenomenon of micrometeorites 0-45415

of interonlectories 0-43413 surface struct., from integrated brightness 0-4853 survey 0-79720 tektite glass in Apollo 12 sample, explanation 0-69438 thermal and i.r. properties of samples 0-48542

Moon continued

thermal diffusivity and conductivity of samples 0-48543

thermal diffusivity and conductivity of samples 0–48543 thermal radiation props, and thermal radiation props, and thermal conductivity of samples 0–45392 thermoluminescence and luminescence in samples, induced by 159 MeV proton bombardment 0–45389 thermoluminescence of samples 0–45388 topographic variations of surface slopes, bistatic radar obs. (with Explorer 35) 0–66580 trace elements in samples, Ga, Ge, In and Ir concentrations 0–45345 trace elements in samples, K, Sr, Ba and rare earth concentrations 0–45342

trace elements in samples, Th-U contents by alpha-particle activity

0—45350
trace elements in samples, abundance of alkali metals, alkaline and rare earths, and \$^{87}Sr/^{86}Sr ratios 0—48495
trace elements in samples, abundance of rare-earth elements 0—45340
trace elements in samples, analytical data 0—45352
trace elements in samples, and accessory minerals 0—48497
trace elements in samples, chemical and emission spectrographic analyses 0—45354

trace elements in samples, emission spectrographic determ. 0-48499 trace elements in samples, instrumental neutron activation analyses 0-45344 trace elem 0-48496 elements in samples, isotopic abundances of actinide elements

trace elements in samples, multielement analysis of soil and rocks 0-45346

trace elements in samples, neutron activation analysis of milligram quantities 0-45347

ties 0–45347 trace elements in samples, semimicro chemical and X-ray fluorescence analysis 0–48498 trace elements in samples, total C and N abundances 0–45343 trace elements in samples of rocks and soil 0–45349 trace elements in samples of surface material 0–45348 trace elements in samples rel. to meteorite infall, solar-wind flux and formation conditions 0–45341 Tranquillity Base regolith, thickness and exposure histories of constituent fragments 0–45333 (Pagents 0–41762)

Mossbauer effect

transient phenomena 0-41762 vacuum level 0-57094 viable organisms in samples, search for 0-45407 wake depend on solar wind plasma characts. 0-51800 C isotopes in lunar fines. ¹³C enrichment by reaction with solar H atoms 0-57096

0-57096
CN molecules in red spot observed in crater Aristarchus 0-45330
H beams, atomic, bombardment of SiO₂ and basalt powder, luminescence spectral distrib. 0-51744
Rb-Sr ages of rocks from Sea of Tranquillity (Apollo 11) 0-45413
S isotopes in lunar fines, ¹³C enrichment by reaction with solar H atoms 0-57096

Morse potential see Kinetic theory; Molecules/intermolecular mechanics
Mosaic structure
see Crystal structure/microstructure

see also Gamma-rays/absorption; Nuclear excitation
AERE Harwell nuclear phys. div. progress report, May-Oct. 1968

0-2033 absolute fraction, exptal, method for determination, resonant-absorber technique 0-79256 absorption spectra evaluation, numerical cales, 0-51276 absorption spectra peak shift and broadening, lack of γ -ray collimation

0-45880

0–45880
acoustic nuclear resonance 0–51277
aftereffect of nuclear reactions in solid 0–54079
alkali halide crystal, solubility and precip, of metal impurities 0–75298
alkali metal nitroprussides, quadrupole splitting obs. 0–41138
Alnico 8. high coercive, examination 0–71759
aminostananes, and quadrupole splittings, obs. 0–41173
rel. to aural meas., amplitude and phase of vibration of basilar membrane of squirrel monkey 0–57190
bauxites, of Fe minerals 0–56507
biological molecules, iron containing, study 0–69094
biological submolecular structure changes due to microwaves, obs. 0–72806
borosilicate glass, complex, with Fe ions 0–76048

borosilicate glass, complex, with Fe ions 0-76048

0—72806
borosilicate glass, complex, with Fe ions 0—76048
Brownian particles suspended in liq. 0—74797
ceramics applic. 0—56506
cerium ethyl sulphate, Ce³* mean square displacement and vel., anomalous temp, depend. 0—43868
conference, India, Dec. 1969 0—38788
conference, nuclear and solid state physics, Powai India, (1968) 0—41919
crystal with interstitial atom, lattice vibrations, calc. 0—50835
cubanite, mag, ordering study 0—79206
data fitting to Lorentzian lines using iterative method 0—38217
diamond with implanted ⁵⁷Co 0—41140
diffusion phenomena and molecular dynamics applications 0—69093
dimethyl tin diffuoride, Gol'danskii-Karyagin effect 0—59383
disordered lattices, double-time Green's function approach 0—40938
Doppler shift, second-order, and mass-change shift, equivalence 0—62626
electric external field effects, theory 0—41134
electronic processes in crystals, exptl. obs. 0—56145
emission, spontaneous, of y-quanta 0—41133
ferricyanides, cubic, effective mag, fields obs. 0—51282
ferricyanides, elec. field gradient temp. depend. obs. 0—48031
ferritin, 2-300 K, mag, props. 0—43198
ferroelectric, K₁,Fe(CN)₆, 3H₂O, rel. to transition temp. 0—41163
ferroelectric, K₁,Fe(CN)₆, 3H₂O, rel. to transition temp. 0—41163 ferroelectric, K₄Fe(CN)₆3H₂O, rel. to transition temp. 0–41163 ferroelectric, KH·PO₄ and KD·PO₄, l.f. mode at transition temp. obs. 0–62630

ferroelectric, SrTiO₂;⁵⁷Fe, multiple charge states obs. 0–41172 ferroelectric with diffuse phase transitions 0–62411 ferroelectrics, perovskite-type with high Curie points, of ⁵⁷Fe and ¹¹⁹Sn 0–72328

ferromagnetic alloy, Fe-Al, comp. depend. 0-79157 ferrous cpds., high spin, in fluctuating environment 0-41157 garnet. CaFe-SiGe(9)C). isomeric shift, temp. depend., 77-800 K 0-62628 garnet. of atoms in three crystallographic non-equivalent lattice sites

glass, borosilicate, complex, with Fe ions 0-76048

Mossbauer effect continued

glass fibre, microstructure 0-43524

Gol'danskii-Karyagin effect in dimethyl tin difluoride 0–59383 haemoglobin, modifications of Fe(II) electronic struct. 0–61186

hyperfine line structure formation, role of spin lattice relax, processes -54072

illite, rel. to Fe coordination and oxidation state, obs. 0-41154 interference from nuclear transitions in crystals 0-48024

internal conversion and photoeffect interference 0-76046

introduction to theory 0 -69092

iron (III) acetate and chloro-derivatives 0-41310

iron acetate and chloro-derivatives 0-56517

isomer shift, reexamination rel. to lattice phonons effect 0-41137 isomer shift studies, electron density at nucleus estimate using SCF wave functions 0-52869

functions 0–52869 isotope effects, equality of temp, shifts for absorpt, of \$7 Fe in \$4 Fe and \$7 Fe in \$6 Fe 0–48034 isotope effects, mag, hyperfine field at \$7 Fe in \$4 Fe, \$6 Fe and \$7 Fe 0–48034 line shape, diffusion broadening 0–41136 line shape of hyperfine spectra, general theory 0–79257 lunar samples, of \$7 Fe 0–48532 lunar samples, of \$7 Fe 0–48532 lunar samples, ptrokenes, of \$7 Fe 0–48531 lunar samples, soils and rocks 0–48518 magnetic cryst. \$7 *ea yield iff, theory for ordering obs. 0–44784 magnetic structure determ, of crystals 0–75917 martensite, containing N, ageing at 40°, for detection of interstitials 0–58792 mass-change shift and second-order Doppler shift, equivalence 0–62626.

martensite, containing N, ageing at 40°, for detection of interstitials 0–58792
mass-change shift and second-order Doppler shift, equivalence 0–62626
measurement instrumentation 0–49342
metal, theory 0–76197
metallic state study 0–66009
molecules, structure, nature of bonding study 0–69096
montmorillonite, rel. to Fe coordination and oxidation state, obs. 0–41154
NH₄Fe(SQ₂)₃, 12H₂O ferroelec, transition obs. 0–40866
organo-Sb cpds. ¹²¹Sb quadrupole moment ratio 0–55132
organoantimony compounds, ¹²¹Sb spectra 0–79265
organoantimony compounds, ¹²¹Sb spectra 0–79267
organoantimony compounds, ¹²¹Sb spectra 0–79265
organoantimony compounds, ¹²¹Sb spectra 0–79266
organoantimony compounds, ¹²¹Sb spectra 0–79265
organoantimo

0 -64561 semiconductor III-V cpds., of Fe impurities 0-72326 smectic mesophase, directional anisotropy 0-71356 solid, conference, Turku, Finland, Aug. 1970 0-74858 spectra, computer code, Fortran IV program for evaluation of complex spectra 0-49495 spectral peak broadening, collimation geometry effect with thick absorbers 0-52589

0–52589
spectrometer, simple, construction and testing 0–52577
spectrometer, time mode operation without precision control of drive waveform 0–46019
spectrometer based on AI 256 analyzer, design and function 0–38743
spectrometer velocity drive using piezoelectric bar 0–49345
spectrometer with large driving force 0–52590
spectrometry, Mossbauer, review 0–54934
spectroscopy, automatic data collection 0–63992
spectroscopy, isomer shift reference standards, criteria 0–77478
spinel, CoAI: "5Fo. 104. ZnAII. "5Feo. 104. 37Fe, electric field gradient
0–45016

steel, austenitic stainless, hyperfine field temp. depend., antiferromag, transitions 0-72331 student's demonstration apparatus 0-66007

superconductivity, strong-coupling theory, parameter determ., and localized impurity modes 0-44104

impurity modes 0-44104 superconductor alloy, Ti-Nb-Fe, annealed, chemical shift correl, with critical current 0-65647 suppression of absorpt, under Laue diffr. conditions 0-69100 surface layer, thin, ⁵⁷Fe backscatt, meas. 0-56508 temperature variation, rigidity and density influence 0-72327 thermal field meas, in solids 0-79255 thermal neutron capture in solids, chemically significant details 0-79460 Ticonal, thermomagnetic treatment obs. 0-58960 transition metal nitroprussides, quadrupole splitting obs. 0-41138 transition metal with dil. ⁵⁷Fe impurity, press, variation 0-79258 trimethyltin cyanide, vibrational anisotropy and Gol'danskii-Karyagin effect 0-78739 vibration calibration systems. 0-47515

effect 0–78739
vibration calibration systems 0–47515
Ag. Au alloys, of ¹⁹⁷Au, isomeric shift following heat treatment 0–54074
Ag. Cd(Zn): ¹¹⁹Sn systems, α-phases, isomeric shifts 0–51278
AgC(I(): ¹¹⁹⁸Sn, spectra. 295 K 0–48025
As. Se-Sn. semiconducting glass. Sn valency comp. depend. 0–48026
Au, V(Mn, Cr) alloys, ordered and disordered, ¹⁹⁷Au obs., mag. behaviour 0–41139
¹⁹⁷Au, from β decay of ¹⁹⁷Pt in Fe matrix, intensities of hyperfine lines, 0.06-20 K 0–49580
¹⁹⁷Au isomeric shift in Cu-Au and Ag-Au alloys obs. 0–54074
BaFeO₄, mag. susceptibility, Neel temp. 0–56513
BaTiO₃, p-ray scatt. by optical phonons 0–62163
Be-Fe di. alloys, mag. behaviour of Fe impurities 0–79259
CaFeSi(Ge)₂O₁; garnets, isomer shift, Neel temp. 0–62629
CaFeSi(Ge)₂O₁; garnets, isomer shift, temp. depend., 77-800 K
0–62628

CaFe₂Si(Ge₂O₁) garnets, isomeric shift, temp. depend., 77-800 K 0-62628 Ca₃Fe₂S₁V₁,5O₁, of ⁵⁷Fe, superexchange interaction of Fe³⁺ 0-41142 CaI₂¹⁷⁹I, and lattice anharmonicity effects, Debye model 0-41162 Ca₃In₂Sn₂O₂ garnet system, cation distrib. 0-41141 CdS, lattice vibrations, generation and relax. Mossbauer scattering applic. 0-43869 in Cd in ice, perturbed ang. correl. determ. of environment 0-59378 CeSn₂ powder, rel. to mae, and structure props. 293.1 feW. 0-44477

CeSn₃ powder, rel, to mag, and structure props., 293-1.6°K 0-44477 CoAl, h.f.s. interactions in ⁵⁷Fe, mag, moments obs. 0-72329 CoCl₂, anhydrous, of ⁵⁷Fe, isomer shift and quadrupole splitting 0-56509

Mossbauer effect continued

CoF₂, of ⁵⁷Fe, charge state and ^{57m}Fe quadrupole moment determ. 0 -48027

Co:GeO4 of 47Co, quadrupole splittings 0-41144

Co(NH₃)₆Cl₂, of ⁵⁷Fe formed by ⁵⁷Co electron capture 0-54073

Con(M1))&Us, of "Fe formed by "Co electron capture 0–54073 $Cos.^{57m}Fe$, 80 and 295K, chemical shift 0–66010 $Cos.^{17}O_4$, of "Co, quadrupole splittings 0–41144 $Cos.^{2}D_{11}$, Fe:04, and internal fields and cation distrib., obs. 0–41143 $^{57}Co.^{2+}$ decay, in $Co.^{17}O_4$ and $Co.^{17}O_5$, Fe valency states determ. 0–41149

0—41149

**7Co implanted in diamond 0—41140

**7Co implanted in diamond 0—41140

**7Co implanted in diamond 0—41140

Cr alloys, of **19Sn and **19Au, hyperfine interactions 0—72330

Cr 03-Fe 03 system, mag. behaviour obs. 0—41146

(Cr 03)₁X(Fe 03)₁-x, antiferromag. cone-spiral, relax. effects, obs. 0—41145

CsFeS- rel. to internal field, obs. 0—41155

Cu Au alloys, of **19Au, isomeric shift following heat treatment 0—54074

Cu-Ni-Fe alloy, phase separation, precipitation, heat treatment effects 0.51279

0.51279
Cu.-Ni-Fe alloys, doublet struct, and clustering cold work effect
Cu.-Ni-Fe alloys, hyperfine intractions at ⁵⁷Fe 0-69097
Cu. of ⁵⁷Fe, force const. changes from fraction calc. 0-40531
Cu_{0.5}Fe_{1.5}O₂ ferrite, saturation magnetization 0-41033
Cu-Mu alloy, mag. behaviour of Fe impurities, 300 and 4.2K
0-48028
Dy, of ¹⁶¹Dy, interference between internal conversion and photoeffect
0-44785

0-44763
DyFeO₃, antiferromag, axis reorientation obs. 0-44770
Er₃Fe₅O₁, of ³Fe, effective mag, fields and isomer shifts 0-41147
Er₁₋₃Gd₃Al₃, of ¹⁶⁶Er, Er³⁺ ground state crystal field splitting determ, 0-41087

0 41087

109 Er beta decay 0-73872

Eu-Ca alloy, rel. to hyperfine fields 0-44786

Eu-Sr alloy, rel. to hyperfine fields 0-44786

Eu. divalent compounds, study of hyperfine interactions, at 0.04 K minimum 0 -51281

mum 0 -51281

Eu. line shapes of γ emitted by ¹⁵²Sm recoiling a 3 eV, lattice pot. effect 0–54075

Eu²- cpds. h.f.s., mag. ordering 0–76053

EuO, critical spin fluctuations and superparamagnetism 0–54016

EuO line shapes of γ emitted by ¹⁵²Sm recoiling a 3 eV, lattice pot. effect 0 54075

Fe²+'/Fe²+' in ice, electron exchange between ions 0–72335

Fe²-Al, ferromag. alloy, comp. depend. 0–79157

Fe Al alloy, b.c.c., hyperfine interactions at final positions of ⁵⁶Fe(n,γ)⁵⁷Fe recoil nuclei 0–41160

Fe-Al alloy, order-disorder transformation, quadrupole interaction 0–43829

Fe Al alloys, order and disorder 0–50527

0–43829

Fe Al alloys, order and disorder 0–50527

Fe Co alloy, hyperfine interactions, meas, of effects of atomic configurational changes 0–44558

Fe H₂SO₄-H₂O system analysis 0–64861

Fe Mn Ge, h.f.s., quadrupole splitting, low field susceptibility 0–41158

Fe Ni alloy particles, supermagnetism, investig. 0–41026

Fe-(3wt.%) Si, anomalous transmission of resonant *y*-rays of ⁵⁷Fe 66011

Fe-(3wt.%) Si, anomalous transmission of resonant *γ*-rays of ⁵⁷Fe 66011 0–66011 Fe, of ⁵⁷Fe, resonant cross-section for 14.4 keV level 0–56512 Fe, oxidation processes 0–41148 Fe carbonyl derivatives and organoiron cpds., of ₅₇Fe, isomer shifts and quadrupole splittings 0–48029 Fe complex, bis(Nr.N-diethyldithiocarbamato)iron(III) chloride, mag. hyperfine interactions 0–41153

nyperine interactions 0—41135
Fe complex, chelates, isomer shifts, quadrupole splittings 0—56510
Fe complex, dimeric 0—59376
Fe complex, Fe acac; Cl, in strong mag, fields, 4K, magnetic dimerisation 0—69098

Fe complex, iron-dibenzoylmethane, isomer shift, quadrupole splitting 0 72332

Fe complex, protoporphyrin ix chloride, magnetic hyperfine interaction 0-44789 O-54787 Fe complexes, hexammine salts 0-59375 Fe compounds, oxides, hydroxides, oxyhydrates prepared from soln. obs. 0-56438

0–36438

Fe dilute impurities in transition metals, lattice dynamics 0–78743

Fe films, 50-10³Å, rel. to internal fields at ⁵⁷Fe^m, obs. 0–56511

Fe valency states, in ⁵⁷Co²⁺ decay, in Co[Cr₂]O₄ and Co[Cr₂]S₄ 0–41149

Fe²⁺ cpds., cubic site symmetry, magneticallly induced nuclear quadrupole interaction 0–44788

Fe³⁺ aqueous solns., effect of Co²⁺ or Fe²⁺ impurities, 20K, rel. to spin relax time 0–48032

FeAl, h.f.s. interactions in ⁵⁷Fe, mag. moments obs. 0–72329

Fe₂Al_{1-x}NH₄(SO₄)₃,12H₂O₅ Fe³⁺ interaction with crystal lattice and other Fe³⁺ ions 0–54076

FeBO₃ single crystal, rel. to critical point behaviour 0–44689

FeC₅, precipitated, effective Debye temp, determ. 0–59105

FeCO₁, siderite, inversion of vibr, anisotropy of Fe atoms 0–53689

FeCO₁, siderite, struct.- mag. phase transitions obs. 0–66012

FeCl₃, 6d charge density distrib, and cryst. field 0–41150

FeCl₃, 6d charge density distrib, and cryst. field 0–41150

FeCl₃, 6H O, spin-spin relax, and Karyagin-Gol'danskii effect 0–41152

FeF₅, isomer shift, recoil-free fraction, and quadrupole splitting for ⁵⁷Fe, 80-300°K 0–41161

FeFe_{2-x}Sc_xO₄ ferrite, crystal lattice, local distortion, X-ray investigation

FeFe_{2-S}C_xO₄ ferrite, crystal lattice, local distortion, X-ray investigation 0-47185

Fe(III) complex, citrate, application, isomer shifts, quadrupole splitting 0-72333

Fe(III) complex, tris(dithioacetylacetonato)iron(III) studies, quadrupole

Fe(III) complex, tris(dithioacetylacetonato)iron(III) studies, quadrupole splitting temperature dependence 0-56574 Fe.N., high resolution spectrum 0-48037 FeNi₃ alloy, order-disorder transformations 0-78698 α -Fe;0;18h, zero point spin deviation 0-48036 Fe;04, magnetite, spectra, rel. to nonstoichiometry 0-69099 Fe;04, permanent defects, pressure and milling effect 0-43673 α -57Fe;03, perfect cryst., line shape and width anomalies measured in Bragg scatt. 0-76050 Fe(P4xPt_{1-x})₃ alloys, mag. behaviour 0-79207 FeS $_{11x}$ system, comp. depend. 0-59377 FeS $_{11x}$ system, comp. depend. 0-44790 FeSO₄(NH₄)₅SO₄,6H₅O, quadrupole splitting and isomer shift 0-44787 FeSO₄(AH₅)O. 57 Fe absorpt. rel. to elec. field gradient params., obs. 0-41156

Mossbauer effect continued

FeSO₄.7H₂O, quadrupole splitting and isomer shift 0_4787 FeSiF₆.6H₂O, divalent.^{57m}Fe quadrupolar coupling consts. 0_41151 FeTa₂O₆, ⁵⁷Fe spectrum, rel. to orbital wave function and mag. moment direction 0–72278

Fe.Ti. ferromag. to antiferromag. transition, rel. to comp. depend. 44559

0–44559
FeTiO₃, ilmenite, quadrupolar hyperfine anisotropy 0–41159
FeFiO₃, ilmenite, quadrupolar hyperfine anisotropy 0–41159
Fe, rel. to charge state study in FoCo-labelled KCoF₃ and K₃CoF₆
0–70558
Fe in FeFe and 5, Fe, mag. hyperfine field, 295K 0_48034
Fe in FeFe and 5 Fe in FeFe, Mossbauer absorpts, equality of temp. shifts
0–48033

Fe in Fe, and 5 Fe in 5 Fe, Mossbauer absorpts, equality of temp, shifts 0–48033
Gd, hyperfine interaction on 5s-p solutes 0–72334
Gd³⁺ epds., h.f.s., mag. ordering 0–76053
GdCa-Sn-Fe₂O₁₂ garnet, temp, depend. 0–79263
Gd₂Fe₁₇, mag. transitions, temp, depend. 0–44796
¹⁸⁸Gd observed after recoil implantation of Coulomb excited nuclei, charge radius change, 2+-0+5 state 0–52703
¹⁸⁶Gd observed after recoil implantation of Coulomb excited nuclei, charge radius change, 2+-0+5 state 0–52703
Ge, complex, iron (III) N,N-dimethyldithiocarbamate, 4.2K 0–76215
H;Fe(CN)₃, anhydrous, spectra, room temp. 0–48035
Hf, recoil radiation damage following Coulomb excitation 0–44791
Hf (A=176, 178 and 189). Mossbauer meas, of quadrupole-moment ratios of first excited 2+ states 0–73836
HfB₃, recoil radiation damage following Coulomb excitation 0–44791
HfO₁, recoil radiation damage following Coulomb excitation 0–44791
HfO₂, recoil radiation damage following Coulomb excitation 0–44791
HfO₃, recoil radiation damage following Coulomb excitation 0–44791
HfO₄, recoil radiation damage following Coulomb excitation 0–44791
HfO₇, recoil radiation famage following Coulomb excitation 0–44791
HfO₇, recoil

Kr. Mossbauer recoilless fraction calc. by quasi-harmonic approx. 0–79261

**Rr solid, 9.3 keV transition. Debye model calc. 0–40532

La³-Me²-Fe₁,³-O₁, 0–72266

Licl, of Sn impurity atoms, emission spectra 0–54077

Li+ Ga,Fe₁,5-,√0, mag. order, h.f.s., Neel temp. 0–41164

Lu,Fe₁, mag. transitions, temp. depend. 0–44796

My|Fe(CN)|, k.H.O, M=Li, Na, Rb, Cs, NH₄ and Ag, spectra, room temp. 0–48035

MgO;Fe²-y, stress-induced ang, momentum quenching 0–44793

Mn-Sn alloy, susceptibility, 119Sn isomer shift 0–56514

(Mn, - Fe₂,Zn,)a(BeSiO₂)₃ Solid solution, 85 and 294 K 0–79262

MnO;Fe²-y, stress-induced angular momentum quenching 0–62631

Mn,Si₁-Fe₂Si₁ system, mag. struct, and bonding 0–59338

Mo-Fe dil, alloys, Kondo effect obs. 0–72336

Mo, of ³¬Fe, force const. changes from fraction calc. 0–40531

NH Fe(SO₂)₃ (2H₂O, anomalous mag. field depend. 0–76051

NHFe²-H(CN)a, spectrum and mag. susceptibility 0–51178

(NH₄)-JrCla, antiferromagnetic, Mossbauer and ENDOR spectra compared 0–75962

(NH₄)-TeCla, 1391 emission spectrum 0–69101

NaCl. of Sn impurity atoms, emission spectra 0–54077

Na,Fe(CNa) single crystal, quadrupole splitting 0–48038

β-NaFeO₁, crystallization from Na₂O-Fe₂O₁-SiO₁ glass 0–47490

NaFeS., rel. to internal field, obs. 0–41155

NdSn, powder, rel. to mag. and structure props., 293-1.6°K 0–44477

Ni-Fe alloys, cold rolled, h.f.s. 0–65918

Ni-Ma solid soln, mag. struct., ³¬Fe obs. 0–41166

Ni-Pd alloys, ferromag. supermag. Fe clusters obs. 0–51284

Ni-Pd alloys, rel. to ⁵⁷Fe impurity clustering and matrix polarization 0–44594
Ni-Pd alloys, ferromag., supermag. Fe clusters obs. 0–51284
Ni-Sn-Sb system, of ¹⁸Sn and ¹²Sb 0–59380
Ni, of ⁵⁷Fe, rel. to temp. 0–51283
NiAl, h.f.s. interactions in ⁵⁷Fe, mag. moments obs. 0–72329
Ni(II) complexes, ⁶¹Ni spectra and quadrupole splittings, obs. 0–41165
NiMnSb magnetic hyperfine interaction 0–72337
NiPd alloy, of ⁶¹Ni, hyperfine field at Ni site, conc. depend. 0–44794
α-Np, of ²²Np, hyperfine interaction and anisotropic lattice vibrs. 0–41167
NpFe₃, ³⁷Fe spectra, at 4K, 77K and room temp. 0–48040
NpFe₅, ³⁷Fe spectra, at 4K, 77K and room temp. 0–48040
NpFe₅, ³⁸No, ³

0-44801
RbFeS₂, rel. to internal field, obs. 0-41155
Rh-Pd-(l wt.%)Fe dil. alloys, h.f.s., mag. ordering 0-76054
α-Sb-Sn solid solns, rel. to interatomic force interaction 0-44795
Sb-O₃, cubic, orthorhombic and amorphous, obs. 0-41169
α-Sb₂O₄, rel. to Sb oxidation state, obs. 0-41169
Sb₂O₅, obs. 0-41169

Sb₂O₅, obs. 0-41169

121Sb quadrupole moment ratio obs. 0-55132

Mossbauer effect continued Si:Cu, of 57 Fe 0—62633 SmB₈, of 149 Sm, isomer shift, valence state determ. 0—44797 Sn:88% 119 Sn. nuclear reaction channel suppression 0—48042 Sn-Sb, solid soln., isomer shifts of 119 Sn and 119 Sn, conc. depend. 0—51285 Sn, β-α transformation kinetics 0—75341 Sn, isomer shift of 119 Sn, pseudopot, approach 0—59381 Sn, isomer shift of 119 Sn, cryst. struct. effects 0—59382 Sn (II) complex, dicyclopentadienyltin(II), of 119 mSn, stereochem, obs. 0—39401 0-39401

0-39401
Sn complexes, aminostannanes, and quadrupole splittings, obs. 0-41173
Sn complexes, organotin(IV) with organic ligands 0-74308
Sn complexes, phthalocyanine and tetraarylporphines, spectra 0-54080
β-Sn isomer shift temp, depend. 0-41170
Sn(II) halide complexes, Mossbauer spectrum obs., quadrupole splitting

Sn complexes, phthalocyanine and tetraaryiporpnines, spectra 0–34080 β. Sn isomer shift temp, depend. 0–41170 Sn(II) halide complexes. Mossbauer spectrum obs., quadrupole splitting 0–48041 SnO, aftereffect of nuclear reactions 0–54079 SnO₂, Fe³⁺ h.f.s., ³⁷Fe obs. 0–41171 SnO₂, surface effects rel. to thermal annealing 0–55705 SnO₂(H-O)₃, stannic acid gel, spectral line broadening 0–55641 ¹¹⁹Sn isomer shift interpret. 0–54081 ¹¹⁹Sn were shift interpret. 0–54081 ¹¹⁹Sn^m level natural linewidth 0–72338 Sn¹/³ compounds, apparatus for simultaneous recording of four time-dependent spectra 0–76055 SrFeO₃, mag. susceptibility. Neel temp. 0–56513 Sr;(FeW)₀-Ba-(FeW)₀C₀ system, phase transition obs. 0–72339 Sr;(FeW)₀-Ba-(FeW)₀C₀ system, phase transition obs. 0–41172 ¹⁸¹Ta 6.25 keV E1 γ rays of Mossbauer absorption spectra, interference of photoelectric and nuclear resonance absorption 0–64059 Te(IV) isoelectronic complexes. ¹²³Te, isomeric shifts 0–44798 Th-Fe₃,ThFe₃,ThFe₄, and Th-Fe₁, 0–44799 ThO₂:Co⁵⁷, low-temp. anharmonicity 0–71833 Ti-Fe₆, α-and β-solid solution, electronic struct. 0–54082 Ti-Nb-Fe₆, superconducting alloy, anhealed, chemical shift correl, with critical current 0–65647 α Tl-Sn solid solns, rel. to interatomic force interaction 0–44795 Tm, ¹⁷²Yb elec.-quadrupole interactions, perturbed-ang,-correl. obs. 0–44800 Tm·OOH, mag. ordering obs., low temp. 0–56515 Tm₃(SO₄)₈,8H-O, mag. ordering obs., low temp. 0–56515 UFe₅, ⁵¹Fe spectra, at 4K, 77K and room temp. 0–48040 UFe₅, ¹⁷Fe spectra, at 4K, 77K and room temp. 0–48040 UFe₅, ¹⁷Fe, force const. changes from fraction calc. 0–40531

0-44801 V_{2.03}, Mossbauer effect study of metal-insulator transition 0–62313 W_{2.03}, Mossbauer effect study of metal-insulator transition 0–62313 W_{2.04}, of ³⁷Fe, force const. changes from fraction calc. 0–40531 W_{2.04}, irrad. effects, resonant absorption following Coulomb excitation obs., anomalous hyperfine interactions 0–76056 ¹⁸²W excited state, following Coulomb excitation by 6.0 MeV α part. 0–57928 ¹⁸⁴W excited state, following Coulomb excitation by 6.0 MeV α part. 0–57928 V₃Al₂Fe₃₋₂O₁₂, garnet, cation distrib. 0–79264 V₃₋₂Ca₃Fe₃₋₂O₁₂, garnet, mag. and elec. hyperfine interactions of ⁵⁷Fe 0–48044

 $Y_{3-2x}Ca_{2x}Fe_{5-x}V_xO_{12}$ garnet, mag. and elec. hyperfine interactions of ⁵⁷Fe 0-48044

0—48044
YCa₃Sn₂Fe₃O₁; garnet, temp. depend. 0—79263
YFe garnet: ¹²¹Sb 0—48043
ZnS: ³¹Cd, spectral obs. 0—56516
Zr:Er, paramag. hyperfine splitting by localized moments 0—44804
Zr:Er, paramag. relax. obs. 4.2-35 K 0—44803
Zr(Fe_{1-x}Mn_x)₂, Laves phase 0—44802

Motors see Electrical machines

Multiple stars see Stars

Muonic atoms see Atoms, mesic and muonic

Muonic molecules see Molecules, mesic and muonic

Muonium

Si, single crystal, hyperfine splitting energy 0-54052

see also Cosmic rays/muons; Nuclear reactions and scattering due to/muons depolarization in mesonic atoms, theory 0-45894 magnetic moment, anomalous, contrib. of terms of order e^2G 0-52448 magnetic moment, anomalous o-70210 magnetic moment, anomalous 0-70210 magnetic moment, sixth order radiative correction to difference between n and e 0-73477 magnetic moment of positive muon meas. 0-45892 magnetic moment precision meas. 0-73476 mass deduced from meas. of magnetic moment 0-73476 mass chery calculation 0-38636 mass energy calculation 0-38636 mass deduced from meas, in $K^+ \rightarrow n^0 u^+ v$ decay 0-38673 storage ring magnet at CERN, proton resonance calibration and field studies 0-52631 transport calc... <18GeV, through Fe shield 0-49212see also Cosmic rays/muons; Nuclear reactions and scattering due

transport calc., <18GeV, through Fe shield 0-49212

capture

low energy theorem 0-77268 radiative, hyperfine effects in impulse approx. 0-55153 ¹²C, in continuum model 0-39021 ¹⁶O, in continuum model 0-39021

photon-neutrino weak coupling 0–38619 two-component and four-component neutrino theories applic. 0–49199

detection, measurement

No entries

interactions

nteractions anomalous behaviour 0–70210 cosmic ray, in Pb at depth of 150 m wat, eq. 0–70283 $^{+}$

Muons continued

interactions continued

 3 He, μ capture rate calc. using quark field algebra and closure approximation 0-57754

production

atmospheric generation mechanism, temperature effect 0–63855 cosmic ray muon intensities, 10¹² to 10¹³ eV, zenith angle depend. 0–38637

pair electroproduction 400 900 MeV masses obs. 0-60524 pairs, photoproduction from carbon between 1300 and 2100 MeV, search for vector bosons 0-49280 pairs with invariant masses between 930 and 1770 MeV, photoprod. 0-77267

The photoproduction, inelastic, Compton terms 0–49210 photoproduction, inelastic, Compton terms

scattering

inelastic, nuclear emulsion study, at high flux 0–60726 μ *e elastic, 10.1 GeV/c, integral cross sections 0–45893 μ p, contribution of Ne eman's fifth χ interaction 0–49211 μ N inelastic 10.1-14.6 GeV/c obs. of N*(1470) resonance 0- μ =e elastic, 5.0-14.5 GeV/c, integral cross sections 0–45893

Music see Acoustics/musical

Musical instruments

bowed strings, negative resistance 0–60055 frequency generation of equally tempered musical scale, RC oscillator applic. 0–52124 applic. 0–52124
guitar design, hologram interferometry tech, applic. 0–49091
Physics of 0–42080

Pnystring, viol vibrations of bodies, application of holographic interferometry

violin, comparison of various test methods 0–60056 violin string, bowed, anal. 0–60054 Navier-Stokes equations see Flow; Hydrodynamics

see also Galaxies
VY CMa, i.r., OH and H₂O source, study of surrounding nebulosity
0-41711

0-41711
BD+30°3639, planetary nebula, physical nature, H_β emission line flux meas. 0-45239
CC H, pure, optical continuum cales. 0-69370
CD-23°12238, moderately high excitation planetary nebula, spectrophotometric study 0-45240
Cetus Arc (Loop 2), further obs. of surrounding filamentary nebulosity 0-54352

Cetus Arc (Loop 2), further obs. of surrounding filamentary nebulosity 0–54352
Crab. X ray emission, search for polarization 0–484844
Crab, X-ray scattering and interstellar dust, rel. to X-ray source 0–57007
Crab, X-ray spectrum. 20 keV to 3 MeV 0_79641
Crab, activity following pulsar spin-up of September (1969) 0–41621
Crab, activity rel. to plasma disturbance, obs. 0–45243
Crab, angular size of source of 25 to 100 keV X-rays 0–57078
Crab, emission lines of 0 I, 0 II, 0 III, N II, S II and H 0–79640
Crab, filament motions and expansion, obs. 0–45244
Crab, jetlike structure detected outside the main body 0–48395
crab, lif. radio source, high spectral index maintained to 10 MHz 0–41735
Crab, polarization at 21.1 cm wavelength 0–79642
Crab, pulsar, optical and X-ray radiation, mechanism 0–66548
Crab, pulsar NP 0532, freq, decay meas. 0–66546
Crab, pulsar NP 0532, req. decay meas. 0–66546
Crab, pulsar NP 0532, occultation, solar corona electron density profile determ. 0–66671
Crab, pulsar 0527 and 0531 and 'runaway' remnant hypothesis 0–51721
Crab, pulsations in X-radiation, ratio to total background radiation, spectral anal. 0–66427
Crab, pulsed X-rays, balloon obs. 0–66429
Crab, pulsed gamma ray emission from its pulsar (NP0531+21)? 0–66534
Crab, pulsed gamma ray emission from its pulsar (NP0531+21) remains venerated 0. 66534

Crab, pulsed gamma ray emission from its pulsar (NP0531+21) remains unproved 0-66533
Crab, radiative ionisation of filaments, excitation conditions 0-59685
Crab, search for polarization in X-ray emission 0-51707
Crab, search for rapid light fluctuations in pulsar NP 0532 0-51724
Crab, small angular diameter source, rel. to pulsar NP 0532 0-57069
Crab, soft X-ray spectrum meas, interstellar absorpt, effect 0-51731
Crab Nebula, Tau x-1, cosmic X-ray source 0-59739
Crab decametric radiation, scattering by solar corona 0-45242
Crab nebula occultation 1967 by solar corona 0-51643
Crab nebula occultation 1967 by solar corona 0-51643
Crab nebula cocultation 1967 by solar corona 0-51643
Crab nebula NP 0532, quasi-sinusoidal oscills, in arrival times of pulses 0-48475
Cygnus loop, Hα halfwidth and radial vels. 0-48397

0-48475 Cygnus loop, $H\alpha$ halfwidth and radial vels. 0-48397 dark, distribution in late-type spiral galaxies 0-56975 diffuse, evolution of 0-72704 formaldehyde, interstellar absorpt., in dark nebulae 0-66513 galactic, interpretation of emitted radio recombination lines 0-76561 Galactic clusters and H II regions, distance determ. 0-56934 gaseous, excitation of forbidden lines, calcs, for $3p^{\alpha}$ ions 0-72703 gaseous, fine structure of emission lines, overestimation of temperature 0-76562

0-76562
gaseous, high excitation. [Ne IV] lines 0-57008
gaseous, level populations of H. calc. 0-54353
gaseous, some forbidden-line intensity ratios 0-45246
gaseous, spectra in yellow-green region, obs. by electronic camera
0-76558

gaseous, tables from which continuous spectra can be calculated 0–45247 HBV 475 planetary, evolution rel. to spectroscopic obs. 0–59686 HIII regions, NGC 2024, W3 and W43, detect. of anomalous recomb. line 166α 0–57011

H II regions, hydrogenic spectral line obs. 0–57012 H II region distrib. in Galactic local spiral arm in Cygnus direction 0–56936

H II region distribution in Galaxy, from radio obs. 0–56917 H II region radial velocities, reinterpretation of Galactic structure 0–56935

0–56935
H II regions, 15, in SMC, kinematics 0–66432
H II regions, props., from radio recomb. lines non-LTE analysis 0–66434
H II regions, ring-type, obs. rel. to Galactic spiral structure 0–56950
Herbit-Haro object No.2, nuclei light vars., 1946-1968 0–62985
IC 2003, moderately high excitation planetary nebula, spectrophotometric study 0–45240

illumination by galactic syst. 0-41618

Nebulae continued

K3-50, planetary, rel, to radio source, microwave obs. 0-59687 K 648, planetary, near centre of globular cluster U15 (NGC 7078), obs.

luminous, near Sco X-1, obs. with H β photometer 0-48393

M16, H II region, 15.4 GHz map, comparison with OB stars in cluster NGC 6611 0-51645

M17, change of He ionization state with position, radio recombination line obs. 0-45324

M17, props., from radio recomb. lines non-LTE analysis 0-66434 M8, [O III] λ 5007 emission line profile, internal kinematics study 0-51646

 $\rm MH\alpha$ 328 116, peculiar continuum corresponding to nebula with thermal collision excitation 0-54351 Magellanic Cloud, Small, neutral H and stars, in wing 0-66430

Magellanic Clouds, member separation from non members, objective prism spectra 0–41623

Messier's Nebulae and Star clusters, annodated, book 0–48398

NGC 1499, electron density 0–41723

NGC 1976, Orion, physical conditions from obs. of radioline of excited H56x 0 72702

H56α 0 72702
NGC 2022, moderately high excitation planetary nebula, spectrophotometric study 0-45240
NGC 2244, Rosette Nebula, determ. of R 0-48394
NGC 4254, H II region colour characteristics 0-56985
NGC 5194, H II region colour characteristics 0-56985
NGC 6164 and 6165, probable ejection from star HD 148937 0-72733
NGC 628, H II region colour characteristics 0-56985
NGC 6888, shell nebula around exciting Wolf-Rayet star, expansion evidence 0-45249
NGC 6888, thin filamentary nebula, interferometric obs. 0-45241
NGC 7027, planetary, absence of H109α recombination line and implications 0-41617
NGC 7027, planetary, obs. at 5 GHz, thermal nature, density fluctuations 0-76559
NGC 7027 planetary, small radio component observation analysis 0-57006

0-57006 Omega, ratio of atomic hydrogen to dust in this direction, 21 cm obs. 0-51702

0-51702 Orion, $5\,\mu$ source observations, spectral energy distribution 0-41619 Orion, $14\,\mu$ photography with half-anstrom filter and Doppler velocity image construction 0-48396 Orion, He triplet spectrum cales, and effect of dust 0-45245 Orion, broadband spectroscopic obs., problems of determining the abundance 0-57009 Orion, change of He ionization state with position, radio recombination line obs. 0-45324

Orion, props.. from radio recomb. lines non LTE analysis 0–66434
Orion, radio obs.. absorpt. and emission of recombination radiation by H I regions effect 0–57062

Orion, very-long-baseline interferometry of associated H_2O source 0-51618

Orion, [O III] $\lambda 5007$ emission line profile, internal kinematics study $0{-}51646$

0–51646
Orion A, H65α-recombination line obs. 0–41622
Orion A, aperture synthesis obs. at 2.695 GHz 0–45248
Orion (NGC 1976) physical conditions from obs. of radioline of excited hydrogen H56α 0–72702
Orion core, recombination lines at λ 3 cm, thermodynamic eqbm. of H₂, He₃, obs. 0–59688
planetaries IC 2003, NGC 2022 and CD-23°12238, spectrophotometric study 0–45240
planetary, 6, search for neutral H in outer parts 0–48392
planetary, BD+30°3639, physical nature, Hβ emission-line flux meas. 0–45239

planetary, NGC 7027, absence of H109 α recombination line and implications 0-41617

planetary, NGC 7027, obs. at 5 GHz, thermal nature, density fluctuations 0-76559

planetary, NGC 7027, small radio component observation analysis 0-57006

0-5/006 planetary, catalogue of all spectral line intensity obs., parameters and chemical abundances determ. 0-45238 planetary, central and spiral arm stars 0-69368 planetary, central stars 0-76560 planetary, comparison of Wolf-Rayet and central planetary nebulae stars 0-69369

0-69369
planetary, electron densities from [O II], [S II], [Ar IV], [K V], [Cl III] emissibilites, results 0-51644
planetary, extinctions and electron temps. 0-66425
planetary, far i.r. and u.v. emission 0-57004
planetary, formation mechanism 0-41616
planetary, in M15 (NGC 7078), obs. 0-69367
planetary, mass ejection rel. to dynamical instabilities of plasma 0-41650
planetary, model atmosphere for central stars 0-41636
planetary, nuclei, multi colour obs. 0-66426
planetary, optical positions 0-41615
planetary, spectroscopic changes 0-57004

planetary, optical positions 0-41615
planetary, spectroscopic changes 0-57004
planetary, symbiotic variables as ancestors 0-62984
planetary, visible distribution 0-72701
planetary K3-50 rel. to radio source microwave observations 0-59687
reflection, BD stars spectra and photometric obs. 0-41620
reflection, colour and polarization, calc, for plane-parallel slab models
0-57010

reflection, colour at 0° offset 0–72705 reflection, colour at 0° offset 0–72705 reflection. light scattering in, grain types 0–79643 reflection, plane-parallel, slab-model B-V, U-B colors, B and V polarization 0–76563

tion 0–76563
reflection. tracing of Galactic spiral arms 0–56937
Rosette, (NGC 2244), determ. of R 0–48394
variable and flare stars in nebulae, survey 0–63025
W3, props., from radio recomb. lines non-LTE analysis 0–66434
W51, props., from radio recomb. lines non-LTE analysis 0–66434
W01F. Rayet stars, mass determ. of associated nebulae using 11 cm obs.
0–54373
C III \(\lambda\) 1909 and other semiforbidden lines, effective collision strengths
0–48467

H, neutral, in outer parts of 6 planetary nebulae, search 0-48392

Nehulae continued

H II region M16, 15.4 GHz map, comparison with OB stars in cluster NGC 6611, 0-51645

H II region stars, colour anomaly, review of explanations 0–45250 H II region stars, interstellar extinction 0–41725 H II regions, (Orion nebula and M8), internal kinematics 0–51646

H II regions, (Orion nebula and M8), internal kinematics 0-51646 H II regions, eleven, electron temps, determ, and summary of similar data 0-41625 H II regions, galactic, existence and effects of compact components 0-48399 H II regions, galactic, interferometric obs. 0-57013 H II regions, galactic and extragalactic, internal motions obs. 0-54354 H II regions. OH sources, fifty new ones 0-66431 H II regions in Large Magellanic Cloud, 10-45251 Perot interferometry 10-45251

0-45251
HII. Hourglass, internal kinematics, OIII \(\lambda\)5007 obs. \(0-41624\)
He triplet spectrum in Orion nebula, cales. \(0-45245\)
K3-50 'planetary', microwave obs. \(0-66423\)
Ne IV forbidden lines in high excitation gaseous nebulae \(0-57008\)
O and He abundances, in planetary₆-ebulae \(0-66424\)

Neel temperature see Magnetic properties of substances

Negatons see Electrons
Negatrons see Electrons

Nematic phase see Liquid crystals

Neodymium

activator in alkali-germanate glass, segregation, electron micrograph 0-39904

u-39904 adsorbed on W. electron emission, work function 0-39979 adsorbed on W. migration and evaporation field emission 0-39980 atom, i.r. spectrum using SISAM spectrometer, Zeeman structure of lines 0-77664

0–77664′ atomic mass difference, precise, and mass systematics in the region of 90 neutrons 0–43014 crystal fields, effect on mag, props. of single cryst. 0–68998 doped laser glasses, refr. index and thermal expansion. 0.4 to 2.3 μ . 0 to 300°C, obs. 0–59360 glass:Nd laser, amplitude and phase struct. of picosec, pulses 0–60233 glass:Nd laser, higher power, obs. 0–67091 glass, monopulse laser 0–38503 glass, thermooptical consts. 0–49113

glass laser, control of generation by u.s. travelling wave diffraction modula-tor 0-42296

tor 0–42296 glass laser, giant-pulse, with diffraction divergence of radiation 0–73246 glass laser, induced polariz, of radiation of excited atoms 0–42295 glass laser, mode locking and bandwidth narrowing 0–60236 glass laser, optical pumping of polymethine dye solns. 0–49063 glass laser, production of polarized radiation 0–45799 glass laser, with smoothly variable emission wavelength 0–73244 glass laser use of Lummer-Gehrke plate-type polarizer 0–42287 glass lasers, calorimeters for power and energy 0–42290 isotope shift const., screening of 5d electron effect 0–77663 laser, axial modes self-locked, radiation dynamics and spectrum changes 0–45798

0-45798
laser, emission spectra structure in free generation regime 0-54877
laser, glass, partial mode locking, spectral-time technique 0-60232
laser, with lenses inside resonator, second harmonic generation 0-49075
laser beam, pulsed, holographic recording 0-42326
laser radiation destruction of thin metallic layers, threshold density of light
current, result 0-53724
lasers, high power pulsed 0-49025
lasers, u.v. generation by sequential freq. conversion method 0-57555
liquid laser, subnanosecond pulse generation 0-73232
luminescence in CaF., X-irrad., growth and decay, thermoluminescence
0-44925

0–44925
magnetic props. of single cryst. 0–68998
magnetic struct., neutron scatt., obs. 0–75885
metastable level lifetime meas., instrument and tech. description 0–49073
photoelectric work function 0–75859
Stark effect in alkali germanates 0–76061
ND³ · POCI, laser, stimulated Raman scatt. 0–69905
Nd: glass laser, travelling-medium, spectral kinetics of radiation 0–49074
Nds² · glass laser, spectral and kinetic characts, in freq. scanning regime 0–69918
Nd³²: glass laser radiation with strong polarizational anisotrony of resona-

0-0916 Nd³⁺: glass laser radiation with strong polarizational anisotropy of resona-tor, forced polarization 0-73253 Nd³⁺: (2aF): YF; laser, construction and characts. 0-42297 Nd³⁺: (2a(NbO₂)); continuous action laser, 300K, absorpt, spectrum

0 - 49071Nd:glass, chemical analysis rel. to laser props. 0-76759

Nd:glass, chemical analysis rel. to laser props. 0–76759
Nd:glass, laser, non-Q switched, intensity correlation functions, second-harmonic generation 0–38507
Nd:glass, thermo-optical characts, direct meas. 0–66006
Nd:glass laser materal, piezo- and thermo-opt, props. 0–79254
Nd:glass in liquid, optically homogeneous mixed laser 0–54870
Nd:Li-Ge-O₁s, glass, laser characts. 0–45797
Nd:Y-POCI, liquid laser, space angular characteristics 0–45792
Nd:YAl garnet Lifo, 0.53 µ harmonic source, repetitively Q-switched 0–69917
Nd:YAl garnet, laser, Q-switched, second harmonic power, computer optimization 0–42294
Nd:YAl garnet laser, continuously operating, energy, spatial and spectral characts. 0–60238
Nd:YAl garnet laser, self-giant-pulsed operation 0–77119
Nd:YAl garnet laser, self-giant-pulsed operation 0–77119
Nd:glass laser rods, microfracturing under monopulse operation 0–60229 $Nd^{+}: Y_3A_1O_1$, laser, electron-phonon interaction manifestation O=6/099 Md-glass laser rods, microfracturing under monopulse operation O=60229 Nd glass laser, saturating absorption at $1.06~\mu$ wavelength O=60227 Nd glass laser radiation, efficient second harmonic conversion O=62582 Nd $^{3+}$, crystal-field shielding parameters O=51247 Nd $^{3+}$, energy-level scheme in LiYF₄ O=62577 Nd $^{3+}$, energy-levels in complexes O=53046 Nd $^{3+}$ approtic solvent laser solns... oscillator and amplifier characts. O=45791

ground state absorption spectrum rel. to laser glass excited state orption 0-38505

Nd* in CaWO₄, spin-orbit and crystal-field parameters for ground term 0–79222 Nd3* in garnets of formula RE_{2.95}Nd_{0.05}Al₅O₁₂ where RE=Ho. Tm. Dy 0–76113

Nd3+ in LiYF4:Yb3+, luminesc., energy transfer 0-76169

Neodymium continued

hymium continued

Nd³+ in SrF₂ with Yb³+, spin-lattice relax, and cross-relax. 0—72291

NdAlO₃, reciprocal mag, susceptibility, temp. depend., 1.7-4.2K 0—41057

POCl₃:SnCl₄, Nd³+ laser system, characteristics 0—60221

POCl₃:ZrCl₄, Nd³+ laser system, characteristics 0—60221

ScOCl₃:SnCl₄, Nd³+ laser system, characteristics 0—60221

YAl garnet:Nd laser, 250W industrial instrument 0—60239

Neodymium compounds

odymium compounds
NdAlO₁, space groups, i.r. obs. 0–61898
NdAlO₂, space groups, i.r. obs. 0–61898
Nd³+:POCl₂:SnCl₂ liq. laser, pulsed, circulating aprotic soln. 0–45790
Nd³+:SeOCl:SbCl₃ liquid laser, active and passive Q switching 0–77113
Nd³+:SeOCl:SbCl₃ liquid laser, active and passive Q switching 0–77113
Nd³+:SeOCl:SbCl₃ liquid laser, pulsed, circulating aprotic soln. 0–45790
Nd:YAl garnet, nonlinear optical props. 0–51258
Nd³+ β-diketonates, spectual intensities 0–58489
Nd³+ complexes, interelectronic repulsion, bonding, electronic energy levels 0–53046
NdCl₃-aq., nonlinear optical absropt, coeff, at 1.064μ obs. with YAL garnet:Nd laser 0–41099
Nd₃NbO₃, monocryst, struct. 0–65252
Nd₂O₃-ZrO₂ system, phase diagram, high temp, study 0–59058
Nd₂SO₃-zrO₂ system, phase diagram, high temp, study 0–59058
Nd₃SO₃), soln., temp, depend, of u.s. abs. 0–64906
NdSn₃-powder, structure and mag, props., 293·1.6°K. Mossbauer and susceptibility meas. 0–44477
Nd³+TFA:POCl₃:ZrCl₄-liq, laser, pulsed, circulating aprotic soln. 0–45790
Nd·Ti-O₂, cryst, structure 0–55847

Nd:Ti₂O₇, cryst. structure 0-55847

Neon

3p4 radiation lifetime Hanle effect obs. 0-4297

3p₄ radiation lifetime Hanle effect obs. 0–42977
in Serra de Mage meteorite feldspar, conc. 0–51781
a.c. discharge. low-pressure, increase of breakdown from 100 Hz to 20 kHz. 0–74626
absorption cell, in alternating magnetic field. for obs. frequency stabilization of He-Ne laser 0–77103
adsorption on Pt, reduction of Pt-H- interaction 0–65107
atom, K absorpt, discontinuity 0–42976
atom, K spectrum, multiple electronic processes 0–49786
atom, autoionization, multiconfiguration close coupling calc. 0–74099
atom, collision with C. Ne and Al. Pauli excitation of atoms in collision 0–43007

atom, configuration interaction wavefunction, 1- and 2-matrices of ground state 0--52921

state 0-52921 atom, dipole polarizabilities calc. 0-60927 atom, elec. field depend, of direct e* annihilation rates 0-55250 atom, electron scatt., 0.37-20 eV, total cross-section meas, by modified Ramsauer technique 0-70792 atom, electron scatt., new calc. of inelastic cross section 0-74141 atom, ground state, electronic wave functions, using CI method 0-42980 atom, metastable, Penning ioniz., cross sections for H₂₁, N₂₁, Ar, Kr, Xe and Hg, 0-70785

atom, pressure broadening of 6074.3 Å line using Zeeman scanning 0-70771

atom, resonance radiation processes and gain coefficient 0-67622 atom, small angle scatt, of 10 keV electrons 0-77698 atom and methane isoelectronic sequence, config. interaction cales.

atom electron shake-off as function of impact electron energy 0-42993 atomic states. lifetimes, metastable, time of flight meas. 0-39298 atomic transitions, new lines, obs in discharges of Ne-SF mixtures 0-52920.

atoms, collisions with slow He^{2+} ions, exothermal capture with ionization 0-7730 atoms, electron scattering, resonances rel. to negative ion formation 0--74142

atoms, long range interatomic potentials, relativistic correction from oscilla tor strength sums 0-74161 atoms, resonance scattering of electrons rel. to electron polarization () \$2444

atoms and ions, collisions with H₂, formation of protons and excited H atoms 0-74185 boiling point, (normal) and triple point temps, and press. 0-50331 boiling point, (normal) and triple point temps, and temps, and press, 0-50331

charge-exchange proton collision. Lyman-17 rad. polarization obs. 0-61030

coexistence curve near triple point, quantum corrections for free energy 0-53395

coexistence curve near triple point, quantum corrections for free energy 0-53395 collisions between ions or atoms and H₂, formation of charged and excited particles 0-46399 crystal, elastic and thermal props, from u.s. propag. vel., 2 20K 0-55941 d.c. discharge, alignment of excited states in weak mag. field 0-42979 diffusion through vitreous silica, effect of prior heat treatment of silica 0-55927

0-539210 discharge. Pe atoms scatt, during postluminesc. 0-53230 discharge, subnormal low pressure column, semi empirical theory with kinetic foundation 0-43360 discharge column, with diffusion, determ, of radial strucuture (Pt.J) 0-43363

discharge in uniform longit, mag. field, moving striations wave nature 0-43359

discharges column with diffusion, radial structure determ (Pt.II) 0-43364 Einstein coefficients and cross-sections for collisions of second kind, laser study 0-73214

electron scattering, abs. total cross sections for low electron energies 0-74293

electron scattering cross sections, total differential, 40 keV electrons () 60980

excitation of reson, lines in collisions with Na*, regular oscillations of total cross section 0–61009 excited levels, transfer of excitation from 2'S level of He, in He+Ne mix ture 0–43030

ture 0-43030 gas, excitation by 600 keV electron beams 0-45963 gas, excitation by 600 keV electron beams 0-42987 gas discharge in mag, field, instability 0-64755 gas interaction with surface, chemisorption through atom probe analysis 0-48188

glow discharge, positive column fluctuations 0-43366 intermolecular potentials from differential cross-section meas. 0-64599 isoelectronic sequence, electric dipole polarizabilities calc, by geometric approx. 0-74097

Neon continued

lamps, resonance, characteristics and design 0-42391

laser, in the infrared, inexpensive, construction 0-67088

laser, pulsed, at 5401 Å, interferometric gas flow studies 0-43384

laser (5401Å), pulsed, for airborne oceanographic remote sensing 0-62898

line spectra, meas. of 1.15μ line under various discharge conditions 0-42978

 $0-4\dot{2}978$ liquid, capture of Σ^- , determination of Λ° trapping probability 0-42861 liquid, u.s. propag., vel. and attenuation 0-74750 outer-shell S-electron ejection by electron impact ionization 0-64769 partial pressure meas, using mass spectrometer 0-74646 plasma, homogeneous. Lorentz type, electron vel. distrib., role of inelastic collision processes 0-71138 plasma discharge, electron drift vel. in positive column 0-61277 plasma discharge, saturation of metastable states rel. to ionization waves existence 0-74522 positive column, constricted, temp, distrib. 0-43365

existence 0—74522
positive column, constricted, temp. distrib. 0—43365
positive column of d.c. discharge broadening, shifts in spectrum 0—42970
positron annihilation 0—73464
solid. Fe-doped, absorpt. spectrum 0—48073
solid. anharmonic effects, applic. of approx. method 0—53674
solid, anharmonicity and potentials 0—47509
solid. film, reflection and transmission spectra in vac. u.v. 0—79288
solid. heat capacity and phonon spectra, dispersion anharmonic effects
calc. 0—40516
solid phonon energies self-consistent, vol. depend. Gruneisen parameter

solid, phonon energies, self-consistent, vol. depend., Gruneisen parameter eqn. 0-47552 eqn. 0–47552
solid, phonon energies and lifetimes, first-order self-consistent approximations 0–53691
solid, thin film, abs. spectrum, 4.2 K 0–79316
solid, trapping of electronic excitations, dynamical investigation 0–75456
solid, with substitutional H- and Li-atom impurities 0–41175
spectra and mean lives of multiply ionized Ne 0–67651
spectral line press. broadening, 0.1-10 torr, rel. to theories 0–52880
spectral line strengths and radiative lifetimes for Ne II 0–67628
spectral line strengths and radiative lifetimes for Ne II 0–67628

spectral transition 2p⁵3p-2p⁵3s, line strengths and transition probabilities 0-55235

0-55235 spectrum, excitation temp, functions calc., appl. to plasma radial temp, distrib, determ. 0-42965 striations, ion-guided and metastable-guided, theory 0-74606 thermal cond. coeff. meas. 0-78217 transition probabilities, absolute of 35 visible and near-i.r. lines 0-64205 vacuum u.v. excitation by electron collisions 0-60962 X-ray absorption spectrum of solid 0-62668 Cs atom scatt., electron energy spectra and autoionizing level excitation 0-64257 H-Ne excitation cross-sections, impact-parameter calc. 0-64216

Cs atom scatt., electron energy spectra and autoionizing level excitation 0–64257
H-Ne excitation cross-sections, impact-parameter calc. 0–64216
H-Ne gaseous mixtures, thermal diffusion. Soret coeff. meas. 0–71270
H- elastic differential scatt., 100 to 2000 eV. obs. 0–77699
He-Ne, d.e. discharge with return or bypass connection, axial press, gradients 0–46768
He-Ne, laser, mode characteristics, theory 0–77100
He-Ne laser, ombination laser, with inhomogeneous elements, pulsed operation investigation 0–67087
He-Ne discharge, optically pumped by He lamp, excitation transfer from He levels to upper Ne levels 0–49793
He-Ne gas, with added Xe, pulse generation under fast electron beam pumping 0–60217
He-Ne laser, 6328 Å, propagation in atmosphere, random fluctuations obs. (Dec 1966 to Jul 1968) 0–59579
He-Ne laser, collisions effect on Ne 6328 Å transition saturation behaviour 0–42274
He-Ne laser, competition of longitudinal modes at 0.63 µm 0–42277
He-Ne laser, current change with interruption of laser beam 0–73225 He-Ne laser, collisions effect on Ne 6328 A transition saturation behaviour 0-42274
He-Ne laser, competition of longitudinal modes at 0.63 μm 0-42277
He-Ne laser, current change with interruption of laser beam 0-73225
He-Ne laser, emission line width meas. 0-67075
He-Ne laser, frequency stabilization by l.f. oscillations of intensity 0-42275
He-Ne laser, frequency stabilization by methane rotational-vibrational transition 0-73226
He-Ne laser, frequency stabilisation by methane rotational-vibrational transition 0-73226
He-Ne laser, intensity of radiation and frequency relationship, non-linear, with absorption cell in magnetic field 0-73218
He Ne laser, optical parameters of components, apparatus and method for determ. 0-67084
He-Ne laser, optical parameters of components, apparatus and method for determ. 0-67084
He-Ne laser, pulsama oscillations and radiated power 0-42278
He-Ne laser, pulsa vel. meas. in Ne absorpt. cell 0-73223
He-Ne laser, radiation modulation using three-mirror resonator using electrooptical effect 0-60216
He-Ne laser, singlet-triplet He metastable transfer 0-77102
He-Ne laser frequency stabilization. rel. to 1, overlapping vibr.-rot. lines near 6330 Å 0-58179
He-Ne laser interferometer, avionic instrument applications 0-60349
He-Ne laser interferometer, avionic instrument applications 0-60349
He-Ne laser noise, dynamic mode competition 0-67085
He-Ne laser parameters 0-54868
He-Ne laser scaliation spectrum, interferometric investigation of magnetic field effects 0-57522
He-Ne lasers, atomic collisions 0-52282
He-Ne lasers, atomic collisions 0-62282
He-Ne lasers, fundamental phenomena, operation, construction and parameter meas. 0-67083
He-Ne lasers, atomic collisions 0-67288
He-Ne lasers, effect of He upon generation 0-67086
He-Ne mixture, electrical and optical characteristics of a hollow cathode discharge 0-64210
He-Ne obs. frequency stabilization by Ne absorption cell in alternating magnetic field 0-67103

K+Ne collision, emission spectra, excitation functions, absolute meas. 0 74156

0 74156
Na, optically pumped, D₁ absorpt., dispersion lines perturbation by Ne, obs. 0-52918
Na atom scatt., electron energy spectra and autoionizing level excitation 0-64257
Ne:Fe, solid absorpt. spectrum 0-48073
Ne-Ar (Kr,Xe) crossed beam differential elastic scatt., intermolecular potentials determ. 0-67844

Neon continued

Ne⁺-Ar collisions, 0.5 to 1.5 MeV, coincidence meas, of inelastic energy losses 0–74153

Ne⁺-Ar single collisions, electron capture meas, 0–74163

Ne-Br₁ gas mixtures, avalanche spark breakdown 0–50120

Ne-He diffusion coefficients, as function of temp., two bulb method 0–78233

0-78233
Ne-He laser, d.c. supplied, operation at 6330 B 0-63621
Ne⁺-He, inelastic, quantum mechanical phase interference effects 0-77727
Ne⁺-He collisions, 10 eV to 5 keV, excitation cross-sections for 3³P0 state of He 0-61027
Ne-N₂ mixtures, electrodeless discharge modes, plasma display panel applic. 0-53158
Ne-Ne elastic-scattering cross section meas. 0-61010
Ne⁺-Ne atomic collision, inelastic energy loss meas. 0-74162
Ne⁺-Ne collisions, 0.5 to 1.5 MeV, coincidence meas. of inelastic energy losses 0-74153
Ne.Ne²⁺ atoms and ions, photoionization cross sections 0-70775
Ne discharge, 1-100 torr, spectroscopic meas, of temp. 0-50121
Ne 1, 2p³3p→2p³3s transitions, probability and lifetimes in simple spectra 0-70768
Ne 1, 2p³3s-2p₃3p transitions, Stark broadening, with weak electrical field

Ne I, 2p³3s-2p³3p transitions, Stark broadening, with weak electrical field depend. 0–46373 Ne I, excited levels, radiative lifetime obs., beam foil technique 0–74108

Ne I, transition probabilities for prominent red lines 0-64204
Ne IV forbidden lines in high excitation gaseous nebulae 0-57008
Ne VII. collisional excitation rate coeffs. for vacuum u.v. lines, obs. 0-60961

0-0961 Ne*, implantation in Si m.o.s. struct., surface characts. 0-47814 Ne* ions. transmission, reflection, absorption in solid thin films 0-39935 Ne₃, absorpt. spectrum u.v. region, discrete band systems anal. 0-74292 Ne₃*, reaction with H at 200°K 0-43205 Ne₃*, reactions with mols. and rare-gas atoms, by flowing afterglow stu-

Ne₂+, reactions with mols. and rare-gas atoms, by flowing afterglow studies 0-46626
Ne+Collision, cross sections for K-shell vacancy prod. 0-46397
Ne_H and Ne-D liquid mixtures, density and sound velocity 0-46909
²⁰Ne, ²²Ne, specific heat obs. 2.2-24K 0-53714
²¹Ne, optical pumping 0-74127
²¹Ne in Serra de Mage meteorites, two-stage irradiation history 0-54449
Ne+Na⁺-Na+*Na, regular oscillations of total cross section of reson, lines excitation 0-61009
0+Ne collisions, 50 to 200 keV, delayed-coincidence study of inelastic energy transfers 0-77702
Rb atom scatt., electron energy spectra and autoionizing level excitation 0-64257

Neon compounds

Ar Ne liq. soln., far-i.r. translational spectrum 0-43456

Neptunium

atom, K-shell binding energies, energies of $K\alpha_1$, $K\alpha_2$, and $K\beta_3$ X-rays 0-49787

0–49787
specific heat meas., from 7 to 300°K, method description 0–68614
α-Np, Mossbauer effect of ²³⁷Np, hyperfine interactions and anisotropic lattice vibrs. 0–41167
Np⁴⁺, crystal-field shielding parameters 0–51247
Np⁴⁺, dynamically induced forbidden elec.-dipole transitions in ThO-0–54101
Np⁴⁺, electronic spectra in various salts 0–58102
Np⁴⁺ in PbMoO₄, free ion and cryst. field params., obs. 0–41078
Np⁵⁺, free-ion and cryst. field spectra for 57° configuration 0–41220
²³⁵Np, half-life, mass-spectrometric determination 0–70557
²³⁷Np fission cross section, neutron induced 0–70677 **putuism compounds**

Neptunium compounds
NpFe₃, magnetically induced elec. field gradients and hyperfine fields
0-44801

NpFe₂, Mossbauer ⁵⁷Fe spectra, at 4K, 77K and room temp. 0–48040 Npres, Mossoauer Trespectia, at 4K, 77K and footh temp. 1.6-300 K, Pd-Np alloy, resistivity, mag. susceptibility, Kondo temp., 1.6-300 K, comp. depend. 0–44066

Nernst effect see Magnetothermal effects

Nernst-Ettinghausen effect see Magnetothermal effects

Neumann algebra see Algebra; Elementary particles; Field theory, auantum

Neutrettos see Neutrinos and antineutrinos

Neutrinos and antineutrinos

see also Cosmic rays/neutrinos; Nuclear reactions and scattering due to/neutrinos

to/neutrinos β decay of polarized neutrons, antineutrino momentum 0–67326 antineutrinos, helicity 0–38627 astrophysical weak neutral currents and neutrino sources in weak and electromagnetic coupling 0–66363 bremsstrahlung, e $_{-}\chi$ -ne $_{-}\nu$ +z, weak interaction with photons, cross section 0–77256 current commutators and 2+ nonet in neutrino-induced production 0–67229

e.m. wave propagation in Fermi sea of neutrinos, investig. for weak-coupling theory 0-48370

ing theory 0–48370 electromagnetic properties and form factor in the presence of weak interactions using two-scalar-boson exchange model 0–57703 emission. from pulsating neutron stars 0–79673 emission in gravitational collapse 0–48364 energy loss rate due to photoneutrino process in hot plasma, comparison of coupling theories 0–45886 forward production cross sections for baryons and baryon resonances 0–49290

four-component field, Pauli and Touschek transformations 0-73402 high energy interac., search of (V+A) currents 0-52435 hypothesis of third neutrino, rel. to β particle polarization characteristics 0-45887

interactions, and electroproduction, connection provided by conserved vec-

interactions, and electroproduction, connection provided by conserved vector current hypothesis 0–63783 luminosity and bremsstrahlung, in a completely relativistic gas in the presence of an intense magnetic field 0–63769 multiple exchange, long-range weak forces and cosmology 0–45210 Oakes's theory, experimental test by bombarding Li 0–55031 P- and T- non-invariant two-component eqn. 0–63768 pair emission by stellar plasma effect in white dwarfs 0–48434 Poincare-like group, applications 0–54995 production, asymptotic weak inelastic, diffraction model 0–49200

```
Neutrinos and antineutrinos continued
                                                                                                                                                                                                                                                                                                                                                                                                                                                                                                                                                                                                                                                                                                                                                  Neutron diffraction examination of materials continued
                                                                                                                                                                                                                                                                                                                                                                                                                                                                                                                                                                                                                                                                                                                                                                              p- azoxyanisole liquid crystals, self-diffusion coeffs. 0–50215 \beta-brass, long-range order 0–75089
                                           production in leptonic decay of {}^{3}H_{\Lambda} hypernucleus, angular lepton-neutrino correlation 0-70416
                                      correlation 0-70416
in quantum electrodynamics 0-52407
reactions, unitarity bounds to T-odd correlations 0-67226
red giants, evolution, photon-neutrino weak coupling 0-54375
solar, and thermonuclear reactions in sun's interior 0-51787
so ar, review 0-57140
solar neutrino capture fluxes with recent corrections to opacity 0-48595
stellar cores, of initial masses 10 and 3M<sub>O</sub>, mixing during advanced evolution 0-76573
                                                                                                                                                                                                                                                                                                                                                                                                                                                                                                                                                                                                                                                                                                                                                                              p-orass, long-range order 0-75089

\alpha-brass, ordering 0-40077

condensed matter, fluctuations from scatt. obs. 0-68583

critical scatt. maxima, temp. shift 0-62484

crystal containing ions with impaired f electrons, thermal scattering theory
                                                                                                                                                                                                                                                                                                                                                                                                                                                                                                                                                                                                                                                                                                                                                                              crystal containing ions with impaired f electrons, thermal scattering theory 0-56426 crystals, mosaic, back-reflection geometry 0-65207 cyclic hydrocarbons, molecular dynamics, cold neutron spectra 0-47511 diatomic crystals with impurities, inelastic scatt., retarded Green's functions 0-61803 eutectic alloy melts 0-68074 ferroconcrete construction, non-destructive testing, apparatus and method 0-50804
                                           tion 0-76573
tetrad equations for the two-component neutrino field in general relativity
0-38170
                                        0-38170 two-component and four-component theories, rel. to weak leptonic and semi-leptonic processes 0-49199 in universe, lepton era 0-76537 mv=per mag, field effect on reaction rate, implication for cosmological He prod. 0-45208
                                                                                                                                                                                                                                                                                                                                                                                                                                                                                                                                                                                                                                                                                                                                                                       eutectic alloy melts  0–68074 ferroconcrete construction, non-destructive testing, apparatus and method  0–50804 ferroelectric. KD-PO4, critical scatt.  0–68943 ferroelectric. NaNO3, oryst. struct. rel. to transition  0–65261 ferroelectric. NaNO3, polarization reversals  0–68945 ferroelectric, soft modes, inclastic scatt. obs. 0–62184 ferroelectric, soft modes, inclastic scatt. obs. 0–62184 ferroelectric, phase transitions  0–53945 ferromagnetic alloy, local moment  0–44578 glass, BeF2, vibr. props. 0–59089 haematite, mag. struct. in strong fields  0–65888 Heisenberg paramagnet, short-range-order effects. applic. to RbMnF3  0–51183 hexamethylbenzene, single cryst., 298 and 130 K, methyl group rotation, transition  0–59087 hydrate, cryst., H.O mol. positions  0–65888 hydrazinium sulphate, cryst. struct., bonds  0–50536 intensity meas. errors of specimen analysis  0–58663 lattice wibrs, theory  0–71832 lattice wave vibr. amplitude from anomalous scatt.  0–47500 liquid, inelastic scatt. theories  0–39730 liquid crystals, self-diffusion coeffs.  0–50215. liquid metals, atomic dynamics  0–61479 magnetic critical phenomena, scaling laws. appl. to β-brass  0–65899 magnetic extinctions determ. from form factor  0–65882 magnetic extinctions determ. from form factor  0–65882 magnetic scattering, covalent spin density, UHF-MO-SCF calc.  0–44485 magnetic struct. in strong fields  0–65888 manganos. inelastic scatt. obs.  0–75886 manganese formate, two-dimens. antiferromag.  0–41067 molecular reorientation in solids, slow scatt. obs.  0–50853 nematic liq. cryst., self-diffusion anisotropy  0–74738 paraelectric NaH3(SeO)3, crystal structure  0–50538 paramagnet, exchange-coupled, with uniaxial single-ion anisotropy, short-range order effects  0–44487 perovskite, K-NaCrF6, 3d electron density determ.  0–65117 perovskite, K-NaCrF6, 3d electron density determ.  0–65888 phonon eigenstates, density determ. from inelastic incoherent scattering  0–47517 phonon spectrometry  0–75384 phonons, inelastic scatt. obs.  0–75886
                                      0−70197  
vN\rightarrow \mu N^*, comparison between Salin's and Adler's models 0−63770  
vN\rightarrow \mu N^*, the comparison between Salin's and Adler's models 0−63780  
vN\rightarrow \mu N^*, the comparison boson prod. 0−60588  
vn\rightarrow \mu p, enhancement due to a resonant effect, implications 0−49312  
v_1N\rightarrow W\Gamma cross-section calc. for W-boson production 0−77345  
v_2N\rightarrow W\Gamma, which energy, appl. of Regge model 0−45884  
v_2N\rightarrow W\Gamma, W boson production in v_2N\rightarrow W\Gamma 0−60561
           Neutron diffraction
    No entries

Neutron diffraction crystallography
see also Crystal structure, atomic
anomalous dispersion, appl. phase problem in Cd compounds 0–61805
anomalous dispersion, appl. phase problem in Cd compounds 0–50505
anomalous scatt., lattice wave vibr. amplitude determ. 0–47500
back-reflection, from mosaic cryst. 0–65207
back-reflection method 0–75073
Bragg intensities, measured integrated, correction for anisotropic thermal
difuse scattering 0–61766
coherent double scatt. 0–58686
collimation corrections in small angle scattering 0–53493
computer control system, time-shared 0–61779
conference, Buffalo, USA, Aug 1969 0–58651
counting system, wide angle position-sensing scintillation principle
0–60667
cryostats, liq. He and N<sub>2</sub> 0–63289
                                                                                                                                                                                                                                                                                                                                                                                                                                                                                                                                                                                                                                                                                                                                                                            0-47517
phonon spectrometry 0-75384
phonons, inelastic scatt. obs. 0-75886
quartz, phonons role in α-β phase transform. 0-40492
rare earth intermetallics, mag, struct. 0-44575
rare earth metals, heavy, mag, anisotropy 0-75885
rare-earth ions, neutron magnetic form factors calc. 0-62486
solution, dil, of small chain-like mols., neutron scatt. obs. of mol. movements 0-39740
spin-correlation effects above curie pt., depolarization meas. 0-40976
spinel, ZnFe<sub>2</sub>O<sub>4</sub> and MnAl<sub>2</sub>O<sub>4</sub>, exchange integrals, paramag, scatt. obs. 0-40948
spinel ferrites mag, struct and eation distrib. 0-41029
                                        0-0061/
cryostats, liq. He and N<sub>2</sub> 0-63289
cryostats, liq. He and N<sub>2</sub> 0-63289
crystal monochromator, integrated reflection and reflectivity rel. to mosaic
spread and thickness 0-47169
diffractometry, computer program for control 0-71559
disorder scattering at long-wavelengths, applic to point defect obs.
0-58744
                                                                                                                                                                                                                                                                                                                                                                                                                                                                                                                                                                                                                                                                                                                                                                     spin-correlation effects above curie pt., depolarization meas. 0–40976 spinel, ZnFe-O2 and MnAI-O2, exchange integrals, paramag, scatt. obs. 0–40948 spinel ferrites, mag, struct. and cation distrib. 0–41029 steel, stainless, non-mag. long-range antiferromag, order 0–51235 p-t-erphenyl, crystal structure refinement 0–61928 AgCI, lattice dynamics 0–50841 AgCrSe(S), mag, struct. and phase transform. 0–62554 AgF; crystal and mag, structure 0–50509 AI-Li alloy, ordering 0–40062 AI-Fey(SiO<sub>2</sub>), almandite, mag, props. 0–62555 Au-Cr alloy, mag, form factor 0–75893 Ba(ClO<sub>2</sub>):H<sub>2</sub>O<sub>2</sub>librational modes of H<sub>2</sub>O mols. 0–40517 BaNiFa; antiferromag, struct. 0–44676 Ba<sub>2</sub>Zn<sub>2</sub>Fe<sub>1</sub>O<sub>2</sub> and Ba<sub>2</sub>Zn<sub>3</sub>Co<sub>3</sub>Cr<sub>2</sub>Fe<sub>1</sub>O<sub>2</sub>Cy(Y), ferrites, 293 and 78 K, spin struct. 0–54007 BeFs, vitrous, vibr. props. 0–59089 C fibres 0–40072 CaF<sub>2</sub>, lattice dynamics, shell model 0–50854 CaF<sub>3</sub>, lattice dynamics, shell model 0–50854 CaF<sub>3</sub>, phonohs, freq. wave vector relations 0–40520 Ca<sub>3</sub>Fe<sub>3</sub>2y<sub>1</sub>Y<sub>3</sub>O<sub>3</sub> ferrite garnet, neutron diffr. exam. 0–51225 CaHPO<sub>3</sub>, H-bonding 0–65116 CaMO<sub>4</sub>, mag, ordering 0–41049 Ca<sub>3</sub>MnO<sub>4</sub>, mag, ordering 0–62557 CdS, perfect crystal, anomalous transmission near resonance excitation energy of ji3Cd 0–75087 Co-Fe alloys, f.c.c., 3d. mag, moment distribution 0–44552 Co., wavenumber depend, susceptibility, anomaly near T<sub>7</sub> 0–41015 CoCO, mag, moment distrib. 0–62524 CoCl<sub>3</sub>.6H<sub>3</sub>O<sub>3</sub>, at temps, above and below Neel temp., magnetic structure, spin direction 0–72275 CoCl<sub>3</sub>.6H<sub>3</sub>O<sub>3</sub>, at temps, above and below Neel temp., magnetic structure, spin direction 0–72275 CoCl<sub>3</sub>.6H<sub>3</sub>O<sub>3</sub>, (0.6≪<1.2), cryst. and mag, struct. 0–44655 Cr<sub>3</sub>T<sub>3</sub>O<sub>3</sub>, erritering or ordering 0–44684 Cu-Zn, β-rass, mag, critical phenomena, scaling laws 0–65899 Cu-MnSn(Ge)S<sub>3</sub> mag, struct. 0–66301 Erc, dilute alloy, Kondo effect 0–44684 Cu-Zn, β-rass, mag, critical phenomena, scaling laws 0–65899 Cu-MnSn(Ge)S<sub>3</sub> mag, struct. 0–66301 ErcO<sub>3</sub>-ErAlp speadobioniary system, mag, struct. lo ordering 0–47936 ErCO<sub>3</sub>, mag, struct, absence of order 0–79125 D
diffractometry, computer program for control 0—71559 disorder scattering at long- wavelengths, applic. to point defect obs. 0—58744 equitorial plane, with plane monochromator, analysis 0—58687 focusing by curved Soller-collimator system 0—71558 incoherent multiple scattering, angular depend. 0—50504 integral intensity meas., equatorial survey scheme 0—65208 lattice wave vibr. amplitude from anomalous scatt. 0—59091 lattice wave vibr. amplitude from anomalous scatt. 0—47500 monochromator, focusing, Fe-Si use 0—61807 monochromator, if or polarized beam 0—58689 monochromator, using ideal curved cryst. 0—68288 monochromators, graphite, singly bent 0—75072 muliple diffr. effects 0—78440 one-phonon neutron groups, artificial splitting due to relaxed vertical collimation 0—71831 small-angle scattering at dislocation in Cu and Ni 0—61806 with specimen production facility 0—74965 spectrometer, scatting-crystal, cold neutron scatt. 0—47511 spectrometer, scriev-flight, for diffr. under h.p., Grenoble 0—60647 spectrometer, fro-of-flight, for diffr. Guinier assembly 0—68289 spinel, ferri- and antiferromagnetic, magnetic interactions obs. 0—47969 structure factors correction for thermal diffuse scatt. 0—71556 techniques, review 0—75049 thermal diffuse scatt., anisotropic, measured integrated Bragg intensities, correction 0—71557 time-of-flight diffr., 100 kbar press. construction of 0—61804 time-of-flight techniques, pseudorandom, use in lattice dynamics and diffr. studies 0—58688 wurtzite struct. cryst., selection rules for inelastic scatt. 0—55825 Fe crystal monochromator, integrated reflection and reflectivity rel. to mosaic spread and thickness 0—47169 Pb crystal monochromator, integrated reflection and reflectivity rel. to mosaic spread and thickness 0—47169 Pb crystal monochromator, integrated reflection and reflectivity rel. to mosaic spread and thickness 0—47169 Pb crystal monochromator, integrated reflection and reflectivity rel. to mosaic spread and thickness 0—47169 Photography of the production of materials allo
                                           antiferromagnet CoF., critical scattering 0-44679 antiferromagnetic alloy. p-Mn, struct. 0-51238
```

S 1138 SUBJECT INDEX Neutron diffraction examination of materials continued Fe-Cr solid solution, decomposition kinetics 0-68566 Fe-Ni-Cr alloy, long-range antiferromag, order 0–51235 Fe-Ni alloy, small angle scattering by spin waves, direct obs. 0–44535 Fe. Ni alloy, small angle scattering by spin waves, direct obs. 0–44535 Fe. anal. of critical scatt. data, dynamical scaling theory 0–69016 Fe. wavenumber depend. susceptibility, anomaly near T_c 0–41015 FeF₂, antiferromag. spin wave dispersion 0–44690 FeF₃, antiferromag. spin wave dispersion 0–44690 FeF₃, mag. props. 0–75885 FeSe₈, ferrimag. ordering 0–72265 FeTiRO₅, R= rare earth, cryst. and mag. struct. 0–51174 Gd. spin wave-dispersion relation 0–62512 169Gd, mag. struct. 0–61807 Ge, randomly distrib. dislocations of low density 0–58815 GeO₂, vitreous, struct. 0–47021 GeO₃, vitreous, struct. 0–47021 GeO₃, vitreous, vibr. props. 0–75370 H₂O molecule. in ionic solutions, low freq. motions 0–61483 Ho_{0.5}En_{6.3} alloy, spin wave excitations. 4.2 K 0–44539 HoIn₃, presence of antiferromagnetism below Neel temp. magnetic structure 0–72284 K₂C₂O₄.H₂O₅ librational modes of H O mols. 0–40517 Holn₃, presence of antiferromagnetism below Neel temp. magnetic structure 0–72284
K.C.O.,H.O. librational modes of H O mols. 0–40517
K.C.U.Cl.,2H.O. crystal structure refinement 0–61873
K.Cu.F., antiferromag. struct. 0–41059
K.D.P.O., ferroelec. critical scatt. 0–68943
K.NaCr.F., 3d electron density determ. 0–65117
K.NiF., antiferromagn. covalency and spin deviation 0–56463
K.NiF., antiferromagnet, effective moment of Ni₂+, covalency, spin deviations 0–44693
K.B.O.(OH)₄12H₂O single cryst., hydrogen position determ. 0–47187
Ll_{0.5}Fe_{2.5} "Al₃O₄, magnetization, temp. depend., 80-650K 0–53988
MgC1.6H, O, cryst. struct. 0–65257
MgO, lattice dynamics 0–53695
MgO, neutron irrad. scattering of long wavelength neutrons 0–43636
p.-Mn- Ni(ZN, Fe) alloys, antiferromag., props., alloying elements influence 0–41060
Mn-M alloys (M=Pd, Rh, Pt, Ir), f.c.c., mag. struct. and exchange interac Mn-M alloys (M=Pd, Rh, Pt, Ir), f.c.c., mag. struct. and exchange interactions 0-62520 Mn-M alloys (M=Pd, Rh, Pt, Ir), f.c.c., mag, struct, and exchange interactions 0-62520
α·Mn, chem. and mag, struct. 0-72281
p·Mn antiferromag, alloys, struct. 0-51238
MnAl·O₄, exchange integrals, paramag, scatt, obs. 0-40948
MnAs_{0.9}·P_{0.08}, crystal and mag, struct. 0-44563
p·MnCn alloy, low-angle, decomposition, ageing 0-40449
MnF₂, quasielastic mag, scatt, in critical region 0-44706
MnF₃, two-magnon scatt, 4.2 K 0-44698
MnPd, phase, antiferromagnetism, atomic ordering and struct. 0-44699
MnSe and MnSe₂, covalency parameters 0-50403
MnSie and MnSe₂, covalency parameters 0-50403
MnTiRO₅, R= rare earth, cryst, and mag, struct. 0-51174
NH₂(L), lattice and mol. vibrs. 0-59081
(NH₃):SO₄, mol. reorientation, slow-neutron scatt, obs. 0-50853
N-H₂SO₄, cryst, struct, and phase transform. 0-6254
NaCrSe₂, mag, struct, and phase transform. 0-6254
NaH₃(SeO₃)₂, paraelectric, crystal structure 0-50538
NaNO₂, cryst, struct, rel. to ferroelec, thenomena 0-68580
NaS₃(O₃,5H₂O₃, cryst, struct. 0-65263
Nb. diffusion of H₃ quasielastic neutron scatt. 0-78582
Nb. D₃, order disorder transitions 0-61807
NbH₃, subthermal neutrons inelastic and quasielastic scatt., mode obs. 0-68582
Ni₂Cu₃ alloys mag scatt, critical phenomena 0-69026 0-0882 Nd. mag. struct. 0-75885 Ni-Cu alloys. mag. scatt., critical phenomena 0-69026 NiFe₂O₄, chem. and mag. struct. 0-62546 Ni₁(Mn.Me). ternary alloys, Me=Fe, Co, Cr, ordering kinetics obs. 0-71809 NISI(WILLIME). terhary alloys. ME=Fe. Co. Cr. ordering kinetics obs. 0-71809

NISs. ordered moment obs. 0-59309

PH.Br(I). cryst. struct. and thermal motion 0-78492

Pb. (4at.%)Bi alloy, disorder scatt. of long-wavelength neutrons 0-58744

Pb. lattice freq. spectra at 90°K 0-59095

Pb. (7b. order) order o Se, amorphous and liquid, vibrational modes from inelastic scatt. 0 -65527

utron spectra carboxylic acids, hydrogen bonding study by neutron energy loss spectra 0-46547 from deuteron breakup by α particles 0-73657 differential fast-n flux determ. in High Flux Isotope Reactor with threshold detectors 0-55186 energy-dependent cross-section data and threshold reaction excitation functions intercalibrated in a pure fission spectrum 0-64147 fast and thermal, pulsed, influence of re-entrant holes on meas. 0-49694 fission, generalized formula for static relative importance 0-39147 fission emission anisotropy, dependence on total kinetic energy of fragments 0-60837 flux, from detection activation, variational approach for determination flux, from detection activation, variational approach for determination 0-46278 flux anisotropy due to arrangement of fast core cell, meas, using emulsion 0-52836graphite moderated lattice, thermal nuetron spectra meas. 0-74050 in homogeneous medium, calculation by direct operational method 0-52823 meas. by two-parameter method using single detector 0–52581 organic scintillator, measurements of intermediate energy neutrons 0–60668 photopeak location and area determination, automatic 0–49327 Q values, reaction near threshold, determ. 0–77552 reactor VPR-S, fast spectra, math. approxs. comparision 0–39218 reactor fast spectrum meas. using threshold detectors, 0.1-10 MeV 0–39245 in reactors, analytical approx. 0–60838 secondary, per steradian from spallation of C, nuclear emulsion obs. 0–73924 solid state track recorder, reactor irrad, facility 0-60710 thermal, at UTR-100 beam hole, meas, using slow neutron chopper 0-49744 soilo state track recorder, reactor irracia ciunty 0–49744 thermal, at UTR-100 beam hole, meas, using slow neutron chopper 0–49744 thermal spectral indexes in reactor cells near plane absorbers 0–39213 from thick target and charged particle beam reaction, differential excitation curves determ. 0–40616 time-of-flight spectroscopy, statistical chopper method 0–45968 Zebra reactor, computer program for calculation 0–42899 zero degree yield from ruli(p.n)? Be reaction near 2.2 MeV 0–52772 27Al, energy distribution of neutrons from proton-nucleus nonelastic collisions for 18 MeV and 15 MeV protons 0–64115 241 Am. Be(r.n) sources as simulated by accelerator produced α-particles, weighting and summation 0–42588 8Pe(r.n.) sources. <1 MeV 0–45973 8Pe(r.n.) are determination 0–60829 Be(r.n.) are determination 0–60829 Be(r.n.) sources. <1 MeV 0–45973 29°Co(p. n), E_p~6.05-6.3 MeV, energy spectra 0–49618 25°Fe, energy distribution of neutrons from proton-nucleus nonelastic collisions for 18 MeV protons 0–64115 Liglass scintillator, 5-inch diameter, time-of-flight technique 0–49377 2Li (*9Be, β-decay, *9Be states obs. 0–38850 25Mn, resonance activation integral, measurement relative to that of 197 Au by absolute counting 0–60816 14N, energy distribution of neutrons from proton-nucleus nonelastic collisions for 18 MeV protons 0–64115 14N(y,p)¹³C+(n)¹²C, de-excitation neutrons obs. 0–60800 0. neutron transport predictions for integral measurements at 14 MeV using sphere transmission and time-of-flight techniques 0–64151 14O(y,n)¹⁵O, 39.3–65 MeV, obs. above giant resonance region 0–52749 16O(γπ -yn), energy spectra 0–46232 181Ta, energy distribution of neutrons from proton-nucleus nonelastic collisions for 18 MeV protons 0–64115 1817a, energy distribution of neutrons from proton-nucleus nonelastic collisions for 18 MeV protons 0–64115 1817a, energy distribution of neutrons from proton-nucleus nonelastic collisions for 18 MeV protons 0–64115 1817a, energy distribution of neutrons from proton-nucleus nonelastic collision 0 -65527
Se, cryst., amorphous and liq., atomic motions 0—75380
SiO2, vitreous silica, conventional and elastic 0—55684
Sn, liq., slow neutrons transverse scatt. cross section obs. 0—39731
SnTe-GeTe alloys, phase transition obs. 0—68950
Sr, amplitude factor for coherent scatt. 0—78801
Sr, applitude factor for coherent scatt. 0—78801
Sr, order-disorder transitions 0—61807
Tb-Ho alloy, magnon energy and lifetime 0—44542
Tb-Ho, single crystal, magnon energy and lifetime 0—44542
TbH₁₃, presence of antiferromagnetism below Neel temp. magnetic structure 0—72284
TbPt₁₃, presence of antiferromagnetism below Neel temp. magnetic structure 0—72284 autron spectrometers
application of proton-recoil proportional counters 0–49739
cross-sections measurements at energies < 10⁻³ eV 0–57845
crystal, time focussed, for pulsed neutron moderator studies 0–70277
fast, identification and energy meas. of recoil protons from hydrogenous radiator 0–49355
fast, using semiconductor detector and small scattering chamber 0–52595
Guinier assembly for powder diffr. 0–68289
for microsecond to infinite duration energy spectra, patent 0–46053
nitrogen cryostat, use for between 80 and 300°K 0–67343
polarization, for thermal neutrons, theory 0–46025
resolution, high energy, for photoneutron angular distrib, meas. 0–45969
scintillator characteristics, stilbene and NE213 0–60663
scintillators, gamma sensitivity of granular, glass and film 0–49376
stilbene for n spectra of ²⁴¹Am-Be(nxn) source 0–42588
stilbene scintillation counter proton recoil application 0–49374
threshold, method, improved, including digital computer for data treat ment 0–77392 Neutron spectrometers TbPt₃, presence of antiferromagnetism below Neel temp. magnetic structure 0-72284 ture 0-72264 Te, cryst. and liq., atomic motions 0-75380 Te, vibrational modes from inelastic scatt. 0-65527 ThH, subthermal neutrons inelastic and quasielastic scatt., mode obs. 0-68582 0–68582
Ti O. solid solution, interstitial order-disorder transformation 0–40499
Ti Zr O system sub-oxides 0–65888
TiO₃, rutile, lattice dynamics 0–59085
TiMnF₃, mag, struct., Paramag, scatt. obs. 0–40952

Neutron diffraction examination of materials continued

utron diffraction examination of materials continued

TmAu₂ and TmAg₂, 300°-1.7°K 0–58760

TmC, 300°-1.7°K 0–58759

α-U, low temp. obs. 0–40103

d-u, low temp. obs. 12 truct. and mag. ordering 0–61913

UAs_{1-x}Se_x, mailerromagnetsim, comp. and temp. depend. 0–79209

UP_{0.75}Se_{x.25}, mag. ordering 0–40936

V-O₃, antiferromagnetism 0–44713

V-O₃ single cryst. and powders, evidence for antiferromag. order 0–69049

V-O₅, thermal expansion and compressibility 0–65560

xMn₃O₄+(1-x)Cu(FeCr)O₄, ferromag, spinels, cryst. struct. 0–61882

Y₃Co_{2x}Ge_{2x}O_{1x}garnet, structure 0–65293

YFeO₃, sublattice magnetization, rel. to hyperfine field, 300-630K
0–44716

VbAu. 0–58760

U-44/16
YbAu, 0-58760
YbC₃, 300°-2°K 0-58763
YbFeO₃, sublattice magnetization, rel. to hyperfine field, 300-630K
0-44716

Zn, phonons obs. 0-62181

ZnFe₂O₄, exchange integrals, paramag, scatt. obs. 0–40948 ZnFe₂O₄, mag. struct., 4.2K 0–41065 ZrN_{0.36}H_{0.80}, call parameters, struct. 0–50557

Neutron radiography see Radiography

Neutron sources see Neutrons/production Neutron spectra

Neutron spectrometers continued

threshold detectors activities, analytical approximations 0–60838 time-of-flight, 5 to 50 MeV, detection efficiency of organic scintillation

time-of-flight, 5 to 50 MeV, detection efficiency of organic scintillation 0-52588 time-of-flight, 5 to 50 MeV, instrumentation 0-52596 time-of-flight, for diffr. under h.p., Grenoble 0-60647 time-of-flight, for scatt. cross section determ. 0-46023 time of-flight, mechanical correlation chopper evaluation 0-49356 time-of-flight, medium energy, detection efficiency of organic scintillators 0-70296

0—70296 time-of-flight, twin rotor, resolution function 0—70290 time of-flight facility for neutron spectra from (p,n) reactions 0—70295 time-of-flight for fast neutrons 0—70294 (n,p), current progress, slow neutron sources, detectors and reaction mechanism 0—73672

⁶Li. solid state sandwich detector in energy range 1 to 100 keV 0-52594

Neutron transport theory

see also Neutrons and antineutrons/diffusion; Neutrons and antineut rons/moderation

26-group cross section set 0-3\(\sigma_21\) angular density representation, generalization and extension 0-46282 angular density representation, generalization and extension 0-46282 anisotropic scattering, one speed transport disadvantage factor calculations 0-42896 Avery's coupled reactor kinetics eqn., mechanics of derivation 0-39196 Boltzmann equation, new solution for time-dependent or stationary processes, integral transform method 0-64149

esses, integral transform method 0–64149
Boltzmann equation in plane geometry, with anisotropic scattering by double P_r method 0–67564
boundary-value problems, numerical soln. 0–39187
boundary-value problems of linear transport theory, Green's function approach 0–72977
Cadilhac thermalization model, asymptotic behaviour 0–60842
collapsing fast reactor cross sections rel. to critical size calcs. 0–58044
continuous slowing down theory calc. of narrow resonance reaction rates in fast-reactor mixtures 0–77593
continuous slowing down theory for anisotropic elastic neutron modera-

continuous slowing down theory for anisotropic elastic neutron modera-tion 0-77594

tion 0-77594 continuous slowing-down theory in fast-reactor assemblies 0-74036 coupled sampling from transport and adjoint transport eqns. for given functional 0-58038 criticality codes and measured values of critical bucklings on multiplying lattices 0-64150 Doppler broadening of cross-sections with temp. and boundary motion 0-52821

equation approximations, finite difference, truncation error analysis 0-74033

equation approximations, finite difference, truncation error analysis 0-74033 equations, linear iterative convergence schemes, a variational rebalancing scheme 0-46281 equivalence relation, lattice dependence 0-49693 fast flux in vicinity of neutron generator target, formula for calculation derivation 0-64153 flux distrib., in-reactor, for temp. depend. cross sections 0-48725 flux spatial distribution in plane heterogeneous critical assembly 0-52840 flux spatial distribution in plane heterogeneous critical assembly 0-52840 flux spectra from detection activation, variational approach for determination 0-46278 function g(c,µ), geometric interpretation 0-77591 for fusion reactor blanket design performance 0-70714 Green function props, in infinite moving medium 0-39180 group of diffusion eqns. comparison of alternating-direction time-differencing methods with implicit methods 0-39182 H-functions, linear integral eqns. and their iterative soln. 0-72877 Helmholtz equation, soln. in one-dimens. multi-region reactors 0-49704 heterogeneous media, diffusion coeff., anisotropy and leakage, and pulsed obs. 0-39179 in heterogeneous systems, Green's function anal. appl. to diffusion eqn. 0-55179 in homogeneous state, initial value problem with perfect reflection, boundary coefficience 0, 52925

0-55179
in homogeneous state, initial value problem with perfect reflection, boundary conditions 0-52825
initial value problem of monoenergetic neutrons for a slab with infinite reflectors, solution for isotropic scattering 0-67567
kinetics, multigroup two-point model for time-dependent analysis of two-zone fast neutron systems 0-64152
kinetics equations in 2 dimensions, multigroup diffusion theory, alternating direction methods for solution 0-77596
monoenergetic pulse description by telegraph equation eigenfunctions 0-46277
multi-group in plane geometry, 0-30186

multi group, in plane geometry 0–39186 multigroup reactor eqns., anal. soln. 0–39192 multilayer systems, heterogeneity effects on space-angle flux distribs, of monoenergetic n 0–52828 nonhomogeneous thermalization eqn., soln. by appl. of Mullikin's method 0–60840

0—60840 in nonuniform slab with ge..eralized boundary conditions 0—49697 one-group transport with anisotropic scatt., non-existence d discrete eigenvalues 0—52822

values 0-32622 one-velocity inhomogeneous transfer equation 0-64155 outer iteration scaling for transport codes 0-58039 in point reactor with weak source, calc. of probability distrib. of n populations 0-60846

propagation in various shielding materials, at intermediate energies 0-39178

pulse (anisotropic) relaxation consts. in uniform moderator 0-46283 pulse propagation in a multiplying medium 0-46297 pulsed distribution decay, integral-transform analytical method 0-49689 pulsed neutron method, appl. to interaction between two moderators 0 - 46309

pulsed source in multiregion reactor, inhour eqn. 0–49692 pulsed thermal and fast n assemblies, influence of re-entrant holes 0–49694

resonance integrals, effective, anal. expression for calc. 0–39177 slab, nonlinear space-time diffusion eqn. comment on iterative approach 0–49695

10—49693 slab-type nonlinear space-time problem, reply to comments on iterative approach 0–49696 slowing down equation. transient solutions 0–46280 slowing down equation for infinite homogeneous monatonic medium, exact. solution 0–74037

slowing down equations of fast neutrons, asymptotic, approximate solution 0-55178 in space dependent noise spectra, deficiencies in diffusion theory 0-39181

Neutron transport theory continued

utron transport theory continued space- and time-dependent neutron slowing down for hydrogen and non-hydrogenous moderators 0-52826 space-time reactor-kinetics analysis, verification by experiment 0-52838 spectra of perturbed semigroups 0-52824 spectral synthesis equations and the general multigroup neutron kinetics equations 0-38036 telegrapher's eqn. for arbitrary infinite plane source 0-39183 thermal flux distrib, in slab with temp, discontinuity 0-39188 thermal neutron distribution in real reactor cell, thermos type method for calc. 0-58041

calc. 0–58041
thermalization. experimental. book 0–42895
thermalization Green-type scattering kernel 0–60841
thermalization egn., time-dependent, nonhomogeneous, soln, by reduction
to a system of Cauchy singular equations 0–58042
time- and space-dependent mutigroup neutron diffusion equations, numeri
cal solution 0–58040
time-dependent, one-velocity eqn., applic, of method of matched asymptotic
expansions 0–49698
time-dependent equation in plane geometry solved numerically for fast
pulsed assemblies 0–74038
transport eqn., numerical soln. 0–52820
transport eqn., numerical soln. 0–52820
transport eqn., symptotic soln. 0–52820
transport eqn., asymptotic soln. 0–5280

transport eqn., numerical soln. 0–52820 transport eqn. asymptotic soln. 0–39185 transport eqn. asymptotic soln. 0–39185 transport equation, one speed, several particular solutions 0–52827 two group, for criticality of finite slab 0–39184 two-group theory with anisotropic scatt. 0–64154 wave analysis in a finite media 0–46279 n age calc., plane fission source in H₂O 0–39190 D₂O-antural uranium subcritical systems, thermal neutron wave propag. props. 0–46276 D₂O moderated UO₂ lattices, reson. escape probab. 0–39189 LiH, Monte Carlo calc. and angular distrib. obs. 0–46275 u. natural, D₂ moderated single rod lattices, buckling obs. rel. to theory 0–39219

0-39219

Neutrons and antineutrons
see also Cosmic rays/neutrons; Nucleons and antinucleons
β decay of polarized neutrons, spin meas. 0-67326
beam intensity amplification by cavities in moderator 0-38735
beam velocity selecting rotor, multi slotted, design 0-55067
benzene, solid, inelastic neutron scatt., 77-270°K 0-75356
bound in matter, analysis 0-45965
CP violating parameter, relationship with electric dipole moment 0-63846
charge, upper limit shown by limits on charges of Cs and K atoms
0-42962
decay, polarized, search for 3-vector correlation 0-45966

decay, polarized, search for 3-vector correlation 0-45966 decay of polarised neutrons, measurement of angular correlations 0-57826

depolarization passing through ferromagnet 0-40612 dipole moments, electric, determination by neutron beam magnetic resonance method 0-52553

nance method 0-52553 dipole moments, electric, experimental meas, techniques 0-52552 electric dipole moment, e.m. T-violation 0-57827 electric dipole moment, relationship with CP violating parameter 0-63846 electric dipole moment, upper limit 0-60616 fast neutron physics, review 0-67327 flux density, 14 MeV, fission track method 0-55063 focusing by curved Soller-collimator system 0-71558 Fokker-Planck eqn., for probability distrib, in multiplying system 0-52818

integral fast flux in irradiation channels of SM-2 reactor 0-46295

integral fast flux in irradiation channels of SM-2 reactor 0–46295 interface conditions for discontinuous flux synthesis methods 0–74049 metal, fission fragments mean range meas, using mica detector 0–78802 moisture gauge, density correction 0–48672 neutron radiography, biomedical applications 0–72807 neutron radiography, fast, inherent problems 0–72812 neutron radiography, fast, inherent problems 0–72813 neutron radiography, slow, rel. to imaging of fatty tissues through deuteration with heavy water 0–72809 neutron radiography, stereoscopic and stop action, rel. to biological objects 0–72810 neutron radiography, thermal biomedical applications 0–72808

objects 0–72810
neutron radiography, thermal, biomedical applications 0–72808
passage through ferromag. film 0–63877
prompt, probability distribution in infinite homogeneous medium due to
uniformly distributed source 0–67566
prompt, probability distribution in infinite homogeneous multiplying
medium 0–67565

pulsed technique with repeated recycling of analyser between bursts 0-74060

solar, decay, proton injection into Earth's radiation belt 0–48317 solar flux 20-160 MeV, meas. 0–76667 n-p mass difference in model of higher baryon couplings 0–70277

s 0-70272 0-46022

n-p mass difference in model of higher baryon couplings 0-70272 n, β -decay angular correl, const. meas., p spectrometer 0-46022 n=pe $^-$ p, mag. field effect on reaction rate, implication to cosmological He prod. 0-45208 ne $^+$ pp mag. field effect on reaction rate, implication for cosmological He prod. 0-45208 nv=pe $^-$ mag. field effect on reaction rate, implication for cosmological He prod. 0-45208 nv=pe $^-$ mag. flowest-order weak amplitudes with e.m. radiative corrections, high-energy behaviour 0-67217 v_{n\varthetarrow\varthetar}

Sb-Be source, neutron spectrum using proton-recoil counting method 0-67330

absorption

see also Nuclear excitation; Nuclear reactions and scattering due to/neut rons

application in cryogenic fuel gauge, patent 0-51859 filter, polycrystalline, transmission of thermal neutrons. Monte Carlo method 0-58037

method [0-58037] resonance, operator formulation 0-52819 resonance, operator formulation 0-52819 resonance absorption at intermediate energy, extrapolation and interpolation in calc. 0-57983 resonance parameter determination of main resonance of Rh by mutual-indication method 0-73675 self-shielding effect in targets for radioisotope prod. 0-38957

Neutrons and antineutrons continued

absorption continued

slowing down equation, transient solutions 0-46280 transmission coefficients for heavy nuclei in energy region 0.05-2 MeV

transmission coefficients for heavy nuclei in energy region 0.05-2 MeV 0-70274

²⁴¹Am resonance integrals 0-70617

Au sphere transmission, 24 keV, capture cross section calc. 0-49637

³⁷Cl(n,y)³⁶Cl, gamma radiation study, neutron separation energy 0-42856

D. cross-section, revised value 0-39232

D-O, cross-section, revised value 0-39232

Er(NO₃), solution, calc. and experiment 0-74031

LiH, spherical, point fission n attenuation, calc. 0-46274

LiH shield, ang. flux spectrum 0.1 eV to 15 MeV 0-55199

FilH, spherical, point fission n attenuation, calc. 0-46274

²³⁹Pu, ²³¹Pu resonance integrals 0-70617

²³⁹Pu milligrm, sample, cross section calc. from irradiation obs. 0-55065

²⁴⁰Pu 1.056 eV resonance, experiment 0-74066

Si. cross sections, thermal neutrons 0-46152

²³¹U milligrm, sample, cross section calc. from irradiation obs. 0-55065

W-LiH laminated sphere, ang flux spectrum and secondary gamma spectrum 0-55199

W-6-LiH laminated shield, spherical, fast reactor n and secondary-p attenuatrum 0-55199 W-6LiH laminated shield, spherical, fast reactor n and secondary-y attenua-

tion, calc. 0-46274

angular distributions

coupled sampling from transport and adjoint transport eqns. by Monte Carlo method 0-58038

cario method 0-58038 photoneutron energy meas, with high n energy resolution spectrometer, facility at Linac Lab. Toronto, method 0-45969 scattered by protons at 24 MeV 0-67329 from scattering, at 1-40 keV by nuclei Sr, Mo, Rh, Cd, Sn, Sb, Te, I, La, Th 0-52785

Th 0-52785 scattering on thick layers, calc. 0-77558 space-angle flux distrib. in multilayer systems, heterogeneity effects for monoenergetic n 0-52828 sr2cf. spontaneous ternary fission, prompt n ang. distribs. 0-49686 LiH, rel. to Monte Carlo transport calc. 0-46275 TLi(d.n)*8e, expt. 0-46242 symn(p, np)*5Fe, <2.5 MeV, n, p ang. correl. meas. 0-46135

capture see Nuclear reactions and scattering due to/neutrons

detection, measurement

see also Dosimetry; Neutron spectrometers against y-ray background, use of highly efficient ³He counters 0–49336 activation analysis for trace elements in normal and cancerous tissue 0–59826

coincident detector distinguishing between (α,n) , (γ,n) and fission products 0-77424

concident detector distinguishing between (r,n), (p,n) and fission products 0–77424 delayed neutron parameter meas, in heavy water reactor 0–39244 detector spherical below 10 keV, sensitivity correction of delayed n and lifetime in moderator 0–49375 detectors and instrumentation for fast reactors 0–49710 differential fast flux (above 0.5 MeV), by threshold detectors, rel. to High Flux Isotope Reactor 0–49746 diffracted, second order contamination measurements by absorbing foil technique 0–63847 fast and thermal, pulsed, influence of re-entrant holes on meas. 0–49694 fission foil-Lexan detector system to monitor reactor n 0–58074 fission-track counting technique, foil Lexan detectors 0–49747 fluctuation analysis, adjoint-weighting, with emphasis on effective detector efficiency 0–46290 flux, slow n integral in reactor core, transmission method 0–46315 flux density in reactor, meas, using threshold detectors 0–74075 flux density in reactor, meas, using threshold detectors 0–74075 flux density in reactor, meas, using threshold detectors 0–74075 flux density standards, internat, comparison using 4πβ-γ coincidence technique 0–38737 flux spectra from detection activation, variational approach for determination 0–46278 liquid activation dosimetry system for 14.7 MeVn 0–66700

lton 0-46278 [liquid activation dosimetry system for 14.7 MeV n 0-66700 low flux meas, by FeSO₄-HCOOH-H₃10BO₃ system 0-69528 n detector of high efficiency 0-77393 neutron flux detectors, counting-type, high temp. and gamma effects 0-63875

neutron flux monitoring 0-64180 neutron flux parameters meas., by combined activation detector method 0-74028

neutron monitoring, boiling water reactors, in-core system 0–64179 neutron monitoring systems, Campbelling, analysis of differences between true-mean-square and average-magnitude-squared detector ccts. 0–63874

nuclear explosions, underground, mag. data recording of neutron cross-section 0-46011

nuclear reactors, thermal neutron flux, in-core meas, using microwave sensors 0-64171

reactor flux meas., correlation method 0–49742 scintillator, Gd loaded mineral oil 0–60669

scintillator. Gd loaded mineral oil 0–60669 solar neutrons near top of atmosphere 0–41510 solid state track recorder 0–60717 source strengths comparison, precision measuring device 0–42589 spectrometer, time-of-flight, for scattering cross section determ. 0–46023 spectrometers, time-of-flight inelastic long wavelength 0–60654 spectrum of beam from thermal column of reactor. Fermi-type chopper for meas. 0–49744 thermal, flux density standard 0–38716 thermal flux spectra incide votes republic color 0, 42908

thermal flux density standard 0-36716 thermal flux spectra inside water annulus, calc. 0-42908 threshold, method, improved, including digital computer for data treatment 0-77392 track detectors, dose response and sensitivity 0-46071 n. α -conversion layers, time dependency of high alpha flux densities, elimination 0-46042

Co, n flux detector, for meas, and control in research and power reactors 0-38757Li glass scintillator, 5-inch diameter, calibration 50 eV to 8 MeV neutron

El grass scintinatori 3-inct vidualitete, cantifatori 30 ev to 8 MeV flettroi energy, neutron spectra 0–49377

Nb crystal permanent-record integrated fast neutron dosimeter, patent 0–60708

235U-235U-232Th mixture forming fission chamber radiator 0–46316

184W as thermal flux monitor at high temps. 0–39200

ZnS:Ag based scintillators, props. 0–48116

Neutrons and antineutrons continued

see also Neutron transport theory
anisotropic transport theory corrections to asymptotic diffusion theory
0-74032

co efficients calc., anisotropic 0-49690

co enicients cate., anisotropic 0–49690 few region problems, nodal approach to solution 0–77592 group of diffusion eqns. comparison of alternating direction time-differencing methods with implicit methods 0–39182 heterogeneous media, anisotropy and leakage, theory and pulsed obs. 0–39179

in heterogeneous systems, appl. of Green's function anal. 0–55179 kinetics equations in 2 dimensions, multigroup diffusion theory, alternating direction methods for solution 0–77596 linear iterative convergence schemes, a variational rebalancing scheme

0 - 46281

microdistribution in a graphite pile with empty channels, pulsed neutron in moderator, neutron density of Pu-Be source, manganese bath method

parameter determ, in heterogeneous acqueous lattice, by pulse method 0-74030

0—74030 time- and space-dependent mutigroup neutron diffusion equations, numerical solution 0—58040 transport eqn., numerical soln. 0—52820 wave analysis in a finite media 0—46279 OM1 in, (mixture of o-, m-, p-terphenyl parameters at different temps. 0—73648

effects

see also Nuclear reactions and scattering due to/neutrons alloys, YuNDK-type, struct. and props. 0–51195 ceramic, structural, fracture behaviour, strength distrib. 0–43761 crystal, irrad., X ray diffuse scatt. obs. 0–58796 para-dichlorobenzene, inelastic neutron scatt. for study of cryst. excitations 0–59090 diodes, gated, neutron irrad., lifetime parameters and I-V characts. 0–47789

10—4/189 ferroelectric, irrad.-induced phase transform. 0—65487 fusion reactor Nb containment vessel, 14 MeV 0—70729 fusion reactor materials damage, 14 MeV 0—70728 fusion reactors, irrad. damage 0—70695 graphite. boronated, control materials, irrad. induced dimens. change 0—58062

graphite, fission product behaviour 0-67586

graphite, inspire release of fission gas 0–67584 graphite, irrad., vacancy and interstitial clusters conc. 0–40134 graphite, isotropic, irrad., ultimate tensile strength, Weibull's theory applic. 0–40346 graphite, pyrolytic and single cryst., irrad., elastic consts. 0-62009

graphite, radiation damage obs., electron microscopy technique applic. 0-40142

0-40142 graphite, vacancies and interstitial clusters 0-75130 image detection for 14.5 MeV n from (d,t) reaction, three techniques, appls. 0-62222 Inconel 625 and 718, post-irrad, creep rupture props. 0-40329 metal, neutron-induced voidage, ion accelerators as simulators 0-78539 methane, solid, near melting pt., neutron scatt., study of lattice vibrs. 0-59092

0–59092 mica, lattice distortion and OH group rupture, obs. 0–40060 n-activation analysis, applic. to epitaxial Si-film's dopants depth distrib. investigation 0–47056 nichrome alloy, 80/20, irrad., tensile props. 0–65405 nuclear material, Be, Fracture toughness 0–40364 nuclear reactor shield, absorbent carbon, physical props. 0–70727 plastics, dielectric, high energy flux detection 0–63869 primary-recoil atom spectra 0–74047 α-quartz, Raman spectra 0–51325 quartz, Positron annihilation, ang. distrib. 0–53732 semiconductor, GaAs, irrad., on refl. coeff. 0–69108 semiconductor, alloyed, n-GeSi, defect prod., elec. characteristics change 0–44198

0-44198

semiconductor, electron removal during fast-neutron irrad., temp, depend, 0-78989

0—44198
semiconductor, electron removal during fast-neutron irrad., temp. depend. 0—78989
semiconductor, induced cond. 0—78931
semiconductor, p-CdTe, recoil-defect, elec. meas., hole removal 0—47229
semiconductor, p-CdTe, recoil-defect, elec. meas., hole removal 0—47229
semiconductor, photocell, 235U coated, neutron irrad., short-circuit currents 0—51156
semiconductor fissionable material coated, bombard., e.m.f. 0—47692
steel, Cr-Al-Y ferritic, fission-fragment irrad, effect on oxidation 0—66183
steel, austenitic stainless, irrad-induced swelling and void form. 0—68802
steel, austenitic stainless, post-irrad, creep-rupture props. 0—40329
steel, irradiation damage, ultrasonic nondestructive meas. 0—47566
steel, rradiation induced high temp. embrittlement, cold working and recrystn. influence 0—40438
steel, stainless, irrad., void form., He effect 0—68347
steel pressure vessel embrittleness, irradiation at 288°C and 393°C, rel. to fracture-safe nuclear reactor design 0—49716
superconducting tubes, mag. flux flow enhancement due to localized hot spots 0—56202
Teflon, inelastic scatt. of low- energy neutrons for meas. of longitudinal acoustic mode 0—59094
1,2,4,5-tetrachlorobenzene, inelastic neutron scatt. for study of cryst. excitations 0—59090
thermoluminescence, fission fragment induced 0—79375
transistors, GaAs junction FET's, degradation of props. 0—47798
Zircaloy, irrad. creep by dislocation climb 0—58903
Zircaloy, irrad. creep by dislocation climb 0—58901
Zircaloy, irrad. creep by dislocation climb 0—58903
Al-(1 ut-6) Ni alloy, irrad. damage 0—58797
Al-(1 ut-6) Ni alloy, irrad. damage 0—58798
Al, damage energy depend., 0.1-15 MeV 0—71882
Al, hardening, low temp. 0—62092
Al, irradiated, internal friction maxima due to relax. of point defects, and shear modulus 0—68406
Al irradiated at 78K with Cu or Ag impurities, appearance of internal friction peaks 0—71736
Au, damage energy depend., 0.1-15 MeV 0—71882
BaSO₄, barite, n-irrad., point defects and annealing, obs. 0—40124

Neutrons and antineutrons continued

effects continued

BaTiO₃-type ferroelectrics, induced phase transitions 0-40854

BaTiO₃, dielectric props. and structural changes on irrad. in single crystals and ceramic 0-47840

BaTiO₃, irrad. induced phase transform. 0-65487

BaTiO₃, irrad.·induced phase transform. 0–65487
Be, fracture toughness 0–40364
Be irradiated with fast n's, props. 0–46311
BeO, irrad. damage, n.m.r. obs. 0–69196
BeO, microcrack formation, annealing behaviour 0–47428
C, absorbent, nuclear reactor shield, physical props. 0–70727
C, absorbing, irrad. effects on phys. props. 0–39227
C, damage energy depend, 0.1-15 MeV 0–71882
C, pyrolytic, fission product behaviour 0–67586
C, pyrolytic, methane and propylene derived, density changes 0–58852
C, pyrolytic irrad., dimensional changes, rate rel. to density and temp. 0.43630 43630

CaWO4 radiation induced paramagnetic centers, ESR, ENDOR investiga-

CaWO₄ radiation induced paramagnetic centers, ESR, ENDOR investigations 0–62753
CdSe-Se photocell, ²³⁵U, coated, short-circuit currents, e.m.f. 0–51156
CdTe, electrical and photoelec, props. 0–40783
p-CdTe, recoil-defect, elec. props., hole removal 0–47229
Cr, induced ageing 0–68516
Cu, 4.6K, step-annealing, longitudinal magnetoresistance, Kohler's rule 0–72188

0-72188
Cu. Cu-(0.001 wt.%)B alloy, irrad. damage and annealing obs. 0-75161
Cu., damage energy depend., 0.1-15 MeV 0-71882
Cu., grain boundary migration in annealed, rolled bicrystal 0-43680
Cu, irrad., defect clusters, X-ray diffuse scattering 0-61934
Cu, nirrad. eff. on grain growth 0-75119
Fe-C alloy, irrad., induced precipitation 0-68509
Fe, irrad. voids, heterogeneous distrib. 0-58801
GaAs, irrad., on refl. coeff. 0-69108
GaAs, p n tunnel junctions, I-V characts. 0-53892
Gd isotopic composition and variation in samples from Apollo 11
0-45414
N-Ge-Te irrad. effects on carrier conc. 0-44249

0-43414
n-Ge:Te, irrad., effects on carrier conc. 0-44249
n-Ge, heavily doped, resistivity, Hall mobility, annealing, compensation effect 0-47752
Ge, irrad., two-beam crystals lattice image exam. of damaged region 0-50580

0-50580
n-GeSi, defect prod., elec. characteristics change 0-44198
Hg. ³He, gas mixture, lasing action 0-73227
InAs, diffusion of Zn, vacancy conc. 0-47293
KBr, thermally stimulated conductivity, 10-300K 0-47863
LiF, TLD-700, TLD-100, TLD-600 powders, thermoluminescent glow curves due to reactor neutrons 0-44932
LiF crystal, annealed, Y-centres, e.p.r 0-41333
LiNbO₃, radiation damage 0-65318
Mg, internal friction at grain boundaries 0-58871
MgO, irrad., secattering of long wavelength neutrons 0-43636
MgO nirrad., energy release of Frenkel defects 0-55876
Mo, elec. resist., thermal emf, lattice parameter, annealing depend. 0-40725
Mo, irrad., defect recovery, isochronal resistivity obs. 0-47231

0-40725
Mo, irrad., defect recovery, isochronal resistivity obs. 0-47221
Mo, microstructural defects, temp. depend., 50-800°C 0-61966
Mo, stage III recovery, dose depend. 0-62094
NaCl, irrad., Young's modulus and internal friction 0-71668
Nb, damage energy depend., 0.1-15 MeV 0-71882
Nb, irrad., radiation hardening, yield stress depend. on dose 0-65461
Nb, single crystal, yield stress, strain-rate, flow stress, temp. depend. 0-78627

0-78627

Nb defect clusters and plastic deformation, transmission electron microscopy 0-50690

Nb fusion reactor containment vessel, 14 MeV 0-70729

Nb Sn superconducting tubes, mag. flux flow enhancement due to localized hot spots 0-56202

Ni-Fe-Cr alloys, radiation hardening, proof stress analysis, mechanism 0-47447

Ni, irrad., vacancy clusters, low temp. 0–78535
PbTiO₃, irrad. induced phase transform. 0–65487
PbTiO₃ ceramic, dielecteic props. and structural changes on irrad. 0–47840

0-47640 Fi. Lir. absorpt. spectra, defect-oxygen complexes 0-48055 Si, irr. ds. diffusion and space-charge generation currents, annealing depend. 0-44262

depend. 0—44.82 p-Si, irrad. damage, photocond. obs. 0—47879 n-Si, neutron-irradiated, resistivity and lifetime meas. 0—51060 Si, photocell. ²³⁹U coated, short-circuit currents, e.m.f. 0—51156 Si, vacancy production near edge absorpt., temp. depend., 145-300°C 0—40136

Si p-n junctions, Scanning Electron Microscopy 0-51079
Si Single crystals, lattice defect production, observation by X-ray topography 0-59123 hy 0-59123
Si solar cells, radiation damage obs. by annealing of photovoltaic parameters 0-75121
Si transistor second breakdown and thermal behaviour 0-44311

 SiO_2 , cristobalite, irrad., structure and thermodynamic props. change 0-62134

SiO₃, enstroonmenter, fraid., Structure and thermodynamic props. change 0–62134
SiO₃, neutron-compacted, Raman scatt, and far-i.r. absorpt. 0–76130
SiO₄, quartr₄, α-β transformation, Raman spectra 0–78702
SnO, aftereffect of nuclear reactions, Mossbauer effect investig. 0–54079
Ta, high-temp, irrad., microstruct., thinning technique 0–75102
U, irradiated, grain growth during annealing 0–47207
UO₃, continuous creep meas, under irrad. 0–68459
UO₅, creepe enhancement during irrad. 0–68459
UO₅, irrad., melting pt, increases and decreases 0–68178
UO₅, re-soln. of gas atoms from bubbles during irrad. 0–67585
V, irrad. induced voids 0–40127
V, vire, thermal hardening, temp, depend. 0–47448
W-(25 wt.%)Re alloy, radiation-induced damage, recovery 0–40146
W, defect recovery process 0–47231
W, vacancy damage production, field ion and electron microscopy 0–75139
Zr alloy, pressure tube, capture cross-section, strength, review 0–43771

Zr alloy, pressure tube, capture cross-section, strength, review 0-43771
Zr alloys, irrad. creep, enhanced ductility obs. 0-71701
Zr alloys, irrad. creep mechanisms 0-78637

Neutrons and antineutrons continued

interactions

with Bloch walls, static and moving 0-73643

capture cross-section meas. using Moxon-Rae detector, precision factors 0-73686

cross-sections resonance structure subgroup method for accounting

pairing correlations, effect on transfer of np pair 0-52649

primary recoil atom spectra 0-74047

s-process neutron capture equations used to calc. abundance of 50 \(A \) \(65 \) nuclides \(0 - 55121 \)

primary recoil atom spectra 0-/4047 s-process neutron capture equations used to calc. abundance of $50\leqslant A\leqslant 65$ nuclides 0-55121 $pn\to pr$, polarization of recoil proton in D for $(\theta\pi)$ c.m.= 90° , in second resonance region 0-77372 $pn\to pr$, phenomenological anal. of π - prod. 0-77322 $pn\to pr$, phenomenological anal. of π - prod. 0-77322 $pn\to pr$, put of 1 GeV, cross sections, evidence for P_1 , resonance 0-60575 $pn\to pr$ - p, diff. cross section meas. at $E_p=600-1250$ MeV using liq. deuterium target 0-38680 $pn\to r^2$ horod. asymmetry 0-55038 $pn\to r^2$ horod. asymmetry 0-52505 $pn\to r^4\Delta^-$ 16 GeV, cross-section meas. 0-73441 $pn\to r^4\Delta^-$ 16 GeV, cross-section meas. 0-73441 k-n, 4.5 GeV/c, final states including A 0-38674 k-n $\to r^*A$ (12°) hypercharge exchange reaction in Reggeized $U(6)\otimes U(6)\otimes U(6)\otimes$

nd \rightarrow pnn, coincidence meas. for 14.4 MeV neutron induced reaction 0-49630

0-49630 m., from two complete exp. on three-nucleon reaction D(n,nnp) at 14.5 MeV 0-73644 m, from two complete exp. on three-nucleon reaction D(n,nnp) at 14.5 MeV 0-73644

14.5MeV 0—73644
np, in three-body reaction p+d→p+p+n with 52 MeV deuterons, exp. investigation 0—73635
np→dp reaction, parity nonconservation 0—49308
np→dπ⁰, differential and total cross sections and a test of charge independence 0—52555

ng-pd, asymmetry of yields compared with pd→np, induced by T-violation 0-45967 npp bremsstrahlung calculated with potential, agreement with experiment 0-57830

0-3/830 vn-μp, enhancement due to a resonant effect, implications 0-49312 pn- Δ - Δ +τ, Δ - in forward direction, possible exotic exchange at 6.98 GeV/c 0-57825 pn-K* $K\pi\pi(K^*K\pi\pi)$ 1=1 enhancement near 2360 MeV, possible obs. of U-meson. 0-45946 double given production at 2.8 GeV/c resolving

 $pn \rightarrow np\pi - n$ interaction, double pion production at 2.8 GeV/c, reaction analysed 0-70248

analysed 0–70248 pn- π $\pi^+\pi^-$ phase-shift model, evidence for daughters 0–57819 pn- $\pi\pi\pi\pi$, in crossing symmetric Regge pole model 0–77366 pn- $\pi\pi\pi\pi$ normalization of amplitude by mass extrapolation 0–55059 $\pi^+\pi^-\pi^-$ d+*(1236), ang. distribs. explained by rescattered model 0–42491

0—42491 ν n→ σ 0n, photoproduction of neutral pions at 500 900 MeV, differential cross-sections 0—52507 K⁻n, E_k=700-1175 MeV/c, cross sections 0—42524 K⁻n→K⁰ σ rn generalized Veneziano model 0—73556 nd—nnp, numerical cales. on 3 separable potential model 0—77370 np ν , meas. at 208 MeV, cross sections 0—77371

moderation

see also Neutron transport theory continuous slowing down theory for anisotropic elastic neutron moderation 0-77594

continuous slowing-down theory in fast-reactor assemblies 0–74036 depletion characteristics of a cylindrical pin containing one isotope or a mixture of burnable poison isotopes 0–52839 entrainment by travelling medium 0–74027 Gauss-Laguerre numerical integration for point kernel shielding calculations 0–55182

uons 0-55182 ice, slowing down time, obs. 0-49691 in mixtures by method of Green's function 0-70276 moderator reactivity coeffs., comparison of four methods of determ.

modulators, pseudo- statistical with different duty cycles, binary sequences and error analysis 0-49305 100 aliaysis 0-49303 nonhomogeneous thermalization eqn., soln. by appl. of Mullikin's method 0-60840

pulsed, joint time and energy depend. of rate of emission using crystal spectrometer 0–70277 pulsed neutron in ice, 21-273°K 0–46302 santowax, slowing down time, obs. 0–49691

Neutrons and antineutrons continued

moderation continued slowing down equation for infinite homogeneous monatonic medium, exact. solution 0-74037

solution 0–74037 slowing down equations of fast neutrons, asymptotic, approximate solution 0–55178 space- and time-dependent neutron slowing down for hydrogen and non-hydrogenous moderators 0–52826 steel sphere in U-metal shell assembly, critical mass irregularity 0–58055 termalisation time in silicons rocks of different moisture content 0–71889 thermalization, theory and expt. 0–60843 water, light, slowing down time, obs. 0–49691 D₂O moderated systems, reactivity coeff, determ., comparison of four methods 0–52844 Pu-Be source, neutron density, diffusing moderator effect, manganese bath method 0–49306 u, natural D₂O moderated single rod lattices, buckling obs. rel. to transport theory 0–39219 nolarization

polarization depolarization in elastic scatt. with ²⁷Al, ⁶³Cu, ⁶⁵Cu, ²⁰⁹Bi, ⁵⁹Co and Ni nuclei 0-42845

depolarization passing through ferromagnet 0–40612 depolarization passing through ferromagnet 0–40612 inelastic, in collision of 3GeV protons with platinum 0–60813 Monte Carlo technique for correcting exptl. fast-neutron polarization data 0–42592

0–42592 scattering on thick layers, calcs. 0–77558 τ " p– τ 0", 310 MeV, neutron polarization meas. 0–73590 11 B(α , n) 14 N, 3.6 3.8 MeV, neutron polarization obs. 0–58007 18 B(α , n) 12 C, polarization for E $_{\alpha}$ =2.4 to 2.9 MeV 0–42593 14 H(n_{por,n}) enriched deuterated benzene solution, En=1.2 MeV 0–49629 14 H(p, n) 14 He, n.3 18 p 18 2.3 MeV 0–39036

production
generator maximum intensity regulation digital system 0–45970
generators, book on principles and applications 0–55066
monochromator system, composite of crystals with gradient of lattice spacing 0–55064
moon's surface interaction with cosmic rays 0–51739
multiplication, using Pu-polystyrene cube 0–49731
photoneutrons, calculations for thick W and Ta targets 0–73913
plasma-focus, intense neutron production from enhanced plasma resistance 0–74542
source of (DD) reactions, D₂O gas target use 0–38719
source plane realized by conversion of horizontal thermal reactor column 0–70735
source strength determination by measures but a contract of the contraction of the

0-70735 source strength determination by manganese bath method, flexibility increase 0-49311 source strengths comparison, precision measuring device 0-42589 yield from 'Li(p,n)'Be reaction near 2.2 MeV 0-52772 Am-Be sources, gamma to neutron ratio 0-49307 'Be(c,n)'2C reaction, polarization of n for $E_\alpha\!=\!2.4$ to 2.9 MeV 0-42593 'S²Cf randomly pulsed neutron source for prompt neutron decay meas. 0-74078 '2³1Pa(n, f) fission, relative delayed neutron group yields with fission neutrons 0-64141 in Pb at depth of 150 m wat. eq. by cosmic ray muons 0-70283 Pu-Be source, neutron density, diffusing moderator effect, manganese bath method 0-49306 Pu Be sources, gamma to neutron ratio 0-49307 '2³8Pu-Be source, activation analysis for partial body obs. of Ca 0-76734 reflection

reflection

scattering

by Bose fluid in restricted geometry 0-71397 air, expressions derived using least square fits to Monte Carlo calcs. 0-45971

0-45971
alkaline earth hydrides, orthorhombic, vibr. spectra from inelastic scatt. of cold neutrons 0-40535
anomalous elastic scatter 0-70273
antiferromagnet, MnF₂, critical mag, scatt. 0-44705
antiferromagnet, semicond., by coupled waves 0-71902
butyl alcohol, tertiary, n scattering study of hydrophobic hydration rel. to H₂O mol. motion in dilute aqueous soln. 0-71314
condensed matter, fluctuations obs. 0-6883
cross section, absolute normalisation of data using organic scintillators as scatterers 0-71373
crystals, mag., exchange integrals meas. 0-40937

scatterers 0–1/3/3 crystals, mag., exchange integrals meas. 0–40937 cyclohexanol, liquid, quasi-elastic incoherent cold neutron scatt., rel. to mol. motions 0–78262 cylindrical targets, corrections for multiple scatt. and flux attenuation 0–42591

Debye spectrum space lattices slow neutron cross sections 0-75353 Debye spectrum space lattices slow neutron cross sections 0-75353 diamagnetic scattering in an atom for an external magnetic field 0-52963 elastic, meas, with moderated bomb source meas. 0-74029 elastic scattering of neutrons by deuterons, investigation of exchange collision Possibility 0-42848 glycerol, quasi-elastic line-broadening meas, using high resolution neutron crystal spectrometer 0-68077 graphite backward by 0, 20, 40, 60 and 80° for semi-infinite thickness 0-45972

hexamethylenetetramine, molecular dynamics, n scattering investigation 0-71069

0–71069 hydrogeneous liquids, of slow neutron, for mol. dynamics 0–39728 liquid, inelastic scatt, theories 0–39730 liquids, slow n scatt, memory function rel. to vel. autocorrel. 0–39729 liquids, stochastic model 0–533150 nethane, gaseous, molecular interaction effect 0–67854 molecular dynamics, obs. using rotating-crystal spectrometer, cyclic hydrocarbon exam. 0–47511

multidetector system using proportional counters with resistance wire 0-55078

paramagnets, short range ordered, model 0–40943 plasma, magnetically confined, with electrostatic ion oscills., cross sections calc. 0–50019 polarized, rel. to optical model of nucleus, 3.2 MeV 0–57878 polyethylene backward by 0, 20, 40, 60 and 80° for semi-infinite thickness 0–45972

polystyrene solns., intermediate concs. 0–53316 propane, methyl group libration meas. 0–43178 rare-earth ions, neutron magnetic form factors calc. 0–62486

Neutrons and antineutrons continued

scattering continued rigid rotor, sum rule for interference scatt. 0–46441 routine for slow neutrons from gas model 0–74035 sample holder corrections 0–60617 semiconductor, antiferromag, by coupled waves 0–71902 slow, quasiclassical approximation 0–71063 in solid cylindrical samples, finite sample corrections 0–53727 solids and liq. rel. to phonons and spin-waves, review 0–46870 thermalization, experimental, book 0–42895 time-of-flight meas, pseudostatistical pulsing method 0–45968 time-of-flight meas, pseudostatistical pulsing method 0–47968 time-of-flight meas, pseudostatistical pulsing method 0–47968 time-of-flight meas, pseudostatistical pulsing method 0–47944 N n→Aπ reaction, difference between Regge cut models, on basis of differing dip systematics 0–45907 K n Kop, Regge-pole model modified by inclusion of lowest order cuts 0–75391 nd, considering exchange collision probability 0–42848

0—73591
nd, considering exchange collision probability 0—42848
nd, elastic scattering at 27 MeV 0—73647
nd, P=1/3* state with tensor forces and repulsion 0—73646
nd, solution of Faddeev equations by Pade approximants 0—52413
nd, variational bounds 0—38717
nd breakup, calc. using Amado's model 0—73645
nd doublet scattering length in 3-boson model 0—52644
nd elastic scattering, semiempirical interpolation formula and cross-section 0—57831
np. mark model 0—73614

0-57831
np. quark model 0-73614
np. charge exchange scatt., one-pion exchange amplitude 0-73636
pn. 1.0-3.5 GeV/c obs. 0_45964
pn. 4p. hard pions and the deuteron equal time commutator with the weak and axial-vector current 0-63850
Al backward by 0, 20, 40, 60 and 80° for semi-infinite thickness 0-45972
Ar, gas, determination of intermediate scattering function 0-68006
inD₃ solid and liq. 0-64854
Fe, dynamics of critical state investigations 0-47938
inH₃ solid and liq. 0-64854
inHD solid and liq. 0-64854
He liquid, high energy neutron scatt., interference and temp. effects 0-46968
He liquid, high energy neutron scatt, interference and temp. effects 0-46968

0-46968

'He liquid, inelastic scattering with high momentum transfers to probe single particle motions 0-43498

Mn² antiferromagnetic salt, electron delocalization effects 0-62566

MnF2, antiferromag, critical mag, scatt. 0-44705

MnF2 antiferromag, inelastic scatt. in critical region 0-47972

MnO, paramag, model 0-40943

Nb-D, solid solns., diffuse scatt., D atom distrib. determ. 0-40463

Ni, small angle critical, as functions of temp, and scatt. vector 0-75914

Niz* antiferromagnetic salt, electron delocalization effects 0-62566

Sn, liq., slow neutrons transverse scatt. cross section obs. 0-39731

Ti backward by 0, 20, 40, 60 and 80° for semi-infinite thickness 0-45972

V, by interstitial H bibrs., inelastic scatt. 0-56095

V₂O₃, inelastic spin-flip scatt., internal mag, field meas. 0-72178

cattering, neutron-proton

scattering, neutron-proton
24 MeV, angular distribution 0-67329
amplitude 0-70268
angular distribution at 24 MeV, differential cross section measurements
0-49309

0—49309
angular distribution data below 10 MeV 0—38718
backward, 1.0-5.5 GeV/c 0—42590
Born approximation for charge-exchange scatt. 0—57823
charge-state oscillations, flipping phenomena 0—60618
cross-section at 14 MeV, high-precision meas, of anisotropy
elastic differential cross sections, 2 to 7 GeV/c 0—52557
Mott-Schwinger interaction 0—39054
phase params, analysis and obs. 0—42586
total cross sections, 8 GeV/c-21 GeV/c 0—49310
Veneziano model for charge exchange scattering 0—52556
without a company of the c

Newtonian fluids see Fluids

Nickel
abundance in lunar samples, emission spectrographic determ. 0–48499
acoustic waves, propag, and attenuation 0–68595
adhesion of Cu, W, oxidized W, quartz to (111) surface, LEED obs.

0 - 43820

0–43820 adsorption by Ge, influence on surface props. 0–72057 adsorption of S. layer structure, formation mechanism, stability 0–39974 alpha-particle bombarded, helium pore growth and dislocations, electron microscopy 0–68343 atom, extended method of calc, applic, to dⁿ shell with N=5–10 0–70764 atomic spectra, classification of new multiplets in extreme u.v. 0–49764 band struct., spin splitting and spin-wave effective mass 0–40666 band struct and Fermi surface rel. to spin-orbit and exchange interactions 0–40728

band struct, and Fermi surface rel. to spin-orbit and exchange interactions band struct, and Fermi surface rel. to spin-orbit and exchange interactions 0–40728

Barkhausen discontinuities, effect of mag, texture produced by elastic deform. 0–75933
cathode, potential drop rel. to press. for inert gases 0–39627
coating on steel, thermoelectric gauging 0–40434
crystal, dislocations, small angle neutron scattering 0–61806
desorption, thermal, of ion-bombanded Ar, obs. 0–56697
desorption, thermal, of ion-bombanded Ar, obs. 0–56697
desorption of HD from active (111) surface, angular dependences 0–65095
dielectric screening, noninteracting band model 0–75496
diffusion in Cu-Ni alloys, volume and grain-boundary diffusion 0–47290
diffusion in Cu-Ni alloys, volume and grain-boundary diffusion 0–47290
diffusion of Cu 0–61995
diffusion to Si surface from bulk 0–78538
disc, ferromagnetic resonance, shape-depend, demagnetizing field 0–56661

0-56661 dislocation dipoles in elastically anisotropic crystals 0-78556 domain wall motion in single-crystal platelet, Kerr effect study 0-41007 e.s.r. in Cd₇Cl₁B₁₆O₃₀ 0–79401 electrical resistivity and thermoelec, power near Curie pt. 0-40727 electroless deposition, mechanism 0-61674 electroless deposits on Be, stress obs. 0-71679 electrolytic, magneto-mechanical damping rel. to recrystallization and recovery 0-47326 electron energy loss spectra obs. and correl, with theory 0-50918 electroplated coatings on steel during brazing, process of soln. 0-68524

Nickel continued

Elinvar prop., high temp., effect of Mn, Ti, Zn additives 0–58856 Elinvar prop., high temp., effects of V, Mo, W, Si, Sn, Cr additives 0–58855

etching by I in organic soln., effect of surface contamination 0-53536 exoelectron emission of surface-oxidized cryst, during plastic deform, in vacuum 0–47891 exploding wires, volt-ampere characteristics in relation to diameter and

length of wire on explosion in air 0-75557 ferromagnetic reson. and relax., 9-54 MHz 0-41304

ferromagnetic resonance transmission in thin sheet, 35 GHz, 4.2 K 0-44972

ferromagnetic thin films existence of dead layers explained by Stoners' theory 0-62539

theory 0–62539 ferromagnetic transmission resonance obs. 0–62745 film, discontinuous struct., elec. and mag. props. 0–72251 film, electrodeposited, metal contamination, appearance and surface topography 0–58576 film. electrodeposited, perpendics a nisotropy 0–62538 film, electrodeposited single cryst., magnetocrystalline anisotropy 0–65942

0-03942 film, electroless growth on plastics, nucleation 0-58596 film, electroplated, recrystallization temp., saccharin conc. depend. 0-47432

film, epitaxial growth, vacuum deposition, electron microscope diffraction patterns 0-43550 film, evaporated, domain wall thickness meas., Lorentz microscopy 0-47955

0-4/955 film, evaporated, thickness depend, of elec, resistance explained by electron refl. and scatt. 0-78822 film, perpendicular anisotropy, stress contrib., and elec, resistivity 0-4639

0-44639 film, prepared by low pressure triode sputtering, stress analysis 0-50674 film, saturation magnetization, rotatonal hysteresis losses, annealing depend. 0-47959 film, saturation magnetization and perpendicular anisotropy 0-41024 film, single crystal, on Cu, accommodation of misfit 0-58567 film, vacuum-deposited, heating effects on substructure and props. 0-47957

0-47957 film, vapour deposition, temp. changes 0-68233 film yapour deposition, temp. changes 0-68233 film growth on (111) Al surface 0-55721 film on transformer steel, influence on bulk mag. permeability 0-51218 films, unencumbered ferromagnetic, spin wave study 0-72250 foil, dynamic and static extension, microhardness, dislocation densities, X-ray investigations 0-50691 foils, strength meas. for thickness $0.51-1.27~\mu m$ 0-50721 Hall effect, spontaneous planar, temp. depend. 0-75929 hydrogenated phases, anodic oxidation 0-56709 hyperfine field of W nucleus determ. 0-57929 inert gas ions burial and thermal release, at surfaces, 100-2400~eV 0-56699 internal friction cathodic hydrogen influence. 0-65370

0-56699
internal friction, cathodic hydrogen influence 0-65370
internal friction, ferromagnetic, torsional deformation effects 0-56019
internal friction, mag, field influence on damping 0-65367
internal friction peaks associated with dislocations, rel. to cold-work, 77700K, 5-50 kHz 0-68410
Invar prop., effect of V, Mo, W, Si, Sn, Cr additives 0-58855
Invar props., effect of Mn Ti, Zn additives 0-58856
ion bombarded, vacancy clustres, spatial distrib. 0-68342
ions, high, ionization equilibria, ionization and recombination rates
0-43343
ions, highly ionized, excitation, equilibria, under solar coronal conditions.

ions, highly ionized, excitation equilibria under solar coronal conditions 0-41817

0-41817
Kerr effect, equatorial and polar, near i.r. 0-51271
kink-point locus and critical phenomena 0-44599
Kondo effect in hydrogenated metal with paramag, impurities 0-78880
LEED determ, of effective atomic scatt, factor and rigid-lattice interference function 0-47518
lattice dynamics, vibration spectra, specific heat and Debye temperature 0-53688
lines, i.r. for faculae and surrounding photosphere, determination of Doppler velocities and damping constants 0-72784
liquid, struct, comparison with liq. Fe 0-71308
magnetic anisotropy of plastically deformed single crystal 0-75925
magnetic cryst. energy temp. depend. 0-79173
magnetic transitions, near Curie pt., transition of second kind 0-75932
magnetization, stress induced 0-51206
magnetization process, reversible, lattice disorders effect 0-51211
magnetomechanical damping, temp. and strain amplitude depend. 0-55935
magnetomechanical damping 0-40279

magnetomechanical damping 0-40279 magnetoresistance, and electron scattering depend on spin orientation

0—44540
magnetoresistance, and electron scattering depend, on spin orientation 0—44540
magnetoresistance, impurity scattering centre effects 0—44064
magnetostriction constants 0—62535
Mossbauer effect of 57Fe, rel. to temp. 0—51283
n.m.r. of 61Ni in bulk metal 0—72512
neutron irradiated, vacancy clusters, low temp. 0—78535
neutron scattering, small angle critical, as functions of temp. and scatt. vector 0—75914
nickel-chrome thin film on mica, internal stresses 0—62029
optical props., visible and near i.r. 0—62602
oxidation. 02 mol. dissoc. as rate determining step during initial stage 0—72540
paramagnet f.c.c., anisotropic a factor of Fermi surface shorter 0—44400

0—72540
paramagnet f.c.c., anisotropic g factor of Fermi surface sheets 0—44499
photoelectric work function 0—75859
photoelectrons, spin polarization obs. 0—75864
photoemission spectra of ferromagnetic (295K) and paramagnetic (678K)
nickel 0—75863

plastic deformation, high temp., oxidation effect, model 0-4374

plastic deformation, high temp., oxidation effect, model 0-43747 plastic deformation, high-speed, slip systems participation 0-40341 plastic flow, acoustically induced, expts. 0-65407 plastic flow threshold meas, and u.s. and static loadings 0-68463 platelet, single-crystal, domain wall motion, Kerr effect study 0-41007 platelet growth, single crystal, conditions 0-55784 polycryst, high temp., effect of plastic deform, on substracture, X-ray diffr. meas. 0-78489

Nickel continued

polycrystalline, dislocation structure, low- and u.s. freq. loading, 77 and 300 K $\,0-75\,166$

K 0-75166
polycrystalline, steady state creep, 0.3-0.55 T_m 0-53601
polycrystalline formation of dislocation networks with point defects, quenching 0-43802
positron lifetimes in shock-deformed polycryst. 0-68674

position meanies in snock-deformed polyeryst. 0–68674 powder, charge density absolute meas., X-ray diffr. 0–61900 recovery after explosive shock-loading 0–75307 reinforced by single cryst, fibres of transition metal carbides, mode of deformation, stress-strain rels. 0–65375

relaxation spectrum, Zr additions effect 0-53576

resistivity, elec., thermoelec. power, temp. depend., Curie point region, anomalies 0-44063

makes 0-44003 resistivity change of wire, annealing temp. depend., impurity effects 0-47651

saturization magnetization, absolute meas., force method 0-62528 scattering of atomic and mol. ions, energy distribs. of emitted particles 0-40912

shock-deformed, positron lifetimes 0-68674

shock-deformed, positron lifetimes 0–68674
single crystal, magnetization in trigonal plane, magnetostriction, galvanomagnetic effect 0–54017
solar abundance from photospheric Ni II lines 0–69474
solid solubility of Ga and Ge, X-ray spectra 0–5980
spin wave spectra 0–62511
spin-wave effective mass, spin splitting and band struct. 0–40666
substructure changes due to fast moving air current 0–61949
substructure misalignment due to high temp. deformation 0–68448
surface, (001), atomic thermal vibr.. LEED obs. 0–74886
surface, (100). C contaminated, photoelectric yield temp. depend.
0 43538
surface, (100), carbon segregation, work functions and LEED obs.

surface, (100), C contaminated, photoelectric yield temp. depend. 0, 43538, surface, (100), carbon segregation, work function and LEED obs. 0–47039, surface, specular electron reflectivity curves, peak widths. 0–61628, surface, trapping and thermal release of 100-300 eV. Ar† and Kr† 0–47038.

surface, trapping and thermal release of 100-300 eV Ar* and Kr* 0-47038
surface cleanliness, work function, argon ion-bombardment, heating, adhesion testing 0-39927
surface comp, analysis by inert gas ions backscatt., 63Cu/65Cu differentiation 0-56717
surface layers, deformation in fast air streams 0-68220
surface scattering of 4He, H₂ and D₂ thermal energy beams 0-65095
susceptibility, differential, existence of two maxima 0-54010
thermal recovery, shock loaded, defect mechanism 0-40450
thermal recovery, shock loaded, defect mechanism 0-40450
thermoremanence, effect of internal stress on 0-69036
trace in atmosphere, atomic absorption spectrochem, analysis 0-56728
trapping and re-emission of fast D ions 0-65880
u.s. attenuation anomalies under stress rel. to magnetization rotation in domains 0-62196
vacancy clusters in neutron irrad, cryst., low temp. 0-78535
valence bands, L-series X-ray spectroscopic study 0-65593
voids on electron irradiation after Ar ion bombardment 0-75149
work-hardened, struct, and creep strength 0-62052
Young's modulus, shear modulus, elastic parameter and coefficient 0-65355
COL decertion or 1000 face 0.47078

Young's modulus change, by magnetic field 0–65355 CO adsorption on (100) face 0–47079 Cr-Ni alloy 2.2%, dynamic properties, annealing conditions effect 0–40927

Cu, energy gap energies determ. from specular electron reflectivities 0-54086

0-54086
Fe in meteorites, with Ge concn. greater than 190 ppm 0-76657
Joints with Cu laser beam welding, metallographic method, physical phenomenon investigation 0-43801
Joints with Ti laser beam welding, metallographic method, physical phenomenon investigation 0-43801
MgO:Ni²*, phonon sidebands in emission spectra 0-62666
inMnF, inpurity magnons, fluorescence 0-44906
Ni.²²Câ hyperfine field meas. 0-75988
Ni.¹⁰Rh, hyperfine field meas. 0-7923
Ni.¹⁰Rh, hyperfine field system studied by NMR/PAC and TDPAC 0-66156
Ni.²Al.O₁ (sapphire) interface, laser beam induced damage, metal vapour effect 0-53528
Ni.²O-Te system at 500°C, stability domain of hexagonal phase 0-65506
Ni.SiO₂-Ni.SiO₂ multilayer coatings on reflectors, black mirror' effect 0-41116
Ni.alumina interface, thermal conductance at elevated temp. 0-71875 Ni-SiO₂-Ni-SiO₂ multilayer coatings on reflectors, 'black mirror' effect 0–41116
Ni-alumina interface, thermal conductance at elevated temp. 0–71875
Ni I, absorption line profiles of multiplets in near u.v. 0–67629
Ni X identification and classification of 3p°3d-3p′3d4s transition 0–39279
Ni⁺c.p.r. in ZnSe 0–41349
Ni⁺, in Ni-Cu ferrite, anisotropy contrib. 0–54036
Ni²⁺, in Ni-Cu ferrite, anisotropy contrib. 0–54036
Ni²⁺, tow-temp. spectrum in CdF₂, site distortions 0–48066
Ni²⁺ absorpt. obs. as nearest neighbour environment meas. in glass 0–56529
Ni²⁺ antiferromagnetic salt, electron delocalization, neutron magnetic form factor 0–62566
Ni²⁺ e.p.r. in CdB₁, 0–62754
Ni₂⁺ in MgO, fluoresc. and absorpt. spectra 0–76170
Ni²⁺ in MgO, Raman relax. rate cales. using shell model of phonons 0–75976
Ni²⁺ single ions and couple pairs, in KMgF₃, effect on thermal conductivity 0–47559
Ni³⁺ e.p.r. in SnO₂ flux-grown cryst., oxidation-reduction effects 0–72492
Ni³⁺ e.p.r. in SnO₂ flux-grown cryst., oxidation-reduction effects 0–72492
Ni³⁺ e.p.r. in SnO₂ flux-grown cryst., oxidation-reduction effects 0–39804
27Np, 2³⁸Np) implanted, hyperfine magnetic field studied 0–69061
S segregation on (110) surface 0–47756
Ni (10), high-resistivity, elec. props. 0–47756
Si doped, contact resistance meas., method 0–51086

Si:Ni, high-resistivity, elec. props. 0-47756 Si doped, contact resistance meas., method 0-51086

Nickel alloys see also Nickel compounds

713C, extruded powder type, heat treatment, strength 0-47378

718, tensile and fatigue props. at cryogenic temps. 0-40354

718, tensile and fatigue props. at cryogenic temps. 0–40354 alloy, plastic deformation following quenching from 1200°C and then annealing 0–55976

Alni, Curie temp. meas. 0–72220

Alnii, effect of alloying elements on Curie point 0–72222

Alnico, Curie temp. meas. 0–72220

Alnico, Ti containing, effect of duplex addition of S and Te 0–71761

Alnico, effect of alloying elements on Curie point 0–72222

Alnico, effect of some alloying elements on structure and magnetic properties 0–71221

Alnico, effect of thermomagnetic treatment on structure changes and properties 0–71767

Alnico, high coercivity, investigations 0–71763

Alnico, magnetic and physical properties, study with changing temp. during technological treatment 0–71769

Alnico, magnetic properties rel. to crystal structure perfection 0–72223

technological treatment 0-71769

Alnico, magnetic properties rel. to crystal structure perfection 0-72223

Alnico, state and distribution of Fe 0-71758

Alnico 450 magnets, problems of heat treatment 0-72170

Alnico 5, structure forming during recrystallization 0-71527

Alnico 5 and 8, magnetic properties at sequential stages of heat treatment in a magnetic field 0-72226

Alnico 5 and 8, structural changes 0-71768

Alnico 8, high coercive, X-ray and Mossbauer study 0-71759

Alnico 8, magnetic properties rel. to crystal structure 0-72224

Alnico type, high coercive, mechanism of periodic distribution of inclusions 0-71765

Chromel-A explosive shock-loading thermal recovery 0-75307

Sions 0—71703 Chromel-A, explosive shock-loading, thermal recovery 0—75307 creep stress and temp, depend. 0—43750 dilute, magnetoresistance, and electron scattering depend. on spin orienta-tion 0—44540

tion 0–44940 electrical resistivity rel. to spin-disorder scatt. 0–78879 Elinvar prop., high temp., effect of Mn, Ti, Zn additives 0–58856 Elinvar prop., high temp., effect of V, Mo, W, Si, Sn, Cr additives 0–58855

0-58855
extruded powder type, 713C and NASA TAZ-8A, heat treatment, strength 0-47378
ferrous, stress corrosion cracking evaluation 0-68488
Hastelloy-N, resistance to embrittlement by thermal neutrons, development 0-39247
high temperature thermomechanical treatment, overheating effects 0-68513

0-68513
high-strength, accelerated stress corrosion test 0-71718
Inconel 600, explosive shock-loading, thermal recovery 0-75307
Inconel 625 and 718, post-irrad, creep-rupture props. 0-40329
Invar, magnetoelastic internal friction, effect of oriented ordering of C atoms, mechanism 0-75233
Invar props., effect of V, Mo, W, Si, Sn, Cr additives 0-58855
Invar props., effect of Mn Ti, Zn additives 0-58856
long range order in γ'-phase superalloys, rupture and heat treatment effects 0-68314
magnetoresistance, and electron scattering depend, on spin orientation in dil, alloy 0-44540
manganin wire, shock piezoresistance coeff, variation rel, to deform, 0-62305
mechanical properties, effects of exposure to Na 0-75275

0-02305
mechanical properties, effects of exposure to Na 0-75275
Monel, mag. transform, effect on ang. distrib, curves during positron annihilation 0-41008
Monel 400, creep, heat treatment and grain size influence 0-71698
NASA TAZ 8A, extruded powder type, heat treatment, strength 0-47378
nichrome, 80/20, tensile props., extension rate and neutron irrad. effect
0-65405

nichrome resistor, reliability under extended temperature storage and high current densities obs. 0–50370 nimalloy, effect of W and Cr additions on permeability 0–59329 nimonic P.E. 16, creep deform, stress depend. 650°C, mechanism 0 - 58896

oxidation and erosion resistance coatings, high temp., patent 0-45067 permalloy, 4-79 Mo, permeability, annealing environment depend. permalloy, 0-41025

Permalloy, ferromagnetic resonance transmission in thin sheet, 35 GHz, 4.2 K 0-44972

permalloy, thin film, plane arrangement of superparamagnetic particles 0-44522 Permalloy 0-51208 79NM, texturing processes effects on mag. anisotropy

79Nm, mag. props. temp. depend., heat treatment effect

Permalloy 0-44630

Permalloy film, 3He-irrad, long range order from uniaxial anisotropy energy meas. 0–44636 permalloy film, 'hypercritical', 'dislocation' domain struct. 0–54030 Permalloy film, biaxial anisotropy development under tensile stress 0–79184

Permalloy film, domain struct., grain size and support surface roughness depend 0-54031

depend 0–54031

Permalloy film, two layers, exchange interactions, spin wave pinning

depend. 0–44967

Permalloy film, iterromag, resonance, line width temp, and mode depend., 4 300 K 0–44968

permalloy film, internal macrostresses, effect of deposition parameters, plasma sputtering process 0–71678

Permalloy film, magnetic coercive force, internal stress, domain pattern, electrodeposition depend. 0–41023

permalloy film, noise characts., thickness depend. 0–65631

permalloy film, opic characts., thickness depend. 0–65631

permalloy film, spin wave resonance, high press, depend. 0–44969

Permalloy film, spin-wave resonance fields, mode number depend. 0–44967

Permalloy film, spin-wave resonance fields, mode number depend. 0–44967

Permalloy film, two layers, exchange interactions, spin wave pinning

Permalloy film, two layers, exchange interactions, spin wave pinning 0-44970

0-44970

Permalloy film in Kerr magneto-optical ammeter 0-65991

Permalloy film structures, ferromag., surface spin pinning 0-44971

Permalloy films, Bloch-wall, I.f. creep, coercive force influence 0-65943

Permalloy films, Cu-diffused, mag. props. improvement 0-65937

Permalloy films, deflection on mag. reversal curve 0-44607

Permalloy films, electrodeposited, uniaxial mag. anisotropy origin 0-62537

Permalloy films, nonuniform rot, threshold field 0-44629

Nickel alloys continued

Permalloy films, orthogonal susceptibility 0-72249

Permalloy films, random anisoropy in crystallites 0-65938 Permalloy powders, insulating film, fluorination method, elec. and mag. props. 0-53430

Permalloy recording head, write field distrib., Fourier analysis 0-44593 permalloy thin film electrodeposition techniques, comp. gradient problem 0-72247

permalloy thin films, spin wave resonance 0-40993

permalloy-Mo, linear magnetostriction, magnetization, permeability 0-51210

Permalloy-Mo, mag. props., sulphur impurity depend. 0-44580

Permalloys, magnetization meas. 0-65909

Permally and EuO films in contact, coupling effects, role of exchange interactions 0-44635

Permany and 200 mins in contact, coupling effects, fole of exchange interactions 0–44635

Permally film, anisotropic, low temp. magnetic reversal. Lorentz microscopy, 4-300K 0–44641

platelet growth, single crystal, conditions 0–55784
resistivity, electrical, at low temperatures 0–75540
resistivity, anisotropy, spontaneous, mechanism 0–62307
rotational, in Ticonal alloy 0–72238
sensitivity coefficients, relative, mass spectrometric studies 0–72565
spin-disorder scatt, rel. to elec. resistivity 0–78879
superalloy, high strength, creep props., high vacuum effect 0–71699
superalloy sheet, creep rupture, 1000 and 1200°F, edge-notch sensitivity, thickness, acuity 0–40372
tensile and fatigue props. at cryogenic temps. in Alloy 718 0–40354
thermoelectric power, absolute, temp. variation 0–47864
Ticonal, thermomagnetic treatment, Mossbauer obs. 0–58960
Ticonal 2000, high coercivity, features of thermal magnetic treatment 0–71764
Ticonal alloys, decomposition, final stages analysis 0–50823
Ticonal alloys, uniaxial anisotropy energy density and local field between

Ticonal alloys, decomposition, final stages analysis 0–50823 Ticonal alloys, uniaxial anisotropy energy density and local field between particles 0–72237 Fe-Ni, effect of rolling on secondary recrystall. 0–62100 Al-Ni-Co-Fe, containing 5 to 10% Ti, columnar castings 0–71762 Al-Ni-Co, microstructure details 0–71766 Al-Ni-Co sintered, improved preparation method 0–71760 Al-Ni-Co high coercive, improvements 0–72225 Al-(1 wt.%) Ni, neutron irrad, damage 0–58798 β-AlNi intermetallic, cold-worked, planar faults 0–65329 Au-Ni-Cr resistor film, vacuum deposited, low-resistance, high stability and low temperature coefficient 0–56178 Au-Ni-Cr recipitation and orientation relations of phases Au-40-4 at %Ni, recipitation and orientation relations of phases Au-40.4 at %Ni, precipitation and orientation relations of phases 0-62103

Au-40.4 at %Ni, precipitation and orientation relations of phases 0–62103
Au-Ni alloy, electrodeposit, heat treated, microstructural and phase changes, X-ray exam. 0–65485
Au-Ni alloys, C contaminated, precipitation phenomena 0–62104
Au-Ni films contaminated with carbon, precip. phenomena 0–56039
Au-Ni films contaminated with carbon, precip. phenomena 0–56039
Au-Ni films contaminated with carbon, precip. phenomena 0–53640
Bi trace determ., emission spectrographic carrier-distillation method 0–56729
CeNi;-CeCu₂, pseudo-binary system, mag. susceptibility. Kondo effect, phase struct. 0–78462
Co-(20wt.%)Ni (20wt.%)Cr, struct. change on mech. deform. 0–78695
Co-Ni, hyperfine field at 119Sn nuclei, anomalous temp. depend. 0–44734
Co-Ni films, with coercive force enhanced values, prod. 0–65936
Co-Ni films, with coercive force enhanced values, prod. 0–65936
Co-Ni films, mith VI B metals, high coercive force 0–54026
Co-Ni martensites, stacking disorder 0–53544
Co-V-Cr-Mn-Ni, mag, moment distrib., neutron diffr. 0–44552
(20wt.%)Cr-(25wt.%)Ni-(1wt.%)Nb austenitic steel. NbC precip., stacking fault contrib. 0–58955
Cr-Ni-B system composition, effects on resistance to scoring 0–58938
Cu-Al-Ni, martensitic transform., temp. and time depend. of internal friction 0–71670
Cu-Al-Ni, memory effect rel. to thermoelastic martensitic transformation 0–59017
Cu-Ni-Fe, dil., low temp. elec. resistivity 0–50983

Cu-Ni-Fe, dil., low temp. elec. resistivity 0-50983 Cu-Ni-Fe, Mossbauer doublet struct. and clustering cold work effect 0-51280

0–51280
Cu-Ni-Fe, Mossbauer spectra, interpretation, constitution depend.
0–51279
Cu-Ni-Mn, development of order 0–56073
Cu-Ni Zn, deformed, stacking faults 0–50601
Cu-Ni, ⁶³Cu nucl. spin-lattice relax. near critical conc. 0–56469
Cu-Ni, clustering effects on photoemission data, and rigid-band model 0–40905

0-40905
Cu-Ni, clustering effects on opt, and photoemission data, and rigid band model 0-40908
Cu-Ni, diffusion of Ni, volume and grain boundary diffusion 0-47290
Cu-Ni, dislocation motion and multiplication in pre-yield micro-plastic deform. 0-58812
Cu-Ni, Hall effect, resistivity, mag. susceptibility 0-40721
Cu-Ni, hyperfine interactions at ⁵⁷Fe 0-6907
Cu-Ni, photoemission and optical reflectivity obs. of electronic struct. 0-79277

Cu-Ni, photoemission and optical reflectivity obs. of electronic struct. 0-79278

0-19218
Cu-Ni, thermal expansion from lattice parameter-temp. curves 0-43919
Cu-Ni 20/80, thermal evolution of ion-bombarded Ar, obs. 0-56697
Cu-Ni 50/50, thermal evolution of ion bombarded Ar, obs. 0-56697
Cu-Ni electron energy-loss spectra 0-78808
Cu-Ni films, ohmic behaviour in ultra-vacuum during heat treatment

Cu-\(\frac{1}{2}\) and consider the constraint of the constraint o

Cu₃-NiMn system, ageing, phase transformations, 300-500°C, X-ray diffr. 0-59018

0–59018
CuNi, electronic struct. 0–75498
Cu_{0.6}Ni_{0.4}, specific heat, variation of anomalous term. 0–68612
CuNiCo dil., microstruct, sideband phenomena obs. 0–68302
(CuO)₃(NiO)_{1-x} solid solns., ordering 0–50526
Fe-Cr-Ni, shock-induced phase-transition press, rel, to comp. 0–47366
(63wt.%)Fe-(32wt.%)Ni-(5wt.%)Co, super-Invar, Young's modulus anisotropy, thermal expansion, _30-600°C 0–75220
Fe (37wt.%)Ni-(8wt.%)Cr, elinvar-type, mag. props., heat treatment effects 0–47943
Ea Ni Al-Co-Ti-effect of Co-S and Tao on liquidus colidus cares. 0, 71775

Fe-Ni-Al-Co-Ti, effect of Co, S and Te on liquidus-solidus gaps 0-71775

Nickel alloys continued

Fe-Ni-Al, influence of elastic stress on precipitation and magnetic properties 0-71776

ttes 0-71776 Fe-Ni-C. diamond crystallization at high pressure 0-47143 Fe-Ni-C, martensite to austenite, shock induced reversal, temp. depend. Fe-Ni-C, r 0-65489

Fe-Ni-C, paramagnetic f.c.c. austenite, plastic deformation-transformation 0-55972

0–55972
Fe-Ni-Co-Mo, preprecip. and reversion 0–59023
Fe-Ni-Co, coercive force temp. depend. rel. to reverse phase transformation 0–44587
Fe-Ni-Cr.-Nb elastic relax. phenomena 0–50650
Fe-Ni-Cr, austenitic, free energy, two y phases, mag. props. 0–43832
Fe-Ni-Cr, leinvar-type, mag. props., heat treatment effects 0–47944
y-Fe-Ni-Cr, long-range antiferromag. order 0–51235
Fe-Ni-Mo, ageing of martensite, 450-500°C, kinetics and mechanism
0–78675

0—786/5
Fe-Ni-Mo(Ti)(-Co) alloys with ageing martensite, recovery 0—50770
Fe-Ni-P film, chemical deposition mag. props., isotropy 0—51217
Fe-Ni-P film, coercive force, induced anisotropy 0—54029
Fe-Ni-Ti-Mo, austenite obs. 0—61865
Fe-Ni, coercivity, plastic strain effect, under applied tensile stress 0—65925

Fe-Ni, coercivity, plastic strain effect, under applied tensile stress 0–65925
Fe-Ni, elastic relax. phenomena 0–50650
Fe-Ni, irreversible, low thermal expansion 0–50896
Fe-Ni, imagnon heat conduction and magnon-electron scattering 0–78792
Fe-Ni, martensite transform. crystallography 0–62131
Fe-Ni, neutron scattering at small angles by spin waves, ang. distrib., direct obs. 0–44535
Fe-Ni, Permalloy range, elec. resist., elastic tensile stress, Mag. field depend. 0–68765
Fe-Ni, phase transformations during low temp. quenching 0–56059
Fe-Ni, polycryst. wires, effect of tensile stress and work hardening on coercivity 0–79170
Fe-Ni, recrystallization. effect of deformation texture 0–75301
Fe-Ni directional ordering rel. to coercivity and loop asymmetry 0–47920
Fe-Ni directional ordering rel. to coercivity and loop asymmetry 0–47920
Fe-Ni film, scattering field above surface 0–75945
Fe-Ni invar, anomalous volume magnetostriction. effect of third component 0–75938
Fe-Ni invar, Curie pt., alloying elements effect 0–65915
Fe Ni particles, supermagnetism, Mossbauer spectroscopy investig. 0–41026
FeNi, order-disorder transformations, Mossbauer spectra 0–78698

0-41026 FeNi, order-disorder transformations, Mossbauer spectra 0-78698 GdNi-GdCu₂, pseudo-binary system, mag. susceptibility, Kondo effect, phase struct. 0-78462 InSb-NiSb eutectic, magneto-sensitive resistance, phase parameters

InSt-NiSb eutectic, magneto-sensitive resistance, phase parameters 0 51037
Mn-Ni, mag. susceptibility at near-equiatomic comp. 0—59339
y-Mn-Ni antiferromag, props., alloying elements influence 0—41060
Ni-Al-Cr-Fe, ZhS6-K type, interdiffusion, local spectral analysis study 0—75208

0-7208
Ni-Al-Nb-Mo solid soln., y and y' phases, investig. 0-47459
Ni-Al-Nb, Ni-rich, phase equilibria, 1200 and 750°C 0-53672
Ni-Al-W alloy WAZ-20, high strength 2000° to 2200°F 0-50787
Ni-Al, ageing precipitate number density, 800°C, dark field electron microscopy 0-53635

Ni-Al, substruct, changes during high-temp, creep, electron microscopy 0–53635
Ni-Al, steady state creep rate, 800°C, u.s. treatment effect 0–50704
Ni-Al, substruct, changes during high-temp, creep, electron microscope and metallographic obs. 0–78488
Ni-Al, work hardening, effect of structural changes 0–71744
Ni-Al and nimonic, critical shear stress rel. to hardening phase particles 0–50747

0–50747
Ni-(6.3 at.%)Al, local order, effect on props. 0–55857
Ni-(11.4wt.%)Al, slip distrib., coherent precipitates75258 0–75258
Ni-Au, internal friction changes during soln. of cryst. phases 0–65369
Ni-Au, precip. initial stages obs. 0–56063
Ni-C, serrated stress-strain curves, temp. and comp. depend. 0–40334
Ni-C solid solution, plastic deformation, internal friction, dislocation damping. 0.4320

Ni-C solid solution, plastic deformation in g 0-40309
Ni-Co-Al-Ti-Cu-Fe permanent magnets, structure 0-71778
Ni-Co, film, substrate constraint contrib. to mag. anisotropy 0-44632
Ni-Co adiabatic elastic stiffness, comp. depend., Debye temp. 0-78601
Ni-Co alloys, electrodeposited stratification of magnetic susceptibility of thin films 0-62540

Ni-Co alloys, electrodeposited stratification of magnetic susceptibility of thin films 0–62540 Ni-Co coatings, influence of current density on composition and coercive force 0–66197 Ni-Co HPG-4, high yield strength, applications to pressure-vessel field

force 0-66197
Ni-Co HPG-4, high yield strength, applications to pressure-vessel field 0-50774
Ni-Co with hexagonal and cubic lattices, Nernst-Ettinghausen effect determ. 0-79199
Ni-Cr-(1 wt.%)ThO:, oxidation, 1200°C 0-56703
Ni-(20wt.%)Cr-(7.5wt.%) Al, slip distrib., coherent precipitates 0-75258
Ni-Cr-Al, elec. resist., plastic deformation and temp, depend., K-state, X-ray exam. 0-47650
Ni-Cr-Al, oxidation behaviour, high temp., Y additives effect 0-51427
SNi-Cr-Mo-V steel, toughness by Charpy V-notch and dynamic tear tests 0-40373
Ni-Cr-Nb, precip.-hardened, plastic deform. mechanisms 0-71689
Ni-Cr-Nb phase solid state phase transformations during long annealing at 700°C 0-56062
Ni-Cr, nichrome film, high temp. ageing 0-71957
Ni-Cr, nichrome film, high temp. ageing 0-71957
Ni-Cr, off-eutectic, Czochralski growth and stability 0-75025
Ni-Cr, photolytic etching, patent 0-39998
Ni-Cr, resistivities and Seebeck coeff. in 50-1000°C range, meas. 0-44037
Ni-Cr, stress-rupture strength, and high temp. props., improvement by adding Mg, patent 0-56021
Ni-Cr, tensile mech. props. after quenching and heat treatment, 25°C 0-40355
Ni-Cr, work hardening, effect of structural changes 0-71744
Ni-Cr base, time-to-rupture, low-temp. annealing effect 0-40371
Ni-Cr crack formation and prevention in heat affected joint zones, during ageing, reasons 0-47414

Ni-Cr crack formation and prevention in heat affected joint zones, during ageing, reasons 0-47414
Ni-Cr doped with Si, contact resitance meas., method 0-51086
Ni-Cr eutectic, directionally solidified, structure 0-50469

Nickel alloys continued

Ni-Cr film, transient oxidation 0-72538

Ni-Cr(Mo, W), thermomag, effect temp, depend. 0–62534 Ni-Cu-C solid solns., equil, temp, depend., vapour transport study 0–71810

0-/1810
Ni-Cu, ferromag., spontaneous Hall coeff. temp. depend., obs. 0-44062
Ni-Cu, giant moment system, elec. resist., temp. depend., 1.5-300 K
0-44061

0—44061 Ni-Cu, giant paramagnetic moments, Ni≤44 at.% 0—44498 Ni-Cu, local mag. moments form. criteria 0—72216 Ni-Cu, low temp. specific heat, magnetisation, temp. and comp. depend.

Ni-Cu, low temp. specific heat, magnetisation, temp. and comp. depend. 0-44497
Ni-Cu, mag. neutron scatt., critical phenomena 0-69026
Ni-Cu, magnetomech. damping, anisotropy effects 0-65928
Ni-Cu, paramag, density-of-states in coherent- pot. approx. 0-59147
Ni-Cu, paramag, giant-moment, elec. resistivity and magnetoresistance 0-50989

0-30989
Ni-Cu, paramagnetic, model, susceptibility 0-62495
Ni-Cu, resistivities and Seebeck coeff. in 50-1000°C range, meas.
0-44037

0-44037

Ni-Cu, rolling texture and stacking fault energy 0-53511

Ni-Cu, Young's modulus and thermal expansion 0-65554

Ni-Cu alloys, electrical resistivity anomaly near ferromagnetic critical composition 0-62308

Ni-Cu ferrite, magnetic anisotropy and anisotropy contrib. of Ni²⁺ ions in tetrahedral sublattice 0-54036

Ni-Fe:Mn film, strain sensitivity and mag. props. 0-44633

Ni-Fe-Co, mag., for space-craft or station components, patent 0-56076

y-Ni-Fe-Co, ordering, neutron diffr. exam. 0-47196

Ni-Fe-Cr, radiation hardening, proof stress analysis, mechanism 0-47447

Ni-Fe-Cu-Mo, magnetic, high permeability, sintering process, resist, variation 0-62089

Ni-Fe-Ci. Tadiation hardeling, proof stress analysis, mechanism 0-4/44/Ni-Fe-Ci. Mo, magnetic, high permeability, sintering process, resist, variation 0-62089
Ni-Fe Mo, thin film, anisotropic field var., with thickness, temp., and Mo conc. 0-79185
Ni-Fe-Mo films, magnetiz., low temp. 0-65944
Ni-Fe, cold rolled, magnetiz. reversal and h.f.s. 0-65918
Ni-Fe, deoxidizing-elements influence on deform, and mag. props. 0-79176
Ni-Fe, electrodeposited, microstruct. 0-61899
Ni-Fe, epitaxial film, oriented growth by vacuum sublimation 0-58629
Ni-Fe, epitaxial film, oriented growth by vacuum sublimation 0-44632
Ni-Fe, hyperfine fields 0-51253
49%Ni-Fe, initial permeability, deoxidizer effects 0-44592
Ni-Fe, initial permeability, deoxidizer effects 0-44592
Ni-Fe, recrystallization activation energy, hardness determ. 0-47433
Ni-Fe, Young's modulus, shear modulus, elastic parameter and coefficient

Ni-Fe, Young's modulus, shear modulus, elastic parameter and coefficient 0-6336 50%Ni-Fe alloy, Rayleigh hysteresis loop, domain wall displacement 0-44564

0-44504 Ni-Fe base coating by vapour deposition, patent 0-44643 Ni-Fe evaporation and deposition, violation of Knudsen's cosine law 0-55674 Ni-Fe film, 1200-2000 Å thick, domain wall strucutre and magnetiz. creep

Ni-Fe film, ferromag, domain wall width, high voltage Lorentz microscopy 0 - 70150

0-79159

Ni-Fe film, flux reversal, Kerr photography 0-44631

Ni-Fe film, induced anisotropy, annealing kinetics, role of atom self-diffusion grain surface regions 0-44637

Ni-Fe film, normal and unconstrained, magnetization-induced uniaxial anisotropy, comp. depend. 0-44634

Ni-Fe film, ripple wavelength, Lorentz microscopy 0-44640

Ni-Fe film, standing spinwave modes and source of volume inhomogeneities 0-47958

Ni-Fe film, double-layer, magnetostriction interaction model 0-65945

ties 0–47958
Ni-Fe films, double-layer, magnetostriction interaction model 0–65945
Ni-Fe films, electrodeposited, uniaxial mag. anisotropy, average stress effect 0–65941

effect 0-65941
Ni-Fe films, h.p. evap.., struct. changes 0-61671
Ni-Fe films, h.p. evap.., struct. changes 0-61671
Ni-Fe strip. mag. domain obs. 0-65903
Ni-Fe tapes, domain patterns, Kerr magneto- optic effect 0-44777
Ni-Fe tapes grain oriented domains and domain wall motion 0-47919
Ni-Ge-Sb system, Mossbauer effect of ¹²¹Sb 0-59380
Ni-Ge-Sb system, Mossbauer effect of ¹²¹Sb 0-59380
Ni-Ge. stacking fault formation, comp. depend. 0-50602
Ni-Ge single crystal, rotatory hysteresis losses, depend. on mag. field magnitude and Ge cone. depend. 0-51209
Ni-Ir system, lattice parameter, electronic sp.ht., mag. susceptibility, Debye temp. 0-40576
Ni-Ma-Mo Nimalloy permesbility comp. depend. 0-75935

temp. 0-40576

Ni-Mn-Mo, Nimalloy, permeability, comp. depend. 0-75935

Ni-Mn, 79 NM, texture effect on mag. props. 0-62529

Ni-Mn, effect of W and Cr additions on permeability 0-59329

Ni-Mn solid soln., mag. struct., Mossbauer obs. 0-41166

Ni-(23at.%)Mo, Ni atom electrotransport 0-47649

Ni-Mo, electrotransport of Mo, 1100-1300°C donor-acceptor interaction 0-50987

U-3087 Ni-Mo, surface layer, mag. props., adsorbed anions depend. 0-59324 Ni-(20at.%)Mo alloy, electrotransport, 950-1300°C, donor acceptor interactions 0-62306 Ni-Mo(W), compressive strength, temp. depend., tensile deformation 0-47377

Ni-Mo(W), compressive strength, temp, depends, tensite deformation 0-4737 Ni-Nb-W phase equilibrium study, 1400-2100°C 0-78334 Ni-O, adherence to alumina 0-50812 Ni-P, 73.8 to 81.4 at % Ni, non-crystalline, structure 0-78491 Ni-P, amorphous film, flash evaporation, crystallization, electron microscopy 0-65085 Ni-P, noncrystalline, structure 0-58531 Ni-P, thin films, variations of props, with temp. 0-44480 Ni-P film, electrodeposited, perpendicular anisotropy 0-62538 Ni-P films, amorphous, prep. and crystn. 0-74917 Ni-P films, elec. cond. and mag. susceptibility 0-40726 Ni-P films, optical props. rel. to struct. 0-51262 Ni-P films, photoelec, emission rel. to struct. 0-51162 Ni-Pd, ferromag. Mossbauer effect, supermag. Fe clusters 0-51284 Ni-Pd, impurity clustering and matrix polarization 0-44594 Ni-Pd, mag. moment distrib. 0-54011 Ni-Pt-P, amorphous, X-ray interference function, elec. resistivity, thermoelec, power 0-53781 Ni-Re, dilute, lattice thermal conductivity, temp, above 400°K 0-68654

Nickel alloys continued

Ni Rh. n.ma., Enght shift line width, spin lattice relocation, 1.4 E 0.45007

Ni 5b system non existence of Sh₃5b = 0 -65507 Ni 5r foss of coherency of p² purifies = 0 -71777 In 5r microstructure, corrosion resist, much props, comp depend

Ni hi hi system. Mossimuer effect of ¹⁷¹th and ¹⁷⁶th . 6 - 59 890.

no in an asystem, wicestoning eigent of "an and "an 0, 59380.

No for contract treat plastic flow obs. 0, 50708.

No for relievation spectrum composite pend. 0, 53576.

No have superally provider, how working ref. to production of high performance material. 0, 65455.

Of the content of the contract of

Lirad ParNb, oxidiation process for diffusion mechanism = 0 -41437 NrAL Lifes, interactions in ³Pe may moments obs = 0 - 17329 γ NrAL plastically deformed, stacking limit origin = 0 -71630 ρ' NrAL 0 -19409 (in Co. Jurromag), n.m.r. spin eigho speciae, crystallographic ordering = 0 - 11236

Exim. active 6 or 38,50m (Ind) effect during ordering 0 65632. Significant effects with the first during ordering 0 65632. No.(Mn Me), terminy. Me Ec. Co. Co. ordering kinetics, neutron difficults 0 /1809. Strong with third 3d transition element or ordering kinetics 0 42461. Significant element or ordering kinetics 0 42461. Significant element or ordering kinetics 0 42461.

Nr.Mn, lerromag, undiried anisotropy, time depend after switching off held 0 7946? t.Mn, mund paraprocess susceptibility behaviour near Carle temp

NuMu, magnetic transitions near Curle pt., transition of second kind 0 75932

On-Min, magnetization and electrosist temp depend, 4.2, 345 K, 0, 68999. Nr.Min, tensile testing, discontinuous yielding, 0, 40,308.

M.M., magnetization into etc. Tassis (emp. nepent., 27, 243.8, 0, 1622).
Mr.M., tensile testing, discontinuous yielding () 46.008.
Nr.M. alloys, domain and magnetization in ordered state. 0, 72245.
Nr.M. alloys, field induced unisotropy at low temperature. 0, 72249.
Nr.M. flin, saturation magnetization, rotational hysteresis losses, annualing depend. 0, 47959.
Nr.M.51, neurest neighbour environment of Sb, anomalous dispersion obs. 0, 65266.

tons, 9 m250 NiAMo, structural changes during isothermal annealing after quenching 0 65269 NiAMo, order induced strengthening 0 47379 NiPd, hyperfine field at Ni site, cone depend, ⁵¹Ni Mossbauer obs

MSE. CoSt, solid solution, electronic struct., X-ray K/β, spectral characts and imag, props obs. 0, 79340.

NISE LeSE, solid solution, electronic struct., X-ray K/β, spectral characts, and imag, props obs. 0, 79340.

NESE, brittle to divide transition, impurity adsorption at grain boundaries 0, 68478.

trace determs, emission spectrographic carrier distillation method 56/29

Pd Ni, dilute, thermal and electresistivities, low temp. Lorenz mumbers,

0 44065 Pd Nt, 4.7 at.⁹5 Nt max., glant moments near critical composition 0 44065
Pd Nt, 4.7 at. 6 Nt max., glant moments bear 0 41009
Pd Nt, compressibility, linear dependence on composition 0 78648
Pd Nt, compressibility, linear dependence on composition 0 78648
Pd Nt, dilute alloy, mag moment destait, neutron diffr. 0 44574
Pd Nt, electron electron scattering effects in low temp. Lorenz numbers, theory addessy 0 65 %
The short image order 0 58745

theory indexp. 0 6; 0 58745
Pd Nr, short range order 0 58745
Pd Nr, shi, sechange endanced, sp. ht. and electresistivity 0 62713
Pt Nr, dil, sechange endanced, sp. ht. and electresistivity 0 62713
Pt Nr, ferromagnetic, resist, comp. and temp. depend., 1.4.4.2 K

determ, emission spectrographic carrier distillation method

0 567/29

The Ni, the NiCi, shock leading thermal recovery () 75307

It is market the front form down as from at 0 79036

It is shape memory effect rel. to witches production () 71856

W. Ni, effect of alloying Ni addition on shitering and self-diffusion () 68544

Zi Fe(Co)(Ni) binary equationic, constitutive props. 0 47423.

Nickel compounds

skel compounds

we also Nickel alloys
boracite, cryst field theory and optical absorpt. 0 66041
complex with metal germanium bond, crystal structure 0 53513
dendrites, electrocrystallization from aqueous solution 0 76270
ferrite, magnetic annualing kinetics, substituent ions effects 0 75951
ferrite application to resistance thermometers 0 72264
ferrite allin, single cryst, mag, props. by ferromag, reson, method

0 2567; Gerromag, resons, obs. 0 41401; lerrites, prophology and surface features, rel. to growth 0 64696. Herrites, morphology and surface features, rel. to growth 0 64696, phosphates, p.m.r. data 0 62718; porphyrin complex, humasec. 0 79434. Au NI solid solutions, thermodynamic interpretation, 1048-12005. 0 56039. BANIS, cryst stone, obe, and man, more, 0 78434.

HaNIS, cryst, struct., else, and mag, props. 0, 78454 Co-B Ni H, ferromag, system, specific heat, low temp, anomalies 0 43901

Niekel compounds continued

Cr.18) steels, austentic, corresion and passivation in H.5O₃, effect of vacuum melting 0, 76268.

Ca.Mr. Pe.Os. (0.1<2<1), orientation superstruct, due to Ca/+ () 44662

(Fe) Mr.). Baystem, magnetocryst, amsotropy 0 54012

In the High system, polarizing props, and optical consts. 0 69074 FeO biO solid solins, struct transform, 0 62433

MnO FitO mixtures, glectrical properties and stability, influence of long period surtering () 78863

1410 (1), and derivatives substituted by PF-, P(McO), and P(Mc), force (motanto () 58191

MrCu Co ferrite, magnetocryst, amsotropy, mag. annealing induced 0-72235

Bit the single cryst, rotational hysteresis losses, temp, and field depend.

10 Mo-phase diagrams 1200-2100°C | 0 | 71408

1a Mo phase diagrams 1700-7109%
 1b Fib Mo, sorbermal section in 1400°C
 7 1408
 1b Nh Phi phase diagrams 1700-7109°C
 7 1408
 1b S Se syst, growth, struct determ.
 6 65265
 1b Zu bernte, nonlinear magnetization theory, domain wall displacement

Ni, complex, histolimethyldithiophosphinato). Nickel(H), crystal structure, X-ray-ohs, 0. 40005.
Ni (CO), photocomization study. 0. 64400.
Ni (H) complex, histisoquinoline 1 carboxaldehyde.
Thiosemi arbazanitopia kel(I) monohydrate, crys), struct. 0. 40094.
Ni (H) complex, a lamidino 2 thiourea, K. absorption spectrum, correlation with proposed cleatronic structure. 0. 61127.
Ni complex, [1-1,N] (NitH-dina)], cryst, and mol. struct. 0. 53512.
Ni complex, insymmetric. 1,2 dinethyl 1,2 dicarbolide racemic, crystal struct, and, config. 0. 47198.
Ni complex, bis (4) 1,7 dicarbolitylinekelate (HI) diamon, crystal and molecular structure. 0. 44640.
Ni complex, bis(4) 4,7 dicarbolitylinekelate (HI) diamon, crystal structure. 0. 783196.
Ni complex, bis(4) third isocyanide) (tetracyanocthylenc)nickel(O), structure. 0. 783196.
Ni complex, eyclopeutadienyl nickel nitrosyl rotational transitions.

Ni complex, cyclopentadienyl nickel nitrosyl rotational transitions () 778/1

Ni complex, eyclopeniadienyl Ni mitrosyl, bond lengths and angles from microwave spectra 0 49883.
Ni complex, dithometylacetone NaH), electronic spectra, MO calc.

Ni complex, ethylenehisbiguinide - Nifff) chloride monohydrate, cryst, and mol struct. 0: 65267.

Ni complex, ethylenehiminetetrancetate Nifff), struct, in aq. soln, from ¹¹C and ¹²O n.in. 0: 78309.

Ni complex, hexamine linkides, critical c.p.r. linewidth transitions 0: 16727.

Ni complex, n alkyl Ni(II) animotroponiminates, ¹⁴C n.m.r. 0 77 Ni complex, N.N ditp tolylaminotroponiminate Ni(II), ¹⁵C 0 77819

O TEP19
Ni complex, Ni(CO)_{4-n} (PA₂)_{ni} force constants, symmetry coords, and G and I matrices (9–49880)
Ni complex, Ni(CO)_{4-n} (PA₁)_{ni} (A=F, OCH₂,CH₁), fundamental vibration freqs. (9–49881)

Nr complex, Nr(C)_{4 n}(PA₄)_n (A=F, OCH₂, CH₃), force constant cale, () 4982.

0.49887
Ni complex, Ni(PE₃)₆ vibr, spectra 0.55309
Ni complex, Ni(PF₃)₆ vibr, spectra 0.55309
Ni complex, Ni(POR)_{1.5}F₃I₆ n.m.r. of ¹⁴P and ¹⁰F, influence of substitution 0.46500
Ni complex, nickel actylacetonate with organic ligands, isotropic contact shifts of ¹⁴C by means of ¹⁴C beteronaclear resonance 0.58190
Ni complex, o phenylenebistdimethylarsine), e.s.r. 0.66434
Ni complex, pentacymonickelate ion, structure Raman spectrum, CN stretching frequencies 0.46504
Ni complexes, phosphines, metal isotope effect on metal figural vibrations 0.77763

Ni ferrite, single crystal, preparation, structure, composition of films Ni II complexes with // ketome thiocarbonamides synthesis 0 55307

0.537/28
Ni H complexes with β ketonic thiocarbonamides synthesis 0.55307
Ni iII thiocyannic complexes, i.r., spectra 0. 49896
S' NiAI, electronic density of states and band structure, rel. to optical properties 0. 65597
EthAl theory of very weak ferromagnetism 0. 75944
NiAI, O., polycryst, a.m.r. spectra of ¹⁷AI 0. 41364
NiASS, skeletti crystallization ii As S glass 0. 75041
NiASS, skeletti crystallization ii As S glass 0. 75041
NiBO₁G (B)(B) crystal, twinning, terroelectric domains, growth anomalies 0. 75099
Patt H C 000 HI O Min* c-pi ob. 0. 41435
NiC NiC NiC ii aqueous solia, mag. circular dichroism and u.v. spectra assignments 0. 71358
NiC c. mussion spectrum 0. 64442
NiC c. e.p.f. sprectrum temp, effects, 49.460 K 0. 48150
NiC c. Sa (Mg C Jg K), terrigonal complex, polarized electronic absorption spectrum 0. 62669
NiC c. Min asker (0. reliax of terromag, precession by excitation of spin waves 0. 44071
NiC c. Min asker (0. reliax of terromag, precession by excitation of spin waves 0. 44071
NiC c. Min asker (0. reliax of terromag precession by excitation of spin waves 0. 44071
NiC c. Min asker (0. reliax of terromag precession by excitation of spin waves 0. 44071
NiC c. Min and complex (0. 79208)
NiC c. Min and complex (0. 10015)

NiCr.S₄(Se₂), magnetic susceptibility temp, depend,, thermomagnetic waves 0 44691
NiCr. Magnons, dispersion relations and selection rules 0-79208
NiL₂ Angiones, dispersion relations and selection rules 0-79208
NiL₂ Angiones, dispersion relations and selection rules 0-79208
NiL₂ Consistency of the consistent fleld study of cluster model 0-70935
NiL₂ Co₁ thermoelec, power and resistivity 0-79198
NiL₂ Co₁ thermoelec, power and resistivity 0-56372
NiL₂ Co₂ them and mag, struct. 0-62546
NiL₂ Co₃, chem, and mag, struct. 0-62546
NiL₂ Co₃, the description of the description of the Co₃ NiL₂ Co₄ the description of the Co₃ NiL₂ Co₄ the description of the Co₃ the Co₄ the description of the Co₃ the Co₄ the description of the Co₄ the Co₄

Null) complexes, of tri-2 pyridylamine, electronic spectra | 0 | 55308

Nickel compounds continued

ckel compounds continued

Ni(H) complexes, thiourea coordinated, paramag, props, ref. to struct, transforms, 90 300°K 0 40949

Ni(H) complex, NiBr (gr/P)-, ligand field spectra 0=47981

Ni(H) complex, 3,3 commo bis lundecarbydro 1,2 dicarba 3 nickela close dodecaboranel, crystal structure, x ray determ. 0 47197

NiMrSD, Mossbauer effect, mag, hyperfine interaction 0 72337

NiMrSD, perfittice, triple dislocation 0 43676

NiNrSD, crystal structure and mag, susceptibility 0 50534

NiO12H, high surface area, mixed saft freeze drying prep. 0 62116

NiO GoO solid solution single crystal with gradient in luttice spacing, production 0 68261

NiO MgO, mixed crystal, mutual diffusion 0 40201

NiO, and diffusion and semiconductivity 0 61996

NiO, cation self diffusion and semiconductivity 0 61996

NiO, cation self diffusion and semiconductivity 0 61996

NiO, defect cone, TGA obs. 0 50579

NiO, critical antiferromag, film, domain struct. 0 69048

NiO, lattice distortion, stoichiometry, paramag, to antiferromag. 0 75963

NiO, mag, semiconductor, energy spectra, cale. 0 44213

NiO, pare Li doped semiconducting, i.r. absorpt. 0 62670

NiO, reflectance spectra, optical consts. 0 79276

NiO, structure and properties, oxygen adsorption 0 68243

NiO (100) face, superstruct, efection diffr. obs. 0 50355

NiO baked pellets and powders, positron annihilation 0 40696

NiO Crystallites with various Cr concentrations, formation and size 0 65268

NiO lim, precipitates with defect struct. 0 71482

NiO film, precipitates with defect struct. 0 71482 NiO Neel transition influence on reactive interface form, during reduction

NiO Neel transition influence on reactive interface form, during reduction 0 62807. MIO & Pe-O₁, polycrystalline, 400 1100°, using new contact method 0 47689. Ni,P Fe-P, lattice parameters, comp. depend. 0 43641. Ni,P, glassy metal, elastic constants 0 78597. Ni(PCl₂), vibrational spectra of solid and in solution force constants, symmetry confirmation 0 64443. NiS, hexagonal, energy bands cale. 0 53761. NiS, mag. transitions, press, effects, 5 kbar anomaly 0 62491. NiS, ordered moment obs., neutron diffr, exam. 0 59309. Ni_{1,2}S, metal semicond, transition, rel. to mag. transition 0 72031. Ni_{1,2}S, thermoelee, power, temp. depend., 83 273 K, semiconductor metal transition 0 79065. MiSeCl₂ and ternary compounds, phase transitions, X ray diffr, thermal

NiSe(Te) and ternary compounds, phase transitions, X ray diffr., thermal analysis 0, 40491

analysis 0 40491
NisTa superlattice, triple dislocations 0 43676
NiTa O₈, magnetic props., susceptibility meas., 14, 16, and 26K 0 72278
NiZn ferrites, complex AE effect 0 79177
NiZn ferrites, cryogenically crushed, mag. props. 0 59336
NiZn ferrites, initial permeability and Curic pt., as function of cation distrib. 0 62548
NiZn ferrites, mag. eqn. of state, obs. 0 44664
NiZn ferrites, magnetooptical and magnetic study of (P,Ni) bonds 0 466499

0. 404.99
MIGOH), cryst, growth from pure water 0. 74984
TiNi, phase transform, kinetics, mechanism 0. 47482
U.N.S. syst., at 800°C, new phases 0. 63852
ZNK.SGOJ.6H.O.NiK.(SOQ).6H.O., crystn. from soln., kinetics, impurities distrib, growth vel. depend. 0. 40020

Night sky see Airglow Nightglow see Airglow

Nilsson's model see Nucleus/models

Niobium

see also Superconducting materials/niohium
see also Superconducting materials/niohium
absorption of Zr 0- 43574
b.c.c., microflow meas, deformation mechanism 0- 75257
band struct, and Fermi surface 0- 44000
collector, in thermionic convertor with single crystal <110 > W emitter,
performance investigation 0- 76989
compatibility with Na containing 0- 0- 45055
crystal, single, high purity flux flow voltages, nonlinear, Kim Anderson
theory modification 0- 50966
Debye temp, and thermal expansion coeff. 0- 78784
defect clusters and plastic deformations, due to neutron irradiation
 0- 50690
deformation, grain size effects 0- 50688

0-50690 determation, grain size effects 0-50688 diffusion of ⁴⁴Ti in single crystal, 994-1492°C 0-40200 diffusion of ¹⁴Ti in single crystal, 994-1492°C 0-40200 diffusion of H. quasieliustic neutron scatt. 0-78582 dislocation damping, freq. depend., 293 GHz, 80K 0-68363 elastic diffusional relixation of H and D 0-68428 electron emission, secondary, ang. distrib. 0-72159 Fermi surface topology 0-43999 film, oxidation, struct., electron diffr. 0-50369 flow stress, temp. depend., neutron irrad. effect 0-78627 Frenkel pair defect annealing cone, depend, in electron irrad, crystals 0-47235 flow stress, temp. depend., neutron irrad, effect 0-78627 Frenkel pair defect annealing cone, depend, in electron irrad, crystals 0-47235 flow stress, temp. depend.

0. 47235
fusion reactor containment vessel, n damage, 14 MeV 0. 70729
hardness, polycryst, grain size effects 0. 71730
mechanical behaviour and twinning, polycrystalline 0. 40353
neutron damage energy depend, 0.1.15 MeV 0. 71882
oxidation, ellipsometry 0. 48197
photoelectric work function 0. 72839
plasma anodisation, ionic current in oxide 0. 72541
plastic flow, strain rate and temp, effect 0. 40307
sputtering by D* and He*, obs. rel. to fusion reactor wall lifetime
0. 70740

sputtering by D* and Nh ions, coeffs, obs. 0 71884 structure, effect of annealing and low temp, rolling X ray diffr, meas, 0 78486

0 / 8486 surface (100), atomic vibr, amplitude, LEED obs. 0 - 43537 surface oxide struct, and supercond, implications 0 - 74885 thermal expansion occiff, and Debye temp. 0 - 78784 X-ray K-absorpt, edge 0 - 41250

Niobium continued

whith continued yield, strain rate and temp, effect 0 -40307 yield, strain rate and temp, effect 0 -40307 yield stress of single crystal, asymmetry 0 -68447 zone refined, redistribution of 1a and W impurities 0 -47139 CaMoO₂Nb, p irrad, e.p.r. 0 - 72478 Li/Nb fusion reactor blanket with Na heat pipes, obs. 0 - 70721 Nb OaAs junction, tunneling anomalies, 10.5 K, differential cond. 10 -790 3.

Nb Zr system, interdiffusion investigation using local X ray spectral analy sis 0 78583

six 0 78883 Nb, recrystillization temp., deformation depend. 0 65454 Nb, thermal X ray sentt, obs., 293-77K 0 - 62175 Nb VII. term analysis of the 4p 4d and 4p 5s transitions 0 SETIO: Nb, effect on semicond, and opt, props. 0 - 47725

SETIO aNb, effect on semicond, and opt, props. 0-47725

Nlobium compounds
alloy, clustering of Zr and N, relaxation penks 0-53575
alloy, creep strength improvement, patent 0-58944
alloy, plastic deformation following quenching from 1200°C and then
annealing 0-55976
base alloys, structural and mechanical effects of interstitual sinks 0-50703
niobates, crystal growth, effects of stoichiometric deviations 0-47110
niobates, rutile structural, ir, absorpt, spectra, vibr, freqs. 0-39393
oxides, X-ray K absorpt, edge 0-41250
solid solutions, Snock relax, peaks, brondening effect 0-68413
superconducting alloys, imagnetization, dimensional effect 0-56205
C+O-Nb-Os-11O+system, phase equil. 0-64987
Co-Nb alloy, struct, changes in decomp, electron microscope obs.
0-71797

Co Nb alloy, struct, changes in decomp, electron microscope obs. 0 / 1/9/ (20wt,%)CF (25wt,%)Ni (1wt,%)Nb austenitic steel, NbC precip, stacking fault contrib. 0 58955 be Nb alloys, ddine, recrystallization characts. 0 58958 Na O BaO Nb Os system, ferroelectric crystal growth, comp. depend., phase diagram 0 39879 15a O Nb Os SiOs glass, i.r. and Raman spectral study, structure 0 0 0 0 0 0 0

Nb Al Ge supercond, films with β W struct, spattering and props. 0, 59171

No Al Ge supercond, finite with *p* w structs, spattering and props.

0.50171
No Al alloy for sheathing fuel elements, prod., patent. 0. 71813
Nb Au system, supercond. 0. 40743
Nb D solid solit. D atom distribution. 0. 40463
Nb H alloy, internal friction peaks in aconstical absorpt, spectrum, 20
400K 0. 68412
Nb Hf Calloys, age hardening. 0. 65453
Nb Hf Calloys, age hardening props., effect of microstructure. 0. 44129
Nb Mo Au system, supercond. 0. 40743
Nb Ho No filoys in air and H-, int. friction and mech. props. 0-55955
Nb Mo N solid solution, N solubility. 0. 58982
Nb Mo alloy, mech. behaviour and twinning. 0. 40353
Nb O, solid solution, yield stress, comp., depend. 0. 65197
Nb O, solid solution, plastic deformation, 4.2.550 K, yield stress, comp. depend. 0. 55975
Nb O bond, nonlinear optical polarizability. 0. 51260
Nb O solid solution, plastic deformation, 4.2.550 K.

Nb O bond, noninear optical politrizability 0 51200 Nb O solid solution, chemical interaction 0 68533 Nb Ru alloy, near equatomic, phase transformations, mechanism 0 78704 Nb Sn, composite superconducting alloy, phase substitution method 0 59475

No Str. composite superconducting alloy, phase substitution method 0.59175.

No Sn, superconducting cast alloy, crystaffization and microstruct, mech. vibration effect. 0.59174.

No Sn'system, constitution diagram. 0.61591.

No Ta C. alloy, effect of Mo and W, phase equilibrium investigation 0.50821.

No Ta alloy, flux flow resistivity by surface resistance meas. 0.56206.

No Ta alloy, thermo electric properties. 0.51136.

No Ta alloy, thermo electric properties. 0.51136.

No Ti Mo alloy, b.e.c., superconducting transition temp., critical field, current carrying capacity. 0.40744.

No Ti, cubic alloy, optical spectra, band struct. 0.54089.

No Ti alloy supercond, incrowave cavity. 0.47676.

No Ti solid solus, supercond, optical props. 0.40740.

No Ti ternary alloy, 6581, struct. 0.61897.

No Ti wires and multiflament composites, energy release by flux jumps. 0.47677.

No Ti wires and multiflament composites, energy release by flux jumps. 0.47677.

No Ti wires for superconducting quadrupole magnet, evaluation of winding.

0. 476/7.
 Nb Ti wires for superconducting quadrupole magnet, evaluation of winding techniques.
 0. 75637.
 Nb HiZri supercond, alloy fabrication method, patent.
 0. 44154.
 Nb W C alloy, phase equilib, constitution, X ray diffr. DTA.
 0. 47491.
 Nb W Hi C, mechanical properties, effects of composition and structure.

0. 65353
Nb (6at/%)W, low temp, thermully activated flow of single crystal, mechanisms 0. 40333
Nb W phase equilibrium study, 1400-2100°C 0. 78334
Nb W single crystal, yield stress, asymmetry 0. 68447
ß Nb (23wt/%)Zr, yield and fracture, temp, depend. 0. 65398
Nb Zr alloy, thermo-electric properties 0. 51136
Nb 1%Zr alloy, in L1, thermal convection loop tests at 1200°C and 1306°C 0. 76.12
Nb 50%Fi, rods, flux jumps, effects of thermal insulation 0.—75616
Nb 1.0 at/%Zr O alloy, substitutional interactions, internal friction 0. 40252
Nb alloy, formability, tensile strength, oxidation resists, comp. depend.

Nb alloy, formability, tensile strength, oxidation resist, comp. depend. 0, 404.77

() 40457

Nh complexes, with peroxides, cryst. struct. () -65264

NhAL NhCiai, mixed crystal series () -50539

Nh₂(AL, Cie), ordering and effect on critical lamp () -50540

Nh₂(AL, Cie) syst., annealed, supercond., phase anal. () -65644

Nh₂(AL, Cie) syst., annealed, supercond. transition temp., upper critical field, 4.2K () 68789

NhC-C composites, labrication temperature lowering, by WC, of NhC-WC examination mechanical properties () 50785

NbC. Composites, hibrication temperature lowering, by W.C., of NbC. We examination mechanical properties 0. 50785.

NbC._{10.706}, supercond., lattice thermal cond. 0. 40742.

NbC._{10.726} × < 0.99) work function at 1800k, obs. 0. 62468.

Nb₂D₁, order disorder transitions 0. 61807.

NbH, subthermal neutrons inelastic and quasiclastic scatt., mode obs. 0. 68582.

MbH., mag, susceptibility, comp. and temp. depend. 0 65886

Niobium compounds continued

Nb_xMo₁ x^{59} Co, dilute alloy, where $0 \le x \le 0.4$, local moment formation, n.m.r. 0-45028

NbO, compressibility and Gruneisen consts. 0–78619 NbO, vacancy filling and removal, effects on electrophysical props. 0 61943

NBO. vacancy nining and removal, effects on electrophysical props. 0 61943
NBO. semicond, metal transitions and transport props. 0-40776
Nb-O. films, photocond., trapping and chemisorption effects 0-65850
Nb-O. anodic film preparation, electron-beam crystallization 0-65080
Nb-O. baked pellets, positron annihilation 0-40696
Nb-O. in Pb(Zr.Ti)O. ceramics, effect on electromech, props. 0-72121
Nb-Os(fr.Pt.Au) alloys, mag. props. 0-51011
NbSe. NbTe., solid soln., lamellar structure, superconductivity 0-62326
NbSe., superconductivity, quasi-two-dimension nature 0-47678
Nb1., Se., non stoichiometric, struct. 0-58743
NbSn cubic-to tetragonal transition, dynamic theory based on electron-phonon interaction 0-78691
NbSn. coating on flexible substrate, superconducting, patent 0-44155
Nb1Sn. low temp. phase transform. 0-65496
Nb1Sn. solution growth in liquid Sn 0-47131
Nb1Sn. superconductivity, hollow cylinders, flux jump behaviour 0-75609
Nb1Sn. tape, superconducting 0-75617

Nb.Sn. tape, superconducting 0--75617
Nb.Sn density of states model rel. to Nb.Sn₁ "Sb₂ system 0-59173
Nb.Sn magnet, superconducting, 51 cm bore solenoid, pumped helium tests 0-44087

Nb₁Sn superconducting tube, map. flux flow enhanced by neutron irrad. 0 56202

Nb.Sn 0-59173

NbTe, domains and dislocations, electron microscopy 0-78555 NbTe, twin like domains, dislocations, electron microscopy and diffraction 0-78487

tion 0–78487
Nb(V) chlorocomplexes, u.v. absorption spectra, estimation of optical electronegativity of OH 0–46498
Nb B system, electrophysical props. of phases 0–65625
Nb—Zr alloys, strengthening by internal oxidation 0–43768
Ni Al-Nb Mo solid soln., p and p' phases, investig. 0–47459
Ni Al Nb alloy, Ni-rich, phase equilibria, 1200 and 750°C 0–53672
Ni Cr Nb precip.-hardened, plastic deform. mechanisms 0–71689
Ni Nb Mo, isothermal section at 1400°C 0–71408
Ni Nb W phase equilibrium study, 1400-2100°C 0–78334
Ni Nb phase diagrams 1200-2100°C 0–71408
Pb(Nb₁, Ta₂)S₁, supercond, transition temps., comp. and thermal history depend., rel. to sp. ht. meas. 0–78901
Ta Nb C alloy, effect of Re and Al, phase equilibrium investigation 0 50822

50823

Ti (Mo,Nb,V) isomorphous alloy, phase transformations 0–53663 Ti Nb Fe, superconducting alloy, annealed, Mossbauer chemical shift rel. to critical current 0–65647

Ti Nb V. ternary system, superconducting resistive critical field, comp. depend. 0–44141 Ti (22 a.1.%)Nb, superconducting alloy, magnetization, Bean model75629 0–75629

Ti Nb alloy, superconducting, longit, critical currents 0-62329

Ti Nb alloys, deform, contrast origin from no contrast line position in micrographs 0–40144
Ti Nb phase boundaries determ, 0–53665
Ti Ta-Nb alloy, superconducting, patent 0–44157
U (7.5 wt.%)Nb (2.5 wt.%)Zr alloy transition phases, cryst. struct.40104
0.4014

40104

0 40104
U Nb Zr alloy, crystal structures of transition phases 0–59041
V Nb alloys, sp. ht. and supercond. 0–78905
Zr Nb alloys, superconducting, longit, critical currents 0–62329
Zr-Nb alloys, exidation in air, dimens, changes 0–45064
Zr Nb alloys, oxidation in air, dimens, changes 0–45064
Zr-Nb alloys increased mechanical resistance following hardening 0–71713
Zr (2.5 wt.%)Nb H system, press, comp. temp. study 0–68570
Zr (2.5 wt.%)Nb alloy, cracking in oxide films 0–40419
Zr (2.5 wt.%)Nb alloy, heat-treated, in-reactor creep rate stress depend. 0–68460

Zr (2.5 wt.%)/No alloy, heat-treated, in-reactor creep rate stress depend. 0 68460
Zr-(2.5 wt.%)/Nb alloys, texture produced on cold rolling and recrystallization 0–68540
Zr-(2.5 wt.)/Nb alloy, heat-treated, stress-rupture props. 0–43775
Zr -(2.5%) Nb thermal expansion, effect of annealing and cold working40586 0–40586

Nitrogen

in e Indi, abundance computed using synthetic stellar spectra 0-72710 absorption system in H-O and solutions of Na-SO₄, KI and Na-SO₄ influence of molecular diffusivity on liquid phase mass transfer obs. 0-68089

0–68089 abundance, elemental and isotopic, in lunar samples 0–45360 abundance in Arcturus 0–57025 abundance in K giants α Boo, α Ser, β Gem, ϵ Peg 0–45262 abundance in lunar samples 0–45343 acoustic velocity, for isotherms from 1 to 70 atm., interaction potential force constants 0–68017 active, reaction with Te atoms, spectroscopic observation 0–46634 adsorption, mixed on W with ethylene, dosing order effect 0–55766 adsorption by active carbon and γ Al₂O₃ at high pressure 0–47087 adsorption on W, successive O₂ adsorpt. 0–58606 adsorption on microporous C, 77 K, Dubinin-Radushkevich characterization 0–61679

adsorption on microporous C. 77 K. Dubinin-Radushkevich characteriza tion 0–61679 afterglow, excitation of added Na atoms 0–46383 afterglow, visible, N atom and pressure depend., e.p.r. meas. 0–53229 afterglow, yellow, first positive band intensities 0–43125 arc. low current, radial temperature, distrib. 0–55530 atmosphere, iodine vapour influence on radial temp, distribution of arc 0–61414

in atmosphere, spectral analysis by laser Raman radar $\,0-69277$ atmospheric, thermal fixation, MHD generator method and apparatus, patent $\,0-54186$

patent 0-54186 atom, autoionization, multiconfiguration close coupling calc. 0-74099 atom, autoionization states predicted with multiconfiguration close coupling calc. 0-74126 atom, binding energy of 1s electron related to potential at nucleus 0-74117

atom, e. scatt., v. small angle 0–39305 atom, h.f.s., spin optimized self-consistent field function 0–46371

Nitrogen continued

atom, in collision with H-like atoms, cross-section calc. for loss of K-shell electrons 0-55251 atom, photoionization cross-sections for Slater-Klein-Brueckner potential

atom, spectra, in He-N mixture, hollow cathode discharge, effect of mag. field 0-43353

atom, spin orbit coupling constants from Gaussian wave functions 0-46353 atom.

atom in simple molecules, chemical shift paramagnetic term 0–53013 atomic; chemisorption on W surface 0–48190 atomic, formation of regular hexagonal pits on graphite cleavage surfaces 0–40176

0-40176
atoms, autoionization, continuum processes 0-77637
cavities vapour filied, dynamics, stiffness, damping, resonance freq. meas.
0-71288
chemisorption on Mo(112), LEED obs. 0-56698
clustering with Zr in dil. Nb alloy, relaxation peaks 0-53575
compressed, meas. of positive ion drift vel. in elec. fields 0-67974
compressibility factor, isothermal, calc. at temp. values from 0 to 150°C
0-67988

0–67988
Compton profile, comparison with theoretical profiles 0–67740 condensation on Cu at 15-100°K, of 300-1400°K N· 0–55668 crystals, α-phase, Raman spectra, assignment of features in intramolecular and lattice regions 0–76126 diffusion and mobility of N+, N+*, N₃+, N₄+ and K+, obs. 0–46765 diffusion and permeability coefficients through low-density polyethylene 0–55928

0-3928 diffusion in Mo and W 0-65342 diffusion in liquid Fe, 1560-1700 °C 0-53328 discharges, stimulated emission, in the range 1-760 torr, introductory study 0-63609

study 0-63609 electron impact excitation, secondary effects 0-64439 electron scattering, meas of total differential cross section at 40 keV, correlation, and binding effects and Bethe corrections 0-74290 electron scattering, plural and multiple 0-70791 electron-collisional ionization rel. to flames 0-69209 first positive and Meinel bands, electron excit, cross-sections, 0 to 700 eV 0-64438

0-04438 fluorescence efficiencies and collisional deactivation rates 0-70931 fragmentation, by 5 to 45 keV He* ions 0-74609 gas, collisional narrowing of vibrational Raman band 0-74279 gas, energy loss of traversing protons 0-45963 gas-methyl cyanide mixtures, in elec, field, meas. 0-78214

glow discharge positive column, meas. of rotational and vibrational temps. 0–67978

0-07978 ionization associative in 800 10500°K, rate const. determination, microwave method 0-58356 ions, ioniz. rates due to electron collisions, calc. 0-43011 ions, solar u.v. lines limb brightening 0-41865 isotope analysis, instrumental system improvements 0-41453

isotopic analysis, instrumental system improvements 0–41453 isotopic analysis by optical spectroscopy 0–41452 Kerr effect, second hyperpolarizabilities, in gas 0–68002 laser, as spark gap trigger, formative times rel. to power 0–53232 laser, pulsed u.v. simple, peak power 10³W 0–42262 lattice dynamics, procedure extendable to more complicated molecular crystals 0–50843

lattice dynamics, procedure extendable to more complicated molecular crystals 0-50843 liquid, automatic disperser, sensing device 0-51854 liquid, boil-off calorimeter, for surface energy measurements 0-78247 liquid, compressed, nuclear spin relaxation 0-78308 liquid, compressed, nuclear spin relaxation 0-78308 liquid, discontinuities of ionic mobilities 0-64945 liquid, generation of cold gas for photomultiplier cooling 0-76766 liquid, level maintenance in cold traps using C-sensor 0-66748 liquid, shock-wave compression 0-58459 liquid, shock-wave compression 0-58459 liquid non-polar, charge injection 0-68131 low pressure generation, controlled, by chem. dissoc. of Ba_3N_2 0-48656 molecular beam, emission spectrum and radiative lifetime of metastable $E^*\Sigma_g^*$ state 0-61120 molecular bond, C-N, polarization increments rel. to tertiary amines, nitriles and heterocyclic compounds 0-58207 molecule. 1PG band system, relative intensities in normal and type-B aurora 0-76426 molecule, de-excitation of Na rel. to initial kinetic energy and final vibrquantum number 0-52950 molecule, electron impact ionization cross-section per unit energy range 0-67972 molecule, overall recombination and dissociation rate coefficients, phase

molecule, overall recombination and dissociation rate coefficients, phase space theory calculation 0–76259 molecule, photoelectron angular distribution 0–64212 molecule, protonation, study using MO SCF calculations, proton affinity 0–64384

molecule, quenching of electronically excited Na atom, calc. 0–67649 molecule, vacuum u.v. absorption cross-sections and oscillator strengths 0 61123

0 61123 molecules proton interaction, cross-sections of elementary charge-exchange processes 0-64420 molecules, electron scattering, resonance, in inelastic channel 0-77817 molecules, emission cross sections of 1st negative band system produced by proton impact 0-70929 molecules excited by 50 to 5000 eV electrons, radiation emission obs. 0-64440

neutron spectra at 14 MeV using sphere transmission and time-of-flight techniques 0-64151 partially ionized, heat transfer determ. in arc heated channel flow 0-53133

0-3133
photoionization meas...rel. to breakdown calc. 0-64768
physisorption on 304 stainless steel, at 10-9 to 10-4 Torr 0-71491
plasma, shock ionized elec. cond. and collision freq. 0-43272
plasma, thermal conductivity determination from electric arc discharge
meas. 0-67910
plasma, transport coeffs., to 13000°K 0-67911
positive column, acoustic and pseudo-acoustic wave propagation
0-53276

pressure effects on vacuum u.v. spectra, rel. to valence shell or Rydberg transitions 0-61057 proton impact, energy loss spectra 0-74289

quadrupole coupling consts., semiempirical calc. 0-43076

Nitrogen continued

Raman spectrum of solid, lattice mode intensities and band assignments 0-51321

refractive index. u.v. interferometric meas. 0-71263

relaxation, vibrational, rel. to absorption of sound in air 0-53277

relaxation, vibrational, ref. to absorption of sound in air 0-53277 solid, cryst, struct, of α , β , and γ modifications at high press. 0-53509 solid, thermal expansion and isothermal compressibility $4.2^{\circ}\text{K} \cdot 40^{\circ}\text{K}$

solid surface, interaction of N beam 0-65567 solubility in glass, effect of Si₂N₄ additions 0-47018

spectral lines, intensities, calculated as functions of axial temp, of discharge channel 0-71169

in steel, Cr-Ni, engineering props, improvement 0-71712

steel, stainless AISI type 304, effect on proportional limit and work hardening rate, 302F 0–43805

ing rate, 302F 0–43805
stimulated brillouin scatt., rel. to hypersonic speed 0–61124
thermal conductivity at 100-1100°C, using column method 0–43398
thermal transpiration, rotational consistion numbers determ. 0–61451
two atoms, interaction at short and medium range 0–67658
ultraviolet induced first negative system 0–70959
vibrational relax, rates meas, behind shock waves 0–77814
viscosity, and density depend... 100 to 25°C ≤250 atm. 0–46835
viscosity meas, at 0-96.38°C, 6500 bars max. 0–61448
A1*-N; electron capture and loss, 0.4 to 4MeV 0–67853
A1*-N; equilibrium charge fractions, 0.4 to 4MeV 0–67852
Ar-N mixture, thermal equilibrium calc, at 1 atmos, and between 5000
35000°K 0–53269
onBa film, chemisorbed, dispacement by O₂, obs. 0–56695

on Ba film, chemisorbed, dispacement by O₂, obs. 0–56695 CO₂/N₂ atmospheric conc. ratio, precise determ, from Raman scatt, meas. 0–51511

0–51511
CO₂ N₂-He amplifier, decomp, influence on 10.6 μ emission 0–77091
CO₂ N₂-He laser, passive Q-switching with CH₂Br gas 0–60213
CO₂ N₂-He lasers, thermal effects and fast flow power scaling techniques role 0–49042
CO₂ N₃ syst., vibrational distrib, of populations and kinetics, in fundamental and harmonic regions 0–70880
CO₂ N₃ atms., radiative transfer on entry, rel. to Mars, Venus 0–54441
CO₃ 15 μ band absorpt, broadening by N₃, obs. 0–50169
CO₂ liq, droplets varporization in N₂ near thermodyn, critical point, theory 0–50329 theory 0–50329
D2-N2 differential scatt. cross-section meas. 0–64604

H atom collisions, total electron-loss cross sections, Born wave calc. 0-64286

0–64286
H atom scatt., electron-loss cross-section calc. 0–64285
H*+N, charge exchange. Balmer-α and N·*(0, 0) simultaneous emission cross section, obs. 0–39479
He·N mixture, thermal equilibrium calc. at 1 atmos. and between 5000 35000°K 0–53269
He*+ N₂→ He + N₂*, mass and optical spectra at 300°K, obs. 0–64612 with Mg. Al polydispersed particles, electroconductivity and radiation 0–50267

molecule, $C^3\pi_{\mu}$, and $B^3\pi_{g}$ vibr. and rot. levels lifetimes, obs. 0–46485

molecule, $C\pi_{u}$, and $B\pi_{g}$ vior, and rot, evels infetimes, obs. 0–46453 N/O/reactive carbon compound systems, chemilluminescence emission of CO fourth positive bands 0–76257 N- methan-ethane system, liq. phase inversion between -255° F and -263° F 0–39882 N+ Ar collisions, Q values determ, by coincidence technique (100 eV 1 keV) 0–39290

Ny-Ar elastic cross-section meas., energy dependence of Rainbow scatt. 0-74445

N₂-Ar laser, as spark gap trigger, formative times rel. to power 0–53232 N₂-CO₂-H₂O (or He) supersonic expansion, population inversion

N-CO gas mixture theoretical and experimental comparison of conductivities 0-50167

N+CO₂ inter- and intra molecular vibrational energy transfer, shock tech nique 0-43096 N₂+N₂ collisions, 2 to 40 eV, symmetric charge exchange and N+ production 0-64611

NO collisional ionization cross section rel. to internal excitation energy 0-64767

N-e collisions studied using single centre wave functions 0–43069
N-e interactions, static potential between molecule and incident electron 0–43067

 N_2 -p collisions, Balmer α and N_2 + first negative emissions, excitation func

N=p collisions. Balmer α and N=V first negative emissions, excitation functions 0=39321 N,N²⁺ atoms, and fons, photoionization cross sections 0=70775 N H-N IV, excited levels radiative lifetimes 0=60925 N II, dense plasma, profiles of 9 lines, Stark broadening 0=39289 N II, meas, of Stark broadening parameters, by laser interferometry 0=60025

0-60902 N V, $2s^2S_{1/2}$ - $2p^2P_{3/2-1/2}$ doublet relative intensities and decay times

0-70766
N V. excitation coeffs. for five transitions, expt. determ. 0-67636
N V. waxitation coeffs. for five transitions, expt. determ. 0-67636
N V multiplets, electron excitation cross-sections 0-43001
N* ionization, by electron impact, relative efficiency vs. kinetic energy, obs. 0-67971
N* mobility, diffusion and reaction rate in N obs. 0-46765
N* reactions with CO and CO ocharge exchange, 0.5 to 25 eV 0-64610
Ns., absorbute fluoresence yields of 3914 A following e bombardment 0.65-1.6 MeV 0-46494
Ns., absorpt. spectrum, rotational anal. of bands in b-X and i-X systems 0-70932
Ns. extrad emission spectra, 0-53043

0-10932N_s, α-irrad., emission spectra 0-53043N_s, coaxial gas laser, generation of short intensive pulses 0-52271γ N_s, cryst. struct. 0-65260N_s, differential elastic scatt. by D₂ in crossed beams 0-39478N_s, emission cross-sections in vac. u.v. by electron impact 0-61114N_s, excitation and relaxation of triplet states by metastable Ar atoms 0 - 64609

N., identification of two low-lying non-Rydberg states

Ns, intercombination for two low-tying non-kyoder states 0--6114 Ns; intercombination transition and intensity distributions, elimination of discrepancy between experimental and theoretical results 0--64434 Ns; ionization, by Li ions, collisions and Li*, Li²* and Li³* ion charge exchange, 0.2-2 MeV 0--61369 e-Ns; lattice dynamics, spectral line widths, using potential of atom-atom form 0-59080

Nitrogen continued

Ns. lifetimes of rotational and vibrational levels of electronic states 0-55303

N., Morse function adjustment, P.E. curve for N121 state 0-46413 No oscillator strengths of Hopfield absorption series ()-61116

Ny, Raman scatt, meas, under ambient atmospheric conditions, atmospheric oxygen balance appl. 0-51511

N scattering cross sections on LiF 0=61203

N₂, small angle electron scattering cross sections, 13, 23, and 43 kV 0-70834

Ns. solid, reflection spectrum at 4.2°K, presence of Rydberg states 0 -76075

N. sound vel. 0-73305

No. threshold excitation spectrum 6.13 eV, excitation of triplet states 0.61118

No, total ioniz, cross section due to e impact 0-67679

N_s, ultrasoft X ray absorpt, meas. 0 – 64818 N_s, vibrational relaxation in collisions with metal atoms = 0 – 74446

Ns and Ns-Ar mixture high pressure discharges, rotational and vibrational temperatures for plasma diagnostics 0 43307

N- autoionizing states, photoelectron spectroscopy: 0 61377

Ny bands excited by soft X rays, fluorescence efficiencies and collisional deactivation rates 0–67739

N- cascade are, meas, of temp, distribs, 26000°K max. 0-39637

N. desorption on (100) W 0-47083

N-electron scatt, resonances, 11 to 12 eV 0-61097 N- electron scattering cross sections, total differential, 40 keV electrons

N. electron scattering cross sections, total differential, 40 keV electrons 0 - 60980
N. ion pair formation by electron beams 0 - 583.54
N. K.-L. Auger spectrum, high energy lines identifications 0 - 4648.7
N. low energy collisons with He, unitarized Borm approximation for rotational excitation 0 - 553.02
N. mol. beam interaction with solid N. surface 0 - 6.556.7
N. mol. electronic struct, from ediffr. 0 - 74116
N. molecule, contraction of Gaussian basis functions effect on molecular calculations 0 - 7426.4
N. molecule, excitation of second positive emission system by fast electrons 0 - 46486
N. molecule, excitation of second positive emission system by fast electrons 0 - 46486
N. molecule, excitation of second positive emission system by fast electrons 0 - 46486
N. mols., pot, energy curves 0 - 64406
N. photoelectron angular distrib, calc. 0 - 61370
N. rot. relax, 0 - 499.50
N. rotational relaxation numbers determ, from u.s. absorption 0 - 77776
N. spectrum, vacuum u.v., a"12g* \(\infty \text{X} \) 2 \(\frac{1}{2} \) (0 absorpt., press, induced 0 39389
N. stimulated Brillouin scatt, freq. shifts meas, and theory, hopestical determinants.

0 39,889 No stimulated Brillouin scatt, freq, shifts meas, and theory, hypersound speed determ. 0 46,824 No visible afterglow spectrum rel. to recombination of atoms. 0 53,041 No shape resonances, local potential. 0 77,818 No electron seatt., molecular orbital calc. of 2 eV shape resonance. 0 46,493

0 ·46493 N·¹, B·Σa¹ vibr. and rot, levels lifetimes, obs. 0 ·46485 N·¹, branch overlapping in first negative bands 0−70927 N·¹, by collisions with He, velocity distributions of fragments 0−77967 N·¹, effective excitation cross section of (0 0) band at 3914 Å in first negative system resulting from collisions between fast electrons and N-molecules 0−46492 N·², excitation of bands in first negative system, by 2¹·¹8 and 2¹·¹9 He atoms 0−58188 N·¹ bands excited by soft X rays, fluorescence efficiencies and collisional deactivation rates 0−67739 N·² first negative emissions, excitation functions, prod. in p N· collisions 0−39321 N·¹ ion, collisionally induced dissociation 0−46603 n·² ionization, by electron impact, relative efficiency vs. kinetic energy,

N-1 ion, collisionally induced dissociation (0.46603) ns⁴ ionization, by electron impact, relative efficiency vs. kinetic energy, obs. (0.4675) Ns⁴ kinetics of emissions and absorptions of Ns⁴ (B² Σ_{n} ⁴ X Σ_{g}) transitions by pulsed radiolysis (0.46486) Ns⁴ mobility, diffusion and reaction rate in Ns, obs. (0.46765) Ns⁴ vibrational states, population, effect of autoionizing transitions (0.46212) and diffusion in Ns, obs. (0.46765)

0=04212 N_3 ! mobility and diffusion in N_3 , obs. 0=46765 N^4 *, Lyelectron loss in H_3 and H_6 , influence of bound state structure on cross section 0=74157 N^4 * charge-exchange autoionization in Ar gas target, long lived states 0=64249

Na+ mobility and diffusion in Na obs. 0-46765

N₄* mobility and diffusion in N₂, obs. 0.46765
N₃(A^{*}Σ_w*), metastable, r.f. spectrum; mag. hyperfine and elec, quadrupole constants 0.70921
N₃(A^{*}Σ_w*) energy transport from, as source of O((S)) in aurora 0.76439
N₃(B^{*}Σ_w*), populations of vibrational levels v'=0 to 7, electron temperature, electron concentration measurements in a He N discharge 0.64435
NII emission due to N₃ simultaneous ionization and dissoc, by 150 eV to 4 keV electrons 0.64203
NV, cross sections, oscillator strengths and inelastic widths for several lines 0.67625
N³ - C collision, cross sections for K shell vucnucy prod. 0.46397
N₃ - CO₃, viscosity meas, of wet and dry mixtures 0.39686
N₃, substitution for ¹⁴N₃ in CO₃-N₃ and N₃-O₃N₄ laser systems 0.42279
N₃ monitoring in heavy water power reactor using Si radiation detector 0.64175

0.-64175 N₃+D₂O₂N₃D³+OD, product angular and velocity distributions, 1.16 eV 0-72522 N₃+H₃+O₂ flame reaction mechanism using 2 computational methods

0-54182 N₂+O³ high energy reaction, simple model (0-41417

N3+O+H; fuel rich flame at atmospheric pressure, structure and reaction kinetics 0-54181
Ne-N; mixtures, electrodeless discharge modes, plasma display panel applic. 0-53158
O-N; atmospheric conc. ratio, precise determ, from Ruthan scatt, meas.
0-51511

O 31311 O electron capture and loss cross sections, 4 to 40 MeV 0 - 67662 in Ta, solid solution hardening 0 - 43806 W(100) adsorption 0 - 47085

Xe-N mixture, thermal equilibrium cale, at 1 atmos, and between 5000 35000°K 0-53269 with Zr. Ti polydispersed particles, electroconductivity and radiation

Nitrogen compounds

auroral, ionic composition, NO+O+ ratio, O+ concentration cales. () ~ 6817

azides, paramag. defects prod., excitons role 0-79406

bis crosslinking agents photodecomposition, two photon absorption 0 70198

cyclophosphazenes, (N P)_n rings, shapes and conformations 0-65259

diphosphatriazine derivatives, cryst. struct. 0–65270 hexaisothiocyanate ions, i.r. and laser Raman spectra, 2200 70cm⁻¹ 0–39376

hydrazinium sulphate, cryst. struct., bonds 0-50536

NOAlBr₄, preparation, Raman spectrum 0-61715

NO interstellar, new spectral lines, 200 to 500 MHz 0-69414

nitrate molten binary and ternary mixtures, cation mobilities 0-79451

nitrate molten binary and ternary mixtures, cation mobilities 0–79451 nitrates, i.r. determ, using Pellet technique 0–54198 nitrates, ionic, laser Raman spectra, band multiplicities 0–72389 nitrates of metals, metals, Raman spectra 0–74759 nitride fuel and cladding materials, Na wetting characts. 0–58555 No. e.p.r., hyperfreq, susceptibility variation with temp. 0–61104 Fe N alloys, prep, technique for homogeneous samples 0–65472 Fe Ti-N alloy, internal friction, heat treatment comp. depend. 0–43721 K NII₃ and ND₂ liq, solns, viscosities 0–43437 Mo N solid soln, low temp. recovery behaviour 0–53634 N-NO collisional ionization cross section rel. to internal excitation energy 0–64767

NCO, radical rotational microwave spectra, transitions, dipole moment, hyperfine const. 0–64429 NCO radical, electronic struct, and spectra, calc. method 0–53073

NCI₁, vibr. anal, and force consts. 0-77815ND mol., A 3H_1 X $^3\Sigma^-$ (0,0) band, rot, anal. 0-64432NF₁, oriented in inert matrices e.s.r. at low temps. 0-61103NF₁, electronic structure calculations 0-70920NF₁, photoelectron spectra presented, assigned, correlated with BF₃ and CF₄ 0-64428

(F₁, 0-04428)
 NF₃, signs of I doubling consts. 0-77812
 NF₁, vibr. anharmonicity 0-55305
 NF₃, vibrational problem, harmonic freqs., potential function, Coriolis coupling consts., centrifugal stretching consts. 0-43128
 NF'Σ⁺ radiative lifetime and rate constant for electronic quenching 0-74281

0 -74281
N-H₄ air bicell 0-67011
NH, potential energy curves and spectra, natural-orbital VC1 studies 0 46490
NH free radical, A(²π₁)-X(²Σ⁻) transition, obs. 0-49878
NH radical, heat of formation 0-41414
NH², electronic states, LCAO MO SCF calc. 0-61077
NH² and NH² radicals, comparison of UHF orbital calculations 0-67743
NH₃ radical, SCF atomic orbitals calculation, hyperfine coupling constants 0-67742
NH₄, abundance in Jupiter's atmosphere 0-57109
NH₃, vibr. harmonic freqs. calc. from observed anharmonic freqs., and ND₁ 0 77816

ND₁ 0 77816

N-H₃, theoretical predictions of structures 0-53044

N-H₃ radicals, ratio of disproportionation to combination 0-54194

NH₃NH₄; antisymmetric wagging band, inversion 0-77813

N-H₃SO₄, cryst. struct., bonds 0-50536

N-H₄+OH-NH₃+NH-O primary products determ. 0-66176

N-H₃+||C(NO₃)||, crystal structure at =-160°C 0-78481

NMe₄, electronic structure calculations 0-70920

NO₃ MAPP gas flame, for atomic obs. spectroscopy 0-66210

NO₄ N-laser, effect of substituting ¹⁵N· for ¹⁴N₃ 0-42279

NO₄ absolute oscillator strength of (0,0) band of y system 0-61119

NO₅ chemisorption on Re at low pressures 0-41428

NO₄ electronegative gas, decaying plasma, diffusion 0-43267

NO₅ fluorescence, dance effect and level obs. 0-61105

NO₆ fluorescence, quenching, energy transfer and predissociation 0-67744

NO₇ gamma system Franck Condon factors and r-centroids 0-74285

0-67744
NO, gamma system Franck Condon factors and r-centroids 0-74285
NO, interaction between sσ and dσ series giving 'deperturbed' Rydberg series 0-67745
NO, interstellar, search at radio freqs. 0-45323
NO, origin in terrestrial atmosphere 0-66270
NO, photochem, and transport 0-79591
NO, relative intensities and Raman shifts of rotational structure 0-53042
NO, spectral and integral absorpt. in 5.3μ band 0-61102
NO adsorbed on zeolites and hydrogen mordenite, e.s.r. at 77°K 0-58192
NO beta band system, RKR Franck Condon factors, rotational contribution 0-74283
NO electron impact. O I and O II emission, decay lifetimes 0-64444

tion 0-74263 NO electron impact, O I and O II emission, decay lifetimes 0-64444 NO gas, i.r. radiation at high temp. 0-70926 NO gas diffusion through liq. films, electrically induced carrier transport 0 61511

NO gas diffusion through liq. hims, electrically induced carrier transport 0 61511

NO radicals in liquid phase, ENDOR obs. 0–70919

NO Raman scatt, cross sections meas. 0–71264

NO 3 and NO 3 aq. soln, radiolysis, transient elec, cond. 0–69225

NO 4, collision induced dissociation at low kinetic energies, effects of internal ionic excitation 0–67827

NO 4, collisional excitation 0–53102

NO 5, by collisions with He, velocity distributions of fragments 0–77967

NO 5, pranck Condon factors and r-centroids 0–74284

NO 6 ion, collisionally induced dissociation 0–46603

NO 5 photoionization rosonance obs. 0–61373

NO 6 photoionization rosonance obs. 0–61373

NO 7, electronic struct. from photoelectron and vac. u.v. spectra 0–61110

(NO) 8, gaseous, i.r. spectrum, structure, and ht. of formation 0–58187

NO 8, ifetime meas, by dye laser excitation 0–77811

NO 8, mol. consts. for (3.0.1) band 0–64431

NO 9, photoelectron spectrum, high resolution, and electron impact energy loss spectrum 0–67741

NO 1, readiative lifetime using tunable organic dye laser 0–70918

NO 1, thermal and recombination emission 0–61109

NO 1, thermal decomposition in shock waves 0–59486

NO 3 adsorbed on synthetic zeolites, hindered motion from e.s.r. obs. 0–70922

0-70922 NO₂ afterglow continuum in O₂·N₂ mixture, intensity study, expt. 0 54262

Nitrogen compounds continued

rogen compounds continued

NO ionization potential by photoelectron spectroscopy effect of traces of
NO, comparison of methods 0-46489

NO oriented in inert matrices e.s.r. at low temps. 0-61103

NO photolysis, quantum yield press, depend. 0-66204

NO reactions with alkali atoms compounds obs. by magnetic and electric deflection analysis 0-46635

NO. | numinescence spectra in KCl rotational fine struct., 1.9-4.2K
0-44919

0-44919
NO-7. molecular luminescence centre in alkali halides, vibrational relaxation, nonradiative transitions 0-44920
NO₂- in alkali halides, Raman and vibronic spectra 0-76089
NO₃- in soln., excited state of n-4π* 0-43194
NO₃- ion, isotopically different forms vibrational band assignment in i.r. and Raman spectra 0-59390
NO₃- ions introposphere, relation to thunderstorms 0-48279
NO₃- polarizability determ, from crystal birefringence 0-49859
N-O, calculated dipole moments and i.r. intensities 0-64403
N₃O, elect. polarizability anisotropies from microwave spectroscopy 0-70923

0-70923
N.O. electron attachment rates, obs. 0-64771
N.O. excited, vibr. relax. 0-39386
N.O. p-radiolysis and vapour phase irradiation with He*, e.s.r. 0-66206
N.O. p-radiolysis and vapour phase irradiation with He*, e.s.r. 0-66206
N.O. mol. parameters, from microwave spectrum 0-64430
N.O. reaction with H* at thermal energies 0-62798
N.O. scatt. and de*excitation coeffs. Calc. 0-61106
N.O. solid, Raman spectra, lattice mode intensities and band assignments 0-51321
N.O. thermal energy reaction rate constants with C* 0-72526
N.O. gas, cross section for slow electrons 0-70886
N.O. laser, Q-switching by Stark effect of NH, 0-42270
N.O. mol. electronic struct. from e diffr. 0-74116
N.O. mol. vibr. Napier relax. time, -H*, -D* collisions effects, 32 and 52°C 0-39390

No laser, Q-switching by Stark effect of NH₃ 0–42270
No mol. electronic struct. From ediff. 0–74116
No mol. vibr. Napier relax. time, -H₃. D₂ collisions effects, 32 and 52°C
0–39390
No molecule. minimal basis STO. SCF and C1 calculations for ionization potentials 0–77808
No vibrational energy transfer from CO₃, rate constant calc. 0–70887
No vibrational spectrum, potential constants 0–43127
No zero angle electron scattering with vibrational excitation 0–43123
No can configuration interaction intensity borrowing in photoelectron spec tra 0–64315
No calculative and non radiative transitions, theory and expt. 0–77773
No calculative and non radiative transitions, theory and expt. 0–77773
No calculative and non radiative transitions, theory and expt. 0–77773
No calculative and non radiative transitions, theory and expt. 0–77773
No calculative and non radiative transitions, theory and expt. 0–77773
No calculative calculation, height of hindering barrier 0–74288
No calculative calculation, height of hindering barrier 0–74288
No calculative calculation, height of hindering barrier 0–74288
No calculation calculation calculation calculation of surface of horizontal tube 0–71250
No calculation calculation

ammonia

on Jupiter's disk, absorption bands (6190 Å), spectrophotometry 0-57107

0–57107 absorption spectra coeffs., 100 to 400 Å 0–55298 adsorption and decomposition on polycryst. W filament 0–54184 adsorption and electro-oxidation at Pt electrode 0–66196 aqueous solutions, solvated electron in pulse radiolysis 0–54195 Franck Condon factors for Å–X transition 0–61112 fuel cell, cracked NH₃-air 0–69823 heat transfer during laminar flow with variable phys. props. 0–58397 hyperfine structure of transition J=K=1, investigation by simultaneous generation of line compounds in beam maser 0–39387 inversion lines, pressure broadening theory 0–43124 liquid, associated, in temperature range –65 to –35, –65 to –10 and –35 to +50°C, comparison with existing data 0–58465

Nitrogen compounds continued

iliquid metal/ammonia solns., interpretation of transport meas. 0–78296 maser, rel. to marginal type oscillator 0–54850 metal-NH₃ solns., excess electrons 0 -61497

metal-ammonia solus, optical consts, determ, by ellipsometric technique

0 39788 metal-ammonia solns., solid, high mobility of electron pairs near metal-non metal transition 0–75541 molecular density matrices 0–64353 molecular spectrum, new hyperfine structure 0–66985 molecule, "NH₁, hyperfine structure and quadrupole coupling 0–43126 molecule, collision induced transitions between rotational levels, microwave studies 6–77810 molecule, electronic struct, and inversion barrier 0–39388 molecule, inner shell correlation energy, invariance with geometry changes 0–43072 molecule, inversion rotation, spectra, 60,200 cm⁻¹ free assignments.

molecule, inversion rotation spectra. 60 200 cm⁻¹ freq. assignments 0. 64433

0. 64433 molecule, microwave inversion spectrum line—width parameters for (1≤√≤8, K=1) lines 0.–55304 molecule, proton magnetic shielding consts. 0.–58171 molecule, u.v. absorption bands intensities of vibrational components 0.–70928

0-10928
molecule Zeeman effect meas, of mag, susceptibility and quadrupole moment 0-46488
molecule photoioniz, photo c energy anal, 0-67706
molecules, charge exchange with H¹ and H¹, cross section meas, 0-77716

photoelectron spectra, and ND₃, using 584Å He resonance 0–64436 photoelectron spectra using He I 584 Å light source, rel. to vibr. fine struct. 0–61121

struct. 0-61121 polar constituent in binary gas mixtures, meas, of thermal conds. 0-53268 polar molecule in H₂, He, N₂ and Ar gases' microwave absorption at high pressure 0-53278 proton polarization up to 40% by dynamic nuclear orientation 0-49302 reaction with Hg(2 P₀), luminescence study by rotating sector method 0-55301

release expts, at high atm., dissociation processes in comets appl. () 69:160

0 69460
Saturn's rings composition, frozen NII₁, i.r. spectrum 0–57116
Stark effect, Q-switching of CO₂ and N₂O lasers 0–42270
Li NH₁ complexes, ab initio SCF MO calc. 0–43120
Li NH₁ solutions, Hall effect 0–55629
ND₂ dissociative electron attachment cross sections 0–64558
NH₃ i.r. microwave double resonance obs. using N₂O laser 0–70924
NH₃ i.r. microwave double resonance obs. using N₂O laser 0–70924
NH₃ i.r. microwave double resonance obs. using N₂O laser 0–70924
NH₃ i.r. microwave double resonance obs. using N₂O laser 0–70924
NH₃ i.r. microwave double resonance obs. using N₂O laser 0–70924
NH₃ i.r. microwave double resonance obs. using N₂O laser 0–70924
NH₃ i.r. microwave double resonance obs. using N₂O laser 0–70924
NH₃ i.r. microwave double resonance obs. using N₂O laser 0–70924
NH₃ i.r. microwave double resonance obs. using N₂O laser 0–70924
NH₃ i.r. microwave double resonance obs. using N₂O laser 0–70924
NH₃ i.r. microwave double resonance obs. using N₂O laser 0–70924
NH₃ i.r. microwave double resonance obs. using N₂O laser 0–70924
NH₃ i.r. microwave double resonance obs. using N₂O laser 0–70924
NH₃ i.r. microwave double resonance obs. using N₂O laser 0–70924
NH₃ i.r. microwave double resonance obs. using N₂O laser 0–70924
NH₃ i.r. microwave double resonance obs. using N₂O laser 0–70924
NH₃ i.r. microwave double resonance obs. using N₂O laser 0–70924
NH₃ i.r. microwave double resonance obs. using N₂O laser 0–70924
NH₃ i.r. microwave double resonance obs. using N₂O laser 0–70924
NH₃ i.r. microwave double resonance obs. using N₂O laser 0–70924
NH₃ i.r. microwave double resonance obs. using N₃O laser 0–70924
NH₄ i.r. microwave double resonance obs. using N₄O laser 0–70924
NH₄ i.r. microwave double resonance obs. using N₄O laser 0–70924
NH₄ i.r. microwave double resonance obs. using N₄O laser 0–70924
NH₄ i.r. microwave double necessariation obs. i.r. microwave 0–70924
NH₄ i.r. microwave double neces

0 - 74282 NH₂-He cale, of intermolecular dispersion potential 0-74444 ¹⁴ND₃, hyperfine interactions of intramolecular fields with ¹⁴N nucleus, determination of constants 0-46491 ¹⁵NH₃, legidud solvent mixtures, study of ¹⁵N n.m.r., shifts rel. to H bonding influence 0-67747 ¹⁵NH₃ pc band, Stark spectra by 10 μ lasers 0-61113 Na NH₃, liquid liquid coexistence and phase separation 0-58454

mamonium compounds
(NH4))H106, nucl. quadrupole interaction, by iodine proton crossover relax. 0-62781 alum, methylammonium chromium, heat capacity 0-71861 ammoniaeal, Raman spectrum evolution with temp. 0-77807 halide, and deutero-ammonium halides, phase transitions 0-75334 halides, irradiated, hydrazinelike defect, production and characterization 0-78525 halides, irradiated, hydrazinelike defect production, theoretical analysis 0-78526

M-/3520 halides with CsCl structure, cohesive energies 0–43577 long range macroscopic order above transition temperature for orienta tional disordering of NH₄+ ions 0–43638 NH₄H-PO₄ optical rectification applie, to giant laser power meas.

oxalate crystal quadratic nonlinearity, second and third harmonics genera-tion, simultaneous, synchronous 0–40540 (CH₁NH₂Al(SO₄)·12H·O) thermal conductivity obs., steady state method

(CH,NH,AI(SO₄)·12H·O) thermal conductivity obs., steady state method 0-75419
FeNH (SO₄).12H·O, mag. temp. calibration against
O, 0.1 to 0.033 K 0-48652
H·O·NH4F liq. solid equilib. 0-64993
ND₄Br, 1=II transition energy 0-75336
ND₄Br, phasq transitions 0-75336
ND₄Cl, I=II transition energy 0-75336
ND₄Cl, A-transition, dilatometric obs. 0-75335
ND₄Cl, A-transition, dilatometric obs. 0-75335
ND₄Cl, pure and X irrad., phonon scattering, thermal conductivity meas., 2 300K 0-40503
ND₄Cl elec. cond. due to cation or anion vacancy form. 0-59258
ND₄F, Raman and far infrared spectra 0-41239
ND₄F, Raman and far infrared spectra 0-41239
ND₄F, X ray determ. of lattice parameters of I, II and III phases, -176 190°C 0-55856
NH₂ radical ion hyperfine coupling const., UHF calc. 0-70930

ND.1, X ray determ. of lattice parameters of I, II and III phases, -176 190°C 0-55856
NH₃* radical ion hyperfine coupling const., UHF calc. 0-70930
NH₄*, in non-cubic cryst. sites, molecular motion, study by laser Raman scatt, and ir. spectroscopy 0-59063
(NH₄)-BcF₄, micromechanism of ferroelec, transition 0-40869
NH₄Br, cohesive energies 0-58614
NH₄Br, ir. determ. of structural and ordering changes 0-62119
NH₄Br, phase transitions 0-75334
NH₄Br, phase transitions 0-75334
NH₄Br lattice dynamics, within rigid ion model 0-71825
(NH₄)-Co₄H₂O, optical rectification 0-51268
(NH₄)-Cc(NO₄)_b, spin isomerism of ammonium group protons, n.m.r. obs. 0-69197
NH₄Cl:Co²*, e.p.r., relaxation, 4.2K, saturation 0-79405

0-69 [97]

NH₄Cl:Co²⁺, e.p.r., relaxation, 4.2K, saturation 0-79405

NH₄Cl:Co²⁺, e.s.r., 77-330 K 0-44991

NH₄Cl:Fe³⁺ zero field energy levels determ. 0-76222

NH₄Cl:M²⁺ single cryst, abs. spectrum, in 293-77°K 0-44849

NH₄Cl, anharmonic potential function for libration 0-65520

NH₄Cl, cohesive energies 0-58614

NH₄Cl, hyper Raman spectrum of lattice modes 0-72390

NH₄Cl, i.r. determ, of structural and ordering changes 0-62119

Nitrogen compounds continued

trogen compounds continued
ammonium compounds continued
NH₄Cl, lattice and mol. vibrs. 0–59081
NH₄Cl, \(\frac{1}{2}\)-transition, dilatometric obs. 0–75335
NH₄Cl, nucleation from aqueous soln., effect of photolytically generated
OH radicals 0–72556

OH radicals 0–72556
NH₂Cl, phase transitions 0–75334
NH₂Cl, pure and X irrad₄, phonon scattering, thermal conductivity meas., 2 300K 0–40503
NH₂Cl, saturated absorpt, spectra using lasers 0–70844
NH₂Cl, solid, spin rotational relax. 0–72290
NH₂Cl, two critical regions, from second harmonic scattering data, order-disorder phase transitions 0–47486
NH₂Cl, u.s. attenuation near λ transition at high pressures, 241-270K
10 680t3
NH₂Cl dendritic growth from aqueous solns. 0–58649

0 68603
NH₄Cl dendritic growth from aqueous solns. 0–58649
NH₄Cl de. cond. due to cation or anion vacancy form. 0–59258
NH₄Cl lattice dynamics, within rigid ion model 0–71825
NH₄Cl(Br.I), aqueous, water structure, Cl⁻, Br⁻, I⁻ effects, X ray scatter ing, radial distribution functions 0–39732
NH₄ClO₄, crystal growth from solution, temp, lowering technique 0–50443

NH₁ClO₁, nucleation rel. to thermal decomposition, photomicrographic and

electron microscopy studies 0-68556 (NH₄)Co₃(OH)₃(SO₄)₃,2H₂O₅ cryst, struct, X-ray powder indexed

(NH₄)Co₃(OH)₃(SO₄)₃,2H₃O₄ cryst. struct., X-ray powder indexed 0-53510 (NH₄).CrO₄, cryst. struct. and bonds 0-61853 (NH₄).CrO₄, crystal structure 0-50542 NH₄F IV. crystal structure 0-71594 NH₄F Raman and far infrared spectra 0-41239 NH₄F-TiF₁ liquid-solid equilibria, pressure effect 0-61590 NH₄F-F₁F₁ (CN)₆, mag, susceptibility and Mossbauer spectrum

0-311/8
NH₄Fe(SO₄).12H·O, ferroelec transition, Mossbauer obs. 0-40866
NH₄Fe(SO₄).12H·O, Mossbauer effect, anomalous mag. field depend. 0-76051

0 - (005) NH₄H-\xSO₄ antiferroelec, transitions and i.r. absorpt. 0-40878 NH₄H-(CO₄). 2H-O, elastic consts. meas. 0-71663 NH₄HF-(electron irrad, e.s.r. of F-2 and H obs. 0-44992 (NH₄)-HPO₄ p irradiated crystals, presence of loosely bound NH* radical

NH₄H₂PO₄, antiferroelec, phase transitions, group theoretical study NH₄H+PO₄, antiterroctec, phase transitions, group theoretical study 0-40877 NH₄H+PO₄, crystal growth, gamma irradiation effects 0-50417 NH₄H+PO₄, e.p.r., of Cr³⁺ in antiferroctec, and paraelec, phase 0-72484 NH₄H+PO₄, electrooptic, solubility of growth 0-71517 NH₄H+PO₄, far i.r. Fourier transform determ, of complex permittivity spec

tra 0-66023 NH₄H-PO₄, far-i.r. refl. spectra 0-69110

NH₄H+PO₄, far-i.r. refl. spectra 0–69110
NH₄H+PO₄, fonlinear optical susceptibilities 0–47991
NH₄H+PO₄, nonlinear optical props. 0–51258
NH₄H+PO₄, optical rectification 0–51268
NH₄H+PO₄, phase diagram to 52 kbar and 400°C 0–55657
NH₄H+PO₄, phase transition, 148 K, antiferroelectric domains 0–79052
NH₄H+PO₄, piezo- optical coeff., temp. and wavelength depend., rel. to electro optical 0–41119
NH₄H+PO₄, sp.ht., deuteration influence, rel. to dielec, transition 0–78779
NH₄H+PO₄ and deuterated isomorphs, sp. ht. 0–65547
NH₄H+PO₄ and deuterated isomorphs, sp. ht. 0–65547
NH₄H+PO₄ downconversion and unconversion, coupled, and parametric with simultaneous phase matching 0–73275
NH₄H+PO₄ laser, free running, thermal self-focusing of radiation 0–49072

0-49072
NH₄H-PO₄ laser modulator crystal, temperature instability 0-47990
NH₄H-PO₄ parametric fluorescence excited by 2573Å pump 0-44907
NH₄H-PO₄ splitting of single photon into two obs. following optical pump ing 0-60191

NH₄H₇PO₄ spinting of stope processing 0-60191

NH₄H₇PO₄ whiskers, growth and mech. props. 0-55801

(NH₄)₄HF₇, nuclear relax., p.p. angular correlation meas., and structure of HF₇, 0-51252

NH₄I, phase transitions 0-75334

NH₄I, X ray determ, of lattice parameters of I, II and III phases, -176-1907C 0-55856

NH₄1, X ray determ. of lattice parameters of I, II and III phases, -176100°C 0 55856

NH₄1 phases, refl. spectra 81°K to 373°K 0-66024

NH₄11, structure refinement 0-68312

NH₄10, spyroelectric, struct, analysis at 298°K 0-61887

(NH₄)·IrCl₆, antiferromagnetic, zero-point spin deviation, ENDOR and Mossbauer spectra obs. 0-75962

(NH₄)·Mg₂(SO₄); Mn³⁺ 0-54159

(NH₄)·Mg₂(SO₄); Mn³⁺ 0-54159

(NH₄)·Mg₂(SO₄); Mn³⁺ 0-54159

(NH₄)·Mg₂(SO₄); Mn³⁺ 0-56669

NI₄(NO₄)·O²⁺ e.s.r. 0-41317

NH₄NO₃, cond. at transitions rel. to O coordination, obs. 0-40831

NH₄NO₃, 2HNO₃, cryst. struct, refinement 0-68313

NH₄NO₃, epr., ferroelec transition of electro optical coeff., 300 750

nm, from 25°C to Curie point 0-41128

(NH₄)·SO₄, epr., ferroelectric transition neutron-scattering study 0-75801

(NH₄)·SO₄, ferroelectric transition, double refraction, electro-optical quadratic coeff. 0-51117

(NH₄)·SO₄, ferroelectric transition, slow-neutron scatt. obs. 0-50853

(NH₄)·SO₄, ferroelectric transition, slow-neutron scatt. obs. 0-50853

(NH₄)·SO₄, ferroelectric transition obs. 0-61888

(NH₄)·SO₄, ferroelectric transition obs. 0-61889

NH₄(H)·H

Nobelium

Nobelium compounds

No entries Noble gases see Inert gases

Noctilucent clouds see Atmosphere/upper; Clouds

cathodes, oxide, anomalous shot noises 0-44427 combustion noise from laminar diffusion flames on kerosene droplet streams 0-72533

Noise continued

diffuse, due to radiation scattering by turbid atmosphere, exptl. study 0-59582

Gaussian, effect on subjective image quality 0-70006

high-intensity, spectral study 0-60059

l.f. in plasma 0-53138 microwave, obs. in rainstorms 0-79533

optical parametric noise pumped by mercury lamp 0-67042 optical parametric oscillators 0-42235

optical parametric oscillators 0-42235

Poisson, effect on subjective image quality 0-70006
reactor, at-power, induced by coolant flow fluctuations 0-77604
reactor, space-dependent formulation based on natural mode approximation 0-39194
source, signal ratio, for ion and metastable detection of neutral molecular beams 0-74227
temperature, fluorescent lamps, influence of cataphoresis 0-45738
thermal, Dragon reactor, primary heat exchangers, spectra meas.
0-42901

thermometry of low temp. 0-42138

triboelectric, generation in commercial cables of underwater electroacoustic transducers 0-72127

transducers 0-7127
Cd_xHg_{1-x}Te solid solns., thermal noise anomalies 0-78681
GaAs CW laser diode, noise, laser-light and current correlation 0-49076
GaAs laser, reduction by KH-PO₄ modulator 0-45804

acoustic

acoustic aerodynamic, fundamental equation for surfaces in uniform translational motion 0–78192 aircraft, duct treatment for, conference 0–73046 ambient level effect on ear-protector attenuation's threshold-shift measures, criteria 0–69537 ambient-noise-spectrum levels as fin of water depth 0–59547 annoyance level, calculation for sounds containing multiple pure tones 0–52139 atmospheric field strength estimation, nonlinear technique 0–51538 attenuation in suppressors of complex configuration, statistical method for calc. 0–48858

cate. 0-48858 auditory system, temporary changes due to prolonged exposure 0-54498 band stop, rel. to two-click auditory thresholds 0-54500 bands, pitch reconsidered, comments 0-66701 broad-band, effect on cats' cochlear microphonic magnitude, study 0-45477

broad band attenuation, in acoustic ducts with airflow 0-69735 by compressors and fans, ground reflection effect on field distrib, results 0-38383

from ejector flows, theoretical and exptl. investigations 0-

engine-powered equipment emission, test-site meas. 0–46/98 engine-powered equipment emission, test-site meas. 0–54735 environmental, intensity meas., standard techs. 0–60058 in flames, turbulent, characteristics and origin 0–54737 flow noise control using nonlinear resistance of orifices 0–60061 flutter in flexible structures, shells and plates immersed in fluid flow 0–42062

0-42062 flutter in shaft whirls, pipelines, role of damping mechanism, analysis 0-38333 rel. to frequency response meas, structures under transient excitation 0-66894

rel. to frequency response meas, structures under transient excitation 0–66894

Gaussian field plus signal, clipped Dimus arrays output, mean, variance, asymptotic expressions 0–57402

Gaussian random stationary, zero-crossing shift as detection method, illustrations 0–52136
of gears of circular arc tooth profile, exptl. results, recommendations for quieter running 0–45650
generation by blade rows due to sound transmission 0–57398
h.f. bands, rel. to masking of l.f. tones 0–54507
hazard meter 0–54499
high intensity, effect on crack propagation of tensioned plates and structural parameters, analysis 0–40390
high-intensity, spectral study 0–60059
in houses low cost, reduction by sound insulation, structural design modifications 0–48862
hydroacoustic, level meter, 100 Hz to 1 MHz range 0–66254
hydroacoustic, level meter, 100 Hz to 1 MHz range 0–66254
hydrodynamic noise reviewed 0–39488
impact noise level, connection with sound transmission loss of floors 0–60066
industrial rel. to hearing imparment, book 0–45464

impact noise level, connection with sound transmission loss of floors 0–60066 industrial rel. to hearing impairment, book 0–45464 intermittent exposures, effects on temporary threshold shift, damage risk criteria 0–66710 jet, influence of retarded time 0–76916 Jet nozzle, reduction due to delta wings vortices flow, meas. 0–43387 in jets, model air, rel. to strip flow spoiler insertion 0–55541 lf. in ocean, theory, dependence on depth, wind vel. 0–62891 loudness level of single and repeated impulses, subjective and objective meas. 0–54490 loudness level subjective meas., choice of sound duration, silent intervals, recommendation to ISO 0–45469 masking thresholds after infinite amplitude clipping 0–57182 measurement, classification of instruments 0–69734 mechanically operated calculating machines, study 0–63455 multipath energy, separation in dispersive media 0–54743 multiple sources, sound field in enclosure 0–54744 in offices large, questionnaire tech., subjective effects, acceptibility criteria model analysis 0–42082 particles counter 0–50272 perceived level, calculation in PLdB 0–52137 photoconductor, CdS, amplification by Mandelshtam-Brillouin scatt. method 0–68609 pink-noise band's pitch, psychoacoustic analysis 0–69531 plate response in supporting elastic medium 0–54684 plumbing appliance emission, test standards 0–54736 pollution level concept 0–54734 quantification of noisiness of approaching and receding sounds 0–73047 reduction, duct lining materials, acoustic behaviour, parametric obs. 0–73045 reduction loss, diffuse sound field method for meas. 0–38380 from rocket exhaust, pressure cross correlation on cylindrical bodies, deterfrom rocket exhaust, pressure cross correlation on cylindrical bodies, deterfrom rocket exhaust, pressure cross correlation on cylindrical bodies, deterfrom rocket exhaust, pressure cross correlation on cylindrical bodies, deterfrom rocket exhaust, pressure cross correlation on cylindrical bodies, deterfrom rocket exhaust, pressure cross correlation on cylindrical bodies, deter

0—73045 reduction loss, diffuse sound field method for meas. 0—38380 from rocket exhaust, pressure cross correlation on cylindrical bodies, determination 0—52065 screech, in hot and cold jets, farfield study 0—55540 sea, vertical directivity investigation using integral eqn. 0—54227 semiconductor, CdS amplifier. us. wave interaction 0—68608 shielding, properties of free-standing wall 0—52144

Noise continued acoustic continued

shock cell in full-scale jet engine flight, Powell's freq. formula extension, results 0-48857

shock-related, in hot and cold jets, farfield study 0-55540

signal energy, dispersive and nondispersive separation through correlation techniques 0-54742

sonic boom, effects 0-38395

sound isolation device, barrier applications 0-52143

sounds containing multiple pure tones, judged noisiness 0-52138 source, obs. in N. Sea 0-79509

spinning-mode theory, exptl. verification 0-54738 test rig, sound-absorbing pad for minimizing acoustical effect of ground 0-54739

thermal, determination in electrodynamic microphones with thermal-electric noise 0–69731

noise 0–69/31 tonal masking, exp. determination of auditory filter shape 0–54504 tone combinations and bandwidth, neurons response in cat's cochlear nuclei to variations 0–45474 tone directivity and cut off 0–76912 traffic noise index, relationship between noise level and subjective reaction 0–48839

trainc noise index, relationship between noise level and subjective reaction 0-48850 traffic noise index 0-48860 of traffic on urban motorways, statistical model applic, for study 0-48856 underwater meas, variance reduction by incoherent hydrophone arrays 0-34740

of underwater towed-body due to streamlined body revolution, meas: 0-71341

urban, limitation criteria 0–57411 vehicle warning devices, optimum sound level 0–52140 whistles, aerodynamic, frequency, intensity, feedback mechanisms 0–42071

0-42071
white, effects on recognition of masked words, expt. 0-57177
white bandwidth effect on loudness of 1 KHz tone 0-69541
CdS, amplification by Mandelshtam-Brillouin scatt. method 0-68609
CdS amplifier, u.s. wave interaction 0-68608
CdSe, photoconducting, current fluctuations, acoustic flux 0-75829
InSb, microwave emission 0-53826

electrical

see also Cosmic radiation, radiofrequency; Sun/radiation, radiofrequency; I/f, in epitaxial Si 0-51066
I/f, of spreading resistances 0-50961
amplifier stage, low-noise linear wideband, for nuclear pulse amplifiers 0-63916
amplifiers, j.f.e.t. nuclear pulse. reduction methods 0-63914
avalanche diodes, review 0-68870
band limit frequencies, influence on distribution of successive zero crossings 0-73131
Barkhausen noise correl. with surface micro-discharges in Seignette salt 0-47836

ings 0–73131

Barkhausen noise correl, with surface micro-discharges in Seignette salt 0–47836
decoupling, rel. to ¹³C resonance spectroscopy 0–67757
diode, Schottky barrier, h.f. shot noise 0–68873
diode, avalanche, microplasma noise, low temp. 0–79009
diode, noise sources in transport eqns, governing carrier flow 0–44282
diode, space-charge limited, Langevin's equation 0–51081
diode, surface barrier, l.f. noise 0–53890
diode struct., GaAs:Cr 0–79011
dipole noise temp. meas. apparatus 0–45737
rel. to electron beam, reduction in low-velocity region, meas. using two fixed cavities 0–54841
galactic, and solar radio bursts, hecto-decametric wave region, Alouette II obs. (Oct. 1966) 0–54483
galactic noise spectrum and solar radio bursts, hecto-decametric wave region, Alouette II obs. (Oct. 1966) 0–54483
hydrophone arrays, towed seismic, for sediment profiling 0–45126
IMPATT Si diode, illum, depend. 0–40812
ionic aqueous solns, 1/f noise in conductance 0–78290
j.f.e.t., ceramic encapsulated 0–65752
Josephson point contacts, current noise 0–75637
junction, I.f. variance noise 0–53868
junction, noise sources in transport eqns, governing carrier flow 0–44282
in lagers, review of problems 0.65734

Junction, noise sources in transport eqns, governing carrier flow 0—44282 in lasers, review of problems 0—65734 m.o.s.f.e.t., Si:Au, generation-recomb, noise and thermal emission rates at acceptor centre 0—68877 m.o.s.t., Si, l.f. noise, theory 0—44312 m.o.s.t., l.f. noise geom, depend, 0—56334 measurement of small signals with correlator 0—42138 Mylar film, thermally stimulated current spectra, traps, low temp. 0—44350

0-44350

narrowband model for statistical properties of image intensity analysis 0-42354

0-42534 nonequilibrium system. I.f. noise, phenomenological approach 0-60129 oscillogram, photographic summation, pulse radiolysis expt. 0-45087 p n diode. flicker noise, surface recombination model 0-68872 Permalloy film. thickness depend. 0-65631 photodiode response obs. using photocurrent shot noise spectrum 0-53967

rel. to photoelectric shadow instrument, with modulating disc, noise spec trum 0-73124

photomultipliers for detection of ultra-weak light fluxes, reduction 0-52255

0-52255
plasma, d.c. spectrum, ion-molecule collision effects 0-67912
polar semiconductors of A_{III}Bv type, current fluctuations in strong elec. fields 0-56248
preamplifier, low-noise, for simultaneous high resolution energy and time meas, with semiconductor detector 0-63898
scanning r.f. spectroscopy, time-averaging method, rel. to resonance line deformation conditions 0-45733
Schottky deviations, periodic, rel. to surface reflection coeffs. 0-47576
Seignette salt, Barkhausen noise and surface micro-discharges correl. 0-47836

semiconductor, 1/f noise 0-78924 semiconductor, ambipolar drift, spectra, mag. field, Green's function method 0-44182

semiconductor, fluctuations, nonequilibrium, correlation functions in electron temp. approx. 0-53813

Noise continued

electrical continued

semiconductor, fluctuations, nonequilibrium, external random forces and eqns. for correlation functions methods 0–56217 semiconductor, quasineutral, transport, conc. and velocity correl. 0–78934

0-/8934 semiconductor, three-level, generation-recombination noise 0-43981 in solid-state devices, review of problems 0-65734 rel. to spectroscopy, nuclear radiation, with semiconductor detectors, S/N 0-38956

superconducting ribbon, flux-transport noise power spectra 0-53811

0—38935
superconducting ribbon, flux-transport noise power spectra 0—53811
in superconductor, flux motion 0—44117
superconductor, magnetic flux 0—50991
superconductor, type-II, flux-flow noise 0—75604
thermometry, absolute noise, low temp., Josephson effect applic. 0—44151
CdS, acoustic, amplification 0—47537
CdSe, photoconducting, current fluctuations, acoustic flux 0—75829
α-Fe₂O₃, n-type with Sn or Ti impurities, g-r noise 0—78917
GaAs-iCr diode struct. 0—79011
GaAs, avalanche photodiodes 0 19012
GaAs diode laser, reduction by optoelectrical feedback 0—63635
I. polycrystalline, ohmic cond., voltage and freq. depend. 0—44035
InSb, noise emission 0—56259
Si:Au m.o.s.f.e.t, generation-recomb, noise and thermal emission rates at acceptor centre 0—68877
Si; Cd compensated S-type diodes, noise oscillations of current 0—72089
Si, epitaxial, 1/f 0—51066
Si m.o.s.t., I.f. noise, theory 0—44312
SiC junctions, elec. fluctuations 0—53883

Noise abatement

see also Absorption/acoustic waves aircraft, architectural modifications for reduction 0–52145 aircraft, duct treatment for, conference 0–73046

aircraft noise, postnatal adaptability, effects during fetal life, statistical study 0-45472

atternation due to exhaust mufflers in piston engines, evaluation 0–57410 attenuation in suppressors of complex configuration, statistical method for calc. 0–48858

broad-band attenuation, in acoustic ducts with airflow 0-69733

broad-band attenuation, in acoustic ducts with airflow 0-69735 of ejector flow noise, theoretical and expl, investigations 0-46798 flanking transmission in buildings, calc. sound insulation barrier construction 0-38393 handbook on noise and vibration control 0-60060 jet, influence of retarded time 0-76916 in jet silencers, reduction 0-61441 mechanically operated calculating machines, use of absorptive treatment 0.63485

0-63455 in offices large, questionnaire tech., subjective effects, acceptibility criteria model analysis 0-42082 reduction by distance from sources of various shapes, geometrical methods, review 0-63454 suppression materials, fatigue evaluation 0-54741

in trains and buses, use of viscoelastic damping layers for plate vibrations 0-38336

transmission prop. of medium, sound wave compensation method, destructive interference 0–38386 urban, limitation criteria 0–57411

Nomenciature and symbols

menctature and symbols see also Units abbreviations and designations, reference book 0–66760 reflectance and directional reflectance and emissivity 0–57420 time, necessity for clarification of meaning 0–72870

Nomograms

see also Graphs see also Graphs
graybody radiometric temperatures, true and apparent in presence of atmosphere 0-4882
for small radioactivity detectability and meas, accuracy 0-46156
spectrophotometers, plot for 0-67183
rel.to thermal conductivity calc., porous materials 0-71871

Non-crystalline state see Amorphous state; Vitreous state Non-Newtonian fluids see Fluids

Nonlinear optics

acentric insulating cryst., coeffs. rel. to Raman scatt. efficiency of phonons 0-59348

0–59348
analytical aspects, review 0–44748
atom, third harmonic generation, theor. calc. 0–55256
boracites. Frequency doubling 0–54055
causality relations in nonlinear systems and optics appls. 0–38519
Cerenkov radiation from light pulses 0–69978
cholesteric liquid crystals, phase-matched, third-harmonic generation 0–55593

conference topic, Charia, Crete, Jul 1968 0–68729 conical refraction in isotropic dielectric in presence of another intense light beam 0–38531

beam 0–38531
crystal defects effect 0–75995
double resonance in solids, theory 0–44753
downconversion and upconversion, coupled and parametric with simul taneous phase matching 0–73275
dye, liquid organic, light absorpt. 0–68107
dye powder, second harmonic of Nd glass laser 0–65978
electron systems, nonlinear parameter due to laser beam interaction 0–42315

equation exact soln. 0-73272 ferroelectric, KH·PO4, second harmonic generation, temp. depend.

0-66069
ferroelectric, NNO₃, phase-matching props. 0-76006
ferroelectric, NaNO₃, second harmonic generation study of phase transition 0-62590
ferroelectric, triglycine sulphate, second harmonic generation and scatt. by domains 0-79229
ferroelectric KTaO₃, anomalous acoustic dispersion with soft optic phonons 0-43873
ferroelectric cryst, props. 0-62584
ferroelectric triglycine sulphate, second harmonic generation and scatt. by domains 0-62592
ferroelectrics, oxygen-octahedra type, models, applies. 0-62619
fluorescence, coherent reson, excited by short light pulses 0-38485
focusing in cubic media, calcs. 0-52349
frequency doubling in mol. cryst. 0-75991

Nonlinear optics continued

frequency mixing in light scatt, by harmonically bound electrons 0-38517 gas, second harmonic generation, d.c. field induced 0-46826

gas, second narmonic generation, d.c. field induced 0–46826 geometrical equations, exact solutions 0–52353 geometrical theory of nonlinear wave propag. 0–60312 glass, laser-irradiated, self-focusing pattern rel. to point-like damage 0–62591

harmonic generation, cascade method, trebling of frequencies 0-42346 harmonic generation, phase-matched, third harmonic in liquid crystals 0-55593

harmonic generation, second, anharmonicity effect in Coulomb subsystem 0-56480

harmonic generation, second, via coupled anharmonic Lorentz oscillator, intuitive theory 0-60315

harmonic generation, third, using hot-electron nonlinearity of semiconductors 0-44750

tors 0–44750 harmonic generation, third, wave pattern in isotropic and anisotropic media 0–49103 harmonic generation, third- and induced second-, and Kerr effect, susceptibilities 0–39317 harmonic generation and multiphoton transitions 0–45734 hexamethylene-tetramine crysts, rectification const. 0–41095 hologram nonlinear off-axis and spurious distortion, study 0–54898 holographic ghost images, analysis using Chebyshev polynomials 0–54888

U-34888 holography, ghost images. Chebyshev polynomial 0-42327 image upconvertor with nonplanar pump beams 0-60413 interference coating types for harmonic generation and parametric amplification 0-62585 amplification 0-62585 iodoform, self-focusing effects of solvent on laser-induced photolysis 0-72557

0-72557
laser beam pulses, self focusing 0-57528
laser beam in glass Q spoiled, self-focusing · 0-59349
laser frequency multiplication using special geometry crystals 0-42317
rel. to lasers, critical evaluation, book 0-42248
lasers, high power pulsed 0-49025
liquid, second harmonic generation, d.c. field induced 0-46826
liquids, Bragg reflection from phase grating induced by non-linear optical
effects 0-71346
lithium formate monohydrate, susceptibility, transmission, and refractive
indices 0-79228

magneto-optic transverse Kerr effect in ferromagnetic metals, theory 0-72310

0—72310
Maker fringes, isotropic and uniaxial crystals, theory and expt. 0—41096
materials, metal oxides with nonbonded electrons 0—62586
materials, review 0—51257
modulation, CO₂ laser-klystron system 0—42236
modulators and tunable oscillators 0—69965
molecular cryst., second harmonic generation rel. to charge transfer 0—75991

0—7991 molecular crystal, second-harmonic generation, quantum theory 0—79226 nematic liq, cryst., transient behaviour in elec. field 0—71349 paraelectric, elec.-field-induced second harmonic generation 0—65976 paramagnetic crystal frequency multiplication and mixing 0—69775 parametric noise pumped by mercury lamp 0—67042 parametric oscillator, optical backward-wave, threshold condition

0-69869

plasma, laser produced, second-harmonic generation 0-71156 polar (pyroelectric) crystals, 6, absolute signs of SHG coeffs. 0-44751 polarizability in resonance interactions. Raman scatt.. Stark effect 0-73274

polarizability tensor near exciton absorpt, band 0-69068 polarization, susceptibility due to resonant non-monochromatic radiation

0-38483 powders, cryst., second harmonic generation 0-44749 principles and applications of quantum electronics, book 0-42234 pulse distortionless propag, in resonant medium 0-49022 pulse propag, in resonant absorber with homogeneously broadened transition 0-56481

tion 0-56481 pulse propagation, coherent, in inhomogeneously broadened attenuator, effect of degeneracy 0-45773 pulses, picosecond, generation and meas. 0-42323 quadratic, crystals, second and third harmonics generation, simultaneous, synchronous 0-40540 rectification const., theory, calc. 0-41095 refractive index, isothermal and isolated susceptibilities 0-75993 resonant scatt., by perturbed atoms, assoc, time-depend, phenomena 0-57505

review of mechanisms and devices 0-67121 scattering, four-photon, in resonant medium 0-54901

scattering, spontaneous parametric three- and four-photon, quantum theory 0-45830

scattering, spontaneous parametric three- and four-photon, quantum theory 0-45830 scattering by static nonuniformities (small particles) 0-69976 scattering in anisotropic media 0-73273 second harmonic generation rel. to charge transfer in mol. cryst. 0-75991 second harmonic generation, cryst. inhomogeneity depend. 0-47985 second harmonic generation, check field induced, in gases and liquids 0-46826

second harmonic generation, phase matching, inhomogeneities effect 0-47986

0-4/860 second harmonic generation, photon correls. 0-62588 second harmonic generation, quantum vs. classical analysis 0-69864 second harmonic generation, refr. index inhomogeneities effects 0-56482 second harmonic generation 0-38520 second harmonic generation by interaction of two basic frequency waves 0-60316

second harmonic generation by ruby laser with dielectric surface scatterer 0-42250

0-42230 second harmonic generation in laser produced plasmas 0-71156 second harmonic generation phase-matching temp. in LiNbO₃ 0-62587 second harmonic generation using LiIO₃ in repetitively Q-switched Nd:YAI garnet laser 0-69917 self-focusing, filament production resulting from focal point motion 0-46014

0 - 46914

self-focusing, thermal, in media with dn/dT<0 0-47987 self-focusing in crystal, spectral broadening 0-79345 self-focusing of high intensity light beams 0-42350

semiconductor, harmonic generation and mixing, free-carrier contrib.

Nonlinear optics continued

semiconductor, indirect band-gap, resonance enhancement of second harmonic generation 0–52352 semiconductor, mixing by mobile carriers 0–47989 semiconductor, second harmonic generation, d.c. electric field 0–47988 semiconductor, third harmonic generation using hot electron nonlinearity 0-44750

0-44/50 spatial filter, linear optimization in synthesis 0-70044 spatial filtering, use of film nonlinearities 0-59839 stimulated Brillouin and Raman effects in liqs, and gases reviewed

0- 43447
susceptibilities, invariants of third-rank cartesian tensor 0-75994
susceptibilities, theory and calc. 0-69069
susceptibility, linear and third order nonlinear, empirical relation 0-79230
theoretical aspects review 0-44748
thermal defocusing of air doped with SF₆ 0-57546
third harmonic elastic scatt, of laser light in gases and liquids, depolariza
tion 0-71259
third harmonic generation, theor, calc. 0-55256
transient-pulse behaviour and self induced transparency 0-38486
triglycine sulphate, ferroelec... second harmonic generation and scatt, by
domains 0-62592
triglycine sulphate, second harmonic generation and scatt, by domains
0-79229
tunable four-photon parametric fluorescence obs... in visible region

tunable four-photon parametric fluorescence obs., in visible region 0-79362

0-79362
tunable oscillators and modulators 0-69965
two-photon absorption, cooperative energy transfer, solids 0-69067
two-photon absorption, cooperative energy transfer, solids 0-69067
two-percation by sequential freq, conversion method 0-57555
two-percation in organic scintillators 0-38506
of ultra-short pulses 0-45815
ultra-short pulse propag., higher conservation laws 0-60310
uniaxial crystals, noncollinear phase-matching cones analysis 0-72299
Agy-AsS, proustite, parametric oscillation 0-77068
Ar. liq., filaments and self phase modulation, Kerr effect nonlinearity 0-53350

Ba-LiNb₂O₁₅, with no microtwinning 0–65974
Ba-NaNb₂O₁₅, parametric fluoresc, for 10 cw pump wavelengths 0–66103

0-66103

BeSO_{1.4}H+O, second harmonic generation 0-68236

CO₂, obs. of optical nutation obs. 0-60311

CS₂ CC₁ mixtures, nonlinear refractive indices 0-39792

CaCO₃, calcite, nonlinear props, meas. 0-51258

CdS thin film's spatial modulation, theory, expt. 0-66005

CdSe semiconductor, absorpt, coeff. at 1.064*u* obs. with YAI garnet: Nd laser 0-41099

CdTe, segond harmonic generation and proceedings.

CdTe, second harmonic generation and sum freq. mixing 0-51259 CdTe semiconductor, absorpt. coeff. at 1.064µ obs. with Yal garnet: Nd laser 0-41099 CdlHg(SCN),I, efficient phase matchable second harmonic generation 0-72300

CsH-AsO₄ crystals, second harmonic generation 0-44754

GaAs, coeffs, determ, rel. to Ag₃SbS₁ 0–65975 GaAs, optical harmonic generation, phase matched, by pulsed u.s. shear wave 0–48022

wave 0–48022
GaAs, optical susceptibility 0–72301
GaAs semiconductor absorpt, coeff, at 1.064 μ obs, with YAI garnet-Nd laser 0–41099
HIO, SHG coeff, d₁₇₃ and nonlinear optical polarizability of 1-O bond 0–44769

0–44769

InAs, optical susceptibility 0–72301
InSb, mixing 0–75998
InSb, optical susceptibility 0–72301

K LiNbO₃, nonlinear properties 0–72302

K vapour, angular distrib, changes of light intensity on laser-beam passage 0–60955

KD-PO₄ laser modulator crystal, temperature instability 0–47990 KH-PO₄, diffraction of moving light waves 0–41097 KH-PO₄, optical second harmonic generation by diverging laser beams 0–42347

0-42347
KH:PO₄, second harmonic generation, temp, depend. 0-66069
KH:PO₄, susceptibility meas. 0-47991
KH:PO₄, susceptibility meas. 0-47991
KH:PO₄ crystal, conversion from low power Nd glass laser radiation to second harmonic 0-62582
KH:PO₄ laser modulator crystal, temperature instability 0-47990
KH:PO₄ optical rectification effect applic, to giant pulse laser power meas. 0-75999

0–73999
KNbO), phase matching props. 0–76006
KTaO), elec.-field-induced second harmonic generation 0–65976
KTaO₃, ferroelectric, anomalous acoustic, dispersions with soft optic phonons 0–43873

LiGaO second-order, nonlinearities and second-harmonic generation 0-59350

LiIO₃, far-i.r. props. 0–69070 LiIO₃, SHG coeffs. d₃₁₁ and d₃₃₃, nonlinear optical polarizability of I-O bond 0–44769

LilO₃, SHG coeffs. d₃₁₁ and d₃₁₃, nonlinear optical polarizability of I·O bond 0 –44769
LilO₃, second harmonic production of ruby laser 0–77120
LilO₃, susceptibilities 0–41098
LiNbO₃, second harmonic openform on solinear phase matching 0–62589
LiNbO₃, second harmonic open-cition phase-matching temp. 0–62587
LiNbO₃, second harmonic generation phase matching inhomogeneities effect 0–47986
LiNbO₃, second harmonic generation, photon correls. 0–62588
NI₄H·PO₄, susceptibility meas. 0–47991
NI₄H·PO₄ downconversion and unconversion, coupled, and parametric with simultaneous phase matching 0–73275
NI₄H·PO₄ poly nonlinear props. meas. 0–51258
NI₄H·PO₄ nonlinear props. meas. 0–51258
NI₄H·PO₄ optical rectification effect applic, to giant pulse laser power meas. 0–75999
NaNO₅, second harmonic generation study of phase transition 0–62590
Nb·O bond, polarizability 0–51260
Nd·Y Al garnet, nonlinear props. meas. 0–51258
Nd·YAl garnet, tollinear props. meas. 0–51258
Nd·YAl garnet, LilO₅ 0.53 μ harmonic source, repetitively Q-switched 0–69917
Nd glass laser, u.v. generation by sequential freq. conversion method

Nd glass laser, u.v. generation by sequential freq. conversion method 0-57555

NdCL₃ aq., absorpt, coeff. at 1.064μ obs. with YAI garnet: Nd laser 0-41099

Nonlinear optics continued

PrCl₁ aq., absorpt coeff, at 1.064*n* obs. with Yal garnet:Nd laser 0–41099 St. rigional, light beam modulation 0–65977 Si semiconductor, absorpt, coeff, at 1.064*μ* obs. with YAl garnet: Nd laser 0–41099

0–41099
SiO₃ quartz susceptibility meas. 0–47991
SrTiO₄ elec.-field-induced second harmonic generation 0–65976
Te, coeffs, determ, rel. to Ag.8bS₄ 0–65975
Te, SHG efficiency, CO₃ laser freq, doubler 0–77104
ZnO₄ nonlinear optical susceptibility, new contribution arising from unequal atomic radii 0–66004
ZnTe, optical susceptibility 0–72301
Zn1Hg(SCN)₃], efficient phase matchable second harmonic generation 0–72300

Novae

see also Stars

RS Oph, spectra, 1959 1968 0-63036

T Pyx, spectra in 1967 maximum 0-63037

T Pyxidis, photometric and spectroscopic obs. two months after December 1966 outburst 0-48450

Cas A, X-ray source, implications for X ray emission from other supernova remnants 0-45327

Cas A, supernova remnant, X ray characts. 0-51689

Crab nebula, X-ray characts., comparison with two other remnants 0-51689

OF Herenitis old noval light curve obs. 0-41694

Crab nebula, X-ray characts... comparison with two other remnants 0–51689
DQ Herculis old nova, light curve obs. 0–41694
Delphini, spectrographic obs. (1967 8) 0–48449
Delphini 1967 spectral and brightness vars. and slow novae characts. 0–63039
HB 21, supernova remnant, assoc, neutral 0–66516
Nova WZ Sge, light curve and model 0–63049
nucleosynthesis in mass range 20≤A≤62 0–69385
plasma shock waves in supernova explosions, book 0–46681
SN 1572. X-ray source, implications for X ray emission from other super nova remnants 0–45327
SN 1572, supernova remnant, X-ray characts. 0–51689
Serpentis 1970, identification with prenova star 0–48447
super, outbursts theory of brightness curves 0–72729
super - positrons and low energy cosmic rays from 0–79672
super-, rotating, mechanism of explosion not connected with nuclear detonation 0–72730
supernova, identification of 15 new remnants, distances and physical properties 0–79698
supernova's garnet composition 0–72740
supernova explosion, in close binary system, effects 0–66500
supernova explosions, heavy element condensation during expansion phase 0–48443
supernova explosions, heavy element condensation during expansion phase 0–48443

supernova neutrino-transport models, nucleosynthesis conditions
0 -48446

supernova plasma shock waves, book 0–46681 supernova remnant features, coincidence with galactic radiosources in 4C catalogue 0–41737 supernova remnants, Cas A, SN 1572 and Crab nebula, X ray characts. 0–51689

supernova remnants Taurus A Cas A, polarization distrib., 9.75 cm 0-41729

supernova remnants γ rays rel. to cosmic rays origin, and Cas A obs. 0 41758

supernova remnants catalogue and distance scale 0–54408 supernova remnants sub-millimeter nightsky radiation background effect on cosmic phenomenon 0–57066 supernova shell origin of cosmic rays 0–79519 supernovae, broad band absorpt, spectra, and intense background 0–41689

0 41689
and supernovae, magnetic fields 0-79671
supernovae, type II, presupernova stage 0-63010
supernovae in random sample of galaxies, search 0-66479
Type I supernovae, from thermonuclear detonations in collapsing white
dwarfs 0-66454
3C10 and 3C58, supernova remnants, polarization props., 1420 and 2880
MHz 0-66559
Novoids see Novae

Nuclear acoustic resonance see Absorption/acoustic waves, ultrasonic; Nuclear magnetic resonance and relaxation Nuclear alignment see Nuclear polarization

Nuclear dignment see Nuclear polarization

Nuclear dignment targets
composite, determ. of partial thickness 0—52582
Doppler shift attentuation meas., vacuum recoil correction 0—60641
mica, 4n geometry, fission detection 0—60711
polarized proton, butanol glycol, intense electron and photon beams
0—60642
radioisotopes prod., shape and arrangement of target materials, self shield
ing effect obs. 0—38957
⁸⁹Co polarized target using ⁹He ⁴He dilution refrigerator 0—49625
Cr foil for medium energy proton scattering experiments 0—77548
D liquid in closed system 0—38740
H liquid in closed system 0—38740
H liquid in closed system 0—38740
H shigh Coold target, prep. 0—46015
La Mg.(NO3); 24H-O proton, polarized, medium sized 0—77386
La Mg.(NO3); 24H-O, polarized proton target for low energy n p scattering 0—52784
¹⁸NH; cold target, prep. 0—46015
242Pu targets, ³³²Cf buildup estimation using underwater neutron counter
0—52583
Zn-T. aerosol parameters obs., inhalation hazard evaluation 0—54487
Nuclear decay theory

Nuclear decay theory
see also Beta decay theory; Nucleus/theory
a penetrabilities deriv. by JWKB approach, accuracy 0–49557
three-body problem, relativistic 0–73437
Nuclear emulsions
see Nuclear track emulsions
Nuclear energy level lifetimes
see Nucleus/energy level transitions

Nuclear excitation

crear exchation see also Mossbauer effect; Nucleus/energy levels β_1 deformation parameter of rare earth nuclei from (p,t) reaction cross section of 4⁺ member 0–49610 analog states, nature of fine structure 0–73753 analog-antianalog gamma, transitions 0–46115

Nuclear excitation continued

analogue resonance in region of overlapping levels of compound nucleus 0-77477 analogue resonances for understanding of excited states 0-67510

analogue resonances for understanding of excited states (-6.75] bound levels, partial radiation widths excited by (p.p') - 0.73894 compound nucleus lifetime meas, using blocking effect 0.-42725 compound nucleus states $(T_0+\frac{1}{2})$, neutron decay 0.-67395 continuum contribution to spectroscopic sum rules 0.-70575

Core excitation model for A=23-35 region 0-70564 Coulomb, of core in Coulomb stripping of heavy ions 0-39130 Coulomb displacement energies in light nuclei rel. to shell model description 0-67408

Coulomb distortion in heavy-ion reactions 0–70669
Coulomb-energy differences of excited mirror nuclei, systematics 0–42720 de-excitation in heavy ion induced reactions, ang. momentum effects

0–39133
deformation lengths of doubly even spherical nuclei near closed shells, 44
MeV α-particle scattering 0–46234
deformed, analogue states 0–67404
deformed nuclei, even, with A≥222, octupole vibrational states, microscopic description 0–55116
deformed nuclei, single particle transfer to highly excited states 0–49583
deformed states in light nuclei, study using single particle representation
0–38829

U=36829 dipole giant resonances of non magic nuclei 0-46117 dipole reson., dwarf type, due to compressional oscillations 0-55115 dispersive effects in elastic electron scattering by vibrational nuclei 0-52755

0-52755 distortion in heavy ion reactions 0-73727 c.m. and weak, of overlapping resons, system, and decay 0-38833 c.m. transition probabilities between excited states of odd nuclei 0-63973 equilibrium deformations in range 28 < Z < 50, 50 < N < 82 0-63978 even quasirotational nuclei, semiempirical description of ground-state band 0-70366 giant dipole reson, gross struct. of N ≈ 90 nuclei 0-67513 giant dipole reson, gross struct.

giant dipole resonance collective correlations model for 4n nuclei 0-67392 heavy nucleus, by electrons subsequent p decay of excited state 0-73911 isobaric analog resonances in N=82 nuclei due to p scatt.. 2₁* mixing 0-64112

10—04112 isobaric analog resonances microscopic theories 0—57891 isobaric analogue reson, description by reson, wave functions 0—49479 isobaric analogue resonances, single particle resonant-state wave functions for descrip. 0—38832

isobaric analogue state, in reactions on even-odd target, three-body model : 0–73893

O=73893 isobaric analogue states, diagrammatic expansions, Coulomb displacement energy 0=63974 isovector excitation, total intensities 0=49481

level widths, from neutron radiative capture 0–73760 mean lifetimes of excited states, in A=15-25 range 0–38857 medium, spherical nuclei study of giant resonance by photon scatt. 0–46194

paired states, by variational approach 0-52653

paned states, by variational approach 0-52653 quadrupole giant resonances in even-even nuclei 0-42728 random phase approximation in terms of eigenvalue problem rare-earth, deformation parameters β_{10} and β_{40} 0-52639 resonance reactions, resolution of paradox in variational formulation 0-73759

resonance struct, function 0–39006 resonances, Mittag-Leffler expansion of S-matrix integral representation 0–73886

rotational excitations, microscopic theory 0-42724 rotations described as intrinsic excitations, without cranking theory 0-63984

 $5U_2$ symmetry group and sum rules for isovector excitation processes 0-67391

S-wave neutron resonances from low-energy capture γ -ray spectrum 0-49493

Schiffer procedure modified for spectroscopic factors from analogue resonances 0-67511 spherical, medium nuclei, study of giant resonance by photon scatt. 0-46194

 $^{\circ}$ 0–46194 states, spin depend, of density 0–52661 strength function of reaction theory, dynamical restrictions 0–73889 transuranium, deformation parameters β_{20} and β_{30} 0–52639 weak coupling model, particle hole excitation in 2s-1d shell 0–70370 (3 He.α) reaction with nuclei in s-d shell, excitation function data analysed 0–67549 (n.2n) fast reaction cross sections in free Fermi gas model, excitation energy 0–39064 14 Cd($\alpha_{cx}\alpha^{cy}$) and Coulomb excitation, interference behaviour 0–49668 1 ε/Tm, n reaction, reson, parameters and spin. E=4–830 eV 0–39073 107 Ag, Coulomb excitation with 10 MeV α particles and 45.5 MeV ions 0–64031 107 Ag, n reaction, reson, parameters and spin, E=4-830 eV 0–39073

¹⁰⁷Ag, n reaction, reson, parameters and spin, E=4-830 eV 0-39073

0-04031
¹⁰⁷Ag, n reaction. reson. parameters and spin. E=4-830 eV 0-39073
¹⁰⁸Ag, n reaction. reson. parameters and spin. E=4-830 eV 0-39073
¹⁰⁹Ag, n reaction. reson. parameters and spin. E=4-830 eV 0-39073
¹⁰⁹Ag Coulomb excitation with 10 MeV α particles and 45.5 MeV oxygen
ions 0-64031
²⁷Al excited levels produced in ²⁶Mg(p.n)²⁶Alm spin-parity assignments
0-17491
²⁷Al T=3/2 analog states excited by ⁹Be(³He.n)¹¹C reaction 0-46121
²⁶Ar*, filterime of 1.970, 4.178, 4.413 MeV 0-46133
²⁶Ar*, analog resonances, level positions and energy integrated total cross-sections 0-39046
⁴⁰Ar quadrupole moments of first two excited states 0-38875
¹⁹⁷Au, Coulomb excitation and 268 keV level 0-64065
²⁶⁷Au, n reaction. reson. parameters and spin. E=1000-2100 eV 0-39079
²⁶⁷Au excited states studied, isomeric decay obs. multipolarity assignments
0-73832
²⁶⁸B 7.01 MeV level width and reson. energy determ. from ⁶Li(α,α)⁶Li
0-39102
²⁶⁸(ELiα,2)α, α-part. continuum spectrum, reson. obs.. E=5-10 MeV

0-39102 in 0-39102 in 0-39102 in 0-39102 in 0-55170 in 0-55170 in 0-46203 in Eq. (a) 0-56170 in 0-46203 in Eq. (a) 0-46203 in Eq. (b) 0-49656 in Eq. (b) 0-49656 in 0-49656 i

Nuclear excitation continued

²⁰⁹Bi, collective septuplet at 2.6 MeV, Coulomb excitation 0-64072 209Bi. Coulomb excitation and the weak-coupling model 0-49551

209 Bi, Coulomb excitation and the weak-coupling model 0–4955 l 209 Bi, obs. of (5 % h₉r.) decuplet, weak coupling 0–77508 l'C giant dipole resonances observed by 108 (p,y) reaction 0–70396 l'C T=3/2 analog states excited by 9 e(14c.n) 1 C reaction 0–46 l21 l'C, of 15.1 MeV level, by inelastic escatt. 0–428 l6 l'C, of giant resonance by inelastic electron scattering 0–739 l4 l'C, struct, in giant reson region, from e scatt, and μ capture in continuum model 0–3902 l l'C (12C, 12C) elastic scattering, excitation functions 0–7067 l'C due to electron scattering at low momentum transfer 0–46195 l'C, level obs. from inelastic electron scatt, between 36 and 65 MeV 0–38856 l'C*—91-12C, following 14Ny.p) l'C*, de-excitation neutrons obs. 0–60800

¹³C*-n+¹⁷C. following ¹4Ny.p) ¹³C*, de-excitation neutrons obs. 0–60800 ⁵¹C. electroexcitation of f_{7/5} proton states 0–70460 ⁴⁰Ca, giant dipole states study from (y.n₀) reaction 0–49594 ⁴⁰Ca, giant resonance, study by inelastic electron scatt. below 60 MeV 0–39018 ⁴⁰Ca 4p-4h model 0–70385

⁴⁰Ca 4p-4h model 0–70385

⁴¹Ca, deduced resonances, from ⁴¹K(p, α₀)¹⁸Ar 0–49616

⁴²Ca, care excitation in ⁴⁴Ca(d,p) stripping reaction 0–49664

⁴⁸Ca, core excitation in ⁴⁴Ca(d,p) stripping reaction 0–49664

⁴⁸Ca, energies, spins decay modes and lifetimes of first 3 excited states determ. 0–77496

⁴⁸Cb, Coulomb, reorientation effect rel. to static quadrupole moment, obs. 0–42757

¹¹⁰Cd, isobaric analog resonances in proton elastic scatt. 0–67475

¹¹²Cd, Coulomb, reorientation effect rel. to static quadrupole moment, obs. 0–42757

¹¹⁴Cd, isobaric analog resonances in proton elastic scatt. 0–67475

¹¹⁴Cd, isobaric analog resonances in proton elastic scatt. 0–67475

14Cd quadrupole moment in first excited state 0-60755 14Ce, lifetimes of excited states at 2083 and 2412 keV 0-52699

49°Ce. lifetimes of excited states at 2083 and 2412 keV 0—52699
 29°2CI primary fission products, experimental information on deformation 0—55176
 3°CI, analog states 0—46132
 3°CI, excited 3.95 MeV level existence from decay scheme for 8.38 MeV isobar-analogous state 0—67502
 3°Co analogue state identified as resonances in (p,γ) and (p,p) reactions on 3°Fe (p,γ) 0—49521
 3°Co, from 3°Fe(p,γ) 0—49521
 3°Co, Coulomb excitation contribution to cross sections for excitation of 2° and 3° levels 0—52797
 4°Cr produced by 3°He, preaction, observation of excitation in low-lying states with T=2 0—73993
 3°Cu, isobaric analog resonances, isospin mixing 0—46137
 3°Cu, isobaric analog resonances, isospin mixing 0—46137
 3°Cu, isobaric analog resonances, isospin mixing 0—46137

⁵⁹Cu. isobaric analog resonances, isospin mixing 0–46137
 ⁶¹Cu, isobaric analog resonances, isospin mixing 0–46137
 ⁶²Cu, isobaric analog resonances, isospin mixing 0–46137
 ⁶³Cu, isobaric analog resonances, isospin mixing 0–46137
 ⁶⁴Cu, isobaric analog resonances, isospin mixing 0–46137
 ⁶⁵Cp, isobaric analog resonances, isospin mixing 0–46137
 ⁶⁶Cp, Coulomb excitation of vibrational and rotational states 0–38932
 ⁶⁶EF coulomb excitation probabilities for 2+ and 4+ levels, bombarded with 3-60 circle of coulomb excitation probabilities for 2+ and 4+ levels, bombarded with 3-60 coulomb excitation probabilities for 2+ and 4+ levels, bombarded with 3-60 coulomb excitation probabilities for 2+ and 4+ levels, bombarded with 3-60 coulomb excitation of rotational and vibrational bands 0–38932
 ⁶⁷EF coulomb excitation of rotational and vibrational bands 0–38932
 ⁶⁷EF excited states studied, isomeric decay obs. multipolarity assignments 0–73832
 ⁶⁸EF isobaric analogue resons, proton polarization meas. 0–38927

¹⁸Er Coulomo excitation of rotational and vibrational and so −36932 or −3832 or −3832 isolaric analogue resons., proton polarization meas. 0−38927 isolaric isolaric analogue resons., proton polarization meas. 0−38927 isolaric analogue resons., proton polarization meas. 0−38927 isolaric analogue resons., proton polarization meas. 0−38927 isolaric analogue stactors of second excited states 11/√−, by differential ang. correlation method 0−73825 isolaric analogue states. 0−52701 isolaric method 0−3825 isolaric analogue states. effect on proton elastic and inelastic scatt. from ¹⁵Fe, core-excitation, effect on spectrum 0−73808 isolaric analogue states, effect on proton elastic and inelastic scatt. from ¹⁵Fe 0−49607 isolaric analogue states of Zn 0−42755 isolaric analogus states of Zn 0−42756 isolaric analogus states of Zn 0−39123 isolaric analogus states of Zn 0−42770 isolaric analogus states of Zn 0−42770 isolaric analogus states of Zn 0−38932 isolaric analogus states of Zn 0−38833 isolaric analogus states of Zn 0−3883 isolaric analogus states states and Zn 0−73836 isolaric analogus states states and Zn 0−73836 isolaric analogus states states and Zn 0−73864 isolaric analogus states of Zn 0−3864 isolaric analogus states of Zn 0−3864 isolaric anal

0—73832

164 Ho, spin determ, of resonances, from low-level occupation probability ratios 0—73964

171 energy levels from Coulomb excitation 0—64035

173 in, Coulomb excitation with oxygen ions, p-ray spectra 0—42759

175 in, Coulomb excitation with oxygen ions, p-ray spectra 0—42759

175 in, Coulomb excitation with oxygen ions, p-ray spectra 0—42759

175 in, n capture resonance p-rays, structure 0—73963

178 ir, Coulomb excitation, angular correlation meas. 0—49544

179 ir excited states studied, isomeric decay obs. multipolarity assignment 0—73832

179 ir, Coulomb excitation, angular correlation meas. 0—49544

179 ir excited states of the course of t

0-46197

37K 0-46197 in a particles 0-70491 FLi, study within excitation range of 17.8-21.1 MeV, by radiative capture reaction 0-49499

6Li, transverse form factor for excitation to 3.56 MeV level by electron scatt. 0-42734

²⁴Mg, by neutron elastic and inelastic scatt, at 14.2MeV 0-73956

Nuclear excitation continued

²⁴Mg, giant resonance, study by inelastic electron scatt, below 60 MeV 0. 39018

²⁴Mg, quadrupole moments, using SU₁ model and projected HF cales. 0.77490

⁰/⁷⁴⁹⁰ ¹/₂Mg(excitation of 3¹, ⁴ levels 0 64132 ²Mg(τ-τ)²Mg, canalog states excited by ⁹Be(¹He.n)¹/₂C reaction 0 46121 ²Mg, giant resonance, study by inclustic electron scatt, below 60 MeV 0 5901:

0. 2001:

Mg inelastic electron scattering, splitting of giant resonance 0. 42741.

Mg inelastic electron scattering, excitation functions 0. 70671.

Mn(4 N), 4 N) elastic scattering, excitation functions 0. 70671.

Mn(4 N), evidence for a tensor effective two body interaction in the 2.31.

MeV excitation 0. 52774.

Nn*, formation of excited levels in capture of μ by O nuclei. 0. 46203.

Na 2.85 keV neutron resonance, radiation width meas. 0. 77489.

Na studied following 3 Ne(p, $p)^{3}$ Na, 300-1300 KeV. 0. 46127.

Nn. levels up to 3.92 MeV, from elastic and inelastic proton scatt, meas. 0. 390.30.

No. 100 Med. 10

Nal, levels up to 3.92 MeV, from elastic and inelastic proton scatt, meas. 0. 39030
Nal, photo excitation of T - ½ states. 0. 67430
Nal by inelastic scattering of electrons. Coulomb excitation of discrete energy levels. 0. 46197
Nd. (A - 144, 146, 148, 150). Coulomb, by He, O and S ions, static quadrupole meas. 0. 64038
Ne grant dipole resonances from ¹⁹F(p,p). 0. 70423
Ni isotopes, of low lying states by α transfer reactions. 0. 46136
Ni 49 4h model. 0. 70385
O giant dipole resonances observed by ¹⁸N(p,p) reaction. 0. 70396
O T = 3/2 analog states excited by ¹⁸F(Fit,n) ¹¹C reaction. 0. 46121
O, electroexcitation of first excited state, monopole sum rule. 0. 70404
O, struct, in giant reson, region, from e-seat, and α capture in continuum model. 0. 39021
O a excitation, ground state correlation effect calc. 0. 73785
O (Φ, ¹⁶O) elsatic scattering, excitation functions. 0. 70671
O from ¹⁹C(F1,d) ¹⁰O and ¹⁰C(F1,d) ¹⁶O rotational bands, giant dipole resonance. 0. 46250
O(Φ, ¹⁰O), low lying negative parity states, from ¹⁸O(p,d) ¹⁷O. 70411
O excited state at 20.4 MeV, assignment from data on ¹⁶O(n,n) ¹⁶O. 49622
²⁹P, p ray transitions, from ²⁸Si(p,p). 0. 73798
O(120) (

0 496.22

"PP, p ray transitions, from 28Si(p,p) 0 73798

"PP, excitation of T 3/2 level by 7/Alc He.n) PP 0 46121

"PP, core exertation, by 28SiCHe.d) 0 70437

"P, exertation of 3 to 6 MeV states, by inclusite scatt, of 14 MeV neutron 0 67437

O 67437

19 photo excitation, lowest T 1/2 state not obs. O 67430

19 photo excitation, lowest T 1/2 state not obs. O 67430

19 photo 202, 200, 198), excited states from decays of BitA 202, 200, 198)

10 49547

PhtA 202, 200, 1760; vactoring to 49547.

²⁰⁸Pb, Coulomb excitation contribution to cross sections for excitation of 2¹ and 3 levels 0 · 52797.

²⁰⁸Pb excitation energies in ³⁰⁷Pb(d,p)⁷⁰⁸Pb 0 · 67492.

²⁰⁸Pb by neutron scattering, RPA and TDA calc., effect of continuum 0 · 73951.

²⁰⁹Pb, 1/2¹ doorway resonance at 500 keV, particle vibration model 0 · 73839.

0. 73839
 10 Pd Coulomb excitation probabilities and quadrupole moments of first excited 2 states. 0. 70481
 10 Pd Coulomb excitation probabilities and quadrupole moments of first excited 2 states. 0. 70481
 14 Pm isobaric analogue resonances, deduced proton decay widths. 0. 46435

0 46125 147Pm, 91 keV level, mag. moment 0- 73827

10. 46125

147 Pm. 91 keV level, mag. moment. 0- 73827

Pl. n reaction, reson, parameters and spin, 1: 4 830 eV 0-39073

158 Pt. strustical approach to deformation. 0-70511

159 Pt., statistical approach to deformation. 0-70511

150 Pt., statistical approach to deformation. 0-70511

150 Pt., statistical approach to deformation. 0-70511

150 Pt., statistical approach to deformation. 0-70511

151 Pt., statistical approach to deformation. 0-8074

152 Pt., statistical approach to deformation. 0-8074

153 Pt., statistical approach to deformation. 0-8074

154 Pt., statistical approach to deformation. 0-8074

155, storing transitions from 15 Pt., p.) to 150 excited state. Fp. 1146 ReV neutron. 0-67437

152 Statistical transitions from 15 Pt., p.) to 150 excited state. Fp. 1146 ReV neutron. 0-67437

153 Stant dipole states study from (p.n.n) reaction. 0-49594

154 Statistical approach to the states of the states of the states of the states. 0-38875

155 Statistical approach to the states of excited states. 0-49511

156 Statistical approach to the states of the states. 0-49594

157 Statistical approach to the states of the states. 0-49594

157 Statistical approach to the states of the s

10 70502 1338m, excitation probabilities 0 64045 1338m, excitation probabilities 0 64045 1338m, multiple Coulomb excitation of ground state rotational band 0 49538 1338m, arababilities 0 64045 0 49538 154Sm, excitation probabilities 0 64045

Sn isotopes, giant dipole and quadrupole resonance, splitting calculated 0 42728 Sn isotopes, giant dipole resonances, exam, by shell model 0 - 70568 ¹¹⁶Sn, by e inclastic scatt., 60 MeV, quadrupole and octupole excitations 0 42761

0 42761 116Sn Coulomb, reorientation effect rel. to static quadrupole moment, obs.

117Sn, of levels from 116Sn (a, 3He) 0-39125

Nuclear excitation continued

¹¹⁸Sn, by c inclusive scatt., 60 MeV, quadrupole and octupole excitations 0, 42761

10/Sn, by e inelastic sentt., 60 MeV, quadrupole and octupole excitations () 12/161

¹⁷⁴Sn, by e inclustic scatt., 60 MeV, quadrupole and octupole excitations 0 42761

0. 42761 ¹²⁴Sn, Coulomb, reorientation effect rel. to static quadrupole moment, obs. 0. 42757

0 42757
Sr isotopes, effective interaction 0 38897
**Sr, mens, of excitation curves for 4 states 0 77579
**Sr, mens, of excitation curves for 4 states 0 77579
**Per, Coulomb excitation, deduction of levels from **Line Coulomb, levels compared with models 0 67476
**Per, Coulomb excitation, deduction of levels from **Line Coulomb, levels compared with models 0 67476
**Line Coulomb,

Gri(S, **JS*p), of first excited 2* states, reorientation measurements of 6404?
**Unir resons, and o_f anal. 0 | 52709
**Unir resons, and o_f anal. 0 | 39080
**V energy of excited levels 0 | 495.19
*!V excited states lifetimes 0 | 38951
**PY h, multiple Coulomb excitation of ground state rotational band 0 | 195.20

10 (1952) 194Yb, multiple Coulomb excitation of ground state rotational band 0 49538 194Yb, multiple Coulomb excitation of ground state rotational band 0 49538

⁶⁰Zn produced by (³He,a) reaction, observation of excitation in low lying states with T=2=0=73993

**States with 1 2 to 75975.

**O'Zn, isospin splitting of giant dipole resonance, (p.np) reaction discussed 0 73810

0 38900

"Port (He d), inhibited transitions to 3810 isobaric analog states 0—73997

"Zr analog resonance studied in "Port (p.p.)" 2Tr 0 38901

"Zr(Tle.d), inhibited transitions to 3810 isobaric analog states 0—73997

"Zr(1,p)" Zr, 4.2 11.2 MeV, charge exchange effects 0—73998

"Zr(1,p)" Zr, 4.2 11.2 MeV, charge exchange effects 0—73998

"Zr(1,p)" Zr, 4.2 11.2 MeV, charge exchange effects 0—73998

"Zr(1,p)" Zr, 4.2 11.2 MeV, charge exchange effects 0—73998

Nuclear explosions | see Explosions/nuclear Nuclear field theory | see Field theory, quantum

Nuclear fission

see also Explosions/nuclear; Nuclear reactors, fission actinide nuclei, intermediate struct, effects 0 74005 adiabatic, by heavy ions 0 38794 adiabatic, by heavy ions 0 38794 adiabatic, development of time dependent Hartree Fock Bogolyubov theory 0 74007 angular anisotropy, effect of fissionability, by statistical theory 0—77587 Coulomb energy, parametric method, liquid drop model calc. 0—39148 cross section calc, in first power reactors 0—39223 cross section meas, total, using solid state track detectors 0—42882 effective cross section, resomnce overlap effect in unresolved resonance region 0 74042 energy levels in potential well deformed by sharp adag. 0—38125

energy levels in potential well deformed by sharp edge 0–38175 hist, ratio obs., determ, of calibration factor P(t) from absolute data 0 77584

0 77584 lisstonability, effect on ang. anisotropy, by statistical theory 0-77587 foil Lexan detectors, reactor neutron meas. 0 49747 fragment detectors, wire to plane spark chamber properties 0 -42628 future development 0 58028 gamma vibration, between equilibrium and saddle pt. 0-74008 heavy nuclei, correlation for cross sections of thermal n fission 0-39155 isobaric spin role for analogue states 0-67561 liquid drop model, surface corrections 0 55172 measurement using solid nucl. track detection 0-77434 mica target, 4π geometry, track detection 0-60711 neutron induced, of actuide nuclei, intermediate struct, effects 0-74005 neutron spectra, energy dependent cross section data and threshold reaction excitation functions interenlibrated in a pure fission spectrum 0-64147 nuclear properties of fissile materials obs., use of nuclear explosives

nuclear properties of fissile materials obs., use of nuclear explosives 0-74015

o 74013 particle characts, decomp, into partial characts. 0=74022 penetrability through 2 peaked fission barriers, exact calculation 0=77585 photofission, ternary, obs. with track recorders of different sensitivity 0=77432

0 77432 in reactor, rate determ, from counting tube signals 0-52847 reactor nuclear data conference, Helsinki, Finland, (1970) 0-74052 rel to reactor technology, cross sections status 0-39202 research tendency in Russian Institute 0-70687 saddle point properties for low temp, aligned nuclei 0-52814 scission barrier existence, static molecular model calc., and consequences 0-46257

seission point, 2 center shell model for two overlapping spheriods with equal mass 0.73745 second minimum systematics. 0.39150

second minimum systematics 0-39150 semi classical estimate of critical charge on ion inducing fission 0-64145 shell energy of deformed nuclei, curvature term 0-42707 shell model 0-46254 spontaneous, ³³Cf, K-X-rays, distribution as a function of mass and atomic number 0-52810 spontaneous, search for elements in nuture 0-52808 status of microscopic data knowledge 0-49688 superheavy elements, their fission and alpha-decay review 0-64079 superheavy elements, their fission and alpha-decay review 0-64079 superheavy elements, their fission and alpha-decay review 0-64079 superheavy elements in meteorites, traces of spontaneous fission 0-41811 ternary, \(\alpha \) particles and 2 main fragments produced, trajectories 0-70684 ternary, heavy fragment emission, high energy 0-42880 ternary fission data, alternative evaluation 0-49675 thermal n fission of heavy nuclei, correlation for cross sections 0-39155

Nuclear fission continued

track visualization dual microscope comparator 0-77428

white noise input sources, auto- and cross- spectral density functions 0-30194

 α -particle accompanied, four-parameter correlation experiment 0-74009 n spectra, generalized formula for static relative importance 0-39147 p.2n, excitation energies of fissioning shape isomers, statistical model 0-74021

p.2n, excitation energies of fissioning shape isomers, statistical model 0–74021

Ag induced by ²⁰Ne ions, 168. 183, 198 MeV cross-sections and fragment distrib. 0–46264

²³⁹Am^m, spontaneously fissioning isomers, fragment mass distribution and kinetic energies 0–39164

²⁴¹Am, by neutrons, 0.3 7.2 MeV, angular anisotropy 0–60835

²⁴²Am, prompt neutron fission yield for thermal neutrons 0–42885

²⁴²Am, prompt neutron fission yield for thermal neutrons 0–42885

²⁴²Am, prompt neutron fission yield for thermal neutrons 0–42885

²⁴²Am, prompt neutron fission in yield for thermal neutrons 0–42885

²⁴²Am, prompt active fission and kinetic energy distribution of 0–58032

²⁹⁰Bi(p.f) at 155 MeV, n energy distribution meas. 0–58034

²⁹⁰Bi(p.f) at 155 MeV, n energy distribution of fragments and nuclear cross-section for E=0.6-1.8 and 4.6 MeV 0–60834

²³²Cf, K X-rays, distribution as a function of mass and atomic number for spontaneous fission 0–52810

²³²Cf, neutron and p-quanta from triple fission, fragment excitation energy 0–46270

²³²Cf, spontaneous, independent yields of ⁸²Br, ⁸⁶Rb, ¹³⁶Cs and ¹⁵⁰Pm 0–39151

²³²Cf, spontaneous fission, emission of particles 3≤Z≤8 0–49677

23°Cf, spontaneous independent yields of ³⁴Br, ³⁸Rb, ¹³⁸Cs and ¹³⁸Pm 0–39151.

23°Cf, spontaneous fission, emission of particles 3≪Z≪8 0–49677.

23°Cf, spontaneous ternary fission, measured prompt gamma yield 0–39154.

23°Cf spontaneous, half life 0–74011.

23°Cf spontaneous, half life 0–74011.

23°Cf study of emitted p-rays, half life and intensity 0–77586.

24°Cm, prompt neutron fission yield for thermal neutrons 0–42885.

24°Cm, spontaneous, frompt neutron fission yield 0–42886.

24°Cm, spontaneous, fission half life 0–46260.

24°Cm, spontaneous, nompt neutron semitted 0–70685.

Em (where A=246, 248, 250), spontaneous, life-times 0–60832.

23°Np, by neutrons, 0.3·7.2 MeV, angular anisotropy 0–60835.

23°Np thermal neutron fission and independent yields of 131 0–52813.

24°Pb, 16°Pb, by α-particles, ang. anisotropy near threshold 0–46263.

24°Pb, He ion induced at 65, 41, 37 and 25 MeV, total cross sections 0–67559.

21°Po effective fission threshold 0–70675.

²⁰⁴Pb, He ion induced at 65, 41, 37 and 25 MeV, total cross sections 0–67559
²¹⁰Po effective fission threshold 0–70675
²¹⁸Pu, prompt neutron fission yield for thermal neutrons 0–42885
²³⁸Pu, prompt neutron fission yield for thermal neutrons 0 feet on energy, 5 keV-1 MeV 0–52809
²³⁹Pu, fission cross-section ratio meas to ²³⁵U, from 0.24 to 24 keV 0–58030
²³⁹Pu, induced by protons of medium energy, charge dispersion studies of Cs isotopes 0–49681
²³⁹Pu, multilevel parameters for fission cross section from 40 100 eV 0–64139
²³⁹Pu, neutron capture fission cross-sections, 0.1-30 keV, error effects on integral parameters in fast reactors 0–77612
²³⁹Pu, neutron induced, angular anisotropy, target spin depend. 0–64142
²³⁹Pu, neutron induced, independent yields of ¹³³I, ¹³⁴I and ¹³⁵I 0–70678
²³⁹Pu, neutron induced fission, fragment angular distributions 0–70682
²³⁹Pu, neutron resonances, cross-sections by statistical methods 0–39156
²³⁹Pu, spin- and energy-dependent fission widths, from channel theory, calc. 0–67558
²³⁹Pu, spontaneous neutron fission and short-lived fisson isomers, deduced

calc. 0-67558
²³⁹Pu, spontaneous neutron fission and short-lived fisson isomers, deduced isomeric a ratios 0-58031
²³⁹Pu, ternary photo-fission, 27.5MeV, study by mica and plastic track detectors 0-42887
²³⁹Pu accuracy of dg/dT rel. to ENDF/B (and other) data files 0-77599

²³⁹Pu accuracy of dg/dT rel. to ENDF/B (and other) data files 0–77599
 ²³⁹Pu fission and capture cross sections 0–39209
 ²³⁹Pu neutron-induced, prompt p meas. 0–77589
 ²³⁹Pu neutron absorption and fission cross-sections in the region 0.02 eV to 30 keV 0–64143
 ²³⁹Pu reaction rates in Pu-recycle fuel lattices 0–74059
 ²³⁹Pu self shielding and Doppler effects, effect of fission width spin dependence 0–74012
 ²³⁹Pu thermal neutron fission and independent yields of ⁸⁰Br, ⁸²Br, ¹²⁸I 0–52813
 ²³⁹Pu thermal neutron fission theoretical neutron representations.

0.-52813 239 Pu thermal neutron fission, theoretical angular momentum of fragments

239 Pu thermal neutron fission, theoretical angular momentum of magnetical 1, 64 148
239 Pu(y, J) and 238 Pu (y, J) angular anisotropy obs. 0—46259
240 Pu fission and capture cross sections 0—39209
240 Pu neutron in duced, near threshold, analysis of cross section and angular anisotropy date 0—70682
241 Pu, cross-section and fission probability from (t,pf) reactions 0—74020
241 Pu, prompt neutron fission yield for thermal neutrons 0—42885
241 Pu, search for ~0.3 yr spontaneous fission isomer 0—77510
241 Pu, spin- and energy-dependent fission widths, from channel theory, calc. 0—67558
241 Pu accuracy of de/dT rel. to ENDF/B (and other) data files 0—77599

²⁴¹Pu, spin- and energy-dependent fission widths, from channel theory, cale. 0–67558
 ²⁴¹Pu accuracy of dg/dT rel. to ENDF/B (and other) data files 0–77599
 ²⁴²Pu reaction rates in Pu-recycle fuel lattices 0–74059
 ²⁴²Pu into three large fragments, obs. 0–39153
 ²⁴²Pu(n,F) En=500, 620, 730, 990 and 1230 keV, fragment angular distributions 0–42884
 ²⁴²Pu(n,F) En=500, 620, 730, 990 and 1230 keV, fragment angular distributions 0–42884
 ²⁴³Pu(n,F) en=500, 620, 730, 990 and 1230 keV, fragment angular distributions 0–42884
 ²⁴³Pu(n,F) en=500, 620, 730, 990 and 1230 keV, fragment distribution 0–46271
 ²⁴⁸Pu(n,F) en=500, 620, 730, 990 and 1230 keV, fragment distribution 0–46271
 ²⁴⁹Pu(n,F) en=500, 620, 730, 990 and 1230 keV, fragment distribution 0–46271
 ²⁴⁸Pu(n,F) en=500, 620, 730, 990 and 1230 keV, fragment distribution 0–46271
 ²⁴⁹Pu(n,F) en=500, 620, 730, 990 and 1230 keV, fragment distribution 0–46271
 ²⁴⁰Pu(n,F) en=500, 620, 730, 990 and 1230 keV, fragment distribution 0–46271
 ²⁴¹Pu(n,F) en=500, 620, 730, 990 and 1230 keV, fragment distribution 0–46271

0.46271

19 Re, compound nucleus, fissionability as function of ang. mom. at excitation energy of 70 MeV 0.39152

Sn induced by ³⁰Ne ions, 168, 183, 198 MeV cross-sections and fragment distrib. 0.46264

20 Th., cross-section and fission probability from (t,pf) reactions 0.74020

20 Th., by 14 MeV neutrons, cumulative yields 0.42883

20 Th. by neutrons, 0.95-2.3 MeV, fragment ang. distribs... channel anal. 0.32811

0-2811
"27th, effective neutron fission cross-section at 14.1 MeV 0-64140
"37th, ternary photo-fission, 27.5 MeV, study by mica and plastic track detectors 0-42887
"37th photofission in symmetric region, cumulative yields 0-42888

Nuclear fission continued

clear fission continued

337Th, cross-section and fission probability from (t,pf) reactions 0-74020

335U reaction rates in Pu-recycle fuel lattices 0-74059

336Um, spontaneously fissioning isomers, fragment mass distributions and kinetic energies 0-39164

238U(p,f) at 155 MeV, n energy distribution meas. 0-58034

products

products

3 ≤ Z ≤ 8 particle emission, from spontaneous fission of ²⁵²Cf 0—49677
angular momentum distributions in primary fragments, theory 0—64148
cascade emission of neutrons from fission fragments 0—46268
chain populations, tables, odd masses, 75 ≤ A≤155 0—39172
charge distribution and recoil properties in ²³⁸U fission 0—74019
concentrations and total neutron absorption of fission product nuclides, calc. by computer program 0—46255
counter, parallel plate avalanche, insensitive to alpha-particles 0—46048
cumulative yields in neutron fission of ²³²Th and ²³⁸U in symmetric region 0—4283
detection in high radiation fields using Si heavy ion detectors 0—52602
detection of fragments by glass detectors as opposed to emulsions 0—39176

detection of 0-39176

detector, low temp., for neutron induced fission cross-section 0-46030 detector, time of flight of very heavy ions 0-52604 detectors, surface barrier, position sensitive, meas, of energy and angular distributions 0-49382

energy and angular distributions of light nuclei, model calculations 0-42881

0-42881 excitation energies of fissioning shape isomers in (p,2n) reactions 0-74021 fragment ang. distrib. in double humped fission barrier framework 0-39173

fragment angular distribs, for low temp, aligned nuclei, predictions 0--52814

0-52814
fragment angular distributions for heavy nuclei fission by 103 MeV helium ions and 51.5 MeV deuterons 0-42890
fragment anisotropy data, from shell effects on level densities 0-63975
fragment energies, measurement using solid-state track detectors 0-46256
fragment kinetic energy, rel. to neutron emission anisotropy 0-60837
fragment mass dispersion and charge distribution, fission process final stage effects 0-46258, prompt ward kinetic appropriate to deforms like

fragment pairs, total prompt y and kinetic energy, scission pt. deforms., liq. drop model cales. 0-39175

fragments, prompt, energy distrib. from renormalized Fermi gas model 0-39174

fragments detection, use of topaz, method 0-49685 fragments detection in α -particle background using fast ionization chamber 0-77397

fragments due to heavy ions, mass distrib, meas, by Ge:Li γ spectrometer 0-46266 -46266

0-46266 fragments energy meas... use of double ionization chamber with increased n-flux use factor 0-49360 fragments track counting in polycarbonates, rel. to meas. of reactor parameter δ^{28} 0-39212 gas bubbles, stationary, behaviour in Na-bond of fuel elements 0-55198 gas release due to fuel cladding failure, simulation expt. 0-64169 halogens and rare gases, apparatus for production and fast separation 0-39163

heavy nuclides, production by rapid multiple neutron capture 0-74023 heavy nuclides, rel. to explosion of Hutch device 0-74024 inert gas release from reactors, detection of fuel element cladding failure 0-49728

0—49/28 irradiated (U.Pu)O₂ and PuO₃. O/M ratio determination, CO/CO₂ gas equilibration method, effect of burnup 0—49738 isomers, spontaneousl fissioning; in U.Pu. Am and Cm isotopes 0—74013 mass spectrometer resolution, pulse height mass assignment 0—52853 neutron coincident detector distinguishing between (α,n), (γ,n) and fission products 0—77424

products 0-77424 neutron detector efficiency correction and neutron multiplicity histograms unfolding 0-49338 neutron emission anisotropy, dependence on total kinetic energy of fragments 0-60837 neutrons emitted by single fragments of fixed mass after ²³⁵U fission 0-77588

photofission of ²³²Th and ²³⁸U in symmetric region, cumulative yields

0-42888 reactor deposition studies using remote gamma spectrometry 0-77600 release from molten pool by thermally induced circulation, estimate of enhancement 0-77590 stationary gas bubbles behaviour, in Na-bonded fuel rod, testing in narrow liquid filled gaps 0-46310 ternary, heavy fragment emission, high energy 0-42880 track ages, thermally lowered, correction method 0-77440 tracks in irrad, plastic films, counting using microscopy or an automatic technique 0-42893 trajectories of α particles and 2 main fragments following ternary fission 0-70684

0-70684 transuranium elements, number of neutrons 0-67562 X-ray emission accompanied by emission of long-range particles 0-46267 zero power reactor, ZR-4 type, study of fission products from fuel elements 0-58051 p-radiation, short time presence of fuel in reactor 0-67575 p, reaction with *Be and D:O with n counting as meas, of fuel burn up 0-46301

0-46301

y spectra application to nondestructive determ. of fuel rod burnup
0-49741

1974u, photon irrad., nucleon comp. and excitation energy 0-70686

1987; independent yield, in 1932Cf spontaneous fission 0-39151

1932Cf, prompt. neutron yields of fission fragments 0-39162

1932Cf, spontaneous ternary fission, prompt name, distribs. 0-49686

1932Cf fragment pairs, correlated emission of K X rays 0-42892

1932Cf primary fission products, experimental information on deformation
0-55176

10-70685

 $^{46}\text{Cm.}$ number of prompt neutrons emitted in spontaneous fission 0-70685

0—70685
Cs isotopes, independent formation cross- section in proton induced fission of ²³⁹Pu 0—49681
¹³⁴Cs, independent yield, in ²³²Cf spontaneous fission 0—39151
³H yield in thernal neutron fission of ²³³U 0—70679
⁴He, priduction rate in nuclear reactor materials 0—46304
I isotopes. ²³⁵U thermal -n fission yields, obs. 0—49687
I isotopes, yield in ²³⁵U fission 0—42894

Nuclear fission continued

products continued products continued products continued [17], [134], [144], independent yeilds, from thermal n fission of [21]U, charge distrib. O 39465

meas. 0 39160 20 Urganeaux energy and angular distrib., thermal < E $_{\!a}<$ 2 MeV 0 39170

0.39170
The uniform induced, fragments energy distribution 0. 49678
W. delayed n groups with t₁₇₇ > 1 min in fission spectrum n fission, abundances 0.39166
W. neutron induced, predicted mass yields 0.39157
W. photo and fast, thermal n fission fragment mass distribs, obs. 0.39167

0. 39167
208U, probability of long range particle emission 0. 74010
208U, prompt n emission, p fission, 12 MeV 0. 42891
208U(n.e.) angular distributions of fragments, analysis 0. 70680
Xe, in motten salt reactor, penalty to breeding ratio and removal process 0. 39248

Xe, optimal control of spatial oscills, in reactor 0 39225 ¹⁰⁸Xe, cumulative yield in proton induced fission of ²¹⁹Pu 0 49681

critical masses, spherical and hemispherical enriched assemblies 0 49730 critical parameters of a uranium solution slab cylinder system 0-55204 discovery, history and props. 0 55177 kinetic energy of fission fragments released from fuel surfaces by recoil

kinetic energy of fission fragments released from fuel surfaces by recoil 0 / 3 98.

1.RA and binary fission for 215U and thermal neutrons, multiparameter study 0 42886 radiation growth with low burn up rates 0 70674 termiry, proton induced, high energy 0 42889 world resources, need for further exploration and development 0 60862 more fragment fission, prompt neutron energy measurement and fragment kinetic energy release for E₀ 9.5 22 MeV 0 58033 for 10 for

MU, thermal neutron fission and independent of the property of

Nuclear fission continued uranium continued

 $^{735}\mathrm{U}_{\rm s}$ absolute ratio of densities due to thermal and epicadmium n fluxes $_{\rm O}$ $_{\rm 4962O}$

1 49620 by medium energy protons, nuclear charge dispersion of light-mass products 0 64144 by U., cross section and fission probability from (t.pf) reactions 0-74020 by enrichment, review of technology 0-52817 by enrichment, review of technology 0-52817 by U., fission cross section ratios 299µ/2391 und 1391/2391 0-58030 by U., neutron induced, angular anisotropy, target spin depend. 0-64142 by U., neutron induced, symmetry meas, from 19Cd/99Mo ratio 0-70681 by U., neutron induced, symmetry meas, from 19Cd/99Mo ratio 0-76819 by U., prods. K X ray yields rel. to Z. obs. 0-39168 by U., prompt gamma rays from thermal neutron fission 0-55175 by U., spin and energy dependent fission widths, from channel theory, calc. 0 67558 by ontaneous neutron fission and short lived fission isomers, deduced

²³⁵U, spontaneous neutron fission and short lived fission isomers, deduced U, spontaneous neutron fission and short lived fission isomers, deduced isomeric σ ratios 0- 58031.

213U, thermal neutron induced, distribution of neutrons emitted by single fragments of fixed mass 0-77588.

213U, thermal n fission, γ ray spectra of products at selected times 0-52816.

213U, thermal neutron fission, isomeric gamma radiation from neutron rich fragments 0-70683.

²³⁵U, thermal neutron fission, isomeric gamma radiation from neutron rich fragments 0. 70683
²³⁵U, thermal neutron fission and independent yields of ⁸⁰Br, ⁸²Br, ¹²⁸J 0. 52813
²³⁵U, thermal neutron fission fine structure of energy spectra 0–46269
²³⁵U, thermal neutron induced, identification of ⁸⁸Se and neutron emission from ⁸⁷Se 0. 49679
²³⁵U, thermal neutrons. LRA fission and binary fission, multiparameter study 0. 42886
²³⁵U, yields of I isotopes and half life and yield of ¹³⁵Te 0–42894
²³⁵U accuracy of dg/dt rel. to ENDF/B (and other) data files 0–77599
²³⁵U and ²³⁶U, with 20 to 85 MeV protons, nuclear charge dispersion 0. 39160
²³⁵U by fission spectrum n, delayed n groups with t₁₀> 1 min abundances

O 39160
3910 by fission spectrum n, delayed n groups with t_{1/8}> 1 min abundances 0 39166
3930 n fission fragments energy and angular distrib., thermal 2 MeV 0 39170
39170 neutron induced, symmetry at individual resonances 0–74017
3910 neutron induced, fragments energy distribution 0–49678
3910 photofission, time behaviour of delayed neutrons, bremsstrahlung endpoint energies 8 and 10 MeV 0–46265
3910 thermal n fission, Fisotopes and Fister fields, obs. 0–49687
3910 thermal n fission, Fistopes and Fister fields, obs. 0–49687
3910 thermal n fission, Fistopes and Fister fields, obs. 0–49687
3910 thermal n fission, Fistopes and Fister fields, obs. 0–49687
3910 thermal n fission, Fistopes and Fister fields, obs. 0–49687
3910 thermal n fission, Fistopes and Fistopes

U thermal n fission, 112Sn half life and fractional cumulative yield 0 74025
 U(d,p) E=13 20 MeV, excitation functions for production of fission isom ers, half lives 0 - 49682
 U(d,p) F=13 20 MeV, excitation functions for spontaneous fission isomer production 0-49683
 U(d, deuteron induced, excitation functions for spontaneous fission isomer production 0-49683
 U(d, nuclear deformation energy in two centre shell model and fission barriers, calculation 0-57936
 U(d, nuclear deformation energy in two centre shell model and fission barriers, calculation 0-57936
 U(d, nuclear deformation probability from (t,pf) reactions 0-74020
 U(d, nuclear deformation probability from (t,pf) reactions 0-74020
 U(d, nuclear deformation probability from (t,pf) reactions 0-74020
 U(d, nuclear deformation energy in two centres sections at 130 1400 keV 0 55162
 U(d, nuclear deformation energy in two centres determ. Of Xe isotope relative yields 0-52812
 U(d, by 14.7 MeV neutrons, mass, spectrometric determ. of Xe isotope relative yields 0-52812
 U(d, by medium energy protons, nuclear charge dispersion of light-mass products 0-64144
 U(d, by nuclear deformation energy surfaces 0-67560
 U(d) neutron induced, predicted mass yields 0-39157
 U(d) neutron induced, predicted mass yields 0-39157
 U(d) neutron induced for various geometrical systems 0-39231
 U(d) resonance integrals for various geometrical systems 0-39231
 U(d) resonance integrals for various geometrical systems 0-39231

³³⁸U, resonance integrals for various geometrical systems 0–39231 ³³⁸U, resonance interaction and analysis of central reactivity worths in fast critical assemblies 0–55205

critical assemblies 0–55205

²¹⁸U, spontaneous neutron fission and short lived fission isomers, deduced isomeric or ratios 0–58031

²¹⁸U, ternary photo fission, 27.5MeV, study by mica and plastic track detectors 0. 42887

²¹⁸U by 11.5 GeV protons, charge distribution and recoil properties of products 0–74019

²¹⁸U by ission spectrum n, delayed n groups with t_{1/2} > 1 min abundances 0. 39166

²¹⁸U photofission, time behaviour of delayed neutrons, bremsstrahlung endpoint energies 8 and 10 MeV 0–46265

²¹⁸U photofission in symmetric region, cumulative yields 0–42888

²¹⁸U(p, IN, E=11.20 MeV excitation functions for production of fission isomers, half lives 0–49682

²¹⁸U(p, I) mass distributions of fragments, analysis 0–70680

²¹⁸U(p, I) mass distribution and kinetic energy distrib. obs. 0–39159

²¹⁸U(t,pf)²¹⁹U, E=12.54MeV, fission threshold, proton spectra 0–74018

²¹⁹U(t,pf)²¹⁹U, E=12.54MeV, fission threshold, proton spectra 0–74018

²¹⁹U(t,pf)²¹⁹U, E=12.54MeV, fission threshold, proton spectra 0–74018

²¹⁹U(t,pf)²¹⁹U, E=12.54MeV, fission threshold, proton spectra 0–74018

Nuclear fission reactors see Nuclear reactors, fission

Nuclear forces

see also Field theory, quantum/meson field
3, 4-nuclear systems, calc. using Jastrow type correlated wave functions
0-67417 nucleon problem, review 0-49450

3 nucleon problem, review 0-43450 16O, binding energy, contribution of central part of Sussex interaction 0 77483

binding energy, doubly magic nuclei, simple lower bound 0-63972 binding energy, form and internal quadrupole moments in even- even binding energy, for nuclei 0-42696

binding energy, model dependence 0–38802 binding energy calc, using separable potentials 0–77472 binding energy for light nuclei, correlation with nuclear radii 0–42716 binding energy formula of identical nucleons in a single j shell, correction term 0 49464

binding energy of nuclear matter calc. of correction of second order in v/c 0 · 77471

Nuclear forces continued

binding energy of triton, effect of Shirovkov corrections. 3-boson model 0-52644

binding potential, line width and level shift, dependence 0-74089

Bloch-Horowitz Brandow expansion, 3rd order terms for A=18 nuclei

Brueckner-Hartree Fock energies in light nuclei 0-70344 c ¹⁴C. ground state binding energies with Tabakin potential as residual interaction 0-67423 central, effective forces, deduced from Thomas-Fermi theory 0-42697 charge, independence, ¹⁰B(n; ⁷Be_{xp})⁷Li_x, Barshay-Temmer theorem verification 0-67550

verification 0–67550 (0–73733 charge independence, survey 0–73733 charge independence, ¹⁰B(α , ⁷Li_{gs}) ⁷Be_{gs}, Barshay-Temmer theorem verification 0–67550

charge independence, ¹⁹B(α, ²Li_s)²Be_{sc}, Barshay-Temmer theorem verification 0–67550 charge independence, deviations 0–42703 configuration interaction matrix elements for D* configurations 0–49477 coulomb displacement energy, calc. 0–67366 Coulomb displacement energy, calc. 0–67366 Coulomb energies, review 0–49457 Coulomb energies, review 0–49457 Coulomb energies rel. to nuclear radii 0–67381 Coulomb interaction for elastic and inelastic scattering of hadrons from nuclei 0–49587 Coulomb potential, in λ-plane, dispersion relations and Levinson's theorem 0–55109 Coulomb interaction impurity effects and violations of isobaric spin symmetry 0–63987 deformed nuclei, use of iterative technique, quadrupole force 0–77467 deformed spin-orbit potential in coupled equations 0–70379 dispersion relation for partial wave scattering amplitude and first Born term 0–67376 effective charges, second-order corrections 0–67379 effective force based on non-local two nucleonic potential 0–52641 effective force for DWBA, many body theory 0–67380 effective interaction from scattering amplitude 0–67315 effective interaction matrix elements from soft-core pot. by Moszkowski-Scott separation method 0–38808 effective potentials in set of coupled eqns., for direct rearrangement colli

effective potentials in set of coupled eqns. for direct rearrangement collisions 0-42805

sions 0-42803 effective two body interaction, charge exchange part 0-42827 energy dependency of effective interactions and matrix elements of the Green operator 0-52651 energy gap calc. using velocity-dependent nucleon nucleon interaction 0-70338

equipotential surfaces in heavy elements 0-49468 even-even, binding energy, form and internal quadrupole moments 0-42696

many-fermion system. R-matrix expansion for ground-state energy 0-77470

nany-terminol system. Remark expansion for ground-state energy 0–77470 finite nuclei in local density approx. 0–73756 hard core potentials, Gilbert Schmidt expansion 0–60744 hard-core potential, local, and the three-body problem 0–52645 Hartree-Fock and related approximations in solvable model 0–70347 Hartree Fock calc. for even-even N=Z nuclei 0–70351 Hartree Fock calcs, and soft core potentials 0–63960 Hartree-Fock calculations, separable potential model 0–67384 Hartree-Fock calculations, separable potential model 0–67384 Hartree-Fock calculations, sotopic spin mixing 0–70349 interaction in finite nuclei, higher order terms and apparent non-convergence of perturbation expansion 0–49462 local nucleon-nucleon potential, non local, for Hartree-Fock calculations 0–70352 local potentials, unitary pole expansion 0–57875

0-70352
local potentials, unitary pole expansion 0-57875
local potentials, use of UPA for calc. .0-77472
local static potential, very soft core 0-67373
long range perturbing forces, by N/D method 0-38653
low-energy theorem for exchange axial-vector currents 0-52718
Majorana field and the relation of spin and statistics, quantum theory of the infinite-component 0-42431
many-body effective interactions from relations among shell model spectra 0-70453

0—70453
many-body problem, self-consistent solution, variational method 0—70348
matrix elements, deduced from N-N phase shifts 0—38801
model dependence of binding energy 0—38802
Morse function type potential velocity and energy dependent, with spinorbit splitting 0—67390

N=Z closed shell nuclei, nuclear surface for simple effective interaction 0-67371

non-local separable potential for α - α interaction 0–42865 non-static two-body potential from relativistic OBE model including δ -mesons 0–67372 nonlocal, and dipole sum rules 0–46100

nuclear Coulomb potential, asymptotic behaviour of Jost function and S-matrix for large complex ang. moments 0-49456 nucleon-nuclear potential, velocity dependent, for Morse function

0 - 49467

one boson exchange potentials rel. to applicability in shell model of ¹⁸O 0–57899

one boson exchange potentials ref. to applicability in shell model of "O 0-5789" one-boson-exchange model, in inner region 0-42702 one-boson-exchange potentials and nuclear matter 0-70363 one-boson-exchange potentials in p-p bremsstrahlung 0-49463 optical potential in terms of nuclear symmetry parameter from proton scattering, isospin dependence 0-57874 optical potentials, for elastic scatt, of t and ³He 0-52793 optical-potential depth from many-body theory 0-49474 pairing and quadrupole forces in nuclear theory search for common symmetry 0-42698 phenomenological 3-body forces 0-70337 potential, local optical model, dispersion relation 0-38804 potential, two-body effective, 2s-1d and 2p nuclei, struct, and scatt, calcs. 0-42732 potential, velocity-dependent, for Morse function 0-49467 potential deduced from N-N scatt. 0-63959 potential energy surface of two heavy nuclei investigated 0-73745 potential field at nucleus in neutral atoms 0-42783

Nuclear forces continued

potential optical, from electrons elastic scattering 0-42818

potentials, Yukawa and separable, comparison of off-shell t matrice 0.--73740

potentials, rank two separable s-state, phase equivalent, central, off shell effects 0-63957

potentials, rel, between, vel, dependent and hard-core appl, to photonuclear sum rules 0–55113 potentials, separable and local, phase equivalent, off-energy-shell behavi our 0–55111

potentials from N-N scattering using Marchenko theory 0-73918

quadrupole, centre-of-mass depend. 0-38805

quadrupole and pairing forces in nuclear theory search for common symmetry 0-42698

quadrupole force from Woods-Saxon potential, radial depend, derivation 0.49460

realistic and delta-function, use for energy gap cales. 0-42700

reansite and cetta-function, use for energy gap cales. 0–42700 repulsive core two-body forces and discrepancy between observed and shell model proton density 0–70341 residual interaction, centrifugal terms 0–73737 residual interaction between nucleons 4 particle levels of even-even spherical nuclei 0–49458

residual interactions effect, analogue state energies, neutron radii 0-67406 residual interactions effect, analogue state energies, neutron radii 0-67406 review of potential concept in N N interactions and limitations of existing models 0-73741 s wave potentials with hard core model 0-70340 saturation, necessary conditions 0-73735 self-consistent calc. for nuclear properties, review 0-70356 self-consistent field, local, in nuclei with large number of nucleons

0 -67368 self-consistent fields, coordinate space study, numerical applications

self-consistent fields, coordinate space study, numerical applications 0–42701 self-consistent shell model potential, finite rank structure 0.–70342 semi realistic effective interactions in shell model 0–70358 short range correlations rel. to displacement energy 0–57876 short-range correlations by means of e scatt, review 0–60801 single-nucleon potential. Bruceckner cales. 0.–63955 single-nucleon potential, definition and width of the single nucleon strength distribution 0–57873 single-particle energies defined as spectroscopic averages 0–70350 single particle potential wells and droplet model nuclear distributions for Thomas Fermi calculations 0–38820 soft-core potential matrix elements, in harmonic oscillator wave functions 0–46099 spin, effect on mag, moments on deformed nuclei 0–52665

Soft-core potential matrix elements, in narmonic oscillator wave functions 0-46099 spin, effect on mag, moments on deformed nuclei 0-52665 structure models, review 0-60738

T=0 realistic forces simulation by phenomenological potentials 0-70343 t-matrix flast convergence by reference spectrum method 0-38807

Tabakin N-N potential 0-73773
tensor, effect in residual pair nucleon interaction 0-52646 theory, important developments 0-77473

Thomas-Fermi calcs, using effective interactions, comparison with Hart ree-Fock calcs, 0-70339 three-body problem, account of core by perturbation theory 0-52648 three and four nucleons in single shell, residual interaction and seniority scheme 0-70346
three-body problem, applic, of Bateman method for factorization of two particle amplitude 0-46118
three-body problem, solution in coordinate space 0-70345
three-body systems, non relativistic, with short ranges interactions 0-63961

three body 0-63961

three-body systems with central local potentials, accurate numerical solns, 0-46101three-particle integral equations, solution by separable expansion method 0-49454

trinucleon binding energies calculated with rank six separable potentials 0-49465

0.-49465
trinucleon energy correction by t-matrix perturbation theory 0.-55110
two-body force through (*He, t) charge exchange reaction on N=28 nuclei
0.-49660
two-body interactions symmetry in relation with their pairing correlations
props. 0.-63958
two-nucleon interaction, charge asymmetry 0.-77469
two-nucleon potentials, for trinucleon form factors 0.-67367
two-nucleon transition matrix, off-energy shell continuation 0.-67377
two-particle interaction, perturbation theory for potentials with core
0.-46104

two-particle two hole admixtures to Hartree-Fock states in 2s 1d nuclei 0 -70334

velocity-dependent, hyperspherical expansion approach to bound states 0-52657

Wood-Saxon potential, quadrupole force, radial depend, derivation 0-49460

0-49400

• particle model interaction pot., energy depend., E<6 MeV 0-55164

• N. S. wave scatt. lengths 0-42596

• N. binding energy in particle matter 0-49496

• binding in nuclear matter, reaction-matrix calc. 0-49461

• in nuclear matter, second Born approx. of self energy 0-73749

• particle, binding energy, calc. with Herndon Tang • N potentials 0-73732

AN, one-boson-exchange potential model 0-73652 A Σ conversion, effect on A particle binding in infinite nuclear matter 0-49459

N-49459
N-N interaction, using G-matrix, effective interaction calc, using variety of approximations 0-73731
N-N potential, isobar intermediate state contributions 0-67374
N-N potential and minimal relativity 0-67369
n-d doublet scattering length and tenergy relationship 0-60743
N interaction amplitude in infinite nuclear matter 0-46102
N pair interactions in nuclei, structure of matrix elements 0-46103
NN effective interactions, density- and momentum-depend. 0-38806
NN force, local, smooth, for nuclear Hartree Fock calcs. 0-73736
NN interaction, velocity dependent determination to fit S. P and D-wave nucleon-nucleon phase shifts 0-57872
NN potentials, reconstruction from nuclear data 0-77466
NN scatt., popular review article 0-49471

Nuclear forces continued

NN scatt, two pion exchange contribution, on basis of pion pion dynamics 0, 73674

nes 0 74624 manufactus from final state interactions 0 42868 NN scattering parameters from final state interactions 0 42868 NN 1 vooluting force from e.m. interaction 0 45955 in effective range parameters from 'H&H,'He)2n and 'H&PH,'H)2p

pu correls, in medium and heavy nuclei 0, 63956, a exchange current in radiative up capture 0, 57974, a nuclear optical potential, from anal of scatt. a = ¹²C 0, 57998, a N., short range interaction, asymptotic behaviours of force functions 0, 55045.

0 57047
Lenergy and red doublet scattering length, relationship 0 60743
letter for Ninteractions, short range correls effects 0 59074
Ba mader implanted in from hyperfine magnetic field 0 69062
Be matable micleus, binding energy of ground state 0 63996
melly, santace micleum potential determ, using clustic \(\alpha\) 5396
0 67544
rings, core renormalization effects in 1 ground state 0 67495
rings shell model with Hamada foliastion potential 0 70530
C binding energy of 1s electron related to potential at nucleus 0 74417
PC, binding energy, contribution of central part of Sussex Interaction
0 77430

6 7743 : ¹⁶C and ¹⁶N, core polarization, agreement between binding energy and β decay 0 60724 ¹⁶C a. Hurtree Lock calculations with semi-realistic interactions 0 70407 ¹⁶C a. neutron separation energies calc, with Morse function type potential 0 67300

0 - 6/390

4°C a lunding energy, from effective NN interactions 0 38806

4°C a effective three body interactions cale 0 70453

4°C before the three body interactions cale 0 70453

4°C before the line of the learner of the large of the larg

0 52664
91 and 41, variation binding energy, second order correction of peturbation theory 0 67444
94 binding energy, relativistic corrections 0 49498
94 binding energy cate, with fustrow type wave functions 0 67447
94 binding energy cate, third order corrections to Hariree Fock approximately

The binding energy, from effective NN interactions = 0, 38806. The binding energy calc, with fastrow type wave functions = 0, 67447. The binding energy calculation using matrix elements of Tabakin's potential = 7,0389.

tral 0 70389

The binding energy of ground state 0 63996

The binding energy of ground state 0 63996

The binding energy of ground state 0 63996

The binding energy of 1562 MeV excited state 0 63996

The binding energy of 1562 MeV excited state 0 63996

The binding energy of 1562 MeV excited state 0 63996

The binding energy of 1562 MeV excited state 0 63996

The binding energy of 1562 MeV excited state 0 63996

The binding energy of 1562 MeV excited state 0 63996

The binding energy of 1562 MeV excited state 0 63996

The binding energy of 1562 MeV excited state 0 63996

The binding energy of 1562 MeV excited state 0 63996

The binding energy of 1562 MeV excited state 0 63996

The binding energy of 1562 MeV excited state 0 63996

The binding energy of 1562 MeV excited state 0 63996

The binding energy of 1562 MeV excited state 0 63996

The binding energy of 1562 MeV excited state 0 63996

The binding energy of 1562 MeV excited state 0 63996

The binding energy of 1562 MeV excited state 0 63996

The binding energy of 1562 MeV excited state 0 63996

The binding energy of 1562 MeV excited state 0 63996

The binding energy of 1562 MeV excited state 0 63996

The binding energy of 1562 MeV excited state 0 63996

The binding energy of 1562 MeV excited state 0 63996

The binding energy of 1562 MeV excited state 0 63996

The binding energy of 1562 MeV excited state 0 63996

The binding energy of 1562 MeV excited state 0 63996

The binding energy of 1562 MeV excited state 0 63996

The binding energy of 1562 MeV excited state 0 63996

The binding energy of 1562 MeV excited state 0 63996

The binding energy of 1562 MeV excited state 0 63996

The binding energy of 1562 MeV excited state 0 63996

The binding energy of 1562 MeV excited state 0 63996

The binding energy of 1562 MeV excited state 0 63996

The binding energy of 1562 MeV excited state 0 63996

The binding energy of 1562 MeV excited state 0 63996

The binding energy of 1562 MeV excited state 0 63996

The binding energy of 1562 MeV excited state 0 63996

The bindin

N binding energy of 1s electron related to potential at nucleus 0 74117 N isotopes, mixed parity Harteee Fock cale, using realism forces 0 76402 N isotopies, intred partry Harriere Fock care, using remain Fock of 7040.

NN, ground state binding energies with Tabakin potential as residual interaction: 0 6742.

BN and BC, core polarization, agreement between binding energy and β decay 0 60754.

BN, 41H calculations with realistic and semi-realistic interactions: 0.70424.

PNe, non-central forces: 0.70426.

appaining correlations, effect on transfer of up pair 0.52649.

O binding energy of b electron related to potential at nucleus: 0.74417.

O asitopes, intexet pairty Hartree bock calc, using realistic forces: 0.7640.

Hartree Fock calculations with semi-realistic interactions: 0.70407.

BO, Hartree Fock calculations with semi-realistic interactions: 0.70407.

O 67490.

SO binding energy, from effective NN interactions: 0.38806.

¹⁸O binding energy, from effective NN interactions 0 38806
 ¹⁸O binding energy calculation using matrix elements of Labakin's potential 0 70389

O binding energy calculation using matrix elements of Tabakin's potential 0 / 00 ft9.
 O, Hartree Fock semi-realistic interactions 0 / 67427
 O, realistic forces, determined state admixtures 0 / 73790
 O'B, realistic forces, determined state admixtures 0 / 73790
 O'B, realistic forces, determined state admixtures 0 / 73790
 O'B, shell model with Hamada Johnston potential 0 / 70521
 D, that ree Fock with Skyrme's interaction 0 / 70522
 D, shell model with Hamada Johnston potential 0 / 70530
 D, shell model with Hamada Johnston potential 0 / 70530
 D, shell model with Hamada Johnston potential 0 / 70530
 D, shell model with Hamada Johnston potential 0 / 70530
 D, shell model with Hamada Johnston potential 0 / 70530
 D, shell model with Hamada Johnston potential 0 / 70433
 D, effective three body interactions calc. 0 / 70433
 E, effective three body interactions calc. 0 / 70433
 S, effective three body interactions calc. 0 / 70433
 S, in isotopes, sell consistent core particle coupling calc. 0 / 70435
 III calculations with realistic and semi-realistic interactions of 0 / 70424
 So isotopes, sell consistent core particle coupling calc. 0 / 70436
 III a, existence of parity non conserving term in nuclear Hamiltonian conformed 0 / 70529
 M, shell model with Hamada Johnston potential 0 / 70521
 D, and D, and D, and D, and C, and C

Nuclear fusion see also Explosions/nuclear; Nuclear reactors, fusion; Thermonuclear

controlled, major facilities, world survey 0 52807 controlled, major facilities, world survey 0 52807 controlled, microwave formation and heating of hydrogen plasmas 0 46687

0. 46687
controlled, review of progress and prospects. 0. 42879
controlled revenich, review. 0. 4625.3
high current techniques in R. & D. 0. 39587
nucleosynthesis by explosive oxygen burning, astrophysical. 0. 48422
review of techniques for unconfined, partially and totally confined plasmas

thermal, functional method for nonlinear problems 0 78047

thermonuclear, of laser produced plasma

Nactear fusion continued

even rusion continued

"C) "C reaction, mechanism via direct transfer of α particle 0–69416

"Kr, 5 to 10.5 MeV/amu projectile, complete fusion cross sections with various targets 0–49676

"Mil, 5 to 10.5 MeV/amu projectile, complete fusion cross sections with various targets 0–49676

"Ke, 5 to 10.5 MeV/amu projectile, complete fusion cross sections with various targets 0–49676

Nuclear induction - see Nuclear magnetic resonance and relaxation

Nuclear Interactions—see Collision processes; Field theory, quantum/interactions; Elementary particles; Nuclear reactions and scattering

Nuclear isomerlam

see also Nucleus/energy levels
Bestoning, spontaneous, in U, Pu, Am and Cm (sotopes 0-74013
level lifetime measurement method for lifetimes 10 4 to 10 2 sec. 0-57892
minoric atoms, effects 0-5296
AL, evidence for 29/2 (sometric level 0-77509)

[97] AL excited states studied, isometric decay obs. multipolarity assignments
[17] [17]

10 T3837

 19 71637
 194 n(n,2n), isomeric ratio analysis, E_n-14.2 (0. 39075)
 195 Gd, 31+2 ms activity produced by ¹⁴⁶ Gd(n,2n) at En-14.15 MeV (0. 52707) ¹⁰ Hr (setn.21), E₀=14.7+0.15 MeV, isomeric ratio determ. 0-73960 m¹⁰ Hr excited states studied, isomeric decay obs. multipolarity assignments 0-73837

184] 3,8 nm (some) obs. 0 38922 ¹⁹⁴Ir excited states studied, isomeric decay obs. multipolarity assignments (i) 7.38-37

(NH4) Ce(NO1)n, spin isomerism of ammonium group protons, n.m.r. obs.

(NH₁), Ce(NO₂)_n, spin isomerism of animonium group protons, n.m.r. obs. 0 69197
(**Not(n,2n), isomeric ratio analysis, E., 14.2 0-39075
(**Not(n,2n), isomeric ratio analysis, E., 14.2 0-39075
(**Not(n,2n), isomeric ratios formed in charged particle and photofission of heavy micleides 0-49684
(**Pr., isomer shifts in 145 keV, Mossbauer obs. 0-73822
(**Pr., isomer shifts in 145 keV, Mossbauer obs. 0-73822
(**Pr., isomer shifts in 145 keV, isomeric ratio determ. 0-73960
(**Setn,2n), E., 1471 0.15 MeV, isomeric ratio determ. 0-73960
(**Setn,2n), E., 1471 0.15 MeV, isomeric ratio determ. 0-73960
(**Setn,2n), E., 1471 0.15 MeV, isomeric ratio determ. 0-73961
(**Sestin,2n), E., 1471 0.15 MeV, isomeric ratio determ. 0-59381
(**Ps), ***Mossbauer isomer shift in Sn. pseudopot, approach 0-59381
(**Ps), ***Mossbauer isomer shift in Sn. 0-59382
(**Ps), ***Pre*, isomeric transitions, multipolarity checked, and E2 admixture determ. 0-5691
(***Indiason, deuteron induced, excitation functions for spontaneous fission isomer production 0-49683
(***Mossbauer isomer shift in Sn. 0-5691
(***Mossbauer isomer shift in Sn. 0-5691
(***Mossbauer isomer shift in Sn. 0-5982
(***Pre*, ***Pre*, isomeric transitions, multipolarity checked, and E2 admixture determ. 0-5691
(***Mossbauer isomer shift in Sn. 0-5982
(***Pre*, ***Pre*, ***Mossbauer isomer shift in Sn. 0-5982
(***Mossbauer isomer shift in Sn. 0-59882
(***Mossbauer isome

MoZr, low level spins of four particle configurations 0 55130
 Nuclear magnetic resonance and relaxation see also Malecules/maclear coupling.
 Spectroscopy, rel. to investigations of preferential solution by diamagnetic carlions in hexamethylphosphorotrainade water mixture 0-68156.
 Pspectroscopy, rel. to investigations of preferential solution by diamagnetic carlions in hexamethylphosphorotrainade water mixture 0-68156.
 RNA manganese complex, p.m.r. study 0-77971.
 UH, and β UD₁, Kinght shift, linewidth and shape, second moment 0-45040.
 (methyl). Notvent systems, ¹⁸N n.m.r. shifts 0-78312.
 AA'MM'X spin systems, heteronuclear double and triple mag, resonance study 0-46443.
 AA'X and AA'B spin systems, spectral props, and exptl. occurrence 0-30359.

ABX spectra analysis 0 67696 acctonitrile in liquid crystal poly p benzyl L glutanate, ¹H and ¹⁴N spectra 0 74321 acctylence, bulogen substituted, J_{th} couplings 0 43446

acid fluorides, vicinal proton fluorine coupling constant, obs. of change of sign with dihedral angle 0 67793

acoustic, effect on resonant y ray absorpt, and emission 0-51277 acoustic, in metals, and e.m. generation of sound 0 68587 acoustic, stimulation by virtual fields of phonons and conduction electrons 0 48157

acoustic mag, reson, spin systems and general principles 0 41358 acoustic mag, reson, in cubic cryst, statistical density matrix cale, 0 40553

0. 40553 meyelic and alicyclic alcohols, $^{13}{\rm C}$ chemical shift obs. by n.m.r. 0. 46534 administration. Overhauser effects and $^{13}{\rm C}$ relaxation times 0. 39407 β adenosine 3' β adenosine 5' phosphoric acid, ${\rm P}^{33}$ n.m.r. spectrum

β adenosine 3' β adenosine 5' phosphoric acid, P³³ n.m.r. spectrum 0.50261 adsorbed inquel layer on carbon, line shift and width 0.50397 adsorbed molecules, self diffusion kineties, spin echo 0.74926 aldopyranoses, pentose and hexose, ¹³C n.m.r. spectra 0.46533 alkali halides, ENDOR obs. of F centres, elect. field effects 0.45039 alkali metals, Knight shifts 0.76238 alkali etals, Knight shifts 0.76238 alkali system, binary, solute Knight shift 0.45013 alkames, substituted, rotational nomerism 0.74327 alkoys strazine, in different solvent 0.64476 alkylphenols 0.74329 allo ocimene, conjugated linear triene 0.77863 alloy, binary f.e.c., effect of atom ordering on quadrupole effects 0.69192 alloy, dil., fields produced by impurities and imperfections 0.75882 alloys, liquid, Knight shifts from clustic scattering 0.61552 alloys, dilute, spin relixation, effect of s d exchange interaction 0.69051 alum, rr and β type p.m.r., H-O mols, position 0.66151 numo acids, ¹⁹N H coupling as source of proton resonance line broaden ing 0.74330 ampere, absolute determination using nuclear magnetic resonance methods 0.63531 antiferromagnet, CoCls.214-O, of ¹⁹Co 0.62773 antiferromagnet, FeFs, phonon effect, near critical point 0.59466

Nuclear magnetic resonance and relaxation continued

antiferromagnet, MnF., frequency shift above Neel temp., hyperfine coupling 0-51410

antiferromagnet, MnO, 4.2 K, ⁵⁵Mn, domain struct. 0–45024 antiferromagnet, kZnF₁:Mn²⁺, ENDOR, unpaired spin density 0–45041 antiferromagnet, linear chain, proton spin-lattice relax. 0–79213

antiferromagnet, manganese formate dihydrate, mag. ordering obs.

antiferromagnetic, MnTe, nucl. acoustic reson. of ⁵⁵Mn 0-59467 antiferromagnetic MnP, of ⁵⁵Mn and ³¹P 0-72511

antiferromagnetic and non-magnetic systems, freq. shift near Neel temp 0-51411

aqueous N-methylpropionamide solutions, structure determ. 0-71383 aromatic hydrocarbons, polycyclic, p-p spin-spin coupling consts., calc. 0-46524

aromatic mol., rot. correl. times by proton spin-lattice relax. 0-61556 autodyne oscillating detector, application of frequency locking and control 0-76972

aza-anions, heteroaromite five memoered, p.m.r. spectra 0-67817 azines, neutral and protonated, H-H and C-H coupling constants azines, nei

benzene, pressure effect on dipolar spin relax, in liquid 0–43478 benzene, proton shielding anisotropy 0–49907 benzene, rotational correlation time in liquid, press, and temp, depend. 0–61482

benzene complexes, temp. effects 0-48168 benzenethiol-d, proton and deuteron mag. reson., liq. cryst. solns. 0-53082

benzenoid hydrocarbons, non-planar overcrowed, proton chemical shifts, comparison between theoretical and experimental determinations 0-67769

benzocycloalkenes and benzocycloalkenediones, strained, proton spectra 0-53063

benzothiacyclene derivatives, spectra discussed, magnetic anisotropy

benzyl fluorides, substituted, structural and solvent effects in ¹⁹F n.m.r. 0-67770

0-67770

N-benzyl tworides, substituted, structural and solvent effects in ¹⁹F n.m.r. 0-67770

N-benzyl oxo-2 piperazines, magnetic inequivalence of protons and intro duction of asymmetry in positions 3 or 6 0-70977

benzylideneoxindoles, geometrical isomerism 0-74339

bicycle compounds, fluoro-substituted, vicinal H-F coupling, combined sub stituent and angular effects 0-49909

bicycle (2.2.2) octane derivatives, proton shielding and coupling consts. 0-39416

bicyclo (2.2.2) octane derivatives, proton shielding and coupling consts. 0-39416

bicyclo (2.2.2) octenes, substituted, bromination products, structure and n.m.r. 0-64489

bifluorenyls, p.m.r. spectra, steric effects 0-67795

1-bromo-2-chloro-2-deuteriothioethane, p.m.r., as example of aa'b sub spectrum 0-39359

2-bromothiazole, double reson. N quadrupole relax. 0-41393

bromovinylcyclopropanes, coupling constants rel. to structure 0-43152

bullvalene, oriented in liquid cryst, solvent 0-77882

1,3 butadienes 0-77883

CIDNP spectra for products of radical pair reactions 0-64356

camphene, plastic flow and self-diffusion 0-62045

cannabinoids, p.m.r. and structure anal. 0-77886

carbothydrates, configurational and conformational influences on ¹³C chem. shifts 0-77885

carbon tetrafluoride, gaseous, Frelaxation 0-58198

carboxylic acids, solvent depend, of C-H proton resonance 0-78311

carotenes, natural-abundance pC spectra 0-53086

celluloses acetate and oligosaccharide homologues, ring proton spectra 0-46550

celluloses, wide line p.m.r. spin-spin and spin-lattice relaxation 0-69199

charcal. ENDOR and dynamic nucl. polarization 0-41389

0-46550 celluloses, wide line p.m.r. spin-spin and spin-lattice relaxation 0-69199 charcoal, ENDOR and dynamic nucl. polarization 0-41389 chlorobenzene, pressure effect on dipolar spin relax, in liquid 0-43478 chloroethanes, proton spin relaxation, as function of conc. in CS-0-77888

chloroform-perfluorobenzene solns., relax. conc. depend., double reson. obs. 0-46953

colors, 0-46953 clathrates, Hofmann-type, p.m.r. in temp. range 80 296°K, motion of quest molecules 0-74352

molecules 0–74352 colemanite, p.m.r., –110-110°C 0–41373 computer applies. 0–66989 conference, India, Dec. 1969 0–38788 copper formate, mag. struct. obs. 0–62558 cross relaxation, pulsed double resonance, via double quantum transitions, relax. times çalc. 0–76242 crystal, four pulse 67 cycle 0–76232 crystallographic and magnetic symmetry, appl. 0–58653 cupric acetate hydrate-d₁₆, n.m.r. in single crystals 0–66153 cycloalkanones, ¹³C chemical shift by n.m.r. spectroscopy 0–46554 cyclobutane in nematic solvent, molec. struct. from proton n.m.r. 0–39420

0–39420 cyclohexane series, 220 MHz spectra 0–67781 cyclohexanes and derivatives, conformational effects on ¹³C carbinyl carbon shieldings 0–39432 cyclopentaldiene trimers, p.m.r. spectra at 220 MHz 0–67782 cyclopropanes, monosubstituted, ¹³C n.m.r. 0–74353 e-cyclopropanic alchohol, effect of pyridine solvent on NMR spectra 0–58502

0–58502
cyclopropene, proton n.m.r. 0–64498
deuterobenzene dissolved in 4,4'n-hexyloxyazoxybenzene at 75.3°C,
relaxation times of deuterium 0–49918
2.4-diacetamidopentane, meso and racemic forms, as model for poly(N
vinyl acetamide), spectra interpretation 0–67838
dialkyl selenides and disclenides, Se and proton resonances 0–77951
diamagnetic, Fe(CO)s, of ³⁷Fe 0–41370
3,4- diazanorcaradiene isomerization, dynamic n.m.r. 0–79439
dibenzo-a-j-acridine in CDC1 soln., assignment of lines 0–55348
dibenzhiepin derivatives, assignments of configuration by nuclear Over
hauser effects 0–43156
1,2-dibromo-1,1 dichloro-2,2 difluoroethylene, of ¹⁹F, double resonance in
presence of chemical exchange 0–70863
2,3 dibromopropene, using double irradiation for assignment of very small
coupling const. 0–77894

Nuclear magnetic resonance and relaxation continued

dicalcium strontium propionate, spin lattice relax, by quasi spin waves 0-72288

2.6-dichlorobenzaldoxime, long range spin spin couplings signs, nonplanar ity degree 0-39424

2.6 dichlorobenzylfluoride, long range spin spin coupling consts. conformational depend. 0-39423

dichlorodifluoromethane, liq., 19F relax, times, temp, and field depend, 0 - 74792

0 - 74/92 dichlorodifluoromethane, solid, ¹⁹F relax, time, field depend. 0 - 76/241 1,2 dichlorofluoroethylenes, solvent depend, of chemical shifts and coupling consts. 0-77897

consts. 0—7897 dichlorotetrafluorocyclopropanes, F F coupling constants 0—67777 2.6 dichlorotetrafluorocyclopropanes, F F coupling constants 0—67777 2.6 dichlorotethuene, partially oriented in nematic phase 0—77898 cisoid dienes, proton coupling constants rel. to mol. config. 0—70987 1.2 difluoroethane, vicinal coupling constants 0—67792 cis. 1.2 difluoroethylene in nematic solvent 0—71043 diflurylmercury isomers, ¹⁹⁹Hg satellite spectra and ¹⁹⁹Hg ¹H long range coupling 0—74361 diglycine nitrate. Ferroelec, transition 0—53942 1.2 dihydronaphthalene, proton coupling constants rel. to mol. config. 0—70987

70987 N. N. dimethyl acetamide, hindered internal rotation, studies solvent effects on N-methyl resonance shifts and activation parameters. 0. 67806
 4 N.N. dimethylaminomitrosobenzene, p.m.r. 0. 77895
 4 m.N. dimethylaminomitrosobenzene, p.m.r. 0. 77895
 4 m.N. dimethylaminomitrosobenzene, p.m.r. 0. 67806
 5 m. dimethyleyelopropylearbinyl cation, double resonance. 0. 67787
 N. N. dimethylformamide, hindered internal rotation, studies solvent effects on N methyl resonance shifts and activation parameters. 0. 67806
 6 phenyl selenides and diselenides, Se and proton resonances. 0. –77951
 6 diphenyl selenides and diselenides, Se and proton resonances. 0. –77951
 6 diphenyl selenides and caicks and esters, distreteromeric 3 substituted, rel. to configuration assignment. 0. 67813
 6 diphosphines, substituent effects in inversion rotation process. 0. –67786
 6 dipolar coupling between nuclei in magnetically ordered systems (antiferromagnets). 0. –75956
 6 finolar broadened spin systems, line shapes, theory. 0. –72504

magnets) 0–75956 dipolar broadened spin systems, line shapes, theory 0–72504 diblens broadened spin systems, line shapes, theory 0–72504 diblensylmercury isomers, ¹⁹⁰Hg satellite spectra and ¹⁹⁰Hg. ¹H long range coupling 0–74361

double irradiation technique for ABX, spectra with very small coupling const. 0, 77894

const. 0-77894
double quantum spectra, strong perturbations 0-76971
double resonance spectra, decoupling, strong oscillatory field 0-42137
double resonance, rot. frame, CaF-dipolar fluctuation spectrum 0-41390
dynamic n.m.r. of complex spin systems 0-79439
ENDOR, nuclear polarization, effect of relax, transitiona 0-67413
ENDOR in external elec. field, line shift, rel. to paramag, centre wave
functions 0-62779
ENDOR studies of V_{ob} centre in CaO 0-50611
e.p.r. saturation effects 0-47976
echo, stimulated quadrupoler, in solids, cross relax, effects 0-56678
echo, stimulated quadrupoler, in solids, cross relax, effects 0-56678
electrolyte solns, conc., chem. shifts and joine nuclei relax, obs. 0-30838

ceho, stimulated quadrupoler, in solids, cross relax, effects 0 56678 effectively solins, conc., chem, shifts and ionic nuclei relax, obs. 0 39838 efectron nuclear triple resonance obs. in KH-AsO₄ 0 76243 efectron nucleus spin system, e.p.r. pumping field amplitude modulation influence 0-63526 efectron spin echo behaviour in high fields 0-75968 enhanced multiple reson, by Overhauser effect in paramag, cryst. 0-41388

O 41182 epichlorohydrin, p.m.r. in benzen and acetonitrile solution; 0-64502 epichlorohydrins, n.m.r. structural correlations 0-64503 ethane, chemical polarization of nuclear mag. moment, meas. 0-71007 ethanes, substituted, p.m.r. and vicinal H H coupling 0-39427 ethanes, substituted, p.m.r. and vicinal H H coupling 0-39427 ethanes, substituted, study of rotational isomerism and barriers to internal rotation 0-67791 ethylene copolymers, n.m.r. study of structure 0-46621 ferroelectric. K.FetCN_{b.3}H O and K.RutCN_{b.3}H.O, phase transitions, water molecules dipole moments 0-54169 ferroelectric, LiN-D-SO₁, deuteron n.m.r. spectra 0-66155 ferroelectric, RiN-PO₁ and CsH-AsO₄, ⁵⁷Rb and ⁷⁵As quadrupolar coupling 0-44366 ferroelectric, hydrogen bonded, deuterated 0-62771

ferroelectric, hydrogen bonded, deuterated 0 62771

ferroelectric, order disorder type, spin lattice relax, by quasi spin waves 0 -72288

ferroelectric diglycine nitrate and trissarcosine CaCl = 0 = 53942 ferromagnet, Cr₂Te₈, spin echo, anomalous depend, on external mag, field 0-72286

0-72286 ferromagnet, Ni.Co, crystallographic ordering 0-41380 ferromagnet, hyperfine field distrib., spin echo meas. 0 72196 ferromagnet with 180° domain wall 0-79155 ferromagnetic Heusler alloys, Cu.Mm/Ni, Cu.Mm/ni, hyperfine fields, spin lattice relaxation 0-51414 ferromagnetic MnP, of 35Mn and ¹¹P 0-72511 ferromagnetic distribution of the spin lattice relaxation rate, local effects

0 45036

0. 4:0.36 ferromagnetic alloys, new reson, spin spin and spin lattice relax. 0. 5946 ferromagnetic film, Co, spin echo, field depend, domain struct. 0. 54168 ferromagnetic metal, enhancement factors distrib, effect. 0. 725.13 ferromagnetic metal, inhomogeneous broadening theory applic. 0. 725.12 ferromagnetic metal, nuclear acoustic resonance. 0. 69190 ferromagnetic metals, theory. 0. 725.02 ferromagnetic, nuclear spin echoes, domain wall enhanced, temp. depend. 0. 75967

fibre, H2O mol. symmetry of orientation obs. 0-66150

fibre, H.O mol. symmetry of orientation obs. 0–66150 field dependent nuclear magnetic shielding in n.m.r. experiments 0.43074 fluorenes, p.m.r. spectra, steric effects 0.67795 fluorides of d¹⁰ elements, of ¹⁹F, chemical shifts 0.51406 fluoroethanes, solvent effects and rotational somerism 0.67794 fluoromethane, ¹⁰CH₁F, partially oriented, anisotropies and absolute signs of indirect spin spin coupling const. 0.46560 fluoropyridines, ¹⁰N relaxation times and tN. F) coupling constants, temperature and medium effects 0.49925 free energies of activation, two exchanging species, coalescence temperature, graphical method. 0–38446 free induction decay in solids, Lowe Norberg theory. 0.41359 Garstens Singer shift in recording nuclear resonance signal using nutation method. 0–48940 gas, perturbed, relax times, rel. to mol. quadrupolar moments. 0.43075

gas, perturbed, relax, times, rel. to mol. quadrupolar moments 0 -43075 gas of regular mols., nucl. mag. relax. 0 78227 glass, struct. obs. 0 -51404 glass, vanadium phosphate, semiconducting, of ⁵¹V 0 48163

Nuclear magnetic resonance and relaxation continued

glycerol+water mixture doped with porphyrexide at 25 and 47.8 kG and at 0.5 $\!\!<\! T \!\!<\! 1.2^o\!\! K$ 0-74791

glycerol/water mixtures, porphyrexide doped, proton polarization times, <1K 0-62770 gradient elastic tensor, stressed cubic crystal 0-51402

gradient elastic tensor, stressed cubic crystal 0-51402 group VIII, aluminides, cubic equiatomic, Knight shift, relax, rate, linewidth and intensity 0-45012 Heisenberg antiferromagnet, rel, to impurity effects 0-51239 heptanols, straight chain, liquids, meas, rel, to extent of association 0-46939

heteroaromatic mol., rot. correl. times by proton spin lattice relax. 0-61556

in heterogeneous systems, comparison with proton and deuteron relaxa

in heterogeneous systems, comparison with proton and deuteron relaxation 0-64885
Heusler alloys, new reson., spin spin and spin lattice relax. 0-59464
hexafluorides, of ¹⁹F. diffusion coefficients determ. 0-72507
hexamethylphosphorotriamide water mixture, preferential solvation by
diamagnetic cations, ¹H and ³¹P spectroscopy investigations 0-68156
hydrocarbons, condensed planar benzenoid, p.m.r. spectra. McWeeny
cales, on hexacyclic mols. 0-43168
hydrocarbons, planar condensed benzenoid, n.m.r. spectra. McWeeny 'ring
current' theory evaluation 0-43167
hydrocarbons, planar condensed benzenoid, p.m.r. spectra in isotropic sol
vent 0-43166
hydrozurea, y-irrad, crysts, NH-CONHO radical 0-79421

vent 0-43166
hydroxyurea, p-irrad, crysts.. NH-CONHO radical 0-79421
hyperfine field interactions effects, theory 0-59463
ice, X-irrad, single crysts.. ENDOR 0-66207
inositols and O-methylated derivatives. ¹¹C spectra 0-46569
interference effect for one- and two spin systems 0-61560
interference effect for three spin system 0-64956
intermolecular Overhauser effect correlation with internuclear distance for ¹H in organic molecules 0-64461
isobutylenes, deuterated, molecular motions in liquid state, d.m.r. study 0-64855

isohalfordin structure from n.m.r. solvent shift in methoxyl groups

isohalfordin structure from n.m.r. solvent shift in methoxyl groups 0–49300 2′.3′-isopropylidene- 3.5′ cycloguanosine, nuclear Overhauser effect and molecular geometry 0–77854 KBr. KCI 0–78566 ketones, β.p.-unsaturated, ¹³C carbonyl carbon shieldings 0–39431 Knight shift, ²³Mg, electric quadrupole coupling 77 503 K 0–51409 Knight shift, Pd-Rh and Ni Rh alloys, 1-4 K, spin lattice relaxation 0–45007 Knight shift, changes on alloying, correlation with soft X-ray emission edge height 0-72506

Knight shift, changes on alloying, correlation with soft X-ray emission edge height 0-72506
Knight shift, rel. to electron density of states, conference, Gaithersburg (1969) 0-65573
Knight shift, rel. to electronic density of states 0-75453
Knight shift, rel. to electronic density of states 0-44733
Knight shift, relax, rate, linewidth and intensity, cubic equiatomic group VIII aluminides 0-45012
Knight shift, solute, in binary alkali system 0-45013
Knight shift and diamagnetic susceptibility of Al₂Pd, AlPd, 77-300K 0-69193
Knight shift and relax, rate in Cd, effect of core polarization, 0-41365

Knight shift and diamagnetic susceptibility of Al₂Pd, AlPd, 77-300K 0-69193

Knight shift in Cd0 0-62772

Knight shift in Cd0 0-62774

Knight shift in Mg 0-62774

Knight shift in Mg 0-62774

Knight shift in India alloys, from elastic scattering 0-61552

Knight shift in liquid alloys, from elastic scattering 0-61552

Knight shift in liquid metals, interference function approach 0-46954

Knight shift in semiconducting vanadium phosphate glasses 0-48163

Knight shift meas: in Cd and Cd-Hg alloys 0-56680

Knight shift of ¹⁰Pk nin Pd Rh alloys 0-41382

Knight shift of 1 Al 7 intermetallics, mag. susceptibility 0-69194

Knight shift of Al Ar intermetallics, mag. susceptibility 0-69194

Knight shift of Id al, alloy, dilation effect 0-78305

Knight shift sand spin lattice relax, rates in Cs and Rb, low-temp. pressure depend, 0-41367

Knight shifts and spin lattice relax, rates in Cs and Rb, low-temp. pressure depend, 0-41367

Knight shifts in transition metals, analyses 0-45011

Kondo system 0-45010

Nondo system 0-501010

Nondo system 0-501010

Nondo system 0-45010

linewidths in high-resolution spectra, intramolec. dipolar relax. effects 0-53012

liquid, meas, of relaxation time of uncoupled protons 0-64955

iquid crystal, nematic. proton spin lattice relax. time, temp. and freq. depend., mechanism 0–78307 liquid crystal, nematic. spin relax. 0–43430 liquid crystal, nematic. spin relax. 0–43430 liquid crystals. modulated spin echo trains 0–58500 liquid crystals. nematic phase. spin lattice relaxation 0–71382 liquid crystals anisylidene p. aminophenylacetate, p.m.r. 0–61558 liquid diute alloy, Knight Shift, dilation effect 0–78305 liquid in porous medium, relax. of spins. grain sizes of medium influence 0–50259 liquid spins. Knight shift, interference function approach 0–46954

0–50259

liquid metals, Knight shift, interference function approach 0–46954
liquid solns, with two nuclear spin species, relax, conc. depend. 0–46953
liquid crystal soln., proton double resonance 0–61557
liquids, rotational diffusion of symmetric top mols. 0–61551
liquids in high magnetic fields (25 to 47.8 kG) and low temperature (0.5 to 1.2°K) 0–74791
Lowe-Norberg theory for free induction decay in solids 0–41359
lunar materials 0–59741
lunar samples, p.m.r. at 60 MHz 0–48487
lunar samples of ²⁷Al, asymmetry parameters and quadrupole coupling 0–48539
2.6-lutidine-water system in critical region 0–46058

2.6-lutidine-water system in critical region 0-46958 magnetic coherence resonances and transitions at zero frequency 0-55245

magnetic material, ordered, nuclear acoustic resonance 0–51403 magnetically dilute metal complexes, ligand ENDOR 0–45040 manganese formate dihydrate, mag. ordering obs. 0–75966 metal, acoustic n.m.r., and e.m. generation of sound 0–68587 metal, ferromag., enhancement factors distrib. effect 0–72513 metal, nonferromagnet, spin echo 0–75969

Nuclear magnetic resonance and relaxation continued

metal, spin lattice relax, time of nuclei, low temp., formulae 0-41071 metal, theory 0-76197

metal, total mag. susceptibility meas. 0-79412

metal, total mag. susceptibility meas. 0–79412
metal complexes. ligand ENDOR in powders 0–45040
metal with mag. impurities. Kondo effect 0–45010
in metals. acoustic eff. 0–75393
methane. chemical polarization of nuclear mag. moment, meas. 0–71007
N-methyl 2-carbomethoxy- 4.6-dinitroaniline, long range spin spin established by p.m.r. 0–55361
methyl acid copolymers. triad assignments 0–43201
methyl alcohol, solid, ar and p-irrad. electron spin echo for spatial radical distrib.. influence of LET and spur effects 0–66133
methylammonium halides, and partially deuterated analogues. p.m.r. 0–62776

0-62776 methylbenzenes, spin lattice relax time, temp variation minima 0-59469 methylbenzenes, spin lattice relax time, temp variation minima 0-59469 methylbroride, in liq, crystal, vibr, corrections on dipole-dipole interactions 0-77919 N- methylpropionanmide aqueous solutions, structure determ. 0-71383 microtechnique, sensitivity enhancement 0-60123 molecular motions in solids, rotating frame 0-48169 mucopolysaccharides, heparin, chondroitins, structure and composition from p.m.r. 0-77978 multi-domain ferromagnetics, local amplification and integral susceptibil itv 0-54166

multi-domain terromagnetics, total amplification, ity 0–54166 multiple pulse spectrum of solid, chem, shift anisotropy absence 0–72503 multiple quantum transitions calc, by second quantization 0–38445 n.m.r., solvent shift in methoxyl groups rel. to isohalfordin structure n.m.r. solv 0-49930

n.m.r. solvent shifts, in polymethoxycoumarins 0–49941 n.m.r. spectra analysis, iterative procedure 0–67708 naphthalene, mononegative ion in DME, proton ENDOR spectra 0-64531

0 -64531 nitrobenzene-1, 3, 5,-d) in liquid crystal poly-γ-benzyl-L-glutamate, ¹H and ¹⁴N spectra 0-74321 nitrobenzenes, fluorinated, ¹⁴N resonance studies 0-67808 nitromethane, in liquid-crystal poly-γ-benzyl-L-glutamate, ¹H and ¹⁴N spectra 0-74321 p-nitrophenol cryst, and α-form, irrad, products 0-72519 nitrophenylhydrazone α-carbonyls, n.m.r. study 0-71024 non-polar molecules in liquids. ¹H chemical shifts, intermolecular effects 0-49849

0–49849
nuclear polarization, dynamic, forbidden transitions saturated 0–56477
nuclear shielding effect rel. to K-shell electron binding energy chemical shifts 0–39357
nuclear spin-spin reservoir, 4.2 K 0–72505
nuclei contribution to particular line in resonance spectrum 0–69810
nucleosides, 13C n.m.r. 0–74395
nucleosides, naturally occurring, 13C spectra' 0–53078
nucleosides, pyrimidine and purine, 13C n.m.r. 0–77947
nucleotides in aqueos soln, 13C spectra 0–53081
organic liquids, self- diff., from spin echo 0–64891
organo metallics, indirect spin coupling, heteronuclear double resonance 0–61142
organometallic 4f and 5f systems, paramagnetic, temp, dependence of

0-61142
organometallic 4f and 5f systems, paramagnetic, temp. dependence of p.m.r. shifts 0-67783
Overhauser effect, intramolecular nuclear, rel. to structure and conformation determination of alicyclic and aromatic compounds 0-67758
Overhauser effect applic, of double reson, apparatus 0-48937
Overhauser effect for determination of molecular geometry in solution 0-77854

0-77854
Overhauser effect in paramag, cryst., enhanced multiple reson. 0-41388
Overhauser effects and ¹³C relaxation times 0-39407
oxetane, analysis of coupling constants 0-49940
5-oxibenzodioxane 1.4 hydrogen bonds, obs. 0-55365
α-oxiranic alchohol, effect of pyridine solvent on NMR spectra 0-58502
para-azoxyanisole liquid crystal, ¹⁴N n.m.r. obs. 0-61559
paramagnet KMnF₁, RbMnF₂ and MnF₃, line shape and spin correlation, exchange narrowing 0-41332
paramagnetic cryst., enhanced multiple resonance by Overhauser effect 0-45038
paramagnetic cryst., enhanced multiple resonance by Overhauser effect 0-45038

0-45038
paramagnetic d⁴ complexes, temp, independent, effect of molecular and local symmetry on p.m.r. spectra 0-67709
penta- and hexadienes, coupling consts. involving methyl protons 0-77883
α, α, 2, 4, 6- pentachlorotoluene, rotational isomerism, p.m.r. obs. 2-4-pentanadiemics.

2.4-pentanediamine, meso and racemic forms, as model for poly(vinyl amine), spectra interpretation 0-67838 perfluoroalkyl-fluoroaromatic compounds. ¹⁹F spectra, F-F coupling constants 0-64536

perfluorocyclohexane, solid, multiple pulse spectrum, chem. shift anisotropy absence 0–72503 peroxides, organic, thermal decomposition, dynamic nuclear polarization of ¹³C nuclei 0–58236 phase-sensitive detectors 0–69191

phase sensitive detectors 0–69191 phenanthridinium compounds, obs. rel. to restricted rotation and magnetic non-equivalence 0–67812 phenol, and methyl, silyl and germyl derivatives, p.m.r. spectra analysis 0–39444

 σ -phenyl-transition metal complexes, $^{19}{\rm F}$ n.m.r. 0-67712 phenyl-phosphine-d₃, proton and deuteron mag, reson., liq. cryst, solns, 0-53082

phenylsilane-d₃, proton and deuteron mag. reson., liq. cryst. solns. 0-53082 photon echo behaviour in high fields 0-75968

piperazines, spectral parameters and ring interconversion 0-74401 polarization magnetometer with measurement sequencing system, patent 0 - 49497

O-49497
poly(vinyl amine), tacticity studies 0-67838
polyamino acids, mol. motions 0-72515
poly(t-butyl ethylene oxide-2-D), struct, study 0-51413
polycrystalline material, asymmetry, n.q.r. and anisotropic shift interactions 0-79422
polyester platicizers, struct, and mol. weight determ. 0-59470
polymers molecular motion study, review 0-64569
polymers, molecular thermal motion study 0-50852
polymers, relaxation times 0-48171
polymers, solid, p.m.r. signal narrowing by magic angle rotation 0-69811

PA 1970 - Part II (July-Dec.) SUBJECT INDEX \$ 1163 Nuclear magnetic resonance and relaxation continued Nuclear magnetic resonance and relaxation continued spin-echo signals obs., thin Co and Co-Fe films, relaxation times meas. 0-45017 polymethoxycoumarins, n.m.r. solvent shifts obs. 0-49941 polypropene-2-d₁ sulphide 0-49950 spin lattice relax, time of nuclei in metals, low temp., formulae 0-41071 polystyrene, atactic, relax. times rel. to glass transition and mol. weight 0-59472 spin-lattice relaxation in nematic liquid crystal phase 0–71382 spin-phonon interaction, magnon-coupled 0–72289 polytetrafluoroethylene relaxation times 0-6277 polyvinyl chloride- β , β -d, in solution, study 0–67832 spin-tickling spectra by second quantization formalism 0--55283 spin-tickling spectra by second quantization formalism 0-55283 spinel, MgAl-O₄, NiAl-O₄, ZnAl-O₄, CoAl-O₄, of ²⁷Al, electric field gradients 0-45016 use in stabilisation of Hall effect regulated electromagnet 0-77027 steroidal androstane, A- and D-ring substituted, of C-18 and C-19 methyl group protons 0-67819 succinic acid, ENDOR of anions in irrad. crysts. 0-41351 succinonitrile, ¹H spin relaxation times, self-diffusion study 0-50630 polyvinylformal, high resolution p.m.r. and i.r. spectra 0-67833 polyvinylpyridines, solutions 0-55632 polyvinylpyrrolidone in deuterated solvents, spin lattice relaxation time of deuterium 0-58263 polywater, p.m.r. spectrum 0-46471 potassium oxalate monohydrate, pulsed deuteron n.m.r., hindered rotation of H₂O 0-66157 succinonitrile. 'H spin relaxation times, self-diffusion study 0–50630 sulphonated cation- exchange resins, ionic solvation study 0–56685 superconductor, spin excitation phenomena 0–47659 terpenes, natural abundance ¹¹C spectra 0–53086 terphenyl, mononegative ion in DME proton ENDOR spectra 0–64531 tetracene, mononegative ion in DME, proton ENDOR spectra 0–64531 2.3.5.6-tetrafluoroaniline, aromatic H-F and F-F coupling constants, relative signs 0–46443 1.1.2.2-tetrafluoroethane, in liquid and solvents, ¹H and ¹⁹F chemical shifts and couplings 0–49938 1.1.2.2-tetrafluoroethane, vicinal coupling constants 0–67792 tetrafluoromethane, ¹⁹F relaxation times 0–56466 tetrafluoromethane, ¹⁹F spin-rotation const. 0–77841 tetramethylammonium bromide, p.m.r., mol. reorientation 100-400°K 0–49931 be, proton, for high field superconducting solenoid calibration 76973 probe. 0-70973 propane, clathrate hydrate, p.m.r., mol. motion 0-64540 propanes, substituted, study of regational isomerism and barriers to internal rotation 0--67791 propanol-water system, proton exchange 0--66166 propanor water system, proton exchange 0-66166 propylene oxide, n.m.r. structural correlations 0-64503 proton, rel. to exchange phenomenon between carbonium ion and patent molecule 0-67775 proton, fluorenes and bifluorenyls, steric effects in spectra 0-67795 proton, spectral study of cyclic ethyleneureas and propyleneureas 0-54165 proton, studies of clostridium pasteurianum rubredoxin 0–645 proton chemical shifts, in liquids, polar effects 0–68152 proton resonance, rel. to Earth's field magnetometer 0–45193 tetramethylammonium chloride, p.m.r., mol. reorientation, 100 400°K proton res 0-45008 resonance affected by cross relax, with quadrupolar nuclei tetramethylammonium iodide, p.m.r., mol, reorientation, 100 400°K protons in water, spin relaxation time and nuclear susceptibility 0—74786 pulsed and Fourier transform 0–63525 pyridine, solvent effects on proton magnetic resonance spectrum 0–49937 pyridine in liq. mixtures, spin lattice relax. time and mol. association 0-49931 0—49931 thiazole series, of ¹³C, chemical shift 0—58247 tri-3-thienylphosphine. ¹H n.m.r. obs. rel. to ¹H.³¹P coupling constant determ. 0—39450 tri-2-thienylphosphine. ¹H n.m.r. obs. rel. to ¹H-³¹P coupling constant determ. 0—39450 tri-2-thienylphosphine. ¹H n.m.r. obs. rel. to ¹H-³¹P coupling constant determ. 0—39450 thietane, analysis of coupling constants. 0—4940 thicactanilides. substituted investigation of cisatrons isomerism. pyridine in 0-71384 0-71384 2-pyridones, delocalization of ring π-electrons proton coupling constants and chemical shifts 0-55370 2-pyridthiones delocalization of ring π-electrons proton coupling constants and chemical shifts 0-55370 2-pyridylphosphine derivatives, coupling constants 0-49936 1-N-pyrrole, 100 MHz p.m.r. spectrum, sub-spectral analysis 0-71029 pyrrole-2-carboxylic acid pyrrole-2-aldehyde, spectral analysis 0-71028 quadrupolar nuclei, multi-site chemical exchange effects in spectra 0.6003 thioacetanilides, substituted, investigation of cis-trans isomerism, 0—04350 2-thioalkylpyridines delocalization of ring π-electrons proton coupling constants and chemical shifts 0—55370 thiodiglycolic acid. ENDOR of anions in irrad. crysts. 0—41351 thiophenes. monosubstituted, ¹³C n.m.r. 0—7.7954 hiophenol, and methyl, silyl and germlyl derivatives, p.m.r. spectra analysis 0—39444 0 - 69203quadrupolar nuclei containing molecules, several spin-1/2 nuclei case 10—49925 quadrupolar spin lattice relax. time.. cryst. rot. effect 0—41072 quadrupolar spin lattice relax. time.. cryst. rot. effect 0—41072 quadrupole interactions in cryst. influence on y-y ang. correls. 0—41088 quinodimethanes, n.m.r. spectra 0—43179 radical ions in soln. resolution enhancement by deuterium n.m.r. 0—58499 rare-earth phosphates, hydrated vs. anhydrous form 0—41381 relaxation, nonexponetial, by quadrupole interactions 0—60125 relaxation of polar mol. in elec. field 0—78270 relaxation times of nuclear spin, rel. to y-y angular correlations 0—41074 Rh (III) complex, rhodium (III)—oxalato-triaquo-monammine oxalate 0—74940 0-49925 sis 0–39444 thiopyranyl-1.1-dioxide anion and related species, p.m.r. spectra analystransition metal complexes. *Irans*-effects 0–64370 transition metal diboride, ¹¹B spin-lattice relaxation times 0–79419 transition metals. Knight shifts, analyses 0–45011 1.2,3 and 1,2,4 tribromobenzene 0–74345 trichloro silyl compounds, chemical shifts and coupling constants 0–64552 0-04332 tricyclopropylborane, n.m.r. spectrum, correlation between coupling constants and substituent electronegativities 0-43184 trifluoro silyl compounds, chemical shifts and coupling constants 0-64552 Rh (III) complex, rhodium (III) oxalato-triaquo-monammine oxalate 0–74940 Rochelle salt, orientations of proton pairs 0–66158 rotating-frame double reson, and cross-relax, in LiF 0–41391 rotational, of symmetric top mols, n.m.r. 0–61551 ruby: Cr³⁺, nominal \(\Delta m = 1.5 \) mag. transition probabilities 0–41362 ruby, of 170, dynamic polarization technique, 1.9K 0–41363 ruby, saturation and population inversion e.s.r. spectra 0–69195 saturational narrowing, theory 0–38447 semiconducting vanadium phosphate glasses, of 51V 0–48163 semiconductor, lead salt. Knight shifts and band struct. 0–56683 semiconductor, magnetic, (La_{1-x}Ca_x)MnO₃, of ³⁵Mn, mag, and elec. props., comp. depend. 0–59307 shielding, gauge invariance and average excitation energy approximation 0–70864 single-spin syst., effects of two reson. 3.3.3-trifluoropropyl tin cpds.. Sn coupling consts. 0–67823 trimethyl silyl compounds, chemical shifts and coupling constants 0–64552 trimethylsilyl cyanide and isocyanide, proton and double reson. spectra 0-55377 0-55377 tri-(5-methyl-2furyl)phosphine derivatives. 'H-3¹P spin-spin coupling constants 0-74384 trissarcosine CaCl-, ferroelec, transition 0-53942 unified theory with n.m.r. rel. to proton polarizations in proton spin refrigerators 0-51381 vicinal coupling constants, in X.CH-CH-Y fragments, effect of substituents 0-67755 0-70864 single-spin syst., effects of two reson, e.m. waves, multiple quantum transitions 0-70836 site factors in solvent effects 0-55284 solid, conference, Turku, Finland, Aug. 1970 0-74858 solid with molecular mobility, spectral calcs. 0-48158 solid-state flux stabilizer for use in conjunction with pulsed expts. 0-73149 ents 0-67755 vinyl compounds, substituent effects on J_{c^+h} Coupling constants 0-58253 vinyl fluoride in nematic solvent 0-71043 vinyleyclopropanes, rotational isomerism studies 0-67825 water, proton relax, time, press, depend., 0^6C 0-61553 water contained in porous medium, relax, of nucl. spins, temp. depend. 0-50260 xylene derivatives, intermethyl proton spin-spin coupling constants signs 0-553790-73149 solvent anisotropy shifts, calculation 0-68151 solvent effect, model for neighbour anisotropy, nonpolar solutes in benzene 0-68149 solvent effects, chemical shift of non-polar solute 0-68150 solvent effects, or proton chem. shifts of nonpolar solutes 0-74790 solvent isotope effect on chemical shift of halide nuclei 0-70444 spectral line forms in presence of equal transitions 0-57471 spectrometer, high resolution. Varian HA-100, solid state spin-echo attachment 0-76231 spectrometer's strange device synchronization, device description 0-48941 spectrometer's transducer, e.m. rate parameter selection, mathematical |Co(NH₁)₄Co₃|Br, p.m.r., thermal motion of ammine groups, 77-383K 0-4[366] [Cu(CD₂CO₂)₂D₂O]₂, D magnetic resonance, CD₃ quadrupole splitting [Cu(CD₂CO₂)₂D₂O]₂, D magnetic resonance, CD₃ quadrupole' splitting 0–66153 Ag-Mn dil. alloys, ¹⁶⁹Ag linewidth 0–79413 Ag alloys containing ≤0.1 at% of Mn or Ni, giant echoes, at 4 MHz, 1.8 to 300°K 0–41360 AgNa(NO₃). ²⁰Na characts. 0–72508 Al-Cr intermetallics, Knight shift, mag. susceptibility 0–69194 Al-Mn alloy, localized spin fluctuations, ⁵⁵Mn and ²⁷Al 0–45015 Al. acoustic, of ²⁷Al, spin-phonon interaction 0–45014 Al spin-lattice relax, times, effects of electron-electron interactions, 1.3-295K 0–51244 Al(III) complex in aqueous solution, p.m.r., hydration numbers 0–58501 Al₂O₃, polycryst., of ²⁷Al, spectra showing local field with asymmetry parameter equal to zero 0–41364 Al₂Pd, AlPd, intermetallics, Knight shift, diamagnetic susceptibility, 77-300k 0–69193 B complexes, solid, molecular motion 0–45009 spectrometer's transducer, e.m. rate parameter selection, mathematical evaluation 0-48942 spectrometer for longitudinal relaxation time meas, of nonequiv nuclei groups 0-48939 groups 0—48939 spectrometer spin-echo timing cet./with improved stability of pulse repetition freq. 0—48938 spectroscopy. conference. Birmingham (1969) 0—63527 spectroscopy. conference. Birmingham (1969) 0—63527 spectroscopy. progressiolation. application to biological compounds examination 0—64465 spectroscopy. p.m.r.. organometallic reference compounds for higher temp. and in aqueous solution 0—66988 spectroscopy. progress in. vol. 5 0—62780 spin 1/s nucleus in polycryst. rigid lattice two-spin system 0—41357 spin dynamics in solids. pulse expts. in two-spin-species systems 0—44718 spin ceho in dipolar broadened solids 0—56679 spin relaxation in dilute alloys, effect of s-d exchange interaction 0—69051 spin relaxation times meas. with HA-100 spectrometer 0—73117 spin-lattice relax, in dynamic orientation of nuclei 0—65967 spin-echo envelope modulation due to transverse interaction 0—41070 300k 0–69193 B complexes, solid, molecular motion 0–45009 B hydrides, volatile, 220 MHz 0–77768 B₁₀H₁₄: ¹¹B and p chem, shifts correl, ring current model 0–74239 B₃H₁₁, anomalous hydrogen 0–77767 ¹²B in Au, Pt, Pd, rel. to nuclear mag, moment, obs. 0+46122 ¹³B polarized, quadrupole effects 0–38855 BaFPO₃, ¹⁹F and ³ ¹P resons, rel. to polycryst, lattice theory 0–41357 Be, hyperfine props., rel. to electronic structure and Knight shift, pseudopotential calc. 0–76234 Be, self-diffusion obs. 0–47288 Be compounds in soln., ³Be and proton n.m.r. 0–77771 BeO, irrad, damage 0–69196

spin-echo envelope modulation due to transverse interaction 0-41070

Nuclear magnetic resonance and relaxation continued

BcO, neutron irrad., e.p.r. ENDOR obs. of F+ centres, hyperfine interaction 0--44985

C, nmr chemical shift, molecular orbital theory in calc, for several mole cules 0-70862

CF₄, solid, of ¹⁹F, spin lattice and spin spin relax., mol. motion 0-75973 (CF₁)₂PF₄, PH and P-F coupling consts. from mag. double reson.

CH.NH.Al(SO₄)-12H-O, ferroelec... of ²⁷Al 0-41361 ¹⁰C-{H}, Overhauser effects and ¹³C relaxation times 0-39407 ¹³C, in thiazoline and its derivatives for determ. of chemical shift 0-58248 ¹³C, resonance spectra, application of field sweep proton decoupling 0 67756

¹⁰C, resonance spectra, application of field sweep proton decoupling 0 67736 ¹⁰C, spectra of proteins, analysis by comparison with computer simulated spectrum 0–66152 ¹⁰C for streutural analysis of steroids 0–64546 ¹⁰C resonance spectroscopy, application of noise decoupling 0–67757 CaB.O₁(OH). H-O, powdered, proton second moment, 4.2-450°K 0 48159 ¹⁰C ar. antiferromagnetism of ¹⁰F nuclei, low temp, production 0–44677 CaF., endor of ¹³Yb at tetragonal sites rel. to cryst. field parameters 0 51251 ¹⁰CaF., free induction decay using Lowe-Norberg theory 0–41359 CaF. dipolar fluctuation spectrum, rot. frame double-reson. obs. 0–41390 CaO, V, centre, ENDOR studies 0–50611 ¹⁰CaO, V, centre, endor of paramagnetic centers, ESR, ENDOR investigations 0–62753 ¹⁰Cd Hg alloys, Knight shift meas. 0–56680

CaWO₁ radiation induced paramagnetic centers, ESR, ENDOR investigations 0-62753
Cd Hg alloys, Knight shift meas. 0-56680
Cd, Knight shift meas. 0-56680
Cd, Knight shift meas. 0-56680
CdF, CdF, 2H-O, of ¹⁹F, chemical shift and second moments. 150 K
0 59465
CdO, of ¹¹⁰Cd, Knight shift 0-62772
ClCN, ¹⁴N quadrupole coupling const. in liquid phase 0-53376
¹⁵Cl, hyperfine structure anomalies 0-49758
¹⁵Cl, hyperfine structure anomalies 0-49758
Co complex, carbonyls containing metal metal bonds, anisotropic chemical shifts for ¹⁵CO 0-74252
Co dil. alloy, ferromagnetic, 4.2K 0-48160
Co film, spin echo, field depend., domain struct. 0-54168
Co hydrates, p.mr., data 0-62778
CoAl-O₄, polycryst., of ¹⁷Al, spectra showing local field with asymmetry parameter equal to zero 0-41364
CoCl-12H-O, antiferromag. of ¹⁵Co 0-62773
Co(II) complex, dichlorobis(picoline)cobalt(II) in CDCl₁, p.m.r. study 0-49861
Co(II) complexes, trigonal, isotropic shifts 0-56681

10 - 49601
Cot(I) complexes, trigonal, isotropic shifts 0 - 56681
Cot(II) complexes, spin decoupling of ⁵⁹Co in p.m.r. 0 - 77782
Cr(II) paramagnetic complexes, p.m.r., hindered methyl rotation 0 - 46465
Cr, Te₈, ferromag., spin echo, anomalous depend, on external mag. field CtrTe₈, ferromag., spin echo, anomalous depend, on external mag. field 0-72286
Cs-O system, liq., of ¹³³Cs, rel. to state of O atoms 0-46956
Cs-bearing perovskites, of ¹³³Cs 0-41399
Cs, Knight shift and spin lattice relax, rate, low-temp, pressure depend, 0-41367

0.-41367
CsCoCl₁, of ¹³Cl 0.-48161
CsF, line shape meas. 0-.72504
CsH-AsO₄, ¹³As quadrupolar coupling, rel. to Curie pt. 0.-44366
CsH₂-AsO₄, ¹³As quadrupole coupling determ. 0.-48161
Cu-base dilute alloys, transient n.m.r. 0.-41368
Cu-Cr alloy, ⁶³CU, Kondo effect suppression, spin relaxation 0.-45035
Cu-Mn dil, alloy, 1st order quadrupole effect, cond. electron density oscillation 0.-45018
Cu-Ni alloys of Cu-spin lattice, relax, page action 1 cond. 0.56460

tion 0–45018

Cu-Ni alloys, 62Cu spin lattice relax, near critical conc. 0–56469

Cu, solid and liq., Knight shift and spin lattice relax, rate 0–41369

Cu foil, elastically deformed 0–79414

Cu-MnA(In), ferromagnetic Heusler alloys, spin lattice relaxation, hyperfine fields 0–51414

D., solid, near orientational ordering transition 0–48162

p.D. solid, relaxation mechanism 0–62769

ErAls, nucl. quadrupole coupling and cryst.-field effects 0–76235

EuFe garnet, of 191Eu and 191Eu, hyperfine field and quadrupole splitting parameters 0–45019

F¹⁹ spectra, radio spectrometer method 0–48943

PF double resonance in presence of chemical exchange 0–70863

Fe-Al alloy, Fe-rich, spin echo meas, rel. to hyperfine field distrib. 0–56682

Fe-Al alloy, retroit spin 0-56682 Fe-Al alloy, ordered, rel. to Al hyperfine fields 0-45020 Fe-Co dil, alloy, of ⁵⁷Fe and ⁵⁹Co 0-41371 Fe-Mo alloy, Fe-rich, spin echo meas. rel. to hyperfine field distrib.

Fe-Mo alloy, Fe-rich, spin echo meas, rel. to hyperfine field distrib. 0-56682 Fe-V alloy, Fe-rich, spin echo meas, rel. to hyperfine field distrib. 0-56682 Fe, dilute alloy, hyperfine fields 0-79415 Fe, of ⁵⁷Fe, rotary saturation 0-72509 Fe allyl complexes, spectra rel. to structure 0-67760 Fe(CO)s, of ⁵⁷Fe 0-41370 FeFs, phonon effect, near antiferromag, critical point 0-59466 FeF.3H.O. ¹⁹Fe, p.m.r., mag, susceptibility, temp, depend, antiferromag, ordering 0-56462 Fe-Oy of ⁵⁷Fe, domain wall resonance, magnetization 0-76236 Ga metal, Knight shift tensor, temp, depend, 0-76233 Ga(III) complex in aqueous solution, p.m.r., hydration numbers 0-58501 Ga·Tes, (i.e., localized electronic states obs. 0-68140 Gd, ferromag., of ¹⁵⁵Gd and ¹⁵⁷Gd, signals depend, on sample type 0-41372 Gd, spin echo obs. 0-6950

0-41372

0-41372

GeH, Spin echo obs. 0-69050

GeF, "F spin rotation const. 0-77841

GeH, spin-rotation const. 0-77841

H, solid, longitudinal relaxation, 4th moment correction to spectral density 0-76240

O H solid, nuclear relax, mechanism 0-62769

HPF d, double reson, expt., P-h and P-F coupling consts. 0-46506

H₂PO₄, aqueous solutions with Al and F ions, n.m.r. study of complexes present 0-68154

H₂SO₄, solid, m and prigrad, electron spin echo for spatial radical distributions.

present 0-06134 P-irrad., electron spin echo for spatial radical distrib., influence of LET and spur effects 0-66133 H-JC heteronuclear resonance of nickel acetylacetonate with organic ligands 0-58190

Nuclear magnetic resonance and relaxation continued

H, uncoupled, in liquid, in homogeneous field, relaxation time 0-64955 ¹H in Mg, Ca, Ba orthophosphates used to study chemistry of dehydration 0.54178

0 54178

²H, ENDOR enhanced n.m.r. 0–51405

²H, isotope and temperature effects in partly deuterated hydrates 0–74261

²H chemical shift, difference for α and β substituents 0–77758

³He ⁴He solid mixtures, 0.3-20 °K 0–78323

³He gas, spin lattice relax, time, density depend., spin-echo obs. 0–78222

HfO₂ (OH)₂,yH₂O amorphous precip., p.m.r. rel. to comp., obs. 0–51412

Hg-In liq. alloys, Knight shift temp, depend. 0-61554 HgF₂, HgF₂2H₂O, of ¹⁹F, chemical shift and second moments, 150 K HgF₂, Hg. 0-59465

HgF₃, HgF₂,2H₂O₃ of ¹⁹F, chemical shift and second moments. 150 K 0-59465

Fr₂AsF₃ solid addition compound, fluorine magnetic resonance study 0-56684

In-Cd(Hg₃, Tl) alloys, of ¹¹⁵In, Knight shift, quadrupole-coupling freq., line-widths 0-45021
In-Te₃, ¹¹⁵In Knight shift, 725-1500 K, liquid and solid 0-46957
KC1:Li²+, stress induced quadrupole splittings of ⁷Li, 1.3-4.2K 0-51408
KF-B₂O₃ glass, coordination number from ¹¹B spectra 0-41374
K₁Fe(CN)₆,3H-O. ferroelectric phase transition, water molecules dipole moments 0-54169
KH-AsO₄, ENDOR observational ferroelectric domains 0-75792
KH-AsO₄, ENDOR observation of ferroelectric domains 0-75792
KH-AsO₄, X-ray irradiated, observation of electron-nuclear triple resonance of AsO₄*-center 0-76243
KH₃(SeO₂), ferroelec, transition, dynamic proton ordering 0-41376
KMnF₁, antiferromag., ¹⁹F₄ acoustic effect 0-41378
KMnF₁, antiferromag., ¹⁹F₄ acoustic effect 0-41378
KMnF₃, paramagnetic, line shape and spin correlation, exchange narrow-

 $KMnF_{3}$, paramagnetic, line shape and spin correlation, exchange narrow ing 0-41332 KPF_{6} . ^{19}F nuclear spin coupling constants, high speed rotation method 0-41377

0-41377 K,Ru(CN)₆,3H-O, ferroelectric, meas. from 6 to 14 kOe 0-41375 K,Ru(CN)₆,3H-O. ferroelectric phase transition, water molecules dipole moments 0-54169 KSbF₆, ¹⁹F nuclear spin coupling constants, high speed rotation method

moments U=34109
KSbF₆, ¹PF nuclear spin coupling constants, high speed rotation intended 0-41377
K₁ZF₇, ¹PF spin lattice relaxation 0-48167
K₂ZF₇, ¹PF spin lattice relaxation 0-48167
K₂ZF₇, ¹Mn²⁺, ENDOR, unpaired spin density 0-45041
(La_{1-x}Ca_x)MnO₃, of ⁵³Mn, mag, and elec. props., comp. depend. 0-59307
LiAlSiO₃:Fe³⁺ ⁷Li spectra, e.s.r. of Fe₃⁺, cryst. struct. 0-45023
LiBD₄, nuclear spin-lattice relaxation times for deuterons, protons and ¹¹B nuclear spin-lattice relaxation times for deuterons, protons and ¹¹B

LiBH₄, nuclear spin-lattice relaxation times for deuterons, protons and ¹¹B nuclei 0–59471
LiBH₄ and LiBD₄, spin lattice relax., hindered rot, obs. 0–75975

LiBr, pure and doped, spin-lattice relax, rel. to diffusive motion 0-41073 Li-D₈O₁, deuteron n.m.r. spectra 0-66155 LiF, ¹⁹F and ⁷Li with single spin-spin reservoir 0-66154 LiF, (111) oriented defect, e.s.r. and ENDOR obs. 0-40125 LiF, ENDOR, F- centre hyperfine interactions, uniaxial stress effect 0-78566 LIF, END 0-78566

0-/8566
LiF, rotating-frame double reson, and cross-relax. 0-41391
LiH, irrad., H- gas bubbles obs. 0-58803
LiNbO₂-LiTaO₃ solid-solution system, of ⁹³Nb 0-72510
LiNbO₃, acoustic dipole and quadrupole saturation of ⁷Li signal, u.s. wave 0-76244

0–76244
LiNbO₃, single cryst., temp. depend. of ⁷Li spectrum, 24-680°C 0–76237
LiSb, quadrupole splitting of spectra of ⁷Li 0–48164
Mg, hyperfine props., rel. to electronic structure and Knight shift 0–44733
Mg, Knight shift, electric quadrupole coupling, 77-503 K 0–51409
Mg, Knight shift 0–62774
Mg, Knight shift and relax, time, pseudopot, calc., 0–79416
MgAl₃, Mn,O₄, polycryst., of ²⁷Al 0–41364
MnBi, of ³⁵Mn, magnetiz, easy axis obs. 0–62775
MnCl₃,2H₂O, CSMnCl₃,2H₂O, KMnCl₃,2H₃O, mag. space groups determ. 0–65966
MnCl₃,2H₂O, proton spin-lattice relax. 0–79213
MnCl₃,4D₂O, d.m.r. spectra and coupling consts., obs. 0–41379
MnF₂, xX, X=V, Fe, Co, Ni, Zn. rel. to impurity effects 0–51239
MnF₃, antiferromag., freq. shift near Neel temp., hyperfine coupling 0–51411
MnF₃, antiferromag., frequency shift above Neel temp., hyperfine coupling

MnFs, antiferromag,, frequency shift above Neel temp., hyperfine coupling 0-51410 MnFs, paramagnetic, line shape and spin correlation, exchange narrowing 0-41332

MoF., paramagnetic, line shape and spin correlation, exchange narrowing 0-41332

MnO, 4.2 K, ⁵⁵Mn, antiferromag, domain struct. 0-45024

MnP, ferromag, and antiferromag., of ⁵⁵Mn and ⁵¹M p 0-72511

MnTe, nucl. acoustic reson. of ⁵⁵Mn 0-59467

⁵⁵Mn Knight shifts, reference epds. 0-45025

N-, compressed liquid, relaxation 0-78308

(NH₄)-Ce(NO₃)s, spin isomerism of ammonium group protons 0-69197

NH₄Cl. solid, spin-rotational relax. 0-72290

(NH₄)-IrCls, antiferromagnetic, Mossbauer and ENDOR spectra compared 0-75962

NO radicals in liquid phase, ENDOR obs. 0-70919

N₃SO₃F₃ isomeric derivatives. ¹⁹F spectra 0-46509

¹⁵N chem. shifts, effect of solvent interactions and H bonding 0-78313

¹⁵NH₃, liquid solvent mixtures, study of ¹⁵N n.m.r. shifts rel. to H bonding influence 0-67747

Na₃As (Sb), quadrupole splitting of spectra of ⁷³Na 0-48164

NaBr.2H-O, polycrystalline, p.m.r. 0-69198

NaCl. Agf, double, sensitivity. Ag conc. depend. 0-48172

NaCl. Fecentres, ENDOR, magnetic hyperfine and quadrupole interactions 0-45042

NaCl. Fecentres. ENDOR, magnetic hyperfine and quadrupole interactions 0-45042

NaCl. Fecentres. ENDOR, representational mobility of NH₄ groups 0-53941

NaNO:²³Na quadrupole spin-lattice relaxation meas, reanalyzed

0-53941 NaNO₁:²³Na quadrupole spin-lattice relaxation meas. reanalyzed

0—79417 NaNbO₃, powder, n.m.r. of ²³Na and ⁹³Nb 0—79417 NaPf₈, ¹⁹F nuclear spin coupling constants, high speed rotation method 0—41377

NaReO₄, aqueous solutions 0-68155

Nb_xMo_{1-x} 0-45028 9Co, dilute alloy, where 0≤x≤0.4, local moment formation

Nb₃Os(Ir.Pt,Au) alloys, mag. props. and electronic struct. 0-51011

Nuclear magnetic resonance and relavation continued

No complet 13 by means of 1H-13C heteronuclear resonance 0-58190 Ni-Rh alloy, Knight shift, line width, spin lattice relaxation, 1-4 K

0-45007 Ni, of ⁶¹Ni, in bulk metal 0-72512

Ni. of °Ni, in bulk metal 0–72512 Ni complex, ethylenediaminetetraacetate Ni(II), struct. in aq. soln. from ¹³C and ¹⁷O n.m.r. 0–78309 Ni complex, n-alkyl Ni(II) aminotroponiminates, ¹³C n.m.r. 0–77820 Ni complex, N,N-di(p-tolyl)aminotroponiminate Ni(II), ¹³C n.m.r. 0–77819 Ni complex, Ni[P(OR)_{3-x} F_x]₄, of ³¹P and ¹⁹F, influence of substitution 0-46500

0-46500
Ni phosphate p.m.r. data 0-62778
NiAl-O₄, polycryst., of Al 0-41364
Ni₂Co₄, ferromag, crystallographic ordering 0-41380
OCS, spin-rot. const. and mag, shielding anisotropy of ¹³C 0-77822
PH₃ in nematic solvent, struct. from p reson, spectrum 0-64445
Pb, Knight shift and relax, time, theory 0-45026
PbS(Se, Te), Knight shifts and balld struct. 0-56683
Pd-Fe, ferromagnetic alloy, spin-lattice relaxation rate, local effects 0-45036

0-45036
Pd-Rh alloy, Knight shift, line width, spin lattice relaxation, 1.4 K 0-45007
Pd-(2 wt.%)Rh alloys, Knight shifts of ¹⁰⁰Rh 0-41382
β-PdH, metallic system, proton relaxation 0-69200
Rb, Knight shift and spin-lattice relax, rate, low temp, pressure depend, 0-41367

(0-41367 Rb-CuCli,2H-O, of ⁸⁵Rb and ⁸⁷Rb, quadrupole interactions 0-41384 RbH,PO₄, ⁸⁷Rb quadrupolar coupling, rel. to Curie pt. 0-44366 RbMnF₃, antiferromagnet, acoustic. ⁵⁵Mn nuclei, 4.2°K 0-45027 RbMnF₃, paramagnetic, line shape and spin correlation, exchange narrowing 0-41332

nig 0-41332 rb. SO₄, p.m.r. rel. to ferroelectricity, 196 to 23°C 0-41383 Rb. SO₄, p.m.r. rel. to ferroelectricity, 196 to 23°C 0-41383 Re nuclear acoustic resonance obs.. Knight shift and zero-field splitting determ. at 4.2K 0-48165 Rh, Knight shift, strain induced 0-59468 Rh, Knight shift, strain induced 0-59468

Rh. Knight shift, strain induced 0–59468 Rh(I) complex with triphenylphosphine, n.m.r. spectra of ³¹P and ¹⁰³Rh, chemical shifts and coupling constants 0–58196 Rh(III) complex with triphenylphosphine, n.m.r. spectra of ³¹P and ¹⁰³Rh, chemical shifts and coupling constants 0–58196 ¹⁰⁰Rh in Ni, hyperfine field system studied by NMR/PAC and TDPAC 0-66156

0-66156

¹⁰Rh Knight shifts, reference cpds. 0-45025

Ru allyl complexes, spectra rel. to structure 0-67760

\$F_6, gaseous, F relaxation 0-58198

\$F_4.ASF_5 solid addition compound, fluorine magnetic resonance study 0-56684 ScB₂, meas. of ⁴⁵Sc 0-79418 ScF₆³⁻ anion in squeeus sola

ScB₃, meas. of ⁴⁵Sc 0—79418
ScF₄³⁻¹ anion in squeous soln. 0—78310
Si-Li, ENDOR, e.s.r. orbital degeneracy 0—56672
Si, uniaxially stressed. ENDOR, piezo-h.f.s., donor ground-state wave function 0—51415
SiF₄, ¹⁹F spin-rotation const. 0—77841
SiF₄, ¹⁹F spin-rotation const. 0—77841
SiF₄, gaseous, F relaxation 0—58198
Sn (II) complex, dicyclopentadienyltin(II), of ^{119m}Sn, stereochem. obs. 0—39401
SnCl₂,2H-O, phase transition obs. 0—62446
¹¹⁹Sn, white, pseudodipolar interaction radial depend. 0—41386
SFF, line shape meas. 0—72504
ThC—H₂, struct., X-ray exam., p.m.r. 0—68317
ThO₂, electron and hole traps rel. to thermoluminesc., e.s.r. and n.m.r. study 0—56650
ThO_{2-x}(OH)_{2x}yH₂O amorphous precip., p.m.r. rel. to comp., obs. 0—51412
Ti-V-C alloy, f.c.c., rel. to electronic structure. 0—40667

0-51412
Ti-V-C alloy, f.c.c., rel. to electronic structure 0-40667
TiFe_{1-x}Co_x alloys, of ⁵⁷Fe, Knight shift, h.f.s. 0-45029
Ti_xMo_{1-x}; ⁵⁹Co, dilute alloy, where 0≤x≤0.4, local moment formation 0-45028

0–45028 TiO_{3-x}(OH_{3x-y}H₂O amorphous precip., p.m.r. rel. to comp., obs. 0–5141; TiII, α - and β -phase, indirect interaction between nuclei and chem. shift 0–54170 TiII, of ²⁰³TI and ²⁰⁵TI, spin exchange interactions and chemical shifts 0–48166

0—48166
TmAl garnet, of ¹⁶⁹Tm and ²⁷Al, paramag, props. 0—45022
TmAl₃, nucl. quadrupole coupling and cryst. field effects 0—76235
2,3,4-trichloronitrobenzene, homonuclear double reson., relax. mechanisms 0—41392

isms 0–41392

UO₂xH₂O₂proton spin-lattice relax. 0–54171

UO₂xH₂O₃proton spin-lattice relax. 0–54171

UP_{1-S}₃, solid solution. ³¹P, mag. ordering depend. 0–45033

V-Co, σ-phase alloy, 5-12 MHz 0–79420

V-B, of ³¹V, localized character of electronic struct. 0–72514

VBe₁₂, of ³¹V, rel. to elec. quadrupole moment determ. 0–46134

V_{1-X}C₁xH₂, of ³¹V, Knight shift and spin-lattice relax. 0–45034

V₂O₃:Cr(Al), metal-insulator transition 0–75570

V₃O₄:P₃O₄ semiconducting glass system, ³¹V n.m.r. of diamag. V³⁺ and paramag. V⁴⁺ ions 0–76239

V₂O₃, of ⁵¹V, 65 kbar. 4.2 K. antiferromag. state suppression 0–45031

Vo₈₈₆, VO_{1.03}, VO_{1.23}, of ⁵¹V, onset of magnetization 0–45032

Ke, self diffusion near critical point and on liq. branch of coexistence curve 0–64890

KeF₄, magnetic shielding of ¹⁹F 0–53052

curve 0-64890

XeF₄, magnetic shielding of ¹⁹F 0-53052

XeF₄ in IF₅, of ¹⁹F 0-74312

YB₂, meas. of ³⁹Y 0-79418

YFe, garnet: Yb. longitudinal relaxation of ⁵⁷Fe, 1.3-140 K 0-45037

YFe garnet: Yb. longitudinal relaxation of ⁵⁷Fe, 2-40 K 0-48170

YO₂, electron and hole traps rel. to thermoluminesc., e.s.r. and n.m.r. study 0-56650

YbAl₃, nucl. quadrupole coupling and cryst.-field effects 0-76235

Zn(NO₃): in anhydrous methanol association, solvation number of Zn 0-58490

U-36490 Zr-H, H diffusion obs., vacancy mechanism 0-47299 ZrO_{2-x}(OH)_{2x-y}H₂O amorphous precip., p.m.r. rel. to comp., obs. 0-51412

bulk susceptibility corrections in expts. using superconducting solenoids 0-69809

decomposition factor, using ENDOR 0-60122 developments rel. to Varian A-60 spectrometer double reson. apparatus 0-48937

Nuclear magnetic resonance and relaxation continued measurement continued

neasurement continued ENDOR, review 0-60120 ENDOR review 0-60120 ENDOR meas, of spectroscopic decomp, factor 0-60122 Fourier transform spectroscopy of slowly relaxing systems, sensitivity 0-73116

Fourier transform technique for double resonance 0-

Fourier transform technique for double resonance 0-60124 line narrowing of p.m.r. by magic angle rotation 0-69811 liquid, spin-lattice relax. times of chemically-shifted protons 0-71386 liquids, high press, sample cell for relax. time meas. 0-78306 magnetometers with dynamic polarization by electronic pumping, perfor mance 0-52224 nutation angle var. suppression in pulsed n.m.r. 0-73118 preforming adiabatic demagnetization in rotating reference frame, frequency modulation method 0-48944 radical ions in soln., resolution enhancement by deuterium n.m.r. 0-58499 space group symmetry determ. 0-65188 spectrometer, broad band, for dynamic proton polarization meas. 0-6981, broad band, for dynamic proton polarization meas.

0-69812 spectrometer, design and accessories 0-66987 spectrometer, variable frequency, patent 0-48945 spectrometer for relaxation studies in solids 0-76969 spectrometer for short relax, time meas, in low fields with small samples 0-60127

0–60127 spin echo relax, times in weak fields 0–38444 spin tickling technique, appl. to liquid-cryst, soln. 0–61557 spin-lattice relax, times of chemically shifted protons 0–71386 spin lattice relax, time determ, elimination of H₁ inhomogeneity and spin spin relax. 0–76970 superconductivity applic. 0–44151 ¹³C Fourier-transform n.m.r., compared with spin echo methods 0–73115 Co nucleus in GdCO₃, Gd₁, xY₂Co₃, Gd₁, xDy₂Co₃ and Gd(Co_{1-x}Ni_x)₃, hyperfine field obs., spin-echo technique 0–51407

Nuclear matter see Nucleus/theory

Nuclear orientation see Nuclear polarization
Nuclear photoeffect see Gamma-rays/effects; Nuclear reactions and scattering due to/ photons

Nuclear physics

AERE Harwell nuclear phys. div., progress report, May-Oct. 1968 0-52633

0–52633
angular correlation meas, with automatic controlling unit 0–60636
annual review, collection of articles 0–46093
computer code for calc. of absolute areas of overlapping peaks in energy
spectra 0–79804
computer-pulse height analyzer interfacing for digital core storage of
nuclear data 0–49329
conference, India, Dec. 1969 0–38788
data acquisition, modular general-purpose system 0–63862
data acquisition using IBM 7094 computer system 0–63860
data acquisition using IBM 7094 computer system 0–72854
data analysis by non-linear least squares procedure, error estimation
0–49328
data handling and analysis by computer 0–73670

0-49328 data handling and analysis by computer 0-73670 dictionary of nucleonics and electronics 0-42612 electronics, basic, book 0-42611 experiments in appl. phys. manual 0-41928 gamma energy standards, new, and computer anal, of nuclear spectra 0-38734 high-energy, exp., data acquisition problems 0-63864

high-energy, exp., data acquisition problems 0–63864 high-energy, modular digital data system, operating experience 0–63863 instrument module system description, from Japan Atomic Energy Research Institute 0–42610 irradiation facility in swimming pool reactor 0–46094 low-energy exp., data acquisition, modular digital interface system utilizing bus structure 0–63865 magnet, dipole, new configuration for use in high energy physics 0–42691 medical applications 0–69521 neutron stars, review 0–72724 parity and time-reversal invariance, review 0–49449 pulse-generators, uniform distributed, for nuclear laboratory 0–60706 pulse-height distributions, convolution analysis 0–38760 relativistic triangle diagram cross-sections 0–49185 review of predictions of stable isotopes 0–70335 review of search for element 114 0–73844 single channel analyzer, peak stabilised 0–49405 thermal neutron flux densities, intercomparison between national laborat ories 0–49326

ories 0-49326 three-body problem, non-local interactions 0-73421

three-body problems, conference, Birmingham (1969) 0–73420 time-to-amplitude converter, transistorized 0–41931 transuranium elements, super heavy, review 0–63942

Nuclear polarization

clear polarization in ENDOR, effect of relax, transitions 0–67413 adiabatic. Coulomb effects 0–38794 atomic levels, excited, orienting, optical pumping 0–46410 biological processes analogous to Overhauser effect 0–63197 charcoal, dynamic polarization and ENDOR obs. 0–41389 Coulomb stripping reactions and DWBA calculations 0–52798 dynamic, saturation of forbidden transitions 0–56477 dynamic, transitions 0–69063 dynamic polarization by solid effect 0–69064 free radicals, spin polarization of reaction product, free diffusion apart proposed 0–79442 glycerol/water mixtures, porphyrexide doped, proton relaxation times, < IK 0–62770 and muonic atoms, review 0–49820

and muonic atoms, review 0–49820 muonic atoms of deformed nuclei 0–49824 organic cryst., dynamic polarization of protons 0–69202 orientation, adiabatic nucl. magnetiz. obs. 0–59345 oriented nuclei intermediate state reorientation, nucl. recoil effect 0–41089

0-41089
paramagnetic cryst., Overhauser effect obs. 0-41388
Rochelle salt, n.m.r., orientations of proton pairs 0-66158
rotational nuclei linear polarization effect 0-63979
spin-lattice relax, in dynamic orientation of nuclei 0-65967
d elastic scatt., 12 MeV, ang. distribs. of vector polarization 0-49645
N emitted in electron interactions with nucleus polarization for study of exchange currents 0-38845
Au-Ce dil. alloys, 137mCe nucl. orientation 0-72298

Nuclear polarization continued

 $^{98}{\rm Au},$ nuclear orientation study of first forbidden β decays to $^{198}{\rm Hg}$ 0-70555

0-7030 (p.p'). effects of core polarization for negative parity transition 0-67529

0-67529
Br. atomic, of ^{79,81}Br 0-43013

¹⁴C and ¹⁴N Core polarization agreement between binding energy and ¹⁵cdeay 0-60754

¹⁶Ca, muonic atoms of spherical nuclei 0-43034

Cd nuclear orientation under vacuum conditions using circularly polarized 3261 A radiation 0-49772

19F orientation following 19F(1007), chemical conservation of alignment 0-39109

19Fe(p.y'), microscopic first-order core polarisation corrections to DWBA 0-42837

3 He exchange currents indicated by polarization of nucleons emitted in electron induced interactions 0–38845
3 H(d.n) He, 3.9 15 MeV, polarization transfer study 0–73987
3 He, 'D levels, orienting, optical pumping 0–46410
3 He exchange currents indicated by polarization of nucleons emitted in electron interactions 0–38845
4 He scattered elastically from He 0–42733
4 He(d, p) He, polarization and asymmetry 0–46241
5 K, by optical pumping, and β-decay asymmetry, obs. 0–52680
4 LiBr, molecular, of 7 sign 0–43013
4 Mn Ag alloys. Kondo effect and relaxation times, influence on nuclear orientation meas. 0–62580
4 N and Me core polarization agreement between binding energy and β-decay 0–60754
5 Na, by optical pumping, and β-decay asymmetry, obs. 0–52680
6 (p.p.) hicroscopic first-order core polarisation corrections to DWBA 0–42837
9 compounds, nuclear polarization in liquid solution containing perchlorot-

P compounds, nuclear polarization in liquid solution containing perchlorot-

P compounds, nuclear polarization in liquid solution containing perchlorotriphenylmethyl radical 0-46955
Pb energy correction for muonic spectra 0-70829

206 Pb(p,p'), microscopic first-order core polarisation corrections to DWBA 0-42837

207 Pb(p,p'), effects of core polarization for even parity transition 0-67529

208 Pb, muonic atoms of spherical nuclei 0-43034

210 Po core polarization in (hg/2) 8+ state 0-64073

139 Tb, dilution refrigeration, search for parity violation in p decay 0-77487

159 Tb, neutron-capture p-rays, ang. distrib. 0-73830

50 Ti(p,p'), effect of core polarization 0-70587

80 Y(p,p'), effect of core polarization 0-70587

90 Zr(p,p'), effect of core polarization 0-70587

90 Zr(p,p'), microscopic first-order core polarisation corrections to DWBA 0-42837

Nuclear power see Nuclear reactors, fission

Nuclear power see Nuclear reactors, fission

Nuclear quadrupole resonance
amines, cyclic, saturated, of "4N, from liq, N, temp. 0–46535
ammonium hydrogen chloracetate, n.q.r., phase transition obs. 0–62448
chalcogenides, of "5As 0–41405
chloranil, cryst., in low Zeeman field, obs. 0–41406
1-chloro-2.4 dinitrobenzene, temp. depend. of Cl pure quadrupole reson.
0–46597

4-chloro-3 methyl phenol, single cryst., Zeeman spectrum of ³⁵Cl 0-66159

cobalticinium salts, 59Co resonance, temp. depend.

1,2-dichloro-3-nitrobenzene, temp. depend. 0–41407
3.4-dichloroaniline, temp. dependence of ³⁵Cl resonance 0–74359
trans-dichlorobis(ethylenediamine)cobalt(III) salts, data interpretations 0–70896

0-7096
trans dichloroethylene, cryst., in low Zeeman field, obs. 0-41406
ethylenimine: \(^{14}\)N, 77°K \(0-66161 \)
ferroelectric, KIO₃ \(0-65813 \)
ferroelectric, SbS1 type \(0-66160 \)
ferroelectric, ammonium hydrogen Chloracetate, phase transition obs.

hexachlorostannate(IV) salts, crystal lattice effects in spectra 0–72518 hexahalometalates, pure n.q.r. 0–77764 line saturation, quantum-statistical theory 0–41395

inte saturation, quantum-statistical intery 0-44395 nitro pyridine, spectra coupling constants 0-55371 paramagnet, K. IrCl₈, spin-lattice relax. 0-56465 pyrimidine, coupling consts. 0-77949 relaxation, two-freq. control method 0-51417 solid, mathematical analysis 0-60119 spectrum for spin 7/2, eigenvalues and Zeeman splitting parameters 0-76245

spinecho, applied electric field effects 0-48173

Stark effect, in solids, investig. 0–51416 superconducting ¹⁹La, double h.e.p., and in normal state 0–41401 transition metal compounds, review 0–76246 1,3.5-trichlorobenzene, temp. depend. of Cl pure quadrupole reson.

1,3.5-trichlorobenzene, temp, depend, of Cl pure quadrupole reson. 0–46597
2,3.4-trichloronitrobenzene, ¹⁴N quadrupole relax. 0–41392 trimethylamine BCl₃ complex, temp, dependence of ³⁵Cl n.q.r. 0–67802 trimethylantimony halides, H-D isotope effects 0–62782 trimethylsilyl pyridine, spectra, coupling constants 0–55371 Zeeman modulator, power-line bidirectional, for n.q.r. spectroscopy 0–73119

2-centar information, power-line bildirectionar, 101 in.q.r. spectroscopy 0-73119 [CO(NH₂)Cl]²⁺, pure n.q.r. of ⁵⁹Co, ³⁵Cl and ³⁷Cl 0-41398 AlBr₃, of ⁵⁹Br, Zeeman effect rel. to bond nature and molecular structure 0-45043

Albris, of "9r, Zeeman effect fet. to both nature and molecular structure 0-45043
Al-SiO₃ (andalusite), ²⁷Al quadrupole coupling tensors 0-54172
As₂X₃ where X=S, Se or Te, of ⁷⁵As 0-41405
BCI₃ and amine and nitrile complexes ³⁵Cl spectra 0-61072
Ba(ClO₃), H₂O₄ Zeeman split n.q.r. spectra 0-41396
Bi₂S₃, of ²⁰⁹Bi 0-72516
Co complex dichlorobis (trimethylenediamine) chloride, hydrochloride dihydrate, ³⁹CO₄, ³³Cl₃ truly 0-79423
CsGeCl₃, ferroelec., calc. elec. field gradients 0-41399
α-Fe₂O₃, haematie, quadrupole moment of ³⁷Fe 0-41084
GaCl₃, ³³Cl₃, ³²Cl₃, ³²C

Nuclear quadrupole resonance continued

crear quadrupole resonance continued

HgX₂ dioxan 1:1 adduct, X=Cl, Br, I, spectra, comparison with pure
halides, Hg-O interaction 0-69201

KlO₁, fercolec, behaviour anomalies 0-65813

KlrCl₆, paramag, and antiferromag, of ³⁵Cl 0-72517

KlrCl₆, spin-lattice relax. 0-56465

KlrCl₆, temperature and pressure variation of the ³⁵Cl n.q.r. frequency
0-54173 35Cl meas., temp, and pressure dependence in high temp, phase

K₂OsCl₆, 3: 0-79424 K:PdCl6, electric field gradient at 35Cl sites, motional averaging by lattice

K.PdCl₆, electric field gradient at ³²Cl sites, motional averaging by lattice vibrations 0–51418
K.PtCl₆, electric field gradient at ³⁵Cl sites, motional averaging by lattice vibrations 0–51418
³⁹La, double h.c.p., superconducting and normal states 0–41401
LiClO₃, ³⁵Cl and ³⁷Cl 0–45044
LiNbO₃, ³³Nb n.q.r. 0–59474
MH₂ASO₄ where M=Li, Na, K, Rb, Cs, Ag, NH₄ and N(CH₃)₄, ferroelec., of ⁷⁵As 0–41400

(NH₄):H₃IO₆, antiferroelec.. by quadrupole interaction iodine-proton crossover-relax. 0-62781

N in 2-bromothiazole, quadrupole relax. 0-41393

¹⁴N in 2-bromothiazole, quadrupole relax. 0–41393
¹⁵N in mol. crysts., lineshapes and widths analysis, obs. 0–41402
RbBr, spin-lattice relax. 0–75978
RbBr spin-lattice relaxation times for ⁷⁹Br, ⁸¹Br, ⁸⁵Rb and ⁸⁷Rb nuclei, 20
K 300 K 0–54174
RbH-PO₃, paraelec., ⁸⁷Rb quadrupolar interaction, obs. 0–41403
³³S hyperfine structure for molecules containing nucleus 0–70866
Sb:S₃, ferroelec., of ¹²¹Sb and ¹²³Sb, coupling consts. eval. 0–41404
SbSBr, ferroelec., of ¹²¹Sb and ⁸¹Br, coupling const. eval. 0–41404
SbSI type ferroelectrics 0–66160
TlAsX; where X=S, Se or Te, of ⁷⁵As 0–41405

Nuclear radius see Nucleus/size

Nuclear radius see Nucleus/stze
Nuclear reactions and scattering
see also Chemical analysis/by nuclear reactions; Fallout; Nuclear
bombardment targets; Nuclear excitation; Nuclear fission; Nuclear fusion;
Nuclear spallation; Radioactivity; Thermonuclear reactions
21+1 rule and channel correlation, relation between 0-73887
R-matrix shell-model cales. of scatt, and reaction cross-sections 0-77529
AERE Harwell nuclear phys. div. progress report, May-Oct. 1968
0.5361

aftereffect in solid, Mossbauer effect study 0-54079 amplitude of nonrelativistic Feynman graph 0-46182 analogue resonances for understanding of excited states 0-67510

analogue resonances for understanding of excited states 0–07310 Breit-Wigner resonances, asymmetric, analysis by accurate graphical methods 0–70561 Brueckner reaction matrix and separable potentials 0–70389 Brueckner reaction-matrix ladders, overcounting problem 0–49585 Brueckner-Hartree-Fock theory, renormalized, empirical validity 0–57939

0-3/939

chamber for energy and angular distrib. meas. 0-46006

charge exchange reactions in light nuclei 0-39003

composite particle reaction, generator co-ordinate treatment 0-39007

compound nuclear-reaction amplitude in soluble model, effect of direct reactions 0-39002

compound nucleus decay independ, of input channel spin, possible violation 0-46186

tion 0-46186 compound nucleus lifetime meas, using blocking effect 0-42725 conference, India, Dec. 1969 0-38788 correlation between group cross-sections to be adjusted by use of integral data 0-64103 coupled channel approach 0-39005 coupled-channel method, review 0-49582 DWBA analysis queried 0-73946 in detectors, stopping, reducing effect by spatial energy loss distribution comparison 0-49333 differential excitation curves from thick target neutron spectra 0-40616

comparison 0–49333 differential excitation curves from thick target neutron spectra 0–40616 diffraction scattering, accuracy of Inopin-Ericson theory 0–60798 diffractional scattering at high and low energies 0–52743 direct directions. time-reversal and reciprocity 0–46188 direct nuclear reactions leading to unbound residual nuclei 0–52745 direct processes, effective potentials in set of coupled eqns. 0–42805 direct reactions, effect on compound nuclear-reaction amplitude in soluble model 0–39002 direct reactions, peripheral model, comparison with expt. data and theories 0–70565 effective interactions, review 0–73890 eigenchannel theory. 0–64102

effective interactions, review 0–73890 eigenchannel theory 0–64102 elastic and inelastic scatt. in A=23·35 region, diff. and integral cross sections, quantum characts. 0–70564 elastic scattering, obs. of nonlocal effects 0–49588 elastic scattering theory, nonrelativistic, time-dependent for Gamow's theory of decay 0–52712 Faddeev equations, extension to complex angular momentum 0–39000 four body theory exact. 2 particle transfer mechanism 0–77525 Friedmann, universe, cold, effects of nuclear reactions 0–41575 generalized Hartree Fock approximation for scattering problem 0–70562 hadron-nucleus and hadron- hadron scatt., high energy, unified model 0–46246

hadron-nucleus forward dispersion relations 0–49603 hadron-nucleus total cross sections 0–52740 hadrons, role of Coulomb interaction for elastic and inelastic scattering 0–49587

Hamiltonian, generalized, and reson. struct. function 0-39006

Hamiltonian, generalized, and reson, struct, function 0–39006 identification of charged particles from nuclear reacts, using magnetic anal, with 4E, E method 0–52742 for impurities meas, in semiconductors 0–78971 inelastic scattlering with photon emission, violation of P-parity 0–77533 ions, heavy, Coulomb distortion for spherical nuclei 0–49671 isobaric analog resonances microscopic theories 0–57891 isobaric multiplet mass equations 0–67512 isospin conservation during direct and transfer reactions 0–38794 K-matrix expansions for elastic scattering by potential of finite range 0–64100 (Sohr's variational, principle to the multi-change reaction, problem

Kohn's variational principle to the multi-channel reaction problem 0-49590

light nuclei, charge exchange reactions 0-39003 many-body aspects shell and optical models, doorway and hallway state 0-60797

mass separation for nuclear reactions, review 0-46183

Mittag-Leffler expansion of S matrix integral representation 0-73886

multiparticle collisions at high energies 0-42809

neutron time-of flight, six-foot long detector 0-46024

neutron time-of flight, six-foot long detector 0–46024 nuclear structure effects described 0–64101 ORNL reactors, irradiation experiments 0–60796 one-particle transfer reactions to highly excited states 0–49583 optical model code for elastic differential cross-section clac., computer program 0–55148 optical potential, generalized 0–77468 optical potential, generalized 0–77468 optical-model potential, surface peaking in the calculated imaginary part 0–38810

0–38810
particle distribution, biased routing system 0–52603
particle identification using on-line PDP-7 computer 0–46013
peripheral model for direct reactions, comparison with expt. data and theories 0–70565
phase shifts for scattering by short-range potentials, upper and lower bounds 0–77527
pick up reactions, diagram approach to polarization effects 0–77534
pickup reactions, spectroscopic factors 0–38999
circular polarization of y-rays from nuclear reactions and form factors 0–70560

position sensitive detector, ratio circuit 0-55092 precompound and compound emission probabilities, quantitative estimate 0-39004

0-39004
RPA theory, partial widths and transition rates 0-64099
R matrix, variation 0-77530
R-matrix and scattering resonances in single channel potential scatt.
0-77528

0-77528

R-matrix expansion, wave-functions near resonance 0-42808
reaction, heavy ion type, distortion of nuclei 0-73727
reaction producing <2 particles, resonance narrowing in two particle interact. 0-73891
reactions, extension of shell model with configuration interactions 0-49591

reactions involving excitation of isobaric analogue state, three-body model 0-73893

0—73893
rearrangement collisions, Kohns variational principle 0—60795
recoil spectrometry obs. 0—38741
Reggeon diagram technique, for asymptotic theory of interactions between hadrons and atomic nuclei 0—52458
resonances, threshold, by R-matrix and S-matrix theories 0—57967
rotational nuclei, scatt. of spin 0 or ½ particles, adiabatic couple-channel calc. 0—52744
SUPERTOG, a program to generate fine-group constants and Pn scattering matrices from nuclear data 0—55149
scattering, energy spread of Gaussian distributed beam 0—77532
scattering, forward amplitude with nuclear correlations and overlapping potentials 0—49589
scattering, new methods and problems in atom, nucleus and particle physics, book 0—54585
Schiffer procedure modified for spectroscopic factors from analogue resonances 0—67511
single particle strength in the continuum and coupling to inelastic channels 0—57964
spectra and energy dependences measurement 0—46009

spectra and energy dependences measurement 0-46009

spectroscopic factors from analogue resonances, modified Schiffer procedure 0–67511 stars, nucleosynthesis 0–48424

stats, nucleosynthesis 0-48424 statistical level density parameter calcs, from renormalized Fermi gas model 0-42807 statistical model including angular momentum and parity conservation 0-67509

0–67509 statistical theory, anal. of $^{32}\mathrm{S}(\mathrm{d},\alpha)$ and $^{40}\mathrm{Ca}(\mathrm{d},\alpha)$ at 7.0 MeV 0–39117 stellar reaction rates, nuclear partition functions calc. 0–52741 stripping and pick up, for excitation of analogue states 0–67394 stripping reaction, to bound and unbound states, unified descrip. 0–70566 stripping reaction theory, Born approx. 0–57966 stripping reactions, diagram approach to polarization effects 0–77534 three body reactions study using 4π -precision vacuum scattering chamber 0–46045

three-body reactions, nucleon-nucleon final state interactions, theoretical study 0–73620 transfer processes, diffraction model formalism 0–49584

transfer reaction spectroscopy, discussion, suggestions 0–42806 transfer reactions involving heavy ion, geometrical polarization effects 0–70559

transmission coeff. related to ratio of average width to average spacing 0-73888

two nucleon transfer in the 1p shell 0-42804

two nucleon transfer in the 1p shell 0-42804 two-nucleon-transfer reactions, theory 0-46189 two-particle random phase approximation for configurations with one particle in the continuum 0-42810 unified reaction formulation, by Fadeev-like method 0-49586 unified reaction theory, examples 0-73892 (p,α) on nuclei from ⁹³Nb to ¹⁰⁹Bi, evidence for α -clustering 0-70610 (p.t) and (p.³He) and nuclear parentage 0-70593 α -particle ang, distrib. meas: using solid track detectors 0-77433 2N transfer reactions, effect on excitation spectrum of final nucleus 0-46185

0 - 46185

0—46.185
n tunneling, use of Hulthen wavefunctions to obtain accurate expression for matrix element 0–77526
A(a,b)B(y)C reaction sequence, particle-gamma correlations, phase conventions 0–46.187
27A(d,a)25Mg, cross-section dependence on collective states of residual nucleus 0–704.29
27A(p,a)24Mg resonance strengths, 1550 to 2650 keV 0–70601
40Ax scattering isobaric analogue resonances fine structure analysis

⁴⁰Ar scattering isobaric analogue resonances, fine structure analysis 0-70368

0-70368

*Be scattering, I-spin analogue states 0-70394
Bi analogue resonant states in deuteron stripping 0-70668

*Bi elastic scattering and isobaric analogue resonances 0-70519

*Bi elastic scattering partial widths of isobaric analogue resonances. microscopic calc. 0-70529

*Bi scattering, and isobaric analogue states in *10*Po 0-70531

*Ca (12°C, 3n)*9*Fe, new delayed proton emitter 0-42752

Ca (d.x)*0*K analogue states in *0+0252

Ca (d.x)*0*K analogue states in *0+0252

Ca (d.x)*0*K analogue states from isobaric analogue states in *0+05c

*Ca scattering, and *0*Ca states from isobaric analogue states in *0+05c

*O-70458

Nuclear reactions and scattering continued

the tractions and scattering continued ⁴⁸Ca(p.n) ⁴⁸Sc total cross-section and isobaric analogue resonance in ⁴⁹Sc 0–70605

48Ca(p,n) 48Sc total cross-section and isobaric analogue resonance in 78Sc 0-70605
37Cl (p,t)38Cl and levels in 35Cl 0-70602
39Co(p,α)39Fe angular distributions, experiment and theory 0-70607
43Ge(n,2)19Fe angular distributions, experiment and theory 0-70607
43Ge(n,2)10, E,=14.7+0.15 MeV, isomeric ratio determ. 0-73960
13H inelastic scattering, isobaric analogue resonances 0-70489
45Kr. core coupled resonances 0-70589
19La scattering and analogue states in 140La 0-70493
3Li, four channel calculation for the 3¹/₂, state 0-49590
4Li (p,34)4He angular distributions meas. and DWBA calc. 0-70595
3Li (p,pα)t at 58.1 MeV, quasi-free cluster knock-out 0-70596
3Li pair prod. in high energy interactions, Monte-Carlo calcs. 0-39001
32Mg(α,γ)37Na, cross-section dependence on collective states of residual nucleus 0-70429
32Mg(α,γ)37Ne, cross-section dependence on collective states of residual nucleus 0-70429
32Ng(α,γ)37Ne, cross-section dependence on collective states of residual nucleus 0-70429
37Ng(α,γ)37Ne, cross-section dependence on collective states of residual nucleus 0-70429
37Ng(α,γ)37Ne, excitation functions 0-67471
Nd(p,t), even isotopes, A=142 to 150, L=0 and 2 transitions 0-70496
30Ne(p,t) 18Ne and energy levels in 18Ne 0-70413
32Ne scattering isobaric analogue resonances, fine structure analysis 0-70368
30Ne(p,t) 18Ne and energy levels in 18Ne 0-70413
32Ne scattering isobaric analogue resonances, fine structure analysis 0-70368

²⁰Ne(p,t) ¹⁶Ne and energy ²¹Ne scattering isobaric analogue resonances, ²²Ne scattering isobaric analogue resonances, ²³Ni(p, α) ²⁵Co, angular distributions, experiment and theory 0–70607 Ni(p,t) and energy levels of even isotopes, comparison with DWBA 0–70472 and ¹⁶O(p, α) and T=³/₂ states in ¹⁷F 0–70420

Ni(p,t) and energy levels of even isotopes, comparison with DWBA 0-70472

16O(p,p) and 16O(p,ax) and T=3/2 states in 17F 0-70420

31P(d,ax)³⁹Si, cross-section dependence on collective states of residual nucleus 0-70429

204 Pb elastic scattering and isobaric analogue resonances 0-70519

206 Pb elastic scattering and isobaric analogue resonances 0-70519

207 Pb, inelastic scattering through ground state analogue, microscopic description 0-70523

208 Pb elastic scattering and isobaric analogue resonances 0-70519

208 Pb, inelastic scattering and isobaric analogue resonances 0-70519

208 Pb, elastic scattering and isobaric analogue resonances 0-70519

208 Pb, compound nucleus, decay, test of independence hypothesis 0-74002

21S elastic scattering, and 33 Cl analogue of 33 Ar ground state 0-70442

22S (i) 209 Pb, 21A, collective correlations model for struct. of giant dipole model 0-67433

29Si(d,ax)²³Al, cross section dependence on collective states of residual nucleus 0-70429

SnO, aftereffect, Mossbauer effect study 0-54079

27c(p,po) ⁹⁰Zr and ⁹¹Zr analogue of ground state 0-73817

Schemical effects

chemical effects

see also Chemical effects of radiations/ionizing radiations thermal neutron capture in solids, chemically significant details 0-79460

thermal neutron capture in solids, chemically significant details 0–79460 high energy >1 GeV electron-photon cascades, calc. of the energy deposited in thick targets at high energy (1 GeV) and comparison with experiment 0–55152 neutron total cross sections, calc. from 5-21 GeV/c 0–77555 recoil escape of nuclei in reactions with high energy particles 0–46184 ω meson photoproduction from complex nuclei at 6.8 GeV obs. 0–45950 π nucleus interactions at 50 GeV, cascade calculations 0–46229 W boson production in neutrino and muon interaction on nuclei 0–60591 Ag, 3 and 29 GeV proton bombardment, yields of stable and radioactive rare-gas isotopes 0–52769 Au, 3 and 29 GeV proton bombardment, yields of stable and radioactive rare-gas isotopes 0–52769 U, 3 and 29 GeV proton bombardment, yields of stable and radioactive rare-gas isotopes 0–52769 U, 3 and 29 GeV proton bombardment, yields of stable and radioactive rare-gas isotopes 0–52769 U, 3 and 29 GeV proton bombardment, yields of stable and radioactive rare-gas isotopes 0–52769 U, 3 and 29 GeV proton bombardment, yields of stable and radioactive rare-gas isotopes 0–52769 U, 3 and 29 GeV proton bombardment, yields of stable and radioactive rare-gas isotopes 0–52769 U, 3 and 29 GeV proton bombardment, yields of stable and radioactive rare-gas isotopes 0–52769 U, 3 and 29 GeV proton bombardment, yields of stable and radioactive rare-gas isotopes 0–52769 U, 3 and 29 GeV proton bombardment, yields of stable and radioactive rare-gas isotopes 0–52769 U, 3 and 29 GeV proton bombardment, yields of stable and radioactive rare-gas isotopes 0–52769 U, 3 and 29 GeV proton bombardment, yields of stable and radioactive rare-gas isotopes 0–52769 U, 3 and 29 GeV proton bombardment, yields of stable and radioactive rare-gas isotopes 0–52769 U, 3 and 29 GeV proton bombardment, yields of stable and radioactive rare-gas isotopes 0–52769 U, 3 and 29 GeV proton bombardment, yields of stable and radioactive rare-gas isotopes 0–52769 U, 3 and 29 GeV proton bombardment, yields of stable and

Nuclear reactions and scattering due to

uclear reactions and scattering due to alpha-particles
40 MeV scatt. on wide range of nuclei, matrix elements calc, and correlated to atomic weight 0-46233 (α .xn), populating rotational levels, spin distributions 0-70375 A=20-68 targets, elastic and inelastic scattering, 12-17 MeV 0-64131 compound nucleus cross-section calcs., parabolic approx. 0-60821 elastic and inelastic scattering, effective interaction and optical potential 0.70630

elastic and inelastic scattering, effective interaction and optical potential 0-70630 inelastic, 44 MeV by nuclei near closed shells with 28 neutrons, 20, 28, 50 and 82 protons 0-46234 isotopic dependence of strong absorption radii, microscopic predictions 0-57999

model interaction pot., energy depend. E<6 MeV 0-55164 neutron coincident detector distinguishing between (α,n) , (γ,n) and fission products 0-77424

neutron coincident detector distinguishing between (α, \mathbf{n}) , (p, \mathbf{n}) and fission products 0–77424 non-local separable potential for α - α interaction 0–42865 reaction, α decay theory 0–60776 scattering, optical-model phase shifts using eikonal approx. 0–77571 scattering by spinless nuclei, Regge pole calc. 0–39091 $(\alpha, 2\alpha)$, break up reaction, mechanism in three-body formulation 0–73982 $(\alpha, 2\alpha)$, break up reaction, mechanism in three-body formulation 0–73982 $(\alpha, 2\alpha)$, final state interaction contrib. 0–60811 $(\alpha, \alpha\alpha)$ reaction on light nuclei 0–58004 $(\alpha, 24e)$ on N=Z nuclei, $(\alpha, 1)$ comparison 0–39104 $(\alpha, 24e)$ on N=Z nuclei, $(\alpha, 1)$ comparison 0–39104 $(\alpha, 24e)$ on N=Z nuclei, $(\alpha, 1)$ comparison 0–39104 $(\alpha, 24e)$ on N=Z nuclei, $(\alpha, 1)$ coulomb excitation 0–64031 $(\alpha, 24e)$ on N=Z nuclei, $(\alpha, 1)$ coulomb excitation 0–64031 $(\alpha, 24e)$, E=10.0 and 10.7 MeV. Coulomb excitation 0–64031 Al. 27.2 MeV. cross-section meas. 0–52803 $(\alpha, 24e)$ on N=Z nuclei states. 5.434, 6.347, 7.28 and 7.50 MeV 0–77479 Al (α, α') , $(\alpha, 24e)$ and angular distributions meas. from 30 to 170° for 20.0 and 27.5 MeV 0–73978 $(\alpha, 24e)$ on N=Z nuclei scattering, effect of (α) particle correlations 0–70636 (α) and 27.5 MeV 0–73978 (α) and pair y assignments 0–38880 (α) relastic scattering, effect of (α) particle correlations 0–70636 (α) Ar elastic scattering, effect of (α) particle correlations 0–70636 (α) (α)

Nuclear reactions and scattering due to continued alpha particles continued

C nuclei of nuclear emulsion, 70 MeV interaction, cross sections for production of Li, Be, B isotopes 0–77572

TC_IN, IFF, emission from IAN irradiation relationship between isotope emission and energy of bombarding particles 0–74000

emission and energy of bombarding particles 0-74000 12 C, absolute differential cross sections, measurement using a photographic method, E_{α} –20-24 MeV 0–64130 12 C, elastic scatt., calc. from S-matrix poles in K-plane 0–39093 12 C, elastic scatt., Regge pole calc. 0–39091 12 C, elastic scattering, 20-24 MeV 0–42864 12 C, inclastic scatt., below 18.0 MeV 0–73979 12 C($(\alpha, 2\alpha)^3$) Be, E_{α} =100 MeV, excitation energy spectrum 0–49657 12 C($(\alpha, 2\alpha)^3$) deduced 6+ level in 16 O 0–52671 12 C($(\alpha, 2\alpha)^3$) deduced 6+ level in 16 O 0–52671 12 C($(\alpha, 2\alpha)^3$) Consistence of 16 C($(\alpha, 2\alpha)^3$) deduced levels and resonances of 18 C for E_{α} =3.5-16.5 MeV 0–57898 16 C($(\alpha, 2\alpha)^3$), deduced levels and resonances of 18 C for E_{α} =4.9-8.5 MeV

 $^{14}\text{C}(\alpha,n)$, deduced levels and resonances of ^{18}O for $\text{E}_{\alpha}{=}4.9{\cdot}8.5$ MeV 0.57898

0. 57898

4°Ca, elastic scatt... 23 MeV, 14-179° 0–52796

4°Ca, elastic scattering, effect of α-particle correlations 0–70636

4°Ca(α-α), angular distribution meas., anomalies in backward-angle 0–77578

4°Ca(α-α), deduced optical model and Regge pole model parameters, 23 MeV, differential cross section 0–39120

4°Ca(α-α)-4°T and 4°T in energy levels and mass 0–70454

4°Ca elastic scattering, effect of α-particle correlations 0–70636

4°Ca elastic scattering, effect of α-particle elastic scattering of α-particle ela

 6 5 Co(α,α) 5 Co optical potential real part calc. by double folding procedure 0 -67543

0 -67543

9°Co(α, p)⁶¹ study 0-58019

6°Cu(α, x) = 19.5 MeV elastic and inelastic (to first excited state scattering angular distributions analysed 0-49646

6°Cu(α, p)⁶²Cn study 0-58019

6°Cu(α, x) = 19.5 MeV elastic and inelastic (to first excited state) scattering angular distributions analysed 0-49646

6°Cu(α, p)⁶²Cn study 0-58019

Eu(α, α') (A=151, 153), energy level study 0-49536

9°F(α, α), differential cross sections, E=20-24 MeV 0_58005

19F(α, α') (MeV) = 10 MeV (MeV)

10 MeV (MeV) = 10 MeV (MeV)

10 MeV

0 39094 19 F(α ,n γ) 12 Na, spin, parity and multipole mixing ratio assignments of low levels in 12 Na 0-77488 4 Fe(α , p γ), 57 Co levels deduced γ -branching, E $_{\alpha}$ =10.71, 11.14 MeV 0-5791

0–57911

*Fe(α, p) 5'Ni lifetimes of low lying levels in Ni 0–64019

*Fe(α, p) 7) 7'S lifetimes of low lying levels 0–64022

*Fe(α, p) 8'Ni, evidence for precompound particles 0–60827

*Fe, optical model analysis for 64.3 MeV scattering 0–70634

"Ga(α,2n) 7'SAs and isomeric state in 7'SAs 0–73813

Ge(α,2n) 7'SE, population of levels in Se isotopes, γ radiation study 0–70476

Ge($\alpha.4\pi\nu$)Se, population of levels in Se isotopes, γ radiation study 0-70476

0-70476

'H(α.αρ)n, at about 160 MeV, theoretical study 0-73935

'H(α.αρ)n, coincidence studies, E=18.0-24.0 MeV 0-39100

('He,p), at low energy, polarization effects 0-73981

He, scattering, separable potential 0-73988

'He, elastic scatt., Regge pole cale. 0-39091

'19ma') H production from irradiated 176 Yb 0-57927

165 Ho(α.2np) (*Tm. γ radiation studied, energies, intensities, angular distributions and py coincidences measured 0-67486

165 Ho(α.2np) (*Tm. γ radiation studied, energies intensities, and collective states 0-64064

1911r, inelastic, and collective states 0-64064

1921r, inelastic, and collective states 0-64064

1931r, inelastic, and collective states 0-64064

1941r, 2π, inpulse distrib. 0-52771

Figure 20, impulse distrib. 0-52771 (Li($\alpha,2\alpha$), impulse distrib. 0-52771 (Li(α,α) (Li, α) (B. 7.01 MeV level width and reson, energy determ. 0-39102 (Li(α,α) (Li, absolute cross section 3.5 5.0 MeV and 4.25 MeV reson, analysis 0-39092

sis 0–39092
6Li($\alpha,\alpha\alpha$)²H, 42.8MeV, mechanism studied, validity of impulse approximation 0–73894
7Li($\alpha,\alpha\alpha$)²H, 42.8MeV, mechanism studied, validity of impulse approximation 0–7384
7Li($\alpha,\alpha\alpha$)²H, ΔT =0 selection rule test 0–67554
7Mg(α,α)²⁸Al, ΔT =0 selection rule test 0–67554
7Mg(α,α)²⁸Mg, excitation of 3+, * 1 levels 0–64132
7Mg(α,β)²⁷Mal and spins of levels in ²⁷Al 0–67432
N nuclei of nuclear emulsion, 70 MeV interaction, cross sections for production of Li, Be, B isotopes 0–77572
7M(α,α) *Modificential cross section meas, for isospin impurities of ¹⁸F states 0–67428
7M(α,α) *Modificential cross section for proton prod. 0–42870
7M(α,α) differential cross-sections and angular distributions for E=20-24
7MeV 0–60824
7MeV 0–60824

MeV 0-60824 "N((κ, α) , differential cross-sections and angular distributions for E=20-24 MeV 0-60824 "N((κ, α)), differential cross-sections and angular distributions for E=20-24 MeV 0-60824 "N((κ, γ))*9F, 13 new resonances in region E=600-3150 keV 0-52801 "N((κ, γ))*9F, 13 new resonances in region E=600-3150 keV 0-52801 "N((κ, γ))*9F, 13 new resonances in region E=600-3150 keV 0-52801 "N((κ, κ))*9Ne obs. Blair Drozdov model 0-77570 "N((κ, κ))*9Ne obs. Blair Drozdov model 0-77570 Ni, 27.2 MeV, cross-section meas. 0-52803 "Ni, optical model analysis for 64.3 and 50.2 MeV scattering 0-70634 69Ni((α))*4Zn compound nucleus formation, neutron emission study 0-77517

Nuclear reactions and scattering due to continued alpha-particles continued

alpha-particles continued
alpha-particles continued
alpha-particles continued
alpha-particles continued
alpha-particles continued
alpha-particles continued
alpha-particles continued
alpha-particles continued
alpha-particles continued
angular distributions analysed 0–49646

64 Ni(p, αγ)⁶¹Co, investigation of low-lying levels 0–64022

16 Q(α, n)⁶⁰Q_π, for spin and parity assignments of ¹⁷O 0–49506

16 Q, absolute differential cross-sections, measurement using a photographic method. E_α=20-24 MeV 0–64130

16 Q, elastic scatt. Regge pole calc. 0–39091

16 Q, elastic scatt. Regge pole calc. 0–39091

16 Q, elastic scattering, 20-24 MeV 0–42864

16 Q(α, α), elastic, 25.4-32.2 MeV, Regge pole analysis 0–46235

17 P, elastic and inelastic scattering, angular distributions 0–70633

17 P(α, pp)³⁴S deduced levels of first two excited states of ³⁴S 0–46131

17 P(α, pp)³⁴S, mean lifetimes of ³⁴S levels, below 5.0 MeV 0–49513

17 P(α, pp)³deduced levels, lifetimes and decay modes of ³⁴S for E_α=6-9MeV, measured Doppler shift attenuation 0–57905

17 P(α, pp) deduced spin of levels in ³⁴S at 4.07 MeV and 4.89 MeV 0–42743

18 Pb, ²⁶Pb, ²⁶Pb, ²⁶Pb, elastic scatt., 14-23 MeV, determ. of surface nuclear potential 0–67544

18 Pb, cross sections for inelastic scattering of 45 MeV α particles 0–52797

28 Pb(α, n)²¹¹Po cross-section below Coulomb barrier 0–70666

Pd(α, xnp) and cd energy levels 0–64032

242 Pu(α, t), deduced levels of ²⁴³Am for E=30 MeV 0–58023

242 Pu(α, t), deduced levels of ²⁴³Am for E=30 MeV 0–58023

243 Pu(α, t), deduced levels of ²⁴³Am for E=30 MeV 0–58023

244 Pu(α, t), and levels in ²⁴³Am 0–70667

17 S, elastic and inelastic scattering, angular distributions 0–70633

29 Si(α, pp)³⁵Cl proton-gamma coincidences measured, energy level structure 0–42746

18 Sis, elastic and inelastic scattering, angular distributions 0–70633

29 Si(α, pp)³⁶Cl proton-gamma coincidences measured, energy level structure 0–42746

18 Sis (elastic and inelastic scattering, angular distributions

0-77576

0-77576

0-77576

0-30Si(απ)³3S investigation of electromagnetic transition rates of ³3S excited states 0-46130

144Sm(α.2π)¹⁴⁶Gd and energy levels of ¹⁴⁶Gd 0-70498

*30Sm(α.2π)¹³²Gd i³2*Gd low-lying states obs. 0-70501

134Sm(α.3π), deduced levels of ¹³⁵Gd for E_α=34 MeV 0-57924

134Sm(α.2π), Te deduced levels 0-38912

134Sn(α.2π), Te deduced levels 0-38912

134Sn(α.2π), Te deduced levels 0-38912

135Sn(α.2π), Te deduced levels 0-38912

232Th(α.1) and levels in ²³³Pa 0-70667

46Ti(α.py)⁴⁹V p branching ratios deduced for levels in ⁴⁹V up to 2.409 MeV, J² assignments 0-49520

48Ti(α.p), ³¹V levels ≤ 6.17 MeV 0ff-3885

48Ti(α.p), ³¹V levels ≤ 6.17 MeV 0-38885

48Ti(α.p), ³¹V levels ≤ 6.17 MeV 0-38885

48Ti(α.p), ³¹V levels ≤ 6.17 MeV 0-38885

48Ti(α.p), ³¹V levels ≤ 6.17 MeV 0-3885

48Ti(α.p), ³¹V levels ≤ 6.17 MeV 0-3885

48Ti(α.p), ³¹V land levels in ³¹Np 0-70667

205Tl(α.t) ³⁰⁰Pb(g.s.) normalization determination, comparison with theoretical 0-70662

195Tu(α.x) ³¹¹Lu, prep. of thin source, for β-ray spectroscopy 0-64078

236U(α.t) and levels in ³²Np 0-70667

238U(α.x) 31 MeV obs. ang. distrib., spin, parity assignments 0-73980

0-13980 MeV obs. ang. distrib., spin, parity assignments 0-73980 66°Zn($\alpha\alpha'$)66°Zn(α) E=19.5 MeV elastic and inelastic (to first excited state) scattering distributions analysed 0-49646

cosmic rays
see also Cosmic rays/effects and interactions
radionuclide production rates in argon in stratosphere 0-60633

deuterons

 4 He(d_{po1},d), tensor polarization $\langle T_{21} \rangle$ and $\langle T_{22} \rangle$ in elastic scattering 0–58003

(d, p), Kohns variational principle for rearrangement collisions 0–60795 (d, pn) DWBA approx. when n is not obs. 0–73985 Coulomb stripping reactions and DWBA calculations 0–52798 differential cross section for radiative capture by protons 0–42866 disintegration, energy distributions of nucleons, energy of incident deuteron 0–46237

dissociation and stripping, high-energy, Glauber-model approach 0-67545

0–67545 elastic scatt. by light nuclei, E_d=13.6 MeV 0–77569 elastic scatt. by light nuclei, spin-orbital coupling influence 0–67541 elastic scatt. of 12 MeV deuterons, ang. distribs. of vector polarization β, meas. and optical model anal. 0–49645 elastic scattering of neutrons, exchange collision 0–42848 elastic scattering of 71.5 Be, ¹¹Bi ¹²B and ¹⁶O, at 28 MeV, optical model analysis 0–52.794

analysis 0–52794
gamma-ray production cross-sections for fast-neutron inelastic scattering, E_n=4.00 to 7.67 MeV for 10 elements 0–64122
reactions, low energy, three-particle model 0–39097
scattering, elastic cross sections, d optical pot. calc. and obs. 0–38844
scattering, optical model potential 0–73984
spectra, meas. using Ge(Li) spectrometer 0–38867
stripping, isospin coupling in (d,p) and (d,n) 0–67547
stripping, multi-step, on deformed nuclei with non-rotational states involved 0–58021
stripping, validity of sudden approximation 0–46239
stripping and dissociation, high-energy, Glauber-model approach 0–67545
stripping below Coulomb harrier, 0–70639

stripping below Coulomb barrier 0-70639

stripping below Coulomb barrier 0-/0639 stripping reactions, spin orbit contributions in DWBA analysis of particle y ang. correlations 0-39095 stripping reactions, theory and expt. 0-57966 three-body model cales. 0-73983 (d, p), for level study in Dy odd-mass isotopes 0-64050 (d, p), S-matrix description of threshold effects 0-49648

Nuclear reactions and scattering due to continued deuterons continued

(d, p) inelastic decay of isobaric analogue resonances, and unmixed states in ²⁰⁸Pb, comparison 0–70526

(d, p) isobaric analogue resonances rel. to proton peak in spectra 0-67548 (d, p) on Ba isotopes, spectroscopic factors comparison with (p, p₀) 0–67543

(d, t) for level study in Dy odd-mass isotopes 0–64050 (d, He) reactions on 13 nuclei from ¹²C to ³²S, and 1-p proton hole states 0–70399

(d,p), by coupled channel theory, props. of interac. kernel, method of numerical soln. 0–49652 (d,p), DWBA, coupled channels, PWBA with Coulomb distortion

nun. (d,p), Dw -70638 (d,p), shipping cross section meas. in nuclear emulsion, at 2.45 GeV/c 0.49647

0-49647

(d.p.) reactions, anomalous behaviour of hole levels 0-46238

(d.p.) reactions in WBP model, effects of D-state of deuteron 0-49650

(d.p.) stripping reactions, Coulomb, polarisation effects 0-52798

p, radiative capture and 20 to 30 MeV 0-42866

Sr(d., opARb study of excited levels of **Rb 0-60762

***belastic scattering, analysis by optical potential 0-67542

**Ag elastic scattering, analysis by optical potential 0-67542

**In 13.6 MeV 0-64011

Al(d., op)Sis, decay of bound isobaric analogue states, ny coincidence recording for E_d=4.0 MeV 0-64011

Al(d., op)Na, excitation function, 0 to 10 MeV 0-39112

**Are leastic and incleastic scattering, suggesting spherical equilibrium

"Al(d,xp)" Na, excitation function, 0 to 10 MeV 0-3112 "Ar elastic and inelastic scattering, suggesting spherical equilibrium 0-70655

²⁷Al(d,αp)²⁴Na, excitation function, 0 to 10 MeV 0-39112
³⁶Ar elastic and inelastic scattering, suggesting spherical equilibrium 0-70655
³⁶Ar(d,t), deduced levels of ³⁵Ar at E_σ=21.6 and 21.0 MeV 0-49661
⁴⁰Ar(d,tp)₄, Ar and energy levels in ⁴¹Ar 0-70452
¹⁹⁷Au(d, 3n)¹⁹⁶Hg, cross sections, 196Hg number obs. 0-39126
¹⁹⁸(d, 3α), 3α emission mechanism, 1 MeV 0-42835
¹⁹⁸(d,αα), angular distribution of the differential cross section from dispersion theory and dynamical cluster structure of ¹⁹⁸B 0-58006
¹⁹⁸(d,α), used to search for lowest T=2 state of ¹²C, no resonance observed 0-73783
¹⁹⁸(d,η)γ), used to search for lowest T=2 state of ¹²C, no resonance observed 0-73783
¹⁹⁸(d,η)γ). Used to search for lowest T=2 state of ¹²C, no resonance observed 0-73783
¹⁹⁸(d,η), stripping reactions of the 1p shell initiated by vector-polarised deuterons 0-55168
¹⁹⁸(d,p), used to search for lowest T=2 state of ¹²C, no resonance observed 0-73783
¹⁹⁸(d,p), ¹⁹⁸Bground state, 2.12, 4.44 and 5.02 MeV levels angular distribution 0-49644
¹⁹⁸(d,p)γ)¹⁹⁸B, 1.5≤E_σ≤3MeV, mechanism, optical model parametrization, DWBA calcs. 0-49655
¹⁹⁸(d,p)γ)¹⁹⁸B, τ stripping reactions of the 1p shell initiated by vector-polarised deuterons 0-55168
¹⁹⁸(d,p)γ)¹⁹⁸B, DWBA calculations of proton angular distribution 0-70637
¹⁹⁸(d,p)γ)(A=130, 132, 134, 136, 138), E_σ=12.0 MeV, proton spectra, ang. distribs. 0-49669
¹⁹⁸(d,e), stripping reactions of the 1p shell initiated by vector-polarised deuterons 0-55168

0-49644

"Be(d,p)"8be ground state and 3.37 MeV level, angular distribution 0-49644

0–49644
"Be(d,p)" Be, isobaric spin doublets at 16.6 and 16.9 MeV 0–57902
"Be(d, α)" Be, isobaric spin doublets at 16.6 and 16.9 MeV 0–57902
"Be(d, α)" Li, production cross section, from 0.67 to 3.0 MeV 0–49656
"Be(d,0)" Be, production cross section, from 2.3 to 12 MeV 0–49656
"Bi(d,3 He)" Be, proton particle-hole states at E_{ϕ} =50 MeV 0–52707
CD gas target, electron capture cross sections for E_{ϕ} =0.3 to 70 keV 0–49653

0=49053 target, electron capture cross sections for E_d=0.3 to 70 keV 0=49653

C₈F₁₆ gas target, electron capture cross sections for E_d=0.3 to 70 keV 0-49653 (CH₄ gas target, electron capture cross sections for E_d=0.3 to 70 keV 0-49653 (IC, ¹³N, ¹⁹F, emission from ¹⁴N irradiation relationship between isotope emission and energy of bombarding particles 0-74000 (¹²C(⁴C₁)¹⁹B(O⁺C, ac-luster pickup reaction E_d=52 MeV 0-58008 (¹²C(⁴d, a)¹⁹B(O⁺C, 1), isospin violating, energy dependence 0-67551 (¹²C(⁴d, a)¹⁹B(O⁺C, 1), isospin nonconserving, comments 0-58019 (¹²C(⁴d, a)¹⁹B(O⁺T=1), isospin nonconserving, comments 0-58011 (¹²C(⁴d, a)¹⁹B(O⁺T=1), isospin nonconserving, comments 0-58011 (¹²C(⁴d, a)¹⁹N, excoil angular distributions, 12, 15 and 17 MeV 0-49654 (¹²C(⁴d, a)¹⁹N, recoil angular distributions, 12, 15 and 17 MeV 0-49654 (¹²C(⁴d, a)¹⁹C, DWBA with spin orbit pot., and obs. 2.8-3.7 MeV 0-39106 (¹²C(⁴d, a)¹⁹C, polarization, ang. distribs., 1.40-2.40 MeV 0-52800 (¹²C(⁴d, a)¹⁹C, asymmetries deuterons, and comparison with DWBA 0-7064 (¹³C, a) (¹³C

"Ca(d,p)*Ca, caics, based on sudden approx, method of d stripping 0-77571 "OCa(d,p)*1Ca, single channel calc. of form factors 0-77531 "OCa(d,p)*1Ca and neutron hole impurities in *OCa 0-70450 "Ca(d,p)*6Ca, core excitation of *Ca, cross section calc. 0-49664 "SCa(d,p)*GCa 0-70657 "SCa(d,p)*GCa calcs, based on sudden approx, method of d stripping 0-77577

Cd (where A=110, 112, 114, 116), elastic and inelastic scatt., from vibr. states, diff. cross sections 0-42863

35Cl(d³He), 34S levels, obs. 0-39119

```
Nuclear reactions and scattering due to continued
```

uclear reactions and scattering documents of the second continued deuterons continued $^{37}\text{CI}(\text{d}.^3\text{He}).^{36}\text{S}$ levels, obs. 0-39119 $^{56}\text{Cr}(\text{d},\text{p})^{51}\text{Cr}, E_d=7.5$ and 8.0 MeV, j-dependence in l=1 transitions

⁵²Cr elastic scattering, analysis by optical potential 0-67542

For the problem of t

0-39121 **2Cr(d,pp)**3Cr and energy levels in **3Cr 0-70465 **2Cr(d,pp)**2Cr used to study levels of **3Cr 0-38886 **5Cr(d,p)**Mn and levels in **6Mn below 1 MeV 0-70467

Cr(d,p) (A=50,52), E=13.6MeV, diff, cross sections 0-73995

⁶³Cu spin dependence of inelastic scattering 0-70635

⁶³Cu spin dependence of inelastic scattering 0—70635

"Cu spin dependence of inelastic scattering 0—70635

(d,t)*Sr at 20.65 MeV, levels study 0—57916

(d,t)*Sr at 20.65 MeV, levels in 169Er studied using 12 MeV deuterons 0—70507

"Fe(d,α)*EFer, levels in 169Er studied using 12 MeV deuterons 0—70507

"F(d,α)*CFE, levels in 169Er studied using 12 MeV deuterons 0—70507

"F(d,α)*CFE, levels in 169Er studied using 12 MeV deuterons 0—70507

"F(d,α)*CFE, levels in 169Er studied using 12 MeV deuterons 0—6135

"F(d,α)*CFE, levels in 169Er studied using 12 MeV deuterons 0—6135

"F(d,α)*CFE, levels using 12 MeV deuterons 0—6135

"F(d,α)*CFE, levels using 12 MeV deuterons 0—6135

0-53171

"FG(d,p), deduced ²⁰F levels up to 6.043 MeV excitation 0-52678

"F(d,p)²⁰F, E_d=600keV, ang. distribs. of ten p groups, DWBA calcs.
0-49659 "P(d,p)"*P, E=000keV, ang. distribs. of ten p groups, DWBA calcs. 0-49659
"F(d,pp) 2°F, single p-ray spectra and pp coincidence spectra, meas, using Ge(Li) spectrometer 0-38867
"Fe elastic scattering, analysis by optical potential 0-67542
"Fe'fe elastic scattering, analysis by optical potential 0-67542
"Fe'fe(d,d') inelastic angular distributions at 11.5 and 11.8 MeV, comparison with DWBA calculations 0-462.36
"Fe(d,d') inelastic angular distributions at 11.5 and 11.8 MeV, comparison with DWBA calculations 0-462.36
"Ga(d,p)"*Ca, 7.1 MeV, study of "Ga levels 0-77499
"4"Gd(d,p)"*Gd, T.1 MeV, study of "Ga levels 0-77499
"4"Gd(d,p)"*Gd, multi-step stripping reaction, 0-58021
"5"Gd(d,p)"*Gd, E=12.1 MeV, ang. distribs. 0-42872
H₂, gas target, electron capture cross sections for E_d=0.3 to 70 keV 0-49653
H₂O gas target, electron capture cross sections for E_d=0.3 to 70 keV

 H_3O gas target, electron capture cross sections for $E_a\!\!=\!\!0.3$ to 70 keV $0\!-\!49653$

0.–49653
'H(d,1)ep, polarization transfer to 0° neutrons 0.–77573
'H(d,n)p); H, E_{ir} =60.505 keV, resonance 0. 42867
'H(d,p); H, E_{ir} =60.505 keV, total cross section, p ray ang. distrib. 0. 39099

O 30099

"H(d,n)He, polarization transfer to 0° neutrons 0-77573

"H(d,n)JHe, rel. to production of 28 MeV neutrons 0-55156

"H(d,n)pd, three-body final state, exp. study at 12.3MeV 0-73986

"H(d,He)2n, final state interaction spectra and \(^1S_0\) neutron-neutron scattering parameters 0-73976

"H(d,He)2n, neutron-neutron interactions in \(^1S_0\) wave 0-70640

³H(d,y)⁵He, cross- section and gamma-ray-neutron branching ratio

3H(d,)*He,2n, neutron-neutron interactions in \(^{1}S_{0}\) wave \(^{0}-70640\)
3H(d,)*He, cross- section and gamma-ray-neutron branching ratio \(^{0}S_{2799}\)
3H(d,n)*He, 3.9-15 MeV, polarization transfer study \(^{0}-73987\)
3H(d,n)*He polarization of neutrons at low deuteron energies \(^{0}-70641\)
3H(d,n)*He rel. to \(^{0}H\) distrib. in Ti determ. \(^{0}-62836\)
3He(d,n)*He rel. to \(^{0}H\) distrib. in Ti determ. \(^{0}-62836\)
3He(d,n)*He, polarization and asymmetry \(^{0}-46241\)
3He(d,1)*P, neutron-neutron interactions in \(^{1}S_{0}\) wave \(^{0}-70640\)
3He(d,1)*P, neutron-neutron interaction spectra and \(^{1}S_{0}\) neutron-neutron scattering parameters \(^{0}-7397\)
3He(d,1)*P, absolute coincidence cross sections and p-p and p-t final state interactions for \(^{0}E=20.7\) MeV \(^{0}-58001\)
4He(d,p)*D, absolute coincidence cross sections and p-p and p-t final state interactions for \(^{0}E=20.7\) MeV \(^{0}-58001\)
4He(d,p)*d, elastic scattering and tensor polarization \(^{1}S_{0}O=58002\)
1n elastic scattering, analysis by optical potential \(^{0}-67542\)
3P1(r, inelastic, and collective states \(^{0}-64064\)
3PK(d, n)*OCa \(^{3}Z_{0}-p^{3}Z\) analogue states \(^{0}-64064\)
3PK(d, n)*OCa \(^{3}Z_{0}-p^{3}Z\) analogue states \(^{0}-64064\)
3PK(d, n)*PL, angular distrib. of \(^{0}A-particles\) and cross-sections for \(^{0}E_{0}=600\)
1200 keV \(^{0}-55166\)
4Li(d,a)*He, polarization of \(^{6}Li-ions\), determination \(^{0}-64134\)
4Li(d,a)*He, polarization of \(^{6}Li-ions\), determination \(^{0}-64134\)
4Li(d,a)*Ple, absolute differential cross-sections, excitation functions, recoil spectrometry obs. \(^{0}-39103\)
3Li(d,n)*Be, recoil angular distributions, 12. 15 and 17 MeV \(^{0}-49644\)
4Li(d,a)*Be, precoil angular distributions, 12. 15 and 17 MeV \(^{0}-49644\)
4Li(d,a)*Be, and alevels in \(^{3}He \) \(^{0}-70392\)
4Li(d,a)*Be, and alevels in \(^{3}He \) \(^{0}-70392\)
4Li(d,a)*Be, and alevels in \(^{3}He \) \(^{0}-70653\)
4Mg(d,p)*2Na, excitation function, 0 to 10 MeV \(^{0}-39112\)
4Mg(d,

0. 49666

Mo(d,t) (A=94, 96, 100), Ed=17 MeV, spectroscopic studies 0-49529

¹³N(d,n)¹³C produced in unstable plasma 0-38958

¹⁴N(d,n)¹³C), and single-particle spectroscopic factors in ¹⁵O 0-70650

¹⁴N(d,p), stripping reactions of the 1p shell initiated by vector-polarised deuterons 0-55168

¹⁵N(d,p)¹³N, for energy separation of doublet at 9.15 MeV in ¹⁵N 0-49502

¹⁵Na(d,a)²¹Ne, cross sections behaviour, E=10-11 MeV 0-39110

¹⁵Nd(d,t)¹⁴Nd and neutron particle-hole states in ¹⁶Nd 0-70494

¹⁶Nd(d,d'), deduced ¹⁶Nd levels, excitation energies and cross-sections 0-60878

146Nd(d,d), deduced 146Nd levels, excitation energies and cross-sections 0-60828

20Ne(d,n)²¹Na reaction studied at 4.5 MeV, energy levels study in ²¹Na

deuterons continued ²⁰Ne(d,p)²¹Ne, excited states in ²¹Ne and comparison with DWBA

 21 Ne(d,p) 22 Ne, excited states in 22 Ne and comparison with DWBA 0 – 104 27

²¹Ne(d,p)²²Ne 0-70652

²³Ne(d,p)²³Ne, excited states in ²³Ne and comparison with DWBA 0-70427

Ni, 13.6 MeV, cross section measurements 0-52803

18. 10.3 MeV-closs section intension linear the second of ¹⁵O(d, ³He)¹⁵N, rel. to ¹⁶O ground state particle hole impurities, 20 MeV

0-38859

¹⁶O₃, spin tensor moments for elastic scatt, absolute cross sections for reactions 0–52802
¹⁶O(d,α)¹⁴N, isospin violating, energy dependences 0–67551
¹⁶O(d,α)¹⁶O, 4.4-8.4 MeV, tensor polarization meas. 0–39108

(6O(d,d))¹⁶O, 4.4-8.4 MeV, tensor polarization meas. 0–39108
 (6O(d,d))¹⁶O study at 4–6 MeV, fit of theoretical curves using DWBA model to exptal. data 0–73991
 (6O(d,n))¹⁷F, 2-4.2 MeV, cross-section meas. 0–73992
 (6O(d,n))¹⁷F study at 4-6 MeV, fit of theoretical curves using DWBA model to exptl. data 0–73991
 (6O(d,p))¹⁶O, (10O(d,α))¹⁸N, 4.4-8.4 MeV, absolute cross-sections meas. 0–39108

¹⁶O(d,p)¹⁷O, analysed using BHMM theory of deuteron stripping

16O(d,p)¹⁷O, analysed using BHMM theory of deuteron stripping 0–70651
16O(d,p)¹⁷O study at 4-6 MeV, fit of theoretical curves using DWBA model to exptal. data 0–73991
16O(d,p)¹⁸O ground state particle hole impurities, 20 MeV 0–38859
16O(d,p)¹⁸O, paraly detection in coincidence with reaction particles and deduced levels of ¹⁶O for E=5.0 MeV 0–57900
18IP(d,p)¹⁸O, p-ray detection in coincidence with reaction particles and deduced levels of ¹⁶O for E=5.0 MeV 0–57900
18IP(d,p)¹⁸O, p-ray detection in coincidence with reaction particles and deduced levels of ¹⁶O for E=5.0 MeV 0–57900
18IP(d,p)¹⁸O, p-ray detection in coincidence with reaction particles and deduced levels of ¹⁶O for E=5.0 MeV 0–64011
18IP(d,p)¹⁸O, possible of the coincidence recording for E=4.0 MeV 0–64011
18IP(d,p)¹⁸O, possible of the coincidence recording for E=4.0 MeV 0–64011
18IP(d,p)¹⁸O, possible of the coincidence recording for E=6.1 MeV 0–64011
18IP(d,p)¹⁸O, possible of the coincidence recording for E=6.1 MeV 0–64011
18IP(d,p)¹⁸O, possible of the coincidence recording for E=6.1 MeV 0–64011
18IP(d,p)¹⁸O, possible of the coincidence recording for E=6.1 MeV 0–64011
18IP(d,p)¹⁸O, possible of the coincidence recording for E=6.1 MeV 0–64011
18IP(d,p)¹⁸O, possible of the coincidence recording for E=6.1 MeV 0–6401
18IP(d,p)¹⁸O, possible of the coincidence recording for E=6.1 MeV 0–64061
18IP(d,p)¹⁸O, possible of the coincidence recording for E=6.1 MeV 0–49661
18IP(d,p)¹⁸O, possible of the coincidence recording for E=6.1 MeV 0–49661
18IP(d,p)¹⁸O, possible of the coincidence recording for E=6.1 MeV 0–49661
18IP(d,p)¹⁸O, possible of the coincidence recording for the coincidence recordi

0-70655

²⁸Si(d, d)²⁸Si, asymmetries measured for vectorially polarised 28 MeV deuterons 0-58009

²⁸Si(d,d)²⁸Si obs. and optical model analysis 0-63851

²⁸Si(d,d)²⁸Si obs. and optical model analysis 0-63851

²⁸Si(d,p)²⁸Si, ²⁹Si deduced levels and spectroscopic factors E=2.00-6.12 MeV 0-58012

²⁸Si(d,t), deduced levels of ²⁷Si at E_a=21.6 and 21.0 MeV 0-49661

²⁸Si(d,a)²⁷Al, cross sections behaviour. E=10-1 MeV 0-39110

³⁸Si(d,p)³ISi, for meas. of mean lives of levels 0-55124

³²Si, elastic and inelastic scattering, suggesting spherical equilibrium 0-70655

Sn (A=112, 116, 118, 120, 122, 124), elastic and inelastic scatt, from vibr.

0-70655
Sn (A=112, 116, 118, 120, 122, 124), elastic and inelastic scatt. from vibr. states, diff. cross sections 0-42863 1¹²Sn(d,p)¹¹³Sn and energy levels in ¹¹³Sn 0-70483 1¹²³Sn(d,p)¹²³Sn and energy levels in ¹¹³Sn 0-70483 (d,p) ¹⁸³St at 20.65 MeV, levels study 0-57916 8⁸Sr(d,p) ⁸⁸Sr at 20.65 MeV, levels study 0-57916 8⁸Sr(d,p) ⁸⁹Sr b study of excited levels of ⁸⁴Rb 0-60762 8⁸Sr(d,n)⁸⁹Y°, threshold region, meas. of excitation curves for ⁸⁸Sr(d,p) ⁸⁹Sr reaction 0-77579 8⁸Sr(d,p) ⁸⁹Sr, excitation curves for 4 states of ⁸⁹Sr in region of ⁸⁸Sr(d,p) ⁸⁹Sr, excitation curves for 4 states of ⁸⁹Sr in region of ⁸⁸Sr(d,p) ⁸⁹Sr, excitation curves for 4 states of ⁸⁹Sr in region of ⁸⁸Sr(d,p) ⁸⁹Sr, polarization effects and ground and first excited state of ⁸⁹Sr (-7058) 8⁸Sr(d,p) ⁸⁹Sr, analysed using BHMM theory of deuteron stripping

88Sr(d,p)89Sr analysed using BHMM theory of deuteron stripping

Te (where A=126, 128, 130), elastic and inelastic scatt., from vibr. states, diff. cross sections 0–42863 ¹²⁴Te(d,d'), deduced ¹²⁴Te levels, excitation energies and cross-sections 0–60828

0-60828 $^{124}\text{Te}(d,d)$, deduced ^{124}Te levels, excitation energies and cross sections

Ti(d,d)Ti (where A=46-50), Ed=13.6 MeV, ang. distrib., optical model anal. 0–60826

233U(d,pf) 8-9.5 MeV. fission characteristics depend. on d energy obs. 0–46262

234U(d,p)²³⁵U E_d=12 MeV, levels of ²³⁵U populated by reaction 0–39111

234U(d,p)²³⁶U^m, fission fragment mass distributions and kinetic energies for spontaneously fissioning isomers 0–39164

236U(d,t)²³⁵U, E_d=12 MeV, levels of ²³⁵U populated by reaction 0–39111

42n(d,n)⁶⁵Ga by time of flight method, differential cross section, spin and parity assignments 0–58020

42n(d,n)⁶⁷Ga by time of flight method, differential cross section, spin and parity assignments 0–58020

42n(d,n)⁶⁷Ga by time of flight method, differential cross section, spin and parity assignments 0–58020

42n(d,n)⁶⁷Ga by time of flight method, differential cross section, spin and parity assignments 0–58020

42n(d,n)⁶⁷Ga by time of flight method, differential cross section, spin and parity assignments 0–58020

42n(d,n)⁶⁷Ga by time of flight method, differential cross section, spin and parity assignments 0–58020

42n(d,n)⁶⁷Ga by time of flight method, differential cross section, spin and parity assignments 0–58020

42n(d,n)⁶⁷Ga by time of flight method, differential cross section, spin and parity assignments 0–58020

42n(d,n)⁶⁷Ga by time of flight method, differential cross section, spin and parity assignments 0–58020

42n(d,n)⁶⁷Ga by time of flight method, differential cross section, spin and parity assignments 0–58020

42n(d,n)⁶⁷Ga by time of flight method, differential cross section, spin and parity assignments 0–58020

42n(d,n)⁶⁷Ga by time of flight method, differential cross section, spin and parity assignments 0–58020

42n(d,n)⁶⁷Ga by time of flight method, differential cross section, spin and parity assignments 0–58020

42n(d,n)⁶⁷Ga by time of flight method, differential cross section, spin and parity assignment of flight method, differential cross section, spin and parity assignment of flight method, differential cross section, spin and pa

⁹²Zr(d,p)⁹³Zr, 4,2-11.2 MeV, charge exchange effects 0-73998

Nuclear reactions and scattering due to continued

electrons

dispersion corrections using harmonic oscillator model of nucleus 0-49596

0–49596
distorted wave calc. for elastic and inelastic scatteing of electrons from partially aligned non-spherical nuclei 0–39022
eigenchannel theory 0–64102
elastic optical potential from dynamic analysis 0–42818
electron-photon cascades, calc. of the energy deposited in thick targets at high energy (1 GeV) and comparison with experiment 0–55152
exchange currents determination by comparison of photon and electron disintegration of nuclei 0–70567
final-state interactions in quasifree electron scattering from nuclei 0–52754
graphite bombard with 87 MeV e 78e and 110 prod. 0–77539

graphite bombard, with 87 MeV e, 7 Be and 11 C prod. 0-77539 heavy nucleus, excitation, subsequent γ decay of excited state 0

neavy nucleus, excitation, subsequent γ decay of excited state 0-73911 inelastic form factors obtained using particle-hole model 0-73907 materials, depth dose distribution meas. 0-59124 melamine bombard, with 87 MeV e, ^{13}N prod. 0-77539 monopole elastic scattering, effect of generalized deformations 0-67518 multiple scattering meas. of $p\beta c$ on electron tracks in nuclear emulsion 0-49423

p-shell nuclei, correlated charge form factors using finite well wave functions 0-42815 quasi-elastic scattering from a finite temperature nucleus 0-52753

quasi-elastic scattering from a finite temperature nucleus 0–52753 radiative corrections to back scattering 0–-70573 scattered e spectra, bremsstrahlung corrections 0–39017 scattering, review of techniques 0–73912 scattering, review of techniques 0–73912 scattering by overlapping resons, system, excitation and decay 0–38833 short-range correlations by means of e scatt, review 0–60801 suggestive approximate dynamical symmetry of electron moving in field of many stationary nuclei 0–73915 virtual nuclear excitations and dispersive effects for vibrational nuclei 0–52755 water hombard with 87 MeV e 150 prod 0–77539

virtual nuclear excitations and dispersive effects for vibrational nuclei 0–52755 water bombard, with 87 MeV e, ¹⁵O prod. 0–77539

*He(e,e)*He assignment of O+ state confirmed, new values of monopole matrix element, evidence for M2 resonance at 24 MeV 0–64107

*Ag, elastic scattering, differences in single, plural and multiple scattering through intermediate angles 0–57970

Al foil, Coulomb scattering, I MeV 0–46198

¹³Al, elastic scattering, differences in single, plural and multiple scattering through intermediate angles 0–57970

²⁷Al(e,e)²⁷Al, M5 magnetic moment determ. 0–64010

Au, thick target bremsstrahlung spectra. E,=0.2-2.8 MeV 0–49598

*Bl(e,e)²⁸Bl elastic and inelastic, calc. of orientation effects 0–77538

Be, thick target bremsstrahlung spectra. E,=0.2-2.8 MeV 0–49598

Bi, elastic scatt... cross section meas. E₃=40-60MeV 0–39023

²⁹Bl(e,e)¹⁰⁸Bl, M9 magnetic moment determ. 0–64010

C. quasi elastic scattering of high energy electrons 0–67519

¹⁰C, alpha-particle model of nucleus and scattering data correlation 0–49500

¹²C, e scatt. spectra in continuum model, struct. in giant reson. region 0–39021

¹²C, electrodisintegration, 15 60 MeV obs. 0–46106

1°C, e scatt. spectra in continuum model, struct. in giant reson. region 0-39021
 1°C, electrodisintegration, 15 60 MeV obs. 0-46196
 1°C, excitation of giant resonance in range 15-30 MeV, longitudinal and transverse form factor spectra 0-73914
 1°C, inelastic scatt... for struct. study 0-42816
 1°C, inelastic scatt... sum rule, expt. and theory 0-73909
 1°C, quasielastic scattering studied within framework of square-well shell model 0-60802
 1°C excitation of ore nucleon continuum by electron scattering, at low momentum transfer 0-46195
 1°C(e, e) 1°C, 28-60 MeV, 0°-O° transitions studied 0-46129
 1°C(e, e) 1°C, 28-60 MeV, 0°-O° transitions studied 0-46129
 1°C(e, e) 1°C, 28-60 MeV, 0°-O° transitions studied 0-46129
 1°C(e, e) 1°C, 28-60 MeV, 0°-O° transitions studied 0-673907
 1°C, inelastic scatt. between 36 and 65 MeV, for energy level study 0-38856
 1°C inelastic scatt., 500 MeV, short range correlations 0-67520
 Ca isotopes, dynamical deformation effects on charge distrib. 0-73910
 1°Ca, elastic scatt., 500 MeV, short range correlations 0-77541
 1°Ca, quasielastic scattering studied within framework of square-well shell model 0-60802
 1°Ca monopole elastic scattering, effect of generalized deformations 0-6512

model 0-00802

**eOCa monopole elastic scattering, effect of generalized deformations 0-67518

**eOCe, e. scatt. up to 3.5MeV 0-77540

**FOCo foils, self-absorption of monoenergetic electrons, 51-58 keV 0-46199

**eOCo foils and transfer of the contraction of

0 -46199

2ºCu, elastic scattering, differences in single, plural and multiple scattering through intermediate angles 0--57970

2H(e,e'n)'H, total cross sections, with BF₃ counter 0-70572

2H(e,e')'H sum rule for spatially symmetric part of 1s shell nuclei 0--64106

3H exchange currents indicated by polarization of nucleons emitted in electron-induced interactions 0--38845

3H(e,e)'H sum rule for spatially symmetric part of 1s shell nuclei 0-64106

3He, scattering at 180° 0-67521

3He exchange currents indicated by polarization of nucleons emitted in

He exchange currents indicated by polarization of nucleons emitted in electron interactions 0–38845 https://doi.org/10.1009/10

He, electrodisintegration cross section calc. 0–73916
He, scattering at 180° 0–67521
He(e,e)*He, sum rule for spatially symmetric part of 1s shell nuclei 0–64106

Hotelef Hotele

Nuclear reactions and scattering due to continued electrons continued

electrons continued

2º Mg, E=225 MeV scatt., anal. in Born approx. 0–60803

2º Mg, inelastic, E_x<60MeV, for study of giant reson. 0–39018

2º Mg inelastic electron scattering, splitting of giant resonance 0–42741

2º Na elastic and inelastic, static characteristics of ground state, excited states 0–46197

2º Ne, scattering at 180° 0–67521

Ni (A=58, 60, 64), elastic scatt., E_e=225 MeV, nuclear charge distr. parameters, charge radius 0–49597

Ni(e,e)Ni elastic scatt. cross-sections at 300 MeV, charge distrib. isotopic depend. 0–64109

1º O, alpha-particle model of nucleus and scattering data correlation 0–49500

1º O, alpha-particle model of nucleus and scattering data correlation 0–49500

10-49500 (60), escatt, spectra in continuum model, struct, in giant reson, region 0-39021 (60), elastic form factor, second diffraction minimum, by α -particle model

0-49601

0–49601

10-Q, electroexcitation of first excited state, monopole sum rule 0–70404

10-Q, glant resonance region, inelastic scattering with primary energies below

60 MeV 0–73908

16-Q(e,e)¹⁶O inelastic, form factor calc, with particle-hole model 0–73907

185-Qs, electron capture and excited states in 185-Re 0–64061

Pb, elastic scatt. E=40-60 MeV, cross section meas. 0–39023

Pb, spectra of bremsstrahlung and secondary e from thick targets, Monte Carlo calcs. 0–46200

187-Pb, elastic scattering, differences in single, plural and multiple scattering through intermediate angles 0–57970

108-Pb, transition density of the octupole vibration for small and high momentum transfer 0–57971

136(e, e)^{31-S}, 28-60 MeV, O*-O* transitions studied 0–46129

1385 in leastic scatt, at high momentum transfer, excitation of particle-hole

momentum transfer U=5/971

³⁸(c), e.³⁸S, 28-60 MeV, O⁺—O⁺ transitions studied 0—46129

²⁸Si inelastic scatt. at high momentum transfer, excitation of particle-hole states 0—73797

²⁸Si(e, e.)³⁸Si, 28-60 MeV, O⁺—O⁺ transitions studied 0—46129

Sn (A=112, 118), elastic scatt., E₌=225 MeV, nuclear charge distr. parameters, charge radius 0—49597

Sn thick target bremsstrahlung spectra, E₌=0.2-2.8 MeV 0—49598

¹¹⁶Sn, inelastic scatt., 60 MeV, quadrupole and octupole excitations 0—42761

¹³⁸Sn, inelastic scatt., 60 MeV, quadrupole and octupole excitations 0—42761

¹³⁶Sn, inelastic scatt., 60 MeV, quadrupole and octupole excitations 0—42761

¹³⁶Sn, inelastic scatt., 60 MeV, quadrupole and octupole excitations 0—42761

¹³⁶Sn, inelastic scatt., 60 MeV, quadrupole and octupole excitations 0—42761

Ta, thick target, bombardment, bremsstrahlung and photonuetron production calculations 0—73913

1a, thick target, bombardment, bremsstrahlung and photonuetron production calculations 0-73913
51V, inelastic scatt. form factors 0-70460
W, bremsstrahlung spectra, ang. distribs. 0-45883
W, thick target, bombardment, bremsstrahlung and photoneutron production calculations 0-73913
90Zr vibrational states from inelastic scattering 0-67522

gamma-rays see Nuclear reactions and scattering due to/photons **heavy ions** see Nuclear reactions and scattering due to/nuclei of Z>2helium-3

imaginary isovector interaction in optical model potential, search 0-67546

0–67546

optical-model analysis of 29 MeV differential and total reaction cross-section data 0–39122

scattering, optical potentials 0–52793

strong absorption for scatt. from various nuclei between C and Sn 0–60822

water, ¹⁸F production 0–58022

(*He, p), O** spin parity obs. in ⁵⁶Co, ⁵⁴Mn, ⁵²V, and ⁵⁰Sc 0–67453

(*He, t) for isospin mixing in nucleus energy levels 0–67396

(*He, *Be) reaction at 30 MeV on light nuclei and states in *Be 0–49649

(*He, α) for study of single neutron hole states in N 49 nuclei 0–38899

(*He, α) with nuclei in s-d shell, angular distributions of α particles. DWBA analysis, cross sections 0–67549

(*He, α) muclei of p shell, stripping reactions with 2 transferred nucleons 0–70629

0–70629 "Mo(³He.d), A=92, 94, 96, 98, inhibited transitions to 3s_{1/2} isobaric analog states 0–73997 ²⁷Al, elastic scatt., 30 MeV, optical model params. 0–42862 ²⁷Al(³He.α') differential cross sections, experimental results compared with theory, energy levels of final nucleus 0–67553 ²⁷Al(³He.d)²⁸Si*. ²⁸Si level lifetimes and excitation energies, ≤11 MeV

²'Al('He.d)²⁸Sf². ²⁶Si level lifetimes and excitation energies, ≤11 MeV 0-38869

²⁷Al('He.n)²⁹P, selectivity for excitation of T=3/2 level of ²⁹P 0-46121

²⁷Al('He.p)²⁹Si and 2p-1h states in ²⁹Si 0-73799

⁴⁰Ar('He.d)⁴¹K deduced levels of ⁴¹K for E=10 MeV 0-57908

⁴⁰Ar('He.d)⁴¹K production of 0⁴ analog and antianalog states at 35 MeV, anomalous L=1 shapes o₁ angular distributions 0-73996

⁸B('He.n) ¹¹C, paired-proton configurations 0-70645

¹⁸B('He.β+He)¹⁰B, 4-18 MeV, differential cross sections, data analysis

⁹B(⁴He.n) ¹¹C, paired-proton configurations 0–70645 ¹⁰B(⁴He.⁴He)⁹B, 4-18 MeV, differential cross sections, data analysis 0–70632 ¹⁰B(⁴He.⁴He)⁹B, 1-10MeV, study of ¹³N levels 0–42736 ¹⁰B(⁴He.⁴) ¹⁰C leading to 8.11 MeV level of ¹¹C and assignment of J^π=¹/₂ for that state 0–73782 ¹⁰B(⁴He.⁴) ¹⁰C singlet deuteron emission by distorted-wave Born approximation 0–42869 ¹¹B(⁴He.⁴α), ¹⁰ dependence of angular distributions 0–70647 ¹³Ba(⁴He.⁴α), ¹³Ta(²Ce, 14-33 MeV, angular distributions, average projected ranges, and cross sections 0–73999 ¹³Be(⁴He.⁴α), ¹⁷C analysis of neutrons, and two-nucleon transfer 0–70646 ¹³Be(⁴He.⁴α), ¹⁷C analysis of neutrons, and two-nucleon transfer 0–70646 ¹³Be(⁴He.⁴α), ¹⁷C, excitation of T=3/2 levels in ¹⁷C 0–43783 ¹⁸Be(⁴He.⁴α) ¹¹C, excitation of T=3/2 levels in ¹⁷C 0–46121 ¹⁸Be(⁴He.⁴α) ¹¹N, paired-proton configurations 0–70645 ¹¹C, ¹¹N, ¹⁸F, emission from ¹⁴N irradiation relationship between isotope emission and energy of bombarding particles 0–74000 ¹²C, elastic, polarization meas. 0–46243 ¹²C(⁴He.²α) ¹⁷C, leading to 8.11 MeV level of ¹¹C and assignment of J^π=¹/₂-for that state 0–73782 ¹²C(⁴He.²α), comparison with (³He.²p) and (t,p) transitions E=9-13.5 MeV 0–42871 ¹²C(⁴He.²n) ¹⁴O, precision meas. of threshold energy by velocity technique (4221)

 ${}^{12}C({}^{14}E_{\rm in}){}^{14}O$, precision meas. of threshold energy by velocity technique 0-46211

Nuclear reactions and scattering due to continued helium-3 continued

redum-3 continued

1²C(³He.p)¹⁴C, at low energy, calc. of polarization effects 0-73981

1²C(³He.py) ¹⁴N, y radiation observed rel. to lifetime of ¹⁴N determ.

0-52670

¹²C(³He,t) and (³He, ³He'), 49.8 MeV, angular distributions 0–39096

"*C(*He.t) and (3He.3He'), 49.8 MeV, angular distributions 0–39096

"*C, T dependence of angular distributions 0–70647

"C(*He.*Belg.s.])*Belg.s.] at 2.0 to 6 MeV 0–39107

"C(*He.n)*O, paired-proton configurations 0–70645

"C(*He.n)*O excitation of T=3/2 levels in "50 0–46121

"C(*He.t) and (*He.3*He'), 39.6 MeV, angular distributions 0–39096

"C(*He.t) and (*He.3*He'), 39.6 MeV, angular distributions 0–39096

70632

¹⁴C(¹He, ¹He)¹⁴C, 4-18 MeV, differential cross sections, data analysis 0–70632

"C(¹He, d)¹⁵N, 14 MeV, ¹⁵N states <6.33 MeV excitation 0–38858

¹⁴C(¹He, d)¹⁵N, 14 MeV, ¹⁵N states <6.33 MeV excitation 0–38858

¹⁴C(¹He, d), deduced shell amplitudes of ¹⁶O, double-stripping study 0–42738

¹⁴C(¹He, d), 44.8 MeV, angular distributions 0–39096

¹⁵C(¹He, d), effective two-body pot. 0–42732

¹⁸C(a)¹He, p), study of decay modes of low-lying levels 0–52674

¹⁶C(a)¹He, d), ¹⁵Sc, 40 MeV, angular distributions of observed levels 0–70656

¹⁶C(a)¹He, d), ¹⁵Sc, single channel calc, of form factors 0–77531

¹⁶C(a)¹He, p), ¹⁵Sc, angular correlation study 0–55127

¹⁶C(a)¹He, p), ¹⁵Sc, angular correlation study 0–55127

¹⁶C(a)¹He, d), ¹⁶Sc, E₁he=15 MeV, energy level study of ⁴⁸Sc 0–38884

¹⁶C(a)¹He, d), ¹⁶In 0–70660

¹¹C(a) elastic scatt., 30 MeV, optical model params. 0–42862

¹¹C(a)¹He, d), ¹⁶Ca, rup to 8.5 MeV, struct. of ¹⁵Ar 0–49514

¹⁷C(a)¹He, d), ¹⁶Ar up to 8.5 MeV, struct. of ¹⁵Ar 0–49514

¹⁷C(a)¹He, d), ¹⁶Ar up to 6.9 MeV, struct. of ¹⁵Ar 7. 0–49514

¹⁷C(a)¹He, d), ¹⁶Ar up to 6.9 MeV, struct. of ¹⁵Ar 7. 0–49514

¹⁷C(a)¹He, d), ¹⁶Ar up to 6.9 MeV, struct. of ¹⁵Ar 7. 0–49514

¹⁷C(a)¹He, d), ¹⁶Ar up to 6.9 MeV, struct. of ¹⁵Ar 7. 0–49514

¹⁷C(a)¹He, d), ¹⁶Ar up to 6.9 MeV, struct. of ¹⁵Ar 7. 0–49514

¹⁷C(a)¹He, d), ¹⁶Ar up to 6.9 MeV, struct. of ¹⁵Ar 7. 0–49514

¹⁷C(a)¹He, d), ¹⁶Ar up to 6.9 MeV, struct. of ¹⁵Ar 7. 0–49514

¹⁷C(a)¹He, d), ¹⁶Ar up to 6.9 MeV, struct. of ¹⁵Ar 7. 0–49514

¹⁷C(a)¹He, d), ¹⁶Ar up to 6.9 MeV, struct. of ¹⁵Ar 7. 0–49514

¹⁷C(a)¹He, d), ¹⁶Ar up to 6.9 MeV, struct. of ¹⁵Ar 7. 0–49514

¹⁸C(a) elastic scatt. 30 and 35 MeV, optical model params. 0–42862

¹⁸Fe(¹He, d), ²Ar and spins of l=1 states in ²⁵Co, 0–67451

"Fe(³He.d)³Ne*, ³®Ne level lifetimes and exentation "Fe(³He.d)³Ne*, ³®Ne level lifetimes and exentation "Fe(³He.d)³SCo and spins of l=1 states in \$\$^C0 0-67451 \$\$^Fe(³He.d)\$SCo and spins of l=1 states in \$\$^C0 up to 4.185 MeV. J* assignments 0-49520 \$\$^He(³He,d)\$PSCo p branching ratios deduced for levels \$\$^C0 up to 4.185 MeV. J* assignments 0-49520 \$\$^H(³He,d)\$Phip, coincidence studies, $E=18.0\cdot24.0$ MeV 0-39100 2 H(3 He, 3 Hp), coincidence studies, $E=18.0\cdot24.0$ MeV 0-39100 3 H(3 He, 3 Hp), 27.7 and 32.3 MeV, differential cross sections, excitation functions for elastic scattering 0-70631 3 He, 3 D, normalization const. in DWBA theory 0-49651 (3 He, 3 D, oharge exchange reaction on N=28 targets, microscopic analysis 0-49660

(³He, α), normalization const. in DWBA theory 0–49651 (³He, t), charge exchange reaction on N=28 targets. microscopic analysis 0–49660 (³He, ³Pe), charge exchange reaction on N=28 targets. microscopic analysis 0–49660 (³He, ³Pe), at low energy, polarization effects 0–73981 (³He, e), isobaric analog states abs. 0–67531 (³He, e), isobaric analog states abs. 0–67531 (³He, e), and comparison to resonating group calculations 0–52795 (³He, optical potentials 0–39089 (³He, ³He, ³Ph, ³Ph

²⁶Mg(³He,n)²⁸Si, observation of excitation in low lying levels with T=2

0.—73993

²⁶Mg(²He.t)²⁶Al, at 16 and 30 MeV 0.—77574

¹⁸N(²He.q.)¹³N, differential cross-sections and deduced ¹³N levels, E.=2.5-8.5 MeV 0.—60825

¹⁸N(³He.d.)¹³O, 14 MeV. ¹⁵O states <8.32 MeV excitation 0.—38858

¹⁸N(³He.d.)¹⁶O, 14 MeV. ¹⁵O states <8.32 MeV excitation 0.—39096

¹⁸N(³He.d.)¹⁶O at 16 and 24.9 MeV, struct. of ¹⁶O 0.—49503

¹⁸N(³He.d.)¹⁶O and 2p.1h contribution in ¹⁷O 0.—73789

¹⁸N(³He.d.)¹⁸O and ²Pel. ³Ne. ³Ne. ³Ne. ³Ne. ³Mg level lifetimes and excitation energies, ≤11 MeV 0.—38869

¹⁸Ne(³He.n.), study of decay modes of low-lying levels 0.—52674

0-38069 is Ne('He.np'), study of decay modes of low-lying levels 0-52674 ²⁰Ne('He.np') Ne. study of levels below excitation energy of 7 MeV 0-77486

0-77486

0-77485

0-77485

0-77485

0-77485

0–77485
²⁰Ne(³He.α) differential cross sections, experimental results compared with theory, energy levels of final nucleus 0–67553
²⁰Ne(³He.n) deduced levels of ²²Mg, between 3.4-9.4 MeV 0–42740
²⁰Ne(³He.η)²²Mg, and low-lying excited states in ²²Mg 0–67429
²²Ne(³He.α) differential cross sections, experimental results compared with theory, energy levels of final nucleus 0–67553
²²Ne(³He.η)²²Na, at 16 and 30 MeV 0–77574
⁵⁸Ni(³He.α)⁵³Ni, obs. of new low-lying states in ⁵³Ni 0–77497

helium-3 continued

58Ni(3He,n)60Zn, observation of excitation in low-lying levels with T=2

60Ni, elastic scatt., 30 and 35 MeV, optical model params. 0-42862 16O(3He, n), comparison with (3He, p) and (t,p) transitions E=913.5 MeV 0-42871

¹⁸O(³He, t)¹⁸F, angular momentum transfer 0-67552

18O(1He. t)18F, angular momentum transfer 0–67552
18O(1He.n)20Ne. 20Ne excited levels, two proton transfer obs. 0–49658
18O(1He.n). deduced 20F levels up to 6.043 MeV excitation 0–52678
18O(1He.n). 18F, at 16 and 30 MeV 0–77574
obs. of energy levels up to 10 MeV excitation, relative spectroscopic factors 0–77494
208*pb(1He.ν). 2079 bat 28 MeV, levels in 207pb 0–49550
242*Pu(1He.d). 2079 bat 28 MeV, levels in 207pb 0–49550
242*Pu(1He.d). 208*Am and levels in 247Am for E=30 MeV 0–58023
242*Pu(1He.d). 208*Am and levels in 247Am 0–70667
104*Rh(1He.t). 208*Am and levels of 31S, E=8.0-12.2 MeV 0–42744
23S(1He.ν) deduced levels of 31S, E=8.0-12.2 MeV 0–42744
23S(1He.ν) deduced levels of 31S, E=8.0-12.2 MeV 0–42744
23S(1He.ν) deduced levels of 31S. E=8.0-12.2 MeV 0–42744
23S(1He.ν) deduced levels of 31S. E=8.0 12.2 MeV 0–42744
23S(1He.ν) deduced levels of 31S. E=8.0 12.2 MeV 0–42744
23S(1He.ν) deduced levels of 31S. E=8.0 12.2 MeV 0–42744
23S(1He.ν) differential cross sections at 12 MeV, energy level study 0–70440
45C(1He.ν) 20 MeV, level structure determ. in 47Ti 0–67446
25S(1He.ν) differential cross sections, experimental results compared with theory, energy levels of final nucleus 0–67553
28S(1He.ν) 20P, 4.3-11 MeV, data analysed using PWBA and DWBA 0–70654

10 – 70654 elastic, angular distribution at 8.0 and 7.0 MeV 0–49662 30 Si(3 He. α) 30 Si at 8.0 and 7.0 MeV, angular distribution of α -particles, excitation curves 0–49662 30 Si(3 He. α) 30 Si MeV, angular distribution of α -particles, excitation curves 0–49662 30 Si(3 He.d) 31 P, 17.85 MeV spectroscopic factors from DWBA analysis 0.75535

0—1773 "Si(i'He.t)³⁰P, at 16 and 30 MeV 0—77574 ¹¹⁰Sn, elastic scatt. 30 and 35 MeV, optical model params. 0—42862 ²³²Th(i'He.d)²³Pa and levels in ²³Pa 0—70667 ⁴⁶Ti(i'He.n)⁴⁸Cr, observation of excitation in low-lying levels with T=2

0 - 73993 **STi(He\arrow \), 13.0 MeV, level structure determ. in ^{47}Ti 0—67446 **STi(He\arrow \), 15 MeV, observation of 54 states in ^{50}V 0—70459 **STi(He\arrow \), 21 Veryles \$11\text{V}\$ tugudy 0—67555 **STi(He\arrow \), 21\text{V}\$ evels \$6.17 MeV 0—38885 **STi(He\arrow \), 21\text{V}\$ peranching ratios deduced for levels in ^{51}V up to 2.699 MeV, J* assignments 0—49520 **23\text{U}(He\arrow \), 22\text{V}\$ U=30 MeV, ang. distribs. of \$\alpha\$ particles, level study of 23\text{U}(He\arrow \), 23\text{U} 0—39128 **

235U (3He.d)²³⁷Np and levels in ²³⁷Np 0–70667
238U(3He.d)²³⁷Np deduced levels of ²³⁷U, E=30 MeV 0–42777
289V, elastic scatt., 30 MeV, optical model params. 0–42862
64 Zn(3He.t)⁶⁴Ga production of 0+ analog and antianalog states at 35 MeV, anomalous L=1 shapes of angular distributions 0–73996
66 Zn(3He.t)⁶⁴Ga production of 0+ analog and antianalog states at 35 MeV, anomalous L=1 shapes of angular distribution 0–73996
67 Zn(3He.t)⁶⁴Ga production of 0+ analog and antianalog states at 35 MeV, anomalous L=1 shapes of angular distribution 0–73996
97 Zr, elastic scatt., 30 MeV, optical model params. 0–42862
97 Zr (3He.t)⁶⁸Nb and spins and excitation energies of Nb multiplet 0–70479

0-7397 °O-7(4)+6,d), inhibited transitions to $3s_{1/2}$ isobaric analog states °O-73997 °O-7(4)+6,d) inhibited transitions to $3s_{1/2}$ isobaric analog states °O-73997 °A-7(3)+6,d) inhibited transitions to $3s_{1/2}$ isobaric analog states °O-73997 °A-7(3)+6,d) inhibited transitions to $3s_{1/2}$ isobaric analog states °O-73997 °A-7(3)+6,d) inhibited transitions to $3s_{1/2}$ isobaric analog states °O-73997

hypernuclei production, by Σ^- absorpt, in emulsion nuclei 0-38843 Λ^o trapping probability from Σ^- capture in liquid neon, hyperfragment production 0-42861 Σ^- capture in liquid neon, hyperfragment production 0-42861 fle(Λ , Λ), 0.1-10 MeV phase shifts, cross-sections and ang. distributions 0-73970

nesons see also Cosmic rays/effects and interactions absorption reactions of neg. II by two N pairs in nucleus 0-49265 cascade, nucleon-meson, energy deposition, Monte Carlo calc. 0-49604 double-closed-shell nuclei, radiative pion capture 0-55154 energy transfer to neutral pions, at >20~GeV 0-73967 G5 nuclear emulsions, hyperfragment emission for $6KeV/cK^-$ 0-49639 Galilean-invariant operator, ambiguity for π absorption by nuclei 0.200640-39084

scattering lengths, related to level shifts and widths in mesonic atoms 0–39083 (π , 2π) in complex nuclei, theoretical aspects, using soft-pion techniques 0–49641

 $(\pi^-,2\pi)$, ang. correl. analysis 0-39086 (π^+,N), self-consistent calc. 0-46228 ($\pi^-\rho^-$), collisions with nuclei with $20 \le A \le 208$ 0-64127 ($\pi^-\rho^0$), collisions with nuclei with $20 \le A \le 208$ 0-64127 $(12C(\pi^-,\pi^-))^{12}C$, 180 MeV, Glauber approx. calc. non-convergent 0-77566

 K^- , emission of hyperfragments from G5 nuclear emulsions at 6GeV/c 0 -49639

0-49039 K interaction on a photographic emulsion at 6 GeV/c, interp. as _{ΛΛ}C¹¹ double hyperfragment 0-49640 K⁻ interactions and kaonic X-rays rel. to neutron distrib. in nucleus 0-49476

K. onteraction with C, Cl, F and Cu at 120 MeV 0-64129 π , double charge exchange, prod. of 8 Li and 8 B, total cross sections 0-42860

0-42800

π charge exchange reactions 0-70628

π absorption, charge exchange and double charge exchange, theory and experiment 0-77565

π absorption, Galilean-invariant operator, ambiguity 0-39084

π absorption, radiative, in medium and heavy nuclei 0-73968

π charge-exchange reaction mechanism and internal bremsstrahlung 0-64128

0-04125 π forward elastic scatt., by dispersion relations 0-49603 π interaction cross sections, eval. by Clauber's theory 0-52765 π interactions with heavy emulsion nuclei, at 60 GeV, prod. of He

π nucleus interactions at 50 GeV, cascade calculations 0-46229

Nuclear reactions and scattering due to continued

 π scatt. by spin 1/2, 1 nuclei, 'elementary particle' nucleus model 0-39082

 π^- absorpt, rate in complex nuclei, shell model calc. 0–39085 π^- capture rate, self-consistent reaction matrix calculation 0–42859 π^- interactions at 3.86 GeV/c, strange particles prod., transverse momenta 0–60820

 π^- interactions at 3.86 GeV/c, strange particles prod., transverse momenta 0–60820 π^+ absorpt. followed by single-nucleon emission 0–39088 π^+ A \to π^- A'..... cross section meas. in 230 to 260 MeV 0–70242 Al. K, θ^- total cross sections at average momenta of 9.0 GeV/c 0–46230 C, K, θ^- total cross sections at average momenta of 9.0 GeV/c 0–46230 °C, charge exchange following pion inelastic scattering, 180 MeV 0–39087 °C, π^+ capture rate, self-consistent reaction matrix calculation 0–42859 °C, π^+ capture rate, self-consistent reaction matrix calculation 0–42859 °C, π^+ absorp. followed by single-nucleon emission 0–39088 °C, π^- scatt., 120–280 MeV, around N* reson. 0–57998 °C(π , π) giant resonance obs. 0–73972 °C(π , π) giant resonance obs. 0–73973 °C(π , π) giant resonance obs. 0–73973 °C(π , 2nd). reaction by (n,p) pair in α cluster 0–77568 °C(π , 2nd). reaction by (n,p) pair in α cluster 0–73971 °C(π , 2nd). Page 3 choice states study 0–73971 °C(π , 2nd). Page 3 choice state interaction effects 0–49642 °C(π , NN) three body partial wave analysis in Born approximation 0–42858 °C(π , 2nd), ang. correl. analysis 0–39086 °C(π , 2nd), ang. correl. analysis 0–39086 °C(π , 2nd), ang. correl. analysis 0–39086

 12 C(π^- ,NN) three body partial wave analysis in Born approximation 0–42858 12 C(π^- , π^-), ang. correl. analysis 0–39086 12 C(π^- , π^-), angular range 40-120 deg. at 30 MeV 0–57997 12 C(π^- , π^-), angular range 40-120 deg. at 30 MeV 0–57997 12 C(π^- , π^-), angular range 40-120 deg. at 30 MeV 0–57997 12 C(π^- , π^-), angular range 40-120 deg. at 30 MeV 0–57997 12 C(π^- , π^-), angular range 40-120 deg. at 30 MeV 0–57997 12 C(π^- , π^-), angular range 40-120 deg. at 30 MeV 0–57997 12 C(π^- , π^-), angular range 40-120 deg. at 30 MeV 0–67997 12 C(π^- , π^-), angular range 40-120 deg. at 30 MeV 0–67997 12 C(π^- , π^-), angular range 40-120 deg. at 30 MeV 0–67997 12 C(π^- , π^-), angular range 40-120 deg. at 30 MeV 0–67997 12 C(π^- , π^-), angular range 40-120 deg. at 30 MeV 0–680 12 CH, spin-isospin formalism for multiple scattering of pions 0–49638 12 He, spin-isospin formalism for multiple scattering of pions 0–49638 12 He(π^- , π^-)3n, rel. to resonant behaviour in three-neutron system within few MeV of threshold 0–52792 12 He, a scatt. 0.826–2.01 GeV 0–60819 12 He, spin-isospin formalism for multiple scattering of pions 0–49638 12 He(π^- , π^-), theoretical aspects, using soft pion techniques 0–49641 12 He(π^- , π^-), spectrum of high-energy p-rays 0–73969 12 Cli(π^- , π^-), Heoretical aspects, using soft pion techniques 0–46231 12 Cli(π^- , π^-), ang. correl. analysis 0–39086 12 Cli(π^- , π^-), Heoretical aspects tracture of Li nucleus 0–46231 12 Cli(π^- , π^-), theoretical aspects, using soft-pion techniques 0–49641 14 N(π^- ,2nd), reaction by (n,p) pair in α cluster 0–77568 16 O, π^- absorpt, followed by single-nucleon emission 0–39088 16 O, radiative capture of π^- , search for giant reson. excitation 0–73974 16 O(π^- , π^-), theoretical aspects, using soft-pion techniques 0–49641 16 O(π^- , π^-), theoretical aspects, using soft-pion t

10-70627 $160(\pi^2,2nd)$, reaction by (n,p) pair in α cluster 0-77568 $160(\pi^2,NN)$ three body partial wave analysis in Born approximation 0-42858

 10 G(π^{-}, η^{-}), n energy spectra 0–46232 16 O(π^{+}, π^{+}), angular range 40-120 deg. at 30 MeV 0–57997 Pb. K./9 total cross sections at average momenta of 9.0 GeV/c 0–46230 S, K mesic interaction in K-mesic atom used to meas. $4f\rightarrow 3d$ atomic transition 0-64307

tion 0-0430I $3^{28}(\pi^{2}-y_{0})$, n energy spectra 0-46232 $5^{1}V(\pi,\pi)^{51}V$. Glauber approx., suppression of scattering amplitude found 0-55163 $0^{2}V(\pi,\pi)^{90}Zr$, Glauber approx., suppression of scattering amplitude found 0-55163

muons

capture by overlapping resons, system, excitation and decay 0-38833 double-closed-shell nuclei, consequence of SU₄ breaking for μ capture 0-55154

double-closed-shell nuclei, consequence of SU₄ breaking for μ capture 0–55154
muon capture, theory, nuclear Coulomb effects on induced pseudoscalar interaction 0–42817
muon capture, time dependence of particle correlations 0–46201
radiative capture, hyperfine effects in impulse approx. 0–55153
scattering, prod. of W 0–42567
total muon capture rates rel. to total forward cross section for neutrino scattering 0–60514
p and n emission capture mechanism 0–60804
μ a absorption by emulsion nuclei Ag, Br, high energy p emission 0–42819
W boson production in neutrino and muon interaction on nuclei 0–60591
²⁷Al(μ-ν) determ. of probability, by activation method 0–46204
¹²C, capture, in continuum model 0–39021
¹³C, μ capture, charged particle emission 0–67524
¹²C(μ-ν)¹³B*, formation of excited levels 0–46203
⁴⁰Ca, capture, n asymmetry. obs. 0–46202
⁴⁰Ca, muon capture rates rel. to breakdown of SU(4) invariance 0–49600
⁴¹He, muon capture rates rel. to breakdown of SU(4) invariance 0–49600
⁴¹He, muon capture rates rel. to breakdown of SU(4) invariance 0–49600
⁴¹L(μ-ν)¹⁹He elementary particle treatment 0–49599
⁴¹Ca, myl⁹He elementary particle treatment 0–49599
⁴¹Ci(μ-ν)¹⁹He, capture rate and the PCAC hypothesis 0–39020
⁴¹L(μ-ν)¹⁹He, capture rate and the PCAC hypothesis 0–39020
⁴¹L(μ-ν)¹⁹He, capture rate and the PCAC hypothesis 0–39020
⁴¹L(μ-ν)¹⁹He, capture, pv ang. correlation 0–46201
⁴¹O, apture, in continuum model 0–39021
⁴¹O, apture, in continuum model 0–39021
⁴²O, capture, in continuum model 0–39021
⁴³O, apture, in continuum model 0–39021
⁴⁴O, determ. of probability, by activation method 0–46204
⁴⁵O determ. of probability, by activation method 0–46204
⁴⁶Cather of probability, by activation method 0–46204
⁴⁷Cather of probability, by activation method 0–46204
⁴⁸Cather of probability, by activation method 0–46204

neutrinos

ross section dependence on mass number 0-70574 cross-section dependence on atomic weight 0-390.19 high-energy, cross sections 0-67517 quasielastic reactions, for \(\nu\) hireraction 0-60512 total elastic cross-section for forward scatt, derived using quark field algebra and closure approximation 0-57754 A(\(\nu\), \(\nu\), \(\nu\), cross-section for W-oson production calc. 0-77345 W boson production in neutrino and muon interaction on nuclei 0-60591

neutrinos continued

Al, v cross-section dependence on atomic weight $0-39019^{-19}$ F(v₁,e-) ¹⁹Ne, as test for lepton charge conservation 0-42472 Pb, v cross-section dependence on atomic weight 0-39019

neutrons

neutrons see also Nuclear fission see also Nuclear fission 208 Pb(n, γ), partial direct and collective cross-sections 0-49619 (n, α) in negative Q-value region, obs. using low background telescopic system 0-42625 capture, p-wave cross sections, 24 keV 0-39057 capture y-rays, high resolution and low Compton background studies 0-39051

capture cross sections at 200 KeV, statistical theory calcs. 0–39063 capture cross-section meas. using Moxon-Rae detector, precision factors 0–73686

capture cross-sections in keV region, calc. of resonance parameters 0-57986

0–57986 capture cross-sections of thermal neutrons and resonance integrals, activation measurements 0–42842 coherent inelastic neutron scattering cross section and dispersion relations for graphite 0–57985 counter telescope design 0–38756 counter telescope for (n,α) reactions 0–49334 cross sections eval. below 2 MeV, optical model parameters 0–39062 cross-section data in a clean fast assembly, integral tests of ENDF/B and GAM 0–46216

GAM 0-46216

cross-section formulae of interaction with nucleus in Coulomb splitting of deuteron 0-64120

cross-section library for reactor design 0-39211

cross-sections and interactions mechanisms for light nuclei 0-49626

elastic scattering, anomalous, at small angles of incidence 0-70615

excited nuclei cross sections meas. 0-39069

fuel analysis, nondestructive radiative neutron capture 0-49727

gamma ray production cross sections meas. using pulsed Van de Graaff

accelerator 0-52782

inelastic cross-section, effective, for fast reactor compositions 0-60848

inelastic scattering, excitation functions, method of meas. 0-46217

inelastic scattering yield measurement via y rays emitted 0-46009

light nuclei, non-elastic processes 0-73954

microdistribution in a graphite pile with empty channels, pulsed neutron meas. 0-42900

Mott-Schwinger interaction effect on neutron-proton scattering 0-39054

microdistribution in a graphite pile with empty channels, pulsed neutro-meas. 0-42900 Mott-Schwinger interaction effect on neutron-proton scattering 0-39054negative Q-value (n,α) studies using low background telescopic system 0-42625

primary-recoil atom spectra 0-74047

primary-recoil atom spectra 0-1404? radioactive capture cross sections for 10-350 keV n, for 11 isotopes with $63 \le A \le 193$ 0-46227 rare earth isotopes. (n.2n), (n, α) and (n,p), statistical model and 14 MeV obs. 0-39077 rare-earth nuclei, configuration mixing from radiative neutron capture 0-64005

0-64005 reactor nuclear data conference, Helsinki, Finland. (1970) 0-74052 rel to reactor technology, cross sections status 0-39202 resonance absorption at intermediate energy, extrapolation and interpolation in calc. 0-57983 resonance self shielding factors for heavy actinides 0-46215 resonance-neutron radiative capture facility at Toronto University 0-77557

resonances statistical construction in unresolved region 0-49620 s-wave neutron bombardment, average level spacing calc. in target nuclei 0 52654

0 52654
S-wave neutron resonances from low-energy capture p-ray spectrum 0 -49493
scattering, 1-40 keV, ang. distribs. 0-52785
scattering on thick layers, polarization and ang. distrib., calcs. 0-77558
self-shielding factors, homogeneity effects for fast reactors 0-58046
single particle states from neutron capture in medium weight nuclei 0-73764

0-73764 slowing down equation, transient solutions 0-46280 target, polarized proton for low energy n-p scattering 0-52784 thermal capture, circular p-polarization and spin determination for compound states 0-49628 thermal neutron capture in solids, chemically significant details 0-79460 total cross section, high energy calc. from 5 to 21 GeV/c 0-77555 total cross sections on Be, C. Al, Cu and Pb, 8-21 GeV/c 0-70619 (n. a), 14.5 MeV, systematics demonstrated from literature 0-52786 (n. p) 14.5 MeV, systematics demonstrated from literature 0-52786 (n. p) 14.5 MeV, systematics demonstrated from literature 0-52786 (n. 2n) absolute cross sections near 14 MeV 0-39061 (n.2n) at 3-7 MeV, cross sections rel. to n excess and single-particle effects 0-39058 (n.2n) fast reaction cross sections in free Fermi gas model, excitation

0–39058
(n.2h) fast reaction cross sections in free Fermi gas model, excitation energy 0–39064
(n.a) cross-sections, prediction 0–55158
(n.p), E.=3MeV. cross sections for ⁶³Cu, ⁷⁴Ge, ⁷⁵As, ⁸⁰Se, ⁸¹Br, ¹⁰³Te, ¹⁴¹Pr, ¹⁸⁵W, ²⁰⁹Bi 0–42847
(n.p), magnetic spectrometer for internal conversion electrons 0–52591
(n.p) for purity of radioisotopes, production 0–64305
(n.n) nuclear temps. rel. to Z, 14 MeV 0–38809
(n.p), nuclear temps. rel. to Z, 14 MeV 0–38809
(n.p) cross-sections, prediction 0–55158
(n.p) cross-sections, prediction 0–55158
(n.p) cross-sections, E.=14.8 MeV 0–39060
(n.p) simultaneous reactions, extension of NEAREX statistical model cross section code 0–46222
prad. prod. by capture, elastic and inelastic scatt. 0–39056

Prad. prod. by capture, elastic and inelastic scatt. 0-39056 98 Mo(n, γ), neutron capture γ -ray spectra measurement and 99 Mo deduced resonances for E=12-818 MeV 0-60817 (n, α), compound-nucleus cross sections and angular distribs., FORTRAN code 0-49621

(n, n), compound-nucleus cross sections and angular distribs., FORTRAN code 0-49621

code 0–49621 (n. p), compound-nucleus cross sections and angular distribs., FORTRAN code 0–49621 np radiative capture and π exchange currents 0–57974 π exchange current in radiative np capture 0–57974 1917 [an, n), optical-model calculations using a spherical and a non-spherical potential for angular distributions, E_m=2.5-8.1 MeV 0–60818 1₀³Ag. reson, parameters and spin obs., E=4.830 eV 0–39073 2³²Th, E=1.5–8.5 MeV, total neutron cross-section measured 0–67539

Nuclear reactions and scattering due to continued

neutrons continued

population in ²³⁶U 0–73965

¹⁰⁷Ag, reson, parameters and spin obs., E=4–830 eV 0–39073

¹⁰⁸Ag, reson, parameters and spin obs., E=4–830 eV 0–39073

Al, total cross section at average momenta of 3.8 GeV/c 0–46230 ²⁷Al, activation cross-sections, (n,p), (n, α) and (n,2n) at 14.8 MeV 0-42854

1.7Al, depolarization parameter, 1.36 MeV 0-42845 1.7Al (m, \u03b2) cross-section determination for 14.43 MeV neutrons, precision measurements 0-64125

The abstraction $S_0 = 04123$ $2^7 \text{Al}(n, d)^{26} \text{Mg}$, $E_\pi = 14.1$ MeV, using counter telescope 0-77560 $2^{41} \text{Am}(n, \gamma)^{242m^2} \text{Am}$ analysis 0-46226

³⁷Ar, thermal neutron capture, energies and intensities of gamma rays

 6 Ar, thermal neutron capture and spins in 47 Ar 6 Ar 6 Ar, hormal neutron capture and spins in 47 Ar 6 Ar 6 Ar (n,p) 41 Ar void space analysis, air irradiation 6 Ar 6 Ar

"Ar(n,p)" Cl. β-decay of "Cl, levels of "Ar 0—7/515" at Ar, thermal neutron capture, energies and intensities of gamma rays 0—57992

0–57992
Au capture cross section, 24 keV, from sphere transmission obs. 0–49637
¹⁹⁷Au, reson. parameters and spin, E=1000-2100 eV 0–39079
¹⁹⁷Au, transmission of 24 keV neutrons by gold spheres, analysis using spin dependent S wave statistics 0–46221
¹⁹⁷Au reaction rates in Pu-recycle fuel lattices 0–74059
¹⁹⁸Au(n, α), energy spectra determination and α part, angular distribution for En=15.1 MeV 0–57995
¹⁹⁸Au(n, γ), neutron reson. capture, γ-ray spectra, using mag. Compton γ-spectrometer 0–73955
¹⁹⁸B thermal-neutron-absorption cross sections by pulsed neutron method 0–57989

0–57989
¹⁰B(n,α) reaction, low energy scattering cross section meas., absorpt. cross section determ. 0–42844
¹⁰B(n,n) elastic and inelastic, 9.72 MeV, differential and integrated cross sections 0–46218
¹¹B(n,n), differential and integrated cross-sections for En=14.1 MeV
0–49631

sections 0-46218

118(n.n.), differential and integrated cross-sections for En=14.1 MeV 0-49631

118(n.n.), elastic and inelastic, 9.72 MeV, differential and integrated cross sections 0-46218

118(n.n.) elastic and inelastic, 9.72 MeV, differential and integrated cross sections 0-46218

118(n.n.) elastic and inelastic, 9.72 MeV, differential and integrated cross sections 0-46218

118(n.n.) elastic and inelastic, 9.72 MeV, differential and integrated cross section problem of the pro

C-(7.0.4) and MeV optical model analysis 0—46220 Cr(n,α) cross-section determ. for natural element using a technique based on the absolute determ. of helium 0—49634 [13] Cs (1.4.8 MeV induced, absolute cross-sections 0—70622 [13] Cs (n,α) praction, level scheme of 13] Cs (0.4.6 Cu, total cross section at average momenta of 3.8 GeV/c 0—46230 [6] Cu, 6] Cu reaction parameter, 1.36 MeV 0—38888 [6] Cu capture p-ray cross section, 25 keV 0—39076 [6] Cu reaction rates in Pu-recycle fuel lattices 0—74059 [6] Cu (n,n/p), gamma ray angular distributions for E_m=2.9 MeV and cross sections 0—57993 [6] Cu reaction resonant neutron capture, gamma-ray spectra 0—42754 [6] Cu reamal- and resonant neutron capture, gamma-ray spectra 0—42754

sections 0–57993

**Cu thermal- and resonant neutron capture, gamma-ray spectra 0–42754

**Cu, inelastic scatt., p-rays and nuclear levels, 2.9 MeV 0–38888

**SCu(n,n'y), gamma ray angular distributions for E_m=2.9 MeV and cross sections 0–57993

**Cu thermal- and resonant-neutron capture, gamma-ray spectra 0–42754

**SEr(n,2n)\(^{16}Er, 14 MeV, and statistical model 0–39077

**SEr(n,2n)\(^{16}Er, 14 MeV, and statistical model 0–39077

**SEu(n,2n)\(^{16}Er, 14 MeV, and statistical model 0–39077

**SEu(n,2n)\(^{15}Er, 1,1 MeV, and statistical model 0–39077

**SEu(n,2n)\(^{15}Er, 1,1 MeV, and statistical model 0–39077

**SEu(n,2n)\(^{15}Er, 1,1 MeV, and statistical model 0–39077

**SEu(n,2n)\(^{15}Er and effective neutron capture cross-section determ. 0–64094

**F(n,n) E=14.1 MeV, elastic and inelastic, angular distributions and cross sections 0–46219

*Pf(n,n) E=14.1 MeV, elastic and inelastic, angular distributions and cross sections 0-46219
 **Fe* cross section 0-39069
 *Fe, neutron elastic and inelastic scattering and gamma-ray-production cross sections from 1.0-7.6 MeV 0-55159
 *Fe capture, and energy level transitions in *TFe 0-73958
 *Fe(n,x) cross-section determ. for natural element using a technique base on the absolute determ. of helium 0-49634

S 1174 SUBJECT INDEX

Gd, elemental, total, elastic and inelastic scatt, cross-sections for $0.3\ to\ 1.5\ MeV\ n\ \ 0-49636$

Gd in Norton County meteorite, neutron capture effects 0-48590

155 Gd thermal neutron capture 0-67344

tiss Gd(n,p) resonance parameters, average capture cross sections up to 20 keV, s-wave strength functions 0-46225

the manufacture of 37342 where 37342 capture cross sections up to 20 keV, s-wave strength functions 0–46225 158Gd (n, α)155Sm, 14 MeV and statistical model 0–39077

157Gd(n, p) resonance parameters, average capture cross sections up to 20 keV, s-wave strength functions 0—46225
158Gd (n, α) 155Sm, 14 MeV and statistical model 0—39077
158Gd capture p-ray cross section, 25 keV 0—39076
159Gd capture p-ray cross section, 25 keV 0—39076
159Gd capture p-ray cross section, 25 keV 0—39076
159Gd (a=70, 72, 74 and 76), inelastic scatt., energy depend, of cross sections 0—52788
13Ge(n, 2n) 17mGe, prod. cross section, half-lives and energies of isomeric activities 0—55129
13Ge(n, p) 14Ge obs. 0—77561
15Ge(n, p) 14Ge obs. 0—77561
15Ge obs. 0—77562
15Ge obs.

CLI cross sections analysis 0-52633

CLi(n,n)°Li(3.56) integral cross sections, from threshold up to 7 MeV
0-39066

6Li(n,p) 6He(O' integral cross sections, from threshold up to 7 MeV 0-39066

**CLi(n,p)6He, study using impulse approx. 0–39067
CLi(n,p) and (p,n), impulse approx. and shell model calcs., 156 MeV 0–39068

7Li total neutron cross-section determ. 100-1500 keV 0-77559
7Li(n, d) He, ang. distrib., comparison with DWBA, cross section calc. 0-49627

2Li total neutron cross-section determ. 100-1500 keV 0—77559
2Li(n, d)+He, ang. distrib., comparison with DWBA, cross section calc.
0—49627
2Li(n, p)+He, ang. distrib., comparison with DWBA calc.
0—49627
2Li(n, p)*SLi, cross section using single particle model for *Li ground state 0—46209
1*SLu(n, p)*ELi, cross section using single particle model for *Li ground state 0—46209
1*SLu(n, p)*ELi mechanism for radiative capture of resonant energy neutrons 0—70623
1*Lu reaction rates in Pu-recycle fuel lattices. 0—74059
2*Mge, elastic and inelastic scatt. E_n=14.2MeV, diff. cross sections 0—73956
2*Mg(n, p)*2*Mg thermal neutron capture cross-sections 0—60815
2*Mg(n, p)*2*Mg thermal neutron capture γ-rays meas. 0—60815
2*Mg(n, p)*3*Mg thermal neutron capture γ-rays meas. 0—60815
3*Mn(n, p)*6*Mn spectra and resonance activation integral, measurement relative to that of *19*Au by absolute counting 0—60816
3*Mn (apulare γ-ray cross section. 25 keV 0—39076
3*Mn(n, p)*6*Mn and spins in *6*Mn from γ-ray angular distribution 0—64041
3*Mn(n, p)*6*Mn and spins in *6*Mn from γ-ray angular distribution 0—64041
3*Mn(n, p)*6*Mn and spins in *6*Mn from γ-ray angular distribution 0—64041
3*Mn(n, p)*6*Mn and capture and energy levels in *6*M0 0—64029
3*Mo, thermal neutron capture and energy levels in *6*M0 0—64029
3*Mo, thermal neutron reactor, rel. of Production 0—49632
1*N(n, T)*C in fission reactor, rel. to T production 0—49632
1*N(n, x), differential cross sections for the production of discrete-energy gamma rays, E_m=8.5-11 MeV 0—64123
Na thermal neutron capture cross-section meas. 0—77489
2*No, inclassic scatt. bos. rel. to levels 0—39055
Nd isotopes, E_m=14 MeV, activation cross sections 0—55161
3*No, (n, 2n), isomeric ratio analysis. E_m=14.2 0—39075

Nuclear reactions and scattering due to continued

neutrons continued

the scheme of 144 Nd, thermal neutron capture, conversion electron spectra, level scheme of 144 Nd 1444 Nd 144 Nd 144 Nd 144 Nd 144 Nd 144 Nd

¹⁸Nd capture γ ray cross section, 25 keV 0–39076 ¹⁵Nd capture γ ray cross section, 25 keV 0–39076 Nd(n, α) (A=143, 145), cross sections 0–42855 ²⁰Ne(n, α), angular distribs, and spectra, 14.1 MeV 0–39081

⁵⁸Ni (ep.) s⁵⁸Co, E_n=14.8 MeV, parent analogues of collective states 58Ni(n,p)58Co. E_m=14.8 MeV, parent analogues of collective states 0–55160
5°Ni* cross section and struct. effects 0–39069
6°Ni(n,p), for 6°Ni excited states study 0–46139
6°Ni(n,p), 6°2Ni and 6°Ni energy levels 0–64023
Ni(n,α) cross-section determ. for natural element using a technique based on the absolute determ. of helium 0–49634
(ap)(n,p) simultaneous reactions, extension of NEAREX programme for nuclear cross-sections 0–57984
16°O, d₂, neutron resonance scatt. 0–64110
16°O(p,n))¹⁵O reaction with 31 MeV bremsstrahlung 0–45969
16°O(n,α) angular distribs. and spectra, 14.1 MeV 0–39081
16°O(n,α) NeV 0–64124
16°O(n,α) neutron scores section between 14 and 19 MeV 0–49622
16°O(n,α) at 5 to 13 keV, differential cross section at narrow levels in 17O 0–57990
16°O(n,α) b, gamma-ray spectra for incident-mean-neutron energies

 $^{10-3/990}$ (Geometric for incident-mean-neutron energies E_n =6.7-11.0 MeV 0-64124 12 O(n,p)¹³N, cross-section for the delayed-neutron yield at 14.1 MeV 0-57991

0–57991
31P. inelastic scatt. of 14 MeV neutrons, excitation of states between 3 and 6 MeV 0–67437
Pb, total cross section at average momenta of 3.8 GeV/c 0–46230
20°9b scattering. RPA and TDA calc., effect of continuum 0–73951
31°Pr, inelastic scatt., γ-rays and nuclear levels, 2.9 MeV 0–38888
31°Pr, inelastic scatt., γ-rays and nuclear levels, 2.9 MeV 0–38888
31°Pr, reson, perage spectra determination and α part, angular distributions for En=15.1 MeV 0–57995
Pt, reson, parameters and spin obs., E =4-830 eV 0–39073
32°Pu, effective capture-to-fission ratio, low flux meas. in fast reactor 0–58056

²³⁹Pu, neutron cross-sections in the unresolved resonance region 0–64121

Language of the control of the control

30 keV 0–64143

240 Pu, neutron cross sections in the unresolved resonance region 0–64121

240 Pu fission and capture cross sections 0–39209

242 Pu total neutron cross section from 0.0015-8000 eV 0–52791

242 Pu(n,2n)²⁴¹ Pu, search for ~0.3 yr spontaneous fission isomer 0–77510

245 Pu(n,2n)²⁴² Pu, search for ~0.3 yr spontaneous fission isomer 0–77510

Rb, activation cross-sections, (n,p), (n,te) and (n,2n) at 14.8 MeV 0–42854

878 Poln, p)⁸⁶ mRb, reaction cross sections between 0.16 MeV and 1.5 MeV 0–73966

87Rb(n,p)⁸⁸ Rb, reaction cross sections between 0.16 MeV and 1.5 MeV 0–73966

87Rb(n,p)⁸⁸ Rb, reaction cross sections between 0.16 MeV and 1.5 MeV 0–73966

103 Rh(n,2n)^{102 m(te)} Rh, excitation functions 0–67471

0-1/3900

10³Rh(n,2)n^{102m(t)}Rh, excitation functions 0-67471

10³Rh(n,2)neutron resonance capture, γ-ray spectra, using mag. Compton γ- spectrometer 0-73955

3¹S, inclastic scatt. of 14 MeV neutrons, excitation of states between 3 and 6 MeV 0-67437

12¹Sh(n,p)¹²⁴Sb thermal and neutron resonance capture 0-77563

13²Sh(n,p)¹²⁴Sb thermal and neutron resonance capture 0-77563

13²Sh(n,p)¹²⁴Sb thermal and neutron resonance capture 0-77563

4³Sc, thermal neutron capture, and low lying states in 4⁶Sc 0-67540

4³Sc(n,p), for study of low-lying odd parity states in 4⁶Sc 0-67840

4³Sc(n,p)¹⁵Se, thermal n, γ ray spectrum 0-52789

8³Se(n,p)¹⁸Se, thermal n, γ ray spectrum 0-52789

8³Sc(n,p)¹⁸Se, the of isomeric cross sections calculation 0-70621

8³Sc(n,n)²Ge 14.7 MeV, half life of product and decay characteristics 0-49570

8³Se(n,p)²⁸As 14.7 MeV, half life of product and decay characteristics 0-49570

Si, elastic scatt. cross section fluctuations, 6.7-13.4 MeV 0-39052

3-Set(n,p)-48-70 (A-7) NeV, final file of product and decay characteristics 0-49570 (Si. elastic scatt. cross section fluctuations, 6.7-13.4 MeV 0-39052 (28), E_m=14.2 MeV, elastic and inelastic scatt., anal. 0-77556 (38) total cross-sections. For energies 3.3-5.2 MeV of neutrons 0-49633 (38) (n,p) deduced levels of 29Si, p transitions and Q values for thermal neutrons 0-42851 (39Si(n,p)) deduced levels of 31Si, p transitions and Q values for thermal neutrons 0-42851 (39Si(n,p)) deduced levels of 31Si, p transitions and Q values for thermal neutrons 0-42851 (31Si(n,p), cross section fluctuations, 6.7-13.4 MeV 0-39052 (31(n,p), cross section fluctuations, 6.7-13.4 MeV 0-39075 (31(n,p), 13(n,p)) (31(n,p), 13(n,p), 14(n,p), 1

 $Sm(n,\alpha)$ (A=147, 149), cross sections 0-42855

Sm(n, α) (A=147, 149), cross sections 0–42855 Sr. activation cross-sections, (n,p), (n, α) and (n,2n) at 14.8 MeV 0–42854 III-1317a, clastic scattering. fast, non spherical optical model 0–70616 III-1317a total cross-sections, for energies 3.3-5.2 MeV of neutrons 0–49633 III-1317a (n, α), energy spectra determination and α part, angular distribution for En=15.1 MeV 0–57995 III-1317a (n, α), neutron resonance capture, γ -ray spectra, using mag. Compton γ -spectrometer 0–73955 III-137b(n, γ) and levels of III-137b(n, γ) and levels of III-137b(n, γ) III-137b(n, γ) and levels of III-137b(n, γ) II

neutrons continued

235U;23PQ, ratios of capture and fission neutron cross-sections at 130-1400 keV 0-55162

235U, cross-sections in the unresolved resonance region 0-64121

235U, effective capture-to-fission ratio, low flux meas. in fast reactor 0-58056

²³⁵U, cross-sections in the unresolved resonance region 0-64121 ²³⁶U, fission, energy dependence of $\overline{\nu}_{\rho}$ below 2.0 MeV 0-70625 ²³⁷U, fission, energy dependence of $\overline{\nu}_{\rho}$ below 2.0 MeV 0-70625 ²³⁸U, fission, energy dependence of $\overline{\nu}_{\rho}$ below 2.0 MeV 0-70625 ²³⁸U, in resons. and σ_{ρ} anal. 0-52709 ²³⁸U, 1-52709 ²³⁸U, enutron cross-sections for range 1 keV to 15 MeV, anal. 0-57996 ²³⁸U, neutron cross-sections in the unresolved resonance region 0-64121 ²³⁸U in UO₂ lattice, neutron absorption resonance, crystal-binding effects on Doppler broadening 0-49624 ²³⁸U total cross-sections, for energies 3.3-5.2 MeV of neutrons 0-49633 ²³⁸U(n, n'p) ²³⁹U thermal neutron residiative capture cross-section 0-52790 ²³⁸U(n, n'p) ²³⁰U thermal neutron residiative capture cross-section 0-52790 ²³⁸U(n, n'p) and levels of ²³⁸U 0-64076 V, inelastic and elastic scatt., $E_e=15-8.1$ MeV 0-49623 V total cross-section, high resolution 0-73953 Xe(n, 2n) activation cross sections, thermal, 21 keV and 14 MeV 0-39071 Xe(n, 2n) activation cross sections, thermal, 21 keV and 14 MeV 0-39071 Xe(n, 2n) activation cross sections, thermal, 21 keV and 14 MeV 0-39071 Xe(n, 2n) activation cross sections, thermal, 21 keV and 14 MeV 0-39071 Xe(n, 2n) activation cross sections, thermal, 21 keV and 14 MeV 0-39071 Xe(n, 2n) activation cross sections, thermal, 21 keV and 14 MeV 0-39071 Ne(n, 2n) activation cross sections, thermal, 21 keV and 14 MeV 0-39071 Ne(n, 2n) activation cross sections, thermal, 21 keV and 14 MeV 0-39071 Ne(n, 2n) activation cross sections, thermal, 21 keV and 14 MeV 0-39071 Ne(n, 2n) activation cross sections, thermal, 21 keV and 14 MeV 0-39071 Ne(n,

0-73966

168 b reaction rates in Pu-recycle fuel lattices 0-74059

168 b thermal neutron capture 0-67344

179 b, thermal neutron capture and regularities in gamma ray spectra 174 b, thermal neutron capture and regularities in gamma ray spectra 0-64126 171 Yb(n,p) 172 Yb, excited K*=0+ bands, study 0-77503 172 Yb, thermal neutron capture and regularities in gamma ray spectra

0-64126

174 Yb, thermal neutron capture and regularities in gamma ray spectra
0 64126

 64 Zn(n, γ) 65 Zn, and 66 Zn, 67 Zn, 68 Zn, γ -spectra obs. transitions studied 0–46724 70 Zn(n,2n), E_n=14.7±0.15 MeV, isomeric ratio determ.

"Zn, activation resonance integral 0-73961

"Zr, activation cross-sections (n,p), (n,a) and (n,2n) at 14.8 MeV 0-42854

Zr, natural and stable isotopes, reson. cross sections 0-42843

"Zr, activation resonance integral 0-73961

"Zr, activation resonance integral, and anomalous integral to thermal activation cross-section ratio 0-73961

nuclei of Z>2

uclei of Z>2 see also Ions/scattering ²⁰Ne(7 Li,t) 24 Mg, search for α -particle structure in 24 Mg 0-46252

0-46232 Coulomb distortion 0-70669 Coulomb stripping of heavy ions, Coulomb excitation of core relative importance 0-39130 DWBA analysis of direct reactions between complex nuclei 0-39132

de-excitation in heavy ion induced reactions, ang. momentum effects 0-39133

elastic and inelastic scattering, grazing collisions at high energy, review 0-73977

heavy ion, conference, La Plagne, March 1969 0-42875

heavy ion, conterence, La Plagne, March 1969 0—42875 heavy ion physics, discussion of some new phenomena 0—77580 heavy ion reactions, review 0—70670 heavy ion scatt., semi-classical Coulomb plus nuclear theory 0—42874 heavy ion-heavy ion scatt, stat, theory applic. 0—39135 heavy ions, products selection using internal symmetry props. 0—39131 heavy-ion collision, fast and slow, potentials within 2 centre shell model 0—77582

heavy-ion scattering, new theoretical approach 0–77581 interaction induced by the exchange of nucleons between the two identical nuclear cores 0–58024
Josephson effect in 2–nucleon transfer in heavy ion scatt. 0–64136
nuclear short-range correls, effects 0–39024
nucleon transfer mechanisms 0–42873
optical-model analysis of elastic scattering of complex nuclei at low energies 0–39134

gies 0-39131 scattering, inclusion of nuclear structure calculations 0-39131 scattering, inclusion of nuclear structure calculations 0-52756 scattering, nuclear density distrib. 0-77583 transfer of α particles, theor. interpret. problems 0-39138 transfer reactions above Coulomb barrier 0-39136 transfer reactions at energies above Coulomb barrier 0-39136

transfer reactions at energies above Coulomb barrier 0–39137 10 O, quasimolecular structure and quasibound molecular states for elastic 16 O- 16 O scattering 0–58027 10 Ag (16 O, 16 Oy) E=45.5 MeV. Coulomb excitation 0–64031 10 Ag (16 O, 16 Oy) E=45.5 MeV. Coulomb excitation 0–64031 27 Al(12 Li, α) 10 Si, search for triton grouping in 30 Si 0–49673 α sub-barrier emission obs. 0–60830 10 Be(11 Li, α), 10 Ag, α -part. continuum spectrum, reson. obs., E=5-10 MeV 0–55170 118 (12 C, 12 D), 13 Ma, radiative capture 0–39145 118 (18 N, 10 O), 12 C, ang. distribs. 0–39143 11 B(14 N, 10 O), 12 C, ang. distribs. 0–39143 118 B(14 N, 10 O), 13 Mc ever range 27-44 MeV, angular distributions average projected ranges, and cross sections 0–73999 98 ee(9 Li, 6 He) 9 Q quasielastic scattering process, experimental results 0–46247

0-46247

*Bet(*Li,p)*4*C, p angular distribs., obs. and statistical cpd. nucleus model 0-39142*

*Bet(*Li,a)*1*2*B triton transfer and excitation of triton states 0-46249

*Bet(*Li,a)*1*2* absolute cross section and angular distrib., obs. 0-39141

*Bet(*Li,b)*5* absolute cross section, angular distrib and *5*C levels, obs. 0-39141

*Bet(*Li,b)*1*C absolute cross section and angular distrib., obs. 0-39141

*Bet(*Li,b)*1*C absolute cross section and angular distrib., obs. 0-39141

*Bet(*Li,b)*1*C absolute cross section and angular distrib., obs. 0-39141

*Bet(*Li,b)*1*C absolute cross section and angular distrib., obs. 0-39141

*Bet(*Li,b)*1*C absolute cross section and angular distrib., obs. 0-39141

10-4958 | 0-4958 | 0-4958 | 0-39146 | 0-2058 | 0-39146 | 0-39146 | 0-39146 | 0-39146 | 0-39146 | 0-39146 | 0-39146 | 0-39146 | 0-39146 | 0-39146 | 0-39146 | 0-39146 | 0-39146 | 0-39146 | 0-39146 | 0-39146 | 0-39146 | 0-39146 | 0-39146 | 0-39146 | 0-39146 | 0-39146 | 0-39146 | 0-39146 | 0-39146 | 0-39146 | 0-39146 | 0-39146 | 0-39146 | 0-39146 | 0-39146 | 0-39146 | 0-39146 | 0-39146 | 0-39146 | 0-39146 | 0-39146 | 0-39146 | 0-39146 | 0-39146 | 0-39146 | 0-39146 | 0-39146 | 0-39146 | 0-39146 | 0-39146 | 0-39146 | 0-39146 | 0-39146 | 0-39146 | 0-39146 | 0-39146 | 0-39146 | 0-39146 | 0-39146 | 0-39146 | 0-39146 | 0-39146 | 0-39146 | 0-39146 | 0-39146 | 0-39146 | 0-39146 | 0-39146 | 0-39146 | 0-39146 | 0-39146 | 0-39146 | 0-39146 | 0-39146 | 0-39146 | 0-39146 | 0-39146 | 0-39146 | 0-39146 | 0-39146 | 0-39146 | 0-39146 | 0-39146 | 0-39146 | 0-39146 | 0-39146 | 0-39146 | 0-39146 | 0-39146 | 0-39146 | 0-39146 | 0-39146 | 0-39146 | 0-39146 | 0-39146 | 0-39146 | 0-39146 | 0-39146 | 0-39146 | 0-39146 | 0-39146 | 0-39146 | 0-39146 | 0-39146 | 0-39146 | 0-39146 | 0-39146 | 0-39146 | 0-39146 | 0-39146 | 0-39146 | 0-39146 | 0-39146 | 0-39146 | 0-39146 | 0-39146 | 0-39146 | 0-39146 | 0-39146 | 0-39146 | 0-39146 | 0-39146 | 0-39146 | 0-39146 | 0-39146 | 0-39146 | 0-39146 | 0-39146 | 0-39146 | 0-39146 | 0-39146 | 0-39146 | 0-39146 | 0-39146 | 0-39146 | 0-39146 | 0-39146 | 0-39146 | 0-39146 | 0-39146 | 0-39146 | 0-39146 | 0-39146 | 0-39146 | 0-39146 | 0-39146 | 0-39146 | 0-39146 | 0-39146 | 0-39146 | 0-39146 | 0-39146 | 0-39146 | 0-39146 | 0-39146 | 0-39146 | 0-39146 | 0-39146 | 0-39146 | 0-39146 | 0-39146 | 0-39146 | 0-39146 | 0-39146 | 0-39146 | 0-39146 | 0-39146 | 0-39146 | 0-39146 | 0-39146 | 0-39146 | 0-39146 | 0-39146 | 0-39146 | 0-39146 | 0-39146 | 0-39146 | 0-39146 | 0-39146 | 0-39146 | 0-39146 | 0-39146 | 0-39146 | 0-39146 | 0-39146 | 0-39146 | 0-39146 | 0-39146 | 0-39146 | 0-39146 | 0-39146 | 0-39146 | 0-39146 | 0-39146 | 0-39146 | 0-39146 | 0-39146 | 0-39146 | 0-39146 | 0-39146 | 0-39146 | 0-39146 | 0-39146 | 0-39146

Nuclear reactions and scattering due to continued nuclei of Z>2 continued

¹²C(¹⁶O₃v)²⁸Si, radiative capture 0-39145

 $^{12}\text{C}(^{6}\text{Li}\alpha)^{14}\text{N}$ at 5.6 to 6.6, 9.0 to 14 MeV, states at different energies 0-8025

 $^{12}\text{C}(^6\text{Li}.\alpha)^{16}\text{O}$ at 5.6 to 6.6. 9.0 to 14 MeV, states at different energies 0-58025

0-38025 1²C(⁶Li,d)¹⁶O, 25-30 MeV, 2 particle transfer 0-46250 1²C(⁶Li,p)¹O at 5.6 to 6.6, 9.0 to 14 MeV, states at different energies 0-58025

0-58025

12C(*Li,t)\(^{15}\)O at 5.6 to 6.6, 9.0 to 14 MeV, states at different energies 0-58025

12C('Li, \(^{2}\))\(^{15}\)N, peaks in the zero degree yield curve, interpretation α)¹⁵N, peaks in the zero degree yield curve, interpretation

0-46248

13C(6Li,6He)13N quasielastic scattering process, experimental results 0-46247

O-4624¹⁷O, E=25.6 MeV, excited states 4p-3h 0-60831 ¹³C(*ELi,d)¹⁷O, 17 MeV, levels discussed within framework of weak-coupling model 0-73787 ¹³C(*ELi,d)¹⁹O and energy levels in ¹⁶O 0-73786 ¹³C(*ELi,d)¹⁹O, E=30.1 MeV, excited states 4p-3h 0-60831 ¹³C(*ELi,d)¹⁹O, 18 MeV, levels discussed within framework of weak-coupling model 0-73787 ¹⁴C(*ELi,d)¹⁹O, 20.4 MeV states in ¹⁸O studied 0-64003 ¹⁴C(*C(*14c))¹⁹OC(*15C) obs. 0-73994 ¹⁴C(*C(*15C))¹⁹Mn obs. 0-73994 ¹⁶C(*15C) obs. 0-73994 ¹⁶

40Ca(6Ld)44Ti 40Ca(7Li,t)44Ti, search for α-particle structure of 44Ti 0-46252
 23°Cf bombardment with 15N ions and creation of new element of atomic number 105, 26°Ha 0-52710
 163 Dy(16O, 16O,>p)163 Dy 36-52 MeV, Coulomb excitation of vibrational and rotational states 0-38932
 168 Er Coulomb excitation probabilities for 2+ and 4+ levels, bombarded with 35°Cl ions 0-70504
 167 Er(16O, 16O, p)167 Er 36-52 MeV Coulomb excitation of rotational and vibrational states 0-38932
 175 Gd(16O, 6O, p) 160 d 36-52 MeV, Coulomb excitation of vibrational rotational states 0-38932
 176 Ce Coulomb excitation of 01* states with 35°Cl ions 0-67460

183 Gd (160, 160', p. 183 Gd 36-52 MeV. Coulomb excitation of vibrational rotational states 0—38932

180 Ge, Coulomb excitation of 0+ state with 35 Clions 0—67460
(34,p), at low energy, polarization effects 0—73981

314 (34) Hely2n, E₂₈=11 MeV, nn effective range parameters 0—55112

314 (34) Hely2n, E₂₈=11 MeV, nn effective range parameters 0—55112

314 (34) Hyly2n, E₂₈=11 MeV, nn effective range parameters 0—55112

314 (34) Hyly2n, E₂₈=11 MeV, nn effective range parameters 0—55112

315 (34) Hyly2n, E₂₈=11 MeV, nn effective range parameters 0—55112

316 (34) Hyly2n, E₂₈=11 MeV, nn effective range parameters 0—55112

317 (41,41) Hyly2n, E₂₈=11 MeV, nn effective range parameters 0—55112

318 (51,41) Hyly2n, effective range parameters 0—5112

319 (41,41) Hyly2n, effective range parameters 0—5112

319 (41,41) Hyly2n, effective range parameters 0—5112

310 (41,41) Hyly2n, effective range parameters 0—5112

311 (41,41) Hyly2n, effective range parameters 0—5112

312 (41,41) Hyly2n, effective parameters effective range parameters 0—5112

313 (41,41) Hyly2n, effective parameters 0—5112

314 (41,41) Hyly2n, effective parameters 0—5112

315 (41,41) Hyly2n, effective parameters 0—5112

316 (41,41) Hyly2n, effective parameters 0—5112

317 (41,41) Hyly2n, effective parameters 0—5112

317 (41,41) Hyly2n, effective parameters 0—5112

318 (41,41) Hyly2n, effective

²⁴Mg(¹Li,α)²³Al, search for triton grouping in ²⁷Al 0–49673 (¹⁴N,Ag) transfer reactions 0–39146 (¹⁴N, ¹⁴N) elastic scattering, excitation functions 0–70671 (¹⁸N(¹⁶O))¹⁴N, gross struct, of excitation functions, optical model anal.

0. 67557 ¹⁵N(¹⁶O)¹⁵N, gross struct, of excitation functions, optical model anal.

¹⁵N₁(¹⁶O₁¹⁶O₁¹⁸N, gross struct. of excitation functions, optical model anal. 0-67557

¹⁶O (¹⁶O₁, pot. scatterer calc. 0-39135

¹⁶O (¹⁶O₁) (¹⁶O₂) elastic scattering: excitation functions 0-70671

¹⁶O₁(¹⁶O₂) (¹⁸S₂, radiative capture 0-39145

¹⁶O₁(¹⁶Li₂, ¹⁸S₂, comparison with (α,d) reaction 0-46251

¹⁶O₁(¹⁶Li₂, ¹⁸O₂Ne, 25-30 MeV levels of ²⁰Ne obs. 0-49672

¹⁶O(¹Cli₂, ²⁰PF, triton band obs. in ground-state based rotational band of ¹⁹F 0-(¹⁶O₁, ¹⁶O₂), ¹⁸O₂, ¹⁸S₂O₃ (¹⁸O₂), ¹⁸O₃O₃ gross struct. of excitation functions, optical model anal. 0-6753

(18Q) (18Q) (18Q) (18Q) gross struct. of excitation functions, optical model anal. 0-67557
(18Q) (18Q) excitation function between 7.5-27.5 MeV c.m. comparison with data from (19Q-16) oscattering 0-64138 (18Q) (15,12) Ne and rotational bands in 22Ne 0-70430 (19Q) (19Q)

288 pt. heavy-ion feactions, production of Thi isotopes of mass 22.1 a. 0. 49581.
 208 pt.(£Li), breakup of ⁶Li 0–67556
 10⁴Pd Coulomb excitation by ⁴He and ¹⁶O ions, and quadrupole moment 0–70481
 10⁶Pd Coulomb excitation by ⁴He and ¹⁶O ions, and quadrupole moment 0–70481
 285i(£Li,d)³PS, ²⁸Si(7Li,t)³²S, search for α-particle structure in ²⁴Mg ³²S 0–46252
 285i(*Li,α)³P, search for triton grouping in ³¹P 0–49673
 188Sm(²⁰Ne,²⁹Ne'y), static quadrupole moments of the first excited states of ²⁰Ne using reorientation effect 0–60757
 184Sm(²²Ne,²²Ne'y), static quadrupole moments of the first excited states of ²¹Ne using reorientation effect 0–60757
 10²Sn(²⁰Ne,²⁰Ne'y), static quadrupole moments of the first excited states of ²⁰Ne using reorientation effect 0–60757
 12⁸Sn(²¹Ne,²⁰Ne'y), static quadrupole moments of the first excited states of ²⁰Ne using reorientation effect 0–60757
 12⁸Sn(²¹Ne,²²Ne'y), static quadrupole moments of the first excited states of ²⁰Ne using reorientation effect 0–60757

S 1176 SUBJECT INDEX

luclear reactions and scattering due to continued
nuclei of Z>2 continued

10°Sn(4°Ar,4n)1°5Er and g-factor of 15°Er 0—70673
12°Sn(4°Ar,4n)1°5Er and g-factor of 15°Er 0—70673
12°Tc(4°N,1°A')r), Coulomb excitation, deduced levels of 123Te for E=44, 48
MeV 0—42763
12°Tc(4°N,1°A')r), Coulomb excitation, deduced levels of 123Te for E=44, 48
MeV 0—42763
12°Tc(4°N,1°A')r), Coulomb excitation, deduced levels of 123Te for E=44, 48
MeV 0—42763
12°Tc(4°N,1°A')r), Sim isomeric state, three quasiparticle 0—38925
12°Tc(2°Ne,7n), 143Sm isomeric state, three quasiparticle 0—38925
12°Tc(2°Ne,2°Ne'p), static quadrupole moments of the first excited states of 2°Ne using reorientation effect 0—60757
12°Tc(2°Ne,2°Ne'p), static quadrupole moments of the first excited states of 2°Ne using reorientation effect 0—60757
12°Tc(2°Ne,7n), 14°Sm isomeric state, three quasiparticle 0—38925
11°Tc(2°Ne,7n), 14°Sm isomeric state, 11°Tc(2°Ne,7n), 14°Sm isomeric state, 11°Tc(2°Ne,7n), 14°Sm isomeric state, 11°Tc(2°Ne,7n), 14°Sm isomeric state, 11°Tc(2°Ne,7n)

U interaction with heavy ions, effect of nuclear deformability on cross section 0-70672

nucleons

angular momentum technique, study of scattering, differential cross-sections 0–77542 continuum contribution to spectroscopic sum rules 0–70575 clastic scatt., complex ang. momentum methods obs. 0–39027 forward clastic scatt., by dispersion relations 0–49603 knockout-exchange mechanism effect in nucleon-nucleus scattering 0–49602

optical potential, high energy, and nuclear correlations 0optical potential, high energy, and nuclear correlations 0–52757 potentials from N-N scattering using Marchenko theory 0–73918 RPA treatment, renormalized, single particle resonances 0–70576 radiative capture, effective charge factor 0–77543 relativistic elastic unitarity, effect on low-energy nucleon-nucleon scattering 0–67369 scattering, quasi free, theory and obs. review 0–39026 scattering, soluble model, study using K-matrix theory of nuclear reactions 0–39002

coattering matrix, struct., in random phase approximation 0–39025 scattering matrix in random phase approximation 0–73917 single nucleon transfer reactions, review 0–73921 single-particle resonances in unified theory of nuclear reactions 0–64110 transfer, single N, multipole sum rules rel. to nuclear spectroscopy 0–39028

two-nucleon transfer reactions, review 0-73922

two-nucleon transfer reactions, inelastic processes, review 0–73920 two-nucleon transfer theory extension to include inelastic processes 0 - 73919

0 -73919 unbound levels spectroscopy from unified reaction theory using quasiparticles 0-70336 ¹⁹⁷Au(p.spall)¹⁴⁹Tb nucleon currents meas., for energies exceeding 600 MeV 0-70577 ¹³C(N.N)¹³C, inelastic scatt., E<9MeV, cross sections for 4.43 MeV p-ray production 0-42820 ¹⁴⁴Dy(⁴⁰Ar,xn)Po, cross-sections for the production of Po nuclides with mass numbers 194 to 200 for ion energies 160 to 280 MeV 0-42876 ¹⁴⁴Dy(⁴⁰Ar,xn)Po, cross-sections for the production of Po nuclides with mass numbers 194 to 200 for ion energies 160 to 280 MeV 0-42876 ¹⁴⁴Dy(¹⁰Ar,xn)Po, cross-sections for the production of Po nuclides with mass numbers 194 to 200 for ion energies 160 to 280 MeV 0-42876 ¹⁴⁴Dy(⁴⁰Ar,xn)Po, cross-sections for the production of Po nuclides with mass numbers 194 to 200 for ion energies 160 to 280 MeV 0-42876 ¹⁴⁴Dy(⁴⁰Ar,xn)Po, cross-sections for the production of Po nuclides with mass numbers 194 to 200 for ion energies 160 to 280 MeV 0-42876 ¹⁴⁴Dy(⁴⁰Ar,xn)Po, cross-sections for the production of Po nuclides with mass numbers 194 to 200 for ion energies 160 to 280 MeV 0-42876 ¹⁴⁴Dy(⁴⁰Ar,xn)Po, cross-sections for the production of Po nuclides with mass numbers 194 to 200 for ion energies 160 to 280 MeV 0-42876 ¹⁴⁴Dy(⁴⁰Ar,xn)Po, cross-sections for the production of Po nuclides with mass numbers 194 to 200 for ion energies 160 to 280 MeV 0-42876 ¹⁴⁴Dy(⁴⁰Ar,xn)Po, cross-sections for the production of Po nuclides with mass numbers 194 to 200 for ion energies 160 to 280 MeV 0-42876 ¹⁴⁴Dy(⁴⁰Ar,xn)Po, cross-sections for the production of Po nuclides with mass numbers 194 to 200 for ion energies 160 to 280 MeV 0-42876 ¹⁴⁴Dy(⁴⁰Ar,xn)Po, cross-sections for the production of Po nuclides with mass numbers 194 to 200 for ion energies 160 to 280 MeV 0-42876 ¹⁴⁴Dy(⁴⁰Ar,xn)Po, cross-sections for the production of Po nuclides with mass numbers 194 to 200 for ion energies 160 to 280 MeV 0-42876 ¹⁴⁴Dy(⁴⁰Ar,xn)Po, cross-sections for the production of Po nuclides with mass numbers

apparatus with diffusion chamber and accelerator for studying photonu-clear reactions 0-49407 bibliography 0-77535 buildup factors in water for gamma rays of 1 MeV and lower energy

dipole oscillator strengths for light elements, between 10 and 80 MeV 0 42812

0 42812
double-closed shell nuclei, production of charged pions 0–55154
elastic scattering of 1.12 and 1.33 MeV γ's through 90° and 124.5°,
deduced Delbruck amplitudes 0–55247
electron-position photoproduction, polarization effects, allowing for e.m.
multipole moments 0–70208
exchange currents determination by comparison of photon and electron
disintegration of nuclei 0–70567
fission product γ reaction with D-O, photo-n counting as meas, of fuel burn
up 0–46301
medium spherical puclei for study of giant resonance, 0–46104

up $0-46301^{\circ}$ medium, spherical nuclei, for study of giant resonance 0-46194 multiple scatt. of Compton photons, depend, on cylindrical scatterer size 0-42811 N ≈ 20 , photoneutron cross sections, giant dipole gross struct. 0-67513 neutral vector meson photoprod, on nuclei 2 H, 3 H and 3 He, by Regge pole and quark model 0-52533 neutron coincident detector distinguishing between (α,n) , (p,n) and fission products 0-77424 photoabsoration, by avarlancing

photoabsorption by overlapping resons, system, excitation and decay photoabsorption cross-section, nonlocal forces and dipole sum rules

0–46 100 photoalpha angular distributions using solid state detectors 0–46027

photodisintegration cross sections determ, independent of detector efficiency and photon spectrum 0–38724 photonuclear cross sections meas, using new photon spectrometer 0–39011

photonuclear disintegration, A≥12, calc., 40 350 MeV 0-49592 Regge trajectories in nuclear photoproduction 0-39010 scattering, excitation of bound nuclear levels, partial radiation widths 0-73894

sum rules, appl. of rel. between hard-core and vel. dependent potentials 0-55113

V-33113

X- and γ-ray elastic scatt, and Compton effect review 0–39009 yield function analysis, cross-sections 0–60799 (γ, p) for ¹⁹⁷La, ¹⁴⁰Ce, ¹⁴¹Pr, ¹⁴³m isobaric analogue states 0–67480 (γ, p) for ⁸⁵⁷ s⁸⁷ γ, ⁸⁰Zr, ⁹⁷Mo isobaric analogue states 0–67465 (γ, pn), microscopic description 0–52746

Nuclear reactions and scattering due to continued

photons continued

 (v,π) , nucl. distortion effects of emitted π 0-39012 v,v' activation analysis and dosimetry 0-73895

ω meson photoproduction from complex nuclei at 6.8 GeV obs. 0-45950

a meson photoproduction from complex nuclei at 6.8 GeV obs. 0–45950 ²⁴²Pu(p,n)→²⁴¹Pu spontaneously fissioning isomer 0–52752 ρ o photoprod. in complex nuclei, anal. by eikonal method 0–42573 ¹⁰⁷Ag(p,2n), photoneutron cross-sections 0–67516 ¹⁰⁸Ag(p,2n), photoneutron cross-sections 0–67516 ¹⁰⁸Ag(p,2n), photoneutron cross-sections 0–67516 ¹⁰⁸Ag(p,n), cross-section o 0–55150 ¹⁰⁸Ag(p,n), cross-secti

¹¹B photodisintegration, explanation of failure to observe all of expected γ rays 0 –70569
Be, photoneutron production for 150 MeV electrons 0–55150
⁹Be(γ .n), with fission product γ , n counting rel. to meas, of irrad, fuel burn up 0–46301
²⁰⁹Bi(γ .μ), E=7637 keV, ²⁰⁹Bi deduced levels 0–39015
C, φ photoprod., 1800 MeV 0–42570
C target, photonuclear absorpt, cross section meas, using new photon spectrometer 0–39011
¹²C(γ .ρ), proton polarization at 650-840 MeV photon energies 0–46190
⁴⁰Ca(γ . n₀) ³⁰Ca differential cross sections, structure at excitation energies corresponding to giant dipole resonance regions 0–49594
¹¹²Cd(γ .γ), E=7632 keV, ¹¹²Cd deduced levels 0–39015
¹²Co(γ .xn) cross-section fine structure 0–77536
¹⁴H, 1.0-6.4 GeV, hadron prod., total cross section 0–73482
¹⁴H, 1.0-6.4 GeV, hadron prod. total cross section 0–73482
¹⁴H, 1.0-6.4 GeV, hadron prod. total cross section 0–73482
¹⁴H, 1.0-6.4 GeV, hadron prod. total cross section 0–73482
¹⁴H, 1.0-6.4 GeV, hadron prod. total cross section 0–73482
¹⁴H, 1.0-6.4 GeV, hadron prod. total cross section 0–73482
¹⁴H, 1.0-6.4 GeV, hadron prod. total cross section 0–73482
¹⁴H, 1.0-6.1 GeV, hadron prod. total cross section 0–7389
¹⁴He(γ .μ)H, ang, distrib, E=16-27 MeV 0–67514
¹⁴He, photodisintegration diff. and total cross section 0–73898
¹⁴He(γ .μ)He, photoneutron cross section from threshold to 31 MeV 0–73897
¹⁴He(γ .μ)He, photoneutron cross section from threshold to 31 MeV 0–73897
¹⁵He(γ .μ)He, photoneutron cross section from threshold to 31 MeV 0–73891

*He(y,n)*He, photoneutron cross section from threshold to 31 MeV 0-73897

*He(y,p)*H. 120 MeV, reaction analysis, total cross section 0–67515

*He(y,p)*H. integrated cross section decomposed into E₁ and E₂ contribs. up to Eye-30 MeV 0–49613

*Is*Ho(y,n)* and (y,2n) cross-sections, 10 to 20 MeV. 0–39016

*Is*In(y,p)*Ils*Im, resonance absorption of gamma rays and gamma flux mapping. 0–64105

*Is*Lo, Liph*Sm*K cross-section, and giant resonance structure. 0–73903

*Is*Lo, Liph*Sm*K cross-section, and giant resonance structure gamma rays and deduced levels. 0–57923

*Li, TLi photonuclear cross-section for disintegration obtained. 0–64108

*Li photodisintegration by 12 MeV Bremsstrahlung. 0–49593

*Li photodisintegration by 12 MeV Bremsstrahlung. 0–49593

*Li photodisintegration at 650-840 MeV photon energies. 0–46190

*In(y,p)*PHe. 620 and 1115 MeV, ang. distrib. of protons obs. 0–46191

*Li(p,p), proton polarization at 650-840 MeV photon energies. 0–46190

*In(y,p)*Is*C+(n)*Is*C, de excitation neutrons obs. 0–60800

*N(y,p)*Is*C and inverse reaction. (*C(p,p)*Is*N calc. 0–46193

*Is*N(y,p)*Is*C and inverse reaction. 4*C(p,p)*Is*N calc. 0–46193

*Is*N(y,p)*Is*C and inverse reaction. 4*C(p,p)*Is*N calc. 0–46193

*Is*N(y,p)*Is*C and inverse reaction. 4*O(x)*Dis*N(y,p)*Is*C and inverse reaction. 4*O(x)*Dis*N

Proposed to the protection of the proposed of

0-42813
²⁰⁸Pb. cross section for neutron prod. in region of giant dipole reson.
0-77537

0—42813
208Pb, cross section for neutron prod, in region of giant dipole reson.
0—77537
208Pb, photoneutron cross section and ang, distrib. meas. 0—77506
208Pb(p,p), photoexcitation of isobaric analogue resonances, E=24.9 MeV
0—57969
208Pb(pn)²⁰⁷Pb energy spectrum of ejected photoneutrons 0—46192
108Pd photoneutron and (p,p) cross-sections and vibrational and isospin splitting of giant dipole resonance 0—73818
14¹Pr(p,m)¹⁴Pr, cross-section meas. from threshold to 24 MeV 0—73906
14¹Pr(p,m)¹⁴Pr energy spectrum of ejected photoneutrons 0—46192
Pu, photon cross sections from 1-600 keV 0—55151
218(p,m)³IS differential cross sections, structure at excitation energies corresponding to giant dipole resonance regions 0—49594
218(p,m)³P, quanta spectra, cross sections of peaks 0—73902
218(p,py'), p quanta spectra, cross sections of peaks 0—73902
218(p,m)³PS differential cross sections of peaks 0—73902
218(p,m)³PS differential cross sections of peaks 0—73902
218(p,m)³PS differential cross sections, structure at excitation energies corresponding to giant resonance, photoabsorpt. 0—38882
218(p,m)³PS differential cross sections, structure at excitation energies corresponding to giant dipole resonance regions 0—49594
Sn. scattering cross section, 6-9 MeV, new method of analysis 0—73896
Sn isotopes, photodisintegration, anal. of expt. results by giant dipole resonance corresponding to giant dipole resonance regions 0—49594
Sn. photoneutron production for 150 MeV electrons 0—70570
Sn(p,p) for isobaric analogue states in Sn isotopes 0—70571
Ta, photoneutron production for 150 MeV electrons 0—55150
Ta, photoneutron production for 150 MeV electrons 0—55150
Ta, photoneutron production for 160 keV 0—55151
2017(p,n), cross section meas. 0—70624
2027(p,n), cross section meas. 0—70624
2037(p,n), cross section meas. 0—70624
2040(p,n), cross section meas. 0—70624
2057(p,n), cross section meas. 0—70624
2057(p,n), cross section meas. 0—70624
2057(p,n), cross section determ. in giant reson. region, expt. and theory 0—

Nuclear reactions and scattering due to continued photons continued

motions continued W, thick target, bombardment, bremsstrahlung and photoneutron production calculations 0-73913 $^{97}Y(y,n)$ and (y,2n) and giant dipole resonance quasibound analogue states 0-73816

(*Y(p,n)) and (p,2n) and grant dipole resonance quasibound analogue states 0—73816
 (*Zn(p,np)), rel. to isospin splitting of giant dipole resonance 0—73810
 Zr, scattering cross-section, 8.5-12.5 MeV, new method of analysis 0—73896
 (*P(p,n))*9*Zr and *9*IZr(p,n)*0*Zr, cross-sections meas. 0—49595
 (*PZr(p, p))*0*Zr(p,+) inelastic, R-matrix analysis through isobaric analog resonance 0—67537

protons

116Sn inelastic scattering effective cross-section, theory and experiment 0-70591

2087b(p,p). partial direct and collective cross-sections 0-49619

2087b(p,p). possible 3.0.3 MeV polarized proton obs., optical model analysis, 2 versions 0-70592

116Sn inelastic scatt. at 580 MeV 0-42824

116Sn inelastic scatt. at 580 MeV 0-42824

116Sn inelastic scatt. at 580 MeV 0-67393

116Sn inelastic scatt. at 580 MeV 0-67393

116Sn inelastic inelastic partial direction, Monte Carlo calc. 0-49604

116Sn inelastic inelastic partial direction, Monte Carlo calc. 0-49609

116Sn inelastic inelastic inelastic postat. for spectroscopic factors through isobaric analogue resonances 0-67399

116Sn inelastic inelastic partial form some struction 0-67532

116Sn inelastic inelastic scatt., analogue resonances study, spectroscopic factors extraction 0-67532

116Sn inelastic scatt., analogue resonances study, spectroscopic factors extraction 0-67532

116Sn inelastic scatt., analogue resonances study, spectroscopic factors extraction 0-67532

116Sn inelastic scatt., inelastic scatt., analogue resonances study, spectroscopic factors extraction 0-67532

116Sn inelastic scatt., inelastic scattering, optical model potential, real part 0-70579

116Sn inelastic scattering, optical model potential, real part 0-70579

116Sn inelastic scattering, real optical potential, real part 0-70579

116Sn inelastic scattering, optical model potential, real part 0-70579

116Sn inelastic scattering, real optical potential, real part 0-70579

116Sn inelastic scattering, optical model potential, real part 0-70579

116Sn inelastic scattering, optical model potential, real part 0-70579

116Sn inelastic scattering, optical model potential, real part 0-70579

elastic scattering, optical model potential, real part 0-70579 elastic scattering, real optical potential, $50\leqslant A \leqslant 70 - 70578$ energy spectra of internal conversion electrons for (p,2n) reactions E0 transitions from $0,1^+\to0,1^+$ states in the Z=82 region 0-52659 even-even nuclei between ⁴⁸Ti and ⁷⁶Ge inelastic scattering, cross-sections 0-70586

even-even nuclei between ⁴⁸Ti and ⁷⁶Ge inelastic scattering, cross-sections 0–70586 inelastic, excitation of one and two phonon like states in medium weight even nuclei 0–46187 inelastic scattc. 6 MeV, of excited levels of ²⁶Mg, ²⁹Si, ³²S, ⁵⁸Ni and ⁶⁰Ni, anal. 0–52652 inelastic scattering cross sections, calc. using computer program on basis of Hauser-Feshbach theory 0–46206 interaction cross sections, eval. by Clauber's theory 0–52765 isobaric analog reson. reactions, for nucl. struct. studies 0–38796 isobaric analog reson. reactions, for nucl. struct, studies 0–38796 isobaric analog reson. reactions, for nucl. struct, studies 0–38796 isobaric analog reson. reactions, for nucl. struct, studies 0–38796 isobaric analog reson neations, for nucl. struct, studies 0–38796 isobaric analog reson neations, for nucl. struct, studies 0–38796 isobaric analog resonance in N=82 nuclei, 2,1 mixing 0–64112 light fragment and p prod. E_{p=}=600 MeV 0–52766 light particle emission, E_{p=}=26 GeV 0–77549 optical potential in terms of nuclear symmetry parameter, isospin dependence 0–57874 peripheral particle generation at high energy, 70 GeV 0–52758 Pt at 3 GeV, inelastic neutron polarization 0–60813 scattering, elfective two body pot, for 2s-1d and 2p nuclei 0–42732 scattering, elfective two body pot, for 2s-1d and 2p nuclei 0–42732 scattering, high-energy, by multiple-diffraction theory 0–64114 scattering by complex nuclei, 16-22 MeV, optical model analysis 0–46205 single particle analog state anomalies in ¹⁹⁷Au, ¹⁹⁶Pt and ¹⁸⁴W 0–67489 spallation of C, nuclear emulsion obs. of secondary neutron spectrum per steradian 0–73924

Ta foil targets, and rotational levels in ¹⁷⁹Ta, ¹⁷⁹W, and ¹⁸⁰W 0–70508 (p. 2p), differential cross-section, effects of distortion, DWBA analysis 0–4521 (p. 2p), final state interaction contrib. 0–60811

(p, 2p), final state interaction contrib. 0–60811 (p, n), isobaric analog states abs. 0–67531 (p, p₀) on Ba isotopes, spectroscopic factors comparison with (d, p) 0–67533

(a, p) 01 of the state of the

(p.n) resonance levels near threshold neutron energies 0–77552 (p.n) resonance reaction with excitation of analogue states in region of overlapping levels 0–77477 (p.p') resonance reaction with excitation of analogue states in region of overlapping levels 0–77477 (p.p') scattering, microscopic quantitative description by D.W.B.A. with antisymmetrization 0–67525 (p.pn), 17 MeV, mechanism 0–49611 (p.i), evaluation of core excitation, use of model with 3 states 0–77551 (p.t), (p. ³He), target with isospin T_i going to analogue final states with T_j=T_j, simultaneous obs. 0–39033 (p.t) cross section analysed for excitation of 4+ member of rare earth nuclei, β_a hexadecapole deformation parameter 0–49610

β₄ hexadecapole deformation parameter 0-49610 ³H production in Al, Sn, Pb and Bi by 0.15-0.66 and 3-10 GeV protons 0 - 42828

0—42828
p. elastic scattering in nuclear emulsions at 3 GeV/c 0—42821
P(p, p)³²S, E_σ=1146 keV and 1151 keV resonances, decays and decay schemes, angular distributions, spin and parity 0—64117
P(p,p)³/2S, spin mixing coeff., 2114 keV resonance 0—77553
Ag, Ep=3 and 29 GeV, yields of stable and radioactive rare-gas isotopes 0—52769

 $^{-2/2}$ Ag(p, α)¹⁰⁴Pd, compound nucleus lifetime using the blocking effect $^{-4/2}$ 775

 $^{109}{\rm Ag}(p,ny),~8.8$ MeV, mean lifetime calc. of 203 keV level in $^{109}{\rm Cd}$ 0-38928

Al, analysing power for 490 MeV protons 0–42839 Al, light fragment and p prod., E_p =600 MeV 0–52766 Al target for 70 GeV protons, 3 He production and observations 0–67415

Nuclear reactions and scattering due to continued protons continued

²⁷Al, energy distribution of neutrons from proton nucleus nonelastic collisions for 18 MeV and 15 MeV protons 0-64115
 ²⁷Al(p_xx)²⁴Mg direct reaction process analysis, E=41.3 MeV 0-39043

 27 Al(p, α)²⁴Mg excitation function rel. to ²⁸Si T=2 state, obs. 0-38876

 27 Al(p,p)²⁸si, branching ratios of bound states determ., spins and parities 0-77492

0-77492

²⁷Al(p,p)²⁸Si, precision meas, of resonance energy by velocity technique 0-4621

²⁷Al(p,p)²⁸Si deduced levels of ²⁸Si for E_p=742 and 1381 keV 0-55122

²⁷Al(p,p)⁶, internal conversion coeffs, precise meas, using in beam spectrometer 0-39044

²⁷Al(p) many charge particles, ¹¹C, ¹³N, ¹⁸F, production angular distribution 0-67534

Ar spallation at 310, 425 and 578 MeV, production rates, theory and expt. 0.49615

0-70598

 $^{11}B(p, 3\alpha)$, 3α emission mechanism, 1.9 MeV 0-42835

¹⁸(p, 3α), 3α emission mechanism, 1.9 MeV 0-42835 ¹⁸(p, α), energy distribs, resonance narrowing 0-73941 ¹⁸(p, α) and de excitation of ¹²C 0-70599 ¹⁸(p, α)2 α , sequential reaction, study of formula derived for differential cross section 0-73942 ¹⁸(p, p') ¹⁸* polarization at 30.3 MeV, poor agreement with shell model 0-67526

¹¹B(p,p') ¹¹B* polarization at 30.3 MeV, poor agreement with shelt model 0–67526 ¹¹B(p,p'y), E_p=5.9 MeV, ang. correlations mens. 0–39039 ¹¹B(p,p) and ¹¹B(p,p'), and de excitation of ¹²C 0–70599 ¹²B(p,p) and ¹¹B(p,p'), and de excitation of ¹²C 0–70599 ¹³B(p,3,a), resonance effect of ¹²C states on α spectra shape 0–73943 ¹³Be(p,p)*B, cross section using single particle model for ³B ground state 0–46209 ¹³Be(p, El), 45 MeV, angular distributions 0–52773 ¹³Be(p, P), 45 MeV, angular distributions 0–52773 ¹³Be(p, p), 45 MeV, angular distributions 0–52773 ¹³Be(p, p), Ep=3.0-12.0 MeV, polarization meas. 0–49605 ¹³Be(p, p), Be=3.0-12.0 MeV, polarization meas. 0–49605 ¹³Be(p, p), Be=3.0-12.0 MeV, polarization meas. 0–49605 ¹³Be(p, p), Bat 20 MeV, neutron spectrum, no evidence for levels 0–57976 ¹³Be(p,p)*Be, 6 MeV used to study 1.67 MeV level 0–77481 Be(p, P)*Be, 6 MeV used to study 1.67 MeV level 0–77481 Be(p, P)*Be, diff. cross sections, near threshold 0–60808 ¹³Bi, scattering through d₃₇ isobaric analogue resonance, cross sections, partial widths 0–77507 ¹³Bi(p, p') ¹³Bi; Ep=39.5 MeV, effect of core polarization, 1.609 MeV ¹¹/, state 0–42826 ¹³Bi(p,2p), events from 1h₉₇ state 0–73949 ¹³Bi(p,2p), events from 1h₉₇ state 0–73949

209Bi(p,2p), events from 1hg/2 state 0 -73949

109 Bi(p,n) mass distribution and kinetic energy distrib. obs. 0—39159
 209 Bi(p,n)²⁰⁹ Po, Coulomb energy difference between ²⁰⁹ Bi and ²⁰⁹ Po

²⁰⁹Bi(p,n)²⁰⁹Po, Coulomb energy difference between ²⁰⁹Bi and ²⁰⁹Po 0.—73840
 ²⁰⁹Bi(p,p), effects of core polarization for negative parity transition 0.—67529
 ²⁰⁹Bi(p,p), investigation to obs. excitation of (5 ⊗h₉,·) decuplet 0.—77508
 C. inelastic scatt., effective cross sections, 200 600 GeV 0.—42830
 ²⁰⁹Cl, PF, emission from ¹⁴N irradiation relationship between isotope emission and energy of bombarding particles 0.—74000
 ²⁰C, 000 MeV interactions, intranuclear cascade, α-cluster model 0.—49609
 ²⁰C, scatt., elastic and inelastic transitions, 100 MeV 0.—39029
 ²⁰C, total cross sections between 10.3 and 21.6 MeV variation 0.—70603
 ²⁰C(p, 2p), differential cross section, effects of distortion, DWBA analysis 0.—7328
 ²⁰C(n, 2n) quasic lastic scatt, at 160 MeV 0.—57975

¹²C(p, 2p), differential cross-section, effects of distortion, DWBA analysis 0-73928
 ¹²C(p,α) quasi-elastic scatt. at 160 MeV 0-57975
 ¹²C(p,ρ)¹³C², 12-14 MeV, spin flip probabilities 0-52760
 ¹²C(p,p)¹²C², elastic scatt., 19-30 MeV, study of ¹³N levels 0-42736
 ¹²C(p,π²)¹²C, 600 MeV, capture cross-sections meas. 0-64116
 ¹²C(p,π²)¹⁴C, 600 MeV, capture cross-sections meas. 0-64116
 ¹²C(p,p)¹²N and inverse reaction ¹³N(p,p)¹⁴C calc. 0-46193
 ¹²C(p,p)¹⁴C, ¹⁶C(f(P,x₀)¹¹B, ¹⁴C(p,n)¹⁴N, ¹⁴C(p,p)¹⁵N rel. to 13.42 MeV level of ¹³N 0-64000
 ¹²C(p,p)¹⁴C, ¹⁶C(f(P,x₀)¹¹B, ¹⁴C(p,n)¹⁴N, ¹⁴C(p,p)¹⁵N rel. to 13.42 MeV level of ¹³N 0-64000
 ¹³C(D(p,p)²p) Cd deduced isobaric analogue levels, E=5.7-7.5 MeV 0-38906
 ¹⁴Ca, elastic and inelastic scattering, deduced resonances of ⁴¹Sc, E=4.8 6.2 MeV 0-42749
 ¹⁶Ca, elastic and cross-sections between 10.3 and 21.6 MeV variation 0-70603
 ¹⁶Ca elastic scattering, energy dependence, optical model 0-70583
 ¹⁶Ca(p,p)¹⁹OCa, levels and transitions obs., 7-9MeV 0-42748
 ¹⁶Ca(p,p)¹⁹OCa, levels and transitions obs., 7-9MeV 0-42748

0–38879 4 °Ca(p,p'p')°Ca and levels in 4 °Ca (0–67439 4 °Ca(p,p'p')°Ca, inelastic, 5.8-6.6 MeV, cross sections for formation of 0°, 3 and 2° states 0–70585 4 °Ca(p,p)°Ca and continuum states in 4 °Sc (0–73804 4 °Ca(p,p)°Ca and parity of 1644 keV state in 4 °K (0–57907 4 °Ca(p,d)°Ca and energy levels in 4 Ca (0–70604 4 °Ca(p,p'p)°Ca and multiplets in 4 Ca (0–67444 4 °Ca(p,n')°Sc, total cross section around isobaric analog state at E_P=1.976 MeV (0–39047 4 °Ca(p,n)°Sc, total cross section around isobaric analog state at E_P=1.976 MeV (0–39047 4 °Ca(p,n)°Sc, total cross section around isobaric analog state at E_P=1.976 MeV (0–39047 4 °Ca(p,n)°Sc, total cross section around isobaric analog state at E_P=1.976 MeV (0–39047 4 °Ca(p,n)°Sc, total cross section around isobaric analog state at E_P=1.976 MeV (0–39047 4 °Ca(p,n)°Sc, total cross section around isobaric analog state at E_P=1.976 MeV (0–19047 4 °Ca(p,n)°Sc, total cross section around isobaric analog state at E_P=1.976 MeV (0–19047 4 °Ca(p,n)°Sc, total cross section around isobaric analog state at E_P=1.976 MeV (0–19047 4 °Ca(p,n)°Sc, total cross section around isobaric analog state at E_P=1.976 MeV (0–19047 4 °Ca(p,n)°Sc, total cross section around isobaric analog state at E_P=1.976 MeV (0–19047 4 °Ca(p,n)°Sc, total cross section around isobaric analog state at E_P=1.976 MeV (0–19047 4 °Ca(p,n)°Sc, total cross section around isobaric analog state at E_P=1.976 MeV (0–19047 4 °Ca(p,n)°Sc, total cross section around isobaric analog state at E_P=1.976 MeV (0–19047 4 °Ca(p,n)°Sc, total cross section around isobaric analog state at E_P=1.976 MeV (0–19047 4 °Ca(p,n)°Sc, total cross section around isobaric analog state at E_P=1.976 MeV (0–19047 4 °Ca(p,n)°Sc, total cross section around isobaric analog state at E_P=1.976 MeV (0–19047 4 °Ca(p,n)°Sc, total cross section around isobaric analog state at E_P=1.976 MeV (0–19047 4 °Ca(p,n)°Sc,

 $^{100}\text{Cd}(p,p'p)$, Cd deduced isobaric analogue levels, E=5.7 7.5 MeV 10 18906

protons continued

108Cd(p,p'y) Cd deduced isobaric analogue levels, E=5.7-7.5 MeV 0-38906 ¹¹⁰Cd, elastic scattering, isobaric analog resonances, E_p=6.0-11.0 MeV

110Cd(p,p'γ) Cd deduced isobaric analogue levels, E=5.7-7.5 MeV 0 38906

¹¹²Cd, elastic scattering, isobaric analog resonances, E_p=6.0-11.0 MeV

0-42841 114Cd, elastic scattering, isobaric analog resonances, E_ρ =6.0-11.0 MeV 0-42841

Cd(p,p'y) enhancement 0-73925

Ce, spallation yields of Xe isotopes 0-77550

¹⁴⁰Ce, structure of generalized neutron particle-hole states 0-38924

 140 Ce(p,d) and (p,t) and one and two neutron hole states 0-70490Ce(p,t) (where A=140,142), for study of strong L=0 and 2 transitions 0-5133

0-55133

**CI, elastic and inelastic scatt., energy level study 0-52764

**CI(p,y)*Ar, cross-sections in the region of giant dipole resonance
0-39045

**CI(p,y)*Ar, y-ray Doppler shift, **Ar excited states lifetimes 0-46133

**CI(p,y)*Ar, y-ray Doppler shift, **SAr excited states lifetimes 0-46133

**CI(p,y)*Ar, cross-sections in the region of giant dipole resonance
0-39045

³⁷Cl(p,n)³⁷Ar, total cross-section meas. 0-39046

Co. elastic scatt., diff. cross section meas. 0–39046
Co. elastic scatt., diff. cross section and polarization 0–70580
5°Co(y.n), cross section determ. in giant reson, region, expt. and theory 0–52747

0-52747

**Co(p.n), E_y-6.05-6.3 MeV, energy spectra of n 0-49618

**Cr, inelastic scatt, polarization 0-77545

**Cr foil target, preparation 0-77548

**Cr(y.n), cross section determ, in giant reson, region, expt. and theory 0-52747

⁵³Cr(p, p), cross section determ. In gasta.
 0-52747
 ⁵²Cr(p, p)⁵³Mn, deduced ⁵³Mn levels and decay of the 2p_{1/2} analogue state, E=1.0·1.8 MeV 0-57979
 ⁵²Cr(p,p)² at 40 MeV, cross section for exciting low lying states 0-57973
 ⁵³Cr(p,p)² Mn, deduced levels of ⁵³Mn at 377.5, 1288.4, 1440.1, 1619.1 keV 0-42753
 Cs, spallation yields of Xe isotopes 0-77550
 Cu, calc. activation by 3 GeV protons 0-77554
 Cu, Ep=3 and 29 Gev. yields of stable and radioactive rare-gas isotopes 0-52769
 ⁶³Cu, elastic scattering, optical model analysis 0-70588

6³Cu, elastic scattering, optical model analysis 0–70588 6³Cu(p)6⁴Zn, compound nucleus formation, neutron emission study 0–77517

 0 - 775 17 6 Cu, elastic scattering, optical model analysis 0–70588 65 Cu(p,n) 65 Zn deduced 65 Zn levels, E_p =3.62, 4.06, 4.50 MeV 0–55155 65 Cu(p,n) 65 Zn deduced 65 Zn levels, E_p =2.80-4.05 MeV 0–55155 Dy. spallation yields of Xe isotopes 0–77550 155 Eu(p,2n) 152 Gd, 152 Gd low-lying states obs. 0–70501 167 F(p,αp)) 16 O at 873 keV and 1374 keV, proton gamma angular distribution meas. 0–60810 167 Gy radiation observed rel. to lifetime of 16 O determ. 0–52670 167 F(p,αp)) 160 O, 1-9 to 4.16 MeV, total cross sections, study of p-rad. 0–46210 167 Gh and 18 MeV. 187 F levels ≤3.36 MeV. 0–38860

0-46210

"F(p, d), 16 and 18 MeV, ¹⁸F levels ≤ 3.36 MeV 0-38860

"F(p, p)¹⁹Ne, and giant dipole resonances in ¹⁰Ne 0-70423

"F(p, p)¹⁹Ye, ang. distrib., 1459 keV level study 0-46123

"F(p, t), 16 and 18 MeV, ¹⁷F levels≤3.86 MeV 0-38860

Fe, elastic scatt., diff. cross section and polarization 0-70580

Fe calc. activation by 3 GeV protons 0-77554

"Fe, inelastic scattering of polarised protons at 30.3 MeV and deduced nuclear deformations 0-52781

"Fee, in microscopic first order core polarization corrections to DWBA

**Ge(p,p'), microscopic first-order core polarization corrections to DWBA 0-42837

0-4283/

*Fe(p,p'y), 10 MeV, diff. cross section, polarizations and py ang. correlations 0-46212

*Fe(p,p), 10 MeV, diff. cross section and polarization meas. 0-46212

*Fe(p,p), 10 MeV, diff. cross section and polarization meas. 0-46212

*Fe(p,p), 10 MeV, diff. cross section and polarization meas. 0-46212

*Fe(p,p), 10 MeV, diff. cross section, polarization meas. 0-46212

Sefe, elastic and inelastic scatt., E=2.6 MeV, role of isobaric analogue states 0.49607
Fe, energy distribution of neutrons from proton-nucleus nonelastic collisions for 18 MeV protons 0.64115
Fe, inelastic scattering of polarised protons at 30.3 MeV and deduced nuclear deformations 0.52781
Fe(p.n)\$6C0 excitation functions, 4.9-39 MeV 0.46213
Fe(p.n)\$6C0 excitation functions, 4.9-39 MeV 0.46213
Fe(p.d), using polarized protons, and DWBA 0.73947
Fe(p.d), using polarized protons, and DWBA 0.73947
Fe(p.d), using polarized protons, and DWBA 0.73947
Fe(p.p)\$6C0 Ep=1175-1675 keV, energy level study of \$6C0 0.49521
Ga(p., ny)\$7Ge E=5.2 MeV, population of 20 ms state 0.64024
Ga(p., ny)\$7Ge, nuclear neutron single hole states in \$157G 0.70499
Ge(p.e, p)\$7Ge, nuclear reaction times and lifetimes of excited states by use of blocking effect E=1.595.91 MeV 0.42803
Ge(p.e, clastic scattering, analysis using optical model for protons of 14.5 MeV 0.42840
Ge(p.p)\$7Ge, nuclear reaction times and lifetimes of excited states by use of blocking effect E=1.595.91 MeV 0.42803
Ge(p.p)\$7Ge, nuclear reaction times and lifetimes of excited states by use of blocking effect E=1.595.91 MeV 0.42803
Ge(p.p)\$73As isobaric analogue states, 3.30.3.37 MeV 0.38893
Ge(p.p)\$746, elastic scattering, analysis using optical model for protons of 14.5
Ge(p.p)\$7476, elastic scattering, analysis using optical model for protons of 14.5

⁷⁴Ge, elastic scattering, analysis using optical model for protons of 14.5 MeV 0-42840

⁷⁶Ge, elastic scattering, analysis using optical model for protons of 14.5 MeV 0–42840

Hi, inelastic scatt., effective cross sections, 20-600 GeV 0–42830 H(p,2p), exp. study at 150 MeV 0–73933 P(p,2p), quasielastic deuteron breakup and cross-sections measurements at 100 MeV 0–60807

at 100 MeV 0–60807 2 H(p,2p)n, asymmetry cross section measurement, 10 MeV, using trochoidal injection 0–60806 2 H(p,2p)n, at 10.5 and 24 MeV, asymmetry meas. 0–73932 2 H(p,2p)n, at about 160MeV, theoretical study 0–73935 2 H(p,2p)n, deduction of cross-section for 2 H(p,d*)p 0–42831 2 H(p,2p)n, p-p quasifree scattering, study of energy dependence 0–73950 2 H(p,2p)n at 35 MeV 0–73936 2 H(p,2p)n reaction 0–42831 2 H(p, γ)³He, exp. and theoretical study at 156MeV 0–73934

Nuclear reactions and scattering due to continued protons continued

 2 H(p,n), using polarized proton of 30 and 50 MeV in polarization determ. 0-39035

²H(p,p)²H 1-10 MeV, cross-section obs. 0-42823

²H(p,pn)¹H, modified impulse approx. calc. of N-N quasi- free scatt. 0 - 67318

²H(p,pp)n, modified impulse approx. calc. of N-N quasi-free scatt.

0–67318 3 H(p, p) 4 He, Ep=3-18 MeV, cross section, ang. distribs. 0–49613 3 H(p, p) 4 He, E_p=156MeV, diff. cross sections meas. 0–52770 3 H(p, p) 4 He, exp. and theoretical study at 156MeV 0–73934 3 H(p, n) 4 He, n polarization, 1.3<p<p<2.3 MeV 0–39036 3 He, n, polarization, 1.3<p<p<2.3 MeV 0–39036 3 He fragment prod. from 6 Li, 9 Be, 12 C, and 16 O, by 665 MeV protons 0–42829

³He(p,n), at 30 and 50 MeV, evidence for broad resonances 0—73937 He, at 46.7 MeV, angular distributions and energy spectra 0—42832 He fragment prod. from Li. Be, L2C and L6O, by 665 MeV protons 0—42829

⁴He(p, ³Hep)n, 47 MeV obs., agreement with Watson-Migdal theory

 4 He(p,d) 3 He excitation functions, 22-46 keV, search for T= $^1/_2$ resonances 0-39037

 4 He(p,p) 4 He)n, meas. at 46 MeV 0-73939 4 He(p,p) 4 He excitation functions, 22-46 MeV, search for $T=^{1}/_{2}$ resonances 0-39037

⁴He(p,pt)p, meas, at 46 MeV 0-73939 ⁴He(p,t)2p, at 156 MeV, interpretation of final state interaction spectra 0-73945

⁴He(p,tp)¹H, 47 MeV obs., agreement with Watson Migdal theory

9K(p,p)¹⁶Ca intermediate structure and continuum states in ⁴⁰Ca 0.73944

0—73944 39 K(p,n) 39 Ca, excess mass calc. from threshold energy 0—57906 41 K, ground state (p,n) Q values 0—77552 41 K(p, α_0) 38 Ar. Ep=1.17-2.10 MeV, resonance and excitation energies, yields, J* values 0—49616 41 K(p, n) 41 Ca, Ep=1.35-1.96 MeV, resonances, partial widths 0—49617 41 K(p, p) 41 K. Fp=1.35-1.96 MeV 0—49617 41 K(p, p) 41 K. Fp=1.35-1.96 MeV 0—49617 48 Kr, elastic and inelastic, isobaric analogue resonances study 0—67463 41 Ci(p, α) 42 Be angular distribution of γ -rays, and calc. 0—70594 41 Ci(p, α) 42 Be_{γ}, charge exchange part of the effective two-body interaction 0—42827

 6 Li(p,n) and (n,p), impulse approx. and shell model calcs., 156 MeV 0-39068

⁶Li(p,n) using polarized proton of 30 and 50 MeV in polarization determ. 0–39035

6Li(p,p'04)*Hf quasi-elastic scattering, Treiman-Yang test 0-73940 6Li(p,p'0Li, differential cross section analysis with collision matrix 0-42833

0-42833

⁶Li(p,pα), impulse distrib. 0-52771

⁶Li(p,pd), impulse distrib. 0-52771

⁶Li(p,pd)*He, distortion and antisymmetrisation effects 0-39038

⁷Li(p,n,)*Be₀, charge exchange part of the effective two-body interaction 0-42827

⁷Li(p,n,)*Be(0.43 MeV) charge exchange part of the effective two-body interaction 0-42827

⁷Li(p,n)*Be, precision meas. of threshold energy by velocity technique 0-46211

⁷Li(p,n)*Be, zero degree neutron yield near 2.2 MeV 0-52772

Nuclear reactions and scattering due to continued

protons continued

15 N(p,n) 15 Q, unified shell model calc. 0—428 14

aclear reactions and scattering due to continued protons continued

15N(p,n)¹⁵O, unified shell model calc. 0–42814

15N(p,p')N* and E1 giant resonance in ¹⁶O 0–70406

15N(p,t), 2 nucleon transfer induced by polarized protons 0–60809

2Na, elastic and inelastic, E_e=6 MeV, meas, of ang, distribs. 0–39030

2Na, proton induced reactions at 1000-1800 keV, resonance detection 0–57977

23Na elastic and inelastic scattering, coupled channel calculation 0–67530

23Na elastic scattering, intermediate structure 0–73796

23Na inelastic scattering, intermediate structure 0–73796

23Na inelastic scattering, intermediate structure 0–73796

23Na(p,α)²⁰Ne direct reaction process analysis 45.5 MeV 0–39043

23Na(p,α)²⁰Ne and spins of states in ²⁴Mg 0–70431

23Na(p,α)²⁰Ne and spins of states in ²⁴Mg 0–70431

23Na(p,α)²⁰Ne leastic cross-sections, fluctuations and model comparisons, 8.0-12.0 MeV 0–42838

23Na(p,α)²⁰Ne verge inelastic cross-sections, fluctuations and model comparisons, 8.0-12.0 MeV 0–42838

23Na(p,α)²⁰Ne in sopin forbidden resonances 0–64119

Nd, spallation yields of Xe isotopes 0–77550

142Nd(p,d) and (p,t) and one and two neutron hole states 0–70490

143Nd(p,t), pairing vibr. states in ³⁴Nd from L=0, 2 transitions 0–70613

25Ne(p,1)²⁸Ne at 50 MeV, differential cross section meas.. DWBA calcs. 0–57904

21Ne(p, p)²²Na, 300-1300 KeV, investigation of ²²Na excited states 0–46127

22Ne, elastic scattering of polarised protons at 30.3 MeV and deduced nuclear deformations 0–52781

25Ni(p,p)³⁵Ni, inelastic scattering of polarised protons at 30.3 MeV and deduced nuclear deformations 0–52781

25Ni(p,p)³⁵Ni, inelastic scattering of polarised protons at 30.3 MeV and deduced nuclear deformations 0–52781

25Ni(p,p)³⁵Ni, and energy levels in ³⁵Ni (p,p)³⁵Ni, in and energy levels in ³⁵Ni (p,p)³⁵Ni, and energy levels in ³⁵Ni (p,p)³⁵Ni, and energy levels in ³⁵Ni (p,p)³⁵Ni and energy levels in ³⁵Ni (p,p)³⁵Ni and energy levels in ³⁵Ni (p,p)³⁵Ni and energy levels in ³⁶Ni (p

10 –77546
6°Ni(p,p'y), 10 MeV, diff. cross section, polarizations and py ang. correlations 0–46212
6°Ni(p,p), 10 MeV, diff. cross section and polarization meas. 0–46212
6°Ni(p,p), 10 MeV, diff. cross section and polarization meas. 0–46212
6°Ni(p,p), 10 MeV, diff. cross section and DWBA 0–73947
6°Ni(p,a) study of 5°Co energy levels 0–52687
6°Ni(p,α), study of 6°Co energy levels 0–52687
6°Ni(p,α), study of 6°Co energy levels 0–52687
6°Ni(p,α), 5°Ni(p,α), 6°Ni(p,α), 6°N

MeV protons U=01/61
Ni(p.p.) differential cross sections and polarizations 0-77547
O. elastic. resonances between 16 and 30 MeV, and optical model analysis 0-70582
16O, scatt., 20-50 MeV, optical model analysis 0-46205
16O (p.p²). resonances in elastic and inelastic scattering between 18.5 and 30 MeV 0-77544
16O elastic scattering, energy dependence, optical model 0-70583
16O(p.716-). Tucleon transfer induced by polarized protons 0-60809
16O(p.d): Quasi- elastic scatt. at 160 MeV 0-57975
16O(p.d): Quasi- elastic scatt. at 160 MeV 0-39041
16O(p.d). 2 nucleon transfer induced by polarized protons 0-60809
17O(p.n). effective two-body pot. 0-42732
18O(p.d): Pfe Factive two-body pot. 0-42732
18O(p.d): Pfe Factive two-body pot. 0-42732
18O(p.d): Pfe Factive two-body pot. 0-42732
18O(p.p): Pfe Factive two-body pot. 0-42732
18O(p.p): Pfe Factive two-body pot. 0-42732
18O(p.p): Pfe Son. yields obs. 0-42732
18O(p.p): Pfe Son. yields obs. 0-42732
18O(p.p): Pfective two-body pot. 0-42733

ingle of coupole one quadrupole phonon states from proton scattering 0–67474 $0-70^{14}$ Au, energy level study by observation of conversion electrons $0-70^{19}$ Au,

0–05.17 0–05.17 0–05.18 0–05.19 0–05.19 0–05.19 040 09.19 040 09.19 05.19 05.19 05.19 07.19

Nuclear reactions and scattering due to continued protons continued

**Sc(p,p'p'), Ep=1.8-4.5 MeV, for level scheme study 0-52683

82Se radiative capture, effect of nuclear charge distribution form and radius 0--64118

radius 0-64118
Se(p,x)*Na (A=22, 24), Ep=100-400 MeV, energy depend. of prod. cross sections 0-49614
Si, 660 MeV p, production of ¹⁸F fragments 0-52778
Si detectors, stacked, promotion bombarded, effect of nuclear reactions on response 0-42641
²⁸Si, scatt., elastic and inelastic, transitions and levels, 100 MeV 0-39029
²⁸Si(p,p), study of 1,381 MeV reson., by Doppler shift attenuation method 0-73798

²⁸Si(p, p), study of 1.381 MeV reson., by Doppler shift attenuation method 0–73788
 ²⁸Si(p, p), ²⁸Si, 100 MeV, ang. distrib. obs., deduced levels of ²⁸Si 0–39031
 ²⁸Si(p, p), ²⁸Si, 100 MeV, ang. distrib. obs., deduced levels of ²⁸Si 0–39031
 ²⁸Si(p, p), ²⁸Si, nuclear reaction times and lifetimes of excited states by use of blocking effect E=1.59-5.91 MeV 0–42803
 ²⁹Si, elastic and inelastic scatt. resonances 0–49606
 ²⁸Si(p, p), ²⁹P, Doppler-shift lifetimes of states populated by decay 0–73800
 ²⁸Si(p, p), ²⁹P, proton capture resonances, yield of 1.27 MeV γ-rays in energy range 1300-1850 keV 0–52777
 ²⁸Si(p, p), ²⁹Si, proton capture resonances, yield of 1.27 MeV γ-rays in energy range 1300-1850 keV 0–52777
 Sm isotopes, elastic scatt. of 50.8 MeV p, ang. distrib. meas. 0–67528
 ¹³Sm(p, d) and (p,t) and one and two neutron hole states 0–70490
 ¹⁴Sm(p, d) and (p,t) and one and two neutron hole states 0–70490
 ¹⁴Sm(p, p) and ¹⁴Sm(p, d) and levels of ¹⁴Sm and ¹⁴Sm (p, p)
 ¹⁴⁸Sm(p, p) and ¹⁴⁸Sm(p, d) and levels of ¹⁴²Sm and ¹⁴³Sm (p) —70495
 ¹⁴⁸Sm(p, p), deformation parameters obtained from coupled-channel analysis of proton scattering 0–73828
 ¹⁵⁹Sm (p, p), deformation parameters obtained from coupled-channel analysis of proton scattering 0–73828
 ¹⁵⁰Sm (p, p), deformation parameters obtained from coupled-channel analysis of proton scattering 0–73828
 ¹⁵⁰Sn (p, p), separation of direct-reaction and compound nucleus contributions 0–60812
 ¹¹²Sn(p, p), separation of direct-reaction and compound nucleus contributions 0–60812

112Sn(p,p'), separation of direct-reaction and compound nucleus contributions 0–60812
112Sn(p,p'), separation of direct-reaction and compound nucleus contributions 0–60812
116Sn(p, n)116Sb, and 117–120Sn, 122Sn, 8.5 MeV, isomeric pair production cross-section 0–46214
117Sn (p,no), struct in p-ray strength function 0–70570
117Sn(p,t)17Sn and low-lying one-quasiparticle states 0–70612
118Sn inelastic scattering effective cross-section, theory and experiment 0–70591
119Sn(p,t)117Sn and low-lying one-quasiparticle states 0–70612
120Sn, inelastic scattering of polarised protons at 30.3 MeV and deduced nuclear deformation 0–52781
120Sn inelastic scattering effective cross-section, theory and experiment 0–70591
120Sn inelastic scattering effective cross-section, theory and experiment 0–70591

129Sn inelastic scattering effective cross-section, theory and experiment 0.—70591
129Sn(p,p)129Sn, 30.3 MeV polarized proton obs., optical model analysis, 2 versions 0.—70592
Sn(p,d), even, targets, angular distrib. J-depend. 0.—52633
Sn(p,d), structure study of odd Sn isotopes 0.—42758
Sn(p,n), A.=117,119,120, 122,124,3-5.5 MeV, cross sections 0.—70611
86Sr(p,p)87Sr, analogue levels study in particle core model 0.—67464
87Sr(p,p), deduced isobaric analog resonances of 88Sr 0.—49527
88Sr(p,p), p)89Sr, resonance structure in octupole transition 0.—67466
88Sr(p,p)89Sr, polarization meas. near isobaric analog resonances 0.—67527

Nuclear reactions and scattering due to continued

protons continued

 $^{90}Zr(p,p_0)^{90}Zr,\ 4.61\text{-}4.83$ MeV, used to study analog resonance of ^{91}Zr 0-38901

⁹⁰Zr(p,p'), effect of core polarization 0–70587 ⁹⁰Zr(p,p,p'), microscopic first-order core polarization corrections to DWBA 0–42837

0–42837 °°Zr(p,p') leading to 1.76 MeV excited state at 6.22 MeV 5/2+ analogue resonance 0–38900 °¹Zr(p,d) using polarized protons, and DWBA 0–73947 °²Zr(p, p)°²Zr, polarization meas. near isobaric analogue resonances 0–67538 °²Zr(p,p)°²Zr*, °²Zr(p,p)°²Zr*, E_p=6.0-10.0 MeV, isobaric analogue resonances, excitation functions 0–39049

tritons

scattering, optical potentials 0-52793 strong absorption for scatt. from various nuclei between C and Sn 0-60822

(t,p) nuclei of p shell, stripping reactions with 2 transferred nucleons 0-70629

0-10029 $^3H(t_{\rm A}/2)2n$, at 90keV, final-state interac. 0-55165 $^3H(t_{\rm A}/n)n$, nucleon- nucleon scattering parameters from final-state interactions 0-42868

³He, optical potentials 0–39089

He, optical potentials 0–39089

³He(I,tr)np, nucleon- nucleon scattering parameters from final-state interactions 0–42868

¹⁴⁸Nd (I,p)¹⁵⁰Nd and L=0 transitions in ¹⁵⁰Nd 0–74001

²⁷Ne(I,p)²⁴Ne, E=33 MeV, low-lying levels of ²⁴Ne, study 0–49509

³⁷Ne(I,p)³⁷P, investigation of bound states of ³³P below 4.3 MeV excitation energy 0–77495

³⁶Pb(I,ta)²⁶TI, E=20 MeV, ang. distribs. 0–39127

²⁶⁸Pb(I,ta)²⁰TI, E=20 MeV, ang. distribs. 0–39127

¹⁶⁴Ru(I,p)¹⁶⁶Ru at 15 MeV, low lying energy levels of ¹⁶⁶Ru investigated 0–49531

²⁵⁸(T,pu)³⁴CL deduced levels below ² MeV and a resy decay accounts for

0–49531

³²S(r,pp)³CI, deduced levels below 3 MeV and *y*-ray decay properties for ³⁴Cl 0–58015

³²S(r,pp)³CI, gamma-ray transition strengths and ³⁴Cl deduced levels 0–58014

³²S(r,pp)³Cl, spin and mean lives of ³⁴Cl levels 0–58013

¹²²Sn(t,p), energy level population investigation 0–39124

³⁴Sn, energy level population investigation 0–39124

³⁴Sn, energy level population investigation 0–39124

³⁶Sr(t,p)³⁸Sr 15 MeV ang. distrib. meas. and compared with DWBA calc. 0–70478

0–70478 130 Te($t_c\alpha$) 130 Sb, configuration mixing in 130 Te and 2p-1h states in 129 Sb 0–70661

Zr(t,p) (A=90,92,94,96), energy level population investigation 0-39124

X-rays see Nuclear reactions and scattering due to/photons

Nuclear reactors, fission

clear reactors, fission

1/v-absorbers, exptl. obs. in 1/E neutron flux 0-74076

878 meas. for three hexagonal pitches by fission fragment counting in polycarbonates 0-39212

BWR fuel assembly, effect of rod spacers and bundle misalignment on critical heat flux 0-39234

boiling water, in-core neutron monitoring system 0-64179

breeder, liquid-metal cooled, pressure meas, instrument 0-64172

buckling correction for experimental power distribution with fuel assemblies in a finite system 0-60852

CANDU, technical and economic aspects 0-55188

carbide fuel elements, compatibility investigation 0-60880

carbide fuel elements, compatibility investigation 0–60880 charcoal confinement filter system, in-place testing with I labelled with 131I 77608

coding, seven-rod cluster, subchannel mixing experiments, using freon 0-42909

0-42909 collision probability criticality calculations 0-52837 conference, nuclear and solid state physics, Powai India, (1968) 0-41919 containment press. reduction system and radioactivity removal system, patent 0-46317 control, direct digital 0-64167 control system stability, testing method 0-46298 core, cylindrical, hot spot factor 0-74045 core, thermal design, hot spot factor and degree of uncertainty studies 0 70713 core design for fast reactors, optimization by linear programming.

core design for fast reactors, optimization by linear programming 0-58049

on-s8049

cores, spatially large, control system stability 0-64165
coupled fission modes, approach to modular reactor kinetics 0-46287
coupled-core, noninteracting control system design 0-64166
critical heat flux in 19 rod cluster, effect of radial power distrib. 0-74056
D.F.R., irradiation rigs 0-60844
D.F.R. irradiation experiments, safety assessment 0-60879
data set and design improvements, fast integral experiments 0-49711
depletion characteristics of a cylindrical pin containing one isotope or a mixture of burnable poison isotopes 0-52839
design, neutron, of fuel elements, cales, and expt. in microlattice, ¹⁵¹Eu simulating ¹³⁹Pu 0-77602
design calculations using UoV, SGHW-type reactors 0-46288
design model, digital, for computation and control 0-60853
discrete meas, analogue signal processor and display 0-64176
Doppler coefficients, calculation using Monte Carlo techniques 0-55181
Dounreay, irradiation techniques developments 0-60874
Dragon, primary heat exchangers, noise spectra meas. 0-42901
Dragon dynamic response meas. and optimum parameter fitting (Apr. 1969) 0-42903
dynamic experiments with Na loop, computer-based data acquisition and

1969) 0-42903 dynamic experiments with Na loop, computer-based data acquisition and pre-elaboration system 0-74064 EBR-II, irradiation techniques development 0-60878 EBR-II and RAPSODIE, fast breeder reactors, operating experience (1967-1969) 0-42904 ESSOR at EURATOM, electrical eqpt, for fuel element manipulation 0-67581

for electricity generation, survey and comparison with other forms of generation 0-70690 energy output, axial distribution, thermophysical criteria 0-74041 failure study discipline, common mode 0-64163

fast, collapsing neutron cross- sections, method rel. to critical size calcs. 0-58044

fast, experimental, future of 0-60847 fast, for electricity generation, survey of Russian developments 0-74040 fast, fuel element temperature field obs., energy flow variable w.r.t. core height 0-67570

Nuclear reactors, fission continued

fast, heterogeneity effects on neutron self-shielding factors 0-58046

fast, neutron detectors and instrumentation, review 0-49710

fast breeder, status and prospects 0-46293

fast flux test facility, design features and testing capabilities 0–60886 fast reactor data, Harwell nuclear phys. div. progress report, May-Oct. 1968 0–52633

fast-neutron temp, fields and heat transfer obs. using exptal, model $0\!-\!74074$

fission product deposition studies using remote gamma spectrometry 0-77600

fission rate determ. from counting tube signals 0-52847

Inssion-fusion hybrid power system 0–70696 fuel element cluster, thermal neutron flux distrib. meas. 0–77605 fuel performance model development, status review 0–74063 fuel rob burnup determ., nondestructive, *y* spectrometer 0–49740 fuel rod burnup determ. nondestructive *y*-spectra of fission products 0–49741

10-49/41 fuel-pin sheaths, creep and plastic behaviour, computer program for evaluation 0-68455 GCR Mark III helium cooled high temp. 0-55189 gamma-ray spectroscopy, Compton electron continuum measurements 0-60651

gas cooled, pyrolytic-C and SiC coated fuel particles, irradiation performance 0-46312 gas-core geometry, air-air fluid flow expt. for curved-porous walls 0-58048

gaseous core type for rockets, use of 'dust curtain' for shielding cavity wall 0-49713

German, fast breeder pin development 0-60851
HTGC Dragon, residual distribution of experimental dynamic responses

0 - 42902

0–42902
Hanford, testing of charcoal confinement filter system using I tagged with Hanford, testing of charcoal confinement filter system using I tagged with 131 0–77608
heat texchanger, counterflow and parallelflow, dynamic analysis 0–77603
heat transfer in vertical annular gas layers 0–50165
heat transfer to liquid metals flowing in closely spaced reactor fuel rods, effects of cladding thickness and thermal conductivity 0–64170
heavy water, ³H production from circulating ¹⁶N 0–49632
heavy water moderated, boiling light water cooled reactor, prototype 0–42905

heavy wat 0-42905

0-42905
heavy water moderated, present status 0-49718
heavy water power, ¹⁶N monitoring using Si radiation detector 0-64175
heavy-water, delayed in parameter meas, accurate determ. 0-39244
High Flux Isotope Reactor, differential fast-n flux determ, with threshold
detectors 0-55186
high power test, optimization of fuel loadings 0-74072
high temperature transients, computer codes 0-49702
IETI-3, out-of-pile facility for testing reactor power channels 0-74053
in-pile colorimetry, ass dumning method and vacuum thermal resistance.

in-pile colorimetry, gas dumping method and vacuum thermal resistance utilization 0–52848 incore thermionic, thermionic convertor development 0–76996 inelastic cross section, effective, for fast reactor compositions 0–60848 inverse kinetics rod-drop measurements, prompt-jump correction 0–52842

0–52842 irradiation facility, tangential in swimming pool reactor 0–46094 irradiation techniques development 0–60874 irradiation techniques development 0–60874 irradiation work at EBR II 0–60878 isothermal irradiators, development and feasibility tests 0–77625 Japan, prototype fast breeder 0–60849 Japan fast breeder reactor, fast flux test facilities 0–60887 liquid-metal cooled, temperature determination based on superposition principle 0–70734 use of maraging steel, ductility and tensile properties changes obs. under neutron irradiation 0–50768 material testing fast reactor designs 0–60855 mechanical properties of steel vessel, changes, neutron spectral analysis, obs. in Big Rock Point Reactor 0–49717 moderator reactivity coeffs., comparison of four methods of determ.

moderator reactivity coeffs., comparison of four methods of determ. 0-52844

0-32644 modular reactor kinetics, coupled fission mode application 0-46287 molten salt breeder fuel-cycle anal. rel. to operation as converter 0-39216 molten salt breeders, history, status and potential 0-39214 molten salt type, design rel. to behaviour of graphite and Xe 0-39248 molten salt type, development of graphite, Hastelloy-N and fluoride salt mats. 0-39247

multiplication factor, subcritical, determ. from counting tube signals 0-52847

n spectrum, 0.1-10 MeV, meas. using threshold detectors 0-39245

neutron anisotropic scattering, one-speed transport disadvantage factor calculations 0-42896 neutron cross-sections, Doppler broadening with temp. and boundary motion 0-52821

neutron energy spectrum calculation for Zebra reactor, computer program

neutron fluctuation analysis, adjoint- weighting, with emphasis on effective detector efficiency 0-46290

neutron flux anisotropy due to arrangment of fast core cell, meas. using emulsion 0–52836 neutron flux in core, from transmission meas. 0–46315 neutron flux monitoring, ex-core, two-range system 0–64180 neutron irradiation facility, spectra meas., solid state track recorder 0–60710

neutron kinetics, book 0-42897 neutron kinetics, non-linear, prompt, space dependent considerations 0 - 70693

u-7/0by3
neutron leakage from TSF-SNAP, Monte Carlo calc. and meas. 0-74039
neutron monitoring with fission foil-Lexan detectors 0-58074
neutron spectrometry by proton-recoil proportional counters 0-49739
noise, at-power, induced by coolant flow fluctuations 0-77604
Nusselt numbers for in-line flow through unbaffled rod bundles, slug-flow
0-46289 Nusser furnices for in the control of the control o

parameter determ. from counting tube signals 0-52847
parameters meas. by zonal characts, of activation y-ray detectors

Nuclear reactors, fission continued

power, dynamics of, analysis 0—74046
power determ. from counting tube signals 0—52847
power distribution, in-core meas. 0—64178
power distribution, space and power dependent, calc. 0—52832
for power generation, water-moderated, water-cooled 0—70712
power monitor based on Cherenkov radiation detection 0—64173
power reactor, controlled, design 0—67569
power station, steam generating heavy water, fuel performance 0—49719
pressure steel vessel, neutron irradiation at 288°C and 393°C Charpy-V
shelf energy degradation and yield strength increase obs. 0—49716
pressure ube nondestructive test results statistical eval. 0—77606
pressure vessel design, steel mechanical and physical properties under
irradiation, steel for nuclear reactor pressure vessel, testing in Big Rock
Point Reactor 0—49715
pressure vessel design and operation, use of stainless steel, austenitic-Cr-Ni
types, properties under environmental effects, radiation and corrosion
0 49714
pressure vessels, fracture 0—39239

types, properties under environmental effects, radiation and corrosion 0-49714
pressure vessels, fracture 0-39239
process control systems, Westinghouse PWR 0-64168
prompt-critical excursions, approximate calculation 0-55183
protection systems, Westinghouse PWR 0-64168
prototype fast breeder in Japan 0-60849
pulsed neutron experiment simulation by analogue computer 0-42898
R2, Studsvik, rebuilding for higher neutron flux 0-74057
radioactivity removal system, patent 0-46317
research tendency in Russian Institute 0-70687
resonance self-shielding factors for heavy actinides 0-46215
rocket propulsion with gaseous core reactors, 'dust curtain' seeding and cavity wall shielding 0-49713
rod-drop obs., tables for evaluation reactivity vs flux density ratios 0-74073
SGHW-type, design calculations using UoV 0-46288
SIEMENS university training, parameter determ. from counting tube signals 0-52847
SM-2 reactor, integral fast n flux in irrad. channels 0-46295
safety assessment of D.F.R. irradiation experiments 0-60879
safety system design, criteria 0-64162
shield shape, optimum, Monte Carlo calc. 0-46294
shielding calc., point kernel, Gauss-Laguerre numerical integration 0-55182
single fuel assembly in organic coolant, meas. of lattice parameters 0-40-40723

single fuel assembly in organic coolant, meas, of lattice parameters 0-49723

0—49/23
space-time reactor-kinetics analysis, verification by experiment 0—52838
spacer grids in rod bundles, drag coefficients 0—52841
status of microscopic data knowledge 0—49688
symposium on nuclear science and power systems 0—46273
TREAT, unradiated EBR II mark I fuel element, Na loop expts. 0—55210
temperature meas, in uninstrumented D.F.R. expts. 0—60888

thermal column, horizontal, conversion into useful neutron source plane 0-70735

thermal disadvantage factor, calc. method 0-39224

thermal disadvantage factor, calc. method 0–39224 thermal neutron flux, in-core meas. using microwave sensors 0–64171 thermal research reactors, max. flux 0–60839 thermal-neutron-activation measurements and Monte Carlo calculations in light-water-moderated uranium cells 0–58045 time-dependent reactivity from flux measurements for a stochastic-point-reactor model using digital Kalman filtering 0–64160 Tokamaks, synchrotron radiation losses 0–70694 transfer functions and period reactivity meas. from rod drop decay 0–39246

U=39246 trends in reactor physics 0-46286 water, pressurised, sources of in-core γ radiation and relation to thermal neutron flux and power density 0-74055 water cooled, economics of blending and diffusion in U-recycle, eqns. 0-46313

water cooled, loss-of-coolant accident, differential press, transients predic-

tion 0-77601

water-cooled, thermoelastic stress due to local heat transfer coeff, transients 0-54667

water-cooled reactors, coolant blowdown model for safety problem evaluation 0-55194

water-moderated, enriched- uranium, for research purposes 0-70723

ZPR-VI assembly 4Z, 26-group cross section analysis 0-39221

Zebra, pulse counting system, electronic with proton recoil proportional counter 0-42916

Zp-III fast critical assembly, 48, 22-group cross section analysis 0-39220

y-radiation of fission products of the cooleans of the coole

p-radiation of fission products, when fuel is present for short time 0-67575

form, prompt, lifetime meas, in fast critical assembly, Rossi α -time correlator 0-42646

n cross sections status rel. to reactor technology 0–39202 n spectra, fast in VVR-S math. approxs. comparison 0–39218 ²⁷Al, threshold detector, determination of fast neutron flux densities 0–74075

Co, n flux detector, for meas, and control in research and power reactors 0-38757

Na cooled fast breeder, possibilities of V alloys 0-49729
Na vapour deposition in inert enclosures, problem in fast breeder reactors 0-53403

0-53403 "5"Ni, threshold detector, determination of fast neutron flux densities 0-74075 "2"Np, threshold detector, determination of fast neutron flux densities 0-74075

0—74075
Pu recycle fuel lattices, reaction rates 0—74059
Pu recycle fuel lattices, reaction rates 0—74059
Pu recycle fuel lattices, reaction rates 0—74075
Pu recycle fuel lattices, reaction rates 0—74075
Put recycle, eqns. 0—46313
Put recycle, eqns. 0—46313
Put recycle, eqns. 0—46313

annealing, linear tempering, of reactor-irradiated crystalline chemical compounds 0–65440
BOR-60, test conditions 0–60871
burn up determination in fuel elements of Novo-Voronezh plant 0–46300
carbide fuel particles, carbon coated, kernel migration 0–58833
carbide powders, characterization 0–58994
cast iron pellet, thermal cond. meas., 0-1000°C, in vac. and gaseous media 0–40608

Nuclear reactors, fission continued materials continued

ceramic, structural, fracture behaviour, strength distrib. 0-43761

ceramic fuel element, annular, optimum configuration for maximum heat

ceramic fuel elements, pore deform, and migration, local thermal stresses influence 0-40194

influence 0–40194 irradiated, autoradiography 0–77620 ceramic fuels, irradiated, autoradiography 0–77620 ceramic fuels, mech. props. 0–55980 ceramic tubes, thermal shock 0–50794 cladding of fuel elements using metal impregnated composite 0–77610 displacement damage interpretation in irradiation effects studies 0–60884 fast, irradiation effects programme 0–60868 fast, irradiation problems 0–60872 fast flux irradiation program in Japan 0–60869 fast reactor irradiation testing, conference, Thurso (1969) 0–60865 fissile fuel distrib. in fast breeders, optimization for min. critical mass 0–58043

0-58043 fissile isotopes, accuracy of dg/dT rel. to ENDF/B (and other) data files 0-77599 fuel, X-ray analysis 0-59515 fuel, axial ratchetting under pressure cycling conditions 0-67591 fuel, bubble-defect configs., migration velocities 0-68344 fuel, coated particles ogas pressure measurement 0-46305 fuel, coated particles, gas pressure measurement 0-46305 fuel, irradiation devices 0-60883 fuel, mixed oxide, simulating performance with Hybrid computer 0-58064

0–58064 fuel, models, fission gas release and statistical fuel swelling 0–77613 fuel, review 0–39238 fuel analysis, nondestructive radiative neutron capture 0–49727 fuel and cladding, models for performance prediction, conference 0–67590 fuel assay, on-line computer system 0–56730 fuel burn up meas. by p fission products reaction with D₂O and 'Be and photo neutron counting 0–46301 fuel burn-up determ. by radiochemical methods 0–55212 fuel cladding, Zr alloy, H distrib, heat flux effects 0–46308 fuel cladding failure, simulation expt. of results of fission product gas release 0–64169 fuel cladding temp. determ. by recording ⁸⁵Kr release during post-irrad.

release 0-04109 fuel cladding temp. determ. by recording ⁸⁵Kr release during post-irrad. heating 0-39229 fuel cooling by water-steam annular flow, dry patch stability 0-78002 fuel clement, EBR-II mark I, TREAT Na loop expts. on performance 0-55210

0-32210 fuel element cladding failure detection by inert gas release 0-49728 fuel element cladding using metal impregnated composite 0-77610 fuel element irradiation in KNK for German fast breeder development 0-60875

0-60875
fuel element out-of-pile testing, use of acoustic transducers 0-42078
fuel elements, cylindrical, mech. and thermal analysis during off-normal
conditions after extended burn-up 0-77616
fuel elements, gas cooled, heat transfer coefficients and friction factor of
tubes 0-58058
fuel elements, small number, three-dimens. heterogeneous anal. in substitution expts. 0-42910
fuel irradiation, clad swelling, Fortissimo project 0-60873
fuel pellets and pins, FFTF, in-process control 0-55200
fuel pellets in hot cell, bulk volume meas. using vacuum pycnometer
0-77621
fuel pin, LMFBR, mixed-oxide, performance analysis. 0-77617

0-77621
fuel pin, LMFBR, mixed-oxide, performance analysis 0-77617
fuel pins, deformation, evaluation of model for prediction 0-74070
fuel pins, irradiation testing 0-60876
fuel pins, prototypic FTR, fabrication 0-58060
fuel pins, radial temp. distrib. effect of different types of void volumes
0-74069

0—74059 fuel pins, swelling, non-steady-state factors in models 0—74071 fuel pins in liquid metal rigs, irradiation 0—60881 fuel rods, irradiated, void volume determination 0—77622 fuel rods, multispan, subjected to axial thrust, inelastic anal. of bowing 0—54635

0—34635 fuel rods, non destructive burnup meas. by *y* spectroscopy 0—58059 fuels, bubble release from dislocations, models 0—39230 fuels, mixed-oxide, fission gas bubbles behavior 0—77614 graphite, boronated, control materials, irrad-induced dimens. change 0—58062

graphite, elastic consts. and anharmonic coeffs. calc. using interatomic pot. 0-40228

pot. 0-40228
graphite, fission product behaviour 0-67586
graphite, free vaporization rates 0-39890
graphite, hot isostatically pressed, creep behaviour 0-40327
graphite, imperfect, hexagonal axis expansion coeff., approx. theory 0-47547 graphite, impurity determ., instrumental activation analysis 0-62835 graphite, in semi-continuum model 0-40581 graphite, in-pile release of fission gas 0-67584 graphite, isotropic, irrad., ultimate tensile strength, Weibull's theory applic.

graphite, isotropic, irrad., ultimate tensile strength, weibuil is theory applic. 0–40346 graphite, life, rad.-induced stresses and permissible geometries rel. to use in molten salt reactor 0–39248 graphite, mech. props. 0–40217 graphite, mech. strength, thermal oxidation by water vapour effect 0–40348

0-40348
graphite, microstruct. changes due to high temp. creep 0-40328
graphite, negative magnetoresistance, field depend. 0-40717
graphite, negative magnetoresistance due to diffuse scatt. at crystallite
boundaries 0-40718
graphite, neutron irrad., dimens. and prop. changes 0-40143
graphite, neutron irrad., vacancy and interstitial clusters conc. 0-40134
graphite, polycryst., anisotropy determ. 0-40069
graphite, polycryst., thermal expansion, model 0-40582
graphite, radiation damage obs., electron microscopy technique applic.
0-40142
graphite radiolytic oxidation effect on plys. props. 0-55946

0-40142 graphite, radiolytic oxidation effect on phys. props. 0-55946 graphite, rethermalization cross-section 0-58072 graphite, stress-strain behaviour under biaxial tension 0-40268 graphite, tensile strength, geom, stress conc. at fillets effect 0-40347 graphite, thermal cond. and diffusivity standards 0-40597 graphite, thermal cond. rel. to elec. resistivity, high temp. 0-40596 graphite, thermal cond. rel. to elec. resistivity, high temp. 0-40596

Nuclear reactors, fission continued materials continued

graphite, thermal shock resistance technique 0-40562

graphite, thermal shock testing using focused electron beam heating

graphite, total hemispherical emittance, high temp. 0-40611 graphite, wetting by molten NaF-ZrF₄-ZrO₂ mixtures in different gases 0 47036

u 47036 graphite in fuels applics. 0–39240 graphite thermal expansion reference for high temp. 0–40580 graphite-Hastelloy-N-fluoride salts, development for molten salt reactors 0–39247

graphite-moderated lattice, thermal neutron spectra meas. 0-74050 HTG, irradiation experiments 0-60854 heat generating circular cylinders, thermal stresses and displacements 0-54664

0–54664
heat generating finite cylinder, thermal stresses and displacements
heat generating finite cylinder, thermal stresses 0–54665
heat transfer in fuel rod bundles with liquid metal cooling 0–58066
hydrogeneous liqs., slow neutron scatt. 0–39728
Inconel 625 and 718, post-irrad. creep-rupture props. 0–40329
ion-exchange resins, thermal stability 0–41410
irradiated fuels, radiographic study 0–58067
irradiation experiments, using fast reactor facility 0–58070
irradiation program, rel. to fast flux test facility 0–58070
LMFBR development, US program 0–60870
LMFBR core irradiation problems 0–60885
liquid metal cooled fuel rod bundles, heat transfer multiregion analysis 0–67580
liquid metal fast breeder, fuel pins irradiation experience. 0, 60876

0-0780 [liquid metal fast breeder, fuel pins irradiation experience 0-60876 liquid metal rigs containing fuel pins, irradiation in BR2 0-60881 MTR plate type fuel elements at Petten, in-core heat transfer 0-55207 magnox type, steel corrosion problems 0-52843

hollow fuel compacts, temperature distribution in graphite

moderators, interaction between two, study using pulsed neutron method 0-46309

moderators, uniform, relaxation consts. of anisotropic neutron pulse 0 46283

0.46283 nitride fuel and cladding materials, Na wetting characts. 0—58555 Novo-Voronezh station, burn up determination in fuel elements 0—46300 Phenix subassembly, irradiation program 0—60867 poison materials, potential burnable, irrad, performance 0—55201 polywater as the mechanism of the pH-reactivity effect in pressurized water reactors 0—46303

reactors 0–46303
porous materials, ellipsoidal yield function 0–55969
power plant component materials obs. 0–77609
radiation shielding and cooling by molten metal, patent 0–58075
Rapsodie, Fortissimo project for fuel irradiation problems 0–60873
remote systems, conference, San Francisco, Califi, USA (1969) 0–77619
review, Chalk River, Canada 0–39238
rod bundles, liquid cooled, mass and heat exchange between adjacent channels 0–55208
SAP channel, study of impact stress 0–55964
seven-pin clusters, 7 EBR-II mark I type, power pulse meltdown expts. 0–55211

Seven-pin clusters, 7 EBR-II mark 1 type, power pulse metidown expts. 0–55211 stationary gas bubbles, behaviour, in Na-bonded fuel rod, testing in narrow liquid filled gaps 0–46310 steel, Cr-Al-Y ferritic, fission-fragment irrad, effect on oxidation 0–66183 steel, call austenitic stainless, post-irrad, creep-rupture props. 0–40329 steel, irradiation damage, ultrasonic nondestructive meas. 0–47566 steel, radiation induced high temp. embrittlement, cold working and recrystn. influence 0–40438 steel, stainless, Na effects on high-temp, creep behaviour 0–42913 steel, stainless, Na high-temp, effects on creep and stress rupture 0–42914 steel, stainless, athigh-temp, effects on creep and stress rupture 0–42914 steel, stainless, diffusion of carbon 0–65341 steel, stainless, diffusion of carbon 0–65341 steel, stainless, high temp. Na effects on mechanical props. 0–42912 steel, stainless, high temp. Na effects on mechanical props. 0–42912 steel, stainless, tirad, void form. He effect 0–68347 steel, stainless, type 316L, carburization in static sodium 0–75331 steel cladding corrosion rate in flowing sodium 0–56705 TRIGA fuel element, radial power distribs. meas. from time and space-depend, temps. 0–55185 thermal neutron fuel irradiation with continuous heat flux meas. 0–60882

depend, temps. 0–55185
thermal neutron fuel irradiation with continuous heat flux meas. 0–60882
thermionic fuel elements, review 0–67014
UO₂ cryst. growth by closed capsule zone melting 0–68259
Zircaloy, β-ω transform. basketweave struct., ZrC effect 0–58767
Zircaloy, irrad. creep by dislocation climb 0–58903
Zircaloy, irrad. creep by dislocation climb 0–58901
Zircaloy, irrad. creep by dislocation climb 0–58902
Zircaloy, low hydrogen content, tetragonal hydride obs. 0–68562
Zircaloy, oxidation in air, dimens. changes 0–45064
Zircaloy-2, cold-worked in-reactor creep rate stress depend. 0–68460
Zircaloy-2, corrosion in steam and oxygen, applied tensile stress effect

Zircalov -2, corrosion in steam and oxygen, applied tensile stress effect

Zircaloy-2, logarithmic creep, temp. effect 0-68461 Zircaloy-2 tubes, radiant heat transfer in bounded annular cavity 0-39228

Zircaloy-2 tubing, irrad. and tested, microstruct. and failure mechanism 0-47209

0-47209 Zircaloy-4, $\beta \rightarrow \alpha$ transform. 0-62140 75% UO_{2-25% PuO₂ fuel pins, irradiated, burst strength obs. 0-77618 Al alloy, XAP-001, dispersion strengthened, fracture initiation and propagation 0-47408 Al and 8001 alloy, thin foil, void shrinkage characts., electron microscopy 0-47237}

 0^{-47221} 4.47 clouds from stack of nuclear reactor, exposure rates of γ -rays, attenuation and build-up 0-55214 B-loaded fuel elements, effective multiplication factors 0-49737 Be, fracture toughness, 77-533 K, heat treatment, neutron irrad. effects

0 - 40364

Be powder, hot-pressing, electron metallography and oxygen impurities role 0-65445 role 0-65445 BeO, annealing of neutron irrad, induced microcracks 0-47428

BeO, melting pt. and phase transform. 0-61593 C. absorbent, neutron shield, manufacture and physical props., neutron irrad. effect 0-7027 C. absorbing, for fast reactor protection, phys. props. 0-39227

Nuclear reactors, fission continued materials continued

C, negative magnetoresistance, field depend. 0-40717

C, pyrolytic, diffusion of actinides, thin-layer expts. 0-78577

C, pyrolytic, fission product behaviour 0-67586

C, pyrolytic, fluidized bed produced, lattice thermal expansion 0–40584 C, pyrolytic, form. from hydrocarbons, growth-inhibition 0–39951 C, pyrolytic, galvanomag. props., 4.2K and high mag. field strengths 0–40716

C, pyrolytic, metha changes 0-58852 methane and propylene derived, neutron-irrad., density

C, pyrolytic, preferred orientation degree, refl. electron diffr. obs. 0-40070

C coatings, pyrolytic, characterization methods 0-40230

C fibres, preferred orientation rel. to elasticity 0-40229

C notes, preferred orientation rel. to elasticity 0–40229

C foam-a cellular structural material 0–39853

C pyrolytic coated fuel particles, irradiation performance, damage study by postirradiation metallography 0–46312

252 Cf randomly pulsed neutron source for prompt neutron decay meas.
0–74078

Co complex, trisethylenediamine nitrate, low temp reactor irradiated, annealing effects 0-65446

D, absorption cross-section, revised value 0-39232

D₂O-natural uranium subcritical systems, thermal neutron wave propag.

D-O-natural uranium subcritical systems, thermal neutron wave propag, props. 0–46276
D-O. absorption cross-section, revised value 0–39232
D-O moderated systems, reactivity coeff. determ., comparison of four methods 0–52844
Fe. irrad. voids, heterogeneous distrib. 0–58801
H-O-moderated lattices of slightly enriched and natural uranium, study of physics parameters 0–58069
H-O moderated systems, reactivity coeff. determ., comparison of four methods 0–52844
He content, production rates, calc. 0–46304
Hf control rods, replacements for BONUS reactor, preparation 0–58057
LiF-BeF-7-ThF4 with 23 UF4 fuel, recycling process for molten salt reactor 0–39226
LiH shields, neutron ane, flux spectrum 0.1 eV to 15 MeV 0–55199

0-37220 LiH shields, neutron ang. flux spectrum 0.1 eV to 15 MeV 0-55199 Mo-UO₂, cermet fuels, determination of postirradiation disposition of ⁸⁵Kr 0-77623

0-/1023
Na/H₂O expts. at Dounreay, review 0-49735
Na-bonded fuels, behaviour of stagnant fission gas bubbles in liq.-filled gaps 0-55198
Na, effects on high-temp. creep behaviour of stainless steel 0-42913
Na, liquid carburization of stainless steel, rel. to grain size and work hardening 0-39242 ing 0-39242 Na carburization of stainless steel 0-42915

Na component walls, thermal transient response and stress obs. 0-39191 Na high-temp. effects on stainless steel 0-42912

Na high-temp. effects on stainless steel creep and stress rupture 0-42914
Na loop 500 kW conceptional design study 0-60877
Na technology, conference argonne (1968) 0-42911
Nb-Al alloy for sheathing fuel elements, prod., patent 0-71813
Nb-1%Zr alloy, in Li, thermal convection loop tests at 1200°C and 1300°C 0-77615

Nd separation from irradiated fuel, determ. of ¹⁴⁸Nd for burn-up 0–55213 Pb as shielding 0–67588 Pb pellet, thermal cond. meas., 0-1000°C, in vac. and gaseous media 0–40608

Pu-polystyrene cube systems, n surface multiplication expt. and theoretical cales. 0-49731

calcs. 0–49731 Pu-(1 wt.%) Ga δ -stabilised alloy, heat content and capacity, 0-685 °C 0–65550

Pu-(1 wt.9) Ga δ-stabilised alloy, heat content and capacity, 0-685 °C 0-65550 Pu-Ti alloys, Pu β phase stabilization 0-68568 (Pu-U)O₂, mixed, creep props. 0-58897 (Pu-U)O₂ mixed fuel in contact with sodium, microprobe exam. 0-59516 α-Pu, self-irrad, length change 0-58827 Pu discharged from Rajasthan CANDU recycling in Tarapur cores, feasibility study 0-39237 Pu fuel, nondestructive assay by γ-ray meas. using on-line computer control 0-55203 PuC_{1-x}, Pu₂C₃, cryst. struct., mag. ordering, neutron diffr. 0-47201 PuO₂, hot-pressing 0-58946 PuO₂ o/M ratio determination, CO/CO₂ gas equilibration method, effect of burnup 0-49738 2¹³⁸PuO₂, self-irrad, activation energy of first stage annealing 0-71742 2¹³⁸PuO₂, self-irrad, activation energy of first stage annealing 0-68620 2¹³⁹Pu, effective capture- to-fission ratio, low flux meas. in fast reactor 0-58056 2¹⁴⁰Pu, beryllia moderated system, resonance capture at 300°K and 219Pu, effective capture- to-fission ratio, low flux meas. in fast reactor 0-58056
240Pu, beryllia moderated system, resonance capture at 300°K and 1500°K 0-42778
240Pu, paphite- moderated system, resonance capture, at 300°K and 1500°K 0-46150
240Pu, in Puc particles in graphite matrix, resonance capture at 300°K and 1500°K 0-46151
240Pu neutron absorption in 1.056 eV resonance 0-74066
Sic coated fuel particles, irradiation performance, damage study by postir-radiation metallography 0-46312
ThO₂-UO₂ fuel pellets, volatile gas release 0-58065
ThO₂-UO₂ solid solution, oxidation behaviour 0-48198
ThO₃ fuel pellets, volatile gas release 0-58065
Tm₂O₃, cold pressed, variables in fabrication 0-58968
Tm₂O₃, high temp. behaviour 0-58961
U-(1.5 wt.%)Mo alloys, continuous and discontinuous precip. reactions68561 0-68561
U-Mo alloys, shear transform, from γ-phase 0-62137
U-Mo alloys, sterse corrosion props. 0-55998
γ-U-Mo fuel alloy, thermal cycling and irrad, stability 0-40467
U-(7.5 wt.%)Nb-(2.5 wt.%)Zr alloy transition phases, cryst. struct.40104 0-40104
U-RD 1003, mixed, bick temp. creen. 0-58900

0-40104

(U-Pu)O₂, mixed, high temp. creep 0-58900 (U-Pu)O₂ fuel pellets, eval. for use in encapsulated fuel pin irrad. tests

(U-Pu)O₂ ruler petiets, eval. for use in circapstractor for part in O-58061 (U-Pu)O₂ fuel petiets, fabrication and characterization 0-56037 (U-Pu)O₂ mixed fuel fabrication for FFTF 0-58962 (U-Pu)O₂ mixed fuels, creep 0-55988 (U-Pu)O₂ mixed fuels, plastic yielding and fracture 0-58992

Nuclear reactors, fission continued materials continued

U-metal spherical shells, steel moderated, critical mass irregularity
0-58055

(U. Pu)₃O₈, lattice parameters rel. to Pu content 0-58762

(U, Pu)O₃, lattice parameters ref. to Pu content 0-38762 (U, Pu)O₃, products emission during irrad. to high burn-up 0-46306 (U, Pu)O₂ solid solns., thermal cond., Pu content effect 0-59116 U, critical masses, spherical and hemispherical enriched assemblies 0-49730

U, Pu)O₂ solid solns., thermal cond., Pu content effect 0.—59116 U, critical masses, spherical and hemispherical enriched assemblies 0.—49730 U, irrad., oxidation and ignition in CO₂, ⁸⁵Kr release 0.—66186 U, oxidation by CO₂, diffusion through CO layer, control 0.—48199 U, quenched, fuel rods, radiation-induced growth 0.—40011 (U, Pu)O₂, irradiated fuels, O/M ratio determination, CO/CO₂ gas equilibration method effect of burnup 0.—49738 U alloys, β-α phase change kinetics 0.—68560 U alloys pile growth 0.—67589 U alloys pile growth 0.—67589 U fuel rods, irradiated mechanical props. 0.—47383 U as shielding 0.—67589 U fuel rods, irradiated mechanical props. 0.—47383 U attices, water-moderated, thermal neutron spectra meas. 0.—74050 U recycling, economics of blending versus diffusion 0.—74068 U rod, texture of quenched mat., effect of external stress 0.—47205 U solution slab-cylinder system, critical parameters 0.—55204 UC-UN solid solns, ideality 0.—68538 UC, carbothermic reduction of UO₂ and oxygen retention 0.—62808 UC, integral transport method and central reactivity worths in fast critical assemblies 0.—55205 UC, rare gas behaviour obs. using helium bubble injection 0.—58842 UC₁-x₁x₂, elastic consts. 0.—71666 UN, Seeback coeff., elec. and thermal cond., 77-400K 0.—47562 UN powders, synthesis and characterization 0.—56051 UO₂-SiO₂, vitroceramics, high burn-up behaviour 0.—39233 UO₂-SiO₂ system vitroceramics, fission fragment irrad. effect on thermal diffusivity 0.—47561 UO₂-SiO₂ vitroceramics, melt props. 0.—46307 UO₂-ThO₂ system, solidus and liquidus temps. 0.—58523 UO₂, 3% enriched, fast fission ratio 0.—39243 1 UO₂, 3% enriched, fast fission ratio 0.—39243 1 UO₂, 3% enriched, fast fission ratio 0.—39243 1 UO₂, creep enhancement during irrad. 0.—68459 UO₂, respenhancement during irrad. 0.—68459 UO₂, respenhancement during irrad. 0.—6864 UO₂, fast londing effect on the effective resonance integral with a simplified phonon frequency distribution 0.—6864 UO₂,

UO₂, in plate issolving as leaves with Third in Lacing UO₂, irrad., melting pt, increases and decreases 0–68178 UO₃, limiting aspects of performance 0–52846 UO₃, polycrystalline, high temp. creep, stress depend., calc. 0–4 UO₂, re-soln. of gas atoms from bubbles during irrad. 0–67585

UO₂, re-soin, or gas atoms from buobles during irrad. U-07585 UO₂, sintering, comp. depend. 0-47434 UO₃, sintering kinetics 0-40442 UO₃, stoichiometric polycryst, strength and fracture 0-40359 UO₂, surface-controlled oxidation-reduction and self-diffusion 0-65344 UO₂, thermal diffusivity meas. during irrad., effect of stored energy 0-49732

0-49732
UO₂, venting and distribution, exp. investigations 0-77624
UO₂ ceramic oxide fuel, importance of radiation heat transfer 0-49733
UO₂ fuel assembly, 28 element water cooled, buckling expt. 0-58073
UO₂ nodules, sintered, electrodynamic vibrocompaction 0-67587
UO₂ pellets, preparation by frittage 0-67592
UO₂ pellets, very high density, fabrication, effect of sintering parameters 0-40471

U-304/1
U₃(1), non-stoichiometric, elec. cond. and defect struct. 0-68351
U₃O₈, phase transitions, elec. cond. study 0-59039
(U_{0.85}Pu_{0.15})C_{1-x}N_x, elastic consts. 0-71666
U₃Si alloy, recovery and recrystn. 0-40443
U₃Si fuel elements, irrad., temp.-depend. swelling 0-55202
U₃Si fuel elements, solid and hollow, irrad. swelling, ≤15000 MWd/te U

U₃Si fuel elements, solid and hollow, irrad. swelling, ≤15000 MWd/te U₀-39236

²³³U fuel in single fluid molten salt breeder reactor 0-39210

²³⁵U, effective capture-to-fission ratio, low flux meas. in fast reactor 0-58056

²³⁶U-³³⁹Pu mixture, influence of resonance interactions on statistical resonance region on effective cross-sections 0-67579

²³⁸U, effective cross sections in resolved reson. region, Doppler broadening

"3" U. effective cross sections in resolved reson. region, Doppler broadening 0–67582
"3" U. resonance integrals for various geometrical systems 0–39231
Uo₂ pellets, oxidation in air, 800–900 °C 0–66187
V, neutron-irrad. induced voids 0–40127
V, radiation hardening 0–47449
V alloy possibilities for Na-cooled fast breeder reactors 0–49729
V alloys as fuel element cladding 0–49734
W (25 wt.%) Re alloy, neutron irrad., damage recovery 40146 0–40146
W, defect recovery process, neutron irrad. 0–47231
W, neutron-irrad. induced voids 0–40127
Xe fission product in molten salt reactor, removal and penalty to breeding ratio 0–39248

13" Xe core conc., in cyclically operated reactors 0–49736
Zr-(1.25 wt.%) Cr- (0.1 wt.%) Fe, quenched, massive grain growth during ageing 0–68369
β-Zr-Mo alloy, quenched, Al influence on stability 0–50826
Zr-Nb alloys, equil. β/α+β transform. temp., oxygen effect 0–47484
Zr-(2.5 wt.%) Nb-H system, press.-comp.-temp. study 0–68570
Zr-(2.5 wt.%) Nb-H system, press.-comp.-temp. study 0–68570
Zr-(2.5 wt.%) Nb-H system, press.-comp.-temp. study 0–68460

0-68460
Zr. Nb(Ti) alloys, oxidation in air, dimens. changes 0-45064
Zr, natural and stable isotopes, reson. n cross sections 0-42843
Zr, resistivity increment of quenched wire, defect come. calc. 0-47232
Zr alloy, pressure tube, capture cross-section, strength, review 0-43771
Zr alloy fuel cladding, H distrib., heat flux effects 0-46308
Zr alloys, corrosion behaviour discussed rel. to use in boiling water reactors at 300°C 0-52845

at 300°C 0–52845
Zr alloys, irrad. creep, enhanced ductility obs. 0–71701
Zr alloys, irrad. creep mechanisms 0–78637
Zr alloys, oxidation, charge transport processes obs. 0–59488
Zr alloys, stress orientation of hydride 0–62139
Zr alloys development 0–39241
Zr anodic oxide and its alloys, growth kinetics in anodizations 0–41441
Zr wires, quenched, defect conc. 0–40128

Nuclear reactors, fission continued materials continued

0 61622

operation

ZrO₂, anodic, morphology 0-45063

boiling water reactor, dynamic behaviour of water-cooled boiling channel with twisted tape 0-55195

ZrO2 amorphous films, crystn, by thermal heating and ion bombardment

boiling water type, control in different system circuits 0-49726

boiling water type, control in different system circuits 0–49726 burn-out of non-uniformly heated channels, flow-instability-induced 0–55191 CANDU, thermal efficiency increase means 0–42907 control of Xe spatial oscillations 0–39225 control rod position indicator, patent 0–58076 control rods, Hf, replacement for BONUS reactor 0–58057 corrosion products build-up in primary circuit, mathematical treatment 0–67572

critical heat flux density under forced convection rel. to artificial roughness 0-49721

data assessment in D.F.R. 0–60859 delayed neutrons in reactor excursions with ramp reactivity insertion 0–58052

0–58052
differential fast neutron flux determination (above 0.5 MeV) by threshold detectors, numerical solution of integral equations 0–49746
Doppler coefficients meas. 0–74077
dosimetry with adiabatic calorimeter 0–49743
fast breeder, coolant cross-mixing in multirod bundles 0–49720
fast-spectrum compact type, meas. of control schemes 0–55190
flow, fluids, hydraulic impedance, boiling loop stability prediction 0–74048

flow, fluid

graphite pile with empty channels, microdistribution, pulsed neutron meas. 0--42900

hot channel and hot spot factors new statistical method for evaluation 0-74061

0-74061 irradiation test facility, data assessment 0-60859 liquid-cooled reactor with pipe rupture model to describe 2 phase critical discharge of saturated or subcooled liquid 0-77607 molten salt breeder type, single fluid, design and performance characts. 0-39210

molten salt reactor, salt handling, chemistry and nuclear characts. 0–39215 molten salt type, history and potential as breeders 0–39214 molten-salt breeder, "LiF-BeF₂-ThF₄ with ²³³UF₄, fuel recycling process

noticen-sait breeder, LIP-Ber₂-1fir₄ with CP₄, fuel recycling process 0–39226 NERVA-type reactor comparison of calc. and meas. energy-dependent activation rate 0–74067 NORA, thermal n spectrum effects of plane boron steel absorbers 0–39213

0-39213
neutron flux meas., correlation method 0-49742
neutron time-of-flight meas., by on-line computer, physical characteristics and programs 0-49745
operational characteristics and analysis 0-70692
power oscillations, Xa induced, spatial 3 dimens. method for design studies 0-67577

O-67577

Down pulse meltdown expts., in mark I TREAT Na loop, on clusters of 7 EBR II mark I type pins O-55211

Down supplies, standby, selection criteria D-64157

Dressure vessel design, book O-43702

Dressurized water reactor, improved model for pressurizer O-55187

Drimary reactor containment, initial response to high-energy excursions O-55196

Dulse characteristics and ramp reactivity insertion and energy-shutdown reactor excursions O-58053

Rapsodie's irradiation expts., fission rates, y heating and dosimetry meas.
O-60860

0-60860 reactivity balance as malfunction as malfunction detector for research reactor 0-60858

tor 0-00838 reactivity changes due to the random vibration of control rods and fuel elements 0-58054 reactivity increases for pressurized water reactors, polywater as mechanism 0-46303

remote systems, conference, San Francisco, Calif., USA (1969) 0-77619 single-pin lattice cells, thermal neutron group constants computation 0-42906

0-42906
stability regions, asymptotic, of thermal neutrons reactors with discrete time control 0-46296
tubular, stability, analysis via Lyapunovs direct method 0-49724
vessel, thermal and radiation shielding 0-38952
voiding of power channels cooled by steam-water mixtures 0-39222
walls exposed to y-rays, transient temp. distrib. during heating up 0-55193

water cooling, two-phase flow problems 0-49722 with water under pressure, primary circuit, activation of corrosion products 0-67574

ZR-4 type, zero power, study of fission products from fuel elements 0-58051

0–58051

Hf-cruciform control rods replacement, for BONUS reactor, selection of material and design 0–46299

Hf control rods replacement for BONUS reactor 0–58057

Hg liquid metal coolant, heat transfer, effect of rod displacement 0–77611

I₂ in coolant circuit of high- temp. gas-cooled reactor, meas. of adsorption isotherms on low Cr alloy steel 0–40003

Pu sphere water reflected, critical mass obs. 0–49725

239Pu, neutron capture fission cross-sections, 0.1-30 keV, error effects on integral parameters in fast reactors 0–77612

Sb-Be, photoneutron start up sources for research reactors 0–74065

UO₂-PuO₂ microlattice with Gd₂O₃ burnable poison, power distributions and reactivity worths 0–67576

Xe poisoning peak reduction with single power pulse VVR-S, obs. 0–39217

Xe spatial oscillations, optimal control 0–39225

Xe spatial oscillations, optimal control 0-39225

theory
Avery's coupled reactor kinetics eqn., mechanics of derivation 0-39196
Boltzmann eqn., energy dependent in plane geometry semianalytical soln.
0-52834

breeder reactor, fast liq. simulation 0–52830 conference, nuclear and solid state physics, Powai India, (1968) 0–41919 continuous slowing down theory calc. of narrow resonance reaction rates in fast-reactor mixtures 0–77593

Nuclear reactors, fission continued

theory continued

creep, non conservative-volume type, relationship under different states of stress 0-55983

critical assembly, plane heterogeneous, neutron flux spatial distrib. 0-52840

dynamic behavior obs. by nodal approximation 0-74044

dynamic systems impulse response, spatially dependent use of cross-correlation technique determination 0–39197 effective cross-section, resonance overlap effect in unresolved resonance region 0–74042

fast, critical size calcs., method of collapsing neutron-cross-sections 0-58044

last, critical size cates, method of conapsing fleation-closs-sections 0-58044
fast, random sampling procedure and statistical uncertainty in Doppler coefficient calculation 0-64158
fast assemblies, very small cylindrical reflected, self-consistent one-dimens. analysis 0-39203
fast critical assembly, high density, params. 0-39208
fast power-reactor life, method of correlation of burnup meas. for physics prediction 0-39223
fast reactors, large, params., intercomparison calc. 0-39209
finite slab, criticality study with two energy group neutron model 0-39184
flux, average, variational principles derivation 0-39204
flux spectra and energy deposition for fast neutrons, FORTRAN code
NEVEMOR 0-77597
fuel cycle studies, calculation model description of MOICANO-2 program
0-67571
fuel element anal. in substitution expts. using three-dimens. heterogeneous method 0-42910
gaseous-core, radiative transport eqn., exact soln. 0-55197

gaseous-core, radiative transport eqn., exact soln. 0–55197 heat transfer crisis under h.p. forced water flow 0–50216 heat transfer in heat generating fluid in tube with cosinusoidal wall temp. distribution 0–55192

distribution 0-35192 heterogeneity effect, anal. by Monte Carlo method 0-67573 information theory applied to in-reactor statistical fluctuations in neutron density 0-77595 interface conditions for discontinuous flux synthesis methods 0-74049

kinetic energy of fission fragments released from fuel surfaces by recoil 0-77598

0-7/398 kinetics equation, on roots and coeff. for general soln. 0-39195 kinetics equations in 2 dimensions, multigroup diffusion theory, alternating direction methods for solution 0-77596 lattices, slab, thermal utilization factor calc. by multiple collision method 0-52831

linear

near homogeneous space-time, stability study, root loci approach 0-64156

lumped parameter kinetics equations, implicit method of solution by repeated extrapolation 0–74048 minimum critical mass in fast breeders with bounded power density 0–58043

moderator, Galerkin method solution of the neutron slowing down equations 0-67568

Monte Carlo calc. of mean free path 0—46285 multi region type, analytical soln. of Helmholtz eqn. over one-dimens. domain 0—49704

domain 0-49704 multigroup reactor eqns., anal. soln. 0-39192 neutron burst thermalization, stochastic simulation 0-52835 neutron density in-reactor statistical fluctuations, application of information theory 0-7595 neutron fluctuation experiments, correlated, on a poorly coupled multiple seed-blanket reactor and on a better coupled cylindrical lattice reactor 0-64159

neutron flux associated with subcriticality, LFEN-FR 5 DIFNE program 0-74051

neutron induced reactions cross-section library 0-39211 neutron transport eqn. with anisotropic scatt., eigenvalues 0-52833 noise, space-dependent formulation based on natural mode approximation 0-39194

nonlinear stability studies, construction of Lyapunov functions 0-49708 pebble bed reactor, effective multiplication constant calc., uncertainty 0-49703

point reactor with periodic reactivity input, kinetic eqns. integration 0-39205

point reactor with weak source, probability distrib. of neutron populations 0-60846

power, bounded and asymptotically stable, dynamic conditions 0-60845 power dynamics of reactor with randomly var. reactivity 0-49705 power reactor stability against bounded external reactivity perturbations 0-49701

pressure cylindrical vessel, thermal and pressure stresses, analytical determination 0–49699 primary reactor containment syst., calc. of hydrodynamic response 0-55209

primary-recoil atom spectra 0-74047 pulsed, fast, Monte Carlo method for geometrical perturbation 0-74054 radiation transport in shield irregularity, calc. 0-49700 reflection and transmission functions, use in problems of slab geometry 0-39199

resonance integral, approx. of $J(\theta\beta)$ function and applic. 0–39198 resonance integral calculations, accuracy of approximations 0–74043 slab type, nonlinear space-depend, neutron diffusion eqn., comment on iterative approach 0–49695

slab type, nonlinear space-time problem, reply to comments on iterative approach 0-49696 space dependent noise spectra from transport eqn., deficiencies in diffusion theory 0-39181 space-correlated fluctuations, measurements and detailed model analysis 0-64159

space-dependent reactor dynamics, weighted residual methods 0-64161 space-energy synthesis, improvement using reaction rate weighting and realistic trial functions 0–49707 space-time kinetics, appl. of finite difference approx. method 0–49706 spectral synthesis of dynamics 0–74034 stability criteria, comments on interpretation in finite dimens. Euclidean state space 0–52829

stability regions, asymptotic, of thermal neutrons reactors with discrete time

steady state temp. in heat generating components, optimum calc. method 0-55184

Nuclear reactors, fission continued

theory continued

superpromptcritical excursions, reactivity feedback and short delay times $0\!-\!39193$

0-39193
Tarapur B.W.R. params. during start-up and fuel burn-up 0-39206 thermal, radially loaded, transport theory calculations 0-46291 thermal design, effective equally limiting hot channels 0-49712 thermal neutron distribution in real reactor cell, thermos type method for calc. 0-58041 thermal reactors, large, stability rel. to spatial Xe oscills. 0-39207 time-profiles as a means of investigating delay time 0-58047 transport equation approximations, finite difference, truncation error analysis 0-74033

sis 0-74033 transport theory function $g(c,\mu)$, geometric interpretation 0-77591 Wigner approximation, accuracy 0-46284 zero-power describing functions, approximate, validity 0-46292 n pulsed source expts. in multiregion reactor, analysis 0-49692

Nuclear reactors, fusion

clear reactors, fusion

θ-pinch pulsed reactor, β=1, feasibility 0-70705

Astron, Li-Na-Be blanket design 0-70720

Astron with p E-layer confinement, 5600 MWe 0-70716

blanket, vacuum wall-free with heat pipes, modular design 0-70721

blankets, design, performance and neutron transport theory 0-70714

conference, Culham, England, 1969 0-70695

design, engineering params. 0-70718

environmental safety 0-70697

fission-fusion hybrid power system 0-70696

fusion torch use for direct appls. of reactor plasma 0-71168

Hall accelerator use for start-up plasma prod. 0-70724

Hall-accelerator, high-current, d.c. two stage, suitability for controlled thermonuclear work 0-70722

ignition using r.f. transit time mag. pumping 0-70725

ion recovery from divertor using moving trapping surface 0-70719

minimum-B, geometry rel. to economics 0-70716

mirror, α-particle heating rel. to energy balance 0-70700

with mirror machine confinement feasibility and end losses reduction 0-39201

mirror systems, economics and energetics 0-70699

mirror systems, economics and energetics 0-70699

mirror systems, economics and energetics 0–70699 mirror systems, fuel cycles, loss reduction and direct conversion 0–70698 non-selfdestructive, plasma confinement times, high density 0–74489 plasma, high temperature energy systems, inductive magnetoplasmadynamic converters 0–60856 plasma confinement, magnetic 0–71160 plasma flow heating 0–70701 power recovery and conversion, charged particle and thermal 0–70726 puised, feasibility, and steady-state mirror energy balance 0–70709 safety research on reactivity accidents, advanced type reactors, programs by pulse reactors 0–74058 selfdestructive, plasma confinement times, high density 0–74489 stellarator, T balance 0–70710 time-dependent behaviour 0–70708 Tokamak, extrapolation, plasma params, and technological problems 0–70703 Tokamak, extrapolation feasibility 0–70702

Tokamak, extrapolation feasibility 0-70702

Tokamak and stellarator, plasma params, for economic reactors 0–70704 toroidal pinch, pulsed, feasibility and economics 0–70707 toroidal pinch, pulsed high- β , plasma and technological problems 0–70706

0–70706
Z-pinch, pulsed high-β, field system and power supply design 0–70717
n damage in Nb containment vessel, 14 MeV 0–70729
n damage to reactor materials, 14 MeV 0–70728
D-T plasma, fuel burn-up and direct energy conversion 0–71132
He cooling, direct, with Brayton gas turbine 0–70711
Li/Nb blanket, vacuum wall-free with Na heat pipes, obs. 0–70721
Li and flibe blankets, neutronics cales. 0–70733
Li and flibe blankets neutronic props. 0–70732
Li blankets, liq., T breeding and energy generation 0–70731
Nb wall lifetime, rel. to D+, He+ sputtering obs. 0–70730
Clear relaxation. see Nuclear magnatic resonance and relaxation.

Nuclear relaxation see Nuclear magnetic resonance and relaxation

Nuclear scattering see Nuclear reactions and scattering

Nuclear spallation

nucleon currents meas., for energies exceeding 600 MeV 0-70577 radionuclide production rates in argon in stratosphere 0-60633 stellar atmospheres, role of spallation reactions 0-41634 Ar, proton spallation at 310, 425 and 578 MeV, production rates, theory and expt. 0-49615 Xe spallation yields from proton irrad. of Cs, Ce, Nd and Dy 0-77550 clear transferance of Northean Company (Northean Company) and the Northean

Nuclear structure see Nucleus/energy levels; Nucleus/theory

Nuclear track emulsions

clear track emulsions
analysis, high flux study of physical processes occurring with small cross sections 0-60726
deformation during final drying of layers, analysis 0-49422
discriminating development of particle tracks by amidol and NaSCN developers 0-38770
discrimination, pretreatment and development 0-38771
electron beam exposed, blackness calc, using recent grain development theory 0-38769
electron prography estimation in beauty media in reconstic field, 0-73711.

theory 0-38769 electron momentum estimation in heavy media in magnetic field 0-73711 electron tracks, multiple scattering meas, of p β c for electron energies 30 to 500 MeV 0-49423 fast neutron film-dosimetry, calibration 0-45459 IFA EN3, electron sensitive, main characts. 0-60725 IIIford K5, p-nucleus interactions at 3 GeV/c lacunarity and blob density methods 0-64113 innorrantic, using polyvinyl alcohol, chemical sensitization for recording

methods 0–64113 ionographic, using polyvinyl alcohol, chemical sensitization for recording RX and a rays 0–52615 ionographic signal analysis 0–49406 isotopic concentrations, cosmic ray carbon determination 0–61039 K scattering factor, multiple Coulomb technique 0–42654 Lexan polycarbonate film, etching 0–73710 luminescence, temperature quenching behaviour 0–63918 neutron flux anisotropy due to arrangement of fast core cell, meas., using emulsion 0–52836 relativistic particles, restricted energy loss 0–63920 restricted energy loss by extremely relativistic particles 0–63920 scanner, automatic 0–46058 spurious scattering 0–70319 track finding with high resolution spark chambers 0–60723

Nuclear track emulsions continued

width calc. of multiply charged ions 0-77427 α_st discrimination, pretreatment and development 0-38771 e, high-energy ionization energy loss 0-78805 p, d discrimination, pretreatment and development 0-38771

Nuclear-solid interactions see Mossbauer effect; Solids Nucleation see Clouds; Crystallization; Freezing

Nuclei with A \leq 5 3, 4-nuclear systems, calc. using Jastrow-type correlated wave functions 0-67417 4He(d_{po},d), tensor polarization $\langle T_{21} \rangle$ and $\langle T_{22} \rangle$ in elastic scattering 0-58003

He($u_{\rm pot}$, d.), tensor polarization $\langle T_{21} \rangle$ and $\langle T_{22} \rangle$ in elastic scattering 0–58003 triton, optical potentials 0–39089 triton, optical potentials 0–39089 $^{\rm He}(\alpha,\alpha)$, separable potentials below 30 MeV 0–42601 $^{\rm He}$ production in beam of negative particles produced by 70 GeV protons on Al target, observation 0–67415 $^{\rm S}$, He resonant states 0–55120 $^{\rm S}$ He (e,e) He assignment of 0 to stay confirmed, new values of monopole matrix element, evidence for M2 resonance at 24 MeV 0–64107 $^{\rm S}$ A, the three-nucleon problem, review 0–49450 $^{\rm S}$ D magnetic resonance in $[{\rm Cu}({\rm CD_3}({\rm CO}_2),{\rm D},{\rm O}]_2$ 0–66153 $^{\rm H-1}$ C heteronuclear resonance of nickel acetylacetonate with organic ligands 0–58190 $^{\rm H-\{^{\rm S}{\rm P}\}}$ double resonance in 2,3,5,6-tetrafluoroaniline 0–46443 $^{\rm H}$ A, amino-ring coupling constants sign in N-ethyl 4-chloro-2-nitroaniline 0–58219 $^{\rm H}$ A, chemical shift in 1,2-dichlorofluoroethylenes 0–77897

H, amino-ring coupling constants sign in N-ethyl -4-chloro-2-nitroaniline 0–58219
H, chemical shift in 1,2-dichlorofluoroethylenes 0–77897
h, chemical shift in fluoranthene, by π-electron 'ring currents' 0–77909
H, in polyvinyl chloride-β,β-d₂ nmr study 0–67832
H, magnetic relaxation in adulterated methane gas system 0–67803
H, n.m.r. in 1-bromo-2-chloro-2-deuteriothioethane 0–39359
H, n.m.r. in 1,1,2,2-terafluoroethane 0–49938
H, n.m.r. in colemanite, meas. from –110 to 110°C 0–41373
H, n.m.r. in difurylmercury and dithienylmercury isomers 0–74361
H, n.m.r. in lunar samples, 60 MHz 0–48487
H, n.m.r. in introphenylhydrazone α-carbonyls 0–71024
H, n.m.r. in organophosphorus cpds., 'H-³1P coupling constants 0–39450
H, n.m.r. in phenol and thiophenol and methyl, silyl and germyl derivs.

1H, n.m.r. in phenol and thiophenol and methyl, silyl and germyl derivs. 0-39444

0-39444
H. n.m.r. in planar condensed benzenoid hydrocarbons, McWeeny calcs. on hexacyclic mols. 0-43168
H. n.m.r. in planar condensed benzenoid hydrocarbons, in isotropic solvent 0-43166

vent 0-43166

H, n.m.r. in polycrystalline NaBr.2H₂O 0-69198

H, n.m.r. in polywater 0-46471

H, n.m.r. in propylene oxide and epihalohydrins 0-64503

H, n.m.r. in pyridine, solvent effects 0-49937

H, n.m.r. in Rb₂SO₂ rel. to ferroelectricity, -196 to 23°C 0-41383

H, n.m.r. of Zn(NO₃)₂ in methanol association 0-58490

H, n.m.r. spectra in epichlorohydrin 0-64502

H, n.m.r. spectra in planar condensed benzenoid hydrocarbons, McWeeny 'ring current' theory evaluation 0-43167

H, n.m.r. spectra of acetonitrile, nitromethane and nitrobenzen-1, 3, 5 d, in liquid crystal PBLG 0-74321

H, n.m.r. spectra of celluloses 0-69199

H, mm in benzyl oxo-2 piperazines with asymmetry in positions 3 or 6 0-70977

H, n.m.r. is solid methylammonium balides 0-62776

H, nmr in solid methylammonium halides 0-62776

H, nmr in solid methylammonium halides 0–027/0
H, nmr spectfa of trimethyl, trifluoro, trichloro silyl compounds 0–64552
H, nuclear spin-lattice relaxation times in LiBD4 and LiBH4 0–59471
H, p.m.r. data in Co hydrates and Ni phosphates 0–62778
H, p.m.r. spectra of 2-pyridones, 2-pyridthiones and 2-thioalkylpyridines 0–55370

0–553/0 H, photoprod. of hadrons, 1.0-6.4 GeV 0–73482 H, photoprod. of ρ^0 and ϕ^0 meson 0–70262 H, uncoupled, nuclear relaxation time in liquid 0–64955 H chemical shifts of non-polar molecules in liquids, intermolecular effects 0 - 49849

0-49849

'H in organic molecules, correlation of Overhauser effect with internuclear distance 0-64461

'H n.m.r. chemical shifts in decaborane ring current model 0-74239

'H n.m.r. in bromination products of some substituted bicyclo[2.2.2]octenes 0-64489

'H n.m.r. of 1'N-pyrrole, sub-spectral analysis 0-71029

'H n.m.r. studies of ionic solvation in sulphated cation-exchange-resins 0-56685

'H radiative transfer of pions, 220-380 MeV/c 0-42857

H n.m.r. of N-pyrrole, sub-spectral analysis 0—1029
H n.m.r. studies of ionic solvation in sulphated cation-exchange-resins 0—56685
Hr radiative transfer of pions, 220-380 MeV/c 0—42857
Hr radiative transfer of pions, 220-380 MeV/c 0—42857
Hr adiative transfer of pions, 220-380 MeV/c 0—42857
Hr spin-rotation consts. in SiH₄ and GeH₄ 0—77841
H(d,'Hey) ang. distrib. of π-d capture cross-section calc. 0—64133
H(d,'n)pp, polarization transfer to 0° neutrons 0—77573
Hr, ENDOR enhanced n.m.r. 0—51405
Hr, n.m.r. in cupric acetate hydrate-d₁6 0—66153
Hr, n.m.r. in cupric acetate hydrate-d₁6 0—66153
Hr, n.m.r. in deuterated isobutylenes in liquid state, molecular motions 0—64855
Hr, n.m.r. in MnCl₂-dD₂ 0—41379
Hr, neutron-induced breakup, n-p coincidence meas. 0—49630
Hr, nuclear spin-lattice relaxation times in LiBD₄ and LiBH₄ 0—59471
Hr, optical potential 0—38844
Hr, photoprod. of hadrons, 1.0-6.4 GeV 0—73482
Hr, photoprod. of hadrons, 1.0-6.4 GeV 0—73482
Hr, photoprod. of p⁰ and p⁰ meson 0—70262
Hr, spin-isospin formalism for multiple scattering of pions 0—49638
Hr, Tabakin N-N potential 0—73773
Hr chemical shift, difference for α and β substituents 0—77758
Hr claxation in deuterobenzene dissolved in liquid crystal 0—49918
Hr spin lattice relaxation time in solutions of polyvinylpyrrolidone in deuterated solvents 0—58263
H('He,'Hep)n, coincidence studies, E=18.0-24.0 MeV 0—39100
H('A, α, ρ)n, at about 160 MeV, theoretical study 0—73935
H('A, α, ρ)n, coincidence studies, E=18.0-24.0 MeV 0—39100
H('A, α, ρ)n, at about 160 MeV, theoretical study 0—73935
H('A, α, ρ)n, coincidence studies, E=18.0-24.0 MeV 0—39100
H('A, ρ)Hr, E_d=60-505 keV, resonance 0—42867
H('A, ρ)He, polarization transfer to 0° nuetrons 0—77573
H('A, ρ)He, polarization transfer to 0° nuetrons 0—77573
H('A, ρ)He, polarization transfer to 0° nuetrons 0—55156
H('A, ρ)Hr, the polarization transfer to 0° nuetrons 0—55156
H('A, ρ)Hr, the polarization transfer to 0° nuetrons 0—55156
H('A, ρ)Hr, the polarization transfer to 0° nuetrons 0—55156
H('A, ρ)Hr, th

Nuclei with A≤5 continued

²H(e,e'n)¹H, total cross sections, with BF₃ counter 0-70572

FIG. e. P.H. total cross sections, with Br3 counter 0 - 76372 FIG. e.) H sum rule for spatially symmetric part of 1s shell nuclei 0 - 64106 FIG. 2. Hungard St. MeV 0 - 57987 FIG. e. P.H. on scattering length determination, En=18.5 MeV 0 - 57987 FIG. e. P.H. on Scattering length determination, En=18.5 MeV 0 - 57987 FIG. e. P.H. on Scattering length determination, En=18.5 MeV 0 - 57987 FIG. e. P.H. on Scattering length determination of the second se

²H(n,n), E=28 MeV, differential cross section 0-42849 ²H(n,n)²H, 28 MeV elastic scatt. studied 0-55156

²H(n_{pol},n) enriched deuterated benzene solution, En=1.2 MeV 0-49629

²H(n,p)2n, 8-28 MeV, p spectra 0-39065 ²H(p,2p), exp. study at 150 MeV 0-73933

²H(p,2p), quasielastic deuteron breakup and cross-sections measurements at 100 MeV 0-60807

at 100 MeV 0-60807

²H(p,2p)n, asymmetry cross-section measurement, 10 MeV, using trochoi dal injection 0-60806

³H(p,2p)n, at 10.5 and 24 MeV, asymmetry meas. 0-73932

⁴H(p,2p)n, at about 160 MeV, theoretical study 0-73935

⁴H(p,2p)n, deduction of cross-section for ³H(p,4*)p 0-42831

³H(p,2p)n, pp quasifree scattering, study of energy dependence 0-73950

³H(p,2p)n at 35 MeV 0-73936

³H(p,4*)p cross-section from the ³H(p,2p)n reaction 0-42831

³H(p,p) polarized protons of 30 and 50 MeV in polarization determ. 0-3935

30-39033 ²H(p,p)²H 1-10 MeV, cross-section obs. 0-42823 ²H(p,pp)n, modified impulse approx. calc. of N-N quasi free scatt. 0-67318

3H-3He, charge asymmetry energy 0-77469
3H, binding energy, effect of Shirovkov corrections, 3-boson model 0-52644

0-52644

3H, r.m.s. charge radii connection with bremsstrahlung weighted cross section of photodisintegration 0-38846

3H, variation binding energy, second order correction of peturbation theory 0-67414

3H, leptonic decays, angular lepton-neutrino correlation 0-70416

3H binding energy, relativistic corrections 0-49498

3H binding energy calc. with Jastrow-type wave functions 0-67417

3H β-spectrum end point energy, ft deduced 0-70540

3H exchange currents indicated by polarization of nucleons emitted in electron-induced interactions 0-38845

3H production in Al, Sn. Pb, and Bi by 0.15-0.66 and 3-10 GeV protons 0-42828

3H yield in thernal neutron fission of 233U 0-70679

0 - 42828

3H yield in thernal neutron fission of ²³³U 0-70679

3H(²H, ²He) 2n, E₂₄=11 MeV, nn effective range parameters 0-55112

3H(²He, ²He), 2.77 and 32.3 MeV, differential cross sections, excitation functions for elastic scattering 0-70631

3H(d, ²He)2n, final state interaction spectra and ¹So neutron-neutron scattering parameters 0-73976

3H(d, ²He)2n, neutron-neutron interactions in ¹So wave 0-70640

3H(d, ²PHe, cross- section and gamma-ray-neutron branching ratio 0-52799

10-52799
14(a,η)*He, 3.9-15 MeV, polarization transfer study 0-73987
14(d,η)*He polarization of neutrons at low deuteron energies 0-70641
14(e,e)*H sum rule for spatially symmetric part of 1s shell nuclei 0-64106
14(e,e)*H sum rule for spatially symmetric part of 1s shell nuclei 0-64106
14(e,p)*He, Ep=-3-18 MeV, cross section, ang. distribs. 0-49613
14(e,p)*He, exp. and theoretical study at 156MeV 0-73934
14(e,p)*He, exp. and theoretical study at 156MeV 0-73934
14(e,n)*He, n polarization, 1.3 < Ep < 2.3 MeV 0-39036
14(e,α) nn, nucleon-nucleon scattering parameters from final-state interactions 0-42868
14-34e, β-decay, corrections due to exchange currents and sensor force 0-73851
14-34e, β-decay, corrections due to exchange currents and sensor force 1-3-34e, β-decay, transition matrix element evaluation 0-49564

³H→³He decay, transition matrix element evaluation 0-49564

⁴H variation binding energy, second order correction of peturbation theory 0–67414

0-0744 He, alpha-particle scattering, separable potential 0-73988 He prod., from interactions of 60 GeV π with heavy emulsion nuclei 0-77567 ³He-³H binding energy difference, contribution of p-n mass difference

U-1/46\)

3He, elastic proton scatt. at 580 MeV 0-42824

3He, elastic scattering and differential cross-sections and comparison to resonating group calculations 0-52795

3He, elastically scattered from 4He, analyzer for polarization 0-42733

3He, electromagnetic structure, charge and magnetic form factors 0-73774

0-13/14

He, electron scattering at 180° 0-67521

He, ground state energy estimation based on dual core model 0-60752

He, liquid, nuclear molar susceptibility between 0.35-2.2°K, 26-37
cm²/mole 0-74825

m³/mole 0–74825

He, liquid, nuclear susceptibility, pulsed NMR obs., 0.035→1°K 0–74826

He, pitical potentials 0–39089

He, π scatt. 0.826–2.01 GeV 0–60819

He, π.m.s. charge radii connection with bremsstrahlung weighted cross section of photodisintegration 0–38846

He, spin-isospin formalism for multiple scattering of pions 0–49638

He, three-body photodisintegration from threshold to 30 MeV 0–52748

He decay in LiD_{0.6}T_{0.4}, lattice expansion 0–50529

He elastic scattering by ⁴He for ³He energies 17.8 to 30.0 MeV 0–58000

He exchange currents indicated by polarization of nucleons emitted in electron interactions 0–38845

He excited levels, exp. investigation 0–73775

He form factor, ε.m., theoretical considerations 0–73776

He spin-lattice relaxation time in liquid ³He and ³He-⁴He mixtures 0–46969

He virtual states using ⁶Li(p,α) and (p,αd) 0–70388

0–46969
The virtual states using °Li(p,α) and (p,αd) 0–70388
He(H,H)H)2p, E₂=11 MeV, nn effective range parameters 0–55112
He(H,H)2p, neutron-neutron interactions in 'S₀ wave 0–70640
He(H,E)P)He total cross section meas, 1100 to 80 keV 0–39101
He(H,E,α)pp, nucleon-nucleon scattering parameters from final-state interactions 0–42868
He(H,E,pp)He, n tunneling use of Hulthen wavefunctions to obtain accurate expression for matrix element 0–77526
He(d,H,E,pp)He, polarization and asymmetry 0–46241
He(d,1)2p, final state interaction spectra and 'S₀ neutron-neutron scattering parameters 0–73976
He(d,pp), absolute coincidence cross sections and p-p and p-t final state interactions for E=20.7 MeV 0–58001

Nuclei with A≤5 continued

³He(e,e) ³He sum rule for spatially symmetric part of 1s shell nuclei -64106

 3 He(γ ,p) 2 H, ang. distrib., E=16-27 MeV 0-67514

 3 He(n,p)T, cross-section meas, 0.3 to 1.16 MeV 0 –57988 3 He(p,n), at 30 and 50 MeV, evidence for broad resonances 0 –73937 3 He(π - π + 1 3n, rel. to resonant behaviour in three-neutron system within few MeV of threshold 0 –52792

 3 He(t, α)np, nucleon-nucleon scattering parameters from final-state interactions 0-42868

⁴He, 2⁺ excited state at 30 MeV, from ⁴He(y,d)d 0-73898

⁴He, 2* excited state at 30 MeV, from ⁴He(ρ,d)d 0-73898
⁴He, α elastic scatt., Regge pole calc. 0-39091
⁴He, charge form factor, microscopic description 0-67416
⁴He, elastic scattering and differential cross-sections for ³He energies 17.8 to 30.0 MeV 0-58000
⁴He, electron scattering at 180° 0-67521
⁴He, first excited 0* state, self-consistent calc. 0-70390
⁴He, ground and first excited states, by shell model 0-73778
⁴He, ground state, realistic nuclear charge-density 0-77480
⁴He, Hartree-Fock calcs. with four-body interaction 0-52667
⁴He, levels, deduced singlet strength, from ³H(ρ, ρ)⁴He and ⁴He(ρ, p) 0-49613

4He, levels 0-49613

0–49613

4He, liquid, ground state energy, variational calculation 0–74819

4He, muon capture rates rel. to breakdown of SU(4) invariance 0–49600

4He, n scatt. and phase shifts, 0.5 and 0.8 MeV 0–39036

4He, photodisintegration, diff. and total cross sections 0–73899

4He, π scatt. 0.826–2.01 GeV 0–60819

4He, π scatt. 0.826–2.01 GeV 0–60819

4He, spin-isospin formalism for multiple scattering of pions 0–49638

4He assignment of 0+ state confirmed, new values of monopole matrix element, evidence for M2 resonance at 24 MeV 0–64107

4He binding-energy calc., third-order corrections to Hartree-Fock approx. 0–73777

0-13717

*He binding energy, size from effective NN interactions 0-38806

*He binding energy calc, with Jastrow-type wave functions 0-67417

*He binding energy calculation using matrix elements of Tabakin's potential 0-70389

He binding energy for Tang soft-core potential 0-63994

He deduced levels from ³He+²H and ⁴He+²H coincidence levels

0-39100

0–39100

He ground state form factor, four particle states 0–63995

He(-He, He), left-right asymmetry of polarized 3 He 0–42733

He(\(A,\A\), 0.1-10 MeV phase shifts, cross-sections and ang. distributions 0–73970

He(d,d)^{4}He, 3-11.5 MeV, vector polarization meas. 0–39090

He(d,b), clastic scattering and tensor polarization $\langle T_{20} \rangle$ 0–58002

He(e,e), the, sum rule for spatially symmetric part of 1s shell nuclei 0–64106

 4 He(γ ,n) 3 He, photoneutron cross section from threshold to 31 MeV 0 –73897

0-/389/
He(y,p)³H, 120 MeV, reaction analysis, total cross section 0-67515
He(y,p)³H, integrated cross section decomposed into E₁ and E₂ contribs. up to Ey=30 MeV 0-49613
He(p, Hep)n, 47 MeV obs., agreement with Watson-Migdal theory 0-73938

 4 He(p,d) 3 He excitation functions, 22 46 keV, search for T= 1 / $_{2}$ resonances 0–39037

 $^4\text{He}(p,p^3\text{He})n$, meas. at 46 MeV $\,0-73939$ $^4\text{He}(p,p)^4\text{He}$ excitation functions, 22-46 MeV, search for T= $^4/_2$ resonances 0-39037

He(p,t)p, meas. at 46 MeV 0-73939
He(p,t)2p, at 156 MeV, interpretation of final state interaction spectra 0-73945

⁴He(p,tp)¹H, 47 MeV obs., agreement with Watson-Migdal theory 0-73938 0-7938 He(π , π), at 46.7 MeV, angular distributions and energy spectra 0-42832 He(π , 2π), theoretical aspects, using soft-pion techniques 0-49641 He(π , ν), spectrum of high-energy ν -rays 0-73969 He energy levels from $\text{Li}(d,\alpha)$ He 0-70392 Li, shell-model calc. 0-46119 Li, shell model calc. 0-46119

5Li, shell model calc. 0—46119
 5Li, study within excitation range of 17.8 21.1 MeV, by radiative capture reaction 0—49499
 5Li energy levels from ⁶Li(³He, α)⁵Li 0—70392
 ⁴He decay, spin depend. of ΛN weak interaction 0—63993
 ⁴He final state interactions in π-mesic decays 0—73791
 ⁵He final state interactions in π-mesic decays 0—73791
 ⁸O energy levels of valence particles calculated using harmonic oscillator intermediate states 0—52634
 ²³⁵U, thermal neutron fission, isomeric gamma radiation from neutron-rich fragments 0—70683

fragments 0–70683

Nuclei with 6≤A≤19

1-p proton hole states in 13 nuclei from ¹²C to ³²S 0–70399

¹⁸O(p,n), effective two-body pot. 0–42732

¹⁹F(d,pp)²⁰F, single y-ray spectra and py coincidence spectra meas. using Ge(Li) spectrometer 0–38867

A=13, 14, 15 compilation of energy levels, structure of systems 0–73784

A=15, 14, 11 a nuclei shell model calculations for non-normal parity states of A=15, 14 and 13 nuclei o–63999

a=15-19, mean lifetimes of excited states 0–38857

A=18 isobaric triplet, energy differences 0–38861

A=19 isobaric quartet, energy differences 0–38861

A=12, photonuclear disintegration, calc., 40-350 MeV 0–49592

1-spin analogue states in A=10 triad 0–70395

shell model, realistic forces, spectra and the effects of correlations in A=6 nuclei 0–57893

(α,αα) reaction on light nuclei 0–58004

¹²C(π⁻, π⁻)¹²C, 180 MeV, Glauber approx. calc. non-convergent 0–77566

¹⁸F, relaxation times in solid tetrafluoromethane 0–56466

¹⁶O, quasimolecular structure and quasibound molecular states for elastic 150-169 centering 0.—58027

 $^{19}\mathrm{F}$, relaxation times in solid tetrafluoromethane 0 —56466 $^{16}\mathrm{O}$, quasimolecular structure and quasibound molecular states for elastic $^{16}\mathrm{O}$ - $^{16}\mathrm{O}$ scattering 0 —58027 12 C, absolute differential cross-sections, measurement using a photographic method, E_{a} =20-24 MeV 0 —64130 $^{99}\mathrm{*AB}$ e resonant states 0 —55120 $^{13}\mathrm{Al}$, elastic scattering, differences in single, plural and multiple scattering through intermediate angles for electrons and positrons 0 —57970

Nuclei with 6≤A≤19 continued

B isotopes, production cross sections on 70 MeV α particle interaction on C and N targets ~0-77572

 8 B, beta-decay meas. by energy distrib. of α -particles from subsequent break up of 8 Be 0–46162

sp. oteratects with the state of the state

10B, thermal-neutron-absorption cross-sections by pulsed neutron method

The thermal neutron absorption cross-sections by pulsed neutron method 0-5798 ^{10}B 7.01 MeV level width and reson, energy determ, from $^{6}\text{Li}(\alpha,\alpha)^{6}\text{Li}$ 0-39102 ^{10}B deuteron induced reactions and scattering, angular distribution 0-49644

10B deuteron induced reactions and scattering, angular distribution 0–49644
10B energy levels, effective interaction calc. 0–38853
10B(i]He, i]He)B, continuous study of i]N levels 0–70632
10B(i]He, i]He)B, 1-10MeV, study of i]N levels 0–42736
10B(i]He, i]N levels 0–42736
10B(i]He, i]N levels 0–42736
10B(i]He, i]N levels 0–42736
10B(i]He, i]N levels 0–43782
10B(i]He, i]N levels 0–55170
10B(α, i] Reg, i]Teg, Barshay-Temmer theorem verification 0–67550
10B(α, i]N leg, i]Reg, Reg, i]Reg, Reg, i]Reg, i

(**B(p,t)**B, differential cross section, to ground and first two excited states of **B 0-70598

"IB, clastic and inelastic scattering of 9.72 MeV neutron differential and integrated cross sections 0-46218
"IB, nuclear spin-lattice relaxation times in LiBD₄ and LiBH₄ 0-59471
"IB, nuclear spin-lattice relaxation times in transition metal diborides 0-79419
"IB, quadrupole moment, Calc. 0-46120

11B, nuclear spin-lattice relaxation times in transition metal diborides 0–79419
11B, quadrupole moment, Calc. 0–46120
11B cusps, threshold states and neutron emission 0–57896
11B n.m.r. chemical shifts in decaborane ring current model 0–74239
11B n.m.r. in KF-B₂O₃ glass, coordination number 0–41374
11B photodisintegration, explanation of failure to observe all of expected γ rays 0–70569
11B proton capture and de-excitation of ¹²C 0–70599
11B(¹²C₂γ²Na, radiative capture 0–39145
11B(¹⁴N, ¹²C)¹²C, ang. distribs. 0–39143
11B(¹⁴N, ¹²C)¹²C, ang. distribs. 0–39143
11B(¹⁴N, ¹⁵C)¹²C, ang. distribs. 0–39143
11B(¹⁴N, ¹⁶C)¹²C, ang. distribs. 0–39143
11B(¹⁴N, ¹⁶C)¹²C, and distribs. 0–39143
11B(¹⁴C₂N)¹⁴N, 3.6-3.8 MeV, neutron polarization obs. 0–58007
11B(A, p)¹²B, γ radiation observed rel. to lifetime of ¹²B determ. 0–52670
11B(A, p)¹²B, p, radiation observed rel. to lifetime of ¹²B determ. 0–52670
11B(A, p)¹²B, angular distribution of photons, DWBA calculations 0 70637
11B(n, p)¹²B, angular distribution of photons, DWBA calculations 0 70637
11B(n, A), differential and integrated cross-sections for En=14.1 MeV 0–49631
11B(p, 3α), 3α emission mechanism, 1.9 MeV 0–42835
11B(p, 3α), αnergy distribs., resonance narrowing 0–73941
11B(p, α)¹²B, energy distribs., resonance narrowing 0–73941
11B(p, α)¹²B, vergential reaction, study of formula derived for differential cross section 0–73942
11B(p, p)¹B polarization at 30.3 MeV, poor agreement with shell model 0–67526
11B(p, p)¹B p polarization at 30.3 MeV, poor agreement with shell model 0–67526
11B(p, p), E_p=5.9 MeV, ang. correlations meas. 0–39039
11B(p, 3α), resonance effect of ¹²C states on α spectra shape 0–73943
11B(p, 3α), resonance effect of ¹²C states on α spectra shape 0–73943
11B(p, 3α), resonance effect of ¹²C states on α spectra shape 0–73943
11B(p, 3α), resonance effect of ¹²C states on α spectra shape 0–73943
11B(p, 3α), resonance effect of ¹²C states on α spectra shape 0–73943
11B(p, 3α)

Nuclei with 6≤A≤19 continued

⁷Be(p,γ)⁸B, cross section using single-particle model for ⁸B ground state

Be, 0^+ , 2^+ , 4^+ states from excitation energy spectrum in $^{12}C(\alpha, 2\alpha)^8$ Be, $E_{\alpha}=100$ MeV 0-496578Be, 0+,

Be, cluster states, reaction matrix theory 0-73781

⁸Be, from 0-46162 from ⁸B beta-decay, energy distrib. of α-particles on breakup

 8 Be, ground state rotational bands, cut off 0-52669 8 Be from 10 B(d, α) 8 Be, isobaric spin doublets at 16.6 and 16.9 MeV 0-57902

⁸Be from ⁷Li(d,n)Be⁸, energy levels and formation 0-55169

⁸Be ground state, α -particle and shell models 0–70393

⁸Be level branching ratio 0-57975

Be level orancing ratio 0-3/9/3
Be, deduced levels from β decay of *Li 0-49567

*Be, low-lying states 0-38849

*Be, mag, form factor calc. with projected Hartree-Fock functions 0-38851

 9 Be, photoneutron counting after fission γ reaction, rel. to fuel burn up

Be, photoneutron counting after fission γ reaction, rel. to fuel burn up meas. 0 – 46301
Be, proton scattering, I-spin analogue states 0 – 70394
Be 1.67 MeV level studied by p scatt 0 – 77481
Be (³He,n)¹¹C analysis of neutrons, and two-nucleon transfer 0 – 70646
Be deuteron induced reactions and scattering, angular distribution 0 – 49644

⁹Be n.m.r. in irrad. BeO 0-69196

Be n.m.r. in irrad. BeO 0-69196
Be states from PLi β-decay obs. 0-38850
Be(He, d), T dependence of angular distributions 0-70647
Be(He, γγ), search for lowest T=2 state of ¹²C 0-73783
Be(He, n)¹¹C, excitation of T=3/2 levels in ¹¹C 0-46121
Be(He, t) and (²He, ³He'), 39.9 MeV, angular distributions 0-39096
Be(El, He) B quasielastic scattering process, experimental results

*Be(*Li,p1*e)*B quasielastic scattering process, experimental results 0-46247

*Be(*Li,p)*C, p angular distribs., obs. and statistical cpd.-nucleus model 0-39142

*Be(*Li,a)*B triton transfer and excitation of triton states 0-46249

*Be(*Li,a)*C absolute cross section and angular distrib., obs. 0-39141

*Be(*Li,b)*C absolute cross section, angular distrib. and *C levels, obs. 0-39141

'Be(TLi,p)'SC absolute cross section, angular distrib. and ¹⁵C levels, obs. 0-39141
'Be(TLi,t_o)'1C absolute cross section and angular distrib. obs. 0-39141
'Be(a,n)'1C reaction, polarization of n for E_a=2.4 to 2.9 MeV 0-42593
'Be(d,a,n)'1C reaction, polarization of n for E_a=2.4 to 2.9 MeV 0-42593
'Be(d,a,n)'1C reactions of the 1p shell initiated by vector-polarised deuterons 0-5168
'Be(d,p)'9Be I-value mixtures 0-70644
'Be(p, He), 45 MeV, angular distributions 0-52773
'Be(p, El), 45 MeV, angular distributions 0-52773
'Be(p, El), 21, 0 MeV, polarization meas. 0-49605
'Be(p, a), quasi-elastic scatt. at 160 MeV 0-57975
'Be(p,n)'Be mechanism 0-70597
'Be(p,n)'Be total cross section, near threshold 0-6080
'Be(p,n)'Be, total cross section, near threshold 0-6080
'Be(p,p)'Be, 6 MeV used to study 1.67 MeV level 0-77481
'Be quadrupole deformation and relative reduced widths from 'Be(d,p) calc. 0-70644
'Be(d,a)'Be, isobaric spin doublets at 16.6 and 16.9 MeV 0-57902
'Be(d,a)'Be, isobaric spin doublets at 16.6 and 16.9 MeV 0-49656
'Be(d,p)'IBe, production cross section, from 0.67 to 3.0 MeV 0-49656
'Be-10B beta decay, second forbidden shell and rotational models calc. 0-73855
'Be, energy of 1st excited level of 'Be, mass excess, from 'Be(d,p) 0-49656
'Be, energy of 1st excited level, mass excess, from 'Be(d,p) 0-49656

0–73855

¹¹Be, energy of 1st excited level, mass excess, from ¹⁰Be(d,p) 0–49656

¹¹Be(¹He,n)¹³N, paired-proton configurations 0–70645

Be(p,p)Be, diff. cross sections, near threshold 0–60808

C, 70 MeV α particle interaction, cross sections for production of Li, Be, B isotopes 0–77572

C, K₁⁰ and neutron total cross sections at GeV energies 0–46230

C, photoprod. of electron-positron pairs, p-ω interference 0–45947

C, φ photoprod. 1800 MeV 0–42570

C, quasi elastic scattering of high energy electrons 0–67519

C total neutron cross-section determ. 100 1500 keV 0–777559

¹⁰C, meas. of T_{ε=3}/₂ masses, using mag. spectrograph 0–67419

¹⁰C, deduced branching ratio for β decay to J⁴=1+ 2.15 MeV state of ¹⁰B

0–38963

¹¹C, assignment of J⁴=3/₂- for 8.11 MeV level 0–73782

9C, meas. of T_e=³/₂ masses, using mag. spectrograph 0-67419
9°C, deduced branching ratio for β decay to J*=1* 2.15 MeV state of ¹⁰B 0-38963
1°C, assignment of J*=³/₂ for 8.11 MeV level 0-73782
1°C, assignment of J*=³/₂ for 8.11 MeV level 0-75382
1°C, assignment of J*=³/₂ for 8.11 MeV level 0-7539
1°C and ³Be prod. from graphite bombard. 87 MeV e. 0-77539
1°C emission on irradiation of ¹⁴N by proton, deuteron, α-particles and ³He ions 0-74000
1°C first excited state, I, from ⁶Li(⁶Li,n), 1.9 MeV 0-39139
1°C giant dipole resonances observed by ¹⁰B(p,p) reaction 0-70396
1°C many charge particle produced by 660 MeV protons on ²⁷Al, angular distribution 0-67534
1°C T=3/2 level excitation in search 0-46121
1°C, ¹⁹F induced transfer reactions, spectroscopic inform. obs. 0-39144
1°C, 2-hole states study using 2- nucleon absorption model 0-73971
1°C, 600 MeV interactions, intranuclear cascade, α-cluster model 0-49609
1°C, α-cluster struct., from (π-,2nd) reaction 0-77568
1°C, α-cluster struct., from (π-,2nd) reaction 0-77568
1°C, α-clustic scatt., reage pole calc. 0-39091
1°C, central, spin-orbit and tensor parts of Sussex interaction, effects on ground state properties 0-77483
1°C, elastically scattered ³He particles 0-46243
1°C, electrodisintegration, 15-60 MeV obs. 0-46196
1°C, excitation of giant resonance by inelastic electron scattering 0-73914
1°C, formation from parity-forbidden α-particle decay from 8.87 MeV 2-state of ¹⁰O 0-73854
1°C, inelastic electron scatt, sum rule, expt. and theory 0-73909
1°C, inelastic electron scatt, sum rule, expt. and theory 0-73909
1°C, inelastic pion scattering, 180 MeV 0-39087
1°C, inelastic pion scattering, 180 MeV 0-739087
1°C, inelastic pion scattering, 180 MeV 0-739087
1°C, inelastic pion s

Nuclei with 6≤A≤19 continued

12C, search for lowest T=2 state using d and ³He induced reactions 0-73783

¹²C. square-well shell model as framework for study of quasielastic electron scattering 0-60802

 $^{12}\mathrm{C},$ struct. in giant reson, region, from e scatt, and μ capture calc. in continuum model 0-39021

continuum model 0–39021

1°C, total cross sections between 10.3 and 21.6 MeV variation 0–70603

1°C, two-nucleon density functions and correlation functions with realistic single-particle functions 0–55119

1°C, 7°C, scatt., 120-280 MeV, around N* reson. 0–57998

1°C (1°C, 1°C) elastic scattering, excitation functions 0–70671

1°C analyzing power for proton polarization determ. 0–55062

1°C cusps, threshold states and neutron emission 0–57896

1°C dee-excitation channels near giant dipole and giant quadrupole resonances 0–70599

nances 0-70599

"In the control of t

¹²C(³He,n)¹⁴O, precision meas, of threshold energy by velocity technique

0-46211

¹²C(³He,p)|⁴C, at low energy, calc. of polarization effects 0-73981

¹²C(³He,py)|⁴N y radiation observed rel. to lifetime of ¹⁴N determ.

0-52670

0-52670

"2C(3He,t) and (3He, 3He'), 49.8 MeV, angular distributions 0-39096

"2C(6Li,α)¹N at 5.6 to 6.6, 9.0 to 14 MeV, states at different energies 0-58025

"2C(6Li,α)¹O at 5.6 to 6.6, 9.0 to 14 MeV, states at different energies 0-58025

"2C(6Li,α)¹O at 5.6 to 6.6, 9.0 to 14 MeV, states at different energies 0-58025

"2C(6Li,α)¹O at 5.6 to 6.6 9.0 to 14 MeV, states at different energies 0-58025

"2C(6Li,α)¹O at 5.6 to 6.6, 9.0 to 14 MeV, states at different energies 0-58025

0-58025 12C(7Li, α 0–58025 " 12 C(7 Li, α) 15 N, peaks in the zero degree yield curve, interpretation 0–58026 " 12 C(7 Li, α) 15 N triton transfer and excitation of triton states 0–46249 " 12 C(7 Li,d) and (7 Li, α) and states in 17 O and 15 N 0–73788 " 12 C(7 Li,t) 16 O, 20-30 MeV, α -particle transfer 0–46250 " 12 C(7 Li,t) 16 O, 16 D, 16

46248

^{1-C}(C(1,1))**(2, U-3-0) MeV, α-particle transfer O-40250*

1°C(TLi,1)**(5), t_{tob}=15, 21.1 and 24 MeV, ang. distribs., ¹⁶O deduced levels 0-46248

1°C(N,N)**(2, inelastic scatt., E<9MeV, cross sections for 4.43 MeV γ-ray production 0-42820

1°C(α, 2α)**Be, Εα=100 MeV, excitation energy spectrum 0-49657

1°C(α, 2α)**deduced 6* level in ¹⁶O 0-52671

1°C(α, α, α), deduced 6* level in ¹⁶O 0-52671

1°C(α, α, α), deduced 6* level in ¹⁶O 0-52671

1°C(α, α, α)**O-24 MeV 0-42864

1°C(α, α, α)**IOC 0-3204 MeV 0-38010

1°C(α, α)**IOC 0-39105

1°C(d, α)**IOC 0-39103

1°C(d, α)**IOC 0-39103

1°C(d, α)**IOC 0-39103

1°C(d, α)**IOC 0-39103

1°C(d, α)**IOC 0-39106

 12 C(p, 2p), differential cross-secuoir, execution on 3928 12 C(p, 2) quasi-elastic scatt. at 160 MeV 0-57975 12 C(p,p) 12 C*, 12-14 MeV, spin-flip probabilities 0-52760 12 C(p,p) 12 C, elastic scatt., 19-30 MeV, study of 13 N levels 0-42736 12 C(p,r) 13 C, 600 MeV, capture cross-sections meas. 0-64116 12 C(π ,p), giant resonance obs. 0-73972 12 C(π ,p) 12 C, 120 ξ T, ξ 280 MeV, comparison of results with Glauber approximation of the comparison of

0–73973 12 C(π - π - π -) 12 N, 4 GeV/c, estimate of cross section 0–73973 12 C(π - π - π) 10 B, analysis, 2-hole states study 0–73971 12 C(π - π) 10 B, final state interaction effects 0–49642 12 C(π - π)N) three body partial wave analysis in Born approximation 0–42858

0-42888 (${}^{12}\text{C}(\pi^-, \pi^-)$), ang. correl. analysis 0-39086 (${}^{12}\text{C}(\pi^-, \pi^-)$), angular range 40-120 deg. at 30 MeV 0-57997 (${}^{12}\text{C}(\pi^-, \pi^-)$)+ ${}^{12}\text{C}(\pi^+, \pi^+)$, angular range 40-120 deg. at 30 MeV 0-57997 (${}^{12}\text{C}(\pi^+, \pi^+)$), angular range 40-120 deg. at 30 MeV 0-57997 (${}^{13}\text{C}$), chemical shift in acyclic and allicyclic alcohols determ. by n.m.r. 0-46534

0-46534

"IC, chemical shift in cycloalkanones by n.m.r. spectroscopy 0-46554

"IC, n.m.r. in thiazoles 0-58247

"IC, props. of levels below 16 MeV 0-38856

"IC, spin-rot, const. and mag. shielding anisotropy in OCS 0-77822

"IC, sudy of resonant state for fast neutrons in C12 elastic and elastic scattering cross-sections 0-49501

"IC, T dependence of angular distributions 0-70647

Nuclei with 6 ≤ A ≤ 19 continued

 13 C, T=3/2 states, isopin forbidden resonance width calcs. 0–67421 13 C⁴⁺, superhyperfine splitting in diamond lattice, e.p.r. obs. 0–48141

¹³C charge radius and form factors from inelastic electron scattering 0-67520

10-12-4*, superhyperhne spitting in diamond lattice, e.p.f. obs. 0—46141
 13C charge radius and form factors from inelastic electron scattering 0–67520
 13C chemical shift in acepleiadene, and acepleiadylene 0—58209
 13C chemical shift obs. in nonalternant hydrocarbons 0—61146
 13C hyperfine interactions in liqs. during photolysis from e.p.f. obs. 0—71381
 13C isotropic contact shifts in complexes of nickel acetylacetonate with organic ligands ¹H-¹¹¹C heteronuclear resonance 0—58190
 13C magnetic resonance for steroids structure 0—64546
 13C n.m.r. (natural abundance) in terpenes and carotenes 0—53086
 13C n.m.r. in β, y-unsaturated ketones, ¹¹3C carbonyl carbon shieldings 0—39431
 13C n.m.r. in cyclohexanols and derivatives, ¹³3C carbinyl carbon shieldings 0—39432
 13C n.m.r. spectra in inositols and their O-methylated derivatives 0—46569
 13C n.m.r. spectra of organic peroxides, dynamic nuclear polarization 0-58236
 13C n.m.r. spectra of organic peroxides, dynamic nuclear polarization 0-53081
 13C n.m.r. spectra of some common nucleotides in aqueous solution 0-53081
 13C n.m.r. spectra of some common nucleotides in aqueous solution 0-53081
 13C + presons. rel. to ¹³N T=3/2 states, obs. 0—42735
 13C + n+¹²C, following ¹⁴N; p) ¹³C*, de-excitation neutrons obs. 0—60800
 13C (¹¹He, ¹³Be[g.s.]) ³Be[g.s.] at 2.0 to 6 MeV 0—39107
 13C (¹¹He, 1)¹G o excitation of T=3/2 levels in ¹³O 0—46121
 13C (¹¹He, 1)³O o excitation of T=3/2 levels in ¹³O 0—60831
 13C (¹¹Li, 1)¹O, E=25.6 MeV, excited states 4p-3h 0—60831
 13C (²¹Li, 1)¹O, E=30.1 MeV, excited states 4p-3h 0—60831
 13C (²¹Li, 1)¹O, 18 MeV, levels discussed within framework of weak-coupling model 0—73787
 13C (²¹Li, 1)¹O, 18 MeV, levels discussed within framework of weak-coupling m

C(t)-C using polarized deuterons, and comparison with DWBA 0-70649 (12C(p,x^{+}))¹⁸C, 600 MeV, capture cross-sections meas. 0-64116 (12C(p,x^{+}))¹⁸C, p-70 MeV, Glauber approx. calc. non-convergent 0-77566 (12C, p-7ay spectrum expt'l evidence of nonstatistical shape 0-77514 (12C, p-7ay spectrum expt'l evidence of nonstatistical shape 0-77514 (12C, p-7ay spectrum expt'l evidence of nonstatistical shape 0-77514 (12C, p-7ay spectrum expt'l evidence of nonstatistical shape 0-77514 (12C, p-7ay spectrum expt'l evidence of nonstatistical shape 0-77514 (12C, p-7ay spectrum expt'l evidence of section of 18C (14C, p-7ay spectrum expt'l evidence of 18C, p-7ay spectrum

¹⁴C($(L_{1,1})^{18}$ O, 20.4 MeV states in ¹⁶O studied 0—64003 14 C((α,α)), deduced levels and resonances of ¹⁸O for E_α=3.5-16.5 MeV 0—57898 14 C((α,π)), deduced levels and resonances of ¹⁸O for E_α=4.9-8.5 MeV 0—57898 14 C((ρ,η)) ¹⁵N and inverse reaction 15 N((ρ,p)) ¹⁴C calc. 0—46193 14 C((ρ,η)) ¹⁶C fective two-body pot. 0—42732 14 C((ρ,η)) ¹⁶C, 14 C((ρ,η)) ¹⁸B, 16 C((ρ,η)) ¹⁸N, 14 C((ρ,η)) ¹⁸N, 14 C((ρ,η)) ¹⁸N, 14 C((ρ,η)) ¹⁸N, 16 C((ρ,η)) ¹⁸N, 18 C((ρ,η)

0-42530 "F, acoustic n.m.r. in antiferromag. KMnF₃ 0-41378 "F, chemical shift in 1,2-dichlorofluoroethylenes 0-77897 "F, chemical shift in 1,2-dichlorofluoroethylenes 0-77897 "F, cleetromagnetic decay of first and second T=3/2 states 0-70415 "F, gamma rad. study in "F(p, $\alpha \gamma$)" by between 1,9 and 4.16 MeV 0 46210 "F, in the biguous weed an explanation for the property of the

¹⁸F, gamma rad. study in ¹⁸F(p,αγ) ¹⁰O between 1.9 and 4.16 MeV 0 46210
 ¹⁹F, iterative technique used, quadrupole force 0–77467
 ¹⁹F, magnetic resonance in CaF₂, absorption spectrum, unsaturated, steady-state 0–41298
 ¹⁹F, magnetic shielding in XeF₄ 0–53052
 ¹⁹F, n.m.r. in 1,1,2,2,-tetrafluoroethane 0–49938
 ¹⁹F, n.m.r. in CaF₂, free induction decay using Lowe-Norberg theory 0–41359

¹⁹F, n.m.r. in CdF₂, CdF₂.2H₂O, HgF₂ and HgF₂.2H₂O, chemical shifts 0-59465 ¹⁹F, n.m.r. in fluorides of d¹⁰-elements, chemical shifts 0-51406

Nuclei with 6≤A≤19 continued

¹⁹F, n.m.r. in fluoromethane, partially oriented 0-46560

¹⁹F. n.m.r. in KPF₆, NaPF₆ and KSbF₆, nuclear spin coupling consts. 0-41377

19F, n.m.r. in LiF, single spin-spin reservoir with 19F 0—66154 19F, n.m.r. in MnF₂:X (X=V, Fe, Co, Ni, Zn), rel. to impurity effects 0–51239

19F, n.m.r. in MnF₂, KMnF₃ and RbMnF₃, line shape and spin correlation, exchange narrowing 0-41332
 19F, n.m.r. in N₃S₃O₃F₃ isomeric derivatives 0-46509

¹⁹F, n.m.r. in Ni[P(OR)_{3-x}F_x]₄, influence of substitution 0-46500

¹⁹F, n.m.r. in solid addition compounds SF₄.AsF₅ and IF₇.AsF₅ 0–56684 ¹⁹F, n.m.r. of XeF₄ in IF₅ 0-74312

 $^{19}\mathrm{F},~\mathrm{nmr}$ spectra of trimethyl, trifluoro, trichloro silyl compounds 0-64552

0-04332

"F, nuclear antiferromagnetism in CaF₂, low temp. production 0-44677

"F, prod. from Si by action of 660 MeV p 0-52778

"F, spin-lattice relax times in liq. dichlorodifluoromethane, temp. and field depend. 0-74792

"F, spin-lattice relaxation time in solid dichlorodifluoromethane, field depend. 0-76241

depend. 0–76241

"9F double resonance in presence of chemical exchange 0–70863

"9F elastic and inelastic scattering of 14.1 MeV neutrons, angular distributions and cross sections, deformation parameters 0–46219

"9F energy levels from ¹⁸O(p,y) at Ep=1764 and 1934 keV 0–70414

"9F n.m.r. in BaFPO₃, and ³¹P reson., rel. to polycryst. lattice theory 0–41357

0-41357

"F n.m.r. in solid CF₄, mol. motion 0-75973

"F n.m.r. in solid hexafluorides, molecular diffusion study 0-72507

"F n.m.r. in solid hexafluorides, molecular diffusion study 0-72507

"F notclear γ-rays following π-capture 0-49643

"F rot.-frame nucl.-double-reson. in CaF₂ 0-41390

"F search for trition cluster structure 0-49673

"F spin-rotation consts. in CF₄, SiF₄ and GeF₄ 0-77841

"F spin lattice relaxation 0-48167

"F spins and parities for 10 levels, produced by "N(α, γ) reaction 0-52801

"FGHe α) "Ne* " "Ne level lifetimes and excitation energies < 11 MeV ¹⁹F(³He,d)²⁰Ne*, ²⁰Ne level lifetimes and excitation energies, ≤11 MeV

 $^{19}F(\alpha,\alpha')^{19}F'$, within gaseous target of SF₆ and CH₄, chemical conservation of alignment of excited nuclei $^{10}G(\alpha,\alpha')^{19}F'$ excitation functions rel. to compound ^{23}Na levels, 3.3-5.0 MeV $^{10}G(\alpha,\alpha')^{19}F(\alpha')^{19$

 $^{19}F(\alpha,\alpha)^{19}F$ excitation functions rel. to compound ^{23}Na levels, 3.3-5.0 MeV 0-39094 $^{19}F(\alpha,np)^{22}Na$, spin, parity and multipole mixing ratio assignments of low levels in ^{22}Na or 0-7488 $^{19}F(d,\alpha)$, $E_{ce}=1-3.95$ MeV, excitation functions and ang. distribs. 0 64135 $^{19}F(d,\alpha)^{17}O$, integrated cross sections and 21+1 rule for $E_{e}=1.6-2.1$ MeV 0-55171

O-5517. Integrated cross sections and z1+1 rule for E_d=1.6-2.1 MeV 0-5517. Integrated cross sections and z1+1 rule for E_d=1.6-2.1 MeV 0-7517. Integrated cross sections and z1+1 rule for E_d=1.6-2.1 MeV 0-7519. Integrated cross sections of ten p groups, DWBA calcs. 0-49659. Integration of the property of the pr

(°Li, *He) quasielastic scattering, charge- exchange spin-flip forces 0-46247
Li isotopes, production cross sections in 70 MeV α particle interaction on C and N targets 0-77572
Li, 'Li electrodisintegration cross- section meas. 0-64108
°Li, 'Li photonuclear cross-section for disintegration obtained 0-64108
°Li, 'Zi photonuclear cross-section for disintegration obtained 0-64108
°Li, 2-hole states study using 2-nucleon absorption model 0-73971
°Li, 5.36 MeV level by e scatt. 0-63998
°Li, α-deuteron model studied 0-63997
°Li, binding energy calc., by considering nuclide as three-body (α-n-p) system 0-73780
°Li, charge form factor 0-38848
°Li, Coulomb breakup on ⁷⁰⁸Pb at 20-, 21-, 24-, and 26 MeV 0-52806
°Li, Hartree-Fock model 0-73779
°Li, incorporation of the residual potentials and nucleon-nucleon correlation effects 0-57894
°Li, incorporation of the residual potentials and nucleon-nucleon correlations 0-38847
°Li, reactions in the even parity, T=0 states, calculation 0-52668
°Li, shell model, realistic forces, spectra and the effects of correlations in A=6 nuclei 0-57893
°Li, thermal-neutron-absorption cross-sections by pulsed neutron method 0-5789
°Li, transverse form factor for excitation to 3.56 MeV level by electron secret in A 27344

0-57989

FLi, transverse form factor for excitation to 3.56 MeV level by electron scatt. 0-42734

FLi, two-nucleon density functions and correlation functions with realistic single-particle wave functions 0-55119

FLI (p.) He) He angular distributions meas. and DWBA calc. 0-70595

FLI binding energy of 3.562 MeV excited state 0-63996

FLI breakup in the field of 369Pb 0-67556

FLI deteron, induced, reactions, and contrained angular, distributions.

⁶Li deuteron induced reactions and scattering angular distribution 0-49644

°Li deuteron induced reactions and scattering angular distribution—049644

°Li photodisintegration by 12 MeV Bremsstrahlung 0–49593

°Li properties predicted from Hamada-Johnston potential 0–67418

°Li("θ-0,p)²-Na, radiative capture 0–39145

°Li("He, d) β-E, E=0.5-1.3 MeV 0–60823

°Li("He,α)²-Li and levels in °Li 0–70392

°Li("He,ρ), below 2 MeV, rel. to °B excited level 0–46240

°Li("He,ρα) β-He, sequential reaction, pick-up by DWBA 0–55167

°Li("He,ρα), below 2 MeV, rel. to °B excited level 0–46240

°Li("Li,α)*Be, final state Coulomb effects 0–74004

°Li("Li,α)*Li, in 1 depend. and cross section to 11 C ground, first excited states, 1.9 MeV 0–39139

°Li(α,2α, impulse distrib. 0–52771

°Li(α,2α,1 impulse distrib. 0–52771

°Li(α,α,2)*Li, in 1 B 7.01 MeV level width and reson. energy determ. 0–39102

°Li(α,2α,2'Li, absolute cross section 3.5-5.0 MeV and 4.25 MeV reson. analysis 0–39092

Nuclei with 6≤A≤19 continued

⁶Li(α , $\alpha\alpha$)²H, 42.8MeV, mechanism studied, validity of impulse approximation 0–73989

tion 0—73989 E_d (id), α) He, angular distrib. of α -particles and cross-sections for E_d =600-1200 keV 0—55166 6 Li(d), α) He, polarization of 6 Li-ions, determination 0—64134

CLi(d,n)7Be, absolute differential cross-sections, excitation functions, recoil spectrometry obs. 0-39103

⁶Li(d,n)⁷Be, recoil angular distributions, 12, 15 and 17 MeV 0-49654

⁶Li(d,p), stripping reactions of the 1p shell initiated by vector-polarised deuterons 0-55168

deuterons (0-55168) $\text{Li}(\mu^-,\nu_\mu)^6\text{He}$ elementary particle treatment (0-4959) $\text{Li}(\mu^-,\nu)^6\text{He}$, capture rate and the PCAC hypothesis (0-39020) $\text{Li}(\mu^-,\nu)^6\text{He}$, renormalization effects in pseudo scalar form factor (0-67523) $\text{Li}(n,n)^6\text{Li}(3.56)$ integral cross sections, from threshold up to 7 MeV

39066 ⁶Li(n,p) ⁶He(O' integral cross sections, from threshold up to 7 MeV 0-39066

6Li(n,p)6He, study using impulse approx. 0–39067 6Li(n,p) and (p,n), impulse approx. and shell model calcs., 156 MeV 0–39068

0–3908 $^{\circ}$ Li(p, α) and $^{\circ}$ Li(p, α d) and $^{\circ}$ He virtual states 0–70388 $^{\circ}$ Li(p, γ) Be angular distribution of y-rays, and calc. 0–70594 $^{\circ}$ Li(p,no) Be_{g.s.} charge exchange part of the effective two-body interaction 0–42827

6.4(p,n) using polarized protons of 30 and 50 MeV in polarization determ.

0 39035 (EL(p,p/d)*Hf quasi elastic scattering, Treiman-Yang test 0-73940 (EL(p,p)*Li, differential cross section analysis with collision matrix 0 42833

0. 42833
©Li(p,p α), impulse distrib. 0–52771
©Li(p,pd), impulse distrib. 0–52771
©Li(p,pd)+He, distortion and antisymmetrisation effects 0–39038
©Li(π ,p η)-TSM description rel. to structure of Li nucleus 0–46231
©Li(π ,nn)+He, analysis, 2-hole states study 0–73971
©Li(π , 2)-He elementary particle treatment 0–49599
©Li- π - 4 -d, vertex function for virtual decay, within three-particle model 0–70541 0--70541

7Li n.m.r. spectra in Li₃Sb, quadrupole splitting 0—48164
7Li photodisintegration by 12 MeV Bremsstrahlung 0—49593
7Li photoproduction of neutral pions 0—55043
7Li resonance temp. depend. on Li-form of H₂O- and D₂O-saturated zeolite Linde 13X 0—43568

Linde 13X 0–43568
Li total neutron cross-section determ. 100-1500 keV 0–77559
Tel transverse form factors calc. with projected Hartree-Fock functions 0–70391
Tel(*0-p)**0*Na, radiative capture 0–39145
Li(*1+e, p)**0*Li, 5-8 MeV 0–70642
Li(α, p)**4 to 43 MeV, quasi-free knock-out of α-particles 0–70643
Tel(α, p)**4 to 43 MeV, quasi-free knock-out of α-particles 0–70643
Tel(α, p)**4 to 43 MeV, quasi-free knock-out of α-particles 0–70643
Tel(α, p)**4 to 46 Li(α, p)**4 to 46 Li(

TLi(n, t), ang. distrib., comparison with DWBA calc. 0-49627
TLi(n,p)PLi, cross section using single-particle model for ⁸Li ground state 0-46209

 $^{7}\text{Li}(p,n_0)^{7}\text{Be}_{g,s}$, charge exchange part of the effective two-body interaction 0-4282710-42827 T.Li(p,n.) Be(0.43 MeV) charge exchange part of the effective two-body interaction 0-42827

⁷Li(p,n) using polarized protons of 30 and 50 MeV in polarization determ.

Li(π, pp), TISM description rel. to structure of Li nucleus 0-46231
Li(π, pp), TISM description rel. to structure of Li nucleus 0-46231
Li(π, pp), TISM description rel. to structure of Li nucleus 0-46231
Li(π, nn)*He, analysis, 2-hole states study 0-73971
Li pair prod. in high energy interactions, Monte-Carlo calcs. 0-39001
Li, β-decay, half-life log ft, branching ratios, study by recoil-particle method and β-n coincidence method 0-49567
*Li-*Be, β-decay, *Be states obs. 0-38850
Λa¹L* Cormation and disintegration, analysis of three centre even for interaction of K- at 6 GeV/c with photographic emulsion 0-49640
Λ²Li final state interactions in π-mesi decays 0-73791
ΛβE decay, α-α interaction, energy distribution 0-52721
*ALF, nucleon correlation on quadrupole transition 0-52676
N, 70 MeV α particle interaction, cross sections for production of Li, Be, B isotopes, mixed parity Hartree-Fock calc. using realistic forces 0-70402
*N, 20-30MeV excited levels, ¹0B(³He, α)³B and ¹²C(p,p)¹²C reactions

 13 N, 20-30MeV excited levels, 10 B(3 He, α) 9 B and 12 C(p,p) 12 C reactions 0-42736

 $(-42736)^{-13}$ N, deduced levels from 14 N(3 He, α), E=2.5-8.5 MeV 0-60825 13 N, paired proton configurations from (3 He,n) 0-70645 13 N, T=3/2 states, isospin forbidden resonance width calcs. 0-67421 13 N, T=3/2 states from 13C+p obs. 0-42735 13 N emission on irradiation of 14 N by proton, deuterons α -particles and 3 He isospin 13 He isospin

¹³N emission on irradiation of ¹⁴N by proton, deuterons α-particles and ¹⁴He ions 0-74000¹³N many charge particle produced by 660 MeV protons in ²⁷Al, angular distribution 0-67534¹³N prod. from melamine bombard. 87 MeV e. 0-77539¹⁴N, α-cluster struct., from $(\pi_*-2\pi d)$ reaction 0-77568¹⁴N, energy distribution of neutrons from proton-neutron nonelastic collisions for 18 MeV protons 0-64115

Nuclei with 6<A<19 continued

14N, ground state, use of perturbation theory and statistical concepts 0-42737

¹⁴N, hyperfine interactions with intermolecular fields of ¹⁴ND₃, determination of constants 0-46491

tion of constants 0—40-49 "N, irradiation by protons, deuterons, α -particles and ³He ions, emission of ¹¹C, ¹³N and ¹⁸F 0—74000 ¹⁴N, lifetime of 8.88 MeV level by Doppler-shift attenuation method 0—52670

¹⁴N, multipolar mixing of 5.83→0 transition 0-67422

14N, μ capture, γν ang. correlation 0-46201

14N, n.q.r. in sat. cyclic amines, from liq. N2 temp.

¹⁴N, quadrupole coupling constant of acctonitrile N-oxide 0-74325 ¹⁴N (¹⁴N, ¹⁴N) elastic scattering, excitation functions 0-70671

¹⁰N ("N,"N) elastic scattering, excitation functions 0—706/1 ¹⁴N and ¹⁴C core polarization, agreement between binding energy and B-decay 0—60754

¹⁴N energy levels, effective interaction calc. 0–38853 ¹⁴N ground-ate binding energies with Tabakin potential as residual interaction 0–67423

tion 0-6/423

14N in ethylenimine, n.q.r. at 77°K 0-66161

14N in fission reactor as source of tritium by 14N(n,T)12C reaction 0-49632

0-49632

14N in mol. crysts., lineshapes and widths analysis, obs. 0-41402

14N n.m.r. in liquid crystal para-azoxyanisole 0-61559

14N quadrupole coupling constants of nitro and trimethylsilyl pyridine 0-5371

14N quadrupole relax. in 2-bromothiazole nuclear double reson. 0-41393

14N quadrupole relax. in 2,3,4-trichloronitrobenzene 0-41392

14N relaxation times and (N, F) coupling constants in fluoropyridines

¹⁸N relaxation times and (17, 17) coapuing
 ¹⁸O₁-49925
 ¹⁸N(¹⁸N, ¹³N)¹⁵N in tunneling, use of Hulthen wavefunctions to obtain accurate expression for matrix element 0-77526
 ¹⁸N(¹⁸O, ¹⁶O)¹⁸N, gross struct. of excitation functions, optical model anal.

¹⁸N(¹⁶O₂)¹⁶O)¹⁶N, gross struct. of excitation functions, optical model anal. 0–67557
 ¹⁸N(¹He,t) and (¹He,³He), 44.6 MeV, angular distributions 0–39996
 ¹⁸N(¹He,t) and (¹He,³He), 44.6 MeV, angular distributions 0–39996
 ¹⁸N(¹He,t)¹⁹N, differential cross-sections and deduced ¹³N levels. E=2.5–8.5 MeV 0–60825
 ¹⁸N(²A, α)¹⁸N differential cross section meas. for isospin impurities of ¹⁸F states 0–67428

states 0-67428 ¹⁴N(α , α) differential cross-sections and angular distributions for E=20-24 MeV 0-60824 ¹⁴N(α , α)¹⁷O, mechanism of reaction, diff. cross section for proton prod. 0-42870 ¹⁴N(α , α)² differential cross-sections and angular distributions for E=20-24 MeV 0-60824 ¹⁴N(α , α)² differential cross-sections and angular distributions for E=20-24 MeV 0-60824 ¹⁴N(α , α)² differential cross-sections and angular distributions for E=20-24 MeV 0-60824 MeV 0-60824 MeV 0-60824 ¹⁴N(α , α)¹⁵N(α , and single-particle spectroscopic factors in ¹⁵O 0-70650 ¹⁴N(α , α)¹⁵N, stripping reactions of the 1p shell initiated by vector-polarised deuterons 0-55168 ¹⁶N(α , α)¹⁵N, for energy separation of doublet at 9.15 MeV in ¹⁵N 0-49502 ¹⁸N(α)¹⁵C α description paytons abs α 0.60800

0-49502

¹⁸N(p,p)¹²C+(n)¹²C, de-excitation neutrons obs. 0-60800

¹⁸N(p,p)¹²C+(n)¹²C, de-excitation neutrons obs. 0-60800

¹⁸N(p,p)¹⁵C, study of ¹⁵O giant dipole resonances 0-70396

¹⁸N(p,p)¹⁵O, study of ¹⁵O giant dipole resonances 0-70396

¹⁸N(p,p)¹⁵O and ¹⁵O(p,p)¹⁸N, reaction and inverse reaction calc. 0-46193

¹⁸N(p,p) effective two-body pot. 0-42732

¹⁸N(p,p) evidence for a tensor effective two-body interaction for E_p=24.8

MeV 0-52774

¹⁸N(p,x¹)¹³N, 600 MeV, capture cross-sections meas. 0-64116

¹⁸N, 2 nucleon transfer induced by polarized protons 0-60809

¹⁵N, angular distribution of de-excitation p-rays from particle decays of giant ¹⁶O resonance 0-70403

¹⁵N, energy separation of doublet at 9.15 MeV, using ¹⁴N(d, pp) reaction 0-49502

0–49502 15 N, of 13.42 MeV T= 3 /₂ state in various reactions 0–64000 15 N, photodisintegration, shell model cales. 0–73900 15 N 3p-4h states from 12 C('Li,2r) 0–73788 15 N level structure determ. by 18 (a,n) 16 N 3.6-3.8 MeV 0–58007 15 N states <6.33 MeV excitation, from 16 C(3 He,d) 15 N, 14 MeV 0–38858 15 NH₃ cold target prep. 0–46015 15 N(16 O) 15 N, gross struct. of excitation functions, optical model anal. 0.6-67557

¹⁵NH₃ cold target prep. 0—46015

¹⁸N(¹⁶O¹⁶O)¹⁵N, gross struct. of excitation functions, optical model anal. 0—67557

¹⁸N(¹He,d)¹⁶O at 16 and 24.9 MeV, struct. of ¹⁶O 0—49503

¹⁸N(¹He,d)¹⁶O at 16 and 24.9 MeV, angular distributions 0—39096

¹⁸N(¹He,t)¹⁷O and 2p-1h contribution in ¹⁷O 0—73789

¹⁸N(¹He,t) and (¹He,¹He), 39.8 MeV, angular distributions 0—39096

¹⁸N(α,p)¹⁸F, new resonances in region E=600-3150 keV 0—52801

¹⁸N(α,p)¹⁸C and inverse reaction ¹⁸C(p,p)¹⁸N calc. 0—46193

¹⁸N(p,p)¹⁸C and partial widths of ¹⁶O transitions 0—52775

¹⁸N(p,p)¹⁹C and partial widths of ¹⁶O transitions 0—67424

¹⁸N(p,p)¹⁹C and partial widths of ¹⁶O transitions 0—67424

¹⁸N(p,p), neffective two-body pot. 0—42732

¹⁸N(p,n), effective two-body pot. 0—42732

¹⁸N(p,n), shell-model calc. 0—39046

¹⁸N(p,p)N** and E1 giant resonance in ¹⁶O 0—70406

¹⁸N(p,p)N** and E1 giant resonance in ¹⁶O 0—70466

¹⁸N(caps), threshold states and neutron emission 0—57896

¹⁸N deduced levels from ¹⁸O(d,α) for E_σ=4.75–11.5 MeV 0—57895

¹⁹N(p, or analogue state, isospin purity 0—67426

¹⁸Ne, edecay modes of low levels from (¹He,ny) reactions 0—52674

¹⁸Ne energy levels from ²⁰Ne(p,t) ¹⁸Ne 0—70413

¹⁸Ne energy levels from ²⁰Ne(p,t) ¹⁸Ne 0—70413

¹⁸Ne half life, second class current problem, ft value for transition to ¹⁸F ground state 0—52722

¹⁸Ne ievels, from ²⁰Ne(p,t) at 50 MeV, differential cross section meas. DWBA calc. 0—57904

¹⁹Ne, investigation of levels below excitation energy of 7 MeV 0—77486

¹⁸Ne, iifetime of 275 keV second excited level from ²⁰Ne(¹He,α) reaction 0—77486

²⁰Ne, excited levels by two proton transfer on ¹⁸O 0—49658

²⁰Ne excited levels by two proton transfer on ¹⁸O 0—49658

²⁰Ne excited levels by two proton transfer on ¹⁸O 0-49658

ewite devels by two proton transfer on "O 0-49658 O, electron scattering, elastic, resonances between 16 and 30 MeV, and optical model analysis 0-70582 O isotopes, mixed parity Hartree-Fock calc. using realistic forces 0-70402 $^{13}\mathrm{O}$, mass excess determ. 0-67420 $^{13}\mathrm{O}$, mass excess determ. 0-67420 $^{13}\mathrm{O}$, mass of $T_{z}=-^{3}/_{z}$ masses, using mag, spectrograph 0-67419 $^{13}\mathrm{O}$ (e, n) "O(e, n) "O(z), if or spin and parity assignments of $^{17}\mathrm{O}$ 0-49506 $^{14}\mathrm{O}$, β decay correction factor and hindered Gamow-Teller allowed transition for a mass-14 system 0-57946

Nuclei with 6≤A≤19 continued

 $^{15}\rm{O},$ angular distribution of the de-excitation of γ -rays from particle decays of giant $^{16}\rm{O}$ resonance $\,0{-}70403$

15O, paired proton configurations from (3He,n) 0-70645

For paired proton configurations from (*He,fi)* 0—70443

So giant dipole resonances observed by ¹⁴N(p,p) reaction 0—70396

So prod. from water bombard. 87 MeV e. 0—77539

So single particle spectroscopic factors from (d,n) 0—70650

So states < 8.32 MeV excitation, from ¹⁴N(³He,d)¹⁵O, 14 MeV 0—38858

So T=3/2 level excitation in search 0—46121

So (d,³He)¹⁵N, rel. to ¹⁶O ground state particle-hole impurities, 20 MeV

"O (1=3/2) [ever exchand in Seatch" 0=40121 [1.5] (a) He) 150 (d) He) 150 (d

10–49001 i¹⁶O, electroexcitation of first excited state, monopole sum rule 0–70404 i¹⁶O, evidence for J*=8+ state 0–70405 i¹⁶O, evidence for parity-forbidden α -particle decay from 8.87 MeV 2⁻ state to i¹⁶C 0–73854

Consider the parity-foroidden α-particle decay from 8.8 / MeV 2⁻ state to ¹²C 0-73854

16O, gamma transitions from ¹⁹F(p,αγ)¹⁶O reaction 0–46210

16O, giant resonance region, inelastic electron scattering with primary energies below 60 MeV 0–73908

16O, ground state, 2 particle-2 hole admixture 0–70410

16O, ground state particle-hole impurities, from ¹⁶O(d.t)¹⁵O and ¹⁵O(d.³He)²N, 20 MeV 0–38859

16O, ground state wavefunction, from ¹⁶O(γ,η) reaction 0–70418

16O, Hartree-Fock calcs of binding, density and single-particle spectra with effective force 0–49470

16O, Hartree-Fock calcs, with realistic potentials 0–38866

16O, Hartree-Fock calcs, with four-body interaction 0–52667

16O, Hartree-Fock calculations with semi-realistic interactions 0–70407

16O, lifetime measurement of 3 excited states 0–64001

16O, lifetime of 6.44 MeV level by Doppler-shift attenuation method 0–52670

16O, muon capture rates rel. to breakdown SU(4) invariance 0–49600

16O, muon capture rates rel. to breakdown SU(4) invariance 0-49600
 16O, negative parity states, effect of ground state correlations 0-70408
 16O, neutron separation energies calc. with Morse function type potential 0-67390

16O, nucleon scatt. by one-particle-one-hole model 0-64111 16O, nucleon scatt. by one-particle-one-hole model 0-64111 16O, odd-parity states, effects of ground-state correlations 0-52672 16O, odd parity spectrum, from interac. between nucleons 0-77484 16O, pscatt., 20-50 MeV, optical model analysis 0-46205 16O, partial widths from $^{12}\text{C}(\alpha, \gamma \gamma)^{16}\text{O}$, $^{15}\text{N}(p, \gamma \gamma)^{16}\text{O}$ and $^{15}\text{N}(p, \gamma \alpha)^{12}\text{C}$ 0-67424

0-6/424 "box or to followed by single-nucleon emission 0-39088 "60, radiative capture of π^- , search for giant reson, excitation 0-73974 "60, renormalization of Brueckner-Hartree-Fock theory using occupation probabilities 0-70330 "160, spin tensor moments and cross- sections for deuteron scatt, and reactive processing of the property of the pr

tions 0-52802 160, states of 2s-1d shell nuclei based on the four-particle—four-hole state 0-49504

0–49504

16°O, struct. in giant reson. region, from e scat.. and μ capture calc. in continuum model 0–39021

16°O, two-nucleon density functions and correlation functions with realistic single particle wave functions 0–55119

16°O 3– excitation, ground state correlation effect calc. 0–73785

16°O (16°O, 16°O) elastic scattering, excitation functions 0–70671

16°O (16°O, 16°O), resonances in elastic and inelastic scattering between 18.5 and 30 MeV 0–77544

16°O binding energy, size from effective NN interactions 0–38806

16°O binding energy calculation using matrix elements of Tabakin's potential 0–70389

ual 0–70389 16 O deduced 6+ level from 12 C(α , α 0) and 12 C(α , α 7) 0–52671 16 O deduced shell amplitudes from 14 C(3 He, n), double- stripping study 0–42738

16O energy levels from ¹³C(*Li,t)¹⁶O 0–73786 16O even-even N=Z nuclei, energy of quartet excited states 0–73807 16O from ¹²C(*Li,d)¹⁶O and ¹²(⁷Li,t)¹⁶O rotational bands, giant dipole resonance 0–46250

beginning the property of the

p-rays 0–70403 (160 ground state, effect of 2p-2h configurations in 16 N on 16 O μ capture rate 0–73975

¹⁶O parity forbidden alpha decay from 2⁻ (8.88 MeV) level 0-46163

Nuclei with 6≤A≤19 continued

 $^{16}\text{O}(d,n)^{17}\text{F}$ study at 4-6 MeV, fit of theoretical curves using DWBA model to exptal. data 0-73991 $^{16}\text{O}(d,p)^{17}\text{O}$, $^{16}\text{O}(d,\alpha)^{14}\text{N}$, 4.4-8.4 MeV, absolute cross-sections meas.

to exptal. data 0-73991 (°O(d,p)¹O, ¹6O(d, α)¹4N, 4.4-8.4 MeV, absolute cross-sections meas. 0-39108 (°O(d,p)¹O analysed using BHMM theory of deuteron stripping 0-70651 (°O(d,p)¹O study at 4-6 MeV, fit of theoretical curves using DWBA model to exptal. data 0-73991 (°O(d,p)¹O, 16O ground state particle-hole impurities, 20 MeV 0-38859 (°O(e,e)¹6O inelastic, form factor calc, with particle-hole model 0-73907 (°O(μ ,n), ground state photoneutron angular distributions in the giant resonance of 16O 0-52750 (°O(μ ,n), two-particle two-hole (2p-2h) correlations 0-70418 (°O(μ ,n)) ¹5O, cross section eval. by statistical method 0-73901 (°O(μ ,n)) ¹5O, cross section eval. by statistical method 0-73901 (°O(μ ,n)) ¹5O, oxoss section eval. by statistical method 0-73901 (°O(μ ,n)) ¹5O, unified shell model calc. 0-42814 (°O(μ ,p)¹)°O, angular distributions of de-excitation ν -rays 0-70403 (°O(μ ,p)²)°N, unified shell model calc. 0-42814 (°O(μ ,p)²)°N, angular distribution of de-excitation ν -rays 0-70403 (°O(μ , μ))°N, formation of excited levels 0-42814 (°O(μ , μ))°N, formation of excited levels 0-46203 (°O(μ , μ))°N, formation of excited levels 0-46203 (°O(μ , μ))°N, formation of excited levels 0-46203 (°O(μ , μ))°N, gamma-ray spectra for incident-mean-neutron energies $E_{\mu}=6.7+11.0$ MeV 0-64124 (°O(μ , μ))°O, gamma-ray spectra for incident-mean-neutron energies $E_{\mu}=6.7+11.0$ MeV 0-64124 (°O(μ , μ))°O, gamma-ray spectra for incident-mean-neutron energies $E_{\mu}=6.7+11.0$ MeV 0-64124 (°O(μ , μ))°O, gamma-ray spectra for incident-mean-neutron energies $E_{\mu}=6.7+11.0$ MeV 0-64124 (°O(μ))°O(μ)°O(μ)°O

0–57990 (-5,7990) gamma-ray spectra for incident-mean-neutron energies $E_{x}=6.7\cdot11.0$ MeV 0-64124 (-5,71.1.0 MeV 0-64124 (-5,71.1.0 MeV 0-64124 (-5,79.5) (-

0-70627 ¹⁶O(π^- ,NN) three body partial wave analysis in Born approximation 0-42858

0–4288 16 O(π - γ n), n energy spectra 0–46232 16 O(π - γ n), angular range 40-120 deg. at 30 MeV 0–57997 17 O, 2p-1h strength contributes only above 7 MeV excitation energy 0–73789

0–73789

1°O, 5p.4h states from ¹²C(²Li,d) 0–73788

1°O, DWBA cales, for stripping to d_{3/2} resonance 0–70419

1°O, effective charge, importance of higher order corrections 0–42726

1°O, low-lying even-parity states, calc. of spectrum 0–52673

1°O, low lying negative parity states, from ¹δ(0[p,d)¹¹O 0–70411

1°O, low lying states, from ¹δ(1(x, p) reaction 0–42870

1°O, n.m.r. in ruby, dynamic polarization technique, 1.9K 0–41363

1°O, with neutron bound to alpha-cluster breathing mode excited core 0–70412

1°O, shell model calculations 0–67425

 10 C, shell model calculations 0 C=67425 12 C, spin and parity assignments from 13 C(α ,n) 17 O_{5.2}. 0 C=49506 12 C, spin and parity of 7.56 MeV level, from 13 C(6 Li,d) and 13 C(7 Li,t) 0 C=60831

0-0031 10 even parity states, shell model extension 0-57897 10 excited state at 20.4 MeV, assignment from data on 16O(n,n)16O

0-49622

"O level structure study from "3C(6Li,d) and "3C(7Li,t) reactions 0-73787

"O levels from "6Q(n,p) at 5 to 13 keV, four narrow resonances 0-57990

"O(n,p)"N, cross- section for the delayed-neutron yield at 14.1 MeV
0-57991

0—57991

1ºO(p,n), effective two-body pot. 0—42732

1ºO(p,n), effective two-body pot. 0—42732

1ºO-18O elastic scattering, comparison with 1ºO-1ºO scattering 0—64138

1ºO, Hay Coold target prep. 0—46015

1ºO, Hay Coold target prep. 0—46015

1ºO, Hay Coold target prep. 0—46015

1ºO, many-particle deformed pot. theory 0—38791

1ºO, states up to excitation energy 12.5 MeV obs., 6+ state at 11.69 MeV belongs to ground state rot. band 0—64030

1ºO and 1ºF mirror transition, ft value 0—52722

1ºO concentration in Greenland ice core rel. to solar activity index 0—63180

O concentration in Greenland ice core rel. to solar activity index 0–63180 ¹⁸O deduced levels and resonances from ¹⁴C(α , α) and ¹⁴C(α ,n) 0–57898 ¹⁸O levels in harmonic oscillator shell model using one boson exchange potentials 0–57899 ¹⁸O(1*0,1*0)1*0, gross struct. of excitation functions, optical model anal. 0–67557 ¹⁸O(3*He,t)*1*F, angular momentum transfer 0–67552 ¹⁸O(3*He,t)*1*F, angular momentum transfer obs. 0–49658 ¹⁸O(3*He,t)*1*F, at 16 and 30 MeV 0–77574 ¹⁸O(1*Li,t)*2*Ne and rotational bands in ¹²Ne 0–70430 ¹⁹O(He,p), deduced ²⁹F levels up to 6.043 MeV excitation 0–52678 ¹⁸O(1*O(4,p)*1*O deduced evels of ¹⁸N for E=4.75–11.5 MeV 0–57895 ¹⁸O(d,p)*1*ON deduced levels of ¹⁸N for E=4.75–11.5 MeV 0–57895 ¹⁸O(d,p)*1*ON deduced levels of ¹⁸O for E=5.0 MeV 0–57900 ¹⁸O(p,p)*1*N, 3-7 MeV, excitation functions obs. 0–39042 ¹⁹O(p,p)*1*P rand energy levels in ¹⁹F 0–70414 ¹⁹O(p,p)*1*P reson yields, obs. 0–42836 ¹⁸O(p,p)*1*P reson yields, obs. 0–42836 ¹⁸O(p,p)*1*P, microscopic first-order core polarization corrections to DWBA 0–42837 ¹⁸O(p,p)*1*O, 3-7 MeV, excitation functions obs. 0–39042 ¹⁸O(p,p)*1*O, 3-7 MeV, excitation functions obs. 0–39042

0-42831 (18²O(p,p' γ)) ¹⁸O, 3-7 MeV, excitation functions obs. 0-39042 ¹⁹O β decay to ¹/₂- state of ¹⁹F, half-life, transition strength 0-73856 ¹⁹O deduced levels and γ -ray detection in coincidence with reaction particles from ¹⁸O(d,pp) for E=5.0 MeV 0-57900 ³¹P(p,p' γ), E_p=5.8 and 6.6 MeV, ang. correlations meas. 0-39039

Nuclei with 20 \leq A \leq 49
1-p proton hole states in 13 nuclei from 12 C to 32 S 0–70399
2 $^+$ and 3 – collective states using schematic forces for Zr 0–55125 20 Ne(6 Li,d) 24 Mg, 20 Ne(7 Li,t) 24 Mg, search for α -particle structure in 24 Mg

²⁰Ne liquid, capture of Σ^- , determination of Λ° trapping probability 0-42861

0—42861

"Mg deduced levels from ²⁰Ne(³He, n) between 3.4-9.4 MeV 0—42740

"Si T=3/2 level excitation in search 0—46121
A=20-25, mean lifetimes of excited states 0—38857
A=23 35, elastic and inelastic scatt., core excitation model 0—70564
A=40, 0-T=2 states, calc. diagonalizing representative nuclear forces

Nuclei with 20≤A≤49 continued A=40, Z=N, density distrib., local density approx. 0–38863

in ⁴⁴Ca(d,p) stripping reaction 0-49664

M2 and E3 transitions, radiative widths and mixing ratios, 33<A<41 0-67438

M2 and E3 transitions, radiative widths and mixing ratios, 33≤A≤41 0–67438
nuclear quadrupole moment in Al₂O₃ determ. 0–62581
β decay, mirror symmetry consideration in A=20 and 25 0–42786
³¹ P(p. p)³²S, E_p=1146 keV and 1151 keV resonances, decays and decay schemes, angular distributions, spin and parity 0–64117
³¹P(p, p)³²S, spin mixing coeff., 2114 keV resonance 0–77553
Ag induced by ³⁰Ne ions, 168, 183, 198 MeV cross-sections and fragment distrib. 0–46264
⁴³Ag, elastic scattering, differences in single, plural and multiple scattering through intermediate angles for electrons and positrons 0–57970
Al, 13.6 MeV d-induced and 27.2 MeV α-particle-induced reactions, cross-section meas. 0–52803
Al, analysing power for 490 MeV protons 0–42839
Al, k, α and neutron total cross sections at GeV energies 0–46230
Al, ρ cross-section meas. 0–52803
Al, p cross-section meas. 0–52803
Al, p cross-section of a model params. 0–46198
²⁸Al, deduced levels, from ²⁶Mg(³He,t) 0–77574
²⁶Al, levels deduced from ²⁴Mg(³He,t) 0–77574
²⁶Al, levels deduced from ²⁴Mg(³He,t) 0–77574
²⁶Al, levels deduced seven, from ²⁶Mg(³He,t) 0–77574
²⁶Al, alevels descay, second forbidden shell and rotational models calc. 0–73855
²⁷Al, ³He elastic scatt, 30 MeV, optical model params. 0–42862
²⁷Al, acoustic n.m.r. in Al, spin-phonon interaction 0–45014
²⁷Al, energy distribution of neutrons from proton-neutron nonelastic collisions for 18 MeV and 15 MeV protons 0–64115
²⁷Al, excitation energies y-branching studied by ²⁶Mg(d,ny)²⁷Al 0–70653
²⁷Al, M5 magnetic moment determ. 0–64010
²⁷Al, n.m.r. in Al-Mn alloy, localized spin fluctuations 0–45015
²⁷Al, n.m.r. in Al-Mn alloy, localized spin fluctuations 0–45015
²⁷Al, n.m.r. in Al-Mn alloy, localized spin fluctuations 0–45015
²⁷Al, n.m.r. in Inlunar samples, asymmetry parameters and quadrupole coupling 0–48539

²Al, n.m.r. in CH₃NH₃Al₄OU₄)₂₋₁2H₂O, terroelec. phase trans. study 0–41361 ²⁹Al, n.m.r. in lunar samples, asymmetry parameters and quadrupole coupling 0–48539 ²⁹Al, n.m.r. in 5pinel aluminates, electric field gradients 0–45016 ²⁹Al, n.m.r. in TmAl garnet 0–45022 ²⁹Al, neutron depolarization in elastic scatt., 1.36 MeV 0–42845 ²⁹Al, spins, partites and mixing factors from ²⁶Mg(p,p')²⁶Mg 0–46207 ²⁹Al 4.41, 4.51 MeV levels studied by ²⁴Mg(α₂)₂₇²⁹Al reaction 0–38873 ²⁹Al angular dependences of many charge particles produced by 660 MeV protons 0–67534 ²⁹Al collective states from (d,α) cross-sections 0–70429 ²⁹Al excited levels produced in ²⁶Mg(p,p)²⁶Al²⁷ spin-parity assignments 0–77491 ²⁹Al in Al₂SiO₂, nuclear quadrupole coupling tensors 0–54172 ²⁹Al levels from ²⁶Mg(p,p)²⁶Mg 0–39032 ²⁹Al n.m.r. in ruby: CF²⁷, nominal Δm=1-5 mag. transition probabilities 0–41362 ²⁹Al neutron activation cross-sections, (n,p), (n,α) and (n,2n) at 14.8 MeV

0—41362 27 Al neutron activation cross-sections, (n,p), (n, α) and (n,2n) at 14.8 MeV 0—42854

0–42854 27 Al search for triton cluster structure 0–49673 27 Al spins of 4.41 and 4.51 MeV levels from 24 Mg(α , $p\gamma$) 0–67432 27 Al states, obs. 0–38898 27 Al states, hold detector, determination of fast neutron flux densities 0–74075

0-14073 $^{-2}$ Al($^{-1}$ He, α) differential cross sections, experimental results compared with theory, energy levels of final nucleus 0-67553 $^{-2}$ Al($^{-1}$ He, d) $^{-2}$ Si*, $^{-2}$ Si level lifetimes and excitation energies, \leqslant 11 MeV

theory, energy levels of final nucleus 0–67553

²⁷Al(²He,d)²⁸Si³, ²⁸Si level lifetimes and excitation energies, ≤11 MeV 0–38869

²⁷Al(²He,p)²⁹Si and 2p-1h states in ²⁹Si 0–73799

²⁷Al(²He,p)²⁹Si, search for triton grouping in ³⁹Si 0–49673

²⁷Al(²Al(x,α)³Si), search for triton grouping in ³⁹Si 0–49673

²⁷Al(α,α), excited states, 5.434, 6.547, 7.28 and 7.50 MeV 0–77479

²⁷Al(α,α)²⁸Si, decay of bound isobaric analogue states, ny coincidence recording for E_α=4.0 MeV 0–64011

²⁷Al(α,α)²⁸Na, excitation function, 0 to 16 MeV 0–39112

²⁷Al(α,α)²⁸Na, excitation function, 0 to 16 MeV 0–39112

²⁷Al(α,α) by determ. of probability, by activation method 0–46204

²⁷Al(η,α) cross-section determination for 14.43 MeV neutrons, precision measurements 0–64125

²⁷Al(η,α)²⁸Mg direct reaction process analysis, E=41.3 MeV 0–39043

²⁷Al(η,α)²⁸Mg derect reaction process analysis, E=41.3 MeV 0–38876

²⁷Al(η,α)²⁸Mg drect reaction function rel. to ²⁸Si T=2 state, obs. 0–38876

²⁷Al(η,α)²⁸Mg excitation function rel. to ²⁸Si T=2 state, obs. 0–38876

²⁷Al(η,α)²⁸Mg resonance strengths, 1550 to 2650 keV 0–70601

²⁸Al(η,d), 16 MeV, ²⁸Al levels≼2.55 MeV 0–38860

²⁹Al(η,b)³⁸Si, spin and parity and branching ratios determ. 0–77492

²⁷Al(η,p)³⁸Si, spin and parity and branching ratios determ. 0–77492

²⁷Al(η,p)³⁸Si, spin and parity and branching ratios determ. 0–55122

²⁸Al(η,p)³⁸Si, spin and parity and branching ratios determ. 0–5122

²⁸Al(η,p)³⁸Si, spin and parity and branching ratios determ. 0–5122

²⁸Al(η,p)³⁸Si, spin and parity and branching ratios determ. 0–5122

²⁸Al(η,p)³⁸Si, spin and parity and branching ratios determ. 0–5122

²⁹Al(η,p)³⁸Si, spin and parity and branching ratios determ. 0–74492

²⁸Al (nerionis coupling model calc. 0–70436

²⁸Al(η,q)³⁸Mg ft value of the superallowed Fer

0–52715
²⁹Al, ang. correl. studies of low-lying levels 0–52682
²⁶MA(β⁺)²⁶Mg ft value of the superallowed Fermi decay 0–38964
Al(α,α')Al*, energy and angular distributions meas. from 30 to 170° for 20.0 and 27.5 MeV 0–73978
Ar, (A=43,44) half-life meas. p-ray specta 0–73857
Ar, proton spallation at 310, 425 and 578 MeV, production rates, theory and expt. 0–49615
³⁵Ar, deduced levels from ³⁶Ar(d,t), at E_d=21.6 and 21.0 MeV 0–49661
³⁵Ar, gas target system for continuous production 0–52994
³⁵Ar energy levels, E2, M1 observables and spectroscopic factors 0–64014
³⁵Ar - 3³C1 study 0–52994
³⁶Ar, excited states mean lifetimes. ³⁵C1(n, p)³⁶Ar, v-ray Doppler shift

³⁶Ar, excite 0–46133 excited states mean lifetimes, 35Cl(p,y)36Ar, y-ray Doppler shift

0–46133 "5eAr, isospin pairing explanation for existence of low-lying vibrational states 0–70327 "5eAr, levels deduced from $^{35}\text{Cl}(\text{He d}), \text{E=}12\,\text{MeV}~0–42747$ ^{36}Ar , expherical, from deuteron scattering 0–70655 ^{36}Ar alpha-particle elastic scattering, effect of α -particle correlations 0–70636

Nuclei with 20 \leq A \leq 49 continued 36 Ar struct. from 35 Cl(3 He,d) 36 Ar up to 8.5 MeV 9 0-49514 36 Ar(d,t), deduced levels of 35 Ar at E_{σ} =21.6 and 21.0 MeV 9 0-49661 36 Ar(p, α) deduced levels of 33 Cl, E=12.0 MeV 9 0-42744 36 Ar(p, γ) 37 K, mean lives of levels measured with Doppler shift attenuation for 75 K 9 0-64016

³⁷Ar, thermal neutron capture, energies and intensities of gamma rays

38Ar, analog resonances, level positions and energy integrated total cross sections 0-39046

³⁸Ar, levels deduced from ³⁷Cl(³He, d), E=12 MeV 0-42747

³⁸Ar, levels deduced from ³⁷Cl(³He, d), E=12 MeV 0-42747 ³⁸Ar excited state half-life, obs. 0-38878 ³⁸Ar struct. from ³⁷(³He,d)³8Ar up to 6.9 MeV 0-49514 ³⁸Ar(p,y)³PK, Ep=1.25-2.35 MeV, y decay of ³⁹K levels 0-73802 ³⁸Ar(p,y)³PK, mean lives of levels measured with Doppler shift attenuation for ³⁹K 0-64016 ³⁹Ar, correlation effect on unique forbidden β decay 0-49562 ⁴⁰Ar, γadioactive dating, precision 0-76345 ⁴⁰Ar, props. obs. in ⁴⁰Ar (n,p)⁴⁰Cl 0-77515 ⁴⁰Ar, thermal neutron capture and spins in ⁴⁷Ar 0-67443 ⁴⁰Ar (α C)⁴⁰Ar, 215-22.2 MeV, spin and parity assignments 0-38880 ⁴⁰Ar alpha-particle elastic scattering, effect of α-particle correlations 0-70636 ⁴⁰Ar levels from ⁴⁰Ar(α C)⁴⁰Ar, spin and parity assignment 0-38880 ⁴⁰Ar levels from ⁴⁰Ar(α C)⁴⁰Ar, spin and parity assignment 0-38880

 40 Ar levels from 40 Ar(α,α') 40 Ar, spin and parity assignment 0–38880 40 Ar proton scattering, isobaric analogue resonances, fine structure 0–70368

0-70368 "0-7074" K deduced levels of 41K for E=10 MeV 0-57908 "0-7074" k, deduced levels of 41K for E=10 MeV 0-57908 "0-7074" k, deduced levels of 61K for E=10 MeV 0-57908 "0-7074" k, deduced levels of 61K for E=10 MeV 0-73996 "0-7074" k, deduced levels of 61K for E=10 MeV, anomalous L=1 shapes of angular distributions 0-73996 "0-70474" k, another of 61K for 10K for 10K

⁴⁰Ar, thermal neutron capture, energies and intensities of gamma rays 0-57992

0-57992

**1'Ar clouds from stack of nuclear reactor, exposure rates of γ-rays, attenuation and build-up 0-55214

**1'Ar spins of levels from thermal neutron capture 0-67443
Ca even isotopes, pairing vibrational states 0-73803
Ca isotopes, dynamical deformation effects on charge distrib. 0-73910

3°Ca, decay modes of low levels from (He.np) reactions 0-52674

3°Ca decay modes of low levels from (He.np) reactions 0-52674

**3°Ca energy levels from **ΦCa(p,d) 0-70604

PCa levels from *X(p,n), excess mass -27281±6 keV 0-57906

**ΦCa, 0+ and 2+ states, description including 0p-0h, 2p-2h and 4p 4h
0-70451

0—70451

«Oca, α elastic scatt., 23 MeV, 14-179° 0—52796

«Oca, α elastic scatt., 23 MeV, 14-179° 0—52796

«Oca, collective effects, lifetimes, spins and decay modes of levels 0—38879

«Oca, comparison of Hartree-Fock and Hamiltonian calculations for single particle energies and rearrangement effects 0—49452

«Oca, deduced levels from 39K/3He,d) and zero DWBA calculations for E=11.0 MeV 0—58016

¹Ca, elastic and inelastic scattering, deduced resonances of ⁴Sc, E=4.8-6.2 MeV 0-42749 ⁴OCa, elastic scatt. of electrons, 750 MeV, short-range correlations 0-77541

0–77541 *0 Ca, from (p,t) reactions, isospin-forbidden decay props. of lowest T=2 states 0–38868 *0 Ca, giant dipole states from study of (γ,η_0) reaction 0–49594 *0 Ca, giant resonance, study by inelastic electron scatt. below 60 MeV 0–39018

0-39018

4ºCa, lifetime of 3734 keV, 3⁻ level 0-67431

4°Ca, muon capture rates rel. to breakdown of SU(4) invariance 0-49600

4°Ca, moun capture; n asymmetry, obs. 0-46202

4°Ca, 0+-O+ transitions studied by inelastic e scatt. 0-46129

4°Ca, odd parity spectrum, from interac, between nucleons 0-77484

4°Ca, square-well shell model as framework for study of quasielastic electron scattering 0-60802

4°Ca, two-nucleon density functions and correlation functions with realistic single particle wave functions 0-55119

4°Ca 4p-4h model of excited states 0-70385

4°Ca alpha-particle elastic scattering, effect of α-particle correlations 0-70636

4°Ca hinding energy, size, from effective NN interactions, 0-38806

⁴⁰Ca binding energy, size, from effective NN interactions 0-38806
 ⁴⁰Ca charge radius larger than that of ⁴⁸Ca from Hartree-Fock calc.
 0-70449

0-70449

**Oca electron scattering, monopole elastic, effect of generalized deformations 0-67518

Oca giant dipole resonance structure from 3S((p,n)*18**mK, 0-73903

**Oca Hartree-Fock cales. of binding, density and single-particle spectra with effective force 0-49470

**Oca Hartree-Fock calculations with semi-realistic interactions 0-70407

Oca levels from 3K(*He,dp') and **Oca(p,p'p) 0-67439

**Oca levels and transitions, 7 9MeV 0-42748

**Oca g.s., neutron hole impurities from DWBA analysis of (d,p) reaction 0-70450

 40 Ca neutron separation energies calc. with Morse function type potential 0-67390

0-67390

**OCa from proton scattering, and continuum states in *ISC 0-73804

**OCa from proton scattering, elastic, energy dependence, optical model 0-70583

**OCa(^12C, ^3He, ^4°Cr obs. 0-73994

OCa(^12C, 1)Mn obs. 0-73994

OCa(^12C, 1)Mn obs. 0-73994

OCa(^14E, d)ISC, 40 MeV, angular distributions of observed levels 0-70566

OCa(^14E, d)ISC, single channel calc. of form factors 0-77531

OCa(^14E, p)ISC, angular correlation study 0-55127

OCa(^14E, d)ISC, angular correlation study 0-55127

0-46252 $^{40}\text{Ca}(\alpha,\alpha)$, angular distribution meas., anomalies in backward-angle 0-77578

Nuclei with 20 < A < 49 continued

 40 Ca(α , deduced optical model and Regge pole model parameters, 23 MeV, differential cross section 0-39120

 40 Ca $(\alpha, \gamma)^{44}$ Ti and 44 Ti energy levels and mass 0-70454

⁴⁰Ca(d, d)⁴⁰Ca, asymmetries measured for vectorially polarised 28 MeV deuterons 0–58009

⁴⁰Ca(d, p), spin dependent deuteron and proton waves and polarisation effects 0–58017 ⁴⁰Ca(d, r), E₂=7.0 MeV, expt. and theory 0–39117 ⁴⁰Ca(d, d) ⁴⁰Ca (E₂=13.6 MeV, ang. distrib., optical model anal. 0–60826 ⁴⁰Ca(d, d) ⁴⁰Ca obs. and optical model analysis 0–63851 ⁴⁰Ca(d, d) ⁴⁰Ca (A₂) ⁴⁰Ca(d, p) ⁴¹Ca, ^{1.95} proton polarisation and γ-ray circular polarisation

0-49663 40Ca(d,p) 41Ca, rel. to angular momentum assignments to 41Ca 0-55126 40Ca(d,p) 41Ca, calcs. based on sudden approx. method of d stripping

0—77577

4°Ca(d,p)*ICa, single channel calc. of form factors 0—77531

4°Ca(d,p)*ICa and neutron hole impurities in 4°Ca 0—70450

4°Ca(e, e)*OCa, 28-60 MeV, 0*O-0* transitions studied 0—46129

4°Ca(e, e)*OCa, 28-60 MeV, 0*O-0* transitions studied 0—46129

4°Ca(p,p)*DCa and energy levels in 3°Ca 0—70604

4°Ca(p,p)*D*OCa, inelastic, 5.8-6.6 MeV, cross-sections for formation of 0*O-10*, 3°Ca 0—70604

4°Ca occupation in the sign of the si

0-70636

2Ca analogue states, study with **1K(p, p)1K and **1K(p, n)**1Ca 0-49617

**2Ca doublet near 4.10 and triplet near 4.44 MeV 0-67444

**Ca in ferromagnetic metals, g factor of 6* state 0-75988

**Ca(p, **1He) spin and parity of 1644 keV state in **0K 0-57907

2Ca(p,d)1Ca and energy levels in **2Ca 0-70604

3Ca(p,d)1Ca and energy levels in **1Ca 0-70604

**3Ca, odd parity states, calc. within shell-model employing **0Ca as core 0-49517

0-49517

**Ca rot.-frame nucl. double-reson. in CaF, 0-41390

**Ca, core excitation in **Ca(d,p) stripping reaction 0-49664

**Ca, excited states, deduced levels, using p-y coincidence meas. 0-55128

**Ca, total cross sections between 10.3 and 21.6 MeV variation 0-70603

**Ca, total cross sections between 10.3 and 21.6 MeV variation dosimetry 0.76732 0 76733

 6 6

0–70636

*4Ca(d,p)*5Ca, core excitation of 44 Ca, cross section calc. 0–49664

**Ca, energies, spins decay modes and lifetimes of first 3 excited states determ. 0–77496

**Ca (d, α)*6K and spins in 46 K. 0–70455

*8Ca alpha-particle elastic scattering, effect of α -particle correlations 0–70636

**Ca charge radius smaller than that of 40 Ca, from Hartree-Fock calc. 0–70449

0-70449
**SCa proton scattering, and **GCa states from isobaric analogue states in **SC 0-70458
Ca(3-74E,t)SC, E_{3hc}=15 MeV, energy level study of **SC 0-38884
Ca(d,p)SCa 0-70657
SCa(d,p)OCa calcs. based on sudden approx. method of d stripping

 48 Ca(d,p) 49 Ca cales, based on sudden approx, method of d stripping 0 77577 48 Ca(p,n) 48 Sc total cross-section and isobaric analogue resonance in 49 Sc 0-70605 48 Ca(p,n) 48 Sc, total cross section around isobaric analog state at E_p=1.976 MeV 0-39047 49 Ca half life, precise measurements by scintillation counting 0-64082 49 Ca spins and parity from isobaric analogue states in 49 Sc 0-70458 33 Cl, levels deduced from 32 S(3 He, d) and 36 Ar(p, α) E≤12.0 MeV 0-42744 33 Cl analogue of 33 Ar ground state from 32 S proton scattering 0-70442 33 Cl half life for β decay 0-52723 34 Cl, deduced spin and mean lives of 34 Cl levels from 31 P(α,np) and 32 S(r,pp) 0-58013 32 Cl, gamma-ray transition strengths and 34 Cl deduced levels from

¹²S(r,py) 0-58013

³⁴Cl, gamma-ray transition strengths and ³⁴Cl deduced levels from ¹²S(r,py)¹⁴Cl 0-58014

³⁴Cl deduced levels and γ-ray decay properties below 3 MeV for ³¹S(r,py)¹⁴Cl 0-58015

³⁵Cl, analog states 0-46132

³⁵Cl, Coulomb excitation of ⁷⁰Ge 0 state 0-67460

³⁵Cl, energy levels, E2, M1 observables and spectroscopic factors 0-6014

0 - 64014

35Cl, excited 3.95 MeV level existence from decay scheme for 8.38 MeV

isobar-analogous state 0-67502

3°Cl, gamma ray transition 0-73801

3°Cl, hyperfine structure anomalies, n.m.r. meas. 0-49758

3°Cl, in K.pPtCl₈ and K.pPtCl₈, elec. field gradient motional averaging by lattice vibrations, n.g.r. 0-51418

3°Cl, Larmor freqs., mag. moments, chem. shift, n.m.r. obs. in aqueous

lattice vibrations, n.g.r. 0—91418

3°CI, Larmor freqs., mag. moments, chem. shift, n.m.r. obs. in aqueous soln. 0—70444

3°CI, NMR in CsMgCl₃ and CsMnCl₃ obs. at 300K 0—48161

3°CI, NMR obs. in CsCoCl₃ 0—48161

3°CI, n.q.r. in CsGeCl₃, calc. elec. field gradients 0—41399

3°CI, n.q.r. in haloacetic acids 0—59475

3°CI, n.q.r. in trichlorophosphazosulphuryl chloride 0—55343

3°CI, n.q.r. spectra of dichlorobis (trimethylenediamine) cobalt (III) chloride, hydrochloride dihydrate 0—79423

3°CI, n.q.r. Zeeman spectrum in 4-chloro-3-methyl phenol, single cryst. 0—66159

3°CI, n.g.r. Zeeman spectrum in 3,4-dichloroaniline, temp. dependence 0—74359

3°CI, niclear quadrupole resonance in 3,4-dichloroaniline, temp. dependence 0—74359

3°CI, proton elastic and inelastic scatt., energy level study 0—52764

3°CI, institutional model 0—64015

3°CI and 3°CI n.g.r. in polycryst. LiClO₃ 0—45044

3°CI cenergy level structure from 3°S(α,pγ)3°CI reaction, spins, branching ratios 0—42746

3°CI first six excited states, spin and parity from 3°CI(p,p/γ)3°CI 0—70445

3°CI in BCI₃ and its amine and nitrile complexes n.g.r. spectra 0—61072

Nuclei with 20 A 49 continued

35Cl intermediate-coupling structure in 2s-1d shell 0-64012

35Cl n.q.r. frequency in K2OsCl6, temp. and pressure dependence 0-79424

³²Cl n.q.r. frequency in K₂OsCl₈, temp. and pressure dependence 0–79424

³⁵Cl n.q.r. in GaCl₃, Zeeman effect, obs. 0–41397

³⁵Cl n.q.r. in paramag, and antiferromag, K₂IrCl₆ 0–72517

³⁵Cl n.q.r. in trimethylamine-BCl₃ complex 0–67802

³⁵Cl spins from ³⁷Cl(p,t) 0–70602

³⁵Cl(³He, d) deduced levels of ³⁶Ar, E=12 MeV 0–42747

³⁵Cl(d, ³He), ³⁴S levels, obs. 0–39119

³⁵Cl(p,p)³⁶Cl, gamma radiation study neutron separation energy 0–42856

³⁵Cl(p,p)³⁶Ar, cross-sections in the region of giant dipole resonance 0–39045

0 - 39045
37Cl, amma ray transitions 0-73801
37Cl, hyperfine structure anomalies, n.m.r. meas. 0-49758
37Cl, Larmor freqs., mag. moments, chem. shift, n.m.r. obs. in aqueous

3°Cl, hyperfine structure anomalies, n.m.r. meas. 0—49/38 3°Cl, Larmor freqs., mag. moments, chem. shift, n.m.r. obs. in aqueous soln. 0—70444 3°Cl, n.q.r. spectra of dichlorobis (trimethylenediamine) cobalt (III) chloride, hydrochloride dihybrate 0—79423 3°Cl (p.t)³Cl and levels in ³5Cl 0—70602 3°Cl excited state half-life, obs. 0—38878 3°Cl(¹He, d) deduced levels of ¹8Ar, E=12 MeV 0—42747 3°Cl(d, ³He), ¹8S levels, obs. 0—39119 3°Cl(p,p)³Ar, cross-sections in the region of giant dipole resonance 0—39045 3°Cl(p,p)³Ar, total cross-section meas. 0—39046 4°Cl, β-decay obs. 0—77515 4°Cr decay, and magnetic moment of 310 state in ⁴8V 0—70456 4°Cr produced by (³He,p) reaction, observation of excitation in low-lying states with T=2 0—73993 4°Cr spin and h.f.s. of ground state meas. 0—73806 Cr(n, n)Cr 0.3-4.1 MeV optical model analysis 0—46220 2°Cu, elastic scattering, differences in single, plural and multiple scattering through intermediate angles for electrons and positrons 0—57970 2°F, deduced levels from ¹80(³He,p) and ¹9F(d,p) for excitation energy up to 6.043 MeV 0—52678
20°F, p.ray transitions, excitation energies, from reaction ¹9F(d,py)²°F

0-32076 0-32076 0-38867

0-32076

0-38867

0–38867 29 F, mirror symmetry in β decay 0–42786 29 F, mer isotope obtained in bombardment of a 232 Th Target with 174 MeV 12 Ne ions 0–52804 49 Fe level from 40 Ca (12 C, 3n), new delayed proton emitter 0–42752 K whole-body γ spectrometry 0–59824 37 K, mean lives of levels measured with Doppler shif attenuation for 36 Ar(p, γ) 37 K 0–64016 37 K polarization by optical pumping, and β -decay asymmetry, obs. 0–52680 38 K energy levels effective interaction calc. 0–38853

NK polarization by optical pumping, and β-decay asymmetry, obs. 0-52680
 18K energy levels, effective interaction calc 0-38853
 18K levels≪2.40 MeV, from 39K (p,d), 16 and 18 MeV 0-38860
 19K, pamma ray transition 0-73801
 19K, y decay of levels, meas, with 39Ar(p,p) 0-73802
 19K, fifetime of 2818 keV, 7/2 level 0-67431
 19K, mean lives of levels measured with Doppler shift attenuation for 38Ar(p, p)39K 0-64016
 19K elastic and inelastic scattering of electrons, charge density distribution, excitation of discrete energy levels 0-46197
 19K giant dipole resonance structure from 39K (y,n)38mK 0-73903
 19K(14e, dy)40Ca, levels and transitions obs. 7-9MeV 0-42748
 19K(14e, dy)40Ca, levels and transitions obs. 7-9MeV 0-42748
 19K(14e, dy)40Ca and levels in 40Ca 0-67439
 19K(14e, dy)40Ca and levels in 40Ca 0-67439
 19K(16, n)40K, y-ray transitions obs. and y-y coincidence matrix 0-42852
 19K(16, n)40K, y-ray transitions obs. and y-y coincidence matrix 0-42852
 19K(p,d) 16 and 18 MeV, 38K levels≪2 240 MeV 0-38860
 19K(p,y)40Ca intermediate structure and continuum states in 40Ca 0-73944
 19K(p,n)40Ca, excess mass calc. from threshold energy 0-57906

0–73944 95 K(p,n) 39 Ca, excess mass calc. from threshold energy 0–57906 40 K, β decay schematic model calculations, particle hole force effect on lifetime 0–70542 40 K, e.m. transitions between odd parity states 0–70446 40 K, from 39 K(n,γ), decay scheme and spins and parities of excited states 0–42852 40 K, spin and parity of 1644 keV state, determination from 42 Ca(p, 3 He) 0–57907

0-57907

"OK anomalous L=1 shapes of angular distributions for (³He,t) transitions to 0+ antianalog states 0-73996

"OK positive parity states from "OAr(p,np)*** reactions 0-70448

"OK-4"OAr beta decay, third-forbidden, shell and rotational models calc. 0-73855

"OK-4"OCa beta decay, third-forbidden, shell and rotational models calc. 0-73855

⁴¹K, deduced levels from ⁴⁰Ar(³He,d)⁴¹K for E=10 MeV 0-57908

 10 (K, deduced levels from 40 Ar(3 He, d) 41 K for E=10 MeV 0-57908 41 K, ground state (p,n) Q values 0-77552 41 K, isobaric analogue states 0-42750 41 K excited state half-life, obs. 0-38878 41 K(41 He, d) 42 Ca, deduced 40 Ca levels and zero DWBA calculations for E=11.0 MeV 0-58016 41 K(p, α_o) 38 Ar, Ep=1.17-2.10 MeV, resonance and excitation energies, yields, 17 values 0-49616 41 K(p, 41 Ca, Ep=1.35-1.96 MeV, resonances, partial widths 0-49617 41 K(p, p) 41 K, Fp=1.35-1.96 MeV 0-49617 42 K, decay, gamma-ray spectra, peaks at 0.692 and 1.228 MeV 0-55143 42 K (ccay, gamma-ray spectra, peaks at 0.692 and form of 5- from (d,α) reactions 0-70455 47 K, β decay, half-life meas, spin and parity of levels 0-77516 71 Li(p,n) 71 Be, precision meas, of threshold energy by velocity technique 0-46211

⁷Li(p,n)/Be, precision meas. of threshold energy by velocity technique 0–46211 Mg (A=24, 25 and 26), proton elastic and inelastic scatt., ang. distribs. near 6MeV, low lying levels -70584 and -70584 and -70884 and -

0–39114

*Mg, analogue of 4 particle-4 hole state in ¹⁶O 0–70422

*Mg, electron scatt., Ee=225 MeV, anal. in Born approx. 0–60803

*Mg, energy level calc. from angular momentum states 0–49504

*Mg, from (p,t) reaction, isospin-forbidden decay props. of lowest T=2 states 0–38868

*Mg, giant resonance study by inelastic electron scatt. below 60 MeV 0–39018

Nuclei with 20 ≤ A ≤ 49 continued

²⁴Mg, inelastic scatt. of protons, polarization 0-77545

²⁴Mg, isospin pairing explanation for axial symmetry 0-70327

²⁴Mg, isospin pairing explanation for axial symmetry 0–70327
 ²⁴Mg, ilifetime of 1369 keV 2+ level 0–67431
 ²⁴Mg, M1 transitikns with ΔT=1 0–70434
 ²⁴Mg, neutron, elastic and inelastic scatt., E_w=14.2MeV, diff. cross sections, level excitation 0–73956
 ²⁴Mg, 0+—0+ transitions studied by inelastic e scatt. 0–46129
 ²⁴Mg, p. scatt., elastic and inelastic transitions, 100 MeV 0–39029
 ²⁴Mg, operation of explanations of explanations.

 44 Mg, p scatt, elastic and inelastic transitions, 100 MeV 0–39029 24 Mg, quadrupole moments of excited states, using SU₃ model and projected HF cales. 0–77490 24 Mg, search for α-particle structure 0–46252 24 Mg, selective population of highly excited states in 16 O(12 C,α) reaction 0–52805

²⁴Mg, selective population of highly excited states in ¹⁶O(¹²C,α) reaction 0-52805
 ²⁴Mg, spin assignment of states from an analysis of Doppler-broadened gamma rays 0-52681
 ²⁴Mg existic and inelastic electron scattering excitation of first (1.37 MeV) level, higher lying levels study 0-46128
 ²⁴Mg ground state rotational bapd, populated preferentially in (p,t), and DWBA 0-70600
 ²⁴Mg ground state shape 0-38872
 ²⁴Mg Hartree-Fock, triaxial, rotational symmetry restoration 0-70353
 ²⁴Mg Hartree-Fock projected spectrum 0-70433
 ²⁴Mg isobaric analogue levels, shell model calc. 0-38870
 ²⁴Mg recoil nuclei in Na alloys, nucl. reson. fluoresc. ¹⁰0-65569
 ²⁴Mg recoil nuclei in Na and NaCl single cryst., effect of anisotropic slowing down on nuclear reson. fluoresc. yield 0-69056
 ²⁴Mg rotational states, lifetimes and branching ratios 0-70432
 ²⁴Mg spins of states at 12.74, 12.85 and 12.97 MeV from Doppler broadened gamma-rays 0-70431
 ²⁴Mg(He,α) E=15 MeV, angular distrib. of α particles ²³Mg levels deduced 0-39114
 ²⁴Mg(He,pp)¹⁶Al directional correlation measurements and deduced levels

 18 18 18 19 19 18 19 19 18 19

Mg(*C1,d)S1, *Mg(*C1,d)**S1, search for \(\alpha \)-particle structure in **Mg**S1 0-46252

**Mg(*C1,\(\alpha \))^2Al, search for trition grouping in **2Al 0-49673

**Mg(\(\alpha \), *\(\alpha \) Al, \(\alpha \) —0 selection rule test 0-67554

**Mg(\(\alpha \), *\(\alpha \) Mg, excitation of \$3^+, *+\$ levels 0-64132

**Mg(\(\alpha \), *\(\alpha \) Mg, excitation of \$1^+, *+\$ levels 0-64432

**Mg(\(\alpha \), *\(\alpha \) Mg, 28-60 MeV, O*+O* transitions studied 0-46129

**Mg(\(\alpha \), *\(\alpha \), *\(\alpha \) leminor crelation and identification of mirror state structure 0-52679

**Mg(\(\alpha \), *\(\alpha \))*Na and level structure of *21Na 0-70428

**Mg(\(\alpha \), *\(\alpha \))*Mg, 100 MeV, ang. distrib. obs. 0-39031

**Mg(\(\alpha \), *\(\alpha \), *\(\alpha \) =0 for 6429

**Mg(\(\alpha \), *\(\alpha \), *\(\alpha \) =0 for 6429

**Mg(\(\alpha \), *\(\alpha \), *\(\alpha \) =0 for 6429

**Mg(\(\alpha \), *\(\alpha \), *\(

0—51409

²³Mg(³He,n)²⁷Si excitation of T=3/2 levels in ²⁷Si 0—46121

²³Mg(³He,n)²⁷Na, cross sections behaviour, E=10—1 MeV 0—39110

²³Mg(n, p)²⁸Mg thermal neutron capture cross-sections 0—60815

²⁸Mg, electron scatt, Ee=225 MeV, anal. in Born approx. 0—60803

²⁶Mg, energy levels from study of ²⁷Al(n,d) at 14.1 MeV 0—77560

²⁸Mg, evidence for isospin splitting of giant dipole state 0—70435

²⁸Mg, gant resonance, study by inelastic electron scatt, below 60 MeV 0—99018

0-39018 26 Mg, resonances of (p,y) reaction between 660 and 1000 keV 0-52776 26 Mg inelastic electron scattering, splitting of giant resonance 0-42741 26 Mg $(^{3}$ He, $\alpha)$ E=15 MeV, angular distrib. of α particles 25 Mg levels deduced

²⁶Mg(³He,d)²⁷Al, 17.85 MeV, spectroscopic factors from DWBA analysis

²⁶Mg(³He,n)²⁸Si, observation of excitation in low-lying levels with T=2

 $^{10-13993}$ ce Mg(14 He,t) 26 Mg(14 He,t) 26 Mg(14 He,t) 26 Mg(12 Mg) 12 Mg(

²⁶Mg(d,α)²⁸Na, excitation function, 0 to 10 MeV 0-39112
²⁶Mg(d,α) reaction, energy spectra and α particle angular distributions 0-46244
²⁶Mg(d,p)²⁷Al, excitation energies and γ-branchings of ²⁷Al 0-70653
²⁶Mg(d,p)²⁷Mg, decay of ²⁷Mg 0-70653
²⁶Mg(d,p)²⁷Mg, decay of ²⁷Mg 0-70653
²⁶Mg(d,p)²⁷Mg, decay of ²⁷Mg 0-70653
²⁶Mg(d,p)²⁷Mg, p-γ-angular correl., 3 MeV 0-39115
²⁶Mg(p,p)²⁸Mg, p-γ-angular correl., 3 MeV 0-39115
²⁶Mg(p,p)²⁸Mg, 1-28 MeV, excited levels produced, spin-parity assignments 0-77491
²⁶Mg(p,p)²⁸Mg, 1-3-3.6 MeV, spins, parities and mixing factors of ²⁷Al determ. 0-46207
²⁶Mg(p,p)²⁸Mg, 1.2-3.0 MeV, ²⁷Al level obs. 0-39032
²⁶Mg(p,p)²⁸Mg, and cistrib. of polarized protons studied 0-52762
²⁶Mg(p,p)²⁸Mg and ground state rotational band in ²⁸Mg 0-70600
²⁷Mg 169, 1.94 MeV levels γ-branching ratios, obs. 0-39115
²⁷Mg decay, β-γ correlation meas. and γ-spectroscopy 0-38965
²⁸Mg decay, β-γ correlation meas. and γ-spectroscopy 0-38965
²⁹Mg excitation energies, γ-branching, β-decay studied by ²⁸Mg(d,pγ)²⁴Mg 0-70653
²⁹Mg low-lying states from ²⁶Mg(d,pγ) p-γ angular correl. obs. 0-38874
²⁹Mg half-life, biological, in humans 0-76727
²⁹Mg half-life, biological, in humans 0-76727
²⁹Mg half-life, biological, in humans 0-76727
²⁹Mg half-life, biological in humans 0-76727
²⁹Mg half-life, biological in humans 0-76727
²⁹Mg half-life, biological, in humans 0-76727
²⁹Mg half-life, biological, in humans 0-76727
²⁰Mg half-lif

0–57947 $^{\circ}$ Na, mirror symmetry in β decay 0–42786 $^{\circ}$ Na, mirror state structure, from angular correlation studies with the e reaction 0–52679 $^{\circ}$ Na energy levels near 2.8 MeV excitation from $^{24}{\rm Mg}({\rm p},\alpha)$ 0–70428 $^{21}{\rm Na}$ lowest negative parity state from $^{20}{\rm Ne}({\rm d.n})^{21}{\rm Na}$ reaction 0–46126 $^{21}{\rm Na}$ polarization by optical pumping, and β -decay asymmetry, obs. 0–52680

Nuclei with 20≤A≤49 continued ¹²Na, deduced levels, from ²²Ne(³He,t) 0-77574

²²Na, deduced levels, from ²²Ne(²He,t) 0-77574

²²Na, energy depend, of prod. cross sections with 100-400 MeV protons, on Mg and Se target 0-49614

²³Na, spin, parity and multipole mixing ratio assignments of low levels from y-ray polarization 0-77488

²⁷Na levels≤3.06 MeV, from ²³Na(p,d), 16 MeV 0-38860

²⁸Na studied following ²³Ne(p, y)²²Na, 300-1300 KeV 0-46127

²³Na, compound, levels rel. to ¹³F(α,α) excitation functions, 3.5-5.0 MeV 0-3994

0-39094 23 Na, elastic and inelastic proton scattering, E_p =6 MeV, meas. of ang. distribs, props. of excited levels, 3.92 MeV max. 0-39030 23 Na, ground state band, collective calculations 0-64009

Na, ground state band, collective calculations 0–64009
 Na, isobaric analogue states 0–42750
 Na, low-lying states, pγ ang. correlations and lifetime meas., from ²³Na(p, p′) 0–49510
 Na, n.m.r in AgNa(NO₂); 0–72508
 Na, n.m.r in polycryst. NaNbO₃ 0–79417
 Na, photo-excitation of T=³/₂ states 0–67430
 Na, proton and α-particle emission for E_m=12.65-18.25 MeV using NaI target 0–42850

target 0-4250

3NA, proton elastic scatt., 8 to 12 MeV, anal. of average cross sections
0-52761

0-52701 3"Na, proton induced reactions at 1000-1800 keV, resonance detection 0-57977

0-5/977

"Na collective states from (d, α) cross-sections 0-70429

"Na elastic and inelastic scattering of electrons, charge density distribution, excitation of discrete energy levels 0-46197

"Na intermediate structure from inelastic proton scattering 0-73796

"Na n.m.r. spectra in Na,As (Sb), quadrupole splitting 0-48164

"Na proton scattering, elastic and inelastic, coupled channel calculation 0-67530

³³Na quadrupole spin lattice relaxation in NaNO₃, results reanalyzed 0-75977

⁴³Na quadrupole spin-lattice relaxation in NaNO₃, results reanalyzed 0-75977

³⁰Na resonance temp, depend, on h₂O- and D₂O-saturated zeolite Linde 13X 0-43568

³¹Na(¹He,d)⁴³Mg*, ⁴⁴Mg level lifetimes and excitation energies, ≤11 MeV 0-38869

³¹Na(μ,α)²¹Ne, cross sections behaviour, E=10-11 MeV 0-39110

³¹Na(μ,α)²¹Ne direct reaction process analysis 45.5 MeV 0-39043

³¹Na(μ,α)²¹Ne and spins of states in ²⁴Mg 0-70431

³¹Na(μ,α), 16 MeV, ²³Na levels≤3.06 MeV 0-38860

³¹Na(μ,p), average inelastic cross-sections, fluctuations and model comparisons, 8.0-12.0 MeV 0-42838

³⁴Na, ²⁴Mg, ²⁴Al isobaric multiplet, study 0-46244

³⁴Na, energy depend, of prod, cross sections with 100-400 MeV protons, on Mg and Se target 0-49614

³⁴Na, half-life in solid NaCl and in aqueous soln, half-life alteration of β-decaying anions and cations 0-56715

³⁴Na source, multicurie, activity meas, by isomeric activation 0-52716

³⁴Nb VIII, term analysis of the 4p-4d and 4p-5s transitions 0-60936

Ne isotopes, 20≤A≤28, static and dynamic quadrupole moments 0-73793

³⁶Ne-induced fission of Sn and Ag, cross-sections and fragment distribu-

²⁰Ne-induced fission of Sn and Ag, cross-sections and fragment distribu-

⁴⁰Ne-induced fission of Sn and Ag, cross-sections and fragment distribution 0-46264
 ⁴⁰Ne, analogue of 4 particle 4 hole state in ¹⁶O 0-70422
 ⁴⁰Ne, electron scattering at 180° 0-67521
 ⁴⁰Ne, energy level calc. from angular momentum states 0-49504
 ⁴⁰Ne, from (p,t) reaction, isospin-forbidden decay props. of lowest T=2 states 0-38868
 ⁴⁰Ne, ground state rotational bands, cut off 0-52669
 ⁴⁰Ne, HF calculations with realistic and semi-realistic interactions 0-70424

²⁰Ne, HF 0-70424

0-70424

2ºNe, p scattering, 1.5-2.4 MeV, p polarization 0-60805

2ºNe, quadrupole moments of first excited states 0-60757

2ºNe energy levels from '9°F(p, ³Be) '¹C 0-73792

2ºNe grant dipole resonances from '9°F(p, °) 0-70423

2ºNe Hartree-Fock constrained calculations for quadrupole genrator coordinate 0-49494

2ºNe isobaric analogue levels, shell model calc. 0-38870

2ºNe level lifetimes and excitation energies from '9°F(²He,d)²ºNe*≤11 MeV

0-38869

No level lifetimes and excitation one gas and one section meas., 0-38869
 No levels, from ²⁰Ne(p,t) at 50 MeV differential cross section meas., DWBA calc. 0-57904
 No equadrupole moment, static, of first excited state 0-70421
 No e studied from (%1,6), (*Li,t) reactions on 160 0-49672
 No to defer one of the section of the section

²⁰Ne(³He,\alpha)¹⁹Ne, study of lifetime of 275 keV second excited level

²⁰Ne(³He,α)¹⁹Ne, study of levels below excitation energy of 7 MeV

0-7486

²⁰Ne(³He,n) deduced levels of ²²Mg, between 3.4-9.4 MeV 0-42740

²⁰Ne(³He,n))²²Mg, and low-lying excited states in ²²Mg 0-67429

²⁰Ne(α,α), 20-24 MeV 0-42864

²⁰Ne(α,α)²⁰Ne obs. Blair-Drozdov model 0-77570

²⁰Ne(d,n)²¹Na reaction studied at 4.5 MeV, energy levels study in ²¹Na 0-46126

²⁰Ne(d,p)²¹Ne, excited states in ²¹Ne and comparison with DWBA 0-70427

0-70427

**ONe(n,x), angular distribs. and spectra, 14.1 MeV 0-39081

**ONe(n,x), 18Ne and energy levels in **Ne 0-70413

**ONe(n,t), 18Ne at 50 MeV, differential cross section meas., DWBA calcs.
0-57904

**INe, mirror state structure from angular correlation studies with the ereaction 0-52679

**INe, non-central forces 0-70429

 21 Ne, non-central forces $\,0-70426$ 21 Ne collective states from (d,p) reactions and DWBA $\,0-70429$ 21 Ne resonances, spin and parity, widths, from 19 F(d, α) at E_d=1-3.95 MeV $\,0-64135$ 21 Ne (d,p) 22 Ne $\,0-652$ 21 Ne (d,p) 22 Ne $\,0-64135$ 21 Ne (d,p) 22 Ne $\,0-70652$ 21 Ne(d,p) 22 Ne, band mixing, computer program calc. $\,0-73794$ 22 Ne, band mixing, computer program calc. $\,0-73794$ 22 Ne, exaded by the We with the constant of 22 Ne 174 MeV ions bombardment of 23 Th target, production of new isotopes 21 N, 23 O, 24 O, 25 F $\,0-52804$ 22 Ne excited states from (d,p) reactions and DWBA $\,0-70427$

Nuclei with 20 < A < 49 continued

²²Ne high spin states, obs. above neutron-decay threshold at 11.01, 11.11 and 11.49 MeV 0-73795

 22 Ne proton scattering, isobaric analogue resonances, fine structure 0-70368

²²Ne rotational bands from ¹⁸O(⁷Li,t)²²Ne 0-70430

²²Ne spectrum, effect of pairing correlations on ground-state band 0-38871

0-38871

²¹Ne(³He,α) differential cross sections, experimental results compared with theory, energy levels of final nucleus 0-67553

²¹Ne(³He,α) differential cross sections, experimental results compared with theory, energy levels of final nucleus 0-67553

²²Ne(⁴He,α) differential cross sections, experimental results compared with theory, energy levels of final nucleus 0-67553

²³Ne(³He,α) differential cross sections, experimental results compared with theory, energy levels of final nucleus 0-077570

²⁴Ne(α,α)²⁴Ne, E,=33 MeV, low-lying levels of ²⁴Ne, study 0-49509

²⁴Ne, level study from ²²Ne(t,p), E,=33 MeV 0-49509

²⁵Ni, level structure from DWBA analysis of (²⁴He,α), (p,p'p), and (³He,p) reactions 0-67446

²⁶O, new isotope obtained in hombardment of a ²³²Th target with 174 MeV ⁹¹Ni, level structure from DWBA analysis of $(^3\text{He}, \alpha)$, (p, p'p'), and $(^3\text{He}, p)$ reactions 0-67446²¹O, new isotope obtained in bombardment of a ²³²Th target with 174 MeV ²³Ne ions 0-52804²⁴O, new isotope obtained in bombardment of a ²³²Th target with 174 MeV ²³Ne ions 0-52804obs. of energy levels up to 10 MeV excitation, relative spectroscopic factors 0-77494²⁹P, ang. moment of 4081 keV excited level 0-38877²⁹P, p-ray transitions of reson and excited states from Si(p,p) 0-73798²⁹P haif life values for β decay 0-52723²⁹P lifetimes and p-ray angular distributions from $^{28}\text{Si}(p,p) = 0-67435$ ²⁹P 1 $^{29}\text{P} = 1-3/2$ level excitation in search 0-46121³⁰P, angular distributions to ground and 4 lowest excited states from $^{28}\text{Si}(^3\text{He}, p)$ reaction 0-70654³⁰P, core excitation, by $^{39}\text{Si}(^3\text{He}, d) = 0-70437$ ³⁰P, lifetimes of levels 0-70438³⁰P levels $\lesssim 2.94$ MeV, from $^{39}\text{P}(p, d)$, 16 MeV 0-38860³⁰P negative parity band, 4 to 8 MeV 0-67436³¹P, alpha-particle elastic and inelastic scattering, angular distributions 0-70633³¹P, excitation of 3 to 6 MeV states, by inelastic scatt. of 14 MeV neutron

³¹P. excitation of 3 to 6 MeV states, by inelastic scatt, of 14 MeV neutron

³¹P_c excitation of 3 to 6 MeV states, by inelastic scatt. of 14 MeV neutron 0–67437

³¹P_c gamma ray transition 0–73801

³¹P_c hyperfine interaction in dithiophosphenes of Cu(II), VO(II), CrO(III), MoO(III), WO(III) 0–70898

³¹P_c n.m.r. in Ni|P(OR)_{3-x}F_x|₄, influence of substitution 0–46500

³¹P_c n.m.r. in UP-US solid solution, rel. to mag. ordering 0–45033

³¹P_c proton elastic scatt, absolute differential cross sections 0–52763

³¹P_c intermediate-coupling structure in 2s-1d shell 0–64012

³¹P_c n.m.r. in anhydrons pare-earth phosphates, obs. 0–41381

³¹P_c n.m.r. in BaFPO₃, and ³⁹F reson., rel. to polycryst. lattice theory 0–41357

³¹P n.m.r. in BaFPO₃, and ⁹⁵F reson., rel. to polycryst. lattice theory 0–41357 [31]P n.m.r. in ferromag. and antiferromag. MnP 0–72511 [31]P n.m.r. in ferromag. And the search for trition cluster structure 0–49673 [31]P search for trition cluster structure 0–49673 [31]P n.m.p. in ferromag. And 4.89 MeV 0–42743 [31]P n.m.p. in ferromag. And 4.89 MeV 0–42743 [31]P n.m.p. in ferromag. And an invest of ³⁴Cl levels 0–58013 [31]P n.m.p. in ferromag. An internation 0–57905 [31]P n.m.p. in ferromag. An internation 0–38910 [31]P n.m.p. in ferromag. An internation 0–38910 [31]P n.m.p. in ferromag. An internation 0–38860 [31]P n.m.p. in ferromag. An internation 0–38966 [32]P n.m.p. investigation of bound states of ³³P below 4.3 MeV excitation energy 0–77495 [32]P, decay period meas. 0–38966 [32]P, internation of the search of the searc 0-42744

0-70633 October 12 and inelastic scattering, angular distributions

3²S, collective nature of second 2⁻ state 0-64013 3²S, decay of reson. levels, from ³¹P(p, y) reaction at 2000-2400 keV 0-67535

³²S, excitation of 3 to 6 MeV states, by inelastic scatt. of 14 MeV neutron 0-67437

0-67437 3^{12} S, from (p,t) reaction, isospin-forbidden decay props. of lowest T=2 states 0-38868 3^{12} S, giant dipole states from study of (p,n₀) reaction 0-49594 3^{12} S, in boson approx. model 0-60758 3^{12} S, isospin pairing explanation for axial symmetry 0-70327 3^{12} S, $0^{+}-0^{+}$ transitions studied by inelastic e scatt. 0-46129 3^{12} S, quadrupole moments of first two excited states 0-38875 3^{12} S, search for α -particle structure 0-46252 3^{12} S proton elastic scattering, and 3^{13} Cl analogue of 3^{13} Ar ground state 0-70442 3^{12} Cl He α) deduced levels of 3^{15} S, E=8.0-12.2 MeV 0-42744

0–70442 $^{32}\text{S}(1+\text{Le},\alpha)$ deduced levels of ^{31}S , E=8.0-12.2 MeV 0–42744 $^{32}\text{S}(1+\text{Le},\alpha)$ deduced levels of ^{31}S , E=8.0-12.2 MeV 0–42744 $^{32}\text{S}(1+\text{Le},\alpha)$ deduced levels of ^{32}C , E=12.0 MeV 0–42744 $^{32}\text{S}(1+\text{Le},\alpha)$ deduced levels of ^{32}C , E=12.0 MeV 0–42744 $^{32}\text{S}(\alpha,\rho)$ $^{32}\text{S}(\alpha,\rho)$ $^{32}\text{S}(\alpha,\rho)$ $^{32}\text{S}(\alpha,\rho)$ ^{32}S and low-lying levels in ^{33}S 0–70439 $^{32}\text{S}(\alpha,\rho)$ ^{32}S (ap) ^{32}S (ap

Nuclei with 20 < A < 49 continued

 $^{32}S(p,np')$, p quanta spectra, cross sections of peaks 0-73902 $^{32}S(p,pp')$, p quanta spectra, cross sections of peaks 0-73902 $^{32}S(p,pp')$, p quanta spectra, cross sections of peaks 0-73902 $^{32}S(p,pp')$ (c), deduced levels below 3 MeV and p-ray decay properties for ^{34}Cl 0-58015

 $^{32}C(\tau,py)^{34}Cl$, gamma-ray transition strengths and ^{34}Cl deduced levels 0-58014

0–58014 $^{12}\mathrm{S}(\tau,\mathrm{py})^{34}\mathrm{Cl}$, spin and mean lives of $^{34}\mathrm{Cl}$ levels 0–58013 $^{31}\mathrm{S}$, $^{34}\mathrm{S}$, proton elastic and inelastic scatta, energy level study 0–52764 $^{33}\mathrm{S}$, electric quadrupole moment calc. 0–74233 $^{33}\mathrm{S}$, energy level study using $^{34}\mathrm{S}(^{3}\mathrm{He},\alpha)$ reaction 0–70440 $^{33}\mathrm{S}$, mean lifetime of 2.94 MeV level using $^{30}\mathrm{S}((\alpha,n))$ reaction 0–70441 $^{33}\mathrm{S}$, multipole migrations and transitions studied from $^{33}\mathrm{S}((\alpha,\mathrm{n}p))^{33}\mathrm{S}$ 0–77576

³S, nuclear quadrupole hyperfine structure of molecules containing nucleus 0-70866

sinches of hypothes stated to the model of the state of the state of the state of the states of the

10—/0440
325S, decay period meas. 0—38966
325S, electric quadrupole moment calc. 0—74233
326S levels from 37Cl(d, 3He), obs. 0—39119
SC isotopes, d_{3/2} hole states, binding energies 0—42751
41SC, deduced resonances from 40Ca(p,p) and 40Ca(p,p'), E=4.8-6.2 MeV
0—42749

10-42/49

"Sc analysis of stripping to quasibound levels 0-70656

"Sc continuum states in "Ca(p,p))"Ca 0-73804

"Sc core-particle interaction and fragmentation of single-particle levels 0-3881

0–38881

*2°Sc, effective three-body interactions calc. 0–70453

*2°Sc, spin assignments for 1.89 MeV level, by studying *4°Ca(3He, pp)*2°Sc at 10.0 MeV 0–49516

*2°Sc energy levels, effective interaction calc. 0–38853

*2°Sc levels from *4°Ca(3'He,pp), angular correlation study 0–55127

3°Sc, K^{}=3'/2[†] rotational band, lifetimes of levels determ. 0–67445

*5°Sc, odd-parity states, calc. within shell-model employing *4°Ca as core 0–49517

*4°Sc, intermediate level in RaTiO, lattice, static elec. quadrupole interactions of the contraction of the contract

⁴⁴Sc, intermediate level in BaTiO₄ lattice, static elec. quadrupole interaction 0–44364

tion 0-443644°Sc, dipole giant resonance, photoabsorpt. 0-388824°Sc, depole giant resonance, photoabsorpt. 0-388824°Sc, excretor and γ transitions, deduced levels, from $(\alpha, \alpha' \gamma)$ and $(p, p' \gamma)$ 0-495184°Sc, ground state (p,n) Q values 0-775524°Sc, in ScB₃, n.m.r. meas. 0-794184°Sc, level scheme, by 4°Sc $(p,p' \gamma)$ at Ep=1.8-4.5 MeV 0-526834°Sc, level scheme, by 4°Sc $(p,p' \gamma)$ at Ep=1.8-4.5 MeV 0-675404°Sc, $(^3He, \alpha)^{44m}$, 46 Sc cross-sections and isomer ratios from 6-19 MeV, recoil range studies for 4m Sc and 44 Sc in 45 Sc 0-580184°Sc $(^3He, \alpha)^{44m}$, 46 Sc and 44 Sc in 45 Sc 0-580184°Sc $(^3He, \alpha)^{44m}$, angular distribs. and spectroscopic factors, 41 MeV 0-496654°Sc $(^3he, \alpha)$, for study of low-lying odd parity states in 46 Sc 0-52685

0-49665

*Sc(p,n), for study of low-lying odd parity states in *6Sc 0-52685

*Sc(p,n), (p,2n), (p,pn), (p,3p) and (p,3pn), cross-sections for energies up to 85 MeV using radiochemical methods 0-57978

*Sc, low-lying odd parity states 0-52685

*Sc, low-lying odd parity states 0-52685

*Sc, low-lying states from thermal neutron capture in *5Sc 0-67540

*Sc, low-lying states from thermal neutron capture in *5Sc 0-67540

*Sc, level struct. from *8Ca(*He.t) at E_{3R}=15 MeV 0-38884

*Sc, level struct. from *8Ca(*He.t) at E_{3R}=15 MeV 0-38884

*Sc effective three-body interactions calc. 0-70453

*Sc isobaric analog resonance, total *8Ca(p,n)*Sc reaction cross-section meas. 0-39047

*Sc isobaric analogue resonance corresponding to *9Ca ground state.* ⁴⁹Sc isobaric analogue resonance corresponding to ⁴⁹Ca ground state 0-70605

0-70005

**Sc isobaric analogue states and **9Ca spins and parities 0-70458

**Sc levels, analogue spin mixing 0-67449

Si, deuteron elastic scattering, analysis by optical potential 0-67542

Si, stable isotopes, thermal neutron absorption cross sections, resonance integrals and resonance parameters 0-46152

integrals and resonance parameters 0-46152 Si, thermal neutron absorption cross sections, resonance integrals and resonance parameters 0-46152 Si elastic scatt. cross section fluctuations, 6.7-13.4 MeV 0-39052 ¹⁸Si, mean lifetime meas, of first excited states 0-49511 ²⁷Si, deduced levels from ²⁸Si(d,t), at E_a=21.6 and 21.0 MeV 0-49661 ²⁸Si, alpha-particle elastic and inelastic scattering, angular distributions 0-70633 ²⁸Si, from (p,t) reaction, isospin-forbidden decay props. of lowest T=2 states 0-38868 ²⁸Si. HF calculations with realistic and semi-realistic interactions 0-70424

²⁸Si, HF calculations with realistic and semi-realistic interactions 0-70424

²⁸Si, M1 transitions with realistic and semi-realistic interactions 0–70424 ²⁸Si, M1 transitions with ΔT =1 0–70434 ²⁸Si, neutron elastic and inelastic scatt., E_m =14.2 MeV, anal. 0–77556 ²⁸Si, 0^+ – 0^+ transitions studied by inelastic e scatt. 0–46129 ²⁸Si, p scatt., elastic and inelastic transitions, 100 MeV 0–39029 ²⁸Si, quadrupole moments of excited states, using SU₃ model and projected HF calcs. 0–77490

HF calcs. 0-77490²⁸Si, quadrupole moments of first two excited states 0-38875²⁸Si, spin and parity and branching ratios 0-77492²⁸Si deduced leads from ²⁷Al(p, p) for E_p =742 and 1381 keV 0-55122²⁸Si deuteron scattering suggesting static oblate deformation 0-70655²⁸Si giant dipole states from study of (ψ, n_0) reactions 0-49594²⁸Si HArtree-Fock constrained calculations for quadrupole generator coordinate 0-40404

dinate 0-49494
dinate 0-49494
issi inelastic scatt. at high momentum transfer, excitation of particle-hole states 0-73797
issi level lifetimes and excitation energies from ²⁷Al(³He,d)²⁸Si*≤11 MeV

0-3886 of Seven interfines and executation energies (0-67434) and (1-67434) and (1-67434) are level obs. at 11.45 MeV in p scatt. expts. 0-39031 and (2-7434) are level obs. at 11.45 meV in p scatt. expts. 0-39031 and (2-7434) are level obs. at 11.45 meV in p scatt. expts. 0-39031 and (2-7434) are level obs. at 11.45 meV in p scatt. expts. 0-39031 are level obs. at 11.45 meV in p scatt. expts. 0-39031 are level obs. at 11.45 meV in p scatt. expts. 0-39031 are level obs. at 11.45 meV in p scatt. expts. 0-39031 are level obs. at 11.45 meV in p scatt. expts. 0-39031 are level obs. at 11.45 meV in p scatt. expts. 0-39031 are level obs. at 11.45 meV in p scatt. expts. 0-39031 are level obs. at 11.45 meV in p scatt. expts. 0-39031 are level obs. at 11.45 meV in p scatt. expts. 0-39031 are level obs. at 11.45 meV in p scatt. expts. 0-39031 are level obs. at 11.45 meV in p scatt. expts. 0-39031 are level obs. at 11.45 meV in p scatt. expts. 0-39031 are level obs. at 11.45 meV in p scatt. expts. 0-39031 are level obs. at 11.45 meV in p scatt. expts. 0-39031 are level obs. at 11.45 meV in p scatt. expts. 0-39031 are level obs. at 11.45 meV in p scatt. expts. 0-39031 are level obs. at 11.45 meV in p scatt. expts. 0-39031 are level obs. at 11.45 meV in p scatt. expts. 0-39031 are level obs. at 11.45 meV in p scatt. expts. 0-39031 are level obs. at 11.45 meV in p scatt. expts. obs. at 11.45 meV in p scatt. expts. obs. at 11.45 meV in p scatt. expts. at 11.45 m

Nuclei with 20< A<49 continued

28Si T=2.0+ state, obs. 0-38876

²⁸Si total cross-sections, for energies 3.3-5.2MeV of neutrons 0-49633

"SI total cross-sections, for energies 3.3-5-2.MeV of neutrons $(0-49633)^2$ "Si(i'He,p)*Pp, 4.3-11 MeV, analysis using PWBA and DWBA $(0-70654)^2$ "Si(i'He α) differential cross sections, experimental results compared with theory, energy levels of final nucleus $(0-67553)^2$ "Si(i'Li,t)*2'S, search for α -particle structure in $(0-24)^2$ Mg $(0-24)^2$ Theorem (10-24) are the section of the

²⁸Si(CLi,d)³²S, ²⁸Si(ZLi,t)³²S, search for α-particle structure in ²⁴Mg ³²S 0 -46252 ²⁸Si(ZLi,α)³¹P, search for triton grouping in ³¹P 0-49673 ²⁸Si(d, d)³⁸Si, asymmetries measured for vectorially polarised 28 MeV deuterons 0-58009 ²⁸Si(d,d)³²Si obs. and optical model analysis 0-63851 ²⁸Si(d,p)³⁵Si, ³⁸Si deduced levels and spectroscopic factors E=2.00-6.12 MeV 0-58012 ²⁸Si(d,p)³⁵Si obs. and optical model analysis 0-63851 ²⁸Si obs. and optical model anal

Si(d,d)Si obs. and optical model analysis U—53851
Si(d,d)Si obs. and optical model analysis U—53851
Si(d,e)2*Si, **Si deduced levels and spectroscopic factors E=2.00-6.12
MeV 0—58012
Si(e,e)Si, 28-60 MeV, O**-O** transitions studied 0—46129
Si(e,e)Si, 28-60 MeV, O**-O** transitions studied 0—46129
Si(e,e)Si, 28-60 MeV, O**-O** transitions studied 0—46129
Si(e,p)PiAI, collective correlations model for struct. of giant dipole model 0—67432
Si(e,p)Discoperation of probability, by activation method 0—46204
Si(e,p)Discoperation of 1.381 MeV reson., by Doppler shift attenuation method 0—73798
Si(p,p)Si, study of 1.381 MeV reson., by Doppler shift attenuation method 0—73798
Si(p,p)PiSN, loo MeV, ang. distrib. obs., deduced levels of 2**Si 0—39031
Si(e,p)PiSN, 100 MeV, ang. distrib. obs., deduced levels of 2**Si 0—39031
Si(e,p)PiSN, 100 MeV, ang. distrib. obs., deduced levels of 2**Si 0—39031
Si(e,p)Si, Coriolis coupling model calc. 0—70436
Si, deduced levels and spectroscopic factors from 2Si(d, p), E=2.00-6.12
MeV 0—58012
**Si, elastic and inelastic proton scatt., resonances 0—49606
Si, from 3Si(i+e,α)**2**Si reaction, obs. up to 10 MeV, relative spectroscopic factors 0—77494
**Si, intermediate-coupling structure in 2s-1d shell 0—64012
**Si, proton capture resonances, yield of 1.27 MeV p-rays in energy range 1300 1850 keV 0—52777
**Si(e,p)*, proton capture resonances, yield of 1.27 MeV p-rays in energy range 1300 1850 keV 0—52777
Si(e,p)*, deduced spin of levels in 3P at 1.755 MeV 0—42743
Si(a,p)*, deduced spin of levels in 3P at 1.755 MeV 0—42743
Si(a,p)*, deduced spin of levels in 3P at 1.755 MeV 0—42743
Si(a,p)*, deduced spin of levels in 3P at 1.755 MeV 0—42743
Si(a,p)*, deduced spin of levels in 3P at 1.755 MeV 0—42743

0. 49662 1951(α , p), deduced spin of levels in 32 P at 1.755 MeV 0—42743 22 Si(α , p), deduced spin of levels in 32 P at 1.755 MeV 0—42743 22 Si(α , p)) 32 S cross section, 3.0-5.4 MeV 0—39116 22 Si(α , p) 32 P, mean lives determ. of 32 P levels from Doppler-shift attenuation meas. 0—49512 22 Si(α , p) 32 A, cross sections behaviour, E=10—1 MeV 0—39110 22 Si(α , p), deduced levels of 32 Si, p transitions and Q values for thermal neutrons 0—42851 22 Si(α , p) 32 P, deduced levels, from 36 Mg(He,t) 0—77574 32 Si, p transitions for thermal neutrons for 22 Si(α , p) 32 Si, ifietimes of levels 0—70438 32 Si, itetimes of levels 0—70438 32 Si, itetimes of levels 0—70438 32 Si, study of excited states using 32 Si(α , α , p) 32 Si 0—55123 36 Si angular distribution from 6 He, α) reaction and 6 He, 3 He) reaction 0—49662 32 Si search for triton cluster structure 0—49673

0-49662

³⁰Si search for triton cluster structure 0-49673

³⁰Si(³He, ³He) elastic, angular distribution at 8.0 and 7.0 MeV 0-49662

³⁰Si(³He, α)³Si at 8.0 and 7.0 MeV, angular distribution of α-particles, excitation curves 0-49662

³⁰Si(³He, α)³¹P, 17.85 MeV spectroscopic factors from DWBA analysis

0–77575

"95(i/4-t,t)³P, at 16 and 30 MeV 0–77574

"95(i(α ,t)³PS, at 16 and 30 MeV 0–77574

"95(i(α ,t)³S study of mean lifetime of 2.94 MeV level of ³³S 0–70441

"95(i(α ,t))³S ang. correlation meas: rel. to multipole mixing ratios in ³³S 0–77576

"95(i(α t))³S investigation of electromagnetic transition rates of ³³S excited

"Sli(ap)" investigation of electromagnetic transition rates of "S excited states 0—46130
"Sli(ap)" Si, for meas, of mean lives of levels 0—55124
"Sli(a, p), deduced levels of "ISi, p transitions and Q values for thermal neutrons 0—42851

³¹Si, γ transitions for thermal neutrons for ³⁰Si(n, γ) 0–42851

 $^{31}\mathrm{Si}$, p transitions for thermal neutrons for $^{30}\mathrm{Si}(n,p)$ 0–42851 $^{31}\mathrm{Si}$, mean lives, branching ratio, excitation energy of lowest six levels, meas. with $^{30}\mathrm{Si}(a,pp)^{31}\mathrm{S}$ 0–55124 $^{32}\mathrm{Si}$, spherical, from deuteron scattering 0–70655 $\mathrm{Si}(n,a)$, cross section fluctuations, 6.7-13.4 MeV 0–39052 $\mathrm{Si}(n,p)$ cross section fluctuations, 6.7-13.4 MeV 0–39052 Ti , even-stable isotopes, octupole and quadrupole transitions 0–67448 $^{42}\mathrm{Ti}$ Gamow-Teller transitions, half-life from β^+ decay 0–64017 $^{44}\mathrm{Ti}$, T=T_+2 level from $^{46}\mathrm{Ti}(p_1)^{44}\mathrm{Ti}$ 0–73805 $^{44}\mathrm{Ti}$ energy levels and mass from $^{46}\mathrm{Ca}(\alpha,p)^{44}\mathrm{Ti}$ 0–70454 $^{44}\mathrm{Ti}$ search for α -particle structure 0–46252 $^{45}\mathrm{Ti}$ mean lives of 1st and 2nd excited states meas. 0–52684 $^{46}\mathrm{Ti}$ isotope, projected Hartree-Fock-Bogolubov calculation 0–52686 $^{46}\mathrm{Ti}$ isotope, projected Hartree-Fock-Bogolubov calculation 0–52686 $^{46}\mathrm{Ti}$ isotope, projected Hartree-Fock-Bogolubov calculation 0–52686 $^{46}\mathrm{Ti}$ reorientation measurements after excitation of first excited 2+ state, quadrupole moment 0–64018 $^{46}\mathrm{Ti}$ isotope, projected Hartree-Fock-Bogolubov calculation 4-52686 $^{46}\mathrm{Ti}$ reorientation measurements after excitation in low-lying levels with T=2 0–73993

 4 Ti(He,n)**Cr, observation of excitation in low-lying levels with 1=20-73993 4 Ti(p,p)*7⁴V, γ ang. distribs. at resonances study of excited states of 4 V 0-49519 4 Ti(p,p)*10-38883 4 Ti(p,p)*0-5.65 MeV. level structure determ. in 4 Ti 0-73805 4 Ti energy levels deduced from 4 Ti(p,p)*0-38883 4 Ti(p,p)*0.65 MeV. level structure determ. in 4 Ti o-67446 4 Ti i d-wave resonance from (n,p) reaction 0-67447 4 Ti i isotope, projected Hartree-Fock-Bogolubov calculation 0-52686 4 Ti quadrupole moment, static, of first excited state 0-70457 4 Ti reorientation measurements after excitation of first excited 2+ state, musdrupole moment 0-64018

**Tire orientation measurements after excitation of mist excited 2 states, quadrupole moment 0-64018 **Ti(4 He α), 13.0 MeV, level structure determ. in 4 Ti 0-67446 **Ti(α , pp)*1V, pray decay properties of states in 5 1V 0-57910 **Ti(4 He α), 51V levels \le 6.17 MeV 0-38885 **Ti(4 He α), 15 MeV, observation of 54 states in 5 1V 0-70459 Ti(4 He α), 16 MeV, ang. distrib., optical model one of 6 10 **Co. 10 **C

11(0,0)11 (where A=40-49), Ed=13.6 MeV, ang. distrib., op anal. 0-60826 Ti(d,p) (A=48.49), E_d=13.6MeV, diff. cross sections 0-73995 Ti(n, n)Ti 0.3-4.1 MeV, optical model analysis 0-46220 Ti(p,t), 27 MeV, inadequacies of DWBA analysis 0-73946 47V energy of excited levels 0-49519 48V magnetic moment of 310 keV state 0-70456

Nuclei with 20 ≤ A ≤ 49 continued

olei with 20 € A € 49 continued

V p branching ratios for levels up to 2.409 MeV J assignments on basis
of decay scheme and I-values 0–49520

*V determ. of probability, by activation method 0–46204

*V determ. of probability, by activation method 0–46204

*Ca isotopes (X = 42 to 50), shell model for low lying states 0–57909

40 Zr VII, term analysis of the 4p-4d and 4p-5s transitions 0–60936 Nuclei with 50<A<89

21et with 50€,A≪89
2+ and 3 collective states using schematic forces for Sn 0-55125
5¹Fe, n.m.r. in Fe-Co dil. alloy, hyperfine field spectra 0-41371
abundance of 50€,A≪65 nuclides from s-process neutron capture equations 0-55121

tions 0–55121
equilibrium deformations in range 28<Z<50, 50<N<82 0–63978
Fe calc, activation by 3 GeV protons 0–77554
fission chain populations, tables, odd masses, 75<A<83 0–39172
fission chain populations, tables, odd masses, 85<A<105 0–39172
proton scattering, elastic, real optical potential, 50<A<70 0–70578
('He, p), O' spin parity obs. in \$6C0, \$4Mn, \$2V, and \$90c 0–67453
*5VCr, decay to levels in \$5Mn investigated using Ge(Li) gamma detectors, deduced \$5Mn levels 0–57948
*5Mn levels deduced from decay of \$5Cr using Ge(Li) gamma detectors 0–57048

⁵Mn levels discovered to the control of the cont

⁵₇Fe, Moss 0-48031

0–40031 8 Sr 3.0, 3.7 MeV levels, obs. 0–38898 2 Zn, (A=65, 67, 68, 69), γ -spectra obs. following thermal neutron capture 0–46224

²Zn, (Å=65, 67, 68, 69), γ-spectra obs. following thermal neutron capture 0–46224

³As isobaric analogue states from ⁷²Ge(p,p) 3.30-3.37 MeV 0–38893

³As isobaric state, g=+1.146±0.007 for 426 keV 0–73813

³As usec isomers, mag. mom. meas. 0–64025

³As-⁷³Ge, γ-ray, K. X-ray and conversion electron spectra investigation using delayed coincidence techniques 0–57953

³As, half-life measurements of levels 0–38894

³As, n.q.r. in AsyX₃, AsXI and TlAsX₇, where X=S, Se or Te 0–41405

³As energy levels from resonance scattering of γ-rays 0–70477

³As excited state lifetimes, obs. 0–38896

³As excited states, transition rates, half life meas, from γ-ray spectrum of

"As excited states, transition rates, half life meas, from γ -ray spectrum of 13 Se 0-73814 "SAs excited states nature 0-73815

As groundstate transition widths from Compton scattered radiation 0-67461

0—67461

"5-As n.q.r. in MH₂AsO₄ where M=Li, Na, K, Rb, Cs, Ag, NH₄ and N(CH₃)₄ 0—41400

"5-As photoneutron cross-section fine structure, dipole-quadrupole coupling effect 0—73905

effect 0-73905 7^3 As quadrupolar coupling in CsH₂AsO₄ rel. to Curie pt. 0-44366 7^7 As, lifetime of the 632 keV⁵/₂+ level by pp delayed coincidence technique

¹⁵As quadrupolar coupling in CsH₂AsO₄ rel. to Curie pt. 0—44366
 ¹⁷As, lifetime of the 632 keV⁵/₂* level by pp delayed coincidence technique 0—42756
 ¹⁸As radioactive nucleide produced by irradiation of ⁸³Se with 14.7 MeV neutrons, half life, decay characteristics 0—49570
 ¹⁵Br—³⁵Se decay, relative intensities of p lines 0—52725
 ¹⁶Br—³⁶Se decay, prepetrum rel. to energy levels in ⁷⁶Se 0—46165
 ¹⁸Br, half-lives and energy of isomeric activity 0—55129
 ¹⁸Br, half-lives and energy of isomeric activity 0—5129
 ¹⁸Br, Larmor freqs., mag. moments, chem. shift, n.m.r. obs. in aqueous soln. 0—70444
 ¹⁹Br, n.q.r. in AlBr₃ rel. to bond nature and molecular structure 0—45043
 ¹⁸Br(n,2n)³⁸Br, p.cod. cross section, half-lives and energies of isomeric activities 0—55129
 ¹⁸Br(n,n)^{7)3m}Br, prod. cross section, half-lives and energies of isomeric activities 0—55129
 ¹⁸Br(n,n)^{7)3m}Br, prod. cross section, half-lives and energies of isomeric activities 0—55129
 ¹⁸Br (n,n)^{7)3m}Br, prod. cross section, half-lives and energies of isomeric activities 0—55129
 ¹⁸Br, Larmor freqs., mag. moments, chem. shift, n.m.r. obs. in aqueous soln. 0—70444
 ¹⁸Br, namor freqs., mag. moments, chem. shift, n.m.r. obs. in aqueous soln. 0—70444
 ¹⁸Br, Larmor freqs., mag. moments, chem. shift, n.m.r. obs. in aqueous soln. 0—70444
 ¹⁸Br, Larmor freqs., mag. moments, chem. shift, n.m.r. obs. in aqueous soln. 0—70441
 ¹⁸Br, decay with ½ ray 2—60779
 ¹⁸Br decay with ½ ray 3 and intense peaks at 1565 keV 0—60779
 ¹⁸Br decay with ½ ray 3 and intense peaks at 1565 keV 0—6779
 ¹⁸Br decay with ½ ray 5 on the complete of th

⁵⁶Co, higher-order effects from isospin- hindered allowed β decay 0.-49569 5°CO, higher-order effects from isospin- hindered allowed β decay 0-49569
5°CO levels from (¹He, p), O⁺ spin parity obs. 0-67453
5°CO, energy level study from Ni(p,α) reactions 0-52687
5°CO, Mossbauer effect in ZnS 0-65516
5°CO²+ decay, in Co[Cr₂|O₄ and Co[Cr₂|S₄, Fe valency states, Mossbauer determ 0-41149
5°CO analogue resonances by use of (p,p) and (p,p) reactions in 5°Fe energy level diagram 0-70469
5°CO deduced levels and γ-branching from 5°4Fe(α, pγ), Ea=10.71, 11.14 MeV 0-57911
5°CO in Y and Pd, hyperfine fields 0-76052
5°CO Mossbauer effect in diamond 0-41140
5°CO-3°TFe, electron capture, chem. effects in solid complexes 0-75982
5°CO, 10,2 sec level magnetic moment, gyromagnetic 0-70470
5°CO, evidence for splitting of bound analog state 0-67456
5°CO, evidence for splitting of bound analog state 0-67456
5°CO, and Fe elastic scatt., 30 and 35 MeV optical model params. 0-42862
5°CO, anternal pair formation coefficient 0-49522
5°CO, internal pair formation coefficient 0-49522
5°CO, n.m.r. in do carbonyls, anisotropic chemical shifts 0-74252
5°CO, n.m.r. in do carbonyls, anisotropic chemical shifts 0-74252
5°CO, n.m.r. in do carbonyls, anisotropic chemical shifts 0-74252
5°CO, n.m.r. in do carbonyls, anisotropic chemical shifts 0-74252
5°CO, n.m.r. in do carbonyls, anisotropic chemical shifts 0-74252
5°CO, n.m.r. in do carbonyls, anisotropic chemical shifts 0-74252
5°CO, n.m.r. in do carbonyls, anisotropic chemical shifts 0-74252
5°CO, n.m.r. in do carbonyls, anisotropic chemical shifts 0-74252
5°CO, n.m.r. in do carbonyls, anisotropic chemical shifts 0-74252
5°CO, n.m.r. in do carbonyls, anisotropic che

Nuclei with 50 < A < 89 continued

50 Co, n.m.r. in Fe-Co dil. alloy, hyperfine field spectra 0-41371

⁵⁹Co, n.g.r. in cobalticinium salts 0-59475

°Co, neutron capture width of 132 eV resonance 0-73959

⁵⁰Co, neutron depolarization in elastic scatt., 1.36MeV 0-42845 ⁵⁰Co, neutron resonance at 132 eV 0-52787 ⁵⁰Co, pulsed neutron determination of thermal neutron absorption cross-section 0-42846

⁵⁹Co, spin-spin effect in total cross-section for 1 MeV polarized neutrons, E=1.1, 1.4 MeV 0-42853

59Co foils, self-absorption of monoenergetic electrons, 51-58 keV 0 - 46199

⁵⁹Co giant dipole resonance and photo neutron cross section 0-77536

°Co investigation of low-lying levels 0–64022 °°Co investigation of low-lying levels 0–64022 °°Co transient n.m.r. in antiferromag. CoCl₂2H₂O 0–62773 °Co(α, α)°Co optical potential real part calc. by double folding procedure 0–67543

0-6/343
⁵⁹Co(α,p)⁶ study 0-58019
⁵⁹Co(η,n), cross section determ. in giant reson, region, expt. and theory 0-52747

0–52747. Octon, p) 9°Fe, E_p =6.3 MeV, energy and ang. distribs. of protons 0–49635. 9°Co(n,p), 6°Co low-lying levels from p-spectra <600 keV 0–38891. 9°Co(n,p), negative energy reson. from p-ray circ. polariz. meas., potential capture 0–70620. 9°Co(n,p) 6°Co, thermal n capture, meas. of p rays in 50 to 1000 keV range 0–39070. 9°Co(n,p) 6°Co, obs. of spin-spin effect 0–60814. 9°Co(p,n), E_p -6.05-6.3 MeV, energy spectra 0–49618. 9°Co(p,n) 9°Fe, angular distributions experiment and theory 0–70607. 9°Co(p,n)p) 9°Ni, p ang. distrib. 0–39048. 9°Co(p,n)p) 9°Ni, p ang. distrib. 0–39048. 9°Co(p,n)p) 9°Ni, p ang. distrib. 0–39070. 9°Co(p,n)p) 9°Ni, p ang. distrib. 0–39070. 9°Co(p,n)p) 9°Ni, p ang. distrib. 0–39070. 9°Co(p,n)p) 9°Ni, p ang. distrib. 0–5900 9°Co(p,n)p) 9°Ni, p ang. distrib. 0–5900 9°Co(n,p) 10°Co(n,p) 10

6ºCo absolute standardization technique for internat. comparison 0–38956

 $^{0-3930}$ e⁰Co decay, velocity depend, of helicity of β particles 0–57951 e⁰Co haif-life meas. 0–64084 e⁰Co low-lying levels from 50 Co(n, γ) γ -spectra < 600 keV 0–38891 e⁰Co source, Compton scattering to give γ -rays for excitation of 75 As 6°Co source, Compton scattering to give *γ*-rays for excitation of ⁷⁵As 0–67461 6°Co, energy level study from Ni(p,α) reactions 0–52687 6°Co investigation of low-lying levels 0–64022 6°Co, deduced levels of °eNi from observed decay 0–52724 6°Co isomeric effect in Szilard- Chalmers recoil in Co (III) complexes, by irradiation at temps. below –80°C 0–77564 6°Co Co isomeric effect in Szilard- Chalmers recoil in Co (III) complexes, by irradiation at temps. below –80°C 0–77564 6°Co Co isomeric effect in Szilard- Chalmers recoil in Co (III) complexes, by irradiation at temps. below –80°C 0–77564 6°Co Co spin and magnetic moment 0–70474 6°Cr(d,p)°1Cr, E_d=7.5 and 8.0 MeV, j-dependence in l=1 transitions 0 39121 6°Cr and Si(Li) detector system for conversion coefficient measurements.

0 59121 FCr, and Si(Li) detector system for conversion coefficient measurements 0-49384

0-49384

**SICR, j-dependence in l=1 transitions, in **SICR, j-dependence in l=1 transitions, in **SICR, j-dependence in l=1 transitions, in **SICR, compound, 2.340 MeV isobaric analogue reson. from **SIV(p,n) obs. 0-38887

**SICR, deuteron elastic scattering, analysis by optical potential 0-67542

**SICR, inelastic scatt. of protons, polarization 0-77545

**CICR, inelastic scatt. of protons, polarization 0-77545

**CICR, inelastic scatt. of protons, polarization 0-77545

**CICR, inelastic scatt. of protons, polarization scattering experiments 0-77548

**CICR, inelastic scatt. of protons, polarization scattering experiments 0-77548

**CICR, inelastic scattering experiments 0-77548

**CIC

0-39121 "Cr(d,pp)5"Cr and energy levels in 5"Cr 0-70465 "Cr(d,pp)5"Cr used to study levels of 5"Cr 0-38886 "Cr(d,np)5"Cr used to study levels of 5"Cr 0-38886 "Cr(y,n), cross section determ. in giant reson. region, expt. and theory 0-52747

0–52747

O'Cr(p, p)3Mn, deduced **53Mn levels and decay of the 2p_{1/2} analogue state, E=1.0-1.8 MeV 0–57979

**3Cr(p,p') at 40 MeV, cross section for exciting low lying states 0–57973

**3Cr, cere-plus-particle model and low lying levels 0–70464

**3Cr, energy levels from **3Cr(d,pp') reaction 0–70465

**3Cr, i-dependence in l=1 transitions, in **3Cr(d,p) 0–39121

**3Cr, N=29, Z=29 nucleus, level calculations using intermediate coupling model, stripping strengths 0–70461

**3Cr transitions below 4.25 MeV obs., spin assignments to levels 0–38886

3Cr(p,p)3Mn, deduced levels of **3Mn at 377.5, 1288.4, 1440.1, 1619.1 keV 0–42753

**4Cr, level scheme for β-decay of **4V 0–49568

keV 0–42753 ⁵⁴Cr, level scheme for β-decay of ⁵⁴V 0–49568 ⁵⁵Cr, level scheme for β-decay of ⁵⁴V 0–49568 ⁵⁵Cr decay, weak β branching 0–73858 ⁵⁵Cr(d,p)⁵⁶Mn and levels in ⁵⁶Mn below 1 MeV 0–70467 Cr(d,p) (A=50,52), E_x=13.6 MeV, diff. cross sections 0–73995 Cr(n,α) cross-section determ. for natural element using a technique based on the absolute determ. of helium 0–49634 Cu, 3 and 29 GeV proton bombardment, yields of stable and radioactive rare-gas isotopes 0–52769 Cu, calc. activation by 3 GeV protons 0–77554 Cu, K, 6 and neutron total cross sections at GeV energies 0–46230 Cu (A=59, 61, 63, 65, 67), M1 transitions and magnetic moments 0–52688 ⁵⁸Cu, decay, energy levels of ⁵⁸Ni, 0–64093

Cu (A=59, 61, 63, 65, 67), M1 transitions and magnetic moments 0-52688

**Cu, decay, energy levels of **Ni 0-64083

**Cu, radioactive decay, \$P-y directional correlations 0-57950

**Su, radioactive decay, \$P-y directional correlations 0-77498

**Cu, isobaric analog resonances, isospin mixing 0-46137

**ICu, isobaric analog resonances, isospin mixing 0-46137

**ICu, N=29, Z=29 nucleus, level calculations using intermediate coupling model, stripping strengths 0-70461

**Cu, Ife-time of short-lived state at 42 keV 0-70475

**2Cu deduced levels of **Ni from observed decay 0-52724

**2Cu-se*Ni, decay, \$p\$ energies and intensities levels deduced in **2Ni 0-46138

**3Cu, **3Cu, low excited states by excited core model 0-52689

**3Cu, n-capture p-ray cross section, 25 keV 0-39076

**3Cu, n-mers, spin-lattice relaxation times in Cu₂MnAl(In), Heusler alloy 0-51414

**3Cu, n-gative parity states, props. in semimicroscopic model 0-49523

⁶³Cu, negative parity states, props. in semimicroscopic model 0-49523

Nuclei with 50 ≤ A ≤ 89 continued

 63 Cu, nuclear spin relaxation in Cu-Cr alloy, Kondo effect suppression 0-45035

 ^{63}Cu 19.5 MeV $\alpha\text{-particle}$ scattering, deduced deformation parameters, elastic inelastic scattering analysis ~0-49646

tic inelastic scattering analysis 0—49446
6³Cu deuteron scattering, spin dependence 0—70635
6³Cu Knight shift and spin-lattice relax. rate in solid and liq. Cu 0—41369
6³Cu proton scattering, elastic, optical model analysis 0—70588
6³Cu radiative capture cross section for 10-350 keV neutrons 0—46227
6³Cu raction rates in Pu-recycle fuel lattices 0—74059
6³Cu spin-lattice relax. near critical conc. 0—56469
6³Cu(n,n)9, gamma ray angular distributions for E_n=2.9 MeV and cross sections 0—57993
6³Cu(n,n)9, gamma ray angular distributions for E_n=2.9 MeV and cross sections 0—57993
6³Cu(p)6³Zn compound nucleus formation, neutron emission study 0—77517

54Fe(μ,η)⁵Ni lifetimes of low lying levels in Ni 0–64019 54Fe(μ,ρ) microscopic first-order core polarization corrections to DWBA 0–42837

0–4283/

*Fe(p,p'y), 10 MeV, diff. cross section, polarizations and py ang. correlations 0–46212

*Fe(p,p), 10 MeV, diff. cross section and polarization meas. 0–46212

*Fe(p,p), 10 MeV, diff. cross section and polarization meas. 0–46212

*Fe, N=29, Z=29 nucleus, level calculations using intermediate coupling model, stripping strengths 0–70461

*Fe electromagnetic decay properties of low lying states, spin assignments 0–60260

"SiPe electromagnetic decay properties of low lying states, spin assignments 0–60760
"Fe from *5Mn(p, np)*5Fe, <2.5 MeV 0–46135
"Fe high spin states from *5Mn(p,np)*5Fe 0–70466
"Fe*n cross section 0–39069
"Fe*n, educed levels from *6Co radioactive decay and energy and intensity of the p-ray transitions 0–57949
"Fe, elateron elastic scattering, analysis by optical potential 0–67542
"Fe, elastic and inelastic p scatt., E=2-6 MeV, role of isobaric analogue states 0–49607
"Fe, energy distribution of neutrons from proton-neutron nonelastic collisions for 18 MeV protons 0–64115
"Fe, inelastic scattering of polarised protons at 30.3 MeV and deduced nuclear deformations 0–52781
"Fe, neutron elastic and inelastic scattering and gamma-ray-production cross-sections from 1.0-7.6 MeV 0–55159
"Fe, quadrupole moments of first excited 2+ states by Coulomb excitation 0–42760
"Fe deduced levels, spin and parity, deformation parameters from inelastic

0-42760

56 Fe deduced levels, spin and parity, deformation parameters from inelastic deuteron scattering 0-46236

56 Fe isobaric analogue states, γ decay 0-70468

56 Fe neutron capture, and energy level transitions in 57 Fe 0-73958

56 Fe(α, p)50 Co, investigation of low-lying levels 0-64022

56 Fe(α, p)50 Ni, evidence for precompound particles 0-60827

56 Fe(α, p)57 Fe recoil nuclei in b.c.c. Fe-Al alloys, hyperfine interactions at final positions 0-41160

57 Fe(p,n)6 Co excitation functions, 4.9-39 MeV 0-46213

57 Fe, anomalous transmission of resonant γ-rays in Fe-3%Si 0-66011

57 Fe, charge states in 57 Co labelled KCoF₃ and K₃CoF₆, Mossbauer study 0-70558

57 Fe, ground state (p,n) Q values 0-77552

0-70558

⁵Te, ground state (p,n) Q values 0-77552

⁵Te, in FeP₂, quadrupole splitting, recoil-free fraction, and isomer shift, Mossbauer studies, 80-300°K 0-41161

⁵Te, internal conversion coeffs, low level, obs. 0-38890

⁵Te, longitudinal relaxation in YFe garnet:Yb, 1.3-140 K 0-45037

⁵Te, Mossbauer effect in anhydrous CoCl₂, isomer shift and quadrupole splitting 0-56509

⁵Te. Mossbauer effect in BaTiO₃, phonon-p-ray scatt. obs. 0-62163

⁵Te, Mossbauer effect in CoF₂, charge state and ^{57m}Fe quadrupole moment determ. 0-48027

⁵Te, Mossbauer effect in Fe carbonyl derivatives and organoiron cpds. 0-48029

⁵Te, Mossbauer effect in Fe carbonyl derivatives and organoiron cpds. 0-48029

⁵Te, Mossbauer effect in Fe carbonyl derivative local lattice distortion X
⁵Te, Mossbauer effect in FeFe₂, Sc₂Q, ferrite local lattice distortion X
⁵Te, Mossbauer effect in FeFe₃, Sc₂Q, ferrite local lattice distortion X
⁵Te, Mossbauer effect in FeFe₃, Sc₄Q, ferrite local lattice distortion X-

O-48029

**Fe, Mossbauer effect in FeFe_{2-x}Sc_xO₄ ferrite, local lattice distortion, X-ray diffr. 0-47185

**Fe, Mossbauer effect in K₂FeO₄, SrFeO₄ and BaFeO₄ 0-56513

**Fe, Mossbauer effect in Inlar samples 0-48532

**Fe, Mossbauer effect in Ni-Mn alloy 0-4166

**Fe, Mossbauer effect in Pd-Au alloys, band filling obs. 0-62260

**Fe, Mossbauer effect in pervoxenes in lunar samples 0-48531

**Fe, Mossbauer effect in pervoxenes in lunar samples 0-72328

**Fe, Mossbauer effect in Pa-Fe, Merchedetrics 0-72328

**Fe, Mossbauer effect in transition metals, press. variation 0-79258

**Fe, Mossbauer meas. of mag. and elec. hyperfine interactions in V and Si garnets 0-48014

**Fe, Mossbauer spectra in spinel aluminates, electric field gradients 0-45016

**Fe, Mossbauer spectra in PuFe₂. NpFe₂ and UFe₃. 0-48040

⁵⁷Fe, Mossbauer spectra in PuFe₂, NpFe₂ and UFe₂ 0-48040

Nuclei with 50 ≤ A ≤ 89 continued

⁵⁷Fe, Mossbauer study of lunar samples 0–45386 ⁵⁷Fe, n.m.r. in diamagnetic Fe(CO)₅ 0–41370 ⁵⁷Fe, n.m.r. in Fe₂O₃, domain wall resonance, magnetization 0–76236

 $^{57}\mathrm{Fe}$, n.m.r. in Fe₂O₃, domain wall resonance, magnetization 0-76236 $^{57}\mathrm{Fe}$, nuclear quadrupole moment in α -Fe₂O₃, haematite 0-41084 $^{57}\mathrm{Fe}$, revaluation of conversion coeff. of 14.4 keV transition 0-67454 $^{57}\mathrm{Fe}$, spin-lattice relax. times in YFe garnet, 2-40 K 0-48170 $^{57}\mathrm{Fe}$, spin-spin relax. in Y₃Fe₂O₁₂, at 77°K 0-79212 $^{57}\mathrm{Fe}$ analogue resonances by use of (p,y) and (p,p) reactions in $^{56}\mathrm{Fe}$ 0-70469 $^{57}\mathrm{Fe}$ containing complexes, Mossbauer effect study 0-72333 $^{57}\mathrm{Fe}$ energy level transitions from $^{56}\mathrm{Fe}$ neutron capture 0-73958 $^{57}\mathrm{Fe}$ in $^{56}\mathrm{Fe}$ and $^{57}\mathrm{Fe}$, mag. hyperfine field, 295 K 0-48034 $^{57}\mathrm{Fe}$ in $^{56}\mathrm{Fe}$ and $^{57}\mathrm{Fe}$ in $^{56}\mathrm{Fe}$, Mossbauer absorpts., equality of temp. shifts 0-480340-48033 ⁵⁷Fe in FeSO_{4.4}H₂O, Mossbauer absorpt, rel. to elec. field gradient params...

57Fe in Sea and 57Fe in Sefe, Mossbauer absorpts, equality of temp. shifts 0–48033
57Fe in FeSO₄.4H₂O, Mossbauer absorpt, rel. to elec. field gradient params., obs. 0–41156
57Fe in V₂O₃, Mossbauer study of metal insulator transition 0–62313
57Fe Mossbauer backscatt. obs. of thin surface layers 0–56508
57Fe Mossbauer effect in Ca-Fe₃S₁V₂O₂D₂ 0–41142
57Fe Mossbauer effect in Cu-Ni alloys, hyperfine interactions 0–69097
57Fe Mossbauer effect in Fe₇O₃, line shape and width anomalies 0–76050
57Fe Mossbauer effect in Fe₇O₃, line shape and width anomalies 0–76050
57Fe Mossbauer effect in Fe₇O₃, line shape and width anomalies 0–76050
57Fe Mossbauer effect in FeAI, CoAl and NiAl 0–72329
57Fe Mossbauer effect in Sic Cu 0–62633
57Fe Mossbauer effect in Sic Cu 0–72509
57Fe Mossbauer obs. in Pt-Fe alloy 0–41168
57Fe m.m.r. in Fe, rotary saturation 0–72509
57Fe n.m.r. in Fe, rotary saturation 0–72509
57Fe n.m.r. in TiFe_{1-x}Co_x alloys 0–45029
57Fe (d.ny)⁵⁸Co, opoulation of 10.2 μsee level 0–70470
57Fe (p.ny)⁵⁸Co population of 10.2 μsee level 0–70470
57Fe (p.ny)⁵⁸Co Ep=1175-1675 keV, energy level study of ⁵⁸Co 0–49521
57Fe, optical model analysis for 64.3 MeV α particle scattering 0–70634
58Fe magnetic moments of first excited 2+ state 0–70471
59Fe β-decay Fermi matrix elements, 273 and 475 keV 0–38967
57Fe p. quadrupolar coupling consts. in FeSiF₆.6H₇O 0–41151
57Fe p. quadrupolar coupling consts. in FeSiF₆.6H₇O 0–41151
57Fe quadrupolar coupling consts. in FeSiF₆O-606010
57Fe quadrupolar coupling consts. in FeSiF₆O-6070
57G₇O 0–4070
57G

0-57949

Ga anomalous L=1 shapes of angular distributions for (³He,t) transitions to 0+ antianalog states 0-73996

Ga levels excitation energies from ⁶⁶Zn(³He,d)⁶⁷Ga obs. 0-39123

Ga retardation of β decay to excited 0+ states 0-64085

Ga, ⁷¹Ga radiative capture cross section for 10-350 keV neutrons 0.46272 69Ga, 71Ga 0-46227

**Ga retardation of β decay to excited 0⁺ states 0–64085
**Ga, ''Ga radiative capture cross section for 10-350 keV neutrons
0–46227
**Ga n.m.r. in liq. Ga;Te3, localized electronic states obs. 0–68140
Ga(ad,p)Ga, 7.1 MeV, study of **OGa levels 0–77499
**OGa levels from (p,n), neutron spectra meas. 0–60759
OGa levels studied in **Ga(ad,p)Ga and **Ozn(p,ny)**OGa 0–77499
**IGa deduced levels from decay of **IZn 0—57901
**IGa n.m.r. in liq. Ga;Te3, localized electronic states obs. 0–68140
**OGa n.m.r. in liq. Ga;Te3, localized electronic states obs. 0–68140
**IGa n.m.r. in liq. Ga;Te3, localized electronic states obs. 0–68140
**IGa n.g. in GaCl3, Zeeman effect, obs. 0–41397
IGa (α, Zn)As and isomeric state in **IAs 0–73813
**IGa decay 0–73861
Ga-7Ge decay scheme 0–38970
**Ge (A=70, 72), shape co-existence, E2 decays 0–73812
**GGe, p-rays accompanying decay 0–46164
**GGe, p-pectrum meas. using Ge(Li) spectrometers 0–73859
**GGe, p-rays accompanying decay 0–46164
**GGe, enoments and hyperfine structure in *IP; state 0–57913
**GGe, Coulomb excitation of 0* state with *ISCl ions 0–67460
**GGe, elastic scattering, analysis using optical model for protons of 14.5
**MeV 0–42840
**GGe(pp?), nuclear reaction times and lifetimes of excited states by use of blocking effect E=1.59-5.91 MeV 0–42803
**I'Ge, half-lives and energy of isomeric activity 0–55129
**I'Ge, elastic scattering, analysis using optical model for protons of 14.5
**MeV 0–42840
**I'Ge, Hartree Fock calcs. of binding, density and single-particle spectra with effective force 0–49470
**I'Ge, elastic scattering, analysis using optical model for protons of 14.5
**MeV 0–42840
**I'Ge, Hartree Fock calcs. of binding, density and single-particle spectra with effective force 0–49470
**I'Ge, elastic scattering, analysis using optical model for protons of 14.5
**MeV 0–42840
**I'Ge, elastic scattering, analysis using optical model for protons of isomeric activities 0–55129
I'Ge(p,p)Poge, direction analogue states, 3.30-3.37
**MeV 0–38893
**I'Ge(p,p)*

⁷⁴Ge, zero spin for 1482.6 keV level, from $\gamma - \gamma(\theta) = 0$ 0-64026 ⁷⁴Ge energy level obs. from ⁷⁴Ga decay 0-38970

Nuclei with 50 ≤ A ≤ 89 continued

**A'Ge levels from Ge(n,n'y) at 0.5 to 2.55 MeV, branching ratios, mixing ratios for four even-AGe isotopes 0-57994

**Ge radiative capture cross sections for 10-350 keV neutrons 0-46227

⁷⁶Ge radiative capture cross sections for 10.350 keV neutrons 0–46227
 ⁷⁵Ge, moments and hyperfine structure in ³P₁ state 0–57913
 ⁷⁶Ge, elastic scattering, analysis using optical model for protons of 14.5 MeV 0–42840
 ⁷⁶Ge(n,2n), E_m=14.7±0.15 MeV, isomeric ratio determ. 0–73960
 ⁷⁹Ge radioactive nucleide produced by irradiation of ⁸⁷Se with 14.7 MeV neutrons, half life, decay characteristics 0–49570
 ⁷⁶Ge(α,2n)Se, population of levels in Se isotopes, γ radiation study 0–70476

0-70470 (Ge(α ,4n γ)Se, population of levels in Se isotopes, γ radiation study 0-70476

0-704⁷6
Ge(n,n'p) and low lying states of Ge isotopes 0-57994
Kr isotopes n activation cross sections, thermal, 21 keV and 14 MeV 0-39071
⁸⁰Kr energy levels from p-spectra 0-64027
⁸¹Kr energy levels from p-spectra 0-64027
⁸²Kr energy levels from p-spectra 0-64027
⁸³Kr energy levels from p-spectra 0-64027
⁸³Kr energy levels from p-spectra 0-64027
⁸³Kr solid. Mossbauer effect, 9.3 keV transition, Debye model calc. 0-40332

6-4032

*«Kr, n-capture γ-ray cross section, 25 keV 0-39076

*Kr content in atmosphere between 1966-1968 in Hungary 0-45159

*Kr release during oxidation and ignition of irrad. U in CO₂ 0-66186 Kr release during oxidation and ignition of irrad. U in CO₂ 0-66186
 Kr release during post-irrad. heating in determ. of reactor fuel cladding temp. 0-39229
 Kr, 5 to 10.5 MeV/amu projectile, complete-fusion cross sections with various targets 0-49676
 Kr, elsatic and inelastic proton scatt. for isobaric analogue resonances study 0-67463
 Kr core coupled resonances in proton reactions 0-70589
 Kr core coupled resonances in proton reactions 0-70589
 Kr decay sheeme, half life meas. 0-52727
 Mn 5°, radioactivity, international comparison in 1968 0-64081
 Mn, β-γ (CP) correl: and isospin conservation, obs. 0-38889
 Mn radioactive isotope prod. in reactions induced by p,d and α's 0-39008
 Mn deduced levels and decay of the 2p_{1/2} analogue states from ⁵²Cr(p, γ).

Solution and the section of the secti

0-51414

53 Mn, neutron spectra and resonance activation integral, measurement relative to that of 197 Au by absolute counting 0-60816

53 Mn, pulse echoes, CsMnF3, antiferromag, resonance, 2°K 0-44977

53 Mn Knight shifts, reference cpds. 0-45025

53 Mn n.m.r. in ferromag, and antiferromag, MnP 0-72511

53 Mn n.m.r. in MnBi, magnetiz. easy axis obs. 0-62775

53 Mn (d,0) 54 Mn, Ed=13.6 MeV, ang. distrib., optical model anal. 0-60826

53 Mn(d,0) 55 Mn magnetic analysis, angular distrib. for 10.1 MeV deuterons 0-40666 "Mn(d,9)" Mn agnetic analysis, angular distrib. optical model anal. 0-00826
"Mn(d,p)" Mn magnetic analysis, angular distrib. for 10.1 MeV deuterons
0-49666
"Mn(n,p)" Mn tannel resonance capture 0-73957
"Mn(n,p)" Fe, <2.5 MeV, n, p ang. correl. meas. 0-46135
"Mn(n,p)" Mn, <2.50 MeV p ang. distrib. obs. 0-46208
"Mn(n,p)" Analysis Mn, <2.50 MeV p ang. distrib. obs. 0-46208
"Mn(n,p)" En, <2.5 MeV, n, p ang. distrib. obs. 0-46208
"Mn(n,p)" En and high spin states in "Fe 0-70466
"Mn (n,p)" Bn (d,p)" Mn with 10.1 MeV deuterons 0-49666
"Mn spins from (n,p) reaction energy from (n,p) and (d,p) 0-70467
"Mn spins from (n,p) reactions 0-64041
Ni, 13.6 MeV d-induced and 27.2 MeV α-particle-induced reactions, cross-section meas. 0-52803
Ni, 2p-2h and 2-quasi-particle excitations 0-70473
Ni (A=58, 60, 64), electron elastic scatt., E_e=225 MeV, nuclear charge distr. parameters, charge radius 0-49597
Ni assessment (p,t) reaction, use of model with 3 states 0-77551
Ni energy levels of even isotopes from (p,t) and comparison with DWBA 0-70472
Ni isotopes, low-lying many-quasiparticle states, expt. 0-46136

No chergy levels of even isotopes from (p.f.) and comparison with DWBA 0-70472
Ni isotopes, low-lying many- quasiparticle states, expt. 0-46136
Ni isotopes ground state rel. to particle number projection effect 0-57920
Ni quasi-particle structure of ground state of pairing Hamiltonian 0-67490
SNi, ¹⁸Ni, positive parity states with prolate deformation constructed by diagonalization 0-67452
Ni) 4p-4h model of excited states 0-70385
Ni, ilifetimes of low lying levels 0-64019
Ni, rew low-lying states observed in ¹⁸Ni(PH,α) reaction 0-77497
Ni, new low-lying states observed in ¹⁸Ni, illetimes of low lying levels 0-64019
Ni, inclusted the state of the state of

0-77546

³Ni, neutron depolarization in elastic scatt., 1.36 MeV 0-42845

³Ni, pairing vibrations, comparison of numerical results with exact solutions 0-77463

³Ni, quadrupole moment, relative static, for first excited state 0-64021

³Ni, shell model continuum in nuclear bound states 0-57890

³Ni, static quadrupole moment of 1st excited state comparison of theoretical and experimental results 0-64020

³Ni energy levels from (p,p'p) reaction 0-67455

³Ni giant dipole resonance, vibrational splitting from photoneutron cross-section 0-73904

³Ni optical model analysis for 64.3 MeV and 50.2 MeV α particle scattering 0-70634

Nuclei with 50 € A € 89 continued

⁵⁸Ni static quadrupole moment of first excited state 0-73809

58Ni threshold detector, determination of fast neutron flux densities 0-74075

58Ni(3He, x)57Ni, obs. of new low-lying states in 57Ni 0-77497

⁵⁸Ni(c)¹He.n)⁶⁰Zn, observation of excitation in low-lying levels with T=2 0–73993 (SNi(d,p)⁵⁸Ni, DWBA analysis 0–39129 (SNi(n,p)⁵⁸Co, E_n=14.8 MeV, parent analogues of collective states 0–55160 (SNi(p,p)⁵⁸Co, angular distributions experiment and theory 0–70607 (SNi(p,p)⁵⁸Cu, baranching ratios for resonance and bound states 0–77498 (SNi(p,p)⁵⁸Cu, gay: analogue resonance 0–70608 (SNi(p,p)⁵⁸Ni(p,p)⁵⁸Ni(p,p)⁵⁸Ni, 30.3 MeV polarized proton obs., optical model analysis, 2 versions 0–70592 (SNi(p,p)⁵⁸Ni, 30.3 MeV polarized proton obs., optical model analysis, 2 versions 0–70592 (SNi⁵⁸Ni(p,p)⁵⁸Ni, 30.3 deV polarized proton obs., optical model analysis, 2 versions 0–70592 (SNi⁵⁸Ni(p,p)⁵⁸Ni, 30.3 deV polarized proton obs., optical model params. 0–42862 (SNi, 1) He clastic scatt., 30 and 35 MeV, optical model params. 0–42862 (SNi, 1) pairing vibrations, comparison of numerical results with exact solu-58Ni(3He,n)60Zn, observation of excitation in low-lying levels with T=2

⁶⁰Ni, pairing vibrations, comparison of numerical results with exact solutions 0-77463

tions 0-77403 (e/Ni, quadrupole moment, relative static, for first excited state 0-64021 e/Ni, resonance fluorescence self-absorption and B(E2) for the first 2' state 0-57912 6°Ni, quadrupole moment, relative static, for first excited state 0–64021
6°Ni, resonance fluorescence self-absorption and B(E2) for the first 2' state 0–57912
6°Ni, static quadrupole moment of 1st excited state comparison of theoretical and experimental results 0–64020
6°Ni igiant dipole resonance, vibrational splitting from photoneutron cross-section 0–73904
6°Ni inelastic scattering of 40 MeV protons, coupled channel analysis 0–77546
6°Ni static quadrupole moment of first excited state 0–73809
6°Ni(a)*2°Ln compound nucleus formation, neutron emission study 0–77517
6°Ni(p,p') inelastic 40 MeV, analysis in terms of coupled-channel approach 0–77546
6°Ni(p,p') in MeV, diff. cross section, polarizations and py ang. correlations 0–46212
6°Ni(p,p), 10 MeV, diff. cross section and polarization meas. 0–46212
6°Ni(p,p), 10 MeV, diff. cross section and polarization meas. 0–46212
6°Ni(p,p), 10 MeV, diff. cross section and polarization meas.
6°Ni in, mr. in bulk Ni 0–72512
6°Ni (n,p), for 6°Ni excited states study 0–46139
6°Ni (n,p), for 6°Ni excited states study 0–46139
6°Ni (n,p), for 6°Ni excited states study 0–46403
6°Ni (p,p) in and 6°Ni energy levels 0–64023
6°Ni(p,p), using polarized protons, and DWBA 0–73947
6°Ni, deduced levels from 6°Ni(p,p), E=7646 keV 0–39015
6°Ni, it deduced levels from 6°Ni(p,p), E=7646 keV 0–39015
6°Ni, it deduced from decay of 6°Co and 6°Cu 0–52724
6°Ni, levels deduced from decay of 6°Co and 6°Cu 0–52724
6°Ni, it levels deduced from decay of 6°Co and 6°Cu 0–52724
6°Ni, it proton elastic scatt... absolute differential cross sections 0–52763
6°Ni, it proton elastic scatt... absolute differential cross sections 0–52763
6°Ni, it proton elastic scatt... absolute differential cross sections 0–52763
6°Ni, it proton elastic scatt... absolute differential cr

⁶²Ni, proton elastic scatt., absolute differential cross sections 0-52763

tions 0–77463

*Ni, proton elastic scatt., absolute differential cross sections 0–52763

*Ni, static quadrupole moment of 1st excited state comparison of theoretical and experimental results 0–64020

*Ni, static quadrupole moment of first excited state 0–73809

*Ni, static quadrupole moment of first excited state 0–73809

*Ni, ground and second excited states, fine structure of isobaric analogues 0–67488

*Ni, T=3½ analogue of ground state of 63C0 for 63Ni, obs. for 27.5 MeV protons in 64Ni(p,d) 0–60761

*Ni first excited state, energy, lifetime g-factor 0–49524

*Ni, 5 to 10.5 MeV/amu projectile, complete fusion cross sections with various targets 0–49676

*Ni, 19.5 MeV a-particle deduced deformation parameters, elastic and ine lastic scattering analysis 0–49646

*Ni(p, ay)**PCo, investigation of low-lying levels 0–64022

*Ni(p,d)**Ni, T=3½ analogue of ground state of 63C0 for 63Ni, obs. for 27.5 MeV protons 0–60761

Ni(e,e)Ni elastic scatt, cross-sections at 300 MeV, charge distrib, isotopic depend. 0–64109

Ni(n,e) cross-section determ, for natural element using a technique based on Ni(n,e) cross-section determ.

depend. 0-64109 Ni(n,x) cross-section determ. for natural element using a technique based on the absolute determ. of helium 0-49634 Ni(p,p), differential cross sections and polarizations 0-77547 8°Pb, elastic scattering, differences in single, plural and multiple scattering through intermediate angles for electrons and positrons 0-57970 Rb, accurate determ. of $P_k\omega_k$ -value and fluoresc. yield ω_k , following e. capture decay of 8°Sr 0-67504 Rb, neutron activation cross-sections, (n,p), (n,t) and (n,2n) at 14.8 MeV 0-42854 8°Rb energy levels from ν -spectra 0-64027

0–42854 ** 8 Rb energy levels from γ -spectra 0–64027 ** 8 Rb energy levels from γ -spectra 0–64027 ** 8 Rb energy levels from γ -spectra 0–64027 ** 8 Rb energy levels from γ -spectra 0–64027 ** 8 Rb, 8 Rb, level determ, using 8 GSr(d, α) 84 Rb and 8 Sr(d, α) 86 Rb reactions

0 - 60762

⁸⁵Rb, g-factors, nuclear and e, obs. 0–52925 ⁸⁵Rb n.m.r. in Rb₂CuCl₄.2H₂O, quadrupole interactions 0–41384 ⁸⁵Rb(n,y)^{86m}Rb, reaction cross sections between 0.16 MeV and 1.5 MeV 85Rb(n,v)86 0-73966

"Robin,p)""Rob, reaction cross sections between 0.16 MeV and 1.5 MeV 0-73966

"Rob, independent yield, in ²⁵² Cf spontaneous fission 0-39151

"Rob,g-factors, nuclear and e, obs. 0-52925

"Rob.n.m.r. in Rob-CuCla,2H₂O, quadrupole interactions 0-41384

"Rob n.q.r. in paraelec. RobH₂PO₄, obs. 0-41403

"Rob quadrupolar coupling in RobH₂PO₄ rel. to Curie pt. 0-44366

"Rob radiative capture cross sections for 10-350 keV neutrons 0-46227

"Rob(n,p)"Rob, reaction cross sections between 0.16 MeV and 1.5 MeV 0-73966

"Sc, β decay, half-life meas., spin and parity of levels 0-77516

"Sc, β decay, half-life meas., spin and parity of levels 0-77516

"Sc, β decay half-life meas., spin and parity of levels 0-77516

"Sc, β devel and γ radiation study 0-70476

"Sc levels, from ("He, p), O" spin parity obs. 0-67453

"Sc, γ ray spectrum n, γ ray spectrum 0-52789

"Sc, γ ray spectrum study, transition rates and half-life meas. of 75 As excited states 0-73814

"Sc, γ transitions, from "Sc(n,p) 0-52789

"Sc, love-energy γ-ray spectrum in radioactive decay 0-49525

"Sc, low-energy γ-ray spectrum, line energies and intensities, transitions 0-38971

⁷⁵Se decay, γ -spectrum, line energies and intensities, transitions 0–38971

Nuclei with 50 ≤ A ≤ 89 continued

⁷⁵Se levels, 3.8 MeV (p,nγ) obs. 0–38895 ⁷⁶Se, energies of levels populated in ⁷⁶Br decay 0–46165

⁷⁶Se, level and y radiation study 0-70476

⁷⁶Se levels, isobaric analogue resonances from neutron decay, spin assignments 0–67462

The superhyperfine splitting in diamond lattice, e.p.r. obs. 0—48141 785e, level and p radiation study 0—70476 80Se radiative capture cross sections for 10-350 keV neutrons 0—46227

 80 Se $(n,y)^{81m.g}$ Se ratio of isomeric cross sections calculation 0-70621*Se irradiation with 14.7 MeV neutrons, to produce radioactive nucleides ³²Ge and ³²As 0–49570

82Se proton radiative capture, effect of nuclear charge distribution form and radius 0-64118

radius 0-64118

**2Se(n,2n), E_m=14.7±0.15 MeV, isomeric ratio determ. 0-73960

**7Se, half-life meas., from ²³⁵U fission 0-49679

**Se, half-life meas., from ²³⁵U fission 0-49679

Se(p.x)*Na (A=22, 24), Ep=100-400 MeV, energy depend. of prod. cross sections 0-49614

Sn induced by ²⁰Ne ions, 168, 183, 198 MeV cross-sections and fragment distrib. 0-46264

Sr, neutron activation cross-sections, (n,p), (n, α) and (n,2n) at 14.8 MeV 0.—4284

Sr, neutron activation cross-sections, (n,p), (n,ν) and (n,2n) at 14.8 MeV 0-42854
Sr conservation of seniority in 1g_{9/2} neutron shell using neutron transfer reactions 0-64028
Sr isotopes, effective interaction 0-38897
(d,p) *Sr at 20.65 MeV, levels study 0-57916
*Sr, props, of levels, from decay of *4Y 0-38972
*Sr levels using (d,t) and (d,p) at 20.65 MeV 0-57916
*Sgr, deduced levels and J, directional γγ correlation measurements from *8Y decay 0-57915
*Sgr, level scheme from decay of *6Y 0-52726
*Sgr, (p,p)*Sgr, analogue levels study in particle core model 0-67464
*Sgr(t,p)*Sgr, 15 MeV ang. distrib. meas. and compared with DWBA calc. 0-70478
*Sgr, kevels from *Sgr(p, p), structure study in particle core model 0-67464
*Sgr levels using (d,t) and (d,p) at 20.65 MeV 0-57916
*Sgr, levels using (d,t) and (d,p) at 20.65 MeV 0-57916
*Sgr, deduced isobaric analog resonances of *8gr 0-49527
*Sgr, excited state half-life, obs. 0-38878
*Sgr from (y, p), isobaric analogue states 0-67465
*Sgr level structure studied in *Sgr(t,p)*Sgr 0-70478
*Sgr (d, γ)*Sgr batdy of excited levels of *Sgr 0-70478
*Sgr(d, γ)*Sgr, excitation curves for 4 states of *Sgr in region of *Sgr(d,p)*Sgr, excitation curves for 4 states of *Sgr in region of *Sgr(d,p)*Sgr, excitation curves for 4 states of *Sgr in region of *Sgr(d,p)*Sgr, excitation effects and ground and first excited state of *Sgr 0-2-70658

Sis Section V = 77.719 sis Section V = 77.719 sis Section V = 77.719 and V = 77.719 sis Section V = 77.719 since V

88Sr(d,p)89Sr analysed using BHMM theory of deuteron stripping 0 -70651

88 Sr(p, p) (89 Sr, resonance structure in octupole transition 0—67466
 88 Sr(p, p) (88 Sr, polarization meas, near isobaric analog resonances 0 - 67527

0.-6752/
**8Sr(p, p) calc. elastic and inelastic analogue state resonances using coupled optical equations 0.-67403 to force of the second of the secon

**Sr ground and first excited state from **Sr(d,p) with polarized d 0-70658 **Sr levels from **Sr(p,p'), particle core states investigation 0-67466 **Sr listotope, projected Hartree-Fock-Bogolubov calculation 0-52686 **Sr listotope, projected Hartree-F

⁵⁰Ti isotope, projected Hartree-Fock- Bogolubov calculation U→2.086
⁵⁰Ti reorientation measurements after excitation of first excited 2⁺ state, quadrupole moment 0—6.4018
⁵⁰Ti('He, d), energy levels ⁵¹V study 0—6.7555
⁵⁰Ti('He, d), ⁵¹V levels ≤ 6.17 MeV 0—38885
⁵⁰Ti(d, d), ⁵¹V, resonances in ⁵¹V study near ⁵¹Ti ground state analogue 0—67536
⁵⁰Ti(p,y), ⁵¹V, resonances in ⁵¹V study near ⁵¹Ti ground state analogue 0—67536

0-67536
"OT(ip.p'), effect of core polarization 0-70587
"OT(ip.p'), effect of core polarization 0-70587
"Ti(ip.p') at 40 MeV, cross section for exciting low lying states 0-57973
"Ti, N=29, Z=29 nucleus, level calculations using intermediate coupling model, stripping strengths 0-70461
"Ti, negative parity levels in various models 0-70462
V, inelastic and elastic n scatt., E=1.5-8.1 MeV, optical-model calcs. 0-49623

0-49623 V neutron total cross-section, high resolution 0-73953

50V, level structure from study of ⁴⁹Ti(³He,d) reaction 0-70459

50V, energy levels deduced from ⁵⁰V(p,e) and ⁵⁰V(p,p) 0-38883

51V, B(M1) and B(E2) reduced transition properties 0-57910

51V, e.s.r. of MoO₃:V, electron hole interactions 0-48149

51V, e.g. and one of the content of the conte

0 -46134
51V, fr₁2 proton states, electroexcitation 0-70460
51V, ground state (p.n) Q values 0-77552
51V, p-decay of lowest 3/2 state, shell model calc. 0-70463
51V, n.m.r. in semiconducting vanadium phosphate glasses 0-48163
51V, n.m.r. in V₂O₃, 65 kbar, 4.2 K, antiferromag, state suppression 0-45031

0-52/47 5¹V(p,p), spin information through analogue resonances decay 0-70606 5¹V(p,n)⁵1Cr, 2.340 MeV isobaric analogue reson. analysis obs. 0-38887 5¹V(p,n)⁵1Cr, y ang. distrib. 0-39048 5¹V(p,p) at 40 MeV, cross section for exciting low lying states 0-57973

Nuclei with 50 < A < 89 continued

 51 V $(\pi,\pi)^{51}$ V, Glauber approx., suppression of scattering amplitude found 0-55163

52V levels, from (3He, p), O+ spin parity obs. 0-67453

Fig. 1. Spin party obs. 0-0.785 5^4V , β -decay, γp - and βp -coincidences, deduced Q_B , log ft, decay scheme and period 0-49568

 3 Ca isotopes (X=42 to 50), shell model for low lying states 0-57909 Xe isotopes in activation cross sections, thermal, 21 keV and 14 MeV

0-39071 0-39071
86Υ, decay, decay scheme 0-38972
86Υ, decay, directional γγ correlation measurements of 86Sr, deduced levels and J 0-57915

and 0-3793 68Y, y-ray spectra, decay scheme 0-52726 87Y, and Si(Li) detector system for conversion coefficient measurements

8⁸Y, and Si(Li) detector system for conversion coefficient measurements 0-49384
8⁸Y, p-spectra of isotope 0-77518
8⁸Y decay, K conversion coefficients for 8⁷Sr 0-49526
8⁸Y, in 48 satis scatt., 30 MeV, optical model params. 0-42862
8⁸Y, in YB, n.m.r. meas. 0-79418
8⁸Y, in YB, n.m.r. meas. by time-of-flight spectrometer 0-39072

6°Y, nelastic scatt. of neutrons neas. by time-of-flight spectrometer 0-39072
8°Y, isobaric analogue states excited from 8°Sr(p,γ) 0-57981
8°Y assignments to levels obtained from inelastic scatt. of neutrons 0-39072
8°Y from (γ, p), siobaric analogue states 0-67465
8°Y giant dipole resonance, quasibound analogue states from (γ,n) and (γ,2n) 0-73816
8°Y proton scattering, inelastic, to first excited state, spin flip 0-70590
8°Y(n,p)°mY, reaction cross sections between 0.16 MeV and 1.5 MeV 0-73966
8°Y(p,p'), effect of core polarization 0-70587
8°Y(p,p'), effect of core polarization of excitation in low-lying states with T=2 0-73993
8'Zn levels from (p,n), neutron spectra meas. 0-60759
8'Zn, spin and parity level assignments 0-73980
8'Zn, compound nucleus formed from p+6°Cu and α+6°Ni, neutron emission 0-77517
8'Zn, isospin splitting of giant dipole resonance, (γ,np) reaction discussed 0-73810
8'Zn product nucleus of various proton-capture reactions, high energy γ-ray

0–73810

**Zn product nucleus of various proton-capture reactions, high energy γ-ray spectra 0–64104

Zn(*He,t)Ga production of 0+ analog and antianalog states at 35 MeV, anomalous L=1 shapes of angular distributions 0–73996

Zn(2,α,γ)Zn, 31 MeV obs. ang. distrib., spin, parity assignments 0–73980

64Zn(α,α')**Zn, 31 MeV Oss. ang.
 64Zn(d,n)65Ga by time of flight method, differential cross section, spin and parity assignments 0-58020
 64Zn(d,n)95Ga by time of flight method, differential cross section, spin and parity assignments 0-58020
 64Zn(y,n), rel. to isospin splitting of giant dipole resonance 0-73810
 64Zn(n, p)*Zn, rel. to isospin splitting of giant dipole resonance 0-73810
 64Zn(n, p)*Zn, and 65Zn, 6*Zn, p-spectra obs. transitions studied 0-462Zd.
 64Zn, 1/K and M/L electron capture ratio 0-67503

 $^{6-35130}$ seeze spins of four particle configurations, nuclear isomerism $^{0-55130}$

0-55130

Nuclei with 90≤A≤149

1341, decay props. from fission products, investig. using NaI(TI) and Ge(Li) detectors 0-38982

A=100, Z=N, density distrib., local density approx. 0-38863 equilibrium deformations in range 28 < Z < 50, 50 < N < 82 0-63978 fission chain populations, tables, odd masses, 107 < A≤127 0-39172 fission chain populations, tables, odd masses, 129 < A≤143 0-39172 fission chain populations, tables, odd masses, 145 < A≤155 0-39172 Fission chain populations, tables, odd masses, 85 < A≤105 0-39172 Fission chain populations, tables, odd masses, 85 < A≤105 0-39172 low-lying opposite parity states in nuclei with Z≈50 0-63988 quadrupole moment of 1st excited state 0-52693 rare earth isotopes, (n,2n), (næ) and (n,p) reactions, statistical model and 14 MeV obs. 0-39077 rare-earth nuclei, configuration mixing from radiative neutron capture

rare-earth nuclei, configuration mixing from radiative neutron capture 0-64005

spherical, $100 \leqslant A \leqslant 124$, self consistent core-particle coupling theory 0-38815

0–38815 (p,α) on nuclei from 93Nb to ²⁰⁹Bi, evidence for α-clustering 0–70610 ¹¹⁴Cd, interference between Coulomb and nuclear excitation by alpha particles 0–49668 ⁹⁴Mo(n,p), neutron capture γ-ray spectra measurement and ⁹⁹Mo deduced resonances for E=12.818 MeV 0–60817 ⁹⁷Te, ⁹⁷Te decay to ³³, ⁹⁴Mo, analysis 0–49528 ¹²⁶Sb^m-1²⁶Te characteristics obs. 0–64090 ¹²⁰ identification of s- and p-levels by moving sample method, neutron cross sections, strength functions 0–49534 ¹¹6Sn proton scattering, inelastic, cross-section, theory and experiment 0–70591 ⁹⁷Nb, from ⁹³Nb(n,2n), 0–67471

¹³₈Nn proton solution from 193 proton solution 93 Nb(n,2n) 0–67471 93 Nb, from 93 Nb(n,2n) 0–67471 93 Mo(94 He,d), A=92, 94, 96, 98, inhibited transitions to $3s_{1/2}$ isobaric analog states 0–73997

Nuclei with 90 ≤ A ≤ 149 continued

Ag, 3 and 29 GeV proton bombardment, yields of stable and radioactive rare-gas isotopes 0-52769

Ag, deuteron elastic scattering, analysis by optical potential 0-67542 ¹⁰²Ag deduced levels from radioactive decay of ¹⁰²Cd 0-52729

¹⁰²Ag deduced levels from radioactive decay of ¹⁰²Cd 0-52729
 ¹⁰³Ag spin meas. 0-77501
 ¹⁰⁴Ag his anomaly and magnetic moment determ. 0-77501
 ¹⁰⁵Ag, decay measurement of internal conversion electrons and ¹⁰⁵Pd decduced levels 0-57954
 ¹⁰⁵Ag, E3 isomer 0-67473
 ¹⁰⁶Ag, n reaction, reson, parameters and spin, E=4-830 eV 0-39073
 ¹⁰⁷Ag(p,2n), photoneutron cross-sections 0-67516
 ¹⁰⁷Ag(p,2n), photoneutron cross-sections 0-67516
 ¹⁰⁷Ag(p,2n), photoneutron cross-sections 0-67516
 ¹⁰⁸Ag(p,2n), photoneutron cross-sections 0-67516
 ¹⁰⁹Ag(p,2n), photoneutron cross-sections 0-67916
 ¹⁰⁹Ag(p,2n), p

107 Ag(p.2) 164Pd, compound nucleus lifetime using the blocking effect 0-42725
109 Ag n reaction, reson. parameters and spin, E=4-830 eV 0-39073
109 Ag Coulomb excitation, energy level deduction 0-64031
109 Ag(p.n.) 190 Cd excitation function, 0-16 MeV 0-46245
109 Ag(p.n.) 190 Cd excitation function, 0-16 MeV 0-46245
109 Ag(p.n.), photoneutron cross-sections 0-67516
109 Ag(p.n.) 164 Ag evidence of (2-) state in 119 Ag level 0-57919
1109 Ag(p.n.) 184 MeV, mean lifetime calc. of 203 keV level in 109 Cd
0-38928
110 Ag levels from 109 Ag(n.), evidence for (2-) state 0-57919
111 Ag levels from 109 Ag(n.), evidence for (2-) state 0-57919
1108 Ag(p.n.) 24 Period 100 Ag(p.n.) 100

0-38918
0-38918
13 Ba, decay scheme and p-spectrum, obs. 0-38920
13 Ba half-life meas. 0-64084
13 Ba-33Cs, multipolarity of 79.6 transition from 161 keV level of 133Cs

"Ba - Cs and corelation to 19.6 transition from 101 keV level of 3.0 Cs 0-42792 (1.3 Ba, p-p-p cascades angular correl., obs. 0-38923 (1.3 Ba, M1/E2 multipole mixing of the 563 and 569 keV transitions using directional correlation techniques 0-42767 (1.3 Ba (He,3n)) (1.3 Cs decay 0-38984) (1.3 Ba (He,3n)) (1.3 Cs decay 0-38984) (1.3 Ba (He,3n)) (1.3 Cs decay 0-38984) (1.3 Ba (He,3n)) (1.3 Cs decay 0-3899) (1.3 Ba (He,3n)) (1.3 Cs decay 0-73999) (1.3 Ba metastable level, 1.3 MeV, agular distributions, average projected ranges, and cross sections 0-73999) (1.3 Ba metastable level, 1.3 MeV, agular distributions, average projected ranges, and cross sections 0-73999) (1.3 Ba (He,3n)) (1.3 Cs decay 0-70490) (1.3 Ba metastable level, 1.3 MeV, agular distributions, average projected ranges, and cross sections 0-73999) (1.3 Ba) (1.3 B

Bald, D) (A=130, 132, 134, 130, 130), proton spectra, and district O-49669

"Br, in RbBr crystal, spin-lattice relaxation times, 20 K-300 K 0-54174

RiBr, in RbBr crystal, spin-lattice relaxation times, 20 K-300 K 0-54174

Cd (where A=110, 112, 114, 116), elastic and inelastic scatt. of deuterons from vibr. states, diff. cross sections 0-42863

Cd deduced levels from Cd(p, p'y) E=5.7-7.5 MeV 0-38906

cd energy levels of even nuclei from Pd(r, xnp) reactions 0-64032

Cd isotopes phenomenological treatment of anharmonic effects 0-38911

10°Cd, radioactive decay deduced levels of 10°Ag 0-52729

10°Cd, quadrupole moment, static, from Coulomb reorientation effect obs. 0-42757

10°Cd (He,d) 110 70660

10°Cd devels and p-spectrum ≤ 2 MeV 0-38907

10°Cd mean lifetime of 203 keV level deduced from 10°Ag (p,np) 0-38928

11°Cd, E2/M1 multipole mixing ratios of p transitions following 110°MAg decay 0-70482 decay 0-70482 110 Cd, elastic scattering, isobaric analog resonances, E_p=6.0-11.0 MeV

 $^{19}\text{Cd}_c$ elastic scattering, isobaric analog resonances, $E_p\!\!=\!\!6.0\text{-}11.0$ MeV $0\!-\!42841$ $^{190}\text{Cd}_c$ isobaric analog resonances in proton elastic scatt. $0\!-\!67475$ $^{190}\text{Cd}_c$ in eapture p-ray cross section, 25 keV $0\!-\!39076$ $^{190}\text{Cd}_c$ deduced levels in ^{190}Cd and search for 0* member of two phonon triplet from decay of $^{1108}\text{Ag}(1^+)$ $0\!-\!57918$ $^{190}\text{Cd}_c$ y-y directional correls. following ^{1909}Ag decay $0\!-\!38977$ $^{190}\text{Cd}_c$ K-LL Auger electron spectra, meas, with mag, β -spectrometer $0\!-\!38997$

111Cd, mean-life of the 343 keV state using delayed coincidence method 0-49532

0–49532
"I'Cd 342 keV state mean life, obs. 0–38909
"I'Cd angular correlation, effect of combined electric and magnetic interaction 0–49574
"I'Cd, elastic scattering, isobaric analog resonances, E_p=6.0-11.0 MeV 0–42841

0-42841 " 112 Cd, isobaric analog resonances in proton elastic scatt. 0-67475 " 122 Cd deduced levels from 12 Cd(γ,γ'), E=7632 keV 0-39015 " 123 Cd, β instability 0-70545 " 123 Cd n.m.r. in CdO, Knight shift 0-62772 " 123 Cd, 134 Cd, 134 Ce elastic scatt., 13 O MeV, optical model params. 0-42862 " 142 Cd, elastic scattering, isobaric analog resonances, E_p =6.0-11.0 MeV

114Cd, elastic scattering, isobaric analog resonances, E_p=6.0-11.0 MeV 0-42841
 114Cd, isobaric analog resonances in proton elastic scatt. 0-67475
 114Cd, quadrupole mom. meas. by Coulomb excitation 0-38913
 114Cd, quadrupole moment, static, from Coulomb reorientation effect obs. 0-42757
 114Cd, quadrupole moments of first excited 2+ states by Coulomb excitation 0-42760
 114Cd quadrupole moment in first excited state 0-60755
 114Cd (3-46.4)¹³In, and first excited states of ¹¹³In 0-70660
 114Cd, 11-20, deta decay, decay scheme 0-49575
 110mCd, gamma-ray cascades angular correl., and 2200 keV level spin, obs. 0-38908

Nuclei with 90 4 4 149 continued

| 132 | 134 | 134 | 134 | 134 | 134 |
| distrib. 0-39165

¹³³I yield in thermal neutron induced fission of ²³³U and ²³⁹Pu 0-70678

S 1200 SUBJECT INDEX Nuclei with 90 ≤ A ≤ 149 continued cele with $90 \le A \le 149$ continued Cd(p,p'y) deduced levels of Cd E=5.7-7.5 MeV 0-38906 Cd(p,p'y) enhancement 0-73925 Ce (where A=140,142), strong L=0 and 2 transitions, study in (p,t) reactions 0-55133tions 0–55133 tions 0–55133 tions 0–42765 tions 0–5134 tions 0–42765 ti ¹⁴⁰Ce, ground-state quasirotational bands and other states 0–42765
¹⁴⁰Ce, lifetimes of excited states at 2083 and 2412 keV 0–52699
¹⁴⁰Ce, cone and two neutron hole states from (p,d) and (p,t) reactions 0–70490
¹⁴⁰Ce, structure of generalized neutron particle-hole states 0–38924
¹⁴⁰Ce, Thomas-Fermi theory calculation of energy per particle, density distribution and single particle potential 0–49451
¹⁴⁰Ce from (p, p), isobaric analogue states 0–67480
¹⁴⁰Ce levels from the decay of ¹⁴⁰Pr 0–52735
¹⁴¹Ce, validity of ξ approximation of 1400 keV β decay 0–70551
¹⁴²Ce, validity of ξ approximation of 1400 keV β decay 0–70551
¹⁴³Ce, validity of ξ approximation of 1400 keV β decay 0–70551
¹⁴⁴Ce decay, deduced levels of ¹⁴⁴Pr and energies and intensities of γ-rays 0–64039
¹⁴⁴Ce+³⁴⁴Pr, γ energies and intensities, ¹⁴⁴Pr excited states 0–70552
¹³⁷⁶Ce, production from ¹³⁷⁸Ba(³He,3n), 14-33MeV, angular distributions, average projected ranges, and cross sections 0–73999
¹³⁷⁶Ce nucl. orientation in dil. Au-Ce alloys 0–72298
¹³⁷⁶Ce production from ¹³⁶Ba(³He,3n), 27-44 MeV, angular distributions, average projected ranges, and cross sections 0–73999
¹³⁷⁶Ce nucl. orientation in dil. Au-Ce alloys 0–72298
¹³⁷⁶Ce, production from ¹³⁶Ba(³He,3n), 27-44 MeV, angular distributions, average projected ranges, and cross sections 0–73999
¹³⁷⁶Ce nucl. orientation in dil. Au-Ce alloys 0–72298
¹³⁷⁶Ce, production from ¹³⁸Ba(³He,3n), 27-44 MeV, angular distributions, average projected ranges, and cross section no proton induced fission of ¹³⁹Pu 0–49681
¹³⁹Cs energy levels, comparison of experimental and calculated results 0–70547
¹³¹Cs energy levels, comparison of experimental and calculated results 0–70547
¹³¹Cs energy levels, from ¹³¹Ba decay obs. 0–32698
¹³²Cs, gadarupole moment, optical h.fs. obs. 0–52698
¹³³Cs, g-factors, nuclear and e, obs. 0–52925
¹³³Cs, g-factors, nuclear and e, obs. 0–52925
¹³³Cs, secited in ¹³³Cs(n,n'y) reaction, levels scheme 0–46145
¹³³C 140Ce, one 0-70490 ¹³Cs, decay, second-order e.m., oos. 0—4.799
¹³Cs, decay, p-ray polariz. meas., depolariz. effects of detector sizes 0–63876
¹³Cs pamma-ray sources, calibration in terms of exposure units 0–48633
¹³Cs half-life meas. 0–64084
¹³⁸Cs, β-decay, ¹³Ba metastable level obs. 0–73868
¹⁴⁵Eu, isobaric analogue resons, proton polarization meas. 0–38927
¹⁴⁶Eu-1⁴⁶Sm high resolution studies of transitions 0–67508
¹⁴⁷Eu, g-factor determ. of 11/2 - excitation states 0–64040
¹⁴⁷Eu, g-factors of second excited states ¹¹/₂ -, by differential ang. correlation method 0–73825
¹⁴⁹Eu, g-factors of second excited states ¹¹/₂ -, by differential ang. correlation method 0–73825
¹⁴⁶Gd energy levels from ¹⁴⁴Sm (α.2np)¹⁴⁶Gd 0–70498
¹⁴⁶Gd energy levels from ¹⁴⁴Sm (α.2np)¹⁴⁶Gd 0–70498
¹⁴⁶Gd energy levels from ¹⁴⁴Sm (α.2np)¹⁴⁶Gd 0–70498
¹⁴⁶Gd energy levels from energy levels

Nb, deuteron elastic scattering, analysis by optical potential 0–0.7342
Nb, neutron activation cross-sections, (n,p), (n,α) and (n,2n) at 14.8 MeV 0–42854

90Nb, four particle levels of 3p,n type 0–55131

90Nb (g₈₇)² multiplet, spins and excitation energies 0–70479

1Nb from 9°Zr(°He, d), spreading of antianalogue states 0–67470

1Nb negative parity levels within a 2-particle 1-hole state 0–70480

92Nb, g₅₇-d₅₇ interactions 0–60763

93Nb, e.s.r. of MoO₃:Nb, electron hole interactions 0–48149

93Nb, n.m.r. in LiNbO₃-LiTaO₃ solid solns. 0–72510

93Nb, n.m.r. in polyeryst. NaNbO₃ 0–79417

93Nb (n,2n)²²mNb, excitation functions 0–67471

93Nb(n,2n)²²mNb, excitation functions 0–67471

93Nb(n,2n)²²mNb, excitation functions 0–67471

93Nb(n,2n)²²mNb, excitation functions 0–67940

"6Nb, g₅₇-d₅₇ config. levels, spin assignment, from 96Zr(³He,t) 0–60763

96Nb, p₅-vircular polarization 0–64087

97Nb, p₇-vircular polarization 0–64087

97Nb, p₇-vircular polarization 0–64087

97Nb, p₇-vircular polarization 0–664087

97Nb level scheme, from ⁹⁷Zr β decay 0–55142

Nd (A=143, 144, 146), energy levels from Pm decay 0–52736

Nd even isotopes, A=142 to 150, L=0 and 2 from (p,t) 0–70496

Nd isotopes, activation cross sections for 14 MeV neutrons 0–55161

141Nd, proton part of wave functions 0–70549

142Nd, generalized neutron particle-hole states from 143Nd(p,t) 0–70494

143Nd, one and two neutron hole states from (p,d) and (p,t) reactions 0–70490 I (A=119, 121, 123), radioactive, level schemes of Te(A=119, 121, 123) 0–49533 I decay and levels in Te isotopes with $117 \le A \le 124$ 0–67476 I isotopes, yield in 235 U fission 0–42894 I isotopes, yield in 235 U fission 0–42894 I isotopes 235 U thermal-n fission yields, obs. from fission of 235 U 0–49687 I isotopes 235 U thermal-n fission yields, obs. from fission of 235 U 0–49687 I isotopes 235 U thermal-n fission yields, obs. from fission of 235 U 0–49687 I isotopes 235 U 1, half life of lying $^{1/5}$ I levels 0–67477 I isotopes 235 U 1 first of edge, 35.48 keV transition conversion coeffs., Te K-fluoresc. yield 0–38980 I isotopes 235 U 1 decay scheme, y rays intensities 0–49577 I isotopes 235 U 1 in Hg1₂, n.q.r. spectra 0–69201 I isotopes in the special point of the

Nuclei with $90 \le A \le 149$ continued ¹⁴²Nd excited levels, ¹⁴²Sm decay obs. 0-70550 ¹⁴²Nd(n,2n), isomeric ratio analysis, $E_n=14.2$ 0-39075 ¹⁴³Nd(d,1)¹⁴²Nd and neutron particle-hole states in ¹⁴³Nd 0-70494

¹⁴³Nd(d,t)¹⁴²Nd and neutron particle-hole states in ¹⁴³Nd 0–70494
¹⁴³Nd(n,e)¹⁴⁴Nd, thermal neutron capture, conversion electron spectra, level scheme of ¹⁴⁴Nd 0–60766
¹⁴³Nd(p,t), pairing vibr. states in ¹⁴¹Nd from L=0, 2 transitions 0–70613
¹⁴⁴Nd, level scheme, from thermal neutron capture by ¹⁴³Nd, conversion electron spectra 0–60766
¹⁴⁴Nd, relative static quadrupole moments of first excited state 0–64038
¹⁴⁴Nd, energy levels and spins from bremsstrahlung resonant scattering 0–70497

relectron spectra 0–60766

144Nd, relative static quadrupole moments of first excited state 0–64038

145Nd energy levels and spins from bremsstrahlung resonant scattering 0–70497

146Nd static quadrupole moment of first excited state 0–73823

144Nd(n,α)14°Ce, 14 MeV and statistical model 0–39077

146Nd, relative static quadrupole moments of first excited state 0–64038

146Nd static quadrupole moment of first excited state 0–73823

146Nd(d,d'), deduced 146Nd levels, excitation energies and cross-sections 0–60828

146Nd(d,d'), deduced 146Nd levels, excitation energies and cross-sections 0–60828

146Nd, n-capture y-ray cross section, 25 keV 0–39076

148Nd, n-capture y-ray cross section, 25 keV 0–39076

148Nd, n-capture y-ray cross section, 25 keV 0–39076

148Nd, relative static quadrupole moments of first excited state 0–64038

148Nd (t,p)150Nd and L=0 transitions in 150Nd 0–74001

148Nd fission product, determination, separation from irradiated fuel 0–55213

148Nd static quadrupole moment of first excited state 0–64038

139Mn, e-decay to three-quasiparticle multiplets in 139Pr 0–70492

141mNd, M4 multipolarity of 756.5 keV isomeric transition 0–60765

141mNd, M4-143, 145), cross sections 0–42855

140Mn, M2-143, 145), cross sections 0–42855

140Mpd, A2-143, 145), cross sections 0–73824

140(n,ω) (A2-143, 145), cross sections 0–42855

140Mpd, decay, allowed β-branch, strong hindrance 0–52797

140Mqd, A2-143, 145), cross sections 0–73824

140Mqd, A2-143, 145), cross sections 0–73862

140Mpd, from decay of 166mRh 0–46167

140Mpd, f

Pd(d,t) (A=108, 110), nuclear structure studies of 107 Pd and 109 Pd $0^{-4}9667$ Pm-Nd (where A=143, 144, 146), inner conversion electron and γ ray spectra 0^{-52736} M²²Pm-M²²Nd, meas of γ transitions, level struct. of 142 Nd 0^{-52700} M²³Pm, obs. in β —decay of 143 Sm 0^{-67507} M²³Pm isobaric analogue resonances, deduced proton decay widths 0^{-46125} M²⁵Pm β emission spectrum, modification 0^{-38632} M²⁷Pm excited state lifetimes, obs. 0^{-38896} M²⁸Pm, ground state, half-life, by γ -ray spectrometry 0^{-46178} M²⁹Pm beta-decay, $1^{-30^{\circ}}$, nuclear matrix elements 0^{-70553} M²⁹Pr, from (γ, p) , isobaric analog states 0^{-67480} M²⁹Pr, isomer shifts in 145-keV, Mossbauer obs. 0^{-73822} M²⁹Pr, isomer shifts in 145-keV, Mossbauer obs. 0^{-73822} M²⁹Pr, inclastic scatt., 2.9 MeV, γ -rays and nuclear levels 0^{-38888} M²⁹Pr energy spectrum of ejected photoneutrons 0^{-46192} M²⁹Pr, 157 and 157 keV levels struct. 0^{-38926} M²⁹Pr, 157 and 157 keV levels struct. 0^{-38926} M²⁹Pr, 157 and 157 keV levels struct. 0^{-38926} M²⁹Pr, 157 and 157 keV levels and intensities of γ -rays for 144Ce radioactive decay 0^{-64039} M²⁹Pr, 157 and 157 keV levels of 157 magnetic moment 0^{-70474} M²⁹Pr, 157 and magnetic moment 10^{-70

radioactive decay 0-64039

14th Prexited states, "4th Ce decay obs. 0-70552

14th Prexited states, "4th Ce decay obs. 0-70474

19th, 19th, 19th, quadrupole mom. meas. by Coulomb excitation 0-38913

19th, in RbBr crystal, spin-lattice relaxation times, 20 K-300 K 0-54174

19th, 19th, in RbBr crystal, spin-lattice relaxation times, 20 K-300 K 0-54174

19th, Knight shift and spin-lattice relax rate, low-temp. pressure-depend. 0-41367

19th, level determ. from 19th decay 0-64086

19th, 19th,

Nuclei with 90≤A≤149 continued ^{102m62}Rh, from ¹⁰³Rh(n,2n) 0-67471 ⁹⁷Ru, excited levels, from y decay of ⁹⁷Rh 0-38974 ¹⁰⁹Ru energy levels from ¹⁰⁹Tc decay 0-64089

¹⁰²Ru, spectroscopic factors, from ¹⁰⁴Ru(d,t) 0–49667 ¹⁰³Ru, spectroscopic factors, from ¹⁰⁴Ru(d,t) 0–49667 ¹⁰³Ru decay, conversion electron spectrum 0–38742

¹⁰³Ru decay, conversion electron spectrum 0–38742 ¹⁰³Ru decay scheme, from ¹⁰³Rh γ -spectrum obs. 0–38904 ¹⁰³Ru decay scheme, from ¹⁰³Rh γ -spectrum obs. 0–48904 ¹⁰³Ru decay to ¹⁰³Rh, and spins of levels in ¹⁰³Rh 0–67505 ¹⁰³Ru→¹⁰³Rh, γ -transitions, level obs. 0–49573 ¹⁰³Ru→¹⁰³Rh β -decay, γ -ray cascades obs. 0–38976 ¹⁰³Ru energy levels from ¹⁰⁶Fic (37 sec) decay 0–64030 ¹⁰⁶Ru lowlying energy levels from ¹⁰⁶Fic (37 sec) decay 0–64030 ¹⁰⁶Ru lowlying energy levels from ¹⁰⁸Tic (8 sec) decay 0–64030 ¹⁰⁶Ru, upcode by photonuclear reactions 0–67472 ¹⁰³Ru, prod. by photonuclear reactions 0–67472 ¹⁰³Ru, prod. by photonuclear reactions 0–67472 ¹⁰³SN, quasiparticle Tamm-Dancoff and random-phase approximations using realistic interactions 0–52694 ¹⁰³Sb, A=115 to A=125, low energy props. of the odd mass isotopes 0–38914 ¹⁰³Sb isotopes, odd-mass low-energy spectra 0–38915

using realistic interactions 0-52694 Sb, A=115 to A=125, low energy props, of the odd mass isotopes 0-38915 Sb isotopes, odd-mass low-energy spectra 0-38915 Sb isotopes decay and levels in 1^{12} .1 1^{12} .1 1^{12} .75C 0-61476 117Sb, deduced levels from 1^{15} In(α ,2np), $E\alpha$ =20.27 MeV 0-42762 117Sb, level scheme, reaction data 0-52695 119Sb, level scheme, reaction data 0-52695 119Sb, excited states and theoretical predictions 0-52731 119Sb, isomer shift in Sn-Sb solid soln., conc. depend. 0-77563 121Sb, isomer shift in Sn-Sb solid soln., conc. depend. 0-51285 121Sb, Mossbauer effect in special solid soln., conc. depend. 0-51285 121Sb, Mossbauer effect in special solid soln., conc. depend. 0-51285 121Sb, Mossbauer effect in Sp Sn idles 0-41169 121Sb isomer shifts in Pd-Sb alloys 0-59380 121Sb, Mossbauer effect in SP Ni alloys 0-59380 121Sb Mossbauer effect in SP Ni alloys 0-59380 121Sb Mossbauer effect in SP Ni alloys 0-59380 121Sb unadrupole moment ratio from Mossbauer obs. of organo-Sb cpds. 0-55132 121Sb radiative capture cross sections for 10-350 keV neutrons 0-46227 121Sb(10-3696) 121Sb hisomer shifts in Pd-Sb alloys 0-59380 121Sb 10-3696 121Sb hisomer shifts in SP Ni alloys 0-59380 121Sb 10-3696 121Sb isomer shifts in SP Ni alloys 0-59380 121Sb 10-3696 121Sb isomer shifts in Pd-Sb alloys 0-59380 121Sb 10-3696 131Sb 10-3696 131Sb 10-3696 131Sb 10-3696 131Sb 10-3696

0–55 134 "-25S 134" and model 0–70495 "-25S menergy levels from 144Sm(p,t), and model 0–70495 "-145Sm $^{+147}$ Nd, 142Nd excited levels obs. 0–70550 "-145Sm energy levels from 144Sm(p,d), and model 0–70495 "-135m three quasiparticle state from Te(22Ne, -70) and Te(20Ne, -70) 0–38925 "-145Sm(n,2n), isomeric ratio analysis, E_n=14.2 0–39075 "-145Sm $^{+147}$ Pm via β -decay, spin and parity assignments 0–67507 "-144Sm, from (γ , p), isobaric analog states 0–67480 "-145Sm $^{+147}$ Pm via β -decay has been states from (p,d) and (p,t) reactions 0–70490 "-145Sm, one and two neutron hole states from (p,d) and (p,t) reactions 0–70490 "-145Sm $^{+147}$ Pm via β -decay has been states from (p,d) and (p,t) reactions 0–70490 "-145Sm $^{+147}$ Pm via β -decay has been states from (p,d) and (p,t) reactions 0–70490 "-145Sm $^{+147}$ Pm via β -decay has been states from (p,d) and (p,t) reactions 0–70490 "-145Sm $^{+147}$ Pm via β -decay has been states from (p,d) and (p,t) reactions 0–70490 "-145Sm $^{+147}$ Pm via β -decay has been states from (p,d) and (p,t) reactions 0–70490 "-145Sm $^{+147}$ Pm via β -decay has been states from (p,d) and (p,t) reactions 0–70490 "-145Sm $^{+147}$ Pm via β -decay has been states from (p,d) and (p,t) reactions 0–70490 "-145Sm $^{+147}$ Pm via β -decay has been states from (p,d) and (p,t) reactions 0–70490 "-145Sm $^{+147}$ Pm via β -decay has been states from (p,d) and (p,t) reactions 0–70490 "-145Sm $^{+147}$ Pm via β -decay has been states from (p,d) and (p,t) reactions 0–70490 "-145Sm $^{+147}$ Pm via β -decay has been states from (p,d) and (p,t) reactions 0–70490 "-145Sm $^{+147}$ Pm via β -decay has been states from (p,d) and (p,t) reactions 0–145Sm $^{+147}$ Pm via β -decay has been states from (p,d) and (p,t) reactions 0–145Sm $^{+147}$ Pm via β -decay has been states from (p,d) and (p,d) and

148Sm(16O₂) 16(2)7, 551 keV first excited state, static quadrupole moment 0-6/7481
 148Sm(20Ne, 20Ne; 2)Ne; static quadrupole moments of the first excited states of 20Ne using reorientation effect 0-60757
 148Sm(20Ne; 20Ne; 2) static quadrupole moments of the first excited states of 22Ne using reorientation effect 0-60757
 148Sm(2) 551 keV first excited state, static quadrupole moment 0-67481
 148Sm(n,p) 148Pm, 14 MeV and statistical model 0-39077
 148Sm(n,p) 148Pm, 14 MeV and statistical model 0-39077
 148Sm(n,p) 16MPm, 14 MeV and statistical model 0-39077
 158Sm(p,p), deformation parameters obtained from coupled-channel analysis of proton scattering 0-73828
 159Sm, 22.494 keV internal conversion subshell transition 0-67482
 159Sm, Mossbauer effect in SmB₆, isomer shift, valence state determ. 0-44797
 159Sm neutron single hole states from (p,d) 0-70499
 15m(n,a) (A=147, 149), cross sections, 150Ne energy levels 0-42855
 15m, 2p-2h and 2-quasi-particle excitations 0-70473
 15m, even isotopes, (p,d), angular distrib. J-depend. 0-52633
 15m, photon scattering cross section, 6-9 MeV, new method of analysis 0-73896
 15m (A=112, 116, 118, 120, 122, 124), elastic and inelastic scatt., of deuterons from vibr. states, diff. cross sections 0-42863
 15m (A=112, 118) electron elastic scatt., E=225 MeV, nuclear charge distr. parameters, charge radius 0-49597

Nuclei with 90 A 149 continued

Sn isotopes, giant dipole and quadrupole resonance, splitting calculated 0-42728

Sn isotopes, photodisintegration, anal. of expt. results by giant dipole reso-

Sn isotopes, self-consistent core-particle coupling calc. 0-70485

Sn isotopes, self-consistent core-particle coupling calc. 0—70485
Sn isotopes (A=111-123) energy levels, angular distribution 0—42758
Sn isotopes ground state rel. to particle number projection effect 0—57920
Sn(12C, xn)136Ba, anal. of n and photon emission from compound-nuclei 0—38918

"Sn proton scattering, inelastic, cross-section, theory and experiment 0-70591

0-70591

1ºSn, decay and the level structure of 1º9In 0-52692

1ºSn, decay and the level structure of 1º9In 0-52692

1ºSn(a,2np). Te deduced levels 0-38912

1ºSn(d,p)¹¹Sn and energy levels in ¹¹¹Sn 0-70483

1ºSn(a,p¹), separation of direct-reaction and compound nucleus contributions 0-60812

1³Sn, energy levels from ¹¹Sn(d,p) 0-70483

1³Sn(a,2np), Te deduced levels 0-38912

1³Sn(b,p²), separation of direct-reaction and compound nucleus contributions 0-60812

1³Sn(b,p²), separation of direct-reaction and compound nucleus contributions 0-60812

1³Sn(b,p²), separation of direct-reaction and compound nucleus contributions 0-60812

11°Sn(p,p'), separation of direct-reaction and compound nucleus contributions 0-60812
 11°Sn, 'He elastic scatt., 30 and 35 MeV, optical model params. 0-42862
 11°Sn, e inelastic scatt., 60 MeV, quadrupole and octupole excitations 0-42761
 11°Sn, quasiparticle Tamm-Dancoff and random-phase approximations using realistic interactions 0-52694
 11°Sn (a,'He), E_a=65.7 MeV, diff. cross sections from 15° to 8° 0-39125
 11°Sn (quadrupole moment, static, from Coulomb reorientation effect obs. 0-42757
 11°Sn(2,3px) Te deduced levels. 0-38912

0 - 42757

116Sn(α,2pγ), Te deduced levels 0—38912

116Sn(α,2pγ), Te deduced levels 0—38912

116Sn(α,n)¹¹⁶Sb, and 117-120Sn, 122Sn, 8.5 MeV, isomeric pair production cross-section 0—46214

117Sn, spectroscopic factors from 116Sn(α,3He) reaction 0—39125

117Sn(p,n)¹¹⁵Sn and low-lying one-quasiparticle states 0—70612

117Sn, e inelastic scatt., 60 MeV, quadrupole and octupole excitations 0—42761

117Sn deduced levels from 118Sn(p,p'), E=6988 keV 0—39015

117Sn, isomer shift in Sb-Sb solid soln., conc. depend. 0—51285

117Sn, Mossbauer effect and isomeric shift in α-phase Ag-Cd(Zn) and Hg 0—51278

117Sn, Mossbauer effect in perovskite-type ferroelectrics 0—72328

117Sn, resonant p scatt., in perfect Sn crystal 0—48042

117Sn, resonant p scatt., in perfect Sn crystal 0—48042

117Sn in Pd-MnSn Heusler alloy, Mossbauer effect rel. to internal field, obs. 0—40939

117Sn isomer shift in Mn Sn alloy, Mossbauer effect, mag. susceptibility 0—56514

0-56514

119Sn^m Mossbauer level natural linewidth 0-72338

119Sn Mossbauer effect in α -Fe₂O₃ 0-76049

119Sn Mossbauer effect in B Ni alloys 0-59380

119Sn Mossbauer effect in Ca₃In₃Sn₃Ge_{3-x}O₁₂ garnet system 0-41141

119Sn Mossbauer effect in Cralloys 0-72330

119Sn Mossbauer isomer shift in Sn 0-59382

119Sn Mossbauer isomer shift in Sn, pseudopot, approach 0-59381

119Sn Mossbauer isomer shift in Sn, pseudopot, approach 0-59381

119Sn Mossbauer isomer shift in Sn, pseudopot, approach 0–59381
119Sn Mossbauer isomer shift in Sn, pseudopot, approach 0–59381
119Sn Mossbauer isomer shift interpret. 0–54081
119Sn(p.n.), Struct, in p-ray strength function 0–70570
119Sn(p.t.)¹¹⁷Sn and low-lying one-quasiparticle states 0–70612
129Sn, i.p-1h states 0–70486
129Sn, i.p-1h states 0–70486
129Sn, Hartree-Fock calcs, of binding, density and single-particle spectra with effective force 0–49470
129Sn, inelastic scattering of polarised protons at 30.3 MeV and deduced nuclear deformations 0–52781
129Sn proton scattering, inelastic, cross-section, theory and experiment 0–70591

1-0-70591

1-20Sn Thomas-Fermi theory calc. of energy per particle, density distribution and single particle potential 0-49451

1-20Sn(2-Ne, 2-Ne'p), static quadrupole moments of the first excited states of 1-20Sn(2-Ne, 2-Ne'p), static quadrupole moments of the first excited states of 1-20Sn(2-Ne, 2-Ne'p), static quadrupole moments of the first excited states of 1-20Sn(2-Ne, 2-Ne'p), static quadrupole moments of the first excited states of 1-20Sn(2-Ne, 2-Ne'p), static quadrupole moments of the first excited states of 1-20Sn(p, 1-2 124Sn, energy level population investigation 0–39124
124Sn quadrupole moment, static, from Coulomb reorientation effect obs.
0-42757

0-4275 124Sn radiative capture cross sections for 10-350 keV neutrons 0-46227 124Sn (40Ar,4n) 160Er and g-factor of 160Er 0-70673 123Sn yield from U thermal n-fission and half life 0-74025 119mSn, Mossbauer effect in AgCl(1) 0-48025 119mSn, Mossbauer and n-m.r. in dicyclopentadienyltin(II) 0-39401 Sn(p,n) A=117,119,120, 122,124, 3-5.5 MeV, cross sections 0-70611 985r/997, j. emission spectrum, modification 0-38632 99Sr, level transitions from decay of 90Rb 0-70543 99Sr, level transitions from decay of 90Rb 0-70543 99Sr, level transitions from decay of 90Rb 0-70543 99Sr, level transitions from decay of 1817a energy distribution of neutrons from proton-neutron nonelastic collisions for 18 MeV protons 0-64115 97Tc*, 97Tc*, symc**, isomeric transitions, multipolarity checked, and E2 admixture determ. 0-52691 91Tc energy distribution of neutrons from proton-neutron nonelastic collisions for 18 MeV protons 0-64115 97Tc*, symc**, isomeric transitions, multipolarity checked, and E2 admixture determ. 0-52691 91Tc capture decay p-spectra and 96Mo levels, obs. 0-38973 91Tc, angular correlation and spin for p-y cascade 0-49530 91Tc, angular correlation and spin for p-y cascade 0-49530 91Tc, angular correlation and spin for p-y cascade 0-49530 91Tc, angular correlation and spin for p-y cascade 0-49530 91Tc, angular correlation and spin for p-y cascade 0-49530 91Tc, angular correlation and spin for p-y cascade 0-49530 91Tc, angular correlation and spin for p-y cascade 0-49530 91Tc, angular correlation and spin for p-y cascade 0-49530 91Tc, angular correlation and spin for p-y cascade 0-49530 91Tc, angular correlation and spin for p-y cascade 0-49530 91Tc, angular correlation and spin for p-y cascade 0-49530 91Tc, angular correlation and spin for p-y cascade 0-49530 91Tc, angular correlation and spin for p-y cascade 0-49530 91Tc, angular correlation and spin for p-y cascade 0-49530 91Tc, angular correlation and spin for p-y cascade 0-49530 91Tc, angular correlation and spin for p-y cascade 0-49530 91Tc, angular correlation an

Nuclei with 90 < A < 149 continued

⁸Tc decay (8 sec) to ¹⁰⁸Ru 0-64030

 96m Tc decay γ-spectra and 96 Mo levels, obs. 0–38973 101m Tc, prod. by photonuclear reactions 0–67472

Te (A=119, 121, 123), level schemes from decays of I(A=119, 121, 123)

Te (A=119, 121, 123), level schemes from decays of I(A=119, 121, 123) 0–49533 Ce (where A=124, 126, 128, 130), variation of charge radii, from data on isotopical shifts of X-ray K α_1 lines 0–52696 Te (where A=126, 128, 130), elastic and inelastic scatt. of deuterons from vibr. states, diff. cross sections 0–42863 Te isotopes, 117 \leq A \leq 130, compared with models 0–67476 "4Te, levels deduced from Sn(α_1 2n β_2) reaction 0–38912 "18Te, levels deduced from Sn(α_2 2n β_2) reaction 0–38912 "18Te levels deduced from Sn(α_2 2n β_2) reaction 0–38912 "12Te, Coulomb excitation, deduction of levels from ¹²³Te(¹⁴N, ¹⁴N' β_2) for E=44, 48 MeV 0–42763

E=44, 48 MeV 0-42763

12³Te magnetic moment and g-factor of ³/₂+ state 0-70487

12³Te(¹⁴N, ¹⁴N'p), Coulomb excitation, deduced levels of ¹²³Te for E=44, 48

MeV 0-42763

12⁴Te angular distribution of elastically and inelastically scattered 12 MeV protons 0-49608

12⁴Te charge radii variations from isotopic shifts of X-ray K. Jinco

124Te angular distribution of elastically and inelastically scattered 12 MeV protons 0-49608
124Te charge radii variations from isotopic shifts of X-ray K_{α1} lines 0-64033
124Te level scheme and spin assignments 0-42791
124Te levels scheme 0-38916
124Te spins from γ-decay of 124Sb 0-73819
124Te(d,d), deduced 124Te levels, excitation energies and cross-sections 0-60828
124Te(d,d), deduced 124Te levels, excitation energies and cross-sections 0-60828
125Te, Coulomb excitation, deduction of levels from 125Te(14N, 14N/γ) for E-44,48 MeV 0-42763
125Te, energy level lifetimes 0-67478
125Te, g factors of 322 and 462 keV levels, obs. 0-38917
125Te, g factors of 322 and 462 keV levels, obs. 0-38917
125Te, Konversion of the M1 and E2 transitions, conversion probability 0-57922
125Te, lifetimes of eight excited states by the delayed coincidence technique 0-57921
125Te, Mossbauer effect in Gd, hyperfine interaction 0-72334
125Te, Mossbauer effect in Te(IV) isoelectronic complexes, isomeric shifts 0-44798

-44798

0-44798 123Te, spin assignment to 525 keV level, from 125Sb decay 0-49576 123Te (*N, **N* γ), Coulomb excitation, deduced levels of 127Te for E=44, 48 MeV 0-42763 125Te, 128Te, 139Te, existence of 2-particle 7- and 5- levels 0-46144 126Te charge radii variations from isotopic shifts of X-ray $K_{\alpha 1}$ lines 0-64033 126Te energy levels deduced from electron capture and β + decay of 126Te everyted states studied in decay of 126Shm, 0-64090

12eTe excited states studied in decay of 12eSp. 0–64090 12eTe(22Ne,5n), 14-Sm isomeric state, three quasiparticle 0–38925 12eTe charge radii variations from isotopic shifts of X-ray K_{a+} lines 0–64033

0-64033 129Te radiative capture cross sections for 10-350 keV neutrons 0-46227 128Te(22Ne, 7n), 143Sm isomeric state, three quasiparticle 0-38925 139Te, neutron particle hole states 0-67479 139Te charge radii variations from isotopic shifts of X-ray K_{a1} lines 0-64033 139Te quadrupole moment of first excited 21 state from Coulomb excitation 0-70481 139Te(3Ne, 29Ne'y), static quadrupole moments of the first excited states of 129Ne using reorientation effect 0-60757 139Te(29Ne, 7n), 143Sm isomeric state, three quasiparticle 0-38925 139Te(29Ne, 22Ne'y), static quadrupole moments of the first excited states of 12Ne using reorientation effect 0-60757 139Te(4xe) 139Sb, configuration mixing in 139Te and 2p-1h states in 129Sb 0-70661 ²²Ne using reorientation effect 130 Tet using reorientation effect 129 Cb (130 Tet 130 Tet 130 Tet 129 Sb, configuration mixing in 130 Te and 2p-1h states in 129 Sb (130 Te) 130 Xe nuclear matrix element for double β decay (130 Te) 130 Xe nuclear matrix element for double β decay (130 Te) 130 Te, half-life and fission yield and half-life, obs. (130 Te) half-life and fission yield 0–42894 Xe isotopes (120 125-129) levels from 124 126. 128 Te (120 3 ny) reactions (124 4764 nucleus half-life) distributions 124 4764 nucleus half-life) 126 4764 nucleus half-life) 126 476577

0–42764

126 Xe energy levels deduced from β- decay of 126 I 0–49577

127 Xe positive parity states and intermediate coupling approach of unified model 0–64034

129 Xe, chemical shift in Xe-other gas mixtures, density depend. 0–71068

129 Xe.^{*}, 196-40 keV transition, γ-γ ang. correl. obs., spin of 236 keV level determined to be 11/2 0–64036

129 Xe positive parity states and intermediate coupling approach of unified model 0–64034

139 Xe excited states from β-decay of 130 I and 130 Cs 0–52697

129 x positive parity states and intermediate coupling approach of unified model 0-64034 model 0-80 mod

0-38902

Zr, natural and stable isotopes, reson. n cross sections 0-42843 Zr, neutron activation cross-sections, (n,p), (n,r) and (n,2n) at 14.8 MeV 0-42854

27, photon scattering cross section, 8.5-12.5 MeV, new method of analysis 0-73896 "2r(p,po) 90Zr and 91Zr analogue of ground state 0-73817 90Zr, 3He elastic scatt., 30 MeV optical model params. 0-42862

Nuclei with 90<A<149 continued

clei with 90 ≤ A ≤ 149 continued

90 Zr, E1 transitions from analogue states 0–67468

90 Zr, four particle levels of 4p type 0–55131

90 Zr, particle-y coincidence meas. for decay of 3.31 MeV state, by high resolution syst. 0–49343

90 Zr, search for double y emission from first excited states 0–70447

90 Zr, spreading of analogue resonances in inelastic proton channels 0–38900

**2r, spreading of analogue resonances in inelastic proton channels 0-38900 polymer. Proton channels 0-38900 polymers and excitation energies of Nb multiplet 0-70479 polymers are consider resonances 0-64119 polymers of the polymers of

0-70651

O*Zr(y, n)*2T and **IZr(y, n)**0Zr, cross-sections meas. 0-49595

O*Zr(p, n)0Zr(0,†*) inelastic, R-matrix analysis through isobaric analog resonance 0-67537

O*Zr(p, p)0Zr(0,†*) inelastic, R-matrix analysis through isobaric analog resonance 0-67537

O*Zr(p, p)0Zr(0,†*) inelastic, R-matrix analysis through isobaric analog resonance 0-67537

3ººZr(p, p,))²ºZr(0,²¹) inelastic, R-matrix analysis through isobaric analog resonance 0-67537
 3ºZr(p,p,)²ºZr, 4.61-4.83 MeV, used to study analog resonance of ²¹Zr 0-38901
 3ºZr(p,p,²), effect of core polarization 0-70587
 3ºZr(p,p,²), microscopic first-order core polarisation corrections to DWBA 0-42837

"Zr(p,p'), microscopic first-order core polarisation corrections to DWBA 0-42837
"Zr(π,π)*0*Zr, Glauber approx., suppression of scattering amplitude found 0-55163
"Zr, weak-coupling states using analog resonance techniques, obs. 0-57917
"Zr analog resonance studied in *0*Zr(p,p₀)*0*Zr 0-38901
"Zr analogue of ground state from *0*Zr proton scattering 0-73817
"Zr(p,d) using polarized protons, and DWBA 0-73947
"Zr, mean lifetimes of the second 0* states 0-52690
*2*Zr, levels populated by β-decay of *2*Y 0-49572
"Zr('He,d), inhibited transitions to 3s_{1/2} isobaric analog states 0-73997
"Zr(p, p)*3*Zr, 4.2-11.2 MeV, charge exchange effects 0-73998
*2*Zr(p, p)*2*Zr, polarization meas. near isobaric analogue resonances / 0-65738
*2*Zr(p,p)*2*Zr*, *2*Zr(p,p)*2*Zr, E_p=6.0-10.0 MeV, isobaric analogue resonances, excitation functions 0-39049
*3*Zr, weak-coupling states using analog resonance techniques, obs. 0-57917
*3*Zr, weak-coupling wave functions for neutrons coupled to excited states of

0-57917

"Zr, weak-coupling wave functions for neutrons coupled to excited states of \$^9Zr, 0-39049

"Zr, activation resonance integral 0-73961

"Zr, activation resonance of the second 0+ states 0-52690

"Zr("3He,d), inhibited transitions to 3s_{1/2} isobaric analog states 0-73997

"Zr("2He,d) inhibited transitions to 3s_{1/2} isobaric analog states 0-73997

"Zr, weak-coupling states using analog resonance techniques, obs. 0-57917 97 Zr, weak-coupling states using analog resonance techniques, 603. 0–57917 96 Zr, activation resonance integral, and anomalous integral to thermal activation cross-section ratio 0–73961 97 Zr, decay scheme, p spectra, pp and pe coincidences 0–70544 97 Zr, 97 Nb, β decay, p ray spectra 0–55142 97 Zr, 97 Nb, decay scheme, β and p spectra 0–38975 97 Zr(p) 97 Z

Zr(t,p) (A=90,92,94,96), energy level population investigation 0–39124

Nuclei with 150≤A

160≤A≤190, K-isomerism systematics 0–38864

230≤A, K-isomerism systematics 0–38864

2³0°pb(n,p), partial direct and collective cross-sections 0–49619

2°pb(n,p), partial direct and collective cross-sections 0–49619

4=161,168,169,170,171) prep. of new isotopes, p spectra anal. of daugh ter isobars. half-lives meas. 0–38989

A=150-190, neutron deficient, deformed, evaluation of half lives of unknown isotopes 0–38989

A=200, Z=N, density distrib., local density approx. 0–38863

critical parameters of a uranium solution slab-cylinder system 0–55204

fission chain populations, tables, odd masses, 145≤A=155 0–39172

as moderator for ²⁴⁰Pu, rel. to resonance capture at 300°K and 1500°K

0–46150

new element of atomic number 105, ²⁶⁰Ha 0–52710

new element of atomic number 105, 260 Ha 0-52710 octupole states of even-even nuclei, $150 \leqslant A \leqslant 176$ in superfluid model 0-63969

0-63969
octupole states of even-even nucleis, 150 €A €176 in superfluid model
0-63969
octupole states of even-even nucleis, 150 €A €176 0-55136
rare earth isotopes, (n,2n), (nα) and (n,p) reactions, statistical model and 14
MeV obs. 0-39077
rare earth new mass difference determinations of separation and pairing
energies 0-67484
review of search for element 114 0-73844
superheavy elements, their fission and alpha-decay review 0-64079
superheavy elements, in closed shell region, props. and prod. 0-38865
transuranium elements, synthesis and search 0-67562
transuranium elements recent research 0-64007

1887Er, level structure and the de-excitation mechanism, study by radiative
capture at thermal energies 0-57925

181Ta(n,n), optical-model calculations using a spherical and a non-spherical
potential for angular distributions, E_m=2.5-8.1 MeV 0-60818

238U, proton-induced fission, prompt neutron energy measurement and fragment kinetic energy release for E₀=9.5-22 MeV 0-58033

238U fission by 11.5 GeV protons, charge distribution and recoil properties
of products 0-74019

172 Lu pairing phenomenon of ½ proton ½ neutron 0-52704

189 Pt, 2¹¹-2¹¹ transition, existence of electric monopole component
0-38940

1972 Pt. $2^{+}\rightarrow 2^{+}$ transition, existence of electric monopole components of -38940 and -38940 deuteron bomardment in energy range 11-20 MeV, excitation functions for production of fission isomers 0-49682 158-8Tb, β -decay, using $4TB^{+}\gamma$ -spectrometer 0-60783 195-8Tl, α ray spectrum, half lives of products from $^{175}\text{Lu}+^{20}\text{Ne}$ 0-49558 ^{175}Cm polarisation effects in $\delta(r^2)$ measurements 0-38929

Nuclei with 150≤A continued

 96 Pb, M1 decay of 1.7 MeV 1* state 0-70520 22 Th, E=1.5-8.5 MeV, total neutron cross section measured 0-67539

 $_{2}^{12}$ Th, E=1.5-8.5 MeV, total neutron cross section measured 0-67539 $_{2}^{12}$ Tm, n reaction, reson. parameters and spin, E=4-830 eV 0-39073 $_{2}^{124}$ Ac α -decay, $_{2}^{120}$ Fr levels obs. 0-60791 $_{2}^{125}$ Ac, electron conversion and $_{2}$ -ray spectra, decay products 0-52739 $_{2}^{127}$ Ac, $_{2}$ -ray spectra, high resolution 0-64075 $_{2}^{127}$ Ac, $_{2}$ -ray spectra, high resolution 0-64075 $_{2}^{127}$ Ac level scheme proposed and interpreted in terms of rotation bands 0-73882 $_{2}^{128}$ Ac $_{2}$ -radiation, low energy 0-60793 $_{2}^{128}$ Ac $_{2}$ -radiation, low energy 0-60793 $_{2}^{128}$ Ac $_{2}$ -radiation, low energy 0-60791 lines, transitions multipolarity 0-42801

228 Ac - 228 Th, p spectra, conversion lines, transitions 10-42801 239 Am², spontaneously fissioning isomers, fragment mass distribution and kinetic energies 0-39164 241 Am, fission by neutrons, 0.3-7.2 MeV, angular anisotropy 0-60835 241 Am, prompt neutron fission yield for thermal neutrons 0-42885 241 Am, urinary excretion during DTPA therapy 0-76726 241 Am alpha particles source, angular distrib, and energies 0-42802 241 Am alpha particles source, angular distrib, and energies 0-42802 242 Am, prompt neutron fission yield for thermal neutrons 0-42885 242 Am, spontaneous fissioning, production by neutron capture 0-58032 243 Am, deduced levels from 242 PCHe, d) and 242 Pu(π, t) for E=30 MeV 0-58032 243 Am energy levels from (3He,d) and (4He,t) 0-70667 232 243 Am energy levels from (3He,d) and (4He,t) 0-7067

²⁴³ Am, deduced levels from ²⁴²P('He, d) and ²⁴³Pu(α , t) for E=30 MeV 0–58023 ²⁴³ Am energy levels from (¹He,d) and ('He,t) 0–70667 ²⁴⁴ Am, spontaneous fissioning, production by neutron capture 0–58032 At (where Λ =209, 210, and 211), fine structure 0 α spectra 0–52738 ²⁶⁵ At. ²⁶⁵Po, decay scheme, deduced log ft 0–55145 ²¹¹ At, 8 excited states of (h_{9/2}) configuration identified 0–67496 ²¹² At excited levels, ²³⁹Fr α -decay obs. 0–60771 ²¹³At excited states lifetimes 0–73841 Au, 3 and 29 GeV proton bombardment, yields of stable and radioactive rare-gas isotopes 0–52769 Au, n capture cross section, 24 keV, from sphere transmission obs. 0–49637 Au isotopes, α -decay, half life meas., spectra 0–49579

0–49637 Au isotopes, α-decay, half life meas., spectra 0–49579 192 Au decay, γ-ray spectra, level transitions 0–70512 194 Au, β+ spectra meas by $4\pi\beta^+$ γ-spectrometer 0–73878 194 Au –194Pt, Εγ, 1γ and γ γ coincidence meas. 0–60788 195 Au energy level, study using 196 Pt(p,2n) and 197 Au(p,t) reactions 0–70517

0-70517

"9-Au level structure, branching ratios, spins and parities, core excitation model 0-46177

"9-Au magnetic moments, hyperfine structure, and similarity with 198 Au 0-57930

0-57930

19°Au neutron single hole states from (p,d) 0-70499

19°Au, 268 keV excited state nature, obs. 0-38941

19°3Au, 16°0m β decay of 19°7Pt in Fe matrix, Mossbauer effect, intensities of hyperfine lines, 0.06 to 20 K 0-49580

19°Au, Mossbauer effect in Pd Au alloys, band filling obs. 0-62260

19°3Au, n reaction, reson. parameters and spin, E=1000-2100 eV 0-39079

19°3Au, single particle analog state anomalies 0-67489

19°3Au 268 keV level from γ-γ coincidence meas. and Coulomb excitation 0-64065

19°3Au excited states studied, isomeric decay obs. multipolarity assignments 0-73832

(0-73832)

197 Au isomeric shift in Cu-Au and Ag-Au alloys obs. 0-54074

197 Au Mossbauer effect in Au₄V(Mn, Cr) ordered and disordered alloys

0-41139

197 Au Mossbauer effect in Cr alloys 0-72330

197 Au photofission fragments, nucleon comp. and excitation energy

0-70686

197 Au Mossbauer eftect in Crainoys 0-72336
197 Au photofission fragments, nucleon comp. and excitation energy 0-70686
197 Au reaction rates in Pu-recycle fuel lattices 0-74059
197 Au transmission of 24 keV neutrons by gold spheres, analysis using spin dependent S-wave statistics 0-46221
197 Au(a, α), energy spectra determination and α part, angular distributions for En=15.1 MeV 0-5795
197 Au(a, α), energy spectra determination and α part, angular distributions for En=15.1 MeV 0-49595
198 Au, disintegration rate, absolute determination by β-γ- and 4πβ-γ- coincidence methods 0-49553
198 Au, half-life, by γ-ray spectrometry 0-46178
198 Au, half-life 0-38996
198 Au, unclear orientation study of first forbidden β decays to 198 Hg 0-70555
198 Au decay rel, to fluorescence and Coster-Kronig yields of L subshells in Hg 0-70767
198 Au(n,γ), neutron reson. capture, γ-ray spectra, using mag. Compton γ-spectrometer 0-73955
199 Au (acay period meas. 0-38966
199 Au, spin and parity of levels, from γ decay of 109 Pd 0-55144
Bi, elastic scatt, of electrons, E=40-60MeV, cross section meas. 0-39023
Bi (A=201, 203, 205, 207), levels deduced from electron capture decays of Po 0-38942
Bi analogue resonant states in deuteron stripping 0-70668
Bi isotopes, study of radioactive props. using e.m. mass separator with

Bi (A=201, 203, 205, 207), levels deduced from electron capture decays of Po 0-38942
Bi analogue resonant states in deuteron stripping 0-70668
Bi isotopes, study of radioactive props. using e.m. mass separator with heavy ion beam 0-73880
Bi-Pb (A=202, 200, 198) 0-49547

20³Bi, intermediate coupling calculations for the unified model 0-57932

20³Bi, intermediate coupling calculations for the unified model 0-57932

20³Bi, core excited states 0-64068

30³Bi, intermediate coupling calculations for the unified model 0-57932

20³Bi (n.e)²0³8Pb, search for E₀ transitions 0-60770

20³Bi (pecay of low lying states from 20³Pb(p,ny) and 20³Pb(d,2ny) reactions 0-64071

20³Bi, collective septuplet at 2.6 MeV, Coulomb excitation 0-64072

20°Bi, colloumb excitation and the weak-coupling model 0-49551

20°Bi, E1 transitions for direct coupling between octupole and dipole states 0-52708

20°Bi, heavy- ion reactions, production of Th isotopes of mass 221-224

0-49581

0-49581

0-30°Bi, isobaric analogue resonances, elastic proton partial widths, microscopic calc. 0-70529

20°Bi, isobaric analogue resonance for inelastic proton decay 0-67493

20°Bi, isobaric analogue resonance for inelastic proton decay 0-67493

20°Bi, neutron depolarization in elastic scatt., 1.36 MeV 0-42845

20°Bi, neutron depolarization in elastic scatt., 1.36 MeV 0-42845

Nuclei with 150 < A continued

 $^{209}\rm{Bi},$ proton scattering through $d_{2/2}$ isobaric analogue resonance, cross sections, partial widths $\,$ 0–77507

 $^{\text{209}}\text{Bi, surface nuclear potential determ. using elastic }\alpha$ scatt., 14-23 MeV $0\!-\!67544$

0-67544
²⁰⁹Bi and ²⁰⁹Po, Coulomb energy difference found 0-73840
²⁰⁹Bi deduced levels from ²⁰⁹Bi(γ,γ'), E-7637 keV 0-39015
²⁰⁹Bi isobaric analogue of ²⁰⁸Pb ground state in (p,n) reaction 0-73948
²⁰⁹Bi isobaric analogue resonances from proton elastic scattering 0-70519
²⁰⁹Bi levels, single particle components of particle vibrational states
0-42776

"0"Bin.q.r.in Bi₂S₃ cryst. 0-72516 "0"Bi photofission fragments, nucleon comp. and excitation energy 0-70686

0–70686 "9081 is cattering, and isobaric analogue states in \$^{210}\$Po 0–70531 \$^{200}\$Bi scattering, and isobaric analogue states in \$^{210}\$Po 10–70531 \$^{200}\$Bi scattuplet, shell model 0–70528 \$^{200}\$Bi scattuplet decay scheme 0–70527 \$^{200}\$Bi(d, ^2he)^{300}\$Pb, proton particle-hole states at E_d =50 MeV 0–52707 200Bi(e,e)^{300}$Bi, M9 magnetic moment determ. 0–64010 <math>^{300}$Bi(p,p)^{300}$Bi, Ep=39.5 MeV, effect of core polarization, 1.609 MeV <math>^{13+}/_2$ state 0–42826 from the state 0–73049

**Sitp.; p. 7 State 0—4826

**PSi(p.2p), events from 1h_{9/2} state 0—73949

**PSi(p.1) at 155 MeV, n energy distribution meas. 0—58034

**PSi(p.1) mass distribution and kinetic energy distrib. obs. 0—39159

**PSi(p.1) mass distribution and kinetic energy distrib. obs. 0—39159

**PSi(p.2p) mass distribution and kinetic energy distrib. obs. 0—39159

**PSi(p.2p) mass distribution and kinetic energy distrib. obs. 0—39159

**PSi(p.2p) mass distribution and kinetic energy distrib. obs. 0—39159

**PSi(p.2p) mass distribution and kinetic energy distrib. obs. 0—39159

**PSi(p.2p) mass distribution and kinetic energy distribution and 200 PO

**PSI(p.2p) mass distribution and kinetic energy distribution and 200 PO

**PSI(p.2p) mass distribution and kinetic energy distribution and 200 PO

**PSI(p.2p) mass distribution and kinetic energy distribution and 200 PO

**PSI(p.2p) mass distribution and kinetic energy distribution and 200 PO

**PSI(p.2p) mass distribution and kinetic energy distribution and 200 PO

**PSI(p.2p) mass distribution and kinetic energy distribution and 200 PO

**PSI(p.2p) mass distribution and kinetic energy distribution and 200 PO

**PSI(p.2p) mass distribution and kinetic energy distribution and 200 PO

**PSI(p.2p) mass distribution and kinetic energy distribution and 200 PO

**PSI(p.2p) mass distribut

209Bi(p,n)³⁰⁹Po, Coulomb energy difference between ²⁰⁹Bi and ²⁰⁹Po 0-73840

209Bi(p,p), investigation to obs. excitation of (5-⊗h_{9/2}) decuplet 0-77508

210Bi, beta decay, K-shell auto-ionization 0-42784

210Bi, core renormalization effects in 1° ground state 0-67495

210Bi, shell model with Hamada-Johnston potential 0-70530

211Bi, intermediate coupling calculations for the unified model 0-57932

211Bi, intermediate coupling calculations for the unified model 0-57932

211Bi, deduced levels from decay of ²¹⁴Pb 0-38998

229Bk, neutron-induced fission, angular distribution of fragments and nuclear cross-section for E=0.6-1.8 and 4.6 MeV 0-60834

239Bk mag, moment, Goudsmit-Fermi-Segre calc. 0-60773

40°Ca, nuclear polarisation of muonic atoms of spherical nuclei 0-43034

Cd isotopes, static quadrupole moments of 1st 2+ states 0-55118

12°Cd de-excitation of 931.1 keV 2-7 state 0-60782

14°Cc→14°3 pr, perturbed ang, correl, and paramag, correction 0-42794

24°Cf bombardment with 1°N ions and creation of new element of atomic number 105, ²⁰⁰Ha 0-52710

24°Cf-y-34°Cm, α-γ ang, correlation, hyperfine interaction 0-55146

23°Cf, neutron and γ-quanta from triple fission, fragment excitation energy 0-46270

23°Cf, neutron source, dose, dose equivalent, and linear energy transfer distributions 0-76736

23°Cf, prompt, neutron yields of fission fragments 0-39162

23°Cf, prompt, neutron siession, emission of particles 3<

Z≤8 0-49677

distributions 0-76736

252°Cf, prompt. neutron yields of fission fragments 0-39162

253°Cf, spontaneous fission, emission of particles 3≤Z≤8 0-49677

252°Cf, spontaneous fission, independent yields of 80°Bf, 86°Rb, 136°Cs and 150°Pm 0-39151

253°Cf, spontaneous ternary fission, prompt n ang. distribs. 0-49686

255°Cf, spontaneous ternary fission, measured prompt gamma yield 0-39154

253°Cf fragment pairs, correlated emission of K X-rays 0-42892

252°Cf K X-rays, distribution as a function of mass and atomic number in the spontaneous fission of 252°Cf 0-52810

252°Cf primary fission products, experimental information on deformation 0-55176

253°Cf randomly pulsed neutron source for

0-55176

0-55176

252Cf randomly pulsed neutron source for prompt neutron decay meas.
0-74078

243Cm, prompt neutron fission yield for thermal neutrons 0-42885

24°Cm, prompt neutron fission yield for thermal neutrons 0-42885
 244°Cm, spontaneous, prompt neutron fission yield 0-42885
 244°Cm, spontaneous fission of 94% sample, partial half life 0-46260
 24°Cm, prompt neutron fission yield for thermal neutrons 0-42885
 246°Cm, number of prompt neutrons emitted in spontaneous fission 0-70685

y isotopes, differences in charge radii, from normalized isotopic shift data 0-73831

Day odd-mass isotopes, level study by (d, p) and (d, t) reactions 0-64050 Dy odd-mass isotopes, level study by (d, p) and (d, t) reactions 0-64050 0-77522

Dy odd-mass isotopes, lever study by (wp. pr. and to. y. 155H) excited level transitions and level scheme, 155Ho decay obs. 0–77522
155Dy excited level transitions and level scheme, 155Ho decay obs. 0–77522
156Dy, conversion e particle params., E. transitions, obs. 0–38930
166Dy, prom 169Ho decay and conversion electron spectra 0–46170
166Dy, polarisation effects in δ(τ) measurements 0–38929
166Dy deduced levels, mixing of gamma vibrational and ground state bands, from decay of 166Tb 0–49542
161Dy Mossbauer effect in Dq, interference between internal conversion and photoeffect 0–44785
161Dy Mossbauer effect in Gd; O₃ 0–79260
161Dy, Coulomb excitation of vibrational and rotational states 0–38932
163Dy(16O, 16O,>y)165Dy 36-52 MeV, Coulomb excitation of vibrational and rotational states 0–38932
164Dy(46A,xn)Po, cross sections for the production of Po nuclides with mass numbers 194 to 200 for ion energies 160 to 280 MeV 0–42876
156Er g-factor from Sn(40A,r4n) reaction 0–70673
165Er g-factor from Sn(40A,r4n) reaction 0–70673
165Er, deduced levels from Dy(α,xn), strongly perturbed positive parity bands 0–42771
165Er, deduced levels from Dy(α,xn), strongly perturbed positive parity bands 0–42771
165Er, deduced levels from Dy(α,xn), strongly perturbed positive parity bands 0–42771
165Er, deduced levels from Dy(α,xn), strongly perturbed positive parity bands 0–42771
165Er, deduced levels from Dy(α,xn), strongly perturbed positive parity bands 0–42771

bands 0-42771

166Er, multiple Coulomb excitation of ground-state rotational band 0-49538

0-49538 $^{166}\mathrm{Er}$, recoilless ν -resonance in $\mathrm{Er}_{1\rightarrow s}\mathrm{Gd}_{s}\mathrm{Al}_{2}$ 0-41087 $^{166}\mathrm{Er}$ Coulomb excitation probabilities for 2^{+} and 4^{+} levels, bombarded with $^{15}\mathrm{Cr}$ in so 0-70504 $^{167}\mathrm{Er}$, S-wave neutron resonances from low-energy capture ν -ray spectrum 0-49493 $^{167}\mathrm{Er}$ Coulomb excitation of rotational and vibrational bands 0-38932 $^{167}\mathrm{Er}$ coiled states studied, isomeric decay obs. multipolarity assignments 0-73832 $^{167}\mathrm{Er}$ ($^{16}\mathrm{O}$, $^{16}\mathrm{O}$,

Nuclei with 150 SA continued

¹⁸Er(d,p)¹⁶⁹Er, levels in ¹⁶⁹Er studied using 12 MeV deuterons 0-70507

clei with 150-2A continued

if SEr(d,p) if SEr, levels in if SEr studied using 12 MeV deuterons 0-70507

if SEr decay, Mossbauer effect 0-73872

if SEr level scheme proposed through if SEr(d,p) and if Cr(d,t) reactions and via thermal-neutron captive in if SEr 0-70507

if Cr(d,t) if SEr, levels in if SEr o-70507

if Er low energy y-spectra 0-64055

if Ex low if SEr studied using 12 MeV deuterons 0-70507

if Er low energy y-spectra 0-64055

if Eu (A=151, 153), deduced levels by clastic scatt. of 12 MeV α 0-49536

if Eu (A=151, 153), deduced levels by clastic scatt. of 12 MeV α 0-49536

if Eu (A=1529 keV internal conversion subshell transition 0-67482

if Eu, e.m. transition probabilities, half-lives of excited states 0-52701

if Eu, e.m.r. in EuFe garnet, hyperfine-field and quadrupole-splitting parameters 0-45019

if Eu, simulating if of SP 383 keV level, meas. in if Eu(n,p) 0-49539

if Eu conversion e spectrum after n capture 0 64042

if Eu, n.m.r. in EuFe garnet, hyperfine-field and quadrupole-splitting parameters 0-45019

if Eu, n.m.r. in EuFe garnet, neas. in if Eu(n,p) 0-49539

if Eu, n.m.r. in EuFe garnet, hyperfine-field and quadrupole-splitting parameters 0-45019

if Eu, n.m.r. in EuFe garnet, hyperfine-field and quadrupole-splitting parameters 0-45019

153 Eu, n.m.r. in EuFe garnet, hyperfine-field and quadrupole-splitting parameters 0-45019

parameters 0—45019

¹⁵³ Eu(n,2n), isomeric ratio analysis, E_n=14.2 0—39075

¹⁵³ Eu(n,2n)¹⁵² Eu, 14 MeV and statistical model 0—39077

¹⁵³ Eu(p,2n)¹⁵² Gd, ¹⁵² Gd low-lying states obs. 0—70501

¹⁵⁴ Eu-1⁵⁴ Gd, y-y perturbed angular correlations 0—73869

¹⁵⁴ Eu-1⁵⁴ Gd revised decay scheme 0 49540

¹⁵⁵ Eu energy levels, from ¹⁵⁵ Sm y-spectrum obs. 0—38904

¹⁵⁵ Eu half-life and effective neutron capture cross-section determ.

0—64094

193Eu half-life and effective neutron capture cross-section determ.
0 –64094
193Eu decay, and energy levels in 193Gd 0 –64095
152mEu, of 152m and 153 Gd, levels obs. 0 –49537
Fm (where A=246, 248, 250), spontaneous fission life-times 0 –60832
120Fr α-decay, 216At levels obs. 0 –60771
1210Fr α-decay, 216At levels obs. from 224 α α-deay 0 –60791
1211Fr, transitions, props. of low-lying levels, from decay of 225 Ac 0 –52739
146 Gd, β decay, meas. 0 –60781
151 Gd, meas. of lifetimes of sort-lived state at 108.1 keV 0 –70475
151 Gd decay to levels of 151 Eu, γ ray study 0 –46169
152 Gd, conversion e particle params., E₂ transitions, obs. 0 –38930
152 Gd, directional correlation of γ rays meas. by two Ge(Li) counters 0 –70500
152 Gd, low-lying states 0 –70501
152 Gd, populated by decay of 152mEu 0 –49537
152 Gd level scheme 0 –38987
152 Gd, in diff. liq. sources, statistically perturbed γγ-ang. correlations 0 –64048
154 Gd, in diff. liq. sources, statistically perturbed γγ-ang. correlations 0 –67483
154 Gd, K =0 – and 1 – octupole bands 0 –64046

0-67483

154 Gd, K*=0- and 1- octupole bands 0-64046

154 Gd from 154 Eu, re- investigation of excited states 0-49540

154 Gd (r) perturbed angular correlations 0-73869

154 Gd (r) perturbed angular correlations 0-73869

155 Gd, 7; 532 | rotational band 0-42769

155 Gd, 31±2 ms activity produced by 156 Gd(n,2n) at En=14-15 MeV

0-52702

155Gd, 3/1- [532] rotational band * O—42769
 155Gd, 31±2 ms activity produced by ¹⁵⁶Gd(n,2n) at En=14-15 MeV 0—52702
 155Gd, deduced levels from ¹⁵⁴Sm(α,3m) for E_α=34 MeV 0—57924
 155Gd, lifetimes of 86.5 and 105.3 keV levels, from ¹⁵⁵Tb decay 0—64049
 155Gd, Nilsson assignments of levels, from ang. distribs. for ¹⁵⁶Gd(d,t) reaction 0—42872
 155Gd, spins of low-energy neutron resonances 0—42770
 155Gd ospitive parity states mixing 0—38931
 155Gd to Coulomb excitation of vibrational and rotational states 0—38932
 155Gd thermal neutron capture 0—67344
 155Gd(16, 16°V, p) ¹⁵⁵Gd 36-52 MeV. Coulomb excitation of vibrational rotational states 0—38932
 155Gd(16, p) stripping reaction, ¹/2- [532] rotational band 0—42769
 155Gd(10, p) resonance parameters, average capture cross sections up to 20 keV, s-wave strength functions 0—46225
 156Gd, energy levels populated by electron capture from ¹⁵⁶Tb 0—70503
 156Gd, energy levels populated by electron capture from ¹⁵⁶Tb 0—70503
 156Gd, K*=0 and 1 octupole bands 0—64046
 156Gd, spins of low-energy neutron resonances 0—42770
 157Gd, spins of low-energy neutron resonances 0—42770
 157Gd, n.m.r. in ferromag, Gd 0—41372
 157Gd thermal neutron capture 0—67344
 157Gd (n.p.) resonance parameters, average capture cross sections up to 20 keV, s-wave strength functions 0—67344
 157Gd (n.p.) resonance parameters, average capture cross sections up to 20 keV, s-wave strength functions 0—4625
 157Gd (n.p.) resonance parameters, average capture cross sections up to 20 keV, s-wave strength functions 0—4625
 157Gd (n.p.) resonance parameters, average capture cross sections up to 20 keV, s-wave strength functions 0—4625
 157Gd (n.p.) resonance parameters, average capture cross sections up to

157Gd thermal neutron capture 0-67344
 157Gd(n,p) resonance parameters, average capture cross sections up to 20 keV, s-wave strength functions 0-46225
 158Gd, elemental, total, elastic and inelastic scatt. neutron cross-sections 0-49636
 158Gd, isomer shift of 2+ state from recoil implantation Mossbauer studies 0-52703
 158Gd, K=0- and 1- octupole bands 0-64046
 158Gd, n-capture y-ray cross section, 25 keV 0-39076
 158Gd(n,a)¹⁵⁵Sm, 14 MeV and statistical model 0-39077
 158Gd(n,a)¹⁵⁷Gd and neutron single hole states in ¹⁵⁷Gd 0-70499
 159Gd energy levels from ¹⁵⁹Eu decay 0-64095
 159Gd energy levels from ¹⁵⁹Eu decay 0-64095
 159Gd, siomer shift of 2+ state from recoil implantation Mossbauer studies 0-52703

160Gd, isomer shift of 2⁺ state from recoil implantation Mossbauer studies 0–52703
 160Gd, n-capture γ-ray cross section, 25 keV 0–39076
 178Hy, γ-γ(θ) meas. of M1 admixture meas. in 2⁺ -2⁺ transition 0–73837
 260Ha, new element of atomic number 105 0–52710
 Hf (A=166,167 and 169), neutron deficient isotopes preparation, γ decay, half-lives 0–38990
 Hf (A=176, 178 and 180), quadrupole moment ratios of first excited 2⁺ states, Mossbauer meas. 0–73836
 Hf ground state, application of generator-coordinate method to rotational spectra 0–77475
 168Hf, half-life meas. 0–38990
 168Hf half-life meas. γ rays det. 0–57958

 168 Hf half life meas. γ rays det. 0-57958

Nuclei with 150 ≤ A continued

aclei with 150 ≤ A continued

169 Hf, half life meas. γ rays det. 0—57958

170 Hf decay scheme, levels of 170 Lu, 170 m and 172 Tm 0—52704

170 Hf half life meas. γ rays det. 0—57958

171 Hf, radioactive decay, deduced rotational levels of 171 Lu 0—60756

171 Hf half life meas., new γ rays 0—57958

172 Hf, lower limit for α-decay half-life 0—46173

174 Hf nuclear quadrupole moment determ. from isotopic shift in Hf I spectrum 0—46363

177 Hf, collomb excited states, Mossbauer effect expts. on Hf and Hf compounds 0—44791

174 Hf, in Fe, mag. hyperfine interaction, obs. 0—44736

177 Hf, metastable decay, internal conversion electron spectra, by β-spectroscope of H√2 type 0—60785

178 Hf, Coulomb excited states, Mossbauer effect expts. on Hf and Hf compounds 0—44791

178 Hf, high spin isomer 179 m² Hf 0—64058

179 Hf high spin isomer 179 m² Hf 0—64058

179 Hf excited states studied, isomeric decay obs. multipolarity assignments 0—73832

179 Hf, Coulomb excited states, Mossbauer effect expts. on Hf and Hf compounds 0—44791

180 Hf, celemental, total, elastic and inelastic scatt. neutron cross-sections 0—49636

180 Hf, nuclear structure effect in internal conversion of 57.54 keV E1 transition 0—60767

181 Hf - 1817 a, search for population of levels above 618.9 KeV 0—46175

¹⁸⁰Hf, nuclear structure effect in internal conversion of 57.54 keV E1 transition 0-60767
 ¹⁸¹Hf-¹⁸¹⁷Ta, esarch for population of levels above 618.9 KeV 0-46175
 ^{179m(2)}Hf high spin isomer, intraband branchings in the ground-state rotational sequence of ¹⁷⁹Hf 0-57927
 ^{179m(2)}Hg isotopes, \(\alpha\) caybox (a-decay), half-life meas., spectra 0-49579
 ¹⁸Hg isotopes, props. of low-lying states, evidence for vibrations 0-55138
 ¹⁸Hg sotopes, short lived 0-73875
 ¹⁹Hg 2- states, excitation probabilities, magnetic moments 'g' factors, energy level deduced 0-49508
 ¹⁹⁸Hg, n.m.r. in difurylmercury and dithienylmercury isomers, satellite spectra 0-74361
 ¹⁹⁸Hg excited state lifetimes, obs. 0-38896

Heg Isotopes, snort invect. (2—7887)

"Heg lectron capture decay of 9.5 h and 40 h isomer 0—46177

"Hig 2" states, excitation probabilities, magnetic moments 'g' factors, energy level deduced. 0—49508

"High, n.m.r. in difurylmercury and dithienylmercury isomers, satellite spectra 0—74361

"High excited state lifetimes, obs. 0—38896

"O'Hg 2" states, excitation probabilities, magnetic moments 'g' factors, energy level deduced 0—49508

"O'Hg 2" states, excitation probabilities magnetic moments 'g' factors, energy level deduced 0—49508

"O'Hg energy levels, low-lying, from decay of ²⁰⁰TI 0—70518

"O'Hg 2" states, excitation probabilities, magnetic moments 'g' factors, energy level deduced 0—49508

"O'Hg, decay, second-order e.m., obs. 0—42799

"O'Hg, decay, second-order e.m., obs. 0—42799

"O'Hg, decay, second-order e.m., obs. 0—42799

"O'Hg, shell model with Hamada-Johnston potential 0—70521

"O'Hg, shell model with Hamada-Johnston potential 0—70521

"O'Hg, shell model with Hamada-Johnston potential 0—70521

"O'Hg, becay, transition multipolarities by magnetic electron and γ-ray spectroscopy 0—73879

Ho, distorted wave cale, for elastic and inelastic scattering of electrons from partially aligned non-spherical nuclei 0—39022

"I'Ho—1***Dy, 1**Dy excited level transitions and level scheme 0—77522

"O'Ho—1**O'Py, obs. 0—46170

"O'Ho decay, fam dy transitions study, decay scheme revision 0—46171

"O'Ho decay, fam dy transitions study, decay scheme revision 0—46171

"O'Ho decay, fam dy transitions study, decay scheme revision 0—46171

"O'Ho decay, fam dy transitions study, decay scheme revision 0—67486

"O'Ho(n,p))**O'Hy, order decay ministions and level scheme 0—77522

"O'Ho (Ho)-1**O'Py, obs. 0—46170

"O'Ho (Ho

Nuclei with 150≤A continued

171Lu, deduced rotational bands from decay of 171Hf 0-60756

¹⁷¹Lu, prep. of thin source, for β -ray spectroscopy, by ¹⁸⁷Tu(α ,x) 0–64078 ¹⁷²Lu, decay, deduced log ft and levels of ¹⁷²Yb 0–57926

11°Lu, decay, deduced log It and levels of 1°Yb 0-5792b
 11°Lu, calculation of k-forbidden p-ray transition probabilities 0-64053
 11°Lu, existence of parity non conserving term in nuclear Hamiltonian conformed 0-70509
 11°Lu-1'3'Dy, internal conversion electron spectrum 0-64096
 11°Lu, conversion electron spectrum, using double-focussing spectrometer

178 Lu, conversion electron spectrum 0—64096
178 Lu, conversion electron spectrum, using double-focussing spectrometer
0—46174
178 Lu, levels up to excitation energy of 1628 keV from 175 Lu(d,t) at E_d=12
179 Lu, 396.3, 282.6 and 144.8 keV p transitions, matrix elements for irregular magnetic transitions 0—46114
173 Lu, retarded transitions, effective mag. moment operator 0—38934
175 Lu(d,t)174 Lu, Ed=12 MeV, energy levels of 174 Lu 0—49543
175 Lu(n,p)176 Lu mechanism for radiative capture of resonant energy neutrons 0—70623
176 Lu reaction rates in Pu-recycle fuel lattices 0—74059
177 Lu, decay, obs. of low energy p-ray spectrum following thermal neutron capture 0—73873
179 Lu, metastable decay, internal conversion electron spectra, by β-spectroscope of II√2 type 0—60785
177 Lu_{x→1}777 Hf, directional p-p correlation studies 0—77523
177 Lu_{x→1}777 Hf, p intensities, E2/M1 mixing ratios, branching ratios 0—38993

13°PLu-3"HI, directional p-p correlation studies 0-7/523 13°PLu-3"THf, p intensities, E2/M1 mixing ratios, branching ratios 0–38993 25°Lw study of α -decay 0–73884 25°Lw study of α -decay 0–73884 21°Lw study of α -decay 0–73824 21°SPA, L=0 transitions to ground and β -vibrational state from 148Nd(t,p) 0–74001 129Nd, n-capture p-ray cross section, 25 keV 0–39076 129Nd, attaic quadrupole moment of first excited state 0–73823 223°Np, half-life, mass spectrometric determination 0–70557 218Np, electron capture decay, KI*=22- state of 21°U obs. 0–38949 21°Np, 009061 21°Np, non-local barrier and anisotropy of alpha emissions for oriented nuclei, for radioactive decay 0–57962 21°Np, threshold detector, determination of fast neutron flux densities 0–74075 21°Np, energy levels from (3He,d) and (4He,t) 0–70667

²³Np, threshold detector, determination of fast neutron flux densities 0-74075 ²³⁷Np energy levels from (³He,d) and (⁴He,t) 0-70667 ²³⁷Np Mossbauer effect in α -Np, hyperfine interactions and anisotropic lattice vibrs. 0-41167 ²³⁸Np thermal neutron fission and independent yields of ⁸⁰Br, ⁸²Br, ¹²⁸I 0-52813

238Np thermal neutron fission and independent yields of 80Br, 82Br, 128I 0-52813
Os prolate-oblate difference in deformation energy 0-64060
185Os, decay, y spectra meas. using Ge(Li) detector 0-73876
185Os, electron capture and excited states in 187Re 0-64061
185Os,=187Re, energies and intensities of transitions in 185Os and internal conversion measurements 0-64097
185Os→185Re, y-y ang. correl. meas. 0-38994
186Os excited state half-life, obs. 0-38878
187Os, S-wave neutron resonances from low-energy capture y-ray spectrum 0-49493
188Os, determination of the electric quadrupole moment of the first 2st states 0-42773
189Os, charge radius determ. from Mossbauer isomer shifts 0-64063
189Os, exevae neutron resonances from low-energy capture y-ray spectrum 0-49493
199Os, determination of the electric quadrupole moment of the first 2st states 0-42773
190Os, determination of the electric quadrupole moment of the first 2st states 0-42773
192Os y-rays, obs. 0-38904
192Os, determination of the electric quadrupole moment of the first 2st states 0-42773
192Os radiative capture cross sections for 10-350 keV neutrons 0-46227
193Os y-ray spectrum and 192Ir levels, obs. 0-38904
PO (where A=200, 201^m, 201, 202, 204), α spectra, half-lives 0-42798
21Pa(n. p. fission relative delayed neutron group yields with fission neutrons)
21Pa(n. p. fission relative delayed neutron group yields with fission neutrons)

0-38947
²³¹Pa, α decay, γ, spectroscopy investigations 0-73882
²³¹Pa(n, f) fission, relative delayed neutron group yields with fission neutrons 0-64141

 13 Pa energy levels from (1 He,d) and (1 He,t) 0-70667 13 Pa level scheme from 23 Th β -decay obs. 0-38948 Pb, elastic scatt. of electrons, E_e =40-60 MeV, cross section meas. 0-39023

D=39023

Pb, K₁° and neutron total cross sections at GeV energies 0-46230

Pb, v cross-section dependence on atomic weight 0-39019

Pb (A=202, 200, 198), v-transitions, excited states, from decays of Bi(A=202, 200, 198) 0-49547

Pb (A=209, 207), single particle components of particle vibrational states 0-42776

Pb forward emitted external bremsstrahlung spectrum, thickness depend. 0-42813

Pb polarization energy correction for muonic spectra 0-70829 204 Pb, 206 Pb, fission by α -particles, ang. anisotropy near threshold

^{26-Pb}, ^{66-Pb}, ^{108-No.} 11881011 by α 20-46263 α 20-46264 α

¹⁰⁴-23 MeV — 0-7344

²⁰⁴Pb He ion induced fission at 65, 41, 37 and 25 MeV, total cross sections 0-67559

²⁰⁴Pb isobaric analogue resonances from proton elastic scattering 0-70519

²⁰⁶Pb, g-factor meas. of states at 803 and 2385 keV 0-49548

²⁰⁶Pb, quasi-particle structure of ground state of pairing Hamiltonian 0-67490

²⁰⁶Pb, shell model with Hamada-Johnston potential 0-70521

²⁰⁶Pb isobaric analogue resonances from proton elastic scattering 0-70519

²⁰⁶Pb isec isomers, mag. mom. meas. 0-64025

²⁰⁶Pb(⁴⁰Ar, ⁴⁰Ar'p), lifetime measurement of first excited state for E=170 MeV 0-60769

²⁰⁶Pb(He,3n), E=32-44 MeV, decay of ²¹⁰Po compound nucleus 0-74002

²⁰⁶Pb(hg), microscopic first-order core polarisation corrections to DWBA 0-42837

²⁰⁶Pb(p,t))²⁰⁶Pb at 22 MeV 0-70614

Nuclei with 150 A continued

 207 Pb, $^{3}/_{2}$ state, from proton inelastic scatt., distorted wave anal. 0-73926 ²⁰⁷Pb, doublet (particle-vibration states), properties by solution of Schrodinger equation 0--57934

²⁰⁷Pb, particle parameters in K, L, and M shells, by e-γ ang. correlations meas. 0–38943

207 Pb, particle parameters in K, L, and M snells, by e-γ ang. correlations meas. 0–38943

207 Pb, shell and collective modes from (p,p'γ) 0–73927

207 Pb from ²⁰⁷ Pb(p, p'), excitation functions meas. 0–67491

207 Pb γ-decay of p_{1/2}-(⊗3- doublet 0–64069

207 Pb γ-decay of p_{1/2}-(⊗3- doublet 0–64069

207 Pb (evels from ²⁰⁸ Pb(He,α)²⁰⁷ Pb at 28 MeV 0–49550

207 Pb(He,3n), E=21-33 MeV, decay of ²¹⁰ Po compound nucleus 0–74002

207 Pb(d,p)²⁰⁸ Pb, excitation energies and γ branching ratios obtained for ²⁰⁸ Pb (0–67492

207 Pb(d,p)²⁰⁸ Pb) isobaric analogue resonances, K-matrix analysis 0–73838

207 Pb(d,p)²⁰⁸ Pb polarization effects near Coulomb barrier 0–70664

207 Pb(d,p)²⁰⁸ Pb(g,s.) distorted wave calculations, polarization effects near Coulomb barrier 0–70664

207 Pb(t,p)²⁰⁶ Pl, E_x=20 MeV, ang. distribs. 0–39127

208 Pb, bombardment with ¹⁶ ions and prod. of ²²¹Th and ²²γTh, decay chains determ. from radioactivity 0–57960

208 Pb, Coulomb breakup of ⁶Li at 20-, 21-, 24-, and 26 MeV 0–52806

208 Pb, Coulomb breakup of ⁶Li at 20-, 21-, 24-, and 26 MeV 0–52806

208 Pb, Coulomb breakup of ⁶Li at 20-, 21-, 24-, and 26 MeV 0–52806

0-77537
²⁰⁸Pb, Hartree-Fock calcs. of binding, density and single-particle spectra with effective force 0-49470
²⁰⁸Pb, Hartree-Fock with Skyrme's interaction 0-70522
²⁰⁸Pb, heavy-ion reactions, production of Th isotopes of mass 221-224
0-49581

0 - 49581

208Pb, inelastic scattering of polarised protons at 30.3 MeV and deduced nuclear deformations 0-52781

208Pb, iso-spin mixing for the 0' analogue of ground state and correction factors to Coulomb displacement energies 0-57935

208Pb, M1 giant reson., from threshold photoneutron meas. 0-77506

208Pb, nuclear polarisation of muonic atoms of spherical nuclei 0-43034

208Pb, nuclear polarisation of muonic atoms of spherical nuclei 0-43034

208Pb, single particle potentials and nucleon density distributions 0-38944

208Pb, transition density of the octupole vibration for small and high momentum transfer for electron scattering 0-57971

208Pb, unmixed states for comparison of analogue resonance studies and Coulomb stripping 0-70526

208Pb analogue ground state, microscopic description 0-70523

208Pb b branching ratios and excitation energies from 207Pb(d,p)²⁰⁸Pb

208Pb energy distribution of neutrons from proton neutron nonelastic colli-

0.-67492

2087b energy distribution of neutrons from proton-neutron nonelastic collisions for 18 MeV and 15 MeV protons 0.-64115

2087b energy spectrum of ejected photoneutrons 0.-46192

2087b excitation by neutron scattering, RPA and TDA calc., effect of continuum 0.-73951

2087b giant dipole resonance damping width calc. 0.-70524

2087b isobaric analogue resonances from proton elastic scattering 0.-70519

2087b isobaric analogue resonances, K-matrix analysis 0.-73838

2087b level from 2078i(n,e), search for E₀ transitions, by neutron capture conversion electrons 0.-60770

2087b photofission fragments, nucleon comp. and excitation energy 0.-70686

0 - 70686
208Pb Thomas-Fermi theory calculations of energy per particle, density distribution and single particle potential 0-49451
208Pb(1.1), breakup of ⁶Li 0-67556
208Pb(1.2), breakup of ⁶Li 0-67556
208Pb(1.2), 10981 0-64071
208Pb(1.2), 10981 0-664071
208Pb(1.2), 10981 0-64071
208Pb(1.2), 10981 0-64071
208Pb(1.2), 10998 0-70663
208Pb(1.2), 10998 0-7064071
20

0-73839

20 Pb, particle-core states 0-38945

210 Pb shell model with Hamada-Johnston potential 0-70530

Pd isotopes, static quadrupole moments of 1st 2 * states 0-55118

10 Pp. de-16 Ag, p decay, study by Ge(Li) and B-ray spectrometers 0-55144

130 Pm, independent yield, in 25 4Cf spontaneous fission 0-39151

130 Pm-150 Sm, energies and relative intensities of p transitions 0-42795

131 Pm, nature of low-lying excited states 0-46146

132 Pm decay, 6-min, β and p transitions obs. 0-38986

Po decay, (A=201, 203, 205, 207) populating levels in Bi odd-mass isotopes 0-38942

20 Po, decay by capture, electron conversion spectrum 0-60789

Transitions obs. 10^{218} m decay, 0-min, β and β transitions obs. 10^{218} m decay, 10^{218} m, 10^{218} m decay, 10^{218} m, 10^{218} m decay of 10^{218} m decay decay

Nuclei with 150 ≤ A continued

Pt (A=189,188), γ spectra meas, using Ge(Li) detector, radioactive decay 0-73876

Pt isotopes α -decay, half life meas., spectra 0-49579 Pt prolate-oblate difference in deformation energy 0-64060

Pt reaction with 3 GeV protons and leading to inelastic neutrons polarization 0-60813

184Pt, first collective levels 0-70510

185Pt, first collective levels 0-70510

185Pt, first collective levels 0-70510

185Pt, existed, statistical approach to deformation 0-70511

185Pt, first collective levels 0-70510

195Pt, flectron capture decay, half-life meas. 0-60787

195Pt, first collective levels 0-70510

195Pt, flectron capture decay, half-life meas. 0-60787

195Pt, first collective levels 0-70510

195Pt, truct, study by e-y and y-y directional correlations 0-49545

195Pt, struct, study by e-y and y-y directional correlations 0-49545

195Pt energy levels from 195Pt decay, by sum peak and sum coincidence studies 0-70513

195Pt g-factor of second excited 2+ state 0-70515

195Pt g-factor of second excited 2+ state 0-70515

195Pt level obs. from 195Pt decay 0-38984

195Pt level obs. from 195Pt decay 0-38984 Pt reaction with 3 GeV protons and leading to inelastic neutrons polariza-

⁹²Pt g-factor of second excited 2° state 10 H₂ 192 flevel obs. from ⁹²Pt decay 0 –38984 9⁹²Pt second excited state, lifetime and g-factor 0 –70516 9⁹²Pt static and transition moments 0 –67488 9⁹⁴Pt, level scheme from ¹⁹⁴Au decay 0 –60788 9⁹⁴Pt static and transition moments 0 –67488 9⁹⁵Pt, internal conversion coeffs. low level, obs. 0 –38890 9⁹⁵Pt, single particle analog state anomalies 0 –67489 9⁹⁶Pt(p,2n) 9⁹⁵Au, energy level study by observation of conversion electrons 0 –70517 9⁹⁷Pt–19⁹⁷Au, oriented nuclei in Fe matrix, β decay study by Mossbauer resonance in ¹⁹⁷Au, 0.06-20 K 0 –49580 Pu (A=242, 244), strong pair correlations in excited 0° states, (p,t) reaction study 0 –60772 Pu fission isomers, systematics 0 –39149 9²³⁸Pu, α emitter, measurement and use of X./α ratios 0 –73883 9²³⁸Pu, prompt neutron fission yield for thermal neutrons 0 –42885 9²³⁸Pu, prompt neutron fission yield for thermal neutrons 0 –42885 9²³⁹Pu, β-decay energy meas. of products 0 –52815 9²³⁹Pu, effective capture-to-fission ratio, low flux meas. in fast reactor 0 -58056 9²³⁹Pu, fission-spectrum n-fission, delayed n groups with t_{1/2}> 1 min abun-

239 Pu, effective capture-to-fission ratio, low flux meas. in fast reactor 0 - 58056
239 Pu, fission-spectrum n-fission, delayed n groups with t_{1/2}> 1 min abundances 0 - 39166
239 Pu, fission products, β-activity obs. at short time after fission 0 - 70539
239 Pu, mission products, β-activity obs. at short time after fission 0 - 70539
239 Pu, multilevel parameters for fission cross section from 40-100 eV
0 - 64139
239 Pu, n-fission fragments, prompt, energy distrib. calc. 0 - 39169
239 Pu, n-group fission cross-sections, 0.1 30 keV, error effects on integral parameters in fast reactors 0 - 77612
239 Pu, neutron capture fission cross-sections, 0.1 30 keV, error effects on integral parameters in fast reactors 0 - 77612
239 Pu, neutron induced fission, fragment angular distributions 0 - 70682
239 Pu, neutron induced fission, fragment angular distributions 0 - 70682
239 Pu, neutron induced fission, charge dispersion studies 0 - 39156
239 Pu, null-reactivity measurements of capture/ fission ratios 0 - 58029
239 Pu, simulated by f31Eu, comparison between calcs. and expts. in microlattice, neutron design of fuel elements 0 - 77602
239 Pu, spin- and energy-dependent fission widths, from channel theory, calc. 0 - 67558
239 Pu, spin- and energy-dependent fission widths, from channel theory, calc. 0 - 6758
239 Pu, ternary photo-fission, 27.5 MeV, study by mica and plastic track detectors 0 - 42887
239 Pu fission, neutron induced, independent yields of fast, fast factors o - 77599
239 Pu fission and capture cross sections 0 - 39209
230 Pu fission and capture cross sections 0 - 39209
230 Pu fission and capture cross sections 0 - 39209
230 Pu fission and capture cross sections 0 - 39209

239 Pu fission, neutron induced, independent yields of ¹³³I, ¹³⁴I and ¹³⁵I O-70678
239 Pu fission and capture cross sections 0-39209
239 Pu fission neutron-induced, prompt ε meas. 0-77589
239 Pu rection absorption and fission cross-sections in the region 0.02 eV to 30 keV 0-64143
239 Pu reaction rates in Pu-recycle fuel lattices 0-74059
239 Pu self-shielding and Doppler effects, effect of fission width spin dependence 0-74012
239 Pu thermal n-fission fragments recoil ranges and energy, obs. 0-39171
239 Pu thermal neutron fission and independent yields of ⁸⁰Br, ⁸²Br, ¹²⁸I O-52813
239 Pu thermal neutron fission, theoretical angular momentum of fragments 0-64148
239 Pu(μ) and ²³⁸Pu(μ) final ²³

 0^{-04146} 328 Pu (γ, f) and 238 Pu (γ, f) angular anisotropy obs. 0-46259 249 Pu, beryllia moderated system, resonance capture at 300° K to 1500° K 0-42778

¹³⁹Pu(p, f) and ²³⁸Pu (p, f) angular anisotropy oos. Under the control of th

Nuclei with 150<A continued

clei with 150 \$\inp A\$ continued

242 Pu("He,d) and ("He,t) reactions 0—70667

242 Pu(α, t), deduced levels of ²⁴³ Am for E=30 MeV 0—58023

242 Pu(n,F) En=500, 620, 730, 990 and 1230 keV, fragment angular dis tributions 0—42884

243 Pu, cross-section and fission probability from (t,pf) reactions 0—74020
Ra fission induced by 14-16 MeV neutrons, abnormal fragment distribution 0—46271

233 Ra, g factor of 50 keV ³/₂- state, magnetic hyperfine fields experienced when imbedded in Ni. Co, and Fe lattices 0—73842

233 Ra, radioactive decay, levels and daughter products 0—60792

233 Ra, radioactive decay, levels and daughter products 0—60792

233 Ra spin and parity of twenty levels 0—64074

233 Ra-²¹⁹ Rn, conversion electron and gamma spectra 0—42800

233 Ra-²¹⁹ Rn, conversion electron and gamma spectra 0—42800

235 Ra from α-decay of ²¹⁸ Th obs. 0—46180

235 Ra from α-decay of ²¹⁹ Th obs. 0—46180

236 Ra, γ ray spectra, decay products 0—52720

Re (A=176,177,178) decay schemea, using several techniques 0—73874

181 Re, compound nucleus, fissionability as function of ang. mom. at excita tion energy of 70 MeV 0—39152

182 Re, life-time of short-lived states at 235.7 and 263.3 keV 0—70475

182 Re, props. levels populated by decay of ¹⁸⁵Os, from γ-γ ang. correl.

185 Re, props. levels populated by decay of ¹⁸⁵Os, from γ-γ ang. correl.

186 Re, at -10.1 % resetting shapes and nuclear matrix elements 0—42772 182Re, props, levels populated by decay of 185Os, from γ-γ ang. correl. meas. 0–38994
 183Re, props, levels populated by decay of 185Os, from γ-γ ang. correl. meas. 0–38994
 183Re spin values from γ-γ angular correlation 0–64061
 186Re, 1-9-0⁺, β spectrum shapes and nuclear matrix elements 0–42772
 186Re, β-particle and γ distributions after polarisation in iron at low temperatures 0–57959
 186Re CVC theory and nuclear matrix elements from β-γ cascades 0–64098
 187Re, transitions, excited state, from β decay of 187W 0–46176
 187Re, transitions, excited state, from β decay of 187W 0–46176
 187Re, transitions, excited state, from β decay of 187W 0–46176
 187Re, transitions, excited state, from β decay of 187W 0–46176
 187Re, transitions, excited state, from β decay of 187W 0–46176
 187Re, transitions, excited state, from β decay of 187W 0–46176
 187Re, transitions, excited state, from β decay of 187W 0–46176
 187Re, transition, excited states from β-γ cascades 0–64098
 261Rf, new isotope of element 104 0–52719
 Rn isotopes, short lived 0–73875
 19Rn, 269 keV transition, spin assignments 0–38946
 219Rn, radioactive decay, levels and products 0–60790
 219Rn excited states lifetimes in 213R α-decay 0–70556
 212Rn, first excited (21) rotational state, from perturbations of α-γ angular correlation in 226Rn decay 0–57961
 Ru isotopes, static quadrupole moments of 1st 21 states 0–55118
 49Sc, hindrance of M1 transition from analogue to antianalogue state 0–73757
 5m isotopes, elastic scatt. of 50.8 MeV p, ang. distrib. meas. 0–67528
 1998m, sin and narity assignments from 199Pn decay 0.42705

0-73757
Sm isotopes, elastic scatt. of 50.8 MeV p, ang. distrib. meas. 0-67528

1995m. spin and parity assignments from 199 m decay 0-42795

1995m excited rotational band from 197 m decay 0-55135

1995m spin from (n, 2) reactions 0-64041

1995m(α, 2n) 1976d 100-4) ying states obs. 0-70501

1995m(α, 2n) 1976d 100-4) ying states obs. 0-70501

1995m, collective states 0-64047

1975m, collective states 0-64047

1975m, conversion e particle params. E₂ transitions, obs. 0-38930

1975m, double Coulomb excitation quantum mechanical corrections. Fellowship of the parameter of the par ¹⁵³Sm, directional correlation of γ rays meas, by two Ge(Li) counters 0.–70500 counters 0.–70500

72. photoneutron production for 150 MeV electrons incident on thick targets 0-55150 and targets 0-55150 and targets 0-55150 and targets 0-55150 and targets 0-70516 model 0-70516 model

181Ta, neutron elastic scattering, fast, non-spherical optical model 0-70616
 179Ta, rotational levels from *p*-ray and conversion electron spectra following proton bombardment 0-70508
 181Ta, decay of 181Hf, search for population of levels above 618.9 KeV 0-46175
 181Ta, existence of parity non conserving term in nuclear Hamiltonian conformed 0-70509
 181Ta, py ang, correlation of 345-136 keV cascades 0-52706
 181Ta, pvel correlation of 345-136 keV cascades 0-52706
 181Ta, pvel crossing in hyperfine interactions, study by perturbed *p*-*p* correlations 0-65971
 181Ta, quadrupole interaction in crystalline HfO₂ 0-62579
 181Ta fo.25 keV E1 *p* rays of Mossbauer absorption spectra, interference of photoelectric and nuclear resonance absorption 0-64059
 181Ta foiis, for spaceflight neutron dosimetry 0-76735
 181Ta foiis, for spaceflight neutron dosimetry 0-76735
 181Ta (a), (a), energy spectra determination and α part, angular distributions for En=15.1 MeV 0-57995
 182Ta(n), (a), energy spectra determination and α part, angular distributions for En=15.1 MeV 0-57995
 182Ta(n), etw. p. energy spectra determination and α part, angular distributions for En=18.1 MeV 0-57995
 182Ta(n), etw. p. energy spectra determination and α part, angular distributions for En=18.1 MeV 0-57995
 182Ta(n), etw. p. energy spectra determination and α part, angular distributions for En=18.1 MeV 0-57995
 182Ta(n), etw. p. etworn erosonance capture p-ray spectra, using mag. Compton p-spectrometer 0-73955
 182Ta(n), etw. p. etworn eventone e-efficients, 351.3 keV line 0-60786
 182Ta(n), etw. p. etworn eventone e-efficients, 351.3 keV line 0-60786
 182Ta(n), etw. p. etworn eventone e-efficients, 351.3 keV line 0-60786
 182Ta(n), etw. p. etworn eventone e-efficients, 351.3 keV line 0-60786</li

Nuclei with 150≤A continued

186Ta→186W decay, excited levels of 186W obs. 0-64062 152 Tb \rightarrow 152 Cd, de-excitation of 931.1 keV 2 + state of 152 Cd obs. 0-60782

¹⁵⁴Tb β ⁺ decay, using $4\Pi\beta$ ⁺ γ -spectrometer 0-60783 155 Tb, rotational bands, non-adiabatic effects 0-73829 156 Tb, 49.630±0.010 keV transition, T_{1/2}=24.4 hr 0-52737

18°Tb, elec. quadrupole moment 0–64206

159Tb, γ decay, search for parity violation 0–77487 159Tb, neutron-capture γ-rays, ang. distrib. 0–73830

1.59 Tb(n, γ) 1.60 Tb, relative intensities and multipolarities of γ -transitions 0.4941

1971b(n, γ)¹⁸⁰Tb, C value determ. 0–73830
196 Tb, 1710 keV β-86 keV γ cascade, β-γ correlation studies 0–60784
197 Tb, 1710 keV β-86 keV γ cascade, β-γ correlation studies 0–60784
196 Tb, β-γ directional correl. 0–38988
196 Tb, radioactive decay, deduced levels of 160 Dy mixing of gamma vibrational and ground state bands 0–49542
196 Tb, spins of 11 levels deduced 0–73830
196 Tb, spins of 11 levels deduced 0–73830
197 Tb, calculation of k-forbidden γ-ray transition probabilities 0–64053
198 Tb, Li ion, 198 bombardment, prod. of ²³⁰Pa, ²³²Pa, ²³³Pa 0–42877
Th (A–221-224), production and decay props. formed in heavy-ion reactions 0–49581
217 Th, α particle decay chains and atomic masses determination 0–57960
217 Th, α particle decay chains and atomic masses determination 0–57960
217 Th, α Particle decay chains and atomic masses determination 0–57960
217 Th, α Particle decay chains and atomic masses determination 0–57960
217 Th, α Particle decay chains and atomic masses determination 0–57960
217 Th, α Particle decay chains and stomic masses determination 0–57960
217 Th, α Particle decay chains and stomic masses determination 0–57960
217 Th, α Particle decay chains and stomic masses determination 0–57960
217 Th, α Particle decay chains and stomic masses determination 0–57960
217 Th, α Particle decay chains and stomic masses determination 0–57960
217 Th, α Particle decay chains and stomic masses determination 0–57960
217 Th, α Particle decay chains and stomic masses determination 0–57960
217 Th, α Particle decay chains and stomic masses determination 0–57960
217 Th, α Particle decay chains and stomic masses determination 0–57960
217 Th, α Particle decay chains and stomic masses determination 0–57960

²²⁹Th, n-fission fragments, prompt, energy distrib. calc. 0–39169 ²²⁹Th α-decay→²²⁵Ra obs. 0–46180

¹²⁹Th α-decay-¹²⁹Ra obs. 0-46180
¹³⁰Th, strong pair correlations in excited 0+ states, (p,t) reaction study 0-60772
¹³¹Th, cross-section and fission probability from (t,pf) reactions 0-74020
¹³²Th, f₂-4f pionic transitions, meas. 0-49552
¹³²Th, effective neutron fission cross-section at 14,1 MeV 0-64140
¹³²Th, fission, by neutrons, 0.95-2.3 MeV, fragment ang. distribs., channel anal. 0-52811
¹³²Th, fission induced by 14 MeV neutrons, ang. distrib. of γ 0-46261
¹³²Th, terruron fission, probability of long range particle emission 0-74010
¹³²Th, terruron fission, 27.5 MeV, study by mica and plastic track detectors 0-42887
¹³²Th, threshold detector, determination of fast neutron flux densities

²⁷Th, threshold detector, determination of fast neutron flux densities 0-74075 0—74075 232 Th energy levels from (n,n'p) reactions 0—64076 232 Th fission by 14 MeV neutrons, cumulative yields 0—42883

detectors U=42887

23°Th, threshold detector, determination of fast neutron flux densities 0–74075

23°Th nergy levels from (n.n'p') reactions 0–64076

23°Th henergy levels from (n.n'p') reactions 0–64076

23°Th hission by 14 MeV neutrons, cumulative yields 0–42883

23°Th photofission in symmetric region, cumulative yields 0–42888

23°Th/Hed, and ("He.1) reactions 0–70667

23°Th, cross section and fission probability from (t.pf) reactions 0–74020

23°Th, cross section and fission probability from (t.pf) reactions 0–74020

23°Th, cross section and fission probability from (t.pf) reactions 0–74020

23°Th, possible oblate shape ½r, some 0–657931

23°Th, lifetime of 279 keV level, two parameter centroid shift meas, method 0–52711, lifetime of 279 keV level, two parameter centroid shift meas, method 0–52711, n.m.r. in 711 0–48166

23°Th play it volation test by an angular correlation between nuclei and chem. shift 0–54170

23°Th parity violation test by an angular correlation method 0–42774

23°Th, n.m.r. in α- and β-TH, indirect interaction between nuclei and chem. shift 0–54170

23°Th parity violation test by an angular correlation method 0–42774

23°Th, parity violation test by an angular correlation method 0–42774

23°Th, parity, longity polarization, obs. 0–38631

23°Th decay rel. to fluorescence and Coster-Kronig yields of L subshells in Hg 0–70767

23°Th, ble-vibration coupling calc. 0–64066

23°Th particle-core coupling from proton scattering 0–64067

23°Th, hole-vibration coupling from proton scattering 0–64067

23°Th, hole-vibration coupling from proton scattering 0–64067

23°Th, shell model with Hamada-Johnston potential 0–70521

23°Th, shell model with Hamada-Johnston potential 0–70521

23°Th, shell model with Hamada-Johnston potential 0–70521

23°Th, parity level study 0–39127

23°Th, acclulation of k-forbidden y-ray transition probabilities 0–64053

14°Th, m. press section meas. 0–70624

23°Th, parity level study from 23°Pb (t.α) properties by solution of Schroding pracile components of particle vibra

Nuclei with 150 A continued
U (A 234, 236, 238), strong pair correlations in excited 0° states, (p,t)
reaction study 0° 60772

U interaction with heavy ions, effect of nuclear deformability on cross section 0 70672

U²¹⁹, half life of ground state 0 -52790

10.4., half life of ground state 0 - 52790

1.2. of sission fragments, prompt, energy distrib, calc. 0-39169

1.2. of sission by neutrons, 0.1 1.5 MeV 0-74014

1.2. of prompt neutron fission yield for thermal neutrons 0-42885

1.2. of 1.2

isomeric a ratios 0 58031 ²¹³U, thermal neutron fission and independent yields of ⁸⁰Br, ⁸²Br, ¹²⁸I

¹³¹U accuracy of dg/dT rel. to ENDF/B (and other) data files 0-77599 ²³¹U fission, neutron induced, independent yields of ¹³³I, ¹³⁴I and ¹³⁵I 0 70678

0. 70678
20 U fission by thermal n, independent yields of ¹³²I ¹³³I and ¹³⁴I, charge distrib. 0. 39165
20 U thermal n fission fragments recoil ranges and energy, obs. 0—39171
20 U thermal neutron fission, tritium yield. 0. 70679
21 U(d,p). 8 9.5 MeV. fission characteristics depend, on d energy obs.

²¹³U(d,p) 8 9.5 MeV, fission characteristics depend, on d energy obs. 0 46262
²¹³U(n, β), fission cross section measurement for neutrons between 0.018 eV and 1.2 keV 0 67563
²¹³U(t,p)2³⁴U, fission threshold meas. 0--74018
²¹⁴U(s,p)2³⁴U, fission threshold meas. 0--74018
²¹⁴U(d,p)2³⁴U F_{at} 12 MeV, levels of ²³⁵U populated by reaction 0--39111
²³⁴U(d,p)2³⁴U³⁴m, fission fragment mass distributions and kinetic energies for spontaneously lissioning isomers 0--39164
²³⁵U; ²³⁹U; ratios of capture and fission neutron cross- sections at 130-1400 keV 0-55162
²³⁵U; absolute ratio of fission densities due to thermal and epicadmium neutron fluxes 0 49680
²³⁵U, by medium energy protons, nuclear charge dispersion of light-mass products 0 64144
²³⁶U, cross section and fission probability from (t,pf) reactions 0--74020
²³⁵U, deduced levels and spteetroscopic factors from ²³⁶U(⁴He, α) at E=30 MeV 0 39128
²³⁵U, effective capture-to-fission ratio, low flux meas, in fast reactor ²¹⁵U, deduced levels and spteetroscopic factors from ²¹⁶U(*He, \$\alpha\$) at E=30 MeV 0 39128 and spteetroscopic factors from ²¹⁶U(*He, \$\alpha\$) at E=30 0 58056 and contains a factor of 58050 and contains a fact

²⁸U, half life measurements of 3/2¹ and 5/2¹ excited levels in 1/2¹ (631) rotational band 0 64077
²⁸U, level assignments from ²¹⁴U(d,p) and ²³⁶U(d,t) 0–39111
²⁸U, neutron cross sections in the unresolved resonance region 0–64121
²⁸U, neutron induced fission, symmetry meas, from ¹¹⁵Cd/⁹⁹Mo ratio 0 70681
²⁸U, neutron induced fission below 2.0 MeV, energy dependence of v_p 0 706.25
²⁸SU, nuclear fission, neutron induced, angular anisotropy, target spin depend. 0–64142
²⁸U, obs. of γ rays emitted from resonance neutron capture, energy level population of ²¹⁶U 0 73965
²⁸U, obs. of γ rays emitted from resonance neutron capture, energy level population of ²¹⁶U 0 73965
²¹⁸U, slow-n fission fragments K X ray yields, obs. 0–39161
²³⁹U, spin and energy dependent fission widths, from channel theory, calc. 0 67558
²⁸U, spontaneous neutron fission and short-lived fission isomers, deduced isomeric σ ratios 0 - 58031
²³U, thermal neutron induced fission, meas of fission fragments 0–77588
²³U, thermal neutron fission and independent yields of ⁸⁰Br, ⁸²Br, ¹²⁸I 0 52813
²³U, thermal neutron fission and independent yields of ⁸⁰Br, ⁸²Br, ¹²⁸I 1 52813

5200, thermal neutron fission and independent yields of \$8B1, \$2B1, \$121.
 5215U, thermal neutron fission fine structure of energy spectra 0-46269
 2325U, thermal neutrons, LRA fission and binary fission, multiparameter study 0-42886
 235U accuracy of dg/dT rel. to ENDF/B (and other) data files 0-77599
 235U and 238U, fission, 20 to 85 MeV proton-induced, nuclides cross-sections meas. 0 39160
 235U deuteron bombardment in energy range 11-20 MeV, excitation functions for production of fission isomers 0-49682
 235U enrichment of metallic U, registration using cellulose nitrate 0-77436
 235U fission, thermal neutron induced, identification of \$8Se and neutron emission from \$5Se 0-49679
 235U fission, yields of I isotopes and half-life and yield of \$135Te 0-42894
 235U fission prods. K X-ray yields rel. to Z, obs. 0-39168
 235U fission prods for several nuclides using comparison method 0-55174
 235Um, transition energy determ, to be 73±5 eV from conversion electron spectrum 0-67497
 235Un fission fragments energy and angular distrib., thermal-2 MeV
 30170

spectrum 0–67497
²³U n.fission fragments energy and angular distrib., thermal-2 MeV
0 39170
10 n.csons. and σ_f anal. 0–52709
²³U neutron induced fission, symmetry at individual resonances 0–74017
²³U photofission, time behaviour of delayed neutrons, bremsstrahlung endpoint energies 8 and 10 MeV 0–46265
²⁴U reaction rates in Pu-recycle fuel lattices 0–74059
²³U thermal-n.fission, 1 isotopes and ²³Te yields, obs. 0–49687
²³U thermal n.fission, ¹³Sn half-life and fractional cumulative yield
0 74025

0 74025 235 U(n,p), 6-40 eV, p emission obs., props. of 236 U resonances 0—39080

Nuclei with 150≤A continued

²³⁶U, energy level, population following resonance neutron capture in ²³⁵U 0 73965 ²³⁶U, low lying 2- state obs. through ²³⁶Np and ²⁴⁰Pu decays 0-38949

²³⁶U, nuclear deformation energy in two centre shell model and fission barriers calculation 0-57936

236U, resonance spin assignments 0–39080
236U, resonance spin assignments 0–39080
236U, resonance spin assignments 0–39080
236U, resonance spin assignments 0–49682
236U fission, deuteron induced, excitation functions for spontaneous fission isomer production 0–49683
236Um, spontaneously fissioning isomers, fragment mass distributions and kinetic energies 0–39164
236Um, spontaneously fissioning isomers, fragment mass distributions and kinetic energies 0–39164
236Um, spontaneously fissioning isomers, fragment mass distributions and kinetic energies 0–39164
236Um, spontaneously fissioning isomers, fragment mass distributions and kinetic energies 0–39164
236Um, spontaneously fissioning isomers, fragment mass distributions and kinetic energies 0–39164
236Um, spontaneously fission fission operations of a particles, level study of 236Um, consistive fission probability from (t,pf) reaction 0–39111
237Um, cross-section and fission probability from (t,pf) reactions 0–74020
237Um, cross-section and fission probability from (t,pf) reactions 0–74020
237Um, ratios of capture and fission neutron cross-sections at 130-1400
238Um, ratios of capture and fission neutron cross-sections at 130-1400
238Um, ratios of capture and fission neutron cross-sections at 130-1400
238Um, conversion ratio, meas, techniques 0–39243
238Um, conversion ratio, meas, techniques 0–39243
238Um, effective cross-sections in resolved reson, region, Doppler broadening 0–67582

218U, 5g-4f pionic transitions, meas. 0—49552
218U, effective cross sections in resolved reson, region, Doppler broadening 0—67582
218U, electron and photofission, yield values 0—64146
218U, fission-spectrum n-fission, delayed n groups with t_{1/2}> 1 min abundances 0—39166
218U, fission by 14.7 MeV neutrons, mass spectrometric determ. of Xe isotope relative yields 0—52812
218U, fission by 3 MeV neutrons, meas. of fis. time by shadow effect 0 60836
218U, fission probability by 2.5, 7.0 and 190 MeV neutrons, emission of long-range particles 0—60833
218U, neutron capture cross sections for 1 keV to 15 MeV, anal. 0—57996
218U, neutron fission, probability of long range particle emission 0—64121
218U, neutron induced, predicted mass yields 0—39157
218U, ne nucleon states and energy surfaces in fission 0—67560
218U, p fission, 12 MeV, prompt. n emission 0—42891
218U, resonance integrals for various geometrical systems 0—39231
218U, resonance integrals for various geometrical systems 0—39231
218U, resonance integrals for various geometrical systems 0—39231
218U, resonance integrals for various geometrical systems of central reactivity worths in fast critical assemblies 0—55205
218U, sonance ous neutron fission and short-lived fission isomers, deduced isomeric α ratios 0—58031
218U, ternary photo-fission, 27.5MeV, study by mica and plastic track detectors 0—42887
218U energy levels from (n,n'p) reactions 0—64076
218U fission, deuteron induced, excitation functions for spontaneous fission

uelectors U-42887

²³⁸U energy levels from (n,n'y) reactions 0-64076

²³⁸U fission, deuteron induced, excitation functions for spontaneous fission isomer production 0-49683

²³⁸U fission, photo- and fast-, thermal-n, fragment mass distribs., obs.

0 39167

0 39167

"38U fission by 14 MeV neutrons, cumulative yields 0-42883

"38U in UO; lattice, neutron absorption resonance, crystal-binding effects on Doppler broadening 0-49624

"38U neutron induced fission, angular distributions of fragments, analysis 0 70680

0 70680
0 70680
188U photofission, time behaviour of delayed neutrons, bremsstrahlung endpoint energies 8 and 10 MeV 0-46265
189U photofission in symmetric region, cumulative yields 0-42888
189U total cross-sections, for energies 3.3-5.2MeV of neutrons 0-49633
189U('He, n') deduced levels of 189U, E=30 MeV 0-42777
189U(n, p) 189U thermal neutron radiative capture cross-section 0-52790
189U(p, f) mass distribution and kinetic energy distrib. obs. 0-39159
189U(p,f) at 155 MeV, n energy distribution meas. 0-58034
189U(p,f) at 155 MeV, n energy distribution meas. 0-74018
189U(p,f) at 155 MeV, n energy distribution meas. 0-74020
191V, cross-section and fission probability from (t,pf) reactions 0-74020
191V, hindrance of M1 transition from analogue to antianalogue state 0-73757
W in Fe. Co and Ni, determ. of hyperfine fields, 300K 0-57929

0—73757
W in Fe, Co and Ni, determ of hyperfine fields, 300K 0—57929
W prolate-oblate difference in deformation energy 0—64060

178 W, deduced levels from Re activity 0—73874
179 W rotational levels from p-ray and conversion electron spectra following proton bombardment of Ta foils 0—70508

180 W rotational levels from p-ray and conversion electron spectra following proton bombardment of Ta foils 0—70508

182 W, life time of short-lived state at 1374 keV 0—70475

183 W expirate states Moschauer resetts 0.57038

 182W, hife time of short-lived state at 1374 keV 0-70475
 182W excited states, Mossbauer spectra 0-57928
 183W in WC, γ irrad. effects, resonant absorption following Coulomb excitation obs., anomalous hyperfine interactions 0-76056
 182W recoil implanted in Fe, mag. hyperfine field by pertubred ang. distribs. of γ-rays 0-44738
 182W triple γ cascade ang. correl. studies from 182Ta decay 0-42796
 183W-1975 spin-spin coupling constant in octahedral Tungsten (VI) derivatives 0-74310
 184W of 34 keV state mags, using hyperfine fields of W in Fe 0. 57020 183W. 19°F spin-spin coupling constant in octahedral Tungsten (VI) derivatives 0—74310

184W, of 364 keV state meas, using hyperfine fields of W in Fe 0—57929

184W, single particle analog state anomalies 0—67489

184W single particle analog state anomalies 0—67489

184W excited states, Mossbauer spectra 0—57928

184W in WC, p irrad, effects, resonant absorption following Coulomb excitation obs., anomalous hyperfine interactions 0—76036

185W, excited states from 185mW and 185Ta 0—68936

185W levels determ, from decay of 185mW and 185Ta 0—38936

186W, energy levels from β decay of 186Ta 0—64062

186W excited states, Mossbauer spectra 0—57928

186W in WC, p irrad, effects, resonant absorption following Coulomb excitation obs., anomalous hyperfine interactions 0—76036

183mW and 187Re, β decay, β-p coincidence meas, decay scheme 0—46176

185mW decay rel. to 185W levels determ. 0—38936

185mW decay scheme and p-spectrum, obs. 0—38937

Yb, L₂ and L₃ subshell- fluorescence yields, COster-Kronig transitions probabilities and K-shell conversion coeff. 0—38992

Yb rotational bands from analysis of analogue resonances, 170≤A≤177

0—73835

168Yb reaction rates in Pu-recycle fuel lattices 0—74059

168Yb thermal neutron capture 0—67344

Nuclei with 150 ≤ A continued

169 th, calculation of k-forbidden y-ray transition probabilties 0—64053 169 th, calculation of k-forbidden y-ray transition probabilties 0—64053 169 th—169 Tm, internal conversion meas. 0—38991 179 th, energy levels from 176 Lu decay 0—46172 179 th, thermal neutron capture and regularities in gamma ray spectra 0—64126

179Yb, thermal neutron capture and regularities in gamma ray spectra 0-64126
179Yb energy levels from internal conversion coefficients and y-y directional correlations 0-64054
171Yb, calculation of k-forbidden y-ray transition probabilities 0-64053
171Yb(n,p) 171Yb, excited K*=0* bands, study 0-77503
172Yb, deduced levels from 172Lu decay 0-57926
172Yb, dererm, of quadrupole ratio Q3*/Q2* 0-67487
172Yb, excited K*=0* bands study 0-77503
172Yb, K*=0* bands at 1043 and 1405 keV 0-64056
172Yb, multiple Coulomb excitation of ground-state rotational band 0-49538

173 b, multiple Coulomb excitation of ground-state rotational band 0-49538 ground-sta

Nucleic acids see Macromolecules

Nucleons and antinucleons

see also Cosmic rays/nucleons; Neutrons and antineutrons; Nuclear reactions and scattering due to/nucleons; Protons and antiprotons
3-nucleon problem, review 0-49450
axial vector form factors, SO₄, group 0-73615
e.m. form factors, best fit to expt. data 0-38709
form factors, elastic and inelastic, bounds 0-57812
form factors, off-mass-shell 0-73616
form-factor, e.m., from sidewise dispersion relations 0-42578
form-factors, electric and magnetic relativistic 0-73481
free, perturbation expansion of wavefunction in a magnetic field 0-51947
like nucleons in large single shell, perturbation treatment 0-73744
magnetic moment, anomalous, from sidewise dispersion relations
0-63842
magnetic moment calculation using Green's function, 0-73346

magnetic moment calculation using Green's function 0-70326 polarization, three-nucleon separable potential model with tensor forces 0 - 73629

0–73629 new state, possible existence 0–67316 three-nucleon problem, method of separable expansion of two-particle t matrix 0–73617 vertex functions, and current algebra 0–45957 KN, new interference model with scatt. amp. consisting of direct-channel resonance amp. and Regge amplitude 0–73559 N*(1460) prod. in $\pi r p \rightarrow \pi \tau \pi \tau \pi' p$ at 3.9 GeV/c 0–42549 π N, veneziano amplitude 0–60582

antinucleons No entries

interactions
at 200 GeV with atomic nuclei 0–45989
absorption reactions of neg. II by two N pairs in nucleus 0–49265
Bethe-Salpeter eqn., three-dimensional 0–38710
effective interac. in infinite nuclear matter 0–67387
hyperon-N, pot., one-boson-exchange model 0–38721
non-relativistic bound states as heavy meson reson. 0–63827
nuclear photoprocesses associated with vector meson dominance
0–60596

0 – 60596
pion photoproduction, continuous sum rules, Regge intercepts 0 – 60568
radiative three-nucleon reactions 0 – 49316
two-nucleon interaction, model descriptions 0 – 67315
vector-meson and dipion production in lepton-nucleon collisions 0 – 49281
pN→π high energy backward reactions and the strong-cut Reggeized absorption model 0 – 52522
pN→π²Δ, quark model explanation 0 – 57774
pN→π²Λ(1236), superconvergence relations 0 – 5493
pN→πλ. Regge-pole description of backward-scatt. data 0 – 57700
pN→p²Δ, minimal gauge-invariant one-vector-meson-exchange model 0 – 52564
KN, 3 GeV/c, cross sections of final states 0 – 38667

¹ O-52564

KN, 3 GeV/c, cross sections of final states 0-38667

KN-3 GeV/c, cross sections of final states 0-38667

KN-3-λ-π, 1-1.85 GeV/c, partial wave analysis 0-77313

A-N, study from binding energy data of p-shell hypernuclei 0-70387

AN, one-boson-exchange potential model 0-73652

AN, weak, spin depend. in hypernuclei decay 0-63993

AN=ΣN transitions in ANN system 0-52675

μN, ang, distrib. and cross section, from underground cosmic ray expt. 0-57839

NK, coupling constant, continuous dispersion sum rule 0-52453 NN, effect of π mass difference, by simple mass-averaging device 0-42703

Nucleons and antinucleons continued

interactions continued

interactions continued

\[\pi\] N at high energy, diffraction association and multipion prod. \[0-67282 \]
\[\pi\] N coupling, derivative and nonderivative, consideration in pion field equation \[0-73573 \]
\[\pi\] N low energy theory, S-wave scatt. \[0-38686 \]
\[\pi\] N partial wave relations from fixed-t dispersion relations \[0-38685 \]
\[\pi\] N review \[0-45932 \]
\[\pi\] N-\[\pi\] high energy backward reactions and the strong cut Reggeized absorption model \[0-52522 \]
\[\pi\] N-\[\pi\] N, B meson exchange contributions \[0--60574 \]
\[\pi\] N-\[\pi\] N vector dominance model, relations for t-channel helicity amplitudes \[0-45933 \]
\[\pi\] N, hyperon-nucleon interaction fit for lower the strong contributions \[0-1000 \]
\[\pi\] N, hyperon-nucleon interaction fit for lower the strong contributions \[0-1000 \]
\[\pi\] N in the strong contributions \[0-1000 \]
\[\pi\] N in the strong contributions \[0-1000 \]
\[\pi\] N in the strong contributions \[0-1000 \]
\[\pi\] N in the strong contributions \[0-1000 \]
\[\pi\] N in the strong contributions \[0-1000 \]
\[\pi\] N in the strong contributions \[0-1000 \]
\[\pi\] N in the strong contributions \[0-1000 \]
\[\pi\] N in the strong contributions \[0-1000 \]
\[\pi\] N in the strong contributions \[0-1000 \]
\[\pi\] N in the strong contributions \[0-1000 \]
\[\pi\] N in the strong contributions \[0-1000 \]
\[\pi\] N in the strong contributions \[0-1000 \]
\[\pi\] N in the strong contributions \[0-1000 \]
\[\pi\] N in the strong contributions \[0-1000 \]
\[\pi\] N in the strong contributions \[0-1000 \]
\[\pi\] N in the strong contributions \[0-1000 \]
\[\pi\] N in the strong contributions \[0-1000 \]
\[\pi\] N in the strong contributions \[0-1000 \]
\[\pi\] N in the strong contributions \[0-1000 \]
\[\pi\] N in the strong contributions \[0-1000 \]
\[\pi\] N in the strong contributions \[0-1000 \]
\[\pi\] N in the strong contributions \[0-1000 \]
\[\pi\] N in the strong contributions \[0-1000 \]

tudes 0–45933 Σ N, hyperon nucleon interaction fit for low energy scattering including Δ p reonance 0–57834 π N, generalized potential, dispersion relations, fixed-t, a new representa

tion 0-38684

777NN five-point function, crossing relations 0-55041

interactions, nucleon-nucleon

interactions, nucleon-nucleon
asymmetry inclasticity in ultrahigh energy reactions 0-77359
bremsstrahlung, low energy, analysis 0-49291
bremsstrahlung, low energy theorem derivation 0-55056
energy gap in nuclear matter calc, using velocity dependent reaction
0 70338

energy gap in nuclear matter catc. using velocity dependent reaction 0 70338 final state, in three-body reactions, theoretical study 0-73620 fireballs, role at cosmic ray energies 0-38726 high energy, uncorrelated meson production, by radiation type eikonal model 0-45915 inelasticity in ultrahigh energy reactions 0-77359 infal state, PWBA treatment, influence of cut-off radii 0-73621 matter- antimatter separation, effect of annihilation 0-48362 NN annihilation up to 5.5 GeV/c, isotopic spin dependence 0-63841 pair, effect of tensor forces on spin 0-52646 Skyrme's interaction used for Hartree-Fock calculations for closed shell nuclei 0-52636
T-violating force from c.m. interaction 0-45955 in three-nucleon system, test of new set of separable potentials 0-73618 ultrahigh-energy, multiplicity, asymmetry, inelasticity, using parton model 0-77359 unitary Pade approximants in strong interactions 0-52542

0–77359
unitary Pade approximants in strong interactions 0–52542
N pair interactions in nuclei, structure of matrix elements 0–46103
NN, nonrelativistic bound states in 1580 1880 MeV region 0–45956
NN \rightarrow NN γ bremsstrahlung, S matrix approach 0–60607
NN \rightarrow W+hadrons, cross sections 0–52544
NN \rightarrow hadrons+ γ \rightarrow hadrons+ μ $^++\mu$ $^-$, cross sections 0–52544

interactions, pion-nucleon see Pions/interactions, pion-nucleon

scattering

15₀ phase shift, by one-boson-exchange model 0-42702 15₁. D₁ scatt. parameters, low-energy, deuteron constraints 0-42579 Compton scatt., Bjorken limit 0-54992 fission fragment detection by glass detectors as opposed to emulsions 0 39176

leptons, polarised, inelastic scattering from polarised nucleons o-52434 low energy, deuteron constraints 0-42579 meson-nucleon, recoil effects in scalar field model 0-60461

meson nucleon and NN cross sections, qualitative differences, explanation 0 -67245

0 - 67245
neutron-deuteron, elastic, dispersion relations 0 - 73628
nuceon-deuteron, elastic channel 0 - 73626
nucleon-deuteron, polarization 0 - 73627
phase shifts calc, using universal theory of primary interactions 0 - 52543
three-N system scatt, states, variational bounds 0 - 38717
vector meson nucleon scatt, amplitude, from quark Regge pole model 0 - 77349
vector meson-nucleon scatt, amplitude, from quark Regge-pole model 0 - 77349

0-77349
dN, review of 3-nucleon problems 0-49450
eN, high energy deep-inelastic, study in a neutral pseudoscalar meson theory 0-73455
eN, inelastic, generalised scaling laws 0-73400
pN, space-time representation and electroproduction cross-section 0-70197
KN, consequences of possible violation of Pomeranchuk theorem 0-52500

KN, duality and non-Pomeranchuk contributions to cross sections 0-67297

N, duality and non-Pomeranchuk contributions to cross sections 0-67297
KN, elastic, anal. with account of Regge cut contribution 0-60563
KN, exchange degeneracy, absorption and loops 0-49254
KN, exchange degeneracy, absorption and loops 0-49254
KN, new interference model with scatt. amp. consisting of direct channel resonance amp. and Regge amplitude 0-73559
KN, Pomeranchuk theorem violation due to unconventional terms in amplitudes 0-45906
KN high energy, multiple rescatterings, accounting Regge poles 0-60557
KN total cross sections, by Pomeranchuk trajectory 0-55047
KN Veneziano model predictions, comparison with exptl. 0-77280
KN-K*(890)N, Regge pole model 0-49257
KN-K*(890)N, Regge pole model 0-49257
KN-N, NAK coupling constant weakly dependent on unphysical region parametrization 0-77314
K*\(^1\)N, NAK coupling constant weakly dependent on unphysical region parametrization of Pomeranchuk theorem 0-38669
K*\(^1\)N, ross sections on hydrogen and deuterium between 0.9 and 2.4
GeV/c 0-52502
K*\(^1\)N, total cross-sections on hydrogen and deuterium up to 3.3 GeV/c K[±]N, total cross-sections on hydrogen and deuterium up to 3.3 GeV/c 0 52503

0 52503 kN, particle-antiparticle total cross section differences at high energies, upper bounds 0-52424 lN scatt., parton model with Poisson distrib. 0-70203 A-N s-wave scatt. lengths 0-42596 A, hyperon-nucleon interaction fit for low energy scattering including Apresonance 0-57834 Nd, K-matrix calc. in energy range 11-40 MeV, polarization 0-77357 vN, highly inelastic, lower bounds for cross section 0-73450 vN inelastic, sum rule for vector axial vector interference form factor 0-63771.

vN scatt., space-time representation and electroproduction cross-section 0-70197 pN, total cross sections on hydrogen and deuterium up to 3.3 GeV/c 0-52503

Nucleons and antinucleons continued

scattering continued π N S_{J1} partial wave analysis, with phenomenological one-pole, multichannel ND $^{+}$ model $^{-0}$

 $net \, ND^{-1} \, model \, 0-42536$ πN , P' pole simulation by two vacuum poles with $\alpha(0) < 0$ 0-67298 πN , by modified interference model, duality concept 0-38693 πN , continuous-moment sum rules, application to analysis of forward scattering 0-73583

tering 0-73583 7N, crossing symmetric pion- nucleon scattering amplitude, Veneziano terms 0-49276

terms 0-492/6
7N, D₁₃ amplitude production model < 700 MeV 0-73584
7N, description at intermediate energies, unitarized interference model 0 42552
7N, duality and non-Pomeranchuk contributions to cross sections 0 67297

 τN , finite energy sum rules in non-forward directions 0-38645 τN , forward scatter and interference models, unitarity and duality

 πN , generalized potentials, particle exchange, Regge pole exchange 0 55048

n. 5,3048 nN, helicity conservation in diffraction scattering and duality 0-57739 nN, high energy, 50-500 GeV/e, predictions of Reggezed multiple-scatter ing quark model 0-67296 nN, high energy, multiple rescatterings, with account of Regge poles 0-60557

0 60557

N. inelastic, chiral dynamics calc. of single # production 0-52508

N. interference of t and u channel amplitudes 0-70253

N. interference of t and u channel amplitudes 0-70253

N. interference of t and u channel amplitudes 0-4593

N. off mass shell corrections to amplitudes 0-38692

N. Pade approximation for S matrix in pion nucleon pseudoscalar field theory above production threshold 0-60583

Theory above production threshold 0-0083 and fifterences at high energies, upper bounds 0-52424 and, phase-shifts solution, resonance parameters 0-77374 and, Pomeranchuk theorem violation due to unconventional terms in amplitudes 0 45906

7N, Pomeranchuk theorem violation due to unconventional terms in amplitudes 0 45906
7N, Rogge and non Regge damping, field theoretic model for high energies 0 42554
7N, s- and p-wave amplitudes, Ward-identity techniques 0-77337
7N, using modified Veneziano model 0-38650
7N, Veneziano model, modified 0-52525
7N at fixed u, finite energy sum rules 0-38694
7N backward charge exchange, Ny contribution 0-77335
7N backward scattering, Regge poles with kinematic cuts 0-52523
7N on mass shell, field theoretic study with currents obeying Gell-Mann Current Algebra 0-73585
7N phase shift analysis for elastic scattering up to 2.8 GeV/c 0-42553
7N Regge cuts and Veneziano model 0-67295
7N review 0 45932
7N Serpukhov results, 30-65 GeV/c, fit to Reggeized quark model 0 57791

0 57791

πN total cross sections, by Pomeranchuk trajectory 0-55047

πN Veneziano type representation for amplitudes 0-38691

πN Veneziano type representation 0-49274

π'N, cross sections on hydrogen and deuterium between 0.9 and 2.4

GeV/c 0 52502

π'N high energy data rel. to violation of Pomeranchuk theorem 0-73581

πN +Nπ coupling and backward scattering 0-57693

πN +Nπ high energy backward reactions and the strong-cut Reggeized absorption model 0-52522

πN +ππN, extraction of ππ scattering information by means of hard pion calc. 0-77336

πN +ρN, application of a dual resonance model for the πππΝΝ-five-point

 $\pi N * \pi^{\prime} N$, extraction of $\pi \pi$ scattering information by means of hard pion calc. 0 -77336 $\pi N * \rho N$, application of a dual resonance model for the $\pi \pi \pi N N$ -five-point function 0 63797 πN , spin independent Pomeron 0-73580 ρN , elastic, anomalous real parts in T matrices 0-63839 ΣN , hyperon nucleon interaction fit for low energy scattering including Λp resonance 0-57834 ΣN inelastic 10.1-14.6 GeV/c obs. of N*(1470) resonance 0-60526 ΣN Collisions in the multi GeV regions 0-55072 ΣN Veneziano model predictions, comparison with exptl. 0-77280 ΣN , crossing symmetric and antisymmetric parts, restrictive assumptions 0.73582

pN, determ, of real part of amplitude 0-77353

scattering, nucleon-nucleon
3.00 GeV/c total cross section, p-p, p-d data compared 0-57814
Chou-Yang model, current current interaction for high energy scattering

cross sections, and meson-nucleon, explanation of qualitative differences 0 67245

0 6/245 double scatt. on polarized proton target 0-49292 cikonal approx. for high energy scatt. 0-49294 fits to data by separable pot. 0-38711 low-energy, rel. to 'universal vector and axial-vector interaction' theory 0 67317

matrix elements nuclear deduced from N-N phase shifts 0-38801 meson resonances standpoint, below 400 MeV, and higher energies, pion pole contribution 0-45954 meson exchange model, based on Nambu Salpeter-Bethe eqn.

3- meson-0 60609

modified impulse approx. calc. in ²H(p,pp)n, ²H(p,pn)¹H 0-67318 multiple rescatterings, with account of Regge poles 0-60557 parameters from final state interactions 0-42868

parameters from final state interactions 0–42868 particle antiparticle total cross section differences at high energies, upper bounds 0–52424 popular review article 0–49471 potentials, hard- and soft core static, elastic scatt. <350 MeV 0–42580 Regge pole theory, Lorentz group appls. 0–38679 Regge pole eikonal theory for small-angle scatt. 0–57815 relativistic, single particle exchange amplitudes, non-local approach 0–57813 sum rules 0–60610 two pion exchange contribution, on basis of pion-pion dynamics 0–73624 Veneziano model 0–67319 Veneziano model consistent with crossing and Regge behaviour 0–73623 Veneziano model for scattering at high energy 0–77358 NN, Regge pole eikonal theory for small-angle scatt. 0–57815 NN, Veneziano model at high energy 0–77358 NN-KK, absorptive Veneziano model 0–677280

Nucleons and antinucleons continued

scattering, nucleon-nucleon continued

NN-NN*, N/D unitary isobar model 0-55057

NN-NN*, N/D unitary isobar model 0-60608

7N duality classes, modified form and interference-model calculation

0-49273 NN Veneziano model consistent with crossing and Regge behaviour 0-73623

scattering, pion-nucleon see Pions/scattering, pion-nucleon

also Elements/origin; Hypernuclei; Radioactivity; Scattering,

charge, critical, fall down to centre at Z>137 0-70329 conference, nuclear and solid state physics, Powai India. (1968) 0-41919 conference, properties of nuclear states. Montreal, Canada (1969) () 63944

cranking model calculations, correction to rotational spectra 0-70374 deformed, M1 transitions between rotational states of deformed nuclei 0-60748

deformed, effect of spin-orbital and spin forces on mag. moments 0-52665

0-32653 deformed, even-even, states I*=1+ 0-60749 deformed, theory of Coriolis interactions by superfluid model 0-38836 density distrib. in Z=N nuclei, A=40, 100, 200, local density approx. 0 38863

effective charges, lower bounds 0-52655

electron density ratios, comparison with ratios for conversion coefficients K/L 0-67411

energy gap parameters, of deformed even-even nuclei in rare-earth region 0 70325

even-even, quasiparticle struct. of ground state 0-70367 even even N=Z type in 2s-Id shell. Hartree-Fock calcs. with Wood-Saxon basis functions 0-46097

basis functions 0-4009 finite, effective interaction, high order terms and apparent non-convergence of perturbation expansion 0-49462 finite nuclei structure in the local density approximation 0-49466 form of light even-even nuclei, and binding energy and internal quadrupole moments 0-42696

heavy equipotential surfaces, shifts of single-particle energy levels 0 49468

intermediate mass, p elastic scatt., diff. cross sections, optical model anal. 0-70581

0-70581 light, correlation between nuclear radii and binding energies 0-42716 mass and deformabilities 0-42714 mass formula, semiempirical, symmetry energy term 0-42715 mass parameter for heavy and superheavy nuclei 0-52677 molecule-like struct, in composite particle reaction 0-39007 moments of inertia, of deformed even-even nuclei in rare-earth region 0-70325

odd, e.m. transition probabilities between excited states 0–63973 odd mass, with major closed shell, one- and three-quasi- particle projected states 0–52656

oscillations, compressional mode 0-55115 quadrupolar, multi-site chemical exchange effects in n.m.r. spectra () 69203

recoupling coefficient calc. using computer program 0–42695 shell struct. and geometric partial differential eqn. theory 0–38/93 spherical, semi-microscopic theory of two-phonon quadrupole-octupole vibrations 0–55117

structure, Harwell nuclear phys. div. progress report, May- Oct. 1968 0-52633

0-2033 structure with realistic interactions, methods and results 0-63947 superheavy elements in closed shell region, props. and prod. 0-38865 temperatures rel. to Z, from (n,p), (n,n') at 14 MeV 0-38809 textbook on nuclear structure comprehensive, from Bohr and Mottelsen 0-55107

0-55107
three-body binding energies, accurate comparison between exact and variational calc. for local potential 0-73752
three-body bound-state energy, dependence on off-shell effects 0-73751
three-body problem, applic. of Bateman method for factorization of twoparticle amplitude 0-46118
three-particle with realistic nuclear forces, theory of dipole sum rule
0 52647

two-nucleon transition matrix with bound state, off-shell continuation 0 - 60740

vibrations, with phonons at low energy, microscopic description 0–55105 or 3840 or 384

electric moment

see also Molecules/nuclear coupling

even-even, internal quadrupole moments, form and binding moments

0 42696

giant dipole resonance, asymmetry of T=0 resonances in light even-even nuclei 0-70382

nuclear quadrupole moment in Al₂O₃ determ. 0–62581 odd nuclei, of ground and excited states, by Bohr model 0–73772 quadrupole, electron cloud effect 0–42729 quadrupole, internal, in even-even nuclei, and form and binding energy 0–42696

quadrupole, static, of first 2+ states of spherical nuclei in schematic model 0-55118

quadrupole, static of first 2+ levels in spherical nuclei 0-52666 quadrupole interaction and birefringent dispersion, relationship with gradient of electric field 0-42730 quadrupole moment, mean values, in phenomenological nuclear theory 0-70381

quadrupole moments calc. from hfs data 0-70761 spherical, odd nuclei, of ground and excited states, by Bohr model 0-73772

0-13712 symmetric top molecule, nuclear electronic quadrupole interaction energy 0-74216 symmetric top molecule, nuclear electronic quadrupole interaction energy 0-74216 symmetric top molecule, nuclear electronic quadrupole interaction energy 0-64018 symmetric particles and symmetric particles are symmetric particles are symmetric particles and symmetric particles are symmetric particles are symmetric particles are symmetric particles and symmetric particles are symmetric particles are symmetric particles are symmetric particles and symmetric particles

Ar E2 observables calc. 0-64014 ⁴⁰Ar quadrupole moments of first two excited states 0-38875

"Ar quadrupole monitors of instructure, dipole-quadrupole coupling effect 0-73905

Nucleus continued

electric moment continued

"Bq. quadrupole moment, calc. 0-46120

"Bq. quadrupole moment, calc. 0-46120

"Bq. quadrupole moment, Calc. 0-46120

"Bq. quadrupole moment 0-38855

"Cd isotopes, static quadrupole moments of 1st 2+ states 0-55118

"Cd, quadrupole static, of first 2+ state, obs. 0-42757

"Cd, quadrupole moment of 1st excited state 0-32693

"ACd, quadrupole moment of 1st excited state 0-52693

"ACd, quadrupole moments of first excited 2+ states by Coulomb excitation 0-42760

14Cd, quadrupole moments of first excited 2+ states by Coulomb excita tion 0-42760
 14Cd, quadrupole static, of first 2+ state, obs. 0-42757
 14Cd quadrupole moment in first excited state 0-60755
 14Cl E2 observables calc. 0-64014
 14Cl E2 observables calc. 0-64014
 15Cl E2 observables calc. 0-64014
 15Cl giant dipole resonance and photo neutron cross section 0-77536
 15Cs, quadrupole moment, optical h.f.s. obs. 0-52698
 15Cs, quadrupole moment, optical h.f.s. obs. 0-52698
 15Cs, quadrupole moments of first excited 2+ states by Coulomb excitation 0-42760
 15TER, quadrupole moments determ, from Mossbauer, splittings in CoEstimates

0-42 57mFe

0-42760
5"mFe quadrupole moment determ. from Mossbauer splittings in CoF₂
0-48027
174Hf nuclear quadrupole moment determ. from isotopic shift in Hf I spec trum 0-46363
127I, hexadecapole moment 0-64458
128 Mg, quadrupole moments of excited states, using SU₃ model and projected HF calcs. 0-77490
145Nd relative static quadrupole moments of first excited state. 0-64038
145Nd relative static quadrupole moments of first excited state. 0-73893

**Not relative static quadrupole moments of first excited state 0—64038

**Not static quadrupole moment of first excited state 0—73823

**Not static quadrupole moment of first excited state 0—64038

**Not static quadrupole moment of first excited state 0—73823

**Not static quadrupole moment of first excited state 0—64038

**Not static quadrupole moment of first excited state 0—64038

**Not static quadrupole moment of first excited state 0—73823

Not static quadrupole moment of first excited state 0—73823

Not static quadrupole moment of first excited state 0—73823

Not static quadrupole moment of first excited state 0—73823

Not static quadrupole moment of first excited state 0—6038

**Not static quadrupole moments of first excited state 0—60757

*Not quadrupole moments of first excited states 0—60757

*Not quadrupole moment constraint imposed on Hartree-Fock calculations 0—49494

**ZNot quadrupole moments of first excited states 0—60757

**ZNot quadrupole moments of first excited states 0—60757

Ne quadrupole moment constraint imposed on Hartree-Fock calculations 0-49494
Ne, quadrupole moments of first excited states 0-60757
Ni, quadrupole, relative static, for first excited state 0-64021
Ni, static quadrupole moment of 1st excited state comparison of theoretical and experimental results 0-64020
Ni, static quadrupole moment of first excited state 0-73809
Ni, static quadrupole moment of 1st excited state 0-64021
Ni, static quadrupole moment of 1st excited state 0-64021
Ni, static quadrupole moment of 1st excited state comparison of theoretical and experimental results 0-64020
Ni, static quadrupole moment of 1st excited state comparison of the theoretical and experimental results 0-64020
Ni, static quadrupole moment of 1st excited state comparison of the theoretical and experimental results 0-64020
Ni, static quadrupole moment of first excited state 0-73809
Ni, static quadrupole moment of first excited state 0-73809
Os, determination of the electric quadrupole moment of the first 2*
states 0-42773
OS, determination of the electric quadrupole moment of the first 2*

states 0-42773 states 0-42773 states 0-42773 states 0-42773

states 0-42773 $^{193}O_{5}$, determination of the electric quadrupole moment of the first 2^{1} states 0-42773

Pd isotopes, static quadrupole moments of 1st 2+ states 0-55118

104 Pd quadrupole moment of first excited 2+ state from Coulomb excitation 0-70481

To duadrupole moment of first excited 2 state from Coulomb excitation 0-70481 [108]2d quadrupole moment of first excited 2 state from Coulomb excitation 0-70481 [193]Pt, existence of electric monopole moment in 2+'-32 transition 0-38940 [194]Pt, 198]Pt, quadrupole mom. meas. by Coulomb excitation 0-38913

0 38913
Ru isotopes, static quadrupole moments of 1st 2* states 0-55118
2*S quadrupole moments of first two excited states 0-38875
3*S, quadrupole moment calc. 0-74233
3*S, quadrupole moment calc. 0-74233
Sb isotopes. odd mass, e.m. moments 0-38915
1*1Sb quadrupole moment ratio from Mossbauer obs. of organo-Sb cpds. 0-55132
2*Si, quadrupole moments of first two excited states 0-38875
2*Si, quadrupole moments of excited states, using SU₁ model and projected HF calcs. 0-77490
3*Si quadrupole moment constraint imposed on Hartree-Fock calculations

**Si quadrupole moment constraint imposed on Hartree- Fock calculations 0:-49494

0-49494

**Sm static quadrupole moment of first excited state 0-73826

**Sm level transition 0-42768

**Sm, polarisation effects in \(\beta(r^2)\) measurements 0-38929

**Sn quadrupole static, of first 2* state, obs. 0-42757

**To, quadrupole moment 0-64206

**To, quadrupole moment of first excited 2* state from Coulomb excitation 0-70481

**Ti static quadrupole moments from excitation of first excited 2* state

0-64018

**Ti, quadrupole, static, of first excited state 0-70457

**Ti static quadrupole moments from excitation of first excited 2* state

0-64018

**Li, quadrupole, dual core fissionable model 0-38950

U, quadrupole, dual core fissionable model 0-38950 U, quadrupole moment magnitude from VBe₁₂ n.m.r. study 0-46134 172Yb, determ. of quadrupole ratio Q³⁺/Q²⁺ 0-67487

content of quadrupole ratio Q²⁺/Q²⁺ 0–67487
cenergy level transitions
2⁺, 3- states e.m. transition rates rel. to quadrupole-octupole coupling anharmonicity 0–38834
β-transitions, anal. of strongly delayed solns. 0–57881
β-transitions, strongly delayed, β, p-ang, correlations 0–57882
analog-antianalog gamma, rel. to struct. 0–46115
cascades, sum and sum-peak coincidence spectroscopy 0–38839
deformed nuclei, Rassey wave functions and gamma transitions 0–46113
Doppler shift measurements of nuclear lifetimes 0–52659
E0 transitions from 0; 4–0; states in the Z=82 region 0–52659
E1 transitions of octupole states in even-even deformed nuclei 0–63991
E1 transitions with N-mixed Nilsson orbitals 0–38817
E2 enhanced interference, possibility in ³⁰Na decay 0–57947

Nucleus continued

energy level transitions continued

E2 matrix elements, reduced isoscalar and isovector, in A=26, T=1 triad 0-57885

E₂ transition probabilities, reduced calc. using single particle-core coupling model 0-38819

ENDOR, nuclear polarization, effect of relax. transitions 0--67413 EO admixture determination by $\gamma - \gamma$ directional correlation meas.

0–57887
EO transitions, competition between electron and electron position pair emission. Fermi functions 0–49563
E(2) interband transition probabilities in deformed even-even nuclei, expression derived 0–63980
e.m., probabilities between excited states of odd nuclei 0–63973
e.m. transition rate, lower bounds for effective charges 0–52655
electromagnetic transition calc. 0–74089
energies and transition probabilities of first 2+ and 3- states for spherical nuclei 0–42727

energies and transition probabilities of first 2+ and 3- states for spherical nuclei 0-42727 even even nuclei, transition probabilities and static moments of excited states 0-73761 excitation functions, automatic measuring system 0-60697 higher order interference effects in hindered allowed β decay, matrix elements ratio 0-67501 internal conversion, higher-order corrections 0-73769 isobaric multiplets, decay rate relation 0-63976 isospin forbidden modes analogue resonances props. 0-67412 isospin states, Coulomb mixing 0-49480 K isomerism systematics, 160≤A≤190 and 230≤A 0-38864 lifetime meas. recoil distance flat target foil preparation 0-49483 lifetime measurements from the analysis of Doppler-broadened shapes 0 52658 M1+E2 transitions, M/L and (N+O+...)/M conversion ratios 0-49490 M1 forbidden, penetration effects on internal conversion for unified model of Sb, I, Pr and Pm 0-42708 M1 transitions between rotational states of deformed nuclei 0-60748 M2 and E3, radiative widths and mixing ratios, 33≤A≤41 0-67438

M1 transitions between rotational states of deformed nuclei: 0-60748 M2 and E3, radiative widths and mixing ratios, 33≤A≤41 0-67438 matrix elements from electromagnetic interactions review 0-73768 mean lifetimes of excited states, in A=15.25 range 0-38857 measurement method for lifetimes 10° to 10°-2 sec. 0-57892 Mossbauer effect, interference in crystals 0-48024 odd-A nuclei, gamma-ray transition probabilities calc. 0-60750 odd-mass spherical nuclei, electric quadrupole transitions 0-73758 overlapping resons, system, after c.m. and weak excitation 0-38833 parity-violating p transitions 0-46114 photon cascade, linearly polarized, angular correlation between first and nth 0-49489 quadrupole transition probabilities, in phenomenological nuclear theory 0-70381

Rassey wave functions and gamma transitions in deformed nuclei 0 46113

0 46113 sspherical nuclei, energies and transition probabilities of first 2* and 3 states 0-42727 states 0-42727 ransition, existence of electric monopole component 0 38940 sph. M1 decay of 1.7 MeV 1* state 0-70520 sph. M1 decay of bound isobaric analogue states, np coincidence recording for E_d = 4.0 MeV 0-64011 sph. from ³²Nb(n,2n) 0-67471 g^{2m}Nb, from ³²Nb(n,2n) 0-67471 cm, (A=65, 67, 68, 69), propertra obs. following thermal neutron capture 0 46224

0. 46133

**Ar excited state half-life, obs. 0—38878

*5As, half life measurements of levels 0—38894

*73As, transition rates, half-life meas, of excited states from 75Se γ-ray spec trum 0—73814

*75As excited state lifetimes, obs. 0—38896

*75As groundstate transition widths from Compton scattered radiation 0. 67461

0 67461

"7As, lifetime of the 632 keV³/₂⁴ level by yy delayed coincidence technique 0 42756

1"At excited states lifetimes 0-73841

19³Au decay, from y-ray spectra 0-70512

19³Au, 191 keV transition, B(E2) estimation 0-64065

19³Au, rel. to 268 keV excited state nature, obs. 0-38941

19³Au excited states studied, isomeric decay obs. multipolarity assignments 0-73832

0-73832

"98Au, half-life of 367.29 keV level 0-49546

"B, lifetimes of 1740, 2154 and 3585 KeV states, obs. 0-38852

"2B, lifetime of 0.953 MeV level by Doppler-shift attenuation method 0-52670

Ba (A=131, 133, 135, 137, 139), spectroscopic factors, for "Ba(d,p) where B=130, 132, 134, 136, 138 0-49669

"29Ba compound nuclei, deexictation by photon and neutron emission 0-38918

0-38918
¹³¹Ba cascades γ-γ correl, rel. to decay scheme and ¹³¹Co levels, obs.
0-38920

131Ba cascades γγ conservations.
0-38920
134Ba, γγ cascades angular correl., obs.
0-38923
134Ba, γγ cascades angular correl., obs.
0-42767
134Ba, γγ conservations of the 563 and 569 keV transitions using directional correlation techniques 0-42767
136, γγ and 136 conservations 0-42767
136, γ decay of low lying states from conservations 0-64071
139Bi, Coulomb excitation and the weak-coupling model 0-49551
139Bi, El transitions for direct coupling between octupole and dipole states 0-52708
139Bi, El transitions for direct coupling between octupole and dipole states 0-52708
139Bi, El ransitions for direct coupling between octupole and dipole states 0-52708
139Bi, El ransitions for direct coupling between octupole and dipole states 0-52708

²⁰⁹Bi, negative parity transition, effect of core polarization in p-p' scatter ing 0-67529

ing 0-67529

²⁰⁹Bi septuplet decay scheme 0-70527

³⁸Br, half lives and energy of isomeric activity 0-55129

³⁹Br, half lives and energy of isomeric activity 0-55129

Nucleus continued

energy level transitions continued

86 Br, 13 \(p \) rays, with intense peaks 1565 keV 0-60779 8⁷Br, 13y rays, with intense peaks 1565 keV 0-60779 12C, in p scatt. elastic and inelastic, 100 MeV 0-39029

19C, in p scatt., elastic and inelastic, 100 MeV 0—39029
19C, 0+-0+ transitions studied by inelastic e scatt. 0-46129
14C from 'Be('Li,p), low-lying levels, obs. 0-39142
13Ca, decay modes of low levels from ('He,ny) reactions 0-52674
14Cc, at 7 to 9 MeV excitation 0-42748
14Cc, at 7 to 9 MeV excitation for bright excitations of 3734 keV, 3- level 0-67431
14Cc, a cate of 19Cc, at 1 decay 0-70482

111Cd, mean-life of the 343 keV state using delayed coincidence method

111Cd, mean-life of the 343 keV state using delayed coincidence method 0-49532 state mean life, obs. 0-38909 114Cd, quadrupole probab. B(E2, 0+-2+), obs. 0-42757 124Cd de-excitation of 931.1 keV 2x* state 0-60782 110mCd, y-ray cascades angular correl., obs. 0-38908 Ce (where A=140,142), strong L=0 and 2 transitions, study in (p,t) reactions 0-55133 149Ce. lifetimes of excited states at 2083 and 2412 keV 0-52699

Ce (where A=140,142), strong L=0 and 2 transitions, study in (p,t) reactions 0-55133

**A¹⁴O_Ce, lifetimes of excited states at 2083 and 2412 keV 0-52699

**A¹⁴O_Ce, semi-magic, γ transitions 0-49507

**A¹⁴Cl, gamma ray transition strengths and 3*Cl deduced levels 0-58014

**Cl excited state, half-life, obs. 0-38878

**Co, L=0 to 0+ states spin parity obs. using (³He, p) 0-67453

Co, decay scheme from 3*Fe(p, p)Co 0-49521

**Co, internal pair formation coefficients 0-49522

**Cr, and Si(Li) detector system for conversion coefficient measurements 0-49534

**Cr, j-dependence in l=1 transitions, in 5*OCr(d,p) reaction 0-39121

**OCr, j-dependence in l=1 transitions, in 5*OCr(d,p) -0-39121

**OCr decay modes of states below 425 MeV studied by 5*2Cr(d,pγ)*3*Cr 0-38886

**OCr from 3*2Cr(d,pγ) reaction 0-70465

**OCs, multipole mixing ratios by γ·γ directional correlations using Ge(Li)-Ge(Li) meas. 0-38921

**3*OCs multipolarity of 79.6 transition from 161 keV level from 13*Ba decay

¹³⁷Cs excited state lifetimes meas. 0–73821
 ¹³³Cs multipolarity of 79.6 transition from 161 keV level from ¹³³Ba decay obs. 0–42792
 Cu (A=59, 61, 63, 65, 67), M1 transitions 0–52688
 ⁶²Cu, life-time of short lived state at 42 keV 0–70475
 ¹⁵⁵Dy, between excited levels, ¹⁵⁴Ho decay obs. 0–77522
 ¹⁶⁷Er excited states studied, isomeric decay obs. multipolarity assignments 0–73832
 ¹⁶⁷Er excited states studied, excited states ¹¹/₂ by differential and correlation

10° Lr excited states studied, isomeric decay obs. multipolarity assignments 0—73825
 14° Eu., g factors of second excited states 11/2-, by differential ang. correlation method 0—73825
 14° Eu., g factors of second excited states 11/2-, by differential ang. correlation method 0—73825
 15° Eu., 1.25° Je Ve internal conversion subshell transition 0—67482
 15° Eu., e.m. transition probabilities, half-lives of excited states 0—52701
 15° Eu, half-life of 89.83 keV level, meas. in 15° Eu(n,p) 0—49539
 17° F. E. 2 transitions, effective charge, importance of higher order corrections 0—42726
 17° F. E. 2 transitions, effective charge, importance of higher order corrections

¹⁷F, E2 transitions, effective charge, importance of higher order correc-

Type 2 transitions, elective charge, importance of higher order consections 0–42/26

"F, E2/MI mixing ratio for 1459→110 keV transition 0–46/123

"F, electromagnetic decay of first and second T=3/2 states 0–70415

"F, p-ray transitions, from reaction "F(d,pp)" of 0–38867

"Fe, ecore-excitation, effect on spectrum 0–73808

"Fe, electromagnetic decay properties of low lying states 0–60760

"Fe isobaric analogue states, p decay 0–70468

"Fe, reevaluation of conversion coeff. of 14.4 keV transition 0–67454

"Fe, reavaluation of conversion coeff. of 14.4 keV transition 0–67454

"Fe, reavaluation of conversion coeff. of 14.4 keV transition 0–67454

"Fe, reavaluation of conversion coeff. of 14.4 keV transition 0–67454

"Fe, reavaluation of conversion coeff. of 14.4 keV transition 0–67454

"Fe, including the states of 14.4 keV transition 0–67454

"Fe, electromagnetic decay properties of low lying states 0–60760

"Fe, p-ray transitions of 14.4 keV transition 0–67454

"Fe, electromagnetic decay properties of low lying states 0–60760

"Fe, p-ray transitions of 14.4 keV transition 0–67454

"Fe, electromagnetic decay properties of low lying states 0–60760

"Fe, p-ray transitions of 14.4 keV transition 0–67454

"Fe, electromagnetic decay properties of low lying states 0–60760

"Fe, p-ray transitions of 14.4 keV transition 0–67454

"Fe, electromagnetic decay properties of low lying states 0–60760

"Fe, p-ray transitions of 14.4 keV transition 0–60760

"Fe, p-ray transitions of 14.4 keV transition 0–60760

"Fe isobaric decay properties of low lying states 0–60760

"Fe, p-ray transitions of 14.4 keV transition 0–60760

"Fe isobaric decay properties of 14.4 keV transition 0–60760

"Fe isobaric decay properties of 14.4 keV transition 0–60760

"Fe isobaric decay properties of 14.4 keV transition 0–60760

"Fe isobaric decay properties of 14.4 keV transition 0–60760

"Fe isobaric decay properties of 14.4 keV transition 0–60760

"Fe isobaric decay properties of 14.4 keV transition 0–60760

"Fe isobaric decay properties of 14.4 keV t

184Gd, beta vibrational band, interband and intraband transitions 0-64048
185Gd, 31±2 ms activity produced by 186Gd(n,2n) at En=14-15 MeV 0-52702
185Gd, lifetimes of 86.5 and 105.3 keV levels, from 185Tb decay 0-64049
185Gd 2+-0+ rotational transition, charge radius change 0-52703
186Gd 2+-0+ rotational Transition, charge radius change 0-52703
Ge (A-70, 72), E2 decays 0-73812
18Ge, lirectional correl of γ-rays 0-46140
18Ge, directional correl of γ-rays 0-46140
18Ge first excited state, coincidence measurements half life of level 0-46141
18Hy, wh(f) meas of MI admixture meas in 2+ 2+ transition 0-73337

¹⁰Ge first excited state, contributions of -46141 (1984), $p \gamma(\theta)$ meas, of M1 admixture meas, in $2^+ \rightarrow 2^+$ transition 0-73837 He, after e.m. and weak excitation, cale. 0-38833 He, shell-model cale. 0-46119 (1974), metastable decay, internal conversion electron spectra, by β-spectroscope of $\Pi/2$ type 0-60785 (1984), from thermal n capture of 197Hf 0-52705 (1984) from thermal n capture of 197Hf 0-52705 (1984) excited states studied, isomeric decay obs. multipolarity assignments 0-73832 (1984) from the nuclear structure effect in internal conversion of 57.54 keV E1 transitive forms of the states of the nuclear structure effect in internal conversion of 57.54 keV E1 transitive forms of the states of the nuclear structure effect in internal conversion of 57.54 keV E1 transitive forms of the states of the states

¹⁸⁰Hr, nuclear structure effect in internal conversion of 57.54 keV E1 transition 0–60767
¹⁹³Hg excited state lifetimes, obs. 0–38896
¹⁹⁷mHg decay, transition multipolarities by magnetic electron and γ -ray spectroscopy 0–73879
¹⁶⁸Ho–1⁶⁸Er, spectral form and transitions analysis 0–73870
¹²¹J1, half life of low-lying l_2 + levels 0–67477
¹²³I, half life of loying l_2 + levels 0–67477
¹²³I, search for isomeric levels of half lives (0.1÷10) μ s 0–73820
¹²⁸I, search for isomeric levels of half lives (0.1÷10) μ s 0–70475
¹⁰⁷In→¹⁰⁷Cd obs. 0–73863

Nucleus continued

Ir, odd A-isotopes, spectroscopic pros. of low lying levels, by model including particle-vibr, and part.-rot. coupling 0-38938

1911r, deduced transition probabilities from Ir(16O, 16O'p) 0-38939

1911r excited states studied, isomeric decay obs. multipolarity assignments 0-73832

191 Ir excited states studied, isomeric decay obs. multipolarity assignments 0-73832

193 Ir, 73 keV *y*-transition, test of time reversal invariance of electromagnetic interaction 0-77505

193 Ir, deduced transition probabilities from Ir(16O,16O'y) 0-38939

1996 Ir decay to 1990 Os, *y*-ray spectra 0-77504

197K, mean lives of levels measured with Doppler shift attenuation for 196 Ar(p,y) 197K 0-64016

197K, y decay of levels, meas, with 18 Ar(p,y) 0-73802

198K, lifetime of 2818 keV, 7/2- level 0-67431

197K, mean lives of levels measured with Doppler shift attenuation for 197K, mean lives of levels measured with Doppler shift attenuation for 197K, interaction of 2818 keV, 7/2- level 0-67431

197K, mean lives of levels measured with Doppler shift attenuation for 197K, interaction of 400 Constant of 197K, interaction of 197K, interact

States V-30000

24Mg, in p. scatt., elastic and inelastic, 100 MeV 0-39029

24Mg, lifetime of 1369 keV 2+ level 0-67431

24Mg, lifetimes and excitation energies from 23Na(3He,d)24Mg*

0-38869

²⁴Mg, lifetime of 1369 keV 2* level 0–67431

²⁴Mg, lifetimes and excitation energies from ²³Na(³He,d)²⁴Mg*≤11 MeV 0–38869

²⁵Mg, M1 with ΔT=1 0–70434

²⁶Mg, O*-O* transitions studied by inelastic e scatt. 0–46129

²⁶Mg, evidence for isospin splitting of giant dipole state 0–70435

²⁷Mg, 194–0.984 MeV multipole mixing ratio, obs. 0–38874

²⁷Mg, 1-94–0.984 MeV multipole mixing ratio, obs. 0–38874

²⁷Mg, 1-94–0.984 MeV multipole mixing ratio, obs. 0–38874

²⁷Mg, 1-95, 194 MeV levels y-branching ratios, obs. 0–38874

²⁷Mg, 1-95, 195 MeV multipole mixing ratio, obs. 0–38874

²⁸Mg 1-69, 194 MeV levels y-branching ratios, obs. 0–38874

²⁹Mg 1-69, 190 MeV levels y-branching ratios, obs. 0–38874

²⁹Mg, 190, 190, 190, pectroscopic study from (d.f) reactions 0–49529

³⁰Mn, 983–126 keV, 1,530–0, mixture of multipole orders 0–46208

Mo (A=94, 96, 100), spectroscopic study from (d.f) reactions 0–49529

³⁰Mo, 204-2 keV transition, E2 admixture determ. 0–52691

³⁰Mo, 204-2 keV transition, E2 admixture determ. 0–52691

³⁰Mo, 204-2 keV transition, E2 admixture determ. 0–52691

³⁰Mo, scheme obs. in ³⁶Nb decay 0–77520

³¹N, lifetime of 8.88 MeV level by Doppler-shift attenuation method 0–52670

³¹N, multipolar mixing of 5.83–0 0–67422

³¹Na, nagular distributions of de-excitation y-rays from particle decays of giant ³⁶O resonance 0–70403

³¹N even parity levels, spectroscopic factors, obs. 0–38858

³⁰Na, anomalous beta alpha anisotropy directional correlation for an allowed ³⁷ decay 0–57947

²¹Na studied following ²¹Ne(p,p)²²Na, 300-1300 KeV 0–46127

²³Na, lifetime meas, for low-lying states, from ²³Na(p,p) 0–49510

⁴¹Nb VIII, term analysis of the 4p-4d and 4p-5s transitions 0–60936

Nd even isotopes, A=142 to 150, Le-0 and 2 from (p.t) 0–70496

⁴²Nd, excited levels, ⁴²Sm decay obs. 0–70550

⁴³Nd, edecay modes of low levels from ⁴³Ne, photophose of the photophose observations of 60765

⁴⁴Ne, lifetime eas of low lying levels using ³⁴Fe(α,m) reaction

16O, lifetime measurement of 3 excited states 0-64001 16O, lifetime of 6.44 MeV level by Doppler-shift attenuation method 0-52670 The difference of 0.444 MeV level by Doppler-sinit attenuation method 0–52670 leO, odd parity spectrum, from interac. between nucleons 0–77484 leO, partial widths from $^{12}\text{C}(\alpha, \gamma \gamma)^{16}\text{O}$, $^{15}\text{N}(\text{p}, \gamma \gamma)^{16}\text{O}$ and $^{15}\text{N}(\text{p}, \gamma \alpha)^{12}\text{C}$ 0–67424

O-67424

1°O, DWBA calcs, for stripping to d_{3/2} resonance 0-70419
1°O, E2 transitions, effective charge, importance of higher order corrections 0-42726
1°O deduced levels and γ-ray detection in coincidence with reaction particles from ¹⁸O(d,pγ) for E=5.0 MeV 0-57900
185 Os→185 Re, energies and intensities of transitions in ¹⁸⁵Os and internal conversion measurements 0-64097
186 Os excited state half-life, obs. 0-38878
1°P, γ-ray transitions of reson and excited states from Si(p,γ) 0-73798
1°P lifetimes and γ-ray angular distributions from ²⁸Si(p,γ) 0-67435

energy level transitions continued

³⁰P, Doppler-shift lifetimes of states populated by 29 Si(p, γ) reaction 0–73800

³⁰P, lifetimes of levels 0-70438

³⁰P, spectroscopic factors below 3.5 MeV excitation 0-70437

³¹P, with p rays, expt. agreement 0–73801
³¹P, with p rays, expt. agreement 0–73801
³²P, lifetime of 77 keV level 0–42745
³³P, pean lives of seven bound states, from ²⁹Si(α,pp) 0–49512
³³P, p-ray decay modes of 8 states below 4.3 MeV 0–77495
²³Pa, p-ray decay modes of 8 states below 4.3 MeV 0–77495
²³Pa, p-ray decay modes of 8 states below 4.3 MeV 0–77495
²³Pb, g-factor meas. of states at 803 and 2385 keV 0–49548
²⁶Pb, g-factor meas. of states at 803 and 2385 keV 0–49548
²⁶Pb, g-p-q-p, lifetime measurement of first excited state for E=170
MeV 0–60769
⁶⁷Pb, e-p ang. correlations involving 570 and 1064 keV transitions 0–38943
²⁶⁷Pb p-decay of p_{1/2}-1⊗3− doublet 0–64069
²⁶⁸Pb, M1 giant reson., from threshold photoneutron meas. 0–77506
²⁶⁸Pb branching ratios below 75 MeV 0–67492
²⁶⁸Pb branching ratios below 75 MeV 0–67492
²⁶⁸Pb from ³⁰Bi(n,e), search for E0, by neutron capture conversion electrons 0–60770

²⁰⁸Pb franching ratios octow 15 MeV over the conversion of th

Pd (A=107, 109), spectroscopic factors, from *Pd(d,t) (where B=108, 110) 0-49667
Pd isotopes, reduced probabilities of direct E2-decay of second 2+ states 0-55118
14Ppm excited state, lifetimes, obs. 0-38896
14Ppo, 272 keV transition, spin assignments 0-38946
14Ppo, 272 keV transition, spin assignments 0-38946
14Ppt, E2/M1 ratios for 3+-2+, 3+-2+ and 4+/-4+, and B(E2) for 2+/ level 0-67488
14Ppt, M1/E2 mixing ratios 0-49545
14Ppt, M1/E2 mixing ratios 0-49545
14Ppt, B(E2) value for excitation of 2+/ level 0-67488
14Pu(A=242, 244) strong pair correlations in excited 0+ states, (p,t) reaction study 0-60772
14Ppt, p-vibrational and ground-state rotational band mixing 0-73843
14Ppt, p-vibrational and ground-state rotational band mixing 0-73843
14Ppt, p-vibrations of levels populated by decay of 14PQ 0-70475
14Ppt, 14Ppt,

Ru isotopes, reduced probabilities of direct EZ-decay of section 2,55118

0-55118

illoRu, spectroscopic factors, from ¹⁰⁴Ru(d,t) 0-49667

illoRu, prod. by photonuclear reactions 0-67472

illoRu, prod. by photonuclear reactions 0-67493

illoRu, prod. by photonuclear reactions 0-67491

illoRu, prod. by photonuclear reactions 0-64013

illoRu, prod. by photonuclear reactions in illoRu, prod. illoRu

33S, multipole migrations and transitions 3.8.6.1.
 34S, multipole migrations and transitions 3.8.6.1.
 34S, mean life of first two excited states 0-46131
 34S, mean life inferimes of levels below 5.0 MeV, meas. by Doppler-shift attenuation method, from 31P(α,p) 0-49513
 35b isotopes, odd-mass low-energy spectra 0-38915
 32Sb existed state lifetimes, obs. 0-38896
 124Sb, low energy y-ray spectra measurement 0-49525
 43Sc, El transition rates using simple phenomenological model 0-38881
 43Sc, el Ireansition rates using simple phenomenological model 0-0-67445

0-6/445 *Sc, electron and p transitions, from $(\alpha, \alpha' p)$ and (p, p'p) 0-49518 *Sc, radiative transitions between low-lying odd parity states 0-52685 *Sc, hindrance of M1 transition from analogue to antianalogue state 0-73757

0-73757

"See from (3He, p), O1 spin parity obs. 0-67453

"Se, from 34Se(n,y) 0-52789

"Se, low energy y-73 spectra measurement 0-49525

"Si, mean lifetime meas. of first excited states 0-49511

"Si, from (p,t) reaction, isospin-forbidden decay props. of lowest T=2 states 0-38869

"Si, in p scatt., elastic and inelastic, 100 MeV 0-39029

"Si, lifetimes and excitation energies from 27Al(3He,d)28Si*≤11 MeV 0-38869

"Si, MI with AT=1 0-70434

²⁸Si, in p scatt., elastic and inclusive, 100 MeV of 180 (24.6) with 27 al (24.6) with 28 si (24.6

Nucleus continued energy level transitions continued

ucleus continued
energy level transitions continued

**PST, K. conversion coefficients from decay of **PY 0-49526

**SST excited state half-life obs. 0-38878

**9SST, first medical points of the state of the stat

O_73757

O_73757

V, p-decay of lowest 3/2 state, shell model calc. O_70463

V, M1E2 mixing ratios for T=7/2 analogue states, from ⁵⁰Ti(p,y)

O_67450

Vexited states lifetimes O_38951

Vexited states lifetimes O_38951

Verited states lifetimes O_48051

Verited states lifetim 0-4938

0-4938

0-4938

0-4938

0-4938

0-4938

0-4938

0-4938

and Si(Li) detector system for conversion coefficient measurements 0—49384
Ye xecited states lifetimes 0—38951
Yb, L; and L₃ subshell-fluorescence yields, COster-Kronig transitions probabilities and K-shell conversion coeff. 0—38992
Yb, Calculation of K-forbidden p-ray transition probabilities 0—64053
Yb, El transitions, branching ratios 0—64057
Yb, Fl transitions, branching ratios 0—64057
Yb, Fl transitions of K-forbidden p-ray transition probabilities 0—64053
Tay Pb, Ford decay of 172Lu 0—64096
Tay Pb, Ford decay of 172Lu 0—64096
To and transitions in inelastic proton scattering 0—67459
Tr, El from analogue states 0—67468
Tr, El from analogue states 0—67468
Tot, El from analogue for decay of 3.31 MeV state, by high resolution syst. 0—49343
Tot, search for double y emission from first excited states 0—70447
Tr, mean lifetimes of the second 0+ states 0—52690
Terrem langles

energy levels

nergy levels see also Radioactivity/decay schemes

1-, 2-, 3-, 4-, 5- quintet splittings rel. to quadrupole-octupole coupling anharmonicity 0-38834

1-p proton hole states in 13 nuclei from ¹²C to ³²S 0-70399

2+ and 3- collective states in Sn and Zr isotopes using schematic forces
0-55125

0-55125
4-nuclei, nature of low-lying even parity even spin states 0-67392
2 Mg deduced levels from 2 Ne(3 He, n) between 3.4-9.4 MeV 0-42740
from 8 Sr(p,p) and 8 Sr(p, p), analogue state resonances using coupled optical equations 0-67403
A=13, 14, 15, compilation of levels, structure of systems 0-73784
A=18 isobaric triplet, energy differences 0-38861
A=19 isobaric quartet, energy differences 0-38861
A=40, 0 T=2 states, calc. diagonalizing representative nuclear forces

A=40, 0*T=2 states, calc. diagonalizing representative nuclear forces 0-49515
analogue fine structure and asymmetry 0-67402
analogue resonances, theory 0-67397
analogue resonances fine structure 0-67398
analogue states, microscopic calculation for escape width 0-67400
analogue states excitation from stripping and pick up reactions 0-67394
analogue states in deformed nuclei 0-67404
anti-analogue state contribution rel. to analogue state decay 0-67401
bound states, hyperspherical expansion approach 0-52657

Nucleus continued

energy levels continued

bound states, hyperspherical-expansion approach 0-63972 combinatorial calculation of nuclear level densities, analytical approximation 0-49486

conference, Asilomar (1969) 0-67393

conference, properties of nuclear states, Montreal, Canada (1969) 0 -63944

0 - 63944 continuum effects on structure, review 0 - 73742 continuum effects on structure, review 0 - 73742 Coulomb energy separation between analogue states rel. to residual interaction effects, n radii 0 - 67406 Coulomb-energy differences of excited mirror nuclei, systematics 0 - 42720

Davydov-Chaban model, anomalous rotational band, spherical even-even nuclei 0–46105 deformed nuclei $A\approx25$, 150<A<190 and A>200, rot. spectra 0–49488

deformed states in light nuclei, study using single-particle representation 0 -38829

densities, calc. by iterative method, from single particle levels 0–38830 densities, excitation energy dependence of shell effects 0–63975 density calc., superfluid and Nilsson models in rare earth elements 0–46124

0-46124 density cates, based on shell models in ²⁰⁸Pb region 0-77474 density for some partially random Hamiltonians 0-73754 density functions, two-nucleon, and correlation functions with realistic single particle wave functions 0-55119 dipole giant resonances of non-magic nuclei 0-46117 displacement energy rel. to short range correlations and charge dependent nuclear forces 0-57876 distribution of spacings between levels, analysis 0-57889 doubly even spherical nuclei near closed shells, 44 MeV α-particle scattering 0-46234

doubly even spherical nuclei near closed shells, 44 MeV α -particle scattering 0–46234 E1 giant resonance splitting, isospin study 0–70380 energy gap calculations using realistic and delta-function forces 0–42700 even nuclei, ground state, application of generator-coordinate method to rotational spectra 0–77475 even quasirotational nuclei, semiempirical description of ground-state band 0–70366 even-even nuclei, deformed to doubly magic ground-state bands of quadrupole type 0–49484 even-even nuclei, rotational energy levels of ground state band in Krutov model 0–67410 even-odd staggering in p-bands, theoretical investigation using collective model 0–52663 excited, spin depend, of density 0–52661 excited state study from analogue resonances 0–67510 excited states, orbiting cluster model 0–38837 Fermi matrix elements, appl. of gross theory of β decay 0–73850 fissionable nucleus, single particle states 0–55173 four-particle proton levels of (1g₉7) (2p₁/2) (1y₁/2) (1y₁/2) (2p₁/2) (2p₁/2) (1y₁/2) (2p₁/2) (2p₁/2

giant dipole resonance, asymmetry of T=0 resonances in light even even nuclei 0 .70382

Hartree-Fock method, using methods of projection 0–73762 Hartree-Fock orbitals with s-state interactions 0–57884 Hauser-Feshbach method for characts. of ²⁶Mg, ²⁹Si, ³²S, ⁵⁸Ni and ⁶⁰Ni

Hartree-Fock method, using methods of projection 0—73762
Hartree-Fock obtitals with s-state interactions 0—57884
Hauser-Feshbach method for characts. of ²⁶Mg, ³⁹Si, ³²S, ⁵⁸Ni and ⁶⁰Ni 0—52652

I'=7/2*, anomalous levels, in nuclei with Z=43, 45, 47 0—57883
I'=1*, in even-even deformed nuclei 0—60749
interaction between 0p-0h and 1p-1h states in 0* calculations with non-Hartree-Fock base 0—57888
isobaric analogus tates from (p, n) and (³He, t) 0—67531
isobaric analogue reson., description by reson, wave functions 0—49479
isobaric analogue resonances widths, distribution of Coulomb mixing strength 0—73755
isobaric analogue resonances, single particle resonant-state wave functions for descrip. 0—38832
isobaric analogue resonances effects in (d, p) and (p, d) 0—67548
isobaric analogue resonances for spectroscopic factors det. 0—67399
isobaric analogue resonances in elastic scatt. of polarized p from ⁸⁸Sr, ⁹⁰Zr, ⁹²Zr, ⁹²Zr, ⁹⁴Zr, ⁹ Mo. ¹⁴Ce, ¹¹Nd, ¹⁴Nd 0 70417
isobaric analogue resonances and spectroscopy applies. -0—46107
isobaric analogue states, review 0—70371
isobaric analogue states, review 0—70371
isobaric analogue states for n spectroscopic factor 0—67405
isobaric multiplet equation, T₂* term 0—77459
isobaric multiplet mass equations 0—67512
isospin impurity in bound state 0—677407
isospin mixing using (*He, t) 0—67396
light nuclei, isospin projected FBCS wavefunction 0—46111
light self-conjugate nuclei, effective interaction calc. 0—38853
line width and level shift, dependence on binding potential 0—74089
low-lying levels, props. by k-harmonics method 0—49487
nearmagic nuclei, effective interaction calc. 0—38853
line width and level shift, dependence on binding potential 0—74089
low-lying levels, props. by k-harmonics method 0—49487
nearmagic nuclei, effective interaction calc. 0—38899
nuclear fission involving spin rel. to isobaric analogue states 0—67361
nucleons in large single shell, perturbation treatment 0—73744
neutron hole states in N=49 nuclei, using ³He, α) reaction 0

octupole states of even-even nuclides, 150 ≤ A ≤ 176 0-55136

octupole vibrational states of even deformed nuclei with A≥222 0-55116 odd nuclei, energy levels discussion 0-46108 one-quasi-particle projected states for odd-mass nuclei with major closed shell 0-52656

orbiting cluster model 0–38837 p-shell nuclei low-lying levels of anomalous parity, in unitary scheme approx. 0–77476 pair states, quasiparticle struct. 0–70367

Nucleus continued energy levels continued

paired states, excited, descrip, by variational approach 0-52653 pairing type states, isospin structure 0-73770

pairing vibration 0-42719

parentage of states simply obtained from two-nucleon transfer reactions 0-70593

Peierls-Yoccoz projection method 0-73762 projection model for ground bands of even-even nuclei 0-38831

proton neutron pairing correlation, T=0, in N≠Z light nuclei 0-38811 quadrupole and octupole in even-even nuclei, inelastic scattering of 11 MeV protons 0-70586

quasirotational energies without perturbation theory 0-70364 rare earths, level density calc. in superfluid and Nilsson models 0-46124 rare-earth nuclei, configuration mixing from radiative neutron capture 0-64005

rare-earth nuclei, one-particle props., effect of deformation parameters $0\!-\!52639$

0-52639 Regge trajectories 0-60747 review of ground state rotational bands, beta vibrations, octupole vibrations 0-73748 rotation, body, of deformed nuclei 0-38838 rotation, unified treatment 0-73767 rotational bands populated by (r,xn) reactions, spin distributions 0-70375 rotational description of states in closed and near-closed-shell nuclei 0-46112 rotational excitations, microscopic theory 0-42724 rotational motion, unified derivation of cranking model and Peierls-Yoccoz method 0-77458 rotational nuclei, linear polarization contributing to isomeric shift 0-63979 rotational spectra, generalized cranking model study 0-70374

totational spectra, generalized cranking model study 0-70374 rotational-vibrational model, two-centre, with phenomenological pot. 0-38818

rotational-vibrational model, two-centre, with phenomenological pot. 0–38818 s-state interactions, Hartree-Fock orbitals 0–57884 shell-model states in seniority scheme, isospin characts., classification, five-dimens, quasispin 0–38821 shells in simple anisotropic harmonic oscillator 0–70365 single particle levels from (p,2p), review 0–73931 single particle levels of heavy nuclei, shifts due to distortion of equipotential surfaces 0–49468 single particle states from neutron capture in medium weight nuclei 0–73764 spacing of states generated by particle hole excitations, relativistic correction 0–38835 spectral distributions 0–63946 spherical model, harmonic vibration, review 0–67361 spherical nuclei, static quadrupole moments of first 2+ levels 0–52666 structural props., set of lectures, book 0–63943 structure calc. by dispersion relation approach 0–55114 structure calcs., projection operators 0–67389 structure studies with isobaric analog reson. reactions 0–38796 structure theory 0–49485 three-nucleon resonances, broad, for a soft-core two-nucleon potential, calculation 0–57886 three-quasi-particle projected states for odd-mass nuclei with major closed shell 0–52656 transuranium nuclei, one-particle props., effect of deformation parameters 0–52656 transuranium nuclei, one-particle props., effect of deformation parameters

transuranium nuclei, one-particle props., effect of deformation parameters 0 -52639

0 - 32639

two-phonon quadrupole-octupole vibrations in spherical nuclei, semi-microscopic theory 0-55117
vibration, pairing, unified treatment 0-73767
vibration-particle coupling, effects on the props. of several light odd-mass nuclei 0-42721

vibrational nuclei, selected topics 0-64070 vibrational nuclei, selected topics 0-64070 vibrations, quadrupole, anharmonic, phenomenological description vibrations, 0 70372

wave functions microscopic theory 0–60745 widths of excited states, from neutron radiative capture 0–73760 ¹⁶⁸Er, level structure and the de-excitation mechanism, study by radiative capture at thermal energies 0–57925 ⁵⁵⁸Mn levels deduced from decay of ³⁵Cr using Ge(Li) gamma detectors 0–57948

capture at thermal energies 0–57925

5 Mn levels deduced from decay of 55 Cr using Ge(Li) gamma detectors 0–57948

n decay of highly excited (T₀+1/2) compound nucleus states 0–67395

n spectroscopic factor rel. to isobaric analogue states 0–67405

N transfer spectroscopy, multipole sum rules appl. 0–39028

5 Mn, weak β branching in 55 Cr decay 0–73858

6 Tm, n reaction, reson. parameters and spin, E=4–830 eV 0–39073

7 See level scheme from decay γ-spectrum obs. 0–38971

27 Ac, scheme proposed and interpreted in terms of rotation bands 0–73882

10 Ag, hfs anomaly determ. 0–77501

10 Ag, hfs anomaly determ. 0–77501

10 Ag, n reaction, reson. parameters and spin, E=4-830 eV 0–39073

10 Ag properties of low lying levels determination by Coulomb excitation 0–64031

110 Ag, n reaction, reson. parameters and spin, E=4-830 eV 0–39073

10 Ag properties of low lying levels determination by Coulomb excitation 0–64031

110 Ag, no reaction, reson. parameters and spin, E=4-830 eV 0–39073

110 Ag prom γ decay of 10 Pd 0–55144

110 Ag, n reaction, reson. parameters and spin, E=4-830 eV 0–39073

110 Ag prom γ decay of 10 Pd 0–55144

110 Ag, n treaction, reson. parameters and spin, E=4-830 eV 0–39073

110 Ag prom γ decay of 10 Pd 0–55144

110 Ag, n reaction, reson. parameters and spin, E=4-830 eV 0–39073

110 Ag from 10 Ag(n,γ), evidence for (2-) state 0–57919

111 Ag, nature, and spins, parities, obs. 0–38910

26 Al, deduced levels from 26 Mg(1+e,t) 0–77574

26 Al deduced from 27 Mg(1+e,pγ) reaction 0–39113

27 Al excitation energies γ-branching studied by 26 Mg(d,nγ) Ag (1-e, γ)

27 Al, excitation energies γ-branching studied by 26 Mg(d,nγ) Ag (1-e, γ)

27 Al excited core model from (d,α) cross-sections 0–70429

27 Al excited core model from (d,α) cross-sections 0–70429

27 Al excited core model from (d,α) cross-sections 0–70429

27 Al excited core model from 6 Mg 0–32682

28 Al, deduced levels from 26 Mg 0–32682

28 Al, deduced levels from 26 Mg 0–36032

28 Al, deduced levels from 26 Mg 0–36032

28 Al, deduced levels from

Nucleus continued energy levels continued

³⁶Ar, isospin pairing explanation for existence of low-lying vibrational states 0-70327

³⁶Ar, levels deduced from ³⁵Cl(³He, d), E=12 MeV 0-42747 ³⁶Ar, levels deduced from ³⁵Cl(³He, d), E=12 MeV 0-42747
 ³⁶Ar struct. from ³⁵Cl(³He, d)³⁶Ar up to 8.5 MeV 0-49514
 ³⁶Ar, levels deduced from ³⁷Cl(³He, d), E=12 MeV 0-42747
 ³⁸Ar struct. from ³⁷(³He, d)³⁸Ar up to 6.9 MeV 0-49514
 ⁴⁰Ar, props. obs. in ⁴⁰Ar (n,p)⁴⁰Cl 0-77515
 ⁴⁰Ar levels from ⁴⁰Ar (a,r,p)⁴⁰Ar, spin and parity assignment 0-38880
 ⁴¹Ar, from ⁴⁰Ar (d,pp)⁴¹Ar, and jj-coupling shell model 0-70452
 ³³As isobaric analogue states from ³²Ge(p,p) 3.30-3.37 MeV 0-38893
 ³³As sexcited states nature 0-73815
 ³⁵As from yray resonance scattering 0-70477

⁷As isomeric state, g=+1.146±0.007 for 426 keV 0-73813
⁷As excited states nature 0-73815
⁷As excited states nature 0-73815
⁷As someric state, g=+1.146±0.007 for 426 keV 0-73813
⁷As excited states of (h₉)³ configuration identified 0-67496
²¹¹At, 8 excited states of (h₉)³ configuration identified 0-67496
²¹²At, 8 excited states of (h₉)³ configuration identified 0-67496
²¹³At, 8 excited states of (h₉)³ configuration 0-60771
¹⁹⁵Au, study using ¹⁹⁶Pt(p,2n) and ¹⁹⁷Au(p,t) reactions 0-70517
¹⁹⁵Au, structure confirmed from eleg-ron capture decay of ¹⁹⁵Hg, branching ratios 0-46177
¹⁹⁶Au neutron single hole states from (p,d) 0-70499
¹⁹⁷Au, excited states studied, isomeric decay obs. multipolarity assignments 0-73832
¹⁹⁷Au, excited states studied, isomeric decay obs. multipolarity assignments 0-73832
¹⁹⁷Au, single particle analog state anomalies 0-67489
¹⁹⁷Au, single particle analog state anomalies 0-67489
¹⁹⁷Au, level scheme from γ-γ coincidence meas. and Coulomb excitation 0-64065
¹⁹⁸Au, level scheme from γ-γ coincidence meas. in ¹⁹⁷Au(n,γ) 0-49546
¹⁹⁸Au, level scheme from ¹⁹Pd 0-55144
¹⁹⁸B, levels deduced from ¹⁹Bp,t) reaction 0-42834
⁸B, ground and 1st two excited states from ¹⁹B(p,t), and DWBA 0-70598
⁸B, from ⁸Li(²He,p) and ⁸Li(²

U=39102

¹¹B cusps, threshold states and neutron emission 0=57896

¹³B*, formation of excited levels in capture of μ- by C nuclei 0=46203

¹³Ba, weak level at 1773 keV, ¹³Cs decay obs. 0=38984

¹³Ba, one and two neutron hole states from (p,d) and (p,t) reactions 0=70490

ba, one and two fleutron finde states from (p,a) and (p,a) feactions 0–70490 19 Ba metastable level, 198m Cs 8 -decay obs. 0–73868 98 Be, ground and first excited state from 9 Li(p,p)'Be 0–70594 98 Be, states from (°He,'Be) reactions on light nuclei at 30 MeV 0–49649 98 Be, 0°, 2°, 4° states from excitation energy spectrum in 12 C(α , 2 α)*Be, 12 Cr=100 MeV 0–49657

E α =100 MeV 0-49657 states from excitation thereby spectrum in G(x, 2x) bc, E α =100 MeV 0-49657 states from atrix theory 0-73781 states, cluster states, reaction matrix theory 0-73781 states, cluster states, reaction and s, cut off 0-52669 states from a transfer in the case in the case of the constraint of the co

16Be quadrupole deformation and relative reduced widths from 9Be(d,p) calc. 0-70644
Bi(A=201, 203, 205, 207), deduced from electron capture decays of Po 0-38942
200 Bi, intermediate coupling calculations for the unified model 0-57932
200 Bi, intermediate coupling calculations for the unified model 0-57932
200 Bi, intermediate coupling calculations for the unified model 0-57932
200 Bi, intermediate coupling calculations for the unified model 0-57932
200 Bi, intermediate coupling calculations for the unified model 0-57932
200 Bi, intermediate coupling calculations for the unified model 0-57932
200 Bi, isobaric analogue resonances for inelastic proton scatt. 0-42826
200 Bi, isobaric analogue resonances, elastic proton partial widths, microscopic calc. 0-70529
200 Bi, isobaric analogue resonances, elastic proton partial widths, microscopic calc. 0-70529
200 Bi, isobaric analogue of 200 Bp ground state in (p,n) reaction 0-73948
200 Bi isobaric analogue resonances from proton elastic scattering 0-70519
200 Bi isobaric analogue resonances from proton elastic scattering 0-70519
201 Bi, intermediate coupling calculations for the unified model 0-57932
201 Bi, intermediate coupling calculations for the unified model 0-57932
201 Bi, intermediate coupling calculations for the unified model 0-57932
201 Bi, intermediate coupling aclulations for the unified model 0-57932
201 Bi, intermediate coupling aclulations for the unified model 0-57932
201 Bi, intermediate coupling aclulations for the unified model 0-57932
201 Bi, intermediate coupling model 0-57934
202 Bi, jew-lying levels, in an intermediate coupling model 0-57914
203 Bi, jew-lying levels in an intermediate coupling model 0-57914
204 Bi, jew-lying levels in an intermediate coupling model 0-57914
205 Bi, jew-lying levels in an intermediate coupling model 0-57914
207 Bi, jew-lying levels in an intermediate coupling model 0-57914
208 Bi, jew-lying levels in an intermediate coupling model 0-57914
209 Bi, jew-lying levels in an intermediate coupling model 0-57914
209 Bi, j

Nucleus continued

energy levels continued ³⁹Ca from ³⁹K(p,n), excess mass -27281±6 keV 0-57906

 $^{40}\text{Ca},\,0^+$ and 2^+ states, description including 0p-0h, 2p-2h and 4p-4h 0-70451

⁴⁰Ca, at 7 to 9 MeV excitation 0-42748

⁴⁰Ca, collective effects, lifetimes, spins and decay modes of levels 0–38879 ⁴⁰Ca, deduced levels from ³⁹K(³He,d) and zero DWBA calculations for E=11.0 MeV 0–58016

E=11.0 MeV 0-58016

*0°Ca, two-nucleon density functions and correlation functions with realistic single-particle wave functions 0-55119

*0°Ca from ³⁹K (³He,dy) and ⁴⁰Ca (p,p'y) 0-67439

*0°Ca from ³⁹K (d,n), d3/2- 'p3/2 analogue states 0-67441

*0°Ca giant dipole resonance structure from ³⁹K (y,n)³⁸M 0-73903

*0°Ca g.s., neutron hole impurities from DWBA analysis of (d,p) reaction 0-70450

0-70450

4°Ca from proton scattering, and continuum states in ⁴1°Sc 0-73804

4°Ca from proton scattering, and continuum states in ⁴1°Sc 0-73804

4°Ca, core-particle interaction and fragmentation of single-particle levels

0-38881

4°Ca, from gamma-ray spectra 0-67442

4°Ca from ⁴Ca(p,d) 0-70604

4°Ca' angular momentum assignment inconsistencies 0-55126

4°Ca, and model continuum in nuclear bound states 0-57890

4°Ca analogue states, study with ⁴1′K(p, p)⁴1′K and ⁴1′K(p, n)⁴1′Ca 0-49617

4°Ca doublet near 4.10 and triplet near 4.44 MeV 0-67444

4°Ca, odd-parity states, calc. within shell-model employing ⁴⁰Ca as core 0-49517

4°Ca, nerraies, spins decay modes and lifetimes of first 3 excited states

**Ca, shell model continuum in nuclear bound states 0—57890
Ca analogue states, study with **K(p, p)*K and **K(p, n)Ca 0—49617
**Ca doublet near 4.10 and triplet near 4.44 MeV 0—67444
**Ca doublet near 4.10 and triplet near 4.44 MeV 0—67444
**Ca, odd-parity states, cale. within shell-model employing **OCa as core 0—49517
**Ca from isobaric analogue states in **Sc 0—70458
cd, even nuclei, from Pd(α, xmy) reactions 0—64032
Cd isotopes, phenomenological treatment of anharmonic effects 0—7349
**Ca from isobaric analogue states in **Sc 0—70458
cd, even nuclei, from Pd(α, xmy) reactions 0—64032
Cd isotopes, phenomenological treatment of anharmonic effects 0—38911
***OCd, deduced levels from Cd(p, γ)*P =5.7-7.5 MeV 0—38906
***OCd, deduced from radioactive y-decay of **Ion 0—55147
***OCd, from y-spectrum c2 MeV 0—38907
***OCd, deduced levels from Cd(p, γ)*P =5.7-7.5 MeV 0—38906
***OCd, deduced levels in **Ion 0 = 40.42841
***OCd, pround and 342 keV state wave functions 0—38907
***In OCd, ground and 342 keV state wave functions 0—38906
***OCd, deduced levels in **Ion 0 = 10.91841
***OCd, deduced levels from Cd(p, γ)*P =5.7-7.5 MeV 0—38906
**Ion 0 = 4.2841
***OCd, and 0 = 10.91841
**Ion 0 = 10.91

energy levels continued ⁵⁹Cu, branching ratios of resonance and bound states 0-77498

⁶¹Cu, N=29, Z=29 nucleus, level calculations using intermediate coupling model, stripping strengths 0-70461

63Cu, from n inelastic scatt. y-rays, 2.9 MeV 0-38888

⁶³Cu, N=29, Z=29 nucleus, level calculations using intermediate coupling model, stripping strengths 0-70461

63 Cu, negative parity states, props. in semimicroscopic model 0-49523

65Cu, from n inelastic scatt. γ-rays, 2.9 MeV 0–38888 65Cu, N=29, Z=29 nucleus, level calculations using intermediate coupling model, stripping strengths 0–70461

Figure 3. The plant of β decay to excited 0+ states 0–64085 Dy odd-mass isotopes, level study by (d, p) and (d, t) reactions 0–64050 155 Dy level scheme, 155 Ho decay obs. 0–77522

66°Cu retardation of β decay to excited 0+ states 0−64085
Dy odd-mass isotopes, level study by (d, p) and (d, t) reactions 0−64050
15°Dy level scheme, 15°Ho decay obs. 0−77522
156°Dy vibrational bands from gamma-ray spectra 0−64052
156°Dy, from 16°Ho decay and conversion electron spectra 0−46170
15°Dy ledeuced levels, mixing of gamma vibrational and ground state bands, from decay of 16°Tb 0−49542
156°Er, multiple Coulomb excitation of ground-state rotational band 0−49538
156°Er excited states studied, isomeric decay obs. multipolarity assignments 0−73832
156°Er scheme proposed through 168°Er (0−9 and 17°Er(d,t) reactions and via thermal-neutron captice in 168°Er 0−70507
Eu (A=151, 153), deduced levels by elastic scatt. of 12 MeV α 0−49536
156°Et, u, isobaric analogue resons., proton polarization meas. 0−38927
157°Eu, g-factor determ. of 11/2− excitation states 0−64040
157°Et, g-factor determ. of 11/2− and (p,α) 0−70420
157°Et, Fr=1/2 states from (p,p) and (p,α) 0−70420
157°Et, From 15°Sm p-spectrum obs. 0−38904
159°Et, from 15°F(p,d), 16 and 18 MeV 0−38860
159°Et, from 150°F(p,d), 16 and 18 MeV 0−38860
159°Et, fedeuced levels, from 160°F(p,d), 16 and 18 MeV 0−38860
159°Et, fedeuced levels, from 160°F(p,d), 16 and 18 MeV 0−38860
159°Et, fedeuced levels from 160°F(p,d), 16 and 18 MeV 0−38860
159°Et, fedeuced levels from 160°F(p,d), 16 and 18 MeV 0−38860
159°Et, fedeuced levels from 160°F(p,d), 16 and 18 MeV 0−38860
159°Et, fedeuced levels from 160°F(p,d), 16 and 18 MeV 0−38860
159°Et, fedeuced levels from 160°F(p,d), 16 and 18 MeV 0−38860
159°Et, fedeuced levels from 150°F(p,d), 16 and 18 MeV 0−38860
159°Et, fedeuced levels from 150°F(p,d), 16 and 18 MeV 0−38860
159°Et, fedeuced levels from 150°F(p,d), 16 and 18 MeV 0−38860
159°Et, fedeuced levels from 150°F(p,d), 16 and 18 MeV 0−38860
159°Et, fedeuced levels from 150°F(p,d), 16 and 1

5°Fe, ground state (p,n) Q values 0-77552 5°Fe analogue resonances of excited states by (p, γ) and (p,p) reactions in 5°Fe 0-70469

Free, ground state (p,iii) yatues 0—7532
Free analogue resonances of excited states by (p, γ) and (p,p) reactions in Free 0—70469
Free 0—70469
Free manetic moments of first excited 2+ state 0—70471
Free recited levels obs. from 224 Ac α-deay 0—60791
Free recited levels obs. from decay of 225 Ac 0—52739
Free analogue resonances of excited 0+ states 0—64085
Free analogue resonances of cast of 225 Ac 0—52739
Free recited levels from decay of 225 Ac 0—52739
Free analogue resonances of cast of 225 Ac 0—52739
Free analogue resonances of 225 Ac 0—52739
Free analogue resonances of 225 Ac 0—60791
Free decay of 792 0—57901
Free decay of 792 0—57902
Free decay of 792 0—

³He, electromagnetic structure, charge and magnetic form factors 0-73774

0–73774

He, ground state energy estimation based on dual core model 0–60752

He virtual states using $^8\text{Li}(p,\alpha)$ and (p,α) 0–70388

He, deduced singlet strength, from $^3\text{H}(p,p)$ 4He and $^4\text{He}(p,p)$ 0–49613

He, first excited 0* state, self-consistent calc. 0–70390

He, ground and first excited states, by shell model 0–73778

He, ground state, realistic nuclear charge-density 0–77480

He, Hartree-Fock calcs. with four-body interaction 0–52667

He assignment of 0* state confirmed, new values of monopole matrix element, evidence for M2 resonance at 24 MeV 0–64107

He deduced levels from $^3\text{He}+^2\text{H}$ and $^4\text{He}+^2\text{H}$ coincidence studies 0–39100

He from $^7\text{Li}(d,\alpha)^5\text{He}$ 0–70392

Hí ground state, application of generator-coordinate method to rotational spectra 0–77475

Nucleus continued energy levels continued

 $^{178}\mathrm{Hf}$, level scheme from conversion electron spectra in thermal n capture of $^{177}\mathrm{Hf}$ 0-52705

¹⁷⁹Hf, high spin isomer ^{179m2}Hf 0-64058

¹⁷⁹Hf excited states studied, isomeric decay obs. multipolarity assignments 0-73832

10-13832
179 Hf photoactivation, level cross-sections 0-55137
179 m(2) Hf high spin isomer, intraband branchings in the ground-state rotational sequence of 179 Hf 0-57927
Hg isotopes, props. of low-lying states 0-55138
178 Hg first 2+ states, excitation probabilities, deduced from γ ray spectra 0-49508

 $^{0-49508}$ of first $^{2+}$ states, excitation probabilities, deduced from γ ray spectra $^{0-49508}$ glow-lying, from decay of 200 Tl $^{0-70518}$ of $^{0-70518}$ or 10 states, excitation probabilities deduced from γ ray spectra 0–49508

200Hg low-lying, from decay of 200T1 0–70518

200Hg low-lying, from decay of 200T1 0–70518

200Hg first 2+ states, excitation probabilities deduced from γ ray spectra 0–49508

204Hg first 2+ states, excitation probabilities deduced from γ ray spectra 0–49508

166Ho, rotational bands studied by neutron capture γ-ray spectroscopy 0–67485

127I from Coulomb excitation 0–64035

109In, level structure from decay of 109Sn 0–52692

113In, levels excited by oxygen ion bombardment 0–42759

114In retardation of β decay to excited 0+ states 0–64085

115In, levels excited by oxygen ion bombardment 0–42759

115In, nucl, photoactivation obs. 0–70484

115In first excited states from 114Cd(2He,d) 0–70660

117In, level scheme from 117Cd and 117Cd decay 0–49575

Ir, odd A-isotopes, spectroscopic pros. of low lying levels, by model including particle-vibr. and part.-rot. coupling 0–38938

1091Ir, collective states 0–64064

1091Ir, excited states studied, isomeric decay obs. multipolarity assignments 0–73832

10–73832

1092Ir, from 1093Os γ-spectrum obs. 0–38904

1093Ir, collective states 0–64064

108K effective interaction calc. 0–38853

1911r, excited states studied, isomeric decay obs. multipolarity assignments 0-73832
1921r, from 193Os γ-spectrum obs. 0-38904
1931r, collective states 0-64064
38K, effective interaction calc. 0-38853
38K, εξ. 40 MeV, from 39K(ρ,d), 16 and 18 MeV 0-38860
39K giant dipole resonance structure from 39K (γ,n)38mK 0-73903
40K positive parity states from 40Ar(ρ,nγ)40K reactions 0-70448
41K, deduced levels from 40Ar(3He,d)41K for E=10 MeV 0-57908
41K, ground state (ρ,n) Q values 0-77552
41K, isobaric analogue states 0-42750
30Kr from γ-spectra 0-64027
31Kr from γ-spectra 0-64027
31Kr from γ-spectra 0-64027
31Kr from γ-spectra 0-64027
31AL, deformation of excited levels 0-64037
313La, deformation of excited levels 0-64037
313La, from n inelastic scatt. γ-rays, 2.9 MeV 0-38888
319La, photoexcitation with thermal neutron capture gamma rays and deduced levels 0-57923
319La from Coulomb excitation by inelastic scattering of α-particles 0-70491
319La from (γ, p), isobaric analogue states 0-67480
40La, beta-decay matrix elements and the implications for isobaric analog states 0-57957
410La analogue states from proton scattering by 139La 0-70493
4Li excited states from γ-11e π-mesic decay interactions 0-73791
51Li, study within excitation range of 17.8-21.1 MeV, by radiative capture reaction 0-49499
51Li from 6Li (14E,α)3Li 0-70392
51Li excited states from γ-11e π-mesic decay interactions 0-73791
51Li, study within excitation range of 17.8-21.1 MeV, by radiative capture reaction 0-49499
51Li from 6Li (14E,α)3Li 0-70392
51Li excited states from γ-11e π-mesic decay interactions 0-73791
51Li, study within excitation range of 17.8-21.1 MeV, by radiative capture reaction 0-49499
51Li from 6Li (14E,α)3Li 0-70392
51Li excited states from γ-11e π-mesic decay interactions 0-73791
51Li, study within excitation and correlation functions with realistic single-particle wave functions 0-55119

scatt. 0–42734

*Li, two-nucleon density functions and correlation functions with realistic single-particle wave functions 0–55119

*Li deduced levels, from *Li(n,p) *He(O) and *Li(n,n')*Li(3.56) 0–39066

*10*Lu pairing phenomenon of */γ* proton */γ* neutron 0–52704

*11*Lu pairing phenomenon of */γ* proton */γ* neutron 0–52704

*12*Lu pairing phenomenon of */γ* proton, */γ* neutron 0–52704

*12*Lu pairing phenomenon of */γ* proton, */γ* neutron 0–52704

*12*Lu, levels up to excitation energy of 1628 keV from *175*Lu(d,t) at E_σ=12

MeV 0–49.543

Mg (A=24, 25 and 26), low-lying levels from elastic and inelastic proton scatt. 0–70.584

*1Mg, meas. of T₂==-3/γ masses, using mag. spectrograph 0–67419

*21Mg, low-lying excited states from *20*Ne(*14e,n'), 0–67429

*21Mg, deduced levels from *4Mg(*14e,α'), 0–15 MeV 0–39114

*21Mg, calc. from angular momentum states 0–49504

*21Mg, selective population of highly excited states in *16O(*12C,α') reaction 0–52805

*24Mg, selective population of states from an analysis of Doppler-broadened

0-52805

²⁴Mg, spin assignment of states from an analysis of Doppler-broadened gamma rays 0-52681

²⁵Mg ground state rotational band, populated preferentially in (p,t), and DWBA 0-70600

²⁶Mg ground state shape 0-38872

²⁶Mg higher lying levels, excitation of 1.37 MeV level by elastic and inelastic scattering 0-46128

²⁶Mg isobaric analogue levels, shell model calc. 0-38870

²⁷Mg deduced levels from ²⁶Mg(³He,α), E=15 MeV 0-39114

²⁷Mg rotational model from (d,α) cross-sections 0-70429

²⁶Mg, from study of ²⁷Al(n,d) at 14.1 MeV 0-77560

²⁷Mg excitation energies, γ-branching, β-decay studied by ²⁶Mg(d,pγ)²⁴Mg

Fig. (16) study of Al(n,a) at 14.1 MeV 0-7/300 2^{8} Mg (d,py) 2^{4} Mg 0-70653

0-70653
53Mn, deduced levels and decay of the 2p_{1/2} analogue states from ⁵²Cr(p, γ), E=1.0-1.8 MeV 0-57979
53Mn feaduced levels from ⁵³Cr(p,nγ)⁵³Mn reaction 0-42753
53Mn from (p,n), neutron spectra meas. 0-60759
53Mn, from n inelastic scatt. γ-rays, 2.9 MeV 0-38888
56Mn, below 1 MeV excitation energy from (n,γ) and (d,p) 0-70467
56Mn, from ⁵³Mn(d,p)⁵⁶Mn with 10.1 MeV deuterons 0-49666
53Mn from ⁵³Mn (d,p)⁵⁶Mn with 10.1 MeV deuterons 0-49666
53Mn from (γ, p), isobaric analog states 0-67465
53Mn, ⁷⁶Mn, analysed from ⁵²Tc, decay 0-49528
53Mo from ⁵²Mo(p,γ), analogue states obs. 0-70609
56Mn from ^{56m,96}Tc decay γ-spectra obs. 0-38973

Nucleus continued energy levels continued

⁹⁶Mo from neutron capture in ⁹⁵Mo 0-64029

¹³No level scheme, from ⁹⁷Nb decay 0–55142 ¹³N, 20-30 MeV, ¹⁰B(³He₁α)⁹B and ¹²C(p,p)¹²C reactions 0–42736 ¹³N, deduced levels from $^{14}N(^{3}He\alpha)$, E=2.5-8.5 MeV 0-60825

¹³N, deduced levels from ¹⁴N(1 He α), E=2.5-8.5 MeV 0-60825 ¹³N, T=3/2 states, isopin forbidden resonance width cales. 0-67421 ¹³N, T=3/2 states from ¹³C+p obs. 0-42735 ¹⁴N, α -cluster struct., from (π -,2nd) reaction 0-77568 ¹⁴N, effective interaction cale. 0-38853 ¹⁴N, ground state, use of perturbation theory and statistical concepts 0-42737

¹⁵N, 13 42 MeV T=³/₂ state obs. in various reactions 0-64000 ¹⁵N, energy separation of doublet at 9.15 MeV, using ¹⁴N(d, py) reaction 0-49502

13N, energy separation of doublet at 37.5 No. 1, 13N, anergy separation of doublet at 37.5 No. 1, 13N, anergy separation of doublet at 37.5 No. 1, 13N, and 39.4h states from $^{12}\text{C}(^{7}\text{Li},\alpha)$ 0–73788 15N level structure determ. by $^{11}\text{B}(\alpha,\eta)^{14}\text{N}$ 3.6·3.8 MeV 0–58007 15N* formation of excited levels in capture of μ^- by 0 nuclei 0–46203 15N<6.33 MeV excitation, from $^{12}\text{C}(^{3}\text{He},q)^{15}\text{N}$, 14 MeV 0–38858 16N, cusps, threshold states and neutron emission 0–57896 16N deduced levels from $^{10}\text{C}(^{3}\text{d},q)$ for E=4.75–11.5 MeV 0–57895 12Na, mirror state structure from angular correlation studies with the e reaction 0–52679 12Na lowest negative parity state from $^{20}\text{Ne}(^{3}\text{d},q)$ 10–70428 12Na, a deduced levels, from $^{22}\text{Ne}(^{3}\text{He},q)$ 0–77574 12Na, a genue of the energy of

PNA, spin, parity and multipole mixing ratio assignments of low levels of PNA, spin, parity and multipole mixing ratio assignments of low levels of PNA, and propound, rel. to **PF(α,α) excitation functions, 3.3-5.0 MeV 0-3094 (2014).

**PNA, excited levels up to 3.92 MeV, from elastic and inelastic proton scatt. meas. 0-3903 (2018).

**PNA, spond state band, collective calculations 0-64009 (2018).

**PNA, isobaric analogue states 0-42750 (2018).

**PNA, isobaric analogue states on the properties of the

Nucleus continued

energy levels continued

neteus continued
energy levels continued
energy levels continued
ei>Ni, excited states related to shell model 0—64023
ei>Ni, level structure from eiNi(n,y) reaction 0—46139
ei>Ni, levels deduced from decay of ei²Co and ei²Cu 0—52724
ei>Ni, first excited state, from ei>Ni(r,y)*, E=7646 keV 0—39015
ei>Ni, first excited state, energy, lifetime and g-factor 0—49524
ei>Ni, ground and second excited states, fine structure of isobaric analogues 0—67458
ei>Ni, T=3/2 analogue of ground state of ei³Co for ei>Ni, obs. for 27.5 MeV protons in ei>Ni(k,d) 0—60761
ei³O, meas. of T==-3/2 masses, using mag. spectrograph 0—67419
ei³O <8.32 MeV excitation, from iin (He,d)iio, 14 MeV 0—38858
ei³O single-particle spectroscopic factors from (d,n) 0—70650
eiO, α-cluster struct., from (π-,2nd) reaction 0—77568
eiO, cluster-model vertex functions, monopole form factors 0—49505
eiO, deduced levels reduced α-widths, from ii²C(i*Li,t) 0—46248
eiO, eluster struct.
eiO, ground state, 2 particle-2 hole admixture 0—70410
eiO, ground state, 2 particle-2 hole aimixture 0—70410
eiO, ground state averfunction, from iiO(μ,n) reaction 0—70418
eiO, ground state wavefunction, from iiO(μ,n) reaction 0—70418
eiO, ground state wavefunction, from iiO(μ,n) reaction 0—70418
eiO, ground state wavefunction, from iiO(μ,n) reaction 0—70418
eiO, ground state states, effect of ground state correlations 0—52667
eiO, ground states, effect of ground-state correlations 0—52672
eiO, states of 2s-1d shell nuclei based on the four-particle—four-hole state 0—49504
eiO, struct. in giant reson. region, from e scatt. and μ capture in continuum model 0—39021 ¹⁰O, states of 2s-1d shell nuclei based on the four-particle—four-hole state 0–49504 ¹⁶O, states of 2s-1d shell nuclei based on the four-particle—four-hole state 0–49504 ¹⁶O, struct. in giant reson. region, from e scatt. and μ capture in continuum model 0–39021 ¹⁶O, two-nucleon density functions and correlation functions with realistic single-particle wave functions 0–55119 ¹⁶O from ¹³C(°Li₁)¹⁶O 0–73786 ¹⁶O 3– excitation, ground state correlation effect calc. 0–73785 ¹⁶O deduced 6+ level from ¹²C(α,α,α) and ¹²C(α,α,α') 0–52671 ¹⁶O deduced shell amplitudes from ¹⁴C(²He, n), double- stripping study 0–42738 ¹⁶O even-even N=Z nuclei, energy of quartet excited states 0–73807 ¹⁶O ground state, effect of 2p-2h configurations in ¹⁶N on ¹⁶O μ capture rate 0–73975 ¹⁶O struct from ¹⁵N(²He,d)¹⁶O at 16 and 24.9 MeV 0–49503 ¹⁶O widths of 6.92 MeV and 7.12 MeV levels 0–64002 ¹⁷O, 2p-1h strength contributes only above 7 MeV excitation energy 0–73788 ¹⁷O, 5p-4h states from ¹²C(⁷Li,d) 0–73788

170, 2p-1h strength contributes only above 7 MeV excitation energy 0—73789
170, 5p-4h states from 12C(*Li,d) 0—73788
170, low-lying, even-parity, calc. of spectrum 0—52673
170, low-lying negative parity states, from 160(p,d)170 0—70411
170, low lying states, shell model extension 0—57897
170 excited state at 20.4 MeV, assignment from data on 160(p,n)160 0—49622
170 from 160(p,p) at 5 to 13 keV, four narrow resonances 0—57990
170 level structure study from 170(*El,d) and 170(*Li,l) reactions 0—73787
180, deformed state admixtures, realistic forces 0—73790
180, of valence particles calculated using harmonic oscillator intermediate states 0—52634
180, states up to excitation energy 12.5 MeV obs., 6+ state at 11.69 MeV belongs to ground state rot. band 0—64003
180 deduced levels and resonances from 140(p, and 140(p, n) 0—57898
180 in harmonic oscillator shell model using one boson exchange potentials 0—57899
0s, prolate-oblate difference in deformation energy 0—64060
1880s, determination of the electric quadrupole moment of the first 2+ states 0—42773
1900s, determination of the electric quadrupole moment of the first 2+ states 0—42773
1900s, determination of the electric quadrupole moment of the first 2+ states 0—42773
1900s, determination of the electric quadrupole moment of the first 2+ states 0—42773

states 0-42773 "9°0 Ir 0-38862 "9°0 Ir 0-38862 "9°0 S levels populated by 1°0 Ir 0-38862 "9°0 S, determination of the electric quadrupole moment of the first 2° states 0-42773 "9°P, ang. moment of 4081 keV excited level 0-38877 "9°P from 3°Si(d,ny), ny angular correlation, branching ratios 0-42742 "3°P, anglar distributions to ground and 4 lowest excited states from 2°Si(He,p) reaction 0-70654 "9°P, search for triton cluster structure 0-49673 "1°P, intermediate-coupling structure in 2s-1d shell 0-64012 "3°P, investigation via 3°P (t,py) 3°P reaction of bound states 0-77495 "3°P, investigation via 3°P (t,py) 3°P reaction of bound states 0-77495 "3°P a level scheme from 23°Th β-decay obs. 0-38948 "Pb (A=209, 207), single particle components of particle vibrational states 0-70776 "9°P b isobaric analogue resonances from proton elastic scattering 0-70519 "1°P (apr) and particle vibrational states 0-67409 b, quasi-particle structure of ground state of pairing Hamiltonian 0-67400 "1°P (apr) and particle vibrational states 0-67409 b, quasi-particle structure of ground state of pairing Hamiltonian 0-674010 "1°P (apr) and particle vibrational states 0-67409 b, quasi-particle structure of ground state of pairing Hamiltonian 0-674010 "1°P (apr) and particle vibrational states 0-674010 "1°P (apr) and particl

0-427/6
204Pb isobaric analogue resonances from proton elastic scattering
0-70519
206Pb, quasi-particle structure of ground state of pairing Hamiltonian
0-67490
206Pb, weak β branching in ²⁰⁶Tl decay 0-73858
206Pb isobaric analogue resonances from proton elastic scattering
0-70519
207Pb, ³/₂-state, from proton inelastic scatt., distorted wave anal. 0-73926
207Pb, doublet (particle- vibration states), properties by solution of Schrodinger equation 0-57934
207Pb, particle parameters in K, L, and M shells, by e-γ ang. correlations meas. 0-38943
207Pb from ²⁰⁷Pb(p, p'), excitation functions meas. 0-67491
207Pb from ²⁰⁸Pb(he.α)²⁰⁷Pb at 28 MeV 0-49550
207Pb isobaric analogue resonances from proton elastic scattering 0-70519
208Pb, iso-spin mixing for the 0+ analogue of ground state and correction factors to Coulomb displacement energies 0-57935
208Pb, proton-particle-hole states from ²⁰⁹Bi(d, ³He)²⁰⁸Pb for E_d=50 MeV 0-52707
208Pb, quadrupole and octupole vibrations 0-64070

0-52707

**Depth quadrupole and octupole vibrations 0-64070

**Depth quadrupole and octupole vibrations 0-64070

**Depth quadrupole and octupole vibration for small and high momentum transfer for electron scattering 0-57971

**Depth quadrupole vibration for small and high momentum transfer for electron scattering 0-57971

**Depth quadrupole vibration for small and high momentum transfer for electron scattering 0-57971

**Depth quadrupole vibration for small and high momentum transfer for electron scattering 0-57971

**Depth quadrupole vibration for small and high momentum transfer for electron scattering 0-57971

**Depth quadrupole vibration for small and high momentum transfer for electron scattering 0-57971

**Depth quadrupole vibration for small and high momentum transfer for electron scattering 0-57971

**Depth quadrupole vibration for small and high momentum transfer for electron scattering 0-57971

**Depth quadrupole vibration for small and high momentum transfer for electron scattering 0-57971

**Depth quadrupole vibration for small and high momentum transfer for electron scattering 0-57971

**Depth quadrupole vibration for small and high momentum transfer for electron scattering 0-57971

**Depth quadrupole vibration for small and high momentum transfer for electron scattering 0-57971

**Depth quadrupole vibration for small and high momentum transfer for electron scattering 0-57971

**Depth quadrupole vibration for small and high momentum transfer for electron scattering 0-57971

**Depth quadrupole vibration for small and high momentum transfer for electron scattering 0-57971

**Depth quadrupole vibration for small and high momentum transfer for electron scattering 0-57971

**Depth quadrupole vibration for small and high momentum transfer for electron for small and high momentum transfer for electron scattering 0-57971

**Depth quadrupole vibration for small and high momentum transfer for electron scattering 0-57971

**Depth quadrupole vibration for small and high momentum transfer for electron scatterin

energy levels continued ⁰⁸Pb isobaric analogue of ground state in ²⁰⁸Pb(p,n) ²⁰⁹Bi 0-73948

208Pb isobaric analogue resonances from proton elastic scattering

0-70519

208Pb isobaric analogue resonances, K-matrix analysis 0-73838

208Pb(p,p'), analog resonances and polarization, E=14.85-15.05 MeV

0-42723

209Pb, 1/2+ doorway resonance at 500 keV, particle-vibration model

0-73839

209 Pb, particle-core states 0-38945

105 Pd, levels deduced from radioactive decay of 105 Ag and measurement of internal contentions (partners) to 5705.4

20°Pp, particle-core states 0—38945

10°Pd, levels deduced from radioactive decay of 105Ag and measurement of internal conversion electrons 0—57954

10°Pd, from decay of 106mRh 0—46167

10°Pd giant dipole resonance, vibrational and isospin splitting from photoneutron and (p.p) cross-sections 0—73818

10°Pd one octupole-one quadrupole phonon states from proton scattering 0—67474

14°Pm, obs. in β—decay of 14°Sm 0—67507

15°Pm, nature of low-lying excited states 0—46146

20°Po, deduced levels from decay of 20°At 0—55145

21°Po isobaric analogue resonances corresponding to 21°Bi states from 20°Bi(p,p') 0—70531

214°Po, deduced from decay of 214°Pb and other 226Ra daughters 0—38998

215°Po, 272 keV transition, spin assignments 0—38946

215°Po, 272 keV transition, spin assignments 0—38946

215°Po, 272 keV transition, spin assignments 0—67480

141°Pr, from (p. p), isobaric analog states 0—67480

141°Pr, from n inelastic scatt, p-rays, 2.9 MeV 0—38888

143°Pr, 57 and 351 keV levels struct. 0—38926

144°Pr, levels determination and energies and intensities of p-rays for 144°Ce radioactive decay 0—604039

144°Pr excited states, 144°Ce decay obs. 0—70552

Pt, n reaction, reson, parameters and spin, E=4 830 eV 0—39073

Pt prolate-oblate difference in deformation energy 0—64060

188°Pt, first collective levels 0—70510

188°Pt, first collective levels 0—70510

189°Pt, first collective levels 0—70510

199°Pt, first first two excited 2+ states 0—70514

192Pt, from 192Ir decay, by sum peak and sum coincidence studies 0-70513
192Pt, from 192Ir decay obs. 0-38984
192Pt, gractors of first two excited 2+ states 0-70514
192Pt, struct. study by e-γ and γ-γ directional correlations 0-49545
194Pt, level scheme from 194 decay 0-60788
196Pt, single particle analog state anomalies 0-67489
240Pu, two-phonon octupole vibrational band for excitation energies of 1410.8 and 1438.5 keV 0-52711
223Ra, radioactive decay, levels and daughter products 0-60792
223Ra, radioactive decay, levels and daughter products 0-60792
223Ra from α-decay of 228Th obs. 0-46180
225Ra from α-decay of 228Th obs. 0-46180
80Rb from γ-spectra 0-64027
83Rb from γ-spectra 0-64027
83Rb from γ-spectra 0-64027
83Rb from γ-spectra 0-64027
83Rb, level determ. using 86Sr(d, α)84Rb and 88Sr(d, α)86Rb reactions 0-60762
90Rb, level determ. from 90Kr decay 0-64086

⁸⁴Rb, ⁸⁶Rb, [evel determ. using ⁸⁶Sr(d, α)⁸⁴Rb and ⁸⁸Sr(d, α)⁸⁶Rb reactions 0–60762

⁹⁰Rb, level determ. from ⁹⁰Kr decay 0–64086

⁹¹Rb, level determ. from ⁹¹Kr decay 0–64086

⁹¹SRb, expin values from γ - γ angular correlation 0–64061

⁹²Rh, anomalous ⁵/₃+ and ⁷/₄+ states from decay of 21 min ⁹⁹Pd 0–38902

¹⁰³Rh, ¹⁰³Ru decay obs. 0–49573

¹⁰⁵Rh from ¹⁰⁴Rh(+let) at 18 MeV and ¹⁰⁸Pd(p, α) at 15 MeV, spectroscopic study 0–57903

²¹⁹Rn, radioactive decay 0–60790

²¹⁹Rn, radioactive decay 0–42800

²¹⁹Rn, radioactive decay 0–57961

⁹⁷Ru, excited levels, from γ decay of ⁹⁷Rh 0–38974

¹⁰⁰Ru, discussion in terms of phonon and rotational models from ¹⁰⁴Ru (t,p) ¹⁰⁶Ru from ¹⁰⁶Tc decay 0–64030

¹⁰⁸Ru from ¹⁰⁶Tc (37 sec) decay 0–64030

¹⁰⁸Ru from ¹⁰⁶Tc (8 sec) decay 0–64030

¹¹S, deduced levels from ¹²S(¹He, α) and ¹³S(He, αγ) E=9.0–12.2 MeV 0–42744

¹²S. collective nature of second 2+ state 0–64013

0 -42744

328, collective nature of second 2* state 0-64013

338, in boson approx. model 0-60758

338, in boson approx. model 0-60758

338, search for α-particle structure 0-46252

338, search for α-particle structure 0-46252

338, staty using 38(3+6,μ) 0-70439

338 study using 38(3+6,μ) 0-70439

338, from 38(1d,3+6) obs. 0-39119

348 deduced levels, lifetimes and decay modes from 31P(α,py) 0-57905

348 lifetimes, branching ratios and excitation energies of first nine excited states 0-70443

348, from 37Cl(d,3+6) obs. 0-39119

349, from 37Cl(d,3+6) obs. 0-39119

340, from 37Cl(d,3+6) obs. 0-39119

341, from 37Cl(d,3+6) obs. 0-39119

342, from 37Cl(d,3+6) obs. 0-39119

343, from 37Cl(d,3+6) obs. 0-39119

344, from 37Cl(d,3+6) obs. 0-39119

345, from 37Cl(d,3+6) obs. 0-39119

346, from 37Cl(d,3+6) obs. 0-39119

347, from 37Cl(d,3+6) obs. 0-39119

348, from 37Cl(d,3+6) obs. 0-39119

349, from 37Cl(d,3+6) obs. 0-39119

340, from 37Cl(d,3+6) obs. 0-39119

340, from 37Cl(d,3+6) obs. 0-39119

340, from 37Cl(d,3+6) obs. 0-39119

341, from 37Cl(d,3+6) obs. 0-39119

342, from 37Cl(d,3+6) obs. 0-39119

343, from 37Cl(d,3+6) obs. 0-39119

344, from 37Cl(d,3+6) obs. 0-39119

345, from 37Cl(d,3+6) obs. 0-39119

346, from 37Cl(d,3+6) obs. 0-39119

347, from 37Cl(d,3+6) obs. 0-39119

348, from 37Cl(d,3+6) obs. 0-39119

349, from 37Cl(d,3+6) obs. 0-39119

0–38914
Sb isotopes, odd-mass low-energy spectra 0–38915
11°Sb, deduced levels from 113 $\ln(\alpha,2n_f)$, $E\alpha$ =20.27 MeV 0–42762
11°Sb, level scheme 0–52695
11°Sb, level scheme 0–52695
11°Sb, level scheme 0–52695
113°Sb, lev

4 Sc analysis of stripping to quasibound levels 0-70656 4 Sc continuum states in 4 Ca(p,py) 4 Ca 0-73804 4 Sc from 4 Ca(3He,py), angular correlation study 0-55127

Nucleus continued energy levels continued

 43 Sc, $K_{\pi}=^{3}/_{2}$ rotational band, evidence for existence 0-67445

43Sc, odd-partiy states, calc. with shell- model employing 40Ca as core 0-49517

0-49517

4°Sc, ground state (p,n) Q values 0-77552

4°Sc, level scheme, by 4°Sc(p,p'p') at Ep=1.8-4.5 MeV 0-52683

4°Sc, low-lying odd parity states 0-52685

4°Sc, low-lying states from thermal neutron capture in 4°Sc 0-67540

4°Sc, struct. from 4°Ca(3°He,t) at E_{3h3}=15 MeV 0-38884

4°Sc analogue spin mixing 0-67449

4°Sc analogue spin mixing 0-67449

4°Sc isobaric analogue resonance corresponding to 4°Ca ground state
0-70605

**Sc analogue spin mixing 0-67449
**Sc isobaric analogue resonance corresponding to **9Ca ground state 0-70605
**Sc isobaric analogue states and **9Ca spins and parities 0-70458
**ZSc, population by Ge(α,2nγ) and Ge(α,4nγ) reaction, study 0-70476
**Sc, population by Ge(α,2nγ) and Ge(α,4nγ) reaction, study 0-70476
**Sc, proposed scheme from decay of **3Br 0-52725
**Sc 3.8 MeV (p,nγ) obs. 0-38895
**Sc, energies of levels populated in **6Br decay 0-46165
**Sc, isobaric analogue resonances from neutron decay, spin assignments 0-67462
**Sc, population by Ge(α,2nγ) and Ge(α,4nγ) reaction, study 0-70476
**Sc, population by Ge(α,2nγ) and Ge(α,4nγ) reaction, study 0-70476
**Sc, population by Ge(α,2nγ) and Ge(α,4nγ) reaction, study 0-70476
**Sc, population by Ge(α,2nγ) and Ge(α,4nγ) reaction, study 0-70476
**Sc, population by Ge(α,2nγ) and Ge(α,4nγ) reaction, study 0-70476
**Sc, population by Ge(α,2nγ) and Ge(α,4nγ) reaction, study 0-70476
**Sc, population by Ge(α,2nγ) and Ge(α,4nγ) reaction, study 0-70476
**Sc, population by Ge(α,2nγ) and Ge(α,4nγ) reaction, study 0-70476
**Sc, population of Ge(α,2nγ) and Ge(α,4nγ) reaction, study 0-70476
**Sc, population of Ge(α,2nγ) and Ge(α,4nγ) reaction, study 0-70476
**Sc, population of Ge(α,2nγ) and Ge(α,4nγ) reaction, study 0-70476
**Sc, population of Ge(α,2nγ) and Ge(α,4nγ) reaction, study 0-70476
**Sc, population of Ge(α,2nγ) and Ge(α,4nγ) reaction, study 0-70476
**Sc, population of Ge(α,2nγ) and Ge(α,4nγ) reaction, study 0-70476
**Sc, population of Ge(α,2nγ) and Ge(α,4nγ) reaction 0-77492
**Si, itage content of Ge(α,2nγ) and Ge(α,2nγ) and Ge(α,2nγ) reaction 0-77492
**Si, itage content of Ge(α,2nγ) and Ge(α,2nγ) reaction 0-49662
**Si, itage content of Ge(α,2nγ) and Ge(α,2nγ) reaction 0-49662
**Si, itage content of Ge(α,2nγ) reaction of Ge(α,2nγ) reaction of Ge(α,2nγ) reactions of Ge(α,2nγ) reactions of Ge(α,2nγ) reactions of Ge(α

U-49538 populated by decay of ^{152m}Eu 0-49537 ¹⁵²Sm populated by decay of ^{152m}Eu 0-49537 ¹⁵⁴Sm, excitation probabilities 0-64045 Sn, 2p-2h and 2-quasi-particle excitations 0-70473 Sn (A=111-123) from Sn (p.d) (cubic A= 112-124), angular distributions 0-42758

Sn, 2p-2h and 2-quasi-particle excitations 0—70473
Sn (A=111-123) from Sn (p,d) (cubic A= 112-124), angular distributions 0—42758
Sn isotopes, isobar analogue states 0—70568
Sn isotopes, particle number projection effect 0—57920
Sn isotopes, self-consistent core-particle coupling calc. 0—70485

113Sn from 112Sn(d,p) 0—70483

117Sn, spectroscopic factors from 114Sn(α,³He) reaction 0—39125

118Sn deduced levels from 119Sn(γ,γ'), E=6988 keV 0—39015

129Sn, 1p-1h states 0—70486

129Sn identification of s- and p-levels by moving sample method, neutron cross sections 0—49534

122Sn 1p-1h states 0—70486

123Sn from 12Sn(d,p) 0—70483
Sr conservation of seniority in 1g_{9/2} neutron shell using neutron transfer reactions 0—64028
Sr isotopes, effective interaction 0—38897

85Sr, log ft values, from decay of 84Y 0—38972

85Sr, log ft values, from decay of 86Y 0—57916

86Sr, level scheme from decay of 86Y 0—52726

87Sr from 85r(p, p), structure study in particle core model 0—67464

87Sr study using (d,t) and (d,p) at 20.65 MeV 0—57916

88Sr, deduced levels and J, directional γγ correlation measurements from 85r study using (d,t) and (d,p) at 20.65 MeV 0—57916

88Sr, revel scheme from decay of 86Y 0—52726

87Sr from (γ, p), isobaric analogue states 0—67465

87Sr, 30, 3.7 MeV levels, obs. 0—38898

87Sr, and 3.0 3.7 MeV levels, obs. 0—38898

87Sr, meas. of excitation curves for 4 states 0—770478

87Sr, yn to 7 MeV, spin assignments to 32 levels above 618.9 KeV 0—46175

18Tr levels deduced from γ-ray and conversion electron spectra following proton bombardment 0—70508

18Tra, decay of 18THf, search for population of levels above 618.9 KeV 0—46175

18Te levels deduced from Sn(α, 2ny) 0—38912

0–49533 Te isotopes, $117\leqslant A\leqslant 130$, compared with models 0–67476 Te isotopes, $117\leqslant A\leqslant 130$, compared with models 0–67476 Te levels deduced from $Sn(\alpha,2np)$ 0–38912 Te, levels deduced from $Sn(\alpha,2np)$ 0–38912 Te/Te, levels deduced from $Sn(\alpha,2np)$ 0–38912 Te/Te, educed levels from $1^{24}\text{Te}(d,d')$ and $1^{24}\text{Te}(d,d)$ 0–60828 Te/Te, scheme 0–38916 Te deduced from differential cross sections of inelastic proton scattering 0–40608

124 Te level scheme from 124 Sb 0–73819 124 Te level scheme from 124 Sb decay obs. 0–42791 125 Te, factors of 322 and 462 keV levels, obs. 0–38917 126 Te, 128 Te, 130 Te, existence of 2-particle 7– and 5– levels 0–46144 126 Te deduced from electron capture and β^+ decay of 126 I 0–49577

```
Nucleus continued energy levels continued in decay of <sup>128</sup>Sb** 0–64090 in order, configuration mixing in (t/α) reaction 0–70661 in order in
              Nucleus continued
                                             energy levels continued
                                                                  <sup>126</sup>Te excited states studied in decay of <sup>126</sup>Sb<sup>m</sup> 0-64090
                                                        <sup>130</sup>Te, configuration mixing in (t,\alpha) reaction 0-70661
                                                               <sup>130</sup>Te, neutron particle hole states 0-67479
                                          Yb rotational bands from the property of the
```

0-49538

1-75 multiple Coulomb excitation of ground-state rotational band 0-49538

1-75 multiple Coulomb excitation of ground-state rotational band 0-49538

1-75 multiple Coulomb excitation of ground-state rotational band 0-49538

0–495.86 ¹⁰Zn from (p,n), neutron spectra meas. 0–60759 ⁶⁵Zn from (p,n), neutron spectra meas. 0–60759 ⁶⁵Zn deduced from ⁶⁵Cu(p,n) and ⁶⁵Cu(p,ny) E_p =2.80-4.50 MeV 0–55155 ⁶⁵Zn, deduced levels from ⁶⁶Ga radioactive decay and energy and intensity of the p-ray transitions 0–57949 ⁶⁷Zn level scheme from ⁶⁷Cu β -decay obs. 0–38969

ucieus continued

energy levels continued

80ZT, low-level spins of four particle configurations 0—55130

88ZT, low-level spins of four particle configurations 0—55130

90ZT, four particle levels of 4p type 0—55131

90ZT, four particle levels of 4p type 0—55131

90ZT, riburational states from inelastic electron scattering 0—67522

91ZT, weak-coupling states using analog resonance techniques, obs.

0-57917 0–57917 °°1Zr analogue of ground state from °°2Zr proton scattering 0–73817 °°1Zr levels populated by β -decay of °°2Y 0–49572 °°1Zr, angular momenta of low lying states 0–67538 °°1Zr, weak-coupling states using analog resonance techniques, obs. 0–57917 °°1Zr, weak-coupling wave functions for neutrons coupled to excited states of °°1Zr 0–39049 °°1Zr, weak-coupling states using analog resonance techniques, obs. 0–57917 excitation see Nuclear excitation magnetic moment see also Gyromagnetic ratio; Molecules/nuclear coupling; Nuclear magnetic resonance and relaxation deformation effect, spin-orbital and spin forces 0–52665 dipole oscillator strengths for light elements, between 10 and 80 MeV 0–42812 electromagnetic moments of extremely short-lived nuclear states, method electromagnetic moments of extremely short-lived nuclear states, method for meas. 0–46367 exchange currents indicated by polarization of nucleons emitted in electron interactions 0–38845 isovector magnetic moment of mirror nuclei 0–63990 odd nuclei, of ground and excited states, by Bohr model 0–73772 polarization magnetic methods and excited states, by Bohr model 0–73772 polarization magnetic methods and the production of the polarization of polarization magnetometer with measurement sequencing system, patent precession in Earth's magnetic field, kinematic relativism 0–52664 spherical, odd nuclei, of ground and excited states, by Bohr model 0–73772 static moments of low lying 2* states review 0–73771 first 2* states, deduced from y ray spectra 0–49508 first 2* states, deduced from y ray spectra 0–49508 first 2* states, deduced from y ray spectra 0–49508 first 2* states, deduced from y ray spectra 0–64010 first 2* states expected for magnetic moment of Co using nuclear orientation 0–62485 first 2* states expected for magnetic moment of Co using nuclear orientation 0–62485 first 2* states expected for moments, form factor calc. 0–38851 first 2* states expected for moments, form factor calc. 0–38851 first 3* state expected for moments, form factor calc. 0–38851 first 3* state expected for moments, form factor calc. 0–38851 first 3* state expected for moments, form factor calc. 0–38851 first 3* state expected for moments, form factor calc. 0–38851 first 3* state expected for moments, form factor calc. 0–38851 first 3* state expected for moments, form factor calc. 0–38851 first 3* state expected for factor factor calc. 0–60773 first 4* state for factor factor calc. 0–64010 first 3* state for factor factor calc. 0–64010 first 4* state for factor precession in Earth's magnetic field, kinematic relativism 0–52664 spherical, odd nuclei, of ground and excited states, by Bohr model 0–73772 Models

4n-nuclei, nature of low-lying even parity even spin states

4n-nuclei, nature of low-lying even parity even spin states

4n-nuclei, nature of low-lying even parity even spin states

4n-nuclei, nature of low-lying even parity even spin states

4n-nuclei, nature of low-lying even parity even spin states

4n-nuclei even factor

4n-nucle

Nucleus continued

cracking and centrifugal stretching models, comparison 0–63966 d" config., interaction matrix 0–49473

Davydov-Chaban model, anomalous rotational band, spherical even-even nuclei 0-46105

nuclei 0-46105
Davydov-Filippov model for deformed even-nuclei 0-42709
deformed, in Hartree-Fock approx. with projection, struct. obs. 0-38795
deformed even-nuclei, Davydov Filippov model 0-42709
droplet and Thomas-Fermi model, average nucl. props. 0-38813
droplet model nuclear distributions and single-particle potential wells for
Thomas-Fermi calculations 0-38820
dual core model for ground state energy estimation of ³He 0-60752
effective interaction and the conditions for weak energy dependence
0-52651
Elliott generalized SU₂ rotons 0-67409

U-2201 Elliott, generalized SU₃ rotons 0–67409 excited core model for ⁶³Cu and ⁶⁵Cu 0–52689 fission energy and angular distributions of light nuclei, model calculations 0–42881

0-42881
generalised harmonic oscillator shell model and generalised oscillator transformation brackets 0-49475
Glauber, for π elastic scatt. on ¹²C 0-70626
harmonic oscillator model, anisotropic, shells 0-70365
harmonic oscillator model, use in calculating electron dispersion correction 0-49596
Hartree-Fock, for study of pion absorption and single nucleon emission 0-46228
hydrodynamical, with surface effects and giant dipole energies 0-57877
intermediate coupling model use in level calc. of N=29, Z=29 nuclei 0-70461

0–70461 intermediate-coupling model for description of 35 Cl nucleus 0–64015 Klein/Jean theory applied to Tl nucleus 0–60768 Krutov for deformed even-even nuclei, rotational energy levels of ground state band 0–67410 liquid-drop cales. for fissionability as function of ang. momentum for 181 Re compound nucleus at 70 MeV 0–39152 macroscopic quadrupole phonon model 0–63971 microscopic description of (γ, pn) reaction 0–52746 Nilsson $\Delta <$ R₂² and $\Delta \beta_p$ relation 0–67382 Nilsson model Hamiltonian, role of j^2 term 0–38816 Nilsson orbitals. N-mixed, El transitions cales. 0–38817 OBE, relativistic, including δ -meson, giving non static two-body potential 0–67372 optical, anal, of d elastic scatt, on 49 Ca $^{46.59}$ Ti and 55 Mp. 0–60826

0–67372
optical, anal. of d elastic scatt. on ⁴⁰Ca ^{46,50}Ti and ⁵⁵Mn 0–60826
optical, anal. of p elastic scatt. on intermediate mass nuclei 0–70581
optical, anal. of polariz. in elastic scatt. of 12 MeV deuterons 0–49645
optical, analysis of elastic scattering of complex nuclei at low energies 0–39134
optical, calc. for n elastic cross sections of V 0–49623
optical, dynamics, role of G-matrix 0–63962
optical, final-state interactions in quasifree electron scattering from nuclei 0–52754

optical, from polarized neutron elastic scattering data, 3.2 MeV 0–57878 optical, local pot., dispersion relation 0–38804 optical, parametrization for ¹⁰B(d,pp)¹¹B 0–49655 optical, proton elastic scattering, real part of potential 0–70579 optical formalism, and method for single particle potential eigenparameters 0–49469

optical model anal, for elastic deuteron scatt, on light nuclei at 28 MeV 0-52794

optical model anal, for polarization of protons elastically scattered from $^{\circ}$ Be 0-49605

optical model code for elastic differential cross-section clac., computer program 0-55148 optical model parameters for neutron cross sections eval. below 2 MeV 0-39062

optical-model phase shifts for α -particle scatt. 0-77571 optical-model potential, surface peaking in the calculated imaginary part 0-38810

optical-potential depth from many-body theory 0–49474 pairing forces, comparison with BCS and BCS+RPA+projection 0–42704

0–42704
pairing model, quasi-particle structure of ground state 0–67490
proton-neutron pairing correlation, T=0, in N≠Z light nuclei 0–38811
quasi-particle approx. and pairing 0–38814
review 0–70360
rotational, SU(3) and SL(3,R) comparison 0–67386
rotational model, Coriolis decoupling 0–63967
rotational-vibrational, two-centre, with phenomenological pot. 0–38818
self consistent cranking model for description of isomeric shift in rotational nuclei 0–63979
self-consistent classical model using Gaussian pot. with Coulomb interac-

self consistent cranking model for description of isomeric shift in rotational nuclei 0–63979 self-consistent classical model using Gaussian pot., with Coulomb interaction and n-p mass difference 0–38812 semimicroscopic model for props. of 6°50 negative parity states 0–49523 semirealistic effective interactions for nuclear shell model 0–42711 separable potential for Hartree-Fock calculations 0–67384 separable-potential, generalized, for treatment of three- and four-nucleon systems 0–38803 shell, as basis for Bethe-Goldstone equation soln. 0–52634 shell, calc. on the N=82 odd-proton nuclei 0–42706 shell, closed and near-closed, rotational description of states 0–46112 shell, comparison with Regge trajectories 0–60747 shell, description of nucleon-transfer form factors 0–77531 shell, effective elec. multipole operators 0–49472 shell, effective elec. multipole operators 0–49472 shell, isospin characts. in seniority scheme, classification, five-dimens. quasispin 0–38821 shell, isospin characts. in seniority scheme, classification, five-dimens. quasispin 0–38821 shell, poor agreement in ¹¹B proton scattering 0–67526 shell, realistic forces, spectra and the effects of correlations in A=6 nuclei 0–57893 shell, relationship of scattering phase shifts 0–67375 shell, review 0–70361 shell, retational spectra, effect of single particle energies 0–70376 shell, self-consistent potential, finite rank structure 0–70342 shell, semi realistic effective interactions 0–70358 shell, semi realistic effective interactions 0–70358 shell, sepicalized for the factor of the factor of

Nucleus continued models continued

shell, transitionally invariant 0-38822

shell, translation-invariant, many-particle fractional parentage coefficients

shell, wave functions, in general method for handling hard core 0-38790 shell, with jj coupling, comparison with results for ⁴¹Ar 0-70452 shell, with ji coupling, companson with results for **At 0.7652*
shell and many-body aspects of nuclear reactions, reviews 0.—60797
shell calculations for non normal parity states of A=15, 14 and 13 nuclei 0.—63999
shell description of level scheme of **27.7 0.—49572
shell effects on level densities, excitation energy dependence 0.—63975
shell energy of deformed nuclei, curvature term 0.—42707
shell model analysis of giant dipole reson. of \$\text{Shi other of the Methods of the M shell and many-body aspects of nuclear reactions, reviews 0-60797 shell calculations for non normal parity states of A=15, 14 and 13 nuclei 0-63999

charge radii, from isotope shifts of K X-rays 0–52877 isotope charge radii vars. from X-ray K shifts 0–38842 mass and deformabilities 0–42714 neutron distribution from kaonic X-rays, K⁻ nuclear interactions 0–49476

0-49476
neutron radii from coulomb displacement energy 0-70384
radii of light nuclei, correlation with binding energy 0-42716

27Al, radius parameter 0-77575
Bi, r.m.s. charge radius from meas. of elastic scatt. of electrons 0-39023

10C charge radius and form factors from inelastic electron scattering 0-67520

 $^{\circ}$ 0–67520 $^{\circ}$ 40°Ca, from effective NN interactions 0–38806 $^{\circ}$ 40°Ca charge radius larger than that of 48 Ca from Hartree-Fock calc. 0–70449 48 Ca charge radius smaller than that of 40 Ca, from Hartree-Fock calc. 0–70449 Dy isotopes, differences in charge radii, from normalized isotopic shift data 0–73831 160 Dy, polarisation effects in δ (r²) measurements 0–38929 158 Gd charge radius change in 2+–0+ rotational transition from recoil implantation Mossbauer effect 0–52703

size continued

cleus continued size contents of photodisintegration 0–38846 size, r.m.s. charge radii connection with bremsstrahlung weighted cross section of photodisintegration 0–38846 size, r.m.s. charge radii connection with bremsstrahlung weighted cross section of photodisintegration 0–38806 size, r.m.s. charge radii connections 0–38806 size, r.m.s. charge radii connections 0–38806 size, si

 128 Te charge radii variations from isotopic shifts of X-ray $K_{\alpha 1}$ lines 129 Te charge radii variations from isotopic shifts of X-ray $K_{\alpha 1}$ lines 128 Te charge radii variations from isotopic shifts of X-ray $K_{\alpha 1}$ lines 128 Te charge radii variations from isotopic shifts of X-ray $K_{\alpha 1}$ lines

to the charge radii variations from isotopic shifts of X-ray $K_{\alpha 1}$ lines 0–64033 (*Ti mass from $^{40}\text{Ca}(\alpha, y)^{44}\text{Ti}$ 0–70454

spin and parity

spin and parity
see also Gyromagnetic ratio; Molecules/nuclear coupling
4*Sc, from (α, α') and (p, p') 0–49518
analogue resonances formed in direct reaction decaying via isospin forbidden modes 0–67412
analogue resonances in isospin forbidden reactions 0–70380
anomalous parity, of low-lying levels of p-shell nuclei 0–77476
compound states formed in thermal neutron capture 0–49628
conference, Asilomar (1969) 0–67393
deformation of parity in sperical nuclei 0–38841
even-odd staggering in γ-bands, theoretical investigation using collective model 0–52663
Franck-Condon principle, extension to nuclear spins 0–58133
Hartree-Fock solutions, isotopic spin mixing 0–70349
I-spin analogue states in A=10 triad 0–70395
isobaric spin mixing in ground states of nuclei 0–63987
isospin incouplings and impurities rel. to Coulomb effects 0–38794
isospin in coupling in (d,p) and (d,n) 0–67547
isospin in coupling in (d,p) and (d,n) 0–67547
isospin mixing in energy levels using (²He, t) 0–67396
isospin structure of pairing vibrations 0–73770
low-lying opposite parity states in nuclei with Z≈50 0–63988
moment-of-inertia theory, formal aspects 0–70377
moments of inertia calc. for deformed nuclei 0–46116
Moszkowski's relation and the second moment of energy for a given seniority or isospin in a single shell 0–49492
multipole precession 0–39258
shell model calculations for non-normal parity states of A=15, 14 and 13 nuclei 0–63999
spin-echo signals obs., thin Co and Co-Fe films, relaxation times meas. 0–45017

spin-echo signals obs., thin Co and Co-Fe films, relaxation times meas. 0-45017

spin-echo signals obs., thin Co and Co-Fe films, relaxation times meas. 0 - 45017
spin-orbit potentials, velocity dependent and quadratic, positivity conditions 0 - 73726
spin-spin effect in neutron scattering on ⁵⁹Co obs. 0 - 60814
spin-vibrational 1 * states, deformed nuclei 0 - 63949
***[*Tm, n reaction, reson. parameters and spin, E=4-830 eV 0 - 39073
**[*2*]*[*3

**Be, lo43 keV level spin assignment from ¹³⁴Cs decay obs. 0–38984

*Be, proton scattering, I-spin analogue states 0–70394

*I*C, assignment of J*=J*/2- for 8.11 MeV level 0–73782

*I*C first excited state, from *Li(*Li,n), 1.9 MeV 0–39139

*I*C T=3/2 states, isospin forbidden resonance width calcs. 0–67421

*I*Ca* angular momentum assignment inconsistencies 0–55126

Ca, assignments, from p-y coincidence study 0–55128

Ca, energies, spins decay modes and lifetimes of first 3 excited states determ. 0–77496

*OC a from isobaric analogue states in *9Sc 0–70458

*I*OCA 2200 keV level 4* spin assignment 0–38977

*I*Om*Cd, 2200 keV level spin, obs. 0–38908

*I*OCA 2200 keV level spin, obs. 0–38908

*I*OCA 2200 keV level spin, obs. 0–38908

*I*OCA is is a scited states from *I*OCA is observed and is obs

Nucleus continued

spin and parity continued

60mCo from atomic beam magnetic resonance 0-70474

⁴⁹Cr meas. by magnetic resonance method 0–73806

⁵³Cr, assignments to 2.227, 3.19, 3.271 and 3.971 MeV levels 0-38886

⁵³Cr, assignments to 2.227, 3.19, 3.271 and 3.971 MeV levels 0–38886 59 Cu, agreement with analysis of results of 58 Ni(p,p) reaction 0–77498 65 Cu, deuteron scattering, spin dependence 0–70635 65 Cu deuteron scattering, spin dependence 0–70635 65 Cu deuteron scattering, spin dependence 0–70635 65 Cu deuteron by the partial partial positive parity bands 0–42771 165 Er, deduced levels from Dy(α,xn), strongly perturbed positive parity bands 0–42771 165 Er, deduced levels from Dy(α,xn), strongly perturbed positive parity bands 0–42771 165 Er, swave neutron resonances from low-energy capture γ-ray spectrum 0–49493 165 Er, levels isospin impurities via 16 N (α, α,) 16 N at 2.311 MeV, 0–67428

O-49493 and the control resonances from 10-40493 per party spectrum 0-49493 and 14 N(α,α) 14N at 2.311 MeV 0-67428 18F, 9.1 MeV T=3/2 state, isobaric spin impurity amplitude, obs. 0-42836 19F, for 10 levels, from 15N(α , γ) 19F reaction 0-52801 19F, for 10 levels, from 15N(α , γ) 19F reaction 0-52801 19F, for 10 levels, from 15N(α , γ) 19F reaction 0-70466 19F expin assignments for some of excited states 0-60760 19G, for 15N at 200 19G, for 15N at 20

131 isobaric analogue resonances 11011 incl. 200. 170489
112In spin cut-off parameter obs. from 113In(n,2n) 0-77562
112In spin cut-off parameter obs. from 113In(n,2n) 0-77562
40K, 1644 keV state, determination from 42 Ca(p, 3 He) 0-57907
40K, from 37 K(n,γ), of excited states 0-42852
40K positive parity states from 40 Ar(p,nγ) 40 K reactions 0-70448
46K ground state spin of 2 and 692keV state spin of 5- from (d,α) reactions 0-70455
47K, from β decay study 0-77516
41C, from atomic beam magnetic resonance 0-70474
51Li, assignments, by radiative capture reaction 0-49499
51Li, reactions in the even parity, T=0 states, calculation 0-52668
24Mg, spin assignment of states from an analysis of Doppler-broadened gamma rays 0-52681
24Mg, states at 12.74, 12.85 and 12.97 MeV, from 23 Na $(p,\alpha\gamma)^{20}$ Ne 0-70431
27Mg low-lying states, from 26 Mg(d,pγ) p-γ angular correl. obs. 0-38874

10-49022 (april 1970). S-wave neutron resonances from low-energy capture y-ray spectrum 0-49493. S-wave neutron resonances from low-energy capture y-ray spectrum 0-49493.

189 Os, S-wave neutron resonances from low-energy capture γ-ray spectrum 0-49493
3Pp negative parity band, 4 to 8 MeV 0-67436
3Pp negative parity band, 4 to 8 MeV 0-67436
3Pp negative parity band, 4 to 8 MeV 0-67436
3Pp negative parity band, 4 to 8 MeV 0-67436
3Pp negative parity band, 4 to 8 MeV 0-67436
3Pp negative parity band, 4 to 8 MeV 0-67436
3Pp negative parity size of 0-42743
3Pp neutron, 1927 neutron session neutron decay, spin assignments 0-38946
102 Net Neutron 1928 neutron 1928 neutron 1929 neu

²⁸Si, certain resonance and bound states from study of ²⁷Al(p, γ) reaction 0–77492

 29 Si T=2 state, obs. 0–38876 29 Si assignments, from elastic and inelastic proton scatt. 30 Si, assignments, study using 30 Si($\alpha,\alpha'\gamma$) 30 Si 0–55123

spin and parity continued

150 Sm., assignments from 150 Pm decay 0-42795

150Sm from (n,y) reactions 0-64041

88Sr spin assignments to 32 levels 0-70478

159Tb, y decay, search for parity violation 0-77487

¹⁶⁰Tb, spins of 11 levels deduced 0-73830

160 Tb., spins of 11 levels deduced 0-73830

9°Tc. angular correlation and spin for γγ cascade 0-49530

124 Te., spin assignments from 1245b decay obs. 0-42791

124 Te from γ-decay of 124 Sb 0-73819

125 Te. of 525 keV level, from 125b decay 0-49576

126 Te. of 125 keV level, from 125b decay 0-49576

127 Te from γ-decay of 124 Sb 0-73819

127 Te. of 525 keV level, from 125b decay 0-49576

128 Te. of 525 keV level, from 125b decay 0-49576

129 Te. of 525 keV level, from 125b decay 0-49576

130 Te. of 125 keV, spins, obs. 0-38885

131 Te. of 125 keV, spins, obs. 0-3885

131 Te. of 125 keV, spins, obs. 0-38885

132 Te. of 125 keV, spins, obs. 0-39886

133 Te. of 125 keV, spins, obs. 0-39886

134 Te. of 125 keV, spins, obs. 0-39886

135 Te. of 125 keV, spins, obs. 0-39886

136 Te. of 125 keV, spins, obs. 0-39886

137 Te. of 125 keV, spins, obs. 0-39886

138 Te. of 125 keV, spins, obs. 0-39886

139 Te. of 125 keV, spins, obs. 0-39886

130 Te. of 125 keV, spins, obs. 0-39886

131 Te. of 125 keV, spins, obs. 0-39886

131 Te. of 125 keV, spins, obs. 0-49576

131 Te. of 125 keV, spins, obs. 0-49576

132 Te. of 125 keV, spins, obs. 0-49576

133 Te. of 125 keV, spins, obs. 0-49576

134 Te. of 125 keV, spins, obs. 0-49576

135 Te. of 125 keV, spins, obs. 0-49576

136 Te. of 125 keV, spins, obs. 0-49576

137 Te. of 125 keV, spins, obs. 0-49576

138 Te. of 125 keV, spins, obs. 0-49576

139 Te. of 125 keV, spins, obs. 0-49576

130 Te. of 125 keV, spins, obs. 0-49576

131 Te. of 125 keV, spins, obs. 0-49576

131 Te. of 125 keV, spins, obs. 0-49576

132 Te. of 125 keV, spins, obs. 0-49576

133 Te. of 125 keV, spins, obs. 0-

model 0–64034

1º9Xe^m spin of 236 keV level determined to be 11/2 0–64036

1º9Xe positive parity states and intermediate coupling approach of unified model 0–64034

1º9Xe positive parity states and intermediate coupling approach of unified model 0–64034

1º9Xe, assignments for 637- and 723 keV levels 0–77502

8º9Y, assignments to levels obtained from inelastic scatt. of neutrons 0–39072

6º4Zn,(6ºZn, level assignments 0–73980

6º4Zn,(d,n)º⁴Ga by time of flight method, differential cross section, spin and parity assignments 0–58020

6º4Zn,(d,n)º⁴Ga by time of flight method, differential cross section, spin and parity assignments 0–58020

6º5Zn,(d,n)º⁴Ga by time of flight method, differential cross section, spin and parity assignments 0–58020

9°2Zn, assignments 0–58020

2s-1d shell, mass systematics analysed by average energy method 0-70378

3, 4-nuclear systems, calc. using Jastrow-type correlated wave functions 0-67417

0-0-0417
A-matrix perturbation theory, applications 0-55110
angular momentum coupling coefficients, computer program 0-69613
anomalous coupling states as new collective modes in spherical odd nuclei 0 - 63950

Bethe Goldstone eqn., new technique for solution 0-77460

0-63950
Bethe Goldstone eqn., new technique for solution 0-77460
Bethe Goldstone eqn., new technique for solution 0-77460
Bethe Goldstone equation, solution using iterative procedure with approximate wavefunctions 0-52634
Bethe Goldstone wave function approximation 0-67378
binding energy of \(\alpha \) with tensor vel. depend, pot. 0-38828
bootstrap EQPC, RPA and the odd-even mass difference 0-63952
bootstrap theory application to pairing vibrations 0-77463
Brueckner reaction-matrix ladders, overcounting problem 0-49585
Brueckner-Hartree-Fock, renormalization with single particle occupation probabilities 0-70330
Brueckner-Hartree-Fock calculation, self-consistent occupation probabilities 0-57871
Brueckner-Hartree-Fock calculations of spherical nuclei in a harmonic oscillator basis 0-52638
charge correction larger for n than for p, rel. to new approach 0-67365
collective coords., rel. to c.m. and collective rot. motions 0-38792
collective motion, microscopic theory 0-67362
collective motion, microscopic theory 0-63948
collective motions, mass quadrupole tensor description 0-77462
collective motions, mass quadrupole tensor description 0-77462
collective states, coordinate transformations 0-63970
compact cluster expansion for finite nuclei 0-38789
compressibility calc. by constrained Thomas-Fermi method 0-46095
compressibility of finite nuclei, calcs. 0-38826
conference, India, Dec. 1969 0-38788
configuration mixing in s.c.s. nuclei, perturbation treatment 0-73724
continuum-continuum interaction by factorization approximation 0-70563.

0 - 70563

0-70563 coulomb displacement energy, calc. 0-67366 Coulomb effects 0-38794 cranking model and Peierls-Yoccoz method energy derivation in unified manner 0-77458 cranking theory of rotation, fixed-particle number corrections 0-63982 decoupling parameters, effect of spin interaction in rare-earth region 0-52642

0-52642
deformed spin orbit potential in coupled equations 0-70379
differential eqn. for logarithmic derivative and applies. 0-38800
dipole sum rule for three-particle with realistic nuclear forces 0-52647
effective charges, second order corrections 0-67379
effective operators in truncated shell model 0-67383
even-even nuclei, proton separation energy analysis 0-57880
exchange currents consistent treatment 0-42717
experimental and the vertical apsects 0-52650
FBCS wavefunction, isospin projected, for light nuclei 0-46111
Faddeev eqns. for realistic 3-nucleon systems, complete angular momentum reduction and antisymmetrization of states 0-73729
fermi liquid, 2-component, stability conditions and other inequalities 0-57297
few-particle system, form factor, relativistic generalization, 0-46006

6-37271 few-particle system, form factor, relativistic generalization 0-46096 four nucleon system, construction of complete sets of translationally invariant states 0-63995 four-nucleon system, treatment by generalized separable-potential model 0-38803

fractional parentage coeffs. in j-j coupling in isospin representation, computer program 0-42699
g-factor in excited state rel. to struct. 0-57869

g-factor in excited state ref. to struct. U-57009

Galilei and translationally invariant spin-orbit interaction in shell model 0-67385

0-0/385 generalized Hartree-Fock approximation for scattering problem 0-70562 generalized symplectic symmetry in identical nucleon systems 0-73734 generator coordinate theory of collective motion 0-63945 generator-coordinate method, application to rotational spectra of ground states of even nuclei 0-77475

Nucleus continued theory continued

ground state charge and matter distributions, macroscopic formulation 0 -63954

ground state correlations, coherent RPA modes contribution 0-70354 hardcore, general handling method with shell- model wave functions 0 38790

Hartree Fock Bogoliubov calc., projected, in p-f shell nuclei 0-38797

Hartree-Fock, triaxial, rotational symmetry restoration 0-70353 Hartree-Fock and related approximations in solvable model 0-70347

Hartree-Fock angular momentum projected, Euler-Lagrange equations derived 0–73730

Hartree-Fock calc., constrained, review 0–73743

Hartree-Fock calc. for even-even N=Z nuclei 0–70351

Hartree-Fock calcs., from smooth realistic local NN force 0–73736

Hartree-Fock calcs., spherical, with Sussex relative matrix elements

0-42694
Hartree-Fock calcs. with density dependent interaction, in local density approx. 0-73756
Hartree-Fock calcs. with s-state interactions in d-s shell 0-42693
Hartree-Fock calculations for closed shell nuclei with Skyrme's interaction

0 - 52636

0–52636
Hartree-Fock calculations with Wood-Saxon basis functions 0–46097
Hartree-Fock calculations with regularized realistic force 0–49470
Hartree-Fock methods, review 0–73723
Hartree-Fock solutions, isotopic spin mixing 0–70349
Hartree-Fock Hoery, use of effective interactions 0–70339
Hartree-Fock-Bogoliubov calcs. in 2s, 1d shell, addendum 0–70357
Hartree-Fock-Bogoliubov equations, solution with realistic forces 0–70327
isobaric analogue resonances, fine structure analysis 0–70368
isobaric multiplet equation, T_s³ term 0–77459
isobaric multiplet mass eqn., evaluation of d from mass excess of ¹³O
0–67420
isobaric multiplet mass eqn., test by meas. of T_s=−3/2 masses of ⁹C.

0–67420 isobaric multiplet mass eqn., test by meas. of $T_z=-^3/_2$ masses of 9 C, 13 O, 21 Mg 0–67419 Jost function, asymptotic behaviour, and S-matrix for large complex angmoments, nuclear-Coulomb potential case 0–49456 Jost function, off-shell T-matrix 0–49455 K harmonics method for cale, props. of low-lying levels 0–49487 Klein-Gordon equation, with external electrostatic potential, spectral theory 0–49453 Levinson's theorem, for Coulomb scatt. in λ plane 0–55109 light nuclei, struct. trends and deformed model obs. 0–38795 Lippmann Schwinger operator, energy dependence of expectation values 0–55109 light nuclei.

52640

local nucleon-nucleon potential, non-local, for Hartree-Fock calculations 0 - 70352

0–70352
many-body description, on formalism of Green's functions 0–77484
many-body problem, self consistent solution, variational method 0–70348
many-berticle deformed pot. theory 0–38791
many-particle deformed pot. theory 0–38791
many-particle fractional parentage coefficients in translation-invariant shell model 0–46098
many-quasiparticle states, bound and unbound, review 0–73766
mass and deformabilities 0–42714
mass relations, review 0–49478
mass systematics of 2s-1d shell analyzed by average energy method 0–38827
matrix elements of one hody operators in odd nuclei and vertex functions

matrix elements of one body operators in odd nuclei and vertex functions 0 60741

0 60741 matter, and n matter, correl. basis function calc. 0–42712 matter, effective NN interactions 0–38806 matter, effective interactions of nucleons 0–67387 matter, effective interactions of nucleons 0–67387 matter, energy gap, from vel. depend. N-N pot. 0–38824 matter, infinite, and phenomenological α-α potential 0-42713 matter, and one-boson-exchange potentials 0–70363 matter, self consistent particle energies and 3-body clusters 0–67388 matter distribution, deformed single-particle model calc. 0–46106 matter transition temp., interacting α-particles, hard-core and long-range pots. 0–38825 microscopic theories of collective motion 0–70333

pots. 0-38825 microscopic theories of collective motion 0-70333 microscopic theory, for rotational excitations 0-42724 microscopic theory, for rotational excitations 0-42724 microscopic theory 0-60745 mirror state structure in 21 Na and 21 Ne from angular correlation studies with the 21 Mg(p, a^{21} Na(p, a^{21} Na) where reaction 0-52679 mixed coupling, stretch scheme and pairing 0-70369 Morse function based on velocity-dependent potential 0-49467 multiconfiguration field theory, difference from Hartree-Fock theory 0-60742 multiplicity of states, calculation method 0-67364 muonic X ray spectra, dynamic E2 hyperfine structure analysis 0-70383 N=Z=even nuclei in 1p shell, Hartree-Fock calc. 0-73738 n-particle fractional parentage coeffs. for anticommuting creation operators 0-77460 neutron matter, cold, superluminal and ultrabaric behaviour 0-48442

tors 0–77464 neutron matter, cold, superluminal and ultrabaric behaviour 0–48442 neutron matter, cold, superluminal and ultrabaric behaviour 0–48442 normal-superfluid transition in nucleus of interacting α-particles 0–38823 nuclear structure theory 0–49485 off shell T-matrix, Jost function 0–49455 orbiting clusters 0–38837 pairing and quadrupole forces, search for common symmetry 0–42698 pairing collective degree of freedom 0–63953 pairing vibration 0–42719 pairing vibration 10–42719 pairing vibrational states, description 0–70373 particle-hole excited states calc, using variational approach for ground state two-body density matrix 0–73763 Pauli principle effect on representation of nucleon pair operators by means of bosons 0–52637 Peierls-Yoccoz method and cranking model energy derivation in unified manner 0–77458 perturbation effects based on velocity-dependent potential 0–49467

perturbation effects based on velocity-dependent potential 0-49467

perturbation theory for degenerate case 0-55106 perturbation theory for degenerate case 0-55106 perturbation theory in core radius for three body problem 0-52648 phase transition from spherical to deformed nuclei 0-67363 phenomenological, for quadrupole transition probabilities 0-70381 properties from droplet and Thomas-Fermi model 0-38813 quasiparticle-phonon interaction in deformed nuclei 0-63977

theory continued

random phase approximation, correction due to particle-phonon interactions 0-55105

review of shapes 0-70386

rotation-particle coupling in odd-mass axially-symmetric nuclei. 0-63981 rotational spectra, effect of single-particle energies 0-70376 rotational spectra of heavy, deformed nuclei, effect of rotational invariance 0-63983

rotations described as intrinsic excitations, without cranking theory 0-63984

0–63984
rotons, three-dimensional microscopic theory 0–63951
SU₃ rotons, generalized, in Elliott model 0–67409
saturation and rotational invariance rel. to microscopic theories of moment of inertia 0–63989
self-consistent field, local, in nuclei with large number of nucleons

0-67368

0-67368
semi-microscopic theory of two phonon quadrupole-octupole vibrations of spherical nuclei 0-55117
single-particle Hamiltonian, from Thomas-Fermi theory, single particle enegies and rearrangement effects 0-49452
single-particle energies defined as spectroscopic averages 0-70350
Slater determinants, solution in which parity projection is performed before variation 0-77461
space symmetry in 2s 1d nuclei, spectral distribution methods 0-70331
spectral distributions 0-63946
spherical nuclei, self consistent core-particle coupling theory 0-38815
spin-orbit potentials, velocity dependent and quadratic, positivity conditions 0-73726
spin-vibrational 1' states, deformed nuclei 0-63949
static field, self-consistent, in the presence of presence of two-particle two-

spin-vorational 1° states, deformed nucle 10°-03949 static field, self-consistent, in the presence of presence of two-particle two-hole admixtures 0–57870 structural props., set of lectures, book 0–63943 structure cales. with realistic NN interactions 0–38798 structure effects in nuclear reactions 0–64101

structure studies with isobaric analog reson, reactions 0–38796 structure with realistic interactions, methods and results 0–63947 superheavy elements in closed shell region, props. and prod. 0–38865 surface neutron and proton densities, evidence of K-mesic X-ray yields 0 - 55104

surface properties using 3-part density- dependent effective interaction 0-70328

symmetry, generalized symplectic, in identical nucleon systems 0-52635 symplectic and quasi-spin groups, generalization of relation 0-70332 Tamm-Dancoff calcs. for N=82 isotones with a realistic interaction 0-64008

third moment of Hamiltonian, in terms of two-body matrix elements

0-60739
Thomas-Fermi calcs, using effective interactions 0-70339
Thomas-Fermi theory, corrections for inhomogeneity 0-77457
Thomas-Fermi theory, effective central forces calc. 0-42697
three particles correlations in nuclear matter 0-57879
three-nucleon system, form factor, relativistic generalization 0-46096
three-nucleon system, perturbation theory 0-77465
three-nucleon system, quasiparticle method, direct application for Lipp
mann-Schwinger operator 0-52640
three-nucleon system, treatment by generalized separable-potential model
0-38803

three-particle integral equations, solution by separable expansion method 0-49454

0-49454 transitional, quadrupole, pairing and spin deformations, review 0-73765 transmission through a real potential barrier, by means of certain phase-integral approximations 0-48723 trinucleus form factors, calc. from realistic local pots. 0-67367 trunneling and super-barrier transmission through a system of two real potential barriers 0-48724 two-nucleon transition matrix, off-energy-shell continuation 0-67377 two-particle two hole admixtures to Hartree-Fock states in 2s-1d nuclei 0-70334

0-70334 unbound levels spectroscopy from unified reaction theory using quasiparticles 0-70336 unified model Peierls-Yoccoz wave functions 0-70335 unified treatment of rotation and vibr. 0-73767 vibration, phenomenological study 0-63971 wave function calc., projected Hartree-Fock states used as representation 0-70377

0—103 II weak coupling model, particle hole excitation in 2s-1d shell 0—70370 α - α potential, phenomenological, and infinite nucl. matter props. 0—42713 α binding energy, with tensor vel. depend. pot. 0—38828 N-d scatt., D-state importance w.r.t. leading S-state of deuteron 0—38799 NN effective interaction components props., Hartree-Fock calcs. 0—42693

0-42693
NN effective interactions in struct. calcs. 0-38798
p separation energy for even-even nuclei 0-57880

8-Ar, spherical, from deuteron scattering 0-70655

198-Au, magnetic moments, hyperfine structure, and similarity with 198-Au
0-57930

 $^9\text{Be},$ mag. form factor calc. with projected Hartree-Fock functions $0{-}38851$

D-38851

10C, central, spin-orbit and tensor parts of Sussex interaction, effects on ground state properties 0-77483

10C grant dipole resonance, particle-hole description, equations of motion method 0-70400

Ca even isotopes, pairing vibrational states 0-73803

140Ce Thomas-Fermi theory calculation of energy per particle, density distribution and single particle potential 0-49451

13Cl, vibrational model 0-64015

13Ce moments and hyperfine structure in 3P₁ state 0-57913

13Ce moments and hyperfine structure in 3P₁ state 0-57913

13Ce moments and hyperfine structure in 3P₁ state 0-57913

14Ce, charge and magnetic form factors separation 0-73774

14Ce, first excited 0° state, self-consistent calc. 0-70390

14Ce, renormalization of Brueckner-Hartree-Fock theory using occupation probabilities 0-70330

15Li, charge form factor 0-38848

15Ce properties predicted from Hamada-Johnston potential 0-67418

15Ce properties predicted from Hamada-Johnston potential 0-67418

15Ce properties predicted from Hamada-Johnston potential 0-67418

0 - 70391

²⁴Mg, analogue of 4 particle-4 hole state in ¹⁶O 0-70422 ²⁴Mg ground state shape 0-38872

Nucleus continued theory continued

and the continued with the continued and continued

N isotopes, increase proceedings of the process of

O 10424
ONe HF spectra, projected 0—70425
ONe HF spectra, projected 0—70425
ONe Hartree-Fock constrained calculations for quadrupole generator coordinate 0—49494

Ni isotopes, pairing correls. 0-38892

18Ni, pairing vibrations, comparison of numerical results with exact solutions 0-77463 tions 0-77403 e⁶0Ni, pairing vibrations, comparison of numerical results with exact solutions 0-77463

tions 0-7/463
Six pairing vibrations, comparison of numerical results with exact solutions 0-77463
O isotopes, mixed parity Hartree-Fock calc. using realistic forces 0-70402

0-70402

16O, renormalization of Brueckner-Hartree-Fock theory using occupation probabilities 0-70330

16O central, spin orbit and tensor parts of Sussex interaction, effects on ground state properties 0-77483

18O, many-particle deformed pot theory 0-38791

2081b analogue ground state, microscopic description 0-70523

 ^{208}Pb analogue ground state, microscopic description $\,0{-}70523$ ^{208}Pb excitation by neutron scattering, RPA and TDA calc., effect of continuum $\,0{-}73951$ ^{208}Pb beginn dipole resonance damping width calc. $\,0{-}70524$ ^{208}Pb Thomas-Fermi theory calculation of energy per particle, density distribution single particle potential $\,0{-}49451$ ^{208}Re CVC theory and nuclear matrix elements from $\beta{-}\gamma$ cascades $\,0$ 64098 ^{188}Re CVC theory and nuclear matrix elements from $\beta{-}\gamma$ cascades $\,0$ 64008

0 64098
 12°SNe CVC theory and nuclear matrix elements from β-γ cascades
 0 64098
 12°SN, quasiparticle Tamm-Dancoff and random-phase approximations using realistic interactions 0-52694
 12°Si, HF calculations with realistic and semi-realistic interactions 0-70424
 22°Si HF spectra, projected 0-70425
 23°Si HF spectra, projected 0-70425
 23°Si HF spectra, brojected 0-70425
 23°Si, spherical, from deuteron scattering 0-70655
 Sn isotopes, self-consistent core-particle coupling calc. 0-70485
 116°Sn, quasiparticle Tamm-Dancoff and random-phase approximations using realistic interactions 0-52694
 12°Sn Thomas Fermi theory calculation of energy per particle, density distribution and single particle potential 0-49451
 4°Ti isotope, projected Hartree-Fock Bogolubov calculation 0-52686
 4°Ti isotope, projected Hartree-Fock Bogolubov calculation 0-52686
 9°Zr particle-hole interactions theory, and comparison with experiment for

³⁰T1 isotope, projected matrice-rock bogolubov calculation ³⁰–32800 oPZr particle-hole interactions theory, and comparison with experiment for 2⁻ state ³⁰–67467 oPZr Thomas Fermi theory calculation of energy per particle, density distribution and single particle potential ³⁰–49451

Oceanography
see also Liquid waves; Seawater
AUTOBUOY, for oceanographic obs., free diving, self controlled device 0 - 76359

acoustic backscattering, volume, meas. in Coral Sea 0-56757 acoustic intensity fluctuations in ocean represented as stochastic medium 0 64912

acoustic path stability, exp. prediction from thermistor-chain data 0-54231

acoustic propag, in isospeed channel with uniform tidal current and depth change 0-58484 acoustic propag, underwater due to explosion across Hawaiian Arch 0 59549

acoustic pulses, 1.f., reflection, from ocean surface, fluctuations 0-56755 acoustic refracted bottom reflected ray propag. in shallow-water channel

0-64913 acoustic reverberation, shallow-water, vertical coherence 0-56756 acoustic signals propagated over long paths, time stability 0-64911 acoustic target strength of single fish over 50-470 KHz, calc., meas.

0-59548 acoustic wave propag., normal mode solns, for abitrary sound speed profiles 0-64910

acoustic wave propag. underwater, effect of geological constructions 0-66256

0-6256
acoustic wave propagation, l.f., in deep water, model 0-56752
acoustic wave propagation, prediction by expt. digital system 0-56751
acoustic wave reflection, from sea surface time and frequency spreading meas. 0-56754
acoustic wave scattering, underwater specular, from anisotropic sea and swell surfaces 0-56754
active layer, vertical struct. of temp. field and depth variation 0-62880
aerodynamic pressure recorder for ocean-atmosphere boundary layer 0.66249

0-66249 air gun velocity surveys, offshore well depths and casing configurations $0\!-\!66266$

air-sea gas exchange, Rn profile meas. 0-66241 air-sea interface, vertical temp. profile 2 m above and below, determ. 0-48223

0-48223
ambient-noise-spectrum levels as fn of water depth 0-59547
arctic seas, pressure systems and dynamic processes 0-66251
Atlantic ocean bottom, viscosity 0-48248
Atlantic rift development and evaporate formation 0-41481
autoprobe, free-floating platform for temperature and pressure meas.
0-69273
Black Sea, sediment and water exam., origin and struct. 0-62888
bottom characteristics, application of earth penetration technology
0-66264

bottom detail, aerial colour photography remote sensing 0–62897 bottom mapping and navigation calibration in real time 0–72605 bottom topography, correl. of scattered acoustic signals 0–52111 bottom topography, effect on wind produced circulation around ocean islands 0–76351

Oceanography continued

Caribbean Sea, suspended-particle distrib. obs. 0-79498

circulation, mass transport vel. induced by free oscillations at single freq.

clouds, fields mapping rel. to equatorial anticyclones 0-48282

coastal and seafloor geometry influence on natural e.m. variations 10-4 to

coastal and seamor geometry inherice on natural c.iii. An addition 10⁴ Hz. 0–45194 coastal effluents, multisensor mapping 0–62900 colour variation, remote sensing 0–72600 continental drift and imperfection of elasticity in Earth 0–41471 current streams in Indian Ocean, caused by planetary-type waves 0–69272

0-69272
currents, Ekman theory applic. 0-76349
currents, steady, induced by oscillations round islands 0-76354
data quality, contributing factors 0-66253
dating of Pacific marine organisms using long-lived γ-ray emitting nuclide Ag-108m 0-69271
deep water search by visual, acoustic and magnetic sensors 0-72601
diffusion models based on instantaneous point source release and slowly
dissolving radioactive source 0-48249
e.m. fields in dissipative half-space, numerical approach 0-45712
eddy diffusivity, scale phenomenon, empirical relationship 0-59545

cady diffusivity, scale phenomenon, empirical relationship 0–59545 electric fields, natural, character and causes of vertical variation 0–66250 rel. to environment, remote sensing, conference Ann Arbor, (1969) 0–54202

explosion signal meas., long-range 0-54230 eaplosion signal meas., long-range 0-54230 fallout nuclides, very low-level gamma analyses, computer applications 0 -66242

fallout traces, survey using Cs absorbers 0-66243

fallout traces, survey using Cs absorbers 0–66243
float platform motions, method for computing 0–64845
flow inertial at low latitude, obs. 0–54229
Geodyne currents meters (1968) 0–48252
glass applic, for submergence struct, stress-corrosion characts. 0–51428
gravity gradient meter on seabottom, effect of microseisms 0–51483
gravity wave eqn. in presence of thermocline, analytic soln. 0–62881
gravity waves, cylindrical, transformations 0–62841
gravity waves, internal, in really stratified ocean, eigencurves and eigenfunctions 0–69269
gravity waves, random, deep-water longcrested, mass transport 0–51499
gravity waves finite height, phase and orbital velocities 0–66246
hydroacoustic noise, level meter, 100 Hz to 1 MHz range 0–66254
hydrodynamics, open-water, Proteus design 0–62887
hydrophone arrays, towed seismic, for sediment profiling, electrical and mechanical characteristics 0–45126
ice mapping, remote sensing using microwave radiometry 0–62894

ice mapping, remote sensing using microwave radiometry 0-62894 ice volumes, curve versus time, changes in earth's orbital parameters 0-79507

insolation changes in deep-sea cores 0-79507 instruments for ocean floor studies, film cameras and magnetometers 0-76358

irregular seas, slow vessel drift oscillation, analysis of peak mooring force 0-66258

Langmuir circulation and vertical momentum flux 0-79500 lithosphere thickness implied from shear velocity in suboceanic mantle 0-51491

0-31491 long waves on rotating earth, calc. 0-79504 magnetic anomalies of crust, matrix method of interpretation 0-79606 magnetotelluric deep sounding in bodies of water 0-62883 marine life damage caused by underwater explosions of dynamite charges 0-79476

meters operations (1968) 0-48252

microwave radiometry, application 0–48253 noise source in N. Sea 0–79509 ocean programs, future of, review 0–66267 off shore technology 0–66257 oil pollution detection, remote sensing using microwave radiometry 0–62894

optical inhomogeneities to 2000m, hydro-optical devices 0-45128 oscillations, free, on hemisphere, bounded by meridians of longitude 0-59540

0 -59540
periodic waves of infinite depth, variance analysis 0-48250
photographic examination, aerial, enhanced imagery 0-62896
photographic techniques, multispectral colour 0-52401
platforms, restrained wave exciting forces and moments in oblique seas,
strip theory 0-66260
pollutant detection, by luminescence sensing using Fraunhofer line discriminator 0-54232
remote sensing, using airborne pulsed Ne laser (5401Å) 0-62898
reverberation derived scattering strength of shallow sea bed 0-62885
ridges on floor, Coriolis force and new global tectonics 0-69270
Rossby-wave refl., western coastal orientation influence 0-79496
rough surface, stochastic boundary theory, perturbation parameter, differential equations 0-72603
salinity, new definition 0-66252
salt fingers, cell structure observations 0-66244
salt fingers, optical distortion of ruled vertical grating, random walk model
0-51498
scattering obs. different depth water samples, relation to dynamic condi-

0-51498 scattering obs. different depth water samples, relation to dynamic conditions 0-62890 scattering strength of shallow sea bed, reverberation derived 0-72604 sea, remote sensing, radar applications 0-62893 sea bed mapping with towed sensors 0-72602 sea conditions, remote sensing with microwave radiometer systems 0-62892

sea rice, remote sensing, radar applications 0–62893 sea noise vertical directivity, integral eqn. for investigation 0–54227 sea state, remote sensing using microwave radiometry 0–62894 sea water salinity changes, effect of temp., temp. salinity plot description 0–59551

0–59551
sea-air interface transport of momentum, heat, humidity, air borne turbulent flux meas. technique 0–76369
seawater light-field fluctuations, differential refraction by surface gravity waves 0–62886
sediment conductivity, in situ, Bullard-type probe 0–59541
sediments, organic-rich, minor metal contents 0–66245
seismic profiling, broadband continuous, hydrophone array 0–45127
seismic proveying, use of explosives 0–66265
shock waves, from detonation amplification in focusing regions at caustics 0–76356

Oceanography continued

canography continued solar refl. from sea surface as surface wind speeds indicator 0-79506 sound absorption, below 10 kHz, quantitative calculations 0-76357 sound forward-scattered from ocean surface, frequency spectra, theoretical analysis 0-71342 sound propagation in ocean, statistics of transmission fluctuation, theoretical study 0-62884 space, time and space resolution requirements 0-66255 spacecraft for ocean exploration 0-66268 spherical waves spreading in turbulent medium, frequency correlation of fluctuations 0-7994 steel, carbon, high strength, mechanical properties for marine applications 0-65468 Stokes drift for developed surface-gravity-wave field, assoc. volume trans-

Stokes drift for developed surface-gravity-wave field, assoc. volume transport 0-41480

sub-bottom profiling, high resolution, development of correlation processor 0-66259

sor 0–66259
submarine pipeline routes, geophysical studies 0–66261
submarines, research 0–79503
surface capillary-gravity waves, phase velocity, experimental test of Kelvin's equation 0–71292
surface response of homogeneous ocean to variable atmospheric force, generation of Kelvin-type waves 0–76353
surface temp. meas, i.r. remote sensing technique 0–62899
suspended-particle distrib. obs. in Caribbean Sea 0–79498
swell meas. from satellite photographs 0–79505
target acquiring angle at source depth in linear-gradient ocean, closed soln. 0–52094.

0-2094. temperature gradient above deep-sea floor 0-72599
Ti alloys for marine applications 0-66263
tidal currents, deposition of fine-grained suspended sediment 0-79499
tidal dynamics equations, finite-difference schemes used in numerical integration 0-72597.

gration 0-72597
trend surface analysis and spatial correl., report 0-79468
tsunami waves accompanying Anapa earthquake of July 12 (1966)
0-79501
turbulence and mixing in stably stratified environments 0-41567
turbulent energy transport and kinetic energy transformation for Indian
Ocean 0-56749
two-layer model, linear response to hurricane 0-79495
underwater target's polarization discrimination contrast improvement

underwater target's polarization discrimination, contrast improvement, particle size effects, comment 0–66240 volcanic characteristics of submarine eruptions, sofar-hydrophone detection 0–54228

water depth determinations, remote sensing techniques 0-62895 water depth penetration, aerial colour photography, remote sensing 0-62897

water movements in surface layer, aircraft obs. 0-79502 wave generation by wind, field study results 0-51522 wave heights, estimating design, extrapolation of historical storm data 0-66262

0-66262
wave modeling by digital computer 0-66248
wave motion, magnetic tape correlation 0-59542
wave parameter determination with ship's radar 0-66247
wave profile meas, use of laser profilometer 0-59550
wave propagation 0-79508
wave setup of nonperiodic wave train and associated shelf oscillation 0-79497

wave transformation from primary to shear mode at ocean bottom 0-56743

wave-drift current induced by random wave motion, formulation 0-48251 waves, capillary-gravity on sloping beach 0-50188 waves, deep-water, 1.96 Hz monochromatic, mean velocity field obs. 0-76355

waves, deep-water, 1.96 Hz monochromatic, mean velocity field obs. 0-76352 waves, internal, resonant generation 0-76352 waves, wind-driven, at small fetches, spectra 0-72598 Western European mean sea levels 0-41478 western coastal orientation influence on large-scale currents 0-79496 wind stress over sea, tangential, computation of 0-79528 Br meas. in seawater salt, p-activation NRL sector focusing cyclotron applic. 0-45130 Ca meas, in sea water salt, p-activation NRL sector focusing cyclotron applic. 0-45130 "He in deep sea, contribution from cosmogenic T 0-76350 In concentrations at different depths and in some sediments 0-41484 ¹⁸O record in deep-sea cores 0-79507 S meas, in seawater salt, p-activation NRL sector focusing cyclotron applic. 0-45130 Sr meas in seawater salt, p-activation NRL sector focusing cyclotron applic. 0-45130 Sr meas. in seawater salt, p-activation NRL sector focusing cyclotron applic. 0-45130

Octet theory see Elementary particles/symmetry; Field theory. quantum

Omegatrons see Leak detection; Mass spectrometers; Vacuum technique

Onsager relations see Statistical mechanics; Thermodynamics

Optical activity see Optical rotation

Optical communication see Laser beams/applications

Optical constants

see also Absorption/light; Reflectivity from ATR data, two prism tech. for calc., accuracy and optimization 0-51261

0–51261
of absorbing isotropic specimen, pseudo- Brewster angle 0–62593
alkali halide, piezo-optic constants dispersion in u.v., deform. pot. constants
of valence band. 0–44782
alkali metal, solid and liq., optical cond., many-electron effects 0–76000
alkaline earth metal, reflectance obs. 0–79273
alloy, disordered binary, in coherent-pot. approx. 0–76001
amalgams, liquid 0–74754
ceramic, scattering and absorbing 0–59351
changes determination for GaAs by double-modulation technique
0–65982
cotton leaves 0–454444

cotton leaves 0-45444 critical angle and generalized principal angle of incidence using CdS 0-44757

crystal, sum rule relating to charge distrib. 0–76002 crystals, metallic, anisotropic, meas. methods 0–44756 diamond, nonlocal-pseudopot. method calc. 0–78841 dielectric, modulation techniques, review 0–72303 of dispersive particles method for calc. 0–39841

Optical constants continued

of dolomite, in Schumann region, from reflectance obs. with polarized light 0 - 69072

ellipsometric meas. 0-71462

from elliptical polarized emission exptl. obs., calc. method 0-76003

ferroelectric trihydrogen selenites 0-62445

ferromagnet, surface impedance in i.r. region 0-62594

films, thin, u.v. consts. from reflectance meas. 0-43540 glasses, photoelastic constants 0-79253

glasses, photoelastic constants 0–79253 glasses, selection method for superachromatic system 0–63699 glasses borosilicate and silicate, thermooptical const. dependence on chem. compositions, exptl. data 0–59352 graphite, dielec. const. in u.v. 0–41104 graphite, pyrolytic 0–44743 high temperature materials 0–56046 laser materials 0–56046 measurement at high temps. 0–41106 measurement simultaneously with magnetooptical parameters, method 0–65080

measurement simultaneously with magnetooptical parameters, memod 0–65980 metal-ammonia solns., by ellipsometric technique 0–39788 NH₂H₂PO₄, nonlinear susceptibilities 0–47991 n and k, calc. from emissivity obs. 0–57421 non-linear susceptibilities, theory and calc. 0–69069 plasma resonance radiation from non- radiative plasmons and decay into photons on a rough surface 0–62273 polarizers zero-angle positions systematic error effect, calc. 0–69075 quartz, determ. at high temps. 0–41106 rare earth metal, reflectance obs. 0–79273 resonance region exact optical indices 0–67133 selenites, trihydrogen, ferroelec. 0–62445 semiconducting materials, determ. with psuedo- Brewster angle technique 0–56483

semiconductor, CdS, i.r. dielectric function 0–62596 semiconductor, Ge, enhancement under giant-pulse irrad. 0–65985 semiconductor, absorption cpefficient, high elec. field, impurities, calc.

0–47995 semiconductor, dispersion 0–44755 semiconductors, n- and i-type, meas. by Beattie-Conn method 0–41103 substrate, 'constant-reflectivity' method of determination using ellipsometry 0–69073 surface, rough, ellipsometry meas. 0–65979 susceptibility, linear and third-order nonlinear, empirical relation 0–79230 thallium-bromide-iodide thin layers, meas., applic. 0–59353 thermo, of silicate, borosilicate glasses, dependence on chem. compositions. exptl. data 0–59352 thermo-optical characts. of laser resonator mats., direct meas. 0–66006 thin films, determ. from reflectance and transmittance meas. by curve fitting 0–41101 thin-film thermochromic effects 0–59358 transfer function meas. of photographic objectives by edge imaging

transfer function meas. of photographic objectives by edge imaging 0-38578

X-ray region, ultrasoft, calculation by graphical solution of Fresnel equations 0-47996

AL₂O₃, co 0-65981 corundum, piezo-optic moduli determ. by interference method

O-65981

Ag, temp. depend., near 4 eV 0-76087
Ag films, thin granular, effective 0-47997
Al, dielectric constant, calculation from exp. Fermi surface 0-65587
Al films, rel. to oxidation, ellipsometric obs. 0-47994
Al, O-3, anodic alumina film, ellipsometry 0-54056
BaF2 photoelastic, cales. 0-44783
CaF2, photoelastic, cales. 0-44783
CaF3, photoelastic, cales. 0-44783
CaF3, photoelastic, cales. 0-44783
CaF2, photoelastic, cales. 0-44783
CaF3, photoelastic, cales. 0-4783
CaF3, photoelastic, cales. 0-4783
CaF3, photoelastic, cales. 0-4783
CaF3, i.r. dielectric function 0-62596
CoO, refectance spectra obs. 0-79276
Cs, above plasma frequency, determ. from meas. of reflectance 0-76013
Eu chalcogenide films, Curie point depend. 0-44758
GaAs, changes determination by double-modulation technique 0-65982
GaAs, anonlinear coeffs. determ. rel. to Ag,SbS3 0-65975
Ge, determ. using pseudo-Brewster angle technique 0-56483
Ge, enhancement under giant-pulse irrad. 0-65985
Ge film, amorphous 0-72304
GeTe, amorphous film, absorpt. coeff., photocond. 0-47873
H plasma, for Nd-glass, ruby and CO2 laser radiation 0-50061
InSb-NiSb system 0-69074
K, testing of interband-transition absorpt. theory 0-79231
KBT, piezo-optical consts. temp. depend. 0-76005
KCI, piezo-optical consts. temp. depend. 0-76005
LaNbO4:Nd single crystals, principle indices of refraction 0-62597
LiO3, nonlinear susceptibilities 0-47991
Na, testing of interband-transition absorpt. theory 0-79231
Nd:Ha-PO4, nonlinear susceptibilities 0-47991
Na, testing of interband-transition absorpt. theory 0-79231
Nd:Ha-PO4, nonlinear susceptibilities 0-47991
Na, testing of interband-transition absorpt. theory 0-79231
Nd:Ha-PO4, nonlinear susceptibilities 0-47991
Nd:Jass, thermo-optical characts, direct meas. 0-66006
NiO, reflectance spectra obs. 0-76074
PTE, calc. from augmented plane-wave k.p. energy bands 0-4798
Pd films, vacuum u.v., photoemissive props. correl. 0-44759
SaSp-Pb, zinkenite, and refractive index, absorpt. coeff. and absorpt. index 0-51265

0-51265
Sb thin film, 5875 Å 0-41105
Se, determ. using dispersion relations 0-54057
Si determ, with psuedo-Brewster angle technque 0-56483
SiC, static dielec. const. 0-79233
SiO₂, quartz, nonlinear susceptibilities 0-47991
Sn. grey, from k.p parameters 0-71926
SrF₂ films, thin 0-47999
Te, lattice vibration contrib. 0-66057
Te, proplices coeff. deeper pel to A+3chSt. 0-65975

Te, lattice vibration contrib. 0-66057
Te, nonlinear coeffs, determ. rel. to Ag₃SbS₃ 0-65975
Ti 0-76759
TiBr film, strain-reduced, and absorpt., Faraday rotation pattern and exciton binding energies 0-44855
TiCl film, strain-reduced, and absorpt., Faraday rotation pattern and exciton binding energies 0-44855
YFe garnet, piezo-optical effect, mag. birefringence 0-69090

Optical dispersion see Dispersion, optical

Optical fibres see Fibres/optical

Optical films see Films/liquid; Films, solid/optical properties

Optical filters see Filters, optical

Optical images

see also Aberrations, optical; Holography; Resolving power, optics analyzer, optical bench error, influence on otf meas. accuracy, method for meas. 0-49133

aperture field of observing opt. instrument, statistical description 0-42355 apodization theory, soln. of integral eqn. 0-42352

blur of fast moved objects illuminated by light flashes, photography 0-70131

0-70131
chromatic image analysis for optical systems, technique 0-38561
coded, from generalized imaging systems (e.g. pinhole arrays), information retrieval 0-38518
complex-amplitude addition and subtraction by diffraction grating interferometric method 0-70003
contrast, loss in reflecting microscope, calculation and meas. 0-49122
in converting system, differences in reproduction of two gray lines lighter and darker than surrounding fields 0-60324
correlation interferometry for incoherently illuminated objects 0-60327
diffraction irradiance distribution circular a precture as periodic rectangular.

correlation interferometry for incoherently illuminated objects 0–60327 diffraction, irradiance distribution, circular aperture as periodic rectangular wave object, Straubel pupil function application 0–38532 diffraction-, of triangular wave grating, formed with slit for sinusoidally transmitting medium 0–54916 diffraction-, of triangular wave grating, formed with spherically aberrating annular aperture 0–54915 digital processing, preliminary expts. 0–60412 direct formation by rapid access photopolymerization 0–77156 distant objects imaged without halo using combination of two Fresnel zone plates 0–60353 edge imaging for calc. meas. of opt. transfer function of photographic objectives 0–38578 electron microscopic modulation transfer for, resolution meas., methods 0–57492

electron microscopic of amorphous thin films, intensity asymmetry around holes 0-52248 electron microscopy, Fourier coefficient, reconstruction methods

electron microscopy, Fourier coefficient, reconstruction methods 0-42216

electronic image recording, electron-storage targets 0-69815 electrophotographic, development technology 0-70008 electrophotographic, resolving power 0-38586 encoding in modulated gratings from 1899-1970, short bibliography 0-60309

enhancement by noise suppression, appl. of statistical props. 0-45839 fibre assembly used as dynamic scanner, image-forming properties 0-60396

field ion micrographs, optical transformation 0-49021 formation, inversion- eye pieces sharpness of edge in microscopic obs. 0-77171 formation, microline application to pattern generation for microelectronics

formation, of photosensitive Hg compounds obs. 0–70121 formation by phase discs in partially coherent contrast microscopy 0–42369

formation by reflecting cone for off-axis 0-60318 formation in differential interference microscopy, theory 0-60390 formation split- eye pieces, sharpness of edge in microscopic obs.

90-1111 ghost in holography, Chebyshev polynomial, analysis 0-42327 glass graded index rods, image aberrations 0-59355 holograms of arbitrary shape, diffraction-limited, scalar image formation 0-60260

nolograms of arbitrary snape, diffraction-limited, scalar image formation 0-60260 holographic, analogy with interferometric image formation 0-42333 holographic image deblurring and optical aperture synthesis 0-69943 holographic theory with partially coherent illumination 0-52344 imagery with Fresnel zone plates, halo eliminating scanning tech. 0-52369

0-52569 improvement of field sources with zone plates, sun in XUV and soft X-ray region 0-69507 information and restorability 0-45820 intensity, statistical properties, analysis from narrowband noise model 0-42354

0-42354 intensity interferometric imaging through diffusing medium 0-77164 interferogram mirror transitive for quasi- Ronchigrams, laser unequal path interferometer 0-67141 internally stabilized, system configurations 0-60325 laser light illuminated through moving diffuser, partial coherence autocorrelation 0-60190 lens form, field obs. 0-49104 liquid cryst., reversible u.v. imaging 0-64917 Lorentz microscopical images of magnetization ripple, Fraunhofer diffr. 0-77188

0 - 77188

0–77188 microscope, polarizing with crossed polarizers, diffraction images of general periodic rectangular wave 0–57620 noncoherent analogue processing, preliminary expts. 0–60411 periodic bar pattern, general, effect of defocussing, rotation symmetric optical system case 0–60350 of periodic rectangular wave object formed by circular aperture with amplitude shading 0–60354 of periodic rectangular wave objects, formed by system in medium with sinusoidal amplitude disturbances 0–60356 in phase contrast microscopy, of phase and amplitude edges in partially coherent illumination 0–42370 phase-object visualization, small shear interference (SSI), phase grating schlieren (PGS), and Wolter's minimum schlieren (WMS) comparison 0–70060 0-70060

0-70060 phase-ring position image contrast on phase contrast objective for partially coherent light 0-63590 photographic, film-grain noise effect 0-70105 pupil and illum, coherence effects and synthetic apertures 0-45814 quality rel. to atmospheric inhomogeneity 0-76390 quality subjective, effect of Gaussian and Poisson noise 0-70006 recording on films with band domains, domain boundaries conservation and temp, effects 0-45817 reflecting prism systems, quality depend, on angle deviations 0-77165 replica optics 0-57569

replica optics 0—57569 restoration of images degraded by spatially variant motion 0—60410 solid-state, electro-optical IC structure, mode of operation and fabrication technique 0—59279 spectrograph blur-free improved for electron energy level meas. 0—42953 stability investigation in ion projectors 0—49019 storage and display devices, fine-grain ferroelec. ceramics applic. 0—52384 sun, in XUV improvement of field sources with zone plates 0—69507

Optical images continued

synthesis in real time by diffraction-grating interferometric method 0-63652

0-05032 from synthetic apertures, analogue of Mills- cross antenna 0-42361 television display, Raster line visibility 0-45482 test object or long focal length lenses, effect of optical bench vibrations, estimation 0-57603 thermal recording, magnetic films, remagnetization curve and energy sensitivity 0-52233 is and heart deflection techniques 0-2004

on thin films, imaging and beam-deflection techniques 0–70004 three-dimensional, real-time transmission, varifocal mirror techniques 0–60326

turbulence-degraded, statistical restoration techniques 0-60409

vibrations, effect on visual, photographic recording, estimation 0-57603 Optical instrument testing

angular surface meas, parabola by scanning-penta-prism test, theory and experiment 0-70056

aspherical surfaces, shape determ. using Newton fringes 0-49125 automatic, for electrooptical systems, operation, techniques, design 0-70046

0-70046
by computer-generated holograms 0-57570
controlled-environment chamber for detuning studies 0-77198
for inspection of interior of smooth or polished cylinders 0-69983
laser pulses, mode-locked for testing ultrafact photodetectors high-speed
electronic cameras 0-77141
lenses, high volume, using modulation comparison techniques 0-69996
microdensitometer evaluation system, automatic method 0-70059
mirrors, plane, in conjunction with concave spherical mirror 0-38558
null lens, variable refractive, for use with rotationally symmetric but nonspherical surfaces 0-38560
test glass surfaces, holograms of, use in place of the test glass 0-49124
transfer function of objectives, Fourier analysis scanning methods
0-70031

0-70031

Optical instruments

tical instruments

Some instruments are listed separately, e.g. Refractometers
absorption meter, seawater 0—41482
achromatic compensator for birefringent wave differences 0—60369
analysis and design, phase-space techniques 0—57609
analysis using three-dimensional vector diagrams, tech. description
0—63700
angle measuring gauge for static or low-frequency meas. 0—70058
atmospheric absorpt., scatt. and turbulence, influence on instruments and
communication systems 0—42381
avionic, He-Ne laser interferometer applications 0—60349
bathyphotometer for deep ocean waters 0—45128

beam splitter, variable transmittance, especially for two-beam hologram recording 0-45836

beam splitters, polarization independent 0–38567 beam steerer, bender-bimorph, piezoelectrically driven, theoretical anal. of performance 0–38563 bench errors, influence on accuracy of off meas. 0–49133

bench errors, influence on accuracy of off meas. 0–49133 bench vibrations effect on testing of long focal length lenses, stability specifications 0–57603 binoculars, 8×20 pocket, description 0–63708 binoculars, Zeiss, history of 0–63707 camera systems, for studies of ocean floor, with magnetometer 0–76358 cell, absorption, white-type multiple pass, for use with Fourier spectrometer 0–73356 colorimetric distortion meas, instrument for colour TV cameras 0–70041 compensator, birefringent, variable wedge 0–60383 coordinates of steel spheres in random packings, optical machine for measurement 0–49131 corner cubes in interferometers, props, of optical centre, simple derivations

corner cubes in interferometers, props. of optical centre, simple derivation 0-45837

correlator, compact, for treatment of coded electronic signals 0–77205 coupler of evanescent-waves 0–54926 cross-correlator with mutual correlation fin., design 0–57604 deflectors, analogue electro-optical, design 0–60379 design, axially symmetrical systems, with spherical and aspherical surfaces, eikonal functions applications, n.r.t. computation 0–38535

detection and ranging systems, actively scanning, threshold relationships 0 .52377

0 - 237/f for dichroism, circular, vacuum u.v. meas. 0 – 76021 dioptometer, for contact lenses meas. in excess of 25 diopters 0 – 73285 ellipsometer, alignment of polarizer and analyzer 0 – 57600 ellipsometer, automatic, based on intensity meas, electrochemical investigation, illustration on thin oxide layer formation on Pt 0 – 51430 ellipsometer, calibration of analyser and polarizer, modified method 0 – 7063.

0-70051 ellipsometer meas. analysis, FORTRAN program 0-45831 elliptical vibr. defining parameters determ. method 0-38552 field view study using diffraction effect, exact formulas 0-67160 filter, interference, bandpass, narrow, temp. controlled, in −20→± range, analysis, assembly configuration performance tests 0-70065 flow light scattering apparatus 0-39787 focometer, Vermier-sighting, design 0-73325 focusing on diffuse edge of luminous object, reproducibility 0-73326 Fourierscope for Fourier transform's interferogram 0-63714 fringe multiplication and photoelastic analysis 0-57602 heterodyne receiver, spatial filtering properties of the reference betterodyne receiver, spatial filtering properties of

heterodyne receiver, spatial filtering properties of the reference beam 0-60381

1... optometer, servo controlled, for producing elec. signal proportional to eye refractive power 0-45481 i.r. polarizers, degree of polarization determination method 0-60432 image storage and display devices, fine grain ferroelec. ceramics applic. 0-52384

0-52384 interference coatings, reduction of polarization effects 0-38567 interference resolution with surface imperfections 0-70029 interference device with gas lasers for small angles, rotations meas. 0-63675

introduction, university textbook 0-38525

large aperture synthesis using successive exposure of single photographic plate in incoherent light 0-70057

lens shutter objective moving in same direction, temporal exposure characts. 0–67164 light detector, high energy, for use with pulsed ruby and glass lasers 0–70048

light guides, thin-film, prism-film coupler, theory 0-73315

Optical instruments continued

light valve arrays, polarization rotating or retarding, matrix addressing method 0-77203

luminance meter for interiors 0-67161

microdensitometer, reflectance, with bright and dark field, phase contrast, spatial filtering and laser optical systems 0-70096 for microdisplacement obs. noncontact devices, photoelectric adaptation

microscope, ultrasonic diffraction, for objects similar to surrounding media 0-70052

microscopes, polarizing i.r., for obs. of domains in thick samples of magnetic oxides 0-73320 modulation transfer function meas., atmosphere 0-66297

modulator transfer function meas., atmosphere 0-06297 modulator wavelength independent for linearly polarized light 0-63704 ocular-focus stimulator, a modification of a Badal optometer 0-42385 PAPA device, pattern classification 0-67163 path length variations recorder for thin transparent objects 0-54923 periscope, furnace, developments and applic. 0-49128 phase-object visualization, small shear interference (SSI), phase grating schlieren (PGS), and Wolter's minimum schlieren (WMS) comparison 0-70060

photo-optical instrumentation, applications and theory, conference, Redondo Beach (1969) 0-60394 polarimeter, double scattering apparatus, for obs. in scattering chamber

polarimeter radiance meter for deep ocean waters 0–45128 prism, Abbe, for convergent and divergent light beams 0–63706 reflectivity, microscopic obs., automatic classifying and histogram plotting equipment 0–76286 reflectometer, Se cell, direct-reading, compact, for reflectance of mineral grains in polished sections 0–73322

reflectometer, vacuum u.v., scanning, designed to minimise mechanical alignment errors 0-73317

reflector design based on power densities transformation, theory, applics. 0 63701

reflectors, conical, props. 0–60389 resolving power, informational statistical approach 0–49134 for sampling and synchronous detection of fast low intensity light signals 0–77204

0-77204

scanner, linear, high resolution, using traveling-wave acoustic lens 0-70045
scanner, multispectral, for Earth Resources Technology Satellite, optimization 0-52380
Schlieren light valve for T.V. projection 0-73335
small path variation meas., photoelectric methods 0-60392
solar concentrator, irradiance distribution in focal plane, photoelectric pulse method 0-63705
solar coronagraph, catadiopbric, design 0-63186
in space vacuum environment, regulation, vacuum chamber design 0-41915

Spectrometer, double-beam, diffraction grating for far i.r. obs. in 250-10 cm $^{-1}$ region, vacuum 0–77219 spectrometer, magnetic, double focusing, for β - γ angular correlation obs.

0-77218 spectrometer derivative, sinusoidally modulated, theory, transfer function

spectrometer grating, two-channel, rapid scan, basic principles, capabilities 0-73350

spectrum analyzer for l.f.-spatial signal detection with aperture tapering 0 63703

0 63703 sun sensor, fine-pointing, choice of spectral region 0–62961 superchromats, optical glasses, considerations on selection 0–70047 telescope, refractive, simple lens systems, mathematics in design, magnification factors 0–76684 transmittance meters for deep ocean waters 0–45128 turbine, quiet for high speed optical applications 0–67162 water wave meas., multiple purpose device 0–42382

Optical materials

tical materials

see also Filters, optical
absorbing uniaxial crystal, complex ellipsoid of indices 0–47982
bonding epoxy resin for i.r. detectors, visible and i.r. transmitting props.,
2-14 µm region 0–41092
cemented optical components, moisture resistance determination 0–57605
ceramic, electro-optic, review and applies. 0–54064
ceramic, hot-pressed ferroelec., electro-optic applies. 0–51272
coating deposit colour-selective, anti reflection of complex configuration
0–57575

Ferroelectric profileger props. 0–62884

ferroelectric, nonlinear props. 0-62584 ferroelectric ceramic, lead zirconate titanate, hot pressing effects rel to electro-opt, applies. 0-62624 glass, borate, for lens system, patent 0-76045 glass, selective absorption in range 1.3 to 1.5 μ , absorption neutrality 0-76042

olass graded index rods, image aberrations 0–59355 glasses, photoelastic constants 0–79253 glasses rel. to fibre optical communications systems, light scattering behaviour 0–48001

our U-48001 holographic image storage media, evaluation by dynamic-range and information efficiencies 0-60271 interference coating types for harmonic generation and parametric amplifications 0-62585 laser, optical and elastic props. 0-76759 for laser recognitors the propositional phase acts of irrect mags. 0, 66006

for laser resonators, thermo-optical characts., direct meas. 0–66006 laser rod, composite, stress analysis, optical path length change 0–42291 lead zirconate titanate ceramic, hot pressing rel. to electro-opt. applics. 0–62624

molecular cryst., second harmonic generation rel. to charge transfer 0-75991

multilayer coatings on reflectors, 'black mirror' effect 0-41116 nonlinear, metal oxides with nonbonded electrons 0-62586 nonlinear, refr. index inhomogeneities effects on second harmonic generation 0-56482

nonlinear crystals, special geometry, for laser frequency multiplication 0-42317

0-42317 photochromic, evaluation for determination of sensitometric, image-decay, resolution and MTF characteristics 0-70109 plastics for optical components manufacture, industrial process 0-57607 powders, cryst., for nonlinear optics 0-44749 shear strain properties to 10⁻¹⁰ 0-50659

Optical materials continued

silica, polished, fused, roughness and slope meas., simple scatter method 0-49130

surface testing by wavefront shearing interferometer, interferograms method 0-60344

surfaces, optical, roughness and slope meas., simple scatter method 0-49130

0—49130
thermal expansion 'zero', meas. 0—62216
vacuum u.v. window, transmittance limit temp., depend. 0—51311
AgCl:AgBr mixed crystals use as an i.r. optical material 0—59346
Al film, highly reflective, fabrication, patent 0—39962
Al₂O₃, vacuum u.v. window, transmittance limit temp. depend. 0—51311
Ba₂LiNb₂O₁₅, nonlinear optical cryst, with no microtwinning 0—65974
FeBO₃, ferromagnet at room temp., transparent in visible, mag. and opt. props. 0—44557

FeBO₃, terromagnet at room temps, transparent in visible, mag. and opt. props. 0–44557
FeF₃, ferromagnet at room temps, transparent in visible, mag. and opt. props. 0–44557
GeO₃, vacuum u.v. window transmittance limit temp. depend. 0–51311
LiNbO₃, growth of high-quality cryst, from congruent melt 0–47136
NaCl.KCl crystals, vitreous, mix.d, ir. optics 0–72345
Nd:glass, thermo-optical characts, direct meas. 0–66006
NiSiO₂-NiSiO₂ multilayer coatings on reflectors, 'black mirror' effect

PbMoO₄, cryst. growth from melt, size and quality optimization conditions 0-61733

SiO₂, vacuum u.v. window, transmittance limit temp. depend. 0–51311 ZnO-type pigments, solar radiation damage, optical props. in u.v. and i.r. 0–41179

0-41179

Optical mode, crystals see Crystals/lattice mechanics
Optical model see Nucleus/models

Optical properties of substances
see also Optical constants; Optical materials
absorbing crystal, theory, exptl. test. 0-62595
alkali halides colour centres 0-47269
alkali metal film, thickness depend., rel. to plasma oscills. and photoelectron diffusion range 0-79224
alkaline earth fluorides 0-54053
amalgams, liquid 0-74754
amorphous semiconductors, conf., Cambridge, England, Sept. 1969
0-47686
antiferromagnets, two magnon props, rel. to spin wave interactions

antiferromagnets, two magnon props. rel. to spin wave interactions 0-40122

p-azoxyanisole, liquid crystal, optical focusing and voltage induced vortic ity 0-53355

ity 0-53355 beam coupling into thin films 0-60340 black polyethylene 3 to 4000 cm⁻¹ 0-44742 cellulose, photochromism obs. in different forms 0-72313 chalcogenide glasses, transmission spectra near absorption edge 0-39906 chalcogenides, ternary, single crystals grown by modified Stockbarger technique 0-50456

coating, thermal control and solar reflector 0-58566 coatings, thermal control, degradation 0-41113 and collective oscillations as function of temperature, i.r. and Raman techniques 0-48085

and collective Schilations as function of temperature, i.f. and Raman techniques 0–48085 critical opalescence, influence of attenuation on the measured angular dependence of intensity in binary liquid mixtures 0–64922 crystals, biaxial, interference figures calc. 0–62625 crystals, metallic, anisotropic, methods for meas. of opt. const. 0–44756 crystals, optically active, frequency change of light waves 0–41090 crystals, uniaxial absorbing, determ, from oblique reflection obs. 0–44743 data calc. from electron energy loss meas. 0–51256 dielectric, Faraday rotation, magnetoplasma reflection 0–72303 dielectrics, effect of h.f. discharge plasma 0–40819 dielectrics, transparent, laser-damage mechanisms 0–58780 dolomite, in Schumann region, optical constants 0–69072 dyes, organic, stimulated emission, study of polarization 0–68105 dyes, sensitising, overcrowding and helicity as indicated by induced optical rotation 0–74752 ellipsometric meas., minimization of errors 0–44767 ferroelectric, oxygen octahedron type, theory 0–40846 ferroelectrics, for applications, survey 0–40850 ferromagnets, transparent, review 0–75907 gas breakdown using single-mode, ruby laser, self-focusing effects

gas breakdown using single-mode, ruby laser, self-focusing effects 0-71261

0-71261
gas mixture, optical clamp 0-78225
gasses, optically thick media, transport of resonance radiation 0-58398
gasses, optically thick media, transport of resonance radiation 0-58398
gasses, optically thick media, transport of resonance radiation 0-58398
gasses of linear mols., Rayleigh light scatt. 0-43050
gelatin, dichromated, hologram etching 0-60272
glass, laser, damage, surface defects 0-57532
glasses, eterm. rel. to production of photosensitive microcrystalline
glasses 0-69065
glasses, laser, travelling wave, surface damage threshold obs. 0-57530
graphite, pyrolytic 0-44743
graphite, variational approach 0-53757
group A^{III}B^V type crystals, and lattice potential energy, piezoelec. and
elastic props. 0-44744
insulator, conference, Turku, Finland, Aug. 1970 0-74858
ionic solids, cubic, longit. modes, effect of lattice anharmonicity 0-44746
laser mat., piezo- and thermo-opt. props. 0-79254
laser mat., piezo- and thermo-opt. props. 0-79254
laser materials 0-76759
laser rod, composite, path length change, stress, end-region analysis

laser rod, composite, path length change, stress, end-region analysis 0-42291

laser rods, ruby, non-destructive damage studies 0–57534 liquid cryst. film of binary mixture 0–58447 liquid crystal, nematic, fluctuations, critical slowing, laser interferometry 0–43446

6 43446
 liquid crystal film, acoustic field mapping, colour changes 0—38391
 liquids, Bragg reflection from phase grating induced by non-linear optical effects 0—71346
 liquids, low-absorption coefficient meas, using laser-transverse modes, beat frequency shift 0—50225
 liquids, possible observation of light inductions and echoes 0—43399
 lunar fines, glassy particles in 0—79719
 lunar samples, polarization characts. 0—48541
 lunar samples, reflectivity, polarization laws and spectrum 0—48540
 lunar samples, rel. to solar radiation effects 0—45398
 macromolecules, activity and statistical zigzag model of struct. 0—58257

Optical properties of substances continued

magnetic-ordered crystals, gyrotropy and birefringence 0–48011 metal, many-electron effects 0–76007 metal ferromagnetic, non-linear transverse Kerr magneto-optic effect, theory 0–72310

molecular reflection, by statistical theory 0–61050 molecules, complex, by appl. of chemical potential 0–67686 nematic-cholesteric mixtures, thermo-optic effects 0–55614

nematic-cholesteric mixtures, thermo-optic effects 0–55614 nitrobenzene-n-anisidine (diphenylamine, diphenyl methane), density, rel. to intermolecular interactions 0–49951 ocean waters to 2000 m, inhomogeneities, hydro-optical devices 0–45128 one-dimensional solids, scalar spectral characteristics 0–44858 optic axis in absorbing crystals, directional determ. 0–65972 organic fluors, tuned laser output power, wavelength depend. 0–50240 organic mixed molecular crystals Green function method 0–40653 perovskite-type cpds., book 0–68293 photochromic solid film, depend. of optical density on time of exposure 0–54067

photochromics 0-51255

photochromics 0-51255 photon-echo theory, superradiant damping effects 0-42920 photoplasticity in ZnO 0-76044 phototropic shutters, nature of residual losses 0-43451 polarization plane, angle of rotation meas, in semiconductors 0-78984 polymers, scalar spectral characteristics 0-44858 polymethine dyes, generation and spectral characts. 0-61523 polystyrene latexes, relationship between coefficient of scattering and cell diameter in multiple light scattering 0-66036 0-66003

rare earth orthochromites, and magnon energies and exchange constants 0-44597

research, Massachusetts Institute of Technology, Sep 1967-Sep 1968 0-38121

ruby laser mat., piezo- and thermo-opt. props. 0–79254 ruby laser with regularly moving crystal, mode-locking effects 0–77122 salt fingers, optical distortion of ruled vertical grating, random walk model 0–51498

salt fingers, optical distortion of ruled vertical grating, random walk model 0 51498 self-focusing, laser glass 0–59349 solids, calculation from adjusted band structures 0–65583 superconductor, Nb-Ti solid solns. 0–40740 surfaces with bestrewed particles, pits, etc., computation method 0–44741 transition metal oxide, and elec. props. 0–75550 1,3,3-trimethylene-dolino-6′-nitro-8′-pyrylospirane, photochromic information storage 0–60451 water, between 1-10° µm 0–43458 Ag.5bS; single crystal, optical props. 0–61709 Ar discharge, high-energy 0–61389 Ar liquid, self-phase modulation in intense electric fields 0–46347 Au, optical density of states, photoemission obs. 0–40907 B/AuZn, rel. to band structure and electronic density of states 0–65597 Ba.Na.Nb₁₀O₁₀, melt stoichiometry effects 0–47983 Ba₂.NaNb₂O₁₃ single crystal, growth striation effects 0–56479 CdIn₂S₄·Yb³⁺, and e.s.r. meas., rel. to site symmetry of Yb³⁺ 0–56473 Cu-Ni alloy, clustering effects, rel. to rigid band model 0–40908 GaAs_{1-x}P_x-rel. to vapour growth and epitaxy 0–47714 Gd₂(MoO₄)₃, ferroelectric, and elec. and mech. meas. 0–47843 Ge specimens, total hemispherical emittance as function of temp., 25-360K 0–54071 Hg. He hollow-cathode discharge, electrical and optical props. obs. 0–43557 InAs. p-n. junction laser, light emission characteristics, temp. depend.

U=52327

InSe films, amorphous 0=56287

K, vapours, at high temperatures and concentrations, with He as expanding gas 0=71260

K vapour, self-frequence of the concentrations of

K vapour, self-focusing of ruby-laser light 0-39675
Kr discharges, h.f., optical and electrical properties 0-43355
Kr liquid and solid, self-phase modulation in intense electric fields 0-46347

Mo photochromatic solns., depend. on composition, conc. and u.v. irrad. strength 0-61520

Mo photochromatic solns., depend. on composition, conc. and u.v. irrad. strength 0–61520
MoS2 single crystals optical anisotropy from obs. of electron energy loss spectra 0–44747
Nb Ti solid solns., supercond. 0–40740
Nd: glass laser mat., piezo- and thermo-opt. props. 0–79254
Nd, glass laser mooptical consts. 0–49113
Ne discharges, h.f., optical and electrical properties. 0–43355
Ni P films, rel. to struct. 0–51262
Ni, visible and near ir 0–62602
β Ni, visible one of the visible of visible of the visible

ZnO photoplasticity 0–76044

Optical pumping
2.13*n* internal optical parametric oscillator 0–69882
absorbing media, light amplification 0–63593
absorbing media, light amplification 0–63592
alkali earths, mechanism, and obs. 0–52937
alkali vapours, light propagation 0–77058
atom in zero field, level-crossing resonances 0–52929
atomic ions free, with h.f.s. oriented in He buffer gas orientation by absorption of circularly polarized light 0–49771
atomic levels, excited, orienting 0–46410
atoms, light shifts and multiple quantum transitions 0–52932
broad-spectrum, excitation of stimulated light scattering 0–55268
conference, optical pumping and at. line shape, Warsaw, 1968 0–52878

Optical pumping continued

diatomic molecule excitation by electron bombardment 0–61051 dye laser, by 200 kW N₂ laser, 3500 to 6000 Å output characts. 0–63622 dye laser, continuous pumping 0–69902 dyes, by flashlamp, wavelength tunability 0–42281 dyes, optical generation intensity and efficiency due to pulsed lamp excitation 0–60222 dynamical eqns., irreducible tensor formalism 0–52959 flashlamp with 20 J capacity and 50 ns rise time 0–42280 gas atoms, extraction of polarized electrons 0–54998 gas dynamic molecular laser 0–77082 gases, relaxation processes 0–52938 generation line splitting in 4-level laser 0–52261 higher order temperatures 0–52257 hyperfine pressure shift, many-body approach 0–70798 intert gas atoms, excitation 0–49795 interstellar masers, stimulated OH emission, pumping mechanisms 0–57060 kryptocyanine, induced Raman spectra by powerful pulse of ruby laser

0-57060
kryptocyanine, induced Raman spectra by powerful pulse of ruby laser 0-43172
laser, gas magnetron diode applie. 0-60195
laser, solid state, pumping energy density 0-49064
of laser by self amplified rad, stability of frequency 0-73213
laser lamps, scientific, engineering information, survey 0-57509
lasing threshold and the quantum yield of the fluorescence of organic phosphors, relationship 0-60220
masers, millimeter range, four models 0-42241
methyl fluoride, methyl alcohol, c.w. submillimetre laser action 0-73207
nonlinear image upconvertor with nonplanar pump beams 0-60413
operator methods, effective 0-52258
organic dye solms, duration of generation 0-42282
organic dye stimulated emission pumped by small coaxial N2 laser 0 63624
parametric noise pumped by mercury lamp 0-67042

parametric noise pumped by mercury lamp 0—67042 parametric oscillator, internal to laser cavity, operation 0—60201 parametric oscillator, proustite, Ag₂AsS₃, by laser 0—77068 phthalimide generation by lamp excitation 0—73233 picosecond pump 0—45815 polymethine dye solns, emission on pumping by Ne glass laser 0—49063 quenching rate meas. method for excited alkali metal atoms 0—67644 relaxation of systems with buffer gases 0—55240 resonance induced by modulated light 0—52941 rhodamine 6G in alcohol solns, under pulsed excitation, effect of induced losses on duration of stimulated emission 0—42285 ruby, non-radiative relaxation time between ⁴T₂ and ²T₁ states, upper limit 0—54123 ruby, nonradiative relaxation ⁴T₂ to ²T₁, 4 ns upper limit 0—44899

0–34123 ruby, nonradiative relaxation 4T_2 to 2T_1 , 4 ns upper limit 0–44899 ruby laser, short-switched giant pulse 0–67098 scintillator laser, by 200 kW N₂ laser, 3500 to 6000 A output characts. 0–63622

semiconductor lasers, bulk, quantum-mechanical rate equations 0-52315 single mode Q-switch operation, influence of spatial hole-burning 0-77072

0-77072
solid laser pump caivity structure with thermal control, patent 0-52333
solid lasers, review 0-77059
spontaneous parametric luminescence 0-74111
Stokes components in stimulated Raman scattering excited by a pulsed laser 0 46429

laser 0 46429
two-frequency generation, phonon processes, theory 0-42252
two-level molecular excitation by ultrashort crossed pulses 0-61054
vapour, at. orientation and alignment rel. to cross-beam propag. 0-52949
vapour, coherence transfer at at. nutation freq. 0-52940
vinyl chloride, c.w. submillimetre laser action 0-73207
X-rays, characteristic, quasistationary population inversion 0-79338
Ag₃As₅, proustite, by laser, optical parametric oscills. 0-77068
Ar laser, role of multi-stage processes in pumping 0-63616
CS, level crossing and double resonance of A¹II state 0-46455
Cd.l²-laser 0 49079
Cs. 6³S_{1/2} hyperfine component selection, mag. filter 0-52946
Cs. ground state spin polarization rel. to 6³P_{3/2} collisional my mixing meas.
0-52945
Cs, photoresonant plasma, ionization 0-53151

0-52945
Cs. photoresonant plasma, ionization 0-53151
Cs. photoresonant plasma, ionization 0-53151
Cs. photoresonant plasma, ionization 0-53151
Cs. photoresonant plasma, ionization 0-52901
Cs atoms, population inversion, hyperfine sublevels, maser, construction 0-52951
iii3 Cs. optically oriented, reson, induced by modulated light 0-52941
ii3 Cs. vapour, coherence transfer at at. nutation freq. 0-52940
F I, visible laser action 0-55232
He. Ne discharge, by He lamp, excitation transfer from He levels to upper Ne levels 0-49793
iHe. 10 levels, orienting 0-46410
iHe, ground state modulated resons, and transverse pumping, obs. 0-52989
He magnetometers, resonance and nonresonance techniques. 0-52229

He magnetometers, resonance and nonresonance techniques 0–52229 Hg isotopes, of 6 P₀ metastable level 0–74139 ²⁰Hg alignment, mag. reson. subharmonic resons. and transients 0–52959

Hg isotopes, of 6 % metastable level 0—74159
20 Hg alignment, mag. reson. subharmonic resons. and transients 0—52959
20 Hg nuclear magnetic moment determination 0—46149
KF, mag. circular dichroism of F band and F-centre spin polarization quenching 0—76027
KH;PO₄ parametric fluorescence excited by 2573Å pump 0—44907
37K, nuclear polarization, and β-decay asymmetry, obs. 0—52680
37K, 479₃₇ level crossing, obs. 0—52913
NH₄H;PO₄ parametric fluorescence excited by 2573Å pump 0—44907
N;O, vibr. relax. 0—39386
21Na nuclear polarization, and β-decay asymmetry, obs. 0—52680
22 Na nuclear polarization, and β-decay asymmetry, obs. 0—52680
23 Na, optically oriented, F=2 multiple quantum transitions, cross-beam obs. 0—52919
24 Ne, levels orientation obs. 0—74127
OH, H;O and H;CO microwave lines, near i.r. stars, i.r. pumping 0—66465
Db. 10₂ metastable state, resonance obs. 0—77671
Bb-vapor, fled reversal signals, experiment's interpretation 0—65995
Rb atoms, population inversion, hyperfine sublevels, maser construction 0—52951
Rb vapour, low-temp. signal detection 0—77672
87Rb, atoms alignment and ground state r.f. Zeman transitions, obs. 0—52954
87Rb maser, theory 0—60193

87Rb maser, theory 0-60193 Sr⁺, optically oriented, relax. in inert gases, obs. 0-52955 Optical pumping continued

ScrF2:Nd3*, laser, spectroscopic study of induced radiation, temp. limit of operation 0-41186

T1, *P1/12 ground state, in presence of buffer gases 0-60964

YAG garnet:Nd lasers, using alkali metal vapour light sources 0-73334

YAI:Nd garnet laser, repetitively Q-switched, continuously pumped, experanalysis 0-77128

Optical quantum generators see Lasers

Optical rotation
see also Magneto-optical effects; Optical constants; Polarimeters;
Polarized light

Polarized light active molecule, origin and development on primordial Earth 0–41476 activity, theory 0–77733 benzil, cryst., theory of optical activity 0–62611 biaxial cryst., activity in directions inclined to optic axis 0–56494 biaxial cryst., activity parameters determ. 0–56493 cholesterol, effective rotary power 0–61522 crystal, activity, theory 0–79239 crystal, and birefringence and absolute config., classical calc. 0–54062 crystals, magneto-optic rotation 0–76019 crystals, rotary power and circular dichroism, dispersion theory 0–41118 trans-cyclo-octene, circular dichroism 0–58213 dispersion, quantitative 0–62608 electro-optical, linear, theory, two-photon effect 0–77192 electrogyration, quadratic, and axial fourth-rank tensors 0–56495 enantiomorphism rel. to H* diffusion in cryst. on pulsed photolysis 0–48202 0 - 48202

0-4202 exciton model for organic crystals 0-62611 Faraday, of EuS, EuF₂ mixture in studies of mag. structures at low temp. 0-51196

0–51196
Faraday rotation, saturated, in mixed crystals, local asymmetry 0–54060 induced, overcrowding and helicity of sensitizing dyes 0–74752 light scattering from optically active fluids 0–46913 liquid crystal mixtures, cholesteric 0–58445 methyl mesityl oxide oxalate, nonenantiomorphous biaxial crystals 0–69079

molecules, exchange theorem calc. 0-55278 piezo-rotatory coeffs. and stress-induced activity, meas., crysts. 0-54061 polarimeter for accurate meas. of rotation of plane of polarization, i.r.

polynucleotides, optical activity of n-\(\pi^*\) transitions \(0-74423\) pyrrolid-2-ones, optically active crysts., atomic parameters \(0-75116\) quarterwave retarders, rhomb-type, critical evaluation \(0-70039\) racemate synthesis, asymmetrical \(0-49829\) suspension of rigid Brownian particles, flow birefringence, rot. scatt. coeffs. determ. \(0-43479\)

determ. 0-43479
uranyl compounds, cubic cryst., gyrotropy 0-44772
CsBr-CsI mixed cryst., Faraday rot. 0-76023
CsFeF3, ferrimagnetic single crystal, Faraday, absorpt. cqeff. 0-44656
MgSO4.7H3O, left-handed epsomite, formation favoured by organic particles 0-78395
NaNO2, nonenantiomorphous biaxial crystals 0-69079
NaSbS4.9H3O, dispersion of rot. of plane of light polarization 0-56496
Si, nonresonant interband Faraday rot. 0-79248
SrMoO4, electric gyrotropy, exptl. detection 0-72323
ligial systems

Optical systems

see also Aberrations, optical; Lenses; Optical images; Optical instruments; Optical materials; Resolving power, optics aberration coeffs, and unusual coords, for specifying rays 0-38536 acousto-optic light deflection devices, material evaluation 0-49117 acousto-optical pattern display with pulse modulation 0-66910 analogue apparatus, coherent correlation techniques in matrix multiplication 0-72852 using three-dimensional vector diagrams, tech. description 0-63700 aspheric surface applications 0-6320

analysis using three-dimensional vector diagrams, tech. description 0–63700 aspheric surface applications 0–60330 atmospheric absorpt., scatt. and turbulence, influence on instruments and communication systems 0–42381 atmospheric scattering and absorption effect 0–48289 autocollimation, use of reflecting prism standards 0–73287 automatic scheme for matching correction of optical systems 0–52374 axially symmetrical, with spherical and aspherical surfaces, eikonal functions applications, n.r.t. computation 0–38535 axicon light collector for foil-excited accelerator beam spectra 0–60737 beam deflection, photoelastic, number of resolvable spots 0–57335 beamguides with few repetitions, radial focusing, theorem 0–38534 birefringent laser beam splitter 0–63596 cavities, degenerate, effect of aberrations, acceptance factors calc, for several cavities 0–60382 chromatic image analysis technique, methods of secondary colour reduction 0–38561 coherent data-processing system, resolution testing by linear gratings 0–70005 coherent light propagation, integral relationship 0–60337

0-70005 coherent light propagation, integral relationship 0-60337 coherent optical processing of 2-dimensional data 0-70043 colour television camera NHK Type 30WM-71, construction and characts. 0 69998 computer simulation for performance evaluation 0-70000 correlator, compact, for treatment of coded electronic signals 0-77205 detection and estimation of incoherent objects, modal decomposition of aperture fields 0-42384 detection and ranging systems, actively scanning, threshold relationships 0-52377 double-beam detection, with pulsed sources of vacuum u.v. radiation

double-beam detection, with pulsed sources of vacuum u.v. radiation 0 -73319

0-60372 electro-optical, optical transfer function applications 0-60372 for film printer, metallic, (OZX 2-35 mm) 0-63738 focus sensor, autocollimating, for systems with high angular resolution 0-60329

focusing glass fibre and rod 0-57610 for focusing and deflection of optical beams by cylindrical mirrors 0-73314

0-73314
Fourier methods for a simple system 0-45819
Gaussian constants rel. to temperature coefficients 0-57571
generalized, (e.g. pinhole arrays), information retrieval from the coded images 0-38518
glasses front protective, parameters calc. 0-57568
guided waves in thin films, grating coupler for efficient excitation 0-52361
for holographic memory, read-write 0-73256
i.r. optical-transfer function analyser for testing 0-70002

Optical systems continued

tical systems continued imaging, effects of near atmosphere anomalies on resolution 0-73288 imaging, using reduction of tetrazolium salts by photoconductor-metal-electrodes cells 0-70007 imaging systems, combined spatial and temporal characteristics 0-77186 intensity interferometric imaging through diffusing medium 0-77164 interference-polarization filter step, phase-shifter errors effects on transmittance 0-77212 kinoform filtering using incoherent illumination 0-70067 large aperture system for low-light-level application, properties and performance 0-69999

laser alignment device for ghost image elimination 0-49028

laser space communications, optical components and technology 0-77173

0-77173
laser-Raman radar, for air pollution probe 0-79544
lens, scanning technique to determine modulation characteristics comparison with standard 0-69996
lens design, Fortran program, user's manual 0-38528
lens design, Fortran program organization and description 0-38529
lens design, Fortran program specifications 0-38527
light modulator, electrooptical, for comparing pulsed sources 0-38556
local det. of distrib. of light at any down-beam range 0-77172
low light level, TV techniques 0-73336
low light level, TV techniques 0-73336
low light level instruments, optical requirements for lens design 0-52355
low spatial frequency, allowable aberrations 0-49105
m.t.f. meas. by photographic technique for comparing sighting system with simulator 0-70138
matching correction through partly automatic scheme 0-52374

matching correction through partly automatic scheme 0-52374 merit function based on extended-range modulation transfer function 0-60322

mignification control using concentric lenses 0-77168 microdensitometer, reflectance, with bright and dark field, phase contrast, spatial filtering and laser optical systems 0-70096 for microdisplacement obs. noncontact devices, photoelectric adaptation 0-73313

moire-holographic interferometry, for three-dimensional stress analysis 0-57327

moire-holographic interferometry, for three-dimensional stress analysis 0—57327
multiple aspheric, manufacturing techniques 0—57563
multiple aspherical surfaces, advantages 0—57562
multiple-lens parallax panoramagraphy 0—70132
multiple-lens parallax panoramagraphy 0—70132
multiples for pattern recognition using point holograms 0—60265
non-redundant array optical analog 0—69975
objectives, optical transfer function determination using scanning methods with Fourier analysis of edge image 0—70031
optimization criteria comparison 0—67132
optimizing, comparison of two criteria 0—57601
oscillation meas., automatic for inverted torsion pendulum 0—75230
otf meas., influence of optical bench errors, method for meas. 0—49133
PAPA device, pattern classification 0—67163
periodic self-focusing, theory 0—73286
photodetection, 4, theoretical and exptl. S/N ratios 0—42392
prism-film coupler, theory by plane-wave analysis 0—73316
prism-film coupler and thin-film light guides, theory 0—73315
protective glasses, parameters calc. 0—57568
for recording schlieren imges with ultrahigh speed framing camera 0—45818
relative absorption measurement, patent 0—60415

relative absorption measurement, patent 0-60415 resolving power of idealized system, physical realizability and constraints 0-38533

restitution of partially known objects, principle of partial deconvolution

restitution of partially known objects, sampling theorem application 0-77210

0-1/210 rotation symmetric, and modulation of general periodic bar pattern 0-60350

0-60350
scanned system's temporal and spatial analysis 0-63712
scanning, efficiency criterion 0-60328
scanning, spatial filter, optimisation 0-57613
signal transfer function of optical components, deriv. 0-45838
single-prism digital light deflector, temperature stabilization of pattern 0 67131
solar concentrator for the content.

0 6/131 solar concentrator for thermionic convertor, patent 0-54817 spectroradiometer, computer based, for light source spectral energy distrib. meas. 0-38569 stabilized periscope systems 0-57573 statistical properties of image intensity, narrowband noise model 0-42354 telescopic, four electrode, diverging, paraxial properties 0-73177 telescopic (pre-electrode, geometric and chromatic aberrations 0-73176 telescopic sights and projection systems, mtf by photographic tech, method 0-49106 testing by computer-generated holographs 0-57570

testing by computer-generated holograms 0–57570 thermo-optical degradation and athermalization 0–57572 tolerancing method 0–57574 transmission using injection light sources 0–77169

two-surface reflecting and refracting module design, astigmatism free 0-700010-70001
ultrasonic beam deflection 0-54925
waveguide, PMMA refr. index photoinduced changes applic. 0-54059
waveguide, dielec. 0-57455
waveguide, glass fibre, with low mode distortion 0-57457
waveguide, glass low loss, prep. 0-57458
waveguide, light cond. along glass surfaces 0-57598
waveguide, sputtered glass 0-57459
waveguide transmission, survey 0-77208
zoom, optically compensated, Gaussian design, thin-lens theory 0-60320
Hg-oil vertical reference pool, portable 0-73323

Optical waveguides see Electromagnetic wave propagation/guided waves

see also Aberrations, optical; Atmospheric optics; Lenses; Mirrors, etc.; Optical images; Quantum optics at A.W.R.E., research in high-speed photography, cameras, laser systems, holography 0–52399 at Goddard Space Flight Center, historical development 0–49127 applied, experiments in manual 0–41928

applied, experiments in manual 0-41920 communication using coherent light beams, possibilities and limitations, expts. 0-60332 cylindrical waveguide mode synthesis 0-60115 in electronics, comparison with electron optics, competitive and complementary technologies 0-73175

Optics continued

eye's image quality performance, visual acuity, rel. to pupil size 0-72840

granularity meas., conversion of semispecular values to diffuse r.m.s. values 0–40472
Huygen's principle for uniaxial medium, use of Green functions 0–69970
hyperboloidal surfaces for reflecting objectives operating in X-ray region, manufacture 0–52376
image encoding in modulated gratings from 1899-1970, short bibliography
0.60300

0 - 60309

0-60309
images, illum, and pupil effects and synthetic apertures 0-45814
information retrieval from coded images formed by generalized systems
(e.g. pinhole arrays) 0-38518
information storage, optical appl. of dichroic absorpt. of M centres in alkali
halides 0-60331
intensity fluctuations at focus of annular aperture 0-60334
introduction, university textbook 0-38525
linear, analogies between ordinary and extraordinary waves 0-69969
luminance gradients, threshold gradients meas. 0-60333
meteorological parameters in launch vehicle environments, new passive
optical detection systems 0-51505
Newton's Opticks, terminological ambiguities 0-67119
nonlinear processes, intensity correlations by photon counting techniques
0-63672
Optical Society of America, meeting, Philadelphia (1970) 0-69977

O-05072
Optical Society of America, meeting, Philadelphia (1970) 0-69977
Optical Society of America annual meeting, Chicago (1969) 0-60313
optical field autocorrelation function from photon counting statistics

photoemission from thin films, role of classical optics 0-47894 pulses compression with periodic gratings and zero plate gratings 0-69926

0—59320 replica, image forming elements 0—57569 screening of the photon propagator in many-body optics 0—38488 second harmonic generation, resonance enhancement 0—52352 space limited functions, simultaneous multiple reproduction method 0—59840

0–59840 surface quality evaluation from interference fringe width 0–38538 test glass surfaces, holograms of, use in place of the test glass 0–49124 video transmission of 3 dimens. images 0–70076 windows (aircraft or spacecraft), angular deviation errors in line of sight, interferograms 0–60380

geometrical axes, nonparallelism of cylindrical lenses, apparatus for determination, design 0-57559 conic surfaces, special ray-trace equations 0-57556 depolarization, 'geometrical', in turbulent atmosphere 0-38549 Fermat's principle, lens design limitation by mock-ray tracing 0-52354 image formation of reflecting cone for off axis source 0-60318 Keller's theory for single strip diffraction, analysis 0-63682 laser beam focusing technique 0-42324 point characteristic of refracting plane, hamiltonian optics 0-60319 propagation over nonparallel stratified medium, geometrical-optical and full-wave solns. 0-69973 rays path difference, high precision meas., tech. 0-67127 surface, spherical, radius of curvature meas. 0-63307 publicar see Nanlingar parties

nonlinear see Nonlinear optics Orbital calculation methods

obital calculation methods
3d orbitals, minimum Gaussian lobe representation 0-70831
AVE CTSCF studies in molecular structure, parameter selection 0-39353
ab initio calcs. for 3d exponent of P and S, insensitivity to molecular environment 0-74098
ab initio calculations for chemical bonds 0-46437
ab initio on HF dimer and mixed H₂O-HF dimer 0-43105
aromatic hydrocarbons, chemical shifts, computation by antisymmetric molecular orbital methods 0-58227
atomic orbitals, calculation of overlap integrals 0-46351
atomic structure, matrix elements of operators calc. for factorized shell 0-49761
atomic virtual orbitals for use in semi-empirical molecular orbital calcular atomic virtual orbitals for use in semi-empirical molecular orbital calcular atomic virtual orbitals for use in semi-empirical molecular orbital calcular atomic virtual orbitals for use in semi-empirical molecular orbital calcular atomic virtual orbitals for use in semi-empirical molecular orbital calcular

0-49761
atomic virtual orbitals for use in semi-empirical molecular orbital calculations 0-46318
atomic wave functions in Hylleraas coords, and Be appl. 0-39283
atoms with one valence electron, Hellman pseudopotentials 0-58093
book 0-58610
Brueckner orbitals for atoms and mols. 0-77626
CI, minimal basis calcs, for ionization potentials of N₂O molecule
0-77808

O-7808
CNDO MO methods for structural and energetic predictions for simple hydrocarbons 0-49928
CNDO calc. of H bond and blue shift in formaldehyde-water 0-74370
CNDO calcs. on hydration of simple ions 0-72520
CNDO/2 CI calc. of electronic states of naphthalene and azulene 0-61145

carbocyclic compounds, calculated orbital energies and ordering 0-64494 closed shell at. pot. representation eff. on e scatt. cross-section 0-74137 conformal groups for Schrodinger eqn. for H atom 0-70810 continuum in config. superposition 0-39348 convergence of Gaussian expansions of Slater-type atomic orbitals 0-58153

U-38133
Correlation coefficients for electronic wavefunctions of atoms in S-states and linear molecules 0-42933
Coulomb Green's function 0-49749
DCSCF energies and orbitals for ground and first excited state of H₂
0-70907

diatomic ion, comparison with one-dimensional model solution 0-49845 diatomic molecules, new approach 0-53028
Dirac form factor for electron vertex in fourth order, calc. of slope at q²=0

Dirac form factor for electron vertex in fourth order, calc. of slope at q=0 0-7645 dual-space-operator technique for building symmetry-adapted wave functions 0-70842 electron correlation, novel perturbative treatment 0-46344 equivalent orbital calculation, ionization potentials of linear alkanes 0.2040

equivalent orbital calculation, ionization potentials of linear alkanes 0—39408 excited-state variational calc, with orthogonality constraint 0—58152 FEMO calcs, on energy levels of polyacene ions 0—74392 FSGO calculation of electric field gradients in mono deuterated methane ethylene and acetylene 0—64524 finite-perturbation method, approximate valence-shell eigenfunctions within framework of CNDO/II theory 0—58155 Floating spherical Double Gaussian Orbital model 0—39251

Orbital calculation methods continued

Gaussian basis functions, contraction of atomic basis sets for water and $N_2 = 0-74264$

Gaussian expansions of SCF atomic orbitals for second-row atoms

Gaussian wavefunctions, integral transform, for H₃²⁺ and H₃⁺ 0-64405

Gaussian wavefunctions, integral transform, for H₃⁺⁺ and H₃⁺⁺ 0–64405 Gaussian-type functions for polyatomic systems 0–58149 generalised free electron molecular orbital method, configuration interaction procedure included 0–74214 HMO calc. of polarizabilities of aromatic hydrocarbons 0–43068 HMO SCF theory with configuration interaction for calc. molecular bands 0–77917

Hamiltonian matrix elements from symmetric wave function 0-77734 two-centre harmonic oscillator integrals, use of second quantization for calc. 0-67593

Hartree-Fock eqns. stability conditions 0-60891

Hartree-Fock first order equation, solution for He atom 0–64290 Hartree-Fock procedure, formulated and applied to polyethylene in CNDO/2 approximation 0–64572 Hartree-Fock theory, virtual orbitals 0–49748 Hartree-Fock theory, virtual orbitals 0–49748 Hartree-Fock time-dependent coupled perturbation theory calc. of optical props. of atoms and diatomic mols. 0–67603 Hartree-Fock valence shell orbitals similar for atoms in the same column of the periodic table 0–58092 Hartree-Fock walence inconsistent field method, calculation on molecular systems 0–39334 Hartree-Fock Bogoliubov self consistent field method, calculation on molecular systems 0–39334 Hartree-Fock Slater calc. for Mn²¹, statistical exchange approximations 0–77661 heterocyclic compounds, calculated orbital energies and ordering

heterocyclic compounds, calculated orbital energies and ordering 0 64494

10 64494

Huckel approximation for electronic structs. of methylallylbenzenes 0–46581

hybrid orbitals construction from irreducible tensors 0–58087

INDO MO method for rationalization of e.s.r. spectrum of Li-naphthale nide anion 0–39433

INDO theory and energy localization 0–39349

immanant wavefunction, properties 0–46319

integral transform trial function for the He like system 0–74102

integral transform Gaussian functions for helium-like systems 0–39250

interaction operators for d° configs., matrix elements 0–55223

Johnson's Hartree-Fock SCF approach to multiple scattering model of polyatomic models 0–64309

Kohn-type variational principles for scattering amplitudes, effect of discontinuous derivative 0–42921

LCAO, cyclobutadiene and derivatives, LCAO study π and σ energies 0–67784

LCAO, optimized, for electronic wave functions calc. in cryst. 0–71898

LCAO, optimized, for electronic wave functions calc, in cryst. 0–71898 LCAO MO SCF calculations for HF₂, HeF₂ and HF₂ radical 0–43106 LCAO MO SCF wave functions for SF₆, ab initio and MZDO treatment

LCAO MO SCF wavefunctions for GaF, GaH1, GeH4, AsH3 and H2Se

LCAO SCF CI, benzyl, and naphthalenic and azulenic homologues elec

tronic structure study 0-67772 LCAO SCF MO, semi-empirical, for treatment of hydrocarbons 0-46564 LCAO SCF MO calculations for ground state of three-membered ring molecular 0-43143

LCAO SCF MO treatment of conjugated N and O containing compounds 0 - 46565

LCAO for crystals, derivation 0-62253

LCAO open shell calcs. on atoms, minimisation of energy functional 0-74090

0–74090 LCAO MO and Hartree-Fock solns, for interaction of inert-gas atoms in region of small overlap, comparison 0–64583 LCAO-MO-SCF two centred function, evaluation of single centre wave function of diatomic molecule 0–43067 LMO, minimizing exchange energy 0–70851 MC SCF wavefunctions, expectation values of one-electron operators, error 0–42918 MINDO SCF, applic, to ionization potential and heat of formation determ, in cyclic hydrocarbons 0–39421 MINDO/2 method, extension to σ bonded mols, containing N and/or O 0–77855

MO SCF study of protonation of CO and N2 using Gaussian basis sets

0—77855

MO SCF study of protonation of CO and N₂ using Gaussian basis sets 0—64384

MO LCAO-SCF-HF, Rittner's potential function discussion 0—53017 methane in CH₂*, near Hartree-Fock energy and equilibrium geometry, orbital energies 0—43173 method of moments for determ. of molec. props. 0—61059 methyl group, single particle wavefunctions satisfying Pauli's exclusion principle 0—64523 methyl radical in pyramidal configuration, temperature dependence of hyperfine splitting 0—46575 molecular integrals by Gaussian transform method 0—39429 molecular orbitals, neighbour atom effects calc. 0—39351 molecules, absolutely inequivalent pure interchange symmetry 0—70857 molecules, an undergraduate textbook 0—60890 numerical soln. of 2-electron Schrodinger eqn. 0—70821 octahedral hybrid orbitals, d'sp' shape 0—67697 open shell at. pot. representation eff. on e scatt. cross-section 0—74143 overlap calc. methods 0—74194 PPP-SCF-MO-CI calcs. for homo-substituted benzenes 0—46540 perturbation theory first order 0—64354 polypeptides, H-bonded, energy parameters 0—64574 polypeptides, study of molecular wavefunctions of monomeric amides 0—64573 pseudopotential theory, LCAO-MO formulation 0—57276 process described were in patomic shell theory. 0, 40760.

pseudopotential theory, LCAO-MO formulation 0-57276 quasi-particles, use in atomic shell theory 0-49760

quinones, ortho and para, electronic structure by improved LCAO method 0-58242

SCF, minimal basis calcs. for ionization potentials of N₂O molecule 0-77808

0-1/808 SCFMO calculations on both minimal and extended basis, SO₂ electronic structure study 0-67753 SCF CI, open-shell calcs., for naphthalene ions 0-74390 SCF LLCAO MO calc. using STO 2G expansions for bond length predic

tions 0-61060

Orbital calculation methods continued

SCF LCAO MO theory, approx., INDO scheme realization on LOAO basis 0-43064

SCF LCAO wave functions, optimization 0-46321

SCF LCAO MO, for one open electronic shell mols., invariant approx. model 0-46432

SCF LCAO MO with CNDO, rel. to electronic struct. of N-heterocyclic benzene analogues 0–39441

benzene analogues 0–39441
SCF MO, electronic structure of CuCl₄²⁻ ion 0–64396
SCF MO, open-shell method, calculation of C nuclear arrangements of cations and anions of heptafulvalene, pentafulvalene, triafulvalene 0–64510
SCF MO, semiempirical, for determ. of ionization potentials and heats of formation of hydrocarbons 0–46563
SCF MO CI treatment, aromatic and heterocyclic compounds, S—containing 0–77923

ing 0–77923 SCF MO LCGO studies on hydrogen bonding in H_2OHOH_2)+ system

0-58168 SCF MO LCGO studies on hydrogen bonding in (FHOH)- system

0-38108

SCF MO LCGO studies on hydrogen bonding in (FHOH)- system 0-53027

SCF MO calculat9ons, variable bases 0-39352

SCF MO theory of nuclear spin coupling 0-74317

SCF MO treatment of conjugated molecules containing bivalent sulphur 0-53088

SCF and CI combined method, for electronically excited states of molecules 0-61163

SCF and k_v wavefunctions, comparison for He isoelectronic series 0-70749

SCF atomic orbitals, use in calculation for NH₂ radical 0-67742

SCF calculations on energy levels and wavefunctions of nucleotide base pairs 0-46610

SCF equations for general open-shell systems, incorporation of quadratic convergence 0-64182

SCF open-shell relectron calcs.. rapid convergence 0-53007

SCF open-shell calcs. on T and V states of ethylene, interpretation 0-64504

SCF wave functions for ground and excited states 0-52869

SCF wave functions for ground and excited states 0-52869 SCF wavefunctions, spin-generalized, for H_2O , OH and O 0-67732 SCF-LCAO-CO method, energy band structures of DNA 0-46609 SCF-LCAO MO method for π electron theory 0-46439 SOGI method for wavefunction determ. in BH 0-39366 STO, minimal basis calcs. for ionization potentials of N_2O molecule 0-77808

self-consistent MO ab initio methods 0-39358 self-consistent MO methods, least-energy minimal atomic orbitals 0 61058

self-consistent methods, energy optimized Gaussian atomic orbitals 0 46433

0 40433 self consistent molec.- orbital methods 0-58153 Slater determinant, projected, for valence-bond functions 0-46435 Slater-type basis for study of charge distribution in organic compounds 0-61140

Slater-type orbitals, expansion techniques for multicentre integrals 0-70738

spin orbit coupling energy, derivation 0-64183 spin-orbitals, natural and generalized overlap amplitudes 0-39268 spin-other-Orbit matrix elements for f⁴ configs. 0-46338

spin-other-Orbit matrix elements for f* configs. 0—46338 spin-spin and orbit orbit interactions, identities relating to spin-orbit interactions 0—77628 steepest-descent method for energy-level densities, extension to higher orders 0—46434 three-centre nucl. attraction integrals. 0—70737 UHF method using LCGO MO approximation comparison of radical ions NH * and NH= 0—67743 universal correlation method 0—67688 valence-bond functions obtained from projected Slater determinant 0—46435

0-404.50
variable bases in SCF MO calculations 0-39352
variable bases in SCF MO calculations 0-39352
wave function, N-body fermion, form investigated by computer 0-60893
wavefunctions calc. for excited states of polyatomic mols. 0-58150
wavefunctions containing first- and second-row atoms, simple basis set

Orbitals see Molecules/electronic structure

Order-disorder transformations see Phase transformations/solid-state

Ordered structure see Crystal/structure; Solids/structure

Organic compounds

sea elso Free radicals; Macromolecules; Plastics; Polymers; Waxes on Mars surface, detection and identification, two approaches 0–57110 D,L-Valine, irradiated, free radical conversions 0–45090 (methyl). "SN-solvent systems, "SN .m.m.r. shifts 0–78312 2-(trimethylsilyl)-tetradeuteropropionic acid, Na salt, as reference compound for p.m.r. spectroscopy 0–66988 sym-dimethylene sulphite, ir. analysis 0–70997 acenaphthylene, librational frequencies calc. 0–47512 accnaphthylene, u.v., absorpt. spectra in vapour, and pure and doped cryst, accnaphthylene, u.v., absorpt. spectra in vapour, and pure and doped cryst.

acenaphthylene, u.v. absorpt. spectra in vapour, and pure and doped cryst. states 0-70965

acenaphthylene, vapour, pure crystal and single matrices, electronic absorption spectrum 0-46531

acenes, solid, electronic spectra at normal and low temperatures in polarised light 0-56555

acepleiadene, ¹³C chemical shift 0–58209 acepleiadylene, ¹³C chemical shift obs. 0–58209

acctaldehyde and derivatives, far u.v. spectra interpretation 0--74326 acctaldehyde and derivatives, far u.v. spectra interpretation 0--74326 acctane, valence force field calc. using vibrational frequencies of isotopic species 0-67759 acctate peel replicas, for electron microscopy, unusual artifacts 0-71554 acctate praseodymium tetrahydrate, Pr³⁺ interaction with medium, transitions 0-62746

acetic acid dimers, far i.r. spectrum of H bond 0-46529

acetic acid dimers, far ir. spectrum of H bond 0–46529 acetic acid in benzene, association const. at surface, from surface tension meas. 0–61472 acetic acid monomers, matrix-isolated, i.r. spectra 0–64470 acetic acid monomers, matrix-isolated, i.r. and Raman spectra, conformation and vibr, assignment 0–53059 acetone, adsorbed on glass, radiage anion, p radiation, e.s.r. 0–39933 acetone, liq., internal refl. spectra, 180 to 200 mµ 0–54940 acetone, rotational Brownian motion from the width of vibrational band contours in molecular spectra 0–61143 acetone, triplet energy transfer to π -bonded mols. 0–77871 acetone, vapour viscosity calc. by free energy average potential model 0–78229

0-78229
acetone in various solns., width of polarized Raman lines as function of conc., effect of intermol. interac. 0-50234
acetonitrile, y-irrad., e.s.r. 0-76228
acetonitrile, ir. band of CC stretching vibr., effect of gas-soln. phase transition 0-43147
acetonitrile, luminesc., low temp. 0-70963
acetonitrile, shift of absorption bands due to dissolved salts with similar anion and cation 0-67846
acetonitrile N-oxide, structure, microwave spectrum, dipole moment, ¹⁴N quadrupole coupling constant 0-74325
acetonitrile hydrogen fluoride complexes, i.r. spectrum, fine struct. 0-43144
acetonitritie in liquid-crystal poly-y-benzyl-L-glutamate. ¹H and ¹⁴N n.m.f.

0–33144 acetonitrite in liquid-crystal poly- γ -benzyl-L-glutamate, 1H and ^{14}N n.m.r. spectra 0–74321 N-acetonyl quinolinium iodide, assignment of bands in i.r. spectrum to different modes of vibration 0–58208 acetophenone, adsorbed on glass, radical anion, γ radiation, e.s.r. 0–39933

0—39933
acetophenone, vibration spectra 0—64474
p.-X-acetophenone anion radicals, hindered rot, of acetyl group 0—64471
acetophenone in benzene, triplet-singlet energy transfer to 9, 10-dibromantracene 0—68117
acetophenone-ds, vibration spectra 0—64474
acetophenone-ds, vibration spectra 0—64474
p- acetotoluidide crystals, X-ray study of orthorhombic modification
0—43647

0-43647

0-43647 acetyl bromide, and deuterated form, Raman spectra 0-55332 acetyl chloride, conductivity of solvent and dil. AlCl₃ solutions 0-55630 N-acetyl-L-tyrosine amide, cryst. struct. 0-78432 acetylacetone, enol form, study of nonplanar vibrations 0-64472 acetylene, adsorption on y-AL₂O₃, i.r. spectra of surface species, effects of S poisoning 0-54106

acetylene, cryst., Raman spectrum in intramol. and lattice vibr. regions 0-72394acetylene, ion-molecule reactions with H2S 0-79438

acetylene, inear and bent, trans and cis isomers found for most low-lying excited states 0–74324 acetylene, in liquid N₂ and O₂, Fermi resonance 0–46530 acetylene, photoionization yields and absorption cross sections, isotope effects 0–70964 acetylene+OH+CO+CH₃, primary products determ. 0–66176 acetylene ¹²C₃HD bands in region 6-10 μ, vibrational energy levels 0–46532

acetylene crystals, normal coordinate calculation, structure, Raman spec tra 0-48093

acetylene mol. photoioniz., photo e energy anal. 0–67706 acetylene-Ar Penning mixture, ionization maximization 0–39618 acetylene-O₂ mixtures, Ar diluted, detonations, transverse wave strength 0-50164

acetylene-O2 reaction in shock tube 0-41426

acetylene-O₂ reaction in shock tube 0-41426 acetylene-O₂ reactions chemi-ionization during induction period 0-79433 acetylene-O₃ reactions chemi-ionization during induction period 0-79433 acetylenes, electric field gradients near deuteron calculated by floating spherical gaussian orbital method 0-64524 acetylenes, i.r. intensities 0-43148 acid fluorides, vicinal proton-fluorine coupling constant, obs. of change of sign with dihedral angle 0-67793 acid-base interactions, protonation and ion pairs obs. 0-79426 acridine, biacetyl phosphorescence quenching, solvent effects, physical energy transfer mechanism 0-39814 acridine in n-alkane matrices at 4°K, vibrational analysis, electronic absorption and fluorescence spectra 0-77866 acridine-acridan mol. complex, e.s.r., prod. of four radical species 0-79411

0 - 79411

acridines, electronic spectra at normal and low temperatures in polarised light 0-56555 acrolein, electric field induced spectra, contour analysis of 3860 Å

ncrolein, spectroscopy, photoisomerism, theoretical considerations 0-43145 acrolein.

u--3.143 acyclic and alicyclic alcohols, ¹³C chemical shift obs. by n.m.r. 0-46534 acyclic phosphates, P-H spin-spin coupling consts. 0-77858 adamantane, Overhauser effects and ¹³C relaxation times 0-39407 adamantane, solid, dynamics of orientational defects 0-59093 β-adenosine-3'-β-adenosine-5'- phosphoric acid, P³¹ n.m.r. spectrum 0-50261

adsorbate on C, desorption kinetic parameters, non-isothermal determ. 0-65103

L-alanine, Cu(II)-doped cryst., e.s.r. 0-62765 β -alanine, semiconductivity, optical transmission and reflection, pure and X irradiated 0-75657alcohol, solid and liq., structural effects near solidification temp., e.s.r. 0 55653

alcohol-water mixtures, u.s. relaxation 0-55611

alcohol-water solutions, static permitivities 0-74774 alcohols, biacetyl phosphorescence, fluorescence quenching, solvent effects. H abstraction mechanism 0-39814

n-alcohol + organic solvent mixtures, u.s. absorption 0-50221 alcohol solutions of Rhodamine 6G, influence of quenchers on threshold of laser effect 0-49060

alcohol-water mixtures, dielec. consts. at low temp.

Organic compounds continued

alcohols, liquid, H bonding h.p. spectroscopy 0–55333 alcohols, self-associated, double excitation in i.r. spectra 0–53060 alcohols, semiconducting, elec. conductivity, temp. dependence 0-62341

alcohols n-butyl, isobutyl, sec-butyl, u.s. relaxation mech. study 0-50222 die and tri-alcoylphosphines addition compounds with borane and monoal-coylboranes magnetooptic properties 0–71040 aldehydes, aromatic. Tr->So radiationless transition 0–46570 aldehydropyridines, monosubstituted, long range coupling consts. 0–77922

aldopyranoses, pentose and hexose, ¹³C n.m.r. spectra 0–46533 alicyclic, structure and conformation determination using intramolecular nuclear Overhauser effect 0–67758

alicyclic hydrocarbons, conformational anal. by MINDO/2 method 0-77915

aliphatic, molecular motion, dielec, abs. 0–59067 aliphatic alcohols in n-heptane soln., dielec, relaxation 0–53367

aliphatic alcohols in h-neptane soin., dielec, relaxation 0-53367 aliphatic long chain, twisting from rate parameters for dielectric relaxation and thermal properties 0-61188 aliphatic polar liquids, vapour pressure, dipole effect 0-68190 aliphatic saturated, C 1s energies meas, by ESCA, binding energy shift 0-74335

0-74335
alkane, linear, ionization potentials, equivalent orbital calc. 0-39408
alkane molecular ions and water vapour, reaction mechanism and rate
constants 0-72530
alkanes, 15 to 30 C atom length, search for in lunar samples 0-48547
alkanes, 1-410m abstraction by CH₃ and OH radicals 0-62803
n-alkanes, MO theory predictions of mass spectra 0-77861
alkanes, atomic and bond charges, calc. from electronegativity 0-64311
alkanes, consistent force field calc. of cryst. structure and props. 0-58608
alkanes, e.s.r. of positive holes in irrad, glasses 0-54161
n-alkanes, homogeneous nucleation 0-43517
alkanes, iliquid, viscosity pressure depend., rel. to branching in molecule
0-61504
alkanes, partially denterated spin lattice relay of CH₂ and CH₂ provide

alkanes, partially denterated, spin-lattice relax. of CH_3 and CH_2D groups 0-79215

0-19215
alkanes, quenching of excited Hg atom 0-70783
alkanes, reactions with OH radicals, kinetic spectra 0-66203
alkanes, substituted, rotational isomerism 0-74327
alkanes, temp, quenching of phosphoresc. in benzophenone 0-51363
n-alkanes + methylformate liq. binary systs. 0-46878
n-alkanes (n-pertane to n-decane), permittivity as function of temp, and pressure 0-68133

alkanes in solution, structure, X-ray diffraction obs. 0-61489 alkanes liquid, azulene, near, i.r. laser Rayleigh, scattering, anisotropic component 0-49897

component 0--49897 alkoys-striagine, in different solvent, u.v., i.r. and n.m.r. spectra 0-64476 alkyl chlorides, dependence of C-Cl stretching frequency on molecular structure 0-77862 alkyl cyanide-HCL (or DCL) mixtures, vapour phase i.r. spectra, H bonding 0-53076 alkyl groups in radicals and ion formed from isomeric phenylpropenes, heteroatomic model 0-46528 alkyl iodides-Cs atom reactions, harmonic forces linear model 0-7252 alkyl restrict leatones and although the dependence of the property of the process of the process

alkyl mesityl ketones and aliphatic and phenyl analogs, dipole moments 0-49901

N- alkyl-N-nitrosoanilines, electronic transitions 0-77860 alkyl-benzenes fluorescence quenching, role of charge transfer complexes 0-50243

0-30243.

Lalkylperoxy, e.s.r. spectra, hyperfine constants 0-49900 alkylphenols, NMR 0-74329 alkylphenols, local section assignment 0-74328.

alkyltriphenylarsonium compounds, neighbouring group effect from i.r. and u.v. spectra 0-64475

u.v. spectra 0–64475
allene, pressure induced i.r. spectrum due to the quadrupole 0–70966
allenic ketones, solvent effects on spin-spin coupling constants 0–43170
allenic phosphines, solvent dependence of ³/₄(P-H) and ⁴/₄(P-H) 0–67761
allo-ocimene, conjugated linear triene, n.m.r. 0–77863
alloxazine, polarized phosphoresc. spectra at 77°K 0–72448
amides, secondary, MO calc. of configuration and H-bonding 0–77864
amides of butyramide series, integrated obs. intensities of carbonyl band
0–67789

0—6/789 aminc+ water solutions, u.s. absorption properties 0—46910 amines, cyclic, saturated, n.q.r. of ¹⁴N, from liq, N₂ temp. 0—46535 amines, effect of solvent interactions and H bonding on ¹⁵N chem, shifts 0—78313

amines, long-chain and large-ring amines, ciannamoyl derivatives, u.v. absorption maxima 0-55618 amines, teritary rotational isomerism 0-58148 amino acid solns. u.s. vel. meas. 0-74751 amino acids, ¹⁵N-H coupling as source of proton resonance line broadening 0-74330

amino acids, X-irrad., correlation of e.s.r. and optical spectra 0-59458 amino acids, free radical production at 77°K by heavy ions, thermal spike theory 0-72534 amino acids in D₂O partial molal heat capacity at infinite dilution

0-46899 acids in H_2O , partial molal heat capacity at infinite dilution 0-46899

U-40079 2-amino-1,4-napthosemiquinones N-substituted in i-propanol, e.s.r. spec tra 0-74331

amino-2 pyrimidine, phosphoresc. and fluoresc., electronic transitions $0\!-\!67762$

4 amino-N, methylphthalimide in propanol, failure of universal relation between absorption and fluorescence spectra, causes 0–50235 amino-acid crystals, study of piezoelec, resonances rel. to cryst, classes 0–40881

aminoalcohols, i.r. spectra as function of CCI4 conc., H bond study

aminoanthracenes, excited states, electron density distrib. 0-49903

aminoazobenzene derivatives, aqueous solns., influence of indifferent substs. on e abs. spectra 0 -50236

aminoindenes, isostructural, optical props. and photosensitivity 0-41227 aminophenols, isomeric, i.r. absorption spectra, vibrational 250-4000 cm-1 range 0-64477

aminophosphines, P-N rotational barriers 0-49902

3-aminophthalimide in propanol, failure of universal relation between absorption and fluorescence spectra, causes 0-50235

aminophthalimides, in glycerine, isobutanol and propyl alcohol, luminesc., anisotropy, effect of temp. 0-71363

aminopyridines and their deuterated analogues, band analysis of i.r. spectra 0-77865 aminostannanes, Mossbauer params. and quadrupole splittings obs. 0-41173

1- amyl alcohol, dilatometric measurements, 1°C interval in range 20°C 70°C 0-68092 ammonium hydrogen chloracetate, n.q.r., phase transition obs. 0-62448

dilatometric measurements, 1°C interval in range

iso- amyl alcohol, dilatometric measurements, 1°C interval in range 20°C-70°C 0-68092 amyl bromide, dielectric relaxation, theory 0-74780 4-anhydro-d-arabino-tetrahydroxybutyl imidiazoline-2-thione, unit cell and space group, by X-ray diffraction 0-61924 aniline, far-i.r. absorpt, spectrum 0-55335 criline designations for the disubstituted. Honding and long-range proton

aniline derivatives, ortho disubstituted, H bonding and long-range proton coupling 0-55334

coupling 0-55334 aniline thin liquid film stabilized with $C_{12}H_{22}OH$, rupture, critical thickness theory 0-64852 aniline-cyclohexane binary solution, relationship between molecular motion and spatial order 0-74722 anilines in cyclohexane at infinite dilution, dipole moments 0-64479 anisole, low-frequency spectra 0-77874 anthracene:tetracene, fluoresc., host-sensitized energy transfer 0-76173 anthracene:tetracene, recombination radiation and fluorescence 0-56619 anthracene, Gruneisen tensor, 0-300 K 0-40589 anthracene, absorption, photocond. Davydov splitting, temp. depend. 0-79323

anthracene, cryst., reflection spectrum, evidence for existence of defects 0-44813

anthracene, cryst., scintillation, channeling effect by α particles, at T=300 and 80°K 0-59444

anthracene, crystalline, non radiative triplet-triplet annihilation rate 59433

0 59433 anthracene, d.c. cond. meas. with large fields 0–44211 anthracene, dielec. const. determ. from photocond. obs. 0–79084 anthracene, drift mobility. high press. effects 0–47723 anthracene, e diff. const. from pulse drop in drift expts. 0–47730 anthracene, elastic const., temp. depend. 0–40237 anthracene, elect. cond., compensation effect 0–47632 anthracene, electroluminesc. 0–56649 anthracene, electroluminescent cells, with tunnel injection cathodes 0–79385 0-79385 anthracene, electroluminescent diode 0-4495 I

anthracene, electron bombard, surface state 0-40669 anthracene, electron-irrad, carrier generation yield, temp. depend. 0-75775 anthracene, exciton surface reaction at electrolyte interface, photocurrent

obs. 0-75839 exciton-phonon interaction, Urbach's rule, low-temp. anthracene.

0-62266 anthracene, fluoresc. excitation obs. using vacuum u.v. synchrotron radia-

tion 0-59426

anthracene, fluorescence and non radiative decay in crystal and solution 0-72438 anthracene, fluorescence modulation by singlet exciton-trapped hole interaction 0-59432

anthracene, fluorescence of localized excitons excited by alpha particles 0-44915

anthracene, heterocyclic derivatives, containing nitrogen, quenching of fluorescence 0-70968

anthracene, in solid solns., luminesc. as function of wave-length of exciting radiation 0-69157

anthracene. 0 -44914 ne, interac. of charge transfer excitons and triplet mol. excitons

anthracene, interaction of triplet excitons at surface with redox couples and

anthracene, interaction of triplet excitons at surface with redox couples and dye molecules 0-40898 anthracene, isotope effect on electron drift mobilities 0-59136 anthracene, monocryst., α -channeling, E α =879 MeV, by transmission expt. at T=130K 0-59120 anthracene, mononegative ion in DME, proton ENDOR spectra 0-64531 anthracene, photocond., excitons 0-75827 anthracene, photocorrent and elec. polarization phenomena 0-44401 anthracene, polycrystalline thin film, conductivity meas. from dielectric loss 0-79036 anthracene, pure and doped cryst., d.c. and pulsed electrolyminaes. 350

anthracene, pure and doped cryst., d.c. and pulsed electroluminesc., 350-100°K 0-79384 anthracene, scintillation and fluorescence of single crystals 0-51367 anthracene, shock wave compression 0-65382 anthracene, single cryst., proton bombardment induced elec. cond. 0-59165

0-39103 anthracene, solubility in compressed methane, ethylene, ethane and CO₂, second cross virial coeffs. using pseudocritical parameters 0-43432 anthracene, spin-orbit coupling and radiative triplet lifetimes 0-67807 anthracene, tetracene-doped, fluoresc. lifetime and energy transfer 0 - 79367

anthracene, tetracene-doped, fusion rate of triplet excitons 0-62267 anthracene, triplet exciton trapping in dislocations formed by plastic bending 0-71930

anthracene, triplet quenching in fluid soln. by Wurster's blue cation 0-39816

anthracene, volume generation and Hall mobility of holes 0-53745 anthracene adsorbed on silica gel, γ -irrad., e.s.r., radical form. 0-39458 anthracene and derivatives, fluoresc., temp. depend., non-radiative transitions 0-77867

anthracene and derivatives, fluorescence lifetimes meas. 30 kbar, 77 K. pressure depend, obs. 0–74334 anthracene and deuterated derivative in n-alkane matrices at 4°K, vibrational analyses, electronic absorption and fluorescence spectra 0–77866

Organic compounds continued

anthracene and its derivatives, vapour, fluoresc. as function of oscillating energy of excited mols. 0-67764 anthracene cryst., delayed fluoresc. spectrum 0-66108

anthracene cryst., delayed nuoresc. spectrum 0–66108 anthracene cryst., scintillation anisotropy as function of energy of bombarded α -part., 1-3 MeV 0–44934 anthracene cryst., width of lowest singlet-singlet transition 0–41228 anthracene crystal, mutual annihilation of triplet excitons, mag. fields effects 0–40673 anthracene crystal. 200, 600 keV.

anthracene crystals, 200-600 keV proton bombarded, scintillation response, directional effects 0-69166

anthracene derivatives, polarization depend. of fluorescence and abs. spectra 0-67763

anthracene derivatives fluorescence quantum yield and duration temp. and wavelength depend. 0–39409 anthracene derivatives in liquids at 293K, fluorescence quenching by addition of naphthalene, singlet triplet energy transfer 0–61533 anthracene e.p.r. studies of optical spin polarization in triplet state 0–74333

0—14333 anthracene in methyl tetrahydrofuran, intersystem crossing, temperature dependence 0—64553 anthracene in naphthalene and phenanthrene, lattice effects on absorpt, and emission spectra 0—72372 anthracene in soln, variations in relative intensities of absorption spectral bands, 0, 24359.

anthracene in soft, variations in relative intensities of absorption spectra bands 0-43459 anthracene ion, use of FEMO theory to calc. transition energies 0-74392 anthracene mixed crysts, intermolec, triplet exciton transfer 0-62728 anthracene single cryst, under α bombardment, scintilliation light yield

anthracene single crystal, basal and non-basal slip 0-71704 anthracene single crystal, photo-enhanced currents, anisotropy in mag. field effects 0-47881 anthracene single crystal, triplet excitons, e.s.r., 35 GHz, 300 and 100 K

0-66144 anthracene triplet-triplet annihilation in fluid solns., mag. field effects

0 - 39815

anthracene-polyvinyltoluene system, fluoresc., anthracene copolymerization effects 0-72439

anthracene-tetracyanoethylene adduct and complex, cryst. struct. 0-47210anthracene/Ca contact, electron photoemission, recombination radiation 0-72156

0-72156
anthracene/perylene layers, fluorescence, exciton diffusion, thickness depend. 0-79366
anthracyl radical, electronic ground states 0-67765
9,10-anthraquinone, decomposed fluoresc. 0-74332
anthraquinone and 1,5-dihaloid derivatives, molecular packing 0-53519
anthraquinone on Ge, effect of illumination on oriented crystallization (photoepitaxy) 0-78378

toepitaxy) 0-78378 9,10-anthraquinone single crystal layers, vibrational bands assignment, of i.r. spectra 0-51295 anthrone, refinement and thermal expansion coefficients of structure (20, -90°C), comparison with anthraquinone 0-53520 anthrone and anthrone-anthraquinone crystals short-range order 0-53521 antimony cpds., Mossbauer effect, ¹²¹Sb quadrupole moment ratio 0-55132

aqueous alcoholic soln., with donors and acceptors, fluoresc. rel. to temp. $0\!-\!78283$

0-78283 aromatic, in vitreous soln., delayed fluoresc. mechanism 0-46926 aromatic, strained, bridged, struct. 0-77869 aromatic, structure and conformation determination using intramolecular nuclear Overhauser effect 0-67758 aromatic carbonyl cpds., T₁-S₀ transitions rel. to vibronic interaction between ππ* and ππ* states 0-70969 aromatic compounds, C Is energies meas. by ESCA, binding energy shift 0-74335

0-74335 aromatic compounds, relative intensities of intramolecular and lattice vibrations in Raman spectra 0-51327 aromatic cpds., nuclear conformation correl, with fluoresc, and absorpt, spectra 0-77868 aromatic cpds. in dichloroethane soln., pulse radiolysis 0-45089 aromatic cryst., Wannier consts. 0-51316 aromatic hydrocarbon cation radicals, monomeric and dimeric, e.s.r. 0-53093

0-53093
aromatic hydrocarbon cryst., electron energy loss spectra 0-71893
aromatic hydrocarbon crysts., charge-carrier transport, theory 0-53746
aromatic hydrocarbons, chemical shifts, computation by antisymmetric
molecular orbital methods 0-58227
aromatic hydrocarbons, intersystem crossing mechanism, effect of deuteration on rate 0-64467
aromatic hydrocarbons in frozen paraffin solutions, To-T* absorption
bands, determination using luminescence excitation spectra 0-46518
aromatic ketones energy transfer mechanism for transfer to rare earth ions.

aromatic ketones, energy transfer mechanism for transfer to rare earth ions in liquid solns. 0-50205

aromatic liqs., Raman bands 250-40cm⁻¹ compared to i.r. absorpt. 0 64928

o 64928 aromatic mol., rot. correl. times by proton spin-lattice relax. 0–61556 aromatic molecules as quenchers of ³P₁ radiation in Hg 0–60981 aromatic mols. in excited state, magnetic anisotropy 0–46536 aromatic nitro cpds., substituted, Kerr effect 0–46931 aromatic photoexcited molecules e.s.r. spectra, hyperfine structure of Δm_x=2 transitions 0–55336 aromatic sulphines, i.r. spectra and mol. structure 0–74320 aromatic vapours, vibra relaxation following inter- system crossing 0–58202

aromatics, excited singlet levels, energy transfer to fluorescent solutes $0\!-\!79360$

aromatics, nitrogen containing zero-field splitting parameters of phosphorescent triplet states 0-46537 aryliodonium and related compounds, u.v. and i.r. spectral study of symmetry 0-53061

aryltricyanoethylenes, dipole moments and electronic abs. spectra 0-61144

ascorbic acid, superadditivity of redox indicators and Weitz radicals 0-70114

0-0714
aza-anions, heteroaromite five-membered, p.m.r. spectra 0-67817
azaporphyrines, oscillatory model 0-67767
azeotropic mixtures, acoustical props. 0-64916
azines, neutral and protonated, H-H and C-H coupling constants azines, ne 0-67766

aziridines, substituted, $v_{0-1}(NH)$ and $v_{0-2}(NH)$ freqs. variation in various solvents 0-39410

azolidon-4, i.r. absorpt. spectra, mutual influence of functional groups 0-64481

azomethane, shock tube decomposition and secondary processes investigation, rate 0-72531

azomethane, structure determ. by electron diffraction 0–77870 azotic acid, dilute solns., Hall effect meas. 0–64943 p-azoxyanisol, nematic, self-diffusion anisotropy 0–74738 p-azoxyanisole, crystal structure 0–40109

p-azoxyanisole, nematic, X-ray diffr. effect on cylindrical distrib. of atoms 0-46873

p- azoxyanisole liquid crystal molecules, elec. field ordering, e.s.r. studies 0-43429

0-43429
p-azoxyanisole liquid crystal voltage induced vorticity and optical focusing 0-53355
p-azoxyanisole liquid crystals, phase transitions, small angle X-ray scattering 0-61496
p- azoxyanisole liquid crystals, self- diffusion coeffs., neutron scatteing method 0-50215
azulene, chemical shift obs. 0-61146

azulene, electron attachement in field of ground and excited electronic states 0-46538

states 0-40336 azulene, electronic states calc. by CNDO/2 CI 0-61145 azulene molecules, plasma effects of π electrons 0-43149 azulene scattering, near i.r. laser Rayleigh anisotropic component 0-49897barbituric acids, 5,5-disubstituted, spectra-polymorphic structure correlations 0-72373

benzaldehydes, substituted, vibrational spectra and torsional barriers

0-778741,2- benzanthracene, fluorescence spectra from second excited π -singlet

state 0-70976 benzanthron, vapour prolonged luminesc. 0-67771 benzanthron, in hydrocarbon solutions, electronic structure and spectra 0-49905

3- benzanthrone, in hydrocarbon solutions, electronic structure and spectra 0-49905

tra 0–49905
1,2-benzcoronene, extinction coeffs. and direction of polarization of T-T absorption spectra 0–74340
benzene, Jahn-Teller effect on vibrational structure of photoelectron spectrum 0–53062
benzene, Rayleigh and depolarization ratios 0–64918
benzene, adsorption by microporous silica gel 0–50398
benzene, and -ds. fluorescence spectra from zero-point level of ¹B_{2n} state 0–46542

benzene, and -d₆, gas phase absorption spectra and decay 0-70975 benzene, and -d₆ vapour excited to single vibronic levels, fluorescence lifetime 0-74342

benzene, azulene, near i.r. laser Rayleigh scattering, dispersion in anisotropy 0–49897 benzene, crystalline, lattice vibrations 0–47513

benzene, crystalline, lattice vibrations 0-47513 benzene, deaerated solutions, varying conc., emission spectra excited by electron pulses, effects of chloroform and oxygen 0-55619 benzene, deuteration eff. on triplet state lifetimes 0-74198 benzene, dielec. dispersion, microwave, Lorentz reson. model 0-43467 benzene, enriched deuterated solution polarization in neutron-deuteron elastic scattering 0-49629 benzene, exact soln. of one-band π -electron theory 0-39413 benzene, fluorescence yields from three vibronic levels in ${}^{1}B_{2w}$ state 0-70974

benzene, frozen in diff. solvents, X-ray and photo-excited, radioluminesc. 0-72468

benzene, high pressure crystal growth 0–50428 benzene, in solvent, distortions of lowest triplet state 0–72446 benzene, induced non-radiative transitions 0–64484 benzene, inexcited singlet state, fluoresc. and nonradiative transitions from single vibr. levels 0–77877

benzene, intersystem crossing mechanism, effect of deuteration on rate 0-64467

benzene, intersystem crossing mechanism, effect of deuteration on rate 0–64467
benzene, isotopic crysts, ground state vibr. struct, and phonons 0–43867
benzene, lattice vibration, further results 0–47514
benzene, liq., I.f. Raman lines in depolarized Rayleigh wing 0–61524
benzene, liq., stimulated Raman scatt., thermospectrum 0–39807
benzene, liq., stap-controlled space charge currents 0–53373
Benzene, liq., acoustic relaxation 0–64907
benzene, liquid, scoustic relaxation 0–64907
benzene, liquid, biphotonic photolysis 0–59506
benzene, liquid, two-photon absorption spectra 0–55267
benzene, lowest singlet-triplet separation, ab initio AMD calc. 0–39414
benzene, mercapto-derivatives, anions spectral calcs. by SCF MO CI method 0–77923
benzene, promittivity, absolute meas. 0–78295
benzene, permittivity, absolute meas. 0–78295
benzene, photolomization resonance obs. 0–61373
benzene, photolomization of second n-iomization potential 0–49926
benzene, proston shielding anisotropy 0–49907
benzene, radiative and nonradiative decay from 3 vibronic levels in $^{1}B_{2n}$ state, absolute rates 0–70970
benzene, rotational correlation time in liquid, press. and temp. depend. 0–61482
benzene, self-focussing and SRS, periodic temp, depend. 0–52335
benzene, self-focussing and SRS, periodic temp, depend. 0–52335

0–61482 benzene, self-focussing and SRS, periodic temp. depend. 0–52335 benzene, self-focussing and SRS, periodic temp. depend. 0–52335 benzene, shock-wave compression 0–58459 benzene, singlet-triplet absorption in pure cryst. 0–41229 benzene, solid, inelastic neutron scatt., 77-270°K 0–75356 benzene, solid, space charge limited currents 0–53831 benzene, spectral study by flash photolysis 0–77935 benzene, spectral study by flash photolysis 0–77935 benzene, spherical cage model for relationship between compressibility and solubility 0–46880 benzene, stimulated Raman lines, lateral optical bands effect 0–50227 benzene, structure of ¹B_{2x} state, influence of substituents 0–64487 benzene, substituted, chemical shift, charge distrib., SCF calc. 0–39415 benzene, surface tension dependence on curvature, correlation between solubility of solute gas 0–71324 benzene, transition energy shifts and polarizabilities of excited states 0–58140 benzene, triplet energy transfer to π-bonded mols. 0–77871

benzene, triplet energy transfer to π -bonded mols. 0-77871

Organic compounds continued

benzene, vibr. relax. and competition with radiationless transitions in ¹B_{2u} state 0-55337

benzene, vibr. relax. in S₁ state 0-77878

benzene, vibrational exciton band profiles •0-70978

benzene, vibrational exciton density for Brillouin zone 0—78847 benzene, vibrational exciton density for Brillouin zone 0—78847 benzene, vibronic overlap calc. from Franck- Condon factors 0—61148 benzene adsorbed on graphite, hindered rotation 0—39970 benzene and benzene-64, cryst, i.r. spectra in polarized light 0—62678 benzene and derivatives, luminescence excitation by vacuum u.v. radiation 0—62706 0-62706

0-62706
benzene and derivatives, spectral study by flash excitation, non-radiative enhancement 0-77879
benzene and ice, reflection technique electron energy loss meas. 0-71890
benzene and monosubstituted derivatives, amplification coeffs. and nonlinear susceptibilities in stimulated Raman spectra 0-50237
benzene complexes, n.m.r. temp. effects 0-48168
benzene crystal, vibronic spectra, dissociation states 0-62677
benzene derivatives, iiq., e-irrad., excimer luminesc. obs. 0-46929
benzene derivatives, m-disubstituted, vibrational spectra 0-70973
benzene derivatives, p-disubstituted, vibrational spectra and fundamental frequencies 0-70971
benzene derivatives, p-disubstituted, vibrational spectra and fundamental frequencies 0-70971

benzene diffusion and permeability coefficients through low-density polye thylene 0–55928 benzene fluorescence quenching, role of charge transfer complexes 0–50248

benzene fluorescence under proton and electron impact 0-74764 benzene in glasses, temperature effect on phosphorescence lifetime 0-56628

benzene in inert solids, u.v. absorption spectrum 0–74343 benzene photoionization, angular distribution of free electrons released 0–52928

0–52928 benzene vapour, excited to single vibronic levels at low press., fluorescence lifetime 0–43150 benzene vapour, fluorescence lifetime 0–39412 benzene vapour, fluorescence lifetime 0–39412 benzene-halogen charge transfer complexes, Raman scatt. 77K 0–74337 benzene-halogen weak complexes, intermolec, interactions 0–58268 benzenes, homo-substituted, semi-empirical PPP-SCF-MO-CI calcs. by π electron approx. 0–46540 benzenes, hydrocarbon monosubstituted and 1, 4- dialkyl series, characteristic features of Raman radiation 0–67773 benzenes, o-disubstituted, vibrational spectra 0–77849 benzenes, nartially deuterated, hospohoresc, lifetimes in rigid media at

benzenes, partially deuterated, phosphoresc. lifetimes in rigid media at 77° K 0-61149

benzenes, substituted, SCF-MO theory of proton-proton coupling 0-74338 benzenes, substituted, electronic structure and props. in excited state 0-64482

0-64482
benzenes, substituted, excited state props., SCF-MO calc. 0-77875
benzenes, substituted, rotational constants of 1st singlet excited state, interpretation in terms of molecular geometry 0-55340
benzenes mono-substituted, PR separations and relative Q-branch intensities in ir. band contours 0-74341
benzenethiol-d, proton and deuteron mag. reson., liq. cryst. solns. 0-53082
benzenoid hydrocarbons, non-planar overcrowed, proton chemical shifts, comparison between theoretical and experimental determinations 0-67769
benzil, Raman spectrum 0-59415
benzil, Raman spectrum 0-59416
benzil, cryst, theory of optical activity 0-62611
benzil, geometrical configurations in various solid-state environments 0-64483
benzil solutions, absorpt. spectra of triplet excited mols. 0-70982

benzoghifluoranthene, chemical shift obs. 0–61146 1,12-benzoperylene, fluoresc. spectrum in methylcylopentane, 77K 0–49904

benzophenone, luminescence in polymers, temp. effects 0-79368 benzophenone, reinvestigation of Raman spectrum using a He-Ne laser 0-49908

benzophenone, temp. quenching of phosphoresc. by alkane materials 0-51363

benzophenone cryst., pure and impure, phosphorescence, effect of lattice struct. 0–69161 benzophenone in solid state, i.r. spectra, freq. assignments 0–46539 benzophenone vapour, prolonged luminesc. 0–67771

benzophenone vapour, prolonged luminesc. 0–67771
benzophenone with mixtures of naphthalenes, luminescence, migration energy 0–71364
benzoporphyrins, spectra and luminescence, effect of azo-substitution 0–43151

benzopurpurine suspensions, optical dispersion of elec. birefringence and dichroism $\,\,0-748\,11$

3.4-benzopyrene, fluorescence spectra from second excited π -singlet state 0–70976 3.4-benzopyrene, quasi-line spectra in n-paraffin matrix, temp. depend. 0–79369

0-79309

para-benzoquinone, CNDO-CI calculations, and charge distributions, electronic structure 0-61147

p-benzoquinone, absorpt. spectrum, 0K 0-56556

benzoquinone, chemisorption on Ge, surface elec. props. 0-40802

p- benzoquinone, chore-derivatives, visible absorption spectra C=O stretching frequency 0-64486 p-benzoquinone, force field calculation pot. energy of fundamental vibrations 0-64466

tions 0-04460
p-benzoquinone, in mixed cryst., T-S emission, n, \(\pi^*\) states 0-64485
p-benzoquinone, triplet-singlet-n\(\pi^*\) luminesc, polarization 0-79358
p-benzoquinone in frozen soln., T-S emission spectrum, 77 K 0-53055
p-benzoquinone solutions, absorpt. spectra of triplet excited mols.
0-70982

benzoselenophene, applic. of Huckel's method for electronic structure determination, u.v. spectra 0-55339

benzothiacyclene derivatives, n.m.r. spectra, stereochemistry 0-46543 benzothiacyclene-S- monoxides and carbonyl derivatives electron absorption spectra 0-46544

benzothiazole, vapour absorption spectrum at 2850 Å 0-74336

benzotniazole, vapour absorption spectrum at 2850 Å U-./4336 benzotrichloride, pure and solution, Rayleigh scatt., i.r. spectra, molecular rotational mobility 0-46924 benzotrifluoride, nuclear spin-internal rotation coupling 0-77876 benzotrifluoride, pure and solution, Rayleigh scatt., i.r. spectra, molecular rotational mobility 0-46924 benzoxazole, vapour absorption spectrum at 2850 Å 0-74336 benzoyl chloride, in liq. and gas phase, i.r. abs. spectra, freq. assignment 0-46541

0 46541
1.12-benzperylene, extinction coeffs, and direction of polarization of T-T absorption spectra 0-74340 benzyl, and naphthalene and azulenic homologues electronic structure study 0-67772 benzyl benzoate, Raman and i.r. spectra, vibration assignments 0-58210 benzyl fluorides, substituted, structural and solvent effects in ¹⁹F n.m.r. 0-67770

0-67770
N-benzyl oxo-2 piperazines, magnetic inequivalence of protons and introduction of asymmetry in positions 3 or 6 0-70977
benzyl radical electronic struct., non-empirical calc., unrestricted SCF method 0-55383
N-benzyl-2-methylpiperidines, para- and meta-substituted, substituent effects on geminal proton-proton coupling constants 0-67768
2-benzylaminopyridine, fluorescence 0-77889
benzylidene-cetazine crystal structure of parameters meas. 0-78512
benzylideneoxindoles, geometrical isomerism 0-74339
biacctyl, luminescence quenching by alcohols, amines, stannane, solvent effects, mechanism 0-39814
biacctyl, quenching of phosphorescence by fluorinated aromatics 0-61150
biacetyl, triplet energy transfer to π-bonded mols. 0-77871

biacetyl, triplet energy transfer to π-bonded mols. 0–77871 biacetyl solutions, absorpt. spectra of triplet excited mols. 0–70982 bicycle compounds, fluoro substituted, vicinal H-F coupling, combined substituent and angular effects 0–49909 bicyclo [1.1.1]pentane, mol. struct., by electron diffr., vapour phase 0–53064

0-53064
bicycloheptadiene (norbornadiene) isomerization to quadricycloheptane, radiation induced 0-79459
bicyclol 2,2,2 loctane derivatives, n.m.r. obs. 0-39416
bicyclol 2,2,2 loctane derivatives, n.m.r. obs. 0-39416
bicyclol 2,1.0 lpent-2-ene, microwave spectrum, molec. struct., moments, and mag. props. 0-77873
bicyclol 2,2,1 octane system, conformation 0-64488
bicyclol 2,2,2 loctanes, substituted, bromination products, structure and n.m.r. 0-64489
bifluorenyls, p.m.r. spectra, steric effects 0-67795
bilirubin in pyridine, spectral properties of solutions and kinetics of formation 0-61525
binary syst, critical temps. 0-64990
biphenyl, luminesc. and molec. geometry in excited electronic states 0-59434
biphenyl, naphthalene doped, vibronic bands and hindered rot, of guest

biphenyl, naphthalene doped, vibronic bands and hindered rot. of guest mol. 0-72379

moi. 0–723/9 biphenyl, perdeuterated and perprotonated, phosphorescence yields in solvents containing heavy atoms 0–58226 biphenyl adsorbed on silica gel, p-irrad., e.s.r., radical form. 0–39458 biphenyl and analogues, identification of lowest excited singlet state 0–46545

biphenyl and biphenylene, electronic spectra 0–39442 biphenyl based heterocyclics, crystals, absorpt, spectra 0–59408 biphenyl crystal, i.r. and Raman spectra, 3100-25 cm⁻¹ 0–72395 biphenyls, symmetrically deuterated, in-plane fundamental frequencies 0–77880 bis(trifluoromethyl) nitroxide, e.p.r. spectrum, temp. dependence, theoretical

bis(trifluoromethyl) nitroxide, e.p.r. spectrum, temp. dependence, theoretical analysis 0-70979 bis(trimethylphosphine) tetrachlorosilicon(IV), crystal structure, X-ray examination 0-71598 p-bis-trifluoromethylbenzol, pure and solution, Rayleigh scatt., i.r. spectra, molecular rotational mobility 0-46924 biscarbazolyl propane intramol. excimers, kinetics 0-64326 5.5' bis isoxazole, molecular struct., non-bonded interaction and PPP calcs. 0-49911

cales. 0-49911

5.5°-bis-isoxazole, molecular structure, vibrational assignment and dipole meas. 0-49910

bonds ionic and covalent studied using K emission spectrum 0-61141

bromine-freen/propane mixtures, thermodynamic props. 18° to 45°C

0-46822

0-58211 bromoacetylene, electronic spectrum 2500 to 900Å 0-74322 bromobenzaldehydes; o, m and p. Raman spectra 0-70980 bromobenzene, rotational band contour analysis in 2700 Å system

0-53065 1-bromo-2-chloro-2-deuteriothioethane, p.m.r., as example of aa'b subspectrum 0-39359 1-bromo-2,2-dichloroethylene band intensities and atomic polarizations

39405

0–39405
2-bromoethanol, microwave spectra, intramolecular hydrogen bonding study 0–43155
bromoethynyl benzene and chloroethynyl benzene, vibr. spectra 0–55342
2-bromothiazole, nuclear double reson., quadrupole relax. 0–41393
bromovinylcyclopropanes, n.m.r. spectra 0–43152
bullvalene, oriented in liquid cryst. solvent, n.m.r. 0–77882
buttadiene, spatial wavefunctions 0–61151
butadiene 1,3, evidence for Cariolis coupling from vibration-rotation bands 0–74346
butadiene-2,3 nitrile, microwave spectrum, rot. and vibr. obs. 0–49912
1,3-butadienes, n.m.r. 0–77883
buttand, praton spin polarization 65 to 70% using continuous flow ³He

butanels 2.3 minute, inicrowave spectrum, 10t. and viol. 508. 0–49912 1,3-butanol, proton spin polarization 65 to 70% using continuous flow ³He cryostat 0–52551 1-butanol in benzene and p-dioxane solns., relax. time distrib. 0–39828

butanone, adsorbed on glass, radical anion, y radiation, e.s.r. 0–39933 1,2,3-butatriene, gas, u.v. absorpt, spectrum 0–61152 cis-2-butene microwave spectrum, internal rotation, conformation dipole moment 0–46546

butyl alcohol, solution in water, I₂ diffusion coefficients 0–71329 butyl alcohol, tertiary, H₂O mol. motion in dilute aqueous soln., neutron scattering study of hydrophobic hydration 0–71314

Organic compounds continued

butyl bromide, density and compressibility from P-V-T relations 0-75250 t-butylcyclohexanes, cryst. struct. 0-78513 butyliodide, tert., rot. spectrum with h.f.s. anal. 0-64490

2.6-di-tbutylphenol in p-xylene, dielectric absorption and dispersion 0-74770

calcium fumarate, trihydrate, cryst. struct. determ. by X-ray exam. 0-58773

calcium tartrate: transition elements, e.p.r 0-41343

camphene, plastic flow and self-diffusion, n.m.r. 0-62045

camphene single crystals of varying purity creep by dislocation climb process, activation energies 0–68327

camphorquinone solutions, absorpt, spectra of triplet excited mols. $0\!-\!70982$

cannabinoids, structure anal., theoretical and p.m.r. 0-77886

carnbathonous, sin deture affair, theoretical and p.int. 0-77886 carbohydrates, configurational and conformational influences on ¹³C chem. shifts 0-77885 carbon disulphide, Rayleigh and depolarization ratios 0-64918 carbon disulphide, dielec. dispersion, microwave, Lorentz reson. model

0 - 43467

carbon disulphide, pure rotational Raman scatt, from excited vibrational levels, obs. 0–61083 carbon tetrachloride, Rayleigh and depolarization ratios 0–64918

carbon tetrachloride, acoustic pulse propagation, large amplitude, transient effect 0-53343

carbon tetrachloride, adsorption by microporous silica gel 0–50398 carbon tetrachloride, band contour of Raman fundamental 0–64344 carbon tetrachloride, dielec. dispersion microwave, Lorentz reson. model 0-43467

carbon tetrachloride, high pressure crystal growth 0–50428 carbon tetrachloride, i.r. spectrum rel. to difference transitions, model 0–43153

carbon tetrachloride, influence on beam current in synchrocyclotron 0-42676

carbon tetrachloride, photolysis in presence of ethyl chloride 0-41447 carbon tetrachloride, pool boiling, pressure effects on bubble growth 0-39891

0–39891
carbon tetrachloride, shock temp. calc. in 100 kbar region 0–64858
carbon tetrachloride, shock-wave compression 0–58459
carbon tetrachloride liquid, discontinuities of ionic mobilities 0–64945
carbon tetrachloride spherical cage model for relationship between com
pressibility and solubility 0–46880
carbon tetrafluoride, gaseous, F relaxation by n.m.r. 0–58198
carbonium ion, exchange interaction with parent molecule, p.m.r. investigations 0–67775

tions 0–67775 carbonyl compounds, C 1s energies meas. by ESCA, binding energy shift 0–74335 carbonyl cyanide, i.r. and Raman spectra of all phases 0–46548 carbonyl fluoride, electronic spectrum 0–39417 carboxylic acids, cryst., radiolysis, CO bond scission 0–72560 carboxylic acids, hydrogen bonding study by neutron energy loss spectra 0–46547

carboxylic acids, solvent depend, of C-H proton resonance 0–78311 β -carotene, resonance Raman effect 0–70983 carotenes, n.m.r., natural-abundance 13 C spectra 0–53086

carotenoid pigments in soln., laser Raman spectra in resonance region 0-78280

B-carotin film, current fluctuations 0–71948 cellobiose, absolute configuration determ. from anomalous scatt. of CuKα X-rays 0–64495 cellophane + H₂O, thermo-osmisis, 10°C to 90°C 0–64894 cellulose, carbonized fibre, X-ray scatt., struct., pyrolysis depend. 0–47026

cellulose, conference, syracuse, Oct.1968 0–46611 cellulose, fibril formation, electron microscopy 0–47013 cellulose, photochromism obs. in different forms 0–72313

acetate and oligosaccharide homologues, n.m.r., ring protons -46550

cellulose acetate and oligosaccharide homologues, n.m.r., ring protons 0-46550 cellulose acetate in reverse osmosis, thin-region resistance model for water transport 0-39767 cellulose fibres, hydrated, electron-microscopy technique for structure investigation 0 68204 cellulose film, light scatt., anisotropy pattern 0-47992 cellulose film, regenerated, gel struct., computer simulation 0-46965 cellulose from cell wall of Velonia ventricosa, and i.r. spectra 0-79325 cellulose nitrate, r particle track visualization, enhancement using electric fields 0-60718 cellulose nitrate, i.r. spectra rel. to heating and evacuation 0-51317 cellulose nitrate, tin sheet, alpha-particle trade enhancement by application of electric field 0-38762 cellulose ritrate solutions, i.r. spectroscopic studies 0-71359 cellulose ritrate solutions i.r. spectroscopic studies 0-71359 cellulose ritrate, tin spectroscopic studies 0-71359 cellulose ritrate, tin spectroscopic studies 0-71359 cellulose ritrate, tin spectroscopic selectra 0-64496 chalcones, substituted, electronic spectra 0-64966 charge transfer complexes, nitrogen and chlorine n.g. 4. spectra 0-46526 chlorasin crest n.g. ris low 7-86764 chalcones, substituted selectronic spectra 0-6496 charge transfer compl

0-387/0 chlorait, cryst., n.q.r. in low Zeeman field, obs. 0-41406 chloranil, semiconductor, field effect obs. 0-47731 p-chloranil single crystal, charge carrier mobility, photocond. meas. 0-51152

1-chloro-2,4-dinitrobenzene, temp. depend. of Cl pure quadrupole reson. 0-46597

4-chloro and 4-bromo-phenylmethylsulphide, vibrational spectra 0-70972

chloro- and fluoro-substituted ethanes, barriers to internal rotation 0-74348

0—74348 chloroalkanes, secondary, liquid spectra and intermolec, vibr. 0—39808 chloroacetic acid, solid and liq. vibr. spectra and structure 0—67776 DL-N-chloroacetylalanine, cryst, struct. 0—47212 chloroacetylene electronic spectrum 3000-1000 Å 0—39418 2-chloroacrylonitrile, vibrational spectra 0—74349

chlorobenzene, density and dielectric constant determination at 30 and 50°C, pressures up to 5000 atm 0-71367

chlorobenzene, dielec. secondary dispersion, Lorentz reson. model 0.43467

chlorobenzene, i.r. and Raman bands, solvent and temp. effect 0-43080 chlorobenzene, i.r. and Raman bands, solvent and temp. effect 0—43080 chlorobenzene, planar ground state vibrs., from 2699 Å electronic band system analysis 0—55344 chlorobenzene, pressure effect on dipolar spin relax. in liquid 0—43478 chlorobenzene, rotational Brownian motion from the width of vibrational band contours in molecular spectra 0—61143 chlorobenzene 2699 Å electronic band system, in-plane vibration modes in excited states 0—49906 chlorobiphenyls, Kerr effect study of conduction and space charge phenomena 0—68142 2-chlorodiphenyl, impregnated paper capacitors, ionic impurity effects 0—44384 chlorodiphenyl, impregnated paper capacitors, ionic impurity effects 0—44384 chlorodiphanes, proton spin relaxation, as function of cone in CSs.

chloroethanes, proton spin relaxation, as function of conc. in CS2

0 - 77888

0-77888
2 chloroethanol, microwave spectra, intramolecular hydrogen bonding study 0-43155
1-chloro-2-fluoroethylenes, cis and trans and deuterated modifications, vibrational assignments of i.r. and Raman spectra 0-64497
chloroform, dipole moment from pressure broadened microwave spectra 0-61179

chloroform, i.r. and Raman bands, solvent and temp. effect 0–43080 chloroform, liq., 25°C, radiolysis, positive ion scavenging 0–76281 chloroform, liquid, Raman spectra, effect of intermolecular interactions

chloroform, surface tension dependence on curvature, correlation between solubility of solute gas 0-71324 chloroform, vapour viscosity calc. by free energy average potential model 0-78229

chloroform and deuterochloroform, vibr. spectra and force consts. 0 55345

chloroform in H₂, He, N₂ and Ar gases, microwave absorption at high pressure 0-53278 chloroform-perfluorbenzene solns. nuclear relax., double reson. obs. 0 46953

chloroform pyridine syst., dielectric abs. meas., relaxation processes

0—71369

chloroform tetrahydrofurane or pyridine, heat of mixing 0—66172
chloroform-trichlorofluoromethane solns., nuclear relax., double reson.
obs. 0—46953

4-chloro-3-methyl phenol, single cryst., n.q.r. Zeeman spectrum of ³⁵Cl'
0—66159

I chloronaphthalene, liquid two-photon absorption spectra 0-55267 α -chloronaphthalene, scatt. light, depolarized component structure

0-64924
α-chloronaphthalene, spectral structure of the anisotropic portion of light scattered 0-61528 α chloronaphthalene, vibrational assignment of frequencies in i.r. 0-74351 ρ-chlorontrobenzene, mag. anisotropies and susceptibilities 0-75892 4 chlorophenol in p-xylene, dielectric absorption and dispersion 0-74770 1 p-chlorophenyl-4, 5-(D-flucofurano) imidazolidine-2-thione, unit cell and space groups, determination by X ray diffraction 0-61923 chlorophyll, mol. energy, fluoresc. 0-67779 3-chloropropene molecule, rotational constants of ground state isomers 0-77889

chloropropenes, rotational isomerism 0-67778

chloroquinoline, anomalous phosphoresc. polarization in durene host 0-41277

0—41277
8-chloroquinoline vapour, electronic absorption spectra . 0—58216
2-chloroquinoline vapour, electronic absorption spectra . 0—58216
chlorostyrenes, isomers, in liquid phase, assignment of vibrational frequencies 0—58212
chloroxylenes, i.r. spectra in liquid state 0—77887
cholesteric liquid crystal films, light reflectivity meas. 0—74755
cholesteric liquid crystals, influence of electric and magnetic fields on dielectric constant 0—58492
cholesterol, effective rotary power 0—61522
cholesterol, 2-72 chopys chopys lepty carbonate, stimulated Brillouin scatt.

cholesteryl 2/2 ethoxy ethoxy) ethyl carbonate, stimulated Brillouin scatt. 0–78277

0—1821/1 cholesteryl 2-(2-ethoxyethoxy) ethyl carbonate and related cpds., liquid crystal props. 0—71309 choline chloride, positron lifetimes temp. and phase dependence 0—44027 chromatography, gas, meas. at concentrations below O.I. parts per billion 0—48208

0-48208
chromium acetate, weak paramagnet, crystal structure 0-61925
cinnamic acid, photopolymerisation, in condensed phase 0-72554
circular dichroism applica. ons 0-49116
clathrates, Hofmann-type, p.mr. in temp. range 80-296°K, motion of quest
molecules 0-74352
cumbustion at low temperature, reviews 0-41422
complexes, charge transfer, absorption spectra in lowest excited single
state 0-74314

conjugated molecules, N and O containing, LCAO SCF MO treatment 0 - 46565

0-46565
copper acetate monohydrate, e.s.r. of γ-irrad, crysts. 0-59459
copper calcium acetate hexahydrate, e.s.r. of Cu²⁺ 0-41352
copper chloride dimethylsulphoxide, ligand field in tetrahedrally co-ord. Cu
(II) ion 0-44731
copper diethyldithiophosphate, e.s.r. 0-41328
copper formate, mag. struct., p.m.r. obs. 0-62558
copper formate tetrahydrate, antiferromagnetic resonance, ordered mag. state 0-44978
copper formate tetrahydrate, ordered mag. state, antiferromag. reson. obs. 0-44980
copper phthalocyanine film. Stark effect, electroabsorption, ferroelectricity

copper phthalocyanine film, Stark effect, electroabsorption, ferroelectricity $0\!-\!62679$

copper propionate, crystal struct., X-ray diffr. 0–50561 copper salts, e.p.r. 0–51400 coronene, lattice energy and equil. struct. calc. by atom-atom pot. method 0–58774

corrins, theoretical analysis of optical spectra 0-67780 coumarin dyes, exciplex laser action evidence from stimulated fluoresc. meas. 0-74763 for counting liquid scintillation of tritium in aqueous samples 0-73684 transcrotononitrile, microwave spectrum, rotational constants 0-39419

Organic compounds continued

cryptocyanine, crystallized solns., light scattering, resonance effect 0-51288

crystal, conference, New Delhi, India, January 1969 0-75650 crystal, conference, New Delhi, India, January 1969 0-75652

crystal, conference, New Delhi, India, January 1969 0–75652 crystal growth by Bridgman method, furnace 0–50414 crystal structure by HEED, anomalous intensity meas. 0–58769 crystals, transport of carriers and energy, quantum-mechanical treatment 0 78823 cupric acetate hydrate-d₁₆, n.m.r. in single crystals 0–66153 cyanethyl cellulose ethers, highly substituted, structural studies using X-ray and i.r. techniques 0–71431 cyanic acid, photodissociation in vacuum u.v., NCO A²Σ and NH(A³πc¹) production 0–74419 cyanides, ionization notentials from photoelectron energy 0. 52005

cyanides, ionization potentials from photoelectron spectra 0-53005 cyanine dyes, high dispersion induced Raman scattering and luminescence spectra of solutions crystallized at liquid nitrogen temperatures 0-62707 spectra of solutions crystallized at liquid nitrogen temperatures 0-62707 cyanine dyes relationship between far i.r. absorption and electrical conductivity 0-64463
2-cyanoethanol, microwave spectrum, ground state assignment of transisomer 0-70986
cyanogen, vibr.-rot. bands obs. 0-61156
cyanogen, vibr.-rot. bands obs. 0-61156
cyanuric acid, electron population parameters by X-ray diffraction 0-46440

cyalinte actu, electron population parameters by X-ray diffraction 0-46440 cyanuric chloride, single cryst. vibr. study with fundamental assignments 0-71829 cyclic, electronic struct. 0-46522 cyclic hydrocarbons, molecular dynamics, cold neutron spectra 0-47511 cyclic hydrocarbons photoelectron spectra, ionization potentials 0-39421 cyclic polyenes, Hartree-Fock solutions instabilities rel. to spin and charge density fluctuations 0-74402 trans- cyclo-octene, circular dichroism 0-58214 trans- cyclo-octene, circular dichroism 0-58214 trans- cyclo-octene, circular dichroism 0-58214 trans- cyclo-octene, circular dichroism 0-58216 cycloalkanones ¹³C chemical shift by n.m.r. spectroscopy 0-46554 cyclobutadiene and derivatives, LCAO electronic structural study 0-67784 cyclobutane, i.r. and Raman spectra, assignment of fundamental freqs. 0-74355 cyclobutane, molec. struct. determ. from proton n.m.r. in nematic solvent

cyclobutane, molec. struct. determ. from proton n.m.r. in nematic solvent 0-39420

cyclobutane, puckering structure, i.r. spectra 0-49914 cyclobutanene, $1A_2$ state, u.v. spectrum, ring puckering and oxygen wagging 0-61157 cyclobutanone, $\pi^* \leftarrow n$ spectra, allowed and forbidden character 0-74354

cyclodecane, doped. single cryst., phosphoresc., influence of lattice mis-match 0-79374

match 0–79374 cycloheptanone, π⁸←n spectra, allowed and forbidden character 0–74354 cycloheptanone, π⁸←n spectra and molec. conformation 0–70984 1,4-cyclohexadiene-1-glycine, cryst. struct. 0–40111 cyclohexane, adsorption by microporous silicia gel 0–50398 cyclohexane, iliq., stimulated Raman scatt., thermospectrum 0–39807 cyclohexane, photon irradiated, dissociation, and reactions of C₆H₁₀+0–79457 Cyclohexane, plastic crystal phase, rate of rotation of individual molecules 0-70850

cyclohexane, polycrystalline, thermal cond., 77-293 K, impurity effects 0-65559

0-05359

cyclohexane, pure-rotational Raman spectra under high dispersion
0-70985

cyclohexane, surface tension dependence on curvature, correlation between
solubility of solute gas 0-71324

cyclohexane, time characteristics of stimulated Raman scattering

0-46552

cyclohexane and related oxanes, vibr. spectra and potential functions 0-58215cyclohexane derivatives, cryst. struct. and absolute configs. 0-78514

cyclohexane derivatives, cryst, struct, and absolute configs. 0–8514 cyclohexane high temp, rotator phase, study of plastic flow 0–68328 cyclohexane series, 220 MHz n.m.r. spectroscopy 0–67781 5-(1-cyclohexane-1-yi)-5 ethyl, crystal structure determ. 0–78515 cyclohexanes, substituted rotational isomerism 0–58148 cyclohexanol, liquid, mol. motions, quasi-elastic incoherent cold neutron scatt, obs. 0–78262

eyclohexanol, liquid, mol. motions, quasi-elastic incoherent cold neutron scatt. obs. 0–78262 cyclohexanol, solid, phase transformation growth rates 0–50827 cyclohexanols and derivatives, ¹³C n.m.r., conformational effects on ¹³C carbinyl carbon shieldings 0–39432 cyclohexanols and derivatives, ¹³C n.m.r., conformational effects on ¹³C carbinyl carbon shieldings 0–39432 cyclohexanole, π*e-n spectra, allowed and forbidden character 0–74354 cyclohexyl iodide, conformational isomerism, i.r. spectra 0–55347 cyclopentadiene, i.r. bands, absolute intensity 0–49915 cyclopentadiene, i.r. bands, absolute intensity 0–49915 cyclopentadiene, iradical and deuterated derivatives, electronic absorption spectrum 0–46553 cyclopentane, crystalline matrix, fluorescence spectra of trapped radicals from xylenes 0–66102 cyclopentane, first ionization energies, vibrational structure in first electronic band 0–55346 cyclopentane, first ionization energies 0–55346 cyclopentane, spectroscopic effects of phase transitions, 80-300K 0–62680 cyclopentane, structure, equilibrium conformation, pseudorotation, electron diffraction determ. 0–77890 cyclopentane solute in n-tridecane, evaporation mass transfer rates into flowing N₂ 0–50325 cyclopentane-carbon tetrachloride solution, excess thermodynamic functions, hard sphere system, first-order perturbation 0–39775 cyclopentane-carbon tetrachloride solution, excess thermodynamic functions, hard sphere system, first-order perturbation 0–39775 cyclopentane, engaged and forbidden character 0–74354 cyclopentanone, π*e-n spectra, allowed and forbidden character 0–74354 cyclopentanone, engetra splene significance, spectra 0–74356 cyclopentanone, ring-puckering pot. functions from i.r. absorpt. spectra 0–74356 cyclopentane oxide, ring-puckering pot. functions from i.r. absorpt. spectra 0–74356

o-viclopentene oxide, ring-puckering pot. functions from i.r. absorpt. spectra 0-74356 cyclopentylamine, i.r. and Raman spectra, vibr. anal. 0-67785 cyclopropane non-dipolar gas, Kerr effect, second hyperpolarizabilities 0-68002

cyclopropane-inert gas collisions, steric effects in translational-vibration energy transfer 0-71062 cyclopropanes, monosubstituted, ¹³C n.m.r. 0-74353

a-cyclopropanic alchohol, effect of pyridine solvent on NMR spectra 0 58502

cyclopropene, proton n.m.r. 0-64498

cylcopentanol, i.r. and Raman spectra, vibr. anal. 0-67785 cytosine, polarization of electronic transition 0-79370 DNA, u.s. beam irradiated, cavitation effects 0-45450

dacron coatings thin, thickness meas, using electron excited γ -ray source, method 0-50362N-decutorated N-methylpropionamide, i.r. and Raman spectra and normal vibrs. 0-53075

N-deuterated N-methylpropionamide, i.r. and Raman spectra and normal vibrs. 0–53075 deuterobenzene dissolved in 4,4'-n-hexyloxyazoxybenzene at 75.3°C, relaxation times of deuterium 0–49918 deuterobenzenes, phorsphoresc. lifetimes, and radiationless transitions, at 77°K 0–61149 deuterobenzenes, phosphoresc. lifetimes in rigid media at 77°K 0–61149 deuterobenoacetylene, electronic spectrum 2500 to 900Å 0–74322 deuterochloroacetylene electronic spectrum 3000-1000 Å 0–39418 dextran aqueous soln., u.s. absorption 0–43443 2,4-diacetamidopentane, meso and racemic forms, as model for poly(N vinyl acetamide), n.m.r. spectra interpretation 0–67838 diacetyl, gaseous and invarious solvent, i.r. bands ν (C=O), effect of hydrogen bonding 0–43171 diacetyl with mixtures of naphthacene, luminescence, migration energy 0–71364 diamagnetic solns., positronium quenching 0–53314

0–71364
diamagnetic solns., positronium quenching 0–53314
diamagnetic susceptibility calculation 0–58204
Diamin's compound, clathrate, cryst. struct. 0–78518
1,2-diaminopropane, liquid, associated, in temperature range –65 to –35, 65 to –10 and –35 to +50°C, comparision with existing data 0–58465
1,4-diaza-bicyclo [2.2.2] octane, vapor state emission 0–70967
1,5-diazanaphthalene, ir. and Raman spectra 0–74358
1,5-diazanaphthalene, vapour, electronic absorpt. spectra 0–61159
2,3-diazanaphthalene, vibronic perturbations and phosphorescence 0–71025

3.4- diazanorcaradiene isomerization, dynamic n.m.r. 0-79439
1.4- diazatriphenylene, high-resolution electronic spectra and electronic states 0-53068

states 0–53068 diazines, magnetic evidence for delocalization of lone pairs 0–58217 diazines, substituted, photoelectron spectra discussion 0–64494 diazomethane, electron relax, and molec, vibr. 0–39361 diazomethane, photolyses with propane and isobutane, kinetics 0–41448 diazomethane, photolyses with propane and isobutane, kinetics 0–41448 diazomethane, wagging and rocking force consts. w.r.t. ethylene, electron relax, effects 0–71005 diazomethane free radical, vibr. spectrum, obs. 0–46571 dibenz (a,h) anthracene, sensitized injection of defect electrons through charge transfer process 0–40897 dibenzalhydrazine, cryst. struct., nature of N-N bond 0–65301 1,2.3.4-dibenzanthracene, extinction coeffs, and direction of polarization of T T absorption spectra 0–74340 dibenzo tetracyclo [4, 3, 1, 0^{4,9}, 0^{5,10}] deca-2, 7-diene, cryst. struct., obs. 0 40110

0 40110

dibenzo-a-j-acridine in CDCl₃ soln., n.m.r. spectra, assignment of lines 0-55348

dibenzoperopyrene, quasi-line spectra in n-paraffin matrix, temp. depend. 0-79369

0-79369 dibenzothiophene and its molecular complexes, photoconductive and photo voltaic effects 0-72141 dibenzolb.flthiepin sulphoxide anion radicals, e.s.r. 0-67788 dibenzhiepin derivatives, assignments of configuration by nuclear Overhauser effects 0-43156 dibenzyl, single cryst., phosphoresc., at large excitations 0-69162 dibenzyl, thermal expansion, Gruneisen tensor, X-ray diffr., 83-297K 0-50898

2,3-dibromo-2,3-dimethylbutane, cryst. struct. 0-58775 dibromo-anthracene in solvents, effective temp. of luminesc. centre 0-66107

0-6107
p-dibromobenzene, absorpt, spectra, 20 K 0-62681
1,2-dibromo-1,1-dichloro-2,2- difluoroethylene, ¹⁹F n.m.r., double reso nance in presence of chemical exchange 0-70863 dibromomethane, microwave spectrum, nuclear quadrupole coupling tensor 0-46555

\$307 0-4032 2,3-dibromopropene, using double irradiation for assignment of very small coupling const. 0-77894 dicalcium strontium propionate, spin-lattice relax, by quasi-spin-waves 0-72288

closo-2, 3-dicarbahexaborane (6), skeletal molecular structure from micro-

wave spectra 0-64500 p-dichalcones, isomers, electronic spectra 0-43157 1.2-dichloro 3,4,5,6-tetramethylbenzene, order-disorder orientation transition 0-59047

tion 0-9904. 2.2-dichloro and 2,2-dibromopropane, vibr. spectra 0-55349 1.2-dichloro-3-nitrobenzene, n.q.r. temp. depend. 0-41407 3,4-dichloroaniline, temp. dependence of ³⁵Cl, nuclear quadrupole resonance 0-74359

g,10-dichloroanthracene films, photocond. 0-72142 dichloroanthracene in solvents, effective temp. of luminesc. centre

2,6-dichlorobenzaldoxime, long-range spin-spin couplings signs, nonplanar

2,6-dichlorobenzaldoxime, long-range spin-spin couplings signs, nonplanarity degree 0-39424 p-dichlorobenzene, absorpt. spectra, $20~\rm K$ 0-62681 1,4-dichlorobenzene, absorption, fluorescence and phosphorescence spectra, $4.2\rm K$ 0-72441 p-dichlorobenzene, dielectric det. α , β transformation, meas. by automatic dielectrometer 0-65834 p-dichlorobenzene, electronic spectra, band assignment 0-70990 para-dichlorobenzene, inelastic n scatt., cryst. excitations 0-59090 p-dichlorobenzene, polarized i.r. spectra of single crystals 0-72374 p-dichlorobenzene, rotational band contour analysis in 2800 Å system 0-43159

2,6-dichlorobenzylfluoride, long-range spin-spin coupling consts. conformational depend. 0--39423 4,4'-dichlorobiphenyl, molec. config. in cryst. and soln. from spectra 0-79324

dichlorodifluoromethane, acoustic velocity, for isotherms from 1 to 70 atm., interaction potential force constants 0-68017 dichlorodifluoromethane, liq., ¹⁹F relax. times, temp. and field depend.

74792

dichlorodifluoromethane, saturated absorpt. spectra using lasers 0-70844

Organic compounds continued

dichlorodifluoromethane, solid, 19F relax, time, field depend. 0-76241 trans-dichloroethylene, cryst., n.q.r. in low Zeeman field, obs. 0-41406 1,1-dichloroethylene, vibr. spectra and cryst. struct., -122 to -250°C 0 - 69133

dichloroethylene photoelimination chemical laser, vibr. energy distrib. 0-77079

dichlorofluoroamine, force field, mean square amplitudes and Coriolis coupling coefficients 0-61160 1,2-dichlorofluoroethylenes, solvent depend, of chemical shifts and coupling consts. 0-77897

dichloromethane, density and dielectric constant determination at 30 and 50°C, pressures up to 5000 atm 0-71367 2,3-dichlorophenol, C_r point group modes of vibration of fundamental

0-49947 2,4-dichlorophenol C_s point group modes of vibration of fundamental 0 - 49942

2,5-dichlorophenol Cs point group modes of vibration of fundamental

0-49942 2,3- dichloroquinoxaline in durene, polarization of mag. zero-field transi-

tions 0-54117 2,3-dichloroquinoxaline in durene host cryst., origin of phosphorescence

dichlorotetrafluorocyclopropanes, F-F coupling constants 0-67777 dichlorotetrafluoroethane-MoF₆ binary mixture liquid-vapour equilibrium at 2600 torr 0—64984

2.5 dichlorotoluene, in liq. phase, Raman and i.r. spectra 0—49919

2.6 dichlorotoluene, n.m.r. partially oriented in nematic phase 0—77898

1.4-bis(dicyanOmethylene)cyclohexane, crystal and mol. structure

0 -40112

dicyanobenzene complexes with methyl substituted benzenes, e.s.r. and phosphorescence spectra 0–46556 dicyanodiacetylene, abs. spectrum, 3100-2300 Å 0–43158 dicyanodiazomethane, vibr. spectrum, obs. 0–46571 dicyclopentadienylnickel, molec. struct. 0–61158 trans-dideuteroethylene molal volume meas, in range 105-175°K 0–74731 dicyclopentadienylnickel, trans-dideuteroethylene molal volume meas, in range 105-175°K 0–74731

dielectric const. variations near transition pt., thermoelec. voltage obs. 0-78288

dielectric relaxation determ, by abs. of microwave radiation in organic compounds 0-39823 cisoid dienes, proton coupling constants rel. to mol. config., n.m.r. spectra

diethyl ether, adsorption kinetics on ThO₂ 0-74930

diethylaniline, adsorbed on glass, radical cation, γ radiation, e.s.r. 0-39933

diethylbenzenes produced radicals, in cryst. matrices, fluoresc. spectra 0 39459

 $\begin{array}{l} \text{4-diethylcarbamoyl-1-cyclohexene-5-carboxylic acid, crystal struct.} \\ 0-78516 \end{array}$

diethylether complexes with metallic halides, low temp. i.r. study 0-70991 diethylthiocarbaminate ion and Se analogur, frequencies and vibration forms 0-67790 diethynyl ketone, i.v. and Raman spectras 0-74360 p-difluorobenzene, rotational band contour analysis in 2710 Å system

N-diffuoroboryl disilizane, mol. struct. from e diffr. 0-64507 diffuorodiazirine, force constants and Coriolis coupling constants 0-58218 -39425

difluorodichloromethane, absolute viscosity at atm. press., -39.7-91.8°C

0-33404 diffuoroethylene, absorpt. line absolute freq. meas. 0-53067 cis-1,2-difluoroethylene, n.m.r. in nematic solvent 0-71043 difluoroethylene, saturation of 890 GHz absorpt. line in HCN laser cavity

0 - 54867

0-54867 difluoroethylenes, dipole moment derivs., appl. to i.r. intensities interpretation 0-74362 difluoromethane, photoelectron spectra 0-61168 difluoromethyl radical in solid Ar, i.r. absorpt. spectrum, rel. to bending and stretching modes 0-66061 1,1-difluoro-3-methylbutadiene microwave spectrum, barrier to internal rotation and dipole moment 0-46557 difluorophosphine borane, microwaves spectrum and rot. consts. 0-70992 1,1-difluoro1,2,2-trichloroethane, pure and in benzene solution, dielectric relaxation time and distribution parameter 0-46938 difurylmercury isomers, ¹⁹⁹Hg satellite spectra and ¹⁹⁹Hg-¹H long-range coupling 0-74361 diglycine nitrate, n.m.r. determ. of ferroelec, transition 0-53942

diglycine nitrate, n.m.r. determ. of ferroelec. transition 0-53942 dihaloacetyl chlorides, i.r. and Raman spectra, vapour, liquid and solid 0-74363

0-14503 dihaloactylenes, vibrational spectra 0-70989 p-dihalobenzene, cryst., T-S emission, n, π^* states 0-64485 dihalobenzenes, ortho- and meta-, far infrared absorption spectra explained by rotational transitions 0-46925 dihalofumaronitriles, vibrational spectra 0-77896 p- dihalogenobenzenes, cryst., mol. motion and l.f. Raman spectra 0-40927

0-44927

p-dihalogenobenzenes, cryst., mol. motion and l.f. Raman spectra 0-44870 0—44-610
4-4'-diheyoxyazoxybenzene, birefringence study by Newtons' rings for students 0—39793
dihydrazinium oxalate, i.r. and Raman spectra 0—71004

dihydrazınıum oxalate, i.r. and Raman spectra 0–71004 2.5, dihydrobenzoquinone, long range coupling, spatial factor associated with π electrons 0–43077 2.3-dihydrofuran, structure study from vibr. spectra 0–64534 1.2-dihydronaphthalene, proton coupling constants rel. to mol. config., n.m.r. spectra 0–70987 4.4, 4b-dihydrophenanthrene oxidation, kinetic isotope effect of deuterium 0–48185

5,10-dihydrophenazine, i.r., u.v. and diffuse reflectance spectra 0–55368 dihydrothymine, irradiation in frozen H₂SO₄ solutions 0–59510 dihydrothymine cryst, p.irrad. e.p.r. study of radical form. 0–77970 dihydrouracil, e.s.r. of p-irrad. single cryst. 0–59460

 β -diketones, triketones, enolized spectroscopic examination of stretch vibrations 0-53069

diketopiperazine, mol. packing from van der Waals and H-bonding energy calcs. 0-43648

dimethycyclopropylcarbinyl cation, n.m.r. double resonance 0-67787 N, N-dimethyl acetamide, n.m.r. studies of hindered internal rotation, solvent effects on N-methyl resonance shifts and activation parameters 0-67806

dimethyl amine, i.r. spectra, vibr. assignments and barrier to inversion 0-70993

dimethyl benzyl carbinol, i.r. and Raman spectra 0-58252 dimethyl ether, molecular Zeeman effect and mag. susceptibility anisotro-pies 0-43160

dimethyl ethers, i.r. spectra in Ar matrices, vibrs. 0–70988 N, N-dimethyl formamide, n.m.r. studies of hindered internal rotation, solvent effects on N-methyl resonance shifts and activation parameters

dimethyl sulphide, molecular Zeeman effect and mag, susceptibility anisotropies 0-43160

ropies 0-43160 20% dimethyl sulphide ethanolic soln., internal refl. spectra, 180 to 200 m μ 0-54940 dimethyl sulphone, single crystals i.r. and Raman spectra, vibrational assignment 0-66074 4.4-dimethyl -1,2-tetralindione anion radical, CH₂ hyperfine splitting

0 - 64515

0-04313 dimethyl tin difluoride, Gol'danskii-Karyagin effect 0-59383 N,N-dimethyl-4-nitroso-aniline, low-frequency spectra 0-77874 dimethyl-4, amine, i.r. spectra, vibr. assignments and barrier to inversion 0 - 70993

dimethylacetylene, liquid and gaseous 0-49920
2-(N,N-dimethylamino)pyridine, fluorescence 0-77899
4-N,N-dimethylaminonitrosobenzene, visible and p.m.r. spectra 0-77895
N,N-dimethylaniline, low-frequency spectra 0-77874
N, N-dimethylbutyramide, Raman and i.v. spectra, freq. assignments 0-67789

0-67789

trans-1, 2- dimethylcyclohexane crystalline matrix, fluorescence spectra of trapped radicals from xylenes 0-66102

dimethylformamide, polarographic reduction of coal extracts 0-62826

N-dimethylfisiobutyramide, piezoelectric effect and crystal growth 0-47855

2 dimethylisiobutyramide, piezoelectric effect and crystal growth

0-4/855
2,3-dimethylnaphthalene, fluoresc, and energy transfer processes 0-62729 dimethylnitrosamine, Raman and i.r. spectra 0-71010
2,4-dimethylphenol vapour, u.v. spectrum, band analysis 0-46558 dimethylphthalate system, heat capacity, calorimetric meas. glass temp. 0-68616

dimethylsulfoxide, solid, lattice fundamentals from i.r. and Raman spectra 0-65525

dimethylsulfoxide- d_6 , solid, lattice fundamentals from i.r. and Raman spectra 0-65525

tra 0-65525
dimethylsulphonimine, mol. struct. by e diffr. at gas 0-64520
dimethylsulphonide, I.f. vibrations 0-41230
dimethylsulphoxide and deuterated derivatives vibrational spectra and autoassociation 0-64501
dimethylthiocarbaminate ion and Se analogue, frequencies and vibration forms 0-67790
p-dimethyoxybenzene attached to spirocyclopropane-norbornane frame, energy transfer 0-77856
dinaphthylalkanes, fluorescence quenching and excimer formation 0-79371
2.6-dinitrobenzaldehyde, spin-spin coupling between aldehydic and ring

0—793/1 2,6 dinitrobenzaldehyde, spin-spin coupling between aldehydic and ring protons, hyperconjugative contrib. 0—39422 p-,m-dinitrobenzene, mag. anisotropies and susceptibilities 0—75892 dioctadecyladipate, cryst. growth and testing for X-ray spectrometer 0-65168

p-dioxane fluorescence 0—74766 p-dioxane fluorescence 0—74765 dioxane-glycerol mixture, chemical relaxation and hydrogen-bonded com-plexes 0—43441

dioxane-glycerol mixture, chemical relaxation and hydrogen-bonded complexes 0-43441 diphenyl, elastic consts. 0-55943 diphenyl, quasiline luminescence and absorption spectra, effect of ethyl bromide 0-62719 diphenyl butadiene, dark conductivity, effects of donor and acceptor groups 0-6563 diphenyl ether-cyclohexane syst., energy transfer of electronic excitation, rel. to viscosity 0-68111 diphenyl mercury-tolan solid solns., lattice energy change at solubility boundary 0-65474 diphenyl mixture, chlorinated thermal variation of viscosity 0-50209 diphenyl propane intramol. excimers, kinetics 0-64326 diphenyl with fluoran, single cryst., phosphoresc., at large excitations 0-69162 diphenyl-1,2-pentanedione-1,4 n.m.r. spectra and conformation 0-77900

diphenyl-1,2-pentanedione-1,4 n.m.r. spectra and conformation 0-77900 diphenylanthracene in solvents, effective temp. of luminesc. centre 0-66107 diphenylanthracene in solvents, effective temp. of luminesc. centre 0–66107
diphenylanthracene in solvents, effective temp. of luminesc. centre 0–66107
diphenylarsine, vibrational spectra 0–74400
1.3-diphenylbutane, from electrical discharge through toluene and ethylbenzene, i.r. and u.v. spectra, physical props. 0–46525
diphenylchlorophosphine, vibrational spectra 0–74399
1.2-diphenylethane, from electrical discharge through toluene and ethylbenzene, i.r. and u.v. spectra, physical props. 0–46525
diphenylphosphine, vibrational spectra 0–74400
2.3-diphenylpropanoic acids and esters, diastereomeric 3-substituted, n.m.r. spectra, configuration and conformation 0–67813
diphenyls, chlorinated, viscosity-temp. relation 0–55598
diphosphines, substituent effects in inversion-rotation process 0–67786
diplicadane anion radical, e.p.r. 0–70994
4.4'-dipyridyl complexes with B and Si halides, u.v. spectra 0–66035
disulphide compounds, reaction with organic ree radicals in aqueous solution, e.p.r. 0–69210
p-dithien ¹³C-H satellite spectrum 0–77901
dithienylmercury isomers, ¹⁹⁹Hg satellite spectra and ¹⁹⁹Hg-¹H long-range coupling 0–74361
p-dithini, ¹³C-H satellite spectrum 0–77901
durene, p-irrad, e.p.r., free radicals 0–62766
durene, napthalene doped, vibronic spectra (¹A1g-¹B2n) 0–72378
durene monoaldehyde, absorption and phosphorescence spectra 0–72375
duroquinone, triplet state, absorption spectrum 0–39406
durosemiquinone in T.H.F. 0–59477
dve, fluorescence and light structure 0–38539
dye excitation, 2-quantum anti-Stokes processes 0–46923
dye laser, high power pulsed 0–49025
dye laser, near u.v. to yellow tunable emission 0–52285
dye laser, high power pulsed 0–49025
dye laser, near u.v. to yellow tunable emission 0–73228
dye laser, high power pulsed 0–49025
dye laser, near u.v. to yellow tunable emission 0–73228
dye laser, high power pulsed 0–63623

Organic compounds continued

dye lasers, high repetition rate, thermal lens effects 0-77112

dye lasers, optical waveguide technique 0-77111

dye molecules in aggregates, extended dipole model for calculation of interaction integrals 0-64578

raction integrals 0–64578
dye powder, second harmonic of Nd glass laser 0–65978
dye soln. laser, c.w. operation 0–73229
dye solns., dimerization on cooling 0–53070
dye solns., lasing, generation power time depend. 0–69903
dye solution, nonlinear light absorpt. 0–68107
dye solution, superluminescent radiation 0–50242
dye solutions, absorpt. coeff., refractive index, calc. 0–39791
dye-polymer complexes, exciton theory of electronic states 0–61187
dyes, fluoresc., excited singlet level lifetime 0–39810
dyes, irrad. by two light beams, fluoresc. blocking 0–39811
dyes, optical generation intensity and efficiency due to pulsed lamp excitation 0–60222
dyes, stimulated emission, study of polarization 0–68105

tion 0-60222
dyes, stimulated emission, study of polarization 0-68105
dyes, transient generation 0-49058
EDTA metal chelates, ionic interaction determ. by u.s. method 0-71304
n-eicosane, cryst. geometry, chemical props. 0-53522
electron donor- acceptor complexes, symmetry classification and selection
rules 0-78511
electron scatt., inelastic, rel. to superconduction possibility 0-75430
electron spectroscopy determ. of 0-C and S-C links 0-55276
electronic struct. of mol. from e diffr. 0-74116
electronic struct. of mol. from e diffr. 0-74116
electronic struct. of mol. from e diffr. 0-74116

electronic struct. of mol. from e diffr. 0-74116 epichlorohydrin,n.m.r., spin-spin coupling constants 0-64502 epihalohydrins, n.m.r., coupling constants, and structural correlations 0-64503 epoxides, isomerisation in bicyclic heptic series, in the presence of zinc bromide 0-70995 epoxy resin, applic. to radial shear distrib. determ. in torsion of nonlinear materials 0-45596

epoxy resins, electrical breakdown development at very high voltages 0-65784

erbium acetate tetrahydrate, absorption spectra of single crystals 0-76114

0—76114 esters, long C chain, polymorphism 0—61921 esters, long C chain, polymorphism 0—61921 esters and diesters, conformational anal. by u.s. relaxation 0—74364 estradiol urea cryst. complex phase determ. 0—78517 ethane, adsorption on C surface 900·1300°C 0—55759 ethane, adsorption on activated charcoal at 77.4 K 0—61680 ethane, bi- and tri-halogen derivatives, isomers, lable products of principal inertia moments 0—43161 ethane, chemical polarization of protons, n.m.r. meas. 0—71007 ethane, gas, laser induced hyper-Raman spectra 0—77918 ethane, indigenous in lunar fines 0—51746 ethane, non-dipolar gas, Kerr effect, second hyperpolarizabilities 0—68002 ethane, positive dimer ion formation 0—61374 ethane, solid and liq., ir. spectra and torsional oscillation 0—70996 ethane and other mols., MO explanation for barrier to internal rotation 0—77902 ethane gas, CO₂ laser, passive O-switching 0—49036

0-17902
ethane gas, CO₂ laser, passive Q-switching 0-49036
ethane mol. photoioniz., photo e energy anal. 0-67706
ethane-methane-N₁ system, liq. phase inversion between -255° and
-263.3°F 0-39882

thanes, substituted, SCF-MO theory of vicinal proton-proton coupling 0-74366

ethanes, substituted, depend. of vicinal H-H coupling on internal rotation 0-39427

ethanes, substituted, depend. of vicinal H-H coupling on internal rotation 0–39427 ethanes, substituted, internal rotation determ. by u.s. relaxation 0–74368 ethanes, substituted, medium effects in rotational isomerism and coupling consts. 0–74367 ethanes, substituted, n.m.r. study of rotational isomerism and barriers to internal rotation 0–67791 ethanes, substituted rotational isomerism 0–58148 ethanol, y-irradiated liquid, electron scavenging 0–45091 ethanoles adsorbed on TiO2, i.r. spectra 0–58605 ethanol, adsorbed on TiO2, i.r. spectra 0–58605 ethanol, adsorbed on TiO2, i.r. spectra 0–78900 ethanol, pool boiling, pressure effects on bubble growth 0–39891 ethanol, solution in water, I₂ diffusion coefficients 0–71329 ethanol and H₂O sat, nucleate boiling, dyn. of vapour bubble 0–55675 ethanol and ethanol-d in Ar matrix, i.r. spectra 20°K 0–74369 ethanolthiol, photodissociation, energy disposal 0–48203 o-ethoxybenzoic acid, crystal struct, at low temp. 0–61922 ethyl acetate, density and dielectric constant determination at 30 and 50°C, pressures up to 5000 atm 0–71367 ethyl alcohol, effect on rf conductivity of air-discharge plasma 0–78072 ethyl alcohol, microwave spectra of isotopic species 0–46559 ethyl alcohol, structure model explaining temp. variation of dielectric constants 0–74776 ethyl alcohol, vapour viscosity calc. by free energy average potential model 0–78229 ethyl alcohol droplets, deformation dynamics in unbound fluid 0–64826 ethyl alcohol in benzene solns., dielectric const. and loss, in microwave freq. region 0–46937 ethyl alcohol in binary solns., variation of Raman scatt. with variation 0–64921 ethyl alcohol in piection into external O₂ flow, heat and mass transfer

0 - 64921

ethyl alcohol injection into external O2 flow, heat and mass transfer 78218

ethyl bromide, density and compressibility from P-V-T relations 0-75250 ethyl bromide, effect on intercombination transitions of aromatic hydrocarbons in frozen n-paraffin solns. 0-59431

bons in frozen n-paraffin solns. 0–59431
ethyl bromide effect on quasiline luminescence and absorption spectra of diphenyl 0–62719
ethyl bromide-n-hexane system, dielectric permittivity, conc. and temp. depend. 0–64937
N-ethyl 4-chloro-2- nitroaniline, signs of long-range amino proton-ring proton coupling constants 0–58219
ethyl ether solute in n-tridecane, evaporation mass transfer rates into flowing N₂ 0–50325
ethyl formate, solid, spectrum rel. to rot. isomers, 3200-250 cm⁻¹ 0–41231
ethyl xanthate on galena, thermodynamics 0–65106
5-ethyl-5-alkyl barbituric acids, molecular assoc. in cryst. struct. 0–58776
ethylamine, microwave spectrum 0–70999
ethyl-p-anisilidene-p-aminocinnamate, nematic, cylindrical domains, elec. field effect 0–78263
ethylbenzene, fluoresc., CCl4 quencher effect, polystyrene comparison

ethylbenzene, fluoresc., CCl₄ quencher effect, polystyrene comparison 0-39817

ethylene, H-atom addition, high press, limiting rate const. 0-62799 ethylene, T and V states, interpretation of open shell SCF cales. 0-64504 ethylene, σ and π electronic structures in ground, triplet, and ionic states 0-77903

ethylene, adsorption on activated charcoal at 77.4 K 0-61680 ethylene, adsorption on artificial zeolite below critical temp. 0-58604 ethylene, comparison of electronic structure with diborane 0-77904 ethylene, excited and cation, isomerization processes, energy barrier cales., semiempirical quantum chemical method 0 39428

ethylene, force consts., semiempirical ASMO SCF calc. 0 61161 ethylene, gas, laser induced hyper Raman spectra 0 - 77918

ethylene, geometric approx. to two particle Green function 0-58220 ethylene, higher-order RPA to system of two π electrons in double bond 0.77852 ethylene, influence of solvents out of plane deformation frequency v_2

0 64505 ethylene, interaction of S atoms 0 -43209

o 64505
ethylene, interaction of S atoms 0 -43209
ethylene, ion molecule reaction product distrib, calc. 0-54179
ethylene, ion molecule reactions with H₂S 0 -79438
ethylene, irreversible adsorpt, displacement by water vapour 0-61678
ethylene, insolvenms to 10 kbar 0 - 64812
ethylene, mixed adsorption on W with N₂, dosing order effects 0-55766
ethylene, molal volume meas, in range 105 175°K 0 -74731
ethylene, molal volume meas, in range 105 175°K 0 -74731
ethylene, saturated absorpt, spectra using lasers 0-70844
ethylene and deuterated derivative, photoelectron spectra, ionization potentials and vibrational structures 0 -64436
ethylene and deuterated derivative, photoelectron spectra, ionization potentials and vibrational structures 0 -64436
ethylene edl used to obtain sequence of laser pulses 0-60219
ethylene edl used to obtain sequence of laser pulses 0-60219
ethylene epixulfoxide, ground state rot, spectra internal splittings and quadrupole coupling consts. 0-77958
ethylene glycol, proton spin polarization 65 to 70% using continuous flow The cryostat 0-52551
ethylene glycol mixtures with water, dielec, const. determ, 0-74775
ethylene glycol water glass, p-irrad, electron traps 0-62821
ethylene molecule, intravalence character of V excited state 0-7098
ethylene molecule, intravalence character of V excited state 0-7098
ethylene molecule, intravalence character of V excited state 0-7098
ethylene oxide, force consts, and mean square amplitudes 0-77905
ethylene oxide, force consts, and mean square amplitudes 0-77905
ethylene oxide, force consts, and mean square amplitudes 0-77905

ethylene oxide, force consts, and mean square amplitudes 0-.77905

ethylene oxide, torce consts, and mean square amplitudes 0-7/905 ethylene oxide in Ar matrix, mol. self assoc, i.r. absorpt, obs. 0-43192 ethylene sulphide, force consts, and mean square amplitudes 0-77905 ethylene sulphide vapour, i.r. absorpt, obs. of mol. self assoc. 0-43192 ethylene sulphide vapour, i.r. absorpt, obs. of mol. self assoc. 0-43192 ethylene Ar Penning mixture, ionization maximization 0-39618 ethylene O2 mixtures, Ar diluted, detonations, transverse wave strength 0-50164

ethylene d, electric field gradients near deuteron calculated by floating spherical guassian orbital method 0 64524 ethylenediamine H₂O system, solvated electron in pulse radiolysis 0 54195

ethyleneimine type mols., rotation inversion problem, exact soln. 0 77906

0 77906 ethylenes, halogenated, ionization potential and vibrational structure from photoelectron spectra 0 49923 ethylenes, perhalogenated, mean amplitudes of vibration 0 49921 ethylenes, substituted, SCF MO theory of vicinal proton proton coupling 0 74366

ethyleneureas and propyleneureas, cyclic, NMR study 0-54165 ethylenimine, i.r. absorpt, spectra comparison in solid Ar and N₂ matrices

0. 49922 ethylenimine, n.q.r. of ¹⁴N, 77°K 0–66161 ethylpyridinium bromide, molten, 130°C, magnetoelectric effect obs. 0. 55633

m ethyltoluene trapped in methyl cyclohexane at very low temperature, photodissociated, fluorescence spectrum 0 44933 europium benzoylacetonate, luminescence decay time press, depend. 0 48106

0 48106 europium benzoylacetonate, symmetry of luminescence centres, pressure induced changes 0-41265 europium benzoylacetonate complexes, absorption spectra in methanol solns. 0-74761 fatty acid monomolecular films deposited on mica in aqueous and nonaqueous media, interfacial energies 0-78363 ferricenium cation, electronic struct, from e.s.r. meas, of cations of ferrocenc derivatives 0-71001 ferrocenc, single crystal absorption spectrum at 4.2 K, 3000 6000 Å 0 76115 ferrocenc, vapour, 30 keV industria.

0 76115
ferrocene, vapour, 30 keV inelastic scatt, obs. of excitation levels 0–58250
ferrocene, vapour, 30 keV inelastic scatt, obs. of excitation levels 0–58250
ferrocene and its derivatives, electronic abs. spectra 0–49924
fluoranthene, chemical shift obs. 0–61146
fluoranthene, proton chemical shift, by τ electron 'ring currents' 0–77909
fluorenes, p.m.r. spectra, steric effects 0–67795
fluorenes, p.m.r. spectra, steric effects 0–67795
fluorescene, fluoresc, yeld, 0–509C, by flash photolysis 0–77908
fluorescene decay of laser excited mols. 0–77850
fluorinated methane, carbon 1s electrons, ionisation potential, chemical substitution depend. 0–39435
fluorinated small ring systems, effect of substituents on chemical shifts and coupling constants 0–67797
fluormethanes, electronic structure and energies 0–71009
4 fluoro and 4 bromo benzenethiol, vibrational spectra 0–70972
fluoroacetylene, mol. Zeeman effect and mag. susceptibility anisotropy 0–77910
p fluoroantiline, dipole moment of lowest singlet π*~ π state 0–71002

0 ·77910
p fluoroaniline, dipole moment of lowest singlet π*←π state 0-71002
p fluoroaniline, electronic bands, rot, analysis 0-53071
o fluoroanisole, vapour, emission, 2765 3000.1, struct, anal. 0-64508
o fluorobenzaldehyde, in vapor phase, n-π electronic emission and absorption spectra 0-39411
fluorobenzene, first excited state π*←π, dipole moment correlation with structure 0-46561
fluorobenzene, fluorescence 0-64506
fluorobenzene, rotational analysis of 0-0 band of 2644 Å system 0-55351
fluorobenzenes, analysis of photo electron and u.v. spectra, ionization potentials 0-49926
fluorocarbon products, O₂-containing, ¹9F chemical shift, 0-67706

fluorocarbon products, O2 containing, 19F chemical shift 0-67796

Organic compounds continued

I fluoro 2,2 dichloroethylene, band intensities and atomic polarizations $0^{-3940^{\circ}}$

fluorodichloromethane, absolute viscosity at atm. press., 39.7 91.8°C 58404

fluoroethanes, n.m.r. spectra, solvent effects and rotational isomerism 0.67794

0 67794
2 fluoroethanol, microwave spectral, study of intramolecular hydrogen bonding 0 46562
fluoroform, second virial coeffs, of Kerr effect 0 68008
fluoromethane, ¹CH₃F, partially oriented, n.m.r. anisotropies and absolute signs of indirect spin spin coupling const. 0 46560
fluoromethane, second dielec, virial coeff. 0 58401
fluoromethane, second dielec, virial coeff. 0 58400
a fluoropaphthalene, emission spectrum analysis 0 58221
p fluorophenol, dipole moment of lowest singlet π*e-π state 0 71002
in fluorophenol in vapour state, vibrational assignment in near u.v.

m fluorophenol vapour, emission, 2765-3000 A, struct, anal. 0 64508 p fluorophenoxy halogenoborane, related systems, bonding study using ¹⁹F chemical shift 0 67798

chemical shift 0 67798
p fluorophenyl hałogenoborane, related systems, bonding study using 1917
chemical shift 0 67798
fluoropyridines, 14N relaxation times and (N, F) coupling constants, temperature and medium effects 0 49925
p fluorothiophenoxy halogenoborane, related systems, bonding study using 1917 chemical shift 0-61798
o fluorothoune, microwave, spectrum, internal rot, barrier, torsion vib. interaction 0-71037
I fluoro 2,4,5 trichlorobenzene, vibr, spectrum 0-55352
fluors, laser output power, funed, wavelength depend, 0-50240
formaldehyde, K resolution spectrum, line obs. 0-49927
formaldehyde, electric dipole moment in 1A2 excited state, Stark effect 0-4 (16.2)

formaldehyde, electronic props., cale, method 0-53073 formaldehyde, interstellar, 1_{11} 1_{10} rotational transition, 4830 MHz obs. 0-45306

0 45306 formaldehyde, interstellar, absorpt, near the galactic centre, 4829 MHz obs. 0 41597 formaldehyde, interstellar, excitation 0 66514 formaldehyde, interstellar absorpt, in dark nebulae 0 66513 formaldehyde, interstellar abundances 0 66511 formaldehyde, interstellar mols., laboratory photolysis studies, 1236 Å and 1470 Å 0 66515 formaldehyde, interstellar mols., laboratory photolysis studies, 1236 Å and

formaldehyde, low lying states, calc. by combined SCF and CI method

formaldehyde, microwave lines, near i.r. stars, i.r. pumping and shock

0 66465 formaldehyde, rotational spectra study by submillimeter microwave spec

formaldehyde, rotational spectra study by submillimeter microwave spectroscopy, rotational and centrifugal constants 0 64509 formaldehyde's radio search in comet Bennett 0 69459 formaldehyde HCHO, HCDO, DCDO, 'A" - 'A₁ spectrum vibr. analysts, obs. 0 39429 formaldehyde (H₁ ¹¹C¹⁶O), interstellar, L₁₂ L₁₀ rotational transition, obs. at 4593 MH2 0 -59729 formaldehyde absorpt. coeffs., 650 to 1850 Å 0=71003 formaldehyde in interstellar clouds, absorpt. spectra ref. to chem. comp. of clouds 0 66521 formaldehyde not beam. Autlet Townsystellar, 0 -61162

formaldehyde mot. beam, Autler Townes effect 0-61162 formaldehyde water system, CNDO study of 11 bond 0-74370 formamide permittivity, electrical, pressure and temp. depend 0-39824 formic acid, // solid, phonon curves and frequency distribution 0-62183 formic acid, crystalline polymorphism first order phase transition obs. 0-75344

formic acid mol. photoioniz., photo e energy anal. 0 67706
Freon 12, o positronium quenching rate, obs. 0 42482
freons liquid, thermal conductivity at normal pressure 0 58483
furan, banmett linear free energy relations tested 0 51419
furan, bond angles by minimizing molecular energies 0 55353
gadolinium ethyl sulphate, e.p.r. relaxation times 0 69182
gelatin, dichromated, u.v. hologram recording 0 67111
germylacetylene, force consts. and Coriolis coupling const. 0 74323
germylcyclopentane, vibr. spectra and barrier to pseudorotation 0 58222
glasses, trapping of electrons at low temp. pulse radiolysis 0 59511
glucose aqueous soln., sonoluminescence 0 61535
glucuronic acid, "Co p-irradiation, effects of radioal scavenger and solute
conc. 0 74371
glycerine water viscous mixture, sonoluminescence from stable cavitation
0 71360
glycerol, dielectric relaxation, theory 0 74780

of 71300 glycerol, dielectric relaxation, theory 0-74780 glycerol, quasi elastic line-broadening meas, using high resolution neutron crystal spectrometer 0-68077 glycerol+water mixture doped with porphyrexide, NMR 0-74791 glycerol/water mixtures, porphyrexide doped, proton polarization times, 1K 0-62770

glycerol/water mixtures, porphyrexide doped, proton polarization times, -1K 0 62770
glycine, internal rotation from low temp, heat capacity data 0 62214
py glycine, long wavelength phonon spectra 0 76133
glycine silver nitrate, cryst, struct. 0 68321
glycol sulphate, pyroclee, current obs. in paraelec, region 0 51129
glycolaldehyde, microwave spectrum and dipole moment 0 58223
glycolaldehyde, microwave spectrum and rot. consts. 0 77913
glyoxal, laser induced emission, band assignment 0 58224
glyoxal, torsional vibration effect on molecular structure 0 70847
glyoxal, vibration rotational analysis of 12 type C bands 0 43163
glyoxid, vibr. rot. anal. of 4540 Å band system 0 -77912
glyoxime in soln, fund, freqs, symmetry and assignment 0 78281
glyoxyl caid, vibr. spectra and free mol. symmetry 0 6 1164
guanidinium aluminium sulphate hexahydrate, e.p.r. of Cu²⁺ mag, com
plexes 0 -72500
It bonded complexes, polarization of C -0 bond 0 - 77857
haloacetic acids n.q.r. of ³⁵Cl 0 59475
halogen derivatives, viscosity meas, using capillary flow method 0 43404
halogen omethylbenzene, lattice modes and thermal motion 0 62182
halogen derivatives, viscosity meas, using capillary flow method 0 43404
halogenoethanes, K ray photoelectron spectra 0 -77914
heavy atom analysis, automatic 0 50558
heme, e.p.r. oriented in organic cryst. 0 -54162
heptafluoriodopropane inert gas mixture, diffusion coefficients 0 -43405

heptafulvalenc, open shell SCF MO calculation of C nuclear cation and anion arrangements, molecular symmetry 0 64540 in heptane, thermoluminescence, exp. investigation 0 72449

heptanols, straight chain, static delect constant, i.e. and n.m.r. spectra 0 460 to

hetero-exemers, fluorescence spectra and bonding 0 58205 heteroaromatic mol., rot. correl. times by proton spin lattice relax.

n heterocyclic benzene analogues, approximate MO theory and electronic structs. O. 19441 N heterocyclic compounds, crystal and mol. struct., X ray diffy, studies

N beterocyclic compounds, crystal and mol, struct. X ray diff; studies () ±011. Studies ()

() 78740

hexachterobenzene single crystals, triplet exciton dynamics. O=A94.16 in hexachterone, positron lifetimes, temp, depend, correl, with viscosity changes. O=74.784 hexafteerone gascous, electron diffraction structure determination.

hosalhoroacetone, vibrational relaxation and radiationless processes in gas phase 0 64543

page V 083 (2) hexallucronzonethane, structure determ, by electron diffraction 0 778 to hexallucrobutyne 2, nuclear spin internal rotation coupling 0 778 (6) hexallucrobutyne 4b), spectra and cryst, structure 0 604 (7) hexallucrobobutene, gascone, electron diffraction structure determination

0. 61165 hexafluoropropylimine, gaseous, electron diffraction structure determina-tion 0. 61165 hexaflydro 1, 3, 5 (finitro s-triazine (RDX), electronic struct, and spectrum, MO calc. 0. 67799 1.1,3,3,5,5 hexakistridenteromethyl) 1,3,5 (tistlacyclositane, as reference compound for pair,c spectroscopy at higher lemp. 0. 66988 hexamethylburzne, single cryst., 298 and 1.30 K, methyl group rotation, transation. 0. 59087

hexamethylene high temp, rotator phase, study of plastic flow 0 - 08328 hexamethylene teiramine cryst,, optical rectification const. 0 - 41025 hexamethylenetetramine, coupling coeffs, and Debys Waller factor 0 - 40529

hexamethylenetetramine, lattice vibr., X-ray scatt. obs. 0 - 62151 hexamethylenetetramine, molecular dynamics, neutron scattering investiga-tion 0 71069

become hylenetetramine, n.q.r. modulation and reorient ational broadening 0.64542

hexamethylphosphorotriamide, mixture with water, 11 1 and 12 0 a.n.r. spectroscopy investigations of preferential solvation by diamagnetic cations 0=68156

O 68156
hexamine, Intitee dynamics, rigid molecule model. O 50008.
hexamine crystal, electro optical props., influence of growth methods, size and operation mode. O 54065
n hexame, electric conduction and breakdown. O 54950
hexame, negative charge injection. O 68136
n hexatic, photoinduced conduction. O 68136
n hexatic, photoinduced conduction. O 6999
hexame diffusion and permeability coefficients through low density polyethylene. O 55928
hexame diffusion and permeability coefficients through low density polyethylene.

hexatine injection into external Oxflow, heat and mass transfer 0 78218 hexatineontane, a ray diffraction maximum as function of temp. 0 65302

O. 63-92. hydrazhium hydrogen oxalate, Lr. and Ruman spectra. 0—71004 hydrazhium hydrogenmols, polurized phosphorescence with reference to photorearrangements. 0—79452. hydrogenidnes, n.v. absorption spectra. 0—58228 hydrogenidnes, n.v. absorption spectra. 0—58228 hydrogenidnes crystals, Hall effect study in triangular model. 0—78664 hydrogenidnes fame, ion density meas, negative electrostatic probestations of the content of the content

hydrocarbon flame bands, rot. struct. 0 49929 hydrocarbon flames formed by opposing jets, fonization 0 78152 hydrozarbon free radicals, in liquid solut, e.s.r. linewidth and saturation studies 0 46666

hydrocarbon fuels, flow through glass fibre fibers, charge generation 0 48948

hydrocarbon liquids, elementary charge carrier models. 0 - 50251 hydrocarbon molecules, auger spectra obs. 0 - 77926 hydrocarbons, MO theory of internal rotation using minimal Slater type

hydrocarbon molecules, auger spectra obs. 0 - 77926
hasis 0 - 77946
hydrocarbons, MO theory of internal rotation using minimal Slater type
hasis 0 - 77946
hydrocarbons, aircmant, oscillator strengths 0 - 40566
hydrocarbons, aircmatic, effect of spin cipit coupling on radiative and non
radiative transitions 0 - 77853
hydrocarbons, aromatic, in frozen a paraffin solns, ethyl bromide effect on
microcombination transitions 0 - 59434
hydrocarbons, aromatic, polarizability in ground and first excited state
0 - 43668
hydrocarbons, aromatic, trans and matrix eff on fluoress 0 - 74449

10-4 0008
Inydrocarbons, aromatic, temp, and matrix eff. on fluoresc. 0-74419
Inydrocarbons, condensed planar benzenoid, p.m.r. spectra, McWeeny
cades, on hexacyclic nois. 0-43468
Inydrocarbons, conjugated, absorption spectra determination: 0-67800
hydrocarbons, conjugated, beats of formation and geometries, LCAO SCF
MO method: 0-46564

hydrogarbons, cyclic, heats of adsorpt, on p Al₂O₁ = 0.5102 hydrogarbons, orcegy loss of slow electrons = 0.78226 hydrogarbons, flow through porous insulation, electrostatic charge genera-tion = 0.44950

hydrocarbons, heats of adsorpt, on MgO 0 65105 hydrocarbons, liquid, electron mobilities 0 46949 hydrocarbons, molecular orbital interpretation of X-ray emission spectra 0 46567

hydrocarbons, p and β bands cale, in accordance with HMO NCF theory with configuration interaction 0, 77917 hydrocarbons, photochemical decomposition into radicals, quenching of excited states 0, 44141

Organic compounds continued

hydrocarbons, planar condensed benzenoid, n.m.r. spectra, McWeony 'ring current' theory evaluation 0 43167

hydrocarbons, planar condensed benzenoid, p.m.r. spectra in isotropic solvent 0.44166

hydrovarbons, polarizabilities, bond additive property 0-85354

hydrocarbons, polycyclic conjugated, LCAO MO calculations for energies of singlet and triplet transitions 0 64464 hydrocarbons, radiolysis, electron scavenging and ion recombination

0 41450 hydrocarbons, saturated, effect of alkyl substituents on fluorescence

0 43105

0. 4.1165 hydrocarbons, saturated, thermoluminese, glow curves and molec, O₂ as electron traps, 0. 4.1283 hydrocarbons, saturated isomerization energies cale,, shape functions method applic. 0. 55.280 hydrocarbons, simple, structural and energetic predictions from NDDo and (NDO MO methods 0. 499.28 hydrocarbons, static charge reduction, device 0. 489.51 hydrocarbons, unsaturated, quenchers of metastable O₂(b¹Σ_g¹), rate constants, 0. 55.140 hydrocarbons, unsaturated, quenchers of metastable O₂(b¹Σ_g¹), rate constants. 0. 55.140 hydrocarbons, unsaturated, quenchers of metastable O₂(b¹Σ_g¹), rate constants.

hydrocarbons, unsaturated polycyclic, ionization potentials and heats of

hydrocarbons, unsaturated polycyclic, ionization potentials and heats of formation 0.46551 hydrocarbons, vapour liquid equilibrium point, use of Redlich Kwong eqn. of state 0.50420 hydrogen bonded, high botting i.r. study, matrix isolation in low temp. inertigas 0.66060 hydrogen complices, i.r. spectra, hydrogen bonding 0.58225 hydroquinone cation, ¹¹O and ¹¹C hyperime interactions in e.p.r. 0.74347 // hydroquinone clathrates, far i.r. spectra at low temp. 0.76116 o hydroxy 9 phenylltucinone, fluoresc, yield, 0.50°C, by flash photolysis 0.75068

hydroxynthrasemiquimones, e.s.r. spectra, solvent effects 0 78302 4 p hydroxyphenyl 2,2,4 trimethylchroman, Diamin's epd., clathrate cryst. struct. 0 78518

hydroxymaga, n.m.r. of p trrad, cryst. 0 79421 hydroxymaga, n.m.r. of p trrad, cryst. 0 79421 undarso p bensequinent anion possible age of proton jump 0 67801 undarsole bond angle dy minimizing molecular energies. 0 55353 undarsole, self diffusion and calleal recombination in single cryst.

1,2 indandione anion radical, CH₂ hyperfine splitting 0 64515 indazole, determ, of dipole moment in excited state 0 64514 lindone, O 0 hand of 2800 Å transition, hybrid character and rotational structure 0 46508 indeed, O become discounted by the original discou

structure () -46568 indego discounter () -55866 indian acetylacetomates, cryst, struct. () -55866 indian acetylacetomates, cryst, struct. () -55866 indian acetylacetomates, cryst at raceted state () -64514 indians, crystal struct. Patterson function interpretation programs () -1811 indians, crystal struct. Patterson function interpretation programs () -61811 indians, crystal struct, patterson function interpretation programs () -64669 intermolecular senti. spectra, temp. phase depend. () -64462 intermolecular Oyenhauser effect, correction with internuclear distance for (1) -6,1161 internuclear distance for () -68660 intermolecular Oyenhauser effect, correction with internuclear distance for () -68660 internuclear distance for () -88660 inte

todoform, laser induced photolysis, nonlinear optical solvent effect 0 72257

0 /2557
Iron (III) acstance and chloro derivatives, Mossbauer effect 0 41310
Iron acetate and chloro derivatives, Mossbauer effect 0 56517
Isobutane, chem. activated, decomp. rates 0 41448
Isobutane, i.r. spectra and internal rotation 0 46584
Isobutanoi dissolving in water, structure 0 39718
Isobutanoi dissolving in water, structure 0 39718
Isobutanoi dissolving in water, structure 0 39718

boobutyfic acid radical in aq. soln., e.a.r. spectra | 0.43196 Isocyanates and ployurethane rubbers, i.r. spectra identification | 0.49947 Isobalfordin structure from n.m.r. solvent shift in methoxyl groups

isonitroso scetaniide derivativss, crystal symmetry rel. to substituents 0.50926

isopentinic, evaporation rates into N₂ in laminar flow system 0-50324 isopropanol, adsorption by microporous silica gel 0-50398 isopropanol cyclohexane mixture, acoustical props. study over temp., press, conc. 0-64916

press, conc. 0 64916
isopropyl alcohol, internal rotation and microwave spectrum 0-43169
isopropyl alcohol in the trans conformation, rotational constants 0-64516
isopropyl alcohol liquid jets, disintegration 0-61466
isopropyl ether, density and dielectric constant determination at 30 and
50°C, pressures up to 5000 atm 0-71367
isopropylamine octallydrate, cryst. struct. determ. 0-75115
27.4 isopropylations 3,3° cyclogranosine, nuclear Overhauser effect and
molecular geometry 0-77854
isoquinoline, i.r., and electronic absorption spectra 0-55372
isoquinoline, vibr. spectra and fundamental assignments 0-64543
isoquinoline, vibr. spectra and fundamental assignments 0-64543
isoquinoline, vibr. spectra and indundamental assignments 0-61557
ksrasoje droplet streams, combustion noise for laminar diffusion flames
0-72531
Ketene, electron relax, and molec, vibr. 0-39361

6 73311
Ketene, electron relax, and molec, vibr. 0 39.361
ketene, wagging and rocking force consts, w.r.t. ethylene, electron relax, effects 0 71005
ketene interstellar, new spectral line, 200 to 500 MHz. 0 69414
ketenes, Bp unsaturated, ¹³C carbonyl carbon shieldings, ¹³C n.m.r. obs. 0 394.11

ketones, aromatic, Γ_1 - S_n radiationless transition =0=46570 ketones, cyclic, angular strain influence on carbonyl stretching vibration =0=53074

kstomes, cyclic mixed in phenol shift of hydroxyl group vibration band to 645.33

ketones, diamagnetic susceptibility meas. O :55356 ketones, apectra structure correl. 400 to 200 cm \(^1\) 0 -55355 kryptocyanine, induced Raman spectra by powerful pulse of ruby laser

lastic acid derivatives, cryst. and mol. structs. 0 - 65303

Instite soid derivatives, cryst, and mot, structs. U- 55305 Immolin, temp, dependence of ultrasonic absorption U- 53345 Ianthanum ethyl sniphate, e.s.r., of nearest neighbour Gd³⁺ pairs 0-41353 Iasser dyes, flash lamp pumped, wavelength tunability U- 52284 Iasser dyes, quenching of molecular triplet states, efficiency effect 0-49059 Iassing dye soines, generation power time depend. U-69903 Imased oil, temp, dependence of ultrasonic absorption U-53345 Iaquid, Raman spectra, energy determ, first Stokes' components U-39798 Iaquid disloctrics, high permittivity, recent developments U-64934

liquid lasers, u.v. emission 0-52286

liquids, pool boiling heat transfer from large array of artificial nucleation sites 0 55673

figuids, pure of low viscosity, thermal conductivity at normal pressures 0.7 U.D.

liquids, relation between adiabatic compress, and viscosity 0-46879

liquids, scintillators, pulse shape discrimination source of delayed fluorescence 0 63890 liquids, self diff. consts. 0 64891 liquids, thermal conductivity in a homologous series or a group 0 64899

liquids dielectrics, radiation induced conductance 0 -64953

liquified natural gas as cryogenic fluid, applicability 0-79812 lithium acetate dihydrate, i.r. and Raman spectra obs. 0-41243

hthum acetare dihydrate, i.r. and Raman spectra obs. 0–41243
hthum formate monohydrate, nonlinear optical susceptibility, transmission, and refractive indices 0–79228
lithium formate monohydrate single cryst., Raman spectra 0–51328
lithium naphthalenide mion structure, e.s.r. study 0–39433
lithium thallium tartrate, ferroelee, props. 0–53943
lithium thallium tartrate, ferroelee, props. 0–53943
in hunar samples, alkanes, 15 to 30 C atom length, search for 0–48547
in lunar samples, bio organic compounds and glassy microparticles
0–48540
in lunar samples, packed detection in

in lunar samples, carbon detection by pyrolysis hydrogen flame ionization 0.45405

0 45405
in lunar samples, organogenic elements and compounds 0 - 45404
in lunar samples, organogenic elements and compounds 0 - 45406
in lunar samples, search and characterization 0 - 45401
in lunar samples, search for 0 - 48548
in lunar samples, search for 0 545409
in lunar samples, search for py mass spectrometry 0 - 45403
in lunar samples, search for porphyrins 0 48549
in lunar samples, search for porphyrins by fluorescence activation 0 - 1540?
lunar samples 0 48551

0 1540.7

Lunar samples 0 48551

2.6 lutidine water system in critical region, n.m.r. study 0-46958 magnesium methoxyl chloride, crystal struct. 0-53518 magnesium phthalocyanine negative ions, mag. circular dichroism and absorpt spectra 0 71023 magnesium phthalocyanine photocells, characts. 0-72146 magnetic resonance spectroscopy of triplet state molecules in zero magnetic field 0 64468.

field 0 64468 mnnganese neetate tetrahydrate, low temp. magnetiz., saturation moment, ordering 0 41041 mnnganese formate, mag. transitions low temp. 0 62569 manganese formate, two dimens, antiferromag. 0 41067 manganese formate dihydrate, mag. ordering, n.m.r. obs. 0 75966 melamine, ¹⁵N prod. by 87 MeV c bombard. 0 77539 melting using electron system 0 78337 mercurous acrylate, photosensitive image formation obs. 0 70121 metal gossypol complexes, spectra 0 39430 metalloporphyrins, Raman spectrum 0 46573 metalloporphyrins, ring geometry effects on triplet and singlet energies 0 74387

0 /4382 meteorite Pueblito de Allende, organic analysis, improbability of contam

meteorite Pueblite de Allende, organic analysis, improbability of contamination 0 - 63157 methane a, rot, struct, of r_b band, 1161cm⁻¹ 0-55357 methane. Zeeman splitting obs. in vibration rotation spectra of ¹Σ, rotational magnetic moment determ. 0-77924 methane, absorpt, spectra coeffs., 100 to 400 Å 0-55298 methane, adsorption on graphite, potential variation with number of layers 0-50396

methane, as counting gas in proportional tube, effect of contaminants 67346

methane, chemical polarization of protons, n.m.r. meas. 0–71007 methane, clathrate hydrate snows in cometary environment 0–57119 methane, d₁, solid, specific heat. Schottky type anomaly, by quantum statistical consideration 0–56110

methane, density depend, of threshold for suppression of stimulated Brillouin sentt. 0-39676

methane, deuterated, fund. v_4 band interpret. 0—74374 methane, deuteron bombard., electron capture cross sections, E_d =0.3 to 70 keV 0 4965.

methane, dissolved in inert solvent, rot. motion and moment anal. of i.r. bands 0 70910 methane, enriched with ¹³C, absorption spectra, rotational and splitting parameters of ν_4 band 0 74381 methane, gas, effective self diffusion coeffs. in transition press. range 0 50172

methane, gas, laser induced hyper Raman spectra 0-77918 methane, gaseous, molecular interaction effect in neutron scattering 0-67854

0 - 67834 methane, hypersonic sound speeds at moderate pressure 0 - 68016 methane, i.r. absorption coeff. 40 500 μ 0 - 55616 methane, indigenous in lunar fines 0 - 51746 methane, indigenous is trystal growth from vapour 0 - 47120 methane, isothermal compressibility factor, calc. at temp. values from 0 to 150°C 0 67988

methane, mixed isotopic crystals, site symmetries from i.r. spectra 0 79269

0 79269
methane, photodissociation 0-53092
methane, photodissociation at 1236 Å 0-77969
methane, photodissociation at 1236 Å 0-77969
methane, photoionization, angular distribution of free electrons released
0 8.2928

methane, polarizability tensor components, CNDO/II calculations 0 64355

methane, proton magnetic shielding consts. 0–58171 methane, rotational vibrational transition, 2947.906 cm⁻¹, frequency stabilisation of He Ne luser 0–73226

methane, self diffusion coeff, near critical point 0–74739 methane, small angle electron scattering cross section 0–43175 methane, solid, James-Keenan model with octahedral symmetry 0–56475 methane, solid, near melting pt., lattice vibrs., study by neutron scatt. methane, sound vel. 0–73305 methane, sound vel. 0–73305 methane, sound vel. 0–73305

methane, stimulated Brillouin scatt, rel. to hypersonic speed 0–61124 methane, stimulated Brillouin scatt, freq. shifts meas, and theory, hyper sound speed determ. 0–46824 methane, ultrasoft X ray absorpt, meas. 0–64818

Organic compounds continued

methane+methyl chloride, polyatomic gas mixture, thermal diffusion as function of temp, and cone. 0-68029

methane + tritium reactions, trajectory studies 0-72525

methane + C+ reactions, 2-200 eV range 0-48178

methane a coustic velocity, for isotherms from 1 to 70 atm., interaction potential force constants 0–68017 methane and deuterated derivative, chromatographic determination of heat and entropy for adsorption on graphitized carbon black 0–71500

methane deuterated molecule photoioniz., photo e energy anal. 0-67706

methane flames, laminar diffusion, stability 0-48888 methane gas, energy loss of traversing protons 0-45963

methane gas system, adulterated, proton magnetic relaxation 0-67803

methane gas system, adulterated, proton magnetic relaxation 0–67803 methane in Jovian atmosphere, high resolution meas. 0–66594 methane ion, CH₄+, geometry, open shell CNDO/2 calcs. 0–71008 methane ion, CH₃+, equilibrium, bond lengths and angles, binding energies, orbital energies, dipole moments, symmetry 0–43173 methane ions, CH+3 and CH-5, STO calculations, electron pair interpretation of stabilities of structure 0–58232 methane molecule photoioniz., photo e energy anal. 0–67706 methane molecules, electron scattering, meas. of total differential cross section at 40 keV, correlation and binding effects 0–74379 methane on Jupiter's disk, absorption bands (6441 Å and 6478 Å), spectrophotometry 0–57107 methane passage of first absorption layer through 3 successive states 0–68240 methane synthesis for radiocarbon dating, catalytic bydrogen converter.

methane synthesis for radiocarbon dating, catalytic hydrogen converter 0 54216

methane through Ne isoelectronic sequence, config. interaction calcs. 0 39437

methane viscosity 293 to 1050°K and intermol, forces 0–74686 methane NH₁ ion-molecule reactions, ion cyclotron resonance 0

methane-d₁, elec. resonance spectra, transitions and elec. dipole moments 0 - 71022

methane-d, electric field gradients near deuteron calculated by floating spherical gaussian orbital method 0–64524 methane ethane N₂ system, liq. phase inversion between –255° and 26.3.3°F 0–39882 methane inert gas mixed crystals, i.r. spectra and structure 0–64522

methane-inert gas mixed crystals, i.r. spectra and structure 0—64522 methane-inert gas mixed crysts., i.r. spectra and structure 1. to methane conc. 0–72377 methane-methane beams, clastic scatt., 0.1 to 2eV 0–74224 methanes, bromine substituted, auger spectra obs. 0–77926 methanes, chlorinated calculation of i.r. band intensities 0–74350 methanes, substituted, self-consistent group calc. 0–58231 methanetlellurol, i.r. and Raman spectra, vibr. anal. 0–64529 methanethiol, 3µ vib. rot. spectra, hindered internal rot. 0–39438 methanol, p-irradiated liquid, electron scavenging 0–45091 methanol, isotopically substituted, in Ar matrix, i.r. spectra 20°K 0–74385 methanol, Lf. vibr. and torsion-rotation spectrum 0–64527

0-14363 methanol, I.f. vibr. and torsion-rotation spectrum 0-64527 methanol, positron lifetime temp. and phase depend., and CD₃OD 0-75533 methanol, rotational spectrum from 550 to 900 cm⁻¹, anal. 0-64528

methanol, saturated with CO, reactions in water photolyisis at 184.9 nm 0 76276

0 /62/6 methanol in benzene and p-dioxane solns., relax, time distrib. 0-39828 methanol jet, r.f. line obs. 0-74375 methanol vapour, CO₂ laser, passive Q-switching 0-49036 methanol-CS₂ binary system, critical phenomena, coexistence curve

0 -39778 methanol-CS2 binary system, critical phenomena, sp. ht. behaviour

0-39777 methanol acetaldchyde ion molecule reactions with H atoms and ions 0-45054

0-45054
methanol-water mixtures, dielec. consts. at low temp. 0-68132
methanol-water mixtures, dielec. consts. at low temp. 0-68132
methoxy benzaldehyde, m- and p-, vapour, n-Π* electronic emission spectra 0-74380
methoxy-substituted benzanthrone, in hydrocarbon solutions, electronic structure and spectra 0-49905
methoxy-substituted benzanthrone, in hydrocarbon solutions, electronic structure and spectra 0-49905
methoxyamine and methoxyammonium ion, i.r. spectra 0-61170
methoxybenzylidene n-butylaniline, liquid crystal, temp. dependence of birefringence 0-74756
methoxyl cation radicals, p splitting consts. in e.s.r. spectra 0-64517
α-methoxyphenylacetic acid, alkali acid salt complexes, structure studies, i.r. spectra 0-46578
N-methyl 2-carbomethoxy- 4,6 dinitroaniline, long range spin-spin estab lished by p.m.r. 0-55361
methyl alcohol, c.w. submillimetre laser action on optical pumping 0-73207
methyl alcohol, solid, α- and p-irrad, spatial radical distrib. by electron spin

neethyl alcohol, c.w. subminimetre laser action on optical pumping 0–3207 methyl alcohol, solid, α - and p-irrad, spatial radical distrib, by electron spin echo, influence of LET and spur effects 0–66133 methyl alcohol, structure model explaining temp, variation of dielectric constants 0–74776 methyl alcohol, vapour viscosity calc, by free energy average potential model 0--78229 methyl alcohol in benzene solns., dielectric const. and loss, in microwave freq, region 0–46937 methyl alcohol mol, photoioniz., photo e energy anal. 0–67706 methyl alcohols, partially deuterated, α depend, of vibr, zero-point energy 0–58230 methyl and other radicals, electronegativity and structure 0–39434 methyl azidoformate, photolytic decomp, in rare-gas matrices near 4°K, i.r. spectra study 0–69222 methyl boron difluoride and deuterated derivative, gas phase i.r. and liquid Raman spectra, vibrational assignments 0–64526 methyl bromide, accidental resonances in fundamentals, anal. 0–71019 methyl bromide, broadening of microwave spectral line of OCS and SO₂ 0–77823 methyl bromide, high resolution spectra anal. rel. to fundamentals

methyl bromide, high resolution spectra anal, rel, to fundamentals 0-71018

methyl bromide gas, passive Q-switching of CO₂-N₂-He laser methyl bromide, microwave absorpt, intensity law, evaluation 0-71016 methyl chloride, second virial coeffs, of Kerr effect 0-68008 methyl chloryde, vacuum u.v. photolysis, i.r. and u.v. study of products 0-76279

methyl chloride, vibr.-rot. band, 2080 cm⁻¹ 0-61166

methyl chloride, vibr.-rot. spectrum between 2700 and 3000 cm⁻¹ 0-71021

methyl chloride, viscosity of binary mixtures with H₂S and SO₂ 0-61449 methyl chloride + Cl⁻ gas phase reaction, potential energy surfaces 0-69204

0-09204
methyl chloride mol., bond behaviour in elec. field 0-64519
methyl cyanide+H₂O, u.s. absorpt, props. 0-68103
methyl cyanide-N₂ gas mixtures, in elec. field, meas. 0-78214
methyl cyanide-d₃, microwave double-photon transitions, obs. by high
power microwave double resonance 0-77925
methyl cyclohexane, crystalline matrix, fluorescence spectra of trapped
radicals from xylenes 0-66102
methyl ethyl ether, isotopic species, i.r. and Raman spectra, isomers
0-46580

0-40380 methyl fluoride, anisotropy of indirect nuclear spin-spin coupling constant, treatment by finite perturbation method 0-74222 methyl fluoride, c.w. submillimetre laser action on optical pumping 0-73207

0—73201 methyl fluoride, photoelectron spectra 0—61168 methyl fluoride, proton magnetic shielding consts. 0—58171 methyl fluoride, reaction with C⁴(P) 0—62797 methyl fluoride, second virial coeffs. of Kerr effect 0—68008 methyl group, motional averaging, e.s.r. hyperfine structure prediction 0—71013

methyl group, vibrational resonances involving E modes 0-7437

methyl group, vinatonal resonances involving Emoties 0-4491 methyl groups in globular mols, barriers to internal rotation 0-64491 methyl halide, mol, vibrs, by hypermatrices commutable in pairs 0-49932 methyl halide positive ions, vibrational frequencies and vibronic interaction 0-55360

methyl halides, deuterated, determ. of A₀ 0–71017 methyl halides, reactions of C⁺, study using mass spectrometer 0–79436 methyl halides, valence-shell ionization potentials by photoelectron spectra 0–55360

methyl halides, valence-shell ionization potentials by photoelectron spectra 0–55360 methyl in pyramidal configuration, temperature dependence of hyperfine splitting 0–46575 methyl iodide, i.r. spectrum and anal. of ν_3 0–77927 methyl iodide, i.r. spectrum and anal. of ν_3 0–77927 methyl iodide, rot. constant A_0 , direct spectroscopic obs. 0–71011 methyl isobutyl ketone, liq., internal refl. spectra, 180 to 200 m μ 0–54940 methyl isobutyl ketone-sulphuric acid, heat of mixing 0–66172 methyl ketene and isotopic molecules including D, ¹³C and ¹⁸O substitutions, of vibration 0–55362 methyl mesityl oxide oxalate, optical activity in nonenantiomorphous biaxial crystals 0–69079 methyl nitrate, molecular structure 0–64521 methyl nitrite, reaction kinetics with alkali atoms 0–46635 N- methyl phosphoramidodichloridothioate and deuterium analogues, assignment of vibrational spectra 0–46579 methyl radical, electron relax, and molec, vibr. 0–39361 methyl radicals, group IVB substituted e.p.r. study evidence for d-p- π bonding 0–43195 methyl rotor, torsional ground state model using single particle wavefunctions. methyl rotor, torsional ground state model using single particle wavefunctions 0-64523 methyl rotor, torsional ground state model using single particle wavefunctions 0-64523 methyl style ther, mol. struct. from e diffr. 0-64518 2-methyl thiophene, microwave spectrum, internal rotation and dipole moment 0-64525 methyl three-top mols., 1.f. vibr. modes 0-55358 2-methyl-1-buten-3-yne, microwave spectra assignments, methyl group barriers to internal rot. 0-77928 2-methyl-4.5-dihydrofuran, ring-puckering pot. functions from i.r. absorpt. spectra 0-74356 3-methyl-4-amino-1, 2-napthtoquinone hydrate, cryst. struct. determ. by X-ray anal. 0-61927 3-methyl-4-bromo-5-carboxamide-pyrazole, crystal and molecular structure 0-78519 1- methyl-4-phospha-3,5,8-trioxabievelo. (2.2.2.) petage 4-evides without

ture 0-78519

I- methyl-4-phospha-3,5,8-trioxabicyclo- (2.2.2.) octane-4-oxide, vibrational spectra 0-74378
methylacetylene, force consts. and Coriolis coupling cost. 0-74323
methylacetylene, mol. Zeeman effect and mag. susceptibility anisotropy 0-77910

0-/910 methylallylbenzenes, Huckel approx. calc. for electronic structs. 0-46581 methylamine, internal rotation and amino- wagging vibr. 0-61171 methylamine, liquid, associated, in temperature range -65 to -335, -65 to -10 and -35 to +50°C, comparison with existing data 0-58465 methylammonium chloride, Raman spectrum of solid state and solution

0 - 62693

methylammonium chloride single cryst., vibr. spectra 0-41233 methylammonium halides, and partially deuterated analogues, p.m.r. 0-62776

methylaniline, adsorbed on glass, radical cation, γ radiation, e.s.r. 0-39933

nethylarinine, adsorbed on glass, radical carton, p radiation, e.s.i. 0–39933 methylarsenic halides, i.r. and Raman spectra 0–71006 methylarsine, microwave spectrum and barrier to internal rot. of methyle group 0–71015 methylacabenzyl radicals, excited electronic states 0–46576 methylbenzenes, spin-lattice relax time, temp variation minima 0–59469 Methylbromodiazirine, microwave spectrum 0–67804 methylchlorobenzenes, hexasubstituted, higher-order transition by progressive decorrelation of mol. orientations 0–71808 methylchlorodiazirine, ground state rot. spectra internal splittings'and quadrupole coupling consts. 0–77958 methylchlorosilanes, integral intensities of vibrational bands in i.r. abs. bands 0–43181 l-methylcyclopentane, first ionization energies, vibrational structure in first electronic band 0–55346 methylcyclopentane crystalline matrix, fluorescence spectra of trapped radicals from xylenes 0–66102 methylcyclopropyl ketone, microwave spectrum rel. to rot. consts. 0–77929 methyldiacetylene, mol. Zeeman effect and mag. susceptibility anisotropy

methyldiacetylene, mol. Zeeman effect and mag. susceptibility anisotropy 0-77910

methyldiboranes, Raman spectra 0-74376

Trans-methyldimide, microwave spectrum 8.43GHz, rel. to struct, and rot. consts. 0–74387 methyldithiocarbaminate ion and Se analogue, frequencies and vibration forms 0–67790

methylene, CH₂, e.p.r. of triplet state 0–61169 methylene, collision-induced singlet-triplet intersystem crossing 0–72558 methylene, nonlinearity of triplet ground state 0–77920

Organic compounds continued

methylene, triplet and singlet, from photolysis of ketene and diazomethane 0-45086 methylene chloride, rotational diffusion in liquid, from i.r. spectrum

methylene chloride, vacuum u.v. photolysis, i.r. and u.v. study of products 0--76279

methylene fluoride, microwave spectrum, centrifugal distortion and molecular structure 0-46577methylene halides, intensity of v₅ band, connection with induced dipole moment 0--49933

methylenecyclobutane, ring puckering pot. function from mid-i.r. combination bands 0-71014

methylenecyclobutane, ring-puckering potential function from mid-i.r. combination bands 0-43174

methylenecyclopentane, first ionization energies 0-55346

methylenecyclopropane, microwave spectrum, struct., and dipole moment 0-53077

3-methyleneoxetane, ring-bending vibr., from microwave spectrum 0--46574

0–465/4 methyllioride, in liq, crystal, n.m.r., vibr. corrections on dipole-dipole interactions 0–77919 methylliormate + n-alkanes liq. binary systs. 0–46878 2-methylliormate + n-alkanes liq. binary systs. 0–46878 2-methylliormate, dipole moment 0–46572 methyl-4-imidazole, Cl- and SnCls²- salts, i.r. study 0–71012 methyliodide, Λ_o determ. by resonance interactions with v_3 0–61167 β -methylnaphthalene, vibrational assignment of frequencies in i.r. 0–74351 L6-dimethylnaphthalene as loaded liquid scintillator 0–60670

0—74331 1,6-dimethylnaphthalene as loaded liquid scintillator 0—60670 1-methylnaphthalene as loaded liquid scintillator 0—60670 2'-methyl4'- nitroazobenzene-2-sulphenyl cyanide, unit cell dimensions and space group, by X ray diffraction 0—47213 3-methylpentane, luminesc. prod. by electron-ion recombination, at 77°K 0—76161

3-methylpentane/O $_2$ glasses, radical formation in photolysis at $\lambda\!>\!190nm$ $0\!-\!62817$

4-methylphenol in cyclohexane, carbon tetrachloride and p-xylene, dielectric absorption and dispersion 0-74770 N-methylpropionamide, i.r. and Raman spectra and normal vibrs. 0-53075

N- methylpropionamide aqueous solns., structure determ. by n.m.r. 0-71383

methylpyridines, monosubstituted, long range coupling consts. 0-77922 methylpyridines and their n-oxides, C-H out-of-plane vibrations, normal coordinate treatment 0-74383

3-methylsydnone, u.v. spectra and electronic struct. using CNDO method 0-58244

methyltetrahydrofuran, photoconductivity of y-irrad. glass at 77°K 0-79134

0—79134
methylthioethyne, i.r. spectrum and force field 0—77921
methyltriphenylphosphonium, EDR spectra of exciton triplets and param
agnetic impurity centres 0—66146
1-methyluracil, polarized single-cryst, absorpt, spectrum 0—72376
methyoxyacetylene, i.r. spectra and chemical structure 0—74386
mineral oil, ultrasonic wave absorption 0—53337
molecular cryst., second harmonic generation rel. to charge transfer
0—75901 0 - 75991

molecular crystal, Davydov splitting 0–40670 molecular crystal, trapping, centres, origin 0–71909 molecular rot, relax, times meas, from gas thermal transpiration obs. 0-39346

molecular rot. relax. times meas. from gas thermal transpiration obs. 0–39346 molecules, review of electronically excited states 0–58206 molecules containing H₂C= group, CH₂ stretch freqs. separation, correlation with HCH angle 0–46527 molecules with low-freq. vibrs., i.r. and Raman spectra, obs. 0–39362 monobutyl naphthalenes, i.r. spectra 0–39439 monocarboxylic cyclobutane acid, dimer forms and config. 0–74388 monohalo-benzenes, liquid and polycrystalline for i.r. study lattice mechanics 0–74760 monohalogenodiacetylenes, molecular constants 0–55364 monomethin cyanine dye, stearyl substituted and long chain hydrocarbon, 1:1 mixture, Scheibe aggregate formation 0–64499 3-monomethylamino-N-methylphthalimide, in glycerine, isobutanol and propyl alcohol, luminesc., anisotropy, effect of temp. 0–71363 morpholine, microwave spectrum, rot. consts. and quadrupole coupling consts. 0–77930 morpholine-water mixture, u.s. velocity, temp. and conc. variation 0–39784 Mylar, shell, oval cylindrical, axially compressed, postbucking characteris-

Mylar, shell, oval cylindrical, axially compressed, postbucking characteristics 0-40284 n-alcohol+organic solvent mixtures, ultrasonic absorption 0-50221 n.m.r. analysis of coupling constants 0-49940 naphthalene:anthracene, fluoresc., host-sensitized energy transfer 0-76173

0—76173
naphthalene, Gruneisen tensor, 0-300 K 0—40589
naphthalene, conjugated ions, optical absorpt, and e.s.r. spectra, open-shell SCF configuration interaction treatment 0—74390
naphthalene, cryst, juminesc., effects of exciting radiation and of impurities 0—68741
naphthalene, cryst, with impurities, localized excitons, obs. from luminesc, and obs. spectra 0—68740
naphthalene, deuteration eff. on triplet state lifetimes 0—74198
naphthalene, dynamics of opt. electron-spin polariz., from mag, field effects on phosphoresc. 0—58233
naphthalene, electronic states calc. by CNDO/2 CI 0—61145
naphthalene, energy transfer between impurity mols. 0—71931
naphthalene, fluoresc. intersyst. crossing, temp. and matrix effects 0—77934

naphthalene, frozen in diff. solvents, X-ray and photo-excited, radioluminesc. 0-72468
naphthalene, in benzene solution, triplet-triplet absorpt., meas. using laser

naphthalene, intersystem crossing mechanism, effect of deuteration on rate 0-64467

naphthalene, mercapto-derivatives, anions, spectral calcs. by SCF MO CI method $\,0-77923\,$

naphthalene, molecule, ionization pot. and electron affinity, open-shell SCF configuration interaction treatment 0–74390

naphthalene, mononegative ion in DME, proton ENDOR spectra

naphthalene, near i.r. laser Rayleigh scattering, anisotropic component

naphthalene, perdeuterated, quenching of phosphoresc, by paramag, ions

naphthalene, perdeuterated and perprotonated, phosphorescence yields in solvents containing heavy atoms 0-58226 naphthalene, singlet-triplet intersystem crossing quantum yields direct determ. 0-39440

determ. 0-39440
naphthalene, spectral study by flash photolysis 0-77935
naphthalene, spin-orbit coupling and radiative triplet lifetimes 0-67807
naphthalene, vibr. rclax. in S₁ state 0-77878
naphthalene adsorbed on silica gel, p-irrad., e.s.r., radical form. 0-39458
naphthalene adsorbed on zeolite, electronic states from fluorescence and
abs. spectra at 77°K 0-46583
naphthalene anion radical, effect of ion pairing on g value 0-46582
naphthalene cryst., delayed fluoresc. spectrum 0-66108
naphthalene cryst., probability for non-radiational transition between
anthracene and naphthacene 0-69159
naphthalene crystal. B_{RM} exciton band structure determ, within Frenkel

naphthalene crystal, 18 _{2a}, exciton band structure determ, within Frenkel limit 0 –78844 naphthalene crystal, i.r. polarization of translational ray parallel to monochine axis, 6 cm $^{-1}$ 0 –48083

clinic axis, 66 cm⁻¹ 0-48083
Naphthalene crystals, excitons, singlet and triplet interacting with impurity molecules 0-44898
naphthalene crysts, elec. charge effect on evap. 0-71426
naphthalene derivatives, liq. e-irrad., excimer luminesc. obs. 0-46929
naphthalene derivatives with carbonamide group, luminescence excited by u.v. irradiation 0-43176
naphthalene dissolved in various organic solvents, viscosity and solubility parameters in terms of theory of regular solutions 0-46886
naphthalene films, surface coating using spraying technique 0-78385
naphthalene in biphenyl cryst., hindered rotation in vibronic spectra 0-72379

naphthalene in durene cryst., vibronic spectra (${}^{1}A_{18}, {}^{1}B_{20}$) 0–72378 naphthalene in toluene, solns, triplet-triplet annihilation 0–68118 naphthalene ion, use of FEMO theory to calc, transition energies 0–74392 naphthalene single crystal, triplet excitons, e.s.r., 35 GHz, 300 and 100 K

naphthalene single crystals, intrinsic photoconductivity 0-72143 naphthalene single crystals, u.s. attenuation, 15-45 MHz, 23 to -180°C

naphthalene solutions, electronic spectra 0-74394 naphthalene sublimation, mass transfer rates, of vertical vibration

0 76859
naphthalene vapour, electronic relaxation 0-77932
naphthalene- rare gas matrices, Wannier type impurity states and quasifree electron state energy 0-59133
naphthalene-air jet, boundary layer flow mass transfer on deflecting surface 0-50155
naphthalene-anthracene(-d-camphor), binary phase diagrams 0-59060
naphthalene-ds, electronic transitions and polarizability 0-74196
naphthalene-ds, vibrational spectra and assignment 0-77931
naphthalene ds in durene cryst., effect of pressure on phosphoresc.
0-59437
naphthalenes, deuterated, impure vibronic absorpt. 0-48082

naphthalenes, deuterated, impure, vibronic absorpt. 0-48082 naphthalenes, fluoro subst. in alcohols, phosphoresc., at 77°K, non-radiative transitions 0–77936 aphthalenes, substituted, triplet state e.p.r. 0–48155 naphthaltrone, quasi-line spectra in n paraffin matrix, temp. depend.

 β naphthol, vibrational assignment of frequencies in i.r. 0–74351 α -naphthol, vibrational assignment of frequencies in i.r. 0–74351 2 naphthol diethylamine in solvents; proton photo-transfer ionization obs.

naphthol triphenylpyrazoline syst., energy transfer of electronic excitation, rel. to viscosity 0–68111 p.naphtholate dissociation in aqueous soln., fast formation of hydrated electron 0–71378

l- and 2-naphthols, crystalline, i.r. and Raman spectra, lattice frequencies 72381

72381
1,4-naphthoquinone, decomposed fluoresc. 0—74332
1,4-naphthoquinone single crystal layers, vibrational bands assignment, of i.r., spectra 0—51295
N-(β-naphthyl) carbazole, electron spectra 0—43154
naphthyl radical, electronic ground states 0—67765
β-naphthylamine fluorescence lifetimes 0—77933
tri-enaphtylboron, properties as solute in organic liquid and plastic scintillators 0—74391

tors 0–74391 arcissidine, cryst. and mol. struct. 0–53523 neopentane, chem. activated, decomp. rates 0–41448 neopentane, i.r. spectra and internal rotation 0–46584 neopentane, liq., p-induced cond. and ion yields obs. at high electric field strengths 0–68146 neopentane, plastic crystalline, molecular motions study by cold neutron scattering 0–68584 neopentane +0(10₂)-neopentanel or neopentyl radical +OH 0–48181 nickel acctate tetrahydrate, e.p.r., irradiation induced spin pairing 0–62767

nitranilic acid hexahydrate, unsymmetric [H₂O.H.OH₂]⁺ ion obs. 0-65304

0-65304
nitrile mixtures, dielectric relaxation 0-64939
nitriles, aromatic, i.r. bands absolute intensities determ, methods 0-78279
nitriles mixtures, dielec, consts, and losses, meas, at 30° 0-61542
nitriles teritary amines, polarization increment of C-N bond 0-58207
p-nitro aniline, mag, anisotropies and susceptibilities 0-75892
p-nitro phenol mag, anisotropies and susceptibilities 0-75892
nitro pyridine ¹⁴N quadrupole coupling constants 0-55371
4-nitro-pyridine anion, i.r. spectra, 1600 to 1100 cm-¹ 0-77939
p-nitroaniline cyclc, adduct, cryst, struct. 0-78520
p-nitroaniline, calc, interpretation of electronic spectra 0-49934
nitroaromatics, polarization of phosphorescence study by photoselection 0-64533

nitrobenze $-1,\,3,\,5\text{-}d_3$ in liquid-crystal poly- γ -benzyl L-glutamate, 1H and ^{14}N n.m.r. spectra $\,$ 0–74321

Organic compounds continued

nitrobenzene, carrier emission phenomena on metallic electrodes, rel. to electrochemical behaviour 0-68143

nitrobenzene, charge injection 0-68138

nitrobenzene, distortion of high-intensity electric fields, electro-optical obs. and meas. 0-64940

nitrobenzene, fluid instability onset when subjected to unipolar injection between plane parallel electrodes 0-68137

nitrobenzene, ionic cond. 0-53374 nitrobenzene, mobilities of charge carriers 0-71377

nitrobenzene, natural conduction 0-64938

nitrobenzene, natural conduction 0-64938
nitrobenzene, photoconduction and ionic relaxation 0-68145
nitrobenzene, pure, photocond. at 300°C, subject to visible rad. 0-71387
nitrobenzene, small part played by Brownian motion in liquid 0-49913
nitrobenzene, torsional vibration effect on molecular structure 0-70847
nitrobenzene anion, i.r. spectra, 1600 to 1100 cm⁻¹ 0-77939
nitrobenzene-n-anisidine (diphenylamine, diphenyl methane), intermolecular
interactions, u.v. spectra and optical density investig. 0-49951

interactions, u.v. spectra and optical density investig. 0–49951 nitrobenzene-n-hexane soln., acoustic relaxation absorption and velocity meas. 0–64908 nitrobenzenes, deuterium quadrupole coupling consts. 0–53080 nitrobenzenes, fluorinated. ¹⁴N resonance studies 0–67808 nitrobenzenes, monosubstituted, vibrational spectra 0–77937 nitrocellulose, thin foil, heavy ion tracks, electron microscopy 0–60709 nitroethane, microwave spectrum model, dipole moments, rotational constants 0–77938 nitrocethylene, microwave spectra of torsionally excited states 0–77941 nitromethane, liquid or solution, vibration bands width, rotation 0–67809 nitromethane, shock temp. calc. in 100 kbar region 0–64858 nitromethane in liquid-crystal poly-v-berzyl-Leglutamate. ¹⁴H and ¹⁴N n.m.f.

intromethane, snock temp. caic. In 100 kbar region 0-04658 mitromethane in liquid-crystal poly-p-benzyl-L-glutamate, ¹H and ¹⁴N n.m.r. spectra 0-74321 p-nitrophenol cryst. and α -form, products, n.m.r. obs. 0-72519 nitrophenols, N-group vibrations with intramolecular H bond in proton acceptor solvents 0-61172nitrophenylhydrazone a-carbonyls, molecule n.m.r. study of configuration 0-71024

4-nitropyridine N-oxide anion, i.r. spectra, 1600 to 1100 cm⁻¹ 0-77939 4-nitropyridine-nitro-N¹⁵N oxide anion, i.r. spectra, 1600 to 1100 cm⁻¹ 0-77939

nitrosobenzene and its radical anions, pot. barriers and reson. energies

introsuberizene and its radical anions, pot. barriers and reson. energies 0-64532 nitroxide radicals, fluoro-substituted, angular dependence of β -fluorine e.s.r. hyperfine coupling 0-55367 7-norbornenyl radical, e.s.r. spectrum 0-43177 nucleosides, ^{13}C n.m.r. 0-74395 nucleosides, naturally occurring, ^{13}C n.m.r. spectra 0-53078 nucleosides in aqueous in aqueous soln., ^{13}C n.m.r. 0-77947 nucleotides in aqueous in aqueous soln., ^{13}C n.m.r. spectra 0-53081 O-alkyl phosphorodichloridothioates, vibr. spectra 0-53530 octa fluorocyclobutane, i.r. and Raman spectra, assignment of fundamental freqs. 0-74355 octachlorocyclobutane, i.r. and Raman spectra, assignments of fundamental freqs. 0-74355 octalkylporphins, vapour absorption spectra 0-74396 n-octane, positron lifetimes, temp. depend., correl. with viscosity changes 0-74784 octanol, liq, and solid, positronium quenching 0-40633

octanol, liq, and solid, positronium quenching 0-40633 oil, insulating, cond, and breakdown processes 0-64933 oils used in vacuum diffusion pump, spectra, sector field mass spectrometer 0-51872

olefins, simple, photolysis, at 185 and 203 nm 0–79456 optical spectra of doped cryst., orientational impurity vibrs. manifestation 0–76064

optically active molecule origin and development on primordial Earth 0-41476organo-metallics, indirect spin coupling, heteronuclear double resonance 0-61142

organoiron compounds, ¹²¹Sb Mossbauer spectra 0–79265 organoiron compounds Mossbauer effect of ⁵⁷Fe, isomer shifts and quadrupole splittings 0–48029 organoilthium complexes, in aromatic solvents, a.c. conductivity 0–64951 organomercuric compounds, Hg (ch₃)₂ and Hg(CD₃)₂, vibrational spectra 0–67805

organometallic 4f and 5f systems, paramagnetic, temp. dependence of p.m.r. shifts 0-67783 organometallic acetylenic compounds, vapour, liquids and solutions 0-64473

0 64473 organometallic crystals, layered structure, superconductivity 0–65640 organometallic crysts., piezoresistance 0–72126 organophosphorous compounds containing P=O group, effect of solvent on spin-spin interac. consts. 0–43433 organophosphorus, P ions charact. i.r. absorpt. freqs. 0–55369 organophosphorus molecules, 1.f. vibrs., mol. structs. and torsional barriers 0–64530

organotin halide complexes, Mossbauer spectra, origin of quadrupole splitting 0–66013 orotic acid, single crystal irradiated, H abstraction, e.s.r. 0–41354 orthonitrophenol solution, for σ phase identification in CrNiMo steel 0–40462

oxacarbocyanine, spectral sensitization of evap. AgBr layers 0-42402 oxalic acid, vibr. spectra, freqs. assignment 0-49935 ac-oxalic acid dihydrate, electron population parameters by X-ray diffraction 0-46440

oxalyl chloride mean square amplitude of vibration and Coriolis coupling constants 0–58235 oxalyl choride mean square amplitude of vibration and Coriolis coupling constants 0–58235 oxalyl fluoride mean square amplitude of vibration and Coriolis coupling constants 0–58235

constants 0—58235

Oxazole, bond angles by minimizing molecular energies 0—55353

2-oxazoline, structure study from vibr. spectra 0—64534

5-oxibenzodioxane-1,4, hydrogen bonds, n.m.r. obs. 0—55365

α-oxiranic alchohol, effect of pyridine solvent on NMR spectra 0—58502

N-oxyphenazine, disorder diffuse scattering, domains of short-range order 0—53525

N-oxyphenazine- phenazine mixed crystals, short-range order 0-53525 para-azoxyanisole liquid crystal, ¹⁴N n.m.r. obs. 0-61559 1,4-parabenzosemiquinone, hyperfine interactions due to ¹³C 0-61550

paraffin, 8 < n < 16, order disorder, specific heat, entropy, phase transformation 0-78706

paraffin, n slowing down time, obs. 0-49691

n-paraffin frozen solns., concentration depend. of spectra 0-62722

n- paraffin liquids, mobility meas, and charge carrier models 0-64952 n paraffins, Rayleigh spectra, fine struct., gas laser appl. 0-53352 paraldehyde, microwave spectrum 0-61173

penta- and hexadienes, coupling consts. involving methyl protons () 77883

pentacene cryst., abs. spectra, 14000-34000 cm $^{-1},$ at 293, 77 and 20 K $_{0.51289}$

pentachlorophenol, $\alpha \rightarrow \beta$ transformations, diamagnetic susceptibility change 0-68547

pentachlorophenol tributylamine complex, H bonded, dielec. absorpt. study 0--61543

pentachloropyridine, solution and crystalline phases, i.r. and Ruman spectra, assignment proposed 0-64%35 $\alpha,\alpha,2,4,6$ -pentachlorotoluene, rotational isomerism, p.m.r. obs. 0-67810

α, α, 2, 4, 6-pentachlorotoluene, rotational isomerism, p.m.r. obs. 0–67810 pentadeuterotetraphenylgermane, low wavenumber vibrations, i.r. and Raman spectra 0–46592
1,3-pentadiene, trans- and cis-, microwave spectra assignments, methyl group barriers to internal rot. 0–77928
pentaerythritol single crystal, polarized ATR spectra 0–48054
pentafulvalene, open-shell SCF MO calculation of C nuclear cation and anion arrangements, molecular symmetry 0–64510
n pentane, evaporation rates into N₂ in laminar flow system 0–50324
n-pentane, liquid-gas critical point, thermal equation of state, gravitational effect 0–74850
n-pentane solute in n-tridecane, evaporation mass transfer rates into flowing N₂ 0–50325
n pentane-Are Penning mixture, ionization maximization 0–39618
24-pentane-Are Penning mixture, ionization maximization 0–39618

amine), n.m.r. spectra interpretation 0–67838
perchloro[4]radialene, crystal and molecular structure 0–77943

perchlorol4|radialene, crystal and molecular structure 0-77943 perdeuterodimethyl amine, i.r. spectra, vibr. assignments and barrier to inversion 0-70993 perfluoro l-methyl-decalin, electric strength 0-68135 perfluoroalkyl-fluoroaromatic compounds, F-F coupling constants from ¹⁹F nmr spectra 0-64536 perfluoroalkylpolyether, electric strength 0-68135 perfluorocyclobutane, unimolecular decomposition boundary layer effects in shock tube studies 0-76252 perfluorocyclobutanone ketyl, e.s.r., long range fluorine coupling and angular dependence of β-fluorine hyperfine splitting 0-55366 perfluorocyclobexane, solid, multiple pulse n.m.r. spectrum, chem. shift anisotropy absence 0-72503 perfluorodecalin, electric strength 0-68135 perfluorotributylamin, electric strength 0-68135 perfluorotributylamin, electric strength 0-68135 perfluorovinyl sulphur pentafluoride SF₆ mixed gaseous dielectric, patent 0-74681

0-74681

peroxides, thermal decomposition, ¹³C dynamic nuclear polarization

peroxyacetyl nitrate, photochemical formation in polluted air, decomposition i.r. spectral studies 0–70839 perylene, adsorbed on glass, radical cation, p radiation, e.s.r. 0–39933 perylene, vapour, 30 keV inclastic scatt., obs. of excitation levels 0–58250 perylene-iodine charge transfer complexes, crystal growth from solution 0 50450

petroleum, crude, combustion 0-76261 phenanthrene, effect of traps on migration and annihilation of triplet excitation 0-41273

phenanthrene, excited state dipole moments by Stark modulation spectro scopy 0-58237

phenanthrene, excited said op-scopy 0-58237
phenanthrene, fluoresc, and energy transfer processes 0-62729
phenanthrene, perdeuterated and perprotonated, phosphorescence yields in solvents containing heavy atoms 0-58226
phenanthrene, shock wave compression 0-65382
phenanthrene, singlet triplet intersystem crossing quantum yields direct determ. 0-39440
phenanthrene, solubility in compressed gases 0-39666

detern. 0—39440

phenanthrene, solubility in compressed gases 0—39666
phenanthrene, solubility in compressed gases 0—39666
phenanthrene, solubility in compressed gases 0—39666
phenanthrene adsorbed on silica gel, p-irsed, e.s.r., radical form. 0—39458
phenanthrene attached to spirocyclopropane-norbornane frame, energy
transfer 0—77856
phenanthridinium compunds, restricted rotation and magnetic non-equi
valence 0—67812
o-phenanthroline, luminesc., Zn ion influence 0—61174
phenazhydrins, i.r., u.v. and diffuse reflectance spectra 0—55368
phenazine, i.r., u.v. and diffuse reflectance spectra 0—55368
phenazine and N-oxyphenazine mixed crystals, crystal structure at 20°C for
various compositions 0—53524
phenazine dyes near i.r. triplet-triplet absorpt. spectra 0—71044
phenazine-N-oxyphenazine system, variation of physical props. with com
position 0—53407
phenol, and methyl, silyl and germyl derivatives, p.m.r. spectra analysis
0—39444
phenol, mol. struct. and rel. to liq., solid struct. 0—39443

phenol, mol. struct. and rel. to liq., solid struct. 0-39443 phenol and 2,6 disopropyl phenol, i.r. study, OH weak intermol. interactions 0-55395 tions 0-55395 phenol mixed with cyclic ketones shift of hydroxyl group vibration band

0 64538

phenol-carbonyl liq. mixtures, Raman effect studies 0-64925

phenol carbonyl liq. mixtures, Raman effect studies 0—64925 phenolic-nylon char, thermal conductivity, degradation temp, and heating rate effects 0—68662 phenols, biacetyl phosphorescence, fluorescence quenching, solvent effects, mechanism 0—39814 phenothiazine dyes, near i.r. triplet triplet absorpt, spectra 0—71044 phenothiazine dyes, near i.r. triplet triplet absorpt, spectra 0—71044 phenyl, 3-oxy, 1,2-benzofluorenone, in polar and nonpolar solvents, electronic absorption spectra 0—67814 phenyl derivatives of group Vb elements, vibrational spectra in solid state 0—76117

phenyl methyl carbinol, carbonyl groups complexing, solvent effect, i.r. obs. 0-46918

phenyl methyl carbinol, i.r and Raman spectra 0-58252 phenyl radical, electronic ground states 0-67765 phenyl rings in ligands of paramagnetic complexes, 'anomalous' spin den sity distribution 0-58238 phenyl salicylate, crystallization, non uniform temp. field of melt 0-65172 Organic compounds continued

9 phenyl thiaxanthyl radical, evidence of restricted rotation from e.s.r. spec 0-67811

phenyl benzyl nitroxides, solvent induced conformational kinetics, study by e.s.r. 0-55281

phenylamine, adsorbed on glass, radical cation, v radiation, e.s.r.

0 399.33
2-(N phenylamino)pyridine, fluorescence 0—77899
phenylarsenic halides, i.r. and Raman spectra 0—71006
phenylarsenic, vibrational spectra 0—74400
4 phenylazo-1-naphthols, in benzene and dioxane soln, dipole moments
and struct. 0—645.37
4 phenylbenzophenone vapour, prolonged luminesc. 0—67771
phenyldichloroapsine, vibrational spectra 0—74399
phenyledichloroapsine, vibrational spectra 0—74399
phenyledidimine derivatives, laterally substituted, two phases with nematic
morphology 0—64871
p phenylenediamine substituted derivatives, inverse relationship between
development rate and developer concentration 0—70119
5 phenyl 2-pentene, intramolecular energy transfer 0—72552
phenylphosphine, vibrational spectra 0—74400
phenylphosphine d₃, proton and deuteron mag. reson., liq. cryst. solns.
0—53082
phenylsilane-d₃, proton and deuteron mag. reson., liq. cryst. solns.

phenylsilane-d₃, proton and deuteron mag. reson., liq. cryst. solns. 0-53082

phosphorescence, laser-induced 0–39404
phosphorous cpds., 'K_{pc} signs 0–39445
phosphorous oxyhalide derivatives, Urey Bradley force consts. 0–70943
phosphoryl absorption band intensities 0–71026
photocathodes with organic coatings for vacuum u.v. region 0–62473
photochromic nitrocompounds, electronic struct., absorpt. bands 0 53079

photoconductivity response curves behaviour 0-62458

photoeconductivity response curves behaviour 0-62458 phthalamide derivatives, lasing threshold and the quantum yield of the fluorescence of organic phosphors, relationship 0-60220 phthalamides in glycerine solvent, relationship between luminescence and absorption at low temp. 0-53053 phthalimide, solns., fluoresc, and obs. spectra, effect of temp. 0-68119 phthalimide derivatives, in non polar solvents, effect of O₂ and water admix tures on luminesc. 0-68120 phthalimide derivatives in solns., native of long-wavelength centres 0-50239 phthalimide generation by lamp excitation 0-73233

0 N0239
phthalimide generation by lamp excitation 0-73233
phthalimide solns, induced radiation polarization 0-43463
phthalimides, fluorescence polarization 0-50244
β phthalocyamine, bulk trapping states in single crysts. 0-40780
phthalocyamine, and metal derivatives, far i.r. spectra 0-74398
phthalocyamine, metal derivatives metal-ligand vibrations in i.r. spectra
0-74307

0 14.337 phthalocyanine, metal free cryst., charge carriers transfer integrals 0 3.76.3

0.33763 phthalocyanine, semiconductor, elec. props. in ferroelec. state 0—44371 phthalocyanine crystal, excitons, photoeffect, temp. depend. 0—79085 phthalocyanine film, nonequilibrium admittance 0—65679 phthalocyanine film, photocurrent decay, lux ampere characts., quasiconti nuous spectrum of levels 0—40899 phthalocyanini, film photo electric effect, quantum yield 0—79067 picoline, Raman spectra, intermolecular interactions for picoline dissoved in water, ethanol and methanol 0—64926 piputacione, r.m.r. spectral parameters and ring interconversion 0—74401 pivalic acid, high temp. rotator phase, self-diffusion and plastic flow study 0—68328 0 68328

polar liquids, yields of ions and excited states produced on radiolysis

10 725.59

polar liquids in dilute benzene solution analysis of Gopala Krishna's method for dielectric relaxation time 0-649.32
polar mol. cryst., energy of intermol. interaction 0-65114
polyarylenes-eyanoethenylenes mol. strict. rel. to optical props. and photo cond. 0-49949
polyenes, self consistent theory of bond alternation 0-64539
polyethylene, black, optical properties from 3 to 4000 cm⁻¹ 0-44742
polyethylene neutron backscattering by 0, 20, 40, 60 and 80° for semi infinite thickness 0-45972
polymethine dye solns, emission on pumping by Ne glass laser 0-49063
polymethine dyes, generation and spectral characts. 0-61523
polyparaaminostyrene, relationship between far i.r. absorption and electrical conductivity 0-64463
polysaccharide, natural, elementary fibrils, chain arrangement 0-47214

cal conductivity 0-64463 polysaccharide, natural, elementary fibrils, chain arrangement 0-47214 polysaccharides, microstructure, conformations, chain folding, fibril struct. 0-47211

polystyrene polybutadiene/toluene, presence of lamellar structure 0 58552

polyvinylidene fluoride, dielectric relaxation and molecular motion 0-75777

porphins with cyanine dyes on methine linkage, excitonic interactions 0.74403

porphyrin, solid-state phenomena, possible superconduction 0–75539 porphyrin molecules, nonradiative transitions 0–58239 porphyrins, mechanisms of fluorescence quenching 0–67816 porphyrins, search for in lunar samples by fluorescence activation 0–45402

porphyrins, vibr. struct, of electronic spectra, using quasi-linear spectral method 0-67815

method 0-67815
porphyrins in lunar samples, search for 0-48549
positron annihilation, time-spectrum long-lived component lifetimes and intensities 0-40692
potassium acid phthalate, cryst. growth and testing for X-ray spec trometer 0-65168
potassium acid phthalate crystals, X-ray spectra 0-69144
potassium acid phthalate crystals, X-ray spectrometric characteristics 0-78420

potassium oxalate monohydrate, pulsed deuteron n.m.r., hindered rotation of H₂O 0 -66157

or H₂O 0-66137
propane, clathrate hydrate, p.m.r. study of motion 0-64540
propane, ir. spectra and internal rotation 0-46584
propane, isotherms to 10 kbar 0-64812
propane, methyl libration meas, by neutron inelastic scatt. 0-43178
propane bubble chamber, track density relativistic increase meas.
0-46062

propanes, substituted, n.m.r. study of rotational isomerism and harriers to internal rotation (0-6779)

propanol water system, proton exchange n.m.r. determ. 0 66166

propargyl mercaptan, microwave spectrum vibrational transitions of torsion mode 0 - 6454)

2 propen I of and 2 propyn I of, fiquid, disless, props. 0 58493 propens, photoiomization yields and absorption cross sections, isotope effects 0 70964

effects 0 70964
prophyrm, mol energy, fluoresc. 0 67779
prophyrm, mol energy, fluoresc. 0 67779
prophonic scid indical in signostic, e.s.r. spectra 0 43196
prophyrm, mol energy temp. 0 70965
propyl alcohol, microwaye spectrum 0 53083
propyl addide, normal, microwaye spectrum rel, to rotational isomers
0 77947
propylene, deuterated, rot. spectra, internal rot. of asymmetric top
0 64541

, internal rotation and electronic struct., CNDO INDO cale propylene, 0 77944

propylene carbonate, equilibrium, dielectric permittivity density and refractive index 0 61544
propylene oxide, n.m.r. 0 64503
propylenes, deaternated, suprour pressure 0 39894

propyne, elec. polarizability anisotropies from microwave spectroscopy 0-70923

propyns, photonomization yields and absorption cross sections, isotope effects () 70964

parme, subst. derivatives, spin orbit coupling induced by \$ atoms () 77946

pyrazine crystal, electronic absorption spectrum, Zeeman effect study 0-76118

0.76118
I pyrazoline, i.r. and Raman spectra, vibr. anal. 0.67785
I pyrazoline, vibr. spectra and ring puckering. 0.58240
pyrene, binderlyl phosphorescence quenching, solvent effects, physical energy transfer mechanism. 0.39814
pyrene, cryst., polarized absorpt, and fluoresc spectra. 0.76119
pyrene, sensitized fluorescence, energy transfer study. 0.72429
pyrene, shock wave compression. 0.65382
pyrene, transferability of simplified vidence force field. 0.74404
pyrene transferability of simplified vidence force field. 0.74404
pyrene single crystals, triplet excimer emission. 0.41274
pyrene d.10, c.s.r. relaxation, temp. dependent measurements on excited triplet state. 0.41394
pyrenyt indical, electronic ground states. 0.67765
pyridine, deform, vibr. freqs., solvent influence. 0.61155

pyrentyl indical, electronic ground states 0, 67765 pyridine, deform, whr. freqs., solvent influence 0, 61155 pyridine, derivatives of raman intensities and depolarizations w.r.t. electro-optical parameters, computer calculation 0, 46585 pyridine, high field linear and quadratic Zeeman effect 0, 46586 pyridine, matrix isolaticd, pair assoc., obs. 0, 71027 pyridine, mercapto derivatives, amons, spectral calcs, by SCF MO CI method 0, 77923 pyridine, tratational Brownian motion from the width of substational brownian motion from the substational forms and the substational from the substational forms and the substational forms and the substational forms are substational forms.

2 pyridthiones p.m.r. spectra study, proton coupling constants, chemical shift 0 35370

shift 0.354/0
2 pyridylphosphine derivatives n.in.r. spectra, coupling constants and energy level diagrams 0.49936
pyrimidine, intercapto derivatives, anions, spectral cales, by SCF MO CI method 0.779.23
pyrimidine, interowave spectra, dipole moment, nuclear quadrupole coupling consts. 0.779.49
pyrimidine, substituted derivatives, spin orbit coupling induced by S atoms 0.779.46
pyrimidine, substituted derivatives, vibrational spectra. 0.74405
pyrimidine, substituted derivatives, vibrational spectra. 0.74405
pyrimidine, substituted derivatives, vibrational spectra. 0.74405
pyrimidine, substituted derivatives, vibrational spectra. 0.74000
0.68108

0 68108

N pyrrole, 100 MHz p.m.r. spectrum, sub-spectral analysis 0 71029
pyrrole, bond angles by minimizing molecular energies 0 55353
pyrrole, rot, fire struct, of NH stretching band 0 77948
pyrrole film, i.r. absorpt, spectrum in polarized light, surface forces effects
0 41234

6 34.234 pyrrole mol., all electron SCF LCAO MO wavefunction 0 39451 pyrrole pyridine hyd., dielectric abs. meas., relaxation processes 0 71.369 pyrrole 2 carboxylic acid pyrrole 2 addehyde, n.m.r. 0 71028 pyrrold 2 ones, optically active crysts, atomic parameters 0 75116 pyrroldide, i.r. and Ruman spectra, vib. mal. 0 67785 quasilment luminese, spectra, impurity centres interaction with environment 0 72410 quindimethanes, n.m.r. spectra 0 43.179 guinoidmethanes, n.m.r. spectra 0 43.179 guinoidmethanes, n.m.r. spectra 0 43.179 guinoidmethanes, n.m.r. spectra 0 43.179 quinoidme, vibr. apectra and assignments 0 64543 quinoline, vibr. apectra and assignments 0 64543 quinoline, vibr. spectra and assignments 0 64543 quinoline, processed as a spectra and assignments 0 64543 quinoidme, processed as a spectra and assignments 0 64543 quinoidmes, hydrated, internal interactions on the basis of absorption spec-

quinolines, hydrated, internal interactions on the basis of absorption spec-tra 0 53084

tra 0 5 3084 quinone crystas, electron injection 0 59.284 quinone crystas, electron injection 0 59.284 quinones, ortho and para, dipole moment calculations, electronic structure by improved LCAO method 0 58.242 quinoxaline, T. So phosphorescence, radiative decay rates of zero field levels of triplet state 0 465.87 quinoxaline, intersystem crossing quantum yield, evidence for high yield of mermal conversion of first excited singlet state to ground state 0 74407 Ramma spectra of liquid solid critical phenomena 0 748.32 Ramma spectra of liquids, energy determ. first Stokes' components 0 19798

1979 reare earth ion aromatic acid complexes, charge transfer bands 0 - 61532 resins, epoxy, assessment as model materials for three dimens, photoelastic ity 0 - 42043

rhodamine, 6G and B, in solvents, effective temp, of luminesc, centre 0 66107

Organic compounds continued

rhodamme 6G dye, long pulse later emission, cyclooctatetraene quenching 0.42284

rhodamne 6G in alcohol solns, under pulsed excitation, effect of induced losses on duration of stimulated emission. 0.42285

rhodamine 6G in glycerol, ultrafast intermolecular electronic energy transfer (0-64576)

rhodamme 6G laser, in aqueous soln. 0 77108

rhodamine 6Zh stimulated radiation due to single and two photon excita-tion cross section 0 -68121

rhodamine derivatives, fluoresc, and obs. spectra, effect of temp. 0 68119 rhodamine derivatives, lasing threshold and the quantum yield of the fluorescence of organic phosphors, relationship 0 60220

rhodamine dye, abs. spectra and luminese,, during interac, with polyanions 0. 68116

rhodamine dyes, associative luminese, at room temp. 0 68114 rhodamine dyes, effect of infromolecular charge transfer on electronic spectra and fluorescence 0 67818

rhodamine dyes, luminescent associates, abs. spectra = 0 = 39446 6ZR rhodamine in ethyl alcohol, laser, operation energy, temporal and spectral characteristics = 0 = 67090 rhodamine lons, excess, effect on luminescent characteristics of Cr(III) complexes = 0 = 67729

complexes 0. 67129

rhodamnes, L-aspectra, mutual influence of functional groups 0. 77950

rhodamnes, L-aspectra, mutual influence of functional groups 0. 77950

rhodamnes, L-aspectra, mutual influence of functional groups 0. 77950

riboflavin, polarized phosphorese, spectra at 77°K 0. 72448

ring compounds, eight, mol. g values, ring, susceptibilities and mol. quadrupole moments 0. 77892

Rochelle Salt crystal growth, undergraduate project 0. 76134

saccharin, Ni electroplating, rel. to recrystallization temp. 0. 47432

salicylaldazinate metal chelates, preparation and i.r. spectra 0. 71036

salich, undergooled, electro-nucleation 0. 61739

santowax, n slowing down time, obs. 0. 49691

samidium neetylacetomates, cryst. struct. 0. 55866

schilllator solutions, R. x. R. 1ype (Re-aryl group, x-oxanzole, oxadiaz ole ring) 0. 39806

schilllators, response data for anthracene, stilbene, NE 213 and Pliot B,

scintillators, response data for anthracene, stilbene, NE 213 and Pilot B, analysis 0 42630

analysis O 42630 semillators for Nd¹¹ glass and N₂ high repetition rate lasers, generation in u.v. region O 38506 selemi oxit cymnia, elec. dipole nature of phosphorese. O 79373 selemicyclopentiane, i.r. and Raman spectra, vibr. anal. O 64544 selemides, dialkyl and diphenyl, Se and proton n.m.r. O 77951 selemium cpds., K_{pri} signs O 39445 selemium dialkylamino compounds, i.r. and Raman spectra force constants

selenium dialkylamino compounds, i.r. and Raman spectra force constants () 46/38 semiconductor, high, regeneration of current carriers () 55622 semiconductor, photosensitivity enhancement () 51445 semiconductor, photosensitivity enhancement () 51445 semiconductor, photosensitivity enhancement () 51445 semiconductors, photosolinic effect wavelength depend. () -72145 semiconductors, binary complex type with charge transfer () 40754 semiconductors are spin lattice relax, time, obs. () -41322 siliacyclobitanes, vibrational spectra, normal coordinate analyses () 46/590

0 46590 subject 2 ene, ring puckering pot, from far i.r. spectrum 0 71032 subject 2 ene, ring puckering pot, from far i.r. spectrum 0 71032 subject 2 ene, restricted of Cie, surface props. 0 40800 subject 2 ene, constants 0 58607 subject 2 ene, constants 0 46589 subject 2 ene, constants 0 46589 subject 2 ene, convection, natural and cellular structure in a cylindrical cell for two different fluids heated from below 0 60080 subject 2 enemals, force constants 0 4659 elements, force constants

nily1 and trimethylsilyl compounds of group 5 elements, force constants 0 46591 advances force constants and Corrolis coupling consts. 0 74323 sodium humate fraction, molecular size determ. 0 69280 sodium hydrogen oxalate monohydrate, crystal structure 0 50563 sodium rubidium tartrate tetrahydrate, ferroelec, phase existence 0 68955 solid, carrier generation yield under electron bombardment 0 62252 solid, carrier generation yield under electron bombardment 0 62252 solid services of a peetrum 0 67089 solitions, semililation, triplet interactions 0 78287 solvents, acronol growth determination, gravinetric method 0 41494 sorption on W, Pt. Kinetics, obs. 0 56693 spiriteria method intercoisomers, monocation struct, from i.r. spectra 0 64545 squalane, thermoluminescence glow curve peaks rel, to phase transitions 0 54130 sterrate multihyers, heavy ion, X ray diffr. 0 50492

o 54140 sterrate multilayers, heavy ion, X ray diffr. 0 50492 steroidal androstane, A and D ring substituted, n.m.r. C 18 and C 19 methyl group protons 0 67819 steroida situeture using ¹⁴C magnetic resonance 0 64546 stilbene, analogues, durk conductivity, effects of donor and acceptor groups 0 65653 stilbene, in diphenylacetylene and dibenzyl, obs. spectra and fluorese, at low temp. 0 68108 trans stilbene crystal, absorpt, and fluorescence spectra 0 62682 stilbene similation counter proton recoil application to fast neutron spectrometry 0 49374 stilbite metastilbite crystalline transf., parameter determ. 0 75345 strontium tarteate transition elements, e.p.r. 0 41343 styrene, vibration spectra 0 64547 styrene da, vibration spectra 0 64547 styrene da, vibration spectra 0 64547 succinic acid, ENDOR of anions in irrad, crysts. 0 41351 succinic acid, ENDOR of anions in irrad, crysts. 0 41351 succinic acid, is struct, and initial component study leg infrared meas.

succinimide, struct, and initial component study leg infrared meas. 0 58243

o 35243.

succinontirile, high temp. plastic phase, self-duffision study 0 68329 succinontirile, mol. cryst., Bullouin and Rayleigh scatt. 0 59417 succinontirile, self-diffusion, n.m.r. study 0 50630 sucrose, aqueous solise, sonoluminescence study 0 61535 sucrose, crystal growth rate, habit, adsorbed impurity effects 0 74989 sulphonylamines, halogen substituted molecules, vibr. spectra, force consts. and struct. 0 53085 and struct. 0=53085 sulphur dialkylamino compounds, i.r. and Raman spectra force constants 0=46588

sulphydryl compounds, reaction with organic free radicals in c.p.r. 0 692 0

superconduction possibility, inclastic electron scattering obs. 0-75430 superconduction possibility, struct, considerations 0-75599 superconduction possibility 0-75597

superconduction possibility in π -electron system, many-body methods applie. 0-75598

superconductor, exciton mechanism, model epds. 0 -75596

superconductor, exciton mechanism 0-75595

superconductors, biosynthesis 0-75633

superconductors, conf. Honolulu, USA, Sept. 1969 0-75632

surface tension of binary solns., Shereshefsky's eqn. appl., obs. 0-55601 sydnone, u.v. spectra and electronic struct, using CNDO method 0 58244

TCNQ film, photocond. spectral response 0 59286

ditartaric acid, deuterated, at 195°K, c.s.r. 0 76229

tartaric acid solns., e.p.r. during photolysis, emission spectrum 0-62823

tartare acid solns, e.p.r. during photolysis, emission spectrum 0–62823. Teflon coating on stainless steel, pool boiling heat transfer 0–3988. terephthal bis (4-n butylaniline), liq. cryst., smeetic C phase, temp. dependent tilt angle 0–71312 terpenes, n.m.r., natural abundance ¹³C spectra 0–53086 p terphenyl, cryst., scintillation, dl.anneling effect by α particles, at T 300 and 80°K 0–59444 p terphenyl, crystal structure, X ray and neutron diffraction refinement 0.6.1039.

0 61928

p-terphenyl, monocryst., a channeling, Ear-879 MeV, by transmission expt. at T=130K 0-59120 terphenyl, mononegative ion in DME, proton ENDOR spectra 0-64531

terphenyl, mononegative ion in DME, proton ENDOR spectra 0–64531 p terphenyl, phonon spectra by Raman spectroscopy 0–78741 p terphenyl as extreme uv. detector 0–60393 p terphenyl fluoresc, and energy transfer processes 0–62729 tert butyl amine, effect of viscos, on dielectric relax, time 0–64941 tertiary amines, polarization increment of C N bond 0–58207 tertiary butyl acetylenes, vib. spectra and force consts. 0–77859 tetra cyano ethylene (TCNE), molecular constants 0–55331 tetra-N-methyl phenylenediamine, adsorbed on glass, radical cation, p radiation, e.s.r. 0–39933 tetra-n butylammonium bromide, u.s. absorption in aq. soin. 0–53346 1,1,2,2 tetrabromoethane, vibrational spectra and internal rotation 0–77953

tetrabutyl ammonium bromide, aqueous solutions, u.s. relaxation 0.53342

tetracene, exciton surface reaction at electrolyte interface, photocurrent obs. 0- 75839

obs. 0-75839
tetracene, mononegative ion in DME, proton ENDOR spectra: 0-64531
tetracene crystal, delayed fluorescence, triplet lifetime: 0-44917
tetracene crystal, exciton fission and flusion, coexistence: 0-44916
tetracene film, photoconductivity, effect of mag. filed: 0-51153
tetracene single crystal, photo-enhanced currents, anisotropy in mag. filed offeets: 0-47881
tetracene use of FEMO theory to calc. transition energies: 0-74392
1,2,4,5-tetrachlorobenzene, absorption, fluorescence and phosphorescence spectra, 42K: 0-72441
1,2,4,5-tetrachlorobenzene, inclusic in seatt,, cryst. excitations: 0-59090
1,2,3,4-tetrachloro-5,6-diphenylcalicene, cryst. and mol. struct. 0-55867
tetraceteracontane, x-ray diffraction maximum as function of temp. 0-65302
s-tetracyanobenzene, laser excitation of EDA complexes, fluorescence and

s-tetracyanobenzene, laser excitation of EDA complexes, fluorescence and absorption spectra 0~72440 tetracyanoethylene, adsorbed on glass, radical anion, y radiation, c.s.r. 0~39933

tetracyanoethylene isomeric π mol. complexes, electronic spectra 0 71034

tetracyanoquinodimethan, conductivity and photoresponse 0-59285

tetracyanoquinodimethan radical anion ammonium salts relationship bet ween far i.r. absorption and electrical conductivity 0 -64463 tetracyanoquinodimethane, As TCNQ, P TCNQ crystals, surface elec. pot. 0-75720

pot. 0-15/20 tetracyanoquinodimethane, As TCNQ and P TCNQ, thermoelec, power anisotropy, in (100), 200 400K 0-79066 tetracyanoquinodimethane, electron electron double resonance of triplet excitons 0-66145

excitons 0 661457 7,7,8,8 tetracyanoquinodimethane (TCNO) and TCNQ da crystals, i.r. and Raman spectra 0-55373 tetracyanoquinodimethane polassium, e.p.r. absorpt, signal anisotropics rel. to temp. 0-41355 tetracyanoquinodimethane salt, Hall effect, thermoelec, power, card 0-78959

7,7,8,8-tetracyanoquinodimethane solubilized in surfactant solns., colour

0. 78959
7,7,8,8-tetracyanoquinodimethane solubilized in surfactant solns., colour changes 0.-74762
tetracyanquinodimethane, FDR spectra of exciton triplets and paramage netic impurity centres 0-66146
tetradeuteroethylene molal volume meas, in range 105 175°K 0-74731
tetraethylammonium bromide, u.s. absorption in aq. soln. 0.-53346
tetraethylammonium ion, effect on Zn electrodeposition, aqueous KOH, dendritic growth 0-72550
2,3.5,6-terafluoroaniline, n.m.r., aromatic H-P and F P coupling constants, relative signs 0-46443
1,1,2,2-tetrafluoroethane, n.m.r. spectrum and rotational isomerism 0-49938
1,1,2,2-tetrafluoroethane, vicinal coupling constants 0-67792
tetrafluoromethane, vicinal coupling constants 0-67792
tetrafluoromethane, acoustic velocity, for isotherms from 1 to 70 atm., interaction potential force constants 0-68017
tetrafluoromethane, neat capacity, 2 20K, phase transformation 0-43914
tetrafluoromethane, nuclear magnetic relaxation and molecular motion in solid 0-56466
tetrahydrofuran, i.r. band absolute intensities, expt., theory 0-39448
tetrahydrofuran, i.r. band absolute intensities, expt., theory 0-39448
tetrahydrofuran, i.r. band absolute intensities, expt., theory 0-39448
tetrahydrofurane-chloroform, heat of mixing 0-66172
tetrahydrofurane-chloroform, heat of mixing 0-66172
tetraiodecthylene solid and in CS, solm, Raman and ir. spectra 0-64548
N,N,N,N tetrakisfdimethyl aminojethylene, chemiluminescent aerosol, patent 0-43491
tetramethylammonium bremide, p.m.r. and mol. reorientation, 100-400°K
0-49931

tetramethylammonium bromide, p.m.r. and mol. reorientation, 100-400°K 0-49931

tetramethylammonium chloride, p.m.r. and mol. reorientation, 100-400°K 0-49931

tetramethylammonium dithioorthoniobate preparation and determ, of symmetry of Nb₂S₂3 · 0-61686

tetramethylammonium iodide, p.m.r. and mol. reorientation, 100 400°K () 49031

Organic compounds continued

tetramethylphenylenediamine TCNQ complex, c.s.r., spin excitations of Heisenberg linear chain 0-41356

tetramethylsilane, chem, activated, decomposition rates 0-41449

tetramethylsilane, integral intensities of vibrational bands in i.r. abs. bands

tetramethylsilane, liquid, electron mobilities 0 46949 tetramethyltitanium, vibrational specira and force consis. 0 7103.3 Tetranonaeontane x ray diffraction maximum as function of temp 0 65302

tetraphenyl p xylene dichloride and zinc dust nature of radical formed 0 43193

tetraphenyldiphosphine, u.v. irrad., c.s.r. 0 76280 tetraphenylgerinane, low wavenumber vibrations, i.r. and Raman spectra 0 46592

tetraphenylporphin, halo derivatives, fluorescence yield with increase of halogen atomic number 0. 67820 tetrathiotetracone films, photoelectron emission, surface state influence 0. 44442

tetrathiotetracene thin layer systems electrophys, and photoelec, props 0.44402

tetrathotetracene thin layer systems electrophys, and photostee, props 0. 4351.4 thallium acetate water binary system, liquid solid phase aquilibrium diagram crystal structure. 0. 78335 thallium acid phthalate, cryst. growth and testing for X-ray spectrometer 0. 65164. 1.3.4 thiadiazoles, absorption spectra in near i.r. 0. 58749 thiazole, deep, abs. spectra and luminese, during interac, with polyanions 0. 68116. 2.4 thiazoleidiadione, i.r. spectra, calc., normal frequencies. 0. 39449 thiazoles, n.m.r., of "C, chemical shift 0. 58747 thiazoldine, i.r. spectra of 2. and 4 thioderavitives, deformation and vibrations. 0. 61176. A 2 thiazolie, chemical shift of "C determ, by NMR 0. 58248 tri. 2 thienylphosphine, "H n.m.r., obs., rel. to "H "P coupling constant determ. 0. 39450 tri. 3 thienylphosphine, "H n.m.r., obs., rel. to "H "P coupling constant determ. 0. 39450 tri. 3 thienylphosphine, "H n.m.r., obs., rel. to "H "P coupling constant determ. 0. 39450 tri. 3 thienylphosphine, "H n.m.r., obs., rel. to "H "P coupling constant determ. 0. 39450 tri. 3 thienylphosphine, "H n.m.r., obs., rel. to "H "P coupling constant determ. 0. 39450 tri. 3 thienylphosphine, "H n.m.r., obs., rel. to "H "P coupling constant determ. 0. 39450 tri. 3 thienylphosphine, "H n.m.r., obs., rel. to "H "P coupling constant determ."

determ. 0 39450

tri 2 thienylphosphine, ¹H n.m.r. obs. rel. to ¹H ¹P coupling constant determ. 0 39450

thietane, n.m.r. analysis of coupling constants. 0 49940

thin films, low energy electron diffraction. 0 74890

thionectanilides, substituted, investigation of cis trans isomerism by nm and i.r. spectroscopy. 0 64550

2 thionkylpyridines p.m.r. spectra study, proton coupling constants, chemical shift. 0 - 55370

thiobenzophenone, 6500 Å transition. 0 - 61175

thiodiglycolic acid, ENDOR of anilons in irrad, crysts. 0 - 41351

thioformaldehyde, interstellar, search for Γ_{ps. 1,1} transition. 0 - 72741

thioformaldehyde microwave detection. 0 - 71035

thiohydantoin, i.r. absorpt, spectra, vibration frequencies, calc. 0 - 46594

thionaphthene, π + π * transition, hybrid character and rotational structure. 0 - 74411 thionaphthene, absorpt, spectrum of 0.0 band, and excited state rot, con-

thionpartners, assorpt, spectrum of 0.0 band, and exercit state for constants, 0.71036.

Thiophene Hammett linear free energy relations tested 0.51449.

Thiophene and thiepine derivatives, SCP MO treatment 0.53088.

Thiophene derivatives, C. H. out of plane vibrations, from force constants, 0.46594.

0. 46594 thiophenes, 2 substituted, i.r. spectra 0. 74410 thiophenes, monosubstituted, ¹C n.n.r. 0. 77954 thiophene (4.5 c) and thiophene (4.5 b) tropones, electronic structures 0. 64549

thiophenol, and methyl, silyl and germyl derivatives, p.m.r. spectra analy sis 0 39444

als 0. 94444 hiophosgene, Zeeman effect in visible spectrum, 5496Å band 0. 58246 thiophosgene, Zeeman effect in visible spectrum, 5496Å band 0. 58245 thiopycanyl 1,1 dioxide anion and related species, p.m.r. spectra 0. 67821 thiosemicanbazide, hydrogen bonding, X ray diffi. 0. 71599 thiosaphosgene, and polymer species, Raman and Lr. spectra 0. 55374 hioureal, seric effects in u.v. and Lr. spectra 0. 53087 thiourea, cryst. struct., phase IV 0. 68372 thiourea, pasted phase transitions mechanism 0. 78747 thiourea, pasted phase transitions mechanism 0. 68956 thiorea, steric effects in u.v. and Lr. spectra 0. 53087 thiourea, posteric effects in u.v. and Lr. spectra 0. 53087 thiourea, paste in u.v. and Lr. spectra 0. 53087 thioxanthone anion radicals, e.s.r. 0. 67788 three membered ring molecules, LCAO SCP MO calculations for ground state 0. 43443 state 0.43143
(hymidine, e.p.r. of radiation damaged deuterated cryst. 0.59461
(hymidine, e.lectronic structure 0.55375
o-m-and p tolialdehydes emission spectra 0.61177
toliuene, Brillouin scatt., undergradiate expt. 0.44873
toliuene, Rhyleigh and depolarization ratios 0.64918
toliuene, dielee, secondary dispersion, Lorentz resum model 0.43467
toliuene, gas phase absorption spectra and decay 0.70975
toliuene, hq., Lf. Rammi lines in depolarized Rayleigh wing 0.61324
toliuene, whr. relax: in 5, state 0.77878
toliuene, whr. relax: in 5, state 0.77878
toliuene, who, relax in 5, state 0.77878 0 43143

toluene, vibr. selection rules 0 - 53089 toluene spherical cage model for relationship between compressibility and solubility 0 - 46880 toluene methylcyclohexane system, diffusion coeff, meas, using birefringent interferometry 0 - 71330 toluene, cryst. struct. 0 - 7195; toluquinone, cryst. struct. 0 - 65305 p toluquinone, cryst. struct. 0 - 65305 p toluquinone, triplet singlet nor luminesc, polarization 0 - 79358 toluquinone, triplet singlet nor luminesc, polarization 0 - 79358 p toluquinone, triplet singlet nor luminesc, polarization 0 - 79358 toluquinone, triplet singlet nor luminesc, polarization 0 - 79358 p toluquinone, triplet singlet nor luminesc, polarization 0 - 79358 p toluquinone, triplet singlet nor luminesc, polarization 0 - 79358 p toluquinone, triplet singlet nor luminesc, polarization 0 - 79358 p toluquinone, triplet singlet nor luminesc, polarization 0 - 40110 transformer oii, pre breakdown conduction current pulses, nanuniform field, press, effects 0 - 53623 translational and vibrational energies exchange efficiencies, velocity dispersion analyses 0 - 53098 transparent, dendrite formation, obs. of initial stages 0 - 50476 tri 2 thienylphosphine and derivatives, "H * 11P * spin coupling constants 0 - 67822 tri 3 thienylphosphine, and derivatives, "H * 11P * spin coupling constants |

tri 3 thionylphosphine, and derivatives. 'H "P spin coupling constants 0 67822 tri n butylstannane, biacetyl phosphorescence, fluorescence quenching, solvent effects, 11 abstraction mechanism 0 39814

triafulvalene, open-shell SCF MO calculation of C nuclear cation and anion arrangements, molecular symmetry 0-64510

13,5- triamino -2,4,6- trinitrobenzene, neutron spectra and vibrational assignments 0—64551 triarylborons, u.v. absorpt. spectra 298° and 77°K 0—64480

triarylmethyl radicals, e.s.r. spectra 0-43185

1,2,3-triazole spectra assignment, by microwave double reson. 0-55376

1,2,3- and 1,2,4-tribromobenzene, n.m.r. 0-74345

1,2,3-trichloro 4,5,6-trimethylbenzene, order disorder orientation transition 0-59047

trichloro silyl compounds, nmr spectra, chemical shifts, coupling constants

2,2,4- trichloro-4,6,6-trisdimethylaminocyclotriphosphazatriene 0-78524 1,3,5-trichlorobenzene, lattice modes and temp. depend. of optical modes 0–78396

1,3,5-trichlorobenzene, temp. depend. of Cl pure quadrupole reson. 0 - 46597

trichlorodiphenyl, dielectric loss at elevated temp., effects of polypropylene

0–68134 trichloroethylene, band intensities and atomic polarizations 0–39405 trichloroethylene, band intensities and atomic polarizations 0–39405 trichlorofluoromethane, SN2 substitution reaction F⁻+CH₃F→FCH₃+F , activation energy 0–45045 trichlorofluoromethane, liquid, Raman spectra, effect of intermolecular interactions 0–43460 trichloromethyl fluoride, dipole moment from pressure-broadened microwave spectra 0–61179 2.3.4-trichloronitrobenzene, homonuclear double reson., relax. mechanisms 0, 41302

2,3,4-trichloronitrobenzene, homonuclear double reson., relax. mechanisms 0–41392 trichlorophosphazosulphuryl chloride, n.q.r. ³⁵Cl spectrum 0–55343 tricyclopropylborane, n.m.r. spectrum, correlation between coupling constants and substituent electronegativities 0–43184 trideuterioacetonitrile, luminesc., low temp. 0–70963 triethylamine, aqueous solution, u.s. absorption near critical solution temp. 0–53344

triethylamine liquid, acoustic dispersion, u.s. attenuation and velocity meas. 0–46911 triethylamine-water soln., near critical soln. temp., u.s. abs. and vel. meas. 0–46912

0-4912 trifluoriodomethane-inert gas mixture, diffusion coefficients 0-43405 trifluoro silyl compounds, nmr spectra, chemical shifts, coupling constants 0-64552

1,1,1-trifluoro-2-butyne, i.r. and Raman spectra, vibrational assignment 0 - 77956

U=1/936 trifluoro acetonitrile, contours of gas phase i.r. bands 0-71038 trifluoroacetic acid, solid, vibrational spectra and structure 0-67824 trifluoroacetic acid bimolecule CF₃COOH-HCOOH, linewidths 0-74412 1,1,1-trifluoroazomethane, structure determ, by electron diffraction 0-77870

1,1,1-trifluoroethane, neutron inelastic scatt. meas. in gaseous phase 0 - 71041

trifluoroidomethane photodissociation laser, optical inhomogeneities of active substance 0-49056 trifluoromethane, photoelectron spectra 0-61168

trifluoromethane, photoelectron spectra 0–61168 trifluoromethylarsenic tetramer, mol. and cryst. struct. 0–78523 3,3.3-trifluoropropyl tin cpds., n.mr., Sn coupling consts. 0–67823 triglyceride series, cryst. growth rel. to mol. chain behaviour 0–61707 triglycine fluoberyllate cryst., meas. of thermal conductivity near order-disorder transition 0–40609 triglycine selenate, ferroelec., phase transition at 13.6 kbar 0–56361 triglycine selenate, nonlinear props., permittivity rel. to field strength and polarization 0–51122 triglycine selenate cryst., meas. of thermal conductivity near order-disorder transition 0–40609 triglycine selenate erryst., meas. of thermal conductivity near order-disorder transition 0–40609 triglycine selenate energy gap, dielec. const. 0–56362 triglycine sulfate, position of fundamental absoption edge as function of temp. 0–62683 triglycine sulphate, Barkhausen effect under continuous X-irrad. 0–53933

temp. 0-62683 triglycine sulphate, Barkhausen effect under continuous X-irrad. 0-53933 triglycine sulphate, Barkhausen jumps and switching current 0-65820 triglycine sulphate, p-irrad, e.p.r., internal motion of H and glycine (I) activation energy 0-62768

activation energy 0-62768 triglycine sulphate, p-irrad., radicals struct. and motions, e.s.r. obs. 0-66147 triglycine sulphate, defect struct. 0-65319 triglycine sulphate, defects influence on dielec. props. 0-65823 triglycine sulphate, dielec. dispersion 0-68957 triglycine sulphate, dielec. dispersion 0-51115 triglycine sulphate, dislocation study 0-40140 triglycine sulphate, domain struct. revealing method 0-59263 triglycine sulphate, elec. constants, pyroelectricity far i.r. spectrum 0-75814

0-7814 triglycine sulphate, equilibrium domain structure near Curie pt. 0-72124 triglycine sulphate, ferroelec., dielectric const., frequency depend., dispersion band obs. 0-75805 triglycine sulphate, ferroelec., second harmonic generation and scatt. by domains 0-62592

domains 0–62592 triglycine sulphate, ferroelec., thermodynamic characts. of phase transition at high pressure 0–40876 triglycine sulphate, ferroelec. eqn. of state from polarization versus field meas. near Curie point 0–51124 triglycine sulphate, ferroelec. sp., ht. 0–65821 triglycine sulphate, ferroelec. transition, molecular mechanism for transition, from i.r. spectra 0–40875 triglycine sulphate, ferroelectric influence of Cu²⁺, Mn²⁺, Cr³⁺ and Fe³⁺ paramagnetic impurities on polarization switching 0–75806 triglycine sulphate, growth regions 0–65822 triglycine sulphate, meas. of thermal conductivity near order-disorder transition 0–40609 triglycine sulphate, paraelec.-ferroelec. phase transition, X-ray critical scatt. 0–68959 triglycine sulphate, permittivity, sp. ht., elec. field depend. 0–62449

triglycine sulphate, permittivity, sp. ht., elec. field depend. 0–62449 triglycine sulphate, phase transition mechanism 0–68958 triglycine sulphate, polarization in absorpt. bands of defective cryst. 0–66062

triglycine sulphate, prep. and quality 0-65169 triglycine sulphate, pyroelec. response in ferroelec. region near Curie pt. 0-44377

Organic compounds continued

triglycine sulphate, second harmonic generation and scatt, by domains $0\!-\!79229$

triglycine sulphate, solid solutions with isomorphous compounds, growth and characterization 0-50429

triglycine sulphate, specific heat near Curie point, constant elec. polarization 0-68615

triglycine sulphate, thermal props. anomalies at phase transition 0—79050 triglycine sulphate, wall motion and nucleation of domains obs. 0—62450 triglycine sulphate and selenate, dielec. consts., pyroelec. and i.r. radiation detection applic. 0—63824

triglycine sulphate crystal, growth twins on faces, annealing effects 0-74968

0-74968 triglycine sulphate crystal, u.s. absorpt., freq. depend. 0-59098 triglycine sulphate crystal and saturated soln., irrad., absorpt. spectra, 220 1500 nm 0-51318 triglycinsulphate, Cr and V doped, single cryst., e.p.r. meas. 0-51401 1,1,1-trihaloethanes and deuterium derivatives, vibrational assignments from Raman spectra 0-43182 2,4,6-trimethyl biphenyl sulphone, space group by intensity statistics 0-53526

2,4,6-trimethyl bipnenyl suphone, space group by intensity statistics 0-53526 trimethyl phosphine borane, microwave spectrum of normal and isotopic species 0-71042 trimethyl silyl compounds, nmr spectra, chemical shifts, coupling constants 0-64552 trimethylacetic acid, mol. cryst., Brillouin and Rayleigh scatt. 0-59417 trimethylamine, ground state rot. spectra internal splittings and qaudrupole coupling consts. 0-77958 trimethylamine, molten, structure, X-ray diffraction pattern, 5°C 0-61490 trimethylamine. BCl₃ complex, temp. dependence of ⁴⁵Cl n.q.r. 0-67802 trimethylene oxide g values, magnetic susceptibilities and quadrupole moments 0-46595 trimethylene selenide, rotational consts. for 7 vibrational states of ring bending mode, microwave spectra 0-74413 trimethylene sulphide g values, magnetic susceptibilities and quadrupole moments 0-46595 1,3,3-trimethylene-dolino-6'- nitro-8'-pyrylospirane, photochromic informa-

1,3,3-trimethylene-dolino-6'- nitro-8'-pyrylospirane, photochromic information storage 0—60451

trimethylsilane reaction with singlet methylene radicals giving chem. acti-

trimethylsilyl ¹⁴N quadrupole coupling constants 0–55371 trimethylsilyl cyanide and isocyanide, constitution, vibr. spectra and proton reson. spectra 0–55377 trimethylsilylmethoxyacetylene, i.r. spectra and chemical structure 0–74386

0-14360 trimethyltin cyanide, vibrational anisotropy and Gol'danskii-Karyagin effect 0-78739 trioxane, high press. effects, i.r. and optical spectroscopic monitoring 0-50828

trioxane, I type doublets in degenerate excited vibr. states 0-61178

trioxane, molecular dipole moment determ, in solid state 0–61930 trioxane, rotational spectrum, ground and several excited vibrational states study 0–46596 triphenylarsine oxide and iodine cyanide complex, charge transfer complex

0-46598 triphenylene, singlet-triplet intersystem crossing quantum yields direct determ. 0-39440

determ. 0–39440 triphenylene, vapour, 30 keV inelastic scatt., obs. of excitation levels 0–58250

triphenylene and triphenylene- d_{12} , crystalline and solution, normal coordinate calculations $0-43\,183$ triphenylphosphine, adsorbed on glass, radical cation, γ radiation, e.s.r. 0-39933

o—39933
triphenylphosphine, assoroed on glass, radical cation, y radiation, e.s.f.
o—39933
triphenylphosphine-(pentahaptocyclopentadienyl)copper(I), crystal and molecular structure 0—61929
triphenylstibine, vibrational spectrum 0—71039
tri-(5-methyl-2furyl)phosphine derivatives, ¹H-³¹P spin-spin coupling constants 0—74384
tris-salicylato-bis-phenanthroline rare earth chelates, u.v., visible and i.r. spectral characteristics 0—71031
trissarcosine CaCl₃, n.m.r. determ. of ferroelec. transition 0—53942
1,3,5- trithiane molecule, i.r. spectra, vibrational assignments 0—49939
DF-trypsin derivatives, cryst. struct. 0—40114
tryptophane, fluoresc. decay rel. to pH 0—46930
unsaturated, H and D bombarded, e.s.r. of radicals produced 0—79410
uranyl chloride, cryst., luminesc. and abs. spectrum, in polarized light, at №2
temp. 0—69175
uranyl compounds, cubic cryst., gyrotropy 0—44772
uranyl hydroxy-formate, orthorhombic unit cell parameters 0—71600
uranyl propionates, single cryst., luminesc, dichroism and dispersion, at room temp. and liq. №2 temp. 0—72430
urazole mol., all-electron SCF-LCAO-MO wavefunction 0—39451
urazole radicals, cation and anion, all-electron SCF-LCAO-MO wavefunction.

urazole mol., all-electron SCF-LCAO-MO wavefunction 0-39451 urea X-irrad., thermoluminescence glow peaks 0-61940 urea X-irrad., thermoluminescence glow peaks 0-61940 urea single crysts., elastic consts. 0-43715 urea single crysts., external vibrs., Raman spectra obs. 0-69138 p-valerolactone, fundamental vibl. assignment from i.r. and Raman spectra 0-46599

vanadyl acetylacetonate nematic liquid crystal, anisotropic pseudo-potential 0-67845

vapours, binary mixtures with inert diluents, thermal conds. 0-53267 vegetable oils in benzene, dielectric properties in radio frequency region 0 - 58491

0-58491
vinyl bromide, pure rotational spectrum of fundamental vibration state, 8-59 GHz 0-46601
vinyl bromide, pure roth, spectra of type ^aR at mm. wavelengths 0-46600
vinyl bronide, c.w. submillimetre laser action on optical pumping 0-73207

0–73207 vinyl compounds, substituent effects on J_{-h} Coupling constants 0–58253 vinyl esters of carboxylic acids. i.r. absorption spectra 0–74365 vinyl fluoride, electronic structure 0–77957 vinyl fluoride, n.m.r. in nematic solvent 0–71043 vinyl fluoride, vacuum u.v. photolysis at 1470 Å 0–66201 vinyl isocyanide, rot. and vibr. spectra 0–55378 vinyl monomer-solvent mixtures, glass transition temperature, specific heat, crystallization 0–47541 vinyl cyclopropanes, rotational isomerism, n.m.r. spectroscopic studies 0–67825

vinylethynylcarbinols, absorption intensity of acetylene bond, i.r.

0-74414 vinyltrifluorosilane, vibrational spectra and structure 0-77952 vitamin B₁₂-5'-phosphate, crystal structure, X-ray diffraction determination 0-71601 water-2-isobutoxyethanol system, u.s. absorption as function of composition, temp. and frequency 0-68102 Wurster's blue cation as anthracene triplet quencher in fluid soln. 0-39816 Wurster's blue perchlorate, electronic absorption at various temperatures 0-56533 xanthene dues pear in triplet triple.

0-5033 xanthene dyes, near i.r. triplet-triplet absorpt. spectra 0-71044 β-D-1,3-xylan, helical struct. 0-46614 o-xylene, far. i.r. spectrum 0-58251 xylene derivatives, intermethyl proton spin-spin coupling constants signs 0-55379

xylene spherical cage model for relationship between compressibility and solubility 0—46880 yttrium ethyl sulphate, Er doped, inhomogeneously broadened e.s.r. line obs. 0–76230

cos. 0=76230

zinc acetate dihydrate, e.p.r. of Mn²+ 0=56676
zinc guandinium sulphate, crystal structure 0=50562
zinc uranyl acetate, vibration level assignment 0=46602
acetylene non-dipolar gas, Kerr effect, second hyperpolarizabilities
0=68002

0-68002
Al-methane-O₂ flames, chem. and phys. kinetics 0-76260
B-methane-O₂ flames, chem. and phys. kinetics 0-76260
B₃H₁₁ in n.m.r., anomalous hydrogen 0-77767
C acids, kinetic hydrogen isotope effects in ionization 0-68144
C K-emission spectrum used to study covalent and ionic bonds of organic compounds 0-61141
C₆D₁₂ pure-rotational Raman spectra under high dispersion 0-70985
C₄F₃- autoionization lifetime by ion cyclotron resonance linewidths 0-74221

CH₂CH-COOH bimolecule, linewidths 0—74412
CF₃COOH-HCOOH bimolecule, linewidths 0—74412
CH₄ thermodynamic properties of and equations of state for 0—39674
CH₄+ ion, geometries, Jahn-Teller distortions, and electronic charge distrib. 0—55359
CH₃+', maximum overlap molec. orbitals 0—77762
C₆H₁₂, pure-rotational Raman spectra under high dispersion 0—70985
CH₃CH₂CH₂Pr vapor solid state, vibrational fundamentals 0—39426
CH₃CH₂CH₂Pr vapor and solid state, vibrational fundamentals 0—39426
CH₃CH₂Pr vapor and solid state, vibrational fundamentals 0—39426
CH₃CH₂Pr vapor and solid state, vibrational fundamentals 0—39426
CH₃CH₂Pr vapor and solid state, vibrational fundamentals 0—39426
CH₃CH₃Pr vapor solid state, vibrational fundamentals 0—39426
CH₃Pr molecules optically pumped, laser action study at 452, 496, 541 μm
0—61153
C₃H₄O molecule, centrifugal distortion constants, calculation 0—49898
CS-CCL₄ mixtures, nonlinear refractive indices 0—39792
C=O, band parameters and profiles of valence vibr. as function of conc. 0—64492
C=O valence vibr. of ketones, band parameters and profiles, (—)30—70°C

C=O valence vibr. of ketones, band parameters and profiles, (-)30-70°C 0-64493

0—64493
Ca tetracetatocopper(II) hexahydrate, estimation of Cu(II) ion orbital reduction factors from spin Hamiltonian parameters 0—70981
d- camphor, elec. cond., phase charge 0—47633
CIF₃-dichlorotetrafluoroethane liquid- vapour equilibrium at constant pressure 0—64983

sure 0-64983
ethylene adsorption on Pt (111) 0-47088
Fe allyl complexes, n.m.r. spectra rel. to structure 0-67760
H atom reactions with n.C.4D10, bond energy effect 0-79425
Kr-methane liquid solns., sound velocity, 110-190°K, adiabatic and isothermal compressibilities 0-43445
LITI-tartrates, simple and deuterated, dielec. props. 0-40856
"N n.q.r. in mol. crysts., line shapes and widths analysis, obs. 0-41402
Na azide, solution growth via precipitant infusion 0-50449
OM1, o., m., p-terphenyl, diffusion parameters for thermal neutrons from 20°C-176°C 0-73648
Ru allyl complexes, n.m.r. spectra rel. to structure 0-67760
X.CH₂CH₂Y fragments, effect of substituents on vicinal coupling constants 0-67755
zanometallic compounds

Organometallic compounds see Organic compounds

Orthicons see Electron tubes

Oscillations

ciliations

see also Electromagnetic oscillations; Liquid oscillations; Plezoelectric oscillations; Vibrations
aeroelastic systems, free oscillatory characteristics, comparison of different assessment methods 0-73030
amplitude jumps, demonstration 0-42060
anode glow in biatomic gas discharge tube 0-67980
atmospheric pressure, periodic, generation of long internal waves 0-56768

boundary layer, turbulent, rel. to heat transfer 0-46784
boundary layer flow, non-uniformly rotating lamina 0-43229
bubble gas underwater, of finite and small amplitude, investigation, comparison 0-71300

parison 0–71300 cylindrical tank of fluid, rotating, anal. of interior flows 0–58301 density wave mode, in two-parallel channel forced-convection boiling upward flow system 0–64648 diode, Read, minority carrier storage and oscillation efficiency 0–72084 discharge with gaseous anode 0–67976 elastic half-space, torsional oscillations due to annular disk 0–66889 flow, two-phase channel type 0–64646 frequency instability and spectral purity relations 0–48825 galactic large-scale, evidence and theoretical calc. 0–56991 Gunn, Stabilization in layered semiconductor structures 0–75756 Gunn diode, microwave oscillations, self-modulation 0–53911 Gunn diodes, concentric electrodes, freq. variation, domain nucleation

Gunn diodes, concentric electrodes, freq. variation, domain nucleation 0–56391

0-50335 hydromagnetic-non radial of incompressible cylinder 0-64657 incompressible fluid in a container, free oscillations 0-71079 lf., effect on radial distrib. of plasma conc. and charged particles escape in hot cathode Penning discharge 0-43277 laser, II to VI semiconductors, complex phonon spectra of mixed crystals 0-52314

laser radiation intensity, forced, resonance phenomena 0-49085 Liapunov instability of the oscillating pendulum, linear stability analysis 0-59947

linear oscillator, probability of random vibr. first crossing threshold 0-73025

Oscillations continued

load moving and fluctuating, distribution on elastic half-plane, Fourier transforms soln. 0–52016 magnetostatic surface 0–75870

mass transport induced by oscill, flow in turbulent boundary layers 0-74475meas., automatic of inverted torsion pendulum with optical system 0-75230

menbrane, symmetrization by identification 0-60003 metal, geometrical, cyclotron resonance, e.m. and u.s. wave interaction 0-78865

0–78865
nonlinear, 1969 International Conference 0–76861
nonlinear of distributed systems, asymptotic method 0–76802
nonlinear oscillation equations, infinite systems, existence and uniqueness of solutions 0–63315
nonlinear systems, mean position under action of random perturbations 0–76840

ocean of uniform depth, on hemisphere bounded by meridians of longitude 0-59540

ocean of uniform depth, on hemisphere bounded by meridians of longitude 0–59540 oscillatory compression of bonded rubber blocks, contribution to effective mass 0–5380 oscillatory flows, axially symmetric, of elastico- viscous liquids, non-Newtonian effects 0–71289 oscillatory radial flow between fixed and free disks 0–53274 parametric, Internal optical 0–41929 perturbations of plane blast waves, thin sheet model 0–39531 power in nuclear reactor, Xe induced spatial, 3 dimens. method for design studies 0–67577 pressure drop, in two-parallel-channel forced-convection boiling upward flow system 0–64648 quantum amomalous, of surface impedance 0–50943 semiconductor, Si-Zh, harmonics of current 0–59231 semiconductor, almost intrinsic Ge, relaxational, in gradient instability obs. 0–47749 semiconductor, forced oscillations of static domain 0–56234 semiconductor, forced oscillations of static domain 0–56234 semiconductor under double injection conditions, kinetic instability and reson. effects 0–56232 spentaneous, in mech. system, paradoxical phenomena 0–57364 stability of Jean's spheroid and Roche's ellipsoid 0–38322 steel, high-C, elastic modulus and oscillation decrement temp. depend. 0–47313 in synchrotron, nonlinear, radiation damping 0–42677 extern with a small linearity, subharmonic, third order oscillations

in synchrotron, nonlinear, radiation damping 0-42677 system with a small linearity, subharmonic third order oscillations 0-52060

torsional, of a rigid convex inclusion embedded in an elastic solid 0-38339

torsional, of earth, frequency equations for model in analytical form. 0-76297

0–76297 transverse, in glass capillary, microsonation at 20 kHz, diverse chemical effects obs. 0–45636 u.s. absorption coeff., in semiconductors in h.f. electric field 0–43874 ultraharmonic, in yielding systems, existence and stability 0–73020 vibrator and rigid bodies, nonlinear connected oscills. for 2, 3, 6 and infinite degrees of freedom 0–38341 of wedges, large amplitude, slow, rel. to hypersonic and supersonic flows 0–55555 Al, induction by penetrating particles 0–60010 Al, quantum, of helicon phase velocity, anisotropy 0–62274 Cd cylinders, magnetomorphic, in Hall resistivity and magnetoresistivity 0–44031 GaAs double-injection devices, thermally induced oscillations and negative

GaAs double-injection devices, thermally induced oscillations and negative resistance 0-75739

GaAs relaxation and hybrid modes 0–44315
Ge, almost intrinsic, relaxational, in gradient instability obs. 0–47749
in He-Cd laser, time delay on 5378 and 5337Å transitions 0–49052
He II, superfluid, surface oscillations, h.f. 0–55645
Hg single crystal, giant quantum in u.s. absorpt. in mag. field, 1.2K
0–50878

n InSb impact-ionized plasma, microwave radiation instability in mag. field 0-72030

Oscillators
35 GHz interferometer, spaced antennas with synchronous oscillators

35 GHz interferometer, spaced antennas with synchronous oscillators 0–72795
3 cm klystron with superconducting resonator 0–45715
avalanche diode, GaAs, high efficiency microwave, theory 0–51082
b.w.t. for submillimetre wavelengths 0–45714
Clapp transistor, starting condition, freq. of oscillation 0–45743
coupled between two spatially extended multimode systems, point excitation, energy flow 0–45611
crystal, anomalous vibrations (activity dips) in AT-cut (R₁) plates 0–53676
demonstration using ring magnets 0–66765

crystal, anomalous vibrations (activity dips) in AT-cut (R₁) plates 0–53676 demonstration, using ring magnets 0–66765 diode, LSA, axial e.m. modes and self-reson. 0–47792 electronic, book 0–63560 frequency instability of oscillator perturbed by internal thermal noise 0–48954 dunn, with varying energy gap 0–79015 Hertzian, radiation on moving through a dielectric medium at superluminal velocities 0–38434 linear, stationary random excitation, displacement first passage of transient response 0–57377 nonlinear optics applications 0–69965 optical parametric, mode locking 0–42240 optical parametric oscillation studies 0–73200 optical parametric oscillation studies 0–73200 parametric, cross-correl. of signal and idler 0–67063 parametric, optical hockward-wave, threshold condition 0–69869 parametric, optical backward-wave, threshold condition 0–69869 parametric gain, momentum mismatch effects 0–69870 phase-locked, discrimination against interfering tones 0–45744 RC for frequency generation of equally tempered musical scale, design description 0–52124 transistor; Clapp, starting condition, freq. of oscillation 0–45743 transistor; clapp, starting condition, freq. of oscillation 0–53337 ultrassistor; calego, parametric, optical backward-wavel of condition 0–69869 parametric gain, momentum mismatch effects 0–69870 phase-locked, discrimination against interfering tones 0–45744 RC for frequency generation of equally tempered musical scale, design description 0–52124 transistor; clapp, starting condition, freq. of oscillation 0–45743 transistor; clapp, starting condition, freq. of oscillation 0–53337

Oscillators continued

Agj.ASS, proustite, optical parametric oscill. 0–77068 CdS electroacoustic, acoustic strain meas. 0–43892 CdS platelet, diffusion of In contacts, electron beam microanalysis 0–40794

GaAs avalanche diode, high efficiency microwave, theory 0-51082 Ge LSA mode, for microwave power 0-72074

85 Rb maser, field-independ. optically pumped 0-73197

Oscillistor effect see Semiconductors Oscillistors see Semiconducting devices Oscillographs see Electrical measurement
Oseen method see Flow; Hydrodynamics

abundance excess in 73 Dra, peculiar A-type variable star 0-41663 atomic mass differences and mass systematics in the region $100 \leqslant N \leqslant 126$

clectron energy loss spectra, 0.6-1.4 keV, 2000 and 1700°C 0-40630 Os⁴⁺ spectra in K₂PtCl₆, Cs₂ZrCl₆, vibronic analysis, obs. 0-41210

Osmium compounds
Cr-Os alloy, elec. resistivity and antiferromagnetism, rel. to temp.
0 44683

0.4063 OsO₄ vapour, absorpt, spectrum and electronic struct. 0–70941 OsO₄ vapour, force constants Raman spectra 0–46503 W-Os solid soln, single crystal, thermionic emission props. of (100) face

Osmosis
cellulose acetate, water transport in reverse systems, thin-region resistance model 0-39767
cochlear perfusion, guinea pigs, significance of osmotic pressure gradients 0-54511

0-34311 electro-osmotic flow, theory and expt. 0-74740 electro-osmotic flow, transport eqn. 0-39766 electroosmotic flow and streaming potential generation in fine capillary slits 0-58475

interaction of sound wave with matter transport across semipermeable membrane 0-64892

osmotic permeability, in homogeneous liquid membranes 0–71332

Pyrex membranes, electroosmotic transport 0–71331

quartz membranes, electroosmotic transport 0–71331

sodium polystyrene sulphonate, NaCl aqueous, osmotic pressure, second virial coefficients 0–39768

Overhauser effect see Nuclear magnetic resonance and relaxation

Oxidation

anodization, conventional and plasma, rel. to field strengths in oxide films

anodization, conventional and plasma, rel. to field strengths in oxide films 0 -61661 anodization, forming voltage 0-66182 anodization, plasma, oxide film production, effects of plasma perturbations 0-61662 carbide materials for rocket nozzle applies. 0-58953 coating, thermal control, reduction, optical props. changes 0-41113 composite, SiC clad graphite, oxidation resistance 0-59003 copper oxide reduction by ethanol vapour rel. to exo-emission characts. 0 44417

4a, 4b dihydrophenanthrene oxidation, kinetic isotope effect of deuterium 0 48185

glass-metal infterface, atmosphere and glass effect on reactions 0–53416 graphite, layer planarity electron microscopy 0–41430 graphite, rel. to diffusion of O₂ 0–71643 graphite, thermal oxidation by water vapour effect on mech. strength

o 40348 graphite, thermal oxidation by water vapour effect on mech. strength o 40348 graphite materials for rocket nozzle applics. 0–58953 graphite reduction of WO₃ and MoO₃, mechanism 0–72547 metal, oxide film growth, stress generation and relief 0–61660 metal oxide layer growth, surface morphology 0–61665 optical surface restoration by rf. excited 0 0–77177 plasma anodization of Ta and Nb, ionic current in oxide 0–72541 plasma anodization of metals and semiconductors, review 0–55734 refractory metals 0–43809 steel, stainless, high temp. behaviour, time lapse photomicrography obs. 0–76265

titanomagnetite, magnetic property changes at low and high temperatures

thanomagnetic, magnetic property changes at low and high temperatures 0—45064

Zircaloy, in air, dimens, changes 0—45064

Zircaloy, 4, anodic in electrolyte bath, morphology 0—45063

of Al, electrode in m.i.m. struct., 1-V characts, variation 0—47625

Al₂O₃, anodic film formation, thickness, ellipsometric determ., ion current efficiency 0—47043

p-Al₂O₃ film growth rate on Al and Al-Cu, dielec, props. 0—53923

Au, mechanism of anodic oxidation with H₂SO₄ 0—76273

CO, by O₂ in shock waves 0—62804

Co, kinetics near α ≠ β transition 0—59487

Co alloy, and erossion resistance coatings, high temp., patent 0—45067

COO, oxidation-reduction kinetics 0—51424

Cr₂O₃ oxidation/vaporization rates 0—51425

Cu-Al alloy, temp. depend. of vel. const., 900-1000°C 0—41431

Cu-Mn alloy, temp. depend. of vel. const., 900 1000°C 0—41431

Cu, low temp. kinetics, dry air, externally applied current depend. 0—45060

Cu, optical study, oxide film thickness measurement 0—47044

0-47040 Cu, optical study, oxide film thickness measurement 0-47044 Cu (100), contact potential meas, during oxidation 0-76264 Cu alloy, internal, effect on coherency 0-43824 Fe-Cr alloy film, transient 0-72538

Fe-Cr alloy lim, transient 0-7238 Fe-Ni films, degree of oxidation and phase comp., var. with annealing temp. and vac. 0-78372 Fe, liq., levitated, kinetics 0-78343 Fe, Mossbauer spectroscopy 0-41148 Fe, polycrystalline and single crystal surfaces, 24-200°C, Kr adsorption, 77K 0-54189

77K 0–54189
Ge surface, struct. and electronic changes, correl. 0–45061
Ge surface in HF:H₂O₂ solns., GeO₂ film growth 0–61670
MO surface oxidation obs. by secondary ion mass spectroscopy 0–72539
Mg and alloys, deform. obs. 0–66184
MnO, oxidation-reduction kinetics, TGA obs. 0–51426
NH₃ at Pt electrode, adsorption 0–66196
Nb, ellipsometry 0–48197
Nb alloy, resist. to comp. depend. 0–40457

Oxidation continued

Nb films, struct., electron diffr. 0–50369

Nb-Zr alloys, strengthening by internal oxidation 0–43768
Ni-Cr-(1 wt.%)/ThO₂ alloys, 1200°C 0–56703
Ni-Cr-Al alloys, Y additives effect on high temp. behaviour 0–51427
Ni-Cr alloy film, transient 0–72538
Ni, effect on plastic deformation at high temp., model 0–43747
Ni, hydrogenated phases, anodic oxidation 0–56709
Ni, O₂ mol. dissoc. as rate determining step during initial stage 0–72540
Ni alloy, and errosion resistance coating, high temp., patent 0–45067
Ni₂Al-Ni₃Nb, ion diffusion mechanism 0–41432
Pt, mechanism of anodic oxidation with H₃SO₄ 0–76273
Si, applic. to sermicond. device technology 0–51076
n.Si, in steam. SiO₂ layer production 0–55748
Si, ion implanted, enhancement during annealing 0–66185
Si surface, thin tunnelable SiO₂ Jayer formation 0–62392
SiC, surface cracks healing 0–58937
SnO₂:Ni³⁺, e.p.r. in flux-grown cryst., oxidation-reduction effects 0–72492
Ta alloy, resist. to, comp. depend. 0–40457

0-72492
Ta alloy, resist. to, comp. depend. 0-40457
ThO₂·UO₂ solid solution 0-48198
Ti, coeff. of oxygen diffusion calc. from kinetic data 0-76266
Ti, thermal effects in initial stages, exptl. conditions effects 0-72542
U, irrad., in CO₂, *8*Kr release 0-66186
UO₂, carbothermic reduction process, oxygen oxygen in uranium carbide 0-62808
UO₂ surface controlled oxidation reduction. 0-65344

0-62808

UO2, surface-controlled oxidation-reduction 0-65344

U+CO2→UO2+2CO, gaseous diffusion control, CO layer 0-48199

UO2 pellets, in air, 800-900 °C 0-66187

W, rel, to CO or N2 adsorbed layers 0-58606

W, study by the ion-ion secondary emission method 0-56704

W surface, effect on electrical contact resistance, meas, by graphite electrode 0-44039

W surface, WO2 and O2 interaction 0-58563

Zn film, I doping effect, 200-390°C 0-76267

Zr. Nb(T1) alloys, in air, dimens, changes 0-45064

Zr., at high temp, low pressure 0-66188

Zr alloys, charge transport processes obs. 0-59488

Zr Bloys, charge transport processes obs. 0-59487

ide cathodes see Cathodes/oxide

Oxide cathodes see Cathodes/oxide

Oxygen

absorption coeff. at Lyman- α line, transmission windows, meas. 0–61066 absorption system in H₂O and solutions of Na₂SO₄, KI and Na₂SO₃, influence of molecular diffusivity on liquid phase mass transfer obs.

0 68089 abundance, in planetary nebulae 0–66424 abundance in Arcturus 0–57025 abundance in He star HD 168476 0–45261 abundance in K giants α Boo, α Ser, β Gem, ϵ Peg 0–45262 abundance in lunar samples, neutron activation determ. 0–45353 abundance of isotopes in lunar samples, $^{18}O/^{16}O$ ratios 0–45358 abundance of isotopes in lunar samples, $^{18}O/^{16}O$ ratios 0–45356 abundance of isotopes in lunar samples, $^{18}O/^{16}O$ ratios 0–45356

abundance of isotopes in lunar samples, fractionation between minerals

addition to solid Kr, effect on self diffusion 0-43696 adsorbed layers on CdS, desorpt, effect on Fermi level and photocond. 0-47739

0-47739
adsorption, dark and photo on NiO from -195·200°C 0-68244
adsorption on Ag (111) face 0-47076
adsorption on Re (0001) face, effect on cryst, surface struct. 0-74928
adsorption on SbSI, effect on ferroelec, phase transition 0-75804
adsorption on Si, from surface cond. vars. obs. 0-55762
adsorption on Si (111), electron beam assisted 0-65108
adsorption on W (110), Auger e spectroscopy obs. 0-55765
adsorption on W (110) plane 0-39982
adsorption on W at room temp., review 0-71498
adsorption on W rel. to N₂ or CO adsorbed layer 0-58606
adsorption on Sylv, work function, thermionic emission 0-74932
adsorption on superconducting Sn film, effect on T₂ 0-65646
adsorption on surface ionization of CsCl molecules on Ir, influence investigation 0-53444
adsorption on tungsten, rel. to work function reduction 0-79093

tigation 0—53444
adsorption on tungsten, rel. to work function reduction 0—79093
assay in natural water, isotope exchange 0—76284
astronomical spectra, emission \$5007 line profile 0—51646
in atmosphere, history of 0—79627
atmospheric, evolution, boundary condition 0—76370
atmospheric, microwave absorpt., resonant and non-resonant 0—59580
atmospheric 1.27 band in twilight airglow, ground based photometric obs.
0—66312

atmospheric red lines, pre-dawn enhancement, theoretical calcs. 0–69298 atom, 'S metastable, production in He-O₂ positive columns 0–39299 atom, 'P₂, spectra in gas phase, lineshapes of multiple quantum transitions 0–55236

atom, binding energy of 1s electron related to potential at nucleus 0-74117

atom, photoionization cross-sections for Slater-Klein-Brueckner potential 0-67638atom, reactive scattering on semiconductor surfaces 0-55704

atom, spin orbit coupling constants from Gaussian wave functions 0-46353

0-46353
atom, spin-generalized SCF wavefunctions using GF method 0-67732
atom in simple molecules, chemical shift paramagnetic term 0-53013
atom inert gas repulsive interactions, 0.3 to 3 eV, obs. 0-77700
atomic, r.f. excited, applic. to optical surface restoration 0-77177
atomic pot, representation eff. on e scatt, cross-section 0-74143
atoms, electron scattering, elastic, differential cross section rel. to compound state formation 0-77706
atoms, interaction with various surfaces 0-58559
auroral, ionic composition, NO+0₂+ ratio, O₂+ concentration cales.
0-56817

0–56817
chemisorbed on tungsten 0–48191
chemisorption on CdS, effects on equilib. conductivity 0–40784
chemisorption on Mo(112), LEED obs. 0–56698
chemisorption on Re 0–45058
chemisorption on Re 0–45058
chemisorption on fresh Mg surface, exo-electron emission 0–39972
d.c. discharge, effect of mag. field on elec. oscillations 0–61394
defect complexes, in neutron irrad., Si crystals, i.r. absorpt. spectra
0–48055

desorption from Mo by electron impact 0-39973

Oxygen continued

desorption on CdS single crystal platelets 0-47077

dielectric obs., liquid and gaseous, capacitor, 55-300°K, 0.2-34 $\rm MN/m^2$ pressure range $\rm \,0{-}74779$

diffusion and permeability coefficients through low-density polyethylene 0-55928

0-55928
diffusion in ZrO₂, 990°C, crystal defect struct. 0-40208
diffusion in aluminosilicate glass, 630-830°C, colour-centre bleaching, optical transmission 0-43691
diffusion in aqueous KOH solns. 0-64887
diffusion in graphite, oxidation effect 0-71643
diffusion in metals, ion analyzer use 0-65345
diffusion in n- and p-CdTe, temp. depend. mass spectrometry 0-43693
dissociative attachment, temperature dependence 0-61184
effect on Fe (001) and (011) surface adhesion, LEED and Auger obs.
0-78688

electron impact excitation cross sections 0-77825 emission, from electron impact on CO, O₂ NO, H₂O, decay lifetimes 0-64444

emission, from electron impact on CO, O₂ NO, H₂O, decay lifetimes 0—64444
flow, ethyl alcohol and hexane injection, heat and mass transfer 0—78218 fragmentation, by 5 to 45 keV He⁺ ions 0—74609
gas, energy loss of traversing protons 0—45963
gas mixutres, O₂ with H₃, acetylene, ethylene, transverse wave strength in detonations 0—50164
glow-arc discharge transition with Ag, Cu electrodes 0—58366
laigh pressure atmosphere effect on PbS film photocond. 0—47877
hypersonic flow, nonequilib. shock layer around cones, expt. and numerical studies 0—53237
1 Ls ²P₂) ²s ³S⁰ level, radiative lifetime meas., beam-foil technique, oscillator strength calc. 0—74122
1.r. emission spectrum, electronic, pressure depend. 0—58085
impurity distrib. in GaP:ZnO liquid phase epitaxy layers 0—62365
influence on W single crystal (110) surface thermionic emission, 1600° to 2200°K 0—51160
ion cluster formation and reactions in flowing afterglow 0—41416
in ionosphere, topside, O²⁺ ion density 0—54288
ions, ioniz: rates due to electron collisions, calc. 0—43011
ions, ionosphere structure, upper, Alouette II obs. Oct. 1966 to Sept. 1967, data analysis 0—54289
ions, monatomic and diatomic, cross sections for charge-exchange reac-

ions, monatomic and diatomic, cross sections for charge-exchange reactions 0-64259

tions 0–64259
ions, solar u.v. lines limb brightening 0–41865
isotopic analysis by optical spectroscopy 0–41452
iv, ions, lifetime obs., beam foil techniques 0–77665
laser, as spark gap trigger, formative times rel. to power 0–53232
liquid, ir. absorption coeff. 40-500 µ 0–55616
liquid, structure factor, from X-ray scatt. obs. 0–46871
low pressure, effect on creep rate of W and 50%W-50%Mo 0–78636
luminescence centers in terbium activated sodium halide crystals 0–56608
in mesosphere, effect of diffusion processes 0–76475
mobility, diffusion and attachment of electrons 0–43349
molecular, in saturated hydrocarbons, as electron trap in thermoluminescence 0–41283
molecule, attachment of slow electron, Bloch-Bradbury mechanism 0–64770
molecule, dissociative electron attachment cross-sections 300° to 10008K

molecule, dissociative electron attachment cross-sections, 300° to 1000°K 0–64559

molecule, electron impact ionization cross-section per unit energy range 0-67972

molecule, partial photoionization cross-sections, ionization potentials 0-64212 molecule.

molecule, predissociation lifetimes of $B^3\Sigma_u$ - state, determ. 0–77830 molecule, thermal energy reaction rate constants with C⁻ 0–72526 molecules, electron scattering, resonance in inelastic channel 0–77817 nebula Hourglass, O III λ 5007 emission rel. to internal kinematics, obs.

0-41624

neutron spectra at 14 MeV using sphere transmission and time-of-flight techniques 0-64151 ozone molecule, rotatory energy levels, comparison with rigid rotor 0-64331

0 –64331
pressure meas. using mass spectrometer 0—74646
photoelectron spectra, resonance wavelength 0—64324
photoionization in photoelectron spectra 0—64325
photoionization meas, rel. to breakdown cale. 0—64768
plasma, atomic recomb, e.p.r. obs. 0—61259
precipitation in Si. effect on surface preparation 0—65729
reaction with H at thermal energies 0—62798
spectral lines, intensities, calculated as functions of axial temp. of discharge channel 0—71169
surface effect on CdS, rel. to barrier height of Au-CdS contact 0—47744
thermal transpiration, rotational collision numbers determ. 0—61451

channel 0—71169
surface effect on CdS, rel. to barrier height of Au-CdS contact 0—47744
thermal transpiration, rotational collision numbers determ. 0—61451
thermodynamic properties, specific heats and sound vel., triple point to
300°K, and P-V-T data 0—46992
thermomagnetic force obs. in gas 0—55566
in thermosphere, lower, effect of diffusion processes 0—76475
trap in group II-VI alloys, photoluminescence 0—72431
triple point and change by noble gas impurities 0—64989
vacancy formation in TiO₂:Cr, rutile, e.p.r. investig. 0—55874
vibrational populations and synthetic spectra of Herzberg bands in night
airglow 0—41515
vibrational relax rates meas., behind shock waves 0—77814
vibrational relax rates meas., behind shock waves 0—77814
vibrational relaxation time, temp. dependence 0—61131
[O]/[O₃] conc., photochemical changes in D-region, rel. to radio propag.
and solar radiation 0—69324
Al-methane-O₂ flames, chem. and phys. kinetics 0—76260
Ar-O plasma afterglow, ion and electron decay rates 0—67894
B-methane-O₂ flames, chem. and phys. kinetics 0—76260
onBa film, chemisorbed N₂ displacement by O₃, obs. 0—56695
CO₂, 15µ band absorpt, broadening by O₃, obs. 0—5669
CaF₂:Eu³⁺, effects on luminescence spectra 0—56589
Fe-C-O₂ isobaric ternary phase diagrams 0—62146
in Ge, concentration determined by i.r. absorption 0—75143
H₂-O₂ flame plasma, Langmuir probes, spectroscopic diagnostic methods 0—71174
H atom collisions, total electron-loss cross-sections, Born wave calc. 0—64286

H atom collisions, total electron-loss cross-sections, Born wave calc. 0-64286

10-04-200 in H₂O, conc., effects of mag. processing 0-68081 in charge exchange cross-section, 1 to 12MeV 0-70805 N/O/reactive carbon compound systems, chemiluminescence emission of CO fourth positive bands 0-76257

Oxygen continued

in Na effect on Nb compatibility 0-45055 $Na^++O\rightarrow Na(3p)+O$, 0.06 -7 eV, cross section determ. 0-61007

 O_2/N_2 atmospheric conc. ratio, precise determ. from Raman scatt. meas. 0-51511

0–515131

O/O₃ conc. photochemical changes in D region, rel. to radio propag. and solar radiation 0–69324

O-CH₃ beams, elastic scatt., 0.1 to 2 eV 0–74224

O-CS₃, mixed in laser cavity, vibrationally excited CO, continuous-wave stimulated emission 0–58162

O+Kr collisions, Q values determ, by coincidence technique (100 eV-1 keV) 0–39290

O-acetylene reactions, chemi-ionization during induction period 0–79433

O-, cluster ion formation and reactions in flowing afterglow 0–41416

«-O. Raman line, previously unobserved due to magnon scatt. 0–62689

O,O³⁺-atoms and ions, photoionization cross sections 0–70775

O1, horadening and shift or i.r. lines by Stark effect 0–77666

O1, λ6300, short-period auroral pulsations 0–41522

O1, wavelengths and oscillator strengths of 2p⁴-2p³3s transition 0–42943

O1 6300 Å line, magnetically conjugate photoelectrons effect 0–79597

O1 auroral and nebular emissions, twilight enhancement rel. to photodis soc. of O₂ 0–45165

O1 emission, from electron impact on CO, O₂ NO, H₂O, decay lifetimes 0–64444

0-64444

0-64444
O I forbidden lines in α Ser, no evidence for abnormal weakness 0-51684
O I oscillator strengths and mean square radii calc. 0-42930
O II in planetary nebulae, emissivity 0-51644
O II lines, spectral intensification in plasma on impulse discharges 0-49788

O VII wavelengths of resonance lines meas. 0-77667

O VII wavelengths of resonance lines meas. 0–7/667 O low-energy ions, electron detachment in collisions with N₂ 0–58360 O production by dissociative attachment of electrons in CO 0–74605 O t, collisions with Ar and Ne, 50 to 200 keV, delayed-coincidence study of inelastic energy transfers 0–77702 O t, implantation in Si m.o.s. struct., surface characts. 0–47814 O and O t beams, vibrational excitation in collisions with neutral mols. 0–53103

O⁺, implantation in St m.o.s. struct., surface characts. 0–4/814
O⁺ and O₂⁺ beams, vibrational excitation in collisions with neutral mols.
0–53103
O⁺2 autoionized reson, states, photo-e spectra rel. to vibr., obs. 0–46502
O₂, cluster ion formation and reactions in flowing afterglow 0–41416
O₂: centres, elastic interaction in alkali halides, e.s.r. 0–69183
O₂: \(^1\sigma_p\); transient species, by high resolution vac. u.v. photoelectron spectroscopy 0–77824
O₂, electron impact, O I and O II emission, decay lifetimes 0–64444
O₃, groundstate, effects of electron correlation on fine-structure constants and spin spin interaction 0–58193
O₂, interastion with W surface 0–58563
O₃, measured transition probabilities for bands of Schumann-Runge (B¹Σ_u – X³Σ_g) syst. 0–70937
α-O₂, phonon sidebands of bimol. transitions 0–62639
O₃, photoelectron spectrum, I2-28 eV, O₂⁺ states 0–55312
O₄, Raman scatt. meas. under ambient atmospheric conditions, atmospheric oxygen balance appl. 0–51511
O₂, total ioniz, cross section due to electron impact 0–67679
O₃, ultrasoft X-ray absorpt, meas. 0–64818
O₃, velocities and interactions of negative ions 0–78155
O₄: \(\frac{1}{2}\sigma_1^{+}\sigma_1^{+}\sigma_1^{+}\copensymbol{eq}\); matmosphere, attenuation at 48 to 72 GHz, calc. 0–62919
α-O₂ cryst., antiferromag., excitation band shift and splitting 0–44851
O₂ dissoc., by shock wave, in 10% O₂ +90% Ar mixture 0–74416
O₂ emission bands obs. at 4784, 5165, 5788 Å in afterglow, assignments to \(^1\sigma_1^{+}\sigma_2^{+}\state \) states 0–74294
O₂ cin A³Z_g* state in upper atmosphere, conc. height profile 0–76413
O₃ ion pair formation by electron beams 0–58354
O₄ mol., fluston to 0–73928
O₅ cond., fluston of 0–74296
O₇ cond. dissoc. on Ni, during oxidation 0–72540
O₇ mols., pot. energy curves 0–64406
O₇ Schumann-Runge bands photographed 0–74296
O₇ condissoc. on Fig. during the profile 0–76413
O₇ mola, pot. energy curves 0–64406
O₇ Schumann-Runge bands photographed

0-74965
0; total electron cross-section 11-12 eV meas. by modified Ramsaucr technique 0-70792
0; trapped in solid matrices, Schumann-Runge bands 0-55311
0; trapped in solid matrices, Schumann-Runge bands 0-55311
0; local mode vibrational constant in alkali halides, luminescence spectra 0-44900
0; molecular luminescence centre in alkali halides, vibrational relaxation, nonradiative transitions 0-44920
0; in alkali halides, luminesce, phonon wing struct. 0-76152
0; in, electronic configuration 0-52923
0; ING band system, relative intensities in normal and type-B aurora 0-76426

O₂+, 1NG 0-76426

0—76426
O₂*, cluster ion formation and reactions in flowing afterglow
O-41416
O₂*, collisional excitation
O-53102
O₂*, by collisions with He, velocity distributions of fragments
O-77967
O₂*, dissociation reactions, collision-induced, at low energies
O-77966
O₂*, excitation of first negative bands by electron impact on O₂
0-43131
O₂*, vibrationally excited, production by solar u.v., effect of autoioniza

 $O_2^{+,\gamma}$, vibrationally excited, production by solar u.v., effect of autoionization 0-77826 O_2^{+} ion, collisionally induced dissociation 0-46603 $O_{2n|Z^2}$ complexes formed in $O_2+O_{2n^2}$ reactions, bond energy determ. 0-72529 O_2^{++} charge-exchange autoionization in Ar gas target, long-lived states 0-64249 O_2^{++} SCF and k, wavefunctions, comparison 0-70749 O_2^{++} Description, metastable helium influence 0-56814 O_2^{++} containing by O_2^{++} , probability of O_2^{++} (O_2^{++}) excitation 0-39398 O_2^{++} (O_2^{++}) upenching efficiency of O_2^{++} relative to other gases 0-41446 O_2^{++} O_2^{++} +neopentane-neopentanol, or -neopentyl radicals +OH 0-48181 O_2^{++} Proposition, rate constant by measurement of intermediate quan

0–48181 Or(D)+H₂O reaction, rate constant by measurement of intermediate quantum yield following flash photolysis 0–45084 O₂(\(^{1}\)_{4}\), summer daytime height profiles, at Fort Churchill 0–45166 O₂(\(^{1}\)_{4}\), auroral i.r. emission, enhancement in <IBC II auroras 0–59633 O₂(\(^{1}\)_{4}\), collisional quenching by gases in atmosphere 0–39396 O₂(\(^{1}\)_{4}\), emission in airglow, production and loss mechanism, O₃-distrib. study 0–54265 O₂(\(^{1}\)_{4}\), emission in aurora, rocket obs. 0–79567 O₃(\(^{1}\)_{4}\), excitation in auroras by electric field 0–69301

Oxygen continued

tygen continued $O_2(^1\Delta_g)$ excited molecules, conc. in upper atmosphere O_72635 OI 1304 A resonance radiation, production rate in dayglow, excitation and radiative transport theory O_76810 OI 6300 Å line nightglow, width variations during mag. storm O_76811 OI auroral 1304 Å resonance radiation, excitation rate, radiative transport calculations O_76820 OI forbidden airglow 5577 Å line emission, diurnal variation at 22 IGY stations O_76809 O: O_76809 O:

 $O_2+N_1+H_2$ flame reaction mechanism using 2 computational methods 0.54182 $O_2+O_{2n}^{1}\rightarrow O_{2n}|_2^{1}$ reactions (n=1-8), equilibrium constants 0-72529 O_2^{+} chemiluminescence in $H_2O_2+OCl^{-}$ reaction 0-79428 $O(2^{1}D_2)$ quenching data in various species, use of OH radical as spectroscopic marker 0-74121 $O_2^{+}(2\Pi_e)$ photoelectron spectra using 736 and 744Å Ne radiation 0.54436 $O_3(b)^{1}Z_g^{+},v'=0)$ flashphotolytic production, reactive lifetime collisional quenching 0-46627 in Si, concentration determination by i.r. absorption 0-75143 in Si, electron irrad. damage obs. 0-43661 in Ta, solid solution hardening 0-43806

Oxygen compounds
OH, Galactic, 47 new sources, distrib, and props. 0–66392
oxide, localized and itinerant electrons, reviews 0–59134
oxide layers on metal substrate, emittance 0–62221
oxides, films, on metal emissive power in relation to structural defects
0–71461
oxides, quantitative electrons, reviews 10–62221

0-71401

oxides, quantitative electron microprobe analysis of oxygen 0-72574

oxides, solid, bulk modulus-volume relationship 0-75215

O₃₊H→OH^{vbr}+O₂, distribution of vibrational population in OH radicals for the H+O₃-atomic flame 0-61132

Al₂O₃ adsorption of H⁺ and OH⁻ in water, equiadsorption acidity point 0-71451

0–71451
Cs-O system, liq., ¹³³Cs n.m.r. rel. to state of O atoms 0–46956
Fe-Cr-O system, phase relations, high temp. and strongly reducing conditions 0–59127
Mg Cr-O system, phase relations, high temp. and strongly reducing conditions 0–59050
Nb-O-N, dilute system, yield stress, comp. depend. 0–65397
Nb-O, solid solution, plastic deformation, 4.2-550 K, yield stress, comp. depend. 0–55975
Nb O solid solution, chemical interaction 0–68533
Nb 1.0 at:%Zr-O alloy, substitutional interstitial interactions, internal friction 0–40252
Ni-O alloys, adherence to alumina 0–50812

tion 0-40252 Ni-O alloys, adherence to alumina 0-50812

non 0-40252

Ni-O alloys, adherence to alumina 0-50812

O₃, relative intensities and Raman shifts of rotational structure 0-53042

O₂, '(As'É_c, paramag, susceptibility, 4.2-300°K 0-72193

OCS, anomalous spectrum assoc, with sudden Stark shifts 0-74298

OCS, elec. dipole moment and mol. quadrupole moment 0-70940

OCS, microwave spectral line width as broadened by methyl bromide, evaluation 0-77823

OCS, mol. second-order force consts. and F- matrix soln. 0-53047

OCS, pressure broadening of rotational lines, theory 0-43124

OCS photolysis as source of S(³P) and S(¹D) 0-72524

OCSe, molecular g-value, magnetic susceptibility anisotropy and quadrupole moment 0-74295

OC1₃, reaction with H atoms, i.r. chemiluminesc. 0-54177

OD free radical, microwave lambda doubling Δ F=0 transitions 0-70939

OD interstellar, new spectral lines, 200 to 500 MHz 0-69414

OD¹, rotational anal. of ${}^3\Pi_{r}$ – ${}^3\Sigma^-$ electronic transitions 0-70938

O₂F₃ radical, i.r. absorpts., prod. by F₇-O₂ photolysis, 20°K 0-39397

O₂F₃ 1.r. spectrum, vibrational potential, and bonding 0-43130

OF(${}^3\Pi$), Hartree-Fock wavefunction, binding energy, ionization potential, electron affinity, moments 0-70936

OH -alkali-halide systems, tunnelling matrix elements strain depend, effect

OH -alkali-halide systems, tunnelling matrix elements strain depend. effect 0-47819

0–47619 0H, 79 μ m electric dipole moment meas. by magnetic resonance absorption method 0–61130 OH, galactic emission and absorption, 18 cm obs. from longitudes 350° to 50° 0–54396

OH, interstellar, 6 cm Λ doublet radiation from ${}^2\Pi_{1/2}$, $J={}^1/{}_2$ state, obs. 0–45305

0–45305 OH, spin generalized SCF wavefunctions using GF method 0–67732 OH, spin generalized SCF wavefunctions using GF method 0–67732 OH A*2+ state, radiative and predissociation probabilities 0–61129 OH absorpt., 18 cm, obs. against galactic continuum sources 0–66406 OH absorption at 1667 MHz near galactic centre 0–54397 OH airglow emission, altitude profile 0–76420 OH emission from ir. stars, search at 1612 MHz 0–45279 OH in sunspots, detection in spectrum between 1.4 and 2.6 microns 0–66650 OH interstellar, obs. OF F=1–0 Λ -doublet transition in ${}^2\pi_{1/2}$ J= ${}^1/_2$ state 0–57061 OH interstellar maser emission 0–79689 OH interstellar molecules, summary of research made so far 0–41728 OH interstellar in doped alkali halide crystals 0–47226 OH microwave lines, near i.r. stars, i.r. pumping and shock waves

OH microwave lines, near i.r. stars, i.r. pumping and shock waves

OH profiles in 4 interstellar dust clouds 0-48457
OH radical abstraction reactions, activation energies 0-62802
OH radical reactions with alkanes, flash photolysis and kinetic spectra

OH radicals, photolytically produced, effect on nucleation of NH₄Cl 0-72556

Oxygen compounds continued

OH source, NML Cygnus, long baseline interferometric meas. 0–66393 OH used as spectroscopic marker for quenching of O(2¹D₂) 0–74121 OH⁻ impurity in alkali halides, vibr. freqs. and lattice alignment 0–72350 OH⁻ in KCl and NaCl at 1.2°K, microwave resonant absorpt, spectra OH- impurity in alkali halides, vibr. freqs. and lattice alignment 0–72350 OH- in KCl and NaCl at 1.2°K, microwave resonant absorpt. spectra 0–79312 OH- ions, fluorescence in alkali halide crysts. 0–41269 OH+, band spectrum of ${}^3\Pi_{1}$ – ${}^3\Sigma_{1}$ transition 0–77827 OH+, rotational anal. of ${}^3\Pi_{1}$ – ${}^3\Sigma_{2}$ electronic transitions 0–70938 OH₃+, oxygen electric field gradient 0–61128 OH(A²Σ⁺) collisions with Ar and N₂, rotation-vibration energy transfer 0–64614 OH+C₃H₂-CO+CH₃ primary products determ. 0–66176 OH+N₂H₄–NH₃+NH₂O primary products determ. 0–66176 ONF₃, electronic structure calculations 0–70920 ONMe₃, electronic structure calculations 0–70920 IsOH, interstellar, search for radio emission at 1584.33 MHz 0–51693 IsOH, lines, absorption in Sgr A and Sgr B2, obs. at 1637 and 1639 MHz 0–79659

0-79659
0+N0+(M)→N02*+(M) at low pressures, chemiluminescence, radiative recombination 0-76421
Ta-O solid solus, e.m.f. meas. 0-75315
Ti-O solid solution, instertial order disorder transformation, neutron diffr.

0–40499
V-O solid solution, elec., mag. and mech. props., comp. depend. 0–58983
V-O system, phase relations below 1200°C 0–59056
Zr-O solid solution, c.p.h., elec. resist., comp. and temp. depend. 0–47829
Zr-Ti-O system, phase obs. on pseudobinaries, subsolidus ternary diagram 0–59057

in D-region concentration above 40 km, sunrise auroral rocket flight meas. 0-69323

in atmosphere, altitude profiles, estimation from O_2 emission in airglow 0--54265

in atmosphere, content effect on l.f. radio wave amplitude fall, pre-sunrise

in atmosphere, distribution, vertical, i.r. method for determination from satellites 0–72618 atmosphere, profiles 0–41493 atmosphere, transport processes in orographically induced gravity waves 0–48278

atmospheric, electrophotometer for observation 0-77197 atmospheric, extreme values obs. in AFCRL ozonesonde network, report 0-79521

atmospheric, externe values obs. in APCRL ozonesonde network, report 0-79521 atmospheric, profile from thermal emission spectra, 400-1500 cm⁻¹, Nimbus 4 Michelson interferometer expt. 0-76367 atmospheric, vertical distrib. measurements and appl. in tracer studies, short review 0-51514 atmospheric, vertical distribution, satellite experiment 0-48274 atmospheric, vertical distribution, satellite experiment 0-48274 atmospheric distrib. obs. from sunlight absorpt. 0-51542 effects on atmospheric electricity in stratosphere 0-66298 atmospheric vertical distribution in the winter subpolar region 0-51513 band origin of v₂ fundamental 0-39395 concentration in mesosphere rel. to collision processes 0-79523 in ionosphere, attachment cross-sections rel. to temp. 0-79576 in mesosphere, vertical profile, diurnal variations 0-56801 millimeter wave spectrum, calc. of dipole moment, g-factor and transition freqs. 0-77829 oxyozone, plane stady Navioer-Stokes detonation 0-45057 photolysis, u.v., effect of molec. O₂ 0-59508 rubber, e.p.r. meas. of strain-induced cracking in ozone environment 0-47417 rel. to spectra, atmos. i.r. emission, balloon-borne radiometer meas.

rel. to spectra, atmos. i.r. emission, balloon-borne radiometer meas. 0-45145

stratosphere and lower mesosphere, O₃ and H reactions, report 0-79520 in stratosphere lower and upper troposphere with tropopause folding, distrimeas. 0-59594

meas. 0-59594 stratosphere vertical distribution model 0-48257 [O]/[O₃] conc., photochemical changes in D-region, rel. to radio propag. and solar radiation 0-69324 O/O₂ conc. photochemical changes in D region, rel. to radio propag. and solar radiation 0-69324

Ozonosphere see Atmosphere

p-n junctions see Semiconducting devices/junctions

P-V-T relations see Equations of state

Pair creation see Electron pairs; and under individual particles, e.g. Mesons Palaeomagnetism see Rock magnetism

Palladium

adsorption of CO on (100) surface, binding energy determ. technique 0-43569 adsorption of CO on (100) surface. binding energy determ. technique 0-43570

band structure 0-50942

Debye temp., model calcs. 0–71862 diffuse layer, on ceramic exoelectron emitters, effect on sensitivity 0–73700

diffusion of dissolved H and D under the action of an electric field 0-78585

film, photoemissive and optical props. correl., vacuum u.v. 0-44759 g factor anisotropy and exchange splitting, in pure and Co-doped samples 0-44502

0-44502 impurity in Ni₃Ga, mag. susceptibility 0-44590 magnetic susceptibility maximum, anomalous peak obs. 0-75888 magnetization, high field, band structure effects 0-44595 magnetization, nonlinear, in semicontinuous fields up to 325 kOe 0-44503

0-44503 microgram level, fire-assay emission spectrographic method 0-54197 paramagnet f.c.c., anisotropic g factor of Fermi surface sheets 0-44499 photoelectric work function 0-75859 photoemission, direct transition analysis 0-65877 polymer formation in organic vapour environment obs., water drop reflection goniometer technique, surface preparation methods comparison 0-5694 sublimation, accelerated, under tensile stress in air 0-47007 thermal expansion, linear, coefficients at low temps., Gruneisen parameters 0-75411 tunnel junction, hydrogenation effects 0-71996 work function and exoemission, effect of deformation 0-75851 Au/Pd bimetal film interface, diffusion annealing, 150-350°C 0-50363

Palladium continued

CO adsorption on (100) face 0-47079 Pd⁴⁷Co, hyperfine fields, low temp. 0-76052 Pd(I), e.s.r. in paramag. complex 0-54160 Xe physical adsorption 0-47080

Palladium compounds

addum compounds
alloy, binary and ternary, giant moments of dilute Fe 0-44501
complex with metal-hydrogen bond, crystal structure 0-53513
porphyrin complex, luminesc. 0-79344
Ag.Pd-Cu contact spring material, age hardenable, characteristics and
performance for relay applications 0-59158
Ag.Pd:Mn.Fe, dilute alloy, mag. susceptibility, s-d exchange scatt.
0-44404

AgPd:Mn.Fe, dilute alloy, mag. susceptibility, s-d exchange scatt. 0–44494
Alpd, AlPd, intermetallics, Knight shift, diamagnetic susceptibility, 77-300k 0–69193
Co-Pd alloy, ferromag, nuclear specific heat meas. rel. to hyperfine fields, 0.4-4.2K 0–56445
Co-Pd alloys, Young's modulus and thermal expansion 0–65551
Co-Pd solid solution, thermodynamic props. 0–68530
Co-Pd system, ordered phase obs. 0–61849
Cr-Pd-Si alloys, amorphous, Kondo-type s-d exchange interaction 0–78877
Cr-Pd siloys disordered antiferromagnetism. 0–62560

C1-ref alloys, almorphous, Kondo-type s-d exchange interaction 0-78877 Cr-Pd alloys, disordered, antiferromagnetism 0-62560 Cu-Pd, sp. ht. comp. depend., 1.5-4.2K, rel. to band structure, ordering effects 0-43903

CuPd:Mn,Fe, dilute system, mag. susceptibility, s-d exchange scatt.

Cu₃Pd, long period ordered alloy, lattice modulation, X-ray diffr. 0-40076

0-40076 Cu₃Pd alloy, periodic antiphase struct. 0-71582 Fe-Pd dil. alloy, ferromag., nuclear specific heat meas. rel. to hyperfine fields, 0.4-4.2 K 0-56445

Tietus, 0.44.2 K 0.30442 Fc(Pd₂Pt)_{2.2}) alloys, mag. behaviour, Mossbauer obs. 0–79207 H-Au-Pd, electrical resistivity as function of H concentration 0–71943 Mn-Pd-Si alloys, amorphous, Kondo-type s-d exchange interaction 0–78877

0-78877

Ni-Pd alloy, impurity clustering and matrix polarization 0-44594

Ni-Pd alloys, ferromag., Mossbauer effect, supermag. Fe clusters
0-51284

Ni-Pd alloys, mag. moment distrib. 0-54011

NiPd alloys, hyperfine field at Ni site; conc. depend., ⁶¹Ni Mossbauer obs.
0-44794

Pd: ⁵¹Co, hyperfine fields, low temp. 0-76052

Pd: Ni, dilute alloy, thermal and elec. resistivities, low temp. Lorenz numbers 0-44065

ers 0.—44065

Pd-Ag alloy, equilib solubility of interstitial H₂, stress effects 0.—53532

Pd-Ag alloy film, homogeneity rel. to prep., X-ray diffr. 0.—47067

Pd-Ag contact alloy, mechanism of tarnishing obs. 0.—55913

Pd-Ag coll alloy, magnetization, high field, band structure effects 0.—44595

Pd-Ag(Au) alloys, resistivity minima 0.—71958

Pd-Au alloy, non-magnetic Elinvar-type, effect of addition elements on mech. props. 0.—65358

Pd-Au alloys, band filling, 'Fe and ¹⁹⁷Au Mossbauer obs. 0.—62260

Pd-Au (Styrem, nonmagnetic Elinvar-type alloy, heat treatment effects 0.—65357

Pd-Au(Ni, Cu, Co) alloys, short-range order 0.—58745

0-65357
Pd-Au(Ni, Cu, Co) alloys, short-range order 0-58745
Pd-B solid solns., low temp. heat capacities 0-62212
Pd-Ba alloy, struct. of Pd₃Ba comp. 0-50544
Pd-Co(Mn), dilute alloy, specific heat, mag. field depend., 1.2-30 K 0 - 43909

Pd-Cu contact alloy, mechanism of tarnishing obs. 0–55913 Pd-Fe, ferromag. alloy, n.m.r., spin-lattice relaxation, local effects 0–45036

0-45036

Pd-Fe dil. alloys, mag. props. 0-44596

Pd-Fe dil. alloys, resistive behaviour at Curie temp. 0-79174

Pd-Gd dil. alloys, g shifts, e.p.r. 0-56660

Pd-H alloys, residual resistivity and low temp. thermopower 0-62310

Pd-H dil. alloys, the resistivity and low temp. thermopower 0-62310

Pd-H dil. alloys, the remopower, virtual recoil evidence 0-59277

Pd-H syst., elec. resist. meas. from room temp. to 55°K 0-65626

Pd-Mn, alloys, ferromag. antiferromag. transition 0-51212

Pd-Mo-Co solid solution, mag. susceptibility, elec. resist., temp. and comp. depend. 0-62309

Pd-Ni, dilute alloy, mag. moment distrib., neutron diffr. 0-44574

Pd-Ni, electron-electron scattering effects in low temp. Lorenz numbers, theory and exp. 0-68535

Pd-Ni alloys, compressibility linear dependence on composition 0-78618

Pd-Ni alloys, 4.7 at.% Ni max., giant moments near critical composition 0-41009

Pd-Ni dil. alloys, magnetostriction and magnetiz. 0-72242

0-41009
Pd-Ni dil. alloys, magnetostriction and magnetiz. 0-72242
Pd-Np alloy, resistivity, mag. susceptibility, Kondo temp., 1.6-300 K, comp. depend. 0-44066
Pd-Pt-Cr alloy, mag. susceptibility and solute resistivity 0-40729
Pd-Pt system, isoelectronic, mag. susceptibility 0-79130
Rd-Rh,Pd-Ag,Pd-H with Fe as impurity, ferromagnetic resonance meas.

0-54157
Pd-Rh alloy, n.m.r., Knight shift, line width, spin lattice relaxation, 1-4 K 0-45007
Pd-Rh dil. alloy, magnetization, high field, band structure effects 0-44595
Pd-(2 wt.%)Rh alloys, Knight shifts of 100Rh41382 0-41382
Pd-Sb alloys, 121Sb isomer shifts, rel. to electronic struct. 0-54078
Pd-Ta alloys, Hall effect and susceptibility temp. depend. 0-75898
α-Pd-X solid solns., lattice spacings, X=particular solute metal 0-75100
Pd complex, dithioacetylacetone Pd(II), electronic spectra, MO calc. 0-67748
Pd complex Pd(PE), wibt spectra 0-55309

Pd complex, Pd(PF₃)₄, vibr. spectra 0-55309 Pd complexes, phosphines, metal isotope effect on metal-ligand vibrations -77763 microcrystals, u.v. results, attributions of absorption bands

0-59406 Pd(CN)₄²⁻ in aqueous soln., mag. circular dichroism and u.v. spectral

Pd(UN) $_{h}^{-}$ in aqueous soin., mag. circular dictronsm and u.v. spectral assignments 0—71358 Pd $_{80-x}$ Fe $_{x}$ Si $_{20}$ alloys, amorphous, superparamag. props. 0—72236 β -PdH, metallic system, nuclear proton relaxation 0—69200 Pd(I) complex produced in γ -irrad. bis(acetylacetonato)Pd(II), e.s.r. 0—54160

0–54160 Pd(II) square-planar tetraamine complexes, polarised u.v. reflection spectra and electronic struct. 0–70944 β -PdIn, energy bands, augmented- plane-wave method, specific heat, mag. susceptibility 0–78840 Pd₃Mn, periodic antiphase domain struct. and defects 0–75137

Palladium compounds continued

Pd₂MnGe(Sn), atomic and mag. ordering 0-41003

PdMnSb, mag. props. 0-72283 Pd₂MnSn Heusler alloy, internal mag. field at ¹¹⁹Sn site, Mossbauer obs.

0-40939

Rh-Pd-(1 wt.%)Fe dil. alloys, Mossbauer obs. 0-76054

Rh-Pd, f.c.c., low-temp. sp. heat 0-71863

capacitors, chlorophenyl-impregnated ionic impurity effects 0-44384

capacitors, chlorophenyl-impregnated ionic impurity effects 0—44384 cellulose, Kraft form, exp. study of electrical properties 0—68886 dielectric props. of pressboard and polyesterfilm treated paper 0—56343 impregnated, high-field conduction 0—68905 impregnated, surface breakdown under impulse voltages 0—68909 insulating, impregnated with liquids of high permittivity, physical factors affecting behaviour 0—68884 insulating, loss tangent and permittivity, 2.5 to 295°K, 47Hz to 89.5kHz 0—68892

oil-impregnated, direct voltage breakdown rel. to temp. gradient 0-68910

oil-impregnated, thermal conductivity meas, transient methods 0–68641 oil-impregnated, thermal conductivity meas, transient methods 0–68639 oil/paper dielectrics, accelerated ageing tests, use of loss angle meas. 0–68893

onionskin, sound velocity, rel. to pressure, temp. and frequency 0-53701

Paraelectric materials see Dielectric properties of substances

Paramagnetic resonance and relaxation
see also Lasers; Masers
acetonitrile, p-irrad., radiation damage 0—76228
p-X-acetophenone anion radicals, hindered rot. of acetyl group 0—64471
acoustic, saturation and instability 0—56666
acoustic e.p.r., self-induced transparency investig. 0—76221
acoustic mag. reson., spin systems and general principles 0—41358
acoustic paramag, relax. 0—50865
acridine-acridan mol. complex, prod. of four radical species 0—79411
L-alanine, Cu(II)-doped cryst. 0—62765
alcohol, solid and liq., structural effects near solidification temp. 0—55653
alkali halides, ENDOR obs. of F centres, elec. field effects 0—45039
alkali halides, ENDOR obs. of F centres, elec. field effects 0—45039
alkali halides, dipole equil. establishment in field-free conditions 0—72486
alkalin metal-ether solns., electron recombination rate constants, e.s.r.
determ. 0—48201
alkali titanate glasses, p-irrad. 0—62748
alkaline earth fluorides, colour centres 0—75176
alkaline earth fluorides, of Ti² 0—79395
alkanes, positive holes in irrad. glasses 0—54161
alkyl radicals, fluorine and chlorine substituted hyperfine splittings
0—53066
t-alkylperoxy radicals, ¹⁷0 enriched, hyperfine constants. 0—49900
amino agide, X-irrad.

0—53066

L-alkylperoxy radicals, ¹⁷O enriched, hyperfine constants 0—49900 amino acids, X-irrad., correlation with optical spectra 0—59458 amino radical and deuterated derivative, ¹⁵N labelled, e.s.r. study, hyperfine splitting 0—64478

2-amino-1,4-naphthosemiquinones N-substituted in i-propanol, e.s.r. spectra 0—74331

anthracene adsorbed on silica gel, γ -irrad., radical form. 0–39458 anthracene e.p.r. studies of optical spin polarization in triplet state 0–74333 anthracene single crystal, triplet excitons 35 GHz, 300 and 100K

anthracene single crystal, triplet excitons 35 GHz, 500 and 100K 0-66144 anthracyl radical 0-67765 antiferroelectric, NH₂PO₄, of Cr³⁺ 0-72484 antimony oxides, of Fe³⁺, spectra and symmetry 0-72488 aromatic hydrocarbon cation radicals, monomeric and dimeric 0-53093 aromatic reduction and symmetry oxides are reductive, and symmetry 0-72488 aromatic hydrocarbon cation radicals, monomeric and dimeric 0-53093 aromatic reductive, and symmetry 0-72488.

aromatic molecules, phosphorescent, hyperfine structure of Δm_s =2 transitions 0-55336

azides, paramag, defects prod., excitons role 0–79406 p-azoxyanisole liquid crystal molecules, rel. to elec. field ordering 0-43429 benzophenone anion radicals, fluorine substituted, $^{19}\mathrm{F}$ hyperfine splittings 0-77872

U = 1/872

n - benzoquinone, chemisorption on Ge, surface elec. props. 0—40802
bicyclic hydrocarbon radicals, coupling, electronic structure 0—74344
bicyclo-octyl radicals, by γ-irradiation of 2,2,2-bicyclo-octane, spectra
0—55341 bicyclo[2,2,1]heptan, γ irradiated, radical production, e.s.r. study 0-74420

biphenyl adsorbed on silica gel, γ -irrad., radical form. 0—39458 bis(trifluoromethyl) nitroxide, temp. dependence, theoretical analysis

0-70979

0—70979
borate glasses, γ-irrad., structure of trapped hole centres 0—62750
borate glasses, γ-irrad., structure of trapped-hole centres 0—59447
tert-butyl radical, study of effect of temp. on hyperfine coupling 0—74409
cation radicals, monomeric and dimeric 0—53093
colloidal suspensions, paramag., hyperfine structure 0—53381
conduction e.s.r. in liquid and solid Na, 293-453°K 0—39837
conference, India, Dec. 1969 0—38788
copper acetate monohydrate, γ-irrad. crysts. 0—59459
copper calcium acetate hexahydrate, Cu²⁺ h.f.s., true ligand field obs. 0—41352
conner diethyldithionhosphate, h.f.s., symmetry 0—41328

copper diethyldithiophosphate, h.f.s., symmetry 0-41328 copper salt of organic acid 0-51400

corannulene, phosphorescent, e.s.r. studies, of pseudorotation, and configuration 0-46551

continguration U=45351 covalent solids, rel. to Jahn-Teller effect for single vacancy 0-44726 cryostat for obs. at 2 300°K 0-72860 CsCoCl₃ obs., g and hyperfine tensors determ. 0-48161 defect centres with g factors close to free spin values, theor. interpret. 0-56665

0–56665
detection of signals, third-derivative 0–73114
diamond, ¹³C⁴⁴, ²⁹Gi⁴⁺, ¹³G⁴⁺ obs. 0–48141
diamond, natural, spectrum analysis 0–59454
diamond, synthetic 0–56667
2,3-diazanaphthalene, in rigid glass solns. at 77K. 0–71025
dibenzo[b,f]thiepin sulphoxide anion radicals 0–67788
dicyanobenzene complexes with methyl substituted benzenes 0–46556
dihydrothymine cryst. *y*-irrad, e.p.r. study of radical form. 0–77970
dihydrouracil, *y*-irrad, single cryst. 0–59460
4,4-dimethyl -1,2- tetralindione anion radical CH₂ hyperfine splitting
0–64515

0-64515

diplieadane anion radical 0-70994

Paramagnetic resonance and relaxation continued

ramagnetic resonance and relaxation continued disulphide compounds, reaction with organic free radicals in aqueous solution, e.p.r. 0–69210 dolomite Mn²⁺, forbidden hyperfine transitions 0–59450 durene, p-irrad, free radicals 0–62766 durosemiquinone system, e.s.r. studies, exchange between triplet ions and parent quinone T.H.F. 0–59477 dynamic polarization by solid effect 0–69064 ENDOR, nuclear polarization, effect of relax, transitions 0–67413 ENDOR in external elec. field, line shift, rel. to paramag, centre wave functions 0–62779

ENDOR in external efect, line shift, fet, to parallag, centre wave functions 0–62779
ENDOR in solids, technique and appls, review 0–41387
ENDOR studies of V_{ob} centre in CaO 0–50611
EPR low temp, reflecting resonator, specimen transport mechanism 0–48935

EPR study of specimen under single axis press., use of low temp. resonators 0-51386

tors 0-51386 ESR, studies of superadditivity in phenidone-hydroquinone system during development 0-70111 in effective field, $T_1 \neq T_2$, $\Delta \omega = 0$ case 0-76968 electron-electron double resonance of triplet excitons 0-66145 electron-nuclear coupled syst. with dipolar interaction, transition probabilities, eigenvalues 0-72474 exciton triplets and paramagnetic impurity centres in crystals of tetracyan-quinodimethane and methyltriphenylphosphonium, EDR spectra 0-66146 F centre production and line at each 06 in 7-6. On the contraction of the contraction and line at each 06 in 7-6. On the contraction is 0.000 and 0.0000 and 0.0000 and 0.0000 and 0.0000 and

0-66146
F centre production and line at g~1.96 in ZnO 0-61981
feldspars, of Fe³- struct. obs. 0-66131
ferrocene derivatives, cations, rel. to electronic structure of ferricenium cation 0-71001
ferroelectric, SrTiO₃, elec. field effect 0-62763
ferroelectric, (NH₀)₃ of Gd³+ 0-72494
ferroelectric, (NH₀)₃ OΔ, transition obs. 0-62758
ferroelectric, guanidinium aluminium sulphate hexahydrate, of Cu²+ mag. complexes 0-72500
ferroelectric, triglycine sulphate, γ-irrad., radicals struct. and motions 0-66147
ferromagnet. FuS. FuOn a. Fa. FuO and Funce Gda a.O. 80-500 K. line ferromagnet. FuS. FuOn and Funce Gda a.O. 80-500 K. line

0-0014′, EuS, EuO_{0.9}, F_{0.1}, EuO and Eu_{0.96} Gd_{0.04}O, 80-500 K, line narrowing, exchange interactions 0-41329 ferromagnet, Sc_{31x}In alloy, magnetization, comp. and temp. depend. 0-44997

fluorene, anion radical, CH₂ hyperfine splitting 0–64515 fluorinated triphenylmethyl radicals, ¹⁹F hyperfine splittings 0–77907 fluorobenzaldehyde radical anions, e.s.r., hyperfine coupling constants 0–49944

0–49944
fluorobenzyl radicals e.s.r., hyperfine coupling constants
forbidden transitions and discrete saturation 0–76205
formaldehyde, multi-photon transitions 0–61062
gadolinium ethyl sulphate, relaxation times 0–69182
general eqns. derivation 0–79211
glass, Na₂O-TiO₂-SiO₂, Ti³+ obs. 0–72487
glass, adsorbed organic radical, p radiation, e.s.r. 0–39933
glass, borate, containing Ti, p-irrad., and optical absorpt. spectra
0–51394 guanidinium aluminium sulphate hexahydrate, of Cu2+ mag. complexes

0 - 72500haemoglobin, conformations 0-43199

haemoglobin, conformations 0–43199
helices, progressive and resonant wave, applic. 0–60121
heme, oriented in organic cryst. 0–54162
heterocyclic multisulphur radical cation 0–64469
hydrocarbon free radicals, in liquid soln., e.s.r. linewidth and saturation
studies 0–46606
hydroquinone cation radical, ¹⁷O and ¹³C hyperfine interactions 0–74347
hydroxyanthrasemiquinones, e.s.r. spectra, solvent effects 0–78302
imidazo p-benzoquinone anion, possible case of proton jump 0–67801
1,2-indandione anion, radical, CH₂ hyperfine splitting 0–64515
inhomogeneously broadened lines, quenching of cross correlation
0–56467
ion pair equilibria exam. 0–59479

1,2-indandione anion, radical, CH₂ hyperfine splitting 0–64515 inhomogeneously broadened lines, quenching of cross correlation 0–56477 ion pair equilibria exam. 0–59479 jons % state in soln, e spin relax. 0–64954 isobutyric acid radical in aq. soln., e.s.r. spectra 0–43196 isolated spin, second harmonic generation at microwave freq., external mag. field depend. 0–79393 Jahn-Teller system, NaCl:Cu²+, spectra at 77 and 95-100K 0–76224 Kramer's doublet in lattice with symmetry axis, mean g value 0–41314 lanthanum ethyl sulphate, of nearest-neighbour Gd³+ pairs 0–41353 laser rods, ruby, non-destructive test technique 0–57534 line broadening, internal stresses, 3d³ ion in T_a symmetry 0–79409 line shape representation, parameters for single line esr spectra 0–66986 line shapes for mol. triplet excitons, temp. effect 0–79392 line shift due to spin-phonon interactions in Fe group ions 0–66132 line width, ang. and temp. depend., theory 0–41313 lines, nonuniformly broadened, relaxation processes 0–76203 lineshapes, effect of anisotropic rotational diffusion 0–68147 liquid crystal, nematic, containing vanadyl acetylacetonate, correl. with n.m.r., rel. to mol. motion 0–78307 liquid during photolysis, hyperfine interactions of ¹³C 0–71381 lithium naphthalenide anion 0–39433 lunar materials 0–59741 lunar samples, 9 and 35 GHz, 4,8 and 300K 0–48539 lunar samples, 9 ond 35 GHz, 4,8 and 300K 0–48541 magnetically dilute crystals, spin-lattice relax. 0–54048 magnezite, Mn²+, forbidden hyperfine transitions 0–59450 matrix interaction for e.p.r. spectrum in paramag, cryst. under external stress 0–76202 metal, spin reson, and relax. 0–54149 metal, spin reson, and relax. 0–54149 metal, theory 0–76197 metal-ammonia solns., solid, high mobility of electron pairs near metal-non-metal transition 0–75541 methyl acetoh, solid, α- and γ-irrad., electron spin echo for spatial radical distrib., influence of LET and spur effects 0–66133 methyl group, motional averaging, e.s.r. hyperfine structure prediction 0–71013 methyl radicals, grou

methyl radicals, group IVB substituted e.p.r. study evidence for d-p- π bonding 0-43195

Paramagnetic resonance and relaxation continued

methylene, CH2, triplet state 0-61169

molecular beam, multi-photon transitions 0-61062 molecular matrices, binary solids, of stabilized Ag atoms 0-72475

molecular matrices, binary solids, of stabilized Ag atoms 0–72475 NH₄Cl:Cr³⁺, 77-330 K 0–44991 naphthalene, conjugated ions, spectra, open-shell SCF configuration interaction treatment 0–74390 naphthalene, dynamics of opt. electron-spin polariz., from mag. field effects on phosphoresc. 0–58233 naphthalene adsorbed on silica gel, p-irrad., radical form. 0–39458 naphthalene single crystal, triplet excitons, 35 GHz, 300 and 100K 0–66144 naphthalenes, fluorinated, cation radicals, spin-density calcs., Q parameters, splitting 0–74393 naphthalenes, substituted, triplet state e.p.r. 0–48155 naphthyl radical 0–67765 nickel acetate tetrahydrate, e.p.r., irradiation induced spin pairing 0–62767 nitrosobenzene and its radical anions, pot. barriers and reson, energies

nitrosobenzene and its radical anions, pot. barriers and reson. energies 0-64532

0-64532 nitroxide radicals, fluoro-substituted, angular dependence of β-fluorine e.s.r. hyperfine coupling 0-55367 nitroxide radicals and biradicals in nematic solvents 0-78304 No, hyperfreq, susceptibility variation with temp. 0-61104 7-norbornenyl radical, e.s.r. spectrum 0-43177 nuclear relaxation under strong e.p.r. saturation 0-47976 organic compounds, unsaturated, H and D bombarded, e.s.r. of radicals produced 0-79410 organophosphorous compounds containing P=O group, effect of solvent on spin spin interac. consts. 0-43433 orotic acid, single crystal irradiated, H abstraction, e.s.r. 0-41354 1.4-parabenzosemiquinone, hyperfine interactions due to ^{13}C 0-61550

orotic acid, single crystal irradiated, H abstraction, e.s.r. 0-41354 1,4-parabenzosemiquinone, hyperfine interactions due to ¹³C 0-61550 anti-1,4,1',4-[2,2] paracyclonaphthane radical anion 0-77942 paramagnetic cryst., under external stress, matrix interaction 0-76202 pectin, polymer, e.s.r. study of effect of X-rays 0-67836 perfluorocyclobutanone ketyl, angular dependence of β -fluorine splitting 0-55366

permethylcyclopolysilanes anion-radicals, electron delocalization

0 - 74408

0—74408
perovskite-type cpds., struct., book 0—68293
phenanthrene adsorbed on silica gel. p-irrad., radical form. 0—39458
phenyl radical 0—67765
9 phenyl thiaxanthyl radical, evidence of restricted rotation from e.s.r. spectra 0—67811

tra 0-67811
phonon width of line and spin-lattice relax., contrib. of crystal lattice anharmonism 0-76204
polyacrylonitrile, pyrolyzed and irrad. 0-72501
poly-3,3-bis(chloromethyl)oxetane, e.s.r. spectra comparison after irradiation with electron beams and u.v. light. 0-54163
poly-3,3-bis(chloromethyl)oxetane, irradiation with electron beams and u.v. light, formation mechanism 0-54163

light, formation mechanism 0—54163
polycarbonate, paramagnetic species produced by p or u.v. irradiation investigated by e.sr. 0—54164
polyethylene, u.v. irrad., e.s.r. spectra, press. depend. 0—53095
polymer, fracture mechanisms, e.p.r. spectra 0—40420
polymers with conjugated system, rel. to electronic struct. 0—75695
propionic acid radical in aq. solm, e.s.r. spectra 0—43196
pyrene-d-10, e.s.r. relaxation, temp. dependent measurements on excited triplet state 0—41394
pyrenyl radical 0—67765
quartz, e.sr. detection of fossil alpha damage 0—50597
quartz, morion, smoky colouring features 0—59407
quartz dissess, p-irrad, capture centre obs. 0—43689
radicals in p-irrad. single crystals 0—62667
radicals in thymine, e.s.r. obs. of single crystals 0—69189
relaxation in nonuniformly broadened lines 0—76203
rubber, e.p.r. meas. of strain-induced cracking in ozone environment 0—47417
ruby: Cr³+, fourth- nearest-neighbour pairs obs. 0—44901

0-47417
ruby: Cr³+, fourth- nearest-neighbour pairs obs. 0-44901
ruby: Cr³+, line broadened by strong hyperfine interactions, second moment 0-51389
ruby: Cr³+, phonon and photon paramag. -response line shapes 0-44984
ruby, X-irrad., isothermal annealing kinetics of Cr ions 0-79396
ruby, n.m.r. saturation and population inversion 0-69195
scheelite cryst., of Yb³+, hyperfine spectra 0-76207
scheelite cryst., of Yb³+ 0-76206
semiconductor, Si-P, d.c. cond. charge 0-72491
semiconductor, n-Si-P, uniaxial compression effect on hyperfine splitting 0-79407
semiounione ions e snip lattice relax time, obs. 0-41322

0—79407
semiquinone ions e spin lattice relax. time, obs. 0—41322
smectic liquid crysts., spin labelled 0—78301
sodalite, photochromic, of F-type centres 0—62760
solvent induced conformational kinetics, study by e.sr. 0—55281
spectrometer, electron resonance spectra recording, mag. field calibration
using p-resonance freq. marks, device 0—48934
spin echo in dipolar broadened solids 0—56679
spin labels, relative to e.p.r. applications 0—48936
spin labels in oriented smectic liquid crysts. 0—78301
spin-lattice relax in F, quartet 0—44724
spin-lattice relax in G, quenching of cross relaxation 0—56467
spin-lattice relaxation, quenching of cross relaxation 0—56467
spin-lattice relaxation in Fe group ions, line shift obs. 0—66132
sulphydryl compounds, reaction with organic free radicals in aqueous solution, e.p.r. 0—69210
surface relax in cond.-e.s.r. 0—62747
of synchrotron oscillations of large amplitude, theory and experiments

of synchrotron oscillations of large amplitude, theory and experiments 0--63524

0-63524
d/tartaric acid, deuterated x-irradiated at 195°K 0-76229
tartaric acid solns., e.p.r. during photolysis, emission spectrum 0-62823
tartrate: transition elements 0-41343
tetracyanoquinodimethane, electron-electron double resonance of triplet excitons 0-66145
tetracyanoquinodimethane potassium, absorpt. signal anisotropies rel. to temp. 0-41356
tetramethylphenylenediamine-TCNQ complex, spin excitations of Heisenberg linear chain 0-41356
tetraphenyldiphosphine, u.v. irrad., e.s.r. 0-76280
thioxanthone anion radicals 0-67788
thymidine, radiation damaged deuterated cryst. 0-59461

0-43912 $CdF_2:V^{3+}(Cr^{3+})$ and impurity centres, 77 K 0-44987

Paramagnetic resonance and relaxation continued Paramagnetic resonance and relaxation continued topaz, parameters correl. with Fe3+ sites 0-79398 Cd(I) formalism in complex CaCd(OOCCH₃)₄.6H₂O e.s.r. evidence 0-48156 transition elements in Sr and Ca tartrates 0-41343 transition ions, book 0-41312 CdIn₂S₄:E³⁺, and absorpt. and fluorescence spectra, energy levels triary/methyl radicals, e.s.r. spectra 0-43185 triglycine sulphate, p-irrad., internal motion of H and glycine (I) activation energy 0-62768CdIn₂S₄:Yb³⁺, and optical meas., rel. to site symmetry of Yb³⁺ 0–56473
CdS:Cu²⁺, paramag, centres and i.r. absorpt, correl. 0–72370
CdS:Gd³⁺, impurity site determ, 7TK 0–44988
CdS:Gd³⁺, two centres 0–79400
CdWO₄:Cr²⁺, 293K, crystal field const. 0–41348
CeO₂ adsorbed on synthetic zeolites, hindered motion obs. 0–70922
ClO₂ in H₂O-butyl alcohol, e.s.r. linewidths 0–68148
Co complex, [Co en₃]Cl₃.Ha²O₂O Cr²⁺; linewidth 0–48143
Co complex, loc en₃Cl₃.Ha²O₃O Cr³⁺ linewidth 0–48143
Co complex, o-phenylenebis(dimethylarsine) 0–66134
Co(II) complexes, pentacyanocobaltate (II) with aromatic nitro cpds. 0–77783
Co(II) low-spin complexe cyanidar. 0–54154 CdIn₂S₄:Yb³⁺, and optical meas., rel. to site symmetry of Yb³⁺ 0-56473 triglycine sulphate, p-irrad., radicals struct. and motions 0-66147 triglycinsulphate, Cr and V doped, fine struct. 0-51401 triplet excitation in molecular aggregates and magnetoselection 0-54148 unified theory with n.m.r. rel. to proton polarizations in proton spin refrigerators 0-51381 D,L-valine free radicals, conversion processes 0-45090 viscous media, line shape, molecular rotational diffusion effect 0-74788 yttrium ethyl sulphate, Er doped, dynamic proton polarization obs. 0-76230 0—76230

zinc acetate dihydrate, e.p.r. of Mn²⁺ 0—56676

ZnO, ESR line at g≈1.96, and F-centre 0—61981

Ag complex, dipyridyl-coordinated ≰ ½²(4d²) 0—41315

Ag in p-irrad, frozen aq. solns, paramag, relaxation 0—45088

Ag Br:Fe_{11,11} defects obs. 0—50578

Ag Cl:Fe_{11,11} defects obs. 0—50578

Ag Cl:Eq. defects obs. 0—50578

Ag Cl:(Se,Cd), Se impurity centre, hyperfine interactions 0—44982

Ag Cl:(Se,Cd), Se impurity centre, hyperfine interactions 0—62820

(Agpy); defects on the second complex p-irrad. 0—62820

(Agpy); complex ion, e.s.r., wavefunctions and ring angle determ. 0—46447

ABB CO_Fe²⁺ chrysophery! X- and O-band frequencies 0—78307 0—77783

Co(II) low-spin complex cyanides 0—54154

Cr³⁺, e.s.r. and electronic relaxation in water and water-glycerol mixtures 0—74787

Cr³⁺ in ruby, props., appl. in a three-level maser 0—69186

Cr³⁺ in single ruby crystal, paramagnetic fine structure spectrum 0—69185

Cr₂O₃, supported on alumina, meas. between —196 and 300°C 0—62487

Cr₂O₃, ground state luminescence transitions investigated by EPR 0—56594 0–56594
Cr₂O₂ powder, pure and Al₂O₃ doped 0–76214
Cs-ethylamine-NH₃ solutions, linewidths 0–55631
Cs-gSO₄:VO²⁺, and i.r. absorpt., rel. to A-, g-tensors, obs. 0–41347
CsCl:Cu²⁺, obs. and spin Hamiltonian analysis 0–41325
CsCl:Cu²⁺, single crysts. e.p.r. 0–59449
CsMgCl₃ obs., g and hyperfine tensors determ. 0–48161
CsNO₃, relaxation times of doped VO²⁺ ion 0–48162
Cs₃ZnCl₃, orthorhombic Fe²⁺ centre obs. 0–56668
Cs+WO₂ CsO formation in ²Σ state obs. 0–46635
Cu- sarcosine, g-tensor and spectral linewidth, obs. 0–41326
Cu-Mn, dil. alloy, 1.4-200 K, s-d exchange scatt. by impurities 0–79402
Cu complex, chelate with aromatic Schiff base 0–59448
Cu complex, base of the chelate of 0-46447

Al₂BeO₄:Fe³⁺, chrysoberyl, X- and Q-band frequencies 0-79397

AlCl₃:Fe³⁺, spin Hamiltonian 0-79399

AlK alum, dynamic proton polarization 0-66136

AlN phosphor, photosensitivity, temp. depend. 0-72477

Al(NH₄) alum, dynamic proton polarization 0-66136

Al₂O₃:Cr²⁺, acoustic, of X-irrad. crystals, effect of elec. fields 0-62749

Al₂O₃:Cr²⁺, acoustic e.p.r. obs. 0-76221

Al₂O₃:Fe³⁺, corrundum, acoustic, rel. to magnetoelastic coeffs. 0-47528

Al₂O₃:Fe³⁺, corrundum, combined e.p.r. and acoustic paramag. reson. 0-72476 0-72476

Al₂O₃:Fe³⁺, line width, temp. depend., 4.2-1100 K 0-66135

Al₂O₃:Fe³⁺, Fe²⁺, acoustic paramag. reson., obs. 0-51393

Al₂O₃:Fe³⁺ corundum, temp. and ang. depend. 0-41316

Al₂O₃:Fl³⁺ corundum, temp. and ang. depend. 0-41316

Al₂O₃:Tl³⁺, corundum, line width and shape 0-51387

Al₂O₃:Tl³⁺, corundum, line width and shape 0-51388

As₃C₄Realgar) powder, u.v. irradiated, an I=3/2 e.sr. center 0-59446

Au-Mn, dil. alloy, 1.4-200 K, s-d exchange scatt. by impurities 0-79402

Au complex, bis(maleonitriledithiolate) dianion, single crystal e.sr. study 0-69184

BaBr₂: electrolytically coloured hyperfine interaction between F centre and Cu complex, tetrakis(dimethylglyoximato)dicopper (II) in glasses, e.p.r. study 0–66148

CuCd(SO₄)₂ mixed cryst., Cu²⁺ line splitting obs. 0–41327

Cu(II) complex, bis(thiosemicarbazone)Cu(II) 0–58164

Cu(II) dialkylselenocarbamate single cryst. 0–41323

CuSO₄-5H₂O:Cd, e.p.r. studies 0–66137

CuZn(SO₄)₂ mixed cryst., g anisotropy, line widths variation 0–41327

Eu_{0.96}Gd_{0.94}O, ferromagnetic, line narrowing, exchange interactions 80-500

K 0–41329

EuO, Eu_{0.9}F_{0.1}, ferromagnetic, line narrowing, exchange interactions 80-500

K 0–41329

FuS. ferromagnetic, line narrowing, exchange interactions, 80-500 K EuO, Eu_{0.6}F_{0.1}, ferromagnetic, line narrowing, exchange interactions 80-500 K 0–41329

EuS, ferromagnetic, line narrowing, exchange interactions, 80-500 K 0–41329

Fe-V_o pairs, epr spectra, for order parameter of SiTiO₃ 0–68567

Fe³⁺¹, e.s.r. and electronic relaxation in water and water-glycerol mixtures 0–74787

Fe³⁺¹ in aq. solns., complex formation and electronic relaxation 0–61549

Fe(1) low spin complex cyanides 0–54154

Fe(1II) complexes, high-spin, powder line shapes 0–41330

GaAs:Fe³⁺¹, ion conc. changes on annealing obs. 0–47234

n-GaP, temp. and impurity conc. effects, 2.5-100K 0–72027

Gd³⁺¹, ss state in soln., e spin relax. 0–64954

Gd³⁺¹ ions in GdMeF₂(Me=Ca, Sr, Ba) site symmetry and crystal field coefficients 0–79403

GdH₂, Gd₂Y₂H₃, linewidths and g-shifts, 100-300 K 0–72481

Ge-As, ultrasonic donor-spin resonance 0–68600

H atoms in flame at atmost, press, e.s.r study of kinetics 0–39320

H₂O-ethylene glycol glass, p-irrad., electron traps 0–62821

H₂SO₄, solid, α- and p-irrad., electron spin echo for spatial radical distrib., influence of LET and spur effects 0–66133

H₃T₂Cd²Te e.s.r., electric dipole excited obs. 0–62755

K-NH₃(ND₃) layer formed by vaporization, obs. following tempering 0–51398 0-69184
BaBr₃, electrolytically coloured, hyperfine interaction between F centre and ions 0-55902
BaF₂:Er³⁺, spin-spin interaction reservoir, absorption spectra saturation, 1.8 K 0-76210
BaF₂:Eu²⁺, 2-360°K, spin Hamiltonian constants 0-76209
BaF₃ trapped holes and excitons investigated 0-51340
Ba(N₃)₂ anhydrous, e.s.r. studies of N₃²⁻ and N₂- molecular ions 0-48140
Ba(NO₃)₂:VO²⁺ 0-41344
Ba(NO₃)₂:VO²⁺ obs. 0-41314
BaTiO₃, Cr valency determ. 0-62751
BaTiO₃ doped with Cr ions, e.p.r. study of temp. dependence of specific resistance 0-71602
Be, spin lattice relaxation time, temp. and impurity conc. depend. resistance 0-71602 Be, spin lattice relaxation time, temp. and impurity conc. depend. 0-79404 BeO, irrad., V₁ centres obs. 0--62752 BeO, neutron irrad., e.p.r.-ENDOR obs. of F⁺ centres, hyperfine interaction 0--44985 tion 0-44985
Be-SiO4, phenacite, identity of PO4⁴⁻ radical 0-62762
C, in transition region and Hennig-Smaller effect 0-41318
C, pyrolytic, graphitization, electronic props. rel. to ambient Cl₂ 0-75545
C black, graphitization kinetics 0-41319
C blacks, paramag, and free radical character 0-41320
Ca-NH₃(ND₃) layer formed by vaporization, obs. following tempering 0-51398
CCO-M²⁺ forbidden transitions (Am=±1) in absentit expectation KBr, KCl, ENDOR, F-centre hyperfine interactions, uniaxial stress effect $CaCO_3:Mn^{2+}$, forbidden transitions ($\Delta m=\pm 1$) in absorpt. spectrum KBr, KSH(:KSeH), nature of centres 0-44989 KBr, KSH(:KSeH), nature of centres 0—44989
KBr(C):Mn²+, soln.; grown, aq. inclusions 0—48146
KCI:H trapped H obs. at 77 K 0—76216
KCI:KSH(:KSeH), nature of centres 0—44989
KCI:Li-1, V, centres obs. 0—76218
KCI:Mn²+, fine struct., temp. depend 0—76219
KCI:Pd, and optical absorpt. and elec. conductivity 0—59403
KCIO₄, X-irradiated, signals from defects due to e and holes trapped on CIO₄ 0—48147 CaCO₃, e.p.r. of CO₂- defects, motional and nonsecular contributions 0-54151 0—34131 CaF₂:Ag²⁺, Jahn-Teller distortions by odd modes, model 0—76213 CaF₃:Ag²⁺, Jahn-Teller distortions by odd modes 0—76212 CaF₂:Dy³⁺, acoustic, orbit-lattice interaction 0—44986 CaF₃:Eg²⁺ 0—59451 CaF₂:Es²⁺ (0-59451
CaF₂:Es²⁺, hyperfine coupling constant, temp. depend. 0-41342
CaF₂:Mn²⁺, new centre obs., field splitting 0-51391
CaF₂:U⁴⁺ obs. to study spin lattice interaction 0-54150
CaF₃, M centre metastable triplet state 0-68370
CaF₃, M centre metastable triplet state 0-68370
CaF₃, orientation kinetics of Gd³⁺-F⁻ interstitial pairs 0-72479
CaF₃, trapped holes and excitons investigated 0-51340
CaF₃, X-ray irradiated, obs. of Gd³⁺ centre, crystal field splitting 0-48145 ClO₄· 0-48147 KD₂AsO₄, observation of ferroelectric domains 0-75792 CO₂+ O₂-46147 CD₂ASO₄, observation of ferroelectric domains O-75792 KH₂ASO₄, observation of ferroelectric domains O-75792 KH₂PO₄·VO²+, and VO²+ orientations, obs. O-41346 KI:Eu²⁺, as function of variation in activator concentration O-59429 KMgF₃:Ni²⁺, spin-phonon interaction, from a.p.r. spectrum O-48154 KMgF₃:Nb²⁺(Gd²⁺), 4.2 K 0-76217 K₃Mg₅(SO₄):VO²⁺ 0-56669 KMnF₃, paramagnetic, line shape and spin correlation, exchange narrowing 0-41332 KN₃, u.v. irrad., exchange coupled paramag. ions, e.s.r. obs. 0-72482 KN₃, u.v. irrad., exchange coupled paramag. ions, e.s.r. obs. 0-72482 KN₃, u.v. irrad., exchange coupled paramag. ions, e.s.r. obs. 0-7482 KN₃, u.v. irrad., exchange coupled paramag. ions, e.s.r. obs. 0-7482 KN₃, u.v. irrad., exchange coupled paramag. ions, e.s.r. obs. 0-72482 KN₃, v. paramagnetic of the decomposition of the deco 0-48145
CanOci.:Nb, Y-irrad., hyperfine struct. 0-72478
CaO:Cu²⁺, temp. changes 0-41321
CaO:Er²⁺, mean g value 0-41314
CaO:Fe_{1,11} defects obs. 0-50578
CaO:Mn²⁺, h.f.s., during carbonation 0-51390
CaO, V_{ob} centre, ENDOR studies 0-50611
Ca(OH)₂, of Cu²⁺, Jahn-Teller effects 0-54152
CaWO:Cc²⁺, 1.8K, saturation, spin-spin temp. concept, verification 0-54153 0—34153 CaWO₄:Cr⁵⁺, e spin lattice relax. time, obs. 0—41322 CaWO₄:Pb, single crystal, X-irrad., hyperfine interactions 0—48142 CaWO₄ radiation induced paramagnetic centers, ESR, ENDOR investigations 0—62753 CdV apour, electron mag, reson. in excited 5³P₁(F=³/₂) state 0-43002 CdBr₂:Ni²⁺, mag, struct. 0-62754 CdCl₂:V²⁺, 77 K 0-44987 Cd₂Cl₂:V³⁺, 79 N 0-79401 CdF₂:Eu³⁺, e spin lattice relax. time, obs. 0-41322 CdF₃:Mn²⁺, Debye temp. determ. from temp.-depend. hyperfine constants 0.43012 K+NO₃, paramagnetic product obs. 0-46635 LaAl₂-Gd dil. alloy, g shifts 0-56660 LaF₃:Yb³⁺, mean g value 0-41314 LaRu₂:Gd⁺ paramagnetic resonance meas., molecular field model

Li-NH₃(ND₃) layer formed by vaporization, obs. following tempering

Li, spin lattice relaxation time, temp. and impurity conc. depend. 0-79404

S 1254 SUBJECT INDEX Paramagnetic resonance and relaxation continued Paramagnetic resonance and relaxation continued LiAlSiO₄:Fe³⁺ β -eucryptite, and LiAlSi₂O₆:Fe³⁺ β -spodumene, n.m.r. of 7 Li crystal struct. 0-45023S₇NH y-irrad., e.s.r. of radicals 0–64450 SO ₇ in H₂O-butyl alcohol, e.s.r. linewidths 0–68148 SO₂⁻ radical ion 0–61555 LiAlSi₄O₁₀, petalite, e.p.r. of Fe³⁺ and Mn²⁺ impurity ions 0–54155 LiAlSi₄O₁₀, petalite, e.p.r. of Fe³⁺, anisotropic broadening of line width 0–54158 So₁₁xIn, ferromagnetic alloy, magnetization, comp. and temp. depend. 0-44997 0-44997 SeVO₄:GO³⁺, parameters and temp. effects 0-44998 Se, charge-transfer state investigation 0-65696 SeD determ. of rotational constant, Λ-doubling, and dipole moment 0-49892 LiCl:Mn², fine struct., temp. depend. 0–76219 LiF:Mn, and F absorption band obs. 0–75186 LiF, (111) oriented defect, and ENDOR obs. 0–40125 LiF, ENDOR, F-centre hyperfine interactions, uniaxial stress effect LIF, ChiDOR, F-centre hyperfine interactions, uniaxial stress effect 0-78566
LiF, irrad., Li colloids, electron microscopy 0-41334
LiF, p-irrad., plastically deformed and annealed, F-centre spectra, H-centre 0-59453 0-49892 SeH determ. of rotational constant, Λ -doubling, and dipole moment 0-49892 Si:Al, Al² interstitial obs. 0-45000 Si:Cr solid solution, precipitation kinetics, diffusion, temp. depend. 0-40454LiF. p-irrad., plastically deformed and annealed, F-centre spectra, H-centre 0–59453

LiF, neutron irrad., ³H production obs. 0–51395

LiF, Y-centre in neutron and p-irrad. cryst., annealed 0–41333

LiNbO₃, of Mn²⁺ 0–62756

LiNbO₃, of Mn²⁺ 0–62756

LiNbO₃, of Mn²⁺ 0–62756

LiNbO₃, of Mn²⁺ 0–64756

LiNbO₃, of Mn²⁺ 0–64756

LiNbO₃, of Mn²⁺ 0–64734

MgO:Ri²⁺, spin-lattice relax. 0–44724

MgO:Ri²⁺, spin-lattice relax. 0–44724

MgO:Ri²⁺, spin-lattice relax. 0–44724

MgO:Ri²⁺, spin-lattice relax. 0–46721

MgO:V³⁺, acoustic e.p.r. obs. 0–76221

MgO:V³⁺, acoustic e.p.r. theory 0–69187

MgO:V³⁺, acoustic e.p.r. theory 0–69187

MgO:V³⁺(Cr³⁺) 0–72483

MgO-Cr₃O₃-(Li₃O):Cr³⁺ cryst, struct, by e.s.r. method 0–65255

MgO of Ir⁴⁺ 0–76220

MgO, spin-lattice relax. of Fe⁺ via excited electronic states 0–56470

MgO of ³²Cr³⁺, line intensities angle depend. 0–56670

MgO of ³²Cr³⁺, line intensities angle depend. 0–48148

MgWO₄:Cr³⁺, 293 K, crystal field const. 0–41348

MnF₂, paramagnetic, line shape and spin correlation, exchange narrowing 0–41332 Si-Cr solid solution, precipitation kinetics, diffusion, temp. depend. 0–40454
Si-Fie, donor and acceptor levels 0–72489
Si-Li, and ENDOR, orbital degeneracy 0–56672
Si-P, conduction electron spin resonance, line shape 0–72490
Si-P, d.c. cond. charge 0–72491
Si-P, d.c. cond. charge 0–72491
Si-P, d.c. cond. charge 0–72491
Si-P, hyperfine splitting, 4.2K. press. depend. 0–41339
Si-P, microwave hot electron effect and resistivity decrease due to donor spin reson. 0–72071
Si-P, rel. to donor pair exchange energy 0–44999
n. Si-P, uniaxial compression effect on hyperfine splitting 0–79407
Si, plastically-deformed 0–48151
Si, signal prod. by plastic deform, annealing behaviour 0–56671
Si film, amorphous, and structural, optical and elec. props. 0–47761
α-SiO::Al, p-irrad., and opt. absorpt., 'Al' centre obs. 0–59456
α-SiO::Ge E' centres, assoc. with Ge impurities 0–43660
SiO::W, Ga, quartz with struct. impurities, solution growth, γ-irrad. 0–71519
SiO-Al₂O₃, e.p.r study of electron donor-acceptor properties and point MnF₂, paramagnetic, line shape and spin correlation, exchange narrowing 0 41332
MnWO₃, anisotropy, 30 GHz, room temp. 0–62757
MnO₃:Cr¹⁺, e.s.r. 0–44990
MnO₃:²¹V(²³Nb), electron hole centre interactions 0–48149
N visible afterglow, N atom and pressure depend, meas. 0–53229
NF oriented in inert matrices e.s.r. at low temps 0–61103
NH₄, halides, irradiated hydrazinelike defect, production and characterization, e.p.r. study 0–78525
NH₄Cl:Co²⁺, relaxation at saturation, 4.2K 0–79405
NH₄Cl:Fe³⁺ zero field energy levels determ, 0–76222
NH₄HF₂, electron-irrad, F₂⁻ and H obs. 0–44992
NH₄H₂PO₄(Cr²⁺, antiferroelec, and paraelec, phase 0–72484
(NH₄):PCl₆, antiferromagnetic, Mossbauer and ENDOR spectra compared 0–75962
(NH₄):Mg₂(SO₄):Mn²⁺, paramagnetic ion position, lattice defects and crystal field parameters 0–54159
(NH₄):Mg₂(SO₄):VO²⁺ 0–56669
NH₄(NH₀):VO²⁺ 0–41344
NH₄NO₃:VO²⁺ 0–41344
NH₄NO₃:VO²⁺ 0–41344
NH₄NO₃:VO²⁺ 0–41317
(NH₄):SO₄, ferroelec, transition obs. 0–62758
(NH₄):SO₄, ferroelec transition obs. 0–6278
(NH₄):SO₄):Mg²⁺, paramagnetic ion position, lattice defects and crystal field parameters 0–54159
NO₂ adsorbed on zeolites and hydrogen mordenite, e.s.r. at 77°K 0–58192
NO₂, in inert matrices e.s.r. at low temps. 0–61103
N₂O₄ p-radiolysis and vapour phase irradiation with He⁺, identification of paramagnetic species 0–66206
Na-NH₄(ND₃) layer formed by vaporization, obs. following tempering 0–51398
Na, liquid and solid, spin lattice relax. time and resistivity, 293-453°K
0–3983 SiO_2 - Al_2O_3 , e.p.r study of electron donor-acceptor properties and point defects 0-59455defects 0-59455

SiO, paramag, centres obs. 0-66141

SiO₃V⁴⁺, cristobalite 0-76226

SnO₂:Ni³⁺ flux-grown cryst., oxidation-reduction effects 0-72492

Sr tartrate: transition elements 0-41343

SrCl₂:La²⁺ e.p.r. observation of Jahn-Teller effect, averaging effects by relaxation, origin of isotropic spectrum 0-44981

SrCl₃: of Am²⁺ and Cm³⁺ 0-56674

SrF₂:Ag²⁺, Jahn-Teller distortions by odd modes 0-76212

SrF₂:Lag²⁺, Jahn-Teller distortions by odd modes, model 0-76213

SrF₂:Eu⁴⁺, hyperfine coupling const., temp. depend., 4-800K 0-41342

SrF₂:Ho³⁺, in trigonal site, non-Kramers doublet obs. 0-41341

SrF₂:Mn³⁺, Debye temp. determ. from temp.-depend. hyperfine constants 0-43912

SrF₃ trapped holes and excitons investigated 0-51340 SrF₂:Mn²⁺, Debye temp, determ, from temp.-depend, hyperfine constants 0-43912
SrF₂ trapped holes and excitons investigated 0-51340
SrTiO₃:Al, rel. to shared holes trapped by charge defects 0-43968
SrTiO₃:N³⁺, dynamic Jahn Teller effect 0-56673
SrTiO₃, 65 K anomaly 0-68559
SrTiO₃, 65 K anomaly 0-68559
SrTiO₃, 65 K anomaly 0-68559
Th with added ²²⁸Th e.s.r. obs. 0-65288
ThO₂:Gd³⁺, spin- lattice strain coeffs. 0-72292
ThO₃, of Pb³⁺ centres 0-79408
ThO₂, study of electron hole traps by e.s.r. and n.m.r. 0-56650
ThO₂: ¹³⁵Gd³⁺, fs forbidden lines obs. 0-62764
TiP²⁺ ions in water, rel. to electronic structure of hydrated ion 0-70955
Ti(III) chelates in aq. soln. 0-78303
TiO₃:Cr, rutile, O vacancies formation 0-55874
TiO₂:Cu²⁺, hyperfine and nucl. quadrupole interactions 0-45001
VO₂:Ti₃, 77-293K, conc. depend. 0-41345
VO₂-P₃-P₃, semiconducting glass system, V⁴⁺/V⁵⁺ ratio determ. 0-76239
VO²⁺ in nitrate single crysts. 0-41344
VO²⁺ in oxide glasses, composition depend., chem. bond nature 0-72493
YAl₂, of Gd³⁺ (erroelece. 0-72496
YFeO₃, spin-cluster reson. 0-72495
YNbO₃:Gd³⁺, ferroelece. 0-72494
VO₃, study of electron hole traps by e.s.r. and n.m.r. 0-56650
Y₁Ti₂O₇:Cr³⁺ pyrochlore crysts., e.s.r. investigation 0-66142
Zn₃B₇O₁Cl. of Cu²⁺ 0-62756
Zn₃BrO₃); esr spectrum, evidence suggesting paramagnetic centre is BrO₂ radical 0-45004 Na, liquid and solid, spin lattice relax. time and resistivity, $293-453^{\circ}$ K 0-39837NaAl(SO₄)₂.12H₂OCr³⁺ oriented magnetic complexes of Cr found 0–62759
NaCl:Co, X-irrad., S-centre obs. 0–75190
NaCl:Cu²⁺, Jahn-Teller system, spectra at 77 and 95-100K 0–76224
NaCl:H trapped H obs. at 77 K 0–76216
NaCl:(Mn²⁺, CN⁻), dielectric absorpt., dopant interactions 0–44993
NaCl:Mn²⁺, dipole-equil. establishment in field free conditions 0–72486
NaCl:Mn²⁺, fine struct., temp. depend. 0–76219
NaCl:Mn²⁺, of Mn²⁺–Na⁺ vacancy pair 0–72485
NaCl:Mn²⁺, X-irrad., Mn centres, and opt. absorpt. bands 0–76104
NaCl:Mn²⁺ itiquid nitrogen temp. obs. 0–62761
NaCl:Mn²⁺ itiquid nitrogen temp. obs. 0–62761
NaCl:Na hasorpt. obs. 0–79315
NaCl:V and absorpt, X-irrad. effects, obs. 0–41217
NaCl, Mn²⁺ solid solution precip. 0–76223
NaClo₃, X-irrad., thermally bleached 0–44994
NaF:Mn²⁺ e.p.r. spectrum, use of power saturation method for relaxation times 0–41338
NaHF2, electron-irrad., F2⁻ and H obs. 0–44992 Y,Ti;O₇:Cr³⁺ pyrochlore crysts,, e.s.r. investigation 0–66142
Zn₁BrO₁;Cl, of Cu²⁺ 0–62756
Zn₁BrO₂); ers spectrum, evidence suggesting paramagnetic centre is BrO₂ radical 0–45004
ZnF₂;Cu²⁺, covalency and electronic struct. of Cu²⁺ 0–41324
ZnG₃;O₄:Cr³⁺, e.p.r. 0–48153
ZnO;Yb³⁺ 0–59457
ZnO, adsorbed I effect 0–45003
ZnO, electron irrad., F⁺ centre obs. 0–45002
ZnO, neutron-irrad., assoc with Zn vacancies 0–72499
ZnO, of V³⁺, spin Hamiltonian and cryst. field parameters 0–45005
ZnO, Zn vacancy obs. 0–76227
ZnO powder, irrad., g-value, paramag. centres obs. 0–41350
ZnO powder, irrad., g-value, paramag. centres obs. 0–41350
ZnO powder, irrad., g-value, paramag. centres obs. 0–72470
ZnS:Fe³⁺, line width broadening, internal stress 0–79409
ZnS:Fe³⁺(Mn³⁺)(Cr⁺), elec. field effect 0–72498
ZnS:I, e.p.r. obs. and defects 0–56675
ZnS Debye temp. determ. using electron phonon state splitting 0–75410
ZnSe:Si, photosensitivity 0–72497
ZnSe, of Ni¹ and Ni³⁺, g-factor, wave function delocalization, super-h.f.s. 0–41349
Zr:Er, Mossbauer effect exam. 0–44804
Zr:Er, Mossbauer effect exam. 0–44804
Zr:Er, Mossbauer effect exam. 0–44803
Zr:Zn₁, exchange enhancement of life-times 0–45006 times 0-41338'
NaHF₂, electron-irrad., F₂⁻ and H obs. 0-44992
NaNO₃:VO²⁺ 0-41344
NaNO₃, VO²⁺ obs. 0-41317
NaN₃X-irradiated, defect identification effect of structure on spectra interpretation 0-75120
Na₂O-TiO₂-SiO₂ glasses, Ti²⁺ obs. 0-72487
Na₃SO₄, X₂, u.v. irrad., rel. to cryst. growth temp., obs. 0-41337
Na₃SO₄, X₂, u.v. irrad., rel. to cryst. growth temp., obs. 0-41336
Ni complex, o-phenylenebis(dimethylarsine) 0-66134
NiCH₂COO)₂-4H₂O:Mn²⁺, obs. 0-41335
NiCl₂, temp. effects on spectra, 49-460 K 0-48150
O atoms, 'P₂ spectra in gas phase, lineshapes of multiple quantum transitions 0-55236
O plasma, atomic recomb. obs. 0-61259 measurement
cavity for low temp. studies 0–57470
Debye temp. determ. from temp. depend, hyperfine constants 0–43912
decomposition factor, using ENDOR 0–60122 tions 0-55236
O plasma, atomic recomb. obs. 0-61259
O₂ adsorption on GaAs and AlSI. 0-47075
PF₂ and PF₄ trapped radicals 0-44995
PbCl₂, of Eu²⁺ and Gd³⁺, second-degree cyrstal field splittings 0-51399
PbF₃: V²⁺ and impurity centres, 77 K 0-44987
Pd(I) complex produced in p-irrad. bis(acetylacetonato)Pd(II) 0-54160
RbCl:Mn²⁺, exchange narrowed line, g-value, peak to peak derivative widths 0-44996
RbMnF₃, paramagnetic, line shape and spin correlation, exchange narrowing 0-41332
S, single line spectra, line shape representation and reliability of parameters 0-66986
S(NH)₂-pirad₂, e.s.r. of radicals 0-64450 dispersion- line-shapes obs. using linearly and circularly polarized r.f. fields 0–38442 double reson, apparatus 0–48937 ENDOR, review 0–60120 ENDOR meas, of spectroscopic decomp, factor 0–60122 g-value measurement of paramagnetic species by simple esr spectroscopy 0–38441

magnetometer, optimization 0-54823 non-linear phenomena, angular momentum detection 0-42135 in r.f. saturating field by torque meas. 0-38443 S₄(NH)₄ y-irrad., e.s.r. of radicals 0-64450

Paramagnetic resonance and relaxation continued

measurement continued

resonator, low temp., for e.p.r. of specimens subject to uniaxial stress 0-54807

review 0-60120

review 0-60120 saturated spin system, transverse relax. time meas. 0-72191 solid, mathematical analysis 0-60119 space group symmetry determ. 0-65188 spectrometer, IFA-type, signal/noise ratio improvement by time averaging 0-63523

spectrometer, using hyperfreq, field amplitude modulation 0–69808 spectrometer, using sample heating to detect magnetic resonance 0–48933 spectrometer bridge superheterodyne attachment of single klystron

spectrometer with flash-correlated 1 µs response for free radical flash photolysis studies 0–63522 X-band spectroscopy, optical irradiation cavity with large aperture 0–42136 .

Na₂OB₂O₃GeO₂ glass, gamma irradiated 0-66140

Paramagnetism

amagnetism
see also Magnetic properties of substances/paramagnetic
crystal nonlinear optical and microwave frequency multiplication and mixing 0-69775

ling 0-05/18. Heisenberg, short-range-order effects in neutron scattering 0-51183 Heisenberg magnet, anisotropic, space-time correls., elevated temp. 0-5390

Heisenberg magnet, dispersion law for propagating modes 0–44520 Ising system, time-depend. fluctuation correl. in Heisenberg-like spin systems, Weiss limit 0–72190

systems, Weiss limit. 0–72190 isotropic, critical, scaling laws for spin motion 0–72192 kinetic, due to temp, gradient in conducting medium 0–52226 kinetic, exptl. obs. in n-InSb Corbino disc 0–73142 kinetic, thermomag, and galvomag, current induced 0–73153 local moment formation model including vertex corrections, parquet-diagram technique 0–44490 moment dynamics 0–40942 neutron scatt. from short range ordered paramagnets, mode 0–40943 nonlinear effects in two-level spin system 0–72191 Pauli, in metals with high densities of states 0–75895 space-time correlations in exchange coupled paramagnets at high temperatures 0–75894 spin motion scaling laws for isotropic magnets in critical region 0–72192 surface stress, derivation from single amperian atomic current model 0–44488 susceptibility meas. 3 to 55 MHz. 1.2 to 77K with tunnel diode oscillators.

susceptibility meas. 3 to 55 MHz, 1.2 to 77K with tunnel diode oscillator 0-48980

Parametric amplifiers see Amplifiers

Parent see Nucleus; Radioactivity

Parity

see also individual particles, e.g. Mesons/spin and parity nuclear physics parity tests, review 0-49449 violation of P-parity in inelastic scatt, with photon emission 0-77533 $K_{L} \rightarrow \pi \pi$ CP violation possibility of kinematic (unitarity) origin 0-70245

Particle accelerators

see also Ion beams

coaxial, current distrib. along accelerating electrodes 0-38777

constant current distrio, along accelerating electrodes 0–38777 deuteron particle beam production for synchrocyclotron 0–63851 electron, in operation and under construction, prospects 0–46083 electron, resonant high frequency discharge in quarter wave coaxial resonator 0–60730

electron, resonant high frequency discharge in quarter wave coaxial resonator 0-60730
electron autoresonant, by e.m. waves in rectangular waveguide 0-49429
electron beam aperture control, patent 0-49448
electron colliding beam devices 0-63921
electron motion, radiation effect 0-38776
electron ring, crossing of an incoherent integral resonance 0-60735
electron ring, research 0-63939
electron ring, stability near initiation of acceleration, self-focusing lower bounds 0-77452
electron ring accelerator, summary of work status to date 0-52624
electrostatic, corona triode characteristics 0-42656
electrostatic, proton, for study of crystalline struct, by shadow effect method 0-63923
emittance and admittance 0-63926
Hall, d.c., high current, suitability for controlled thermonuclear fusion work 0-70722
Hall, use for fusion reactor start-up plasma prod. 0-70724
for heavy ions, of electron-ring type 0-42685
heavy-ion, Oak Ridge APACHE project 0-63927
ion, 100-600 keV 0-42655
ion, collective effect acceleration 0-42232
ion, heavy, problems 0-42658
ion, low energy, for hot atom chemical research 0-74165
ion ILU to 100 KeV with separation of ions by mass, description 0-49427
ion acceleration processes in electron beam, max. energies 0-46075
of ions heavy, choice of system 0-55094

0-49427 ion acceleration processes in electron beam, max. energies 0-46075 of ions, heavy, choice of system 0-55094 ions acceleration by collective methods 0-49425 linear, high current, image instability in coherent lateral motion 0-73715 low-energy accelerator industry, <100 MeV, review 0-63924 magnetic field struct, distortion by conducting coatings on chamber 0-63934

0-3934
microtron with inhomogeneous mag. field 0-42678
multimomentum, 600keV high current density, long focal length 0-73713
multiperiodic standing wave accelerating structure, interaction with beam.
'transient and steady-state conditions 0-49428
multisectional tube, design and advantages 0-38774
on-line control, analogue data break interface 0-63922
orbital, bunched cavity system, equivalent cct. 0-70322
plasma, with e.m. waves, mean velocity calc. 0-50072
proton, electrostatic, for study of cryst. struct. by shadow effect method 0-63923
proton, high-energy, reduction of the residual photon dose rate 0-57861

0—63923 proton, high-energy, reduction of the residual photon dose rate 0—57861 proton, in operation and under construction, prospects 0—46083 proton linear, synchrocyclotron and synchrotron, work of Radio Engineer ing Institute, USSR 0—57863 review of accelerator physics, present status 0—42657 superconducting, cryogenic developments 0—55093

Particle accelerators continued

synchrocyclotron beam current enhancement on injection of carbon tetrachloride 0-42676

tandem, at Erlangen, source of polarized protons and deuterons description 0-42660

temperature field distrib. on chamber walls with conducting coatings

0-6395 Van de Graaff, CISE 8 MeV tandem, stabilization system 0-73712 e, pulsed 40 keV 0-73714

accessories

accumulator ring, input of electron beam with 100 MeV energy 0-63941 axicon light collector for foil-excited beam spectra 0-60737 beam analyzer-magnetic spectrograph combination, energy calibration 0-52629

0-52629
beam division device, patent 0-57868
beam transfer channels, optics, computer programme 0-49446
bremsstrahlung production rate from internal targets of electron synchrotron, servo correction system 0-52630
cathode, boride, vacuum hot pressing 0-73720
chopper, fast, slit arrangement to simplify background time dependency
0-49442 circuit for 0-46082 magnetic field corrections in high energy synchrotrons

Co-Ax connectors, shorting modification 0-49444 colliding-beam expts., diagonal and nondiagonal e.m. interactions colliding-beam expts., 0-60736

door alarm and interlock system at Los Alamos tandem accelerator facil ity 0-46091

electrostatic generator design for CISE 8 MeV tandem Van de Graaf 0 - 52617

electrostatic separator with oxide glass semiconductor cathode, test results 0 - 49440

energy calibration of analyzing magnet using ⁵⁸Ni(p,n)⁵⁸Cu reaction 0-46092

energy calibration of analyzing magnet using ³⁸Ni(p,n)³⁸Cu reaction 0–46092 · Faraday cup, milliohm resistance subnanosecond risetime for obs. electron beams 0–77456 fast kickers, analysis of magnets and pulsing circuits, components description, characteristics 0–63940 focusing, automatic with tracking rectifier for e.s. accelerator 0–77454 gas flow valve, stabilized for heavy ion source 0–46090 gradient magnets, core material, low carbon steel, mag. and mechanical properties 0–57867 helical beam rotation suppression device, patent 0–42690 injector design for CISE 8 MeV tandem Van de Graaf 0–52618 interdigital structures, H type 0–42687 ion source for cyclotron 0–38775 magnet, concrete insulated, design for European 300 GeV type 0–49438 magnet, quadrupole doublet system, optical parameters 0–42689 muon storage ring magnet at CERN, proton resonance calibration and field studies 0–52631 NAL-200 MeV linear, pre-accelerator, linac systems, diagnostic equipment, computer control system 0–52620 neutron time-of-flight facility for neutron spectra from (p,n) reactions 0–70295 nuclear resonance flux meter frequency, control by on-line computer for

Various of the various of v

proton resonance magnetometer for use with muon storage ring 0-52631 r.f. ion source, of low consumption for pressurized accelerators 0-49439 radiation - safety instrumentation, for small fractional beam spills radiation - safety instrumentation, for small fractional beam spills 0–76716 resonator structure, single 0–42688 scintillation counter telescope, four-channel, circuits 0–46088 septum coil of Bevatron extraction magnet M1 mark 4, design and fabrication description 0–55101 storage rings intersecting at CERN, resonant extraction 0–49445 synchrocyclotron meson canal beam analysis by star detector 0–46089 synchrotron radiation from electrons in storage device, interference expt. and photon statistics 0–60507 tandem accelerator, source of polarized H⁻ ions 0–73721 threshold Cherenkov counters for proton synchrotron 0–46087 waveguides, disk-loaded, matching mode-transformers using r.f. pulses, for linear electron accelerators 0–48925 D source, polarized, for a 28 MeV synchrocyclotron 0–42686 e storage ring for electroexcitation expts. on nuclei 0–49447 Cu and Fe magnet, activation by 3 GeV p 0–73722

betatrons

betatrons
beam front dynamics rel. to e capture 0—38786
electron beams transverse instability 0—60734
electron motion in perturbed mag. field, extraction process 0—73716
focusing, theory, stable adjoin trajectories 0—42681
frequency shift formulae, space charge effect with crossing angle 0—49436
iron-free high-current, principle dimensions, determ. 0—49435
oscillations, quantum fluctuations 0—52623
plasma betatron, acceleration of electrons, mechanism 0—67357
plasma linear, electron acceleration energy spectrum study 0—52625
strong-focusing, horizon, damping coeffs. 0—63930
e beam energy absolute meas. <5 MeV 0—38779

beam bursts repetition rate-reduction using gated ion source $\,0-57864$ beam ourrent limits based on residual radiation for protons, deuterons, He-3 and α -particles $\,0-52627$ beam transport system for Harwell variable energy cyclotron $\,0-49434$ crossed-field motion of electron, effect of travelling RF wave $\,0-73717$ electron motion, quantum theory $\,0-55097$ Harwell variable energy, beam transport system $\,0-49434$ heavy ion, gas-discharge ion source for e.m. mass-separator $\,0-46076$ ion source on axis, at positive bias potential $\,0-73718$ ions ource on axis, at positive bias potential $\,0-73718$ ions, very heavy, series pair arrangement $\,0-42674$ irradiating tablets with $\,p$ -beams using remotely controlled apparatus, description $\,0-77450$ use for irradiation activation, uniform of metal ball $\,0-53726$ isochronous, $\,685$ mm, deuteron-beam deviation $\,0-42684$ isochronous, phase compression and dilation effects $\,0-77451$ isochronous, with separated hard-edge magnets, orbital properties $\,0-57865$

isochronous 0-57865

Particle accelerators continued evelotrons continued

Julich isochronous, use of automatic beam-emittance-measuring device,

results 0-46085
magnetic channels, geometry calculation 0-60731
multicharged heavy ions accel. in IPCR (Riken) 160 cm ordinary cyclotron 0-63936
NRL sector focusing for p, d, h, applic, to oceanographic investigations 0-45130

0-45130
Nimrod operation and development quarterly report (Jan-Mar 1969)
0-38785
parametric 'cooling' of slow cyclotron wave of electron beam in crossed fields 0-67356
proton beam anti- resonant phase effects in rot. fields 0-52628
SIN ring cyclotron, extraction efficiency and energy spread, Monte Carlo simulation 0-42682

simulation 0-42682 separated orbit machine, patent 0-52632 separated sector isochronous, isochronism adjustment 0-57866 synchro cyclotrons, capture efficiencies 0-52616 synchrocyclotron, CERN 600 MeV 0-67355 synchrocyclotron, Lyon, achromatic optical focussing 0-55102 U120 systems, malfunction diagnosis 0-42679 variable energy, Orsay, stripping study 0-38787 variable frequency, Saclay, heavy ion accel, using trochoidal injector 0-42679

Li-ion acceleration 0-77453

linear

140 MeV, data handling and analysis by computer 0-73670
beam dispersion, horizontal, influence of fluctuation of radiation 0-63931
beam emittance enhancing, theory of mechanism 0-70321
data acquisition system, ORELA facility 0-63928
e, in short travelling wave linac, eqns. of motion, analytical solution 0-46079
electron. Oak Ridge, pulse-shape meas, using gamma-ray detection tech e, in short travelling wave linac, eqns. of motion, analytical solution 0.46079
electron, Oak Ridge, pulse-shape meas, using gamma-ray detection tech niques 0-77449
electron, beam transport system design 0-49432
electron, having diaphragm wave-guide 0-60729
electron, radial movement of particles, reflected wave influence 0-55099
electron bunches of short duration, production for injection, in adjustable numbers 0-46080
electron linac, by alternating periodic struct. 0-67354
electron radial motion and beam focussing taking account of electric field asymmetry 0-38782
helix, for heavy ions 0-42667
induction high current, coherent instabilities, stability criteria and mechanism 0-55098
ion, accelerating structures 0-42665
ion, delay line with metallic supports, theory of structure 0-52621
ion, heavy, Lyon project 0-42671
ion, heavy, accel. method 0-42668
ion, heavy, conference, La Plagne, March 1969 0-42875
ion, heavy, dynamic problems 0-38783
ion, heavy, new model 0-42670
ion gun, 750 keV, high gradient 0-63929
ion prestripper accelerator with electrostatic quadrupole focusing 0-42669
ions, atomic, any mass, variable energy 0-42661
ions multi-charved beam focussing in basic section by impulsive magnetic

0-42669 ions, atomic, any mass, variable energy 0-42661 ions, atomic, any mass, variable energy 0-42661 ions, multi-charged, beam focussing in basic section by impulsive magnetic quadrupoles 0-63933 linac gap, p beam dynamics and fields 0-49430 modulator, transverse instability, theory 0-67352 multiperiodic accelerating structures, dispersive props. 0-42666 NAL-200 MeV, 10 MeV section's operation performance 0-52620 Oak Ridge 140 MeV e linac, ORELA 0-63927 p-beam, transverse motion computation 0-46078 plasma betatron, electron energy meas., spectra study 0-52625 positron source, 10 to 50 MeV monoenergetic, design and analysis 0-49433

progressive wave, energy and phase of injected electrons, calc. method 0-49431

0–49424 and continuous and phase of injected electrons, catc. Intention of the continuous accelerating structure with washers and drift tubes, radiotechnical parameters determination 0–52622 proton beam dynamics calc., new approach 0–49424 proton momentum spread in linac injector of synchrotron 0–46081 relativistic electron beam, Cornell University 0–42673 resonators, coupled chains transient response 0–73084 space-charge limited current derivation, for various parameters, injection condition and types of particle 0–67353 Stanford University research, review 0–42662 strong-focusing, horizon, damping coeffs. 0–63930 tandem, He ion source, production technique 0–42664 tandem, Van der Graff, new Florida machine 0–42663 tandem Van de Graaff 0–63932 theory, calc. of horizon, dispersion of beam influence of fluctuation of radiation 0–63931 theory, horizontal osc., damping coeffs. 0–60728

Tadiation 0-0531 theory, horizontal osc., damping coeffs. 0-60728 theory, vertical oscillations, damping coeffs. 0-60727 Van de Graaf, CISE 8 MeV, design of injector 0-52618 Van de Graaf, CISE 8 MeV tandem design of electrostatic generator 0-52617

0-52617
Van de Graaff, 5 MV, Groningen, description 0-77448
Van de Graaff, pulsed, (n,xy) cross- sections meas. 0-52782
Van der Graff, 30 MeV, at Brookhaven Nat. Lab. 0-52619
weak focusing, horizontal osc., damping coeffs. 0-60728
weak-focusing vertical oscillations, damping coeffs. 0-60727
X-ray beam stability for radiotherapy 0-57862
e beam profile meas. technique 0-42672
p, 25 and 100 MeV, work of Radio Engineering Institute AN SSSR
0-57863

p, high-energy, residual photon dose rate 0-38773

p. high-energy, residual photon dose rate 0–38/73
synchrotrons
200 GeV at National Accelerator Laboratory 0–67358
300 GeV, proton, CERN, design 0–73719
70 GeV proton, starting and complex tuning 0–46086
beam ejection theory, resonant 0–52626
bremsstrahlung production rate from internal targets, spill servo correction
system 0–52630
Dubna synchrocyclotron, meson-channel beam formation 0–45917
electron 1.5 GeV synchrotron at Tomsk, some improvements 0–42680

Particle accelerators continued

synchrotrons continued

Frascati, electron synchrotron radiation, spectral distrib. in 80-1200 Å range 0-77262

range 0-77202 gradient magnets, core material, low carbon steel, mag, and mechanical properties 0-57867 impulse, FIAN, intensity stabilisation 0-63938 isotope-separator on-line, study of short lived nuclides spallation produced

0–61041
magnetic channels geometry calculation 0–60731
magnetic field corrections, multipurpose circuit 0–46082
oscillations, quantum fluctuations 0–52623
p-current booster for Princeton Pennsylvania accelerator, design 0–55095
Princeton-Pennsylvania accelerator for heavy ion acceleration, p-current booster synchrotron coupling 0–55095
proton, CERN 28 GeV, and intersecting storage rings 0–67355
proton, conversion linear accelerator as injector 0–77447
proton, particle separation in clusters by threshold Cherenkov counters 0–46087

proton, starting and complex tuning of 70 GeV machine 0-46086 Saxonburg synchrocyclotron conversion to heavy-ion isochronous cyclot ron 0-70323

strong-focusing, horizon, damping coeffs. 0–63930 synchrocyclotron, Lyon, achromatic optical focusing 0–55102 synchrophasotron, mode of acceleration of d and He++, expt., calc. 0–49437

0-49437
vibrations, non-linear radiation damping 0-42677
wave guide non-ferrous synchrotron, investigation of an accelerating
system 0-38784
e synchrotron, 2.5 GeV, of Bonn, description 0-60732
p, 10 GeV weakly focused, work of Radio Engineering Institute AN SSSR
0-57863
p, Serpukhov 70 GeV, closed orbit, geodetic survey 0-42683
p, Serpukhov 70 GeV, closed orbit, geodetic survey 0-42683

p, CERN, resonant extraction from intersecting storage rings 0-49445

Particle beams

ricle beams
acceleration by a.c. fields, without phase relation between field and incoming part, or accel, cycle 0-55100
channelling, applic, in solid state physics 0-68668
characteristics determination with multielectrode spark chamber 0-77443
charged, current meas, using Hall effect 0-48999
charged, injection into mag, traps, method 0-38464
charged, interacting with thick target, differential excitation curves from neutron spectra 0-40616
chemical reactions, merging beam technique for study 0-76256
coherent instabilities in high current linear induction accelerators, resonance effect 0-55098
cyclotron, variable energy, at Harwell, beam transport system 0-49434
deflection systems, stigmatic and achromatic, necessary conditions 0-42194
direction stabilizer system, simple 0-77034

direction stabilizer system, simple 0-77034

direction stabilizer system, simple 0-77034 envelope calculation of initially uncorrelated ellipsoidal beam 0-49000 fast, transport problems soln. using analogue hybrid computer 0-60162 focussing, optimal mag. system 0-38465 linac gap, p beam dynamics and fields 0-49430 negative, transport channel, with momentum up to 60 GeV/c 0-69851 neutron, from thermal column of UTR-100 reactor, meas. of energy spectrum 0-49744 phase separator, optimal, for division of 3 component beam 0-38778 photon, polarized, obtained from diamond crystal subject to electron beam 0-45875

plasma-beam system, finite, instabilities 0-58347

polarized proton and deuteron source for the Erlangen- tandem accelerator 0-42660

tor 0–42660 proton linac beam dynamics cales, new approach 0–49424 protons, symmetric rotational, transverse motion computation 0–46078 protons from duoplasmatron ion source, phase density redistribution processes 0–45761 radiation field of clustered beam in irregular retarding system 0–63564 relativistic, charged, some limitations 0–63925 secondary particles, tracking system, based on scintillation counter telescopes 0–42629 in superconducting resonator, beam loading and rad, from particle clusters 0–73166 synchrocyclotron, enhancement on injection of carbon telescoles.

synchrocyclotron, enhancement on injection of carbon tetrachloride 0 -42676

0 -42676
synchrotrons, resonant beam ejection theory 0-52626
transport system for Harwell variable energy cyclotron 0-49434
/n generators, book on principles and applications 0-55066
, from charge exchange accelerator, polarization meas. 0-46077
d particle beam production for synchrocyclotron 0-63851
e linac beam profile meas. technique 0-42672
N, rotors, multi-slotted for velocity selection, design 0-55067
n 28 MeV, production from 'H(d,n)'He 0-55156
p, low energy, inelastically scattered:- a source of circularly polarized photons 0-42469
Au, film, back scatter of projectiles 'H, 4He, 7Li, ''B of energy 50-110 keV 0-65563

Particle detectors

see also Bubble chambers; Cloud chambers; Counters; Ionization chambers; New January Counters; Ionization chambers; New January Counters; Ionization chambers; New January Counters (New January Counter) Counters (New January Counter) Counters (New January Counter) Counters (New January Counter) Counter (New January Counter) Counter) Counter (New January Counter) Counter (New January Counter) Counter (New January Counter) Coun

distributions in nuclear reactions, biased routing system 0–52603 electron multipliers, efficiency for H atom detection 0–77414 electron-capture type, for gas chromatography, basic parameters 0–63871

electrostatic analyser with no fringe field for use in space vehicles $0\!-\!73676$

fabrication method, patent 0-46054 for fission fragments 0-46030

Particle detectors continued

rticle detectors continued fission neutron detector efficiency correction and neutron multiplicity histograms unfolding 0-49338 guide to current literature and teaching aids 0-49332 h.v. hermetic seal for lead-in 0-46008 using high vacuum gas discharge in electrostatic field 0-60700 high-energy, detection problems 0-60634 hodoscope of Si surface barrier detectors, data analysis and recording by electronic systems 0-49390 identification of charged particles using on-line computer 0-46012 ion optical condensor structure to increase number of usable secondary particles 0-57502 ionized charged particle monitoring on Apollo VIII 0-63907 for ions, positive 0 to 10 keV, nonsimultaneous, using Daly-type conversion detector 0-73190 multidetector, stabilization system, rel. to scintillation spectrometer 0-42618

0-42018 multidetector system for asymmetry parameter meas. 0-70310 multiplier, channel, straight, ion feedback, exptal. obs. 0-77046 n-detector spherical below 10 keV, \$\mathbb{E}\$_1\sitivity meas., time-of-flight method 0-49375

neutrons, CdS, radiation damage annealing 0-73692 neutrons, pulsed source, health physics monitoring 0-73697 nucleon currents meas., for energies exceeding 600 MeV 0-70577 pattern recording, fast buffer memory 0-63861 perturbed angular correlation meas., frequency spectra, random signal analysis 0-49335 ysis 0-49335 position sensitive, using multiple semiconductor diode arrays 0-60696 position sensitive detector, ratio circuit 0-55092 positron emitters, low-level counting using p-p coincidence detector 0-52607

quantameter Wilson-type, calibration using electron synchrotrons

0-46047
recoil spectrometry for nucl. reactions study 0-38741
relativistic energies, identification using secondary emitters 0-60637
with resonance absorbers, evaluation of neutron spectral effects 0-57854
scanners, multichannel, airborne, applications 0-77411
self-powered, for mixed neutron-gamma radiation fields 0-70312
solid state, for conversion electrons 0-52580
solid-state, intrinsic region thickness meas. 0-46046
stopping, reducing effect of nuclear reactions by spatial energy loss distribution comparison 0-49333
surface barrier, position sensitive, response to fission fragments and heavy ions 0-49382
surface barrier detectors, radiation damage effects, 4.5 MeV α particles 0-49383
technical problems involved in particle physics, review 0-38602

0–49383
technical problems involved in particle physics, review 0–38602
time-of-flight of very heavy ions 0–52604
topaz for detection of nuclear fission fragments, description 0–49685
transition radiation for detection of super-high energy particles 0–60695
ultrahigh energy, using transition X-radiation 0–55077
(n,p) spectroscopy, current status of progress 0–73672
for n-reactions angular distribs. meas. scatt. chamber with emulsions 0–38763

BeO exoelectron emitters, ceramic sensitivity increase by diffused layers of Pt, Pd, Au, effects as function of diffusion 0-73700 Co, n flux detector, for meas. and control in research and power reactors 0-38757

0–38/57
LiF dosimeter, calorimeter design, calibration and obs. of energy dependence, in 5-15 keV energy range of X-rays 0–73701
MgO exoelectron emitters, ceramic sensitivity increase by diffused layers of Pt, Pd, Au, effects as function of diffusion 0–73700
Nal:TI wrapped crystal, characteristics determining, reflection coefficient meas. 0–41112

Particle focusing see Particle optics

Particle optics

see also Electron optics; Ion optics
'blurred' charge eigen-energy 0-63561
beam deflection systems, stigmatic and achromatic, necessary conditions
0-42194

0-42194
beam transport systems, differential matrices 0-48994
charged, energy and momentum, electrostatic and magnetic quadrupole
channels 0-60161
charged particles trajectories tracing in mag. sectors 0-38739
charged particles, injection into mag. traps 0-38464
circular polarizations of horiz, harmonics in weakly perturbed cyclotron
field 0-48993
forecurrents bullow and continuous 0-6363

for currents, hollow and continuous 0-63563 electrostatic lenses, slit-aperture, axial potential distribution calc. method

0 - 73164focusing, automatic with tracking rectifier for e.s. accelerator 0-77454 fringing field effect of deflecting magnet on charged particle trajectory 0-73165

0-73165
image aberrations, influence of magnetic field meas. errors 0-48996
iens, magnetic quadrupole, useful aperture determination by floating wire
method 0-48995
lens, superconducting quadrupole coils, trapezoidal cross-sections, optimization of geometric parameters 0-52244
mag. quadrupole field with higher multipolarity error fields, effect on
charged particle trajectories 0-77031
mag. quadrupole lens systems, minimum aperture aberrations 0-48998
quadripolar triplet, phase acceptance in convergent-divergent-convergent
plane 0-60160
quadrupole lens parameters meas. by spinning-coil method 0-48997
thin-lens, waist-to-waist transfer, graphical calc. 0-42193
Z-focusing in cylindrical electrostatic analyser 0-77033
riticle range see Energy loss of particles

Particle range see Energy loss of particles

Particle size

see also Surface measurement
15 microns in suspension, heat transfer investigation, heated duct application 0-74796

aerosol, β -active 'hot' particle, effect on spontaneous unipolar charging 0-39846

aerosols, distribution changes during flow through vessels 0–78316 alloy film, flash evaporation technique 0–61663 β -alumina powders, densification and microstruct. 0–53650

aluminas, distrib. determ. from computer-processed scanning electron microscope images 0–68543 analyser for airborne dust, portable 0–78315

Particle size continued

crimet, UN/W(Mo), fabrication from mixed powders, effects 0–40470 colloid, mass and shape determ. by small angle x-ray scatt. 0–61565 colloid stability, effect on 0–46963 colloid stability, effect on 0–46963 colloid stability, effect on 0–46963 diduction colloids, spherical, angular scattering diagram study 0–68161 dielectric constant, particle size dependence 0–44745 diffusion creep, grain size depend. 0–40323 disperse system, non-Newtonian, apparent viscosity rel. to distrib. 0–61563

disperse systems use of transparency to determ. particle size 0-58506 distribution, influence on high-speed flow of gas-solid suspension pipe 0-64965

distribution, influence on high-speed flow of gas-solid suspension pipe 0–64965
distribution in cryst., calc. method 0–61759
distribution obs. in polydisperse settling aerosol, second and higher order scattering of light 0–74812
distribution transformation. sample-size induced errors 0–71783
effect in crystal structure transformations 0–40479
ferrite grain size effects on fatigue strength, acoustical testing 0–65419
flow light scattering determ. 0–39787
flog drops, distributions, measurement methods and evaluation 0–41503
holographic meas., forward-scatter, Fresnel 0–60261
lunar samples, grain size distribution 0–45380
magnetite, mechanically activated, cryst. anisotropy 0–72217
measurement by X-ray fluorescence 0–47469
measurement by laser photometer 0–57597
measurement methods, comparison 0–47468
metal powder, effect on burning time, statistical analysis 0–41424
micromeritic instrumentation development 0–76791
Permalloy film, domain struct., grain size and support surface roughness
depend 0–54031
polyethylene, semicrystalline, X-ray diffr. determ. 0–58545
powders, determ. by X-ray abs. method 0–50335
probability theory 0–50799
serrated yielding, activation energy, grain size depend. 0–43736
silica, colloidal, Ludox HS, small-angle X-ray scatt. 0–53382
submicron by resistive pulse technique, counting, in conductive fluid 0-74795
suspension, distribu, applic of electro-opt, effects 0–39845
X-ray diffr meas limit of coherent regions 0–443606

submicron by resistive pulse technique, counting, in conductive fluid 0 -74795 suspension, distrib., applic of electro-opt. effects 0-39845 X-ray diffr. meas., limit of coherent regions 0-43606 Ag, lattice contraction, electron microscopy 0-71566 Ag particles, size dependence of dielectric constant 0-44745 Al-Si eutectic, rolled, Si particle size distrib. meas. using extraction technique 0-58973 Al, subgrain coalescence in recrystallization, grain size meas. 0-58951 Al₂O₃ powders, size and shape distrib. 0-58997 B'-AuZn(50%Zn), effect on martensitic transformation 0-71793 BaSO₄C rystallized from aqueous soln. 0-61721 BaTiO₃, powders, effect on i.r. absorpt. spectra 0-48061 Cu, grain size effects on strain hardening curves 0-62076 Fe compounds obs. of superparamagnetism in ultra fine particles using Mossbauer effect 0-56438 ar-Fe₂O₃ powders, and distrib., particle shape, temp. depend. 0-75320 Fe₃O₄, magnetite, subdomain disperse colloidal, magnetization 0-43483 HTiO₄ powders 0-58999 Nb, polycryst. grain size effects on hardness 0-71730 Ni-Al alloys and nimonic, critical shear stress rel. to hardening phase particles 0-50747 NiO, less than 80 Å due to paramagnetum at 77 K 0-68243 STTiO₃ powders, effect on i.r. absorpt, spectra 0-48061 Ti alloy, powder 0-40473 UN/W(Mo) mixed powder, effect on ermet fabrication 0-40470 WC-(10wt.%) Co alloy, transverse-rupture strength depend. 0-47384 YFe garnet, polycrystalline, microwave props., grain size depend. 0-41307 rticle spectrometers

Particle spectrometers

see also Alpha-particle spectrometers, etc.

A/D convertors with digit by-digit weighting 0-46017

Auger electron, preamplifer, design 0-46020

background correction, automatic, instrum. 0-73678

Bloch-Siegert modulation correction 0-77388

Compton, summing, operation of separately housed Ge(Li) detectors 0-60682

0-60682
design, from information on spatial trajectories of ions in 2 dimens. magnetic fields 0-63587
electron, Auger, repetitive multichannel monitor, application to surface composition changes 0-79463
electron, development of parallel plate channel multipliers 0-60179
electron peam, with mag. deflection system to meas, electron scattering angle 0-49354

electron beam, with mag, deflection system to meas, electron scattering angle 0-49354 electron energy meas, from secondary electron intensity at cascade shower maximum 0-70292 electron impact spectrometer 0-45097 electron and ion microprobes, review 0-45098 electron transporter, mag, solenoid type for meas, energy of conversion electrons 0-49349 flat, design and description, evaluation of reliable paameters 0-49347 score for polar-cap-absorption events 0-63878 image detector for dispersed fluxes of energetic particles using fibre-optics delay, multi-channel counting 0-70301 induced electron emission spectrometer 0-45096 ion optical condensor structure to increase number of usable secondary particles 0-57502 ion optical condensor structure to increase number of usable secondary particles 0-57502 ion optical condensor structure to increase number of usable secondary particles (design using digital computer 0-52587 magnetic, charged particle trajectories tracing in sectors 0-38739 magnetic, design using digital computer 0-52587 magnetic, flash tube information, vidicon digitalizing system 0-42622 magnetic, high resolution, broad range, for MP tandem 0-77389 magnetic focusing device design, numerical optimization 0-69852 magnetic focusing device design, numerical optimization 0-69852 magnetic resolution increase using external electronic circuit 0-49344 Mossbauer, time-mode operation without precision control of drive wave-form 0-46019 Mossbauer beak broadening, collimation geometry effect with thick absorbers 0-52589 Mossbauer with large driving force 0-52590 neutron, telescope, proton-recoil, obs. of neutron spectrum between 50 and

Mossbauer with large driving force 0--52590 neutron, telescope, proton-recoil, obs. of neutron spectrum between 50 and 450 keV 0-73681

S 1258 SUBJECT INDEX Particle spectrometers continued neutron time of flight with fast chopper 0—52593 neutron time-of-flight, six-foot long detector 0—46024 nuclear, multichannel, peak parameter determination as function of channel width, statistical errors 0—42633 on-line systems, communications control, small computer application 0–63882 photoalpha angular distributions using solid state detectors 0-46027 photoelectron, applic. to ethylene and O_2 ionization potential determ. photoelectron, for chemical analysis, computer regulated system, design 0-46021 polarization, for thermal neutrons, theory 0-46025 proton, for Apollo applications programme 0-63884 proton-recoil, energy sensitivity calibration using neutrons 0-42620 recoil spectrometry for nucl. reactions study 0-38741 scintillation, multidetector, stabilisation system 0-42618 space-borne, digital closed-loop calibration system 0-63880 spark range for electrons and photons energy resolution investigation 0-49412 0-49412 testing by multipurpose pulse generator 0-46016 total body radiation spectrometer in est. neutron dose from induced ²⁴Na activity 0-41884 wire spark chamber, capacitor memory and f.e.t. readout 0-60644 α particle semiconductor counting 0-49357 c, internal conversion following thermal neutron capture, magnetic spectrometer for meas. 0-52591 forn β-decay angular correl. const. meas... p spectrometer 0-46022 n time-of-flight, inelastic long wavelength 0-60654 He I photoelectron spectrometer calibration 0-74124 Particle symmetry see Elementary particles/symmetry Particle track visualization see also Bubble chambers; Cloud chambers; Luminescence chambers; see also Bubble chambers; Cloud chambers; Luminescence chambers; Nuclear track emulsions; Spark chambers apparatus with diffusion chamber and accelerator for studying photonuclear reactions 0-49407 cosmic ray track meas. in plastic detectors 0-77438 damage track detection in thin foils, rapid reading technique 0-77435 decay points determination, without track reconstruction in space 0-52613 0–52613 in emulsion plates spark chambers, high resolution 0–60723 etch pit diameters correl, with fission fragment energy 0–60714 fission meas, using solid track detectors 0–77434 fission track ages, thermally lowered correction method 0–77440 fission tracks in irrad, plastic films, counting using microscopy or an automatic technique 0–42893 in glasses, track erasure by shock waves 0–70315 hodoscope arrays of scintillation counters, appl, and performance of small, fast photomultiplier tube 0–42647 holograms, information storage and depth of construction, bubble chamber tracks appl. 0–38515 ions, heavy, interaction in emulsions and dielec., models 0–40618 Lexan plastic prints formation 0–77429 Lexan polycarbonate detector, etching enhancement by spark discharge 0–60712 Lexan polycarbonate film, etching 0–73710 Lexan polycarbonate film, etching 0-73710 mica, 4π geometry, fission detection 0-60711 microscope comparator, dual, for fission studies 0-77428 mitrocellulose, thin foil, heavy ions, electron microscopy 0-60709 organic nuclear charged particle track detectors, latent track formation 0-46072photofission, ternary, obs. with track recorders of different sensitivity 0-77432 0 -77432 plastic, sensitivity enhancement through photo-oxidation 0-63870 plastic detector, track registration in critical energy region 0-77431 plastic detector, track registration in critical energy region 0-77431 plastic track detector, track registration in critical energy region 0-77431 plastic track detector, calibration for use in cosmic ray expts. 0-77430 plastic track detectors, calibration for use in cosmic ray expts. 0-77430 plastics, etched, cone length and range meas. 0-77441 plastics, etching parameters 0-60713 plastics, etching parameters 0-60715 polyvinylchloride track detector 0-77439 proportional wire chamber designs, computer evaluation facility 0-52609 reactor neutrons, monitoring with fission foil-Lexan detector system 0-58074 silicates in glasses, track erasure by shock waves. 0-70315

0–58074
silicates in glasses, track erasure by shock waves 0–70315
simulation in spark chamber, method 0–77446
solid state recorder, environmental neutron meas. 0–60717
solid state recorder for neutron spectra, reactor irrad. facility 0–60710
streamer chamber, self-triggering, applications 0–49417
streamer chamber experimental set-up, logic control unit 0–70318
supersaturated vapours of crystals applic. 0–73706
wire chambers, proportional, system of, performance 0–42648
α-particle ang. distrib. meas. in nucl. reactions using solid track detectors
0–77433

 α , track enhancement in cellulose nitrate using electric fields 0-60718

for n-reactions angular distribs. meas. scatt. chamber with emulsions 0-38763 $\begin{array}{l} 0.-38763 \\ 2^{235}U \text{ enrichment of metallic U, registration using cellulose nitrate} & 0-77436 \end{array}$

Particle tracks

rticle tracks
see also Energy loss of particles
alpha-particles, enhancement of tracks in cellulose nitrate by applic. of
electric field 0-38762
near axis of EAS, exam of normal tracks in cloud chambers rel. to reinterpretation 0-38764
in bubble chamber, ionisation density measuring device 0-60721
charged pairs, passage through matter producing lightly ionized tracks
0-57857

0–57857 damage track detection in thin foils, rapid reading technique $\,0-77435$ development in emulsions by amidol and NaSCN developers $\,0-38770$ in dielectric inorg, solid, identification $\,0-38761$ distortion due to gas convection in Wilson cloud chamber, calcs. $\,0-49410$ electron scattering, multiple, in gas sequence bias for observed and expected track shapes $\,0-42999$ fission track ages, thermally lowered correction method $\,0-77440$ formation, ionization energy due to δ -rays $\,0-62227$

Particle tracks continued

formation in mica, Ar ion irrad., x-ray small-angle scatt. 0-58781

formation in fined, Ar form trad, x-ray small-angrescatt. 0-35781 fossil in extraterrestrial materials, cosmic ray 0-63156 fragments track counting in polycarbonates, rel. to meas. of reactor parameter δ^{28} 0-39212 heavy-ion, formation mechanism in minerals 0-62235

ideaty/soli, formation inclination in liquid-hydrogen bubble chamber, effect of ultrasound 0–46063

ionographic signal analysis 0–49406 localization method for wide-gap spark chambers 0–42653 lunar samples, density meas. 0–45363 lunar samples, tracks of cosmic ray and solar origin 0–48508

measurement, digitized co-ordinate recording device, for nuclear brakes and bubble chamber photograms 0-60720 measurement in emulsions 0-46070

in mica, Ar ion irrad., formation mechanism, small angle X-ray scatt. 0-61935

neutron detectors, sensitivity and dose response 0–46071 nitrocellulose, thin foil, heavy ion, electron microscopy 0–60709 nuclear, fossil, in extraterrestrial matter, high voltage electron microscope studies 0–72778

orientation meas, with parallel plate ionization chamber with gas multiplication 0–49361

tion 0-49361
photographs, rapid semi-automatic meas, using laser beam steered by computer controlled mirrors 0-49408
plastic detector, track registration in critical energy region 0-77431
in polymer, form, mechanism 0-78803
position sensitive detector, ratio circuit 0-55092
propane bubble chamber, track density relativistic increase meas.
0-46062

separated beam of secondary particles, tracking system 0-42629 in solids, review 0-40613 thermal conductivity determination for gas impinging on hot plate 0-74672

u.s. effect on form. in liq. H bubble chambers 0-52612 ultasound formation in hydrogen bubble chamber 0-52610

Particle velocity analysis

rticle velocity analysis

see also Alpha-particle spectrometers; Beta-ray spectrometers;

Energy loss of particles; Ion velocity; Mass spectrometers
atmospheric precipitation, Doppler radar meas. 0–56776
exact drift velocity soln, for charged particle in static axially symmetric
magnetic field 0–52240
high-energy, problems 0–60634
hypervelocity, hologram recording, Fourier transform method 0–49095
ion acceleration due to electron beam injection into low-pressure H₂-filled
region 0–73171
time-of-flight analyser, 16000 channel 50 MHz, for high data rates
0–63879
Cu. particles ejected from surface under bombardment by Artions

Cu, particles ejected from surface under bombardment by Ar^+ions 0-65039

Particles see Elementary particles; Energy loss of particles; Scattering, particles; and under individual particles, e.g. Protons and antiprotons

Paschen-Back effect see Spectra
Patterson diagrams see X-ray crystallography/calculation methods
Peierls-Nabarro force see Crystal imperfections/dislocations; Internal

Peltier effect see Thermoelectricity

Pendellosung fringes see X-ray crystallography

Pendulums

0-75230 torsion, oscillations, automatic meas. using optical system

Liapunov instability of the oscillating pendulum, linear stability analysis $0\!-\!59947$

swings, pumping 0-48777 transient, torsion, analysed as device for obtaining data on viscoelastic materials 0-59993

Periodic system
see also Elements

transuranic metals rel. to rare earths 0-41409 vapour pressure straight lines in the periodic table 0-39893

Permalloy see Iron alloys; Nickel alloys

Permeability, magnetic see Magnetic properties of substances; Magnetization

Permeability, mechanical
see also Diffusion in solids
anisotropic in porous media 0-67857
ceramic fuel elements, pore deform, and migration, local thermal stresses influence 0-40194

osmotic/tracer permeability ratio, in homogeneous liquid membranes

Fe, of cathodic H, effect of physicochemical surface treatment 0-65340

Permittivity see Dielectric properties of substances

Perturbation theory see Field theory, quantum; Quantum theory

pH see Electrochemistry

Phase diagrams see Phase equilibrium; Phase transformations

Phase equilibrium

ase equilibrium

see also Solubility; Solutions

alkaline earth fluorides-oxides-oxides of silicon/aluminum/titanium

0-62144

alkaline earth vanadate systems, cpd, form. and polymorphism 0-50831

alloy, binary, liquid phase composition on contact fusion 0-71410

alloy, binary liquid phase composition on contact fusion 0-71410

alloy, systems, homogeneous monotonic, liquidus-solidus gap 0-50300

alloys, multiphase, constitution determ. using mag. methods 0-75311

Bethe-lattice gas, 2-component, or 3-component Bethe-lattice soln.

0-41987

binary vapour-liquid equilib... numerical integration of co-existence equilibrium processions.

binary vapour-liquid equilib., numerical integration of co-existence eqn. 0-50319

boundary determ, for binary equilib, diags, using free-energy/conc, functions 0-64991

boundary movement kinetics 0-78325 critical systems, long-range correl. length 0-57291 cryogenic mixtures, multi-component, vapour- liquid equilibria prediction methods 0-55666 crystal growth, flux method, solubility, saturation point 0-74978 diagram, multicomponent, computer mapping 0-78331

```
Phase equilibrium continued
```

diagrams, graphical calc. 0-64992

dichlorotetrafluoroethane-MoF6 binary mixture liquid-vapour equilibrium

at 2600 torr 0–64984 electro-optic K₂O-Kl₂O-Nb₂O₅, tungsten bronze field 0–61588 ferromagnetic alloy, Co-Mn, Young's modulus, thermal expansion 0–57413

fluid-crystal, theoretical confirmation of Simon eqn. describing temp.-pres sure relation 0-51989

sure relation 0—51989 gas-gas, 2-component lattice-gas model explanation 0—55557 gas liquid interface, dynamics near critical point 0—71404 glass, critical immiscibility meas. by viscosity drift method 0—55680 glass, liquid liquid phase separation rel. to bending strength 0—53607 glass, lithia-silica, separation, effect of P₂O₅, transmission electron microscopy meas. 0—50340 glass, phase separated, ball indentation strength, heat treatment time depend. 0—53608 glass, separation, ougnitiative meas, using transmission electron microglass, separation, ougnitiative meas, using transmission electron microglass, separation, ougnitiative meas, using transmission electron microglass.

glass, phase separated, oall indentation strength, neat treatment time depend. 0–53608 glass, separation, quantitative meas, using transmission electron microscopy, exptl. technique and analysis method 0–50339 isopropanol-cyclohexane mixture, im estigation over temp., press., conc. range 0–64916 liquid metals and vapours under press. 0–46989 liquid phase composition on contact fusion 0–71410 liquid-gas critical pt., sp. ht. anomaly rel. to sound vel. 0–50321 lunar samples, electron-microprobe analyses 0–45351 lunar samples, lectron-microprobe analyses 0–45351 metal solutions, binary 0–55594 metal solutions, binary velocitical phenomena, coexistence curve 0 39778 molecular crystals, binary phase diagrams 0–59060 moving boundary problem, 3-phase system, 2 moving boundary, math. soln. 0–55912 multi-component interface system, entropy production 0–74877 multi-component tierface system, entropy production 0–74877 multi-component tierface system, entropy production from liquid boiling tem-incomponent vapour-liquid system, calculation, from liquid boiling tem-

tion data 0–68184
multicomponent vapour-liquid system, calculation, from liquid boiling temperature data 0–68185
PbO.PbCrO₄-PbO.PbXO₄, X=Mo, W, S, rel. to crystal growth 0–58522
n-pentane, liquid-gas critical point, thermal equation of state, gravitational effect 0–74850
rare-earth intra-alloys, review 0–71779
semiconductor, HgTe, crystal-vapour, Hall effect, Seebeck coeff. 0–78344
semiconductor, defective diamond like, intermediate phase 0–47174
sodium borosilicate glasses, thermal shock resistant, effect on production 0–68199

sodium borosilicate glasses, thermal shock resistant, effect on production 0-68199 steel, Cr-Ni, austenitic, determ. of low concs. of α -phase (ferromag.), effect of austenite (paramag.) 0-78697 steel, N36Kh12TYu, microhardness in regions of continuous and discontinuous deposition of y'-phase 0-50782 steel, stainless ATSI type 304, proportional limit and work hardening rate, effect of N, 302F 0-43805 sulphates, high-temp. cubic phase props. 0-75412 superconductor, Ce, phase boundary determ., high press., 77-480K 0-43823

sulphates, high-temp. cubic phase props. 0—75412 superconductor, Ce, phase boundary determ., high press., 77-480K 0—43823 thallium acetate-water binary system, liquid-solid phase equilibrium diagram 0—78335 transition metal-B-C-Si systems, phase diagrams 0—50833 triple point coords. rel. to cohesive energy 0—71424 triple point of water, cell production 0—50301 vapour-liquid, appl. of Redlich-Kwong equ. of state 0—50320 vapour-liquid surface, motion of He ions 0—50322 vapour-liquid with Redlich-Kwong equation of state 0—68183 Ag-Ca syst., differential thermal anal. 0—56049 Ag alloys, body-centred cubic structure, stability 0—78448 Al-Zn alloys, metastable states, diffuse X-ray obs. 0—58974 Al effect in Ta-Mo-C and Ta-Nb-C system, equilibrium investigation 0—50822 Al2-0;-Cr₂O₃ system, spinodal microstructures 0—50511 Ar, liquid, triple-dipole dispersion forces at critical state 0—50197 As-Sb-Se system, phase relations and liq. struct. 0—5091 Au-Al system intermetallic form 0—71794 Au alloys, body-centred cubic structure, stability 0—78448 B-Sc system, struct., comp. depend. 0—55830 Ba-Cs 400-1300°K, thermodyn. anal. 0—55606 BaBr₃ with alkali bromides, thermodyn balaviour 0—65479 BaF₂-rare earth fluoride system, phase relations 0—56023 BaF₂-liff-3 syste, new phases detected 0—62145 Ba₂NaNb₂O₃, constitutional obs. 0—50298 BaSnGe₂O₃, prep. of new phase 0—53668 Ba-Al-Ti system, liquidus surfaces 0—58520 Bi-Sn alloys, interface instability and microsegregation 0—74835 Bi-Tl, diag. and thermodynamic eqns. of state 0—74838 Bi-Tl alloy system under press. 0—40500 Bi, 4.2-300 K, 50 kbar 0—43811 CO₃, long-range coherence length near critical pt. 0—53401 CS₂-methanol binary system, critical phenomena, coexistence curve 0—39778 CaC-SiO₂ system immiscibility, free energy model obs. 0—58540 CaO-TiO₃, at liquidus temps. 0—43510 CG-CRO₃), "AppO₃ system one of capsO₃ cervice energy model obs. 0—5840 CaO-TiO₃, at liquidus temps. 0—64987 CaO-GiO₂, appoint phase evidence 0—65502 Ca(PO₂), "AppO

CIF₃-MoF₆ liquid-vapour equilibrium at 2600 torr, dew and boiling curves 0-64981

CIF₃-dichlorotetrafluoroethane liquid- vapour equilibrium at constant pressure 0-64983

Co-Ho system, thermal analysis, microscopy, X-ray diffr. 0—58521 Co-Mn, ferromag, alloy, Young's modulus, thermal expansion 0—75 CoBr₂-KBr-H₂O system, solid-liq., vapour pressure meas. 0—55654 Cr-Fe system, and thermodynamic props. 0—56041 Cu-Ni-Mn, development of order 0—56073

Phase equilibrium continued

CuCl, crystal growth, Stockbarger method, annealing, melt phase diagrams 0-75003

CuO-Ga₂O₃-Cr₂O₃, spinel phase, evidence 0-65503

DyBO₃-Dy₂O₃, liquid region, rel. to DyBO₃ prep. 0-76258

DyBO₃-Dy₃O₃, iquid region, rel. to DyBO₃ prep. 0—76258
F, vapour-liquid coexistence boundary critical parameters 0—71417
Fe-C-O₃ isobaric ternary phase diagrams 0—62146
Fe-Co-V, magnetically hard, rel. to magnetic properties 0—72227
Fe-Cr-O system, phase relations, high temp. and strongly reducing conditions 0—59127
Fe-Ni-C, rel. to diamond crystallization at high pressure 0—47143
Fe₃O₄-Te₃O₄ 0—75348
0—75348

Fe-N-C, rel. to diamond crystallization at high pressure 0-47143
Fe304-xF, (where 0≤x≤0.5), from oxygenated homologue Fe304
0-75348
Ga-GaP-GaAs system 0-58519
Ga-In-Sn system, liquidus isotherm 0-71412
Ga-In-Sn system, ternary eutectic, 10.7°C 0-78333
Ga, β-metastable phase, electron diffr. obs. 0-50832
Ga, triple metastable iquid-β-Ga-Ga III pt. obs. 0-53399
GaF-SrF₂ syst., liq.-solid equilibrium diagram, formation of ternary fluorides 0-65284
Ga₂0₂-Pb syst., formation of three compounds 0-65481
GaP-InP pseudobinary system, solidus boundary, electron microprobe, lattice parameter, Vegard's law 0-53396
GaSe-InSe, diag. obs. 0-46979
Gd₂Fe₃C_{12-x}F_x (0≤x≤0.60), new oxyfluoride phase of garnet 0-56075
Ge-Si-Sn(Pb) ternary diags., quasi-chem. calcs. 0-71407
HCl-H₂O system, vapour-liqid equilibria 0-74849
H₃O-NH₄F liq.-solid equilib. 0-64993
He-CO₂ system, vapour-liqd, data and dielec. constants 0-50323
HfO₂-Hf system, phase relations 0-59049
HgTe, crystal-vapour, Hall effect, Seebeck coeff. 0-78344
In-Sn system, state diagram rel. to comp-prop. diagrams 0-65505
InSb-NiSb eutectic alloy, rel. to magnetosensitive resistance 0-51037
KH₃ASO₄, diagram to 52 kbar and 400°C 0-55657
KNbO₂-Sr(Ba)Nb₂O₆ system, dielectric and struct, props. 0-47489
K₂O-Li₂O-Nb₂O₅, tungsten bronze field 0-61588
KPO₃-Mg(PO₃)₂ and KPO₂-Zn(PO₂)₃ systems, diagram 0-62149
K₃SO₄.2MgSO₄, langbeinite, effects of K replacement by Na and Mg by Ca on stability 0-68310
La-Be-Al, investigations 0-50790
Lil-LiBr-H₂O system, solid-solid, vapour pressure meas. 0-55654
LisPO₃-Mg(PO₃)₂ and KPO₃-Zn(PO₃)₃ system, solid-solutions 0-61589
LisSiO₄-Zn₂SiO₆ system, getic forms studied 0-55850
Mg-Al-Sh, diag, for Mg-rich region 0-50303

props. 0–78412 MNbSe₃, phases, lattice forms studied 0–55850 Mg-Al-Sn, diag, for Mg-rich region 0–50303 Mg-Cr-O system, phase relations, high temp. and strongly reducing condi-tions 0–59050

MgO-H₂O, high temp., press. 0–59027 Mn-Ge system 0–59051 MnF₂, magnetic phase diagram from u.s. and differential magnetization meas. 0–51240

MnF₂, magnetic phase diagram from u.s. and differential magnetization meas. 0–51240
MnO-ZrO₂-SiO₂ system, phase relations 0–58517
Mo effect on V-Ta-C and Nb-Ta-C system, equilibrium at high temperature investigation 0–50821
NH₄F-TiF, liq.-solid, pressure effect 0–61590
NH₄H₂PO₄, diagram to 52 kbar and 400°C 0–55657
Na-Bi system, diagram 0–39869
Na-NH₃, liquid-liquid coexistence and phase separation 0–58454
Na-Rb system, solid-liq. phase diagram 0–53398
Na-NO₂-Al₂O₃ diagram 0–58518
Na-NO₂-BaO-Nb₂O₅ system, ferroelectric crystal growth, comp. depend., phase diagram 0–39879
Na₂O-BaO-Nb₂O₅ system, ferroelectric crystal growth, comp. depend., phase diagram 0–39879
Na₂O-Fe₂O₃-SiO₂ glass, crystallization of β-NaFeO₂, Mossbauer spectra, x-ray diffr. 0–47490
NaOH-BaGOH₃ solid-liq. syst. 0–64994
Na₂U₂O₇-V₂O₅ syst., 400-1000°C, prep. and identification of 3 new phases 0–53671
Na₂O-BaO₃-Li₂O.SiO₂-SiO₂ syst., phase separation, metastable liquation

Na₂0.4B₂O₃-Li₂O.SiO₂-SiO₂ syst., phase separation, metastable liquation

0-68557
Nb-Sn system, constitution diagram 0-61591
Nb-W-C alloy, constitution, X-ray diffr., DTA 0-47491
Nb-W by phase equilibrium study, 1400-2100°C 0-78334
Nb-B system, electrophysical props. of phases 0-65625
Ne. co-existence curve near triple point, quantum corrections for free energy 0-53395
Ni-Al-Nb alloy, Ni-rich, 1200 and 750°C 0-53672
Ni-Co-Te system at 500°C, stability domain of hexagonal phase 0-65506
Ni-Cu-C solid solns, equil. temp. depend., vapour transport study 0-71810
Ni-Ga-B, during solidification and at 800°C 0-47455

0-71810
Ni-Ga-B, during solidification and at 800°C 0-47455
Ni-Nb-W phase equilibrium study, 1400-2100°C 0-78334
Ni-Sb system non-existence of Ni₁₃Sb 0-65507
PbO-SiO₂ system, liquidus obs. in SiO₂-rich region 0-61594
Pu-Ti alloys, Pu β phase stabilization 0-68568
RbBFa, high pressure relations 0-55658
Rb₂CO₃, high pressure relations 0-55658
Rb₂CO₃, high pressure relations 0-55658
Rb-CO₃ high pressure relations 0-50682
Rb-CO₃ high pressure relations 0-50682

0-3082Z
Ru-O system, thermodynamic obs. 0-50304
Se, thermodynamic props. 0-50305
SiO₂-B₂O₃-Na₂O₃ system glasses, phase separation mechanism 0-58544
Sn-Pb(-SnAg₃,-Zn) eutectics, solid-solid interface energies, laminar growth theories 0-39923
Snapper (Snapper 0-50206)

theories 0–39923
Sn-Sb-Te system 0–50306
SnAs₁-SnAs-SnTe subsystem, eutectic obs. 0–74836
SrBr₂ with alkali bromides, thermodyn. behaviour 0–65479
SrF₂-InF₃, new phases detected 0–62145
Ta-H system, diagram, and electronic structure 0–47492
Ta₂VO₆-VO₂ solid solns., calc. for appearance of order 0–55860
Te-Se melts, miscibility, cpd. formation, surface tension and density 0–50210

0-50210
TeO₂-V/O₃-CdO, phase diagram for glass formation, properties 0-68201
Ti-C system, precip. bands below stoichiometry 0-59034
Ti-O system, intermediate oxide phases 0-71811
Ti-V(Nb,Mo) phase boundaries determ. 0-53665

S 1260 SUBJECT INDEX nase equilibrium continued

TiO, polymorphs, stability, comp. and temp. depend. 0-65508

Ti-Sb, thermodyn. anal. 0-65477

Ti-CO₃, high press, phase boundaries 0-62136

TiPO₃-Ca(PO₃)₂, diagram, rel. to new compounds 0-50834

TiPO₃-Co(PO₃)₂, diagram, rel. to new compounds 0-50834

TiPO₃-Co(PO₃)₃, diagram, rel. to new compounds 0-50834

U.C-Si phase diagram, U.Si-C section obs. 0-64988

U-Ce O ternary phase diagram constructed 0-47483

U-Ni-S syst., at 800°C, new phases 0-63852

U-Ru-C system, phase identification, microhardness, electron microprobe 0-56057

UC-UC₂ equilibrium diagram revised following X-ray diffraction examination at. 1790°C 0-536657

UC-UC₂ equilibrium diagram revised following X-ray diffraction examination at. 1790°C 0-53669

UO-PuO₂-Pu₂O₃ system, phase diagram 0-62147

UO₂-SiO₃ vitroceramics, liquidus curve 0-46307

UO₂-ThO₂ system, solidus and liquidus temps. 0-58523

UO-UC₃ system, 0-0.5<x<0.2), solidus-liquidus temps. 0-58523

UO-U₅ system, 0-0.5<x<0.2), solidus-liquidus temps. 0-58524

U₃O₃ phase diagram, elec. cond. study 0-59039

U₄O₃-v₄O₃-v₅O Phase equilibrium continued Y Cd and Y-Cd-Zn systems, phase diagrams and relations, intermetallics obs. 0–18707
Y-Sb alloy system, phase diagram 0–64995
YFe garnet, high-press, stability 0–62138
YF- garnet, high-press, stability 0–62138
Yb-Ag system, phase struct., melting, comp. depend. 0–64996
Zn, Cd-1, xTe solid solution, phase diagram 0–47493
Zn, Hg1, xTe solid solution, phase diagram 0–47493
Zn-Hg1, xTe solid solution, spinel phase, evidence 0–65503
ZnSb CdSb system, elec. resistance and activation energy extremums and anomalies, model explanation 0–75349
ZnSb-CdSb system, existence of phase ZnCdSb₂ 0–75111
ZnTe-ZnSe, liquid-solid, rel. to single crystal growth from melt 0–50462
Zn,WJOs, formation and props. 0–65473
Zr-Ti-O system, phase obs. on pseudobinaries, subsolidus ternary diagram 0–59057
ZrO₂-Nd₂O₃, high temperature study 0–59058 0-59057
ZrO₂-Nd₂O₃, high temperature study 0-59058
ZrO₂-WO₃-P₂O₃ 0-47494
ZrO₂ polymorphs, i.r. and Raman spectra obs. 0-54112
ZrO₂ stabilization by MnO and partial substitution of Ti, Nb or Ta
0-59059 ZrO2 system, diag. 0-61587 Phase flow see Flow/two-phase
Phase meters see Electrical measurement Phase transformations acetonitrile, gas-soln. transition, effect on i.r. band of CC stretching vibr. alcohol, structural effects near solidification temp., e.s.r. 0-55653 alcohol, structural effects near solidification temp., e.s.r. 0—55653 alloys, concentrated experiments, solid-liquid interface temp. meas. and stability 0—50776 alloys, liq., second-order transform. rel. to cluster struct., obs. 0—39726 p-azoxyanisole, liquid crystals, small angle X-ray scattering 0—61496 benzene, shock-wave compression 0—58459 binary liquid, decoupled-mode dynamical scaling theory 0—46865 binary system, specific heat peak splitting and discontinuity, calorimetry inhomogeneity 0—53393

binary system, specific near peak splitting and discontinuity, calorimetry inhomogeneity 0.–53393

Bose-Einstein, quasiparticle interactions, gas 0.–66846

boundary movement kinetics 0.–78325

condensation of liquid metals 0.–58527

conference, growth points of physics, Florence (1969) 0.–45504

correlators, high order, behaviour near transition of second kind 0.–48738

critical indices and lattice models 0.–51970

critical phenomena, fluctuons 0.–68715

critical phenomena, model 0.–58516

critical phenomena, research, review 0.–46975

critical region, Orstein-Zernicke theory extension 0.–43509

critical region correlation functions, asymptotic form 0.–46976

critical region correlation functions, asymptotic form 0.–46865

cyclopentane, spectroscopic effects, 80-300K 0.–62680

density of states function, conditions 0.–71921

dynamical scaling, sum rules 0.–59934

electron fluid 0.–57299

eutectic solidification, oriented microstructures, Al₂O₃/ZrO₂ system 0.–61597

ferro/paramagnetic, of triglycine sulphate, effect of parameters 0.–74837

0-0137/ ferro/paramagnetic, of triglycine sulphate, effect of parameters 0-74837 first-order, of magnetic model, stable and metastable thermodynamic states 0-72955 first-order, rel. to radial distrib. function 0-51983 in flow channel, heat and mass transfer rel. to surface mass addition 0-71081

0-71081
fluids, one-dimensional, correlation functions 0-50297
fluids, one-dimensional, simple lograrithmic model 0-50296
fluids, one-dimensional, thermodynamics 0-50294
fluids with several transitions 0-46642
free energy expansion near transitions 0-48747
gas, 1st order transition and critical pt. from isotherms 0-43393
glass, oxide, molten, liquid-liquid phase transitions, viscosity meas.

glass, phase separation, coalescence of second phase particles 0-74863 glass, soda-silica, phase-separated, heat treatment influence 0-74868 glass systems, phase separated, conf., Bristol, England Sept. 1970 0-74859

10 14639 heat transfer in triangular channels with and without phase change 0-78341 model, phase transition as function of applied transverse field 0-63354

Lennard-Jones system, high temperature part of coexistence curve investigated by Monte Carlo calc. 0-71425

Phase transformations continued

Lennard-Jones system. Monte Carlo calc. 0-46977 liquid, binary, decoupled-mode dynamical scaling theory 0-46865

liquid crystal, isotropic nematic transf., mol.-field description 0-68078 liquid crystal, nematic, pretransitional phenomena in isotropic phase 0-68079

0–68079

liquid crystals, p-azoxyanisole, critical thermodynamic derivs. 0–58451 liquid crystals, nematic, possible uniaxial- biaxial transition, rel. to corr. n.m.r. and e.p.r. studies 0–78307 liquid metals, surface tension and critical props. 0–58470 liquid depase nucleus, critical size, electric field strength depend. 0–50326 liquid-gas, Green's function approx. for eqn. of state 0–74846 liquid-gas azeotropic critical point, diffusion theory 0–74848 liquid-gas transition near Te, Fisher droplet model 0–55667 liquid-solid, Landaus' argument on nonexistence of critical point, rigorous basis 0–54600 macromolecular polymers, in solns., conformal transf., study by polarized luminesc. 0–67830 membranes, porous, charged, transition between 2 steady states 0–66840 methane, gas, effective self-diffusion coeffs. in transition press. range 0–50172 methanol, liq.-solid, effect on positron lifetime, and CH₃OH 0–75533

methanol, liq.-solid, effect on positron lifetime, and CH₃OH 0-75533 Monte Carlo method applic. to grand canonical ensemble of real gas 0-38201

Mott transitions, effect of correlations 0–75537
neutron scatt. meas. near critical transforms. 0–46870
non-negative interactions, bounds, successive approximations and limits for distribution functions 0–57292

nuclear matter, interacting α -particles, hard-core and long-range pots. 0-38825

0–38825 nucleus of interacting α-particles, normal-superfluid transition 0–38823 paraffin, 8≤n≤16, order-disorder, specific heat, entropy 0–78706 pertubation effect, application to anisotropic Ising model 0–72961 phase transition, correlation functions, scaling laws violation 0–72952 phenomenological model 0–54604 polypropylene oxide, multiple melting transitions 0–65006 porous substances during melting, determ. by shock compression 0–46980

quasithermodynamic theory, comparison with molecular theory 0-64982 Raman spectra of liquid-solid critical phenomena in organic cpds. 0-74832

0-74832 second-order, without divergences in second derivs. of thermodynamic potential .0-68548 sharp in two-dimensions, without long range order .0-71403 solid, dielectric conductivity, high press. and temp. effects study using chamber .0-79039 solid-liquid growth fronts, non-planar, solute distrib., steady-state and transient conditions, no stirring .0-39868 solid-vapour equilibria in cryogenic systems, review .0-47002 solidification, surface, in axisymmetric fluid flow in tubes .0-49977 solidification of molten metal pool during pulsed are welding, thermal condi-

solidification of molten metal pool during pulsed arc welding, thermal conditions 0-47475

solidification of molten metal pool during pulsed arc welding, thermal conditions 0-47475
spherical bodies, heat cond. 0-78324
spherical lattice gas, 1-dimensional phase transitions from inverse power law potentials 0-57283
Stephan problem approx. soln. 0-55652
substituted arylidine amino-cinnamates, liquid crystal transitions 0-64870
thermodynamic, pure, as extremal KMS states 0-73065
thermodynamics, statistical, analytic props. 0-5186
of triglycine sulphate influence of different parameters, surface condits.
sample thickness, composition, electrode area 0-74837
upper mantle, Earth's crustal structure 0-45109
water adsorbed on ice-nucleating two-dimens. transitions 0-53397
Ag-Ge alloy, heavy faulting on rapid solidification, electron microscope
obs. 0-40141
Ar, rel. to Lennard Jones system 0-46977
Be-Al-Ti system, liquidus surfaces 0-58520
BeO, meas. using thermal arrest technique 0-61593
Bi-Sn alloys, interface instability and microsegregation 0-74835
Bi-Tl alloys, solid-liquid, struct. obs., conductivity meas. 0-64864
CO₂, effective self-diffusion coeffs: in transition press. range 0-50172
CO₂, long-range coherence length near critical pt. 0-53401
CS₂, shock-wave compression 0-58459
Co-In system, phase diagram, thermal analysis, microscopy, X-ray diffr.
0-58521
D₂, shift in vibr. frequencies caused by gas-soln, phase transition 0-43111
D₂O, positron lifetime temp, depend, melting nt. obs. 0-43512

0-35221 D₂, shift in vibr. frequencies caused by gas-soln. phase transition 0-43111 D₂O, positron lifetime temp. depend., melting pt. obs. 0-43512 Fe-Ni-Al-Co-Ti alloys, effect of Co, S and Te on liquidus-solidus gaps 0-71775

0-11775
GeO₂-GeO glasses, phase separation 0-74864
H₂, shift in vibr. frequencies caused by gas-soln. phase transition 0-43111
H₂O, critical exponent δ, Kiang's formula 0-39881
H₂O, positron lifetime temp. depend, melting pt. obs. 0-43512
H₂¹⁸O, fractional factor of ¹⁸O between water vapour and ice, -33.4 to 0°C 0-65011
³He-4He liq. mixture, thermodynamic behaviour of model Hamiltonian 0-74818

Hg, liquid formation in gas discharge tubes 0-61383

In-Ga-Sn eutectic, elec, resistance in melting region, 280-310K 0-74842 In-Sn, In-Bi alloys, solid-liquid, struct. obs., conductivity meas. 0-64864 In film, vacuum deposition, liquid-like behaviour, electron microscopy 0-74915

 N_{2^-} methane-ethane system, liq. phase inversion between $-255^{\circ}F$ and $-263^{\circ}F$ 0-39882

~263°F 0-39882
NaCl due to shock waves 0-47481
Nb₃(Al, 6e), critical temp., effect of crystal ordering 0-50540
Ne, coexistence curve near triple point, quantum corrections for free energy 0-53395
Ni-Mo phase diagram 1200-2100°C 0-71408
Ni-Nb-Mo isothermal section at 1400°C 0-71408
Ni-Nb-Mo isothermal section at 1400°C 0-71408
Ni-Nb phase diagram 1200-2100°C 0-71408
Ni-Nb phase diagram 1200-2100°C 0-71408
Ni-Nb phase diagram 1200-100°C 0-71408
Ni-Nb phase diagram 1200-100°C 0-71408
So₂, triple point to 300°K, thermodynamic props., specific heats and P-V-T data 0-46992
Ru-O system, thermodynamic obs. 0-50304
SF₆, Rayleigh scatt., critical region obs. 0-71405
Se, thermodynamic props. 0-50305
Ti-Te, molton alloy, thermoelectricity, elec. cond., comp. depend., semiconductor-metal transition 0-46948
Zn-Al alloy, supersaturated near-eutectoid, decomposition 0-61599

Phase transformations continued solid-state

see also Ageing

 $y=\alpha$, induced uniaxial anisotropy 0-54013

 $A_2B_2O_7$ -type cpds., displactive-type, systematic correlation with crystal structs. 0-58730alkali fluoroborates, volume changes at transition temp. 0-43435

alkali nitrates, cond. vars. rel. to 0 coordination 0-40831

alkali sulphates, cond. vars. rel. to 0 coordination 0-40831

alkaline earth vanadate systems, cpd. form. and polymorphism 0-50831 alloy, binary, kinetics 0-78690

alloy, domain struct. during ordering, field ion microscope obs. 0-58971

alloy, effect of transition temp. on mag. moments 0-75879

alloy, metastable phases, strain induced, deformation hot stage metallographic facility 0-40481 alloy, oxide-dispersion-strengthened, high temp. material instabilities prediction 0-75324

alloy, quantitative dilatometry 0-59013 alloy, supercond, 35BT, cold-worked specimen annealed 0-78692 alloy, without comp. change 0-59045 alloy AMG6 welder, phase composition, electrolytic investigation method 0-43827

anoy Awdo whete, phase composition, electrolyte investigation method 0-43827 ammonium and deutero-ammonium halides 0-75334 ammonium and deutero-ammonium halides 0-75334 amorphization rel. to sputtering mechanism 0-40624 antiferroelectric, perovskite-type, phase transitions 0-75807 antiferroelectric ferroelectric termodynamics 0-75808 d-camphor, electrical conductivity 0-47633 conference, Buffalo, USA, Aug 1969 0-58651 critical phenomena, fluctuons 0-68715 cubic cryst., rel. to soft librational modes 0-71789 cyclohexanol, growth rates 0-50827 cyclopentanol, anomalous dielectric behaviour 0-56070 diamagnetic susceptibilities change at transition point 0-68547 1,2-dichloro 3,4,5,6-tetramethylbenzene, order-disorder orientation transition 0-59047 diffuse, for ferroelectrics, determ. sizes of Kanzig regions 0-40847 diffusion-limited, math. approxs. comparison and crit. evaluations 0-78689 diffusionless transform., conditions determ. 0-56071

0–78689
diffusionless transform., conditions determ. 0–56071
disorder, bombardment- induced, measurement, interpret. model 0–50829
duplex massive, growth of feathery structures 0–56056
e.m. wave field induced rel. to electron-phonon interaction 0–68549
earth's const., geophysics record 0–54206
in electrolytic deposition of metals 0–56707
electron microscopy, transmission, applic. 0–75066
enstatite, X-ray study of phase transformations 0–56058
eutectoid and solid solution decomposition, unidirectional, aligned composite material prep. 0–53656
f.c.c. cryst., complex, rel. to soft librational modes 0–71789
Fe, α-γp, enthalpy meas. with automatic spherical high-temperature calorimeter 0–73078
FeCO₃, siderite, Mossbauer obs. 0–66012
ferroelectric, BaTiO₃ type struct. disorder 0–65501
ferroelectric, NaH₃(SeO₃)₂, specific heat, configurational entropy change
0–43907

0 - 43907

ferroelectric, diffuse transf., determ. sizes of Kanzig regions 0-40847

lerroelectric, difluse transt, determ. sizes of Kanzig regions 0–40847 ferroelectric, effect of changes of electrostatic constraints 0–47837 ferroelectric, electron-phonon nature 0–40841 ferroelectric, netreband theory of spontaneous polarization 0–40843 ferroelectric, radiation induced transform. 0–65487 ferroelectric material, ion beam microscopy, shadow-effect 0–40478 ferroelectric perovskite-type mats., influence of Kanzig regions on dielectrophysics, with budgagen bonds electric neutrality violation. 0–75794

props. 0-40848 ferroelectric with hydrogen-bonds, electric neutrality violation 0-75794 ferromagnet, Fe-Ni-Co alloy, martensite-to-austenite, coercive force, temp. depend. 0-44587 ferromagnetic alloy, Co-Al, coercive force rel. to microstructure, ageing depend. 0-54008 first-order transition front, nucleation models 0-62127 formic acid, crystalline, obs. 78-300 K first order phase transition obs. 0-75344

o-75344
glass, LiAlSi; O₆ 0-59026
Gorskii-Bragg Williams model, analysis 0-47485
granite transformations due to underground nuclear explosions oraphite-diamond-graphite, shock-induced, microstruct. effects 0-78693
graphitization, internal friction applic. 0-65366
graphitization, role of internal tensions 0-40483
graphitization winder press, accelerating effect of coexisting Ca cpds. 0-40482
graphitization under press, accelerating effect of coexisting Ca cpds. 0-40482
graphitzation in annealed pyrolytic graphite, irreversible dimens. changes

u-40402
graphization in annealed pyrolytic graphite, irreversible dimens. changes and kinetics 0-40484
Halloysite, with gradual dehydration, mechanism 0-59015
hexamethylbenzene, single cryst., at 298 and 130 K, from n diffr. studies 0-59087

0-59087

Hg, martensitic transform., 77-4.2 K 0-56060
high pressure technique and apparatus 0-61744

Homopolymers and copolymers with alkyl side chains, glass transition temperatures 0-65021
interacting elementary excitations 0-40634
introduction for students 0-56022
in beam microscopy, ferroelectrics, shadow effect 0-40478
low temperature X-ray powder diffractometry, cryostat., 1.5K 0-61777
lunar samples, impact metamorphism 0-48528
lunar samples, minerals-> glasses transformation due to shock effects 0-45379

0-45379
lunar samples, shock metamorphism 0-48527
lunar samples, shock metamorphism evidence and implications 0-45384
magnetite, powdered synthetic, specific heat singularity in phase transitions
near second kind transitions, effect of inhomogeneity 0-50891
martensite, nucleation as coherency-loss problem 0-75317
martensite in Fe-Ni-Mo alloy, ageing at 450-500°C, mechanism 0-78675
martensite steel, struct. defects effect on decomp. 0-62129
martensitic, crystallography and electron microscopic obs. 0-75325
martensitic, in maraging alloy, by interval friction meas. 0-62130
martensitic shape strain determ. methods 0-71681
martensitic transformation point study in steel with 18% Ni 0-78696

Phase transformations continued solid-state continued

metal, civil-type, obs. by new photoemission-electron microscope 0-71555

metal, effect of transition temp. on mag. moments 0-75879

metals, body centred cubic low temp. transitions 0-40480

metais, body centred cubic low temp. transitions: 0—40480 methane, d₁, specific heat anomaly: 0—56110 methane, solid, James-Keenan model with octahedral symmetry: 0—56475 methanol, effect on positron lifetime, and CH₂OH 0—75533 methylchlorobenzenes, hexasubstituted, higher-order transition by progressive decorrelation of mol. orientations: 0—71808 molecules, dissolved, observed under different crystallization conditions: 0—64319 melcoite, debudyation physical conditions: 0—64319

nekoite, dehydration obs. of cryst. struct. 0–58720 nuclei growth and interactions, diffusion controlled rate 0–50814 order-disorder transitions, critical exponents from second-harmonic scattering 0–47486

ing 0-47486 ordering of hanges, short-range, vacancy-quenching effects 0-75346 paraffin, 8≤n≤16, order-disorder, specific heat, entropy 0-78706 particle size effects and thermal hysteresis 0-40479 pentachlorophenol, α-γβ transformation, diamagnetic susceptibilities change 0-68547 perovskite, CspbCl₃ 0-65488 perovskite, CspbCl₃ 0-69031 perovskite, Sr₂WNiO₆, tetragonal-cubic, influence on heat capacity 0-40577

0–40577
perovskite, Sr₂(FeW)O₆-Ba₂(FeW)O₆ system, Mossbauer obs. 0–72339
perovskite, SrTiO₃, interaction with elastic strain 0–56067
perovskite, displacement-type phase transitions 0–71788
perovskite type cryst., theory, interaction with elastic strain 0–53657
perovskite-type cpds., book 0–68293
β- phase, resistivity anomaly near critical region 0–50982
rel. to phonon instabilities and interactions 0–56084
physical mechanisms, basic thermodynamics, applicability 0–39875
poly-y-benzyl-L-glutamate. Helix-coil transition press. depend., model 0–39473

polybutadienes, trans- and cis-, glass transition, by various methods 0 - 47023

polybutene-1 crysts., glass transition in surface layers 0-53415 poly-e-carbobenzoxy-L- lysine, helix-coil transition press, depend., model 0-39473

polyesterurethane block-polymers, phase composition, -100-100°C 0-68611

poly-L-lysine, helix-coil transition press. depend., model 0--39473 polymers, glassy, transition between liquid or rubbery state to glassy state 0-65019

0–65019 polymorphic transitions in thin cryst. plates 0–62123 polypropylene, isotactic, paracrystal-crystal transition 0–62142 polystyrene, atactic, glass transition, o-positronium decay obs. 0–78349 polytetrafluoroethylene, Raman spectra 0–41244 polyvinylchloride-diotylphthalate system glass transition temp. 0–68616 polyvinylchloride-diotylphthalate system glass transition temp. 0–68616 potassium halides, Fm3m=Pm3m transition, thermodynamics 0–43826 quartz, α-β transform, phonons role, neutron scatt. obs. 0–40492 quartz, fracture in alkali silicate and borate melts 0–40387 arae earth molybdate, high-temp. X-ray exam. 0–78701 rare earth molybdate, high-temp. X-ray exam. 0–78701 rare carth perovskitelike cpds. 0–75337 refractory carbides, hemicarbide and dicarbide transforms. 0–59014 resins, thermoactive, anomalies in thermal expansion at glass transition temp. 0–59113 reversible, interfacial energies 0–39920

temp. 0–59113
reversible, interfacial energies 0–39920
review 0–75323
rocksalt type struct, order- disorder, i.r. spectra obs. 0–53670
rubidium halides, Fm3m=Pm3m transition, thermodynamics 0–43826
second-order, close, unified theory 0–47364
semiconductor, Si, surface layer amorphisation by ion bombardment, at. no. depend. 0–68558
shadow effect in ion scattering 0–62122
solid, conference, Turku, Finland, Aug. 1970 0–74858
solid solution, interstitial, by elastic relax. methods 0–68527
solid solutions, multicomponent, early-stage ordering and clustering 0–58970
specific heat singularity in phase transitions near second kind transitions.

specific heat singularity in phase transitions near second kind transitions,

specific heat singularity in phase transitions near second kind transitions effect of sample inhomogeneity 0—50891 spinel, low temp., X-ray obs. 0—62124 spinel, order-disorder transitions on octahedral sites 0—59046 squalane, shown by thermoluminescence glow curve peaks 0—54130 steel, Mo-bearing, diffusional y→α, carbide formation 0—47480 steel, α→by process, effect of original condition of steel 0—75332 steel, austenite stabilization 0—40487 steel, austenite, 18%Cr-9%Ni type, deformation-induced 600 to -190°C 0—68553 steel austenitic, stainless ferrite, sigma phase and carbides precin

steel, austenitic stainless, ferrite, sigma phase and carbides precip. 0-40488

0-40488 steel, bainite reaction, kinetic anomaly 0-71801 steel, cementite phase particles, diffusional coalescence, kinetics 0-50817 steel, diffusional $y-\alpha$, Nb_xC formation 0-50818 steel, hypereutectic, bainite structure formation mechanism 0-47479 steel, maraging, electron diffr. obs. 0-62108 steel, martensite crystallography theory 0-40485 steel, martensite transformation, dilatometric determ. of M_s and M_f 0-65491 where s and phase composition effects of heating and prolonger

0-65491 steel, mech. props. and phase composition, effects of heating and prolonged isothermal holding 0-59020 steel, plastic deformation, χ-carbide, Fe₅C₂, formation 0-53587 steel, rel. to fracture-safe design 0-40411 steel, secondary structure formation under impulse loading 0-71802 steel, stainless, ferrite sigma phase and carbides precip. 0-40489 steel, stainless, rel. to corrosion resistance and mech. strength, patent 0-47495

 $0^{-4.493}$ steel, stainless, type 316L, carburization in static sodium 0-75331 Steel, with 18% Ni, martensitic transformation point study 0-78696 steel 35G18, multiple $y=\varepsilon$, $y=\varepsilon$, transforms. effect on mech. props.

0-40350 0-40350 steel -6% Re, quenched, elec. resist., -196 to -100°C 0-50986 steel wires, amorphous martensite formation, friction testing 0-68552 steel-Ni-Cr-Ti, austenitic, age hardening, reversion 0-53631 stiblite-metastilbite transformation, parameters determ. 0-75345 sulphates, high-temp. cubic phase props. 0-75412

Phase transformations continued solid-state continued

superconducting composite alloy Nb-Sn, substitution method 0-59175 superconductor, Ce, phase boundary determ., high press., 77-480K 0-43823

0–43823 superconductor, V₃Si and Nb₃Sn, low-temp. transform. 0–65496 superconductor, alloy 35BT, cold-worked specimen annealed 0–78692 tetrafluoromethane, heat capacity, 2-20K 0–43914 transition metal alloys, optic mode instabilities associated with second-order structural phase transition 0–78814 1.2.3-trichloro 4.5,6-trimethylbenzene, order-disorder orientation transition 0–59047 triglycine sulphate, ferroelec., molecular mechanism for transition, from i.r. spectra 0–40875 triglycine sulphate, ferroelec., thermodynamic characts. of phase transition at high pressure 0–40876 trioxane, high press. effects, i.r. and optical spectroscopic monitoring 0–50828 u.s. attenuation and soft-mode damping at displacive transition, model

U.s. attenuation and soft-mode damping at displacive transition, model Hamiltonian 0-43876 Vicalloy, annealed, omnidirectional press. effect, rel. to mag. props. 0-79153

0–79153 vinyl monomers, by X-ray, i.r. and thermal anal. study 0–47024 welding wire quality determination immediately after melting 0–68550 Zircaloy, $\beta \rightarrow \alpha$ transform. basketweave struct., ZrC effect 0–58767 Zircaloy-4, $\beta \rightarrow \alpha$ transform. 0–62140 Ag-In alloy system 0–75313 Ag-halides, press. induced, X-ray diffr. 0–62126 AgBr, specific heat, temp. depend., 70-550°C, defect depend. 0–40567 AgCrSe(S), neutron diffr. obs. 0–62554 AgS(Se), specific heat, temp. depend., -70–550°C, defect depend. 0–40567 Al-(15w %) Ag alloy, p plates, surface relief effects. 0–65483

Ags(se), specific heat, temp. depend., —70—350°C, defect depend. 0-40567
Al-(15wt.96)Ag alloy, p plates, surface relief effects 0—65483
Al Cr, Al-Mn alloys 0—50815
Al Fe solid soln, supersaturated, decomp, during annealing 0—40437
Al, embrittlement by liquid metals, temp., pressure effects, deformation hot stage metallographic facility 0—40481
Al-03/2rO₂ system, oriented eutectic microstructure 0—61597
α-Al₂O₃, (0001) face heat treatment, surface struct. 0—65046
Al₂O₃, electron diffr. obs. 0—58616
Ar O₂ mixtures 0—62210
Au-(50at.96)Cd alloy, splat-cooled, martensitic 0—71791
Au-Ni, Au-Co alloys, electrodeposits, heat treated, microstructural changes, X-ray exam. 0—65485
Au-40.4 at/Ni, orientation relations of phases formed by precip. 62103
0-62103
AuCd, β-phase alloy, martensite instability, rel. to elastic anisotropy 0—43822
β'-Au-Zn(50%Zn), martensitic, particle size effect 0—71793

0-43822 \$\text{B'-AuZn(50\text{\ti}\text{\texi

BaMnP₃, microwave elastic and u.s. props., Ireq. and temp. depend. 0–78611
Ba₂NaNb₂O₁₅, elastic anomaly 0–71795
BaTiO₃-type, mechanism of dynamic polarization in phase transf. region 0–40849
BaTiO₃-type, neutron irradiated, induced phase transitions 0–40854
BaTiO₃, first-order transition front, nucleation models 0–62127
BaTiO₃, high resistivity, cubic-tetragonal transition 0–65486
BaTiO₃, adiation induced transform. 0–65487
BaTiO₃, adiation induced transform. 0–65487
BaTiO₃ single cryst., induced transf. 0–40857
Bi, 4.2-300 K, 50 kbar 0–43831
Bi, temperature coeff. of I-II transition press. meas. 0–47477
C, pyrolytic, graphitization, electronic props., ambient Cl₂ effect 0–75545
CH₃NH₃Al(SO₄), 1/2H₂O₃ ferroelec., study by n.m.r. of ²⁷Al 0–41361
Ca₃P₂O₃, displacive-type, systematic correlation with crystal structs. 0–58730
CaSO₄ > β transition due to anhydrous precipitation 0–78694

0-58730
CaSO₄ γ→β transition due to anhydrous precipitation 0-78694
Cd₂Nb₂O₇, 80 K, X-ray diffr. 0-75328
Cd₂CdF₂, order-disorder 0-69206
CdS(Se,Te), h.p. polymorphism, kinetics 0-53659
CdTiO₃, perovskite modification, X-ray diffr., 0-1200°C 0-50522
Ce, superconducting phase boundary electron, high press., 77-480K
0-43823
²⁴⁴Cm₂O₃, temps., laser heating, thermal diffusivity and conductivity 0 47557
Co-Al, ferromagnetic alloy, coercive force rel. to microstruct agein.

Col-20xt. Phys. Tasac Teating, thermal diffusivity and conductivity 0 47557

Co-AI, ferromagnetic alloy, coercive force rel. to microstruct., ageing depend. 0–54008

Co-(20wt.%)Ni (20wt.%)Cr alloy, mech. deform. induced 0–78695

Co, spark eroded, surface struct. 0–58560

CoCO,(NH₃)₄2SO₄.3H₁O, thermal transform. 0–59016

Co₅Sm-Cu₅Sm, ternary phase diagram 0–71772

Cs-PbCl₁, perovskite 0–65488

CsSH low temperature structure, transition temperatures 0–47478

Cu-Al-Ni alloys, martensitic, interphase boundary migration, internal friction 0–71670

Cu-Al-Ni alloys, thermoelastic martensitic, memory effect 0–59017

Cu-Al-Ni alloys, bothermal decomposition of β phase 0–53661

Cu-Al alloys, β phase ordering isothermally in 400-560°C range 0–53667

Cu-Be system β phase, ordering 0–75347

Cu-Ni-Fe alloy, Mossbauer spectra, interpretation 0–51279

Cu₃-NiMn system. ageing, 300-500°C, X-ray diffr. 0–59018

Cu-Sn alloys, martensitic, interphase boundary migration, internal friction 0–71670

0-71670

0-71670

Cu-Zn, retardation of diffusion -controlled phase formation 0-47291

Cu-Au, ordering, strengthening and kinetics 0-40497

Cu-Cr-S₂, neutron diffr. obs. 0-62554

Cu-Fe-S₄, bornite 0-75090

Cu-Pt, order-disorder transform as classical phase transform 0-56074

Cu-S₄, specific heat, temp. depend., -70-550°C, defect depend. 0-40567

Cu-S₄, digenite 0-75090

Cu-S(Te) and ternary compounds, X-ray diffr., thermal, elec. and mag. analysis 0-40491

D₂, pressure changes with temp. and para conc., thermodynamic props. 0-47540

DR rordering 0-59024

DBr, ordering 0-59024 DCl, rel. to mol. motion 0-59079

Phase transformations continued solid-state continued

DyF₃, high press. form., 11.6 kbar, 265°C, struct. 0–55837 Dy VO_4 , rel. to magnetically controllable distortion at 14K 0–44728 Eu₂S₄, at 168K 0–71798

Eu₂SiO₄, structural and energy-related changes 0–62128 Fe-Al alloy, order- disorder, Mossbauer spectra, quadrupole interaction 0–43829

Fe-Al alloys, order and disorder, Mossbauer effect 0-50527

Fe-C-Si, complementary shear during 420°C martensitic transformation 0-71800

e-C-Si alloy, orientation relations between ferrite and carbon enriched austenite, 420°C, e. microscope and e. diffraction studies 0-65490 Fe-C-Si alloy,

Fe-(8wt.%)Cr- (1wt.%)C alloy, martensite platelet growth rel. to austenite stacking faults 71799 $\,$ 0–71799 6-Cr-Ni alloys, shock-induced phase-transition press. rel. to comp. 0-47366

Fe-Cr alloys, shock- induced phase-transition press. rel. to comp. $0\!-\!47366$

Fe-Mn alloys, b.c.c., shock-induced martensitic transform. 0–59022 Fe-Mn alloys, martensitic rel. to elec. resist., temp. depend., –196-300°C

Fe-Mi alloys, martensitic rel. to elect resist, temp, depend., —199-300°C 0-50985

Fe-Ni-C alloy, martensite to austenite, shock-induced reversal, temp, depend. 0-65489

Fe-Ni-C alloy, paramagnetic austenite, f.c.c., plastic deformation 0-55972

Pe-Ni-C alloy, paramagnetic austenite, 1.e.c., plastic deformation 0-55972
Fe-Ni-Co alloy, martensite-to-austenite, rel. to coercive force temp. depend. 0-44587
Fe-Ni-Cr, alloy, austenitic, free energy, mag. props. 0-43832
Fe-Ni-Mo(Ti)(-Co) alloys with ageing martensite, recovery 0-50770
Fe-Ni alloy, low. temp. quenching 0-56059
Fe-Ni alloy, irreversible, low thermal expansion 0-50896
Fe-Ni films, degree of oxidation and phase comp., var. with annealing temp. and vac. 0-78372
Fe, h.c.p., pressure effects 0-59033
Fe, p→a transformation, impurity effect 0-50819
Fe, non-equilibrium, p-v calcs., elementary model 0-39875
Fe alloy G20, multiple p≠e, p≠e' transforms. effect on mech. props. 0 40350
FeCo alloy, order-disorder changes, 550°C anomaly resistivity meas. 0-68565
FeN₁3 alloy, order-disorder, Mossbauer spectra 0-78698

FeO_{1,ly}, wustite, phase boundaries rel. to temp. O₂ partial pressure and composition 0-71854

composition 0–71854
Fe₂O₃, γ-α transform kinetics 0–40486
Fe₂O₃, γ-α transform kinetics 0–40486
FeOOH, β- and δ-, thermal transition to α-Fe₂O₃, 100-600C 0–75330
γ-FeOOH and decomposed product, electron microscope observation of thermal transformation 0–61863
δ-FeOOH–α-Fe₂O₃, annealed, 23-650°C, cryst. struct., mag. props., Mossbauer spectra 0–65492
Fe₃Pt alloy, ordered, martensitic transform., electron microscope obs. 0–65493

0—03493 Ga, polymorphic transitions, h.p. 0—53399 GaAs, ion bombarded, induced, and inert gas mobility 0—65494 Ge-Pd diagrams 0—53669 Ge, amorphization rel. to sputtering mechanism 0—40624 Ge, ion bombarded, induced, and inert gas mobility 0—65494

Ge film, amorphous to crystalline, elec. and opt. props., 77-750K 0-44254

0-44234
Hcl, struct. and ferro-paraelectic 0-62440
Hf, h.c.p.-b.c.c. rel. to changes in electronic density of states 0-75494
HfO₂-CaO(Y₂O₂,MgO), solid solns., cyclic heating and thermal shock effects on stability 0-59025
Hg1₂, high press. decomposition 0-62132
H₂p- to o conversion in adsorbed layers on Gd₂O₃ and Y₂O₃ 0-50820
InTe film, thickness change on annealing in high vacuum 0-39939
K₂Cr₂O₃ displacive-type systematic correlation with crystal structs

displacive-type, systematic correlation with crystal structs.

K₂Cr₂O₃, displacive-type, systematic correlation 0-58730 KH₂PO₄, phase diagram to 40 kbar 0-62114 KH₂PO₄ and KD₂PO₄, from i.r. spectra 0-62115

Mg-Zn-Cu(Ag) system, structural changes rel. to Friauf-Laves phases

0-05333
Mg-Zn-Cu(Ag) system, structural changes rel. to Friauf-Laves phases 0-61877
Mg3Cd, ordering process 0-59028
Mn-and Re-steels, low temp. quenching 0-56059
Mn_{2-x}A₂B₃Sb_{1-y} system, ferromag, struct. 0-75921
p-MnCu alloy, low-angle neutron diffr., decomposition, ageing 0-40449
MnO₂ surface layer structure variations during phase transformation, 200-400°C 0-59029
Mn₂O₃ Sc³⁺, Cr³⁺ and Ga³⁺ substituted, ordering 0-56464
MnSe, neutron diffr. obs. 0-59030
Nn₂O₃ Sc³⁺, Cr³⁺ and Ga³⁺ substituted, ordering 0-56464
MnSe, neutron diffr. obs. 0-59030
Nn₂Cl, I=II transition energy 0-75336
Nn₂Cl, I-II transition energy 0-75336
Nn₄Cl, I-II transition dilatometric obs. 0-75335
Nn₄Cl, I-II transition dilatometric obs. 0-7535
Nn₄Cl, I-II determ. of structural and ordering changes 0-62119
NH₄Cl, I-II determ. of structural and ordering changes 0-62119
NH₄Cl, I-II determ. of structural and ordering changes 0-62119
NH₄Cl, I-II caterm. of structural and ordering changes 0-62119
NH₄Cl, I-II caterm. of structural and ordering changes 0-62119
NH₄Cl, I-II caterm. of structural and ordering changes 0-62119
NH₄Cl, I-II caterm. of structural and ordering changes 0-62119
NH₄Cl, I-II caterm. of structural and ordering changes 0-62119
NH₄Cl, I-II caterm. of structural and ordering changes 0-62119
NH₄Cl, I-II caterm. of structural and ordering changes 0-62119
NH₄Cl, I-II caterm. of structural and ordering changes 0-62119
NH₄Cl, I-II caterm. of structural and ordering changes 0-62119

Phase transformations continued

solid-state continued

NH₄Cl long range macroscopic order above transition temperature for orientational disordering of NH₄+ ions 0.–43638
NH₄ClO₄, nucleation rel. to thermal decomposition, photomicrographic and electron microscopy study 0.–68556
NH₄H₂ASO₄ antiferroelec. transitions and i.r. absorpt. 0.–40878

NH₄H₂AsO₄ antiferroelec. transitions and i.r. absorpt. 0–40878
NH₄H₂PO₄, antiferroelec., accompanied by displacements of atoms, group theoretical study 0–40877
NH₄H₂PO₄ antiferroelec. transitions and i.r. absorpt. 0–40878
NH₄I, X-ray study of I, II and III modifications between -176°-190°C 0–55856
NH₄NO₃ cond. vars. rel. to O coordination, obs. 0–40831
NaCrSe₂, neutron diffr. obs. 0–62554
Na(H₁,=D₂)₂(SCO₃)₂, thermal expansion, isotope effect 0–56111
NaH₃(SCO₃)₂, ferroelectric, specific heat, configurational entropy change 0–43901

0 - 43907

NaH₃(SeO₃)₃, ferroelectric, specific heat, configurational entropy change 0–43907

NaNO₃, Raman line broadening, rel. to order disorder transform. 0–76127

NaNbO₃, perovskite 0–59031

NaNbO₃, X-ray exam. 0–71805

Na₂O-Fe₂O₃-SiO₂ glass, crystallization of β-NaFeO₂, Mossbauer spectra, x-ray diffr. 0–47490

Nb-Ru alloy, near- equiatomic, mechanism 0–78704

Nb-Sn, composite superconducting alloy, substitution method 0–59175

Nb₃(Al,Ge) syst., annealed, anal. of supercond. phase 0–65644

NbSn, cubic-to-tetragonal transition. dynamic theory based on electron-phonon interaction 0–78691

Nb₃Sn₁, low-temp. transform. 0–65496

Nb₃Sn₁, low-temp. transform 0–65496

Nb₃Sn₁, sb₂ system, rel. to density of states model for Nb₃Sn 0–59173

Nb₄O₃, order-disorder transitions 0–61807

Ni-Cr-Nb phase solid state phase transformations during long annealing at 700°C 0–56062

Ni-Cr-Ta solid state phase transformations during long annealing at 700°C 0–56062

Ni-Cr-Ta solid state phase transformations during long annealing at 700°C 0–56062

Ni-Cr-Ta solid state phase transformations during long annealing at 700°C 0–56062

Ni-Cr-Ta solid state phase transformations during long annealing at 700°C 0–56062

Ni-Cr-Ta solid state phase transformations during long annealing at 700°C 0–56062

Ni-Cr-Ta solid state phase transformations during long annealing at 700°C 0–56062

Ni-Cr-Ta solid state phase transformations during long annealing at 700°C 0–56062

Ni-Cr-Ta solid state phase transformations during long annealing at 700°C 0–56062

Ni-Cr-Ta solid state phase transformations during long annealing at 700°C 0–56062

Ni(II) complexes, thiourea coordinated, rel. to paramag. props., 90-300°K 0-40949

Mi(II) complexes, thiourea coordinated, rel. to paramag. props., 90-300°K 0-40949
Ni₃Mn-Ni₃Fe(Co) solid solns., ordering, Hall effect changes 0-65632
Ni₃(Mn,Me), ternary alloys, Me=Fe, Co, Cr, ordering kinetics, neutron diffr. obs. 0-71809
Ni₃Mn, effect of alloying with third 3d-transition element or ordering kinetics 0-47461
Ni₄Mo, order-induced strengthening 0-47379
Ni(NH₃)₆Cl₂, specific heat and thermal conductivity meas. 0-56108
NiO₂ lattice distortion, stoichiometry, paramag, to antiferromag. 0-75963
NiSe(Te) and ternary compounds, X-ray diffr., thermal, elec. and mag. analysis 0-40491
Pb, h.e.p., pressure effects 0-59033
Pb(CoW)₀₋₅O₃-PbTiO₃-PbZrO₃ system 0-65773
PbF₂-TiF₃ three new phases 0-56065
PbNb₃O₆ transition from ferroelec. to nonferroelec. type 0-56050
Pb(Ti, Zr)O₃ solid solutions, morphotropic boundary, dielectric polarization, comp. depend. 0-62403
PbTiO₃, radiation induced transform. 0-65487
Pb(Zn_{1/3}Nb_{2/3}O₃, ferroelectric props. 0-44368
PrAlO₃, 205 and 151 K, X-ray diffr. 0-53662
PrAlO₃, first- and second-order, X-ray obs. 0-59032
Pr_{1-x}Nd_xAlO₁, system, rel. to dielec. const. anomalies, 300-5K 0-51106
Re, h.e.p., pressure effects 0-59033
Sb, rhombohedral-cubic, p=70 kbar 0-71806
Sb₂S₃, calorimetric study 0-40874
SbS1, existence of critical point, from optical and dielectric props. 0-40873
Se, crystn. mechanism obs. 0-58631
Se, monoclinic-hexagonal 0-65161
Se, red amorphous and monoclinic 0-75338
Si, ion bombardment induced amorphisation of surface layers, at. no. depend. 0-68588
SiO₂, cristobalite, neutron irrad. effect 0-62134
SiO₂, quartz, α-β transition, neutron irrad. Raman spectra 0-78702

depend. 0–68558
SiO₂, cristobalite, neutron irrad, effect 0–62134
SiO₂, cristobalite, neutron irrad, Raman spectra 0–78702
Sm, high temp. rel. to resistivity changes 0–58749
Sm₂(MoO₄)₃, M-modification 0–65498
SmZn₃, xz-l1, crystal structure of high temp. form 0–50549
Sn-Pb alloys, dendrite-eutectic, during solidification with low temp. gradient 0–65003
Sn, β-α, kinetics, Mossbauer effect 0–75341
Sr₃(FeW)O₆-Ba₂(FeW)O₆ system, Mossbauer obs. 0–72339
Sr_{1-x}PO_{3|b}, high press. phases with perovskite-related struct. 0–62135
Sr_{1-x}Po_{3-R}RuO₃ system, pyrochlore to perovskite, 1400°C, press. induced 0–56066
SrTiO₃-107 K transition, u.s. meas. 0–75342

0-36066
SrTiO₃, 107 K transition, u.s. meas. 0-75342
SrTiO₃, 65 K anomaly, e.s.r. obs. 0-68559
SrTiO₃, order parameter, variation with uniaxial stress 0-68567
SrTiO₃, rel. to u.s. propag. 0-75389
SrTiO₃, rel. to u.s. propag. 0-75389
SrTiO₃ solid solution, decomposition and precipitation, 225K, neutron diffr. 0-30830
Ta₂D₃, order-disorder transitions 0-61807
Ta₃O₅ films, electron diffr. obs. 0-55719
Th₂CH₃, cubic and hexagonal structure, X-ray, neutron diffr., n.m.r. 0-58755
ThO₂-La₂O₃ syst., new phases 0-65499

0-58755Th-102-12-12-13 syst., new phases 0-65499 β -Ti:(Mo,Nb,V) isomorphous alloy 0-53663Ti-Hg-Zn syst., X-ray studies 0-40465Ti-Mo-Zr-Sn alloy, β -III, as-quenched, stability 0-71807Ti-O, solid solution, interstitial order-disorder, neutron diffr. 0-40499Ti, effect on thermal cond. and phys. props. meas. 0-75421Ti, h.c.p.-b.c. c. rel. to changes in electronic density of states 0-75494Ti, shock wave induced, X-ray diffr. 0-40493Ti alloy, metastable β -phase decomposition, ageing, 480 °C, electron microscopy 0-53664 α + β Ti alloy, metastable phase decomp. 20-500°C, resistivity var., rel. to electron structure and band charge 0-78882

Phase transformations continued solid-state continued

Ti alloy TA6V6E2 kinetic study of transformations under isothermal condi-

Ti alloy TA₆V₆E₂ kinetic study of transformations under isothermal conditions 0–56068
TiH₃, struct., comp. depend. 0–50551
TiNi, kinetics, mechanism 0–47482
TiNi, martensitic change, effect on u.s. wave propag. 0–56069
TiNi, martensitic transform, atomic mechanism 0–59036
TiO₂SnO₂, tetragonal system, separation by spinodal decomposition 0–59035

0-59035
TiO₂ polymorphic transform, topotaxy 0-59037
Tl, α=β polymorphic, impurity effects 0-68554
TiCrO₂, reversible transformation at 610°C 0-78505
TiFeO₂, transition point at 750° 0-78505
TiI, orthorhombic to CsCl-type struct, i.r. and Raman spectra study 0 72393

0 /2593 Tl₂O new form stable between 354°C and melting point and binary phase diagram from Tl₂O to Tl₂O.B₂O₃ 0-59038 U-(1.5 wt.%)Mo alloys, continuous and discontinuous precip. reactions 0-68561

0–68561 U-Mo alloys, shear transform. from γ -phase 0–62137 γ -U-Mo fuel alloy, thermal cycling and irrad., stability 0–40467 U-Nb-Zr alloy, crystal structure 0–59041 U alloys, β - α phase change kinetics 0–68560 α -U single crystal, low temp., effect of hydrostatic pressure, elastic moduli meas. 0–40495 U₃O₈, elec. cond. study 0–59039 U₄O₉, dielec. const. change obs. 0–56352 U₄O₉, quenching effects, X-ray exam. 0–43833 (UO₂AsO₄)H₃O₃H₂O₄, trogerite, synthetic 0–59042 UP₃, cryst. struct., thermal expansion 0–61912 UP₃, cryst. struct., thermal expansion 0–61912 UIn₃, nonstoichiometry, cryst. struct., x-ray diffr. 0–50824 V-O system 0–59056 V₃Oa foil, martensitic 10–300°K 0–40496 V₂O₅, decomp., electron microscope obs. 0–59043

Uns, nonstotichometry, cryst. struct., x-ray chift. 0—50824
V-Os, system 0—59056
V₃Ga foil, martensitic 10-300°K 0—40496
V₂O₃, decomp., electron microscope obs. 0—59043
V₂O_{4.80}nH₂O, 2 values of n, phases prepared, transformation into one another 0—78703
V₃Si, cubic-to-tetragonal transition, dynamic theory based on electron-phonon interaction 0—78691
V₃Si, low-temp, transform. 0—65496
W, evaporated films, supercond. transition temp. 0—51016
WO₃, antiferroelec., accompanied by displacements of atoms, group theoretical study 0—40877
Y-Sb alloy system, phase diagram 0—64995
12Mol.96 Y₃O₃-ZrO₃, destabilization by electrolysis 47465 0—47465
Yb, flow-stress temp. depend., 78-525K 0—65406
Yb polymorphic transformation discovered 0—75343
YbC_∞, system, 0.33 ≤ 2.00 comp. range 0—53653
Zn, embrittlement by liquid metals, temp., pressure effects, deformation hot stage metallographic facility 0—40481
α-Zn₂P₃O₇, X-ray obs. 0—58765
ZnS film, and recrystallization, electron microscope obs. 0—50825
β-Zr-Mo alloy, quenched, Al influence on stability 0—50826
Zr-Nb alloys, equil. β/α+β transform. temp., oxygen effect 0—47484
Zr, h.c.p.→b.c.c. re.1 to changes in electronic density of states 0—75494
Zr, shock wave induced, X-ray diffr. 0—40493
Zr 3 components on oxidation in pure oxygen at 850°C 0—71597
Zr alloys, stress orientation of hydride 0—62139
ZrO₂, monoclinic-tetragonal transition, X-ray diffr. 0—62141
ZrO₂, unstabilized, rel. to deform. substruct. 0—50822
ZrO₂ polymorphs. i.r. and Raman spectra obs. 0—54112
Phase transitions see Phase transformations
Phase-contrast microscopy see Microscopy
Phonon drag see Crystal electron states/transport processes; Crystals/lattice mechanics

Phonon-electron interactions see Crystal electron states/transport processes; Crystals/lattice mechanics

Phonons see Crystals/lattice mechanics Phosphorescence see Luminescence

Phosphors see Luminescence; Luminescent devices

Phosphorus

ab initio calcs, for 3d exponent, insensitivity to molecular environment 0-74098

ab initio calcs. for 3d exponent, insensitivity to molecular environment 0.–74098 atomic transition tables 0–39284 cathodoluminescent spectroscopy, demountable excitation unit 0.–44940 diffusion and deposition in Si, technology for advanced microelectronic processing 0–65719 diffusion in Si, conc.-depend. 0–55926 diffusion in Si, highly controllable source material, patent 0.–40209 diffusion in Si, using PH₃. 0–65343 diffusion in Si using PH₃. 0–65343 diffusion in Si using POCl₃ as source 0–78587 diffusion in p-Si, surface density depend. 0–61999 diffusion into Si (100) sand (111) slices 0.–44221 diffusion of Si, microscopic study 0.–51050 doping of Si, PH₃ process, sheet resistance conc. 0–56299 doping of Si from gaseous source (PH₃). 0–47743 e.p.r. in .7si, hyperfine splitting, 4.2K, press. depend. 0–41339 in ferrophosphorus and slag from electric-reduction furnace, determination using X-ray fluorescence analysis 0.–51452 ions production using ion-source, description 0–51163 red, i.r. and Raman spectra, structure 0.–4986 reflection spectrum, 1-12.5 Ev 0–62646 Pr-Ar, meas. of Q values at keV energies 0–77691 P³¹ n.mr. spectrum, of β-adenosine-3'-β-adenosine-5'-phosphoric acid 0.–50261 sphere and troposphere obs. 0–76403 sphere and troposphere obs. 0–76403 sphere and troposphere obs. 0–76403 Si-P, microwave hot electron effect and resistivity decrease due to donor spine reson. 0–72071 Si-P layered struct, ion implanted, P conc. distrib. 0–56297 in Si, donor pair exchange energy, from e.p.r. spectrum 0–44999 in Si, ion implantation, profile, treatment depend. 0–44256 Si diffusion microscopic study 0–51050 X-ray K-, absorpt. spectra of red P 0–41251

Phosphorus compounds

cyclophosphazenes, (N-P)_n rings, shapes and conformations 0–65259 diphosphatriazine derivatives, cryst. struct. 0–65270 ion implanted in St, 400 keV, carrier conc., mobility, resistivity and impurity conc. 0–65713

metal P-s compounds, crystal growth, by vapour transport 0-71513 molecules, 2p electron binding energies, correlation with extended Huckel charges 0-46504

nuclear polarization in liquid solution containing perchlorotriphenylmethyl radical 0-46955

charges 0–46504
nuclear polarization in liquid solution containing perchlorotriphenylmethyl radical 0–46955
organophosphorous compounds containing P=O group, effect of solvent on spin-spin interac, consts. 0–43433
oxyhalides and derivatives, Urey Bradley force consts. 0–70943
phosphate glass: Yb³, ion coordination obs. 0–51310
phosphites, i.r. and Raman spectra electronic structure 0–70906
phosphoryl absorption band intensities 0–71026
BP, X-ray K-absorpt, spectra 0–41251
Be;SiO₄ radical, e.p.r. in phenacite 0–62762
Bi-O₃ P₂O₅ system glasses, props. rel. to comp. 0–58539
Co P film, mag. annealed, uniaxial mag. anisotropy var. with annealing conditions 0–79183
Co P film, mag. behaviour, 80-300K 0–59304
Co P films, chem. deposited, induced uniaxial anisotropy 0–56451
Co P thin film, electroless plating for video tape recording 0–72248
CoP X-ray K absorpt, spectra 0–41251
Fe Ni P film, chemical deposition, mag. props., isotropy 0–51217
Fe-Ni P film, coercive force, induced anisotropy 0–54029
Fe P-C alloy, amorphous, struct. 0–39903
FeO P₂O₃ glass, dielectric loss, d.e. cond., devitrification, electron micro scopy 0–53925
GaAs P degradation, criteria for design and operation 0–48121

Fe P-C alloy, amorphous, struct. 0–39903
FeO P₂O₉ glass, dielectric loss, d.e. cond., devitrification, electron micro scopy 0–53925
GaAs-P degradation, criteria for design and operation 0–48121
Mi-P, amorphous film, flash evaporation, crystallization, electron micro scopy 0–65085
Ni-P alloy, noncrystalline, structure 0–58531
Ni-P film, electrodeposited, perpendicular anisotropy 0–62538
Ni-P films, electrodeposited, perpendicular anisotropy 0–62538
Ni-P films, electrodeposited, perpendicular anisotropy 0–62538
Ni-P films, optical props. rel. to struct. 0–51262
Ni-P films, optical props. rel. to struct. 0–51262
Ni-P films, photoelec. emission rel. to struct. 0–51162
Ni-P films, photoelec. emission rel. to struct. 0–51162
Ni-P tilms, optical props. rel. to struct. 0–51262
Ni-P tilms, optical props. rel. to struct. 0–51162
Ni-P tilms, optical props. rel. to struct. 0–51162
Ni-P tilms, optical props. rel. to struct. 0–51262
Ni-P tilms, optical props. rel. to struct. 0–51162
Ni-P tilms, optical props. rel. to struct. 0–51162
Ni-P tilms, optical props. rel. to struct. 0–51313
PCL-F₃, molecular constants from spectroscopic data 0–55313

PD₄Cl, far i.r. spectra of thin films and Raman spectra of polycrystalline sample 0-48092
PD₄Cl, lattice vibrs, and barrier to torsional oscills, from i.r. and Raman spectra 0-65521
PF₃ and PF₄, trapped radicals, e.s.r. 0-44995
PF₄, i.r. spectra, β₃ band recorded 0-74300
PF₄, ligand properties, exptl, and theoretical study 0-70942
PF₁, vibr, anharmonicity 0-55305
PF₃ microwave double photon transitions, obs. by high power microwave double resonance 0-77925
PF₅, force constants and normal modes of vibration 0-70871
PF₅, saturated absorpt, spectra using lasers 0-70844
PF₄O, electronic struct., ab initio SCF MO calcs., rel. to ligand props. of PF₁, 0-70942
PH₃, rotational analysis of V₂¹ bands 0-77832

PH₃, rotational analysis of V₃¹ bands 0-77832 PH₃, source for Si doping, process 0-56299 PH₃, vibr. harmonic freqs. calc. from observed anharmonic freqs., and PD₃ 0-77816

PD3 0-77816
PH3 ground state SCF wave functions and molecular properties 0-77842
PH3 in nematic solvent, struct. from p reson, spectrum 0-64445
PH3br(I), cryst. struct, and thermal motion 0-78492
PH3CI, far i.r. spectra of thin films and Raman spectra of polycrystalline sample 0-48092
PH3CI, lattice vibrs, and barrier to torsional oscills, from i.r. and Raman spectra 0-65521
PNCI, electron diffr. obs. 0-64446
P4O10-V3O5 system glasses, elec., cond. 0-59169
P4O10-W3O1 system glasses, elec., cond. 0-59169
PO, B²³H₂ transition established in new system in region 4800-3800 Å 0-74299
PO, new bands in the visible and their relational analysis.

PO, new bands in the visible and their rotational analysis 0-58194
PO degenerate band of N²Σ'·B²Σ' transition rotational analysis 0-77831
PO radical, rot. obs. of Rydberg-Rydberg transition 0-49884
PO radical, rotational anal, of new visible electronic band system 0-55315

0-55315
PO radical, rotational study and spectroscopic data 0-55314
PO radical, spectra, rot. analysis, new state obs. 0-49885
PO₃⁴, general valence force field force constants 0-55316
PO₃⁴, general valence force field force constants 0-55316
PO₅⁴, general valence force field force constants 0-55316
POCl₃:SnCl₄,Nd⁴¹ laser system, characteristics 0-60221
POCl₃:SnCl₄, Nd⁴¹ laser system, characteristics 0-60221
POCl₃:SnCl₄, liq₄, Tb¹⁴ fluoresc. 0-64931
POCl₃:SnCl₄, liq₄, Tb¹⁴ fluoresc. 0-70873
Pf₁, E' force field 0-61133
V₂O₅:P₂O₅, glass d.c. and a.c. conductivity, thermoelectric power, comp. depend. 0-47630
ZrO; WO; P₂O₅, phase equilibria 0-47494

Photochemistry
see also Photographic process

see also Photographic process acrolein, photoisomerism 0–43145 actinometer, digital, for reaction cell absorb, monitoring 0–73308 alkali metals in ether solvents, anion ionization by light to yield solvated electrons 0–48201 atmosphere, lower, popular article 0–51502 azides, paramag, defects prod., excitons role 0–79406 benzene, liquid, biphotonic photolysis 0–59506 biochemical control photoreactions rel. to metabolism 0–76711 carbon tetrachloride, photolysis in presence of ethyl chloride 0–41447 colour production and emission, ionic cryst., rel. to dislocation rate of movement determ. 0–61955

Photochemistry continued

cyanic acid, photodissociation in vacuum u.v., NCO $A^2\Sigma$ and $NH(A^3\pi c^1)$ production 0-74419

cyclohexane, photon irradiated, dissociation, and reactions of $C_6 H_{10}{}^+ \\ 0{-}79457$

cyclopentadienyl radical and deuterated derivatives, flash, photolysis 0.-46553

diatomic molecule dissociation states, radiation probability, laser possibili-

diatomic molecule dissociation states, radiation probability, laser possibilities 0–55269 diazomethane, photolyses with propane and isobutane, kinetics 0–41448 diazomethane and ketene, flash photolysis, production and reaction kinetics of triplet and singlet methylene 0–45086 e.p.r. of liquids during photolysis, hyperfine interactions of ¹³C 0–71381 electron-transfer reactions at surface of organic crystals 0–79453 ethanothiol, photodissociation, energy disposal 0–48203 m. ethyltoluene trapped in methyl-cyclohexane at very low temperature, photodissociated, fluorescence spectrum 0–44933 flash photolysis, for study of internal conversion in xantho colourants

flash photolysis, for study of internal conversion in xantho colourants

fluorescent lamp processes 0–56711 formaldehyde vapour, photolysis, 1236 Å and 1470 Å 0–66515

gas, photodissociation wave propagation 0–76278
hexachlorobenzene, triplet exciton phosphorescence 0–59436
hydrazo compounds, polarized phosphorescence with reference to photocarrangements 0–79452
hydrocarbons, decomposition into radicals, quenching of excited states
0-43141

iodoform, laser-induced photolysis, nonlinear optical solvent effect 0 -72557 ionosphere, E region, ion composition determining reactions 0-51584

ionosphere, E region, ion composition determining reactions 0-51584 ketene and diazomethane, flash photolysis, production and reaction kinetics of triplet and single methylene 0-45086 magnetophotoselection expts., for triplet-triplet energy transfer 0-76277 methane, photodissociation at 1236 Å 0-77969 methyl azidoformate, photolytic decomp. in rare-gas matrices near 4°K, i.r. spectra study 0-69222 methyl chloride, vacuum u.v. photolysis, i.r. and u.v. study of products 0-76279

methylene, collision induced singlet→triplet intersystem crossing 0–7258 methylene, triplet and singlet, from photolysis of ketene and diazomethane 0-45086

methylene chloride, vacuum u.v. photolysis, i.r. and u.v. study of products 0-76279

3- methylpentane/O, glasses, radical formation at λ >190nm 0-62817 molecular decay in condensed state, rel. to electronic structure 0-43070 2 naphthol-diethylamine in solvents; proton photo-transfer ionization obs.

0-5351
non-radiative processes 0-79454
olefins, simple, photolysis, at 185 and 203 nm 0-79456
5-phenyl 2-pentene, intramolecular energy transfer 0-72552
photobleaching, ultra-high speed 0-72553
photochromism, Ag halide glasses 0-49157
photodissociation, molec. dynamics 0-43191
photolysis, flash, using Ne pulse laser, for study of naphthalene and benzene 0-77935
photolysis lamp, pulsed vacuum u.v. 0-79455
photolytic hot atom expts., applic. of collision density calcs. for hot H atoms in Xe mediums 0-67673
photopolymerisation, initiation obs. 0-72555
photopolymerisation, initiation obs. 0-72553
photorearrangement products of phenethylamine derivatives, phase determination, X-ray diffr. 0-66202
photosensitive, fee-radical optically developed, rel.to photography 0-49156
polymerization, cyclic dimerization 0-54185

polymerization, cyclic dimerization 0-54185

pyridines, phosphoresc. 0-41278 RNA mol., irrad., limiting proportions of hydrations 0-66205 radical production in single crstals, polarised absorpt., e.s.r. spectra 0-62667

0-52667 reineckate ion, photoaquation, role of doublet and quartet states 0-58088 resonance application of i.r. laser radiation 0-56710 shpolsky system, multiplets and phonon band 0-56534 tartaric acid solns, e.p.r. during photolysis, emission spectrum 0-62823 tetraphenyldiphosphine, u.v. irrad., e.s.r. 0-76280 transformations, nonlinear, in complex organic molecules, effect on light generation in allowed transitions 0-46520

generation in anowed transitions 0-4520 trimethylsilane reaction with singlet methylene radicals giving chem. activated tetramethylsilane 0-41449 triplet triplet absorpt, meas, using laser 0-39799 two-quantum photoionization, role of highly excited triplet mols. 0-72551 unimolecular reactions, photochemical excitation at low pressures 0.46607

0 46607 vinyl fluoride, vacuum u.v. photolysis at 1470 Å 0–66201 Ag salts sensitised photolysis on semiconductor surfaces 0–56712 AgBr evap. layers, spectral sensitization by oxacarbocyanine 0–42402 Ag,SBr and Ag,SI solid electrolytes, photoelec. effects 0–68981 C-lamp intense line source at 1931 Å for analysis 0–62814

C-lamp intense line source at 1931 A for analysis 0–62814
C₃F₁, photodissociation, accumulation of I₂ molecules, breakdown of laser generation 0–73212
CO₃, Xe sensitized photolysis 0–62815
CO₄ in Martian atmosphere 0–48576
CdS, traps, photochem. changes 0–47871
GeCl₄, HGeCl₃ and H₂GeCl₂, vacuum u.v. photolysis, i.r. spectra of GeCl₃ and GeCl₁ 0–66200
HCl₁ isolated in Ar matrix, vacuum u.v. photolysis, ClHCl⁻ production 0–64391

HCl. isolated in Ar matrix, vacuum u.v. photolysis, CIHCl⁻ production 0-64391 H $^{\circ}$ diffusion on pulsed photolysis, rel. to enantiomorphism 0-48202 Hg atom reaction with 1 atoms from photolysis of CF $_{11}$ 0-45085 Hg vapour in silica envelope, as light source 0-54929 Hg(P)+H $_{2}$, absolute cross-section and imprisonment lifetimes for Hg(P)+O-56713 ICN, photodissociation, quasidiatomic model 0-43191 IO $_{7}$ radicals trapped in boric acid glass 0-59507 NyH $_{7}$ radicals, ratio of disproportionation to combination 0-54194 NO prod. and diffusion 0-79591 NO, photolysis, quantum yield press, depend. 0-66204 NO+(X/ Σ^{+}) reaction with C_{3} - C_{7} hydrocarbons, high pressure photoionization 0-62816

Photochemistry continued

O-H model with vertical eddy diffusion, use in determ. OH emission diurnal var. 0-59561

var. 0–59561
O₃ photolysis, energy emission meas., quenching with O(¹D) 0–39398
O₃, u.v. photolysis, effect of molec, O₃ 0–59508
OCS photolysis as source of S(¹P) and S(¹D) 0–72524
O(¹D) quenching efficiency of O₃ relative to other gases
O(¹CD)+H₂O reaction, rate constant by measurement of intermediate quantum yield following flash photolysis 0–45084
OH radical reactions with alkanes, flash photolysis and kinetic spectra
0–66203

0-66203

0–66203 OH radicals, photolytically produced, effect on nucleation of NH₄Cl 0–72556 O₃(b\(^1\)\(^2\)_s\(^1\)\(^1\)\(^2\) flash photolytic production from O₂ 0–46627 ZnO u.v. photolysis in vacuum, prevention by Fe surface states, obs. 0–56714

Photoconducting devices

book on photoelectronic devices 0-44395

book on photoelectronic devices 0–44395 detector, p-GaAs:Cu, operating at 1C.6 µm 0–79090 diode, S-type, photoelect. processes 0–79069 diode, surface-barrier, 1f. noise 0–53890 ferroelectric-photoconductor, hologram storage 0–67112 fibres, in i.r. image convertor and amplifier for night observation equipment, patent 0–52260 film converters based on Si, CdTe, CdS and GaAs 0–65859 image converter based on high field domains 0–79088 junction, surface-barrier p-n, in high-resistivity CdTe 0–56379 photocathodes sensitivity variations, long-term 0–65857 photodetector, sminature avalanche diode 0–53964 photodetector, semicond, investigation methods under photographic conditions 0–79089 photodiode, Ge, planar p-n junction, for microwave modulation freqs. 0–68984

0-68984

D=0884
photodiode, avalanche, multiplication factor optimization 0-65858
photodiode, avalanching, threshold sensitivity and light receiver performance 0-65856
photodiode, prep. by ion bombardment of CdS films 0-53954
photodiode response 0-53965
photodiode response obs. using photocurrent shot noise spectrum

0-53967

0–53967
photodiodes, survey 0–47010
photoelectret state in semicond, with p-n junctions 0–56315
photomemory of surface-barrier junctions in CdTe 0–56318
photoresistor, PbS, effective diffusion and drift tengths 0–79082
photoresistor, Si:B(Ga, In) applic. 0–56397
photoresistor, prep. by ion bombardment of CdS films 0–53954
photoresistors with neutral contacts, photocurrent amplification 0–53968
photoresistors, PbS, localization of trapping centres 0–56406
photothyristor, multicollector, operating principle 0–56407
pyrometer, for are electrode temperature measurement 0–55531
radiation detectors, spectral sensitivity meas. accuracy, effect of scattered light 0–49148
radiation detectors and emitters solid-state, pomenclature 0–75848

radiation detectors, spectral sensitivity meass, accuracy, effect of scattered light 0-49148
radiation detectors and emitters solid-state, nomenclature 0-75848
semiconductor, illuminated, in open resonator, detection of i.r. and optical radiation 0-51154
solid-state imaging, IC structure, mode of operation and fabrication tech nique 0-99279
survey 0-47010
tunnel diodes, photoresponse at 6328 Å, obs. 0-59290
Asy,Sey-SnO₂ image pickup tube with resistive film 0-75849
n-CdS-p-Cu_{3-x}S photocells, changes in recombination losses due to thermal treatment 0-72147
CdS exposure control system for cine camera 0-77229
CdS film, ion bombarded, photodiode and photoresistor prep. 0-53954
n-CdSb, ir. detector, spectral distrib. characts, 80K 0-444410
CdSe-Se, photocell, ²³⁵U coated, neutron irrad., short- circuit currents, e.m.f. 0-51156
CdTe surface-barrier junctions photomemory 0-56318
Cu₃S-CdS heterojunction, light microprobe investigation, minority carrier diffusion length 0-40902
Cu₃S-CdS mechanism and obs. heterojunctions, photovoltaic effect

 Cu_3S -CdS mechanism and obs. heterojunctions, photovoltaic effect 0-56401

0-56401

GaAs:Cu, detector operating at 10.6

m 0-79090

GaAs:Cu, detector operating at 10.6

m 0-79090

GaAs-In, Ga_{1-x}As p-n heterojunctions, photosensitivity spectra and electroluminesc. 0-56387

GaAs, avalanche photodiodes, noise meas. 0-79012

GaAs, avalanche photodiodes, noise meas. 0-79012

GaAs, junction, p-n, impurity photoeffect 0-53955

GaP junctions, p-n, impurity photo-e.m.f. 0-56408

Ge-Hg i.r. radiation detector, wideband optical heterodyne performance, parameters calc. 0-68977

Ge photodiode, planar p-n junction, for microwave modulation freqs. 0-68984

0-68984

"InP photocells, photo-e.m.f. and short-cct. photocurrent 0-53966
InSb, n-p junction photodetector, proton bombard. fabrication 0-44411
PbO members, production, patent 0-65860
PbS photoresistor, voltage sensitivity, effect of background illumination obs. 0-75835
PbS photoresistors, localization of trapping centres 0-56406
PbTe i.r. multiplier with amorphous Se insulator, feasibility 0-51149
Se/As₂Se₂, system, high performance target for vidicon 0-47884
Si-SnO₃ heterojunctions, elec. and optical props. 0-72080
Si, photocell, ²³²U coated, neutron irrad., short-circuit currents, e.m.f. 0-51156
Si photocell, with multilayer heat-reflecting coatings 0-75823

U=51136
Si photocell, with multilayer heat-reflecting coatings 0-75823
Si photocells, reflection reduction, temp. stabilization and radiation protection by optical films 0-44409
Si photodiodes contact to metals, u.s. welding, apparatus description 0-53636

Photoconductivity

otoconductivity

see also Photoconducting devices
alkali halides magneto-photocond., band symmetry, spin-dependent polaron
transport, F-centres 0-44397
alkali metal metaselenoarsenites, elec. cond., -50-190°C 0-51032
anthracene, Davydov splitting, absorption, temp. depend. 0-79323
anthracene, elecc. const. obs. 0-7984
anthracene, exciton-surface reaction at electrolyte interface 0-75839
anthracene, excitons 0-75827
anthracene, interaction of triplet excitons at surface with redox couples and
dye molecules 0-40898
anthracene, photocurrent and elec. polarization phenomena 0-44401

Photoconductivity continued

anthracene single crystal, photo-enhanced currents, anisotropy in mag. field effects 0-47881

antiferromagnet, EuTe, absorpt. edge, temp. depend. 0-59400

p-chloranil single crystal, charge carrier mobility 0-51152
Debye length, freq, depend. in compensated extrinsic photoconductors 0-40880

0-40889 dibenz (a,h) anthracene, sensitized injection of defect electrons through charge transfer process 0-40897 dibenzothiophene and its molecular complexes, exp. investigation 0-72141

0—72142

9,10-dichloroanthracene films 0—72142

dielectric, transient space-charge-limited currents 0—79038

diode, probe method using light-shadow boundary scanning 0—47787

europium chalcogenides, band struct. 0—59399

exciton recombination mechanism 0—41254

ferroelectric semiconductor, influence on phase transform. 0—59262

ferromagnet, EuO, magneto-photocond. near Curie temp. 0—56383

frequency response with reduced background 0—59278

gain in strong elec. fields 0—79070

Ge, photon drag 0—65848

group II-VI cpds., temp.-elec. instability, theory 0—72132

n-hexane, distinction between photoionization and cathode photostimulation 0—64949

1.r. quenching of excited photoconductors 0—56377 i.r. quenching of excited photoconductors 0-56377

ice, alkaline, y-irrad., photocurrent temp, depend, and trapped electrons levels location 0-40894

ice, alkaline, p-irradiated 0—65849 induced, and recombination luminescence of diamonds 0—56373 instability 0—56249 insulator, discharge characts, and mobility meas. 0—62460 ionic crystals, effect of charged dislocation elec. field, on colour centres 0—51143

local, as function of injection level 0-79068 m.i.m., Al-Al₂O₃-Au, film system, photocurrent spectra, pot. barrier 0-44324 m.i.s. struct., barrier energy determ. from photoinjected currents voltage depend. 0-47806

materials, prod. and techniques, patent literature review 0-75826 measurement, spectral dependence, metal cell with precise temp, control

0–65844
methyltetrahydrofuran, γ-irrad, glass at 77°K 0–79134
molecular crystal, lattice vibrations contrib. 0–44396
molecular solids, field control, model 0–47867
maphthalene, single crystals, intrinsic photocarrier generation 0–72143
negative photocond. in quantizing mag, field 0–72137
nitrobenzene, exp. study 0–68145
nitrobenzene, pure, at 300°C, subject to visible rad. 0–71387
opto-electronics, review and prospects 0–69814
organic cryst., response curves behaviour 0–62486
organic semiconductor, photosepsitivity enhancement, 0–51145

organic cryst., response curves behaviour 0–62458
organic semiconductor, photosensitivity enhancement 0–51145
oscillatory, Boltzmann-eqn. model, exact soln. 0–75824
photo-e.m.f. generation, transverse, by unpolarized radiation 0–56375
photocurrent detection in simple polymer systems 0–65853
of photographic coatings using pulsed d.c. single flash apparatus 0–70127
phthalocyanine conditions, doping degree influence 0–77227
phthalocyanine, crystal, excitons, temp. depend. 0–79085
phthalocyanine film, photocurrent decay, lux-ampere characts., quasicontinuous spectrum of levels 0–40899
poly-N-vinylcarbazole, dye sensitized 0–72442
polyarylense-evanoethenylense mol, strict, rel, to optical props, and photo-

polyarylenes-cyanoethenylenes mol. strict. rel. to optical props. and photo-cond. 0-49949

cond. 0–49949
polyethylene, investigation using monochromatic light 0–65843
polymer systems, simple, photocurrent detection 0–65853
polyvinyl carbazole, photocurrent action spectra study 0–75500
polyN-vinylcarbazole, effect of crystallinity 0–65023
quinone crysts, electron injection 0–59284
semiconductor, CdGeP₃, crystal growth by vapour transport, forbidden
band width 0–74971
semiconductor, CdS-type, impurity, linear and nonlinear relax, kinetics
0–65846

semiconductor, CdS-type, impurity, linear and nonlinear relax, kinetics 0—65846
semiconductor, EuTe, absorpt, edge, temp, depend. 0—59400
semiconductor, GaAs, in surface region 0—56384
semiconductor, Ge, in fund, absorpt, region 0—56388
semiconductor, P-InSb, impurity, photo-Hall effect, spectral oscillation, 5-20K 0—56393
semiconductor, Sb₅S-Sb₅Se, solid solution, spectral distrib. 0—51150
semiconductor, amorphous, and switching 0—78939
semiconductor, amorphous, and switching 0—78939
semiconductor, pulk trapping effect on carrier diffusion length by surface photovoltage method 0—44184
semiconductor, foreclece, influence on phase transform. 0—59262
semiconductor, imperfection centres, thermal and optical emission, capture rates, cross section 0—53839
semiconductor, imperfection centres, thermal and optical emission, capture rates, cross section 0—53839
semiconductor, local inhomogeneities influence on spectral photosensitivity 0—56374
semiconductor, magnetic, europium chalcogenides, band struct. 0—59399
semiconductor, p. Fis, electron irrad. 0—65852
semiconductor, photoelec. effects due to photon momentum in photoioniz. of impurity centres 0—65841
semiconductor, photoelec. effects due to photon momentum in photoioniz. of impurity centres 0—65841
semiconductor, photoelec. effects due to semiconductor, photoelec. effects due to photon momentum in photoioniz.

semiconductor, photo capture by surface states, cross sections 0–56376 semiconductor, photon capture by surface states, cross sections 0–56376 semiconductor, vitreous, local states, thermoelec. 0–79071 semiconductor II-VI cpds., book 0–62342 semiconductor film, field effect 0–68974 semiconductor high resistance, apparatus for effect study 0–59288 semiconductor panel, illuminated, rel. to millimetre wave attenuation 0–45719

U-45719
semiconductor photodetection, active transmission line analogue 0-72133
semiconductor under double injection conditions, kinetic instability and reson. effects 0-56232
silver halides, photoelectric and photographic sensitivity, Urbach rule, exciton absorpt, region 0-47870
solar cell materials, dopant effects on carrier lifetimes 0-59280
spectral oscillations 0-75825
surface properties of single crystal using ultrahigh vacuum cryostat 0-51857

Photoconductivity continued survey 0-47010

TCNO film, spectral response 0-59286

tetracene, exciton-surface reaction at electrolyte interface 0-75839

tetracene film, effect of mag. field 0-51153 tetracene single crystal, photo-enhanced currents, anisotropy in mag. field effects 0-47881

tetracyanoquinodimethan, conductivity and photoresponse 0–59285 tetrathiotetracene thin layer systems 0–44402 transient photocurrent due to pulse illumination in presence of trapping 0–62459

transition-metal dichalcogenides, optical absorpt. spectra, excitons 0-47875

0-47875 work function meas, on high resistivity photoconductors 0-51144 xeroradiography, principles and characteristics 0-70141 Al-Al₂O₃-Au film system, photocurrent spectra, pot. barrier 0-44324 As-Te, As-Te-Ga, As-Te-Ga Ge-Si chalcogenides, amorphous semicond, and switching 0-78939 As.S₂, vitreous, spectra 0-53816 As.Se, amorphous and cryst., rel. to thermal transitions of carriers 0-72134 As.Se, single crystal and amorphous film 0-47705

0-/134 $A_{S_1}Se_3$, single crystal and amorphous film 0-47705 $A_{S_1}Te_3$, amorphous film 0-47706 $A_{S_1}Te_3$ film, amorphous, and opt, absorpt, and conductivity, 200-400°K

AS₂1e₂, first, amorphous, and opt. assorpt. and conductivity, 200-400 K 0-44187 CdCr₂Se₄, spectral sensitivity, 300 and 77 K 0-79077 CdGeP₂, crystal growth by vapour transport, forbidden band width 0-74971

0-4971 CdN, thin film, meas. in range 1900 7000 Å at 298 and 77 K 0-65973 CdS:P. As, acceptor obs. 0-66090 CdS-type semiconductor, impurity, linear and nonlinear relax, kinetics 0-65846

0-65846
CdS, acoustoelectric phenomena, large signal gain and current saturation expressions applic. 0-43891
CdS, carrier excitation, i.r. absorpt. 0-44830
CdS, chemisorption influence 0-68976
CdS, current filaments, acoustoelec. origin 0-68820
CdS, effect of desorption of O surface layers 0-47739
CdS, effect of u.v. on spectral distrib. for low temperatures 0-53953
CdS, hole traps evidence 0-51147
CdS, insulating influence of chemisorption on dark current 0-75831
CdS, ion-implanted 0-51146
CdS, rel to u.s. absorption. 2.5-50 K 0-47530
CdS, threshold field for current saturation, crystal inhomogeneity effects 0-59281
CdS, traps, photochem, changes 0-47871

CdS, traps, photochem. changes 0-47871

CdS, traps, photochem. changes 0-47871
CdS, ultra high vacuum treatment depend., O₂ desorption, annealing, electron bombard. 0-79078
CdS, undoped single crystal, 280 keV electron irrad. 0-44398
CdS electroacoustic oscillator, acoustic strain meas. 0-43892
CdS in combination with luminophore layer in u.v. region temp. dependence of photocurrent of photoresistance 0-68975
CdS solar cell. elisive mechanism 0-73137
(CdS)₂(CdSe)_{1-x} multilayer systems, photoelec, props. 0-74911
CdS(Se) films, induced impurity photocond. 0-79073
CdS_{0.995}Se_{0.005}, Ar laser excitation intensity depend., exciton interaction 0-79076
CdS.Se. ... films, adsorption influence. 0-56380

0–79076

CdS_xSe_{1-x} films, adsorption influence 0–56380

CdSe, current fluctuations, acoustic noise flux 0–75829

CdSe, electron irrad., Cd vapour firing, defect production 0–75830

CdSe, illum. effects 0–53952

CdSe, Non-uniform illum., electrothermal domains 0–56381

CdSe film, residual, applied field depend. 0–75828

CdSe films, field effect for surface pot. changes case, illumination influence 0–78944 CdSe film, residual, applied field depend. 0—75828
CdSe films, field effect for surface pot. changes case, illumination influence 0—78944
CdSe films, field effect for surface pot. changes case, illumination influence 0—78944
CdSe films, vapour evaporating-reactive sputtering prepared 0—72135
CdSe photosensitive films, trap parameters determ. 0—79075
CdT2, 300-100K, and reflectivity 0—56382
CdTe, deep impurity levels and photomemory effect 0—78973
CdTe, effect of thermal treatment, 450°C max. 0—62466
CdTe, high-resistivity, surface-barrier p-n junctions, props. 0—56379
p-CdTe, photosensitivity spectrum, temp. influence 0—79072
p-CdTe, photosensitivity spectrum, temp. influence 0—79074
CdTe,CdSe_{1—x} solid solns. 0—65845
CTB_{T3}, Seebeck voltage and resist, temp. depend. 0—75547
CsF, F-centre, Schottky ionization. bleaching 0—55904
Cu complex, chlorinated phthalocyanines, temp. depend. 0—65621
EuO, magneto-photocond. near Curie temp. 0—56383
EuSe, transient, meas. magnetic impurity state model 0—79079
EuTe, absorpt. edge, temp. depend. 0—59400
GaAs:Au. dopant behaviour temp. depend. 0—56385
GaAs:Cr, current oscillation, —80°C, spectra and optical quenching 0—47868
GaAs:Fe, Hall coeff., elec. resist., deep levels 0—40791
GaAs-GaSb photoconductivity obs. 0—65847
n-GaAs, epitaxial, donor-state spectrum 0—44838
GaAs, photocarrier multiplication due to impact ionization 0—75832
GaAs, relax. kinetics 0—56386
GaAs, photocarrier multiplication due to impact ionization 0—75832
GaAs, relax. kinetics 0—56386
GaSb, oscillatory photocond. under mag. field 0—59922
GaSe under two-photon excitation conditions 0—72136
GaTe, layer-type semiconductor, absorpt. coeff., reflectivity 0—62661
n-Ge:Co, transient photocond., recomb. of electrons and holes 0—40893
n-Ge:Ni, 80K, elec. field quenching 0—47872
n-Ge:Te rel. to recomb., 145-300 ° K 0—44250
Ge, in fund. absorpt. region 0—56388
Ge, kinetics under cyclotron reson. conditions 0—56389
Ge, photon drag of free current carriers, mag. field effect 0—75833
Ge, spectra, elec. field effec

Photoconductivity continued

otoconductivity continued

Ge, surface props., silane treatment depend. 0–40800

GeTe films, amorphous, density of states obs. 0–53957

GeTe(Se), amorphous film, high-field, edge shift 0–53956

HgI-xCd₃Te, intrinsic carrier conc. using k.p. calc. 0–59201

HgI, photopolarization, exposure-illuminance characts. 0–53958

HgI, photopolarization in ir. region of photocond. quenching 0–56392

HgN₆ thin film, meas. in range 1900-7000 Å at 298 and 77 K 0–65973

HgO, surface, spectral response 0–40895

n-InAs, and photomag. effects 0–40900

n-InAs, and photomagnetic effects, quantum oscillations, 1.8-4.2°K

0–40901

n-InAs, electron heating, 1.8-4.2K 0-68983
n-InAs, negative photocond. in quantizing mag. field 0-72137
InSb:Fe, carrer lifetime, 80-270K, transport props. 0-47716
n-InSb, and photomag. effects 0-40900
n-InSb, and photomagnetic effects, quantum oscillations, 1.8-4.2°K
0-40901

0-40901

n-InSb, electron heating, 1.8-4.2K 0-68983

P-InSb, impurity, photo-Hall effect, spectral oscillation, 5-20K 0-56393

n-InSb, negative photocond. in quantizing mag. field 0-72137

p-InSb, oscillating photocurrent spectra, 4.2 K, 15 kOe, absolute negative cond. 0-75834

cond. 0–75834
p-InSb, photomagnetoelectric effect, electron irrad. effect 0–79081
n-InSb, pel. to electron heating 0–79080
p-InSb, two step photocond. decay by laser irrad. 0–68978
InSe, single cryst., influence of preparation procedure 0–59226
In₃Te₄ films, coarse-grained 0–56258
KCl:Eu²+ multiphoton excitation of single crystals by ruby and neodymium laser light 0–56600
KCl, coloured crystal, a.c., relaxation 0–62462
KCl, during F-centre photochemical conversion and elec. conductivity 0–75179
MoS₂, ontical absorpt, spectral excitons 0–47875

KCI, during F-centre photochemical conversion and elec. conductivity 0-75179
MoS₂, optical absorpt. spectra, excitons 0-47875
MoSe₃, optical absorpt. spectra, excitons 0-47875
MoSe₅, optical absorpt. spectra, excitons 0-47875
MoTe₅, optical absorpt. spectra, excitons 0-47875
Nb₂O₅ films, trapping and chemisorption effects 0-65850
(Pb,Sn)O mixed cryst. 0-56394
Pb azides, 1900 to 7000 Å, 298° to 100°K 0-51307
PbO doped with organic donors and acceptors, effect on photocurrent 0-75840
PbS optiaxial films 0-53959
PbS film, current establishment kinetics 0-53960
PbS film, O₂, high press. atmos., effect 0-47877
PbS films, photosensitive, recomb. mechanism 0-53961
PbS photoresistor, effective diffusion and drift lengths 0-79082
PbSe films 0-65851
Sb₂S₃-St₂Se₃ semiconducting solid solution, spectral distribution, specific resist., 18-150°C 0-51150
Sb₃S₃ excited photocoond, i.r. quenching 0-56377
SbSI, -170-100°C 0-75836
SbSI, influence on ferroelec. props. 0-68949
Sb₂Se₃, Se vapour press. depend., temp. depend., elec. cond. 0-40896
Se:As, electrophotographic and fatigue props., var. with As conc. and temp. 0-75837
Se, amorphous, anomalous, temp. depend., 120-170 K 0-75838
Se, amorphous, anomalous, temp. depend., 120-170 K 0-75838

Se:As, electrophotographic and fatigue props., var. with As conc. and temp. 0—75837
Se. amorphous, anomalous, temp. depend., 120-170 K 0—75838
Se. amorphous, optical absorpt., transport props. 0—47724
Se. amorphous, short-range order influence 0—72138
Se. amorphous, short-range order influence 0—72138
Se. amorphous film, emission- to space-charge-limited 0—44399
Se. α- and β-red monoclinic cryst. 0—65161
Se, temp. depend, i. quenching 0—56395
Se, vitreous binary alloys, transport props., valency depend. 0—47722
Se films, amorphous, trapping of minority carriers, photocond. transient-decay obs. 0—56396
α-Se monoclinic, charge transport 0—51151
Se single cryst., hexagonal, non-ohmic effects 0—47878
Se single cryst., hexagonal, optical quenching 0—53962
Si:B(Ga.In), photosensitivity, rel. to photoresistor applic. 0—56397
Si:Ga impurity optical absorption cross-section obs. 0—59283
Si:Zn optoelectronic devices applic. 0—53697
Si:Ga impurity optical and Al interstitial defects 0—43662
p-Si, electron irrad. 0—65852
p-Si, extrinsic 0—44408
p-Si, neutron-irrad. 0—47879
Si, surface recombination velocity, surface trapping and surface photovoltage 0—68979
Si films, amorphous, glow-discharge deposited 0—59227
Si surface layers phenomena 0—72139
SrTiO₃, anomaly, local ferroelec, phase transition obs., 47K 0—68952
ZnO-resin binder layers, dye-sensitized, quantum efficiency and photocond. 0—72140
ZnO electrophotographic layers, effect of degassing desorbed O₂ on photoconductive patterns. 0—73376

cond. 0-72140

ZnO electrophotographic layers, effect of degassing desorbed O₂ on photoconductive patterns 0-73376

ZnS:Ag:B crystal, photodepolarization current 0-68980

ZnS-GaAs heterojunctions, spectral distrib., and photoelectroluminescence spectrum 0-51351

ZnS films, props. 0-47880

ZnSe on Ge heterojunction, prep. by epitaxial deposition, elec. characts. 0-68868

0-68868

0-0888 ZnTe-CdTe, crystals, negative, intrinsic and impurity 0-44400 ZnTe. doped, ir. quenching 0-79083 ZnTe, photosensitivity spectrum, annealing effect 0-56398 p-ZnTe, under combined excitation conditions 0-56399

Photodisintegration see Deuterons/photodisintegration; Nuclear reactions and scattering due to/photons

Photodissociation see Photochemistry

Photoeffect, nuclear see Gamma-rays/effects; Nuclear reactions and scattering due to/photons

tering due to/ photons

Photoelasticity
see also Double refraction/mechanical
alkali halide, constants, and Clausius-Mossotti field 0-55953
alkali halide, piezo-optic constants dispersion in u.v., deform. pot. constants
of valence band 0-44782
alkali halide crystals, influence of annihilating dislocations 0-48010
analysis of fracture dynamics 0-48651
Cranz Schardin modified system 0-48811
dynamic propagating cracks expt. 0-47405
e.m. plane wave propag. in mat. with finite deformations 0-38277

Photoelasticity continued

ferroelectric, BaTiO₃, critical polarization fluctuations influence 0–72.309 ferroelectric, strain-induced energy shifts and strain-depend. oscillator strengths in nonmetallic cryst. 0–41132 with finite deformations, propag. of plane e.m. waves 0–54645 flexural waves in bar, optical stress analysis 0–71675 glasses, optical, mechanical and photoelastic props., high and low temp. meas. in vacuum, instrument 0–53573 interference fringes in a sheet of photoelastic material 0–42035 ionic crystals 0–76038 laser mat., piezo- and thermo-opt. props. 0–79254 optical glasses, photoelastic constants 0–79253 photomechanical effect kinetics, microhardness meas. 0–50746 piezo-optic effects on transmission in electro-optic shutters 0–77194 piezo-optical effect and mag. birefringence in YFe garnet 0–69090 piezoreflectance, modulated, in semiconductors, shear deform. potentials determ. 0–43727 plexiglass, apparent colours when stressed 0–55988 polymers, amorphous, stress/birefringence curves and stress-optical coeffs. 0–71655 principles and applications 0–38264 pyrex, apparent colours when stressed 0–55958 quartz, vibrating at resonance, rel. to synchronization of pulsed laser 0–47300 rubbers, synthetic, stress/birefringence curves and stress-optical coeffs. 0–71655.

rubbers, synthetic, stress/birefringence curves and stress-optical coeffs. 0-71655

U-1653
ruby, photoelastic constants determ. 0-62004
ruby laser mat., piezo- and thermo-opt. props. 0-79254
semiconductor, GaSb, piezoreflectance 0-76015
semiconductor, Ge and Si, piezo-absorption in absorption edge region

semiconductor, Ge and Si, piezo-absorption in absorption edge region 0-41121 semiconductor, piezoreflectance, modulated, shear deform potentials determ. 0-43727 strain-induced energy shifts and strain-depend oscillator strengths in non-metallic cryst. 0-41132 stress analysis and a universal instrument for fringe multiplication 0-57602

0-57602 stressmeters for biaxial stress and strain meas. 0-50668 styrene-butadiene-styrene block copolymer, rheo-optical props., morphology effect 0-40273 tension bar, comparison of stress cones, due to semicircular grooves and circular hole 0-38236 three-dimensional modelling, assessment of three epoxy resins as materials

0-42043

0-42043 valency crystal, rel. to vibrational absorpt. by charged impurity 0-48057 , rel. to wave analysis, continuous media 0-52079 zincblende-type materials, contrib. of piezoelec. strain to electroreflectance 0-76037

 AL_2O_3 , corundum, piezo-optic moduli determ. by interference method 0-65981

Ag-Au alloy, piezo-optical props., reflectance change due to strain 0-48003

Ag single crystal, piezo-optical props., reflectance change due to strain 0-48003

Ag single crystal, piezo-optical props., reflectance change due to strain 0-48003
BaF₂ stress- and strain-optical constants 0-44783
BaTiO₃, critical polarization fluctuations influence 0-72309
CaF₂, stress- and strain-optical constants 0-44783
CdS, photomechanical effect kinetics, microhardness meas. 0-50746
GaAs, split-off valence-band parameters from stress-modulated magneto-reflectivity 0-72315
GaSb, piezoreflectance 0-76015
Ge, photomechanical effect kinetics, microhardness meas. 0-50746
Ge, stress-modulated magnetoreflectance for direct transitions 0-76026
Ge, piezo-absorption in absorption edge region 0-41121
InSb, photomechanical effect kinetics, microhardness meas. 0-50746
KBr, piezo-optical consts. temp. depend. 0-76005
KCI, piezo-optical consts. temp. depend. 0-76005
KCI, piezo-optical consts. temp. depend. 0-76005
KH,PO₄, temp. depend., wavelength depend. contrib. to electro-optical phenomena 0-41119
LiNbO₃, secondary (electro) photoelastic effect 0-76033
LiNbO₃ Brillouin scattering, photoelastic constants 0-72397
NH,H,PO₄, temp. depend., wavelength depend. contrib. to electro-optical phenomena 0-41119
NaCI, plastic bending, stress distrib., dislocation density 0-43746
Nd:glass laser mat., piezo- and thermo-opt. props. 0-79254
Sb, photomechanical effect kinetics, microhardness meas. 0-50746
Si:Mg, excitation spectra and piezospectroscopic effects of neutral and singly ionized donors 0-51287
Si piezo-absorption in absorption edge region 0-41121
TiO₃, rutile, difference in coeffs., confirmation of rotational contribution to Brillouin scattering 0-79335
ZnS cubic crystal, exciton piezoreflection, 77K 0-56491

Photoelectrets see Electrets; Photography

Photoelectric cells see Photoconducting devices; Photoconductivity; Photoelectricity; Photovoltaic effects

Photoelectric effect, atomic see Atoms

Photoelectric emission see Electron emission/photoelectric

Photoelectricity

see also Electron emission/photoelectric; Photoconductivity; Photovol-taic effects

aminoindenes, isostructural, photosensitivity 0–41227 charge transfer complexes, rel. to cryst. struct. 0–58770 counting distributions for determination of intensity correlation functions 0–77055

demonstration for physics student by inexpensive apparatus 0-45739 detectors, e.m. field effects statistical optics considerations 0-63692 m.i.s. structure, capacitor, photo-e.m.f., carrier generation distrib. 0-47804

0–47804 membranes, lipid, bilayer, appearance of e.m.f. on illumination 0–76686 n-quantum photoeffect, minimum light current density, calc. 0–47866 optical image recording, electron-storage targets 0–69815 opto-electronics, review and prospects 0–69814 p-n, Ag-PbO-SnO₂, thermally stimulated current, trapping levels 0–40809 photocathodes with organic coatings for vacuum u.v. region 0–62473 photodipole effect, high-temp, kinetics 0–78811 photoelectrets, efficiency improvements due to heat treatment in various gas atmospheres 0–65854 photoelectronic imaging devices, detective quantum efficiency 0–69816 photometer, dual-channel, for stellar obs. 0–45834

Photoelectricity continued

phthalocynanin, film photo-electric effect, quantum yield 0-79067 polyethylene, photoelectric response as function of wavelength 0-68973 semiconductor, p-Si, photothermoelec. effect, anomalous 0-78995

semiconductor, photoelec. effects due to photon momentum in photoioniz. of impurity centres 0–65841

semiconductor, work function determ. from photoelec. meas. 0-53841 shadow instrument with modulating disc noise spectrum at output calculation 0-73124

solar cells, energy concentrator, mirror-and-lens 0-48961 spectral distribution of radiant losses in pulsed plasma accelerators 0-71154

water pump, solar, tests 0-42167
water-pumping unit, solar, control system 0-42168
Ag PbO-SnO₂, p-n junction, thermally stimulated current, trapping levels 0-40809

Ag. PbO-SnO₂, p-n junction, thermally stimulated current, trapping levels 0—40809

Ag.SBr and Ag,SI solid electrolytes, photoelec. effects 0—68981

As.S₃—Sb₂S₃, evaporated layers 0—40890

As.S₃—Sb₂S₃, evaporated layers 0—40890

As.S₃—Sb₂S₃, evaporated layers 0—40707

Au-SiO₄GaAs electroluminescent diodes, photoelection applic. 0—40814

CdTe, electron and neutron irrad. effects 0—40783

GaAs Au surface barrier diode characteristics 0—51155

GaAs₂P₁—, local levels obs. 0—65682

GaP:Cu, local level obs. 0—65682

GeS monocrystals produced by sublimation in vacuo 0—50432

InAs p-n junction fabrication and props. 0—62385

InAs p-n junction fabrication and props. 0—62385

InSe single crystal, photovoltaic props. 0—75845

PbS film, high voltage photo-e.m.f., effect of external voltage 0—51142

p-Si/Al surface-barrier diode, field-induced photoelectron emission, energy distrib. 0—44421

p-Si/Al surface-barrier diode, field emission of photo-induced conduction electrons 0—4420

p-Si, photothermoelec. effect, anomalous 0—78995

Sil, surface-barrier photo effect during polarization in electrolyte 0—65842

Isl Ta 6.25 keV El y rays of Mossbauer absorption spectra, interference of photoelectric and nuclear resonance absorption 0—64059

otoelectromagnetic effects

Photoelectric and nuclear resonance absorption 0-04059

Photoelectromagnetic effects
n-quantum, minimum light current density, calc. 0-47866
semiconductor, anisotropic, minority carrier mobility determ. 0-75661
semiconductor, n-InSb, n-InAs, photomag, and photothermomag, effects, electron heating, photocond. 0-68983
CdTe APV film, miniature magnetometer 0-44405
n-InAs, and photoconductivity, quantum oscillations, 1.8 4.2°K 0-40901
n-InAs, photomag, photothermomag, effects and photocond, electron heating, 1.8-4.2K 0-68983
n-InAs, photomagnetic effect and photocond. 0-40900

heating, I.8.4.2K 0–68983

n-In As, photomagnetic effect and photocond. 0–40900
InSb:Fe, carrer lifetime, 80 270K, transport props. 0–47716

n-In Sb, and photoconductivity, quantum oscillations, 1.8-4.2°K 0–40901

p-In Sb, photocond, electron irrad. effect 0–79081

n-In Sb, photomag. and photocond. 0–40900

n In Sb, photomag. and photothermomag. effects 0–79080

n-In Sb, photomag. effect, 7TK 0–75847

n-Si:Au, low-temp. props. 0–79086

p Si, 300°K and model 0–44406

Photofission see Nuclear fission

Photographic light sources see Light sources; Photography

Photographic materials

see also Nuclear track emulsions
Agla-Gevaert Scientia 14 C 75, 10 e 75, 8 E 75 emulsions, diffraction efficiency of gratings, meas. 0–42367 coatings, photoconductivity obs. using pulsed d.c. single flash apparatus 0 70127

0 70127
developers, colour, oxidized, in gelatine, computing of effective diffusion coefficients 0-73312
developers, inverse relationship between development rate and developer concentration 0-70119
developers, superadditivity of redox indicators and Weitz radicals with hydroquinone, ascorbic acid and sodium dithionite 0-70114
emulsion, contrast transfer fn. 0-67185
emulsion, neutral, gelatine substituted by polyvinyl alcohol 0-60449
emulsion, optical path variation, relationship with variation of Ag on film
0 73362
emulsion, photopolymerisation system, molecular structural requirements

emulsion, photopolymerisation system, molecular structural requirements $0\!-\!70112$

emulsion grains, opto-electronic tech. for classification 0–49158 emulsion shrinkage reduction for real-time holographic interferometry 0–63656

emulsion-developer systems, images of triangular wave gratings 0-60450

emulsion-developer systems, images of triangular wave gratings 0-60450 emulsions, sensitivity to X-rays and variation with exposure 0-57638 equidensity production, one operation, new photographic layer 0-60454 film, constant MTF investigation of existence 0-70115 film, effect of heat on characteristic curves 0-70122 film, information content and channel capacity 0-57642 film, as radiometric imaging detector 0-60453 film photochromic organic, hologram 0-57553 film-grain noise, photographic image enhancement study 0-70105 films, interferences 0-63674 films, reciprocity failure in vacuum, room air and other gases 0-70123 films, threshold modulation curves, history, measurement and accuracy 0-38583 films, vesicular, distribution and quantity of thermal energy utilized is

0-3888 films, vesicular, distribution and quantity of thermal energy utilized in development 0-73370 films for holography, evaluation 0-69956 films for holography, evaluative test results 0-69957 filter, glass, calculation and preparation for photographic sensitometry 0-57614

0-57614

free-radical photosensitive, optically developed 0-49156
glasses, photochromic Ag haide 0-49157

Herschel effect rel. to photoelec. effect 0-77224
for holography, scattered flux spectrum of Agfa 14C70, 10E70, 8E70,
Kodak 649 F, analysis 0-52347
Itek RS flin, high-resolution contact printing process 0-70107
lens, objective, conveying properties, image modulation 0-57544
negative emulsions, meas. of modulation transfer function 0-63737
phenidone-hydroquinone system, superadditivity obs. by ESR during development 0-70111
p-phenylenediamine substituted derivatives, inverse relationship between

p-phenylenediamine substituted derivatives, inverse relationship between development rate and developer concentration 0-70119

Photographic materials continued

photochromic, evaluation for determination of sensitometric, image-decay, resolution and MTF characteristics 0-70109 photopolymer recording of holograms 0-60273 photopolymers, rapid access, for direct formation of images 0-77156 photoresist layers, use in high precision gratings 0-42366 scattering, coherent optical power spectra 0-57639 transparent table for H₂ bubble chamber's photographs processing 0-77442 [1,3,3-trimethylena-doling-64 city-92]

transparent table for Fig. 0000c channels.

0-77442

1,3,3-trimethylene-dolino-6'- nitro-8'-pyrylospirane, photochromic information storage 0-60451

AgBr EMC and AgBr-1 photoemulsion microcrystals additional band due to Ag centers 0-51296

AgBr surface, contact phenomena rel. to development process 0-73365

Hg comps., photosensitive, image formation obs. 0-70121

Se:As, electrophotographic and fatigue props., var. with As conc. and temp. 0-75837

sensitivity

emulsion, contrast transfer function 0–57641 emulsion, high speed Ektachrome, at -50°C rel. to astrophotography 0–41873

layers, effect of radiations 0-63734

light-sensitive, new, for image recording process 0-70116 modulation transfer-function evaluation using laser speckle pattern 0 - 57640

0-7/640 noise spectral power density at high spatial frequencies 0-70104 sensitometric exposure of daylight films, use of glass filters 0-67170 silver halide emulsions 0-73366 silver halides, and photoelectric, Urbach rule, exciton absorpt. 0-47870 spectral region, 1.5 to 23.6Å, UF-2T, UF-R and SC-5 films 0-38582 X-ray film response to 9-70 keV range for 3 nsee exposures 0-42404 ZnO-resin binder layers, dye-sensitized, quantum efficiency and photo-cond. 0-72140

Photographic process

see also Photochemistry

contact-printing process, image degradation, near-field diffraction analysis
0-70108

0-70108 image recording, new light sensitive material 0-70116 imaging, migration new concepts 0-70117 ltek RS film, high-resolution contact printing 0-70107 Lippmann colour method for undergrad. lab. 0-73361 modulation transfer function of negative emulsion, two methods of meas.

modulation transfer function of negative entities, and the control technology 0-70126 photofinishing, progress in processing technology, development of equipment and chemistry 0-70125 photofinishing progress in equipment technology 0-70124 plate processing system in Cabot Spectrographic Lab. 0-63736 primary, obs. by transient measurements of photocharge 0-73369 semiconductor, image contrast meas. 0-77228 semiconductor layer based 0-77226 semiconductor optimal doping role 0-77227 technique for vertical lunar orbital photography 0-70128 AgBr, simultaneous capture of 2 photoelectrons by a sensitivity centre 0-54949

AgBr evap. layers, spectral sensitization by oxacarbocyanine 0-42402

development
concentration effect, inverse relationship between rate and developer concentration for substituted p-phenylenediamine derivatives 0-70119
electrochemical mechanism, fundamental, deviations from electrode theory 0-73367
image amplification characteristics in Ag-complex diffusion-transfer processes 0-70113
image transfer characteristics in Ag complex diffusion-transfer processes 0-70113
image transfer characteristics in Ag complex diffusion-transfer processes 0-70113

induction period, visible 'massive reduction' period 0-70118 initiation and continuation, views and correlations 0-70110 masking of negatives, comparison of various methods 0-60452 mechanism, by metal complexes, inner and outer sphere 0-73368 nuclear emulsions, discriminating development by amidol and NaSCN developers 0-38770

developers 0-36170 printers, image acuity determination 0-54950 rate limiting steps, solvent effects 0-70120 superadditive, phenidone-hydro-quinone system, ESR obs. 0-70111 track emulsion discrimination improved by use of solvatant amidol developer 0-57859

vapour deposition on latent image of electron beam, patent 0-42405 of vesicular films, distribution and quantity of thermal energy utilized 0-73370

Photography

also Cameras; Cinematography; Lenses/photographic; Radiogra-

phy airborne time-lapse, for cloud photogrammetry 0–72619 celestial, with fiber-optics image tubes 0–76675 chamber for 3MV electron microscope 0–49002 composite and cancellation problem, quantitative investigation, applic. to galaxies 0–38579 conference on scientific and engineering aspects, New York (1970) 0–70095

deblurring of photographic images by holography 0-42338 deconvolution of blurred photographs, by scanning in spatial domain

deconvolution of blurred photographs, by scanning in spatial domain 0-42337 electro-, photoconductive gain 0-73364 electro-, photoconductive gain 0-73364 electron-beam-recorded patterns on photographic plate, distortion due to charge-up 0-70140 electrophoretic development of electrostatic charge patterns 0-54952 electrophotographic images, resolving power 0-38586 electrophotography, sensitivity concept 0-38585 evaporography, obs. and theory 0-70094 holographic recording using completely incoherent light and single exposure 0-42334 holographic storage media, figures of merit 0-42335 image intensifier, of ultrahigh energy cascades in ionization spectrometer 0-73338 of ionizing radiations, book 0-38581

of ionizing radiations, book 0-38581 laser beam photography by multiple beam technique 0-57544 of laser rod internal stresses 0-45795

Photography continued

long-wavelength, semicond. applic. 0-54948 low temp. of substance under quasihydrostatic press., use of high press. X-ray camera, method 0-50488

parallax panoramagraphy, multiple lens system 0-70132 planetary, high resolution at midday, Mars, Jupiter, Saturn, Moon 0-63089

printer, metallic, (OZX 2-35 mm), development of optical system 0-63738

rasters made of cylindrical microlenses, optical capacity 0-73372 recording of electro optical images 0-57585

semiconductor applic. to long-wavelength photography 0-54948 semiconductor photodetector under photographic conditions, investigation methods 0-79089

methods 0-79089 sensitometer for obs. of reciprocity failure in vacuum and gaseous mixtures with controlled temp, and humidity 0-70103 stellar, sky background reduction by using polarizer, and new magnitude determ, method 0-45441 substances under quasihydrostatic press., use of high press. X-ray camera, method 0-50488 system design, Cobb chart resolution method for performance prediction 0-77225 time-lapse, use of motor-driven cam-controlled cameras 0-63735 xerography, amorphous Se films light absorpt., effect of charging 0-60421

ZnO electrophotographic layers, effect of degassing desorbed O₂ on photoconductive patterns 0-73376

applications

applications
rel. to Moon surface obs., use of Range probes 0–59747
aerial colour rel. to remote sensing of ocean bottom detail and water depth
penetration 0–62897
for analysis, rel. to flexural waves in bar 0–71675
benzene, high pressure crystal growth study 0–50428
bubble chamber negatives, automatic measurement 0–46061
carbon tetrachloride, high pressure crystal growth study 0–50428
colour, electron microbeam probe samples, comments 0–49161
colour i.r film, high-altitude use 0–51609
computer display photographs of shock wave structure in gas, bimodal
model 0–39662
entomology, lenses assessment by experts 0–38584

model 0–39662 entomology, lenses assessment by experts 0–38584 explosive anode erosion in high current sparks, tree shape optical phenomenon study 0–61405 film photochromic organic, hologram 0–57553 fluorescent penetrant images of cracks 0–42403 galaxies southern unreported clusters and groups, Yale observatory Argentina double astrograph results 0–41614 hologram image reconstruction, nonlinearity of photographic process causing undesired images 0–38516 hologram recordings initiation of photopolymerisation obs. 0–72555 holograms low noise improved efficiency, production on AgH emulsion 0–63643 holography, multi-image recording by superposition 0–77152

holography, multi-image recording by superposition 0-77152 i.r. mammary carcinoma detection comparison with thermography 0-76717

image blur of fast moved objects illuminated by light flashes 0-70131 isophote recording in negative 0-49160 large screen display systems, initiation of photopolymerisation obs. 0-72555

0—72555 laser beam, in engineering 0—49159 laser beam, in engineering 0—49159 laser rod internal stress determ. 0—73235 lenses kinoform, tech. for accurate figuring 0—67186 lightning spectroscopy, photographic techs., review 0—66299 lunar orbital, vertical, optimum processing technique 0—70128 microcyntography and photoengraping, rel. to IC fabrication 0—57647 mtf obs., comparison of sighting system and simulator 0—70138 mtf study of large optical systems, method 0—49106 multispectral colour, agricultural and oceanographic 0—52401 ocean depth determination, by water wavelength examinations 0—62895 off-eutectic mixtures, controlled solidification process examination 0—47102 oceanograph moise summation, pulse radiolysis expt. 0—45087

oscillogram noise summation, pulse radiolysis expt. 0-45087 photochromic film, optical procedure for processing electric signals

0-70139
photogrammetry, checking of building structures 0-73374
photogrammetry, photogrammetric system engineering 0-73373
photomicrography, study of nucleation rel. to thermal decomposition in NH₄ClO₄ 0-68556
photoresists, standing waves and absorption 0-45822
planets, various methods 0-72793
polymer solidification, interface morphology studies 0-46988
solar u.v. part of photospheric network spectrum 0-54481
space, enhanced multiband, rel. to inventory of earth resources 0-52400
space photography, scientific potentialities and analytic framework
0-56867

space pho 0-56867

spectrograms, photographic prism, reduction by combined computational and graphical method $\,0-60419$ spectrophotometry elimination of systematic errors with slotted steel foil 0-60435

star field photographs, photometric calibration using calcite polaroid filter 0-59812

sters, precise identification non-homographic method 0–63187 stellar magnitudes using modern 35mm panchromatic films Tri-X, HP4, preparation of sky charts 0–69506 stereophotographs, three-dimensional restitution with stereocomparator 0–73375

time-lapse, rel. to electrical contacts, material transfer obs. 0-56177 time-lapse from high altitude balloons, camera arrangement 0–66290 time-lapse from high altitude balloons, camera arrangement 0–66290 time-lapse of atmos. clouds, procedure, equipment 0–66291 underwater, analytical techniques and standards 0–70136 underwater, system, engineering considerations 0–70135 underwater system, effect of physical nature of water on recording phase 0–70134

InSb film micro-zone crystallization, macrophotographic examination of growth process 0-47065 NH₄ClO₄, nucleation rel. to thermal decomposition, photomicrographic studies 0-68556

NaNO₃, morphology of solid-melt interface, holographic study 0-47138

Photography continued applications continued

3%Si-Fe grain boundary demagnetizing fields, domain struct., high speed Kerr cinematography 44566 0-44566

aerial colour rel. to remote sensing of ocean bottom detail and water depth penetration 0-62897

penetration 0–62897 application to electron microbeam probe samples, comments 0–49161 astrophotography at Flagstaff Station 0–41873 close-up, stereo lunar surface, Apollo 11 and 12 0–76622 Lippmann method for undergrad. lab. 0–73361 multispectral, agricultural and oceanographic applications 0–52401 spatial-frequency coding implementation features 0–70042 xerographic reproduction 0–70137

high-speed at A.W.R.E., research activities 0–52399 application, apparatus, technique, review 0–38580 camera for dense plasma diagnosis 3–52398 cameras with image intensifier tubes 0–52397 droplet formation obs., 20 kHz ultrasonic atomisation of oil 0–78248 electrical contact breaking events obs. using ultra high-speed camera 0–63739

0-63739
electron camers, employing close focusing shutter tubes 0-52395
electronic photoflash meter 0-57594
electronics systems applications, development limitation 0-52392
electronics systems applications 0-52393
geological fault displacement and motion studies 0-41465
image blur, illuminated by light flashes 0-57645
image blur of fast moved objects illuminated by light flashes 0-70131
Kerr effect shutters in high-speed applications 0-52396
objective lenses, design and fabrication 0-57646
schlieren images, optical system for recording 0-45818
spectrograph shutter, 70 m.sec⁻¹ event triggered 0-73358
time function in electron cameras 0-52394

Photoionization
acetylene, yields, isotope effects 0-70964
alkali metal atoms, review 0-58105
amorphous state, recombination luminescence following photoionization
0-72408

atomic beams, polarized alkali, rel. to production of polarized electrons

atoms, one- and two-electron, theory and exptl. investigations 0-52935 benzene, angular distribution of free electrons released 0-52928 benzene, angular distribution of free electrons released 0–52928 computer program for calc. of cross sections for atomic systems with (np)² configuration 0–74131 double, threshold behaviour 0–52956 heavy atoms, resonance widths 0–74134 n-hexane, rel. to photoinduced conduction 0–64949 liquids and solutions, potential measurement apparatus 0–50257 methane, angular distribution of free electrons released 0–52928 molecules, polyatomic, temp. depend. of cross section 0–43073 nitrobenzene, ionic relaxation 0–68145 propene, yields, isotope effects 0–70964 propyne, yields, isotope effects 0–70964 rel. to resonance lamps, rare gas, quantum yields ane extinction coefficients 0–42391 solids, potential measurement apparatus 0–50257 two-quantum, role of highly excited triplet mols. 0–72551 Ar., angular distribution of free electrons released 0–52928 Ar., cross-section, many-body corrections 0–60967

two-quantum, role of highly excited triplet mols. 0–72551
Ar, angular distribution of free electrons released 0–52928
Ar, cross-section, many-body corrections 0–60967
Ar double photoionization, resonance mechanism 0–64227
Ar final-state correlation effect 0—70779
C,C+,N,N²+,O,O³+,Ne,Ne²+ cross sections, atoms and ions 0–70775
Cs, polarization effect 0—74130
Cs, polarization effect 0—74130
Cs atoms, photoionization in first excited state 0—77669
Fe (CO), fragmentation process studied 0–64400
GaP-Te, absorpt, spectra obs. 0—76101
H,O angular distribution of free electrons released 0—52928
He and He-like ions, Resonant photoionization calc, method 0—74188
K, polarization of the atomic core, effect on the oscillator strengths and photoionization cross-sections 0—60923
Li, cross-section, polarized orbitals method 0—64228
Li, polarization of the atomic core, effect on the oscillator strengths and photoionization cross-sections 0—60923
Na isoelectronic sequence, cross-section calc. 0—64229
Ni(CO), fragmentation process studied 0—64400
S-photodetachment cross-section above threshold, obs. 0—78159
Xe, angular distribution of free electrons released 0—52928
Xe atom final-state correlation effect 0—70779
Xe atom in plasma, threshold investigation 0—67895
Xe²+ direct production cross-section obs. 0—60968
Xe³+ direct production cross-section obs. 0—60968
Xe³+ direct production cross-section obs. 0—60968
Xe³+ direct production cross-section obs. 0—60968
Ty, double ionization, threshold behaviour 0—52956
Zn²+ direct production cross-section obs. 0—60968
Type of the production cross-se

air, rel. to breakdown calculations, exp. meas. 0–64768
atmosphere, upper, photoionization rate of O, O₂, N₂ temp. depend.
0–51576
benzene, photoionization resonance obs. 0–61373
chamber, at high density, theory 0–63888
at laser beam focus, anomaly in multiphoton ionization rate 0–61358
methyl halides, valence-shell ionization potentials by photoelectron spectra
0–55360

u=35380

Ar, cross-sections for Slater-Klein-Brueckner potential 0-67638

Ar photoelectron angular distrib. obs. 0-61366

C atoms, cross sections for Slater-Klein-Brueckner potential 0-67638

H - free-free absorption coeff. calc. from adiabatic exchange wave functions 0-78157

H₂, correlated pseudopotential treatment 0-64765 H₂, Ly-β geocoronal irradiation influence on electron density in E-region 0-56842

H₂ autoionizing states, photoelectron spectroscopy 0-61377 H₂ photoelectron angular distrib. calc. 0-61370

H₂ photoelectron angular distrib. calc. 0–61370
He, interstellar, cross section 0–63076
Hg atoms, 10.5-72 eV 0–52947
Kr photoelectron angular distrib. obs. 0–61366
N atoms, cross-sections for Slater-Klein-Brueckner potential 0–67638

Photoionization continued

gases continued

Reses continued

N₂, rel. to breakdown calculations, exp. meas. 0–64768

N₃ autoionizing states, photoelectron spectroscopy 0–61377

N₄ photoelectron angular distrib. calc. 0–61370

NH₃ and ND₃, photoelectron spectra using molec. beams 0–58186

NO[†] photoionization resonance obs. 0–61373

O atoms, cross sections for Slater-Klein-Brueckner potential 0–67638

O₂, rel. to breakdown calculations, exp. meas. 0–64768

O₂^{*}, vibrationally excited, production by solar u.v., effect of autoionization 0–77826

O₃(2₂-), validity of Franck-Condon factor for photoionizing transitions

0–74297

Xe photoelectron angular distrib. obs. 0-61366

Photolysis see Photochemistry

Photomagnetic effects see Photoelectromagnetic effects

Photomagnetoelectric effects see Photoelectromagnetic effects

otomaters
see also Spectrophotometers
actinometer, digital, using thermistor bridge 0-73308
colour spot, for colour TV studio 0-38551
electronic photoflash meter 0-57594
electrophotometer for obs. of ozone content in atmos. 0-77197
with graduated light source, industrial use 0-77196
iris, automatic determ. of radial luminosities 0-67156
laser, for particle size measurements 0-57597
light scatt., low angle, design 0-54919
luminous efficiency meter for Ar-electric arc, on-line meas., analogue method 0-49119
microphotometer, recording, double-beam, design and operation 0-73309
photoelectric; dual-channel, for stellar observations 0-45834
photon-counting, for light scatt. meas. in optical bulk glass 0-67157
polarization, use of analogue cct. for meas. 0-63687,
for skylight polarization, spectral distribution, automatic 0-79540
small area, sensitive, description 0-54918
Sofica, light scattering from cylindrical cells 0-73307
stellar, synchronous three-colour 0-6298
ultraviolet, 100-1300 A wavelength region, for space research 0-76424
universal automatic integrating instrument 0-54920
for winds, high altitude, daytime meas. using Li trails 0-76414
otometry

Photometry see also Brightness; Densitometry; Illumination; Spectropho-

see also Brightness; Densitometry; Illumination; Spectro tometry of HD 211853, binary, Wolf-Rayet eclipsing 0–63055 atmospheric constituents vertical distri., method description 0–59599 aurora, far u.v. photometry from OGO 4 0–48307 binary star detection 0–41703

calibration of direct photographs of star field using calcite polaroid filter 0-59812

detectors, e.m. field effects statistical optics considerations 0-63692

detectors, e.m. field effects statistical optics considerations 0-63692 filter error calc., simple mathematical model 0-77195 flame photometric determinations of diff. coeffs. 0-61422 flux losses by diffraction 0-63695 H α , obs. of galactic H II regions 0-79644 i.r., narrow-band, obs. of α -Ori 0-72717 integrating sphere, effect of centrally, located samples 0-42378 introduction, university textbook 0-38525 late-type spiral galaxies, angular momentum calc. 0-56976 line-blanketing effect on indices of uvby β photometric system 0-41667 luminance, inhomogeneous, visual acuity in separate fields of adaptation 0-60375 luminance coefficient, payements, aperture of illumination and observation

luminance coefficient, pavements, aperture of illumination and observation 0-57595

0-3793

rel. to luminescent screens, book 0-44935
photocathodes sensitivity variations, long-term 0-65857
retro-reflective, for screen efficiency evaluation 0-60376
retroreflective, for screen efficiency evaluation analytical treatment

star size and colour obs., variables 0-79660 stellar photographic photometry, appl. of fibre optic image intensifier 0-48622

0–4802 surfaces, rough, average height of microirregularities determ. 0–61614 two-colour, obs. of Wolf-Rayet binary (CV Ser) 0–63054 UBV, of β -cephei type variable stars, γ Pegasi 0–63000 of weakly scattering objects 0–42379 H_{β} and four-colour photometry of B and A stars, calibration 0–56949

light sources automobile headlamp, illumination test employing TV camera 0-60374 fluorescent lamps, considerations and measurements of luminance distribution 0-57596

laser, pulsed, for shadow instruments 0-45846 photometric error analysis, enriched energy calc. for annular apertures

o-03073 temperature scale derivation, Planck's equation application, gold melting joint determination 0-38419 Ar arc lamp, luminous input and output efficiency, Hall-effect multiplier, Se cell, applic. 0-49119

Photomultipliers

area sensitivity, effect on obs. of integrated spectral line intensities 0-73182

channel, straight, ion feedback, exptal. obs. 0-77046 current mag. modulation using solenoid and e.m. modulators, results 0 - 49009

0-49009 dynode, GaP, gain variation 0-49012 dynode high-gain, statistics and timing of first photoelectron 0-62472 electron, efficiency for H atom detection 0-77414 electron, response to H atoms in 30 eV to 10 keV energy range electron current control 0-42222 electron with separated dynodes and magnetic focussing, construction description 0-49008 fast high gain small, tube for scintillation counter hadrens.

fast, high gain, small tube for scintillation counter hodoscope arrays 0-42647

0-42047 gamma-ray counter using far-u.v. photomultipliers 0-49391 for high speed physics, new design 0-60177 hybrid Cockroft Walton multi-dynode, power supply for space applica-tions 0-63584 i.r. laser as point detector for sensitivity and high speed 0-47895 noise reduction when used to detect ultraweak light fluxes, 200-850nm 0-5225

Photomultipliers continued

operation in heterodyne detection mode, optimization employing external electrode 0-73183

parallel-plate, channel, for use in electron spectroscopy 0-60179 photocathode quantum yield, temp. coeff. determ. 0-47899

pulse's time fluctuations investigation using plastic scintillators 0-49011 quantum efficiencies >50% from commercially available type 0-42223 RCA 31000E, photocathode quantum efficiency enhancement at 6328 Å 0-67037

0-67037

S/N ratio of 4 light detection systems, theoretical and exptl. 0-42392 single electron, improving signal to noise ratio 0-60180 spectral sensitivity as function of voltage and ir. illumination 0-38473 spurious response following short intense over-exposure 0-77047 statistics, edge effect 0-57497 time and threshold characteristics investigation 0-49010 tubes, new developments 0-60178 weak light pulse meas, by photoelectron counting 0-45770 XP1021, time resolution meas, with differential time-to-amplitude converter and compensator 0-49371 GaP(Cs) dynode, recent developments 0-60176

Photons

see also Cosmic rays/photons; Gamma-rays; Nuclear reactions and scattering due to/photons; X-rays absorption, in photodecomposition of bis-crosslinking agents 0-70198 absorption, multiphoton, field correlation effects 0-42989 atomic excitation, rel. to spectroscopy of excited states 0-52934 beam, polarized, obtained from diamond crystal subject to electron beam 0-45875

bunching effect, extended, glauber theory calc., spectroscopy application 0-38571

0-38571
count distribs. for lasers near threshold 0-42253
counter, crystal with N impurity centres superradiation, emission of coherent signal with intensity N² 0-60192
counting, correlation functions in critical region 0-63591
counting, treatment by noise covariance function method 0-77057
counting distribs., relaxed and triggered, for laser and pseudo-thermal sources 0-38487
counting fluctuations, digital, autocorrelation, statistical, accuracy

fluctuations, digital autocorrelation, statistical accuracy

counting photometer for scatt. meas. in optical bulk glass 0-67157 counting photometer for scatt. meas, in optical bulk glass 0–67157 counting statistics of harmonic signal mixed with thermal light 0–69867 counting techniques, in intensity correlation of optical non-linear processes 0–63672 decay, two-photon, of metastable He ions 0–52986 detection using high vacuum gas discharge in e.s. field 0–60700 dose rate, residual, around high energy p accelerators 0–38773 dose rate, residual, reduction, around high-energy proton accelerators 0–57861

0–57861 fourth order radiative corrections to electron-photon vertex 0–42475 gauge invariance with non zero bare mass 0–67222 in insulator, simultaneous propag, with phonons 0–68571 mass, and light vel. freq. depend. test using pulsar emission, and photon mass, obs. 0–38522 model, based on broken symm. 0–38609 monochromatic beam by positron annihilation in cyclic accelerators 0–3863

0 - 38623

0–38623 noise spectrum, Bose-Einstein statistics continuity 0–57424 nuclear transitions, angular correlation of 1st and nth linearly polarized photons in a cascade 0–49489 optical field autocorrelation function from photon counting statistics 0–69868

0-69868
origin, investigation within framework of Goldstone theorem 0-67198
phase meas., probability distrib. 0-73196
photon-matter interaction energy relationship to refr. index 0-52348
photons tachyons in Fresnel evanescent wave 0-48697
positrons (monochromatic) annihilation in flight, photon spectrum computer calc. 0-38634
radiation model development and comparison of photons and wave models 0-45813

models 0–45813
scattering, by phonons, under condtions of stimulated induction 0–45775
source of circularly polarized photons: scattered low energy polarized proton beam 0–42469
spin inertia effect 0–49107
spititing in strong magnetic field 0–73439
spititing in strong magnetic field 0–73439
spititing of single photon into two obs. (parametric fluorescence) 0–60191
statistics and counting 0–45774
statistics of Gaussian light scatt. by Gaussian medium 0–67043 transitions, spontaneous two-photon, in H and He 0–52974
transport calc., Monte Carlo programs 0–72853
two-photon absorption of tumbling molecules, polarization depend. 0–55267
two-photon counting distrib. for modulated laser beam 0–60251
two-photon transitions, effect on frequency and threshold of two-frequency generation 0–52261
ultra-weak light fluxes 200-850 nm, reducing photomultiplier noise 0–52255
virtual, timelike, emitted in hadron-hadron collisions, helicity 0–38620

0-32233 virtual, timelike, emitted in hadron-hadron collisions, helicity 0-38620 virtual-photon mass limit, gauge invariance condition 0-77257

virtual, timelike, emitted in hadron-hadron collisions, helicity 0–38620 virtual-photon mass limit, gauge invariance condition 0–77257 X ray tube, flash, photon energy spectrum determ. 0–48661 n-Ge-Te, irrad, effects on carrier conc. 0–44249 NH₄H,PO₄ splitting of single photon into two obs, following optical pumping 0–60191

interactions

baryon-antibaryon pair production 0–57810 with cosmic rays, very high energy, decomposition and energy degradation 0–59680 forward Compton scattering and photon-proton total cross-sections 0–52432

kinematical struct, by vector dominance model 0-42467

kinematical struct. by vector dominance model 0–42467 linearly polarized, for vector meson photoproduction, associated with vector meson dominance model 0–60597 M-functions, antisymmetric tensor wave functions 0–38622 meson production, resonance obs. method 0–45914 multibody photoprod. between 2 and 16 GeV 0–45874 neutral-boson photoprod. on hydrogen, at high energies 0–42516 nuclear photoprocesses associated with vector meson dominance 0–60596

pair producing collisions with high energy cosmic rays, energy loss 0-55074

Photons continued

interactions continued

photon absorption cross section on hadrons, vector dominance and sum rule 0-70196

photon-neutrino weak coupling for weak interactions 0-38619 photoproduction, inelastic, for muon pairs, Compton terms 0-49210 photoproduction, multipion, hyperons and K^0K^0 channels in π -p interactions 0–52517

photoproduction and ρ⁰-ω interference 0—49287 photoproduction of charged pions, vector dominance for high energy exchange reactions 0—49260

photoproduction of vector mesons, relative phase angle for leptonic decay 0-5231 photoproduction process, absence of fixed poles, compositeness of external particle 0-73508

photoproduction sum rules, quark model 0-73442

photoproduction sum rules testing operator Schwinger terms 0-42470 pseudoscalar mesons photoproduction and vector meson dominance 0-60595

O-60595
QQQ model for photoproduction processes 0-52430
vector mesons e.m. prod. 0-52532
vector-meson photoproduction, phase calc. 0-73606
weak, with neutrino bremsstrahlung, cross section 0-77256
A,º photoproduction on proton, PCAC, Dalitz process and Primakoff
effect 0-73611
d, photodisintegration, 220-340 MeV 0-49318
Δ(1238) isobar photoproduction 0-77377
e-e+ photoproduction, 2.3 and 5.6 GeV 0-57711
ey in intensive flux, time delay and saturation 0-52442
pd photoabsorption cross-section meas. 3.7-17.9 GeV 0-73440
pd processes and existence of exotic states 0-57697
yd→NPx, three body final state, relativistic corrections 0-52511
pd→npa, asymmetry of yields compared with np→pd, induced by T-violation 0-45967
yd→ppp-, between 1 and 5 GeV 0-63837

γγ→e⁻e⁻e⁺ 0−60506

 $pp \rightarrow e^+e^-$, polarization phenomena, proposal for expt. study 0–52431 $pN \rightarrow N\pi$ high energy backward reactions and the strong-cut Reggeized absorption model 0–52522

 $pn\to \rho^-\rho$ cross-section rel. to vector meson exchange 0—52532 $p^+N\to \rho^+\Delta$, minimal gauge-invariant one-vector-meson-exchange model 0—52564

0-52564
γNN+, π electroprod, vertex momentum-transfer depend. 0-42538
γN, diffractive two-pion production, dual reson, anal. 0-52506
γp, photoabsorption cross-section meas. 3.7-17.9 GeV 0-73440
γp→Δ⁺⁺π⁻, study at 2.8 and 4.7 GeV, cross-sections, Δ⁺⁺ parity asymmetry 0-77376
γp→K⁺Λ, 1. GeV range, differential cross-sections and Λ polarization 0-67273
γp→K⁺Λ, 1.3-1.45 GeV meas. cf. with Regge-cut model 0-77259
γp→K⁺Σ⁰, 1.45 GeV meas. cf. with Regge-cut model 0-77259
γp→K⁺Σ⁰, diffractive kaon photoproduction, dual resonance model 0-49244
γp→N⁺γπ⁻, decay N⁺⁺→γπ⁺ and spin-3/γ polarisation 0-52562
γp→Nπρ, Nππρ, 0.3-5.8 GeV, cross-section obs. for ρ production

 τ^- , decay N*++→p π^+ and spin- 3 /2 polarisation 0-52562 Nππρ, 0.3-5.8 GeV, cross-section obs. for ρ production

0-30021 pp→pp, differential cross section at 4 and 6 GeV 0-77297 pp→pη, quark model classification of I=1/2 nucleon isobars 0-60622 pp→pω, 2.8 and 4.7 GeV, cross section 0-49194 pp→pπ^α differential cross section at photon energies 4.0 and 5.8 GeV 0-49261

0-49261
pp-ppθ, E_p=2.8 and 4.7 GeV, conservation of s-channel helicity 0-38705
pp-ppθ, E_p=2.8 and 4.7GeV, linearly polarized photon beam, cross sections 0-38704
pp-π Δ+* 16 GeV, cross-section meas. 0-73441
pp-πθp Prod. analysis, E_p<500 MeV 0-55038
pp-πθp Regge cuts due to absorption, numerical study 0-67277
pp-πτΔ*, 16 GeV, cross-section meas. 0-73441
pp-πτβ, 5 and 16 GeV, measurement of asymmetry in produced pions 0-73563

0-/3563 $pp\rightarrow\pi^+n$, Reggeized $U(6)\otimes U(6)\otimes O(3)$ and absorption model 0-57696 $pp\rightarrow\pi^+n$ with linearly polarized 3 GeV photons, natural parity exchange dominance 0-73564 $pp\rightarrow\pi p$, s^2 dependence of differential cross section and asymmetry ratio 0-52475

0-324/5 $pp-\rho^0$ p, determ. of $\rho\pi\gamma$ coupling const. 0-70264 $pp-\rho^0$ p cross-section rel. to s-channel resons. 0-52532 $pp\phi p\pi^+\pi^-$, photoproduction in 2.6-6.8 GeV 0-60508 $p\pi-\Delta\pi\pi$ in Veneziano model and π^0 lifetime 0-57801 $pp-\Delta\pi\pi$, $\Delta\pi\pi\pi$, $\Delta\pi\pi\pi\pi$, to 5.8 GeV, cross-section for Δ production obs. 0-38621

008. 0–38621 $\gamma \rho \rightarrow 0.3621$ $\gamma \rho \rightarrow$

Photons continued

interactions continued

7 photoproduction, phenomenological model with diffr. correction 0-49262

 π photoproduction, polarization theorems 0-73572

π photoproduction, polarization theorems 0—/35/2
 π photoproduction on p, polarized photon cross section asymmetry, 230-380 MeV 0—55037
 π0, photoproduction at backward angles, Regge analysis 0—52510
 π⁺, photoproduction, at backward angles, Regge analysis 0—52510
 π[±] photoproduction, cross-section behaviour 0—42543
 π[±] photoproduction from hydrogen at backward angles in the energy range 1:3 GeV 0—52509
 π⁰ photoproduction on N, dip structure mechanism, Regge theory confirmed 0—60574

1.3 GeV 0—52509

π° photoproduction on N, dip structure mechanism, Regge theory confirmed 0—60574

πΔ photoproduction and conspiracy relations 0—49314

ρ neutral photoproduction from complex nuclei 0—60603

ρ photoproduction from C and H at 3.5 GeV 0—63838

ρ°, photoproduction, anomalous real parts in T matrices 0—63839

γπ→π°n, photoproduction of neutral pions at 500 900 MeV, differential cross-sections 0—52507

γN→π²N, quark model explanation 0—57774

Li photoproduction of neutral pions 0—55043

polarization

polarization two-photon absorption of tumbling molecules, polarization depend. 0-55267 $pp-\pi^+n$ with linearly polarized 3 GeV photons, natural parity exchange dominance 0-73564 τ photoproduction, polarization theorems 0-73572 Ge(Li) detectors, single planar, as gamma-ray polarimeters 0-73688

backscatter energy calc. 0-70200
commutators of current-density operators, asymptotic expansion with fixed negative photon mass squared 0-57698
Compton, by polarized electrons, radiative correction calc. 0-73443
Compton energy exchange, relativistic 0-57708
dose transmission and reflection probability, 0.2-10.0 MeV obliquely incident on concrete barriers 0-54488
four-photon, in resonant medium 0-54901
linear optical birefringence effects on polarization density matrix 0-42375
linewidths, Hameka theory 0-38189
multiple scatt., polarization and frequency change 0-70194
multiple scatt. of Compton photons, depend, on cylindrical scatterer size 0-42811
photon-neutral scalar particle, differential cross-sections calc. by gravita-

photon-neutral scalar particle, differential cross-sections calc. by gravita tional interaction 0-60509

photon-photon, differential cross-sections calc. by gravitational interaction 0-60509

tion 0-60509
photoproduction rel. to diffractive features at high energy 0-60510
polarization density matrix description of optical birefringence incorporat
ing non-linear phenomena 0-38548
polarized scatt., in nuclear field, with prod. of e⁺e- pair and several photons 0-77260

tons 0-77260
Reggeized pole approx. 0-49198
pp elastic scattering, amplitudes close to forward direction, quantum electrodynamic explanation 0-60506
pn, cross-section evaluated, Regge pole fits, 3.7-17.9 GeV 0-73444
p Compton scatt., in terms of quark model 0-70257
H atom, at resonance fluorescence 0-43022
Photonuclear reactions see Nuclear reactions and scattering due to/photons

Photophoresis No entries

Photoproduction see Gamma-rays/effects; Nuclear reactions and scattering due to/photons; Photons/interactions

Photoresistors see Photoconducting devices; Semiconducting devices

Photosphere see Sun

Photovoltaic effects

CdTe, effect of thermal treatment, 450°C max. 0–62466 cells, surey 0–47010 dibenzothiophene and its molecular complexes, exp. investigation 0–72141

epitaxial films, rel. to investigation of layer parameter reproducibility 0-78377

on the parameter reproductionary of the parameter reproductionary 0-78377 opto-electronics, review and prospects 0-69814 organic semiconductors, wavelength depend. 0-72145 photocell, magnesium phthalocyanine, characts. 0-72146 semiconductor, graded band gap 0-44403 semiconductor, prinsb, surface response 0-62465 semiconductor, optical ioniz. cross sections determ. 0-75844 Ag.S layers, contact potential effect 0-75841 n-CdS-p-Cu_{3-x}S, solar converter, long-wave sensitivity 0-75842 CdS-Cu_{3-x}S cells, preparation and properties 0-47883 CdS solar cells, simulated space environmental tests 0-48973 Cu₃S-CdS heterojunctions, mechanism and obs. 0-56401 Cu₃S-CdS heterojunctions, heat treatment effect 0-75843 GaAs diodes for low irradiance use 0-72144 GaP, optical ioniz. cross sections determ. 0-75844 n-InSb surface response 0-62465 Pb₂Sn_{3-x}Te detectors for 8-14μ atmospheric window, spectral response 0-52987 Se, amorphous, short-range order influence 0-72138

Se, amorphous, short-range order influence 0–72138
Si:Au, donor level effect 0–44404
Si:Au, intrinsic photovoltaic effect 0–75846
Si:Au acceptor centre, rel. to recombination- generation, 200-300°K
0–44892

0 -44892
Si, solar cells with titanium-silver contacts, environmental tests 0-42165
Si solar cells, effect of annealing rel. to radiation damage obs. 0-75121
Si solar cells, radiation-hardened, recovery by lithium 0-57481
Si solar cells, radiation damage obs. 0-75122
ZnS, growth atmosphere effects 0-79087
ZnTe film, polarity, substate depend. 0-47882

Physical chemistry
alkaline earth metal dimers, equilibrium properties, calculation 0-74230
geo-, in book on physics of the earth 0-45200
Hammett linear free energy relationships tested for foran and thiophene

0-51419

pyrolysis, surface, mass transfer induced in multicomponent gaseous boundary layer 0-66164

Physical chemistry continued

relaxation method of studying vacancies in metals under quasiequilibrium conditions 0–47223 stochastic processes in chemical physics, book 0–51959

Physical effects of radiations see also Under individual radiations, e.g. Neutrons and antineutrons/

see also Under individual radiations. e.g. Neutrons and antineutrons/effects
alkali halides films, exoelectron emission 0–65863
alkali halides, far u.v. irrad., F centre prod. 0–50614
alkali halides, radiation colloids 0–58793
amorphization of Ge due to ion irradiation 0–62243
azides, paramag. defects prod., excitons role 0–79406
b.c.c. metal, α-Fe, defect annihilation and clustering effects on displacement spike annealing 0–47230
channelling and blocking, ion camera for spatial distribution 0–53492
charge carriers, radiation- produced, recombination 0–62229
charge carriers produced by u.v. 0–59817
charged particles, fast, density effect in ionization energy loss 0–62234
chloropropene rubber, effect of u.v. irradiation on structure 0–50344
chlorosodalite, photochromism, mechanism from optical data 0–76096
coated-particle irrad. testing, microsphere test particle prep. 0–62112
coatings, thermal control, degradation due to u.v. irrad. 0–39941
creep, non conservative-volume type, relationship under different states of stress 0–55983
crystal, photon emission by fast charged particle scatt. 0–66117
degradation i.r. detector by sky radiation 0–62463
degradation of m.o.s. structures and transistors, mechanism and its validative transparent, destruction by alsers's impulse duration, dependence

degradation of m.o.s. structures and transistors, mechanism and its validity 0-47808 dielectric transparent, destruction by laser's impulse duration, dependence on threshold energy 0-53915 dielectrics, organic liquid, radiation-induced conductance 0-64953 diodes, gated, neutron irrad., lifetime parameters and I-V characts. 0 47789

e.m., stress-wave generation in temperature-dependent absorbing solid 0-69699

0-9699
lelectrical insulating materials 0-59246
electrification of solids by gamma radiation 0-71881
electron, proton and u.v., thermal control coatings, spectral reflectance changes meas. 0-50912
electron beam modulation by light wave 0-54842
fracture-safe pressure steel vessel design, obs. at 288°C and 393°C 0-49716

glass, irradiated and etched, temporal dependence of fragmentation mode 0 - 68666

glass, radiation-induced colour-centers, review 0-61978

0–68666
glass, radiation-induced colour-centers, review 0–61978
glass dosimeter perturbation by radiation-induced fading 0–49394
heat transfer, laminar, in a circular tube under solar radiation in space,
temp. distrib. and Nussel number variation 0–66937
i.r. stimulating radiation in CaS, SrS phosphors 0–56588
inert gases, damage in pure gold thin films 0–62240
insulating materials, effects of steady-state radiation 0–56345
ion processing and penetration characteristics, device using differential
pumping system, design 0–57860
ionizing, degradation phenomena of bipolar and m.o.s. transistors, theoretical model 0–47800
ionizing, on thermally oxidized Si surfaces 0–68845
irradiation damage in glass, ion-beams effect 0–49132
laser beam self trapping and damage in transparent glass, electrostrictive
transient and steady state 0–72305
laser irradiation, laws governing ejection of material 0–61308
liquid structure induced by non-linear interaction with high-intensity ruby
laser beam 0–71346
lunar samples, rock, breccia and soil, radiation weathering 0–48524
macrosonic deformation processes, physical phenomena 0–65529
maraging steel, ductility and tensile properties changes obs. 0–50768
mechanical properties changes, Charpy V and tensile specimen testing, in
Big Rock Point Reactor 0–49717
metal, irrad-, point defects aggregation, chem. reaction rate theory applic.
0–68330
metal ball, uniform activation, irradiation using cyclotro 0–53726
metal damage by high-speed pulsed plasma iets 0–53726

metal hall, uniform activation, irradiation using cyclotron 0–53726 metal ball, uniform activation, irradiation using cyclotron 0–53726 metal damage by high-speed pulsed plasma jets 0–53728 metal surface, exo-emission efficiency, light radiation effect 0–72148 metalls thin layer destruction by laser radiation, threshold formula derivation 0–53724 on metals, growth and stability of voids 0–75424 metals, review of damage, techniques, Frenkel defects 0–59118 in metals, void formation and creep, neutron bombardment 0–68341 mica, etching, pore growth 0–39994 microelectronic circuits in reactor radiation 0–74079 Mylar, corona charged, thermal currents 0–47823 naphthalene derivatives with carbonamide group, luminescence excited by u.v. irradiation 0–43176 nuclear e.m. cascades in glass, iron and tungsten absorbers 0-59119 optical surface degradation from combined u.v. radiation o–54907 optical surface degradation from combined u.v. radiation sed units of the combined of the combined

0–54907
optical surface degradation from combined u.v. radiation and outgassed materials, further comments 0–54908
particle tracks. charged, in solids, review 0–40613
perovskite type cpds, coloration by light, book 0–68293
photographic layers, mechanism of interaction 0–63734
photomechanical effect, annealing, ambient atmosphere effect 0–75289
point contact, superconducting, irrad., I-V characts. 0–51017
polyethylene, branched, radiothermoluminescence 0–41282
polyethylene, u.v. irradiated, free radical formation, pressure dependence 0–33095
nolymers, creen and electrocond, rel. to intensity and temp. 0–50706

0–53095
polymers, creep and electrocond. rel. to intensity and temp. 0–50706
polymers, organic, radiation induced trapped charge carriers and thermoelectric current generation model 0–47865
polypropylene, isotactic, radiothermoluminescence 0–41282
pulsed ionzing, on laser action in YAI garnet:Cr-Nd 0–42300
pyrrone polymer, elec. characts. 0–47634
quartz, coloured synthesis 0–74966
RNA mol., irrad., limiting proportions of hydrations 0–66205
RNA molecules, dimer equilib. distrib. 0–43200
radioactive source, rel. to lightning stroke path 0–45155
radioluminescence buildup kinetics, indistinguishability of electron-hole and
exciton processes 0–56583
resistivity variation, ion bombarded, thin metal layer 0–62294
Rochelle salt, absorpt. spectra, 220-1500 nm 0–51318

Physical effects of radiations continued

rubber, chloropropene, effect of u.v. irradiation on structure 0-50344 on ruby laser 0-77118

semiconductor, photocell, ²³⁵U coated, neutron irrad., short-circuit currents 0--51156

semiconductor, radiation damage 0–75714
semiconductor, radiation ionization energy and Fano factor 0–78926
semiconductor devices, neutron hardness assurance, irradiate-anneal
screening, technique without reliability degradation 0–47777
semiconductor devices damage 0–75738
semiconductor fissionable material coated, neutron bombard., e.m.f.

0 - 47692

0-47692 semiconductor junctions, high-low, damage math. simulation 0-47782 semiconductor lattice disorder, penetration depth ionic bombardment, channeling technique, thickness of amorphous region 0-62363 semiconductors, binary, ion implantation damage 0-62362 slip band growth mechanism in irrad. crystats 0-40172 solar arrays output power, charged-particle irradiation effect, computer program 0-48979 colid discoluted has capture by moving hubble 0-43690

program 0-45/19 solid, dissolved gas, capture by moving bubble 0-43690 solid, nuclear bombardment research techniques 0-68667 solid solution, nucleation stimulated by non-equilibrium electrons 0-78801

solid solution, nucleation stimulated by non-equilibrium electrons 0-78800

solid-radiation interaction obs., scanning electron microscopy applics., conf., Chicago, USA, April 1970 0–68276 on stainless steel, mechanical props. and dimensional stability 0–68531 steel, stainless, austenitic, growth mechanism of voids in fast reactor irradiated material 0-53725

steel for nuclear reactor pressure vessel, testing in Big Rock Point Reactor 0--49715

surface transparency destruction of dielectrics (K-8 glass), by laser beam 0-65562

thymidine, e.p.r. of radiation damaged deuterated cryst. 0–59461 transistors, GaAs junction FET's, neutron irrad., degradation of props. 0–47798

u-v-1788 u.v. on electrodes, glass and Ag-AgCl 0-66198 u.v. on electrodes, glass and Ag-AgCl 0-66198 AgCl:(Se,Cd), e.s.r. of Se⁻ centre, hyperfine interactions 0-44982 AgCl-Mn phosphors, red and blue luminescence, temp. and i.r. radiation effects 0-54128.

effects 0-54129 Al, energy deposition by electron beams, dynamic response meas., laser interferometer method 0-59126 Al, quenched, void form., preinjected helium effects 0-68345 Al, Zn segregation to vacancy sinks 0-71608 Al film, secondary electron emission, fission fragments and α -particle reflection 0-40915 As,Sq. (Realgar) powder, u.v. irradiated, transformation into orpiment 0-59446

As_{3.84} (Kealgar) powder, u.v. Irradiated, transformation into orpiment 0-59446 Au coherent film light-activated deposition, patent 0-78388
Ca halophosphate luminophors, colour centre formation under X-ray, u.v. irradiation 0-55903
CaCO₃, artificial calcite, optical spectra, morphology 0-78398
CaS phosphor i.r. stimulated emission and trapping center depth 0-56588
CaWO₄:Cu, u.v. irrad., paramagnetic centres, thermoluminescence glow peaks 0-79377
Cd, irrad., damage prod., low temp. 0-78542
CdS i.r.-induced emission of green luminescence in crystals 0-56591
CdSe-Se, photocell, ²³⁵U coated, neutron irrad., short-circuit currents, e.m.f. 0-51156
CsBr thermostimulated electron emission, thermostimulated concentration e.m.f., thermostimulated luminescence, and radioluminescence 0-56636
CsI thermostimulated electron emission, thermostimulated concentration e.m.f., thermostimulated luminescence, and radioluminescence 0-56636

e.m.f., thermostimulated luminescence, and radioluminescence 0--56636 Cu, characteristic X-ray generation by heavy particle irrad. 0-69566 Cu, irrad, slip band growth mechanism 0-40172 Cu film 300 to 1000Å, electrical conductivity, wavelengths 0.6 to 2.0µ

Cu, Irrad, stip band growth mechanism 0-401/2 Cu film 300 to 1000A, electrical conductivity, wavelengths 0.6 to 2.0μ 0-40706 Fe, b.c.c. low-temp, irrad, internal friction 0-68411 α -Fe, defect annihilation and clustering effects on displacement spike annealing 0-47230 Ge/anthraquinone, illumination of substrate effect on oriented crystallization of layer 0-78378 Ge amorphization due to ion irradiation 0-62243 KBr:Eu radioluminescence temp, depend. 0-56603 KCI:TI, colour centres, radiative creation, Coulomb interaction 0-40184 KCl, pure and Ag*, Sr2* doped, study of photothermal destruction of F centres 0-43688 KI, sputtering due to electron and u.v. irrad. 0-68709 LiF, e.p. r. and electron microscopy of Li colloids 0-41334 LiF, hardening, impurity effects, thermoluminescence, thermoelec, emission 0-50771 LiH:LiT, rel, to volume expansion due to tritium β -decay 0-47217 MgO, neutron irradiated, absorption bands with zero phonon lines 0-72363 Mo, b.c. low-temp, irrad, internal friction 0-68411

0-12363 Mo, b.c.c. low-temp, irrad., internal friction 0-68411 Mo, polycrystalline, effect on slip and twinning 0-40353 NH₄ halides, hydrazinelike defect production and characterization 0-78525

0-75148
NaCl, radiational defects, stored energy release during annealing 0-75148
NaCl, u.v. irrad., effect on breakdown and time lags 0-65783
NaCl monocryst., effect on attenuation of u.s. waves 0-65325
NaCl pure and Agr, Sr²⁺ doped, study of photothermal destruction of F centres 0-43688

Nb-Mo alloy, effect on slip and twinning 0-40353
Nb, polycrystalline, effect on slip and twinning 0-40353
Nh, halides, hydrazinelike defect production theoretical analysis 0-78526

Ni, substruct, changes due to fast moving air current 0-61949 pb, longitudinal development of electron initiated cascades, 0.5-4.0GeV energy range 0-62232

pbs photoresistor, effect of unmodulated illumination on voltage sensitivity obs. 0–75835 obs. 0-75835 Pt. dislocation cutting of depleted zones, activation energy, annealing effects 0-53541

α-Pu, self-irrad., length change 0-58827

Physical effects of radiations continued

ysical effects of radiations continued PuO_{1.7}, metallic inclusion formation at high burnups, electron microprobe analysis 0–71885 PuO_{2.0}, metallic inclusion formation at high burnups, electron microprobe analysis 0–71885 Se, ang. distrib. of annihilation quanta, illumination influence 0–62283 Si:Li, radiation damage, kinetic eqn. of annealing 0–61950 Si, average triton energy required for electron-hole pair prod. 0–47577 Si, crystalline perfection rel. to ion dose, depth below surface and annealing treatment 0–68350 Si, photocell, ²³⁹U coated, neutron irrad., short-circuit currents, e.m.f. 0–51156 Si lifetime degradation, electron irradiation by 2-MeV Febetron, sensitivity to sample surface. 0–51068 Si solar cells, radiation damage and annealing behaviour, impurities effect 0–69836

0-69834

0-69834
SiO₂, model for radiation induced paramagnetic defect 0-75191
SiO₂, model for radiation, change in thickness, optical props. 0-62604
SrS phosphor, i.r. stimulated emission and trapping center depth 0-56588
Tm₂O₃, sintered wafers, fabrication 0-58992
P-U-Mo fiel alloy, stability, thermal cycling 0-40467
U, quenched, fuel rods, radiation-induced growth 0-40011
U fuel rods, irradiated, mechanical props. 0-47383
UC, high temp, irradiation behaviour 0-78799
UN, high temp. irradiation behaviour 0-78799
UO₂, SiO₂, vitroceramics, high burn-up behaviour 0-39233
UO₂, high temp. irradiation behaviour 0-78799
UO₂, typt temp. irradiation behaviour 0-78799
UO₃, bigh temp. irradiation behaviour 0-78799
UO₄, typt temp. irradiation damage, annealing and bubbles formation

 UO_2 bombardment, radiation damage, annealing and bubbles formation 0-62244

w, vacancy loops, electron microscopy 0-61969 ZnO-type pigments, solar radiation damage, optical props. in u.v. and i.r. 0-41179

0-41179
ZnO film, u.v. degraded, elec. cond., Hall mobility, optical transmission 0-40778
ZnO powder, photodamage, e.s.r. 0-66143
ZnO pure single crystals, electrical props. temp. depend., effect of u.v. irrad. 0-47729
ZnS:Cu(Cl), phorphors, effect of i.r. on electrolumines. 0-41289

Physics

ssics see also Biographies; History; Nuclear physics; Teaching applied, expts. manual 0–41928 applied, training for technologist 0–63300 book, junior college attempting to explain concepts of physics 0–54530 book, multi-author dealing with an assortment of topics 0–57228 CAI in physics 0–72865 college introduction book for non-science major 0–45508 college introduction book for non-science major 0–45508 college introduction book for non-science major 0–65508

college introduction book for non-science major 0–45508 college introductory textbook for non-science major 0–57230 college level text-book for the non science major 0–54529 computer based instruction, anthology 0–41926 computer controlled experimenta and on-line analysis 0–62102 conference, Singapore Nat. Acad. Sci. Congress, (1968) 0–4864 conference on Advancement of Science, Montreal, Canada (1969) 0–41920 conference on mechanical analyses and the following the science of the sc

0-41920 conference on mechanical engineering, Haifa, Israel (1970) 0-72863 conference on theoretical physics, Syracuse, USA (1969) 0-63298 course, oriented to specific educational needs of Colombian students

0-48665
Czechoslovak Journal of Physics, in retrospect and comparison 0-48665
Czechoslovak Journal of Physics, in retrospect and comparison 0-48665
developments, in 20th century, review 0-63299
education and the use of computers 0-54528
forces, overlapping points of view 0-51883
game theory for introductory physics 0-41923
gnosiological problems 0-72864
high temperature of material, bibliography, April-June 1969 0-57194
high-energy, equations of motion applicability 0-63758
IEEE International Convention, New York (1970) 0-69571
and industry, review 0-45505
insect flight, physics and physiology 0-57159
interlingual scientific dictionaries, a bibliography 0-51885
introductory approach based on the conservation laws 0-54525
ionospheric, physical processes applicable to ionosphere, book 0-59648
journal, in retrospect and comparison 0-48665
language, informal, new, to describe relativistic quantum field theories 0-57658
and music 0-42080

and music 0-42080 perspective drawing using computers, spherical projection method 0-63282

0–63282 superconductivity, Resource Letter 0–56194 teaching, applic. of educational technology 0–38123 teaching by television to engineering students 0–41924 text book of modern physics 0–54531 theoretical, conference, Syracuse, USA (1969) 0–63298 undergraduate course, use of computer 0–76787 variational principles and techniques for solving radiation and scattering problems 0–63368

Physics fundamentals

see also Cosmology; Elementary particles; Field theory, classi-cal; Field theory, quantum; Indeterminacy; Mechanics; Parity; Probability; Quantum theory; Relativity; Thermodynamics;

astronomy and laboratory science, interaction 0–72862 axiomatics and computers 0–42012 causality, retarded, compatibility of faster than light particles 0–76805 causality violation, and faster-than-light group vels. 0–51930 conservation laws, geometrical derivation 0–51923 conservation laws 0–59945

conservation laws 0–59945
conservation laws rel. to invariant transformations 0–57303
Coulomb's law balance for physics majors and nonscience students 0–73125
e/h determ. using macroscopic quantum phase coherence in superconductors 0–71970
finite principle and concepts of time and space 0–66757
Machs' principle, compatibility with scalar-tensor theory 0–51924

Physiology
see also Biological technique and instruments; Blood; Hearing; Vision
barbituric acids, correlation between structure and action on central
nervous system 0-72373

electrostimulation of hearing, test results 0-63244

Physiology continued

eye's image quality performance, visual acuity, rel. to pupil size 0-72840 parameters normalization by potassium meas. of whole body 0–59824 vascular, lumped hydraulic impedance analysis of vascular bed 0–76725 diagnostics, y-ray cameras, design, isotope distribution changes recording 0–45455

Piezo-optical effects see Photoelasticity

Piezoelectric oscillations

accelerometer description 0–59867
accoustic microwave propag, in layered piezoelectrics 0–47524
acoustic surface-waves, nonlinear effects 0–47523
Bleustein-Gulyaev waves, generation, excitation efficiency 0–79054
crystal anisotropic, elastic layer modes propagation, symmetry consideration 0–65829

deflection of compound discs and single disc with passive metal carriers 0 - 47852

0-47852 disks, thin, microwave acoustic rearmances obs. 0-47854 ferroelectric, SbSI crystal, piezomechanical waves 0-56364 N-electrode piezoelectric bar, disturbances under electrical and thermal excitations 0-63418 piezoelectric plate thick, circular, response investigation interferometric tech applic, results 0-42069 plate, admittance formulation for parallel field excitation 0-68961 plates under perpendicular field excitation, admittance calc. 0-63416 potential pulse in piezoelectric plate, transient analysis 0-38376 quartz, acoustic surface-waves nonlinearities and third-order elastic consts. 0-47523 quartz, effect on scanning electron micrographs 0-68964 quartz bar, influence of vac. deposited electrodes on frequency 0-51126

quartz, effect on scanning electron micrographs 0—68964 quartz bar, influence of vac. deposited electrodes on frequency 0—51126 quartz plates, X-ray diffraction topography 0—68268 quartz vibrating at resonance, photoelastic props. rel. to synchronization of pulsed laser 0—47300 resonator, circular, electric equivalent circuit 0—51125 shells, cylindrical, vibrational analysis, significance of coupled solutions 0—52081 shells of revolution, vibration analysis, coupled theory, applic. to ferroelectric ceramic vibration analysis 0—52080 surface waves interdigital devices, diffraction pattern determination, method 0—45622 surface-wave propag, at piezoelec.-fluid boundary 0—50856

surface-wave propag, at piezoelec.-fluid boundary 0-50856 surface-waves parametric amplification in hexagonal piezoelecs,, theory

0 - 50876

0-50876 thickness vibrating plates, electromechanical coupling factors and fundamental material constants evaluation, effect of anisotropy 0-47848 CdS, electromech, coupling factors rel. to dislocations, obs. 0-47853 LiNbO₃, acoustic surface-waves nonlinearities and third-order elastic consts. 0-47523

sts. 0-47523
LiNbO₃-fluid boundary, surface-wave propag. 0-50856
LiTaO₃, length expander bars, zero temp. coeff. of resonant frequency 0-63417
PbZrO₃-PbTiO₃ solid solns, circular plates, contour oscillations 0-53948
SbSI cystal, piezomechanical waves 0-56364
SiO₂, quartz rod, torsional vibrations, overtones 0-79057
ZnO, heteroepitavial, on sapphire, fund. Rayleigh wave mode dispersive props. 0-59271
Revision and Lorent waves records above 0-47524 props. 0-59271 ZnS films an Al_2O_3 , Rayleigh and Lamb waves propag., obs. 0-47524

Piezoelectricity

see also Electrostriction; Piezoresistance
acoustic surface wave propag, and amplification 0–75386
acoustic surface wave propag, on cubic and hexagonal cryst. 0–56097
acouste-optical interactions in piezoelec. crysts, theory 0–51275
acoustoelectric device applications of piezoelectric and semiconducting thin
films 0–56103

films 0-56103 admittance formulation for parallel field excitation of plates 0-68961 amino-acid crystals, resonances study rel. to cryst. classes 0-40881 bender elements, effect of clamping and damping 0-72125 bone, in dry and wet state 0-68963 ceramic, ferro-(piezo)-ceramics, electrophys. parameters rel. to struct. parameters 0-65793 ceramic Pb(Zr,Ti)O₃, elec., piezoelec. and elastic props. field depend. 0-65843

coupled semicond.-piezoelectric system, conductance modulation 0–79053

crystal manufacturing 0-65176
crystal surface elastic waves, excitation, detection and dispersion 0-44374
crystal with divided electrodes, elec. response by Laplace transform
0-47850

cubic cryst., surface waves 0-47849 deflection of compound discs and single disc with passive metal carriers 0-47852

deformation of rotating inhomogeneous piezoelectric thick disc 0-42025

, deformation of rotating inhomogeneous piezoelectric thick disc 0–42025 N-dimethylisobutyramide and crystal growth 0–47855 e.m. scattering by cylinder 0–42132 elastic waves, calcs. 0–47328 elastic waves viscous absorpt, anisotropy 0–68596 elastodielectric interactions, invariant form of linear twin-property constitutive eqns. 0–65827 ferroelectric, temperature autostabilization region, piezoelec. nonlinearities applies. 0–65795 ferroelectric ceramics, effects 0–53947 ferroelectric ceramics, effects wave as h.f. limit of shear-horizontal piezoelec. wave 0–62408 ferromaenetic piezo-semiconductor amplifier, for nonpolarized transversal

ferromagnetic piezo-semiconductor amplifier, for nonpolarized transversal wave 0-44268

wave 0-44268 glass, optical, elastic and piezoelectric consts. from single diffractogram 0-50637 group A^{III}B^V type crystals, and lattice potential energy, opt. and elastic props. 0-44744 Gunn effect oscillator coupled to piezoelectric, elastic wave generation 0-44375

0-44373
layered medium, u.s. amplification, mag. field 0-47531
muscle, piezoelec. effects 0-68962
piezo-semiconductor amplifier, continuous action, with CdS and cond.
surface layer 0-40879
piezoelectric-semiconductor system, amplification of u.s. surface waves

0 - 78763poly(y-methyl L-glutamate), temperature variation of piezoelectric moduli 0-47856 Piezoelectricity continued

pressure probe, calibration using plane Chapman-Jouguet detonations, in $1-30~\mathrm{atm}$ range ~0-72872

pressure probe, high speed, design 0-46734 α -quartz, coeff, meas, method 0-51127

quartz, strain coeff. meas. using dilatometer

quartz, stain coen: nieas, using unatometer 0-75818 quartz plates, symmetrical thermal bending 0-76879 Rayleigh surface waves, parametric amplification 0-47851 Rayleigh wave's scalar electric potential calc. using computer iterative method 0-65828 reflector for laser f.m cancellation, patent 0–42258 resonator, piezo-semiconductor, based on surface wave 0–44373 semi-infinite medium, coated with perfectly conducting thin film, disturbances 0–79055

bances 0–79055 semiconductor, InSb, const. meas. by electromech. reson. 0–51039 semiconductor, acoustoelect. effects 0–75400 semiconductor, acoustoelectric amplification 0–40555 semiconductor, acoustoelectric amplification 0–40555 semiconductor, acoustoelectric gain, non-linear theory, Gaussian electron distrib. 0–51026 semiconductor, acoustoelectric interactions 0–43887 semiconductor, acoustoelectric interactions 0–43887 semiconductor, modulated piezoreflectance, shear deform. potentials determ. 0–43727 semiconductor, nonlinear amplification of sound 0–47536 semiconductor, propagation of ultrasound, effect of varying elec. field 0–62186

0 - 62186

semiconductor plates, u.s. interaction with charge carriers 0-68812

semiconductor piates, u.s. interaction with charge carriers 0-08812 semiconductors, acoustoelectric amplification, non-linear theory 0-51030 Stewart-Tolman effect, microscopic theory 0-53738 surface potential on monocrystals, production by shock waves 0-47847 surface waves in cubic cryst. 0-47849 transducer, ZnO film, hypersonic, losses rel. to texture, resist. thickness 0-68605

0-68605

transducer, annular disk, mechanical response due to step input with prescribed temp, field 0-45642

transducer, inhomogeneous, subjected to static charge, electromech, response 0-44381

transducer ceramic, radiation in radially symmetric modes, calc. 0-62452

transducer material, whisker reinforced piezoelectric ceramic, production and props. 0-63444

transducer with divided electrodes subject to constant heat flow, mechanical response 0-56363

u.s. wave generation in semiconducting, platelets by drift electrons 0-75385

wurtzite group crystals, perfect piezo-semicond. resonator based on surface wave 0--44373

wave 0-44373
of BaTiO₃, application to vibration detection, transducer design and operation 0-45608
BaTiO₃, consts. calc. method 0-65801
BaTiO₃, rel to layered domain structure 0-47311
BaTiO₃ piezoelectric cylinder, shear and compressional waves scattering numerical results 0-59270
BaTiO₃ single cryst., pure and containing CoO, modulus near Curie point 0-40888

40858 BeSO₄.4 H_2 O, nonlinear polarizability tensors and piezoelec. moduli 0-68236

0-0220 Bi₁/GeO₂₀, metallized and unmetallized, acoustic surface wave velocity 0-78748 CdS, piezoelec, stiffened u.s. vel. enhancement by electron trapping 0-50884

0-50884
CdS, Rayleigh surface waves, parametric amplification 0-47851
CdS, with cond. surface layer, continuous action piezo-semicond. amplifier with net gain 0-40879
CdS epitaxial transducer, freq. characts. 0-44383
CdS film, evap., piezoelec. const., deposition rate depend. 0-68965
CdS films, polycryst. 0-51128
CdSe f.e.t., effects of stress and strain, application to ultrasonic transducer 0-44310

0–44310
CdTe, piezosemiconductor, Rayleigh wave amplification 0–75399
GaAs, Rayleigh waves amplification, analytical eqns. 0–62197
Ge, amorphous and polycrystalline, piezoresistance 0–47754
InSb, const. meas. by electromech. reson 0–51039
LiNbO₃/CdSe film system, acoustic surface waves amplification 0–75398
LiNbO₃, acousto-optical interactions, theory 0–51275
LiNbO₃, elastic const., acoustic wave vel. meas. 0–79056
LiNbO₃, elastic exporting vector, generalised form 0–65831
LiNbO₃, leaky surface wave 0–75810
LiNbO₃, LiTaO₃ resonators in med. freq. range with low capacitance ratios, temp. coeff., design 0–65830
LiNbO₃ blates Z-cut, high overtone mode thickness-dilational resonances LiNbO₃ plates Z-cut, high overtone mode thickness-dilational resonances 0-47854

LiTaO₃, Curie pt. behaviour 0-65814

LiTaO₃, Curie pt. behaviour 0–65814
LiTaO₃ oriented crystal for transducer, patent 0–44385
Pb(Co₁₃Pb(2₂₃D₃-PbTiO₃-PbZrO₃ solid soln. ceramics, and dielecttic props. 0–65766
PbTiO₃ ceramics, polarization and piezoelectric. props. 0–65832
PbTiO₃ ceramics, production and application 0–44376
(1-x)(0.6PbTiO₃+0.4PbMg_{0.3}W_{0.3}O₃)+xPbZrO₃ ferroelectric ceramic properties 0–75811
Pb(Zr,Ti)O₃ piezoceramics, elec., piezoelec. and élastic props. field depend. 0–65833
SbSI, dark cond., hydrostatic press. depend., piezoresistance coeff. 0–62443
SbSI, doped, props. meas. by resonance-antireson method. 0–40880

0-62443
SbSI, doped, props. meas. by resonance-antireson. method 0-40880
Se, tensors for textures of co-type 0-75813
Se film on Te, electromech. coupling factors 0-68966
Se layer, props., effect of texture 0-75812
SrKLiNb₁₀O₃, elastic and piezoelectric constants 0-72123
SrTiO₃, elastic compliance press, depend. near transition temp. 0-47315
TeO₃, const. temp. depend. 0-47317
TeO₂, props. of single crystals 0-78593
TiO₃+BaCO₃, shock compression, piezoelec. props. 0-75774
V₂O₃, semiconductor-metal transition temp., switching effect, elec. field depend. 0-65678
ZnO₃ is attenuation freq. depend., room temp. 0-53705
ZnO₃ film, hypersonic transducer, losses rel. to texture, resist. thickness 0-6805
ZnO₃ film deposition 0-76221

ZnO film deposition 0-76221 ZnS(Se,Te), piezosemiconductor, Rayleigh wave amplification 0-75399

Piezomagneto-optical effects see Magneto-optical effects

Piezoresistance see also Piezoelectricity

see also Piezoelectricity accelerometer, subminiature piezoresist. Si beam 0–72131 organometallic crysts. 0–72126 semiconductor, anisotropic, minority carrier mobility determ. 0–75661 semiconductor β -rhombohedral B, elastoresist., 180-500K 0–78942 β -B, rhombohedral, elastoresist., 180-500K 0–78942 Si beam accelerometer, subminiature piezoresist. 0–72131

Piles, nuclear fission see Nuclear reactors, fission

Pinch effect see Discharges, electric; Plasma/confinement; Semiconducting

Pions

e.m. form factor, calc. of ρ-exchange contribution 0-42536
e.m. form factor, from high energy electroproduction 0-73566
e.m. form factor, rel. to Veneziano amplitude for ππ scatt. 0-77320
e.m. form factor derived using PCAC, current algebra and Veneziano model 0-57756
e.m. form factor evaluation 0-57772
e.m. form factor in a Veneziano-type representation 0-52504
e.m. mass difference of π and K, by appl. of Veneziano amplitude 0-42537
e.m. mass difference of zero-mass pions fourth order contribution and

e.m. mass difference of zero-mass pions, fourth order contribution and possible sources of divergence 0–57773 electric form factor, by Weinberg sum rules with Veneziano residues 0–70247

 $0{-}70247$ electromagnetic form factor with dipion unitarity $0{-}73562$ $f_{kl}/f_{\pi_1}\,f_{k0}/f_{k\parallel}$ sum rules $0{-}70235$ form factor, Veneziano like, via hard-pion current algebra $0{-}57770$ form factors, superconvergence, status of KSFR relation $0{-}73561$ hard-pion techniques, current-field equal time commutators $0{-}73397$ mass difference effect in N-N scatt. phase parameters $0{-}60573$ six charged, exorcized factorising dual amplitude $0{-}57771$ soft, theorems, SW(3) broken chiral symmetry and finite mass corrections $0{-}60567$ ${m^+}{\cdot}\pi^0$ e.m. mass differences using form factors from nonlocal field theory $0{-}52546$

decay

decay lifetime of π^0 and $\gamma \pi \to \pi \pi$ in Veneziano model 0–57801 β decay, three-point functions and a sum rule from radiative corrections, a unified description of low-energy meson phenomena 0–49259 $\pi^+ \to \Gamma \nu$, e.m. form factors 0–73571 $\pi^+ \to \pi^0 + \nu \nu$, axial vector part, appl. of PCAC 0–55036 $\pi^0 \to \nu \nu$, axial vector part, appl. of PCAC 0–55036 $\pi^0 \to \nu \nu$. SU(3) symmetry breaking 0–60556 $\pi^0 \to \nu \nu$, sum rule analysis for decay amplitudes 0–70237 $\pi^0 \to \nu \nu$ sum rule analysis for decay amplitudes 0–70237 $\pi^0 \to \nu \nu$ vector meson dominance model predictions 0–77295 $\pi^+ \to \Gamma \nu \nu$, T-violation and the B meson 0–60572 $\pi^- \to \nu \nu$, non-linear spinor theory 0–73543 $\pi \to \nu \nu$, Pagels's sum rule, exact version 0–57799 $\pi \to \mu \nu \nu$, form factor sensitivity 0–55042 $\pi \to \nu \nu$, form factor sensitivity 0–55042 $\pi \to \nu \nu$, form factor sensitivity 0–55042 $\pi \to \nu \nu$, form factor sensitivity 0–55042 interactions

interactions at 200 GeV with atomic nuclei 0–45989 axial-vector field-current identity for interacting π and A_1 fields, rigorous lower bound 0–60474 energy density distribution in Sn from 8 GeV beam using linear internuclear

tower bound 0-04/4 / energy density distribution in Sn from 8 GeV beam using linear internuclear nucleonic code 0-77324 final state, scalar boson disentanglement from background, rel. to low-energy production theory 0-73567 many pion, possible Veneziano amplitude 0-63812 pion conspiracy and Regge cuts, at high energy 0-67281 A^μπ→ππ, non-vector-dominance Veneziano models for the axial-vector-current three-pion amplitudes 0-63818 pπ→ππ in Veneziano model and π⁰ lifetime 0-57801 ωπ→ππ, bootstrap calc. of ρ trajectory 0-60602 π⁺→pp, 142, 165, 187, 230 and 262 MeV, cross-section meas. 0-55044 πα+ππβ, high-energy behaviour of chiral Lagrangians 0-45938 π⁻d, 20-65 GeV/c, total and abs. cross-sections 0-77332 π⁻d-K*(Σ¬n), expt. search for bound (Σ n) dibaryon state 0-60604 π⁺d, 1.1 to 2.4 GeV/c, strange particle production 0-67280 π⁺d, nonstrange boson production at 9 GeV/c 0-73601 π⁺d-9pp, 150-300 MeV phenomenological cross-section calc. 0-49252 π⁺d-9pπ π⁻π, 5.4 GeV/c, evidence for structure in dipion mass region 0-63833 π⁺d-ππ Glaviano constants of the section to the section of the

0–05853 π^+ 14–374 π^+ 27 , 4.2 GeV/c, prominent features 0–45928 π^- 3He- π^+ nnn, Glauber's eikonal approx. used for analysis 0–57777 π^- 4He, double charge exchange, anal. 0–38681 π^+ n- $\pi^ \Delta^+$ +1(1236), ang. distribs. explained by rescattered model

0–2491 τ^- p, comparison of models for neutral and charged pion multiplicities observed in 25 GeV/c collisions 0–49266 π^- p $-\eta\eta^0$ for determ. of expt. limit of η decay mode 0–70240 π^+ p, strange particle production at 1.7 GeV/c 0–67289 $\pi^2 p^0 \rightarrow \tau^2 p^0$, factorization props. 0–57771 $\pi\pi\pi$ NN five-point function, crossing relations 0–55041

interactions, pion-nucleon

absorption reactions of neg, II by two N pairs in nucleus 0-49265 chiral SU(2)×SU(2) transformations, curved isospin space with torsion

coupling, derivative and nonderivative, consideration in pion field equation 0-73573

0–73573 coupling, nonderivative, transformation to derivative, effect 0–73384 D_{11} phase shift, relativistic three-body calc. 0–73574 diffraction association and multipion prod. 0–67282 diffractive processes at high energy 0–67286 dispersion relations, fixed-t, a new representation 0–38684 low-energy theory, S-wave scatt. 0–38686 multiplicity distributions at energies >1 GeV 0–45931 on nuclei, complex, diffraction generation of π 0–45926 partial wave relations from fixed-t dispersion relations 0–38685 review 0–45932 short-range interaction, asymptotic behaviours of force functions.

short-range interaction, asymptotic behaviours of force functions 0-55045

N₃₃* production, prediction by quark model 0-52561

Pions continued

interactions, pion-nucleon continued

 $\pi\text{-N},$ two- and three- prong, azimuthal anisotropy and diffr. dissoc., 17.2 GeV/c 0--38683

 $7N \rightarrow N\rho$ in ligh energy backward reactions and the strong-cut Reggeized absorption model 0-52522 $\pi N \rightarrow \omega N$, B meson exchange contributions 0-60574 $\pi N \rightarrow \pi \pi N$, effective Lagrangians, by chiral dynamics 0-70251 $\pi N \rightarrow \rho N$ vector dominance model, relations for t-channel helicity amplitudes 0-45933

interactions, pion-pion rel. to meson dynamics developments 0–60581 resonance recognition in a Veneziano model 0–73578 secondary particle production of 4.0 GeV/c, longitudinal and transversal momentum 0–67292 N*, Δ, search for strange particle decay 0–52563 P-p-ππ, ρ trajectory doubling 0–63823 π-π collision, applic. of principle of self-colliding orbits 0–55096 π-p, 20-65 GeV/c, total and abs. cross-sections 0–77332 π-p, hyperon and K⁰K⁰ channels π-p interactions and multipion photoproduction 0–52517 π-p, 1=0 π-π⁺ enhancement, at 1.07 GeV 0–63836 π-p-3π-2π⁺pπ, N^{*++} (1236), ξ⁰ and A₁-prod., 6 GeV/c 0–42546 π-p-3π 2π⁺pπ⁰, ω°, B-, N^{*++} (1236) and N*(1688) prod., 6 GeV/c 0–42546 π-p-ηη, differential cross sections and polarizations 0–52475

0–42546 π-p-ηπ, differential cross sections and polarizations 0–52475 π-p-ηπ, differential cross sections and polarizations 0–52475 π-p-ηπ 2 , E_{π} = 6GeV/c, ang. distrib., cross sections 0–38690 π-p-ηπ 2 , K_{π} = 70 max 2 = 70 max $^{$

0-0.290 τ^2 p, 11.2 GeV/c, evidence for A₁(1070) and other structures 0-49284 π^- p, 20 GeV, cross section for strange particle production 0-57789 π^- p, 3.2 GeV/c, six- prong channels, kinematical and dynamical struct. 0-38688

0—38688
π⁻p, 4 and 5.1 GeV/c, mass spectrum of ΛK system 0—45977
π⁻p, 5.1 GeV/c, Ξ hyperon production 0—45976
π⁻p, 6.7 GeV/c, four and five body final states 0—49271
π⁻p, at 11.2 GeV, quasi-three-body state production, by double Regge-pole model 0—52514
π⁻p, at 6 BeV/c, six-pronged interactions 0—45936
π⁻p, high sparse york of gross section in Regge-pole fit. 0—60569

 π^- p, high energy total cross section in Regge pole fit 0-60569 π^- p, KK pair final states, three- to six body, 6BeV/c 0-42547

7 p. KR pair final states, three- to six body, 6BeV/c 0-42547
π-p, ρ° production rel. to vector-dominance-model 0-57784
π-p, ρ° production rel. to vector-dominance-model 0-57784
π-p-K°C₂p-pole model, 16 GeV/c 0-49268
π-p-K°K-p, crossing symmetric description of data with the generalized Veneziano model 0-49227
π-p-K°C₂(Σ°), Hypercharge exchange reaction in Reggeized U(6) ⊗ U(6) ⊗ U(3) model 0-57778
π-p-K°A-K*-n, 11.04 GeV/c, K+K- system obs. over all decay orientations 0-77331
π-p-K°A, generalized 3-body Veneziano model description 0-57760
π-p-ΛΚ°, 4 and 6.2 GeV/c, ang. distrib. obs. 0-49269
π-p-N*++(1236)π-π-, at 4.45 GeV/c, anal. by pion-Regge pole and three one-pion exchange models 0-60580
π-p-ΛΣ-K*, angular distribs., by rescattering model 0-42598
π-p-ηπ, Regge poles amplitude for charge-exchange 0-63835
π-p-ηπ, nolarization parameters at 5.9 and 11.2 GeV/c 0-57779
π-p-ηπ, Regge-pole model modified by inclusion of lowest order cuts 0-73591
π-p-ηπ, total and diffic cross sections for η prod., η decay 0-42513

0–73591 π – $p\rightarrow\eta n$, total and diffr. cross sections for η prod., η decay 0–42513 π – $p\rightarrow\eta n$, total and diffr. cross sections for η prod., η decay 0–42513 π – $p\rightarrow\eta n$, Veneziano model 0–57786 π – $p\rightarrow\eta n$, veneziano model study of M° 0–60590 π – $p\rightarrow\eta n$, at $p\pi$ –15-3.8 GeV/c, in U channel 0–60578 π – $p\rightarrow\eta n^2\pi^-$ 8 GeV/c, evidence for structure in dipion mass region 0–63833

 $\pi^- p \rightarrow n \pi^+ \pi^+ \pi^- \pi^-$, 8 GeV/c cross sections, resonance parameters 0–49272

 π p \rightarrow n π $^{+}$ π $^{+}$ π $^{-}$ π m π 0, 4 GeV/c, expt. study 0–52519 π p \rightarrow pX $^{-}$, multi-Regge model, relation with missing-mass spectrum 0–57750

 $\pi^- p \rightarrow p(\pi \rho)^-$, double-Regge- pole model used to investigate $\pi \rho$ mass enhancement 0-57783

emindement $0^{-31/85}$ and 20 GeV and N*++(1236), ρ^o and ρ^o meson production 0^-63822 $\pi^-p \rightarrow p\pi^+\pi^-\pi^-$ at 3.9 GeV/c, constructive interference effect between 2π decays of ω and ρ^o 0^-52516

 $\pi^-\pi^-$ partial wave analysis of 3π decay of A_2 in this reaction π⁻p→pπ⁺π 0-73610

0–57785 $\pi^- p \rightarrow \pi^- \pi^- \pi^+ p$, 3.9 GeV/c, dominant processes 0–42549 $\pi^- p \rightarrow \pi^- \pi^0 p$, at 339 MeV 0–60579 $\pi^- p \rightarrow \pi^- \pi^+ n$, 247 MeV, cross-section meas. 0–67288 $\pi^- p \rightarrow \pi^- \pi^+ n$, 7 GeV/c used to study $\pi^- \pi$ scattering up to 1.4 GeV dipion mass 0–57797 $\pi^- p \rightarrow \pi^- \pi^+ n$, at 339 MeV 0–60579 $\pi^- p \rightarrow \pi^- \pi^+ n$, at 539 MeV 0–60579 $\pi^- p \rightarrow \pi^- \pi^+ n$, at 6 GeV/c, ρ^0 and $\Delta^{++}(1236)$ production domination, evidence of Λ_1 , Λ_1 , mesons in 3π mass spectrum 0–60577 $\pi^- p \rightarrow \pi^0 n$ at 70 GeV/c, Reggeized U(6) \otimes U(6) \otimes O(3) absorption model 0–60570 $\pi^- p \rightarrow \pi^0 n$, ephancement of $2\pi^0$ means $2\pi^0 n \pi^0 n \pi^0 n$, ephancement of $2\pi^0$ means $2\pi^0 n \pi^0 n \pi^0 n \pi^0 n$, ephancement of $2\pi^0$ means $2\pi^0 n \pi^0 n$

 $^{-0.370}$ networks a constraint and $^{-0.370}$ networks a spectrum at 10 GeV/c 0–77350 $^{-0.370}$ $^{-0.370}$ $^{-0.370}$ $^{-0.370}$ $^{-0.370}$ $^{-0.370}$ $^{-0.370}$ negge poles amplitude for charge-exchange 0–63835 $^{-0.370}$ networks a scattering. Chew-Low extrapolation 0–49267

 $\pi^- p \rightarrow \pi^0 n$, polarization parameters at 5.9 and 11.2 GeV/c 0-57779 $\pi^- p \rightarrow \rho^- p$, 8 GeV/c, vector dominance and current conservation 0-45933

Pions continued

interactions, pion-pion continued

 $\pi^- p \rightarrow \rho^0 n$, vector meson dominance 0-60597

 $\pi^- p \rightarrow \rho^0 n$ coherent droplet model 0-57782

 τ^- p $\to \rho \omega n$, 2.3 GeV/c, interference $\omega \to \pi \pi$ and $\rho^0 \to \pi^+ \pi^-$ decay modes 0–73576

 π^+ p, 8 GeV/c, cross-sections of strange-particle production 0–57788

 π^+ p, 8 GeV/c correlation between transverse and longitudinal momenta of secondaries 0–57787

secondaries 0–57787 \$\pi^+\text{p}\$ Regge pole model at 8 GeV/c 0–49268 \$\pi^+\text{p}\$-K+\Sigma^+\text{p}\$ reross section and polarization at 3, 4 and 5 GeV/c, momentum transfers up to 3 (GeV/c)^2 0–49270 \$\sigma^+\text{p}\$-K+\Sigma^+\text{p}\$ hypercharge exchange reaction in Reggeized U(6) \$\sigma^+\text{p}\$-K+\Sigma^+\text{Y}_1^*(1385), Regge trajectory exchange model 0–73655 \$\pi^+\text{p}\$-K+\Sigma^+\text{p}\$, weak, pole model calc. of cross-section 0–67287 \$\pi^+\text{p}\$-K+\Sigma^+\text{A}\$ cossed reaction, appl. of dual multiparticle model for \$V_0.0...\sigma^+\text{p}\$-\$\text{A}\$ \(\text{A}\$ \(\te

 $\pi^*P \rightarrow N^* + \Lambda$ crossed feaction, apply of dual interparative invariants $K \rightarrow \pi^* \pi^* \Lambda$ 0–368.9 at $\pi^+P \rightarrow N^* + \eta$ from 2.95 to 4.08 GeV/c, differential cross sections 0–60576 $\pi^+P \rightarrow N^* + \iota$ from 2.95 to 4.08 GeV/c, differential cross sections 0–60576 $\pi^+P \rightarrow N^* + \iota$ from 2.95 to 4.08 GeV/c, differential cross sections #p→N*+** from 2.95 to 4.08 GeV/c, differential cross sections 0-60576
π*p→N*+* from 2.95 to 4.08 GeV/c, differential cross sections 0-60576
π*p→N*+* ω from 2.95 to 4.08 GeV/c, differential cross sections
0-60576
π*p→N*+* ω from 2.95 to 4.08 GeV/c, differential cross sections
0-60576
π*p→Y, **(1385)K+, quasi-two body reaction at 1.7 GeV/c, channel cross section 0-7328
π*p→P*Δ+*, 8 GeV/c, absence of anomaly explained in coherent droplet model 0-57782
π*p→ω*π*η*, 2.9 GeV/c, channels, branching ratios, expt. 0-45937
π*p→pπ*πy, 2.9 GeV/c, channels, branching ratios, expt. 0-45937
π*p→pπ*π*η*, evidence for three boson structs. 0-63819
π*p→π*α*Δ+*(1236), Lorentz pole analysis 0-42548
π*p→π*μ*π*π*π, 1.13 GeV, cbs. of N*(1720)-Δ+*π+μπ*π*π 0-45982
π*p→π*π*π*π, 1.13 GeV, obs. of N*(1720)-Δ+*π+μπ*π*π 0-45982
π*p→π*π*η*ρ*p 1.3.1 GeV, double Regge exchange model 0-73577
π*p→π*ρ*p*p 1.3.1 GeV, double Regge exchange model 0-63816
π*p→ρ*Δ+**, coherent droplet model 0-57782
π*p→ρ*Δ+*, coherent droplet model 0-57782
π*p→ρ*p, coherent droplet model 0-52515
πp→N+amything, cross-sections, approximately constant for 8, 11, and 16
GeV incident π energy 0-49279
πp→pπππππ, Chan-Loskiewicz-Allison model applic., 8 GeV/c 0-45934
πp→π +anything cross-sections, approximately constant for 8, 11, and 16
GeV incident π energy 0-49279
πp→πππππ, Chan-Loskiewicz-Allison model applic., 8 GeV/c 0-6580
ππ-ηχ, Veneziano models with X a boson of any spin 0-52520
ππ-ηχ, Veneziano models with X a boson of any spin 0-52520
ππ-ηχ Veneziano models with X a boson of any spin 0-52520
ππ-ηχ Veneziano models with X a boson of any spin 0-52520
ππ-ηχ Veneziano models with X a boson of any spin 0-52520
ππ-ηχ Veneziano models with X a boson of any spin 0-52520
ππ-ηχ Veneziano models with X a boson of any spin 0-52520
ππ-ηχ Veneziano models with X a boson of any spin 0-52520
ππ-ηχ Veneziano models with X a boson of any spin 0-52520
ππ-ηχ Veneziano models with X a boson of any spin 0-52520
ππ-ηχ Veneziano models with X a boson of any spin 0-52520
ππ-ηχ Veneziano m

interactions, pion-proton

production

10--70 BeV, new scaling law and empirical formulas rel. to Serpukhov data 0--77327

0-1/321 chiral-dynamics calculations of single-pion production in π -N inelastic scattering 0-52508 diffraction dissociation, high-energy, dual resonance model 0-49226 diffraction dissociation from nuclei in independent-particle Glauber model 0.73600

0 - 73609diffraction generation, by nucleon and π interac. on complex nuclei 0-45926

0-43926 e.m. prod., low energy theorem 0-77268 electroproduction, T-violation effects, final state interactions 0-42535 electroproduction, high energy 0-73566 electroproduction, in vector meson-dominance model, choice of frame 0-63815

electroproduction, multipoles prediction 0–49258 electroproduction of charged π using fixed-momentum-transfer dispersion relations 0–57776

relations 0-51/16 electroproduction on protons, $1000\cdot1170$ MeV obs. 0-45930 hyperon and K^0 channels in π -p interactions and multipion photoproduction 0-52517 location and Dalitz pairs, simultaneous detection 0-77319

location and Dalitz pairs, simultaneous detection 0-77319 low-energy, disentangling scalar bosons from background of final state interactions 0-73567 matrix elements for emission and absorption of soft pions 0-67278 multiparticle from high energy pp and Kp interact., expts. 0-67279 multipion production, factorization, difference between elastic and inelastic cases 0-42542 one-pion process in pp collision at 0.97 eV, in terms of one-boson-exchange model 0-38713 photoproduction, Regge cuts due to absorption, numerical study 0-67277 photoproduction, 0-55047 photoproduction, 0-55047 photoproduction, 0-55047 photoproduction, 0-55047 photoproduction, 0-55047 photoproduction, assist for isotensor current 0-73409 photoproduction, evidence for isotensor current 0-73409 photoproduction, evidence for isotensor e.m. current 0-45927 photoproduction, extension pseudomodel 0-77326 photoproduction, multiple, energy dependence of partial cross-section 0-63821 photoproduction, nucl. distortion effects of emitted π 0-39012

0–63821 photoproduction, nucl. distortion effects of emitted π 0–39012 photoproduction, phenomenological model with diffr. correction 0–49262 photoproduction, polarization theorems 0–73572 photoproduction, vector dominance model 0–38677 photoproduction, vector-dominance model, dispersion relations for invariant amplitudes 0–67276 photoproduction by real and virtual photons and electroprod., low energy theorems 0–38662 photoproduction form ¹⁵Ω 0–39013

photoproduction from ¹⁶O 0-39013

Pions continued

production continued

photoproduction from N, Regge pole theory, Lorentz group appls. 0-38679

photoproduction of π^0 from neutrons, 500-900 MeV differential cross section 0-52507

photoproduction of charged pions, low-t theorems 0-57800 photoproduction of charged pions, vector dominance at high energies 0-49260

photoproduction on deuteron, three-body final state, relativistic treatment 0-52511

photoproduction on hydrogen, 4 and 5 GeV 0-49261 photoproduction on nueleons, E₂<500 MeV 0-55038 single, photoprod, electroprod, and neutrino induced prod., T-violation effects 0-42535

single, photoprod., electroprod. and neutrino induced prod., T-violation effects 0-42535
two-pion photoproduction, diffractive, dual reson. anal. 0-52506
D⁰ π π τ, Daliz polo cale. 0-52520
dd→ddπ, 7.9 GeV/c obs. and comparison with Reggeized one-pion-exchange model 0-55071
e⁻c⁺ τ π τ ψ used to study ππ scatt. for dipion states of even charge conjugation 0-57712
e⁺c⁻π π τ vacuum polarization effects 0-49209
pn-γπ 1 vacuum polarization effects 0-49209
pn-γπ 1 vacuum polarization effects 0-49209
pn-γπ 1 vacuum polarization effects 0-49209
pn-γπ 2 naround N(1518) resonance 0-70250
pNN+, electroprod. vertex depend. 0-42538
pγψρπ 1π , photoproduction in 2.6-6.8 GeV 0-60508
p induced production, T-violation effects, final state interactions 0-42535
PP-ppπ 0 σ -γρπ 1 σ - npπ 1 at 2.7 GeV/c 0-38712
gd-γρd 1π τ, 5.5 GeV/c cross-section obs. 0-73633
pn-γρπ π- at 2.8 GeV/c incident p laboratory momentum, reaction analysed 0-70248
pn-γρπ π at 2.8 GeV/c incident p laboratory momentum, reaction analysed 0-70248
pn-γρπ π at 2.8 GeV/c incident p laboratory momentum, reaction analysed 0-70248
pn-γρπ π at 2.8 GeV/c incident p laboratory momentum, reaction analysed 0-70248
pn-γρπ π at 2.8 GeV/c incident p laboratory momentum, reaction analysed 0-70248
pn-γρπ π at 2.8 GeV/c incident p laboratory momentum, reaction analysed 0-70248
pn-γρπ π at 2.8 GeV/c incident p laboratory momentum, reaction analysed 0-70248
pn-γρπ π at 2.8 GeV/c incident p laboratory momentum, reaction analysed 0-70248
pn-γρπ π at 2.7 GeV/c receive m 2 × 80000 pp. 2 × 800

pp annimation into 8 and more pions at 6.94 GeV/C $\,^{\circ}$ U=49303 pp collisions proton momentum spectra compared $\,^{\circ}$ 0=63844 pp $\,^{\circ}$ KKn π (n=1,2...), 2.7 GeV/c cross-section, K*(890), ρ^{0} , ω° production obs. $\,^{\circ}$ 0=38720 pp=np π 7, 740 MeV explanation in terms of Mandelstam resonance model $\,^{\circ}$ 0=73634

pp-pp $\pi^+\pi^+$, 2.4 and 2.9 GeV/c, $\bar{\Delta}^-$, Δ^{++} production 0–57820 pp- $\pi^+\pi^+\pi^-\pi^-$ 2.5 GeV/c, abundant resonance production obs. 0–77869 π- photoproduction in second resonance region, phenomenological anal.

π, photoprod. on hydrogen, at high energies 0-42516 π photoproduction on p, polarized photon cross section asymmetry, 230-380 MeV 0-55037

0-13563

π[†] photoproduction, quark model explanation 0-57774

π[‡] photoproduction from hydrogen at backward angles in the energy range
1-3 GeV 0-52509

π° photoproduction on N, dip structure mechanism, Regge theory confirmed 0-60574

πΔ photoproduction and conspiracy relations 0-49314

π⁻¬¬π¬π†η, 247 MeV, cross-section meas. 0-67288

π†π- photoproduction on neutron in deuterium bubble chamber, up to 900

MeV 0-77318

π†π photoproduction on neutron in deuterium bubble chamber up to 900

MeV 0-77318 $\pi^{+}\pi^{0}$ photoproduction on neutron in deuterium bubble chamber, up to 900 MeV 0-77318⁷Li photoproduction of neutral pions 0-55043

scattering

cattering

rd, use of new dispersion relations in Glauber formalism 0-52512

Compton, exchange degeneracy consequences 0-49264

Compton scatt. in Veneziano model 0-42540

dual resonant amplitude for many pions 0-73568

dual-resonance models and six- and eight- charged-pion amplitudes, construction from dual models 0-73497

interference amplitudes, construction from dual models 0-73497

multiple, spin-isosonic formalism 0-49638

multiple, spin-isospin formalism 0-49638
Regge trajectory 0-73570
S-wave lengths for π-hadron collisions calc. 0-70249
Veneziano amplitude and model for the isoscalar-current three-pion ampli-

S-wave lengths for π -hadron collisions calc. 0–70249 Veneziano amplitude and model for the isoscalar-current three-pion amplitude 0–63814 A π -A π , amplitude with crossing symmetry, proper asymptotic behaviour and pole structure 0–49283 p3 π coupling const. in Veneziano model 0–60571 p π -p π double-helicity-flip amplitude and Regge effects in weak amplitudes and final-state strong interactions 0–63795 K π , I= 1 /₂ p-wave amplitude, three-channel model 0–57809 K π elastic, in T=3/2 state, studied in K $^{-}$ d-K π $^{-}$ pp, 0–63810 $\omega \pi$ - $\omega \pi$ Veneziano model, invariant amplitudes, signature and amplitude conspiracy relations 0–45948 π A₁, Veneziano amplitudes 0–77325 π A₁, Veneziano model and chiral algebra 0–42534 π $^{\pm}\alpha$, strong scattering with electromagnetic corrections 0–49277 π $^{\dagger}\alpha$ low-energy reanalysis with Coulomb corrections 0–55046 π d, high energy, inelastic processes and duality 0–73579 π d, inelastic effects at high-energy, in composite model 0–42541 π d high-energy total cross-sections Serpukhov meas. 0–63824 π d nuclear screening at 16 GeV, inelastic screening at 65 GeV 0–63820 π d using Bakamjian-Thomas transformation theory 0–77333 π π d, 16 GeV/c, nuclear screening 50% higher than elastic shadow effect 0–52513 π -d π d, Glauber's eikonal approx. used for analysis 0–57777

 $\pi^- d \rightarrow \pi d$, Glauber's eikonal approx. used for analysis 0-57777

Pions continued

scattering continued

πη degeneracy in context of duality 0-73565

π³He, small angle, by Regge-pole eikonal theory 0-49263

 πK , evidence for current divergences belonging to (3,3*)+(3*,3) representation of SU(3)×SU(3) 0–42485

πK, Veneziano amplitudes and chiral symmetry breaking 0-67303

 πK dispersive sum rule approach, off-shell corrections 0–67294 πK low energy, analysis on basis of dispersion relations for s and p waves 0–67285

0-6/285

πK Veneziano model calc. of absorption parameters <2 GeV using partial wave dispersion relation 0-73599

πω-πω, Veneziano-type model 0-45929

πρ scattering amplitudes and A₁ meson width from current algebra 0-49286

πd, elastic, calc. via impulse approx. at intermediate energies 0-77334

πα, elastic, calc. via impulse approx. at intermediate energies 0–77334 scattering, pion-nucleon angular distrib, interference of t and u channel amplitudes 0–70253 backward charge exchange, N_P contribution 0–77335 chiral-dynamics calculations of single-pion production in π-N inelastic scattering 0–52508 continuous-moment sum rules, application to analysis of forward scattering 0–73583 crossing symmeteric pion-nucleon scattering amplitude, Veneziano terms 0–49276

crossing symmetric and antisymmetric parts, restrictive assumptions 0-73582

D₁, amplitude production model < 700 MeV 0-73584 determinantal optimal approx. technique appl. 0-38659 duality and non-Pomeranchuk contributions to cross sections 0-67297 duality classes, modified form and interference-model calculation 0-49273

0-49273
finite energy sum rules in non-forward directions 0-38645
finite-energy sum rules, appl. at fixed u 0-38694
forward, interference models, unitarity and duality 0-52524
generalized potentials, particle exchange, Regge pole exchange 0-55048
helicity conservation in diffraction scattering and duality 0-57739
high energy, 50-500 GeV/c, predictions at Reggeized multiple-scattering
quark model 0-67296
high energy backward reactions and the strong-cut Reggeized absorption
model 0-52522
at intermediate energies, description, unitarized interference model

at intermediate energies, description, unitarized interference model 0-42552

at intermediate energies, description, unitarized interference model 0–42552 low energy, p meson contribution 0–45939 on mass-shell, field theoretic study with currents obeying Gell-Mann Current Algebra 0–73585 model, absorptive optical, for all scattering angles 0–60500 model for amplitudes, applic. 0–52463 multiple rescatterings, with account of Regge poles 0–60557 off-mass shell corrections to amplitudes 0–38692 P'-pole simulation by two vacuum poles with \(\alpha(0) < 0 \) 0–67298 Pade approximation for S-matrix in pion-nucleon pseudoscalar field theory above production threshold 0–60583 particle-antiparticle total cross section differences at high energies, upper bounds 0–52424 phase shift analysis for elastic scattering up to 2.8 GeV/c 0–42553 phase-shift solution, resonance parameters 0–77374 Pomeranchuk theorem violation due to unconventional terms in amplitudes 0–45906 process anal. by modified interference model, duality concept 0–38693 rediative corrections to forward scatt. obs. 0–42423 Regge and non-Regge damping, field theoretic model for high energies 0–42554 Regge cuts and Veneziano model 0–67295

Regge and non-Regge damping, field theoretic model for high energies 0-42554 Regge cuts and Veneziano model 0-67295 Regge poles with kinematic cuts for backward scattering 0-52523 review 0-45932 S_{11} partial wave analysis with phenomenological one-pole, multichannel ND-1 model 0-42556 s- and p-wave amplitudes, Ward-identity techniques 0-77337 threshold behaviour of Regge parameter for nuclear trajectories for mass-zero pions 0-49275 total cross sections, by Pomeranchuk trajectory 0-55047 Veneziano model, modified 0-32525 Veneziano model, modified 0-38650 Veneziano-type representation 0-49274 Veneziano-type representation 0-49274 Veneziano-type representation 0-49274 Veneziano-type representation for πN amplitudes 0-38691 $\pi - \rho$ scatt. in the Veneziano model 0-42555 πN , veneziano amplitude 0-60582 πN Serpukhov results, 30-65 GeV/c, fit to Reggeized quark model 0-57791 $\pi^{\pm}N$, cross sections on hydrogen and deuterium between 0.9 and 2.4 GeV/c 0-52502 $\pi^{\pm}N$ high energy data rel. to violation of Pomeranchuk theorem 0-73581 $\pi N - \pi \pi N$, extraction of $\pi \pi$ scattering information by means of hard-pion calc. 0-7736 application of a dual resonance model for the $\pi \pi \pi N \bar{N}$ -five-point function 0-63797 scattering, pion-pion

scattering, pion-pion S-wave amplitudes, derivatives, rigorous inequalities 0–57795 absolute bound to scattering amplitude and Herglotz functions 0–67300 absorption model applic. to obtain unique s-wave I=0 phase shift from π -p \rightarrow π - π ⁺ π 0–67302 amplitudes, ratio of real to imaginery, model 0–73586 amplitudes from positivity, constraints above and below threshold 0–60586

analysis of information up to 850 MeV using forward dispersion relations 0-67301

0-0701 cross section upper bounds, rigorous calc. 0-70255 cross-sections, total and charge exchange, 70 to 290 MeV 0-73592 crossing-symmetry sum rules applied to Brown and Goble's model 0-73597

0–73597 current algebra amplitudes construction, illustration of method 0–49179 current divergences belonging to (3,3*)+(3*,3) representation of SU(3)×SU(3), evidence for 0–42485 duality among leading trajectories 0–63825 e.m. form factor and the Veneziano model 0–52527 elastic, backward, 875-1580 MeV/c, diff. cross sections 0–73589 elastic, compared with phase shift analysis, 1225-2070 MeV/c 0–42550

Pions continued

scattering, pion-pion continued elastic, differential cross section from condition of conformal invariance $0\!-\!77343$

electromagnetic form factor from Veneziano model and current algebra 0-57793

 $0-\frac{1}{193}$ celectromagnetic form factor with dipion unitarity 0-73562 hard-pion calc. on $\pi N \rightarrow 2\pi N$ reaction for $\pi \pi$ scattering information, models 0-77336 high energy, rotation of nucleon spin, in Regge-pole model 0-42503

inelastic cross sections according to Reggeized multiperipheral model 0-52521

0–52521 inverse of crossing-even amplitude structure, dispersion relation 0–73595 length predictions by current algebra 0–73492 low boundaries for scatt. lengths 0–77344 low energy amplitude, numerical approach 0–42562 model and extrapolation procedures of phase shifts 0–52526 model for amplitudes, applic. 0–52463 multi-Regge model rel. to ABFST π-exchange multiperipheral model 0–67249 N/D equations, fixed-angle amplitudes and threshold behaviour 0–57736 nonparallel daughter trajectories model 0–73594 partial-wave amplitudes, inequalities on left hand discontinuities 0–57779 partial-wave expansions, crossing-symmetric, positivity constraints 0–57727 partial-wave expansions, crossing-symmetric, positivity constraints 0–37893 phase contours 0–57792

0-73593
phase contours 0-57792
phase shift, T=J=0, analytical hard-pion calc. 0-55050
phase shifts, P-wave and isoscalar S-wave, determ. 0-77341
Pomeranchuk term, crossing symmetry, dual models 0-73522
resonance interpretation 0-73558
S- and P-waves, models from analyticity, unitarity and crossing symmetry

5- and p-wave partial amplitudes, integral inequalities due to crossing symmetry and positivity 0-45943

S-wave, isoscalar, phase shift from unitary current algebra model 0-77342

0–77342 S-wave amplitudes, unitarized and nearly crossing symmetric 0–42551 s-wave phase shifts, current algebra calc. 0–77339 S-wave phase shifts, low energy, total cross sections analysis 0–45944 s-wave scatt. lengths, current algebra calcs. 0–42559 s-wave scattering, Chew-Low extrapolation from study of $\pi^- p \rightarrow \pi^0 \pi^0 n$ 0–49267

0-49267 S-waves, crossing-symmetric and unitary 0-57796 sum rule, finite-energy 0-38648 total cross sections analysis, low energy S-wave $\pi\pi$ -phase shifts 0-45944 Veneziano amplitude, for π e.m. form factor 0-77320 Veneziano amplitude, off-shell extension 0-73596 Veneziano amplitude, unitarized, asymptotic behaviour 0-57794 Veneziano amplitude rel. to e.m. form factor 0-57772 Veneziano amplitudes and chiral symmetry breaking 0-67303 Veneziano model, elastic unitarity low-energy parameters, S,P-wave phase shifts 0-73600 each summitarization method 0-47560

Veneziano model, elastic unitarity low-energy parameters, S,P-wave phase shifts 0–73600
Veneziano model, new unitarization method 0–42560
Veneziano model, new unitarization method 0–42560
Veneziano model, two-term amplitude 0–42497
Veneziano model unitarized, with satellites 0–73598
Veneziano model predictions that satellites 0–73598
Veneziano model predictions, comparison with exptl. 0–77280
Veneziano model predictions, comparison with exptl. 0–77280
Veneziano model with secondary terms 0–42561
Veneziano partial-wave amplitude in complex s plane, dispersion relations and asymptotic behavior 0–67304
ere'-ππ*π*p used to study ππ scatt. for dipion states of even charge conjugation 0–57712
K+ππ*π*e*y decay, current algebra applications 0–70246
π+p elastic scatt., 893 to 1.03 BeV/c 0–38696
π+μ-α+ππ*π*, 8 GeV/c used to study ππ scatt. in ρ mass region 0–77340
π+p. 2.77 GeV/c, production and differential cross-sections, three-body final-state reactions 0–77329
π-p, elastic, 6-14 GeV/c 0–38695
π-p, elastic, between 1.7 and 2.5 GeV/c, partial wave anal. 0–45941
π-p, forward charge exchange scatt, 2-18 GeV, by interference model 0–73587
π-p, high energy, backward peaks, by reflection model 0–42464

0-73587

¬P, high energy, backward peaks, by reflection model 0-42464
¬P, phase-shift anal. solns, comparison 0-45942
¬P backward elastic from 2.38 to 3 GeV/c differential cross section for fine momenta 0-60585
¬P diffractional model for elastic scattering, high energy 0-52743
¬P → π ¬+n, 7 GeV/c used to study ππ scattering up to 1.4 GeV dipion mass 0-57797
¬P → π ∘ η, 310 MeV, neutron polarization meas. 0-73590
¬P → π ∘ η, Regge-pole model modified by inclusion of lowest order cuts 0-73591

0-73591 $\pi^-p \to \pi^+\pi^-n$, comparison of data with models of $\pi\pi$ scattering 0-77336 $\pi^-p \to \pi^0n$, convergence of finite energy sum rules in non-forward directions 0-57728 π^+p , at 2.50 and 2.75 Bev/c, first phase-band description 0-70254 π^+p , elastic at large angles, structure at 5 GeV/c 0-49278 π^+p , expt. comparison between on and off-mass shell inelasticity 0-42558 π^+p , polarization in backward- angle scattering between 2.5-3.75 GeV/c 0-73588

 π^+ p blackward ang. distribs., test of duality 0–42557 π^+ p blastic scattering, partial wave amplitudes in the 2-5 GeV/c region 0–60584

 π^2 p, elastic, polarization at 2.74 GeV/c 0–67283 π^2 p, shower enhancement of branch-point contrib., total cross section increase, $A \rightarrow \infty$ 0–45940 π^2 p differential cross sections for scattering over wide energy range 0–70192

0-70192 $\pi^2 p$ dispersion relation calc. of real parts of forward scatt. amplitude 0-57790 $\pi^2 p$ clastic, polarization meas. 2.75 and 5.15 GeV/c 0-67284 p prod. rel. to S-matrix inputs, N/D calc. 0-38701 π -p, topologic cross-sections, a regularity 0-49297 $\pi^2 p$, high-energy total cross- sections Serpukhov meas. 0-63824

scattering, pion-proton

Pitch detection see Acoustical measurement: Hearing Plages see Sun Planetary nebulae see Nebulae; Stars

Planets

nets

see also Solar system

12 Victoria, orbital elements 0-41798

13 Egeria, orbital elements 0-41798

30 Urania, orbital elements 0-41798

30 Urania, orbital elements 0-41798

433 Eros, motion anal. rel. to solid parallax and mass of earth-moon system 0-45417

1620 Geographos, minor planet, obs. during recent close approach 0-54445

57 Mnemosyne, motion and orbit rel. to mass determ. of Jupiter 0-41788

12 Victoria, asteroid, photometric obs. of light variation, and pole co-ords. 0-41787

0–41787′ absorption spectra computation for multiply scatt. atmospheres 0–51754 asteroid capture, a rate expression 0–51692 atmosphere, composition determination from X-ray glow 0–72767 atmosphere, determination of presence of chemical compounds 0–76635 atmosphere, dissipation problems 0–69444 atmosphere, energy balance 0–79728 atmosphere, external radiation fields for scattering 0–76634 atmosphere, inhomogeneous, semiinfinite, pure scatt. 0–48567 atmosphere, interaction with solar wind 0–41799 atmosphere, plane parallel Mie, multiple scattering of radiation, modified Fourier transform method 0–59578 atmosphere, polarization in scattered radiation 0–76633 atmosphere, radiative transfer, reciprocity relations for diffuse reflection and transmission 0–79726 atmosphere and surface obs., symposium, Woods Hole (1969) 0–59765

and transmission 0–79726
atmosphere and surface obs., symposium, Woods Hole (1969) 0–59765
atmosphere and surfaces, AU-URSi symposium 0–45418
atmosphere lower motions, Venus, Mars, Jupiter 0–72771
atmospheres, diffuse reflection and transmission of light, three-term scatt.
indicatrix case 0–48563
atmospheres, line formation, simple reflecting model 0–66586
atmospheres, pransmission absorption spectroscopy probing techniques
using satellites 0–51753
atmospheric albedos, accuracy of Eddingtons approx. 0–41784
atmospheric refraction, rel. to optical systems for grand tour space probes
0–63091
bibliography (third quarter of 1969) 0–76630

0-63091 bibliography (third quarter of 1969) 0-76630 Bode's law and dynamic relaxation of planetary systems 0-41783 climatology, convective heat exchange 0-79729 convection in mantles, depend, on magnitude of Rayleigh number 0-41782

cratered surfaces, distrib. and covariance function of elevations, derivation 0-48562

dynamic constants from Mariner 5 data 0-63127

dynamic constants from Mariner 3 data 0-63127 Earth, early, surface temp. and nature of atmosphere 0-57104 Earth, satellites, natural, obs. 0-79730 exosphere temps. of Earth, Mercury, Venus, Mars, Jupiter and solar corona 0-72768 formation, quantitative evidence monist theory 0-76636

formation, quantitative evidence monist theory 0–76636 fragmentation, collisional, and the evolution of meteoritic and asteroidal mass distribs. 0–54447 i.r. spectra, molecular line identification 0–49855 inferior including earth, treated as cold bodies, geophysical approach 0–72769 inner, radar obs. combined with Icarus obs. to determine several astronomical consts. 0–54325 interior, radiative thermal conductivity, i.r. spectra of minerals 0–72592 interior density-depth relations, Emden's eqns. applic. 0–57103 ionosphere, integral electron conc. determination from satellite ionogram 0–51577 ionospheres, beaming of electromagnetic radiation. 0–76631

ionospheres, beaming of electromagnetic radiation 0–76631 Irenaea, position determination rel. to identified stars from SAO catalogue 0–69445

Jovian decameter source, interplanetary scintillations, solar wind streams

Jovian accameter source, interplanetary scintillations, solar wind streams deduction 0–66643
Jovian satellite systems, obs. commensurabilities 0–66388
Jovian satellites I to IV, albedo and thermal emission 0–79731
Juno, perturbation coeffs, for orbit due to all large planets of solar system 0–79738

0-79738

Jupiter, Red Spot in 1968-1969, photographic obs. 0-69448

Jupiter, Red Spot longitude, three-months period oscillation 0-54436

Jupiter, S-burst activity, broadband obs. 0-66592

Jupiter, Saturn, Uranus, and Neptune, params. survey 0-48568

Jupiter, Venus and 3C 273 obs., at wavelengths 2 and 8 mm 0-41781

Jupiter, abundance of ammonia in atmosphere 0-57109

Jupiter, atmosphere, lower, motions 0-72771

Jupiter, chemical composition and internal structure, review 0-69446

Jupiter, circular polarization meas. at 13 cm and magnetosphere rotation period determ. 0-51758

Jupiter, convection, Red Spot Iongitudinal motion, 0-69449

period determ. "0–51758
Jupiter, convection, Red Spot longitudinal motion 0–69449
Jupiter, decametre source, non-10 controlled 0–45420
Jupiter, decametric radiation, 12-year periodicities 0–66591
Jupiter, decametric radiation, 12-year periodicities 0–63093
Jupiter, decametric radiation, long-term variations 0–63095
Jupiter, decimeter radiation, synchrotron radiation model 0–54437
Jupiter, decimetric radiation, synchrotron model 0–63097
Jupiter, diam., polar and equatorial optic meas. 0–54432
Jupiter, effect on short-period comets, of repeated close approaches 0–76653
Jupiter, hectometric continuum radiation, investigation using RAE-I satel

0—76653

Iupiter, hectometric continuum radiation, investigation using RAE-I satel-lite 0—66590

Jupiter, limb darkening and magnitude of internal energy source 0—69447

Jupiter, line positions and intensities in methane band of atmosphere 0—66594

0-66594

Jupiter, magnetosphere, radio emissions, deductions, interactions between mag. field and plasma 0-72773

Jupiter, mass determ. from motion of 57 Mnemosyne 0-51756

Jupiter, mass determ. from motion of (57) Mnemosyne 0-41788

Jupiter, methane and NH₃ absorption bands, spectrophotometry 0-57107

Jupiter, microwave rad. in 0.8-1.5 cm range, atmos. broad-absorpt. feature 0-45419

Jupiter, microwave spectrum, polarimetric obs. 0–63096 Jupiter, millisecond bursts at 18 MHz, interferometric obs. with 52800 λ baseline 0–41789 Jupiter, models, thermal histories 0–76637

Planets continued

Jupiter, occultation by Moon obs., by radiotelescope 0-63094

Jupiter, r.f. spectrum, dipolar model 0-79732

Jupiter, red spot, darkness parameter 1891 to 1947, solar activity relation-ship 0-66589

Jupiter, red spot motion, new theory 0-51757

Jupiter, rocket u.v. obs. 0-66593

Jupiter, sixth satellite, photoelectric obs. and photographic positions 0 66595

Jupiter, solid-state convection in molecular hydrogen mantle 0-76638 Jupiter, spectral obs. 18.5-24.0 GHz, near 1968 opposition 0-48570

Jupiter, thermal radio emission meas. 0-63092

Jupiter's atmosphere, H abundance from 6367.8 Å line 0-48569

Jupiter's decametric radio emission, modulation by Io, d.c. cct. model 0-59768

0-59768

Jupiter C/H value compared with solar value 0-48569

Jupiter atmosphere composition 0-59769

Jupiter features, photographic obs., 1960-1967 0-57108

Jupiter features 1967-68, latit. and longit. meas. 0-51755

Jupiter interaction with comet Ryves 1931 IV, changes in total energy 0-41807

Jupiter photographic obs., international patrol program 0-76632 Lagrangian planetary eqns., Encke-type, special perturbation method applic. 0-56907

Dagrangan panetary eqnis, Encke-type, special perturbation method applic. 0–56907

Limpopo, position determination rel. to identified stars from SAO catalogue 0–69445

magnetic fields 0–57106

Mars, thermal conditions in south polar region 0–48572

Mars, 1967 photographic map 0–76639

Mars, CO₂ abundance and surface press. 0–48575

Mars, Mariner 1971, TV expt. 0–54307

Mars, Mariner 1971, i.r. radiometry expt. 0–54308

Mars, Mariner 1971, i.r. radiometry expt. 0–54308

Mars, asymptotic velocity vector from computer program 0–69338

Mars, atm., radio occultation meas. by Mariners 6 and 7 0–51760

Mars, atmosphere, ion-molecule reactions involving N₂+, N+, O₂+ and O+ ions, from 300°K to ~1 eV 0–43006

Mars, atmosphere, origin of ionized carbon dioxide u.v. spectrum 0–59766

Mars, atmosphere, photochemistry of CO₂ 0–48576

0–59766
Mars, atmosphere, photochemistry of CO₂ 0–48576
Mars, atmosphere, significance of Mie scatt. 0–51766
Mars, atmosphere 0–57115
Mars, atmosphere and ionosphere, struct., temp. distrib., effects of CO₂ photochem. 0–41795
Mars, atmosphere obs. by Mariner 4 and 5 and Venera 4, review 0–59770
Mars, brightness variations (opposition effect), cubic crystals in the clouds mechanism 0–48573
Mars clouds obs using area scanning photometer. 0–51763

Mars, clouds, obs. using area scanning photometer 0–51763
Mars, detection and identification of surface organic compounds, two approaches 0–57110
Mars, exospheric temps., solar cycle var., predictions for Mariner 6 and 7
0–51759

0-51759
Mars, figure, from Mariner radio occultation meas. 0-66597
Mars, gamma ray spectroscopic measurement possibilities 0-57111
Mars, ionosphere, space vehicle investigation 0-57105
Mars, ionospheric features and methods of obs., comparison with Venus and Earth 0-69450
Mars, lower atmosphere, radio occultation meas. 0-63098
Mars, mascons beneath circular basins, rel. to dynamical asymmetries 0-41774
Mars, mass rel. to earth/moon ratio from obs. of Mariners 6 and 7.

Mars, mass, rel. to earth/moon ratio from obs. of Mariners 6 and 7 0-51751

Mars, mass and dynamical oblateness soln. using Mariner IV Doppler data 0-51764

data 0-31764
Mars, multispectral imaging from landing vehicle 0-59771
Mars, oases, frequency-size distrib. supports crater hypothesis 0-48577
Mars, occurrence of liq. water 0-66596
Mars, parhelic halo brightness rel. to ice crystal quantity in atmos. 0-48578

Mars, parhelic halo brightness rel. to ice crystal quantity in atmos. 0–48578

Mars, photographic obs., international patrol program. 0–76632

Mars, photographic obs. and scientific potentialities of space photography in general. 0–56867

Mars, polar cap, Mariner 7 obs., i.r. absorpt., 3µ. 0–41793

Mars, polar cap boundaries seasonal vars., obs. 0–41791

Mars, polar caps, convective heat exchange. 0–79729

Mars, radar obs. (1969), preliminary results. 0–63102

Mars, radative transfer on atm. entry. 0–54441

Mars, radio and radar studies, review. 0–63112

Mars, satellites, relative obs. 0–76644

Mars, satellites, relative obs. 0–76644

Mars, soil surface, 'Hellas' region anomalies. 0–41790

Mars, solar wind flow round atmosphere. 0–79754

Mars, solar wind flow round atmosphere. 0–79754

Mars, solar wind flow round atmosphere. 0–79754

Mars, surface coloration rel. to C,0, polymers i.r. spectra. 0–41792

Mars, surface studies review. 0–63100

Mars, surface topography and roughness, radar meas. 0–63101

Mars, surface cheight variations, radar-time delay and Doppler obs. 0–6313

Mars, topography and surface features. 0–63103

Mars, topography and surface features. 0–641794

Mars, topography and surface features. 0–641704

0-63113

Mars, topography and surface features 0-63103

Mars, topography large-scale vars., obs. 0-41794

Mars, ubvy and near i.r. photometric obs. near the opposition 0-51765

Mars, upper atmosphere, occultation meas. 0-63099

Mars, upper atmosphere and ionosphere, model calculations including transport effects, Mariner 4 obs. 0-76640

Mars, upper cover matter, props. determ. from radio radiation 0-48571

Mars and Venus atmospheres, review paper 0-51762

Mars surface, thermophysical model, thermal conductivity of particulate basalt as function of density in simulated temp. and pressure 0-75416

Mars surface obs., from radio emission 0-63104

Martian blue-clearing during 1967 apparition 0-54440

Martian blue-clearing during 1967 apparition 0-54105

Martian blue-clearing during 1967 apparition 0-54105

Martian topography from Mariner 6 and 7 i.r. spectra 0-79733

Planets continued

Mehiboen, position determination rel. to identified stars from SAO catalogue (0-69445)

Mercury, epilith physical parameters and hermocentric longitude dependence of 3.3 mm radiation 0 63108

Mercury, image resolutions of 1km for solving problems 0 76641

Mercury, mascons beneath circular basins, rel. to dynamical asymmetries 0 - 41774 Mercury, miscours beneath circular basins, ref. to dynamical asymmetries 0. 41774

Mercury, microwave spectrum, departure from thermal spectrum, explanation 0. 51764

Mercury, perihelic precession, heuristic derivation 0. 79727

Mercury, perihelic precession, heuristic derivation 0. 79727

Mercury, perihelic precession 0. 765.34

Mercury, photographs of transit on 9th Mny, 1970. 0. 76642

Mercury, present knowledge on orbit, diameter, mass, density, rotation, surface features, atmosphere, polarisation, colour, abedo. 0. 76641

Mercury, apin orbit reson, ref. to core mantle coupling. 0. 57114

Mercury, spin orbit reson, ref. to core mantle coupling. 0. 57114

Mercury, surface struct. From integrated brightness. 0. 48553

Mercury, thermal models and microwave temps. 0. 48580

Mercury's rotation, thermal and tidal effects. 0. 57112

Mercury's rotational velocity, fluctuation. 0. 57113

Mercury and Venus transits. 0. 41796

Mercury interaction with Comet. Perrine Chofardet. 1898. IX, changes in total arcty. 0. 11897

Mercury Biration, thermal and tidal effect. 0. 51767

measularry. 0 11207
Mercury libration, thermal and tidal effect 0 51767
Mercury libration, thermal and tidal effect 0 51767
Mercury nucrowave spectrum, disk temp, at 1.95 and 6 cm 0 1857/9
mmor, 57 Mnemosyne motion, appl. to Jupiter mass determ. 0 517/6
mmor, Juno, perturbation coeffs, for orbit 0 79738
motio. Vesta, i.e. damateta 0 63151
mmor, general perturbations to, appl. of Hansen's method 0 45422
mmor, rel. to defunct cometry nucleic 0 57721
motion's vectorial elements, zero rank effects, Hill's method of perturbation application 0 56904
Neptune, Meridian observation investigation from comparison with photoelectric occultation obs. 0 59773
Neptune, dimn. polar and equatorial optic meas. 0 54432
Neptune, ann. obs. relative to Mars, Jupiter and Saturu, 9.5 3.5 mm, brightness temperature 0 79736
Neptune, motion, cometary belt effects, caic. 0 51770
Neptune, photoelec, obs. of occultation of BD 1794388, April 1968, ann.l. 0 45434
Neptune, thermal radio emission meas. 0 63092

ABBL 0. 43-92.

Reptune, thermal radio emission meas. 0. 63092.

Reptune's orbit, inexplained residuals. 0. 6945.2.

Reptune's orbit, inexplained residuals. 0. 6945.2.

Reptune's rotating, properties of haddey regimes. 0. 63090.

Reptune orbits, Frojan manifold, survey and conjectures. 0. 59767.

Reptune orbits, recent theories. 0. 66588.

patrol program, international photographic Network, obs. of Mars and Jupiter 0 -76632 photography, high resolution, midday, Mars, Jupiter, Saturn, Moon 0 -63089

photography methods 0 72793

Photo albedo between 3400 and 5900 AA wavelengths 0 79735

polarization, optical, of planetary radiation, meas, using high resolution

Lourier spectroscopic method 0 51752

Rockefellia, position determination rel. to identified stars from SAO catalogue 0 69345

rotating, properties of hadley regimes 0 63090 satellite orbital evolution, under radiation press, influence, secular effects investigation 0 57102

myestigation 0-57102
Saturn, dinm., point and equatorial optic meas. 0-54432
Saturn, mm., wave spectrum 0-66598
saturn, rinm., wave spectrum 0-66598
saturn, rings, dynamical model for radial structure 0-76643
Saturn, rings, dentification of water frost 0-54433
Saturn, thermal radio emission meas. 0-63092
saturn, stater vapour in ring, Greenhousen effect on surface 0-63109
Saturn's rings, Interrul dimensions 0-54432
saturn's rings, meteoroidal bombard, eades. 0-51769
Saturn's rings, structure 0-54442
Saturn's rings, structure 0-54442
Saturn's rings composition, frozen NH, i.r. spectrum 0-57116
second order perturbation in reetangular coords., computation method 0-54435
solids, volume at high press. 0-51490

strongly interacting systems, computer simulations, and Bode's law 0 66388

sunspot number prediction from dyn, rel, of sun and planets 0 - 54471 surfaces, radar studies, factors controlling the reflection coefficient rough ness 0 72770

triton, methane atmosphere, lack 0- 41797

triton, methane atmosphere, lack 0-41797
Trojan asteroids, density and magnitudes near the preceding Lagrangian point 0-54444
Uranus, Diam., polar and equatorial optic meas. 0-54432
Uranus, min. obs. relative to Mars, Jupiter and Saturn, 9.5-3.5 mm, bright ness temperature 0-79736
Uranus, motion, cometary belt effects, calc. 0-51770
Uranus, reciprocal mass, based on 1913-1968 obs. of Saturn 0-66899
Uranus, satellites, relative obs. 0-76644
Uranus, Hermal radio emission meas. 0-63092
Venus, 70 cm radar obs., delay Doppler analysis 0-63115
Venus, CO, absort, bands, interpretation 0-41802
Venus, CO, accumulation and runaway greenhouse effect in atmosphere 0-57118
Venus, Mariner V flight, gravitational field, atmosphere, ionosphere,

Venus, Mariner V flight, gravitational field, atmosphere, ionosphere, hydrogen corona solar wind 0 63122 Venus, Venera 4 flight, cosmophysical investigations and probing Venus, Ve

Venus, absolute spectrum, 2.8 to 14µ 0 -63135 Venus, atmos. comp. obs. on automatic stations, Venera 5, Venera 6 0 63116

Venus, atmosphere, absorption of radar signals 0--63130 Venus, atmosphere, chemical composition, Venera 4 landing probe 0-63123

Venus, atmosphere, ionosphere, Mariner V S band radio occultation measurement 0 - 63125
Venus, atmosphere, lower, motions 0 72771
Venus, atmosphere, minor constituents spectra 0--63133
Venus, atmosphere, particulate medium 0--63140

Planets continued

Venus, atmosphere, polymerised water in quasi equilibrium with its vapour 0 76648

Venus, atmosphere, refraction of radio waves and field intensity 0-69456

Venus, atmosphere, upper, C atoms detection 0–54443 Venus, atmosphere 0–57115

Venus, atmosphere composition, temperature and pressure, data survey 0 59776

Venus, atmosphere data, estimate of deep mantle degassing rate 0-76645

Venus, atmosphere interaction with solar wind 0-41799
Venus, atmosphere interferometric obs. 0-59778
Venus, atmosphere obs. by Mariner 4 and 5 and Venera 4, review 0-59770

Venus, atmosphere obs. by space probes Venera 5 and 6, parameters from temperature and pressure meas, analysis 0-59775 Venus, atmospheric parameter determination from microwave spectrum 0-76646

Venus, atmospheric water content rel. to temp. and lithosphere composition 0-63110

Venus, chemistry of volatile elements 0 48583 Venus, clouds structure 0 59780

Venus, cloudy atmosphere, curve of growth, phase effects 0–63136 Venus, evolution of water vapour in atmosphere, loss rate through photodis sociation 0–63119

Venus, exospheric temps, solar cycle var., prediction for Mariner 6 and 7 () =51759

Venus, external cloud layer retrograde rotation 0-48581

Venus, geochemistry, radar data interpretation 0-59779

Venus, heat transfer in atmosphere 0 6311

Venus, high dispersion spectroscopic obs. CO₂ band at 10362 Å 0-76647

Venus, hydrogen corona, Mariner V obs. 0-63122

Venus, intrinsic magnetic dipole moment, upper limit, absence of radiation belt 0 63149

Venus, ionosphere, Mariner 5 obs. electron density profiles 0–63118
Venus, ionosphere, space vehicle investigation 0–57105
Venus, ionosphere and atmosphere, dual frequency radio occultation
Mariner 5 obs. 0–63141
Venus, ionosphere structure, calculations on Mariner 5 and Venera 4 obs.
0–63146

Venus, ionospheric features and methods of obs. comparison with Mars and Fauth 0 69450

Venus, lower atmosphere structure, brightness temp, spectrum 0–57117 Venus, mass, oblateness, centre of mass, Mariner 5 obs. 0–63131 Venus, microwave brightness at 11 cm, surface temp, distrib, determ, 0–51772

Venus, mass, oblateness, centre of mass, Martiner 5 obs. 0–63131 Venus, microwave brightness at 11 cm, surface temp. distrib, determ. 0–51772 Venus, mm. wavelength obs., with Josephson junction detector 0–66649 Venus, monochromatic phase curves, albedos 0–63137 venus, nature of interplanetary mag. field 0–51771 Venus, near i.r. reflectivity compared with ice clouds 0–63139 venus, obs., at wavelengths 2 and 8 mm 0–41781 Venus, obs. 8 to 13/n brightness temperature 0–63134 Venus, phase curve, nature of clouds 0–63138 Venus, plasma and magnetic fields, Mariners 0–63148 Venus, plasma flux measurements 0–63160 Venus, plasma flux measurements 0–63160 Venus, radar and radio obs., interpretation 0–76649 Venus, radar backscattering props. at 70 cm, theory 0–48586 Venus, radar backscattering props. at 70 cm, theory 0–48586 Venus, radar mapping, interferometric resolution of range Doppler ambiguity 0–63114 Venus, radio and radar studies, review 0–63112 Venus, radio and radar studies, review 0–63112 Venus, radio interferometry meas. of temperature variation at 11.1 cm wavelength 0–59777 Venus, radio interferometry meas. of temperature variation at 11.1 cm wavelength 0–59777 Venus, radio planetary radar, Mariner 5 radio tracking data 0–63127 Venus, radio interferometry meas. of temperature variation at 11.1 cm wavelength 0–59777 Venus, refraction, optical and radio 0–63132 Venus, solar wind flow round atmosphere 0–79755 Venus, seattering of solar X-rays, Rayleigh and Compton fluxes and K fluoresc. flux 0–57135 Venus, solar wind flow round atmosphere 0–79729 Venus, surface height variations, radar time delay and Doppler obs. 0–6313 Venus, thermal H¹ and/or D¹ in ionosphere, origin and behaviour 0–41800

Venus, the 0 41800 thermal H1 and/or D1 in ionosphere, origin and behaviour

Venus, ultraviolet emissions, Mariner 5 obs. 0—63142 Venus, upper atmosphere, Lyman alpha obs. 0—63143 Venus, upper atmosphere, bulk rotation from cloud displacement obs. 0—69457

0.69457
Venus, upper atmosphere, ionosphere, Mariner 5 obs. 0—63145
Venus, upper atmosphere, ionosphere at night, escape of water 0—63147
Venus, water loss mechanism 0—63117
Venus and Mars atmospheres, review paper 0—51762
Venus and Mercury transits 0—41796
Venus atmosphere, CO, band at 8689 Å 0—48584
Venus atmosphere, Mariner V obs. 0—63122
Venus atmosphere, conference 0—63120
Venus atmosphere dynamics from meas, of radial vel. of Venera-4 probe 0—56870
Venus atmosphere; composition, temps and press, determ, from Venera-4
Venus atmosphere; composition, temps and press, determ, from Venera-4
Venus atmosphere; composition, temps and press, determ, from Venera-4

Venus atmospheric composition, temp-and press, determ, from Venera 4 and Earth 0-63129

and Earth 0–63129

Venus lower atmosphere, model based on Venera 4 obs. 0–63124

Venus obliquity, synodic spin resonance with earth, atmospheric tidal torque, mechanism investigation 0–41785

Venus radius determ, by Mariner 5 tracking 0–63128

Venus resonant rotation role of atoms, tides 0–48582

Venus rotation problem 0–66600

Venus solar wind interaction, Mariner V obs. 0–63122

Venus solar wind interaction, Mariner V obs. 0–63122

Venus surface dust and send transportation and denosition equations

Venus surface dust and sand, transportation and deposition equations 0 69454

Venus, far u.v. Venera 4 obs. 0–63144 Venusian atmospheric turbulence, microwave signal fading 0–48585 X and gamma radiation production at surface 0–54434

see also Discharges, electric; Electrons; Ions; Space charge; Thermonu-

acceleration mechanism for neutron production in focus and z-pinch discharges 0-78057

acoustic wave attenuation, at ion-plasma frequency 0-46679 acoustic wave propag. in one- and two-dimens. plasma 0-46705

acoustic wave propag, in one- and two-dimens, plasma 0-46705 acoustic wave propag, with transverse inhomogeneity 0-55460 adiabatic eqns. for slow movement in electric and mag, fields, three sets of higher order eqns. comparison 0-43262 afterglow, columns, non-uniform rare gas (Ar, Ne, He) echoes at upper hybrid resonance 0-61347

hybrid resonance 0–61347 afterglow, dust induced quenching 0–50043 air-discharge, effect of ethyl alcohol on rf conductivity 0–78072 analog computer simulation 0–61262 anisotropic, nonlinear characts, elec. field of particle 0–53155 anisotropic, relativistic, stability to perpendicular magnetosonic waves 0–74594

anodisation of Ta and Nb, ionic current in oxide 0-72541 anodization, forming voltage 0-66182 anodization in oxide film production, effects of plasma perturbations

anodization in oxide film production 0–61661 arc, disc stabilized, in multi-component plasma, spectroscopic temp. meas., 3000-17000K 0–58309 argon, total and total line radiation, 2000 to 60,000A 0–46712

argon, total and total line radiation, 2000 to 60,000A 0-46712 atomic line identification method using Doppler shift in coaxial plasma source 0-42939 back-diffusion type, control of ion-energy distrib. 0-61269 beam, nonuniform collisionless, anomalous decay in u.h.f. field 0-46759 beam interaction, frequency, intensity and direction of electric fields 0-64866

0-64686 beam systems, dispersion equations soln. 0-61258 beam-plasma system, numerical soln. 0-43253 beams, spatially separated, instability 0-39611 betatron linear, electron acceleration energy spectrum study 0-52625 blobs, equilibrium configurations in magnetic field of two-dimensional dipole 0-51548 boundary as a Mach surface, motion of ions 0-39555 boundary layer, hydromagnetic, structure of current sheet, solns. 0-53176

0-53176
boundary value problems for the integro-differential equations of nonlocal wave interaction 0-48683
breaking, turbulent, experiments 0-67902
cathodic interaction of electrode with dense plasma 0-78067
cesium, research, book 0-46681
charge separation, application of external voltage 0-39554
charged particle motion, in self-consistent, continuous spectrum of waves
0-71134
chemical composition and kinetics of dissociation in CO-laser, role in

charged particle motion, in self-consistent, continuous spectrum of waves 0–71134
chemical composition and kinetics of dissociation in CO₂ laser, role in formation of inverse population 0–73217
classical system of charged particles, applic. of dielectric theory of Singwi, particle correlations 0–45550
clouds, spherical ionized artificial in uniform anisotropic plasma 0–51580
cold, condensation on to solid supports, synthesis of thin films 0–39539
cold, homogeneous, exact fields of pulsed dipole 0–55462
cold, interaction with solid tetraamminecopper(II) sulfate hydrate and nitrate, decomposition mechanism study 0–54175
cold, non-uniform, in uniform magnetic field, echoes at upper hybrid resonance 0–61346
collective excitations of two-dimens. plasma in mag. field 0–46705
collision-free, turbulent shock waves 0–64690
collisional, non-uniform, thermal conductivity and l.f. waves 0–61339
collisionless, flow, steady, planar effect of dissipation due to weak firehose instability 0–74498
collisionless, theory of resistivity 0–74519
column, axisymmetric bulged region formation 0–78170
column, dense, radiation and temperature 0–61397
columns with self-absorption, radial temp, distrib. 0–39643
compressible, between two parallel planes, magnetohydrodynamic wave 0–74511
conductivity, elec., high field, field independence suggested 0–78076
conductivity, elec., high field, field independence suggested 0–78076

0-74511
conductivity, elec., high field, field independence suggested 0-78076
conductivity, elec. in steady state discharge 0-61274
conductivity nonlinear h.f. influence of ion-ion correlations 0-39564
conductor and irradiation effects in electric arc plasma 0-78091
conference, growth points of physics, Florence (1969) 0-45504
convection pattern in asymmetric electric fields, shear effect anomalous transport in Q-machine 0-39588
convex bodies, thermal study Rayleigh-Gans-Born approximation
0-64664

0-64664

cumulation under concentric pressure impulse, approx. integral determ.

current carrying, linear mechanism for thermal energy transport 0-74486 currents sheet structure in rail gun 0-61443 currents, mag, induced, and thermoelec. effects, in non-uniform stream 0-39563

cylindrical column, propag. of fast magneto-acoustic waves 0-39600 d.c. arc, spectrochemical determination of traces as function of arc current 0-61276

in d.c. are with non-uniform mag. field 0-50137

d.c. discharge float zoning, hollow cathode, rel. to growth of materials with high melting points 0-50473 decay, anomalous, of nonuniform collisionless beam in u.h.f. field 0-46759

decaying, diffusion in 0-43267 deflagration, theory and expt. properties of coaxial deflagration gun 0-74495

dense, formed in pulsed electric arcs, parameters 0-71158 dense, prod. by laser, characts. 0-67945 dense, thermodynamics 0-74497 density, electron, measurement using e.m. wave in extraordinary mode 0-67914

0-0714
density, magnetospheric rel. to very low frequency electric field antenna impednance 0-66310
density in afterglow of axial discharge, meas. using double electric probes 0-55488
density measurement in open barrel shaped resonators 0-74567
density of toroidal O-pinch, by laser scatt. 0-58329

```
Plasma continued
```

diffusion, anomalous, geometric factor dependence 0-64674 diffusion, anomalous, rel. to l.f. self-excited oscills. 0-61342

diffusion, anomalous, rel. to weak turbulence 0-64673

diffusion, anomalous, rel. to weak turbulence 0–64673 diffusion, of separate charged particles across magnetic field 0–64675 diffusion, turbulent, in toroidal systems 0–50033 diffusion ambipolar and dissociative recombination of electrons with mole cular Ar₂* ions, exptl. investigation 0–35149 diffusion and instability in cold cathode PIG discharge 0–39553 diffusion eqn. numerical soln. 0–78052 diffusion in toroidal resistive plasma, equilibrium equations 0–50031 diffusion in toroidal systems with anisotropic press. 0–67937 diffusion of decaying densities across a magnetic field 0–74503 dipole field configuration, moment equation 0–58307 discharge, Penning hot cathode, radial distrib. of conc., effect of Lf. oscillations 0–43277 discharge, beam current instability and plasma heating by electron beam

discharge, beam current instability and plasma heating by electron beam 0-46699

0-46685 discharge, h.f., with skin current, turbulent heating 0-46685 discharge, h.f., with skin current, turbulent heating of ions 0-39543 in discharge, high pressure impulsed, characteristics 0-61255 discharge, inductive electrodeless, numerical study 0-64684 discharge, plasmoidal, r.f., delayed-emission theory of dark sheath 0-55463

0-3463 discharge, r.f., capacitive, dynamic instability, retuning effects 0-46697 discharge, r.f. field propag. 0-71146 discharge column, high-power constricted, theor. analysis 0-64685 discharge in laser, electron temp. meas. through bremsstrahlung X-ray spectral distrib. 0-43278

discharge positive column, enhanced light emission by current modulation 0-64701

dispersion velocity, formed by explosion of microspikes under action of autoelectron current of large density 0-74500 drift instabilities in low β plasma, non-uniform electric field effect

0-61264new drift mechanism found in nonstatic anisotropic plasma found by analog

computer simulation 0-61262 drift waves, nonlinear, in collisionless anisothermal plasma 0-50026 e.m. and particle fields interaction, first order versus reduced formulation 0-71147

e.m. and particle neios interaction, first order versus reduced formulation 0–71147
e.m. field transmission through slab having specified electron density—collision frequency profiles, integral 0–46707
e.m. wave echo, perturbation theory 0–50054
echo, three-momentum oscillations 0–46750
echo theory, spatial 0–67893
elastohydrodynmic models, coupling of monochromatic waves 0–55440
electric arc, combined irradiation and conduction effects 0–78091
electrical discharge rel. to controlled turbulence influence 0–53224
electrode behaviour in low pressure tubes 0–53163
electrondepartic T-tube, electron temp. determination, spectroscopic and laser light scattering 0–78051
electron, long-range interactions, computer study 0–45546
electron, stochastic heating in mag, mirror field 0–50022
electron Maxwell-Vlasov, quasi-particle description 0–46683
electron beam, intense relativistic, injection, equilib. and stability 0–46700
electron beam cyclotron interaction, distrib. function transformation 0–74507 electron beam in quiescent plasma, multiple scattering and energy loss

0 - 78042electron beam interaction, hot electron component formation mechanism 0 - 71191

electron beams intense relativistic propagation, effect of mag. guide field 0 - 39556

electron bremsstrahlung, nonrelativistic, in strongly magnetized plasma 0-64663

electron conc. determ. by interferometric study using He-Ne laser $0\,\text{--}5008\,\text{I}$

electron concentration, temp., excited atoms distrib., spectral lines intensity 0-58339

electron concentrations from atomic temps. 0–43311 electron cyclotron heating, resonant particles 0–50021 electron density and transverse electron temperature meas., of magnetoactive plasma 0–43273

electron density determ, by the number of the extreme resolved line 0-395590–3955) electron density determ. by the humber of the exterior teastres and 0–3962 electron density profile calc, using diffusion eqn. 0–78052 electron diffusion in magnetic bottle of cusped geometry 0–50028 electron distrib. of weakly ionized plasmas in arbitrarily time-depend, e.m. fields 0–43254 electron distribution function, in pre-electrode layer, influence of inelastic collisions 0–74508 electron echo expt., relation between echo frequency and wavelength determined by ballistic properties of electrons 0–50014 electron energy exchange, in thermionic convertors 0–77001 electron-cyclotron heating, numerical simulation 0–71135 electrostatic pot. of hot electron plasma confined in mag. bottle 0–50070 electrostatic shocks, collisionless 0–50035 electrostatic wave coupling in nongyrotropic plasma, dispersion relation 0–53157

0 - 53157

electrostatic wave coupling in nongyrotropic plasma, dispersion relation 0–53157
electrostatic waves growth rates, maximum linear, comparison for large domain of physical parameters 0–67924
electrostatic waves in plasma column in strong mag, field, linear and non-linear theory 0–55464
emissivity determ., of electrically nonconducting mats. 0–39578
end effects in alkali plasma, book 0–46682
energy, electron, distribution function in presence of noise 'following' probe method 0–64677
energy balance equation, exact deriv. 0–50025
engineering course, importance description 0–59855
equilibrium plasma, non-ideal, Monte Carlo investigation 0–53137
equilibrium relations, collision coeffs. 0–46694
excitation by He-Ne laser, transport processes 0–71133
excited states mean lifetimes absolute meas. using correlated photons in cascade 0–60941
finite-β, warm, structure of shock waves and solutions 0–64691
flash generator of tubular pinch discharge type 0–67977
flow, collisionless, around a cylinder, hybrid calculus to compute coulombian drag on body 0–67906

```
Plasma continued
```

flow, inmagnetic nozzle, experimental study 0-67915 flow, shear, divergent growth of mol. fluctuations 0-78050

flow, steady, planar effect of dissipation due to weak firehose instability 0-74498

flow, unsteady, one-dimensional, well-posedness criteria for anisotropic plasma 0-55459

flow dynamical equations, strong mag. field 0-53144 Focus, dense, laser driven axial flow pinch 0-71145

formation and dispersal in e.m. accelerators with dielectric erosion, monochromaticity coeff., calc. method 0-53136 fusion devices, new methods of driving plasma current 0-50027 gas, above 15000°K, from pulsed discharge tube 0-53223

general-relativistic collisionless 0–53140
h.f. discharge, interaction with surface of dielectrics 0–40819
heat transfer due to instability buildup of nonconducting electrons 0–39542

0-39542 heating, electron cyclotron, resonant particles 0-50021 heating, electron-cyclotron numerical simulation 0-71135 heating, resonant, in beam discharge 0-64667 heating, temporal and spatial origin of hot ions 0-74496 heating, turbulent, in discharge with skin current 0-46685 heating, turbulent, of ions in h.f. discharge with skin current 0-39543 heating, turbulent, to broadening of H spectral lines 0-50113 heating, turbulent, stochastic kinetic theory 0-78049 heating by electron beam prod. in linear discharge, beam current instability 0-46699 heating by exciting drift-beam instability, feedback system 0-64670 heating by opposed beams of coherent radiation 0-64669 heating by ultrashort laser pulses in electronic heat cond. process 0-78053 heating in high current gas discharge 0-64779

heating in high current gas discharge 0-64779
high pressure, with increased density of energy and radiation 0-43274
in high-current coaxial accelerator, interferometric study using He-Ne
laser 0-50081
high-pressure, ionization measurements using pulsed Langmuir probe
0-53175

high-temperature, neutral particle density determ. 0–61312 of hydrocarbon flame with alkali metals, effect of positive ions increase 0–58351

inert gas, stationary, non-equilibrium effects under normal pressure 0-74487

inhomogeneous, decay processes, generation of second harmonic 0-64700

 $0{-}64700$ inhomogeneous, magnetised, transport coefficients, derivation using quasi-linear approximation $0{-}67905$ inhomogeneous, ohmic resistance $0{-}50045$ injection, high- β_1 into mag. field from θ -pinch gun, obs. $0{-}46726$ interaction, nonlinear, with low density relativistic electron beam $0{-}50097$ interaction in microwave cylindrical cavity, TM_{010} reson. freq. $0{-}64711$ interaction with electron beam, h.f. instability threshold $0{-}46760$ interplanetary, lab. simulation $0{-}76658$ interplanetary flow properties at different meridional distances from active region centre $0{-}51783$ interstellar, wave phenomena, book $0{-}48461$ ion acoustic waves, apparent non-linear, effects of bunched ion bursts $0{-}78128$ ion bursts, series, generated by single voltage pulse on grid $0{-}50044$

0–78128 on bursts, series, generated by single voltage pulse on grid 0–50044 ion collection by spherical d.c. probe 0–58349 ion energy balance in Tokamak machine 0–61301 ion extraction, space charge layer parameters 0–43252 ion heating, laser pulse induced 0–74494 ion heating by h.f. electron beam-centrifugal instability 0–64751 ion recombination, review 0–58361 ion source, radial, Penning discharge 0–67940 ion sources, with hollow cathode 0–57499 ion-cyclotron vibrations in ion beam formed plasma, excitation 0–39603 ionised, weakly, conductivity, as related to particle diffusion in μ space 0–78075 ionised, weakly, response to turbulent gas flow 0–78056

ionised, weakly, response to turbulent gas flow 0-78056 degree of ionization, kinetic energy corrections for partially ionized plasma 0-50038

0-50038
ionization and recomb. functions of low temp. plasma 0-55506
ionization non-equilib. during cooling in pulse discharge 0-39544
ionization wave front, propag, and structure 0-53213
ionospheric, disturbances due to moving space vehicle, electron density obs. by gyro-probe 0-76477
ionospheric, interaction with satellite frontal surface 0-66331
ionozation inequilibrium, on input of current to magnetic field 0-64687
ions heating by fast magnetosonic waves, mechanism 0-53199
jets, interference holographic investigation using second harmonics of Rb-laser, results 0-53183
kinetic equation, unified 0-43260
kinetic equation of fully ionized plasmas 0-43257
kinetic theory for many body correlation and conditional probability fns, test particle method 0-43261
kinetic theory of completely ionized plasmas 0-43256

test particle method 0-43261 kinetic theory of completely ionized plasmas 0-43256 kinetic theory of fast processes 0-46693 kinetic theory with considerations of transverse plasma waves 0-43258 l.f. noise 0-53138 Lagrangian and Hamiltonian formulations 0-74493 Lagrangian inter radius, effects on perturbation flow of collisionless plasma 0-53145 from learn from a processing the process of the pr

0–53145
from laser beam interaction with solid surface 0–45805
laser created, stimulated emission 0–50060
laser irradiated solid particle, confined by mag, field 0–78094
laser produced, e.m. radiation expanding into uniform mag, field 0–74516
laser produced, second-harmonic generation 0–71156
light scattered by turbulent medium, mutual coherence function 0–53170
line broadening, ion motion effects 0–64703
linear absorption method, use of lines with initial Doppler profile 0–74491
longitudinal waves radiation pattern, from monopole and dipole antenna 0–58323
Lorentz, suppression of runaway of electrons, crossed electric and mag.

Lorentz, suppression of runaway of electrons, crossed electric and mag-fields 0-74514

Licitis 0-74514 Lorentzian gas, response to a.c. pulse 0-55455 low \(\text{low} \), streaming, column, stationary convective cells 0-61263 low density, resistive, m.h.d. equilibrium in model stellarator, theory effect of inertia and influence on loss 0-71141

Plasma continued

low-density, rel. to galactic HII regions, Investigations using hydrogenic spectral line obs. 0-57012

low-temperature in e.m. fields, instability region, non-linear theory 0 - 71136

magnetic, difference freq. harmonic ion heating using Whistler modes 0-55456

magnetized, fluctuation levels and reactive marginal instabilities 0-39608

magneto-active, effect of magnetic perturbation 0-55454

magneto-ionic theory, wave polarization 0-71131 magneto plasma, nonlinear resonant ion heating 0-64727

magnetoactive, excitation of waves by inhomogeneous electron beam 0-71178

magnetoactive, structure of relativistic solitons 0-46680

magnetoactive, synchrotron emissivity functions, rel. to the coeffs. of the dispersion equation 0–61287 magnetohydrostatic equilibrium 0–78073 magnetohydrostatic flux, current-eddy blob energy 0–51784 magnetoplasma, modulation due to magnetic perturbations 0–67897 magnetoplasma, synchrotron radiation, effect of plasma inhomogeneity and

magnetoplasma, intofulation due to magnetic petrobations of 50-7697 magnetoplasma, synchrotron radiation, effect of plasma inhomogeneity and drift 0-67896 magnetoplasmas, thermally ionized, enhanced ion surface recombination, theory 0-50016 magnetoplasmas, thermally ionized, particle losses, expts. with Cs. Ba. Sr and Li plasmas 0-50017 in magnetosphere, flow structure in vicinity of frontal point 0-51544 magnetospheric ring currents theory 0-51555 mass transfer processes on electrodynamic acceleration 0-64676 microwave, right-hand circularly polarized, through plasma with axial mag. field, damping 0-39537 microwave abs., effect of d.c. elec. field 0-71128 microwave emission from Maxwellian magnetoplasma 0-71144 microwave scatt. from nonuniform plasma 0-74527 models stable 1 and 2 dimens, thermal relaxation, particle-in-cell numerical computation 0-46684 monatomic partially ionized, excited levels population, nonelastic collisions effects 0-39540 motion in axially symmetric coordinate system 0-67904

motion of newly created non-uniform collisionless magnetoplasma 0–78048

0—78048
multi-component, Boltzmann eqns., linearization method 0—39541
nitrogen, total and total line radiation, 2000 to 60,000A 0—46712
noise, random, generation by electrons and ions 0—71129
noise spectrum, d.e., ion-molecule collision effects 0—67912
with non-Maxwellian velocity distrib., light spectra, study 0—46715
non-neutral, magnetically confined, rotor equilibria 0—78093
non-relativistic, nonlinear-cond-ternary correl. relations, transverse contrib. 0—78054

non-thermal arc, balance equations and transport coefficients 0-74499 nonequilibrium in MHD channel, Joule heating 0-45748 nonlinear theory, explanation in terms of three basic interactions, book 0--- 58308

nonuniform, normal-mode approach to linear oscillations 0-67949

information in marrious approach to miser oscinations 0-07949 obmic resistance of inhomogeneous sample 0-50045 opacity, direct laser measurement 0-67927 optical absorption coeffs, and half-widths of lines with combined levels 0-77641

optical scatt. spectra, cooperative parameter 0–61292 optical transparency, criterion 0–46714 optically dense, absorption and emission coeffs., calc., experimental error 0–50057

O-3003/0 oxygen, total and total line radiation 2000 to 60,000A 0-46712 PIG discharge, charged particle diffusion, obs. 0-39552 particle calculations in 2 and 3 dimensions, optimization, GALAXY computer program 0-39538 particle diffusion along elec. field transverse to non-uniform mag. field

0 - 53146phase relations between charact, variables of separately excited layers 0-43255

phase transition and negative clusters, imperfect system of metal vapour $0\!-\!74510$

pinched beams, r.f. defocusing, theory and experiment, comparison 0-43292

plasmoidal discharge, r.f., delayed-emission theory of dark sheath 0-55463

0-55463
popular article on plasma cluster during acceleration 0-55451
popular article on plasma physics and its application 0-50013
positiv column thermal inhomogeniety electrons balance eqn., Laplace
transform method 0-53227
pressure anisotropic and dielectric tensor, velocity moment and Vlasov
eqns., results 0-53143
quartz, plasma gas discharge heating of the surface of a solid 0-62207
pussing translations of the plasma gas discharge negative plasma

eqns., results 0–53143
quartz, plasma gas discharge heating of the surface of a solid 0–62207
quasineutral, charge separation, external voltage application 0–39554
radial temperature distribution, Fowler-Milne method, some He and Xelines 0–39549
radiation and conduction losses, analysis 0–39546
radiation from pulsed arc 0–58314
radiative transfer, stationary number density in excited state 0–42011
rare gas ion recombination, review 0–58361
reactive, high-temp, time-depend, behaviour 0–70708
refractive index determ, propag, method 0–43289
relativistic, Boltzmann collisionless eqn. 0–39557
relativistic, dispersion relation for longitudinal waves 0–50098
relativistic thermodynamic fluid, properties 0–39489
relativistic thermodynamic fluid, properties 0–39489
relaxation, in ignited-mode thermionic convertor, general theory 0–77007
resistance, anomalous, computations 0–67916
resistance anomaly rel. to ion-acoustic turbulence 0–53206
resistivity, anomalous, from ion-wave instabilities 0–64748
resonance, at 790 Å in reflection from thin Zr films 0–69078
resonance excitation by small pulsed dipole in weakly inhomogeneous plasma 0–59651
resonance radiation from non-radiative plasmons and decay into photons on a rough surface 0–62273
resonant electrons interaction with turbulent ion-acoustic oscillations 0–64743
review of current developments in theory and research including controlled thermonuclear fusion 0–74429

thermonuclear fusion 0-74492 second harmonic generation in laser produced plasmas 0-71156

Plasma continued

semi-infinite, correlation effects equilibrium and non equilibrium theory 0-61253

semiconductor low-temperature in e.m. fields, instability region, non-linear theory 0-71136 sheath, ion space-charge, time evolution from solid electrode, computer simulations 0-78096 sheath criterion for growing sheath 0-74541

shock wave in weakly ionized plasma, e temp. distrib. 0-55468

simulation, theory, using finite-size particles 0-61257

skin effect, anomalous, in magnetized plasma 0-43265 solar outflow equations with allowance for ion composition 0-51799 solar wind, measurement near earth's bow shock 0-59612

solar wind, plasma instabilities associated with heat, conduction and their consequences 0-51804

consequences 0–51804
solar wind, turbulence, viscosity and dissipation 0–48607
solar wind hydromag, obs. of velocity distribution function 0–59798
solid-state carrier waves, transmissic 1-line analogue 0–50024
soliton, relativistic, structure in magnetoactive plasma 0–46680
sources, coaxial, for identification of atomic spectra 0–42945
spectra, electron-broadening shift functions, exact calc. 0–50059
spectra, influence of pinch effect 0–74544
spectra of scattered laser light, effect of impurities 0–64702
spectral line intensity increase in d.c. arc discharge with applied nonhomogeneous magnetic field 0–48215
spectral lines press, broadening and shifts 0–52887
stimulated emission by laser created plasma 0–50060
stratified, transition radiation 0–78088
stream motion, stability in mag, field 0–64752
supersonic flow around dipole, convergence of method of successive

stream motion, stability in mag. field 0-04/32 supersonic flow around dipole, convergence of method of successive approximations 0-51552 surface heating, radiative by dense gas discharge plasma absorption of black body radiation 0-62207 surface waves excitation on Hg positive column, microwave scattering 0-53192

surface waves excitation on Hg positive column, microwave scattering 0-53192 surface waves on plasma half-space, dispersion relation, temp. and density gradients effect 0-55465 synchrotron radiation from thermonuclear plasma for electron temps. up to 200 keV, cales. 0-50018 temperature distrib, radial, possibility of determ. from excitation temp. functions, rare gases appl. 0-42965 temperature in afterglow of axial discharge, meas. using double electric probes 0-55488 temperature of ions in rarefied, multicomponent plasma, meas. by long ion tube 0-50020 temperature relaxations, Fokker-Planck coefficients in terms of spectral function of electric field fluctuations 0-78074 temperature relaxations, Fokker-Planck coefficients in terms of spectral function of electric field fluctuations 0-78074 temperature susceptibility, anisotropic 0-53143 test ion energy loss in plasma with homogeneous magnetic field 0-53141 textbook on plasma physics for undergraduate students 0-55453 theory, non-linear, one-dimensional, homogeneous, collisionless, three papers, report 0-64666 thermal conduction, radial, losses, analysis 0-39545 local thermal equilibrium assumption validity in electromagnetic shock tubes 0-78051 thermal induction, radiation and conduction losses report 0-64671 in thermionic convertors, analysis 0-77000

thermal induction, radiation and conduction losses report 0–64671 in thermionic convertors, analysis 0–77000 in thermionic convertors, electron energy exchange 0–77001 thermionic convertors, radiation intensities, spectroscopic meas. in several regions of 1-V characteristic 0–77008 thermionic with magnetic shear, convective losses, Q- machine anomalous transport, expt. 0–39588 thermodynamic equil. in Debye approx., distrib. function 0–43250 thermodynamic frozen props. of high temp. gases 0–61261 thermonuclear, synchrotron radiation for electron temps. up to 200 keV, calcs. 0–50018 thermonuclear explosion conditions in expanding sphere 0–49674 toroidal diffusion, effect of longitudinal electric field, pinch effect 0–78058 transparency, calc. based on interference-pattern contrast 0–50058 transport, unified theory, for partially ionized nonisothermal system 0–43264 transport mechanisms on excitation with He-Ne laser 0–71133

transport mechanisms on excitation with He-Ne laser 0–71133 transport model for converting charged species in drift tubes, mathematical modification 0–43251 transport phenomena, analysis, improved formalism 0–78059

transport phenomena, electron and ion., thermionic converters, report 0-63546

0-63546
transport phenomena, highly non-equilibrium conditions 0-67907
transport processes in mag. field, electron gas transport eqns. 0-62250
transport processes in mag. field, gauge-independent formalism 0-59131
transport properties, in strong external mag. field 0-78055
transport props. in strong mag. field 0-46690
turbulence, Dupree's perturbation and quasilinear theory comparison
0-50029
turbulence, accelerating mechanism for relativistic particles, spectrum
0-56887
urbulence, quiescent, weak and strong states, fluctuations theory

turbulence, quiescent, weak and strong states, fluctuations theory 0-50030

0–50030 turbulence, statistical theory Vlasov equation solution 0–67898 turbulence, strong, theor. method 0–46761 turbulent, anisotropic, e.m. radiation 0–71150 turbulent, frequency spectrum of microwaves scattered by 0–78086 weak turbulent computational study of correlation functions 0–55461 turbulent heating, rel. to broadening of H spectral lines 0–50113 turbulent heating in discharge with skin current 0–46685 two-component, one-dimensional, steady-state Vlasov equations for monotonic electric potential 0–74518 two-component, transport processes on the basis of Landau equation

two-component, transport processes on the basis of Landau equation 0-46691

two-temperature, population of excited levels, degree of ionization, formulae 0-74490

value to -74490 v.h.f. pulse discharge, source for exciting molecular spectra 0-74532 velocity distribution function of electrons in gas in electric field, 'stationarization' 0-53139 Doppler broadening 0-78045 Venus, changes in properties, Mariner 5 obs. 0-63148 Venus vicinity flux measurements, charged particle traps 0-63150

Plasma continued

very-high-density, for thermonuclear fusion, focus, axial flow-pinch, inertial confinement 0-74489

viscosity of argon from 3500 to 8500°K at atmospheric pressure 0-74685 Vlasov eqn., test particle method in kinetic theory, conditional probability for 0-43261

0-71130

for 0-43261
Vlasov-BGK eqn., method of normal soln. 0-71
Vlasov-BGK equation, linearized 0-43259
Vlasov-BGK equation, linearized 0-5198
wake feature study of OGO-2 satellite 0-64665

warm, dispersion relations 0-61260
wave conversion and resonance below second electron cyclotron harmonic

0 - 50095wave propagation, longitudinal, in partly ionized viscous plasmas 0-78127

wave resonances, kinetic theory, test in inhomogeneous plasma column $0-53156\,$

waveguide comprising two separated isotropic layers, leaky wave propagation 0-42127

weakly ionized, in arbitrarily time-depend. e.m. fields, electron distrib. 0-43254

0-43254
weakly ionized strong interaction, semiconducting props. 0-55466
wings of Stark-broadened lines, profiles of forbidden components, objections to method of calc. 0-61019
wire explosion, temperature and electron density in late stage, spectroscopy 0-43341
a-particle heating rel. to mirror reactor energy balance 0-70700
Al, laser-produced, temperature decay 0-64672
Ar-K cylinder, energy loss due to K resonance radiation 0-39547
Ar-K streaming through channel with segmented electrode array, current distribution 0-39567
Ar-Na rotationally symmetric, neutral Na partial pressure distribution

distribution 0-39567
Ar-Na, rotationally symmetric, neutral Na partial pressure distribution 0-61254
Ar-O plasma afterglow, ion and electron decay rates 0-67894
Ar-jet, temp. and velocity distrib. 0-67903
Ar, Cs seeded non-equilib., preionization, obs. 0-48969
Ar, electrodeless rf discharge, electron temp., density and cond. 0-39566
Ar, equilibrium 0-78063
Ar, in supersonic cooling under electronic supersonic supersonic supersonic cooling under electronic supersonic supersonic supersonic super

Ar, in supersonic cooling, under elec. discharge, elec. cond. increase 0-78077 Ar, radial temp. distrib. determ. from excitation temperature functions 0-42965

0-42965
Ar, shock produced, absolute line intensities and continuous background meas. 0-78092
Ar, supersonic flow, local electron vel. and density, under accelerator forces 0-61284
Ar, temp., electron density, optical thickness, under press. 0-39561
Ar, transition from three-body to dissociative electronion recomb. 0-61266

0-61266
Ar, transport properties, exp. determination 0-67909
Ar breakdown moving between cold electrodes in crossed mag. and elec. fields 0-39565
Ar conductivity under pulsed field, effect of preliminary ionization, data 0 58327

U 58321
Ar ion, spectral lines press, broadening and shifts 0-52887
Ar low temp, continuous radiation at 12000 and 16000°K 0-55474
Ar plasma afterglow, ion and electron decay rates 0-67894
Ar plasma in supersonic flow, electron temp, and density determ.
0-61256

Ar radial distribution of electron density, spectroscopic investigation

Ar supersonic flow, under Laplace accelerating forces, aerodynamic parameters variation 0-67908
Ar, st clusters in high pressure plasmas, icosahedral symmetry 0-74501
CO₂-N₃, 90%-10%, total radiative intensity calcs. 1×10³-2×10⁵ °K
0-43288

CO₂, total radiative intensity calcs., 1×10⁵-2×10⁵ °K 0-43288

CO₂, total radiative intensity calcs, 1×10° 2×10° 0K 0–43288 Cs, emission lines, intermediary electrode polarization influence 0–53172 Cs, equilibrium composition estimate 0–58310 Cs, photoresonant, optical pumping, ionization 0–53151 Cs, spectral lines press, broadening and shifts 0–52887 Cs, transport phenomena 0–64678 Cs, transport phenomena 0–64678 Cs, transport phenomena 0–50046 Cs discharge, ionic species 0–50046 Cs I lines shift due to const. elec. and mag. fields acting simultaneously 0–49774 Cs plasma research, book 0-46682

Cs plasma research, book 0-40682
Cs vapour, discharge electron-energy distribution function 0-74614
D-T thermonuclear, fuel burn-up and direct energy conversion 0-71132
FeXVII, intensities of 2p-3d, 2p-3s lines in a rarefied plasma 0-42964
H, fully ionized, optical consts. for Nd-glass, ruby and CO, laser radiation 0-50061

H, in supersonic spherical source, parameters 0-55452
H, ion density from Stark broadening meas. 0-78065
H, nonisothermal, influence of surface emissivity on conduction, convection and radiation 0-67899

and radiation 0-0-1899
H, radiative energy transfer 0-46689
H, reaction kinetics, study by short-time spectroscopy 0-71175
H, spectra, close collisions in Stark broadening 0-61294
H, spectral lines press broadening and shifts 0-52887
H, thermal conductivity, determination from electric arc discharge exp.

0 - 67910

Hoptically thin, self-consistent e vel. distrib. 0-78064 H₂, density of negative glow, in longitudinal mag. field 0-50126 H₂, fully ionized, of mean density, quantum statistical equation of state 0-53142

O-39548

H. estimated expansion due to laser impulse produced thermal shock O-39558
He.K. thermal props., mass transfer due to contact with cold wall O-39548

0–39548
He, diffusion of decaying densities across a magnetic field 0–74503
He, electropositive gas, decaying, diffusion 0–43267
He, model for nonequilibrium arc plasma 0–67900
He, rotating, magnetoacoustic waves excitation and detection 0–43324
He, spectral emissivity, at 20000-5000° and 1-100 atm. 0–42973
He, spectral imes press. broadening and shifts 0–52887
He, Stark broadening of neutral line 5876 Å, electron density and temp. determ. 0–49815
He, Stark profiles of 4471 Å line and forbidden components, calc. 0–39325

Plasma continued

He, stationary, non-equilibrium effects, expt. and theory 0–74488
He, turbulent heating, satellites 0–53173
He, variation of density of accelerated electrons behind diaphragm 0–53150
He I 5016Å computed profiles at high electron densities 0–74531
He I \(\text{1.4471}, \text{1.4470}, \text{1aboratory plasma obs. rel. to astrophysical spectra 0–61018}

0-61018

He II line λ =4686 Å, broadening 0-64293

Hg, afterglow, electron density and temp. decay, meas. using microwave cavities 0-64789

Hg, free-fall theory for decay of average electron density 0-53164

Hg diffusion velocity 0-74502

Kr spectral lines, excitation temp. functions 0 46368

Li, exploded-wire, He-Ne laser radiation absorption 0-46716

Li, spectral emissivity, at 20000-50000° and 1 100 atm. 0-42973

LiH, laser-produced, spectroscopic meas. 0-61295

LiI 2P 4F and 2P-4D lines, relative intensities and shifts, rel. to electron conc. 0-74534

N. mag. confined column, e temp. spectroscopic obs. 0-46217

N, mag. confined column, e temp., spectroscopic obs. 0-46717 N, thermal conductivity, determination from electric arc discharge exp. 0-67910

0-67910
N, viscosity determination 0-61265
N and N, shock ionized, elec. cond. in mag. field 0-43272
N*, Stark broadening of line spectra 0-39289
N; transport coeffs, to 13000°K 0-67911
NO, electronegative gas, decaying, diffusion 0-43267
Ne-N; mixtures, electrodeless discharge modes, plasma display panel applic. 0-53158
Ne discharge, electron drift vel. positive column 0-61277
Ne Lorentz plasma, electron vel. distrib., role of inelastic collision processes 0-71138
O, atomic recomb. en.r. obs. 0-61259

esses 0-71138
O, atomic recomb., e.p.r. obs. 0-61259
Sr, density meas. by reson. fluorescence scatt. method 0-42995
U-II temp. and partial press. meas. using Boltzmann plot tech. and relative intensity method 0-50023
X, variation of density of accelerated electrons behind diaphragm 0-53150

Xe, absorptivity and emissivity of pulsed discharge plasma 0-53174
Xe, continuous spectrum calculation 0-67895
Xe, effects of pressure, input energy, and magnetic field on spectral properties 0-55473

Xe, electroconductivity of impulse discharge, temperature dependence 0-64688

Xe, ionization behind shock wave front, i.r. diagnostics 0-53189 Xe, laser produced, electron density, spatio-temporal evolution 0–78066 Xe, pulse discharge, radiation absorption 0–50062 Xe, pulsed, two wavelength laser interferometry, refractive index investigation 0–71157

collision processes

collision processes
binary, simulation mirror mode problem in θ-pinch geometry 0–61267
Boltzmann eqn. for relativistic plasma 0–39557
Boltzmann transport eqn., for perturbation in Maxwellian vel. distrib. function 0–55454
boundary layer model for weakly ionized plasma 0–43271
Cerenkov radiation affected by electron collisions 0–43268
coefficients, rel. between forward and inverse reactions 0–46694
collisionless shock, meas. of turbulence by collective scatt. of light 0–67918

0-67918

Compton interaction of a photon gas with a plasma 0-58311
cyclotron echoes, E-H, for relax, and diffusion meas. 0-74505
diffusion, enhanced collisional, and an exact energy balance equation deriv. 0-50025
e.m. wave penetration into hot plasma slab, electron transit time-wave period ratio 0-50052
e.s. coherent plasma waves, growth and decay, nonlinear interaction study 0-67955

elastic and non-elastic, effects, thermodynamic balance 0-78060 elastic scattering, of fast charged particles in a background plasma 0-43269 electron ion, diffusion broadening effect on clusters in longit. mag. field 0-74540

0-74540 electron collisions during passage of radiowaves through magnetized inhomog, plasma, investig. 0-53166 electron impact broadening, theory 0-74533 electron-atom energy exchange 0-78061 electron energy exchange 0-78061 electron-sollision frequency in plasma, influence of finite dimensions of ions, exptl. determination 0-53147 electrons runaway suppression in Lorentz plasma, diffusion eqn., expt. 0-53148 finite sized particles in one two end that its light of the control of th

electrons runaway suppression in Lorentz plasma, diffusion eqn., expt. 0–53148 finite sized particles, in one-, two- and three-dimensions dynamics and kinetics 0–61268 with gas, neutral in magnetic field obs. 0–67913 heavy particle, influence on population and ioniz. equil. 0–74506 inelastic, influence on distribution function of electrons in pre-electrode layer 0–74508 instability, collision-induced, nonlinear 0–67965 ion-molecule, effect on d.c. noise spectrum 0–67912 in ion-wave echoes spatial, numerical study 0–55493 ionosphere, F2 region cooling by inelastic collisions of electrons with O(P) 0–54287 kinetic theory of transport processes for Coulomb interactions 0–43270 laser-produced from Al, Cu-metal surfaces, study 0–67946 Lorentzian magnetoplasma in external magnetic fields presence, transport phenomenon, electron distrib. for 0–39560 losses in mirror confined plasma, spatial variations effects 0–43294 magnetoplasma, freq. dependent transport eqn., Fokker-Planck collision terms 0–46692 mirror machine, hot electrons and residual neutral particles interaction, end loss theoretical analysis 0–50068 model integral, for particles of different masses 0–64743 neutrons (slow) scattering by magnetically confined plasma with electrostatic ion oscills, cross sections 0–50019 nonelastic, in monatomic partially ionized gas rel. to excited levels population 0–39540 positron production and equilib. conc., optically thin relativistic system 0–74504 radial structure of collision-dominated plasma column 0–50034 resistive diffusion in axially symmetric Tokomak geometry 0–50032

Plasma continued collision processes continued

sheath in weak mag, field ion-electron pair generation fn. 0–43290 solar wind, effective frequency and thermal state 0–41836 supercooled dense, possibility of metastable state's existence, ball lightning hypothesis 0–58344 three-wave interaction, resonant, effect of collisions, kinetic approach 0–61343

0-61343
transport equations, hydrodynamic for weakly ionized plasma of gas discharge 0-39551
wave particle interaction in magnetosphere, viscous magnetopause, boundary layer behavior 0-56805
waves absorption in mag. field 0-74571
Ar, neutral atom collision freqs. 0-71137
CO, laser plasma, populations, mass spectra 0-46695
H, neutral atom collision freqs. 0-71137
H, spectra, close collisions in Stark broadening 0-61294
He, recombination rate coeff. of He²⁺ with electrons, depend. on electron density 0-78046
Li, elastic electron scatt. by Li⁺, resonance effects, plasma electric props. 0-50037
Mg, u.s. jet, charge exchange of cluster 0-74509

Mg, u.s. jet, charge exchange of cluster 0-74509 N and N₂ shock ionized, electron collision freq. 0-43272

3 equilibrium bifurcation problem in E-layer, methods for solution 0-46723

 0^{-40723} θ pinch, multichannel energy anal, of ion flux 0-46730 θ pinch for plasma with high ion temperature, stationary collisionless shock waves 0-39570 θ -pinch, electron velocity distribution function, deviations from Maxwellian,

 θ -pinch, electron velocity distribution function, deviations from Maxwellian, laser radiation scattering 0–78113 θ -pinch, electron-density profiles by holographic interferometry 0–64668 θ -pinch, microwave scattering by I.f. oscillations 0–71163 θ -pinch model for spontaneous mag. field reversal at high temps. in compression phase 0–78099 θ -pinch, stable curved, in series of caulked cusp fields 0–46719 θ -pinch, toroidal, with superposed hexapole, plasma losses 0–67939 θ -pinch two-dimensional model for buildup drive current, symmetric method of energy feeding 0–43293 afterglow hydrogenic plasma, particle distribution 0–64705 alkali plasmas, book 0–46682 Astron, equilibrium mag. field associated with E-layer, eqn., methods for soln. 0–46723 astron-like devices, injection phase 0–74546

sonii. 0–40723 astron-like devices, injection phase 0–74546 beam plasma discharge in magnetic mirror, experimental studies 0–39584 bounded, spherical electrostatic, probe charact., asymptotic continuum theory 0–58336 cavity resonator, cylindrical, partially filled with magnetized plasma

cavity res 0-63497

0–549/7 clusters with parabolic particle distribs., diffusion broadening in longit. mag. field 0–74540 column, high- β , sharp-boundaried with helical fields, feedback stabilization 0–78101

0-78101 column, streaming, low β , surface-ionized, at low mag. fields 0-78105 configurations, ellipsoidal, in gas discharge 0-74548 control-theoretic approach 0-53179 diffuse screw pinch, magnetohydrodynamic stability 0-55498 Doublets, parameter obs., scaling laws 0-78104 drift model, rigid for high temperature containment 0-67934 electron-hole pinch, oscillations 0-62271 ellipsoid, equilibrium in external h.f. field 0-61296 excitation of surface wave, waveguide bounded with perfect magnetic wall 0-43249

0 - 43249

flow process, exptal. obs. of magnetic flux transfer at hyperbolic neutral point 0-78097 rel. to fusion, controlled, mag. confinement and microinstabilities 0-46253

0–46253
fusion reactor conference, Culham, England, 1969 0–70695
heating, stochastic, in mag. mirror field, electron plasma 0–50022
and heating by nonlinear interaction with laser radiation 0–50085
Heliotron-P field with buried ring conductors, expt. 0–71164
high current techniques in R & D 0–39587
and instabilities, review 0–46753
interaction between fully ionized plasma and neutral gas blanket 0–55475
ion energy balance in Tokamak machine 0–61301
ion source, heavy, high charge state, for accelerators 0–38780
ionized gas-solid suspended in electric field, thermal effect 0–65866
laser-produced, optical interferometric meas. 0–53190
lenses using superconducting magnets 0–47680
linear multipole fields as guide fields for high-β output of plasma gun
0–78103
loss structure from hot electron plasmas in Princeton linear guadruscole.

loss structure from hot electron plasmas in Princeton linear quadrupole device 0-67933 mag. field, of laser irradiated solid particle plasmas 0-78094

magnetic, and thermonuclear reactor appl. 0–71160
magnetic, ion charge/mass ratio analyser 0–46718
magnetic, non-neutral plasma, rotor equilibria Vlasov-Maxwell model 0–78093

0-78093
magnetic bottle, electrostatic pot. of hot electron plasma 0-50070
magnetic bottle of cusped geometry, electron diffusion 0-50028
magnetic bundles in reacting flowing plasma 0-71162
by magnetic field, concentration, probing by atomic beams for determination of core displacement 0-64710
magnetic mirror traps, critical adiabatic parameters for stable-unstable transition 0-46721
magnetic systems, closed, theoretical analysis of toroidal field configurations 0-74550
magnetic trap, self-diffusion paradox 0-55478
mirror confined, press. anisotropy meas, using external method 0-46724
mirror onfined plasmas, role of end regions in the steady state 0-61300
mirror machine, charged particle injection 0-38464
mirror machine, end loss due to interaction with residual gases, theoretical analysis 0-50068

analysis 0-50068
mirror system, collisional losses, effects of spatial variations, Fokker-Planck eqn. applic. 0-43294

mirror-confined, feedback suppression of collisionless, multimode drift waves 0-46743 mirror-trap, ion-cyclotron instability 0-39610 multipole, linear, convective cells in quiescent region 0-58328

Plasma continued confinement continued

multipole device, effect of trapped particles on drift-cyclotron instability 0-39609

negative V¹¹ system without use of toroidal solenoid coils 0-50065

O-pinch, toroidal, with superposed hexapole field 0-58329 pinch, direct in quadrupolar h.f. field, stability rel. to electrode separation 0-64757

pinch effect, magnetohydrodynamics theory, in dense plasma focus 0-74545

pinch effect, trapped particle, explanation of Tokamak toroidal discharges

pinch effect due to driving toroidal electric field 0–78100 pinch effect for trapped particles in Tokamak 0–55476 pinch-theta, stability, exptal. and theoretical obs. 0–78098 puff generated by θ -pinch, consequences of rotation in logit. mag. field 0–39581

0–39581
puff in mag, guide fields, analysis of extracted ions 0–64706
Q machine with magnetic shear for thermionic plasma convective losses, anomalous transport, expt. 0–39588
Q-machine plasma, temp. gradient effects 0–55479
quadrupole, levitated toroidal, effect of introducing supports 0–55477
reactor using mirror machine confinement feasibility and end losses reduction 0–39201
sheath, inhomogeneous, stability study 0–55496
sheath boundary, a Mach surface 0–67936
sheath low density in weak mag, field, theory 0–43290
sheet pinch stability, computer models for motion simulation, expt. 0–46758
shield clouds surrounding test particles, conditional probability and many-body correlation fns. 0–43261
by small superconducting magnets 0–67930
stabilisation, dynamic in static mag, field with small alternating e.m. field 0–71165

stabilization of trapped particle mode by cool plasma component 0 - 61349

0-61349
stationary magnetic and high frequency fields, ratio of magnetic mirror length to skin depth arbitrary 0-50069
stellarator, effect of electrostatic field on particle motion 0-74547
stellarator, finite β, magnetohydrostatic |=1, equilibrium 0-61302
stellarator, min. B field drift and magnetic surfaces 0-58331
stellarator, sharp surface, equilibrium and stability with longitudinal current 0-39586

current 0–39586 stellarator, stochastic heating, obs. 0–64719 stellarator, stochastic heating, obs. 0–64719 stellarator equilibrium conditions 0–46722 stellarator field, minimum B, magnetic and drift surfaces 0–39580 stellarator with sharp surfaces, stability limitations 0–43335 Stix coil, use in ion cyclotron resonance heating 0–64707 thermal induction plasma, maintenance voltage direct meas. 0–64715 thermoisolation in stellarator Uragan 0–74604 theta-pinch, shock and current sheet structure 0–50066 Tokamak, parameter obs., scaling laws 0–78104 tokamak discharges, adiabatic compression 0–78102 Tokamak 3, large values of β_1 0–74553 Tokamak 3 machine, ion energy lifetime 0–74552 tornado trap, structure of the magnetic field, photographs of visualisations 0–64708 toroidal, axisymmetric, systematic, shaping of |B| flux surfaces 0–39585

toroidal, axisymmetric, systematic, shaping of |B| flux surfaces 0–39585 toroidal, high- β , rotating plasma, perturbation of magnetic surfaces 0–74537

toroidal high-\$\beta\$ device, plasma behaviour 0-50067 toroidal octupole, obstacle, induced convection, effects of hoop supports 0-43291

0—43291 toroidal octupole, single-particle diffusion due to magnetically guarded hangers 0—53181 toroidal resistive, diffusion, equilibrium equations 0—50031 toroidal system, trapped particle modes in multipoles, finite press. effect 0—74579 toroidal systems by hydrogen 0, 74551

toroidal systems, turbulence 0–74551 toroidal systems with anisotropic press, diffusion 0–67937 torosatron config., mag. screw type in presence of axial current 0–39583 Torsatron system combined with Vintotron system 0–50063

torus, axially symmetric, steady flow using guiding-centre equations 0-67932

trap, magnetic, quadrupolar, retention and injection in 0-64709 turbulence studies using Stark broadening 0-50064 two-setting spiral magnetic configurations with spatial axes 0-61297 in unsymmetric mag. field configurations, motion and equilibrium obs.

0-71142
Z-pinch, conical, effect of axial mag. field 0-61298
Z-pinch, time-dependent electron densities calc. by improved optical resonator 0-43305
Ar, Z-pinch discharge, props. and laser effects 0-43276
Ar confined-arc plasma, non-equilibrium behaviour 0-53208
He, Z-pinch discharge, time-correlated study 0-46720
He confined-arc plasma, non-equilibrium behaviour 0-53208
Li ion heating in Penning discharge in mag. mirror geometry 0-46688

devices acceleration of neutrons in z-pinch and focus discharges, model 0-78057 accelerator, 20MW, design and operational charac. 0-53182 accelerator, for gas with Cs impurity, parameters in crossed E, H fields at intermed, pressure 0-71166 accelerator, impulsive, end-type, structure of discharge, effect of pinch effect 0-74544 accelerator, optimum parameters 0-71159 accelerator end-face type, heat fluxes to electrodes, electrodes erosion, meas. method 0-58330 accelerator impulsive with dielectric erosion, current distrib. investigation 0-53178

0-53178 accelerator two stage impulsive of coaxial type with electrode, investigation 0-53177

tion 0-53177
accelerator with harmonic e.m. waves, plasma mean vel. calc. 0-50072
accelerators, pulsed, spectral distribution of radiant losses 0-71154
are excitation source, economical design, emission characts. 0-53234
arcs, pulsed constricted for producing high temp. 0-50135
astron-like devices, injection phase 0-74546
beam melting installation, layout and application 0-39589
burner applic. to coating fabrication 0-58588

Plasma continued devices continued

cavity resonator partially filled with non-uniform plasma, TM₀₁₀ reson. freq. 0-64711

coaxial sources, fast particles formation 0–61304 convertor, thermionic plane geometry, radial distribution of parameters 0–42159

0—42139
cyclic magnetic apparatus with irises, azimuthal border fields formed by mobile mag. screens 0—74554 diode, two-emitter, pot. distrib. 0—45752 diode with cylindric symmetry, thermoelec, theory 0—73136 diodes, ionosonic vibrations freq., wavelength determination, expressions 0—53198 display panel, electrodeless, discharge modes in Ne-N $_2$ mixtures applic. 0-53158

0-3138
divertor magnetic surfaces, influence on toroidal drift 0-74549
flow heating for fusion 0-70701
frequency multiplier with vacuum region in coaxial metallic channel
0-78095

0-8095 (usion torch, direct appls. of reactor plasma 0-71168 gun, θ -pinch, and high- β injection into mag. field, obs. 0-46726 gun, θ -pinch, for high- β injection 0-67938 gun, deflagration, coaxial properties 0-74495 hf. plasmatron, jet characts. of controlled and combined discharge 0-39641

h.f. plasmatron, jet characts. of controlled and combined discharge 0—39641

Hall-accelerator, high-current, d.c. two stage, suitability for controlled thermonuclear work 0—70722
heating, with combined r.f. and steady mag. fields 0—78106
hollow-cathode, plasma ion source 0—42225
homopolarnik, nonstationary processes, in discharge 0—43362
injector, coaxial, charge concentration and spatial distribution 0—61307
injector, quasi stationary, pressure distrib. in current 0—61306
ion source, profiles of outlet opening, determination 0—57498
jet, high-speed (4-6 cm/usec) propag. 0—71167
jet, spectroscopic temperature meas. 0—66952
Jet, supersonic, spectroscopic investigation 0—46727
jet formation by laser beam radiation 0—61308
jets, high speed, study of metal damage 0—53728
jets interstreaming, collisionless interaction 0—55480
Knudsen thermoemission converter in transverse mag. field, plasma state in gap investigation 0—52217
Langmuir probes for Ar-tenuous plasma jet meas., peculiarities 0—58337
light plasmotron based on continuous operation CO₂ laser 0—53191
linear crossed field generators and accelerators, circulating currents velocity and distributions 0—50040
nebulizing plasma arc system for alloy analysis 0—53638
optical plasmatron, feasibility 0—64721
particle analysers, space charge effects on energy resolution, report 0.64720

particle analysers, space charge effects on energy resolution, report 0 64720

plasma-focus, intense neutron production from enhanced plasma resis tance 0-74542

plasmatron outlet spectroscopic investigation of plasma parameters 0-64704

0-64704
plasmotron, electrodeless, review 0-78107
plasmotron, power requirements 0-46739
power generation systems, ionizing fronts 0-64713
probe electrostatic spherical for chemically frozen plasma, continuum theory applic, description 0-53187
probe multinet characteristics, influence of outer net, quantitative examination 0-53185

tion 0-53185
probes magnetic small-dimension cooled, construction 0-58334
Q machine, book using alkali-plasma 0-46682
Q machine with magnetic shear for thermionic plasma convective losses, anomalous transport, expt. 0-39588
Q-device, production and applic. of Li and Sr 0-64723
Q-machine, interaction between plasma ions and grid-excited pulses 0-6731.

O-67931
Q-machine's thermally ionized plasma, stable state investigation 0-58345
reactors, high temperature energy systems, inductive magnetoplasma
dynamic converters 0-60856
source of great intensity, balance of negative ions 0-43296
stellarator, Sinus, effect of divertor mag. field configurations on toroidal
drift, in closed mag. traps 0-74549
stellarator, drift waves and plasma diffusion 0-74538
stellarator, finite β, magnetohydrostatic l=1, equilibrium 0-61302
stellarator Uragan, thermoisolation and confinement of plasma 0-74604
stellarator WIIa, operation 0-64712
thermoanemometer Langmuir probe for tenuous plasma diagnostics
0-58332
thrusters, continuously working, investigation 0-61309

0-3532 thrusters, continuously working, investigation 0-61309 Tokamak, pinch effect for trapped particles 0-55476 Tokamak TM-3 machine, plasma probing with beam of fast H atoms 0-74555

0-74555
Tokamak extrapolation as fusion reactor 0-70703
Tokamak extrapolation as fusion reactor 0-70702
Tokamak machine, ion energy balance 0-61301
Tokamak3 machine, ion energy lifetime 0-74552
torch, induction, for high power levels 0-61305
torch with converging moveable jet generators, patent 0-58338
toroidal configuration of Tokamak type, stability of ballooning modes 0-46725

0–46725
u.h.f. pulse generator for slow e.m. wave's phase vel. meas. in plasma waveguide 0–58318
Z-pinch, deuterium, electrode metal effects 0–61299
Ar jet, weakly ionized, axial and radial temperature profiles 0–61310
Ar supersonic jet, Langmuir probe meas. 0–58337
N₂ jet, rel. to heat transfer to cylinders at high temp. 0–69745
Se-amorphous and polycrystalline layers plasma contact, volt-ampere characteristics investigation 0–53159

diagnostics θ pinch, multichannel energy anal. of ion flux 0–46730 air, breakdown, laser induced, temp. meas. by X-ray emission 0–43308 alkali metal, with negative ions, ion and electron density 0–61325 aperture effect on axial velocity distribution function meas. 0–64682 arc physics, book 0–50138 atomic and ionic transfer temp. meas. using X-ray meas. 0–78108 atomic temperatures for diagnostics at medium pressures 0–43311 beam-plasma discharge meas. and properties 0–39584 boundary as a Mach surface, motion of ions 0–39555

Plasma continued

diagnostics continued bounded, spherical electrostatic, probe charact., asymptotic continuum theory 0–58336

concentration determ. from probe characts. over wide press. range

concentration determ. in TM-3 apparatus using H beam 0-74555

conductivity, complex, rp. meas. by external probes 0-43303 conductivity meas. rf. apparatus, patent 0-78118 current sheet propagating structure, press. distrib., high speed piezoelectric press transducer applic. 0-39582 density meas. in closed system using u.h.f. oscillations at $\lambda=8$ mm 0-71171

0-71171
density meas, using series of fast ion bursts produced by single voltage pulse 0-50044
discharge inductive stationary at atmospheric press, in air, Ar, parameters meas, by mag. probes 0-58315
double electric probes for meas, of radial profiles of density and temp.
0.55498

double electric probes for meas, of radial profiles of density and temp. 0-55488 dual time of flight mass spectrometer 0-43301 electrode temperature in region of spot radial distribution 0-43312 electron's temp, and energy distrib, charged particles conc. in Ar discharge, probe meas, method 0-53149 electron densities, time-dependent, meas, by improved optical resonator 0-43305

0-43305 electron densities and temp. of Ar with moving striations, simultaneous meas. 0-67941 electron density, conditions necessary for obtaining given density 0-55483

0-55483
electron density by laser self-heterodyne 0-50077
electron density determ. using skin effect 0-56199
electron density determ. using surface wave probe method 0-39594
electron density meas., low value (to 10°/cm⁻³) microwave interferometer, simple and inexpensive design 0-50080
electron density meas. by TM_{0.00} cavity method 0-67942
electron density measurement using electromagnetic wave in extraordinary mode 0-67914 and inches the design of the desi

electron density of post-discharge plasma, hyperfreq. interferometer design 0-43299

0-43299
electron energy distrib., time-resolved meas., method 0-74559
electron energy distrib in gas discharge, meas. 0-43376
electron temp. estimation from mag. probe signal difference 0-64693
electron temp. from incoherent scatt. of mm waves 0-55469
electron temp. meas., refinements in He line ratio method 0-74558
electron temperature in standing microwave, spatial dependence meas.
0-39574

0–39574 electron temperature meas., in flowing high-density plasma, by Langmuir-probe 0–64714 electron velocity distribution function of θ -pinch plasma fron incoherent laser radiation scattering 0–78113 electron-density profiles in θ -pinched plasma by holographic interferometry 0–64668 with electrons, hot, obtained on cyclotron resonance 0–74562 electrostatic probe and cct. for low-temp. meas. 0–46731 energy, electron, distribution function in presence of noise 'following' probe method 0–64677 energy, analyser in axial magnetic field report 0–50075

method 0-640/7
energy analyser in axial magnetic field, report 0-50075
energy-mass analysis for highly ionized steady state plasma 0-71173
flow vel. meas. with total head tube 0-55485
fluctuations, electron-beam echo applic. 0-50079
in gas-discharge cells transparent, use of three-mirror laser interferometer 0-49112

0-49112
h.f. density meas., laser interferometer, Schlieren system 0-46735
harmonic generation, by Landau-damped ion acoustic waves, experimental study 0-50074
high-pressure discharges, rotational and vibrational temps. 0-43307
high-pressure plasma under thin-sheath conditions, ion current to spherical probe 0-61315
holographic investigation of laser sparks, electron concentration and temperature 0-63612
hydrocarbon flame, ion density meas., negative electrostatic probe 0-56690

0-5690 1.r. technique, Xe ionization and recombination behind shock wave 0-53189

0-53189 inhomogeneous, light irrad., temp. and density determ. by scatt, light intensity method 0-74560 interferometer, fast far i.r. 0-46726 interferometer, hyperfreq., for post-discharge plasma electron density meas. 0-43299 interferometric study in high-current coaxial accelerator using He-Ne laser 0-50081

interplanetary space and magnetosphere 0-62930 ion current from flowing plasma to sheath-surrounded cylindrical electrode 0-64716

ion sheath modification by electron emitting probe 0-50076 ion temp. determ. method in laser-produced plasmas 0-58335 ion temp. in Tokamak-3 device, determ. from Doppler broadening 0-46728

ion temp, in Tokamak-3 device, determ. from Doppler broadening 0—46728
Langmuir double-probe, stationary sheath-probe capacity 0—53188
Langmuir probe, directional 0—78110
Langmuir probe, ion flow effects 0—50082
Langmuir probe meas. in Cs plasma, for determ. of Cs⁺→Cs collision cross section 0—64255
Langmuir probe meas. in glow discharges, contamination effects 0—61313
Langmuir probes, cross spectrum of density fluctuations in abnormal glow discharge plasma 0—61316
Langmuir probes, effect of surface conditions 0—43310
Langmuir probes, effect of surface conditions 0—43310
Langmuir probes for Ar-tenuous plasma jet meas., peculiarities 0—58337
Langmuir probes for Ar-tenuous plasma jet meas., peculiarities 0—58337
Langmuir probes for Ar-tenuous plasma in measure of the surface of the surface

Plasma continued

diagnostics continued microwave, appl. to constricted rare gas discharges, electron temp. determ, 0-43298

microwave, of dense cylindrical plasma columns, inclusion of skin effect 0-43297

microwave cavity, eigenvalues 0-46732 microwave cavity method for high electron density meas. 0-67942 microwave meas. electron conc. profile in supersonic arc jet 0-74640 microwave method for the measurement of the relative phase and relative amplitude of variations of the electron density and collision frequency 0-55482

multiple-pass holographic interferometer 0-61319 nebular, density and temperature from forbidden lines of ionized S and Ar 0-74128

neutral particle density determ. 0-61312 noise amplitude, dependence on potential of cylindrical probe, obs. 0-74565open barrel shaped resonators for density meas., theory and expt. 0-74567

oscillation, induced scattering in strong mag. field, sounding wave 0-74577

parameters by multi-grid probes description and analysis 0-64718 particle analysers, space charge effects on energy resolution, report 0-64720

piezoelectric pressure probe, high speed, acoustic impedance matching 0-46734potential calc. from measured values of electron temperature and floating potential 0-43306

potential calc. from measured values of electron temperature and floating potential 0–43306 potential in strong mag. field, meas. using individual emitting electrostatic probe 0–74566 potential meas. by reducing experimental Langmuir probe data, collisionless probe theory comparison 0–46733 probe, Langmuir, ion current response rel. to plasma flow speed and props. 0–41536 probe, electrostatic, time-depend. theory 0–43300 probe, electrostatic, time-depend. theory 0–43300 probe, entiting, floating potential 0–53186 probe charact, second derivative meas. method 0–74559 probe electrostatic spherical for chemically frozen plasma, continuum theory applic., description 0–53187 probe sheath thickness r.f. meas. 0–43304 probe sheath thickness r.f. meas. 0–43304 probe senhique in intermediate press. region 0–67943 probes, multigrid, for obs. with directed flow of charged particles 0–74563 probes, spaturation ion current for large intermediate press. 0–39593 probes, spherical and cylindrical, ion saturation currents calc. 0–39592 probes magnetic small-dimension cooled, construction 0–58334 probes plane, cylindrical, spherical, ion currents 0–61317 puff in mag. guide fields, analysis of extracted ions 0–64706 in pulsed light source, use of holography 0–69938 quadripolar probe behaviour, isotropic hot plasma 0–74557 r.f. floating double probe 0–43309 radiation spectra in mm range using interference filters, meas., results 0–53184 resonance probe, planar, in free mol. arc-heated flowing plasma 0–71172 using resonance probe, planar, in free mol. arc-heated flowing plasma 0–71172 using resonance probe, planar, in free mol. arc-heated flowing plasma 0–71172 using resonance probe, planar, in free mol. arc-heated flowing plasma 0–71172 using resonance probe, planar, in free mol. arc-heated flowing plasma 0–71172 using resonance probe, planar, in free mol. arc-heated flowing plasma 0–71172 0-3184 resonance probe, planar, in free mol. arc-heated flowing plasma 0-71172 using resonator, cylindrical limited, open 0-74564 rotational and vibrational temperatures for high pressure discharges 0-43307

0-43307

Schlieren method, for density gradient determ. 0-74556
sheath with a monotonic potential profile, at an electrode close to plasma
potential 0-55487
shock wave front layer using e.s. probes 0-61318
short-time spectroscopy for study of reaction kinetics of H₂ plasma
0-71175
space potential meas. using heavy-ion-beam probe 0-50078
spectra, line contours, recording by IKL-1 instrument 0-38576
spectral method for determ. of internal props. of asymm. plasmas
0-50073

spectroscopic, ultra-rapid, by focusing of laser beam in a gas 0-67928 spectroscopic meas, of isothermal plasma at various pressures, arc source 0-50136

spectroscopic meas. of isothermal plasma at various pressures, arc source 0–50136 spectroscopic temp. determination, local thermal equilibrium assumption validity in electromagnetic shock tubes 0–78051 Stark effect applic., h.f. 0–78112 surface wave probe method for electron density determ. 0–39594 temperature, by scanning spectral lines 0–67944 temperature determ. by i.r. laser beam absorption 0–64717 temperature determination, along axis of discharge channel as function of time of discharge 0–71169 temperature distrib. meas. using excitation temp. functions of Kr spectral lines 0–46368 temperature measurement by X-ray emission of laser induced air break-down 0–43308 temperature measurement for time resolved spectra in spark produced plasma 0–53171 temperature obs. using two different methods 0–71176 tenuous, thermoanemometer - Langmuir probe applic. 0–58332 thermal induction plasma, maintenance voltage direct meas. 0–64715 thermally perturbed heavy components, electron temperature distribution by relatively cold probe 0–71170 toroidal mag. field shape meas. technique 0–61311 u.h.f. waves right and left polarized applications 0–55490 ultra-speed camera application 0–52398 velocity, multichannel registration of radiation spectra of laser-jet high-temp. plasma 0–78109
X-ray meas. of atomic and ionic transfer temp. 0–78108
Al¹ outflow velocity, obs. of Doppler shift of spectral lines, in impulse plasma accelerator 0–74668
Al¹ outflow velocity, obs. of Doppler shift of spectral lines, in impulse plasma accelerator 0–746768
Ar discharge, electrostatic probe, electron density determ. 0–46737

plasma accelerator U-74508 Ar, afterglow, density, time depend., mass spectrometry 0-46736 Ar discharge, electrostatic probe, electron density determ. 0-46737 Ar dynamic z pinch, current sheet structure, press. distrib. high speed piezoelectric press. transducer applic. 0-39582 Ar spectral methods for internal props. determ. 0-50073

Plasma continued

diagnostics continued

C++ outflow velocity, obs. of Doppler shift of spectral lines, in impulse plasma accelerator 0-74568

Cs, prod. by contact ionization 0-43314

H₂-O₂ flame plasma, spectroscopic methods 0-71174

He enriched, interplanetary shock due to solar flare, obs. 0-41813

He rotating, input current, gas velocities and electrical conductivity 0-43324

Hg discharge, positive column, Langmuir probe, ion flow effects 0-50082 N_2 and N_2 -Ar mixture high pressure discharges, rotational and vibrational temperatures for plasma diagnostics 0-43307

Ne discharge, electron drift vel. in positive column 0-61277 Xe, electron density determ. 0-78114

electromagnetic waves
alkali plasma, h.f. and l.f. propagation, book 0–46682
anisotropic, inhomogeneous, column, interaction with extraordinary wave
at lower hybrid resonance 0–618/1
antenna system using isotropic plasma column 0–52177

antenna system using isotropic plasma column 0–52177 with arbitrary polarization, propagation in nonlinear media 0–43281 attenuation, collisionless, in regions of strong inhomogeneity 0–46713 bremsstrahlung radiation from weakly ionized lab. plasma 0–53168 charged particle radiation, non-equilib. magnetoactive case 0–53169 collisionless, anomalous absorption interpreation 0–64697 colloidal plasma, analytical study 0–67919 columns positive propagation of nanosecond pulses in TM mode mercury vapour 0–61400 Compton scatt, induced 0–61286 on conducting, wire, in magnetoplasma, phase constant meas. 0–78083 on conducting wave, in general magnetoplasma, propagation 0–78081 coupling, transverse em and longitudinal, quasilongitudinal propagation in drifting magnetoplasma 0–67925 coupling of different types of plasma waves and equations describing plasma behaviour 0–67923 cyclotron, oblique propagation in warm magnetoplasma, instabilities occur-

plasma behaviour 0–67923 cyclotron, oblique propagation in warm magnetoplasma, instabilities occurrence, ring, Maxwellian rel. distribution 0–55503 cyclotron second harmonic emission and absorpt. in non-uniform density plasma 0–46704 dependence on surface electron reflection mechanism 0–64695 directivity of scattered waves, diagrammatic diagnosis 0–61290 dispersion of waves in lower exosphere with multiple ionic species 0–66309

0-6309
dispersion relation concept for periodic plasma 0-46706
Doppler shift due to electron motion 0-43282
echo, perturbation theory 0-50054
electron temperature in standing microwave, spatial dependence meas.
0-39574

0-39574
exact analysis, TEM wave as example, Poynting theorem 0-55470
excitation by magnetic current ring source round compressible plasma
column 0-67920
force exerted in 'sharp' plasma-vacuum boundary by e.m. wave, vol. of
bounded plasma 0-50049
generation by jet flows 0-64696
generation of second harmonic, decay processes 0-64700
generation of vl.f. waves as a result of nonlinear mixing of 2 microwaves
0-67929

growth rates, maximum linear, comparison for large domain of physical parameters 0-67924 guide, absorption and linear transformation 0-39573

gyro-synchrotron radiation, influence of magnetoplasma 0–71148 gyrotropic plasma, dynamic potentials 0–46710 h.f., nonlinear interaction with cyclotron es. oscillations 0–78080 harmonic generation, optimum second in inhomogeneous plasma 0–43287

0-43287
helicon-wave propagation, analysis 0-61285
hot magnetoplasma, theory and physical processes 0-50056
hydromagnetic waves, approx. dispersion relations 0-64699
incoherent scatt. of mm waves 0-55469
instabilities investigation 0-61354
interaction, with material frequencies 0-61288
interaction of plane e.m. waves with moving compressible plasma
0-58317
instruction moving plasma radiation from mag line source 0-45718

0--8311'
isotropic, moving plasma, radiation from mag. line source 0-45718
Lf., interaction with plane non-isothermal layer in one dimensional case average potential, perturbed parameter determination 0-71149
Lf., ionospheric inhomogeneous layer 0-76452
loop impedance in magnetoplasma, theory and expt. 0-57467 magnetic field conversion coeff., analysis 0-74528
magneto-acoustic, weak nonlinear, effective electron-ion collisions

magneto-acoustic, 0-43284

magneto-plasma, stratified horizontally, exact solns. for vertically polarized waves 0-58316

waves 0-58316
magnetoactive, Booker theorem inapplicability 0-64698
magnetoplasma, group velocity computation 0-58325
magnetoplasma, loop impedance, theory and expt. 0-57467
magnetoplasma, radiation resistance of electric dipole 0-58322
magnetoplasma, solid state, for millimetre wave mode conversion 0-73098

0-73098
magnetoplasma nonuniform columns, scattering spectra in upper hybrid resonance, Maxwell eqns. solns. 0-43285
in magnetosheath, a.c. fields, wave particle interactions 0-59621
in magnetoshere, a.c. fields, wave particle interactions 0-59621
magnets, bounded, whistler propagation 0-58326
microwave radiation from reflective discharge plasma in inhomogeneous mag. field 0-39571
microwaves, scattered, frequency spectrum 0-78086
microwaves in periodically varying plasma, amplitude modulation 0-55472
modes of bounded plasmas, effect of inhomogeneous magnetic field 0-67922
moving, isotropic plasma, radiation from mag. line source 0-45718

0-6/9/22 moving, isotropic plasma, radiation from mag. line source 0-45718 mutual coherence propagation, scalar-wave equation 0-71152 nonlinear interaction in cold magnetized plasma 0-43286 nonlinear interaction in solid-state plasma 0-71932 nonlinear low frequency parallel propagation 0-64745 normal modes in magnetized plasma, existence criteria, electrostatic approx. 0-46711 oblique E wave propag, in warm plane stratified plasma 0-58321 oblique incidence on slab, boundary-value treatment 0-78090

Plasma continued electromagnetic waves continued

optical mixing, excitation of electrostatic oscillations in strong mag, field

optical wave in turbulent medium, modulation transfer and phase structure

optical wave in turbulent medium, modulation transfer and phase structure functions 0-50055 parallel-plate waveguide, plasma-air interface theory 0-67921 parametric excitation of extra-ordinary waves 0-43283 penetration into hot slab, calc. using thermal electron motion 0-50052 penetration into plasma as function of wave polarization 0-43273 periodic plasma, dispersion relation concept 0-46706 in plasma waveguide, phase velocity meas., u.h.f. pulse generator applic. 0-58318

plume attenuation anal. and calc. using flame diagnostic data 0-63520 propagation along const. inag. field, transverse waves dispersion relations 0-50108

0-50108
propagation in cold plasma in Coriolis force presence 0-67926
propagation instability of e.m. modes in external mag. field electron cyclotron frequency 0-43334
radiation, total and total line, 2000 to 60.000 for nitrogen, argon, oxygen plasmas 0-46712
radiation from heterogeneous plasma 0-71150
radiation from heterogeneous plasma 0-78082
radio waves, conditions for neglecting ion motion 0-46708
resonance absorpt. scatt. by uniform cylinder 0-39575
scattered power, multiple, upper bound 0-46709
scattering, microwave, from surface waves excited on Hg plasma column 0-53192
scattering, turbulent plasma 0-71151
scattering from random plasma slab, electron density fluctuations and statistical properties 0-46703
scattering on ellipsoidal plasma formation in atmos., eqns., soln. method 0-53165
scattering within plasma in radiation transport approximation 0-78084

scattering on ellipsoidal plasma formation in atmos., eqns., soln. method 0–53165
scattering within plasma in radiation transport approximation 0–78084
second-order linear inhomogeneous wave equation, solution 0–67923
semiconductor, amplification 0–44174
simulating of transfer function; network sysnthesis 0–50048
in solar wind a.c. fields, wave particle interactions 0–59621
surface waves on fluctuating columns 0–50051
synchrotron emission from hot electron plasma, plasma effects 0–50053
transformation coefficients (Transverse to or from longitudinal) at vacuum boundar 0–39604
transient wave reflection from inhomogeneous plasmas 0–58320
transition radiation in periodically stratified plasma 0–78088
transmission coeff. of radiowaves through magnetized inhomog, plasma, relationship with electrons conc., collision 0–53166
transverse, beam, acoustic instabilities, low-frequency 0–78087
turbulent plasma, scattering 0–71151
u.v. absorption, continuum, for laser generated metallic plasma 0–58319
u.v. emission from plasma produced by laser input on Al solid 0–39579
VHF field distrib. in plasma waveguide in mag. fields, discharge region of existence 0–39572
v.h.f. from electron beam interaction with magnetosonic waves 0–61289
warm drifting uniaxial, guided wave propagation 0–39576
v.h.f. from electron beam interaction with magnetosonic waves 0–61289
warm drifting uniaxial, guided wave propagation 0–39576
waves coupling in a viscous plasma between electron-acoustic, ion-acoustic

warm drifting uniaxial, guided wave propagation 0-39576 wave coupling in a viscous plasma between electron-acoustic, ion-acoustic and e.m. plane waves 0-46701 waveguide, heat fluctuations of amplitudes of surface charge waves 0-78089

U-78089 waveguide, interaction 0-74529 waveguide, non-linear interaction 0-74530 waveguide bounded with perfect magnetic wall, excitation of surface wave 0-43249

0-43249
waveguides, kinetic theory of e.m. field excitation 0-71153
X-ray spectra from dense plasma focus devices 0-78085
Ar plasma, v.h.f. absorpt., larger than cyclotronic mag. fields, discharge region of existence 0-39572
K thermally ionized in pyrex tube, upper hybrid resonance scattering calc. 0-43285

N, mag. confined column, spectrum rel. to e temp., obs. 0-46717

magnetohydrodynamics

adiabatic eqns. for slow movement in electric and mag. fields, three sets of higher order eqns. comparison 0-43262 Alfven and cylindrical magnetoacoustic waves, Weinberg method of study 0-58313

Alfven wave propagation in an inhomogeneous medium, effect of gravitational field 0-39569

Alfven wave refl., compressional, from mag. 'cliff' 0-61270
Alfven wavelength, depend. on geometry of nonhomogeneous plane mag. field 0-61271

field 0–61271

Alfven waves, parametric amplification 0–71188
alkali metal seeded, interaction with metallic electrodes 0–52198
aperture effect on axial velocity distribution function meas. 0–64682
arc transition in generator 0–50041
in astrophysics, stability and equilib. of rotating, turbulent convective
zones 0–41650
blast wave propag. 0–39562
cluster motion in axially symmetric variable sign mag. field, model, computer applic. 0–53152
combustion plasma, magneto-viscous effects 0–43248
convertors, construction, process analysis and applications 0–52187
core with current in strong longitude mag. field, instability 0–39612
crossed mag. and electric fields, suppression of runaway of electrons
0–74514
cyclotron waves and MHD modes, coupling 0–46745

0-74514
cyclotron waves and MHD modes, coupling 0-46745
diamagnetic plasma in mag, field of two-dimensional dipole, equilibirum
configurations 0-74512
dielectric permeability tensor- operator of inhomogeneous relativistic
stream of cold plasma expressions 0-46698
diffusion of 1.f. mag, field into moving plasma, theory and exptal obs.
0-78068
discharge phenomenon near cathode in crossed E-H fields presence, electrodynamic eqns. 0-50039
e.m. radiation expanding into uniform mag, field 0-74516
echo, relativistic synchrotron, Vlasov equation treatment 0-74515
electrical conductivity 0-53153
fast electron inhomogeneities, trapped in magnetosphere, non-linear dynam
ics 0-76416

magnetohydrodynamics continued

magnetohydrodynamics continued
equilibrium, in model stellarator, theory, effect of inertia on motion, and influence on loss 0–71141
flow, high-speed, in cusped mag, field 0–71139
flow in self field of arc discharge 0–78069
generation by shock tube with controlled diaphragm burst 0–42154
generator, Faraday type, image converter photographs in generator channel 0–63542
Hall coefficients in molecular gases 0–53154
Hall volt-amp, charact, in nonequilib, inhomogeneous plasma 0–54811
hydromagnetic waves guided by mag, field, scattering cone 0–74513
induction eqn, integral of mag, field for flow of dissipative plasma
0–71143
instability, simulation 0–53211

instability, simulation 0-53211

ion acoustic waves propagating in collision-free gravity-supported plasma in static mag. field 0–74576 linear crossed-field generators and accelerators, circulating currents velocity and distributions 0–50040 lorentzian magnetoplasma in external magnetic fields presence, transport phenomenon, electron distrib. for 0–39560 magnetoplasma, freq. dependent transport eqn. 0–46692 magnetoplasma weakly inhomogeneous, electrostatic instability convective and absolute, analysis 0–46757 in magnetosphere, motion near axis of symmetry, quasi-hydrodynamic equations solution 0–76415 motion and equilibrium in unsymmetric fields 0–71142 motion and equilibrium in unsymmetric mag. field, report 0–64746 non-linear resonant interaction between three waves propagating in direction of constant mag, field 0–74517 nonequilibrium, ionization instability, numerical simulation 0–43327 normal modes existence 0–64681 oscillations, hydromagnetic, of tangential discontinuity, linear modes 0–50042 plane gyrotropic waveguide excitation, fields determination 0–46696 latement of the properties of tangential discontinuity.

plane gyrotropic waveguide excitation, fields determination 0–46696 plasmoid motion in duct with variable inductance, analytical dependence on time, determination 0–48964 puff generated by θ -pinch, consequences of rotation in logit, mag, field 0–39581

radiational retardation influence on motion in inhomogeneous mag. field 0-74539

0-74539
resistance, anomalous 0-74521
stability of laminar flow in strong mag, field 0-43275
stabilization, dynamic, of unstable MHD equilibria 0-53200
theory with resistivity, application to rotation of Tokamak equilibria
0-64750

0-64750
turbulence, steady state frequency spectra for Alfven and m.h.d. waves stability conditions 0-71140
turbulence as mechanism for pulsar radiation 0-57075
wave propagation along the magnetic field in a two component warm plasma 0-58312
waves in compressible plasma 0-74511
Weinberg method of study of Alfven and cylindrical magnetoacoustic waves 0-58313
H arc radial press, profile, 13-moments approx. 0-78071
H arc radial press, profile, 5-moments approx. 0-78070
magnificant technique. see Plasma/diagnassics

measurement technique see Plasma/diagnostics

oscillations

oscillations
3 longitudinal waves, coupling coefficients which account for nonlinear interaction 0–74583
3-wave interaction in well defined phase description with regard to nonlinear explosive instabilities 0–53204 acoustic waves, continuous pseudo, excitation and damping 0–61329 Alfven waves, parametric amplification 0–71188 auroral micropulsation instability 0–59667 axially symmetric waves in vacuum channel 0–67956 azulene molecules, plasma effects of π electrons 0–43149 ballistic echo, spatial 0–61334 in beam discharge, electron temperature and density 0–64741 in beam discharge, mechanism of resonant heating 0–64667 beam mystem, ion-acoustic wave, Langmuir wave excitation, stationary regime 0–78124 beam-plasma system, inhomogeneous, electrostatic waves propag, and amplification 0–43319 Bernstein mode excitation due to helical electron beam 0–50093 bounded magnetoactive, non-linear wave theory 0–46748

Bernstein mode excitation due to helical electron beam 0-50093 bounded magnetoactive, non-linear wave theory 0-46748 cavity resonators, containing magnetoplasmas, r.f. fields and resonant freqs. 0-78121 compression waves, solitary, in three component plasma with neg. ions 0-74589 correction term of Landau damping, due to trapped particles 0-74591 coupling, nonlinear of modulated wave and low-frequency mode producing resonant interaction and instability 0-46745

resonant interaction and instability 0-46745 cyclotron, perpendicular propagation in warm magnetoplasma, dispersion characteristics 0-53203 cyclotron, tenuous plasma in inhomogeneous mag. field 0-64732 cyclotron e.s., nonlinear interaction with h.f. e.m. waves 0-78080 cyclotron instability, stat. elec. field 0-53209 cyclotron vibration stability 0-61344 cyclotron wave in computer expt., obs. of self-trapping instability 0-46756

0-46756
cylindrical, drift wave propagation 0-78122
damped, eigenfrequency derivation 0-67947
damping, spatial, of large amplitude waves 0-78129
decay, luminescence max. in spectral line 0-58339
discharge positive column, effect of ionized oscillations on current-interchange instability 0-46772
dispersion, decay and growth of 1-f. quasi-neutral waves 0-74590
dispersion relation for plasma of 2 crossed electron beams in a magnetic
field 0-58342
drift, nonlinear excitation 0-39601
drift waves, multimode, feedback suppression in mirror-confined plasma
0-46743
drift waves due to press. gradient in collisionless plasma 0-78120

drift waves due to press. gradient in collisionless plasma 0-78120 drift waves in Q machine, min. B stabilization 0-43295 e.s. coherent plasma waves, growth and decay, nonlinear interaction study

echo, high and low frequency, oscillation conversion theory 0-74578

Plasma continued

oscillations continued

echo, spatial, electron-neutral collisions effect 0-71182

echo, spatial, in collisionless plasma, impulse length influence 0-71180

ecno, spatial, in collisioniess plasma, impulse length influence 0–71180 echo, three-momentum oscillations 0–46750 electron, excitation by ion acoustic waves 0–71184 electron, large amplitude with trapped particles, computer expts. on stability 0–78144 electron, longit. subharmonic excitation by beam modulation 0–74536 electron beam, wave generation peculiarities, non-uniform influence 0–74584

electron beam interaction, fine struct. distrib. function 0-78125

electron beam interaction, hot electron component formation mechanism 0-71191

electron beam repelling with local cyclotron reson. 0–61336 electron cyclotron resonance induced, h.f. instability obs. 0–71194 electron cyclotron waves, drift instability 0–78149 in electron gas of metal film in optical frustrated total reflection filters

electron resonance, main, of bounded plasma at high mag, fields 0-78131 electron waves, quasilinear equations 0-78132 electron hole pinch 0-62271 electron-ion plasma, instability production above threshold amplitude

0-78136

0-18130 electron-ion wave coupling due to scatt. by electrons 0-61331 electrostatic, collisional damping 0-46742 electrostatic, flute-lke instabilities in plasma with cylindrical relativistic electron beam 0-55495 electrostatic, unstable, in inhomogeneous plasma, theory 0-78141 electrostatic energy waves, positive and negative, nonlinear interaction 0-74515

0 - 74535electrostatic from non-linear interactions of two electromagnetic waves

0-53195

electrostatic ion cyclotron wave, dispersion 0-74574 electrostatic ion waves, dispersion obs. in uniform magnetic field 0-61337 electrostatic wave energy, l.f., reson. absorpt., in nonuniform mag. field 0 - 71185

electrostatic wave instabilities excited by high-frequency electric field 0-50099

0-50099
electrostatic waves, l.f., in mag. field, collisional effects 0-71190
electrostatic waves, refl. and absorpt. 0-78126
electrostatic waves propag, and amplification in electron beam-inhomogeneous plasma system 0-43319
energy density determ. using ion beam scatt. 0-78138
entropy waves, gyro-relaxation effect rel. to stability 0-74586
evolution to non linear saturation of instabilities, observation of spatially
growing ionization waves 0-43336
excitation, h.f. on interaction with electron beams 0-64737
excitation, parametric, of purely growing modes in magnetoplasma
0-78134
excitation, resonance, of high-amplitude waves 0-467449

excitation, resonance, of high-amplitude waves 0-46749 excitation by magnetic current ring source round compressible plasma column 0-67920

in field of standing H-waves stability 0-74588

in field of standing H-waves stability 0-74588 fluctuating columns, e.m. surface waves 0-50051 fluctuations, electron-beam echo applic. 0-50079 flute instability, suppression, feed-back system 0-53205 generated by electron beam, hollow, spiraling 0-67952 generation of harmonics and combination frequencies, review 0-58343 growing in hot plasma for symmetrical double-humped vel. distribution, calc. 0-53193 h.f., turbulence and electron heating during beam instability 0-50112 h.f., two types in beam generated plasma, as function of cyclotron freq. 0-50086 h.f. excitation by e-beam interaction, 0-30596

0 50986 h.f. excitation, by e. beam interaction 0--39596 heating by large-amplitude long wavelength electric field oscillating near plasma frequency 0--43263 high-amplitude waves, resonance excitation 0--46749 hot bounded with and without mag. field, ion-electron resonances study

0 -46744

hydromagnetic, of tangential discontinuity, linear modes 0-50042

induced scattering in strong mag. field, sounding wave 0–74577 instability, ion cyclotron, in cylinder, dispersion equations 0–71192 interaction, nonlinear, with low density relativistic electron beam, wave propag. 0–50097

propag. 0-50097 interaction of test waves and trapped particles in collisionless electron plasma 0-50091 interactions, 3-wave, nonlinear resonance conditions 0-64730 ion, acoustic Landau-damped, nonlinear mixing, external excitation 0-61341

ion acoustic modes of hot electron plasma, nonlinear Landau damping 0-78130

0-78130
ion acoustic wave-sheath interaction 0-58341
ion acoustic waves, damping, electron drift effect 0-58340
ion acoustic waves, self-excited 0-61335
ion cyclotron, excitation in crossed electric and mag, fields 0-61348
ion cyclotron harmonic wave propagation 0-78135
ion distributions, perturbed, in ion waves and ion wave echoes 0-67950
ion wave, slow, new mode obs. in turbulent plasma without mag, field
0-74582 ion wave, slowing down of velocity in nonisothermal plasma 0-

ion waves, slowing down of velocity in nonisothermal plasma 0–78119 ion waves, continuous pseudo, excitation and damping 0–61329 ion waves, l.f. trapped, propagation in warm cylinder 0–78133 ion waves electrostatic, propagation in uniform mag. field, dispersion, electron Landau damping 0–43321 ion waves finite amplitude without mag. field, linear instability 0–39613 ion waves propagation, wave-wave coupling 0–43322 ion-acoustic, effect of high-frequency electric field on development 0–74592

ion-acoustic turbulent, interaction of resonant electrons 0-64733 ion-acoustic waves, non-linear resonance excitation by external elec. field

0-0797 i ion-acoustic waves, quasilinear effects 0-55492 ion-cyclotron, alkali, light ions 0-61345 ion wave echoes, spatial collisional effects numerical study 0-55493 ionization rate variations, in ionization waves 0-50088 ionization waves, ionization rate variations 0-71179 ionization diffusion 0-74587 ionization diffusion 0-74587 indexes disclarate the inverse of the control of the control

ionosonic vibrations in plasma diode, freq., wavelength increment expressions 0-53198

Plasma continued oscillations continued

ionospheric waves, l.f. 0-62944

isotropic layer, surface waves, absorption effect on characteristics 0-74573

l.f., drift type, effect on anomalous diffusion 0-64673

0-443/3

If., drift type, effect on anomalous diffusion 0-64673

If., in θ-pinch plasma, microwave scattering 0-71163

If., in bounded low press. plasma in mag. field 0-78139

If., self-excited, rel. to anomalous plasma diffusion 0-61342

If. electrostatic non-uniform collisional 0-61339

If. interchanges, stability 0-67964

If. relaxation in inhomogeneous h.f. field 0-64728

If. spectra in stellarator 0-46722

Landau damping, heuristic approach and dimensional arguments 0-71187

Landau damping due to trapped particles, correction term 0-61330

linear, of nonuniform plasma, normal mode approach 0-67949

longitudinal, in uniform magnetic field, with bi-Maxwellian distribution function, numerical study 0-67%C1

longitudinal waves, dispersion relation in relativistic plasma 0-50098

low-density, He generation by gas-discharge tube, correlation with electrical power 0-46751

magnetic sound excitation in cylinder by spiral wave propagation 0-64742

magnetized, excitation by transverse e.m. wave 0-67958

magnetized and unmagnetized, parametric excitation by oscillating electric field 0-53194

field 0-53194 magneto-active plasma, semi-limited, plane wave nonlinear interactions at the boundary 0-39602 magnetoacoustic wave propag, in cylindrical column, study by geometrical optical techn. 0-39600 magnetoacoustic waves in solid-state plasmas, light scatt, theory 0-41102 magnetoactive, surface wave excitation by gyrating particles beam 0-67954

0-67954
magnetoplasma, l.f. waves 0-71189
magnetoplasma, l.f. waves 0-71189
magnetoplasma, l.f. waves 0-71189
magnetoplasma, waves propagation 0-39605
magnetosonic waves, excitation in cylinder 0--64734
magnetosphere, electron precipitation pulsations 0-59605
Maxwellian distribs. approx. using simple functions 0-39597
model integral in three component plasma 0-64743
neutrons (slow) scattering by magnetically confined plasma with electrostatic ion oscills... cross sections 0-50019
non-linear, behaviour in vicinity of marginally stable state, theoretical analysis 0-50087
non-uniform finite-amplitude non-linear decay and instability. 0-61338

ysis 0-50087 non-uniform, finite-amplitude non-linear decay and instability 0-61338 nonharmonic loss-cone flute mode, nonlinear dynamics 0-43320 nonlinear evolution of multiple-finite amplitude resonant loss-cone modes 0-61340 nonlinear low frequency waves, parallel propagation 0-64745 nonlinear wave, stochastic heating 0-54553 nonlinear waves in relativistic electron beam 0-61333 parametric excitation of low frequencies 0-46741 parametric excitation of unmagnetized and magnetized plasmas by oscillating electric field 0-53194 parametric in magnetic field, instability investigation, dispersion relation 0-50108 plane-wave solutions of two-component hydrodynamic plasma 0-78140

0-30106
plane-wave solutions of two-component hydrodynamic plasma 0-78140
potential fluctuations for 2 interacting jet streams, probe obs. 0-64729
potential variations meas. 0-43306
quasilinear theory, new derivation, neglecting wave-wave interactions

0 - 74575

O-74575 regular, caused by beam instability on light radiation 0-64740 relaxation, non-linear in Q-machine, mechanism frequency, criteria for excitation and density variations 0-71183 resonance conditions in mag. field 0-53196 second-order theory, computer test 0-39606 solitons, ion-acoustic, formation and interaction 0-55494 spectral width 0-50092 stability, limitations for stellarator with sharp surfaces 0-43335 stochastc, caused by beam instability on light radiation 0-64740 superluminous waves in streaming relativistic plasmas not exciting instability 0-46752 surface, of small \(\lambda\) compared with characteristic dimensions of inhomogeneities 0-64736 surface wave propag, and electrostatic reson. 0-71181 surface waves, boundary equations 0-64744 surface waves excitation on Hg plasma column, microwave scattering 0-53192

temporal echo, rectangular pulse case 0-61327 three-wave interaction, resonant, effect of collisions, kinetic approach 0-61343

Tokamak toroidal discharges, trapped particle pinch effect explanation 0-74543

transformation coefficients (transverse to or from longitudinal at vacuum boundary 0-39604 transient beam-plasma interaction study by beam-switching electron gun

transfert beam-plasma interaction study by beam-switching electron gain 0-57485 transient region obs. 0-50089 trapped particle modes in multipoles, finite press. effect 0-74579 turbulent, fluctuation level optical meas. 0-61332 on turbulent heating, ionic sound obs. in toroidally-shaped plasma 0-46747

on turbulent neating, ionic sound oos. In toriotally-shaped plasma 0-46746 turbulent positive column in axial magnetic field, particle transport rate, Dupre-Kadomtsev theories 0-39632 turbulent systems, weakly, general kinetic eqn. 0-43323 two-stream suppression by beam modulation 0-43331 v.h.f., short Cs and Hg are discharges at low pressure 0-67959 vibrations, surface, equations for energy and damping 0-64735 Vlasov non-linear eqn. numerical soln., temp. renormalization 0-39598 Vlasov one-dimens. plasma, harmonics selective excitation by counterstreaming e beams 0-39599 warm, semi-infinite, surface wave propag., low-freq. ion modes 0-74581 wave, If., in magnetoplasma 0-71189 wave, If., in magnetoplasma 0-71189 wave, transverse, in relativistic plasma, stability 0-71161 wave coupling, transverse em and longitudinal, quasilongitudinal propagation in drifting magnetoplasma 0-67925 wave echo, second order perturbed distribution 0-67953 wave echo in one-dimensional weakly turbulent electron plasma 0-50094

oscillations continued

wave excitation in magnetoactive plasma by inhomogeneous electron beam 0-71178 wave motion, in collisionless plasma with anisotropic pressure 0-64726 wave transformation in magnetoactive plasma 0-54477 wave-particle interactions, nonlinear 0-58308

wave-particle interactions, nonlinear 0–58308
wave-particle interactions 0–58308
wave-wave, interactions, non-linear 0–58308
wave-wave, interactions, non-linear 0–58308
waves. Cerenkov type, generation by fast electrons in solar corona 0–76674

waves, Cerenkov type, generation by fast electrons in solar corona 0–76674 waves, diffusion and transformation in cylindrical inhomogeneous electron currents 0–64739 waves, interacting, shock instability 0–58348 waves, ion-acoustic, long-wavelength, in gravitational field, linearised Vlasov equations 0–74576 waves, longit. excitation near ion cyclotron harmonics 0–61328 waves, nonlinear Landau damping in mag. field, expt. 0–78137 waves, ponlinear interaction, general kinetic eqn. 0–43323 waves, pseudo-sonorous and drift, in h.f. discharge 0–61273 waves absorption rel. to collisions 0–74571 waves discussion, property of amplification 0–78060 waves in two-temp. plasma with periodic elec, field 0–50090 waves inosiation-diffusion, in gap in induced electric field 0–64738 weakly ionized afterglow, mag. field, short tube 0–53202 Ar discharge, saturation of metastable states rel. to ionization waves existence 0–74522 CO₂, acoustic wave excitation by Q-switched CO₂ laser 0–78123 He Ne laser, excited by direct current 0–42278 He afterglow, thermal conduction energy loss, acoustic standing wave, microwave interferometry 0–55457 He discharge, saturation of metastable states rel. to ionization waves existence 0–74522 Use yapour, pulsed discharge, large amplitude ionic waves in decay 0–4329 Hg vapour, pulsed discharge, large amplitude ionic waves in decay 0–4329 has a control of the cont

Hg vapour, pulsed discharge, large amplitude ionic waves in decay 0-43325

Li ion heating in Penning discharge in mag. mirror geometry 0-46688 Ne discharge, saturation of metastable states rel. to ionization waves existence 0-74522

production

production
by V-groove cathode discharge, parameters 0-46738
alkali metal, with negative ions, in Q-device 0-61325
by beam on solid target 0-46729
continuous discharge maintenance by laser beam 0-64721
electron, turbulently heated plasma which shields against Franck-Condon
neutrals 0-61323

electron and ion waves, growth and decay, nonlinear interaction study 0--67955

0-67955 formation time, crossed fields in millisecond region, cylindrical magnetron diode, hot cathode 0-61387 formation time, influence of hot cathode in crossed fields 0-61324 ion source, hollow-cathode, optimization 0-61303 ion stream composed of two components in vel. distrib. 0-61326 laser, 1.06µm emission 0-39577 by laser, for thermonuclear fusion 0-744006 laser, ionization obs. 0-74569 by laser, mono-impulsive radiation, on solid target in vacuum conditions formation 0-74570 laser induced, from metal surface, spectral study of plasma produced 0-78117 laser interaction with solids, bibliographical review 0-71177

laser induced, non-metar surface, spectral study of plasma produced 0–78117
laser interaction with solids, bibliographical review 0–71177
laser irradiated solid particle, formation and heating 0–78115
laser production, oinz, and heating mechanism 0–43315
laser production of dense plasmas 0–67945
laser pulse on solid, multiply-charged ions prod. 0–61322
laser system, multibeam for spherical plasmas 0–50083
laser-induced continuous discharge 0–64721
laser-induced evaporation, onset of screening, theory 0–65010
laser-induced evaporation of metals, onset of screening 0–65012
laser-produced, containment, optical interferometric meas. 0–53190
laser produced from Al, Cu-metal surfaces, study 0–67946
by magnetic fields, impulsive, multipolar, short clusters 0–64725
metals, interaction of intense laser beams 0–43316
microwave formation and heating for, in controlled fusion research 0–46687
microwave formation and heating process 0–46686

0-4067/microwave formation and heating process 0-46686 optical plasmatron, feasibility 0-64721 by photoionisation, u.v. radiation from linear z pinch in Xe for shock wave experiments 0-64722

plasmotron, power requirements 0-46739 Q-machine, Te/Ti ratio >10 by electron cyclotron resonance heating

0-50071 r.f. struct. device analysis 0-63516

rd. struct. device analysis 0-63316 by radiation, laser spark propagation maintenance threshold 0-53191 by rail accelerator, structure, energy characteristics of impusive acceleration 0-64724 source, construct, and performance 0-61321 spherical, extended homogeneous, field free device for production 0-78116

0—78116
stellarator WIIa, operation 0—64712
T-tube, behind reflected shock front, spectroscopic obs. of D₂ 0—61282
Tokamak-3 machine, ion energy lifetime 0—74552
in toroidal octupole by microwave heating, cold ion plasma behaviour 0—50084 0-50084
Al-surface plasmas laser-produced, study 0-67946
Al by laser impact on solid, u.v. emission 0-39579
Ar, due to high press, pulsed arc 0-58314
Cs, shock tube, at pressures up to 10 atm. pressure 0-69736
Cs vapour, laser-induced breakdown two-photon ionization 0-78158
Cu surface plasmas lase-produced, study 0-67946
H plasma, giant pulse lasers action on solid H₂ 0-39595
H₂ solid foils irrad, with giant pulse ruby laser 0-46740
Li in Q device 0-64723
Na vapour, laser-induced breakdown, two-photon ionization 0-78158
Sr in Q device 0-64723
U-II high press. in 0.1-1.0 atmos. range 0-50023
U cutting by laser beam 0-43318
hock waves

shock waves

Alfven wave propagation in an inhomogeneous medium, effect of gravitational field 0-39569

```
Plasma continued
```

shock waves continued

Bernstein waves of negative energy giving rise to instability 0–67917 Boltzmann eqn. nonlinear numerical soln. 0–74526 classical gas dynamic, theoretical, m.h.d., ionizing, theoretical review 0–46702

Boltzmann eqn. nonlinear numerical soln. 0—74526 classical gas dynamic, theoretical, m.h.d., ionizing, theoretical review 0—46702 cold, theory, applic. to transverse resistive shock wave's existence and structure 0—43279 collisionless, front structure and propagation character exam-in relation to M_g 0—61280 collisionless, in magnetized plasma 0—53162 collisionless, magnetostatic, turbulence level, Balmer Hβ line, Stark broadening 0—64689 collisionless, meas. of turbulence by collective scatt. of light 0—67918 collisionless, one dimensional electrostatic shock solution to steady state Vlasov equations and Poisson's equation 0—74524 current shelf structure in theta pinch configuration 0—50066 e.s. probes for front layer thickness meas. 0—61318 electron, in collisionless plasma 0—74525 electron density, laser interferometric meas. 0—61278 electronic turbulent 0—78078 electrostatic laminar, solns, to Poisson's eqns. 0—39568 due to flow interactions with large mag, fields 0—64680 formation, pulsed plasma travelling in stationary gas-discharge plasmas, H, Ar 0—50047 front layer thickness meas. using e.s. probes 0—61318 heating, by reflected conising shock waves 0—67901 hydromagnetic, propagation along mag, field, dissipation discontinuities effect on shock structure 0—53161 ion acoustic waves with Landau damping, nonlinear theory 0—53160 ion-acoustic, weak nonlinear, perturbation analysis 0—74523 ionizing normal in H-D-He mixtures 0—64694 from laboratory shocks to supernova explosions, book 0—46681 MPD expts. in inductive hydrodynamic shock tube 0—53163 magnetospheric, collisionless 0—59613 plasma, magnetized, anisotropic, jump relations for shocks 0—64692 production in tube with controlled diaphragm burst 0—42154 propagation of cylindrical blast wave 0—39562 relaxation effects behind fronts generated through plasma-flow interaction 0—61279 solar wind, lunar limb shock, formation of lunar conducting islands 0—48560

solar wind, lunar limb shock, formation of lunar conducting islands 0-48560

0-48560 spectroscopic obs. of D₂ behind front 0-61282 stationary collisionless, in initial plasma with high ion temp. 0-39570 strong, front temperature meas. 0-61281 structure, propagating oblique to magnetic field 0-64691 turbulent, collisionless, electrostatic shocks, conditions per occurrence 0-43280

0-43280 turbulent waves in collision-free plasma 0-64690 wave coupling in a viscous plasma between electron-acoustic, ion-acoustic and e.m. plane waves 0-46701 Ar. supersonic flow, local electron vel. and density, under accelerator forces 0-61284 'H, estimated expansion due to laser impulse 0-39558 Hg, ionization and excitation of atoms ahead of shock front, kinetics 0-78079

stability

stability
a.c. electric-arc discharges, design criteria 0–46775
Alfven type waves with finite press. in inhomogeneous plasma, stirring results to instability 0–53197
anisotropic rel. distrib., eyelotron instabilities 0–74602
beam instability, use in heating ions in trap with mag, stopper 0–39550
beam system, influence of electron collisions, expt. and theory 0–74601
beam-plasma finite system, instabilities 0–58347
beam-plasma system, inhomogeneous, unstable modes, phase vel. and growth rate 0–43319
beams, spatially separated 0–39611
Bernstein mode excitation due to helical electron beam 0–50093
Bernstein waves of negative energy giving rise to instability 0–67917
Bernstein-Green-Kruskal large amplitude periodic wave in collisionless plasma, method 0–43333
boundary conditions, generalized, ion-sound waves, drift waves 0–67963
bunching instability in bounded system 0–43329
collective excitations in mag, field, two-dimens, plasma 0–46705
column, high-β, sharp-boundaried with helical fields, feedback stabilization 0–78101
column, streaming, low β, surface-ionized, at low mag. fields 0–78105

column, streaming, low β , surface-ionized, at low mag. fields 0–78105 convective and nonconvective instability, frequency cusp discrimination 0–43338

core with current, instability in strong longitudinal mag. field 0–39612 Coulomb collisions influencing non linear effects 0–61355 counterstreaming electron-ion, linearly polarized mode instability

0-55497
coupling, nonlinear of modulated wave and low-frequency mode producing resonant interaction and instability 0-46745
cyclotron, antisymmetrical mode in OGRA-2, feedback system 0-50101
cyclotron, in adiabatic magnetic traps 0-74600
cyclotron, low density, in two component electron plasma 0-78145
cyclotron instabilities, perpendicularly propagating, one-dimensional computer model simulation 0-55499
cyclotron instability of Alfven waves in plasma with anisotropic distribution of hot protons 0-51597
cyclotron oscillations, stat. elec. field 0-53209
cyclotron resonance instability in rotating plasma 0-61348
decay, anomalous, of nonuniform collisionless beam in u.h.f. field 0-46759
decay-type, backward scattering instabilities of cyclotron harmonic waves

decay-type, backward scattering instabilities of cyclotron harmonic waves 0-78147

dense, thermodynamics 0-74497 diffuse, radially constricted, between electrodes, criterion for stability of interchanges 0-53201 diffuse screw pinch, magnetohydrodynamic stability 0-55498 of direct pinch, in quadrupolar h.f. field, influence of electrode separation 0-64757

discharge, Penning, relax. instability in output current 0-64683 discharge, cold cathode PIG, instability 0-39553 drift, effect of magnetic perturbations in axisymmtric tori 0-67961

Plasma continued stability continued

drift dissipative instability in e.m. field 0-50107 drift instability, collisionless shocks 0-61283

drift wave instability suppression, by r.f. electric field 0-74603

drift-cyclotron instability in a multipole, effect of trapped particles 0-39609

drift-dissipative, non-linear theory, analysis in semi-infinite slab geometry 0-78146

0-78146 drift-dissipative instability in afterglow plasmas 0-43332 drift-wave instability suppression by rf electric field 0-43337 e.m. ordinary mode instability in high β -plasmas in mag. field 0-43334 e.m. waves, instabilities investigation 0-61354 echo, spatial, electron-neutral collisions effect 0-71182 electron and ion acceleration to walls during instabilities 0-38958 electron beam, plane parallel isolated from metallic walls 0-38470 electron beam interaction, nonlinear stabilisation 0-74599 electron beam relax., ultrarelativistic, plasma inhomogeneity influence 0-67948 electron beam with linear velocity profile, criteria rel. to retaining magnetic profiles of the stability of the profile of the retaining magnetic profile of the pro

0-67948 electron beam with linear velocity profile, criteria rel. to retaining mag. field 0-38469 electron cyclotron resonance induced-, h.f. instability obs. 0-71194 electron cyclotron waves, drift instability 0-78149 electron gas, uniform density, charact, instability 0-58346 electron gas in uniform mag. field, Vlasov equilibria, stability to electrostatic perturbations 0-50109

fast electron inhomogeneities trapped in magnetosphere, non-linear dynamics 0-76416

electrostatic counterstreaming instabilities in ion beams, numerical simulation 0-61352electrostatic modes stabilization by reverse feedback in confined plasma

0-39607 electrostatic plasma wave instabilities excited by high frequency electric field 0-50099

field 0–50099
electrothermal, condition derivation 0–50110
electrothermal, critical condition for partially ionized plasma 0–46755
entropy waves, gyro-relaxation effect 0–74586
explosive, nonlinear, in well- defined phase description 0–53204
explosively unstable plasmas, phase-locking of coupled modes 0–78151
feedback stabilization, phase relations necessary for differing classes of
electrostatic instability 0–50096
feedback stabilization of surface instabilities, lightly conducting, report
0–64760
in fields combined theory 0–64756

0-64760 in fields, combined, theory 0-64756 flow, laminar inhomgeneous in strong mag. field 0-43275 flute instability, suppression, feed-back system 0-53205 flute instability stabilization using controlled electron beams 0-67960 flute-like instability driven by field inhomogeneities 0-64754 rel. to fusion, controlled, microinstabilities in mag. confinement 0-46253 gravitational instability of rotating anisotropic plasma with Hall's effect 0-50111 h.f., excited by electron beam, turbulence and electron heating 0-50112 h.f. threshold in interaction with electron beam 0-46760 Hastie-Taylor guiding-centre criterion for magnetic-well equilibria, extension 0-78148 heating by exciting drift-beam, feedback system 0-64670

heating by exciting drift-beam, feedback system 0-64670 helical instability in cylindrical column rel. to anomalous diffusion 0-64759

0-64759
helicon effect on loss-cone and drift loss-cone instabilities 0-61353
hot ion, microinstability modes Harris, finite length 0-61350
hydrodynamic non-uniform mag, field 0-71195
hydromagnetic, of axisymmetric bulged region in midplane of theta-pinch
0-78098

0—78098
hydromagnetic cold in presence of ext. mag. field 0—56856
inhomogeneous, formed by hollow ion beam, I.f. 0—43339
inhomogeneous sheath 0—55496
instabilities, dissipative, variational methods 0—61356
instabilities, explosive, soln. of eqns. 0—55501
instabilities in warm magneto-plasma, oblique cyclotron wave propagation,
collision effect 0—55503
instabilities pon lipser of Langmuir waves rel. to Coulomb collisions

instabilities non linear of Langmuir waves rel. to Coulomb collisions 0-61355

instability, linear of finite amplitude ion waves without mag. field parametric resonance method 0-39613instability, self-trapping, of plasma cyclotron wave in computer expt. 0-46756

instability nstability in parametric oscillations in mag. field, dispersion relation 0-50108

instability in warm magnetoplasma, longitudinal wave propag., collision effect 0-53203 instability of finite amplitude waves in limited plasma, mechanism study 0-53199

instability production above threshold amplitude by oscillations, anomalous

0—53199
instability production above threshold amplitude by oscillations, anomalous damping 0—78136
interaction of test waves and trapped particles in collisionless electron plasma 0—50091
interchange instability in collisionless low-β plasma, temp. gradients, wave-guiding centre resonance effects 0—78142
ion acoustic instability due to electron drift driven by applied constant electric field 0—74519
ion acoustic waves, self-excited, stabilization 0—61335
ion heating by hf. electron beam-centrifugal instability 0—64751
ion-acoustic, effect of high-frequency electric field on development 0—74592
ion-acoustic instability, anomalous resistance of plasmas in sub-critical electric fields 0—50104
ion-acoustic turbulence, anomalous resistance 0—53206
ion-cyclotron, in mirror trap 0—39610
ion-cyclotron, of oscillation in cylinder, dispersion equations 0—71192
ion-sound instability, remote feedback stabilization, at electron-cyclotron reson. freq. 0—64749
ion-wave instability, simulation 0—53211
ionization instability, simulation 0—53211
ionization instability, ele to boundary conditions 0—55502
ionosonic vibrations in plasma diode, freq., wavelength increment expressions 0—53198
isotropic, Lif. interchanges 0—67964
kinetic instability development in high current discharge 0—64779
lf., in inhomogeneous plasma formed by hollow ion beam 0—43339
lf., ion heating and diffusion with electron beam 0—64758

Plasma continued stability continued

lamination in quasi-static h.f. electric field 0-43328 limitations for stellarator with sharp surfaces 0-43335

linear to non linear saturation of instabilities evolution, change in zeroth-order conditions 0-43336

order conditions 0-43336 low- β equil. in linear multipole mag. fields 0-64747 MHD generator, ionization instabilities meas. 0-54814 MHD nonequilibrium, ionization instability, numerical simulation 0-43327

MHD unstable equilibria dynamic stabilization 0-53200 macroscopic and microscopic, and confinement, review 0-46753 magnetic mirror traps, critical adiabatic parameters for stable-unstable transition 0-46721

magnetic confinement, instabilities 0-71160
magnetized, fluctuation levels and reactive marginal instabilities 0-39608
magnetoplasma, collisional drift-like instability 0-50100
to magnetosonic, perpendicular waves, near ion cyclotron frequency
0-74594

metastable state's existence in supercooled dense plasma, ball lightning hypothesis 0-58344 micro-instabilities driven by density gradient, h.f. elec. field effects 0-74593

microinstabilities in inhomogeneous plasma, theory 0-78141 microinstability absolute and convective, Bers-Briggs criterion, analysis

microinstability absolute and convective, Bers-Briggs criterion, analysis 0-46757 in mirror trap, ion-cyclotron 0-39610 negative mass instability, loss cone modes interactions 0-61351 non-linear interaction of waves, shock 0-58348 nonhomogeneous, collisionless, magnetoactive, effect of high-frequency electromagnetic field 0-50105 nonhomogeneous nonequilib. solid state, interacting nonlinearly with strong elec, and mag, fields 0-62270 nonlinear behaviour of waves, in vicinity of marginally stable state, theoretical analysis 0-50087 parametric instability, for phased oscillators interaction 0-61357 Penning modified discharge Q-PIG, temp. instability 0-64753 Penning modified discharge Q-PIG, temp. instability 0-43330 plasma current multipole, theory 0-50102 plasmoid, high- β , global stability problem 0-50106 positive column spiral instability calc. including mode-coupling and He $^{\circ}$ and He $^{\circ}$ mixtures 0-78169 Q machine drift waves, min. B stabilization 0-43295 Q machine, stable state, electrons-ions distrib, fin., potential 0-58345 Rayleigh-Taylor, effect of gyro-viscosity, finite ion-Larmor radius of 0-74595 Rayleigh-Taylor instability of rotating plasma, finite ion-Larmor radius effect 0-50103 remote feedback stabilization of ion-sound instability, at electron-cyclotron reson-freq. 0-64749 rotating plasma, Rayleigh Taylor instability, finite ion-Larmor radius effect 0-50103

rotating plasma, Rayleigh Taylor instability, finite ion-Larmor radius effect 0-50103

Shafranov's type equilibrium configuration for finite β toroidal plasma 0–71193

0—71193
sheet pinch, computer models for motion simulation, expt. 0—46758
sideband computer expts., trapped particles 0—78144
simulation of 2 stream instability, transform and particle-in-cell methods
comparison 0—55500
stellarator, unstable drift waves, magnetic shear effects 0—74538
stellarator equilibrium conditions 0—46722
stream motion in mag. field 0—64752
stream goollision plasmas, transverse instabilities 0—74598

superluminous waves in streaming relativistic plasmas not exciting instability 0-46752

Ty 0-46/32 Tokamak equilibria, instability towards rotation about magnetic axes due to resistivity 0-64750 Tokamak-3, large values of β_1 0-74553 toroidal configuration of Tokamak type, stability of ballooning modes 0-46725

transverse wave instability—driven by shear flow in unmagnetised, collision-less plasma 0-78143

less plasma 0–78143
trapped particle mode stabilization by cool plasma component 0–61349
trapped particle modes in multipoles, finite press. effect 0–74579
turbulence, strong, theor, method 0–46751
turbulent heating, determ. by broadening of H spectral lines 0–50113
turbulent ion heating in Oak Ridge Mirror Machine 0–71196
two-stream, classification into absolute and convective for hot plasmas
0–74596

two-stream instability in ionos., nonlinear stabilization 0–41532 two-stream suppression by beam modulation 0–43331 unmagnetized collisionless anisotropic plasmas, strong stabilizing effect 0–53207

0-33207
variational methods for dissipative instabilities 0-61356
velocity space, with freqn. near electron cyclotron frequency, obs. of freqn. shift 0-78145
velocity-space instabilities, due to self-interaction of single species 0-78150
Vlasov eqn. integration using Bernstein-Greene-Kruskal distrib. fn., trapping effects 0-43333
wave, transverse, in relativistic plasma 0-71161
wave growth populipses limit induced by low density, cold electron beam.

wave growth, nonlinear limit, induced by low density, cold electron beam 0-67962

0-6/962 weakly ionized afterglow, mag. field, short tube 0-53202 weakly-inhomogeneous, two ion species, instabilty in absence of mag. field (0-46754 Ar-Cs, electrothermal instability with current flow parallel to magnetic field 0-53212

Ar, in duoplasmatron, mag. field depend., obs. 0-42230 Ar, time-averaged density profile, finite amplitude helical instability 0-43326

10-43220 H model plasma, thermal stability anal. 0-50114 He-Cs, electrothermal instability with current flow parallel to magnetic field 0-53212 Ne positive column instability in mag. field 0-64755

Plasma diodes see Electricity/direct conversion; Electron tubes;

Plasma/devices Plasma guns see Plasma/devices Plasma in solids see Crystal electron states/plasma; Electron gas; Semiconductors; Solids

Plasma jets see Plasma/devices

Plasma sheath see Plasma confinement

Plasma thermocouples see Electricity/direct conversion; Plasma/devices

Plasma torches see Plasma/devices Plasma waves see Plasma oscillations

Plasmoids see Plasma

Plasmons see Crystal electron states/plasma

Plastic deformation

acrylonitrile-butadiene-styrene (ABS) polymers, birefringence obs. 0-78629

activation areas in high temp. deform., reln. between theory and expt. 0-50680alkali halide, strain hardening, theory, dislocation mechanism, simple slip 0-40447

alkali halide crystals, slip lines, generation and propagation, $1.4~\mathrm{K}$ 0-62055

0-62055
alloy, KhN77TYuR, ageing 0-68503
alloy, KhN77TYuR, ageing 0-68503
alloy, two-phase, continuum and microscopic theories 0-65385
alloys, and dislocations rel. to low temp. magnetoresist. 0-40713
angular, orthotropic glass reinforced up to 373°K 0-78622
anisotropic mats. under biaxial stress 0-62034
anodic coating on Al, buckling 0-62032
anthracene, dislocation production due to bending, triplet exciton trapping
0-71930

0-71930
b.c.c. metals, strain rate, temp. depend. 0-43738
beam-support system, oblique impact, rel. to collision of automobile with protective system 0-72997
bending of transversely anisotropic circular plates 0-45598
brass, M63, yield surface, prestraining history effect 0-43735
α-brass, affeorm. under explosive shock 0-78625
buckling, matrix eigenvalue problems, algorithms 0-38249
buckling creep, simply supported moderately thin circular cylindrical shells 0-38298
buckling during etching of thin thermally grown SiO₂ films 0-65052
buckling of cylindrical shell reinforced by spiral stiffeners under external pressure 0-48812
buckling of shallow spherical shells, asymmetric nonlinear dynamic response 0-45600
buckling stresses in spherical shell 0-73017
camphene single crystals of varying purity creep by dislocation climb

camphene single crystals of varying purity creep by dislocation climb process, activation energies 0-68327

process, activation energies 0–6532 (circular cylinder non-symmetrical collapse modes under symmetrical loading 0–38294 (circular cylindrical shells, moderately thin, simply supported, creep buckling 0–38298 (circular hole expansion in disc, effects of anisotropy and work hardening 0–54653

circular bole expansion in disc, effects of anisotropy and work hardening 0–54653 circular plates, axisymmetric deformation under combined lateral load and membrane force 0–38263 of circular sheet, by punch stretching 0–69695 composite, metal-matrix, interface region role 0–75267 compound cylinders, max. internal press., for specified deform. 0–52045 constitutive equ. for ideal plasticity, derivation 0–38295 constitutive equations at finite strain kinematical viewpoint 0–52038 Cottrell-Stokes law, and for b.c.c. and f.c.c. metals 0–75255 covalent cryst., Ge 0–62033 rel. to cracks, static and moving 0–40396 creep damage theory, linear, for thermal fatigue 0–40397 crystalline aggregate, mechanics 0–47350 under cyclic loading, work-hardening model 0–40444 cylinder, strain analysis, digital computer program 0–38308 diamond, deformation tvinining obs. 0–43741 dipoles, dislocation, positions derived 0–78556 dislocation, mobile, density 0–47246 dislocation and loop density tensors contribs. 0–47249 dislocation velocity and density meas. 0–55884 displacement bounding principle, cylindrical shell 0–52049 dynamic loading, rigid-plastic structures 0–54654 elastic-plastic thin-walled cylinder incremental and total strain theories and obs. 0–40302 elasto-plasticly deformed flat strip, residual stresses 0–52009 elastomers, strength characts, shear resist. 0–55993 ethylene-vnyl acetate polymer, flow props. and softening pt. 0–62048 ferrite, forging, mag.-crystallographic orientation obs. 0–78669 fllm, sheeting, elongation meas. in tensile testing 0–43762 glass, indentation and scratch expts., crack splinter formation 0–40310 glasses 0–62033

plass, muchation and scratch expts., crack splinter formation 0–40310 glasses 0–62033 grain boundary sliding as deformation mechanism in creep 0–75262 high temperature microdynamics, dislocations, effective stresses 0–65394 high temperature model, dislocation dynamics, rate theory, internal stress 0–43733

0-43/33 high-velocity, of visco-plastic rectangular disc in compression test 0-69690 hole in nonuniform disc, twisting and expansion 0-48817 impact, spherical and cylindrical cavities expansion, finite element approach 0-50679 impact between a rigid sphere and a thin layer on a rigid substrate 0-57353

0–57353 incremental, unified theory based on dislocation distrib. 0–40297 indentation experiments correlation 0–43734 inhomogeneous, criterion 0–68439 insulating layers on steel, as result of tensile stress and bending 0–62031 inverse strain-rate effects 0–65383 inverse strain-rate effects 0–65383 unar samples, revealed by chemical etching 0–48546 martensite, C behaviour 0–62040 martensite, liq. N temp., effect on crystal struct., X-ray diffr. meas. 0–78474

measuring method, at high strain rates 0–71682 metal, b.c.c., f.c.c., anal. of Cottrell-Stokes law 0–75255 metal, b.c.c., high temp. work hardening, theory 0–40445 metal, by 10⁻⁸ sec. laser pulse 0–47354 metal, cubic, determ. of symm. groups of deform. textures 0–71688 metal, under cyclic loading, work-hardening model 0–40444

Plastic deformation continued

metal, dislocation, density estimation from small angle scattering data 0-47253

metal, f.c.c., effect of stacking fault energy on deform. characts. 0-78621 metal, f.c.c., sensitivity to deformation velocity, stacking fault energy 0-68437

metal, f.c.c. and h.c.p., strain bursts and coarse slip during cyclic deform. 0-71703

metal, localization and fracture under alternating loads 0–75252 metal, polycrystalline, phenomenological theory 0–53582 metal, polycrystalline, phenomenological theory 0–53582 metal, polycrystalline, phenomenological theory 0–53582 metal, strain hardening eqns. 0–68438 metal, strain hardening eqns. 0–68438 metal, thermodynamic theory 0–40294 metal crystals near yield point, X-ray topographic examination 0–40291 metal system, two-phase, continuum and microscopic theories 0–65385 metals, and dislocations rel. to low temp. magnetoresist. 0–40713 metals, self-diffusion 0–75196 metals at elevated temp., vacancies under nonequilibrium conditions, relaxation method 0–47224 nylon 6-10, anhydrous, stress ageing 0–78628 oval cylindrical shell, axially compressed, postbuckling characteristics 0–40284 plane strain problems, applic. of an orthogonal net of circles 0–38302

plane strain problems, applic, of an orthogonal net of circles 0–38302 plastic, glass-reinforced, unidirectional prestressed, in uniaxial tension 0–40288

plastomechanical principles, cold working 0-40446 plate, circular, by distributed time-var. load 0-38304 plates, impulsively loaded, plastic behaviour, large deformations, mid-plane forces 0-38307

forces 0-38307 polyethylene terephthalate), oriented, crazing behaviour 0-62047 polyethylene, spherulitic, deform. obs. 0-75260 polyethylene, spherulitic, deform. obs. 0-75260 polyethylene, stretched, annealed, superstructures, small-angle X-ray scatt. 0-61932 polyethylene sheets, formation of mech. twins, rel. to tensile modulus 0-50641

polyethylene terephthalate fibres, structural morphological transitions 0-71692

0−1052 polymer, cryst., cold drawing 0−40452 polymer in nonuniform omnidirectional compression 0−40287 polymers, 130 150°C 0−62046 polymethylmethacrylate, formation of micro shear bands 0−68452

polymentymentary lact, formation of micro shear bands 0—68432 poly-4-methylpentene-1 crysts, and slip, obs. 0—40316 polystyrene, formation of micro shear bands 0—68452 polyvinyl chloride, yield-stress in glass transition region, obs. 0—40317 polyvinylchloride, yield condition and propagation of Luders' lines 0—68453

pulsar crust 0-48481

quartz, mechanical, constant strain-rate compression expts. 0-68449 quartz, mechanical, stress relaxation and thermal activation parameters 0-71690

recovery meas, using modulated thermopower system 0–40292 refractory alloys, ductility, ductile creep resisting, hardening, softening kinetics 0–43809 reversibility in cyclic tension and compression 0–62038 rigid cylindrical shells, impulsively loaded, influence of large deflections 0–69693

rotating disc, ratio of velocities for central and radial yield 0–69691 semiconducting crystals, surface layer, anomalous behaviour 0–40289 semiconductor, n-Ge, transverse magnetoresistance, 77 K, dislocations, electron scatt. 0–44252

serrated yielding, activation energy, temp. and strain rate depend. 0-43736

sheet-type tensile specimens, elongation thickness effects 0-43763 shell, cylindrical, elastic and plastic buckling under impulsive loads

shell, eccentrically stiffened multilayered cylinder, transcendental stability 0-54658

0-34038 shell, flexible axisymmetric, finite deform, in plastic flow theory 0-38300 shells, cylindrical, under internal impulsive press, theor. 0-54657 shells, cylindrical Cu, under internal impulsive press, expt. 0-55970 shells, cylindrical and spherical with cracks 0-65387

shells, rotationally symmetric, yield-point load, numerical method of anal.

shells, rotationally symmetric, yield-point load, numerical method of anal. 0–59954
shells, rotationally symmetric, yield-point load, numerical method of anal. 0–59954
shells, truncated conical, axially compressed, plastic buckling 0–38305
solid solution, non-random configurational changes, calc. 0–40338
spaceframes, semirigid, buckling, finite element analysis 0–38283
spherical shell, thick-walled, calc. of large isothermal non-strain hardening deforms 0–76873
steel, SAE 1035 and SAE4340 hollow cylinders rel. to theories 0–40302
steel, y-carbide phase, Fe₃C₃, formation 0–53587
steel, austenitic, 18%Cr–9%Ni type, effect on phase transformations, 600 to –190°C 0–68553
steel, carbon and high-temperature, cyclic elastic-plastic deformation diagram, strength 0–40299
steel, internal residual stresses in cementite phase, X-ray meas. 0–40280
steel, internal residual stresses in cementite phase, X-ray meas. 0–40280
steel, mild, low yield pts, ferrite grain size depend. 0–53589
steel, mild, vield pt. 0–53588
steel, pearlitic, flow stress and work hardening mechanism, microscopic obs. 0–65395
steel, secondary structure formation under impulse loading 0–71802

steel, secondary structure formation under impulse loading 0-71802 steel, transformer, effect on mag. props. and struct. 0-62518 steel, void formation, effect on austenite grain growth 0-50816 steel, yielding rel. to fractography, scanning electron microscopy 0-68490 steel, polycrystalline, particle size and lattice distortion, radiographic determination 0-40461

steel stainless, Cr-Ni, engineering props., improvement by nitrogen addition 0–71712 steel tempering, programmed loading rel. to mech. props. 0–68445 steel thin plates elasto-plastically bent, unloading and inverse loading 0–55963

strain, second order, applied to cyclic loading of columns 0–48815 strain hardening curves, grain size effects 0–62076 stresses internal, measurement recovery effect 0–40277

Plastic deformation continued

succinonitrile, high temp. plastic phase, self diffusion controlled 0-68329

succinonitrile, high temp. plastic phase, self diffusion controlled 0–68329 superconductor, Nb, critical current anisotropy 0–62325 superconductor, Nb, traction instability, 4.2K 0–44128 superconductor, Pb, yield point, flow and shear stress 0–47355 superplastic sheet bulging by lateral pressure, analysis 0–66872 surface notches and protrusions, interaction of dislocations 0–61951 tensile plastic instability, elevated temp., strain rate depend. 0–62041 thin films of thermally grown SiO₂, buckling during etching 0–65052 time-dependent, in metals, structure of stress/strain relations 0–50671 torispherical drum heads under internal pressure loading, computer survey 0–50671

orspherical drum heads under internal pressure loading, computer survey 0–50671 transition conditions, yield conditions 0–73016 twinning, shape strain determ. methods 0–71681 vinyl rods, torsion tests 0–40361 yield condition allowing second-order extension, theory 0–38297 yield surface, prestraining history effect 0–43735 yield-point phenomena in substitutional alloys 0–65386 yielding systems, ultraharmonic oscillations 0–73020 Ag, effect on work function and exoemission 0–73020 Ag, effect on work function and exoemission 0–75851 AgCl pure and Tl doped, potential difference occurring 0–51097 Al-Ag solid solns, rel. to hardening and slip 0–53883 Al-Cu, role of deformation twinning 0–65389 Al-Cu, superplasticity data, numerical anal, using multidimens, regressional techniques 0–75253 Al-(0.042wt.%)Fe, supersaturated and deformer, annealing, micromechanisms 0–75299 Al-(3wt.%) Li alloy, yielding phenomena, annealing depend., lattice const., electron microscopy 0–47353 Al-Mg single cryst., 290K 0–68443 Al-Mg,Si alloy, serrated, yielding, strain rate depend. 0–43739 Al-Mn alloy, 3003 type, strain rate sensitivity, initial struct, effects 0–68442 Al-Zn alloy, age-hardening structure, effects produced by hydrostatic extruction of the produced of the produced by hydrostatic extruction of the produced by hydrostatic extruction of the produced by hydrostatic extruction.

Al-Zn alloy, age-hardening structure, effects produced by hydrostatic extrusion 0-47442 Al-(6.8 at.%)Zn alloy, quenched, effect on pre-precip., -196°C 50779 0-50779

Al-stainless steel composites, yielding, Uniaxial, substructure correlation 0-43787

0-43787
Al, cube texture, tensile deform, cryst. geom. 0-71613
Al, dislocation loop formation on quenching during deformation under creep 0-78552
Al, f.c.c, due to pulsed high mag. fields 0-53584
Al, multiplication of dislocations 0-55886
Al, neutron irad, cavities, formation, stability and effect on yield stress 0-62036

0-62036
Al alloy, yielding, rel. to heat treatment and age hardening 0-40298
Al alloy 2024-T4 hollow cylinder, rel. to theories incremental and total strain theories and obs. 0-40302
Al alloys, cyclic elastic-plastic deformation, diagram, mechanical strength 0-40299

0—40299
Al cylindrical vessels with cutouts and branches 0—40296
Al pure, low-temp. deform., study of recovery by X-ray diffraction, effect of annealing 0—47441
Al single crystal, u.s. attenuation, deform. rate effects during loading, unloading and reloading 0—68598
Al strain changes rel. to dislocation density 0—40297
Al,O₃, double bicrystal, twinning and slip 0—50683
Al,O₃, due to abrasion 0—58890
Al,O₃, nine grained, at high strains and repeated loads 0—50682
Al-78%Zn alloy, superplasticity mechanism 0—50684
Au. effect on work function and exoemission 0—75851
Au, energy absorpt. 0—62037
Au, quenched, initial hardening 0—78624
a-Fe, plastic deformation at low temp., origin of cleavage in twinning 0 58891
BOO.6Fe₂O₃ platelets, defects nature 0—65952

0 58891
BaO.6Fe₂O₃ platelets, defects nature 0-65952
Be, polygonised and cellular structure formation, annealing and temp. depend. 0-50516
Bi, crystal, Bauschinger hardening of twin boundaries 0-47420 depend. 0–50516
Bi, crystal, Bauschinger hardening of twin boundaries 0–47420
Bi, dislocation density, impurity interaction 0–40159
Cd, polycrystalline, elec. current pulses effect 0–40313
Cd whisker, surface film depend. 0–40300
Co-(20wt.%)Ni-(20wt.%)cr alloy, struct. change production 0–78695
Co, effect on mag. props. 0–79168
Cr. pressurization, compressibility, yield drop, hardening, electron microscopy dislocations 0–62030
Cu-(29.9 at %)Au alloy, crystal twinning 62039
Cu-Al alloy, Cu-rich, rel. to short-range order 0–68529
Cu-Al alloy, deformation bands produced in tension 0–43743
Cu-Al alloy, dislocation behaviour 0–58813
Cu-Ni-Zn alloys, stacking faults 0–50601
Cu, Ni-Zn alloys, stacking faults 0–50601
Cu, anisotropy predictions using pole-inversion figures 0–65384
Cu, Cu-O (tough-pitch copper), comparison 0–65391
Cu, deformed in tension, stage III recovery of resistivity 0–78878
Cu, during creep, substruct, analysis, single cryst. 0–65233
Cu, during creep, substruct. and dislocations, etch-pit obs., single cryst. 0–68362
Cu, effect on transverse magnetoresistivity 0–47644
Cu, high-purity, torsional stress, annealing, point defects, elec. resist. 0–75304
Cu, reversibility in cyclic tension and compression 0–62038

Cu, reversibility in cyclic tension and compression 0–62038 Cu, strain cycling, modulus changes dislocations-point defect interaction 0–50686

O-50686
Cu, sub surface dislocation struct. 0-43671
Cu alloys, effect on thermal cond. 0-50906
Cu and Cu-Zn with Al₂O₃ particles, work hardening theory and macrostruct. 0-65392
Cu and Cu-Zn with Al₂O₃ particles, microstruct. 0-65393
Cu cylindrical shells under internal impulsive press. expt. 0-55970
Cu f.c.c., due to pulsed high mag. fields 0-53584
Cu film, condensed, stress rel. to microstrain 0-65390
Cu film, vacuum-deposited, yield stress rel. to struct. 0-61645
Cu films, weak deform. influence on proton channelling 0-71888
Cu polycrystalline, elevated temp., substructure misalignment 0-68448
Cu rods, soft, prestressed, small strain wave propag. 0-53585
Cu single crystal, and dispersion hardened, constant strain amplitude fatigue deform. 0-56005

Plastic deformation continued

Cu single crystal, deformed, Hirth locks 0-40162

Cu single crystals, influence of deformation temp. ion dislocation arrangement 0-75162

Cu single crystals, influence of deformation temp. ion dislocation arrangement 0-75162

Cu₃Au, rel. to low temp. magnetoresist. 0-40713

D₃, solid, stress relaxation, 1.4-17.5K 0-40304

Fe/Ag composite wires, anomalous props. 0-59005

Fe-Ni-C alloy, paramagnetic austenite, f.c.c., transformation 0-55972

Fe-Ni-C alloy, paramagnetic austenite, f.c.c., transformation 0-5087

Fe-Si alloy, slip temp., microdynamics, minimum effective stresses, dislocations 0-65394

Fe-Si, alloy, deformation and primary recrystn. textures 0-75254

Fe-Si alloy, slip singularities in single crystal 0-53603

Fe-Si single crystals, rolling, active slip systems determ. 0-78640

Fe-Si single crystals, rolling, active slip systems determ. 0-62054

Fe-Si single crystals, rolling, active slip systems determ. 0-62054

Fe-Si single crystals, rolling, active slip systems determ. 0-62054

Fe-Si single crystals, rolling, active slip systems determ. 0-78640

Fe-Si single crystals, rolling, active slip systems determ. 0-78640

Fe-Si single crystals, rolling, active slip systems determ. 0-62054

Fe-Si single crystals, rolling, active slip systems determ. 0-62054

Fe-Si single crystals, rolling, active slip systems determ. 0-62054

Fe-Si single crystals, rolling, active slip systems determ. 0-78640

Fe-Si single crystals, rolling, active slip systems determ. 0-62054

Fe-Si single crystals, rolling, active slip systems determ. 0-62054

Fe-Si slip, or yet all serves. 10-6404

Fe-Fe-Ti alloy, yield stress, flow stress, Luders strain, grain size and interstitials effects 0-50689

Fe, internal friction and modulus change, low temp. 0-71671

Fe, zone velocity depend. on stress, using single Luders band propag. 0-35586

Gd, h.c.p., by twin partial dislocation form., obs. 0-40303

Ge-Si alloy and Si, simultaneous, prod. of semiconductor thermocouples 0–43748

Ge, p-n junction, diffusion of Ga 0-53876 n-Ge, transverse magnetoresistance, 77 K, dislocations, electron scatt. 0-44252

Hg, crystal, twinning, characts. 0-53545 In-Pb alloys, tensile plastic instability, elevated temp., strain rate depend.

0-62041

In, polycrystalline, elec. current pulses effect 0-40313
KCl, F centre growth, thermoluminescence 0-50613
KCl, under u.s. wave exposure 0-62042
KCl v-irrad. crysts., luminesc. 0-76195
LiF, charge on dislocations and elec. signal 0-53590
LiF, dislocation forest and resistance 0-68446
LiF, e.s.r., H-centre in F-centre spectra 0-59453
LiF, fracture surface energy, dislocation processes, dynamical cleavage, theory 0-47412
LiF, fracture surface energy and dislocation processes, dynamical cleavage, expt. 0-47413
LiF, velocity, stress relaxation, 309, 78 and 4.2K, dislocation velocity 0-40305
LiF crystal, M-centre persistence after appealing 0-47290

0-40305
LiF crystal, M-centre persistence after annealing 0-47280
MgO single crystal, rolling-contact deform, track props. rel. to dislocations and slip 0-40306
Mg-Al eutectic, superplastic, grain boundary sliding contrib. 0-55974
Mn-Ga alloys, effects on mag. props. 0-47914
MnTe, MnTe-MnSe solid solutions, and fracture 0-62043
Mo-Re alloy, 78-425 K, dislocation velocity depend. 0-43745
Mo, annealed and deformed, X-ray exam., Kossel lines, local distortions 0-68348

0 - 68348

0-08348 Mo, interaction of moving dislocations with interstitial impurities, stress relaxation, 300-600K 0-50575 Mo, yield and flow, strain rate and temp. effect 0-40307 Mo-Ti-C, carbide precipitation, strengthening 0-40331 NaCl, bending, stress distrib., photoelasticity, dislocation density 0-4331 MaCl, bending, stress distrib. Mo-Ti-C, carbide precipitation, strengthening 0-40331 NaCl, bending, stress distrib., photoelasticity, dislocation density 0-43746 NaCl, effect on elec. strength 0-65783 NaCl single cryst., effect on transmission and reflection at 2000-950 Å 0-44766

0-44766
Nb-N, solid solution, yield stress 0-65396
Nb-O-N, dilute system, yield stress, comp. depend. 0-65397
Nb-O-N, dilute system, yield stress, comp. depend. 0-55975
Nb-(6at.%)W, single crystal, low temp., thermally activated, mechanisms 0-40333
Nb-W single crystal, yield stress, effect of orientation and sense of applied stress 0-68447
β-Nb-(25wt.%)Zr, yield and fracture, temp. depend. 0-65398
Nb, b.c.c., microflow meas. mechanism 0-75257
Nb, grain size effects 0-50688
Nb, neutron irrad., radiation hardening, yield stress depend. on dose 0-65461
Nb, recrystallization temp. 0-65454

Nb, recrystallization temp. 0-65454 Nb, superconducting, effect on magnetic props. and resistive transitions 0-75605

0-75605
Mb, superconductor, critical current anisotropy 0-62325
Nb, traction instability, 4.2K 0-44128
Nb, yield and flow, strain rate and temp. effect 0-40307
Nb neutron irradiation, transmission electron microscopy and tensile testing 0-50690
Nb single crystal, yield stress, effect of orientation and sense of applied stress 0-68447

Nb single crystals, struct., effect of low-temp. rolling X-ray diffr. meas. 0–78486
Ni-C solid solution, tensile testing, internal friction, dislocation damping 0–40309

0-40309

Ni-Cr-Al alloy, elec. resist., temp. depend., K-state, X-ray exam. 0-47650

Ni-Cr-Nb alloy, precip.-hardened, deform. mechanisms 0-71689

Ni-Cr-Nb alloy quenched from 1200°C and then annealed by slip, shearing and twinning 0-55976

Ni-Cu alloys, rolling texture and stacking fault energy 0-53511

Ni-Ge alloy, stacking fault formation, comp. depend. 0-50602

Ni-Mo(W) alloys, temp. depend. 0-47377

Ni-base alloys, effect of structural changes on hardening of single crystals 0-71744

Ni effect on magnetomechanical damping. 0-55935

0—71/44
Ni, effect on magnetomechanical damping 0—55935
Ni, effect on transverse magnetoresistivity 0—47644
Ni, high-speed deform, sips systems participation 0—40341
Ni, oxidation effects, high temp. model 0—43747
Ni, polycryst., high temp., effect on substructure, X-ray diffr. meas. 0—78489

Ni, single crystal, mag. anisotropy 0-75925 Ni, surface-oxidized, in vacuum, effect on exo-emission 0-47891

Plastic deformation continued

Ni, work-hardened, creep strength 0-62052

Ni dipoles, dislocation, positions derived 0-78556
Ni foil, dynamic and static extension, microhardness, dislocation densities,
X-ray investigation 0-50691

(18wt.%)Ni maraging steel, tensile ductility and press-forming props. up to 300°C 0-58928

Ni polycrystalline, elevated temp., substructure misalignment 0-68448 p'-Ni₃Al, stacking fault origin 0-71630

Ni₃Fe, Ni₃Fe-Al alloys, discontinuous yielding 0-40308

Ni₁Mn alloy, tensile testing, discontinuous yielding 0-40308 Ni₁Mn alloy, tensile testing, discontinuous yielding 0-40308 Ni₁Mo, twins, cold rolled, quenched 0-5895 Pb-Sn eutectic alloys, superplastic, mechanism, direct obs. using scanning electron microscope 0-71687 Pb, microstructural changes rel. to self-diffusion activation energy 0-61997

Pb, normal and superconducting states 0-47355

Pb, normal and superconducting states 0–47355
Pb, polycrystalline, electric current pulses effect 0–40313
Pd, effect on work function and exoemission 0–75851
Pt, effect on work function and exoemission 0–75851
Pt, irrad, dislocation cutting of depleted zones, activation energy, annealing effects 0–53541
Pt, positron annihilation ang. correl. obs. 0–59155
Se, vitreous, influence on crystn. 0–53412
Si-Fe welds, strain behaviour of heat affected zones 0–71725
Si, e.p.r. spectrum 0–48151
Si, internal friction, temp. depend., damping mechanism 0–68417
Si, production of e.p.r. signal, annealing behaviour 0–56671
Si and Ge Si alloy, simultaneous, prod. of semiconductor thermocouples 0–43748
Si surface, –196 to 550°C, metallographic and transmission electron.

Si and Ge Si alloy, simultaneous, prod. of semiconductor thermocouples 0–43748
Si surface, −196 to 550°C, metallographic and transmission electron microscope obs. 0–40311
SiO₃, thin, thermally grown films buckling during etching 0–65052
Sn, polycrystalline, elec. current pulses effect. 0–40313
SFF, crystal, slip etching, dislocations 0–43758
Ti-Al alloys, modes, strength and fracture characteristics 0–47382
TiO₂, ≈21, temp. and comp. depend. 0–50692
U, energy release kinetics during annealing 0–56034
UO₃, polycrystalline, high temp. creep, calc. 0–47361
V wire, neutron irrad, thermal hardening, temp. depend. 0–47448
VC, crystal, dislocation etch pits 0–61968
WC-Co alloy, effect on strength and hardness 0–43770
Zn-(0.4 wt.%)Al superplastic sheet, anisotropic effects 0–40315
Zn, crystal, Bauschinger hardening of twin boundaries 0–47420
Zn, dislocation forests role 0–40312
Zn, in pyramidal slip, mechanism 0–62044
Zn, single crytal and polycrystalline, electric current pulses effect 0–40313
Zn cold-stretched single cryst., mechanism rel. to twin formation 0–68450

0-40313 Zn cold-stretched single cryst., mechanism rel. to twin formation $\,0-68450$ Zn crystals, deformed, dislocation struct. investigation by electron transmission microscope $\,0-78558$ Zn whisker, surface film depend. $\,0-40300$ ZnO, photoplastic effect, dislocations and interstitials, coulomb interaction $\,0-40337$ ZnO whiskers, and fracture $\,0-62071$ ZrB $_2$, and ZrB $_2+SiC$, behaviour above $1400^{\circ}C$ $\,0-55977$ ZrO $_2$, unstabilized, deform. substruct. $\,0-50582$

setic flow

see also Rheology
alkali halide single crysts., work hardening theory 0–68515
alkali halide single crysts., work hardening theory 0–65460
brass, M63, yield surface, prestraining history effect 0–43735
buckling of cylindrical shells due to impulsive loading 0–57354
camphene, self-diffusion, n.m.r. 0–62045
Cosserat theory 0–52048
crystalline solids, athermal component of flow stress, expt. methods and theory 0–78639
crystals, mechanisms 0–47362
cyclohexane high temp. rotator phase, study 0–68328
diffusional flow in polycryst. 0–65399
dislocation motion, thermally activated, in Peierls pot., internal stress influence 0–78630
ductile fracture, continuum models 0–47403
ductile brittle transition temp. obs. of intermetallic single and polycryst. 0–40385
epoxy moulding compounds, properties under transfer moulding pressure

0-40385 epoxy moulding compounds, properties under transfer moulding pressure obs., rel. to reliability of electrical and electronic components packaging 0-47365 fuel pin sheaths, computer program for evaluation, CRASH 0-68455 glass tube drawing technique 0-57193 hexamethylene high temp. rotator phase, study 0-68328 intermetallic single and polcryst., ductile-brittle transition temp. obs. 0-40385

0 - 40385

0-40385 ionic powders, eff. on sintering 0-75297 martensite, strain ageing by hydrostatic extrusion 0-53633 metal, f.c.c., Cottrell-Stokes ratios, stacking fault energies 0-43678 metal, f.c.c., flow stress irreversible component 0-47349 metal, flow stress at low temp., long-range internal stress contrib. 0-40320 metal, flow stress theory rel. to spurt-like dislocation movement 0-58888

metals, ductile, yield, initial, macroscopic criteria 0—40400 metals, ductile, yield, initial, macroscopic criteria 0—40400 metals, dynamics rel. to ductile crack propagation speed 0—50738 metals and magnetostrictive materials, acoustically induced 0—65407 NaCl crystal, dislocation motion in slip bands, stress depend. 0—68462 nichrome alloy, 80/20, ductility rel. to extension rate and neutron irrad. 0—65405

0-65405
oxide film growth, stress generation and relief 0-61660
pivalic acid, high temp. rotator phase, study 0-68328
plane, in material description 0-59950
plane flow, lagrangian co-ords. used to derive fundamental eqns. 0-38301
plastomechanical principles of cold working 0-40446
residual stresses for growing crack, BCS model 0-53617
rigid plastic structures, displacement fields loaded beyond point of plastic
flow 0-45602
shell, flexible axisymmetric, flow theory applied to finite deform. under
loading 0-38300
steel, 20 Cr/25Ni/Nb stabilized austenitic, ductility and fracture, effects of
heat treatment 0-43757

Plastic flow continued

steel, ductile-to-brittle transition temp., crack nucleation and growth $0\!-\!53613$

steel, low-C and Ti-stabilized, between ambient and liquid N temps. 0-47363

steel, mild, low yield pts., ferrite grain size depend. 0-53589 steel, mild, plastic stress concentration factor, cyclic load, method comparison 0-43737

steel, mild, yield pt. 0-53588 steel, pearlitic, flow stress and work hardening mechanism, microscopic obs. 0-65395

obs. 0-65395 steel, stainless, ductility, pre-strain effect 0-78634 steel, yielding rel. to fractography, scanning electron microscopy 0-68496 steel 35G18, ductility multiple p=e, $p=e^*$ transforms, effect 0-40350 stress azimuthal component determ, method comparison 0-50693 superconducting In, changes in flow stress 0-78635 turbo-generator retaining rings, yield strength, cold working 0-40345 viscoplastic flow between fixed and moving plates, self-modelling soln. 0-52050 yield criteria singular angles are free to the strength of t

0–52050
yield criteria, singular surfaces in plastic solids 0–38306
yield stress at low temps., cryst. orientation depend., slip geometry, unified model 0 58889
yield surface, prestraining history effect 0–43735
yielding, serrated, activation energy grain size depend. 0–47351
Al-Mg alloys, Portevin-Le Chatelier effect 0–58862
Al, flow stress rel. to strain, strain-rate and temp., comment on dimensional homogeneity of eqns. 0–40326
Al, pure, low-temp. deform, study of recovery by X-ray diffraction, effect of annealing 0–47441
Al single crystal, flow-stress temp. depend. stage II deformation 0–55985
Cd single crystal, torsional deformation effect 0–58905
Cr. polycrystalline, ductile brittle transition temp., press. effect, 5-31 kbars 0–53598
Cr wire, ductile/brittle transition 0–40453

Cr. polycrystalline, ductile brittle transition temp., press. effect, 5-31 kbars 0-35398
Cr wire, ductile/brittle transition 0-40453
Cu-Al bicryst., anomalous hysteresis loop shape 0-71716
Cu-Ti Al alloys, temp. depend. 0-55986
Cu-Ti alloys, temp. depend. 0-55986
Cu. Cottrell Stokes ratio, dislocation distrib. 0-75263
Cu. Cottrell Stokes ratio, dislocation distrib. 0-65391
Cu., flow stress rel. to strain, strain-rate and temp., comment on dimensional homogeneity of eqns. 0-40326
Fe, Fe-Ti alloy, yield stress, flow stress, Luders strain, grain size and interstitials effects 0-50689
Fe, thermally activated, orientation depend. single cryst. 0-68444
Fe alloy G20, ductility, multiple y=xe, y=xe' transform. effect 0-40350
Fe single crystal, orientation and temp. depend. 0-53599
In, normal and supercond., changes in flow stress 0-78635
LiF, dislocation forest and deformation resistance 0-68446
LiF, LiF:Mg, yield stress, slip mechanism, 77-450K 0-40340
Mg0, stress, impurity effect, dislocation mobility, microscopy 0-55987
Mo, ductile brittle transition temp. annealing temp. effect 0-58895
Mo, polycryst., ductile-brittle, microyielding and failure mechanisms 0-75256
Mo, yield and flow, strain rate and temp, effect 0-40307 0—13230 Mo, yield and flow, strain rate and temp. effect 0—40307 Nb-N, solid solution, yield stress 0—65396 Nb-O-N, dilute system, yield stress, comp. depend. 0—65397 Nb-(6at.%)W, single crystal, low temp., thermally activated, mechanisms

100-(00.1%) w. Single crystal, low temp, thermany activated, mechanisms β-Nb-(25wt.%)Zr, yield and fracture, temp. depend. 0–65398 Nb, single crystal, flow stress, temp. depend., neutron irrad. effect 0–78627

No, single crystal, now sitess, temp. depend., neutron final. effect 0-4862 7 Nb, yield and flow, strain rate and temp. effect 0-40307 Ni-C alloy, serrated stress-strain curves, temp. and comp. depend. 0-40334 Ni-Cr alloy, ductility after quenching and heat treatment, 25°C 0-40355 Ni-Ti alloy, microstructural obs. 0-50708 Ni, acoustically induced, expts. 0-65407 Ni, threshold meas. and u.s. and static loadings 0-68463 (18wt.%)Ni maraging steel, tensile ductility and press-forming props. up to 300°C 0-58928 Ta alloy, ductility, mech. strength, hardness, comp. depend. 0-55997 Ti-Al-V alloy, u.s. yield stress and internal friction 0-68419 a-Ti, stress azimuthal component determ, method comparison 0-50693 TiFe, TiCo, TiNi and ternary solid solution, ductility 0-40336 (U-Pu)O₂ mixed fuels, yielding 0-58892 UO₂, stochiometric polycryst., fracture at macroscopic yield stress 0-40359 Vb, polycrystalline, temp. depend. 78-525K 0-65406

0-40359
Yb, polycrystalline, temp. depend., 78-525K 0-65406
Zn-(0.4 wt.%)Al superplastic sheet, anisotropic effects 0-40315
ZnO, photoplastic effect, dislocations and interstitials, coulomb interaction 0-40337
Zr alloys, irrad. creep, enhanced ductility obs. 0-71701
ZrB₂, and ZrB₂+SiC, behaviour above 1400°C 0-55977

Plasticity

see also Viscoelasticity

after-effect, rel. to cold working peaks 0-40248
anisotropic, anomalous behaviour of aluminium sheet under balanced biaxial tension 0-59959
anisotropic disc, expansion of circular hole, effects of work hardening 0-54653

u-34933
anisotropic plasticity, strain hardening hypothesis 0-45599
anisotropic plate plastic bending study 0-48813
arches, elastic plastic, appl. of theory of finite deflections 0-54628
beam-column, inelastic, elastic-plastic behaviour, general solution
0-66880

0-66880 boundary value problem for elastic-plastic materials 0-59986 a-brass, anisotropy prediction using pole-inversion figures 0-65384 circular cylinder non-symmetrical collapse modes under symmetrical loading 0-38294 composites, polycrystalline, elastic-plastic behaviour 0-71676 condition for isotropic and orthotropic acicular polycrystals 0-47368 constitutive eqn. for ideal mat., derivation 0-38295 deformation theory study of propagation of unloading shock waves in elastic-plastic strain hardening medium 0-45601 disc, plastic anisotropic, similarity solns, for expansion of hole 0-38303 elastic-perfectly plastic stress problems, computerized relaxation method 0-47339 elastic plastic bar with moving heat source, stress wave propagated felatic-plastic bar with moving heat source, stress wave propagated felatic-plastic bar with moving heat source, stress wave propagated felatic-plastic bar with moving heat source.

elastic-plastic bar with moving heat source, stress wave propag. and field anal. 0-38317

Plasticity continued

elastic-plastic boundaries, effect on propag. of plane and cylindrical com-bined stress waves 0-48838

elastic-plastic hollow cylinder, unloading effect under monotonic twist 0-4584

0-45584 elastic-plastic materials, acceleration waves 0-48826 elastic-plastic plane-strain solns, with separable stress fields 0-42049 elastic-plastic rings and cylinders, transient response rel. to strain-hardening and strain-rate sensitivity 0-38260 elastoplastic analysis of plane-strain and axisymmetric flat punch indentation by finite-element method 0-59960 elastoplasticity, minimum theorems in boundary value problems 0-38265 exploitation, conference, Eastbourne (1969) 0-62035 flow, plane, in material description 0-59950 rel. to forming processes 0-62098 graphite, artificial, elastic-plastic continuum theory for small deform. 0-43740 illimit theorems, extension of applicability 0-69696

0-43740
limit theorems, extension of applicability 0-69696
Luders bands in Al-Mg alloys 0-50631
membrane, elasto-plastic, motion under shock loading 0-45594
metals, theory 0-78623
models and theory of complex media 0-59989
optimal design of structures of composite materials, internal and external
reinforcement 0-48806
photoplasticity in ZnO 0-76044
plane elasto-plastic problems, modelling by photoplastic method 0-45595
plane flow, lagrangian co-ords, used to derive fundamental eqns. 0-38301
plane strain problems, applic. of an orthogonal net of circles, or Ringleb's
theorem 0-38302
plane-strain finite deformation in strain-rate sensitive elastic-plastic
materials and shock thickness 0-57360
plastic-strain waves, dispersive, gauge length errors in strain meas.
0-40290
plastomechanical principles of cold working 0-40446

0-40290 plastomechanical principles of cold working 0-40446 plates, impulsively loaded, plastic behaviour, large deformations, mid-plane forces 0-38307 Poisson's ratio var., elastic to plastic range 0-48798

polymer rod, longit. elastoplastic wave propag. 0–40254 prismatic solid, modified plane strain, discrete-element plastic analysis 0–40265

response of circular blanks to underwater explosions 0-54760 rigid cylindrical shell, impulsive loading, influence of large deflections 0-69693

rigid cylindrical shell, impulsive loading, influence of large deflections 0–69693 rigid plastic structures, displacement fields loaded beyond point of plastic flow 0–45602 semiconducting crystals, surface layer, anomalous behaviour 0–40289 shell, cylindrical, buckling under impulsive loads 0–59974 shells, flexible, orthotropic, finite deformations 0–54655 shells, slender, axisymmetric, subjected to plastic flow in large deform, numerical procedure 0–54656 shells, spherical elastic-plastic, significance of strain-hardening and strain-rate effects on transient response 0–69675 soils, finite deformation theory of elastic-plastic behaviour 0–63390 solid, book 0–43702 soilds, singular surfaces, for yield criteria 0–38306 stacking fault energy depend. 0–50598 steel, 17-4PH and 15-5PH, ductility, microstructure and mech. strength 0–40330 steel, hot-rolled, study by statistical method 0–62063 steel, nickel chrome, strain analysis under various cyclic loading 0–50717 steel, stainless, ductility, pre-strain effect 0–78634 strain, small, anisotropic: discretized variational formulation 0–52046 superplastic metal forming, theory and expt. 0–68525 superplasticity, microstructural changes, similarities and differences rel. to hot working and creep 0–68504 superplasticity, microstructural changes, similarities and differences rel. to hot working and creep 0–68504 superplasticity, numerical anal. by multidimens. regressional techniques 0–75253 superplasticit, rictability, elevated temp. strain rate depend 0–62041

0-71684 superplasticity, review 0-71684 tensile plastic instability, elevated temp., strain rate depend. 0-62041 theory, minimum energy, for sliding forces of rigid cones over metals 0-53626

theory, second-order effects 0–38297 thermodynamics of crystalline materials, macroscopic and microscopic 0–40293

0-40293 thin structures, computation method 0-48816 time dependent in wedge shaped ring surrounding crack, shortening of time to failure compared with time-independent 0-47401 vinyl rods, torsion tests 0-40361 visco-plastic disc, rectangular, high-velocity deformation in compression test 0-69690 viscoplastic rod, thermally sensitive, elastoplastic wave propagation 0-69692

0-69692
viscoplasticity, basic problems 0-52047
viscoplasticity, basic problems 0-52047
wave propagation in two-dimensions, allowed directions 0-39875
working processes, rel. to exploitation 0-68441
Al-Mg alloy, Luders bands 0-50631
Al, f.c.c., viscoplasticity 0-53584
Cr, ductile-brittle transition 0-61741
Cr wire, ductile-brittle transition 0-40453
Cu, anisotropy predictions using pole-inversion figures 0-65384
Cu, f.c.c. viscoplasticity 0-53584
Cu, polycryst, quantitative anal. of anisotropy 0-55968
In-Pb alloys, tensile plastic instability, elevated temp., strain rate depend.
0-62041
Mo-Rh alloys, props., 78°-425°K, and elastic props. 0-43711

0-02041
Mo-Rh alloys, props., 78°-425°K, and elastic props. 0-43711
Sn-Pb alloy, superplastic 0-71691
UO₂, stoichiometric polycryst, ductile-brittle transition 0-40359
Zn-Al eutectoid, copper additions rel. to superplasticity 0-68451
ZnO, photoplastic effect, dislocations and interstitials, coulomb interaction 0-40337

ZnO photoplasticity 0-76044

stics see also Polymers for Cherenkov detectors, spectral transmission description 0–49378 p-ray detector, dielectric, for high exposure applic. 0–49397 black polyethylene, optical properties from 3 to 4000 cm⁻¹ 0–44742 carbon-phenolic material, charring 0–47539 dielectric, high energy neutron flux detection 0–63869

Plastics continued

elastically different samples joining, strain pattern examination 0-47340 electrical, specific resistance and temp. coeff. relationship, meas., instru. 0-59159

encapsulation for semiconductor devices, design and evaluation w.r.t. reliability 0-47771 epoxide resins set with different anhydrides, dielectric relaxation 0-72103

epoxies, application to packaging semiconductor devices, moisture resistance 0-47772

tance 0-47772
epoxy resin, tensile strength, drop weight test machine 0-50658
films, thin, permittivity meas at 1 MHz 0-68889
fission fragment counting in control of personnel neutron doses 0-77423
fission track registration, etching parameters influence on sensitivity
0-77437
glass fibre reinforced laminates, shear characteristics determination,
method 0-47321
glass fibre reinforcement, mech. props. 0-47471
glass reinforced, laboratory testing of electrical and mechanical properties
0-68911

glass reinforced up to 373°K, angular deformations 0–78622 glass-reinforced, as reinforcement in metal shells, prestress effect on strength 0–40343

glass-reinforced, deform. in tension stress- strain curve discontinuity 0-40262

0-40262
glass-reinforced, filament-winding and prestress variation 0-40451
glass-reinforced, unidirectional prestressed, deform, and fabrication technique 0-40288
glass-reinforced AG-4S, elastic characts, under short-time and long-time loads 0-40222

loads 0-40222
IC encapsulation, failure mechanisms, reliability testing 0-51069
IC encapsulation reliability evaluation and analysis 0-47770
Iaminates, glass fibre reinforced, fatigue strength investigation 0-47394
Iaminates reinforced by fiber, behaviour under uniaxial, biaxial and shear loadings obs. 0-50712
Lexan plastic prints formation 0-77429
Lexan polycarbonate, heavy ion tracks, etching enhancement by spark discharge 0-60712
melinex, X-ray absorpt., 44-85Å 0-66085
moulding of high performance thermally stable matrices by reactive hotpressing 0-50347
Mylar film, thermally stimulated currents depolarization, high terms because the property of the property

Mylar film, thermally stimulated currents, depolarization, high temp., low field 0-44351

nuclear track detectors, sensitivity enhancement through photo-oxidation

0 - 63870

0-5870 for optical components manufacture, industrial process 0-57607 particle track detectors for particle indentification 0-46073 particle tracks, etching parameters 0-60713 particle tracks, solvent development 0-60715 perspex, capacitance variation due to thermo-electret formation 0-59273 Perspex, development of discharge channels under impulse conditions 0-68904

plastic/composite materials, reinforced, nondestructive test methods 0-40475

Plexiglass, moving crack, Rayleigh wave generation 0-75241 pollutants, biologically recalcitrant, photomodification processing 0-63217

poly(ethylene terephthalate), oriented, deformation, crazing behaviour 0-62047

polybutylmethacrylate, structure obs. from u.s. velocity and refr. index at 6328 Å 0-61613 polyburybonate film, track etching rates rel. to atmosphere and u.v. irrad.

0-60716
polyethylmethacrylate, structure obs. from u.s. velocity and refr. index at 6328 Å 0-61613
polymethylmethacrylate, structure obs. from u.s. velocity and refr. index at 6328 Å 0-61613
polymethylmethacrylate-BaTiO₃ mixture, electret effect 0-40883
polystyrene, fluoresc., CCl₄ quencher effect, ethylbenzene comparison 0-39817

polyvinyl chloride, orientated, residual optical birefringence 0–51269 polyvinyl fluoride, d.c. and a.c. cond., dielec. loss, temp. depend. 0–75781 radiation dosimeter using peroxy radicals in irrad. polytetrafluoroethylene 0–70313

radiation dosimeter using peroxy radicals in irrad. polytetrafluoroethylene 0–70313
reinforcement by glass fibres, mech. props. 0–47471
scintillators, polystyrene based, ageing characteristics 0–77399
scintillators with increased transparency 0–46029
sheet, thickness meas., gauging head assembly, patent 0–55751
silicone resins as encapsulants in timing circuits, H₂ evolution, absorption
by Evanohm resistors resistance increase causing malfunction 0–47620
silicones, application to packaging semiconductor devices, moisture resistance 0–47712
stepl-resin composite, fibre-matrix adhesive bond, press. effect 0–62118
strain measurement, appl. of grids for moire fringe method 0–40263
substrate for metal film nucleation and growth 0–58596
textile fibre, fractography, scanning electron microscopy 0–62059
thermoplastic Hostadur, mechanical, chemical and electrical properties, engineering applications 0–58844
thermoplastic s, cyclic thermal softening and fatigue 0–47337
thermoplastics, stress analysis w.r.t. long-term behaviour, deflections prediction and component dimensions estimate 0–58877
track detectors, calibration for use in cosmic ray expt. 0–77430
track meass, cone length and range meas. 0–77441
transient comparison methods of simultaneous thermal properties meas. 0–50885
two-layer laminated, apparent Young's modulus, freq. effect 0–40221
u.s. complex transmission coeff. for plastic specimen immersed in water 0–68597
vinyl, structure, hydrostatic pressure effect 0–58549
vinyl rods torsion tests. 0–40361

vinyl, structure, hydrostatic pressure effect 0-58549 vinyl rods, torsion tests 0-40361 C fibre reinforced structures, design and manufacture 0-47025 polypropylene, X-ray absorpt., 44-85Å 0-66085

Platinum

dsorption of H₂ transient stage, field ion microscopical obs., effect of Ne adsorption 0-65107 adsorption of ethylene on Pt (111) 0-47088 anodic oxidation with H₃SO₄, mechanism 0-76273 band structure shift for f.c.c. metal, non-muffin-tin potential 0-44067

Platinum continued

crystal, low temp. electron irrad., defect production and recovery 0-50576

diffuse layer, on ceramic exoelectron emitters, effect on sensitivity 0-73700

0-73700
diffusion in Si 0-40204
electrode, adsorption and electro-oxidation of NH₃ 0-66196
electrodes, Cu monolayers form. 0-54192
electron energy loss spectra obs. and correl. with theory 0-50918
film, 'island' condensate, anomalous struct, elec. cond. 0-75568
film thermometer on Pyrex glass, meas. of surface temp. in nucleate boiling
of water 0-48894
Frank loops, field-ion microscopy, computer simulation and exptl. obs.
0-75167

0-75167
g factor anisotropy and exchange splitting 0-44502
gamma-rays inelastic scatt. by K shell electrons 0-39302
hyperfine fields at dil. Fe and Co impurities, below 4.2K 0-48039
impurity in Ni₅Ga, mag, susceptibility 0-44590
ion desorption induced by e bombard, study 0-55761
irradiated, dislocation cutting of depleted zones, activation energy, annealing effects 0-53541
microgram level, fire-assay emission spectrographic method 0-54197
Mossbauer fraction of 37Fe, force const. changes obs. 0-40531
paramagnet f.c.c., anisotropic g factor of Fermi surface sheets 0-44499
photoelectric work function 0-75859
polymer formation in organic vapour environment obs., water drop reflection goniometer technique, surface preparation methods comparison 0-5694
positron annihilation from electron-irrad. or plastically deformed ang.

son 0-30094 positron annihilation from electron-irrad. or plastically deformed ang. correl. material 0-59155 scattering of atomic and mol. ions, energy distribs. of emitted particles 0-40912

0–40912 sorption of organic cpds., kinetics obs. 0–56693 specific ht., 1.3° to 90°K, high purity Pt. 0–53713 spectrographic analysis in gold beads from fire assay. 0–66213 sublimation, accelerated, under tensile stress in air. 0–47007 surface scattering of He and D₃ beams, LEED meas. 0–74887 thermal conductivity meas., 380-610 K. 0–40594 thermal conductivity meas., 380-610 K. 0–40594 thermal expansion rel. to vacancy formation. 0–47550 thermometer, resistance rugged, stable, differential construction, calibration and testing. 0–48895 work function and exoemission, effect of deformation. 0–75851 CO¹ desorption induced by e bombard, study. 0–55761 Cl and Br¹ bombardment, electron emission, ions scattering. 0–59292 H² desorption induced by e bombard, study. 0–55761 Pt;3°CA, hyperfine fields, low temp. 0–76052 197Pt;197Au, Debye-Waller factors of Au atoms. 0–78744 Si:Pt., energy levels in forbidden band. 0–53847 tithum compounds.

Platinum compounds
alloy, dil., Matthiessen's rule deviations 0—53847

Platinum compounds
alloy, dil., Matthiessen's rule deviations 0—59167
porphyrin complex, luminesc. 0—79344
CoPt alloys, annealing, internal friction 0—62079
CuPt, order-disorder changes as classical phase transform 0—56074
Fe(Pd, Pt_{1-x}), alloys, mag. behaviour, Mossbauer obs. 0—79207
FePt, coercive force rel. to ordering 0—47942
Fe₃Pt alloy, ordered, martensitic transform, electron microscope obs. 0—65493
Ni-Pt-P alloys, amorphous, X-ray interference function, elec. resistivity, thermoelec. power 0—53781
Pd-Pt:Cr alloy, mag. susceptibility and solute resistivity 0—40729
Pd-Pt system, isoelectronic, mag. susceptibility 0—79130
Pt-3°Co, hyperfine fields, low temp. 0—76052
Pt-(1.3 wt.%)BA alloy, field-emission microscope obs. 0—47040
Pt-Ba alloy, struct. of Pt-Ba comp. 0—50544
Pt-Co, dilute alloy, specific heat, mag. field depend., 1.2-30 K 0—43909
Pt-Co, stress directed ordering 0—79131
Pt-Co dil. alloy, high field susceptibility 0—41018
Pt-Cu-Zn system, struct. 0—65273
Pt-Fe dil. alloys, magnetostriction and magnetiz. 0—72242
Pt-Ni alloy, ferromagnetic, resistance comp. and temp. depend., 1.4-4.2 K 0—44068
Pt-Ni dil. alloys, exchange-enhanced, sp. ht. and elec. resistivity 0—62213
Pt-Rh alloy, Co activity-comp. relationships 0—78682
Pt-Rh alloy, cottivity-comp. relationships 0—78682
Pt-Rh alloy, co activity-comp. relationships 0—78682
Pt-Rh alloy, co activity-comp. relationships 0—78682
Pt-Rh alloy, exchange-enhanced, sp. ht. and elec. resistivity 0—62213
Pt-Rh alloy, co activity-comp. relationships 0—78682
Pt-Rh alloy, co activity-comp relationships 0—78682
Pt-Rh alloy, exchange-enhanced poly platinum (IV) dihydrate, crystal structure, X-ray obs. 0—40095
Pt complex, dihidinely, i.r. spectra confirming trans structure 0—64447
Pt complex, ammonium tristonetasulphido) platinum (IV) dihydrate, crystal structure, X-ray obs. 0—40095
Pt complex, by the development of the platinum (IV) dihydrate, crystal structure, X-ray obs. 0—40095

0-67748
Pt complex, Pt(PF₃)₄, vibr. spectra 0-55309
Pt complexes, [Pt(L)(SCN)₂], L=ethylenediamine or C- or N-substituted ethylenediamine, electronic spectra 0-55317
Pt dialkyl cpds., i.r. spectra rel. to spectra of chemisorbed hydrocarbons 0-77834
Pt(CN)₄²⁻ in aqueous soln., mag. circular dichroism and u.v. spectral assignments 0-71358
PtF₆²⁻, electronic absorption spectra 0-46508

assignments 0—71358

Pt(II) square-planar tetraamine complexes, polarized u.v. reflection spectra and electronic struct. 0—70944

Pt139kRh/Pt, thermocouple, revised reference tables 0—63487

Pt199kRh/Pt thermocouple, revised reference tables 0—63487

PtSn intermetallic compound, de Haas-van Alphen effect determ. of Fermi surface 0—44024

Pt₅TeAs, deformed c.p. struct. with constitutional vacancies 0—75135

Pleochroism alkali halide: Pb2+, Ag-, mag. circular dichroism curve, resolution 0-48009

alkali halide d¹0s² complexes, mag. circular dichroism spectra 0-69080 benzopurpurine suspensions, optical dispersion of elec. dichroism 0-74811

charge transfer bands, study using magnetic circular dichroism 0-55271 circular dichroism, measuring instrument 0-58214 circular dichroism and rotary power of crystals, dispersion theory circular di 0-41118

copolymers rubbery, dichroism 0–59367 Cotton-Mouton dichroism, use in crystal spectroscopy 0–56518

Pleochroism continued

crystals, magnetic circular dichroism 0-76019

crystals, magnetic circular dichroism 0-76019
trans-cyclo-octene, circular dichroism 0-58213
trans-cyclo-octene, circular dichroism 0-58214
dichroism, circular, chemical applications 0-65986
dichroism, circular, instrum. for vacuum u.v. meas. 0-76021
dichroism, circular, instrum. for vacuum u.v. meas. 0-76021
dichroism, circular, circular, cleterm. of organic cyds. 0-49116
ferrimagnetic, RbNiF₃, Cotton-Mouton effect, birefringence, dichroism
0-44775
flow dichroism for light flow viewellingting and control of the control of

flow dichroism for liq. flow visualization 0-71278

ions, ground state, ns² configuration, magnetic circular and linear dichroism 0-56519 linear dichroism meas. using electro-optic device in spectropolarimeter 0-49154

ilinear dichrosim meas. in vacuum u.v., apparatus 0-76020 magnesium phthalocyanine neg. ions. mag. circular dichroism spectra 0-71023

magnetic circular dichroism, meas. by modified spectropolarimeter 0.38550

0 38550
magnetic circular dichroism curve, resolution 0-48009
photodichroism, nonlinearity of reversible orientation 0-60335
polymers, idealized helical, circular dichroism associated with vibrational transitions 0-74424
polypeptides, amorphous, one state solns., circular dichroism 0-71052
polypeptides, exciton states and hypochromism 0-74431
polystyrene, amorphous, molecular orientation study by i.r dichroism 0-47022

0-47022 or polytrifluorochloroethylene film, extruded, dichroism and struct. anisotropy 0-50371 rubbery copolymers, dichroism and birefringence 0-41122 ruby, magneto circular dichroism of octahedral Cr III 0-72312 uranyl compounds, cubic cryst., circular dichroism 0-44772 uranyl propionates, single cryst. at room temp. and liq. N₁ temp. 0-72430 AlLaO₂:Pr³+, mag. circular dichroism study of ³H₄→³P₀ transition 0-72311 CaWO₄:Nd³+, mag. circular dichroism study of ⁴I₀/₂→²P₁/₂ transition 0-72311

0-72311 CaWO₄:Nd³⁺, Na⁺, Cotton-Mouton Dichroism and perpendicular g factors 0-69081 Eu³⁺ in vitreous matrix, local symmetry and mag. circular dichroism 0 44773

0.44773 [IFBr₆²⁻, magnetic circular dichroism, in host crystals at room and liq. He temps. 0–74276 [KF, mag. circular dichroism of F band and F-centre spin polarization quenching 0–76027 [KI, circular dichroism in Urbach region 0–44774 [RbNiF] Ferrimagnet, cotton Mouton effect, birefringence, dichroism 0–44775 [IFBRIGHT of the control of the con

V₂O₃ suspensions, optical dispersion of elec. dichroism 0–74811 YFe garnet: Si, optical dichroism and photo-induced uniaxial mag. anisotropy 0–44598

Plexiglas see Plastics

Plutonium atom, K-shell binding energies, energies of $K\alpha_1$, $K\alpha_2$, $K\beta_1$ and $K\beta_3$ X-rays 0-49787 reactor fuel, nondestructive assay by γ -ray meas, using on-line computer

reactor fuel, nondestructive assay by p-ray meas, using on-the computer control 0-55203 specific heat meas., from 13° to 300°K, method description 0-68614 sphere, water reflected, critical mass, obs. 0-49725 Pu-polystyrene cube systems, n surface multiplication expt. and theoretical cales. 0-49731 239,240 pu and 238 Pu deposition from 1958 to 1969 in Tokyo and Japan Sea 0 -59593

0 59593 α-Pu, self-irrad, length change 0–58827 ²⁴⁰Pu, beryllia moderated system, resonance capture at 300°K and 1500°K 0–42778 ²⁴⁰Pu, graphite-moderated system, resonance capture, at 300°K and 1500°K 0–46150 ²⁴⁰Pu, in PuC particles in graphite matrix, resonance capture at 300°K and 1500°K 0–46151 ²⁴⁰Pu, hypothesis in graphite matrix, resonance capture at 300°K and 1500°K 0–46151

²⁴⁴Pu abundance in the early solar system 0-45329

Plutonium compounds

carbides, vap. pres. meas. 0-74855 Pu-(1 wt.%) Ga δ-stabilised alloy, heat content and capacity, 0-685 °C65550 0-65550

°C65550 0–65550 Pu-Ga solid soln., δ -phase, cryst. parameter rel. to Ga conc. 0–65274 Pu-Ti alloys, Pu β phase stabilization 0–68568 (Pu-U)O₂, mixed fuel in contact with sodium, microprobe exam. 0–59516 Pu₂AlGa₃ and related cpds., cryst. struct. 0–78495 PuC particles in graphite matrix, rel. to resonance capture at 300°K and 1500°K 0–46151 PuC₁₇₇ Pu₂C₃, cryst. struct. and magnetic ordering, neutron diffr. 0–47201

PuCl₃, thin films, absorption spectrum, new assignments 0-76110 PuFe₂, magnetically induced elec. field gradients and hyperfine fields

PuC1,3, thin limis, assorption spectrum, new assignments 0—4801

PuFe3, magnetically induced elec. field gradients and hyperfine fields

0—44801

PuFe4, Mossbauer 57Fe spectra, at 4K, 77K and room temp. 0—48040

PuFeAl and related cpds., cryst. struct. 0—78495

PuO2-UO2, polyerystalline, elastic and anelastic response 0—58859

PuO1,718, cryst. struct. X-ray and neutron diffr. obs. 0—78496

PuO1,718, cryst. struct. X-ray and neutron diffr. obs. 0—78496

PuO2, hot-pressing 0—58946

PuRhGa and related cpds., cryst. struct. 0—78495

238PuO3, self-irrad, activation energy of first stage annealing 0—71742

238PuO3, self-irrad, activation energy of first stage annealing 0—71742

238PuO2, plasma-formed microspheres, thermal expansion 0—68620

puO2.0, irradiated, metallic inclusions formed at high burnups, electron microprobe analysis 0—71885

(U-Pu)O2, mixed, high temp. creep 0—58900

(U-Pu)O2 fuel pellets, eval. for use in encapsulated fuel pin irrad. tests 0—58061

(U-Pu)O2 fuel pellets, fabrication and characterization 0—56037

0-58061 (U-Pu)O, fuel pellets, fabrication and characterization 0-56037 (U-Pu)O, mixed fuel fabrication for FFTF 0-58962 (U-Pu)O, mixed fuels, creep 0-55988 (U-Pu)O, mixed fuels, plastic yielding and fracture 0-5892 (U, Pu)₃O₈, lattice parameters rel. to Pu content 0-58762

Plutonium compounds continued

 $(U,Pu)O_2$, fission products emission during irrad, to high burn-up 0-46306

(U,Pu)O₂ solid solns., thermal cond., Pu content effect 0-59116

UO₂-PuO₂-Pu₂O₃ system, phase diagram 0-62147 (U_{0.8}-Pu_{0.15})C_{1-x}N_x, elastic consts. 0-71666 (U_{0.75}-Pu_{0.25})C₂ mixed fuel processing using 9-variable fractional factorial expt. 0-58969

Zr-Pu dil. alloys, resistance minima and 5f levels obs. 0-75571

Pockels effect see Electro-optical effects Point defects see Crystal imperfections
Point groups see Crystal structure, atomic Poiseuille flow see Flow; Hydrodynamics Poisson ratio see Elastic constants

Polar cap absorption see Electromagnetic wave propagation/ionosphere

Polar cap flow see Airglow

Polarimeters

double scattering apparatus, for obs. in scattering chamber 0-77191 ellipsometer meas. analysis, FORTRAN program 0-45831 gamma-ray, use of single planar Ge(Li detectors 0-73688 linear dichroism meas. using electro-optic device in spectropolarimeter

0-49154

microscope polarizing with crossed polarizers, diffraction images of general periodic rectangular wave 0-57620 using photoelectric effect 0-49115 photographic for solar eclipse emission lines linear polarization meas. 0-69492

proton double scattering with Si detector as analyzer 0-60698

three-channel, for atmospheric meas. 0–59588 twinned cryst. behaviour as light analyzer 0–63686 X-ray, asymmetric Bragg cosmic polarimeter 0–48619 X-ray astronomy, use of highly reflecting crystals 0–45328

Polarized light

see also Polarimeters Double refraction; Optical rotation; Photoelasticity; 0 - 52164

atmosphere, reflected and transmitted radiation polarization, calc. 0-59587

0-59587
atomic collisions and line radiation 0-55227
atomic ions free, with h.f.s. oriented in He buffer gas, orientation by absorption of circularly polarized light 0-49771
beam, narrow, depolarisation of back-scattered radiation 0-73306
Brewster angle, pseudo-rel. to optical constants 0-62593
carbon black suspensions, HAF, depolarization of scatt. light 0-50275
characteristics of radiation passed through scattering layer 0-60367
circular, of thermal radiation in mag. field 0-76924
cubic crystal, duplex modulation, single sideband modulation and light freq.
change 0-44768
depolarization, "segmetrical" in turbulent atmosphere 0-38549

depolarization, 'geometrical', in turbulent atmosphere 0–38549 diffraction efficiency of gratings in photographic layers 0–42367 ellipsometer, calibration of analyser and polarizer, modified method

ellipsometric meas, minimization of errors 0-44767 ellipsometric optical surface anisotropy, azimuthal misalignment error, analysis 0-69075

analysis 0–69075
ellipsometric technique for substrate optical consts. meas. 0–71462
ellipsometry, measurement of circular dichroism 0–62612
ellipsometry, transients intensity meas. applic. 0–63685
ellipsometry meas. of film thickness, polarizer ellipticity effects 0–55709
ellipsometry of rough surface, optical consts. meas. 0–65979
ellipsometry of thin films on fused quartz 0–74891
elliptical emission, determ. of optical constants 0–76003

elliptical emission, determ, of optical constants 0—76003 elliptical vibr. defining parameters determ, method 0—38552 Faraday rotation angle meas. 0—41124 ferroelectric, polarization in absorpt. bands of defective cryst. 0—66062 film on Cu electrode, electropolishing, ellipsometry 0—65058 in filters, optical resolution study 0—59365 flow dichroism for liq. flow visualization 0—71278 glass, frosted, polishing of rear surface, effect on polarization of radiation 0—62609

o-0203 glass, optical, scattering, Krishnan effect 0-56492 holography, high-quality 0-52340 i.r., Ge prism as converter from linear to circular polarization 0-48008 i.r., Ge prism as converter from linear to circular polarization 0–48008 i.r., Ge prism as converter from linear to circular polarization 0–48008 i.r., Ge prism as converter from linear to circular polarization 0–60432 incandescent bodies in magnetic field, magnetoemission 0–48014 interference coatings, reduction of polarization effects 0–38567 isolator, depolarization effects of magneto-optically active specimen on decoupling magnitude 0–45833 laser beam interference experiment for student laboratory 0–67139 laser radiation reflected by water 0–49087 laser triangular ring with discharge tube, Brewster-angle windows, polarization props, investigation 0–63599 linear, rotation meas, using wavelength-independent modulator 0–63704 linearly, propagation in variable-length one-dimensional cavity 0–69769 luminescence polarization meas, using analogue cets. 0–63687 mica polarizing prism, design 0–60391 molecular nonlinear spectroscopy 0–55270 p-nitroaniline cryst., ir. absorpt., band assignments 0–48084 particulate systems, optically active, differential scatter of left and right circularly polarized light 0–55635 photon beam, polarized, obtained from diamond crystal subject to electron beam 0–45875 phthalimide solns, induced radiation polarization 0–43463

phthalimide solns., induced radiation polarization 0–43463 planetary atmosphere, scattered radiation 0–76633 from planets, meas. using high resolution Fourier spectroscopic method 0–51752

Pockels effect in light commutator with finite apertures, analysis 0-59371 polarimeter for accurate meas. of rotation of plane of polarization, i.r. 0-63688

0–63688 polarization discrimination for underwater targets, contrast improvement, particle size effects, comment 0–66240 polarization plane, angle of rotation meas, in semiconductors 0–78984 polarizer's absolute alignment determination, reply to comments 0–63690 pressure-induced depolarization of Rayleight scatt, from gas 0–71262 prism polarizer's absolute alignment determination, comments 0–63689 pseudo-Brewster angle technique for determ, optical constants of semiconductors, a suitable reflectometer 0–56483 pyrene, cryst., polarized absorpt, spectra 0–76119

Polarized light continued

Raman depolarization meas, of liquids in capillary cells, divergence errors cales, 0-50224

reflection, total, of beam, perpendicular shift in incident plane 0–49107 resonance fluorescence, theory of frequency and polarization modulation 0 - 68018

ring laser with circularly anisotropic resonator, polarization of radiation 0-42264

0-42264 Rochelle salt, polarization in absorpt. bands of defective cryst. 0-66062 rotation angle over wide range and accuracy, method of recording 0-57592

rotation angle over wide range and accuracy, method of recording 0-57592
sample depolarization ratio meas. by Raman spectrometry 0-54938 scattering, by polydisperse systems of irregular particles 0-53377 scattering by semielliptic groove in ground plane, planewave, low-frequency limit 0-42374
skylight, spectral distribution using automatic photometer 0-79540 from solar corona during the November 12, 1966 eclipse 0-41864 from solar disk, broad-band measurements, interpretation 0-79740 southern OB-star polarization, galactic diagram 0-56963 stars, early type, upper limit to Chandrasekar polarization 0-59706 from stars, red variables of high luminosity, polarimetric obs. 0-69396 Stokes parameters, definition in terms of e.m. theory 0-60366 transfer of partially polarized light in Rayleigh-scattering atmosphere with true absorption 0-69972 triglycine sulphate, polarization in absorpt. bands of defective cryst. 0-60602
in turbid media, degree of polarization, relationship with incidence flux, depth 0-59544 twinned cryst. behaviour as light analyzer 0-63686 two-photon absorption of tumbling molecules, polarization depend. 0-55267
p-rays from nuclear reactions, circular polarization 0-70560

0-55267
p-rays from nuclear reactions, circular polarization 0-70560
Ag, adsorbed gases, optical props., ellipsometry 0-39967
Ag, adsorbed gases, optical props., ellipsometry 0-39966
Al, optical consts., rel. to oxidation, ellipsometric obs. 0-47994
Al, optical consts., rel. to oxidation, ellipsometric obs. 0-47994
CsBr(1), two-photon spectroscopy 0-79300
GaSb band parameters determ. using Hall effect and rotary polarization of i.r. radiation 0-59216
Hin 2s, 2p states, calc. of optical polarizability 0-43021
HIO₃ SHG coeff. d₁₂₃ and nonlinear optical polarizability of I-O bond 0-44769

He, ion impact excited, polarization of light of de-excitation 0–77720 Hg vapour fluorescing in oscillating magnetic field, frequency and polarization modulation 0–68020

tion modulation 0–68020
InSb-NiSb polarizing props. 0–69074
LilO₃. SHG coeffs. d₃₁₁ and d₃₃₃, nonlinear optical polarizability of I-O bond 0–44769
(NH₄), C₃O₄.H₃O, optical rectification 0–51268
NA₅NSA₅.9H₂O, dispersion of rot. of plane of light polarization 0–56496
NA₅NSA₅.9H₂O, dispersion of rot of plane of light polarization 0–56496
Na₅NSA₅.9H₂O, dispersion of rot. of plane of light polarization 0–56496
Na₅NSA₅.9H₂O, dispersion of rot. of plane of light polarization 0–56496
Na₅NSA₅.9H₂O, dispersion of rot. of plane of light polarization 0–56496
Na₅NSA₅.9H₂O, dispersion of rot. of plane of light polarization 0–56496
Na₅NSA₅.9H₂O, dispersion of rot. of plane of light polarization 0–56496
Na₅NSA₅.9H₂O, dispersion of rot. of plane of light polarization 0–56496
Na₅NSA₅.9H₂O, dispersion of rot. of plane of light polarization 0–56496
Na₅NSA₅.9H₂O, dispersion of rot. of plane of light polarization 0–56496
Na₅NSA₅.9H₂O, dispersion of rot. of plane of light polarization 0–56496
Na₅NSA₅.9H₂O, dispersion of rot. of plane of light polarization 0–56496
Na₅NSA₅.9H₂O, dispersion of rot. of plane of light polarization 0–56496
Na₅NSA₅.9H₂O, dispersion of rot. of plane of light polarization 0–56496
Na₅NSA₅.9H₂O, dispersion of rot. of plane of light polarization 0–56496
Na₅NSA₅NH₂O, dispersion of rot. of plane of light polarization 0–56496
Na₅NSA₅NH₂O, dispersion of rot. of plane of light polarization 0–56496
Na₅NSA₅NH₂O, dispersion of rot. of plane of light polarization 0–56496
Na₅NSA₅NH₂O, dispersion of rot. of plane of light polarization 0–56496
Na₅NSA₅NH₂O, dispersion of rot. of plane of light polarization 0–56496
Na₅NSA₅NH₂O, dispersion of rot. of plane of light polarization 0–56496
Na₅NSA₅NH₂O, dispersion of rot. of plane of light polarization 0–56496
Na₅NSA₅NH₂O, dispersion of rot. of plane of light polarization 0–56496
Na₅NSA₅NH₂O, dispersion of rot. of light polari

Polarography see Chemical analysis/electrochemical

Polarons see Crystal electron states/polarons Polishing see Surface structure

Polonium

No entries

Polonium compounds

No entries

Polyelectrolytes see Electrochemistry; Polymers; Solutions Polymerization

cationic, vinyl ethers and cyclic acetals, electronic structures of active centre models 0-70960 cooperative interaction of growing chains and macromol. matrices 0-72337

Cooperative interaction of growing chains and macroniol. matrices 0–72537 cross linkage problem, dilute cross-linked systems 0–48195 cyclic dimerization 0–54185 dye solns., dimerization on cooling 0–53070 photopolymerisation, initiation obs. 0–72555 polyimide solutions, cyclization from 2,4-diaminoisopropylbenzene and pyromellitic dianhydride 0–41429 polymer, cross linkage problem, dense cross linked system, method of second quantization 0–48196 polymer, cross linkage problem, method of second quantization 0–48194 polyoxymethylene crysts. grown within irrad. trioxane crysts. 0–78352 polyvinyl alcohol, aqueous soln., effect of degree of polymerization on critical shear rate 0–53292 polyvinylchloride, with dialkylphthalates, vitreous or viscoelastic system effect on u.s. velocity 0–40542 polyvinyldinenfluoride, rel. to structure 0–71439 products from electrical discharge through toluene and ethylbenzene 0–46525 water, possible existence of strong OHO bonds 0–50199

water, possible existence of strong OHO bonds 0-50199

Polymers

see also Plastics alkane-imide extruded wire insulation 0-58551 allyl, interrelation between current, breakdown voltage and hardness 0-68914

0-68914
amine-cured epoxy relation between network structure and dynamic mechanical properties 0-55945
amorphous, h.p. effects, densification 0-55685
amorphous, stress/birefringence curves and stress-optical coeffs. 0-71655
amorphous, thermal conductivity changes on change from vitreous to high-elastic state 0-68664
amorphous, visco-elastic behaviour, effect of vibrations 0-40243
amorphous linear, subjected to orientational stretching, reticulate struct. parameters determ. 0-39912
anthracene-polyvinyltoluene system, fluoresc., anthracene copolymerization effects 0-72439
birefringence, dispersion, correlation with transmittance spectra 0-65989

birefringence, dispersion, correlation with transmittance spectra 0-65989 bisphenol A polycarbonate solns., temp. coeff. of intrinsic viscosity 0-39754

branched, normal modes of ring and star shaped mols. 0–64566 breakdown strength, effect of aperiodic and vibratory impulses 0–75786

Polymers continued

butadiene-styrene copolymer filled with carbon-black thermal expansion, free volume and molecular mobility 0-65555

butyl acrylate-acrylic acid copolymer, effect of microstructure on tensile behaviour 0-71714

carbopol, dilute aqueous solns., wall shear stress meas., in laminar flow 0-43407

0—43407
cellodextrins interpretation of diffraction patterns 0—65306
cellulose, in Kraft paper form, exp. study of electrical properties 0—68886
cellulose, crystallimity, linear relation to dielectric constant 0—40115
cellulose acetate phthalate, surface props. 0—74430
cellulose from cell wall of Velonia ventricosa, and i.r. spectra 0—79325
celluloses, wide line p.m.r. line widths, second moments and spin-spin, spin-lattice relaxation 0—69199
chain, intramolecular energy, excluded volume effect 0—74426
chain, relaxation and dynamics of three-dimens, cubic and tetrahedral lattice models 0—50656
chain entanglement in linear polymers, molecular approach 0—64568
chain folding aspects of structure 0—65307
chain length and helical conformation, effect on optical properties 0—74424
chain molecule dynamics, stochastic model 0—67828

0—14424 chain molecule dynamics, stochastic model 0—67828 chain type molecules with random force constant defects, distrib. of eigenvalues and eigenvectors 0—77976 chains in dilute soln., transport processes, hydrodynamic interaction 0—58460

0—38460 charged spheres, secondary electroviscous effect, including theoretical values of Huggins coeff. 0—71318 chemical structure, rel. to engineering applications 0—66162 coatings, diffusion of water, prod. of internal stress, means of meas. coeff. 0—50676

0–50676
cold drawing in cryst. 0–40452
cold-drawn, retraction and annealing behaviour 0–56035
comonomer and stereosequence distributions in high polymers 0–78353
complex branched mols. and ring systems, normal modes 0–64567
conference, Kingston, Canada (1969) 0–71054
conjugated, electronic struct., e.p.r., semiconduction 0–75695
copolymer (dAT), helix-coli transition determ. by light scatt. 0–54180
copolymers rubbery, birefringence and dichroism 0–59367
copolymers with long side branches, X-ray and thermographic study
0–58548
creen modelling allowing for vibration and temp effects. 0–58904

creep modelling allowing for vibration and temp. effects 0-58904 cross linkage problem, dense cross linked system, method of second quantization 0-48196

cross linkage problem, dilute cross-linked systems 0–48195 cross linkage problem, method of second quantization 0–48194 cross-linkage, quadrupole lens system for electron beam curing apparatus 0–54843

0-54843
cross linked p.v.c. wire insulation systems 0-58553
crystal, simple chain refolding scheme for annealing behaviour 0-71739
crystalline, effect of flexibility of main chain on struct., X-ray and thermographic 0-58548
crystalline, melting, lattice theory 0-39870
crystalline, melting, lattice theory 0-39870
crystalline, structure 0-39913
crystals, single, grown in films 0-47133
deformation, exponential extension ratio 0-40245
deformation calorimeters 0-46615
density, processing conditions influence 0-74428
deoxyribonuclei acid, normal and tumour, i.r. at different relative humidities 0-48626
dielectric relaxation, non-symmetrical, study of empirical decay function

dielectric relaxation, non-symmetrical, study of empirical decay function 0-53926 diffusion of penetrant, time lag needed to reach steady state 0-40193

dilute solutions, mechanism for turbulent drag reduction 0-64844 dilute solutions, rheology and hydrodynamics for flow in annulus 0-46842

dilute solutions, turbulent flow in pipes, correlation of pressure drop data 0-71284 disclination loops 0-78544

discination loops 0–78544 disordered, equations for density of electronic states 0–71896 (dye-)polymer films, sample holder for polarized fluoresc. meas. 0–73360 dye-polymer complexes, exciton theory of electronic states 0–61187 dynamic elastic behaviour exam. 0–74427 dynamic alsatic behaviour exam. 0–74427 dynamic model for locally stiff ring and straight chain polymers 0–39468 elastic deformation peculiarities in viscous state 0–68392 elastic deformation peculiarities in viscous state 0–68392 elastic ity, stimulated-elasticity limit temp.-time relationship 0–50642 elastoriaties, stimulated-elasticity limit temp.-time relationship 0–50642 elastoplastic longit, wave propag. in long rod 0–40254 electrical conduction mechanism 0–79042 electrical conduction mechanism 0–79042 electroadhesive props. in elec. field 0–75815 enthalpy of mixing of soln., calc. from considerations of free volume 0–71315 enthalpy of diffusion of water, prod. of internal stress., means of epoxide coatings, diffusion of water, prod. of internal stress., means of

0–71315
epoxide coatings, diffusion of water, prod. of internal stress., means of meas. coeff. 0–50676
epoxide resin-stainless steel system, adhesion and internal stress 0–50677
epoxy, glass filled, relative modulus temp. depend. 0–40238
ethyl acrylate-acrylic acid copolymer, effect of microstructure on tensile behaviour 0–71714
ethylene, secondary dispersion due to motion of chain branches 0–47327
ethylene copolymers, n.m.r. study of structure 0–46621
ethylene copolymers and branched polyethylenes, melting behaviour 0–65000

0-5000 ethylene propylene terpolymer wire and cable insulation 0-58550 ethylene-methacrylic acid copolymer, and salts, dynamic and steady shear viscosities 0-58408 ethylene-methacrylic acid copolymers, relax, birefringence obs. 0-78613 ethylene-methacrylic acid copolymers, cryst. struct. rel. to composition 0-50343

ethylene vinyl acetate polymer, flow props, and softening pt. 0–62048 excluded volume effect on helix-to-coil transitions in n-stranded mols. 0–64564

excluded-volume problem, distribution function 0–64565
F-actin, semi-flexible polymer, Doppler broadening of scatt. light 0–71348
fabric, adhesion of Al film, vacuum evap., reflectivity 0–58594
fatigue crack propagation 0–62072
fibres, micropropagation 0–62072
fibres, micropropagation 4, scholaring 0–50000

fibres, microporous struct. obs. technique 0-50809

fibrillous structures in oriented crystalline polymers, cross-sectional dimensions 0-78355

fibrous, deformation behaviour modulus functions 0-40239

filament cooling and solidification, numerical calc. of temp. profiles and interface position 0-50311

filled, relative modulus temp. depend. 0-40238

filled materials, Poisson's ratio and shear dynamic Young's modulus study at sonic freqs. 0-50640

film, for semiconductor passivation 0-44272

film formation on electrodes in glow discharge 0-65091

films, for irradiation doses by fast neutrons and gamma radiation 0-51839

films, luminescence accompanied mechanical deformation and rupture 0-51379

films, luminescence accompanied mechanical deformation and rupture 0–51379 films, rel. to particle track detection 0–57856 films and fibres failure strength, mechanical testing instrument 0–47372 films having nonrandom orientation fluctuations, light scattering 0–79235 films structural changes corresponding to changes in their fluorescence spectra 0–48110 flow, in capillary rheometer reservoir, patterns, exp. study 0–68042 flow in capillary rheometer reservoir, patterns, exp. study 0–68042 flow birefringence of real polymer chains, theory 0–78278 fluoropolymers, surface tension, London dispersion term 0–50211 foils, charge storage investigations 0–65835 folded chain lamelae in selenium spherulitic crystallization 0–50413 foiled-chain crystals, with irregular fold surfaces, stability, statistical-mechanical study 0–71437 formation on Pt group contacts in organic vapour environment, effect of surface preparation methods obs. 0–56694 fracture, nucleation and propagation, dislocation mechanisms 0–40362 free vibrating reed for obs. of internal friction and Young's modulus down to 4°K 0–78607 fusion of crystalline polymers, intramolec. contrib, to entropy 0–43514 glassy, mech. characts., reson. method at audio freqs. 0–40211 glassy, mech characts., reson. method at audio freqs. 0–40211 glassy, transition between liquid or rubbery state to glassy state 0–65019 Gruneisen parameter calculation from thermal conductivity meas. under pressure 0–75415 guanine:cytosine helices, interbase vibr. coupling 0–39472 heat resistance, with temp, and stress 0–65543 helical, polariton modes 0–44008 hexafluoropropylene and vinylidene fluoride copolymers, dielec. relaxation 0–67830 high, thermal diffusivity, use of hyperbolic heat equation in data analysis 0–66943

high, thermal diffusivity, use of hyperbolic heat equation in data analysis

Homopolymers and copolymers with alkyl side chains, glass transition temperatures 0-65021

temperatures 0-65021 hydrocarbon polymers, thermoluminescent props. 0-48115 i.r. emission spectra 0-71053 inorganic, viscoelasticity 0-40249 insulating, charge transport carrier mobility 0-47822 insulating materials, elec. cond. 0-65769 internal stress relax. elastomer introd. effect 0-40276 intrinsic viscosity, extension of theory to short chains 0-61506 intrinsic viscosity, extension of theory to short chains 0-61507 introductory book for 6th formers 0-46618 ion clustering, theoretical approach 0-49948 ion track form. mechanism 0-78803 ionenes, aliphatic, glass transition temps. 0-78347 irradiation, use in nuclear engineering 0-49945 KTFR (Photoresist) film, electron beam exposure characteristics obs. 0-57490 Langevin theory of polymer dynamics in dilute solutions 0-53322

0–57490
Langevin theory of polymer dynamics in dilute solutions 0–53322
layer, bidimensional, thermodynamic props. 0–61619
light scatt. from deformed regions round voids and inclusions in amorphous polymers 0–41094
light scattering by anisotropic shells 0–76120
linear, amorphous, molecular approach to chain entanglement 0–64568
long chain effect of small quantities on point of maximum density of H₂O
0–68083

0–68083

low temp, lit. survey 0–39914

luminescence, quenching by oxygen 0–51355

macromolecules in solutions, mobility and conformal transformation, study by polarized luminesc. 0–67830

mechanical properties, following deformation between 130 and 150°C 0–62046

0-62046
mechanical properties at large strains 0-71654
melts, comparison of methods of making normal stress meas. 0-58411
melts, flow in circular tube 0-68048
melts, shear-dependent relax. spectrum, conversion from steady-flow viscosities 0-68053
melts in tube flow, temperature profile 0-68047
methacrylate plastics, sound vel. 0-73305
methacrylic acid-2-methyl-5-vinylpyridine copolymers, aqueous solutions, flow birefringence and viscosity at different ionic strength and pH
0-71354

0–71354
methyl methacrylate-methacrylic acid copolymers, n.m.r. triad assignments 0–43201
methyl polymethacrylate, u.s. absorption between 1.6-100 MHz, temp. variation 0–58487
modulus and damping rel. to structures 0–55929
molecular complex detection from mass spectra of neg. ions 0–61189
molecular reorientation and deform, optical meas. on deform, band 0–41110

molecular reorientation and deform, refractive indices calc. 0–41109 molecular weight averages and distributions, glass transition temperature range from 100° to -73° 0–55385

molecular weight distribution effect on shear dependence of viscosity 0 58466

0 58466 molecular weights, abnormal, from light scattering experiments 0-53348 mucopolysaccharides, heparin, chondroitins, structure and composition from p.m.r. 0-77978 Mylar, corona charged, thermal currents 0-47823 n.m.r., relaxation times 0-48171 n.m.r., spectrum, paramagnetic center effects 0-49946 n.m.r. studies of mol. motion, review 0-64569

Polymers continued

natorsol, dilute aqueous solns, wall shear stress meas, in laminar flow 0-43407

non-oriented, temperature-time dependence of strength under cyclic loading 0-47386

ing 0-47386
nuclear charged particle track detectors, latent track formation 0-46072
nucleate pool boiling, heat transfer 0-61600
nylon 6-10, anhydrous, stress ageing 0-78628
olefin type, applic, to dosimetry of ionizing radiations, patent 0-55090
optical props., scalar spectral characteristics 0-44858
orientation distribution function, analysis 0-78354
rel, to oxyluminescence meas. 0-76143
PVC thermoelecter term, depend, surface charge formation and deca

PVC thermoelectret, temp. depend., surface charge formation and decay characts. 0-44379 characts. 0-44-379
p.m.r. signal narrowing by magic angle rotation in solid 0-69811
paracrystalline struct. on electron-irrad. induced lattice distortion

paracrystalline struct. 0-78527

pertin, effect of X-rays, e.s.r. study 0–67836
penton, struct, and physicomech. props. 0–39917
peptides, H-bonded, energy parameters 0–64574
permethylcyclopolysilanes anion-radicals, electron delocalization 0–74408

0-1440o perspex, glassy, fracture props., effect of pre-orientation 0-71729 perspex, heat treated, β^+ lifetime rel. to density, cryst. struct., obs. perspex, h 0-40700

phase holograms in thick photopolymer films 0-69961 photocurrent detection 0-65853

photocurrent detection 0-65853
photoelastic props. of amorphous polymers 0-71655
photopolymer recording of holograms 0-60273
photopolymer recording of holograms 0-60273
photopolymerisation, in condensed phase 0-72554
pipe flow of dilute solution; turbulent ultimate asymptote and mean flow structure 0-71281
plastic, wear resistance, surface deformation, abrasion, composition effects, friction, strength, ductility 0-40425
plastic based, manufacture method, bioengineering applic. 0-71438
plastic deform. in nonuniform omnicitrectional compression 0-40287
Plexiglas column, curved, transverse vibrs. under periodic axial loading 0-38343
poly(2,3,4-chlorostyrene), dielec. loss, 0.1-20 kHz, 4-300°K 0-40830
poly(3,4-chlorostyrene), dielec. loss, 0.1-20 kHz, 4-300°K 0-40830
poly(ethylene terephthalate) fibres, chain folding characterization 0-78351
poly(ethylene terephthalate) films, oriented, lamellar domains size

poly(ethylene terephthalate) films, oriented, lamellar domains size 0-78376

poly(vinyl amine), n.m.r. studies of tacticity 0-67838 poly (α-methylstyrene), n.m.r. spectra rel. to methly resonances and tacticity 0-39839

poly (terlicent) says (poly benzyl-L-glutomate in dioxan, aggregation due to applied electric field,

poly benzyl-L-glutomate in dioxan, aggregation due to applied electric field, rates of deaggregation 0–64942 poly (trans-1, 4-butadiene) crysts., chain folding, obs. 0–39915 poly-L-alanine, rhythmic crystn. of spherulites 0–68254 poly-L-proline, epitaxial growth on quartz single crystal surfaces, characterization 0–50482 poly-N-vinylcarbazole, dye sensitized, fluoresc. quenching and charge transfer 0–72442 poly-y-benzyl-L-glutamate, concentrated solutions, light scattering, application of correlation function methods 0–71353 poly-n-vinyl carbazole, steady state and transient photoemission, energy levels, transport props. 0–47897 polyacrylamide, N,N-disubstituted, i.r. spectra, basicity, amide repeat unit 0–74429 polyacrylamide solns., dil., flow stabilization and destabilization 0–74708

polyacrylamide solns., dil., flow stabilization and destabilization 0-74708 polyacrylonitrile, pyrolyzed and irrad., e.s.r. 0-72501 polyacrylonitrile fibres, stretch during wet-spinning effect on mech. props. of C fibres 0-40231

polyacrylonitrile films, structure and orientation degree measurements, i.r. spectroscopic method 0-53413 polyalanine, planar zig and chlical chains vibr. spectra calc. 0-39470

polyamines, transition and relaxation phenomena, i.r. spectroscopic studies 0–67835 polyamino acids, n.m.r., mol. motions 0–72515 polyarylenes-cyanoethenylenes mol. strict. rel. to optical props. and photocond. 0–49949

polyazophenylenes, semicond., cond. 0–75696 poly-y-benzyl-L-glutamate, helix-coil transition press. depend., model 0–39473

poly-3,3-bis(chloromethyl)oxetane, e.s.r. spectra, radical formation, electron beam and u.v. light irradation 0-54163 polybisphenol-A-carbonate, toughness rel. to molecular movements 0-5599

0-55999
polybutadiene, branched, melt viscosity, effect of dilution 0-58467
1,4-polybutadienes, elastic props. as functions of microtacticity and molecular weight 0-58846
cis-polybutadienes, polydisperse, rheological behaviour 0-47367
polybutadienes, temperature dependence of viscosity, density and rubbery deformation, microstructure 0-55386
polybutadienes, trans- and cis-glass transition and melt temp., by various methods 0-47023
polybutene-1, solidification, interface morphology 0-46988
polybutene-1, crysts., glass transition in surface layers 0-53415
poly(t-butylethylene oxide-2-D), n.m.r. study of struct. 0-51413
polycaproamide, crack formation, submicroscopic, under cyclic loads 0-56015
polycaproamide, crack nucleation fibrillar struct. X-ray scatt. 0-43793

polycaproamide, crack nucleation, fibrillar struct., X-ray scatt. 0—43793 polycaproamide, radiation creep and electocond. 0—50706 poly-e-carbobenzoxy-L-lysine, helix-coil transition press. depend., model 0—39473

polycarbonate, amorphous, supermolecular structure obs. 0–50336 polycarbonate, deformation and fracture characteristics under high pressure 0–55991 polycarbonate, hydrostatic press. effects on elasticity, strength deform, and fracture 0-43716

polycarbonate, paramagnetic species produced by γ or u.v. irradiation investigated by e.s.r. 0-54164 polycarbonate, yield-stress in glass transition region, obs. 0-40317 polycarbonate films, effect of impregnants on dielectric loss 0-68899

polycarbonates, use in fission fragment track counting and meas. of reactor parameter δ²⁸ 0-39212

trans-polychloroprene, thermodynamic melting temperature 0-68179

trans-polychloroprene, thermodynamic melting temperature 0-68179 polydiallylphthalates, structure of monomeric unit 0-68202 poly(2,6-dimethylphenylene oxide), dielectric props. 0-79031 polyelectrolyte salts, mica and asbestos filled, relative modulus temp. depend. 0-40238 polyenes, linear, correlation effects on $\pi\pi^*$ transition energies 0-58260 polyenes, linear, correlation effects on $\pi\pi^*$ transition energies 0-46620 polyenes, single and double bonds 0-62253 polyestes, plasticizers, struct. and mol. weight determ. by n.m.r. study 0-59470

polyesterfilm treated paper, dielectric props. 0-56343 polyesterurethane block-polymers, thermal behaviour of phase state 0-68611

0–0011 polyethleneterephtalate, crystallization temp. region determ., temp. dependence of dielectric loss 0–59255 polyethyl acrylate, α -dielec. relax. behaviour, expt. compared with empirical curve 0–53926

curve 0-53926
polyethylene, CNDO/2 approximation, Hartree-Fock procedure formulation and application for electronic structure 0-64572
polyethylene, absorption, acoustic waves, ultrasonic, to above melting point, curve shape, model 0-40550
polyethylene, alpha mechanical losses, X-ray diffr., optical props.

0-4023 polyethylene, alpha relax. 0-78612 polyethylene, annealing under elevated pressure, extended chain crystals, structure analysis 0-47215 polyethylene, branched, radiothermoluminescence 0-41282

polyethylene, branched, radiothermoluminescence 0-41282 polyethylene, branched metals, viscoelastic properties 0-55580 polyethylene, breakdown strength, effect of aperiodic and vibratory impulses 0-75786 polyethylene, cable insulator, tensile strength improvement at increasing temps. by p-irradiation 0-43772 polyethylene, chain twisting from rate parameters for dielectric relaxation and thermal properties 0-61188 polyethylene, creep above room temp. 0-75268 polyethylene, creep modelling allowing for vibration and temp effects 0-5804

0-58904

polyethylene, crystal, mosaic-structure, lattice distortions and surface energy 0–65308 polyethylene, crystallization at elevated press. to extended-chain morphology 0–40013 polyethylene, crystallization from melt by jet stretching, spherulitization 0–71526

polyethylene, crystallization under orientation and pressure effects of capillary viscometer 0–78350

polyethylene, degree of crystallinity, atomic positions, particle size and lattice disorder 0–58545 polyethylene, deuterated target, preparation 0–57963 polyethylene, dielectric behaviour rel. to gamma and electron irrad. 0–40828

polyethylene, dielectric properties, ageing effects 0-68887 polyethylene, electron irrad. and partial discharges effect on struct. 0-78358

0—78338 polyethylene, epitaxial growth on graphite single crystal surfaces, characterization 0—50482 polyethylene, extended-chain crysts., melting, thermal anal. of multiple prepeaks and superheating 0—40015 polyethylene, extended-chain crysts., melting under equilib. conditions

polyethylene, extended-chain crysts., nucleation, growth conditions and press. crystn. 0-40012 polyethylene, flow instability, mol. depend. 0-53290 polyethylene, friction, He bombard. effect. 0-56020 polyethylene, heat treated, β^+ lifetime rel. to density, cryst. struct., obs. 0-407000-40031

0-40700
polyethylene, high density, cold-drawing 0-47453
polyethylene, high density, relationship between mechanical behaviour and mol. weight distrib. 0-65409
polyethylene, hydrostatic press. effects on elasticity, strength, deform. and fracture 0-43716
polyethylene, irradiated, tangential and normal stresses investigation 0-68464

0–68464
polyethylene, linear, drawing of single cryst, mats 0–39957
polyethylene, linear, precip. by soln. stirring, melting behaviour 0–58525
polyethylene, low-density, annealing effects on struct., rel. to tensile stress
and hydrostatic press. 0–58546
polyethylene, melt reloolgical props., low-shear behaviour, molecular structure dependence 0–46853
polyethylene, mixed crystal ir. study of chain segregation 0–58261
polyethylene, mixed crystal ir. study of chain segregation 0–40116
polyethylene, oxidation induction period meas. using differential thermometry 0–69212
polyethylene, phosphorylated, mechanical and thermal props. 0–55932
polyethylene, photoconductivity, investigation using monochromatic light
0–65843
polyethylene, photoelectric response as function of wavelength 0–68973

0–65843
polyethylene, photoelectric response as function of wavelength 0–68973
polyethylene, positron annihilation spectra rel. to energy transfer 0–40829
polyethylene, radiation creep and electrocond. 0–50706
polyethylene, size distrib. of extended-chain crysts. 0–40014
polyethylene, solidification, interface morphology 0–46988
polyethylene, spherulitic, deform. obs. 0–75260
polyethylene, static electrification, decay by cond. processes 0–72101
polyethylene, stretched, annealed, superstructures, small-angle X-ray scatt. 0–61932
polyethylene, temp-time dependence of strength, effect of additives 0–43760
polyethylene thermolyminese, dose kinetics. 0–69165

0-43760 polyethylene, thermoluminesc., dose kinetics $\,0-69165$ polyethylene, thermoluminesc. glow curves and electron traps $\,0-59442$ polyethylene, thermoluminesc. glow curves and molec. O_2 as electron traps $\,0-41283$ polyethylene, thin-layer, thermal conductivity and specific heat polyethylene, u.v. irrad., e.s.r. spectra, press. depend. $\,0-53095$ polyethylene, wollastonite filled, relative modulus temp. depend. $\,0-40238$ polyethylene and deuteroderivatives, vibr. spectra $\,0-39471$ polyethylene cable insulation, lapped, thermal resistivity $\,0-68665$

Polymers continued

polyethylene crystal, radiation damage in high voltage electron microscope 0-65317

polyethylene crystals, annealing under elevated press. 0-40016

polyethylene crystals, annealing under elevated press. 0–40016 polyethylene dendrites, nucleation from soln. 0–43592 polyethylene filute solutions, crystallization kinetics 0–68255 polyethylene fibre, acoustic vel. and absorpt. coeff., effect of mech. and thermal treatment, 93-363K 0–71839 polyethylene fibres, polarized Raman spectra assignment of bands to symmetry classes 0–46622 polyethylene filled comp., adhesion to steel 0–40477 polyethylene film, structure effect on tensile deform, and strength 0–50694

polyethylene film, surface elec. charges, decay process 0–68898 polyethylene films, crystallite shape effects on low-angle X-ray diffraction patterns 0–40056 polyethylene films drawn from mats of single crystals, structure and proper-

polyethylene glycol, molten, vibr. spectrum rel. to conformation, obs. 0–39469

polyethylene glycol aqueous soln., u.s. absorption 0–43443 polyethylene glycol aqueous solns., u.s. absorption 0–43442 polyethylene low-density, diffusion and permeability coefficients of CO₂, O₂, N₃ hexane and benzene 0–55928

polyethylene melt, under high pressure, capillary flow rel. to mol. struct. 0-53305polyethylene melt viscosity, effect of molecular structure variables 0-46854

polyethylene melts, filled, relaxation spectra 0-58424

polyethylene oxide, dilute soln, heat transfer in rough pipe flow 0–68093 polyethylene oxide, dilute soln, heat transfer in rough pipe flow 0–68093 polyethylene oxide, solidification interface morphology, interlamellar solidification and diffusion layer obs. 0–46988 polyethylene oxide chains, rotational state populations, for bonds, effect of "OH" end groups and temp. variations 0–55387 polyethylene sheets, effect of mech. twinning on tensile modulus 0–56641 relayethylene sizeds, effect of mech. twinning on tensile modulus 0–56641

polyethylene sheets, effect of mech. twinning on tensile modulus 0–50641 polyethylene single crystal, mosaic structure change during degradation by hot fumic nitric acid 0–61931 polyethylene single crystals, annealing 0–50760 polyethylene solutions, intrinsic viscosity, Huggins constant 0–68084 polyethylene solutions, intrinsic viscosity, Huggins constant 0–68084 polyethylene strips, effect of bending and stretching on adsorption of surface active substabces 0–65111 polyethylene structure, hydrostatic pressure effect 0–58549 polyethylene terephthalate, charge transport 0–68908 polyethylene terephthalate, glass point, effect of elec. field strength 0–74870

0-/4870 polyethylene terephthalate, molecular reorientation and deform, optical meas, on deform. band 0-41110 polyethylene terephthalate fibres, structural-morphological transitions during deformation 0-71692 polyethylene unit cell, thermal expansion lamella thickness effect 0-78785 polyethylene-perdeuteropolyethylene mixed crysts., chain folding, i.r. obs. 0-39916

0-39916
polyethyleneterephtalate, fibre crystallization and orientation, u.s. effects, density determ. 0-50345
polyfluoroethylene structure, hydrostatic pressure effect 0-58549
polyflormaldehyde, microhardness of filled and unfilled supermolecular structures 0-50748

structures 0–50748 polyglycine, Raman spectra and phonon dispersion 0–44871 polyglycine chain, vibrational props. 0–71051 polyglycolic acid, crystallization from melt, optical and morphological props. of different habits 0–74991 polyhexamethylene adipamide (66-nylon), crystallization from glycerol solutions 0–50451 poly(β-hydroxyethyl methacrylate), crosslinked solns. creep compliance in robbery zone, obs. 0–39706 P13N polyimide composites, C fibre-reinforced, fractography, scanning electron microscopy 0–68497 polyimide solutions, cyclization and inherent viscosities 0–41429 polyisobutene correlation between max. strength and anomalous viscosity 0–58458

polyisobutlene in viscous state, peculiarities of high elastic deformations 0--68392

0—68392
polyisobutylene, heat evolution at high rates of shear deform. 0—50667
polyisobutylene, in decahydronaphthalene soln., shear depend of intrinsic
viscosity and ion formation 0—58468
polyisobutylene, rheological characteristics determ. 0—46855
polyisobutylene in viscous state, peculiarities of high elastic deformations
0.68302

0 - 68392polyisobutylene solns in transformer oil, flow through short capillaries

0—50183
trans: 1,4-polyisoprene cryst. phases, melting, obs. 0—39871
polyisoprenes, deuterated, i.r. absorption spectra 0—77977
poly-L-lysine, helix-coil transition press. depend., model 0—39473
polymer film growth under electron bombardment 0—43557
polar polymers, analytical method for calc. of dielectric relaxation
0—59248

0–71317
polymethacrylic esthers, internal rotation of side chains discovered by method of dipole moments 0–58262
polymethine dyes, energy characts, of generation in longitudinal transverse variants of excitation 0–49061
polymethoxycoumarins, n.m.r. solvent shifts obs. 0–49941
poly(y-methyl L-glutamate), temperature variation of piezoelectric moduli 0–47856

polymethyl methacrylate, Kerr effect 0-66002 polymethyl methacrylates isotactic and syndiotactic, dielectric process of β relaxation 0-51108

polymethylene dye laser, mode locking by excitation from Ne laser 0-42283polymethylmethacrylate, craze growth, fracture mechanics approach 0-71728

polymethylmethacrylate, formation of micro shear bands 0-68452 polymethylmethacrylate, h.p. effects, densification 0-55885 polymethylmethacrylate, hydrostatic press. effects on elasticity, strength deform, and fracture 0-43716

polymethylmethacrylate, laser irrad., struct defects 0-78543

polymethylmethacrylate, photoinduced refr. index changes and applics.

polymethylmethacrylate, shock amplitude variation rel. to strain gradient $0\!-\!62023$

polymethylmethacrylate, shock wave propag. characts. 0-71672

polymethylmethacrylate, shock wave propag. characts. 0–71672 polymethylmethacrylate, steady shock wave propag., anal. based on viscoelastic theory 0–78614 polymethylmethacrylate, thermoelectric current generation model, radiation-induced trapped charge carriers 0–47865 polymethylmethacrylate, vitreous, relax. behaviour rel. to shear and compression strain states 0–50657 polymethylmethacrylate surface layers under friction, elastic deform. 0–40429

poly-4-methylpentene l crysts., plastic deform., obs. 0–40316
polymethylphenylsiloxamers, dilute solution parameters 0–64872
polymethylsobate, dielectric const. and loss tangent, relax, processes
0–53927

0-53927 poly-α-methylstyrene, dielectric behaviour rel. to gamma and electron irrad. 0-40828 poly-α-methylstyrene, normal stress effects in steady shear flow 0-64840 polyα methylstyrene solns., particle scatt. factor and segment-segment distance distrib. 0-71347 polynucleotides, crystal growth investigations 0-50430 polynucleotides, optical activity of $n-\pi^*$ transitions 0-74423 poly-α-olefins, optical activity and statistical zigzag model of struct. 0-58257

polyox, dilute aqueous solns, wall shear stress meas,, in laminar flow 0-43407

0-43401 Polyox WSR 301 drag reducing soln., shear thinnning treatment 0-50269 polyoxyethylene high-molecular, press fluctuations in boundary layers, exptl. investigation 0-61456

polyoxymethylene, epitaxial growth on graphite and quartz single crystal surfaces, characterization 0–50482 polyoxymethylene, needle-like, structure 0–78356 polyoxymethylene, solidificaton, interface morphology 0–46988

polyoxymethylene crystal, radiation damage in high voltage electron micro-

polyoxymethylene crysts, grown within irrad, trioxane crysts., morphology 0-78352 ogy 0-78352 polypeptide chains, vibrs. and conformations 0-39466

polypeptides, amorphous, one state solns, opt, props. 0–71052 polypeptides, exciton states and hypochromism 0–74431 polypeptides, exciton states and hypochromism 0–74431 polypeptides, molecular wavefunctions of monomeric amides study, to account for polarization and spectral splittings 0–64573 polypeptides, synthetic, crystal growth investigations 0–50430 polyphenylacetylenes, paramagnetic center effect on NMR spectrum 0–49946

polypropene-2-d₁, n.m.r. spectra 0-49950 polypropylene, chain length and helical conformation, effect on optical properties 0-74424

polypropylene, crack formation, submicroscopic, under cyclic loads 0–56015

polypropylene, crack nucleation, fibrillar struct., X-ray scatt. 0-43793 polypropylene, dielectric behaviour rel. to gamma and electron irrad. 0-40828

polypropylene, effects on dielectric loss of trichlorodiphenyl at elevated temp. 0-68134

polypropylene, isotactic, paracrystal-crystal transition 0–62142 polypropylene, isotactic, radiothermoluminescence 0–41282 polypropylene, o-positronium annihilation on nitric acid etching 0–75534 polypropylene fibre, acoustic vel. and absorpt. coeffs., relaxation processes, 93-433K 0–71851

polypropylene film, impregnated, dielectric behaviour at l.f. and m.f. rel. to capacitor applications 0-68968 polypropylene film, structure effect on tensile deform and strength 0-50694

0-3094
polypropylene films and fibres, deformation characterization 0-71686
polypropylene oxide, chain length and helical conformation, effect on opti
cal properties 0-74424
polypropylene oxide, multiple melting transitions 0-65006

polypropylene oxide, multiple melting transitions 0-65006 polypropylene oxide in methyl cyclohexane soln., max. dielec. loss freq. rel. to concentration 0-50252 polypropylene oxide solns, dielec. props. rel. to conc. 0-39829 polypyromellitimide films with metal and salt admixtures, electron phonon optimization 0-68756 polyquinone, chemical struct, dependence of electrical cond. 0-59254 polyropylene films, effect of impregnants on dielectric loss 0-68899 polysiloxanes, fractionated, electron microscope examination of morphology 0-50565 polystyrene, Kerr effect 0-66002 polystyrene, amorphous, molecular orientation study by hirefringence and

polystyrene, amorphous, molecular orientation study by birefringence and i.r. dichroism 0-47022

polystyrene, amorphous, supermolecular structure obs. 0-50336 polystyrene, amorphous, supermolecular structure obs. 0–50336 polystyrene, atactic, glass transition, o positronium decay obs. 0–78349 polystyrene, atactic linear, spin lattice relax, times in lab. frame and rotating frame 0–59472 polystyrene, charge transport 0–68908 polystyrene, concentrated solutions, normal and shear stress under steady and oscillatory shear flow 0–55572 polystyrene, crack propag., effect of crazes 0–47419 polystyrene, deuterated derivatives, 1r. spectra 0–64575 polystyrene, dielec. p. relax. 0–68900 polystyrene, dielec. p. relax. 0–68900 polystyrene, dielec. p. telax. 0–68900 polystyrene, dielec behaviour rel. to gamma and electron irrad. 0–40828 polystyrene, films fluorescence rel. to structural props. 0–48110

polystyrene, films fluorescence rel. to structural props. 0-48110 polystyrene, fluoresc., CCl₄ quencher effect, ethylbenzene comparison

polystyrene, formation of micro shear bands 0-68452 polystyrene, glass point, effect of elec, field strength 0-74870 polystyrene, glassy, fracture props., effect of pre-orientation 0-71729 polystyrene, light scattering measurements 0-64919 polystyrene, markings on fracture surface 0-65426 polystyrene, multiple melting 0-65007 polystyrene, rubber reinforced high impact, gel phase shear modulus, obs. 0-39855

polystyrene, sp. ht., cross-linking effect, 1.6-4K 0-62215 polystyrene, u.s. absorption between 1.6-100 MHz, temp. variation 0-58487

Polymers continued

polystyrene crystallite orientation distribution refinement procedure, X-ray diffraction 0-47170

polystyrene derivatives, glassy state, dielec. relax. 0-65775

polystyrene foam solar concentrator reflector substrate 0-69555

polystyrene latex, diffusion through millipore filters, temp. and pore diameter depend. 0–50276 polystyrene latexes, relationship between coefficient of attenuation, coefficient of scattering and cell diameter in multiple light scattering 0–66003

polystyrene melt, prediction of tensile behaviour 0-78243 polystyrene molecular beam, microions in beam, magnitude and nature 0-43079

polystyrene moulding techniques for liquid nitrogen Dewar 0–51845 polystyrene solns, coherent neutron scatt. 0–53316 polystyrene Pu cube systems, n surface multiplication expt. and theoretical cales. 0–49731

polystyrene-polybutadiene/toluene, presence of lamellar structure 0-58552

polytetrafluorethylene, lattice distortions and crystallite sizes, X-ray diffr. determ., 20°C 0-58778 polytetrafluoroethylene, Raman scatt. and thermal defects 0-41244

polytetrafluoroethylene, Raman scatt. and thermal defects 0–41244 polytetrafluoroethylene, compression stress relax. processes 0–40282 polytetrafluoroethylene, fractography 0–40375 polytetrafluoroethylene, hydrostatic press. effects on elasticity, strength, deform. and fracture 0–43716 polytetrafluoroethylene, n.m.r., relaxation times 0–62777 polytetrafluoroethylene, positron annihilation spectra rel. to energy transfer 0–40829 polytetrafluoroethylene, positron annihilation spectra rel. to energy transfer 0—40829
polytetrafluoroethylene, r.f. sputtering using diode system 0—50366
polytetrafluoroethylene, valence force field calc. by damped least-squares
method 0—53094
polytetrahydrofuran, degree of crystallinity, determination using X-ray and
i.r. techniques 0—68324
polythene, carrier injection and transport 0—68901

polythene, discharge channel propagation, effect of additives 0–68907 polythene, space charge effects on breakdown 0–68915 polytrifluorochloroethylene film, extruded, struct., dielec. losses, dichroism and birefringence 0–50371

polyurethane, creep modelling allowing for vibration and temp. effects 0-58904polyurethane, duration of memory determination 0-71673

polyuretnane, duration of memory determination 0–71673 polyurethane, linear, effect of thermal treatment and crystallization conditions, on struct. 0–58547 polyurethane, nonlinear creep, linear compressibility assumption for multiple integral representation 0–71702 polyurethane, relationship between creep of solid and foam resulting from combined stresses 0–55989 polyurethane—polyether foam acoustical wedges, use in semianechoic chambers 0–52134

chambers 0-2134
polyurethane elastomer, rate-sensitive fracture energy 0-50726
polyurethane foam, sound absorption tests rel. to anechoic enclosure applications 0-43489
polyurethane foams, sound absorpt. rel. to anechoic enclousres applic. 0-58511

polyurethane rubber, Solithane 113-50/50, stable crack propag. 0—47399 polyurethane rubbers, dielectric props., variation with temp., freq., and X-ray dose 0—65776

polyurethane rubbers, i.r. spectra identification 0-49947 polyurethane-polyether foam acoustical wedges, use in semianechoic chambers 0-52135

polyurethane-polyfurfuryl alcohol foam system, carbonization 0-39853 polyurethanes, molecular motion, study by nmr and dielectric methods 0-67837

0-0/83/
polyvinyl acetate thermoelectret, temp. depend., surface charge formation and decay characts. 0-44379
polyvinyl alcohol, aqueous soln., effect of degree of polymerization on critical shear rate 0-53292
polyvinyl alcohol, fractionation, by shearing force solution 0-53293
polyvinyl alcohol, use in preparing ionographic emulsion, sensitization for recording RX and \(\alpha\) rays 0-52615
polyvinyl alcohol film, i.r. study of tensile strength behavior 0-68473

polyvinyl alcohol films, deformation under joint action of solvent and static load 0-68205load 0–68205
polyvinyl alcohol solns. containing low molecular additive spectroscopic study of gelation 0–58512
polyvinyl carbazole, solid, excitons, interaction with trapped holes, photocurrent action spectra study 0–75500
polyvinyl chloride, branched, new macromol. model 0–64560
polyvinyl chloride, containing mass defects, vibr. spectra 0–39471
polyvinyl chloride, plasticized, rheological and thermodynamic interaction
effects 0–71656
polyvinyl chloride, positronium lifetime meas, and thermal degradation
0–41420
polyvinyl chloride, unplasticized melts relayation modulus and spectra in

0—41420 polyvinyl chloride, unplasticized melts relaxation modulus and spectra in temp. range 150-220°C 0–68033 polyvinyl chloride, yield-stress in glass transition region, obs. 0–40317 polyvinyl chloride and non-linear viscoelastic behaviour 0–57358 polyvinyl chloride $β_b β_c d_c$ mm study 0–67832 polyvinyl fluoride, structure i.r. spectra 0–46623 polyvinyl-p-methoxybenzoate and poly-p-methoxystyrene, dielectric props. meas., secondary relaxation mechanism 0–79032 polyN-inylcarbazole, effect of crystallinity on photoconductivity 0–65023

polyvinylchloride, plasticized, correlation between struct. and props. 0-58554

0-3834
polyvinylchloride, thermoelectric current generation model, radiation-induced trapped charge carriers 0-47865
polyvinylchloride, u.s. velocity, density and adiabatic compressibility after plasticizing with dialklylphthalates 0-40542
polyvinylchloride track detector 0-77439

polyvinylchloride track detector 0—77439 polyvinylchloride-dibutylphthalate system heat capacity, calorimetric meas. glass temp. 0—68616 polyvinylchloride-dioctylphthalate system, heat capacity, calorimetric meas. glass temp. 0—68616 polyvinylformal, high resolution p.m.r. and i.r. spectra 0—67833 polyvinylidene fluoride, crystallinity 0—78357 polyvinylidene fluoride, dielectric relaxation and molecular motion 0—75777

polyvinylidenefluoride, structural changes at deformation 0-58847 polyvinylpyridine solns., u.s. absorption between 1.6-100 MHz, temp. variation 0-58487

polyvinylpyridines, solutions, n.m.r. study 0-55632

polyvinylpyrrolidone in deuterated solvents, spin lattice relaxation time of deuterium 0-58263

polyvinylpyridines, solutions, n.m.r. study 0—55632
polywinylpyrrolidone in deuterated solvents, spin lattice relaxation time of deuterium 0—58263
polywater, lattice models, dynamics 0—39720
polywater, measurements 0—58457
polywater, properties 0—58455
polywater, structure 0—58456
polywater, structure 0—58456
polywater, structure 0—58456
polywater, structure 0—58456
polywater, structure 1—58456
polywater, structure 0—58456
polywater structural model proposed 0—46867
porous, accessible surface determ, sorption transient isotherm. 0—53445
o-positronium decay in glass transition of atactic polystyrene 0—78349
pyrrone, elec. characts., irradiation effects 0—47634
quantum mechanical tunneling in viscoelastic relaxation, energy dissipation mechanism 0—74425
Raman spectroscopy 0—69136
refractive index determ. from meas. of refractive increment using Dale-Gladstone eqn. 0—41111
relaxation, from n.m.r. results 0—57688
relaxation behaviour, freely jointed chain model 0—46616
resins, cross-linked, shear strength and deform. 0—40360
resins, thermoactive, anomalies in thermal expansion at glass transition temp. 0—59113
reticulate struct. parameters determ. for amorphous linear materials subjected to orientational stretching 0—39912
reloological eqns., statistical interpret. 0—40210
rubber-like, hermoelasticity at high strain 0—78590
rubber-like, thermoelasticity at high strain 0—78590
rubber-like, thermoelasticity at high strain 0—78590
rubber-like, mech. characts., reson. method at audio freqs. 0—40211
rubber-like, mech. characts., reson. method at audio freqs. 0—40211
rubber-like, mech. characts., reson. method at audio freqs. 0—40211
rubber-like, mech. characts, reson. method at audio freqs. 0—40211
rubber-like, mech. characts, reson. method at audio freqs. 0—40211
rubber-like, mech. characts, reson. method at audio freqs. 0—40211
rubber-like, mech. characts, reson. method at audio freqs. 0—40211
rubber-like, mech. characts, reson. method at audio freqs. 0—40211
rubber-like, mech. characts, reson. method at audio freqs.

suicones 1SE 200 and SH 410 hims, electron beam exposure charecteristics obs., application to electron microscope image recording 0-57490 sodium poly(acrylate) in NaBr solutions, intrinsic, viscosity, molecular weight, degree of ionization depend. 0-39765 sodium polystyrene sulphonate, NaCl aqueous, osmotic pressure, second virial coefficients 0-39768 solid high polymers, 3-terminal cell for meas, dielectric properties 0-56341

solutions, dilute, heat capacity calc. 0–58478 solutions, dilute, laminar flow around circular cylinders, heat transfer, drag 0–71279

orag 0-11219
solutions, dilute, turbulent flow drag reduction 0-53299
solutions, dilute, two parameter model for viscosity 0-64878
solutions, effect of high shear rate of flow on rigidity 0-58410
solutions, expansion in solvent, interfacial free-energy effects 0-39743
solutions, laminar flow, stress relationships from symmetry conditions
0-55573 solutions light scatt., Zimm plot fitting 0-46917 spectra, vibrational, allowance for interac. of non-neighbouring units 0-43061

spectroscopy, high temp. i.r. cell design 0-67184 sperulites films effect on birefringence on low-angle light- scattering patterns 0-65987 spherical particles, behaviour under conditions of stretch deformation 0-68388

spherulite morphology, computer models 0—78348 spherulitic deformed films, effect of birefringence on light scattering 0—65988

0-65988 statistical segments, 2, probability distribution of radius of gyration, analytical solution 0-77974 stiffness, rel. to chain folding 0-71705 strength, rel. to chain folding 0-71705 stress and deformation relations 0-50643 stress-strain relations 0-78615 structure, hydrostatic pressure effect 0-58549 structure, relation to properties illustrated by simple models 0-77975 structure and mech props. of solids, review 0-50342 structure and orientation measurements, i.r. spectroscopic method applic. 0-33413 structure-to-property relations and future applications. 0-65020.

styrene-butadiene-styrene block copolymer, mech. and rheo-optical props., morphology effect 0-40273 styrene-butadiene-styrene block copolymer, viscoelastic behaviour 0-58873

0–58873 styromal based coatings, physico mech. props. 0–40281 surface layers mechanical behaviour studies by transition processes in u.s. vibration 0–50360 surface tension, critical, calculation from chemical structures 0–68087 Teflon, heat treated, β* lifetime rel. to density, cryst. struct., obs. 0–40700 Teflon, longitudinal acoustic mode, meas. by inelastic scatt. of low-energy neutrons 0–59094 hermoelectric current generation model, radiation-induced trapped charge 'carriers 0–47865 thin sheets manufacture, film-blowing process, model 0–68072 thin-film, deposition techniques and materials 0–78386 hiophosgene, Raman and i.r. spectra 0–55374 triethyleneglycoledimethacrylate structure study, i.r. spectra 0–67834 3.3-3-trifluorogropylene-ethylene copolymers, cryst. struct. rel. to composition 0–50343 vinyl alcohol and N-vinylpyrrolidone copolymer i.r. study of tensile strength

0–50343 vinyl alcohol and N-vinylpyrrolidone copolymer i.r. study of tensile strength behaviour 0–68473 vinyl monomers, struct. and phase transitions, X-ray, i.r and thermal anal. study 0–47024 vinyl plastic, wear, friction, temp. depend., rubbed on steel 0–40425 vinyl plastics structure, hydrostatic pressure effect 0–58549

Polymers continued

vinylidene fluoride and hexafluoropropylene copolymers, dielec. relax. 0-47830 viscoelasticity, Poisson coefficient as function of stress- strain state

0 - 50647

0–50647 viscoelasticity, Voigt and Maxwell models generalization 0–40247 viscoelasticity, quasilinear theory and small parameter method 0–40246 viscoelasticity of inorg, polymers 0–40249 volatilization 0–76759 water, covalent, structural scheme 0–71316 wormlike chains, sedimentation and diffusion constants 0–67831 C, glassy, formation from thermosetting resins, crosslinking effect 0–71435 of C₃O₂, spectra 0.2-1.6 μ rel. to Mars coloration 0–41792 H₂O, MO calc. of energies and configurations 0–53033 (KPO₃)_n, γ irradiated at 77°K e.s.r. spectra, components radicals structure, temperature effect 0–59462

temperature effect 0–59462

Polymorphism
see also Crystal structure
alkaline earth vanadate systems 0–50831
alkaline earth vanadate systems 0–50831
alkaline earth-chalcogenide crystals, influence of short-range three-ion interactions 0–75214
barbituric acids, 5,5-disubstituted, spectra-polymorphic structure correlations 0–72373
chloroacetic acid, three polymorphic forms and distinct spectra 0–67776
and compressibility 0–40285
diamorphism, rel. to coloured symmetry 0–58652
enantiomorphous symmetry groups 0–61746
esters, long C chain 0–61921
formic acid, crystalline, obs. 78-300 K first order phase transition obs. 0–75344
liquid cryst. 0–58450

esters, long C chain 0-61921 formic acid, crystalline, obs. 78-300 K first order phase transition ob 0-75344 liquid cryst. 0-58450 rare earth disilicate, 900-1800°C 0-58746 rare earth double tungstate hydrothermal synthesis 0-74986 structural stability 0-43622 transitions in thin cryst. plates 0-62123 CdS(Se,7e), h.p. phase transform. 0-53659 Ga, polymorphic transitions, h.p. 0-53399 HfO₂ films, evap. 0-58575 K.NO₃, single crystal, rhythmic growth, $\alpha \rightarrow \beta$ transformation 0-78403 MgM, (where M=Zn, Cu, Ni), ternary Laves, polytypes 0-58737 (NaPO₃), Polymorphic modifications obs. 0-55859 S and other divalent elements, theory and actuality 0-50405 SiC. Sec crystal Sc melt growth, 4H polytype 0-58619 SiC, polytypism rel. to but emp. photoluminescence spectra 0-54141 SiC polytype 69R, cryst. struct. 0-65280 Ta₂O₄, polymorphs, growth, unit cells and space groups 0-65285 TbNi, heat treatment depend. 0-65286 TiO₄, stability, comp. and temp. depend. 0-65508 TiO₄ polymorphic transform, topotaxy 0-59037 Tl, $\alpha = \beta$ transformation, impurity effects 0-68554 XeF₆ 0-65123 Yb polymorphic transformation discovered 0-75343 Zn-In-S system ternary phases, polytypism 0-78810 ZnIn,S₄(1) polytypic form, cryst. struct. 0-65296 ZnS, vapour-phase grown, mechanism of polytype formation 0-50825 ZnS, polytypes, low-order 0-71506 ZrO₂, i.r. spectra of different polymorphic powders 0-72371 ZrO₂ evap. films, 30 to 1400°C 0-71506 ZrO₂, films, evap. 0-58875 **lytypoints**

Polynomials see Algebra; Functions

Polytypism see Polymorphism
Pomeranchuk rule see Elementary particles/scattering
Population inversion see Lasers; Masers; Optical pumping

Porosity see Porous materials

Porous materials

see also Permeability, mechanical; Surface measurement adsorbant with constant diameter channels, measurement of porosity 0-65097

adsorbant with constant diameter channels, measurement of porosity 0–65097
adsorption kinetics 0–65094
alumina, porosity effects on electric strength 0–68960
capillary action, physics and thermodynamics 0–68050
capillary porous, moist, thermal conductivity 0–68623
characterization in terms of gas transmission props. 0–78571
disc, submerged in liquid, bubble formation mode transitions 0–68066
disperse bodies, contact strength between crystals 0–78687
electrodes, flow rate through, meas, device 0–62812
fibres, microporous struct. obs. technique 0–50809
Fingero-imbibition in slightly dipping porous medium 0–64876
with fluid, heat and mass transfer, stability criteria 0–67860
gas flow, laminar, in porous pipe with wall injection, pressure drops, exit centerline velocities 0–78180
granular materials, sheared, critical porosity, applic. of geometrical probability 0–56048
graphite, artificial, density and struct. distribs. 0–71651
heat transfer in air bubbling through porous graphite cylinder into water including vaporization 0–46995
heat transfer in porous medium filled with gas and bounded by plane rectangular sheets, natural convection 0–46816
insulator, vol. resistivity, water vapour effect 0–51093
insulators, hydrocarbon flow through, electrostatic charge generation 0–48950
kaolin sediments, homoionic, pore struct. 0–59006
melting phase transformations determ. by shock compression. 0–46980

0-48950 kaolin sediments, homoionic, pore struct. 0-59006 melting phase transformations determ. by shock compression 0-46980 metal membranes with uniform submicron size pores 0-43818 permeability, anisotropic methods of meas. 0-67857 polymer, accessible surface determ, sorption transient isotherm. 0-53445 polymer fibres, microporous struct, obs. technique 0-50809 pore size, micromeritic instrumentation development 0-76791 pore size distrib, meas. techniques comparison 0-56052 pore structure analysis by water vapour adsorption 0-61831 porosity, minimum, of assembles of identical spheres 0-47467

S 1300 SUBJECT INDEX sitrons continued annihilation in metals, dislocation effects 0–50956 annihilation in metals, role of electron-electron interaction 0–71941 annihilation in metals 0–75529 annihilation in single crystals, temp. depend. 0–40625 annihilation in synthetic zeolites 0–56166 collision processes, with H, He atoms, theory 0–52976 cosmic rays, annihilation radiation 0–48367 crystal, many-beam cales. on fast charged particle propag. 0–75432 detector (p-p coincidence) for cosmogenic positron emitters 0–52607 electron capture from H₂, rel. to positronium formation 0–77266 in electron gas, Green's function calc., annihilation applic. 0–44010 energy loss, average, empirical relation 0–42476 Green's function, cold single crystal 0–40627 Green's function and positron annihilation probability in an electron gas 0–55000 n-hexadecane, lifetimes, temp. depend. correl. with viscocity collection and positron annihilation probability in an electron gas 0–1000 n-hexadecane, lifetimes, temp. depend. correl. with viscocity collection and positron annihilation correl. Positrons continued Porous materials continued porosity determination, use of thermal-neutron irradiated air (41Ar) 0-46223porosity determination, use of thermal-neutron irradiated air (41Ar) 0–46223 porosity investigation, choice of base meas. 0–62120 powder, grain size distrib., comparison of Hg porosimetry, sedimentation and microscopy 0–56047 powder diffr. porosity effect 0–71538 powder diffr. porosity effect 0–71538 powder diffr. porosity effect determ. 0–61789 semi-infinite, heat and mass transfer, well- stirred fluid 0–42100 silica gel, microporous, adsorption of benzene, cyclobenzene, isopropanol and carbon tetrachloride 0–50398 silica gels, pore struct. determ. by electron microscopy and low-temp. N₂ adsorpt. 0–78318 sorbents, diffusion coeffs., calc., adsorption isotherm 0–50616 sound absorption as humidity fin, meas. 0–65532 synthetic aggregate, sandblast abrasion testing 0–71731 t-plot characterization of microporosity 0–74924 thermal conductivity meas. methods 0–71872 thermal conductivity theoretical prediction 0–55634 two-phase flow, constitutive equations for force per unit volume 0–68049 UO₂, surface free energy anisotropy 0–61633 Al, theor. shock props. 0–55959 Al₂O₃/Al, anodic film, transport numbers, structure 0–53922 Al₂O₃, film anodic, struct. development 0–58571 β-Al₂O₃ sintered sodium ceramics 0–58985 As₃Se₃ layers, optical reflection obs. 0–76012 Au-Al₂O₃ alloys, electrodeposited, porosity effects on creep strength 0–59007 Au, electrodeposit on Cu, porosity, scanning electron microscope exam. 0–5872 n-hexadecane, lifetimes, temp. depend., correl. with viscosity changes 0-74784 lifetime, trapped in F-centres in KC1 0–75457 low-energy, total cross-section, direct meas, technique 0–73463 metal, annihilation, meas, technique 0–47571 in metals, effective mass 0–40701 methanol, lifetime temp, and phase depend., and CD₃OD 0–75533 n-octane, lifetimes, temp, depend., correl. with viscosity changes 0–74784 in plasma, equilib. conc. 0–74504 production in coulomb field with Z>137 0–73852 slow, annihilation and diffusion in He gas 0–77265 source, monoenergetic 10 to 50 MeV, design and analysis 0–49433 from supernovae 0–79672 e⁺p, ep scatt. cross sections, comparison 0–38633 e⁺p scattering, comparison with e⁻p scattering at small angles 0–49207 CSCl, solid and liq., annihilation time spectra, 295-1223 K 0–47616 Cu, anisotropic annihilation, with high-momentum components of conduction band 0–47615 FeO, Fe₂O₃, Fe₂O₃, Fray, ang. distrib., valence state depend. 0–40629 lifetime, trapped in F-centres in KCl 0-75457 Au, electrodeposit on Cu, porosity, scanning electron microscope exam. 0-58572Au electrodeposit on Cu, effect on substrate pretreatment on porosity 0-585730-58573 Au electrodeposits, pore obs. 0-53652 (Ba_{0.8}Pb_{0.12}Ca_{0.08})TiO₃, influence of porosity on sound velocity investigation 0-50860 C, active, pore structure, H₂O vapour adsorption 0-75322 C, adsorption of CO₂, 195K, N₂ and Ar, 77K, Dubinin-Radushkevich characterization 0-61679 C, glassy, formation from thermosetting resins, crosslinking effect 0-71435 tion band 0–47615 FeO, Fe,O₄, Fe,O₃, y-ray, ang. distrib., valence state depend. 0–40629 He-e+ bound state 0–39329 KCl, solid and liq., annihilation time spectra, 295-1223 K 0–47616 MgO, annihilation, Brillouin zone boundaries effect 0–53775 NaCl, solid and liq., annihilation time spectra, 295-1223 K 0–47616 Si, positron channeling 16-28 MeV, forward bremsstrahlung obs. 0-71435 C, graphitized, pore growth, CO₂ reaction 0-40177 Cu sinters, rel. to elastic modulus determination 0-40271 Fe sinters, rel. to elastic modulus determinations 0-40271 β-FeOOH tubular subcrystals, presence and structure of pores, atomic formulation 0-65237 MgO, polycryst, effect of temp., grain-size, porosity and surface condition on strength 0-40352 Si surface barrier semiconductor detector, pulse height distributions, $100 \text{ to } 1200 \text{ keV} \quad 0-49388$ UO₂, annihilation, Brillouin zone boundaries effect 0-53775 abundance in lunar rocks and separated phases 0-45342 adsorbed on W, surface diffusion activation energy, field emission method 0-39977 Nb bicrystals, welded, boundary porosity sintering 0-40440 (Pb_{0.6}Ba_{0.4})Nb₂O₆, influence of porosity on sound velocity investigation 0-50860 atom, cross sections on rare gases, in velocity range 300-15000 m/s 0-77694(F0)₂, Sagary (F0)₃, minuses (P0)₃, minuses (P0)₃ atom, elastic scattering from I and I $_2$ at thermal energies $\,$ 0-70797 atom, electric charge upper limit rel. to electron-proton charge difference $\,$ 0-42962 Porterin-LeChatelier effect see Stress/strain relations atom, ionization by He collisions, Penning electron energy distribs., interaction potentials 0-74159 Positive column see Discharges, electric atom, minima of generalized oscillator strengths for continuum transitions 0-67627 Positive ray sources see Ion sources Positive rays see Chemical analysis/by mass spectrometry; Ion 0-67627 atom, oscillator strengths of high terms of principal series 0-49780 atom, polarization of the atomic core, effect on the oscillator strengths and photoionization cross-sections 0-60923 atom, quadratic Stark shifts of Zeeman levels in ground state 0-77662 atom, rotationally inelastic scatt. from CO₂, crossed-beam obs. 0-67850 atom, scattering from halogen compounds at hyperthermal energies 0-46632 beams Positons see Positrons sitions see Positrons sitronium 2S hyperfine structure, level shift, depend. on field strength between atom and medium 0–74092 atom, in ionic crystals, props. 0–75440 in benzene, liq. and solid, quenching 0–40633 emission of photons in excited state transitions 0–42941 formation, by electron capture by positrons from H₂ 0–77266 formation in interacting electron gas 0–71934 formation in oxides rel. to forbidden band width 0–47614 free, properties and atomic collision aspects 0–52447 ground state, precision determ. of fine struct, interval 0–77635 hyperfine structure of order α²lnα⁻¹, corrections 0–42948 Lyman α⁻radiation, from positrons stopped in inert gases, search 0–64186 Lyman-α⁻radiation, attempt at detection, apparatus, results 0–77416 in molecular materials, o-positronium form, quenching 0–40691 in octanol, liq, and solid, quenching 0–40633 in organic diamag. solns, lifetimes 0–53314 ortho-, quenching in Ar and Freon-12, obs. 0–42482 in oxides, o-positronium two- and three- photon lifetimes 0–40694 paramagnetic quenching of 0-positronium by H, Li impurity atoms 0–40690 parapositronium, direct meas. of decay rate 0–77635 Positronium atom, spin exchange scattering by Cs 0-49805 atom, spin-orbit perturbation from photoionization experiment 0-60914 atom and ion, collisions with Na and K vapour and inert gases, 20-155 keV 0-39316 keV 0-39316 atom scattering by inert gases, total cross-sections 0-61202 atomic transition tables 0-39284 atomic transition tables 0-39284 atomic, collisional my mixing in 4²P_{3/2}, 4²P_{1/2}, selection rules, obs. 0-55244 atomic, polarized, spin exchange collision with electrons to produce polarized electron beams 0-52443 atomic escatti, elastic spin exchange, 0.5-1.2 eV 0-39306 binding energy, elastic consts. and derivatives, eqns. of state, and phonon spectrum 0-56088 spectrum 0-56088 cyclotron resonance, relaxation time, mass anisotropy and magnetic field tipping, relationship 0-62275 diffusion in Na₃O-K₂O glasses 0-55921 discharge, low-pressure, population mechanism 0-74644 electron mean free path from r.f. size effect meas., 1.9-4.2°K 0-43956 electron scattering, elastic differential and differential exchange cross sections 0-74140 electron scattering, spin-analysed differential cross section meas. 0-52958 excited atomic states, mean lives of K I, II and III, beam-foil excitation technique 0-67648 excited atoms, inelastic collisions with slow electrons 0-60958 ion, desorbed from W-surface, residence time meas, using correlation tech. 0-68239 ion collisions with inert gases, 12 keV to threshold, resonance lines obs. 0-40690 parapositronium, direct meas, of decay rate 0-77635 polypropylene, o-positronium annihilation on nitric acid etching 0-75534 polystyrene, atactic, o-positronium decay obs. of glass transition 0-78349 polyvinyl chloride, lifetime meas, and thermal degradation 0-41420 quenching by org. diamag, mols. 0-53314 quenching of orthopositronium in He 0-38635 scalar model. Pade approximants, test in Coulomb bound-state problem 0-72924 0-72924 Z_{op}, effective number of singlet annihilation electrons for ortho-positronium in molecular liquids 0-42937 MgS, decay, τ_2 obs. 0-40699 ortho, decay rate, obs. 0-42482 Zns, decay, τ_2 obs. 0-40699ion collisions with inert gases, 12 keV to threshold, resonance lines obs. 0-61003o-61003 ion-inert gas interactions, 150 to 4000 eV, obs. 0-77701 liquid, solubilities of V, Ti, Zr 0-39741 liquid, solubility of refractory metals and alloys 0-39742 liquid, spin lattice relax. 0-74789 magnetoresistance, linear 0-71938 optical constants, testing of interband-transition absorpt, theory 0-79231 photocathode, pairs of photoemitted electrons 0-68988 photoelectric yield and photoelectron energy distrib. 0-40910 plasma thermally ionized in pyrex tube, upper hybrid resonance scattering calc. 0-43285 r.f. size effect, rel. to cyclotron reson., helicon and sound waves 0-44016 resonance radiation energy loss in Ar-K plasma cylinder 0-39547 seeded Ar discharge tube, electrode potential drop 0-53225 spectral line press. broadening, 0.1-10 torr, rel. to theories 0-52880 spin lattice relax. in liq. and solid, 253-433K 0-74789 Stark effect, laser field 0-39288 u.s. attenuation due to electron-phonon interaction 0-53704 u.s. generation, direct, mag. field depend., obs. 0-50879 vacancy pairs, asymptotic interaction energies 0-43657 Positrons see also Electron pairs; and Electrons, which include both negative and positive electrons when the differences between them are of no special significance annihilation, in He, Ne, Ar 0-73464 annihilation, continuum atomic process, quantum theoretical approach 0-52860 annihilation, rel. to electron states in α and β brass 0–65615 annihilation, positron-electron many-body system 0–54999 annihilation cross-sections in various atomic shells, second-order calc. 0 - 463870-4638/ annihilation in He, Ne and Ar 0-55250 annihilation in He and e* He bound state 0-39329 annihilation in He gas, 4.6-30°K 0-64263 annihilation in flight of monochromatic positrons, photon spectrum com-puter calc. 0-38634

Potassium continued

vapour, atomic, angular distrib. changes of light intensity on laser-beam passage 0-60955

vapour, optical properties at high temperatures and concentrations 0-71260

O-71260
vapour, ruby laser excited, emission spectra, fine structure 0-74118
vapour, self-focusing of ruby-laser light by K vapour 0-39675
vapour diode study under high pressure 0-52216
whole-body p counter 0-59825
whole-body p spectrometry 0-59824
Ar:K, doping by reactor irrad., absorpt. spectra 0-40175
Ar isochron method for radioactive dating of samples 0-45120
atom, collisions with diatomic mols., excitation and ionization, role of ion-pair states 0-60957
atom, electronic excitation in collisions with diatomic mols., thresholds and energy dependence 1-5 eV 0-60956
He-K mixture, non-equilib., transport props., 1000-5000K 0-55567
He-K plasma, thermal props., mass transfer due to contact with cold wall 0-39548
K+-Ar, meas. of Q values at keV generies (0-77691)

K+Ar, meas of Q values at keV energies 0-77691
K-NH₃ and ND₃ liq. solns., viscosities 0-43437
K-NH₃(ND₃) layer formed by evaporation, EPR obs. following tempering

0-51398 K+-Ne collision, emission spectra, excitation functions, absolute meas.

0-74156

0–74156
K-Xe collisions, 4²P_{1/2}-4²P_{3/2} mixing, exp. evidence for absence of long-lived K-Xe complex 0–77695
K II lines prod. in collisions between k* and He atoms, excitation functions absolute meas. 0–39297
K V in planetary nebulae, emissivity 0–51644
k*, injection and mobility in He II 0–43505
K* mobility and diffusion in N₂, obs. 0–46765
K*+ Rb collisional excitation transfer cross-sections, obs. 0–67643
K. radiative lifetime of BI/II, state 0–74277

K+ + Re consistant excitation transfer cross-sections, obs. 0–67645 K₂, radiative lifetime of B¹II_u state 0–74277 ³⁹K, optically pumped, 4²P_{3/2} level crossing, obs. 0–52913 K+HBr→KBr+H reaction, mechanism 0–72523 K+NO₂, paramagnetic product obs. 0–46635 K. II (3p⁵4p) life-times of nine of the ten levels, meas. using beam-foil to technique, comparison to ArI levels 0–64222

Potassium compounds
acid phthalate, cryst. growth and testing for X-ray spectrometer 0–65168
electro-optic crystals, KTN, reproducible growth techniques 0–50440
halides, Born model, u.s. parameters 0–43706
halides, Fm3m=Pm3m transition, thermodynamics 0–43826
halides, Schottky defect energies calc., NaCl struct. 0–40135
halides, high mobility of heavy inert gases at low temps. 0–43695
halides, i.r. absorption due to H ions, anharmonic side bands 0–72359
halides, vibronic spectra of O₂°, S₂- and NO₂°, rotational degrees of freedom 0–53535
K₃Li₂(Ta₂Nb₁₋₂)₂O₁₅, structural and ferrolec. props., comp. depend.
0–62441
muscovite, cryst. struct. 0–65250

0—02441
muscovite, cryst. struct. 0—65250
AgNO₃-K.NO₃ system, molten, internal transport numbers and ionic mobilities of Ag and K ions 0—59494
GeO₂-K.O glass system, diffuse Raman spectra 0—56564
K.Hg dil. alloy, liquid, elec. resistivity, comp. depend., 100-260°C
0—50255

K-LiNbO₃, nonlinear optical properties 0-72302 K-Pb dil. alloy, liquid, elec. resistivity, comp. depend., 100-260°C

50255

U=0025 K-Rb liquid alloy, u.s. absorpt. and vel. obs. 0−64915 K-Tl dil. alloy, liquid, elec. resistivity, comp. depend., 100-260°C 0−50255 (K,Na)TaO₃ mixed cryst., soft phonon modes 0−65518 K₄ Re(CN)_{6.3}H₂O space group symmetry and unit cell dimensions 0−65249

(K,Na)TaO, mixed cryst., soft phonon modes 0-65518
K₄ Re(CN)₆ 3H₂O space group symmetry and unit cell dimensions 0-65249
KAl(MoO₄)₂, synthesis, cryst. struct., X-ray diffr. 0-78476
K,B₂O₆, bond lengths and thermal parameters 0-68309
K,B₄Nb₁₀O₃₀, polycrystalline, with K-W bronze structure, test of ferroelectric and physical properties 0-75800
KBa₃TiNb₂O₃₀, tungsten-bronze type struct. and dielec, props. 0-53924
K,C₂O₄,H₂O, librational modes of H₂O mols. 0-40517
K,C₂O₄,H₂O, librational modes of water mols. 0-43851
K,C₂O₄,H₂O, cryst. structure, symbolic addition method 0-68307
KC₂O₃,H₂O, cryst. structure, symbolic addition method 0-68307
KC₂O₃, prep. and struct. 0-55844
KCl, plasmons, volume and surface, evidence in secondary electron emission spectra 0-75867
KClO₂ annealing of chemical radiation damage 0-65450
KClO₄, Xi rradiated, e.s.r. signals from defects due to e and holes trapped on ClO₄ 0-48147
KCoF₃, *7Co-labelled, Mossbauer study of charge states of *7Fe formed by electron capture decay 0-70558
K,CoF₆, *7Co-labelled Mossbauer study of charge states of *7Fe formed by electron capture decay 0-70558
K,Co₃(OH)₂(SO₄)₃,2H₂O, cryst. struct., X-ray powder indexed 0-53510
K,Cr(CN)₆, *A₂-*T₂ transition 0-62664
K,Cr(CN)₆, *O₃-*T₂ transition 0-62664
K,Cr₂O₃, cryst. absorpt. spectra 0-72360
K,Cr₂O₃, cryst. growth irregularities and symmetry, supersaturation depend. 0-40084
K,Cr₂O₃, eptromage, struct., neutron diffraction refinement 0-61873
KCuCl₃, antiferromag, struct., neutron diffraction refinement 0-61873
KD,PO₄, deuteron motion obs. 0-79285
KD,PO₄, devented transition in dodekahedral cryst. field 0-41177
K,CuCl₄, 2H₂O, crystal structure, neutron diffraction refinement 0-61873
KD,PO₄, devented transition of ferroelectric domains 0-75792
KD,PO₄, devented transition of 0-40867
KD,PO₄, devented transition of 0-40867
KD,PO₄, ferroelectric mode motion 0-40867
KD,PO₄, leteromic decertic excited Raman sp

KD₂PO₄, Raman scatt. by ferroelec. mode 0–79330 KD₂PO₄ laser modulator crystal, temperature instability 0–47990

Potassium compounds continued

KF.B₂CO₃ glass, n.m.r. of ¹¹B, coordination number 0–41374 KF, F centre, X-irrad., 100 K, radiative lifetime 0–79364

KF, F centre, X-irrad., 100 K, radiative lifetime 0-79364
KF, mag. circular dichroism of F band and F-centre spin polarization quenching 0-76027
KF film, electron diffraction study of bonding forces 0-74938
K₃Fe(CN)₆, change in crystalline state, temp. depend. quadrupole splitting meas. 0-47188
K₃Fe(CN)₆, Mossbauer spectra for electron-phonon instability at ~130 K
0-59379
KFC(N)₆, OD transity 6-64266

0-393.99

K₃Fe(CN)₆, OD-struct. 0-61875

K₄Fe(CN)₆, 3H₂O, ferroelec transition, Mossbauer obs. 0-40866

K₄Fe(CN)₆, 3H₂O, ferroelectric, Mossbauer spectra at transition temp. 0-41163

G-41163

K₄Fe(CN)₆.3H₂O, ferroelec. phase transition, water molecules dipole moments, n.m.r. 0–54169

K₄Fe(CN)₆.3H₂O and isomorphous ferroelec. phase transitions rel. to ordering of dipole moments 0–65808

KFe(MoO₄), 0–78476

K,FeO₄, mag. susceptibility, Neel temp., Mossbauer effect 0–56513

KFeS₂, Mossbauer spectrum rel. to internal field, obs. 0–41155

KFe(SO₄), and KFe(SO₄), 4H₂O, cryst. struct. 0–65251

KH₂ASO₄, e.p.r. and ENDOR observation of ferroelectric domains 0–75792

KH₂ASO₄ phase discrept to S2 beyon and 400°C, 0, 55677

KH₂ASO₄ phase discrept to S2 beyon and 400°C, 0, 55677

KH₂ASO₄ phase discrept to S2 beyon and 400°C, 0, 55677

KH₂ASO₄ phase discrept to S2 beyon and 400°C, 0, 55677

KH₂ASO₄ phase discrept to S2 beyon and 400°C, 0, 55677

KH₂ASO₄ phase discrept to S2 beyon and 400°C, 0, 55677

KH₂ASO₄ phase discrept to S2 beyon and 400°C, 0, 55677

KH₂ASO₄ phase discrept to S2 beyon and 400°C, 0, 55677

KH₂ASO₄ phase discrept to S2 beyon and 400°C, 0, 55677

KH₂ASO₄ phase discrept to S2 beyon and 400°C, 0, 55677

KH₂ASO₄ phase discrept to S2 beyon and 400°C, 0, 55677

KH₂ASO₄ phase discrept to S2 beyon and 400°C, 0, 55677

KH₂ASO₄ phase discrept to S2 beyon and 400°C, 0, 55677

KH₂ASO₄ phase discrept to S2 beyon and 400°C, 0, 55677

KH₂ASO₄ phase discrept to S2 beyon and 400°C, 0, 55677

KH₂ASO₄ phase discrept to S2 beyon and 400°C, 0, 55677

KH₂ASO₄ phase discrept to S2 beyon and 400°C, 0, 55677

KH₂ASO₄ phase discrept to S2 beyon and 400°C, 0, 55677

KH₂ASO₄ phase discrept to S2 beyon and 400°C, 0, 55677

KH₂ASO₄ phase discrept to S2 beyon and 400°C, 0, 55677

KH₂ASO₄ phase discrept to S2 beyon and 400°C, 0, 55677

KH₂ASO₄ phase discrept to S2 beyon and 400°C, 0, 55677

KH₂ASO₄ phase discrept to S2 beyon and 400°C, 0, 55677

KH₂ASO₄ phase discrept to S2 beyon and 400°C, 0, 55677

KH₂ASO₄ phase discrept to S2 beyon and 400°C, 0, 55677

KH₂ASO₄ phase discrept to

0-75792

KH₂AsO₄, phase diagram to 52 kbar and 400°C 0-55657

KH₂AsO₄, X-ray irradiated, observation of electron-nuclear triple resonance of AsO₄* center 0-76243

KH₃(CsO₄), 2H₁O, elastic consts. meas. 0-71663

KH₅C, phys. 2H₁O, elastic consts. meas. 0-71663

KH₅P₀, 2H₁O, elastic consts. meas. 0-75548

KH₄F₃, prigration in elec. field, pres. up to 60 kbar 0-75548

KH₄PO₄-type ferroelectrics, proton dynamics from ir. absorpt. 0-40864

KH₂PO₄-type ferroelectrics, proton dynamics from ir. absorpt. 0-40864

KH₂PO₄-type ferroelectrics, proton dynamics from ir. absorpt. 0-65812

KH₂PO₄-type ferroelectrics, proton dynamics from ir. absorpt. 0-65812

KH₂PO₄-type ferroelectrics, proton dynamics from ir. absorpt. 0-40864

KH₂PO₄-type ferroelectrics, proton dynamics from ir. absorpt. 0-40864

KH₂PO₄-type ferroelectrics, proton dynamics from ir. absorpt. 0-40864

0—65812
KH₂PO₄, dielec. const. rel. to coupled p tunnelling, 9.4 GHz
0—47844
KH₂PO₄, diffraction of moving light waves
0—41097
KH₂PO₄, electrocaloric effect, u.s. attenuation meas. 0—56371
KH₂PO₄, electrooptic, solubility of growth 0—71517
KH₂PO₄, far i.r. Fourier transform determ. of complex permittivity spectra 0—66023

tra 0-66023 KH₂PO₄, far-ir. refl. spectra 0-69110

KH₂PO₄, far-1.F. reft. spectra 0-09110 KH₂PO₄, prirrad, dielec. props. 0-68941 KH₂PO₄, prirrad, dielec. props. 0-68941 KH₂PO₄, laser excited Raman spectral study of quasi-spin wave hydrogen tunneling modes 0-47845 KH₂PO₄, modulator for excess noise reduction in GaAs laser beam 0-45804

KH₂PO₄, nonlinear optical susceptibilities 0-47991

KH₂PO₄, optical second harmonic generation by diverging laser beams 0-42347

KH₂PO₄, paraelec. phase, struct. of H₂PO₄ ion, from Raman spectra study 0-40862

0-42347
KH,PO4, paraelec. phase, struct. of H₂PO₄ ion, from Raman spectra study 0-40862
KH₂PO4, phase front motion obs. 0-65809
KH₂PO4, phase transformations and melting to 40 kbar 0-62114
KH₂PO4, phase transition origin 0-68942
KH₂PO4, phase transition origin 0-68942
KH₂PO4, phase transition origin 0-65810
KH₂PO4, polarization and phase transition 0-65810
KH₂PO4, polarization and phase transition 0-65810
KH₂PO4, Raman spectrum and second harmonic generation, temp. depend 0-66069
KH₂PO4, specific heat, phase transition anomaly 0-40572
KH₂PO4, specific heat, phase transition anomaly 0-40572
KH₂PO4, temp. and wavelength depend. of electro-optical coeff., 300-750 nm, from 25°C to Curie point 0-41128
KH₂PO4, thermal cond. meas. near Curie point 0-40605
KH₂PO4 and deuterated isomorphs, sp. ht. 0-65547
KH₂PO4 and KD₂PO4, phase transitions obs. from i.r. spectra 0-62115
KH₂PO4 coupled order-disorder phonon system with damping 0-62171
KH₂PO4, crysta, polariz. and domain struct. in static elec. field 0-40863
KH₂PO4 crystal, conversion from low power Nd glass laser radiation to second harmonic 0-62582
KH₂PO4 ferroelectric, normal vibrations, symm., Raman spectra 0-40523
KH₂PO4, laser, free-running, thermal self focussing of radiation 0-49072
KH₂PO4 laser, free-running, thermal self focussing of radiation 0-49072

KH₂PO₄ laser, free-running, thermal self focussing of radiation 0–49072 KH₂PO₄ laser modulator crystal, temperature instability 0–47990 KH₂PO₄ optical rectification effect applic to giant pulse laser power meas.

0-75999 KH.;PO₄ p migration in elec. field, pres. up to 60 kbar 0-75548 KH;PO₄ parametric fluorescence excited by 2573Å pump 0-44907 KH;PO₄ Pockels cell, performance in Q-switched laser, transient elastooptic effects 0-66766 KH;Po₄, ferroelec. phase, internal vibrs. spectra 0-79308 KH;GeO₃), ferroelec. dynamic proton ordering during transition, from n.mr. meas. 0-41376 KI:Ag⁺, far ir. absorpt. temp. depend. rel. to lattice resonant modes 0-44843 KI:Cu recombination luminescence investigated 0-56601

K1:Ag*, 1ar 17. absorpt. temp. depend. Fel. to lattice resonant modes 0-44843
K1:Cu recombination luminescence investigated 0-56601
K1:Eu, additively coloured in Na vapour, luminescence studied 0-56602
K1:Eu, luminescence, activator centres investigated 0-56630
K1:Eu²+, absorption, excitation, luminescence and e.p.r. spectra 0-59429
K1:Eu²+, phosphorescence and captrue centre determ. 0-66110
K1:Na, luminescence 0-66096
K1:Yb, additively coloured in Na vapour, luminescence studied
K1:Yb, additively coloured in Na vapour, luminescence studied
K1:KB r solid solns, with Sr²+ impurities, ionic cond. 0-65778
K1, additively coloured with K, colloidal absorpt bands 0-75183
K1, aqueous inclusion migration during centrifugation 0-61994
K1, circular dichroism in Urbach region 0-44774
K1, colloidal colour centre, e.m. wave absorpt. 0-65332
K1, dispersion curves, deformable shell model calc. 0-40524
K1, electroluminesc. due to internal field emission 0-59445
K1, electron centres, differently charged forms 0-68372
K1, exciton absorpt, band, non-elementary long-wave, rel. to luminescence 0-66046
K1, F-centre accumulation, proton beam intensity depend. 0-40190

KI, F-centre accumulation, proton beam intensity depend. 0-40190 KI, F-centre accumulation under proton irradiation, temp. depend. of kinet

ics, 90-300 K 0-50612

Potassium compounds continued

KI, F₂⁺ centres form. 0-71634

KI, F₂ centres form. 0-71634
KI, formed in K/I and K/I₂ collisions, electronic hamiltonian between covalent and ionic states 0-70797
KI, intrinsic luminesc., 80K 0-44889
KI, ionic cond. 0-65777
KI, quenched in colour centre, photoluminescence, optical absorpt. 0-47281

KI, ionic cond. 0–65777
KI, quenched in colour centre, photoluminescence, optical absorpt. 0–47281
KI, Raman spectrum and assignments 0–72362
KI, sputtering due to electron and u.v. irrad. 0–68709
KI, thermal expansion, 100:300 K 0–43920
KI, V_k centres, optical absorpt. and thermal reorientation, small polaron theory 0–47277
KI host lattice for 1º0₃- and 1º80₃- ions, i.r. spectra 0–66045
KI measurement of thermostimulated current and luminescence, nature of conductivity 0–51366
KI resistivity and conductivity variations at high concentrations, temperature and pressure effects 0–46944
KI single crystal, F centre growth curves, nonuniform electron irrad. effect, and electron penetration 0–53552
KI surface, Se decorated, active epitaxial vacancy cluster centres, electron diffr. 0–74881
KIO₃, ferroelec. behaviour anomalies 0–65813
KIO₃, Holy, cryst, struct. 0–78477
K, IrCl₆, sparamag, and antiferromag, n.q.r. of ³⁵Cl 0–72517
K, IrCl₆, sparamag, and antiferromag, n.q.r. of ³⁵Cl 0–72517
K, IrCl₆, sparamag, and antiferromag, n.q.r. of ³⁵Cl 0–72517
K, IrCl₆, temperature and pressure variation of the ³⁵Cl n.q.r. frequency 0–54173
KLa, Ti₆Nb₆O₃₀, tungsten-bronze type struct. and dielec. props. 0–53924
KLiBef₁, crystal structure 0–75095
KLa, Ti₆Nb₆O₃₀, new phase of hexagonal bronze type 0–71803
K, Li₆(Te₈Nb₁)₂-₂O₁₅, dielec. and struct. obs. 0–68940
K, M^{*} (*CrO₄)₂-2H₂O, X-ray crystallographic determ. of lattice parameters (M=metal) 0–65248
KMF₃, Ni²⁺, spin- phonon interaction, from a.p.r. spectrum 0–48154
KMgF₃;Ni²⁺, spin- phonon interaction, from a.p.r. spectrum 0–48154
KMgF₃;Ni²⁺, spin- phonon interaction and energy transfer for 3d³ ions, ⁴A₂-²E transition 0–41085
KMgF₃;N²⁺, single cryst., in excited state, absorp. spectra 0–41209
KMgF₃;N²⁺, spin- phonon interaction and energy transfer for 3d³ ions, ⁴A₂-²E transition 0–41085
KMgF₃;N²⁺, single cryst., in excited state, absorp. spectra 0–41209
KMgF₃;N²⁺, spin- phonon int

0–41270 KMnF₃, antiferromag., ¹⁹F, acoustic n.m.r. 0–41378 KMnF₃, antiferromag., n.m.r. freq. shift near Neel temp., hyperfine coupling 0–51411 KMnF₃, antiferromag., two magnon scatt. of light 0–66112 KMnF₃. Hartree-Fock molecular orbital calc., covalency parameters 0–43583

0-43583 KMnF₃, i.r. active mode below phase transition 0-56525 KMnF₃, paramagnetic, e.p.r. and n.m.r., line shapes and spin correlation, exchange narrowing 0-41332 KMnF₃, superexchange, theory 0-41058 K₂MnF₆, solid and in solns. of anhydrous HF, i.r. and Raman spectra, force const. 0-64373 KMnF₃ E dill antiferromagnetic true and three dimensional

const. U=043/3 K₂)Mn_pB_{1-p}F₂₄₀ dil. antiferromagnets, two- and three-dimensional Heisenberg, ordering 0=44694 K₂Mn(NH₂)_a lattice parameters determ., thermal degradation 0=55843 K₂MoO₄, crystal parameters 0=55842 K₄MoO₂(CN)₄.6H₂O, crystal struct., geometry of complex anion

K₄MoO₂(CN)₄.6H₂O, crystal struct., geometry of complex anion 0-55845. KN₃, crystal, melt growth technique 0-61732 KN₃, u.v. irrad., exchange coupled paramag. ions, e.s.r. obs. 0-72482 KNCO single crystals, vibrational spectrum at room temperature 0-69132 KNO₂-Ca(NO₃)₂, vitreous mixture, conductance temp. depend., 65-235°C 0-62288 KNO₂-Ca(NO₃), glass network struct determ, using transition metal ion

No₃-Carto₃-y, who in initial conductance temp. depend. $0.5233 \cdot C_{0} - 62288$ KNO₃-Ca(NO₃), glass, network struct, determ, using transition metal ion spectroscopic probes 0.-62676 KNO₃-KNO₂, mixed crystal, phase transition, comp. depend. 0.-40865 KNO₃, cond. at transitions rel. to 0 coordination 0.-40831 KNO₃, ferroelect, lattice dynamics model 0.-78732 KNO₃, ferroelectric modification, thermal expansion from lattice parameter vs. temperature curves 0.-53717 KNO₃, i.r. spectra during phase transition 0.-66016 KNO₃, in water-dioxane at 25° C, electrical conductance meas. 0.-68902 KNO₃, single crystal, rhythmic growth, $\alpha \rightarrow \beta$ transformation 0.-78403 KNO₃, in determination using Pellet tech. 0.-54198 KNO₃ in methanol dioxane at 25° C, electrical conductance meas. 0.-68903 KNO₃ in methanol dioxane at 25° C, electrical conductance meas. 0.-68903 KNO₃ in methanol dioxane at 25° C, electrical conductance meas. 0.-68903 KNO₃ in methanol dioxane at 25° C, electrical conductance meas. 0.-68903 KNO₃ in methanol dioxane at 25° C, electrical conductance meas. 0.-68903 KNO₃ in methanol dioxane at 25° C, electrical conductance meas. 0.-68903 KNO₃ in methanol dioxane at 25° C, electrical conductance meas.

0-68903
K,NaCrF₆, 3d electron density determ. 0-65117
KNaThF₁, cryst. struct. 0-68308
KNbO₃:KMgF₃ solid solution, results of dielectric study 0-75772
from KNbO₃-LiNbO₃-BaNb₂O₆ pseudosystem, tungsten bronze-type electro-optic cryst. growth 0-58644
KNbO₃-Sr(Ba)Nb₂O₆ system, phase equilib., dielectric and struct. props. 0-47489

0-4/467
KNbO₃, dielec. const. and cond. behaviour 0-40868
KNbO₃, optical props. 0-76006
KNiF₃, antiferromag., covalency and spin deviation, neutron diffr. meas. 0-56463

0-56463 KNiF3, antiferromagnetic, effective moment of Ni²+, covalency, spin deviations, neutron diffr. 0-44693 KNiF3, two-magnon Raman scatt. 0-44867 KNiF3, two-dimens. antiferromagnet, transitions and mag. correls. 0-44696 K2NiF4, two-dimensional antiferromagnet, phase transitions and mag. correlations 0-44695 KNi_xZn_{1-x}F3, heat capacity rel. to mag. ordering, $80\text{-}300^\circ\text{K}$ 0-40573 K20-Li₂O-Nb₂O₅, phase relationships, tungsten bronze field 0-61588

Potassium compounds continued

ASSUM compounds continued

K,O-SrO-SiO₂ system, interdiffusion 0–50623

KOAc-Ca(OAc)₂ glass, network struct. determ. using transition metal ion spectroscopic probes 0–62676

KOH aqueous solns, diffusion of H₂ and O₂ 0–64887

KOH aqueous solns, transport processes 0–39752

 KO_2PO_4 , ferroelec. transition region, polarization relax. and susceptibility 0-53940

0-53940
IOK, 0.402nO.50P₂O₃.Cr³⁺ e.p.r. spectra obs. 0-54156
IOK, 0.402nO.50P₂O₃.Mo³⁺ e.p.r. spectra obs. 0-54156
K₂OSCl₆, temp. and pressure variation of ³⁵Cl n.q.r. frequency 0-79424
KPF₆, n.m.r. of ¹⁹F₁, nuclear spin coupling constants, high speed rotation method 0-41377

K,OSC, lemp. and pressure variation of **CLin.qr. frequency 'O--/94.24 KPF₆, nmr. of ¹⁹F, nuclear spin coupling constants, high speed rotation method 0-41377 K,PdCl₆, pressure effects on vibrational modes 0-56086 K,PdCl₆, electric field gradient at ³⁵Cl sites, motional averaging by lattice vibrations, n.g.r. meas. 0-51418 KPrO₃, prep. and structure refinement, bond length 0-65247 K,PtCl₆, average frequency of rotary lattice mode 0-79424 K,PtCl₆, electric field gradient at ³⁵Cl sites, motional modes 0-56086 K,PtCl₆, electric field gradient at ³⁵Cl sites, motional averaging by lattice vibrations, n.g.r. meas. 0-51418 K,PtCl₆, electric field gradient at ³⁵Cl sites, motional averaging by lattice vibrations, n.g.r. meas. 0-51418 K,ReBr₆, crystal structure refinement, bond length 0-65247 K,ReCl₆, soft librational modes rel. to phase transitions 0-71789 K,ReCl₆, crystal structure refinement, bond length 0-65247 K,Ru(CN)₆,3H₂O, ferroelec. phase transition, water molecules dipole moments, n.m.r. 0-54169 K₄Ru(CN)₆,3H₂O, n.m.r. spectra, meas. from 6 to 14 kOe 0-41375 KSCN motion, stotope eff. of thermal diff. 0-64888 K,SO₄:Cu²⁺, e.p.r., 77K 0-41331 K,SO₄:Cu²⁺, e.p.r., 77K 0-41331 K,SO₄:Cu²⁺, e.p.r., -66149 K,SO₄-Zh₂SO₄ polycryst. mixtures, thermal expansion 0-65553 K,SO₄-Zh₂SO₄ polycryst. mixtures, thermal expansion o-65553 K,SO₄-Zh₂SO₄ polycryst. mixtures, thermal bleaching on paramagnetic centres 0-75189 K,SO₄, anisotropic elec. cond. 0-40825 K,SO₄, effect of optical and thermal bleaching on paramagnetic centres 0-75189 K,SO₄, deat contents, specific heats and latent heats of phase transformations 0-65548 (SSD₆, num.r. of ¹⁹F, nuclear spin coupling constants, high speed rotation method 0-41377 KSC(MO₄)₂, sryst. struct., synthesis, K-ray diffr. 0-78476 KSC(WO₄)₂, cryst. struct., synthesis, K-ray diffr. 0-78476

method 0-41377

KSc(MoQ₄)₇, synthesis, cryst. struct., X-ray diffr. 0-78476

KSc(Wo₄)₂, cryst. struct., synthesis, X-ray diffr. 0-78476

K₂SeO₄, y-irrad., e.s.r., phase changes and paramag. species identification 0-66138

K₂SnC₄, order-disorder transition 0-78705

K₂Sr₄Nb₁₀O₃₀, polycrystalline, with K-W bronze structure, test of ferroelectric and physical properties 0-75800

KSr₄TiNb₂O₃₀, ungsten-bronze type struct. and dielec. props. 0-53924

K(Ta,Nb)O₃, mixed cryst., soft phonon modes 0-65518

KTa₂Nb_{1-x}O₃, morphic electro-optic effects, dielectric constant, polarization 0-76030

KTaO₂-Fe, e.s.r. spectra rel. to cubic or tetragonal field 0-59452

KTa,Nb_{1-x}O₃ morphic electro-optic effects, dielectric constant, polarization 0-76030
KTaO₃:Fe, e.sr. spectra rel. to cubic or tetragonal field 0-59452
KTaO₃ PbTiO₃ system, cryst. struct. and dielec. props. 0-56360
KTaO₃, anomalous acoustic dispersion with soft optic phonons 0-43873
KTaO₃, coupled modes in phonon spectra 0-71828
KTaO₃ single crystal, dielec. const., loss tangent and conductivity, and optical absorpt. 0-59250
KTaO₃,NaTaO mixed crystal, dielec. const., loss tangent and conductivity, and optical absorpt. 0-59250
K₂MO₄, crystal parameters 0-55842
KY(MoO₄):Nd⁴⁺, absoption and luminescence spectra, lifetime of excited state 0-62715
KZnPO₄ crystal, prep., patent 0-43595
K₂TF₇, n.m.r. ¹⁹F, spin lattice relaxation 0-48167
K[B₂O₆(OH₃|2]t₁O₅ single cryst., hydrogen position determ. by neutron diffraction method 0-47187
K₄|Ni₃(CN₈), lattice disorder and polytypes 0-58820
K₂|PdCl₄|, absorpt. spectra, low temp. 0-79310
K₂|RuCl₃NO₁|, i.r. spectra, low temp. 0-79310
K₂|RuCl₃NO₁|, i.r. spectra, vibrs. obs. 0-79309
KcN, cubic, orientational disorder 0-78460
Ki:Eu formation and luminescence of Eu²⁺ centers 0-65334
kZnF₃·Mn²⁺, antiferromag, ENDOR, unpaired spin density 0-45041
LiBr-KBr fused binary systems, ionic transport and self-diffusion 0-39826
LiCl-KCl eutectic, equilib. between V, Mo and Ta in dilute solns.

DIST-KBT 108 of one of the control o

potassium bromide

aqueous solution, ultrasonic absorption anomaly 0-74748
Brillouin spectra, sound velocity, elastic onstants of cubic crystal 0-51329

0–51329
colour centre, colloidal, e.m. wave absorpt. 0–65332
colour centre generation, heating, impurity effects 0–40183
colour centre prod. rel. to intersitial stabilization 0–75181
colour centres, F' type and ionized F aggregate, 77K 0–75180
comparison of colour center formation 0–47268
crystal, dispersion curves, deformable shell model cale. 0–40524
defects created by low energy X-rays, volume change 0–40121
dielectric properties, 1.f., single crystals and pressed discs 0–68896
diffusion, thermal, isotope eff. in mothen salt 0–64888
diffusion and mobility of 10 Ag 0–61993
elastic constant and Debye temp., temp. depend. 0–75222
elastic distortions and interactions of point defects and elastic distortions
0–58782

0–38/82 electronic behaviour, exciton and polaron roles 0–75506
F centre formation, role of K shell ionization, 78K 0–47271
F centre growth curves, nonuniform electron irrad. effect, and electron penetration, single crystal 0–53552
F centre prod. by far u.v. irrad. 0–50614
F-centre hyperfine interactions, ENDOR, uniaxial stress effects 0–78566
H' centre formation and structure 0–43686
holographic information storage in U-centres 0–65333

Potassium compounds continued potassium bromide continued

i.r. absorption band parameters with NO_2 -, NO_3 - impurity ions, 100-300K 0-62665

0-62665
Interstitial stabilization, rel. to colour centre prod. 0-75181
Jahn-Teller effect, influence on U-centre local mode absorption 0-58828
phosphorescence, Eu²+ activated, and capture centre determ. 0-66110
piezo-optical consts, temp. depend. 0-76005
shock compressed, 150-350 Kbar 0-47993
solution, critical supersaturation, ultracentrifuge meas. rel. to crystal growth 0-50439
Te epitaxial film 0-43553
thermal emissivity, far i.r., 80-600 K, meas. rel. to vibr. modes 0-76106
thermally stimulated conductivity, 10-300K, γ- and neutron irrad. crystal 0-47863

thermally stimulated conductivity, 10-300K, \$p\$- and neutron irrad. crystal 0—47863 thermopower meas. 0—59276 U band pressure shifts 0—44844 U-centre local mode absorption, influence of Jahn-Teller effect 0—58828 i.r. vibrational absorpt. of Hp- and Pp- centres, near and far i.r. 0—44841 KBr:BO₂-, i.r. absorpt. spectra, doublet struct. 0—44845 KBr:CrO₂²-, i.r. absorpt. spectra, 120-800 K 0—41208 KBr:Eu radioluminescence temp. depend. 0—56603 KBr:In, radiative recombination, thermoluminescence 0—62714 KBr:KCl, Brillouin spectra, sound velocity, elastic constants of cubic crystal 0—51329 KBr:KSH(:KSeH), e.s.r. 0—44989 KBr:Li²-, far i.r. absorpt. temp. depend. rel. to lattice resonant modes 0—44843 KBr:Mg, optical absorpt. temp. depend. rel. to lattice resonant modes 0—44846 KBr:(Na*,Li*), X-irrad., interstitial centres interactions 0—53531 KBr:Sm²-, lattice dynamics, vibronic spectra obs. 0—78731 KBr:Tl, luminescence and abs. spectra, effect of external electric field 0—56550 KBr:Tl, stimulated emission, M-centres 0—51342 KBr-KCl, diffusion pair, misfit dislocations 0—75164 KBr-Tl, stimulated emission, M-centres 0—51342 KBr-KCl, diffusion pair, misfit dislocations 0—75164 KBr-Tl, quick-response energy transfer, optical flash 0—66094 KBr-Tl, quick-response energy transfer, optical flash 0—66094 KBr-Tl, quick-response energy transfer, photoscintillations 0—66095 NO₂-, NO₃- impurity ions, temp. effect on i.r. absorption band parameters 0—62665 SO₄²- impurity centers studied from vibrational absorption spectra

 SO_4^{2-} impurity centers studied from vibrational absorption spectra 0-56549

potassium chloride

 γ -irradiated, dose rel. to dislocation mobility, and absorpt. spectra 0-43675

bombardment by 40 keV ions, mass analysis of secondary ions 0-62478 Brillouin spectra, sound velocity, elastic onstants of cubic crystal 0-51329

colloid centres and elec. props. of additively coloured crystals 0-75182 colloidal centre dimens. obs., absorpt, spectra 0-48072

colloid centres and elec. props. of additively coloured crystals 0-/5182 colloidal centre dimens. obs., absorpt. spectra 0-48072 colour centre, colloidal, e.m. wave absorpt. 0-65332 colour centre, quenched in, photolum, optical absorpt. 0-47281 colour centres, F' type and ionized F-aggregate, 77K 0-75180 colour centres, diffusion, applic. of electrolytic coloration kinetics 0-47270

0-47270

creep and time to rupture of crystal, ambient medium depend. 0-40332 crystal growth from Pb- and Sn-containing aqueous solns., additives incorporation 0-58639

bebye. Waller factors 0-53692

defects created by low energy X-rays, volume change 0-40121

deformation luminescence of photochemically coloured crystals, KCl and KCl:Cu, mechanism 0-41292

dielectric loss, microwave propag., crystal chemistry 0-53919

dielectric properties, I.T., single crystals and pressed discs 0-68896

dielectric relaxation of sample containing Ba²⁺, Pb²⁺, Sr²⁺ and Ca²⁺ impurities 0-44343

dielectric relaxation of sample containing 8a-1, Po-1, Sr-1 and Ca-1 impurities 0—44343 diffusion, thermal, isotope eff. in molten salt 0—64888 diffusion of Trl+ in single and bicryst. 0—50624 dislocation density rel. to anomalous X-ray transmission 0—61964 dislocations in cryst. grown from melt with [110] seen orientation, obs. 0 - 40166

elastic constants and Debye temp. of single crystal, 300-80 K 0-65354 electron-trapping centers, low-temperature 0-55907 epitaxial growth on mica 0-65069 F centre formation, role of K shell ionization, 78K 0-47272 F centre growth, plastic deformation, thermoluminescence 0-50613 F centre growth and thermoluminescence in X-tirrad, additively colonization, the contract of the contraction of th

F centre growth, plastic deformation, thermoluminescence 0-50613

F centre growth and thermoluminescence in X-irrad., additively coloured crystals 0-61979

F centre growth curves, nonuniform electron irrad. effect, and electron penetration, single crystal 0-53552

F centre prod, by far u.v.irrad. 0-50614

F centres growth, effect of heat treatment and background divalent cation impurity 0-43685

F centres rel. to conductivity and rectification 0-43687

F-centre, photoconductivity and elec. conductivity during photochemical conversion 0-75179

F-centre hyperfine interactions, ENDOR, uniaxial stress effects 0-78566
fracture, mechanism and time-depend. rel. to stress rate, obs. 0-40370

H' centre formation and structure 0-43686

ir. absorption band parameters with NO₂-, NO₃- impurity ions, 100-300K
0-62665
in-electron secondary emission coefficients and the incidence angle of slow

0-62665 ion-electron secondary emission coefficients and the incidence angle of slow inert-gas ions 0-56422 ion-electron secondary contrib. 0-75782 luminescence and absorption features of alkali halide crystals containing mixed impurities 0-56548 luminescence due to plastic deform. and light irrad, p-irrad, cryst. 0-76195

M centre, mechanism of triplet-singlet transition 0-53551
M centre formation and destruction, statistical analysis 0-40186
M centres, study of triplet state 0-53550
M-centers, reorientation 0-47275

Mossbauer effect of Sn impurity atoms 0–54077
optical material, crystals, mixed with NaCl, i.r. optics 0–72345
paraelectric resonance spectra of Li⁺ impurities, orientation depend.
0–40836

phosphorescence, Eu²⁺ activated, and capture centre determ. 0-66110 photoconductivity, a.c. relaxation, of coloured crystal 0-62462

Potassium compounds continued potassium chloride continued photothermal destruction of F centres in pure and Ag⁺, Sr²⁺ doped crystals 0–43688 piezo-optical consts. temp. depend. 0–76005 plastic deformation under u.s. wave exposure 0–62042 porous layers, secondary electron emission 0–59298 positron annihilation, defects role 0–50957 positron annihilation time spectra in solid and liq., 295-1223 K 0–47616 positron lifetime, trapped in F-centres 0–75457 refractive index of soln., interferometer calibration applic. 0–39790 SCF calc. on molec. props. 0–58180 screw dislocations in whiskers and thin rods, X-ray intensity meas. 0–61965 shock compressed, 150-350 Kbar 0–47993

shock compressed, 150-350 Kbar 0–47993 slip, thermally activated, 77-560 K, anisotropy 0–78642 surface struct., (100), LEED obs. 0–68219

sylvite, elastic constants meas. using Schaefer-Bergmann method 0-50637

0–50637 Te epitaxial film 0–43553 thermal conductivity of γ -irrad, crystals, 0.4-4 K, defect model 0–47560 thermal emissivity, far i.r., 80-600 K, meas, rel. to vibr. modes 0–76106 thermal expansion, and law of corresponding states 0–47549 thermoelectric power, with reversible electrodes 0–66195 U-centers, local oscillations 0–68371

u.v. absorpt. rel. to colour centres, X-irrad. crysts., 200-1700 m_µ 0-41211

 V_3 band formation under electron irrad., saturation at room temp. 0-47278

vacancies, single and pairs, migration barriers calc. 0-40135 whiskers, colour center accumulation, effect of Sr impurities 0-55906 X-irrad, additively coloured, F centre growth and thermoluminescence 0-61979

0–61979
X-ray reflection spectrum, long-wavelength, analysis by Kramers-Kronig method 0–62699
Zeeman anisotropy fluorescence, third-nearest-neighbour, Sm⁺-K⁺ vacancy pair 0–56623
H trapped in single crystals at 77 K, E.S.R. obs. 0–76216
KCL:Tl+ configuration coordinates study from Raman scattering 0–41235

KCI: 11° configuration coordinates study from Kanian scattering 0-41235 KCI: Ag, X-irrad, V_k centres, Raman spectra, 77K 0-40185 KCI: Ag⁻, emission and absorption spectra 0-44842 KCI: Ba⁺⁺, Pb⁺⁺, Sr²⁺, Ca²⁺, impurity-vacancy complexes, reorientation 0-44343 KCI: Ca²⁺ dielectric measurements temp. range 50°→−179°C, effects created by impurities 0-79033 KCI: Ce absorption and luminescence spectra 0-56551 KCI: Cu additively coloured, colloidal absorpt. band 0-72361 KCI: Cu, additively coloured, colloidal absorpt. band 0-72361 KCI: Cu thermoluminescent X-ray dosimeter 0-73702 KCI: Eu²⁺, single crystals, multiphoton excitation of luminescence and photoconductivity by ruby- and neodymium laser light 0-56600 KCI: F, ir. absorption after gamma irrad, internal vibration 0-79311 KCI: In: Ag, radiative recombination thermoluminescence 0-62714 KCI: KSH(:KSeH), e.sr. 0-44889 KCI: Li⁺, paraelectric resonance, internal strains effect 0-44355 KCI: Li⁺, paraelectric resonance, internal strains effect 0-44355 KCI: Li⁺, stress- induced quadrupole splittings of ⁷Li n.m.r. line 1.3-4.2 K 0-51408

KCl:Li⁺, Stress-induced qualified 0–51408
CCl:Li⁺, V₁ centres, e.p.r. and absorpt. obs. 0–76218
KCl:LiCl, microwave spectroscopy of Li⁺ 0–72407
KCl:Mn²⁺, e.p.r., fine struct., temp. depend. 0–76219
KCl:Mn²⁺ soln.-grown, aq. inclusions, e.p.r. obs. 0–48146
KCl:NO₂-, luminescence spectra, rotational fine struct., 1.9-4.2K

KCl:OH-, electric dipole system, ferroelectric state, quantum theory 0-790470-7904 KCI:OH

KCI:OH-, microwave resonant absorpt. spectra from 8 to 40 GHz 0--79312

KCl:Pd, optical and e.s.r. absorpt. and elec. conductivity 0-59403 KCl:Sm²⁺ fluoresc., nonlinear mag. field depend. and polarization

KCI:Pd, optical and e.s.r. absorpt. and elec. conductivity 0—5940. KCI:Sm²⁺ fluoresc., nonlinear mag. field depend. and polarization 0—76168 KCI:Sr²⁺, dielectric absorpt. intensity, conc. depend. 0—51104 KCI:Tl, cathodoluminesc. yield 0—41284 KCI:Tl, colour centres, radiative creation, Coulomb interaction 0—40184 KCI:Tl irradiated cryst., thermoluminesc. by simultaneous intensity and spectral distr. meas., between 30 and 400°C 0—48129 KCI:Tl(Br), lattice reson. modes, sp. ht. meas. 0—75374 KCI:Tl(IX, Tirrad, rel. to absropt rel. to colour centres, 200-1700 mμ 0—41211 KCI:Tl(Pb⁺), additive coloration, dopant ion reduction 0—58830 KCI-In, KCI-Tl phosphors, long and short term components of X-ray luminescence 0—54128 KCI-KBr solid solns., Debye temp. 0—65546 KCI-KBr solid solns., Debye temp. 0—65546 KCI-NaCI solid-solution alloys, creep, 600°C 0—65404 KCI, gBr_x, Raman spectrum and assignments 0—72362 NO_{2-x}, NO₃- impurity ions, temp. effect on i.r. absorption band parameters 0—62665 Pb²⁺ centre, tetragonal, and trigonal R centre 0—51343 PbCl₃ + KCI molten mixtures, specific, electrical conductance, 500 to 800°C, PbCl₂ conc. depend. 0—39834 tential energy, gaseous molecules see Molecules/intermolecular mechanics

Potential energy, gaseous molecules see Molecules/intermolecular mechanics Potential energy, single molecules see Molecules/internal mechanics; Mole cules/vibration

Potentiometers see Electrical measurement

Powder diffraction cameras see X-ray crystallography/apparatus

Powder metallurgy see Metallurgy; Sintering

Powders

see also Granular structure; Particle size; Sintering; Surface measure

ment aggregates, strength characterization 0–58910 β-alumina, densification and microstruct. 0–53650 antiferromagnetic, polycrystalline, magnetoelectric effect 0–44675 calcite, X-ray refl. integrated intensity anomaly 0–58721 carbide, characterization for nucl. applic. 0–58994 for cermet, UN/W(Mo), fabrication, particle size effects 0–40470 cohesion, temp. and compression effects 0–50798 cold compaction 0–75318

Powders continued

crystalline, depolarization ratios in Raman spectra 0-72383 cubic, integrated X-ray intensities, correction for preferred orientiation 0 61768

dye, second harmonic of Nd glass laser 0-65978 ferromagnetic, use of magnetic susceptibility to determ. grain size 0-56452

flow in pneumatic conveyor, particle velocity and mass flow meas: 0-43482

0-43482
glass, emission spectra, diffuse reflectance effects 0-66098
grain size distrib., comparison of Hg porosimetry, sedimentation and microscopy 0-56047
grain size distrib. by X-ray scatt. 0-75035
harmonic generation, second, optical 0-44749
ionic, plastic flow eff. on sintering 0-75297
metal, combustion, particle size rel. to burning time, statistical analysis
0-41424

0-41424 metal, sintering, compaction kinetics 0-65475 metallurgy homogenisation time estimation 0-50756 metallurgy products, formation and mech, props. 0-65459 mixing presintering, quantitative analysis, X-ray exam. 0-50797 nonoriented maser-amplifier material 0-42242 oxide, crystallite size, X-ray line broadening meas. 0-40909 packing structure of a fine powder and bulkiness, experiments 0-55678 particle statistics 0-50799 rermalloy, insulating film, fluorination method, elec. and mag. props. 0-53430

0-53430
plane deformation, general yield conditions 0-58995
porosity, minimum, of assembles of identical spheres 0-47467
prealloyed, extruded, Ni-based, 713C and NASA TAZ-8A, heat treatment, strength 0-47378
preparation of powders exhibiting marked cleavage for counter diffractometer exam. 0-50494
quartz, extinction of Debye-Scherrer lines, crystal domain radius determ. 0-61904

tometer exam. 0—50494 quartz, extinction of Debye-Scherrer lines, crystal domain radius determ. 0—61904 reactor fuels, X-ray analysis 0—59515 rock, proton bombardment-induced target temperatures and thermal accommodation coefficients meas, by I.r. pyrometry 0—50800 spectrochemical analysis, flame spectroscopy, scintillation recording mechanism 0—41454 vibrocompaction, energy parameter 0—58996 wetting, rel. to geometry 0—74872 white oxide, colour centre formation rel. to spacecraft thermal control coatings 0—47267 Al, integrated X-ray intensities, correction for preferred orientation 0—61768 Al,0g, alumina, size and shape distrib. 0—58997 Al,0g, alumina, size and shape distrib. 0—58997 Al,0g, ligh density, sintering 0—58998 Al,0g particles, sintered and fused, strain obs. 0—58882 As,5x (Realgar) powder, u.v. irradiated, an I=3/2 e.s.r. center 0—59446 BR, thermoluminesc. 0—59440 BaTiO3, i.r. absorpt. spectra, particle size and shape effect 0—48061 Be, hot-pressing, electron metallography and oxygen impurities role 0—65445 CaF₂, strace thermoluminesc, yield, crushing effect 0—66113 CeSn₃, structure and mag. props., 293-1.6°K Mossbauer and susceptibility meas. 0—44477 Cr.Qo, pure and Al₂Q₃ doped, e.p.r. absorpt. spectra 0—76214 Cu, compaction, sintering, prep. for high conductivity use 0—65476 y Fe₂Q₃; in nonmagnetic matrix, alternating and rotational hysteresis losses 0—72174 arFe₂Q₃ temp. depend. of characts. props. 0—75320 Ge adsorption of water vapour obs. 0—53446 He II, liquid, isothermal flow through fine grained powder 0—39865 HfB₃, hot-pressed, fabrication and characterization, SiC and C effects 0—50801 HfTiO₄, prep. and characterization 0—5899 KCl pressed discs, 1f. dielectric properties 0—68896

HfB₃, hot-pressed, fabrication and characterization, SiC and C effects 0–50801

HfTiO₄, prep, and characterization 0–58999

KCl pressed discs, 1.f. dielectric properties 0–68896

LiF, surface thermoluminesc, yield, crushing effect 0–66113

LiF TLD-700, TLD-100, TLD-600 powders, thermoluminescent glow curves, reactor neutron and gamma ray irrad. 0–44932

MgO, crystallite size, X-ray line broadening meas. 0–40090

Mn-Zn ferrite heat treatment effect on magnetic permeability 0–62549

Mo-Cu mixture, explosive heating 0–75302

Mo, hot pressing, 1400-1600°C 0–65451

NdSn₃, structure and mag. props., 293-1.6°K, Mossbauer and susceptibility meas. 0–44477

Ni-Fe-Cu-Mo, mag. alloy, high permeability, sintering process 0–62089

Ni, charge density absolute meas., X-ray diffr. 0–61900

PrSn₃, structure and mag. props., 293-1.6°K, Mossbauer and susceptibility meas. 0–44477

STF1O₃, i.r. absorpt. spectra, particle size and shape effect 0–48061

Tm₂O₃, cold pressed, variables in fabrication 0–58968

UN/W(Mo) mixed, particle size effect on cermet fabrication 0–40470

UN, synthesis and characterization 0–56951

VF₂, magnetic short-range order 0–44481

W-Mo-Ag based, pseudo-alloy production for elec. contact making 0–68544

W, vibration-condensation kinetics 0–47470

W and allyus bot pressing process 0–78680

W- 0-0.344
W, vibration-condensation kinetics 0-47470
W and alloys, hot pressing process 0-78680
WC, formation from W powder, microstruct. obs. 0-65478
ZnO, chemisorption of hydrogen, conductivity, electrical, 30 to 300°C 0-40708

ZnO, photodamage, e.s.r. 0-66143 ZnS grains for TV screen, surface treatment to improve uniform coating 0-54845

 ZrB_2 , hot-pressed, fabrication and characterization, SiC and C effects 0-50801

Praseodymium

conductivity, h.p. effect 0-65633 crystal fields, effect on mag. props. 0-68998 diffusion of Zn, diffusivities in b.c.c. and double h.c.p. phase 0-68382 f.c.c., energy bands, and density of states, mag. susceptibility and Fermi surface 0-4397

Magnetic props. of single cryst. 0-68998 magnetic struct., neutron scatt., obs. 0-75885

Praseodymium continued

specific heat, nucl., due to hyperfine interactions 0–43910
Pr IV 4F(8S)5d, energy level calc. 0–42972
Pr³*, crystal field levels in paramagnetic metallic PrBi 0–44730
Pr³*, energy levels in Pr(NO₃), 6H₂O 0–62673
Pr³* in acetate praseodymium tetrahydrate, spectrum obs., interaction with crystal 0–62746
Pr³* in AlLaO₃, Zeeman decomp. of energy levels 0–51297
Pr³* in on pair in aqueous solution, electronic-transitions observation 0–64221

Pr³+ spectrum, hypersensitive transitions 0–77833 PrAlO₃, reciprocal mag. susceptibility, temp. depend., 1.7-4.2K 0–41057

Praseodymium compounds

PrAIO3, reciprocal mag. susceptibility, temp. depend., 1.74.2K 0-41057 aseodymium compounds alloy, conductivity, h.p. effect 0-65633 crystal fields, by neutron spectroscopy 0-69059 Pr-Gd alloy, mag. and crystallographic props., 2-500°K 0-44484 Pr. complexes, Pr³ ½ Gilketonates, spectral intensities 0-39399 Pr III complexes, hypersensitivity of spectral bands 0-77833 PrAIO3, phase transform, X-ray obs. 0-59032 PrAIO3, phase transform, X-ray diffr. 0-53662 PrBi, crystal field levels of Pr³ , neutron spectroscopy 0-44730 PrCl3, aq., nonlinear optical absorpt. coeff. at 1.064µ obs. with YAL garnet:Nd laser 0-41099 PrCo., PrCu3 galoys, mag., props. 0-75936 PrF3, far-ir. absorpt., 1f. lines 0-51308 Pr,Fe17, Mossbauer effect, mag., props., temp. depend. 0-44796 Pr(III) complexes, interelectronic repulsion, spin-orbit interaction and bonding 0-43132 Pr₂(MoO₄), N-modification obs. 0-55858 Pr(NO₃), 6H₂O, optical absorption and energy levels of Pr³+ 0-62673 Pr₃, Nd₄AlO₃, system, dielec. const. anomalies, 300-5K 0-51106 PrO₂, structure and mag. props. 0-56434 PrPt₃, nuclear adiabatic demagnetization, from 60 to 3 mdeg K 0-48653 PrSn₃ powder, structure and mag. props. 293-1.6°K, Mossbauer and susceptibility meas. 0-44477 PrTJ₃, nuclear adiabatic demagnetization, from 60 to 3 mdeg K 0-48653 PrSn₃ powder, structure and mag. props. 293-1.6°K, Mossbauer and susceptibility meas. 0-44477 PrTJ₃, nuclear adiabatic demagnetization, from 60 to 3 mdeg K 0-48653 Pr₃, Wo₆Cl₃, cryst struct. 0-4096 Pr₂Wo₆Cl₃, cryst struct. 0-4096 Pr₃Wo₆Cl₃, cryst struct. 0-4096

Pr; WO₆Cl₃, crystal, hydrothermal synthesis, struct. U=14985

Precipitation

see also Atmosphere/precipitation

alkali halide crystal, and solubility of metal impurities, dielec., Mossbauer and optical meas. 0=75298

alloy, cluster theory 0=71753

alloy, diffusional interaction of edge dislocations with new phase precipitates 0=62101

alloys, bond energy calc., impurities and grain boundaries during form. of equilib. segregations 0=78536

in alloys, solution kinetics by torque magnetometry 0=43825

ceramics, processes and effects and electronic props. 0=50795

cluster theory of solns. 0=71753

coalescence along a line defect, diffusion kinetics 0=65482

diffusion-limited, math. approxs. comparison and crit. evaluations

diffusion-limited, math. approxs. comparison and crit. evaluations 0-78689and dispersion hardening, Mg base alloys, transmission microscopy 0-50784

ferrite, coprecip. of Li, prep. process 0-65495 in ferromagnetic matrix, of nonferromag, inclusions effect on mag. ageing 0-69014

gases, rare, in solids during annealing following ion bombardment 0-61985

0-61985 intermetallic phases out of welded joints in AMg6 alloy, electrolytic method 0-43827 ionic cryst., precip. and dissolution pot., zeta pot. 0-59492 martensite, nucleation as coherency-loss problem 0-75317 nuclei growth and interactions, diffusion controlled rate 0-50814 particle kinetics under Ostwald ripening conditions 0-59012 polyvinyl alcohol, from aqueous soln., by non-solvent addition method 0-53293

0-53293 refractory, high-alumina, bauxite-based-phase development and cryst. growth 0-59011 segregation, vacancy flux induced, to grain boundaries during cooling, model 0-47454 solid solns., X-ray scatt., anomalous diffr. effects 0-65215 solid solns., cluster theory 0-71753 solid solution, nucleation stimulated by non-equilibrium electrons 0-78801 solution, pushed to stimulated by non-equilibrium electrons o-78801 solution, pushed to stimulated by non-equilibrium electrons

0–78801 solid solution, nucleation stimulated by non-equilibrium electrons 0–78800 steel, Mo-bearing, carbide formation during diffusional $p\rightarrow\alpha$ transform. 0–47480 steel, Nb-treated, carbonitride precipitates obs. 0–40080 steel, Ni-Cr-Ti austenite, reageing rate, reversion 0–53632 steel, SAE 4340, tempered martensite embrittlement and fracture toughness 0–43780 steel, austenite grain growth kinetics 0–58726 steel, austenite grain growth on working, void effects 0–50816 steel, austenitic, and recrystallization 0–58956 steel, austenitic stainless, ferrite, sigma phase and carbides precip. 0–40488 steel, cementite phase particles, diffusional coalescence, kinetics 0–50817

0–40488
steel, cementite phase particles, diffusional coalescence, kinetics 0–50817
steel, hypercutectic, bainite structure formation mechanism 0–47479
steel, microsegregation, chem. and metallographic study 0–58977
steel, stainless, ferrite sigma phase and carbides precip. 0–40489
steel-Ni-Cr-Ti, austenitic, age hardening, reversion 0–53631
steels, stainless, with Co and Mo, hardening by precipitation 0–53646
Ticonal alloys, decomposition, final stages analysis 0–50823
from turbulent stream, assumptions of theory 0–46961
vacancy-interstitial impurity interaction effects 0–62125
Zircaloy, low hydrogen content, tetragonal hydride obs. 0–68562
AgCl, growth kinetics 0–55778
Al-Ag solid solutions, second stage decomposition, diffuse X-ray scatt. 0–68564
Al-(20 wt. %)Ag alloy, cold working effect on subsequent precip.

0-68564
Al-(20 wt. %)Ag alloy, cold working effect on subsequent precip.
0-47476
Al-Cu-Cd alloy, differential calorimetry 0-75326
Al-Cu-In, quenched alloy, differential calorimetry 0-75327
Al-Cu, dil. alloy, vacancy jump freqs. ratio around and away from Cu impurities 0-75129
Al-Cu alloy, grain boundary, interfacial energies, growth kinetics 0-58950

Precipitation continued

Al-Cu alloy, kinetics, vacancy and dislocation migration 0-43821 Al-(0.42wt.96)Fe, supersaturated and deformer, annealing, micromechanisms 0-475299

Al-Fe alloys, supersaturated, splat cooled 0-68528

Al-Fe solid soln., supersaturated, decomp. during annealing 0-40437 Al-Ge alloys, Ge nucleation, obs. by modified small-angle X-ray camera

Al-Fe alloys, supersaturated, splat cooled 0–68528
Al-Fe solid soln, supersaturated, decomp. during annealing 0–40437
Al-Ge alloys, Ge nucleation, obs. by modified small-angle X-ray camera 0–75044
Al-Mn alloys, supersaturated, splat cooled 0–68528
Al-Si, alloys, precip. nucleation rel. to excess vacancies 0–68551
Al-Ti alloy, showly, precipitate struct, and morphology 0–75137
Al-Zn-Mg alloys, precipitate struct, and morphology 0–75137
Al-Zn-Mg alloys, precipitate struct, and morphology 0–75137
Al-Zn-Mg alloy, two-stage deposition effects 0–685484
Al-Zn alloy, rhombohedral distortion of transition precipitates 0–58972
Al-Ge at-196°C50779 0–50779
Al-Zn-Mg alloy, two-stage deposition effects 0—65484
Al-Zn segregation to vacancy sinks 0–71608
Al alloys, nucleation and growth, heat treatment effects 0—50761
7075 Al rolled plate, precipitate distribs. rel. to stress corrosion cracking sensitivity 0–43670
Au-Vi, Au-Co alloys, electrodeposits, heat treated, microstructural and phase changes, X-ray exam. 0–65485
Au-Ni alloys, C contaminated, precipitation phenomena 0–62104
Au-Ni films contaminated with carbon, precip. phenomena 0–56039
Au-Ni films contaminated with carbon, precip. phenomena 0–56030
Au-Ni solid soln., complexes form. influence 0–71792
Be-Fe alloys, during quenching and ageing 0–68508
CaSO₄ γ-γ transition due to anhydrous precipitation 0–78694
Co-Nb alloy, struct. changes in decomp., electron microscope obs. 0–71797
Co-(9/at.96/Ti alloy, morphology, electron microscopy 0–53660
Co-27Cr-7Mo alloys, C-free, hardening 0–53642
(20wt.%)Cr-(25wt.%)Ni-(1wt.%)Nb austenitic steel, of NbC, stacking fault contrib. 0–58955
CrM.oh, on low alloy creep-resisting steel 0–58959
CrN. in low alloy creep-resisting steel 0–58959
CrN. in low alloy creep-resisting steel 0–58959
CrN. in low alloy creep-resisting steel 0–58959
CrV. Ti-Fa alloy, Mossbauer spectra, interpretation 0–51279
Cu-Ti-Fa alloy, high temps softening, electron microscopy 0–47444
Cu-Ti-Fa alloy, high temps softening, electron microscopy 0–47444
Cu-Ti-Fa all

tion 0–43779

Fe-Ni-Al, influence of elastic stress 0–71776

Fe-Ni-Co-Mo alloy, preprecip, and reversion 0–59023

Fe-Ni-Mo(Ti)(-Co) alloys with ageing martensite, recovery 0–50770

Fe-Si-Ti(Nb), effect on age hardening 0–65428

Fe alloys, microsegregation 0–59021

Ge:As solid solution, anomalous X-ray transmission 0–75333

Ge:O, solid solution, defect structure, anomalous X-ray transmission 0–75142

Ge-As solid solution, kinetics 0–53648

Ge:O, solid solution, defect structure, anomalous X-ray transmission 0-75142 Ge-As solid solution, kinetics 0-53648 Mg-(1.8wt.%)Al alloy, and pre-precip.71804 0-71804 Mg-Al alloys, precipitate struct. and morphology 0-75137 p-MnCu alloys, ageing, low angle neutron diffr. 0-40449 Mo-Ti-C, carbide on dislocations, creep at 1800°F 0-40331 NaCl:MnCl, solid solution, kinetics, dislocation nuclei 0-75314 NaCl:MnCl, solid solution, e.p.r. 0-76223 Ni-Al alloy, ageing, number density, 800°C, dark field electron microscopy 0-53635 Ni-Cr-Al alloy, hyperfine, electron microscope obs. 0-62090 Ni-Galloy, loss of coherency of p' particles 0-71777 x10NiCrWTi36.15, high temp, and stress hardened 0-40490 Ni₁Mo alloys, during isothermal annealing after quenching 0-65269 NiO film, precipitates with defect struct. 0-71482 O₂, in Si, effect on surface preparation 0-65729 SiCr- solid solution, kinetics, diffusion temp, depend., e.p.r. 0-40454 Si, heavily doped, homogeneity disturbance 0-65497 Si, of Li 0-53563 SiO₂, rosettes of crystolbalite 0-61903

Si, of Li 0–53563
SiO₃, rosettes of crystolbalite 0–61903
Ta-D solid solution, decomposition, neutron diffr., 225K 0–50830
Ti-C system, precip. bands below stoichiometry 0–59034
Ti alloy, metastable β-phase decomposition, ageing, 480 °C, electron microscopy 0–53664
β-Ti alloys, of carbides 0–43828
TiO₂-SnO₃, tetragonal system, spinodal decomposition in phase separation 0–59035

wt.%)Mo alloys, continuous and discontinuous precip. reactions 0-68561

0-68561
U alloy, alpha crystallization, B impurity depend. 0-40494
U dil. alloy, isothermal growth of secondary-phase particles 0-59040
UO₃, Fe ion bombarded, effect on Xe migration 0-43697
V-H system, low temp. diffuse X-ray scatt. 0-59044
V-Ti alloy, cubic phase, TiO, electron microscopy 0-65500
V, cubic phase, VO, electron microscopy 0-65500
Zr-{1 wt/%)V alloys, martensite phase age-hardening 0-68517
Zr alloys, stress orientation of hydride 0-62139

see also Atmospheric pressure and density; High pressure phenomena and effects; Radiation pressure; Vapour pressure alkali halide crystals, hydrostatic pressure effects on absorption and luminescence of emission centers 0–56606 axial and radial distribution in current sheet structure propagating in dynamic z pinch of Ar 0–39582

Pressure continued

axial rarefaction wave in radially expanding tube of pressurized gas $0\!-\!74645$

boundary layer induced on flat plate in unsteady hypersonic flight 0-53249

buckling, cylindrical shell reinforced by spiral stiffeners 0-48812 in compound cylinders, max., for specified plastic deform. 0-52045 cone-cylinder-flare configs., supersonics speeds, distrib. data, report 0 - 78205

0–78205
discharge, critical, in annular two-phase flow 0–64963
distributions, comparison of brass and nylon pipelines conveying polystyrene powder 0–64966
drop, spherical caps motion in low Reynolds number tube flow 0–67872
drop, velocity field in entrance region for laminar flow 0–39490
drop in single phase water, heat transfer characteristics 0–39772
flow in suction duct, straight with porous walls 0–64631
fluctuating, induced by three-dimensional protuberances 0–53245
fluctuation in boundary layer, influence of polymer additives, exptl. investigation 0–61456
fluctuations, supersonic turbulence-induced 0–53261

tigation 0-61456
fluctuations, supersonic turbulence-induced 0-53261
fluctuations, turbulent boundary-layer, over rough walls 0-53297
fluid mixtures, in generalized Percus-Yevick approximation 0-43217
gradients, prediction, in pipeline systems during two-phase flow 0-64962
hydrostatic, effects on galvanomagnetic properties of graphite 0-75528
hypersonic flow past some central surfaces of second order 0-58376
jet impinging on deflecting surface, distrib. rel. to nozzle height 0-50154
pulse transmission in flowing mixtures rel. to two phase critical flow and
sonic velocity 0-39696
punch coupled with isotropic visco-elastic semi-plane, pressure calc.
0-76892

saturation, rel. to vapour growth of Cd crystals, effects 0-55783 shear strength and sliding friction, pressure dependence 0-58941 on slender cylinder in hypersonic viscous flow, effects of transverse curvature 0-53258

sound, distrib. over rigid sphere from point source on sphere, theory, expt. 0-38384

Stirling cycle, pressure drop effects in heat-exchange components 0-52157

0-52157
stress in reactor cylindrical vessel, analytical determination 0-49699
subsonic convected in flexural wave propagation in periodically supported
infinite beams 0-38363
surface distrib., from shock wave envelopes round conical bodies, M=4.0,
report 0-78204
turbulent boundary-layer, wavenumber-frequency spectra, microphone
array meas. 0-53296
vacuum gauge calibration of ion current measurements for partial pressures 0-51867

sures 0-3186/ and velocity fluctuations, non-turbulent region, rel. to jet flow 0-44407 wall pressure fluctuations beneath turbulent boundary layer on cylinder 0-53114 N2, fixed low press. in vacuum region, generation by chem. dissoc. of Ba₃N₂ 0-48656 ZrBr₄, sublimation pressure 0-53404

ZrBr₄, sublimation pressure 0–53404

Pressure measurement see also Manometers; Vacuum gauges; Vapour pressure measurement 0.1 to 50 torr, oil manometer, rapidly degassed 0–45515 acoustical meas. of supersonic transitional boundary layer press. fluctuations 0–69733 anisotropy in mirror-confined plasma using ext. method 0–46724 blood, digital with strain gauge 0–72805 in breeder reactors, liquid-metal-cooled 0–64172 fluid, subdural cerebrospinal, with epidural transducers 0–76723 in fluid flow using conductive rubber pressure transducers 0–49987 gas discharge lamp filling 0–55511 gauges, Bayard-Alpert, modulation characts. 0–66752 gauges, partial press. for analysis of residual gases in high vacuum systems 0–45498 in impact probes, diffused diaphragm sensors. 0–66768

U-45498 in impact probes, diffused diaphragm sensors 0-66768 ionization gauge, high pressure, operation and control 0-48675 manometer absolute, for gas pressure in 10⁻³ to 10⁻² torr range 0-79826 mechanism, bubble chamber, circular thin-walled capsule as deformable separating element 0-42650 noise free, ionization converter for changing range to 10-7-10-3 torr 0-79825

0—79825
oceanographic, autoprobe, free-floating observation platform 0—69273
in particle fuels, coated 0—46305
piezoelectric probe, calibration using plane Chapman-Jouguet detonations,
in 1–30 atm range 0–72872
transducer, fast-response, 1/20-100 psi 0—69575
transducer, micro-differential, constructed by combination of diaphragm
and advance wires 0—51897
transducer, ultra-miniature piezoresistive, for wind tunnel models, development 0—72129

transducer, ultraminiature piezoresist., for wind tunnel models, fabrication 0 72130

transducers primary calibration to 10,000 Hz 0-69576

transducers primary calibration to 10,000 Hz 0-69576 wind tunnel models, low press. data acquisition system 0-72851 CO₂, using mass spectrometer 0-74646

³He exchange energy from effect of spin ordering on pressure 0-50293 Na, neutral, distribution in Ar-Na plasma 0-61254

Ne, using mass spectrometer 0-74646

O₂, partial pressure using mass spectrometer 0-74646

U-II plasma using Boltzmann plot tech. and relative intensity method 0-50023

Prisms, optical

sms, optical

Abbe, for convergent or divergent light beams 0–63706 digital light deflector, temperature stabilization of pattern 0–67131 direct vision, mode of single glass 0–38562 laser reflector, high power, design and performance 0–77202 mica polarizer, design 0–60391 pentaprisms, appl. to laser beam alignment 0–60248 polarizer, Lummer-Gehrke plate-type, for Ne glass laser 0–42287 polarizing, absolute alignment determination 0–63689 quartz, with total internal reflection, laser cavity obs. 0–73279 reflecting, angle deviations effect on image quality 0–77165 reflecting, standards in optical autocollimation systems 0–73287 sapphire, for internal refl. spectra of solvents, 180 to 200 mμ 0–54940 spectrograms, photographic prism, reduction by combined computational and graphical method 0–60419

Prisms, ontical continued

Au thin film on LiNbO₃, refraction and reflection of ultrasonic surface waves obs. 0–65538

Probability

see also Random processes; Statistical analysis conditional fn. for shield clouds surrounding test particles, Vlasov eqn., kinetic theory 0-43261 density fn. of time-average power and log 0-66860 distribution functions, one-dimensional, of random processes, error in meas. 0-38218

meas. 0–38218
error analysis, disappearing filament pyrometers 0–38420
harmonic oscillator in random electrodynamics framework 0–38183
in information theory foundation of statistical thermodynamics independent
of ensembles, validity 0–38202
measurement and dependence of information content on time 0–54535
PAPA device, pattern classification 0–67163
particle system analysis 0–50799
Poisson distrib, rel. between average and most probable value 0–41982
random noise, response maxima results display, probabilistic shock spectra 0–54590

Procopiu effect see Films, solid; Magnetoelectric effects; Magnetomechanical

Programming see Calculating apparatus/digital computer programmes

Projectiles see Ballistics

Projectors, optical
condensing system, three-element 0-38553
electro-optical systems, image converter and secondary electron amplifier
types, methods of calculation 0-7339
ion, image stability investigation 0-49019
lenses for integrated circuit production 0-69988

atomic mass difference, precise, and mass systematics in the region of 90 neutrons 0–43014

147Pm diffusion in Si 0–53564

Promethium compounds No entries

Prominences, solar see Sun/prominences

Propagation see Acoutsic wave propagation; Electromagnetic wave propaga-

Propagators see Field theory, quantum; Quantum electrodynamics
Proportional counters see Counters/proportional
Prospecting see Geophysical prospecting

Protactinium No entries

Protactinium compounds

No entries Proteins

adsorption, on metals, using capacitance techniques 0—74933 albumin, human serum, electrolytic complexation of 99m Tc at constant current, clinical applications 0—41882 crystal structure analysis, phase probability distrib. representation for simplified combination of independent phase information 0—40040 crystallography, electron density function, Fourier coeffs. determ. 0—50559

Crystallography, isomorphous replacement, calc. 0-50560 DNA, electron and heavy particle emission 0-72798 DNA, structure anal. by Fourier method and electron density functions 0-39463

0-39463
DNA, turbulent drag reduction rel. to stability of double helix struct.
0-71283
0-46612 u-11283 enzymes, at. struct., and catalytic mechanism 0-46612 ferritin, X-ray crystallography, Patterson functions 0-61828 free radical production at 77°K by heavy ions, thermal spike theory 0-72534

globular, far i.r. absorpt. spectra, rel. to dielec. props. 0–51315 haemoglobin, low temp. mag. susceptibility, e.p.r. 0–43199 haemoglobin, modifications of Fe(II) electronic struct., Mossbauer determ. 0–61186

0-61 86
heme, e.p.r. oriented in organic cryst. 0-54162
heme, e.p.r. oriented in organic cryst. 0-64465
hemo-proteins, d-d transitions of Fe, from near i.r. circular dichroism studies 0-71050
parameters, macromolecular, low-angle X-ray scattering data 0-43197
polar energy states in spatial lattice of peptide groups 0-55384
poly-L-leucine, vac. u.v. absorpt. spectra, conformation depend. 0-77973
polypeptide chains, vibrs. and conformations 0-39466
polypeptides film surface absorpt., Auger emission obs. 0-61636
polypeptides, amorphous, one state solns. opt. props. 0-71052
polypeptides in solution, X-ray small angle scatt. 0-61498
RNA, transfer, cryst., three dimens. Patterson function, 12 Å resolution 0-50564
Raman spectrum, in aqueous soln. 0-39462

0-50504
Raman spectrum, in aqueous soln. 0-39462
solid, Raman spectrum 0-76122
spectra, C¹³ n.m.r. by comparison with computer simulation 0-66152
starch products, non-soluble, y-irradiated, i.r. spectra 0-39464

Proton magnetic resonance
see Nuclear magnetic resonance and relaxation

Proton magnetic resonance see Nuclear magnetic resonance and reproton spectra
high energy in abs. of μ - by Ag, Br 0–42819
recoil, neutron spectra expansion method 0–49339
n-n final state region for nd-nnp interaction 0–77370
Ba(d,p) (A=130, 132, 134, 136, 138), E_d=12.0 MeV 0–49669
²H(n,p)2n, 8-28 MeV 0–39065
²BU(t,pf)²³⁹U, E=12.54MeV 0–74018
Protonium see Protons and antiprotons
Protonium see Protons and antiprotons

Protonosphere see Atmosphere/upper

Protons and antiprotons
see also Cosmic rays/protons; Nuclear reactions and scattering due to/protons; Nucleons and antinucleons
alkali halide, channelling, 1.5 MeV 0—78807
in atmospheric inner radiation belt, rocket obs. of time variations
0-41527
heam from diverse.

beam from duoplasmatron ion source, phase density redistribution processes 0-45761

coses 0-45701 blocking patterns, effects of lattice vibrations 0-40507 charge exchange with multielectron atoms, effect of inner shells 0-74147 e.m. structure, phenomenological model 0-45959

Protons and antiprotons continued

earth's radiation belt, injection from solar neutron decay 0-48317

electromagnetic form factor determ. 0-77364

electromagnetic form factor determ. 0-//1564 form factor, explanation of asymptotic behaviour using relativistic quantum field theory 0-49169 form factor extrapolation into timelike region 0-55058 form factor in timelike region, large deviations from scaling law 0-77365 forward matrix element of current commutator, singularities on light cone in terms of scaling functions 0-49178 gas mixture, freq. distrib. of energy deposition in very small pathlengths 0-8804

0 - 68001

0-68001 geomagnetically trapped, observations 0-41526 linac beam dynamics cales, new approach 0-49424 mass, comparison 0-77632 momentum spread for large and small currents in linac injector of synchrotron 0-46081

ron 0-46081
mono-energetic pitch- angle distri., interaction with cyclotron resonance, expressions 0-56807
proton collision ionization of H and He, energy distribution of ejected electrons 0-55255
proton struct., correction to Fermi formula 0-52545
protons, low energy intensity contours in earth's radiation zone at magnetic equator 0-48315

equator 0—48315
radiation belt protons, time variations 0—79572
outer radiation zone, low-energy proton omnidirectional intensity contours at magnetic equator 0—48319
outer radiation zone, ring current proton intensities, asymmetric increases during magnetic storms 0—48318
solar, 100-1000 MeV, increase in intensity at 4.55 7 July 1966 0—54467 from solar flare, February 5, 1965, heliocentric longitude intensity profile

0-48617 solar halo and energetic storm protons, comment on previous paper

0-41840

0-41840
in solar wind, mean free path 0-66642
source of polarized protons for the Erlangen-tandem accelerator 0-42660
spin refrigerator, theory and operation, rel. to proton polarization in crystals, yttrium ethyl sulphate nonahydrate:Yb³+ 0-51381
Van Allen radiation belt, source of high energy protons 0-56828
Venus, ionosphere, thermal origin and behaviour 0-41800
e-p charge difference, from upper limits on charges of Cs and K atoms 0-42962

 $pn \to p\pi$, of recoil proton, in D for $(\theta\pi)$ c.m.=90° in second-reson. region 0-77372

n-p mass difference in model of higher baryon couplings 0-70272 p-n e.m. mass differences using form factors from nonlocal field theory 0-52546

0-52546 p formation, in collisions of inert gas ions and atoms with H₂ 0-74185 Au, sputtering, 500 eV-8 keV 0-40622 CaF₂, channel stopping power and escape of protons 0-68710 Cu films, channelling, weak deform. influence 0-71888 in H₁8O₂ migration in elec. field, pres. up to 60 kbar 0-75548 in KH₂; migration in elec. field, pres. up to 60 kbar 0-75548 SiO₂ film, range, 15-50 keV 0-71891

attenuation of 2.5 keV beam by inelastic collisions in Cs vapour 0-39315 energy loss in N₂, O₂, air, Ar, Ne, Kr, CH₄, CO₂ 0-45963

energy loss in N₂, O₂, air, Ar, Ne, Kr, CH₄, CO₂ 0–45963 angular distribution statered by neutrons at 24 MeV 0–67329 11 B(d,p)¹²B, DWBA calculations 0–70637 11 B(p,p'p), E_p=5.9 MeV, ang. correlations meas. 0–39039 Ba(d,p) (A=130, 132, 134, 136, 138), E_q=12.0 MeV 0–49669 9 Be(p, p), Ep=3.0-12.0 MeV, of polarization, optical model anal. 0–49605 12 C(d,p)¹³C, 1.4-2.4 MeV, of polarization 0–52800 59 Co(m, p)⁵⁹Fe, meas. 0–49635 19 F(d,p)²⁰F, E_q=600 keV, DWBA calcs. 0–49659 11 P(p,p'p), E_p=5.8 and 6.6 MeV, ang. correlations meas. 0–39039 artificators.

antiprotons

maprions production, 10-70 BeV, new scaling law and empirical formulas rel. to Serpukhov data 0–77327 pp scatt, elastic, 6-14 GeV/c 0–38695 pp—KKnr(n=1,2...), 2.7 GeV/c cross-section, K*(890), ρ^0 , ω^o production obs. 0–38720

detection, measurement

beam current meas, from residual gas ionization current density 0—46028 low-energy protons, recording by scintillation counter 0—38751

activation of seawater salt to measure Ca, Sr, Br, S content, NRL sector focusing cyclotron applic. 0–45130 alkali halides, anisotropic X-ray excitation 0–53729 alkali halides, channelling and X-ray production 0–68711 anthracene crystals, 200-600 keV proton bombarded, scintillation response, directional effects 0–69166 atomic collision phenomena in solids, conf., Brighton, England, Sept. 1969 0–68676

charge exchange cross sections, on $(C_3H_4)_n$, Al, Ag, Au and Pb targets, 20-43 MeV 0-75434

charge exchange cross sections, on (C_3H_4)_n, Al, Ag, Au and Pb targets, 20-43 MeV 0–75434 crystalline solid, defects, i.r. absorpt. 0–40139 dechanneling, Si, dependence on penetration depth 0–62230 dechanneling along 111 axis of Si at different temps. 0–78796 glass, solar cell cover materials, low-energy irradiation, effects on spectral transmission in 0.3 to 2.2 µ region 0–71433 ionization and excitation of N₂ 1 to 25 keV 0–41518 metal, radiation damage 0–75146 mixing of 29 states of positive ions 0–60942 photodetector fabrication, n-p junction in InSb 0–44411 powder rock, bombardment-induced target temperatures and thermal accommodation coefficients, meas, by i.r. pyrometry 0–50800 silicates, paramagnetic defect on electron and proton irradiation 0–61941 soil, long-lived induced activity, calculation of 0–78797 straggling of 20 and 49 MeV protons in thick absorbers 0–50914 thermoluminescence in thick targets 0–62731 Al single crystal, channelling investigation, refl. from atomic or ionic chains 0–40615 Au, channelling, energy loss 0–56131 Au, channelling, energy loss 0–56131 Au single crystal, channelling investigation, refl. from atomic or ionic chains 0–40615

Protons and antiprotons continued

effects continued

CaF2:Eu scintillation cryst., protons channelling effects on luminesc

Car₂-Eu schillation cryst., protons channeling effects on luminesc. response 0–62712 Cu and Fe accelerator magnet, activation by 3 GeV p 0–73722 Cu single crystal, channelling investigation, refl. from atomic or ionic chains 0–40615 chains 0-4013 n.-GaAs, absorpt. spectra, $1/6 \mu m$, Hall mobility, temp. depend. 0-41202 InSb, n-p junction photodetector, proton bombard. fabrication 0-44411 KI, F-centre accumulation 0-40190

KI, F-centre accumulation under irrad., temp. depend. of kinetics, 90-300 K 0-50612 LiF single crystal, channelling investigation, refl. from atomic or ionic chains 0-40615

thains 0-40615

MgO, channelling and X-ray production 0-68711
MgO single crystal, channelling investigation, refl. from atomic or ionic chains 0-40615

chains U=40615 Mo, irrad., emitted Lyman α radiation, Doppler shift 0=40620 Si, channelling, 6.72 MeV, 100-800 K 0=65570 Si, damage annealing, fluence depend., minority carrier lifetime 0=43803 Si, surface-barrier type, operation under 10-70 keV p irradiation 0=42632 Si crystals, 60 μ m, 240 μ m thick, channeling and blocking of 31.5 MeV p 0=43939

0.033 solar cells, borosilicate glass and SiO_2 integral coverslips evaluation 0.698356 solar cells, radiation damage obs. from photovoltaic parameters 0-75122

Si solar cells, radiation damage obs. by annealing of photovoltaic parameters 0-75121

interactions

see also Nuclear reactions and scattering due to/protons
1-2 GeV, effects of form factors, in terms of one-boson-exchange model
0 38713

annihilation interactions producing eight or more pions at 2.7 GeV/c

bremsstrahlung, by one-boson-exchange potentials 0-49463 bremsstrahlung, unitary gauge invariant formulation 0-42471 bremsstrahlung cross section at 99 MeV, angular distribution 0-45958 characteristics deduced from data below 30 MeV 0-49296 forward Compton scattering and photon-proton total cross-sections 0-52432

multiparticle production, 100 to 800 GeV, ang. distrib. 0-67323 pp \rightarrow n $\Delta^{++}(1236)$ pion exchange dominance at high energies 0-42584 production in K $^+$ p interac. at 9 GeV/c 0-42525 in three-body reaction p $+d\rightarrow$ p+p+n with 52 MeV detuerons, exp. investigation 0-73635

two temperature model of high-energy interactions, interpretation and evaluation 0-49188

evaluation 0-3160 A₁° photoproduction on proton, PCAC, Dalitz process and Primakoff effect 0-73611 ep-eN*, e.m. inelastic form factors, in relativistic extended particle model 0-70205

0-70205 pp, diffractive two-pion production, dual reson. anal. 0-52506 pp $\rightarrow \Delta^{++}\pi^-$, study at 2.8 and 4.7 GeV, cross-sections, Δ^{++} parity asymmetry 0-77376 pp $\rightarrow K^+\Lambda$, 1 GeV range, differential cross-sections and Λ polarization 0-67273

 ν 0–0.1213 ν 0–0.1213 ν 0–0.1213 ν 0–0.1213 ν 0–0.12145 GeV meas.cf. with Regge-cut model 0–7.7259 ν 0–4.024 ν 0–0.4924 ν 0–0.4924

 γp -N⁺⁺π⁻, decay N⁺⁺→ $p\pi$ ⁺ and spin⁻³/, polarisation 0–52562 γp -Nπ ρ , Nπ $\pi \rho$, 0.3-5.8 GeV, cross-section obs. for ρ production 0–38621

0-38021 γρ→ρη, differential cross section at 4 and 6 GeV 0-77297 γρ→ρη, quark model classification of I=1/2 nucleon isobars 0-60622 γρ→ρμο, 2.8 and 4.7 GeV, cross section 0-49194 γρ→ρπο differential cross section at photon energies 4.0 and 5.8 GeV 0-49261

0-49261
pp-pp⁹, E_p=2.8 and 4.7 GeV, conservation of s-channel helicity 0-38705
pp-pp⁹, E_p=2.8 and 4.7GeV, linearly polarized photon beam, cross sections 0-38704
pp-π²Δ+16 GeV, cross-section meas. 0-73441
pp-π²9 prod. analysis, E_p<500 MeV 0-55038
pp-π⁹9 Regge cuts due to absorption, numerical study 0-67277
pp-π⁴Δ, 16 GeV, cross-section meas. 0-73441
pp-π⁴Δ, 5 and 16 GeV, measurement of asymmetry in produced pions 0-73563
pp-π⁴η, Reggeized U(6)⊗U(6)⊗O(3) and absorption model. 0-57606

pp-n⁺n, Reggeized U(6)⊗U(6)⊗O(3) and absorption model 0-57696 pp-n⁺n with linearly polarized 3 GeV photons, natural parity exchange dominance 0-73564 pp-np, s² dependence of differential cross section and asymmetry ratio 0-52475

pp- $ρ^p$ ρ, determ. of ρπν coupling const. 0–70264 $ppφpπ^*π^*$, photoproduction in 2.6-6.8 GeV 0–60508 pp- $\Delta λππ$, $\Delta πππ$, $\Delta ππππ$, to 5.8 GeV, cross-section for Δ production

 $\nu\rho\rightarrow\Delta\pi\pi$, $\Delta\pi\pi\pi$ obs. 0–38621

'obs. 0–38621
γρ→Δρ cross-section for Δρ production obs. 0–38621
γρ→Νπππ, Νπππππ, Νπππππ, 0.3-5.8 GeV distributions of effective masses obs. 0–38621
Κ, π production, proton momentum spectra compared 0–63844
Κ-ρ→Κθη, Regge poles amplitude for charge-exchange 0–63835
Κ-p, 20-65 GeV/c, total and abs. cross-sections 0–77332
Κ-p-κ-π'π-p, 4.6 GeV/c, 1. meson production 0–55055
Κ-p-y, *πη,980) properties of peripherally produced π_n 0–67305
Κ-p, 10 GeV/c, Regge-pole model 0–49268
Κ-p, 4.6 and 5.0 BeV/c, Κ*(1420) prod. and props. 0–42574
Κ-p, cross section, between 440 and 800 MeV 0–63800
Κ-p, K-matrix S-wave fit below 280 MeV/c 0–63806
Κ-p-Κ,°+neutral baryon, 4.1, 5.5 GeV/c obs. rel. to Regge and quark models 0–38675

K⁻p→K,°+neutral baryon, 4.1, 5.5 GeV/c obs. rel. to Regge and quark models 0–38675 K₋p→K°n, anal. with account of Regge cut contribution 0–60563 K₋p→K°n, anal. with account of K₋p-K°n, system 0–73555 K₋p→K°n, final-state cross sections and amplitudes near Λ(1520) at 330-430 MeV/c 0–52499 K₋p−K°n, final-state cross sections and amplitudes near Λ(1520) at 230-430 MeV/c 0–52499 K₋p−K°n, crossing symmetric description of data with the generalized Veneziano model 0–49227 K₋p→K°n, use of 3-body generalized Veneziano model 0–57760 K₋p→K°n (890)p, coherent droplet model 0–57782 K₋p→K°(890)n, coherent droplet model for spikes and dips 0–57782

Protons and antiprotons continued

interactions continued $K^-p \rightarrow K^+\pi^+n$, generalized Veneziano model application 0–63807 $K^-p \rightarrow \Lambda$ +neutral meson, 4.1, 5.5 GeV/c obs. to Regge and quark models 0-38675

0-42491

73644

see also reaction D(n,nnp) at 14 5MeV np, from two complete exp. on three-nucleon reaction D(n,nnp) at 14.5MeV 0-73644 np, in three-body reaction p+d \rightarrow p+p+n with 52 MeV deuterons, exp. investigation 0-73635

np-dp reaction, parity nonconservation 0-49308 np-dp, differential and total cross sections and a test of charge independence 0-52555

np \rightarrow pd, asymmetry of yields compared with pd \rightarrow np, induced by T-violation 0-45967 npy bremsstrahlung calculated with potential, agreement with experiment 0-57830

0-3/630 νρ- μ Γρ π ⁺, high energy, appl. of Regge model 0-45884 νρ- μ Wp, W boson prod. 0-60588 Λγ- μ K+K*K*, possible use for Ω ⁺ parity determ. 0-57833 PP γρ π ⁰ or \rightarrow pp π ⁺ or \rightarrow pp π ⁺ or \rightarrow pp π ⁻ at 2.7 GeV/c 0-38712 PP γρ Φ ⁰+ π ⁺ studied at 19 GeV/c in pp \rightarrow np π ⁺ π ⁺ π ⁻ and pp \rightarrow pp π ⁺ π ⁻ π ⁰ 0-57816

0-3/610 p+d-3/He+p, obs. cross section and p-ray ang. distribution 0-73656 pd at 3.7 GeV/c, cross sections for N*(1238) production 0-77362 pd-3/He+ missing mass, evidence for η^0 and ω^0 production 0-38666 pd-p,ppp- study at 5.5 GeV/c, cross section, Regge pole models

pd \rightarrow pd $\pi^+\pi^-$, 5.5 GeV/c cross-section obs. 0–73633 pd \rightarrow ppn, break-up reaction Ed=52 MeV 0–49298

low energy pp quasi-free scattering at E_p=4.5-13.0 MeV pd→ppn, 1 0--77363

0-77363
pn-Δ-Δ++, Δ- in forward direction, possible exotic exchange at 6.98 GeV/c 0-57825
pn-K*Kππ(K*Kππ) I=1 enhancement near 2360 MeV, possible obs. of U-meson. 0-45946
pn-npπ-π- interaction, double pion production at 2.8 GeV/c, reaction analysed 0-70248
pn *pnπ+π-, N* production 0-77362
pn-pnπ+π- interaction, double pion production at 2.8 GeV/c, reaction analysed 0-70248
pn-pnπ+π- interaction, double pion production at 2.8 GeV/c, reaction analysed 0-70248

pn→ppπ^{-π+} interaction, double pion production at 2.8 GeV/c, reaction analysed 0-70248

analysed 0-70248
pn→π-π¹π- phase-shift model, evidence for daughters 0-57819
pn→πππ, in crossing symmetric Regge pole model 0-77366
pn→πππ, normalization of amplitude by mass extrapolation 0-55059
pp, 20-65 GeV/c, total and abs. cross-sections 0-77332
pp 6-prong annihilation at 6.4 GeV/c, heavy-boson production 0-55060
pp annihilation into 8 and more pions at 6.94 GeV/c 0-49303
pp annihilations into kaons and pions at 5.7 GeV/c 0-60615
Pp→π²π, ρ rajectory doubling 0-63823
pp→ lepton-pair+hadrons off- mass-shell bootstrap model, predictions 0-38613
pp→Δ¹+M, role of pion exchange at 28.5 GeV/c and cross sections 0-52547
pp→KeVc, spin depend of ampibilation cross sections

0-52547
pp-K°K°, spin depend of annihilation cross sections 0-60614
pp-K*Kπ, spin depend of annihilation cross sections 0-60614
pp-KKππ(n=1,2...), 2.7 GeV/c cross-section, K*(890), ρ°, ω° production obs. 0-38720
pp-K*ππ(K*ππ, I=1 enhancement near 2360 MeV, possible obs. of U-meson 0-45946
pp-ΛΛ, use of K exchange amplitude in explaining angular distributions and total cross-sections 0-77299
pp-Λnk*π*, K*(890), N*(1236), Y*(1385) production at 6BeV/c 0-60613

 $pp \rightarrow \Lambda nk^{+}\pi^{+}, 0-60613$

pp→ΛpK⁰ π ⁺, K*(890), N*(1236), Y*(1385) production at 6 BeV/c 0-60613

pp $\to \Lambda p K^+ \pi^0$, K*(890), N*(1236), Y*(1385) production at 6BeV/c $_0-60613$

pp $\to \Pi\pi\pi\pi$, normalization using dual six-point function 0-73631 pp $\to d+MM$ search for T=1 bosons near 1 GeV, missing mass spectrum measured 0-63830 pp-e+e-, anapole and elec. dipole moments obs. 0-73642

```
73644 continued
```

 $pp^--e^+e^-(\mu^+\mu^-)$ dependences of cross section on initial particles polarizations 0-63843 $pp^-n\Delta^{++}$ 0-57782

 $pp \rightarrow np\pi^+$, 740 MeV explanation in terms of Mandelstam resonance model 0-73634

pp \to np $\pi^+\pi^-\pi^-$ study of pp $\to \rho\Delta$ N, pp $\to \rho^o\Delta^{++}$ n 0-57816 pp \to pM, diff. cross section for $\sharp |< 0.8 (\text{GeV/c})^2$ at 29 GeV/c 0-73632 pp \to pn π^+ use of relativistic triangle-diagrams 0-49186 pp \to pn $\pi^+\pi^-\pi^-$, non-strange baryon and meson resons. prod., 6 GeV/c 0-38699

0-38699
pp→pp+lepton pair/pp→π+lepton pair, ratio of cross-section→0 0-38613
pp→ppπ⁺π-π⁰ study of pp→pΔN, pp→pσ⁴+n 0-57816
pp→ppπ⁺π-, 8.1 GeV/c, multi-Regge anal. 0-57818
pp→ppπ⁺π-, at 2.7 and 2.9 GeV/c, interpretation of pπ⁺π⁻ and pπ⁺π⁻ mass spectra 0-42585
pp→ppπ⁺π⁻, non-strange baryon and meson resons. prod. 6 GeV/c 0-38699

pp-pp $\pi^+\pi^-\pi^0$, non-strange baryon and meson resons. prod., 6 GeV/c $_0^-0-38699$ pp \rightarrow pp $\pi^+\pi^-\pi^0$, pn $\pi^+\pi^+\pi^-$ and np $\pi^-\pi^-\pi^+$ at 2.4 and 2.9 GeV/c 0-57820

 $_2$ — $_2$ 7820 $_2$ Pp \rightarrow pp $\pi^+\pi^+$, 2.4 and 2.9 GeV/c, \bar{A} — A^{++} production 0–57820 $_2$ Pp \rightarrow p $\pi^-p\pi^+$, 2.8–3.5 GeV/c, examination of low mass $_2$ P $\pi^-\pi^+$, $_2$ Pr $\pi^-\pi^+$, $_3$ Pr $\pi^-\pi^+$ enhancements 0–60612 $_3$ Pp $\pi^+\pi^-$ pn, 660 MeV, energy spectrum, expt. and theory, reaction mechanism 0–42581

ISM $0^{-4}2381$ pp $\rightarrow\pi^+\pi$, spin depend, of annihilation cross sections 0-60614 pp $\rightarrow\pi^+\pi^-\pi^+\pi^-$, annihilation at rest, analysis 0-60625 pp $\rightarrow\pi^+\pi^+\pi^+\pi^-$ 2.5 GeV/c, abundant resonance production obs. $0^{-7}7369$

0–77369 pp→ π -anything, scaling behaviour 0–67322 π electroproduction on protons obs. 1000-1170 MeV 0–45930 π photoproduction, extension pseudomodel 0–77326 π - π - π 0n, polarization parameters at 5.9 and 11.2 GeV/c 0–57779 π -p, 20–65 GeV/c, total and abs. cross-sections 0–77332 π -p, hyperon and K°[6 C channels in π -p interactions and multipion photoproduction 0–52517 π -p, 1=0 π - π + enhancement, at 1.07 GeV 0–63836 π -p- π n0, differential cross sections and polarizations 0–52475 π -p- π pπ0, E $_{\pi}$ =6GeV/c, ang. distrib., cross sections 0–38690 π -p- π - π - π 1, backward ρ 0 production at 2.3 BeV/c 0–52538 π -p- π 0, differential cross sections and polarizations 0–52475 π -p- π 0, and ifferential cross sections and polarizations 0–52475 π -p- π 0, amplitudes for reaction from single-pion photoproduction 0–67290 π 5.0 GeV/c, search for strange particle decays of Δ , N* 0–52563

0-67290
 πp, 5.0 GeV/c, search for strange particle decays of Δ, N* 0-52563
 πp, recording particle production at 4.0 GeV/c, longitudinal and transversal momentum 0-67292
 πp, 11.2 GeV/c, evidence for A₁(1070) and other structures 0-49284
 π-p, 2.0 GeV, cross section for strange particle production 0-57789
 π-p, 3.2 GeV/c, six- prong channels, kinematical and dynamical struct.
 38688

π p. 20 GeV/c, six- prong channels, kinematical and dynamical struct.
0 38688
π-p, 4 and 5.1 GeV/c, mass spectrum of ΛK system 0–45977
π-p, 5.1 GeV/c, Ξ hyperon production 0–45976
π-p, at 11.2 GeV, quasi-three- body state production, by double Regge-pole model 0–52514
π-p, at 6 BeV/c, six- pronged interactions 0–45936
π-p, comparison of models for neutral and charged pion multiplicities observed in 25 GeV/c collisions 0–49266
π-p, high energy total cross section in Regge pole fit 0–60569
π-p, po production rel. to vector-dominance-model 0–57784
π-p Regge-pole model, 16 GeV/c 0–49268
π-p→K°N-p, crossing symmetric description of data with the generalized Veneziano model 0–49227
π-p-K°Λ(Σ°), Hypercharge exchange reaction in Reggeized U(6) ⊗ U(6) ⊗ O(3) model 0–57778
π-p-K°Λ(Σ°), Hypercharge exchange reaction in Reggeized U(6) ⊗ U(6) ⊗ O(3) model 0–57778
π-p-K°Λ, generalized 3-body Veneziano model description 0–57760
π-p-K°Λ, and 6.2 GeV/c, ang. distrib. obs. 0–49269
π-p-M°N-1(236)π-π, at 4.45 GeV/c, anal. by pion-Regge pole and three one-pion exchange models 0–60580
π-p-Σ-K*, angular distribs., by rescattering model 0–42598
π-p-ηπ, Regge poles amplitude for charge-exchange 0–63835
π-p-ηπ, Regge poles amplitude for charge-exchange 0–63835
π-p-ηπ, Regge poles amplitude for charge-exchange 0–63835
π-p-ηπ, electromagnetic study of M° 0–60590
π-p-ηπ, at pπ-=15-3.8 GeV/c, in U channel 0–60578
π-p-ηπ, π-π π π , 8 GeV/c, evidence for structure in dipion mass region 0–63833
π-p-ηπ+π-π π π , 8 GeV/c cross sections, resonance parameters 0–49272

 $\pi^- p \rightarrow n \pi^+ \pi^+ \pi^- \pi^-$, 8 GeV/c cross sections, resonance parameters 0-49272

 $\pi^- p \to n \pi^+ \pi^+ \pi^- \pi^- m \pi^0$, 4 GeV/c, expt. study 0—52519 $\pi^- p \to p X$, multi-Regge model, relation with missing-mass spectrum 0—57750

0–57750 $^{\circ}$ π-p- $^{\circ}$ ης, double-Regge- pole model used to investigate $\pi\rho$ mass enhancement 0–57783 $^{\circ}$ π-p- $^{\circ}$ μπ-π-π, reaction at 13 and 20 GeV and N*++(1236), ρ^o and ρ^o meson production 0–63822 $^{\circ}$ π-p- $^{\circ}$ μπ-π at 3.9 GeV/c, constructive interference effect between 2 $^{\circ}$ π decays of $^{\omega}$ and $^{\circ}$ 0–52516 $^{\circ}$ π-p- $^{\circ}$ μπ-π partial wave analysis of $^{\circ}$ π decay of $^{\circ}$ Λ₂ in this reaction 0–73610

 τ^{-} p→p $\pi^{+}\pi^{-}$ 0—73610 $\pi^- p \to p \pi^+ \pi^- \pi^- \pi^0$, 13 and 20 GeV/c, Reggeized miltiperipheral model 0–77330

 0^-77330 $\tau^ P^ T^ K^0\Sigma^+$, final-state interaction effects analyzed in a perturbation model 0^-52518 $\tau^ P^ T^ N^+$, 8, 16 GeV/c, obs. 0^-73575 $\tau^ P^ T^ P^ N^ T^ N^ N^-$ 170 to 1050 GeV/c 0^- 38663 $\tau^ P^ T^ T^$

0-57/85 $\tau p \rightarrow \pi \tau \pi^+ p$, 3.9 GeV/c, dominant processes 0-42549 $\pi^- p \rightarrow \pi \tau \pi^+ p$, 247 MeV 0-60579 $\tau p \rightarrow \pi \tau \pi^+ n$, 247 MeV, cross-section meas. 0-67288 $\tau p \rightarrow \pi \tau^+ n$, 7 GeV/c used to study $\pi \pi$ scattering up to 1.4 GeV dipion mass 0-57797

 $\pi^- p \rightarrow \pi^- \pi^+ n$, at 339 MeV 0-60579

73644 continued

 $\pi^- p \to \pi^- \pi^+ \pi^- p$ at 6 GeV/c, ρ^0 and $\Delta^{++}(1236)$ production domination, evidence of A_1 , $A_{1.5}$ mesons in 3π mass spectrum 0–60577

π⁻p→π⁰n at 70 GeV/c, Reggeized U(6)⊗U(6)⊗O(3) absorption model 0-60570

 $\pi^- p \to \pi^0 \eta^0$, enhancement of $2\pi^0$ mass spectrum at 10 GeV/c 0-77350 $\pi^- p \to \pi^+ \pi^- \pi^-$, double Regge pole model at 13 and 20 GeV/c 0-57780

π p→πon, Regge poles amplitude for charge exchange 0-63835 $\pi^- p \to \pi^0 \pi^0 n$, rel. to s-wave $\pi \pi$ scattering, Chew-Low extrapolation 0-49267

0–55261 np pairing correlations, effect on transfer of np pair 0–52649 npp, meas. at 208 MeV, cross sections 0–77371 π -p, 6.7 GeV/c, four and five-body final states 0–49271 π -p $\rightarrow\pi$ -N*(1730), 6 GeV/c reaction, principal decay mode and properties of N*(1730) 0–57781 π -p $\rightarrow\pi$ - π - θ -p, 2.77 GeV/c, production and differential cross-sections, three-body final-state reactions 0–77329 π -p $\rightarrow\pi$ - π +N, 2.77 GeV/c, production and differential cross-sections, three-body final-state reactions 0–77329

Protons and antiprotons

magnetic moment

omegatron meas, in terms of nuclear magneton 0-49295

polarization

polarization
in ammonia up to 40% by dynamic nuclear orientation 0–49302
at 2.74 GeV/c by elastic scatt. 0–67283
beam measurement, from charge exchange accelerator 0–46077
in butanol, 65 to 70% using continuous flow ³He cryostat 0–52551
cross sections in proton Compton scattering 0–52548
in crystal, yttrium ethyl sulphate nonahydrate: Yb³+, by spin refrigerator method, theory and operation 0–51381
in ethylene glycol, 65 to 70% using continuous flow ³He cryostate 0–52551

0-32531
polarimeter for energy of 300 MeV and made from graphite plate spark chambers 0-55062
source, polarized, ionizer, principle 0-38772
ep elastic scattering 0-60517
ep scatt., 1.5, 1.9 (GeV/c)², meas. of polarization of recoil proton 0-63845

0-63845

K²p, elastic scatt. at 2.74 GeV/c 0-67283

π²p elastic scatt. at 2.74 GeV/c 0-67283

π²p elastic scatt. at 2.75 and 5.15 GeV/c 0-67284

AlK alum, dynamic proton polarization 0-66136

Al(NH₂) alum, dynamic proton polarization 0-66136

Be(p, p), Ep=3.0-12.0 MeV, ang. distribs., optical model anal. 0-49605

¹²C analyzing power determ. using graphite polarimeter 0-55062

¹²Cd, p)¹³C, 1.4-2.4 MeV 0-52800

Co, of elastic scattering 0-70580

²³Cr, of inelastically scattered 0-77545

Fe, of elastic scattering 0-70580

²⁴Mg, of inelastically scattered 0-77545

²⁶Mg(p,p)²⁶Mg ang. distrib. of polarized protons studied 0-52762

²⁶Ng scatt. at 1.5-2.4 MeV 0-60805

²⁸Ni, of inelastically scattered 0-77545

in H₂'-electron collisions, proton energy spectrum 0-74272 polarized source, ionizer, principle 0-38772 p production, 10-70 BeV, new scaling law and empirical formulas rel. to Serpukhov data 0-77327

scattering backward, 1.0-5.5 GeV/c 0-42590

Protons and antiprotons continued

scattering continued

Compton forward scattering and continuous dispersion sum rules 0-57699

Compton scatt., in terms of quark model 0-70257

Compton scattering, high energy wide-angle and applic. of bootstrap theory 0-52549

crystallography applic. 0-65209

high energy, model approach involving flat Pomeron 0-77368

model approach involving flat Pomeron 0-77368

ep, Compton amplitude constraints and conformal symmetry reduction of independent covariants 0-60518

ep, cross sections at 4 momentum transfers 0-77364

ep, deep inelastic range of virtual photons 0-63776

ep, implications of data for vector meson dominance 0-63777

ep, inelastic, deep, model 0–38630 ep, inelastic, geometrical interpretation of scale invariance 0–67218 ep, inelastic, geometrical interpretation of scale invariance 0–67218 ep, inelastic, multiperipheral model with scalar couplings, scale invariance 0–70206

0-70206
ep, inelastic, parton model 0-57710
ep, inelastic, polarized p, up-down asymmetry 0-67231
ep, phenomenological model 0-45959
ep, T-violation effects, simulated in elastic scatt. 0-73458
ep, two-photon exchange contribution 0-42479
ep and et p scattering, comparison at small angles 0-49207
ep deep-inelastic, model to describe structure function W, 0-73459
ep elastic, proton polarization calcs. 0-60517
ep elastic cross sections meas. by coincidence technique 0-57707
ep inelastic, cross section formula 0-70207
ep renormalized weak interaction theory, experimental verification 0-45890
ep scatt. 1.5, 1.9 (GeV/c), meas, of polarization of recoil proton

ep scatt., 1.5, 1.9 (GeV/c)², meas. of polarization of recoil proton 0-63845

0–63845
ep scart., inelastic, small-angle eikonal model and application to weak (neutrino-induced) inelastic production 0–49200
e¹p, ep scatt. cross sections, comparison 0–38633
e¬-eN*, differential cross-section for inelastic scattering in the polarized case 0–49204
pp→K 'Σ°, 1.45 GeV meas. cf. with Regge-cut model 0–77259
K-p, Regge cut contribution to high-energy cross sections 0–70270
Kp, fixed u continous moment sum rules 0–45920
Kp, pkarization and differential cross-section data between 982 MeV/c and 1732 MeV/c 0–77315
K-p→K*n, Regge-pole model modified by inclusion of lowest order cuts 0–73591
K-p→K*p, angular distributions at various angles, rescattering model 0–38706

p-K*p, angular distributions at various angles, rescattering model

0—38/06
K⁺p, 0.9-1.5 GeV/c, elastic scatt. phase shift analysis 0—55034
K⁺p, backward differential cross-section, Regge-pole description 0—38676
K⁺p, evidence for constructive interference in small-angle scattering at 5
GeV/c 0—77300

 K^+p , forward elasc-scattering peaks study using the diffraction model 0-45925

0-43923 (hg. inelastic, 864-1585 MeV/c, ang. distribs. for prod. and decay of quasi two-body final states 0-38668 K*p, oscillatory behaviour by Regge-pole exchange 0-38670 K*p, phase shift analysis to 2.5 GeV/c, no evidence for existence of Z* 0-63809

0–63809

K*p, Regge cut contribution to high-energy cross sections 0–70270

K*p <1.5 GeV/c using a new method of analysis 0–57766.

K*p > 0.7 GeV/c, Regge-pole analysis 0–49255

K*p elastic, 12.7 GeV/c obs. 0–49256

K*p elastic, 12.7 GeV/c obs. 0–49256

K*p elastic, 12.7 GeV/c obs. 0–52501

K*p Serpukhov data contradiction of Pomeranchuk theorem 0–67248

K*p Serpukhov data contradiction of Pomeranchuk theorem 0–67248

K*p, analysis using Regge pole parametrization plus duality 0–73557

K*p, elastic, at 180°, 0.41-0.72 GeV/c 0–67275

K*p, dispersion relation calc. of real parts of forward scatt. amplitude 0–57790

K*p leastic scatt., determ. of forward amplitudes 0–55033

 K^2 p elastic scatt., determ. of forward amplitudes 0–55033 K^2 p= K^* (890p, Regge-pole model 0–52515 K_2^0 p- K_1^0 p, K_2^0 p, Regge-pole eikonal model to calc. differential cross sections 0–57767

tions 0–57767

K†p<600 MeV/c; s and p wave scattering lengths obtained 0–77317 μ p, contribution of Ne'eman's fifth χ interaction 0–49211
np, 24 MeV, angular distribution 0–67329
np, angular distribution data below 10 MeV 0–38718
np, charge-state oscillations, flipping phenomena 0–60618
np, elastic differential cross sections, 2 to 7 GeV/c 0–52557
r.p, quark model 0–73614
np, Veneziano model for charge-exchange scattering 0–52556
np angular distribution at 24 MeV, differential cross section measurements 0–49309
np charge exchange scatt. One-pion exchange amplitude 0–73636

0-49309

np charge exchange scatt., one-pion exchange amplitude 0-73636

np cross-section at 14 MeV, high-precision meas, of anisotropy 0-67328

np total cross sections, 8 GeV/c-21 GeV/c 0-49310

pd, and effective range expansion 0-70271

pd, elastic, 50 MeV, triple scattering parameter meas. 0-73641

pd 3.00 GeV/c, cross section found to be lower than previously assumed

0-57822
pd 3.00 GeV/c total cross section meas. 0-57814
p³He polarization, 10-20 MeV 0-38714
pn, 1.0-3.5 GeV/c obs. 0-45964
pn, amplitude 0-70268
pn, Born approximation for charge-exchange scatt. 0-57823
pN, total cross sections on hydrogen and deuterium up to 3.3 GeV/c
0-52503

0-52503
pπ-dp, hard pions and the deuteron equal time commutator with the weak and axial-vector current 0-63850
pp, elastic, 6-14 GeV/c 0-38695
π+p elastic scatt., 893 to 1.03 BeV/c 0-38696
π+σ-4+π+π-π, 8 GeV/c used to study ππ scatt. in ρ mass region 0-77340
π-p-π+π-π-p, 5 GeV/c, multi-Regge model analysis 0-67293
πp, cross-sections, total and charge exchange, 70 to 290 MeV 0-73592
πp, high energy, rotation of nucleon spin, in Regge-pole model 0-42503
πp elastic, compared with phase shift analysis, 1225-2070 MeV/c
0-42550

Protons and antiprotons continued

scattering continued

πp elastic, intermediate-angle, 3.0-5.0 GeV, diff. cross section meas. 0-67299

 πp inelastic cross sections according to Reggeized multiperipheral model 0-52521

U=2521
 π-p, 2.77 GeV/c, production and differential cross-sections, three-body final-state reactions 0-77329
 π-p, backward elastic scatt., 875-1580 MeV/c 0-73589
 π-p, elastic, between 1.7 and 2.5 GeV/c, partial wave anal. 0-45941
 π-p, forward charge exchange scatt., 2-18 GeV, by interference model 0-73587

m⁻p, high energy, backward peaks, by reflection model 0-42464 m⁻p, phase-shift anal. solns., comparison 0-45942 m⁻p backward elastic from 2.38 to 3 GeV/c, differential cross section for

fine moment 0-60585 $\pi^-p\to\eta n$, Regge-pole model modified by inclusion of lowest order cuts 0-73591

0-73591 π^- p $\rightarrow \pi^0$ n, 310 MeV, neutron polarization meas. 0-73590 π^- p $\rightarrow \pi^0$ n, Regge-pole model modified by inclusion of lowest order cuts 0-73591

0—73591

π⁻p→π⁺π⁻n, comparison of data with models of ππ scattering 0—77336

π⁻p→π⁰n, convergence of finite energy sum rules in non-forward directions 0—57728

π⁺p, at 2.50 and 2.75 Bev/c, first phase-band description 0—70254

π⁺p, elastic at large angles, structure at 5 GeV/c 0—49278

π⁺p, expt. comparison between on and off-mass shell inelasticity 0—42558

π⁺p, polarization in backward- angle scattering between 2.5-3.75 GeV/c
0—73588

 π^+ p backward ang. distribs., test of duality 0–42557 π^+ p elastic scattering, partial wave amplitudes in the 2-5 GeV/c region 0–60584

 α -00004 ar²b, shower enhancement of branch-point contrib. total crosss section increase, $A\to\infty$ 0–45940 ar⁴p dispersion relation calc. of real parts of forward scatt, amplitude 0–57790

0-57790

2-p, elastic, obs. 0-67335

H, pseudo-state expansion calc. 0-64281

from H atoms, cross section evaluation 0-49814

He+p system elastic differential scattering expts., cross section 0-74184

K*p, shower enhancement of branch-point contrib. total cross section increase, A→∞ 0-45940

N₂, proton impact, energy loss spectra 0-74289

np, effect of Mott-Schwinger interaction 0-39054

¬p, topologic cross-sections, a regularity 0-49297

¬²p, high-energy total cross-sections Serpukhov meas. 0-63824

SiC phases identification by proton blocking patterns 0-50548

scattering, proton-proton 3.00 GeV/c, cross section found to be lower than previously assumed 0-57820

0-37622 3.00 GeV/c total cross section meas. 0-57814 9.96, 9.918, 13.6 MeV results 0-55061 angular distribs, of secondaries produced, Hagedorn's model analysis 0-42582

0-42582 bremsstrahlung, relativistic spin corrections 0-49301 contact interaction evaluated, differential cross section discussed 0-67321 D-parameter meas, at 90° near 1 GeV 0-45960 data below 30 MeV, deduced characts, of pp interaction 0-49296 differential cross sections for scattering over wide energy range 0-70192 differential peak at super-high energy, based on isobar pionization 0-42460

dispersion sum rules, superconvergent, saturation 0–45962 eikonal model, high-energy scatt. 0–49299 eikonal model, slope of Pomeranchuk trajectory 0–77367

eikonal model, slope of Pomeranchuk trajectory 0–77367 elastic, at high energy, bremsstrahlung model 0–67325 elastic, relation connecting it with ep scattering by means of Bremsstrahlung 0–77361 elastic, strong s dependence requiring energy-dependent potential 0–57824

elastic, triple scatt. depolarization transfer parameter 0-49292 forward elastic- scattering peaks study using the diffraction model 0-45925

forward peak structure above 18 GeV $\,$ 0–49300 high energy, rel. between total cross section and slope of $\ln \left(d\sigma/dt \right)$ 0–73637

ngn energy, ret. between total cross section and slope of in (do/ds) 0–73637 high energy, using bilocal-field-exchange model 0–70267 high energy study in terms of one-boson-exchange model 0–73630 inelastic, as test for models of diffractive processes 0–67324 inelastic collisions, multiplicity 0–38715 at large momentum transfer, consistency conditions 0–45961 multiplicity, inelastic collisions 0–38715 optimized polynomial expansions, applic, to analysis 0–60611 phase params, analysis and obs. 0–42586 quasi-free scattering in pd--ppn reaction for Ep-=4.5-13.0 MeV 0–77363 quasifree, in reaction ²H(p,2p)n, study of energy dependence 0–73950 Regge cut contribution to high-energy cross sections 0–70270 repulsive core and interaction energy for scatt, at 60° and 90° 0–52550 scaling, study of existence in elastic scattering 0–77360 thermodynamical model analysis of ang. distribs, of secondaries produced 0–42582 topologic cross-sections, a regularity 0–49297

0-42582 topologic cross-sections, a regularity 0-49297 pp, polarization cross sections in proton Compton scattering 0-52548 pp, Born approximation for charge-exchange scatt. 0-57823 pp, elastic, high-energy, simple model 0-42587 pp, Regge cut contribution to high-energy cross sections 0-70270 pp <70 MeV, differential cross-sections 0-49304 pp and pp, crossover in differential cross sections, Regge-pole eikonal theory 0-57815 $pp-4\pi^+$, hard pions and the deuterons equal time commutator with the weak and axial-vector current 0-63850 pp- $pp\pi^+\pi^-\pi^0$, $\eta(549)$ and $\omega(783)$ production at 6.6 GeV/c 0-52537

scattering proton-deuteron elastic, differential cross-section, E=9.7, 12.8 and 15.8 GeV/c for t values up to 2 GeV² 0-57821 elastic, results of experimental study at 4 GeV, Re/Im ratio for scattering amplitude 0-70268

Pseudopotential methods see Crystal electron states

```
S 1310 SUBJECT INDEX
   Pulsars see Cosmic radiations, radiofrequency
   Pulse generators see Circuits
    Pulse-height analysers see Counting circuits
   Pumps
                  see also Vacuum pumps
peristaltic, fluid mechanics 0-76697
                peristante, num mechanics 0-76697
water, photoelectric solar unit as drive, control system 0-42168
water, photoelectric solar unit as drive 0-42167
water, thermoelectric, solar radiation concentrator, calorimetric investiga-
tion 0-48976
                   water, thermoelectric solar unit, optico-mechanical section 0-48975
    Purkinje effect see Vision
  Plyroelectricity
glycol sulphate, current obs. in paraelec. region 0–51129
polar crystals, 6, absolute signs of nonlinear optical coeffs. 0–44751
triglycine sulphate, and far i.r. spectrum 0–75814
triglycine sulphate, pyroelec. response in ferroelec. region near Curie pt.
0–44377
                   BaTiO<sub>3</sub> detector, for optical and i.r. radiation, characteristics 0-76929
   Pyrolysis see Chemical reactions
Pyrolysis see Chemical reactions
Pyrometers
for 100-600°C, i.r. range, with laminated bimetallic thermopile sensing element 0-42098
i.r., photoelectric, for measuring flame temps. 0-52163
i.r., proton bombardment-induced target temperatures and thermal accommodation coefficients meas., rock powders 0-50800
optical, high speed 0-73075
optical density flame pyrometry 0-38422
photoelectric, for arc electrode temperature meas. 0-53231
radiation, light pipe, theory 0-70050
total radiation, ambient temperature effect on thermal e.m.f., automatic bimetallic compensation method 0-42096

Ouadrupole crystal field interactions see Crystals/hyperfine field inte-
    Quadrupole moments, molecular see Molecules/moments
    Quadrupole moments, nuclear see Nucleus/electric moment
     Quanticule theory (of chemical binding) see Bonds
   Quantization see Field theory, quantum/quantization; Quantum theory/quantization
   Quantum chemistry
three-body rearrangement scattering 0—38187
university second or third year book based on author's lecture notes
0-48175
     Quantum counters see Photons; Radiation detectors
   Quantum counters see Photons; Radiation detectors
Quantum electrodynamics
see also Electrodynamics; Electromagnetism
Bjorken limit in model theory 0-54967
charge, by infinitesimal nonlinear interactions 0-42427
coherent states and infrared divergences 0-70163
constraints and the canonical quantization procedure 0-42191
cosmology, steady state, framework formulation 0-79625
diffraction scattering for inelastic processes 0-42462
dipole ghost, interpretation 0-42411
Dirac equ., symmetry 0-38600
Dirac form factor for electron vertex in fourth order, calc. of slope at q²=0
0-77645
electron, free, optically induced level struct, and mass shift 0-52440
              Dirac form factor for electron vertex in fourth order, calc. of slope at q²=0 0-77645 electron, free, optically induced level struct, and mass shift 0-52440 electron charge renormalization in metals 0-40638 rel. to electron pairs, photoproduction, at high energies, comparison with exptl. results 0-52446 fermion propagator in arbitrary gauge 0-42425 Feynman diagrams, ir. divergences 0-52409 gauge invariance and renormalization 0-42424 gauge invariance of transition amplitudes 0-38598 Goto-Imamura-Schwinger term, investigation in connection with gauge and renormalization 0-73389 high-energy production processes, production amplitudes 0-42429 hyperquantization, of spin ½ field 0-54968 ir. divergences in S-matrix amplitudes 0-52408 ir. divergences in S-matrix amplitudes 0-52409 limits of breakdown from muon pair photoproduction from carbon between 1300 and 2100 MeV 0-49280 and many-body quantum mech, relationship 0-38599 massive, applic, to very high energy pp scatt. 0-73639 Maxwell field, quantization 0-52408 model, qualitative, involving electrically interacting neutrinos 0-52407 new aspects 0-52408, infinitesimal 0-42427 pair production in vacuum by an alternating electric field 0-73385 pair-creating field, simplest processes 0-45853 relativistic invariance, gauge transformations 0-42426 renormalization group postulate, exact content 0-70162 renormalization group postulate, exact content 0-70162 renormalization field in nonlinear gauge 0-73380
              73393 restricted theory, survey 0–52411
S-matrix for gravitational field in nonlinear gauge 0–73380 scattering amplitudes due to multiphoton exchange 0–73392 scattering cross sections calc. and i.r. divergence 0–42423 self-mass, by infinitesimal nonlinear interactions 0–38601 spinor, nonexistence of Schwinger terms 0–38601 spinor, renormalization of the axial-vector vertex 0–42428 spontaneous emission and classical Wheeler-Feynman theory status, review 0–45856 for strong fields and superheavy nuclei 0–73388 strong interactions, corrections 0–70183 theory, relativistically and gauge invariant, unitary and free of divergences 0–73390 e bremsstrahlung, wide-angle 0–45882
 0-73390
e bremsstrahlung, wide-angle 0-45882
e'e scattering at 2×510 MeV, test 0-45857
pp scatt., massive quantum electrodynamics applic. to very high energy scatt. 0-73639
Quantum electronics see Lasers; Masers; Photons; Quantum optics
Quantum field theory see Field theory, quantum
   Quantum fluids
                  crystal, many-body perturbation theory 0–45548
crystal, many-body theory, ladder approx. 0–45549
crystalline ordering, absence, in one dimensional systems 0–41999
```

Quantum fluids continued crystalline ordering in one and two dimensional classical systems gas, cluster coefficients, formulation of closed theory 0–41994 hard ellipse, two dimens., structure factor 0–45557 one dimensional classical syst., impossibility of crystalline ordering 0–45547 0-4554/
one-dimensional syst., absence of crystalline ordering 0-41999
paragas, spinless particles 0-72962
paraparticles, classification 0-57684
paraparticles, indistinguishability 0-69646
quantum crystals, Bose-Einstein condensation with crystalline ordering 0-69651 superfluid syst., microscopic derivation of transport eqns. 0-50292 two dimensional classical syst., impossibility of crystalline ordering weak-coupling limit for transport coefficients of classical or quantum gases 0-39680

³He, validity of the Landau theory, evidence 0-53386 ³He, validity of the Landau theory, evidence 0–53386

boson systems
32 bosons interacting through Lennard-Jones potential integration of Schrodinger equation 0–69650
with attractive interactions, low temperature properties 0–38212
Bogolyubov transformation in terms of SU(1,1) group 0–72971
Bose liquid, approx. scheme based on small flucutations in density and currents 0–69649
Bose-Einstein condensation with crystalline ordering 0–69651
bosons and bose condensates, two types, in material systems 0–38214
correlated basis functions, analysis 0–45552
correlation functions of charged particles 0–42004
degenerate, quasiparticle ensemble, microscopic theory 0–48554
degenerate Bose fluid, applic. of Hartree-Fock theory 0–45554
degenerate and nondegenerate, calc. of pair distrib. function 0–48761
differential conservation equations derived for the mass-, momentumenergy-density operators for a 1-component simple fluid 0–67859
dilute, hard-sphere gas, energy spectrum, using linear response theory
0–45553
gas, Bose-Einstein phase transition, quasi particle interactions 0–66846 0-45553
gas, Bose-Einstein phase transition, quasi particle interactions
gas, Bose-Einstein phase transition, quasi particle interactions
gas, fluctuation in ground state occupation number 0-69647
gas, nonideal, Green's functions, asymptotic properties 0-69653
gas, nonideal, Hartree-Fock method generalization 0-69652
gas, rotating two-dimensional ideal, condensation 0-48763
Goldstone theorem and collective excitations from condensed Fermi systems 0-42005
hard-core formalism, applic, to Heisenberg ferromagnet 0-40988
hard-sphere, dilute gas, energy spectrum, using linear response theory 0-45553
indistriputional policy 0-69646 indistinguishability 0-69646 indistinguishability 0-69646 interacting bosons, partition function, derivation of Bell-Hirota representation 0-72972 low temperature properties 0-38212 mass splitting mechanism of degenerate particles 0-73381 one-and two-particle distrib. functions anal. props. 0-48762 one-dimensional, with repulsive δ-function interactions at a finite temperature T 0-69648 partition function derivation of Bell-Hirota representation 0-69645. ure T 0-69648
partition function, derivation of Bell-Hirota representation 0-69645
phase transition, correlation functions, scaling laws violation 0-72952
quarks, non-leptonic weak interactions 0-60529
quasi-free states, C* algebras, application 0-54615
restricted geometry, high energy neutron scattering 0-71397
shielded potential in Hartree approx., sum of self-energy diagrams
0-72970
spatial distribution, high energy neutron scattering control of the self-energy diagrams
spatial distribution. spatial distribution, by quantum field theoretical methods 0-48760 thermodynamics 0-76856 fermion systems

condensed, collective excitations, rel. to Goldstone theorem

condensed, collective excitations, rel. to Goldstone theorem

differential conservation equations derived for the mass-, momentum- and energy-density operators for a 1-component simple fluid 0-67859

Fermi system in random scatt. centres, independent electrons, varying field, strong single-centre potentials

-42007

Fermi-gas interacting with localized perturbation possessing internal degrees of freedom

-48764

fields, functional quantum theory

-63364

fourfermion interaction composite states

-63365

gas, in disordered one- dimensional lattice, elec. resistance

-40677

gas, perfect, eqn. of state

-54616

gas, with Coulomb interaction, collision integral

-51991

gas mixture with Coulomb interaction, collision integral

-51992

gas model, free, rel. to fast (n,2n) reactions

-39174

gas model, renormalized, rel. to nucl. reactions

-42907 two kinds of bosons and Bose condensates 0-38213 0–39174 gas model, renormalized, rel. to nucl. reactions 0–42807 hard-core, method of point transforms 0–45555 ideal Fermi gas, behaviour of reduced density matrices 0–42006 indistinguishability 0–69646 interaction in general relativity, using covariant Dirac eqn. 0–48708 liquid, 2-component, stability conditions and other inequalities 0–57297 liquid, anomalous props., low temp. 0–57298 liquid, hard sphere, criterion for ferromag. 0–72200 many-fermion syst., normalization problem assoc. with homogeneous vertex part eqn. 0–72974 melting theory, analysis of model system 0–71411 N-body antisymmetric wave function, N+2 spin orbital approx. 0–66812 perturbation theory, single particle energies, factorization problem 0–66848 0-66848
quasi-free states, C* algebras, application 0-54615
R-matrix expansion for ground-state energy 0-77470
spatial distribution, by quantum field theoretical methods o-48760
spin diffusion and echoes 0-43494
thermodynamics 0-76856 Quantum generators see Lasers; Masers Quantum mechanics see Quantum theory amulin opecs amplification and freq. conversion, with trilinear Hamiltonian 0-38482 coherence function, unimodular, and density matrix 0-73195 coherent indices 0-73192 conference, growth points of physics, Florence (1969) 0-45504 coupled systems, master eqn., higher order effects 0-38480

Quantum optics continued

detectors, e.m. field effects statistical optics considerations 0-63692 fluorescence, coherent reson., excited by short light pulses 0-38485 two-frequency generation, effect of two photon transitions on frequency and threshold 0-52261

generator, quantum single-mode, of travelling wave, noise 0-60189 light beams, propagation in continuously focusing lens-like media -42360

light beams, propagation in continuously focusing lens-like media 0–42360 light propag, in optically pumped vapour 0–52258 mixing effects in multilevel quantum systems 0–38481 multiphoton and photon-phonon transitions 0–45734 oscillations in syst. comprising N two-level mols. 0–77053 parametric limitation calc. method 0–63597 parametric oscillators, noise calculations 0–42235 picosecond pulse structure, mode-locking 0–73194 principles and applications of quantum electronics, book 0–42234 propagation in 2-level system, functional quantum statistics 0–57503 propagation of linearly polarized light in variable-length one-dimensional cavity 0–69769 pulse distortionless propag, in resonant medium 0–49022 pulse propag, in resonant media, superradiant effects 0–38484 radiation interaction theories and at. spontaneous emission 0–52879 resonant non-monochromatic radiation, nonlinear polarization 0–38483 scattering, spontaneous parametric three- and four-photon, quantum theory 0–45830 screening of the photon propagator in many-body optics 0–38488 second harmonic generation, quantum vs. classical analysis 0–69864 second harmonic generation, statistical properties, dynamical description 0–69865

second harmonic generation, statistical properties, dynamical description 0-69865 statistics of one-photon interaction of light with two-level atoms 0-70787 stimulated emission and elastic scatt. of resonance photons in two-level system 0-52256 Stokes radiation pulses, gigantic in Raman radiation, generation theory 0-52254

superradiance, coherence brightening and amplified spontaneous emission 0-42314thermal blooming in gases 0-38479 thermal defocusing of air doped with SF₆ 0-57546 X-rays, characteristic, quasistationary population inversion 0-79338

Quantum statistics see Statistical mechanics/quantum Quantum theory

Electron theory; Field theory, quantum; Elementary

antum theory
see also Electron theory; Field theory, quantum; Elementary
particles
3-level system, absorption spectrum in field of two intense nonmonochromatic beams 0-60911
action-angle variables and relation with second quantization 0-66814
advanced, graduate level textbook 0-54571
angular momentum coupling coefficients, computer program 0-69613
anharmonic oscillator, by Borel summability 0-69621
atoms, bounds to overlap between true and approx. wavefunctions
0-64197

0-64197
binding energies using Kohn-Hulthen variational principles 0-72920
Boolean algebra, quantum families 0-59871
Brillouin-Wigner perturbation theory, upper bounds 0-76828
C*-algebra and quantum logic, comparison 0-66811
causality and wave packet scattering 0-45537
classical mechanics with a quantum-like structure 0-57304
Clebsch-Gordan coeffs. of unitary groups, isoscalar factors 0-70217
conservation laws rel. to invariant transformations 0-57303
Coulomb bound-state problem, test of Pade approximants approach 0-72924
de Broglie's hidden thermodynamics and the isolated particle, new formulation 0-66824
detection and estimation theory, applications to signals in optical frequen-

tion 0-66824
detection and estimation theory, applications to signals in optical frequencies in presence of thermal radiation analysis 0-48756
diffusion of metal interstitials 0-55911
Dirac bracket, symmetric partner obtained 0-52003
Einstein's, Podolsky's and Rosen's objection 0-48714
Einstein-Bohr box expt. 0-76821
electric multipole radiation operator 0-48719
electron moving in field of many stationary nuclei, suggestive approximate dynamical symmetry 0-73915
energy levels in potential well deformed by sharp edge 0-38175
epistemelogical meaning, interpretation through Lenin's philosophy 0-51944
Galilean transformation in quantum mechanics 0-76820

epistemelogical meaning, interpretation through Lenin's philosophy 0–51944
Galilean transformation in quantum mechanics 0–76820 gauge invariance and regularization 0–54579 gear wheels as classical analogue 0–69619 generalized for phase transitions and fundamental particles 0–41972 groups, limitable, dynamical, a model including arbitrary spin 0–38174 Hamiltonian form of Maxwell's egns. in vacuum 0–52168
'iarmonic oscillator, phase ambiguity in ladder operator soln. 0–72932 harmonic oscillator, superradiant states 0–51957 harmonic oscillators, first order perturbation theory 0–5912 harmonic oscillators, first order perturbation theory 0–5912 harmonic oscillators, superradiance, algebraic approach 0–76834 Heisenberg's correspondence principle for non-relativistic matrix 0–66822 Heisenberg pressure, gauge invariance and charge operator 0–72928 Heisenberg uncertainty principle, generalisation 0–54577 history of its founders, book 0–45529 hydrogen wave functions, computer-animated film 0–54573 hyperplane formalism, localized states reconstructed as superposition of canonical states 0–48716
'immanant wavefunction, properties 0–46319 interacting particles, two-body pot. transform. in hyperspherical formalism 0–54582 kinetic equation, applic. of Wigner distrib, function 0–72919 Lande interval rule. Zeynansion corrections.

kinetic equation, applic. of Wigner distrib. function 0-72919 Lande interval rule, Z-expansion corrections 0-60906 logics, generalised, (orthocomplemented weakly modular σ lattice) 0-57264

0-57264 logics, generalised, and bounded vector-valued Borel measures, integration theory of observables 0-57265 logics, projective representations and the superpoint in principle logics, projective representations and the superpoint in principle O-57263 Lorentz group, dynamical 2+1, generators construct. 0-76831 Lorentz-invariant localization for elementary systems 0-48717 Mackey and Segal models, comparison 0-66811 macrocausality, propagation of observables 0-54961 many-body problems, quantum mechanical 0-48742

Quantum theory continued

many-fermion perturbation series with attractive forces, summability 0-66847

measurement process 0-76819

mechanics, history and interpretation 0-63342

mechanics, instory and interpretation 0-03342 mechanics, many-body, and quantum electrodynamics, relationship 0-38599 mixing effects in multilevel quantum systems 0-38481 modular variables, non-local aspects of interaction 0-41971 nonrelativistic, based on local currents, description of spin and statistics

0-54974 oscillator, N-dimens. non-stationary forced, coherent states and excitation

u=39910 oscillator, harmonic nonadiabatic 0=66857 oscillator phase operators, cosine and sine, props. 0=51949 particle density of mass zero bosons, energy density of mass zero fermions 0=54977

0-54977
path integrals in curvilinear coordinates 0-66816
perturbation, two equivalent centres problem 0-63350
perturbation expansion, singular, simple example 0-38186
perturbation expansion of bound state energy, nth order coefficients, new formulae 0-48727
perturbation problems, wide class, applic, of transform 0-77788
perturbation theories, symmetry adapted, derivation 0-51955
perturbation theory, three nucleon system 0-77465
perturbation theory, time-dependent 0-76818
perturbation theory and phase transition, application to anisotropic Ising

perturbation theory and phase transition, application to anisotropic Ising model 0-72961

perturbation theory applied to relation of ionization potential with atomic number 0-64348

number 0-04348 perturbation theory estimate of 3 body term, effect on T₂3 term in isobaric multiplet eqn. 0-77459 perturbation theory evaluation of double time spin Green functions, rel. to eqn. of motion 0-59923 phase shift derivatives using Kohn-Hulthen variational principles 0-72920

0–72920
phase space distributions 0–59901
phonons as thermal energy quanta 0–71853
physical theories and correlations between measurements, a 'mathematical logic' approach 0–66773
Planckeon, scalar, spherical wave 0–59905
potential barrier diagrams 0–76827
pressure effect on material behaviour, cellular methods 0–69374
quantum mechanical model for interaction of spinless bound particle in e.m. field study 0–74089
quaternions, use in direct integration of systems of partial differential equations by separation of variables 0–69614
Racach coeffs, new symmetry derived 0–72921
radial integrals and bound electron states denumeration in Coulomb pot. 0–54569
radiation, adiabatic theorems for oscill. systems 0–38182

u-34369
radiation, adiabatic theorems for oscill, systems 0-38182
radiation from collision-damped two-level system 0-70753
Regge pole theory formulation from two body scattering amplitude 0-69596

Negge pote theory forminator from two body scattering ampirated 0–69596 relativistic contraction, consequence of relativistic Doppler shift in de Broglie waves 0–48715 relativistic quantum mechanics of elementary particles, new dynamical group 0–57266 resonance tunnelling reactions, theory of phase shifts 0–43206 Riemann tensor with functionally constant invariants 0–66815 rigid rotator with arbitrary deformation, dynamical group approach 0–72923 SU(1,1) existence of rotation-invariant representation 0–72891 scattering pot operator, integral representation 0–48729 scattering states, N-particle, relativistic kinematics, quantum mechanical treatment 0–72925 Schwinger functionals, existence 0–63749 second-order energy, on upper and lower bounds in Schrodinger's perturbation theory 0–63349 spin and polarization of particles 0–59921 spin statistics theorem, non-relativistic proof 0–54572

spin and polarization of particles 0—59921 spin statistics theorem, non-relativistic proof 0—54572 spin-1/2 particles and hidden variables 0—54568 spin-orbit potentials, velocity dependent and quadratic, positivity conditions 0—73726 spinors and other quantum systems coupled to external rotating field, dynaical rotations 0—66810 spontaneous decay and level shifts by soln. of Maxwell's eqn. with Dirac's or Schrodinger's 0—42931 stationary states, nodal structure, nodal flux fields and flux quantization 0—66820 statistical basis embedding formalism. 0—69615

statistical basis, embedding formalism 0-69615

statistical basis, embedding formalism 0–69615 statistical electron-positron equilibrium in a magnetic field 0–69618 Stokes polarization parameters 0–41970 structure of physical theory and its 'ideal form' 0–51942 text-book on the foundations of quantum mechanics 0–54570 textbook for undergraduates 0–57267 thermodynamic theory applic. 0–51945 three-particle Coulomb systems, ground state from Faddeev equations 0–72922

0-72922 transition probability, variational method for calc. lower limit 0-45536 unbounded functionals in group algebra, applic. 0-41940 uncertainty packets, unitarily equivalent to coherent states, operator approach 0-59904 uncertainty principle, momentum meas. using Compton effect 0-54567 uncertainty principle according to hydrodynamic model 0-51943 uncertainty relations, canonically conjugate pairs and phase operators 0-66813

0-66813

uncertainty relations, generalized set, rel. to nature of uncertainty principle 0-66819

unstable particles defined in terms of representations of a semigroup con-

taining the Lorentz group 0–59896 unstable systems, decay theory, further contribution 0–45535 unspectable systems, decay theory, further contribution 0–45535 upper and lower limits for the number of bound states of physical systems 0–59913

Vavilov-Cerenkov rad. emitted by electron in transparent uniaxial cryst. 0-43951 second virial coefficient for square well potential, quantum corrections 0-54583

virial theorem, methods of proof and applications 0-42016 wave packet scattering, causality 0-45537

Quantum theory continued

wavefunction determination 0-58077X-Y model, relaxation of longitudinal magnetization, examination 0-72163

application methods

recoustic wave scattering, by spherically symmetric inhomogeneities 0-54716

0–54716
analytic mathematical physics, conference, Bloomington (1968) 0–66858
anharmonic oscillators, coupling const. analyticity 0–48728
anharmonic oscillators, high-order calc. 0–59909
anharmonic oscillators, numerical integration method 0–59908
barrier penetration discussed 0–59907
binding energy of two particles, Schrodinger eqn. with screened Coulomb potential 0–38181
bond, chemical, expt. data anal. 0–64357
Borel summability, appl. to anharmonic oscillator 0–69621
Born cross sections, with local approximation for Green function, normalization 0–76829
Clebsch-Gordan coeffs. and nonrelativistic multiparticle reactions

Clebsch-Gordan coeffs. and nonrelativistic multiparticle reactions 0-38190 communication theory, structure and performance of ideal receiver finding 0-76832

0-76832 correlated wave functions and the shell model of the nucleus, realistic forces, spectra and the effects of correlations in A=6 nuclei 0-57893 critical micromass of classical particle, criterion for appraisal 0-59900 de Sitter group, inhomogeneous, and the relation to the quantum mechanics of elementary particles 0-66826 diamagnetic susceptibility of infinite bands, II electron ring currents, quantum mechanical calculations 0-53058 per turbation and extramolation states and the second control of the correction of the corr

diatomic molecules, rot.- vibr. energies, perturbation calc., systematic approach 0-64340 discrete double groups of symmetry elements, eigenvalue approach 0-57262

0–57262
disjointness of the KMS states of different temperatures 0–38200
dye molecules, struct. study 0–58159
eigenvalue problems, nonlinear, branching of solutions 0–48725
eigenvalues of 2 and 3-dimensional systems by matrix methods 0–66821
electromagnetic field in one-dimensional variable-length cavity 0–69769
excited-state wavefunctions, calc. by variational method 0–58078
expectation values for one-dimensional problems using WKB quantization
condition 0–72931
Faddeev method, to three-spin deviation problem for Heisenberg model
0–40970

Faddeev method, to three-spin deviation problem for Heisenberg model 0–40970

Feynman path integrals in imaginary time and spherical polar coords., Monte Carlo evaluation 0–38173

first- and second- quantized theories of paraparticles, correspondence 0–48749

generalised free electron molecular orbital method, configuration interaction procedure included 0-74214 generalised harmonic oscillator shell model and generalised oscillator transformation brackets 0-49475

gravitational field, quantum model with positivity requirements and transformation invariance 0-63326

HF wave functions, spin-unrestricted, for atomic hyperfine struct. 0-77644

harmonic oscillator coupled to scalar field, irreversible behaviour for simple model 0-63359 harmonic oscillator representation, general soln. 0-46424 harmonic oscillator representation in two dimensions, matrix elements 0-46425

harmonic oscillator with extra cubic force, algebraic treatment of H-atom 0-58124

harmonic oscillator with extra cubic force, algebraic treatment of H-atom 0–58124
Hartree-Fock method, extension, to many-body variation theory 0–54612
Hartree-Fock Stater model calc, for K-LM Auger intensities 0–77675
helium liquids, microscopic quantum theory 0–43492
inelastic collisions, WKB-type general solutions 0–38128
linear systems analysis, steady state 0–76833
magnetic substance, macroscopic props. 0–44449
many body-theory 0–59906
n.m.r. multiple quantum transitions calc. by second quantization 0–38445
network model for electrons in solids, solvable model which may have several bound states per node point 0–68717
nonuniqueness of the energy correction in application of the WKB approximation to radial problems 0–48726
nucleon-nucelon interactions, final state, PWBA treatment, influence of cut-off radii 0–73621
oscillator strength, MO formulations in one dimension using double well potentials 0–43052
particles with hard cores, statistical mechanics 0–38199
partitioning perturbation theory, applic. to electron exchange 0–57275
partitioning perturbation theory, sease of almost degeneracy 0–51952
partitioning perturbation theory, sease of almost degeneracy 0–57274
perturbation method for boundary-value problems in dynamic elasticity 0–76884
perturbation dopential 0–70741

perturbation theory, higher order, for one-electron ion in generalized central-field potential 0-70741 perturbation theory, unified, necessary condition for applicability 0-66374

perturbation theory, unified, necessary condition for applicability 0–66374
perturbation theory for spin Green's functions 0–51953
perturbation theory through spin systems, teaching 0–41979
phase shift calc, use of it, iterative method 0–60984
phase-amplitude method for electron in ionic potential 0–64188
potential scattering, eikonal approximations and impact-parameter approximation, relationship 0–59917
potentials, separable 0–72930
projection methods for ang. moments 0–41946
quantum probability, operational approach 0–51978
quasiparticle lifetime, Green function decoupling scheme 0–66823
radiative transfer eqns. in spectral line regime 0–69656
reduced density matrices for ground-state energy of atomic syst. 0–64195
relativistic quantum mechanics for scattering by an external e.m. field identical bosons 0–45912
resonant state lifetimes due to particle scatt., comparison of Fermi and Smith estimates 0–45538
scattering, atomic and molecular, long-range interaction processes, variational method 0–74082
scattering in terms of the Abelian subalgebras of observables and the S matrix 0–59916
scattering theory, density matrices in the many-body problem 0–42002

matrix 0-59916 scattering theory, density matrices in the many-body problem 0-42002

Quantum theory continued application methods continued

solid, rate theory, N-dimens. tunnelling effects 0-43650

solid, rate theory, N-dimens, tunnelling effects 0–43650 stabilization method, for calculating resonance energies, applic. to model potentials 0–76830 ultradense matter, quantum system of particles interacting via neutral vector-meson exchange, noncausality and instability 0–59911 united atom perturbation theory of the interaction of two atoms at small separation and Hartree-Fock wavefunctions 0–67659 van der Waals constant for two H atoms 0–63349 variational method and principle 0–51954 wave function zero in some region of space, justification 0–70841 Wigner-Weisskopf atom, relaxation in one-dimensional radiation field 0–38184

0-38184
Hatom, Stark effect 0-63349
He liquid, quasiparticle Hamiltonian 0-43496
many-particle systems see Helium/liquid; Quantum fluids; Statistical
mechanics/quantum; Superconductivity; Superfluidity

quantization

see also Field theory quantum/quantization atomic collisions, binary encounter theory, initial state m-quantization 0-67661

flux quantization in stationary quantum states 0-66820

oscillators, by generalized perturbation theory 0-54580 photoionization cross-section, second quantization formalism 0-64225 second-quantization picture for fermion system, non-invariance groups 0-51956

Wheeler-Feynman electrodynamics, spontaneous emission 0-38185 wave equations

wave equations adiabatic exchange, calc. of H- free-free absorption coeff. 0—78157 analogy to spin waves 0—63341 atomic 3- and 4-particle systems, regular wave functions 0—52862 Born and Rytov expansions, interrelationship 0—57272 bound state eigenvalues and props. of radial Schrodinger eqn., iteractive determ. 0—41976 bounds to eigenvalues for overlap between approximate and exact wave functions 0—51946 current algebra commutation relations on the space of solutions of finite-or infinite-component wave equations 0—42434

infinite-component wave equations 0-42434 Dirac, nonrelativistic limit in the continuum 0-76823

Dirac eqn., exact solution for electron moving in nonuniform magnetic field 0-76825

Dirac equ., new exact solutions 0-63344 Dirac equation, solution for oblique electric and magnetic fields 0-73453 Dirac equation, tensorial representation using a geometrical approach 0-66817

0–66817
Dirac quadratic equation, generalization 0–57273
Dirac-Fierz-Pauli equation, reformulation for spin 3/2 0–76824
eigenvalues, prolate spheroidal coords, tables 0–45530
electron fluid, degenerate, of metals 0–47606
electron-electron interaction in energy level determ. 0–77640
energy spectrum by phase integral approximation for Green's function
0–48778

0–48778
errors, weighted mean, bounds, theory 0–38178
Galilean-invariant, introduction of minimal coupling for computation of magnetic moments, particle of ranges spin 0–49184
generalized, infinite component fields for SL(2,C) ⊗ Dirac 0–48721
Hamilton-Ostrogradsky's principle, modification for initial value problems
0–41977

0–41977
Hamiltonians and wave equations for particles of spin O and spin ½ with nonzero mass 0–54574
Hartree theory, extension to time dependent problems 0–69616
hydrodynamic regime, damping constant of collective mode 0–44517
identical particles and paraparticles 0–41974
infinite-component, leading to families of linear trajectories 0–59903
integral-transform electronic wave functions, range relaxation 0–77627
Kemmer eqn., reduction and singular behaviour of integer-spin Hamiltonians 0–49177
Klein-Gordon, with external potential, asymptotic behaviour 0–76822
Lorentz group, (1, ½)⊕(½, 1) irreducible representation study 0–76824
Lorentz-invariant in form of supermultiplets, hadron energy levels description 0–49289
lower bounds for overlap, derivation of Eckart formula 0–57270
lower bounds for overlap of approximate wavefunctions 0–48720

lower bounds for overlap of approximate wavefunctions 0-48720 N-body antisymmetric wave function, N+2 spin orbital approx. 0-Nambu Takabayasi equation and transition form factors, Schrodinger picture 0-51951

ture 0-51951 non-inear, spinor wave-mechanical field theory of elementary measurement 0-57269 nonlinear, stationary states 0-72927 periodic Hilbert space, mathematical structure, and the one-dimensional structure constant in the Green Function method 0-54575 perturbation expansion, for free nucleons in a magnetic field 0-51947 quasi-stationary state, asymptotic behaviour of wave function 0-38180 relativistic particles, interaction, with or without spin 0-59898 Rytov and Born expansions, interrelationships 0-57272 Schrodinger, 1-dimensional, replacement by a pair of coupled integral equations and solution 0-63345 Schrodinger, conformal groups, H atom 0-70810 Schrodinger, chact solution for three-and four-body problems 0-72968 Schrodinger, exact solution for three-and four-body problems 0-72968 Schrodinger, generalized, axially symmetric, analytic theory and uniqueness problems 0-38177 Schrodinger, soln. using separable-potential-subtraction method 0-38179

problems 0–38177
Schrodinger, soln. using separable-potential-subtraction method 0–38179
Schrodinger, time independent, mechanical analogues 0–41973
Schrodinger, with nonlocal potential, numerical solution 0–45534
Schrodinger, with screened Coulomb potential, application to two particle binding energy 0–38181
Schrodinger's eqn. for 2-plate system interacting through static screened Coulomb potential, accurate numerical solns. 0–46350
Schrödinger's perturbation theory, unper and lower bounds to second-order.

Schrodinger's perturbation theory, upper and lower bounds to second-order energy 0-63349

energy $^{\circ}$ 0-63349 Schrodinger eqn, 2-electron, numerical solution 0-70821 Schrodinger eqn., amplitude-phase approach to bound states, superper-turbation theory 0-54576 Schrodinger eqn., nonrelativistic, for one-electron ion in generalized cen-tral-field potential 0-70741 Schrodinger eqn., one-dimensional, transformation to integral eqn. 0-72954

Schrodinger eqn., radial, transform. to differential eqn. 0-38800

Quantum theory continued

wave equations continued

Schrödinger eqn. rel. to electron band structure, numerical solutions review 0-65579

Schrodinger eqn. resolution for diatomic mol. 0-77743

Schrodinger eqn. resolution for diatomic mol. 0–77743
Schrodinger eqns., e.m. struct. 0–63355
Schrodinger equation, many- body, generator-coordinate theory as a flexible formulation 0–48722
Schrodinger equation analysis for spherical, cylindrical and plane-layer samples, for a particle moving in a thin layer sample 0–63343
Schrodinger equation for hydrogenic atom in nonuniform field, eigenvalues correction 0–70808
Schrodinger equation radial for nonlocal potential, transformation to local potential 0–59899
Schrodinger equation soln. of Mathieu potential, mass-velocity correction 0–56138
Schrodinger equations, separable, for 2 interacting particles in external

Schrodinger equations, separable, for 2 interacting particles in external fields 0-51950

Schrodinger for electrons in highest atomic energy level, equivalence to statistical atomic model 0-49765
Schrodinger one-dimensional eqn., step function method of soln. 0-45533
Schrodinger operator, nonself-adjoint, eigenfunctions, expansions 0-69617

Schrodinger operators, new method for pointwise estimation of wavefunctions 0-72926

Schrodinger picture for Nambu-Takabayasi equation and transition form factors 0-51951

Schrodinger relativistic eqn. of a four-vector derived 0–57268 Schrodinger wave function, nodal structure, for description of N-particle system in stationary state 0–66820 Schrodinger wave functions for an N-particle system, nodal structure 0–45531

singular integral operator encountered in scattering theory and application

singular integral operator encounters. Singular integral operator encounters. O-63347 spheroidal, eigenvalues and eigenfunctions using oblate and prolate spheroidal coordinates 0-63346 spin wave eqn, relativistic, Hwa's method of reduction 0-38611 spinor eqn. removed from 4-vector eqn. 0-57268 spinor-theory, non-linear, study of composite states for 4 fermion interactions 0-77241 thermal decomp. principle demonstration 0-38176

spinor-theory, non-linear, study of composite states for 4 fermion interactions 0–77241
thermal decomp, principle demonstration 0–38176
three-body problem, effective moment of inertia 0–42003
transmission through a real potential barrier, by means of certain phaseintegral approximations 0–48723
tunneling and super-barrier transmission through a system of two real
potential barriers 0–48724
unstable particles, kinematical description in terms of invariant equations
under broken IO(4,1) 0–57244
wave and scattering operators in terms of singular integral operators
derived for an interaction of rank one 0–66818
wave functions, with discontinuous derivative, Kohn-type variational principles for scattering amplitudes 0–42921
wavefunction construction for nonlocal potentials 0–51948
wavefunctions, accuracy assessed by overlap integral S, discussion of literature available 0–57271
zero mass particles with spin ½ 0–41975

'He liquid many-body wavefunction constructed by antisymmetrization
0–50285
H, ionization problem, asymptotic form of wave function 0–52979

0-50285 $H_1, ionization problem, asymptotic form of wave function <math display="inline">0-52979$ H_2^+ integral transform Gaussian wavefunction, ground state energies at various internuclear separations 0-58170 Ne, configuration interaction wavefunction, 1- and 2-matrices of ground state 0-52921

Ouarks

arks
algebraic model, Schwinger terms 0–70215
baryon-antibaryon scatt. in quark model 0–73614
Bethe-Salpeter eqn. with near harmonic interaction 0–70143
binding mechanism in hadrons 0–77269
bose, non-leptonic weak interactions 0–60529
charge ½e and ½e, search in cosmic radiation near sea level 0–49322
commutators, current algebra and field algebra, validity 0–73398
cosmological estimates for abundance in stellar sources 0–67238
Dirac model of hadrons, mass dependence for eigenvalue hadron mass 0–60530
dual model Pemeranchuk term. 0–57715

dual model, Pomeranchuk term 0-57715

dual model, Pomeranchuk term 0-57715 elementary, existence rel. to high energy scatt. 0-38647 elementary particles constructed with integral spin and $B \neq 0$ 0-42435 evidence in high-energy cosmic-ray bubble chamber picture 0-38640 hadron decays, weak, refined model 0-42484 hadron model, three-body vertices 0-49217 rel. to hadron spectrum 0-45895 harmonic mode, extra nonspatial association from new harmonic-oscillator model 0-49215 1=1/2 nucleon isobar prod. in $\gamma p \rightarrow \eta p$, quark model 0-60622 mass and separation in the hadron core estimated 0-77272 masses of bare quarks from asymptotic SU(6), spectral sum rules 0-386410 - 38641

meson model which yields square of mass proportional to spin 0-52480 mistaken identity of tracks produced by high-energy particle pairs 0-57857

0–5/85/model, chiral transformations 0–55002 model, chiral transformations 0–55002 model, for $yN\rightarrow\pi^{\pm}N$ and $yN\rightarrow\pi^{\pm}\Delta$ 0–57774 model, hadron mass dependence 0–63780 model, polarization predictions 0–57713 model, relativistic, based on Veneziano representation, baryon trajectories 0-55006

10—55006
model, relativistic, based on Veneziano representation, general trajectories
0—55005
model, relativistic, based on Veneziano representation, general trajectories
0—55005
model, rest-frame sum rules and field algebra 0—77285
model, to high energy asymptotic limit scatt. processes 0—73526
model, treatment of spins 0—55007
model description of high energy photoprod. of vector mesons
model for backward N₃₁* prod. in 7N collisions 0—52561
model for high energy scattering 0—70216
model for mesons 0—73538
neutrino reactions on nuclei total elastic cross section for forward scatt.
derived using quark field algebra and closure approximation 0—57754
non-local field theory of quark model 0—52452
photoproduction sum rules, quark model 0—73442

Quarks continued

quark model for $K\rightarrow 2\pi$ rel. to $\Delta I=^{1/2}$ rule 0—63804 quark-quark scalar interaction between 0.3 and 0.4 fm 0—77273

relativistic, of charge e/3, search in cosmic ray showers at sea level 0-49325

0—49325
relativistic SO(4,2) model, current algebra representation, at infinite momentum 0–52451
relativistic field-theoretical model 0–73387
SU₃/Z₃, irreducible unitary representations, existence of projective realizations 0–73483
SU₆ model, differential cross section relations in region of second diffraction max. 0–77282
Sakata-Yukawa model unifying quarks and leptons in SO(6,1) 0–38626 search in ordinary matter using simultaneous meas. of mass and charge 0–40216

o-49/16 spin, consistent treatment valid for high energy small angle scatt. 0-55007 star, hypothesis 0-76582 supermultiplet meson coupling constant g, in SU(6)×O(3) quark model 0-73542

symmetric model, e.m. decay of baryon resonances 0–45980 three-quark baryons, configuration mixing SU(6)⊗O(3) 0–42575 three-triplet quark model, exotic mesons and baryons 0–55004 track in high-energy cosmic ray bubble chamber picture, evidence 0–67235

unified field theory fo quartz and electrons 0-42413
vector meson decay selection rule in quark model 0-57804
weak interaction model with currents constructed out of 4 basic quark

helds 0-73426

np scatt, quark model 0-73614

pp scatt, quark model 0-73614

np scatt, and scatt, 30-65 GeV/c, fit to Reggeized quark model 0-57791

U−57/91
W, generalizations of W spin to orbital extensions of quark model 0−57802
Y*(1385) production in multibody final states and quark model 0−70282
Y₁*(1385) two-body production processes and quark model 0−49315
³He,µ capture rate calc. using quark field algebra and closure approximation 0−57754

artz α, shear-wave phase velocity, linear wave-vector dispersion 0–54070
μ-irradiated, 'Al' centre obs., opt. absorpt., e.p.r. 0–59456
accelerometer for tidal to seismic freq. investigation 0–51484
acoustic harmonic generation and third order elastic coeffs., obs. acoustic 1 0-40538 acoustic surface-wave vel. temp. depend., obs.

acoustical rotary power meas, \(\alpha\) -quartz \(0 - \gamma\) -79252 adhesion to Ni(111), LEED obs. \(0 - 43820\) (3140) bent crystal, elastically, plastically, reflectivity, continuous X-ray spectrum \(0 - 41115\)

spectrum 0—4113 coloured, synthesis, impurity doping, radiation effects 0—74966 crystal growth vel. under hydrothermal conditions, Li influence 0—55782 crystal surfaces, epitaxial growth of poly-L-proline and polyoxymethylene, characterization 0—50482

characterization 0-30462 cylindrical waveguide, 10GHz waves propagation 0-57460 damage, pre-catastrophic laser produced, Raman spectrum 0-59409 deformation, mechanical, constant strain-rate compression expts. 0-68449

0-68449
deformation, mechanical, stress relaxation and thermal activation parameters 0-71690
diffusion of ²²Na, 330-910°C 0-62001
diffusion of Ca below 1000°C 0-50627
electric pulse breakdown, orientation depend. 0-44354
electrooptical activity, quadratic effect 0-48021
fibre, adhesion to Re, LEED studies 0-50813
fossil alpha damage, e.s.r detection 0-50597
fracture and stimulated Mandel'shtam-Brillouin scatt., giant ruby laser pulses 0-43773
fracture in alkali silicate and borate melts. mech. stresses and phase trans-

ses 0-45/13. Fracture in alkali silicate and borate melts, mech. stresses and phase transformation 0-40387 fracture press, dynamic, obs. 0-40357 fragments, abrasion and wear resistance exposed to hydroabrasive medium, lab. testing 0-47422 fused, as substrate for optical studies of thin films 0-74891

glasses, γ -irrad., capture centre, e.p.r. obs. 0–43689 growth rate of rhombohedra, effect on external form of vertices 0–40010

glasses, p-irradi, capture centre, e.p.r. obs. 0-43089 growth rate of rhombothedra, effect on external form of vertices of hydrothermal growth, computerized process control 0-47111 hydrothermal recrystallization 0-78413 hypersonic attenuation, transverse modes, low temp. 0-50873 i.r. reflectivity, 380-640 cm⁻¹, extraordinary phonon dispersion 0-78737 light beam deflection by longit, acoustic waves at 800 MHz. 0-49118 luminescence, physiochemical studies 0-56581 melting of natural and synthetic crystals kinetics, 1500-1650°C 0-50309 membranes, electroosmotic transport 0-71331 morion, smoky colouring features 0-59407 natural and synthetic, imperfections, X-ray topography 0-75169 neutron irradiated, α - β transformation, Raman spectra 0-78702 optical absorption coeff. determ. at high temps. 0-41106 optical susceptibilities, nonlinear 0-47991 Paschen-Back effect for muonium atom 0-49826 phase transform, α - β , phonons role, neutron scatt. obs. 0-40492 phase transition, first-order α - β , u.s. investigation 0-75340 photoelastic props, vibrating at resonance, rel. to synchronization of pulsed laser 0-47300 piezoelectric bar, influence of vac. deposited, electrodes on frequency 0-51126

0-51126

piezoelectric oscillations, effect on scanning electron micrographs 0-68964

piezoelectric plates, symmetrical thermal bending 0-76879 piezoelectric strain coeff. meas. 0-75818 piezoelectric surface-waves nonlinearities and third-order elastic consts. 0-47523 plate's Y, AC, BC cuts, high overtone mode thickness-shear resonance 0-47854

plates, thin, deformation on chemical deposition of interference films 0-53581

polaritons, stimulated rel. to i.r. radiation obs. 0-41222 positron annihilation, fast neutron irrad. effect 0-53732 positron annihilation, positronium-like Bloch states obs. 0-53776 powder, extinction of Debye-Scherrer lines, crystal domain radius determ.

Quenching, thermal see Heat treatment Racah coefficients see Quantum theory

```
Radiation
Quartz continued
            prism, total internal reflection, laser cavity obs. 0-73279
             α quartz, acoustical activity direct obs. 0-78750
             \alpha-quartz, electrostriction and piezoelec. coeffs. meas. method 0-51127
             aquartz, surface acoustic wave vel. temp. depend. 0-59096
             Raman scattering cross-section 0-62688
             Raman spectra, inherent electric and anisotropic forces effect 0-56565
           Raman spectra, u.s. stress, impurity motion 0–79319
Raman spectra of \( \alpha \) type, neutron irrad, effect 0–51325
resonator-excited, X-ray diffr. topography 0–47027
rod, torsional vibrations, overtones 0–79057
sound vel., first and zero sound 0–78751
            structural defects, moire topography 0–58804 surface, high-power laser interaction 0–77157
           surface heating, radiative by dense gas discharge plasma absorption of black body radiation 0-62207 synthetic, Al entry during growth, temp. and supersaturation effects 0-75012
             synthetic, hydrothermal growth, computerized process control 0-61719
             with thin metallic film, dispersive Rayleigh waves propagation, attenuation obs. 0-65533
             transparency, visible and u.v., effect of heating to 1100°C 0-41107
             u.s. attenuation, low temp., three-phonon interaction model 0-71844
             vertices, external form, rhombohedra growth rate effects 0-40010
           in NaF melt, dissolving of spheres, diffusion and convection processes 0–39764

• SiO; Ge, E' centres assoc, with Ge impurities, e.p.r. 0–43660 with W, Ga struct, impurities, solution growth 0–71519
Quartz resonators see Piezoelectric oscillations; Resonators; Transducers
 Quasars
           see also Cosmic radiations, radiofrequency; Cosmology; Galaxies; Stars
3C273B, 'galactic flare' model 0-45312
3C 273 scintillation obs., effect of medium near Earth 0-45317
3C 273 spectrum, power and light fluctuations 0-59732
3C 298, angular dimensions at 60 MHz 0-45314
3C 273, angular dimensions of the scintillating component at 60 MHz 0-45314
4C 05 34, unusually large radebit 0-54403
          0-45314
4C 05 34, unusually large redshift 0-54403

'galactic flare' model and physical props. 0-45312
absorption lines, rel. to radio polarization 0-66523
absorption lines in QSO's 0-45315
absorption lines with zehox-zem redshifts 0-79695
accretion of metagalactic gas clouds into galactic nuclei and quasar like phenomena 0-48383
anisotropy of radio emission, mechanism 0-45310
blue stellar objects (408 MHz observations 0-79693
blue stellar objects (BSOs), recent identifications with faint radio sources questioned 0-48478
Compton process, inverse, and Seyfert-type nuclei 0-41731
dissolution of early clusters of galaxies by strong QSS's 0-45230
electrodynamical rotating gas cloud model of radiogalaxies and quasars 0-51713
energetic activity origin 0-72751
            energetic activity origin 0-72751 energy spectrum of expanding relativistic particle clouds 0-72742 fragmentation into groups and clusters of galaxies 0-45313 as images formed by clusters of galaxies acting as gravitational lens 0-51710
         as images formed by clusters of galaxies acting as gravitational tens 0–51710 linear size distrib. relation with redshift 0–48470 mass determination from spectra 0–72743 maximum efficiency of energy release in spherical collapse, and gravitational energy stars 0–62997 mechanism rel. to matter-antimatter separation at black body kT>350 MeV 0–51626 mechanism rel. to matter-antimatter separation at black body kT>350 MeV 0–51624 nature and properties 0–48468 optical variability, obs. 0–63079 PHL 938 spectra, absorption 0–59731 PKS 0237-23, Lamb shift enhancement hypothesis for multiple redshifts 0–79694 PKS 0237-23 pectra, absorption 0–59731 Parkes 2700 MHz survey, 132 objects found, identifications 0–79692 photographic photometry of QSO's 0–51712 polarization, circular at \lambda 49 cm 0–66524 polarization, inear as function of wavelength for high redshifts 0–51709 polarization, radio rel. to presence of absorption line spectra 0–66523 pulsar distances rel. to spiral structure and interstellar electron density 0–56930
         pulsar distances rei. to spiral structure and interstellar electron density 0–56930 pulsars, observable, longitude distrib. in Galaxy 0–56929 quasi-stellar objects, Bowen resonance fluorescence lines 0–79691 red shift distribution, explanation 0–45311 red shifts, explanation 0–45316 redshift distribution of OSO's 0–66528 redshifts reducing distribution of OSO's 0–66528 redshift reparent magnitude relation for 147QSO 0–54402 redshifted 21-cm absorption, in QSOs, cause 0–48469 redshifts, multiple absorption, in QSOs, cause 0–48469 redshifts and apparent magnitudes rel. to cosmological models and evolution 0–41573 review 0–59730 review of developments (1967-8) 0–72744 spectra, multiple absorpt. redshifts 0–66525 spectral index-flux density relation 0–63078 spectrum, power, light fluctuations of 3C 273 0–59732 structures of 74 quasars, 2695 MHz interferometric obs. 0–51711 supermassive stars, rapidly rotating, as QSO model, nonuniform rotation 0–51688
           0–51688
3C 9, struct. 408 MHz and 2695 MHz
0–66526
C III \( \text{L} \) 1909 and other semiforbidden lines, effective collision strengths in QSOs
0–48467
Quasi-particles see Excitons; Magnons, Phonons, Polarons, etc.
Quenching, optical see Luminescence
```

```
PA 1970 - Part II (July-Dec.)
             auon
see also Acoustic radiations; Bremsstrahlung; Cherenkov radiation; Elec-
tromagnetic waves; Electrons/radiation; Emissivity Radiative transfer;
Stars/radiation; Sun/radiation; Sunlight
     from Jupiter, decametric, twelve-year periodicities 0-63093
     of Jupiter, decimetric, synchrotron model 0-63097 of Jupiter, long-term variations obs. 0-63095
     or Jupiter, long-term variations obs. U=63095 from N-atom syst., general formalism 0=77636 γ, calculation of backscattering, generalization of results using similarity theory 0=67224 0=52164
 theory 0–67224
0–52164
0–52164
0–52164
0–52164
0–52164
0–52164
0–76374
0–76374
by atom located between two parallel mirrors 0–70740
back-scattered, of narrow polarised light beam, depolarisation 0–73306
black body, matter-antimatter separation, effect of annihilation 0–48362
black body, non-Planckian spectral density, thermodynamics and temporal coherence, for small cavities 0–66932
black body heating of surface layer of quartz 0–62207
black-body, classical theory 0–73068
blackbody, relativistic thermodynamics, formulation 0–52153
book elementary on radiation physics 0–57161
cavity radiator with temp. gradient, radiance calc. 0–66931
charges moving in cylinder with anisotropic conducting surface 0–38461
from circumferential gap in circular waveguide 0–73102
coherent, spontaneous, from two-level atoms 0–64189
crystal, molecular, field theory including Umklapp processes 0–75990
current ring source around compressible plasma column 0–67920
damping formula re-derived using Wheeler-Feynman formalism 0–67025
dipole rotator, plane, rigid, classical, in e.m. zero-point radiation, specific heat 0–60071
discontinuous, temperature problem 0–66953
dislocation reradiation of elastic waves and viscous damping 0–68354
distribution, in solar energy units with mirror concentrators 0–42169
dose to patient in cardiac radiology 0–59828
e.m., from slots in moving media, analysis 0–52170
e.m., areno-point, third law of thermodynamics 0–54605
reaching earth rel. to electric discharges in solar, stellar and galactic atmo-
e.m. waves, boundary value problems, modern mathematical treatment, textbook 0–42113
e.m. zero-point, third law of thermodynamics 0–54605
reaching earth rel. to electric discharges in solar, stellar and galactic atmosphere 0–62967
from electron, classical, spinning 0–48990
electron beam modulation by laser beam, production of monochromatic radiation 0–60154
fast neutron and y ray damage on Si devices 0–72075
field, functional integration calcs. 0–41981
field, oscillations in syst. comprising N two-level mols. 0–77053
fields amplitude in waveguides 0–54799
flame, 'soot' diameter meas. 0–52161
flow, turbulent, effects on heat transfer, for small optical depths 0–55415
forced harmonic vibration of clamped circular plate in acoustic field 0–69716
friction force in uniformly accelerated motion of charge 0–73161
gas, dynamics of radiating gases 0–46804
gaseous, nonisothermal, band absorptance formulation 0–55565
glass laser, near-infrared, space-resolved intensity 0–63626
gravitational, effect on secular stability of Maclaurin spheroid 0–59673
gravitational, effect on secular stability of Maclaurin spheroid 0–59673
gravitational, evolution of Jacobi ellipsoid 0–59675
harmonic oscillator, superradiant states 0–51957
heat transfer calc. by Monte Carlo method 0–69752
i.r., rel. to Moon thermophysical properties of surface obs. 0–59754
i.r., and visible, solid state devices using semicond, properties of PbTe, PbSe, PbS and PbO 0–47690
i.r. far, detection and spectral resolution, electron cyclotron resonance 0–68748
i.r. from GaAs diode, for distance meas. 0–51083
i.r. tropical storm cloud pattern data rel. to max, wind speed estimation
    i.r. from GaAs diode, for distance meas. 0-51083 i.r. tropical storm cloud pattern data rel. to max, wind speed estimation
    interaction with matter, dynamic theory 0-45713 irradiation, focused in materials by electron beams, temp. distribution 0-43935
    irradiation meas. at welding processes, eye-protection against i.r. hazard 0-66930
    Jovian, hectometric continuum, investigation using RAE-I satellite 0-66590
    l.f. spatial freq. signals enhancement with optical aperture tapering 0-63703
  0-63703 localized direct, oscillating shock wave productions, response of cylindrical shell 0-54757 loss in e.m. wave propagation in dielectric or optical fibres 0-66968 lunar radiation meas. in 1.2 mm wavelength range, surface roughness effect 0-51745 Lyman-\alpha, detection, from positronium atom 0-77416 magnetic, K^{\pm} \rightarrow \pi^{\pm} \pi^{0} \gamma decays 0-55030 magnetic line source in moving isotropic plasma 0-45718 master equation, expansion, with applications to coupled atom-radiation systems 0-57290 models, development and comparison of photons and wave models 0-45813 nonelectromagnetic, headlight effect. 0-48704
    nonelectromagnetic, headlight effect 0-48704 partially polarized multiply scattered, exact soln. of integral eqns. 0-51997
    pattern investigation, from dipole in randomly nonuniform medium 0\!-\!57464
  0–57464
pattern of longitudinal waves in plasma, by antenna 0–58323
photodetection, many-quantum, statistical peculiarities 0–42238
plasma resonance radiation from non- radiative plasmons and decay into photons on a rough surface 0–62273
in plasmas, thermal induction, analytical treatment, report 0–64671
polarization, kinetics 0–48920
polarization state of quasi-monochromatic, fields 0–67155
propagation of finite beam in random medium 0–41947
resonance, capture in gas 0–46827
resonance, self reversal by re-emission 0–42954
scattering by turbid atmosphere, diffuse noise level investigation 0–59582
scattering from point source in finite spheroidal atmosphere 0–66789
scattering isotropic from asymmetric spherical source in finite atmosphere 0–66788
```

Radiation continued

seismic, from series of line charges, directivity 0-76318 semiclassical theory, adiabatic theorems for oscill. systems 0-38182 semiclassical theory, for Stokes polarization parameter for quantum systems 0-41970

systems 0-41970 semiconductor laser, dynamic instabilities 0-42301 shock waves induced in gases by nonequilib, radiation 0-53263 spheres and infinitely long cylinders, evaluation of configuration factors, analytical approach 0-45661 spherical, symmetrical body, slowly rotating, Kerr-Vaidya metric 0-57261

0-57261 structure dependent, upper limit for K⁺→e⁺ν_eγ 0-55029 superradiation spectrum from a Ne pulse laser, fine structure 0-63608 temperatures, true and apparent, of graybodies in presence of atmosphere, nomogram relation 0-48872 transition, applic to detection of super-high energy particles 0-60695 transition, in periodically stratified plasma 0-78088 transition, relativistic charged particles traversing thin foils at oblique incidence 0-50915

transport, in solar energy units with mirror concentrations 0-42169 u.v. generation by sequential freq. conversion method 0-57555 uniformly accelerated charge 0-73158 variational methods applicable for approx. solns., error estimates

variational principles and techniques for solving radiation and scattering problems 0-63368

problems 0–63368
Ar-K plasma cylinder, K resonance radiation energy loss 0–39547
Ar plasma, source strength, exp. determination 0–67909
LiF, sound, from mobile dislocation walls, freq. depend. 0–68588
Mg, Al particles in N₂, integral radiation 0–50267
NaCl, sound, from mobile dislocation walls, freq. depend. 0–68588
SiLi, solar cells, effects on annealing times and carrier removal 0–45753
Zr, Ti particles in N₂, integral radiation 0–50268

heat

rel. to Mars, nature of surface material determining, from radio emission 0-63104

0-63104 in Zircaloy-2 tubes, in bounded annular cavity 0-39228 air-water interface, thermal emission, from Fresnel eqns. 0-43448 black body, isothermal cavity in grey scatt. material, apparent emission factor determ. 0-66929 in black body radiation at kT<10²MeV, baryon number instabilities 0-51625

0–51625
black radiator, variable for temp. to 4000 K 0–38406
black-body source isothermal cavity, prototype 0–66927
blackbody. Einstein derivation without assuming Maxwell-Boltzmann energy distribution 0–38198
blackbody absorptive power meas. 0–54767
blackbody calibration with thermocouples, accuracy 0–60073
blackbody isothermal cavity source 0–60072
cavity, hemispherical, absorption 0–45665
circular polarization in mag. field 0–76924
conduction interaction, surface emittance and approx. kernels 0–50166
Einstein's formula for fluctuations, verification 0–76926
emittance, total hemispherical measurement 0–48873
evaporography, obs. and theory 0–70094
flame turbulent diffusion buoyant, radiative heat transfer 0–48887
gas, on expansion, transient energy transfer in hot and cold layers 0–39667
gas-filled spherical cavity, transport eqn. soln. 0–76927

0-39667
gas-filled spherical cavity, transport eqn. soln. 0-76927
on insulation, effect on thermal conductivity w.r.t. thickness 0-68636
liquid, viscous, in vibr. pipes, heat emission at surface vibr. 0-39769
from major planets, meas. 0-63092
measurement, reflectance of blackened Cu, 300 to 2500 nm wavelength

measurement, renectance of blackened Ct, 300 to 2500 mm wavelength 0-57423 metal film/dielectric, temp., phonon radiators 0-47564 metals, thermal and radiative props. meas., 1000-2500°K, instrum. 0-65545

0-5545
nongrey transfer, correction to thermal cond. meas. 0-57437
plane problem soln., radiative heat exchange in infinite channel 0-54765
plasma, losses, analysis 0-39546
polarization in a symmetric cavity 0-66926
in randomly inhomogeneous medium 0-60926
in randomly inhomogeneous medium 0-60926

in randomly inhomogeneous medium 0-60098 solar concentrator, irradiance distribution in focal plane, photoelectric pulse method 0-63705 solar concentrator, paraboloid, energy distribution in focal plane, geometrical interpretation of mathematical model 0-67130 solar concentrator, paraboloid, radiant flux distribution, algorithm for statistical solution 0-67128 solar concentrators, Cassegrain system, modified, energy concentration 0-63667

olar cylindrical receiver, radiant flux distribution over walls, calc. method 0-63666 solar flux distrib. in penumbra 0-66928

solar flux distrib. in penumbra 0-66928 solar heater-receiver, concentration ratio relation to surface shape for parallel-ray flux 0-63664 spherical particles, physical parameters, particle emissivity 0-66933 temperature scale derivation, Planck's equation application, gold melting joint determination 0-38419 thermal diffusion of solid disk meas., w.r.t. radiation losses from all faces, transient heating method 0-47283 transfer in duct, medium of variable temp. 0-42102 Al₂O₃ cloud of small, spherical micronsized particles absorption and scattering 0-58503 Mo. in ranse 1900 to 2800°K, high speed meas. 0-47546

Mo, in range 1900 to 2800°K, high speed meas. 0—47546 UO₂ ceramic oxide fuel, rad, transfer importance in fast reactor 0—49733

Radiation belts see Atmosphere/radiation belts Radiation chemistry see Chemical effects of radiations/ionizing radiations;

Radiochemistry

Radiation damage see Physical effects of radiation

Radiation detectors

see also Bolometers; Photometry; Radioactivity measurement for Lyman-a from positronium atom, results 0-77416 black-body-cavity bridge radiometer, patent 0-57443 black-body-cavities directional spectral emittance, meas. tech., applic. 0-63472

cavity radiometer, absolute, solar irradiance meas. 0–57425 direct and heterodyne detection systems for lasers 0–69966 disturbance suppression, patent 0–60095

Radiation detectors continued

energy balance in cooling, thermal influx from outside, exptl. determination 0-57418

extreme u.v., use of paraterphenyl 0-60393 fission foil-Lexan, reactor neutron meas. 0-49747 gamma camera using NaI or Ge detectors, spatial resolution degradation 0-60699

gamma-ray spectrum, comparison of folding and unfolding techniques for determination from neutron capture in Al 0-77390 gravitation 0-72902

gravitation 0–72902 heat flux, boundary properties of oblique layer device 0–76925 i.r., Bose-Einstein photon noise statistics and Fermi electron statistics, continuity 0–57424 ir., D**degradation by sky or cloud radiation 0–69744 ir., blackbody objects, frequency convsersion into visible images by optical mixing 0–70074 ir., bonding material, visible and ir. transmitting props., 2-14 µm region 0–41092

0-41092
i.r., cel. to multisensor mapping of coastal effluents 0-62900
i.r., rel. to multisensor mapping of coastal effluents 0-62900
i.r., rel. to remote meas. of horizontal temp, gradients in atmos. 0-54237
i.r., semiconductor measuring system, patent 0-57444
i.r., as turbulence detector, clear air, inflight testing results 0-54244
i.r., as turbulence detector, clear air, inflight testing results 0-54245
i.r., and particles, visual detection using heat sensitive papers, description 0-49421
i.r. and visible, solid state devices using semicond. properties of PbTe, PbSe, PbS and PbO 0-47690

PbS and PbO 0-47690 i.r. for remote detection of clear air turbulence, instrumentation, tech. 0-66278

0–66278
i.r. laser rad., based on negative electron affinity 0–47895
i.r. low temperature, using Ge:Ga and InSb 0–76928
i.r. photoconductive, wideband optical heterodyne performance, parameters calc. 0–68977
i.r. remote sensors, rel. to ocean and water surface temp, meas. 0–62899
i.r. scanner, rel. to biothermography in 8 to 14μ spectral region 0–72800 lag reduction method 0–60639
laser power meter, for large or divergent beams, design and calibration 0–45668

laser pulse, propagation data analysis technique 0–49099 light detection systems, 4, theoretical and exptl. S/N ratios 0–42392 light receiver, avalanching photodiode based 0–65856 millimetre wave, rel. to atmos., stability meas. 0–54239

millimetrewave, low noise characts., using hot electron effect in Si:P 0-76964

0–76964
Nernst effect based 0–63474
optical heterodyne detection of 10.6μ radiation by metal-metal point contact diodes 0–67120
optical scanning system, spatial filter, optimisation 0–57613
photocathodes with organic coatings for vacuum u.v. region 0–62473
photocateric, accuracy of meas. of spectral sensitivity, effect of scattered light 0–49148 ir., visible and u.v. range, classification and characteristics

photon, ia 0-59296

0-59296
photon tagging system, high resolution, wide range 0-77412
pyroelectric for laser radiation's time and energy characteristics determination, description 0-49026
pyroelectric triglycine sulphate and selenate detectors 0-65824
radiometer, employing frequency domain coding 0-63191
radiometer, net, polythene shielded, relative sensitivities for short and long
wave radiation 0-76930
radiometers, blackbody, two high accuracy cavity types 0-48912
radiometers, methods for determination of spatial response nonlinearities
0-69742
radiometric imaging, photographic film applications 0-60453

o-09/142 radiometric imaging, photographic film applications 0-60453 radiometric target detection, pattern recognition application 0-45667 semiconductor, charge collection process 0-70309 semiconductor, illuminated, in open resonator, i.r. and optical radiation

0-51154

0–51154
semiconductor, introduction 0–60689
with superconducting weak links, response to photons 0–78909
surface barrier, window thickness meas. 0–73691
TGS pyroelectric detectors, performance characteristics 0–68967
threshold, High Flux Isotope Reactor, differential fast neutron flux determination (above 0.5 MeV) 0–49746
X-ray, Si surface-barrier type, Fano factor meas. 0–42640
BaTiO₃, pyroelectric, for optical and i.r. radiation, characteristics 0–76929
Ge:Li well-type detectors for y-rays activity meas. 0–46041
Ge-Hg, operational characteristic calc. 0–68977
Ge n-type for y rays, surface barrier, characts. 0–60688
Ge(Li), charge collection mechanism in high mag, fields 0–73687
Ge(Li), coaxial, pulse shape distrib., applicability for nanosecond half-life meas. 0–42638
GeLi, in-vivo counting, radionuclide depositions in humans 0–73695

GeLi, in-vivo counting, radionuclide depositions in humans 0-73695 Ge(Li), selection of the Ge by obs. of etch- pit distribs. 0-42637 Ge(Li) and Si(Li) biased detectors with cooled FET input, capacitance meas. method 0-42634

meas. method 0-42634

HgCdTe, thermal sensitivity meas. 0-63473

InAs, sensitivity improvement by clarifying coating 0-45666
n-InSb, appl. to submillimeter laser radiation meas. 0-67118
InSb, sensitivity improvement by clarifying coating 0-45666
InSb, thermal sensitivity meas. 0-63473

MgO-Fe²+, microwave photon-phonon double-quantum detection, performance and applic, 1.5 K 0-68602

Si surface-barrier X-ray detector, Fano factor meas. 0-42640

Si(Li) and Ge(Li) biased detectors with cooled FET input, capacitance meas. method 0-42634

T, in air, monitor, portable, down to 10µCi/m³ 0-73694

Te garnet radiometer and temperature controller 0-76931

YFe garnet radiometer and temperature controller 0-76931

Radiation effects see Biological effects of radiations; Chemical effects of radiations; Physical effects of radiations
Radiation monitoring

see also Dosimetry

boiling type atomic power station environments 0-70688 fuel detection, residual, in leached hulls, neutron counting eequipment 0-64174

monitor, portable semiquantitative with linear or logarithmic output 0-49555

neutron flux, ex-core two-range system for nuclear reactors 0-64180

Radiation monitoring continued

diation monitoring continued neutrons, Campbelling systems, analysis of differences between true mean-square and average-mangitude-squared detector ccts. 0–63874 neutrons, in-core system for boiling-water reactors 0–64179 nuclear instrumentation for fast reactors, review 0–49710 personnel, developments 0–76732 photons obliquely incident on concrete barrier, dose transmission and reflection probabilities 0–54488 for radionuclides, airborne, portable air sampling monitors 0–76408 reactor neutron meas, fission foil-Lexan detectors 0–49747 reactor neutrons, with fission foil-Lexan detector system 0–58074 reactor power, based on Cherenkov radiation detection 0–64173

Radiation pressure

diation pressure

see also Acoustic streaming

1 atm. and above, microsonation using transversely oscillating capillary.
chemical and biological effects obs. 0-45636

acoustic in medium, destructive interference method for reduction, noise
abatement, analysis 0-38386

balloon satellite acceleration, report 0-72671

dynamic theory 0-45713

far-field of unbaffied one side disc radiators, axial field values 0-60031
isotropic, on spherical particles, dynamical effects 0-67126
nearfield acoustic, meas. for 7.7 kHz free flooded cylindrical ring 0-69719
satellite orbital evolution under radiation press, influence, secular effects satellite orbital evolution under radiation press. influence, secular effects 0-57102

solar, artificial satellite orbit perturbations long period formulation 0-48350

on Al foil, focused picosecond light pulses effects 0-69981

Radiation protection
see also Radiation monitoring
book elementary on radiation physics 0-57161
contamination of vacuum system in electromagnetic isotope separator for
short lived fission products 0-45495
decontamination facility at Whiteshell Nuclear Research Establishment

0-45451 door alarm and interlock system at Los Alamos tandem accelerator facil ity 0-46091 electronics, miniature, techniques used in instrument design, report 0-66691

electromics, miniature, techniques used in instrument design, report 0–66691 fusion reactors environmental safety 0–70697 gamma ray dose-rate distribs. in slab phantom 0–73449 i.r. transmission factor of welding filters, eye-protection 0–59822 instrumentation for high-intensity, high duty accelerator 0–76716 instrumentation for measurement, European trends 0–76708 laser safety 0–57504 nuclear, transport in shield irregularity, calc. 0–49700 photon dose rate, residual, around high energy p accelerators 0–38773 photon dose rate, residual, reduction, around high-energy proton accelerators 0–57861 radiothermoluminescent dosimetry, current and future research and applications 0–48635 reactor building during loss-of-coolant accident, differential press. transients prediction 0–77601 reactor shield shape, optimum, Monte Carlo calc. 0–46294 reactor shielding and cooling by molten metal, patent 0–58075 self-shielding factors, homogeneity effects for fast reactors 0–58046 shielding and penetration of monoenergetic neutrons in multilayer systems 0–52828 shielding in reactor vessels, survey 0–38952

0-52828 shielding in reactor vessels, survey 0-38952 shielding in reactor vessels, survey 0-38952 shielding materials, propagation of neutrons, at intermediate energies 0-39178 shielding of reactor using uranium 0-67589 shielding of reactor using uranium 0-67589 shielding of reactor using uranium 0-67589 shielding of reactor using uranium advantage of the property of the property

thermal skin simulants for studies 0-/6/15 whole body counting, arrangement with tilting chair, arc or scanning bed geometry, operational parameters evaluation 0-55081 whole body counting, tilting chair and scanning geometries, relative photopeak efficiencies calculated, optimal operational parameters determination 0-55080

X-rays spectral transmission and attenuation rel. to glasses and resins in colour TV 0-51829 γ , photoelec. absorpt. in composite mats., effective atomic numbers calc. 0-45878

0-45878
p, photoelectric absorpt. by 14 elements, energy depend. 0-45877
LiH shields, neutron ang. flux spectrum 0.1 eV to 15 MeV 0-55199
Pb as shielding material 0-67588
Pb targets, spectra of bremsstrahlung and secondary electrons after e interaction 0-46200
Si photocells, by optical films 0-44409
U as shielding material 0-67589
W-LiH laminated sphere, neutron ang. flux spectrum and secondary gamma spectrum 0-55199
W, thick, ang. distribs. of bremsstrahlung prod. by 8.8 MeV e 0-45883
Zn-T targets in neutron generators Zr-T aerosol parameters obs., T gas inhalation hazard evaluation 0-54487
distribe recombination.

Radiative recombination see Luminescence

Radiative transfer

on Mars, Venus atms. entry 0-54441 in Rayleigh-scattering atmosphere with true absorption 0-69972 in absorbing and emitting medium, multidimens, transfer, approx, calc 0-45679

0–45679
in anisotropically light scattering and absorbing medium, radiation flux investigation 0–57590
annular fins of trapezoidal profile, radiation heat transfer 0–45662 atmosphere, Venus 8-14 \(\mu\) limb darkening particulate medium 0–63140 atmosphere, inhomogeneous, semiinfinite, pure scatt. 0–48567 atmospheric surface layer temp. from, meas. 0–66277 averaged eqns. for gas-dynamic problems 0–78215 cavities, cylindrical and annular, angular coeffs. 0–54766 for chromospheric lines, eqn. of transfer solved by Fourier transformations 0–57154 in cylindrical medium, Monte Carlo simulation 0–38216 discharges, high current 0–43297 disintegrating body in gas stream 0–71302 Eckert's technique rel. to radiation view factors for toroid 0–38410

Radiative transfer continued

diative transfer continued in enclosure with plane isothermal and adiabatic surfaces 0–57433 of energy, in gases non-diffusive in strong explosion 0–64823 equation, emittance obs. by thermal decay integration method 0–66940 equations, solns. by invariant imbedding method 0–66853 equations in spectral line regime, quantum theoretical deduction 0–69656 exchange problems, solution by least squares techniques 0–57301 finite slab, conservative, with internal source 0–69749 from flame, turbulent diffusion buoyant 0–48887 flames and gases radiative transfer in a cold wall combustion chamber 0–45673

0-45673
gas-filled spherical cavity, transport eqn. soln. 0-76927
in gaseous-core reactor, exact soln. of transport eqn. 0-55197
gases, resonance, optically thick media 0-58398
gray medium between concentric spheres, variational calc. 0-66856
H-functions, linear integral eqns. and their iterative soln. 0-72877
heat exchange between grey surfaces, iteration method 0-45681
heat transfer accompanying high temp., accelerating shock wave characteristics in decreasing atmosphere 0-43380
inverse mean free paths and lub. frame absorption coeffs. 0-69601
Lorentz lines in nonisothermal gases 0-78223
MHD generator, eff. on ioniz. relax. length 0-54812
metal damage by high-speed pulsed jets 0-53728
Mine problem, perturbation soln. 0-48771
Milne problem, soln. in picket-fence model 0-69659
molecules, energy transfer 0-55279
Monte Carlo method applic. to γ radiation transport, efficiency improvement 0-72979
nongray, in planar medium exposed to collimated flux 0-66854

nongray, in planar medium exposed to collimated flux 0-66854 nongray cylindrical medium 0-45660 nongray surfaces, radiative interchange, new mathematical formulation 0-45663

0–45663
nongrey planar medium, effect of band or line shape 0–668.55
plane problem soln., radiative heat exchange in infinite channel 0–54765
in planetary atmosphere, reciprocity relations for diffuse reflection and transmission 0–79726
planetary atmospheres, external radiation fields for scattering 0–76634
plasma, hydrogen, radiative energy transfer 0–46689
radiation, terrestrial, in 10-12 µ range, satellite meas., results 0–59574
radiative heat-exchange in large scale atmospheric dynamics 0–59575
radiative ionization in cold precursor of detached shock 0–71198
resonance radiation in purely scattering media 0–72980
resonance radiation in purely scattering media 0–72981
scattering medium with inhomogeneous absorption model 0–57591
semitransparent body with uniform wall thickness, radiation characts.
0–57432
shock waves, dispersion by energy transfer 0–54750
spectral line formed in multidimen, atmosphere 0–51675
spherical (stellar) atmosphere of free electrons 0–59708
in spherical shell atmosphere, externally illuminated, probabilisite model 0–51999

0 - 51999

0-51999
spontaneous decay and level shifts in semiclassical theory 0-42931
stationary, non-equilibrium, entropy production 0-51998
stationary number density in excited state 0-42011
statistical electrodynamic content 0-63692
steady and transient heat transfer in a medium bounded by two coaxial
cylindrical surfaces 0-45670
stellar atmospheres, finite, inhomogeneous, partially polarized radiation
transfer 0-57019
in stellar atmospheres that are spherical 0-54361
troposphere's radiative fluxes and influxes, approx. method for calc.
0-59575
CO₂-N₂ atms., on entry, rel. to Mars, Venus 0-54441
H plasma, effect of surface emissivity 0-67899
diators. See Electromagnetic waves/radiators. Transcheers

Radiators see Electromagnetic waves/radiators; Transducers

Radicals see Free radicals

Radicals see Free radicals

Radioactive dating
apatites, fission track ages 0-72596
chondrites, carbonaceous, 8⁸Rb-8⁹Sr dating 0-45426
feldspar in meteorites, ²⁶Al-²⁶Mg dating 0-45425
fission track annealing method for epidote and allanite mineral's age determination 0-51497
fission tracking of volcanic glasses and thermal history of rocks 0-45119
fossil bones, unsuccessful appl. of uranium-helium method 0-48239
ground water, ¹⁴C dating, evaluation and application 0-54215
lunar samples, Rb-Sr, U and Th-Pb dating 0-48492
lunar samples, age determ. from radioactivity 0-48510
lunar samples, concentrations of U, Th and Pb rel. to age determination 0-45334

lunar samples, crystalline rock, ⁴⁰Ar/³⁹Ar dating 0-48491 marine organisms, Pacific, using long-lived *y*-ray emitting nuclide Ag-108m 0-69271

nethane synthesis for radiocarbon dating, catalytic hydrogenation converter 0–54216 natural, 106-108 years half life, information on early history of solar system 0–62878 sand, age determinations of size fractions of monazite and zircon 0–48240

0—48240

tektites, fission-track ages, effect of strain 0—45103

*0Ar/³9Ar, precision of technique 0—76345

*0Ar-³9Ar versus *0K.³8Ar isochron plots of samples, analysis 0—45120

*14C method foe Iceland's volcanic material 0—66269

*1291-*129Xe, evidence for cold assembly of unequilibrate chondrite 0—72776

K-Ar isochron method and initial Ar-ratios 0—45120

*18O concentration in Greenland ice core rel. to solar activity index 0—63180

*1.-He method unsuccessful anal to fossil bones. 0—48239

U-He method, unsuccessful appl. to fossil bones 0-48239 U geochemistry, nuclear methods 0-66239

Radioactive tracers

fin vitro' procedures, review 0–66693
atmospheric, conference Heidelberg (1969) 0–54241
rel. to blood flow, pulmonary, spatial distribution, with computer-generated three-dimensional oscilloscopic images 0–63205
dissolved complexes, correlation times from rotational tracers 0–58256
for hemodynamics function studies, multichannel for test device applic.
0–45454

0 - 45454reactors in series, distribution functions analysis from radioisotope tracer expts. 0-45048

198 Au for marking fine deposits 0-77524

Radioactive tracers continued

113Sn, rel. to flow pattern and velocity determination of liquid Sn 0-50174 99mTc, electrolytic complexation with human serum albumin at constant current, clinical applications 0–41882
204Tl, rel. to flow pattern and velocity determination of liquid Sn 0–50174

Radioactivity

toactivity
see also Alpha-particles; Beta-rays; Gamma-rays;
Atmosphere/radioactivity; Beta-decay theory; Chemical analysis, radioactive; Chemical effects of radiations/ionizing radiations;
Fallout; Geophysical prospecting; Nuclear decay theory;
Nuclear bombardment targets; Nuclear excitation; Nuclear reactions and

Nuclear bombardment largets; Nuclear excitation; Nuclear reactions amscattering; Radiochemistry
α decay, accuracy of JWKB approach for deriv. of penetrabilities
0-49557
β-active 'hot' aerosol particles, spontaneous unipolar charging 0-39846
β-active 'hot' aerosol particles, unipolar charging in electric field, kinetics
0-39847

charge of recoil atoms after α decay 0-38961 conversion electron γ coincidences, conversion ratios used solid state detectors 0-70534 cosmogenic radionuclide production rates in argon in stratosphere 0-60633

Cosmognic consideration of the production rates in agon in statosphere 0-6063 crystals, ionic, calc. of surface elec. charge from decay 0-40817 decay theory, based on nonrelativistic time-dependent elastic scattering theory 0-52712 decay theory by Gamow, validity of exponential law 0-52713 Earth, by antineutrino induced K-capture, meas. 0-42473 earth, gamma radiation spectra, airborne meas., comparison with field verification meas. 0-52714 element 104, effect of α -radioactive background on α -decay 0-73846 elements, α -radioactive, thin films, diffusion coeff. determ. from activity meas. 0-78574 experiments for schools 0-38953 Gamow's theory of decay, based on nonrelativistic time-dependent elastic scattering theory 0-52712 Gamow's theory of decay, validity of exponential law 0-52713 halos, giant 0-70538 hyperfragments, heavy, lifetimes, Monte Carlo calculations 0-67498 induced in plasma by electron and ion acceleration to walls during instabilities 0-38958 irradiations experiment in ORNL 0-60796

ites 0-36936 irradiations experiment in ORNL 0-60796 lunar samples, Ar radioactivities from cosmic ray bombardment 0-48504 lunar samples, Th-U contents by alpha-particle activity 0-45350 lunar samples, bombardment-produced radionuclides, in rock and soil

-48509

0-48509

lunar samples, cosmogenic and primordial radionuclides, γ-ray spectrometry 0-45365

lunar samples, of tritium and argon 0-48507

lunar samples, radioactivity induced by solar flare protons 0-66581

lunar samples, radionuclides determ. by γ-ray spectrometry 0-48510

lunar samples, rel. to meteorite infall, solar-wind flux and formation conditions 0-45341

natural, dating history of rocks, early history of meteorite parent body and solar system 0-62878 nuclear crater ejecta, postshot distribution and movement of radionuclides

0-7305

0—73057 once-forbidden β transitions at 72 \leq A \leq 86. β γ correlations 0—46161 radioisotopes prod., shape and arrangement of target materials, self-shielding effect obs. 0—38957 radionuclides, separation, application of high voltage electrophoresis 0—73853

rare-earth isotopes, short lived, 150 Dy, 151 , 152 , 153 Ho, 153 , 154 , 155 Er, α spec

0–1/3833 rare-arth isotopes, short lived, ¹⁵⁰Dy, ¹⁵¹. ¹⁵². ¹⁵³Ho, ¹⁵³. ¹⁵⁴. ¹⁵⁵Er, α spectra 0–49561 reactor containment, removal system, patent 0–46317 review of expt. work 0–57938 source, uniform γ , disc, using short lived isotopes 0–63767 superheavy elements, their fission and alpha-decay review 0–64079 Szczawno mineral waters, long-lived α and β activity 0–59538 α decay, of even deformed nuclei, r.p.a. pairing correlation 0–38960 ¹⁵⁶Tb, β + decay, using $4\Pi\beta^*\gamma$ -spectrometer 0–60783 ²²⁵Ac, internal electron conversion spectra, decay products, γ spectra 0–52739 ²²⁷Ac, α branching ratio determ. 0–73881 ^{110m}Ag, oriented, new technique for study of β -ray asymmetry 0–67506 ³⁵Ar- β -12 study 0–52994 ³⁹Ar, correlation effect on unique forbidden decay 0–49562 ⁴¹Ar, correlation effect on unique forbidden decay 0–49562 At (A=209, 210, and 211), fine structure of α spectra 0–52738 ¹⁹²Au, γ -ray spectra meas. 0–70512 ²⁹⁴Au, β -decay, spectra study 0–73878 ¹⁹⁸Au, nuclear orientation study of first-forbidden β decays to ¹⁹⁸Hg 0–70555 ¹⁹⁸Au, rel, to fluorescence and Coster-Kronig yields of L subshells in Hg

0-70555

198 Au, rel. to fluorescence and Coster-Kronig yields of L subshells in Hg
0-70767

0–3898
³⁰Br decay to excited 0+ states, retardation 0–64085
³⁴C, β-ray spectrum expt'l evidence of nonstatistical shape 0–77514
³⁴C and ³⁴N core polarization, agreement between binding energy and β-decay 0–60754
³⁴Ca, Gamow-Teller, half-life 0–64017
¹¹¹Cd, K-LL Auger electron spectra, meas, with mag. β-spectrometer

0–38997 ... 0–38997 ... 0–70551 ... 0

56Co, higher-order effects from isospin-hindered allowed β decay 0-49569

0–49569 $^{\circ}$ °Co²+ decay, in Co[Cr₂]O₄ and Co[Cr₂]S₄, Fe valency states, Mossbauer determ. 0–41149 $^{\circ}$ °Co, energy-dependent beta-gamma circular polarization 0–57956 $^{\circ}$ °Co, velocity dependence of helicity of β particles 0–57951 13 °Cs comparison of experimental and calculated results 0–70547 13 °Cs $_{\circ}$ - 13 °Ba, $_{\rho}$ Py directional correlation studies 0–70548 13 °Cs $_{\circ}$ -ray polariz, meas., depolariz, effects of detector sizes 0–63876 13 °Cs, $_{\circ}$ -decay, $_{\circ}$ -Ba metastable level obs. 0–73868 Cu, calc. activation by 3 GeV protons 0–77554

Radioactivity continued

⁵⁸Cu, decay, energy levels of ⁵⁸Ni 0-64083

dioactivity continued

58Cu, decay, energy levels of 58Ni 0—64083

66Cu decay to excited 0+ states, retardation 0—64085

146Eu, β+ decay, meas. 0—60781

148Eu, β+ decay, meas. 0—60781

149Eu, energy levels of 159Gd 0—64095

Fe calc. activation by 3 GeV protons 0—77554

68Ga decay to excited 0+ states, retardation 0—64085

146Gd, β+ decay, meas. 0—60781

147Gd—147Eu, gamma spectrum meas., y transitions 0—64093

66Ge, γ spectrum meas using Ge(Li) spectrometers 0—73859

67Ge, γ rays produced investigated 0—46164

3H, β-decay in LiH rel. to volume expansion 0—47217

3H, β spectrum, end point energy, ft deduced 0—70540

3He and 3H possible delayed emission discussed 0—46160

3He decay in LiD₀.6T_{0.4}, lattice expansion 0—50529

Hg isotopes, α-decay 0—49579

197mHg, transition multipolarities by magnetic electron and γ-ray spectroscopy 0—73879

1(A=119, 121, 123), level schemes of Te(A=119, 121, 123) 0—49533

13H, activity determ. after perturbation of reactor 0—64091

13H, β-decay, autoionization of k-shell and outer shells 0—52732

13H, internal conversion ratios of 364keV transition 0—49578

14In, β-decay, autoionization of k-shell and outer shells 0—52732

13H, internal conversion ratios of 364keV transition 0—49578

14In, β-decay, pectra study 0—73878

18BIr, β+ decay, spectra study 0—73878

18BIr, γ-bectra meas. 0—73876

199Ir, rel. to population of levels in 199Os 0—38862

192Ir, level struct. study of 192Pt by sum-peak and sum-coincidences 0—70513

192Ir decay, β—pranular correlation 0—73877

194Ir, β-particle and γ distributions after polarisation in iron at low tempe

0-70315¹⁹²Ir decay, $\beta-\gamma$ angular correlation 0–73877 ¹⁹⁴Ir, β -particle and γ distributions after polarisation in iron at low temperatures 0–57959

ratures 0-57959 '

*2'K, gamma-ray spectra, peaks at 0.692 and 1.228 MeV 0-55143

*9'Kr, decay energy determ. 0-70543

*9'Kr decay to 50'Rb, energy level determ. 0-64086

*9'Kr decay to 9'Rb, energy level determ. 0-64086

*40'La, beta-decay matrix elements and the implications for isobaric analog states 0-57957

*40'La, energy-dependent beta-gamma circular polarization 0-57956

*6'Li→α+d, vertex function for virtual decay, within three-particle model 0-70541

0-10341 in Lu, prep. of thin source, for β -ray spectroscopy, by 169 Tu(α ,x) 0-64078 in Lu- 173 Yb, internal conversion electron spectrum 0-64096 in Lu, conversion electron spectrum, using double-focusing spectrometer 0-46174

0=401/4 235 Lw study of α -decay 0=73884 236 Lw study of α -decay 0=73884 257 Lw study of α -decay 0=73884 257 Lw study of α -decay α -particle energy distribution calculated

237Lw study of α-decay 0—73884 $_{\Lambda}^{9}$ Be \rightarrow α- $_{\Lambda}^{2}$ Pe \rightarrow α- $_{\Lambda}^{2}$ Periodic meas. and $_{\Lambda}^{2}$ -spectroscopy 0—38965 Mm⁵s, international comparison in 1968 0—64081 $_{\Lambda}^{2}$ PM prod. in reactions induced by p, d and $_{\Lambda}^{2}$ s 0—39008 $_{\Lambda}^{2}$ PM og amma spectra, radioactive decay 0—64088 $_{\Lambda}^{3}$ N and $_{\Lambda}^{4}$ C, core polarization, agreement between binding energy and $_{\Lambda}^{2}$ PM of $_{\Lambda}^{2}$ PM of $_{\Lambda}^{2}$ Periodic offect on unique forbidden decay $_{\Lambda}^{2}$ PM of $_{\Lambda$

Na, β' decay, anomalous beta-aipna anisotropy directional correlation 0–57947

"Nb β γ circular polarization asymmetry 0–64087

**I¹/₂mNd, allowed β-branch, strong hindrance 0–70549

**I²Np, non-local barrier and anisotropy of alpha emissions for oriented nuclei 0–57962

***¹/₂O, β decay correction factor and hindered Gamow-Teller allowed transition for a mass-14 system 0–57946

***¹/₃O, φ-vidence for parity-forbidden α-decay from 8.87 MeV 2⁻ state, transition width 0–73854

***¹/₃O parity forbidden alpha decay from 2⁻ (8.88 MeV) level 0–46163

***¹/₃O, β decay to ¹/₂- state of ¹ºF, half life, transition strength 0–73856

***²/₃O, β decay to ¹/₂- state of ¹ºF, half life, transition strength 0–73856

***²/₃O₂ s psectra meas. 0–73876

***²/₃O₂ s psectra meas. 0–38994

***²/₃Pa, α decay, γ, spectroscopy investigation 0–73882

***²/₃Pa, α decay, γ, spectroscopy investigation 0–73882

***²/₃Pa, α decay, γ, spectroscopy investigation 0–738998

***³/₃Pm-Nd (A=143, 144, 146), inner conversion electron and γ ray spectra

2-38998 Pm→Nd (A=143, 144, 146), inner conversion electron and γ ray spectra 0-52736
1-22 Pm→1-42 Nd, meas. of γ transitions, level struct. of 1-42 Nd 0-52700
1-48 Pm, 1-0-1 β-decay, nuclear matrix elements 0-70553
2-11 Po, fine structure of α spectra 0-52738
2-12 Po, α-decay reduced with contribution of 2 proton excitation from ground state to uppermost occupied neutron orbit 0-49559
Pt (A=189,188), γ spectra meas. 0-73876
1-37 Pc, 1-37 Au, oriented nuclei in Fe matrix, β decay study by Mossbauer resonance in 1-37 Au, 0.06-20 K 0-49580
2-39 Pu, β-decay energy meas. of products 0-52815
2-39 Pu, β-decay energy meas. of products 0-52815
2-39 Pu, β-decay energy meas. of products 0-52720
2-38 Particle and γ distributions after polarisation in iron at low temperatures 0-57959
1-38 Re (CVC theory and nuclear matrix elements from β-γ cascades 0-64098

0 - 64098¹⁸⁸Re, β -particle and γ distributions after polarisation in iron at low tempe-

ratures 0-57959 188 Re CVC theory and nuclear matrix elements from β - γ cascades

0-64098 and indetail matrix elements from ρ - ρ cascades 0-64098 228 Rn, perturbations of α - ν angular correlation 0-57961 21 Sb, K-LL Auger electron spectra, meas, with mag. β - spectrometer 0-38997

0-38971 238b, nuclear matrix elements of 437 keV β transition 0-73867 2138b -125Ce, $\gamma - \gamma$ directional correlations for two cascades 0-49576 89sr, meas. of β spectrum shape, anal. using electron radial wave functions 0-49571

0–495/1 Ta (Δ =167,168,169,179,171), prep. of new isotopes, γ spectra anal. of daughter isobars Hf, Lu, Yb 0–38989 186 Ta $_{\pm}$ 186 W decay, excited levels of 186 W obs. 0–64062 154 Tb β + decay, using 4Π β + γ -spectrometer 0–60783 160 Tb, 1710 keV β →86 keV γ cascade, β - γ correlation studies 0–60784 130 Te $_{\pm}$ 130 Xe nuclear matrix element for double β decay 0–70546

Radioactivity continued Th (A=221-224), α -decay properties, produced in heavy-ion reactions with ^{209}Bi and ^{208}Pb 0–49581

²²⁷Th→²²³Ra, conversion electron spectra of 29.9 and 31.6 keV transitions

0 -70767 of L subshells in Hg 0 -70767

0 -70767 "25'U enrichment of metallic U, registration using cellulose nitrate 0-77436 "25'U enrichment of metallic U, registration using cellulose nitrate 0-77436 (4V, β -decay, γ -and β -coincidences, deduced Q_{β} , log ft 0-49568 (2Pd, 21 min decay, anomalous $^5/_2$ + and $^7/_2$ + states in 99 Rh investigation 0-38902

dating see Radioactive dating

decay periods
β, double, in regions far removed from β-stable band 0–42785
half-life, statistical considerations 0–60794
half-life estimation statistical and systematic error, factors affecting
0–46159
half-life meas., statistical error and systematic bias factors 0–49556
half-lives, short, determination, using pulsed activation, information loss
0–52714 lifetime meas. in 100 ps range, two parameter centroid shift method

0. 52715 microwave method for short lifetimes meas. in α -decay 0–70556 neutron deficient, deformed nuclei, 150<A<190, classification, eval. of half lives of unknown nuclei 0–38989 rare-earth isotopes, short lived, ¹⁵⁰Dy, ^{151, 152, 153}Ho, ^{153, 154, 1}/₅°Er, α decay 0-49561

0 - 49561 rare-earth nuclides, half-lives and gamma-ray abundances 0 – 52717 review of predictions of stable isotopes 0 – 70535 total half-life predictions for neutron deficient actinide isotopes 0 – 57944 $\rm X/\alpha$ ratios, measurement and use for transurance α emitters 0 – 73883 $\rm ^{195}$ $\rm ^{87}$ l, α ray spectrum and product identification from $\rm ^{175}Lu + ^{20}Ne$ 1 $\rm ^{196}$ Ag half-life 0 – 73864 $\rm ^{28}$ Al, lifetime of 31.2 keV level, two parameter centroid shift meas. method 0 – 52715 $\rm ^{15}$ Ar ($\rm ^{16}$ $\rm ^{16}$ $\rm ^{15}$ $\rm ^$

²⁻⁸Al, inetime of 31.2 keV level, two parameter centroid shift lineas: hiethod 0-52715 Ar (A=43,44), from Ti, V (p, spallation) 0-73857 ⁹⁹As decay 0-73860 ⁸²As half life from irradiation of ⁸²Se with 14.7 MeV neutrons 0-49570 Au isotopes, α -decay, half-life meas. 0-49579 ¹⁹⁸Au, half-life 0-38966 ¹⁹⁹Au, 0-38966 ¹⁹⁹Au, 0-38966 ¹⁹¹Bi \rightarrow 20°T1 α -decay, excited states lifetimes 0-70556 ⁴⁰Ca half-life meas. 0-64084 ²¹¹Bi \rightarrow 20°T1 α -decay, excited states lifetimes 0-70556 ⁴⁰Ca, half-life meas. by following decay of γ rays emitted 0-77516 ¹¹³Cd, β instability, half-life 0-70545 ¹¹³Cl, half-life value 0-52723 ²⁴⁴Cm, spontaneous fission of 94% sample, partial half life 0-46260 ⁶⁰Co half-life meas. 0-64084 ¹³⁷Cs half-life meas. 0-64084 ¹³⁷Cs half-life meas. 0-64084 ¹³⁷Cs half-life and effective neutron capture cross-section determ. 0-64094

2³⁴Cm, spontaneous fission of 94% sample, partial half life 0—46260 (⁹⁴Co half-life meas. 0—64084 (³⁷Cs half life meas. 0—64084 (³⁷Cs half life meas. 0—64084 (³⁸Eu half-life and effective neutron capture cross-section determ. 0—64094 (³⁸F), half-life, mirror symmetry in β decay 0—42786 (³⁸Ge half life from irradiation of ⁸²Se with 14.7 MeV neutrons 0—49570 Hf (A=166,167 and 169), neutron deficient isotopes 0—38990 (³⁸Hf, half-life meas. p rays det. 0—57958 (³⁶Hf half life meas. p rays det. 0—57958 (³⁷Hf, lower limit for α-decay half-life 0—46173 (³⁷Hg isotopes, α-decay, half-lives meas. 0—49579 Hg isotopes, short lived 0—73875 (³⁸Hg half-life meas. by following decay of p-rays emitted 0—77516 (³⁸HK, half-life meas. by following decay of p-rays emitted 0—77516 (³⁸HK, half-life meas. by following decay of p-rays emitted 0—77516 (³⁸HK, half-life in solid NaCl and in aqueous solution 0—55140 (³⁸HK, half-life in solid NaCl and in aqueous soln., half-life alteration of β-decay in an and cations 0—73873 (³⁸MgCl half-life, biological, in humans, dose calculations 0—76727 (³⁸HgCl half-life, biological, in humans, dose calculations 0—76727 (³⁸HgCl half-life, mass-spectrometric determination 0—70557 (³⁸Pp, half-life walue 0—52722 (³²Pp, half-life, mass-spectrometric determination 0—70557 (³⁸Pp, half-life, and cations 0—56715 (³⁸Pp, half-life, and cations 0—56715 (³⁸Pp, half-life, and cations 0—46718 (³⁸Ppm, ground state, half-life, by p-ray spectrometry 0—46178 (³⁸Ppm, half-life, and cations 0—52723 (³⁸Ppm, half-life, and cations 0—52723 (³⁸Ppm, half-life, and cations 0—60787 (³⁸Ppm, paround state, half-life, by p-ray spectrometry 0—46178 (³⁸Ppm, half-life, and cations of 0—60787 (³⁸Ppm, paround state, half-

decay schemes
β-decay, EO transitions, competition between electro and electron-position pair emission, Fermi functions 0-49563 cascades, sum and sum-peak coincidence spectroscopy 0-38839

Radioactivity continued decay schemes continued

nuclides, disintegration rate, absolute determination by β - γ - and $4\pi\beta$ - γ -coincidence methods 0-49553 in radiation dose estimation 0-51840

review of search for element 114 0-73844

in radiation dose estimation 0–51840 review of search for element 114 0–73844 β decay, mirror symmetry consideration in A=20 and 25 0–42786 δ decay, mirror symmetry consideration in A=20 and 25 0–42786 δ decay to levels in δ Mn investigated using Ge(Li) gamma detectors, deduced δ Mn levels 0–57948 levels 0–57948 levels 0–57948 levels 0–60791 levels 0–60791 levels 0–60791 levels 0–60791 levels 0–60793 lines, transitions multipolarity 0–42801 levels 0–57954 levels 0–60793 lines, transitions multipolarity 0–42801 levels 0–57954 levels 0–57954 levels 0–57954 levels 0–57954 levels 0–57950 levels 0–57950

0–38963 102 Cd, deduced levels of 103 Ag 0–52729 117 Cd, 117m Cd, beta decay 0–49575 141 Ce, β - γ directional correlations 0–57950 142 Ce, β - γ directional correlations 0–57950 142 Ce decay, deduced levels of 144 Pr and energies and intensities of γ -rays

0-64039

144 Ce-144 Pr, y energies and intensities, 144 Pr excited states 0-70552

35 Cl, isobar-analogous state, 8.38 MeV level, rel. to excited 3.95 MeV level

o-576Co, energy and intensity of the X-ray transitions, deduced 56Fe levels 0-57949

6-379.2 y-ray spectra 0-42787 6-36-6-57.1, 15 min, γ obs. 0-38968 6-36-6-6-7.1 spectra of the X-ray transitions, deduced 6-2π levels 0-57949

and intensity of the X-ray transitions, deduced δ⁸Zn levels 0–57949

¹³Ga 0–73861

¹⁴Ga→¹⁴Ge, energy level obs. 0–38970

¹⁴Gd-1¹⁴Eu→1¹⁶Sm, high resolution studies of transitions 0–67508

¹⁴⁹Gd, electron capture, γ-rays studied 0–77521

¹⁵¹Gd→1⁵¹Eu, from γ-ray energy and intensity meas. 0–46169

¹⁵²Gd, γ spectra, level scheme obs. 0–38987

¹³H→¹He, transition matrix element evaluation 0–49564

¹⁶⁹H, neutron deficient isotope 0–38990

¹⁷⁰Hf obs. rel. to levels in ¹⁷⁰Lu, ¹⁷⁰Tm and ¹⁷²Tm 0–52704

¹⁷¹Hf, deduced rotational levels of ¹⁷¹Lu 0–60756

¹⁸¹H(→1⁸¹Ta, search for population of levels above 618.9 KeV 0–46175

²⁰⁶Hg, levels in ²⁰⁶Tl, (s₁₇-¹p_{1/2}-¹) 0–49549

¹⁵⁵Ho→1¹⁵⁵Dy, ¹⁵⁵Dy excited level transitions and level scheme 0–77522

¹⁶⁰HO→1¹⁶⁰Dy, obs. 0–46170

¹⁶²Ho decay, β and γ transitions study, decay scheme revision 0–46171

¹⁶⁵Ho→1¹⁶⁶Ho→1¹⁶⁶Er, spectral form and transitions analysis 0–73870

I isotopes, and levels in Te isotopes with 117≤A≤124 0–67476

¹⁸⁵H→1¹²Te, 35.48 keV transition conversion coeffs., Te K-fluoresc. yield 0–38980

1251—125Te, 35.48 keV transition conversion coeffs., Te K-fluoresc. yield 0–38980

1261, p-radiation, intensities of p-rays 0–49577

1301 and 139Cs β-decay, 139Xe excited states 0–52697

1321—132Ke, excited levels scheme 0–49535

1341, decay props. from fission products, investig. using NaI(Tl) and Ge(Li) detectors · 0–38982

1351, deduced levels of 135Xe 0–52733

107 In→107Cd, p-radiation and conversion electron obs. 0–73863

109 In→109Cd p spectrum and 109Cd deduced levels 0–55147

1111n, anisotropy of pp angular correlation 0–49574

1321—1321, p-1821, p-1821, p-1821, p-1824

109Gr decay to 190Cs, p-ray spectra 0–77504

40K, from 19K(n,p), scheme for observed p-ray transitions 0–42852

40K, 40Ca, schematic model calculations, particle hole force effect on lifetime 0–70542

40K–40Ca, third-forbidden, shell and rotational models calc. 0–73855

89Kr studied by means of Li drifted Ge detector, energies and relative intensities of p-transitions 0–52727

140La β-decay, obs. 0–38985

1Li, β-decay, study by recoil- particle method and β-n coincidence method 0–49567

2Li→9Be, β-decay, 9Be states obs. 0–38850

⁹Li→⁹Be, β-decay, ⁹Be states obs. 0-38850

```
Radioactivity continued
                                                                                                                                                                                                                                                                                                                                                                                           Radioactivity continued electron capture continued
           decay schemes continued
                <sup>169</sup>Lu, conversion e spectra meas. 0–73871

<sup>170</sup>Lu→<sup>170</sup>Yb, energy levels of <sup>170</sup>Yb 0–46172
                                                                                                                                                                                                                                                                                                                                                                                                           Retain Capture Communication Rb, accurate determ. of P_8\omega_k-value and fluoresc. yield \omega_k, following e. capture decay of {}^{88}\text{Sr} - 0-67504 {}^{189}\text{Tb}, population of energy levels in {}^{186}\text{Gd} - 0-70503 {}^{65}\text{Zn}, L/K and M/L ratio 0-67503
       178Lu, deapy, deduced log fr and levels of "77b 0—57926
177Lu, "17Hf, directional y-y correlation studies 0—77523
177Lu, "17Hf, y intensities, E2/M1 mixing ratios, branching ratios 0—38993
17Mg β-decay 0—70653
17Mg β-decay 0—70653
17Mg β-decay 0—77519
18Ng β-decay 0—70819
18Ng β-decay 0—70829
18Ng β-decay 18Ng 
               172Lu, decay, deduced log ft and levels of 172Yb 0-40172
172Lu, decay, deduced log ft and levels of 172Yb 0-57926
177Lu-177Hf, directional p-p correlation studies 0-77523
177mLu-177Hf, p intensities, E2/M1 mixing ratios, branching ratios
                                                                                                                                                                                                                                                                                                                                                                                                      protection see Radiation protection
                                                                                                                                                                                                                                                                                                                                                                                            Radioactivity measurement see also Dosimetry; Radiation monitoring; and the specific radiation,
                                                                                                                                                                                                                                                                                                                                                                                                          see also Dosimetry; Radiation monitoring; and the specific radiation, e.g. Gamma rays
p-radioactive nuclides quantitative analysis, amplitude summing Compton spectrometer applic. 0-49340
in air and raim, to middle of 1969, results 0-45158
in biological microsamples, using quaternary ammonium base 0-76718
fuel analysis, nondestructive radiative neutron capture 0-49727
half-lives, by p-ray spectrometry 0-46178
internal conversion electrons, detection in charged particle spectra using Si(Li) detector 0-38840
isotopes initial counting rate, short-lived, during multichannel analyzer lifetimes 0-387318
lifetimes in 100 ps range, two parameter centroid shift method, 0-57715
                                                                                                                                                                                                                                                                                                                                                                                                           lifetimes in 100 ps range, two parameter centroid shift method 0-52715 microwave method for short lifetimes meas. in \alpha-decay 0-70556 preset-count and preset-time determ. 0-77511
                                                                                                                                                                                                                                                                                                                                                                                                          preset-count and preset-time determ. 0–77511 relative intensities, internal conversion coefficients 0–60775 in surface air, turbulent exchange and wash-out obs. 0–76404 60°Co absolute standardization technique for internat. comparison 0–38956 60°Co isotope in Alandroal, Allende and Sprucefield fallen meteorites 0–54451 134Cs p-rays, applic. of stilbene crystal p-ray scintillation spectrometer 0–49400
                                                                                                                                                                                                                                                                                                                                                                                                           <sup>3</sup>H isotope in Alandroal, Allende and Sprucefield fallen meteorites 0-54451
                                                                                                                                                                                                                                                                                                                                                                                                           ^{0-54451} K whole-body \gamma spectrometry 0–59824 ^{22}Na+^{26}Al isotope in Alandroal, Allende and Sprucefield fallen meteorites 0–54451
                                                                                                                                                                                                                                                                                                                                                                                                           <sup>30–3431</sup> as ource, multicurie, by isomeric activation 0–52716
Ra, comparison of four national standards, exptl. procedures and results 0–57841
                                                                                                                                                                                                                                                                                                                                                                                                           Nature 100-37842 (2008) The manation of four national standards, statistical analysis 0-57842 (2008) The manation from soils 0-45117 (2008) The manation, meas. by disintegration chamber and by nuclear emul-
                                                                                                                                                                                                                                                                                                                                                                                                           ron 0-76346

Zn-T targets in neutron generators, T gas inhalation hazards evaluation, Zr-T aerosol parameters obs. 0-54487
                                                                                                                                                                                                                                                                                                                                                                                                      apparatus
                                                                                                                                                                                                                                                                                                                                                                                                           see also Particle detectors \beta-activity, use of low-background system of 1.2 pulses/min. and 4\pi geometry 0-49358
                                                                                                                                                                                                                                                                                                                                                                                                           calorimetry, applications and instrumentation, review 0-70536 environmental signatures, rapid evaluation using airborne platform
                                                                                                                                                                                                                                                                                                                                                                                                          0-63867 halogens, in liquid samples, neutron activation analysis, patent 0-57943 multiscaler with ferrite memory 0-55139 nuclear excavation, meas, system for deposition and resuspension of radioactive particulate 0-63866 nuclear half-lives, long period, meas, using time-to-pulse height converter
                                                                                                                                                                                                                                                                                                                                                                                                                0 - 42644
           electron capture
            electron capture
detector for gas chromatography, basic parameters 0–63871
exchange effect, relativistic evaluation, correction factors 0–70532
functions for analysis, from atomic K and L shells 0–46153
K capture, relative probabilities, K/β+ branching ratios 0–70533
K- and L-shell electrons, relative capture probabilities 0–57937
ratios meas. by multi-wire prop. counters, correction 0–42779
review of expt. work 0–57938
strength function phenomena 0–73848
<sup>37</sup>Co-<sup>37</sup>Fe, chem. effects in solid complexes 0–75982
<sup>37</sup>Fe, charge states in <sup>37</sup>Co-labelled KCoF<sub>3</sub> and K<sub>3</sub>CoF<sub>6</sub>, Mossbauer study 0–70558
<sup>48</sup>Gd decay scheme studied 0–77521
```

⁵Fe, charge states in "Co-tablish" (1975):
149Gd decay scheme studied 0–77521
159 Hg₂-159Au 9.5 h and 40 h isomer decay study 0–46177
1154π]n, K-X-ray-y-ray directional correlation obs. 0–60780
216Np KI*=22- state of ²¹⁶U obs. 0–38949
Po (A=201, 203, 205, 207) populating levels in Bi odd-mass isotopes 0–38942
204Po, electron conversion spectrum 0–60789
151Pt decay, half-life meas. 0–60787

0–4264 muclides, disintegration rate, absolute determination by β - γ - and $4\pi\beta$ - γ -coincidence methods 0–49553 radionuclide analyses, gamma-ray spectrometer, NaI(TI), anticoincidence shielded, total absorption 0–57942 separation of radioactive series elements by successive alpha recoils under vacuum, automatic device 0–42781 sources, line, production, simple method 0–77512 rel. to whole body counting, arrangement with tilting chair, arc or scanning bed geometry, photopeak efficiency for print source evaluation 0–55081 whole body counting, tilting chair and scanning geometries, relative photopeak efficiencies calculations, optimal operational parameters determination 0–55080 whole body γ counter for potassium meas. 0–59825 whole-body p counter for potassium meas. 0–59825 whole-body monitors, counting-rate variation 0–42616 p point source calibrator, automatic, design and statistical procedures for evaluation 0–57840 evaluation $0^{-3}/640$ (Ge(Li) coaxial detector, pulse shape distrib., applicability for nanosecond half life meas. $0^{-4}2638$ NaI(Tl), anticoincidence shielded, total absorption, for radionuclide analyses $0^{-5}7942$ T, in air, monitor, portable, down to $10\mu\text{Ci/m}^3$ 0–73694 Radioastronomy
see also Cosmic radiations, radiofrequency; Sun/radiation, radiofrequency 1-30 mm range, review of observations 0-41743
35 GHz interferometer, spaced antennas with synchronous oscillators 0-72795 atmospheric attenuation and emission at 90 GHz, rel, to solar radio obs. atmospheric attenuation and emission at 90 GHz, rel. to solar radio obs. 0–62921
attenuation and emission of atmosphere at 3.3 mm 0–79550
attenuation at 3.9 GHz rel. to oblate raindrops 0–59591
Cassiopeia-A, radio intensity 3 to 15 cm. obs. 0–79706
correlation antenna array configurations, comparison 0–63189
Cygus-A, radio intensity obs. 3 to 15 cm. 0 –79706
detection practices 0–45443
discrete source intensity meas., statistical estimation 0–66675
estimation practices 0–45443
frequency allocations 0–79774
high efficiency parabolic antennas 0–63190
information from radio sources, extracting method from noise 0–41744
Jupiter, microwave absorpt. by atmosphere, and possible temp. inversion feature 0–45419
Jupiter, r.f. spectrum, dipolar model 0–79732
Mariners 6 and 7. occultation meas. of Mars atm. 0–51760
maser radiometer system design and theory 0–49023
millimeter wave interferometer, appl. to solar and galactic rad. 0–76666
Moon surface material chemical composition determination comparison with chemical analysis by Surveyor 0–66579
Moon surface slopes, topographic variations, bistatic radar obs. 0–66580
National Acad. Sci. annual meeting, Washington (1970) 0–66677
parametric amplifier applications 0–79775 Radioastronomy continued

phase measurements, interferometric, with 11.3 km baseline 0-51815

pulsar obs., using swept-freq. local oscillator 0-66550 pulsars rel. to neutron stars 0-66522 radar polarization meas., exploitation of ionospheric Faraday rotation 0-76679

0-76679
radar return attenuation meas. at 15 GHz 0-59590
radio sources, high resolution obs. 0-72796
radio telescopes, synthetic-aperture 0-76680
radiotelescopes, fundamentals and design, book 0-45442
refractive corrections in high-accuracy radio interferometry 0-51534
review of observations in 1-30 mm range 0-41743
satellite obs. ionospheric influence on radiowave refraction 0-72672
scintillation of extended radio sources, with finite bandwidth reciever
0-54487

solar corona structure obs. at 80 MHz, two-dimensional pictures 0-79770 solar radio bursts, obs. at Arcetri Observatory, Sept. 1965-Dec. 1967 0-51798

source dimensions, obs. with radiointerferometer with base Green-Bank-Crimea 0–72748 space observations, advantages over conventional techniques, future plans 0–51814

0—51814
Spectrograph, data acquisition and control using computer 0—76681
Taurus-A, radio intensity obs. 3 to 15 cm. 0—79706
telescope, 6 GHz for solar observation 0—57158
waves absorption calc. in ionosphere D-region 0—76484
weak sources detection near strong sources with Cambridge One-mile Telescope 0—41867
O¹6H molecule, 18-cm transition frequencies 0—79704

Radiocarbon dating see Radioactive dating

Radiochemistry
see also Chemical analysis/radioactive; Chemical effects of radiations/

see also Chemical analysis/radioactive; Chemical effects of radiations/
ionizing radiations; Radioactive tracers
analysis, qualitative, quantitative and structural, Mossbauer spectroscopy,
nuclear instrumentation and radioisotope techniques, application to NBS
Standard Reference Materials 0–51453
chloroform, liq., radiolysis, at 25°C 0–76281
ethanol, p-irradiated liquid, electron scavenging 0–45091
fluorocarbon gases, irradiated, direct obs. of electron disappearance
0–78153

0—/8153 hot atom reactions, moderation processes 0—59513 methanol, p-irradiated liquid, electron scavenging 0—45091 nuclear fuel burn-up determ. by radiochemical methods 0—55212 ²²⁰Rn emanation from soils, meas. 0—45117 T hot-atom exchange reactions with H₂ and D₂ 0—41451 T+HR hot-atom reactions, distrib. of products 0—48204

Radiography
see also Luminescent devices; X-ray tubes
abdominal radionuclide aortography with gamma scintillation counter
0-51833

alpha autoradiography, nonphotographic alpha and neutronlinduced autoradiography 0–57164 autoradiography, study of irradiated nuclear fuels 0–58067 autoradiography in scanning electron microscope 0–69223 back-reflection or transmission diffraction dual-purpose apparatus, patent 0–45503

0-45503
book elementary on radiation physics 0-57161
coal bore cores, X radiograph unit 0-48246
differential, electro optical means 0-72815
displays, full-colour and three-dimensional 0-72817
dose reduction, with magnetic disc recorder 0-76729
electron beam recording with vapour-deposition development, patent
0-42405

0-42405 electron-beam-recorded patterns on photographic plate, distortion due to charge-up 0-70140 fluorometallic intensifying screens, characts and applies. 0-49162 gamma, analysis if digitally processed colour readouts from scintillation cameras and scanners 0-66692 gamma spectrometry, health physics meas. methods 0-63207 grain boundary diffusion 0-61983 grid projection with large y sources 0-51828 histoautoradiography, nuclear emulsion, liftord G₅ and IFA EN₃ comparison 0-66699 neutron. biological systems. Monte Carlo simulation 0-72811

histoautoradiography, nuclear emulsion, Ilford G₅ and IFA EN₅ comparison 0–66699
neutron, biological systems, Monte Carlo simulation 0–72811
neutron, biological systems, Monte Carlo simulation 0–72811
neutron, find statistical modulation transfer functions and dosimetry 0–72813
neutron, front screen thickness optimization, calc. 0–51837
neutron, front screen thickness optimization, calc. 0–51837
neutron, meas. automation circuit 0–45848
neutron, slow, rel. to imaging of fatty tissues through deuteration with heavy water 0–72809
neutron, stereoscopic and stop action, rel. to biological objects 0–72810
neutron, study of limiting planar heat pipe performance 0–57428
neutron, thermal, biomedical applications 0–72808
nuclear ceramic fuels, irradiated, autoradiography 0–77620
pathological change diagnosis, single tissue, influence of exposure parameters 0–72819
photographic action of ionizing radiation, book 0–38581
radiographs, viewing conditions 0–63741
screens, intensifying, fluorometallic, tests 0–63740
solder joint and component X-radiography 0–76758
steel, polycrystalline plastically deformed, particle size and lattice distortion 0–40461
steel, transformer, distrib. of C by autoradiography 0–62107

steel, transformer, distrib. of C by autoradiography 0-62107 transmission diffraction or back-reflection dual-purpose apparatus, patent

0 - 45503Weissenberg photograph, X-ray intensity meas. using TV cameras

Weissenberg photograph, X-ray intensity meas. using TV cameras 0-55816

X-ray, rel. to fine structure resolution of insulation 0-69565

X-ray, three-dimensional imaging 0-72818

X-ray inage intensifier, solid-state, electroluminescent-photoconductor type 0-48630

X-ray medical, book 0-45456

X-ray pictures information content study 0-59827

xeroradiography, principles and characteristics 0-70141

Co units and betratron, building effects rel. to irrad. params. obs. 0-41887

LiH₂PO₃ radiocrystallographic study 0-55848

Radiolysis see Chemical effects of radiations/ionizing radiations

Radiometer gauges see Vacuum gauges

Radiosondes see Meteorological instruments

Radiosources see Cosmic radiations, radiofrequency

Radiostars see Cosmic radiations, radiofrequency; Stars

Radiotelescopes see Radioastronomy

Radiowave propagation see Electromagnetic wave propagation

Radiowave spectra see Nuclear magnetic resonance and relaxation; Paramagnetic resonance and relaxation; Spectra

Radium No entries

Radium compounds No entries

Radium emanation see Radon

concentration, low level measurement, ionization chamber 0-54200 exhalation from vast areas, w.r.t. vertical distribution of its short lived decay products in atmos. 0-76402

deeay products in atmos. 0–76402 sublimation pressure predicted from law of corresponding states 0–71427 siblination, meas. by disintegration chamber and by nuclear emulsion 0–76346 siblination of the product of the control of the product of the control of the

in see also Condensation; Snow attenuation parameters affecting millimetric radiolink design 0-54251 capacitive rate sensor 0-51504 drop size, rel. to its conc. of trace elements 0-51524 fisson products meas, to middle of 1969, results 0-45158 frequency association with extraterrestrial magnetic spherules in tropo sphere 0-45424 hail detector, dual wavelength radar, report 0-79514 oblate raindrop attenuation at 30.9 GHz 0-59591 radio waves at 15 GHz propagation, amplitude variations 0-59590 radioactivity capture during precipitation, model 0-76400 radiothermal and radar meas. 0-59569 rainstorms, microwave noise obs. 0-79933

Raman spectra see Scattering/light, Raman spectra

Ramsauer effect see Electron beams; Electrons/absorption; Energy loss of

Random functions see Random processes

Random processes

see also Brownian motion; Fluctuations; Statistical analysis

continuous systems, stability, random excitation 0–38192 exciton migration model 0–75502 lattice sites visited in a random walk with infinite invariance 0–38195 Monte Carlo methods, rel. to diodes, thermionic, emission rate calculation

0-42220
Monte Carlo methods, rel. to electron attenuation rates in atmos.
0-41538
nonlinear systems, thermal fluctuations 0-51963
packing, dense, of hard spheres as structural model for noncryst. metals
0-43625

probability distribution functions, one-dimensional error in meas. 0-38218

0–38218 radio transmission, level-crossing intervals prop. of random functions 0–69770 stochastic, symmetry rel. to group theory 0–69594 surface profiles, height distrib. and auto-correl. function, props. 0–47032 transport process statistical model 0–76842 ransport process statistical model 0–76842 walk, non-self interacting with nearest neighbour interactions 0–51972 walks, self-avoiding, Ising and Heisenberg models 0–41985 waveform of random signal used to study profile of surface contact 0–47032

Range of particles see Energy loss of particles

Range of particles see Energy loss of particles

Rare earth compounds

see also the compounds of the individual metals; Ferrites
alloy, RFe₂ and R_xY_{1-x}Fe₂ type, cubic, mag. props. 0–72184
alloys, intra-type, behaviour and structure, review 0–71779
alloys, magnetism 0–72175
aluminates, rhombonedral space groups, i.r. obs. 0–61898
antimonides, growth by halide vapour transport 0–58636
argentides, mag. struct. 0–62530
arsenides, growth by halide vapour transport 0–58636
aurides, mag. struct. 0–62530
bonding, 4f contribution 0–58611
bromo-sulfides, classification into 3 crystal types 0–78478
chelate complex, ionic-covalent, parameters determining luminescence spectra intensity 0–51337
cobaltides, RCo₃, magneto-crystalline anisotropy, spin struct. 0–44482
cobaltides, permanent magnet development 0–62506
complexes, metal-ligand spacing from spectral bands positions 0–70915
copper alloys, RCu₆, crystal structure 0–43642
dielectric, indirect exchange, many-electron theory 0–72183
disilicates, polymorphism, 900–1800°C 0–78746
double tungstate, hydrothermal synthesis, polymorphism 0–74986
ferrite garnet, induced noncollinear struct, magnetothermal struct. 0–54037
ferrite garnet, substituted, exchange interactions 0–69041

ferrite garnet, substituted, exchange interactions 0-69041 ferrite garnets, magnetiz. process, near compensating temperature 0-79163

0-79163 fluorides, far-i.r. absorpt., I.f. lines 0-51308 fluorides, far-i.r. absorpt., I.f. lines 0-51308 in glass lasers, doped, electron spin resonance measurements 0-57529 halides, lattice vibrs., force const. models 0-59082 intermetallic, RZn, type, mag. characts. 0-75890 intermetallic, representation of truct., neutron diffr. 0-44575 intermetallic, reversible room temp. hydrogen absorpt. 0-50395 intermetallic, intermetallic, ternary, mag. and struct. characts. 0-75889 intermetallics, indirect exchange interaction 0-44565 luminescence, efficient i.r. excitation 0-72435 magnetic and optical props. of dilute complexes, theory 0-40924 manganites, magnetostatic props. 0-44710 molybdate, phase transformation, high-temp. X-ray exam. 0-78701 monoselenides, gaseous, mass spectrometric determ. of dissociation energies 0-61180

Rare earth compounds continued Rare earth metals continued trivalent ions in crysts., mean g values 0-41314 u.s. relaxation in spin spiral phase 0-47527 Di atoms, effect on decay and thermoluminescence of CaS:Bi phosphor 0-72446 monotellurides, gaseous, mass spectrometric determ, of dissociation energies 0-61180 orthochromites, exchange constants, magnon energies and opt. props. orthoferrite, Faraday rot. and birefringence, visible and irr. 0-59369 orthoferrites, Faraday rot. and birefringence, visible and irr. 0-59369 orthoferrites, absorption and transmission bands, 0.5-50µ. 0-69125 orthoferrites, domain wall interactions with twin and grain boundaries Y₃Al₅O₁₂:R³⁺, R=rare earth, X-ray fluorescence 0-44926 Rare gases see Inert gases Rayleigh scattering see Scattering/light Rayleigh waves see Elastic waves; Seismic waves 0-54046 orthoferrites, exchange interaction of rare eath ions and Fe ions 0-79189 orthoferrites, mag. domains, X-ray obs. 0-79192 orthoferrites, mag. structures 0-40951 orthoferrites, magneto-optical props. 0-72317 orthoferrites, magneto-optical props. 0-72317 orthoferrites, magneto-optical props. 0-59340 orthoferrites, magneto-optical props. Re(h)binder effect see Mechanical strength; Surface phenomena Reaction kinetics see also Catalysis; Chemical reactions; Exchanges, chemical; Exploorthoferrites, magnetic parameter answings feet to comp. 6–35300 orthoferrites, preparation for memory application, magnetic and optical properties 0–79191 orthoferrites, wall energy anisotropy 0–54044 orthorhodites, MRhO₃, perovskite, cell dimens. 0–50545 orthovanadates, Bi³⁺ activated, fluoresc., excited states lifetimes meas. alkane molecular ions and water vapour, mechanism and rate constants alkanes, H atom abstraction by CH₃ and OH radicals 0–62803 aromatic cpds. in dichloroethane soln., molec. cations in pulse radiolysis 0–45089 0-45089
bimolecular association reactions and microscopic reversibility 0-66167
bimolecular microcanonical activated complex theory 0-59482
boundary layer effects in shock tube studies 0-76252
collision theory of reactive hard spheres 0-41411
computer program for spectrophotometric obs. 0-51442
conformational changes in molecules, conference 0-74218
constants in nonisothermal reaction, obs. by calorimetric method
0-79435
constants in horisothermal reaction, obs. by calorimetric method orthovanadates, Bi³⁺ activated, fluoresc., excited states lifetimes meas. 0—4489] orthovanadates, Bi³⁺ activated, fluoresc. decay consts., low temp. 0—56624 oxides, Bi³⁺ activated, fluoresc. decay consts. low temp. 0—56624 oxides, LnLiO₂ type, Eu³⁺ luminesc. 0—76156 oxides, activated, X-ray induced fluoresc, of rare earth ions 0—76171 oxides, catalysts, effect of low mag. field on p.H₂ conversion rate 0—79443 oxides, cubic, mag. struct. 0—62492 oxysulphides, mag. props., 2–700k 0—44504 perovskitelike, phase transition 0—75337 phosphates, anhydrons, ³¹P n.m.r., obs. 0—41381 phosphates, n.m.r., hydrated vs. anhydrous form 0—41385 polycrystalline, optical spectra by scattered transmission, using teflon powder 0—76057 pseudo-binary with 3d transitional metals, structural and magnetic properties 0—51181 pyrosilicates, cryst. struct. 0—47202 selenates, from Sm—Lu, cryst. struct. determ. by X-ray exam. 0—53514 silicides, LnM_xSi_{1-x} (where Ln=La—Gd, M=Ni, Co, Fe), lattice consts., comp. depend. 0—58747 stannates, mag. props. 0—40935 0-79435 copolymer (dAT), helix-coil transition determ. by light scatt. 0-54180 direct reactions, model 0-62788 energetic atoms, integrodifferential form of Boltzmann eqn. 0-48177 ethylene, ion-molecule reaction product distrib. calc. 0-54179 hot-atom reactions, moderation processes 0-59513 ion molecule reactions, complex-stripping transition energies 0-59481 ion-exchange resins, thermal stability 0-41410 ion-molecule, isotope effects on collision dynamics 0-62788 ion-molecule reaction product distrib., calc. using quasiequilibrium theory 0-54179 ion-molecule reaction rates, sources of error; in drift tube mass spectrometer. ion-molecule reaction rates, sources of error in drift tube mass spectrometer determ. 0-45046 ion-molecule reaction rates meas., with drift-tube mass spectrometer, error sources 0–56688 ion-polar-molecule reactions 0–45054 comp. depend. U—38/4//
stannates, mag. props. 0—40935
sulphate hydrates, ir. spectra, low temp. behaviour 0—41178
sulphide and selenide, specific resist., thermo e.m.f., 300-1500K 0—75686
tellurides, growth by halide vapour transport 0—58636
trichlorides, isomorphous series, electronic and phonon-Raman-spectra
0—72348 ions, positive, gas-phase reaction rates with H₂O₂ at 296°K 0-79434 isobutane, chem. activated, decomp. rates 0-41448 isobutane, chem. activated, decomp. rates 0-41448 isokinetic temperature, determ., least squares method of formulation 0-62791 10-02/91
Lanthanides, reduction to lower valence states in ionic crysts. 0-66175
light scattering studies 0-54180
methane-NH₃ ion-molecule reactions, ion cyclotron resonance 0-79440
methyl nitrite, reaction kinetics with alkali atoms 0-46635
neopentane, chem. activated, decomp. rates 0-41448
nonequilibrium contrib. to rates, perturbation of velocity distrib. function 0—72348 vanadate and phosphate, magnetization, 1.9K-630K 0—40950 Au-Zn5:NdF₃-Ta₂O₃-Ta composite films, pulse excited electroluminescence characteristics 0—44950 Au-rare earth alloys, mag. susceptibility and elec. resistivity 0—72179 Co-rare earth alloys, as permanent magnet materials, recent developments 0—72171 0-2171
Co intermetallics, permanent magnets, review 0-44572
Fe garnets, superexchange interaction, model calc. 0-79200
Pr₁₀S₁₄O type, β-phase, crystal struct. 0-61830
RCo₂ (R=rare earth metal) and related compounds, exp. rel. to permanent magnet properties 0-72176 0 - 414120-41412 organic molecules, configuration changes by rotation about single bond, reactivity 0-43142 perfluorocyclobutane, unimolecular decomposition boundary layer effects in shock tube studies 0-76252 rate, and activation energies distrib. 0–45047
rate, radiative attachment of electrons on H and alkali atoms 0–62793
rate constants determination, cyclotron resonance spectroscopy application, trapped ion analyzer cell 0–45735
reactants stochastically distributed, decay, closure stochastic soln. 0–45051 Rare earth metals see also the individual metals in Allende meteorite, abundances 0-69465 in Allende meteorite, abundances 0—69465 abundance in lunar rocks and separated phases 0—45342 abundance in lunar samples 0—45340 abundance in lunar samples 0—48495 atoms, X-ray spectra, h.f. satellite Ly,' 0—70747 band struct., 4f states location 0—75491 cerium subgroup, ordering and Neel temps. 0—75957 conductivities, elec. and thermal, meas., between 77-400°K, 1000 G to 20 kG 0—53777 0-45051 recombination and diffusion kinetics, nonlinear initial-boundary-value prob-lems analysis 0-66169 redox reactions in cryst. lattices 0-66175 relation between cross-sections of endothermic and rate consts. of exother mic reactions 0-59482. exchange interaction, crystal field, one-ion anisotropy energy 0–43947 exchange interaction, indirect, in strong mag. fields 0–62480 ferromagnets, lattice contribution to thermal conductivity 0–68651 galvanomagnetic effects, meas., between 77-400°K, 1000 G to 20 kG 0–53777 relaxation in gas reacting with flow of particles, numerical integration relaxation in gas reacting with flow of particles, numerical integration 0-66174 steel corrosion by liquid Na 0-41434 stochastic theory 0-56687 surface reactions, by field pulse desorpt, and mass spectrometry 0-56693 tetramethylsilane, chem. activated, decomposition rates 0-41449 transition-state theory, test using H+H; reaction 0-62800 unimolecular, incomplete energy equilibration in activated complexes 0-62790 as impurities in YB_6 and ZrB_{12} , depression of superconducting transition 0-441430–44143 impurity diffusion in Cu 0–75202 ion, deuteration eff. on triplet state lifetimes 0–74198 ions, in alkaline earth fluorides, cryst. field obs. 0–79218 ions, spectra and theory of electronic Raman transitions 0–70868 ions in liquid solns., energy transfer to aromatic ketones 0–50205 isotopes, separation and pairing energies 0–67484 isotopes, short-lived, ¹⁵⁹Dy, ¹⁵¹. ¹⁵². ¹⁵³Ho, ¹⁵⁵. ¹⁵⁴. ¹⁵⁵Er, α -decay, half-lives 0–49561 0 - 62789unimolecular rate, effect of exclusion of disallowed states from state den sity 0-76253 unimolecular reactions, vibrational relaxation and dissociation 0-46607 DL-valine, free radical conversions 0-45090
Al-methane-O₂ flames 0-76260
Ar*+H₂-ArH*, isotope effects on collision dynamics 0-62788
Ar*+H₂-ArH*+H, cross- section, rotational kinetic energy dependence • 0_49561

lanthanides, reduction to lower valence states in ionic crysts. 0_66175
magnetic anisotropy, meas. 0_75924
magnetic anisotropy mechanism, neutron scatt. obs. 0_75885
magnetic behaviour 0_75878
magnetic props. 0_79132
magnetic form factors calc. for ions 0_62486
nuclear decoupling parameters, effect of spin interaction 0_52642
nuclear energy level density calc. in superfluid and Nilsson models
0_46124
0_753977 Ar'+H₂→ArH'+H, cross-section, rotational kinetic energy dependence 0-62794
B-H compounds, cryogenic stability 0-62795
B-methane-O₂ flames 0-76260
C₇H₃, no reaction observed 0-72526
CO, oxidation by O₂ in shock waves 0-62804
CO'+D₂→COP'+D, crossed beam study 0-79437
C⁺(P)+CH₁F 0-62797
C⁺+CO, thermal energy rate constant meas., production of free electrons and neutral products 0-72526
C⁺+CO₂, thermal energy rate constant meas., production of free electrons and neutral products 0-72526
C⁺+CO₂, thermal energy rate constant meas., production of free electrons and neutral products 0-72526 and neutral products 0-72526 C $^-+N\cdot O$, thermal energy rate constant meas., production of free electrons and neutral products 0-72526 C ^-+O), thermal energy rate constant meas., production of O^- 0-72526 C1+Br, in crossed beams, differential cross-section 0-41415 Co, oxidation, near $\alpha=\beta$ transition 0-59487 Cs-alky loidides, harmonic forces linear model 0-72527 Cs+NO₃, CsO formation in $^2\Sigma$ state, paramagnetic obs. 0-46635 Cu-(2 wt.%)Co alloy, precip. kinetics by torque magnetometry 43825 Cu-Ni 20/80 alloy, thermal evolution of ion-bombarded Ar, obs. 0-56697 Cu bermal evolution of ion-bombarded Ar, obs. 0-56697orbital exchange 0–53977

oxide phosphors, activated, cathode-ray efficiency, 10kV 0–44942 paramagnetic susceptibility of single crystals, anisotropy 0–47924 physical properties, survey 0–71430
Raman scattering by magnons 0–56557 reflectance obs., optical constants, interband cond. 0–79273 spectra, atomic, analysis 0–58095 spin-phonon relax time temp. depend. 0–75974 spin-wave excitation energies temp. depend. 0–44541 thin films, 130Å to 2500 Å resistivity obs. at 4.2°K to room temperature, magnetoresistance obs., transverse fields up to 15 KOe, longitudinal fields up to 10KOe 0–51175 trivalent ion activators in La₂O₂S, excitation and relax. characts. 0–76153 trivalent ions in Yb³⁺-sensitized cryst., cooperative and stepwise excitation of luminesc. 0–41264 orbital exchange 0-53977 Cu, thermal evolution of ion-bombarded Ar, obs. 0-56697 D+D+D $_{2}-2D_{2}$, rate constant, calc. by orbiting resonance theory 0-7252

Reaction kinetics continued

Dy₂O₃ + B₂O₃-DyBO₃, sintering processes, 600-1400C 0-76258 F-A₇-F+A₇+e, F-Cs⁺+F+Cs⁺+e, in shock-heated mixtures 0-71058 Fe oxides, comparative reactivity for Zn ferrite synthesis 0-72269 GaAs, epitaxial, kinetics, {001} orientation 0-58583 H-atom addition to ethylene, high-press. limiting rate const. 0-62799 H and D atom reactions with SCl₂ and S₇Cl₂, vibr. populations of HCl products 0-54176 H atom and ion transfer in methanol-acetaldehyde molecule system 0-45054

H atom and ion transfer in methanol-acetaldehyde molecule system 0 45054 H atom reactions with SCl₂, S₂Cl₂, SOCl, SO₂Cl₂, and OCl₂, i.r. chemiluminesc. 0-54177 H, thermal energy reactions with O₂, NO, CO, and N₂O 0-62798 H₃⁺ ion-molecule reactions 0-59484 H₃⁺ simple exchange reaction, mechanism 0-48186 H₃O, proton affinity 0-62785 H₃S, ion-molecule reactions with ethylene and acetylene 0-79438 H+C₂H₃, absolute rates of reactions 0-72569 H+C₃H₃, absolute rates of reactions 0-72569 H₂+N₃+O₂ flame, mechanism using 2 computational methods 0-54182 H₃+O₃+N₃ fuel rich flame at atmospheric pressure, structure 0-54181 K+NO₂, paramagnetic product obs. 0-46635 N/O/reactive carbon compound systems, mechanism of production of CO fourth positive bands 0-76257 N₂, phase space theory calculation of overall recombination and dissociation rate coefficients 0-76259 N₂H₃ radicals, ratio of disproportionation to combination 0-54194 NO₂, thermal decomposition in shock waves 0-59486 N₂O₄ thermal decomposition in shock waves 0-59486 N₂O₄ dissociating, viscosity investigation by vibrating disk method 0-58406 NOC (XXX) reaction with Alkali atoms compounds bish pressure photoionization OCC (XXX) reaction with Alkali atoms compounds bish pressure photoionization-10 NOC (XXX) reaction with C₂-C₂ hydrocarbons high pressure photoionization-10 NOC (XXX) reaction with C₂-C₃ hydrocarbons high pressure photoionization-10 NOC (XXX) reaction with C₂-C₃ hydrocarbons high pressure photoionization-10 NOC (XXX) reaction with C₂-C₃ hydrocarbons high pressure photoionization-10 NOC (XXX) reaction with C₃-C₄ hydrocarbons high pressure photoionization-10 NOC (XXX) reaction with C₃-C₄ hydrocarbons high pressure photoionization-10 NOC (XXX) reaction with C₃-C₄ hydrocarbons high pressure photoionization-10 NOC (XXX) reaction with C₃-C₄ hydrocarbons high pressure photoionization-10 NOC (XXX) reaction with C₃-C₄ hydrocarbons high pressure photoionization-10 NO N₂O₄ dissociating, viscosity investigation 0.58406
NO+(X¹Σ⁺) reaction with C₃-C₇ hydrocarbons, high pressure photoionization 0.62816

tion U-62816
Na, liquid corrosion of steel 0-41434
Na+NO₂, formation of NaO in ²Π state obs. 0-46635
Ni, thermal evolution of ion bombarded Ar, obs. 0-56697
O₂-, and O₂-, cluster ion formation and reactions in flowing afterglow 0-41416

0-41416
O₂*, cluster ion formation and reactions in flowing afterglow 0-41416
O¹(D)+H₂O reaction, rate constant by measurement of intermediate quantum yield following flash photolysis 0-45084
OH radical abstraction reactions, activation energies 0-62802
OH radical reactions with alkanes, flash photolysis and kinetic spectra

0-66203
OH reaction with ethylene, kinetic spectra 0-62805
O+CO, 0-59485
O+N, high-energy reaction, simple model 0-41417
Pb5+CdO, solid state double decomp, conductivity meas. 0-66173
Pt, sorption of organic cpds. obs. 0-56693
SO₄-, rate constant determination, photolytic 0-76275
T+HR hot-atom reactions, distrib. of products 0-48204
UCy, high temp. thermodynamic properties, cqns. 0-59109
W, sorption of organic cpds., obs. 0-56693
Reactors see Nuclear reactors, fission; Nuclear reactors, fusion
Recombination see Ions, recombination; Semiconductors
Recombination radiation see Luminescence

Recombination radiation see Luminescence

Recording

electro-optical images 0-57585 electron beam, latent image development by vapou deposition, patent 0 - 42405

0-42405 electron beam on film, high-resolution magnetic deflection system 0-42214 of electron microscope images, use of crosslinking phenomenon of silicone resin film, interference colour obs. 0-57491 geomagnetic micropulsations, by saturated-core magnetometers 0-54299 holographic-recording device, cyclically reusable 0-69955 i.r., using SPECORD 71 IR and SPECORD 72 IR spectrophotometers 0-57636 magnetic holography, reconstruction effects. 0-63659

0–57636
magnetic holography, reconstruction effects 0–63659
magnetic medium, orientation of mag, particles 0–52239
magnetic tape layer, orientation process of acicular oxides 0–52238
mass spectrometer, simultaneous recording of three mass peaks 0–46322
microphotometer, double-beam, design and operation 0–73309
of multitrack occurrences, by acoustic spark chambers 0–38767
seismic data, s/n enhancement, optimum digital filters 0–41469
seismic digital instruments 0–51469
seismic waves refraction, analysis and interpretation thorough reflection
technique, digital processing 0–48227
sound, 8 mm variable density, using SiC light emitting diode 0–54137
temperature inhomogeneities in sea 0–51501
video tape, applic, of Co-P electroless plating 0–72248
crystallization (metals) see Heal treatment

Recrystallization (metals) see Heat treatment

Rectifiers

see also Electron tubes; Semiconducting devices
charging, with magnetic amplifiers, e.m. processes
thermal, design 0-63480
KCl. F-centre effect on rectification 0-43687
Sa:Ag, capacitance curves under pulse operation 0-68862
SiC, high-temp, for reverse voltages 0-53866
Ta:Ta;O;-electrolyte system, study of rectification 0-79006

Red shifts see Astronomical spectra; Cosmology; Relativity/general Reflectance see Reflectivity

flection
see also Neutrons/reflection; X-ray reflection
core waves, precursors, multiple paths in upper mantle 0--62851
diffuse reflectance comparative study of Kubelka-Munk and Girin Stepanov theories 0-45821
electron from W crystal faces, {100} and {110}, 80-300 K 0-74888
electrons, on insulator surfaces, kinetics 0-78362
low-energy electron-reflection, application to study singlet and triplet molecular states 0-74890
multipath from random surfaces, reflections counting method 0-51917
of seismic waveless, by thin layers and layered boundaries plane-wave theory 0-41468

theory 0-41468 shock waves, plane, from rigid cylindrically-concave wall 0-73049 He and H_2 beams, from LiF(001) surface 0-47034

Reflection continued

acoustic waves see also Echo; Reverberation

anechoic chamber, reflective surfaces for hearing speech and music 0-52132

by blade rows of arbitrary spacing and stagger soln. 0-57398 from blade spacing effect, flow Mach number, super-resonant condition 0-38382

in compressors duct axial flow through blade row, semi-actuator disk theory applic. 0-38381 in electric field at crystal boundary, and refraction and self-focussing 0-56096

0-3096 ferroelectric material, domain boundaries 0-78766 from ground, effect on field distrib. of localised source distrib. 0-38383 harmonic source sound field about infinite thin plate in homogeneous medium, analysis 0-60032 lamellar media, magnetoacoustic wave 0-54711

from layers plane-parallel moving, expression in terms of tangential discontinuities 0-45631

tinuities 0-45631
from liquid cylinder imbedded in another liquid, study 0-53336
from nonlinear absorber, computational techniques 0-71843
from ocean surface, model tank expt., freq. spread of surface reflection, determination 0-71342
panels layered with absorbent material. sound insulation, predicted and measured values, discrepency investigatio 0-40544
plane wave pattern det. using slowness diagram 0-52109
reflective surfaces, rel. to reinforcement of unamplified speech in lecture room and thrust-stage theatre 0-52146
at sea surface, literature review 0-52091
sonic boom, pressure-time history prediction 0-76908
sonic boom simulation device 0-60045
specularly reflected pulses from soft cylinders, creeping wave formulation of

specularly reflected pulses from soft cylinders, creeping wave formulation of scatt. theory 0–66902 from stochastic surface, time varying, signal spectrum 0–54712 and transmission characteristics, visual structure walls, method of calculating reverberation time 0–42084 from water due to sonic boom penetration; pressure analysis 0–52093

acoustic waves, ultrasonic conical, from liquid-solid boundaries, optical obs. 0–52110 electrically controlled surface-wave refl. in quartz delay line, 120 MHz

quartz delay line, elec. controlled surface-wave refl. , 120 MHz $\,$ 0–48846 size and orientation of reflectors from freq. anal., expts. and model $\,$ 0–63433 $\,$ by Au thin film layer on LiNbO₃, surface-wave phenomena obs. 0-65538 Cu, reflectivity of single and polycryst. at water-Cu boundaries 0-43872

electromagnetic waves
air-water interface, microwave reflection 0-43448
auroral radio reflection signals, polarization characteristics 0-76436
coefficients, effective, in forward scatter from dielectric slightly rough
surface 0-63514
coefficients from broken theorem inapplicable when magnetic field present

0-64698

from conducting media, electrodynamics, perturbation technique for solving boundary value problems 0-67024 diffuse, of radiative transfer in planetary atmosphere, reciprocity relations 0-79726

0-79726 evanescent, standard invariance in total refl. on dioptre plane 0-45721 ferrite, moving domain wall 0-75946 film, resonance value calc. 0-41100 i.r. spectrum in 1.1 to $3.0~\mu$ region, rel. to multilayer coatings for Si photocells 0-75823 at interface of two dielectric media, in relative motion perpendicular to plane of incidence 0-54793 from ionosphere, field intensity measurement of radiowaves 0-51568 ionosphere, sporadic-E reflection coefficient, frequency depend., method using AIS ionosonde attachment 0-76491 ionosphere anomalous multiple reflec. 0-72644 by ionospheric 0-region, at steep incidence, of low-frequency pulses, during

tonosphere anomatous multiple reliec. 0=12044 by ionospheric D-region, at steep incidence, of low-frequency pulses, during eclipse 0-66335 ionospheric E and F layers, for v.l.f. and l.f. 0-66332 ionospheric models, reflection coefficients of v.l.f. and l.f. radio waves, full-wave studies 0-45171 ionospheric reflection of radio signal, frequency spread measurement

0-45174

from layer, nonuniform, differential eqns. 0–63503 in layered anisotropic media, method for calc. 0–48915 from lunar rock bare surfaces, quasi-specular scattering, radar echo studies 0–51743

metal, in anomalous skin effect 0–71939 meteor trails, diffraction patterns of radioechoes 0–51778 oblique, from isotropic media with limiting Epstein-type stratifications 0–69779

0-097/9
oblique wave from striated impedance surface 0-42116
plane, vertically or horizontally polarized, Fresnel coefficients calculation,
computer programme 0-69780
polarized horizontally wave at imperfectly conducting surface, approx.
step-function response 0-76959
radiar backscatter intensities 0-76963
radio wave \$\lambda\$ 3.8 cm, 12.5 cm, 23 cm Venus, atmosphere, radar signals
0-63130

0–63130 radio waves, at low angles of elevation by ionos, focusing 0–62935 radio-waves 16-3000 kHz, by ionospheric models 0–76483 rectangular waveguide characteristics 0–76960 resonant dielectric sphere, in waveguide 0–57451 resonator, astigmatic, analytical calc. of the complex natural frequencies and field distribution at reflecting surfaces 0–60203 spherically laminared anisotropic layer, coeff. calcs. by impedance and field scalings 0–38436 in substances with negative electrical conductivity 0–69781 transient wave reflection from inhomogeneous plasmas 0–58320 troposphere, calc. 0–57449 n-GaAs, coeff. and phase angle, mm. range 0–76014

n-GaAs, coeff. and phase angle, mm. range 0-76014

light

see also Films, solid/optical properties; Mirrors β -alanine, semiconductivity, optical transmission and reflection, pure and X-irradiated 0–75657

albedo problems, analytical soln. 0–51961 alkali iodides, fund. absorpt., strain effects 0–62644 amorphous semiconductors 0–47721

Reflection continued

light continued

anisotropic medium, new formulae 0-69982 antiferroelectric, NH₄H₂PO₄, far-i.r. spectra 0-69110

antireflecting film, three-layer, accelerated process of formation 0-74908

antireflection folim, three-layer, accelerated process of formation 0—74908 antireflection coatings, two-layer, achromatic 0—49135 by cholesteric liquid crystal, thin film, Bragg reflection 0—71351 cholesteric liquid crystal films, light reflectivity meas. 0—74755 multilayer coatings, highly reflecting, with large dispersion of phase discontinuity 0—45843 coefficient meas., rel. to scintillation detectors, NaI:TI wrapped crystals, characteristics determining reflection coefficient meas. 0—41112 crystal surface facet angles, evaluation technique 0—78361 crystalline samples, small, meas. with Zeiss MM monochromator 0—62606

of diffuse reflectance of anisotropically scattering material, calc. 0–67135 of diffuser with nonuniform absorption, total reflectance calc. 0–67154 ellipsometer, calibration of analyser and polarizer, modified method 0–70051

0—70051
ellipsometric technique for substrate optical consts. meas. 0—71462
ellipsometry meas. of film thickness, polarizer ellipticity effects 0—55709
ellipsometry of rough surface, optical consts. meas. 0—65979
ellipsiometry of rough surface, optical consts. meas. 0—65979
ellipsiometry of rough surface, optical consts. meas. 0—65979
elliptical vibr. defining parameters determ. method 0—38552
ferroelectric, KH₂PO₄, far-ir. spectra 0—69110
ferromagnetic semiconductors, EuO, EuS, EuSe, spectra, mag. ordering effects 0—44816
film, optical index and thickness determ. 0—69071
film covered substrate obs. and meas. of differential phase shift 0—45823
films on Cu electrode, electropolishing, ellipsometry 0—65058
films, thin, approx. expression for coeffs. 0—44763
Fresnel, losses at boundaries, diffraction efficiency of photographic layers, meas. 0—42367
Fresnel formulas derived from dispersion theory 0—60339
Gaussian beam freq. shifting by u.s. surface waves 0—63683
glass surface obs. i.r. spectroscopy involving multiple total internal reflection 0—71457
i.r., rel., to thickness meas. of semiconductor epitaxial layer 0—65064

reflection 0–71457 i.r., rel. to thickness meas. of semiconductor epitaxial layer 0–65064 image formation of reflecting cone for off axis source 0–60318 interferometry, multiple-beam, fringes profile 0–63678 luminosity coefficients for diffuse reflection, analytical expression 0–67123 lunar rocks albedo, pulverization effects 0–48559 metal, liquid, binary mixtures, critical opalescence, conc. depend. 0–74753 metal, nearly free electron, sensitivity to interband transitions broadening 0–48050

0-48050

metal, surface impedance meas, technqiue 0-44965 metal's reflectance calc. for inclined incident light, ellipsometric meas. 0-69077

0-69077
metal reflectivity at any angle of incidence, ellipsometric determ. 0-59362
metal surface, incoherent scatt. 0-62640
minerals, i.r. spectra 0-66017
by mirrors, thermally deformed 0-70014
MnSe-CdSe solid solution, spectra, energy gap 0-54087
multiple, in thin crystalline plates, rel. to Faraday effect 0-48013
optical surface degradation from combined u.v. and outgassed materials
0-54907

0-54907 optical surface degradation from combined u.v. radiation and outgassed materials, further comments 0-54908 from pavements, luminance coeff meas. 0-67137 pentaerythritol single crystal, polarized ATR spectra, comparison with X-ray diffraction analysis 0-48054 perovskite, KMnF₃, i.r. active mode below phase transition 0-56525 phase shift of spherical wave at total refl. 0-38537 of plane wave by rough regular interfaces from stratified medium 0-77184

planetary atmospheres, diffuse reflection and transmission of light, three-term scatt, indicatrix case 0–48563 polarized beam, elliptically, total refl., perpendicular shift in incident plane 0–49107

0-49107
reflectographic method for inspection of internal surface of smooth cylinders 0-69983
reflectometer, Se-cell, direct-reading, compact, for reflectance of mineral grains in polished sections 0-73322
reflectometer, vacuum u.v., scanning, designed to minimise mechanical alignment errors 0-73317
reflectometer for pseudo-Brewster angle technique for determining optical constants 0-56483
reflector design based on power densities transformation, theory, applies.
0-63701

0-63701

0-63/01 rough surface, ensemble-averaged coherence function, correl. length determ. 0-67136 semiconductor, GaAs, neutron irrad., influence on refl. coeff. 0-69108 semiconductor, InSb, spectra, electron effective mass, band struct. 0-47736

semiconductor, InSb, spectra, electron effective mass, band struct. 0–47736 semiconductor, Si, epitaxial, carrier conc. non-destructive determ. using total internal refl. 0–44266 semiconductor, effective mass, carrier relaxation time 0–40759 semiconductor, electrorefl. in exciton absorpt. region 0–66021 semiconductor, electroreflection spectra, expt. methods 0–66019 semiconductor, modulated piezoreflectance, shear deform. potentials determ. 0–43727 semiconductor film, plasma edge 0–44762 semiconductor plasma refl. minumum, carrier density and effective mass determ. 0–72015 semiconductors, III-V, density of conduction states 0–75699 from shock front at grazing incidence 0–52360 shock wave, at grazing incidence 0–61429 specular, for in situ obs. of electrodes 0–59498 surface influencing laser range finder 0–42322 thin metal film on dielectric substrate, anomalous behaviour in relative phase difference 0–70015 total, rel. to quartz prisms, laser cavity obs. 0–73279 water wave meas, multiple purpose instrument 0–42382 Ag, adsorbed gases, optical props., ellipsometry 0–39967 n-Ag, adsorbed gases, optical props., ellipsometry 0–39966 n-Ag, Te, i.r. spectra, elec. props., carrier effective mass 0–44186 Al film, highly reflective, fabrication, patent 0–39962 Al films, specular refl. 0–51266

Reflection continued

light continued

ight continued

AIN, band structure 0–76065

AIN, spectra 5-12.5eV at 293K and 1.5-4eV at 77K 0–59388

AI₂O₃, corundum, abnormal phonon distrib, i.r. refl. spectrum 0–53685

As, energy spectrum in range 1-12.5 eV 0–62646

As₂Se₂ porous layers, obs. 0–76012

B, β-rhombohedral crystal, spectra lattice vibrations, impurity bands 0–51291

BP, vacuum u.v. spectra 0–79272

Ba(NO₃), i.r. spectra, internal vibrs. anharmonicity 0–69118

Bi-Ga liquid mixtures, critical opalescence, conc. depend. 0–74753

Bi, energy spectrum in range 1-12.5 eV 0–62646

CdGeAs₃, crystalline and vitreous state, electronic and vibrational spectra 0–47505

CdS:Li, spectra, 77k, dopant conc. depend. 0–56622

0—47505
CdS:Li, spectra, 77k, dopant conc. depend. 0—56622
CdS:Li, spectra, 77k, dopant conc. depend. 0—56622
CdSiAs₂, crystal, i.r. spectra, 300 and 83K 0—48064
CdSnP₂, i.r. spectra, permittivity and refr. index calc. 0—72341
CdTe, cxciton thermorefl. 0—56522
CdTe, fund. absorpt. region spectra struct. 0—79274
Cu, oxide film, thickness meas. 0—47044
Cu, Oxide film, thickness meas. 0—47044
Eu chalcogenides, spectra, multiplet struct., mag. field effect 0—44816
EuO, ferromag, semiconductor, spectra, mag. ordering effects 0—44816
EuS, ferromag, semiconductor, spectra, mag. ordering effects 0—44816
EuSe, ferromag, semiconductor, spectra, mag. ordering effects 0—44816
EuTe, antiferromag, spectra, mag. ordering effects 0—44816
GaAs, electroreflectance spectra at hydrostatic pressure, 6800 kg/cm²
0—59389
GaAs, i.r. spectra, room temp., 2-60u, optical phonon lifetime. 0—48051

0-59389
GaAs, Ir. spectra, room temp., 2-60µ, optical phonon lifetime 0-48051
GaAs, neutron irrad. influence on refl. coeff. 0-69108
GaAs absolute reflectance meas. using sensitive spectrophotometer 0-67178
GaN, thin films, optical absorption and vacuum ultraviolet reflectance 0-6262
GaS(Se, Te), electrorefl. in exciton absorpt. region 0-66021
GaSb, and electronic props., local pseudopotential model 0-43994
Ge, cathodoreflectance, depend. on modulation freq., excitation density 0-51267
Ge, surface physicochem, state influence. 0-79283

0–51267
Ge, surface physicochem, state influence 0–79283
Ge film, amorphous, reflectance and transmission, and elec. props. and structure, 77-750K 0–44254
Hg,Cl, diffuse refl. spectra 0–76073
β-HgS, film, prep., temp. depend. 0–48005
n-HgTe, spectra, 80K, phonon-plasma interaction, band-band transitions 0–41180
Letyst, spectra, back at the Company of the company

0-41180

I cryst., spectra, band struct. 0-56524

InAs film, i.r., and related elec. props. 0-44764

In_{2(1-x)}Cd_xSn_xAs_x, reflectance spectra determ. 1.5-6.0 eV by reflectance, thermoreflectance and electroreflectance 0-76063

In₂O_x films, heavily doped, i.r. refl. obs. 0-79284

InP absolute reflectance meas. using sensitive spectrophotometer 0-67178

InP assolute rehectance meas. using sensitive spectrophotometer 0-67178
InSb.InTe, spectra, comp. depend. 0-48071
InSb, spectra, electron effective mass, band struct. 0-47736
InSe, electrorefl. in exciton absorpt. region 0-66021
KD₂PO₄, deuteron motion obs. 0-79285
KH₂PO₄, far-ir. spectra 0-69110
KMnF₃, ir. active mode below phase transition 0-56525
Kr, solids, reflectance for photon energies from 8 to 25 eV 0-79286
Mg(H₂PO₂),6H₂O, ir. spectra, optical consts. 0-76074
MgO₂, ir. spectrum, rel. to abnormal phonon distrib. 0-79287
Mn₂O₃, diffuse spectra, 200-1000m 0-54088
NH₄H₂PO₄, far-ir. spectra 0-69110
NaCl single cryst. 2000-950 Å, effect of plastic deformation and X-ray irradiation 0-44766
Ni-SiO₂-Ni-SiO₂ multilayer coatings on reflectors, 'black mirror' effect 0-4116
P, energy spectrum in range 1-12.5 eV 0-62646

Ni-SiO₂-Ni-SiO₂ multilayer coatings on reflectors, 'black mirror' effect 0–41116
P, energy spectrum in range 1-12.5 eV 0–62646
Pb(NO₃)₂, i.r. spectra, internal vibrs. anharmonicity 0–69118
PbS(Se) (Te), spectra and band structure, 1-14eV 0–69111
Sb. energy spectrum in range 1-12.5 eV 0–62646
Si. epitaxial, carrier conc. non-destructive determ. using total internal refl. 0–44266
Si photocells, reduction by optical films 0–44409
Si with high density nonequilib. carriers, i.r. 0–56489
α-SiC:N, 6H polytype, and absorpt. spectra, 300 and 550 K 0–56553
SiO₃ layer, ellipsometry, refractive index, thickness 0–76016
Sr(NO₃)₂, i.r. spectra, internal vibrs., anharmonicity 0–69118
VO₂, elec. cond., transmission spectra, temp. depend., semiconductor-semimetal transition 0–75690
Xe, solid, reflectance for photon energies from 8 to 25 eV 0–79286
Zn₂Cd₁-Ze single crystal, and luminescence spectra, rel. to exciton spectra 2nd English exciton piezoreflection, 77K 0–56491
ZnS, thermoreflection, rel. to band structure 0–56151
ZnS cubic crystal, exciton piezoreflection, 77K 0–56491
ZnSe films, elec. field influence 0–69076
ZnSe single crystal, and luminescence spectra rel. to exciton spectra 0–44897
ZnTe, fund. absorpt. region spectra struct. 0–79274

ZnTe, fund. absorpt. region spectra struct. 0-79274

Reflectivity

see also Diffusion/light; Films, solid/optical properties; Optical constants
absorbing crystal, theory, exptl. test. 0–62595
alkali halides, deform, potentials 0–79271
alkaline earth metal, reflectance obs., optical constants, interband cond.
0–79273

alloys, meas. by compositional modulation 0-62607 antireflective glass coating, two-layer, with inhomogeneous first layer 0-76011

0-76011
bent crystal, elastically, plastically, continuous X-ray spectrum, method, equipment, 50 to 80 keV 0-41115
chalcogenide, quaternary, opt. reflectance, thermoelec. power, Hall coeff., elec. conductivity and microhardness 0-75821
chalcogenides, quaternary, and thermoelec. props. 0-47860
coatings, thermal control, degradation 0-41113
crystal neutron monochromator, rel. to mosaic spread and thickness 0-47169

Cu, blackened, reflectance, 300 to 2500 nm wavelength 0-57423 Cu, specular electron reflectivities, energy gap edges determ. 0-54086

Reflectivity continued

electrolyte-surface barrier technique, electroreflectance at fund, direct threshold 0-76072

asymptotic convolution integral, interband dielectric electroreflectance function 0-59385

europium chalcogenides, band struct. 0-59399

europium chalcogenides, mag. ordering effects, obs. 0-59322

ferroelectric, SbSI, far-i.r. spectra, temp. depend. 0-66025 ferroelectric, SbSI, far-i.r. spectra, temp. depend. 0-66025 ferroelectric, SbSI, far-i.r. spectra. 0-66026 films, thin, thickness and complex refractive index, determ. from reflectance and transmittance meas. 0-43540 i.r. (near), 5-25 µ range for sample temps. 4°-400°K, meas. tech. 0-56488 item infrared ration. 0. 66487

ice, infrared region 0-56487

laser mirror loss meas, using low finesse scanning interferometer 0-38490

lasers, GaAs injection, external quantum efficiency 0-52303 lunar samples, irradiation and vitrification effects 0-45391 lunar samples, spectral reflectivity of samples 0-48544 lunar spectral reflectivity, implications for remote mineralogical analysis 0-79723

metal surface, rough 0-76018 metal surface, rough 0-76017 metal surfaces, any angle of incidence, by opt. ellipsometric measurements 59362

0-39.02 metals, thick samples, surface plasmon effect on reflectance 0-48002 oxide solid solns, with Ni and Co ions, reflectance spectra 0-72343 photoreflectance line shape at fund. edge in ultrapure GaAs 0-76069 quartz (3140), bent, elastically or plastically, continuous X-ray spectrum 0-41115

rare earth metal, reflectance obs., optical constants, interband cond. 0-79273

reflectance nomenclature and directional reflectance and emissivity 0 - 57420

reflectance parameters, assessment of effectiveness in absorption study $0\!-\!76078$

0–76078 resonant reflectance anomalies, surface irregularities effect 0–44761 semiconductor, BiTel, band struct. obs. 0–44828 semiconductor, CdSb, plasma, i.r., 3-30 μm 85-300K, hole effective masses 0–75679 semiconductor, CdSnP₂, electroreflectance, optical transitions 0–76066 semiconductor, GaAs, photoreflectance line shape a fund. edge 0–76069 semiconductor, GaAs, surface damage due to ion implanatation, reflectance meas. 0–78366 semiconductor, GaAs, surface damage due to ion implanatation, reflectance semiconductor.

semiconductor, CaAs, surface damage due to for implanatation, renectance meas. 0–78366
semiconductor, GaSb, piezoreflectance 0–76015
semiconductor, Ge, enhancement under giant pulse irrad. 0–65985
semiconductor, InSb, electroreflectance spectrum, inter-conduction band transitions 0–44818
semiconductor, SiAs, transition band gap energy determ., 300K 0–44854
semiconductor, SiAs, transition band gap energy determ., 300K 0–44854

semiconductor, doped polar, coupled magnetoplasma- phonon modes obs. 0-54084

semiconductor, electroreflectance in space charge region 0-65984 semiconductor, europium chalcogenides, mag. ordering effects, obs. 0-5932

0—3932 semiconductor, group V and IV-VI, band structure 0—79270 semiconductor, layer-type, GaTe, absorpt. coeff., photocond. 0—62661 semiconductor, magnetic, europium chalcogenides, band struct. 0—59399 semiconductor, p-GaP, doped, ir., effective mass of holes determ. 0 - 79280

solar absorptances and spectral reflectances, 12 metals, 250° to 550°K 0-51294

solid, rel. to electronic struct., conference, Charia, Crete, Jul 1968 0-68729

spectral, of particulate materials, quantitative theory 0-62641

surfaces slightly tarnished, dirty or rough, computation method 0-62642 surfaces with bestrewed particles, pits. etc., computation of optical props. 0 - 44741

0–44741
thermal control coatings, effect of electron, proton and u.v. radiation investigation, spectral reflectance changes meas. 0–50912
thin film optical consts. from reflectance and transmittance meas. by curve fitting 0–41101
Venus, near ir. ice clouds 0–63139
Venus spectral rel. to wavelength, phase angle 0–63137
zincblende-type materials, contrib. of piezoelec. strain to electroreflectance 0.–76037

0-76037

Ag-Au alloy, reflectance change due to strain 0–48003 Ag-Zn(Cd) alloys, α -phase, reflectance and band struct. obs. 0–75996 Ag foils, thick, photon-surface-plasmon coupling, reflectance obs. 0–41114

Al overcoated with MgF₂ or LiF₂ obs. 0-59363
Al (200), bent, elastically or plastically, continuous X-ray spectrum 0-41115

As, i.r., rel. to energy band structure 0-65613
As, i.r., rel. to energy band structure 0-65613
As, S₃, vitreous, spectra 0-53816
Au, reflectance, rel. to band struct. 0-62645
BiTeI, band struct. obs. 0-44828
CdS, electroreflection, 300K, field strength depend., Lorentzian broadening 0-69107

CdS, electrorenection, stock and consider the consideration of the consi

CuO, diffuse reflectance spectra of pure and diluted samples, to 200 m μ 0-56523

0-50.23 Fe crystal neutron monochromator, rel. to mosaic spread and thickness 0-47169 Ga film, 0.25-25µm 0-48004 Ga_{1-x}Al_xAs mixed crystals, i.r. lattice-vibration spectra 0-44817 GaAs:Cd⁺, ion implantation damage, optical spectra, annealing effect 0-79279

0-19219 GaAs, derivative spectra, 5°K, 2.8-6.0 eV 0-51292 GaAs, split-off valence-band parameters from stress modulated magnetoreflectivity 0-72315

Reflectivity continued

GaAs, surface damage due to ion implantation, reflectance meas. 0-78366

0-78366
GaAs, ultrapure, photoreflectance line shape at fund. edge 0-76069
GaAs_{1-x}Sb, long wave optical phonon modes 0-76070
Ga_{1-x}In_xAs, long wave optical phonon modes 0-76070
GaN, i.r. spectra, phonons and electrons obs. 0-62648
p-GaP, doped, i.r., effective mass of holes determ. 0-79280
GaSb, electroreflectance spectra 0-79282
GaSb, piezoreflectance 0-76015
GaTe, layer-type semiconductor, absorpt. coeff., photocond. 0-62661
Ge-Si, amorphous alloy, fundamental absorpt. 0-48069
Ge-electrolyte interface, electroreflectance at fund. direct threshold 0-76072 0-76072

O-76072

Ge, amorphous, fundamental absorpt. 0-48069

Ge, enhancement under giant-pulse irrad. 0-65985

Ge, semiconductor, magnetoreflectance at 1.7 K., effect of mag. field modulation 0-79247

Ge, stress modulated magnetoreflectance for direct transitions 0-76026

GeSe_{0.75}Te_{0.25}, reflectance spectrum, band struct. obs. 0-76071

HgS, far i.r., Raman scatt., lattice vibrations 0-56085

HgS, plasma edge and band struct. obs. 0-69109

InAs_{1-x}Sb_xlong wave optical phonon modes 0-76070

InSb-NiSb system 0-69074

InSb, electroreflectance spectrum, inter-conduction-band transitions 0-44818

Li halide, low-temp., 5-10 eV, fine struct., excitons 0-76076

LiF(200), bent, elastically or plastically, continuous X-ray spectrum 0-41115

Na halide, low-temp., 5-10 eV, fine struct., excitons 0-76076

0-41115

Na halide, low-temp., 5-10 eV, fine struct., excitons 0-76076

NaH₃(SeO₃)₂, far i.r. spectra, 16-400 cm⁻¹, 300 and 202K, complex dielectonst. 0-56526

Na_xWO₃ measurements in energy range 1.75 to 6 eV, energy band structure 0-44765

Ni, specular electron reflectivities, energy gap edges determ. 0-54086

NiO, reflectance spectra, optical consts. 0-79276

Pb crystal neutron monochromator, rel. to mosaic spread and thickness 0-47169

PbSe, free electron effective mass. 0-51046

0-47169
PbSe, free electron effective mass 0-51046
Pb_{1-x}Sn_xSe mixed cryst., free electron effective mass 0-51046
SbSI, far-i.r. spectra, temp. depend. 0-66025
SbSI, far-ir. spectra 0-66026
Se, trigonal, interband region obs. 0-66051

Se, Ingonal, Interband region obs. 0–66051 semiconductor, Ge, magnetoreflectance at 1.7 K., effect of mag. field modulation 0–79247 Si, derivative spectra, 5°K, 2.8-6.0 eV 0–51292 Si, thermoreflectance spectra 0–41181 Si amorphous, fundamental absorpt. 0–48069 SiAs, transition band gap energy determ., 300K 0–44854 SiO₂, α-quartz, i.r., 380-640 cn⁻¹, extraordinary phonon dispersion 0–78737

0-78737
Sn, grey, spectra, critical-pt. analysis 0-71926
SnO₂-F films on glass, spectral reflectance 4 to 20 μ 0-69104
Te. lattice vibration contrib. 0-66057
Te(Ge,As) based amorphous semiconductor 0-56490
ZnAs; films, vacuum evap. 0-65983
ZnO₂, u.v. spectra, charact. energy-loss spectra comparison 0-54090
ZnSe, spectra, 15 and 300K, calc. and meas. 0-48007
ZnTe, spectra, 15 and 300K, calc. and meas. 0-48007

records, analysis and interpretation thorough siesmic waves reflection technique, digital processing 0-48227

acoustic waves

see also Dispersion/acoustic in constant-gradient media, refraction correction by ray tracing, graph 0-53272 in electric field at crystal boundary, and reflection and self-focussing

0-56096

0-56096 harmonic source sound field about infinite thin plate in homogeneous medium, analysis 0-60032 from inhomogeneities, large weak, relations with plane waves 0-52104 jet temperature profile variation obs. 0-64816 by jets, numerical study 0-55539 lens, mechanical Luneberg, comparison of theory and experiment 0-54701

acoustic waves, ultrasonic by Au thin film layer on LiNbO $_3$, surface-wave phenomena obs. 0-65538

electromagnetic waves see also Electromagnetic wave propagation rel. to Venus atmosphere, r.f., structure of field intensity obs. 0–69456 atmosphere, 35, 70, 97 and 135 GHz, comparison with optical refraction

atmosphere, 35, 70, 97 and 135 GHz, comparison with optical refraction 0-62922 radar ducting, frequency dependence 0-59553 refractive corrections in high-accuracy radio interferometry 0-51534 semiconductor, isotropic, in mag. field, refraction of e.m. waves, Abeles treatment extension 0-45722 stratified anisotropic media, extension of Abeles treatment 0-45722 Venus, radio and optical 0-63132 Venus atmosphere, Mariner V S-band radio occultation measurement 0-63125

refraction

ight

see also Double refraction
anisotropic medium, new formulae 0-69982
conical, in isotropic nonlinear dielectric in presence of another intense light beam 0-38531
of contact lens meas, in excess of 25 diopters 0-73285
eye, servo-controlled optometer for producing elec. signal proportional to refr. power 0-45481
focused beam, rel. to acoustic imaging 0-52130
Fresnel formulas derived from dispersion theory 0-60339
gas, atmospheric, near 22 GHz H₂O vapour rot. line 0-64820
Kerr cell, frequency shift in He-Ne laser beam 0-73252
liquid birefringence, acoustically induced, optical discrimination between two mechanisms 0-53349
in planetary atmospheres, rel. to optical systems for grand tour space

two mechanisms 0-53349 in planetary atmospheres, rel. to optical systems for grand tour space probes 0-63091 seawater light-field fluctuations, differential refraction by surface gravity waves 0-62886

refraction continued light continued

self-focusing, periodic of light beams, theory 0-57558 in statisted anisotropic media, Abeles formalism extension 0-60338 water vapour 0-64820

water vapour 0-64820

Refractive index
film, X-ray reflection 0-74894
garnets, isolated in lunar rock 0-79725
and group velocity in moving dispersive media 0-58324
moving dispersive media, group velocity 0-58324
phenazine-N-oxyphenazine system, variation with composition 0-53407
radio, over India and neighbourhood, microwave propagation 0-59592
rel. to radiowave propagation in atmosphere, distribution field obs. to 2 km,
fluctuation parameters 0-51536
v1.f., in ionosphere 0-72642
X-ray, of LiF, interferometry, forward scatt. amplitude 0-79234
Kr gas determ. in vacuum region spectrum 0-43401
LiF, X-ray interferometry, forward scatt. amplitude 0-79234
LiNbO₃, from electro-optical effect obs. in 126-132 GHz range 0-48020
SiO₂ layer, ellipsometry 0-76016
Xe gas determ. in vacuum region spectrum 0-43401
Xe pulsed plasma, two wavelength laser interferometric study 0-71157
ZnS thin films, deposited on glass substrates, abnormal dispersion caused
by inhomogeneity 0-62599
light

see also Disperions, optical; Double refraction; Optical constants air, variation, correction for in optical interferometry 0-54913 atmospheric, average structural characteristics meas. 0-79542

aur, variation, correction for in optical interferometry 0–54913 atmospheric, average structural characteristics meas. 0–79542 dielectric or semiconducting media, evaluation from interference-fringe transmission spectra 0–48000 dye solutions, calc. 0–39791 ellipsoid, complex, of absorbing uniaxial crystals 0–47982 from elliptical polarized emission explt. obs., calc. method 0–76003 ferroelectric, KNbO₃, birefringence temp. depend. 0–76006 ferroelectric, LTaO₃, Curie pt. behaviour 0–65814 ferroelectric, SbSI, rel. to phase transition 0–65826 ferroelectric, SbSI 0–62603 film, dielectric, rel. to ageing 0–51264 film, inhomogeneous, bilayer structure form 0–51263 fluids, 'heavy', rel. to density, appl. to particle density determ. 0–47466 glass, Corning 9025, for cathode ray tube faceplate 0–59354 glass, La₂O₃-BaO-B₂O₃ system 0–58541 glass, mercury oxide containing 0–39908 glass graded index rods, image aberrations 0–59355 glass rods, cylindrical graded-index, as image relays 0–60397 high melting pt. crysts. 0–58625 lithium formate monohydrate, nonlinear optical susceptibility and transmission indices 0–79228 nonlinear medium, random inhomogeneities rel. to light beam narrowing 0–73289 nonlinear optical material, inhomogeneities effect on second harmonic ageneration. 0.5640

0-73289
nomlinear optical material, inhomogeneities effect on second harmonic generation 0-56482
photon-matter, interaction energy relationship 0-52348
polybutylmethacrylate, structure obs. from u.s. velocity and refr. index at 6328 Å 0-61613
polyethylene terephthalate, molecular orientation and deform, meas. in deform bands 0-41110
polyethylmethacrylate, structure obs. from u.s. velocity and refr. index at 6328 Å 0-61613
polymer, molecular orientation and deform, meas. in deform bands 0-41110
polymer, molecular reorientation and deform, calc. 0-41109

polymer, molecular reorientation and deform, calc. 0–41109 polymers, determ, from meas, of refractive increment using Dale-Gladstone eqn. 0–41111 polymethylmethacrylate, photoinduced refr. index changes and applics. 0–54059

polymethylmethacrylate, structure obs. from u.s. velocity and refr.

0-61613 polywater identification, measurement in glass capillaries using interference

polywater identification, measurement in glass capillaries using interference microscope 0–50198 propylene carbonate, liquid, equilibrium meas. 0–61544 pyroelectric, laser-induced index damage 0–62601 pyrrhotite, hexagonal, complex ellipsoid of absorbing crystal 0–47982 random medium with refractice index variations, laboratory model 0–69994

reflecting surface determination using ellipsometric method 0-69075 rubber, fluctuations in index, crosslinking inhomogeneity determ. rubber, fluctuations in index, crosslinking inhomogeneity determ.

0–390/5
semiconductor film, and extinction coeff. 0–44762
semiconductors with population inversion 0–540/58
thin-film thermochromic effects 0–593/58
tropospheric refractivity profile for satellite data correction 0–48286
turbulence measurement 0–780/11
variations meas. in large glass blank, dual interferometer 0–72306
AIF, film, vacuum evaporated, tensile strength 0–47061
AI,O₃ film on Si, r.f. sputtering power density effect 0–65081
AIP, absorpt. obs. 0–69115
Ar, solid and liquid, meas. 0–71263
BaF₃, calc. 0–44783
BaFiO₃, optically induced changes, obs. 0–62600
BeSO₄AH₂O, dispersion 0–68236
CS₂-CCl₄ mixtures, nonlinear using laser 0–39792
CaF₃, calc. 0–44783
CdSnP₃, i.r. ref. and absorpt. obs. 0–72341
CSCu₂Cl₃, large index obs. 0–40006
Dy, and absorpt. coeff., 1.13-3.96 eV 0–76009
Gd, and absorpt. coeff., 1.13-3.96 eV 0–76009
n-lnAs, as function of carrier conc. 0–44840
KCl soln., interferometer calibration applic. 0–39790
KNbO₃, temp. depend. rel. to structure and ferroelectric props. 0–76006
Kr, solid and liquid, meas. 0–71352
LaNbO₄:Nd single crystals, principle indices of refraction 0–62597
LiO₃, far-i.r. props. 0–69070
LiNbO₃, laser-induced index damage 0–62601
LiTaO₃, Curie pt. behaviour 0–65814
MgF₂ deposited A/4 film in ultra high vacuum, determination, mass spectrometric analysis 0–72307 rubber, fl 0-39905

Refractive index continued

light continued

ight continued

MnAs film, complex, and Kerr rotation, Faraday effect, and complex dielectensor 0-44628

N₂, u.v. interferometric meas. 0-71263

N₃-0.SiO₂ glasses, water retention effect 0-58542

Nd doped laser glasses, 0.4 to 2.3 μ, 0 to 300°C, obs. 0-59360

Pb.MoO₃, single crystal, visible region, room temperature, 0.19-2.5 μ 0-76010

S₂Sb₂Pb, zinkenite, and absorpt. coeff. and absorpt. index 0-51265

SbSI, ferroelec. 0-62603

SbSI, rel. to phase transition 0-65826

Se, amorphous, variation with byressure to 7 kbars 0-59361

Se amorphous, variation with pressure to 7 kbars 0-59361

Se amorphous, variation with hydrostatic press., obs. and interpretation 0-48023

0-48023 SiO₂ films u.v. irradiation, change 0-62604 Sm, and absorpt. coeff., 1.13-3.96 eV 0-76009 Xe, solid and liquid, meas. 0-71352 ZnAs, films, vacuum evap. 0-65983 ZnSe films, elec. field influence 0-69076

Refractive index measurement

for dispersive particles 0–39841 gases, meas, with multi-purpose instrument 0–66948 glass, index distrib. meas. apparatus 0–49129 introduction, university textbook 0–38525

Refractometers

cratcioneters — capacitor, instabilities rel. to temp. transients — 0—42383 — critical angle linear, opt. props. — 0—38554 — dual cavity, instabilities rel. to temp. transients — 0—42383 — Fourier far i.r. interferometric system using double beam — 0—63723 — microwave, meso cavity specular integrating, obs. of dynamic characteristics of atmos. — 0—45138

Refractories see High-temperature phenomena and effects
Refrigerators see Low-temperature production

Regge poles see Elementary particles/scattering Relativity

bremsstrahlung, gravitational 0–54994 bremsstrahlung, relativistic electron, elementary process, theory and obs. 0–52439

0–52433 circular orbits in classical relativistic two-body systems with 2 interacting charges 0–72905 classical Newtonian mechanics and Mach's principle, union, development of relational mechanics 0–54620 dynamical systems, abstract theory and hereditary 0–69665 dynamical systems, no-interaction theorem 0–72994 clinstein's eqns. reformation using techniques similar to those for strong interactions 0–72903 clinstein's priority in recognizing time dilation 0–59880 clinstein-Bohr box expt. 0–76821 electromagnetic fields, their relativistic symmetry groups 0–76953 endomorphisms, quasi-stochastic semi-groups formalism, physical content 0–54555 energy-momentum tensor construction to include property of scale

0—34555
energy-momentum tensor construction to include property of scale invariance 0—12901
faster than light particles, compatibility with retarded causality 0—76805
faster-than-light group vels. and causality violation 0—51930
Foldy-Wouthuysen transf., rel. problems 0—66795
Gaillean, equations of motion of a spin-one particle and the Bargmann-Wigner method 0—59881

hydrodynamics, vorticity application of general theory of space-like congruences 0-41953

ences 0–41953 interaction angular momentum and conservation laws 0–42190 Mercury perihelic precession, heuristic derivation 0–79727 Mossbauer effect measurement 0–69095 most general field representation, discussed from symmetry principles 0–48698

0–48698
particle systems in gravitational interaction 0–54557
photons-tachyons in Fresnel evanescent wave 0–48697
scattering amplitude parametrization, definition of crossing symmetric
measure and inertial tensor 0–76811
scattering states, N-particle, relativistic kinematics, quantum mechanical
treatment 0–72925
space-time absoluteness proof, crucial expt. 0–54559
statistical-covariance of velocity and gradients for e.m. radiation 0–66796
tachyons, classical motion in external field 0–51928
theoretical aspects 0–41568
double time scale for expanding model of uniform universe 0–72681
transformation to rotating coordinates 0–76810
two-particle system, relative position representation 0–72906
world model, homogeneous, anisotropic, with negative space curvature
0–69604

0-69604

general

see also Cosmology; Gravitation; Space-time configurations axially symmetric fields and static metrics, particular solution for the interior of a body 0-63336 bibliography of works rel. to Einsteins unified field theory 0-54566 Brans-Dicke, relation to Jordan theories, transformation of units and interpretation 0-57260 charge moving with the speed of light, Einstein-Maxwell equations, solution 0-66802 charged-dust distributions 0-38169 chronometric invariants, use in distinguishing classes of gravitational fields 0-76807

0-76807 cultsters of spin-1/2 particles, relativistic description 0-73481 collapse, critical parameters for isentropic objects with rest masses 10² to 10² M_☉ 0-76571 complex 2-dimensional internal space, calculus of vectors from the concept of existence of local basis systems 0-66804 composite particles, description, wave functions and form factors 0-7271 comparation laws integral 0-66806

0-77271
conservation laws, integral 0-66806
conservation laws in Minkowski space 0-41968
conservation of matter 0-66800
continuous matter eqns. of state, invariant forms 0-48705
covariant derivative in the affine approach 0-41966
curvature tensor, algebraic classification 0-76814
curved space, definition of multipole moments for static, asymptotically flat,
source-free solutions of Einstein's equations 0-66805

```
Relativity continued
  general continued
```

de Sitter spinning manifold 0-63330

differential forms in use in gravitational theory, introduction 0-72910

Einstein's field eqns., from metric tensor 0-69605

Einstein's field equations with incoherent matter and electromagnetic radia-

Einstein's field equations with incoherent matter and electromagnetic radiation, solution 0–63339 Einstein's theory prediction of deflection of radiation on passing sun, exptl. test 0–48711 Einstein's theory prediction of deviation of 9.602-GHz radiation in solar gravitational field exptl. test 0–51723 Einstein field exptl. test 0–51723 Einstein field exptl. test 0–518162 Einstein field exptl. test 0–38162 Einstein field exptl. test 0–38162 Einstein field exptl. test for explanation of the field exptl. test 0–28164 Einstein field exptl. test for explanation of the field exptl.

gravitational field exptl. test 0–51725
Einstein field eqns, solns. conform classified to embedding class 1 0–38162
Einstein field eqns, shear-free solns with fluid eqn. of state 0–38161
Einstein field eqns, shear-free solns with fluid eqn. of state 0–38161
Einstein spaces with symmetry groups 0–69609
Einstein universe, point mass in, exact solution 0–51936
Einstein Maxwell equations, class of solutions corresponding to stationary null electromagnetic fields 0–66803
Einstein-Maxwell field equations, null field solutions 0–41960
elasticity theory formulated 0–48712
electrodynamics, invariance, gauge transformations 0–42426
electromagnetic field in isotropic space-time 0–76815
for energy transformation analysis 0–42160
equations of motion, in gravitational field of system 0–54240
equivalence principle, development of quantum field theory 0–63747
experiment on Mariner Mars (1971) 0–54337
Fermions interaction, using covariant Dirac eqn. 0–48708
fields interaction, electromagnetic and gravitational, dependence on electromagnetic field frequency 0–63335
fluid sphere, static charged, exact interior soln. 0–51939
Friedman-Lobachevskii space, gravitational pressure 0–76816
gauge fields, local 0–54563
global singularities and Taub-NUT metric 0–69579
gravitation, linear theory 0–69607
gravitational and inertial mass of bodies of interacting electrical charges,
Einstein and Brans Dicke theories 0–57257
gravitational field synamical variables, SL(2,C) symmetry 0–69608
gravitational field synamical variables, SL(2,C) symmetry 0–69608
gravitational redative interactions of elementary particles, at high energy 0–70181
gravitational redative interactions, non-linear 0–48710
gravitational redastive interactions, non-linear 0–48710
gravitational redostive interactions, non-linear 0–7622
gyroscope, precession, another effect of earth's quadrupole moment 0–72904
gyroscope, precession, another effect of earth's quadrupole moment 0–72904
gyroscope, superfluid 0–76809

90-12904
Gyroscope, superfluid 0-76809
Hamilton-Jacobi eqn., gauge invariance 0-77238
Hamilton-Jacobi functional, new props. 0-54564
Helmholtz vorticity theorum, Boltzmann form. 0-72911
homogeneous anisotropic models with shear, Newtonian analogies 0-62968

hydrodynamic equations in $2^{1}/_{2}$ -post- Newtonian approx., deriv. and anal. 0-49961

0-49961 interplanetary radar time delays, general relativistic calc. 0-48620 Kirchhoff equations, generalised 0-38168 Lagrangian, quadratic action, its uniqueness 0-63334 light, escape from within massive object 0-62970 light deflection for complete celestial sphere 0-79621 Lorentz-covariance and generalisations of the Ricci calculus and spinor calculus 0-66801 Mach's principle, differentiable manifolds 0-51932 Mach's principle, discontinuity of first derivatives of metric tensor 0-69605 Mach's principle, two trials 0-51931 magnetic field, gravitationally induced 0-59891 matrix space theory, invariance and differentiation 0-72881 multipole moments in flat space 0-48709 neutral stability against convection, stars in hydrostatic equilibrium 0-79649

0-79649

non-static matter distribution of spherical symmetry, eqn. 0–72915 null field solutions of the Einstein-Maxwell field equations 0–41960 observational tests 0–41568 orbits, circular, in stationary axisymmetric space times, stability criteria 0–48706

0-48706
perfect fluid space-times, algebraically special 0-38163
photon charged and Maxwell's equations solution 0-63325
plasma, nonrelativistic collisionless model, generalization to general-relativistic domain 0-53140
point mass in an Einstein universe 0-41569
pulsars, electrodynamics 0-66562
quantum, in framework of Feynman sum-over- histories quantization 0-38167.
Reissner-Nordstrom solution generalized for Einstein-Maxwell equations

Reissner-Nordstrom solution generalized for Einstein-Maxwell equations

0–41963
Riemann tensor, symbolic computation, compact method 0–38165
Romer's method of speed-of-light determ., possibility of yielding unidirectional speed 0–51935
scale invariance and gravitational coupling 0–63333
Schwarschild metric, stability against small perturbations after gravitational collapse 0–57259
Schwarzschild metric, differential equations for perturbations 0–59894
Schwarzschild field, spin precession 0–45528
Schwarzschild sphere, evolution of charged sphere after collapse 0–59893
singularities, influence of rotation 0–45526
space-time configuration static spherically symmetric, optical point characts. determination 0–69611
spin connection and gauge potentials in Riemann space, use of anholonomic

acts. determination 0-69611 spin connection and gauge potentials in Riemann space, use of anholonomic bases 0-57258 stability of relativistic gas spheres and clusters of point masses with large central redshifts 0-45205 star in hydrostatic equilibrium, inequalities 0-41637 stars, ultrarelativistic, stability, two new theorems 0-57022 static spherically symmetric charged mass distribution, exact solns. 0-69610

0-09610 static system, closed, energy momentum complex 0-41962 static universes in Fridman space 0-51937 surface density, definition 0-41961 surface layer theory 0-51938 tachyons, review 0-38160

Relativity continued general continued

tetrad equations for the two-component neutrino field 0-38170 theories and possible high precision tests 0-59890 theory, role of Eotvos expt. 0-38164 thermodynamics, 2nd law, chronometric invariant formulation 0-76817 time, setting up of initial conditions on 'a priori' basis 0-41964 topology 0-41961 unified treatment of the Kerr and Vaidya solutions, based on the Schild-Kerr metric 0-51940 vacuum metrics without symmetry 0-41956

vacuum metrics without symmetry 0–41956
special
'twin' of 'clock' paradox, treatment based on invariance of metric interval
and concept of proper time 0–48700
appearances, geometrical, at relativistic speeds 0–54560
atomic clocks in a moving frame of reference, discrepancy 0–57255
e.m. wave interaction with moving mirror 0–48904
elastic body motion tetrad formulation 0–54647
ether theory revived 0–45525
faster-than-light particles, further evidence against 0–76812
force in special relativity, paradoxical behaviour 0–66799
headlight effect for nonelectromagnetic radiation, anomalous 0–48704
instantaneous interaction for two particles in one dimension, Lorentz
invariance 0–48701
kinematics, from Lorentz transformations 0–63329
light, its velocity, not invariant in Galillean co-ordinates 0–76813

kinematics, from Lorentz transformations 0-63329 light, its velocity, not invariant in Gallilean co-ordinates 0-76813 light velocity, ellipsoid theory, shrinking orbital radii 0-59885 light velocity, moon laser experiment 0-57256 light velocity definitions of seven velocities of light and the introduction of the centrovelocity 0-54903 light velocity in moving medium, 'extinction' theory of Fizeau experiment 0-41958

0–41938 light velocity in space, radar testing 0–54562 lorentz contractions of rot, discs 0–63332 Lorentz transform, generalization, significance 0–48702 Lorentz transforms and linearity, deduction 0–57254 Lorentz-Dirac equations, extraction of spin effects 0–60153 media in non-inertial frames, electrodynamics, tensor and Lorentz transforms 0–38431 meter stick in a matchbox, obtaining a photograph 0–66797 microelectromagnetism, theory 0–48905 moving terrestrial clocks, rate relative to stationary ones 0–59882 particles travelling faster than light, theory and implications 0–54561 photons-tachyons in the evanescent wave assoc, with total refi. 0–41957 radial velocity calc. of relativistic atom from spectral line shift 0–57037 right-angled lever and Thomas precession 0–63328 tachyons, detection and Tolman's paradox 0–59884 tachyons, paradox, anticausality 0–54972

tachyons, noncausal behaviour and classical-particle description 0-59883 tachyons, paradox, anticausality 0-54972 tachyons, reply to objections 0-48699 tachyons, self-energy problem when charged, theoretical basis 0-63331 tachyons, simple model 0-48703 theory, review 0-51934 time and the principle of Caratheodory for a space-proper-time representation 0-41959 transformation of force, validity of conventional expression 0-72908 transformation of force in static conditions 0-72909 vertical line, visual appearance at varying speeds 0-66798

vertical line, visual appearance at varying speeds 0-66798

unified field theories block diagrams and the extension of timelike two-surfaces and schematic representation of 2-dimension metrics 0—63337

Bonnors form reduction to Einstein-Maxwell eqns. of general relativity

0 - 59886

0-39600 charged line mass, general relativistic solution 0-54565 Einstein-Maxwell equations, class of exact solutions from solutions that formally satisfy the two-dimensional Newtonian Laplacian equation 0-63340

0-03340
Einstein Maxwell field equations, null field solutions 0-41960
Einsteins equations, bibliography for general relativity-gravit. theory cosmology facet 0-54566
electromagnetic tensor in Riemannian space-time 0-38171
gravitational theory of particles with variable mass, formalism 0-63338
gravitational theory of particles with variable mass, physical consequences

higher-dimensional field theory for macroscopic and microscopic properties of matter 0-41969 Newman-Penrose formalism of the geometrodynamics of electromagnetic

Newman-Penrose formalism of the geometrodynamics of electromagnetic fields 0-51941 α nonlinear theory 0-59888 particle-like behaviour of a non-linear theory 0-59887 Rainich's Aiready Unified Field Theory for spherically symmetric, electrically charged body 0-76567 Rainich's theory 0-72917 weak field approx. in already unified theory 0-69612 Weyl's rel. to Rainich's 0-38172 availing

Relaxation

see also Acoustic wave propagation. Dielectric phenomena; Elastic relaxation; Ferroelectric phenomena; Ferromagnetic relaxation; Mole-cules/relaxation; Nuclear magnetic resonance and relaxation; Paramag-

cules/relaxation, Nuclear magnetic resonance and relaxation, Paramagnetic resonance and relaxation acoustic in nitrobenzene-n-hexane soln., study 0-64908 alkali, silicate glasses, ion-exchanged, mech. relax. 0-62020 alkali, silicate glasses, ion-exchanged, mech. relax. 0-62021 alkali halide aqueous soins., dielec. relax. time 0-39825 alkali silicate glasses, mixed 0-58870 anelastic and dielectric, due to reacting point defects, kinetics 0-68429 atom, in coherent optical field 0-39256 l-butanol in benzene and p-dioxane solns., relax. time distrib. 0-39828 chemical, dioxane-glycerol mixture, ultra-sonic absorption 0-43441 crystals, dipolar relax. rel. to defects and disorder 0-40823 cyclotron resonance, relaxation time, mass anisotropy and magnetic field tipping, relationship in metals 0-62275 l-decanol in benzene and p-dioxane solns., relax. time distrib. 0-39828 decay laws, non-exponential 0-38150 dielectric, at high frequencies, theory based on use of interpolation function 0-74777 dielectric, critical slowing-down process in H-bonded cryst. 0-65798

tion $0-(4/7)^2$ dielectric, critical slowing-down process in H-bonded cryst. 0-65798 dielectric, distribution functions 0-53920 dielectric, epoxide resins set with different anhydrides 0-72103 β , dielectric, in isotactic and polymethyl methacrylates 0-51108

Relaxation continued

dielectric, in nitrite mixtures 0-64939

dielectric and anelastic, due to reacting point defects, kinetics 0-68429 duration of memory determination, for viscoelastic materials 0-71673

duration of memory determination, for viscoelastic materials 0–71673 ethylene-methacrylic acid copolymers, birefringence obs. 0–78613 ferroelectric, AgNa(NO₂)₃, dielec. relax. 0–62429 ferroelectric, dielec. relax. 0–72111 ferroelectric, distrib, near Curie temp. 0–68921 and hybrid modes in GaAs 0–44315 ionic, in nitrobenzene 0–68145 ions in liquid He, momentum relaxation times 0–46967 liquid, u.s. relax. as rate process 0–39725 liquids, u.s. shear and compressional, dynamical model 0–53311 liquids, ultrasonic 0–71338 mechanism, by new Lf. anelasticity measurement technique 0–75231 metal, b.c.e. single crystal, dislocation, 77-450K 0–68355 methanol in benzene and p-dioxane solns, relax. time distrib. 0–39828 method for metal vacancies study under nonequilibrium conditions of plastic deformation 0–47224 method of studying vacancies in metals under quasiequilibrium conditions 0–47223

0 - 47223

0-47223 of optically pumped systems with buffer gases 0-55240 pentachlorophenol-tributylamine complex, H-bonded, dielec. absorpt. study 0-61543 phonon, applic. of Peierls' phonon-Boltzmann eqn., eigenvalue spectrum of linearized collision operator 0-41996 photon-echo theory, superradiant damping effects 0-42920 plasma, nonequilibrium electronic behaviour 0-68742 plasma, transient relaxation of velocity distrib. function of electrons 0-55458

plasma in solid, dielec. relax. 0–40681 plasma temperature, Fokker-Planck coeffs. rel. to spectral function of elec. field vars. 0–78074

polyethylene, alpha relax. 0–78612 polyethylene melts, filled, relaxation spectra 0–58424 polymer, internal stress relax., elastomer introd. effect 0–40276 polymers, dynamics of three dimens. cubic and tetrahedral lathe models 0–50656

polymers, rubber like, low temp. phenomena at low deformation 0–68387 polymethylmethacrylate, vitreous, rel.to interaction of shear and compression strain states 0–50657 Polypropylene fibre, acoustic vel. and absorpt. coeffs., processes, 93-433K 0–71851

conjungment tone, acoustic vei, and absorpt, coeffs., processes, 93-433K 0-71851

polystyrene, dielec. y-relax. 0-68900

polystyrene derivatives, glassy state, dielec. relax. 0-65775

polytetrafluoroethylene, compression stress relax. processes 0-40282

polyvinyl chloride, unplasticized melts, modulus in temp. range 150-220°C, spectra calculated 0-68033

polyvinyl-p-methoxybenzoate and poly-p-methoxystyrene, dielectric props. meas., secondary relaxation mechanism 0-79032

polyvinyl-p-methoxybenzoate and poly-p-methoxystyrene, dielectric props. meas., secondary relaxation mechanism 0-79032

polyvinyl-dene fluoride, dielectric, and molecular motion 0-75777

quartz, mechanical deformation, stress relaxation and thermal activation parameters 0-71690

rare-earth metals, u.s. relax. in spin spiral phase 0-47527

reversible and irreversible, in gases, and photon echo 0-61436

rubber-like polymers, stress-relaxation 0-50675

ruby, "T. to "T, nornadiative, 4 ns upper limit 0-44899

ruby, non-radiative relaxation time between 4T2 and 2T1 states, upper limit 0-54123

semiconductor, effect on coherent interaction between electrons and strong

semiconductor, effect on coherent interaction between electrons and strong e.m. wave 0-75674

semiconductor, energy-depend. relax. times in electroacoustic absorpt. 0-43888

0-43888 shock waves in atmosphere 0-76374 sodium borosilicate melts, viscous, anomaly observed above critical points 0-74734 solid, book 0-43702 spectra from experimental data 0-69598 statistical kinetics special class called relaxed motion 0-54587 stress-relaxation in network rubber-like polymers 0-50675 structural dynamics in liquids, distributed relaxae local liquid structure. This is used to predict both time spectrum, physical model, analysis 0-53313 superconductor, Pb, stressed, dislocation motion and electron drag 0-78645 0 - 78645

0-78645
theory of lightning stepped leader 0-59589
thermal, temp. coeff. resist. obs., metals 0-71950
thermal in one and two dimensional plasma models, particle-in-cell numerical computation 0-46684
and thermodynamics, general relativistic 0-38405
time longitudinal of nonequiv. nuclei groups, meas. using NMR spectrometers 0-48939

time longitudinal of nonequiv. nuclei groups, meas. using NMR spectrometers 0—48939
us., in aqueous solutions of tetrabutyl ammonium bromide 0—53342
us., in alcohol—water mixtures 0—55611
u.s. in n-butyl, isobutyl, sec-butyl alcohols, mechanism study 0—50222
viscoelastic linear materials 0—73019
viscoelastic materials, linear one-dimens., monotonicity 0—57355
viscoelasticity, linear, theory, admissible functions 0—38312
AgNa(NO₂)₂, dielec. relax. 0—62429
CaF₂, dipolar relax., 1.f. 0—62429
D₂, solid, stress relax., plastic deform., 1.4-17.5K 0—40304
n-GaAs, small-signal relax. times for lattice scattering 0—44193
LiF, stress curves, 300, 78 and 4.2K, dislocation velocity 0—40305
LiF, stress relax., internal stress. work hardening 0—68436
Mn-Ag alloys, influence of time on nuclear orientation meas. 0—62580
NaCl:Co, X-irrad., dielectric loss 0—44344
NaCl. stress relax., internal stress. work hardening 0—68436
NaNO₂, static electric susceptibility near transition points 0—44356
Nb solid solution, Snoek peaks, broadening effect 0—68413
Ni, Zr addition effect 0—53576
O₂, vibrational time, temp. dependence 0—61131
Pb, stressed, supercond. transition effect, dislocation motion and electron drag 0—78645
Si:Li,B single crystal, anelastic, internal friction peak, 150C, 1.2 kHz
0-68418
SiO₂, excess vibr. modes, anelastic and dielec. relax. 0—59084 0 -68418

0.58418 SiO₃, excess vibr. modes, anelastic and dielec. relax. 0.59084 SrTiO₃, mech. relax. and nonlinearity 0.65819 SrTiO₃ containing rare-earth ions, dielec. relax. 0.59253 TiO₃, blue, dielec. relax. and assoc. defects 0.40827 V:H, cold-worked, anelastic effects, 4.2-450K 0.68422

Remanence see Magnetization state

Renner effect see Molecules Replica techniques see Electron microscopy

Reproduction see Sound reproduction

Resistance, electrical see Conductivity, electrical

Resistance thermometers see Thermometers/resistance

Resistivity see Conductivity, electrical

Resolving power, optics see also Optical instrument testing

aperture field of observing opt. instrument, statistical description 0-42355 coherent data-processing system, resolution testing by linear gratings 0-70005

detection and estimation of incoherent objects, modal decomposition of aperture fields 0-42384

aperture neids 0—42384 electron microscopes, scanning transmission, construction 0—42215 electrophotographic images 0—38586 gratings high precision with laser light and photoresist layers, 100×100 mm, 90% resolution sq. 50% efficiency 0—42366 hologram wavelet reconstruction with increased resolution, patent 0—42342

0-42342 of idealized system, physical realizability and constraints 0-38533 imaging with optical synthetic apertures, f/30 system, Mills-cross antenna analogue 0-42361 interferometers, Michelson and Fabry-Perot, rel. to background intensity 0-52385

introduction, university textbook 0—38525 of microscope, partial coherence effect 0—77201 telescopic sights and projection systems, mtf by photographic tech., method 0—49106

Resonance, elementary particles see Baryons/resonances; Hyperons/resonances; Mesons/resonances Resonance, magnetic see Magnetic resonance and relaxation

Resonance spectra see Spectra

Resonators

2.13µ internal optical parametric oscillator 0-69882 anisotropic cavity, magnetooptic mode splitting 0-52265 astigmatic, analytical calc. of the complex natural frequencies and field distribution at reflecting surfaces 0-60203 covity, containing magnetoplasmas, r.f. fields and resonant freqs. 0-78121

0–78121
cavity, dissipative ponderomotive effects of e.m. radiation 0–48913
cavity, dissipative ponderomance in LiNbO₃, KH₂PO₄ Pockels cells, transient elastooptic effects 0–66766
circularly anisotropic, in ring laser 0–42264
complex, symmetric fields calc. 0–38495
coupled chains transient response 0–73084
with curved mirrors, oscillatory behaviour 0–77075
dielectric, at microwave, temperature stable ceramics 0–75316
difluoroethylene in HCN laser cavity, saturation of 890 GHz absorpt. line 0–54867
dispersive, retunable, appl. to solid state lasers 0–67068
EPR low temp. reflecting resonator, specimen transport mechanism 0–48935
Fabry-Perot, disturbed, made calculation using Weinstein theory

Fabry-Perot, disturbed, made calculation using Weinstein theory 0 45779

Fabry-Perot, passive, in anisotropic optical medium calc. of modes 0-69878

70–09076
Fabry-Perot laser cavities immersed in homogeneous moving medium, resonant modes 0–77071
Fabry-Perot with electron-tube for mm. wave generation 0–76956

Helmholtz for earmold vents resonance pattern, damping effect, investigation 0-45463

tion 0-43403 laser, anisotropic cavity, magnetooptic mode splitting 0-38494 laser, degenerate vernier interferometric 0-63600 laser, mutual coherence function separation, cross-spectral purity applic. 0-69883

laser, nonlinear processes for reflection into resonator by moving reflector 0-38502

laser output coupler, Fabry Perot displacement detector 0-45780 low temp. for EPR study of specimens under single axis press., description 0-51386

0-3186 microwave, crossed cylinder 0-54790 mode volume and radiation power of a laser 0-63601 multilayer, natural vibrs. 0-42257 multilayer media, with uniform structure, resonance frequencies 0-45781 multimode, method for electron conc. determination in electron beams 0-52361 0 - 52245

open, hemi-spheric, reflective diffraction grate, spectra, field distrib., natural oscillations 0-45717

open with reflective diffraction gratings 0–54853 optical, experiment with a nonabsorbing diffraction selector of longitudinal modes 0–60204

optical, improved, for measuring time-dependent electron densities 0-43305

optical, improved, for measuring time-dependent electron densities 0–43305 optical, stimulated Raman emission, generation of several Stokes component 0–42256 optical, with 'edge coupling' through reflector aperture, patent 0–49033 optical parametric internal oscillation 0–41929 optical standing wave, thin film diffraction grating for 0–42254 optical transverse mode selection methods compared 0–52264 output coupler, Fabry Perot displaceent detector 0–45780 piezo-semiconductor phaser based on surface waves, for wurtzite crysts. with cond. surface layer 0–44373 piezoelectric, circular, electric equivalent circuit 0–51125 polarized anisotropy, effects on output of Nd laser 0–42295 Q-modulator of laser cavity based on variable abs. Fabry-Perot interferometer 0–38496 Raman oscillator, quasi-CW, low power 0–42245 ring, travelling wave mode with external mirror 0–42255 ring with discharge tube, Brewster-angle windows, polarization props. investigation 0–63599 rotating ring, in gravitational field 0–48914 for rotational laser transitions realization 0–52268 spherical, single pulse evolution, effect of transversal structure of field 0–69774 superconducting for 3cm klystron oscillator 0–45715 superconducting for 3cm klystron oscillator 0–6707

superconducting for 3cm klystron oscillator 0-45715 superconducting r.f. cavity, problems 0-68797

Reviews continued Resonators continued rews continued ferroelectric phase transitions, critical zone-centre mode obs., i.r. and Raman spectra 0–68917 ferroelectric phase transitions, elec. conductive, surface and electro-optic props. 0–75791 ferroelectric phenomena 0–75790 three-mirror, for He-Ne laser radiation modulation using electrooptical effect 0-60216 three-mirror non-coordinated, laser oscillations 0-60202 X-ray freq., characts. 0-60188 LiNbO3 in med. freq. range with low capacitance ratios, temp. coeff., design 0-65830ferroelectric phenomena 0-75793 ferromagnets; transparent 0-7593 fluid spramings; 1968 0-58289 fluid mechanics, book by several authors 0-39486 fluid mechanics, book by several authors 0-66795 free radicals in astrophysics 0-54320 fusion, controlled, research 0-66293 free radicals in astrophysics 0-54320 fusion, controlled, research 0-6253 geomagnetic pulsations, diagnostics of magnetosphere 0-76513 glass, radiation induced colour centers 0-61978 h.f. discharges, induction, at high pressures, appl. 0-78107 hard magnetic materials 0-79170-73743 Hartree-Fock method in nuclear theory 0-73723 heat and mass transfer, Polisis works 0-66938 heat transfer, 1968 literature 0-48879 heat transfer, 1978 heat transfe LiTaO₃ in med. freq. range with low capacitance ratios, temp. coeff., design 0-65830 PbZrO₃-PbTiO₃ solid soln., piezoelec. ceramics, circular plates, contour oscillations 0–53948 YFe garnet epitaxial film, rel. to magnetically tunable microwave bandstop filters 0–44667 acoustic see Acoustic resonators electromagnetic see Electromagnetic oscillations Reverberation reflectation see also Architectural acoustics; Echo chambers, acoustical modelling 0–52133 explosive in shallow sea-bed, meas. 0–62885 reverberent sound field, discrete versus continuous space averaging, analysis 0–57386 sis 0-5/386 shallow-water, vertical coherence 0-56756 theory refinement using digital simulation of sound transmission in reverberant spaces 0-66916 time calculations, visual structure walls, slat- and grid- transmission and reflection characteristics 0-42084 Reviews 3-nucleon problem 0—49450 ablation 0—71733 acoustic waves, reflection and scattering from sea surface literature survey 0—52091 0-52091 acoustics 0-38377 acoustoelectric device applications of piezoelectric and semiconducting thin films 0-56103 adsorption of 02 on W at room temp. 0-71498 aircraft in space research 0-79613 alkali halides, growth and physical props. 0-58646 alloys, of high susceptibility, magnetic props. 0-53979 antiferromagnetic dielectrics, abs. of light 0-76081 astronomical instrument design, review of literature 0-66673 astronomy and astrophysics (1969) book 0-72677 atom-atom scattering models 0-60985 atom-electron scattering 0-60972 atomic X-ray emission spectra in K, L, and M regions, review of elements 0-60907 atomic Collisions, impulse and Vainshtein approximation, matheds atomic collisions, impulse and Vainshtein approximation methods 0-58114 atomic collisions, impuse and Vainsntein approximation methods 0—58114 atomic collisions 0—58115 atomic energy levels, relativistic Z-dependent corrections 0—74114 atomic spectra analysis 0—58095 avalanche diodes, noise characts. 0—68870 300 binary-encounter and classical collision theories for atoms 0—58116 biological effects of magnetic fields 0—69523 blood flow in heart and arteries 0—41880 bosons and Bose condensates, two kinds 0—38213 boundary layers transition from laminar to turbulent flow 0—39495 chemical reactions and molecular collisional excitation 0—59476 chromatography, liquid 0—72562 coincidence measurements for atomic collisions 0—58117 collision theory, quantum mechanical 0—59922 colloidal electro-optic effects 0—55638 combustion at low temperature, reviews 0—41422 continuous media, mechanics for non-canonical regions 0—45561 cosmic ray electrons studies, contributions to cosmic ray astrophysics 0—45215 cosmic ray electrons studies, contributions to cosmic ray astrophysics 0–45215 Coulomb energies 0–49457 Coulomb energies 0–49457 coupled channel method in nuclear reaction studies 0–49582 critical phenomena research 0–46975 cryogenic techniques for solid state properties 0–74857 cryogenic techniques for solid state properties 0–74857 cryogenic techniques for solid state properties 0–74857 cryotal structure determ. by X-ray diffraction 0–53482 Crystallization from the melt 0–40022 damping, dislocation effects 0–43720 dielectrics, antiferromag., abs. of light 0–76081 dielectrics, multiquantum photoemissive effects 0–75860 diffusion coeff. determ. for metals using solid electrolytes 0–65339 discharges, reflex and Penning 0–55510 dislocations near ends of cracks 0–78649 drift tube technique for study of mobility, diffusion, and reactions of slow ions in gases 0–60986 Earth's interior, equations of state at high pressures 0–45110 electrochydrodynamics, role of interfacial shear stresses 0–39487 electron breakdown in solids 0–62406 electrohydrodynamics, role of interfacial shear stresses 0–39487 electronoliminescent materials, production 0–62738 electron baam investigation of atoms 0–60973 electron microscopy, scanning, image contrast 0–75061 electron microscopy, scanning 0–78439 electron microscopy, scanning 0–78439 electron microscopy, scanning 0–78439 electron microscopy, scanning, image contrast 0–75061 electron microscopy, scanning, image contrast 0–75061 electron microscopy, scanning 0–78439 electron microscopy, scanning 0–78439 electron microscopy, scanning 0–786716 electron microscopy 0–58676 electron microscopy 0–58676 electron microscopy 0–58676 electron microscopy 0–582644 0-70790 electronic and vibrational energy transfer between atoms and molecules in the gas phase 0-58264 electronic materials film production 0-61664 elementary particle properties 0-38605 elementary particle scattering 0-60502 elementary particle scattering 0-60504 elementary particles current exptl. and theoretical activity 0-38603 elementary particles, current exptl. and theoretical activity 0-38603 elementary particles, current exptl. and theoretical activity 0-38603 elementary particles, ourrent exptl. and theoretical activity 0-38603 elementary particles props, tables and listings 0-70171 embrittlement by hydrogen of iron and steel 0-68477 Euclidean quantum field Theory 0-70161 europium chalcogenides, optical props, review 0-59399 excitation of atoms and molecules, shock waves 0-58104 fatigue, thermal, test methods 0-65418 ferroelectric phase transitions, Mossbauer obs. 0-68918

Reviews continued

physics education, secondary school and univ. 0—45506 physics in 20th century 0—63299 plasma, theory of generation of harmonics and combination frequencies 0 - 58343

plasma anodization of metals and semiconductors 0-55734

plasma anodization of metals and semiconductors 0–55734 plasma instabilities 0 –46753 plasmotron, electrodeless 0–78107 plumes and thermals in the atmosphere 0–41497 polymers, molecular motion, n.m.r. studies 0–64569 positron collisions with atoms 0–58109 potential in nucleon-nucleon interactions and limitations of existing models 0–73741

potential in nucleon-nucleon interactions and limitations of existing models 0--73741 programmed learning 0-59854 pulsar research 0-59730 pulsars, review of electrodynamic emission 0-66540 pulsars and neutron stars 0-59738 quantum electrodynamics status 0-45856 quasar research, present state 0-59730 quasi-stellar objects (1967-8), developments 0-72744 r.f. quadrupole field mass spectrometers 0-55218 r.f. sputtering 0-65566 radiation chemistry, energy loss of particles 0-59505 radiation chemistry, energy loss of particles 0-59505 radiation damage in metals 0-59118 radioactive decay, expt. work 0-57938 radioastronomical observations in 1-30 mm region 0-41743 rare-earth intra-alloys behaviour and structure 0-71779 rarefied gas flow 0-39644 reactor experiments, Na/H₂O at Dounreay, review 0-49735 recombination of rare gas ions in plasma 0-58361 relativity, general and special 0-51934 scanning electron microscope and its applic, to thin film meas., review 0-55820 search for element 114 0-73844

scanning electron microscope and its applic. to thin film meas., review 0-55820 search for element 114 0-73844 self-consistent calc. for nuclear properties 0-70356 semi-classical scatt. theory 0-63352 semiconducting chalcogenides, of groups II, IV, V 0-72002 semiconducting polymers 0-75694 semiconductor doping and junction formation 0-59220 shell model 0-70361 shock waves and radiation 0-38396 single-nucleon transfer reactions 0-73921 Solar Proton Flare Project (1969) 0-63171 solar neutrinos 0-57140 solar research at Ondrejov observatory 0-59786 solid-vapour equilibria in cryogenic systems 0-47002 solidification and casting, lit. 0-58947 space symmetry in 2s-1d nuclei, spectral distribution methods 0-70331 specific heat of elec. conductors at high temp., high-speed method 0-56105 spectrochemical analysis in criminalistics 0-72570

spectrochemical analysis in criminalistics 0-72570

spectrochemical analysis in criminalistics 0–72570 spectrometry, Mossbauer 0–54934 spectrometry, Raman 0–57628 spectrometry, emission 0–54936 spectrometry, i.r. 0–54936 spectrometry, i.r. 0–54935 spectrometry, i.r. 0–54937 spectrometry, u.r. 0–54937 spectrometry, u.r. 0–57629 stable isotopes, predictions 0–70535 static moments of low lying 2+ states 0–73771 stratified flows, discussion in terms of incompressible fluid with gravity 0–41498 superconducting magnetometers and cryogenics 0–52227

0-41498 superconducting magnetometers and cryogenics 0-52227 superconducting materials 0-68773 superconductivity at high pressures 0-71961 superconductivity theories and applications 0-44096 superconductors, their thermal conductivity and acoustic absorption 0-71962 superconductors, their thermal conductivity and acoustic absorption 0-71962 superheavy elements, their fission and alpha- decay review 0-64079 superplasticity 0-71684 surface-tension induced phenomena 0-39713 thermoelectric materials production 0-75820 thin film analysis by mass spectrometry 0-56722 transition matrix elements from electromagnetic interactions 0-73768 transition metal complexes, absolute configs. 0-74309 transition metal complexes, absolute configs. 0-74309 transition metal compounds, n.q.r. spectra, review 0-76246 transition metal oxides, electronic transport 0-59210 transitional nuclei, quadrupole, pairing and spin deformations 0-73765 transuranium elements, super-heavy 0-63942 triboelectricity 0-59272 turbulence, shear flow 0-39700 turbulence, survey of analytical theories 0-53113 two-nucleon transfer reactions, inelastic processes 0-73920 two-nucleon transfer reactions 0-73922 ultrasonics and physical acoustics, Poland 0-45624 upper atmospheric density and models 0-59730 Venus and Mars atmosphere 0-63147 vibrational energy exchange in molecular collisions 0-58146 wave functions, prolate spheroidal 0-66784 wave mechanic, history and interpretation 0-63342 weak interactions, leading divergences, algebra of compound fields 0-42452 X-and p-ray nuclear elastic scatt, and Compton effect 0-39009 X-ray, low energy, and electron analysis. 0-6244

0-42452
X- and p-ray nuclear elastic scatt. and Compton effect 0-39009
X-ray, low energy and electron analysis 0-69244
X-ray absorption and emission 0-56572
X-ray absorption spectra, extended fine struct. 0-44874
X-ray absorption spectra, extended fine struct. 0-44874
X-ray crystallography using divergent beam 0-65190
X-ray diffraction 0-55808
X-ray diffraction 0-55808
X-ray satellite lines, theories 0-39262
yield-point phenomena in substitutional alloys 0-65386
(p.2p) and single particle levels 0-73931
πN interactions, scattering 0-45932
Li induced α-particle transfer reactions 0-73922
Pb_{1-x}Sn_xSe semiconductors 0-56224
Pb_{1-x}Sn_xTe semiconductors 0-56224
208 Pb shell model 0-70525
Si-Ge thermocouple Air-Vac converters 0-67016

Reynolds number see Flow; Hydrodynamics

Rhenium

adhesion of quartz, LEED studies 0-50813
adsorption of CO, by electron probe mass spectrometry 0-47081
anomalous isotopic ratio in solar wind, detection at nanogram level 0-41838

atomic mass differences and mass systematics in the region 100≤N≤126

0-43015

0-43015 chemisorption of NO, low pressure obs. 0-41428 chemisorption of O₂ 0-45058 dispersed on high area oxides, morphology 0-55718 effect in Ta-Mo-C and Ta-Nb-C system, equilibrium investigation 0-50822

0-50822
Fermi-surface topology changes rel. to supercond. T_c, h.p. 0-40746 films, electrical properties and superconductivity 0-71944 h.c.p., CO covered, field emission obs. 0-43571 heat capacity, 0.02-0.4K, 0-75623 ion bombarded with Ar¹ and He⁺, radiation damage enhanced trapping of He¹ 0-65309 lattice parameters, effects of pressure and temp. 0-47203 nuclear acoustic resonance obs., Knight shift and zero-field splitting determ. at 4.2K, 0-48165

at 4.2K. 0—48103 specific heat in normal and supercond. states 0—44138 sputtering, ang. distrib., fine struct., Ar† bombard. single cryst. 0—75438 superconducor, high purity, electron-phonon interaction, u.s. investigation 0—75580

0-7580 superconducting, heat capacity, 0.02-0.4K 0-75623 surface struct. of (0001) face, effect of O₂ adsorption 0-74928 thermionic convertor, 0001 crystal, performance characteristics 0-76988 u.s. attenuation anomalies, 2-band model of electron-phonon interaction 0-50930

Work functions, cesiated, for 0001 crystal, exp. meas. 0—79103 MO cathodes for thermoemission converters, optimal electrical power, interelectrode separation fn, Cs, pressure 0—38453 Ref+ in Cs₂ZrCl₆ and Cs₇ HfCl₆, sharp-line luminesc. 0—44883

Rehium compounds
[ReCl₆]² - salts, i.r. spectra, 350 to 250 cm⁻¹ 0–55319
Ag-Re dispersion electric contact, patent 0–71949
Co-Rh dii alloys, elec. resist and thermal cond., 293° to 1123°K 0–56118
Cr-Re alloy, antiferromagnetism, high pressure depend. 0–44681
Cs. [ReF₆] force consts. on basis of D_{6h} symm. 0–39402
LaB₆-Re alloy, elec. resistance, temp. depend. 0–50971
LaB₆-Re alloy, elec. resistance, themp. depend. 0–50970
Mo-Re alloy, plastic deformation, 78-425 K 0–43745
Ni-Re, dilute, lattice thermal conductivity, temp. above 400°K 0–68654
ReF₆, negative ion formation 0–64763
ReF₆, Raman spectrum in vapour state 0–58183
ReF₆, struct. from electron diffraction exam. heavy atom corrections
0–70945
ReF₇, polar distortions 0–55318

ReF7, polar distortions 0-55318

ReF₇, polar distortions 0–55318
ReO₃, crystal growth, vapour transport method 0–55785
ReO₃, high elec. cond. 0–44069
Re–Mo(W,Os) dil. solid solns., Fermi-surface topology rel. to T_c, h.p. 0–40746
W-10 at.%Re, streaking obs. in field-ion microscopy images 0–58562
W-3wt.%Re/W-(25wt.%)Re, thermocouple, reliability and stability, e.m.f. vs. temp. 0–75822
W-Re-HfC alloys, effect of 4 at.% Re on mech. props. 0–47385
W-Re solid soln. single crystal, thermionic emission props. of (100) face 0–53972
W-(25 wt.%)Re alloy, neutron irrad., damage recovery 40146 0–40146
W-25%Re, sublimation between 1550 and 1950°C in low pressure O₂ 0–78345
75%W-25%Re electrodes, bare and cesiated, characterization for thermionic convertor applic. 76987 0–76987

Rheology
see also Plasticity; Viscoelasticity
acrylonitrile-butadiene-styrene (ABS) polymers, rheo-optical props.
0-78629
heoretical and applied mechanics and mech. engng., Haifa

0-78629
conference on theoretical and applied mechanics and mech. engng., Haifa, Israel (1969) 0-42023
constant stretch history, most general motion 0-78019
cylindrical shell with longitudinal rib reinforcements limit analysis 0-45572
disc struct., dense lattice-type, edge effect 0-42028
divinyl rubber, viscosity temp, depend, at high shear strain rates 0-50709
of earth's mantle, presence of molten zone 0-76331
edge effects on obs. theory of flow generation in elastico-viscous liquid 0-69671

0-69671
epoxy moulding compounds, flow properties under transfer moulding pressures obs. rel. to reliability of electrical and electronic components packaging 0-47365
ethylene-methacrylic acid copolymer, and salts, dynamic and steady shear viscosities 0-58408
extrusion, plane-strain and axisymmetric vel. field calc. 0-38237
flow, stratified of viscoelastic liquids, stability rel. to elasticity 0-53289
glass, critical oxide mixtures, viscous relax, topological model 0-74712
influence coeffs., by assumed stress method 0-72999
material fibres with prescribed deformation path, motion of plastic body
0-38299
Maxwell orthogonal rheometer flow, molec, interpretation for steady state

Maxwell orthogonal rheometer flow, molec. interpretation for steady state 0-48783

mineral oils, during impact 0-53303 model for spherical cavity's collapse in viscoelastic fluids, non-linear integro-differential eqns. for motion 0-43411 mirile rubber, behaviour at high rates of shear deformation, 50-150°C 0-58906

optimal design of structures of composite materials, internal and external reinforcement 0-48806

cis-polybutadienes, polydisperse, behaviour study 0-47367 polyethylene, irradiated, tangential and normal stresses investigation 0-68464

polyethylene, melt rheological props., low-shear behaviour, molecular structure dependence 0-46853 polyethylene melt viscosity, effect of molecular structure variables 0-46854

polymer, statistical calc. of elementary micromechanisms 0-40210 polymer melts, shear-dependent relax. spectrum, conversion from steady-flow viscosities 0-68053

polymer solutions, dilute, drag reduction for flow at pipe inlet 0-46842

Rheology continued

polystyrene melt, prediction of tensile behaviour 0-78243

polystyrene met, prediction of tensile behaviour 0-78243 polyvinj (ehoride, plasticized, rheological and thermodynamic interaction effects 0-71656 rheogoniometer, for second normal stress difference meas. 0-63386 rheometer, high temp, high shear rate, for molten glass 0-58537 rheometer reservoir, capillary, flow patterns of polymer fluids, exp. study

silicone fluids, during impact 0–53304 suspensions, spherical particles in non-Newtonian pseudo-plastic liquids 0–48788

0-40708 thermo-rheologically simple solid, linearized theory with infinitesimal deform, systematic derivation 0-42030 Toms' phenomenon, ultimate asymptote and mean flow structure 0-71281

0-/1281 vessel, mechanics of arteries, blood flow 0-66684 water/petroleum interphase film, properties 0-53307 weighing of speimens during long duration mechanical testing, two aids 0-48787

SiO₂-H₂O suspension, data study using viscometer 0-68160

Rhodium

odium
creep, high-temp. 0–62053
electron energy loss spectra, reflection meas. 0–56134
Knight shift, strain induced 0–59468
Knight shifts of 1¹⁰⁹Rh, reference cpds. 0–45025
microgram level, fire-assay emission spectrographic method 0–54197
positron annihilation radiation correl, in single cryst. 0–44026
spectrographic analysis in gold beads from fire assay 0–66213
surface structure, clean (111), LEED, Auger electron spectroscopy
0–65042

0-05042 thermal conductivity, at liquid He temp. and in magnetic fields 0-68655 thermal expansion, linear, coefficients at low temps., Gruneisen parameters 0-75411 NaCl:Rh, optical and e.s.r. absorpt. spectra 0-79315 Rh²+ e.s.r. in MGO 0-51396 Rh4+ e.s.r. in MgO 0-51396

Rh** e.sr. in MgU 0-51396

Rhodium compounds

Fe-Rh, alloys, anomalous hyperfine field at 103Rh following low energy Coulomb excitation 0-44739

Fe-Rh alloys, antiferro-ferromag. transition, excess entropy, exchange inversion 0-69024

Fe-Rh first-order mag. phase transition, press. depend. 0-75960

Feas-3Rh_{50.5}, mag. transitions, press. depend., >25 kbar 0-79129

Mo-Rh alloys, elastic and plastic props., -190°C to +100°C 0-43711

Ni-Rh alloy, n.m.r., Knight shift, line width, spin lattice relaxation, 1-4 K
0-45007

Pd-Rh alloy, n.m.r., Knight shift, line width, spin lattice relaxation, 1-4 K 0 - 45007

Pd-Rh alloy, n.m.r., Knight shift, line width, spin lattice relaxation, 1-4 K 0-45007
Pd-Rh dil. alloy, magnetization, high field, band structure effects 0-44595
Pd-(2 wt,%)Rh alloys, Knight shifts of 100Rh41382 0-41382
Pt-Rh alloy, accelerated sublimation under tensile stress in air 0-47007
Pt-Rh alloy, accelerated sublimation under tensile stress in air 0-47007
Pt-Rh alloy, coactivity-comp. relationships 0-78882
Pt-Rh alloy, effective atomic number for differential K-shell photoelectric effect 0-64230
Rh-Co dil. alloys, resistance anomaly 0-62312
Rh-Co mixed cryst., ferromag. props. rel. to Co concentration 0-72210
Rh-Fe alloys, interactions between anomalous local moments and mag. ordering 0-69028
Rh-Fe mixed cryst., antiferromag. props. rel. to Fe conc. 0-72210
Rh-Pd, (c.c., low-temp. sp. heat 0-71863
Rh (III) complex, rhodium (III) oxalato-triaquo-monammine oxalate, separation, i.r. and n.m.r. obs., chem. props. 0-74940
Rh (III) complex, rhodium (III) oxalato-triaquo-monammine, prep., identification, props. 0-58748
Rh³⁺ complexes, cryst. field transitions, intensities 0-44729
RhBe_{6.5}, crystal structure 0-40097
Rh(I) complex with triphenylphosphine, n.m.r. spectra of ³¹P and ¹⁰³Rh, chemical shifts and coupling constants 0-58196
Rh(III) complex with triphenylphosphine, n.m.r. spectra of ³¹P and ¹⁰³Rh, chemical shifts and coupling constants 0-58196
Rh(III) complexes, prediction of luminescence properties 0-43133
Ru-Rh, f.c.c., low-temp. sp. heat 0-71863
Riemann-Cristoffel tensors see Relativity: Tensors
Righi-Leduc effect see Magnetothermal effects
Ring currents see Almosphere; Ionosphere
Riometers see Ionosphere measuring apparatus
Rochelle salt

Riometers see Ionosphere measuring apparatus

Rochelle salt

Barkhausen effect under continuous X-irrad. 0–53933
Barkhausen jumps starting field rel. to critical polarization 0–51121
crystal and saturated soln., irrad., absorpt. spectra, 220-1500 nm
0–51318

0-31318
crystal growth, gamma irradiation effects 0-50417
dielectric behaviour, microwave range, defects influence 0-65790
dielectric relax. due to struct. defects 0-65772
dielectric relax. due to proton pairs 0-66158
optical absorption and defects in p irradiated crystals 0-41184
piezoelectric loudspeaker crystal growth, undergraduate project 0-76789
relaxation absorption of sound, influence of electrical boundary conditions
0-75790

Rock magnetism basalt ferromag, fraction rel. to lava formation conditions 0-62953

basalts ferromag, fraction rel. to lava formation conditions 0–62953 basalts, hopkinson effect, blocking temp, and Curie points 0–48347 basalts, out of crust of different type 0–75884 book on physics of the earth 0–45200 book on physics of the earth 0–45200 Earth's mantle and core evolution 0–76520 Earth's non-dipole mag, field over Upper Tertiary times, permanent aspects 0–51607 exchange anisotropy of red sedimentary rocks 0–62954 horizontal displacement according to data 0–76521 magnetite, and magnetite- bearing rocks, low temperature treatment 0–76517

0—76517
magnetite remanence, effects of elastic and plastic deformation and fracturing 0—48348
natural remanent magnetization 0—45199
palaeographic reconstructions of Gondwanic continents based on palaeomag, and sea-floor spreading data 0—48238
Permian time paleontologic data to test Permian latitude models for Northern Hemisphere 0—76516

Rock magnetism continued

pressure effects, on mountainous rocks, seismomagnetic effects 0–76523 remanence, stable, in magnetite-bearing igneous rocks, origin 0–72667 secondary natural magnetizations, in igneous and baked rocks, nature 0–72669

0-/2669 sedimentary, viscous remanent magnetization, resistance to alternating mag. field 0-56866 sedimentary rocks, origin of depositional remanent mag., model 0-54306 stress, mechanical, effects on reversible and irreversible magnetisation 0-76522

0-76522 structure, rifts, extinct, between symmetric magnetic anomalies 0-72666 thermally activated and hysteresis-induced processes at various temp., relationship, study 0-51605 titanomagnetite and ilmenohematite series, stresses and magnetostrictive effects of lamellae 0-72668 titanomagnetites, multidomain, coercive force, effect of dislocation density and inclusions from domain structure 0-69337

volcanic, viscous remanent magnetization, resistance to alternating magnetid 0-56866

Zma field and geomorphology and geotectonics of earth's crust 0-51608

Rockets

Aerobee, Orion region electronographic photography 0-66501 Aerobee 150, Sagitarius X-ray sources location, with rot, modulation collimator 0-66566

ekhaust noise, pressure cross correlation on cylindrical bodies, determination 0–52065 holography, pulsed laser, of liq. rocket combustion 0–69941 impulsive transfer between neighbouring circular orbits, geometrical soln.

0–56871 infrasound long range 0–59596 motion, fundamental eqns., for teaching 0–41558 nozzle, carbide and graphite, material characterization 0–58953 nuclear reactor (gaseous core) propulsion, 'dust curtain' seeding and cavity wall shielding 0–49713 pulsed, motion 0–72995 sounding, passive cone angle amplifier 0–63450 trajectories, optimum with specified transfer angle 0–79614 Hβ, production measurement in H aurora 0–41517

Rolling see Forming processes

Rotating bodies

see also Angular velocity measurement; Centrifuges; Earth/rotation;
Gyroscopes

beam, slender in centrifugal force field, coupled vibrations 0–45618 body with gyroscope in Newtonian field of force, stability of motion body with 0-59948

disc, acceleration stress 0-48784

disc, effect of vapour drag on condensation 0-74851 disc, ratio of velocities for central and radial yield under plastic deformation 0-69691

tion 0–69691
e.m. suspension system, temperature near interface meas., vacuum technique design 0–48892
fluid, contained, spin-up and viscous diffusion 0–46646
gyrocompass model, statistical error analysis 0–45513
Kepler motion, simplified treatment 0–42021
liquid masses, homogeneous, book 0–39693
Mercury, fluctuation of angular velocity 0–57113
Mercury, thermal and tidal effects 0–57112
rigid body motion about fixed point under attractive force 0–72991
shells of revolution with asymmetrical stiffness, computer analysis 0–38225

skewed boundary layer flow around, velocity profiles 0-58294 stresses, elastic, disks of variable thickness, annular and circularly mounted 0-63385

Rotation, molecular see Molecules/rotation

Rotatory power, dispersion see Optical rotation

RS coupling see Atoms; Spectra/atoms

Rubber

borded blocks of infinite length, effective mass, effect of oscillatory compression 0–53580 bonding with steel non destructive testing by ultrasonics 0–45646 butyl, in viscous state, peculiarities of high elastic deformations 0–68392 carbon black filled, stress relaxation mechanism 0–68430 chloropropene, u.v. irradiation, effect on structure 0–50344 conductive, mechanical and electrical properties 0–68757 cracking in ozone environment, e.p.r. meas. 0–47417 crosslinking inhomogeneity determ. by light scatt. 0–39905 crosslinking inhomogeneity determ. by light scatt. 0–39910 divinyl isoprene type, heat evolution at high rates of shear deform. 0–50667 divinyl rubber, viscosity temp, denend, at high shear strain rates. 0–50709

0-50667 divinyl rubber, viscosity temp, depend. at high shear strain rates 0-50709 elastic constants 0-43703 elasticity, energy contribution 0-71653 elasticity volume change accompanying extension, theoretical and experimental comparison 0-71432 elastomers, bubble growth under high degree supersaturation with inert gas 0-65022 elastomers cliber reinforce cilicone, mechanism of their energy expenses

gas 0-65022 elastomers, silica reinforce silicone, mechanism of strain energy storage 0-55933 friction meas. in vacuum under high normal pressures 0-78662 hardness tester indenter forces 10 gf to 10 kgf, load cell for verification 0-65427

natural, mechanical characterization 0-68433 natural vulcanizates mechanical properties under orthogonal biaxial stretching 0-68386 polymers rubber-like thermal effects during shear deformation 60-120°C 0-53414

polyurethane, Solithane 113-50/50, stable crack propag. 0–47399 polyurethane, dielectric properties, variation with temp., freq., and X-ray dose 0–65776

siloxane elastomers, stength and supermol. struct. 0–43759 siloxane rubbers, X-ray studies of secondary crystalliz. 0–50346 stress-relaxation in network rubber-like polymers 0–50675 styrene butadiene, experimental study of nonlinear viscoelasticity

0-50651 synthetic, deforms, due to simple shear and bending 0-38233 thermoelasticity at high strain 0-78590

Rubidium

578 J₁₂-58 P₃₂ mixing induced in collisions with molecules 0–77703 abundance in lunar crystalline rocks 0–45338 abundance in lunar rock samples 0–48493 abundance in lunar rock samples 0–48492 abundance in lunar rock and separated phases 0–45342 abundance in lunar rocks and separated phases 0–45342 abundance in lunar rocks and separated phases 0–45342

abundance in lunar rocks and separated phases 0–45342 abundance in lunar samples from Tranquillity Base 0–45337 atom, D, line hyperfine spectrum temp. depend. 0–67632 atom, double s.h.f. resonance 0–49797 atom, ground states interacting with nonresonant r.f. field, modified Zeeman hyperfine spectra 0–39318 atom, spin-orbit perturbation from photoionization experiment 0–60914 atom collision with He and Ne, electron energy spectra and auto-ionizing level excitation 0–64257 atom ground state g, shift, He induced 0–52888 atom quenching of first excited state doublet by N, obs. 0–49818 atomic beam emerging from cell, flux dependence on spin polarisation 0–43016

0–43016 atomic level $5P_{3/2}$ excited by laser pumping 0–67652 atoms, collisional m_j mixing in $^2P_{W_j}$, time-reversal selection rule, obs. 0–55243 discharge, low-pressure, population mechanism 0-74644 elastic constant calc. using modified Mie-Gruneisen eqn. state 0-78595 ion collisions with inert gases, 12 keV to threshold, resonance lines obs.

0 - 61003liquid, positron annih., electron momentum distrib. obs. 0-40698

magnetometer, gradiometer-connected, design and application 0–54297 melting pt. and melting ht. 0–56109 neutron coherent scatt, amplitude determ. 0–43643 neutron coherent scatt, amplitude determ. from diffr. meas. on KCl

optical pumping, population inversion, hyperfine sublevels, maser construction 0-52951

optical pumped, field reversal signal detection 0-77672 optically pumped, field reversal signals, experiment's interpretation 0-65995

positron annihilation in liq. and solid, electron momentum distrib. obs. 0 - 40698

to 40096 ines for Rb II 0-70773 in seawater and interstitial solns., determ. using flame spectrophotometry 0-48247

vapour, stimulated radiation by laser excitation, frequency adjustable 0-77660

Vapour, scinnated Tadiation by laser excitation, requency adjustable 0–77660 vapour arc lamps, spectral radiance 0.42- $1.1~\mu$, varying power input and press. 0–49138 K^* + Rb collisional excitation transfer cross-sections, obs. 0–67643 Rb I thin films, complex refractive index and thickness from reflectance meas. 0–43540 Rb+quadrupole polarizability, using H-F wave functions 0–39260 Rb+0-70-71, crystal struct. by single crystal X-ray diffraction 0–43645 Rb+0-87Rb, nuclear and e g-factors, obs. 0–52925 Rb+0-87Rb maser-oscillator 0–57508 Rb+0-87Rb maser-oscillator field-independ, optically pumped 0–73197 Rb+0-87Rb-0-77704 Rb+0-77704 Rb+0-77705 Rb+0-77704 Rb+0-77704 Rb+0-77704 Rb+0-77704 Rb+0-77704 Rb+0-77704 Rb+0-77704 Rb+0-77704 Rb+0-77704 Rb+0-77705 Rb+0-77704 Rb+0-77705 Rb+0-

**Rb optically pumped, at. alignment and ground state r.f. Zeeman transitions, obs. 0–52954

Rubidium compounds
halide films, extreme u.v. absorpt. 0–76098
halides, Smm+Pm3m transition, thermodynamics 0–43826
halides, Schottky defect energies calc., NaCl struct. 0–40135

K. Rb liquid alloy, u.s. absorpt. and vel. obs. 0–64915
Na-Rb system, solid-liquid phase equilib. diagram 0–53398
Rb-Na silicate glasses, internal friction and alkali diffusion 0–55956
RbAgals, single crystal and polycrystalline, ionic conductivity 0–40834
RbAgals, single crystal growth from non-stoichiometric melts, Czochralski process 0–50471
RbBF4, phase relations, high pressure 0–55658
RbBr, F. centre formation, role of K shell ionization, 78K 0–50609
RbBr, Nucl. quadrupole spin-lattice relax. 0–75978
RbBr, Rb* Miv., absorption spectra, fine structure 0–72400
RbBr, rotational state distrib. of molecular beam 0–77835
RbBr molien, isotope eff. of thermal diff. 0–64888
RbBr spin-lattice relaxation times for 79Rr, 81Br, 85Rb and 87Rb nuclei, 20
K.300 K 0–54174
Rb-CO3, high press. phase boundaries 0–62136
RbCl:Eu luminescence obs. 0–56607
RbCl:Mn²²+, e.p.r. and absorpt. spectra 0–44996
Rk-Cl, diffusion of ion implanted Kr, radiation damage effects 0–61998
RbCl, diffusion of Na, 377-707°C 0–75209
RbCl, elastic constant calc. using modified Mie-Gruneisen eqn. state 0–78595
RbCl, elastic constant, adiabatic, 140-300K 0–71665
RbCl; honon dispersion relations, 80 K 0–53696
RbCl, Rb-My, absorption spectra, fine structure 0–72400
RbCl, vacancies, single and pairs, migration barriers calc. 0–40135
RbCl molten, isotope eff. of thermal diff. 0–64888
RbCl od, phase relations, high pressure 0–55658
RbCl, phase relations, high pressure 0–55658
RbCl, phase relations, night pressure 0–55658
RbClod, phase relations, night pressure 0–55658
RbClod, phase relations, night pressure 0–55658
RbCl, phonon dispersion relations, 8

Rb.CuCl_{4.2}H₂O, n.mr. of ⁸⁹Rb and ⁸⁷Rb, quadrupole interactions 0–4134 RbF, phonon dispersion relations, 80 K 0–53696 Rb.FeF₄ two-dimens. antiferromagnet, transitions and mag. correls. 0–44696 RbFeS₃, Mossbauer spectrum rel. to internal field, obs. 0–41155 RbH.PO₄, n.mr.₄, ⁸⁷Rb quadrupolar coupling, rel. to Curie pt. 0–44366 RbH.PO₄, paraelec., ⁸⁷Rb n.q.r., obs. 0–41403 RbH.PO₄ and deuterated isomorphs, sp. ht. 0–65547 RbHSO₄, cryst. struct. of paraelec. and ferrolec. phases, transition mechanisms 0–78497

RbH₃(SeO₃)₂ and RbD₃(SeO₃)₂, phase transition, thermo- and electro-optical effects 0-65999

Rubidium compounds continued

RbI-AgI solid electrolyte system, high conductivity 0–62811 RbI, additively coloured with K, colloidal absorpt, bands 0–75183 RbI, Brillouin spectra, sound velocity, elastic constants of cubic crystal 0–51329

RbI, Gruneisen parameter, low temp., from elastic constants press. derivs.

Rbl, Gruneisen parameter, low temp., from elastic constants press. derivs. 0-43923
Rbl, lattice dynamics, 80 K 0-78736
Rbl, Raman spectrum and assignments 0-72362
Rbl, undoped and Na-doped cryst., colour centres, optical and reaction-kinetic props. 0-53554
Rbl layers, ion penetration depth 0-47572
RbLiBeF4, crystal structure 0-75095
RbMnF3, Ni, Raman scatt. from localized magnons 0-41238
RbMnF3, antiferromag, and paramag, phases, Raman spectra, magnon-pair modes 0-44708
RbMnF3, antiferromagnet, 55Mn nuclear acoustic resonance, 4.2°K 0-45027
RbMnF3, applic. of short-range-order effects in neutron scattering from

0-4302/ RbMnF₃, applic. of short-range-order effects in neutron scattering from Heisenberg paramagnets 0-51183 RbMnF₃, exciton absorpt. line, Zeeman effect, Davydov splitting 0-66050

O-66050

RbMnF₃, magnetic scattering of neutrons near critical point 0-44709

RbMnF₃, paramagnetic, e.p.r. and n.m.r., line shapes and spin correlation, exchange narrowing 0-41332

RbMnF₃, spectral density, kinetic theory calc. rel. to neutron scattering cross section 0-44505

RbMnF₄, two-dimens. antiferromagnet, transitions and inag. correls. 0-44696

RbNO₃-NaNO₃ melt, interdiff. coeff. 0-64889

RbNO₃, in water-dioxane at 25°C, electrical conductance meas. 0-68902

RbN₃N₃, yrep., struct., chem. props. 0-71580

RbNiCl₃, mag. struct. 0-56460

RbNiF₃, induced ferrimagnetism 0-72268

RbNiF₃ ferrimagnet, Cotton-Mouton effect, birefringence, dichroism 0-44775

RbOD, matrix isolated, i.r. spectra rel. to bending and stretching modes and

RbOD, matrix isolated, i.r. spectra rel. to bending and stretching modes and RbOH, matrix isolated, i.r. spectra rel. to bending and stretching modes and struct. 0–69126

Struct. U-09126 RbPr(MoQ₄), polymorphic modifications obs. 0-55859 Rb₂SO₄, p.m.r. rel. to ferroelectricity, -196 to 23°C 0-41383 RbT:Tl, emission spectra for excitation in A, B, C, and D absorpt. bands 0-44890

acoustic paramagnetic resonance spectra of X-irrad. crystals, effect of elec. fields 0-62749

acoustoelectric resonance in laser pulse field 0–47535 colour centres, effect on the spectrum of Cr³⁺ in ruby 0–55899 crystal growth, Geneva flame fusion process, examination of boules and stones 0–50459

stones 0-50459 crystals growth, in thermal image furnace, improved techniques 0-50460 dislocation struct. rel. to high temp. annealing 0-68366 e.p.r. of Cr³+, line broadened by strong hyperfine interactions, second moment 0-51389 e.p.r. of isothermal annealing kinetics of Cr ions in X-irrad., cryst. 0-79396

0—7396 electronic spectrum, excited-state 0—69114 energy levels of Cr ion pairs 0—59152 fluorescence, R' optical transitions of Cr³+, linewidths, broadening mechanisms 0—76166 fluorescence, excitation by near and vacuum u.v. synchrotron radiation 0.4405.

0-44905
fluorescence of Cr³+, 4T₂, state lifetime 0-62723
fluorescence line narrowing, laser-induced 0-76162
ground state luminescence transitions investigated by EPR 0-56594
high purity, synthesis 0-47106
laser, 0-switched, rel. to stimulated Raman scattering in cyclohexane, time
characteristics 0-46552
laser, continuous giant pulse operation 0-63627
laser, continuous-wave nonspiking single-mode 0-49069
laser, dielectric layer surface scatterer, operation 0-49065
laser, emission spectra structure in free generation regime 0-54877
laser, free generation operating conditions, dynamics 0-45796
laser, giant pulse, mode-locking 0-49070
laser, giant pulse generation method 0-52289
laser, high power pulse generation by means of u.s. traveling wave
0-42298
laser, holography applic. 0-60258 0-44905

laser, holography applic. 0-60258 laser, mode excitation, spatial coherence and free oscillation kinetics 0-60231

U=00231
laser, mode-controlled, Q-switched, tuneable 0-60224
laser, monopulse, with phototropic shutter 0-52291
laser, monopulse 0-38503
laser, narrow line 0-60230
laser, narrow line 0-60230
laser, orange degradation, sub-cryst. misalignment, chem. analysis 0-76759

laser, orange degradation, \$40-cryst. Inisanginient, chem. analysis 0-76759 laser, output power as function of pumping power 0-38504 laser, partial mode locking, spectral-time technique 0-60232 laser, periodic operation, giant pulse 0-73333 laser, periodic operation, giant pulse 0-73333 laser, regular relaxation pulses obs. 0-77121 laser, second harmonic, 25% generation 0-73243 laser, second harmonic production by LiIO₃ crystal 0-77120 laser, second harmonic production by LiIO₃ crystal 0-77120 laser, series of multiple plates inside cavity laser 0-42292 laser, spingle-freq., radiation field coherent combination 0-73242 laser, single-frequency with electrooptical Q-modulation 0-60237 laser, spatial modulation of level populations, light diffraction investig. 0-42288 laser, spiking behaviour, effect of saturable absorber concentration laser, spiking behaviour, effect of saturable absorber concentration 0-52290

laser, spontaneous giant pulsing 0–54876
laser, thermal parameters in repeated pulse regime 0–73241
laser beam, pulse formation and power increased using u.s. modulated travelling wave diffraction in a phototropic medium 0–45807

S 1332 SUBJECT INDEX laser beam as auxiliary ionization factor 0–53222
laser coagulator of eye tissue 0–59835
laser giant pulse prod. >500MW, methods 0–69914
laser irrad. of vitreous solids 77°K, emission spectra 0–56652
laser material, piezo- and thermo-opt. props. 0–79254
laser operating between plane mirrors, beam divergence 0–38511
laser pulse, picosecond, breakdown of Ar and He, threshold flux 0–50131
laser with optical delay line inside resonator 0–67097
laser with regularly moving crystal, mode-locking effects 0–77122
lasers, high power pulsed 0–49025
light absoprition, laser beam pulses, shock wave 0–54054
light scattering small angle indicatrix, rational characteristics, empirical fn. 0–59356
magneto circular dichroism of octahedral Cr. III. 0–73312 resonances, overlapping, production and decay 0–45872 scattering, problem of existence 0–42412 scattering S-matrix existence problem 0–42406 scattering amplitudes, covariance and analyticity 0–70154 space time properties and physical region analyticity 0–70155 strong interactions, low energy amplitudes, single particle exchange model 0–38592 S-matrix theory continued Ruby continued 0–38592
threshold resonances anal. 0–57967
two-particle random phase approximation for configurations with one particle in the continuum 0–42810
two-resonance problem, overlapping, prod. and decay 0–45872
variational description of a resonance curve 0–52427
weak interaction transition amplitudes 0–73425
(d, p) reactions, description of threshold effects 0–49648 magneto circular dichroism of octahedral Cr III 0–72312 maser, push-push pumping mode 0–69871 microwave generation and amplification produced by optical absorpt. 0–67049 Safety precautions see Radiation protection Sakata model see Elementary particles marium abundance in lunar samples, and Sm/Eu ratios 0—45340 atomic mass difference, precise, and mass systematics in the region of 90 neutrons 0—43014 film, existence of h.c.p. phase, electron diffr. 0—71467 gamma ray scatt., incoherent, by K-shell electrons 0—58120 optical props., 1.13 3.96 eV 0—76009 photoelectric work function 0—78859 vapour, i.r. laser lines 0—49778 void formation due to thermal diffusion during film annealing 0—50581 Sm I, level crossing and optical double reson. obs. 0—52916 Sm II, 4f° 85_{7/2}° term identification 0—52926 Sm² fuoresc. in KCl, nonlinear mag. field depend. and polarization 0—76168 Sm² in KBr, lattice dynamics, vibronic spectra obs. 0—78731 marium compounds Samarium n.m.r. of ¹⁷O, dynamic polarization technique, 1.9K 0-41363 n.m.r. saturation, electron cross-relaxation and inversion, e.s.r. spectra 0-69195 phonon-photon scattering, under conditions of stimulated induction 0-45775photoelastic constants determ. 0–62004 relaxation, 4T_2 to 2T_1 nonradiative, 4 ns upper limit 0–44899 relaxation time, nonradiative between 4T_2 and 2T_1 states, upper limit 0–54123 ruby: Cr^{3+} , fluoresc., fine struct. from fourth-nearest-neighbour pairs 0-449010-44901 ruby: Cf³⁺, n.m.r., nominal Δm=1-5 mag. transition probabilities 0-41362 ruby: Cf³⁺, phonon and photon paramag. -response line shapes 0-44984 second harmonic generation by ruby laser with dielectric surface scatterer 0-42250 Samarium compounds
SmB₆, Mossbauer effect in ¹⁴⁹Sm, isomer shift, valence state determ.
0-44797 0-42250
shock compressibility 0-75248
spin-lattice relax.props. 0-56468
spin lattice relaxation times at 34.6 Gc/s 0-69053
spin-phonon transition probabilities, X-band frequencies of relax. times, meas. 0-47977
surface destruction by laser radiation 0-39924
X-ray irrad, isothermal annealing kinetics of Cr ions, e.p.r. obs. 0-79396
Cr³+ in ruby, e.p.r. props., appl. in a three-level maser 0-69186
Cr³+ in single ruby crystal, paramagnetic fine structure spectrum 0-69185 Co-Sm permanent magnets prep. and props. 0—65919
SmB_s(Eu,Gd), paramag. susceptibility, elec. cond., low temp. 0—44506
SmCo_s-SmCu_s system alloy, directional mag. props. rei. to structure 0—65920 0-65920
SmCo₃ permanent magnets, preparation techniques 0-72177
SmCo₅ permanent magnets, prep. and props. 0-54019
SmCo₅ powder, domain wall motion, hysteresis loops 0-44568
SmCo₅ powders, domain-wall processes 0-79160
SmCrO₃, exchange constants, magnon energies and opt. props. 0-44597
SmFe garnet, Curie temp. variation with press. 0-51227
SmSi₅O₇, low temp. form, crystal struct. 0-50550
Sm_{0.35}Tb_{0.45}FeO₃ platelet, interaction of planar domain wall and individual dislocations, obs. optically 0-75922
SmTe, pressure-induced metal-semiconductor transition and 4f electron delocalization 0-65634 Russell-Saunders coupling see Atoms; Spectra/atoms Ruthenium electrical resistivity, meas. to 2000°C 0–68753 Ru⁴⁺ spectra in K₂PtCl₆, Cs₂ZrCl₆, vibronic analysis, obs. 0–41210 ¹⁰⁶Ru, self diffusion coefficients in ionic and colloidal states 0–46891 Ruthenium compounds Cr-Ru alloy, antiferromagnetism, high pressure depend. 0-44681 Cr-Ru alloy, elec. resistivity and antiferromagnetism, rel. to temp. Sampling see Statistical analysis 0-44681

Quality of the solution of the soluti age determination of size fractions of monazite and zircon 0–48240 beds, erodible, stability in alluvial channel, model based on vorticity transport equations 0–72595 gamma-ray build-up factor coefficient determination 0–73446 quartz, in turbulent water, model for prediction of settling velocities and vertical diffusion 0–50264 sand-compressed air mixtures, dense phase horizontal flow 0-74793 Satellites, artificial aerodynamic characteristics with regard to position and orientation in orbit 0-56879 orbit 0-56879 aerodynamic force and moment coefficients, calculation 0-54314 aerodynamics, environment, information processing; symposium, Toulouse, France, (1970) 0-54312 Alouette I, data analysis, for delineating rapid changes in foF2 with position, report 0-79594 Ariel III, data analysis, for ionosphere characts. 0-79594 atmosphere meas, ozone vertical distribution and cloud studies 0-48274 atmospheric transparency studies in u.v., photometering of Pageos and Echo-2 0-76387 automatic location methods 0-69344 balloon high altitude radiation pressure effects on acceleration reports. Rutile see Titanium compounds Rutile see Titanium compounds

S-matrix theory

see also Dispersion relations
amplitudes, cancellation of i.r. divergences 0–52409
analytic, explicit realization of E(2) symmetry 0–42444
approximations, Pade and Cini-Fubini equivalence 0–42466
asymptotic states, in quantum electrodynamics 0–54969
book defining basic principles of unsolved problems and some applications
of S-matrix theory 0–38595
book on unsolved problems and applications 0–54962
boson system, spinless neutral, dynamical eqns. on mass-shell formation
0–49236
cluster decompositions, generalization for arbitrary mess 0–52428 balloon, high altitude, radiation pressure effects on acceleration, report 0-726710-72671
balloon, rotation, obs. Ondrejov observatory, photometric determination of rotation 0-62960
beacon, Faraday rotation of signals, in presence of travelling ionos. disturbances, simulation and analysis 0-72645
beacon frequencies, proposal for use in measurement of ∫Nds for ionosphere and magnetosphere 0-76470
communication, low-noise amplifier subsystem 0-72674
DODGE, gravity-gradient stabilized, magnetic sample-and-hold damping 0-48349
density of upper atmosphere, determination 0-48299 confluent-hypergeometric function model with complex trajectories 0-42447 connuent-hypergeometric function model with complex trajectories 0—42447 conformal invariance proof 0—72895 coupled channels on two-particle amplitudes, physical effects and analytic structure 0—42502 crossing symmetric Regge behaviour, idea of duality 0—70185 currents and off mass shell extension of scatt, amplitudes 0—42465 discontinuity around arbitrary physical-region singularity, Cutkosky-type formula 0—70144 electrodynamics, Wheeler-Feynman, quantum theory 0—67200 gravitational field in nonlinear gauge 0—73380 Kadyshevsky's prepresentation, renormalization problems 0—54971 Mittag-Leffler expansion 0—73886 models for weak interactions 0—57690 mutual commutation relations and unitarity condition 0—49171 non degenerate thresholds, exact S-matrix 0—52426 nonlinear analysis application 0—70156 nuclear-Coulomb potential case, for large complex ang. moments 0—49456 density of upper atmosphere, determination 0–48299 drag meas. 0–76528 dual-spin, with nutation damping, motion and stability 0–56882 Earth, motion determination using second order derivatives, method 0–56873

Earth, perturbed motion during short time interval calculation 0–66862
Earth, prediction of corrected period of revolution, systematic errors estimation 0–56878

Earth Resources Technology, optimization of multispectral scanner 0–52380
Earth resource observations from orbiting spacecraft 0–66223
Earth resource observations from orbiting spacecraft 0–66223
Echo I, balloon, rotation, obs. Ondrejov observatory, photometric determination of rotation 0–62960
Echo II, balloon, rotation, obs. Ondrejov observatory, photometric determination of rotation 0–62960
Echo-type, induction drag, obs. 0–66359
Explorer 36(Geos-B) 1968-02A flashing light, obs. 0–69340
Explorer 4, magnetic coordinates, recalculation 0–59668
Explorer-22, radio signal scintillation rel. to ionosphere inhomogeneities 0–62947 -56873 0-49436
Pade approximation appl. to s-wave matrix elements 0-77254
Pade approximation for S-matrix in pion-nucleon pseudoscalar field theory above production threshold 0-60583
parameters in terms of R-matrix 0-77255
perturbation theory series summation for scattering matrix 0-42432
quantum-mechanical scattering as an isomorphism for Abelian subalgebras 0-59916
Regge-pole theory, eigenchannels and unitary separation of background parts 0-70232 0-0294/GEOS-II, reson, with 13th-order terms of the geopotential, anal. 0-45201 geosynchronous, meteorological applications 0-59554 ground traces of Earth satellites, perturbation effects 0-41561 ITOS-1 meteorological satellite 0-59669 ice cover obs., surface meas. for correlation 0-41502 ionosphere meas., total electron content 0-41533

Satellites, artificial continued

ionosphere sounding critical frequencies f0F2 obs. by Alouette II, comparison with ground based sounding 0–54281 ionospheric interaction study by Poisson- Vlasov equations solution 0–51612

U-51612
Langley Lunar Orbiters, lunar gravit. harmonics, from secular and long period effects 0-66585
lunar, theory and semianalytical soln. of motion 0-41562
magnetic moment meas. rel. to attitude 0-54313
magnetometer, proton, obs. of magnetic anomalies 0-76529
meteorological, tropospheric refractivity profile for data corrections
0-48286

meteorological applic. 0-72614 meteorological research potential of manned Earth-orbiting spacecraft 0-66276

meteorological research potential of manned Earth-orbiting spacecraft 0–66276 motion, Earth's gravitational effects 0–51466 motion near mass centre, characts. 0–56880 NIMBUS, i.r. grating spectrometers 0–76330 navigation and communications vth.f. systems, and ionospheric propag., conference (1970) 0–79577 near Earth, geopotential harmonics effects on motion 0–56883 OGO, wake structure deduced from antenna impedance obs. 0–76478 OGO 3 and ATS 1, intensity correlation and substorm electron drift effect measurements in outer radiation belt 0–41524 OGO 4, observations of geomagnetically trapped protons and α 0–41526 OGO-V, fast-drift solar burst obs., Nov. 18, 1968 0–66636 ORBIS CAL exp., ionosphere ducting of radio signals 0–76461 OSO VI, solar surges, flares and active regions development, obs. 0–66653 OSO-VI, Harvard expt. 0–66360 OSO-VI, KUV spectrum, solar active regions 0–66630 OV4-1 dual satellite exp., results on guided ionos. propagation 0–72647 ocean exploration by spacecraft 0–66268 optical data relay link, for ultra-wide bandwidth laser communications, comparison with microwave link 0–79617 orbit's tracking meas, error in computed values, evaluation method 0–56877

-56877

orbit perturbation due to earth's oblateness, Hansen's method for calc. 0--56872

orbit perturbations due to solar radiation pressure and lunar and solar gravitational forces, long period formulation 0-48350 orbit theories, error bounds and initialization 0-66356 orbit theories, error bounds and initialization 0-66356

orbital motion, computation of spherical harmonic terms needed during numerical integration 0–66384 orbital perturbation due to arbitrary geopotential zonal harmonies 0–56876

orbital perturbation due to solar radiation pressure 0–66357 orbital plane rotating, by reactive thrust, solution of absolute minimum and minimising sequences 0–69342

orbital trajectories with small eccentricities, analysis by perturbation techniques 0–52007

Orbiting Astronomical Observatory, summary of Smithsonian Observatory's results 0–66353

Orbiting Solar Observatory, fifth, hard solar X-rays obs. 0–66628 orbits, formulae calc, under action of secular perturbations 0–79616 orbits, perturbed intermediaries, mixed secular terms investigation 0–54315

orientation and motion of Earth satellites determ., new computer method 0 - 56874

0-56874
Pageos I, balloon, rotation, obs. Ondrejov observatory, photometric determination of rotation 0-62960
of planets (inner), orbit evolution, report 0-66358
positions, determination of accuracy of visual estimates 0-69339
proton-2, orientation determination, motion description with respect to center of mass 0-56875
protons, high energy, trapped on low L shells, measurement of intensity 0-41525
RAE I, rel. to investigation of Jovian hectometric continuum radiation 0-66590
rf, scintillation, low angle, 20-360 MHz 0-79584

0-6590
rf, scintillation, low angle, 20-360 MHz 0-79584
radio signals, scintillation studies at low-latitude station 0-76460
radiowave refraction, ionospheric effects 0-72672
relative motion of two particles in elliptic orbits 0-63373
relativistic cosmic ray LH nuclei, meas, of relative abundance 0-76545
resonance of GEOS-II with 13th order terms of the geopotential 0-45201 short wave polarization fading period, fluctuations, rel. to ionosphere structure 0-56884

signal scintillation by ionosphere 0-62948

signal scintilations, rel. to irregularities in ionos. F-region, low latitude studies 0–76501 spow conver obs., surface meas, for correlation 0–41502 spherical, spinning, thermal design, nonlinear three-nodes analysis, numerical solution 0–45202 synchronous, orbit calculation 0–59670 transitional forms established the durantic mathe.

terrestrial gravity field from satellite data, dynamic method 0-41462 theory, main problem for small and moderate eccentricities 0-66352 thermal balance in nighttime protonosphere, observations 0-45160 theory, final protein to sinal and moderate eccentricities 0-0332 thermal balance in nighttime protonosphere, observations 0-45160 thermo-electric generator as energy source, patent 0-60141 Tiros 10, obs. of Bay of Bengal cyclotronic storm 7-15 December (1965) 0-66285

transmission, applic. of atmos. studies, conf., Boston (1969) 0-72673

0-41492

transmission, applic. of atmos. studies, coil., Boston (1909) 0–12 transmission experiment, wide-band, proposals 0–72646 Vela, X-ray source birth, obs., July 1969 0–66567 water-vapour-height profiles determ, satellite techniques 0–41492 OAO-A2, interstellar Lyman-alpha absorpt., obs. 0–66517 OSO-III, Sco X-1 X-ray emission obs., time variability 0–66569

SC (sudden commencement) see Magnetic storms

Scalers see Counting circuits

Scandium

photoelectric work function 0-75859 Sc XIII, X-ray lines, gf-values 0-66375

Scandium compounds
acetylacetonates, cryst. struct. 0—55866
halides, gaseous, thermodynamic functions at 293.5-3000°K 0—71249
Sc-Hf alloys, Hall effect, susceptibility and elec. resist. temp. depend.
0—75898 ScB2, n.m.r. meas. of 45Sc 0-79418

Scandium compounds continued

ScBO₂:Ce²⁺;Tb³⁺, energy transfer between dopant ions

ScCd₃, absorpt. spectra of V³⁺ and Cr³⁺, level splitting

0-79306

ScCl₃, electronic-vibr-rot. spectrum, 2200-9000 A

0-49891

ScCl₃, sheliding of cryst. fields at rare-earth ions

0-79307

ScF₆³⁻ anion in aqueous soln., n.m.r.

0-78310

Sc_{31x}In, ferromagnetic alloy, e.s.r, magnetization, comp. and temp. depend.

0-44997

ScRu₂, Laves phase, supercond. transition temp. meas.

ScVO₄:Gd³⁺, e.p.r. parameters, temp. effects

0-44998

Scattering

abstract scattering theory for system more general than quantum mechan-ics 0-41950

ics 0-41950
amplitude, determination of phase from differential cross section 0-48732
amplitudes, covariance and analyticity 0-70154
amplitudes, covariance and analyticity 0-70154
amplitudes, relativistic, theory of 2-variable expansion based on Lorentz
group 0-48718
amplitudes, for unphysical energies variational bounds 0-48733
analytic mathematical physics, conference, Bloomington (1968) 0-66858
anisotropic exact soln. of family of integral eqns. 0-48692
atmosphere, inhomogeneous, semifinite 0-48567
atom-diatom, statistical anal. of matrices in strong coupled rotational
excitation 0-55389
atomic, long-range interaction processes, variational method 0-74082

atomic, long-range interaction processes, variational method 0-74082 book, new met and problems in atom, nucleus and particle physics 0-54585

0-34385 classical, computer simulation as teaching expt. 0-59856 conformal-invariant scattering amplitudes for the two-dimensional world model 0-52418 of cosmic X-rays by atmosphere, effect on spectrum at balloon altitudes 0-76409

Coulomb functions, many dimensional 0-76838 Coulomb potential, phase eqn. for scattering length 0-69622 coupled channel problem, principal value integrals in dispersion relations 0-76835

0—76835
coupled open channels and eigenvalues, noniterative solns. of integral eqns. 0—63351
Dirichlet problem for prolate spheroid and plane scalar wave 0—66787 distorted wave Born series for inelastic scatt., pole contributions 0—57278 elastic normal modes in plate with two-dimensional surface roughness, Fourier transform 0—60026
of gravitational waves by Schwarzschild black-hole 0—69354 hyperplane dependence of amplitude 0—72933 inert-gas beams, from W(110) surface 0—65043 integral eqns., noniterative solutions 0—59915 integral eqns., noniterative solutions 0—59914 lattice theoretic formulation 0—66829
Legendre series, amplitude behaviour 0—66790
Lennard-Jones fluid, molecular dynamics investigation of coherent scattering function 0—77990 light atoms from solid surrace 0—39921

light atoms from solid surrace 0–39921 linewidths, Hameka theory 0–38189 Lorentz-poles into unequal mass scatt. amplitudes 0–38148

Love wave by periodically uneven surface, propagating in a half-space 0-62847

microwave, from surface waves excited on Hg plasma column 0-53192 molecular, long-range interaction processes, variational method 0-74082 molecular beams, apparatus using electron bombardment detection 0-49852

0–49852
multichannel, field theor, formulation 0–41949
multiple scatter, comparison of theory with expt. 0–59942
Neumann problem for prolate spheroid and scalar plane wave 0–63321
noniterative solns, of integral eqns. 0–38188
optical model, semiclassical, potential inversion 0–66827
Pade method for phase eqn. with singular potentials 0–76836
phase shift calc., use of it, iterative method 0–60984
phase shift derivatives using Kohn-Hulthen variational principles
0–72920
phonon in disordered alloys of GaSh-InSh at 300°K 0–68532

0—72920
phonon, in disordered alloys of GaSb-InSb at 300°K 0—68532
phonon, magnetic field dependent, by Mn³¹ ions in Al₂O₃ 0—68326
phonon-photon, under conditions of stimulated induction 0—45775
polyatomic molecules, model using Johnson's Hartree-Fock SCF
approach 0—64309
potential, WKB solution of inversion problems 0—72934
potential, wKB solution of inversion problems 0—72934
potential, eikonal approximations and impact-parameter approximation, relationship 0—59917
potential, large-angle, impact-parameter amplitudes 0—69624
potential, s-wave phase shift 0—45522
potential, variable phase approach 0—59918
potential and scattering data exact relationships for nonrelativistic S-wave scatt. 0—59920

potential and scattering data exact relationships for nonrelativistic S-wave scatt. 0–59920 potential inversion for semiclassical optical model 0–66827 potential off-shell T-matrix elements 0–38191 potential operator, integral representation 0–48729 potentials, exponentially singular, peratization 0–57279 quantum nonrelativistic, particle conservation theorem 0–48731 R-matrix and scattering resonances in single channel potential scatt. 0–77528 rediation isotropic from asymmetric suberical source in finite atmosphere

radiation, isotropic, from asymmetric spherical source in finite atmosphere 0-66788

0-66788
reactive, with activation energy, empirical model 0-64586
resonances in scattering cross sections, unified model 0-64181
second-harmonic, rel. to critical exponents for order-disorder phase transitions 0-47486
semi-classical theory reviewed 0-63352
from separable nonlocal potential, using cordinate representations 0-41980
singular integral or activation of the control of

singular integral operator encountered in scattering theory and application singular potential problems in scattering theory 0–59919 by spherically symmetric inhomogeneities 0–69625 of stress waves, by circular elastic cylinder embedded in elastic medium 0–69712

0-09712 theory, asymptotic states 0-54969 three-body, configuration-space theory 0-66828 three-body, theory in configuration space 0-72967 three-body problem, solution in 1 dimension for classical and quantal cases 0-52425

```
Scattering continued
```

three-particle Coulomb syst., Faddeev approach 0-77683 unitarity equation, approximate solution for phase of scattering amplitude 0-54584 methods applicable for approx. solns., error estimates

variational variational principles and techniques for solving radiation and scattering problems 0-63368

velocity dependence of total cross-section 0-61196 second virial coefficient for square well potential, quantum corrections 0-54583

0–54583
wave, parameter, probability distrib. functions, statistical analysis
0–38155
wave and scattering operators in terms of singular integral operators
derived for an interaction of rank one 0–66818
wave packet, causality 0–45537
Ar atomic beams, from (111) face of Ag crystals, intensity and speed
distributions 0–47035
Ar epithermal beams, from Ag(111) surfaces 0–53419
Cs atoms, by He, Kr, and Xe, low velocity 0–61000
D₂ by N₃, differential elastic, in crossed beams 0–39478
Li, glory scattering by spherical top molecules 0–64616
LiF on Ar, Kr and N₂, total cross-sections 0–61203
Pt (111) surfaces, of He and D₂ beams, LEED meas. 0–74887

acoustic waves
air-filled targets, cylindrical and spherical, freq. response 0–63435
rel. to atmospheric density structure investigations 0–54238
backscatter, in air, from rough surfaces, meas, using f.m.pulses 0–54717
backscattering, volume, meas, in Coral Sea 0–56757
backscattering from plane surface, relationship with pulsed radiation, reception 0–57400

creeping wave pulses propag, on soft cylinders 0–42073 creeping waves, experimental verification and visualization, rigid bodies in air 0–76910

air 0-76910
fm. pulse scattered from Al-sphere in water, echoes analysis 0-58486
in ferromagnet, stimulated Raman 0-47520
forward-scattered from ocean surface, frequency spectra, theoretical analysis 0-71342
high frequency at random rough surfaces, energy conservation 0-73041
by inhomogeneities, spherically symmetric, quantum theoretical solution 0-54716

inhomogeneous media, exptl. obs. 0–64901 liquids, critical, binary mixtures of, 0–64901 near specular, from three-dimensional travelling sinusoidal surface, spectra 0–54719

prolate spheroid coated with acoustic material, exact solution 0–48849 pulse, multiple scattering from a random collection of volume scatterers 0–54714

Raman, stimulated, in ferromagnet 0–47520 reverberation-derived scattering strength of shallow sea bed 0–62885 by rigid spheres, method of variables separation in spherical coordinates 0–45635

0-45635
at rough surface, cross-correlation and covariance 0-52111
from rough surfaces, soluble problems 0-54713
at sea surface, literature review 0-52091
signal return cale. from rough pressure-release surface 0-73040
sound by sound due to nonlinear interaction of two finite sources in water, expt. 0-58485
specular, from three-dimensional travelling sinusoidal surface, spectra 0-54719
specularly reflected pulses from a flow the

0–54719
specularly reflected pulses from soft cylinders, creeping wave formulation of scatt. theory 0–66902
by spin waves 0–71845
underwater, by gas bubble, multiple near-field sound scatt. 0–42075
underwater sound forward scattered from statistically rough surface, spatial and temporal correlation, theory 0–53333
underwater sound forward scattered from statistically rough surface, spatial, temporal correlation 0–53334
underwater specular, from anisotropic sea and swell surfaces 0–56753
in vapour, condensing, acoustic attenuation 0–78339
in waveduct with irregular boundary 0–57399
from waveguides having irregularities at normal-mode critical freqs., analysis 0–45634

acoustic waves, ultrasonic backscattering, near 28 kHz, statistical studies 0–54720 from cavities in solids, number density of scatt. centres calc. 0–68585

electromagnetic waves

antiferromagnet, semicond, by coupled waves 0-71902 atmospheric aerosol scattering coeffs. in the i.r., prediction method 0-56783

0-36783 backscatter fron rough sphere irradiated by moving source 0-45725 backscattering, axial, from absorbing finite cone 0-45726 on bodies of revolution, computation of surface currents 0-73093 from circumferential gap in circular waveguide 0-73102 complex shapes, perfectly reflecting, theory 0-45724 Compton scattering, nonlinear, boundary conditions, plane-wave packets, limitation for a monochromatic radiation field 0-60505 cylinder, infinite, dielectric-needle limit 0-63511 from cylinder of infinite length in oblique incidence 0-73096 cylinders, circular, concentric, infinite, plane waves obliquely incident, interstellar grain model appl. 0-45309 cylinders, parallel circular, arbitrary ensemble 0-66970 cylindrical objects of arbitrary physical properties and cross sections 0-57453 dielectric coated square prism, cross-section reduction 0-47815

dielectric coated square prism, cross-section reduction 0–47815 from dielectric steps in waveguides, residue calculus techniques 0–73097 electron density profiles from backscatter obs. and ionogram analysis 0–63515

0-63515
from expanding dielectric slab 0-48921
by ferrite column, axially magnetized with perfectly conducting core, dipolar resonances 0-42123
by ferrite sphere in d.c. magnetic field, theory 0-73094
finite tubular cylinder, numerical solutions 0-57469
forward, from dielectric slightly rough surface, effective reflection coefficients 0-63514
h.f. radio waves by spherical electron cloud, ray optics solution 0-57454
i.r. backscattering, by fog, ice and water 0-45143
inhomogeneities, statistical ensembles, theory 0-48928

Scattering continued

electromagnetic waves continued

electromagnetic waves continued
on inhomogeneities in a medium whose dielectric permeability changes
linearly with distance along on its surface 0-54796
inhomogeneous media, theory 0-63512
rel, to ionized meteors traces 0-51779
from ionized turbulent underdense gas, power spectrum from radar returns,
autocorrelation fn., analysis 0-43347
from ionospheric irregularities, oblique incidence of spherical wave, amplitude and phase fluctuations, variance formulae 0-45176
If, oblate spheroids and disks 0-66971
multiple, by spheres 0-69787
multiple, from plasma, upper bound 0-46709
piezoelectric cylinder, theory 0-42132
from piezoelectric isotropic cylinder, general soln. 0-59270
plane, from conical bodies 0-42122
plane, by moving objects 0-42122
plane, by moving objects 0-42125
plasma, incoherent scatt. of mm waves 0-55469
in plasma formations ellipsoidal with electric and mag. anisotropy, eqn.,
soln., method 0-53165
in plasma in radiation transport approximation 0-78084
polarized radiation, resonance fluorescence, general function 0-69785
by polydispersions, spherical, in planetary and terrestrial atmospheres, Mie
theory 0-48283
power spectrum from radar returns and autocorrelation fn. in underdense
turbulent ionized gas 0-43347
radiation, partially polarized, in finite inhomogeneous atms. 0-66365
radio, on track of body moving in the ionosphere 0-56844
radiowave scattering cross section on trail of rapidly moving body, in
ionosphere, sphericity allowance 0-51563
radiowave scattering cross-section on trail of vertically travelling body in
ionosphere 0-51562
radiowave scattering effects on ionosphere investigations by radiophysical
methods 0-76449
radiowave scattering in homogeneous, turbulent, gyrotropic medium
0-76448
radiowave scattering on trail of body moving in ionosphere near caustic

radiowave scattering in homogeneous, turbulent, gyrotropic mediani 0-76448 radiowave scattering on trail of body moving in ionosphere near caustic curve 0-76450

random plasma slab, electron density fluctuation and statistical properties 0-46703rectangular waveguide involving metallic obstacles, Green's function methods 0-54800

resonance upper hybrid by nonuniform magnetoplasma column 0-43285 resonant dielectric sphere, in waveguide 0-57451 rough plane-backed layer, extension of Rice small-perturbation method 0-60109

rough surface: shadowing and multiple-scatter effects 0-73095 rough surfaces in Fraunhofer zone 0-38439 scattered field co-efficients from near field meas. 0-69786

scintillation of extended radio sources, with finite bandwidth reciever 0-54482

0–54482 semiconductor; antiferromag., by coupled waves 0–71902 solar radiation, by atmos., calculation methods 0–54247 sphere, Mie soln. applic. to constitutive parameters meas. 0–63496 in substances with negative electrical conductivity 0–69781 Thomson, determ. of F-region vertical drifts 0–59658 turbulent medium, statistical optics treatment 0–42124 wavefunctions in uniformly moving media 0–48922 by wire, thin finite, theoretical investigation 0–42121 wires configuration, numerical computation using analytical methods 0–66972

see also Diffusion, light see also Diffusion, light for Brownian motion study of suspensions 0–43480 absorbing media, light amplification 0–63593 absorbing media, light amplification 0–63592 by acoustic waves with complex amplitude distrib., far-field diffr. patterns 0–60363

0 -60363 in aerosol, polydisperse settling, second and higher order, particle size distribution 0—74812 albedo problems, analytical soln. 0—51961 alkanes liquid, near i.r. laser Rayleigh, anisotropic component 0—49897 angular functions for spherical water droplets, using computer 0—64923 anisotropic, in boundary layers of turbid medium with narrow beam illumination 0—59543 anisotropic media 0—73273 anisotropically turbid medium, radiation transport investigation 0—57590 antiferromagnet, semicond, by coupled waves 0—71902

anisotropically turbid medium, radiation transport investigation 0-57590 antiferromagnet, semicond, by coupled waves 0-71902 atmosphere, influenced on optical instruments and communication systems 0-42381 atmosphere bounded by reflector, source functions 0-79537 atmosphere effect on optical sensors 0-48289 atmospheric aerosol scattering coeffs. in the i.r., prediction method 0-56783

0-56783
atmospheric angle scatt, fin. from sky brightness obs. 0-59576
by atom, two or more level system 0-39272
azulene, near i.r. laser Rayleigh, anisotropic component 0-49897
benzene, Rayleigh and depolarization ratios 0-64918
benzene, near i.r. laser Rayleigh, dispersion in anisotropy 0-49897
benzotrichloride, pure and soln., Rayleigh, i.r. spectra, molecular rotational mobility 0-46924
benzotrifluoride, pure and solution, Rayleigh scatt., i.r. spectra, molecular rotational mobility 0-46924
biological suspension, absorption and multiple scattering 0-66694
birefringence, effect in spherulite films 0-65987
bis-trifluoromethylbenzol, pure and soln., Rayleigh, i.r. spectra, molecular rotational mobility 0-46924
Brillouin, stimulated, thermal, in fluids, theory 0-39484
from bubbles growing in viscoelastic liquid, theory 0-78249
carbon black suspensions, HAF, mol. wt. and g-factors from Zimm plots 0-50274
carbon disulphide, Rayleigh and depolarization ratios 0-64918

0–302/4 carbon disulphide, Rayleigh and depolarization ratios 0–64918 carbon tetrachloride, Rayleigh and depolarization ratios 0–64918 cells, mammalian, rel. to size, Hodkinson scatt. model appl. 0–42373 cellulose film, anisotropy pattern 0–47992 ceramic, ferroelec. 0–62618 ceramic, hot-pressed ferroelec., props. 0–54064

```
Scattering continued light continued
```

chemical reaction kinetics determ. 0-54180

α-chloronaphthalene, depolarized component structure 0-64924

by cloud, phase function polynomial representation 0-72623

to cloud, phase function polynomial representation 0-/2023 coherent, on moving diffusion surfaces 0-38546 coherent radiation scattered by moving diffuse reflector, space time statistical props. 0-42237 colloid system, cales: for two spherical Rayleigh particles over all orientations 0-74805 colloidal spherical particles, size from angular scattering diagram study 0-68161

0–68161 colloids electro-optical props., review 0–55638 combination, asymmetric line contours, parameter values 0–73302 combinational and Rayleigh, in field of intense wave 0–39272 conference topic, Charia, Crete, Jul 1968 0–68729 cooperative effects in a scattering volume, expl. detection 0–60364 copolymer (dAT) helix-coil transition determ. 0–54180 critical binary mixture of dielec. liq. 4½, e.e. field effect 0–71355 cryptocyanine, crystallized solns., resonance effect 0–51288 deformed spherulitic films, effect of birefringence 0–65988 depolarized component in α-chloronaphthalene 0–64924 dielectric liq. binary mixture, elec. field effect 0–71355 by diffraction gratings using different ruling engines 0–73298 disperse syst. with power law distrib., struct. determ. by light scatt. 0–50270 in disperse system, ang. distrib. intensity 0–39842

disperse syst. with power law distrib., struct. determ. by light scatt. 0–50270
in disperse system, ang. distrib. intensity 0–39842
Doppler shift, fluid velocity measurement 0–46847
Doppler shift fluid velocity measurement 0–46847
Doppler shift in Bragg cells 0–70036
double-scattering into fundamental and second harmonic waves by materials of finite dimension 0–57589
effect on accuracy of meas. of spectral sensitivity, photoelectric radiation detectors 0–49148
elastic, number phase relation 0–45829
by electrons, harmonically bound, study of frequency mixing 0–38517
extraordinary wave, by inhomogeneous, anisotropic plasma column, at lower hybrid resonance 0–61291
F-actin, semi-flexible polymer Doppler broadening 0–71348
ferroelectric ceramics 0–62618
field fluctuations in a turbid medium for a spatially coherent emission source 0–60365
by films with nonrandom orientation fluctuations 0–72324
films with nonrandom orientation fluctuations 0–72325
first order, by ordered spin systems, temp. depend. 0–48045
flow light scattering, theory and apparatus 0–39787
forward, in settling aerosol, extinction, optical depth 0–74813
gas, monatomic, Rayleigh scatt., depolarization ratio virial expansion 0–78224
gas, third harmonic scatt., depolarization 0–71259
gases from thermal fluctuations call to determination of density density.

0-78224
gas, third harmonic scatt., depolarization 0-71259
gases, from thermal fluctuations, rel. to determination of density-density correlation function 0-53281
gases of linear mols., Rayleigh light 0-43050
Gaussian light scatt. by Gaussian medium, statistics, photon-counting probability distrib. 0-67043
gels, swollen 0-58510
glass, phase-separated, struct. obs. 0-74861
glass etched matt. surface 0-41117
glass fibres for light guidance, scatt. losses 0-57456
glasses rel. to fibre optical communication systems 0-48001
by groove, semielliptic in ground plane, low-frequency scatter of plane wave 0-42374
holography, forward-scatter, Fresnel, particle size measurement 0-60261

holography, forward-scatter, Fresnel, particle size measurement 0-60261 homogeneous medium with moving boundary, theory 0-42371 index determ. of low-abs. medium, from meas. of multiple scatt. characts. 0-42376

0-42376 with inhomogeneous absorpt., radiative transfer model 0-57591 laser, Brillouin scatt. spectroscopy 0-46729 laser beam, water-and ice-cloud discrimination 0-72620 laser beam scatt. by free electrons, classical theory 0-67021 laser inelastic scatt. spectra analysis 0-73344 laser-radar, from atmos. molecules and aerosols 0-54236 liquid, Zimm diagram and calc. program 0-39794 liquid, polar and nonpolar, and solns., anisotropic Rayleigh scatt. 0-53353 liquid, stimulated entropy 0-50226 liquid, stimulated entropy 0-50226 liquid, third harmonic scatt, depolarization 0-71259 liquid cryst., reversible u.v. imaging 0-64917 liquid droplets holography, Mie scattering 0-50223 liquid-vapour critical point, isothermal compressibility, temp. depend. 0-55665

0-55665 liquids, weak depolarized Rayleigh wing obs. 0-43450 macromolecular solns., Doppler broadening 0-71348 macromolecular solns., quasi-elastic scatt., Doppler broadening 0-61530 macromolecules, small-angle scattering, expansion allowance 0-77972 macromolecules in soln., particle scatt. factor and segment-segment distance distrib. 0-71347 magnetically ordered cryst. 0-44807 metal, liquid, binary mixtures, critical opalescence, conc. depend. 0-74753

0—74753 metal surface, rough 0—76018 metal surface, rough 0—76017 methane, stimulated Brillouin scatt, freq. shifts meas. and theory, hypersound speed determ. 0—46824 micelles in aqueous solutions of C₁₂H₂₅CONNMe, structure and polydispersity 0—64957 molecular spectroscopy, polarization phenomena 0—55270 molecular weights, abnormal, for polymers 0—53348 Moon's continental regions, spatial scattering function 0—51738 multiple, in plane parallel Mie atmosphere 0—59578 multiple, relationship between coefficient of attenuation, coefficient of scattering and cell diameter in polystyrene latexes 0—66003 multiple by large, low-refracting, absorbing particles, interface effects 0—52372 multiple scattered laser radiation, transient response laboratory obs. 0-52372 multiple scattered laser radiation, transient response laboratory obs. 0-77144 control laser Payleigh anisotropic component 0-49897

naphthalene, near i.r. laser Rayleigh, anisotropic component 0-49897 nonlinear, by static nonuniformities (small particles) 0-69976 oceanic, related to dynamic conditions different depth water samples 0-62890

in optical bulk glass, meas. by photon-counting photometer 0-67157

Scattering continued light continued

optically active fluids, theory 0-46913

orientation dependence of Rayleigh and Raman scattering 0-43043

n-paraffins, Rayleigh spectra, fine struct., using gas laser 0-53352

particulate systems, optically active, differential scatter of left and right circularly polarized light 0–55635 nepenthane, scaling method including gravitational effect, and critical indices determ. 0–71350

periodic structure, resonant absorpt., spatial distrib., holography appl. 0-77146

periodic structure, resonant aosorpt, spatial distrio, nolography appl. 0–77146
perturbation theory approach to scattering from rough surfaces or thin films using smooth surface and surface current sources model 0–62.583
photoconductor, CdS, acoustic noise amplification, Mandelshtam-Brillouin method 0–68609
photographic materials, coherent optical power spectra 0–57639
photometer, Sofica, from cylindrical cells 0–73307
planetary atmosphere, polarization in scattered radiation 0–76633
planetary atmospheres, external radiation fields 0–76634
plasma, cooperatively scatt., exptl. spectra interpret. 0–61292
plasma, inhomogeneous, temp. and density determ. by scatt. light intensity method 0–74560
plasma, of soft-state, from magnetoacoustic waves 0–41102
by plasma, turbulent, mutual coherence functions 0–53170
plasma parameter determ. from satellite shift and half-width obs. 0–39591
from plasmas with non-Maxwellian velocity distrib. spectral study 0–46715
polariton, coupled photon-polarization excitation modes 0–69134

polariton, coupled photon-polarization excitation modes 0–69134 by polaritons, parametric luminescence 0–48126 polarization characteristics of radiation passed through scattering layer 0–60367

0-60367
poly-y-benzyl-L-glutamate, concentrated solutions, application of correlation function methods 0-71353
polydisperse systems of irregular particles, polarized light scatt. 0-53377
polymer, deformed regions about voids and inclusions 0-41123
polymer anisotropic shells 0-76120
polymer solns., Zimm plot fitting 0-46917
polymers, amorphous, from deformed regions round voids and inclusions 0-41094

0-41094
polya-methylstyrene solns., particle scatt. factor and segment-segment distance distrib. 0-71347
polystyrene, measurements 0-64919
quantum electrodynamics 0-52256
Raman, stimulated, transient, theory of Stokes pulse shapes 0-77190
Rayleigh, anisotropic, of polar and nonpolar liq. and soln. 0-53353
Rayleigh, fine struct. for n-paraffins using gas laser 0-53352
Rayleigh, from gas of optically isotropic mols., pressure-induced depolarization 0-71262
Rayleigh, from monatomic gases, depolarization ratio virial expansion 0-78224
Rayleigh, laser optical saturation effects 0-46417

Nayleigh, 100m individue gases, depolarization ratio virial expansion 0—78224
Rayleigh, laser optical saturation effects 0—46417
Rayleigh, nonlinear changes due to electric and magnetic fields 0—38545
Rayleigh, relaxation theory 0—55615
Rayleigh, stimulated, thermal, in fluids, theory 0—39484
Rayleigh, stimulated, thermal, in fligs, thermally relax, and near crit, point 0—39484
Rayleigh and combinational, in field of intense wave 0—39272
Rayleigh in liquids, use of Frenkel model for molecular rotation 0—43447
resonance, in static magnetic and electric fields, rel. to investigations of excited atomic energy levels 0—52934
resonance radiation transfer in scattering media 0—72981
resonance radiation transfer in scattering media 0—72980
resonance radiation transfer in scattering media 0—72980
resonance by perturbed atoms, assoc. time-depend, phenomena 0—57505
rod assembly, orientated, theory 0—38547
rubber, crosslinking inhomogeneity determ, by light scatt. 0—39905
rubber, swollen, determ, of inhomogeneity in cross-linking 0—39910

rubber, wollen, determ. of inhomogeneity in cross-linking 0–39910 ruby crystals, quantitative characteristics, empirical fn. 0–59356 secaling method including gravitational effect, and critical indices determ. 0–71350

scattered flux spectrum of photographic materials for holography, analysis 0-52347

screening of the photon propagator in many-body optics 0-38488 second harmonic generation by ruby laser with dielectric surface scatterer 0-42250

0-42250 semiconductor, antiferromag., by coupled waves 0-71902 semiconductor, by sound 0-48094 semiconductor, impurity centres fluctuations, effect 0-68837 semiconductor electron-hole plasma in applied elec, field 0-72319 from semiconductor plasma, in mag. field 0-40757 from semiconductor plasma, rel. to coupled e.m.-magnetoplasma modes 0-40756 from semiconductor plasma, ed. 60135. from semiconductor plasmons 0-69135

from semiconductor plasmons 0–69135 short pulses, by laser-produced plasma 0–39577 simulated thermal scattering, of short pulses 0–45832 single component systems under gravitational effect, intensity distribution in precritical region 0–61209 small molecules dissolved in CS₂ diffusion coeff. meas. by quasi elastic light scattering 0–64884 solutions, fluctuations of dielectric constant 0–61538 by sound waves, in fluid, three-dimensional wave theory 0–70034 speckle patterns, random, intensity fluctuations power spectrum for coher ent illumination 0–73303 spherical particles, generation of angular distrib. coeffs. 0–70035 by spherulites, disordered 0–79236 spontaneous parametric three- and four-photon, quantum theory 0–45830 stimulated, by surface waves on liq. or solid 0–46915 stimulated, effect of spectral line anomalous broadening in nonlinear liqs. 0–39797

0-39797
stimulated, excitation by broad-spectrum pumping 0-55268
stimulated, from surface of liquid of arbitrary viscosity 0-61519
stimulated, in liquids and gases, review 0-39676
stimulated, ultra-short pulses 0-45815
stimulated and spontaneous scatt. 0-73305
stimulated combinational, rel. to laser self-focusing, observational possibilities 0-38492

ties 0-3649/, stimulated combinational, plane wave method applic. 0-46419 stimulated entropy scatt., theory and expt. 0-76135 stratospheric dust layer, particle concentration from scattered radiator observations 0-69275

PA 1970 - Part II (July-Dec.) S 1336 SUBJECT INDEX Scattering continued Scattering continued light, Raman spectra continued light continued succinonitrile, mol. cryst., Rayleigh scatt. 0–59417 sunlight, by atmosphere, energy distribution model 0–41506 third harmonic, in gases and liquids, depolarization 0–71259 tobacco mosaic virus particle solns., quasi elastic scatt., Doppler broadencrystal surface effects 0-66063 crystals, role of optical phonons 0-76123 defect cryst., cross section temp. depend. and no-phonon line 0–72382 depolarization meas. divergence errors of liquids in capillary cells, calc. tobacco mosaic virus particle solns., quasi elastic scatt., Doppler broadening 0–61530 tobacco mosaic virus solution, Doppler shift 0–78314 toluene, Rayleigh and depolarization ratios 0–64918 trimethylacetic acid, mol. cryst., Rayleigh scatt. 0–59417 turbid atmosphere, diffuse noise level investigation 0–59582 twilight, atmospheric dust content changes 0–48292 Bi-Ga liquid mixtures, critical opalescence, conc. depend. 0–74753 CO₂, at gas/liquid interface near critical temp., rel. to surface tension and viscosity 0–39757 CO₃ stimulated Brillouin scatt. freq. shifts meas. and theory hyperson of the content of th 0–50224
depolarization ratio spectrometry 0–54938
depolarization ratios, excitation in a continuance of states, resonance with single discrete state 0–58137
depolarization ratios of cryst. powders 0–72383
diamond, cross-section 0–62688
N, N-dimethylbutyramide, freq. assignments 0–67789
excitation by Ar-Kr multi-line laser 0–74199
ferroelectric, KH₂PO₄, symm., normal vibrations 0–40523
glass, selection rule breaking and density of states 0–62685
hyper Raman effect, nonlinear phenomenon 0–67692
intensities, vibration, theory 0–43042
intensities, vibration, theory 0–43042
intensity, angular dependence for random fluids 0–77736
ion-lattice relaxation processes and spectroscopic linewidths 0–56558
Jahn-Teller effect, influence on line intensity 0–49833
laser Raman spectroscopy oltra-fast 0–70081
line intensities, temp. depend., effect of electrooptical anharmonicity 0–43048
line parameters, determ. of true characteristics with computer from 0 - 50224CO₂ stimulated Brillouin scatt. freq. shifts meas. and theory, hypersound speed determ. 0–46824 CdS, acoustic noise amplification, Mandelshtam-Brillouin method 0–68609

GaAs, enhancement by heating electrons 0–41093

³He, liq., critical, opalescent light scatt., obs. 0–43495

³He, liq., described by account of the property of the pr 0-68609 0-43048 line parameters, determ. of true characteristics with computer from experimental data 0-49835 linear molecule, role of intermediate electronic states 0-43043 liquid, linewidth corres to totally symmetrical vibr., determ. 0-61526 liquids, effects of Brownian motion 0-49913 liquids, stimulated radiation, time-behaviour and self-focusing effects upon output power 0-46919 of liquids sample holder at temps. between -196° to +200°C, description 0-50228 molecular coherence effects in stimulated Raman scatt. 0-39340 light, Brillouin spectra
absorbing media, stimulated scatt., time-resolved obs., phonon lifetimes
0-39789 0–50228 molecular coherence effects in stimulated Raman scatt. 0–39340 molecular coherence effects in stimulated Raman scatt. 0–39340 molecule, line profile calc. from corres. i.r. band 0–55265 multiphonon combinational, excitons and impurity levels 0–56560 nonlinear phenomenon, theory of hyper Raman effect 0–67692 nonlinear polarizability in resonance interactions 0–73274 odd-parity Raman effect, mol. depolarization and rot. struct. study 0–70856 absorbing media, stimulated scatt., time-resolved obs., phonon lifetimes 0–39789 cholesteryl 2 (2 ethoxy ethoxy) ethyl carbonate, backward stimulated scatt., threshold power discontinuity 0–78277 for elastic constants determ, applic, to solid Xe 0–78598 in fluid media, extended, interaction between components 0–53356 fundamental aspects 0–56569 gas, hypersound vel. meas. 0–50168 gas under press, u.s. dispersion obs. 0–61440 glass, stimulated Mandel'shtam-giant ruby laser pulses 0–43773 lattice vibrations effect, molecular crystal 0–75989 line breadth meas. by Fourier-transform spectroscopy 0–60424 liquid cryst., backward stimulated scatt., threshold power discontinuity 0–78277 liquids, high viscosity 0–53357 Mandel'shtam-Brillouin scatt., stimulated, theory and expt. 0–76135 meas. by Fourier-transform spectroscopy 0–67175 methane, stimulated Brillouin scatt., rel. to hypersonic speed 0–61124 quartz, fused, stimulated Mandel'shtam-, giant ruby laser pulses 0–43773 resonance-enhanced, in crystals 0–56571 semiconductor, propagating acoustoelec, domains obs. 0–78768 stimulated, low-temp, applications 0–53383 stimulated, quantitative investigations 0–56570 stimulated effects in the nonlinear optics of light with sound 0–53000 stimulated molecular, rel. to interaction of light with sound 0–53000 0—70856
piezoelectric orthorhombic cryst., by polar phonons 0—43837
in polar crystals, in resonance with exciton transition 0—62686
from polaritons, localized-mode 0—44859
polarization dependence of scattering intensity relationship with each
Raman tensor 0—70838
polymeric mats. 0—69136
pressure broadening calc. 0—57632
profiles of lines, true from observed calc. 0—58143
quantum mechanical analysis of higher order processes 0—66064
quantum-mech treatment taking coherence into account 0—60889
quartz, cross-section 0—62688
radar technique, spectroscopic detection of SO₂ and CO₂ mol. in polluted atmosphere 0—67105
ruthenocene single crystals Raman spectra 0—76134
semiconductor, electronic Raman scatt. 0—41236
spectrometry, Raman, review 0—57628
spherical top molecules, Raman band contours, computer programme 0—64618
stimulated, excitation by broad-spectrum pumping 0—55268 0 - 434470-46418 stimulated, excitation by broad-spectrum pumping 0-55268 stimulated, in field of ultra-short laser pulses 0-73304 stimulated, in optical cavity, simultaneous generation of several Stokes components 0-43049 stimulated, in self-focusing liquids, time behavior 0-53347 stimulated, simultaneous excitation of two different vibrs. 0-64332 stimulated effects in the nonlinear optics of liqs. and gases, review 0-43447 stimulated molecular, rel. to interaction of light with sound 0-53000 strong driving field effect, on the frequency shift of stimulated Brillouin scattering in gases 0-53280 sociationing in gases 0-33200 succinonitrile, molecular cryst., spectral and intensity changes 0-59417 toluene, expt. for undergrad. lab. 0-44873 transparent media, stimulated scatt., time-resolve obs., phonon lifetime 0-39789 trimethylacetic acid, molecular cryst., spectral and intensity changes 0-59417 0 - 434470-43447
stimulated emission in optical reson, generation of several Stokes component 0-42256
stimulated in self focusing liquids, time behaviour 0-39786
stimulated scattering inside and near absorption bands 0-62684
Stokes components in stimulated Raman scattering excited by a pulsed laser 0-46429
Stokes components in stimulated scatt, in lossy medium, intensity calc. 0-61056 79-79-71/2, obs. 0-46829
n-GaAs, propagating acoustoelec. domains obs. 0-78768
He superfluid, h.f. first sound waves attenuation and velocity meas.
0-61578

0-61578

He, superfluid, thermally excited first sound 0-43500

KBr, KbR:KCl, cubic crystals, sound velocity and elastic constants
0-51329

KCl, cubic crystals, sound velocity and elastic constants 0-51329

LiNbO₃, Mandel'shtam spectra 0-41245

LiNbO₃, Motoelastic constants 0-72397

MgO:Ni, rel. to phonon bottleneck obs. 0-54113

NgCiN, rel. to phonon bottleneck obs. 0–54113
N₂, stimulated Brillouin scatt., rel. to hypersonic speed 0–61124
NaClO₃, elastic consts. determ. 0–53572
Nd³·POCl₃:SnCl₄ aprotic soln., rel. to pulsed laser appls., obs. 0–45790
Nd³·SeOCl₂:SnCl₄ aprotic soln., rel. to pulsed laser appls., obs. 0–45790
Nd³·TFA:POCl₃:ZrCl₄ aprotic soln., rel. to pulsed laser appls., obs. 0–45790

0-45790
Pb(NO₃), acoustic vel. and elastic consts. obs. 0-79334
RbI, cubic crystal, sound velocity and elastic constants 0-51329
SF₆, near critical point, sound velocity deductions 0-54114
STiO₃, rutile, cross sections, rotational contribution 0-79335
Xe, adiabatic elastic consts., determ. at 156° K by Brillouin spectroscopy 0-78598

Xe, meas, of sound velocity dispersion in critical region 0-78328 Xe, near critical point, analysis using hydrodynamic model 0-78326

light, Raman spectra

acetone in various solns., width of polarized lines as function of conc., effect of intermol. interac. 0–50234 air pollutant molecules density meas. 0–72608 air pollutants detection by Raman effect in far u.v. 0–72609 air pollutants meas. using single-ended remote Raman spectrometric techniques 0–72610

air pollution, spectroscopic detection of mols. by radar technique 0-67105amorphous materials, selection rule breaking and density of states 0-62685

cell, low temperature, for meas. 0-60438

cross sections determ. in reson. region, photoelec, method 0–49832 crystal, effect of anisotropy rel. to interpret. 0–54107 crystal plate, theory 0–56559

530kes pulse shapes in stimulated Raman scattering 0–69928 symmetric top molecules, degenerate vibration-rotation bands, computer program calc. 0–74204 symmetric- and spherical-top mols., rot. struct. of novel Raman effect 0–46423

temperature-jump heating, using stimulated Raman effect 0-77143 valency crystal, vibrational absorpt. by charged impurity, and photoelastic consts. 0-48057

consts. 0–48057
variation with concentration in binary solns. 0–64921
vibrational and electronic effects 0–67695
CO₂ under ambient atmospheric conditions, atmospheric oxygen balance appl. 0–51511
CaCO₃, calcite, cross-section 0–62688
KH₂PO₄ ferroelectric, normal vibrations, symm. 0–40523
N₂, under ambient atmospheric conditions, atmospheric oxygen balance appl. 0–51511
NaNO₃, cross-section 0–62688
O₃, under ambient atmospheric conditions, atmospheric oxygen balance appl. 0–51511
Pb TiO₃, ferroelectric, temp. dependent Raman spectra of underdamped soft modes 0–59414

modes 0–59414

light, Raman spectra, inorganic acentric insulating cryst., scatt. efficiency of phonons rel. to nonlinear coeffs. 0–59348
alkali halides, anharmonic renormalization of phonon freqs. 0–79326
alkali halides, of nitrite ion, freq. obs. 0–76089
alkali halides, with mol. impurities, rotational Raman effect 0–79331
alkali metal nitrates, crystalline field effects 0–59404
alkali-metal carbonates, molten 0–53358
alum, methylammonium aluminium sulphate/selenate dodecahydrate, rel. to ferroelec. behaviour 0–66066
ammoniacal, rel. to temp. 0–77807
antiferromagnet, KMnF₃, two-magnon scatt. 0–66112
antiferromagnet, KNiF₃, two-magnon 0–44867

PA 1970 - Part II (July-Dec.) Scattering continued light, Raman spectra, inorganic continued Scattering continued light, Raman spectra, inorganic continued antiferromagnet, MnF₂:Co, impurity magnons 0-44697 antiferromagnet, MnF₂, two-magnon line shape 0-44848 Ca_(1-x)Sr_xF₂, phonon vibrs. rel. to disordering, obs. 0-48087 Ca_{(1)-∞}Sr_xF_x, phonon vibrs. rel. to disordering, obs. 0–48087
Cd (II) complexes with thiourea 0–74313
CdCr₂Se₄(S)₄, ferromag., phonons and mag. order 0–72386
CdF₂, first order spectra, at 300, 77 and 4.2°K 0–48088
CdF₂, pure and semiconducting, polaron models 0–44864
CdS, insulating crystal, resonance scatt., polariton theory 0–44860
CdS, insulating crystal, resonance scatt., polariton theory 0–44860
CdS, eneironductor, decrease in TO scattering efficiency as direct energy gap approached 0–76125
Cl₂, lattice and mol. vibrs., obs. 0–48089
Cl₂ low temp. laser excited, lattice and molecular modes assigned, isotope effects distinguished 0–72387
Cl₂+, rel. to struct. and force field consts. 0–70893
ClF₂+, rel. to struct. and force field consts. 0–70893
ClF₃+, rel. to struct. and force field consts. 0–70893
ClF₃+, rel. to struct. and force field consts. 0–70893
Coisonitrile complexes, study 0–61085
Co(CO)₄- tetrahedral ion 0–46922
CoF₂, from phonons 0–56562
CoF₃, from phonons 0–56562
CoF₃, from phonons 0–56562
Cs₂Cr₃O₇, i.r. spectra, space group 0–56563
Cs₃MnF₆, solid and in solns. of anhydrous HF 0–64373
CuSO₄, hydrated and anhydrous, SO₄²- obs. 0–44866
Cs₃MnF₆, solid and in solns. of anhydrous HF 0–64373
CuSO₄, hydrated and anhydrous, SO₄²- obs. 0–44866
D, anti-Stokes Raman scatt. from metastable atoms 0–74170
p-D₂, roton spectra calculation, J=3 0–48091
EuAlO₃, electronic transitions to states of ⁷F₁, ⁷F₂ and ⁷F₃ manifolds 0–72380
Eu(III) complexes, β-diketonates, i.r. and Raman spectra 0–48090
F₃S₃O₄ molecular, i.r. and Raman spectra 0–55294 Cd (II) complexes with thiourea 0-74313 antiferromagnet, RbMnF₃, FeF₂, magnon-pair modes 0–44708 antiferromagnet, from localized magnons 0–41238 antiferromagnet, from localized magnons 0–41238 benzene-halogen charge transfer complexes, vibrs. analysis 0–74337 ceramics, review 0–51364 deuterium, ordered state, rotational excitations 0–59412 diamond 0–44862 electrolyte solns., conc. aqueous 0–39795 ferroelectric, BaTiO₃ by phonons and polaritons 0–66068 ferroelectric, KD,PO₄, isotopic shift 0–79329 ferroelectric, KD,PO₄ 0–79330 ferroelectric, KD,PO₄ temp. depend. 0–66069 ferroelectric, zone-centre mode obs. at phase transitions 0–68917 ferroelectric alum, methylammonium aluminium sulphate/selenate dodecah-ydrate. 0–66066 terroelectric alum, methylammonium aluminium sulphate/selenate dodecahydrate 0-66066 ferromagnet, CdCr₂Se₄(S)₄, phonors and mag. order 0-72386 ferromagnetic transition metal, magnons and Stoner excitations, thermal Green's function 0-76121 glass, silicate, vibr. spectra 0-76128 glasses, alkaline silicates, spectral interpretation 0-72392 graphite 0-62687 hexabologicalists 0-73764 graphite 0–62687
hexahalometalates 0–77764
hexaisothiocyanate ions, 2200-70cm⁻¹ 0–39376
hydroxyapatites, hydrothermally prepared, vibr. obs. 0–54110
HI-V and II-VI semiconductors, inelastic scattering at resonance 0–72384
insulating crystal, CdS, resonance scatt., polariton theory 0–44860
ionic cryst., from polaritons in presence of lattice damping 0–54108
metal surface, incoherent scatt. 0–62640
molecules with low-freq, vibrs., and i.r. spectra, obs. 0–39362
molten carbonates 0–53358
nitrates, ionic, laser spectra, band multiplicities 0–72389
nitrates of metals, melts 0–74759
optical properties and collective oscillations as function of temperature 0–48085
phosphites, i.r. and Raman spectra, electronic structure, 0–70906 0-72380 Eu(III) complexes, β -diketonates, i.r. and Raman spectra 0-48090 F,55,0 molecular, i.r. and Raman spectra 0-55294 FSSF 0-70902 FeF₂, magnon-pair modes, antiferromag, and paramag, phases, temp. depend. 0-44708 GaAs, photoexcited hot LO phonons 0-59410 GaAs, surface scatt. by localized mode of P impurities 0-79328 GaN, phonons and electrons obs. 0-62648 GaP, obs. of high-frequency localized vibrational modes of impurities 0-78729 GaP local-mode lattice vibrations obs. in Raman scatt. and as cooperating 0-48085 phosphites, i.r. and Raman spectra, electronic structure 0-70906 polyhalide ions 0-70901 protein, in aqueous soln. 0-39462 α -quartz, inherent electric and anisotropic forces effect 0-56565 α -quartz, neutron irrad. effect 0-51325 rare earth ions, spectra and theoretical background 0-70868 rare earth metals, by magnons 0-56557 rare earth trichlorides, isomorphous series, phonon-Raman-spectra 0-72348 GaP, obs. of high-frequency localized vibrational modes of impurities 0-78729

GaP local-mode lattice vibrations obs. in Raman scatt. and as cooperating phonon in optical transitions 0-78716

Gd₂(MoO₂), ferroelastic-ferroelectric, rel. to anomalous phonon behaviour near phase transition 0-40861

GeO_{-K-2}O glass system, diffuse spectra 0-56564

GeO₂, optical phonons freqs. and symmetries, temp. depend. 0-59411

GeO₂, vitreous, and i.r. absorpt. from low lying modes 0-51326

α-GeTe, soft phonon mode and ferroelec. 0-69120

H₂, line-narrowing, gas laser obs. 0-49954

0-H₂, roton spectra calculation, J=3 0-48091

H₂, solid, ordered state, rotational excitations 0-59412

p-H₃ solid, lattice dynamical effects in frequency anal. 0-72388

HCl, condensed phases, mol. motion 0-72357

α-HIO₃, freqs. variation with orientation of scatt. elastic waves 0-51323

H₃O₂+ClO₄-, i.r. 0-41195

H₃PO₂, i.r. and Raman spectra, electronic structure 0-70906

Hg (II) complexes with thiourea 0-74313

HgI, lattice vibrs. anal., Raman scatt. study 0-43863

HgS, cinnabar, fund. vibrs. obs. 0-41237

HgS, lattice vibra anal., Raman scatt. study 0-67720

I₂ Raman spectra laser-excited of low temp. polycrystalline sample 0-72387

IBr gas, resonance scatt. with Ar ion laser excitation 0-67720 rare earth metals, by magnons 0—36357 rare earth trichlorides, isomorphous series, phonon-Raman-spectra 0—72348 rare-earth oxides, phonon and electronic Raman spectra 0—62692 rocksalt type crystals, by polaritons, mechanism 0—51319 rocksalt type struct., order-disorder, i.r. obs. 0—53670 semiconductor, CdF2, polaron model 0—44864 semiconductor, First-order effect in plasma in mag. field 0—44924 semiconductor, propolar Raman tensor, pseudopot, calc. 0—51320 semiconductor, mechanisms, laser application 0—54109 silica fused, spectral interpretation 0—72392 silicate glasses, vibr. spectra 0—76128 solids damage, laser produced, obs. 0—59409 spinels, rel. to force consts. of octahedral and tetrahedral bonds 0—70869 tetravinyl-lead, liquid 0—77847 tetravinylgermanium, liquid 0—77847 tetravinylgilicon, liquid 0—77847 tetravinylgermanium, liquid 0—77847 tetravinyltin, liquid 0—77847 tetravinyltin, liquid 0—77847 tetravinyltin, liquid 0—77847 tetravinyltin, liquid 0—39800 AgNO3, crystalline field effects 0—59404 AlBr₄—0—74235 AsF₅, findamentals and overtones, force constants 0—70871 AsI₃ single cryst. 0—66067 Au₂Cl₆ I.r. and Raman spectra, normal coordinate calculations 0—46481 B₃Ce₄, B₃F₄, liquid-phase obs., mol. vib. 0—70876 BF₃-(CH₃),So isotopically substituted coordination compounds 0—74238 B₃Ce₄, B₃F₄, liquid-phase obs., mol. vib. 0—70876 BF₃-(CH₃),So powdered crysts. 0—66065 Ba₄-3Sf₄F₇, phonon vibrs. rel. to disordering, obs. 0—48087 BaTlO3, by pinonns and polaritons 0—66068 Ba₄-3Sf₄F₇, phonon vibrs. rel. to disordering, obs. 0—48087 BaTlO3, by pinonns and polaritons 0—66068 BaTlO3, polariton lines 0—72385 Be single crystal, symmetry 0—48086 Bil (III) halide complexes with DMSO, i.r. amd Raman assignments 0—4890 Bil₃ cryst. powder 0—66067 Br. gas, simultaneous obs. of resonance Raman effect and resonance 15. Rainan Spectra laser-excited of low tellip. Polycrystamine Sample 0-72387

18. gas, resonance scatt, with Ar ion laser excitation 0-67720

15. Clg as, resonance scatt, with Ar ion laser excitation 0-67720

15. Clg as, resonance scatt, with Ar ion laser excitation 0-67720

15. Clg as, resonance scatt, with Ar ion laser excitation 0-67720

15. Clg as, resonance scatt, with Ar ion laser excitation 0-67720

15. Clg as, resonance scatt, with Ar ion laser excitation 0-67720

15. Clg as, resonance scatt, with Ar ion laser excitation 0-67818

16. Clg as, resonance scatt, with Ar ion laser excitation 0-4681

16. Clg as, resonance scatt, with Ar ion laser excitation 0-4681

16. Clg as, resonance scatt, with Ar ion laser excitation 0-67930

16. Clg as, resonance scatt, with Ar ion laser excitation 0-7930

16. Clg as, resonance scatt, with Ar ion laser excitation 0-67930

16. Clg as, resonance scatt, with Ar ion laser excitation 0-67930

16. Clg as, resonance scatt, with Ar ion laser excitation 0-67930

16. Clg as, resonance scatt, with Ar ion laser excitation 0-67930

16. Clg as, resonance scatt, with Ar ion laser excitation 0-67930

16. Clg as, resonance scatt, with Ar ion laser excitation 0-67930

16. Clg as, resonance scatt, with Ar ion laser excitation 0-67930

16. Clg as, resonance scatt, with Ar ion laser excitation 0-67720

17. Clg as, resonance scatt, with Ar ion laser excitation 0-67720

17. Clg as, resonance scatt, with Ar ion laser excitation 0-67720

17. Clg as, resonance scatt, with Ar ion laser excitation 0-67720

17. Clg as, resonance scatt, with Ar ion laser excitation 0-67720

17. Clg as, resonance scatt, with Ar ion laser excitation 0-67720

17. Clg as, resonance scatt, with Ar ion laser excitation 0-67720

17. Clg as, resonance scatt, with Ar ion laser excitation 0-67720

17. Clg as, resonance scatt, with Ar ion laser excitation 0-67720

17. Clg as, resonance scatt, with Ar ion laser excitation 0-67720

17. Clg as, resonance scatt, with Ar ion laser excitation 0-67720

17. Clg as, resonance scatt, w B₁, grs, simultaneous obs. of resonance Raman effect and resonance fluoresc. 0-64382 Br., gas, suttutaneous obs. of resonance Raman effect and resonance fluoresc. 0–64382
Br., lattice and mol. vibrs., obs. 0–48089
Br. gas, resonance scatt. with Ar ion laser excitation 0–67720
Br. low temp., laser excited, lattice and molecular modes assigned, isotope effects distinguished 0–72387
Br. vapour, contour of fundamental 0–64344
BrCl gas, resonance scatt. with Ar ion laser excitation 0–67720
CCla, Fermi resonance of Raman spectra in gas, liquid phases 0–43094
CNBr, polarized spectrum rel. to lattice dynamics 0–78725
CO, solid, band assignment and lattice mode intensities 0–51321
CO gas, collisional narrowing of vibrational band 0–74279
CO solid, \(\alpha \) phase at 18K, assignment of features in intramolecular and lattice regions 0–76126
CO₂, solid, band assignment and lattice mode intensities 0–51321
CO₂ pure rotational scatt. from excited vibrational levels, obs. 0–61083
CS₂, Fermi resonance of Raman spectra in gas, liquid phases 0–43091
CS₂, self-focusing effect on stimulated scatt., due to vibrational states
0–44861
CS₂ self-modulation of stimulated light, phase modulation 0–67721 KH, Po₄, ferroelec. phase, internal vibrs. spectra 0–79308 KI, assignments of peaks to two-phonon combinations and overtones 0–72362 KI, assignments of peaks to two-phonon combinations and overtones 0–72362. KMnF₃, antiferromag, two-magnon scatt. 0–66112 KyMnF₄, solid and in solns. of anhydrous HF 0–64373 KNiF₃, two-magnon 0–44867 K(Ta,Nb)O₃ mixed cryst., soft phonon modes 0–65518 L₃C₇O₇, 1.r. and Raman spectra 0–46483 LiF:Mn²⁺, Mg²⁺, normal modes obs. 0–51324 LiF defect structs. 0–66070 LiO₃, uniaxial and optically active, scattering meas. problems 0–72391 LiYF₄, single cryst. 0–40525 MgBr₃ and MgI, diethyl ether complexes 0–74278 Mm₃(CO)₀, and i.r. spectrum, vibr. analysis, obs. 0–39391 MnF₂:Co, impurity magnons 0–44697 MnF₂:Fe, from localized magnons 0–44238 MnF₂, two-magnon line shape, i.r. absorpt. spectra 0–44848 MoF₆, vapour state 0–58183 N₂, solid, \$\alpha\$ phase at 18K, assignment of features in intramolecular and lattice regions 0–76126 N₂, solid, \$\alpha\$ phase at 18K, assignment of 74279 N₂, solid, \$\alpha\$ phase at 18K, assignment of 74279 N₃, solid solid saignment and lattice mode intensities 0–51321 N₂, solid, \$\alpha\$ phase spectral analysis by laser-Raman radar 0–69277 N₂, gas, collisional narrowing of vibrational band 0–74279 ND₄F, Raman and far-infrared 0–41239 NH₄-in non-cubic cryst. sites, study of molecular motion 0–59063 NH₄Cl, hyper-Raman spectrum of lattice modes C–72390 NH₄F, Raman and far-infrared 0–41239 NO, cross section meas. 0–71264 NO, relative intensities and Raman shifts of rotational structure 0–53042

Scatt. 0–313/2 CaCO₃ cryst., ang. distrib. of components of stimulated Raman scatt. 0–44863 CaF₃:Ce, impurity scatt. 0–79327 CaMgSi₂O₆, diopside, cryst. and vitreous 0–56561 Ca(NO₃)₂, powdered crysts. 0–66065 Ca_{1-x}Sr_xF₂, phonon contrib., Green-function method calcs. 0–44809

0—44861
CS₂ self-modulation of stimulated light, phase modulation 0—67721
CS₃ self-trapped filaments of liquid, molecular coherence effects in stimulated Raman scatt. 0—39340
CaCO₃, supplementary emission of Stokes components in stimulated scatt. 0—51322 stimulated scatt. 0—51322 stimulated Raman scatt.

```
Scattering continued light, Raman spectra, inorganic continued
                                                                                              ion, isotopically different forms vibrational band assignment
                                                                  -59390
                         0–59390

N<sub>2</sub>O, solid, band assignment and lattice mode intensities 0–51321

NOAIBr<sub>4</sub> 0–61715

NO<sub>2</sub>SO<sub>3</sub>F ionic character, structure 0–70925

NO<sub>2</sub>(SO<sub>3</sub>), F ionic character, structure 0–70925

NaCl, from Ag* pairs 0–59413

NaCl, second-order, 90K 0–54111

NaCl cryst., Ag* doped, impurity induced and 2nd order 0–66071

NaClO<sub>3</sub>, at high press., rel. to changes in freqs. of vibr. modes 0–66072

NaClO<sub>3</sub>, cubic and optically active, scattering meas. problem 0–72391

Na<sub>2</sub>Cr<sub>3</sub>(CO'<sub>10</sub>, and i.r. spectrum, vibr. analysis, obs. 0–39391

NaHCr<sub>3</sub>(CO)<sub>10</sub>, and i.r. spectrum obs. 0–74291

NaNO<sub>3</sub>, line broadening, i.r. and Raman spectra, force constants of complex ion 0–46497

NaNO<sub>3</sub>, biaxial, scattering meas. problems 0–72391

NaNO<sub>3</sub>, line broadening, rel. to order-disorder transform. 0–76127

NaNO<sub>3</sub> mine broadening, rel. to order-disorder transform. 0–76127

NaNO<sub>3</sub>, bine broadening, rel. to order-disorder transform. 0–76127

Na<sub>2</sub>O-N<sub>2</sub>O<sub>3</sub>CiO<sub>3</sub> glass, structure study 0–69139

Na<sub>2</sub>[Fe(CN)<sub>3</sub>NO], 2H<sub>2</sub>O, 0–76105

Na<sub>3</sub><sup>3</sup>·POCl<sub>3</sub>:SnCl<sub>4</sub> aprotic soln., rel. to pulsed laser appls., obs. 0–45790

Nd<sup>3</sup>·POCl<sub>3</sub>:SnCl<sub>4</sub> aprotic soln., rel. to pulsed laser appls., obs. 0–45790

Ni<sub>2</sub>O-RD-2Cl<sub>2</sub>:ZrCl<sub>4</sub> aprotic soln., rel. to pulsed laser appls., obs. 0–45790

Ni<sub>2</sub>O-RD-2Cl<sub>3</sub>:ZrCl<sub>4</sub> aprotic soln., rel. to pulsed laser appls., obs. 0–45790

Ni<sub>2</sub>O-RD-2Cl<sub>3</sub>:ZrCl<sub>4</sub> aprotic soln., rel. to pulsed laser appls., obs. 0–45790

Ni<sub>2</sub>O-RD-2Cl<sub>3</sub>:ZrCl<sub>4</sub> aprotic soln., rel. to pulsed laser appls., obs. 0–45790

Ni<sub>2</sub>O-RD-2Cl<sub>3</sub>:ZrCl<sub>4</sub> aprotic soln., rel. to pulsed laser appls., obs. 0–45790
                                   N<sub>2</sub>O, solid, band assignment and lattice mode intensities 0-51321
                                 0-45/90
Ni, Pd and Pt complexes, Ni(PF<sub>3</sub>)<sub>4</sub>, Pd(PF<sub>3</sub>)<sub>4</sub> and Pt(PF<sub>3</sub>)<sub>4</sub> 0-55309
Ni complex, pentacyanonickelate ion, structure Raman spectrum, CN stretching frequencies 0-46501
Ni(PCl<sub>3</sub>)<sub>4</sub>, solid and in solution in organic solvents, polarization data 0-64443
                            0-64443
α-Q, previously unobserved line 0-62689
O<sub>3</sub>, relative intensities and Raman shifts of rotational structure 0-53042
O<sub>5</sub>, relative intensities and Raman shifts of rotational structure 0-53042
O<sub>5</sub>, relative intensities and Raman shifts of rotational structure 0-53042
O<sub>7</sub>, red i.r. and Raman spectra, structure 0-49886
PBr<sub>2</sub>, F<sub>3</sub>, ionic form 0-62690
PD<sub>4</sub>Cl, polycrystalline sample, -170°C 0-48092
PH<sub>4</sub>Cl, polycrystalline sample, -170°C 0-48092
PbF<sub>3</sub>, first order spectra, at 300, 77 and 4.2°K 0-48088
Pb(NO<sub>3</sub>)<sub>3</sub>, powdered crysts. 0-66065
PbTiO<sub>3</sub> ceramic platelets and oriented single crystals, investigation 0-71826
PbTi<sub>1</sub>, xZr<sub>2</sub>O<sub>3</sub>, ceramic ferroelectric-antiferroelectric system, meas. of soft
                              U=71826
PbTi<sub>1</sub> ZI<sub>2</sub>O<sub>3</sub>, ceramic ferroelectric-antiferroelectric system, meas. of soft E(TO) optical phonon modes 0-79332
Pd complexes, phosphines, isotope effects on metal-ligand vibrations 0-77763
                                 RbI, assignments of peaks to two-phonon combinations and overtones 0\!-\!72362
                              0-72362
RbMnF<sub>3</sub>:Ni, from localized magnons 0-41238
ReF<sub>6</sub>, vapour state 0-58183
S<sub>2</sub><sup>2</sup>, rel. to struct. 0-70948
S<sub>3</sub><sup>2</sup>, rel. to struct. 0-70948
S<sub>4</sub><sup>2</sup>, rel. to struct. 0-70948
S<sub>4</sub><sup>2</sup>, rel. to struct. 0-70948
SF<sub>6</sub>, vapour struct. 0-70948
SF<sub>6</sub>, vapour state 0-58183
SO<sub>2</sub>, cross section meas. 0-71264
SSF<sub>7</sub>, 0-70902
Rb (III) halide complexes with DMSO in and Raman assignments.
                                 SSF: 0-70902
Sb (III) halide complexes with DMSO, i.r. and Raman assignments
0-49890
                              0 -49890
SbCl<sub>3</sub>, temp. changes, low frequencies 0-49888
Sbl<sub>3</sub> cryst. powder 0 -66067
Se, trigonal, α-monoclinic, amorphous 0-66073
SeF<sub>6</sub>, vapour state 0-58183
Si, semiconductor, decrease of F<sub>2g</sub> mode as resonance with indirect energy gap approached 0-76125
Si, spontaneous-Raman-scatt. efficiency and stimulated scatt. 0-79333
Si, temp. depend., 20-770°K, linewidth and freq. meas. 0-44868
Si, vitreous, heat capacity calc. 0-78781
Si,Cl<sub>6</sub>, Si<sub>2</sub>Br<sub>6</sub> and Si<sub>2</sub>I<sub>6</sub> 0-55325
SiH<sub>4</sub>, condensed phases, interpretation rel. to site and factor groups 0-70952
(SiH<sub>4</sub>), CH<sub>2</sub> and (SiD<sub>4</sub>)-CH<sub>2</sub> 0-77845
                         S1;Cl<sub>6</sub>, S1;B<sub>6</sub> and S1;l<sub>6</sub> 0—55325
SiH<sub>4</sub>, condensed phases, interpretation rel. to site and factor groups 0–70952
(SiH<sub>3</sub>);CH<sub>2</sub> and (SiD<sub>3</sub>);CH<sub>2</sub> 0—77845
SiO<sub>2</sub>, neutron-compacted, l.f. modes 0—76130
SiO<sub>3</sub>, quartz, neutron irrad., α-β transformation 0—78702
SiO<sub>3</sub>, quartz, u.s. stress, impurity motion 0—79319
SiO<sub>2</sub>, vitreous, and i.r. absorpt. from low lying modes 0—51326
SmAlO<sub>3</sub>, 10-970K, phonon freq., temp. depend. 0—56566
SnO<sub>2</sub>, crystal 0—62691
Sr(NO<sub>3</sub>)<sub>2</sub>, powdered crysts. 0—66065
Sr(NO<sub>3</sub>)<sub>3</sub>, vibrs. assignment, space group 0—56567
Sr, VO<sub>4</sub>Cl(Br) spodiosite-type struct. 0—58750
Ta<sub>2</sub>Cl<sub>10</sub>, mode obs. 0—70954
TcF<sub>6</sub>, vapour state 0—58183
TeF<sub>6</sub>, vapour state 0—58183
TeF<sub>6</sub>, vapour state 0—58183
UO<sub>2</sub>-2+ salts, vib. assignments 0—41241
VF<sub>3</sub> frundamentals and overtones, force constants 0—70871
XeO<sub>4</sub> vapour and solid force constants 0—46503
Yb<sub>2</sub>O<sub>3</sub>-26, Raman luminescence obs. 0—44894
Zn (II) complexes with thiourea 0—74313
Zn(II) halide complexes, of NH<sub>3</sub> and mindazole 0—58490
ZnO<sub>3</sub> u.v. resonant scatt. 0—76131
ZnS resonant scatt. using a UV Cd-He laser, obs. 0—44869
ZnSe, temp. depend. of optical phonon linewidths and freqs. 0—76132
ZnSe resonant scatt. using a UV Cd-He laser, obs. 0—44869
ZnSe, lattice vibrations 0—41242
```

```
ZnTe, temp. depend. of optical phonon linewidths and freqs. 0-76132\ ZrO_2 polymorphs., phase obs. 0-54112
light, Raman spectra, organic acetic and perdeuteroacetic anhydrides, liq. 0—53059 acetyl bromide, and deuterated form, absolute intensities and depolarizations 0—55332
       ons 0-55332 acetylene, cryst., in intramol. and lattice vibr. regions 0-72394 acetylene crystals, normal coordinate calculation, structure 0-48093 alkanes, substituted, rotational isomerism 0-74327 aromatic compounds, relative intensities of intramolecular and lattice vibrations 0-51327 aromatic ligs., Raman bands 250-40cm<sup>-1</sup> compared to i.r. absorpt. 0-64928
   aromatic ligis., Raman bands 250-40cm<sup>-1</sup> compared to 1:r. absorpt. 0–64928
benzaldehydes, substituted 0–77874
benzene, liq., 1:f. Raman lines in depolarized Rayleigh wing 0–61524
benzene, liq., stimulated scatt., thermospectrum 0–39807
benzene, stimulated lines, lateral optical bands effect 0–50227
benzene and monosubstituted derivatives, amplification coeffs. and non-linear susceptibilities 0–50237
benzene derivatives, m-disubstituted 0–70973
benzenes, hydrocarbon monosubstituted and 1, 4-dialkyl series, characteristic features 0–67773
benzenes, o-disubstituted 0–77849
benzil crystal 0–59415
benzil crystal 0–59416
benzophenone, reinvestigation using a He-Ne laser 0–49908
benzyl benzoate 0–58210
biphenyl crystal, 3100-25 cm<sup>-1</sup> 0–72395
5,5'-bis-isoxazole, in crystal state and soln. 0–49910
2-bromo ethyl benzene, correlation between ground and excited state frequencies 0–58211
bromobenzaldehydes; o, m and p 0–70980
bromoethynyl benzene and chlorocthynyl benzene, liq. phase 0–55342
carbon disulphide, pure rotational scatt. from excited vibrational levels, osbs. 0–61083
       obs. 0-61083 carbon tetrachloride, contour of fundamental 0-64344 carbonyl cyanide, i.r. spectra all phases 0-46548 \beta carotene, resonance Raman effect 0-70983 carotenoid pigments in soln., excitation profiles in resonance region 0.7829
              0 - 78280
     0-78280
cellulose from cell wall of Velonia ventricosa, and i.r. spectra 0-79325
4-chloro- and 4-bromo-phenylmethylsulphide 0-70972
2-chloroacrylonitrile 0-74349
chlorobenzene, band intensity, solvent and temp. influence 0-43080
1-chloro-2-fluoroethylenes, cis and trans and deuterated modifications, vibrational assignments 0-64497
chloroform, band intensity, solvent and temp. influence 0-43080
chloroform, liquid, effect of intermolecular interactions on spectra 0-43460
     chloroform and deuterochloroform, small part played by Brownian motion in liquid 0-49913 chlorostyrenes, isomers, in liquid phase, assignment of vibrational frequencies 0-58212
   cies 0-58212
critical, liquid-solid 0-74832
cyanine dyes, high dispersion induced Raman scattering and luminescence spectra of solutions crystallized at liquid nitrogen temperatures 0-62707
cycloheptene 0-70984
cyclohexane, liq., stimulated scatt., thermospectrum 0-39807
cyclohexane, pure-rotational Raman spectra under high dispersion 0-70985
 0 -70982
cyclohexane, pure-totational Ramair Spectra direct high caspassion 0 -70982
cyclopentanol, vibr. anal. 0 -67785
cyclopentanone, deuterated isomers, laser spectra 0 -77891
cyclopentylamine, vibr. anal. 0 -67785
N-deuterated N-methylpropionamide, and normal vibrs., obs. 0 -53075
1,5-diazanaphthalene, polarizations 0 -74358
2,2-dichloro and 2,2-dibromopropane, liq., and polarization data 0 -55349
2,5-dichlorotoluene, in liq. phase 0 -49919
dicyanodiazomethane, vibr. spectrum, obs. 0 -46571
diethynyl ketone, liquid, rel. to freqs. of fundamentals 0 -74360
dihaloacetylenes 0 -70989
dihalofumaronitriles 0 -77896
pdihalogenobenzenes, cryst., 1.f., vibr. assignments, intermol. forces variations 0 -44927
pdihalogenobenzenes, 1.f., mol. motion obs. 0 -44870
 p dinalogenobenzenes, cryst., 11., vlor. assignments, intermol. forces variations 0—44927
p dihalogenobenzenes, 1.f., mol. motion obs. 0—44870
dihydrazinium oxalate, interpretation in terms of frequencies of functional groups 0—71004
2,3-dihydrofuran, structure study 0—64534
dimethyl benzyl carbinol, qualitative intensity calculation 0—58252
dimethyl sulphone, single crystals, vibrational assignment 0—66074
dimethylacetylene, liquid and gaseous, symmetry 0—49920
dimethylsulfoxide, and -d<sub>6</sub>, rel. to lattice fundamentals 0—65525
dimethylsulfoxide and deuterated derivative, new assignments 0—64501
dimethylsulphoxide and deuterated derivative, new assignments 0—64501
diphenylarsine 0—74400
diphenylchlorophosphine 0—74490
diphenylchlorophosphine 0—74490
diphenylchlorophosphine 0—74400
 ethyl alcohol in binary solns., variation of Raman scatt. with variation 0–64921 ethylene, gas, laser induced hyper-Raman spectra 0–77918 4-fluoro- and 4-bromo-benzenethiol 0–70972 1-fluoro-2,4,5-trichlorobenzene 0–55352 germylcyclopentane 0–58222 p-glycine, long wavelength phonon spectra 0–76133 glyoxime in soln., fund. freqs. symmetry and assignment 0–78281 hexachlorobenzene, polarized spectrum rel. to lattice dynamics 0–78740 hydrazinium hydrogen oxalate, interpretation in terms of frequencies of functional groups 0–71004 kryptocyanine, induced spectra by powerful pulse of ruby laser 0–43172 liquid, energy determ. first Stokes' components 0–39798 liquid, excitation upon Q-switching of laser by investigated liquid 0–53354 liquids, bandwidths, comparison with i.r. bandwidths 0–46519
     liquids, bandwidths, comparison with i.r. bandwidths 0-46519
```

Scattering continued light, Raman spectra, inorganic continued

Scattering continued light, Raman spectra, organic continued

lithium acetate dihydrate cryst., vibr. and internal modes obs. 0-41243

lithium formate monohydrate, cryst. chem., bonds 0-51328

metalloporphyrins, Raman spectrum 0-46573 methane, gas, laser induced hyper-Raman spectra 0-77918

methanetellurol, vibrational anal. 0-64529

methyl boron difluoride and deuterated derivative, depolarization measurements in liquid state 0-64526 methyl ethyl ether, isotopic species, i.r. and Raman spectra, isomers 0-46580

N- methyl phosphoramidodichloridothioate and deuterium analogues, assignment of vibrational spectra 0-46579

N-methyl propionamide, and normal vibrs., obs. 0–53075 1- methyl 4-phospha-3,5,8-trioxabicyclo-(2.2.2.) octane-4-oxide 0–74378

methylammonium chloride, solid state and solution 0-62693 methylarsenic halides 0-71006

methylcyclopentane, vibr. anal. 0-67785 methyldiboranes 0-74376 methyl-4-imidazole spectra of aqueous solution of chlorohydrate 0-71012

molecules with low-freq. vibrs., and i.r. spectra, obs. 0–39362 monocarboxylic cyclobutane acid, dimer forms and config. 0–74388 naphthalene-d₈ 0–77931 1- and 2-naphthols, crystalline, below 250 cm⁻¹ 0–72381

nitrobenzene, small part played by Brownian motion in liquid 0-49913 nitrobenzenes, monosubstituted 0-77937

O-alkyl phosphorodichloridothioates 0-55350

octachlorocyclobutane, with polarizations, rel. to fundamental freqs. 0-74355

octafluorocyclobutane, with polarizations, rel. to fundamental freqs. 0 - 74355

octahydroxycyclobutane, with polarizations, rel. to fundamental freqs. 0-74355

organometallic acetylenic compounds, vapour, liquids and solutions 0-64473

oxalic acid, vibr. assignment 0-49935 oxalyl chloride 0-58234

2-oxazoline, structure study 0-64534

pentachloropyridine, solution and crystalline phases, assignment proposed $0\!-\!64535$

phenol-carbonyl liq. mixtures 0-64925

phenyl derivatives of group Vb elements in solid state 0-76117

phenyl methyl carbinol, qualitative intensity calculation 0-58252

phenylarsenic halides 0-71006

phenylarsine 0-74400

phenyldichloroarsine 0-74399 phenyldichlorophosphine 0-74399 phenylphosphine 0-74400

picoline, intermolecular interactions for picoline dissolved in water, ethanol and methanol 0-64926

cis-1,4- polybutadiene crystalline laser excited 0-56568

polyethylene, fibres assignment of bands to symmetry classes 0-46622

polyethylene, fibres assignment of bands to symmetry classes 0—46622 polyglycine, cryst. 0—44871 polytetrafluoroethylene, temperature effects 0—41244 proteins, solid 0—76122 1-pyrazoline, vibr. anal. 0—67785 1-pyrazoline 0—58240 pyridine, derivatives of intensities and depolarizations w.r.t. electro-optical parameters, computer calculation 0—46585 pyrimidine, substituted derivatives 0—74405 pyrrolidine, vibr. anal. 0—67785 selenacyclopentane, rel. to symmetry and struct. 0—64544 selenium dialkylamino compounds, i.r. and Raman spectra force constants 0—46588

0 - 46588

silacyclobutanes, vibrational spectra, normal coordinate analyses 0-46590

silico-organic cpds., [(CH₃)₃Si]₄El^{IV} (El^{IV}=C, Si, Ge, Sn), vibrational spec tra and force constants 0-46589 silyl and trimethylsilyl compounds of group 5 elements, force constants

0-46591 succinic acid in saturated aqueous soln., freqs. assignment, symmetry and bonds 0-39447 sulphonylamines, halogen-substituted 0-53085 sulphur dialkylamino compounds, i.r. and Raman spectra force constants 0-46588

5—46588
p-terphenyl, phonon spectra obs. 0—78741
l₃!,2,2-terrabromoethane 0—77953
7,7,8,8-tetracyanoquinodimethane (TCNQ) and TCNQ-d₄ crystals, i.r. and Raman spectra 0—55373
tetraiodoethylene solid and in CS₂ soln., laser excitation 0—64548
tetramethyltitanium 0—71033
thiophosgene, and polymer species 0—55374
thiourea, rel. to lattice vibrs. of each polymorphic form 0—78742
toluene, liq., l.f. Raman lines in depolarized Rayleigh wing 0—61524
1,3,5-trichlorobenzene, partial identification of lattice modes 0—72396
trichlorofluoromethane, liquid, effect of intermolecular interactions on spectra 0—43460
1,1,1-trifluoro-2-butyne, vibrational assignment 0—77956
trifluoroacetic acid, solid, vibrational spectra 0—67824
1₄·1,1-trihaloethanes and deuterium derivatives, vibrational assignments 0—43182
trimethylsilyl cyanide and isocyanide, with polarization data 0—55377

0–43182 trimethylsilyl cyanide and isocyanide, with polarization data 0–55377 triphenylene and triphenylene-d₁₇, crystalline and solution, normal coordinate calculations 0–43183 urea single crysts., external vibrs. 0–69138 p valerolactone, fundametnal vibl. assignment 0–46599 vinyltrifluorosilane 0–77952 zinc uranyl acetate, vibration level assignment 0–46602 C₆D₁₂ pure-rotational Raman spectra under high dispersion 0–70985 C₆H₁₂, pure-rotational Raman spectra under high dispersion 0–70985

X-rays see X-ray scattering Scattering, elementary particles see Elementary particles/scattering

Scattering, nuclear see Nuclear reactions and scattering

Scattering, particles

see also Collision processes; Energy loss of particles; Field theory, quantum/interactions; Elementary particles/scattering; Nuclear forces; Nuclear reactions and scattering; Particle tracks; S-matrix theory; and under individual particles, e.g., Alpha-particles Clebsch-Gordan coeffs, and nonrelativistic multiparticle reactions 0–38190

close-coupling theory in eikonal approximation for atomic collisions 0-64252crystals, spatial distributions of heavy charged particles, ion camera 0-53492

density matrices in the many-body problem 0-42002

Dirac particles, inverse scattering problem 0-42002
Dirac particles, inverse scattering problem 0-51958
discontinuity eqns. for many particle scatt, amplitudes 0-38614
elastic scattering, of fast charged particles in a background plasma 0-43269

0-43209 electron energy loss processes usually masked by plural scattering of fast electrons 0-68708 fns. of spherical particles, Fourier, Legendre series coeffs. computation 0-63322

inelastic, particle on bound system of identical particles, model 0-76837 multicollision theory, threshold cusps and resonance phenomena, review -59922

0–59922 nuclear emulsions, spurious scattering 0–70319 nuclear particles of spin 0 or ½, by rotational nuclei, adiabatic couple-channel calc. 0–52744 in nuclear track emulsions, small angle meas. 0–60724 particle-bound-state, eigenvalue theory 0–77682 by plasma, electron beam, multiple scattering and energy loss 0–78042 protons and α-particles, high energy, from H, cross section evaluation 0–49814

0-49814

relativistic amplitude parametrization, definition of crossing symmetric measure and inertial tensor 0-76811

relativistic kinematics for N-particle scattering states 0-57249
relativistic polarization and angular correlation 0-59921

resonant state lifetimes Fermi and Smith estimates compared 0-45538
spinless, by central potential, phase determ. of scatt. amplitude from differential cross-section 0-59874

two-body, spinless, unique determ. of non-local potential 0-48730

Schizons see Elementary particles; Field theory, quantum/interactions,

hlieren systems
aberration elimination by holographic method 0–54895
colour techniques, extended range 0–45841
gas dynamic flows, discontinuity surfaces determ. 0–71221
image recording optical system 0–45818
interferometric method of studying heat transfer 0–45684
optical inhomogeneity, production of shearing interferogram and schlieren
pictures from singly exposed hologram 0–45810
plasma diagnostics, density gradient determ. 0–74556
rel. to u.s. reflection, conical, from liquid-solid boundaries, obs. technique
0–52110

Schottky defects see Crystal imperfections/vacancies

Schottky effect (noise) see Electron tubes; Noise/electrical; Semiconducting

Schrodinger equation see Quantum theory/wave equations

Schwarzschild space see Cosmology; Gravitation; Relativity/general

Scintillation see Luminescence

Scintillation chambers see Luminescence chambers Scintillation counters see Counters/scintillation

alumina, anodic film, sealing effects at barrier-porous layer interface 0-76274

0—76274
alumina, anodic film, structure sensitization for sealing 0—72549
ceramic-metal, in travelling wave tubes, problems 0—57494
ceramic-metal adhesion bonding 0—50810
ceramic-metal adhesion bonding sintering conditions effect 0—53654
ceramic-to-metal joiningtechniques 0—47463
glass-metal adhesion bonding 0—50810
grease, apiezon N, thermal conductivity at 4.2 to 1.4 K 0—47563
plastic, fluorocarbon, confined, for movable and fixed modular vacuum
devices 0—76777

devices 0—76777

u.h. vacuum, gasket coating materials 0—76776

u.s. bonding of Cu lead to Ta film on glass or ceramic, patent 0—59062

Al₂O₂ ceramics to metals 0—43817

Ti joint to artificial sapphire 0—48659

awater absorption coefficient, optical, meas. 0–41482 concentrates, heat capacity, meas. up to 200°C 0–45124 extinction coeff., solar altitude influence 0–62882 floor sediments, mechanical properties estimation, underway acoustics technique 0–41479 heat capacity, meas. up to 200°C 0–45124 ice crystals, growth parameter effect on substructure spacing 0–45125 light-field fluctuations, differential refraction by surface gravity waves 0–62886 sound velocity, random components, statistical analysis, 0–54710

sound velocity, random components, statistical analysis 0-54710 surface temperature, remote sensing using microwave radiometry 0-62894

0-62894
temperature inhomogeneities, spatial geometry and dynamics 0-51501
tidal forcing, undular bores 0-51500
tides in shallow irregular estuaries, simulation 0-41483
In concentrations at different depths and in some sediments 0-41484
Li content, determ. using flame spectrophotometry 0-48247
Rb content, determ. using flame spectrophotometry 0-48247
Second sound see Helium/liquid, sound propagation
Secondary electron emission see Electron emission/secondary

Sedimentation

Concentration dependence at theta state 0-39851
Liesegang phenomena, one-dimens, theory 0-74815
photosedimentometer, centrifugal disc type, line start method stability 0 - 39844

salt melts, rel. between diff. and sedimentation 0-46893 saturated sediments, acoustic wave attenuation, mathematical model, analysis 0-53335

sedimentometer, X-ray 0-50263

Sedimentation continued

turbulent water, settling velocities and vertical diffusion, laboratory meas., theoretical model $\,0-50264$ In of Au, centrifugal field, 10^{5} g $\,0-66163$

Seebeck effect see Thermoelectricity Seidel theory see Aberrations, optical Seignette salt see Rochelle salt

Seignettoelectric materials see Ferroelectric materials

Seignettoetectre interest.

Seismic waves

see also Seismology

P, travel times using Joint Epicentre Method 0—48229

acoustic coupling into ionosphere during Kurile Islands earthquake August

11 (1969) 0—66229

amplitude prediction fro future man made lunar impacts
attenuation, physical mechanisms, theoretical and exptal evidence

u-79481 body-wave spectra anal, for earthquake energy determ. 0-56742 chalk, amplitude increase, rel. to granite 0-41467 compressional, in marine sediments, velocities, obs. in situ from research submersible 0-76313 deformation, by thin layers and layered boundaries, plane-wave theory 0-41468

0-41468
discontinuity variations near 600 km, France obs. 0-51472
dispersion of phase velocity in absorbing media in limited frequency range, calculation method 0-51478
dispersion of phase velocity in absorbing media in limited frequency range, calculation method 0-51478
frequency, relation with tidal waves, investigation with quartz accelerometer 0-51484

G-, propagation theories, energy concentration due to low velocity layer 0-69260

0-69260
generation, explosion in heterogeneous media 0-62843
granite, amplitudes, rel. to chalk 0-41467
head waves, in two-dimensional seismic models 0-66225
information on Earth's interior 0-69261
interpretation of Earth's interior, review 0-45110
layered media, surface waves 0-54693
Lg-, propagation theories, low period energy concentration 0-69260
long period, upper mantle investigation by obs., in Europe 0-76308
longitudinal emergence angles in earth's crust and upper mantle, velocity
distrib. 0-62872
Love, explosion generated, source mechanism interpretation 0-45107

Love, explosion generated, source mechanism interpretation 0-45107 Love, long-period, property in medium with layers of varying thickness 0-76314

0-76314

Love, propagation in medium containing a heterogeneous layer 0-66228

Love due to point source in inhomogeneous medium 0-59531

Love wave dispersion for a homogeneous crust overlying continuous mantle with vertical inhomogeneity 0-51488

Love wave dispersion in laterally heterogeneous layer over homogeneous semi-infite medium 0-51489

Love waves propagation across ocean-continent type boundary, finite difference calc. 0-51485

Love waves propagation in anisotropic inhomogeneous n-layered medium 0-51482

0-51482
magnitude determination, correction for focal mechanism 0-76312
microseisms, from storms over deep sea 0-69260
microzoning under conditions of two-layer model for ground 0-62864
nuclear explosions P-wave amplitude decay rate with epicentral distance 1°
to 98° 0-54758
P, plane, multiple reflection by dipping layer 0-66226
P, remote, relative delay time in Iceland 0-66227
PKiKP, upper bound to density jump at boundary of Earth's inner core
0-76315

PS polarized converted recordings for crystal anisotropy study 0-51479 P and S displacement field, dependence on earthquake foci characteristics 0-51477

0-514/1/
P wave amplitudes, long and short period, comparison of least squares analysis 0-514/16
p-, travel time gradient obs. 0-45112
P-type, focal mechanism solutions, comparison with S-wave data

p-, tr. P-type, 1. 0-76311 wave e

P-wave explosively generated, 3 dimens. models, energy coupling 0-69256

0-0230
P-waves, vertical array of triaxial seismometer, data processing results
0-72590
p-waves 1968 tables accuracy, analysis 0-51473

p-waves 1968 tables accuracy, analysis 0–51473
period 10-100 seconds, symmetrical triaxial seismometer 0–62842
prediction from contained and excavation nuclear detonations 0–76317
processing, fan filtration method, analysis 0–62861
pulses, primary, generated by explosions in boreholes, experiments 0–62858
Q-, P-, and S wave velocity depth variation obs., upper mantle and lower crust studies 0–76321 in quarter and three-quarter plane, motion at corners 0–76901 radiation patterns of surface and body waves, eff. on magnitude estimates 0–56740
Rayleigh, dispersion in crust rel to sedimentary thickness and low velocity.

Rayleigh, dispersion in crust, rel. to sedimentary thickness and low velocity channels 0-59530
Rayleigh, explosion generated, source mechanism interpretation 0-45107
Rayleigh, possibility of propag in isotropic orthorhombic material 0-59527

0-59527
Rayleigh in wedge models, photoelastic analysis 0-76309
rays intensities computation, time integration method 0-56737
refracted-diffracted, interpretation, due to dykes 0-62855
refraction records, analysis and interpretation thorough reflection technique, digital processing 0-48227
Rg-, propagation theories, low period energy concentration 0-69260
SV, plane, multiple reflection by dipping layer 0-66226
SV waves in plane layered medium, discrete time soln. 0-69255
S and SKS travel times, arc distances 30° to 126° 0-56738
S to P conversion, base of crust of waves, deep earthquakes, crystal studies 0-59529
S-type, focal mechanism solutions, comparison with P-wave data 0-76311
sea, refractive influence of islands, calc. 0-45129

sea, refractive influence of islands, calc. 0-45129 shear in marine sediments, velocities, obs. in situ from research submersible 0-76313

shell, spherical, inversion of layer matrix 0-54691

Seismic waves continued

silicate minerals, P- and S-wave velocities, relation between Debye temp, and thermal conductivity 0-43911 source depth, determ, using spectral, cepstral and pseudo-autocorrel, anal.

0 - 79480

spectral amplitudes, high and low frequency, earthquake stresses, ridges or trenches 0-59528 structural effects on nuclear power plants, dynamic analysis 0-52078

structural effects on nuclear power plants, dynamic analysis 0–52078 surface, excitation by earthquakes and underground explosions 0–62848 surface, generation from seismic sources 0–48230 surface, resolution at intermediate distances, effects of obs. error 0–76310 surface wave dispersion, inversion of phase and group slowness, dispersion relations 0–54209 surface wave rad, from circular sources 0–56741 surface-wave dispersion computations 0–54692 time signal extraordisting inversettly posed linear problems in Hilbert

surface-wave dispersion computations 0–54692 time-signal extrapolation, incorrectly posed linear problems in Hilbert-space, approx. soln. applic. 0–51481 toroidal free oscillations of earth, factorization method 0–51486 travel times equalization, error influence minimization, soln. 0–59534 velocity distribution rel. to travel time for spherical earth, ray simulation 0–62834

velocity rel. to rock density 0-51487

Seismographs see Seismology

Seismology

see also Geophysical prospecting; Seismic waves for Earth's interior composition, review 0-45110 in USSR, research and observational techniques 0-79479 activity map for S.E. Siberia, rel. to relief, gravitational anomalies 0-59532

activity map for S.E. Siberia, rel. to relief, gravitational anomalies 0–59532
amplitude increase on chalk, rel. to granite 0–41467
amplitude meas, in seismic research at sea, accuracy estimation 0–62865
anisotropy crystal, use of recordings of converted seismic waves 0–51479
Apollo 12 lunar module impact, lab. simulation and possible downrange ballistic effects 0–79722
body waves, as normal leaking modes, pseudo modes and partial derivatives on (+ –) sheet 0–79482
bottom seismographs, explosion study of earths crust 0–79492
brittle fracture initiation under triaxial stress conditions 0–51475
Cagniard seismograms computation and theory 0–48232
conference, Madrid (1969) 0–76296
crust, lower, methods of study 0–76321
crustal layer of seismic velocity 6.9 to 7.6 km/sec under deep oceans 0–62868
data processing, prediction theory application 0–48228
data recordings, s/n enhancement, optimum digital filters 0–41469
depth soundings, isostasy testing 0–66233
dielectric constants determination 0–76339
directivity of seismic radiation, from series of line charges 0–76318
disclocations finite-Volterra-type, P and S waves displacement fields 0–51477
dykes, refracted-diffracted waves, interpretation 0–62855

0-31477 dykes, refracted-diffracted waves, interpretation 0-62855 earth, motion picture 1961 1967 period 0-62853 earth strain in 66 dB range, portable 30 day unattended system for obs.

0 - 76320

o-76323 earth structure, internal, mechanical properties 0-76323 earthquake, 28 March 1970, Gediz (Turkey) 0-66230 earthquake Parkfield, California, 1966, acceleration parallel to fault

0 - 628440-02644 earthquake energy determ, from body-wave spectra anal. 0-56742 earthquake focal mechanism determ, from surface waves 0-48230

earthquake foci characteristics, elastic wave dependence, displacement field study 0-51477

study 0-51477
earthquake prediction and control 0-51470
earthquake prediction and severity reduction by artificial means 0-76316
earthquake prediction or modification 0-79473
earthquake seismogram recordings of converted transmitted waves of PS
type, crystal anisotropy study 0-51479
earthquake sizes measures integrated and frequency-band magnitude
0-62850

earthquakes, source parameter determination, using frequency spectrum of waves 0–66232 earthquakes, source parameter determination, using frequency spectrum of waves 0–66232 earthquakes, strong-motion, evolutionary (time dependent) power spectral density 0–62849 earthquakes above Benioff zones, crustal, symmetry obs. 0–41470 earthquakes and the Chandler wobble 0–79472 earthquakes of various energies, spatial relations, disturbances sizes estimates 0–62860 elastic shock activity during crack growth in brittle materials 0–40392 elastic wave equation on the surface of a homogeneous half-space derived by the Fourier transformation and Green's function use 0–66896 energy efficiency of underground nuclear detonations 0–41466 energy source control via radio link, patent 0–48254 explosions, underwater, dynamite, seismic effects 0–79476 fan filtration method for processing seismic waves, theory, analysis 0–62861 fault displacement and motion rel. to underground nuclear explosions

fault displacement and motion rel. to underground nuclear explosions 0-41465

fault model, kinematic, particle motion 0-56739

France, propag. layer contour discontinuity and signal amplitude variations, correl. 0–48235
France, upper mantle, heterogeneities 0–51471
gross earth data, free period partial derivatives, correlation properties 0–62869

ground motion studies, bilinear Z-transform method recursive relationship 0 - 62846

instrument, symmetrical triaxial seismometer, long period seismometry 0--62842

0-62842 instruments and devices in Japan, development and production 0-59535 interior of earth, lattice thermal conductivity from seismic data 0-43911 large-array, applications of detection and estimation theory 0-45108 Love waves, scattering, surface layer with irregular boundary 0-62847 Love waves in nonuniform waveguides, seismograms, Fourier transform, finite diff. approx. 0-51485 Lunar models travel times, variational parameters and Love Nos. 0-63085 lunar regulith layer seismogram, Apullo, 12 avet, application parameters.

0-53085 Unar regolith layer seismogram, Apollo 12 expt., anelastic parameters values, analysis 0-51740 unar seismogram and anelasticity from Apollo 12 LP, Q-regolith layer model, analysis 0-51741

marine, air guns, seismic signatures 0-66237

Seismology continued

marine, explosive charges as reflection and refraction sources 0–66265 microseism's effect on sea-bottom gradient meter on moving base, testing model 0–51483

model 0-51485 microzoning under conditions of two-layer model for ground 0-62864 moon, Apollo passive seismic experiment 0-76626 Moon, anomalous energy propag, as elastic waves, represented as diffusive process 0-51747

process 0-51747
moon, seismic energy coupling using untamped surface charge 0-488556
moon, seismic energy coupling using untamped surface charge 0-488556
moon, seismic energy coupling using untamped surface charge 0-488556
mootion of fluid sphere, seismograms for distributed force 0-43210
multiply-reflected wave intensity study using seismic profiling, expt.
0-62862
nonlinear elasticity in free oscillations revealed by spectral and bispectral
analysis 0-48233
offshore, surveys, processing of data, for petroleum exploration 0-76319
p-wave travel time gradient obs. rel. to lower mantle structure 0-45112
processor array, iterative synthesis 0-62859
profiling, ocean bottom, continuous configuration hydrophone array
0-45127

0-45127
propagation layer contour discontinuity and signal amplitude variations, correl. 0-48235
prospecting, time-travel curves, of reflected waves, non-Gaussian distrib. of normal components 0-51480
Q-solids, constant, pulse propagation in, predicted pedestal effect 0-79474 radiation fields, elastodynamic, stress relation sources, theoretical study 0-48234

0-48234
random components isolation in observations, models 0-62866
Rayleigh wave radiation from vertical directional charge 0-48236
reflection seismograms, wavelet maps for analysis 0-79478
refraction experiments on Rockall Bank 0-66231
representation theorem using seismic reciprocity, derivation 0-56744
response spectra, digitised seismic acceleration records 0-62852
rotation of Earth, perturbation by major earthquakes and explosions,
spherical theory 0-51457
S to P conversion, base of crust of waves, deep earthquakes, crystal studies 0-59529
seismic data, statistically optimal stacking 0-79477
seismic digital instruments 0-51469
seismic digital processing units 0-51468
seismograms, algorithm for inversion, implications w.r. to field techniques
0-79475

0-79475

signal and noise statistics determination using correlation theory 0-51474 signals comparison for missile impact on earth and lunar module impact on moon, structure differences 0-57099

source depth, determ. using spectral, cepstral and pseudo-autocorrel. anal. 0-79480

0-79480 source dimensions, aftershock sequences, m=4½-6 magnitude 0-62848 spinel, elastic constants, pressure depend. from lattice model 0-40240 steady state response, elastic half space 0-62845 strains, residual, associated with underground nuclear explosion 0-41464 surface wave resolution at intermediate distances, effects of obs. errors 0-76310 tidal dip, weak components obs. 0-45106 tidal to seismic frequency investigations with quartz accelerometer of new geometry 0-51484 triaxial vertical array, data processing results 0-72590 underground nuclear explosions obs., magnitude determination 0-73062 upper bound to density jump at boundary of Earth's inner core, PKiKP waves 0-76315

Wares 0-76515
VIBROSEIS method, continuous sweep 0-66236
velocity spectra, use in stratigraphic and lithologic differentiation, geological models 0-62856

vibratory surface sources coupling with ground, harmonic distortion effect, analysis 0-69257 volcanic glasses and thermal history of rocks, fission track dating 0-45119

wavelet maps, analysis tool for reflection seismograms 0-79478

Selenium

enium amorphous, anomalous photocond., temp. depend., 120-170 K 0-75838 amorphous, atomic motions 0-75380 amorphous, dielectric constant calc. 0-79232 amorphous, elec. cond. rel. to crystallization 0-47628 amorphous, i.r. vibrational analysis 0-66054 amorphous, i.r. active lattice vibs. 0-66052 amorphous, optical absorpt., photocond., transport props. 0-47724 amorphous, optical absorpt., photocond., transport props. 0-47724 amorphous, photocond. and photovoltaic effect, cryst. analogues and short-range order 0-72138 amorphous, piezo-optic props. at 1.15 μ wavelength 0-48023 amorphous, red, and monoclinic, phase transform. 0-75338 amorphous, refr. index nonlinear variation with pressure to 7 kbars 0-59361 amorphous, xeroradiographic properties. X-ray spectra, applied field amorphous, xeroradiographic properties, X-ray spectra, applied field depend. 0-44876

depend. 0—44876
amorphous and liquid, internal defect structure from i.r. microscopy and spectrometry 0—66053
amorphous and polycrystalline layers plasma contact, volt-ampere characteristics investigation 0—53159
amorphous film charging by Auger neutralization of positive ions 0—47045

amorphous insulator, steady state and transient photoemission, energy levels, transport props. 0–47897 amorphous insulator for PbTe i.r. photoconductor multiplier, feasibility 0–51149

0–51149
amorphous semiconductor, optical and elec. props. 0–47721
amorphous thin layers, I-V characts., high field 0–56263
atomic motions in cryst., amorphous and liq. 0–75380
band structure, pseudopotential approach 0–65600
band structure cales. 0–65684
band structure obs. from optical spectra, trigonal 0–66051
charge-transfer state investigation by e.p.r. 0–65696
coating on glass, light transmission 0–44780
conductivity mechanism in monocrystalline Se 0–68827
conference, Montreal, Canada, Oct. 1967 0–65652
crystal, coarseness determination using photoelectric device 0–61621

Selenium continued

crystal growth, perfection and damageability 0-65163

crystal growth, struct., photoconductivity, α - and β -red monoclinic 0-65161

0-65161 crystal growth and morphology, trigonal modifications 0-65160 crystal growth from Se saturated CS₂, α -monoclinic cryst. 0-65143 crystal growth from aq. Na₃S, solubility determ. 0-65142 crystal growth from impurity-doped melts, hexagonal single cryst. 0-65159

0-65159
crystal structure, coordination and thermal motion 0-65278
crystallization, polymeric morphology 0-50425
crystallization mechanism 0-58631
density of α-monoclinic cryst. 0-58943
epitaxial film on Te, morphology and elec. props. 0-65675
epitaxial growth and struct., single-cryst. film 0-65070
etch pit obs. on melt-grown hexagonal crystals 0-65125
film, Br doping determ, by radioactive isotopes 0-68843
film, amorphous, emission- to space-charge-limited photocond. 0-44399
film, local levels, activation energies 0-40704
film on Te, piezoelec, props. 0-68966
films, amorphous, in xerography, effect of charging on light absorpt.

films, amorphous, in xerography, effect of charging on light absorpt. 0--60421

heat capacity and heat of fusion, hexagonal, meas. with differential scanning calorimeter 0-78780 i.r. vibrational analysis, trigonal, α -monoclinic amorphous 0-66054 impurity characterization techniques 0-65695 isoelectronic sequence, oscillator strengths of resonance lines 0-49789 lattice vibrational modes from inelastic neutron scatt., amorphous and liquid state 0-65527 layer, piezoelectric props., effect of texture 0-75812 light beam modulation in trigonal crysts. 0-65977 liquid, atomic motions 0-75380 luminescence, 2-50K 0-66097 optical parameters determ. using dispersion relations 0-54057 phonon spectra calcs. using force constant model 0-65522 photocoll, 235 U coated, neutron irrad., short-circuit currents, e.m.f. 0-51156 photoconductivity, hexagonal single cryst., non-ohmic effects 0-47878

0–51156
photoconductivity, hexagonal single cryst., non-ohmic effects 0–47878
photoconductivity in hexagonal single cryst., non-ohmic effects 0–47878
photoconductivity in hexagonal single cryst., optical quenching 0–53962
photoclectret layers, oriented crystallization, elec. struct. of substrate
surface reproduction 0–71446
photoelectric props. of trigonal single cryst. 0–56395
photoemission yield meas. on amorphous material 0–62476
piezoelectric tensors for textures of co-type 0–75813
positron annihilation ang. distrib., illumination influence 0–62283
Raman spectra, trigonal, α-monoclinic, amorphous 0–66073
rectification mechanism rel. to C4-Se contact behaviour 0–65740
refractive index of amorphous Se, variation with hydrostatic press., obs.
and interpretation 0–48023
semiconductor glasses, elec. conductivity meas. up to 1000°C 0–68828
spherulitic crystallization folded chain lamellae formation 0–50413
switching element, thin-film, capacitance characts. 0–56314
hermodynamic props. of vitreous, liq. and cryst. phases 0–50305
thickness on Ni substrate meas., bremsstrahlung radiation method
0–65055
viscosity rel. to crystallizability of alloys 0–65162

0-65055 viscosity rel. to crystallizability of alloys 0-65162 viscosity rel. to crystallizability of alloys 0-65162 vitreous, crystn., plastic deform. influence 0-53412 vitreous, hole transport temp, depend. 0-78953 vitreous and trigonal, drift mobility, high press. effects 0-47723 in KCl(Br):KSeH crystals, e.s.r. 0-44989 Se:Ag rectifiers, capacitance curves under pulse operation 0-68862 Se:As, electrophotographic and fatigue props., var. with As conc. and temp. 0-75837 Se/As,Se, system, high performance photoconductive target 0-47884 p-Se/n-CdSe heterojunction diodes, vacuum-deposited 0-44301 Se, Se:K(TI), trapping level determ. 0-65685 Ser, e.s.r. h. agCl(Se,Cd), hyperfine interactions 0-44982 "Se diffusion in PbS(Se,Te) 0-55922 "Se diffusion in PbS(Se,Te) 0-55922 "Se diffusion in PbS(Se,Te) 0-65912 viscosity of the proposition of the

Selenium compounds
alloy, vitreous binary, transport props., valency depend. 0—47722
coloured glass, by Cd, S and Se compounds, structure of fundamental
absorption band edged 0—76040
selenate ion, in monodentate selenato complexes, vibrs. 0—55324
double selenates, including Tutton's salts, i.r. spectra, 2000 to 40 cm⁻¹ 0-55321

selenates, spectra, 4000 to 250 cm⁻¹, and structs., high and low temp. forms 0-55322 Ag.Se single crystal phase production by pulse annealing film couples 0-58642

Ag.Se single crystal phase production by pulse annealing film couples 0—58642

As-Sb-Se system, phase relations and liq. struct. 0—50302

As-Se-Sn semiconducting glass, Mossbauer effect, Sn valency comp. depend. 0—48026

As-Se alloy, glass-like, semiconducting, l.f. conductivity 0—65667

Cu-Se-Te, Cu,SeTe phase, investigation by X-ray diffraction and differential thermal analysis 0—71773

M MojSe, where M=Fe, Co, Ni, synthesis and X-ray diffraction patterns 0—58740

Se-Te, Se-Ar alloys, crystallizability rel. to viscous Se viscosity 0—65162

Se-Te alloys, liq. thermal cond. 0—58482

Se, Se-Te mixed cryst., 2-50K 0—66097

Se hexahalide ions, mol. force fields 0—43136

Ses-Cl. and Se₂Br₂ ir. spectra 220-700 cm⁻¹ 0—64449

SeD, rot. const., A-doubling, hyperfine struct. and dipole moment 0—49892

SeF, Hartree-Fock binding energies, ionization potential, electron affinity, dipole and quadrupole moments 0—74304

SeF₆, cryst., struct. and mol. motion m.p. to —160°C 0—50546

SeF₆, negative ion formation 0—64763

SeF₆, Raman spectrum in vapour state 0—58183

SeH rot. const., A-doubling, hyperfine struct. and dipole moment 0—49892

Se₆(HS₂O₇)₇, cryst. struct. 0—65279

Se₄(HS₂O₇)₂, cryst. struct. 0-65279

SeO₂ matrix violated, evidence for slow internal conversion between excited states 0-46512

Section Section 12 Sec

SeOCl₂:SnCl₄,Nd³⁺ laser system, characteristics 0-60221

radiation damage 0-75738

```
Selenium compounds continued
                  SeOF<sub>2</sub>, molecular force field, Se-F stretching force constant 0–49893 SeO<sub>2</sub>F<sub>2</sub>, molecular force field, Se-F stretching force constant 0–49893 Se<sub>x</sub>Te<sub>1-x</sub>Hg, solid solution, crystal growth, morphology and dislocations 0–74988
                    Te-Se alloy, liquid, conductivity switching phenomena in elec. field obs.
                                        78300
                    Te-Se melts, surface tension and density rel. to miscibility and cpd. forma
  tion 0–50210

Te-Se molten alloy, mutual diffusion, 500°C, comp. depend. 0–39765

Self-diffusion see Diffusion in gases, in liquids, in solids
  Semi-insulating materials (high-resistivity semiconductors) see Semiconduct
 Semiconducting devices

Semiconducting devices

See also Counters/semiconductor; Lasers/semiconductor; Masers
alloyed contacts to thick large area devices 0—79002
amplifier, ferromag. semicond., based on polarized transversal wave
0—44269
                    0—42097
avalanche bolometer, heat pulse detection in mag. field 0—42097
book 0—53850
book 0—53854
                  book 0–53854
bulk switching, of Si<sub>3</sub>Ge<sub>4</sub>As<sub>38</sub>Te<sub>55</sub> 0–79004
chalcogenide glass, Si<sub>3</sub>Ge<sub>4</sub>As<sub>38</sub>Te<sub>55</sub>, bulk switching properties 0–79004
chip stripe buried in passivation overlay, nondestructive failure analysis, by
scanning electron microscope 0–47776
component reliability, assessment of environmental screening 0–53864
components attachment to packages, techniques, rel. to hybrid IC, physics
of failure 0–51071
                  of failure 0–51071
contact, anomalous barrier capacitance 0–56310
contact, semiconductor-metal, acoustoelec, interaction 0–53855
contacts and multilayer interconnections fabrication 0–56307
doping by ion implantation 0–78969
energy convertors, solar 0–42166
epitaxial layers, doping profile meas. 0–75649
and fabrication, conference, New Delhi, India, January 1969 0–75652
and fabrication, conference, New Delhi, India, January 1969 0–75650
ferromagnetic piezo-semiconductor amplifier, for nonpolarized transversal wave 0–44268
formation by masking and diffusion, patent 0–51092
fundamental aspects, lecture 0–71894
fundamental aspects, lecture 0–71894
fundamental of electronic devices and circuits, book 0–47978
Ge thermometer, computers fitting of characteristics 0–76946
glass, chalcogenide, film switches, switching behaviour and bulk props. 0–44276
Gunn, shielded-eathode mode 0–44313
                      Gunn, shielded cathode mode 0-44313
Gunn effect oscillator coupled to piezoelectric, elastic wave generation
0-44375
                    Hall effect domain detector 0–42181

IC, electro-optics application, structure, mode of operation and fabrication technique 0–59279
                    IC. plastic encapsulation, reliability evaluation and analysis 0-47770 IC, reliability functional and pin-to-pin screening methods evaluation program 0-51074 IC fabrication, microphotography and photoengraving, techniques 0-57647
                  IC fabrication, microphotography and photoengraving, techniques 0-57647
IC fabrication, oxidation and diffusion technology, theoretical and practical aspects 0-59237
IC masking process and results 0-79003
IC production, step coverage of metal stripes 0-50387
IC reliability, evaluation using test patterns 0-4774
IMPATT, Si, noise, illum. depend. 0-4774
IMPATT, Si, noise, illum. depend. 0-40812
ir. radiation measuring system, patent 0-57444
impurities, feasibility of obtaining general distributions by diffusion 0-72073
impurity diffusion source and method, patent 0-43701
impurity profile plotter 0-65694
integrated circuits, ion implantation mechanism and conditions 0-78970
integrated circuits, in-firm, Si on sapphire substrate 0-56311
integrated electronic systems, book 0-59238
MOS integrated circuits, fabrication, review 0-56339
m.is. structure, impurity of insulation film obs., slow charging of meas. capacitor method 0-75759
m.o.s., voltage thermal instability 0-79024
m.o.s. IC, ion implementation technique application, performance improvement 0-59219
m.o.s.st. structure, umerical method of investigation 0-79026
measurement methods, review 0-68847
                    measurement methods, review 0-68847
measurement methods of nevesugation 0-79020
measurement methods 0-53818
measurement methods and process control 0-56313
measurement methods development 0-44165
measurement methods program 0-44273
metal-SiNi-SiO<sub>2</sub>-Si capacitor structures, charge storage, automatic meas.
                  metallization integrity determination, by scanning electron microscope 0–47775 microelectronic, diffusion and deposition of P in Si rel. to device processing technology 0–65719 microwave, avalanche and transferred electron 0–53852 multilayer, employing ion bombardment 0–60184 neutron hardness assurance, irradiate anneal screening, technique without reliability degradation 0–47777 noise, electrical, review of problems 0–65734 oscillation mechanism 0–47691 p*pn* struct., transient cond., low temp. 0–56309 passivation by polymer films 0–44272 performance, rel. to Al metallization deposition parameters 0–65737 photoconverters, film, based on Si, CdTe, CdS and GaAs 0–65859 photoelectret state in semicond, with p-n junctions 0–56315 photoresistor with neutral contacts, photocurrent amplification 0–53968 photothyristor, multicollector, operating principle 0–56407 physics, models and circuits, book 0–44267 planar, SiO<sub>2</sub> surface, phosphosilicate glass passivation, evaporated metal interconnection, failure analysis 0–47772 plastic-encapsulation, design and evaluation w.r.t. reliability 0–47711 processing, meas, and control of dielectric film properties 0–65735 quality control, use of scanning electron microscope in production line 0–05736 radiation damage 0–75738
                      metallization integrity determination, by scanning electron microscope
```

Semiconducting devices continued radiation damage 0-75714 reliability, IEEE conf., Las Vegas, April (1970) 0-47768 resonator, piezo-semiconductor, based on surface wave 0 selfheating and thermal runaway phenomenon 0-44270 0-44373 selfheating and thermal runaway phenomenon 0-44270 semiconductor device, implantation 0-53853 shift register, 8-bit, charge coupled 0-60132 surface passivation, charge instability mechanisms review 0-47769 switches, glassy, transient behaviour 0-44271 switching, double injection initiation pulse meas. 0-53851 switching device based on glassy CdGeAs, 0-65739 switching element, thin film, capacitance characts. 0-56314 thermistor, NTC, using PbO.PbCrO₄ 0-59239 thermistor thermometer linearity 0-44274 thermistors based on polymers with conjugate double bonds, electrophys. props. 0-75741 thermocouple, non-homogeneous, thermoelec, theory 0-44200 props. 0-13/41 thermocouple, non-homogeneous, thermoelec, theory 0-44390 thermocouple, prod. by simultaneous plastic deform, of Si and Ge-Si alloy 0-43748 thermocouple, prod. by simultaneous plastic deform. of Si and Ge-Si alloy 0-43748
thermoelements, bridging solders for moderate temp. operation 0-51141
thermoelements, electroplating rel. to bridging 0-44394
thin films, epitaxial growth and related processes 0-58579
thin layer, applie. of preferential electrochem. etching 0-65758
thin-film failure modes 0-56312
thyristor, critical turn-on charge 0-53858
thyristor, critical turn-on charge 0-53856
thyristor, multicollector 0-53860
thyristor, n-p-n-p type struct., as control elements in switching devices 0-53861
thyristor, tyristor, n-p-n-p type struct., as control elements in switching devices 0-53861
thyristor, static turn-on current, temp. depend. 0-53857
thyristor, tatic turn-on current, temp. depend. 0-53857
thyristor, turning on by short gate current pulses 0-53859
thyristor, turning on by short gate current rise increase 0-65738
transducer, mechanical response, by Laplace transforms 0-42077
transducer ultrasonic with exponential conductivity-thickness distrib., transformation characts., expression 0-63443
traxial strain-gauge anemometer 0-48262
tunnelling across metal/carbon/metal sandwich 0-79022
u.s. bonded wire interconnections, comparison of 1% Mg-Al and 1% Si-Al 0-51072
vapour pressure sensor 0-47008
wire bonding ultrasonic Al-Sit wire with Al bonding pads and Auralated vapour pressure sensor 0-47008 wire bonding, ultrasonic Al-Si wire with Al bonding pads and Au-plated headers obs., by pull-strength distributions, rel. to reliability testing 0-51073 0-51073
Al-quartz-Ti Pt-Au interconnections fabrication 0-56307
CdGeAs,, glassy, switching device 0-65739
CdS piezo-semicond. amplifier for surface waves, using cond. surface layer 0-40879
GaAs:Si, amphoteric diode, electroluminescence steady state response 0-44946 0-44946
GaAs/Ag-In contact, I-V curves, thermal processing depend. 0-51075
GaAs, parameter effects rel. to bulk domain dynamics 0-44196
GaAs, resistance thermometer for low temp. 0-63488
GaAs double-injection devices, thermally induced oscillations and negative resistance 0-75739
GaAs Gunn oscillators, growth and evaluation of epitaxial layers 0-61647 0-01047 (Ge film thermocouples, p- and n-type, prep. 0-63485 InSb, InSb-NiSb eutectic, microwave emission 0-44240 n-InSb radiation detectors, appl. to submillimeter laser radiation meas. 0-67118 0-07118
Mn-SiO₂-Si, voltage thermal instability 0-79024
PtSi contacts fabrication 0-56307
Se switching element, thin-film, capacitance characts. 0-56314
Si:P, millimetrewave radiation detector with low noise characts. 0-76964
Si-detector diffused small rod shaped for medical applications, spectra
0-46038 0-4038
Si-on-sapphire space-charge-limited thin-film triodes 0-47778
Si, activation analysis in processing 0-65725
Si, annealing of radiation produced defects 0-72075
Si, diffused, donor-type generation-recombination centers 0-75740
Si, epitaxial and diffused, structural faults introduced during fabrication 0-65723
Si sphiration local existation 0-51076 Si, fabrication, local oxidation 0–51076
Si, fabrication, preparation of stabilized surfaces 0–65727
Si, passivation with SiO₂ 0–56308
Si, processing, conference, Gaithersburg (1970) 0–65716
Si, radiation resistant, patent 0–44333
Si depletion layer magnetometer 0–48982
Si integrated circuits, thin-film, on sapphire-substrate 0–56311
Si photothyristor, spectral characts. 0–44277
Si thin layer, applic. of preferential electrochem. etching 0–65758
SiC crystals with improved Cr contacts, patent 0–75761
TI-Te-Ge, bistable system with elect. switching, patent 0–44336
V₂O₄, critical temperature resister, oscillation and switching phenomena 0–51070 Si, fabrication, local oxidation 0-51076 0-51070

diodes
avalanche, GaAs, high-efficiency oscillations, theory
avalanche, I.f. and h.f. mode mechanism 0-72082
avalanche, microplasma noise, low temp. 0-79009
avalanche, miniature, photodetector 0-53964
avalanche, noise characts., review 0-68870
avalanche breakdown control 0-62383
base resistance, total, calc. 0-44290
capacitance, total equiv., depend. on injection level 0-44291
carrier density, longit. mag. field effect 0-79008
carrier lifetime, equilib. conc. and basic range length determ. 0-65745
carrier lifetime meas. by injection-extraction method 0-65733
chalcogenide glass, metal electrodes, I-V characts., switching, memory
0-47803
current filamentation in long diode 0-72081 0-47803 current flamentation in long diode 0-72081 current-voltage characts., hysteresis, optical feedback 0-47793 diode Schottky effect with metal semiconductor contact, physical and electrical parameters relationship 0-69177 electroluminescent, GaAs_{1-x}P_x, electron irrad., defect centres 0-69170 electroluminescent, GaAs, degradation mechanism 0-56644 electroluminescent, GaAs, small-area high-current-density, improved degradation characts. 0-62739

Semiconducting devices continued

```
diodes continued
```

electroluminescent, GaAs, with light-activated negative resistance 0 - 69171

electroluminescent, GaP, anomalous capacitance 0-76192 electroluminescent, GaP red-emitting, recomb. kinetics from photocurrent and decay characts. 0-72458 electroluminescent, minority carrier lifetime determ, method 0-69168

electroluminescent, GaP red-emitting, recomb. kinetics from photocurrent and decay characts. 0-72458
electroluminescent, minority carrier lifetime determ. method 0-69168 emission, spontaneous, amplitude-freq. characts. 0-79388 epitaxy in vapour state, Gunn diodes 0-43594 flicker noise, surface recombination model 0-68872
GaAs, Gunn oscillations temp. depend. 0-65748 gated, neutron irrad, lifetime parameters and I-V characts. 0-44799 glass, chalcogenide, I-V characts. 0-44294 glass, memory and switching 0-44169
Gunn, S-shaped I-V characts. and current pinching 0-56336
Gunn, current filament motion in mag. field 0-79019
Gunn, current filament motion in mag. field 0-79019
Gunn, current filamentation 0-796.8
Gunn, feld-depend. carrier trapping influence 0-65743
Gunn, filed-depend. carrier trapping influence 0-65743
Gunn, microwave cavity spectrometer, design 0-48932
Gunn, microwave cavity spectrometer, design 0-48932
Gunn, microwave oscillations, self- modulation 0-53911
Gunn, space charge wave propagation, one-dimensional approach and its validity 0-47710
Gunn, ultrasound generation 0-65742
Gunn device, heavily doped, I-V characts. 0-68878
Gunn diodes, gamma radiation effects 0-44314
Gunn effect, concentric electrodes, oscillation frequency, domain nucleation 0-56335
Gunn effect, pr.f. shielding 0-59241
Gunn effect, threshold power, theoretical calc. 0-47786
IMPATT, p-n junction resistance 0-10 Mc freq. 0-53891
LSA, axial e.m. modes and self-reson. 0-47792
laser, with Gaussian impurity zones, radiative generation 0-42302 light-emitting, radiation hysteresis 0-44957
luminescent, jr.n. ZnTe-CoBe heterojunction based 0-72469
m.i.m. tunnel diodes, Al-I-Al, Mn-doped, coherence effects 0-72093
magnetodiode, principles and applications 0-44275
memory, using amorphous material 0-53888
microwave backward, InAs 0-44300
microwave physics, book 0-47794
noise sources in transport eqns. assoc. with ambipolar diffusion and Shock-ley-Read recomb. 0-44282
p+3-7-1, long struct., double injection neg. resistance, mag. field effects

p-i-n, base modulation by carrier drift under double injection conditions 0-79010

0-/9010
p-i-n, double injection, I-V characts., breakdown voltage 0-53887
p-i-n, double injection, multivalent trapping centres 0-75711
p-i-n long, with one trapping level, double injection currents 0-44293
p-n junction, I-V characts., mag, field effects 0-44299
photodiode, Ge, planar p-n junction, for microwave modulation freqs.

0–68984
photodiode, avalanche, multiplication factor optimization 0–65858
photodiode detectors automatic linearity testing, device 0–68871
probe method using light-shadow boundary scanning 0–47787
pulsed p-i-n, appl. to X-band permittivity meas. of lossy liqs. 0–50246
Read, avalanche, multifrequency operation, nonlinear analysis 0–47790
Read, minority carrier storage and oscillation efficiency 0–72084
Read, saturation current and large-signal operation 0–72083
Read avalanche oscillator, effects of load conductance on operation
0–44292

0-44292
recombination radiation, conversion efficiency, thermodynamics 0-41257
S-type, photoelec. processes 0-79069
Schottky, physical fundamentals for characteristics calc. 0-75749
Schottky barrier, C-V relationship, impurity level distrib. 0-47791
Schottky barrier, h.f. shot noise 0-68873
Schottky barrier, metal-GaAs, elec. props. 0-65747
Schottky barrier, metal-Silicide, reverse IV characts. 0-62388
Schottky barriers, review of physics 0-56316
Schottky barriers, review of physics 0-56316
Schottky barriers on n-GaP, deep centres effect 0-65746
semiconductor-electrode boundary, tunneling forced by temp. gradient 0-68874

space-charge limited, thermal noise, Langevin's equation 0-51081

space-charge limited, thermal noise, Langevin's equation 0–51081 surface-barrier, 1.f. noise 0–53890 switching, using Ge-As-Te system glasses 0–78938 thermometer, low temp 30-300°K 0–76947 tunnel, GaSb, diffused p-n, elec. field temp. depend. 0–56331 tunnel, InP, IV characts., current density 0–53901 tunnel, heterojunction, IV charact. 0–53900 tunnel, with heterojunction, field obs. 0–53899 tunnel transitions, trap-assisted, temp. effect 0–53898 voltage-current characts., thin heterogeneous base 0–51080 whisker, in ir. laser beam, improved coupling using antenna theory 0–56323

Zener, as hydrostatic press. transducer 0–59240
Au-Nio-ZnO-In film structure, I-V curves, rectifying behaviour 0–75752
Au-ZnO-In(Ag) film structure, I-V curves, rectifying behaviour 0–75752
Cs current, influence of transverse mag. field, results 0–53886
(Ga,Al)As, light emitting, Zn-Te compensated, with negative resistance 0–72459

GaAs:Cr struct., noise props. 0-79011
GaAs:Ge, radiative recomb. 0-54136
GaAs:Si, amphoteric diodes, transient response 0-41287
p-GaAs:Si, long lifetime (laser) states 0-48119
GaAs:Si, S-type IV characts. 0-56325
GaAs, avalanche, photodiodes, noise meas. 0-79012
GaAs, avalanche photodiodes, noise meas. 0-79012
GaAs, diodes, integrated array 0-79013
GaAs, electroluminesc., small-area high-current-density improved degradation characts. 0-62739
GaAs, electroluminesc., with light-activated negative resistance
GaAs, electroluminescent, degradation mechanism 0-56644
GaAs, epitaxial, electroluminesc., y-irrad. effects 0-51371
GaAs, infrared radiation for distance measurement 0-51083

Semiconducting devices continued

diodes continued

GaAs, p-n junction, temperature dependence of power output 0-44297

GaAs, p-n tunnel junctions, I-V characts., neutron irrad. effects 0-53892 GaAs, pulse, electron irrad. influence on parameters 0-56326

GaAs duplex diodes polarizable junction exhibiting duplex or multiplex de current-voltage characteristics 0-75751

GaAs illuminators with high average power 0-52382

n,p-GaAs luminescent diode, patent 0-54142

GaAs Schottky barrier, fabrication by fluxed wetting of Sn, In and In-Zn alloy, and characts. 0-44296

GaAs_{1-x}P_x, electroluminesc. GaAs_{1-x}P_x, electron irrad., defect centres 0-69170 GaP(:Zn,Te), electroluminescence, rel. to radiative recombination kinetics

GaP(:2.n,1e), electrolumnescence, ref. to radiative recombination kinetics 0-4484 n-GaP-metal Schottky barriers, deep centres effect 0-65746 GaP, electroluminescent, anomalous capacitance 0-76192 GaP, red-emitting, liq. phase epitaxy fabricated, high quantum efficiency 0-54132

GaP, red-emitting, photo- and electroluminesc. time decay correl. 0-62740GaP red-emitting, recomb. kinetics from photocurrent and decay characts. 0-72458

0—72458
GaSb, tunnel, diffused p-n, elec. field temp. depend. 0—56331
GaSb tunnel diode electromechanical, transducer, miniature, theory, fabrication and performance 0—44295
Ge:Au, double injection, potential vis. distance, prebreakdown square law region 0—40811
Ge, depletion layer capacitance, mag. field effects <12 kOe 0—44298
Ge, phonon-assisted tunnelling, obs. of differential conductance 0—56293
Ge p-n junction, I-V characts, mag. field effects 0—44299
Ge photodiode, planar p-n junction, for microwave modulation freqs. 0—68984

0—68984
Ge photodiode with extended long-wavelength response 0—65749
InAs microwave backward diodes 0—44300
InP-GaAs solid solns, IV characts. 0—53893
InP, tunnel, IV characts., current density 0—53901
Pb_xSe_{1-x}, stimulated recomb, radiation 0—79356
PbTe, from epitaxial layers, fabrication, characterization 0—61656

Pb,Se_{1-x}, stimulated recomb. radiation '0-79356
PbTe, from epitaxial layers, fabrication, characterization 0-61656
p-Se/n-CdSe thin-film heterojunction, vacuum-deposited 0-44301
Si:Au, current filaments 0-53894
Si:Au, long, IV charact. temp. depend. 0-56328
Si:Ni, P, magnetodiode, I-V characts. 0-47795
Si:Zn(Cd) with negative resistance, transient characts. 0-65750
p-Si/Al surface-barrier, field- induced photoelectron emission, energy distrib. 0-44421
p-Si/Al surface barrier, field- induced photoelectron emission 0-44420
n-Si:Ni, Schottky barrier, Si surface conditions influence 0-72085
Si, array targets for TV tube, n* layer effect on gain 0-79014
Si, avalanche, switched on microplasma growth 0-47779
Si, Cd-compensated, long, transient processes 0-56329
Si, depletion layer capacitance, mag. field effects <12 kOe 0-44298
Si, forward-biased p-n_t-n IV characts. 0-53895
Si, IMPATT, noise, illum. depend. 0-40812
Si, prep. by alloying Al to n-type, props. 0-62389
Si, thin slices, fabrication 0-56324
Si, X-irrad. effect on IV and CV characts. 0-53896
Si avalanche, high efficiency microwave oscillations, design and performance, TRAPATT approach 0-47788
Si epitaxial on low Al-rich spinel, vertical junction device characts. 0-62395
Si p-n junction, I-V characts., mag. field effects 0-44299
Si vidicon, electrometer for current meas. in 10-16 to 10-15 A range 0-73122.
SiC, negative-resistance 0-72086

0-7312 SiC, negative-resistance 0-72086 Ti-Si Schottky barrier, fabrication and props. 0-44302 n-ZnSe, avalanche breakdown and light emission at low-angle boundaries 0-44209

ZnTe-CdSe p-n heterojunction based luminescent diode 0-72469

ZnTe-CdSe p-n heterojunction based luminescent diode 0—72469
junctions
avalanching p+nn+, with carrier trapping, temp. coeffs. 0—53867
doping and junction formation, review 0—59220
e.m. wave generator-detector, patent 0—52172
electroluminescent, diffused GaP p-n 0—66109
electroluminescent, polarization of recomb. radiation 0—79382
ferroelectrics, low temp., p-n junctions and p and n regions study by frost
method 0—40855
high-low, operation and radiation damage, math. simulation 0—47782
m.o.s., photoelec. emission, Si band struct. obs. 0—44257
n'-n-p struct. with deep levels, capacitance characts. 0—53871
noise, 1f. variance 0—53868
noise sources in transport egns. assoc. with ambipolar diffusion and Shockley-Read recomb. 0—44282
p-i-n Si structure, double-carrier injection, recombination oscillations
0—53879
p-n, Ag-PbO-SnO₂, thermally stimulated current, trapping levels 0—40809

p-i-n Si structure, double-carrier injection, recombination oscillations 0-53879
p-n, Ag-PbO-SnO₂, thermally stimulated current, trapping levels 0-40809
p-n, Ge, plastic deform, and Ga diffusion 0-53876
p-n, Sior Ge, I-V characts, p-irrad, and press. depend. 0-44286
p-n, asymmetrical, inversion layers 0-53869
p-n, avalanche breakdown, mechanisms 0-56317
p-n, book 0-53854
p-n, doping profile meas. 0-75742
p-n, electric and magnetic field, influence 0-44281
p-n, electric and magnetic field, influence 0-44281
p-n, februation by diffusion, donor-acceptor pair form, and space charge influence 0-68864
p-n, formation by ion beam bombardment 0-68667
p-n, heavily-doped, tunnelling probability cales. 0-75743
p-n, microwave admittance, breakdown nature influence 0-69086
p-n, pressure transducer, feasibility 0-47783
p-n, space-charge field, electron transport, Boltzmann equation 0-47784
p-n, thin-base, thermal equil. 0-72077
p-n, under electron beam bombardment, carrier profiles and collection efficiency 0-44280
p-n, under steady-state conditions 0-79005
p-n abrupt, capacitance, freq. depend. 0-44279

Semiconducting devices continued junctions continued

formation by successive double diffusion of impurities, p-n hyperabrupt, patent 0-44334

p-n-n $^+$ struct, at high injection levels, differential resistance and diffusion capacitance 0-53870

p-n-p-n struct., static IV charact. in on-state 0-53889

p-n-p-n struct, state 1V characts, in on-state 0-3369 p-n-p-n structures, 1-V characts, temp, depend, turn-on and turn-off currents 0-47780 passivated, manufacture, glass former diffusion, patent 0-44335 passivation by \$i_1N_4 layer deposition 0-75745 photoelectret state in semicond, with p-n junctions 0-56315

photovoltaic effect induced by two-photon excitation in p-n device 0-56400

Schottky, GaAs, zero-bias tunnelling struct., temp. and bias depend. 0-68863

Schottky barriers, n-Ge, one-electron and phonon-assisted tunnelling 0-44285

0-44285 steady-state junction- current distribs. in resistive films, nonlinear eqns. solns. 0-65744 surface-barrier, GaAs, Tamm states role in form. 0-56319 surface-barrier p-n, in high-resistivity CdTe 0-56379 thyristor, minority carrier density, recombination radiation intensity 0-44278

0-44278
tunnel, InP, p-n, elec. props. temp. depend. 0-56332
tunnel junction, phonon and plasmon interactions 0-79016
tunnelling spectroscopy in ferromag. semiconductors 0-59214
Ag-PbO-SnO₂, p-n, thermally stimulated current, trapping levels 0-40809
Al-Si Schottky barriers, LSI arrays reliability 0-47785
Al₂Ga_{1-x}As-GaAs, heterojunction, electroluminescence 0-41286
Al₃Ga_{1-x}As-GaAs heterojunctions, band model and injection luminesc.

 $Al_xGa_{1-x}As$ h.v. p-n, electron probe recording current method obs. 0-75744

 $Al_xGa_{1-x}As$ heterojunction structure, optoelectronic cold cathode 0-44416

As: Te₃ and Ge, Si and InSb single crystals, rectifying props. of junctions 0-62387

BiSb-Al₂O₃-BiSb symmetric thin film, tunnelling characts, at low temp.

o-08865 CdTe, high-resistivity, surface-barrier p-n, props. 0-56379 CdTe surface-barrier, photomemory 0-56318

Cu₂S-CdS heterojunction impurity profile, red, blue light, energy band-diagram 0-44283
Cu₂S-CdS heterojunctions, heat treatment rel. to photovoltaic effects 0-75843

0—75843
Cu,S-CdS heterojunctions, photovoltaic props. 0—65855
EuS:Eu/In junctions, tunnelling spectroscopy 0—59214
GaAs:Zn, polarization of recomb. radiation 0—79382
GaAs-Ge heterojunctions, fabrication and props. 0—44284
GaAs-In_xGa_{1-x}As p-n heterojunctions, photosensitivity spectra and electroluminese. 0—56387
GaAs-ZnSe heterojunctions, fabrication and props. 0—44284
GaAs, diffused p-n, recomb. radiation intensity and voltage drop distrib.

0-54133
GaAs, p-n, electroluminesc. and cathodoluminesc. 0-54135
GaAs, p-n, low-energy recomb. radiation 0-54134
GaAs, p-n, low-energy recomb. radiation 0-54134
GaAs, Schottky, zero-bias tunnelling struct., temp. and bias depend. 0-68863
GaAs electroluminesc. and photoluminesc., density of-states tails role 0-72420
GaAs h.v. p-n, electron probe recording current method obs. 0-75744
GaAs n*1-n* step junctions, anomalous layers interpret. 0-68866
GaAs p-n, epitaxial, prod. in closed iodine system, I conc. depend 0-53873
GaAs surface-barrier. Tamm states role in form. 0-56310

GaAs surface-barrier, Tamm states role in form. 0–56319
GaAs_{xr}P_{1-x}, liquid epitaxial growth, parameters, electroluminescence 0–43549

0-43549

GaP-GaAs diffused heterojunctions, conc. profiles, microprobe analysis 0-53874

GaP, n-on-p, doping profile meas. 0-75742

GaP, p-n, diffused, green and red electroluminesc. 0-66109

GaP, p-n, electroluminescent, high efficiency, prep., patent 0-48130

GaP, p-n, impurity level positions thermally stimulated current obs. 0-53875

GaP, p-n, impurity photo-e.m.f. 0-56408

Ge-GaAs epitaxial heterojunction, liquid phase deposition, I-V characts. 0-56321

α-Ge-GaAs heterojunctions, IV characts., pot. barrier 0-53877

Ge-Si n-n heterojunctions, IV characts, pot. barrier 0-53877 Ge-Si n-n heterojunctions, fabrication method influence on elec. characts. 0-56320

6-5320
 6e-Si p-n heterojunctions, tunnel transitions, trap-assisted, temp. effect
 0-53898
 6e, p-n, I-V characts., γ-irrad. and press. depend.
 0-44286
 6e γ spectrometer, working parameters, impurity compensation technology of securing drift of Li in Ge, preparing crystals, vacuum chamber construction
 0-38744

n-Ge Schottky barriers, one-electron and phonon-assisted tunnelling 0-44285

0—44285
InAs, diffused p-n, I-V characts. 0—53878
InAs, diffused p-n, fabrication, elec. and photoelec. props. 0—62385
InP-InAs diffused heterojunctions, conc. profiles, microprobe analysis 0—53874
InP, tunnel, p-n, elec. props. temp. depend. 0—56332
p-n, double diffused, doping profile determination 0—65741
Si-Ge ISO-type heterojunctions, characts., mechanism 0—51078
Si-SnO₂ heterojunctions, elec. and optical props. 0—72080
Si-SnO₂ heterojunctions, props. of controlled structures 0—75746
Si, diffused p-n, ioniz. rates meas. 0—44287
p+ph*-Si, forward-biased structures, cond., low temp. characts. 0—79007
Si, p-i-n structures, double-carrier injection, recombination oscillations 0—53879
Si, p-n, avalanche and tunnel breakdown, recomb. radiation characts.

Si, p-n, avalanche and tunnel breakdown, recomb. radiation characts. 0-54139

0-34139 Si, p-n, breakdown voltage depend. on surface pot. 0-53880 Si, p-n, deep diffused, surface breakdown time characts. 0-7: Si, p-n, I-V characts., y-irrad. and press depend. 0-44286 Si, p-n, impurity interaction I-V characts. 0-40805 0-72079

Semiconducting devices continued

junctions continued

junctions continued

Si, p-n, nonuniform deform. influence on current 0-53881

Si, p-n, nonuniform deform. influence on sensitivity 0-53882

Si, p-n, tunnel breakdown, radiation power 0-53884

Si, p⁺π tunnel breakdown, radiation power 0-53884

Si, p⁺π struct., long, double injection temp. depend. 0-62386

Si p-n, channel currents on surface 0-40810

Si p-n, low voltage, isothermal I-V characts. of mesoplasma 0-51077

Si p-n, microplasma light emission characts., temp. effects 0-51349

Si p-n, nuclear radiation effects 0-51079

Si p-n, siO₂ precipitates influence on I-V characts. 0-56327

SiC-Al, diffused and epitaxial p-n, elec. and luminesc. props. 0-53885

p-SiC-Be, alloyed p-n, electroluminesc. 0-54138

SiC-CdS p-n, IV characts., features 0-75477

SiC, diffused p-n, electroluminescence, current-brightness characts. 0-41288

SiC, elec. fluctuations 0-53883

SiC, elec. fluctuations 0-53883

SiC, etc. nuctuations 0-53883 SiC p-n, reverse biased, use as ionization gauge e source 0-57212 SiC p-n, tunnel breakdown 0-56322 Tl₂Se and Ge, Si and InSb single crystals, rectifying props. of junctions 0-62387

0-62387

ZnS-GaAs heterojunctions, photoconductivity spectral distrib. and photoelectroluminescence spectrum 0-51351

ZnSe-Ge heterojunctions, switching and meory 0-68867

ZnSe-Ge heterojunctions, fabrication and props. 0-44284

ZnSe-ZnTe heterojunctions, interface obs. 0-79383

ZnSe on Ge heterojunction, prep. by epitaxial deposition, elec. characts.

2nde of General States of the Column States of Column Sta

transistors

bipolar, avalanche breakdown characts, rel. to high current densites 0-56333

bipolar, base width modulation and Early effect 0-53903 bipolar, degradation phenomena under ionizing radiation, theoretical model 0-47800

model 0-47800 bipolar, h_p, degradation mechanisms and their characteristics 0-47801 bipolar IC, self-isolated transistor structures 0-68875 degradation, avalanche, of h_pe 0-72090 diffused junction, statistical approach to design and fabrication 0-65755 dislocations effect, diffusion-induced emitter edge 0-44225 diffi. flux-method calc. of characts. 0-53908 electrometers, d.c. logarithmic, for low-current meas. 0-63530 feet, ref. to counting circuits, charge amplifeation, without charge leaf

electrometers, d.c. logarithmic, for low-current meas. 0–63530 f.e.t., rel. to counting circuits, charge amplification without charge leak resistor 0–60635 f.e.t., in overload recovery cct. for charge amp. 0–63915 f.e.t., theory and applications, book 0–47799 f.e.t. readout, rel. to wire spark chamber spectrometer with capacitor memory 0–60644 fabrication technique, patent 0–40816 field effect, Schottky-barrier, dynamic performance 0–53904 formation by masking and diffusion, patent 0–44332 formation using diffusion process, patent 0–44331 h.f. behaviour, lateral zone influence 0–44309 heterojunction, cut-off frequency 0–44307 i.g.f.e.t., channel thickness definition and shape 0–65760 impurity concentration profile in heterojunction 0–44307 j.f.e.t., ceramic encapsulated, noise studies 0–65752 j.f.e.t. amplifiers, nuclear pulse, methods of reducing noise 0–63914 junction f.e.t., theory, linear and switching circuit, applications and LSI 0–59243 junction transistors, prediction of rise-time using charge control equation 0–53905

0 - 53905

junction triode, use in linear scale ohmmeter 0-76977 m.i.s., characts. 0-53907

m.i.s. f.e.t., theory, linear and switching circuit, applications and LSI $0\!-\!59243$

m.i.s.t., current-multiplication 0-53906
m.i.s.t., current-multiplication 0-53906
m.i.s.t., carrent-multiplication 0-53906
m.i.s.t., carrent-multiplication 0-65754
m.n.o.s., characteristics and applications 0-65754
m.n.o.s. memory, direct-tunnelling mode, effect of SiO₂ thickness variation (15 to 30Å) on charge storage 0-51085
m.o.s., ionising radiation degradation mechanism and its validity 0-47808
m.o.s., time instabilities, disymmetric behaviour 0-44305
m.o.s.t., degradation phenomena under ionizing radiation, theoretical model 0-47800
m.o.s.f.e.t., Si:Au, generation-recomb. noise and thermal emission rates at acceptor centre 0-68877
m.o.s.f.e.t., carrier distrib. and inversion layer thickness, quantum mech. calc. 0-68876
m.o.s.f.e.t., drift velocity saturation 0-44327
m.o.s.f.e.t., small-signal-pulsed field effect obs. of Au impurities in Si 0-72068
m.o.s.t., Si, l.f. noise, theory 0-44312

0-72068
m.o.s.t., Si, I.f. noise, theory 0-44312
m.o.s.t., Si determination of interface-state density and mobility ratio in surface inversion layers 0-72097
m.o.s.t., epitaxial Si on low Al-rich spinel 0-62395
m.o.s.t., instability due to hot electron and hole injection into gate oxide 0-72091
m.o.s.t., I.f. noise geom. depend. 0-56334
m.o.s.t., pre-irrad, high temp. stability 0-62390
m.o.s.t. structure, numerical method of investigation 0-79026
microwave, bipolar, characterization 0-44308
preavalanche region, weak collector current characts. 0-53902
pressure-sensitive, collector and base current depend. on mech. stress 0-53909
Schottky-barrier, field effect, dynamic performance 0-53904

0-33909
Schottky-barrier, field effect, dynamic performance 0-53904
structure, patent 0-75762
thin-film, theory and circuit techniques, textbook 0-51084
Au gettering rel. to P diffusion and influence on parameters 0-72087
CdSe, polycrystalline, unit conductivity model 0-62343
CdSe f.e.t. piezoelectric effect, application to ultrasonic transducer
0-44310

CdSe fe.t. piezoelectric effect, application to ultrasonic transducer 0-44310
GaAs junction FET, neutron irrad., degradation of props. 0-47798
GaAs junction f.e.t., I-V characts. in hot electron range 0-72088
GaAs structures, correlation of emission and electrical properties 0-75754

Si:Au m.o.s.f.e.t., generation-recomb. noise and thermal emission rates at acceptor centre 0-68877 n-p-n-Si, anomalous diffusion, emitter dip effect, dislocations 0-75755

Semiconducting devices continued

transistors continued

Si, bipolar, application to functional electronic blocks, aspects of design 0-59242

Si, double diffused, mobility influence on carrier distrib. in base 0-53910 Si, neutron irradiation effects on second breakdown and thermal behaviour 0-44311

Si m.o.s.t., determination of interface-state density and mobility ratio in surface inversion layers 0–72097
Si m.o.s.t., 1f. noise, theory 0–44312

Si microwave, from ion implantation 0-62391

SnO₂ thin film 0--65751

TiO₂ gate insulator for m.o.s.t. 0-62397 n-ZnSe-p-Ge- n-Ge, current gain, doping depend., optical props. 0-44289

tunnel and interface devices

barrier, potential trapezoidal, tunnelling conductance, asymmetry 0-44323

0-44323
barrier energy determ, from photoinjected currents voltage depend.
0-47806
capacitor, Al-Al₂O₃-Al, base influence on stability 0-59274
capacitor m.o.s., deeply depleted 0-44328
colloquium, Ilmenau, Germany, (1970) 0-79000
diodes, negative diffusion capacitance 0-53897

i.g. f.e.t., single-layer, gamma-irradiation, thermal activation obs. techniques, rel. to stability invest., comparison with doubly insulated gate 0-47802

mi.m., Al-Al₂O₃-Au, film system, photocurrent spectra, pot. barrier 0-44324

0-44324 mi.m., Al-Al₂O₃-Au struct., IV characts. rel. to gas atmosphere 0-53914 mi.m., Au-MgO-Au, IV characts. for cond. through oxide film 0-62393 mi.m., metal-ferroelectric-metal, space-charge-limited currents 0-44319 mi.m. tunneling currents, E-k relation 0-72005 mi.m. capacitor, silicon oxynitride dielectric, props. vel. to reactive sputtering prep. 0-53932 mi.m. cermet struct. form. by ion bombardment 0-44320 mi.m. struct., Al-Al₂O₃-Al, tunnel current, for non-uniform dielec. layer thickness 0-44325 mi.m. struct., cortect limited currents. 0-65359

thickness 0-44325
mi.m. struct., contact-limited currents 0-65759
mi.m. struct., transport coeff. for oxide layer 0-44318
mi.m. struct. transport coeff. for oxide layer 0-44317
mi.m. systems, and mechanism oxide evap. mode influence 0-51087
mi.m. thin film structure, resonance tunnel current 0-44321
mi.m. tunnel diodes, Al-1-Al, Mn-doped, coherence effects 0-72093
mi.m. tunnel diodes, inelastic tunnelling due to vibr. modes 0-75758
mi.s., Al-Si₂N₄-Si₃, C-V and I-V characts, hysteresis 0-44326
mi.s., two-layer structures (Al₂O₃ or Si₂N₄ on SiO₂), bias instability 0-47807
mi.s. capacitor, metal-Al₂O₃-Si parameters 0-75760

m.is. capacitor, metal-Al₂O₃-Si parameters 0-75760 m.is. capacitor, pulsed, transient response 0-72094 m.is. devices, electronic instabilities 0-47805 m.is. electroluminescent diode in ZnTe, red and green spectral output 0-54140

m.i.s. electroluminescent diodes, photodetection applic. 0-40814 m.i.s. struct., barrier energy determ. from photoinjected currents voltage depend. 0-47806

m.i.s. struct., surface recomb. vel. determ. from transient response 0-62394

m.i.s. structure, capacitor, photo-e.m.f., carrier generation distrib. 0-47804

nis. structures and C-V meas. technique 0-75721
mis. transistors, characts. 0-53907
mis. tunnel junctions, electron local-mode phonon interaction 0-79025
mis.t, urrent-multiplication 0-53906
mis.t, urrent-multiplication 0-63906
mis.t, near saturation, drainfield and source to drain resistance 0-44306 n.o.m. systems, electron conductance control by mobile impurities 0-44322

mo.m. systems, electron conductance control by mobile impurities 0-44322 m.o.s., Al₂O₃ film characts, rel. to prep. by AlCl₃ hydrolysis 0-59247 m.o.s., Al-Al₂O₃-Bi_{1-x}Sb_x, cond. anomaly, zero-bias, 4.2-1.8 K, 10 katm. press. 0-47813 m.o.s., Al-SiO₂-Ge, negative surface charge after annealing 0-72096 m.o.s., Si gate, room temperature threshold shift obs. 0-51091 m.o.s., ionising radiation degradation mechanism and its validity 0-47808 m.o.s. and bipolar integrated circuits, effect of insulator surface-ion migration, review 0-47812 m.o.s. capacitor, Si/SiO₂, thermally stimulated charge release, interface states obs. 0-47809 m.o.s. capacitor, Si/SiO₂, thermally stimulated charge release, interface states obs. 0-47809 m.o.s. capacitor, pulsed, for bulk and surface components of lifetime separation 0-44224 m.o.s. junction, photoelec. emission, Si band struct. obs. 0-44257 m.o.s. struct., Ag SiO₂-SiC (P-type) I-V characts, temp. depend. 0-40815 m.o.s. struct., Ag SiO₂-SiC (P-type) I-V characts, temp. depend. 0-40815 m.o.s. struct., Ag SiO₂-SiC (P-type) I-V characts, temp. depend. 0-40815 m.o.s. struct., Mo film for partial diffusion masking, applic. to device

Mo.s. struct., Mo film for partial diffusion masking, applic. to device processing 0–79027 m.o.s. struct., Pt influence at Si-SiO₂ interface 0–62396 m.o.s. struct., Si, ion implantation of O+ and Ne⁺, surface characts.

m.o.s. struct., SiO₂ pyrolytic films obs. 0–56340 m.o.s. struct., SnO₂-semiconductor heterojunction 0–75748 m.o.s. struct., avalanche injection of electrons into insulating SiO₂ 0–56338

m.o.s. struct., irrad., interface barrier energies, photoemission obs. 0-59245

0—59245
m.o.s. structure, InSb based, image converter possibilities
0—51088
m.o.s. structure, SiO₇ film deposited by r.f. glow discharge
0—51090
m.o.s. structures, Al₂O₇ on Si-Si, exp. obs. 0—72095
m.o.s. structures, r.d. to surface study of anodized InSb 0—47746
m.o.s. transistors, time instabilities, disymmetric behaviour
0—44305
m.o.s.f.e.t, passivation by polymer films
0—44272
m.o.s.f.e.t, Si.Au, generation-recomb. noise and thermal emission rates at acceptor centre
0—68877
m.o.s.f.e.t, carrier distrib. and inversion layer thickness, quantum mech. calc. 0—68876

Semiconducting devices continued

tunnel and interface devices continued

m.o.s.f.e.t. small-signal-pulsed field effect obs. of Au impurities in Si $0\!-\!72068$

m.o.s.t., Si, l.f. noise, theory 0-44312 m.o.s.t., epitaxial Si on low Al-rich spinel 0-62395

m.o.s.t., instability due to hot electron and hole injection into gate oxide 0-72091

m.o.s.t., lf. noise geom. depend. 0–56334 m.o.s.t., pre-irrad., high temp. stability 0–62390 metal contact to semiconductor, u.s. welding, apparatus description 0–53636

0—40813 metal-semiconductor interface, elementary excitations 0—40813 metal-ferroelectric-metal, space-charge-limited currents 0—44319 metal-semiconductor barriers, carrier transport 0—53912 metal semiconductor junctions, tunneling models, review 0—56330 microwave physics, book 0—47794

microwave physics, book 0–4/194 radiacmeter for dose rate meas, using m.o.s. field effect transistor electrometer 0–49396 rectifying contact, Al-CdS-Al, negative resistance under unidirectional voltage pulse excitation 0–59244 semiconductor- dielectric-semiconductor film system, pair correl, of electrons and holes 0–53913

superconducting tunnel junction, phonon emission by quasiparticle decay 0-44147 switching device based on charge-controlled double injection 0-44330

switching device based on charge-controlled double injection 0–44330 tunnel diode, GaSb, diffused p-n, elec. field temp. depend. 0–56331 tunnel diode, I-V characts. Fermi level depend. 0–44303 tunnel diode, I-V characts. Fermi level depend. 0–4303 tunnel diode, heterojunction, IV charact. 0–53900 tunnel diode, heterojunction, field obs. 0–53890 tunnel diodes, bentoresponse at 6328 Å, obs. 0–59290 tunnel diodes, tunneling meas., conductance bridge 0–75753 tunnel junction, InP, p-n, elec. props. temp. depend. 0–56332 tunnel junction, phonon and plasmon interactions 0–79016 tunnel transitions, trap-assisted, temp. effect 0–53898 tunnel-diode binary counter to 20 MHz 0–45742 tunneling between two one-dimens. periodic potentials, WKB theory generalization 0–79021 tunnelling in Cr-Cr₂O₂-metal junctions 0–78910 tunnelling, spin-flip, Ni electrodes. rel. to conductance-voltage charact. 0–75469

Ag-SiO₂-SiC m.o.s. struct., (P-type), I-V characts., temp. depend. 0-40815

0-4013
Al-Al₂O₃-Al capacitor, base influence on stability 0-59274
Al-Al₂O₃-Al struct., tunnel current, for non-uniform dielec, layer thickness
0-44325

0-44325

Al-Al₂O₃-Au film system, photocurrent spectra, pot. barrier 0-44324

Al-Al₂O₃-Au struct., attenuation depth of electrons in Al and Au 0-51157

Al-Al₂O₃-Au struct., IV characts. rel. to gas atmosphere 0-53914

Al-Al₂O₃-Bu, <u>sb</u>, tunnel structure, anomalous cond., zero bias, 4.2-1.8 K, 10 katm. press. 0-47813

Al-CdS-Al structure, negative resistance, under unidirectional voltage pulse excitation 0-59244

Al-CeO₂-Al system, permittivity, loss tangent and elec. strength 0-51103

Al-Si₃N₄Si, mis. structure, C-V and I-V characts, hysteresis 0-44326

Al-SiO₂-Al struct., IV characts, charge in dielec. influence 0-56337

Al-SiO₂-Si system, model rel. to m.o.s. processes 0-65761

Al₂O₃-SiO₂ double layer struct., electron-gun evap., Na migration 0-44341

O-44341
Al₂O₃ layer, electron-gun evap., Na migration 0-44341
Al₂O₃ on Si-Si, m.o.s. structure, exp. obs. 0-72095
Au MgO-Au, IV characts. for cond. through oxide film 0-62393
Au-SiO-Al cold cathode, hot-electron emission, coherent scatt. 0-53971
Au-SiO,GaAs electroluminescent diodes, photodetection applic. 0-40814
CdS-metal, tunnelling mechanism 0-56330
CdS-metal junctions, phonon tunnelling and e-collective excitation interactions 0-56330
CT-Cr₂O₂-metal tunnel diodes, inelastic tunnelling due to vibr. modes 0-75758
GaAs metal junctions plasmon tunneling and e-collective excitation interac-

GaAs metal junctions plasmon tunneling and e-collective excitation interactions 0-56330

tions U=36330
GaSb tunnel diode, diffused p-n, elec. field temp. depend. 0=56331
GaSb tunnel diode, I-V characts., 10, 80 or 300K, band structure
0=47796
n-Ge/BaTiO₃ structure, surface conductivity 0=44316
Ge-SiO₂ interface, C-V characts. freq. and temp. depend., BT treatment
0=68880

0-0880
Ge-metal junctions, tunnelling rel. to Ge phonon spectra 0-56330
InP tunnel diodes 0-53901
InP tunnel junction, p-n, elec. props. temp. depend. 0-56332
Nb-GaAs junction, tunneling anomalies, 10.5 K, differential cond. 0-79023
with Ni electrodes, spin flip tunnelling rel. to LV characts. 0-75460

0-79023 with Ni electrodes, spin-flip tunnelling rel. to I-V characts. 0-75469 Pt. Si, I-V meas. 0-47797 SizAu m.o.s.f.et., generation-recomb. noise and thermal emission rates at acceptor centre 0-68877 Si/SiO₂ m.o.s. structure, SiO₂ film deposited by r.f. glow discharge 0-51090 Si-SiO₂-Al₂O₃, m.o.s. capacitance, interface props. 0-44329 Si-SiO₂ interface, characts., control, review 0-65715 Si-SiO₂ interface, electron states and hole mobility changes on γ-irrad. 0-65714 Si-SiO₂ interface, I-EED obs. 0-39929

0-65714
Si-SiO; interface, LEED obs. 0-39929
Si-SiO; interface, localized recombination-generation sites, capacitance mapping technique 0-44263
Si-SiO; pinversion layers, effect of temperature on magneto-electrical properties 0-68881
Si-SiO; based, water contamination in device technology 0-58841
Si-metal junctions, phonon tunnelling and e-collective excitation interactions 0-56330
Si, m.o.s. struct., ion implantation of O+ and Ne+, surface characts. 0-47814
Si.-p.n junction, growth, I-V characts, impurity effects 0-39955

10-4/814 Si, p-n junction, growth, I-V characts, impurity effects 0-39955 Si m.o.s.t., 1.f. noise, theory 0-44312 Si oxidized structure, interface states 0-47765 SiO₂-Si, tunnelable layer formation by Si oxidation 0-62392

 SiO_2 pyrolytic films in m.o.s. struct., surface state and charge densities 0-56340

SnO₂-semiconductor heterojunction m.o.s. struct. 0-75748

PA 1970 - Part II (July-Dec.) S 1346 SUBJECT INDEX Semiconducting materials continued Semiconducting devices continued tunnel and interface devices continued Y-Y₂O₃-metal tunnel diodes, inelastic tunnelling due to to vibr. modes 0-75758 film, conduction behaviour 0-68807 film, intermetallic, growth, props. and device applies., book 0-44162 film, magnetoresistance, size anisotropy effect, in weak mag. field 0-72009 ZnTe, mis. electroluminescent diode, red and green spectral output 0-72009
film, photocond., field effect 0-68974
film, size quantization, band structure 0-75697
film, size-quantized, cond. in quantizing mag. field 0-72016
film, thickening rate influence on conc. profile and p-n transition region
position 0-55714
films thin, Hall coeff. meas. by Pauw's method 0-59182
glass, As;Se;, Ohm's law deviation 0-75677
glass, Ge-8-8-Te system, elec. cond. and switching diode applic. 0-78938
glass, Hall and drift mobility, meas. 0-40777
glass, chalcogenide, conductivity, thermolec. power, optical absorpt. and
carrier mobility 0-44200
glass, chalcogenide, film switches, switching behaviour and bulk props.
0-44276
glass, chalcogenide, thermal pinching effect 0-51033 0-54140 niconducting materials

see also Magnetoelectric effects; Photoconductivity; Photovoltaic effects; Semimetals

A_{III}-B_V compounds, chemical binding, spin-orbit splitting 0—53450

A_{III}-B_V compounds with zinc blende structure, chemical binding, spin-orbit splitting 0—55770

A^{III}B^V cpds., potential distrib. rel. to band struct. 0—59217

A^{RB,n}, dispersion energy proportional to ionicity 0—75992
acoustic wave amplification in presence of external electric and magnetic fields 0—43889

acoustoclectric device applications of pleased exterior and complex distributions. Semiconducting materials fields 0–43889
acoustoelectric device applications of piezoelectric and semiconducting thin films 0–56103
β-alanine, semiconductivity, optical transmission and reflection, pure and X irradiated 0–75657
alcohols, elec. conductivity, temp. dependence 0–62341
alkali metal metaselenoarsenites, elec. cond., –50-190°C 0–51032
alloy, amorphous, carrier kinetics 0–59187
alloy, amorphous, localized states 0–75712
alloy, band structure 0–59212
alloy epitaxial film, X-ray diffr. characterization 0–58580
amorphous, As₂Se₃, u.s. velocity and attenuation, doping depend. 0–47529
amorphous, conduction and switching 0–78939 0-44276
glass, chalcogenide, thermal pinching effect 0-51033
glass, electronic switching mechanism, electrothermal initiation 0-51028
glass, memory phenomena, elec. and calorimetric analyses 0-72020
glass, oxide, struct. prop. correls. 0-59185
glass, reversible switching, time delay 0-56246
glass, reversible switching effect, switching cycle 0-53812
glass, sid state switches, transient behaviour 0-44271
glass, vanadium phosphate, n.mr. of 51V 0-48163
glass arsenic chalcogenide, fundamental absorpt. edge, carriers, effective mass 0-44827
glasses, amorphous germanium and silicon, vitreous selenium chalcogenide. amorphous, confuction and switching 0–78939 amorphous, conf., Cambridge, England, Sept. 1969 0–47686 amorphous, electronic dielectric constant calc. 0–75765 amorphous, in memory diode 0–53888 amorphous, optical spectra, elec. cond., thermoelectricity 0–53821 amorphous, switching effects 0–62347 amorphous film, switching phenomena and differential negative resistance 0–75663 glasses, amorphous germanium and silicon, vitreous selenium chalcogenide glasses and transition metal-oxide glasses, properties and interpretation 0–62337 glasses, threshold switching, mechanism 0-56244 group, IH-V appoint plants growth technique and system 0-58632 group III-V, amphoteric impurities behaviour, thermodynamic analysis group III-V appoints growth technique and system 0-58632 group III-V, amphoteric impurities behaviour, thermodynamic analysis group III-V appoints group III-V appoin anthracene, d.c. cond. meas, with large fields 0–44211 anthracene, drift mobility, high press, effects 0–47723 anthracene, e diff. const. from pulse drop in drift expts. 0–4730 anthracene, electroluminesc. 0–56649 group III-V, amphoteric impurities behaviour, thermodynamic analysis 0–68838 group III-V compounds, covalent charge, correlation with reduced microhardness 0–43575 group III-V cpds., Mossbauer effect of Fe impurities 0–72326 group III-V cpds., direct-gap, electron mobility 0–75671 group III-V cpds., lattice mobility of holes 0–75670 group III-V cpds., scatt., ang. depend. of matrix elements 0–75464 group III-V cpds. scatt., ang. depend. of matrix elements 0–75464 group III-V pds. polaxial film prep. 0–61649 group III-V pds. polos. operation in semitransparent mode 0–59295 group II-VI, IV-VI, and V-VI cpds., review 0–72002 group II-VI, cpds., book 0–62342 group II-VI cpds., isothermal linear compressibilities 0–71680 group II-VI cpds., vapour-phase growth in sealed tube, kinetics 0–61718 group IV, pseudopot. form factors and band struct. 0–53832 group IV-VI compounds, data tables 0–68806 growth of single cryst., use of moulds from refractive non-oxidizable materials 0–65127 high surface area, mixed salt freeze drying prep. 0–62116 homopolar, cubic, directional depend. of photoconductivity 0–47869 III-V and II-Vi compounds, inelastic light scattering at resonance 0–72384 impact ionization, transverse, n-type 0–44181 anthracene, electroluminescent cells, with tunnel injection cathodes 0-79385antiferromagnet, p-MnTe₅ and p-MnTe₅:Na, transport props. and magnon drag 0-44205 benzene, solid, space charge limited currents 0–53873 benzene, solid, space charge limited currents 0–53831 book 0–53850 chalcogenide, quaternary, thermoelec. power, Hall coeff., elec. conductivity, microhardness and opt. reflectance 0-75821 chalcogenide film, switching phenomena and differential negative resistance 0-75663 tance 0-75005
chalcogenide glass, Si₃Ge₄As_{3s}Te_{5s}, bulk switching properties 0-79004
chalcogenide glass, band or hopping conduction, d.c. and a.c. 0-47700
chalcogenide glass, bond type, polarization, electron cond., switching phenomena 0-47703 nomena 0-47/03 chalcogenide glass, struct., threshold and memory switching 0-56243 chalcogenide glass, thermal pinching effect 0-51033 chalcogenides, quaternary, thermoelec, props. 0-47860 chalcogenides of groups II, IV, V, review 0-72002 characterisation ir, techniques, free charge carrier conc., mobility 0-72055 impact ionization, transverse, n-type 0-44181 imperfection centres, thermal and optical emission and capture rates 0-53839 chloranil, field effect obs. 0-47731 impurity diffusion source and method, patent 0–43701 impurity spectra, valley-orbit interaction, effect on donors 0–54091 interface, misfit dislocations 0–65320 ion implantation, apparatus and technique 0–53853 ion implantation, applic. of channeling 0–43933 layer, interband transitions in quantum size effect 0–71912 layered medium, u.s. amplification, mag. field 0–47531 lead chalcogenides, carrier scatt. mechanisms 0–47720 liquid, In, Te3, n.m.r., 1151n Knight shift, pseudogap 0–46957 liquid, org., regeneration of current carriers 0–55622 liquid, transport phenomena rel. to Mott model 0–71372 magnetic, CdCr, Se4, electron and hole bands 0–59213 magnetic, EuO, conductivity temp. and mag. field depend. 0–59194 magnetic, Hall mobility meas. rel. to electron ordering, 65-373K 0–59195 magnetic, (La_{1-x}Cu_x)MnO₃, elec. and mag. props., comp. depend. 0–59307 magnetic, band struct. 0–59207 impurity diffusion source and method, patent 0-43701 p-chloranil single crystal, charge carrier mobility, photocond. meas. 0-51152compound-type, epitaxial, deposition by fused salt electrolysis, patent 0-436020.—43602

conference, Dallas, Texas, USA, (1970) 0.—62286

conference, Moscow, USSR, July 1966 0.—74949

conference, Moscow, USSR, July 1966 0.—74949

conference, Moscow, USSR, July 1966 0.—74946

crystal growth, IIIB-VB compounds, patent 0.—43600

crystal manufacturing 0.—65176

cubic, homopolar, directional depend, of photoconductivity 0.—47869

diamond, Li, ion bombarded, cond. distrib. with depth 0.—65676

diamond, synthetic, electron irrad, influence on electron and optical props.

80 450K 0.—75678 diamond, synthetic, electron irrad, influence on elec, and optical props. 0--66099 0-66099
diamond doped by ion implantation, electrical properties 0-78972
diamond-type, band struct., K.R.-Z. calc. 0-71972
diodes, glass, memory and switching 0-44169
diphenyl butadiene, dark conductivity, effects of donor and acceptor groups 0-65653
disordered structures, carrier mobility 0-56168
electrical breakdown, review 0-62406
electrical properties, variational methods for experimental investigations 0-44238 magnetic, band struct. 0-59207 magnetic, band struct. 0–59207
magnetic, chalcogenide spinels, spin-disorder scatt., band struct. 0–59190
magnetic, conf., Yorktown Heights, USA, Nov. 1969 0–56237
magnetic, europium chalcogenides, optical props., band struct. 0–59399
magnetic, indirect transitions, mag. field depend. 0–56532
magnetic, p-Ag_xCd_{1-x}Cr₂Sa₄, high-field nonohmic behaviour 0–59188
magnetic, paramag. polaron stability conditions, appl. to Eu chalcogenides
0–78851
magnetic tuppelling spectages of 5024 0-44238
electron-effective-mass dependence and higher band interactions for HgSe and HgTe 0-59222
elemental, evaporation using work-accelerated electron beam source for thin film growth 0-50333
epitaxial film, bulk lifetime meas, by insulated cryst, method 0-78921
epitaxial film, bulk lifetime meas, by insulated cryst, method 0-78921
epitaxial film, to HIV-2 cpds., prep. 0-61649
epitaxial flims of HIV-2 cpds., prep. 0-61649
epitaxial layers, doping profile meas, 0-75649
etch monitoring by internal reflection interferometry 0-50411
europium chalcogenides, band splitting mag, ordering effects, reflectance obs. 0-59322
europium chalcogenides, optical props., band struct. 0-59399
europium chalcogenides, transport props. rel, to behaviour at T_e 0-59193 magnetic, tunnelling spectroscopy 0–59214
measurement methods, process control and devices 0–56313
measurement methods, review 0–68847
measurement methods development 0–44165
metal oxide glass, bond type, polarization, electron cond., switching phenomena 0–47703 metal-semiconductor contact, resist., capacitance, abrupt boundary potential 0-65699 micro-fields, electric and magnetic, electron emission microscope obs. 0-53490 0-53490 microhomogeneity, integrated absorption inspection, nondestructive express method applic. 0-47698 monomolecular layers, organic molecules, physical, optical and electrical properties 0-78920 n-type, transverse impact ionization 0-44181 optical constant determ. with pseudo-Brewster angle technqiue, a reflectometer 0-56483 organic, binary complex type with charge transfer 0-40754 organic, conduction mechanism 0-72056 oxides, chemisorption and catalysis meas, apparatus. Hall effect 0-44237 europium chalcogenides, transport props. rel. to behaviour at T_c 0–59193 europium chalcogenides, transport props. rel. to behaviour at T_c 0–59193 examination using scanning laser i.r. microscope 0–49123 F_{elix}Cr_{2-x}S₄, resistivity, ferrimag. props., cryst. struct., comp. depend. 0–44657 ferroelectric, AvBvICvII, phase transition, nonequil. carriers influence 0 - 68931oxides, chemisorption and catalysis meas. apparatus, Hall effect 0–44237 oxides, production of low resistance contacts 0–44232 perovskite-type cpds., book 0–68293 phosphides of groups I, II and III, X-ray emission spectra, valence bands ferroelectric, SbSI, transport phenomena 0-68826 ferroelectric, elec. cond., anomaly near Curie point 0–44358 ferroelectric, elec. cond., anomaly near Curie point 0–44358 ferroelectric cryst., theory of elec. induction waves 0–40845 ferromagnet, Eu₃P₂ and Eu₃As₂, structure and Curie pts. 0–47687

photoconducting II-VI cpds., temp.-elec. instability, theory 0-72132

photoexcited carrier, non equilib., theory 0-56378

 β - phthalocyamine, bulk trapping states in single crysts. 0-40780

phthalocyanine, elec. props. 0—44371 phthalocyanine film, nonequilibrium admittance 0—65679

piezoelectric, acoustoelec, effects 0-75400

piezoelectric, acoustoelectric amplification 0-40555

piezoelectric-semiconductor system, amplification of u.s. surface waves

0-18/03
pinch effect, theory, transducer potentials 0-44164
plasma anodization of metals and semiconductors, review 0-55734
polyacrylonitrile, pyrolyzed and irrad., e.s.r. 0-72501
polyazophenylenes, cond. 0-75696
polycrystalline, non-degenerate, electron gas model 0-48765
polymer with conjugate double bonds, thermistor props. 0-75741
polymers with conjugated system, relational porphyrin structure based, semiconduction and possible superconduction
0-75539

0—155.39
quaternary alloy, (II-VI)-(III-V), band gap variation 0—40787
radiation damage 0—75714
rare earth sulphide and selenides, specific resist., thermo e.m.f., 3001500K 0—75686
refractive index evaluation from interference-fringe transmission spectra

0-48000 resistivity, carrier life time, Hall effect, measurement methods 0-53818 rutile, reduced, 2-370K 0-75688

ruthe, reduced, 2-3 fok 0-7588
Se epitaxial film on Te, morphology and elec. props. 0-65675
specific resistance meas. in wide temp. range using noncontact cavity
resonator method 0-51052
sphalerite, ZnS, structure, elastic constants, theory 0-55938
stilbene, analogues, dark conductivity, effects of donor and acceptor
groups 0-65653

groups 0–65653
superconductor, SrTiO₃, type II phenomena 0–68791
surface layer characterization by X-ray topography 0–65666
surface layer plastic deformation anomaly 0–40289
surface scattering reactive oxygen atoms 0–55704
surface scattering reactive oxygen atoms 0–55704
surface states, fast, m.o.s. capacitance obs. 0–75717
surface states in complicated band struct. material 0–75606
susceptibility, non-linear, of semiconducting of CdTe 0–47984
tetracene crystal, exciton fission and fusion, coexistence 0–44916
tetracyanoquinodimethan, conductivity and photoresponse 0–59285
tetracyanoquinodimethane, As-TCNQ, P-TCNQ crystals, surface elec.
pot. 0–75720
tetracyanoquinodimethane salt, Hall effect, thermoelec. power, card

tetracyanoquinodimethane salt, Hall effect, thermoelec. power, card 0-78959

tetrathiotetracene films, photoelectron emission, surface state influence 0-44442

tetrathiotetracene thin-layer systems electrophys, and photoelec, props.

thermal properties, variational methods for experimental investigations 0-44238

thin films, deformation effect on conductivity 0-65049 transferred-electron, assessment criteria 0-51020

transferred-electron, assessment criteria 0-51020 transition metal dichalcogenides, IVB-VIB, thin single crysts, cond. 0-75689

transition metal oxides, electronic transport, review 0-59210 u.s. absorption by conduction electrons, oscillations in h.f. electric field 0-43874

vapour pressure sensing 0-47008 vitreous, As-S-Te system, bond-structural approach to elec. conduction 0-75676

wurtzite-type, spin-lattice relax. of shallow donors 0-47590 zinc-blende, direct, band edge optical transitions, uniaxial strain effects 0-44806

U-44800
AS,S, glassy, indirect transitions 0-47733
p-Ag,Cd₁-Cr₂Se₄, high-field nonohmic behaviour 0-59188
n-Ag,Te, carrier effective mass, i.r. reflection spectra, elec. props. 0-44186

AgTISe₂, liq. and solid, elec. cond., thermal cond. and thermopower 0-78937

(U-1895) Al SI, O₂- adsorption through e.p.r. evidence 0-47075 AlAs, vapor-grown, photo- and cathodoluminesc. 0-72450 Al_xGa_{1-x}As junctions, h.v. p-n, electron probe recording current method obs. 0-75744

obs. 0-75744

Al₃Ga_{1-x}As, indirect bandgap mat., luminesc., opt. ionization energies of Sn., Te., Zn.-impurities 0-76147

(Al₃Ga_{1-x})As, ionization rates, Al content depend. 0-75675

Al₃Ga_{1-x}As Fabry Perot injection lasers with room-temp. threshold current densities of 2530 A/cm² 0-67101

Al₂Ga₁, alumina, conductivity, d.c., in single crystal and polycryst., 600-1573K 0-44033

AlP, band gap and refr. index, absorpt. obs. 0-69115

AlP, intrinsic absorpt., indirect bandgap obs. 0-76091

Al-S-S-Te system, vitreous, bond-structural approach to elec. conduction 0-75676

As-Se-Sn glass, Mossbauer effect. Sn valency comp. depend. 0-48026

0-75676

As-Se-Sn glass, Mossbauer effect, Sn valency comp. depend. 0-48026

As-Se alloy, glass-like, l.f. conductivity 0-65667

As-Te-Ge-Si, amorphous film, non-ohmic props., 77-350K 0-56242

As-Te-Ge glass, filament formation, electron probe analysis, radiometric microscopy 0-56285

As-Te, As-Te-Ga, As-Te-Ga-Ge-Si chalcogenides, amorphous, conduction and switching 0-78939

As-Si, optical abs. and mag. susceptibility with temp., localized states 0-69116

As-Si, vitreous, reflectivity, absorpt., photocond. spectra, I-V characts.

As,S,, vitreous, reflectivity, absorpt., photocond. spectra, I-V characts. 0-53816AsyS₃, vitreous and single crystal, radiative recombination, photoexcitation 0-48099

 $As_{7}Se_{2};As_{2}O_{3}$ chalcogenide glass, prep., i.r. spectrum and conductivity $0\!-\!59184$

0-59184

0-59184

As, Se3, amorphous, local states, thermally stimulated depolarization method 0-40788

As₂Se₃, amorphous, optical and elec. props. 0–47721 As₂Se₃, amorphous and cryst., photocond. and thermal transitions of carriers 0–72134

Semiconducting materials continued

 As_2Se_3 , cryst. and glassy, electroabsorpt., elec.-field-induced shift of absorbent edge 0-66034

 As_2Se_3 , single crystal and amorphous film, absorpt. spectra, elec. props. 0-4705

As₂Se₃, vitreous, freq. depend. cond. 0-78940

As,Se₃, vitreous and single crystal, radiative recombination, photoexcitation 0-48099 As₂Se₃, vitreous elec. cond., photoelectricity, photopolarization 0–47707 As₂Se₃, glass, Ohm's law deviation 0–75677 As₂Se₅, vitreous, switching and memory props. 0–56250

As;Se, chalcogenide glass, prep., ir. spectrum and conductivity 0–59184
As;Se, chalcogenide glass, prep., ir. spectrum and conductivity 0–59184
As;Te, amorphous film, non-ohmic props., 77-350K 0–56242
As;Te, amorphous film, photocond., elec. cond. 0–47706
As;Te, film, amorphous, conductivity, opt. absorpt., and photoconductivity
meas., 200-400°K 0–44187
B, amorphous film, current filament formation switching, liquid cryst. obs.
0–47709

0-47709

B, doped, elec. props. 0-72021

β-B, elec. props., high temp. 0-56251

β-B, elec. props., high temp. 0-56252

β-B, rhombohedral, cond. mechanism, electron and hole trapping levels
0-78941

0—78941
β-B, rhombohedral, elastoresist., 180-500K
0—78942
BAs, electronic struct. and optical spectrum
0—59189
BN, plasma oscillations anisotropy, interband transitions determ. applic.
0—40782

BN, plasma oscillations anisotropy, interband transitions determ. applic. 0–40782
BP, self-consistent energy bands and related props. 0–53834
BaO, deterioration rel. to strong local electric field, reduction of 0–56220
BaTiO₃, reduced crystal, elec. cond. Seebeck coeff., Curie point, polaron to hopping 0–62349
BaTiO₃ crystals, resistivity. Seebeck coef. and optical absorption meas., conduction processes obs. 0–51054
n-BiTe, thermal conductivity, Wiedemann-Franz relationship and carrier scattering mechanism 0–56117
Bi-Sb, helicon reson. 0–56256
Bi-Sb alloy, Sb-rich, semiconductor-metal electron transitions in strong mag, field 0–75703
Bi-Sb alloys, Nernst effect 0–68819
Bi₈Sb₅:Te crystal, elec. resist., Hall coeff., magnetoresist., Seebeck coeff. 80 K 0–51034
BiSb-Al₃O₃ BiSb symmetric thin film junctions, tunnelling characts. at low temp. 0–68879
Bi₁₋₈Sb₂ alloy, transition to 'quasimetal', press. and comp. depend. 0 53835

0 53835

Bi_{0.3}Sb_{1.5}Te_{2.4}Se_{0.6} solid solution, forbidden band width, temp. depend., 80 700 K, transport props. 0-62361

Bi₂Se₅ band structure and transport coefficients 0-78977

Bi₂Te₃ Sb₂Te₅ Hall constant and mobility of free charge carriers measurement with voltage comparator 0-44239

Bi₂Te_{3.5} Se₅ solid structure and transport coefficients 0-78977

BiTel, optical absorpt. and reflectivity, band struct. 0-44828

Bi₂Te_{3.5}Se₅ solid solution, thermoelec. figure of merit, elec. cond. 0-62457

6.62457
C, diamond, charge density, Fourier transforms using self-consistent orthogonalized plane-wave method 0-44212
CaS phosphor, negative thermally stimulated cond. 0-40767
Cd₃As₇-Cd₃P₃ solid solutions, physical and electronic properties, thermoelectric figure of merit 0-65469
CdAs₈, glass, structure and electronic props. 0-47020
Cd₃As₇, conduction band model 0-68833
Cd₃As₇, polycrystalline, magnetoresistance and magneto-Seebeck meas. second conduction band in doped samples 0-75704
CdCr₂Sd₄, CdIn₂Sq₂Cr, absorpt. edge, magneto-optical obs. 0-56540
CdCr₂Sd₈, cylical transitions and band struct. model 0-68832
n-CdCr₂Se₄, electron and hole bands 0-59213
CdCr₅Se₄, Faraday effect, mag, ordering effects 0-56501
n-CdCr₅Se₄, mixed-cond. model for charge transport 0-75680
CdCr₅Se₄, transport processes, band struct., spin-disorder scatt. 0-59190
CdF₇: Y, polaron effects 0-50951
CdF₇, polaron model for transport processes, Raman spectra 0-44864
CdGeAs₂, crystalline and vitreous state, electronic and vibrational 0-47505
CdGeAs₂, glassy, switching device 0-65739

0-47003 CdGeAs₂, glassy, switching device 0-65739 CdGe_xAs₂, amorphous, Seebeck coeff, resist., temp. depend. 0-79063 CdGe_xAs₂, vitreous, Hall effect, thermoelec. power and elec. cond. 0-75681

0-73061 CdGeAs₂(P₂), amorphous film, I-V characts., switching and memory effects 0-40768 CdGeP₂, vapour transport growth, photocond., forbidden band width 0 74971

0 /49/1 Cd₄Hg_{1-x}Te dust, electrification 0-58508 Cd_xHg_{1-x}Te solid solns, thermal noise anomalies 0-78681 CdIn.S₄, band struct, pseudopot. calc. 0-75705 CdIn.S₄, magnetoresist, ang. depend., conduction band anisotropy 0-78945

0-78945
Cd3-P₄ laser, optically pumped 0-49079
Cd5-Bi laser, electron beam pumping 0-42305
Cd5-P₄As, acceptor levels, photocond., absorpt. and luminesc. 0-66090
CdS-S defect centres origin and behaviour obs., i.r. luminescence method, curve fitting technique 0-51048
n-nCdS-CdS-GaAs alloy, intrinsic absorpt. edge 0-66039
CdS, acoustoelec. current oscillation, transverse mag. field effect 0-71850
CdS, acoustoelec surface wave domains 0-62201
CdS, acoustoelectric gain, large signal characts., and current saturation 0-40556
CdS, acoustoelectric phenomena, large- signal gain and current saturation

0-40556
CdS, acoustoelectric phenomena, large- signal gain and current saturation expressions applic. 0-43891
CdS, cnd. electron hyperfine interaction 0-75987
CdS, constancy of charge at minima of dark current 0-62350
CdS, current filaments, acoustoelec. origin 0-68820
CdS, deterioration rel. to strong local electric field, reduction of 0-56220
CdS, effects of O chemisorpt, states on equilib. conductivity 0-40784
CdS, high-field domain modes 0-51031
CdS, hole traps evidence 0-51147
CdS, luminescence band of first phonon repetition of exciton A, damping time meas. using ruby laser picosecond pulses 0-72418
CdS, negative magnetoresistance temp. depend. 0-53822

CdS, neutron-irrad., β - and γ -induced cond. 0–78931 CdS, nonlinear attenuation of microsound 0–68599

CdS, optical modulation by acoustoelectric domains 0-75997

CdS, optical modulation near intrinsic absorpt, edge due to acoustic domain

Cds, piezoelec, acoustoelec effects 0-75400 CdS, piezoelec stiffened u.s. vel. enhancement by electron trapping 0-50884

CdS, Raman scattering, resonant cancellation, Loudon theory extension 0-76125

0-76125
CdS, single cryst., electroreflectance spectrum near fundamental abs. edge, at room temp. 0-66018
CdS, surface treatment influence on luminesc. 0-72417
CdS, thin-film, conduction, mechanism by field ionization or tunnelling 0-78946

0-78946
Cds, traps, photochem, changes 0-47871
Cds, u.s. amplification, nonlinear interaction 0-43890
Cds filaments, acoustoelec, domain incubation 0-71849
Cds film, vacuum-deposited, photoluminescent props. 0-79349
Cds films, vacuum deposited, resist, vars., 250-400°K 0-56253
Cds Hall effect and associated phenomena, obs., parameters of imperfection centres determination 0-56271
Cds laser, electron beam pumping 0-42305
Cds layer, elec, props. and surface structure changes after thermal processing 0-75718
Cds platelet oscillator, diffusion of In contacts, electron beam microanalysis 0-40794
Cds platelets, effect of O desorption on Fermi level and photocond.

sis 0-40794 CdS platelets, effect of O desorption on Fermi level and photocond. 0-47739

0-47739
CdS surface potential rel. to barrier height of Au-CdS contact exposed to 0 0-47744
CdS thin film, current decay and trap evaluation, temperature dependence obs. 0-68831
CdS thin film, effect of deposition rate, obs. at 2, 9, 16 Å/sec 0-50389
CdS(Se), additional birefringence 0-72314
CdS(Se) (Te) film, epitaxial growth, temp. depend., elec. props. 0-50376
CdS(Se) films, induced impurity photocond. 0-79073
CdS_xSe_{1-x} films, adsorption influence on elec. and photoelec. props. 0-56380
CdS(Se)(Te) films absorpt spectra in 36-150 eV region 0-48080

0-5380
CdS(Se)(Te) films, absorpt, spectra in 36-150 eV region 0-48080
CdSb, conduction and thermoelectric properties, effect of donor and acceptor impurities 0-65840
n-CdSb, electroconductance, anisotropy 0-68814
CdSb, ir. plasma reflectivity, 3-30 \(mm\), 85-300K, hole effective masses 0-75679

CdSe-CdTe alloy films, characts, rel. to prep. by flash evaporation 0-59191

0-59191
CdSe-GaAs alloy, intrinsic absorpt. edge 0-66039
CdSe-Se, photocell, ²³⁵U coated, neutron irrad., short- circuit currents, e.m.f. 0-51156
CdSe-SiO_x thin film conductivity 0-72003
CdSe, deterioration rel. to strong local electric field, reduction of 0-56220
CdSe, elec. cond., Hall effect, Cd vapour press. depend., 558-835°C 0-78947
CdSe, represents, current oscillation, 0-56238

CdSe, elec. cond., Hall effect, Cd Tape 2.

0–78947

CdSe, monocryst., current oscillation 0–56228

CdSe, photoconducting, current fluctuations, acoustic noise flux 0–75829

CdSe, polycrystalline, unit conductivity model 0–62343

CdSe, undamped acoustoelec. oscillations 0–78767

CdSe film, Lamb waves 0–75396

CdSe film, surface potential and cond., doping depend. 0–62370

CdSe films, field effect for surface pot. changes cases 0–78943

CdSe films, field effect for surface pot. changes case, illumination influence 0–78944

CdSe films, vapour evaporating-reactive sputtering prepared, photocond.

CdSe films, vapour evaporating-reactive sputtering prepared, photocond. 0–72135

CdSe lasers, spontaneous and stimulated carrier lifetime, spectral output 0–57539

0–57539
CdSe nonlinear optical absorpt. coeff. at 1.064μ obs. with YAL garnet: Nd laser 0–41099
CdSe photosensitive films, trap parameters determ. 0–79075
CdSe thin film conductivity 0–72003
CdSiAs₃, hole conc., stoichiometry depend. 0–78948
CdSiP₃, semiconductor with chalcopyrite lattice, energy zone structure 0–65683

0–65683
n-CdSnAs₂, cond. band struct. 0–56270
CdSnAs₂, Hall mobility temp. depend. 0–72054
CdSnP₂, electroreflectance, optical transitions 0–76066
CdSnP₂, i.r. refl. and absorpt., permittivity and refr. index calc. 0–72341
CdSnP₂, negative crystal-field splitting of valence bands 0–47734
CdTe, deep impurity levels and photomemory effect 0–78973
p-CdTe, diffusion of In, Cd v.p. influence 0–53559
CdTe, electron and neutron irrad., electrical and photoelec, props., defects 0–40783
p-CdTe, electron mobility temp. depend, impurity effect. 0–40769

CdTe, electron and neutron irrad., electrical and photoelec, props., defects 0–40783

n-CdTe, electron mobility, temp. depend., impurity effect 0–40769

CdTe, exciton thermorefi. 0–56522

n-CdTe, Faraday effect in ir. 0–66015

CdTe, high-resistivity, surface-barrier p-n junctions, props. 0–56379

CdTe, non-linear susceptibility 0–47984

p-CdTe, nuetron-irrad., hole removal, recoil defect interaction, Hall effect, conductivity meas. 0–47229

p-CdTe, photosensitivity centres parameters 0–79072

CdTe, piezosemiconductor, Rayleigh wave amplification 0–75399

CdTe, second harmonic generation and sum freq. mixing 0–51259

CdTe, surface barrier detector, material inhomogeneities correlation with resolution 0–57851

CdTe as y spectrometer 0–60643

CdTe are sy spectrometer 0–60643

CdTe effective mass from plasma edge reflection measurements 0–72041

CdTe are 104099

p-CdTe photosensitivity spectrum, temp. influence 0–79074

CdTe radiation counter 0–52600

CdTe surface-barrier junctions photomemory 0–56318

CdTe₂Se_{1-x} valust, electrification 0–58508

n-Ce₁₁₀O₂, electron mobility at high temps. 0–51035

CoSi₁, thermal and elec. cond. 0–78791

CrSi₂, transport props. anisotropy 0–72022

CsAu, electronic struct., photoemission obs. 0–75706

CuCl, radiative recomb. and form. of free excitonic mol. by laser excitation 0–72419

Semiconducting materials continued

CuMSe₂, (M=Ga, In, As), liq. and solid, elec. props. 0-78298

CuNbO₃, high press. prep., struct. 0-55836 Cu₂O, bulk cond., thermal variation 0-68821

Cu₂O, cond. and space charge limited currents 0-72023 Cu₂O, grain-boundary cond. and rectifier obs. 0-62351

Cu₂O, hole trap level, thermally stimulated current obs. 0-75715 Cu₂O crystals, high resistance, surface layers and their conductivity 0-53843

Cu₂S-CdS heterojunctions, photovoltaic props. 0-65855

CuSbSe2, liquid, transport props. 0-46947

CubbSe₂, liquid, transport props. 0–46947
CuTaO₃, high press. prep., struct. 0–55836
Cu,Te, absorpt. spectra, rel. to intrinsic semicond. behaviour 0–79301
CuTlSe₂, liq. and solid, elec. cond., thermal cond. and thermopower 0–78937
Eu₂As₂, ferromagnet, structure and Curie point 0–47687
EuO:Gd, transport props., 123 K, resistive anomaly 0–44189
EuO, conductivity temp. and Mag. field depend. 0–59194
EuO, magneto-photocond. near Curie temp. 0–56383
EuO pressure and temperature dependence of electrical resistivity

O pressure and temperature dependence of electrical resistivity 44214

O-44214
EuO(S), energy spectra, calc. 0-44213
EuO(S), energy spectra, calc. 0-44213
Eu,P. ferromagnet, structure and Curie point 0-47687
EuS:Eu/In junctions, tunnelling spectroscopy 0-59214
Eu;S.4, elec. cond., thermoelec., 100-1000°K, electron hopping 0-40770
EuS(Se, Te):Gd, paramag. Curie temp., rel. to cond. band 0-40944
EuTe, photocond., absorpt. edge, temp. depend. 0-59400
EuTe, resistivity, antiferromag. ordering effect 0-62352
Fe;O₁, magnetite, Hall mobility meas. rel. to electron ordering, 65-373K
0-59195
ar-Fe;O₃, n-type with Sn or Ti impurities, electrical conduction, g-r noise and Seebeck coeff. 0-78917
Fe;O₄, magnetite, metal-semiconductor transition, band model 0-44034
(Ga,Al)As-GaAs heterojunction laser, carrier and radiation confinements 0-5326
(Ga,Al)As diddes, light emitting, Zn-Te compensated, with negative resis-

(Ga,Al)As diodes, light emitting, Zn-Te compensated, with negative resis-

(Ga,Al)As diodes, light emitting, Zn-Te compensated, with negative resistance 0-72459
Gal-xAl,As-GaAs heterojunction lasers, internal Q-switching 0-69923
GaAs-Al,As-GaAs heterojunction lasers, internal Q-switching 0-69923
GaAs-Al,Gal-xAs heterostruct. lasers, wave-guiding props. 0-57540
GaAs-Al,Gal-xAs injection lasers, continuous operation, room temp. 0-60244
GaAs-CdS solid solns., elec. and thermoelec. props. 0-65669
GaAs-ZnSe heterojunctions, fabrication and props. 0-44284
GaAs, epitaxial growth, liquid phase, under transient thermal conditions 0-47151

0.47151
GaAs, low temp. non ohmic transport, electron temp. model 0-44194
GaAs injection laser, optical loss control, heterojunction introduction, theory and experiment 0-42306
GaAs_{1-x}P_x electroluminesc. diodes, electron irrad., defect centres 0-69170

GaAs, P_{1-x}, local levels obs. 0–65682
GaAs, P_{1-x}, local levels obs. 0–65682
GaAs, P_{1-x}, photoluminescence obs. of inhomogeneities 0–56229
GaAs, P_{1-x}, photoluminescence obs. of inhomogeneities 0–56229
GaAs, P_{1-x}, photoluminescence obs. of inhomogeneities 0–56229
GaAs, Diquid epitaxial growth, use as high-efficiency, long-wavelength threshold photoemitter 0–47896
GaN, low temp. photoluminesc., band gap obs. 0–76151
GaN, optical absorpt. 0–76100
GaN, photoluminesc., low temp. 0–72434
GaP:Cu, local level obs. 0–65682
GaP:D_{v1}, d_{v1}=group VI donor, impurity binding energies 0–44230
GaP:Si(S) (Te), conductivity, Hall effect, 4.2-293K, scatt., mechanism 0–72027
GaP:Te, effective mass calcs. from spectroscopic study 0–44810
GaP:Te, photoioniz. energy, absorpt. spectrum obs. 0–76101
GaP:Te, photoioniz energy, absorpt. spectrum obs. 0–62364
GaP:Zn.O, liquid phase epitaxyal layers, impurity gradients 0–62364
GaP:Zn.O, c, photoluminescent saturation 0–69151
GaP:Zn.O, o, photoluminescent saturation 0–69151
GaP:Zn.O, o, radiative recombin, time decay and temp. depend. 0–66093
GaP:Zn.O, ir. emission luminescent intensity and decay time, oxygen donor role 0–77428
p-GaP:Zn.O, luminesce. and minority carrier recomb. 0–79355
GaP:Zn.O, luminescent time decay of excitons bound to Zn-O complexes 0–79351

0-/9431 GaP:Zn(O), recomb. kinetics of electrons and holes at isoelectronic impuri-ties 0-59423 GaP-GaAs diffused heterojunctions, conc. profiles, microprobe analysis 0-53874

0–53874
GaP, metal Schottky barriers, deep centres effect 0–65746
GaP, absorpt. and luminescence of excitons at neutral acceptors 0–56543
p-GaP, doped, i.r. reflectivity, effective mass of holes determ. 0–79280
n-GaP, e.p.r. obs., 2.5-100K 0–72027
GaP, electro- and photoluminescen, oxygen influence 0–56646
GaP, electroluminescent, preparation and applications 0–59424
GaP, interimpurity radiative recomb_i.r. radiation influence 0–56596
GaP, ion implantation profile 0–75716
GaP, luminescent efficiency, effects of plasma screening and Auger recombination 0–48103

GaP, luminescent efficiency, effects of plasma screening and Auger recombination 0–48103 n-GaP, optical absorpt. by free carriers, surface effects 0–66043 GaP, optical ioniz. cross sections determ. using photovoltaic effect 0–75844 GaP, Raman scattering obs. of high-frequency localized vibrational modes of impurities 0–78729 n-GaP, thermoluminesc., trapping levels obs. 0–66114 GaP diodes, red-emitting, photo- and electroluminesc. time decay correl. 0. 62740

GaP electroluminescent p-n junction device, high efficiency, prep., patent

0 - 48130GaP electroluminescent p-n junctions, anomalous capacitance 0-76192 GaP epitaxial layers, thick, doping profiles meas. using Schottky barrier C-V data 0-72046

C-V data 0-72046

GaP heteroepitaxial growth on Si substrates by evap. method 0-58582

GaP junctions, p-n, impurity level positions, thermally stimulated current obs. 0-53875

GaP junctions, p-n, impurity photo-e.m.f. 0-56408

GaP p n junctions, diffused, green and red electroluminesc. 0-66109

GaP pair spectra, capture modes from line intensities obs. 0-79354

GaP red-emitting diodes, liq-phase epitaxy fabricated, high quantum efficiency 0-54132

GaP red-emitting diodes, recomb. kinetics from photocurrent and decay characts. 0-72458

(GaP)_{0.95}(ZnSe)_{0.05} alloy, electronic transport props., Hall mobilities 0-44188

GaS(Se) with metal contacts, barrier energies and I-V characts. 0-44235

Gas_se(Te)_{1-x} layered cryst., electroluminesc. 0–56643 n-GaSb:Te, inversion-asymmetry splitting of conduction band, Shubni-kov-de Haas meas. 0–44216 GaSb:Te, n- to p-type conversion by electron irrad., thermal cond. obs. 0–44190

0-44190
n-GaSb:Te, photoluminesc, spectra 0-56595
GaSb:Te donor level 0-51049
GaSb-GaAs solid soln, films, elec, and optical props. 0-78950
GaSb, cond, bands energy difference variations with hydrostatic press.
0-44217

GaSb, cond. bands energy difference variations with hydrostatic press. 0-44217

GaSb, crystal growth from solution, excess Ga 0-74983
GaSb, diffusion of Zn 0-78581
GaSb, doped, Fermi surface, and effective mass 0-59215
GaSb, electron mobility, 4.2K 0-44236
GaSb, electron mobility, 4.2K 0-44236
GaSb, electroreflectance spectra, spin-orbit splitting 0-72037
GaSb, etching anisotropy, light figure method 0-50412
n-GaSb, bot electron transfer, ir. Faraday effect 0-62621
GaSb, i-V characts., high field, 300K, magnetoresist., avalanche breakdown 0-75682
GaSb, injection electroluminesc. 0-72460
GaSb, local pseudopotential model, electronic and optical props. 0-43994
GaSb, socillatory photocond. under mag. field 0-59282
GaSb, piezoreflectance 0-76015
n-GaSb, Shubnikov-de Haas freq. anisotropy 0-44168
GaSb, zero bias conductance anomaly, uniaxial stress effect on subsidiary band minima 0-72026
GaSb band parameters determ. using Hall effect and rotary polarization of ir. radiation 0-59216
GaSb epitaxial vapour growth 0-71474
GaSb film, strain effect 0-53825
GaSb tunnel diode, diffused p-n, elec. field temp. depend. 0-56331
GaSb tunnel diode, I-V characts., 10, 80 or 300K, band structure 0-47796
GaSb tunnel diode, electromechanical transducer, miniature, theory, fabrication and performance 0-44295

GaSb tunnel diode electromechanical transducer, miniature, theory, fabrication and performance 0-44295

GaSe-InSe, phase systems analysis 0—46979
GaSe, electroabsorption spectra, 80-395 K, exciton annihilation 0—62659
p-GaSe, exciton mechanism of short-wavelength electroluminesc. peak
0—56645

0-30645
GaSe, forbidden gap, E-k relation 0-72005
GaSe, laser emission under two-photon excitation conditions 0-72422
GaSe, photocond. and luminesc. under two-photon excitation conditions 0-72136

O-72136
p-GaSe, photomag, effects 0-56402
GaTe, magnetic susceptibility of holes, 4.2-290K 0-40934
GaTe, reflectivity, absorpt. coeff., photocond. 0-62661
GaTe, thermal cond. 0-55608
Ga,Te, jid., n.m.r., localized electronic states obs. 0-68140
n-Gap, free-carrier absorpt. 0-44197
n-Gd,S, single crystal, growth by chemical transport reaction 0-40007
n-Ge:Te, recombination, 145-300°K 0-44250
Ge-As-Te system glass forming regions and elec. cond. 0-75683
Ge-As-Te system glasses, elec. cond. and switching diode applic. 0-78938
Ge-Si alloy and Si, simultaneous plastic deform., prod. of semiconductor thermocouples 0-43748
Ge-Si solid solns, Hg impurity states 0-56281
Ge-Li) detector, 120 cm³, characts. and comparison with smaller detectors 0-42639
Ge-Se film, elec. props., rel. to structure 0-75655

Ge(Li) detector, 120 cm³, characts. and comparison with smaller detectors 0-42639
GeSe film, elec. props., rel. to structure 0-75655
GeSe_{0.75}Te_{0.25}, reflectance spectrum, band struct. obs. 0-76071
GeSi, neutron irrad., conductivity, Seebeck coeff., thermal conductivity, Z-parameter 0-44198
GeTe-Ga(In)Te solid solns., elec. props. 0-72028
GeTe, amorphous, negative magnetoresistance 0-47719
GeTe, properties rel. to suitability as thermoelectric material 0-51133
GeTe film, amorphous and cryst., elec. props. and band structure 0-44199
GeTe film, elec. props., rel. to structure 0-75655
GeTe films, amorphous, photocond. and density of states 0-53957
GeTe(Se), amorphous films, high-field photocond., edge shift 0-53956
HfC_{0.9}, magnetoresistance and Hall effect, mag, field depend. 0-65677
HgCdTe surface, field-effect mobility 0-68824
Hg_{0.9}Cd_{0.1}Te, helicon reson. 0-56256
Hg_{1.-}Cd₂Te, Auger recomb. 0-62366
Hg_{1.-}Cd₂Te, auger recomb. 0-62366
Hg_{1.-}Cd₂Te, turinsic carrier conc. using k.p. calc. 0-59201
Hg_{0.-}Cd₂Te, transport props. at ferromag. reson. 0-59200
Hg_{0.-}Tsama edge and band struct., reflectivity and absorpt. obs. 0-69109
Hg_{0.5}Te_{1.-}s solid solns., galvanomag. and thermoelec. props. 0-51031
Hg_{0.-}Ce_{0.-}Te_{0.-}Cetric. singularity 0-78963
HeTe-In_{0.}Te_{0.-} cinnabar-structure, high pressure Hall meas. to 65 kbar

U-59222 HgSe(Te), dielectric. singularity 0-78963 HgTe-In-Te₃, cinnabar-structure, high pressure Hall meas. to 65 kbar 0-56255

N=5625 HgTe, anomalous mag. susceptibility, rel. to energy spectrum and impurity pot 0-56431 HgTe, cinnabar-structure, high pressure Hall meas. to 65 kbar 0-56255 HgTe, crystal-vapour equilib., Hall effect, Seebeck coeff. 0-78344 HgTe, electron-effective-mass dependence and higher band interactions 0-59222

HgTe, electron mobility, temp. depend., 1.7-300K, carrier scatt. theory 0-40774

HgTe, electron scatt. mechanism 0-65670
HgTe, helicon reson. 0-56256
HgTe, intrinsic conc. temp. depend. 0-53837
n-HgTe, permittivity, freq. depend., phonon-plasma interaction, reflection spectra, 80K 0-41180
In_{1-x}Al_xP, electron- microprobe cathodoluminesc., cond. bands and alloy comp. 0-72455
LACTOR CAYES. depres, impurities, electron density and mobility, conc.

comp. 0-72455 InAs:Te(Se)(S), donor impurities electron density and mobility, conc. depend. 0-47742

Semiconducting materials continued

InAs-GaAs system InAs-rich solid solns., effective mass of cond. electrons 0-72039

n-lnAs, absorpt. coeff. at different doping levels '0-56546 lnAs, effective mass press depend. 0-56272 lnAs, excitonic effects on E_1 and $E_1+\Delta_1$ transitions 0-48048 lnAs, films for device appls., elec. props. rel. to coevaporation conditions 0-55745

In As, interband transitions in valence band 0-72358 n-In As, mag. freezeout and band tailing 0-78964 n-In As, magnetophonon minima in Hall coeff. 0-68825

n-InAs, magnetophonon minima in Hall coeff. 0–68825
n-InAs, magnetoresistance magnetophonon peaks, temp. depend. of bandedge effective mass 0–53838
n-InAs, mobility of hot electron 0–62357
n-InAs, negative photocond. in quantizing mag. field 0–72137
n-InAs, optical props. as function of carrier conc. 0–44840
n-InAs, photomagnetic effects and photoconductivity, quantum oscillations, 1.8-4.2K
0–68983
n-InAs, wavelength modulation spectra, 1.75.6.0 aV, 0.44811

0-6893
InAs, wavelength-modulation spectra, 1.75-6.0 eV 0-44811
InAs effective mass from plasma edge reflection measurements 0-72041
InAs film, elec. and related optical props. 0-44764
InAs film, elec. and related optical props. 0-44764
InAs film, mobility, carrier conc., cond., explosion growth 0-47064
InAs film, mobility, carrier conc., cond., explosion growth 0-47064
InAs junctions, diffused p-n, I-V characts. 0-53878
InAs laser, time consts. 0-52328
InAs laser, diode, radiative transitions 0-52329
InAs microwave backward diodes 0-44300
InAs,P_{1-x}, epitaxial deposition on GaAs and GaP substrates 0-71475
In_{1-x}Ga_xAs alloy, growth, Czochralski techniques, Hall effect 0-75009
InGaP alloys, photoluminese. excitation spectroscopy obs. 0-66105
In₀₋₅Ga_{0-x}Sb-Te, elec. cond., thermoelec., magnetothermoelec., Hall coeff., 300K, cond. bands 0-40785
In₁₋₂O_x films, heavily doped, i.r. refl. obs. 0-79284
InP·GaAs solid solns, diodes, IV characts. 0-53893
InP-InAs diffused heterojunctions, conc. profiles, microprobe analysis 0-53874
InP, Gand structure, high-field transport props. 0-56261

InP, band structure, high-field transport props. 0-56261

InP, epitaxial layers, vapour reaction prep., electron mobility, 77 K 0-58586

InP, hip press., conduction band struct., Hall effect 0-59218
InP, interband radiative and impact recomb. 0-56282
n-InP, intra- and interband free- carrier absorpt. and fund. absorpt. edge 0-54099

InP laser, injection, spectral narrowing of radiation 0-52330

InP laser, injection, spectral narrowing of radiation 0—52330
InP photocells, photo-e.m.f. and short-ect. photoceurrent 0—53961
InP tunnel diodes 0—53901
InP tunnel junction, p-n, elec. props. temp, depend. 0—56332
InP_{1-x}As, laser, injection, spectral narrowing of radiation 0—52330
InSb-InTe, reflection and transmission spectra, comp. depend. 0—48071
InSb-NiSb eutectic alloy, magneto- sensitive resistance 0—51037
InSe, liquid, transport props. 0—46947
InSe, prep. and elec. props. 0—74973
InSe films, amorphous, elec. and optical props. 0—56287
In₂Se, recomb. radiation, laser emission 0—72424
In₃Te₄/metal contact, nonreversible props. 0—68844
In₂Te₃, liquid, ¹¹SIn Knight shift, pseudogap 0—46957
In₃Te₄ films, coarse-grained, props. and struct. 0—56258
(La_{1-x}Ca₂, MMO₃, elec. and mag. props., comp. depend. 0—59307
La₂O₃ Cr₂O₃-Al₂O₃ systems, conductivity and thermoelec. power 0—75685
Mg Bi, liquid alloy, conducting props., comp. depend. 0—46945

Mg-Bi, liquid alloy, conducting props., comp. depend. 0–46945 MgO, deterioration rel. to strong local electric field, reduction of 0–56220 MgSiP₂₃ semiconductor with chalcopyrite lattice, energy zone structure

MgSiP₃, semiconductor with chalcopyrite lattice, energy zone structure 0-65683
Mg₂Sm, elec. and thermal cond., Hall coeff., forbidden band width, 80-800 K 0-44203
MnO:Li₂, conductivity, thermoelectric force and dielectric losses temp. depend. 0-44204
MnO, MnO:Cr²⁺, effects of stoichiometry and defect conc. on elec. props. 0-51042
MnO, MnO, resistivity. Hall mobility. LiV characts. Seeback coeff

MnO₂, Mn₂O₃, resistivity, Hall mobility, I-V characts., Seebeck coeff. meas. 0–65673 p-MnTe₅:Na, antiferromag., transport props. and magnon drag 0–44205

Na₂KSb(Cs), multialkali photocathode, from Hall effect and cond. meas. 0-53817

0–53817

NbO₂, semicond-metal transitions and transport props. 0–40776
Nb₂O₃ films, photocond., trapping and chemisorption effects 0–65850
Ni₂Fe₃ ₂O₄, transport props. 0–59206
NiO-type, Hall and drift mobilities, temp. depend. 0–65661
NiO, energy spectra, calc. 0–44213
NiO, pure and Li-doped, band struct. 0–59207
NiO, semiconductivity and cation self-diffusion 0–61996
NiO-α-Fe₃O₃, polycrystalline, 400-1100°, using new contact method 0–47689

0-47689
Ni_{1-x}S, metal-semicond. transition, rel. to mag. transition 0-72031
Ni_{1-x}S, thermoelec. power, temp. depend., 83-273 K, semiconductor-metal transition 0-79065
Pb chalcogenides, interdiffusion, conc. depend. 0-40202
PbO, review, use in solid state devices, detection of i.r. and visible radiations 0-47690
PbS, fsum rule analysis of band edges, values of energy gaps and electron and hole effective masses 0-44220
PbS, review, use in solid state devides, detection of i.r. and visible radiations 0-47690
PbS effective mass from plasma edge reflection measurements 0-72041
PbS film, current carrier lifetime, 200-300 K 0-65674
PbS film, polycrystalline, electroluminescence and photoluminescence, 290K, radiative recombination mechanism 0-48123
PbS(Se, Te), band struct., relativistic Green's function method calc. 0-78965

290K, radiative recombination mechanism U-46123 PbS(Se, Te), band struct., relativistic Green's function method calc. 0-78965 PbS(Se, Te), Knight shifts and band struct. 0-56683 PbS(Se, Te), interband Faraday effect 0-69085 PbS_xSe_{1-x} diodes, stimulated recomb. radiation 0-79356 PbS(Se)(Te), epitaxial film formation mechanism 0-43551 PbS(Te) films, absorpt. spectra in 36-150 eV region 0-48080 PbSe, f-sum rule analysis of band edges, values of energy gaps and electron and hole effective masses 0-44220

PbSe, free electron effective mass 0-51046

PbSe, interdiffusion, p-n junction movement 0-40792

PbSe, review, use in solid state devices, detection of i.r. and visible radiations 0-47690
PbSe, transverse g-factors, magnetoacoustic quantum oscillations

0-78764

PbSe films, photocond. 0-65851

PbSe injection laser diodes, props., 77K 0-63636

Pb₁₋₂Sn_xSe, props., band struct. and fabrication, review 0-56224

Pb_{1-x}Sn_xSe mixed cryst., free electron effective mass 0-51046

Pb₀₋₈Sn_xTe, props., band struct. and fabrication, review 0-56224

Pb_{1-x}Sn_xTe, props., band struct. and fabrication, review 0-56224

Pb_{1-x}Sn_xTe, films, eptiaxial, transport and elec. props., obs. 0-59208

Pb_{1-x}Sn_xTe films, eptiaxial, transport and elec. props., obs. 0-77138

Pb_xSn_xTe, laser diode, Sb diffusion prep., emission characts. 0-77138

Pb_xSn_xTe, alloy films, single cryst., elec. props. rel. to shoichiometry 0-59209

PbTe:Mn alloys, carrier scatt, by mag. Mn impurities 0-53744

D=3/209
PbTe:Mn alloys, carrier scatt. by mag. Mn impurities 0-53744
PbTe:SnTe. solid solution, Hall coeff., thermoelec., elec. cond., Nernst-Ettingshausen 0-44206
PbTe, band-gap temp. depend. and Debye-Waller factors 0-78735
PbTe, degenerate, elastic constants, magnetoelastic quantum oscills. obs. 0-78602

0-/8602
PbTe, epitaxial layer growth, characts, diode fabrication 0-61656
PbTe, f-sum rule analysis of band edges, values of energy gaps and electron and hole effective masses 0-44220
p-PbTe, Fermi surface anisotropy 0-78966
PbTe, magneto-phonon oscillations and magnetoresistance behaviour 0-40764

0-40/64PbTe, Pb_{0.8}Sn_{0.7}Te, metal-semiconductor barriers, low threshold laser emission, 4.2K 0-52331PbTe, review, use in solid state devices, detection of i.r. and visible radiations 0-47690

ston, 4.2R. 0–32331
PbTe, review, use in solid state devices, detection of i.r. and visible radiations 0–47690
PbTe bonding and segmentation, PbTl-MnTl systems analysis, junctions testing 0–53669
PbTe(Se), epitaxial film, growth microstructure, electron microscopy 0–61654
Pd-Si-Ge system, Ge-Pd phase diagrams, alloy chemistry of germanides and silicides 0–53669
Sb-S₃-Sb-Se, solid solution, photocurrent spectral distribution, specific resist. 18-150°C 0–51150
Sb-S₃, field emission as function of illumination and temp. 0–51158
Sb-S₃, switching to metallic conducting, elec. field, temp. depend. 0–44207
SbSI, doped, elastic and piezoelec, props. 0–40880
SbSI, ferroelec, u.s. absorpt. near Curie pt. 0–75394
SbSI, transport phenomena 0–68826
Sb-Se, is amorphous film, local states, thermally stimulated depolarization method 0–40788
Sb-Se, liquid, transport props. 0–46947
Sb-Ses, photoconductivity and elec. cond., Se vapour press. and temp. depend. 0–40896
Se:Ag rectifiers, capacitance curves under pulse operation 0–68862

depend. 0-4086 Se:Ag rectifiers, capacitance curves under pulse operation 0-68862 Se-amorphous and polycrystalline layers plasma contact, volt-ampere characteristics investigation 0-53159 Se, amorphous, on Al, Au contact, space-charge-limited currents 0-72010

0-/2010
Se, amorphous, optical absorpt., transport, photocond. 0-47724
Se, amorphous, optical absorpt., photocond., transport props. 0-47724
Se, amorphous, optical and elec. props. 0-47721
Se, amorphous thin layers, I-V characts., high field 0-56263
Se, charge-transfer state investigation by e.p.r. 0-65696
Se, electrical and electronic props., conf., Montreal, Canada, Oct. 1967
0-65622

0-65652

o-Se, monoclinic, charge transport 0-51151
Se, monocrystalline, conductivity mechanism 0-68827
Se, Se:K(Tl), trapping level determ. 0-65685
se, switching element, thin-film, capacitance characts. 0-56314
Se, vitreous, hole transport temp. depend. 0-78953
Se, vitreous and trigonal, drift mobility, high press. effects 0-47723
Se, vitreous binary alloys, transport props, valency depend. 0-47722
Se film, Br doping determ. by radioactive isotopes 0-68843
Se film, local levels, activation energies 0-40704
Se films, amorphous, trapping of minority carriers, photocond. transient-decay obs. 0-56396
Se films, surface charging by Auger neutralization of positive ions.

Se films, surface charging by Auger neutralization of positive ions 0-47045

0-4/045
Se,Te_{1-..}Hg, crystal growth, morphology and dislocations 0-74988
Si SnO₂ heterojunctions, elec. and optical props. 0-72080
Si, local oxidation, semicond-device technology 0-51076
Si, photocell, ²³⁵U coated, neutron irrad., short-circuit currents, e.m.f. 0-51156

Si, photocell, ²³³U coated, neutron irrad., short-circuit currents, e.m.f. 0–51156
Si devices, radiation resistant, patent 0–44333
SiC:Al junctions, diffused and epitaxial p-n, elec. and luminesc. props. 0–53885
p SiC:Be alloyed p-n junctions, electroluminesc. 0–54138
SiC:N.B., injection electroluminesc. and radiative recomb. 0–72425
SiC:CdS junctions, p-n, IV characts., features 0–75747
SiC, cubic, Zeeman effect of recomb. radiation 0–76158
n-α-SiC, elec. props. 0–56265
β SiC. electron irrad., 'red' cathodoluminesc. band fine struct. 0–56641
n-SiC, m.i.s. tunnel junctions, electron local-mode phonon interaction 0–79025
SiC, prep. and purification, bibliography 0–43590
SiC, thermoluminesc. and optical charge exchange 0–79380
SiC crystals with improved Cr contacts, patent 0–75761
β-SiC epitaxial film form. by reactive deposition 0–58587
SiC junctions, elec. fluctuations 0–53883
SiC negative-resistance diodes 0–72086
SiC p-n junctions, tunnel breakdown 0–56322
SiC rectifiers, high-temp., for reverse voltages 0–53866
Sig Ge, As₃₈ Te₃₅, bulk switching properties 0–79004
SiO. /Si surface recombination vel. field. effect. planar technology control.

61–44208
SiO_x/Si, surface recombination vel., field- effect, planar technology control 0–75733

0-75733 SiO₂ amorphous layer, stored charge under high electrical stresses 0 68808

with SiO₂ coating, etchant comp., patent 0—43585 SmTe, pressure-induced metal-semiconductor transition 0—65634 α -Sn, dielec. enhancement and mobility 0—78956

Semiconducting materials continued

 α -Sn, interband magnetorefl. 0-76028

Sn_{1-x}Bi_xTe solid solns., energy spectrum of carriers 0-78954 SnO₂-semiconductor heterojunction m.o.s. struct. 0-75748

 SnO_2 films with In and Sb impurities, elec. props. 0–72049 SnO_2 thin film transistors 0–65751

n-SnO₃ film on ferroelec. ceramic, ferroelec. field effect studies, 300-78°K 0-47846

SnS₂, mobility of electrons 0–75687 SnTe-MnTe system, spec. ht., 2-25K rel. to electronic and magnetic props. 0–59108 9-SnTe, elec.-susceptibility mass of free holes 0-75709 SnTe, thermal cond. 0-55608 (SnTe)_{1-x}(GdTe)_x solid solution, elec. cond., Hall effect, lattice thermal cond. 0-78955

cond. 0-78955
SrTiO₃, band structure theory and experiment 0-68835
SrTiO₃, conductivity, Hall effect, temp. depend., effect of Ce and Nb dopants 0-47725
SrTiO₃, type II superconducting phenomena 0-68791
Te-As-Ge-Si, glass film, switching characts. 0-56266
Te-As-Si-Ce film, prep. by explosion method, negative resistance curves 0-51025

0–51025
Te-Cu-Au, amorphous alloy 0–47727
Te-Ge alloys, amorphous, valence electron config. of Te 0–75710
Te-S, Te-Se alloys, liq., switching obs. 0–78300
Te, acoustoelec. domain movement, 77-250K 0–78771
Te, amorphous, optical and elec. props. 0–47721
p-Te, cyclotron reson. and impurity transitions in valence band 0–56274
Te, electrical and electronic props., conf., Montreal, Canada, Oct. 1967
0–65652 0 - 65652

0-65652
Te, Hall effect, magnetoresistance, 150-350K 0-78957
p-Te, Landau levels in valence band 0-56273
Te, magnetophonon resonances 0-68829
p-Te, microwave emission, 77K 0-72033
Te sound attenuation, 60-600MHz, 77-300K, free carrier interaction 0-68610

0–68610

Te₈₁Ge₁₅As₈ glass, d.c. resistivity, 4-300K, ac. cond., 300K, Hall effect, magnetoresistance 0–47726

Ti_{C0.98}, magnetoresistance and Hall effect, mag. field depend. 0–65677

Ti₁O₃,Ti₁O₃,Ti₅O₉,Ti₆O₁₁, metallic transition, mag. susceptibility meas. 0–44711

Ti-Te-Ge glass, comp. for bistable system with elec. switching, patent 0–44336

Ti-Te, molten alloy, thermoelectricity, elec. cond., comp. depend., semiconductor-metal transition 0–46948

TlAsSe₂, glassy, current-voltage, characts. 0–47694

TlSe, valence band separation 0–68836

Tl₂Se, As₂Se₂, amorphous, local states, thermally stimulated depolarization

Ti,Se,As₃Se₃, amorphous, local states, thermally stimulated depolarization method 0–40788 Ti,Te,As₃Te₃, vitreous, elec. resist., Hall effect, thermoelec., temp. depend. 0–47728

 $V_{1-x}Nb_xO_2$ solid soln., semicond.-metal transitions and transport props. 0-40776

VO₂, P₂O₅ glass system, electrical conductivity, implications of n.m.r. and e.p.r. data 0–76239
VO₃, doped, cryst, growth and elec. props. 0–56267
VO₂, elec. and optical props., insulator-metal transition 0–78958
VO₃, elec. cond., optical reflection and transmission spectra, temp. depend. 0–75690

0-75690
VO2, metal-insulator Mott transition, mag. field depend. 0-51043
VO20; metal-semiconductor transition, symmetry change, effects 0-44072
V203, metal-insulator, transition characterization 0-62359
V203, metal-insulator transition in strong elec. field 0-75691
V203, metal-insulator transition 0-59211
V203, semiconductor-metal transition temp., switching effect, elec. field depend. 0-65678
V6017, elec. resist., thermoelectric power, temp. depend. 0-72034
V7013, elec. resist., thermoelectric power, temp. depend. 0-72034
V1-xYix02 solid soln., semicond.-metal transitions and transport props. 0-40776

YFe garnet:Si, negative resistance, conductive switching and memory effect 0-75692

ZnGeAs₂, amorphous film, I-V characts., switching and memory effects 0-40768

0–40768
ZnGeP₂, semiconductor with chalcopyrite lattice, energy zone structure
0–65683
Zn_xHg_{1-x}Te, crystal growth, morphology and dislocations 0–74988
Zn_xHg_{1-x}Te solid solns., prep., band struct., transport props. 0–51047
ZnO:Li, field effect cond., slow relaxation 0–75693
ZnO, acoustoelec. current saturation due to off-axis shear waves 0–50883
ZnO, electron-beam pumped laser action and luminesc., 15-250K
0–76160

ZnO, elec 0-76160

ZnO, acoustoelec. current saturation due to off-axis shear waves 2nO, electron-beam pumped laser action and luminesc., 15-250K 0-76160

ZnO, oxidation of Zn film, I doping effect, 200-390°C 0-76267

ZnO, piezoelec., acoustoelec. effects 0-75400

ZnO, us. attenuation freq. depend., room temp. 0-53705

ZnO epitaxial layers on sapphire, growth and props. 0-50378

ZnO film, u.v. irrad., Hall mobility, cond., optical transmission 0-40778

ZnO film. Hall effect, growth and struct. 0-61673

ZnO films, elec. cond., ambient oxygen influence 0-33829

ZnO surface barrier systems 0-65687

ZnS. Cu.Mn.Cl films, electroluminesc. 0-66123

ZnS. Cu.Mn.Cl films, electroluminesc. and related props. 0-69173

ZnS, deterioration rel. to strong local electric field, reduction of 0-56220

ZnS, electroluminesc., deviation from neutrality influence 0-56647

ZnS, illuminated, screening of threshold field 0-69172

ZnS, photovoltaic props., growth atmosphere effects 0-79087

ZnS film, vapour-deposited, electron-induced conductivity 0-44210

ZnS (se) (Te) film, epitaxial growth, temp, depend., elec. props. 0-50376

ZnS(Se) (Te) film, epitaxial growth, temp, depend., elec. props. 0-50376

ZnS(Se) Ge heterojunctions, switching and meory 0-6867

ZnSe-Ge heterojunctions, fabrication and props. 0-44284

ZnSe-ZnTe heterostruct., recomb, radiation 0-56648

ZnSe, appearance of self-activated photoluminescence accompanied by increase in n-type conductivity 0-56615

n-ZnSe, avalanche breakdown and light emission at low-angle boundaries 0-44209

0-44209
ZnSe, change density, Fourier transforms using self-consistent orthogonalized-plane-wave method 0-44212
ZnSe, crystal growth, vapour transport reaction 0-74976
ZnSe, dielectric function, wave-vector-dependent 0-78962
ZnSe, electroabsorpt. 0-72369
ZnSe, laser, props. 0-52332
ZnSe films, photoluminesc. and electroluminesc. 0-51374
ZnSe(Te) films, absorpt. spectra in 36-150 eV region 0-48080
ZnSiAs₃, semiconductor with chalcopyrite lattice, energy zone structure 0-65683
ZnSiP, spectra in photoluminesc. spectra 0-54122 ZnStAs₂, senuconatector 0-65683
ZnSiP₂, sharp-line photoluminesc. spectra 0-54122
ZnTe-CdSe p-n heterojunction based luminescent diode 0-72469
ZnTe, doped, photocond. 0-79083
ZnTe, m.i.s. electroluminescent diode, red and green spectral output 0-54140
ZnTe, photocond, under combined excitation conditions 0-56399

0–54140 p-ZnTe, photocond. under combined excitation conditions 0–56399 ZnTe, photosensitivity spectrum, annealing effect 0–56398 ZnTe epitaxial vapour growth on InAs 0–68230 ZnTe films, vacuum-deposited, space-charged-limited-current 0–53830 ZrC_{1.0}, magnetoresistance and Hall effect, mag. field depend. 0–65677 (ZrO)_{0.913}(Y₂O₃)_{0.087}, elec. cond. at 1000–2000°C 0–56268

gallium arsenide

(110) planes, photoemission and contact potential meas., bulk dopings from p to n-type 0-56286 acoustoelectric domains, propagating, Brillouin scatt. obs. 0-78768 acoustoelectric domains in n-type, microwave emission, freq. spectrum obs. 0-47538 acoustoelectric domains spectral comp., microwave emission, obs.

0-43893

acoustoelectric effects 0–75400 application as window material for high power 10.6 μ CO₂ laser operation 0–54861

u-34801 avalanche diode, high- efficiency oscillations, theory 0-51082 avalanche photodiodes, noise meas. 0-79012 band structure, crystal potential derivation, expts. 0-44218 band structure, self-consistent orthogonalized-plane-wave method 0-44215

chemical analysis for Cr, o, Si, Ge, by neutron activation 0–45100 conducting layer formation by ion bombard. 0–40796 conductivity, anisotropy, rel. to electron distrib. in satellite (100) energy minima, n-type 0–78978

contact with Ag-In electrode, I-V curves, thermal processing depend. 0-51075

contact with Au, space charge layer, photosensitivity, elec. field depend 0-40795

counter, carrier lifetime 0-70306

devices, manufacturing process and application 0–68861 dielectric function, wave-vector dependent 0–78962 diffusion of impurities, surface polarity depend. 0–61990 diffusion phenomena of electrons including thermal diffusion obs. 0–56254

diffusion of impurities, surface polarity depend. 0–61990 diffusion phenomena of electrons including thermal diffusion obs. 0–56254 diode, epitaxial, electroluminesc., γ-irrad, effects 0–51371 diode, pulse, electron irrad, influence on parameters 0–56326 diode struct., noise props. 0–79011 domain dynamics, bulk, device parameter effects 0–44196 doping, single crystals heavy ions of Ne, Cd and Te energy spectrum 0–62362 doping by Zn ion implantation 0–78974 double-injection devices, thermally induced oscillations and negative resistance 0–75739 e.m. reflection coeff. and phase angle, mm range, n-type 0–76014 effective mass from plasma edge reflection measurements 0–72041 electro-optical props. at λ=10.6 μ 0–72321 electroluminescent diode of or optical information transmission 0–62741 electroluminescent diode for optical information transmission 0–62741 electroluminescent diodes, degradation mechanism 0–56644 electroluminescent diodes, small-area high-current-density, improved degradation characts. 0–62739 electron, hot, effect, rel. to current oscillations 0–44202 electron flow, laminar, in thin slabs 0–78951 electron hobility in high-purity material 0–59197 electron transport, non-ohmic, from conductivity and Hall effect elec. field depend., 1.2-300°K, n-type 0–44192 electron hotpair props., Monte Carlo determ. 0–72061 electron-holo pair prod. by hot electrons, threshold energy 0–53836 epitaxial growth, asiotropy 0–50480 epitaxial growth, asiotropy 0–50480 epitaxial growth, selective, anisotropy in etching and deposition 0–71473 epitaxial growth, selective, anisotropy in etching and deposition 0–71473 epitaxial growth, selective, anisotropy in etching and deposition 0–65757 epitaxial layer, spontaneous and stimulated carrier lifetime meas. 0–72045 epitaxial layer growth, liq-phase, under transient thermal conditions 0–58584 epitaxial layer growth on insulating substrates using vapour transport 0–63068

epitaxial layer growth on insulating substrates using vapour transport 0-65068

0-65068 epitaxial layers, dislocation structure, growth depend. 0-50377 epitaxial layers, impurity concentration, Schottky barrier characts., space charge effect 0-59221 epitaxial layers for Gunn oscillators, growth and evaluation 0-61647 epitaxial n-type, high-temp. transport props. 0-47711 epitaxy, doping process, patent 0-44242 etch monitoring by internal reflection interferometry 0-50411 growth from supercooled melt dislocations 0-75004 Gunn domain behaviour high-field, in dielectric-surface-loaded bulk device 0-78918 Gunn oscillations in diodes, temp. depend. 0-65748

0-78918
Gunn oscillations in diodes, temp. depend. 0-65748
Hall coeff., elec. resist., photocond., deep levels, Fe doping 0-40791
Hall coeff. factor for polar mode scattering, temp. and mag. field depend., 300-77K, n-type 0-51036
Hall mobility absorpt. spectra, proton irrad. effect in n-type 0-41202
hole velocity in p-type 0-53823
i.r. reflection spectra room temp., 2-60u, optical phonon lifetime 0-48051 impurity ionization energy for residual donors 0-78975 ion bombarded, induced phase transform. and inert gas mobility 0-65494 ion implantation profile 0-75716

```
Semiconducting materials continued
```

gallium arsenide continued ionization energy of Mg and Be acceptors 0-44227

ionization mechanism of shallow donor centres 0-40790

junction, diffused p-n, recomb. radiation intensity and voltage drop distrib. 0-54133

0-54133

junction, h.v. p-n, electron probe recording current method obs. 0-75744
junction, p-n, electroluminesc., density-of-states tails role 0-72420
junction, p-n, electroluminesc. and cathodoluminesc. 0-54135
junction, p-n, impurity photoeffect 0-53955
junction, p-n, low-energy recomb. radiation 0-54134
junction, p-n low-energy recomb. radiation 0-79382
junction field. The first probability of the first probabilit

laser, emission spectrum, spontaneous transient processes 0-77137 laser, injection, electromagnetic theory 0-73250 laser, injection, frequency stabilization using Fabry-Perot resonator 0-54882

laser, room-temp, close-confinement technique, 40% external quantum efficiency 0–67103 laser, second-harmonic generation 0–60245 laser, short-time mode behaviour 0–73247 laser, spectral and threshold characts, cond. type and carrier density depend. 0–69921

laser, transducer in low-temp. storage 0-42184 laser conversion from infrared to blue light by second harmonic generation 0-69924

0-69924 laser diode, channel chemically etched, local mirror formation 0-45803 laser diode, waveguide props. of p-n junction 0-42307 laser emission characts. rel. to photoluminescent props. 0-72421 laser nanosecond pulsed emission characts. 0-63634 magnetophonon maxima in Hall coeff., n-type 0-68825 magnetoreflectivity, stress-modulated, split-off valence-band parameters 0-72315

0–72315 magnetoresistance magnetophonon peaks, temp. depend. of band-edge effective mass, n-type 0–53838 microhardness, effect of surface treatment, meas. 0–58939 microwave devices, material selection 0–47747 microwave emission due to round-trip gain in cavity, obs. 0–66042 mobility effects due to dil. multilevel impurities 0–62354 n¹-n² step junctions, anomalous layers interpret. 0–68866 n,p-type luminesenct diode, patent 0–54142 ntype, Hall coeff. factor for polar mode scattering, temp. and mag. field depend, 300-77K 0–51036 ntype, Hall mobility, absorpt. spectra, proton irrad, effect 0–41202 ntype, Shubnikov-de Haas oscillations, 1.3 4.2°K 0–44191 ntype, absorpt. due to free carriers, far-f.r. 0–51030 ntype, acoustoelec. domains, microwave emission, freq. spectrum obs. 0–47538 ntype, acoustoelect domains, microwave emission, Brillouin scatt, obs.

n-type, acoustoelectric domains, propagating, Brillouin scatt. obs. 0-78768

0-78768
n type, conductivity, anisotropy, rel, to electron distrib. in satellite (100) energy minima 0-78978
n-type, e.m. reflection coeff. and phase angle, mm range 0-76014
n-type, elec. conductivity and Hall effect, elec. field depend., 1.2-300°K, rel. to non-ohmic electron transport 0-44192
n-type, electron heating contrib. to transport props. 0-40772
n-type, electron heating contrib. to transport props. 0-47711
n-type, low-temp, heat treatment, carrier density obs. 0-78949
n-type, magnetophonon maxima in Hall coeff. 0-68825
n-type, resistivity and Gunn effect uniaxial stress depend. 0-47713
n-type, semi-insulating, impurity centers characts, determ. 0-68842
n-type heavily doped and degenerate, Fermi energy and bandtail parameters 0-51045
negative magnetoresistance of p-type, ang. depend. 0-59199

negative magnetoresistance of p-type, ang. depend. 0-59199 nonlinear optical absorpt, coeff. at 1.064μ obs. with YAL garnet:Nd laser 0-41099

ohmic contact, prep. techniques 0-44167 ohmic contacts prep. 0-62384 p-n junction, epitaxial, prod. in closed iodine system, I conc. depend. 0-53873

0-53873
p-n junction diodes, temperature dependence of power output 0-44297
p-n junction diodes, temperature dependence of power output 0-44297
p-n tunnel junctions, I-V characts., neutron irrad. effects 0-53892
p-type, electrolytic removal from thin n-type layers 0-72004
p-type, hole velocity 0-53823
p-type, thermally converted, heat treatment effect on elec. props. 0-53824
p-type Cu-doped as photoconductive detector at 10.6 µm 0-79990
photocarbrier multiplication due to impact ionization 0-75832
photocathode, semitransparent, quantum yield 0-65875
photoconductivity, surface region obs. 0-56384
photoconductivity kinetics 0-56386
photoconductivity of Cr doped crystals, 77-300K 0-40891
photographic process applic. 0-77226
photoluminescence, elec. field effect 0-41267
photoluminescence of n-type, hot electron carriers, radiative recombination 0-41259
photoluminescent props. rel. to laser emission characts. 0-72421

tion 0-41259 photoluminescent props. rel. to laser emission characts. 0-72421 photoreflectance line shape at fund. edge 0-76069 photothermoelec. effects, two-carrier 0-62461 radiative recomb, compensation influence 0-72420 resistance thermometer for low temp. 0-63488 Schottky barrier diode, fabrication by fluxed wetting of Sn, In and In-Zn alloy, and characts. 0-44296 Schottky barrier diode, metal-GaAs, elec. props. 0-65747 Schottky junction, zero-bias tunnelling struct, temp. and bias depend. 0-68863 Submitleon-de-Haps oscillations in n-type sample, 1.3-4.2°K 0-44191

Shubnikov-de Haas oscillations in n-type sample, 1.3-4.2°K 0-44191 space-charge region, high-resistance, near cathode, formation mechanism 0-47745

stripline, domains and guided electromagnetic waves 0-69792 surface carrier conc., rel. to heating liq. epitaxial crystals in As vapour 0-44234

```
S 1352 SUBJECT INDEX
                                                                                                                                                                                                                                                                                                                                  Semiconducting materials continued
 Semiconducting materials continued
                                                                                                                                                                                                                                                                                                                                            germanium continued
          gallium arsenide continued
surface damage, mech. induced 0-65040
                                                                                                                                                                                                                                                                                                                                                application as window material for high power 10.6 \mu CO<sub>2</sub> laser operation 0–54861
               surface damage due to ion implantation reflectance meas. 0–7 surface-barrier junctions, Tamm states role in form. 0–56319 thin film, epitaxial growth 0–65066
                                                                                                                                                                                                                                      0-78366
                                                                                                                                                                                                                                                                                                                                                 band struct., heavy doping effect 0-65702
                                                                                                                                                                                                                                                                                                                                               bulk negative differential conductance in n-type 0-65706 bulk-gradient e.m.f., current depend. 0-65704 carrier density, field depend. under intrinsic photoexcitation conditons 0-56292
                                                                                                                                                                                                                                                                                                                                                 breakdown, in p-type rel. to impurity ioniz. in strong mag. fields 0-59228
              thin slab, space-charge wave propagation, laminar electron flow, theoretical relations 0-44195 transistor structures, correlation of emission and electrical properties 0-75754
             0-75754
transport, low temp. non-ohmic, electron temp. model 0-44194
transport props. temp. depend., Monte Carlo calc. 0-68822
trapped centres, photocapacitative obs. 0-40789
vacuum-evaporated thin films, props. 0-72006
velocity-field characteristic, microwave meas. 0-75722
wavelength-modulation spectra, 1.75-6.0 eV 0-44811
AlAs-GaAs heterojunction injection lasers, spatial distrib. of emitted radiation 0-77135
AlAs GaAs heterostruct, parameters influence on laser threshold current and continuous emission 0-77136
Al,Ga<sub>1-x</sub>As-GaAs, heterojunction, electroluminescence 0-41286
Al,Ga<sub>1-x</sub>As-GaAs heterojunctions, band model and injection luminesc. 0-53872
Cs<sub>5</sub>O covered, work function shifts 0-47886
                                                                                                                                                                                                                                                                                                                                                carrier lifetimes, excess, hydrostatic press. effect 0-78992
                                                                                                                                                                                                                                                                                                                                                 carrier lifetimes, thermal defects influence 0-56289
                                                                                                                                                                                                                                                                                                                                                 carrier temp. elec. field depend. in p-Ge, warm-e range 0-44161
                                                                                                                                                                                                                                                                                                                                               carrier temp. elec. field depend. in p-Ge, warm-e-range 0-44161 charge density, Fourier transforms using self-consistent orthogonalized-plane-wave method 0-44212 chemical shifts of acceptor binding energies, g factors calc. 0-47758 conductivity, high-field, of \(\frac{111}{111}\) vallleys 0-75726 conductivity changes in X-irrad. p-ty, 0-44248 current instabilities in p-type 0-75731 current instability in n-type subjected to bending deform. 0-78987 current oscillations, large amplitude, 77K, 1GHz, elec. field depend. in n-type 0-44243
                                                                                                                                                                                                                                                                                                                                               current oscillations, targe amplitude, 7/K, 16/H<sub>2</sub>, elect. field depend. In 1/type 0–44243 current-voltage characts. of n-type, static domain formation 0–44245 cyclotron reson. in valence band, under uniaxial stress 0–72060 cyclotron resonance, 0.5-4.2 K, 71 GHz, phonon and impurity scatt., spin polarization 0–75725
               Cs<sub>2</sub>O covered, work function shifts 0-47886 epitaxial film-substrate interface, deep levels in high resistance region
               (Ga,Al)As-GaAs heterojunction laser, carrier and radiation confinements
             (Ga,Al)As-GaAs heterojunction laser, carrier and resultation 0-52326
Ga<sub>1-x</sub>Al<sub>x</sub>As-GaAs heterojunction lasers, internal Q-switching 0-69923
Ga<sub>x</sub>Al<sub>1-x</sub>As-GaAs laser diode, wave confinement analysis 0-69922
p-GaAs:Ag, photoluminesc., emission band obs. 0-69152
GaAs:Au, dopant behaviour temp. depend. 0-56385
GaAs:Cd<sup>+</sup>, implantation damage, reflectivity spectra, annealing effect 0-79279
n-GaAs:Cr, current oscillation, -80°C, spectra and optical quenching
                                                                                                                                                                                                                                                                                                                                               polarization 0—75725
cyclotron resonance, carriers spatial distrib. 0—68851
cyclotron resonance, holes at non-local magnetic critical points 0—72038
Czochralski and epitaxial growth 0—65176
dielectric function, wave-vector-dependent 0—78962
diffusion, self- and impurity-, doping effects 0—75205
diffusion of Ga in p-n junction, plastic deform, effect 0—53876
diffusion of In and Sb in electron irrad, sample 0—55919
dissipative processes, suppression in mag. field carriers in cycloidal paths
0—47748
dopon binding energies for group V dopants. 0—44229
                                                                                                                                                                                                                                                                                                                                              dissipative processes, suppression in mag. held carriers in cycloidal paths 0–47748
donor binding energies for group V dopants 0–44229
dopant in homogeneities meas. by spreading resistance 0–65708
doping by ion bombardment 0–56291
doping with B using BI<sub>3</sub> source prepd. in situ 0–72047
doping-level determ. in impurity-striations 0–75729
double injection diode, Au doped, potential vis. distance 0–40811
effective mass from plasma edge reflection measurements 0–72041
elastic constants rel. to doping in n-type 0–47314
electrical properties of single cryst. grown by Stepanov's method 0–65701
electron, hot, effects, rel. to conductivity 0–44202
electron capture, hot, from trapping and Hall mobility data in n-Ge:Pt, Sb
compensated 0–44247
electron irradiated, 3.5 MeV, annealed, carrier density and mobility, temp.
depend., P-type 0–40799
electron irradiation, 28 MeV, 88K, of n-type, Hall e.m.f., conductivity
0–51055
electron-electron and electron-hole type scatt. 0–72058
electrons vel.-field charact., under uniaxial press. 0–51059
electrons vel.-field charact., under uniaxial press. 0–51059
electron-tent live beautiful threshold of Ge-electrolyte interface
0–76072
             0-47868
GaAs:Cr, mixed cond. temp. depend. 0-68823
n-GaAs:Cu, acceptor level population at 0.13 eV after diffusion doping 0-56279
GaAs:Fe, current pulses 0-72024
GaAs:Fe, e.p.r. of Fe<sup>1+</sup> optical charge exchange, thermally stimulated current 0-48144
GaAs:Fe, Cr, injection breakdown 0-78927
GaAs:Ge diodes, radiative recomb. 0-54136
n-GaAs:S(Se,Te), absorption coeff. 0-76102
GaAs:Si, amphoteric diode, electroluminescence, transient response 0-41287
GaAs:Si, amphoteric diode, electroluminescence, steady, state, response
               GaAs:Si, amphoteric diode, electroluminescence steady state response
                               44946
              0-44946
GaAs:Si, luminescent props. of energy-band-tail states 0-79353
GaAs:Si, net carrier conc. 0-62353
n GaAs:Si, vapour-grown, growth, elec. and opt. props. 0-44228
p-GaAs:Si diodes, long lifetime (laser) states 0-48119
GaAs:Ti diodes, S-type IV characts. 0-56325
GaAs:Ti diodes, S-type IV characts. 0-56325
GaAs:Zn, exciton recombination radiation 0-44887
GaAs:Zn, exciton recombination adiation 0-44887
GaAs:Alas salidadas pages and physical gases 0. 75037
                                                                                                                                                                                                                                                                                                                                                 electroreflectance line shape, light and heavy holes 0-75707 electroreflectance spectra, polarization dependent, effect of band degenerac-
               0-40773
GaAs-AlAS solid soln., prep. and physical props. 0-75027
GaAs-Al<sub>x</sub>Ga<sub>1-x</sub>As heterostruct. lasers, wave-guiding props. 0-57540
GaAs-Ge heterojunctions, fabrication and props. 0-44284
GaAs-In<sub>x</sub>Ga<sub>1-x</sub>As p-n heterojunctions, photosensitivity spectra and electroluminesc. 0-56387
                                                                                                                                                                                                                                                                                                                                               electroreflectance spectra, polarization dependent, effect of band degeneracies 0–48052 emittance, total hemispherical, as function of temp., 25-360K 0–54071 epitaxial and Czochralski growth 0–65176 epitaxial growth, patent 0–39958 epitaxial growth, sapphire substrate, patent 0–43563 epitaxial layer, B doping resistivity, anomalous thermal, behaviour 0–44246 Fano factor 0–46039
               p GaAs-Pb point contacts, electron tunneling characts, through GaAs 0-47735
              0-47735
GaAs-ZnSe, heterojunctions, fabrication and props. 0-44284
n-GaAs, epitaxial, impurity conduction, mag. field effect 0-47712
n-GaAs, lattice scattering, small-signal relax. times 0-44193
GaAs,Te, Hall density, carrier mobility, annealing depend. 0-40771
p- GaAs (100), work function and photoemission meas., LEED-Auger spectroscopy correlation 0-47885
GaAs<sub>1-x</sub>P<sub>x</sub> growth and dislocation props. 0-47714
GaAs<sub>x</sub>P<sub>1-x</sub>, liquid epitaxial growth, parameters, electroluminescence 0-43549
                                                                                                                                                                                                                                                                                                                                              0-44246
Fano factor 0-46039
Faraday rotation anisotropy, elec. field depend. 0-48019
field effect mobility temp. depend., n-Ge, 27-65°C 0-40803
field emission kinetics of p-type 0-44418
film, amorphous, glow-discharge deposited, props.
film, amorphous, resistivity, optical transmission and reflectance, rel. to
structure, 77-750K 0-44254
film, struct. and carrier mobility rel. to deposition 0-62375
film, transmission of electrons 0-65568
galvanothermal instability of current, 77 and 300 K 0-75724
gauss-ampere characts. in strong elec. fields, p-type material 0-65712
growth of single cryst., use of moulds from refractive non-oxidizable
materials 0-65127
Hall coefficient and I-V characts., current density depend. in strong elec.
and mag. fields, n-type 0-53846
Hall effect, quadratic, in n-type single crystals 0-44255
Hall effect anisotropy in n-type p-irrad. sample with 0 impurities, 77K
0-68853
helical instability, strong mag. field 0-40798
                GaP-GaAs diffused heterojunctions, conc. profiles, microprobe analysis
               O-53874 Ge-GaAs epitaxial heterojunction, liquid phase deposition, I-V characts. 0-56321
              Ge-GaAs heterojunctions, IV characts., pot. barrier 0–53877
Ge doped, acceptor concentration investigations 0–56280
InP-GaAs solid solns., diodes, IV characts. 0–53893
n-type, epitaxial, growth parameter effects on Ge doping 0–47741
n-type, epitaxial far ir. donor-state absorpt. and photoconductivity
0–44838
                                                                                                                                                                                                                                                                                                                                                 helical instability, strong mag. field 0-40798
               Nb-GaAs junction, tunneling anomalies, 10.5 K, differential cond. 0-79023
                                                                                                                                                                                                                                                                                                                                                hop cond., phonon assisted, transverse magnetoresist. 0–53845 impurities, shallow, ground state energies, corrections 0–40804 impurity conc. determ. from cyclotron reson. 0–65705 impurity deform.-pot. consts., spectroscopic obs. 0–79304 insulator-metal transition, dopant conc. depend. 0–75728 interface with SiO<sub>2</sub>, C-V characts. freq. and temp. depend., BT treatment 0–68800.
               O<sub>2</sub>- adsorption, through e.p.r. study O
P, visible lamps and arrays 0-48120
               n-, piezo-absorption electron population, relative, in valleys, uniaxial stress, i.r. absorption 0-41121
              p-radiation defects form and annealing 0-65703

n-type, current oscillations, large-amplitude, 77K, 1GHz elec. field depend. 0-44243

absorption of light by carriers in heavily doped layers 0-56544

absorption spectrum in p-type sample, effect of doping, 94 and 295 K

0 66044
                                                                                                                                                                                                                                                                                                                                                    0-68880
              acoustic scattering anisotropy, cyclotron resonance, 4.2 K 0-75723 acoustic phonon attenuation by bound donor electrons in p-type sample, temp, depend. 0-43882 amorphization, caused by ion bombardment, model modified hot spike concept 0-62243
```

amorphous, fundamental absorpt., reflectivity, transmission, ellipsometry $0\!-\!48069$

amorphous, i.r. absorpt. spectra, 0.02-0.7 eV 0-48070 amorphous, negative magnetoresistance 0-47719 amorphous, optical and elec. props. 0-47721 amorphous and polycrystalline piezoresist. 0-47754 amorphous thick film, conductance, 300K, ambient gas comp. depend. 0-78993

PA 1970 - Part II (July-Dec.) 0-68880
interface with electrolyte, electroreflectance at fund, direct threshold 0-76072
intervalley scattering, selection rules 0-47755
intrinsic, relax, oscils, obs. in gradient in stability investig. 0-47749
ion bombarded, induced phase transform, and inert gas mobility 0-65494
ion bombardment damage annealing 0-61948
ion implantation profile 0-75716
ion implanted layers, elec. meas. 0-75730
as ionization chamber material, Cu-compensated 0-70300
junction, p-n, formed by B ion bombardment 0-56291
lattice disorder, B ion bombardment, 56 keV, dose and temp. depend. 0-61938
lattice disorder, penetration depth ionic bombardment, channeling tech-0–61938 lattice disorder, penetration depth ionic bombardment, channeling technique, thickness of amorphous region 0–62363 lattice vibr. spectrum under press., singularities 0–78730 magnetic susceptibility of holes, 4.2K 0–40934 magnetoreflectance at 1.7 K, effect of mag. field modulation 0–79247 magnetoresistance, abnormal, surface recomb. vels. calc. 0–47750 microwave cond. of n-type in high elec. field 0–68852

```
Semiconducting materials continued
  germanium continued
```

microwave conductivity during impact ionization of impurities at 4.2°K 0-75736

minority-carrier lifetime, stress effects 0-62373 n-type, 28 MeV, electron irrad., 88K, Hall e.m.f., conductivity 0-51055 n-type, Schottky barriers, one-electron and phonon-assisted tunnelling 0-44285

n-type, γ-irrad, with O impurities, Hall effect anisotropy 77K 0-68853 n-type, annealing at low temperatures 0-75118 n-type, bulk negative differential conductance 0-65706

n-type, but negative differential conductance 4-0-5/06 n-type, electron capture by neutral donors 0-72063 n-type, electron irrad., thermal stability of disordered regions 0-68850 n-type, electron removal during fast-neutron irrad., temp. depend. n-type, ele 0-78989

0-18989
n-type, far i.r. recombination emission, 4.2°K 0-44888
n-type, heating of electrons, mag. fieldi. fluence 0-78985
n-type, heavily doped anisotropic scatt. of electrons by ionized impurities 0-68849

0-68849
n-type, magnetoresistance, Hall effect and carrier transfer 0-78994
n-type, microwave cond. in high elec. field 0-68852
n-type, microwave conductivity during impact ionization of impurities at 4.2°K 0-75736
n-type, nonlinear phenomena in strong elec. and mag, fields 0-53846
n-type, optical mixing due to cond. electrons 0-79268
n-type, under bending deform, current instability 0-78987
n-type, under bending deform, current instability 0-78987
n-type electrodynamic instabilities in deformation-potential interaction 0-72059

n-type electrodynamic instabilities in deformation-potential interaction 0-72059
n-type microwave Faraday effect due to hot electrons 0-56502
n-type single crystals, quadratic Hall effect 0-44255
optical absorpt, longit, distrib, of optically created carriers, recomb, centre levels 0-76103
optical consts., enhancement under giant-pulse irrad. 0-65985
oscillations, relax, obs. in gradient instability investig., almost intrinsic mat. 0-47749
p-n junction, I-V characts., press. depend., p-irrad. depend. 0-44286
p-n junction diode, mag. field effects 0-44299
p-type, absorption spectrum, effect of doping, 94 and 295 K 0-66044
p-type, acoustic-phonon attenuation by bound donor electrons, temp. depend. 0-43882
p-type, correct of the company of the compa

0-47874 photodiode, planar p-n junction, for microwave modulation freqs.

O-68984

photoelectric emission from Al₂O₂-coated n-type cryst. 0-72155
photoelectric emission from Ba-coated cryst. 0-72157
photoepitaxial deposition of anthraquinone 0-78378
photoluminescence, biexcitons obs. 0-56598
photon drag 0-65848
photon drag 0-65848
photon drag of free current carriers, mag, field effect 0-75833
plasma, electron-hole, h.f. stabilization of helical instability 0-50953
potential distrib. rel. to band struct. 0-59217
recombination emission, far ir., in rtype sample, 4.2°K 0-44888
recombination radiation, condensed phase of nonequlibrium carriers, 2-4 2K 0-48102

recombination radiation, condensed phase of nonequlibrium carriers, 2 4.2K 0–48102 recombination radiation, laser excitation, efficiency 0–41260 Schottky barriers, one-electron and phonon-assisted tunnelling 0–44285 self-diffusion, chemical bond photoexcitation effect 0–50618 surface, oxidation, struct, and electronic changes, correl. 0–45061 surface elec. props., CO, CO₂, NO molecule adsorpt. depend. 0–40801 surface elec. props., n-benzoquinone, chemisorption depend. 0–40801 surface ercomb. vels. calc. using abnormal magnetoresistance effect 0–4750 surface recombination velocity SiO₂ film deposition effect 0–51056

surface recombination velocity SiO₂ film deposition effect 0–51056 surface states; calc. by methods of effective mass and variational procedure 0–53844

dure 0.53844
surface transverse impedance 0.–72064
surface barrier photo effect during polarization in electrolyte 0.–65842
thermoelectric effect 0.–79064
u.s. attenuation, donor electron interaction 0.–56101
u.s. attenuation by neutral donors, mag. field depend. 0.–43883
wavelength-modulation spectra, 1.75.6.0 eV 0.–44811
X-irraciation induced cond. changes in p-type 0.–44248
electron-phonon interaction in p-type, noise temp. meas. 0.–51057
GaAs-Ge heterojunctions, fabrication and props. 0.–44284
efe:Au, neutral acceptor level electron statistics 0.–65710
Ge:Au, with moving elec. domains, weak perturbation influence 0.–68848
Ge:Be cond., temp. and microwave radiation influence, low temp. 0.–78986
n. Oe:Co, recombination and trapping 0.–51148

0-78986

n-Ge:Co, recombination and trapping 0-51148

n-Ge:Co, transient photocond., recomb. of electrons and holes 0-40893

p-Ge:Cu, recomb., elec. field influence 0-78988

Ge:Hg, Sb, radiative capture of electrons by neutral Hg 0-72423

p-Ge:Li, drift velocity of Li, electron irrad. effect 0-75204

p-Ge:Li, drift velocity of Li, electron irrad. effect 0-75204

p-Ge:Li detectors, negative differential resistance 0-77406

Ge:Li interstitial donor ground state struct. 0-47751

n-Ge:Ni, 1-Y characts, instability, elec. field 0-44244

n-Ge:Ni, intrinsic photoconductivity, 80K, elec. field quenching 0-47872

Ge:Ni, recomb. of hot electrons at Ni atoms 0-56288

```
Semiconducting materials continued
```

germanium continued

n-Ge:Pt, Sb compensated, hot electron capture from trapping and Hall mobility data 0-44247

Ge:Sb, electron-phonon interaction, phonon conductivity 0-78991 n-Ge:Te, irrad. by electrons, photons and neutrons, effects 0-44249 Ge-GaAs epitaxial heterojunction, liquid phase deposition, I-V characts.

α-Ge-GaAs heterojunctions, IV characts., pot. barrier 0-53877

Ge-Si n-n heterojunctions, fabrication method influence on elec. characts. 0-56320

Ge-Si p-n heterojunctions, tunnel transitions, trap-assisted, temp. effect 0-53898

GeSt p-n heterojunctions, tunnel transitions, trap-assisted, temp. effect 0-53898
n-Ge, d.c. magnetoresistance of hop conduction, calc. 0-47753
n-Ge, heavily doped, transport props., neutron irrad., isochronal anneal, compensation effect 0-47752
n-Ge, magnetoresistance, 77 K, rel. to plastic deformation, dislocations, electron scatt. 0-44252
Ge, silane treated, fast surface states 0-40800
n-Ge film on BaTiO₁, surface conductivity 0-44316
Ge(Li) biased radiation detectors with cooled FET input, capacitance meas. method 0-42634
Ge(Li) detector, pulse shape distrib., applicability for nanosecond half-life meas. 0-42638
Ge(Li) counter, charge collection 0-63896
Ge(Li) detector, double-drift thin-window planar 0-63903
Ge(Li) detector, revaluation techniques 0-63899
Ge(Li) detector, variation of effective Fano factor 0-63902
Ge(Li) detectors, reduction of losses using gated integrator 0-52599
Ge(Li) detectors, total-absorption and double-escape peak efficiencies, approx. calc. methods 0-63904
Ge(Li) detectors, total-absorption and double-escape peak efficiencies, approx. calc. methods 0-63904
Ge(Li) detectors, stotal-absorption and double-escape peak efficiencies, approx. calc. methods 0-63904
Ge(Li) detectors, stotal-absorption and double-escape peak efficiencies, approx. calc. methods 0-63904
Ge(Li) detectors, stotal-absorption and double-escape peak efficiencies, approx. calc. methods 0-63904
Ge(Li) detectors, stotal-absorption and double-escape peak efficiencies, approx. calc. methods 0-63904
Ge(Li) detectors, stotal-absorption and double-escape peak efficiencies, approx. calc. methods 0-63904
Ge(Li) detectors, stotal-absorption and double-escape peak efficiencies, approx. calc. methods 0-63904
Ge(Li) detectors, stotal-absorption and double-escape peak efficiencies, approx. calc. methods 0-63904

Ge(Li) radiation detectors, selection of Ge by cost of 0–42637 Li drifted, y-ray detector, materials problems, characts. 0–46037 n-type, long wavelength i.r. absorpt. spectra, 1.5K 0–41204 Si-Ge ISO-type heterojunctions, characts., mechanism 0–51078 ZnSe-Ge heterojunctions, fabrication and props. 0–44284 ZnSe-Ge heterojunctions, switching and meory 0–68867 ZnSe on Ge heterojunction, characteristics 0–44288

indium antimonide

acoustic wave amplification in n-type, 77 K, transverse mag. field 0-62198

acoustoelectric amplification coeff. calc. in n-type $\,0-78769$ amorphous, negative magnetoresistance $\,0-47719$ amorphous, optical and elec. props. $\,0-47721$ anodized, surface state charges $\,0-47746$ application as window material for high power $\,10.6\,\mu$ CO $_2$ laser operation $\,0-54861$

brass contact, resistance meas., effect of magnetic field obs. 0-47619

conduction band, from i.r. cyclotron resonance 0-44219 conductivity, high electric field, n-type material 0-65732 conductivity, thin film, elec. field depend., volt-ampere characts. obs. 0-78979

conductivity, thin film, elec. held depend., volt-ampere characts. obs. 0–78979 current and voltage pulse meas. at 77°K 0–78981 cyclotron resonance, i.r., rel. to conduction band 0–44219 cyclotron resonance transmission spectrum, in n-type sample, using HCN laser 0–47688 diffusion of impurities, surface polarity depend. 0–61990 e.m. radiation, freq. tripling, 4 mm range, 77 K, conduction band nonparabolicity 0–75684 effective mass from plasma edge reflection measurements 0–72041 electrical props., effect of four point bending, n-type 0–44170 electronacoustic amplification at microwave frequencies 0–78770 electron, hot, effects, rel. to conductivity 0–44202 electron density of states, variations near conduction band edge 0–72042 electron effective mass, reflection spectra, band struct. 0–47736 electron effective mass anomaly and mobility, low temp. obs. 0–43995 electron tunnelling, in contact, differential resist, and second derivative meas. 0–75719 electron note plasma, electron energy loss 0–53827

electron-hole plasma, electron energy loss 0-53827 electron-hole plasma instability and hot-electron microwave cond.

0-59204
electron-phonon interaction in n-type 0-51041
electron-phonon interaction in n-type 0-51041
electroreflectance spectrum, inter-conduction-band transitions 0-44818
field effect exprs. at 77% on anodized surface 0-44171
film, evaporated, effects of strain on resistance 0-78919
film, getter evaporation 0-43556
film, mobility, carrier conc., cond., explosion growth 0-47064
film, strain effect 0-53825
film deposition by electric explosion, resistivity, Hall mobility, n-type
0-62358
film in microwave field cond. as 4.4

film deposition by electric explosion, resistivity, Hall mobility, n-type 0–62358
film in microwave field, cond. and d.c. e.m.f. 0–59202
forbidden band width press. coeff. 0–72040
Gunn effect in n-type, mag. field effect 0–51040
Hall coefficient and resistivity changes under hydrostatic pressure up to 40
kbar 0–47718
Hall effect meas. by self-mag. field 0–62372
hole scatt. mechanism 0–56257
i.r. absorption in highly alloyed n-type, 80°k 0–69121
i.r. cyclotron resonance, variations near conduction band edge 0–72042
impurity photoconductivity and photo-Hall effect of p-type, spectral oscillation, 5-20K 0–56393
intrinsic carrier conc. of holes, Hall coeff. 0–40775
laser, coherent radiation, mag. field tuning 0–38510
layers, evap. conditions effect on elec. props. 0–47717
m.o.s. structure, image converter, possibilities 0–51088
magnetic susceptibility of holes, 4.2-290K 0–40934
magnetophonon minima in Hall coeff., n-type 0–68825
magnetoresistance. Hall coeff., freeze-out effects in n-type 0–44201
magnetoresistance magnetophonon peaks, temp. depend. of band-edge
effective mass, n-type 0–53838
microwave acoustic noise emission 0–53826
microwave emission, high-field, contacts influence 0–78952
microwave emission characts., device applies. 0–44240

```
Semiconducting materials continued indium antimonide continued
```

microwave emission from n-type, sample prep. and spatial depend. influence 0-65671

n-p junction photodetector, proton bombard, fabrication 0-44411

n-p transition under hydrostatic pressure up to 40 kbar 0-47718

n-type, Gunn effect, mag. field effect 0-51040 n-type, acoustoelec, amplification coeff. calc. 0-78769

n-type, cyclotron resonance transmission spectrum, using HCN laser 0 47688

0 47688
n-type, electron energy relax, under quantizing mag, fields 0-78928
n-type, electron mobility in thin films 0-72029
n-type, electron-phonon interaction 0-51041
n-type, four-point bending, effect on elec, props 0-44170
n-type, high electric field conductivity 0-65732
n-type, high field transport phenomena, high temp. 0-51038
n-type, highly alloyed, i.r. absorption measured 0-69121
n-type, impact-ionized plasma, microwave radiation instability in mag. field 0-72030
n-type, light absorpt, by injected holes for CO, laser modulation 0-52273
n-type, localized electron-hole plasma, optical probing 0-75665
n-type, magnetophonon minima in Hall coeff. 0-68825
n-type, microwave emission, sample prep. and spatial depend, influence 0-65671
n-type, negative photocond, in quantizing mag, field 0-72137

0-65671
n-type, negative photocond, in quantizing mag, field 0-72137
n-type, photomag, effect and photocond, 0-79080
n-type, photomagnetic effect, 77K 0-75847
n-type, photomagnetic effects and photoconductivity, quantum oscillations, 1.8-4.2°K 0-40901
n-type, photovoltaic response in surface 0-62465
noise emission 0-56259
non-equilibrium plasma production 0-78080

non-equilibrium plasma production 0–78980 optical mixing 0–75998 oscillating photocurrent spectra, 4.2 K, 15 kOe, absolute negative cond. 0–75834

0-75834
p-type, anodized surface, field effect expts, at 77°K 0-44171
p-type, far i.r. recombination emission, 4.2°K 0-44888
P-type, high density injection, 77K 0-53840
p-type, thermoelec power temp, depend. 0-65672
p-type, two step photocond, decay by laser irrad. 0-68978
p-type, vel. field characts, of electrons, high field 0-62355
photoconductivity and photomagnetoelectric effect in p-type, electron irrad, effect 0-79081
photomagnetic effect, 77K, n-type 0-75847
photomagnetic effects and photoconductivity, quantum oscillations, n-type, 1.8-4.2°K 0-40901
photomagnetic phenomena and electron heating, 1.8-4.2K 0-68983

1.8-4.2°K 0-40901
photomagnetic phenomena and electron heating, 1.8-4.2K 0-68983
piezoelectric const., electromech. reson. meas. 0-51039
plasma, localized electron-hole, in n-type, optical probing 0-75665
plasma surface waves, electron beam interaction 0-62371
polar optical mode mobility, quantum mech. treatment 0-75459
recombination emission, far i.r., in p-type sample, 4.2°K 0-44888
surface, n-type, photovoltaic response 0-62465
surface mobility, cuspidal behaviour 0-59203
thermal cond. decrease due to phonon scatt. by free current carriers
0-50908

0-50908
thermoelectric power temp, depend, in p-type 0-65672
twist mode propagation at 70 GHz 0-66967
u.s. amplification in high elec, field under transverse mag, field 0-62202
wavelength-modulation spectra, 1.75-6.0 eV 0-44811
absorpt, spectra and band struct. 0-56547
InAs film, evaporated, effects of strain on resistance 0-78919
InSb:Cd, acceptor levels ionization energy 0-44231
InSb:Fe, carrer lifetime, photocond., Hall effect, elec, cond., photomagnetic, effect 0-47716
InSb-NiSb eutectic, microwave emissions with and without magnetic.
0-44240

InSb, relationship between microwave emissions with and without magnetic fields 0-51334

n-InSb(As) film deposition by electric explosion, resistivity, Hall mobility 0–63758

l/f noise in epitaxial layers 0-51066 absorption, i.r., laser induced 0-69129 absorption edge, valley-orbit splitting of free excitons 0-41223 absorption of light by carriers in heavily doped layers 0-56544 accumulation layer, application to acoustic surface wave amplification 0-76911

acoustic scattering anisotropy, cyclotron resonance, 4.2 K 0-75723 amorphous, fundamental absorpt., reflectivity, transmission, ellipsometry

0 - 48069

amorphous, fundamental absorpt., reflectivity, transmission, ellipsometry 0–48069
amorphous, negative magnetoresistance 0–47719
amorphous, optical, electrical and structural props. 0–47757
amorphous film, I-V characts., switching phenomena, conducting filament formation 0–47708
avalanche diode, switched-on microplasma growth 0–47779
band struct., heavy doping effect 0–65702
band struct., non-muffin-tin bands by KKR method 0–59148
band structure, orthogonalized plane wave method calc. 0–78996
band structure calcs. using self-consistent OPW 0–44265
book 0–44260
buried layers, spreading resistance meas. 0–65722
charge density, Fourier transforms using self-consistent orthogonalizedplane-wave method 0–44212
chemical shifts of acceptor binding energies, g factors calc. 0–47758
chemisorptive luminescence of o₂ 0–48125
conduction band effective mass, i.r. free carrier dispersion and Faraday rot. meas. 0–56300
conductivity of hot holes, 77K 0–75737
contact, Si-metal, ion bombarded, induced stress-sensitivity 0–53865
counters, p-n junction and Li drifted, resolution rel. to recomb. and trapping 0–38754
cyclotron resonance, 0.5-4.2 K, 71 GHz, phonon and impurity scatt., spin polarization 0–75725
Czochralski and epitaxial growth 0–65176
defects, induced by device processing 0–65724
defects during ion implantation 0–43655

Semiconducting materials continued

silicon continued

detector, surface-barrier, direct and inverse characts. in avalanche region

detectors, stacked, proton bombarded, effect of nuclear reactions on response 0-42641

detectors, surface barrier, energy resolution counting α -particles, gamma flux effect 0-46043

flux effect 0—46043
device processing, activation analysis 0—65725
device processing, activation analysis 0—65725
device processing, conference, Gaithersburg (1970) 0—65716
delectric function, wave vector-dependent 0—78962
diffused, structural faults introduced during device processing 0—65723
diffusion, from doped oxide sources 0—65720
diffusion, self- and impurity-, doping effects 0—75205
diffusion, solubility and elec. props. of Co 0—40806
diffusion and deposition of P, technology for advanced microelectronic processing 0—65719
diffusion coefficients, determination and accepted values 0—65718
diffusion current and space- charge generation current, neutron irrad., annealing 0—44262
diffusion diffusion into P, microscopic study 0—51050
diffusion kinetics, effect of diffusion-induced defects 0—65721
diffusion of 14°Pm 0—53564
diffusion of Au, radiation- accelerated 0—78586

diffusion of Au, radiation accelerated 0—78586 diffusion of Au, radiation accelerated 0—78586 diffusion of Au, radiation accelerated 0—78586 diffusion of Au, radiation accelerated 0—68385 diffusion of B, P, As and Sb into (100) and (111) slices 0—44221 diffusion of P, bulk diffusion in hydrogen atmosphere 0—68383 diffusion of P using PH, 0—65343 diffusion of P using POCI, as source 0—78587 diffusion of Pt 0—40204 diffusion of Sb, P in p-type and B in n-type, surface density depend. 0—61999 diffusion of Zn, by closed-tube two-temp. technique 0—62000 diffusion of Zn, influence on elec. propst. 0—55924 diffusion of radiophosphorous, effects of free surface and redox reactions 0—75210 diffusion profile and evap. vel. of As 0—53562

0–75210 diffusion profile and evap. vel. of As 0–53562 diffusion profiles, radiochemical determination methods 0–65717 diode, S-type Cd-compensated, noise oscillations of current 0–72089 diode, X-irrad. effect on IV and CV characts. 0–53896 diode, forward-biased p-n_Fn, IV characts. 0–53895 diode, long, from compensated n-type, transient processes 0–56329 diode array targets for TV tube, n* layer effect on gain 0–79014 diodes, vidicon, electrometer for current meas. in 10⁻¹⁶ to 10⁻¹⁵ A range 0–73122

0—1312z donor binding energies for group V dopants 0—44229 donor ground-state wave function and piezo-h.f.s., ENDOR obs. 0—51415 donor levels, deep, hydrostatic press. and temp. effect 0—78999 donor type generation-recombination centres in device technology

donor type 0-75740

doped, Gaussian distrib., Hall effect meas., numerical corrections 0-62378

0-62378
doping, PH₃ process, sheet resistance conc. 0-56299
doping, employing ion bombardment 0-60184
doping degree influence on equil. vacancy conc. 0-71610
doping from gaseous source (PH₂) by P 0-47743
double injection at high operating pts. 0-68856
drift mobility of dislocations in p-type Si 0-68855
effective mass from plasma edge reflection measurements 0-72041
elastic constants rel. to doping in p-type 0-47314
electron drift vel., saturation values, 300-4.2 K 0-59235
electron emission, secondary, under ion bombardment 0-53975
electron energy and momentum loss rates 0-78998
electron irradiation and low temperature annealing, B and Al doped
0-75118
electron saturated drift velocity from 77°K to 500°K 0-51065

0—75118 electron saturated drift velocity from 77°K to 500°K 0—51065 electron-electron and electron-hole type scatt. 0—72058 electron-hole pair prod., average triton energy required meas. 0—47577 electron-phonon scatt. anisotropy 0—56303 emittance, total hemispherical, as function of temp., 25-360K 0—54071 epitaxial, carrier conc. non- destructive determ. using total internal refi. 0—44266

epitaxial, on low Al-rich spinel, m.o.s. and vertical junction device characts. 0-62395

acts. 0–62395 epitaxial, structural faults introduced during device processing 0–65723 epitaxial, structural faults introduced during device processing 0–65723 epitaxial film on \(\alpha \cdot Al_2 \O_2 \), interface reactions 0–55726 epitaxial films, diffusion of boron 0–55923 epitaxial growth, rel. to device processing technology 0–65177 epitaxial growth, sapphire substrate, patent 0–43563 epitaxial layers, N on N⁺, impurity profile 0–72069 epitaxial layers on sapphire substrates, chem. interaction effects on electrops. 0–59232 epitaxial p-type layers on sapphire, superlinear current density obs. 0–51062 pitaxial p-type layers on sapphire, superlinear current density obs. 0-51062

0-51062 epitaxial structure, electrochemical thinning 0-53432 etch monitoring by internal reflection interferometry 0-50411 etching, preferential electrochemical, applic to thin layer device fabrication 0-65758 exciton and excitonic molecule recombination kinetics, intrinsic semicond.

0–51350
fano factor 0–49387
Fano factor meas. in n-type Si in surface barrier detector 0–42640
Faraday rot., nonresonant interband 0–79248
field evaporation, surface electron states depend. 0–62382
film, amorphous, electronic transport, 290-85°K 0–68857
film, amorphous, glow-discharge deposited, props. 0–59227
film, amorphous, structural, optical and elec. props. 0–47761
film, electrochemical etching, concentration profile determ. 0–72067
film, epitaxy, initial nucleation and growth, molecular beam technique
0–74905

0-/4905 film, growth, I-V characts, of tunnel p-n junction 0-39955 film, on sapphire, Hall mobility and carrier conc. temp. depend. 0-53828 film, transmission of electrons 0-65568 free carrier (bipolar) relaxation time, semiconductor parameter dependence, 10.6 micron laser radation 0-44261

silicon continued

galvanomagnetic effects of hot carriers in n-type 0-51063

growth of single cryst., use of moulds from refractive non-oxidizable materials 0-65127

heteroepitaxial layers, dopant transfer 0–65711 hole mobility, temp. depend., non-parabolicity, of valence band 0–47759 holes, temp. depend. of combined effective mass, model from 40-400°K 0–75734

0-75734 hot-hole anisotropy 0-51061 IC fabrication, doped SiO₂ film formation, oxidation and diffusion technology 0-59237 ir. reflection from sample with high density nonequilib. carriers 0-56489 implantation of B ions in n-type by bombardment with 30 and 100 keV ions, distrib. profile 0-56298 impurities, shallow, ground state energies, corrections 0-40804 impurities effect on carrier lifetime, electron irradiation by 2-MeV Febetron 0-51068 impurity cone, and location, ion-scatt obs. 0-55740

tron U=51068
impurity conc. and location, ion-scatt. obs. 0-55749
impurity diffusion, properties and techniques 0-65337
impurity interaction, p-n junction, I-V characts. 0-40805
insulator-metal transition, dopant conc. depend. 0-75728
interface characterization, ellipsometric techniques 0-65731
interface states in Si-SiO₂ interfaces, elec. props. energy depend. 0-56294
internal acceptor states of Group III impurities, configuration interaction
0-75732

interstitial defects in p-type electron irrad, sample, i.r. photoconductivity

interstand defects in p-type electron triad sample, its photoconducting study 0-43662 intervalley scattering, selection rules 0-47755 inversion layers, electron mobility, field and temp. depend., oscillatory magnetocond. 0-40808 ion bombarded, induced phase transform, and inert gas mobility 0-65494 ion bombardment induced amorphisation of surface layers, at. no. depend.

0-68558
ion bombardment induced damage by Bi and I 0-68340
ion implantation, P, As, Sb, profiles, treatment depend. 0-44256
ion implantation, annealing characts. rel. to damage 0-59233
ion implantation of B, lattice location, annealing effects 0-43943
ion implanted, B, lattice disorder obs. 0-68339
ion implanted, B and Cs, channelling and Hall effect obs. 0-72070
ion implanted layers, elec. meas. 0-75730
ion implanted technique application, rel. to m.o.s. IC fabrication 0-59219
ion-implanted, annealed, minority carrier lifetimes. 0, 62334

0—59219
ion-implanted, annealed, minority carrier lifetime 0—62374
junction, diffused p-n, ioniz, rates meas. 0—44287
junction, diffused p-n, ioniz, rates meas. 0—44287
junction, p-n, SiO₂ precipitates influence on I-V characts. 0—56327
junction, p-n, avalanche and tunnel breakdown, recomb. radiation characts. 0—54139
junction, p-n, beep diffused, surface breakdown time characts. 0—72079
junction, p-n, nonuniform deform. influence on current 0—53881
junction, p-n, nonuniform deform. influence on sensitivity 0—53882
junction, p-n, tunnel breakdown, radiation power 0—53884
lapping, rel. to crystallographic damage 0—65726
lattice disorder, penetration depth ionic bombardment, channeling technique, thickness of amorphous region 0—62363
lattice disorder and Hg location due to ion implantation 0—61945
light emission characts. of microplasma in p-n junctions, temp. effect
0—51349
luminescence and electron tunnelling characts., irrad, effects 0—56610

0-51349 luminescence and electron tunnelling characts., irrad. effects 0-56610 m.i.s. tunnel junctions, electron local-mode phonon interaction 0-79025 m.o.s. struct., Mo film for partial diffusion masking, applic. to device processing 0-79027 m.o.s. struct., Pt influence at Si-SiO₂ interface 0-62396 m.o.s. structure, surface characts., O+ and Ne+ implantation effect 0-47814

0-47814
m.o.s.f.e.t., Si:Au, generation-recomb. noise and thermal emission rates at acceptor centre 0-68877
m.o.s.t., determination of interface-state density and mobility ratio in surface inversion layers 0-72097
m.o.s.t., 1f. noise, theory 0-44312
magnetometer, depletion layer 0-48982
magnetoresistance, transverse, in n-type film, anisotropy, 20-77K
0-51064

metal film conductor on Si, failure due to electromigration, time prediction 0-47635

u=4/635 microdefects, effect on device technology obs. 0–75735 microhomogeneity, integrated absorption inspection, nondestructive express method applic. 0–47698 minority carrier life-time, 10 MeV electron irrad. effect 0–40807 minority current lifetime, effect of Au, Fe, Mn and Cu impurities 0–53848 minority-carrier lifetime, stress effects 0–62373 n type, bombarded with 30 and 100 keV B ions, distrib. profile of implanted B 0–56298

n-type, cond. anisotropy, population redistrib., high elec. field 0—44258 n-type, conduction band effective mass, i.r. free carrier dispersion and Faraday rot. meas. 0—56300 n-type, electron capture by neutral donors 0—72063 n-type, electron removal during fast-neutron irrad., temp. depend. 0—78989

0—18989
n-type, galvanomagnetic effects of hot carriers 0—51063
n-type film, transverse magnetoresistance, anisotropy, 20-77K 0—51064
n-type heavily doped, density of states function, metal-semiconductor barrier junction tunnelling study 0—72048
nonlinear optical absorpt. coeff. at 1.064µ obs. with YAL garnet:Nd laser (0—4109)

0—41099
Ohmic mobility of holes, 40-400°K
0—56302
optical transition obs. 0—47811
oxidation, thin tunnelable SiO₂ layer formation
oxidized structure, interface states
0—47765
p⁺-π-n⁺ struct., long, double injection temp. depend. 0—62386
p⁺pn⁺, forward-biased structure, cond., low temp. characts. 0—79007
ptype, surface conductivity without and with Cs covering 0—47766
p-i-n structure, double-carrier injection, recombination oscillations
0—53879
p-n junction. I-V characts.

0-3819
p-n junction, I-V characts., press. depend., prirrad. depend. 0-44286
p-n junction, channel currents on surface 0-40810
p-n junction, isothermal I-V characts. of mesoplasma 0-51077
p-n junction diode, mag. field effects 0-44299
p-n junctions, nuclear radiation effects 0-51079

```
Semiconducting materials continued
```

silicon continued

p-type, p-irrad., elec. props., damage obs. 0-44264 p-type, boron content determination using nuclear activation method p-type, bo

p-type, combined-resonance theory 0-78990

p-type, electron irrad. prod. of interstitial defects, i.r. photoconductivity study 0-43662

p-type, extrinsic photoconductivity 0-44408 p-type, neutron-irrad. damage, photoconductivity 0-47879 p-type, photothermoelec. effect, anomalous 0-78995

p-type, photothermoelec. effect, anomalous 0—78995 p-type epitaxial layers on sapphire, superlinear current density obs. 0–51062 p-type high-field electron drift vel. 0—62380 permittivity meas., contacts influence 0—51058 phonon conductivity 0—75727 phonon limited electron mobility, theory 0—59236 photocell, ²³⁵U coated, neutron irrad., short-circuit currents, e.m.f. 0.51156

photocell, 0 -51156

0 51156
photoconductivity in neutron-irrad. p-type 0-47879
photoconductivity of electron irrad. p-type 0-65852
photoelectric emission 0-59297
photoelectric emission from Ba-coated cryst. 0-72157
photoelectric phenomena in surface layers 0-72139
photoelectric phenomena in surface layers 0-72139
photoelectric phenomena in p-Si, 300°K and model 0-44406
photothyristor, spectral characts. 0-44277
piezo-absorption in absorption edge region 0-41121
piezo-electric-semiconductor system, amplification of u.s. surface waves
0-78763

plastic deformation simultaneously with Ge-Si alloy, prod. of semiconduc-

phastic deformation simultaneously with Ge-Si alloy, prod. of semiconductor thermocouples 0-43748 polishing, rel. to crystallographic damage 0-65726 potential distrib. rel. to band struct. 0-59217 proton damage annealing, fluence depend, minority carrier lifetime 0-43803

radiation detector, rel. to ¹⁶N Monitoring in heavy water power reactor 0-64175

0-04175 radiative recomb. of condensed phase of nonequil. carriers 0-62716 radiative recombination, two-phonon processes, peak shapes 0-44893 radioactive ion implantation, range distrib. 0-68858 Raman scattering, resonant cancellation, Loudon theory extension 0-76125

0-16125 recombination generation and photovoltaic props. of Au acceptor centre, 200-300°K 0-44892 resistivity profile, radial, rel. to semiconductor counter applications 0-65709

0-57/09
Schottky barrier contact, n-Si-Ni, Si surface conditions influence 0-72085 self-diffusion, chemical bond photoexcitation effect 0-50618 silicide-silicon contacts, field dependent barrier 0-47767 slicing, rel. to crystallographic damage 0-65726 solar cells, p-irrad induced recomb. centres, effects 0-54815 solar cells, radiation damage and annealing behaviour, impurities effect 0-69834

0-69834
solar cells, radiation damage obs. from photovoltaic parameters 0-75122
solar cells with solderless contacts, environmental testing 0-57480
surface, ionised impurity scattering 0-53849
surface, photoanodic engraving of holograms 0-73262
surface bands of (111) slabs, LCAO obs. 0-56304
surface caracterization, ellipsometric techniques 0-65731
surface contamination studies 0-65728
surface doping with metallic impurities in chemically active electrolytes 0-56296

0-56296
surface examination, Auger spectroscopy techniques 0-65730
surface impurities study with Auger electron spectroscopy 0-47764
surface layers, photoelec. phenomena 0-72139
surface preparation, effect of O₂ precipitation 0-65729
surface preparation, mechanical damage considerations 0-68859
surface preparation, stabilized, for device fabrication 0-65727
surface preparation, stabilized, for device fabrication 0-65727
surface combination velocity, surface trapping and surface photovoltage, photoconductivity meas. 0-68979
surface recombination velocity, surface the photoconductivity meas. 0-68979
surface state density of \$i/\$iO₂ interface, thermal treatments effect 0-62381
surface states; cale, by methods of effective mass and variational processors.

surface states; calc. by methods of effective mass and variational procedure 0-53844

dure 0–53844
surface states, fast, m.o.s. capacitance obs. 0–75717
surface states effective density at Si/Si₁N₂ interface 0–62379
surface-barrier photo effect during polarization in electrolyte 0–65842
surfaces, inverted p-type, elec. quantum effects 0–56301
surfaces, thermally oxidized, ionizing radiation influence 0–68845
switching and temperature effects in lateral films 0–62377
thin slices, diode fabrication 0–56324
transient conductivity 0–51067
n-p-n-transistor, anomalous diffusion, emitter dip effect, dislocations 0–75755
transistor, double diffused, mobility influence on carrier distrib. in base 0–53910
transistor second breakdown and thermal behaviour, effects of neutror

transistor, double diffused, mobility influence on carrier distrib. In base 0—59310 transistor second breakdown and thermal behaviour, effects of neutron irradiation 0—44311 us. attenuation, donor electron interaction 0—56101 valence band and probability of occupation of quantum states 0—72065 wafer for functional electronic block, fabrication process 0—59225 wavelength-modulation spectra, 1.75-6.0 eV 0—44811 work function of clean and Au-coated (111) faces 0—68986 Al-Si contacts, current crowding effects obs., reliability testing 0—47641 Al doping process, by Ar ion bombardment, billiard ball model 0—59230 Au compensated, bulk sample instabilities obs. 0—47714 B diffusion-induced imperfections, X-ray topographic study B diffusion formation of insoluble surface layer 0—47296 B doped solar cells, effect of Ni 0—57479 C contamination on surfaces 0—47763 Co compensated, bulk sample instabilities obs. 0—47714 Ga impurity optical absorption cross-section obs. 0—59283 Ge-Si n-n heterojunctions, fabrication method influence on elec. characts. 0—56320 Ge-Si p-n heterojunctions, tunnel transitions, trap-assisted, temp. effect

Ge-Si p-n heterojunctions, tunnel transitions, trap-assisted, temp. effect 0-53898 Li compensated detector manufacture 0-46036 Mn-SiO₂-Si struct., voltage thermal instability 0-79024 n-type, neutron-irradiated, resistivity and lifetime meas. 0-51060

N layer, additional doping using r.f. glow discharge 0–56295
P ion implanted, 400 keV, carrier conc., mobility, resistivity and impurity conc. 0–65713
Pt contact, current transport by thermally assisted tunnelling 0–47797
Sb doping process, by Ar ion bombardment, billiard ball model 0–59230
Si:Au, intrinsic photovoltaic effect 0–75846
n-Si:Au, low-temp., photomagnetoelec, props. 0–79086
Si:Au, thermal emission rates of electrons and holes at Au centres 0–72068
Si:Au, lique long, IV charget, tamp, depend. 0–56329

0 72068
Si:Au diode, long, IV charact. temp. depend. 0—56328
Si:Au diodes, current filaments 0—53894
Si:Au m.o.s.f.e.t., generation-recomb. noise and thermal emission rates at acceptor centre 0—68877
Si:(B,As) layers, sublimation, 430-600°C, elec. and cryst. props. 0—65086
Si:B, Hg ion implantation, lattice disorder, He ion backscattering, annealing effect 0—53537

Si:B epitaxial films, impurities distrib. 0-55728

Si:B epitaxial films, impurities distrib. 0-55728
Si:B', ion penetration profile, computer simulation 0-68854
Si:B(Ga,In), photosensitivity, rel. to photoresistor applic. 0-56397
Si:Be, acceptor diffusion, energy level and distrib. coeff. 0-59234
Si:Fe, e.s.r. of interstitials 0-72489
Si:In, ion implanted, Hall effect meas. 0-59229
Si:Li, high-temp, props., donor effect 0-62376
n Si:Li, neutron irrad., minority carrier lifetime degradation and anneal 0-47762
Si:Li, radiation damage, kinetic eqn. of annealing 0-61950
Si:Me_excitation_spectra_and_piezospectroscopic_effects_of_neutral_anneal_a

Si-Li, neutron irrad., minority carrier lifetime degradation and anneal 0–47762
Si-Li, radiation damage, kinetic eqn. of annealing 0–61950
Si-Li, radiation spectra and piezospectroscopic effects of neutral and singly ionized donors 0–51287
Si-Na. donor parameters obs. 0–78997
Si-Ni, high-resistivity, props. 0–47756
Si-Ni, P magnetodiode, I-V characts. 0–47795
Si-Ni, high-resistivity, props. 0–47756
Si-Ni, P, magnetodiode, I-V characts. 0–47778
Si-P, donor pair exchange energy, from e.p.r. spectrum 0–44999
n-Si-P, e.p.r., hyperfine splitting, 4.2K, press. depend. 0–41339
n-Si-P, e.p.r., uniaxial compression effect on hyperfine splitting 0–79407
Si-P, e.s.r. d.c. cond. 0–72491
Si-P, hot electron effect, millimetrewave radiation detection with low noise characts. 0–76964
Si-P, microwave hot electron effect and resistivity decrease due to donor spin reson. 0–72071
Si-Playerd struct., ion implanted, P conc. distrib. 0–56297
n-Si-Pl(As)(Sb), thermal cond., thermoelec. power, 4-300 K, phonon drag 0–50909
Si-Pt, energy levels in forbidden band 0–53847
Si-Zn, narmonics of self-oscillations of current 0–59231
Si-Zn optoelectronic devices applic. 0–53697
Si-Zn(Cd) diodes, with negative resistance, transient characts. 0–65750
p-Si/Al surface-barrier diode, field emission of photo-induced conduction electrons 0–44420
p-Si/Al surface-barrier diode, field emission of photo-induced conduction electrons 0–44420
p-Si/SiO₂ interface, reaction between epitaxial film and substrate 0–55726
Si/SiO₂ interface, characts, control, review 0–65715
Si-Gi-ISO-type heterojunctions, characts, mechanism 0–51078
Si-SiO₂ interface, characts, control, review 0–65715
Si-SiO₂ interface, localized recombination-generation sites, capacitance mapping technique 0–44263
Si-SiO₂ heterojunctions, elec- and optical props. 0–72080
Si-SiO₂ heterojunctions, elec- and optical props. 0–72080
Si-SiO₂ heterojunctions, props. of controlled structures 0–75746
Si-On-sapphire films, deep levels within forbidden gap 0–444259
Si-On-sapphire films, deep l

Si(Au), surface barrier detector to 44 KeV to resolution for α particles 0-57850

0-57830 Si(Li) biased radiation detectors with cooled FET input, capacitance meas. method 0-42634 Si(Li) detectors, trapping and detrapping effects 0-38753 SiO₂-Si interface photoinjection spectra correction for optical interference 0-62369

With SiO₂ film, water contamination in device technology 0–58841 Ti-Si Schottky barrier diodes, fabrication and props. 0–44302 Zn compensated, bulk sample instabilities obs. 0–47714 ZrO₂ film deposition at 250° to 350°C 0–78375

Semiconductor lasers see Lasers/semiconductor

Semiconductor lasers see Lasers/semiconductor
Semiconductors
see also Crystal electron states; Magnetoelectric effects; Photoconductivity; Photovoltaic effects
absorption coefficient, high elec. field, impurities, calc. 0–47995
absorption of radiation by locally excited charge carriers 0–51273
acoustic phonons, high energy, amplification 0–71848
acoustic waves propagation, gain mechanisms, sound velocity changes
under two limiting conditions 0–47697
amorphous, absorpt. edge and internal elec. fields 0–79290
amorphous, band structure, theory 0–47732
amorphous, conf., Cambridge, England, Sept. 1969 0–47686
amorphous, covalent, energy gaps 0–72036
amorphous, electronic structure transport props. 0–47704
amorphous, localized states 0–73654
amorphous, metal-insulator transition, nucleation of conducting phase
0–73658
amorphous, metal-insulator transition, nucleation of conducting phase

amorphous, metal-insulator transition, nucleation of conducting phase 0 -56245

0 -56245 amorphous, modelling of structure 0-47014 amorphous, optical and elec. props. 0-47721 amorphous, optical spectra, elec. cond., thermoelectricity 0-53821 amorphous, structure and bonding 0-53409 amorphous, study 0-53735 amorphous, switching effects 0-62347 amorphous, switching effects 0-62347 amorphous undulatorily graded band-gap systems 0-78915 amorphous covalent, short-range order role in producing energy gap 0-75702

Semiconductors continued

anisotropic, minority carrier mobility determ. 0-75661 antiferromagnet, current carriers in sample with narrow band 0-47702 antiferromagnetic, scatt. of light and electrons by coupled waves 0-71902

auger recombination in mag. field, inverse population of Landau levels 0-59183

0–59183 avalanche region, carrier diffusion 0–59186 avalanches, quasistatic approx. 0–47699 band struct., calc. methods and models 0–68830 band struct. of diamond-type, KKR-Z calc. 0–71972 band structure of tetrahedral cpds., orthogonalized-plane-wave convergence 0–53833 bandgaps, thermochem. approach 0–47591 binary, band gap prediction chem. approach 0–59138 binary, implantation of Ne, Cd, Te heavy ions in GaAs and GaP 0–62362 biological, small polarons 0–75647 bound hole states, vibronic coupling, dynamic Jahn-Teller effect 0–40762 breakdown in alternating elec. field 0–51024 bulk, e.m. and space-charge wave propag. and amplification 0–43886 bulk, wave instabilities rel. to field-depend. drift vel. and carrier temp. 0–65656

0-65656 bulk and surface components of lifetime separation using pulsed m.o.s. capacitor 0-44224

capacitor 0-44224 carrier diffusion length by surface photovoltage method, bulk trapping effect 0-44184 carrier lifetime meas by injection-extraction method 0-65733 carrier lifetime reduction by Au doping, and final product, patent 0-44163

carrier lifetimes in samples with two interacting or two independ, recombination levels 0-44180

carrier lifetimes in samples with two interacting or two independ. recombination levels 0—44180 carrier mobility, meas, in nonhomogeneous samples 0—78982 carrier mobility and density, determination, bimodal microwave resonator, analysis 0—47621 carrier mobility determ. using bimodal resonator 0—78960 carrier mobility determ. using bimodal resonator 0—78961 carrier temp. elec. field depend., warm-e-range 0—44161 cathode oxide glass for electrostatic separator, test results 0—49440 chalcopyrite lattice structure, energy zone structure 0—65683 chalcopyrite lattice structure, energy zones structure 0—65683 charge carrier scatt. length determ. 0—75673 charge carriers energy relax. time in harmonic mixing expts. 0—47701 charge transport in non-crystalline 0—53820 charge transport props. from nucl. pulse shape meas. 0—40765 compensated, ambipolar drift and recomb-drift mobility 0—78930 compound, in sputtering ion source for ion implantation 0—60183 compound-type, epitaxial, deposition by fused salt electrolysis, patent 0—43602 III-V compounds, growth 0—47103 conductivity, β- and γ-induced 0—78931 conductivity, elec. and thermal, and thermal e.m.f. under high pressure 0—64944

0 - 64944

0-49494 conductivity, mag, field orientation depend. 0-47695 conductivity, radiation induced, after bombardment with medium energy particles 0-56353 conference, New Delhi, India, January 1969 0-75650 Conference, New Delhi, India, January 1969 0-75652 coupled e.m.-magnetoplasma modes, light scattering obs. 0-40756

coupled semicond.-piezoelectric system, conductance modulation 0-79053

covalent, with aribtrary band struct., electron momentum distrib. function $0\!-\!56225$

covalent alloy, high field breakdown, conduction and switching phenomena 0-56241 crystal, growth, impurity adsorption and segregation anisotropy 0-74996 crystal chemistry, struct., octahedral and mixed atomic coordinations 0-50508

crystal growth, floating zone melting technique, patent 0–43601 crystal growth, solution and travelling solvent zone technique 0–47129 current calculation, strong alternating elec. field, inelastic electron scatt. 0–44173

current column motion in mag. field in samples with S-like I-V characts. 0-40763

0–40763
current controlled negative resistance, model 0–72013
current oscillations, low surface recombination velocity 0–44177
current oscillations due to recomb. centres 0–44185
current oscillations in external cct. containing low surface recomb. vel. semicond. 0–72007
cyclotron resonance line shape, optical photons effect 0–56221
Czochralski growth, high pressure techniques 0–47126
deep-level defect, diamond with nitrogen donor, electron band structure 0–75485
defect vibrs. 0–75360
defective, diamond like, intermediate between vitreous and crystalline states 0–47174
degenerate, Faraday and Voigt effects 0–79244
degenerate, cyclotron-phonon absorpt. 0–51021

degenerate, Faraday and Voigt effects 0–79244
degenerate, cyclotron-phonon absorpt. 0–51021
degenerate, optical absorpt. near Burstein edge 0–41187
degenerated, evaluation of transport processes 0–56230
density of states in forbidden band, heavy doping 0–40781
diamond structure, direct exciton spectrum 0–66014
diamond type, sputtering ejection pattern, Ar ion bombardment, 5-15 keV
0–68706
diffusion, double-stream, partial differential eqns. soln. 0–55910
diffusion eqn. soln. for non isothermal diffusion 0–68373
diffusion from heterogeneous solid, impurity distrib. 0–71635
diffusion phenomena, concentration dependent 0–68839
diffusion processes, bond predissoc. role 0–78568
diffusion profiles, determination using incremental sheet resistivity technique 0–65689
direct-gap polar, electron mobility 0–75671

direct-gap polar, electron mobility 0-75671 disc resistivity meas., two-probe method 0-47685 dislocations, diffusion-induced emitter edge, obs. using Sirtl etchant 0-44225

0-44Zc3 dislocations generated for dislocation vel. meas. Burgers vector 0-58805 disordered, carrier-carrier interactions effect on transport props. 0-7566-disordered, e.m. wave absorption, elec. cond. freq. depend. 0-75653 disordered systems, polaron hopping conduction 0-56240

Semiconductors continued

domain oscillations, forced 0-56234

domain oscinations, forced 0-56,234 dopant injector for crystal pulling furnaces 0-74992 doped, cond. and intervalley redistrib. anisotropy, low temp. 0-65649 doped, effective masses from holes influence on elastic moduli 0-56269 doped, static residual conductivity, theory rel. to impurity interactions 0-44179

doped polar, coupled magnetoplasma-phonon modes obs. from refl. spec tra 0-54084

doped surface layers, high-energy ion-beam analysis 0–65690 doping, ion implantation process, techniques 0–44222 doping, monatomic ion beam, analyzing magnet, patent 0–44241 doping profiles, meas. using capacitance-voltage technique 0–65691 double injection, multivalent trapping centres 0–75711 double injection at high operating pts. 0–68856 double injection in semicond. heavily doped with two-level traps 0–72044 e.m. wave amplification in plasma 0–44174 e.m. wave propagation, carriers, nonlinear effects 0–47683 e.m. wave propagation, phonon heating effect 0–75646 effective mass and carrier relaxation time, i.r. reflection spectra 0–40759 Einstein relation, validity for nonequilibrium conditions 0–65665 electrical conductivity meas. Landau levels collision induced broadening electrical conductivity tensor. Landau levels collision induced broadening

0-76314 conductivity tensor, Landau levels collision induced broadening 0-68758

electrical instabilities 0-56249

electrical instabilities 0–56249
electrical properties, apparatus for determination 0–51053
electrical properties, contactless meas. method for thin films 0–78983
electro-absorption, excitonic absorpt. edge 0–59372
electroabsorption, excitonic sefects 0–48017
electroacoustic absorption, energy-depend, relax. times 0–43888
electron concentration theory of instability phenomena 0–51023
electron excitation by ion and electron bombardment 0–68815
electron exact states theory, strongly doped system, band structure, impurities 0–75701
electron transitions from impurity to band in strong e.m. field, 0–56277

0-3701 electron transitions from impurity to band in strong e.m. field 0-56277 electron-donor recombination in mag. field 0-56278 electron-phonon and electron-impurity interactions, laser beam effect 0-40758

electron-ghonor ecombination in mag., held 0-362/8 electron-ghonor and electron-impurity interactions, laser beam effect 0-40758 electron-phonon interaction, localized potential method 0-47580 electron-ghonon interaction, localized potential method 0-47580 electron-ghonon interaction, Charia, Crete, Jul 1968 0-68729 electroreflectance in space charge region 0-65984 electrostatic field, positive pt., line or plane charges potential 0-68810 epitaxial growth, liquid phase 0-47149 epitaxial growth, liquid phase 0-47149 epitaxial layer, high-resistance, Hall mobility of current carriers, meas. by probe method 0-65662 epitaxial layer deposition on semicond. substrate, including baffling of source, substrate and interspace from environment, patent 0-43560 epitaxy, impurity profile plotter 0-65694 excited locally, e.m. radiation transmission 0-78923 exciton anisotropy, rel. to effective mass tensor 0-68802 exciton differential spectrum in crossed and parallel fields 0-79266 exciton luminese. assoc. with excited exciton state 0-72409 exciton recomb. of electrons and holes, statistical theory 0-56226 excitons bound to axially symmetric defects, stress effects 0-44160 fabrication technique pertmitting examination of epitaxially grown layers, patent 0-40797

Faraday effect, interband, impurity conc. depend. 0-48012

Faraday effect, method of meas. 0-78984

Faraday effect, method of meas. 0-78984

Faraday effect, we photon spectroscopy 0-79242

Faraday effect, method of meas. 0-7804

Farriet, local inhomogeneities, prod. and investig. 0-51019 ferroelectric, AVBVCVII, phase transform., photocond. effect 0-59262 ferroelectric, single domain polarization, theory 0-40840 ferromagnetic, electron-magnon interaction 0-72000 field singularity due to charged electrode edge, model 0-68800 field-effect relax, charact. features 0-72018 film, intermetallic, growth, props. and device applics., book 0-44162 film, intermetallic, growth, props. and device applics., book 0-44162 film, intermetallic, defect o-68974 film, photocond, field effe

film, intermetallic, growth, props. and device applies., book 0—44162 film, magnetoresistance, size anisotropy effect, in weak mag. field 0—72009 film, phonon drag contrib. to thermopower 0—56233 film, photocond., field effect 0—68974 film, plasma reflection edge 0—44762 film, superconductivity 0—44118 film, thin, quantized, electron-phonon carrying theory 0—65663 film, thin, quantized, electron-phonon carrying theory 0—65664 films, speriaxial, thickness meas. by interference method 0—55707 films, thin single cryst., condensation and nucleation, obs. 0—47069 fissionable material coated, neutron bombard., e.m.f. 0—47692 fluctuations, nonequilibrium, correlation functions in electron temp. approx. 0—53813 fluctuations, nonequilibrium, external random forces and eqns. for correlation functions methods 0—56217 forbidden energy gap meas. diffuse reflectance technique 0—75700 fundamental aspects, lecture 0—71894 galvanomagnetic effects, low temp., in strong elec. fields 0—78935 galvanomagnetic effects in strong elec. fields 0—78935 galvanomagnetic effects in strong elec. fields 0—72011 galvanomagnetic phenomena, theory, elec. cond. tensor, impurity conc. depend. 0—50975 glass, model and switching behaviour, frequency dependence 0—62338 glassy, conf., Bristol, England Sept. 1970 0—74859 graded band gap, photovoltaic effect 0—44403 group III-V, density of conduction states meas. of absorption and reflection spectra 0—75699 Gunn domains vel. 0—62344 Gunn effect, internal mag, field effect 0—56231 Gunn effect, internal mag, field effect 0—56231 Gunn effect, internal mag, field effect 0—56231 Hall effect, inhomogeneous mag. field, equations 0—44178 Hall effect in long plate in homogeneous mag, field 0—72001 Hall tensor components meas. in anisotropic specimens 0—56236

Semiconductors continued

harmonic generation, third, using hot-electron nonlinearity 0-44750 helical and magnetoacoustic waves, parametric excitation 0-72008

helical wave, Lf., nonlinear propagation 0–75667 helicon mode, hot-electron, conversion 0–65657 high-resistance, galvanomagnetic thermal and photo effects, apparatus for study 0–59288 homopolar, Raman tensor, pseudopot. calc. 0–51320 illuminated, in open resonator, detection of i.r. and optical radiation

0 - 51154

0-51154
illuminated panel, millimeter wave attenuation 0-45719
impact ionization in covalent material with ellipsoidal const-energy surfaces 0-78922
imperfection centres, thermal and optical emission and capture rates 0-53839

imperrection centres, thermal and optical emission and capture rates 0–53839 impurities, in single crystals, microdistribution 0–47737 impurity, hydrogen-like, screened, in strong mag field 0–78976 impurity atom activation energies 0–56276 impurity atom activation energies 0–56276 impurity band conduction, mag. field, Green function calc. 0–40761 impurity centre, deep-level, determ. 0–78967 impurity centres fluctuations, effect on light scatt. 0–68837 impurity centres fluctuations, effect on light scatt. 0–68837 impurity diffusion eqn. solns. 0–72051 impurity diffusion eqn. solns. 0–72051 impurity levels, deep 0–68841 impurity levels, shallow 0–68840 impurity problem kq representation 0–75713 impurity profile, spreading resistance probe applications 0–65688 impurity profiles, variations of capacitance-voltage determination technique 0–65693 impurity screening charge density in elec. current 0–62339 indirect band-gap type, resonance enhancement of second harmonic generation 0–52352 indirect exchange, mag. defects method 0–62481

indirect varies aprype, resonance emancement of second narmonic generation 0-52352 indirect exchange, mag. defects method 0-62481 inhomogeneous, space-charge-limited currents, thermally stimulated cond. obs. 0-65654 interaction, coherent, between electron and strong e.m. wave, effect of relax. processes 0-75674 interface-wave instability in parallel arrangement of sheets with transverse mag. field 0-72053 intermetallic structure and n-type diffusion method, patent 0-56275 inversion layers with many occupied subbands, screening and impurity scatt. 0-75660 ion implantation, electron microprobe study 0-62223 ion implantation, monatomic beam, analyzing magnet, patent 0-44241 ion implantation, scatter of range and distrib. profile of ions 0-56122 ionic alloying using ILU ion accelerator, results 0-49427 ionization and drift-temp. waves 0-74590 Kadomtsev-Nedospasov instability, external- circuit current oscills. 0-62345 kinetic instability and reson. effects under double injection conditions

kinetic instability and reson. effects under double injection conditions 0-56232

kinetic instability and reson. effects under double injection conditions 0–56232 lattice dynamics and band struct., group theory appl. 0–40508 lattice parameters, fully automated high precision X-ray obs. 0–58711 lattice vibration in II-VI compounds 0–40509 layer and interface props. determ., C-V technique 0–75721 layered structure, stabilization of Gunn oscillations 0–75756 light scatt. by electron-hole plasma in applied elec. field 0–72319 light scatt. by sound 0–48094 light scattering by plasmons 0–69135 liquid, classification, comp. depend. 0–46945 liquid, conductivity, correlation function calc. 0–46942 liquid, conf., Bristol, England Sept. 1970 0–74859 liquid, elec. and thermal conductivity and thermal e.m.f. under high pressure 0–64944 liquid, theory and expt. 0–46943 low-ohmic, fluctuations in non-equilib. plasma 0–44166 luminescence, i.r. radiation quenching and enhancing effects, centres level depths obs. 0–66086 luminescence and abs. spectra, analogy to complex molecules 0–44822 magnetic, Curie temp., resonance shift 0–40755 magnetic, exchange coupling effects 0–44453 magnetic, mobility of large paramag. polaron theory 0–78849 magnetic, properties and applications, review 0–71997 magnetic, review 0–59181 magnetic, with degenerate d-bands, allowance for Coulomb interaction 0–72035 magnetization state, Hubbard Hamiltonian, bandwidth to Coulomb integral ratio 0–44451

magnetization state, Hubbard Hamiltonian, bandwidth to Coulomb integral

0—72035
magnetized, with degleriest devidings, allowance to the Coulomb interaction
0—72035
magnetization state, Hubbard Hamiltonian, bandwidth to Coulomb integral
ratio 0—44451
magneto-optic absorption, interband, polaron effect 0—56498
magneto-optical effects, anisotropic, rel. to cubic symmetry 0—69082
magneto-optical effects, anisotropic, rel. to cubic symmetry 0—69082
magneto-optical effects, of hot electrons in high mag. fields 0—79241
magnetoconductivity tensor calcs. rel. to warped energy surface 0—68816
magnetoresistance, anomalous effects and rel. to band struct. 0—40764
magnetoresistance, negative, scatt. by imperfections associated 0—75524
magnon specific heat rel. to phonon-magnon interaction 0—40978
many-valley, Faraday effect of hot electrons 0—79245
many-valley, in diffusion phenomena of electrons including thermal diffusion
obs. 0—56254
many-valley, hot electron transfer, i.r. Faraday effect obs.
many-valley, hot electron transfer, i.r. Faraday effect obs.
many-valley, the splitting of donor impurity pairs 0—40786
many-valley, the reg. depend., equations 0—47526
microwave emission 0—56222
molten, thermo-e.m.f. meas. cell 0—46941
Mott transition theory 0—68804
multivalley model, weak-field magnetoresistance 0—75526
n-type, field of negative point, line or plane charges 0—72012
n-type, negative conductivity in strong mag, field 0—47696
n-type two-valley, high-field galvanomag. effects 0—68813
narrow-band, localized states 0—75654
negative differential resistance, formation mechanism during impurity
breakdown 0—53819
noise, 1/f 0—78924

```
Semiconductors continued
Semiconductors continued
                                                                                                                                                                                                                                                                                                                                                                                                                                                                                                                                                                                                                      recombination in material with macroscopic defects 0-65655 with recombination levels, two interacting or two independ., carrier life
                        noise, ambipolar drift spectrum, mag. field, Green's function 0-44182
                        non-radiative recombination obs. via detailed balance 0-68730
                      non-stoichiometry, fully automated high precision X-ray obs. 0–58711 with nonconstant impurity profiles, Poisson's eqn. soln. 0–44223 nondegenerate, resistivity, effect of heating of phonons by hot electrons 0–56216
                                                                                                                                                                                                                                                                                                                                                                                                                                                                                                                                                                                                                             times 0-44180
                                                                                                                                                                                                                                                                                                                                                                                                                                                                                                                                                                                                                      recombination eartre capture-probability temp. depend. determ. method
                                                                                                                                                                                                                                                                                                                                                                                                                                                                                                                                                                                                                  recombination-centre capture-probability temp. depend. determ. method 0–72043 reflectivity, current-induced changes 0–59387 reflectivity, current-induced changes 0–59387 reflectivity, current-induced changes 0–59387 reflectivity spectra, band structure, group V and IV-VI materials 0–79270 refractive index changes with population inversion 0–54058 resistance, current controlled negative, model 0–72013 saturation state in strong e.m. wave field and mag. field 0–78913 screening of bound states 0–62346 second harmonic generation, d.c. electric field 0–47988 semiconductor, U.S. 'superheterodyne' amplification 0–62199 shallow donor energy, subsidiary minimum correction 0–78968 soiid, conference, Turku, Finland, Aug. 1970 0–74858 space charge measurement 0–56219 space-charge-limited current, I-V characts., theory 0–47693 spin waves on dislocations 0–47911 spin-lattice relax. of shallow donors in wurtzite-type 0–47590 sputtering target, Ar+ bombarded, 40 keV, positive and negative ion yields 0–68688 stability of static domains, effect of boundary conditions 0–54540
                      0-56216
nonhomogeneous, carrier mobility measurement 0-78982
nonisothermal meas. in presence of thermoelect., thermomag, and galvano-
magnetic effects 0-68846
nonlinear harmonic generation and mixing, free-carrier contrib. 0-59347
nonlinear props. due to shallow impurities 0-65650
nonparabolic, microwave cond., hot-electron anisotropy 0-56238
one-carrier, space charge wave excitation at jump in doping density
0-78936
optical absorpt, size quantization and phonor discontinuities. 0-72344
                    one-carrier, space charge wave excitation at jump in doping density 0—78936 optical absorpt., size quantization and phonon discontinuities 0—72344 optical absorption in degenerate sample 0—41187 optical and electro-optical coeffs., dispersion 0—44755 optical consts. determ. of n and i-type by Beattie-Conn method 0—41103 optical mixing by mobile carriers 0—47989 optical transitions in impure 0—48058 organic, photosensitivity enhancement 0—51145 organic, photosensitivity enhancement 0—51145 organic, pre-exponential factor, theory 0—40779 organic, small polarons 0—75647 oscillation mechanism 0—75647 oscillation mechanism 0—47691 oscillation mechanism 0—47691 oscillation mechanism in strong elec. field 0—72154 parametric excitation of helical and magnetoacoustic waves 0—72008 phase transition to semimetal, two critical temps. 0—44159 phonon instability, pulsed elec. field 0—44175 photoconductivity, oscillatory, Boltzmann-eqn. model, exact soln. 0—75824 photoconductivity, spectrum local inhomogeneities influence 0—56374
                                                                                                                                                                                                                                                                                                                                                                                                                                                                                                                                                                                                            spin waves on uslocations 0-4/91 spittering target, Ar+ bombarded, 40 keV, positive and negative ion yields 0-68688 stability of static domains, effect of boundary conditions 0-54540 stimulated emission under electron and optical excitation 0-79343 surface, electron mirror microscopy 0-72052 surface, interaction with adjacent parallel electron beam 0-65697 surface, large unit cells, two-centre theory 0-65025 surface barrier, metal-semiconductor system 0-65700 surface helical instability in electron-hole plasma in strong mag. field 0-56283 surface layer, intrinsic, impedance, calc., diffusion region charge 0-53842 surface oscillistor effect, theory 0-40793 surface scattering reactive oxygen atoms 0-55704 surface space charge layers, cond. 0-78929 surface states characterization by laser probe 0-44233 surface state characterization by laser probe 0-44233 surface states chectron depletion 0-50946 surface states in complicated band struct. material 0-75606 surface wave amplification, surface states effects 0-75395 switching, double injection initiation pulse meas. 0-53851 Tamm surface states 0-65698 tetrahedral, self-consistent orthogonalized-plane- wave eigenvalues and binding energies, comparison 0-43950 tetrahedrally bonded, theoretical electron density of states study 0-65681 tetrahedrally coordinated, cohesive energies and heats of form. 0-78392 thermal properties, apparatus for determination 0-51053 thermoelectric effect of hot carriers in samples with nonparabolic energy bands 0-44388 thermomagnetic effects, quantum theory 0-56367 thermoreflection spectra, expt. methods 0-66019 thin film, monocryst., theory of space-charge region 0-75666 thin films, electrical properties meas, contactless method 0-78983 three-level, generation-recombination noise 0-43981 transport processes, soln., displaced distrib. method 0-72014 tunneling currents, E-k relation 0-70505 two-photon transitions at saddle points, peaks in freq. depend. 0-44821 two-valley, with traps, Gum effect 0-65688 u.s. absorption, in many-valley, freq. d
                      photoconductivity, oscillatory, Boltzmann-eqn, model, exact soln. 0–75824
photoconductority spectrum local inhomogeneities influence 0–56374
photoconductor, I-V characts, two trapping levels, calc. 0–44172
photodection, active transmission line analogue 0–72133
photolipole effect, high temp, kinetics 0–78811
photoelectron mission of p-type, in strong elec. field 0–72154
photoexcited carrier, non-equilib, theory 0–56378
photography applic., long-wavelength 0–54948
photon capture by surface states, cross sections 0–56376
photovoltaic effect in graded band gap semicond. 0–44403
photovoltaic effects 0–62464
physics and devices, book 0–44267
piezoelectric, acoustoelectric amplification, non-linear theory 0–51030
piezoelectric, acoustoelectric amplification 0–40555
piezoelectric, acoustoelectric amplification 0–40555
piezoelectric, acoustoelectric amplification 0–40555
piezoelectric, acoustoelectric interactions 0–43887
piezoelectric, cacustoelectric interactions 0–43887
piezoelectric, nonlinear effect of the propagation of sound 0–47536
piezoelectric, nonlinear amplification of sound 0–47536
piezoelectric, nonlinear electroacoustic conversion 0–7865
piezoelectric, nonlinear amplification of sound 0–47536
piezoelectric, nonlinear electroacoustic conversion 0–78765
piezoelectric, nonlinear electroacoustic onversion 0–78765
piezoelectric, was was generation in platelets by drift electrops 0, 75385
                          0-62186
piezoelectric, u.s. wave generation in platelets by drift electrons 0-75385
piezoelectric plates, transverse u.s. waves interaction with charge carriers
                      0-68812
piezoreflectance, modulated, shear deform, potentials determ. 0-43727
pinch effect, theory, transducer potentials 0-44164
pinch effect for degenerate and non- degenerate electron-hole plasma with
bimolecular vol. recombination 0-53815
pinch effect for high degeneracy of electron-hole plasma 0-62360
Pinch effect in samples with bipolar conductivity at electron-hole scattering 0-68805
pinch-effect, bipolar cond., external mag. field 0-53814
plasma, Θ pinch 0-71998
plasma, convective instability in cross elec. and mag. fields 0-47604
plasma, electron-hole, helical instability, excitation and h.f. stabilization in
strong mag. field 0-62272
plasma, first-order Raman effect in mag. field 0-44924
plasma, helical instability 0-62340
plasma, helical instability of electron-hole plasma in parallel fields
0-75659
plasma, helical instability suppression, mag. field 0-47684
                                                                                                                                                                                                                                                                                                                                                                                                                                                                                                                                                                                                                      CdS-type, impurity photoconductivity, linear and nonlinear relax, kinetics 0\!-\!65846
                                                                                                                                                                                                                                                                                                                                                                                                                                                                                                                                                                                                                    0-05840 CdSiP<sub>3</sub>, single crystal growth by vapour transport and from solution 0-47123 Te(Ge,As) based, amorphous, reflectivity 0-56490 ZnSiP<sub>3</sub>, single crystal growth by vapour transport and from solution 0-47123
                        0-75659
plasma, helical instability suppression, mag. field 0-47684
plasma, light scattering, inelastic, in mag. field 0-40757
plasma, non-equilib., stationary state for finite cross-section 0-75648
plasma injection, diffusive current 0-40766
plasma low-temperature in e.m. fields, instability region, non-linear theory
0-71136
plasma oscillations, ambipolar, u.s. interaction 0-68811
plasma refl. minimum, carrier density and effective mass determ. 0-72015
plasma wave instability under intervalley transition conditions 0-78925
plate in waveguide, elec. field distrib. 0-68809
Poisson's equation soln. for samples with nonconstant impurity profiles
0-44223
polar, current fluctuations in strong elec. fields, A<sub>III</sub>B<sub>V</sub> type, band struct.
                                                                                                                                                                                                                                                                                                                                                                                                                                                                                                                                                                                            Semimetals
                                                                                                                                                                                                                                                                                                                                                                                                                                                                                                                                                                                                                    diamagnetic susceptibility 0–40941
electronic states, effective Hamiltonian 0–71929
electronic states, effective Hamiltonian 0–71928
                                                                                                                                                                                                                                                                                                                                                                                                                                                                                                                                                                                                                electronic states, effective Hamiltonian 0-71928 exciton formation in extremely high mag, fields 0-47599 film, cond. during form. 0-62296 film, imperfect surface, free carrier optical absorption spectrum 0-76082 film, superconductivity 0-44118 film, thermal cond. under size quantization conditions 0-71868 heat capacity singularities in mag, field 0-53712 layer, interband transitions in quantum size effect 0-71912 multivalley model, weak-field magnetoresistance 0-75526 nuclear quadrupole interaction, sp. ht. meas. 0-75986 phase transition to semiconductor, two critical temps. 0-44159 As, charge density, covalent features 0-39991 As, de Haas-van Alphen effect on nearly ellipsoidal Fermi surface 0-44021
                          polar, current fluctuations in strong elec. fields, A_{\rm III}B_{\nu} type, band struct 0{-}56248
                      0–56248
polar, degenerate, helicons-TO phonons coupling 0–71999
polar, necrowave cond. anisotropy 0–56239
polar one-valley, hot electron h.f. behaviour 0–51029
polar optical mode mobility, quantum mech. treatment 0–75459
polarization, migrational 0–65762
polaron effective mass in mag. field 0–56162
polymer, review 0–75694
polymers with conjugated system, rel. to electronic struct. 0–75695
Poole-Frenkel effect, free-carrier, in crystalline solids 0–72019
positive conductance, generalized proof of Shockley's theorem 0–78933
potential barrier limited current in non-homogeneous p-type 0–75662
quasineutral, transport noise, conc. and vel. correl. 0–78934
radiation damage 0–75714
radiation recombination rel. to carrier distrib. under varying plasma pinch 0–41255
radiation ionization energy and Fano factor 0–78926
                                                                                                                                                                                                                                                                                                                                                                                                                                                                                                                                                                                                                      As, de H
0-44021
                                                                                                                                                                                                                                                                                                                                                                                                                                                                                                                                                                                                                O-44021

As, Seebeck coeffs, and Fermi energies 0-51135
Bi, ang. correl. of annihilation photons, electronic props. obs. 0-40697
Bi, diamag. susceptibility 0-40941
Bi, film, single crystal, thermoelec. power 0-56370
Bi, photoemission, temp. and polarization depend. 0-62475
Bi, resistivity, even transverse field 0-62298
Bi, resistivity, quadratic temp. depend., liq. He temp. 0-44055
Bi, Shubnikov-de Haas meas. 0-75527
Bi, sound vel., giant quantum oscillations 0-71837
Bi cyclotron reson. Linewidth 0-62276
Bi film, magnetoresistance, quantum oscillations 0-75563
Bi film, magnetoresistance, quantum oscillations props., Fermi surface 0-75562
                          radiation-ionization energy and Fano factor 0-78926
radiative recomb. kinetics of electrons and holes at isoelectronic impurities
0 59423
                            Raman scatt., electronic 0-41236
                          Raman spectroscopy, laser application 0–54109 recombination emission, pinch effect 0–54120
```

Bi films, thin, resistivity and Hall coefficient 0-75564

Bl_{1...}50_x alloy, semiconductor—'quasimetal'—semiconductor transition, pressure and comp. depend. 0—53835
Sb, de Haas-van Alphen effect on nearly ellipsoidal Fermi surface 0—44021

0-44021 Sb, magnetoresistance anisotropy, 4.2-77 K 0-78881 Sb film, cond. during form. 0-62296 VO₂, elec. cond., optical reflection and transmission spectra, temp. depend. 0-75690 Series

Bessel, in elasticity problems, summation 0-66870 finite, ways of summing 0-54538 power, as solns. of differential equations, extension of radius of convergence 0-38139 power, divergent, vacuum expectation values of exponential operators 0-72880

Sferics see Atmospherics

Shadow universe see Cosmology; Elementary particles

Shear strength see Mechanical strength/shear Shell model see Nucleus/model

Shielding see Radiation protection Shock tubes

diaphragm burst control 0-42154

electrical for blast waves, shock wave energy and front trajectory calc. 0-42088

electromagnetic diaphragm 0-73050

experiments on snow, Hugoniot curves 0–50655 glass particles in air, drag coefficients of flow 0–58505 hypersonic shock wind tunnel, new technique for high speed testing 0–45651

0-45651 implosion-driven, performance, computer program 0-48865 magnetically driven, effect of diffusion on current-sheet speed 0-76917 magnetodynamic, luminous phenomena obs. 0-53131 molecular vibration, relaxation rate shock tube meas. review 0-58147 precursor, electron temp. meas. by He line ratio method 0-74558 as spectroscopic light source, review 0-52391 techniques and instrumentation survey 0-48864 thermal fluxmeter design for surface meas. 0-38397 Cs vapour, production of plasma up to 10 atm. pressure, shock wave absorption spectra 0-69736

Shock waves

see also Detonation; Explosions; Plasma/shock waves; Supersonic flow in MHD supersonic channel flows 0–50001 acetylene-O₂ mixtures, Ar diluted, detonations, transverse wave strength 0–50164

air, radiating inviscid shock layers round hyperbolic speed spheres 0-50157

air-breathing jet engine channels, supersonic flow closing shock wave position 0-74667

air-glass particle suspensions, effective drag coeffs. behind shock front 0-58507

uirblast from exploding spherical charges, closed-in scaling 0-45656 auroral arc in supersonic motion, generation of bow wave 0-54275 axial rarefaction wave in radially expanding tube of pressurized gas 0-74645

blast, shape and strength distn., finite element method, calc. 0--60068 blast plane infinite, disturbance by surface ripples, thin sheet model, differential eqns. 0-39531

ferential eqns. 0-39531 blast waves, spherical, stability 0-57416 blast waves, spherical, stability 0-57416 blast waves produced in electric shock tubes, energy, shock front trajectory calc. 0-42088 blast waves spherical scaling laws, study with intermediate strength formalism scaling relations 0-42091 Boltzmann eqn. nonlinear numerical soln. 0-74526 Brinkley-Kirkwood theory 0-66917 composites Laminated transient stress-wave expts. dispersive pulse pro-

Brinkley-Kirkwood theory 0-66917 composites, laminated, transient stress-wave expts., dispersive pulse propag. 0-40256 compression wave formation behind weak shock front in combustible 2-phase mixture 0-66920 converging, uniformly, trajectory derivation 0-42085 in crystal, damping by dislocations 0-68424 curved boundary interaction 0-42086 cylindrical, propagation, exploding wire generation, mag. field effect 0-42090 density slope thickness, molecular model effect. Mott-Smith theory predices

density slope thickness, molecular model effect, Mott-Smith theory prediction 0-39662

detonation, external below 0 order struct. 0–52149 detonation, marginal, microwave velocity meas. 0–52150 pre-detonation accelerated front, shape 0–45652 detonation produced in CH₄+2O₂ mixture in tube, front structure 0–45654

diffraction round a small angle, soln. 0-78199 discontinuities, nonuniform propag. behaviour, astron. applications

0-34734 dispersion by radiative energy transfer 0-54750 earth's bow shock preheating near leading edge, obs. 0-59612 elastic brittle material, crack growth, rel. to earthquakes 0-40392 envelopes, round conical bodies, M=4.0, for surface press. distrib., report 0-78204

ethylene- O_2 mixtures, Ar diluted, detonations, transverse wave strength 0-50164

0–50164 evolution, thermal disturbances generated by fractionally accommodating surfaces 0–64801 excitation of solar bursts, type IV moving and type II 0–79746 explosive material, XTX-8003 and PETN, shock initiation 0–66180 explosively generated, for sonic bang simulation in structural forcing, spatial distrib. technique 0–38401 in flow field from impact of two plates, analytical solution 0–50145 flow in m.h.d. generator 0–43244 fluidization, transition from homogeneous to heterogeneous, criterion 0–64630.

0-64635

0-40455 formation, by moving piston, study by kinetic theory of gases 0-68007 functions, shock, relations between response and Fourier spectra 0-57414 gas, emitting, struct. of shock waves 0-55551 in gas flow, in divergent duct, viscous quasi-one-dimens, difference soln. 0-58379

in gas of point center molecular repulsion structure study, Monte Carlo simulation method, molecular model 0-39662

Shock waves continued

in gases, binary mixture, formation of stationary weak waves 0-61434 generation, energy-conserving Bhatagar-Gros-Krook kinetic equation 0-46799

graphite, thermal shock resistance technique 0-40562

graphite, thermal shock testing using focused electron beam heating 0-40563

hypersonic flow past some central surfaces of second order 0-58376 immobile, prod. upon stationary evaporation of metal by laser radiation 0-48866

0-48866 internal, perfect gas flow around blunt cone 0-74662 interplanetary, interaction with solar cosmic rays 0-57137 interplanetary, review of various treatments 0-57128 ion acoustic, formation and interaction one dimensional hydrodynamic equations 0-6919 ionization and radiation induced in gases 0-53263 ionizing, generation by high explosive 0-38402 laminar boundary layers in entropy gradient, integral calc., method 0-39657.

laminar b

0–39657 from line sources, numerical solns, and exptal. obs. 0–76919 luminosity and brightness 0–38396 Mach speed, optical emission and microwave attenuation on converging and diverging taper sections 0–78175 magnetospheric, collisionless 0–59613 magnetostatic, collisionless, turbulence level, Balmer Hβ line, Stark broadening 0–64689 mechanical, frequency analysis, analogue methods 0–52148 model bimodal of structure in gas of point center of molecular repulsion 0–39662 in monatomic, gas, structure, study, using, modified, moment, method, in monatomic, gas, structure, study, using, modified, moment, method.

in monatomic gas, structure study using modified moment method 0--46801

0-46801

Navier-Stokes detonation, plane steady, applic. to oxyzone 0-45057
rel. to nuclear explosion fluid flow in distending tunnels computation, w.r.f. mass, momentum and energy exchange with walls 0-74664
obliquely incident on steady supersonic flow, refraction by upstream disturbances 0-78194
optical refl. at grazing incidence 0-61429
perturbation of similarity soln., for propag. 0-43388
plane, diffraction by moving thin wing 0-68000
plane, front, stability at small magnetic Reynolds no. 0-69737
plane, reflection from rigid concave wall, Mach (1.21-1.35) 0-73049
plane, thermal radiation effect on propagation 0-53270
plane front generation by incorporation of metallic lens in explosive 0-57413
plasma, weakly ionized, e temp, distrib. 0-55468

plasma, weakly ionized, e temp. distrib. 0-55468

plasma, weakly forfized, e temp. distrib. 0—53466 plexiglass, pre-stressed sheet, stress wave propag from internal explosive source 0—55958 polymethylmethacrylate, propag. characts. 0—71672 polymethylmethacrylate, shock amplitude variation rel. to strain gradient 0—62023

polymethylmethacrylate, shock amplitude variation rel. to strain gradient 0-62023 in polymethylmethacrylate, steady propag., anal. based on viscoelastic theory 0-78614 pressure, dissipative magnetohydrodynamic propagation 0-67889 propagating upwards in decreasing exponential atmosphere, Lagrangian eqn. of motion 0-43380 propagation in gas in channel with non-uniform magnetic field 0-78035 propagation in medium of decreasing density 0-45653 propagation in modium of decreasing density 0-45653 propagation in solids 0-38396 propagation in solids 0-38396 propagation in solids 0-38396 propagation in thomogeneous media 0-76918 pseudo-shock, \(\lambda\)-type 0-54752 pyrex, pre-stressed sheet, stress wave propag. from internal explosive source 0-55958 and radiation, review 0-38396 radiation gas dynamics, point explosion similarity soln. 0-73052 radiative ionization in cold precursor of detached shock 0-71198 reflection, Mach weak and strong in shock tubes 0-63470 reflection from heat conducting wall, contact region structure 0-78190 reflection of light from shock front at near grazing incidence 0-52360 resistive transverse, existence and structure, two fluid theory applic., critical Mach number effect 0-43279 rotor pressure field and sound power under supersonic conditions 0-67987 ruby, laser beam pulse absorpt. 0-54054 in shock tubes magnetically driven using air separation from purpose these.

0-67987
ruby, laser beam pulse absorpt. 0-54054
in shock tubes magnetically driven using air, separation from current sheets,
comments 0-43390
solar atmospheres, frequency and strength 0-63183
in solar wind, interplanetary 0-59797
in solar wind due to p-flare of 7 July 1966, satellite magnetometers obs.
0-57151

0-57151
solid, precursor decay and rel. to dislocation dynamics 0-47332
solid, shock adiabat eqn. 0-65361
sonic boom, pressure fields caused in rooms with open windows 0-54745
sonic boom, simulation model study, implications for full-scale simulation tests 0-63471
sonic boom rise times, theory 0-54756
sonic boom simulation device 0-60045
source characteristic meas., from small TNT charges exploded in deep ocean 0-52152
soark emitted, four-metre 0-54753

ocean 0–52152

spark emitted, four-metre 0–54753
in stellar atmospheres, emission from region behind them 0–45273
in stellar atmospheres, gravitational, propagation 0–48421
stress pulse propag, in poroelastic solid, dissipation mechanisms 0–38398
strong, dispersion by radiative energy transfer 0–54750
strong, laminar boundary layers created by 0–63469
strong shock wave propagation, self-consistent soln, of second kind for energy losses 0–78198
structure, non-equilib-kinetic description 0–53247
structure connected with radiant heat exchange 0–38396
supersonic, Smyrl's results correction 0–50160
supersonic waves from rockets, coupling with infrasonic waves 0–59596
switch-on, structure, magnetohydrodynamic, precursor ionization effects
0–46678
transverse wave instability in solid explosive 0–45655

transverse wave instability in solid explosive 0-45655 turbulent mixing of test gas with driven gas at contact surface 0-39663 underwater, from detonation, amplification in focusing regions at caustics 0-76356

unloading, 0-45601 propagation in elastic-plastic strain hardening medium S 1360 SUBJECT INDEX velocity enhancement in explosively driven tubes 0-60067
Venus vicinity, inferred from Venera 4 plasma obs. 0-63150
Whitham's rule 0-66917
Al-methane-O₂ flames, propag. 0-76260
Al, porous, theor, shock props. 0-55959
Al₂O₃, sapphire, propag. characts. 0-71672
in Ar-He mixtures, vel. distrib. functions 0-53262
Ar c.w. laser holographic interferometry 0-60069
B-methane-O₂ flames, propag. 0-76260
D₂ gas at 50mTorr shock waves at 10⁸ cm/sec in coaxial shock tube 0-74647 Shock waves continued 0-1404/1 H₂-O₂ mixtures, Ar diluted and undiluted, detonations, transverse wave strength 0-50164 H₂, study rel. to struct. and radiative transfer in stellar atmospheres 0-54361 U=34501

He Ar turbulent test mixture with He driver, effects 0-39663

He discharge, at high initial pressures 0-46720

N; and O; vibr. relax. rates meas. 0-77814

NaCl, shock-velocity, u.s. obs. 0-71667

O; shock layer, nonequilib. around cones in hypersonic flow, expt. and numerical studies 0-53237

SiO, fixed propers 0-71672 SiO₂, fused, propag. characts. 0-71672 effects
acetylene-O₂ reaction in shock tube 0–41426
airstreams, two supersonic, crossing shock waves, mixing 0–46788
alumina, impact fracture tests 0–43786
anthracene, compression 0–65382
atmospheric, nonequilibrium radiation behind 0–76374
axisymmetric supersonic flow about blunt body, transient flows 0–43389
benzene, compression effects 0–58459
brass, defect microstructure, shock-induced, mechanical properties correla
tion, electron microscopy 0–40079
β-brass, deform, under explosive shock 0–78625
carbon tetrachloride, compression effects 0–58459
Chromel-A, explosive shock-loading, thermal recovery 0–75307
cold precursor of shock in monatomic gas, radiative ionization patterns
0–53218
combustion initiation in heterogeneous unmixed systems 0–41421
compressibility of cubic lattice metals, analytical model 0–58887
crystals, ionic, optical absorption for 150 to 350 Kbar shock compression
0–47993
deformation, non-linear elastic material 0–48837 compressionity of cubic lattice metals, analytical model 0—58887 crystals, ionic, optical absorption for 150 to 350 Kbar shock compression 0—47993 deformation, non-linear elastic material 0—48837 droplet agglomeration induced by weak shock waves 0—50278 electric field structure near front in weakly ionized gas 0—39678 excitation of atoms and molecules, review 0—58104 flow, self-similar one-dimensional behind shock propagating upward in decreasing atmosphere 0—43380 galactic large-scale phenomena and star formation 0—57001 in galaxies, Sc, spiral arms and dark lanes 0—72695 gas, cond., three-dimens. flow behind shock wave 0—53134 graphite-diamond-graphite, transform. 0—78693 heat transfer accompanying high temp., accelerating shock wave charac teristics in decreasing atmosphere 0—43380 Inconel 600, explosive shock-loading, thermal recovery 0—75307 interplanetary, on comet brightness 0—72775 ionization in Ar for different values of pressures, Mach numbers, eqbm. investigation 0—53215 ionizing, incident upon transverse mag. field, interaction study 0—42087 ionizing, interaction with transverse mag. field 0—46763 liquids, C₄(T) eqn. of state for shock temp. calc. 0—64858 lunar minerals, impact metamorphism 0—48528 lunar samples, shock metamorphism 0—48528 lunar samples, shock metamorphism 0—48527 lunar samples, shock metamorphism 0—48528 membrane, elasto-plastic, motion under shock loading 0—45594 metal, compressibility under shock, parameters determ. 0—40587 metal, f.c.c., shock-deformed, stacking fault energy influence on dislocation configs. 0—40148 monocrystal surface elec. potentials 0—47847 noise, acoustic, in hot and cold jets, farfield study 0—55540 nuclear craterings, digital computers application 0—73061 one dimensional waves, structure foundation interaction and damping effects 0—52077 oscillating, produced by localized direct radiation, response of cylindrical shell 0—54757 effects 0–52077
oscillating, produced by localized direct radiation, response of cylindrical shell 0–54757
particle track erasure in glass and silicates 0–70315
phenanthrene, compression 0–65382
plasma, electronic heating at front, probe obs. 0–64693
plasma, electrostatic shocks, collisionless 0–50035
plasma, electrostatic shocks, collisionless 0–50036
plasma heating by reflected ionising shock waves 0–67901
pyrene, compression 0–65382
seismic excitation on nuclear power plants structural behaviour dynamic analysis 0–52078
seismic waves generated by sonic booms, theory 0–66235
shell elastic in light fluid medium, response study, approx. analytical expressions 0–66895
ship and submarine models exposed to underwater explosion, flevural sions 0-66895 ship and submarine models exposed to underwater explosion, flexural modes, expt. 0-60012 solar chromosphere, low, heating 0-66657 in solid, effect of short laser pulses on absorbing substance 0-40617 sonic boom, diffraction and reflection 0-76908 sonic boom effect on panel-cavity system's vibrations, theory, expt. 0-38364 0–38364 sonic boom generated seismic waves, theory 0–66235 sonic boom generated seismic waves, theory 0–66235 sonic boom penetration into water, pressure analysis 0–52093 steel, Hadfield, hardness and microstructure, effect of stress amplitude and duration 0–43794 steel, stainless, defect microstructures, shock-induced, mechanical properties correlation, electron microscopy 0–40079 stress wave propagation in hollow circular cylinders, safe impact velocity determination 0–69711 structures subject to earthquake, Portugal (28 Feb 1969) 0–57415 surface disintegration kinetics under shock heating 0–40393 thermocouple, abnormal thermo-e.m.f. 0–40888 rel.to underground, nuclear explosions, dimensional analysis of mechanical effects 0–73063

effects continued rel, to underground nuclear explosions origins of displacements 0-75240 viscoplastic solid, plane shock propag., nonlinear constitutive relns. 0-573560-7330
Al₁O₃, ruby and corundum, shock compressibility
0-75248
Ar, radiative ionization patterns in cold precursor
0-53218
B₄C, shock compressibility
0-75248
CN molecules, decomposition reaction chain following shock wave CN molecules, decomposition reaction chain following shock wave 0-48182 CO-F₂O reactions following a shock wave 0-48183 CO, oxidation by O₂ 0-62804 CS₂, compression effects 0-58459 CaF₂, fluorite, dynamic compression 0-40257 Cu, defect microstructure, shock-induced, mechanical properties correlation, electron microscopy 0-40079 Cu, impact loads effects on work hardening 0-47439 F₂O-CO reactions following a shock wave 0-48183 Fe-Cr and Fe-Cr. Ni alloys, phase transitions 0-47366 Fe-Mn, deformed, transverse magnetoresistance 0-5619 Fe-Mn alloys, b.c., induced martensitic transform. 0-59022 Fe-Ni-C alloy, martensite to austenite induced reversal, temp. depend, Fe-Mn, actormed, transverse magnetoresistance 0—36191
Fe-Mi-C alloy, b.c.c., induced martensitic transform. 0—59022
Fe-Ni-C alloy, martensite to austenite induced reversal, temp. depend. 0—65489
Fe-Ni, deformed, transverse magnetoresistance 0—56191
Fe, deformed, transverse magnetoresistance 0—56191
No., liquid, compression effects 0—58459
NO., thermal decomposition 0—59486
N,O4, thermal decomposition 0—59486
N,O4, thermal decomposition 0—59486
N,O4 thermal decomposition 0—47481
Ni, deformed, positron lifetimes 0—68674
Ni, ceplosive shock-loading, recovery 0—75307
O, dissoc., in 10% O₂ +90% Ar mixture 0—74416
"O atom exchange reactions with CO₂, SO₂ 0—48176
TaC, shock compressibility 0—75248
ThO₂ Ni, ThO₂ NiCr, explosive shock-loading, recovery 0—75307
Ti, phase transition, 120-500 kbar, X-ray diffr. 0—40493
TiO₂+BaCO₃, shock compressibility 0—75248
Xe ionization at shock-wave front for 6-10 Mach numbers, meas. 0—53216
Xe plasma, ionization, i.r., diagnostics 0—53189 0-33216 Xe plasma, ionization, i.r. diagnostics 0-53189 Zr, phase transition, 120-500 k bar, X-ray diffr. 0-40493 ZrO₂, coatings, plasma sprayed, thermal shock resistance 0-53577 Shot noise see Noise/electrical Showers see Cosmic rays/showers and bursts Shubnikov-de Haas effect see Magnetoresistance see also Semiconducting devices; Semiconducting materials/silicon absorption, i.r., laser-induced 0-69129 absorption of light by carriers in heavily doped layers 0-56544 absorption of light by carriers in heavily doped layers 0–56544 abundance in lunar samples, neutron activation determ. 0–45353 abundance of isotopes in lunar samples, ³⁰Si/²⁸Si ratios 0–45356 adsorption and desorption of water, on single cryst., study by desorption spectrometry 0–74929 adsorption of O₂, or [110] and [111] faces of Si 0–39976 adsorption of O₂, or [111] surface cond. vars. obs. 0–55762 adsorption of O₃ on (111) surface, electron beam assisted 0–65108 amorphous, fundamental absorpt., reflectivity, transmission, ellipsometry 0-48069 amorphous films, meas. of photoelectric yield and energy distribution $0\!-\!75850$ annealing of proton damage, fluence depend., minority carrier lifetime 0-438030-43803
atomic mean square displacements at (III) surface 0-78738
atomic scatt. factors accurate determ. using Pendellosung and interferometry fringes 0-78428
atomic transition tables 0-39284
avalanche diode, high efficiency microwave oscillations, design and performance, TRAPATT approach 0-47788
backscatter currents under keV ion bombardment 0-68704
band structure calcs. using self-consistent OPW 0-44265
in chrome concentrates and ores, n-activation analyzer for process control 0-48220 0 - 482200-48220 conduction electron spin resonance, line shape 0-72490 conduction electron spin resonance, line shape 0-72490 conductivity (thermal) obs., low temp., irradiated with fast neutrons at 80°K 0-75417 creep characteristics 0-75266 crystal, hyperfine splitting energy of muonium 0-54052 crystal growth by Stepanov's method 0-65165 crystal growth from Al-Si-Zn alloys, instabilities, obs. by scanning electron microscope 0-68258 crystal growth from melt, calc. of thermal field 0-65158 crystal noncentrosymmetric thermal oscills., neutron diffraction obs. 0-62177 crystal vibration, valence force potentials calc. 0-75378 crystal vibration, valence force potentials calc. 0-75378 crystals, dislocation-free [111], vacuum float zoned, non-circular cross section 0-50472 crystals, dislocation-free [111], vacuum float zoned, non-circular cross tion 0-50472 cyclotron resonance at split-off valence band, obs. 0-75520 defect, radiation-induced, annealing, atomic freq, and entropy 0-5056 defect structure on As-diffusion 0-65326 diffusion of light by laser generated free carriers 0-62605 diffusants, surface concentration, determination techniques 0-65338 diffusion of 14Pm 0-3564 diffusion of Au, X-ray stimulation 0-78589 diffusion of Au, xdissociative mechanism 0-78588 diffusion of Au, radiation- accelerated 0-78586 diffusion of Au in thin slices, mechanism 0-68385 diffusion of B, concentration profiles for two-step diffusion of B, orientation depend. 0-68384 diffusion of B, and P, conc.-depend. 0-55926 diffusion of B glass layers on surface 0-39950 diffusion of B in single cryst., 1000-1200°C 0-40203 diffusion of P, bulk diffusion in hydrogen atmosphere 0-68383 diffusion of P, bighly controllable source material, patent 0-40209 diffusion of P using POCl₃ as source 0-78587 diffusion of P using POCl₃ as source 0-78587 0-50567

Shock waves continued

Silicon continued

diffusion of Sb, P in p-type and B in n-type, surface density depend. 0-61999

diffusion of Zn, by closed-tube two-temp, technique 0-62000

diffusion of Zn, influence on elec. props. 0–55924 diffusion of radiophosphorous, effects of free surface and redox reactions

0-75210
diffusion profile and evap. vel. of As 0-53562
diode depletion layer capacitance, mag. field effects, <12 kOe 0-44298
dislocation motion in deformation, X-ray topography obs. 0-47261
dislocations, X-ray topographic obs. 0-58816
dislocations, direct vel. meas. 0-68364
dislocations, dissociated, electron microscope obs. 0-75168
dislocations, dynamic behaviour, transmission electron microscope exam.
0-88866

0-58806

0-3806 dislocations, dynamical diffr. images 0-75150 divacancy and near edge absorpt. production, neutron irrad., temp. depend. 0-40136 durability and creep rel. to bonding 0-43795 ENDOR spectra, donor ground-state wave function and piezo-h.f.s. 0-51415

c.0–5|415
e.p.r. in plastically-deformed crystals 0–48151
e.p.r. signal prod. by plastic deform, annealing behaviour 0–56671
elastic const. determ. by Debye-Sear eff. 0–62005
electron irrad-damaged, effect on annealing, fractionation expt. 0–75303
electron-phonon scatt., anisotropic 0–75470
epitaxial, highly uniform and defect-free, deposition techniques 0–68260
epitaxial film, misfit dislocations, distrib. and character 0–53434
epitaxial film on α-Al₂O₃, interface reactions 0–55726
epitaxial films, Si (111), surface struct, impurities influence 0–61657
epitaxial films, diffusion of boron 0–55923
epitaxial films, limitations of evaluation techniques 0–65075
epitaxial films, grown by silane and chloride methods, Sb distrib. 0–55727
epitaxial growth, on Si surfaces near (100), step motion anisotropy 0–50481
epitaxial growth, comparison of resistance heated reactor with other epitaxia.

epitaxial growth, comparison of resistance heated reactor with other epitaxial systems 0-65179

pitaxial growth, selective, using SiH₄ 0–47153 epitaxial growth, stacking fault nucleation 0–55802 epitaxial growth from SiH₄ in horizontal reactor stagnant layer model 0–65071

0-65071
epitaxial layers, N on N*, impurity profile 0-72069
epitaxial layers, N on N*, impurity profile 0-72069
epitaxial layers thickness meas. by i.r. interference 0-61638
epitaxial structure, electrochemical thinning 0-53432
epitaxially grown layers, thickness obs. by i.r. multiple reflection 0-75339
epitaxy submicron single and multilayer growth 0-65073
epitaxy reactors, equipment considerations 0-65178
exciton and excitonic molecule recombination kinetics, intrinsic semicond.
0-51350 Faraday rot., nonresonant interband 0-79248

in ferrophosphorus and slag from electric-reduction furnace, determination using X-ray fluorescence analysis 0–51452 film, epitaxial, deposition on Si in horizontal reactor, system and growth 0–74904

film, epitaxy, initial nucleation and growth, molecular beam technique 0-74905

0-14905 (ilm, growth, I-V characts, of tunnel p-n junction 0-39955 (ilm, growth by Stepanov's method using different moulds 0-65164 (ilm, heteroepitaxial deposition on insulating substrates, stress 0-39946 (ilm, transmission of electrons 0-65568)

film epitaxial, dopants depth distrib. investig. n-activation analysis method 0-47056 film photoconverter, investigation 0-65859

him photoconverter, investigation 0-65859 films, epitaxial, impurity distribution 0-43552 films, epitaxially grown from SiH₄, control 0-65072 films, homoepitaxial doped, low temp. vacuum deposition, LEED and transmission electron microscopy studies 0-47057 films, thin, preparation for transmission electron microscopy by photolithography and dynamic etching 0-78379 gate m.o.s. devices, room temperature threshold shift obs. 0-51091 Gruneisen parameter, low temp., from elastic constant press. derivs. 0-43924 impurity cone, and location, ion-scatt. obs. 0-55749 impurity conc. and location, ion-scatt. obs. 0-55749 internal friction, temp. depend., damping mechanism, plastic deformation

0 - 68417ion bombarded, depth profiles of lattice disorder 0-68349

ion bombardment induced amorphisation of surface layers, at. no. depend. 0-68558

0-68558
ion bombardment induced almol pinsation of surface layers, at. no. depond.
0-68558
ion bombardment induced damage by Bi and I 0-68340
ion implanted, B, lattice disorder obs. 0-68339
ion implanted, account for sputtering below 200 eV 0-71886
ion-implanted, oxidation enhancement during annealing 0-66185
ions, solar u.v. lines limb brightening 0-41865
ions cattering and secondary electron emission influence of radiation defects in target on angular effects 0-56133
isotopes, stable, thermal neutron absorption cross sections, resonance integrals and resonance parameters 0-46152
LEED intensity-voltage curves, maxima interpret. 0-43613
lattice disorder, penetration depth ionic bombardment, channeling technique, thickness of amorphous region 0-62363
lattice disorder and Hg location due to ion implantation 0-61945
lattice parameters, device design and tech. for meas, description 0-50499
layer crystallization on polycryst, substrates by zonal melting method 0-65088
low temperature thermometer and bolometer, doped surface layer, prepara-

low temperature thermometer and bolometer, doped surface layer, prepara-

tion and applications 0–45669 molten, acoustic wave vel. and compressibility 0–55613 monocrystal nuclei, substrate for SiO₂ films 0–39954 neutron absorption thermal, cross sections 0–46152 neutron irradiated, defect-oxygen complexes, i.r. a 0–48055 absorpt. spectra

o-48050 optical constant determ, with pseudo-Brewster angle technqiue, a reflectometer 0-56483 oxidation in steam to SiO₂ 0-55748 particle size distrib, in rolled Al-Si eutectic, meas, using extraction technique 0-58973 photoabsorption near L_{II,IIII} edge 0-79299

Silicon continued

photocell, with multilayer heat-reflecting coatings 0-75823

photodiodes contact to metals, u.s. welding, apparatus description

0-3636
plastic deformation, prod. of e.p.r. signal, annealing behaviour 0-56671
plastic deformation, surface, -196 to 550°C, metallographic and transmission electron microscope obs. 0-40311
plastically-deformed crystals, e.p.r. 0-48151
positron channeling 16-28 MeV, forward bremsstrahlung obs. 0-56125
precipitation of Li 0-35563
proton channeling, 6.72 MeV, 100-800 K, 0-65570
proton channeling, 6.72 MeV, 100-800 K, 0-65570
proton deformed to the strength of the control of the channeling detection of the control of the channeling detection of the control of the channeling detection of the channel of

proton channeling, 6.72 MeV, 100-800 K. 0-65570 proton dechanneling, dependence on penetration depth 0-62230 proton dechannelling along 111 axis at different temps. 0-78796 radiation damage to lattice rel. to ion dose, depth below surface and annealing treatment 0-68350 Raman scatt. efficiency, spontaneous, and stimulated scatt. 0-79333 Raman scattering, resonant cancellation, Loudon theory extension 0-76125

Raman scattering, temp. depend., 20-770°K, linewidth and freq. meas. 0-44868

0-44868
Rayleigh wave propag. on (111) face 0-43723
resonance integrals, absorption 0-46152
resonance parameters 0-46152
Schottky effect, thermionic and photoelectric emission, work function 0-75855

0-73533 secondary electron emission, for single crystals 0-44446 semiconductor devices, passivation with SiO₂ 0-56308 in solar 3b flare decay, resonance, intercombination and forbidden transitions, He-like 0-69497

solar cells, borosilicate glass and SiO₂ integral coverslips evaluation

solubility of Zn, influence on elec. props. 0-55924 spectrum, using grazing-incidence spectrometer 0-52912 spherulite growth and morphology in Na-modified Al-Si eutectic alloys 0-75083

spin-lattice relaxation process in phosphorous donor pairs 0-44725 steel, low-alloy, high-strength, effect on stress corrosion resistance 0-56001

0-56001 strain generated surface patterns 0-65045 surface, Au-coated (111) faces, vibrs. of atoms 0-71456 surface, (111)-7 struct., by cleavage at room temp. 0-61632 surface, protection by thermal oxidation, suitable conditions 0-39944 surface cleaning and Au-stabilization, LEED obs. 0-55703 surface patterns, strain generated 0-65045 surfaces, (111) cleaved, Auger e spectroscopy, rel. to (111)7 struct. impurities 0-56721 thermal conductivity, lattice, four-phonon processes contrib., 300-1300°K 0-43932

thermal conductivity, lattice, transverse and longit. phonon contrib. 0-40590

thermal conductivity, single crystals, in boundary scattering regime from 1 to 4°K 0-68656

to 4°K 0-68656
thermoreflectance spectra 0-41181
vacancy, single, in SiC, electronic levels 0-58791
vacancy conc., doping degree influence 0-71610
vacancy equil. config. refinement 0-71611
valence band structure, from soft X-ray emission spectra 0-65601
valence charge density and covalency. Fourier components 0-43582
vitreous, heat capacity calc. from Raman spectra 0-78781
wavelength modulation spectra, 5°K, 2.8-6.0 eV, derivative reflectivity
spectra 0-51292
whiskers group from soft, growth features, 0-61672

spectra 0-51292
whiskers grown from soln., growth features 0-61672
X-ray L₂ emission spectra 0-56577
X-ray emission spectra, rel. to energy band structure, transition probabilities and lifetime effects 0-44877
X-ray photoelectric emission from perfect single cryst., ang. depend. 0-75868

Young's modulus and internal friction of thermally treated samples 0-50639 p channeling and blocking, 31.5 MeV in 60 μm and 240 μm crystals 0-43939

O-43939

Al-Si, noise with Al bonding pads and Au-plated Kovar headers, ultrasonic bond integrity meas. by pull-strength distributions 0-51073

Al-SiO₂-Si system, model rel. to m.o.s. processes 0-65761
nucleation on (111) substrates at u.h.v., induction period kinetics 0-55747
O₂ concentration, determination by i.r. absorption 0-75143

Si:Al, e.p.r. of Al²⁺ interstitial 0-45000

Si:Al, i.t. or electron irrad. compensated, one-phonon absorpt. 0-44853

Si:Al, impurity photovoltaic effect of Au donor level 0-44404

Si:Ba, alsylayers, sublimation, 430-600°C, elec. and cryst. props. 0-65086

Si:Ba, glayers, sublimation, 430-600°C, elec. and cryst. props. 0-65086

Si:Cu, Mossbauer spectra of ³⁷Fe 0-62633

Si:Cu, Au, crystal growth, crucible-free zone melt method, impurity distrib. 0-75144

Si:Fe, e.s.r. 0-72489

Si-Cu,Au, crystal growth, crucible-free zone melt method, impurity distrib. 0-75144
Si-Fe, e.s.r. 0-72489
Si-Fe(Ni), diffusion to surface 0-78538
Si-Li, ENDOR, e.s.r., orbital degeneracy 0-56672
Si-Li, B single crystal, internal friction peak, 150C, 1.2 kHz 0-68418
Si-Mg, excitation spectra and piezospectroscopic effects of neutral and singly ionized donors 0-51287
Si-O, absorption in the near and far infrared 0-54102
Si-P, conc.-depend. spin-lattice relax. times, low temp. 0-79214
n-Si-P, e.p.r., uniaxial compression effect on hyperfine splitting 0-79407
Si-Sb, crystal, dislocations, dope substructure, acicular deposits, x-ray exam., ir. microscopy 0-75170
Si-Si-O, interface, LEED obs. 0-39929
Si-metal junctions, tunnelling mechanism 0-56330
Si, with C and O impurities, radiation damage obs. 0-43661
Si I and Si II lines, relative transition probabilities 0-70772
Si I oscillator strengths and mean square radii calc. 0-42930
Si II, relative f-values 0-67624
Si II broadening parameters meas. 0-60929
Si II electron collisional excitation cross sections of u.v. resonance transitions 0-42994
Si II spectral lines in 56 Arietis 0-62993
Si XIII. mar, diople degrace of 235 state, 0-67617

Si II spectral lines in 56 Arietis 0–62993 Si XIII, mag.-dipole decay of 2'S₁ state 0–67612 Si, new band systems discovered, rotational and vibrational constants 0–77844 Si(Li) detector, transverse field 0-60686 Si(Li) detectors, rel. to behavioural studies 0-60684

```
Silicon continued
```

Si(Li) detectors, coaxial 0-60679

with SiO_x film, water contamination in device technology 0-58841 ²⁹Si⁴⁺, superhyperfine splitting in diamond lattice, e.p.r. obs. 0-48141

TiO2:Si, decorated dislocations 0-58818

Silicon compounds

see also Quartz

 α -SiC pure cryst., prep. method 0-61716 arsenide, vapour growth of crystals 0-65139 axinite, H(Fe,Mn)Ca₂Al₃BSi₄O₁₆, cryst. stru n)Ca₂Al₃BSi₄O₁₆ axinite, cryst. struct. 0-50528

axinite, H(Fe,Mn)Ca₂Al₃BSi₄O₁₆, cryst. stru n)Ca₂Al₂BSi₄O₁₆ axinite, cryst. struct. 0–50528
brass, corrosion resistance, thermal conductivity 0–43789
complex permittivity at microwave freqs. high temp. meas. 0–47825
halide complexes with 44'-dipyridyl, .u. v. spectra 0–66035
oils used in vacuum diffusion pump, spectra, sector field mass spectrometer 0–51872
opal-cristobalite tridymite, submicron structures 0–50547
oxide, effect of alkaline earth fluoride additive 0–62144
oxynitride, dielectric for mi.m. capacitor, props. rel. to reactive sputtering prep. 0–53932
photoluminescence, α-SiC(6H) crystals, emission bands and internal recombination of donor-acceptor pairs at 20 K 0–66124
sheet, cold-rolled, secondary recrystal, as result of annealing 0–62086
SiF₄, gaseous, F relaxation by n.mr. 0–58198
silica, colloidal, Ludox HS, small-angle X-ray scatt. 0–53382
silica, colloidal, tability 0–74809
silica, fureous, diffusion of He and Ne, effect of prior heat treatment of silica 0–55927
silica gel, microporous, adsorption of benzene, cyclobenzene, isopropanol and carbon tetrachloride 0–50398
silica gel, wiration of dielectric constant with activation at different temperatures 0–68165
silica gel with adsorbed ammoniac, relax, regions obs. 0–39854
silica gels, rel. to Cu₂O crystal growth at near ambient temp. 0–50436
silica gels, pore struct, determ, by electron microscopy and low-temp. N. adsorpt. 0–78318 silica gels, rel. to Cu₂O crystal growth at near ambient temp. 0–50436 silica gels, pore struct, determ, by electron microscopy and low-temp. N. adsorpt. 0–78318 silica glass, diffusion of water. OH-content effects 0–62002 silica minerals, submicron structures 0–50547 silica phases, polymorphous, in (NaPO₃)₈, Na₂SiO₃ 0–59053 silica surface wave spreading, nonlinear phenomena 0–78761 silica surfaces, i.r. spectra obs. 0–50357 silicate, interstellar absorption bands in direction of galactic centre 0–76595 silicate glass: Mn²⁺ absorpt, greater and livrigory

silicate glass: Mn²⁺, absorpt. spectra and luminesc. conc. depend. 0-62674

0-626/4 silicate glass: Yb³⁺, ion coordination obs. 0-51310 silicate glass. NBS 710 viscosity standard, diffusion of ²⁴Na 0-62003 silicate glass films, chemical vapour deposition thermal densification, dielec. props. 0-53440 silicate glasses, Hertzian fracture processes, quantitative evidence 0-65424

silicate glasses, chemical vapour deposition, 300-500°C 0-53439 silicate minerals, heavy ion tracks, annealing characts. 0-78540 silicate minerals in interstellar grains, recent identification questioned 0-51703

silicate particles, interstellar, absorpt. band, 4430Å 0–66519 silicates, hydrate, structon theory applic. 0–40099 silicates, interstellar, absorpt. spectra, low temp. 0–66520 silicates, laminated, thiophene mols. adsorption by cation exchange 0–62786

0-02780 silicates, paramagnetic defect on electron and proton irradiation o-61941 silicates in interstellar matter, along with Fe and graphite grains 0-66508 silicone fluids, rheology during impact 0-53304 silyl halides, mol. struct. and rot. consts., from microwave spectra

tetravinylsilicon, vibr. spectra and molec. struct. 0–77847 transition metal-B-C-Si systems, phase diagrams 0–50833 Ag. SiO₂-SiC m.o.s. struct., (P-type), I-V characts., temp. depend.

0 - 40815

0-40815
Al-Mg,Si alloy, ageing behaviour, Si excess effect, resist., hardness, electron microscopy 0-47443
Al-Mg,Si alloy, serrated yielding, strain rate depend. 0-43739
Al-Si, Silumin solid solution, of Cu, influence of Ni, Fe, Mn 0-50778
Al-Si alloys, cast, strength, effects of composition and microstructure 0-75272

0-/52/12
Al-Si alloys, precip, nucleation rel. to excess vacancies 0-68551
Al-Si eutectic, rolled, Si particle size distrib, meas, using extraction technique 0-58973
Al-Si eutectic alloy, Na-modified, Si spherulite growth and morphology 0-75083

0-75083
Al-Si Schottky barriers, LSI arrays, reliability 0-47785
Al-Si O₂-Al struct., IV characts., charge in dielec, influence 0-56337
Al-SiO₂-Si system, model rel. to m.o.s. processes 0-65761
Al-O₃-SiO₂ double layer struct, electron-gun evap., Na migration 0-44341

0–44341
As-Te-Ge-Si, amorphous film, non-ohmic props., 77-350K
0–56242
As-O₃-SiO₂ glasses, struct, changes with heat treatment 0–68198
Au-Al-5%Si, diffusion couple, ageing at 200°C to 460°C intermetallic phases and their kinetics rel. to wire-bonds reliability 0–50769
Au-Si solid soln, precip., complexes form, influence 0–71792
Au-SiO₂ cermet film, transport props., microstructure 0–44353
BaO-SiO₂-H₂O system cpd, form, identification and struct. 0–68298
C-Si, chemical vapour deposition, 1340-1630°C, comp., temp. depend. 0–74910

C-Si, chemical variable of the control of the control of the capacitors of the capac

0–78877
Cu-Si-Mn f.c.c. filings, X-ray diffr. pattern, Fourier analysis applic.
0–71586
Cu-Si solid soln., X-ray L₃₃ emission spectra 0–56577
Cu-ZrCuSi alloy, unidirectional solidification, mech. and elec. props. of composite 0–40476
Fe-C-Si, complementary shear during 420°C martensitic transformation 0–71800
Fe-C-Si alloys, phase transf. at 420°C, e. microscope and e. diffraction studies 0–65490

Silicon compounds continued

Fe-C-Si alloys, rapid cooling by casting, effect of composition on struct, of graphite 0–65504
Fe-Cr-Si-Ti hardening on heating to 600°C 0–58957

Fe-(3.25 wt.%)Si, mag. permeability, thermal demagnetiz, below Curie pt. influence 0-44586 Fe-(3.25 wt.%)Si alloys, coercive field temp. depend.65917 0-65917 Fe-Si-Al, nonoriented electrical sheet, ductility, mag. props. 0-43811 Fe-(3wt.%) Si, anomalous transmission of resonant y-rays of ⁵⁷Fe

7-62519 (2519) 17-62519 (2519) 27-62519 (2519) 27-62519 (2519) 27-62519 (2519) 27-62519 (2519) 27-62519 (2519) 27-62519 (2519) 27-62519 (2519) 27-62519 (2519) 27-62519 (2519) 27-62519

0-0219
Fe-(3.4wt.%)Si, slip planes temp. depend.78641 0-78641
Fe-(3wt.%)Si, high temp. plastic deformation, microdynamics, minimum effective stresses, dislocations 0-65394
Fe-Si, annealing in mag. field or under applied stress, magnetostriction 0-62533

0-62533
Fe-Si, coercive force, theory 0-44547
Fe-Si, Cr or Mo coated, plastic deform. characts., var. with grain size 0-78626
Fe-Si, domain width, thickness-dependence, var. with sample crystallographic orientation 0-75919
Fe-Si, struct. of primary recrystn. 0-61867
Fe-Si alloy, grain growth rate, orientation depend. 0-53628
Fe-Si alloy, mag, props, surface film influence, anisotropy 0-65926
Fe-Si alloys, angolic popularization behaviour 0-66194
Fe-Si alloys, corrosion characts. 0-41437
Fe-Si alloys, grain growth in ribbed texture formation, effect of annealing 0-62096
Fe-Si as focussing neutron monochromators 0-61807

Fe-Si as focussing neutron monochromators 0-61807 Fe-Si sheet, mag. props., treatments producing directional props. effect 0-65923

Pe-Si sheet, mag. props., treatments producing directional props. effect 0−65923
Fe-Si single crystals, rolling, active slip systems determ. 0−78640
Fe-Si single crysts., asymm. of slip on {112} planes 0−62054
Fe-Si single devists., asymm. of slip on {112} planes 0−62054
Fe-Si system, ordering, X-ray obs. 0−61866
Fe-(3.25wt.96)Si alloy, coercive field, initial susceptibility, plastic deformation effect44588 0−44588
Fe-(3.2 wt.96)Si alloy, deformed, dislocation struct., electron microscope obs. 0−47260
Fe-(3.5 at.%)Si alloy, single cryst., domain structure, study by X-ray topograhy61861 0−61861
Fe-∓7.963 single cryst., recrystal., effect of low temp. annealing 0−61859
Fe(3 wt.%)Si, total loss, tensile stress effects 56449 0−56449
Ga-As-Si liquidus-solidus phase diagram 0−62353
Ge-Si-As-Te, amorphous alloy, fundamental absorpt., reflectivity, transmission, ellipsometry 0−48069
Ge-Si colons, Hg impurity states 0−56281
KyO-SrO SiO, system, interdiffusion 0−50623
Liy-SiAy, system, phase transformations 0−56061
LiyO-AlyO, SiO, glasses, nucleation efficiency of TiO, 0−74866
LiO-SiO3, glasses immiscibilities, neutron-induced autoradiography obs. 0−605051
Ge-Si objects of the structure of the structure

0-46877

Li₂O-SiO₂ glass, crystn., hot stage transmission electron microscopy obs. 0-50341

Li₂O-SiO₂ glasses, cryst. nucleation 0-74865

Ln_CCdSi₂S₁₄ solid soln. where Ln=La...Gd, cryst. struct. 0-71780

Mn-Co-Si system, X-phase, crystal struct. 0-50535

Mn-Pd-Si alloys, amorphous, Kondo-type s-d exchange interaction 0-78877

Mn-SiO₂-Si struct., voltage thermal instability 0-79024 MnO-ZrO₂-SiO₂ system, phase relations 0-58517 Na₂O-BaO-SiO₂ system, immiscibility, nucleation and cryst. growth

Na2O-Nb2O5-SiO2 glass, ix. and Raman spectral study, structure

Na₂O-ZnO-SiO₂ system glasses, ZnO structure role 0–58543 Ni-Si alloy, loss of coherency of p' particles 0–71777 Ni-Si alloy, microstructure, corrosion resist, mech. props., comp. depend. 0–43815

Ni-SiO₂-Ni-SiO₂ multilayer coatings on reflectors, 'black mirror' effect 0-41116

OSiCN mol. obs. by mass spectroscopy 0–66177
Si:Cr solid solution, precipitation kinetics, diffusion, temp. depend., e.p.r.
0–40454

Si/SiO; interface states, nature 0–56305 1%Si-Al, u.s. bonded wire interconnections, comparison with 1% Mg-Al 0–51072

Si-Al contacts, interface films and their effects on product performance

Si-Fe, domain struct., alternating mag. field 0-54009 Si-Fe, grain orientated, low temp. fracture behaviour, -196°C, planar anisotropy 0-56008

Si-Fe, grain orientated, low temp. fracture behaviour, -196°C, planar anisotropy 0-56008
Si-Fe, magnetization, stress induced 0-51206
Si-Fe, single crystal and rolled sheet, elastic moduli, internal friction, anisotropy 0-68416
3.2%Si-Fe alloy, mag. annealed, domain struct. 0-44567
Si-Fe alloys, antiphase domain boundaries 0-55702
3%Si-Fe grain boundary demagnetizing fields, domain struct., high speed Kerr cinematography 44566 0-44566
Si-Fe sheet, crack retardation by twins 0-68491
Si-Fe sheets with oriented grains, mag. domain pattern determ. 0-40998
Si-Fe weld's heat affected zones, plastic strain behaviour study 0-71725
Si-Ge-Sn(Pb) ternary phase diags., quasi-chem. calcs. 0-71407
Si-SiO₂ interface, LEED obs. 0-39929
Si-SiO₃ interface, Localized recombination-generation sites, capacitance mapping technique 0-44263
Si-As, absorpt. and reflectivity spectra, 300K 0-44854
Si-As, vapour growth of crystals 0-65139
Si-BF₇, mol. struct. determ. by electron diffraction 0-67751
Si-BF₇, struct. 0-64455
β-SiC:Al, photoluminescence, 77K 0-54141
P-SiC:Al film, line luminescence, 80K, electron beam excitation, 3-5 keV 0-44941
SiC:Al junctions, diffused and epitaxial p-n, elec. and luminesc. props.

SiC:Al junctions, diffused and epitaxial p-n, elec. and luminesc. props. 0-53885

p-SiC:Be alloyed p-n junctions, electroluminesc. 0-54138

Silicon compounds continued

SiC:N, 4H, 8H, 27H, 15R and 21R polytypes, photoluminescence, 20 and 77K $0\!-\!54141$

 α -SiC:N, 6H polytype, absorpt. and reflection spectra, 300 and 550K 0-56553

 α -SiC:N, (6H) crystal, absorpt. spectra, 0.7-1.1 μ 0-69128

α·SiC:N, (6H) crystal, absorpt, spectra, 0.7-1.1μ 0-69128
SiC:N,B, injection electroluminesc, and radiative recomb. 0-72425
SiC:Sc crystal Sc melt growth, 4H polytype 0-58619
SiC/metal composites, wettability and reactivity 0-50808
SiC-CdS junctions, p·n, IV characts., features 0-75747
α·SiC, 6H, i.r. luminescence and conduction band structure 0-72467
SiC, 6H polytype, photoluminescence, 77 0-54141
SiC, (6H), fundamental absorpt. edge, 4.2-600K, excitons, impurity effects 0-69127

SiC. (6H), fundamental absorpt. edge, 4.2-600K, excitons, impurity effects 0–69127
SiC. cathode, cold, of low power for direct modulation, characteristics, growth, geometry 0–79094
2HSiC, crystal growth 0–47119
SiC, cubic, optical absorpt. and reflectivity 0–48006
SiC, cubic, Zeeman effect of recomb. radiation 0–76158
SiC, diffused p-n junction, electroluminescence, current-brightness characts. 0–41288
n-α-SiC, elec. props. 0–56265
β-SiC, elec. props. 0–56265
β-SiC, elec. props. 0–56265
β-SiC, epitaxial growth, struct. and topography 0–53433
β-SiC, isopeitaxial deposition method 0–61658
SiC, isopeitaxial deposition method 0–61658
SiC, polycrystalline, sintered, microstructure 0–78498
SiC, polycrystalline, sintered, microstructure 0–78498
SiC, prep. and purification, bibliography 0–43590
α-SiC, solubility of B 0–71781
SiC, static dielec. const. 0–79233
SiC, surface cracks healing by oxidation 0–58937
SiC, thermoluminesc, and optical charge exchange 0–79380
SiC, work function meas. by thermoemission and contact potential difference 0–65867

SiC, work function meas, by thermoemission and contact potential difference 0–65867
SiC, X-ray emission spectra, Van Hove singularities 0–41246
n₋₂α-SiC 6H, spectrum analysis, 86 K, four-particle nitrogen-exciton complexes 0–48074
SiC coated with fuel particles in nuclear reactors, irradiation performance 0–46312

0-4012 SiC diode for 8 mm variable density sound recording 0-54137 β-SiC epitaxial film form, by reactive deposition 0-58587 SiC fibres, fracture after heat ageing, rel. to WC formation at core 0-50725

0-50725
β-SiC film, formed by chem. conversion, growth morphology and crystallographic orientation 0-58600
β-SiC films, formed by chemical conversion, surface characteristics and electrical conduction 0-68754
β-SiC films, formed by chemical conversion, surface characteristics and electrical conduction 0-68754
β-SiC films, formed by chemical conversion, surface characteristics and electrical conduction 0-68754
SiC junctions, elec. fluctuations 0-53883
SiC negative-resistance diodes 0-72086
SiC p-n junctions, tunnel breakdown 0-56322
SiC phases identification by proton blocking patterns 0-50548
SiC polytype-69R, cryst. struct. 0-65280
SiC rectifiers, high-temp., for reverse voltages 0-53866
SiC semiconducting crystals with improved Cr contacts, patent 0-75761
SiCN mol. obs. by mass spectroscopy 0-66177
α-SiC(6H), low-temp. photoluminescence (20 K) emission bands and internal recombination of donor-acceptor pairs 0-66124
SiC(6H), luminescence through bombardment by medium-energy charged

nal recombination of donor-acceptor pairs 0-66124 SiC(6H), luminescence through bombardment by medium-energy charged particles 0-56655 SiCl vibrational and rotational spectra analysis 0-61137 Si₂Cl₄, Si₃Br₄, and Si₂I₄, vibr. spectra and force consts. 0-55325 SiD₄, solid, i.r. spectra, in region of v_3 and v_4 fundamentals 0-69130 SiF, Franck-Condon factors and r-centroids 0-74284 SiF molecule, matrix element of dipole moment of A²-X² electron transition 0-53050 SiF, Franck-Condon factors and r-centroids 0-74284
SiF molecule, matrix element of dipole moment of A²-X² electron transition 0-53050
SiF, nature of excited state and transition involved during emission spectrum of SiF₄ vapour 0-46514
SiF₄, "PF spin-rotation const. 0-77841
(SiF₃)-S molecular structure determined by electron diffraction 0-53056
SiGGe, As₃, Te₅, bulk switching properties 0-79004
SiH₄, sondensed phases, i.r. and Raman spectra 0-70950
SiH₄, condensed phases, i.r. and Raman spectra 0-70950
SiH₄, condensed phases, i.r. and Raman spectra 0-70952
SiH₄, photoelectron spectra 0-61168
SiH₄, proton spin-rotation const. 0-77841
SiH₄, rel. to selective epitaxial growth of Si 0-47153
SiH₄, solid, i.r. spectra in region of P₃ and P₄ fundamentals 0-69130
SiH₄, solid, mol. motions from meas. of thermodynamic props. 0-59083
SiH₃, Srand SiD₃AsD₂, vibrational spectra 0-74307
(SiH₃), CH₂, and (SiD₃), CH₂, wibr. spectra and structure 0-77845
SiHO₃, and SiDC₃I, i.r. spectra and force constants 0-70951
SiHD₃, solid, mol. motions from meas. of thermodynamic props. 0-59083
SiH₃NCH₃H₃, mole. struct. 0-77843
(SiH₃)+O, i.r. spectra and frequencies 0-77846
SiH₃H₃PO₄, i.r. spectra and frequencies 0-77846
SiH₃H₃CeH₃, long-range H-H coupling 0-70950
SiH₃X SeedeH₃, long-range H-H coupling 0-70950
SiH₃X SeedeH₃, long-range H-H coupling 0-70950
SiH₃X SeedeH₃, long-range force constants and frequencies 0-67752
SiN(-oxide) films, vapour deposited, conduction from I-V characts. 0-44208

0-44208

0-44208
SiN, epitaxial deposition in radiantly-treated multiwafer reactor 0-65074
SiN, reaction-sintered, strength and oxidation 0-47380
Si₂N₄, effect on glass chem. and phys. props. 0-47018
Si₃N₄, single and two-layer coatings, thickness measurement by i.r. spectroscopy 0-50364 scopy 0-50364 Si_1N_4 film, breakdown, chemical vapour phase reaction deposition 0-58599

0-36374 film deposited on thermally grown SiO_2 , bias instability obs. 0-47807

Si₃N₄ films, prep. and dielec. props. 0-65774

Si₁N₄ thin layer deposition, semiconductor junction passivation 0–75745 Si₁N₂ thin layer deposition, semiconductor junction passivation 0–75745 Si₀N₂Si₁Si₁Si₁Si₁Care recombination vel., field-effect, planar technology control 0–75733

10-73/35 SiO₂-Al₂O₃, e.p.r study of electron donor-acceptor properties and point defects 0-59455 SiO₂-B₂O₃-Na₂O system glasses, phase separation mechanism 0-58544 SiO₂-CaO systems, molten, effect of alkali and alkaline-earth fluorides on surface tension 0-53326

Silicon compounds continued

SiO2-H2O, suspension, rheological study, electrophoretic mobility 0-68160

SiO, e.s.r., paramag. centres 0-66141

SiO, evaporated film, d.c. characts., conduction process model 0-79030 SiO, film, permittivity and loss tangent, 102-106 Hz, 77-573K 0-79035

SiO, passivating film, i.r. spectra, thermal treatment depend. 0-51309

SiO films, dielectric properties 0-65765

SiO mol, band oscillator strengths for $A\Pi$ -X¹ Σ ⁺ system 0–58197 SiO molecule, ${}^{3}\Sigma$ - ${}^{3}\Pi$ transitions, rotational constants determ. 0–61136 SiO on W. field emission obs. 0–44419 SiO₃, amorphous layer on Si, S-shift curve characts. of Si-O stretching band 0–72367

SiO₂, cristobalite, growth and stacking faults, X-ray powder diffr. 0-55894

0-33694
SiO₂, cristobalite, neutron irrad., structure and thermodynamic props. change 0-62134
SiO₃, densified, vol. relax. 0-58845
SiO₃, excess vibr. modes, anelastic and dielec. relax. 0-59084
SiO₂, fused, polished, roughness and slope meas., simple scatter method 0-49130

SiO₂, fused, u.s. attenuation meas. by Bragg diffr., obs. 0–50874 SiO₂, fused silica, u.s. beam mixing as meas. of nonlinear parameters 0–75223

0-15223 SiO₂, insulator film, r.f. sputtered, metal edbe coverage, charge accumulation control 0-53438 SiO₂, model for radiation induced paramagnetic defect 0-75191 SiO₂, neutron-compacted, Raman scatt, and far-i.r. absorpt. 0-76130 SiO₂, non-crystalline film, defect model, elec. and optical props., etching 0-47049

0-47049
\$iO₃, paramagnetic impurity centres in y-irradiation 0-75117
\$iO₃, passivation of \$i\$ semicond, devices 0-56308
\$iO₃, postety ciching, patent 0-39999
\$iO₃, rosettes of crystolbalite 0-61903
\$iO₃, sosettes of crystolbalite 0-61903
\$iO₃, silica, shock wave propag, characts. 0-71672
\$iO₃, silica, surface struct, Auger electron spectroscopy obs. 0-78368
\$iO₃, silica, vitreous, fine struct. 0-68200
\$iO₃, silica, evert, secondary electron emission and depend 0-44445

SiO₂, silica, vitreous, fine struct. 0–68200
SiO₃, single cryst, secondary electron emission, ang. depend. 0–44445
SiO₃, sputtered film, re-emission during growth, rel. to quality 0–53437
SiO₃, vacuum u.v. mats., transmittance limit temp. depend. 0–51311
SiO₃, vitreous, atomic vibrs. 0–75379
SiO₃, vitreous, filmision of sodium, thermal history effects 0–55925
SiO₃, vitreous, far-i.r. spectrum, vibrs. obs. 0–76129
SiO₂, vitreous, hydroxyl content rel. to vol. temp. relation 0–39909
SiO₂, vitreous, Raman scattering and i.r. absorpt. from low lying modes 0–51326
SiO₃, vitreous silica, conventional and elastic neutron diffr. 0–55684
SiO₃ bombardment by atomic H beams, lunar luminescence study, spectral distrib. 0–51744
SiO₂ coatings on semiconductor, etching, comp., patent 0–43585

distrib. 0–51744
SiO₂ coatings on semiconductor, etching, comp., patent 0–43585
SiO₂ film, high rate radio-frequency sputtering 0–57217
SiO₂ film, range of low energy protons 0–71891
SiO₂ film on Si, structure and porosity, infrared absorption technique 0–39944

0-39944
SiO₂ film on Si and Ge, surface recombination velocity depend. 0-51056
SiO₂ films, chem. deposited, behaviour during annealing in N₂ 0-39945
SiO₂ films, h.f. discharge plasma deposited, struct. 0-65087
SiO₂ films, preparation on Si monocrystal nuclei 0-39954
SiO₃ films, pyrolytically deposited, ionic instabilities 0-59260
SiO₄ films, r.f. glow discharge sputtering deposited, elec. and optical props. 0-75780

0—75780
SiO; films, struct, analysis, electron diffr, and i.r. absorpt. 0—71483
SiO; films u.v. irradiation, change in thickness, optical props. 0—62604
SiO; gel, y-irrad, luminesc, during gas sorption 0—43490
(96 wt.%) SiO; glass, divalent rare activation 0—59430
SiO; growth on n.Si by oxidation in steam 0—55748
SiO; integral coverslips for Si solar cells 0—69835
SiO; layer, ellipsometry, refractive index, thickness 0—76016
SiO; layers, thickness meas, by interference method 0—61639
SiO; proylytic films in m.o.s. struct., surface state and charge densities 0—56340

SiO₂ sample's transport efficiency determination from electrode cavity to gas stabilized d.c. arcs excitation zone, eqns. 0-51449 SiO₂ solid soln., decomp., in dislocation-free Si 0-40464

SiO₂ sublimation, continuous, vacuum using electron beam 0–50334 SiO₂ surface, polished fused, roughness effects on elasticity 0–65359 SiO₂ thermally grown, Al₂O₃ os Si₃N₄ films deposition, bias instability obs. 0–47807

0–47807
SiO₂ thin layer, tunnelable, formation by Si oxidation 0–62392
SiO₃, dielectric film, breakdown mechanism 0–75787
SiO₄ film on Si, stress determ, by dynamical X-ray diffr. 0–58577
SiO_x on Si, water contamination in device technology 0–58841
SiO₅, fused, i.r. spectra, vibrational analysis 0–48075
SiO₃1v⁴, cristobalite, e.p.r. 0–76226
Te-As Ge-Si, glass film, switching characts. 0–56266
Te-As-Si-Ge film, prep. by explosion method, negative resistance curves 0–51025

0-51025
Ti-Si system, unidirectional solidification 0-71525
U-C-Si phase diagram, U,Si-C section obs. 0-64988
U-Si, phase identification 0-68539
U-Si system, phase identification, microhardness, electron microprobe 0-56057
UO₂-SiO₂ fuel element, vitreous-ceramic power density calc. 0-39235
UO₂-SiO₂ system vitroceramics, fission fragment irrad. effect on thermal diffusivity 0-47561
UO₂-SiO₂ vitroceramics, melt props. 0-46307
U₃Si alloy, recovery and recrystn. 0-40443

adsorption of gases, LEED and ellipsometric obs. 0–39966 adsorption of gases, LEED and ellipsometric obs. 0–39967 adsorption of oxygen on (111) face 0–47076 aerosol particles in distilled water, light transmission 0–44780 atom, core polarization of 4d*95s* 2D states 0–70761 atoms comparison of calculated and obs. transition probabilities 0–60953 backscatter currents under keV ion bombardment 0–68704 band struct, Fermi surface and de Haas-van Alphen freq. APW calc. 0–40653 0-40657

band struct. and Fermi surface, Green's function calc. 0-40656 coating on glass, light transmission 0-44780

```
Silver continued
```

colloidal particles stacking faults, twinning obs. by electron diffraction

concentration in an aluminium silver specimen by small angle X-ray diffrac-

contacts, sintered Ag-faced, brazed joints with brass or Cu contact holders, mechanical strength 0–58850 crystal, single, channelling of protons and α -particles 0–40615 crystal growth from melt, use in electrocrystallization studies 0–50455 crystal growth from supersaturated metallic solns., initial cryst. obs. 0–55788

cyclotron reson., discrete spectrum waves 0-75517 de Haas-van Alphen effect, absolute amplitudes of neck oscillations 0-75522

diffusion in CdS single crystal, temp. depend. and activation energy 0 - 75200

diffusion in Pb, and electrotransport 0-47295 diffusion in single crystals, dislocation enhanced, 300-800°C 0-53558 diffusion of ¹¹⁰Ag in Cu at 400 to 1050°C, eff. of added Cr, Ti and Zr

e.p.r. of stabilized atoms in binary matrices 0~72475 elastic guided waves in films on Cu, Al, Ni, vel. dispersion, 5 45 MHz 0-47336

rel. to electrical contacts, switch material transfer obs., time lapse photogra-

phy 0-56177 dectrical resistivity due to vacancies 0-68764 electrodeposition in porous glass 0-41444 electrodeposition of ¹¹⁰Ag, ¹⁰⁹Cd, ^{114m}In, ¹¹³Sn and ¹²⁴Sb, valence effect 0 - 71640

0-71640 electron energy loss spectra, calc. and meas. comparison, retardation and foil structure influence 0-68701 electron energy loss spectra obs. and correl. with theory 0-50918 electron mean free paths 0-43965 electrotransport in liq. Zn-Ag alloys 0-39835 epitaxial film, resistivity strain depend. 0-75559 evaporation from Al Ag alloy, effect of β -particle bombardment 0-53405 Fermi surface, properties at normal volume and as function of pressure 0-65590

0-05390
Fermi surface and band-struct. determ., normal volume results and Herman-Skillman potentials 0-44047
film, epitaxial growth, elec. field effect 0-74901
film, epitaxial growth on NaCl crystal, effect of u.s. agitation of substrate 0-47051

0-47051
film, internal stresses, thickness depend. 0-47346
film, longit. plasmons excitation by photons 0-76088
film, optical plasma-reson. absorpt. 0-44823
film, radiative surface plasmons 0-62637
film, vacuum deposited, annealing technique 0-71478
film, vacuum-deposited, growth and orientations, rel. to air pressure, thickness, deposition rate and substrate temp. 0-43543
film, vacuum-deposited, point defects, recovery process 0-71604
film, vapour deposited, structure rel. to substrate comp., annealing depend.
0-61642
film on alkali halide substrates effect of Classical Company.

film on alkali halide substrates, effect of Cl exposure on epitaxy 0-74900 films, slow electron m.f.p. 0-68703 films, thin granular, complex permittivity and effective optical constants 0-47997

films, slow electron mi.p. 0-68/03 films, thin granular, complex permittivity and effective optical constants 0-47997 films epitaxy on LiF, MgO, rel. to lattice misfit and e irrad., obs. 0-55722 foils, thick, photon-surface-plasmon coupling, reflectance obs. 0-41114 growth, epitaxial, on electrically heterogeneous NaCl surfaces 0-53431 ions diff. in cubic high temp, phase of AgI 0-40196 lattice contraction rel. to paticle size, electron microscopy 0-71566 lattice dynamics, study on basis of angular force models 0-71820 lattice wave dispersion rel. to freq. 0-71821 liquid, struct. components 0-74723 liquid, struct. components 0-74723 liquid, struct. components 0-74723 liquid, struct. components 0-74723 molecular beam, diffraction by edge and cylinder 0-53104 molecular spectra in high temp, discharge, u.v. region 0-53015 nucleation on W substrate, contact angle 0-55741 optical consts. temp. depend., near 4 eV 0-76087 particles, size dependence of dielectric constant 0-44745 phonon dispersion relations, three symmetry directions, theory 0-50845 phosphor activation, in solution, absorpt. and emission 0-39813 photoelectric work function 0-75859 photon-surface-plasmon coupling in thick foils 0-41114 polymer formation in organic vapour environment obs., water drop reflection goniometer technique, surface preparation methods comparison 0-56694 pseudopotential form factors 0-40723 reflectance change due to strain in single crystal 0-48003 resistivity tensor, anisotropic, meas. using heliconlike waves 0-75560 self-diffusion, dislocation pipe, single cryst., obs. 0-47286 silica and alumina supported, pretreated with O₂ and H₂ adsorption of CO, ir. spectra 0-39971 solid, mean surface energy, Kelvin equation 0-68186 solubility of Cu, X-ray spectral analysis 0-61835 surface scattering of 4He, H, and D, thermal energy beams 0-65095 surface scattering of 1eV Ar atoms 0-39919 surface scattering of 1eV Ar atoms 0-39919 surface scattering of 5eV Ar atoms 0-39919 surface scattering of 5eV Ar atoms 0-39919 surface scattering of

thermal, conductivity and electrical resistivity precisely determ. 80-350 K $0\!-\!65557$

thermal expansion, linear, c.c.p., monovacancy formation 0-43916 for vacuum solders, impurity trace determ., spectrochem. analysis 0-76288

0-76288
vaporization wave, superheated 0-74853
vapour discharge with hot hollow cathode, nature of radiation 0-50122
work function and excemission, effect of deformation 0-75851
X-ray thermal diffuse scatt. 0-59075
Young's modulus of polycryst. wire, temp. depend. 0-71661
Ag-O-Cs photocathode, temp. depend. of work function 0-44435
Ag-O-Cs photocathodes, Cs donor impurity concentration determ. 0-44434
Ag-Si(O-SiC m.e.s. estreet. (D. work). The

Ag-SiO₂-SiC m.o.s. struct., (P-type), 1-V characts., temp. depend. 0-40815

Ag I 4d⁹5s6s level, intermediate coupling calc. 0–46375 Ag thin film, bombardment by keV beams of ¹H, ¹⁴N and ⁴⁰Ar, backscatter current yield 0–47042

Silver continued

Ag thin film, granular, covered with Al, characts. of interference 0-44781 Ag-, emission and absorpt. spectra in KCl 0-44842

Agr, mag. circular dichroism and complex absorpt. curves, resolution in alkali halides 0–48009

Agr centres in alkali halides, optical transitions 0–44846

Ag^o and Ag²⁺, in p-irrad. frozen aq. solns., paramag. relaxation 0–45088 Ag⁺ doped NaCl crysts., Raman spectra 0–66071

Ag+ impurity in NaCl, nuclear mag. double reson., conc. rel. to sensitivity 0-48172

0-48172
Ag* pairs in NaCl, Raman scatt. 0-59413
Ag*, Jahn-Teller distortions in CaF2 and SrF2. 0-76212
Ag**, Jahn-Teller distortions in CaF3 and SrF3. model 0-76213
110-Ag diffusion and mobility in KBr 0-6193
Ag(111), scattering of epithermal Ar beams 0-53419
Cs* ion bombardment for negative ion sputtering 0-57500
Cu₂O:Ag, effect on optical absorpt. spectra, and annealing effects
0-41197

He atms, diffr. from Ag (001) surface, obs. 0-55692

Silver compounds

Ag-Au alloy, elec, and thermal cond., thermoelec., 3-300k, comp., depend. 0-62456

0–62456
alloy, with group B impurities, Gorter-Nordheim rel. deviation, impurity-impurity interactions 0–51137
alloys, body-centred cubic structure, stability 0–78448
alloys, dil, Lorenz no. 0–47556
alloys, dilute, with V, Cr, Mn, Fe, Co, resistance anomaly 0–68751
alloys, elastic constants, precision meas., solute conc. effects 0–68397
alloys, solubility of Cu, X-ray spectral analysis 0–71743
alloys containing \$0.1\$ at% of Mn or Ni, giant echoes, at 4 MHz, 1.8 to 300°K 0–41360
halide, diffusion of impurity tracer, model 0–75198
halide emulsions, photographic sensitivity 0–73366
halide glasses, photochromic, behaviour and applications 0–49157
halide solutions, absorpt., excitation and luminescence spectra, effect of base cations 0–64927
halides, electron-phonon interactions in optical transitions 0–76084

base cations 0-64927
halides, electron-phonon interactions in optical transitions 0-76084
halides, induction of i.r. absorpt. by bound polaron 0-76086
halides, photoelectric and photographic sensitivity, Urbach rule, exciton absorpt. region 0-47870
halides, photoemission, anomalous temp. dependence, 80-295°K 0-79106
halides, sensitized photochromic glasses, high resolution holographic-image recording 0-76041
photolysis, sensitised, on semiconductor surfaces 0-56712
A-Ag system, Kirkendale effect, interdiffusion coeff. calcs. 0-78575
A-In liquid system, integral molar enthalpy 0-64898
Ag-Ag-Cl. electrode potential, effect of u.v. radiation 0-66198
Ag-Al alloy contact, resistance failures of Ag contacts due to corrosion 0-56174
Ag-Au-Yb, dilute alloy, mag, susceptibility, thermoelec. power, Kondo

Ag-Au:Yb, dilute alloy, mag. susceptibility, thermoelec. power, Kondo effect 0-44457

G-Ag-Au-Sn alloy, axial ratio changes 0-71565 Ag-Au, 3 alloys, Mossbauer isomeric shift of ¹⁹⁷Au, order dependence 0-54074

Ag-Au, electron density of states, photoemission study technique 0-71901

 0—1/1901
 Ag. Au alloy, reflectance change due to strain 0—48003
 Ag. Au (Cd, In) alloy films, optical plasma-reson, absorpt. 0—44823
 Ag. Bi alloy films vacuum evaporated on rock salt, growth obs. 0—55739
 Ag. Ca syst, differential thermal anal. 0—56049
 Ag. Cd solid solns., thermal vibrs. of atoms 0—71819
 Ag. Cd(Zn): 198n systems, α-phases, Mossbauer effect, isomeric shift 0—51278
 Ag. Ge alloy, heavy faulting on rapid solidification electron microscope obs. 0—40141
 Ag. Ge alloys, X-ray line broadening analysis 0—61835 heavy faulting on rapid solidification electron microscope

obs. 0-40141
Ag-Ge alloys, X-ray line broadening analysis 0-61835
Ag-In, electron density of states, photoemission study technique 0-71901
Ag-In alloy system, phase transformations 0-75313
Ag-M(III) binary alloys, thermodynamic behaviour 0-64898
Ag-Mn alloy, dilute, e transport props. low-temp, anomalies 0-40711
Ag-Mn alloy, thermal expansion from lattice parameter-temp. curves 0-43919
Ag-Mn dil. alloys, n.m.r. 0-79413
Ag-Pd-Cu contact spring material, age hardenable, characteristics and performance for relay applications 0-59158
Ag-Re dispersion electric contact, patent 0-71949
Ag-Sn alloy contact, resistance failures of Ag contacts due to corrosion 0-56174
Ag-Zn, Ag-Cd, Ag-Hg solid solutions, α-, temp. and conc. depend. of lattice parameters 0-78447
Ag-Zn, alloy, equiatomic, β' and ζ° phases, low temp. sp. ht. 0-78775

Ag-Zn alloy, equiatomic, β' and ζ^0 phases, low temp. sp. ht. 0–78775 Ag-Zn alloy contact, resistance failures of Ag contacts due to corrosion 0–56174 Ag-Zn alloys, lattice termal cond. 0–71874

Ag-Zn sliolys, lattice termal cond. 0–71874
Ag-Zn solid solns, thermal vibrs. of atoms 0–71819
Ag-Zn(Cd) alloys, α -phase, reflectance and band struct. obs. 0–75996
Ag Cl, thermal conductivity, 1.2-80 K, effect of substitutional impurities, and far i.r. absorpt. 0–43927
Ag complex, $\{(CH_3)_4N_{12}Ag_{13}I_{15}$, crystal structure from X-ray diffraction data 0–47175

data 0-4/11/5
Ag complex, C₆H₆AgAlCl₄, i.r. spectra of solid 0-76085
Ag complex, dipyridyl-coordinated Ag²⁺(4d*), e.p.r. 0-41315
Ag salts, soln. containing halogens and oxygen, 290-20°K, luminesc. and obs. spectra 0-68115
Ag;Al single crystal phase production by pulse annealing film couples 0-58642

O-58642
Ag3AsS3, proustite, optical parametric oscillation 0-77068
AgBi absorpt. band system in visible 0-61068
AgBr:Clr, AgBr, exciton absorption, photoluminescence 0-76163
AgBr:Fe_{1,III} defects, e.p.r. obs. 0-50578
AgBr:Na⁺(Lt⁺), exciton luminescence 0-76164
AgBr, AgBr I, thermoelectret state, ionic cond., temp. depend., calc. 0-44346
AgBr, agastic conets, press, and temp. derivatives, 0-68401

AgBr, elastic consts., press. and temp. derivatives 0–68401
AgBr, electronic behaviour, exciton and polaron roles 0–75506
AgBr, emulsion, dielectric meas., Maxwell- Wagner effect 0–43488
AgBr, simultaneous capture of 2 photoelectrons by a sensitivity centre

Silver compounds continued

AgBr, specific heat, -70 to 550°C, temp. depend., phase transition, defect effect 0-40567

AgBr EMC and AgBr-I photoemulsion microcrystals additional band due to Ag centers 0-51296

AgBr evap. layers, spectral sensitization by oxacarbocyanine 0-42402 AgBr surface, contact phenomena rel. to photographic process 0-73365 AgBr(Cl), optical absorpt. of self-trapped holes 0-79297 AgBr+ alkali bromides fused, thermoelec. power 700°C 0-64948

α-AgCd, Hall resistivity meas., 4.2-80K, anisotropic relaxation 0-75558 AgCl:AgBr mixed crystals, properties, use as an i.r. optical material 0-59346

AgCl:Fe_{II,III} defects, e.p.r. obs. 0–50578 AgCl:Hg, Na, doping effect on mech. and optical props. 0–50713 AgCl:(Se, Cd), e.s.r. of Se⁻ impurity centre, hyperfine interactions 0–44982 V =44962 AgCl:Ti³⁺(V³⁺,Cr³⁺), dipolar point de^cect relaxation, ionic thermo-current 0-75127

AgCl: 197 (AgCl: 1) dipolar point agreet relaxation, ionic thermo-current 0-75127

AgCl Mn phosphors, red and blue luminescence, temp. and i.r. radiation effects 0-54129

AgCl: AgCl: thermoelectret state, ionic cond., temp. depend., calc. 0-44346

AgCl, AgCl.I, thermoelectret state, ionic cond., temp. depend., calc. 0–44346
AgCl, diffusion of Li ions, isotopic effect 0–61986
AgCl, distrib. coeff. of S ions 0–54199
AgCl, elastic consts., press. and temp. derivatives 0–68401
AgCl, lattice dynamics 0–50841
AgCl, non-stoichiometric, hole conduction, 50-300°C 0–79034
AgCl, phonon freq.-wave vector relation, n scatt. obs. 0–40534
AgCl, photoluminescence after X-ray irradiation 0–56653
AgCl, precipitation and growth kinetics 0–55778
AgCl, specific heat, Debye temp., 2-12K, lattice vibration model 0–47544
AgCl monocrystal sheets, applications to the study of photographic sensitivity 0–65128
AgCl pure and Tl doped potential difference occurring during plastic deformation, meas. of stress at yield point 0–51097
AgCl single crystals, electroluminescence 0–51370
AgCl thermal conductivity at 300 K to 35 kbar 0–78789
AgCl(1): 1198n, Mossbauer spectra, 295 K 0–48025
AgCl(1): 1198n, Mossbauer spectra, 295 K 0–480

Agl. Rpl. solid electrolyte system, high conductivity 0–62811 Agl, cryst. growth 0–74981 Agl, m

AgI, cryst. growth 0–74981 AgI, m α-AgI cation cond. in microwave and i.r. region 0–62289 Ag(0) complexes, linear, ligand field second-order stabilization 0–51249 Ag(1) complexes, linear, ligand field second-order stabilization 0–51249 AgI cubic high temp. phase, self diff. of Ag ions. 0–40196 AgI epitaxial layer growth 0–61650 AgI epitaxial layer growth 0–61650 AgI nuclei remain on surface of drops 0–68069 Ag(II) complex, silver(II)-bis (pyridine-2,3-dicarboxylate dihydrate, crystal structure X-ray analysis 0–55827 α-AgIn, Hall resistivity meas., 4.2-80K, anisotropic relaxation 0–75558 Aga-In₁3, optical absorption and photoelectron energy distribution for electronic structure 0–65577 AgMeF₃ (Me-Mg, Mn, Co, Ni, Zn), crystal parameter related to electronic structure 0–55826 AgMg, line broadening rel. to stacking faults or antiplane domain boundaries 0–53542 Ag₃NG, long period order 0–75082 AgNO₃-KNO₃ system, molten, internal transport numbers and ionic mobilities of Ag and K ions 0–59494 AgNO₃-NaNO₃ melt, interdiff. coeff. 0–64889 AgNO₃, rystalline field effects on i.r. and and Raman spectra 0–59404 AgNO₃, molten, diffusion coefficient of Ag⁺ in Ca(NO₃)₂,4H₂O, chronopotentiometric 0–39762 AgNO₃ frozen aq. solns., p-irrad., paramagnetic relaxation 0–45088 AgNO₃ in methanol-water mixtures, rel. to electrostriction at 30°C 0–61541 AgNa(NO₂)₂, dielec. relax. 0–62429

O-01941 AgNa(NO₂)₂, dietec. relax. 0-62429 AgNa(NO₂)₂, ferroelec. transition pt. sp. ht. anomaly 0-65799 AgNa(NO₂)₂, n.m.r of ²³Na 0-72508 AgPd:Mn.Fe, dilute alloy, mag. susceptibility, s-d exchange scatt. 0-44494

 Ag_2S , thermal conductivity at high temperatures including liquid phase 0-71873

Ag₃SB layers, contact potential photovoltaic effect 0–75841
Ag₃SB and Ag₃SI solid electrolytes, photoelec, effects 0–68981
Ag₂S(Se,Te), ion and electron mobilities 0–71945
Ag₃S(Se), specific heat, –70 to 550°C, temp. depend., phase transition, defect effect 0–40567
α-AgSb, Hall resistivity meas, 4.2-80K, anisotropic relaxation 0–75558
Ag₃SbS₃, stephanite, crystal structure 0–40061
Ag₃SbS₃, stephanite, crystal structure 0–40061
Ag₃Se, formation by electrolysis of SeO₂ soln. on Ag cathode 0–72548
Ag₃Se film, vapour-deposited on single crystal substrates, electron diffrexam. 0–58593
Ag₃Se single crystal phase production by pulse annealing film couples 0–58642
α-AgSh, Hall resistivity meas, 4.2-80K, anisotropic relaxation 0–75558

0-3642
 α-AgSn, Hall resistivity meas., 4.2-80K, anisotropic relaxation 0-75558
 n-Ag₂Te, carrier effective mass, i.r. reflection spectra, elec. props.
 0-44186

 $\mathrm{Ag_2Te}$ film, vapour-deposited on single crystal substrates, electron diffr. exam. 0-58593

exam. U->8393 Ag_Tle₂, formation by electrolysis of TeO₂ soln. on Ag cathode 0-72548 AgTlSe₂, liq. and solid, elec. cond., thermal cond. and thermopower 0-78937 AgX-Ag₂S luminescence, flash and burst spectra at liquid nitrogen temperatures 0-56587 AgX luminescence flash and burst spectra at liquid.

AgX lluminescence, flash and burst spectra at liquid nitrogen temperatures 0-56587 Ag₃[Fe(CN)₆].xH₂O, Mossbauer spectra, room temp. 0-48035

Silver compounds continued

 $(Agpy_2)^{2+}$ complex ion, e.s.r., wavefunctions and ring angle determ. 0-46447

Al-(0.64 at.%)Ag alloy, clustering kinetics 0-50571

Al-Ag, Ag concentration by X-ray diffraction 0-53447Al-Ag, soft X-ray L_{2.3} spectra of Al constituent 0-66079Al-Ag alloy, evaporation of Ag, effect of β -particle bombardment 0-53405

U-53403 Al-Ag alloy, ordering, X-ray diffr. pattern, central diffuse spot, origin 0-53502

Al-Ag alloys, lattice ht. capacity enhancement by 1f. resonance modes 0-43900

Al-Ag solid solns., deform. 0-53583
Al-Ag solid solution, second stage decomposition, diffuse X-ray scatt.
0-68564
%\Ag alloy, cold working effect on subsequent precip.

0–68564
Al-(20 wt. %)Ag alloy, cold working effect on subsequent precip.
0–47476
Al-(15wt.%)Ag alloy, surface relief effects, γ plates, diffusional phase transformation 65483 0–65483
Al-Zn-Ag alloy flims, vapour phase nucleation 0–65060
Au-Ag alloys, impurity potentials rel. to nuclear spec. ht. 0–62256
Au-Ag contact alloy, mechanism of tarnishing obs. 0–55913
Au-Fe alloys, dilute, resistance anomaly 0–68751
Ca(PO₃)₇-AgPO₃ syst., equil. diagram, cryst. parameters 0–65502
Cu-Ag alloy, cold worked, heated, 600-800°C, hardness, recovery 0–58965

Cu-Ag all 0-58965

Cu-Ag alloys, recrystallization comp. depend. 0-50781 CuTISe₂, liq. and solid, elec. cond., thermal cond. and thermopower 0-78937

0-1893/ Fe/Ag composite wires, deformation, anomalous props. 0-59005 Fe-Ag, sintered, thermal e.m.f. in microscopic regime, role of parasitic thermoelements 0-40886

Mg-Zn-Ag system, structural changes rel. to Friauf-Laves phases 0-61877

Mn-Ag alloys, Kondo effect and relaxation times influence on nuclear orientation meas. 0-62580
Pd-Ag alloy, equilib. solubility of interstitial H₂, stress effects 0-53532
Pd-Ag alloy, flim, homogeneity rel. to prep. X-ray diffr. 0-47067
Pd-Ag alloys, resistivity minima 0-71958
Pd-Ag contact alloy, mechanism of tarnishing obs. 0-55913
Pd-Ag dil. alloy, magnetization, high field, band structure effects 0-44595
W Mo Ag based powder metallurgy, pseudo- alloy production for elec. contact making 0-68544
Yb-Ag system, phase diagram, struct. 0-64996
Zn-Ag, alloys, liq., electrotransport of Ag, effective charge determ. 0-39835

Sinanoglu's theory see Atoms/structure

Sinanogh's theory see Atoms/structure

Sintering
actinide oxides, hot-pressing 0-58946
β-alumina powders, densification 0-53650
β-alumina powders, densification and microstruct. 0-53650
carbide materials for rocket nozzle applics. 0-58953
ceramic dielectric sintered mixture, high dielec. const. and Q value and low temp. coeff., patent 0-44387
ceramic oxide cpds., transparent, fabrication by press. sintering 0-50793
ceramic-metal bond strength, sintering conditions effect 0-53654
cermet, UN/W(Mo), fabrication from mixed powders, conditions
0-40470
densification, volume diffusion as rate-controlling step 0-78684
ferrites, for h.f. and v.h.f. bands, relation between conditions and magnetic properties 0-51222
ferroelectric ceramic lead zirconate titanate, hot pressing effects rel. to electro-opt. applics. 0-62624
furnace; modification for continuous monitoring high-temp. kinetics
0-78666
graphite materials for rocket nozzle applics. 0-58953

graphite materials for rocket nozzle applies. 0-58953 graphite materials for rocket nozzle applies. 0–58953 hot-pressing as means of synthesizing pure materials 0–50759 initial stage analysis, time and length corrections 0–47438 initial stage analysis, time and length corrections 0–47437 ionic powders, plastic flow eft. 0–75297 iron ore, reduction cracking 0–58935 lead zirconate titanate, ceramic, hot pressing rel. to electro-opt. applies. 0–62624 metal powders, compaction kinetics 0–65475 model, diffusion, with surface energy and press. effects as driving forces 0–78665 powder mixing presintering quantitative analysis. X-ray even. 0–50797

model, diffusion, with surface energy and press. effects as driving forces 0–78665
0–78665
powder mixing presintering, quantitative analysis, X-ray exam. 0–50797
spinal ferrites effect of cooling on electrical and magnetic properties after sintering 0–44644
stresses, photoelasticity 0–65442
thermodynamic characteristics rel. to technological parameters 0–78663
Al-Ni-Co alloys, improved preparation method 0–71760
Al₂O₃-TiO₂, comp. depend. 0–47427
Al₂O₃ ceramics, characterization 0–58988
Al₂O₃ upstrates, prep. by isostatic pressing process 0–53637
BaTiO₃ ceramic, oxide additives effect 0–58990
BaTiO₃ ceramic, sintered and press.-sintered, additives influence on densification and strength 0–58989
Be, under pressure phys. props. surface chemistry effects 0–47464
Be powder, hot-pressing, electron metallography and oxygen impurities role 0–65445
CaF₂ powders, first-stage densification under pressure and temp. 0–58954
Cu compacts from powders, prep. for high conductivity use 0–65476
Cu wire, dispersion-hardened 0–68546
Cu wire, dispersion-hardened 0–68546
Fe, sintered and mild steel, adhesion props. rel. to void fraction 0–56053
HfB₃, with SiC and C additives, densification 0–50801
HfO₃-refractory oxide solid solns., comp. changes 0–50783
Li_{0.3}Fe_{2.3}O₄, effect on mag. and cryst. props. 0–65956
MgA₂O₄O₄, vol. diffusion depend., 1300-160°C 0–50764
MgO₂CliF₁ liquid phase process, densification 0–47452
MgO₂CaO-Ga₂O₃ system, sinterability and resistivity to hydration 0–586bility and 1500 mixtures, for long periods, influence on electrical properties and stability 0–78863

0-53629

MnO-NiO mixtures, for long periods, influence on electrical properties and

Stability 0—78863 Mo powder, hot pressing, 1400-1600°C 0—65451 Nb-Ti(Zr) supercond. alloy fabrication method, patent 0—44154 Nb bicrystals, welded, of boundary porosity 0—40440

Slip continued Sintering continued Ni-Fe-Cu-Mo, magnetic alloy, high permeability, resist. variation 0 -62089 Fe single crystal, plastic flow, orientation and temp. depend. 0-53599 KCL, thermally activated, anisotropy, 77-560 K 0-78642 Fe single crystata, plastic how, offendation and tenja. depends, VCI, thermally activated, anisotropy, 77-560 K 0-78642

LiF, bands rel. to crack deceleration 0-40416

LiF, dislocation forest and deformation resistance 0-68446

LiF, Lif's, mechanism, yield stress, temp. depend., 77-450K 0-40340

MgO single crystal, rolling- contact deform. rel. to track props. 0-40306

Mo, deformed, stress-strain characts. 0-78643 0 - 62089
PuO₂, hot-pressing 0 - 58946
SiC, polycrystalline, microstructure 0 - 78498
TiN, in N₂ 0 - 65456
TiN, 0₃, high temp, behaviour 0 - 58961
(U Pu)O₃ mixed fuel fabrication for FFTF 0 - 58962
UN/W(MO) mixed powder, conditions for cermet fabrication 0 - 40470
UN powders, synthesis and characterization 0 - 56051
UO₂, comp. depend. 0 - 47434
UO₃, kinetics, isothermal shrinkage obs. 0 - 40442
UO₃, clubes, electrodynamic vibrocompaction 0 - 67587 Mo, polycryst., ductile-brittle, microyielding and failure mechanisms 0-75256 Mo, polycrystalline, inhibition in brittle region, on irrad. and alloying 0 40353 0 40353
NaCl, bands rel. to crack deceleration 0-40416
NaCl single crysts. rel. to dislocation glide bands and hardening due to dynamic impacts, obs. 0-40168
Nb-Mo alloy, inhibition in brittle region, on irrad. 0-40353
Nb, polycrystalline, inhibition in brittle region, on irrad. and alloying 0-40353 UO₂ nodules, electrodynamic vibrocompaction 0–67587 UO₂ pellets, very high density, fabrication, effect of sintering parameters 0-40471 0-40471 (U_{0.71}Pu_{0.75})O₃ mixed fuel processing using 9-variable fractional factorial expt. 0-58969 W-Mo-Ag based alloy powders, for elec. contacts 0-68544 W, Ni additive effect 0-68514 YFe garnet, additive effect 0-50766 YFe garnet, grain growth, comp. depend., rel. to magnetic props. 0-47435 12Mol.% Y₂O₃-ZrO₃, stabilization, monoclinic content 0-47465 ZrB, with SiC and C additives, densification 0-50801 Ni-(11.4wt.%)Al alloy, distrib. rel. to coherent precipitates 0—75258 Ni-(20wt.%) Cr-(7.5wt.%) Al alloy, distrib. rel. to coherent precipitates Ω-Ni, high-speed deform., slip systems participation 0-40341 Str₂, dislocation etch pits, room-temp, microplasticity 0–43758 TaC₂, single crystal, and mech, props. 0–47308 TaC₂, single crystal, and mech, props. 0–47308 Zn.(0.4 wt.%)Al superplastic sheet, anisotropic effects 0–40315 Zn, in pyramidal slip, plastic deform, mechanism 0–62044 Skin effect n effect
anomalous, in cylindrical conductor in mag. field 0–65614
anomalous, skin-effect fields enhancement beneath rough surface 0–71940
boundary value problems for the integro differential equations of nonlocal
wave interaction 0–48683
conduction electrons, boundary condition, diffuse 0–47612
Fermi velocity and a new mechanism for anomalous field penetration in
metals 0–53774 Smectic phase see Liquid crystals Smokes see Aerosols Snoek effect see Crystal imperfections/interstitials; Elastic relaxation metals 0-35/14
low frequencies (0.3-15.0) Hertz, four point probe technique 0-40686
metal, anomalous effect, nonlinear e.m. wave reft. 0-71939
metal, cyclotron resonance for arbitrary skin effect anomaly 0-47610
metal, electromagnetic wave echo under anomalous skin-effect conditions
0.47613 shock tube experiments, Hugoniot curves 0-50655 terrestial cover, surface meas, for correlation with aerial obs. 0-41502 thermal cond. meas, of frost by transient hot-wire technique 0-79551 Sodium $3^{2}P_{1/2}$ - $3^{2}P_{3/2}$ mixing induced in collisions with molecules 0-74160 metal, surface impedance, variable field amplitude depend. 0-56164 metal, surface impedance in anomalous-skin-effect regime, Fermi liq. effects 0-71935 absorption, phonon contrib. 0–51336
absorption on W(112) surface 0–50359
in atmosphere, conc. determination from twilight observations 0–54242
atom, 3²P_{3/2} level crossing, obs. 0–52889
atom, ²³Na polarization of resonance lines excited by electron impact calc. metal cylinder, anomalous, in mag. field 0-65614 Sky brightness see also Airglow; Twilight
angle scattering fn. determination, obs. 0–59576
elliptical polarization 0–51529 atom, ⁴³Na polarization of resonance lines excited by electron impact calc. 0–46369 atom, (3²S→3²P) electron excitation cross sections for light atoms using Slater wavefunctions 0–67605 atom, de-excitation by N₂ rel. to initial kinetic energy and final vibr.-quantum number 0–52950 atom, excitation in nitrogen afterglows 0–46383 atom, hyperfine struct. from Stark eff. investigation of 3²P_{3/2} state 0–39291 computer potalization (V-3)527 Milky Way, inference of Galactic structure (0-56938) night, and atmospheric transparency, obs. on March 1965 at Bamako (0-59629) night, rel. to interstellar radiation field, 2000-5560 Å 0-41594 night sky light continuum in atmosphere, data 0-54266 u.v. spectral radiance meas. of horizon-sky between 3000 Å - 4200 Å 0-62912 atom, ionization by He collisions, Penning electron energy distribs., interac. potentials 0—74159 atom, isolation of flat level-crossing signal 0—60926 atom, minima of generalized oscillator strengths for continuum transitions 0—67627 Sliderules see Calculating apparatus Slip alkali halide crystals, lines, generation and propagation, 1.4 K 0–62055 alkali halide single crysts., work hardening theory 0–68515 alkali halide single crysts., work hardening theory 0–65460 alloy with coherent precipitates, distrib. 0–75258 alloy with coherent precipitates, distrib. 0–75258 anodic coating on Al, buckling 0–62032 anthracene single crystal, basal and non-basal 0–71704 b.c.c. metal, single crystal, stress effects, critical shear 0–43756 band, retarded, distrib. of dislocations, calc. 0–78546 band growth in irrad. crystals, mechanism 0–40172 composite materials, theory 0–47472 conditions for occurrence in brittle solids, specially under hydrostatic pressure 0–78651 diamond, natural crystals, in growth mechanism, contrary evidence for twin diamond, natural crystals, in growth mechanism, contrary evidence for twin 0-0/627 atom, quadratic Stark shifts of Zeeman levels in ground state 0-77662 atom 0-67649 atom absorpt. spectra in solid Ar, Kr, Xe, obs. 0-49783 atom and ion, collisions with Na and K vapour and inert gases, 20-155 keV 0-39316 atom collision with He and Ne, electron energy spectra and auto-ionizing level excitation 0-64257 atom vapour, atomic absorption method for determining pressure 0-67621 atomic transition tables 0-39284 atoms, 2P m_J mixing in inert gas collisions, D_2 optical pumping, obs. 0-529530-52953
atoms, light emission meas, at simulated meteor conditions 0-49785
atoms diffusion coeff. in H₂+O₂+N₂ flame, 1920-2520K 0-64799
atoms in arc discharge, spatial distribution 0-74613
binding energy, elastic consts, and derivatives, eqns. of state, and phonon spectrum 0-56088
boiling, nucleate pool, mechanism and stability criterion 0-39892
bond in reactor fuel elements, behaviour of stationary fission gas bubbles 0-55198 diamond, natural crystals, in growth mechanism, contrary evidence for twin lamellae 0-74958 diffusive, in polyatomic gas mixtures 0-46807 dislocation, interaction with twin boundaries 0-78551 fretting fatigue, stress distrib., component strength, finite element tech nique 0-40377 h.c.p. metla, dislocation-deformation twin interactions, decomposition 0-61958 0—33198
consider and compressibility in body-centred cubic phase 0—43579
combustion of liquid at pressures below atmospheric 0—56689
Compton scattering, rel. to ground state momentum distribution function of conduction electrons 0—65576 metal, b.c.c., high temp. work hardening, theory 0-40445 metal, b.c.c. and h.c.p., strain bursts and coarse slip during cyclic deform. 0-71703 0-71703 microslip, creep and wear in rolling contact 0-43755 particle slip surfaces in bubbling gas fluidised beds 0-50271 poly-4-methylpentene-1 crysts. in plastic deform., obs. 0-40316 rarefied gas flow over wedge, low-speed soln. 0-71229 rolling texture, brass-type, development 0-50757 solid solution, non-random, deformation, configurational changes, calc. 0-40338 steel, low-carbon microcracks by slip deformation 0-50741 viscous, in polyatomic gas mixtures 0-46807 Al-Ag solid-solns. 0-53583 Al single crystal, fatigued, X-ray topography examination of slip bands 0-40339 Al₂O₃, double bicrystal, high temp. deformation 0-50683 Al₂O₃, fine grained, deform, at high strains and repeated loads 0-50682 CsCl type compounds, anisotropic elasticity theory, predictions 0-47012 Cu-Zn crystal, fatigued, dislocations, slip bands, electron microscopy 0-78549 Cu-(12at.%)Al, strain burst in single crystal, cyclic stress-strain curve 0-40269 condensed phase, electrical resistance up to 1300° K, as function of temp. 0-71374corrosion of stainless steel, with 4 and 12 p.p.m. O, up to 760°C 0-41435 dayglow over Fritz Peak Observatory, seasonal, diurnal variations, obs. 0-54261 diffusion in RbCl, 377-707°C 0-75209 diffusion in SiO_2 glass, anomalous behaviour, superimposed processes 0-559200-55920
diffusion in quartz, 330-910°C 0-62001
diffusion in silicate glass, NBS 710 viscosity standard 0-62003
diffusion in vitreous silica, thermal history effects 0-55925
doping of AgCI, effect on mech. and optical props. 0-50713
electrical resistivity, 4.2 to 15 K, obs. 0-56185
excited atomic states, mean lives of Na I, II and III, beam-foil excitation technique 0-67648
film on (011) face of W, struct., 77-400 K, electron diffr. 0-39943
g shift of cond. electrons 0-79227
heat pipes, in Li/Nb fusion reactor blanket, obs. 0-70721
helicon waves propag. 0-47608
high temperature effects on stainless steel creep and stress rupture 0-42914
high-temperature effects on reactor stainless steel 0-42912 0-40269 Cu, high temp, creep behaviour of single crystal, orientation depend. 0-437510-43751
Cu, irrad., band growth mechanism 0-40172
Fee (3.4wt.%)Si, slip planes temp. depend.78641 0-78641
Fee Si alloy, singularities in plastic deform. of single crystal 0-53603
Fee Si single crystals, rolled, determ. of active slip systems 0-78640
Fee Si single crysts, asymm. of slip on (112) planes 0-62054
Fee, slip induced cleavage crack nucleation 0-50741
Fee, strain-rate sensitivity and thermally activated flow, orientation depend., single cryst. 0-68444
Fee macroscopic structure, single crystals, obs. by optical microscopy, etch pits, X-ray topography 0-75269 high-temperature effects on reactor stainless steel 0-42912 high-temperature effects on stainless steel creep behaviour 0-42913 impurity in Si crystal, effect on growth at twin boundaries and on surface steps 0-61717

interstellar, lines in spectra of 9 stars in galactic centre direction 0-48435 ion-atom combinations, resonant and nonresonant charge transfer cross sections 0-77696 ion-ion potential calc, using one-orthoganalized plane wave bare electron-ion matrix element 0-65118

Sodium continued

isoelectronic sequence, photoionization cross-section calc. 0-64229 liquid, carburization of stainless steel, rel. to grain size and work hardening

liquid, cavitation damage to Co alloy, effect of temperature and pressure,

obs. 0-50749 liquid, collective atomic motions 0-39721

liquid, collective atomic motions 0-39721 liquid, collective atomic motions 0-43421 liquid, corrosion of V and alloys 0-45066 liquid, corrosion of steel, kinetics 0-41434

liquid, corrosion of steel, kinetics 0—41436 liquid, flowing corrosion of stainless steel at high heat flux 0—41436 liquid, flowing corrosion of stainless steel 0—39749 liquid, new mass transfer of stainless steel 0—39748 liquid, permanent-magnet flowmeter, end-effect theory 0—46845 liquid, permanent-magnet flowmeter performance meas. 0—46846 liquid and solid, spin lattice relax. time and resistivity, 293-453°K 0—39837 liquid at 160-800°C, viscosity determination, exptl. unit and investigation method 0—58461 luminescence activator in KI 0—66096 luminescence of atoms in solid argon at 4.2°K 0—56605 mass transfer and wear corrosion of stainless steel 0—45065 methigs, hp. 0—74843 model lattice, b.c.c. and h.c.p. phases, stacking fault energies and screw dislocations 0—50594

optical absorpt. near i.r. to far u.v., calc. 0-41219 optical constants, testing of interband-transition absorpt, theory 0-79231 optically pumped, D₁ absorpt, dispersion lines perturbation by He, Ne, obs. 0-52918

overlayers on W(112), LEED obs. 0-65109

overlayers on W(112), LEED obs. 0-65109 phonon dispersion curves, pressure depend. 0-47507 photoabsorption meas., L_{II,III} edges 0-66049 photoelectric yield and photoelectron energy distrib. 0-40910 photoemission, angular dependence, band structure determination by electron distribution 0-44433* reactor, Na-cooled, corrosion rate of steel cladding 0-56705 reactor component walls, thermal transient response and stress obs. 0-39191

reactor experiments, Na/H₂O at Dounreay, review 0–49735 reactor technology, conference, Argonne (1968) 0–42911 spectral radiant energy of Mg-NaNO₃ pyrotechnic flare, 3800 to 7400 Å

0-67626
stacking fault energies and screw dislocations in b.c.c. and h.c.p. model lattice 0-50594
surface diffusion on metal substrates, meas. techniques, numerical simulation 0-47282
thermal resistivity, 4.2 to 15 K, obs. 0-56185
twilight intensity variation enhancement study 0-54267
vacancy pairs, asymptotic interaction energies 0-43657
vapour, laser-induced breakdown, two-photon ionization 0-78158
vapour, enew pair potential for virial coeff, data 0-74671
vapour, undergoing double quantum transitions, radiofreq. coherences
0-74120
vapour denosition in inert englesses.

vapour deposition in inert enclosures 0–53403
X-ray emission spectra, conduction electron scatt. pot. 0–79339
Br. quenching of 3²P state of atom, calc. 0–67650
I₂ quenching of 3²P state of atom, calc. 0–67650
I₂ quenching of 3²P state of atom, calc. 0–67650
I₂ quenching of 3²P state of atom, calc. 0–67650
I₂ quenching of 3²P state of atom, calc. 0–67650
I₂ quenching of 3²P state of atom, calc. 0–67650
Na-Ar collision, depolarization of 3²Py, state 0–58119
Na-NH₁, siquid-liquid coexistence and phase separation 0–58454
Na-NH₃(ND₃) layer formed by evaporation, EPR obs. following tempering 0–51398
Na-NaCl molten solutions, magnetic susceptibility, 800-970°C 0–74785
Na I, mean lifetime measurements and spectra for isoelectronic sequences using beam-foil techniques 0–64213
Na I λ5889 line, pressure broadening by high temp. neutral helium 0–52917
Na I redshifted D lines, identification in compact galaxy IV Zw 150

Na I redshifted D lines, identification in compact galaxy IV Zw 150 0-48388

0-48388
Na II, 2p³3p configuration mean lives of fine structure states 0-42975
Na, laser-induced fluorescence at 632.8 and 640.1 nm 0-58189
²²Na concentration in ground-level air meas, air exchange between stratosphere and troposphere obs. 0-76403
²²Na+²⁶Al isotope, radioactivity meas. in Alandroal, Allende, and Sprucefield fallen meteorites 0-54451
²³Na, atomic constants meas. using level-crossing signals of 3²P_{3/2} state 0-58100

John Complexity oriented, F=2 multiple quantum transitions, cross-beam obs. 0-52919
 Na cosmogenic radionuclides, production rate meas. at 19 Km. and over

²⁸Na cosmogenic radionuclides, production rate meas, at 19 Km. and over 0-59595 Na±NO₂, formation of NaO in ²II state obs. 0-46635 Na±NO₂, formation of NaO in ²II state obs. 0-46635 Na+N-N-Na+Ne*, regular oscillations of total cross section of reson, lines excitation 0-61009 Na++O+Na(3p)+O, 0.06-7 eV, cross section determ. 0-61007 Nb compatibility rel. to O content 0-45055 O₂ conc. and mass transfer coeffs, determ. using uranium 0-69231 Si:Na, donor parameters obs. 0-78997 V-Ti alloy corrosion resistance rel. to Ti content 0-40468

Sodium compounds

alloys, ²⁴Mg recoil nuclei nucl. reson. fluoresc. 0–65569

analoite, elec. cond. 0–59251

borosilicate glasses, thermal shock resistant, effects of viscosity, phase stability and crystallization in production 0–68199

borosilicate melts, viscous relaxation anomaly observed above critical points 0–74734

cryolite sola, with Al-O, at 1025°C, anode effect 0–66193

points 0–74734
cryolite soln. with Al₂O₃ at 1025°C, anode effect 0–66193
glass soda-lime -silica, Na content determ. by X-ray fluorescence 0–41456
halide, low temp. reflectivity, 5-10 eV, fine struct., excitons 0–76076
halide crystals, terbium activated, presence of 0 centers 0–56608
halides, Born model, u.s. parameters 0–43706
halides, i.r. absorption due to H⁻ions, anharmonic side bands 0–72359
loeweite, disordered sulphate group 0–65262
niobate hydrates, crystal chemistry 0–55771
soda sources for fint glasses 0–58536
soda-lime-silica melt, dissolution of vitreous silica by forced convection 0–58452
sodalite, photochromic, e.p.r. of F-type centres 0–62760
sodium tungsten bronze, pure and doped, single crystal growth 0–74964

Sodium compounds continued

tantalate hydrates, crystal chemistry 0-55771 zirconsilicate: Dy(Gd,Eu), luminescence and exoemission 0-76154 [Na₆F(OH₂)₁₈](NaH₂)(AsO₄)₂, crystal structure, polycation 0-58741 Ca(PO₃)₂-NaPO₃, phase equilibrium diagram, existence of CaNa(PO₃)₃ 0-47487

CdCl₂-NaCl molten system, self-diffusion coeffs., using capillary method 0-39763

CoCl₂-NaCl fused system, Co²⁺ mag. moment 0–62490 LiCrSi₂O₆-NaCrSi₂O₆ system, synthesis and solubilities 0–56044

Na-Bi system, phase diagram 0-39869 Na-Cs liquid alloy, u.s. absorpt. and vel. obs. 0-64915

Na-Cs liquid alloy, u.s. absorpt. and vel. obs. 0–64915
Na-Hg, exo- and dark-emission correls., obs. 0–40904
Na-Kalloy, liquid, electromigration 0–43473
Na-Rb system, solid-liquid phase equilib. diagram 0–53398
Na, montmorillonite, b dimension changes with water content 0–61891
Na₂, laser induced reson. fluoresc. of X \(\mathbb{L}_2\), \(\mathbb{L}_3\) \(\mat

NaAls(OH)₄(PO₄)₇.2H₂O, wardite, cryst. struct. 0—61896
NaAls(O₄)₈.12H₂O.²Ch² e.s.r. studies 0 62759
(NaAlSiO₄)₈.2NaCl, sodalite, single crystal, hydrothermal growth 0—40009
Na₃As (Sb), quadrupole splitting of ²³Na n.m.r. spectra 0—48164
NaBa₃Nb₂O₁₅, optical quality crystals, growth from alkali-rich melts 0—50468
Na₂Ba₄Nb₁₉O₁₉, polycrystalline, with K.-W bronze structure, test of ferroelectric and physical properties 0—75800
NaBr:Eu luminescence obs. 0—56607
NaBr-NaCl, diffusion pair, misht dislocations 0—75164
NaBr, Debye temp, elastic constants, temp. depend., 80-300 K, u.s. velocity meas. 0—62012
NaBr, elastic compliances and stiffnesses, 293-573 K 0—50638
NaBr, multiphonon X-ray scattering calc. 0—62173
NaBr, phonon frequencies 0—47508
NaBr, rhermopower meas. 0—59276
NaBr comparison of colour center formation 0—47268
NaBr, 2H₂O, polycrystalline, p.m.r. 0—69198
NaCNS in conc. aqueous solns, elec. conductance, diffusion, viscosity and density meas. at 25° 0—71375
Na₂CO₃H₂O, crystal structure 0—78482
NaCl-K Cl solid-solution alloys, creep, 600°C 0—65404
NaClO₃, elastic consts., Brillouin scatt. obs. 0—53572
NaClO₃, growth from solution, convection- induced rate-depend. habit 0—61725
NaClO₃, growth from solution, convection- induced rate-depend. habit 0—61725
NaClO₃, growth from solution, convection- induced rate-depend. habit 0—61725
NaClO₃, thermally bleached, e.s.r. absorpt. spectrum 0—44994
NaClO₃ cubic and optically active, scattering meas. problems 0—72391
NaClO₄ in conc. aqueous solns., elec. conductance, diffusion, viscosity and density meas. at 25° 0—71375
NaCoF₃, cryst. struct. from X-ray powder patterns 0—65218
Na₃Co₄O(OH)₅(SO₄), 4H₂O, cryst. struct., X-ray powder indexed 0—53510
Na₃Cr₃Cr₃Cryst. struct. from X-ray powder patterns 0—65218
Na₂Cr₃CO(OH)₅(SO₄), 4H₂O, cryst. struct. in A Raman spectra, vibr. analysis, obs. 0—39391
Na(Cl)₄Cr₄Cr₅Cry₅Cryst. struct. the A Raman spectra, vibr. analysis, obs. 0—393

Na* 0-39827
NaF, multiphonon X-ray scattering calc. 0-62173
NaF, potential distrib. and electron density in lattice, atomic scattering factors 0-43998
NaF, role in Ti-Al alloy stress corrosion cracking 0-50744
NaF, sleaved, thermal etch pit terracing, obs. 0-39996
NaF, specific electrical conductivity in molten state 0-58496
NaF, thermal emissivity, far ir., 80-600 K, meas., rel. to vibr. modes 0-76106

NaF containing substitutional divalent cation impurities, ionic thermocurrents 0-75783
NaF films, dielec. breakdown, in Al-NaF-Al capacitors, 80-380K

0-53931 NaF melt, dissolving of quartz spheres, diffusional convection processes

Nat melt, dissolving of quality spinots,

0-39764

NaF second sound anomaly at high temp. 0-56100

NaFe(CN), aqueous solutions, photoelectron emission 0-74778

NaFe(CN), single crystal, mossbauer spectra, quadrupole splitting

Na₄Fe((N_8)) single crystal, mossbauer spectra, quadrupole splitting 0-48038 NaFeS₂, Mossbauer spectrum rel. to internal field, obs. 0-41155 NaFe($(WO_4)_2$, cryst. struct., unit wolframite motive variation 0-40087 NaGdSiO₄, cryst. struct. 0-78485 NaH, equilibrium conc. in earth's upper atmosphere during night-time 0-79554

NaH*, hyperfine coupling constants for Na and H for various bond lengths 0-49854
NaHCr₂(CO)₁₀, i.r. and Raman spectra, vibr. analysis, obs. 0-39391
NaHCr₂(CO)₁₀, i.r. and Raman spectra, vibr. analysis, obs. 0-39391
Na(H_{1-x})₁₀(SeO₃)₂, thermal expansion, phase transitions, isotope effect 0-56111

0-56111

NaHF₂, electron-irrad., e.s.r. of F₂⁻ and H obs. 0-44992

NaHF₂ i.r. and Raman spectra 0-74291

NaH₃(SeO₃)₂, far i.r. reflectivity, 16-400 cm⁻¹, 300 and 202K, complex dielec. const. 0-56526

NaH₃(SeO₃)₂, H bonds rel. to thermal expansion 0-68619

NaH₃(SeO₃)₂, paraelectric, crystal structure, neutron diffr. study 0-50538

NaH₃(SeO₃)₂ and NaD₃(SeO₃)₂, ferroelec. phase transitions, thermal props. obs. 0-65816

Sodium compounds continued

 $NaH_{3}(SeO_{3})_{2}$ ferroelectric, phase transitions, specific heat, configurational entropy change $\,0{-}43907$

NaI:Eu luminescence obs. 0-56607

Nal:TI, energy loss spectra for gamma rays, Monte Carlo calc. 0–52584 Nal:TI, scintillation response to ⁴He and ¹⁶O ions, channelling effect 0–72456

NaI:T1 crystals, scintillation counter, lone-energy protons recording 0-38751

Nal:TI plastic scintillation counter, props. of arrangement for time and energy obs. 0-77402 NaI:Tl scintillator, incomplete optical contact, light collection coeff. calc.

0 - 46032

NaI:TI wrapped crystals, reflection coeff., meas., rel. to scintillation detectors, characteristics determining 0-41112

NaI:Tl+, impurity, transport ionic conduction, diffusion 0-40199 NaI, Fourier components, instantaneous premittivity, lattice vibrations 0 -40527

Nal, in metallic iodide lamps, patent 0-53226 Nal, quenched in colour centre, photoluminescence, optical absorpt. 0 47281

NaIAICH₃Cl₃ complex, i.r. and Raman spectra, force constants of complex ion 0-46497

NaI(TI), y-ray spectrometers, semi-automatic generation of response function matrices 0-60649

tion matrices 0-60649

Nal(TI), y-ray spectrometer, anticoincidence, shielded, total absorption, for low level radionuclide analysis 0-73679

Nal(TI), scintillators, comparison of constant fraction and leading edge timing 0-63895

Nal(TI) counters, whole-body, calibration 0-55081

Nal(TI) scintillation counters, delayed coincidence time resolution 0-63893

Nai(Ti) spectrometer, total absorption, for electrons and y-rays at GeV energies 0-60653
Nai,KSb(Cos), multialkali photocathode, semiconducting props. 0-53817
Na; KSb(Cs), multialyer cathode, attenuation length of photoelectron

0-0220 NaN₂ crystal, soln., growth 0-71518 NaN₃, far i.r. absorpt. spectra, lattice modes 0-56089 NaN₃ e.p.r. identification of a defect, effect of structure on interpretation 0-75120

NaNH₄SO₄.2H₂O, ferroelec., domain struct. 0–62442 NaNH₄SeO₄.2H₂O, ferroelectric, orientational mobility of NH₄ groups, p.m.r. investig. 0–53941 NaNH₄So₄.2H₂O, ferroelec. phase transitions, thermal props. obs.

NaINT4504.2H₂O, ferroelec. phase transitions, thermal props. obs. 0–65816
NaNO₃:Ca, d.c. conductivity a.c. conductivity and anisotropy 0–56184
NaNO₃:²¹Na quadrupole spin-lattice relaxation meas. reanalyzed 0–75977

0-159/1/ NaNO;·YO²⁺, e.p.r. 0-41344 NaNO;-AgNO₃ melt, interdiff. coeff. 0-64889 NaNO₃-Mg, illuminating flare flame, visible spectra, strong emission features 0-64821 features 0–64821 NaNO₃ RbNO₃ melt, interdiff. coeff. 0–64889

NaNO₃, RbNO₃ melt, interdiff. coeff. 0–64889

NaNO₃, dielectric relaxation time, static susceptibility, near transition points 0–44356

NaNO₂, far-i.r. reflectivity spectra, temp. depend. 0–66025

NaNO₂, ferroelec. polarization reversals, neutron diffr. obs. 0–68945

NaNO₂, force consts. from isotopic substitution in NO₂-radical 0–69124

NaNO₂, i.r. spectra during phase transition 0–66016

NaNO₂, l.f. electro-optic response analysis 0–62623

NaNO₂, lattice dynamics rel. to ferroelec. phase transition 0–51118

NaNO₂, lattice vibr. and ferroelec. phenomena 0–68580

NaNO₂, long wavelength absorpt. spectrum, Zeeman line splitting 0–62667

NaNO₂, optical activity in nonenantiomorphous biaxial crystals. 0–69070

NaNO₂, long wavelength absorpt, spectrum, Zeeman line splitting 0–62667

NaNO₂, optical activity in nonenantiomorphous biaxial crystals 0–69079

NaNO₂, second harmonic generation study of phase transition 0–62590

NaNO₃, use, attenuation near transition pts. 0–65817

NaNO₃, X-ray diffr, topographic method applic. 0–62413

NaNO₃, crystal growth from melt, holographic study of solid-melt interface morphology 0–47138

NaNO₃, crystal growth from melt, holographic study of solid-melt interface morphology 0–47138

NaNO₃, ideec const. temp. depend. 0–40826

NaNO₃, ideec const. temp. depend. 0–40826

NaNO₃, ir. spectra rel. to temp., press., polarization, propag. direction and isotopic comp. 0–72364

NaNO₃, ir., spectra rel. to temp., press., polarization, propag. direction and isotopic comp. 0–72364

NaNO₃, ir., precison lattice parameter and thermal expansion 0–43639

NaNO₃, Raman line broadening, rel. to order disorder transform 0–76127

NaNO₃, Raman scattering cross-section 0–62688

NaNO₃, two-phonon absorpt, spectra at low temp. 0–76107

NaNO₃, VO²⁺, e.s.r. 0–41317

NaNO₃ biaxial, Raman scattering meas, problems 0–72391

NaNO₃ biaxial, Raman scattering meas, problems 0–72391

NaNO₃ ir. determination using Pellet tech. 0–54198

NaNO₃ ir. determination using Pellet tech. 0–54198 NaNO₃ in conc. aqueous solns, elec. conductance, diffusion, viscosity and density meas. at 25° 0–71375 NaNO₃ in methanol dioxane at 25°C, electrical conductance meas.

0-68903

0-68903
NaNO₃ in water-dioxane at 25°C, electrical conductance meas. 0-68902
NaNO₃ molten, Raman spectrum 0-39805
NaNO₃ pure and doped, electrical conductivity, under atmospheric ahd hydrostatic pressure 0-50973
NaNbO₃, perovskite, phase transform. 0-59031
NaNbO₃, phase transitions, high temp, X-ray exam. 0-71805
NaNbO₃, powder, n.m.r. of ²³Na and ⁹³Nb 0-79417
Na₃Nb₄O₁, cryst. struct. 0-61895
NaNd₃(GeO₄)₂(OH)₃, crystal structure 0-47195
NaNiF₃, cryst. struct. from X-ray powder patterns 0-65218
Na₃Ni¹CO¹¹F₃, of weherite struct., ferrimag. 0-65258
Na₃O-B₃O₃-P₃O₃:Cu(II) glass, colour comp. depend. 0-44850
Na₂O-B₂O₃-SiO₂ glass, metastable immiscibility surface 0-50337

Sodium compounds continued

Na₂O-BaO-Nb₂O₅ system, ferroelectric crystal growth, comp. depend., phase diagram 0-39879 Na2O-BaO-SiO2 system, immiscibility, nucleation and cryst. growth

0 - 74869

0-/4869 Na₂O-Fe₂O₃-SiO₂ glass, crystallization of β-NaFeO₂, Mossbauer spectra, x-ray diffr. 0-47490 Na₂O-GeO₂ glasses, internal friction 0-58872 Na₂O-Nb₂O₃-SiO₂ glass, i.r. and Raman spectral study, structure 0-69139

Na2O-SiO2 glass, colour centres annealing and thermoluminescence

0—76183 Na₂O-SiO₂ glasses, water retention effect on optical, elec. and mech. props. 0—58542 Na₂O-TiO₂-SiO₂ glasses, Ti³⁺ e.s.r. 0—72487 Na₂O-TiO₂-SiO₂ glasses, elastic consts. 0—55947 Na₂O-ZnO-SiO₂ system glasses, ZnO structure role 0—58543 NGO envillation once in earths upper atmosphere during night-time

NaO, equilibrium conc. in earth's upper atmosphere during night-time 0-79554

NaO, gas, dissociation energy, from condensed Na₂O 0 -79554

NaO, gas, dissociation energy, from condensed Na₂O 0 -77968

Na₂O, gas, heat of atomization, from condensed Na₂O 0 -77968

Na₂OB, O₃GeO₂ glass, gamma irradiated e.p.r. meas. 0 -66140

NaOD, matrix isolated, i.r. spectra rel. to bending and stretching modes and struct. 0-69126

NaOH-Ba(OH)₂ solid-liq, phase equilib. 0-64994

NaOH, matrix isolated, i.r. spectra rel. to bending and stretching modes and struct. 0-69126

Na₂OsCl₆ in LiGI-KCl eutectic melt at 450°C, spectrum 0-46496

NaPF₆, n.m.r. of ¹⁹F, nuclear spin coupling constants, high speed rotation method 0-41377

(NaPO₃)₂. Na₂SiO₃, polymorphous silica phases 0-59053

NaReO₄, n.m.r. of aqueous solutions 0-68155

Na₃S-S fluxes, growth of dendritic and prismatic HgS 0-47147

NaSCN, developer for charged particle tracks in nuclear emulsions 0-38770

Na₃SO₄-Li₃SO₄ polycryst. mixtures, thermal expansion 0-65553

Na;SO₄, Effect of optical and thermal bleaching on paramagnetic centres 0–75189

Na₃SO₄, trick of optical and thermal obtaching on paramagnetic centres 0–75189

Na₅SO₄, X-, u.v. irrad., e.p.r. and absorpt., cryst. growth temp. effects, obs. 0–41337

Na₅SO₄, X-irrad. crystal, e.s.r., Sr²⁺ impurity depend. 0–41336

Na₅SO₄, SH₂O₅, cryst. struct. 0–65263

Na₅SO₄, SH₂O₅, cryst. struct. 0–65263

Na₅So₄, eryst. struct. 0–78484

Na₅Sr₄Nb₁₀O₁₀, polycrystalline, with K.W bronze structure, test of ferroelectric and physical properties 0–75800

NaTh₂(PO₄), cryst. struct. 0–61894

Na₅(TiO)[GeO₄], cryst. struct. 0–61892

0-65526 Na₃W(CN)₈,4H₂O, crystal structure, second configuration 0-61890

Na; W(CN)₃, 4H;O, crystal structure, second configuration 0–61890 Na_xWO₃, cubic, thermal conductivity meas. at low temp. 0–68653 Na_xWO₃, electrolytic crystal growth technique 0–50445 Na_xWO₃ x=0.157 and 0.72, energy band structure from optical reflectivity in energy range 1.75 to 6.0 eV 0–44765 Na₂XFsiO₅, cryst. struct. 0–61893 Na;ZrSiO₅, rare-earth activated luminescence 0–56609 Na;0.4B;O₃-Li₂O SiO₂-SiO₂ syst., phase separation, metastable liquation 0–68557

Na₂[Fe(CN)₅NO],2H₂O, Raman spectrum vibrs. assignment, 20K 0 - 41240

0-41240 Na; Fe(CN); NO].2H₂O, i.r. and Raman spectra 0-76105 Rb-Na silicate glasses, internal friction and alkali diffusion 0-55956 SiO₂-B₂O₃-Na₂O system glasses, phase separation mechanism 0-58544

sodium chloride y-irradiated, dose rel. to dislocation mobility, and absorpt. spectra

0-43675

0-43675 absorption, i.r., of finite cryst. 0-59405 anharmonic eqn. of state, fourth-order, ambiguities 0-68572 bombardment by 40 KeV ions, mass analysis of secondary ions 0-62478 cleavage planes, evaporation and pitting in vacua, 454-593°C 0-61703 colloidal centre dimens. obs., absorpt. spectra 0-48072 colour centre bleaching, negative ion vacancy, electron capture cross-section 0-40189 colour centres due to ion bombardment 0-75184 crack deceleration by slip bands 0-40416 creep, u.s. obs. 0-71697 creep and time to rupture of crystal, ambient medium depend. 0-40332 crystal, step structure resulting from decrystallization, high-vac. evaporation 0-74884 crystal prep. and purity determ. from elec. props. 0-78410

ton 0-74664
crystal prep. and purity determ. from elec. props. 0-78410
Debye temp. pressure depend. to 30 kbar 0-62174
defects, from conductivity, transport numbers and self-diffusion of ions
0-47222

dielectric breakdown and time lags, u.v. irrad. effects 0–65783 dipole moments and hyperfine consts. from mol. r.f. spectra 0–70933 dislocation density rel. to compression stress-strain relations, obs. 0-40169

0-40169 dislocation glide bands and hardening due to dynamic impacts, obs. single crysts., obs. 0-40168 dislocation motion in slip bands, stress depend. 0-68462 dislocation patterns assoc. with cleavage cracks 0-40167 dislocation pinning, study by u.s. attenuation waves, irradiated monocryst. 0-65325

0-65325 dislocation struct. of single cryst. grown from melt 0-65324 dislocation substruct., hydrostatic press. effect 0-47258 doped with Ba, Pb, light scattering peculiarities 0-56484 ESC A spectra from single cryst., ang. distrib. of electrons 0-62833 e.p.r. of Mn²+ solid solution precipitation 0-76223 elastic constants, adiabatic, 190-300K 0-71665 elastic constants, third order 0-75217 elastic constants and Debye temp. of single crystal, 300-120 K 0-65354 elastic consts., u.s. beam mixing meas. 0-75223 elastic consts. press. depend., low temp. 0-71667 elastic consts. var. with temp. from u.s. waves propag. speed 0-55934

Sodium compounds continued sodium chloride continued

```
PA 1970 - Part II (July-Dec.)
Sodium compounds continued sodium chloride continued
              elastic limit, Hugoniot 0-62028
              electric pulse breakdown, orientation depend. 0-44354
              electroluminescence 0-66121
            electroluminescence 0--06121 vertical electroluminescence of thin layer, voltage-brightness characts. 0-44948 electroluminescence temp. depend. 0-48122 electron beam coloured crystals for holographic recording 0-63644 electron emission following MgK\alpha, AlK\alpha irradiation, ang. distrib. 0-76282
             electron emission of freshly formed surfaces bombarded with ions 0-53974
             equation of state for P-V isotherms of solns. 0–43423
F centre formation in X-irrad. samples, temp. depend. 0–58831
F centre growth curves, nonuniform electron irrad. effect, and electron penetration, single crystal 0–53552
F-centre, ENDOR, magnetic hyperfine and quadrupole interactions 0–45042
             6-43042
F-centre electronic struct., pseudo-pot. treatment 0-40179
film, electron diffraction ring pattern, intensity variation with energy loss
0-40047
             ir. absorption band parameters with NO<sub>2</sub>-, NO<sub>3</sub>-, impurity ions, 100-300K 0-62665
            300K 0-62665 ice, growth parameters, effect on substruct, spacing 0-58742 in ice ingots, macrosegregation on brine solidification 0-65001 internal friction, neutron irrad, effect 0-71668 ion-electron secondary emission coefficients and the incidence angle of slow inert-gas ions 0-56422 Kelkrmann's model, detailed study 0-50850 luminescence, recombination, mechanism 0-51348 luminescence of rock salt, strong elec. field, glow discharge contact 0-6742
            0-62742
M and F centre growth in \gamma-irradiated NaCl, kinetics 0-50615 microhardness reduction under illumination, effect of impurities 0-56017 molecule, theoretical study of 12^+, 32^+, 31, 11 states 0-43129 Mossbauer effect of Sn impurity atoms 0-54077 multiphonon X-ray scattering calc. 0-62173 n.m.r. line shape meas. 0-72504 nuclear reson. fluoresc. yield, effect of anisotropic slowing down of 2^4Mg recoils 0-69056
             recoils 0–69056 optical material, crystals, mixed with KCl, i.r. optics 0–72345 phase transformation of rock salt under shock wave action 0–47481 phonon dispersion spectrum 0–75376 phonon relax. due to impurities 0–62155 phosphorescence, Eu²+ activated, and capture centre determ. 0–66110 photothermal destruction of F centres in pure and Ag²+, Sr²+ doped crystals 0–43688 plastic bending, stress distrib., photoelasticity, dislocation density 0–43746
              0-43/40
point defect and dislocations binding energy determ. by internal friction
meas. 0-75165
polarization studies 0-59257
             polarization studies 0—59257
positron annihilation time spectra in solid and liq., 295-1223 K 0—47616
r.f. Stark spectra, mol. beam elec. reson. obs. 0—39392
r.f. spectra by molec.-beam electric resonance 0—61126
Raman scatt. from Ag* pairs 0—59413
Raman scattering of light, second-order, 90K 0—54111
Raman spectra of Ag* doped crysts. 0—66071
reflection at 2000 950 Å, effect of plastic deform. and X-ray irradiation 0.44766
                   0 - 44766
             0-44766
resistivity and conductivity variations at high concentrations, temperature and pressure effects 0-46944
sound radiation from mobile dislocation walls, freq. depend. 0-68588
stress relax., internal stress, work hardening 0-68436
substrate, ZnS epitaxial film, vacuum-evaporated, structure 0-47058
substrate, epitaxial growth of Ag film, effect of u.s. agitation of substrate 0-47051
              surface, electrically heterogeneous, epitaxial growth of Ag 0-53431 surface vacancy clusters, PbS condensation, electron microscopy 0-75133
             0=75135
Te epitaxial film 0=43553
thermal emissivity, far i.r., 80-600 K, meas., rel. to vibr. modes 0=76106
thermal expansion, and law of corresponding states 0=47549
transmission at 2000-950 Å, effect of plastic deform. and X-ray irradia-
tion 0=44766
              u.s. beam mixing meas of nonlinear parameters 0-75223
u.s. third harmonic amplitude changes, recovery after small plastic
deform. 0-40548
               vacancies and vacancy pair diffusion, contrib. to ionic conductivity 0-44348
             0–44348

vacancy pair diffusion contrib. to ionic conductivity
0–44349

Weigert effect and anisotropy of colloidal particles of Na 0–53380

work hardening characts. 0–43804

Young's modulus, neutron irrad. effect 0–71668

H trapped in single crystals at 77 K, E.S.R. obs. 0–76216

Mn²+ impurity ions e.s.r. spectrum at liquid N temp. 0–62761

NO<sub>2</sub>-, NO<sub>3</sub>- impurity ions, temp. effect on i.r. absorption band parameters
0–62665

NaCl:Ag excitons diffusion controlled.
              NaCl:Ag excitons, diffusion and self-localization, luminescence, temp. depend. 0-41262
NaCl:Ag+, nuclear mag. double reson., sensitivity, Ag conc. depend. 0-48172
              0-48172
NaCl:Au, colloidal system, interaction with high power ruby laser ligh 'pulses 0-41218
NaCl:Ca<sup>2+</sup>(Mn<sup>2+</sup>), dielectric absorpt, intensity, conc. depend. 0-51104
NaCl:Cc absorption and luminescence spectra 0-56551
NaCl:Co, S-centre formation on X-irrad., e.s.r. and absorpt. obs. 0-75190
NaCl:Co, X-irrad., dielectric relaxation loss 0-44344
NaCl:Cu thermostimulated luminescence and thermal bleaching, role of activator ions 0-56638
NaCl:Cu<sup>+</sup>, far ir. absorpt. temp. depend. rel. to lattice resonant modes 0-44843
NaCl:Cu<sup>+</sup> reson mode freq. stress influence 0-68579
```

0-44843

NaCl:Cu⁺, reson, mode freq., stress influence 0-68579

NaCl:Cu⁺, resonant bandmode shape, influence of uniaxial stress and dislocations 0-79314

NaCl:Cu²⁺, Jahn-Teller system, e.p.r. spectrum 0-76224

NaCl:MgCl₂, dislocation distrib. prod. by identation, obs. 0-40170

NaCl:(Mn²⁺,CN⁻), e.s.r., dielectric absorpt., dopant interactions 0-44993

```
NaCl:Mn<sup>2+</sup>, dipole-equil. establishment in field-free conditions 0–72486
NaCl:Mn<sup>2+</sup>, dislocations, pick-up and loss of charge 0–50593
NaCl:Mn<sup>2+</sup>, e.p.r. of Mn<sup>2+</sup>—Na<sup>+</sup> vecancy pair 0–72485
NaCl:Mn<sup>2+</sup>, e.p.r. of Mn<sup>2+</sup>—Na<sup>+</sup> vecancy pair 0–72485
NaCl:Mn<sup>2+</sup>, X-irrad., optical absorpt. and e.p.r. spectra, Mn centres
              0 - 76104
           NaCl:MnCl<sub>2</sub> solid solution precipitation kinetics, dislocation nuclei 0-75314
            NaCl:PbCl<sub>2</sub>, electron microscope decoration determ, of impurity distrib.
              0 - 78537
          NaCl-Ag phosphors, long and short term components of X-ray lumines cence 0-54128
            NaCl-BaCl<sub>2</sub>, super-saturated solid soln., ageing, solubility determ.
              0-62095
           0-62095
NaCl-Na, molten solutions, magnetic susceptibility, 800-970°C 0-74785
NaCl-NaBr, diffusion pair, misfit dislocations 0-75164
NaCl bicrystal, tilt boundary migration, driving force, misorientation angle 0-58821
NaCl radiational defects, stored energy release during annealing 0-75148
NaCl(Au) colloidal syst., extinction spectra, computation by IBM 360-65
           NaCl(Na) colloidal syst., extinction spectra, computation by IBM 360-65 0-51286
           NcCl:OH-, microwave resonant absorpt. spectrum from 8 to 40 GHz
              0 - 79312
Sofar see Sound ranging
Sogicons see Semiconducting devices
          analysis, spectroscopic detection of Tl traces, using SnCd eutectic mixture 0-69240
         0-69240nd, friction of solids, effect of ultrahigh vacuum 0-78661 elastic moduli by dynamic method 0-48242 freezing and enlargement 0-74845 frozen, thermal conductivity Leda clay, Sudbury silty clay 0→−22°C, obs. by thermal probe 0-78786 induced activity, long-lived from 200 MeV protons, calculations 0-78797 lunar, mechanical properties, Surveyor obs. 0-59750 lunar from Apollo 11, Gd isotopic composition and variation, neutron capture effects 0-45414 plane deformation, general yield conditions 0-58995 radioisotope concentration, gamma radiation spectra, airborne meas., comparison with field verification meas. 0-54214 stress-strain relations, experimental and analytic program 0-59539 water, transfer to atmos. ref. to soil properties, plant characteristics, weather 0-45122 <sup>220</sup>Rn, emanation meas. 0-45117
           <sup>220</sup>Rn, emanation meas. 0-45117
Solar activity see Sun; Sunspots
Solar batteries see Electricity, direct conversion
Solar cells see Electricity, direct conversion/solar cells
Solar constant see Sunlight
Solar corona see Sun/corona
Solar corpuscular streams see Sun/radiation corpuscular
Solar eclipses see Sun/eclipses
Solar flares see Sun/flares
Solar furnaces see Heating; High-temperature phenomena and effects
Solar noise see Sun/radiation, radiofrequency
Solar prominences see Sun/prominences
Solar system
         ar system
see also Planets, etc.

12 Victoria, minor planet, orbital elements 0-41798
13 Egeria, minor planet, orbital elements 0-41798
30 Urania, minor planet, orbital elements 0-41798
433 Eros, motion anal. rel. to solid parallax and mass of earth-moon system 0-45417
12 Victoria, asteroid, light variation obs., and pole co-ords. 0-41787
asteroidal-gired bodies, melting hy mipolar induction from primardial T
         asteroidal-sized bodies, melting by unipolar induction from primordial T Tauri sun 0-54446 astroidal-spatial density in elliptic plane 0-54448 astronomical unit, determ. from H-line radial vel. meas. 0-45203 cosmic rays, convection, diffusion and adiabatic deceleration in solar wind 0-41759
         Earth-Comet Encke orbital system giving validity to Hansen's method of partial anomalies 0-41806
          Earth-moon system mass relative to Sun, from anal. of motion of 433 Eros 0-45417
       Earth-moon system mass relative to Sun, from anal. of motion of 433 Eros 0–45417

formation from relativistic encounter between galactic nuclei and cold earthlike body 0–54426

formation interval, nucleosynthetic chronology 0–79619

genesis, role of non-central, motional-gravitational fields 0–54425

gravitational tides, effect on Venus obliquity 0–41785

gravitational to inertial mass ratios of bodies, meas. 0–54424

history, early 0–51735

mass spectroscopic study symposium 0–79466

melting of asteroidal-sized bodies by unipolar induction from a primordial T

Tauri sun 0–54446

origin, by contraction of interstellar cloud 0–72759

planets, satellites, small bodies, properties, tidal effects 0–79717

radar obs. of inner planets and Icarus used to determine several astronomical constants 0–54325

radar time delays, interplanetary, general relativistic calc. 0–48620

structure and evolutionary history, stability method of obs. 0–79717

three body problem, restricted, taking into account solar radiation pressure 0–45216

three-body capture of interstellar dust 0–76594

<sup>244</sup>Pu abundance in the early solar system 0–45329

lar wind see Sun/radiation, corpuscular
Solar wind see Sun/radiation, corpuscular
```

Solid solutions

see also Alloys; and under compounds of the individual elements. Solid solutions such as Au-Cu, Au-Cu-Zn are indexed under compounds of the named elements, i.e. 'Gold compounds', 'Copper alloys', 'Zinc compounds' in these examples

b.c.c. dilute, solvent self-diffusion 0-40195

binary, orderable, correlation allowance 0-40455

binary alloys, soft X-ray emission, electronic struct. 0-79336

binary system, continuous series, interdiffusion, local X-ray spectral analy sis 0-47284

sis 0-47284
CC Ca(PO₃)₂-LiPO₃ system study 0-65470
cluster theory 0-71753
component redistrib. on quenching, X-ray and electron microscope analysis 0-50773

by electronic meas. 0-62121

component redistrib. on quenching, X-ray and electron microscope analysis 0–50773
concentration determ. by elec. resistance meas. 0–62121
crystal growth, solution and travelling solvent zone technique 0–47129
decomposition, unidirectional, aligned composite material prep. 0–53656
diffusion anomalies rel. to solubility saturation 0–58832
dil. alloy, clustering of Zr and N, relaxation peaks 0–53575
dilute, positron annihilation, impurity effect 0–62281
diphenyl mercury-tolan, lattice energy charge at solubility boundary 0–65474
dislocations thermodynamics at start. 0–53539

0-65474
dislocations, thermodynamics at start 0-53539
disordered, ordered zones 0-58710
electrolyte, sulphide, ionic cond., elevated temp. 0-59491
entropy mixing of solids with retrograde solidus 0-43830
f.c.c. hardening, effects of electron conc. 0-56032
glass-ceramic materials, microcryst, phases characterization 0-78685
grain size refinement by scraping solid-liquid interface during freezing
0 61596

group II-VI alloys, photoluminescence of isoelectronic O and Te traps 0-72431

0-72431 hardening, Frank theory applicability to b.c.c. metals with high interstitial contents 0-43806 interstitial, dil., elastic free energy 0-53639 interstitial, thermodynamic props. by elastic relax. methods 0-68527 interstitial diffusion and lattice strains contrib. 0-61944 lattice vibrs., X-ray scatt. 0-75355 molecules, dissolved, observed under different crystallization conditions 0-64319

0-64319
Monel 400, creep, heat treatment and grain size influence 0-71698 multicomponent, early-stage ordering and clustering 0-58970
Nb-O, chemical interaction 0-68533
nonrandom, deformation, configurational changes, calc. 0-40338
nucleation stimulated by non-equilibrium electrons 0-78801
nucleation stimulated by non-equilibrium electrons 0-78800
ordering and size effect, X-ray scatt. obs. 0-75081
oxide, with Ni and Co ions, reflectance spectra 0-72343
oxides, absorption and luminescence 0-56586
perovskite, La_{1-x}Ca_xFe_{1-x}Mn_xO₃, structure, elec. and mag, props. 0-43635

photoluminescence, self-depolarization theory 0–48098 precipitating, X-ray scatt., anomalous diffr. effects 0–65215 quenching, component redistrib., X-ray and electron microscope analysis 0–50773

rare-earth intra-alloys, behaviour and structure, review 0-71779 short-range-order, X-ray line intensity profiles, mathematical analysis 0-53500

spinel-ferrite, cation vacancy distrib. between sublattices, thermodynamics 0-43656spinel-ferrite, cation vacancy distrib, between sublattices, thermodynamics 0-43656 stabilization of impurity defects 0-75141 stilbene-diphenylmercury, lattice binding energies 0-58777 substitutional, local order, lattice vibrations 0-75351 substitutional, local order lattice vibrations 0-75352 surface tension of solid metal, effect of impurity forming fusible eutectic 0-71750

Surface tension of solid metal, effect of impurity forming fusible eutectic 0–71750 triglycine sulphate, with isomorphous compounds, growth and characterization 0–50429 tungsten-bronze ferroelectrics, cryst. chem. and lattice dynamics 0–65796 uranium monochalcogenides and monopnictides, long range mag. interactions 0–44712 X-ray scatt. by lattice vibrs. 0–75355 Ag-Cd, thermal vibrs. of atoms 0–71819 Ag-Cu, solubility obs. from X-ray spectral analysis 0–71743 Ag-Zn, Ag-Cd, Ag-Hg, α -, temp. and conc. depend. of lattice parameters, X-ray diffr. meas. 0–78447 Ag-Zn, thermal vibrs. of atoms 0–71819 Ai-Cr, precipitation kinetics, diffusion, temp. depend., e.p.r. 0–40454 Al-Ag, deform. rel. to hardening and slip 0–53583 Al-Ag, second stage decomposition, diffuse X-ray scatt. 0–68564 Al-Fe, internal friction rel. to dislocations, condensation temp., grain boundaries 0–68423 Al-Si, Silumin, solubility of Cu, influence of Ni, Fe, Mn 0–50778 Al-transition metals, lattice parameter variation with impurity conc. 0–47458 Al binary alloys with Mn, Fe, Co and Ni, volume lattice distortions

Al binary alloys with Mn, Fe, Co and Ni, volume lattice distortions 0-50777

Al binary alloys with Mn, Fe, Co and Ni, volume lattice distortions 0-50777

AlAs-GaAs, epitaxial film, photoluminescence spectra 0-51356
Al₂O₃-Cr₂O₃ system, spinodal microstructures 0-50511
Au-Al(Ge₂), hardening 0-58975
Au-Cu, solubility obs. from X-ray spectral analysis 0-71743
Au-Ni, thermodynamic interpretation, 1048-1200°K 0-56038
Au-Si, precip., complexes form. influence 0-71792
BaTiO₃·SnO₃, truncated cone capacitor, semiconducting props. nonlinearity 0-44370
BaTiO₃·SnO₃, truncated cone capacitor, semiconducting props. nonlinearity 0-44370
BaTiO₃·SnO₃, truncated cone capacitor, semiconducting props. nonlinearity 0-44370
BaTiO₃·SnO₄, frorbidden band width, transport props, temp. depend, 80 700 K 0-62361
Bi₂To₃-Se_{0.6}, forbidden band width, transport props, temp. depend, 80 700 K 0-62361
Bi₂To₃-Se_{0.6}, forbidden band width, transport props, temp. depend, 80 700 K 0-62361
Bi₂To₃-Se_{0.6}, forbidden band width, transport props, temp. depend, 80 700 K 0-62457
Bi₂Tl₃·Bi₂Sl₃ Seebeck coefficient, effect of magnitude of initial particles, quantity of additives and production technology obs. 0-51132
C, incomplete solution in 38CrMoV21.14 steet, metallographic examination and contact thermal e.m.f. meas. 0-40458
CaF₂-RF₃, R-rare earth metal, structure 0-47180
CaO-MnO, activity-composition relns., 1100-1300°C 0-71771
Cd-Mn, axial ratios and solubility limits of h.c.p. η and e phases 0-40073
Cd-Ms. Te thermal noise anomalies 0-78681 Cd₃As₂-Cd 0-65469

 $Cd_xHg_{1-x}Te$, thermal noise anomalies 0-78681

Solid solutions continued CdSnp₂-CdSnAs₂, i.r. absorpt. spectral forbidden band width 0-41192 CdTe_xCdSe_{1-x}, prod. and photoelec. props 0-65845

CdTe_xZnTe_{1-x}, prod. and photoelec. props. 0-65845

Co-Pd, thermodynamic props. 0–65845 Co-Pd, thermodynamic props. 0–68530 Co-Si, thermal diffusivity and cond. 0–40599 Co₂Ba₃Fe₂₄Q₄-Co₂Sr₃Fe₂₄Q₄₁, mag. props., comp. depend. 0–62543 CoO-NiO single crystal with gradient in lattice spacing, production 0–68261

(0-68261 COSi₃-NiSi₃, electronic struct., X-ray K β_5 spectral characts. and mag. props. obs. (0-79340 Cr_{1-x}Fe_xSi, Hall coeff. temp-conc. depend. (0-68755 Cu₋(10.37 at.%)Al alloy, small domain superlattice, electron microscopy (0-71585)

Cu-Al, system, near-order, hardening temp. depend., X-ray scatt. 0-53644

0-53644
Cu-Mo, form by explosive heating 0-75302
Cu-Si, X-ray L₂₃ emission spectra 0-56577
Cu-Zr-Cr alloy, high temp, softening, electron microscopy 0-47444
Cu wire, dispersion-hardened 0-68546
(CuO)_x(NiO)_{1-xx} ordering 0-50526
Fe-Al, diffusion and self-diffusion of Fe, 320°C, X-ray diffuse scattering method 0-53561
Fe-Cr-C system, phase relations, high temp, and strongly reducing conditions 0-59127
Fe-Cr, decomposition kinetics, neutron diffr. 0-68566

tions 0–59127 Fe-Cr, decomposition kinetics, neutron diffr. 0–68566 Fe-Si, theraml diffusivity and cond. 0–40599 FeSi;-NiSi;, electronic struct., X-ray K β_5 spectral characts. and mag. props. obs. 0–79340 Ga-Cu(Ni), solubility, X-ray spectra, K absorpt. edge shift 0–58980 Ga-Sa-Al-Al-Sa, prep. and physical props. 0–75027 Ga-Sc-GdS, elec. and thermoelec props. 0–65669 Ga-Fj-PbF₂ system study 0–56042 GaSb-Ga-Sa films, elec. and optical props. 0–78950 Ge-As-Reavily doped, precipitation rel. to anomalous X-ray transmission 0–75333

0-75333

Ge-As-Ga, dissociation, rel. to effect of impurities of structure changed and dislocation mobility 0-43674

Ge-As, crystal lattice parameters 0-55841

Ge-As, precipiation kinetics 0-53648

Ge-Cu(Ni), solubility, X-ray spectra, K absorpt. edge shift 0-58980

GeTe-Ga(In)Te, elec. props. 0-72028

H in bcc early transition metals, theoretical interpretation 0-58981

HfO₂-CaO(Y₂O₃,MgO), cyclic heating and thermal shock effects on stability 0-59025

HfO₂-refractory oxide, stabilized, comp. and cryst. struct. 0-50783 Hg_{0.86}Cd_{0.14}Te solid solution, thermomagnetic and galvanomagnetic props., low temps. 0-53951

incomposition of the property of the property

0 - 71780

0–71780
M₂"Mo₃-xW_xO₈ (M=Mg, Mn, Fe, Co, Ni, Zn, Cd), formation and props.
0–65473
MgO-CoO, struct. and mag. characts. 0–75097
MgO-Cr₂O₃-(Li₂O) struct. by e.s.r. method 0–65255
MgO.Al₂O₃-xSiO₂, superstructure X-ray reflections 0–58733
(Mn_{1-x-y}Fe₂Zn_y)₄(BeSiO₄)₅S, Mossbauer effect, 85 and 294 K 0–79262
MnS-MnSe crystals, degree investigations 0–47117
MnSe-CdSe, transmission and reflectance spectra, optical energy gap
0–54087
MnSe-MnTe deformation fracture hardness 0–62043

MnSe-CdSe, transmission and reflectance spectra, optical energy gap 0-54087

MnSe-MnTe, deformation, fracture, hardness 0-62043

Mo-N, low temp. recovery behaviour 0-53634

NaCl:Mn⁻², precipitation kinetics, dislocation nuclei 0-75314

NaCl:MnCl₂, precipitation kinetics, dislocation nuclei 0-75314

NaCl-KCl alloys, creep, 600°C 0-65404

Na₂O-BaO-Nb₂O₃ system, ferroelectric crystal growth, comp. depend., phase diagram 0-39879

Nb-D, distribution of D atoms 0-40463

Nb-Mo-N, solubility of N 0-58982

Nb-N, yield stress 0-65396

Nb-O, Henry's law, emf. meas. 0-75315

Nb-W C alloy, phase equilib., constitution, X-ray diffr., DTA 0-47491

Nb, Snoek relax, peaks, broadening effect 0-68413

NbC-C composites, fabrication temperature lowering, by WC, of NbC-WC examination mechanical properties 0-50785

NbSe₂-NbTe₂, lamellar structure, superconductivity 0-62326

Ni-Al-Nb-Mo system, p and p'phases, investig. 0-47459

Ni-Cu-C, equil. temp. depend., vapour transport study 0-71810

Ni₂Co₁₋₂C1,6H₂O₃ antiferromag., susceptibility, specific heat, Neel temp., conc. depend. 0-75965

Ni₃(Fe,V), ternarry, Young's modulus, elec. resist., ordering, magnetization 0-75218

Ni₃Mn-Ni₃Co(Fe) disordered alloy, specific resist., Hall effect 0-50988

0–75218
Ni₃Mn-Ni₃Co(Fe) disordered alloy, specific resist., Hall effect 0–50988
Ni₃Mn-Ni₃Fe(Co) systems, Hall effect during ordering 0–65632
Ni₃Mn-Ni₃Fe(Co) systems, Hall effect during ordering 0–65632
Ni₃Mn-Ni₃Fe₃P₃ lattice parameters, comp. depend. 0–43641
α-Pb-Sn, Mossbauer effect, rel. to interatomic force interaction 0–44795
Pb(Co₁₃Nb₂₃)O₃- PbTiO₃-PbZrO₃ ceramics, dielectric and piezoelectric props. 0–65766
PbO-SnO, formation 0–53649
PbSe with SnSe, review, use in solid state devices, detection of i.r. and visible radiations 0–47690
Pb₃Sr_{1-x}TiO₃, solvent zone growth technique 0–61735
PbTe-SnTe, elec. props., temp. depend., 80-300K 0–44206

Solid solutions continued

PbTe based, thermal cond. 0-71878

PbTe based, thermal cond. 0–71878 PbTe with SnTe, review, use in solid state devices, detection of i.r. and visible radiations 0–47690 Pb(Ti, Zr)O₃, dielectric polarization, morphotropic phase boundary, comp. depend. 0–62403 Pbx_Ti,Zr, $_{-x}$ O₃ solvent zone growth technique 0–61735 Pd-Ag alloy, equilib. H₂ solubility, tensile and compressive elastic stress effects 0–53532 Pd-B, low temp. heat capacities 0–62212 Pd-Mo:Co, mag. susceptibility, elec. resist., temp. and comp. depend. 0–62309 α -Pd-X, lattice spacings, X=particular solute metal 0–75100 Pu-Ga, δ -phase, cryst. parameter rel. to Ga conc. 0–65274 α -Sb-Sn, Mossbauer effect, rel. to interatomic force interaction 0–44795 Sb,S₃-Sb,Se₃, photocurrent spectral distribution, specific resist., 18-150°C 0–51150 Se₃-Te,_xHg, crystal growth, morphology and dislocations 0–74988

0-51150
Se,Te,_Hg, crystal growth, morphology and dislocations 0-74988
SiO₂, decomp., in dislocation-free Si 0-40464
Sn-Zn dilute alloy freezing, distrib. coeff. rel. to growth velocity and initial conc. tracer method 0-68536
Sn₁-sB₁-Te, energy spectrum of carriers 0-78954
(SnTe)₁₋₂(GdTe)₂, elec., cond., Hall effect, lattice thermal cond., defect-phonon scatt. 0-78955

(SnTe)_{1-x}(GdTe)_n, elec. cond., Hall effect, lattice thermal cond., defect-phonon scatt. 0–78955
Ta-D, decomposition and precipitation, 225K, neutron diffr. 0–50830
Ta-O, Henry's law, e.m.f. meas. 0–75315
Ta, hardening by O and N O–43806
Ta₂VO₆, VO₂, calc. for appearance of order 0–55860
ThO₂-UO₂, oxdiation behaviour 0–48198
Ti-O, interstitial order-disorder transformation, neutron diffr. 0–40499
α-Ti-Sn, Mossbauer effect, rel. to interatomic force interaction 0–44795
UC-UN, equil. and ideal behaviour 0–68538
UC-UN, Vegards law, validity, possible causes of disagreement, O₂ contamination 0–71752
UC_{1-x}N_x, mag. susceptibility and electronic sp. ht. 0–53994
UP_{1-x}S_x, n.m.r. rel. to mag. ordering 0–45033
UC_{1-x}N₂, phase, X-ray and chem. analysis 0–47462
V-N(O), elec. resist., thermoelec. power, mag. susceptibility, lattice parameter, mech. props. 0–58983
W-Ir single crystal, thermionic emission props. of (100) face 0–53972
W-Os single crystal, thermionic emission props. of (100) face 0–53972
W-Os single crystal, thermionic emission props. of (100) face 0–53972
Y2i₂O₂-Y₂Ce₂O₃ system, i.r. spectral analysis 0–41226
Zn-Mn, axial ratios and solubility limits of h.c.p. η and ε phases 0–40073
Zn₂Cd_{1-x}Te, phase diagram 0–47493
Zn₂Hg_{1-x}Te, crystal growth, morphology and dislocations 0–74988
Zn₂Hg_{1-x}Te, crystals, negative photoconductivity, intrinsic and impurity 0–44400

-44400 Zr-O, c.p.h., elec. resist., comp. and temp. depend. 0-47829

Solidification see Freezing

Solids

ids

see also Crystals; Films, solid; Metals; Plastics; Powders; Semiconductors; Vitreous state
conference, India, Dec. 1969 0–38788
conference, Turku, Finland, Aug. 1970 0–74858
density meas., apparent 0–48713
diffusivity, thermal, meas. methods 0–40593
electromagnetic wave interaction with charge carriers 0–38438
experiments in appl. phys. manual 0–41928
flow, gravity, of bulk mats., book 0–55435
high pressure apparatus for research, book 0–57198
laser interaction to produce plasma, bibliographical review 0–71177
nonmetallic tubes, heat conductivity coefficient, determination 0–65556
particulate, gravity flow down vertical pipes 0–64960
phenomenology rel. to materials science, engineering and technology
0–68194

0 -68194 photoionization potential measurement, apparatus 0-50257 quantum, molecular field approx. 0-78346 research in materials, M.I.T., annual report, 1968-1969 0-55677 spin-lattice relaxation time meas. by absorption mag. resonance signal decay method 0-65968 viscoelastic, deformation rel. to boundary value problem 0-59970 volume at high press. 0-51490

see also Crystal structure; Electron diffraction examination of materials; Electron microscope examination of materials; Granular structure; Neutron diffraction examination of materials; X-ray exam-ination of materials

mation of materials acicular polycrystals, isotropic and orthotropic, conditions of plasticity and strength 0-47368 cellulose fibres, hydrated, electron microscope examination 0-68204 chloroacetic acid, distinct vibr. spectra rel. to three polymorphic forms

cyanethyl cellulose ethers, highly substituted, X-ray and i.r. investigations 0-71431

0–71431
discontinuous association theory 0–74831
field-ion microscopy, basic principles and range of applications 0–61801
h.c.p. lattice, non-ideal, energy 0–50399
inert gas crystals, development of molecular theory of solids 0–39898
lunar fines and rock, Apollo II samples, morphological obs., scanning electron microscopy 0–68291
Madelung's constant co-ordination algorithm for calculation 0–58612
Madelung potential and elec. field intensity for NaCl and for CsCl lattice, computer program 0–43581
poly (trans-1, 4-butadiene) crysts., chain folding, obs. 0–39915
polycarbonate, amorphous, supermolecular structure obs. 0–50336
polymeric materials, hydrostatic pressure effects 0–58549
polymers, folded-chain crystals with irregular fold surfaces, stability 0–71437
polymers, macromolecular networks, classification and structural theory

0-71437
polymers, macromolecular networks, classification and structural theory
0-39911
polymers, orientation analysis 0-78354
polyoxymethylene, needle-like 0-78356
polystyrene, amorphous, molecular orientation study of birefringence and
i.r. dichroism 0-47022
polystyrene amorphous, supermolecular structure obs. 0-50336
polystyrene-polybutadiene/toluene, presence of lamellar structure
0-58552

Solids continued

structure continued

polyvinylidenefluoride, dependence on polymerization conditions 0-71439

0=71439
rocks of Pechanga series, internal structure determination 0-62871
rubber, crosslinking inhomogeneity determ. by light scatt. 0-39910
steel, high-speed, structure examining using potential-polarization method
0-68511

steel microscopic inhomogeneities obs., contact thermoelectric power meas. 0-68262

meas. 0-68262
theory, book 0-39901
u.s. holographic imaging 0-57406
Bi-T1 alloys, elec. conductivity meas. 0-64864
Fe ingot, macrostruct., supercooling depend. 0-71414
In-Sn, In-Bi alloys, elec. conductivity meas. 0-64864
Mg₃Cd alloy, X-ray study of ordering process at 26-170°C 0-55851
Ni-P, noncrystalline alloy 0-58531

adjoint plane waves and Green's function methods 0-50934 alkaline earth chalcogenide crystals, Born-Mayer model extension 0-75214

adjoint plane waves and Green's function methods 0–50934 alkaline earth chalcogenide crystals, Born-Mayer model extension 0–75214 alloys, disordered, electronic structure 0–71755 Anderson model, ground state, effect of external mag, field 0–53749 atomic-like excitations theory of structure and props. 0–40639 Bloch density matrix with inclusion of spin 0–41989 book 0–39901 book 0–39900 Born model, us. parameters 0–43706 boundary conditions for relativistic Kronig-Penney model 0–43953 brittle, crack propagation, dynamic theories 0–40401 cell-model prediction of thermodynamic properties, comparison with Monte-Carlo and lattice dynamics 0–75402 conference on theoretical physics, Florence (1969) 0–45504 conference on theoretical physics, Syracuse, USA (1969) 0–63298 crystal, anharmonic, microscopic theory of electronic contributions to lattice dynamics 0–50840 conference medium, electron distrib. and internal energy, high temp. 0–40635 diamagnetic high susceptibility 0–40940 diamond, cohesive energy, from OPW cales. 0–43709 dielectric, second sound 0–74856 dielectric dipolar relax. rel. to defects and disorder 0–40823 disordered one dimensional lattice, elec. resistance of Fermi gas 0–40677 disordered system, density of states, Green's function 0–47015 e.m. dipole interaction in condensed medium, quantum electrodynamics treatment 0–47009 electron correlation at metallic densities, formalism 0–71897 electron excitation transfer via phonons, perturbation theory 0–53741 electron levels, density for small particles 0–75449 electron correlation at metallic densities, formalism 0–71897 electron excitation transfer via phonons, perturbation theory 0–53741 electron levels, density for small particles 0–75449 electron correlation at metallic densities, formalism 0–71897 electron excitation transfer via phonons, perturbation theory 0–53741 electron bevels, density for small particles 0–75449 electron correlation at metallic densities, formalism 0–71897 electron excitation 1–668722 finite elastic deformation 0–66875 fluctuatio

Inflict easistic deformation 0—00873 fluctuation theory for space charge limited currents for ideal nonmetallic solids 0—51110 h.c.p. lattice, non-ideal, energy 0—50399 hard-square solids at high densities 0—65113 inert gas, exp-6 cell model calc., characterization of pair potential parameters 0—47496

ers 0-4/496 inert gas, exp-6 cell model calc., triple-dipole term effect on thermodynamic props. 0-47497 interacting elementary excitations 0-40634 Kronig-Penney model, relativisite, boundary conditions 0-43953 melting, compression, Hugoniot for mixed phase, equation of state 0-39875

0–39875
melting temperatures, pressure effects 0–39872
micropolar, elasticity, thermodynamics 0–40212
molecular field approx. for quantum solids 0–78346
molecular theory, by solidified inert gases 0–39898
non-Kramers doublets, effective Hamiltonian, irreducible tensor operators
method 0–47578
ordered and disordered systems, electronic struct., one-dimensional
0–47016 ordered as 0-47016

0-4/016
principles, introduction 0-68193
quantum rate theory, N-dimens, tunnelling effects 0-43650
relativistic Kronig-Penney model, boundary conditions 0-43953
Schrodinger equation in extended crystal momentum representation

0-47575 second sound in dielec.cryst. 0-74856 stability and order in one and two-dimens. 0-39986

Solions see Transducers

see also Colloids; Sedimentation
Liesegang phenomena, one-dimens., theory 0-74815
silica, amorphous, stability 0-74810

Solubility

see also Phase equilibrium alkali halide crystal, and precip. of metal impurities, dielec., Mossbauer and optical meas. 0-75298 anthracene in compressed methane, ethylene, ethane and CO₂, second cross

antinacene in compressed methane, euryteine, etinate and 602, second cross virial coeffs, using pseudocritical parameters 0–43432 benzene, spherical cage model for relationship between compressibility and solubility 0–46880 bivalent admixtures in NaCl, from self diffusion and ionic cond. meas. 0–53451

0-53451
carbon tetrachloride spherical cage model for relationship between compressibility and solubility 0-46880
condensed substances in dense gases, effect on PVT props. 0-46803
crystal growth, flux method, phase equilib., saturation point 0-74978
diphenyl mercury, of tolan, conditions analysis 0-65474
electrolytes in water, thermodynamic props. 0-68080
glass, of N and S, effect of Si₂N₃ additions 0-47018
glass, of gases, monatomic model 0-53411
low-holling liquids, solubility of gases, application of hard-sphere model

low-boiling liquids, solubility of gases, application of hard-sphere model 0-74729

metals, of H, rel. to structure and d-vacancies 0-58834

Solubility continued

naphthalene, solubility parameter in various organic solvents, calc. 0-46886

phenanthrene in compressed gases 0-39666

refractory oxides in fused melts 0-43593

Rh (III) complex, rhodium (III)- oxalato-triaquo-monammine oxalate 0-74940

0-14940 toluene spherical cage model for relationship between compressibility and solubility 0-46880 xylene spherical cage model for relationship between compressibility and solubility 0-46880 Ag and alloys, of Cu, X-ray spectral analysis 0-71743 Al-Si, Silumin solid solution, of Cu, influence of Ni, Fe, Mu 0-50778

Alg and anoys, of Cu, X-ray spectral analysis 0–71743
Al-Si. Silumin solid solution, of Cu, influence of Ni, Fe, Mu 0–50778
Al, solute induced grain boundary hardening 0–71790
Au, and alloys, of Cu, X-ray spectral analysis 0–71743
CdCl₂, liquid, of Cd, 873, 943, and 1021K 0–58453
Cu, liquid, of solid Fe, rate equation 0–74730
Cu(Ni) of Ga, Ge, X-ray spectra, solid state 0–58980
β-FeSi₂, solid solubility of CoSi₂ 0–40460
HfO₂, of refractory oxides 0–50783
K, liquid, of refractory metals and alloys 0–39742
K, liquid, of V, Ti, Zr 0–39741
KH₂PO₄, electrooptic crystals, rel. to growth 0–71517
Li, liquid, of refractory metals and alloys 0–39742
NH₄H₂PO₄, electrooptic crystals, rel. to growth 0–71517
NaCl-BaCl₂, supersaturated solid soln., from ageing obs. 0–62095
Nb-Mo-N solid solution of N 0–58982
Nb-O solid solution of N 0–58982
Sh-O solid solins, e.m.f. meas. 0–75315
Pd-Ag alloy, of interstitial H₂, tensile and compressive elastic stress effects 0–53532
Se in aq. Na₂S solns., rel. to cryst. growth technique 0–65142

0–53532
Se in aq. Na₂S solns., rel. to cryst. growth technique 0–65142
Si, of Co, diffusion coeff., band struct. 0–40806
Si, of Zn, influence on elec. props. 0–55924
α-SiC, of B 0–71781
Ta-H system, limits of Ta-rich solid soln. 0–47492
Ta-O solid solns., e.m.f. meas. 0–75315
Te-Se melts, miscibility, cpd. formation, surface tension and density 0–50210

O-50210 a·V. of O 0-59056 ZnS liquidus, in Zn, 1000 to 1300 °C, rel. to solution growth of crystals 0-50448

Solution energy see Heat of solution

utions
see also Heat of solution; Liquids; Solid solutions
alcohol solutions of Rhodamine 6G, influence of quenchers on threshold of
laser effect 0-49060
alcohol-water, static permittivities 0-74774
amine+water, u.s. absorption properties 0-46910
anthracene in soln., variations in relative intensities of absorption spectral
bands 0-43459
aqueous, of bovine haemoglobin, u.s. absorption 0-55612
aqueous, of tetrabutyl ammonium bromide, u.s. relaxation 0-53342
aqueous N-methylpropionamide solns., structure determ. by n.m.r.
0-71383

aromatic ketones, energy transfer mechanism for transfer to rare earth ions in liquid solns. 0-50205

bilirubin in pyridine, spectral properties of solutions and kinetics of forma-tion 0-61525 binary, Eberhart model and surface tension new critical solution temp. 0-64881

0—04881 binary, hydrostatic effect near critical dissolution point 0—53321 bisphenol A polycarbonate solns, temp. coeff. of intrinsic viscosity 0—39754 butyl alcohol, tertiary, H₂O mol. motion in dilute aqueous soln., neutron scattering study of hydrophobic hydration 0—71314 t-butyl alcohol-water, l₂ diffusion coefficients 0—71329 cellulose nitrate, i.r. spectroscopic studies 0—71359 complexes, behaviour, methods of study 0—53319 concentrated, theory of elec. conductivity 0—78293 conformal solution theory of mixing 0—39738 cyclopentane-carbon tetrachloride, excess thermodynamic functions, hard sphere system, first-order perturbation 0—39775 α-cyclopropanic alchohol, effect of pyridine solvent on NMR spectra 0—58502 diffusivity variation with conc. and temp. 0—78269

diffusivity variation with conc. and temp. 0-78269 dilute, of small chain-like mols., neutron scatt. obs. of mol. movements 0-39740

0–39740
dispersion of a solute in a fully developed laminar tube flow 0–53286
dye, organic, laser, duration of generation 0–42282
electrolyte, Monte Carlo study of thermodynamics 0–53320
electrolyte, concentrated aqueous, viscosity using Thomas eqn. 0–50207
electrolyte, primitive model, exact soln. of integral eqn. 0–39739
electrolyte, rotational correlation times and viscosity coeffs. 0–78271
electrolytes, aqueous, ultrasonic parameters and hydration numbers
0–74746

0-14/40 1:1 electrolytes, dissociation consts. meas. 0-43431 electrolytic, osmotic pressure and density 0-56706 electronic energy transfer between donor and acceptor molecules

electron

0-50202

ethanol-water, I_2 diffusion coefficients 0-71329 ethylenediamine- H_2O system, solvated electron in pulse radiolysis 0 - 54195

0—34193 excess electrons in polar solvents 0—61497 fluorescence dependence on solvent and temp. 0—71362 interstitial, Li and Rb content, determ. using flame spectrophotometry 0—48247

Kerr const. of rigid conducting dipolar macromols.

Kerr const. of rigid conducting dipolar macromols. 0–78276
Langevin theory of polymer dynamics in dilute solutions 0–53322
light scatt., Zimm diagram and calc. program 0–39794
macromolecules, X-ray exam. by heavy atom distances 0–61484
of macromolecules, X-ray exam. by heavy atom method rel. to disordered
system analysis 0–61764
magnetoelectric effect meas. method for aqueous solutions 0–71371
metal metls, of solid and liq. metals, rate of solution, alloy formation
0–50203

metal melts, of solid and liq. metals, rate of solution, alloy formation 0-50204

metal-ammonia solns., excess electrons 0-61497 metals, thermodynamic interpretation, Gibbs-Duhem eqn. 0-55594

methacrylic acid-2-methyl-5-vinylpyridine, aqueous, flow birefringence and viscosity at different ionic strength and pH 0-71354 methylformate + n-alkanes binary systs. 0-46878 multi-component, intermol. interactions and spectra of mols. 0-49834 multicomponent, failure of universal relationship between absorption and fluorescence spectra 0-50231 n.m.r. spectra, solvent effects, chemical shift of non-polar solute 0-68150 2-naphthol-diethylamine in solvents; proton photo-transfer ionization obs. 0-33351 non-electrolyte, excess thermodynamic functions.

0-53351
non-electrolyte, excess thermodynamic functions, hard sphere system, first-order perturbation 0-39775
organophosphorous compounds containing P=O group, effect of solvent on spin-spin interac. consts. in p.m.r. spectra 0-43433
α-oxiranic alchohol, effect of pyridine solvent on NMR spectra 0-58502
photoionization potential measurement apparatus 0-50257
poly benzyl-L-glutomate in dioxan, saturation effect due to application of electric field 0-64942
polybutadiene, branched, effects of diluents on melt viscosity 0-58467
polyimides, cyclization and inherent viscosities 0-41429
polyisobutene correlation between max. strength and anomalous viscosity 0-58458
polymer, dilute, mechanism for turbulent drag reduction 0-64844

polymer, dilute, mechanism for turbulent drag reduction 0-64844 polymer, dilute, turbulent flow drag reduction 0-53299 polymer, dilute, turbulent flow in pipes, correlation of pressure drop data 0-71284

0-71284
polymer, flow birefringence, theory 0-78278
polymer, free enthalpy of mixing of soln., calc. from considerations of free
volume 0-71315
polymer, heat capacity calc. 0-58478
polymer, sedimentation at theta state 0-39851
polymer chains in dilute soln., transport processes, hydrodynamic interaction 0-58460

tion 0–58460 polymer drag reducing solns., and fibre suspensions, shear thinning treatment 0–50269 polymer shear and first normal stress difference 0–39704 polymerhacrylic acid, deformation, structural changes and shear strength appearance 0–71317 polymethacrylic acid-N₂N-diethylaminoethylmethacrylate copolymer, deformation, structural changes and shear strength appearance 0–71317 polymethylphenylsiloxamers, dilute solution parameters 0–64872 polypeptide, X-ray small-angle scattering 0–61498 Raman scatt. variation with concentration in binary solns. 0–64921 sheared, deformation of macromolecule, effect of internal viscosity 0–43436

0-43436

soda-lime-silica melt, of vitreous silica, forced convection dissolution 0-58452

soda-lime-silica melt, of vitreous silica, forced convection dissolution 0–58452 sodium poly(acrylate) in NaBr, intrinsic viscosity, molecular weight, degree of ionization depend. 0–39755 specific heat, thermistorized calorimeter meas. 0–42108 spectrum, van der Waals potential effects 0–43453 supercritical viscosity anomaly in oxide mixtures 0–61503 surface active substances, surface tension meas., automatic drop counting stalagmometer applic. 0–46890 ternary systems, aspects of diffusion 0–71326 7,7,8,8-tetracyanoquinodimethane solubilized in surfactant solns., colour changes 0–74762 theory, cluster component method 0–39737 thermionic emission from solns. of solvated electrons 0–61548 thermodynamics, applic. of ion-exchange membrane electrodes 0–43440 water-friethylamine, u.s. absorption near critical solution temp. 0–53344 Cs-ethylamine-NH_x, e.s.r. linewidths and soln. stability 0–55631 Cu-Au, Cu-Ag, Cu-Pt, Co-Ni, Cu-Co and Cu-Fe alloys with dissolved O₂, thermodynamic props. 0–64873 Fe-H₂SO₄-H₂O system structure analysis Mossbauer spectroscopy application 0–64861 Fe³⁺ in aq. solns., complex formation and electronic relaxation, e.s.r. determ. 0–61549 HNO₃, aqueous, sp. ht. in temp. range -196 to 20°C 0–68091 H₂O₄, aqueous, with Al and F ions, n.m.r. study of complexes present 0–68154 H₂SO₄ aqueous, sp. ht. in temp. range -196 to 20°C 0–68091 KBr, ultracentrifuge meas. of critical supersaturation rel. to crystal growth 0–50439 KI in H₂O₄ absorption systems of O₂, N₂, Ar₂ and He₂, influence of molecular diffusivity on liquid phase transfer obs. 0–68089

KI in H₂O, absorption systems of O₂, N₂, Ar₂ and He₂, influence of molecular diffusivity on liquid phase transfer obs. 0–68089 LiO₂-SiO₂, glasses immiscibilities, neutron-induced autoradiography obs. 0–46877

Mg-Al-spinel in alkaline solns., hydrothermal dissolution reactions 0-62801

0–62801

Mo, photochromatic, optical props., depend. on composition, conc. and u.v. irrad. strength 0–61520

NH₁ aq. solns., solvated electron in pulse radiolysis 0–54195

Na-NH₃, liquid-liquid oceasistence and phase separation 0–58454

NaF melt, of quartz spheres, diffusional convection processes 0–39764

Na₂O BaO-SiO₂ system, immiscibility 0–74869

Na₃SO₃ in H₂O, absorption systems of O₂, N₃, Ar₂ and He₂, influence of molecular diffusivity on liquid phase transfer obs. 0–68089

Na₃SO₄ in H₂O, absorption systems of O₂, N₃, Ar₃ and He₂, influence of molecular diffusivity on liquid phase transfer obs. 0–68089

Nd³⁺/SeOCl₂, laser props. 0–54873

Te-Se melts, miscibility, cpd. formation, surface tension and density 0–50210

U soln. in H₂O, on-stream trace activation analysis based on nuclear and

U soln. in H2O, on-stream trace activation analysis based on nuclear and flow phenomena 0-48221 Zn-Bi, Zn-Pb, Zn-Bi-Pb systems, effect of ternary additions on thermodynamic props. 0-68082

Sonar see Sound ranging

Sonic boom see Aerodynamics; Shock waves/effects

Sonoluminescence see Luminescence/liquids and solutions

Soret effect see Diffusion in liquids, thermal

see also Adsorption
alkali halide (100) surface, electron stimulated desorption 0–65036
alloy, Ceto, with Ti and Zr 0–55753
Bayard-Alpert gauge sensitivity vars, due to chemisorpt, on collector 0–57209

chemisoption rel. to surface at. struct. 0-56692

Sorption continued

chemisorption, He of NO, low pressure obs. 0—41428 chemisorption, MO model, small metallic regions 0—41427 chemisorption, for thermokinetics meas., Calvet microcalorimeter chemisorption, for 0-51422

chemisorption, frictional polymer studies effect of contact surface prepara-tion technique, characterization using water drop reflection goniometer technique 0-56694

chemisorption and catalysis measurement apparatus for semiconductor oxides by Hall effect 0-44237 chemisorption thermokinetics, Calvet microcalorimeter appl. 0-51423

degassing quantity meas, method 0–41916 desorption, field pulse, for surface reaction kinetics meas. 0–56693 electron impact desorption, auger electron impact desorption, Auger electron spectroscopy determ.

0-37671 electron-impact desorption effects in vacuum gauges and mass spectrometers 0-57208 flash desorption data for activation energy linearly dependent on coverage

0-47071 glass, ionic pumping of inert gases $\sim \! 100$ eV, energy states distinguished $0 \! - \! 43566$

graphite, chemisorption of Cl₂, atomically pure surface, 300 K, mechanism 0-72535

hydrocarbons, i.r. spectra compared with i.r. spectra of alkyl Pt cpds. 0-77834

0-77834
metals, chemisorption of CO, i.r. spectra comparison for Ag, Cu, Au, Co and Ni films 0-59394
phosphor, radical recombination luminescence, chemisorption 0-51376
polyvinyl alcohol, of solvent, rel. to deformation of films 0-68205
porous polymers, transient isotherm, determination of accessible surface 0-53445
radionuclides, by anion exchangers, effect of pH values 0-71484
rare earth intermetallic compounds of H, reversible, room temp. 0-50395
zeolite, Linde 13X, H₂O- and D₂O-saturated, TLi, ²³Na and ¹³³Ca resonances 0-43568
Ag, allumina and silica supported, of CO, O₂ and H, prepretated, i.r. spectra

Ag, alumina and silica supported, of CO, O₂ and H₂ pretreated, i.r. spectra 0-39971

0–39971
p-Al₂O₃, of acetylene, i.r. spectra of surface species, effects of S poisoning
0–54106
Al₂O₃ corundum, growth, epitaxial tungstate melt chemisorption effect
0–50458
p-al₂O₃-supported Pt, of acetylene, i.r. spectra of surface species, effects of S poisoning 0–54106
Ba film, chemisorbed N₂ dispacement by O₂, obs. 0–56695
C, desorption of organic adsorbate, kinetic parameters, non-isothermal determ. 0–65103
CdS, chemisorption of O, effects on equilib. conductivity 0–40784
CdS, chemisorption influence on photocond. 0–68976
CdS, desorption of O, effect on Fermi level and photoconductance 0–47739
Cl, chemisorbed on Cu, effect on Cu surface self diff. 0–55915

0-47739
Cl., chemisorbed on Cu, effect on Cu surface self diff. 0-55915
Cu-Ni 20/80 alloy, ion-bombarded Ar thermal evolution, obs. 0-56697
Cu-Ni 50/50 alloy, ion-bombarded Ar thermal evolution, obs. 0-56697
Cu, ion-bombarded Ar thermal evolution, obs. 0-56697
Ge, surface elec. props., n-benzoquinone, chemisorption depend. 0-40802
H₂ chemisorption, geometry of precursor state in terms of MO-method 0-69211

We advanted film contribution of description to best capacity. 0, 78300

0-9211 He adsorbed film, contribution of desorption to heat capacity 0-78390 I₂, ion low Cr alloy steel, in vac. 0-40003 Mg, chemisorption of O₂ and H₂O on fresh surface, exo-electron emission 0-39972

0-39972

Mo, desorption of H₂, O, and H₂O by electron impact 0-39973

Mo(12), chemisorpt. of O₂, N₃, H₃, CO, LEED obs. 0-56698

Nb₂O₃ films, photocond., trapping and chemisorption effects 0-65850

Ni, inert gas ions burial and thermal release, 100-2400 eV 0-56699

Ni, ion-bombarded Ar thermal evolution obs. 0-56697

Ni surface, trapping and thermal release of 100-300 eV Ar⁺ and Kr⁺ 0-47038

0-47038
O₂ desorbed, effect of degassing on photoconductive patterns, obtained in electrophotographic ZnO layers 0-73376
Pt, desorption of H⁺, CO⁺ induced by electron bombardment 0-55761
Pt, of organic cpds., kinetics, obs. 0-56693
Re, h.c.p., of CO, field emission obs. 0-43571
Re, of O₂, reactive 0-45058
Ru, h.c.p., of CO, field emission obs. 0-43571
Si single cryst., desorption of water, study by desorption spectrometry 0-74929

0-74929
Si surfaces of o₂, chemisorptive luminescence 0-48125
SiO₂ gel, y-irrad., luminesc. during gas sorption 0-43490
W, chemisorption of 5d atoms 0-72536
W, desorption of residual gases in strong elec. fields 0-74931
W, desorption of U neutrals 0-55764
W, field desorption of Li at 20, 77 and 112 K 0-43573
W, O chemisorbed, isotope effect in electron stimulated desorption 0-45059

W, of organic cpds., kinetics, obs. 0–56693 ZnO, chemisorption of H atoms 0–56700 Zr, chemisorption of C on surface 0–56701

Sound see Acoustics

Sound field see Acoustic radiators; Acoustics; Intensity measurement/acoustics

Sound ranging
adaptive arrays 0-73036
in constant-gradient media, refraction correction by ray tracing, graph
0-53272

0-32/12 intertansducer NEFBRACS (nearfield bearing and range accuracy calibration system), design, construction 0-63445 rocket, passive cone angle amplifier 0-63450 sonar system range predictions, supporting studies 0-45645

Sound recording see Recording

Sound reproduction see also Acoustic radiators; Recording; Transducers No entries

Space charge
of atmosphere, value and polarity below 50 km 0-51530
benzene, liq., trap-controlled space charge currents 0-53831
benzene, solid, space charge limited currents 0-53831
betatron frequency shift formulae with crossing angle 0-49436

Space charge continued

ace charge continued effect on Cu evaporation by electron beam 0-43522 effect on paraxial electron trajectories 0-42211 field distortion, rel. to avalanche breakdown in solids 0-65781 influence on fogs and clouds 0-76384 insulating liq., space charge induced turbulence 0-74769 ion extraction from plasma, space charge layer parameters 0-43252 magnetron, electron space charge and tangential current density distribs.

0—43/68
nematic liq. cryst., elec. field distrib. assoc. with dynamic scatt. 0—53362 in positive corona, impulse type, in rod/earthed plane gaps 0—50133 in thermionic emitter sheath, theory 0—77005 wave excitation, in one-carrier semiconductor at jump in doping density 0—78936

wave propagation, in microwave tubes, effects of electrostatic focusing 0-77045

wave propagation in GaAs thin slab, laminar electron flow, theoretical relations 0-44195

wave propagation in thick Gunn diode, dispersion relation, one-dimensional approach and its validity 0-47710 waves, diffusion and transformation in cylindrical inhomogeneous electron currents 0-64739

waves in electron beams with velocity distribution 0-73167 Si-on-sapphire space charge-limited thin-film triodes 0-47778

electron beam intense relativistic, effect of background ions on propagation 0-39556

formation in pre-cathode region of elec. discharge 0-74620 r.f. discharge in planar diode, space charge instabilities 0-55508

alkali halide, time-depend. polarisation 0-53921 alkali halide crystal, formation mechanism, temp. depend. 0-47831 amorphous, monostable structures, electrical 0-56180 switching processes

0 - 56180
conduction, dimensional effects 0-72104
dielectric, photocond, transient space charge-limited currents 0-79038
fluctuation theory for space charge limited currents for ideal nonmetallic solids 0-51110
insulator, amorphous film 0-53928
p-n junction, electron transport, Boltzmann equation 0-47784
permittivity, complex, dispersion due to space-charge polarization 0-72102
photoconducting- dielectric struct., transient space-charge-limited currents 0-2-7938

photoconducting dielectric struct, transient space charge 0.–79038 polyethylene, static electrification, decay by cond. processes 0–72101 polythene, effects on electrical breakdown 0–68915 rectifying contact, Al-CdS-Al, negative resistance under unidirectional voltage pulse excitation 0–59244 sand grains, dispersion due to mutual repulsion 0–51109 semiconductor, electroreflectance 0–65984 emiconductor, inhomogeneous, space-charge- limited currents, thermally

semiconductor, inhomogeneous, space-charge- limited currents, thermally stimulated cond. obs. 0-65654 semiconductor junction, p-n, influence on fabrication by diffusion

0–68864
semiconductor surface space-charge layers, cond. 0–78929
semiconductors and photodieletrics, meas. 0–56219
Al-CdS-Al structure, negative resistance under unidirectional voltage pulse excitation 0–59244
Cu₂O, space charge limited currents 0–72023
n-GaAs/Au contact, photosensitivity, elec. field depend. 0–40795
n-GaAs, epitaxial layers, majority carrier profile, Schottky barrier characts. 0–59221

GaAs, high-resist. region near cathode, formation mechanism 0-47745

Se, amorphous, on Al, Au contact, space-charge-limited currents 0-72010

Si, amorphous film, photoconductivity 0-44399
ZnS:Cu,Mn, film condenser, electroluminescence, development mechanism 0-44949
ZnTe films, vacuum-deposited, space-charged-limited-current 0-53830

Space groups see Crystal structure, atomic

Space research

see also Atmosphere
aerodynamics of re-entrant-craft 0-66347
aircraft use, review 0-79613
Apollo lunar surface and sample expts leading utilization of extraterrestrial resources 0-66349
apparatus motion in normal gravitational field subject to secondary forces

0–51611
astronomy, OAO-II, present reality, future prospects 0–76527
camera calibration using uniform variable light source 0–49139
cloud cover statistics in planning of remote sensing missions 0–51525
collection efficiency for inertial impaction and sounding rocket collection of meteoric dust 0–76524
conjunction, superior, of Pioneer 6 0–41560
cosmic ray experiment, adaptive data compression method 0–77381
film, colour i.r., high-altitude use 0–51609
LSI logarithmic counters for space physics applications 0–77408
laser communication systems, optical components and technology 0–77173
lung grayimetry and mascons 0–76619

0-77173 lunar gravimetry and mascons 0-76619 manned laboratories in space, book 0-66355 Mariner Mars (1971), TV expt. 0-54307 Mariner Mars (1971), ir. rsdiometry expt. 0-54308 Mariner Mars (1971), ir. rsdiometry expt. 0-54309 Mariner Mars (1971), ir. spectroscopy expt. 0-54309 Mariner Mars (1971) 0-54439 Mariner Mars (1971) 0-54439 Mariner Mars (1971) clestial mechanics expts. 0-54310 Mariner Mars (1971) clestial mechanics expts. 0-54337 meteorological parameters in launch vehicle environments, new passive optical detection systems 0-51505 micrometeorite detection in space and interpretation of results 0-41812 minimum velocity vector three impulse maneuvers on to constrained asymptotic velocity vector 0-69338 occultation of Pioneer 6, measurement of transient Faraday rotation 0-41559 optical data satellite link, for ultra-wide bandwidth laser communications

optical data satellite link, for ultra-wide bandwidth laser communications 0-79617optical instrument regulation, vacuum chamber design 0-41915 orbital plane of satellite determining, statistical method 0-69341

Space research continued

organic compounds detection and identification on Mars, surface, two approaches 0–57110 particle analyzer, electrostatic, with no fringe field 0–73676 partitioning of energy in hypervelocity impact against loose sand targets, lunar craters 0–76525

photography in space, scientific potentialities and analytic framework 0-56867

0-56867 photometer, far ultraviolet 100-1300 Å wavelength region 0-76424 radioastronomy from space, advantages over conventional techniques, future plans 0-51814 re-entry, radar obs., survey of noise in S. sky at 55 MHz with radar receiving equipment 0-54410 weak magnetic fields, colloquium, Paris (1969) 0-52222

Space vehicles

see also Rockets; Satellites, artificial

15.3 GHz communication link, propagation obs. 0–69343
acoustic tests of flexible spacecraft model 0–63451
acoustical meas. of laminar-turbulent transition on reentry vehicles
0–71243

0-71243
aerodynamics, environment, information processing; symposium, Toulouse, France. (1970) 0-54312
aerodynamics, re-entry problems 0-66347
Apollo 12 lunar module impact, lab. simulation and possible downrange ballistic effects 0-79722
Apollo 13, lunar heat flow meas. 0-57098
artificial gravitation calc. for living compartments 0-51614
branched trajectories, optimal 0-56881
debris clouds, water vapour nucleation 0-79615
heat transfer simulating devices, review 0-59671
impulsive transfer between neighboring circular orbits, geometrical soln. 0-56871
low magnetic field technology 0-54317

0 - 56871

low magnetic field technology 0 - 54317

magnetic disturbance torque for determination of attitude motion, control actuator sizing, fuel requirements and spin decay 0 - 51613

Mariner, radio occultation meas. of figure of Mars 0 - 66597

Mariner of and 7, Mars and Venus exospheric temps., solar cycle var., prediction 0 - 51759

Mariners 6 and 7, radio occultation meas. of Mars atm. 0 - 51760

meteoroid impacts, on Gemini windows, data interpretation 0 - 69467

navigation, continuous observation processing and effective estimates determ. by maximum likelihood method 0 - 56868

OSO-V, solar X-ray spectrum obs., 1 Å to 400 Å 0 - 66629

Orbiting Astronomical Observatory II, geophysical applications 0 - 76301

Pioneer 6, solar occultation, measurement of transient Faraday rotation 0 - 41550

Pioneer 6, superior conjunction 0 - 41560

Pioneer 6, superior conjunction 0-41560 refractory pigments for white thermal control coatings, developments 0-62080

0-02000 rotation, stable, effect of elastic rod vibrs. 0-56869 space station, manner, for remote sensing of earth resources 0-62839 spinning cavity, specular, axisymmetric; solar radiant energy exchange, ray tracing method 0-62959 structural members, vibratory response to vehicle acoustic fields, simula

tion 0-66900 table listing satellites and probes launched between Nov.1 1968 and Dec.31 (1969) 0-62955 temperature prediction and other heat conduction problems, perturbation theory 0-66351 thermal reflectance, bidirectional, for three-dimensional diffuse surfaces

0 - 66350

thermodynamics and thermophysics of space flight, conference, Palo Alto, Ca., USA (1970) 0-62958 trajectory height reduction above lunar surface, lunar relief correlation function appl. 0-57091

Tunction appl. 0—3/091
instrumentation
see also Rockets; Satellites, artificial
aerospace instrumentation conference, Las Vegas USA, (1969) 0—72670
Apollo, proton spectrometer 0—63884
counters, variable prescaling, design techniques 0—48351
heater using 2Al+3CuO→3Cu+Al₂O₃+1750 Btu/lbm solid-solid reaction
0—72675

0-72675
interferograms, window wavefront deformation relating angular deviations to line of sight 0-66348
mag. analyzer of primary cosmic rays, superconducting mag. system with field 20 kOe 0-51615
magnetometers, USSR developments 0-54318
Mars, multispectral imaging from landing vehicle 0-59771
meteoroids, luminescent-detector 0-51616
multispectral scanner, for Earth Resources Technology Satellite, optimization 0-52380
OGO-IV airglow photometer, in-flight radiometric calibration 0-59627
OSO-VI, Harvard expt. 0-66360
particle detectors, in-flight, calibration systems 0-63872
particle spectrometer, digital closed-loop calibration system 0-63880
photometric calibration changes in EUV solar satellite instruments 0-60373
photomultiplier, hybrid Cockroft Walton multi-dynode, power supply

photomultiplier, hybrid Cockroft Walton multi-dynode, power supply

pressure gauges aboard Explorer 32, outgassing and surface adsorption during rotation 0-56885

solar-energy concentrator, rotating film reflector, connection without rigid shaft 0-69345

shaft 0–69345 spectrometer for solar extreme u.v. obs. from OSO-1 satellite 0–51789 spectrometers, review 0–66361 star sensors on Mariner spacecraft, development history 0–51610 sun sensor, fine-pointing, choice of spectral region 0–62961 wide range magnetometers 0–54316 X-ray detection system, non-dispersive, for analysis of lunar X-rays 0–69441 He-Ne laser interferometer applications 0–60349

Space-time configurations

3-dimensional chronometrically-invariant 2-metric formalism, sequential three-dimensional modification 0-51905 absoluteness proof, crucial expt. 0-54559 asymptotically flat space-times, analysis of Newman-Unti integration procedure 0-38166

commutation property of a stationary, axisymmetric system 0-51922 cosmology, energy theorem and choice of clocks 0-72678

Space-time configurations continued

ace-time configurations continued
curved space, definition of multipole moments for static, asymptotically flat,
source-free solutions of Einstein's equations 0-66805
Einstein Rosen matter 0-69606
electromagnetic flet in isotropic space time 0-76815
electromagnetic tensor in Riemannian space-time 0-38171
flat and asymptotically flat, Newman-Penrose consts. 0-41952
in high energy interactions 0-70182
Hilbert spaces, automorphism group for anticommutation relations
0-76799
Hilbert spaces continuous

Hilbert spaces, continuous tensor product, translated representations 0-69585

hyperbolic velocity space, cosmological basis 0–57250 invariant of spherically symmetric space-times 0–63323 isotropy principle formulation, 4-dimensional space-time deduction 0–51927

Kerr metric, source 0-66793

Mach's principle, differentiable manifolds 0–41934
Mach's principle, differentiable manifolds 0–51932
Mach's principle, two trials 0–51931
Minkowski diagram, useful form 0–76803
position operators 0–45524

position operators 0–45524 pseudo-Riemannian manifolds, global isometric embedding 0–41951 Riemannian, dimensionally dependent identities, generalization 0–69589 Riemannian, polynomial conformal tensors 0–72890 Riemannian, tensor expressions for acoustic ray tracing 0–52084 Riemannian space-times, groups of curvature collineations which admit fields of parallel vectors 0–48695 SO+ (n,1)-invariant finite component wave equations and reflection invariance 0–38158 SO(3,R) (Bianchi Type IX) homogeneous cosmologies, dynamics 0–48209

SU(2) spinor calculus for stationary space-times 0-76808

Schwarzchild space-time, generalized singular em. field 0–48707 spatially homogeneous anisotropic cosmological models containing relativistic fluid and magnetic field 0–54338 static spherically symmetric, optical point characts, determination 0.69611

0 69611 static vacuum solutions of Einstein's eqns., analyticity 0—57252 symmetric, spherical, invariant 0—63323 Taub and NUT spaces and extensions of their tangent bundles 0—51933 transition from continuous to discrete space-time scheme 0—41954 type (22), geodesic equations, quadratic first integrals 0—69602 and unstable particle production and decay 0—45862

Spallation see Nuclear spallation

Spark chambers

acoustic, multitrack occurrences recording 0-38767

acoustic, multitrack occurrences recording 0–38767 book, various kinds and applic. 0–49419 data acquisition and monitoring, computer system 0–73709 datum markers, method of plotting using Scotchlite film 0–77445 efficiency, (multi-track), and other props, influence of transmission-line behaviour 0–42651 high resolution, use in track finding in emulsion plates 0–60723 magnetostriction, specifications of non-overloading preamplifier 0–52614 multileactrode for charged particle beam characteristics 0–77443 multigap, 980×490 mm thin foil electrodes preparation, description 0–49414

0-49414 multigap, with plexiglas plates for electrons and photons energy resolution investigation 0-49412 multilayer, electron and γ quantum energy spectra meas. 0-46064 multispark recording by flat ribbon microphone 0-46066 multispark proportional, operation, amplification limits, mag. fields effects measurements 0-46068 pulser construction using stripline as feeder cable and storage capacitor 0-42669.

0-42652

0-42652 shower, for cosmic ray electron registration, 0.1 to 1.5 GeV 0-42607 small gap, determ., ionizing capacity of particle 0-46065 spark-coordinates, rapid information determination using filmless optical method 0-77444 streamer, He-filled, p and π ionization rel. to momentum, obs. 0-46067 streamer, developments 0-73689 streamer stable operation, power supply description 0-49415 system for recording and outputting to digital computer from 32-wire chamber 0-49420 track simulation charged particles, method 0-77446 wire, p-ray detection 0-49418 wire, in magnetic fields, read-out by lumped delay line 0-60722 wire, optical digitization 0-46069 wire chambers, proportional mode, amplifier/discriminator/limiter, low cost 0-49416 wire rel. to spectrometer with capacitor memory and f.e.t. readout 0-60644 for α particles from radioactive nuclei 0-49357

for α particles from radioactive nuclei 0-49357 for γ-ray astronomy, digitized spark chamber 0-54422 Pb electrodes for recording high-energy electrons and photons, properties 0 - 49413

Spark counters see Counters/spark

Sparks, electric

irks, electric see also Breakdown, electric; Lightning atoms, mean residue time 0-50134 discharge, cathode vaporization 0-39635 discharge, impulse breakdown of air gaps in nanosec time range, commutation process 0-50128 discharge, spark, low-pressure, description of current growth processes 0-71214

formation mechanism spark chamber 0-64794 gap laser triggered, effect of various gases on formative times obs. 0-61406

gaps, laser-triggered pressurised with subnanosecond risetime 0-74639

gaps, laster-friggered pressurised with submanosecond risetime 0-4639 gaps at atmospheric pressure, low inductance high voltage, flashover avoidance 0-74638 in gas, similarity and dimension method 0-64793 multichannel vacuum gap 0-46773 nanolight at high current densities and gas pressures, static model, energy balance eqn. 0-64791

optical phenomenon tree shape in explosive anode erosion, time resolved photography, spectroscopy 0-61405

Sparks, electric continued

plasma production and temperature measurement for time resolved spectra 0-53171

pulsed, time-controllable continuum photon emission, applic. to vac. u.v.

spectroscopy 0-43369 spectroscope for time and spatial light distrib. meas. 0-43371 trigatron gap, breakdown, voltage reduction, effect of triggering energy 0-74629

triggered by laser beam, formative times rel. to voltage for different press., gaps and laser power 0-53232 vacuum, triggering device using auxiliary spark produced by rectangular pulse 0-74637

Fe spark spectrum (10-18 Å), line list 0-49776 H₂ spark channels, thermalisation and e density and temp. rel. to time 0-43372

Specific heat

see also Thermodynamic properties binary system, critical point discontinuity, calorimetry inhomogeneity 0-53393

0-53393
calorimeter meas, thermistorized 0-42108
calorimetric measurement 0-48899
capacity of small particles, impulse method 0-57436
critical liq.-gas pt., anomaly, rel. to sound vel. 0-50321
dipole rotator, plane, rigid, classical, in e.m. zero-point radiation 0-60071
electronic, rel. to determination of electronic density of states 0-71900
ferromagnet, Ni-Cu alloys, temp. and comp. depend. 0-44497
fluids, dense, Cv. PY theory of extrema and comparison with expt.
0-43216

gas liquid critical point, gravity effects on meas. 0-46990 Gruneisen parameter, low temp., from elastic constants press derivs. for RbI 0-43923

Gruneisen parameter, low temp., from elastic constants press derivs. or RbI 0-43923

Gruneisen parameter calculation from thermal conductivity meas. under pressure 0-75415

Ising system, random, mol.-field theory in external mag. field 0-40966

low-temp. data, rel. to electron density of states 0-75452

negative value for some systems 0-45657

series for f.c..c. and b.c.c. lattices 0-51964

tetramethylgermane, lt. capacity 15-300°K 0-43513

transition metal tris(accetylacetonato) complexes, heat capacity 0-75409

CsSO₄ heat contents, specific heats and latent heats of phase transformations 0-65548

K₂SO₄ heat contents, specific heats and latent heats of phase transformations 0-65548

Ni-Cu alloy, low temp. magnetisation, comp. depend. 0-44497

O₂, triple point to 300°K, at const. vol. and press. 0-46992

RbI, Gruneisen parameter, low temp., from elastic constants press. derivs. 0-43923

Si, Gruneisen parameter, low temp., from elastic constant press. derivs.

Si, Gruneisen parameter, low temp., from elastic constant press. derivs.

0-43924 0—43924
ZnSe Debye temp., compounds of same Gruneisen constant, linearity of log (Debye temp.) with log (molar vol.) 0—50900
ZnTe Debye temp., compounds of same Gruneisen constant, linearity of log (debye temp.) with log (molar vol.) 0—50900

singularity of C_p and C_p at critical point 0-74834 χe , C_p/C_v from Brillouin scatt. near critical pt., obs. 0-46829 χe , C_p/C_v ratio, temp. dependence 0-78326

liquids

amino acids in D2O partial molal heat capacity and infinite dilution

amino acids in H_2O , partial molal heat capacity at infinite dilution 0-46899

0-46899
Gruneisen coeff. rel. to intermol. force constants 0-64853
and loose or plastic media, determination, dynamic method 0-39774
methanol-CS₂ binary system, critical phenomena 0-39777
polymer solns, heat capacity calc. 0-58478
pseudo-Gruneisen parameter 0-55604
supercooled, heat capacity 0-64896
Al, calorimetric meas., thermodyn. anal. 0-78776
Al, result 0-59110
Ar and structure 0-43424

Al, result 0-59110
Ar, and structure 0-43424
CS₂-methanol binary system, critical phenomena 0-39777
CS₂, heat capacity evaluation from partition function 0-78260
Cu, result 0-59110
HNO₃, aqueous solutions, in temp. range -196 to 20°C 0-68091
H₃SO₄, aqueous solutions, in temp. range -196 to 20°C 0-68091
H₂CO₄, aqueous solutions, in temp. range -196 to 20°C 0-68091
H₂CO₄, aqueous solutions, in temp. range -196 to 20°C 0-68091
H₃CO₄, aqueous solutions, in temp. range -196 to 20°C 0-68091
H₃CO₄, adueous solutions, in temp. range -196 to 20°C 0-78319
³He⁴He mixtures, near junction of λ and phase separation curves
0-74824
Kr at const. volume along holling line. 0-55607

P-14624 Kr at const. volume along boiling line 0-55607 Pb, result 0-59110 W, result 0-59110

alkali halide cryst., Debye temp. rel. to formation energy of vacancies 0-71605 alkali halide crystals, calc. of Gruneisen constant 0-56104

alkali halides, Debye temp. rel. to physical history 0-50669 alkali halides, X-ray Debye temp. rel. to Schottky defects form. energy

0-40132

0-40132 alloy, dil., electronic contrib. 0-71857 alloy, dil. mag. 0-43963 alloy, dilute, rel. to force constant changes in metals with impurities alloy, din. 0-43896

0—43896
alloys, noble metal-transition metal, dilute, low-temp. anomalies 0—40711
alloys dil, rel. to density of states calc. 0—43985
alum, methylammonium chromium, heat capacity 0—71861
anthracene, Gruneisen tensor, 0-300 K 0—40589
antiferromagnet, magnon-phonon interaction effect 0—40566
antiferromagnet, short-wavelength magnon freqs. temp. depend. rel. to heat
capacity 0—44674
antiferromagnet Cs₃Cu₂Cl₃.2H₂O, ht. capacity below 4.2°K in mag. fields
0—43906

0-43906 antiferromagnetic solid solution, Ni_xCo_{1-x}Cl₂.6H₂O, susceptibility, Neel temp., conc. depend. 0–75965 conductors, electrical, at high temps., high-speed method 0–56105

Specific heat continued

solids continued

Crystals, appl. of minimax approx. 0—78774

Debye's theory, solution of integral in terms of Fourier series 0—50889

Debye temp., zero point motion role 0—40565

Debye temp. calc. from temp.-depend. hyperfine constants, e.s.r. determ. 0—43912

Debye temp. determ. using electron phonon state splitting 0-75410
Debye temp. in V, Nb, Ta from X-ray meas. new T_c 0-62179
Debye temp. pressure depend, to 30 kbar in NaCl 0-62174
Debye temperature of cubic elements from elastic constants, comparison of

methods 0-43898 dibenzyl crystal, thermal expansion, Gruneisen tensor, X-ray diffr., 83-297K 0-50898 dimethylphthalate system, heat capacity, calorimetric meas. glass temp. 0-68616

electron rel. to electron density of states, conference, Gaithersburg (1969) 0-65573

0-0573

ferrites, temp. variation, expt. 0-59102

ferroelectric, AgNa(NO₂)₂, transition pt. anomaly 0-65799

ferroelectric, KH₂PO₄, phase transition anomaly 0-40572

ferroelectric, NaH₃(SeO₃)₂, phase transitions, configurational entropy change 0-43907 ferroelectric, NaH₃(SeO₃)₂, phase transitions, configurational entropy change 0–43907
ferroelectric, rel. to phase transitions 0–65816
ferroelectric, triglycine sulphate, anomalies at transition 0–79050
ferroelectric, triglycine sulphate, constant electric polarization 0–68615
ferroelectric, triglycine sulphate, elec. field depend. 0–62449
ferroelectric, triglycine sulphate 0–65821
ferromagnet, Co₃B-Ni₃B, FeB-CoB, systems, critical conc. range, low temp.
anomalies 0–43901
ferromagnet, EuO, 0.37-4.4K, spin wave theory 0–43904
ferromagnet, tauC, 0.37-4.4K, spin wave theory 0–43904
ferromagnet, mag. sp. th., external field near critical pt.
ferromagnet, mag. sp. th., external field effect 0–47542
ferromagnetic films, surface corrections 0–40564
films, quenched, In, Pb and Bi, specific heat at 5-8 K 0–62208
glycine, internal rotation from low temp. heat capacity data 0–62214
goethite, heat crapacity, 51 to 298% 0–71858
graphite surface, Debye temp. 0–59104
graphite surface, Debye temp. 0–59104
Gruneisen parameter depend. M, method 0–56114
Gruneisen parameter, offs, method 0–56114
Gruneisen parameter, effect of anharmonicity 0–40588
Gruneisen parameter, edos, for several models 0–43922
Gruneisen parameter eqn., soln, rel. to vol. depend. of self consistent pho-

Gruneisen parameter eq.n., soln. rel. to vol. depend. of self consistent phonon energies 0-47552
Gruneisen parameter for Born-von Karman lattices 0-56113
Gruneisen parameter, mode, calc. for Al₂O₃ 0-50899
heat capacity, anharmonic effect up to critical temp. of lattice instability 0-43899

heterophase fluctuation during melting 0-74839 inert gas, short-range three-body pot. interaction, dispersion curves, elastic const. 0-75357

const. 0—75357 heat capacity, anharmonic effects calc. 0—40516 low-temperature crystal, anharmonic contribs. 0—40558 lunar samples, 90-350 K 0—45400 lunar samples, direct meas. 0—48542 magnetic alloy, dil. 0—43894 magnetic dilute alloy, Cu-Fe, heat capacity, 0.06-1 K, spin-compensated crates 0—5308

magnetic dilute alloy, Cu-Fe, heat capacity, 0.06-1 K, spin-compensated states 0–59308 magnetite, powdered synthetic, effect of inhomogeneity on singularity in phase transitions near second kind transitions 0–50891 magnon specific heat rel. to phonon-magnon interaction 0–40978 metal, Debye temp. rel. to physical history 0–50669 metal, Gruneisen coeff. determ., compressibility parameters applic. 0–40587

0–40587 metal, cubic, Gruneisen parameters 0–53718 metal, cubic, Gruneisen parameters 0–53718 metal, normal, in pseudopot. model, electron-phonon-Coulomb interactions effect 0–43897 metal, surface mag, levels contrib. 0–47543 metals, Mie-Gruneisen scheme, extended 0–65544 metals, rare earths, calc. from estimation of radiation losses 0–53777 metals, spin fluctuations in nearly antiferromagnetic metals 0–54038 metals, thermal and radiative props. meas., 1000-2500°K, instrum. 0–65545

metals, th

of metals for vacancy studies in metals under quasiequilibrium condition, relaxation method 0-47223 methane, d₁, solid, Schottky-type anomaly, by quantum statistical consideration 0-56110

minimax approximation applied to evaluation of sp. ht. of crystals 0-78774

0—18/14
naphthalene, Gruneisen tensor, 0-300 K 0—40589
paraffin, 8≤n≤16, order-disorder, phase transformations, entropy
0—78/706
perovskite, Sr, WNiO₆, cryst. transition influence on heat capacity behaviour 0—40577

phonon spectrum and lattice specific heat including leading anharmonic corrections to self-consistent harmonic approximation of b.c.c. ³He

corrections to self-consistent harmonic approximation of b.c.c. ?He 0–59106 polyesterurethane block-polymers, heat capacity, -100-100°C 0–68611 polyethylene, thin-layer, 32°C 0–78773 polystyrene, cross-linking effect, 1.6-4K 0–62215 polyvinylchloride-dibutylphthalate system, heat capacity, calorimetric meas. Glass temp. 0–68616 polyvinylchloride-dioctylphthalate system, heat capacity, calorimetric meas. glass temp. 0–68616 pyrophyllite, heat capacity, 51 to 298 °K 0–71858 pyroxylin, thermal capacity, 51 to 298 °K 0–71858 pyroxylin, thermal capacity, high temp. meas. 0–75404 rare earth metal, nucl. sp. ht. due to hyperfine interactions 0–43910 rare earth metals, calc. from estimation of radiation losses 0–53777 refractory metals, b.c.c., high temp. specific heat 0–56106 semiconductor alloy system, SnTe-MnTe, 2-25K, rel. to magnetization state 0–59108 semimetal, heat capacity singularities in mag. field 0–53712 semimetal, nucl. quadrupole interaction obs. 0–75986 singularity in phase transitions near second kind transitions, effect of sample inhomogeneity 0–50891 superconducting alloy, type-II, highly reversible 0–71976 0 - 59106

```
Specific heat continued
  solids continued
```

superconductor, Pb(Nb_{1-x}Ta_x)S₃, meas. rel. to transition temp., comp. and thermal history depend. 0–78901 superconductor, Re, heat capacity, 0.02–0.4K 0–75623 superconductor, Re 0–44138 superconductor, dil. alloy 0–44099 superconductor, singularities near T_c 0–71967 superconductor, singularities near T_c 0–76761 tetrafluoromethane, heat capacity, 9.2-20K, phase transformation 0–43914 thermal capacity of spin waves in domain Bloch wall 0–40975 transition metal semi-borides, first series, low temp. meas., ferromagnetism 0–78782 triglycine sulphate, anomalies at transition.

0-78782

triglycine sulphate, anomalies at transition 0-79050

triglycine sulphate, constant electric polarization 0-68615

triglycine sulphate, ferroelect. sp. ht. 0-65821

triglycine sulphate, ferroelectric, elec. field depend. 0-62449

vinyl monomer-solvent mixtures glass transition temperature, crystallization 0-47541

Ag-Mn alloy, dilute, low-temp. anomalies 0-40711

Ag-Mn alloy, equiatomic, ß' and \(\cappa \) phases, low temp. 0-78775

AgBr, temp. depend., -70-550°C, defect effect, phase transition 0-40567

AgCl, Debye temp., 2-12K, lattice vibration model 0-47544

AgNa(NO₂), ferroelec transition pt. anomaly 0-65799

Ag₂S(Se), temp. depend., -70-550°C, defect effect, phase transition 0-40567

Al-Ag alloys, lattice ht. capacity enhancement by 1.f. resonance modes

Al-Ag alloys, lattice ht. capacity enhancement by l.f. resonance modes $0\!-\!43900$

0–55939
Co-Mn alloy, ferromag., nuclear component, 0.4-4.2K, rel. to hyperfine fields 0–56445
Co-Pd alloy, ferromag., nuclear component, 0.4-4.2K, rel. to hyperfine fields 0–56445
Co₃B-Ni₂B, ferromag. system, low temp. anomalies 0–43901
CrTe, heat capacity rel. to ferro-paramag. transition, 300-570°K 0–40568
Cs, below 3°K, meas. 0–56109
CsBr(Cl₁), Gruneisen const. 0–78727
Cs₁Cu₂Cl₁-2H₂O single crystal, rel. to antiferromag. ordering 0–41054
Cu-Au alloys, below 3 K 0–43902
Cu-Fe. dilute alloy, heat capacity. 0.06-1 K, spin-compensated states

Cu-Fe, dilute alloy, heat capacity, 0.06-1 K, spin-compensated states 0-59308

Cu-Fe, dilute alloy, heat capacity, 0.06-1 K, spin-compensated states 0–59308

Cu-Pd alloys, comp. depend., 1.5-4.2K, rel. to band structure, ordering effects 0–43903

Cu-5.87%Al, Debye temp., temp. depend. 300-800°K 0–40569

Cu, 1.5 to 20K, residual resistivity ratio depend. 0–50890

Cu, Debye temp., temp. depend. 300-800°K 0–40569

Cu, Debye tempender and specific heat 0–53688

Cu, high purity, 1.3° to 90°K obs. 0–53713

Cu, result 0–59110

Cu, S, temp. depend., -70-550°C, defect effect, phase transition 0–40567

Dy, temp. depend., -70-550°C, defect effect, phase transition 0–40567

Dy, temp. depend., -70-550°C, defect effect, phase transition 0–40567

Er-Tm, h.c.p., low temp. meas. 0–75406

Er-As, double peak at low temp. 0–40571

ErSb, double peaks, low temp., rel. to mag. ordering 0–75407

ErSb, double peaks, low temp., rel. to mag. ordering 0–75407

EuO, 0.37-4.4 K, mag. spin wave theory 0–43904

Fe-Pd dil. alloy, ferromag, nuclear component, 0.4-4.2K, rel. to hyperfine fields 0–56445

Fe, electron heat capacity, temp. depend. at Curie point 0–78777

FeB-CoB, ferromag, system, low temp. anomalies 0–43901

Fe-C, precipitated, effective Debye temp. determ. 0–59105

Fe₃(PO₄), 4H₂O, Ludlamite, 2.4-68 K, Ising linear-chain model 0–51194

Gd-Lu alloys, low temp., rel. to mag. transition 0–78408

Gd, heat capacity near Curie pt. 0–72214

GdAlO₃, at liq. He temps. 0–69047

GdFeO₃, 0.5-12°K, and mag. interactions 0–44692

GdFeO₃, 0.5-12°K, and mag. interactions 0–44692

GdFeO₃, 0.5-12°K, and mag. interactions 0–62562

GdI, at low temperatures, 1.3°-4.4°K magnetic transition 0–71859

34e, b.e.c., phonon spectrum and lattice specific heat including leading anharmonic corrections to the self-consistent harmonic approximation 0–59106

34e adsorbed film, heat capacity meas. 0–78390

annarmonic contections of the content of the conten

Specific heat continued solids continued

HgSe, polycrystalline, temp. depend., 15-290K 0-68613

In-Sn dil. alloys, electronic contrib., 0.5-1.7 K 0-43905

In, heat capacity study; application of electron-ion interaction model 0-71823

0–71823

KBr, elastic constant and Debye temp., temp. depend. 0–75222

KCl:Ti(Br), lattice reson. modes obs. 0–75374

KCl:KBr solid solns., Debye temp. 0–65546

KCl single crystal, Debye temp. and elastic constants, 300-80 K 0–65354

KH₂PO₄, ferroelec., phase transition anomaly 0–40572

KH₂PO₄ and deuterated isomorphs 0–65547

KMF₃ M=divalent transition metal, heat capacity and superexchange consts. 0–40573

KNi₂Zn_{1-x}F₃, heat capacity rel. to mag. ordering, 80-300°K 0–40573

LiF, Gruneisen parameter, 0K 0–56114

Mg, data analysis 60-150K, freq. distrib. function even moments calc. 0–40574

MgO, Gruneisen parameter, 0K 0–56114

MgO, Gruneisen parameter, OK. 0–56114
MgO, Gruneisen parameter, OK. 0–56114
MgO heat capacity anal. 0–62211
Mn₁B, MnB, MnB₂, electronic sp. hts. obs. 0–40575
MnBr₂, 4H₂O, ht. capacity in mag. fields at liquid He temp. 0–65549
a/MnCl₂,4H₂O, ht. capacity below 4.2°K in mag. fields 0–43906
Mn(NH₃)₈C(Br₃)₈, heat capacity, mag. phase transitions obs. 0–62565
Mo, heat capacity in range 1900 to 2800°K, high speed meas. 0–47546
NH₄H₂PO₄, deuteration influence, rel. to dielec. transition 0–78779
NH₄H₂PO₄ and deuterated isomorphs 0–65547
NaBr₄, Young's modulus, Poisson's ratio, hydrostatic compressibility, Debye temp. u.s. velocity 0–62012
NaCl, Debye temp. pressure depend. to 30 kbar 0–62174
NaCl, mode Gruneisen parameters 0–71667
NaCl single crystal, Debye temp. and elastic constants, 300-120 K
0–65354
NaH₃(SeO₃)₂, ferroelectric, phase transitions, configurational entropy

NaH₃(SeO₃)₂, ferroelectric, phase transitions, configurational entropy change 0–43907 NaH₃(SeO₃)₂ and NaD₃(SeO₃)₂, rel. to ferroelec. phase transitions

0-65816

NaNH₄SO_{4.2}H₂O, rel. to ferroelec. phase transitions 0-65816

Nb-Ta alloys, rel. to supercond. T_c 0-78905

Nb, Debye temp., X-ray diffr. obs. 0-78784

Nb surface, effective Debye temp. 0-74855

NbO, Gruneisen consts. 0-78619

Ne, heat capacity, anharmonic effects calc. 0-40516

Ne crystal, Debye temp. and Gruneisen coeff., from u.s. vel. of propag., 2-20K 0-55941

²⁰Ne, ²²Ne, obs. 2.2-24K 0-53714

Ni-Co alloy, Debye temp., adiabatic elastic stiffness, comp. depend 0-78601 0-78601

0-7801 Ni-Ir alloy system, electronic sp. ht. and Debye temp. 0-40576 Ni-Sb system, non-existence of Ni₁₅Sb from thermo-magnetic obs. 0-65507

Ni-fa alloy system, electronic sp. ht. and Debye temp. 0–40576
Ni-Sb system, non-existence of Ni₁₈Sb from thermo-magnetic obs. 0–65507
Ni, Debye temperature and specific heat 0–53688
Ni₁₈Co₁₋₂Cl₁, 6H₂O, solid solution, antiferromag., susceptibility, Neel temp. conc. depend. 0–75965
Ni(NH₃)₆Cl₂, and thermal conductivity, rel. to phase transition 0–56108
Ni(001) surface Debye temp., LEED obs. 0–74886
Np meas. from 7.5°K to 300°K, method description 0–68614
Pb, result 0–59110
PbF₃, cubic, Gruneisen param. low temp. limit calc. 0–40235
Pb(Nb_{1-x}Ta₂)S₃, supercond. transition temps., comp. and thermal history depend., rel. to sp. ht. meas. 0–78901
PbTI(Bi) alloys, rigid-band behaviour, electron-phonon enhancement effects 0–43908
Pd-B solid solns., low temp. heat capacities 0–62212
Pd, Debye temp., model calcs. 0–71862
β-PdIn, energy bands, augmented- plane-wave method, mag. susceptibility calc. 0–78840
Pr. nucl. sp. ht. due to hyperfine interactions 0–43910
Pt-Ni dil. alloys, exchange-enhanced 0–62213
Pt, high purity, 1.3° to 90°K obs. 0–53713
Pu-(1 wt.%) Ga δ-stabilised alloy, heat content and capacity, 0-685 °C65550 0–65550
Pu meas. from 13° to 300°K, method description 0–68614
Rb, below 3°K, meas. 0–56109
RbH, PO₄ and deuterated isomorphs 0–65547
Re, heat capacity, 0.02.0 4K 0–75623
Re, normal and supercond. 0–44138
Rh-Pd, f.c., low-temp. meas. 0–71863
Sb, 0.03–0.8 K 0–50893
Se, hexagonal, heat capacity meas., 320-480 K, with differential scanning calorimeter 0–78780
Si, vitreous, heat capacity calc. from Raman spectra 0–78781
Sn, result 0–59110
SnTe-MnTe system, 2-25K, rel. to magnetization state 0–59108
SrF;-Mn², Debye temp. calc. from temp.-depend. hyperfine constants, e.s.r. determ. 0–43912
SrO heat capacity anal. 0–62211
Sr₂WNiO₆, perovskite type, cryst. transition influence on heat capacity behaviour 0–40577
Ta-H, system, rel. to electronic structure 0–47492
Ti-V-C alloy, f.c.c., rel. to electronic structure 0–47667

Sr₃WNiO₆, perovskite type, cryst. transition innuence on near checkwise, percentage of the second of the secon

Xe, heat capacity, anharmonic effects calc. 0-40516 ZnS Debye temp. determ. using electron phonon state splitting 0-75410

Specific heat continued

solids continued

ZnTe, mode Gruneisen parameters 0-75383 ZrH_x, electronic contrib. 0-44001

Spectra see also Absorption/light; Astronomical spectra; Atmospheric spectra; Chemical shift; Colour; Mass spectra; Scattering/light, Raman spectra; Spectrohemical analysis; Spectroscopy; Stark effect; X-ray spectra; Zeeman effect

absorption, of covalent solids, rel. to Jahn-Teller effect for single vacancy 0-44726

0-44726
absorption coefficient models, parameters reducing discrepancies between expt. and theory 0-58079 acoustic propagation data at sea from transient and continuous sources, analysis using fast Fourier transform algorithms 0-69720 alkali metal lamps, operation in strong mag. field 0-64192 analysis, computerized 0-41907 analyzer, af. signal-processing system using hybrid time-compression techniques 0-72856 authorized the payedox splitting. 0-62636

niques 0-72856
antiferrodielectric, Davydov splitting 0-62636
Auger, \(\alpha\) excited 0-68213
auroral, artificial, Starfish in northern conjugate region, first 5 seconds spectrogram 0-56821
autoionizing spectral lines, curves of growth 0-67176
band struct, calcs. 0-75478
in band struct, calcs. 0-75480
beam-foil, line identification of foil spectrum 0-38575
bearene, liquid, transient absorption spectrum and fluorescence of excimer 0-59506
charge transfer transitions, molecular orbital theory 0-54083

charge transfer transitions, molecular orbital theory 0-54083 computation from interferograms obtained on IT-69 Fourier spectrometer

0 - 52386continuous, optical reconstruction using Fourier spectroscopy method

0-45847

0-45847
and cross-spectra, estimation of two-dimensional field, fast digital of Fourier transform, techniques 0-41542
crystal, line broadening of impurity mol., microscopic theory 0-72340
crystal with dislocations, localized states 0-62154
crystal with interstitial atom, lattice vibrations, calc. 0-50835
crystals, use of magneto-optics 0-56518
cyclopentane, i.r. absorpt. bandwidth temp. depend. rel. to phase transitions, 80-300K 0-62680
discharge, pulsed in mag. field, time resolved spectra 0-61384
disordered systems, with a slowly varying random field, interband transitions 0-48046
dynamic hyperfine structure in the spectra of deformed nuclei in muonic

tions 0—48046 dynamic hyperfine structure in the spectra of deformed nuclei in muonic atoms 0—43035 Einstein coefficient, method of determination using spontaneous emission spectra of condensed media 0—43046 electron energy-loss due to impact on N₂, calc. 0—53045 electroreflectance, asymptotic convolution integral, interband dielectric function 0—59385 emission in v-u.v. region from noble gases excited by protons 0—74123 emission in v-u.v. region from noble gases excited by protons 0—74123 emergy intrinsic, space-time correlations of velocity and pressure, role of

emission in v-u.v. region from noble gases excited by protons 0-74123 energy intrinsic, space-time correlations of velocity and pressure, role of convection for homogeneous turbulence 0-43220 energy substruct, prod. using metal/semicond. plate system 0-69102 estimation using fast Fourier transform algorithm 0-72983 exciton, non-Hermitean splitting terms 0-79291 exciton levels, lower, behaviour in strong mag. field 0-50950 exciton phonon complexes and temp. depend. of fundamental absorpt. edge 0-69112 ferroelectric, i.r., free carriers effect 0-66020 ferroelectric mats, influence of free carriers on i.r. spectrum 0-41174 Fourier transform's spectral analysis using real-time computer 0-72855 frequency of extensional vibration of infinite plate strips, Kane-Mindlin eqns. applic. 0-38337 galactic radio radiation at 610 MHz, obs. 0-56966 high resolution, algorithmic assignment and anal. 0-71018 hydrogen-like broadening by electron collision 0-72347 hyperfine, photon echo applic. 0-42946 i.r. absorption in crystal with line defect, harmonic lattice, theory 0-79294 i.r. emission, rel. to airborne geological mapping 0-54221 ir. emission, rel. to airborne geological mapping 0-54221 ir. emission, and absorption measurements convergence. Corrections

0-79724

i.r. far region, absorption measurements convergence corrections
0-57631 information theory, 'non-classical', determ. of most probable line shape

0-57246 infrared, location of hydrogen bond stretching frequencies in crystals 0-67704

0-67704 interband transitions in disordered systems with a slowly varying random field 0-48046 laser, solid, amplification line broadening 0-73236 laser junction, compensated epitaxial GaAs, spontaneous emission and band tailing 0-52299 laser light scattered by plasma, effect of impurities 0-64702 laser sparks in air, He and Ar, energy distribution in spectrum 0-63611 lasers, semiconductor, emission, stimulated and spontaneous, densities of states 0-52300 light scattered fields meas, during diffusion 0-38546 line contours, parameter values calc. 0-73302 line intensity increase by arc compression in mag. field or heating 0-49141 liquid, simple, broadening of localized transitions, model 0-46921

0-49141
liquid, simple, broadening of localized transitions, model 0-46921
liquids and solutions, electronic vibrational absorption bands, broadening, role of fluctuation processes 0-61527
Lorentz lines, radiative transport in nonisothermal gases 0-78223
luminescence, meas. apparatus with digital storage 0-56620
lunar environment, enhancement of diagnostic features of ix. emission 0-79724
lunar samples operated collections from the Control of the contr

lunar samples, spectral reflectivity of samples 0-48544 molecular cryst., excitation spectrum of interacting polariton waves 0-59384

u-39.84 noise high intensity, analysis 0-60059 optical phonons and plasmons in superconductor, dispersion law 0-56520 phonon, calc. rel. to tunnelling meas. of superconducting quasi-particle density of states 0-71964 phonon, of mixed crystals in oscillation processes of II to VI semiconductor lasers 0-52314 photon-erby theory superradiant damping affects. 0. 42020

photon-echo theory, superradiant damping effects 0-42920

Spectra continued

planetary atmospheres, absorpt, spectra computation 0–51754 plasma, electron-broadening shift functions, exact calc. 0–50059 plasma, laser created, stimulated emission 0–50060 plasma decay, luminescence max. in spectral line 0–58339 plasma radiation, total and total line, 2000 to 60,000A for nitrogen, oxygen, argon plasmas 0–46712 polar cryst., optical phonons in presence of Landau quantization 0–75354 polymeric mats., high temp. ir. cell design 0–67184 power, magnetic field irregularities, radio intensity scintillations 0–59783 power of radar returns from underdense ionized turbulent gas, electron density decay 0–43347 production by concave transmission grating, theory 0–38543 radicals in p-irrad. single crystals, polarized absorpt. 0–62667 radio of E and SO galaxies 0–56967 radiowaves, v.l.f. and e.lp. atmospherics 0–51532 Raman, measurement by low temperature cell 0–60438 refractive index evaluation from interference-fringe transmission spectra 0–48000

0-48000

0-48000
relaxation, from experimental data 0-69598
scattered, of ion feature 0-61320
scattering of upper hybrid resonance of thermally ionized K-plasma column, Langmuir probes obs. 0-43285
seismic pseudo relative vel. for digitized acceleration records 0-62852
semiconductor, impure, optical transitions 0-48058
semiconductor, reflection, effective mass., carrier relaxation time 0-40759
semiconductors, abs. spectra, analogy to complex molecules 0-44822
semiconductors, two-photon transitions at saddle points, peaks in freq. depend. 0-44821
sine-wave signal components spectral analysis using complex exponent algorithms 0-69600
small splittings determ. by light echo technique 0-69103

small splittings determ, by light echo technique 0–69103 solid, multiphoton transition, phonon-assisted 0–47589 solids, line-shape representations and broad bands 0–76059

solids, two-photon interband transition rate in mag. field 0-44820 solutions, effect of van der Waals forces on spectrum 0-43453 solutions, highly diluted, absorpt, and fluoresc, yield 0-64929 solutions, multicomponent, failure of universal relationship between absorption and fluorescence spectra 0-50231 solvent cavity shape and size, effects on i.r. band shape and intensities 0-39796

0–39796
spin-orbit coupling, analysis and applications 0–59128
superconductor, optical phonons and plasmons, dispersion law 0–56520
turbulent energy, atoms. surface layer 0–45139
wironically coupled orbital triplet, band-shape 0–62635
waves, wind driven, at small fetches 0–72598
Al plasma produced by laser impact on solid, u.v. emission 0–39579
Ar plasma, shock produced, absolute line intensities and continuous background meas. 0–78092
Ce ternary peroxide complexes with carboxylic acids, abs. spectra 0–56535

Cu vapour discharge with hot hollow cathode, nature of radiation 0-50122

Mg. NaNO₃, illuminating-flare flame, visible spectra, strong emission features 0-64821 MgO₃ flame and arc lamp, use in colour and luminance temp. determ.

atoms

see also Atoms/excitation; Atoms/structure

3-level system, absorption spectrum in field of two intense nonmonochromatic beams 0-60911

matic beams 0-60911
g-factors, proton and electron, ratio meas. in atomic H 0-52969
absorption lines, quasars, rel. to radio polarization 0-66523
absorption meas. using graphite cell and spectrophotometer 0-57635
actinides, 5/3, electronic spectra various salts 0-58102
air high temp., at. lines and absorpt. coeff., obs. 0-46339
alkali metal, excited by electron impact, polarization of resonance line
radiation 0-64208
alkali metals, wavelengths of 4f-5g transitions meas. 0-77646
alkali-like, influence of electron core polarization on hyperfine struct.
0-67602
analysis, review 0-58005

analysis, review 0-58095

analysis, review 0—58095 are generator, powerful, type C-2, for atomic spectra 0—53233 As, vacuum u.v. emission, source 0—61070 aspiration system, variable flow, forced feed, for atomic absorption spectro-photometry 0—48212 for atom-absorption meas. using graphite cell, test model 0—57635 atomic absorption bibliography 0—46331 Auger electron spectrometer, preamplifier, design 0—46020 Balmer's series, construction from manuscripts 0—49763 Balmer & first negative emissions, excitation functions, prod. in p-N₂ collisions 0—39321 beam-foil spectroscopy applic. 0—39276 bibliography on analyses of optical spectra. ⁴²Mo-³⁷La, ⁷²Hf.⁸⁹Ac 0—39275 collective oscills. of electrons, statistical theory 0—74104

0-39275
collective oscills, of electrons, statistical theory 0-74104
collisional excitation, ionization and charge transfer assoc. 0-60909
complex, semiphenomenological Green's function of optical electron
0-39271
conference, optical pumping and at. line shape, Warsaw, 1968 0-52878
dielectronic recombination, time-dependent theory of overlapping resonances interacting with electron and photon continua 0-46345
double resonance spectroscopy in gas lasers 0-49037
effective operators and energy-dependent parameters, comparison
0-60912
electron energy levels determination, blue feet incomparison continual continua

electron energy levels determination, blur-free images spectrograph applic. 0-42953

0—42933 emission and absorption in strong field and recoil effect 0—74112 emission and absorption spectra, changes in a strong field 0—46346 emission lines in spectrographic are burning in inert gas atmosphere 0—46378

energy-dependent parameters and effective operators, comparison 0-60912

excited levels, orienting, optical pumping 0-46410

excited states, electronic impact excitation technique 0–52933 excited states, photon excitation 0–52934 excited states mean lifetimes absolute meas. using correlated photons in cascade 0–60941 FORTRAN IV program for line-by-line calc. 0–60901

Spectra continued atoms continued

fine structure constant, Sommerfeld, experimental meas, methods and numerical value 0-52873

fluorescence, coherent reson., excited by short light pulses 0-38485 fluorescence, hot wire loop atomiser, for analysis of volatile metals 0-73355

no-73355
heavy, vacuum u.v. emission, source 0–61070
i.r. laser transitions, spectroscopic obs. 0–67601
identification, using coaxial plasma sources 0–42945
inert gas atomic transitions induced in two-component mixtures by voltage
pulses 0–60922
inert gas mixtures, excitation mechanisms in elec. arc 0–49780
intensification in plasma of an impulse discharge 0–49788
ion beams, excited, as spectroscopic sources 0–52876
ionisation, ultraviolet inner shell transitions, wavelength overlap 0–58084
ionized emission lines due to transitions from singly and doubly excited
levels in Na, Mg, Al, Si, P, S and Cl 0–67637
isoelectronic series O I to Fe XIX, wavelengths and oscillator strengths of
2pt-2p13s transition 0–42943
isotope effects review 0–55263
isotope shifts in light elements 0–52885
K₃/K_B/I (ransition probabilities in elements of medium and high atomic
number 0–46348
K-shell fluorescence yield for low atomic number elements 0–70757
Lamb shift, confirmation of new theoretical value 0–42949

K-shell fluorescence yield for low atomic number elements 0-70757 Lamb shift, confirmation of new theoretical value 0-42949 Lamb shift, theory 0-52875 Lamb shift in n=2 state of C54 0-77655 Lamb shift obs. in H beam 0-64289 Lamb shift energy, integral representation and variational estimates of upper and lower limits 0-64194 Lande interval rule, Z-expansion corrections 0-60906 line broadening by charged particles, review 0-55228 line broadening by foreign gases, classical path approximation 0-39261 line identification method using Doppler shift in coaxial plasma source 0-42939 line intensity increase in decage discharge with applied prohomography.

0-42939 line intensity increase in d.c. arc discharge with applied nonhomogeneous magnetic field 0-48215 line radiation, polarization in atomic collision processes 0-55227 line shape, effect of transitions induced by non-adiabatic collisions 0-39280 line shifts by electronic collisions, semi-classical calc. 0-52961 line strength, transitions in multi-ionized case, perturbation theory calc. 0-39293 line shape dispension and observation Fourier coefficients.

Lorentzian line shpae, dispersion and absorption Fourier coeffs. relation

0 - 52884magnetic scanning method for meas. of broadening and displacement 0-42940magnetic

magnetron discharge, pulsed gas 0–61398 multi-electron atom, model Hamiltonian charact. wave-functions 0–74105

multiphoton processes, Green's function of optical electron 0-39271 muonic, Lyman and Balmer series, static and dynamic h.f.s. interactions 0-52996

0—52996
muonic, in lead region, nuclear polarization energy correction 0—70829
Na I, mean lifetime measurements and spectra for isoelectronic sequences using beam-foil techniques 0—64213
non-hydrogenic atoms, continuous absorpt. coeffs., extension of earlier lists 0—77638
non-hydrogenic atoms, continuous absorpt. coeffs., extension of earlier lists 0—39282
optical double reson, line shape in time resolved meas. 0—52891
optical resonance in vapour excited by modulated light beam 0—52890
Paschen-Back effect for muonium in quartz and corundum 0—49826
photon echo applied to hyperfine spectroscopy 0—42946
photon echoes, mixing collisions effects 0—39270
polarization model of Waller derived from perturbation theory 0—70820
positivo column of d.c. discharge broadening, shifts in spectrum 0—42970
positronium, 2¹S₁, existence in matter, hyperfine structure level shift 0—74092
positronium emission of photons in excited state transitions 0—42941

positronium emission of photons in excited state transitions 0-42941 quantized radiation-field-N-molecule Hamiltonian, approx. solns. 0 - 39336

positronium emission of photons in excited state transitions 0–42941 quantized radiation-field-N-molecule Hamiltonian, approx. solns. 0–39336
r.f., ground and excited states, optical methods 0–52872
r.f. study of free at. ions 0–49762
radiation due to discrete level transition, oscillator strength calc. of upper spectral series 0–58091
radiation from collision-damped two-level system 0–70753
radiative electron capture, damping in optical continuum 0–77648
radiative lifetimes in vac. u.v., nanosec., meas. with multichannel time interval recording system 0–52870
radiative transition probabilities for vacancies in M sub-shells 0–58094
rare earth, analysis 0–58095
rare gases, electric light gain, transport phenomenon 0–74680
Rayleigh and combinational scattering in field of intense wave 0–39272
resonance broadening, density depend. 0–70751
resonance light absorption, errors in meas. atomic concentration 0–64190
resonance radiation, self-reversal by re-emission 0–42954
resonance radiation apture, in gas 0–46827
resonance radiation apture, in gas 0–46827
resonance radiation processes and gain coefficient 0–67622
Rydberg series, perturbed, graphic analysis 0–70754
secondary-standard wavelengths from Th 1 energy levels 0–42982
shift and broadening by collision with foreign gas atoms 0–74109
shock wave, collisionless magnetostatic, turbulence level, Balmer Hβ line,
Stark broadening 0–64689
spectral distributions of elements in arcs 0–46777
spectral line formation in Wolf-Rayet envelopes, escape probability method 0–59707
spectral series upper terms, oscillator strength calc. 0–58091
spontaneous emission by syst. of identical atoms 0–70758
stark broadening, isolated ion lines in plasma 0–60913
time-resolved spectra in spark produced plasma 0–53171
transition probability calc., review of methods 0–74113
vacuum, u.v. from microwave discharges in inert gases, report 0–74115
vacuum u.v. lines, continuum-continuum emission struct. in low energy wings 0–52892
wavelength measurement using an Ebert mounting 0–46336
wings of Sta

Spectra continued atoms continued

X-ray emission spectra in K, L, and M regions, review of elements 0-60907

OI $3s^3S_1-3p^3P_{021}$ line complex intensities for different excitation conditions 0-55226

Ag I, hyperfine structure of 4d95s² $^2D_{3/2}\text{-}4d^{10}5p^2$ $P_{1/2}$ $\lambda{=}19372$ Å transition 0–70761

Ag I, intermediate coupling calc. of 4d°5s6s level 0–46375
Al, using grazing-incidence spectrometer 0–52912
Al atomic transition tables 0–39284
Al foil particles, ejection and electronic excitation by heavy-ion impact 0–60905

0-0905
Al II, mean lifetime measurements and spectra for isoelectronic sequences using beam-foil techniques 0-64213
Al III, mean lifetime measurements and spectra for isoelectronic sequences using beam foil techniques 0-64213
AmO₂²⁺, electronic spectra various salts 0-58102
Ar, absorption in vacuum u.v. region 0-67610
Ar, bich pressure pulsed discharge continuous spectrum absorption of

Ar, high pressure pulsed discharge, continuous spectrum absorption of radiation 0-61380
Ar, positive column of d.c. discharge broadening shifts in spectrum 0-42970

O-42970

Ar, in supersonic plasma jet, level populations 0-46727

Ar, vacuum u.v. absorption, obs. 0-60915

Ar ¹P₂ metastable, collision-induced emission 0-67639

Ar excitation temperature functions of some spectrum lines 0-42965

Ar gas, compressed, stimulated backscatt. 0-42955

Ar I, equilibrium in arc plasma 0-78063

Ar I, radiative transition probabilities between 3p⁵4p and 3p⁵4s configurations 0-67611

Ar I, Stark consts. and oscillator forces for Thomas-Fermi-Dirac pot. 0-70762

Ar I and II, line profile analysis, Fabry-Perot interferometer 0-64198
Ar II, meas. of Stark broadening parameters 0-49770
Ar II, new lines in 2050-1870 Å region 0-49769
Ar II, transition probabilities 0-70763
Ar II new lines in far and vacuum ultraviolet region, 1870-1700 Å 0-42956

0-42956
Ar transition tables 0-39284
Ar XVII, helium-like, relativistic mag. dipole emission 0-77649
Ar XVII, mag.-dipole decay of 2³S₁ state 0-67612
ArII and III levels, radiative lifetime meas by beam-foil technique 0-52893

0-52893
Ar+He⁺-Ar⁺, 4610 and 4765 Å lines of Ar⁺, energy depend. 0-39294
Au I, line profile analysis, Fabry-Perot interferometer 0-64198
B I extra-photographic infra red obs. 0-77651
B I to IV, electronic transitions 450-5000 Å, beam-foil spectra 0-67613
B II, spectrum obs., 33 new lines identified 0-77652
B(2s2p²¹D), isotopic shift and fine structure 0-28855
Ba, even A, 685d Zeeman substates r.f. transitions, obs. 0-52895
Ba, i.r. laser lines 0-58097
Ba I, abs., in autoioniz. region from 2382 to 1700 Å 0-77653
Ba I and Ba II, critically evaluated transition probabilities 0-46355
Be foil particles, ejection and electronic excitation by heavy-ion impact 0-60905 0-60905

Be I isoelectronic sequence, level lifetimes 0–55229 Bi hyperfine structure, interferometric meas. 0–46357

Bi I mixed multipole lines, interference effects in the Zeeman pattern 0-42957

0-42957
Br, h.f.s., 79.81Br polarization 0-43013
C, ionized, oscillator forces of u.v. transitions 0-42959
C ³P.³D isoelectronic sequence, transition probabilities 0-77654
C foil particles, ejection and electronic excitation by heavy-ion impact 0-60905
C in Venusian upper atmosphere 0-54443
C X-ray emission spectrum used to study bonds of organic mols. 0-61141
C ⁵+ Lamb shift in p-2 attacks.

C³·, Lamb shift in n=2 state, meas. 0–77655 CI oscillator strengths and mean square radii calc. 0–42930 CO₂·N₂, 90%-10%, plasma, total radiative intensity calcs., 1×10⁵–2×10⁵ °K 0–43288

Co₂, plasma, total radiative intensity calcs., $1 \times 10^{3} - 2 \times 10^{5}$ °K 0-43288 Ca, g_{g} values of metastable ${}^{3}P_{2}$ and ${}^{4}D_{2}$ levels 0-52896 Ca 15 MeV 0⁴⁺ bombardment, K X-ray spectra obs. 0-77693 Ca II oscillator strengths and mean square radii calc. 0-42930 Ca transition tables 0-39284

 Ca^+ impact excitation of 3d ^2D 4p ^2P levels, polarization of emitted radiation $0{-}60917$

tion 0-60917
Cd, in solid AT, Kr, Xe, absorpt. rel. to at. interactions, obs. 0-49783
Cd, optical ionization-excitation by electron impact 0-60966
Cd,5³P₁ mag, dipole transition induced by elec. field, obs. 0-52898
Cd 5³P₁, optical double reson. line shape in time resolved meas., obs. 0-52891
Cd 6³S₁, state, stepwise excitation, zero field level-crossing technique 0-52944
Cd absorption resonant line in flame. 0, 52011

Cd absorption resonant line in flame 0-52911 Cd II, cw laser oscillations in hollow cathode C

Cd II, cw laser oscillations in hollow cathode 0-64199 Cd vapour, triple radio-optical reson 0-43002 Cl. Stark line broadening 0-67614 Cl., Stark broadening parameters 0-60916 Cl K α and K β emission spectra in free molecules 0-52899 Cl transition tables 0-39284 Co I optical determ. of hyperfine splitting 0-49773 Co II, oscillator strengths of elec. dipole and quadrupole transitions 0-67615

Co IX identification and classification of 3p63d-3p53d4s transition 0-39279

0–39279
Cr I absolute gf-values, shock tube meas, extended to higher excitation potentials 0–52900
Cr³⁺ absorption spectrum in ruby, effect of colour centres 0–55899
Cs, absorpt, inert gas press, effects, obs. 0–52903
Cs, hyperfine sublevels, population inversion, optical pumping, maser construction 0–52951
Cs, laser field Stark effect, calc. 0–39288
Cs, optically pumped, r.f. hyperfine transitions, light beam modulation obs. 0–52901
Cs. profiles of Xe broadened atomic lines and satellite bands 0–74106

Cs, profiles of Xe broadened atomic lines and satellite bands 0-74106

Cs absorpt, bands observed between two components of 1st and 2nd doublets perturbed by rare gases 0-42963

```
Spectra continued
  atoms continued
```

Cs at. ion, r.f. study 0-49762
Cs 1, g, factors in np ²P_{3/2} series 0-70765
Cs I, wavelengths of 6s-5d and 5d-nf transitions, meas. with Czerny-Turner spectrograph 0-55231
Cs I lines shift due to const. elec. and mag. fields acting simultaneously 0-49774

 Cs^+ collisions with He and Ar, 3000 to 6000 Å, 4 to 80 keV, obs. 0-61001

Cs+ collisions with inert gases, 12 keV to threshold, resonance lines obs. 0-61003

0-5003

33 Cs, optically oriented, reson. induced by modulated light, obs. 0-52941

Cs+He, excitation functions for 3 resonance lines, threshold behaviour obs. 0-61002

coss. 0-51002
Cu, in a.c. arc discharge, curves of spectral lines 0-39273
Cu classification of new multiplets ig extreme u.v. 0-49764
Cu II, 3d⁹ 5g configuration, meas. of hyperfine struct. 0-39286
Cu line profiles, from low temp, arc, interferometric anal. 0-49775
Cu XI identification and classification of 3p⁶3d-3p⁵3d4s transition 0-39279

0—39279
Dy I and Dy II temperature classification 0—77656
Dy II, Zeeman structures at 49,430 Oe of 129 transitions 0—67616
²⁵³Es, emission, hyperfine structure, nuclear spin, nuclear mag. dipole moment and energy levels 0—74107
Eu, expl. identification of a missing term and configuration interaction explanation 0—46360

explanation 0—46.500 Eu I, level crossing and optical double reson. obs. 0—52916 Eu vapour, ir. laser lines 0—49778 F, beam-foil, 1050-4000 Å mean lives of excited levels 0—77707 F I. visible laser action 0—55232 F VII 22²S_{1/2}-2p²P_{3/2,1/2} doublet relative intensities and decay times 0—70766

0–70766 Fe, Kα satellite-type lines from 2p→1s transitions with 1s, 2s vacancies, wavelength calc. 0–77657 Fe emission lines in Seyfert galaxies 0–76551 Fe spark spectrum (10-18 Å), line list 0–49776 Fe+, dipole transitions 36^44 p→ $3d^2$ 0–67618 Fe+, dipole transitions 36^44 p→ $3d^4$ s 0–55233 Fe²+ ions, tetrahedrally coordinated absorption spectrum in ZnS crystals with stacking faults 0–49777 FeXVII, intensities of 2p-3d, 2p-3s lines in a rarefied plasma 0–42964 Gd II, arc spectrum, multiplets and even levels obs. 0–39285 Gd II energy levels of three newly identified configurations 0–46362 H- free-free absorption coeff., calc., astrophysical appls. 0–51617 H, Balmer series lines, beam foil excitation, periodic modulation 0–52975 H, beam-foil excited, Lamb shift with circularly polarized r.f. field 0–61012

0-61012 H, fine struct, interval $2^2S_{1/2}$ - $2^2P_{3/2}$, energy separation meas. 0-39322 H, fine structure constant, Sommerfeld, meas, by level crossing 0-52968 H, h.f.s., H maser investigations 0-52971 H, h.f.s. in ground state 0-52970 H, in flame at atmos. press., e.s.r. study of kinetics 0-39320 H, Lamb shift effects on interference of excited states 0-64267 H, Ly α -radiation generation from microwave powered discharge 0-64266

H, microwave recombination lines, analysis method 0–64264 H, prod. using gas discharge lamp 0–60441 H, recombination continuum rel. to lowering of ionization energy 0–71201

0 –71201
H Balmer series in afterglow of H_2O vapor, excitation mechanism spectroscopic study 0-56813
H beam, obsrvation of Lamb shift 0-64289
H ground states interacting with nonresonant r.f. fields, modified Zeeman hyperfine spectra 0-39318
H hyperfine spectra 0-39318
H hyperfine splittings, second order calcs. 0-70807
H in 2s, 2p states, calc. of optical polarizability 0-43021
H $Ly-\alpha$, He broadened, continuum-continuum emission struct. in low energy wing 0-52892
H-, stripping inert gases, 5-40 keV, Lyman α -line 0-52981
H $_{\alpha}$ and H $_{\gamma}$ lines, Stark broadening calculations 0-74169
H $_{\gamma}$ Balmer line, Stark splitting in fields <20 kV/cm 0-67665
H $_{2}O$ vapor atomic emission mechanism in afterglow, spectroscopic study 0-56813

H₂O vapor atomic emission mechanism in afterglow, spectroscopic study 0–56813

Hz zero-field quantum beats subsequent to beam-foil excitation 0–64265

Hβ zero-field quantum beats subsequent to beam-foil excitation 0–64265

He-like ions, dielectronic recombination, spectroscopic obs. 0–78163

He, 33P-23Ps, zero-field quantum beats subsequent to beam-foil excitation 0–64265

He, 4026 Å line and forbidden components, Stark profiles 0–55258

He, absorption, occupation inversion 0–77719

He, tondening of 5876 Å line in shock wave plasma, in He-H gas mixture 0–49815

He, continuous spectra, for medium pressure plasma diagnostics 0–43313

0-49815

He, continuous spectra, for medium pressure plasma diagnostics 0-43313

He, high resolution electron impact techniques 0-55259

He, Hopfield continuum, prod. using gas discharge lamp 0-60441

He, ion impact excited, polarization of light of de-excitation 0-77720

He, ionized, high resolution study of line complex emitted from cooled hollow cathode 0-43028

He, isoelectronic sequence, 2p² ³P and 2p³p¹P states eigenvalues and radiative lifetimes, wavelength predictions 0-42950

He, photoabsorpt. cross section, polarization effects 0-74175

He, Stark profiles of 4471 Å line and forbidden components, calc. 0-39325

die, in supersonic plasma iet. level populations 0-46727

0-39325
die, in supersonic plasma jet, level populations 0-46727
He, vacuum u.v. lines, continuum-continuum emission struct. in low energy wings 0-52892
He 2³S excitation by He⁺ impact 0-61034
He excitation temperature functions of some spectrum lines 0-42965
He gas, compressed, stimulated backscatt. 0-42955
He I, polarization model for excited states 0-70820
He I ir. laser lines, isotope shift 0-39323
He I λ4471, λ4470, laboratory plasma obs. rel. to astrophysical spectra 0-61018
He II line λ=4686 Å, broadening in plasma 0-64293

He II line λ =4686 Å, broadening in plasma 0-64293 He ion beams, excited by Au single cryst., channelling influence on emission spectra 0-78798

He isoelectronic sequences, 1s21S-1s np ¹P transitions, matrix elements 0-46340

He plasma, emissivity, at 20000-50000° and 1-100 atm. 0-42973

Spectra continued atoms continued

He plasma, turbulent heating, satellites 0-53173

He+-Ar collision excitation He I and Ar I spectra 0-55260

³He, ¹D levels, orienting, optical pumping 0-46410

³He, fine and hyperfine structure meas., level-crossing technique 0-52984 ³He, ground state modulated resons., obs. 0–52989 ³He⁺, h.f.s. in storage collision technique 0–52983 ³He II n=4–5 (10124 Å) and n=4–6 (6560 Å) transitions, obs. 0–61020

He II n=4-5 (10124 Å) and n=4-6 (6560 Å) transitions, obs. 0-61020 ⁴He, fine and hyperfine structure meas, level-crossing technique 0-52984 ⁴He II n=4-5 (10124 Å) and n=4-6 (6560 Å) transitions, obs. 0-61020 Hf I, isotope shift effects on spectrum obs., determ. of ¹⁷⁴Hf nuclear quadrupole moment 0-46363

pole moment 0-46363

Hg, 2537 Å, Ar, He broadened, intensity distrib. and shift calc. 0-52907

Hg, generalized oscillator strengths for 6 S₀-6 P₁ transition 0-60954

Hg, in solid Ar, Kr, Xe, absorpt. rel. to at. interactions, obs. 0-49783

Hg, isotopic shift of 1.5295 P₂ line obs. 0-42966

Hg, optical ionization-excitation by electron impact 0-60966

Hg 2537 Å reson. line, Kr press. effects, obs. 0-52908

Hg I, absorption cross section and oscillator strength of autoionizing line
1126.6 Å 0-67619

Hg in solid rare gases, ³P₁-S₀ transition 0-46364

Hg resonance radiation trapping and quenching 0-67642

198 Hg 1850 Å line mag. depolarization, anomalous dispersion, Hanle effect obs. 0-52906

199 Hg, reson. fluoresc. Larmor modulation, foreign gas effects 0-52905

obs. 0–52906

"99 Hg, reson. fluoresc. Larmor modulation, foreign gas effects 0–52905

"90 Hg, mag. reson. lines optically induced shifts, obs. 0–52960

Ho, emission, Fourier spectroscopy using 106 samples 0–70086

"1231, 1271, cascade transitions, y-y ang. correl. perturbation obs. following formation of I by e capture in Xe 0–46366

In, in solid Ar, Kr, Xe, absorpt. rel. to at. interactions, obs. 0–49783

In I, hyperfine struct. of 5d²D_{5/2} state, level crossing investigations 0–42969

0-42969
K+Ne collision, emission, excitation functions, absolute meas. 0-74156
K, laser field Stark effect, calc. 0-39288
K, mean lives of excited atomic states of K I, II and III 0-67648
K, minima of generalized oscillator strengths for continuum transitions 0-67627

0-67627
K II lines prod. in collisions between K_{II} and He atoms, excitation functions absolute meas. 0-39297
K oscillator strengths of high terms of principal series 0-49780
K transition tables 0-39284
K vapour, angular distrib. changes of light intensity on laser-beam passage 0-6955 K vapour, emission, fine struct., ruby laser excitation 0-74118 K+ collisions with inert gases, $12~{\rm keV}$ to threshold, resonance lines obs.

K⁺ collisions with inert gases, 12 keV to threshold, resonance lines obs. 0-61003

K. II (3p²4p) life-times of nine of the ten levels, meas, using beam-foil to technique, comparison to ArI levels 0-64222

Kr, absorpt. line displacements due to perturbation by rare gases 0-49781

Kr 86 i.r. transitions, wavelength meas, and calibration of Kr 86 electrodeless lamp 0-49137

Kr excitation temperature functions of some spectrum lines 0-42965

Kr lines, excitation temp, functions 0-46368

⁸⁰Kr I wavelengths meas, using electrodeless lamp 0-74119

La I, appl. of nuclear quadrupole interaction for spd configurations 0-70769

Mn I, hyperfine splitting, meas, level-crossing technique 0–52915 Mn I, level crossing and optical double reson. obs. 0–52916 Mn II, analysis, apparent discrepancies between theoretical and experimental results 0–58099

Mo levels population in hollow cathode 0-64202
Mo VI, spectrum 6800-2200 Å in Penning type arc discharge, 4 new levels determ. 0-42974
Mo VII, vacuum spark, u.v., meas. 0-55238
Mo VIII, term analysis of the 4p-4d and 4p-5s transitions 0-60937
N, in He-N mixture, hollow cathode discharge, effect of mag. field

N, in He-N mixture, nonlow cannote discharge, effect of flag. field 0-43353

N II-N IV, excited levels radiative lifetimes 0-60925

N II, dense plasma, profiles of 9 lines, Stark broadening 0-39289

N II, meas. of Stark broadening parameters, by laser interferometry 0-60902

N III lines, from cascade arc, partially double ioniz. 0-39637 N V, 25²S_{1/2}-2p²P_{3/2,1/2} doublet relative intensities and decay times 0 70766 NII emission due to N_2 simultaneous ionization and dissoc. by 150 eV to 4 keV electrons 0-64203 Na, 2 P fine structure transitions in collisions with He 0-61006

Na, ² F line structure transitions in Consistons with the O-61000 Na, ²F_{3/2} level crossing, obs. 0.–52889 Na, ²F_{3/2} state, Stark eff. investigation of hyperfine struct. 0.–39291 Na, in solid Ar, Kr, Xe, absorpt. rel. to at. interactions, obs. 0.–49783 Na, mean lives of excited atomic states of Na I, II and III 0.–67648 Na, minima of generalized oscillator strengths for continuum transitions 0.–67627

Na, optically pumped, D₁ absorpt., dispersion lines perturbation by He, Ne, obs. 0-52918
Na, radiant energy of Mg-NaNO₃ pyrotechnic flare, 3800 to 7400 Å
0-67626

Na atomic transition tables 0-39284Na D-line in afterglow of H_2O vapor, excitation mechanism spectroscopic study 0-56813

Spectra continued atoms continued

Na I $\lambda 5889$ line, pressure broadening by high temp. neutral helium 0-52917

Na light emission meas, at simulated meteor conditions 0-49785

Na light emission meas, at simulated meteor conditions 0–49785

Na oriented vapour, undergoing double quantum transitions, radiofreq. coherences 0–74120

Na vapour, atomic absorption method for determining pressure 0–67621

Na vapour, atomic absorption method for determining pressure 0–67621

Na vapour, atomic absorption method for determining pressure 0–67621

Na vapour, atomic absorption method for determining pressure 0–67621

Na vapour, atomic absorption method for determining pressure 0–67621

Na vapour, atomic absorption method for determining pressure 0–67621

Nb VI, vacuum spark, u.v., meas. 0–55238

Nb VII, term analysis of the 4p-4d and 4p-5s transitions 0–60937

Nd, i.r. spectrum using SISAM spectrometer, Zeeman structure of lines 0–77664

Nd, isotope shift const., screening of 5d electron effect 0–77663

Nd, isotope shift const., screening of 5d electron effect 0-77663 Nd³* ground state absorption rel. to laser glass, excited state absorption 0-38505

Ne, $2p^53p-2p^53s$ transition, line strengths and transition probabilities 0-55235

Ne, contour of 1.15μ line, meas. under various discharge conditions 0-42978 Ne, positive column of d.c. discharge broadening shifts in spectrum 0-42970

Ne, pressure broadening of 6074.3 Å line using Zeeman scanning 0-70771

Ne, radiation lifetime of 3p₄ state, Hanle effect obs. 0–42977 Ne atomic transitions, new lines obs. in discharges of Ne SF₆ mixtures 0–52920

0-52920

Ne excitation temperature functions of some spectrum lines 0-42965

Ne I, 2p³3p-2p³3s transitions, probability and lifetimes in simple spectra 0-70768

Ne I, 2p³3s-2p³3p transitions, Stark broadening, with weak electrical field depend. 0-46373

Ne I, transition probabilities for prominent red lines 0-64204

Ne I, transition probabilities, absolute of 35 visible and near-i.r. lines 0-64205

0-64205
Ne II, line strengths and radiative lifetimes 0-67628
Ne IV forbidden lines in high excitation gaseous nebulae 0-57008
Ne resonance radiation processes and gain coefficient 0-67622
Ne VII, collisional excitation rate coeffs. for vacuum u.v. lines, obs. 0 - 60961

Ne vacuum u.v. excitation by electron collisions 0-60962
Ni classification of new multiplets in extreme u.v. 0-49764
Ni I, absorption line profiles of multiplets in near u.v. 0-67629
Ni X identification and classification of 3p⁶3d 3p⁵3d4s transition

Ni X identification and classification of 3p63d 3p53d4s transition 0-39279
Np4+, dynamically induced forbidden elec.-dipole transitions in ThO2 0-54101
Np4+, electronic spectra various salts 0-58102
O, expl. transition probabilities for some lines of astrophysical interest 0-52922
O, u.v., 12s ²2p³ 3s ³50 level, radiative lifetime meas., beam-foil technique, oscillator strength calc. 0-74122
O1, broadening and shift or i.r. lines by Stark effect 0-77666
O1 emission, from electron impact on CO, O2 NO, H2O, decay lifetimes 0-64444

0 II emission, from electron impact on CO, O₂ NO, H₂O, decay lifetimes 0-64444

O II lines, spectral intensification in plasma on impulse discharges 0-49788

Oir. emission, electronic, pressure depend. 0–58085 Oiv, beam foil, ionised beam lifetimes for transitions 1200-5000 Å 0–77665

0-77665
O(1D) excitation, metastable helium influence 0-56814
O(1 304 Å resonance radiation, production rate in dayglow, excitation and radiative transport theory 0-56810
OI 6300 Å line nightglow, width variations during mag. storm 0-56811
OI attroral 1304 Å resonance radiation, excitation rate, radiative transport calculations 0-56820
OI forbidden airglow 5577 Å line emission, diurnal variation at 22 IGY stations 0-56809
OI oscillator strengths and mean square radii calc. 0-42930
O(II and III) ions, radiative lifetimes of some energy levels 0-52924
O(2¹D₂) quenching data in various species, use of OH radical as spectro scopic marker 0-74121
Os⁴+ in K₂PtCl₆, Cs₂ZrCl₆ single crysts., vibronic analysis, 4.2°K
0-41210
Patomic transition tables 0-39284

P atomic transition tables 0–39284 Pb $(6p)^2$ 1D_2 level, G_j factor meas, and hyperfine structure of 1D_2 in 207 Pb 0-46374

0-46374

Pb vapour in h.f. electrodeless lamps 0-49155

Pbl vapour in h.f. electrodeless lamps 0-67630

Pu²+, electronic spectra various salts 0-58102

Rb, hyperfine sublevels, population inversion, optical pumping, maser construction 0-52951

Rb D₁ line hyperfine spectrum temp. depend. 0-67632

Rb ground states interacting with nonresonant r.f. field, modified Zeeman hyperfine spectra 0-39318

Rb II, resonance lines 0-70773

Rb yapour, powerful stimulated radiation, laser excitation, ediustable frequency

Rb vapour, powerful stimulated radiation, laser excitation, adjustable freq. 0-77660

Rb+ collisions with inert gases, 12 keV to threshold, resonance lines obs. 0-61003

8°Rb, optically pumped, ground state r.f. Zeeman transitions, obs. 0-52954
Ru⁴⁺ in K₂PtCl₆, Cs₂ZrCl₆ single crysts., vibronic analysis, 4.2°K

0-32934 Ru4+ in K₂PtCl₆, Cs₂ZrCl₆ single crysts., vibronic analysis, 4.2°K 0-41210 S, 4f-3d transition in K-mesonic atom, meas. using K-mesonic interac-

tions 0-64307 S transition tables 0-39284

S transition tables 0-39284
S XV, mag.-dopole decay of 2³S, state 0-67612
Se isoelectronic sequence, oscillator strengths of resonance lines 0-49789
Si, using grazing-incidence spectrometer 0-52912
Si atomic transition tables 0-39284
Si I and Si II lines, relative transition probabilities 0-70772
Si I oscillator strengths and mean square radii calc. 0-42930
Si II, relative f-values 0-67624

Spectra continued atoms continued

atoms continued

Si II broadening parameters meas. 0–60929

Si XIII, mag.-dipole decay of 2³S, state 0–67612

Sm I, level crossing and optical double reson. obs. 0–52916

Sm II, 47⁸ 59₁₇° term identification 0–52926

Sm vapour, i.r. laser lines 0–49778

Sn, isotopic shifts in u.v. 0–60930

Sr, absorption spectrum in vacuum u.v. 0–58101

Sr, gy values of ¹D, level 0–52896

Sr 5³P₁ optical double reson. line shape in time resolved meas. obs. 0–52891

Sr, II oscillator strengths and mean square radii calc. 0–42930

Sr 5°P₁ optical double reson. line shape in time resolved meas. obs. 0–52891
Sr III oscillator strengths and mean square radii calc. 0–42930
Sr III, resonance lines 0–70773
Ta, wavelengths and transitions, table 0–46337
Te isoelectronic sequence, oscillator strengths of resonance lines 0–49789
Th, emission, Fourier spectroscopy using 106 samples 0–70086
Th I energy levels computation and proposed secondary-standard wavelengths 0–42982
Ti-He atomic collision, possible complex obs. by level- crossing spectroscopy 0–77705
TI atom in 7°S_{1/2} state, effect of collisions with foreign atoms on polarized emission 0–42983
Tm 1, level crossing and optical double reson. obs. 0–52916
Tm 1, optical double resonance expts., g, values determ. 0–39287
Tm 1, oscillator strengths of lines in 6000-2450 Å region 0–42944
Tm III, 848 low-excitation lines and their analysis 0–42984
Tm III, serengy levels and Slater parameters, obs. 0–60931
Tm vapour, i.r. laser lines 0–49778
U³⁺, electronic spectra various salts 0–58102
UF₆, i.r., obs. of v_e band, gas determination 0–67633
V, (VIII), 37'd spectrum 0–58103
V, (VIII), 37'd spectrum 0–58103
V II, oscillator strengths of elec. dipole transitions 0–67634
Va 15 MeV 0⁴⁺ bombardment, K X-ray spectra obs. 0–77693
Xe, absorpt, 1,250-1300 Å, new bond obs. 0–39292
Xe, absorpt, 1,250-1300 Å, new bond obs. 0–39292
Xe, absorpt, line displacements due to perturbation by rare gases 0–49781
Xe, Lisotope vol. shifts 0–52927
Xe excitation temperature functions of some spectrum lines 0–42965
Xe I, isotope vol. shifts 0–52927

Xe, laser lines, isotope shifts 0–49779
Xe excitation temperature functions of some spectrum lines 0–42965
Xe I, isotope vol. shifts 0–52927
Xe lifetimes of certain levels meas. 0–42985
Xe plasma effects of pressure, input energy, and magnetic field on spectral properties 0–55473
Xe plasma ionization behind shock wave front, i.r. diagnostics 0–53189

136 Xe, interferometric wavelength obs. 3949-11088 Å and 12626-35079 Å
0–70746

136 Xe second spectrum, wavelength interferometry 0–60933
Y IV, resonance lines 300 to 4000 Å, obs. 0–60934
Y2· 4/136 configuration 0–42971
Yb I, oscillator strengths of spectral lines in 6000-2450 Å region 0–42944
Yb vapour, i.r. laser lines 0–49778
Zn, observation of Zn II, Zn III and other unkown spectral lines, 2300a-3000a 0–55237
Zn, optical ionization-excitation by electron impact 0–60966
Zn classification of new multiplets in extreme u.v. 0–49764
Zn I, 4p² configuration, autoionization probability for ¹S₀ and ¹D₂ levels 0–60935
Zn II, cw laser oscillations in hollow cathode 0–64199

0-00952
Zn II, cw laser oscillations in hollow cathode 0-64199
Zn II, intermediate coupling calc. of 3d⁹4s5s level 0-46375
Zn II, new vacuum u.v. wavelengths and revised energy levels 0-46376
Zr V, vacuum spark, u.v., meas. 0-55238
Zr VI, term analysis of the 4p-4d and 4p-5s transitions 0-60937

inorganic liquids and solutions condensed media, Einstein coeff. spectra from observed spectra 0—43454 dye solutions, absorpt. coeff., refractive index, calc. 0—39791 electrolytes, luminescent, absorpt. and excitation spectra 0—43455 far i.r. spectroscopy using interferometers 0—49147 halogen acids with CN⁻, SCN⁻ and SeCN⁻ admixtures, obs. and excitation spectra 0—68106

in absorption bands, broadening due to fluctuation processes 0-43047 induced i.r. absorption of symmetric triatomic mols. in soln. 0-74757 luminescent soln., Stepanov's relation for abs. and emission spectra

0—64930 metal carbonyls, M₂(CO)₁₀ type, band polarizations 0—77765 polarization determ, in nematic liq. cryst. solvent 0—77765 salts, aqueous solutions, continuous Rayleigh spectrum 0—46446 silver halide solutions, effect of base cations 0—64927 solutions, Stepanov's relation for abs. and emission spectra 0—64930 water, adsorbed on TiO₂ 0—58605 water, adsorbed on TiO₂ 0—58605 water, adsorbed on TiO₂ 0—78605 water, adsorbed on TiO₃ 0—78605 water, dispersion and abs. in i.r. and r.f. spectra 0—43458 water, i.r., abs., at 2130 cm⁻¹, assignment 0—50230 Ag-activated phosphor containing, absorpt. and emission 0—39813 Ag-astivated phosphor containing, absorpt. and emission 0—39813 Ar:Xe, liquid, vac. u.v., Wannier type exciton states 0—46916 Ar:Ne, far-i.r. absorption coefficient, 40-500 μ 0—55616 halide complexes with 4,4'-dipridyl. 0—66035 BrO₁ aqueous ions in solution, electronic spectra, assignment of bands 0—50229

CO is. absorption coefficient, 40-500 u 0-55616

CO i.r. absorption coefficient, $40\text{-}500~\mu$ 0-55616 CO₂, collision induced i.r. absorpt. spectrum in gas and liq. state 0-74250 CIF₃, i.r., assignment rel. to known struct. 0-70894 CIO₃ aqueous ions in solution, electronic spectra, assignment of bands 0-50229 Co₃CO₄- tetrahedral ion, i.r. spectrum 0-46922 Cs₃MnF₆ in solns. of anhydrous HF, i.r. 0-64373 DCl, dissolved in inert solvent, rot. motion and moment anal. of i.r. bands 0-70910 DCl dissolved in liquid SF₆, far i.r. spectrum 0-39803 D₂O₄ i.r., differential technique 0-68110 Fe complex, bis-(1,10-phenthroline) biscyanoiron (II), solvent effects 0-71357

0-/135/ Fe complex, bis-(2,2'-bipyridyl) biscyanoiron (II), solvent effects 0-71357 Fe₂(CN)*₋₁₀ electron transfer bands of binuclear iron (II, III) complexes containing 2 cyanide bridges 0-55617 Fe₂(CN)*₋₁₀ electron transfer bands of binuclear (II, III) complexes contain-ing 2 cyanide bridges 0-55617 H i.r. absorption coefficient, 40-500 μ 0-55616

inorganic liquids and solutions continued

 H_2 in liq. Ar and N_2 , abs. spectra, 7800-8900 cm⁻¹, $0\rightarrow 2$ vibr. transition 0-43457

HBr, dissolved in inert solvent, rot. motion and moment anal. of i.r. bands 0-70910

HCl, dissolved in inert solvent, rot. motion and moment anal. of i.r. bands 0-70910

HCl, solution in CCl₄, temp. dependence of i.r. spectrum 0-46477

HCl, solution in CCl₄, temp. dependence of i.r. spectrum 0-46477 HCl dissolved in liquid SF₆, far i.r. spectrum 0-39803 HDO in water and NaCl soln., i.r., molar absorptivity between 10 and 85°, 4000 to 2000 cm⁻¹ 0-43452 H₂O, i.r., differential technique 0-68110 H₂PO, far u.v. absorption of ions present 0-50232 He liquid, dispersion of phonon spectrum 0-43493 IO₃ aqueous ions in solution, electronic spectra, assignment of bands 0-50229 K₂MpF₆ in solute of aphydrous HF 4 u. 0-64373

0–50229

K₂MnF₆ in solns of anhydrous HF,11. 0–64373

Kr:Xe, liquid, vac. u.v., Wannier type exciton states 0–46916

LiNO₃-alkaline earth nitrate molten mixtures, u.v. absorpt. 0–50233

MgBr₂ and MgJ₂ diethyl ether complexes in solution 0–74278

Nir. absorption coefficient, 40–500 μ 0–55616

NH₃ aq. solns., solvated electron in pulse radiolysis 0–54195

N₂O₃, transitions between torsional levels, rel. to barrier to internal rotation 0–74288

N₂O₃C₄ in Ligh-KC entectic melt, at 450°C 0–46496

Na; OSCI, in Lici-KCl eutectic melt, at 450°C 0—46496 Na; OSCI, in Lici-KCl eutectic melt, at 450°C 0—46496 Nd³⁺: POCI; SnCl, aprotic soln, rel. to pulsed laser appls., obs. 0—45790 Nd³⁺: \$\frac{1}{2}\text{McHonates}, intensities in various solvents 0—58489 Nd³⁺FA: POCI; ZrCl₄ aprotic soln., rel. to pulsed laser appls., obs. 0—45790

Ni(CN)₄²⁻ in aqueous soln., mag. circular dichroism and u.v. spectral assignments 0–71358 Ni(II) in molten ZnCl₂-CsCl mixtures, coordination geometry 0–39804

N(t) in motien 2nc. 3-C-SC instatres, coordinator geometry 0-39804 Ni(PCl₃), i.r. spectra in organic solvents 0-64443 O i.r. absorption coefficient, $40-500~\mu$ 0-55616 Pd(CN)₂²⁻¹ in aqueous soln., mag. circular dichroism and u.v. spectral assignments 0-71358 Pt(CN)₂²⁻¹ in aqueous soln., mag. circular dichroism and u.v. spectra assignments 0-71358

SO₃ aqueous ions in solution, electronic spectra, assignment of bands 0-50229

Se, internal defect structure from i.r. microscopy and spectrometry 0 - 66053

Si halide complexes with 4,4'-dipyridyl. 0-66035

Sill4 ir. 0-70932 ZnCl₂, far-ir., Raman, probe ion electronic and vibrational spectra 0-68076 Zn(NO₃); in anhydrous methanol i.r. spectrum, association 0-58490

inorganic molecules

see also Molecules see also Molecules acetylacetone and deuterioacetylacetone, absorption bands of nonplanar vibrations 0-64472 aminoalcohols, i.r. spectra as function of CCl₄ conc., H bond study

-43122

chlorobenzene, electronic and i.r. analysis, planar ground state vibrs.

dihydrazinium oxalate, interpretation in terms of frequencies of functional groups 0-71004

groups 0-71004
far ir. spectroscopy using interferometers 0-49147
halogens, photodissoc. translational spectroscopy 0-77963
hydrazinium hydrogen oxalate, interpretation in terms of frequencies of functional groups 0-71004
ir. and Raman spectra of mols. with low-freq. vibrs., obs. 0-39362
inert gas mixtures, translational spectra, 16-250 cm⁻¹, mass and temp.
effect 0-43081

kinetic intensity variations of spectral lines and bands for individual mole-cular gases and mixtures in lasers 0-64321 polyhalide ions, i.r. spectra 0-70901 rhodamine dyes, effect of intramolecular charge transfer on electronic spec-tra 0-67818 Ag vapour discharge with hot hollow cathode, nature of radiation 0-50122

Al-Mg, optical absorption peaks at 4.2 K, 0.2-5.0 0-59393 Al vapour discharge with hot hollow cathode, nature of radiation 0 - 50122

0-3012Ca vapour discharge with hot hollow cathode, nature of radiation 0-5012C Cl K α and K β emission spectra in free molecules 0-52899Ne, multiply ionized, and mean lives in vacuum u.v. 0-67651

CI Kα and Kβ emission spectra in free molecules 0–52899
Ne, multiply ionized, and mean lives in vacuum u.v. 0–67651
inorganic molecules, diatomic
As O and AsO+ radicals, vacuum u.v. emission, source 0–61070
FORTRAN IV program for line-by-line calc. 0–60901
heavy, vacuum u.v. emission, source 0–61070
hydride band, with wide rot. struct. near 7666Å 0–70870
N₂, fluorescence efficiencies and collisional deactivation rates 0–70931
radiation probability, dissociation states, rel. to laser possibilities 0–55269
Ag₂, in high temp. discharge, u.v. region 0–53015
AgBi absorpt, band system in visible 0–61068
AlD 'II+-1Σ+ perturbation obs. in mol. spectrum 0–73349
AlD+, emission, study of band with wide rot. struct. near 7666Å 0–70870
AlH+ emission, study of band with wide rot. struct. near 7666Å 0–70870
AlO C²Σ+.X²Σ+ syst, rot. anal. 0–61069
Ar₂, absorption spectrum in vacuum u.v. region 0–67714
Ar₂, vacuum u.v. emission, time resolved study 0–58176
As₂, rotational anal. of strongly perturbed 'II-1Σ system 0–70872
AsO+, rotational anal sion of far u.v. 0–61071
AsP, u.v. emission, vibr. and rot. anal. 0–70873
AsS(AsS+) radicals, emission 2500-to-8000Å 0–39457
AsSb, u.v. emission, vibr. and rot. anal. 0–70873
Au₂, in high temp. discharge, u.v. region 0–53015
BCI, Franck-Condon factors and r-centroids 0–74284
BaF, Franck-Condon factors and r-centroids 0–74284
BaF, Franck-Condon factors for A-X, B-X and D'-X bands, intensity 0–70878
BaI, emission spectrum in u.v. 0–61074

BaI, emission spectrum in u.v. 0-61074

Spectra continued

inorganic molecules, diatomic continued

Bi₂ vapour, emission spectrum, 3 new band systems, vibrational analysis 0-74242

Bil, observation of bands in absorption in region $\lambda\lambda$ 5300-4650 abscribed to A–X and A′–X systems 0–64381

Br₂, Ig (³Π_{1g}) - 2u (³Δ_{2u}) bands in avalanche spark breakdown of Ne-Br₂ mixtures 0-50120

Br₂, anal. of four abs. bands of weak A ${}^{3}\Pi(1u)$ —x ${}^{1}\Sigma_{g}^{+}$ syst. 0—67718 Br₂, two photon spectroscopy of dissociative states 0—61183

⁷⁹Br³⁵Cl, ⁸¹Br³⁵Cl, rotational analysis of absorption bands 0-67719

C2, Phillips system, new vibrational and equilib. consts. 0-53022

C₂, Phillips system, new vibrational and equilib. consts. 0–53022
C₂, Phillips system, new molecular consts. 0–43090
CBr radicals, new absorption systems 0–74421
CCI radicals, new absorption systems 0–74421
CF, absorpt. 1500 to 2500 Å, rot. anal. of A and B states 0–70890
CF, B-X system obs. in emission 0–46458
CN, Ar induced red shift of violet bands 0–43089
CN, vacuum u.v., rotational and vibrational analysis 0–43085
CN red system, improved molecular consts. with perturbation anal. 0–55292

-55292 CO, adsorbed on copper, i.r. spectra 0-46453 CO, adsorbed on polished metal surfaces, i.r. spectra 0-67724 CO, Cameron bands, correl, with bands attributed to F_2 CO 0-61078 CO, collision-broadened, half-width variation interpretation 0-61082 CO, compressed, vibr.-rot. lines of v_{0-3} band 0-49858 CO, compressed by N_2 and HCl, vibr.-rot. lines of v_{0-3} band 0-49858 CO, fund, band linewidths 0-74243 CO, Herzberg bands, isotope shift studies 0-64393 CO, i.r. line intensities and dipole moment functions 0-70888 CO, i.r. vibr.-rot. bands, absorption coeffs. calc: 0-77774 CO, perturbed by A_1 , v_{0-3} band vibr-rot. lines 0-39368 CO, pure rotational lines, self-broadened semi-halfwidths 0-70889 CO, radiative lifetime of $b^*\Sigma^*$ state 0-67727 CO, vib. population inversion in free-burning CS₂/O₂ flame 0-70884 CO accorbed on Ni and Rh (110) surfaces in vac., i.r. reflectance spect

CO adsorbed on Ni and Rh (110) surfaces in vac., i.r. reflectance spectra 0-46457

CO adsorbed on SiO₂-supported Pt, i.r. spectrum 0–67723 CO⁺, comet-tail and Baldet-Johnson bands, isotope shift studies 0–64393 CO⁺, emission cross sections of A² Π and B² Σ ⁺ states, for 0.05-5 keV electrons 0–77777

CO⁺, emission cross sections of A²Π and B²Ē⁺ states, for 0.05-5 keV electrons 0-77777
CO₂ absorpt. and emission spectra at 25, 300 and 800°C, windowless gas cell appl. 0-49153
CP, Franck-Condon factors and r-centroids 0-74284
¹²C¹⁶O, Ångstrom bands, rotationless vibr. levels rot. perturbations 0-46454
¹²C¹⁸O Angstrom system, vibr. and rot. consts., perturbation shifts, electronic shifts, determ. 0-77781
¹²C¹⁶O, Angstrom system spectral lines and band origins 0-43084
CaBr, u.v. emission spectrum 0-46459
CaF A-X system in region 6300-5830 Å investigated by CaF₂ excitation in a carbon arc 0-43093
CdBr u.v. spectrum, vibrational analysis 0-46549
CdS, photoconductivity at low temperatures, effect of u.v on spectral distribution 0-53953
Cly visible, absorption band spectrum 0-39371
ClCN gas phase i.r. 0-46461
Cs, transient species, absorpt. spectra in vacuum u.v. 0-53020
Cu₂, in high temp. discharge, u.v. region 0-53015
CuBi, visible, line obs. 0-53025
D₂, excited by 0 to 500 eV electrons, extreme u.v. emission obs. 0-64441
D₂, i.r. absorpt. induced by CO collisions 0-70899
D₃ in solid Ar, fundamental i.r. absorption, molecular and lattice transitions 0-54098
D₂ + vibrational constants of ground state from photoelectron spectra
0-8169
DBr electronic spectra and structure of b³Π, and C ¹Π states 0-46475
DCI, solvent effects on infra-red band shapes and intensities 0-3802

D₂+ vibrational constants of ground state from photoelectron spectra 0–58169

DBr electronic spectra and structure of b³H₁ and C ³H states 0–46475

DCl, solvent effects on infra-red band shapes and intensities 0–39802

DCl b³H₁ and C ³H states from absorption spectra 0–39377

DCl dissolved in liquid SF₆, far i.r. spectrum 0–39803

DI absorption spectra, analyses of 'B'-X and C-X transitions, molecular constants 0–46476

F₂-H₂O photolysis in N₂ matrix, 20°K, i.r. absorpts. 0–39397

FeBr emission spectrum, new system of violet-degraded bands 0–43097

FeCl isotope shift studies 0–49865

Fe(III) complex, u.v. abs. spectrum 0–58165

GdO, band spectrum 0–64402

GeCl, u.v. absorption spectrum 0–49867

H halides, i.r. vibrational spectra, effect of intermolecular forces 0–43112

H₂, discrete absorption and photodissociation 0–49872

H₃, excited by 0 to 500 eV electrons, extreme u.v. emission obs. 0–64441

H₃, Lyrman and Werner systems, isotope effects 0–64407

H₄, Lyrman bands, stimulated emission, in vac., at 1000 Å 0–67081

H₃, photoabs, channel-interaction treatment 0–64411

H₃, pressure-broadened linewidths in electric-field induced spectrum 0–46478

H₂, pure rotation i.r. spectra, elec. field induced 0–61096

0—30476 H₂, pure rotation i.r. spectra, elec. field induced 0—61096 H₂, Rydberg absorpt, series converging to $V\geqslant 0$ levels of H₂⁺ 0—74268 H₂ in solid Kr, fundamental i.r. absorption, molecular and lattice transitions 0—54098

H₂- compound state formation effect on vacuum u.v. excitation 0-64424 H₂+, absorption spectrum in vacuum-u.v. region, Rydberg series obs. at liquid N temp. 0-46474

vibrational constants of ground state from photoelectron spectra

0—38169

HBr, electronic spectra and structure of b³Π₁ and C ¹Π states

0—46475

HBr, i.r., in Ar and other matrices, 20°K

0—49869

HBr, i.r., in doped Ar matrices, 20°K

0—49871

HCN vibrational transitions in emission spectrum

0—74262

HCI-CI-Ar in glow discharges, i.r. absorpts., 956 and 696 cm⁻¹ 0—39397 HCl, collision-broadened, half-width variation interpretation 0—61082 HCl, fundamental band, self-broadened, intensity, variation with pressure 0-74200

0-74200 HCl, i.r., in Ar and other matrices, 20°K 0-49869 HCl, i.r., in doped Ar matrices, 20°K 0-49871 HCl, i.r. line intensities and dipole moment functions 0-70888 HCl, solvent effects on infra-red band shapes and intensities 0-39802 HCl $\mathrm{b}^3\Pi_1$ and $\mathrm{C}^3\Pi$ states from absorption spectra 0-39377

inorganic molecules, diatomic continued

HCl compressed gas, vibr.-rot. spectrum, intensities and widths in $v_{0^{-2}}$ band 0-43109

HCl dipole moment matrix elements of vibration-rotation bands 0-77790

HCl dissolved in liquid SF₆, far i.r. spectrum 0-39803 HCl in solid Ar and Kr. far i.r. spectra 0-77789 HD* vibrational constants of ground state from photoelectron spectra

0-46479
HF, strength and width in first overtone band 0-53029
HI, i.r., in Ar and other matrices, 20°K 0-49869
HI, i.r., in doped Ar matrices, 20°K 0-49871
HI absorption spectra, analyses of 'B'→X and C←X transitions, molecular constants 0-46476
Hel, rot. lines press. broadening and shift 0-43098
Hd, Lyman system 0-53034
He., absorption and emission, between ground state and first excited singlet 0-77800
Hes, emission near 600Å, theoretical investigation 0-77801

giet 0-7/800
He₃, emission near 600Å, theoretical investigation 0-77801
He₅, vacuum u.v. emission, time-resolved study 0-58176
HgD band spectrum analysis extended 0-77802
HgH, band spectrum analysis extended 0-77802
HgI 0-45085
HgI 0-45085

HgT spectrum produced and partially analyzed 0–77802 I₂, absorpt. linewidths in B $^3\Pi_{ou}^+$ -X $^1\Sigma_g^+$ system, alternation with J 0–70914

0-70914

I₁, and ground-state dissociation energy 0-53039
I₂, laser excited reson. fluoresc. 0-46482
I₃, two photon spectroscopy of dissociative states 0-61183
I₃, u.v., in vacuum, Rydberg transitions 0-46480
I₂ overlapping vibr. rot. lines near 6330 Å, rel. to He-Ne laser freq. stabilization 0-58179
LaO, emission spectrum, u.v., vibr. struct. 0-61101
La¹⁸0 band spectra, vibrational analysis of green-yellow system 0-43119
LiBr, h.f.s.^{2,98}Br polarization 0-43013
LiH A-X system, intensity distribution in rotational structure 0-58181
Mg₂, abs. spectrum, meas. with high resolution spectrograph 0-46484
MgF, r-centroids and Franck-Condon factors for C¹2⁵+X²2⁵ system 0-70917
MgO, Franck-Condon factors and r-centroids for D¹Δ-A¹Π and C¹1Σ-

MgO, Franck-Condon factors and r-centroids for D¹ Δ -A¹ Π and C¹1 Σ -A¹ Π systems 0.49877 N₂, absorpt., rotational anal. of bands in b-X and i-X systems 0.70932 N₂, beam, emission and radiative lifetime of metastable E³ Σ_R state 0.61120

 N_2 , e bombardment 0.65-1.6 MeV obs. absolute fluoresence of first negative (0.0) band 0-46494

 N_2 , electron beam excited, spreading of first and second positive bands 0--61117

0–61117 N_2 , emission cross-sections in vac. u.v. by electron impact 0–61114 N_2 , excited by 0 to 500 eV electrons, extreme u.v. emission obs. 0–64441 N_3 , from second positive emission system excited by electrons 0–46486 N_2 , of visible afterglow, rel. to recombination energy 0–53041 N_3 , oscillator strengths of Hopfield absorption series 0–61116 N_3 , rel. to arcs spectroscopic obs. in u.v. region 0–55527 N_2 , vacuum u.v., $a^{m/2} \Sigma_g^+ \leftarrow X^1 \Sigma_g^+ (0-0)$ absorpt., press. induced 0–39389 N_2 , vacuum u.v. absorption cross-sections and oscillator strengths 0–61123

N₂, yellow afterglow, first positive band intensities 0–43125 N₂, excited by 50 to 5000 eV electrons, radiation emission obs. 0–64440 N₂ first positive and Meinel bands, electron excit. cross-sections, 0 to 700 eV 0–64438

eV 0–64438 N; K-LL Auger spectrum, high energy lines identification 0–46487 N₂+, branch overlapping in first negative bands 0–70927 N₂+ first negative emissions, excitation functions, prod. in p-N₂ collisions 0–39321 N₂(A³ Σ_a +), metastable, r.f. spectrum, mag. hyperfine and elec. quadrupole constants 0–70921 ND, A³ Π_f -X³ Σ^- (0,0) band, rot. anal. 0–64432 NF12+ radiative lifetime and rate constant for electronic quenching 0.–74281

ND, $A^3 \Pi_{r} X^3 \Sigma^-(0,0)$ band, rot. anal. 0-64432 NF1 Σ^+ radiative lifetime and rate constant for electronic quenching 0-74281 NH. natural-orbital VCI studies 0-46490 NH free radical, $A(^2\pi_l) - X(^2\Sigma^-)$ transition, obs. 0-49878 NO, absolute oscillator strength of (0,0) band of γ system 0-61119 NO, emission, rot. struct. of pair of $^2A^{-2}II$ bands 0-67746 NO, opama system Franck-Condon factors and r-centroids 0-74285 NO, interaction between $s\sigma$ and $d\sigma$ series giving 'deperturbed' Rydberg series 0-67745 NO, spectral and integral absorpt. in 5.3μ band 0-61102 NO $^+$, Franck-Condon factors and r-centroids 0-74284 NS radical, Franck Condon factor for $B^2II X^2II$ transition 0-74280 NSe, rot. struct. of bands of A-X system 0-49879 NSe, vibr. and rot. study 0-61107 NSe rot. anal. of 0.5 and 0.6 bands for $^5/_2 - X^2II_{3/2}$ syst. 0-67738 NSe transition from rotational analysis 0-61108 NSe, $^{18}N^{18}O$, electronic, vibrational isotope effect 0-39385 NSe $^{18}N^{18}O$, electronic, vibrational isotope effect 0-39394 Nd 3* complexes, bonding inferred from nephelauxetic effect 0-39394 Nd 3* complexes, bonding inferred from nephelauxetic effect 0-39394 Ne 2 , absorpt, in u-x region, discrete band systems anal. 0-74292 NiCl, emission spectrum 0-64442 O2, intensity meas. on $A^3\Sigma_u^+ - X^3\Sigma_g^-$ Herzberg I band system 0-67749 O3, measured transition probabilities for bands of Schummann-Runge (B $^3\Sigma_u - X^3\Sigma_g^-$) syst. 0-70937 O3, photoelectron spectra, resonance wavelength 0-64324 O5, photoelectron spectrum, 12-28 eV, O2 $^+$ states 0-55312 O3, photoelectron spectrum, 12-28 eV, O2 $^+$ states 0-55312 O3, photoelectron spectrum, 12-28 eV, O2 $^+$ states 0-55312 O3, photoelectron spectrum, 12-28 eV, O2 $^+$ states 0-55312 O3, photoelectron spectrum, 12-28 eV, O2 $^+$ states 0-55312 O3, photoelectron spectrum, 12-28 eV, O2 $^+$ states 0-55312 O3, photoelectron spectrum, 12-28 eV, O2 $^+$ states 0-55312 O3, photoelectron spectrum, 12-28 eV, O2 $^+$ st

0–61066 O₂ emission bands obs. at 4784, 5165, 5788 Å in afterglow, assignments to $^{1}\Delta_{g}$, $^{1}\Sigma_{g}$ states 0–74294 O₂ Schumann-Runge bands photographed 0–74296 O₂ trapped in solid matrices, Schumann-Runge bands 0–55311 OD+, electronic transitions $^{3}H_{I}^{-3}\Sigma_{-}$, rotational anal. 0–70938 O₂($^{1}\Delta_{g}$), summer daytime height profiles, at Fort Churchill 0–45166 O₂($^{1}\Delta_{g}$), auroral i.r. emission, enhancement in <IBC II auroras 0–59633 O₂($^{1}\Delta_{g}$) trapped in solid O₂ at 4.2°K, emission spectra 0–62671

Spectra continued inorganic molecules, diatomic continued

forgain infectios, diatomic constants 0-70936 OH⁺; electronic transitions ${}^{3}\Pi_{1}$ – ${}^{3}\Sigma^{-}$, rotational anal. 0-70938 OH⁺; ${}^{3}\Pi_{1}$ – ${}^{3}\Sigma^{-}$ 0-77827

O₂* chemiluminescence in H₂O₂+OCl⁻ reaction 0-79428 O₂*(2 Π_2) photoelectron spectra using 736 and 744Å Ne radiation 0-64436

O₂ (211₈) pnotoelectron spectra using /35 and /44A Ne radiation 0–64436
PCl, A-X band syst. in visible region 0–46507
PO, emission spectrum, new system in region 4800-3800 Å 0–74299
PO degenerate band of N²Σ+B²Σ+ transition rotational analysis 0–77831
PO radical, rot. analysis, new state obs. 0–49885
PO radical, rot. obs. of Rydberg- Rydberg transition 0–49884
PO radical, rot. obs. of Rydberg- Rydberg transition 0–49884
PO radical, rotational study and spectroscopic data 0–55314
PSb, u.v. emission, vibr. and rot. anal. 0–70873
PtO emission spectra in 4000-7000 Å region, band analysis 0–74301
S₂ transient species, absorpt. spectra in vacuum u.v. 0–53020
S₂-z, i.r. rel. to struct. 0–70948
SF₆, i.r. double resonance study of relaxation 0–46510
SH radical, microwave obs. of first electronically excited state 0–70962
SbF, new band system in 4050-5450 Å region 0–49889
SbF, rotational anal. of C₃ system 0–67750
SbN molecular flash absorption spectrum obs. 0–77839
ScCl, electronic-vibr. rot. spectrum, 2200-9000 Å 0–4981
Si₂ new band systems discovered, rotational and vibrational constants 0–77844
SiCl, B-X system, vibrational and rotational analysis 0–61137

S1, new band systems discovered, rotational and vibrational constants 0–77844
SiCl, B-X system, vibrational and rotational analysis 0–61137
SiF, Franck-Condon factors and r centroids 0–74284
SiF, Pranck-Condon factors and r centroids 0–74284
SiF, molecule, matrix element of dipole moment of A²-X² electron transition 0–53050
SiO, band oscillator strengths for A¹Π-X¹Σ⁺ system 0–58197
SiO ³Σ⁻³Π transitions, rotational constants determ. 0–61136
SnO, matrix-isolated, i.r. spectrum 0–61138
SrS, ¹Σ⁻⁴⁻Σ⁺ syst. rot. anal. 0–70953
TiBr absorption and emission spectra 0–49895
TiF, emission spectrum from Δν=0 sequence of ⁴π⁻⁴Σ transition 0–55326
TiN, rotational analysis of the red electronic emission system 0–53051
TiO, meas. of intensities of α and β band systems 0–46515
VCl, spectra obtained under photodissociation and He bombardment of VCl4, 0–77848
Xe-Hg(³P₀) complex emission band obs. during irradiation of Xe-Hg gas mixture rate constant for reaction determ. 0–74274
ZrBr, band spectrum, in visible and u.v. regions 0–70958
Inorganic molecules, diatomic, radiofrequency

inorganic molecules, diatomic, radiofrequency

see also Nuclear magnetic resonance and relaxation; Paramagnetic resonance and relaxation

nance and relaxation

14N16O, A-doubling transitions, hyperfine constants, predicted frequencies
0-58184
AIF, mm and sub mm spectrum 0-39364
AIF absorpt. spectra 0-67713
BaS, Stark, mol. beam elec. reson. obs. 0-39392
CS, optical-r.f. double reson. on A¹Π state, dipole moments and lambda doublings 0-70891
GaF absorpt. spectra 0-67713
HBr, coupling consts. from hyperfine struct. of submm. spectrum
0-70913

HE and DF h fs constants 0-53035

0-70913HF and DF, h.f.s. constants 0-53035HF and DF, h.f.s. constants 0-53035InF absorpt, spectra 0-67713NaBr. Stark, mol. beam elec. reson. obs. 0-39392NaCl, by molec.-beam electric resonance method 0-61126NaCl, quadrupole coupling consts. from r.f. spectrum 0-70933NaCl, Stark, mol. beam elec. reson. obs. 0-39392OD free radical, microwave lambda doubling $\Delta F=0$ transitions 0-70939TIBr, h.f.s. 0-64457TIF absorpt. spectra 0-67713TII, h.f.s. and elec. hexadecapole moment of ^{127}I 0-64458

inorganic molecules, polyatomic air, due to pre-breakdown phenomena 0-39360 alkali metal chlorates, bromates and iodates, powders, i.r. absorpt., vibrs. 0-53016

alkali metal hexafluoromanganates (IV), electronic spectra 0-64375 alkaline earth metal hexafluoromanganates (IV), electronic spectra 0-64375

antimonates, rutile struct., i.r. absorpt., vibr. freqs. 0-39393 arsenates and selenates, 4000 to 250 cm⁻¹, high and low temp. forms 0-55322

asymmetrical top mol., centrifugal distortion effects, Kivelson-Wilson theory applic. 0–61064 halides, groups III, IV, V and VI, photoelectron spectra, interpretation in terms of orbital structure 0–64368 hexahalometalates 0–77764 hexaisothiocyanate ions, 2200-70cm⁻¹ 0–39376 langbeinites, M₂IM₂II(SO₄)₃, i.r. forbidden transitions 0–64374 lanthanide complexes, metal-ligand spacing from spectral bands positions 0–70915 metal carbonyl deginations.

lanthanide complexes, metal-ligand spacing from spectral bands positions 0–70915
metal carbonyl derivatives, anomalies in i.r. spectra 0–74231
metal halides (II A) absorption spectra, stretching vibrations 0–49860
NaHCr₁CO₁₀, i.r. and Raman spectra, vibr. freqs. 0–39391
niobates, rutile struct., i.r absorpt., vibr. freqs. 0–39393
ozone, band origin of ρ₂ fundamental 0–39395
phosphites, i.r. and Raman spectra electronic structure 0–70906
photoelectron spectram, high resolution, and electron impact energy loss
spectrum of NO₂ 0–67741
silyl halides, microwave spectra, rot. const. 0–64454
double sulphates and selenates, including Tutton's salts, i.r. 2000 to 40
cm⁻¹ 0–55321
antalates, rutile struct., i.r. absorpt., vibr. freqs. 0–39393
tetravinyl-lead, i.r. spectra in liquid and solid states 0–77847
tetravinylegremanium, ir. spectra in liquid and solid states 0–77847
tetravinylegremanium, ir. spectra in liquid and solid states 0–77847
tetravinyltin, i.r. spectra in liquid and solid states 0–77847
tetravinyltin, i.r. spectra in liquid and solid states 0–77847
tetravinyltin i.r. spectra in liquid and solid states 0–77847
tetravinyltin i.r. spectra in liquid and solid states 0–77847
tetravinyltin i.r. spectra in liquid and solid states 0–77847
tetravinyltin i.r. spectra in liquid and solid states 0–77847
tetravinyltin i.r. spectra in liquid and solid states 0–77847
tetravinyltin i.r. spectra in liquid and solid states 0–77847
tetravinyltin i.r. spectra in liquid and solid states 0–77847
tetravinyltin i.r. spectra in liquid solid states 0–77847
tetravinyltin i.r. spectra in liquid states 0–77847
tetravinyltin i.r. spectra in liquid states 0–77847
tetravinyltin i.r. spectra in liquid solid states 0–77847

transition metal-\sigma-phenyl complexes, i.r. spectra 0-67712

inorganic molecules, polyatomic continued

[ReCl₆]²⁻ salts, i.r., 350 to 250 cm⁻¹ 0-55319 AgSb(OH)₆, i.r. absorpt., vibrs. 0-61125

Al complex, AlCl₃, 2EtOAC, i.r. spectra 0-46448

AlBr₄-, i.r. 0-74235

Al₂O₂ gaseous, bending freq. in i.r. absorpt. 0-64376

AsN, photographed at dispersion of about 0.4 Å/mm 0-46450

Au₂Cl₆ i.r. and Raman spectra, normal coordinate calculations 0-46481 B₂Ce₄, B₂F₄, matrix-isolated, i.r. and config., liq., Raman scatt. 0-70876 BCl₃, vibrational, dissociation, recombination radiation, CO_2 laser excited 0-46604

0-46604
BF₃-(CH₃)₂SO isotopically substituted coordination compounds, i.r. spectra 0-74238
(BFHN)₃, photoelectron spectra 0-64378
BF₃-(CH₃)₂CO isotopically substituted coordination compounds, i.r. spectra 0-77770
B₂H₆, photoelectron spectra 0-64378
(BHNH)₃, photoelectron spectra 0-64378
BN.H₆ initiation properties by hypotoelectron spectroscopy, and INDO

B₂H₆, pnotoelectron spectra 0-64378
B₁N₁H₆, ionization potentials by photoelectron spectroscopy and INDO theory 0-39367
BeB₂H₈, i.r. spectrum and structure 0-67717
Bh₄ (d_n), i.r. spectrum on-33019
C₁ lines obs. in carbon cathode discharge spectrum 0-61391
CF₂, centrifugal distortion effects in microwave spectra 0-74249
CH₁, i.r., resolution enhancement 0-42396
CO, X-ray photoelectron spectroscopic determ. of ionization potentials 0-70882
CO²₂, radiative transitions, theory and expt. 0-77773
CO₂, 001-100 band, temp. depend. of seff-broadened half-width of P20 line 0-61084
CO₂, calc, of high-temp. steradiancy for vibr-rotation bands 0-43088
CO₂, collision induced i.r. absorpt. spectrum in gas and liq. state 0-74250
CO₂, emissivity in region 2100-2500 cm¹³ 0-61079
CO₂, excited, amplification coeff. in b₂-b₁ laser transition 0-74244
CO₂, i.r., rel. to line identification in planetary spectra 0-49855
CO₃, i.r., rel. to line identification in planetary spectra 0-49855
CO₃, i.r., rel. to line identification in planetary spectra 0-49855
CO₃, relative populations of vibr. energy levels from i.r. emission spectra

 ${
m CO}_2$, relative populations of vibr. energy levels from i.r. emission spectra 0-67725

CO₂, solvent effects on infra-red band shapes and intensities 0–39802 CO₂ absorber gas, standing-wave saturation reson. in 10.6 μ transitions 0–61076

CO₂ and CO₂+, electronic, calc. 0–53073 CO₂ compressed, temp. variation of far i.r. absorption quadrupole moment 0–43086 C₃O₂, absorpt. spectrum of 1780 Å band and strength of transition 0–61080

0-61080
C₃O₂ polymers, 0.2-1.6 μ rel. to Mars surface coloration 0-41792
COS, i.r. spectra at 2400-7000 cm⁻¹ 0-64383
CS₂, radiative transitions, theory and expt. 0-77773
CS₂, solvent effects on infra-red band shapes and intensities 0-39802
β-Ca₃(PO₄)₂, assignment of i.r. bands 0-77778
Cd (II) complexes with thiourea, i.r. 0-74313
CIHCl⁻ ion isolated in argon matrix, i.r. spectrum 0-64391
ClO₂, 4750 Å band syst., rot. anal., force field and intensity calc. 0-64392
Co (II) complex, utrea and thiourea sulphates, diffuse reflectance spectra 0-39374

0-39374

Co complex, nitrosyltricarbonylcobalt and monosubst. derivatives, i.r. intensity meas. 0-64394

Co isonitrile complexes, low-frequency i.r. study 0-61085

CoCl₂ matrix-isolated molecules 0-39373

Cr complex, [Cr(bipy)₃]*, z=+3, +2, +1, 0, electronic spectra 0-46462

Cr(CO)₅, vacuum u.v. spectra 0-70867

(CrF₈)*- electronic spectrum investigation of ion 0-64395

Cr(III) complexes, fluorides, assignments of configurations from i.r. spectra 0-49862

tra 0-49802 Cr(III) complexes, of tri-2-pyridylamine, electronic spectra 0-55308 Cu complex, with triethanolamine, i.r. spectra and structure 0-64397 CuBr₃²- ion, electronic spectrum 0-55293

CuCl₂, electronic spectrum 0—5293 CuCl₂, electronic spectrum assignment 0—61086 Cu(II) complexes, of tri-2-pyridylamine, electronic spectra 0—55308 CuSeO₃.2H₂O and its deutero-analog ir. spectra 0—53024 DCN, submm. mol. beam maser spectroscopy study of rot. consts. 0—74269

0-74269
D₂O, abs. lines near 600 GHz 0-77792
D₂O, abs. lines near 600 GHz 0-77792
D₂O₃+ ion, vibrational, at -180°C 0-58175
F₂CO, correlation with Cameron bands of CO 0-61078
F₂CS, 4500Å band system 0-77772
F₂CS, molecule, 'A₂-'A₁ transition, spectra analyzed 0-74255
F₃SO₄ molecular, i.r. and Raman spectra 0-55294
FSSF, i.r. 0-70902
FeCl., i.r. matrix spectra studied by effusion technique, assignment 0-74257

FeCl₃, i.r. matrix spectra studied by effusion technique, assignment 0-74257

Pecl₃, 11. Inatix spectra studied by effusion technique, assignment 0-74257
Fe₂Cl₄, i.r. matrix spectra studied by effusion technique, assignment 0-74257
GeCl₂, i.r. spectra in solid Ar matrix, vibrational assignment and force constants 0-49866
GeCl₃, matrix-isolated i.r. spectra 0-66200
GeCl₃, matrix-isolated i.r. spectra 0-66200
GeCl₃, mothix-isolated i.r. spectra 0-61680
GeH₄, photoelectron spectra 0-61168
HCN, absorpt. meas. rel. to vibr. and ro-vibr. consts. 0-61094
HCN, electric field induced 0-61095
HCN, electronic, calc. 0-53073
HCN, submm. mol. beam maser spectroscopy study of rot. consts. 0-74269
HCN 337 μm maser line, identification of molecular coincidences

HCN 337 μm maser line, identification of molecular coincidences 0-67733

HDO, absorpt., in regions 2400-3495 and 4022-4400 cm⁻¹ 0-64416 HDO in C₂Cl₃F₃-CS₂ mixtures, valence vibrs., contact complexes obs. 0-49873

HN₃ photoelectron spectra, orbital identification by comparison with other spectra 0-64409

Spectra continued

inorganic molecules, polyatomic continued HNCS photoelectron spectra, orbital identification by comparison with other spectra 0-64409

HNF, absorpt. spectrum of \overline{A}^2A' - X^2A'' system 0-77796 H₂O, abs. lines near 600 GHz 0-77792

13.0, abs. nnes near 600 GHz 0-77792 H₂O, absorpt. coeffs., 100 to 400 Å 0-55298 H₂O, asymmetric top, line intensities, Δk effect 0-74212 H₂O, line intensity, 6.3 μm band, vibratory-rotatory interactions 0-53032 H₂O in C₂Cl₃F₃-CS₂ mixtures, valence vibrs., contact complexes obs. 0-49873

H₂O in C₂Cl₃F₂CS₂ mixtures, valence vibrs., contact complexes obs. 0–49873
H₂O line strengths in v₃ band 0–39382
H₂O vapour, absorption, 23 cm⁻¹ at low temps. 0–74275
H₂O vapour, absorption coeffs. 10-22 μ at high temps. 0–67734
H₂O vapour, ix., rel. to line identification in planetary spectra 0–49855
H₂O₃+ ion, vibrational, at −180°C 0–58175
H₃PO₃, i.r. and Raman spectra, electronic structure 0–70906
H₂S, i.r. spectra in solid N₂ matrix 0–58174
H₃S, i.r. spectra in solid N₂ matrix 0–58174
H₃S, photoelectron spectra rel. to vibr. fine struct. in electronic states 0–61121
Hg (II) complexes with thiourea, i.r. 0–74313
I₂Cl₆ i.r. and Raman spectra, normal coordinate calculations 0–46481
IFBr₆²⁻, electronic absorption spectrum, in host crystals at room and liq. He temps. 0–74276
Li₂Cr₁O₃, ir. and Raman spectra 0–6483
LiO₂, i.r., rel. to struct., vibr. potential and bonding 0–70916
LiO(1) (X=A), Ga, Co, Cr, Rh, Sc), i.r., Li⁶-Li⁷ isotopic shifts 0–55300
Me₁LX₃ absorption spectra, stretching vibrations 0–49860
Me₂CO₁O₁, i.r., and Raman spectra, vibrations of B-O, Mg-O bonds 0–53040
Mn₃(CO)₁₀, i.r., and Raman spectra, vibrational-fine structure of bands 0–58182
MnO₃²⁻¹ i.r., electronic transitions, vibrational fine structure of bands 0–68182
MnO₃²⁻¹ i.r., electronic transitions, vibrational fine structure of bands 0–68182

0-58182 MnO₄²· ir., electronic transitions, vibrational fine structure of bands 0-58182

0–58182

Mo(CO)₆, vacuum u.v. spectra 0–70867

NCO radical, electronic, calc. 0–53073

NCO radical, rotational microwave spectra 0–64429

NF₃, photoelectron spectra presented, assigned, correlated with BF₃ and CF₄ 0–64428

NH₃, absorpt. coeffs., 100 to 400 Å 0–55298

NH₃, Franck-Condon factors for A-X transition 0–61112

NH₃, hyperfine structure on inversion transition for various rotl. states 0–43126

0-43126 NH₃, ir.-microwave double-resonance obs. using N₂O laser 0-70924 NH₃, photoelectron spectra rel. to vibr. fine struct. in electronic states 0-61121

NH₃, thermally excited, inversion-rotation spectrum, 60-200 cm⁻¹ 0-64433 0-NH₃, u.v. 0-70928 u.v. absorption bands, intensities of vibrational components

NH₃ and deuterated derivative, photoelectron spectra using 584Å He reso-

NH₃ and deuterated derivative, photoelectron spectra using 584A H nance 0–64436
NH₃ and ND₃, photoelectron spectra using molec. beams 0–58186
NH₃ microwave spectrum, new hyperfine structure 0–66985
NH₄Cl., saturated absorpt., using CO₂ and N₂O lasers 0–70844
NH₂D, rotational-vibrational spectroscopy, transitions of v₂
0–74282

0-74282
NH₂, fine struct. of 937 cm⁻¹ band 0-77813
NO₂- ion isolated in Ar matrix, ir. spectrum 0-41215
(NO)₂, ir. 0-58187
NO₂, ir. absorpt. spectra of isotopic species 0-64437
NO₂, of (3,0,1) band, mol. consts. 0-64431
NO₂, photoelectron and vac. u.v. 0-61110
NO₂, thermal and recombination emission 0-61109
N₂O, microwave spectrum, 125-302 GHz, mol. parameters 0-64430
N₂O ir., resolution enhancement 0-42396
N₂O ir., resolution enhancement 0-42396
N₂O virtual spectrum, potential constants 0-43127

NyO. ir., resolution enhancement 0–42396
NyO vibrational spectrum, potential constants 0–43127
NyO*, configuration interaction intensity borrowing in photoelectron spectra 0–64315
NyO*, configuration interaction intensity borrowing in photoelectron spectra 0–64315
NyO*, Soy; Fi.r. spectrum, ionic character structure 0–70925
No*, Soy; Fi.r. spectrum, ionic character structure 0–70925
No*, Soy; Fi.r. spectrum, ionic character structure 0–70925
No*, Soy; Fi.r. spectrum, ionic character structure of vibra intended in the signal of t

NaIA(CH₃CI; complex, it is not 0-61125 Nb(V) chlorocomplexes, u.v. absorption spectra, estimation of optical electronegativity of OH - 0-46498 nf₃, i.r. band contours, using 1-resonance band contour 0-77812 Ni, Pd and Pt complexes, Ni(PF₃)₄, Pd(PF₃)₄ and Pt(PF₃)₄, ix. 0-55309 Ni (II) complex of 1-amidino-2-thiourea, K-absorption spectrum, correlation with proposed structure 0-61127 Ni complex, dithioacetylacetonato Ni(II), electronic spectra, MO calc. 0-67748 Ni complex, dithioacetylacetonato spectrum in an E₁ vibrational state Ni complex, nitrosyl microwave spectrum in an E₁ vibrational state

Ni complex, nitrosyl microwave spectrum in an E₁ vibrational state 0-77821

Ni complexes, phosphines, far i.r. spectra (600-100 cm⁻¹)

Ni complexes, phosphines, far i.r. spectra (600-100 cm⁻¹) 0–77763 Ni II complexes with β-ketonic thiocarbonmides 0–55307 Ni trithiocyanate complexes, i.r. spectra 0–49896 Ni(II) complexes, of tri-2-pyridylamine, electronic spectra 0–55308 Ni(PCl₂)₄ i.r. spectra 0–64443 O₃ millimeter wave spectrum, calc. of transition freqs. 0–77829 OCS, rel. to elec. dipole and mol. quadrupole moments 0–70940 O₂F radical, i.r. absorpts., prod. by F₂-O₂ photolysis, 20°K 0–39397 O₂F₂, i.r. 0–43130 OH, in nightglow 0–59628 ONF₂, photoelectron spectra presented, assigned, correlated with BF

Ork, in highigiow 0-39026
ONF3, photoelectron spectra presented, assigned, correlated with BF3 and CF4 0-64428
OSCl62 in LiClF KCl eutectic melt at 450°C 0-46496
OSO4, absorpt., rel. to electronic struct. 0-70941
P, red i.r. and Raman spectra, structure 0-49886

Spectra continued inorganic molecules, polyatomic continued

PCL,F₃, molecular constants from spectroscopic data 0–55313 PCL,F₃, molecular constants from spectroscopic data 0–55313 PF₃, i.r. spectra, v_3 band recorded 0–74300 PF₃, photoelectron spectra, change in ligand geometry on co-ordination 0–70942

0-70942
PF₁, microwave double-photon transitions, obs. by high power microwave double resonance 0-77925
PF₃, saturated absorpt., using CO₂ and N₃O lasers 0-70844
PF₁O₂, photoelectron spectra, change in ligand geometry on co-ordination 0-70942

PbCl₂, i.r. spectra in solid Ar matrix, vibrational assignment and force constants 0-49866

Pd complex, dithioacetylacetone Pd(II), electronic spectra, MO calc. 0-67748

0–67/48 Pd complexes, phosphines, far i.r. spectra (600-100 cm $^{-1}$) 0–77763 Pr complexes, Pr $^{1+}$ β -diketonates, spectral intensities 0–39399 Pr III complexes, hypersensitivity of spectral bands 0–77833 Pt complex, (histidine), i.r. spectra confirming trans structure 0–64447 Pt complex, dithioacetylacetone Pt(II), electronic spectra, MO calc. 0–67748

Pt complex, unmoacetyractone Pt(II), electronic spectra, MO calc. 0.67748

Pt complexes, [Pt(L)(SCN)₂], L=ethylenediamine or C- or N-substituted ethylenediamine, electronic 0-55317

Pt dialkyl cpds., i.r. spectra rel. to spectra of chemisorbed hydrocarbons 0-77834

Pt₆-2, electronic absorption spectra 0-46508

RuO₄, absorpt., rel. to electronic struct. 0-70941

S₁-2, i.r. rel. to struct. 0-70948

S₂-2, i.r. rel. to struct. 0-70948

SCO₄, radiative transitions, theory and expt. 0-77773

S₂Cl, and S₂Br₂ i.r. spectra 220 700 cm⁻¹ 0-64449

SF₆, saturated absorpt. using CO₂ and N₃O lasers 0-70844

SO₃, iB₁-4N₂ region, at 4.2°K 0-79317

SO₃, broadening of rotational lines by dipolar gases 0-64448

SO₂, electronic transitions 0-39400

SO₃, i.r., dipole moment obs. 0-55320

SO₃, photoelectron spectra rel. to vibr. fine struct. in electronic states 0-61121

0 -61121
SO₂, photoelectron, interpretation using results of extended basis SCFMO calculation 0-67753
SO₃, i.r., and mol. struct., obs. 0-43134
SOC1, solvent effects on infra-red band shapes and intensities 0-39802
SOC1)s Solvent effects on infra-red band shapes and intensities 0-39802
SOC1)s The struct of the structure of

SeO₂, microwave spectrum, 8000 36000 MHz, equil. struct, parameters 0-64453

SeO₃, Interowave spectrum, 8000 30000 MHz, equil. Struct. parameters 0-64453 Si₂Cl₆, Si₃Br₈ and Si₃I₆, ir. 0-55325 Si₅Cl₆, Si₃Br₈ and Si₃I₆, ir. 0-65325 SiF₂ emission in near u.v. from electrodeless discharge of SiF₄ vapour, ground and excited states 0-46514 SiH₄, photoelectron spectra 0-61168 SiH₄, photoelectron spectra 0-61168 SiH₄, photoelectron spectra 0-74307 (SiH₄)₅CH₂, ir. 0-74845 SiHCl₇ and SiDCl₈, ir. spectra and force constants 0-70951 (SiH₄)₅O₄ir. 0-74846 SiH₂PH₂ and SiD₄PD₂, ir. 0-74307 SnCl₅, ir. spectra in solid Ar matrix, vibrational assignment and force constants 0-49866 SnF₄ diadducts with 4-subst. pyridine 1-oxides and 4-subst. quinoline 1-oxides, l.f. i.r. spectra 0-49894 Sn₂O₃, Sn₃O₃, Sn₄O₄, matrix isolated, i.r. spectra 0-61138 TeO₃, absorption spectra 5000-2000 Å 0-64456 Ti complex, [Ti(bipy)₃] and Li[Ti(bipy)₃] 3.7THF, electronic spectra 0-46464

TiBr band spectrum excited in emission in radio-frequency discharge

0-43137

TiCl₄ vapour, absorpt, spectrum at 20, 300 and 700°C, windowless gas cell appl. 0-49153 TiF₄ diadducts with 4-subst, quinoline 1-oxides, l.f. i.r. spectra 0-49894

appl. 0–49153

TiF₄ diadducts with 4-subst. quinoline 1-oxides, l.f. i.r. spectra 0–49894

TiSbCl₆ ir. study and assignment 0–67754

UF₄, i.r. spectra, force constants 0–64459

UO,F₅ complexes, i.r. absorpt. 0–58199

V complex, [V(bipy)₁]², z=+2, +1, 0, -1, electronic spectra 0–46463

(VF₆)² electronic spectrum investigation of ion 0–64395

V(IV) complexes, VF₄ para substituted pyridine N-oxides, N-O stretching mode obs. 0–39403

W(CO)₆, vacuum u.v. spectra 0–70867

Zn (II) complexes with thiourea, i.r. 0–74313

Zn hexathiocyanates, i.r. spectra 0–46517

Zn trithiocyanate complexes, i.r. spectra 0–49896

ZnCl₃ vapour, absorpt. and emission spectra at 700°C, windowless gas cell appl. 0–49153

Zn(II) halide complexes, of NH₃ and imidazole, i.r., 500 to 40 cm⁻¹₃ 0–55329

Zr(SO₄)₂ hydrates, i.r. absorpt. data and H bonding 0-55330

inorganic molecules, polyatomic, radiofrequency

see also Nuclear magnetic resonance and relaxation; Paramagnetic resonance and relaxation

B₃H₃Br₄ rotational spectra of 8 isotopic species, 10-27 GHz 0-70875 COS, elec. polarizability anisotropies obs. 0-70923 COS in H₂, He, N₂ and Ar gases, microwave absorption at high pressure 0-53278

0-33218 CD₁, struct. obs. 0-70892 D₂O, microwave spectrum, rotational levels of ground vibrational state 0 74254

0 74254
D₂O₂ rot. spectra, microwave 0-53030
D₃O₂ rot. spectra, microwave o-53030
D₃O₃ rot. spectra mand submm wave spectra rel. to Q-branch transitions 0-70900
H₃O₄ rel. to quadrupole moment and sign of elec. dipole moment 0-70912
NH₃, microwave inversion spectrum line-width parameters for (1≤J≤8, K=1) lines 0-55304
NH₃ in H₃, He, N₂ and Ar gases, microwave absorption at high pressure 0-53278
N₃O₄ elec. polarizability anisotropies obs. 0-70923

0-3278 Ni₂O, elec. polarizability anisotropies obs. 0-70923 Ni complex, cyclopentadienyl Ni nitrosyl, bond lengths and angles from microwave spectra 0-49883

Spectra continued

inorganic molecules, polyatomic, radiofrequency continued

OCS, anomalous spectrum assoc. with sudden Stark shifts 0-74298

inorganic solids absorption, light metals, cancellation effects 0-66031

actinide 5f compounds 0-58102

actinides, crystal field spectra 0-41220

alkali halide, F-centre emission, Stark effect, 2-150K 0-56536 alkali halide, for i.r., of colour centres 0-75364

alkali halide, valence band deform. pot. constants from piezo-optic const. u.v. dispersion 0-44782

alkali halides, de colour centres, optical transitions of OH- and SH- impurities of OH- impurities of

0-72350
alkali halides, irrad., colloidal colour centres obs. 0-40178
alkali halides, paraelec. defects, lattice resonant modes 0-76080
Alkali halides, transient optical absorption by self trapped excitons
0-66029
alkali halides absorption and emission spectra review 0-58646
alkali iodides, fund. absorpt., strain effects 0-62644
alkali metal, optical absorpt., many-particle approach 0-79292
alkali metal, thin film, abs. rel. to electronic struct. 0-62643
alkali metal oxides, matrix isolated, i.r. spectra and force consts. 0-66033
alkali metal nitrates, crystalline field effects on ir. spectra 0-59404
alkaline earth borate glass, charge transfer absorpt. by ferric iron
0-59392
alkaline earth fluorides, absorpt., colour centres 0-75176

alkaline earth fluorides, absorpt., colour centres 0-75176 alkaline earth sulphides, fundamental absorption, excitation 0-56538 alkaline-earth halides, orthorhombic, i.r. transmission and lattice vibr. 0-40535

alloys isotopic, vibration spectra calc. using Green's functions methods 0-76058

alum, methylammonium aluminium sulphate/selenate dodecahydrate, rel. to ferroelec. behaviour 0-66066

amorphous semiconductors, Ge, InSb, Se, Te and As₂Se₃, elec. props. 0-47721 andradite, oscillator strength, effect of next-nearest neighbour interaction 0-44826

0-4820 anthophyllite-gedrite series, hydroxyl stretching freqs. in i.r. spectra 0-48060 antiferrodiclectric, Davydov splitting 0-62636 antiferroelectric, NH₄H₂PO₄, far-i.r. Fourier transform. determ. of complex permittivity spectra 0-66023 antiferroelectric, NH₄H₂PO₄, far-i.r. reft. 0-69110

permittivity spectra 0–66023 antiferroelectric, NH₄H,PO₄, far-ir, refl. 0–69110 antiferroelectric transitions in NH₄H,PO₄ and NH₄H₂AsO₄, i.r. absorpt. 0–40878 antiferromagnet, Cr and alloys, absorpt. obs. 0–72356 antiferromagnet, cr-O₂, phonon sidebands of bimol transitions 0–62639 antiferromagnet, two-magnon spectra 0–62658 antiferromagnetic α-O₂, double excitation band shift and splitting 0–44851 apatite, i.r. obs. of PO₄ vibrations 0–62655 apatite single cryst, polarized ir. reflectance 0–69106 apatites, CO₂²-containing, i.r. absorpt. 0–69119 apatites, synthetic, i.r. absorpt. 0–55768 rel. to arcs spectroscopic obs., Aul lines analysis 0–55527 arsenates and selenates, 4000 to 250 cm⁻¹, high and low temp. forms 0–55322 ascharite, i.r. obs. 0–41214 in band struct. calcs. 0–75480 band struct. calcs. 0–75480 band struct. calcs. 0–75480 bentonite structures, transformed i.r. analysis 0–62649 boracites, ferroelec., absorpt. 0–79302 β-brass, disordered, density of states for electrons, T matrix calc. 0–43993 Ca₁. Sin absorption, photoexcitation and luminescence spectra at 90, 250 K. 0–62654 chalcogenide glass, i.r., O impurities and defects. 0–47238

K 0-62654
chalcogenide glass, i.r., O impurities and defects 0-47238
chalcogenide glasses, transmission near absorption edge 0-39906
crystal, absorpt., ionicity 0-79295
crystalline, proton bombard, i.r. absorpt. 0-40139
Cs₂ZrCl₂:05⁴⁺, Ru⁴⁺, vibronic analysis, 4.2°K 0-41210
cubic crystalls, ⁴T₂ excited states of d^{3,7} ions, dynamic Jahn-Teller effect
0-41077

0–41077 diamond, GR I absorpt. band lineshape, rel. to vacancy centres 0–48063 diamond, electron irrad., ND I absorpt. centre, symmetry props. 0–51298 diamond, i.r. and u.v. nitrogen impurity conc. 0–54094 diamond absorpt. of N3-centres, Stark effect, point symmetry 0–62653 emission, light metals, cancellation effects 0–66031 europium chalcogenides, mag. ordering effects, obs. 0–59322 europium chalcogenides 0–59399 far i.r. spectroscopy using interferometers 0–49147 ferroelectric, KH₂PO₄, far-i.r. Fourier transform. determ. of complex permittivity spectra 0–66023 ferroelectric, KH₂PO₄, far-i.r. reflectivity, temp. depend. 0–66025 ferroelectric, i.r., free carriers effect 0–66026 ferroelectric, i.r., free carriers effect 0–66026 ferroelectric, zone-centre mode obs. at phase transitions 0–68917 ferroelectric alum, methylammonium aluminium sulphate/selenate dodecahydrate 0–66066 ferroelectric boracites, absorpt. 0–79302

ydiate 0-00000 ferroelectric boracites, absorpt. 0-79302 ferroelectrics, KH₂PO_x-type, i.r. absorpt. and proton dynamics 0-40864 ferromagnetic semiconductors, EuO, EuS, EuSe, reflectance, mag. ordering effects 0-44816

GaAs, neutron irrad. influence on refl. coeff. 0–69108
Ge, amorphous semiconductor 0–47721
germanate glass: Yb³⁺, ion coordination obs. 0–51310
glass, Ni²⁺ absorpt. obs. as nearest neighbour environment meas.

glass, Ni²⁺ 0-56529

glass, defect induced far infra-red absorpt., lattice vibrations 0-41221 glass, extinction coeff. of ferrous ion, environment influence 0-56528 glass, nitrate-containing, Cu(II), visible and i.r., ligand fields 0-51300 glass, silicate, absorpt. of d and f transitions 0-56552 glass, silicate, vibr. spectra 0-76128 glass arsenic chalcogenide, fundamental absorpt. edge, carriers, effective mass 0-44827

glass surface obs. i.r. spectroscopy involving multiple total internal reflection 0-71457

inorganic solids continued

glass u.v. absorption investigation for selection of filters for lasers 0-67065

graphite, transverse dielectric function, band struct, calc. 0-41190

hexafluoferrites, i.s. studies 0-71504 hexahalometalates 0-77764

hydroxyapatites, hydrothermally prepared, vibr. obs. 0-54110

i.r. absorpt., room temp. 0-48065

ix. and Raman, optical properties and collective oscillations as function of temperature 0-48085

ir. sources, wide waveband apparatus 0-76060 inert gas-methane mixed crysts., ir., rel. to struct. and methane conc. 0-72377

inorganic ions in alkali halide matrices, i.r. integrated intensities rel. to mech. anharmonicity 0-69113

ionic and semiconductor, i.r. absorpt, impurity complexes, localized vibra

ionic and semiconductor, i.r. absorpt. impurity complexes, localized vibration modes 0-56527 ionic cryst., extreme-u.v. absorpt. 0-79296 ionic crystal slab, surface modes, i.r. absorpt. 0-59391 ionoxation spectroscopy of surfaces 0-47906 lanthanide ternary complexes, i.r. spectra 0-66032 lattice resonant modes rel. to far i.r. absorpt. temp, depend. 0-44843 magneto-optical peak profile rel. to spin-phonon interaction constant 0-48015

metal, surface impedance meas. technque 0-44965

metali, surface impedance meas, technique 0–44965 metallic phthalocyanines in alkali halide matrices, i.r. integrated intensities rel. to mech, anharmonicity 0–69113 metals, free-electron like, plasmon-induced structure in optical interband absorption 0–66030 metals, light, cancellation effects in emission and absorption spectra 0–66031

0-66031 metals with chemisorbed CO, i.r. spectra comparison for Ag, Cu, Au, Co and Ni films 0-59394 mica, n-irrad., rel. to OH group rupture, i.r. obs. 0-40060 minerals i.r. refl. 0-66017 molecular, lattice-vibrational review 0-76062 molecular crystal, HCN (DCN), far i.r., l.f. vibs. 0-59402 molybdates, tungstates and periodates, 2000 to 40 cm⁻¹ 0-55323 olivine minerals, cation ordering from crystal field spectra 0-61880 optical transitions in impurity centres between local and energy band states 0-56530 orthoferites, i.r. spectra, 1-2.5 µm 0-79267

optical transitions in impurity centres between local and energy band states 0—56530 orthoferrites, i.r., spectra, 1-2.5 μm 0—79267 oxide solid solns, with Ni and Co ions, reflectance spectra 0—72343 oxide solid solutions, absorption and luminescence 0—56586 perovskite, K.MnF₃, i.r. active mode below phase transition 0—56525 perovskite, fluorides, electron-transfer states of pairs of unlike transition-metal ions 0—72346 perovskites, rare earth, electronic and i.r. spectra 0—66027 phosphate glass: Yb³⁺, ion coordination obs. 0—51310 photoconductor, i.r. absorpt. rel. to carrier photoexcitation 0—44830 photoconverter, n-CdS p-Cu_{2-xS}, long-wave sensitivity 0—75842 photoemulsion microcrystals additional band due to Ag centers 0—51296 polar cryst, optical phonons in presence of Landau quantization 0—75354 polycrystalline actinide and lantamanide compounds, using teflon powder 0—76057 pure and Li-doped semiconducting, i.r., small polaron model 0—62670 quartz, infrared radiation obs. from stimulated polaritons 0—41222 quartz, morion, smoky colouring features 0—59407 rare earth complexes, dilute, and mag. props., theory 0—40924 rare earth orthoferrites, Zeeman effects, spin Hamiltonian for even-electron singlet states 0—51313 rare earth orthoferrites, absorpt. and transmission bands, 0.5-50μ 0—69125

0--69125

Tare earth sulphate hydrates, i.r. low temp. behaviour 0-41178 rare earth trichlorides, isomorphous series 0-72348 Rh (III) complex, rhodium (III)- oxalato-triaquo-monammine oxalate 0-74940

O /4940 Rochelle salt, y irradiated abs. spectra 0-41184 Rochelle salt, absorption edge, position as a function of temp. 0-62683 rocksalt type struct, order-disorder, i.r. obs. 0-53670 ruby, excited-state electronic spectrum 0-69114 ruby, spin-forbidden line spectra and ⁴A₂₋₃⁴T₂ band obs. by magneto circular dichroism 0-72312

schorlomite, oscillator strength, effect of next-nearest neighbour interaction 0-44826

tion 0-44826 semiconductor, AlAs(P), fundamental absorpt. edge, 2-300K 0-44825 semiconductor, CdSh, i.r. plasma reflectivity, 3-30 µm, 85-300K, hole effective masses 0-75679 semiconductor, CdSnP2, electroreflectance, optical transitions 0-76066 semiconductor, CdSnP2, electroreflectance, optical transitions 0-769108 semiconductor, GaAs, neutron irrad, influence on refl. coeff. 0-69108 semiconductor, GaAs, photoreflectance line shape at fund. edge 0-76069 semiconductor, GaS(Se,Te) and InSe, electroabsorpt. and electrorefl.

semiconductor, GaSc, electro-reflectance spectra, 1.97-2.13 eV 0-79281 semiconductor, III-IV cpd., AlSb, deformation potentials of absorpt. edges 0-44824

semiconductor, InSb, electroreflectance spectrum, inter-conduction band transitions 0-44818

semiconductor, InSb, reflection, electron effective mass, band structure

semiconductor, Li-doped NiO/CoO, i.r., small polaron model 0–62670 semiconductor, SiAs, transition band gap energy determ., 300K 0–44854 semiconductor, amorphous, Ge, i.r. absorpt., 0.02-0.7 eV 0–48070 semiconductor, amorphous, absorpt. edge and internal elec. fields 0–79290

0—79290
semiconductor, amorphous 0—53821
semiconductor, arsenic chalcogenide glass, fundamental absorpt. edge, carriers, effective mass 0—44827
semiconductor, deform.-pot. consts. of group-III impurities 0—79304
semiconductor, direct zinc-blende, band-edge optical transitions, uniaxial strain effects 0—44806
semiconductor, doped polar, coupled magnetoplasma phonon modes obs. 0—54084

0 - 54084semiconductor, europium chalcogenides, mag. ordering effects, obs. Spectra continued inorganic solids continued

semiconductor, exciton differential spectrum in crossed and parallel fields

semiconductor, group V and IV-VI, reflectivity, band structure 0-79270 semiconductor, magnetic, CdCr₂S₄, CdIn₂S₄:Cr, absorpt. edge, magneto-optical obs. 0-56540

semiconductor, magnetic, conf., Yorktown Heights, USA, Nov. 1969 0-56237

semiconductor, magnetic, europium chalcogenides 0-59399

semiconductor, magnetic, europium chalcogenides 0—59399 semiconductor, magnetic, indirect transitions, mag. field depend. 0—5632 semiconductor, n-CdTe, Faraday effect in i.r. 0—66015 semiconductor, n-Ge, optical mixing due to cond. electrons 0—79268 semiconductor, p-GaP, doped, i.r. reflectivity, effective mass of holes determ. 0—79280

semiconductor, quaternary alloy, (II-VI)-(III-V), band gap variation

0 40187 semiconductor, thermoreflection, expt. methods 0-66019 semiconductor, valley-orbit interaction, effect on donors 0-54091 semiconductor SrTiO₃, Ce and Nb dopants effects 0-47725 semiconductor or semimetal film, free carrier absorption, imperfect surface

semiconductors, diamond and zinc-blende struct, direct exciton spectrum 0-66014

u-ob014
silica surfaces, i.r. obs. 0-50357
silicate glass: Mn²⁺, and conc. depend. luminesc. 0-62674
silicate glass: Yb²⁺, ion coordination obs. 0-51310
silicate glasses, absorpt. of and f transitions 0-56552
silicate glasses, vibr. spectra 0-76128
silver halides, electron-phonon interactions in optical transitions 0-76084
spinels, i.r., rel. to force consts. of octahedral and tetrahedral bonds
0-70869

double sulphates and selenates, including Tutton's salts, i.r. spectra, 2000 to 40 cm⁻¹ 0-55321

transition metal complexes, dilute, and mag. props., theory 0-40924 transition metal dichalcogenides, optical absorpt. photocond., excitons 0-47875

transition metal ions in crysts., absorpt. from metastable excited stress 0-54092

0—54092
transition metals, Auger-electron spectra 0—43533
transition metals, 1 period, K- and L_{III}-absorpt., band structure 0—79318
vacuum u.v. window mats., transmittance limit temp. depend. 0—51311
vibronically coupled orbital triplet, band-shape 0—62635
[PbBr₆]⁴- complex, abs. 0—72365
[PbCl₆]⁴- complex, abs. 0—7687
[PbCl₆]⁴- complex, abs. 0—7687
[PbCl₆]⁴- complex, abs. 0—7687
[PbCl₆]⁴- complex, abs. 0—7688
[PbCl₆]⁴- complex, abs. 0—7687
[PbCl₆]⁴- complex, abs. 0—7688
[PbCl₆]⁴- complex, abs. 0—7687
[PbCl₆]⁴- complex, abs. 0—7688
[PbCl₆]⁴- co

tronic structure 0–65577
AgNO₃, crystalline field effects on i.r. spectra 0–59404
n. Ag, Te, i.r. reflection, elec, props., carrier effective mass. 0–44186
Al, peaks at L₂₁ absorpt. edge, room and liq. N; temp. obs. 0–44832
Al, vibrational spectra 0–53688
Al film deposited from AlCl₃, NH₃, i.r. 0–61666
Al low energy absorptivity at 4.2K, 0.2-5.0 eV 0–59393
AlAs(P), fundamental absorpt. edge, 2-300K 0–44825
AlLaO₃:Pr²¹, Zeeman decomp. of energy levels 0–51297
AlN, band structure, reflection peaks 0–76065
AlN, reflection, 5-12.5 eV at 293K and 1.5-5 eV at 77K 0–59388
Al₂O₃, corundum, abnormal phonon distrib., i.r. refl. spectrum 0–53685
Al₂O₃, corundum, with transition- metal ions, charge-transfer spectra 0–41188
Al₂O₃, vacuum u.v. window mats., transmittance limit temp. depend.

 Al_2O_3 , vacuum u.v. window mats., transmittance limit temp. depend. 0-51311

0-51311

Al₂O₃3WO₃, absorption, 4.2, 77 and 290 K 0-79298

AlSb, deformation potentials of absorpt, edges 0-44824

Ar:Li, Na, In, Hg, Cd, absorpt, rel. to at, interactions, obs. 0-49783

Ar, solid, with substitutional H- and Li-atom impurities 0-41175

As₂S₃, abs., with temp. 0-69116

As₃S₄, vitreous, reflectivity, absorpt., photocond. 0-53816

As₃Se₄:As₅O₅ semiconducting chalcogenide glass, i.r. spectrum 0-59184

As₃Se₅:As₅O₅ semiconducting chalcogenide glass, i.r. spectrum 0-59184

As₅Se₅, single crystal and amorphous film, absorpt., photocond., elec. cond. 0-47705

As₅Se₅: single crystal and amorphous film, absorpt., photocond., elec. cond. 0-47705

As₅Se₅: As₅Se₆: amorphous film, absorpt., photocond., elec. cond. 0-47705

As;Se₃, single crystal and amorphous film, absorpt., photocond., elec. cond. 0–47705
As;Se₃ semiconducting chalcogenide glass, i.r. spectrum 0–59184
Au, reflectance, rel. to band struct. 0–62645
Au, dispersed layers, relationship between absorption selectivities in visible and i.r. 0–69117
B, β-rhombohedral crystal, reflection and transmission, lattice vibrations, impurity bands 0–51291
B halide complexes with 4,4′ dipyridyl. 0–66035
BP, refl., vacuum u.v. 0–79272
Ba zaide, i.r. assignments and cryst. struct. 0–72352
BaFs, in Kr matrix at 20°K, i.r., rel. to mol. geometry and vibr. modes 0–54095
BaFy in solid Kr matrix, i.r. rel. to apex angles and force consts. 0–77779
BaN₆, i.r. spectra 0–54093
Ba(NO₃)₃, i.r. refl., internal vibrs., anharmonicity 0–69118
BaN(0₃)₃, i.r. refl., internal vibrs., anharmonicity 0–69118
BaN(0₃)₃, i.r. refl., internal vibrs., anharmonicity 0–6918
Ba₃Sr_{1-x}Nb₂O₆ crystal, transmission 0,3-1.3μm, Czochralski prep., goniometry, dielec. permittivity 0–65148
BaTiO₃ doped with Cr ions, transmission spectra in visible and i.r. regions 0–71602
BaTiO₃ powderes, i.r. absorption 0–59420
BrCN, absolute absorpt. intensities of i.r. librational modes 0–41194
BrCN, absolute absorpt. intensities of i.r. librational modes 0–70895
CO, chemisorbed on Ag, Cu, Au, Co and Ni films, i.r. spectra comparison 0–59194
CO adsorpt. complexes on MgO, i.r. spectra 0–65104

CO adsorpt. complexes on MgO, i.r. spectra 0-65104

Spectra continued inorganic solids continued

CO2, i.r. intensities of lattice modes 0-48062

CO2, longitudinal i.r. bands 0-59395

C₃S₂, vibrational, fundamental, first and second overtones of ν_7 , and potential function 0–72353 CaCO₃:Mn²⁺, forbidden transitions (Δ m=±1) in absorpt. e.p.r. spectrum

0-76211
CacO₃, artificial calcite, morphology, optical parameters, irrad. effects 0-78398
CacO₃, ir., meas. of uniaxial spectral dielec. response 0-72354
CacO₃, ir. transmission and reflection, anisotropy of limiting freqs. 0-54107

CaCO₃, ir. transmission and reflection, anisotropy of limiting freqs. 0–54107
CaCO₃, two-phonon absorpt, at low temp. 0–76107
CaF₂: Ca colloidal system, high power ruby laser pulses 0–41218
CaF₃: CaC₃: energy level cales. 0–41080
CaF₃: Mn²⁺, new centre, field splitting obs. 0–51391
CaF₃: M₂: poptical spectra determ, of cause of different colorations 0–68249
CaF₂, in Kr matrix at 20°K, i.r., rel. to mol. geometry and vibr. modes 0–54095
CaF₃, M centre metastable triplet state 0–68370
CaF₃, optical absorption of single crystals, Smakula and Mollwo spectra 0–56537
CaF₂, X-irrad, colour centres 0–40181
CaF₃: nisolid Kr matrix, i.r. rel. to apex angles and force consts. 0–77779
Cal₃: Pb, absorption, photoexcitation and luminescence spectra at 90, 250 K 0–62654
CaMg(CO₃), two-phonon absorpt, at low temp. 0–76107
Ca(NO₃), powdered crysts, i.r. spectra 0–66065
Ca₃(PO₄); Tl spectra obs. 0–51341
Cal₃(PO₄); Tl spectra obs. 0–51341
Cal₃(PO₄); Agsignment of i.r. bands 0–77778
Cal₃(PO₄); F₃ hydroxyl ion in 4000-1800 cm⁻¹ region, impurity orientation 0–51302
Cal₃(Sr₄F₂, phonon contrib, Green-function method cales. 0–44809

 $^{O-31502}_{Ca_{1-s}Sr_{p}T_{2}}$, phonon contrib., Green-function method calcs. 0–44809 $^{Ca}W_{0,i}H_{0}^{3+}$, ground term energy levels of H_{0}^{3+} 0–62663 $^{Ca}W_{0,i}N_{0}^{3+}$, Na*-compensated, absorpt. and luminesc., 1.06 μ region 0–44829

0—44829
Cdi n solid Xe, u.v. absorpt. spectra 0—41207
CdCr,S4, CdIn,S4:Cr, absorpt. edge, magneto-optical obs. 0—56540
CdF₂:Ni²⁺(Cr³⁺), low-temp. spectra, site distortions 0—48066
CdF₂:2H₂O, i.r., struct, thermal stability 0—58729
CdGeAs₃, crystalline and vitreous state, electronic and vibrational 0—47505

0-47505
CdGeAs₂, reflectance spectra determ. 1.5-6.0 eV by reflectance, thermoreflectance and electroreflectance 0-76063
CdGeP₂, CdGeAs₂, i.r. absorpt., room temp. 0-48065
Cd₁, trapping centres, spectra and luminescence 0-56592
CdO-CdF; system. compound formation 0-69206
CdS:Cl, exciton and impurity absorpt. 0-59397
CdS:Cu**, paramag. centres and i.r. absorpt. correl. 0-72370
CdS:Li, reflection and luminescence, 77k, dopant conc. depend. 0-56622
n-CdS-p-Cu_{2-x}S, photoconverter, long wave sensitivity 0-75842
CdS, Cl donor excited states obs. 0-76067
Cds. electro-absorption, 85-300K 0-41193
CdS, electro-effection, 300K, field strength depend., Lorentzian broadening 0-69107
CdS, exciton absorpt., deformation effects 0-76095

Cds, exciton absorpt, deformation effects 0—76095
Cds, i.r. absorpt, rel. to carrier photoexcitation 0—44830
Cds, light-modulated reflectance and detailed structure 0—54085
Cds, thermoreflectance near fund. absorpt, edge 0—79275
Cds crystal, absorption, optical densities, doublet structure, exciton bands 0—48068

0-48068
CdS single crystal, electroreflectance spectrum near fundamental abs. edge at room temp. 0-66018
CdS,Se_{1-x} mixed cryst., vibr., props., doping effect 0-43858
CdS(Se)(Te) films, absorpt., in 36-150 eV region 0-48080
CdSb, ir. absorpt. edge. 295 and 130 K, band struct. 0-76094
CdSb, ir. plasma reflectivity, 3-30 μ m, 85-300K, hole effective masses 0-75679
CdSiAs, crystal ir reflection and absorpt. 300 and 83K, 0-48064

CdSb, i.r. absorpt. edge, 299 and 130 k, vanious constitutions of the constitution of

Co-complexes, monodentate selenato, i.r. 0-55324 Co²⁺ in tetrahedral crystals with axial distortion, MO approach 0-76097 CoHPO₄.1.5H₂O, and dehydrated and deuterated products, i.r. absorption spectra rel. to state of H₂O molecule 0-62656 CoO, pure and Li-doped semiconducting, i.r., small polaron model 0-62670

0-62670
CoO, reflectance, optical consts. 0-79276
Cr and alloys, antiferromag., absorpt. obs. 0-72356
Cr₂O₃, supported on alumina, reflectance spectra at room temp. 0-62487
Cs₃CO₄·VO²⁺, ir. absorpt. and e.p.r. rel. to A. g. tensors, obs. 0-41347
CsBr: NH₄+, pressure-scanned Fermi resonance at 100°K 0-48047
CsBr with distributed colloidal Ga, In, absorption bands 0-56542
CsBr(I), two-photon spectroscopy 0-79300
Cs₂Cr₂O₇, ir. and Raman, space group 0-56563
Csl:Ti+, resonant bandmodes, shape rel. to uniaxial stress and dislocations 0-79314

0-19314
Csl, multiplet absorpt. band, extreme u.v. 0-66040
Csl with distributed colloidal Ga, In, absorption bands 0-56542
Cs₃(Mg_{1-x}Ni_xCl_xCl_xCl_y polarized electronic absorption spectrum 0-62669
CsMnF₃, absorpt., exciton, magnon and phonon structs., 3900Å 0-54096

Spectra continued inorganic solids continued

CsNpF₆, crystal-field diagram for 5f²Np⁵⁺ 0-41220 CsUO₃Cl₄, absorpt, interpret. 0-41232 Cs[UO₃(NO₃)₃] cross-section for excited absorption of uranyl ions 0-44921

Cs[UO₂(NO₃)₃] cross-section for excited absorption of uranyl ions 0–44921 Cu-(½25at.%)Ni-(25at.%)Zn alloy, absorpt. edge from reflectance meas, 1.55-5.18 eV 0–44815 Cu, arc close-electrode effects in magnetic field 0–43374 Cu, vibrational spectra 0–53688 Cu halides, thin film, absorption in 185-3500 nm region 0–41198 CuCl, excitonic electroreflectance 0–76068 Cu₃₄Ge₆, optical absorption and photoelectron energy distribution for electronic structure 0–65577 Cu(III) in nitrate-containing glass, i.r. and visible, ligand field effect 0–51300 Cu(KSO₄)₂.6H₂O single crystals, diluted with Zn(KSO₄)₂.6H₂O, optical absorption spectra 0–76099 CuO, diffuse reflectance, down to 200 mμ, pure and diluted samples 0–56523 Cu₂O, diffuse reflectance, down to 200 mμ, pure and diluted samples 0–56523 Cu₂O, diffuse reflectance, semicond. behaviour 0–79301 CuS, hydrated and anhydrous, SO₄2- obs. 0–44866 Cu₂Te, absorpt, rel. to intrinsic semicond. behaviour 0–79301 Cu₂(Fe(CN)₂) i.r., rel. to struct. and Fe-C stretching motion 0–72349 D₂ in solid Ar, fundamental i.r. absorption, molecular and lattice transitions 0–54098 D₂O₃ in Solid N₂ matrix at 20°K, i.r., rel. to struct. and bonding 0–70911 Dy, absorpt. and refraction, 1.13-3.96 eV 0–76009 Dy_{2,8} NA₁O₂, garnet, absorption of Na³ 0–76113 ErCrO₃, ground state splitting, temp. depend., 1.5-140 K 0–59398 Eu chalcogenides, reflectance, multiplet struct., mag. field effect 0–44812 Eu chelates, absorption in u.v. 0–66028 EuAlO₃, absorpt., 17100-21500 cm⁻¹, crystal field splitting 0–41200 EuAlO₃, absorpt., 17100-21500 cm⁻¹, crystal field splitting 0–41200 EuAlO₃, absorpt., 17100-21500 cm⁻¹, crystal field splitting o–41200 euCl(III) complexes, β-diketonates, i.r. and Raman spectra 0–48090 EuO, ferromag. semiconductor, reflectance, mag. ordering effects 0–44816

Eu(III) complexes, PeuO, ferromag. semiconductor, renectate, 0—4816
EuOF:Eu³+ rhombohedral, absorpt. and fluoresc. 0—51301
EuS, ferromag. semiconductor, reflectance mag. ordering effects 0—44816
EuSe, ferromag. semiconductor, reflectance, mag. ordering effects

EuSe, ferromag, semiconductor, reflectance, mag, ordering effects 0-44816
Eu;SiO₄, energy gap change on phase transition 0-62128
EuTe, antiferromag, reflectance, mag, ordering effects 0-44816
fe complex, bis (N, N dialkyl dithiocarbamato) Fe (III) halides, far ix. spectra 0-62657
FeF₂, antiferromag, two-magnon spectra 0-62658
α-FeOOH conversion to hematite by heat treatment, ix. investigation 0-68512
FeS-9 uranyl glass, cross-section for excited absorption of uranyl ions 0-44921

Fes. 9 uranyl glass, cross-section for excited absorption of uranyl ions 0-44921

Fe₄[Fe(CN)₆]₃, rel. to struct. and Fe-C stretching motion 0-72349

Ga_{1-x}Al₂As mixed crystals, i.r. lattice-vibration spectra 0-44817

GaAs:Cd⁺, ion implantation damage, reflectivity, annealing effect 0-79279

n-GaAs, absorpt., 1-6 μ m, Hall mobility proton irrad. and temp. depend. 0-41202

GaAs, electroreflectance spectra at hydrostatic pressure, 6800 kg/cm² 0-59389

n-GaAs, epitaxial, far i.r. donor-state absorpt. and photoconducting 0-44838

0-44838
GaAs, i.r. reflection room temp., 2-60, potical phonon lifetime 0-48051
GaAs, interband piezo-absorption 0-44835
GaAs, ultrapure, photoreflectance line shape at fund. edge 0-76069
GaAs, wavelength-modulation, 1.75-6.0 eV 0-44811
GaAs, wavelength modulation, 5°K, 2.8-6.0 eV 0-51292
GaAs with Nd and Mn impurities, meas. 0-51258
GaAs_{1-x}Sb, fari.r. reflectivity, long wave optical phonon modes 0-76070
Ga_{1-x}In_xAs, fari.r. reflectivity, long wave optical phonon modes 0-76070
GaN, thin films, optical absorption and vacuum ultraviolet reflectance 0-62662

0-62662
GaP:Mg, pair spectra involving shallow acceptor 0-62660
GaP:Te, photoioniz. energy, absorpt. spectrum obs. 0-76101
GaP:Te, rel. to effective mass calcs. 0-44810
GaP, absorpt. coeff., 530-1100 nm 0-59401
p-GaP, doped, i.r. reflectivity, effective mass of holes determ. 0-79280
GaP local-mode lattice vibrations obs. in Raman scatt. and as cooperating phonon in optical transitions 0-78716
GaS(Se,Te), electroabsorpt. and electrorefl. in exciton absorpt. region 0-66021
GaS(Se) i.r. absorpt. 50-300K phonon struct. 0-41203

GaS(Se, Te), electroabsorpt, and electrorefl. in exciton absorpt. region 0–66021
GaS(Se), i.r. absorpt., 50-300K, phonon struct. 0–41203
GaSb, electroreflectance, spin-orbit splitting 0–72037
GaSb, electroreflectance spectra 0–79282
GaSb, rel. to electronic structure, local pseudopotential model 0–43994
GaSb, wavelength-modulation, 1.75-6.0 eV 0–44811
GaSe, absorpt., 77K, exciton region, elec. field effect 0–41201
GaSe, absorption, 77 and 292 K, hyperbolic excitons 0–79303
GaSe, electro-reflectance spectra, 1.97-2.13 eV 0–79281
GaSe, electro-absorption, 80-395 K, exciton annihilation 0–62659
Gd, absorpt, and refraction, 1.13-3.96 eV 0–76009
Ge:Sb, far i.r. absorpt., conc. depend. 0–54097
Ge-Si, amorphous alloy, fundamental absorpt., reflectivity, transmission, ellipsometry 0–48069
Ge, amorphous film, i.r. absorpt., 0.02-0.7 eV 0–48070
Ge, deform-pot. consts. of group-III impurities 0–79304
Ge, electroreflectance line shape, light and heavy holes 0–75707
Ge, i.r. absorpt., surface props., silane treatment depend. 0–40800
n-Ge, long wavelength i.r. absorpt., 1.5K, impurity effect 0–41204
n-Ge, optical mixing due to cond. electrons 0–79283
Ge, wavelength ir. shorpt., 1.5K, impurity effect 0–41204
n-Ge, optical mixing due to cond. electrons 0–79283
Ge, wavelength modulation, 1.75-6.0 eV 0–44811
GeO₂, vacuum u.v. window mats., transmittance limit temp. depend. 0–51311
GeSe_{0.75} Te_{0.25}, reflectance spectrum, band struct. obs. 0–76071
H halides, charge transfer effect 0–66022

U=1511 GeSe_{0.75}Te_{0.25}, reflectance spectrum, band struct. obs. 0-76071 H halides, charge transfer effect 0-66022 H solid, lattice-vibrational spectra 0-76062 p-H₂, i.r., lattice dynamical effects in frequency anal. 0-72388

Spectra continued inorganic solids continued

 H_2 in solid Kr, fundamental i.r. absorption, molecular and lattice transitions $0\!-\!54098$

HCN, DCN, far i.r., l.f. vibs. 0-59402 HDO in solid N₂ matrix at 20°K, i.r., rel. to struct. and bonding 0-70911

HDO in solid N₂ matrix at 20°K, i.r., rel. to struct. and bonding 0-70911 HlO₃, vibr. spectra 0-51304 H,O in solid N₂ matrix at 20°K, i.r., rel. to struct. and bonding 0-70911 H₃O₂·ClO₄-, i.r. 0-41195 H₂S, i.r. spectra in solid N₂ matrix 0-58174 HfO₂·₂(Dh₂x-H₂O₃ omorphous precip., rel. to comp., i.r. obs. 0-51312 Hg in solid Xe. Ar and Kr, u.v. absorpt. spectra 0-41207 Hg.Cl., diffuse refl., absorpt., emission and excitation spectra 0-76073 HgF₂, 2H₂O, i.r. struct. thermal stability 0-58729 HgS, cinnabar, fund. vibrs. obs. 0-41237 HgS, far i.r. reflectivity, Raman seatt., lattice vibrations 0-56085 HgS, plasma edge and band struct., reflectivity and absorpt. obs. 0-69109 HgS, trigonal and cubic, i.r. lattice bands 0-41206 n-HgTe, reflection, 80K, phonon-plasma interaction, band-band transitions 0-41180 HoFe gamet, absorption spectrum of Ho ions, characteristics 0-51305 HoFeO₃, Zeeman effects, spin Hamiltonian for even-electron singlet states 0-51313

HoPeU₃, Zeeman effects, spin Hamiltonian for even-electron singlet states 0–51313 HoGa garnet, absorption spectrum of Ho ions, characteristics 0–51305 Ho_{2.93}Nd_{0.05}Al₂O₁₂ garnet, absorption of Nd³⁺ 0–76113 I., refl., band struct. 0–56524 IO₃ solid solution in K1 lattice, i.r. spectra. 0–66045 In in Xe, absorpt. spectra at 4.5°K 0–41213 n-InAs, absorpt. coeff. at different doping levels 0–56546 InAs, excitonic effects on E₁ and E₁+Δ₁ transitions 0–48048 InAs, wavelength-modulation, 1.75-6.0 eV 0–44811 nAs_{1-x}Sb_x, far i.r. reflectivity, long wave optical phonon modes 0–76070 InCl₃, absorpt. spectra of V³⁺ and Cr³⁺; level splitting 0–79306 InP:B, i.r. absorpt. bands, rel. to localised B vibrations 0–79305 n-InSb.Te, absorpt. band struct. obs. 0–56547 InSb-InTe, reflection and transmission comp. depend. 0–48071 InSb, electroreflectance, rel. to band population effects 0–75489 InSb, electroreflectance spectrum, inter-conduction-band transitions 0–44818

InSb, highly alloyed n-type, i.r. absorption measured 0-69121 InSb, magneto-optical peak profile rel to spin-phonon interaction constant 0-48015 0-75656 nicrowave emission obs. 77K in d.c. magnetic and electric fields

0—75656
InSb, reflection, electron effective mass, band structure 0—47736
InSb, wavelength-modulation, 1.75-6.0 eV 0—44811
InSe, electroabsorpt, and electrorefl, in exciton absorpt, region 0—66021
In_{2(1-x)}Zn_xSn_xAs_x, reflectance spectra determ, 1.5-6.0 eV by reflectance, thermoreflectance and electroreflectance 0—76063
K halides, vibronic spectra of O₂-, S₂- and NO₂-, rotational degrees of freedom 0—53355

Treedom U-53335
K halides i.r. 435375
K halides i.r. 43507tion due to H⁻ ions anharmonic side bands of the local mode 0-72359
KBr:BO₇, i.r. absorpt., doublet struct. 0-44845
KBr:CrQ₄²-, i.r. absorpt., 120-800K 0-41208
KBr:Li⁺, far i.r. absorpt. temp. depend. rel. to lattice resonant modes 0-44843

KBr:NO₂-,NO₃-,i.r. absorption band parameters, 100-300K 0-62665 KBr:Tl, abs. and emission spectra in external elec. field 0-56550

KBr, KCl, thermal emissivity, far i.r., 80-600 K, meas., rel. to vibr. modes 0-76106

WBr, near and far i.r. vibr. absorptive of H_i⁻ and D_i⁻ centres 0-44841 KBr, SO₄² impurity centers studied from vibrational absorption spectra 0-56549

KBr, SO₄?— impurity centers studied from vibrational absorption spectra 0–36549
KBr, U band pressure shift 0–44844
KCl:Ag⁻, emission and absorption 0–44842
KCl:Ca basorption and luminescence spectra 0–56551
KCl:CrO₄?⁻, i.r. absorpti, 120-800K 0–41208
KCl:F, gamma irrad., i.r. absorption, internal vibration 0–79311
KCl:Li⁺, paraelectric resonance, internal strains effect 0–44355
KCl:NO₂-, NO₂- i.r. absorption band parameters, 100-300K 0–62665
KCl:OH-, microwave resonant absorpt. 0–79312
KCl:TCl, X-irrad., rel. to colour centres, absorpt. 200-1700 mμ 0–41211
KCl, colloidal centre diemss. obs. 0–48072
KCl, tetragonal Pb²⁺ centre, symmetry and structure, and trigonal R centre 0–51343
KCl, X-irrad., rel. to colour centres, absorpt. 200-1700 mμ 0–41211
KCl crystals containing quantities of AgCl and KOH, features of absorption 0–56548
K₂Cr(CN_b, ⁴Δ_γ-²T_γ transition 0–62664
K₃Cr(CN_b, ⁴Δ_γ-²T_γ transition in dodekahedral cryst. field 0–41177
KD₂PO₄, deuteron motion obs. 0–79285
K₃Cr(O₃)₄, electronic transition in dodekahedral cryst. field 0–41177
KD₂PO₄, far-i.r. Fourier transform determ. of complex permittivity spectra 0–66023
KH₂PO₄, far-i.r. Fourier transform determ. of complex permittivity spectra 0–66023
KH₂PO₄, far-i.r. absorpt. temp. depend. rel. to lattice resonant modes 0–44848
KI:Eu²⁺, absorption, as function of variation in activator concentration 0–59429

KI:Eu2+, absorption, as function of variation in activator concentration

K1:Eu²+, absorption, as function of variation in the control of variation of of

brooks 0-020/NgSO₄, langbeinite, effects of K replacement by Na and Mg by Ca on stability 0-68310 K₂[PdCl₄], absorpt., low temp. 0-79310

Spectra continued

inorganic solids continued

K₂[RuCl₅NO], i.r., vibrs. obs. 0-79309

Kr:Li, Na, In, Hg, Cd, absorpt. rel. to at. interactions, obs. 0-49783

Kr, reflectance for photon energies between 8 and 25 eV 0-79286

Kr. reflectance for photon energies between 8 and 25 eV 0—79286 LaCl₃:Nd³⁺, multiphonon radiationless relaxation 0—48049 LaF₃:Ho³⁺, absorption and fluorescence spectra, He³⁺ energy levels 0—79313 LaF₃:Nd³⁺, laser excitation, relaxation rates 0—76108 LaF₃:Nd³⁺ concentration broadening of absorption lines, contrib. of resonance interactions 0—44847 LaF₃:Tm³⁺, absorption 0.2-2.0 u 0—41212 LaF₃:Ir., meas. of uniaxial spectral dielec, response 0—72354 LaNbO₄:Nd single crystals, absorption spectra in polarized light 0—62597 Li halide, low temp. reflectivity, 5-10 eV, fine struct, excitons 0—76076 Li nXe, Kr and Ar, absorpt. spectra at 4.5°K 0—41213 LiCN, matrix isolated in Ar, i.r. spectra and vibr. freqs. 0—69122 LiF:Mn, F absorpt. band and es.a. obs. 0—75186 LiF, absorpt., neutron irrad. and thermal transformation of defects 0—40188 LiGeO₃:Nd glass, spectroscopic and laser characts. 0—57535

LiF, absorpt., neutron irrad. and thermal transformation of defects 0-40188
Li₂GeO₃:Nd glass, spectroscopic and laser characts. 0-57535
LiNO₃, attenuated total reflections 0-48053
LiNO₃, attenuated total reflections 0-48053
LiNO₃, i.r., rel. to temp., press, polarization, propag. direction and isotopic comp. 0-72364
Li₃NO₃, 10-72364
Li₃NO₄, O., X-, u.v. irrad., absorpt. rel. to cryst. growth temp., obs. 0-41337
Li₂UO₄, i.r. spectrameas., force constants and U-O lattice vibrations 0-65526
LiYF₄, Yb(Ho), i.r. to visible conversion, simple model 0-76155
LiYF₄, i.r. emittance and absorption 0-40525
LuAl garnet:Nd³⁺, absorpt. and luminesc, laser radiation 0-69123
Mg, radiative decay meas. of intrinsic damping rate and vol. plasmon energy 0-62638
Mg peaks at L₂₃ absorpt. edge, room and liq. N₂ temp. obs. 0-44832
MgBr₃, and MgI, diethyl ether complexes 0-74278
Mg(H,PO₃),6H,O, i.r. refl., optical consts. 0-76074
MgO₃:V²+(Ni²), emission, phonon sidebands 0-62666
MgO₃:r. refl., rel. to abnormal phonon distrib. 0-79287
MnF₂:Co₃:mupurity magnons, far i.r. absorpt. Raman scatt. 0-44697
MnF₂:Co₃:mupurity magnons spectra. 0-62658
MgE₃:antiferromas. two,magnon spectra. 0-62658 0-44843

0-44843
MnF₂, antiferromag, two-magnon spectra 0-62658
MnF₂, MnF₂:Fe³⁺, far i.r. transmission, antiferromagnetic resonance, two-magnon absorpt. 0-44979
MnF₂, two-magnon inc shape, ir. absorpt., Raman scatt. 0-44848
Mn₂O₃, diffuse reflectance, 200-1000nm 0-54088
MnSe-CdSe solid solution, transmission and reflectance, energy gap 0-54087

0-54087

MoS₂, optical absorpt., photocond., excitons 0-47875

MoS₂, optical absorpt., photocond., excitons 0-47875

MoTe₂, optical absorpt., photocond., excitons 0-47875

MoTe₂, optical absorpt., photocond., excitons 0-47875

N₂-H₂ in microwave discharge tube, afterglow effects 0-55306

N₂, reflection spectrum at 4.2°K, presence of Rydberg states 0-76075

ND₄F, Raman and far-infrared 0-41239

NH₄* in non-cubic cryst. sites, it. spectra for study of molecular motion 0-59063

NH₂ Re it. determ of structural and ordering changes 0-62119

http://december.com/december.co

Na, absorptin, near ir. to far u.v., calc. 0–41219
Na halide, low temp. reflectivity, 5-10 eV, fine struct., excitons 0–76076
Na halides, ir. absorption due to H⁻ ions, anharmonic side bands of the local mode 0–72359

Na inXe, absorpt, spectra at 4.5°K 0-41213 NaCl:Au, colloidal system, high power ruby laser pulses irrad. 0-41218

Na in Xe, absorpt. spectra at 4.5°K 0–4.1213

NaCl:Au, colloidal system, high power ruby laser pulses irrad. 0–41218

NaCl:Ce absorption and luminescence spectra 0–56551

NaCl:Co, X-irrad, S-centre obs. 0–75190

NaCl:Cu⁺, far i.r. absorpt. temp. depend. rel. to lattice resonant modes 0–44843

NaCl:Cu⁺, resonant bandmodes, shape rel. to uniaxial stress and dislocations 0–79314

NaCl:Nor, Noy-, i.r. absorption band parameters, 100-300K 0–62665

NaCl:OH⁻, microwave resonant absorpt. 0–79312

NaCl:Rh, absorpt. and e.p.r., X-irrad. effects, obs. 0–41217

NaCl, colloidal centre dimens. obs. 0–48072

NaCl(Au) colloidal syst., extinction spectra, computation by IBM 360-65
0–51286

NaCl(Na) colloidal syst., extinction spectra, computation by IBM 360-65
0–51286

NaF:Mn⁻²⁺, absorpt., 300 and 80°K and analysis 0–41216

NaF, NaCl, thermal emissivity, far i.r., 80-600 K., meas., rel. to vibr. modes 0–76106

NaH₃(Seo₃)₂, far i.r. reflectivity, 16-400 cm⁻¹, 300 and 202K, complex dielec.const. 0–56526

NaMgF₃, Sm²⁺, single cryst., in excited state, absorpt. spectra 0–41209

NaMgF₃, Sm²⁺, single cryst., in excited state, absorpt. spectra 0–69124

NaNO₂, force consts. from isotopic substitution in NO₂- radical 0–69124

NaNO₂, ir., during phase transition 0–66016

NaNO₂, long wavelength band, singlet-triplet No₂- transition 0–62667

NaNO₂, long tentral transition 0–6803

NaNO₂, 1r., during phase transition 0—60016
NaNO₃, nong wavelength band, singlet-triplet No₂- transition 0—62667
NaNO₃, attenuated total reflection 0—48053
NaNO₃, ir., rel. to temp., press., polarization, propag. direction and isotopic comp. 0—72364
NaNO₃, two-phonon absorpt. at low temp. 0—76107
Na₂O.Nb₂O₃-SiO₂ ir., and Raman spectra and structure 0—69139
Na₂O.SiO₂ glasses, water retention effect 0—58542
NaOD, matrix isolated, ir., rel. to struct., bending and stretching modes 0.6016

inorganic solids continued

NaOH, matrix isolated, i.r., rel. to struct., bending and stretching modes 0 - 69126

Na₂SO₄, X-, u.v. irrad., absorpt. rel. to cryst. growth temp., obs. 0-41337 B-Na₂UO₄, i.r. spectrameas., force constants and U-O lattice vibrations 0-65526

Na₂|Fe(CN)₂NO].2H₂O 0-76105 β-Nb-Ti, cubic alloy, band struct. 0-54089 Nb, superconducting, for i.r. absorption, energy gap width and critical temperature 0-44130 Nd³⁺ glass laser, energy levels, and spectral broadening 0-54879

temperature 0-44130 M3¹ :glass laser, energy levels, and spectral broadening 0-54879 Nd lines in glasses, inhomogeneous broadening, magnitude 0-62651 Nd¹* in garnets of formula RE_{2.95}Nd_{0.05}Al₃O₁₂ where RE=Ho, Tm, Dy 0-76113 Nd¹* laser ion in soda-lime glass, absorption, excited state and saturation

0-54100

Nd³⁺ laser ion in soda-lime glass, absorption, excited state and saturation 0–54100

Ne, film, abs. spectrum, 4.2 K 0–79316
Ne, solid, with substitutional H- and L-atom impurities 0–41175
Ne film, reflec, and transmission, in vac. u.v. 0–79288
Ni, vibrational spectra 0–53688
NiCl₃- Cs/(MgCl₃)Cl₃ tetragonal complex, polarized electronic absorption spectrum 0–62669
NiO₁ reflectance, optical consts. 0–79276
α-O₂, phonon sidebands of bimol. transitions 0–62639
α-O₃ cryst., antiferromag., excitation band shift and splitting 0–44851
O₂(1_A) trapped in solid O₂ at 4.2°K, emission spectra 0–62671
O₂F₁, i.r. 0–43130
PD₃Cl, far i.r. spectra of thin films and Raman spectra of polycrystalline sample 0–48092
PD₄Cl, i.r., rel. to lattice vibrs. and torsional oscills. 0–65521
PH₄Cl, i.r., rel. to lattice vibrs. and torsional oscills. 0–65521
Ph₃Cl, i.r. rel. to lattice vibrs. and torsional oscills. 0–65521
Ph₄Cl, i.r., rel. to lattice vibrs. and torsional oscills. 0–65521
Ph₅Cl, i.r. absorptivity, using Holstein-Boltzmann eqn. 0–72366
Ph, superconducting and normal, phonon contribution to far i.r. absorptivity 0–44852
Pb azides absorpt., 1900 to 7000 Å, 2978 to 100°K 0–51307

ity 0-44852
Pb azides absorpt., 1900 to 7000 Å, 298° to 100°K 0-51307
pb film, ellipsometry, absorpt., 0.6-6eV 0-62672
Pb films, band struct. obs. 0-76109
Pb(II) complexes in mixed solutions KCl-KI 0-76077
PbMoO₄:Np⁴⁺, absorpt., cryst. field and free ion params., obs. 0-41078
Pb(NO₃)₂, i.r. refl., internal vibrs. anharmonicity 0-69118
Pb(NO₃)₂, powdered crysts., ir., spectra 0-66065
PbS(Se) (Te), reflection spectra and band structure, 1-14eV 0-69111
PbS(Te) films, absorpt., in 36-150 eV region 0-48080
PbTiO₃ ceramic platelets and oriented single crystals, i.r investigation 0-71826
Pd(CN)₂²⁻⁻ microcrystals, u.y. results, attributions of absorption bands 0-71826
Pd(CN)₄?= microcrystals, u.v. results, attributions of absorption bands 0-59406
Pd(II) tetraamine complexes, square-planar, polarized u.v. refl. spectra 0-70944
PfF₃, far-i.r. absorpt., l.f. lines 0-51308
Pr(NO₃)₃.6H₂O, energy levels of Pr³⁺ 0-62673
Pt(CN)₄?= microcrystals, u.v. results, attributions of absorption bands 0-59406

0-39406 Pt(II) tetraamine complexes, square-planar, polarized u.v. refl. 0-70944 PuCl₃, thin films, absorption spectrum, new assignments 0-76110 pyroborates of Mg, Mn and Fe, with B₂O₃⁴⁻ and B₃O₆³⁻ radicals, i.r. spectra 0-41176

spectra 0-411/6 RbBr, absorption, soft X-ray, fine structure near Rb⁺M_{IV,V} edges 0-72400 RbCl:Mr¹⁻, absorption, cubic field parameters 0-44996 RbCl, absorption, soft X-ray, fine structure near Rb⁺M_{IV,V} edges 0-72400

Non-12400. Rbl cryst., undoped and Na-doped, abs. and emission spectra of colour centres 0-53554. RbMnF3, excition absorpt., Zeeman effect, Davydov splitting 0-66050. RbOD, matrix isolated, i.r., rel. to struct., bending and stretching modes

0-69126 RbOH, matrix isolated, i.r., rel. to struct., bending and stretching modes

0–69126
RbOH, matrix isolated, i.r., rel. to struct., bending and stretching modes 0–69126
Rh, clean (111) surface, Auger electron spectroscopy, LEED 0–65042
Ru, clean (0001) surface, Auger electron spectroscopy, LEED 0–65042
SO₂, 'B₁='A₁ region, at 4.2°K 0–79317
SO₂, singlet-triplet absorpt. and emission 0–69154
SbS1, far-i.r. reflectivity 0–66026
SbS1, far-i.r. reflectivity, temp. depend. 0–66025
ScBO₁:Ce³⁺, Tb³⁺, energy transfer between dopant ions 0–72436
ScCl₃, absorpt. spectra of V³⁺ and Cr³⁺, level splitting 0–79306
Se, amorphous, i.r. active lattice vibs. 0–66052
Se, amorphous, i.r. active lattice vibs. 0–66052
Se, amorphous, irr active lattice vibs. 0–66052
Se, amorphous, irr and effect structure from i.r. microscopy and spectrometry 0–66053
Se, amorphous, internal defect structure from i.r. microscopy and spectrometry 0–66053
Se, i.r. vib. analysis, trigonal, α-monoclinic, amorphous 0–66054
Se, i.r. vib. analysis, trigonal, α-monoclinic, amorphous 0–66054
Se, trigonal, energy band struct. obs. 0–66051
Si-Mg, excitation spectra and piezospectroscopic effects of neutral and singly ionized donors 0–51287
Si-O, absorption in the near and far infrared 0–54102
Si, amorphous fundamental absorpt., reflectivity transmission, ellipsometry 0–48069
Si, derivative abs. spectrum, abs. edge 0–41223
Si, neutron irrad., defect oxygen complexes, i.r. absorpt. 0–48055
Si, thermoreflectance 0–41181
Si, wavelength modulation, 1.75-6.0 eV 0–44811
Si, wavelength modulation, 1.75-6.0 eV 0–6035
SiAs, absorpt. and reflectance, 300K 0–44854
α-SiC:N, (6H) crystal, absorpt. 0.7-1.1μ 0–69128
Si-C. (6H), fundamental absorpt. edge, 4.2-600K, excitons, impurity effects 0–69127
n-α-SiC 6H, absorpt. analysis, 86 K, four-particle nitrogen-exciton complexes 0–48074

 $-\alpha$ -SiC 6H, absorpt. analysis, 86 K, four-particle nitrogen-exciton complexes 0-48074

SiD₄, in region of fundamentals v_3 and v_4 0-69130

SiH₄, i.r., interpretation rel. to possible site and factor groups 0–70952 SiH₄, i.r. gion of fundamentals ν_1 and ν_2 0–69130 (SiH₃):CH₂ and (SiD₃):CH₂, i.r. 0–77845 (SiH₃):O, i.r. 0–77846

Spectra continued inorganic solids continued

 α -SiO₂:Al, ν -irrad., absorpt. and e.p.r., 'Al' centre obs. 0-59456

SiO, passivating film, i.r. absorpt., thermal treatment depend. 0–51309 SiO₂, amorphous layer on Si, S-shift curve characts. of Si-O stretching band 0–72367

ound 0—72307 SiO₃, α-quartz, i.r. reflectivity, 380-640 cm⁻¹, extraordinary phonon dispersion 0—78737 SiO₃, far-i.r. absorpt.1.f. modes 0—76130 SiO₃, vacuum u.v. window mats., transmittance limit temp. depend. 0—51311

0-3111 SiO₂, vitreous, far-i.r. obs. of vibrs. 0-76129 SiO₂, fused, i.r., vibrational analysis 0-48075 Sm, absorpt. and refraction, 1.13-3.96 eV 0-76009 SmTe, obs., effect of pressure 0-65634 SnO₂-F films on glass, transmittance 0.3 to 2.5 μ and reflectance 4 to 20 μ

 500_2 : F mms on glass, transmittance 0.3 to 2.3 μ and renectance 4 to $20 \,\mu$ 0-69104 SrF_2 :Nd³⁺, obs., in wide temp.range 0-41186 SrF_2 , in Kr matrix at 20°K, i.r., rel. to mol. geometry and vibr. modes 0-54095

0-54095
SrF, in solid Kr matrix, i.r. rel. to apex angles and force consts. 0-77779
Sr(NO₃), i.r. refl., internal vibrs. anharmonicity 0-69118
Sr(NO₃), powdered crysts., i.r. spectra 0-66065
SrTiO₃, 3500cm⁻¹ absorp. band due to H impurities, temp. and elec. field depend. 0-66055
SrTiO₃, abs. below fundamental edge, near liq. N₂ temp. 0-79289
SrTiO₃, semiconducting, effect of Ce and Nb dopants 0-47725
SrTiO₃ powders, i.r. absorpt., particle size and shape effect 0-48061
β-SrUO₄, i.r. spectrameas., force constants and U-O lattice vibrations 0-6526
Sr₂VO₂(I/Br), i.r. Raman and fluorescence 0-58750

β-SrUO,, i.r. spectrameas, force constants and U-O lattice vibrations 0-65526
Sr₂VO₂Cl(Br), i.r., Raman and fluorescence 0-58750
Ta, superconducting, for i.r. absorption, energy gap width and critical temperature 0-44130
Tb³⁺, relaxation between excited levels, resonance transfer in glassy matrix 0-51358
Tb³⁺ in TbAlG, Zeeman-Raman transitions obs. 0-48097
Te, absorpt., 18-460 cm⁻¹, 300, 77 and 4 K 0-79320
Te, amorphous semiconductor 0-47721
Te, i.r. absorpt., valence band struct. 0-41225
Te, interband transition of holes 0-66056
Te, lattice vibration contrib. 0-66057
Th with added ²²⁸Th, i.r. and u.v. absorption 0-65288
ThO₂:Np⁴⁺, dynamically induced forbidden elec.-dipole transitions 0-54101
ThO_{3-x}(OH)_{2x}, yH₂O, amorphous precip., rel. to comp., i.r. obs. 0-51312
TiO₃, two-photon absorpt. spectrum struct. 0-54104
TiO_{3-x}(OH)_{2x}, yH₂O, amorphous precip., rel. to comp., i.r. obs. 0-51312
Til azide, i.r. assignments and cryst. struct. 0-72352
Tll, i.r., study of orthorhombic to CSCl-type struct. transition 0-72393
TlNO₃, crystalline field effects on i.r. spectra 0-59404
TiSbS₃, fundamental absorpt. edge, forbidden band width 0-69131
TmCl₃.6H₂O, Tm₃(SO₄)₃.8H₂O, Zeeman splitting between Stark levels of Tm³⁺ (4f²) 0-76111
TmFeO₃, Zeeman effects, spin Hamiltonian for even-electron singlet states 0-51313
Tm_{2xys}Nd_{40,65}Al₅O₁, garnet, absorption of Nd³⁺ 0-76113
Tm(ReO₄)₃.4H₂O, single crystals, absorption spectra 0-48078

Tm_{2.98}Nd_{0.05}Al₅O₁₂ garnet, absorption of Nd³⁺ 0-76113 Tm(ReO₄)₃4H₂O, single crystals, absorption spectra 0-48078 UO₂ in silicate glass, spectral-kinetic characts, at high excitation power 0-44856

UO₂ in silicate glass, spectral-kinetic characts, at high excitation power 0-44856
8-UO₃ ir. spectra 0-65524
UO₂Cl₂ crystal, ir. spectra in polarized light 0-51290
UO₂SO₃3H₂O, cross-section for excited absorption of uranyl ions 0-44921
²³³U hyperfine structure 0-72368
VCl₃.2N(CH₃)₂, absorption spectra interpretation using energy level diagram of V¹⁺ 0-79321
Y₂O₃:Cr, optical cond. spectra, metallic, insulating, and antiferromag, phases, rel. to electronic spins 0-79238
VO₂, reflection, transmission, elec. cond., temp. depend., semiconductor-semimetal transition 0-75690
VO²⁺ in oxide glasses, composition depend., chem. bond nature 0-72493
Y₂O₃ single cryst, reflection spectra 0-51293
W₂O₄-0.76 µ at 1200 to 2600°K, emissive power 0-56120
WO₃ i.r. spectra 0-65524
Xe₂I.i., Na, In, Hg, Cd, absorpt. rel. to at. interactions, obs. 0-49783
Xe₃ reflectance for photon energies between 8 and 25 eV 0-79286
YA I garnet: Pt³⁺, absorption spectra 0-62675
YCl₃O₄H₂O₃Tm³⁺, Y₃(SO₄)₃, 8H₂O₃Tm³⁺, Zeeman splitting between Stark levels of Tm³⁺ (4P²) 0-76111
YFe garnet: Ho³⁺, energy levels rel. to laser transitions 0-44857
YFe garnet, energy levels of Ho³⁺ and Ho³⁺. Fe³⁺ exchange interaction 0-51248
YGa garnet: Ho³⁺, energy levels rel. to laser transitions 0-44857

0–51248
YGa garnet: Ho³⁺, energy levels rel. to laser transitions 0–44857
YGa garnet, energy levels of Ho³⁺ 0–51248
Y₂Si₂O₇-Y₂Ce₂O₃ solid-solns, i.r., crystal chemistry 0–41226
Y₂Ti₃O₇ pyrochlore crysts. Cr³⁺ doped, absorpt, spectrum 0–66142
Yal garnet: Pd, Rh, absorpt, spectra 0–66058
Zn acetate dhydrate: Co³⁺ single cryst. 0–56541
ZnCl₂ glass, network struct, detect, using transition metal ion probes 0–62676

0-20/0 EV by reflectance spectra determ. 1.5-6.0 eV by reflectance, thermoreflectance and electroreflectance 0-76063 Znl₂, anhydrous and hydrated, absorption in far i.r., effect of Kr and H₂O 0-66059

ZnO-type pigments, solar radiation damage, optical props. in u.v. and i.r. 0-41179

ZnO-type pigments, solar radiation damage, optical props. in u.v. and i.r. 0.—41179
ZnO, 2 photon magnetoabsorption 0—76079
ZnO, u.v. reflectivity, charact. energy- loss spectra comparison 0—54090
ZnS:Cl effect of Fe, Ni, Co on stimulated absorption 0—56531
ZnS:Cr, identification of transitions, 2-0.34 µm, 4.2-500K 0—76112
ZnS:Cu, Cl effect of Fe, Ni, Co on stimulated absorption 0—56531
ZnS:Cu²⁺, paramag. centres and i.r. absorpt. correl. 0—72370
ZnS-CdS-Ag-Ni phosphors, excitation and emission spectra 0—56617
ZnS u.v. emission from sublimed films 0—56554
ZnS(SeXTe) Ilms absorpt. in 36-150 eV resion 0—48080

ZnS(Se)(Te) films, absorpt, in 36-150 eV region 0-48080
ZnS(se)(Te) films, absorpt, in 36-150 eV region 0-48080
ZnSe, electroabsorpt. 0-72369
ZnSe, reflectivity, 15 and 300K, calc. and meas. 0-48007
ZnSiAs₂, ir. absorpt, room temp. 0-48065
ZnSiAs₂, reflectance spectra determ. 1.5-6.0 eV by reflectance, thermoreflectance and electroreflectance 0-76063

```
Spectra continued
```

inorganic solids continued

ZnSiP₂, chalcopyrite struct., i.s. absorpt. 0-79322 ZnSnAs₂, reflectance spectra determ. 1.5-6.0 eV by reflectance, thermoreflectance and electroreflectance 0-76063

thermoreflectance and electroreflectance 0–76063
ZnSnP₂, i.r. absorpt, room temp. 0–48065
ZnTe, multiphonon i.r. spectrum 0–75383
ZnTe, refl. in fund. absorpt. region 0–79274
ZnTe, reflectivity, 15 and 300K, calc. and meas. 0–48007
ZnWO₄:Cr³⁺, Li⁺, absorption, reductive colouring, pair substitutions, annealing 0–48081
Zn₂[Fe(CN)₂], i.r., rel. to struct. and Fe-C stretching motion 0–72349
ZrO₂ polymorphs, phase obs. 0–54112
ZrO₂ powders, i.r. spectroscopic study of struct. 0–53516
ZrO_{2-x}(OH)_{2x}, Jr., spectroscopic study of struct. 0–53516
ZrO_{2-x}(OH)_{2x}, Jr., amorphous precip., rel. to comp., i.r. 0–51312
increanic solids. radjofrequency

inorganic solids, radiofrequency see also Nuclear magnetic resonance and relaxation; Paramagnetic reso-

see also Nuclear magnetic resonance and relaxation; raramagnetic resonance and relaxation silica gel with adsorbed ammoniac, relax. regions obs. 0–39854 spin wave modes, permalloy thin films surface pinning 0–40993 InSb, relationship between emission with and without magnetic fields 0–51334

KCl:LiCl, microwave spectroscopy of Li⁺ 0-72407

molecules

ω, universal halide bond parameter, use in spectroscopy 0-64317 0-55267

ABX, analysis 0-67696

ABX, analysis 0-67696
absolute intensities calc. of i.r. absorpt. bands 0-74201
absorption, damped oscillator model for determ. of Einstein coeff. spectra
of condensed media 0-43454
absorption, integral, breakdown of relationship to life-times of excited
states 0-67689
absorption in gases, collisionally induced 0-46420
adsorption infrared spectroscopy 0-47072
anisotropically polarized molecules, relation between observed and true
absorption spectra 0-64320
asymmetric rotor, i.r. intensity perturbations and selection rule breakdown
0-70848
asymmetric ton, line intensities. Ak effect. 0-74212

asymmetric top, line intensities, Δk effect 0-74212 atmospheric transmittance, comparison of Elsasser and static models 0-54248

0–54248
beam, spectroscopic number 0–46445
beam-foil spectroscopy applic. 0–39276
carbocyclic, photoelectron spectra, use of different light sources 0–64494
charge transfer bands, study using magnetic circular dichroism 0–55271
complex molecules as harmonic oscillators with damping 0–61053
complex molecules as harmonic oscillators with damping 0–61052
complex molecules as harmonic oscillators with damping 0–61054
complex molecules as harmonic oscillators with damping 0–61054
complex molecules as harmonic oscillators with damping 0–61045
complex molecules as harmonic oscillators with damping 0–61053
complex molecules as harmonic oscillators with damping

correlations and structural group anal. using symbolic logic methods 0-58134 coupled systems with loosely connected fragments, transition energies, oscillator forces 0-53009 diatomic, Schrodinger eqn. resolution 0-77743 diatomic, angular distrib. of ejected photoelectrons in photoelectron spectroscopy 0-64327 diatomic, angular distribution and intensity in photoelectron spectroscopy 0-64323

0-04323 diatomic, homologous, relationship between reduced mass and vibration freq. 0-5299 diatomic, level-crossing spectroscopy and excited state coupling parameters 0-74197 diatomic, photoelectron spectra, Franck-Condon factors and autoionization 0-64324

tion 0-643.24 diatomic, photoionization in photoelectron spectra 0-643.25 diatomic molecule excitation by electron bombardment 0-61051 Dicke effect and perturbation of internal energy levels 0-67691 dissolved in solid solutions observed under different crystallization conditions 0-64319

Einstein coefficient, method of determination using spontaneous emission

Einstein coetincient, method of determination using spontaneous emission spectra of condensed media. 0–43046 electron spectroscopy for chemical analysis. 0–66214 electronic, solvent effects, microscopic model. 0–58140 group IV tetrahalides, bonding studied by photoelectron spectroscopy. 0–64369

group IV tetrahalides, bonding studied by photoelectron spectroscopy 0-64369

0-04309 heterocyclic, photoelectron spectra, use of different light sources 0-64494 i.r., 1-type resonance in perpendicular bands, perturbations 0-64316 i.r., resolution enhancement by numerical spectrometer distortion correc-tion 0-42396

tion 0-42396

it. vibr.-rot. bands, absorption coeffs. calc. 0-77774
intensity of spectra in gas, liquid phases, differences 0-43045
inversion, natural system in discharges, broadband gain 0-39339
isotope effects review 0-55263
Lamb dip in high-precision mm-wave spectroscopy 0-61052
line splitting for optical transitions in gases induced by resonant external fields 0-49836

low temperature, vapour-deposited molecules in inert matrices 0-64336 Lyman- α radiation from electron collisions with H-containing mols. 0-64329

0-04329 maser quantum mechanical model, exact analysis 0-42244 microwave, centrifugal distortion data, numerical anal. 0-74249 microwave, numerical treatment of general vibr-rot. Hamiltonian *3-67693

microwave absorption by gas mixtures at high pressure, exptl. technique 0-53278microwave spectroscopy, calculation of nuclear quadrupole splittings $0\!-\!39347$

multicomponent solns., intermolecular interactions and spectra, composition of solvate sheath 0-58266 non-rigid molecules in crystal 70 K, singlet and triplet state differences 0-5298

0-52998
nonlinear, polarization phenomena 0-55270
oscillator strength, MO formulations in one dimension using double well potentials 0-43052
phosphorescence spectrum zero-field origin of each vibronic band, new technique for identification 0-73107
photoelectron, configuration interaction intensity borrowing 0-64315
photoelectron spectra, He 584Å, principle features 0-64322

Spectra continued molecules continued

photoelectron spectra of C≡N group containing molecules 0—53005 photoelectron spectra of open-shell molecules, band intensities 0—77735 photon echoes, mixing collisions effects 0—39270 photon irrad, homogeneous system, photon and electron energy spectra 0—55266

0-35266
polar, in condensed phase, r.f. and far-i.r. absorpt. 0-43040
polar molecules in condensed phases, microdynamics studied by dielec,
dispersion and vib.-rot. spectra 0-43054
polarization of mag. zero-field transitions, optical detection 0-54117
polyatomic, radiationless transitions 0-74210
polyatomic molecules, line shape of inhomogeneously broadened resonance 0-58136

naince 0-58136
polyatomic molecules, optical and u.v., line shapes 0-58135
pressure shift in microwave region 0-68005
protonic spectra similar to electronic spectra 0-70835
qualitative structural group analysis, use of computer 0-43044
rf.-rf. double reson. of gases at l.p., 'dressed' Hamiltonian formalism
applic. 0-39335
Raman intensities, vibrational, theory 0-43042
Raman scatt. semi-classical calc. of 3-level system 0-39340
rotation spectra, Zeeman effect theory 0-39345
rotation-coupled vibr. states, selection roles and line strengths calc. 0-39429

0-39429

0-39429 rotational, molecules with C₃, symmetry in excited state v_i=2 0-43055 rotational line strength doublet transitions, calculation 0-67700 rotational relaxation and broadening rates, equivalence in MRR spectroscopy 0-70854 rotational transition reson. freq. shift due to non-resonant microwave pumping 0-53003 saturated absorpt., using CO₂ and N₂O lasers 0-70844 saturation and Stark effect in optical freq. fields 0-64310 single-spin syst., effects of two reson. e.m. waves, multiple quantum transitions 0-70836 singlet and triplet states studied using low-energy electron-reflection 0-74890 starch products, non-soluble, v-irradiated it respects 0-39464

0-74890 starch products, non-soluble, p-irradiated, i.r. spectra 0-39464 statistical theory of mol. reflection 0-61050 symmetric top molecules, degenerate vibration-rotation bands, computer program calc. 0-74204 symmetric top type, AK-3 rotational transitions 0-64346 symmetric tops, intensity distrib. within rotational struct. vibrational of bands 0-74213

bands 0-742.13 tetrahedral XY₄ molecules, energy levels and the v_2 band 0-49837 v.h.f. pulse plasma excitation 0-74532 vacuum u.v., effects of small press. of He or N₂ on valence shell or Rydberg transitions 0-61057 vapour, rarefied, method of meas. fluoresc. duration 0-39337 vibrational, of periodic mols. of finite length, allowance for interac. of non-neighbouring units 0-43061 vibrational intensities, intermolecular interactions effects 0-46920

vibrational intensities, intermolecular interactions effects 0–46920 Yaris and Shain method for calculating lineshapes 0–39338 HNCO photoelectron spectra, orbital identification by comparison with other spectra 0–64409 SF₆, rotational-vibrational transitions, narrow reson, within Doppler line during absorpt, saturation 0–70947

organic molecules and substances

organic molecules and substances see also Molecules absorption and luminescence of complex molecules, relationship at low temp. 0–53053 acenaphthylene, u.v. absorpt. spectra in vapour, and pure and doped cryst. states 0–70965 acenaphthylene, vapour, pure crystal and single crystal matrices, electronic absorption 0–46531 acenes, solid, electronic spectra at normal and low temperatures in polarised light 0–56555 acetaldehyde and derivatives, far u.v. spectra interpretation 0–74326 acetate praseodymium tetrahydrate, in Pr¹⁺, absorption spectrum 0–62746 acetone, lig., internal refl., 180 to 200 mu 0–54940

0-62/46 acetone, liq., internal reft.. 180 to 200 mu 0-54940 acetone, rotational Brownian motion from the width of vibrational band contours in molecular spectra 0-61143 acetonitrile, shift of absorption bands due to dissolved salts with similar anion and cation 0-67846

acetophenone, vibration spectra 0–64474 acetophenone-d₃, vibration spectra 0–64474 acetophenone-d₃, vibration spectra 0–64474 acetophenone-d₃, vibration spectra 0–64474 acetophenone-d₃, vibration spectra 0–64474 acetylene ¹²C₂HD bands in region 6-10 μ , vibrational energy levels

0-46532

acridine in n-alkane matrices at $4^{\circ}K$, electronic absorption spectra 0-77866

0–77866
acridines, electronic spectra at normal and low temperatures in polarised light 0–56555
acrolein, electric field induced, contour analysis of 3860 Å band 0–49899
acrolein, spectroscopy 0–43145
alcohols, liquid, H bonding h.p. spectroscopy 0–55333
alkoxy-s-triazine, in different solvent, u.v. spectra 0–64476
N-alkyl-n-nitrosoanilines, electronic absorpt, spectra 0–77860
amides of butyramide series, integrated obs. intensities of carbonyl band 0–67789
amines, long-chain and large rise

amines, long-chain and large-ring amines, ciannamoyl derivatives, u.v.

amines, long-chain and large-ring amines, clannamoyi derivatives, u.v. absorption maxima 0-55618
amino acids, X. irrad., correlation with e.s.r. spectra 0-59458
4 amino-N, methylphthalimide in propanol, failure of universal relation between absorption and fluorescence spectra, causes 0-50235
aminoanthracenes, absorpt., fluoresc. and phosphoresc. 0-49903
aminoanthracenes, absorpt., fluoresc. and phosphoresc. 0-49903

aminoanthracenes, absorpt., fluoresc. and phosphoresc. 0—49903
aminoacobenzene derivatives, aqueous solns, influence of indifferent substs.
on e abs. spectra 0—50236
aminoindenes, isostructural, electronic and vibr. absorpt. 0—41227
3- aminophthalimide in propanol, failure of universal relation between
absorption and fluorescence spectra, causes 0—50235
anthracene, absorpt. and emission in phenanthrene and naphthalene, lattice
effects 0—72372
anthracene, cryst., reflection spectrum, evidence for existence of defects
0—44813

0-44813
anthracene and deuterated derivative in n-alkane matrices at 4°K, electronic absorption spectra 0-77866
anthracene cryst., width of lowest singlet-singlet transition 0-41228
anthracene derivatives, polarization depend. 0-67763

organic molecules and substances continued

anthracene derivatives fluorescence quantum yield and duration temp. and wavelength depend. 0-39409

anthracene in soln., variations in relative intensities of absorption spectral bands 0-43459

sands 0-434.99 aromatic and heterocyclic compounds, S-containing u.v. absorpt., calc. by SCF MO CI method 0-77923 aromatic carbonyl cpds., T_1-S_0 transitions rel. to vibronic interaction between $n\pi^*$ and $n\pi^*$ states 0-70969 aromatic cpds., nuclear conformation correl. with fluoresc. and absorpt. spectra 0-77868

aromatic cpds., nuclear conformation correl, with fluoresc, and absorpt. spectra 0–77868 aromatic cryst., Wannier consts. 0–51316 aromatic hydrocarbons in frozen paraffin solutions, T₀-T* absorption bands, determination using luminescence excitation spectra 0–46518 aryliriodonium and related compounds, u.v. spectra, symmetry 0–53061 aryltricyanoethylenes, electron abs. spectra 0–61144 aziridines, substituted, v₀₋₁(NH) and v₀₋₂(NH) freqs. variation in various solvents 0–39410 benzanthrone, in hydrocarbon solutions, electronic 0–49905 3-benzanthrone, in hydrocarbon solutions, electronic 0–49905 3-benzanthrone, extinction coeffs, and direction of polarization of T-T absorption spectra 0–74340 benzene, and -d₀, gas phase absorption spectra and decay 0–70975 benzene, eaciton band profiles for entire Brillouin zone 0–70978 benzene, exciton band profiles for entire Brillouin zone 0–70978 benzene, intensity effects governed by vibronic overlap 0–61148 benzene, liquid, two-photon absorption 0–55267 benzene, singlet-triplet absorption in pure cryst. 0–41229 benzene, study by flash photolysis 0–77935 benzene, transition energy shifts and polarizabilities of excited states 0–58140 benzene and derivatives, study by flash excitation 0–77879 benzene and derivatives, study by flash excitation 0–77879

0–58140
benzene and derivatives, study by flash excitation 0–77879
benzene crystal, two-particle absorpt, band 0–62677
benzene in inert solids, u.v. absorption spectrum 0–74343
benzil, in various solid-state environments 0–64483
benzil solutions, absorpt, of triplet excited mols. 0–70982
benzimidazole, vapour absorption at 2850 Å 0–74336
benzonhenone in benzene solution, triplet-triplet absorpt., meas. using laser 0–39799
henzonhenone in solid state, i.r. spectra freq. assignments 0–46539

benzophenone in solid state, i.r. spectra, freq. assignments 0-46539 benzoporphyrins, spectra and luminescence, effect of azo-substitution 0-43151

p-benzoquinone, chloro-derivatives, visible absorption spectra 0-64486 p-benzoquinone, excitonic struct. of ${}^{1}B_{1g} \leftarrow {}^{1}A_{g}(\pi \leftarrow n)$ transition, 1.5 K 0-56556 p-benzoquinone, excitonic struct. of ¹B₁₈···A₈(π-n) transition, 1.5 K 0–56556 benzoquinone, in mixed cryst., T-S emission and abs. spectra 0–64485 p-benzoquinone solutions, absorpt. of triplet excited mols. 0–70982 benzoselenophene, u.v. spectra 0–55339 benzothiacyclene-S- monoxides and carbonyl derivatives electron absorption spectra 0–46544 benzothiazole, vapour absorption at 2850 Å 0–74336 benzotrichloride, pure and soln., Rayleigh scatt., molecular rotational mobility 0–46924 benzoatazole, vapour absorption at 2850 Å 0–74336 1.12-benzperylene extinction coeffs. and direction of polarization of T-T absorption spectra 0–74340 benzyl benzoate, vibrational, i.r. 0–58210 biacetyl solutions, absorpt. of triplet excited mols. 0–70982 bilirubin in pyridine, spectral properties of solutions and kinetics of formation 0–61525 biphenyl and biphenylene, electronic spectra 0–39442 biphenyl and biphenylene, electronic spectrum of vapour and solid 0–58211 bromoaetylene, electronic spectrum 0 vapour and solid 0–58211 bromoaetylene, electronic spectrum 2500 to 900Å 0–74322 bromobenzene, rotational band contour analysis in 2700 Å system 0–53065 butadiene-2,3 nitrile, microwave spectrum, rot. and vibr. obs. 0–49912 1,2,3-butatriene, gas, u.v. absorpt, spectrum 0–61152 camphorquinone solutions, absorpt, of triplet excited mols. 0–70982 carbonyl fluoride, electronic spectrum 0–39417 carboxylic acids, hydrogen bonding study by neutron energy loss spectra 0–64646 chloroacetic acid, vibr. spectra of solid and lig, rel. to struct. 0–67776

0—46547
chalcones, substituted, electronic spectra 0—64496
chloroacetic acid, vibr. spectra of solid and liq, rel, to struct. 0—67776
chloroacetylene, electronic spectrum 3000-1000 Å 0—39418
chlorobenzene, rotational Brownian motion from the width of vibrational band contours in molecular spectra 0—61143
chlorobenzene 2699 Å electronic band system, in-plane vibration modes in excited states 0—49906
1- chloronaphthalene, liquid, two photon absorption 0—55267
α-chloronaphthalene, spectral structure of the anisotropic portion of light scattered 0—61528
8-chloroquinoline vapour, electronic absorption spectra 0—58216
2-chloroquinoline vapour, electronic absorption spectra 0—58216
corrins, theoretical analysis 0—67780
cryptocyanine, crystallized solns, resonance effect 0—51288
cyclic hydrocarbons, photoelectron, ionization potentials 0—39421
cyclobutanone, ¹A₂ state, u.v., rel. to ring puckering and oxygen wagging 0—61157
cyclobutanone, π*+-n spectra, allowed and forbidden character 0—74354

0 -61157 cyclobutanone, π*←n spectra, allowed and forbidden character cyclobutanone, π*←n spectra, allowed and forbidden character cyclohexanane, π*←n spectra, allowed and forbidden character cyclopentadienyl radical and deuterated derivatives electronic spectrum 0-46553 cyclopentanone, π*←n spectra, allowed and forbidden character 0-74354

cytosutane, puckering structure, vibration, i.r. 0–49914 cytosine, polarized reflectance spectra 0–79370 DNA base pair, hydrogen-bound, optical excitation, absorpt. luminescence 0–74422

deuterobromoacetylene, electronic spectrum 2500 to 900Å 0–74322 deuterobromoacetylene electronic spectrum 3000-1000 Å 0–39418 1,5-diazanaphthalene, vapour, electronic absorpt, spectra 0–61159 1,4-diazantiphenylene, fluoresc, and absorpt, high resolution 0–53068 1,2,3,4-dibenzanthracene, extinction coeffs, and direction of polarization of T-T absorption spectra 0–74340

Spectra continued

organic molecules and substances continued dibenzoperopyrene and 3.4-benzopyrene in n-paraffin matrix, quasi-line, luminescence, temp. depend. 0-79369 p-dibromobenzene, absorpt., 20 K, excitonic struct. 0-62681

p-dichalcones, isomers, electronic spectra 0-43157

p-dichlorobenzene, absorpt., 20 K, excitonic struct. 0–62681 1,4-dichlorobenzene, absorption, fluorescence and phosphorescence, 4.2K 0–72441

p-dichlorobenzene, rotational band contour analysis in 2800 Å system 0-43159 p-dichlorobenzene, vapour phase near u.v. absorption spectra 0-70990 dichlorodifluoromethane, saturated absorpt., using CO₂ and N₂O lasers 0-70844

0-70644 2.5-dichlorotoluene, in liq. phase, i.r. spectra 0-49919 dicyanodiacetylene, abs. spectrum, 3100-2300 Å 0-43158 p-difluorobenzene, rotational band contour analysis in 2710 Å system 0-39425

0-39425
difluoromethane, photoelectron spectra 0-61168
p-dihalobenzene, cryst., T-S emission spectra 0-64485
dihalobenzenes, ortho- and meta-, far infrared absorption spectra explained
by rotational transitions 0-46925
5,10- dihydrophenazine, i.r., u.v. and diffuse reflectance 0-55368
β-diketones, triketones, enolized spectroscopic examination of stretch vibrations 0-53069

tions 0–53069 dimethyl sulphide ethanolic soln., internal refl., 180 to 200 mµ 0–54940 4-N,N-dimethyl aminonitrosobenzene and methyl derivatives 0–77895 2,4-dimethylphenol vapour, u.v. spectrum, band analysis 0–46558 diphenyl ether-eyclohexane syst., energy transfer of electronic excitation, rel. to viscosity 0–68!!! 1.3-diphenylbutane, from electrical discharge through toluene and ethylbenzene, i.r. and u.v. spectra 0–46525 1.2-diphenylethane, from electrical discharge through toluene and ethylbenzene, i.r. and u.v. spectra 0–46525 p-dithiene ¹³C-H satellite spectrum 0–7790! p-dithinin, ¹³C-H satellite spectrum 0–7790! p-dithinin, ¹³C-H satellite spectrum 0–7790! durene mongaldehyde, absorption and phosphorescence 0–72375

p-dithin, "C-H satellite spectrum 0—7901 durene monoaldehyde, absorption and phosphorescence 0—72375 duroquinone, triplet state, absorption spectrum 0—39406 dye, aggregates, light abs. 0—58159 erbium accetate tetrahydrate, absorption spectra of single crystals 0—76114

0-76:14 ethylene, saturated absorpt., using CO₂ and N₂O lasers 0-70844 ethylene and dueterated derivative, photoelectron spectra using 584Å He resonance 0-64436 ethylene episulfoxide, ground state rot. spectra 0-77958 ethylenediamine-H₂O system, solvated electron in pulse radiolysis 0-54195

0-34193 europium benzoylacetonate complexes, absorption spectra in methanol solns. 0-74761 ferrocene, single-crystal absorption spectrum at 4.2 K, 3000-6000 Å 0-76115

0-76!15 ferrocene and its derivatives, electronic abs. spectra 0-49924 p-fluoroaniline, near u.v. absorpt., rot. struct. 0-53071 p-fluoroaniline, rot. fine struct. rel. to dipole moment changes 0-71002 o-fluoroanisole, emission, $2765\cdot3000~\lambda~0-64508$ o-fluorobenzaldehyde, $n-\pi$ electronic emission and absorption, meas.

fluorobenzene, rotational analysis of 0-0 band of 2644 Å system 0–55351 fluorobenzene, rotational fine structure of 0-0 band of π^* - π state

0 - 46561

fluorobenzenes, photo-electron and u.v., analysis 0-49926

huoropenzenes, photo-electron, electron is tructs. 0-49926 fluoromethanes, photoelectron, electronic structs. 0-71009 α -fluoronaphthalene, emission spectrum analysis 0-58221 m-fluorophenol, emission, 2765-3000 λ 0-64508 p-fluorophenol, rot. fine struct. rel. to dipole moment changes 0-71002 m-fluorophenol in vapour state, vibrational assignment in near u.v. 0-53072

o-fluorotoluene, microwave, internal rot. barrier, torsion-vib. interaction 0-71037

formaldehyde, K resolution spectrum, line obs. 0–49927 formaldehyde, electronic, calc. 0–53073 formaldehyde HCHO, HCDO, DCDO, ¹A"←¹A₁ spectrum vibr. analysis, obs. 0–39429

formaldehyde absorpt. coeffs., 650 to 1850 Å 0-71003

glasses, low-temp., resolution of structure in trapped electron spectra 0-59512

0-99512
glycolaldehyde, microwave, determ. of rot. and centrifugal distortion consts. 0-58223
glycoxal, laser induced emission 0-58224
glyoxal, vibration-rotational analysis of 12 type C bands 0-43163
glyoxal-d₂, vibr.-rot. anal. of 4540 Å band system 0-77912
glyoxylic acid, vibr. spectra and free mol. symmetry 0-61164
heme proteins, n.m.r. spectroscopy application 0-64465
hemoproteins, i.r. circular dichroism studies of d→d transitions of Fe
0-71050
hexachlorobenzene, absorpt., 20 K, excitonic struct 0-62681

hemoproteins, i.r. circular dichroism studies of d→d transitions of Fe 0−71050 hexachlorobenzene, absorpt. 20 K, excitonic struct 0−6268! hexachlorobenzene, high field Zeeman effects of vibronic transitions in lowest triplet states 0−6451! hexachlorosenzene, high field Zeeman effects of vibronic transitions in lowest triplet states 0−6451! hexachlorosenzenzene method physical phosphorescence with reference to photograrian description of the physical physical phosphorescence with reference to photograrian description physical ph

```
Spectra continued
```

organic molecules and substances continued

isoquinoline, vibrational spectra and assignments 0-43180

laser-excited phosphorescence 0-39404

magnesium phthalocyanine negative ions, mag. circular dichroism and absorpt. spectra 0-71023

absorpt. spectra 0–71023
of metal-gossypol complexes 0–39430
methane_d, rot. struct, of v_b band, !16!cm⁻¹ 0–55357
methane_d, rot. struct, of v_b band, !16!cm⁻¹ 0–55357
methane, absorpt. coeffs., !00 to 400 Å 0–55298
methane, deuterated, fund, v_b band interpret. 0–74374
methane, enriched with 13 C, absorption spectra, rotational and splitting parameters of v_b band 0–7438!
methane, photoelectron spectra 0–61168
methanes, bromine substituted, auger spectra obs. 0–77926
methanethiol, 2 avib. rot. spectra, hindered internal rot. 0–39438
methanol, I.f. vibr. and torsion-rotation spectrum 0–64527
methanol, rotational, anal. of regions 5 Co to 900 cm⁻¹ 0–64528
methoxy benzaldehyde, m- and p-, vapour, n- II^* electronic emission spectra 0–74380
3- methoxy-substituted benzanthrones, in hydrocarbon solutions, electronic 0–49905
methyl acetylene, fine struct. in vibr.-rot. bands 0–71020
methyl bromide, high resolution spectra anal. rel. to fundamentals 0–71018

methyl br

methyl chloride, vibr.-rot. band, $2080~\rm{cm^{-1}}~0-61166$ methyl chloride, vibr.-rot. spectrum between 2700 and 3000 cm⁻¹ 0-71021

0-71021 methyl cyanide-d₂, microwave double-photon transitions, obs. by high power microwave double resonance 0-77925 methyl fluoride, photoelectron spectra 0-61168 methyl halides, deuterated, study of v_4 and $2v_4$ bands, determ. of A_0 0-71017

methyl halides, photoelectron spectra 0-55360

methyl halides, photoelectron spectra 0—55360 methyl iodide, rot. constant A₀, direct obs. 0—71011 methyl isobutyl ketone, liq., internal refl., 180 to 200 mµ 0—54940 methylammonium chloride single cryst., vibr. spectra 0—41233 methylchlorodiazirine, ground state rot. spectra 0—77958 3—methylsydnone, u.v., rel. to electronic structure 0—58244 1-methyluracil, polarized single-cryst. absorpt. spectrum 0—72376 methyoxyacetylene, i.r. spectra and chemical structure 0—74386 molecular, review of lattice vibrational spectra 0—74386 molecular, review of lattice vibrational spectra 0—76062 molecular, exciton band impurity, effect, optical absorpt. 0—44805 maphthalene, conjugated ions, optical absorption, open-shell SCF configuration interaction treatment 0—74390 naphthalene, study by flash photolysis 0—77935 naphthalene adsorbed on zeolite, fluorescence and abs. spectra 0—46583 naphthalene cryst., probability for non-radiational transition between anthracene and naphthacene 0—69159 naphthalene derivatives with carbonamide group, thin film, u.v. irradiated, luminescence 0—43176 naphthalene in benzene solution, triplet-triplet absorpt., meas. using laser 0—37999 naphthalene in biphenyl cryst., hindered rotation in vibronic spectra

naphthalene in biphenyl cryst., hindered rotation in vibronic spectra 0-72379

naphthalene in biphenyl cryst., hindered rotation in vibronic spectra 0–72379
naphthalene in durene cryst., vibronic spectra (¹A₁₈-¹B_{2u}) 0–72378
naphthalene solutions 0–74394
naphthalenes, deuterated, impure, vibronic absorpt. 0–48082
naphthantrone in n-paraffin matrix, quasi-line, luminescence, temp. depend. 0–79369
naphtholt-triphenylpyrazoline syst., energy transfer of electronic excitation, rel. to viscosity 0–681!1
N-(β-naphthyl)- carbazole, electron spectra 0–43154
β-naphthyl- carbazole, electron spectra 0–43154
β-naphthylamine fluorescence lifetimes 0–77933
nitroanilines, calc., interpretation of electronic spectra 0–49934
nitrobenzene-n- anisidine (diphenylamine, diphenyl methane), u.v., rel. to intermolecular interactions 0–49951
nitrophenols, N-group vibrations with intramolecular H bond in proton acceptor solvents 0–61172
octalkylporphins, vapour absorption spectra 0–74396
oils used in vacuum diffusion pump, spectra, sector field mass spectrometer 0–51872
one-dimensional solids, scalar spectral characteristics 0–44858
pentacene cryst., abs., 14000-34000 cm⁻¹, at 293, 77 and 20 K 0–51289
pentaerrythritol single crystal, polarized ATR spectra 0–48054
phenanthrene, Stark modulation spectroscopy, excited state dipole moments 0–58237

pentaerythritol single crystal, polarized ATR spectra 0–48054 phenanthrene, Stark modulation spectroscopy, excited state dipole moments 0–58237 phenazhydrins, i.r., u.v. and diffuse reflectance 0–55368 phenazine, i.r., u.v. and diffuse reflectance 0–55368 4-phenyl, 3-oxy, 1,2-benzofluorenone, in polar and nonpolar solvents, electronic absorption spectra 0–67814 phthalimide, solns, influence of temp. 0–68119 polar liquids, for infrared absorption spectra explained by rotational transitions 0–46925 poly-L-alanine, alpha-helix, vibration spectra 0–64571 poly-L-leucine, vac. u.v. absorpt., conformation depend. 0–77973 polyalanine, planar zig and helical chains vibr. spectra calc. 0–39470 polyarylenes-cyanoethenylenes mol. strict. rel. to optical props. and photocond. 0–49949 polyethylene and deuteroderivatives, vibr. 0–39471

cond. 0–49949
polyethylene and deuteroderivatives, vibr. 0–39471
polyglycine-chain, dispersion curves and vibration spectra 0–64570
polymers, scalar spectral characteristics 0–44858
polypeptides, amorphous, one state solns. 0–71052
polyvinbonucleotides, u.v. absorpt, electronic struct. 0–39467
polyvinyl alcohol containing low molecular additives, abs. spectra
0–58512

polyvinyl chloride, containing mass defects, vibr. 0–3947! porphins with cyanine dyes on methine linkage, excitonic interactions 0–74403

porphyrins, vibr. struct. of electronic spectra, using quasi-linear spectral method 0-67815 prolate asymmetric top molecules, band contours in electronic spectra 0-46430

propylene, deuterated, appl. of internal rot. of asymmetric top theory 0-6454!

0-6434! propyne, elec. polarizability anisotropies obs. 0-70923 pyrazine crystal, electronic absorption spectrum 0-76118 pyrene, cryst., polarized absorpt. spectra 0-76119 pyridine, rotational Brownian motion from the width of vibrational band contours in molecular spectra 0-61143

Spectra continued

organic molecules and substances continued

cetra continued organic molecules and substances continued pyrine, in hexane and heptane, obs. spectra, at low temps. 0–68108 pyrrole, rot. fine struct. of NH stretching band 0–77948 quasi-line, impurity centre interaction with surroundings 0–79369 β-quinol clathrates, far ix., molecular motion 0–58241 quinoline, vibra-spectra, and assignment of fundamentals 0–64543 quinolines, hydrated, internal interactions on the basis of absorption spectra 0–53084 quinoxaline, intersystem crossing quantum yield, evidence for high yield of internal conversion of first excited singlet state to ground state 0–74407 rare-earth ion-aromatic acid complexes, charge-transfer bands 0–61532 rhodamine derivatives, influence of temp. 0–68119 rhodamine dye, interaction with polyanions, abs. spectra 0–68116 rhodamine dyes, ilminescent associates 0–39446 Rochelle salt, irrad., absorpt., 220-1500 nm 0–51318 shpolsky system, multiplets and phonon band 0–56534 solution laser, absorption and generation spectra 0–67089 stilbene, in diphenylacetylene and dibenzyl, obs. spectra, at low temps. 0–68108 trans-stilbene crystal, absorpt. and fluorescence 0–62682

0-68108 trans-stilbene crystal, absorpt, and fluorescence 0-62682 styrene, vibration spectra 0-64547 styrene-ds, vibration spectra 0-64547 sydnone, u.v., rel. to electronic structure 0-58244 1,2,4,5-tetrachlorobenzene, absorption, fluorescence and phosphorescence, 4,27,6,7,3441.

1,2,4,3-terracnioropenzene, absorption, nuorescence and phosphorescence, 4.2K 0-72441
s-tetracyanobenzene, laser excitation of EDA complexes, fluorescence and absorption spectra 0-72440
tetracyanoethylene isomeric π-mol. complexes, electronic spectra 0-71034

7,7,8,8-tetracyanoquinodimethane solubilized in surfactant solns. 0-74762

thiazine dye, interaction with polyanions, abs. spectra 0-68116 thiobenzophenone, 6500 Å transition 0-61175 thiopaphthene, absorpt. of 0-0 band, rel. to excited state rot. consts. 0-71036

thionapittiene, absorpt. of 0-0 band, rel. to excited state rot. consts. 0–71036
thiophosgene, 5142 Å transition 0–58245
thiophosgene, Zeeman effect in visible spectrum, 5496Å band 0–58246
thiophosgene, Zeeman effect in u.v. and i.r. spectra 0–53087
thiourcal, steric effects in u.v. and i.r. spectra 0–53087
thiourca, steric effects in u.v. and i.r. spectra 0–53087
o-m- and p-tolualdehydes emission spectra 0–61177
toluene, gas phase absorption spectra and decay 0–70975
transitions, radiative and non-radiative, review 0–58206
1,3,5- triamino -2,4,6- trinitrobenzene, neutron spectra and vibrational assignments 0–64551
triarylborons, u.v. absorpt. spectra 298° and 77°K 0–64480
trifluoromethane, photoelectron spectra 0–61168
triglycine selenate energy gap, dielec. const. 0–56362
triglycine sulfate, position of fundamental absoption edge as function of temp. 0–62683
triglycine sulphate, irrad., absorpt., 220-1500 nm 0–51318
trimethylamine, ground state rot. spectra 0–77958
trimethylamine, ground state rot. spectra and chemical structure 0–74386
triplet-triplet absorpt., meas. using laser 0–39799

(-14.386) triplet absorpt., meas. using laser (-39799) tris-salicylato-bis- phenanthroline rare earth chelates, u.v. and visible, study of characteristics (-71031) uranyl chloride, cryst., in polarized light at liq. N_2 temp. (-69175) vinyl bromide, pure rotational spectrum of fundamental vibration state. (-8.59) GHz (-0.4660)1

Wurster's blue perchlorate, electronic absorption at various temperatures 0-56533

Bi (III) halide complexes with DMSO, i.r. and Raman assignments 0-49890

O-47870 C X-ray emission spectrum used to study bonds of organic mols. 0-6!141

0-0144; CCI, free radical, produced from photolysis of methylene chloride, u.v. absorption 0-76279 C=O, band parameters and profiles of valence vibr. as function of conc. 0-64492

Sb (III) halide complexes with DMSO, i.r. and Raman assignments

organic molecules and substances, infrared

organic molecules and substances, infrared sym-dimethylene sulphite, vapour and dilute solutions in polar and non-polar solvents 400-4000 cm⁻¹ 0-70997
ATR, low temp. 0-69105
absorption in soln. tunnelling p eff. 0-74758
acenaphthene, librational frequencies calc. 0-47512
acetic acid dimers, far i.r. spectrum of H bond 0-46529
acetic acid dimers, far i.r. spectrum of H bond 0-46529
acetic acid dononmers, matrix isolated 0-64470
acetic and perdeuteroacetic anhydrides, gaseous, liq. and cryst., 200 to
4000 cm⁻¹ 0-53059
acetonitrile, gas-soln. phase transition effect on i.r. bands 0-43147
acetonitrile hydrogen fluoride complexes, fine struct. 0-43144
N-acetonyl quinolnium iodide, assignment of bands 0-58208
acetylene, in liquid N₂ and O₃. Fermi resonance 0-46530
acetylene adsorbed on y-AL₂O₃ and y-Al₂O₃-supported Pt, effects of S
poisoning 0-54106
acetylenes, i.r. intensities 0-43148
alcohols, self- associated, double excitation 0-53060
alkanes, substituted, rotational isomerism 0-74327
alkoxys-s-triazine, in different solvents 0-64476
alkyl cyanide- HCL (or DCL) mixtures, vapour phase, H bonding
0-53076
alkyltrip-tolyl arsonium compounds, and u.v. neighbouring group effect
0-64475
alkene, pressure induced due to the quadrupole 0-70966
aminophenols, isomeric, vibrational spectra 0-64477

allene, pressure induced due to the quadrupole 0-70966 aminophenols, isomeric, vibrational spectra 0-64477 aminopyridines and their deuterated analogues, analysis of spectra 0-77865

o=/1003 aniline, absorpt. freqs. 0=55335 anisole 0=77874 9,10-anthraquinone single crystal layers, vibrational bands assignment 0=51295 aromatic liqs., Raman bands 250-40cm⁻¹ compared to i.r. absorpt. 0-64928

aromatic sulphines, rel. to mol. structure 0-74320

S 1392 SUBJECT INDEX Spectra continued organic molecules and substances, infrared continued aryliodonium and related compounds, symmetry from spectra 0-5306! azyliodonum and related compounds, symmetry from spectra 0—33061 azolidon-4, absorpt., mutual influence of functional groups 0—64481 barbituric acids, 5,5-disubstituted, spectra-polymorphic structure correlations 0—72373 benzaldehydes, substituted 0—77874 benzene and benzene-da, crystal spectra in polarized light 0—62678 benzene derivatives, m-disubstituted 0—70971 benzene ring, low-energy collective electron excitation obs. 0—50238 benzenes, o-disubstituted 0—77849 benzenes mono-substituted, PR separations and relative Q-branch intensities in i.r. band contours 0—74341 benzends management of the contours 0—74341 benzentifuoride, pure and solution, Rayleigh scatt., molecular rotational mobility 0—46924 benzenes holded the contours 0—741183 biphenyl crystal, 3100-25 cm⁻¹ 0—72395 p-bis-trifluoromethylbenzol, pure and solution, Rayleigh scatt., molecular rotational mobility 0—46924 5,5'-bis-isoxazole, in crystal state and soln. 0—49910 1-bromo-2,2-dichloroethylene band intensities and atomic polarizations 0—39405 bromoethynyl benzene and chloroethynyl benzene, liq. and vapour phase 0—55342 azolidon-4, absorpt., mutual influence of functional groups 0-6448! bromoethynyl benzene and chloroethynyl benzene, liq. and vapour phase 0-55342 carbon tetrachloride, rel. to difference transitions, model 0-43153 carbonyl cyanide, all phases, and Raman spectra 0-46548 cellulose from cell wall of Velonia ventricosa, and Raman spectra 0-79325 0-79325 cellulose nitrate, rel. to OH and CH groups, effects of heating 0-51317 cellulose nitrate solutions, rel. to nitrate group interaction studies 0-71359 4-chloro- and 4-bromo phenylmethylsulphide 0-70972 chloro-alkanes, secondary, liquid spectra and intermolec. vibr. 0-39808 2-chloroacrylonitrile 0-74349 chloroberzene, and electronic analysis, planar ground state vibrs. 0-55344 0-55344 chlorobenzene, band intensity, solvent and temp. influence 0-43080 l-chloro-2-fluoroethylenes, cis and trans and deuterated modifications, vibrational assignments 0-64497 chloroform, band intensity, solvent and temp. influence 0-43080 chloroform and deuterochloroform, gaseous 0-55345 α-chloronaphthalene, vibrational assignment of frequencies 0-74351 chloroxylenes, ground state fundamentals, assignments 0-77887 coal, i.r. absorption spectra 700 to 500 cm⁻¹, dead rock content influence 0-44819 cyanine dyes relationship between far i.r. absorption and electrical conductions of the content influence of the cyanine dyes relationship between far i.r. absorption and electrical conductivity 0-64463 cyanogen, vibr.-rot. bands obs. 0-61156 cyclobutane. assignment of fundamental freqs. 0-74355 cyclohexane and related oxanes, vibr. spectra and potential functions 0-58215
cyclohexyl iodide, conformational isomerism 0-55347 cyclopentadiene, absolute intensity of bands 0—45915
cyclopentadiene, absolute intensity of bands 0—49915
cyclopentanone, dueterated isomers, vibr. spectra 0—77891
cyclopentanone, rel. to ring-puckering pot. functions 0—74356
cyclopentene oxide, rel. to ring-puckering pot. functions 0—74356
cyclopentene oxide, rel. to ring-puckering pot. functions 0—74356
cyclopentylamine, vibr. anal. rel. to out-of-phase ring deforms. 0—67785
cyclotpentanol, vibr. anal. rel. to out-of-phase ring deforms. 0—67785
cyclotpentanol, vibr. anal. rel. to out-of-phase ring deforms. 0—67785
deoxyribonuclei acid, normal and tumour, relative humidity hydration
0—48626 0–48626 N-deuterated N-methylpropionamide, and normal vibrs., obs. 0–53075 deuterated solvents 0–53054 diacetyl, gaseous and invarious solvent, i.r. bands ν (C=O), effect of hydrogen bonding 0–4317! diazomethane free radical, vibr. spectrum, obs. 0–4657! 2.2-dichloro and 2,2-dibromopropane, gaseous and liq., 5000 to 200 cm⁻¹ 0–55349 y-dichlorobenzene, polarized i.r. spectra of single crystals 0–72374 4,4'-dichlorobiphenyl, cryst. and soln., rel. to molec. config. 0–79324 1,1-dichloroethylene, from –122 to –250°C, rel. to cryst. struct. 0–69133 2,3-dichlorophenol, C₅ point group modes of vibration of fundamental 0-49942 2,5-dichlorophenol C_s point group modes of vibration of fundamental 2,4-dichlorophenol C_{s} point group modes of vibration of fundamental 0-499420-4942 diezynodiazomethane, vibr. spectrum, obs. 0-46571 diethylether complexes with metallic halides, low temp. study 0-7099! diethylthiocarbaminate ion and Se analogur, frequencies and vibration forms 0-67790 diethynyl ketone, solid and gas, rel. to fundamental freqs. 0-74360 diluoroethylene, intensity interpretation, appl. of dipole moment derivs. 0-74362 diffuoromethyl radical in solid Ar, absorpt. rel. to H bending and C-F difluoromethyl radical in solid Ar, absorpt. rel. to H bending and C-I stretching modes 0–66061 dihaloacetyl chloride, in vapour, liquid and solid states 0–74363 dihaloacetylenes 0–70989 dihalofumaronitriles 0–77896 2,3-dihydrofuran, rel. to struct. 0–64534 dimethyl amine, rel. to vibr. assignment and barrier to inversion 0–70993 dimethyl benzyl carbinol, qualitative intensity calculation 0–58252 dimethyl ethers, in Ar matrices, vibrs. 0–70988 dimethyl sulphone, single crystals, vibrational assignment 0–66074 N,N-dimethyl-4-nitroso-aniline 0–77874 dimethyl-4₆ amine, rel. to vibr. assignment and barrier to inversion 0–70990 dimethyl-d₆ amine, rel. to vibr. assignment and barrier to inversion 0-70993
N,N-dimethylaniline 0-77874
N,N-dimethylbutyramide, freq. assignments 0-67789
dimethylether at 3.508 µ He-Xe laser line 0-55363
dimethylnitrosamine 0-71010
dimethylsulfoxide, and -d₆ type, rel. to lattice fundamentals 0-65525
dimethylsulphoxide and deuterated derivative, new assignments 0-64501
dimethylthiocarbaminate ion and Se analogue, frequencies and vibration forms 0-67790
-67790
-67790 forms 0-67790 diphenylarsine 0-74400

diphenylchlorophosphine 0-74399

Spectra continued organic molecules and substances, infrared continued diphenylphosphine 0–74400 ethane, solid and liq., rel. to torsional oscill. 0–70996 ethanol, adsorbed on TiO₂ 0–58605 ethanol and ethanol-d in Ar matrix, 20°K 0–74369 ethyl formate, solid, rel. to rot. isomers, 3200-250 cm⁻¹ 0–41231 ethylene oxide in Ar matrix, absorpt., mol. self-assoc. obs. 0–43192 ethylene sulphide, absorpt., mol. self-assoc. obs. 0–43192 ethylene sulphide, absorpt., mol. self-assoc. obs. 0–43192 ethylene sulphide, appour and dilute solutions in polar and non-polar solvents 400 4000 cm⁻¹ 0–70997 ethylenimine, absorpt. comparison in solid Ar and N₂ matrices 0–49922 far ir. spectroscopy using interferometers 0–49147 4-fluoro- and 4-bromo-benzenethiol 0–70972 1-fluoro- 2,2-dichloroethylene, band intensities and atomic polarizations 0–39405 1-fluoro-2,4,5-trichlorobenzene 0–55352 diphenylphosphine 0-74400 0-39405
1-fluoro-2,4,5-trichlorobenzene 0-55352
germylcyclopentane 0-58222
p-glycine, long wavelength phonon spectra 0-76133
glycine, matrix-isolated, structure study 0-74372
guanine:cytosine helices, interbase vibr. coupling 0-39472
H-bonded complexes, polarization of C=0 bond 0-77857
heptanols, straight chain, liquids, meas. rel. to extent of association 0-46939 hexafluoroethane, rel. to vibr. spectra interpretation and cryst. struct. 0-69137 hydrogen-bonded, high-boiling cpds., matrix-isolation in inert gas 0-66060 hydrogen-complexes, hydrogen bonding 0-58225 β -hydroguinone clathrates, far i.r. spectra at low temp. 0-76116 ionic and semiconductor, i.r. absorpt. impurity complexes, localized vibraionic and semiconductor, 17. absorpt. impurity complexes, location modes 0–56527 isobutane, rel. to potential barrier to internal rotation 0–46584 isocyanates and polyurethane rubbers, identification 0–49947 isoquinoline, 700 to 4000 cm⁻¹ 0–55372 ketones, spectra-structure correl. 400 to 200 cm⁻¹ 0–55355 ketones, spectra-structure correl. 400 to 200 cm⁻¹ 0-35355 liquids, bandwidths, comparison with Raman bandwidths 0-46519 lithium acetate dihydrate cryst., vibr. and internal modes obs. 0-41243 methane, dissolved in inert solvent, rot. motion and moment anal. of i.r. bands 0-70910 methane, mixed isotopic crystals, site symmetries 0-79269 methane, mixed isotopic crystals, site symmetries 0-79269 methane, mixed provides theme and provides theme and provides theme. methane inert gas mixed crystals, temp. and methane conce. influence on vibration band 0-64522methane-inert gas mixed crysts., rel. to struct. and methane conc. 0-72377 methanes, chlorinated calculation of i.r. band intensities 0–74350 methanetellurol, vibrational anal. 0–64529 methanol, isotopically substituted in Ar matrix at 20°K 0–74385 methoxyamine and methoxyammonium ion 0–61170 α-methoxyaphenylacetic acid, alkali acid salt complexes, structure studies 0–46578 0-40578 methyl azidoformate in rare-gas matrices near 4°K, study of photolytic decomp. 0-69222 methyl boron difluoride and deuterated derivative, gas phase spectra 0-64526 methyl bromide, accidental resonances in fundamentals, anal. 0-71019 methyl ethyl ether, isotopic species, i.r. and Raman spectra, isomers 0-46580 0-46580 methyl iodide, anal. of ν₅ 0-77927 N- methyl phosphoramidodichloridothioate and deuterium analogues, assignment of vibrational spectra 0-46579 methyl three-top mols., 1f. vibr. modes 0-55358 2-methyl-4,5-dihydrofuran, rel. to ring-puckering pot. functions 0-74356 1- methyl-4-phospha-3,5,8-trioxabicyclo-(2.2.2.) octane-4-oxide 0-74378 methyl-phosphorus compounds, rel. to 1f. vibrs. and torsional barriers 0-64530 methylarsenic halides 0-71006 methylchloroxilanes integral integrality integrity integral integral integrity integral integral integrity integral integra methylchlorosilanes, integral intensities of vibrational bands 0-43181 methylcyclopentane, vibr. anal. rel. to out-of-phase ring deforms. 0-67785 methyldithiocarbaninate ion and Se analogue, frequencies and vibration 0—67785
methyldithiocarbaminate ion and Se analogue, frequencies and vibration forms 0—67790
methylenecyclobutane, ring puckering pot. function from mid-i.r. combination bands 0—71014
methylenecyclobutane, ring-puckering potential function from mid-i.r. combination bands 0—743174
methylenecyclobutane, ring-puckering potential function from mid-i.r. combination bands 0—43174
methylenemidazole, Cl. and SnCl₂-salts, study 0—71012
β-methylnaphthalene, vibrational assignment of frequencies 0—74351
N- methylpropionamide, and normal vibrs., obs. 0—53075
methylthioethyne 0—77921
molecules with low freq. vibrs., and Raman spectra, obs. 0—39362
of monobutyl naphthalenes 0—39439
monocarboxylic cyclobutane acid, dimer forms and config. 0—74388
monochloromethyl radical, assignment of absorptions 0—74389
monohalo-benzenes, liquid and polycrystallino phases, study 0—74760
naphthalene-d₈ 0—77931
β-naphthol, vibrational assignment of frequencies 0—74351
α-naphthol, vibrational assignment of frequencies 0—74351
1- and 2-naphthol, vibrational assignment of frequencies 0—74351
1- and 2-naphthols, crystalline, below 250 cm-1 0—72381
1,4-naphthoquinone single crystal layers, vibrational bands assignment 0—51295
neopentane, rel. to potential barrier to internal rotation 0—46584 neopentane, rel. to potential barrier to internal rotation outlines, aromatic, absolute intensities determ, methods outlines, aromatic, absolute intensities determ, methods outlines, aromatic, absorpt, in polarized light outlines, assignments outlines, and outlines outlines, assignments outlines, assignments outlines, as of the control of the contro 0—48084
nitrobenzene anion 0—77939
nitrobenzenes, monosubstituted 0—77937
nitromethane, liquid or solution, vibration bands width 0—67809
4-nitropyridine N-oxide anion 0—77939
4-nitropyridine anion 0—77939
4-nitropyridine nion 0—77939
9-nitrotluene anion 0—77939
O-alkyl phosphorodichloridothioates 0—55350
octachlorocyclobutane, assignment of fundamental freqs. 0—74355
octafluorocyclobutane, assignment of fundamental freqs. 0—74355
octafluorocyclobutane, assignment of fundamental freqs. 0—74355
organomercuric compounds, Hg (ch₃)₂ and Hg(CD₃)₂, vibrational spectra
0—67805

```
Spectra continued
```

organic molecules and substances, infrared continued

organometallic acetylenic compounds, vapour, liquids and solutions 0-64473

organophosphorus cpds., Pions charact. absorpt. freqs. 0-55369 oxalyl chloride 0-58234

oxaryt enioride 0-58234
2-oxazoline, rel. to struct. 0-64534
pentachloropyridine, solution and crystalline phases 0-64535
pentadeuterotetraphenylgermane, low wavenumber vibrations, i.r. and Raman spectra 0-46592
perdeuterodimethyl amine, rel. to vibr. assignment and barrier to inversion 0-70993

peroxyacetyl nitrate, from NO_2 and 2-trans-butene in polluted air 0-70839

phenazine dyes, triplet-triplet absorpt. 0–71044 phenol, vapour, liq. and solid rel. to mol. structs. 0–39443 phenol and 2,6-diisopropyl phenol, OH weak intermol. interactions 0–55395

phenothiazine dyes, triplet-triplet absorpt. 0-71044 phenyl derivatives of group Vb elements in solid state 0-76117 phenyl methyl carbinol, carbonyl groups complexing, solvent effect phenyl me 0-46918

phenyl methyl carbinol, qualitative intensity calculation 0-58252

phenyl methyl carbinol, qualitative intensity calculation 0–58252 phenylarsenic haides 0–71006 phenylarsine 0–74400 phenyldichloroarsine 0–74399 phenyldichlorophosphine 0–74399 phenyldichlorophosphine 0–74399 phenylphosphine 0–74400 phosphoryl absorption band intensities 0–71026 phthalocyanine, and metal derivatives, far i.r. spectra 0–74397 phthalocyanine, metal derivatives, metal-ligand vibrations 0–74397 polyacrylamide, N.N-disubstituted, basicity determ. 0–74429 polyamides, rel. to transition and relaxation phenomena 0–67835 polyethylene, mixed crystal i.r. study of chain segregation 0–58261 polyethylene glycol, molten, vibr. analysis rel. to conformation, obs. 0–39469

polyethylene glycol, molten, vibr. analysis rel. to conformation, obs. 0–39469
polyethylene-perdeuteropolyethylene mixed crysts., rel. to chain folding obs. 0–39916
polyisoprenes, deuterated 0–77977
polymers, emission spectra 0–71053
polymers, study of molecular thermal motion 0–50852
polyparaaminostyrene, relationship between far i.r. absorption and electrical conductivity 0–64463
polystyrene, deuterated derivatives 0–64575
polyurethane rubbers, identification 0–49947
polyvinyl alcohol film, ir study of tensile strength behaviour 0–68473
polyvinyl fluoride, structure 0–46623
polyvinylidenefluoride, rel. to investigation of structure dependence on polymerization conditions 0–71439
propane, rel. to potential barrier to internal rotation 0–46584
protein, globular absorpt., rel. to dielec. props. 0–51315
1-pyrazoline, vibr. anal. rel. to out-of-phase ring deforms. 0–67785
1-pyrazoline, substituted derivatives 0–74405
pyrrididine, substituted derivatives 0–74405
pyrrole film, absorpt. in polarized light, surface forces effects 0–41234
pyrrolidine, vibr. anal. rel. to out-of-phase ring deforms. 0–67785
quinhydrone type complexes 0–74406
rhodanines, mutual influence of functional groups 0–77950
salicylaldazinate metal chelates, rel. to vibration studies 0–71030
selenaeyclopentane, rel. to symmetry and struct. 0–64544
selenium dialkylamino compounds, i.r. and Raman spectra force constants 0–46590

0-40500 silacyclobutanes, vibrational spectra, normal coordinate analyses 0-46590

0-46590 silacyclopent-2-ene, far i.r. absorpt. rel. to ring-puckering pot. 0-71032 silanol adsorption of water, i.r. spectra 0-58607 silico-organic cpds., [(CH₃)Sil₂El²V (El²=C, Si, Ge, Sn), vibrational spectra and force constants 0-46589 silyl and trimethylsilyl compounds of group 5 elements, force constants 0-46591

0-46591 sparteine and stereoisomers, monocation struct. 0-64545 succhimide, for struct. study 0-58243 sulphonylamines, halogen-substituted 0-53085 sulphur dialkylamino compounds, i.r. and Raman spectra force constants 0

sulphur dialkylamino compounds, i.r. and Raman spectra force constants 0-46588 1,1,2,2-tertabromoethane 0-77953 tetracyanoquinodimethan radical anion ammonium salts relationship between far ir. absorption and electrical conductivity 0-64463 7,7,8,3-tetracyanoquinodimethane (TCNQ) and TCNQ-d₄ crystals, i.r. and Raman spectra 0-55373 tetrahydrofuran, band absolute intensities 0-39448 tetraiodoethylene solid and in CS₂ soln., laser excitation 0-64548 tetramethylsilane, integral intensities of vibrational bands 0-43181 tetramethylitanium 0-71033 tetraphenylgermane, low wavenumber vibrations, i.r. and Raman spectra 0-46592 1,3,4-thiadiazoles, absorption spectra in near i.r. 0-58249

tetramethylttanulm ——1093
tetraphenylgermane, low wavenumber vibrations, i.r. and Raman spectra 0—46592
1,3.4-thiadiazoles, absorption spectra in near i.r. 0—58249
2,4-thiazoleidindione, calc., normal frequencies 0—39449
thiazolidine, i.r. spectra of 2- and 4-thioderavitives, deformation and vibrations 0—61176
thioacetanilides, substituted, investigation of cis-trans isomerism 0—64550
thiohydantoin, vibration frequencies, calc. 0—46593
thiophenes, 2-substituted 0—74410
thiophosgene, and polymer species 0—55374
torsional data, analysis 0—74208
trichloroethylene, band intensities and atomic polarizations 0—39405
trichlyleneglycoledimethacrylate polymer study 0—67834
1,1,1-trifluoro-2-butyne, vibrational assignment 0—77956
3,3,3-trifluoro-1,2-epoxypropane differences between variously prepared polymers 0—68203
trifluoro-acetonitrile, contours of gas phase i.r. bands 0—71038
trifluoro-acetonitrile, contours of gas phase i.r. bands 0—71038
trifluoro-acetonitrile, spectra determ, for molecular mechanism of ferroelec. transition 0—40875
triglycine sulphate, and pyroelectric detector applic. 0—75814
triglycine sulphate and selenate, dielec. consts., pyroelec. and i.r. radiation detection applic. 0—65824
trimethylsilyl cyanide and isocyanide, 33 to 4000 cm⁻¹ 0—55377

trimethylsilyl cyanide and isocyanide, 33 to 4000 cm⁻¹ 0-55377

Spectra continued

0-49939

behaviour 0-68473
vinyl esters of carboxylic acids 0-74365
vinyl isocyanide, 200 to 4400 cm⁻¹ 0-55378
vinyl frifluorosilane 0-77952
xanthene dyes, triplet-triplet absorpt. 0-71044
o-xylene, far i.r. 0-58251
zinc uranyl acetate, vibration level assignment 0-46602
CH₂CH₂Fir vapor and solid state, vibrational fundamentals 0-39426
CH₂CH₂CI vapor and solid state, vibrational fundamentals 0-39426
CH₃CH₂F vapor and solid state, vibrational fundamentals 0-39426
CH₃CH₂I vapor and solid state, vibrational fundamentals 0-39426
CH₃CH₂I vapor and solid state, vibrational fundamentals 0-39426
C=0 valence vibr. of ketones, band parameters and profiles, (-)30-70°C

triphenylarsine oxide and iodine cyanide complex, charge transfer complex 0--46598 0-40.98 triphenylene and triphenylene-d₁₂, crystalline and solution, normal coordinate calculations 0-43183 triphenylstibine 0-71039

trips salicylato-bis-phenanthroline rare earth chelates, study of characteristics 0-7103!

1,3,5 trithiane, vibrational assignments and normal coordinate treatment

p valerolactone, fundametnal vibl. assignment 0–46599 vinyl alcohol and N-vinylpyrrolidone copolymer ir study of tensile strength behaviour 0–68473

0-64493

organic molecules and substances, infrared continued

organic molecules and substances, radiofrequency see also Nuclear magnetic resonance and relaxation; Paramagnetic reso-nance and relaxation acetonitrile N-oxide, microwave spectrum, structure determination 0-74325

0-74325 bicyclo[2.1.0]pent-2-ene 0-77873 2-bromoethanol, microwave spectra, intramolecular hydrogen bonding study 0-43155 cis-2-butteen microwave, internal rotation, conformation 0-46546 butyliodide, tert., rot. spectrum with hf.s. anal. 0-64490 2-chloroethanol, microwave spectra, intramolecular hydrogen bonding study 0-43155 eitherform dipole moment determ, and pressure-broadened spectra

chloroform, dipole moment determ. and pressure-broadened spectra 0-61179

0-61179 chloroform in H₂, He, N₂ and Ar gases, microwave absorption at high pressure 0-53278
3-chloropropene, microwave spectrum, rotational constants, nuclear quadrupole coupling constants 0-77889 transcrotononitrile, microwave spectrum, rotational constants 0-39419
2-cyanoethanol, microwave spectrum, ground state assignment of transisomer 0-70986 dibromomethane, microwave spectrum nuclear quadrupole coupling 0-46555 close-2.3-dicarbahexaborane (6), skeletal molecular structure from micro-

0–46555
closs-2, 3-dicarbahexaborane (6), skeletal molecular structure from microwave spectra 0–64500
2,3- dichoroquinoxaline in durene, polarization of mag. zero-field transitions 0–54117
1,1-difluoro-3-methylbutadiene microwave spectrum, barrier to internal rotation and dipole moment 0–46557
difluorophosphine borane, microwaves spectrum and rot. consts. 0–70992
ethyl alcohol, microwave spectra of isotopic species 0–46559
ethylamine, microwave spectrum rot. consts. 0–70992
ethylene sulfone, microwave spectrum rot. consts. 0–71000
2-fluoroethanol, microwave spectral, study of intramolecular hydrogen bonding 0–46562
formaldehyde, rotational spectra study by submillimeter microwave spectroscopy, rotational and centrifugal constants 0–64509
glycolaldehyde, microwave, rot. consts. and vibr. state assignments 0–77913
isopropyl alcohol, detection of 2 rotational isomers by microwave spec-

isopropyl alcohol, detection of 2 rotational isomers by microwave spectrum 0-43169methane-d₁, elec. resonance spectra, transitions and elec. dipole moments

methanol jet, line obs. 0-74375
methyl chloride, microwave absorpt, intensity law, evaluation 0-71016
2-methyl thiophene, microwave spectrum, internal rotation and dipole moment 0-64525
2-methyl-1-buten-3-yne, microwave, methyl group barriers to internal rot. 0-77928
methyl-arcine, microwave, methyl group barriers to internal rot.

u=1/928 methylarsine, microwave spectrum and barrier to internal rot. of methyl group 0-71015 methylbromodiazirine 0-67804 methylcylopropyl ketone, microwave, assignments and rot. consts. 0-77929

trans-methyldiimide, microwave, rel. to struct. and rot. consts. 0-74387 methylene fluoride, microwave, centrifugal distortion and molecular structure 0-46577

ture 0-40517 methylenecyclopropane, microwave 0-53077 methylenecyclopropane, microwave spectrum, ring-bending vibr. 0-46574 microwave rotational spectra, series of broad bands, interpretation 0-70961

morpholine, microwave, rel. to rot. consts. and quadrupole coupling 0-77930

u=77930 nitroethane, microwave spectrum, molecular model 0-77938 nitroethylene, microwave of torsionally excited states 0-7794! paraldehyde, microwave spectrum 0-61173 1,3-pentadiene, trans and cis, microwave methyl group barriers to internal rot. 0-77928

rot. 0–77928

propargyl mercaptan, microwave spectrum 0–64542

propyl alcohol, microwave spectrum 0–64542

propyl iodide, normal, microwave, effects of rotational Isomers 0–77945

pyrimidine, microwave spectra, 8000–18000 MHz 0–77949

thioformaldehyde detection 0–71035

1,2,3- triazole assignment, by microwave double reson. 0–55376

trichloromethyl fluoride, dipole moment determ, and pressure-broadened spectra 0–61179

trimethyl phosphine borane, microwave spectrum of normal and isotopic species 0–71042

trimethylene selenide, microwave spectra, 7,3-32 GHz 0–74413

trioxane, Itype doublets in degenerate excited vibr. states 0–61178

trioxane, rotational, ground and several excited vibrational states study 0–46596

vinyl bromide, pure rotn, spectra of type aR at mm, wavelengths 0–46600

vinyl bromide, pure rotn, spectra of type °R at mm, wavelengths 0-46600 vinyl isocyanide, microwave 0-55378

Spectral line breadth

see also Doppler effect; Stark effect; Zeeman effect Anderson exchange narrowing model soln. for I>1/2 0-59343 anthracene cryst., width of lowest singlet-singlet transition 0-41228 atom, effect of transitions induced by non-adiabatic collisions 0-39280 atomic, foreign gas interaction, classical path approximation 0-39261 atomic collisions, violent, discrete energy loss spectra 0-74148 atoms, broadening by charged particles, review 0-55228

atoms, collision broadening by foreign gas atoms 0-74109 bicyclo-octyl radicals, e.p.r. spectrum, line width changes as function of temp. compared with n.m.r. results 0-55341

Brillouin, meas. by Fourier-transform spectroscopy 0--60424

broadening, anomalous, in nonlinear liqs, and effect on stimulated scattering processes 0-39797

ing processes 0–39797
broadening, nonuniform, resonance energy transfer 0–44808
chloroform, pressure-broadened microwave spectra 0–61179
collisional broadening, classical oscillator analog 0–77685
collisional broadening used for determ. of interatomic potential 0–70796
conference, optical pumping and at. line shape, Warsaw, 1968 0–52878
contour distortion by second order recording system, analysis 0–60423
contours recording, by IKL-1 instrument 0–38576
corrections, dynamical, to Holtsmark's theory of spectral line broadening
from linear Stark effects 0–58089
crystal self-focusing, laser irradiated 0–79345
dibenzoperopyrene and 3,4-benzopyrene in n-paraffin matrix, quasi-line,
temp. depend. 0–79369
Dicke effect and perturbation of internal energy levels 0–6769!
e.p.r., ang. and temp. depend., theory 0–41313
e.p.r. of ferromagnetic compounds of Eu, 80-500 K, exchange interactions 0–41329
edge recombination radiation, inhomogeneous broadening 0–44880

edge recombination radiation, inhomogeneous broadening 0-44880 effect of band or line shape on radiative transfer in nongrey planar medium 0-66855

medium 0-66855
electron impact broadening, treatment of correlations 0-70788
electron-impact broadening, non-Markovian theory 0-70789
Hameka theory of linewidths 0-38189
hydrogen-like broadening by electron collision 0-72347
i.r., resolution enhancement by numerical spectrometer distortion correction 0-42396
impurity centre interaction with surrounding, quasi-line 0-79369
inert gase broadening of at. lines, theory 0-52883
inert gases, rel. to interat. reson. coupling 0-52881
inhomogeneously broadened line, frequency modulation in the spectroscopy 0-42919
laser He-Ne, threshold bandwidth of the 0.63*u* laser 0-60208

inhomogeneously broadened line, frequency modulation in the spectroscopy 0-42919 laser, He-Ne, threshold bandwidth of the 0.63*u* laser 0-60208 laser, solid, generation spectra, line struct. 0-73236 lines with combined levels, half-widths and absorption coeffs. 0-7764! liquid, simple, broadening of localized transitions, model 0-4692! liquids and solutions, electronic-vibrational absorption bands, broadening, role of fluctuation processes 0-61527 magnetic resonance, spin spin reservoir 0-41297 magnetic scanning method for meas. of broadening and displacement 0-42940

microscopic theory of broadening of impurity mol. lines in crysts. 0-72340

0-72340
n.m.r., in presence of equal transitions 0-57471
n.m.r., a saturational narrowing 0-38447
n.m.r. high-resolution spectra, intramolec. dipolar relax. effects 0-53012
n.m.r. linewidths homogeneous broadening due to intermolecular relaxation 0-46442
naphthantrone in n-paraffin matrix, quasi-line, temp. depend. 0-79369
nitromethane, liquid or solution, vibration bands 0-67809
optical density flame pyrometry 0-38422
optical double reson. line shape in time resolved meas. 0-52891
oxide powders, X-ray line broadening meas. of crystallite size 0-40090
p.m.r. line narrowing by magic angle rotation 0-6981?
Permalloy film, ferromag, resonance, temp. and mode depend., 4-300K
0-44968
plasma, electron impact broadening, theory 0-74533

Permalloy film, ferromag, resonance, temp. and mode depend., 4-300K 0-44968

plasma, electron impact broadening, theory 0-74533

plasma, press, broadening and line shifts 0-52887

plasma line broadening, ion motion effects 0-64703

pressure broadening, 0.1-10 torr, theories and obs. 0-52880

pressure broadening, Eleisenberg model 0-52882

pressure broadening, calc. for i.r. and Raman spectra 0-57632

pressure broadening of at. lines, quasi-mol. theory 0-52886

resolution improvement by Fourier transform techniques 0-70079

resonance broadening, density depend. 0-7075!

ruby: Cr³+, e.p.r. line broadened by strong hyperfine interactions, second moment 0-51389

ruby, R' optical transitions of Cr³+ linewidths, broadening mechanisms 0-76166

satellite half-width obs. rel. to plasma parameter determ. 0-39591

shock wave, collisionless magnetostatic, turbulence level, Balmer Hβ line, Stark broadening 0-64689

splitting for optical transitions in gases induced by resonant external fields 0-49836

stochastic theory 0-55215

thin film ferromag, reson, temp, dependence 0-44963

triochloromethyl fluoride, pressure- broadened microwave spectra 0-61179

0-61179 velocity distribution effect in pressure broadened lines 0-77647 wings of Stark-broadened lines, profiles of forbidden components, objections to method of calc. 0-61019
Al₂0₃:Fe³⁺ e.p.r., temp. depend., 4.2-1100 K 0-66135
Al₃0₃:Ti³⁺, corundum, e.p.r. line shape 0-51387
Ar, pressure broadening, 0.1-10 torr, rel. to theories 0-52880
Ar, self-broadening due to 3p³4-s3p³4p transitions, obs. 0-52894
Ar positive column of d.c. discharge 0-42970
CP₃COOH-HCOOH bimolecule 0-74412
CO, collision-broadened, half-width variation interpretation 0-61082
CO, self-broadened semi-halfwidths of pure rotational lines 0-70889
CO gas, collisional narrowing of vibrational Raman band 0-74279
CO₃, 001-100 band, temp. depend. of self-broadened half-width of P20 line 0-61084
Ca, 4¹P₁, 4¹D₂ and 5¹D₂ Hanle curves broadening by He, obs. 0-52897
Cd 5³P₁, optical double reson. line shape in time resolved meas. obs. 0-52891
Cl0₂ in H₂O-butyl alcohol, e.s.r. linewidths 0-68148

ClO₂ in H₂O-butyl alcohol, e.s.r. linewidths 0-68148

Spectral line breadth continued

Co complex, [Co en₃]Cl_{3.n}H₂O, paramag. reson. linewidth of Cr³⁺ 0 - 48143

0-48!43
Co(II) complex, dichlorobis(picoline)cobalt(II) in CDCl₃, electron spir relaxation times from data for ligand and solvent protons 0-4986!
Cs, profiles of Xe broadened atomic lines and satellite bands 0-74!06
Cs absorpt. line broadening by inert gases, obs. 0-52903
Cs reson. line broadening by Ar, Kr, calc. 0-52904
EuFe garnet, ferromag, resonance, anisotropic exchange interactions 0-44966

H, Stark broadening calc. by unified classical path theory 0-77659
H line broadening due to electrodynamical, Doppler and Zeeman effects 0-46402

H plasma, close collisions in Stark broadening 0-61294

H₂, pressure-broadened linewidths in electric-field induced spectrum 0-46478

0-46478

H_o and H_y lines, Stark broadening calculations 0-74169
HCl, collision-broadened, half-width variation interpretation 0-61082
HCl, inert-gas pressure-induced, impact theory 0-70909
HCl, inert-gas pressure-induced, impact theory 0-70908
HCl, rotational lines perturbed by monoatomic gases 0-61089
HCl pressure broadening and spectral line shift of pure rotational lines perturbed by noble gases 0-67735
HF, strength and width in first overtone band 0-53029
HF gas, line broadening and shifting in 2-0 band by Ar, Kr and Xe 0-77797

Hel, rot. lines press. broadening and shift 0–43098
He, pressure broadening, 0.1-10 torr, rel. to theories 0–52880
He, rel. to interat. reson. coupling 0–52881
He I 5016A computed profiles at high electron densities 0–74531
He I 34471, 34470, laboratory plasma obs. rel. to astrophysical spectra 0–61018

0–61018
He II line λ=4686 Å, broadening in plasma 0–64293
He ionized, anomalously large lines observed due to large momentum transfer in excitation process 0–43028
Hg 2537 Å reson line, Kr press. effects, obs. 0–52908
Hg atom 2537 Å, Ar, He broadened, intensity distrib. and shift calc. 0–52907
198 Hg ³P₁ crossing curves self-broadening, obs. 0–52910
1₂, absorpt. linewidths in B ³H_{out}+X¹Σ_g+ system, alternation with J 0–70914
K pressure broadening 0.1.10 torr, rel. to theories. 0–52880

 $^{\circ}$ 0-70914 K, pressure broadening, 0.1:10 torr, rel. to theories 0-52880 Kr, pressure broadening, 0.1:10 torr, rel. to theories 0-52880 Kr, pressure broadening, 0.1:10 torr, rel. to theories 0-52880 LiAlSi₄O₁₀, petalite, e.p.r. of Fe³⁺, anisotropic broadening of line width 0-54158 MgO powders, X-ray line broadening meas. of crystallite size 0-40090 MnF₂, e.p.r. line width, critical broadening 68-380K 0-51397 N II, dense plasma, profiles of 9 lines, Stark broadening 0-39289 α-N₂, using potential of atom-atom form 0-59080 N₂ gas, collisional narrowing of vibrational Raman band 0-74279 NH₃, microwave inversion spectrum line width parameters for (1≤J≤8, K=1) lines 0-55304

N=1) lines 0-53304 NH₃, pressure broadening of inversion lines, theory 0-43124 NV, cross-sections, oscillator strengths and inelastic widths for several lines 0-67625 Na I A5889 line, pressure broadening by high temp. neutral helium 0-52917

Nd lines in glasses, inhomogeneous broadening, magnitude 0-6265! Ne, pressure broadening, 0.1-10 torr, rel. to theories 0-52880 Ne, pressure broadening of 6074.3 Å line using Zeeman scanning 0-7077!

No. 70771

Ne positive column of d.c. discharge 0-42970

Ni I, absorption line profiles of multiplets in near u.v. 0-67629

Ni I, absorption line profiles of multiplets in near u.v. 0-67629

Ni I, absorption line profiles of multiplets in near u.v. 0-67629

Ni I, absorption line profiles of multiplets in near u.v. 0-67629

Ni I, absorption line profiles of multiplets in near u.v. 0-67629

Ni I, absorption line profiles of multiplets in near u.v. 0-67629

Ni I, absorption line profiles of the line by Stark effect 0-77666

OCS, microwave parameters, as broadened by methyl bromide 0-77823

OS, broadening of rotational lines by quadrupolar gas 0-43135

SO₂, broadening of rotational lines by dipolar gases 0-64448

SO₂, microwave parameters, as broadened by methyl bromide 0-77823

Si II broadening parameters meas. 0-60929

SnO.(H,O₂), stannic acid gel, nuclear gamma resonance 0-55641

Sr 5³P₁ optical double reson. line shape in time resolved meas. obs. 0-52891

Ke, Rayleigh linewidth meas. near critical point 0-78329

Xe, Rayleigh linewidth meas, near critical point 0-78329

Spectrochemical analysis also Chemical

analysis/by mass spectrometry; Spectro-

ATR, low temp. applic. 0–69105 air type atmosphere, major components analysis using emission techniques 0–45095 arc and complementary spark excitation method for miscellaneous materials 0–56724

aspiration system, variable flow, forced feed, for atomic absorption spectro-photometry 0-48212 atmosphere, Cr, Ni, Mn, Cu trace determ., atomic absorption method 0-56728

atomic absorption, lead determinations in air-borne particulates over Morton Grove, Illinois 0-66212

Morton Grove, Illinois 0—66212 atomic absorption, metallic constituents at macro and trace levels in nuclear fuel, remote analyses 0—76287 atomic absorption, ring burner and absorption tube technique 0—62829 atomic absorption bibliography 0—46331 atomic absorption spectrophotometry with air-acetylene flame overexcitation interferences 0—69238 atomic fluorescence, detecting system with interference filter 0—69235 atomic fluorescence, spectroscopy, influence of flame composition

atomic fluorescence spectroscopy, influence of flame composition 0 52867

d 3/280/a atomic fluorescence spectroscopy, interference studies with a continuum source 0–52868 conference, Chicago, USA, May 1968 0–69237 conference, Chicago, USA, May 1968 0–66215 correlation spectroscopy application 0–67177 in criminalistics review 0–72570

d.c. arc, 'cathode region' method, determination of impurities in plutonium 0-66211

Spectrochemical analysis continued

detection limits, experiments and theories 0-72572

diffusion layer concentrations for high concentrations 0-41196

direct electron excitation and comparison with X-ray fluorescence of geological samples 0-48213

ESCA, NaCl crystal electron emission following MgK α , AlK α irradiation, ang. distrib. 0–76282

electrode heaters for analysis, design description 0-51446

electron spectroscopy for chem. anal., appl. to electron escape depth determ. in Au 0-7586!

electron spectroscopy for chemical analysis 0–66214 emission, transition lifetime influence on meas. reproducibility 0–51447 emission spectroscopy, internal standardization 0-56725 flame spectroscopy, powder specimens, scintillation recording method 0-41454

fluorescence, hot wire loop atomiser, for analysis of volatile metals $0\!-\!73355$

glass, anal. with use of sliding discharges 0–51448 glass soda-lime-silica, Na content determ, by X-ray fluorescence 0–41456 Hadamard-transform optical encoder for automobile-exhaust analysis

0-72573 impurities in metals and alloys, parts per billion 0-72571 with laser or tungsten sources, slit function rel. to absorption law 0-63733 line intensity increase in d.c. arc discharge with applied nonhomogeneous magnetic field 0-48215 luminescent, polarization method for delimiting photoluminescent radiation from exciting rays 0-69233 lunar samples, X-ray fluorescence analysis 0-48498 lunar samples, igneous-type rocks and spherules, X-ray fluorescence 0-45369

10-45369 lunar samples, major and minor constituents, emission spectrographic analysis 0-45354 lunar samples, search for porphrins by fluorescence activation 0-45402 lunar samples, search for porphyrins by fluorescence spectrometry 0-48549

10-40-349 lunar samples, trace elements, emission spectrographic determ. 0-48499 microelements content of surface air, above continent and ocean 0-76372 mineral, powder specimen, flame spectroscopy, scintillation recording method 0-41454

molecular structural group anal., symbolic logic methods 0–58134 monitoring atmospheric contaminants during W-inert gas are welding, parameters involved 0–76285

Mossbauer effect used to determ. Fe content in alumina and corundum 0 - 56726

neutral atom spatial distribution in long pathlength cell, influence of temp. gradients 0-69232 optical emission, analysis for Pt, Pt, and Rh in gold beads from fire assay

0-66213

plasma, d.c., trace determ. 0-61276

plasma, d.c., trace determ. 0-61276 plasma jet, streaming analysis by evaluation of spectral lines of atoms and molecules 0-66952 plasmas, laser induced, for analytical spectroscopy 0-78117 pulse-height analysis network method comparison with cryst. spectrometry 0-41457 quantitative using gas transport and arc discharge 0-62830 reaction rates, computer program for spectrophotometric obs. 0-51442 sensitivity of emission spectra for free running and pulsed laser regimes

sensitivity of emission spectra for free running and pulsed laser regimes 0-69236

of soil, determination of T traces using eutectic metal mixture SnCd 0-69240

spark emission method for detecting $\rm H_2$ contamination in compounds on Al surfaces 0–51443 spectrographic arc, electrical and optical properties for graphite 0–48214 spectrographic arc burning in inert gas atmosphere, atomic excitation mechanisms 0–46378 spectrographic evaporating dish, improvement 0–62828 spectrographic evaporating dish, improvement 0–62828 spectrophotofluorometer-gas chromatograph combination, patent 0–76295 spectrophotometric, high property of the pro

spectrophotometric high press, cell for chemical reactions direct obs. 0-69234

spectrophotometric high press. cell for chemical reactions direct obs. 0–69234
surfaces and reaction products, X-ray emission analysis 0–65031
time-resolved spectra in spark produced plasma 0–53171
X-ray dispersion techniques, ultrasoft, total reflection at critical angle 0–66217
X-ray fluorescence anal., internal standard method, overcoming particle size effect 0–66221
X-ray fluorescence determ. S in mineralised rocks 0–66218
X-ray line wavelength shift voltage depend. 0–66077
Ag and alloys, Au and alloys, with dissolved Cu, X-ray analysis of solubility 0–71743
Ag for vacuum solders, impurity trace determ. 0–76288
Au microgram level, fire-assay emission spectrographic method 0–54197
Ba determination in biological materials by atomic absorption spectroscopy 0–51444
BaNO₃ i.r. determination using Pellet Tech. 0–54198
C content in steel determination using direct reading spectrometer, single calibration curve 0–51445
C in charcoal, h.f. spark excitation spectrum of sintered tablet of 96% Fe, 4% charcoal 0–69239
F determ. in standard rocks 0–56727
Fe-H,SO₂-H₂O system, system structure analysis Mossbauer spectroscopy application 0–64861
Ga impurity ultra-trace determination, electrodes evaluation and pre-treatment 0–41455
KNO₃ i.r. determination using Pellet tech. 0–54198
N. in atmosphere, spectral analysis of laser-Raman radar 0–69277

Ga impurity ultra-trace determination, electrodes contained ment 0-41455 ment 0-41455 No. 1 i. determination using Pellet tech. 0-54198 Nj. in atmosphere, spectral analysis of laser-Raman radar 0-69277 NO.-MAPQ gas flame, for atomic obs. spectroscopy 0-66210 NaNo, i.r. determination using Pellet tech. 0-54198 Nj. base alloys, Pb, Bi, Sn trace determ, emission spectrographic carrier-distillation method 0-56729 Pd microgram level, fire-assay emission spectrographic method 0-54197 Pt microgram level, fire-assay emission spectrographic method 0-54197 Rh microgram level, fire-assay emission spectrographic method 0-54197 Rh microgram level, fire-assay emission spectrographic method 0-54197 SiO, sample's transport efficiency determination from electrode cavity to gas-stabilized d.c. arcs excitation zone, eqns. 0-51449 Sr determination in biological materials by atomic absorption spectroscopy 0-51444 SrNO, i.r. determination using Pellet tech. 0-54198

Spectrochemical analysis continued

Th in rare earth, determination using γ -ray spectrometry, method description 0-51450

Spectrometers

see also Mass spectrometers; Monochromators; Particle spectrometers; Spectrophotometers; X-ray spectrometers

2m Universal Reflecting Telescope, spectrograph in Cassegrain focus, plane grating, desing and operation 0-51816

ATR, for low temp. applic. 0-69105

astronomical slitless spectrograph for flash spectrum 0-69515

atomic-fluorescence, detecting system with interference filter 0-69235

for automobile-exhaust analysis using Hadamard-transform optical encoder 0-72573

centriflusal strugglagers of pages 0.76211

aromobile-exhaust analysis using Hadamard-transform optical encoder 0–72573 encoder 0–72573 entroing Hadamard-transform optical encoder 0–76371 correlation, for remote detection of atmospheric pollutants 0–56763 Czerny-Turner, high resolution 1.5 m in-plane, geometrical aberrations obs., astigmatism, residual coma 0–73348 Czerny-Turner, wavelength distribution of stray light 0–54942 derivative, sinusoidally modulated, theory, transfer function 0–77217 derivative, sinusoidally modulated, theory, transfer function 0–77217 derivative, wide frequency range 0–66999 direct-reading 2000 channel spectrograph 0–60436 direct-reading spectrometer DSA 240, suitability for analysis of alloys and impurities 0–42398 dispersive, doubly multiplexed, performance 0–60427 double resonance modulation microwave spectrograph, description 0–70085 double-beam, diffraction grating for far i.r. obs. in 250-10 cm⁻¹ region,

double-beam, diffraction grating for far i.r. obs. in 250·10 cm⁻¹ region, vacuum 0-77219 dual-channel, for rotational temp. meas. 0-60093

duochromator, (polarization Fabry-Perot), for meas. of small spectral line displacements 0-60426 e.s.r., IFA-type, signal/noise ratio improvement by time averaging 0-63523

0.-63523 earth's radiance near 4.3 μ , meas, using grating spectrometer, calibration and performance 0.-41786 echelle spectrograph, astronomical 0.-66679 electron, electrons, electrons, electrons, electrons and spherical, optimum deflection angle 0.-52247

0-32247 electron, sealed-off vacuum device, fabrication of fine slits 0-76775 electron impact, for chemical analysis of gases and vapours 0-67179 with electron microscope combined in instrument with $<10\text{\AA}$ resolution

0-43/63
electron spectrographs of electrostatic cylindrical type, soft X-ray tube construction 0-79828
Fabry-Perot, high luminosity, for night airglow studies 0-62934
Fabry-Perot, universal, plate separation control by piezoelectric effect, design and applications 0-49145
Fabry-Perot photoelectric, analytical expression's numerical results 0-60429 0-60429

far i.r. interferometric Fourier system, using double beam methods 0-63723

0-03/23 Fourier, IT-69, computation of spectra from interferograms prod. by this spectrometer 0-52386 Fourier transform, derivate traces 0-38570

Fourier transform, derivate traces 0-38570 grating, Ebert type, astigmatism and coma free 0-70090 grating, role of coherence 0-57637 grating, two channel, rapid scan, basic principles, capabilities 0-73350 ix., for remote sensing of air pollution 0-7261! ir. grating, NIMBUS satellite expt. 0-76530 ix. grating spectrometer for low-frequency modes of organic and inorganic mols. 0-63717 ir. near, digital with ice-cooled photomultiplier for airglow; auroral emission study 0-63718 ir. satellite for atmospheric temp., radiative transfer meas., design 0-66277 ir. spectra, resolution enhancement by numerical spectrometer distortion

0-6277

1. spectra, resolution enhancement by numerical spectrometer distortion correction 0-42396
infrared, calibration using alkali halide solid soln. spectra 0-70088
interferential, for ultra short light pulse obs. 0-49150
interferential, spatially and chromatically compensated 0-67181
interferometer, far Fourier spectroscopy using 10° samples 0-70086
interferometer, i.r., on NIMBUS III satellites, thermal emission spectra of Earth and atmosphere 0-76531
interferometric based on polarising beam splitters 0-67180
ion cyclotron resonance principle, ion-molecule reactions research 0-59483
magnetic, cylindrical, rel. to solid surfaces, electron impact desorption of

0–59483
magnetic, cylindrical, rel. to solid surfaces, electron impact desorption of ions and neutrals 0–68238
magnetic, double focusing, for β-γ angular correlation obs. 0–77218
Michelson interferometer, spectral density modulation 0–70084
microwave, slowly-sweeped, device for automatic obs. and transcription of frequency 0–73110
multinuclear resonance, new type 0–49152
 NMR's transducer, e.m. rate parameter selection, mathematical evaluation 0–48042

0 - 48942NMR for longitudinal relaxation time meas. of nonequiv. nuclei groups

-48939

NMR storage device synchronization, device description 0-4894! n.m.r., for short relax. time meas. in low fields with small samples 0-60127

0-0127 n.m.r., high resolution, Varian HA 100, solid state spin-echo attachment 0-7623! nuclear, digitally stabilized, resolution function 0-6388!

nuclear, agitally stabilized, resolution function 0-388: rel. to ocean colour, remote sensing 0-72600 for phonons, acoustic, 10 to 300 GHz 0-53684 photoelectron spectrometer for molecules 0-61168 Raman, design criteria and performance 0-54941 recording for isotopic N analysis, conversion of Zeiss Q 24 spectrograph 0-60445

SISAM for absolute wavelength meas., standardisation 0–60428 scanning for 1050-3800 Å obs. on board OAO 0–59811 for solar extreme u.v. obs. from OSO-1 satellite 0–51789 spectrograph improved image blurred-free focusing for energy levels of atomic spectra 0–42953

spectropolarimeter, modification for magnetic circular dichroism meas. 0-38550

spin-echo timing cct. with improved stability of pulse repetition freq. 0-48938

Spectrometers continued

step-scanning, vacuum u.v., computer controlled, for beam foil spectroscopy 0-38577

scopy 0-38577 stroboscopic time-resolved nanosecond instrument 0-60437 time delay, for acoustic and e.m. radiation meas., patent 0-48863 u.s., self-modulated marginal oscillator spectrometer 0-48855 for varying light source examination, 200-850 nm, thermoluminescent emission spectra appl. 0-49151 Ge(Li)-Ge(Li) sum-peak (integral-bias summing coincidence) spectrometer

Si(Li), photon response characteristics between 5 and 280 keV 0-49387

accessories

automatic devices for obs. and transcription of frequency 0-73110

automatic devices for obs. and transcription of frequency 0—73110 cell, absorption, white-type multiple pass, for use with Fourier spectrometer 0—73356 cell, diamond window, i.r. short path length, for corrosive liquids 0—63727 cell, gas short path, i.r. for compounds unstable in normal cells 0—63728 cell for far-i.r. spectroscopy, vacuum type, demountable 0—70091 data acquisition system for Raman spectrometer 0—63731 demountable excitation unit for cathodoluminescent spectroscopy

-44940

0-44940 diffraction grating, concave, mounting with fixed focal curve, small astigmatism of spectral image 0-45827 for diffractive efficiency meas. on 3-dimens. holograms 0-77153 Fastie vacuum spectrograph, grating order sorter for separation of high orders 0-73349 gas cell, windowless, for high temp.ix. appl. 0-49153 high-temperature cell for ix. emission of high polymers 0-71053 ix. cell for high temp. exam. of polymeric mats. 0-67184 image intensifier photography apparatus, for ultrahigh energy cascades 0-73338 infrared, grating table rotation detecting technique with Michelson interfe-

infrared, grating table rotation detecting technique with Michelson interferometer 0-49114
King furnace for metal vapour absorption, high-temp, version 0-60440
line contours, recording by IKL-1 instrument 0-38576

line intensity ratio, photoelectronic attachment for meas. of logarithm

0 - 52387Mossbauer drive, velocity sweep, electronic feedback mechanism prob-lems 0-60646

Raman and i.r. with time sharing computer, on-line data acquisition 0-63729

0-03729 reference beam cell for i.r. spectra of absorbed substs. 0-73357 refrigerator, thermoelec., for cells 0-63730 shutter, 70 m.sec⁻¹ event triggered, for spectrograph 0-73358 solid state spin-echo attachment for n.m.r. Varian HA-100, high resolution 0-76231

spectral slit width with servocontrol, analog inversion and correction loading 0–49149 spectrofluorometer sample holder for (dye-)polymer films polarized fluoresc. meas. 0–73360

spectrophotometer cell, u.v., with sub- μ path length 0-73359 thermostat jacket for capillary cells in laser-Raman-spectrometer 0-63726

triggering device for vacuum sparks, using auxiliary spark produced by rectangular pulse 0-74637 unitary sample cell for absorption spectrophotometry, patent 0-59843

unitary sample cell for absorption spectrophotometry, patent 0–59843

Spectrometers, radiofrequency

see also Nuclear magnetic resonance and relaxation/measurement;

Paramagnetic resonance and relaxation/measurement

e.p.r., bridge superheterodyne attachment of single klystron 0–69807

e.p.r., using hyperfine field amplitude modulation 0–69808

e.s.r., using sample heating to detect magnetic resonance 0–48933

e.s.r., with flash-correlated 1 µs response for free radical flash photolysis studies 0–63522

emission spectrum analyzer for submillimeters.

emission spectrum analyzer for submillimeter and millimeter ranges 0-42133

0-42133

Byromagnetic resonance, with sample rotation rate meas., patent 0-38448

Hewlett-Packard type, calibration of signal strength rel. to meas. of absolute intensities 0-76966

magnetic resonance, thermal detection, square wave modulation 0-42134

microwave, high resolution, depending on high energy emission of NH₃ molecules in high-Q cavity 0-66985

microwave RE-1301, semiautomatic calibration of mag. field using p-resonance device 0-48934

microwave cavity, Gunn diode application 0-48932

microwave saturation, for obs. of linewidth and absolute intensity 0-73111

modulator solid-state microwave Stark for microwave spectroscopy.

reflection-interferometer 8mm, aerial construct. 0-66983 variable resolution employing time scaling 0-69806 Varian A-60, developments in n.m.r. meas. 0-54808

Varian A-ou, developments in n.m.r. meas. 0—34808

Spectrophotometers
air type atmosphere, major components analysis 0—45095
astronomical, filter type for 1200-4200 Å, obs. on board OAO 0—5981!
for atom-absorption meas. using graphite cell, test model 0—57635
automatic single-beam precision instrument 0—63719
cell, high pressure, for direct observation of chemical reactions 0—69234
chemiluminescence meas. using stabilized, dual detector instrument
0—70082

0 - 70082

0-70082
digital output triggering, photomechanical device 0-60439
double-beam recording, construction 0-57634
electrophotometer for obs. of ozone content in atmos. 0-77197
G.E., photomechanical device for triggering digital output 0-70083
i.r., optical null modification for phase sensitive detection 0-73352
i.r. reflection, variable-angle attachment, patent 0-54947
i.r. for investigation of Martian surface 0-63105
kinetic, versatile, manual Zeiss PMQII 0-63721
with laser or tungsten sources, slit function rel. to absorption law 0-63733
nomogram plot 0-67183
rel. to ocean colour, remote sensing 0-72600
photoelectric radiation detectors, accuracy of meas. of spectral sensitivity,
effect of scattered light 0-49148
for plasma meas., photomultiplier cooling 0-46717

for plasma meas,, photomultiplier cooling 0-46717

Spectrophotometers continued

with pulsed photoexcitation for photosynthesis studies 0-41879 readout device, patent 0-54946

for reflectance and transmittance meas, of samples using transparent refracting chopper 0-67178

resonance lamp apparatus and method, patent 0-60444

rocket-borne, for starlight meas., pulse counting and encoding systems 0-70087

SPECORD 71 IR and SPECORD 72 IR, recording ir. instruments 0 - 57636

0-57636 scanning type, comparison with Fourier transform spectrometers 0-63725 single beam, with concave diffraction grating, for u.v. region design and methods for adjusting 0-73353 single-channel emission flame, produced in different contries, basic characteristics, service 0-73354 for spark discharge light distrib. meas. 0-43371 spectrophotofluorometer-gas chromatograph combination, patent 0-76295 for thermodynamic props. meas. allows automated at absorpt spectrophotograph of the production of the property of the production o

for thermodynamic props. meas., alloys, automated at. absorpt. spectrophotometer 0-75403 unitary sample cell, patent 0-59843

Spectrophotometry

see also Colorimetry
absorption for air pollutants conc. detection, physical principles, apparatus 0-60430
aspiration system, variable flow, forced feed, for atomic absorption spectrophotometry 0-48212
atomic absorption, metallic constituents at macro and trace levels in nuclear

atomic absorption, metallic constituents at macro and trace levels in nuclear fuel, remote analyses 0–76287 atomic absorption spectrophotometry with air-acetylene flame overexcitation interferences 0–69238 bandpass-correction terms for dual-beam, ratio-measuring spectrophotometer 0–60431 calibration of objective prism spectra using calcite-polaroid filter 0–59814 correlation, principle and application to analytical procedures 0–67177 in dosimetry, Perspex H.X. megarad, spectrophotometry error 0–46049 double beam, background correction technique for furnace or flame atomic absorption 0–70077 flame, appl. to determ. of Li and Rb in seawater and interstitial solns.

flame, appl. to determ, of Li and Rb in seawater and interstitial solns. 0-48247

line intensity ratio, photoelectronic attachment for meas. of logarithm 0-52387

perturbed total internal reflection, possibilities for studying liquid-crystals

photographic elimination of systematic errors with slotted steel foil 0-60435

0-0433 ultra-micro, rel. to concentration change meas, across growth striae in electronic single crystals 0-47099 weighing flask for manipulation of volatile solutes and solvents in i.r. spectrophotometry 0-48650 Co(PO₃)₂, glassy, structure study 0-39907

Spectroscopy
see also Spectra; Spectrometers; Spectrophotometry
absorption, air-pollution meas. 0—72606
analytical emission, internal standardization 0—56725

analytical emission, internal standardization 0-36725 arcs obs., meas. u.v. region, Au electrodes, AuI lines analysis 0-55527 astronomical, lasers applic., optical mixing for absolute monochromatic flux, expts. 0-5181! atomic, excitee states, electronic impact excitation technique 0-52933 atomic, with excited ion beams 0-52876 atomic absorption bibliography 0-4633! atomic energy levels meas. improved blurred-free spectrograph applic. 0-42953

atomic excited states, photon excitation 0-52934 atomic fluorescence spectroscopy, influence of flame composition atomic fluor-52867

0-52867 atomic fluorescence spectroscopy, interference studies with a continuum source 0-52868 atomic obs., nitrous oxide-MAPP gas flame 0-66210 Auger, LEED technique, work function and photoemission meas. correlation for p type GaAs (100) 0-47885 Auger, rel. to Si surface examination 0-65730 Auger electron, chemical effects 0-47030 Auger electron, impurities in Si crystal surface 0-47764 beam-foil, computer controlled step-scanning vacuum u.v. spectrometer 0-38577

beam-foil, computer controlled step-scanning vacuum u.v. spectrometer 0–38577
blackbody cavities direction spectral emittance, meas. tech., applic. 0–63472
Brillouin spectra meas. by Fourier-transform spectroscopy 0–67175
bunching effect, extended, glauber theory calc. 0–38571
cathodoluminescent, demountable excitation unit 0–44940
collision, heavy particle, rel. to one- and two-electron systems 0–52964
conference, Chicago, USA, May 1968 0–69237
conference, Chicago, USA, May 1968 0–66215
contours of spectral lines, distortion by simple RC filter, determ. using trigonometric approx. 0–60422
correlation, principle and application to analytical procedures 0–67177
deconvolution with experimental error 0–66776
depolarized light mixing for light beating spectroscopy 0–73343
discharge, pulse, study of temporal scans 0–38573
e.p.r. X-band, optical, irradiation cavity with large aperture 0–42136
electron, development of parallel plate channel multipliers 0–60179
electron impact, high resolution, rel. to He atom 0–55259
electron spectrometer, high sensitivity 0–42219
explosive anode erosion in high current sparks, tree shape optical phenomenon study 0–61405
explosive charges underwater, energy spectra, depth variation effects 0–66921
far i.r., interferometric instruments, applications to different types of compound 0–49147
far i.r., interferometric instruments 0–49146
filters, optical interference, for adjustment of spectral response and power distribution 0–57611

iar 17. Interferometric instruments 0–49146 filters, optical interference, for adjustment of spectral response and power distribution 0–5761! flame, using two lamps and Fabry-Perot interferometer 0–5291! flame spectrometry, review 0–54933 Fourier, resolution limit investigation 0–52385 Fourier, spectral recovery using asymmetric interferogram multiplicative technique 0–57633

Spectroscopy continued

Fourier method, rel. to optical reconstruction of continuous spectrum 0-45847

Fourier transform, i.r. and far-i.r., theory 0-60420 Fourier transform, real-time calculator 0-52390

Fourier transform and conventional scanning techniques, comparison 0-63725

Fourier-transform method for Brillouin line breadth meas. 0-60424 Fourierscope for Fourier transform's interferogram 0-63714

fractional glow technique for trapping spectroscopy, computer simulation 0-56585free jet and nozzle beam sources, use with microwave spectrometer 0-70089

furnace 0.2 MW for oscillator strength meas., absorption method, design

criteria 0-60418 gamma with multiplying semiconductor detectors 0-60640

Gamma-ray, Compton electron continuum measurements 0–60651 group theory application 0–42394 i.r., double-beam hot cell 0–41909 i.r., far, interferometric methods 0–38572 i.r., temperature regulating devices 0–60094

ir, u.v., visible region, high speed electro-optic spectral scanning, tech. 0-65998

0-5998
i.r., use in air pollution research and monitoring 0-49142
i.r. Fourier transform, derivate traces 0-38570
i.r. Fourier transform type, complex number computation and 'phase error' correction 0-63724
i.r. airglow, auroral emission study using digital near i.r. spectrometer 0-63718

0-63718 i.r. and optical, monitoring of high press, effects on trioxane 0-50828 i.r. far, obs. of ν_4 band of UF₆ determination of this gas 0-67633 i.r. for molecule on adsorption 0-47072 i.r. for polymers structure and orientation meas. 0-53413 i.r. in 50-2000 microns region, bibliography 0-57630 i.r. on Mariner Mars (1971) 0-54309 i.r. polarized of hydroxyl ion in $Ca_{10}(PO_4)_6F_2$, impurity orientation 0-51302 industrial instrumentation in USSP, 0-40143

0-51302 industrial instrumentation in USSR 0-49143 integrating cavity, application to absorption coeff. obs. of material introduced into cavity 0-70078 integrating-sphere method for paint reflectivity and absorption 0-60425 interferential, spatially and chromatically compensated 0-67181 interferentic, meas. of ir. emissivity 0-42393 interferentic, using beat technique 0-67174 ion-neutralization, rel. to study of solid surface electronic structure 0-65606

ir. liquid cell, temperature measurements with thermocouple in aqueous solutions 0-63482

solutions 0-63482
laser Raman and Brillouin scatt, spectroscopy 0-46729
laser inelastic scatt, spectra analysis 0-73344
laser-Raman, ultra-fast 0-70081
level-crossing, of diatomic molecules and excited state coupling parameters 0-74197

light echo method for determining small splittings 0-69103 line intensity increase by arc compression in mag. field or heating 0-49141

intensity increase by are compression in mag. neid of neating 0-49141 liquid scintillation, chemical quenching effect 0-38749 low-energy electron-reflection, application to study singlet an triplet molecular states 0-74890 luminescence, measurement, error analysis 0-63715 luminosity, three criteria, intercomparison 0-66499 mass spectrometry, review 0-54932 metal vapour absorption, high-temp. King furnace 0-60440 microwave pulse flash-spectroscopy apparatus 0-63716 molecular beam time-of-flight 0-74226 Mossbauer effect, automatic data collection 0-63992 multipletts, chromatic defects correction 0-38526 neutron, threshold, improved method, digital computer for data treatment 0-77392 nuclear, calibration source of 95Nb by electrodeposition from aqueous bath 0-57940 nuclear radiation, with semiconductor detectors, S/N and time-resolving

bath 0-57940
nuclear radiation, with semiconductor detectors, S/N and time-resolving power 0-38955
optical, of Cr, rel. to crystal growth co-ordination identification 0-47104
optical, on-line computer system 0-69552
optical equipment construction, development trends 0-42397
optical phenomenon tree shape in explosive anode erosion, time resolved photography, spectroscopy 0-61405
photoelectron, for chemical analysis, computer regulated system 0-4602!
photoelectron, principles and applic. 0-73340
photomultiplier, spectral sensitivity as function of voltage and i.r. illumination 0-38473
planetary atmospheres, transmission absorption spectroscopy probing techniques using satellites 0-51753
plasma, alkali, book 0-46682
of plasma, isothermal at various pressures using wall stabilized arc source 0-50136
polarization of ir, and electronic absorpt. bands, determ. in liq. cryst.

0–50136
polarization of i.r. and electronic absorpt. bands, determ. in liq. cryst. solvent 0–77765
Raman, depolarization ratio meas. 0–54938
Raman laser for liquids sample holder at temps. between –196° to +200°C, description 0–50228
Raman tunable spin-flip laser for i.r. spectroscopy 0–54939
reference lines establishment, use of optical frequency measuring method (0–42395)
research. Massachusette. Institute of Texas research, Massachusetts Institute of Technology, Sep 1967-Sep 1968 0-38121

0–30121 resolution improvement by Fourier transform techniques 0–70079 resolution of overlapping line spectra with digital filter 0–73341 Sc II $\lambda 4320/Y$ II $\lambda 4309$, criterion for detection of metallic line stars (Am) 0–72715

semiconductor, forbidden energy gap meas. diffuse reflectance technique

semiconductor, forbidden energy gap meas, clittuse renectance technique 0-75700 short-time, for study of reaction kinetics of H, plasma 0-71175 signal density by statistical modulation of pulse sequences 0-49144 simultaneous filming of synchronously excited spectra of analysed and reference specimens 0-73345 slow electron, optical surface phonons in zinc oxide single crystals, detection 0-53694

Spectroscopy continued

spark emission method for detecting H_2 contamination level on Al surfaces 0-51443spectra computation from interferograms obtained on IT-69 Fourier spectrometer 0-52386

spectra visualization system using program computer connected to memory of ordinator 0-77221

spectral comparison method for temp. meas. of gas and condensed phase in flames 0-5142!

spectral irradiance meas. at welding processes 0-66930 spectral line contour distortion by second order recording system, analysis 0-60423

0-60423
spectral line intensity, integrated, effect of area sensitivity of photomultiplier tubes obs. 0-73182
spectral scanning of i.r., u.v., visible regions, tech. 0-65998
spectrograms, photographic prism, reduction by combined computational and graphical method 0-60419
spectrometry, Mossbauer, review 0-54934
spectrometry, Raman, review 0-57628
spectrometry, emission, review 0-54936
spectrometry, i.r., reviews 0-54935
spectrometry, light absorption, review 0-54931
spectrometry, u.v., review 0-57629
spectrometry, u.v., review 0-57629
spectrometry, u.v., review 0-57629
spectrometry analyzer for 1f-spatial signal detection with aperture tapering 0-63703
stellar, high dispersion, with schelle grating 0-73346

o-63703
stellar, high dispersion, with schelle grating 0-73346
surfaces composition through electron impact ionization 0-47906
thermal emissivity, opaque materials, technique without black body ref.
source 0-76106
rel. to thermionic convertors, plasma radiation intensity meas. in several
regions of I-V characteristic 0-77008
time resolved, with image-converter streak camera, detection of mode hopping and tuning in CdSe lasers 0-69915
time-domain, dielectric relaxation obs. 0-79029
time-resolved, for exploding wire source, temporal and spatial information
0-63713
time-resolved in visible region for identification display of emission, absorbe-

0-63713
time-resolved in visible region for identification, display of emission, absorption features 0-66299
u.v. near vacuum, vacuum aspects 0-43041
u.v. on Mariner Mars (1971) 0-54310
u.v. photoelectric, rel. to investigations of W 5d band structure 0-65605
u.v. photoelectric, rel. to optical density of states 0-65584
unfolding of spectra by Fourier transformation, numerical filter application 0-73342
wavelength measurement with ZnS-cryolite coatings and phase retardation 0-41108
y for body potassium meas. 0-59825

y for body potassium meas. 0-59825

light sources

ight sources are excitation source, economical design, emission characts. 0–53234 atomic, obs. on preparation and operation of microwave excited electrodeless discharge tubes 0–64778 discharge lamps, electrodeless, containing Cd, Hg and Mn 0–63732 electrodeless discharge tubes, comparison with hollow cathode lamps for atomic absorpt, spectroscopy 0–42401 flash generator of tubular pinch discharge type 0–67977 gas discharge lamp for extreme u.v. 0–6044! hf. electrodes lamps with vapour of Pb and its salts, spectral characts. 0–49155

0 - 49155

0—9155
hf. inductive discharge as light source for emission spectroscopy
high current hollow cathode, excitation mechanism 0—71211
inert gas resonance lamps, design, filling procedure and characts.
0—54945

0-54945
laser and tungsten lamp, slit function rel. to absorption law 0-63733 lightning, photographic techs, review 0-66299
Penning, in far u.v. region, contribution to design 0-77222 power peak width for high-resolution spectroscopy using a laser with an absorption cell 0-60442 power spectrum analysis using interferential set-up 0-49150 of radiation in 1-2000 Å range 0-54944 shock tube applications, review 0-52391 spark, vac. u.v., time-controllable 0-43369 spectrophotometric resonance lamp apparatus and method, patent 0-60444

storage ring, 240 MeV, for extreme u.v. spectroscopy in 40-400 Å range 0-77223

u.v., far, capacitor discharge in capillary tube 0-70093
vac. u.v. atomic-beam light source 0-42400
C-lamp as intense line source at 1931 Å for photochemistry 0-62814
Pb_{0.88}Sn_{0.17}Te diode laser, current tunable, high resolution is. absorpt. 0-42399 Xe lamp, rel.to luminescence spectra meas. 0-54943

Spectroscopy, radiofrequency
see also Nuclear magnetic resonance and relaxation; Paramagnetic resonance and relaxation; Spectrometers, radiofrequency
absolute intensities meas. in microwave spectroscopy 0—76966
conference, optical pumping and at. line shape, Warsaw, 1968 0—52878
cyclotron resonance, trapped ion analyzer cell 0—45735
gas, lp., rf.rf. double reson, 'dressed' Hamiltonian formalism applic.
0—39335

level crossing curves resolution improvement by delayed meas. 0–52889 microwave, numerical treatment of general vibr.-rot. Hamiltonian 0–67693

0-67693
microwave, single shot analysis 0-73112
microwave, in undergraduate labs. 0-66984
microwave study of internal rotation in molecules 0-74209
millimetre and submillimetre, review 0-73108
molecular microwave oscillator/spectrometer 0-66985
multiphoton transitions 0-45734
n.m.r., conference, Birmingham (1969) 0-63527
n.m.r., high-resolution, application to biological compounds examination 0-64465
n.m.r., pulsed and Fourier transform 0-63525

0-64465
n.m.r., pulsed and Fourier transform 0-63525
n.q.r., power-line bidirectional Zeeman modulator 0-73119
optical methods, rel. to a torms, ground and excited states 0-52872
p.m.r. line narrowing by magic angle rotation 0-69811
phosphorescence-microwave double resonance spectroscopy, polarized modulated new technique 0-73107
reflection-interferometer 8mm, aerial construct. 0-66983

Spectroscopy, radiofrequency continued

resonance line determination conditions, rel. to noise scanning by time-ave-

raging method 0-45733 solid, mathematical analysis 0-60!19

sond, matternated analysis 0-0012, sepectrum analyzer for pulse processes in microwave region 0-48931 stored ions, spectroscopic techniques 0-73109

3He⁺, h.f.s. spectrum, ion storage collision technique 0-52983

Speech

see also Hearing absorpt. coeff. of acoustic materials, development and appl. 0–63466 air-pressure variations, lingual and intraoral, rel. to vocal intensity 0–54493

0-34493 analysis, using analogue, cochlea 0-76740 CV syllables dichotical, monotical syllables, delayed channel's opposed effects on perception 0-69544 cousonant's lenis-fortis opposition rel. to physiological parameters, analysis 0-57172

sis 0-57172 divers correction, in pressurised helium-oxygen atmospheres using homomorphic deconvolution 0-72827 duration of /s/ in /s/-plosive blends of females, differential influence of vowels and consonants 0-45461 formant-frequency trajectories in selected CVČ-syllable nuclei, meas., analyses 0-54491 frequency contours, fundamental, analysis of 0-72828 glottal air flow waveform, derivation by inverse-filtering technique 0-76738 human yogal tract, cross-sectional area function determ method, 0-60523

0-76738 human vocal tract, cross-sectional area function determ, method 0-69532 identification of selected sounds, minimum number of necessary glottal pulses 0-66705 intelligibility in partitioned rooms 0-38392 intelligibility monaural, effect of forward and backward masking 0-41888 loudness, acoustic intensity and vocal effect as loudness correlates 0-66704

perception, comparison using monotonic and dichotic modes of listening $0\!-\!66724$

perception, dichotic and monotic time-staggered speech 0–63234 perception, hemispheric specialization 0–69534 perception of the repeating word, evidence for a universal feature detector system 0–66703

phonation time, maximum, effects of frequency, intensity and vowel-type 0-69535

phonations, vocal fry and modal register, comparison of aerodynamics $0\!-\!54495$

pitch extraction system, exptl. harmonic identification, performance characteristics study 0-57173 processing, running memory-span technique demonstrating syntactic and perceptual units relationship 0-66702

perceptual units relationship "0-66702" reading rate, perceptual judgments, significance of intra- and intersentence pause times 0-69536 reading rates, temporal patterns 0-66706 recognition, author's reply to comments 0-57176 recognition, author's reply to comments 0-57176 recognition and production, comments 0-5830 recognition studies implications, comments 0-57174 recognition studies implications, comments 0-57175 spectrum, long-term, effect of Helium and depth 0-76739 spectrum, long-term, effect of Helium and depth 0-76739 specd-level measurement with VU meter, reduction of observer bias, method 0-54492 subglottal air pressure changes with fundamental frequency, analysis 0-72825 synthesizer, parametrically controlled terminal analog with resonators,

synthesizer, parametrically controlled terminal analog with resonators, crosspoint programming matrices applic. 0-45460 vocal fry phonation, intensity variations, relationship with fundamental freq. 0-72826

vocal tract length calc, from labial impedance 0–69533 voice, normal, EMG aerodynamic study 0–54494 voice pitch rate patterns, on analogue ear, stimulation response 0–72829 waveforms, voiced, unvoiced and clicks, combinational tones effects on perception 0–72831 words paced recognition masked in white noise, expt. 0–57177

Spherical aberration see Aberrations, optical

Spicules see Sun/prominences

Spin see Elementary particles; Hyperons/spin and parity; Mesons/spin and parity; Nucleus/spin and parity; Rotating bodies Spin echo see Nuclear magnetic resonance and relaxation Spin waves see Ferromagnetism/spin-wave theory

Spin-lattice relaxation see Crystals/lattice mechanics; Magnetic resonance and relaxation

Spinors see Quantum theory, wave equations
Spions (pions with spin) see Pions
Spirality see Elementary particles; Field theory, quantum

Sporadic-E see Ionosphere/E-region **Sprays**

see also Aerosols; Drops; Jets No entries

Spurions see Elementary particles

Spurious see Elementary particles

Sputtering
alkali halide surfaces, low energy irradiation 0–62238
alloy, homogeneous, smooth deposit thickness profiles prod. from parallel strip sources 0–7838!
alloy films, mechanism 0–48655
amorphization rel. to mechanism 0–40624
angle of incidence depend. 0–68686
angular distributions of atoms sputtered from polycrystalline targets by inert-gas ions 0–57199
anisotropy in cathode sputtering of polycrystalline materials 0–57200
anode of mercury arc valves 0–4222!
arrival energy effect on properties of Au films 0–50380
cathode, conditions for obtaining Si₃N₄ coatings, analysis of films 0–79447
cermet struct., m.i.m., form. by ion bombardment 0–44320
composite metal films, etching, scanning electron microscopy 0–68224
compound films, mechanism 0–48655
computer simulation 0–62224
d.c. bias sputtering for depositing films of refractory metals 0–74918
d.c. reactive, Al₂O₃ thin films 0–78371
dielectric film prep., cond. phenomena obs. 0–79037
efficiency, energy and incidence angle depend. 0–68885

Sputtering continued

energy distribs. of particles, from Al, Ti, Ni, Cu and Ag targets by Ar^+ 0-74895

energy distributions, applications 0-62236

film, oxide, stoichiometric variations determ. 0-71477

film growth, arrival energy effect on structual and electrical properties 0-50388

nim growth, artival energy effect on structual and electrical properties 0–50388 film prep. by reactive cathodic sputtering of cold plasma 0–39947 film quality improvement techniques 0–57219 films tress analysis, prepared by low pressure triode sputtering 0–50674 films, thin, vacuum deposition techniques 0–53435 films in r.f. planar diode gas discharge, nonuniformity rel. to space charge instability 0–55508 gases, high-purity, importance in process 0–50386 glass optical waveguide 0–57459 Harwell sputtered ion gun 0–54847 ion products, use of MI-1305 mass spectrometer for study 0–50916 low energy, angular distrib, surface roughness 0–68683 metal, angle of incidence depend. 0–75437 metal, b.c.c., angular distrib, anomalies 0–50911 metal, lon energy depend. for polycrystalline and single crystals 0–40614 metal films, mechanism 0–48655 metallic thin films, structural analysis 0–78679 metals, light ion bombardment, product energy spectra 0–68675 neutral particle energy distribs, from AI, Ti, Ni, Cu and Ag targets by Ar+0–74895 non-metals, mechanism, by slow multiply charged ions 0–68687

0-74895
non-metals, mechanism, by slow multiply charged ions 0-68687
optical multilayer coating deposition, automatic apparatus 0-77176
oxide film, stoichiometric variations determ. 0-71477
particle ang. distrib. characts. after ion bombardment of single cryst.
0-75433
particle flux mass, energy meas. system for planar diode 0-76782
polycrystalline solids, efficiency 0-65561
polytetrafluoroethylene 0-50380
r.f., film property control through substrate tuning 0-53427
r.f., ion etching of soft biological material, scanning electron microscopy
0-51831

0-51831
rf., non-grounded double electrode system 0-50380
rf., process parameters, review 0-65566
rf., substrate bombardment 0-50380
rf., substrate bombardment with electrons, ions and neutral particles 0-50382

rf. discharge application 0-53426 rf. planar diode, substrate heating reduction 0-57218 rf. system, high rate 0-57217

rf. system of non-grounded double electrode configuration, disc and annulus 0-5038!

lus 0–5038! rf. vacuum sputtering module, inline 0–57223 reactive and r.f., for preparation of ferroelectric Bi₄Ti₂O₁₂ films 0–71472 semiconductor, diamond type, Ar ion bombardment, 5-15 keV, ejection pattern 0–68706 silicon oxynitride, m.i.m. capacitor dielectric, props. rel. to prep. 0–53932 single crystal, ion beam planar channelling depend. 0–68684 of stainless steel, 304L, microstructure obs. 0–71464 steel, stainless, deposited from bias sputtering, reduced Ni CONC. 0–62834

0–62834 steel, stainless, under Hg ion bombardment, 15-100 keV 0–71883 superconducting film, r.f.-sputtered, with β-tungsten struct. 0–78900 theory, depend. of angle of incidence of bombarding particles 0–47567 thermionic converter electrodes prep. by ion sputtering 0–67015 thin films depositions analysis 0–45500 transition metals, ion irrad, ion form. from ejected atoms in superexcited states 0–43944 triode, highly reliable, applications for very low pressure 0–47060 vacuum deposition apparatus, patent 0–50394 vacuum system, oil diffusion pumped, operation examination w.s.t. cleanliness 0–69560 vields, thin film targets 0–62237

ness 0–69560
yields, thin film targets 0–62237
Ag by Cs², negative ion source 0–57500
Al, ang. distrib., fine struct. obs. 0–75431
Al bronze, Ar² energy distrib. and H contamination, obs. 0–76782
Al, O₃ thin films, d.c. reactive method 0–78371
Au, 500 eV·8 keV protons 0–40622
Au, channeling effects on sputtering and backscatt. process 0–40621
Au, low energy 0–68705
Au self-diffusion, microsectioning and profiling 0–78576
Au by Cs², negative ion source 0–57500
Au film, arrival energy effect on structural and electrical properties 0–50388
BaTiO, film prep. by d.c. diode sputtering 0–47063

Au film, arrival energy effect on structural and electrical properties 0–50388
BaTiO₃ film prep. by d.c. diode sputtering 0–47063
Bi₂O₃-Ta₂O₃ glass films for capacitor appls., r.f. sputtering 0–58595
Bi₂O₃-TiO₃ glass films for capacitor appls., r.f. sputtering 0–58595
Bi₂O₃-Y₂O₃ glass films for capacitor appls., r.f. sputtering 0–58595
CdS r.f. sputtered thin crystals, deposition and X-ray and e-diffraction examination 0–55742
Cu, \(\text{100} \) face, Ne ion bombardment 0–40623.
Cu, ang. distrib., fine struct. obs. 0–75431
Cu, Arf energy distrib. and H contamination, obs. 0–76782
Cu, single crystal, Arf bombard., ang. distrib., fine struct. 0–75438
Cu by Cs², negative ion source 0–57500
Cu face, angle of incidence depend. 0–75437
Cu monocrystal specific orientations sputtering ratio, dechanneling model for temp. behaviour, under Ne² and Arf bombardment 0–62242
GaAs by Ar-ions, use of MI-1305 mass spectrometer for study 0–50916
p-GaP films, obs. 0–55743
Ge, amorphization rel. to mechanism 0–40624
Ge, atom ejection patterns from (1!1) and (!10) surfaces 0–65565
Ge, single crystal, Arf bombard., ang. distrib., fine struct. 0–75438
Hf film prep. 0–71481
HfN film prep. 0–71481
HfN film prep. 0–71481
HfN film prep. 0–71481
IfN film prep. 0–71481
IfN film prep. 0–71481
IfN film prep. 0–71481
No. 1972
No. 1972
No. 1974
No.

Sputtering continued

Nb, by D+ and Nb ions, sputtering coeffs., obs. 0-71884

Nb, by D* and Nb ions, sputtering coeffs., obs. 0–71884
Re, single crystal, Ar* bombard., ang. distrib., fine struct. 0–75438
Sb, single crystal, Ar* bombard., ang. distrib., fine struct. 0–75438
Si, (11) Ar content, ion implanted, 50-2200 eV 0–71886
Si-SiC epitaxial film form. by reactive deposition 0–58587
SiO, film, re-emission during growth, rel. to quality 0–53437
Sin, solid and liquid, low-energy Ar* sputtering yields 0–78809
Ta, metal films onto Teflon discs up to 5.1 cm diameter, modification of d.c. sputtering diode geometry 0–7678!
Ta film, growth, 13-525°C, crystal phases, resist., superconductivity 0–47068

U=4/008
Ta film, in O₂, orientation effects in resistivity 0-75569
Ta film, phase forming processes 0-65089
Ta film deposition by d.c. bias sputtering 0-74918
W, under Hg ion bombardment, 15-100 keV 0-71883
Zn single crystal, emission patterns 0-68713
Stacking faults see Crystal imperfections

Standards

ndards
see also Constants; Units
for Mossbauer spectroscopy, isomer shift reference standards, criteria
0-77478
activity, for ion-selective electrodes 0-45077
calibration uncertainties 0-57235
ceramics for electronics, ASTM 1969, book 0-38455
dielectric films, thin, high molecular weight, electrical test methods
0-62399

0–62399
frequency, Cs beam cavity design 0–633!0
frequency, proposed, H storage beam tube 0–63595
gamma ray point-source calibrator, automatic, design and statistical procedures for evaluation 0–57840
Geiger-Muller counters, test procedures 0–70298
graphite thermal cond. and diffusivity 0–40597
graphite thermal expansion reference for high temp. 0–40580
high pressure scale establishment, reference-point determ. 0–76770
high-temperature thermal conductivity 0–50903
humidity, calibration facility 0–66281
laboratory work in aircraft maintenance 0–51887
magnetic properties, ASTM 1969, book 0–38455
materials for electron devices and microelectronics, ASTM 1969, book 0–38455
mechanical vibration and shock 0–60011

mechanical vibration and shock 0-600!!

methanical vibration and shock 0-60011 metallic materials for thermostats and elec. resistance, heating, contacts, ASTM 1969, book 0-38455 metals, die-cast, ASTM book (1969) 0-40432 metals, light, ast material comparison using $4\pi\beta$ -p coincidence technique 0-38737 noise, acoustic testing, emission by plumbing appliances 0-54736 optical frequency, for gas lasers with stable radiation 0-69884 radiochemical analysis, Mossbauer spectroscopy, nuclear instrumentation and radioisotope techniques 0-51453 reflecting prism, rel. to optical instruments working on autocollimation principle 0-73287 thermal cond. of pyrometric Pb, elec. cond. correl. 0-59861 thermal conductivity reference materials, 4 to 300° K, Armco iron 0-68650 thermal neutron flux density standard 0-38716

0-68530
thermal neutron flux density standard 0-38716
wavelength of superradiant radiation 0-54534
Cs beam atomic clock 0-5812!
Cs beam frequency, at NBS, improvements to raise figure of merit to >500 0-51886
in consideration of the standard self-scenario of the standard self

87Rb frequency standard cell formation 0-66742

alkali germanates, with Nd ions 0–7606! alkali halide, F-centre emission spectra, 2-150K 0–56536 atom, two-level, perturbation coherence role in dynamic effect 0–67635 atomic spectra, linear and quadratic broadening by ions and electrons, review 0–55228 beam-plasma interaction, frequency, intensity and direction of electric

fields 0-64686

fields 0–64886 copper, phthalocyanine film, electroabsorption, ferroelectricity 0–62679 corrections, dynamical, to Holtsmark's theory of spectral line broadening from linear Stark effects 0–58089 diamond, N3-centre, point symmetry, absorpt. spectra 0–62653 excitonic, CuCl, and electroreflectance 0–76068 p.βuoroaniline, in rot. fine struct., meas. of dipole moment change on excitation 0–71002 fluorobenzene, rotational fine structure of 0-0 band of π*←π state 0–46561.

0 -46561
p-fluorophenol, in rot. fine struct., meas. of dipole moment change on excitation 0-71002
formaldehyde rotational lines in ³A₂ excited state 0-43162
group IV/VI compounds, meas. on pure rotational transitions 0-70866
ion lines, isolated, in plasma, evaluation of half widths 0-60913
n.q.r. in solids, investig. 0-51416
nonlinear polarizability in resonance interactions 0-73274
plasma confinement, turbulence studies using Stark broadening 0-50064
plasma diagnostics applic. of h.f. effect 0-78112
propyne, elec. polarizability anisotropies obs. 0-70923
rigid linear top rotor, Stark perturbed rotational energy levels 0-46414
and saturation, in optical freq. fields 0-64310
shock wave, collisionless magnetostatic, turbulence level, Balmer Hβ line,
Stark broadening 0-64689
Wasserstoff's linear Stark effect constant, precessional determination
0-67599
wings of Stark-broadened lines, profiles of forbidden components, objec-

wings of Stark-broadened lines, profiles of forbidden components, objections to method of calc. 0–61019
Ar I, Stark consts. and oscillator forces for Thomas-Fermi-Dirac pot. 0–70762

0-70/62
Ar II, meas, of Stark broadening parameters 0-49770
COS, elec, polarizability anisotropies obs. 0-70923
CdInGaS₄:Er³⁺, splitting of luminescence spectra, rel. to crystal field

Stark effect continued

Cl I lines, isolated neutral atom lines 0-60916

Cl I lines, isolated neutral atom lines 0–60916
Cl spectral line broadening 0–67614
CuCl, excitonic, electroreflectance meas. 0–76068
H, Stark broadening calc. by unified classical path theory 0–77659
H atom, for nonuniform fields 0–70808
H plasma, close collisions in Stark broadening 0–61294
H plasma ion density, broadening of H_B line 0–78065
H Stark broadening calc. with unified classical path theory 0–74171
H_a and H_y lines, Stark broadening calculations 0–74169
H_B Balmer line, Stark splitting in fields <20 kV/cm 0–67665
HBr, hyperfine structure of rotational transitions 0–46473
HI hyperfine structure of rotational transitions 0–46473
He, 4471 Å line and forbidden components, Stark profiles calc. 0–39325
He, broadening of 5876 Å line in shock wave plasma, in He-H gas mixture 0–49815

He, broadening of 38 /6 A line in shock wave plasma, in He-H gas mixture 0-49815
He, profiles of 4026 Å line and forbidden components 0-55258
Ke, qaudratic Stark shifts of Zeeman levels in ground state 0-77662
LiF:U luminescence spectra, linear Stark effect 0-51344
N II, dense plasma, profiles of 9 lines, Stark broadening 0-39289
N II, meas. of Stark broadening parameters, by laser interferometry 0-60902
NH₂, Q-switching of CO₂ and N₂O lasers 0-42270
NH₂D, exhibition by transitions of ν₂ band 0-74282
N₂O, elec. polarizability anisotropies obs. 0-70923
¹³NH₃ ν₂ band, Stark spectra by 10 μ lasers 0-61113
Na, 3¹²γ₂ state, Stark eff. investigation of hyperfine struct. 0-39291
Na, quadratic Stark shifts of Zeeman levels in ground state 0-77662
NaF:U luminescence spectra, linear Stark effect 0-51344
Nd in alkali germanate glasses 0-76061
Nel 1, 29²3s-2p²3p transitions, Stark broadening, with weak electrical field depend. 0-46373
O I, broadening and shift of i.r. lines 0-77666.
OCS, anomalous spectrum assoc, with sudden Stark shifts 0-74298

O1, broadening and shift of ir. lines 0–77666.

OCS, anomalous spectrum assoc. with sudden Stark shifts 0–74298
Sn 1, (5p₁y₂5d₅y₂)₂₋₂ state, energy shifts in elec. field 0–64223
Tl, consistent with electric dipole moment 0–43003
TmCl₃.6H₂O, Tm₂(SO₄)₃.8H₂O, Zeeman splitting between Stark levels of Tm³⁺ (4ft²) 0–7611!
YCl₃.6H₃O:Tm³⁺, Y₂(SO₄)₃.8H₂O:Tm³⁺, Zeeman splitting between Stark levels of Tm³⁺ (4ft²) 0–7611!
Znln₂S₄:Er³⁺, splitting of luminescence spectra, rel. to crystal field 0–56593

Stars

rs
see also Nebulae; Novae; Sun
HD 137569, halo B, high dispersion spectral analysis 0-72725
66 Oph, probable early type flare 0-79674
T Aurigae, additional times of minima 0-79677
VY CMa, i.r., OH and H₂O source, study of surrounding nebulosity

VY CMa, very-long-baseline interferometry of associated H₂O source 0-51618

O-51618

DICar—a cepheid? New photoelectric data 0—48448

UV Ceti, flare properties 0—63016

S Cnc, UBV limb darkening coeffs. 0—66496

V444 Cygni binary system, light curve for eclipsing stars with scattering envelopes 0—72736

73 Dra, (HD 196502), existence of stellar spots 0—72706
nearF stars, spatial motions and rotation speed 0—57021

WY Geminorum, eclipsing system 0—62988

U Geminorum, period increase 0—79677

DQ Her, rate of mass exchange 0—54391

68 Her, rotational velocity study of B2 components 0—57056

Ex Hydrae, additional times of minima 0—79677

VZ Hydrae, eclipsing binary, UBV curves for mass-luminosity diagram 0—6489

16 Lac, ß CMa star, tidal resonances in some pulsation modes 0—63040

VZ Hydrae, eclipsing binary, UBV curves for mass-luminosity diagram 0–66489

16 Lac, β CMa star, tidal resonances in some pulsation modes 0–63040 AD Leo, low intensity flares, 1-11 March, 1970 monitoring obs. 0–63004 in Magellanic Cloud, Small, wing 0–66430 α-Ori, narrow-band ir. photometric obs. 0–72717

BM Orionis, eclipsing binary in the Trapezium, photoelectric UBV obs. and anal. 0–57055 γ and h Persei association, dynamical instability 0–69403 RW Piscis Austrini, eclipsing binary, W-Ursae Meyoris-type 0–66490 ISco cluster, new distant supergiant stars 0–45298 RZ Scuti, period, elements and UBV light curves, obs. 0–41714 δ Scutivariables, two new southern stars, periods 0–41628 near South Galactic Pole, spectral types and radial velocities 0–66438 β UMa, similarity with Sirius 0–51665 θ Ursae Majoris, atmospheric analysis 0–51666 HD 36695, VV Orionis, eclipsing triple system, spectroscopic obs. 0–69402 γ Vel, study using stellar intensity interferometer 0–45292 15 Vulpeculae, metal abundance 0–45260 α Cen, binary system chemical composition, post in two-colour diagram 0–76588 α Ursae Majoris, binary system, mass ratio and combined mass 0–57051 Visited of the state of the state

0-76588
α Ursae Majoris, binary system, mass ratio and combined mass 0-57051
α Virginis A radial vel. obs. and physical props. 0-66480
α-Lyrae, spectral energy distribution 0-72727
β-Lyrae, mass exchange, polarimetric obs. 0-72726
γ Pegasi, UBV photometric obs. 0-63000
γ-Cas, stellar envelopes, rotationally extended, spectral resolution obs. 0-69301

0-9391
 δ Scuti, an interpretation 0-54381
 ε Vir. line blanketed model atm. 0-66444
 v Indi, N₂ abundance, computed using synthetic stellar spectra 0-72710 (globular) cluster, M92, luminosity function from star counts 0-72734 (open) clusters, red supergiants spectral types and UBV photometry 0-76586

0-76586 ages, consequences of time-varying physical constants deduced from Dirac's hypothesis 0-45256 Ap, diffusion processes responsible for the peculiar abundances 0-41647 Ap, solar motion from radial velocities, properties, including galactic rotation effects 0-41629 Ap, spectrum-variable, radio obs. at $6.2 \text{cm}~\lambda~0-72728$ Arcturus, convective energy transport in atm., model 0-41643 Arcturus, radial velocity from interferometric spectra 0-62986 artificial, for use in teaching laboratory 0-69509 association III Cephei, photometry, four colour and $\mathrm{H}\beta~0-79678$ associations in Large Magellanic Cloud 0-79632 atmosphere, convective energy transport, model 0-41643

Stars continued

atmosphere, determination of presence of chemical compounds 0-76635 atmosphere, inhomogeneous, semiinfinite, pure scatt. 0-48567

atmosphere, pressure behaviour, quantum-mechanical cellular methods 0 - 69374

atmosphere models for central stars of planetary nebulae 0-41636 atmosphere non-LTE, variable Eddington factors for computation 0-59697

atmosphere rotating, meridional circulation velocities, expressions 0-51658 atmospheres, finite, inhomogeneous, partially polarized radiation transfer 0-57019

atmospheres, gravitational, of $3\,M_\odot$ stars, propag. of shock waves 0-48421

0-48421 atmospheres, line formation by noncoherent scatt., an invariant imbedding approach 0-48406 atmospheres, model, grid of line-blanketed, He line profiles calc. 0-45264 atmospheres, polytropic, low frequency oscillatory convection in strong mag. field 0-48419 atmospheres, thermal-convective instability 0-41635 atmospheres of cool, oxygen rich stars, ZrO₂, TiO₂ and VO supersaturation 0-51657

atmospheric convective energy transport, convective thermal model 0-48418

BE Vulpeculae eclipsing variable, photometric obs. 0–63001
BW Agr, photoelectric obs. rel. to secondary minima determination
0–59720

U-39/ZU
B-type, model atmospheres, blanketing by ultraviolet lines 0-59696
Barnard's, two planet model, stability 0-5969!
Be, radial vel. rel. to galactic rot., obs. 0-41589
Beta Cephei, radial oscills., linear non-adiabatic analysis 0-66484
binaries, 142 visual, MK classifications 0-41716
binaries, eclipsing, BV 419, 9 Chamaeleontis, AU Puppis, orbital elements

0 4!699
binaries, eclipsing, Z Draconis and W Ursae Minoris, light curves and orbital elements 0-4845!
binaries, eclipsing, irregular vars. and period changes 0-63067
binaries, eclipsing, light curve atlas 0-69412
binaries, eclipsing, orbital elements determ, from limb darkening laws 0-66497

binaries, numerical investigation of geometry of Roche coords, for various mass ratios 0-54336 binaries, spectroscopic, observational effects, interpretation of the B-effect 0-45297

binaries, visual, period rel. to eccentricities 0–41703 binary, HD 49798, O-type, spectroscopic orbit 0–76589 binary, Perseus arm, mean velocities 0–59717 binary, eclipsing, TW Cas, orbital elements and photometric obs. 0–41877

0–41877
binary, eclipsing, light curves, computer solution 0–72737
binary, statistical study 0–41703
binary AS Cam, eclipses, eccentric orbit, and ephemeris, photometric obs. 0–41708
binary HD !84552, short-period vars. and orbital elements 0–41710
binary encounters in n body gravit. system, rigorous treatment 0–41630
binary system, close, effects of supernova explosion 0–66500
binary systems, close, eacous ring dimensions 0–69407
binary systems, close, intrinsic polarization 0–66495
binocular variables, new branch of British Astronomical Society, obs. and techniques 0–41698
branched-horizontal in 1 HLF 2 area, radial velocities measurements 0–45255

branched-horizontal in 1 HLF 2 area, radial velocities measurements 0–45255
CP 0950 pulsar, obs. for solar coronal electron distrib. 0–66670
CV Ser, Wolf-Rayet binary, two-colour photometric obs. 0–63054
C-M diagrams for globular clusters, a bibliography 0–51696
Capella meas, with stellar interferometer 0–57034
Car OB 2 association, photometric obs. 0–56945
carbon burning rate, ¹³C+¹⁴C reaction cross-section 0–79654
Carina, space distrib. of 436 OB stars 0–66437
Carina region, nine new faint Wolf Rayet stars 0–48408
Catalogue, Greenwich first (1950.0) 0–57018
catalogue, Greenwich first (1950.0) 0–57018
catalogues, photographic, overlap algorithm for reduction 0–69379
cetalogues, brot graphic, overlap algorithm for reduction 0–69378
cepheid HR 8157, spectra 0–66461
cepheid S Nor, in NGC 6087, pulsation and radius 0–66502
Cepheid S Nor southern in galactic cluster NGC 6087, pulsation and radius meas. 0–41696
Cepheid envelope models, pulsation constants 0–79667
Cepheid instability strip, pulsation constants, densities, double-mode variables 0–59712
Cepheid models, static and hydrodynamic, comparison 0–54390
cepheid, formula relating amplitude of radius variation with phase shift 0–72731
Cepheids, long-period, of Galaxy spherical component, light-curve and neriod vars. 0–63045

O-72731
Cepheids, long-period, of Galaxy spherical component, light-curve and period vars. 0-63045
Cepheids in globular clusters 0-48423
classification, early type, photometric and spectral, away from galactic plane 0-69377
close-binary systems, intrinsic polarization obs. 0-76587
cluster, M53, spatial distributions, diameter and structure 0-69411
cluster, NGC 5053, spatial distributions, diameter, structure 0-69411
cluster, globular, M4 metal rich, blue horizontal-branch 0-59718
cluster, very young, associated with \(\) Sculptoris and having moderate metal deficiency 0-51695
clusters, Hyades, Praesepe and Coma, ages 0-41717
clusters, Kron 3, in Small Magellanic Cloud, electronographic magnitude and colours 0-76585
clusters, globular, bulk props., by models comparison with obs. 0-66503

clusters, globular, bulk props., by models comparison with obs. 0–66503 clusters, globular, in Fornax galaxy, magnitudes and colour indices 0–41713

clusters, globular, magnitude of brightest as galactic dist. meas. 0-41605 clusters, isotropic, instability against radial perturbations, sufficient condition 0-45301

tion 0-4530! clusters, open, selective absorption and distance modulus determination from colour-magnitude diagram 0-57050 clusters, open, visible distribution 0-7270! clusters, relativistic, truncated, isothermal, stability criteria 0-48453 clusters IC 2944, new spectral types and UBV photometry 0-76586

Stars continued

clusters NGC 3293, red supergiant spectral type and UBV photometry $0\!-\!76586$

clusters NGC 3766, red supergiant new spectral types and UBV photometry 0-76586

clusters NGC 4755, red supergiant new spectral types and UBV photometry 0-76586 clusters in Galaxy, H obs. in four regions 0-56928 clusters in Milky Way, two-colour photographic photometry 0-41719 Collinder 399, nearby loose cluster 0-51698

collisions, in dense stellar systems, coalescence vs. disruption 0-66449

colour distance calcs., photometric, obs. 0-79660

comet capture, a rate expression 0-51692

convective energy transport, model atmosphere calc. 0-54364

Darwin ellipsoids, congruent, resonant oscills, and instability 0–48452 dead-cold, fully degenerate, normal radial vibrations 0–57020 density inversion in convective zones 0–51659 double, close, photometric and astrometric meas., with Kron electronic camera 0–66494

camera 0–66494
double, meas, with quantitative interferometer 0–66678
double, orbital plane orientation, statistical study 0–41623
double, physical peculiarities of the components 0–63056
double, visual and photographic meas., systematic errors 0–66493
doubles in astrographic zones +34° and +35°, list 0–76590
dwarf, comparison with supergiants of same spectral type through u.v.
flux-deficiency 0–69390
dwarf, type A, in large Magellan cloud direction 0–76556
dynamics, haloing effect of the third integral 0–48405
early-type, emission line, catalogue 0–76548
early-type, formation problems of neutral He lines 0–79658
early-type, radial velocities in Galaxy 0–56952
early-type emission line stars, collation of extant lists 0–51649
effective temps, and gravities for A and F stars near lower instability strip
0–48415
electrically charged body, spherically symmetric, in Rainich's Already

0-49435 (electrically charged body, spherically symmetric, in Rainich's Already Unified Field Theory 0-76567 electron scattering opacity of stellar interiors, collective interactions effects 0-57031

energy loss rate, due to neutrino pair emission 0-77256 equation of state, highly condensed zero-temp, stars, stability and vibr. periods 0-48411

very low to 11 evolved, continual photoelectric monitoring 0-59701 flare, EV Lac and UV Cet, continual photoelectric monitoring 0-59701 flare, as X-ray sources 0-79668 flare, distrib. in T-assoc. near NGC 7023 0-63023 flare, in Pleiades 0-45252

0-45232 (0-45232) O-45253 (0-45253) Orion association

flare, positions and magnitudes in Pleiades region and Orion complex 0-41684

0-41064 flare, radioastronomy, obs. 0-41750 flare, search for new ones, Gliese's catalogue 0-63003 flare stars, young, group in solar vicinity 0-63022 Galactic clusters and H II regions, distance determ. 0-

giant, G-K, in large Magellan cloud direction 0-76556 giants, intermediate age, motions and distribution, study program

giants, intermediate age, motions and distribution, study program 0–51648 giants, red, heavy metal, Li/Ca ratio 0–72735 globular cluster NGC 6637 (M69), containing two Mira variables 0–51691

0-51691
globular cluster black holes as gravitationally collapsed cores, observational aspects 0-45299
globular clusters, bibliography of C-M diagrams 0-51696
globular clusters, third catalogue of contained variable stars 0-63073
globular clusters, two, statistical anal. of 12 colour photometry 0-45224
globular clusters of Formax dwarf galaxy, UBV colour indices 0-41718
gravitational field arising from random distrib. stars, two point statistics 0-51650 0-51650

groups, moving, numerical investigation of possible origins 0-66436 HD 12881, spectroscopic binary, orbital soln. deriv. and other props. 0-41706 HD 148937, ejection of nebulosities, NGC 6164 NGC 6165

HD 161701, spectrographic binary, orbital elements 0-41701 HD 191765 line intensities, level populations of He II ions in envelope

0-59702 HD 192163 line intensities, level populations of He II ions in envelope

0–39/02

HD 192163 line intensities, level populations of He II ions in envelope 0–59702

HD 196502 (73 Dra), stellar spots, existence of 0–72706

HD 204613, peculiar high velocity G-type star 0–48403

HD 211853, binary, Wolf-Rayet eclipsing, two colour photometry 0–63055

HR 8880, δ Saiti star, low amplitude 0–63006

horizontal branch models obtained for wide composition range 0–54368

horizontal-branch, at high Galactic latitudes, positions, B magnitudes and spectra 0–79646

Hu 1597, visual binary, graphically deduced orbital elements 0–41705

Hyades and Wolf 630 group members, chemical homogeneity and absolute magnitudes 0–48409

Hyades binaries, parallaxes 0–41709

hyades giant stars ε and γ Tau, effective temperatures and hydrogen-tometal ratio 0–69408

in hydrostatic equilibrium, general relativistic inequalities 0–41637

i.r., anal. of observations using physics of radiation processes 0–45204

in hydrostate equinorium, general relativistic inequantes 0-41637 i.r., anal. of observations using physics of radiation processes 0-45204 identification, precise, non-homographic method 0-63187 index of discontinuity in $\Delta \delta_8$ (FK4-GC) between Northern and Southern hemisphere positions 0-69379 initial horizontal branch models for six compositions 0-51656 interiors, dense, thermal and vibrational energy losses due to URCA shells 0-54374

interiors, electron scatt. opacity, collective interactions effects 0-

interiors, plasmon neutrinos emission in strong mag, field 0–57031 interiors, plasmon neutrinos emission in strong mag, field 0–57030 Jacob double star, relative movements for 1845-2000 0–66440 K stars, seventh magnitude, 87, accurate photoelectric radial vels. 0–48420

Lacerta OB1 region, statistics 0–51694 with large proper motions, in astrographic zones +34° and +35° 0–69376 late-type, finding list for regions of intermediate galactic latitude 0–57015 local distribution rel. to Galactic spiral structure 0–56932

```
Stars continued
```

lunar occultation measurements, interpretation of traces with special reference to limb effects 0-54357

lunar occultation measurements, photoelectric, review of methods and applications 0-54355

lunar occultation measurements at McDonald University, instrumentation 0-54356

0-54356
M51, stellar velocity field in outer regions, obs. 0-57052
M5 globular cluster, period changes of RR Lyrae variables 0-54394
M82 emission region, spectroscopic evidence for rotation of the ionized gas 0-57053
M92, globular cluster, luminosity function from star counts 0-72734
M dwarf, +4°4048 B (=VB 10) infrared and photometric obs. 0-59704
M dwarf Wolf 359, infrared and photometric obs. 0-59704
M supergiants in Perseus arm, radial vels., spectrograms and UBV photometry 0-51661
magnetic, irregular variations, observational data 0-63032
magnetic, model and application 0-57027
magnetic, model and application 0-63033
magnetic braking by stellar wind, oblique rotator with quasi-radial field 0-66442

-66442

magnetic braking by stellar wind, oblique rotator with quasi-radial field 0–66442
mass, of red giants, rel. to use of K-line luminosities 0–41676
mass determ., fallacy in previously used method 0–48415
mass loss: a hydrodynamic envelope for stellar models 0–57026
massive, pulsational stability in He burning phase 0–69401
massive, with uniform chemical composition, pulsational stability, influence of opacity 0–48425
Merak (βUMa), similarity with Sirius 0–51665
metal-deficient, search using objective prism plates 0–51662
metallic-line, detection, ratio Sc II λ4320/ V II λ4309 as criteria 0–72715
Microturbulence in λ-type supergiants 0–41646
Mira variables, two in the globular cluster NGC 6637 (M69) 0–51691
Mira variables companions, radial velocities 0–41691
model, magnetic, radial oscillations 0–79652
models, dynamical, long-period variable 0–59711
models, partially mixed stars 0–66446
models, relativistic, isentropic, construction by method which automatically detects instabilities 0–57023
models, rotating spherical shell, nonaxisymmetric convection 0–76565
motion of groups of early stars and Orion variables with respect to galactic plane 0–57017
NGC 6637 (M69), globular cluster, containing two Mira variables 0–51691
NP 0532 pulsar, freq. decay meas. 0–66546

plane 0—57017
NGC 6637 (M69), globular cluster, containing two Mira variables 0—51691
NP 0532 pulsar, freq. decay meas. 0—66546
NP 0532 pulsar, occultation, solar corona electron density profile determ. 0—66671
NP 0532 pulsar, period, radio obs. 0—66549
neutron, co-rotating mag. field pulsar model 0—79664
neutron, conductivity in crusts, calculations and comparisons 0—76581
neutron, electrical and thermal conductivity in interior, calc. 0—54388
neutron, electrical and thermal conductivity in interior, calc. 0—54388
neutron, electron gas, mag. moment and mag. fields 0—76564
neutron, ionization zones, H_a luminosities, heating of interstellar matter, influence on accretion 0—72723
neutron, magnetic, self-excitation of oscillation possibility 0—54389
neutron, neutrino synchrotron radiation 0—79663
neutron, of small masses, cooling time and interior characts. 0—45294
neutron, neutrino synchrotron radiation 0—79663
neutron, pulsar distributions without surface mag. field decay 0—79665
neutron, pulsars, obs. of intensity variations 0—69422
neutron, review 0—59730
neutron, review 0—59730
neutron, review 0—59730
neutron, review 0—59738
neutron, rotating, objections to this as pulsar model 0—59736
neutron, stability rel. to central densities, and mass range 0—66476
neutron matter, cold, superluminal and ultrabaric behaviour 0—48442
neutron-core stars, models using realistic nuclear matter calcs. 0—66474
neutron matter, cold, superluminal and ultrabaric behaviour 0—48442
neutron-core stars, models using realistic nuclear matter calcs. 0—66474
neutron matter, cold, superluminal and ultrabaric behaviour 0—48442
neutron-core stars, models using realistic nuclear matter calcs. 0—66474
neutron matter, cold, superluminal and ultrabaric behaviour 0—48442
neutron-core stars, models using realistic nuclear matter calcs. 0—66474
neutron matter, cold, superluminal and ultrabaric behaviour 0—48442
neutron-star models for pulsars, ionization energy of atoms increases with Z 0—64187
nuclear partition functions for stellar reaction ra

O-51655 open clusters, old, obs. of red giants, colour magnitude diagrams 0—69410 Orion OB1 association, $H\beta$ obs. of Northern Sword and i Orionis subclusters 0—51699 Orion association, percentage of flare stars among the RW Aurigae type variables 0—45253 Orion constellation, electronographic photography 0—66501 Orion variables, motion with respect to galactic plane 0—57017 oscillations, adibatic 0—79675 oscillations, radial, density distributions which lead to three-term recurrence relations 0—79676 PZT, Tokyo observation program 0—59690 parallaxes, trigonumetric, in right ascension and declination, comparison 0—66439 parallaxes and proper motions of 22 faint red dwarfs 0—48404

parallaxes and proper motions of 22 faint red dwarfs 0-48404 peculiar, noted on objective-prism plates 0-62987 photography, sky background reduction by using polarizer, and new magnitude determ. method 0-45441 photometry, photographic, in fields with variable background density 0-51647

0-51647
physics of, mass M≥10 M_☉ 0-72707
Pleiades, occultation obs., March 1969 0-66498
Pleiades, relative proper motions for 92 stars, cluster mass and luminosity determ. 0-54392
Pleiades cluster, age determination, rotation considerations
polarisation meas. in Magellanic clouds, results 0-69388

Stars continued

polytropes, composite, with some central condensation, radial pulsations $0\!-\!69375$

positions of 502 stars in 1.5 deg. sq. in Pleiades cluster, unconventional procedure, astrometric tech., discussion 0-54359 proper motion data processing 0-41870

procedure, astrometric tech., discussion 0–54359
proper motions, absolute, determination referred to galaxies 0–57016
proto-, OH emission 0–79651
protostars of 10, 10², 10² and 10²M_O, collapse 0–45272
pulsar, Vela, spin-up, microscopic description 0–66477
pulsar, Vela, spin-up, two component model 0–66478
pulsar, oblique rotators, alignment 0–66547
pulsar dispersion measure statistics, interpretation 0–66552
pulsar obs., using swept-freq local oscillator 0–66550
pulsar phenomenon, discussion 0–66542
pulsar quantum electrodynamics 0–66542
pulsars, 13, accurate dispersions 0–66551
pulsars, sitrib. in space, statistical investigation 0–63081
pulsars, general relativistic electrodynamics 0–66562
pulsars, magnetic decay and maximum period 0–51726
pulsars, nulling phenomena obs. of short term behaviour 0–76605
pulsars, optical obs. 0–66475
pulsars, optical search techniques 0–66545
pulsars, possibility as neutron stars 0–59716
pulsars, possibility as neutron stars 0–59716
pulsars, stellar wind torques 0–51725
pulsars, vortex-lattice vibrations, Ruderman's theory 0–66473
pulsars as 'runaway' remnants of binary systems, appl. to Crab Nebula
pulsars as 'runaway' remnants of binary systems, appl. to Crab Nebula
pulsations, nonlinear, and stability of slowly rotating stars 0–48412
pulsations, nonlinear periodic, new numerical soln. 0–66448

pulsars as 'runaway' remnants of binary systems, appl. to Crab Nebula pulsars 0—51721 pulsations, nonlinear, and stability of slowly rotating stars 0—48412 pulsations, nonlinear periodic, new numerical soln. 0—66448 quark, hypothesis 0—76582 quarks, cosmological estimates for abundance in stellar sources 0—67238 RR Lyrae variables, period changes, in M5 globular clusters 0—54394 R Muscae, (123668), obs. of variations in luminosity 0—76584 radial oscillations of composite polytropes 0—48400 radial vels., catalogue, 0½-12½ Mount Wilson obs. 0—6644! radio, pulsating chronological and short story of discovery of first 14 objects 0—66530 random variable, computer simulated light curves 0—66488 red dwarfs, faint, 22, parallaxes and proper motions 0—48404 red giants, masses, rel. to use of K-line luminosities 0—41676 red-giant model, influence of relativistic gas characts. 0—45267 relativistic, spherically symmetric Taylor instabilities 0—72708 relativity, general, neutral stability against convection 0—79649 rings, rel. to Galactic structure 0—56951 rotating, energy transfer in convective envelope, rel. to solar differential rotation 0—54365 rotating, escape of photons, in stationary gravitational field 0—48439 rotating, rapidly, coupling of Henyey and self consistent-field methods 0—59693 rotating (slowly, differentially) relativistic stars, energy and moment of inertia 0—51654

rotating (slowly, differentially) relativistic stars, energy and moment of inertia 0-51654 rotation, age determination of Pleiades 0-79650

rotation, angular momentum dissipation by gravitational radiation 0-59675

0–59675
rotation, problems in theoretical study 0–72713
rotational velocities compilation 0–72711
runaway, remnants of binary systems, pulsar hypothesis 0–51721
Sagittarius, X-ray sources, location 0–66566
scintillation, correlation with jet-streams 0–69381
scintillation, saturation, atmospheric dispersion 0–79538
scintillation, wavelength depend. 0–69286
Sgr A, Sgr B2, ¹⁸OH absorption spectra, obs. at 1637 and 1639 MHz
0–79659

Sgr A, Sgr B2, ¹⁰OH absorption spectra, obs. at 1637 and 1639 MHz 0-79659 shock wave propag, in gravitational atmospheres of 3M_☉ stars 0-48421 Sirius, photoelectric obs. and for u.v. model fittings 0-51664 Sirius, similarity with UMa (Merak) 0-51665 size, distance calcs., photometric, obs. 0-79660 space distrib., galactic latitude +45° 0-66407 spectral types A and F, radial velocities 0-51660 Spica, occultation on June 24, 1969 0-41627 stability, models, upper end of main sequence 0-66445 stability of equilibrium of isentropic spherically symmetric relativistic star, static criterion 0-69373 stars, radial, field horizontal branch in 1 HLF 2 area 0-45255 static velocity distribution 0-54541 stellar assocs. development, model 0-66377 superdense tertiary stars family, stable, eqn. of state 0-41642 supergiant, comparison with dwarfs of same spectral type through u.v. flux-deficiency 0-69390 supergiants, A-type, 10, anal. of small scale velocity fields 0-41646 supergiants, distribution and kinematics 0-66512 supergiants, distribution and kinematics of all spectral types 0-54358 supergiants, red, mass loss, rotation and location in H.R. diagram 0-76566 supermassive, rapidly rotating, as QSO model, nonuniform rotation

supermassive, rapidly rotating, as QSO model, nonuniform rotation 0-51688

survey of intermediate galactic latitude, catalogue of stars later than class F2 $^{\circ}0-57015$

F2 0–57015 systems, inhomogeneous, linear stability, necessary and sufficient energy principle 0–45300 TW Cassiopeia, eclipsing binary, orbital elements and photometric obs. 0–41877 T Tau variables, $H\alpha$ emission profiles, obs. 0–63015 thermodynamic parameters of matter in electronic degeneration conditions, correct analytical expressions 0–69380 third integral, quasi-isolating, existence for family of high velocity stars 0–48407 these bedy problem periodic objects asymptotic solution. 0–48488

U-3-040/t three-body problem, periodic obrits asymptotic solution 0-48488 u.v. excess stars, variable matter infall 0-63014 ultrarelativistic, stability, two new theorems 0-57022 underlying Sco X-1, acoustic oscills. in plasma atm. rel. to periodic 'flickering' 0-63083

Ursa Major group, rotational vels. for 49 members 0-66458 VW Cygni, orbital elements, photometric 0-79679

S 1402 SUBJECT INDEX Stars continued Stars continued variable, 80 in region of CPD-31°5547 brightness periods of light variation 0-63002 composition continued uon 0-63002 variable, Ap, radio obs. at 6.2cm λ 0-72728 variable, β -cephei-type, γ -Pegasi; UBV photometry 0-63000 variable, cepheids, formula relating amplitude of radius variation with phase shift 0-72731magnetic stars, atmospheric conditions from magnetic null line list 0-41640magnetic metals, photometric variability, Ap 0-59695 nucleosynthesis at stellar surface 0-48424 shift 0-72731
variable, eclipsing triple system VV Orionis (HD 36695), spectroscopic obs. 0-69402
variable, freq. depend. of speed of light in gravitational field 0-72676
variable, in galactic window in Saggitarius I. obs. 0-69400
variable, long-period, period changes 0-69398
variable, long-period, proper motions, precise stellar positions from micrometric obs. 0-72732
variable, magnetic, oblique rotator model 0-69384
variable, non-periodic phenomena, 1968 Budapest conference 0-63007
variable, non-periodic phenomena, statistical meas. and interpretation 0-63008
variable, size distance calcs, photometric, obs. 0-79660 opacity tables, Rosseland, for 10 Population I compositions 0-41655 opacity tables, Rosseland, for 10 Population I compositions 0-41656 opacity tables, Rosseland, for 19 Population II mixtures 0-41657 origin of Li, Be and B, due to galactic cosmic ray implications 0-56893 origin of Li, Be and B, due to galactic cosmic ray implications 0–56893 peculiar A, light-element abundances 0–76570 Population I, Rosseland opacity tables for 10 compositions 0–41656 Population I, Rosseland opacity tables for 10 compositions 0–41655 Population II, Rosseland opacity tables for 10 compositions 0–41655 Population II, Rosseland opacity tables for 19 mixtures 0–41657 supergiants, M-type, metal abundances in atmospheres, curve-of-growth analysis of spectrograms 0–72738 Ba abundance of 56 Pegasi 0–59699 Be°, surface layers, events affecting observed chemical abundances 0–72712 C isotope ratio in cool carbon stars using lines of (2.0) band of CN variable, size distance cales, photometric, obs. 0-79660 variable HD 116994, orbital elements 0-41699 variable Lyr RR with very high vel., photometric, spectroscopic investigations 0-57048 variable RY Sagittarii, light curve from June 1967 to August 1969 0-41688 C isotope ratio in cool carbon stars using lines of (2,0) band of CN 0-51653c C isotope ratio in cool carbon stars using lines of (2,0) band of CN 0–51653 R Cyg., Zr relative isotopic abundances 0–41645 He abundance in early-type stars, departures from local thermodynamic equilibrium 0–76580 He abundance in population I B stars, statistical study 0–54369 Li content in late-type giants 0–41648 Li isotopic abundances in F and G type stars 0–54367 Li§, Li³, surface layers, events affecting observed chemical abundances 0–72712 Mn star, t Coronae Borealis, abundance anal. 0–54371 Mn star ϕ Her, abundance anal. 0–54370 N₂, abundance in He star HD 168476 0–45261 O, abundance in He star HD 168476 0–45261 O I forbidden lines in α Ser, no evidence for abnormal weakness 0–51684 Pu lines, search for in 73 Dra and other Ap stars 0–66460 α Ser, no evidence for abnormal weakness of [O I] 0–51684 Si II intensity variations in the Ap stars CU Vir and 56 Ari 0–45258 Zr relative isotopic abundances in R Cyg. 0–41645 0–41688 variable and flare stars in nebulae, survey 0–63025 variable colour distance calcs., photometric, obs. 0–79660 variables, T Tau, $H\alpha$ emission profiles, obs. 0–63015 variables, α -Lyrae, spectral energy distribution 0–72727 variables, β -Lyrae, mass exchange, polarimetric obs. 0–72726 variables, amplitude ratios of several groups 0–76583 variables, eclipsing, Nurnberg and Izmir observatories research program 0–63072 variables, calipsing, light ourses 0–59713 0-63072
variables, eclipsing, light curves 0-59713
variables, long period, dynamical models 0-59711
variables, lutrashort period in old disk population 0-63005
variables in globular clusters, third catalogue 0-63073
velocity field in M51, obs. 0-56984
velocity variations of zero mass stars, a purely discontinuous random process 0-45254
Vulpeculae-S, Wachmann suggestion as classical Cepheid, UBV obs. 0-41697
WNA line intensities level populations of He II jons in envelope. 0-59702 0-41097
WN6, line intensities, level populations of He II ions in envelope 0-59702
W UMa, photoelectric times of primary min., interpretation of period variations 0-41685
white dwarf CoD 38° 10980, physical system with G-type star HR 6094 β Cephei phenomenon due to semiconvective zone within star 0–51671 associations, extended, with low mean density, formation from low temp. interstellar gas 0–48427 interstellar gas 0–48427
associations, formation by Rayleigh-Taylor instability 0–54393
binaries contact W Ursae Majoris system, nature investigation 0–59722
binary, origin 0–41703
binary formation rate due to stellar three-body collisions 0–51692
binary systems pre-main-sequence mass transfer, investigation 0–59724
Cepheid variables and He content rel. to red giant phase mass loss
0–57047 white dwarfs, convection in envelopes 0-66447 white dwarfs, convection in envelopes 0-66447 white dwarfs, core conductivity elec. and thermal 0-59709 white dwarfs, electron gas, mag. moment and mag. fields 0-76564 white dwarfs, hot white dwarfs, and 10Mo, models, nonradial oscills. 0 66485 Cepheids in globular clusters, He shell burning phase computation white dwarfs, models, implications of coulomb cryst. vibr. results 0 65514 Cepheids in globular clusters, He shell burning phase computation 0-5168 cluster, consisting of 25 protostars, numerical soln. of motion 0-45296 clusters, computing method 0-69409 clusters galactic, obs. suggesting photoneutrino process in m-supergiants 0-59719 0 65514
white dwarfs, neutrinos synchrotron radiation 0–79662
wind, influence on accretion 0–57014
wind, stellar, relativistic analytical solns, to a previous model 0–48402
Wolf-Rayet, conference 0–41631
Wolf-Rayet, luminosities, masses, ages, distributions, summary of available information 0–41632 0–59719

corlapsing star, optical appearance in terms of scalar-tensor theory of gravitation 0–45271

cores of initial masses 10 and 3M_☉, in advanced phases 0–76573

dynamical instability, critical parameters for isentropic objects with rest masses 10² to 10⁷ M_☉ 0–76571

energy conservation equation and the inclusion of chemical potential terms 0–51669

exploding stars, damping effect of beta processes 0–66450

formation from galactic large-scale shock phenomena 0–57001

globular cluster Cepheids, He shell burning phase computation 0–51668

in globular clusters 0–41653

HII region investigations, obs. of hydrogenic spectral lines 0–57012 information 0-41632
Wolf Rayet, nine new ones in Carina 0-48408
Wolf Rayet, nine new ones in Carina 0-48408
Wolf-Rayet, obs. rel. to Galactic spiral structure 0-56950
Wolf-Rayet, six WN-type, effective temp. determ. 0-51672
Wolf Rayet HD 211853 eclipsing binary, 2 colour photometric obs. 0 63055
Wolf-Rayet and central planetary nebulae stars comparison 0-69369
Wolf-Rayet binaries, negligible transit-time effect 0-45302
Wolf-Rayet target were determed of experience when he were transited and the second of the property of Wolf-Rayet stars, mass determ. of associated nebulae using 11 cm obs. 0-54373 HII region investigations, obs. of hydrogenic spectral lines 0–57012 HR 72, a super-metal-rich G dwarf, curve of growth anal. 0–48426 Henyey-type code, computation of single star or component of close binary 0–62990 0-34373 CH Cygni, variations, nature 0-66487 G 44-32, short period variability 0-66486 H II region stars, interstellar extinction 0-41725 He line profiles for grid of approx. line-blanketed model atmospheres 0-45264 onnary 0-0.2990 iron stars in gravitational contraction phase 0-45270 life history of stars, book 0-45257 low mass, structure, pre-main- sequence and main sequence models 0-76568 Composition

see also Elements/origin

56 Pegasi, Ba abundance 0–59699

56 Ari, (Ap star), surface conditions and Si II spots 0–45258

µ Arietis, Fe and V content 0–51678

ι Coronae Borealis, Mn star, abundance anal. 0–54371

3 Dra, peculiar A-type variable, high Os/Fe abundance ratio 0–41663

φ Her, Mn star, abundance anal. 0–54370

Ap stars CU Vir and 56 Ari, surface conditions and Si II spots 0–45258

Arcturus, CO bands, anal. of equivalent width obs. 0–51676

Arctururs, relative abundance of Mg isotopes in atmosphere 0–45266

B stars, population I, He abundance, statistical study 0–54369

binaries, eclipsing, metal abundance obs. 0–41680

binaries W UMa type system using Lucy model 0–59723

CU Vir, (Ap star), surface conditions and Si II spots 0–45258

chemical, α Cen A, α Cen B pos⁴ in two-colour diagram 0–76588

circumstellar grain material, some possible components 0–51657

F and G type stars, 12, Li isotopic abundances 0–54367

F dwarfs, late, 12, from curve-of-growth analysis 0–54366

giants, late-type, Li content 0–41648

HD 196502, (73 Dra), peculiar A-type variable, high Os/Fe abundance ratio 0–41663

HD 205805, B-type subdwarf, atmospheric He abundance from He line strengths 0–45265

HR 72, a super-metal-rich G dwarf, curve of growth anal. 0–48426 iron stars in gravitational contraction phase, decomposition of Fe 0–45270

K, projected and observed densities of molecular constituents 0–59692

K giants α Boo, α Ser, β Gem, ε Peg, C, N and O abundances 0–45262 late-type stars, 17/Zr atomic abundance ratio 0–54362 low-mass, X=0.68, X=0.29, Z=0.03, evolution, contraction to main sequence 0–59700 low-mass, Y=0.1, 0.2, 0.3 and Z=−3, −4 metal-poor, horizontal branch 0–62989

M, projected and observed densities of molecular constituents 0–59692 composition 0—76568
low-mass, contraction to main sequence 0—59700
lower main sequence, outer boundary conditions 0—66456
m-supergiants obs. suggesting photoneutrino process 0—59719
main sequence to white dwarf, carbon ignition 0—66451
main-sequence, density gradients in different Galactic latitudes, comparison 0—56941
Markovian process used in stellar dynamics 0—54377
mass loss in early-type supergiants, mechanism 0—48410
massive, Stromgren zones 0—45269
massive, Stromgren zones 0—45269
massive stars (12 Mo) 0—51670
metal-poor, horizontal branch 0—62989
mixing between stellar envelope and core in advanced phases 0—76572
neutrinos in red giants, photon-neutrino weak coupling 0—54375
nucleosynthesis by explosive oxygen burning, abundance distribs. calc.
0—48422
OB type from main sequence to He exhaustion phase 0—79655 0-48422
OB type from main sequence to He exhaustion phase 0-79655
OB-type space distrib. in Carina Spiral Features 0-56944
Paczynski degnerate C-O cores as structs. preceding pulsar phase 0-57076 partially mixed, models 0–66446
Population I, 30M_☉ 0–41649
Population I, 50 solar masses, calcs. 0–66452
pre-main sequence, low mass, grey and non-grey boundary conditions 0–66457

M, projected and observed densities of molecular constituents 0-59692

protostars, rapid contraction to stage of quasi-hydrostatic equil. 0–45272 protostellar cluster consisting of 25 bodies, numerical soln. of motion 0–45296 pulsars, nature and origin 0-69427

0-0437 pre-main sequence, low mass stars 0-66455 proton-proton chain termination, importance of ${}^{7}\text{Be}(\mathbf{p}, \gamma)^{8}\text{B}(\beta^{+}, \nu)^{8}\text{Be}^{*}(\alpha)^{4}\text{He}$ sequence 0-46209 protostars, rapid contraction to stage of quasi-hydrostatic equilibrium

Stars continued

evolution continued

red giant, $1 m_{\odot}$ 'extreme Pop II', model, using He flash hydrodynamics 0--54360

0—34360 red giants, after rapid mass loss, comparison with Harman-Seaton sequence 0—41651 rotation effect on shape and struct. of turbulent convective zones 0—41650 Schwarzschild black-hole, scattering of gravitational radiation 0—69354 self-gravitating syst., numerical models, plane parallel layers 0—57029 self-gravitating systems, numerical models, point masses 0—57044 supermassive, origin from the non-elastic evolution of stellar system 0—45268

0-45258
WZ Sge binary, ultrashort period, origin 0-41707
white dwarfs, collapsing, thermonuclear detonations 0-66454
white dwarfs, non-equilib. beta processes as source of thermal energy
0-45259

white dwarfs, rotating 0-41652 white dwarfs near Chandrasekhar's 4i.nit, rotating, period of pulsation 0-69386

Wolf-Rayet, clues regarding evolutionary stage 0-41644
Wolf-Rayet, planetary nebula excitation, HVB 475 spectroscopic obs.
0-59686
young Cepheid variables, Galactic distribution 0-56942
He-shell burning termination, in solar mass stars 0-66453
He core flash phase, hydrodynamical effects 0-79653

magnetism

see also Sun/magnetism β CrB, variations of mean surface field 0-48413 Ap stars, four, double lined, Zeeman obs., absence of strong mag. fields

0-45281 assembly of neutrons with hard cores being magnetic, assumption raised by pulsars 0-69394 field generation by partially ionized convective envelopes 0-69469 HD 126515, large variable field, implications for mag. stars rigid rotator model 0-48414 HD 9996, very slow spectrum, magnetic and photometric variations 0-45280 kinetic diagraph.

0-45280 kinetic dia- and para-magnetism due to temp. gradient 0-52226 models, field effect on structure 0-59694 neutron, stars existence of B~10¹² G magnetic fields ionization energy of atoms 0-64187

stars, magnetic axis alignment, effect of crystalline mantle neutron st 0-48440

rotating stars, thermal generation of mag. fields with radiation press. 0-51704

variable β GrB, brightness variation 0-57035 variations, irregular, in magnetic stars, observational data 0-63032

radiation

radiation see also Cosmic radiations, radiofrequency; Sun/radiation TT Ari, light vars. rel. to close binary struct. 0-63048 14 Aur, short-period vars., obs. 0-63043 RW Aurigae, six southern, UBV obs. 0-63012 RX Boo, polarization, brightness and wavelength, connection 0-45277 YZ CMi, flare periodicity, obs. 0-63017 RS CVn, photometric vars., obs. 0-63017 RS CVn, polarization, brightness and wavelength, connection 0-45277 ω Cen. RR Lyrae stars, anal. of published photometry 0-57041 RS Cep, UBV photometry, appl. of Huang disk model 0-57058 β Cephei, variability period from blue- and visual-band photometry 0-79670 UV Cet flare stars, flare polarization meas. 0-63024

UV Ceti flare stars, flare polarization meas. 0–63024 γ Coronae Borealis, classification confirmation and light variation obs. 0–48436

0-48436
AB Cyg, polarization, brightness and wavelength, connection 0-45277
31 Cyg and 32 Cyg, binary, photoelec. obs. in 1968 eclipse, colour variation 0-41704
CG Cygni, O'Connell effect, obs. and origin 0-63070
RX Gem, UBV photometry, appl. of Huang disk model 0-57058
U Gem, eclipse light curves irregularity, obs. 0-63060
U Gem, hot, short-period eruptive binary, photometric and spectroscopic data interpretation 0-63058
U Gem stars, anal. of light curves 0-63062
VZ Hya eclipsing binary, UBV light curves and M-L position, obs. 0-41715

0–41715

RT Lac, O'Connell effect, obs. and origin 0–63070

EV Lac, flare star, synchronous UBV photometric obs. 0–62998 β Lyrae, differential UBV photometry 0–63057 β Lyrae, light curve changes, 1958-1959 0–63069

RR Lyrae halo variables, discrepancy in magnitude 0–69392

RR Lyrae stars in M3 and ω Cen. anal. of published photometry 0–57041

0-5/04! RR Lyrae variables in M5, O-C diagrams, rel. to period vars. 0-63044 UMon, RV Tauri star, polarization obs. 0-45282 in NGC 6791, M92 and M13, photometry obs. 0-41712 SU Ori, brightness, rel. to variable matter infall in u.v. excess stars 0-63014

XX Ori, brightness, rel. to variable matter infall in u.v. excess stars 0-63014

0-63014

© Ori, spectroscopic binary, light variations 0-41702

V429 Orionis, variability 0-41692

V429 Orionis, variability 0-41692

AG Peg, light variations from 1962-1967, explanation 0-45275

AK Peg, polarization, brightness and wavelength, connection 0-45277

Ber, sudden period changes, 1920-1965 0-63071

RW PsA binaries, eclipsing, photoelec. obs. 0-66492

V1216 Sag, photometric obs. 0-41661

RSct, RV Tauri star, polarization obs. 0-45282

RZ Scuti, UBV light curve asymmetries rel. to struct. obs. 0-41714

RY Sgr, vars. in 1967-68 minimum, obs. 0-63035

BL Telescopii, supergiant eclipsing variable, photographic light curve 0-54380

W UMa binaries with low mass ratio, light vars., model 0-63064

W UMi, eclipsing binary, two independent multicolour photoelectric light curves and solns. 0-48454

y² Vel, study using stellar intensity interferometer 0-45292

δ Scuti stars, consistent absolute magnitudes and period-colour-luminosity relation determ. 0-54381

A and F stars, u.v. features study, spectral type and colour relationship

and F stars, u.v. features study, spectral type and colour relationship leterm. 0-45284determ.

Algol, sudden period changes, 1920-1965 0-63071

Stars continued

radiation continued

from atmosphere, plane-parallel, grey, radiation transfer equations solution with Rayleigh's law scattering 0-76576
BL Lac photographic magnitudes (Jun-Nov 1969) 0-59714

BL Lac photographic magnitudes (Jun-Nov 1969) 0—59714
BV 845, eclipsing binary, photoelectric obs. 0—66491
BV 845 and RW PsA binaries, eclipsing, photoelec studies 0—66492
Be stars, 50 which recently showed large photometric changes 0—48437
binaries, W UMa type with low mass ratio, light vars, model 0—63064
binaries, close, radiation transfer and refl. effect 0—63065
binaries, close dwarfs system, rapid brightness vars. origin 0—63063
binaries, eclipsing, BV 419, 9 Chamaeleontis, AU Puppis, photometric obs. 0—41699
binaries eclipsing BV Convall effect origin, 0, 63070

binaries, eclipsing, O'Connell effect origin 0-63070 binaries, eclipsing, Z Draconis and W Ursae Minoris, light curves, obs. 0-4845!

0-48451 binaries visual in southern hemisphere, mass luminosity relationship, U, B, V photometry, results 0-59726 binary, eclipsing, TW Cas, photometric obs. 0-41877 binary 31 and 32 Cyg, photoelec. obs. in 1968 eclipse, colour variation 0-41704

0-41704 binary systems, close, effects of highly distorted while dwarf secondary, calc. 0-63059 blue stars, high latitude, photometric classification methods 0-54385 bright stars in Southern hemisphere, four colour and H β photometry 0-54378

brightnesses, 1216 Å band obs., Orbiting Astronomical Observatory results 0-66353

results 0-06353 (Capella, absolute u.v. flux from high altitude photographs 0-51687 Cassiopeia-A, radio intensity 3 to 15 cm. obs. 0-79706 cepheid variable of small amplitude HR 4768, period and light curve 0-51683

0–51683 cepheids, absolute period-luminosity relations deriv. 0–57049 cepheids, absolute period-luminosity relations deriv. 0–57049 cepheids, classical, radiation excess in the brightness maxima 0–45286 Cepheids, long-period, of Galaxy spherical component, light-curve and period vars. 0–63045 Cepheids, southern, 29, UBV obs. 0–45288 Chandrasekhar polarization, upper limit in early type stars 0–59706 chromospheric emission from 65 Hyades stars, bolometric luminosity depend. 0–48429 circular polarization of thermal radiation in mag. field 0–76924 cluster M92, colour-colour diag., interpretation 0–59725 cluster globular, intermediate bandpass photometric u.v. color meas. 0–56970 clusters, globular, in Fornax galaxy, magnitudes and coloour indices

clusters, globular, in Fornax galaxy, magnitudes and coloour indices 0-41713

clusters, globular, photometry 0-41680 clusters, globular, seven-colour intermediate band photometry obs. 0-41670

0-41677 colour anomaly of stars in H II regions, review of explanations 0-45250 colour-colour diagram of M92, interpretation 0-59725 colours, intrinsic, Cepheids, periods and light amplitudes 0-59705 Cygnus, a region, spectrophotometry of cool stars in near ir. 0-66459 Cygnus-A, radio intensity obs. 3 to 15 cm. 0-79706 distant OB stars, photometric and spectroscopic data 0-56946 double stars, 874, photovisual magnitude differences between components 0-57054

0-57054

early type, with extended atmospheres, intrinsic polarization 0-48430 emergent flux from rotating atmosphere, effect of turbulence 0-51658 field-horizontal branch stars, 39, intrinsic colours determ. 0-51686 flare, UV Ceti type, flare light curves classification 0-63018 flare, UV Ceti-type, flare properties 0-63016 flare polarization meas. of UV Ceti type flare stars 0-63024 flare stars, Orion, UBVR photometry 0-63019 flare stars, photoelec. obs. 0-63020 G44-32 blue variable, obs. of flare activity 0-48444 globuler clusters in Andromeda Nebula, photoelec. and spectroscopic obs. 0-45295 eravitational. Jacobi ellipsoid evolution 0-59675

0-45295
gravitational, Jacobi ellipsoid evolution 0-59675
HD 152667, eclipsing variable, three colour obs. 0-41659
HD 160202, flares, obs. 0-6302!
HD 173650, period of light and magnetic variations 0-41672
HD 17514, binary, nearly contact, light and radial vel. curves 0-63066
HD 9996, very slow spectrum, magnetic and photometric variations 0-45280
HR 4768, cepheid variable of small amplitude, period and light curve 0-51683
HR 6283, eclipsing variable, three colour obs. 0-41659
HV 13055, similarity to symbiotic variables 0-48438
h and χ Persei, short period light vars, of stars 0-66408
Hyades stars, 65, chromospheric emission depend. on bolometric luminosity 0-48429
i.r. of 32 stars in A0 to M7 spectral range, CO, CN, C2, CH, TiO, H2O, AlH identification 0-69382

AlH identification 0-69382 ir. sources, galactic 0-66414 ir., stars, 6, photometric and spectroscopic obs. and their interpretation 0-45278

interstellar radiation field 2000-5560 Å, from night sky brightness 0-41594

0–41594 large-scale stellar statistics, usefulness and feasibility 0–56955 late-type, (M, N, R, S spectral types), intrinsic polarization obs. 0–62999 light, r.f. intensity modulation by ionosphere 0–41681 light meas, rocket-borne spectrophotometer, pulse counting and encoding systems 0–70087 luminosity function, initial, secular variations 0–76579 luminosity function, initial, secular variations 0–76570 M R R Lyrae stars, anal. of published photometry 0–57041 MK and MtW spectral-luminosity classification comparison 0–41658 MWC 84, line identifications, emission line intensities and energy distrib. in continuous spectrum 0–45276 M-type, high luminosity, photometric observations to 3.4μ 0–79656 magnetic stars, photometric obs. 0–63034 magnetic variable βGrB, brightness variation 0–57035 magnitudes, meas., Wilson-Bappu method appl. at moderate dispersion 0–41868

0-41868

main sequence, 20-100 M., rapid differential rot., rel. to colour, magnitude 0-41641 0-304: maximum efficiency of energy release in spherical collapse, and gravita-tional energy 0-62997 Mira Ceti, periodicity of light vars. 0-63047 Mira stars, 40, UBV obs. at or near max. light 0-54379

radiation continued

Mira variables, period variations, correl, with other props. 0–63046
Mira variables, period variations, correl, with other props. 0–63046
NGC 6611 OB stars, comparison with 15.4 GHz map of M16 0–51645
NP 0532, Crab pulsar, X-rays, balloon obs. 0–66429
neutrino energy loss rate due to photoneutrino process in hot plasma, comparison of coupling theories 0–45886
neutrino synchrotron, application to neutron stars 0–79663
neutrino synchrotron, application to white dwarfs 0–79662
neutron, pulsars, Crab, NP 0532, irregularities in wobble 0–79708
neutron, pulsars, defunct, obs. consequences of accretion 0–79701
neutron stars, gas accretion accompanied by gamma and radio radiation 0–45293 0 - 45293

neutron stars in state of accretion, generation of relativistic particles

0-69393 nova, old, DQ Herculis, light curve obs. 0-41694 novalike variables, C-M relation 0-51685 OB stars in cluster NGC 6611, comparison with 15.4 GHz map of M16 0-51645

O-51645
O and Of stars luminosity criteria defined using narrow band photoelectric photometry 0-48431
O and early B stars, non LTE multi-line hydrogen-helium model atmospheres calcs. 0-48416
opacity tables, Rosseland, for 10 Population I compositions 0-41656
opacity tables, Rosseland, for 10 Population I compositions 0-41655
opacity tables, Rosseland, for 19 Population II mixtures 0-41657
Orion flare stars, UBVR photometric obs. 0-63019
P Cygni, total light and spectral vars. 0-63028
photometry, photographic, appl. of fibre optic image intensifiers 0-48622
photometry, seven-colour intermediate band obs. 0-41677
plasma neutrino pairs emission, effect in white dwarfs 0-48434
polarimetric obs. of long period variable stars 0-45277
polarization, intrinsic, of 40 Be and shell stars with extended atmospheres
0-da109

0–48430
polarized, from plane-parallel non-gray atmosphere 0–57040
polarized, from plane-parallel non-gray atmosphere 0–57040
population I, Rosseland opacity tables for 10 compositions 0–41655
Population II, Rosseland opacity tables for 10 compositions 0–41656
Population II, Rosseland opacity tables for 19 mixtures 0–41657
pulsar, Cab, optical and X-ray synchrotron radiation calc. 0–54412
pulsar, NP 0532 polarization of strong pulses at 430 MHz, obs. with 300
kHz bandwidth 0–72752
pulsar CP 0834, spectra showing modulation of pulse period
pulsar CP 1919, spectra showing modulation of pulse period 0–41662
pulsar CP ab nebula, optical polarisation obs. 0–72722
pulsar rota nebula, optical polarisation obs. 0–72722
pulsar signals, 21 cm absorpt. 0–66554
pulsars, and laser process 0–66564
pulsars, mechanism 0–66548
VX puppis, beat period 0–41665
RR Lyrae stars and dwarf Cepheids, intermediate-band photometry
0–41680
RU Cam, light variation and period, (1967-68) 0–41686

0-41680
RU Cam, light variation and period, (1967-68) 0-41686
RX And light standstill, UBV obs., rapid brightness vars. 0-6306!
R Coronae Borealis, variable, obscuration rel. to C condensation in ejected gas shell 0-41695
red giants, K-line luminosities rel. to mass underestimation 0-41676
red southern giants, narrow and broad band photometry 0-51673
red supergiants, i.r. emission from circumstellar mineral grains, models
0-54386

U=54386
red variable stars of high luminosity, polarization 0-69396
scintillation, wavelength dependence obs. 0-59586
Sco X-1, short term periodic variations following optical flare 0-41753
Southern Milky Way fields, 4, UBV photoelectric photometry 0-54401
southern OB-star polarization, galactic diagram 0-56963
spectral line formation in Wolf-Rayet envelopes, escape probability
method 0-59707
stellar lines analysis analysis and the star polarization and th

stellar lines analysis, applic. of laser line shifts, Doppler shifts meas. 0-51811

supernova remnants Taurus A Cas A, polarization distrib., 9.75 cm 0-41729

0-41729
symbiotic stars, brightness, colour vars. and model 0-63050
TW Cassiopeia, eclipsing binary, photometric obs. 0-41877
T Tauri stars and other objects, spectral anal. of light curves 0-63009
Taurus-A, radio intensity obs. 3 to 15 cm. 0-79706
transfer in free electron spherical atmos. 0-59708
UBV photometry of 137 stars near south galactic pole 0-41660
U Geminorum stars, outburst mechanism 0-57043
us y flux-deficiency, in currections compared to dwarfs of came spec

u.v. flux-deficiency in supergiants compared to dwarfs of same spectral class 0-69390 variability in the lower Hertzsprung gap, obs. of 213 bright field stars 0-51690

0-21690 variable HD 116994, photometric obs. 0-41699 variable R CrB, obscuration rel. to C condensation in ejected gas shell

variable R CrB, obscuration rel. to C condensation in ejected gas shell 0-41695 variable VY Canis Maj., OH emission, 1612 MHz 0-48445 variables, RR Lyrae, in M5, O-C diagrams, rel. to period vars. 0-63044 variables, RW Aurigae, six southern, UBV obs. 0-63012 variables, TTauri, light curves power spectrum analysis 0-63009 variables, eclipsing, RZ Scuti and ZZ Bootis, photometry 0-41680 variables, young, contracting 0-6301! W₃ (OH), 3.8 cm spectrum, low-noise search, lab. meas. 0-69387 wind, and magnetic braking, oblique rotator with quasi-radial field 0-66442 winds supersonic in early type stars effect of mechanical force due to

winds, supersonic, in early type stars, effect of mechanical force due to radiation 0—4840! Wolf-Rayet envelopes, spectral line formation, escape probability method 0–59707

Z Cam light standstills, UBV obs., rapid brightness vars. 0-6306! H_{β} and four-colour photometry of B and A stars, calibration 0-56949

ispectra
15 UMa, metallic lines characts, obs. 0–72716
HD 4174, vars., obs. 0–63052
44 i Bootis, Hβ obs. 0–66462
56 Ari, (Ap star), surface conditions and Si II spots 0–45258
μ Arietis, Fe and V content 0–51678
RW Aur, emission and absorpt. lines and line intensities, catalogue, 3250–4900Å 0–45283

14 Aur, short-period vars., obs. 0-63043

```
Stars continued
```

spectra continued

γ Boo, short-term spectral vars., obs. 0-63042 R Canis Majoris, spectroscopic elements and orbit computation, two models proposed 0-48433

 γ Cas, continuum long-term vars., obs. 0–63030 μ Cas, line intensities in visual region 0–54383

W Cep, vars., obs. 0-63052

X Cnc, identification of i.r. CN bands 0-51677 V 1016 Cyg, spectral evolution, 1965-67 0-63051 BC Cygni, possible OH source 0-41673

BC Cygni, possible OH source 0–41673
BX Delphini, photoelectric photometry 0–41668
73 Dra, and other Ap stars, search for Pu lines 0–66460
73 Dra, peculiar A-type variable, high Os/Fe abundance ratio 0–41663 χDra,, H_β line, photometric variations 0–51680
U Gem, hot, short-period eruptive binary, photometric and spectroscopic data interpretation 0–63058
WY Gem, vars., obs. 0–63052
112 Her, spectrosopic binary, mass ratio 0–48455 φ Herculis, line intensities 0–76578
U Hya, identification of i.r. CN bands 0–51677
λ Lep, (B0.5 IV), continuous and line spectra obs., anal. using model atmosphere techniques 0–41654
R Lep, long-period, variable CN rot. lines doubling and H_α profile rel. to struct. 0–41693
RR Lyrae, interstellar reddening 0–62994

struct. 0–41693
RR Lyrae, interstellar reddening 0–62994
for Magellanic large cloud membership, Butler and Norris method of determination 0–54350
W Ori, identification of i.r. CN bands 0–51677
SU Ori, rel. to variable matter infall in u.v. excess stars 0–63014
XX Ori, rel. to variable matter infall in u.v. excess stars 0–63014
S 5114– K3π 5235 Pavonis, flare, late-type dwarf from spectra, colour indices 0–41674
y Peg, line widths and profiles var., obs. 0–6304!
{ Per, and \$\epsilon\$ Per, comparison to determine interstellar extinction in the u.v. 0–57063
} Psc, identification of i.r. CN bands 0–51677

{ Per, and ε Per, comparison to determine interstellar extinction in the divides of the constraint of the constraint of the divides of the constraint of the co

Algol, K line 0-62996 Ap, search for plutonium lines 0-66460

Ap stars, four, double lined, Zeeman obs., absence of strong mag. fields 0-45281

Ap stars, round, double lined, Zeenhan obs., absence of strong rings, fields 0–45281. Ap stars CU Vir and 56 Ari, surface conditions and Si II spots 0–45258 Arietis, He I and Si II lines 0–62993 B2 class, theoretical profiles of H₂ and H₃ hydrogen lines 0–62991 BD, in reft. nebulae, obs. 0–41620 B-stars, peculiar, with colour-spectrum discrepancies, characts. 0–66470 Barnard's star, 6900·11000Å 0–41666 Be stars, rapid spectral variations, obs. 0–63026 Be type, emission lines variation, long-term behaviour patterns 0–69389 binaries, close, continuous and line spectra, calc. 0–41720 binaries, visual, three luminosity criteria, intercomparison 0–66499 binary HD 184552, short-period vars. and orbital elements 0–41710 binary ε Lupi, double line spectroscopic orbit derivation 0–5972! C, M and K, 1 to 4 micron 0–66468 CH Cygni, obs., 1968 0–59715 CN bands, 3883Å and 4215Å, G and K stars, absorpt. strengths 0–66466

CN bands, 3883A and 4215A, G and K stars, absorpt. strengths 0-66466 CPD-74°214(BV 1041), photometric and spectroscopic obs. 0-57048 CU Vir, (Ap star), surface conditions and Si II spots 0-45258 CU Vir (HD 124 224), spectrum variable Ap star and oblique rotator model 0-69397

model 0-69397
calibration of Cambridge obs. of G and K giants, synthetic spectra computation 0-45289
η car. reddening from permitted Fe II lines 0-41664
carbon stars, infrared colour indices 0-41671
central and spiral arm stars of planetary nebulae 0-69368
Cep OB3 and comparison region, interstellar reddening law, 3360 A to 8400 A 0-41727
cepheid HR 8157 0-66461
classification of A and F stars, colour-spectral type relationship 0-45284
collapsing star, optical appearance in terms of scalar-tensor theory of gravitation 0-45271
colour-colour diagram of M92, interpretation 0-59725

itation 0-45271 colour-colour diagram of M92, interpretation 0-59725 computer programs for automatic reduction of spectrograms, application to K-type giant stars 0-72718 diffuse interstellar absorpt. band at 4430 Å, rel. to Fe³+ 0-57038 distant OB stars, photometric and spectroscopic data 0-56946 Draconis, ν_1 and ν_2 , comparison with normal stars of approx. same temp. 0-51681 dwarfs, cool, Wolf 359 and Barnard's star, and M giants, 6900-11000Å.

0-41666 early-type, 0-41669 Hr equivalent widths, photoelectronic spectrophotometry

0–41669
early-type, in south galactic pole region, objective prism survey
emission from behind shock waves in the atmosphere 0–45273
with emission lines, catalogue of early-type stars 0–62992
energy distribution in 8 stars 0–57046
extreme u.v., Japan 1948-68 0–54321
F2-G5 stars, 166, MK classifications, erratum to original paper
field horizontal-branch, radial rels. determ. 0–51663

Stars continued

spectra continued

flare UV Cet-type stars, chromospheres, solar comparison from spectro-photometric investigations 0-69395

flares, dMe, time resolved low resolution 0-59703

G and K stars, 225, photoelectric meas. of λ 6495 Fe I line 0-54387 globuler clusters in Andromeda Nebula, photoelec. and spectroscopic obs.

globuler clusters in Andromeda Nebula, photoelec. and spectroscopic obs. 0-45295 HBV 475, emission spectrum, near i.r. 0-51679 HD 109387, H_{β} line, photometric variations 0-51680 HD 12881, binary, deriv. of orbital soln. and other props. 0-41706 HD 160529, component of interstellar Na perhaps indicating gas flowing from galactic centre 0-48435 HD 196502, (73 Dra), peculiar A-type variable, high Os/Fe abundance ratio 0-41663 HD 204075, Ba II star, double differential curve of growth analysis 0-51667 HD 204075, atmospheric abundances for 37 elements 0-51667 HD 205805, B-type subdwarf, atmospheric He abundance from He line strengths 0-45265 HD 37202 envelope, periodic and short-term vars., obs. 0-63031 HD 9996, very slow spectrum, magnetic and photometric variations 0-452800-45280

0-45280
HR 2142, rel. to shell ejection, obs. 0-41639
Hd 217050, variation of absorption and emission lines 0-45287
hot stars, neutral He lines and the He anomaly 0-41683
i.r., spectral distribution 0-72719
i.r. \(\lambda \) 9000 \(\text{A review} \) 0-72721
i.r. of 32 stars in A0 to M7 spectral range, CO, CN, C2, CH, TiO, H2O, AlH identification 0-69382
i.r. stars, 60, search for OH emission at 1612 MHz 0-45279
i.r. stars, 60 becomes the analysis of the stars of the

i.r. stars, 6, photometric and spectroscopic obs. and their interpretation 0-45278

0-45278 interstellar diffuse bands, polarization and extinction shapes 0-66519 interstellar lines, new, 200 to 500 MHz 0-69414 interstellar silicates and 'ices', absorpt. low temp. 0-66520 iris photometer readings reduction to stellar magnitudes, computer programmes 0-41623 Lacerta OB1, ratio of K to A stars, objective-prism survey 0-79645 late-type K and M, H₂O and TiO bands rel. to spectral class, 7900-12000 A 0-41678

A 0-41678 line formation by noncoherent scatt., an invariant imbedding approach

0-48406
Lyman-alpha absorpt., interstellar, OAO-A2 obs. 0-66517
MHα 328-116, spectral evolution, 1965-67 0-63051
MK and MtW spectral-luminosity classifications comparison 0-41658
MWC 84, line identifications, emission line intensities and energy distrib, in continuous spectrum 0-45276
M giants, 6900-11000 Å 0-41666
M supergiants in the Perseus arm, radial vels. from i.r. spectra 0-45263
main-sequence, Ca emission intensities as age indicators 0-54382
Nandy's interstellar extinction laws, kink at 4300 Å 0-57033
non-L.T.E. analysis of lines 0-79657
Novae Delphini, H.R. Del, in first two months following discovery 0-66481

Novae De 0-6648!

O-66481

OB stars, southern, emission line profiles o-45291
Os stars, southern, emission line profiles 0-45291
Os stars, apid spectral variations, obs. 0-45291
Os stars, rapid spectral variations, obs. 0-63026
Oracity calc. allowing for light absorpt. in spectral lines 0-72720
PKS 0237-23, line-shifts in absorption spectrum 0-63077
P Cygni, and brightness, vars. 0-63028
P Cygni vars., obs. 0-63029
P Cygni line profiles emission, absorption components separation, rectification procedure 0-57036
peculiar emission-line stars, southern, 24, observational data 0-45274
Persei cluster, \(\chi a\text{dh}\) f, four-colour and H\(\beta\) photometry, obs. 0-69404
Perseus OB1 association, study of constituent supergiants 0-45263
uvby\(\beta\) photometric system, line-blanketing effects on indices for \(\beta\) Pegasi, 50 Andromedae, HD19445 0-41667
Population I main sequence stars, singlet-triplet anomaly of neutral He lines 0-45285
pulsars, power spectra of intensity fluctuations, 378 MHz 0-66554

pulsars, power spectra of intensity fluctuations, 378 MHz 0-66554 radiative transfer for spectral line formed in multidimen, atmosphere 0-51675

0-51675

red shift, gravitational of O stars 0-48428
reflection, curves of growth in plane-parallel atmosphere 0-51674
S stars, reproduction of spectra in the blue region 0-48466
Sco X-1, optical photometry and charact, variation 0-57079
Sirius, 1 to 4 micron 0-66468
Sirius components magnitude difference, relative photographic positions, tech. development 0-69405
sky-suppressing, automatic trailing device 0-41670
spectral line formation in Wolf-Rayet envelopes, escape probability method 0-59707
spectral line width, effect of uniform rotation in pole-on case 0-76575
symbiotic stars, vars, and model 0-63050

spectral line width, effect of uniform rotation in pole-on case 9-76575 symbiotic stars, vars. and model 0-63050 theory, book 0-7966!

U Cephei, hydrogen-line emission 0-41675 near u.v., comparison between expt. results and stellar atmosphere models 0-57032 variables, Ag and HR Carinae 0-62995 variables, B and Be, photoelec. line scanning obs. 0-63027 variables, OF and Be, rapid spectral vars., obs. 0-63026 variables, long period, comparison stars, photoelectric observations 0-51682 variables, young, contracting 0-6301!

Von Zeipel 1128 bright O star in globular cluster M3, analysis 0-57042 W3, (OH), 3.8 cm spectrum, low-noise search, lab. meas. 0-69387 wavelength determination using electronic figure computer 0-57157 lota Coronae Borealis, equivalent widths element by element 0-76577 Wolf 359 cool dwarf, 6900-11000Å 0-41666 Wolf-Rayet, planetary nebula excitation, HVB 475 spectroscopic obs. 0-59686

Wolf-Rayet, planetary nebula excitation, HVB 4/7 spectroscopic obs 0-59686
Wolf-Rayet, spectroscopic characts, and diagnostic processes 0-41644
Wolf-Rayet, survey of spectroscopic features 0-41679
Z Cam, light standstill obs. 0-63061
Arcturus, CO bands, anal. of equivalent width obs. 0-51676
Be and B, Balmer lines, first three, equiv. widths 0-6469
C_z, Phillips system, new molecular consts. 0-43090

Stars continued spectra continued

CN bands, i.r., identified in several carbon stars 0-51677 CO bands in Arcturus, anal. of equivalent width obs. 0-51676 Ca emission intensities of 325 main- sequence stars as age indicators 0-54382

Fe I excitation temps. in A stars and systematic errors in gf-scale 0-57039

Fe I λ 6495 line in 225 G and K stars, photoelectric meas.

H₂, interstellar, obs., from vibr.rot. emission lines 0—45304 H₂, interstellar, obs., from vibr.rot. emission lines 0—45304 He lines and the He anomaly in hot stars 0—41683 He neutral lines, formation problems in early type stars 0—79658 M31, emission lines, in nuclear region 0—66471 Na lines, interstellar, in specta of 9 stars in galactic centre direction 0—48435

0—48435
O- and Of-type, central stars of planetary nebula 0—66472
O, expt. transition probabilities for some lines of stellar interest 0—52922
OH, H₂O and H₂CO microwave lines, near i.r. stars, i.r. pumping and shock waves 0—66465
OH emission, interstellar, polarization 0—41726
OH emission from i.r. stars, search at 1612 MHz 0—45279
iiiOH absorption in Sgr A and Sgr B2, obs. at 1637 and 1639 MHz 0—79659

Si II intensity variations in the Ap stars CU Vir and 56 Ari 0-45258 structure

structure

\$\textit{B}\$ Cephei phenomenon due to semiconvective zone within star 0-51671 RLep, long-period variable, rel. to CN rot. lines doubling 0-41693 atmosphere models, non-LTE, including bound-bound transitions, multi-line computations 0-51651 atmospheres, T_e depend, on quantity versus quality of radiation field 0-54372

0-54372
binaries, close, effect of rotation and tidal interaction, double-approx. method 0-41721
binaries W UMa type system using Lucy model 0-59723
binary contact and close, polytropic models constructed using Laplace approx., perturbation tech. 0-51697
binary systems, close, rapidly rotating, polytropic theory 0-45303
binary systems, rapidly rotating, close, polytropic theory 0-57057
classical Cepheids, hydrodynamic model and hydrostatic constant flux atmospheres 0-54363
cool stars, atmospheric structure with and without graphite-particle opacity 0-79648
cool stars, atmospheric structure with and without graphite-particle opacity 0-79648
cool stars, atmospheric structure with and without graphite-particle opacity 0-79648
degenerate stars, model atmosphere computation 0-57028

ity 0-79648
degenerate stars, model atmosphere computation 0-57028
dipole magnetosphere, possible emission of cosmic rays 0-62972
envelopes, instability due to radiation pressure 0-51652
HR2142, shell ejection, obs. 0-41639
life history of stars, book 0-45257
low mass, evolution, pre-main sequence and main sequence models
0-76568

0—76568
neutron, crustal strength and shape rel. to pulsar wobble 0—41638
O and early B stars, non LTE multi-line hydrogen-helium model atmospheres cales. 0—48416
Persei cluster, χ and h, four-colour and Hβ photometry, obs. 0—69404
pressure rel. to envelope instability 0—51652
pulsars, neutron and white dwarf models 0—41733
rotation, and viscous fluid rot. about fixed axis 0—39491
spherical atmospheres, radiative transfer and gas dynamic motions
0—54361

static, long-period variable, static-model calculations 0-59710 supermassive, and formation by non-elastic evolution of stellar system 0-45268

0-45.208 variables, long period, static model calc. 0-59710 white dwarfs, atmospheric boundaries of convection zones 0-72709 white dwarfs rapidly rotating, second- order perturbation analysis 0-57024

Wolf-Rayet, summary of current problems, ideas and conclusions 0-41633 Wolf-Rayet atmosphere model 0-41644

Stars (nuclear) see Particle track visualisation

Stars (nuclear) see Particle track visualisation

Statistical analysis

see also Measurement/errors; Probability; Random processes
counting statistics, student experiment 0-66859
e.m. wave propag, in turbulent medium, optical method 0-42124
of errors in gravimetrically computed vertical deflections 0-76299

histogram storing on magnetic discs using pulse height analysis systems 0-55089

0-5089 international scientific meetings, participation 0-57229
Lagrangian time correlations comparison from dispersion experiments and space-time correlation functions 0-39502
Liouville's eqn., characteristic function derivation 0-76839
Markoffian master eqn., exact, derivation and comparison with non-Markoffian type 0-45539
mathematical statistics, textbook 0-52001
Monte Carlo calc. of NaI crystals' energy response to gamma-radiation 0-57849
Monte Carlo calculations of lifetime of heavy hyperfragments 0-67498

0-57849

Monte Carlo calculations of lifetime of heavy hyperfragments 0-67498

Monte-Carlo thermodynamic properties, comparison with lattice dynamics and cell-model approx. 0-75402

noise level in large offices, acceptibility criteria 0-42082

PAPA device, pattern classification 0-67163

point stochastic series, spectral anal., theory, computation and appl.

0-72986

Poisson distrib., rel. between average and most probable value 0-41982 polynomial and time invariant systems, identification from higher order spectra 0-72939

probability distribution functions, one-dimensional, or random processes, error in meas. 0–38218 radiative transfer, in cylindrical medium, Monte Carlo simulation 0–38216

uncertainty in Doppler

0-38216
random sampling procedure and statistical uncertainty in Dopple coefficient calculation for fast reactors 0-64158
regression, third degree, expts., optimal design 0-42014
spectra and cross-spectra estimation with fast Fourier transform algorithm 0-72983

spectra of perturbed semigroups 0–52824 transport process model 0–76842 transport process model 0–76843 trend surface and spatial correl., report 0–79468

Statistical analysis continued

upper atmospheric turbulent velocity distributions 0-41513

applications

ee also Counters/statistical analysis

p-ray low energy, applic. of gas Cerenkov detector, detectors efficiency, angular response 0-46035

P-ray scintilation spectra, multiple linear regression analysis, automatic candidate selection 0-46158
p-ray scintillation spectra, multiple linear regression analysis 0-46157
p-rays flux-to-dose rate conversion, Monte Carlo method applic. 0-45876 acoustic backscattering, near 28 kHz 0-54720

acoustic backscattering, near 28 kHz 0-54720 acoustic field's statistical moments in randomly inhomogeneous medium, parabolic eqn., local method 0-45562 acoustic mode in ideal elastic fluid, sampling statistics 0-39529 adsorbed layer ordering, Monte-Carlo treatment, LEED 0-65098 atmospheric turbulent kinetic energy from wave-number frequency Fourier analysis of velocity distributions 0-41499 biology, microphysical model 0-6668! boundary layer turbulent, large-scale motion in intermittent region sampling measuring tech. 0-49968 brittle bodies, micro-non-homogeneous, size effect, probability analysis 0-4378!

0–43781
clipped Dimus arrays output in Gaussian noise plus signal field, mean, variance, asymptotic expressions 0–57402
comets long-period during 1800-1970, total energy changes 0–41807
computer studies of particle dynamics in condensed matter 0–45346
correlation function methods, light scattering, by concentrated solutions of poly-p-benzyl-L-glutamate 0–71353
correlation methods in nuclear physics 0–57844
detailed balancing for derivation of distrib. functions 0–41992
distribution function of degenerate hot electrons 0–50929
energy distribution function, electrons in nonuniform positive column
0–46769

o-46769 error analysis, disappearing filament pyrometer 0–38420 errors, systematic, statistical model 0–41930 error systematic, statistical model 0–41930 errors systematic at lines intersection of aeromagnetic survey data, statistical estimation 0–51593 excluded-volume problem, distribution function 0–64565 ferrite polycryst, media characterization 0–65949 fracture, brittle, probability models 0–40402 gamma-ray spectra, polyenergetic, variance-covariance calcs. 0–5794! gravitational fields separation correlation tech, applic. 0–51494 Ising model two-dimensional 0–69633 isokinetic temperature determ., using method of least squares 0–6279! Lagrange factor for subst. under high pressure 0–63353 least squares fitting of data to pseudolinear relationships 0–45560 light scattering, by concentrated solutions of poly-γ-benzyl-L-glutamate, correlation function methods 0–71353 liquid structure factor S(k) and velocity autocorrelation function ψ(t) computation, Monte Carlo and molecular dynamics technique 0–50196 magnetic tapes, Preisach-representation and statistical instability 0–42186 material strength, composites 0–58914

magnetic tapes, Presacia- representation and statistical instability 0–42186 material strength, composites 0–58914 maximum likelihood, electron motion in inhomogeneous magnetic field, parameters determination 0–42187 mean-square responses in structural systems subject to white noise excitation, theoretical computation 0–57365 metal powder combustion parameters 0–41424 meteorology, stochastic dynamic prediction 0–41488 model of traffic noise in city and motor ways 0–48856 molecular conductance from curved surface through cylindrical hole, Monte Carlo calc. 0–58373 Monte Carlo calc. of GaAs transport props, temp, depend. 0–68822 Monte Carlo calc. of magnetization 0–79151 Monte Carlo calc. of thermodynamics of electrolyte solutions 0–53320 Monte Carlo determ, of GaAs electron transport props. 0–72061 Monte Carlo evaluation of Feynman path integrals in imaginary time and spherical polar coords. 0–38173 Monte Carlo method, neutron transmission through polycrystalline filters 0–58037 Monte Carlo method, test on fast simulation of Ising lattice 0–51966

Monte Carlo method, test on fast simulation of Ising lattice 0-51966 Monte Carlo method applic. to γ radiation transport, efficiency improvement 0-72979 Monte Carlo method applic to grand canonical ensemble of real gas

Monte Carlo method applic, to grand canonical ensemble of real gas 0–38201

Monte Carlo method for generating peripheral events 0–38612

Monte Carlo method for geometrical perturbation and applic, to pulsed fast reactor 0–74054

Monte Carlo method for radiative heat transfer calcs. 0–69752

Monte Carlo methods, rel. to calc, of plane electron beam in intersecting fields 0–73170

Monte Carlo percolation-probability 0–72950

Monte Carlo simulation, biological neutron radiography 0–72811

Monte-Carlo, ordering of adsorbed layers, LEED 0–65098

Monte-Carlo calcs., molecular orientation freedom in crystals 0–71808

noise attenuation in suppressors of complex configuration, statistical method for calc. 0–48858

nuclear motions, collective coords, formalism 0–38792

observations random component non-Gaussian distrib expt. data analysis 0–51480

orbital plane of satellite determining 0–69341

U→3:480 orbital plane of satellite determining 0–69341 particle size distrib. transform, sample-size induced errors 0–71783 particle systems, probability theory 0–50799 particles, small, coercivity size depend. 0–72161 photomultiplier, high gain dynode, statistics and timing of first photoelectron 0–62472

photomultipliers and electron multipliers, edge effect 0–57497 polymer rheological eqns. interpret. 0–40210 prediction theory, seismic data processing 0–48228 properties of image intensity, analysis from noise signal in electrical model 0–42354

0-42534 radial velocities in Galactic anticentre region 0-56926 radiation, error estimates for variational methods applicable to approx. solns. 0-48691

radioastronomy, discrete source intensity meas. 0-66675 radiography, fast neutron, Monte Carlo calculation of theoretical modulation transfer functions 0-72813

Statistical analysis continued applications continued

stochastically distributed, decay, closure stochastic soln. reactants 0 - 45051

reactor, nuclear, Dragon dynamic response meas, and optimum parameter fitting (Apr. 1969) 0-42903

resonance forces in four-body ion-molecule reactions 0-64592

scattering, error estimates for variational methods applicable to approx. solns. 0-4869!

scattering matrices in strong coupling 0-55389

service load distribution simulation, use of stationary, non-Gaussian random time histories 0-54591 shock waves structure in gas, Monte Carlo simulation method 0-39662

signal multimodal detection, statistical and probabilistic addition models 0-45466

0-45466
since waves having random phases and amplitudes, probability density approx. 0-60029
sound propagation in ocean, statistics of transmission fluctuation, theoretical study 0-62884
sound radiators system, field, influence of phase scatter and amplitude 0-45627
sound velocity in seawater, random components 0-54710
spectral line shape, stochastic theory 0-55215
spectrometry, nuclear multichannel, peak parameter determination as function of channel width, errors 0-42633
stars, variable, non-periodic phenomena meas. 0-63008
stochastic theory of chem. kinetics 0-62790
strength minimum of spot welded joints in thin walled structures of high strength alloys, determination 0-58912
thermal network models, digital, errors estimation and elimination

thermal network models, digital, errors estimation and elimination 0-45680

thermodynamic non-negative interactions, bounds, successive approximations and limits for distribution functions and phase transitions 0–57292 transistors, diffused junction, design and fabrication 0–65755 turbulence, fully developed, new approach 0–55436 turbulent shear flow, simplification of the direct interaction equations 0–39523

vapour deposition on two-dimensional lattices, computer simulation 0-39922

0–39922 variational methods applicable for approx solns., error estimates 0–48691 wave scattering parameter, probability distrib. functions 0–38155 weighted residual methods, space-dependent reactor dynamics 0–64161 wind velocity time fluctuations near sea surface 0–5672 X-ray diffraction intensities, systematic error 0–58694 Ge(Li), sum-coincidence mode, Monte Carlo analysis 0–60685 KCl, M centre formation and destruction 0–40186 Ra, comparison of four national standards, statistical analysis 0–57842

Statistical mechanics

see also Lattices, theory and statistics; Quantum fluids
alloy, binary one-dimens., with Heisenberg interactions 0-57284
back with deductive structure suitable for undergraduates 0-45545
Boltzmann's H function, successive time derivatives 0-57289
Boltzmann eqn. for Lorentz model, exact and Chapman-Enskog solns.

Boltzmann eqn. for Lorentz model, exact and Chapman-Enskog solns. 0-39496
Born-Yvon-Green and Kirkwood hierarchies in equilibrium 0-61207
Brillouin-Wigner expansion for ground state energy at finite temperature, partition function 0-48764
chain molecule dynamics, stochastic model 0-67828
classical, superstable interactions for particles in v dimensions, correlation functions and density functions 0-59936
classical fluid dense, collective and single-particle effects in autocorrelation functions 0-71074
classical lattice gas, thermodynamic equilibrium states, equivalence of different definitions 0-59924
conjecture by Dyson for distribution of energy levels, short proof

conjecture by Dyson for distribution of energy levels, short proof 0.48746

0 48/46 correlation functions, asymptotic time behaviour 0-76858 correlation functions, reduced 0-51974 correlation functions of weakly relativistic systems, Gibbs ensemble, chains of eqns. 0-41997 correlation length, finite, without 3-body collisions, physical basis 0.38205 0 - 38205

crystal ordering impossibility in 1- and 2-dimens. systems

0–38205
crystal ordering impossibility in 1- and 2-dimens, systems 0–59933
Darwin-Fowler method and geometric programming 0–63358
density matrix, nonequilibrium, inclusion of interactions 0–69641
dynamical critical phenomena, critical slowing down characts. 0–51984
dynamical scaling, sum rules 0–59935
dynamical scaling concept 0–59934
dynamical scaling concept 0–59934
dynamical scaling concept 0–59934
dynamics of classical hindered rotator 0–57286
electronic props. of disordered systems by tight-binding method 0–59931
elementary, university level book 0–54609
equilibrium, information theory 0–41991
equilibrium ensembles, asymptotic equivalence at thermodynamic limit,
Laplace transforms 0–48750
error bounds and spectral densities 0–51960
evolution of reduced distribution functions 0–42009
evolution of reduced distribution functions 0–42009
evolution of reduced distribution functions 0–42008
Fermi-Dirac statistics, elementary explanation 0–76846
flow field turbulent chemically reacting with uniform velocity gradient, statistical theory 0–39701
fluctuation kinetics and coeff. determ. 0–45544
fluid mixtures, Ornstein-Zernike relation and Percus-Yevick approximation 0–43214
Fock space, creation and annihilation operators 0–66839
Fourier transform of density-density correlation function expressed as function of 43214
Fock space, creation and annihilation operators 0–66839
Fourier transform of density-density correlation function expressed as function of specific particle distribution 0–41993
functional integrals 0–41981
gas-liquid interface, dynamics near critical point 0–71404
gas/liquid two phase flow, pulsation phenomena 0–49976
Gibbs method for calc. of trajectory probabilities of Brownian particle 0–76844
hard spheres, dynamical theorems 0–71056

0—76844
hard spheres, dynamical theorems 0—71056
hard spheres, momentum moments of one-body function 0—42009
hard-sphere model for self-diffusion in liq. metals 0—53327
hard-square solids at high densities 0—65113
Heisenberg, finite model, thermodynamic props. calc. 0—40960
Heisenberg model, finite 0—4554!

Statistical mechanics continued

ideal gas of 2-atom molecules having dipoles with constant electric and magnetic moments and in parallel electric and magnetic fields 0-53266 indistinguishability of identical particles, entropy 0-48743

magnetic moments and in parallel electric and magnetic fields 0–53266 indistinguishability of identical particles, entropy 0–48743 information theory foundation independent of use of ensembles 0–38202 interstitial pairs, M3+-F-, in fluorite-type lattice, Maxwell- Boltzman distrib. 0–50573 irreversible processes, extremum principles 0–72958 Ising model, one-dimens., scaling theory 0–54593 Ising model, singularities 0–54594 Ising model, singularities 0–54594 Ising model with perpendicular field, order parameter and ground state energy 0–69627 Ising system, random, mol.-field theory in external mag. field 0–40966 Jacobi coordinates for identical particle systems 0–57296 kinetics, statistical, relaxed motion 0–54587 Kondo model, scaling theory, qualitatively correct soln, and one-dimens. statistical models 0–72204 lattice gas, mag., one-dimensional, diffuse phase transition 0–57284 lattice gas, zeros of grand partition function 0–69630 lattice systems, classical, location of zeros of partition function 0–59927 many possible systems, boundary conditions 0–48757 many-body perturbation theory for non-orthogonalized basis 0–48759 Markov processes with interactions 0–54613 master equation, generalized for the time evolution of the reduced-density distribution function 0–48736 matter, many-body problem in classical and quantum forms, statistical basis 0–66843 Maxwell-Boltzmann distrib. of M³+-F- interstitial pairs in fluorite-type lattice 0–50573 memory function approach, equivalence to linear response theory, spin

Maxwell-Boltzmann distrib. of M³⁺-F- interstitial pairs in fluorite-type lattice 0–50573
memory function approach, equivalence to linear response theory, spin diffusion 0–51975
mixtures, perturbation calc. of eqn. of state 0–43213
mode expansion for classical equilibrium system 0–57288
momentum autocorrelation function of particle in one-dimensional box 0–63357

0-63357
monomer-dimer system, free energy for an arbitrary system 0-51969
multiparticle interaction, generating function 0-38208
non-Hamiltonian description from generalized transformation theory, relation between dynamics and statistical mechanics 0-54622
non-electrolyte solution, excess thermodynamic functions, hard sphere system, first-order perturbation 0-39775
non-equilibrium statistical operator and its applications to irreversible processes 0-51979
nonequilibrium, Green's functions and perturbation theory 0-51962
one-dimensional gas, Yang-Lee distrib. of zeros 0-69655
one-dimensional gas of particles, in the limit of vanishing external potential 0-69637
one-dimensional systems, time-dependent correlation, thermodynamic

one-dimensional systems, time-dependent correlation, thermodynamic

one-dimensional systems, time-dependent correlation, thermodynamic limit 0–72957
Onsager systems, microscopic and phenomenological effects 0–6684!
Onsanger systems, linear, phenomenological state variables, regression fluctuation theorems and phenomenological state variables 0–54607 order parameter fluctuations at critical pt. 0–48752
Ornstein-Zernicke systems, mean-field aspect 0–48751
oscillations, nonlinear systems, mean position under action of random perturbations 0–76840
pair correlation functions, moment method 0–48748
Green's paraparticles in unified theory of identical particles72963
0–72963
particle density matrices, integral equations 0–38209

0—72963
particle density matrices, integral equations 0—38209
particle identity entropy and Maxwell-Boltzmann counting 0—48744
path integrals, new series expansion for calculation 0—54608
perturbation theory, Bjorken limit breakdown in the 'gluon' model of strong interactions 0—60532
phase space of N classical particles with the equivalence class of points, derivations 0—57287
hase transition description using formalism of equilib statistical classical

derivations 0 – 57287
phase transition, description using formalism of equilib. statistical classical mechanics 0–38201
plasma, non-relativistic, nonlinear-cond. ternary correl. relations, transverse contrib. 0–78054
plasma in thermodynamic equil. in Debye approx. 0–43250
polymer crystals, folded-chain, with irregular fold surfaces, stability
0–71437

0-71437

pressure virial coeffs. for nonspherical hard-core molecules 0-43037
quantum fluids thermodyn. 0-76856
quantum mechanical particles with hard cores 0-38199
in quantum theory 0-51945
quasiparticle transformation theory 0-72960
radial distribution function, nonadditivity correction 0-64619
relativistic kinematics for N-particle scattering states 0-57249
repulsive interatomic potential calc. 0-77687
rigid sphere Longuet-Higgins-Widom model, applic. to melting of argon 0-46983
scaled particle theory for mythyres of head-

0-46983 scaled particle theory for mixtures of hard convex particles 0-41995 scaling hypothesis exhibiting asymmetry, variant 0-66837 single-occupancy systems of spheres, disks and rods 0-59930 spin correlation and entropy 0-48754 stable potentials and non-negative functions 0-51976 stochastic excitation, one class nonlinear system, analysis 0-48835 stochastic processes, collection of articles book 0-51959 stochastic signals, time behaviour 0-38206 stochastic theory with particular reference to the Langevin and master eqns. 0-54588 symmetry number in classical statistical mechanics 0-66835

symmetry number in classical statistical mechanics 0–66835 thermodynamic potential expression as stationary functional of occupation numbers 0–54598

numbers 0-54598 thermodynamics, progress in different fields 0-38203 Thirring's model, asymptotically exact solution 0-51980 Thomas-Fermi-Weizsacker eqn., March-Young plane wave variational density matrix derivation 0-72947 time correlation functions in binary gas mixture 0-78210 time translations in C* algebraic formulation 0-72959 turbulent systems, weakly, general kinetic eqn. 0-43323 van der Waals gas, one-dimensional with long but finite potential 0-72976 velocity autocorrel. function, long time behaviour 0-66849 weak-scaling theory, critical exponents derived 0-48753 H*-H collisions, classical 'charge-exchange probability theory and expt. 0-64280

Statistical mechanics continued

auantum

A transformation, greatly simplified, obtained 0–45554
atomic structure, one-, two- and many-electron problems 0–52871
atoms, electron impact ionization, threshold law calculation 0–55249
Bloch density matrix with inclusion of spin 0–41989
Boltzmann eqn., quantum mech., for gas with rot. states 0–39683
Bose gas, correlated basis functions 0–45552
Bose-Einstein photon noise statistics and Fermi electron statistics, continuity 0–57424
become fields with he marked interaction desired.

nuity U-5/424
boson fields with bounded interaction densities 0-51977
Brownian movement, dielectric constant 0-45540
coherence function, unimodular, and density matrix 0-73195
convolution approximation for the n-particle distribution function

cooperativity, phenomenological model 0–54604 crystal ordering impossibility in 1-dimens, quantum system 0–41998 density operator for oscillator syst., by generalized perturbation theory 0–54580

density operator for oscillator syst., by generalized perturbation theory 0-54580 detection and estimation theory, applications to signals in optical frequencies in presence of thermal radiation analysis 0-48756 differential conservation equations derived for the mass-, momentum- and energy-density operators for a 1-component simple fluid 0-67859 disjointness of the KMS states of different temperatures 0-38200 dispersion relations, double and spectral density functions 0-59932 e.m. fields, continuous space time dependent anal. by functionals 0-38430 electron detachment collisions of slow negative ions 0-77688 electron impact broadening, treatment of correlations 0-70788 electron impact broadening, treatment of correlations 0-70788 electron microscope, mirror, treatment 0-77036 electron mobility in randomly located hard-core scatterers, appl. of Kubo's theory 0-48766 embedding formalism of statistical basis for quantum theory 0-69615 equation of motion method in many-body systems, pairing, lifetime, and renormalization effects 0-38211 Euclidean symmetry breaking, critical point in liquid-solid phase transition 0-54600 flux equil, in systems far from thermal equil. 0-5188

0–54600 flux equil. in systems far from thermal equil. 0–51988 Fokker-Planck eqn. derivation for Brownian particle motion 0–72953 gas, fully ionized, multicomponents, theory 0–78154 gas-surface scattering, cubes model 0–71443 Gibbs' inequalities, unified, presentation, generalizations 0–48745 Green's function, classical, for the ideal gas 0–51985 Hartree-Fock theory applied to Lee-Yang theory 0–45554 hydrodynamic model 0–57293 inertial potentials 0–54602 intermediate statistics 0–69636 irreversible processes, continuously representable correl. functions 0–38204

0 - 38204

Ising syst., rectangular, effect of impurity configurations on critical temp. 0-69632

kinetic eqn., effect of initial correlation 0–76848 Kramers-Fokker-Planck equation by non-equilibrium statistical operator 0–66838

0-66338
Liouville's eqn., anal. of perturbation series 0-76845
Liouville energy eigenvalue problem 0-76854
Liouville eqn. for XY model 0-76852
many-body problem, linked cluster expansion theorem, proof 0-57295
many-body problems 0-48742
many-body systems, pairing, lifetime, and renormalization effects, eqn. of
motion method 0-3821!

Markovian processes in Englishean space, and a mestingth of Schrodinger.

motion method 0—382.11 Markovian processes in Euclidean space and e.m. struct. of Schrodinger eqns. 0—63355 maser model, exact analysis 0—42244 master equation, expansion, with applications to coupled atom-radiation systems 0—57290 molecular quantum mechanics, constrained variation method 0—43066 n.q.r., line saturation theory 0—41395 non-Markovian irreversible behaviour in simple model 0—63359 nonadiabatic transitions, multi-term system 0—69635 nonlinear theory of thermal fluctuations, contrib. 0—48755 one-dimensional quantum mechanics, integral eqn. formulation 0—72954 paraparticles, first- and second-quantized theories, correspondence 0—48749 parastatistics, physical content of a para-Fermi field theory, alternatives to

0-48749,
parastatistics, physical content of a para-Fermi field theory, alternatives to Bose or Fermi statistics 0-63356
polymer, cross linkage problem, dense cross linked system, method of second quantization 0-48196
polymer, cross linkage problem, method of second quantization 0-48194
pressure continuity as a function of the density for Boltzmann particles and bosons at low density 0-51990
propositions, validity 0-69634
quantum probability, operational approach 0-51978
RRKM unimolecular rate theory, centrifugal factor 0-46628
relativistic form of statistical thermodynamics, formalism using 'sums over states' 0-66836
spin diffusion coeff. calcs. 0-45543
stochastic processes, quantum, importance of Markovian, to quantum and quantum field theory 0-48740
temporal evolution, equilibrium of noninteracting quantum particles 0-76850
temporal evolution, equilibrium of quantum particle in suddenly expanded

temporal evolution, equilibrium of quantum particle in suddenly expanded box 0–76849 tetradics formulation of two-time Green's function method, Heisenberg ferromagnet 0–51982 theory of electron diffraction pattern modulation by laser interaction 0–44779

0-44779
Thomas-Fermi theory, proof of Hellmann-Feynman theorem 0-69654
three-particle system, trace eqn. 0-45551
unbounded local observables for C* algebra 0-54601
second virial coefficient, quantum corrections, applic. to hard-core-plussquare-well potential at high temperatures 0-45542
virial coefficients, low temp. behaviour 0-69643
Wigner-Weisskopf atom, relaxation in one-dimensional radiation field
0-38184
XY model, Liouville eqn. 0-76852
fistical thermodynamics. see Statistical mechanics

Statistical thermodynamics see Statistical mechanics

Steady-state theory see Cosmology Steam

bubbles in water, collapse 0-46862

Steam continued

condensation in subcooled liquid, exptl. investigation 0-71420 condensation on a rotating vertical cylinder, heat transfer coeffs. 0-46994 condensation on curved surface 0-78338

equations of state, characteristics calc. by thermodynamic consistency 0–74720

0-74720 silica-steam system, thermodynamic properties, rel.to nuclear cratering and cavity formation 0-76248 steam-water mixture, pressure pulse model rel. to critical flow and sonic velocity 0-39696 superheated, heat take-up in tubes and annular channels 0-69753 thermal conductivity meas, at atm. press., 100-700°C 0-43397 viscosity at high temperature and high pressure 0-50208 water-steam mixtures flowing in heated channel, density transients 0-39222

Steel

17-4PH and 15-5PH, microstructure and ductility 0-40330
α-γ transformation process, effect of original condition of steel 0-75332
A302-B, A533, A543, effect of neutron irradiation at 288°C and 393°C
obs., rel. to fracture-safe nuclear reactor design 0-49716
AFC 77, deform, voids in refining austenite grain size and improve mech.

AISI 1045, fractured under high pressures, natural strain rel. to hardness

AM 350 stainless, fatigue lifetime rel. to high-temp. outdoor exposure 0-50730

adhesion between surfaces of porous metal and mild steel 0-56053 ageing in Kh16N6 type, carbon content depend. 0-47445 antiferromagnetic order, long-range, in stainless non-mag. sample 0 - 51235

0-51235
austenite, tattice parameter, effect of alloying additions 0-58725
austenite, retained, X-ray diffr. determ. 0-40081
austenite, thermodynamics, statistical model 0-53641
austenite grain growth, effect of deformation voids 0-50816
austenite grain size refining using deform. voids 0-43813
austenite stabilization 0-40487
austenite, 18%Cr-9%Ni type, deformation-induced phase transformations, 600 to -190°C 0-68553
austenitic, C film. carburized, structure, zone cracking under load austenitic, C film, carburized, structure, zone cracking under load 0-40410

austenitic, C film, carburized, structure, zone cracking under load 0—40410
austenitic, Ni-Cr-Ti, reageing rate, reversion, precipitation 0—53632
austenitic, radiation induced high temp. embrittlement, cold working and recrystn. influence 0—40438
austenitic, recrystallization and precip. 0—58956
austenitic, total emissivity meas. 0—71879
austenitic NbC precip., stacking fault contrib. 0—58955
austenitic recep-resisting, welding technique 0—58978
austenitic stainless, ferrite, sigma phase and carbides precip. 0—40488
austenitic stainless, ferrite, sigma phase and carbides precip. 0—40488
austenitic stainless, prost-irrad, induced swelling and void form. 0—58802
austenitic stainless, substructure texture 0—71588
austenitic stainless, substructure texture 0—71588
austenitic stainless, substructure texture 0—71581
barifor reinforced concrete, bending tests 0—40366
bonding with rubber non-destructive testing by ultrasonics 0—45646
bonding with rubber non-destructive testing by ultrasonics 0—45646
bonding with rubber non-destructive testing by ultrasonics 0—45646
brittle fracture susceptibility 0—40275
temper brittleness, application of scanning electron microscopy, and microfractography 0—56007
brittleness at high temp, microstructural, mech. and theor. factors 0—62064

calcium aluminate inclusions, thermal expansion, rel. to tessellated stresses 0-59112

carbide formation during diffusional $y{ o}\alpha$ transform, in Mo-bearing steel 0-47480

0-47400 y-carbide phase, Fe₅C₂, formation, plastic deformation 0-53587 low carbon, core material for gradient magnet of proton synchrotron, magnand mechanical properties 0-57867 carbon, high strength, mechanical properties for marine applications

carbon, high strength, mechanical properties for marine applications 0-65468 low- carbon and titanium stabilized, yielding and plastic flow between ambient and liquid N temps. 0-47363 carburization of type 316L stainless, in static sodium 0-75331 carburized, stress factor determ. using X-ray two-exposure technique

carburized gear, impact fatigue resistance testing 0-43778 cementite phase, X-ray meas, of tensile residual stresses after plastic deform. 0-40280

cementite phase particles, diffusional coalescence, kinetics 0–50817 changes due to heat treatment, obs., thermal and electrical conductivity meas. 0–65449 cleanliness rating using ultrasonics 0–65441

coated with insulating layers, behaviour on stretching and bending 0-6203!

coil products, low-carbon hot-rolled, with low finishing and coiling temp., mechanical properties 0-65352 cold rolled elec. sheet with improved transverse mag. props., patent 0-5906!

composite, metal-matrix, interface region role in mech. behaviour 0-78638

composite, metal-matrix, interface region role in mechanical behaviour 0-75267

0—75267
cooling rate depend. on bar diameter, heat treatment, heat conduction theory 0—40439
corrosion by liquid Na., kinetics 0—41434
corrosion in magnox type reactors, problems arising 0—52843
Cr-Co-Mo-W-V alloy-type, comp., structure, hardness, patent 0—43834
crack growth rate in distilled water with loading 0—47410
crack propagation, corrosion-fatigue, obs. in new high-strength structural steels 0—40413
crack propagation, corrosion-fatigue in high strength steels 0—47409
creep tests, effect of different gas environments 0—47360
crystallization of low C, Al and Ca deoxidized steels 0—65443
cubic texture of transformer steel, structural prerequisites 0—61862
cyclic elastic-plastic deformation diagram, strength, carbon, high-temperature 0—40299
decarbonization in moist N₂-H₂O mixtures, of transformer steel 0—62188

decarbonization in moist N_2 - H_2O mixtures, of transformer steel 0-62148 decarbonization of transformer steel, in gaseous mixture of N_2 + H_2 , $800-850^{\circ}C$ 0-62083

```
Steel continued
```

deformation and fatigue, nonmetallic inclusions effects, obs. 0-65351 diffusion of H2, structure effects 0-5062!

diffusional $\gamma \rightarrow \alpha$ transformations, Nb_xC formation 0-50818

dislocations, effect on mag. props. of transformer-steel 0-62526 dissimilar, residual stresses in pipe joints 0-58884

ductile-to-brittle transition temperature, crack nucleation and growth

ductility, microstructure, and mech. strength in 17-4PH and 15-5PH sample 0-40330

ple 0–40330 ductility of 35G18, multiple $p \neq \epsilon$, $p \neq \epsilon'$ transforms, effect 0–40350 dynamic loading behaviour, data summary 0–47335 EN58J for surgical implants, tensile strength, corrosion fatigue characts, study 0–71757 eddy current phenomena in plates 0–56179 electrical resistivity, -196 to -100° C, in quenched 6% Re specimens 0–50986

0-50986
embritlement by hydrogen 0-68477
epoxide resin-stainless steel system, adhesion and internal stress 0-50677
eutectoid carbon, controlled rolling and cooling 0-65465
fatigue crack growth in maraging sample, fractographic obs. 0-58936
fatigue crack growth rates, temperature effects 0-56010
fatigue crack propag, low cycle fatigue testing 0-53620
fatigue crack propagagion anisotropy in hot rolled banded plate 0-56013
fatigue endurance, high strain, of 0.5% Mo steel, environment and hold time
effect 0-62019
fatigue fracture, initial stages, obs. by photoelastic coating technique
0-75285
fatigue fractures at high and low stress levels 0-50720

0-75285
fatigue fractures at high and low stress levels 0-50729
fatigue limits, rapid determination, u.s. oscillations applic. 0-47325
fatigue loading, stress conc. 0-75279
fatigue low cycle, in torsion, axial compression effects 0-47324
fatigue strength, sub-surface, En 40B 0-40381
fatigue tests of low carbon samples 0-62061
fault detection, utilizing Compton scatt. 80-400 kV 0-53527
fault detection using X-ray Compton scatt, 80-400 kV 0-53527
faritic, stress corrosion cracking, trans-granular 0-62070
fractography, scanning electron microscopy, yielding phenomena 0-68490

0-68490 fractography using scanning electron microscopy 0-71447 fracture, ductile, in stainless sample, continuum models 0-47403 fracture initiation in normalized and cold-worked mild steels 0-65422 fracture resistance, strengthening method effects 0-53606 fracture surface topography and toughness, AISI 4340 0-40367 fracture surface topography and toughness of AISI 4130 0-40283 fracture toughness and crack propagation, thickness depend. 0-40383 fracture toughness characts. of maraging steel welds 0-40412 fracture-safe design, coupling of fracture mech. and transition temp. 0-40411

0-40411

friction and wear, effects of surface treatments 0-7529!

Hadfield, hardness, effect of shock stress amplitude and duration, and Hugoniot eqn. of state 0–43794 hardened thermally low alloy, stress concentration zones failure, exptl. investigation 0–47391

hardening by precipitation, stainless steels with Co and Mo 0–53646 hardness, effect of shock stress amplitude and duration, and Hugoniot eqn. of state 0–43794 hardness indentation testing, recovered depth using interference methods

hardness inucritation (2016), 50 – 50745 high-C, elastic modulus and oscillation decrement temp. depend. 0–47313 high-Mn, O₂ cutting rel. to crack formation 0–58979 high-speed, structure examining, potential-polarization method applica-

high-Mn, O₂ cutting rel. to crack formation 0—58979 high-speed, structure examining, potential-polarization method application 0—6851! high-strength, failure-safe design rel. to stress-corrosion cracking 0—78654 high-strength, low alloy, stress corrosion resistance, Si effect 0—43791 high-strength, stress corrosion crack branching 0—43790 high-strength, stress corrosion crack branching 0—56002 hypereutectic, bainite structure formation mechanism 0—47479 hysteresis losses in rotating mag. field, effect of anneal 0—62521 impact fatigue resistance meas. apparatus, applic. to carburized gear steels 0—43778 internal stresses appuniform distrib. 0—40275

internal stresses nonuniform distrib. 0-40275

irradiation damage, ultrasonic nondestructive meas. 0–47566 joints, mechanically heterogeneous high-tensile, in uniaxial and biaxial tension, mechanical strength 0–58926 laminated core, thermal conductivity meas. using transient methods 0–68639

ilightly alloyed, cold working, obs. using constant temperature dilatometer obs. 0-68510 liquid, composition of non-metallic inclusions, reln. with interfacial tension

liquid, composition of non-metallic inclusions, reln. with interfacial tension 0–61480 low C, Cu-bearing, microstructure and mech. props. 0–58924 low C, fatigue slip-bands limit rel. to strain-ageing 0–68476 low alloy creep-resisting, precip. of CrN and (CrMo)₂C 0–58959 low alloy quenched and tempered, grain boundary segregation of impurities, and integranular brittle fracture 0–53614 low carbon, effect of local work hardening and ageing 0–58963 low carbon, varying Si content, effect of small deformation on recrystallization and texture 0–62082 low-alloy, high-strength, stress corrosion resistance, effect of Si 0–56001 low-carbon microcracks by slip deformation 0–50741 magnet, gradient of protons synchrotron, low carbon steel as core material.

low-carbon microcracks by slip deformation 0-50741 magnet, gradient of protons synchrotron, low carbon steel as core material, properties 0-57867 magnetic characts. improving by diffusion alloying, patent 0-69034 magnetic properties, meas. by a.c. bridge 0-62497 magnetic props. of E44 transformer steel, effect of anneal 0-62508 magnetization, stress induced 0-51206 maraging, (18wt.%)Ni, tensile and press-forming props. up to 300°C 0-58928

maraging, electron diffr. obs. 0–62108 maraging, fatugue crack growth, fractographic obs. 0–58936 maraging, welds, fracture toughness characts., ratio analysis diagram interpret. 0–40412

martensite, amorphous, formation in wires, obs. by friction testing 0-68552

martensite, dislocation/C interactions 0-40164 martensite, electron bombarded, C atom migration, ageing effect, X-ray diffr. 0-68337

martensite, liq. N temp., effect of plastic deform. on crystal struct., X-ray diffr. meas. 0-78474

Steel continued

martensite, low-C tempered, fracture rel. to microstructure 0-65423

martensite, nucleation as coherency-loss problem 0-75317 martensite, plastically deformed, C behaviour 0-62040

martensite, strain ageing by hydrostatic extrusion 0-53633 martensite, strain tempering, structural changes and strengthening

martensite, 0-71740

martensite, struct. defects effect on decomp. 0-62129 martensite crystallography theory, transformations, applications 0-40485 martensite embrittlement, tempered, and fracture toughness, SAE 4340 0-43780

martensitic structure study by electron microscope 0-61864 martensitic transform., crystallography and electron microscopic obs. 0-75325

martensitic transform. in maraging alloy, by internal friction meas. 0-62130

0-02300 martensitic transformation, dilatometric determ. of M, and M $_f$ 0-65491 martensitic transformation point study in steel with 18% Ni 0-78696 mechanical behaviour in Cu-contaminated Na of stainless, type 304 sample, 950-1300F 0-55996

950-1300F 0-55996 mechanical properties changes, Charpy-V and tensile specimen testing in Big Rock Point Reactor 0-49717 mechanical props. and phase composition, effects of heating and prolonged isothermal holding 0-59020 mechanical props. improvement of AFC 77 using deform. voids 0-43813 mechanical props. of 35G18, multiple γ=ε, γ=ε' transforms. effect 0-40350

mechanical strength behaviour, repeated non-elastic loading 0-4035! mechanical strength of austenitic steel at 1200 F in air, helium and sodium atm. 0-47376

atm. 0-4/3/0 microcracks surface, growth in fatigue 0-47397 microchardness in regions of continuous and discontinuous deposition of γ' -phase 0-50782 microscopic inhomogeneities obs. contact thermoelectric power meas.

0 - 68262

microsegregation, chem. and metallographic study 0-58977 microsegregation, crient and netanographic study 0–3597/ microsegregation, estimation by electron beam microanalyser 0–68305 microstructure and mech. props. in low C, Cu-bearing sample 0–58924 mild, behaviour under dynamic incremental shear loading 0–40259 mild, low yield pts., ferrite grain size depend. 0–53589 mild, plastic stress concentration factor, cyclic load, method comparison 0–43737

0-43737
mild, yield pt. 0-53588
moderation of U-metal spherical shell assembly, and critical mass irregularity 0-58055
molten, viscosity, non-metallic inclusions effects 0-64877
N36Kh12TYu, microhardness in regions of continuous and discontinuous deposition of y-phase 0-50782
non-magnetic, high strength age hardening type containing C, Mn, Cr, Ni and V; properties 0-55992
notched, mild, discontinuity in S/N curve, microstructure, plastic deformation, monotonic straining 0-40295
for nuclear reactor construction, 12Ni-5Cr-3Mo maraging, ductility and tensile properties changes obs. under neutron irradiation 0-50768
for nuclear reactor pressure vessel, testing in Big Rock Point Reactor 0-49715
oriented Si, simultaneous obs. of grain struct. and orientation 0-65239

oriented Si, simultaneous obs. of grain struct. and orientation 0-65239 oxidation of Cr-Al-Y ferritic steel, fission-fragment irrad. effect 0-66183 oxidation of stainless steel, high temp. behaviour, time lapse photomicrography obs. 0-76265 pearlite, flow stress and work hardening mechanism, microscopic obs. 0-65395

0-6395
pearlitic whiteband, strength and ductility, results 0-68467
plastic deformation by 10-8 sec. laser pulse 0-47354
plastic strain energy and low cycle fatigue strength 0-50717
plastic stress concentration factor, cyclic load, method comparison, mild 0-43737

0-43737
plates, exptl. buckling load determ. 0-50685
polycrystalline, plastically deformed, particle size and lattice distortion, radiographic determination 0-40461
precipitate form, carbonitride, in Nb-treated steel 0-40080
proportional limit and work hardening rate, AISI type 304 stainless sample, effect of N, 302F 0-43805
reactor cladding, corrosion rate in flowing Na 0-56705
rod and plate, notch strengths meas. 0-50716
SAE 1035, elastic-plastic deform. of hollow cylinder rel. to theories 0-40302
SAF 4340, elastic-plastic deform of hollow cylinder rel. to theories SAE 4340, elastic-plastic deform. of hollow cylinder rel. to theories

0-40302 SAE 4340 4340 controlled fatigue crack growth rates, temperature effects

0 - 56010

secondary recrystallization, effect of surface active impurities in annealing atm. 0-62087

secondary terrystanication, effect of surface active impulses a annualing atm. 0–62087 secondary structure formation under impulse loading 0–71802 for ships' hulls, temp, fields and thermal cycles during CO, welding, investigation 0–47430 spheres in random packings, optical machine for coordinates meas. 0–49131

0-49131 sputtering and electron emission under Hg ion bombardment, 15-100 keV 0-71883 stabilized 20 Cr/25 Ni/Nb austenite, high temp. ductility and fracture, effects of heat-treatment 0-43757 stainless, 304, 316, effect of fast flux irradiation on mechanical props. and

stainless, 304, 316, effect of fast flux irradiation on mechanical props. and dimensional stability 0–6853! stainless, 304, 316, irradiated and unirradiated, low cycle fatigue and short term tensile behaviour 0–6847! stainless, 304, N₂ physisorption, at 10-9 to 10-4 Torr 0–71491 stainless, 304, surface comp. analysis by inert gas ions backscatt. 0–5671? stainless, 304L, sputter deposited, microstructure obs. 0–71464 stainless, AISI 316, ion irrad, faults formed in assoc. with voids 0–47240 stainless, AISI type 304, proportional limit and work hardening rate, effect of N, 302F 0–43805 stainless, AIC composites, fracture, uniaxial yielding, substructure, stress state correlation 0–43787 stainless, Cr-Ni, engineering props., improvement by nitrogen addition 0–71712 stainless, austenitic, Mossbauer effect, antiferromag, transitions 0–72331

stainless, austenitic, Mossbauer effect, antiferromag, transitions 0-72331 stainless, austenitic, fast reactor irradiated growth mechanism of voids 0-53725

Steel continued

stainless, austenitic-Cr-Ni types, rel. to nuclear reactor pressure vessel, properties under environmental effects, radiation and corrosion discussion 0-49714

stonine 0-43714 stainless, carburization by Na 0-42915 stainless, carburization by liquid Na, rel. to grain size and work hardening 0-39242

stainless, coated with Teflon, pool boiling heat transfer 0-39888

stainless, corrosion by Na with 4 and 12 p.p.m. O, up to 760°C 0-41435 stainless, corrosion in flowing Na at high heat flux 0-41436

stainless, defect microstructures, shock-induced, mechanical properties correlation, electron microscopy 0-40079

stainless, deposited from bias sputtering, reduced Ni conc. 0-62834

stainless, diffusion of carbon 0-65341 stainless, ductile fracture, continuum models 0-47403

stainless, duchle tracture, continuum models 0–47403 stainless, elevated temp. irrad. effects 0–40560 stainless, ferrite sigma phase and carbides precip. 0–40489 stainless, in Na, mass transfer and wear tests 0–45065 stainless, irrad., void form. He effect 0–68347 stainless, irrad., void form. He effect 0–68347 stainless, low cycle fatigue in torsion 0–47395 stainless, oxidation, high temp. beahviour, time lapse photomicrography obs. 0–76265

stainless, sputtering and electron emission under Hg ion bombardment, 15-100 keV 0-71883 13-10-KeV 0-/1883 stainless, stress-cracking corrosion immunity, electrochemical technique 0-50742

0-30/42 stainless, thermal recovery, shock loaded, defect mechanism 0-40450 stainless, treatment for corrosion resistance and mech. strength, patent 0-47495

stainless, type 304, mech. behaviour in Cu-contaminated Na, 950-1300F 0-55996

stainless, type 316L, carburization in static sodium 0-75331 stainless 20 Cr/25 Ni austenitic cavity growth during creep, kinetics 0-43812

stainless austenitic, substructure texture 0-71588 stainless for nuclear reactors, Na effects on high-temp, creep behaviour 0 - 42913

stainless for nuclear reactors, high-temp. Na effects on creep and stress rupture 0-42914 stainless for nuclear reactors, high-temp. Na effects on mechanical props.

0 - 42912

stainless for nuclear reactors, fign-temp. Na effects on friedmandar props. 0–49212 stainless mass transfer and corrosion in liquid Na 0–39748 stainless mass transfer and corrosions in liquid Na 0–39748 stainless non-mag, long-range antiferromag, order 0–51235 steel, fatigue life, nonmetallic inclusions us. detection 0–40382 steel, stainless, ductility, pre-strain effect 0–78634 steel, stainless, mass transfer in liquid na loop 0–39749 steel-resin composite, fibre-matrix adhesive bond, press. effect 0–62118 strain and hardness in AISI 1045 sample, fractured under high pressures 0–47421 strength of 35C18, multiple y=e, y=e' transforms. effect 0–40350 stress analysis, X-ray methods, ret to strain dependence of lattice stress/strain relations 0–40270 stress corrosion crack branching in high-strength steels 0–56002 stress corrosion crack branching in high-strength steels 0–473790 stress corrosion crack branching in high-strength steels 0–47411 stress corrosion crack detection by internal friction meas. 0–47411 stress corrosion crack in the stress of lattice stress corrosion crack detection by internal friction meas. 0–47411 stress corrosion reack letter to the stress corrosion crack branching in high-strength sample, effect of Si 0–56001

0 - 5600!

stress corrosion resistance of low-alloy high-strength steels, Si effect 0-43791stress-strain and limiting strain, in stretching of low C anisotropic sheets $0\!-\!53578$

stress-strain curve, serrations and Portevin-Le Chatelier phenomenon in $18\%~\mathrm{Ni}$ steel ~0-65376

structural, high-strength, corrosion-fatigue crack propag, tests 0-40413 superheater tubes, microstructural changes after prolonged services 0-65236

surface with lubrication, exoelectronic emission 0-65864 tempering, programmed loading rel. to plastic deformation resist. 0-68445

0-68445
tensile props. rel. to resilience 0-75274
tensile testing, high-speed, using high explosives 0-40342
tension compression tests, uniaxial 0-55963
thermal conductivity of 400 stainless steels 0-47558
thermal state, transient, in solid construction elements, in strong e.m. field, analysis 0-62218
thick plates, eddy current obs. 0-56179
thin circular plates, bending analysis of unloading and inverse loading 0-55963
transformer. Fe 3% Si. X-rev. diffe. photography.

transformer, Fe 3% Si, X-ray diffr. photographs rapid graphical interpreta-tion 0-65210 transformer, Ni film covered, hysteresis loops form, elastic deform. effect

0 - 65927

0-03927 transformer, cold-rolled, loss ratio, effect of structural factors 0-62517 transformer, cryst., plastic deformation and recovery, effect on mag. props. and struct. 0-62518

transformer, decarbonization in gaseous mixture of N2,H2, 800-850°C 0-62083

transformer, decarbonization in moist N2-H2O mixtures

transformer, decarbonization in moist N₂-H₂O mixtures 0–62148 transformer, effect of dislocation on mag. props. 0–62526 transformer, effect of rolling on secondary crystall. 0–62100 transformer, effect of surface struct, on props. 0–61629 transformer, effect of temperature of secondary rolling on recryst, and deformation texture 0–62099 transformer, for h.f. machines, processing principles 0–62084 transformer, grain growth rate, orientation depend., secondary recrystallisation 0–50762

transformer, high-temp. annealing, effect on structure and mag. props. 0-62507

transformer, hot-rolled, causes of brittleness, by statistical method 0-62063

transformer, influence of cold-rolling on texture and mag. props. 0–61860 transformer, mag. losses, temp. depend. 0–47945 transformer, magnetic and struct. props. 0–62525 transformer, magnetic permeability, surface Ni film effect 0–51218 transformer, mark E44, effect of anneal on mag. props. 0–62508 transformer, new grades, production techniques 0–62081

transformer, primary recrystallization, stabilized matrix, influence of inclusions 0-62106

transformer, sheet, straightening annealing, effect on magnetic props. 0 - 62111

transformer, sheets, hot-rolled, study of residual stresses 0-62027 transformer, structural prerequisites for cubic texture 0-61862 transformer, structure formation as result of rolling and annealing 0-61962 u.s. attenuation rel. to austenitic grain growth, 1% C-steel 985-200°C

0-50867

unalloyed, transformer, effect of annealing on mag, props. 0-62509 VNS2 and VNS5 welding by electron beams after strengthening by heat treatment 0-43799

viscoelastic circular plates, impulsive loading 0–48814 welded, crack obs. using scanning electron microscopy 0–71723 welding, cold cracking, fracture, H₂-influence investigation 0–71721

welded, crack obs. using scanning electron microscopy 0—71723 welding, cold cracking, fracture, H₂-influence investigation 0—71721 welds, maraging, fracture toughness characts., ratio analysis diagram interpret. 0—40412 wetting by Na-Fe-silica glasses 0—53423 wire stainless steel reinforcement in Al sheet, tensile strength 0—71710 work hardening propag, under impact loads 0—62091 yielding and plastic flow between ambient and liquid N temps. of low carbon and itianium-stabilized steel 0—47363
Al fault detection, utilizing Compton scatt. 80-400 kV 0—53527
Ar ions injected into various minerals and steel, retention coefficients and thermal release profiles 0—65564
C-Mn, contact wear of Cu-Sn bronzes, obs. 0—50750
C, annealed, stress effect in fatigue strength behaviour 0—50718
C, cycle frequency rel. to fretting fatigue life 0—50648
C, service load and fatigue strength 0—50720
C annealed, crack propagation under impulsive load 0—50719
C content determination using direct reading spectrometer, single calibration curve 0—51445
C distribution, determ. by autoradiography 0—62107
Cr-Mn alloyed, brittleness after electroslag welding, reason 0—58932
Cr-Mo, tubular stress rupture testing in high pressure hydrogen 0—47390 (20wt.%)Cr-(25wt.%)Ni-(1wt.%)Nb austentic, NbC precip., stacking fault contrib.S8955 0—58955
Cr-Ni, austenitic, corrosion and passivation in H₂SO₄, effect of vacuum melting 0—76268
Cr-Ni, austenitic, determ. of low concs. of α-phase (ferromag.), effect of austenite (paramag.) 0—778697
38 CrMoV 21.14 steel, incomplete solutions of C. metallographic examination and contact thermal e.m.f. meas. 0—40458
Cr-Nii, austenitic, care propagation using orthonitrophenol solution 0—40462
Fe-(10wt.%)Al-(1.S0wt.%)C, martensite, twin and stacking faults, lattice structure, electron microscopy 0—75092
Fe-Mn auloys, martensitic transformations, elec. resist. temp. depend., —196-300°C 0—50985

0-11/24
Mn-Cr austenitic, non-magnetic, containing V; structural changes during tempering 0-56027
Mn, phase transformations during low temp. quenching 0-56059
0.5%Mo, high strain fatigue endurance, effect of environment and hold time 0-62019

time 0-62019

Ni-Co-C, strain tempering of bainite 0-40435

Ni-Co-Mo-Ti maraging, mechanical strength, effect of Duplex ageing treatments 0-43767

5Ni-Cr-Mo-V, fracture toughness by Charpy V-notch and dynamic tear tests 0-40373

Ni-Cr-Ti, austentitic, age hardening, reversion 0-53631

Ni coating, thermoelectric gauging 0-40434

(18wt.%)Ni maraging steel, tensile ductility and press-forming props. up to 300°C 0-58928

x10NiCrWTi36.15, precipitation behaviour, high temp. and stress hardening 0-40490

Re, phase transformations during low temp, quenching 0-56059

Si, mag, annealing effect on props. and domain struct. 0-65924

Stellar atmospheres see Stars Stellar clusters see Stars

Stellar composition see Stars/composition

Stellar evolution see Stars/evolution

Stellar motion see Celestial mechanics; Stars Stellar structure see Stars/structure

Stellarator see Plasma/devices Stereoisomerism see Isomerism

Stereophonic sound see Acoustics

Steroscopy see Vision

Stimulated emission see Lasers; Luminescence; Masers

Stimulated Raman scattering see Lasers; Scattering/light, Raman spectra
Stochastic processes see Probability; Random processes; Statistical anal-

Stokes flow see Flow; Hydrodynamics Stokes law, fluids see Flow; Viscosity Stokes law, optical see Luminescence

Stokes lines see Luminescence; Scattering/light, Raman spectra; Spectra/ molecules

Stopping power see Energy loss of particles

Storage devices

rage devices
ferroelectric-photoconductor, hologram storage 0–67112
gas chromatographic data storage and retrieval system 0–62825
high capacity holographic memory 0–54890
hologram storage in ferroelectric-photocond. device 0–67112
m.n.o.s. memory, direct-tunnelling mode, effect of SiO₂ thickness variation
(15 to 30Å) 0–51085
magnetic bubble technology 0–79118
magnetic domain bubble technique 0–72213
magneto-ptical, physical aspects 0–60370
memory diode using amorphous semicond. 0–53888
photomemory of surface-barrier junctions in CdTe 0–56318
sodalites, colour centres 0–61977
thermoplastic hologram write-read-erase optical memory array 0–60274

Storage devices continued

Co-P thin film, electroless plating for video tape recording 0-72248

Storage rings see Particle accelerators/accessories

Storms see Atmosphere/movements; Magnetic storms; Thunderstorms Strain effects see Deformation; Elastic deformation; Plastic deformation

electrical, use in reinforced concrete slbas 0-43728 electrical resistance pressure dependence 0-75542 evaluation with different cement combinations for long use at elevated temps. 0-43729 gauge factor evaluation with simple circuit giving digital read-out 0-41932

0-41932
length effect on dynamic measurement 0-41933
optical diffraction technique 0-54848
quartz-bar, meas. after underground nuclear explosion 0-41464
semiconductor films, InSb and GaSb, temp. depend. 0-53825
stress gauge, omnidirectional, design 0-60004
surface strain meas. by holographic interferometry 0-62025
telemetering system. simple short range type, for use with gauge, and appls. 0-38129
transient response due to incident stress-wave analysis, transducer design 0-52044

Strain hardening see Work hardening

Strange particles production $\pi^+ d$ interactions from 1.1 to 2.4 GeV/c 0-67280 production in channels of $\pi^- p$ reaction at 4.0 GeV/c 0-67292 κ meson mass rel. to parameters of K_D decay 0-67265 πp , 5.0 GeV/c, search for strange particle decays of Δ , N* 0-52563

Strangeness see Elementary particles; Field theory, quantum
Stratosphere see Atmosphere

Streamers see Discharges, electric

Strength see Electric strength; Mechanical strength

Stress analysis

see also Bending; Photoelasticity; Strain gauges; Torsion

arches, elastic-plastic, appl. of theory of finite deflections 0-54628

beam resting on elastic foundation, eigenfunction soln, for end problem

beam resume on classic foundation, organization, organization of the state of the s

brittle tensile specimens, fracture 0-75280 buckling, column, thick, stability theory 0-38255 buckling loads of axially compressed cylindrical shells subject to relaxed boundary conditions 0-57325

buckling of plate girder webs under partial edge loadings, influence of flange members 0-45582 buckling of radially constrained thin spherical shell under edge load 0-57313

buckling of thin cylindrical shells under uniform axial compression 0-63382

cantilever plate, bending 0-54646

0—63382
cantilever plate, bending 0—54646
cap, shallow spherical, collapse under partial load 0—45577
ceramic, structural, nuclear environment 0—43761
ceramics, crack- initiation under thermal stress test 0—62065
circular hole in conical shell with torsional loading analysis 0—63394
circular hole in thin plate, creep behaviour in vicinity 0—52040
in circular plate with ring of eccentric holes 0—54633
coefficient matrix of a cross-section of a vibrating curved and twisted non-prismatic space thin beam 0—59958
composite materials 0—50634
concrete frames, reinforced, relative variation of unit stress 0—45574
concrete pressure vessels, prestressed, ultimate pressure analysis of deep end slabs 0—52019
contact problem for elastic half-plane with semi-infinite elastic rod coupled to it 0—54640
contact problem for elastic infinite cone 0—54639
contact stresses in elastic half-plane with stiffened boundary 0—48808
crack at vertex of wedge, stress intensity factor at tip, closed soln. 0—38262
crack extension in linear viscoelasti body, distrib. anal. 0—48818
crack in elastic half-plane perp. to free surface 0—54648
crack in elastic half-plane perp. to free surface 0—54648
crack systems, two and three dimensional, strain energy, various loading conditions, calc. 0—40386
creep, calculation methods, study of single cases and use of computers in deriving solutions 0—54641
cyclic shear and normal on spherical shells, energy dissipation, method for investigation 0—45573
cylinder, anisotropic rotating, and cylindrical shell, dynamic response 0—57332

cylinder, anisotropic rotating, and cylindrical shell, dynamic response 0-57332

cylinder, elastic and semi-infinite, partially surrounded by moving sleeve 0-76880

cylinder, elastic-plastic deformation, creep strain, digital computer program 0-38308 cylinder, long circular, transversely isotropic material, co-axial cylindrical inclusion, symmetric deformation 0-57311

cylinder, transversely isotropic non-homogeneous, plane strain problems 0-57334

0-57334
cylindrical block, compressible dielectric, radial deformations 0-42031
cylindrical block, compressible dielectric, radial deformations 0-42031
cylindrical shell, buckling under longitudinal shear load 0-38251
cylindrical shell weakened by elliptic hole with major axis perpendicular to shell axis 0-69687
cylindrical shell with longitudinal rib reinforcements limit analysis 0-45572

in cylindrical shells with reinforced circular holes 0–63376 deformation, finite, plane curved beams under static loading, solution using rate equations 0–57330 deformations around spherical cavity in semi-infinite elastic body

deformations around spherical cavity in semi-infinite elastic body 0–63379 diagrid, uniform simply supported, lateral buckling 0–45564 dislocation pile up at cylindrical inclusion 0–40274 dynamic and static, propagating cracks expt., dynamic photoelasticity 0–47405

dynamic response of an infinite cylindrical shell reinforced with elastic rings and submerged in an acoustic medium 0-57341 dynamical stresses in members subjected impulsive loads 0-63381

Stress analysis continued

earthquakes, on ridges compared with trenches 0-59528

edge-cracked sheet, elasto-plastic strain distrib. 0-55962

edge-cracks, growth or dormancy, effect of a tensile mean stress on the alternating stress, for various materials 0-59963

effect of stress wave diffraction on stress meas, omnidirectional dynamic gauge 0-52044

elastic anisotropic body with exterior crack, stress distrib. 0-59979

elastic curvilinear inclusion problem, general form of soln. 0-76874 elastic expansion bellows 0-57322

elastic half-plane with variable Poisson's ratio, traction boundary problem 0-42038

elastic quarter plane, algorithmic solution 0-57350

elastic quarter plane, with circular inclusion 0-69685

elastic shell theory, bending equilib. eqns. under Kirchhoff-Love hypothesis 0-45579

elastic strain measurement, X_sray diffraction and line displacement 0-53475

elastic stresses in rotating anisotropic disks of variable thickness, annular and circularly mounted 0–63385 elastic torispherical drum heads, under internal pressure loading, computer survey 0–50670 elastic waves, interaction with penny-shaped crack in elastic medium 0.52070

elastic way

elastic-perfectly plastic stress problems, computerized relaxation method 0-47339

computer survey 0-50671 elastic plastic bar with moving point heat source, thermal stress field anal. 0-38317

0-3017 elastical continuum, harmonic and finite-element perturbation studies, comparison 0-3826! elastically different plastics, strain pattern in joined pair examination

0-47340

0-4/340 elasto-plasticly deformed flat strip, residual stresses 0-52009 elastoplastic analysis of plane-strain and axisymmetric flat punch indentation by finite-element method 0-59960 around elliptic hole symmetrically centred in long plate under uniform tension 0-76868 equatorial segment of a spherical shell, buckling under own weight

-38250

o-3220 extended stress bonded in rigid plates 0-57315 extended stress bonded in rigid plates 0-57315 extensometer, strain meas, for tensile creep testing machine 0-40322 fatigue, biaxial, tests with zero mean stresses using tubular specimens fatigue, bia

0-5384
fatigue cracks in metals, propagation theories 0-52017
fiber composites, unidirectional, shear loading in axial direction 0-50663
fibre reinforced composites, with imperfect bonding, stresses due to broken
fibres or cracks 0-38273

fibrous composites, stress and deflection analysis under external load $0\!-\!7532!$

6-1332.1 film/crystal interfacial strain, asymmetric diffr. use in X-ray topography 0-68206

finite element method described 0-52014 finite element method, static and dynamic analyses of complex shells 0-38246

0-38246
flawed structure design 0-65349
flexibility coeff. analysis, EIC Conf., Canada, Sep 1969 0-57347
flexibility coefficient method for indeterminate structure analysis 0-57348
fracture mechanics, plasticity corrections, graphical method 0-73002
fracture semiempirical analysis for small surface cracks 0-48791
fretting fatigue, component strength, finite element technique 0-40377
fuel rods, multispan, subjected to axial thrust, inelastic anal. of bowing
0-54635

glass, surface-compressed, stress-corrosion characts. in sea-water 0-51428

granular cohesionless mat, in bins 0–69670 graphite, artificial, elastic-plastic continuum theory for small deform. 0–43740

0-43740
half-space, effect of closely embedded fibre 0-48793
harmonic wave analysis in a longitudinally reciprocated bar, steady-state solution by Fourier analysis 0-60016
impulsively loaded, inelastic structures and continua, approximate solutions 0-57314

inclusion, axisymmetrical, subjected to uniform tension in an elastic solid, numerical method 0–63383 inclusion, spherical, inhomogeneous, on axis of circ. cylinder in torsion 0–66863

inclusion method, for materials with inaccurately known elastic moduli 0-50664

0-50664
incompressible elastic media, nonlinear stress- strain equations 0-38235
infinite plate with elastic rectangular inclusion 0-52010
influence coeffs., by assumed stress method 0-72999
internal loads acting on the members of a statically indeterminant mechanism 0-59967
isotropic body, limiting states, general theory 0-45566
Lame-Maxwell equations, generalization 0-42026
laser rod, composite, end-region, optical path length change 0-42291
loading of cantilevers, beams and frames, magnetomotive method 0-69661

0-9061 longitudinal impact of two thin viscoelastic rods stress and strain distribution 0-69697 lubricant film, combined compression and shear for two-dimens. deform. case 0-40427 macrostresses, residual, theoretical aspects for X-ray diffractometry

0-54644 mechanical and thermal, distribution in nozzle-to-flat plate connection,

mechanical and thermal, distribution in nozzle-to-flat plate connection, arbitrarily loaded 0–5066! membrane, elasto-plastic, motion under shock loading 0–45594 membrane stresses on non-spherical domes 0–57316 membrane with hole, in-place displacement measurement by holographic interferometry 0–69672 metal, annealed, surface residual stress, changes during fatigue 0–40261 metals and alloys, creep exam. 0–50698

Stress analysis continued

moire fringe method, plate, two circular holes, inclusions, equal size, pure torsion 0-40264

moire fringes in strain analysis, book 0-38242

Moire strain analysis of bent plates, in-plane 0-59962

moving cracks in finite strip under tearing action 0-76869 nondestructive testing using pulsed laser holography, tech. 0-63646

nonlocative two testing using pulsed laser nolography, tech. 0-63046 nonhomogeneous elastic media, axi-symmetric stress eqns. of motion, integration 0-57333 nonlinear, incremental complementary energy method 0-38239 nonlinear theory, geometrically, for elastic anisotropic sandwich-type plates 0-57317 nonlinear viticostestic collinear with obtains inner curfoce and faith

nonlinear theory, geometrically, for elastic anisotropic sandwich-type plates 0–57317
nonlinear viscoelastic cylinder with ablating inner surface, small finite deformation 0–57320
nonlinearity elastic bar, finite deflections 0–57337
optical, flexural waves in bar 0–71675
optical diffration-strain relations 0–54627
panel cylindrically curved with damped, elastic boundaries, eigenfrequency analysis, mathematical model 0–60019
photoelastic analysis and fringe multiplication instrument 0–57602
piezoelectric probes, high speed acoustic impedance matching, rel. to gas dynamics and plasma physics 0–46734
pipe bends, bounding and flexibility factors 0–52018
pipe bends, mitred, under in-plane bending 0–52022
plane stress, structural anal. using Legendre polynomial expansions, higher order theories 0–38268
plane-strain finite deformation in strain-rate sensitive elastic-plastic materials and shock thickness 0–57360
plastic laminates glass fibre reinforced, shear characteristics determination, method 0–47321
plate, bent, polygonal, boundary equil. eqns. 0–57319

method 0-4732! plate, bent, polygonal, boundary equil. eqns. 0-57319 plate, circular holes, inclusions, two, equal size, pure torsion, moire fringe method 0-40264 plate at buckling load, reactive forces at edges 0-69669 plate bending, using annular and circular sector finite elements 0-45567 plate containing circular hole with notch 0-63377 plate deflection, bi-harmonic eqn. soln. using polar finite-difference approx. 0-45581 plates, circular, variable thickness, elastic bending

plates, carected to plane stresses at infinity 0-63380 plates and shells under high-temp. external loading 0-45576 polymer, internal stress relax, elastomer introd. effect 0-40276 polymer melts, comparison of methods of making normal stress meas.

0-58411

0–58411
polymer solutions, laminar flow, stress relationships from symmetry conditions 0–55573
polymer solutions, shear and first normal stress difference 0–39704
polystyrene, concentrated solutions, normal and shear, under steady and oscillatory shear flow 0–55572
polytetrafluoroethylene, compression stress relax. processes 0–40282
pressure vessels, computer program for stress and strain calcs. 0–76890
reduction of stress conc. near circular cutouts in tension field without sheet reinforcement 0–42041
of reinforced circular holes in cylindrical shells 0–63376
rings and tubes, plastic and linear strain hardened, rate sensitivity 0–5931
rotating disk, acceleration stress 0–48784

rotating disk, acceleration stress 0-48784 rubber, styrene butadiene, experimental study of nonlinear viscoelasticity

0-5065

0-30031 Saint-Venant Principle for Neumann problem with non-thin two-dimensional domain 0-52033 Sanders-Koiter linear shell equations, simplification and reduction 0-76870

second-grade materials, singular stress concentrations 0–73013 seismic excitation on nuclear power plants structural behaviour dynamic analysis 0–52078 semi-infinite medium, dynamic press. on boundary, couple stress 0–76872 shallow shell finite element of triangular shape developed, application 0–52015

0-32015 shape strain determ, methods for deformation twinning 0-71681 shear, effect on nonlinear behavior of elastic bars 0-57343 shear, in laminar flow along flat plate 0-53123 shear, solid-liquid interface for climbing film flow in an annular duct 0-39744

shear, transverse, of asymmetric stiffened shell type structures, finite element method 0-54625 shear and first normal stress difference for polymer solutions 0-39704 shear loading, longitudinal, of unidirectional fiber-reinforced composites 0-57328

0-57328 shear pulse propagation parallel to the interfaces of a periodically laminated medium 0-57329 shear stress measurement at the exit of a burner port prior to computation by a mass transfer technique 0-66864 shell, circular cylindrical, supported along generator, subject to arbitrary forces 0-38275 shell, cylindrical, and anisotropic rotating cylinders, dynamic response 0-57332

0-57332
shell, shallow spherical, under eccentrically applied load 0-48795
shell, spherical, ring-stiffened, transient response to pressure increase in acoustic medium 0-48792
shell configurations to suppress bending and transverse shears 0-59966
shell of revolution, axially symmetric deforms., applic, to circular plate and membrane theory 0-38240
shells, cylindrical, normally intersecting, subjected to internal pressure 0-54637

0–5463/s shells, rotationally symmetric, numerical methods for limit anal. 0–59954 shells, shallow, by point matching method 0–73001 shells, shallow, relative variation of unit stress 0–45574 shells, stiffened, cylindrical, parametric instability 0–42039 shrinkage stresses, numerical determination for rectangular elastic plates 0–57326

o-37226 skew plates, simply supported, buckling 0-42040 in slab solidification, study of thermal stress and displacement distribs. 0-39878

0-39878
sols, anisotropic, yield criterion 0-50280
sphere restrained hyperelastic, stress distribution 0-42036
spheroical shell, crack-line imperfections, theoretical analysis 0-48790
spheroidal inclusions and cavities in a transversely isotropic material under
pure shear, stress concentration 0-57324

Stress analysis continued

spirally corrugated shell subjected to torsional deformation 0–63378 spit cylinder tension test for concrete 0–57349 steel, X-ray determinations rel. to strain dependence of lattice stress/strain relations 0–40270

steel, mild, plastic stress concentration factor, cyclic load, method comparison 0-43737

strain, remnant radial in half space containing isotropic source 0-59956 strain gauges, effect of cross-sensitivity on the determination of stress 0-54643

strain measurement, direct measure, by an extension of moire theory 0-57318

0-37318 stretch forming over hemispherical punch heads, theory 0-59957 stretching of a cylindrical membrane 0-57312 strip compressed oppositely with elastic flat punches, time-depend. var. of stress distrib. 0-42027

strip containing unsymmetrically located infinite row of circular holes 0-54629

0-346.29 structures during creep, reference stress concepts 0-68454 structures subject to broad freq. band, spatial variation of stress, strain, acceleration, theory, expt. 0-57370 symmetric U-shaped notches in tension strips, stress-conc. factors

tensile testing, high-speed, using high explosives 0-40342

tensile testing, high-speed, using high explosives 0–40342 tension bar, photoelastic comparison of stress cones, due to semicircular grooves and circular hole 0–38236 thermal, near prolate spheroidal inclusion 0–69700 thermal and pressure, rel. to nuclear reactor, cylindrical vessel, analytical determination 0–49699 thermo-elastic, in unrestrained rectangular plate subjected to known temperature distribution method, extension of Kantorovich method 0–63399 thermo-elastic strain in a composite shell, radical and shearing stresses 0–63402

thermoelasticity, infinite slab of an anisotropic material of constant finite thickness 0-60000 thermoelasticity, non-linear, stress relation from general theory of incompatible deformations of elastic media 0-38315

patible detormations of easier fields 0-38313 of nonconservative elastic continuous systems 0-45580 thermoplastics, long-term behaviour, deflections prediction and component dimensions estimate 0-58877

thick walled permeable cylinders under internal, external and axial pressures 0–66883 three-dimensional, moire-holographic interferometry 0–57327 toroidal shell, circular, with uniform internal press., stresses and deforms. 0–38241

transient motion of an elastic half space due to a semi-infinite surface line load 0-57342 transerse flexure of strip with double row of circular holes 0-38258

trajezoidal structures, natural coordinate system 0–48794 tri-layers, pressure-bonded, during fabrication 0–78617 tube to annulus stretching, exact solns. for Mooney and neo-Hookean mats. 0–48800

mats. 0–48800 turbulent fluctuating in noise producing region of jets with and without delta wings 0–43387 viscoelastic circular ring under impulsive loading and heat additions, dynamic membrane stress 0–38324 viscoelastic disk, compression 0–45603 viscoelastic materials with small distantinal changes linear and populsers.

viscoelastic materials with small dilatational changes, linear and nonlinear problems 0–42054 viscoelastic strip with propagating central crack, stress intensity factor calc. 0–48821

viscoplastic solid, plane shock propag., nonlinear constitutive relns. 0-57356

wave generation, in temperature-dependent absorbing solid, by impulsive e.m. radiation 0-69699

e.m. radiation 0–69699
wave propagation, shear, study on mild steel, Cu and Al 0–40259
waves, spherical and cylindrical, conservation relations 0–50653
waves in one-dimensional media, relaxation at wave fronts, description
using non-linear models 0–73018
wedge, anisotropic, loaded on vertex by concentrated moment 0–54630
welded joints, by moire method 0–54642
Al-alloy L73, sinusoidal and random loadings, stress pattern, Rayleigh's
criterion, resonance method 0–40378
Al, strain distribution inhomogeneities during creep and extension
0–50699

Al alloy L73, sinusoidal and narrow band random loading, fatigue testing 0-40378

0-40578
Al alloys, stress corrosion testing in seawater using smooth and precracked specimens 0-47457
Cu sinters, rel. to deformation 0-4027!

Cu sinters, rel. to deformation 0–40271

a.-Fe, high temp. creep, super jog mechanism 0–75264

Fe sinters, rel. to deformation 0–4027!

LiF, LiF:Mg, slip mechanism, yield, temp. depend., 77-450K 0–40340

Mo-Ti-C, tensile properties, creep, 1800 to 3200°F, dislocation precipitation 0–4033!

Nb-(6at.96)W, low temp., thermally activated flow of single crystal, mechanisms 0–40333

Pb-Cd-Sb alloys, tensile and rupture properties 0–50724

Zr-(2.5 wt.)Nb alloy, heat-treated, stress-rupture props. 0–43775

Stress effects
alkali halide:OH-, tunnelling matrix elements, strain depend. effect
0-47819

0-47819
alkali halide, absorpt. spectral line shifts, piezo-optic. constants dispersion 0-44782
alkali halides, deform. potentials 0-79271
alkali iodides, fund. absorpt., strain effects 0-62644
alloy, metastable phases, transformation, strain induced, deformation hot stage metallographic facility 0-4048!
alloy, stress-corrosion cracking, susceptibility, machining and grinding influence 0-40403
b.c.c. metal, single crystal, slip movement, nucleation shear 0-43756
brass, M63, prestraining history effect on yield surface 0-43735
brass, notched specimens, stress corrosion cracking under bending stress 0-68487
brittle fracture initiation, theory 0-58931

brittle fracture initiation, theory 0–58931 buckling of clamped isotropic parallelogrammic plates under combined loading 0–42045

Stress effects continued

ceramic fuels, thermal stress cracking 0-55980

ceramics, biaxial fracture strength, combined stresses effect 0-50711 combined stresses and plane elastic-plastic wave propag, in half-space

composites, laminated, transient stress-wave expts, dispersive pulse propag. 0-40256

corrosion cracking obs. using scanning electron microscopy 0-68482 crack arrest under transverse loading in elastic plates 0-56012

crack fatigue in metal 0-50736 crack generation by laser, pre-stressing effects 0-47418

crack propagation at void in elastic mat., initiated by horiz. polarized shear wave 0-78653

crack response, equation of motion, Lagrangian method 0–43784 cracked plate bendings, arbitrary stress distribution, influence of thickness theoretical analysis 0–45575 cumulative damage concept based on French's damage line 0–43776 cylinder, circular, thick-walled, stress-redistribution, by creep, axial and thermal loading 0–38248 cylindrical inhomogeneous medium, disturbances due to transient forces and twists on surface 0–38330 cylindrical shell, composite, buckling under axial and radial loading, effect of boundary conditions 0–38270 damping capacities of plates and beams 0–54632 decelerating point surface load on elastic half space, study of surface displacement field 0–38369 dislocation concentration, effect of amplitude of varying stresses 0–55879 dislocation emergence from tilt boundaries 0–47245 disperse systems, flow props., shear rate effects 0–55637 elastic half-space, pulse generation by uniform normal loading of circular surface segment 0–60021 elastic half-space, transient excitation by point load travelling on surface 0–42047 crack response, equation of motion, Lagrangian method 0-43784

elastic plate, separation of smooth circular inclusions under uniaxial tension 0-76875

sion 0-76875 elastic medium, combined stresses propagation, plane and cylindrical wave, boundaries 0-38374 elasticity, 2 dimensional linearized, complex potentials 0-52031 fc.c. metals, low temp. creep, attractive junctions, stacking fault energy depend. 0-40325 failure of high-tensile steel in stress conc. zones, mechanism, exptl. investigation 0-47391

fatigue crack propagation under constant stress amplitude 0–50719 ferromagnet, Barkhausen effect meas. 0–72212 ferromagnet, Ni, Co, u.s. attenuation anomalies rel. to magnetization rotation in domains 0–62196

tion in domains 0-62196 ferrous alloys, high-strength, accelerated stress corrosion test 0-71718 field ion emitter tip, calc. 0-44447 film, enhancement of diffusion 0-75199 film, resistance strain coeff. 0-62292 film, resistance strain coeff. 0-62926 film, resistance strain coeff. 0-63296 glass, stress corrosion cracking, chem. interpret. 0-58933 glass, stress-induced binary diffusion 0-50337 gradient-elastic tensor, cubic crystal, n.m.r. 0-51402 Granato-Lucke internal friction theory for variable strain amplitudes, asymptotic expressions 0-47322 granular material, shear along bordering surface, coeff. of friction 0-71735 granular materials, sheared critical porceity, applies of accordingly

o-71735
granular materials, shear along bordering surface, cochi. of friction o-71735
granular materials, sheared, critical porosity, applic. of geometrical probability 0-56048
graphite, polycryst., premium grades, characterization 0-58923
graphite, stress-strain behaviour under biaxial tension 0-40268
graphite, thermal expansion coeff, variation rel. to prestressing 0-40583
insulating layers on steel, effect of tensile stress bending 0-62031
interrupted stressing technique for crack propagation data on notched rotating beam specimens 0-5601!
iron, grey cast thermal fatigue resistance 0-40368
irregular load sequences, fatigue life estimation 0-47393
lattice defects, diffusion in stress field 0-43664
loading, plastic and elastic, and acceleration waves 0-48826
low cycle fatigue strength 0-50660
on magnetic characteristics of crustal rocks, reversible and irreversible 0-76522
magnanin wire, shock piezoresistance coeff. variation rel. to deform.

manganin wire, shock piezoresistance coeff. variation rel. to deform. 0-62305

martensite, strain ageing by hydrostatic extrusion 0–53633 metal, clastic relief wave vels. 0–50654 metal, f.c.c., under shear, band struct. 0–71919 metal, on mobile and immobile dislocations 0–40147

metal, stress-corrosion cracking, susceptibility, machining, and grinding influence 0–40403 metal film, different surface props., strain coeff. of resistivity derived 0–78874

0–78874 metal film, temp. coeff. resistance, thermal strain effects 0–65628 metal shells reinforced with glass-reinforced plastic on strength 0–40343 metal surface, contact-pot. changes due to tensile stresses 0–58556 metals, fatigue data analysis using real-time computer system 0–75232 multiring structures, multi layered, bonded and non-bonded, non-linear response, high intensity blasts 0–38223 multiring structures, multilayered, bonded and unbonded, non-linear response, high intensity blasts 0–38222 Newtonian fluid, suspension of force-free particles 0–50266 nimonic P.E. 16, creep deform, stress depend, 650°C, mechanism 0–58896

0-58896

0–58896 rel.to nuclear explosions, dynamic elastic moduli of rocks under pressure determination 0–75219 rel.to nuclear explosions, influence of environment on inelastic behaviour of rocks obs. 0–75238 nylon 6-10, anhydrous, stress ageing 0–78628 periodic axial loading of curved viscoelastic column, study of transverse vibrs. 0–38343 photoplasticity in ZnO 0–76044 plastic deformation at high strain rates 0–71682

plastic deformation at high strain rates 0—71682 polycaproamide, crack formation, submicroscopic under cyclic loads 0—56015

polymer, breakdown strength, effect of aperiodic and vibratory impulses 0-75786polymer, fracture, e.p.r. spectra 0-40420 poly- α -methylstyrene, steady shear flow 0-64840

Stress effects continued

polypropylene, crack formation, submicroscopic, under cyclic loads 0-56015

polyurethane, relationship between creep of solid and foam 0-55989 polyvinylchloride, yield condition and propagation of Luders' lines in tension-torsion expts. 0-68453

quartz, mechanical deformation, constant strain-rate compression expts. 0-68449

quartz, mechanical deformation, constant strain-rate compression expts. 0-68449
quartz, mechanical deformation, stress relaxation and thermal activation parameters 0-71690
quartz fracture in alkali silicate and borate melts 0-40387
rectangular orthotropic panels subjected to uniform in-plane loads and deflection-depend, lateral loads, static instability 0-42044
redistribution by creep, circular cylinder thick walled, axial and thermal loading 0-38248
on rocks, rel. to nuclear explosion, numerical simulation of stress wave propagation 0-75239
rubber-like polymers, stress-relaxation 0-50675
semiconductor, GaSb, piezoreflectance 0-76015
semiconductor, amorphous, elaste, sistivity 0-78932
semiconductor, amorphous, elaste, sistivity 0-78932
semiconductor, deform-pot. consts. of group-III acceptors, spectroscopic obs. 0-79304
semiconductor, exitons bound to axially symmetric defects 0-44160
semiconductor, n-GaAs, resistivity and Gunn effect changes 0-47713
semiconductor, plastically bent, transverse magnetoresistance, 77 K, dislocations, electron scatt. 0-44252
shear pulse propagation in dispersive medium 0-45565
shell, cylindrical, elastic and plastic buckling under impulsive loads 0-59974
stain, arising from welding moire method of measurement 0-70022

0-399/4 stain, arising from welding moire method of measurement 0-70022 steel, AISI 1045, natural strain rel. to hardness during fracture under high pressure 0-47421 steel, Cr-Mo, tubular stress-rupture testing in high pressure hydrogen 0-47390

teel, austenite, corrosion cracks, internal friction detection 0–47411 steel, fatigue fractures 0–50729 steel, ferritic, stress corrosion cracking, trans-granular 0–62070 steel, fracture toughness and cracks propagation 0–40383 steel, high-strength, failure-safe design rel. to stress-corrosion cracking 0–78654

tsteel, high-strength, strength, stress corrosion crack branching 0-56002 steel, high-strength, stress corrosion crack branching 0-43790 steel, low-C, strain-ageing rel. to fatigue limit 0-68476 steel, low-alloy, high-strength, stress corrosion resistance, effect of Si

steel, low-alloy, high-strength, stress corrosion resistance, effect of Si 0-56001 steel, low-alloy high-strength, stress corrosion resistance, Si effect 0-43791

steel, stainless, ductility, pre-strain effect 0-78634 steel, stainless for nuclear reactors, high-temp. Na effects on rupture 0-42914

0-42914
strain variations in shear belts 0-79483
strain ageing rel, to fatigue limit 0-68476
strain-hardening hypothesis in anisotropic plasticity 0-45599
strain-hardening yield condition allowing second-order effects 0-38297
straining attachment for X-ray diffractometer specimens 0-47348
stress-acoustic law verification, 190-400 kHz 0-50857
stress-corrosion cracking characterization procedures and failure-safe
design interpret. 0-78654
superconductor, Nb, critical current anisotropy 0-62325
surface patterns, strain generated in Si 0-65045
tektities, fission-track ages, effect of strain 0-45103
thermal, in solid, effect of short laser pulses on absorbing substance
0-40617
thermonlastics, cyclic laodine, fatigue and softening 0-47337

thermoplastics, cyclic laoding, fatigue and softening 0-47337 toroidal shell under uniform internal press., struct. behaviour of middle surface 0-38241

on transition temperature, superconducting of SrTiO₃ 0-71965 transverse compression loading on elastic plate, and running crack arrest

tunnelling matrix elements in OH--alkali-halide systems, strain depend. effect 0-47819

effect 0-47819 viscoelastic material under finite strain and variable strain rate 0-42055 viscoelastic plate, separation of smooth circular inclusions under uniaxial tension 0-76875 yield surface, prestraining history effect 0-43735 zincblende-type materials, contrib. of piezoelec. strain to electroreflectance 0-76037

Zircaloy-2, corrosion in steam and oxygen, applied tensile stress effect 0-69216

Zircaloy-2, corrosion process 0-71726

 AL_2O_3 , corundum, piezo-optic moduli determ. by interference method 0-65981

AL205, corunaum, piezo-optic moduli determ. by interference method 0-65981.

Ag-Au alloy, reflectance change due to strain 0-48003.
Ag, epitaxial film, resistivity strain depend. 0-75559.
Ag single crystal, reflectance change due to strain 0-48003.
AgCl pure and Tl doped, plastic deformation, stress measurements at yield point 0-51097.

Al-Zn-Mg alloys, stress corrosion cracking effect of added Cr and Li 0-50740.
Al, elastic relief wave vels. 0-50654.
Al, multiplication of dislocations 0-55886.
Al alloy, corrosion, crack initiation phenomena 0-40407.
Al film, enhancement of diffusion of Be 0-75199.

7075. Al rolled plate, corrosion cracking sensitivity rel. to microstructure 0-43670.
Al single crystal, u.s. attenuation, deform. rate effects during loading, unloading and reloading 0-68598.
Al-O3, fine grained, deform. at high strains and repeated loads. 0-50682.
Al-O3, adherent layers, fracture rel. to substrate strain and environment afforce.

Al₂O₃, fine grained, deform, at high strains and repeated loads 0–50682 Al₂O₃ adherent layers, fracture rel. to substrate strain and environment effects 0–65421 AlSb, deformation potentials of absorpt, edges 0–44824 Be, velocity of sound, Landau quantum oscillations 0–56148 C steel, cracks propagation 0–50720 C steel, cycle frequency rel. to fretting fatigue life 0–50648 C steel annealed, fatigue strength behaviour 0–50718 CaCO₃, calcite, twinning dislocation motion 0–58810 CaCO₃ calcite, twinning dislocation mobility 0–40161 Cd single crystal, flow, plastic torsion 0–58905

Stress effects continued

CdTe single crystal, birefringence induced by uniaxial stress 0-56497 Co, u.s. attenuation anomalies rel. to magnetization rotation in domains 0-62196

0-62196
Cr, compressibility, microstructure, dislocations, yield drop, hardening, electron microscopy 0-62030
Cu-Zn alloys, Sn and As effects on stress corrosion cracking 0-40409
Cu, elastic relief wave vels. 0-50654
Cu, strain cycling effect on Zn diffusion 0-40197
Cu film, condensed, stress rel. to microstrain 0-65390
Cu single crystal, edge dislocations mobility, stress and temp. depend. 0-50590 Cu stress-deform, rels., effect of grain size 0-68432

Cu stress-deform. rels., effect of grain size 0–68432
Fe-Ag sintered, strain deformation X-ray obs. 0–40301
Fe-Cu sintered, strain deformation X-ray obs. 0–40301
Fe-Ni-Al, influence on precipitation and magnetic properties 0–71776
Fe-Ni-C alloy, paramagnetic f.c.c. austenite, plastic deformation-transformation 0–55972
Fe-Ni alloy, Permalloy range, elec. resist. rel. to mag. field 0–68765
Fe-Ni alloy, polycryst. wires, effect of tensile stress on coercivity 0–79170
Fe-Ni alloys, coercivity, plastic strain effect, under applied tensile stress 0–65025

Fe-Si alloy, annealing, magnetostriction 0-62533
Fe, propagation during deformation in tension, electron microscope obs. 0-75286

76.2 - 75.286 γ and magnetoresistance 0—440.58 Fe, resistivity and magnetoresistance 0—440.58 Fe elloys, stress corrosion cracking evaluation 0—68488 Fe polycrystalline wire, magnetization, tensile stress effects in elastic deformation region 0—65914 α-Fe polycrystals with different carbon contents, temperature dependence of flow stress in microstrain region 0—50707 Fe(3 wt.%05), total loss, tensile stress effects 56449 0—56449 GaAs, interband piezo-absorption 0—44835 n—GaAs, resistivity and Gunn effect changes 0—47713 GaAs, split-off valence-band parameters from stress-modulated magnetoreflectivity 0—72315 GaP, uniaxial, effect on photoluminescence spectrum of excitons bound to Bi impurities 0—48128 GaSb, piezoreflectance 0—76015 GaSb, zero bias conductance anomaly, uniaxial stress effect on subsidiary

GaSb, piezoreflectance 0-76015
GaSb, zero bias conductance anomaly, uniaxial stress effect on subsidiary band minima 0-72026
Gd, Curie temp. 0-40945
Ge, deform-pot. consts. of group-III acceptors, spectroscopic obs. 0-79304
Ge, minority-carrier lifetime 0-62373
Ge, stress-modulated magnetoreflectance for direct transitions 0-76026
n-Ge, transverse magnetoresistance, 77 K, dislocations, electron scatt. 0-44752

n-Ge, transverse magnetoresistance, 77 K, dislocations, electron scatt.
0-44252
H₂, embrittlement of high-strength alloys 0-50775
HfO₂-CaO(Y₂O₃,MgO), solid solns, cyclic heating and thermal shock effects on stability 0-59025
InAs film, evaporated, effects of strain on resistance 0-78919
InSb film, evaporated, effects of strain on resistance 0-78919
KCl:Li+*, induced quadrupole splittings of 7Li n.m.r. line, 1.3-4.2K
0-51408

0-5/408 (KH,PO₄, piezo-opticial coeff., temp. and wavelength depend., rel. to electro-optical phenomena 0-41119 LiF plastically deformed crystal, M-centre persistence after annealing 0-47280

Mg structure changes due to explosive loading, invert. by X-ray Laue patterns, diffractometric meas. and Fourier analysis of line profiles 0-53508

MgO, plastic flow, impurity depend., dislocation mobility, microscopy 0-55987

MgO, polycrystalline, compressive creep, 1200°C 0-43752 MnO:Fe²⁺, angular momentum quenching Mossbauer spectroscopy 0-62631

Mo int. friction peaks rel. to stress- deform. curve 0-65368 NH₄H₂PO₄, piezo-optical coeff., temp. and wavelength depend., rel. to electro-optical phenomena 0-41119 NaCl:Cu⁺ reson. mode freq. 0-68579 NaCl, us. third harmonic amplitude changes recovery after small plastic deform. 0-40548

Nb-W single crystal, yield stress, effect of orientation and sense of applied stress 0-68447

stress 0–68447
Nb, superconductor, critical current anisotropy 0–62325
Nb single crystal, yield stress, effect of orientation and sense of applied stress 0–68447
Ni-Cr alloy, stress-rupture strength and high temp. props., improvement by adding Mg, patent 0–5602!
Ni-Fe films, electrodeposited, uniaxial mag, anisotropy, average stress effect 0–6594!
Ni, u.s. attenuation anomalies rel. to magnetization rotation in domains 0–62196
Ni allovs, stress corrosion cracking evaluation 0–68488

0-62196
Ni alloys, stress corrosion cracking evaluation 0-68488
Ni film, contrib. to perpendicular anisotropy, and elec. resistivity 0-44639 x10NiCrWTi36.15, precipitation behaviour, high temp. 0-40490
Pb bar, single-cryst., step-function press-loading and longit. strain pulse propag. 0-43725
Pd-Ag alloy, equilib. H₂ solubility 0-53532
Pd, accelerated sublimation under tensile stress in air 0-47007
Pt-Rh alloy, accelerated sublimation under tensile stress in air 0-47007
Pt, accelerated sublimation under tensile stress in air 0-47007
Rh, Knight shift 0-59468
Si, minority-carrier lifetime 0-62373
Si, strain generated surface patterns 0-65045
SrTiO₃, uniaxial stress to (111) face, phase transitions, order parameter 0-68567
steel, Ni-Co-C, strain tempering of bainite 0-40435

0-68567

Ta alloy, T-111, creep behaviour under continuously varying stresses influence 0-71700

ThO₂:Gd³⁺, e.p.r., spin-lattice strain coeffs. 0-72292

Ti-Al, stress corrosion cracking, in aqueous solutions at ambient temperatures 0-68492

Ti 6Al-4V flaw growth, testing in Freon TF environment 0-47392

Ti alloys, stress-corrosion-cracking characterizations procedures 0-47415

Ti alloys, stress corrosion cracking mechanism 0-78656 Ti alloys, stress corrosion cracking 0-65425 TiC, fracture under static and sliding contact 0-40417

Stress effects continued

U-Mo alloys, stress corrosion props. 0–55998
U, stress corrosion cracking and hydrogen embrittlement 0–40388
U rods, external stress during quenching rel. to final texture 0–47205

UO2, polycrystalline, high temp. creep, calc. 0-4736!

CO₂, polycrystalline, light temp. creep, calc. 0—4/361

VPc garnet, piezo-optical effect, mag. birefringence 0—69090

ZnO photoplasticity 0—76044

Zr-(2.5 wt.)Nb alloy, heat-treated, stress-rupture props. 0—43775

Zr alloys, corrosion cracking, environmentally induced in methanolic solutions 0—55948

Zr alloys, stress corrosion cracking in methanolic solutions, topography 0-71727

Zr alloys, stress orientation of hydride 0-62139 ZrB₂ with SiC additive, strain hardening 0-55977

Stress measurement see Strain gauges

Stress/strain relations

see also Elastic constants
b.c.c. metals, strain rate, temp. depend. 0–43738
composite material, fibre reinforced theory 0–40321
composites, polycrystalline, elastic-plastic behaviour 0–71676
concentration factors in notched members in plane stress 0–57323
concrete reinforced slabs, strain meas, by bonding in elec. gauges
0–43728

constitutive eqn. for ideal plasticity, derivation 0-38295 constitutive equations from impact data 0-40266 curves in plastic region, from new apparatus to shear bulk materials 0-55994

deformation, high temp., reln. between theor. and exptl. activation areas $0\!-\!50680$

0-50680 deformation, inverse strain-rate effects 0-65383 diffusion creep, grain size depend., vacancy sources or sinks 0-40323 dislocation pile-up formation dynamics, nonlinear stress-velocity reln. for dislocation motion 0-55883 edge-cracked sheet, plane stress model finite element method 0-55962 elastic-plastic rings and cylinders, transient response rel. to strain-hardening and strain-rate sensitivity 0-38260 elastodynamic problems, two-dimensional, method of initial functions 0-57339 around elliptic hole symmetrically centred in long plate under uniform

around elliptic hole symmetrically centred in long plate under uniform tension 0-76868 fatigue crack propag, under shear loading, discrete dislocation model 0-40394

fatigue crack propag, under shear loading, discrete dislocation model 0—40394 filamentary composites, stress-wave amplitudes, calc., theory 0—68426 glass fibre, strength, clastic moduli 0—40344 glass-epoxy composite beam in flexure, failure- time characts. 0—40384 graphite under biaxial tension 0—40268 inelastic granular medium, experimental and analytic program 0—59539 layered structure, displacement due to nucleus of torsional strain 0—38234 membrane, circular deform. by abrupt press., meas. of displacement, strains and strain rates 0—38321 metal, b.c.c., high temp. work hardening, theory 0—40445 metal, f.c.c., tensile-tested, effect of grain-size on curve 0—58876 metal, f.c.c., tensile-tested, effect of grain-size on curve 0—58876 metals, fracture and breaking 0—50723 metals, polycrystalline, clastic-plastic behaviour 0—71676 metals, structure for time-dependent plastic deformation 0—50697 moire effect appls. to stress and problems, advantages over conventional grid techniques 0—43730 rel.to non linear cracks, model analysis, numerical solution 0—40389 nonlinear, and the large deflection of an annular plate 0—59965 nonlinear equations for incompressible elastic media 0—38235 notch roots in sheet specimens, elastoplastic behaviour under constant-amplitude loading 0—47341 notched tension specimen, circumferential notch 0—40267 optical materials, shear strain properties 0—50659 panel structures, stability and vibr., computational problems in matrix anal. 0—38332 penton 0—39917 plane-strain indenter, computerized relaxation 0—47339 plastic, glass-reinforced, in tension, discontinuity in curve 0—40262

penton 0–39917
plane-strain indenter, computerized relaxation 0–47339
plastic, glass-reinforced, in tension, discontinuity in curve 0–40262
plastic deformation, inhomogeneous, criterion 0–68439
plasticity theory, second-order effects 0–38297
plastics, grid appls. for moire fringe method of strain meas. 0–40263
plastomechanical principles, cold working 0–40446
plexiglass pre-stressed sheet, stress wave propag. from internal explosive source 0–55958

polymeric materials, dynamic 0–78615 polymers, interlaced elastic 0–50643 polymers, interpretation in terms of molecular structures and conformations 0–71654

polymethylmethacrylate, formation of micro shear bands 0-68452 polymethylmethacrylate, vitreous, relax. after combined shear and compression strains 0-50657

polystyrene, formation of micro shear bands 0–68452 polyvinyl alcohol, aqueous soln., effect of degree of polymerization on critical shear rate 0–53292 prismatic solid, modified plane strain, discrete element plastic analysis 0–40265

pyrex pre-stressed sheet, stress wave propag. from internal explosive source 0-55958 quartz, mechanical deformation, constant strain-rate compression expts.

0-68449
refractory material, bauxitic alumino-silicate 0-58879
rubber, natural, mechanical characterization 0-68433
shear fatigue crack model, effect of mean stress on cyclic shear crack growth 0-40395
shearing mechanism in 2.2% Cr-Ni alloy, annealing conditions effect 0-40927

0-40927 shells of revolution, circumferentially stress and strain 0-48807 steel, nickel chrome and low carbon, cyclic loop in low cycle fatigue tests 0-50666 steel 18% Ni, stress-strain curve serrations and Portevin-Le Chatelier phe nomenon 0-65376 steel lattice, strain dependence, X-ray internal stress determination 0-40270

50-40270 steel sheets, low C, anisotropic and limiting strain, in stretching 0-53578 steel thin plates elasto-plastically bent, unloading and inverse loading 0-55963

Stress/strain relations continued

strain gauge use for long times at high temp., evaluation of different cement combinations 0-43729

strain hardening in polycrystalline Indian commercial aluminum 0-47342 for stress components in porous medium, soil-water interaction 0-75242 stress relaxation in combined torsion-tension 0-57321

stream reason to the strength of the strength

tubing, hollow drawn, wall thickness changes and bulk strain behaviour 0-47370

0–47370
viscoelastic flow, two-dimens., constitutive eqns. 0–48820
in viscoelastic flow, two-dimens., constitutive eqns. 0–48820
in viscoelasticity nonlinear theory 0–59990
yield stress, strain-rate depend., comment on dimensional homogeneity of eqns. 0–40326
Al-(3wt.%) Li alloy, yielding phenomena, annealing depend., lattice const., electron microscopy 0–47353
Al-Mg alloys, Portevin-Le Chatelier effect 0–58862
Al, cyclic loop in low cycle fatigue tests 0–50666
Al, polycrystalline Indian commercial, strain hardening 0–47342
Al, strain-rate depend. of yield stress, comment on dimensional homogeneity of eqns. 0–40326
Al, strain distribution inhomogeneities during creep and extension 0–50699
Al, tensile load, torsional vibrations effect, dislocation theory. 0–50665

0-50699
Al, tensile load, torsional vibrations effect, dislocation theory 0-50665
Al 1100, cyclic hysteresis loop behavior 0-55961
Al alloy, 296, 77 and 4 K 0-40272
Al₂O₃, double bicrystal, high temp. deformation 0-50683
Bi spherical single crystal, strain-free, prep., any desired orientation and thickness 0-40004
Co matrix reinforced by single cryst. fibres of transition metal carbides 0-65376 0 - 65375

Cr-Ni 2.2% alloy, shearing mechanism, annealing conditions effect 0-40927

O-40927
Cu-(12at.96)Al, maxima rel. to slip band propagation 0-40269
Cu, effect of grain size and temp. 0-65374
Cu, from high temp. creep meas. 0-62051
Cu, resistivity, impurity and grain size depend. 0-47646
Cu, strain-rate depend. of yield stress, comment on dimensional homogeneity of eqns. 0-40326
Cu alloy, 296, 77 and 4 K 0-40272
Cu and Cu-Zn with Al₂O₃ particles, work hardening theory and macrostruct. 0-65392
Cu rods, soft, prestressed, small plastic strain wave propag. 0-53585
Cu whiskers, characts, and internal friction, in uniaxial tension 0-47343
D₂, solid, plastic deformation, relaxation, 14-17.5K 0-40304
a-Fe, dislocation model, density variation 0-47255
Fe, Luders band propag, and vel. rel. to stress 0-53586
Fe, strain-rate sensitivity, orientation depend., single cryst. 0-68444
Fe alloy, 296, 77 and 4 K 0-40272
Fe expt. determ. of dynamic stress-strain characteristics 0-53567
Fe matrix reinforced by single cryst. fibres of transition metal carbides 0-65375

Per matrix reinforced by single cryst. nores of transition metal carbides 0-65375

Mo-Rh alloys, plastic and elastic props., -190°C to +100°C 0-43711

Mo, deformed, slip behaviour 0-78643

NaCl compression, rel. to dislocation density, obs. 0-40169

Nb, single crystal, flow stress, temp. depend., neutron irrad. effect 0-78627

Ni-C, serrated flow, temp. and comp. depend. 0–40334
Ni matrix reinforced by single cryst. fibres of transition metal carbides
0–65375

Zn single crystals, high strain rate compression 0-75244

Stresses, internal

alkali halides, microstrain rel. to physical history 0–50669 anisotropic media, curved dislocations, numerical analysis, linear elasticity range 0–75156 b.c.c. metal, residual stress level rel. to fatigue damage 0–68484

anisotropic media, curved dislocations, numerical analysis, linear elasticity range 0–75156
b.c.c. metal, residual stress level rel. to fatigue damage 0–68484
biaxial stress and stain meas. using photoelastic meters 0–50668
bond, in composites with overlapping fibres 0–71677
brittle material, elastic shock activity during crack growth, earthquake mechanisms 0–40392
buckling stresses in spherical shell 0–73017
cavity growth, conc. and vacancy interaction 0–47388
coatings, residual stresses determ. from flexture of flat cathode 0–43542
composite, glass-matrix, Griffith flaw limitation 0–58929
composite materials, fibre-matrix interaction 0–68434
composite materials, interfacial tractions 0–43732
compound cylinder, using accelerated direct search technique 0–66865
condensation in annular flow 0–39885
conoid shell, circular, bending deformation, numerical analysis 0–38245
conoids, circular, bending deformation, numerical analysis 0–38244
contact problems in elasticity, solution for thick layer on Winkler type foundation 0–38286
creep, steady-state diffusional 0–55984
creep, strain component caused by grain boundary sliding 0–71694
creep, strain component caused by grain boundary sliding 0–71694
creep, strain component caused by grain boundary sliding 0–71694
creep, transient, phenomenological theory 0–55979
crystals, thin film, grown from melt, thermal stresses 0–65373
cubic media, elastic field of point defect 0–71603
curved beams with variable section, normal unit stresses det. using cylindrical section hypothesis 0–53579
deformation, structural properties change 0–40277
diamond, ion bombarded, thin surface region form. and elastic stresses 0–55887
dislocation motion in ensemble, computer modelling 0–68353
dislocation pileup producing stress at barrier 0–47252
dislocation sinduced in anisotropic media 0–43666
dislocations near free surfaces in anisotropic cubic crysts., stress fields and interaction stresses 0–55885
e.p.r. line width broadening for 3d³ ions in T_d symmetry 0–79409
edge cracks, stress intensity f

elastic strain measurement, X-ray diffraction and line displacement 0-53475

Stresses, internal continued

elastic-plastic plane-strain solns, with separable stress fields 0-42049 epoxide coatings, internal stress due to water content 0-50676

epoxide resin-stainless steel system, adhesion and internal stress 0-50677

epoxuce resin-staintess steet system, adhesion and internal stress 0-50677 f.c.c. lattice, mechanical interaction of point defects 0-75123 fibre-reinforced elastic composite material, interfacial tractions 0-43732 films, thin metal, condensed 0-62029 glass-crystal composites, residual stresses 0-75245 glasses, optical, mechanical and photoelastic props., high and low temp. meas. in vacuum, instrument 0-53573 graphite, geom. stress conc. at fillets effect on tensile strength 0-40347 inclusion, cavity problem, thick plate with eccentric spherical inclusion 0-38293

inclusion, spherical, inhomogeneous, on axis of circ. cylinder in torsion 0-66863inclusion/cavity problem thick plate with eccentric spherical cavity 0-38292

laser rod, photography 0-45795 laser rod, photography 0-73235 macrostresses, residual, theoretical aspects for X-ray diffractometry 0-54644

0-54644
magnetomechanical effects, distrib, theory 0-44466
magnetomechanical hysteresis model applic. 0-62532
measurement, X-ray diffr. technique 0-55965
measurement by reversed stress relax. method 0-58881
metal, b.c.c., high temp. work hardening, theory 0-40445
metal, b.c.c. and h.c.p., strain bursts and coarse slip during cyclic deform.
0-71703
metal long-range contrib to flow stress at low temp. 0-40370

metal, long-range, contrib. to flow stress at low temp. 0-40320 metal, microstrain rel. to physical history 0-50669 metal, thermoelastic response to relativistic electron beam absorpt.

0—78609
metal working, reduction by applic. of vibrations 0—47424
metals, residual stress meas., instrum. 0—65378
microcrack formation, activation energy 0—68480
micropolar body, thermal stresses induced by action of discontinuous temp.
field 0—63401
moon, internal strain and fissions due to tidal force, calcs. 0—66575
oxide film, stress generation and relief during growth 0—61660
Permalloy film, electrodeposition, thickness, current density and temp.
denend. 0—41023 Oxide limit, sites generation and reiner during growth 0-51000 Permalloy film, electrodeposition, thickness, current density and temp. depend. 0-41023 permalloy films, macrostresses, effect of deposition parameters, plasma sputtering process 0-71678 perovskite, SrTiO₃, elastic strain interaction with struct. transform. 0-50067

in pipe joints between dissimilar steels 0-58884 plastic deformation, high temp, dislocation dynamics, rate theory 0-43733

0-43733
plate, elastic, infinite, response to axisymmetric initial velocity distrib. with applic. to hypervelocity impact 0-38288
plate, thick, with eccentric spherical inclusion, or cavity 0-38293
plate, thick, with eccentric spherical inclusion or cavity 0-38292
plate strip extensional vibrations curve, frequency spectra from Kane-Mindlin eqns., comparison 0-38337
polyerystals with dislocation struct., statistical approach 0-47309
polymer, internal stress relax., elastomer introd. effect 0-40276
polytetrafluoroethylene, compression stress relax. processes 0-40282
in prisms, optical triangular rotating, associated deformation 0-38530
quartz, shear amplitudes from scanning electron micrographs of oscillating crystals 0-68964
residual, caused by plastic flow for growing crack BCS model 0-53617

crystais 0-68964 residual, caused by plastic flow for growing crack BCS model 0-53617 rook, various determination techniques 0-48244 in rotating disks, plane, without rotational symmetry, meas. and calc. 0-76871

shell, spirally corrugated, subject to internal pressure 0-5463! shells, cylindrical, normally intersecting, subjected to internal pressure 0-54637

u=3403/ sintering model, photoelasticity 0-65442 soldered assemblies, automobile 0-55950 sphere, non-homogeneous, incompressible, thermal stresses in periodic temp. field 0-54662 steel, calcium aluminate inclusions, thermal expansion, rel. to tessellated stresses 0-59112

steel, carburized, stress factor determ. using X-ray two-exposure technique 0-68435

steel, fatigue loading, stress conc. 0–75279
steel, nonmetallic inclusions effects, obs. using photoelastic coating
0–65351

steel, nonuniform distrib. 0-40275

steel, nonuniform distrib. 0–40275
steel, residual stresses in cementite phase after plastic deform. 0–40280
steel, stresses due to entry of cathodic H₂ 0–40278
steel, transformer, study of residual stresses 0–62027
steel lattice, strain dependence, X-ray determination 0–40270
styromal based coatings, form. mechanism obs. 0–40281
superconductor, quasidislocations, elastic and dielastic interactions
0–75579
surface patterns, strain generated in Si. 0–65045

Super-conductor, quastusiocadons, etasuc and decastic interactions 0-75579 surface patterns, strain generated in Si 0-65045 thermal, in circular disc, transient behaviour 0-48824 thermal, in finite heat-generating circ. cylinders 0-54664 thermal, of finite heat generating cylinder 0-54665 thermal, et. to heat transfer in skin of hypersonic vehicle 0-38411 thermal stresses in rectangular plate cooled along one edge, Green's function prediction 0-47345 thermoelastic layers media, transient stresses due to impulsive e.m. energy depositon 0-38319 thermoelastic material stability, appl. of invariance principle for systems on Banach space 0-52059 thermoelasticity, micropolar, plane problem of strain and stress 0-57361 torispherical drum heads, elastic analysis, computer survey 0-50670 torispherical drum heads, elastic analysis, computer survey 0-50670 torispherical drum heads, elastic-plastic analysis, computer survey 0-50671 two-phase mats., conc. at edge-dislocation pile-ups 0-50587

two-phase mats, conc. at edge-dislocation pile-ups 0-50587 work hardening by non-deforming particles and fibres 0-65458 Ag film, thickness depend. 0-47346 Al-Mn alloy, 3003 type, strain rate sensitivity, initial struct. effects 0-68442

Al₂O₃, residual stresses produced by quenching 0-58883

Stresses, internal continued

Al₂O₃ particles, sintered and fused, strain obs. 0–58882
Co-Au alloy films, rel. to amorphous and solid son. phases, obs. 0–5966
Co, effect on mag. props. 0–79168
Cu, electrodeposited, mechanical, elec. and thermal props., struct., treatment depend. 0–71662
Cu, minimal critical shear stress 0–61731
of Cu electrodeposits, effect of concentrations of CuSO₄ in CuSO₄·H₂SO₄
bath and of benzotriazole as addition agent obs. 0–69220
Fe, slip surface distortion production 0–75269
Fe₃O₄, magnetite, ground sample, microstrains and stacking faults
0–58819

Fe₃Si films, non-stoichiometric, parameter variations rel. to stresses

Fe,Si films, non-stoichiometric, parameter variations rel. to stresses 0–61668
GaAs, dislocation generation, thermal stress 0–78554
Ga,Te, Ga,Se, Ga,S,, stoichiometry, vacancies and impurities 0–61942
KCl:Li⁺, effect on paraelectric resonance 0–44355
LiF, and stress. relax., work hardening 0–68436
LiF, dislocation velocity depend., dipole, annealing kinetics 0–47257
MgO, active, X-ray line broadening analysis 0–62110
MgO, critical resolved shear stress, impurities effect 0–65379
Mo film deposited from carbonyl decomp., rel. to device technology 0–58597

0-58597

MoSi₂ film on Mo, meas. using X-ray method 0-75246

NaCl, and stress relax, work hardening 0-68436

Ni-Al alloys and nimonic, critical shear stress rel. to hardening phase particles 0-50747

Ni, stresses due to entry of cathodic H₂ 0-40278

Ni electroless deposits on Be 0-71679

Si, strain generated surface patterns 0-65045

p- Si epitaxial layers on sapphire, superlinear current density obs. 0-51062

0-310b2
Si film, heteroepitaxial deposition on insulating substrates 0-39946
SiO_x on Si, determ. by dynamical X-ray diffr. 0-58577
V, decremental unloading test meas. high temp. 0-55967
W film deposited from carbonyl decomp., rel. to device technology

w lim deposited from carbonyl decomp, ret. to 0-58597 WC-Co alloy, effect of small plastic deform. 0-43770 YFe garnet epitaxial films on YAI garnet 0-65380 ZnS:Fe³⁺, e.p.r. line width broadening 0-79409

Striations see Discharges, electric Stripping reactions see Nuclear reactions and scattering

Stroboscopes

electronic, flash burst operation light source for multiflash photography 0-77215

Strong interactions see Elementary particles/interactions, strong; Field theory, quantum/interactions, strong

Strontium

ontium
abundance and isotopic composition in lunar crystalline rocks 0–45338
abundance and isotopic compositions in lunar rock samples 0–48492
abundance in lunar rocks and separated phases 0–45342
abundance of isotopes in lunar igneous rock samples 0–48493
abundance of isotopes in lunar samples, "Sr/MSF ratios 0–48495
abundance of isotopes in lunar samples from Tranquillity Base 0–45337
amplitude factor for coherent neutron scatt. 0–7850!
atom, absorption spectrum in vacuum u.v. 0–5810!
atom excited levels radiative lifetimes, Hanle effect obs. 0–52943
atoms, even A, 5³P, optical double reson, lineshape in time resolved obs. 0–52891
band structure, theoretical approach, 0–68732

band structure, theoretical approach 0–68732 in biological materials, determination by atomic absorption spectroscopy 0–51444

g, values of ¹D₂ level 0-52896 Langmuir S-curves, exp. for Sr adsorbed on (110) Mo monocrystal 0-79102

0-/9102
resonance lines for Sr III 0-70773
resonance lines for Sr III 0-70773
rRb-87Sr chondrites, carbonaceous, age determination 0-45426
Sr II oscillator strengths and mean square radii calc. 0-42930
Sr*, optically oriented, relax. in inert gases, obs. 0-52955
Sr* oscillator strength of reson transitions from plasma density meas. 0-42995

Strontium compounds

fluor collectine, crystal morphology rel. to environmental conditions 0–65122 fluorophosphates, Th substituted, Sb and Mn activated, optical and structural 0–79359 rai 0-79359 orthophosphate and pyrophosphate compositions, mixed alkaline earth, Eu²⁺ activated, luminescence 0-72432 Sr₂GeS₄, crystal structure determ. 0-65283 (Ba,Sr)TiO₃, ferroelectric, polycrystalline specimen, investigation in 50-80 GHz frequency range 0-75796 (Ba₂Sr_{1-x})TiO₃ solid solns, transition temp. shifting by hydrostatic press. 0-68937

(Ba₁,Sr_{1-x})TiO₂ solid solns., transition temp. shifting by hydrostatic press. 0–68937

BaO_{0.75}SrO_{0.25}.6Fe₂O₃ with group III admixtures, mag. props. 0–69040
Eu-Sr alloy, Mossbauer effect meas. rel. to highest of the description of the description

SrF₂:Gd³⁺ with Ce³⁺ as codopant, 6P(7/2) fluorescence enhancement 0-76172

0-/61/2 SrF₂:Ho²⁺, e.p.r. in trigonal site 0-4134! SrF₂:Mn²⁺, Debye temp. calc. from temp.-depend. hyperfine constants, e.s.r. determ 0-43912 SrF₂:Nd³⁺, laser, spectroscopic study of induced radiation, temp. limit of operation 0-41186

Strontium compounds continued SrF₂:Nd³⁺, Yb³⁺ system, spin-lattice relax. and cross-relax. 0—72291 SrF₂:InF₃ syst., new phases detected 0—62145 SrF₂, elastic moduli, third-order 0—47316 SrF₂, electron-irrad., electron photo-emission spectra rel. to colour centres 0—75177 $\rm SrF_{2}, excitons$ and holes, self-trapped, study by e.p.r. and optical absorpt. spectra 0–51340 SrF₂, i.r. spectra and mol. geometry in solid Kr matrix 0-54095 SrF_2 , i.r. spectrum, apex angle and force consts., in solid Kr matrix 0-77779SrF₂, N.M.R. line shape meas. 0-72504 SrF₂, phonon scattering by point defects, low temp. thermal conductivity meas. 0-43855 meas. 0—43853 SrF₂, thin films, optical constants 0—47999 SrF₂ crystal, etched, dislocations, room temp. microplasticity 0—43758 SrFeO₄, mag. susceptibility, Neel temp., Mossbauer effect 0—56513 Sr₂(FeW)O₆-Ba₂(FeW)O₆ system, phase transition, Mossbauer obs. 0—72339 Gr₂(FeW)O₆ Ba₂(FeW)O₆ system, phase transition, Mossbauer obs. 0–72339
Sr₂GeS₄, cryst. struct. determ., by X-ray powder diffraction 0–61845
Sr₁, HrO₃₁, high press. phases with perovskite-related struct. 0–62135
Sr₄KLiNb₁₀O₃₀, elastic and piezoelectric constants 0–72123
Sr₄KLiNb₁₀O₃₀, type ferroelectrics, electro-optical props. 0–66000
SrMoO₄, electric gyrotropy, exptl. detection 0–72323
SrNO₅ i.r. determination using Pellet tech. 0–54198
Sr(NO₃), i.r. reft. spectra, internal vibrs., anharmonicity
Sr(NO₃), i.r. spectra of powdered crysts. 0–66065
Sr(NO₃), Raman spectra, vibrs. assignment 0–56567
Sr₄NaLiNb₁₀O₃₀ type ferroelectrics, superlattice struct. 0–71595
Sr₄NaLiNb₁₀O₃₀ type ferroelectrics, electro-optical props. 0–72318
SrO, layers, O evaporation, effect of electric field 0–43520
SrO heat capacity anal. 0–62211
SrO single crystal, F-band 0–76093
SrO(6–x)Fe₂O₃xAl₂O₃, uniaxial single crystals, temp. dependence of domain structure, high anisotropy field 0–72259
SrO.2B₃O₃, enthalpy of fusion 0–55664
Sr₇bO₃, perovskite, struct, X-ray diffr., 0-800°C 0–50514
Sr₁, xPb₂RuO₃ system, pyrochlore to perovskite transformations, 1400°C, press. induced 0–56066
SrS-Cu phosphors, electroluminescence at 77°K 0–76194
SrS-Cu, Eu phosphors, phosphoroseence following electroluminescence 0–62737
SrS gaseous, 1Σ+1Σ+ syst. rot. anal. 0–70953 SrS:Eu, Sm, ir. stimulable phosphor 0–59435
SrS-Cu, Eu phosphors, phosphorescence following electroluminescence 0–62737
SrS gaseous, ½+1½+3 syst.rot. anal. 0–70953
SrS phosphor ir. stimulated emission and trapping center depth 0–56588
Sr,Ti,Nb₈O₃₀, tungsten-bronze type struct. and dielec. props. 0–53924
SrTiO₃:Al, shared holes trapped by charge defects 0–43968
SrTiO₃:Cr³⁺(Mn⁴⁺), fluorescence spectra, temp, depend. 0–41271
SrTiO₃:Ni³⁺, dynamic Jahn-Teller effect 0–56673
SrTiO₃, SrNi³⁺, dynamic Jahn-Teller effect 0–56673
SrTiO₃, anomalous us. attenuation at 105K transform. 0–43884
SrTiO₃, anomalous us. attenuation at 105K transform. 0–43884
SrTiO₃, coypted modes in phonon spectra 0–71828
SrTiO₃, crystal, solvent zone growth technique 0–61735
SrTiO₃, elsec, field effect 0–62763
SrTiO₃, elsec, field effect 0–62763
SrTiO₃, elsec, field effect 0–62763
SrTiO₃, elsec, field induced optical second harmonic generation 0–65976
SrTiO₃, elec, field induced optical second harmonic generation 0–65976
SrTiO₃, elec, field induced optical second harmonic generation 0–65976
SrTiO₃, elec, field depend. of H impurity mode in 3500 cm-1 absorp. band 0–66055
SrTiO₃, ferroelectric, single crystals and polycrystalline specimen, investigation in 50-80 GHz frequency range 0–75796
SrTiO₃, optical gap, deviation from Urbach tail behaviour 0–79289
SrTiO₃, perovskite, sublattice atomic displacements 0–40528
SrTiO₃, phase transitions, order parameter, variation with uniaxial stress 0–68567
SrTiO₃, phase transition, 107 K, u.s. meas. 0–75342
SrTiO₃, phase transition, order parameter, variation with uniaxial stress 0–68567 SrTiO₃, photocond. anomaly, local ferroelec. phase transition obs., 47K 0-68952SrTiO₃, piezoelectric, elastic compliance, press. depend. near transition temp. 0–47315 SrTiO₃, piezoelectric, elastic companies, p. 103, piezoelectric, elastic comp. 0–47315
SrTiO₃, quadratic electro-optic coeffs., interferometric determ. 0–72322
SrTiO₃, relative atomic displacements of sublattices 0–53675
SrTiO₃, semiconductor, conductivity, Hall effect, temp. depend., effect of Ce and Nb dopants 0–47725
SrTiO₃, single-domain direct obs. 0–75789
SrTiO₃, single-domain direct obs. 0–75789
SrTiO₃, single crystals, dielectric properties at low temperatures 0–44342
SrTiO₃, truncated cone capacitor, nonlinear semiconducting props. 0–44370
SrTiO₃, u.s. propag. rel. to struct, phase transition 0–75389
SrTiO₃, u.s. propag. rel. to struct, phase transition 0–75389 Sulphur compounds 0—44370
STTiO₃, u.s. propag. rel. to struct. phase transition 0—75389
STTiO₃ containing rare-earth ions, dielec. relax. 0—59253
STTiO₃ Cr³⁺ polarized fluoresc. through phase transition 0—62726
STTiO₃ powders, i.r. absorpt. spectra, particle size and shape effect 0—48061 0-4806: STiO, semiconductor, type II superconductivity 0-6879! STiO; single cryst., 5°-300°K, Brillouin scatt. 0-44872 STiO; single cryst., dielectric const. and loss, 40-10°° c/s 0-47828 STiO; single crystal, elastic constants, third order, temp. depend., 106-300°K 0-40236 STIO; straight of temperature, superconducting effect of stress, 0-71965 74681

see also Heat of sublimation; Vaporization
in cryogenic systems, review 0-47002
elements, monatomic, model 0-47004
Lennard-Jones system, high temperature part of coexistence curve investigated by Monte Carlo calc. 0-71425
naphthalene, mass transfer rates, effect of vertical vibration 0-76859
rare-gas solids, applic. of law of corresponding states 0-71427
transition metals, of atomic ions, positive and negative, in 1800 to 2600°K
range 0-47005
50%-5096Mo, in low-pressure O₂, rate correlation with creep rate78636
Ar, model 0-47004
Ar solid, vibrational lattice modes effect 0-47006 Ar, model 0-47004
Ar solid, vibrational lattice modes effect 0-47006
CdS cryst., surface struct. rel. to sublimation model 0-50353
GeS monocrystals produced by sublimation in vacuo 0-50432
Kr, model 0-47004 Pd, accelerated, under tensile stress in air 0-47007 Pt. Rh alloy, accelerated, under tensile stress in air 0-47007 Pt. accelerated, under tensile stress in air 0-47007 Rn sublimation pressure predicted from law of corresponding states 0-71427 0-71427
SiO₂ continuous vacuum sublimation using electron beam 0-50334
SnSe, coeff, determ. 0-61604
W-25%Re, between 1550 and 1950°C in low pressure O₂ 0-78345
W, in low-pressure O₂, rate correlation with creep rate 0-78636
Xe, model 0-47004
ZnS cryst., surface struct. rel. to sublimation model 0-50353
ZrBr₄, pressure from effusion rates rel. to orifice size 0-53404 Sudden commencement see Magnetic storms Suhl effect see Hall effect; Semiconductors Sulphur
in Alnico alloys, Ti containing, effect on crystal growth 0–71761
ab initio calcs. for 3d exponent, insensitivity to molecular environment
0–74098 abundance, elemental and isotopic, in lunar samples 0–45359 adsorbed layer on Ni, structure, formation mechanism, stability 0–39974 allotropy and structural aspects 0–50405 atom, K-mesonic, 4f→3d transition meas. using K-mesic interactions 0–64307 atom, ground-state and electronically excited, reaction study using OCS photolysis as source 0-72524 atom, interaction with ethylene 0-43209 atom ionized, forbidden lines rel. to diagnostics of nebular plasmas 0-74128 atomic transition tables 0-39284 atoms 3¹S₀, collisional deactivation of excited state by Xe, Ar and He 0-60963 offfusion in metal, rel. to sulphurization in H₂S-H₂ mixtures 0-75207 impurity effect in Mo-Permalloy, mag. props. 0-44580 ions in AgCl, distrib. coeff. 0-54199 magnetoelectrets, photo-depolarization in polycrystalline samples 0-79058 magnetoelectrets, photo-depolarization in polycrystalline samples 0–79058
orthorhombic, drift mobility, high press. effects 0–47723
segregation on Ni(110) surface 0–47031
in solar 3b flare decay, resonance, intercombination and forbidden transitions, He-like 0–69497
solubility in glass, effect of Si₃N₄ additions 0–47018
vibration-rotation consts. of isotopic species OCS 0–49887
X-ray fluorescence determination in mineralised rocks in Utah 0–66218
Fe-Ni-Al-Co-Ti in alloys, effect on liquidus-solidus gaps 0–71775
in KC(Br):KSH crystals, e.s.r. 0–44989
Na₅>S fluxes, growth of dendritic and prismatic HgS 0–47147
S⁺-Ar, meas. of Q values at keV energies 0–77691
S-photodetachment cross-section above threshold, obs. 0–78159
S II in planetary nebulae, emissivity 0–51644
α-S single cryst, growth from solns, with org, cpds. 0–74987
S XV, mag.-dopole decay of 2³S₁ state 0–67612
S₂, transient species, absorpt. spectra in vacuum u.v. 0–53020
S₂⁻⁻ molecular luminescence centre in alkali halides, vibrational relaxation, nonradiative transitions 0–44920
S₃²⁻⁻, i.r. and Raman spectra 0–70948
S₄²⁻⁻, i.r. and Raman spectra 0–70948
S₈, mol. orbitals and charge-carrier transport 0–75492
S₈, mol. orbitals and charge-carrier transport 0–75492
S₈, mol. orbitals and charge-carrier transport 0–75493
S₈ molecule, electronic energy levels, MO calc. 0–77837
3*S⁴⁺, superhyperfine splitting in diamond lattice, c.p.r. obs. 0–48141
[phur compounds] alkaline earth sulphides, fundamental absorption, excitation 0–56538 coloured glass, by Cd, S and Se compounds, structure of fundamental absorption band edged 0–76040 hexaisothiocyanate ions, i.r. and laser Raman spectra, 2200-70cm⁻¹ 0-39376 metal-P-s compounds, crystal growth, by vapour transport 0-71513 molecules, correlation of electron binding energy with structure 0-77752 perfluorovinyl sulphur pentafluoride-SF₆ mixed gaseous dielectric, patent 0-/4681 double sulphates, including Tutton's salts, i.r. spectra, 2000 to 40 cm⁻¹ 0-55321 0-3321 sulphates cryst. chem. classification 0-61688 sulphide phosphors, annealing effects on luminescence, and X-ray lumines-cence 0-56631 sulphosalts, struct. classification 0-65276 As-S-Te system semiconductors, vitreous, bond-structural approach to electood. 0-75676

Fe-S melt, activity vs. comp., 1100-1300°C, heat and entropy of solution 0-74743 0-74743 . H₂SO₄-methyl isobutyl ketone, heat of mixing, two-step equilib. model 0-66172 H₂SO₄, aqueous soln., water vapour pressure control 0-43519 N₃S₄O₃P₃ isomeric derivatives, ^{19}F n.m.r. spectra 0-46509 S₈(AsF₆)₂, mol. config. of S₈ $^{2+}$ 0-77838 S₃BrCl Raman spectrum 0-64449 SCO⁺, radiative and non-radiative transitions, theory and expt. 0-77773 SCl₂ and S₂Cl₂, reactions with H atoms, vibr. populations of HCl products 0-54176 SCl₂ and S₂Cl₂, reactions with H atoms, i.r. chemiluminesc. 0-54177 S₂Cl₂ and S₃Br₂1r. spectra 220-700 cm $^{-1}$ 0-64449

Structure of matter see Crystal structure; Liquids/structure; Solids/structure

SU(3) group theory see Elementary particles/symmetry; Field theory, quantum/interactions, strong; Group theory

Structure factors see Crystal structure, atomic; X-ray crystallogra-

SrTiO₃ transition temperature, superconducting, effect of stress 0-71965 \$\textit{\beta}\subseteq 1.jr. spectrameas., force constants and U-O lattice vibrations 0-65526

0-65526
SrU₂S₂, preparation and crystal properties 0-55832
Sr₂VO₃C(lBr), prep. and props. 0-58750
Sr₂WNiO₆, perovskite type, cryst. transition influence on heat capacity behaviour 0-40577
SrWO₄, scheelite, elec-field-induced g shift for loose Yb³⁺ ions 0-51392
SrZrO₃, replacement of Sr by Ca or Ba, mech. behaviour rel. to diff. phases and reorientation 0-47307

Sulphur compounds continued

phur compounds continued
SD, chem. excitation of A²E⁺, X²II system 0--74306
SF, Hartree-Fock binding energies, ionization potential, electron affinity, dipole and quadrupole moments 0--74304
SF₂, centrifugal distortion effects in microwave spectra 0--74249
SF₄, Raman spectrum and force consts. 0--53049
SF₄, viscosity 293 to 873°K and intermol. forces 0--74686
SF₄ gaseous, electronic struct. exam. by soft X-ray spectroscopy 0--46511
SF₅- autoionization lifetime by ion cyclotron resonance linewidths 0--74221
SF₆ attachment rate for a literal constant of the second constant o

0-74221 SF₆, attachment rate for electrons 0-64772 SF₆. Brillouin scattering near critical point 0-54114 Brillouin scattering near critical point, sound velocity deductions

SF₆, Brillouin scattering near critical point, sound velocity deductions 0–54:114
SF₆, cryst., struct. and mol. motion, m.p. to –160°C 0–50546
SF₆, density from -40 to +200°C, 4 to 500 kbars 0–71220
SF₆, gas, CO₁ laser 10-6 μ pulse reshaping, obs. 0–49954
SF₆, gaseous, F relaxation by n.m.r. 0–58:198
SF₆, i.r. absorption saturation at 10.59μ CO₂ laser wavelengths 0–77840
SF₆, i.r. double resonance study of relaxation 0–465:10
SF₆, ionization attachment and bgr\(^{\text{s}}\)down 0–64773
SF₆, ionization attachment and bgr\(^{\text{s}}\)down 0–64773
SF₆, laser induced 16μ fluoresc., acoustic effects 0–77836
SF₆, laser induced 16μ fluoresc., acoustic effects 0–77836
SF₆, mobility and diffusion of negative ions 0–50116
SF₆, mobility and diffusion of negative ions 0–50116
SF₆, staurated absorpt. spectra using lasers 0–70844
SF₆, staurated absorpt. spectra using lasers 0–70844
SF₆, turbidity near critical point using an optical analog of the Wheatstone bridge 0–58488
SF₆ gaseous, electronic struct. exam. by soft X-ray spectroscopy 0–465:11
SF₆ molecule, rotational-vibrational transitions, narrow reson. within Doppler line during absorpt, saturation 0–70947
SF₆ molecule interaction with positive and negative ions 0–64615
SF₆ sy vibr. mode fluoresc. lifetime 0–53048
SF₆ stimulated Brillouin scatt. freq. shifts meas. and theory, hypersound speed determ. 0–46824
SF₆ use in Q switching N₂O laser 0–54869
SF₄ AsF₃ solid addition compound, fluorine magnetic resonance study 0–56684
SH, chem. excitation of A²Σ⁺-X²Π system, 0–74306

SF₄-AsF₅ solid addition compound, fluorine magnetic resonance study 0–56684
SH, chem. excitation of A²Σ⁺·X²Π system, 0–74306
SH radical, matrix-isolation spectrum 0–61135
SH⁻ impurity in alkali halides, vibr. freqs. and lattice alignment 0–72350
S₄(NH₂)-irrad, e.s.r. of radicals 0–64450
S₇NH γ-irrad, e.s.r. of radicals 0–64450
S₇NH γ-irrad, e.s.r. of radicals 0–64450
SO₇- in H₂O-butyl alcohol, e.s.r. linewidths 0–68148
SO₇, in H₂O-butyl alcohol, e.s.r. linewidths 0–68148
SO₂, in H₂O-butyl alcohol, e.s.r. linewidths 0–68148
SO₂, ibroadening of rotational lines by quadrupolar gas 0–43135
SO₃, broadening of rotational lines by dipolar gases 0–64448
SO₂, dipole mom ir. spectra obs. 0–55320
SO₃, electronic structure study using SCFMO calculations on both minimal and extended basis 0–67753
SO₃, exchange reaction with ¹⁰O atoms in shock waves 0–48176
SO₂, microwave spectral line width as broadened by methyl bromide, evaluation 0–77823
SO₂, molecular properties, theoretical study 0–74233
SO₂, photoelectron spectra using He I 584 Å light source, rel. to vibr. fine struct. 0–61121
SO₂, polar constituent in binary gas mixtures, meas. of thermal conds. 0–53268
SO₂, solid, singlet-triplet absorpt, and emission 0–69154
SO₂ additional frequencies 0–74303

0-53268
SO₂, solid, singlet-triplet absorpt, and emission 0-69154
SO₂ adsorbed, vibrational frequencies 0-74303
SO₂ and SO₂F₂ mixtures thermal conductivity and viscosity measurements, self diffusion and interdiffusion estimation 0-50171
SO₂ laser, far i.r. 0-77107
SO₂ Raman scatt. cross sections meas. 0-71264
SO₂ solvent effects on infra-red band shapes and intensities 0-39802
SO₂ radical ion, e.s.r. spectrum 0-61555
SO₃, i.r. spectrum and mol. struct. obs. 0-43134
SO₃ ions in aqueous solution, electronic spectra assignment of bands 0-50229

SO₃ ions i 0-50229

 $S_2O_3^{-2}$ in aqueous solns, of HF, HCl and HBr, luminescence at room temp, and $77^{\circ}K$ 0-68113

and 77°K 0–68113

\$_{Q_{2}^{-2}} in aqueous solns. of HF, HCl and HBr, luminescence at room temp. and 77°K 0–68113

\$_{Q_{2}^{-2}} in aqueous solns. of HF, HCl and HBr, luminescence at room temp. and 77°K 0–68113

\$_{Q_{2}^{-2}} in aqueous solns. of HF, HCl and HBr, luminescence at room temp. and 77°K 0–68113

\$_{Q_{2}^{-2}} in aqueous solns. of HF, HCl and HBr, luminescence at room temp. and 77°K 0–68113

\$_{Q_{2}^{-1}} (SOCl₂) solvent effects on infra-red band shapes and intensities 0–39802

\$_{Q_{2}^{-1}} (SOCl₂) solvent effects on infra-red band shapes and intensities 0–39802

\$_{Q_{2}^{-1}} (SOCl₂) solvent effects on infra-red band shapes and intensities 0–39802

\$_{Q_{2}^{-1}} (SOCl₂) solvent effects on infra-red band shapes and intensities 0–39802

\$_{Q_{2}^{-1}} (SOCl₂) solvent effects on infra-red band shapes and intensities 0–39802

\$_{Q_{2}^{-1}} (SOC) solvent effects on infra-red band shapes and intensities 0–39802

\$_{Q_{2}^{-1}} (SOC) solvent effects on infra-red band shapes and intensities 0–39802

\$_{Q_{2}^{-1}} (SOC) solvent effects on infra-red band shapes and intensities 0–39802

\$_{Q_{2}^{-1}} (SOC) solvent effects on infra-red band shapes and intensities 0–39802

\$_{Q_{2}^{-1}} (SOC) solvent effects on infra-red band shapes and intensities 0–39802

\$_{Q_{2}^{-1}} (SOC) solvent effects on infra-red band shapes and intensities 0–39802

\$_{Q_{2}^{-1}} (SOC) solvent effects on infra-red band shapes and intensities 0–39802

\$_{Q_{2}^{-1}} (SOC) solvent effects on infra-red band shapes and intensities 0–39802

\$_{Q_{2}^{-1}} (SOC) solvent effects on infra-red band shapes and intensities 0–39802

\$_{Q_{2}^{-1}} (SOC) solvent effects on infra-red band shapes and intensities 0–39802

\$_{Q_{2}^{-1}} (SOC) solvent effects on infra-red band shapes and intensities 0–39802

\$_{Q_{2}^{-1}} (SOC) solvent effects on infra-red band shapes and intensities 0–39802

\$_{Q_{2}^{-1}} (SOC) solvent effects on infra-red band shapes and intensities 0–39802

\$_{Q_{2}^{-1}} (SOC) solven

U-Ni-S syst., at 800°C, new phases 0-63852

Sum rules see Elementary particles/theory

see also Sunspots

active region, development and flaring, exhibiting unusual mag. structure 0-79762

active regions, survey and neutral line spectra rel. to flare productivity 0-41852

0-41852 active regions in chromosphere and corona, EUV obs., ion emission enhancement calc. 0-41863 active regions polarimetry, line selection and data interpretation 0-41854 activity, Aurora Borealis correl., obs. 0-41516 activity, cosmic ray variations, periodic 0-54304 activity, during 1968, obs. Belgian Royal Observatory 0-63163

Sun continued

activity, influence on ionosphere total electron content 0-76469

activity, mm. wavelength obs., with Josephson junction detector 0-66649 activity, origin of cycles, quasiaxisymmetric models of magnetic dynamo 0-72786

activity and Jupiter's great red spot darkness parameter 1891 to 1947, relationship 0-66589

activity centres, variation of principle characts, with drift of 11 year cycle 0-63178

0-63178
activity cycle amplitude 0-48612
activity in 1968 optical and ratio obs. 0-72780
activity in 1968 optical and ratio obs. 0-72780
activity index, validity supported by oxygen isotope dating 0-63180
activity maximas, effect on 27-day variation and long term modulation of cosmic rays 0-41820
activity rel. to microwave and soft X-ray slowly var. components, obs.

0-48600 atmosphere, convective energy transport, model 0-41643 atmosphere, isotope ratio of Eu 0-41860

atmosphere, thermally driven motion, nonlinear eqns., num. soln. 0-59808

0-59808
atmosphere circulation, models rel. to flare forecasting 0-48618
atmosphere model, non-LTE line-blanketed 0-59806
atmosphere vortex ring, class 1B flares 0-59807
atmospheric shock waves, frequency and strength 0-63183
bursts, type II, excited by shock waves 0-79746
bursts, type II, positions of fundamental and harmonic sources 0-79744
bursts, type III, associated scattering in position of sources 0-79747
bursts, type IV, moving, excited by shock waves 0-79746
bursts, type IV, moving March 1, 1969 80 MHz obs. 0-79767
chromosphere, Los Alamos airborne obs. during March 7 1970 eclipse 0-66617
chromosphere, brightness temperature distributions of the control of the con

0-66617
chromosphere, brightness temperature distribution, radio obs. during March 7 1970 eclipse 0-66654
chromosphere, coupling of radiative transfer and thermal cond. 0-51807
chromosphere, dark and bright mottles, lifetime 0-41861
chromosphere, low, effect of density scale height on shock-wave heating 0-72788
chromosphere, low, shock wave heating 0-66657
chromosphere, models 0-54479
chromosphere, thermally driven motion, analysis 0-59808
chromosphere's fine structure, observational results 0-57153
chromosphere active regions EUV obs., ion emission enhancement calc. 0-41863
chromosphere structure, relationship with coronal structure during eclipse

chromosphere structure, relationship with coronal structure during eclipse $0\!-\!69500$

0–69500 chromosphere-corona transition region 0–63184 chromospheric brightening plage-like obs. due to sudden disappearance of quiescent prominence 0–54472 chromospheric fine structure, obs. by 53-cm Lyot coronagraph 0–63181 chromospheric mottles, mechanical fluxes in and outside, ratio 0–69489 chromospheric spicule, model 0–38216 chromospheric supergranules, filtergrams at $H\alpha$ +0.65Å over 62 hours 0–41844

0-41844 control of stratospheric circulation 0-45133 convection cells existence rel. to simple model 0-66612 convection cells existence rel. to simple model 0-66612 convection large-scale, effects of rotation, study 0-54453 core opacity, effect of comp. uncertainty 0-66647 cosmic-ray intensity fluctuations, short-period at geomagnetic equator, photosphere frequency relationship 0-59664 electron density in chromosphere, chromospheric flares and prominences, determ. method 0-39559 faculae, turbulent velocities and damping constants from i.r. Ni and Fe lines 0-72784

Fe photospheric abundance, effect on core opacity 0-66647 granules, inside flow pattern 0-66645 gravitational field, selective modelling 0-59892 interior, thermonuclear reactions and solar neutrinos 0-51787 interior rot. convective damping, density stratified liq. spin-down obs. 0-45428 model, atm., line-blanketed 0-66656

model, atm., line-blanketed 0–6656 modulation and heliocentric gradient characts. for low energy cosmic rays 0–56899

0-56899
modulation of galactic cosmic rays 0-41577
morphology of individual features, comparison of multichannel magnetograph obs. with spectroheliograms 0-54454
motion, and galactic rot. from Be stars radial vel. obs. 0-41589
neutrino capture fluxes with recent corrections to opacity 0-48595
neutrinos, solar, and interior thermonuclear reactions 0-51787
OSO-VI, Harvard expt. obs. 0-66360
oblateness rel. to relativity 0-41568
opacity of solar core, influence of individual heavy elements 0-54452
photosphere, magnetic field position determination using interference filter 0-69487
hotosphere, magnetic fields on March 7 1970 eclipse 0-66644

photosphere, magnetic fields on March 7 1970 eclipse 0–66644 photosphere, motions in region of faint mag. fields 0–63175 photosphere, velocities (vertical) and horizontal wave propagation 0–79757

photosphere, wave propagation, horizontal and vertical velocities 0-79757

photosphere and chromosphere, small-scale motions 0-41819
photosphere five-min vel. oscills. and supergranulation, obs. 0-41845
photosphere model, homogeneous, includes line blanketing due to neutral
and ionized metals 0-41822

photosphere turbulent velocities and damping constants from i.r. Ni and Fe lines 0-72784

pinotospiele tunient velocites and valaring constants from 17.14 and relines 0-72784 plages, H_{α} , config. rel. to large flares prediction 0-48614 plages, with only small or no spots, major $H\alpha$ flares 0-79759 position, in local spiral arm 0-66396 prominence, $H\alpha$ spectroscope construction 0-69513 quiet, new moon centre, brightness temp. and brightness temp. ratio at 3.3- and 5.7-mm λ 0-76671 quiet and disturbed, influence on ionospheric absorption 0-45179 radar echo, possible role of maser effect 0-72790 radio telescope, 6 GHz for solar observation 0-57158 research at Ondrejov observatory 0-59786 rotation, differential, driven by baroclinic stratification 0-54365 rotation, differential, in hydrogen convection zone, caused by anisotropic turbulent viscosity 0-69470 rotation, spectroscopic determination 0-57129

Sun continued

seeing effects, image motion and blurring obs. 0-6947! short period oscills. of photosphere and Doppler velocity gradients 0-4!843

solar parallax, dynamical determ. from motion of 433 Eros 0-45417 sunspot number prediction from dyn. rel. of sun and planets 0-54471 supergranular network, time and shape changes, K_{232} spectroheliograms 0-79758

supergranulation, at centre of disk 0-66646

surges, temporal correlation with flares 0-69494

telescopes, glancing incidence, for extreme u.v. obs., optical design 0-51818

U=31818 temperature, photospheric, difference between equator and poles 0-69486 temperature-minimum region, model 0-66655 U-bursts, at metre wavelengths dynamic spectra, radio heliograph maps 0-79748

0-19/48
C/H compared with value in Jupiter's atmosphere 0-48569
CO, molecular layer, temp. constancy 0-57141
12C/13C ratio possibility of determ. from line strengths in new 13C14N search regions 0-45432

regions U-4.94.2 Eu isotope ratio in solar atmosphere 0-41860 Fe/H ratio and new system of oscillator strengths for Fe I lines 0-41824 Ga and rare metals abundances 0-66613 He atoms stationary distrib, for atomic levels occurring in solar atmosphere 0-63162

Mg isotopic abundance, determ. from line profiles anal. 0-57131 Ni abundance from photospheric Ni II lines 0-69474

active regions in chromosphere and corona, EUV obs., ion emission enhancement calc. 0–41863 chromosphere transition region 0–63184 coronagraph, catadioptric, design 0–63186 coronagraph, catadioptric, design 0–63186 coronagraph obs., monochromatic, at 5303 Å and 6563 Å, photographic, isodensity, isophotal data during eclipse 0–6658 coronagraph obs. of coronal condensation during 1962 eclipse, anal. 0–41866

Crab nebula occultation 1967 by solar corona 0–51643 density structure, connection with magnetic fields 0–69501 Doppler temperature and motion 0–66665 of eclipse, 12 November 1966 0–51806

electron density determ. by radio interferometric meas, of light bending near sun 0-487!!

sun 0–487!! electron density profile, from pulsar occultation 0–6667! electron density profile, from pulsar occultation 0–66670 emissions, U burst and type III, polarized, theory 0–76674 expansion phenomena, flare-associated Sacramento Peak obs. 0–66668 inhomogeneities, corotating, velocity driven perturbations to determine solar wind structure 0–59795 ion excitation equilibria for highly excited Fe, Ni and Ca 0–41817 ions, acceleration and motion 0–66639 limb, image motion, at Norikura corona station 0–79771 Los Alamos airborne obs. during March 1970 eclipse 0–66617 magnetic bottle, at 10 solar radii, evidence 0–63185 microwave, X-ray and Type-3 emissions, modulation into 10 sec pulses 0–79772 model, steady-state, with neutron decay as main energy source 0–54480

model, steady-state, with neutron decay as main energy source 0–54480 model with spicules to explain limb brightening of u.v. lines of C, N, O, Si ions 0–41865 models 0–54479

occultation of Pioneer 6, measurement of transient Faraday rotation 0-41559

0-41539
occultation of Pioneer 6, spectrogram 0-41560
occultation studies, 1969 Taurus A 0-66659
outer, F and K separation at March 7 1970 eclipse 0-66666
photograph during March 7, 1970 eclipse 0-66614
photographs, Lockheed Aerospace eclipse expedition, March 7 1970
0-66616

0-06616
photographs, from Apollo 11, analysis 0-66672
photometric obs., Mexico March 7 1970 solar eclipse 0-66663
photometric study, K and F during March 7 1970 eclipse 0-66664
plasma, e.m. waves, different modes of amplification 0-72790
plasma, non-linear processes, rel. to types I and III radio bursts interdependence 0-37126

dence 0-57136

plasma, regions of rapid acceleration, vel. profile of solar wind determ. 0 - 54466

plasma wave radiation by electron stream in corona 0–54476 plasma wave transformation in magnetoactive plasma 0–54477 polarimetric obs., Mexico March 7 1970 solar eclipse 0–66663 polarization and intensity at the November 12, 1966 eclipse 0–41864 radar echoes, observed characteristics, implications, results 0–54478 radio emission, pulsating, analysis of three such outbursts at 239 MHz 0.41832 0 - 41832

0–41832 rocket obs, on March 7 1970 eclipse, photographic records 0–66662 scattering of decametric radiation from Crab nebula by corona 0–45242 solar eclipse emission lines, 7 March 1970, linear polarization meas. using photographic polarimeter 0–69492 spectroscopic obs., Mexico March 7 1970 solar eclipse 0–66663 spectrum 3500 to 6000 Å at eclipse of March 7, 1970 0–66666 streamers, energy transport and ineterstreamer regions 0–69503 streamers, evolution of discrete features from sun to 1 AU 0–69502 streamers disk locations, determination from eclipse, K-coronameter, balloon-borne coronagraph, obs. 0–59809 structure, associated with structure of chromosphere during eclipse 0–69500 structure, predicted and observed during March 7 1970 eclipse 0–66660

o-69500
structure, predicted and observed during March 7 1970 eclipse 0-66660
structure, predicted and observed during March 7 1970 eclipse 0-66661
structure, predicted and observed during March 7 1970 eclipse 0-66661
structure, radio obs. at 80 MHz, two-dimensional pictures 0-79770
structure evaluation from rocket obs. Feb. 15, 1961 0-72791
structure prediction in eclipse of March 7, 1970 0-48598
temperature determination, from flux of soft X-radiation 0-72789
temperature rel. to exosphere temp, of Earth 0-72768
x-ray obs. of forbidden line in helium isoelectronic sequence 0-66669
X-ray photographs during eclipse on March 7, 1970 0-66667
Ca II fine structure on solar disc, high dispersion spectra, line profiles variations 0-59799
Ca(XV), forbidden spectral lines, intensity ratio line to continuum ratio 0-41826

excitations equilibria for highly ionized Fe, Ni and Ca ions 0-41817

Sun continued

corona continued

Fe lines, Ca XV λ 5694 line, anal. of February 4, 196, coronagraph obs. 0-41866

He isoelectronic sequence, x-ray obs. of forbidden lines 0-66669

clipses
1896, Aug 9, total, obs. at Hokkaido, Japan 0-59788
1896, Aug 9, total eclipse, 4 cm obs. 0-63164
1966, Nov. 12, description of aircraft expedition 0-51806
1966, Nov. 12, instrumentation and observational programmes at Bage
(Brazil) 0-51812
1966, Nov. 12, radioastronomical instruments and observation 0-51788
1970, March 7, antural VLF radio signals obs. in Newfoundland 0-66300
1970, March 7, partial phases 0-63165
1970, March 7, prediction of coronal structure 0-48598
1970, March 7, radio burst at three wavelengths, at onset of totality
0-69481

1970, March 7, radio obs. with 7 GHz polarimeter 0-66634
1970, March 7, radio obs. with 7 GHz polarimeter 0-66634
1970, March 7, rocket u.v. flash spectra 0-48597
1970 March 7, Lockheed aerospace expedition, coronal photograph experiments 0-66616

httens 0-00010 1970 March 7, Los Alamos airborne chromospheric coronal, geophysical obs. 0-66617 1970 March 7, VLF propagation effects 0-66615 1970 March 7, atmospheric gravity waves generation, possible detection

0-66308

0-65306 1970 March 7, radio obs. at 16 GHz 0-66633 1970 March 7, radio obs. at Sagamore Hill solar radio observatory 0 - 66618

air temperature variations during eclipse on May 20, (1966) 0-41490 coronagraph obs. of coronal condensation during 1962 eclipse, anal. 0-41866

coronal polarization and intensity during the November 12, 1966 eclipse 0-41864

ionospheric 100 kHz pulse propagation comparison of July 1963 and March (1970) 0-66325

ionospheric changes, solar radiation, electron densities, Canada obs. 0–66321

0-66321
ionospheric effects, trends in study 0-66320
March 7, 1970 ionospheric total electron content changes along three paths 0-66326
March 7, 1970 rocket density measurements at Florida 0-66306
March 7, 1970 rocket density measurements at Florida 0-66306
March 7, 1970, information on corona, from photographs 0-66614
meteorological obs. rockets 0-66275
partial on 1968 September 22, radio observations 0-41818
radio obs., 16 and 30 GHz, March 7 (1970) 0-76665
Taurus A absorption spectrum change 0-59787
total, effects on equatorial F₂-region, calculations 0-72655
total, greyish light obs. 0-69499
X-ray source identification using D-layer ionization 0-41830
X-ray source identification using D-layer ionization 0-41829
Bares

flares

1968, July 6 and 8, anal. of obs. 0-45439 18 class, vortex ring 0-59807 1N, 1968 April 25, development of young bright region with loops 0-79762

0-79762 active regions neutral line spectra rel. to flare productivity 0-41852 activity, solar X-rays as indicators 0-48615 area, peak intensity and integrated intensity meas. by videometer 0-41858 aurora following solar flare, emission structure deviations 0-54276 chromospheric, electron conc. and structure 0-45437 chromospheric, enhancements in EUV, relationship with solar abundances, report 0-69498

report 0–69498
chromospheric, solar wind disturbances distribution 0–69493
class lb, X-ray spectrum 4 to 16 keV 0–79764
w.r.t. coronal expansion phenomena 0–66668
cosmic ray acceleration before Forbush decreases, depend. on solar longitude of chromospheric flare 0–51627
3b decay, Ca, Si and S resonance, intercombination and forbidden transitions, He like 0–69497
development, phase of particle acceleration 0–79769
electron density profile meas. at Pennsylvania in D-region 0–69325
electrons ~40 keV events during Aug. 1966-Dec. 1967, obs., emission, propagation 0–59805
energetic particles, props. and propagation characteristics, findings since

p. opagation 0-39803 energetic particles, props. and propagation characteristics, findings since 1966, review 0-79755 forecasting, solar atm. circulation models 0-48618 rel. to geomagnetic storms, sudden-commencement families 1957 to 1964 0-76514

 $H\alpha$, major, in plages with only small or no spots 0–79759 homologous, optical and radio, observed from $H\alpha+4.00\text{\AA}$ to $H\alpha-4.26\text{\AA}$ and 10-cm radio 0–41859

interplanetary shock He-enriched driver gas, obs. 0–41813 rel. to ionosphere, sudden disturbance, recombination coefficients 0–45181

ionosphere effects at Lindau 0-69308

ionospheric electromagnetic wave propagation, v1f. and e1f. 0-62927

ionospheric electromagnetic wave propagation, v1f. and e.1f. 0–62927 mechanisms, critical account of current theories of origins 0–72787 microwave and soft x-ray, burst component correl., obs. 0–48601 neutron flux, obs. 0–41842 observations at the Swedish Astrophysical station in Anacapri for the years 1965-1968 0–57152 October 30, 1968 and associated active dark filaments 0–54473 optical, association with type III radio bursts from 4 to 2 MHz 0–51795 p-flare of 7 July 1966, oblique shock initiation in solar wind, satellite magnetometers obs. 0–57151 plages, H_a, config. rel. to large flares prediction 0–48614 prominences, ascending, correl. with flares 0–45438 proton, of July, August, September 1966, polar cap absorption, anomalous cosmic radio noise 0–51575 Proton Flare Project (1969), review 0–63171 proton flares, characts. of assoc. X-ray emissions rel. to ionospheric disturbances 0–54474 15 MeV protons, heliocentric longitude intensity profile, (February 5, 1965) 0–48617 spectra, Fe1 x4063 anomalous enhancement obs. 0–41856

spectra, soft X-ray, recombination edges 0-69496

```
Sun continued
```

flares continued

ares continued

3b spectra, soft X-ray 0.7-8.5Å 0—69495
spectrum of microwave bursts usig coherent plasma emission mechanism for v~v,≥v, 0—66651
rel. to sunspot group area and flariness, flare probab. 0—41855
and surges and active regions development, OSO VI obs. 0—66653
temporal correlation with surges 0—69494
type II burst, shock wave induced solar radio emission, evidence 0—59804
type IV burst, shock wave induced solar radio emission, evidence 0—59804
VERBY (August 17, 1966) 0—48416

0-39804
X-ray, (August 17, 1966) 0-48616
X-ray, temp. and emission-measure profiles 0-79765
X-ray enhancement, soft, quiescent and flare tune temps. 0-79768
Fe I y³F₂ level, selective excitation in spectrum of two flares 0-54475
Fe line emission at 1.9 Å during flares 0-51793

magnetism

active regions, survey of mag. meas. and deduced results 0–41853 chromosphere field determ. from fitergrams 0–63182 corona bottle at 10 solar radii, evidence 0–63185 field distrib. in sunspot observed in October (1963) 0–59800

netd aistrib. in sunspot observed in October (1963) 0—59800 field generation by partially ionized convective envelope, polar field strength calc. 0-69469 field measurement using 4-image spectroheliograph 0—54459 fields, connection with density structure of corona 0—69501 fields in asymmetric pores, distinction between pores and sunspots 0—69488

fields rel. to convection 0-54453

hetes ref. to convector 0—34433 kinetic dia- and para-magnetism due to temp, gradient 0—52226 photospheric fields on either side of quiescent filaments 0—48613 photospheric mag, field and brightenings, relation with large quiescent pro-minence 0—54472

photospheric mag. field postion determination using interference filter 0-69487

0-69487
polarmag. fields of July and August 1968 0-69472
spectral line formation in mag. field, magnetographic meas. 0-54470
sunspot with photospheric bridge, mag. field structure 0-45435
surface, meas. techniques used at San Fernando observatory 0-63188
toroidal mag. fields, and differentially rot. sun 0-66619
variations obs. at Abinger, estimation by spectral analysis via Fourier
transform 0-66611

prominences

prominences
ascending, limb-SD type, apparent motions 0–45438
mag, fields line formation, role of atomic level polarization, magnetograph
meas, comments 0–59792
quiescent, photospheric mag, fields obs. on either side of filament 0–48613
quiescent, with helical structure, model 0–41857
quiescent large on solar disk, sudden disappearance, obs. 0–54472
solar eclipse emission lines, 7 March 1970, linear polarization meas. using
photographic polarimeter 0–69492
spicule energy balance, sources of energy 0–45436
spicules, cylindrical, spinning emission of CaII K line 0–79766
stability, thermal and dynamical hydromagnetic and radiavtive instabilities
0–66652

radiation

radiation
see also Sunlight
1968, Jul. 13 to Aug. 9, u.v. flux var., nonrandom, report 0-76662
effect on D-region ion conc., u.v. and visible sensors 0-69323
y-, during active and quiet periods 0-76664
absorption by atmos., calculation methods 0-54247
brightness meas. using 4-image spectrohediograph 0-54459
chromosphere, low, dark band arising from unwanted photospheric light
0-41862

coronal polarization and intensity at the November 12, 1966 eclipse 0-41864

density of upper atmosphere, determination 0-48299 earth incident, conversion factor values for mean daily total calc. 0-41505

0-41505 flare, optical and radio homologies, correl. 0-41859 gamma-ray lines, 30 keV to 6.3 MeV, search 0-59794 hot regions on solar disk, obs. at 1.2 mm 0-54464 ion emission enhancement from active regions in chromosphere and corona 0-41863 in onosphere, lower, eclipse effects 0-66321 $L\alpha$, absorbtion obs. in upper atmosphere 0-72638 limb spread fn. for stray light, determination 0-59810 line formation in prominences mag. field, role of atomic level polarization, comments 0-59792 lunar samples, solar radiation effects 0-45398 Mars and Venus variation of exospheric temp. with solar u.v. radiation 0-51759 mm, region, slowly varying component, props. 0-66637

0-51759
mm. region, slowly varying component, props. 0-66637
optical polarization of solar disk, broad band measurements 0-79740
Ottawa River Solar Observatory project 0-69505
plasma wave radiation by electron stream in corona 0-54476
polar brightness study, temp. distribs. and thermal currents 0-48596
polarimetery in active regions, line selection and data interpretation
0-41854

0-41854
proton events in 20th solar cycle 0-51801
quite sun, ionospheric effects of X-rays 0-59740
scattering by atmos, calculation methods 0-54247
solar const., Balloon obs. 0-48594
solar wind, interaction with geomagnetic field, review 0-41551
spatial structure of brightness field from earth's reflection, statistical charact, satellite meas. 0-59552
thermotidal modes excitation in dynamo region of ionosphere, Joule heating estimate 0-56840

estimate 0-56840
u.v., extreme, spectrometer for obs. from OSO ! satellite 0-51789
u.v., percentage in total radiant flux, depend. on solar hour angle and atmospheric haze 0-66622
u.v. continuum 1450-2100Å, transition of solar temp. minimum at 1700Å study 0-54458
u.v. flux, nonrandom variations (Jul. 13 to Aug. 9, 1968), report 0-76662
X-radiation, review 0-54461
x-ray, control of ionospheric E-region ionization 0-56841
X-ray bursts at energies less than 10 keV, OSO-4 obs. 0-41828
X-ray control of ionosphere E-region electron density 0-41540
X-ray emission above 3 keV, localization, spatial distrib. expt. 0-69477
X-ray emission assoc. with proton flares, rel. to ionospheric disturbances
0-54474

radiation continued

Author continued

X-ray emission from iron line at 1.9 Å during flares 0-51793

X-ray emission rel. to ~40 keV flare electrons events 0-59805

X-ray flux in selected emission lines over the disk 0-51792

X-ray fluxes, from Solrad 9 satellite, data 0-69478

X-ray fluxes, telemetering from SOLRAD 8 satellite, from December 1965

to November 1967 0-57133

X-ray fluxes from Solrad 9 satellite (1968-17A), March 1968-Dec. 1968

0-57134

0-57134

X-ray photographs during eclipse on March 7, 1970 0-66667

X-ray spectrum 4 to 16 keV of class 1b solar flare 0-79764

X-rays, Rayleigh and Compton scatt. fluxes and K fluoresc. flux for Venus, Mars and the Moon 0-57135

X-rays, as flare activity indicators 0-48615

X-rays, saning spectroheliograph 0-54485

x-rays, soft, and microwaves, burst components correl., obs. 0-48601

X-rays, soft, and microwaves, burst components correl. 0-48604

X-rays, soft, slowly var. component rel. to microwave vars. and solar activity, obs. 0-48600

X-rays from 3 sources above sunspot groups, comparison with microwave emission 0-48602

H Lyman α line, high-resolution profile, atmos. altitude depend. 0-59558

addation. corpuscular

radiation, corpuscular activity in Proton Flare Project Retrospective Interval (5-18 June 1969) 0-63172

o-03172 artificial satellite perturbation effects 0-66357 cosmic ray acceleration before Forbush decreases, depend. on velocity of solar wind 0-51627

solar wind 0–51627
cosmic ray anisotropic, propagation in inhomogeneous medium, model, effect of solar shell 0–59802
cosmic ray entry into earth's magnetosphere 0–62931
cosmic ray, high energy, modulation by solar wind 0–59678
cosmic rays, high energy, modulation by solar wind 0–59678
cosmic-ray intensity 11-year modulation, depend. on heliolatitudinal sunspot distribution 0–76668
electron scattering opacity, effects of electron correls. on calc. of neutrino flux 0–63174
electrons ~40 keV events during Aug. 1966-Dec. 1967, obs., emission, propagation 0–59805
filaments, fluid dynamics, radial dependence of flow parameters 0–79756
high atmosphere ionization by solar cosmic rays, generalization of solns.
0–48321
interaction with earth, moon. Mars. Venus, review of findings since (1066)

interaction with earth, moon, Mars, Venus, review of findings since (1966) 0-79755

interaction with earth, moon, Mars, Venus, review of findings since (1966) 0–79755 interaction with planetary atmos. 0–41799 ionospheric penetration at low altitudes 0–76443 L_a, role in ionization of lower ionosphere 0–56832 neutrino flux, theoretical calc., effects of electron correls. rel. to scatt. opacity 0–63174 neutron decay, proton injection into earth's radiation belt 0–48317 neutron decay, proton injection into earth's radiation belt 0–48317 neutrons, flare and quiet-sun fluxes, obs. 0–41842 neutrons, flare and quiet-sun fluxes, obs. 0–41842 neutrons near top of atmosphere, meas. 0–41510 one-fluid equations, solution with modified thermal conductivity 0–69483 p-flare of 7 July 1966, oblique shock initiation in solar wind, satellite magnetometers obs. 0–57151 plasma, findings since 1966, review 0–79755 plasma, traveltime and variability of geophysically effective flux responsible for magnetospheric storm 0–72783 plasma magnetic field, relationship with geomagnetic field 0–56860 plasma outflow equations with allowance for ion composition 0–51799 plasma waves 0–59621 polar cap absorption, particle spectrometer, high-sensitivity, for measurements 0–63878
Proton Flare Project (1969), review 0–63171
Proton Flare Project (1969), summary of June events 0–63173 proton emission, advanced warning from 10.7 cm radio and 0-8 Å X-ray wavelengths 0–54469 proton events, bibliography rel. to forecasting 0–59796 proton events, during 1964-67, rel. to electrons ~40 keV flare events during Aug. 1966 Dec. 1967 0–59805 protons, halo and energetic storm, comment on previous paper 0–41840 protons.

protons, 100-1000 MeV, increase in intensity at 4.55 7 July 1966 0–54467 protons, halo and energetic storm, comment on previous paper 0–41840 protons, halo and energetic storm, comments on a previous note 0–41841 protons, low-energy, phenomenological classification 0–51802 protons, solar flare, inducing radioactivity in lunar samples 0–41835 protons, solar flare, inducing radioactivity in lunar samples 0–66581 shock, reverse hydromagnetic 0–69484 solar wind, tangential discontinuity causing magnetospheric disturbance, ionosphere current effects 0–51595 solar wind flow behind interplanetary shock fronts, Mariner 5 and Explorer 34 days 0–60488

34 obs. 0-69485 solar wind flow past Venus and Mars 0-79754 solar wind flow past Venus and Mars 0-79754 obs. 0-57139

solar wind shock wave at lunar limb, lunar conducting islands theory 0-48560

solar wind streams, from amplitude scintillation in Jovian decameter emis sion 0-66643

solarwind velocity relation to geomagnetic activity, empirical equations 0 - 51598

thermal state and effective collision frequency 0-41836

thermal state and effective collision frequency 0—41836 v.1f. radio noise wave characts, meas, using multiple receivers 0—45186 wind, Het flux, Apollo 1! expt. 0—48606 wind, α-particles in magnetosheath, obs. 0—76670 wind, cosmic ray convection, diffusion and adiabatic deceleration in this wind 0—41759 wind, density fluctuations, structure from interplanetary scintillation of radio sources 0—41746 wind, discontinuity due to solar flare, He-enriched driver, gas, obs. 0—41813 visit believe physicages and playing appropriate 0—48410.

wind, helium abundances and plasma properties 0-48610 wind, history of scientific discover, lecture 0-41839 wind, hydromagnetic aspects of flow past moon 0-48555

```
Sun continued
```

radiation, corpuscular continued

wind, hydromagnetic observations 0-59803 wind, hydromagnetic observations 0-59798

wind, instabilities associated with heat conduction, consequences 0-41837

0–41837
wind, interaction with planetary atmosphere, dynamics 0–63161
wind, interactions, appl. of Knudsen number concept 0–48609
wind, ions, acceleration and motion 0–66639
wind, model including viscosity, rotation and mag. field effects and with two temps. 0–51803
wind, non-spherical, velocity field model 0–66638
wind, plasma instabilities associated with heat conduction and their consequences 0–51804
wind, rel. to geomag. activity semi-annual variation 0–41552
wind, relative He abundance and plasma props. 0–54468
wind, reverse hydromagnetic shock, report 0–66640
wind, theoretical investigation including fluctuations 0–48608
wind, velocity profile in regions of rapid acceleration of coronal plasma

wind, velocity profile in regions of rapid acceleration of coronal plasma 0-54466

wind, velocity profile in regions of rapid acceleration of coronal plasma 0-54466 wind disturbances due to chromospheric flares, distribution 0-69493 wind flux, implications from trace elements and radioactivity meas. in lunar samples 0-45341 wind interaction with earth's mag, field, lab. simulation 0-76658 wind interaction with interstellar H, and anisotropic distrib. of H in interplanetary space 0-41814 wind interaction with magnetosphere and Moon 0-56862 wind interplanetary shock waves 0-59797 wind plasma characts, lunar wake depend. 0-51800 wind plasma turbulence, viscosity and dissipation 0-48607 wind positive ion spectrum near earth's bow shock 0-48302 wind structure, ion-temp, anisotropies, mechanism for limiting 0-57138 wind structure determinedly corotating coronal inhomogeneities, velocity driven perturbations 0-59795 x-ray, y and particle sources 0-66641 H-H scatt., H at, in cold H gas, for solar wind calcs. 0-64277 H atoms, reaction with C and S isotopes in lunar fines 0-57096 He-H, density ratios in solar wind, variations 0-54468 Re, anomalous isotopic ratio, detection at nanogram level 0-41838 radiation, radiofrequency

radiation, radiofrequency storm', type III, exciter speed, direction, and plasma distance scale 0-6635 burst, at three wavelengths, at onset of phase of totality of solar eclipse

0-6948!

burst, fast-drift, type III, 3.5 MHz to 50 KHz 0-66636 burst, fast-drift, type III, 3.5 MHz to 50 KHz 0-66636 bursts, U-like, trajectories followed by the disturbing agency 0-41831 bursts, microwave and meterwave, correl, with X-ray bursts 0-66628 bursts, microwave impulsive, centre-to limb variation, gyrosynchrotron emission in mag, dipole field appl. 0-45433 bursts, obs. at Arcetri Observatory, Sept. 1965-Dec. 1967 0-51798 bursts, sohort duration, associated with type-III activity, high resolution obs. 0-54465

bursts, sympathetic, at mm λ 0–69482 bursts, type 2 and 3, coherent synchrotron deceleration mech. 0–51796 bursts, type III, dynamic spectra from 4 to 2 MHz, OGO-III obs. 0–51794

0-51794
bursts, type III, from 4 to 2 MHz, association with optical flares 0-51795
bursts, type III, plasma wave conversion into main tone and second
harmonic radiation 0-51797
bursts, type IV, influence of magnetoplasma on gyro-synchrotron radiation 0-71148
bursts, types I and III, interdependence, explanation 0-57136
bursts I and IV mB-type and noise storms mode coupling in warm plasma,
interpretation 0-54462
bursts in Proton Flare Project Interval (May-July, 1969), Alouette II obs.
0-66632

0 - 66632

0–66632 coronal microwave emissions, modulation into 10 sec pulses 0–79772 eclipse of March 7, 1970, 16 GHz observing frequency 0–66633 eclipse of March 7, 1970, obs. with 7 GHz polarimeter 0–66634 during eclipse of March 7, 1970, residual emission and spectrum of McMath 607 region 0–66618 emission, 4.4 cm, polarisation of local sources 0–72747 flares, microwave bursts, spectrum using coherent plasma emission mechanism for ν~ν_ε»ν_ρ 0–66651 galactic noise spectrum and solar radio bursts hecto-decametric wave region, Alouette II obs. (Oct. 1966) 0–54483 line source fn. in continuum, dependence on freq., error analysis 0–54463 microwave (10.7cms), correlation with X-ray (2-12Å), nonflaring source 0–76663 0 - 76663

0–76663
microwave and soft X-ray burst components correl. 0–48604
microwave and soft X-ray slowly var. components correl., obs. 0–48600
microwave and soft x-ray, burst component correl., obs. 0–48601
microwave bursts, polarization reversal, possible explanation 0–48603
microwave emission from 3 sources above sunspot groups, comparison
with X-ray emission 0–48602
microwave impulsive bursts centre-to- limb variation, gyro-syncrhtron
emission in mag. dipole field appl. 0–45433
millimeter emission, slowly varying component, report 0–76673
millimeter wave region, techniques and instrumentation 0–76666
noise storm, May 20, 1966, two dimen. structure determ. from eclipse data
0–45434
polarization at 74 MHz, May 18-26 (1967) 0–41834

polarization at 74 MHz, May 18-26 (1967) 0-41834 polarization characts, at metre wavelengths observed in reflection 0 - 48605

polarization during passage of McMath plage region over visible disk, 74 MHz obs. 0-41834 prominences, ascending, correl, with radio emission 0-45438 pulsating emissions at 239 MHz, analysis of three such outbursts 0-41832 quiet, 3.3-mm centre to limb brightness distribution 0-63176

quiet, 3.3-inm centre to limb brightness distribution 0-63176 radio type II, IV emission rel. to ~40 keV flare electrons events 0-59805 s-component, significance of energetic electrons 0-66631 sources of type I and III, structure, polarization and spatial relationship 0-41833

type II burst, solar radio emission from flare induced shock waves 0-59804

type $\overline{\text{IV}}$ burst, solar radio emission from flare induced shock waves 0-59804

type IV event, 1970, March 2. two peculiar phases 0-69480

Sun continued

radiation, radiofrequency continued

U-bursts, relative intensity of second branches 0-7975! X-ray (2-12Å), correlation with microwave (10.7cms) nonflaring source 0-76663

spectra
see also Sun/corona; Sun/flares; Sun/prominences
10 microns to 1 cm, theoretical, from temp-minimum region model
0-66655

0–6655 absorption filter, magnetic beam, elementary theory for different experimental conditions 0–41875 active regions 10830 i.r. line, photoelectric obs. Doppler width 0–72785 active regions neutral lines spectra rel. to flare productivity 0–41852 Ca II H and K lines, core residual intensity ratios 0–4543! Ca II H and K lines emission cores, asymmetries in K₂ and K₃ 0–41825 chromosphere, variations in line profiles to chromosphere during eclipse 0–66624

chromospheric lines, soln. of line transfer eqn. 0-57154 damping consts. of i.r. Fraunhofer lines, variation with optical depth 0-41821

outpung consts. of 1r. Fraunnofer lines, variation with optical depth 0–41821 detection of water vapour in sunspots from absorpt. bands 0–57145 EUV, Fe XIV theoretical intensities 0–66627 Einstein effect, and the observed red shifts 0–69473 emission, line intensities, effectively thick approximation 0–59789 extreme u.v., Japan 1948-68 0–54321 Fe XIV line in corona, using Fabry-Perot interferometers 0–66665 flares, soft X-ray, recombination edges 0–69496 flares, Fe I A4063 anomalous enhancement obs. 0–41856 3b flares, soft X-ray 0.7-8.5Å 0–69495 Fraunhofer, Re I lines search 0–69475 Fraunhofer, Re I lines search 0–69475 Fraunhofer, determination of profiles of selected lines 0–59790 Fraunhofer lines, centre-to-limb variation in photosphere 0–48599 Fraunhofer lines, i.r., damping consts. and their variation with optical depth 0–41821 Fraunhofer lines per frequency and per equivalent width, counts and statis-

Fraunhofer lines per frequency and per equivalent width, counts and statistics 0-54457

Fraunhofer lines without Zeeman splitting, results 0-57132 gamma-ray lines, 30 keV to 6.3 MeV, search 0-59794 ir. from 4 to 14.3 microns, variation with attitude of meas. 0-54460

 K_2 emission peaks, violet, enhancements due to motions in the atmosphere 0-41825

0-41825 limb brightening of XUV reson. lines of Li-like ions, obs. 0-45440 limb brightening of u.v. lines of C, N, O, Si ions, coronal model with spicules 0-41865 line at solar limb, dependence on freq. 0-54463 line blanketing, (depth dependent), by neutral and ionized metals, model photosphere appl. 0-41822 line formation in mag. field 0-54470 line formation in mag. field 0-54470 line formation in prominences mag. field role of atomic level polarization.

line formation in mag. field 0-54470 line formation in prominences mag. field, role of atomic level polarization, comments 0-59792 line shifts, analysis 0-63166 line-blanketing, in model solar atm. 0-66656 moustaches, asymmetry of emission photometry 0-41823 photoelectric, of photosphere and sunspot umbra and penumbra. 3900-8000Å 0-72781 uvby β photometric system, line-blanketing effects on indices 0-41667 photosphere, centre-to-limb variation of 9 Fraunhofer lines 0-48599 photosphere, opacity 2000 to 3500Å, temp. and wavelength depend., role of H_3^+ ion 0-41827 photosphere, variations in line profiles to chromosphere during eclipse

photosphere, variations in line profiles to chromosphere during eclipse 0-66624

0–6624
photospheric, variations in line profiles to chromosphere during eclipse 0–66624
photospheric, spectrum in 5881 Å region, HOH lines existence, use of rapid scanning spectrometer 0–57147
profile analysis for photoelectric observations of carbon molecules 0–63167
rf., variations in emission at 3.3 mm λ, and relation to flares 0–79749
radio, dynamic, comparison of Sept 2 1966 complex burst obs. at Culgoora and Wessenau 0–79752
radio bursts, U-like relative intensity of second branches 0–79751
radio pulsation, theory, whistlers 0–79750
red shift, gravitational, atomic beam study 0–63169
red shift, gravitational, atomic beam study 0–63169
red shifts obs., Einstein effect 0–69473
simulation in 0.25-2.5μ region using individual and combinations of inert gases 0–51785
simulators at the Jet Propulsion Laboratory, development 0–51786
spectroheliograms, from OSO VI 0–66653
sunspot spectrum in 5881 Å region, HOH lines existence, use of rapid scanning spectrometer 0–57147
telluric absorpt. effect, sub-millimeter obs. at Mauna Kea observatory 0–51813
u.v. C II resonance line profiles, broadening mechanisms 0–63170

u.v. C II resonance line profiles, broadening mechanisms 0-63170 u.v. continuum intensity between 1700Å and 1D limit of Si at 1682Å 0-54458

0—54458
u.v. flash, 1400° Å-1960 Å in total eclipse 0—66623
u.v. part, photography method, Herschel effect, results 0—54481
extreme-u.v. spectroheliograms from OSO-iv, atlas 0—76660
umbra flash, in CaII lines, as magneto-acoustic wave phenomenon
0—79741.

0—19/14: XUV, active regions, OSO-VI obs. 0—66630 X-ray, 1 Å to 400 Å, OSO-V obs. 0—66629 X-ray, and diffuse cosmic X-ray spectra, satellite meas. August 7-8 (1967) 0—48483

X-ray, obs. techniques, interpretation of data 0-72782 X-ray, of active regions, 3 Å-15 Å, electron density determination 0-79742

3 -19

X-ray source identification using D-layer ionization behavior during eclipse 0-41829

B abundance, absorption band spectra of BH, BN, BO in sunspots 0-41849

0—41049
Ba II excitation and ionization equilibrium in the chromosphere 0—54456
C II u.v. resonance line profiles, broadening mechanisms 0—63170
CN molecular bands in photosphere, formation mechanism 0—45429

13C 18N ten new rotational line positions in near ix. spectrum, calc.

0-45432 Ca II H and K lines, profiles 0-63168

Sun continued

spectra continued

ca II i.r. triplet, obs. at three positions on solar disk 0-51791
Ca II ion, five-level, statistical equilib, and radiative transfer eqns. soln.
0-66655
Ca II K line on solar disc, fine structure 0-59799
CaII K line, formation in spinning cylindrical spicule 0-79766
Ca(XV), forbidden coronal lines, intensity ratio and line to continuum ratio 0-41826

ratio U-41820
Eu isotope ratio in atmosphere, from spectral line profiles 0-41860
Fe I excitation temps, and systematic errors in gf-scale 0-57039
Fe I lines, new system of oscillator strengths and iron abundance determ.
0-41824
Fe I yFr, evel, selective excitation in spectrum of two flares 0-54475
Fe II, Ti II and Cr II lines in umbra, excitation by penumbra radiation field 0-66626

field 0-66226
Fe II 3938 line in plages near limb, behaviour 0-63177
Fe line emission at 1.9 Å during flares 0-51793
Fel 6569.2A line, exam. For granules inside motions 0-66645
Ga abundance 0-76661
H 21 cm line, detection in quiet Sun and in prominence 0-54479
Ha, rotation broadening limb darkening, non-LTE model atmospheres 0-76574

0-76574 4 and two FeI lines profiles for differentially moving atmos., velocity effects, meas. 0-59791 4 4 chromospheric network, lifetime 0-69476 4 4 filtergrams, March 7 1970 eclipse 0-66625 4 He like ion forbidden line emission 0-59793 4 He isoelectronic sequence, X-ray obs. of forbidden lines 0-66669 4 He line, 10830 Å, line profile obs. and models 0-45430 K line, 7699Å gravitational red shift, atomic beam, study 0-63169 Li ike ions, limb brightening of XUV reson. lines 0-45440 Ni II lines, photospheric, abundance 0-69474 $\frac{1}{11694}$

Sunlight

see also Sky brightness albedo energy, terrestrial, scattering atmosphere model 0—41506 daily total solar radiation, conversion factor values for calc. 0—41505 radiant flux distrib. in penumbra 0—66928 solar absorptances and spectral reflectances, 12 metals, 250° to 550°K 0—51294

o-31294 solar constant irradiance standard 0-59573 solar constant variations, aerostatic investigations 0-56782 u.v., depend. on solar hour angle and atmospheric haze 0-66622

Sunspots

absorption band spectra of BH, BN, BO, solar abundance of B 0–41849 active centre interaction effects on growth, proper motion, mag. configuration 0–41850 activity, during 1968, obs. Belgian Royal Observatory 0–63163 curves of growth, magnetic and turbulent effects comparison 0–57149 distribution, heliolatitudinal, and 11-year modulation of cosmic-ray intensity 0–76668 distribution, hemispherical inequality 0–41846 electric current of 3.8×108 amp. per km height obs. 0–57148 electric currents, azimuthal in surface layers 0–57142 flare probab. rel. to sunspot group area and flariness 0–41855 form and size, photometric obs. 0–59801 formation, rel. to mag. flux trapping in moving Al conductor, obs. 0–38428 formation by magnetic buoyancy' 0–76672

formation by 'magnetic buoyancy' 0-76672 groups, in different latitude intervals, character of variations of mean importance 0-63179 intensity minimum, dependence on area 0-57146

intensity profiles, near solar limb, photoelectric obs. 0–79761 ionospheric D-region, lunar tide near mag. equator, seasonal variation 0–45189 latitude distribution during solar cycle, Maunder's butterfly diagram

0—45189
latitude distribution during solar cycle, Maunder's butterfly diagram 0—69490
magnetic field and radial velocity distrib. in sunspot observed in October (1963) 0—59800
magnetic field structure of a spot with a photospheric bridge 0—45435
magnetic splitting of line Fel \$\lambda\$ 6302.508 Å 0—57143
magnetostatic model of sunspot with 'twisted' fields 0—57150
number depend. of semiannual Sq(H) variations 0—56861
observation quality, comparison with reference observations 0—41847
overlapping, 1968 December 10, 11, 12, photographs 0—66648
penumbrol mag. fields 0—41848
spectra, photoelectric, penumbra and umbra 3900-8000Å 0—72781
spectra for (0,0) band of SiH, A*\(^2\)\(^2\

Li abundance, from Zeeman effect, interferometric obs. 0-41851

Superconducting devices
bridge, thin-film, harmonic generation 0-51018
bridges, current-phase, relations 0-75638
circuit, multiply connected self interacting 0-56211
coherent matter waves, de Broglie-wave diffraction and interference
0-71995
coils, application to electron lenses for electron microscope, patent
0-6181

coils, application to electron lenses for electron microscope, patent 0-60181

0-0181 coils, current carrying, a.c. losses, electrical methods for obs. 0-75641 coupling system for microwave resonators 0-63498 films, type 1, flux flow velocity by passage time obs. 0-68776 force-cooled coil system 0-56210 hollow cylinder, mag. flux meas. by electron interferometry 0-44146 Josephson contact, fluctuations 0-40750 Josephson coupling theory in thermal fluctuations presence 0-71989

Superconducting devices continued

Josephson effect at point contacts in superconductor-normal metal-super-conductor system 0–59179 Josephson effect in ring 0–75639 Josephson junction, inductive coupling to external circuit 0–44152

Josephson junction, maximum zero-voltage current, junction geom. effect 0 - 53808

Josephson junction detection of vortex motion 0-56197

Josephson junction detector, mm. wavelength obs. of solar activity, Moon and Venus 0-66649

Josephson junction with Cu barrier for magnetometry 0–54827
Josephson junctions, Nb/Pb, fabrication techniques 0–44151
Josephson junctions, c.c. switching characts, hysteresis 0–68793
Josephson junctions, o.c. switching characts, hysteresis 0–68793
Josephson junctions, noise voltage 0–59180
Josephson oscillation harmonics and subharmonics generation 0–78906
Josephson small tunnel junction, I/V characts. 0–68799
Josephson tunnel junctions, mixing 0–62335
Josephson tunnel junctions, mixing 0–62331
levitron, stabilized by feedback and eddy currents, stability analysis 0–62331
mi.m. tunnel diodes, Al-I-Al, Mn-doped, coherence effects 0–72093
magnetic flux detector 0–75642
magnetic shields 0–52234
magnetometer, point-contact, for magnetocardiograms 0–40749

m.im. tunnel diodes, Al-I-Al, Mn-doped, coherence effects 0—72093 magnetic flux detector 0—75642 magnetic shields 0—52234 magnetometers, principles and limitations 0—54826 magnetometers, principles and limitations 0—54826 magnetometers and cryogenics, review 0—52227 magnetometers for 10-10 gauss 0—52227 magnetometers for 10-10 gauss 0—52227 magnetometers for 10-10 gauss 0—52228 magnetothermal power generation, patent 0—57482 microwave cavity, Nb-Ti alloy 0—47676 Nb₃Sn ribbon solenoid, high pressure performance 0—75643 point contact assembly, phase transition obs. 0—78908 point contact weakly connecting two superconductors 0—56212 point-contacts, IV characts. 0—62332 point-contact, quantum, rf. based, design and operation 0—40751 potentiality at 30 GHz and higher frequencies 0—56213 power cables, vacuum production and maintenance 0—51864 quantum interference device, metals resist. meas. appl. 0—75554 rf. cavities superconducting, source of residual power loss 0—73100 rf. cavity, problems 0—68797 radiation detectors involving weak links, response to photons 0—78909 resistive quantum interference, phase fluctuations 0—40752 resonator for 3cm klystron oscillator 0—45715 ribbon, flux-transport noise power spectra 0—53811 solenoids, determ. of regions of cooperation 0—44145 solenoids in n.m.r. spectrometers, bulk susceptibility corrections 0—69809 strips, inductive obs. of flux transport across, resistivity 0—75640 superconducting-normal-superconducting, proximity effects 0—68794 thin-film bridge, between pure- and resistive-superconductive states, switching 0—47682 transmission line, model for current flow 0—73123 tunnel diodes, m.i.m., Al1-Al, Mn-doped, coherence effects 0—72093 tunnel diodes, m.i.m., Al1-Al, Mn-doped, coherence effects 0—72093 tunnel diodes, m.i.m., Al1-Al, Mn-doped, coherence effects 0—72093 tunnel junction, phonon emission by quasiparticle decay 0—44147 tunnel junction, phonon emission by quasiparticle decay 0—44147 tunnel junction, service-insulator-supercond, transition temp. and tunnelling

weak point contact, d.c. and a.c.interference 0-68796

Nb-Ti alloy microwave cavity 0-47676

Nb, TM₀₁₀ mode cavity, electron-beam welded 0-44153

Nb₃Sn tube, mag, flux flow enhanced by heating due to neutron irrad.

0 - 56202

0-56202

Pb-Pb tunnel junction, d.c. Josephson current temp. variations 0-78911

Pb-Pb Unrel junctions, maximum de Josephson current 0-75622

Pb magnetic shield 0-52235

Pd tunnel junction, hydrogenation effects 0-71996

Sn-Ag-Sn system, point contacts, Josephson effect 0-59179

Sn SnO-Sn tunnel junctions, microwave-photon-assisted tunnelling 0-71992

Ta-Ag-Sn system, point contacts, Josephson effect 0-59179

Ta-Ag-Sn system, point contacts, Josephson effect 0–59179

Superconducting magnets
apparatus for MHD generator, patent 0–56214
application to elec. power generation, charge particle lenses and plasma confinement 0–47680
coil, mag. field prod. by discharge of stored e.m. energy 0–69841
composite conductors, twisted, magnetization meas. 0–78893
construction of 100 kOe device 0–59178
constructional problems 0–68795
in primary cosmic ray mag. analyzer on artificial Earth satellite 0–51615
flux instabilities in high field wires 0–71991
force-cooled coil system 0–56210
high-field generation, use review 0–38125
inductive coils with dust cores 0–44150
instabilities rel. to ferromagnetic materials 0–62333
pool boiling heat transfer to helium from treated surfaces, applic. 0–46966
quadrupole, 10 cm, winding and testing 0–75634
semistabilized wires, bare and insulated, quenching propag. 0–62330
small coil, applic, to plasma physics 0–67930
solenoid, Nb₂Sn ribbon wound, mag. image effects on vibrating sample magnetometer 0–48985

```
Superconducting magnets continued
                                                                                                                                                                                                                                                                                                                                                                                                                                                                                                                                                                                                                                                                                                                                                                                                    Superconducting materials continued
                                                                                                                                                                                                                                                                                                                                                                                                                                                                                                                                                                                                                                                                                                                                                                                                                           Al film, fluctuations in resistive transition, purity depend. 0–62321
Al film, nonlinear excess cond. above T<sub>c</sub> 0–78898
Al film, unnelling 0–53800
Al films, pair cond. above T<sub>c</sub> 0–44121
Al films, pair cond. above T<sub>c</sub> 0–44121
Al films, pair cond. above T<sub>c</sub> 0–44123
Al thin film link, Josephson effect 0–68766
Al thin films, first-order magnetic transition, exptl. evidence 0–44122
Ba, high pressure modification 0–47675
Bi-TI alloys, f.c.c., Fermi surface-Brillouin zone interaction 0–51007
Bi, amorphous, energy gap temp, depend. 0–78899
Bi and alloys, amorphous, transition temp. 0–75611
Bi film, amorphous, flarit, transmission 0–40739
Bi IV(V), 30-100 kbar 0–56200
Cd-S, lamellar eutectic, rf. surface permeability 0–75612
Ce, phase boundary determ, high press. 77-480K 0–43823
CuS(Se, Te)s, pyrite-type, de Haas-van Alphen effect 0–62280
Ga, amorphous, Iransition temp. 0–75611
Ga, film and β-phase, far-i.r. transmission 0–40739
Ga, thin amorphous films, superconductivity increase in mag. field, explanation by order parameter fluctuations 0–75611
Ga, film and β-phase, far-i.r. transmission 0–40739
Ga, thin amorphous films, superconductivity increase in mag. field, explanation by order parameter fluctuations 0–75613
Ga isotropically and metallurgically pure, fluctuation effects above T<sub>c</sub>, evidence 0–44088
HRcs, HTCs, transitions temps, and lattice struct, determ. 0–71985
Hg, cryst., u.s. attenuation 0–75614
Hg, energy gaps and transition temps, as functions of mean free paths of electrons 0–68787
Hg, films, electron tunnelling, below 0.4 K 0–44124
Hg, strong coupling effects in pressure depend. 0–44134
Hg with admixtures, transition temps. 0–59177
In-Bi, flux flow resist, temp, and field depend. 0–5801
In, surface impedance in mag. field 0–44127
In, flim, superheating and supercooling 0–5880
In, duratic intermediate state, domain movement 0–5801
In, surface impedance in mag. field 0–44127
In film, optical currents 0–7199
In film, nonlinear props. in u.h.f. field, 1.5-4.2°K 0–44137
In films, magnetic flux penetratio
                                   solenoid, made of deformable alloys, 90 kOe at 4.2 K, 115 kOe at 2 K
                                                                                                                                                                                                                                                                                                                                                                                                                                                                                                                                                                                                                                                                                                                                                                                                                                       Al film, fluctuations in resistive transition, purity depend. 0-62321
                                               0 - 53807
                                                                                                                                                                                                                                                                                                                                                                                                                                                                                                                                                                                                                                                                                                                                                                                                                                          Al film, nonlinear excess cond. above T<sub>c</sub> 0-78898
                                0-380/s solenoid calibrating n.m.r. proton probe 0-76973 stabilized systems, reliability testing 0-44149 suspension systems, persistent mode operation 0-73120 wire, high field, flux instabilities 0-71991 Al, super purity, technology aspects analysis, electrical resistivity changes due to internal defects meas. at 4°K 0-50964
                                                                                                                                                                                                                                                                                                                                                                                                                                                                                                                                                                                                                                                                                                                                                                                                                                          Al film, tunnelling 0-53800
                                   Nb:Tl, 98 and 102 kG, design and performance, comparison with Nb÷Sn 0-47681
                                   Nb Ti quadrupole, wires, evaluation of winding techniques 0-75635
Nb<sub>3</sub>Sn, 51 cm bore solenoid, pumped helium tests 0-44087
Superconducting materials alloy, 35BT, phase transforms, on annealing cold-worked specimen
                                alloy, 35BT, phase transforms. on annealing cold-wor 0-78692 alloy, A-15, T, strain depend, and related effects 0-51000 alloy, dil, density of states rel. to impurities 0-44099
                                alloy, dil, with paramag, impurity, current-carrying film, e.m. props. 0-47657
                           alloy, dil., with paramag. impurity, current-carrying film, e.m. props. 0-47657 alloy, dil. mag., proximity effect, tunnelling obs. 0-50999 alloy, strong coupling, \kappa_1(\Gamma) calc. 0-75590 alloy, type-II, Highly reversible, sp. ht. in mag. field 0-71976 alloy with Ce impurities, pair breaking parameter press, depend. 0-53795 alloys, generalised diffusion eqn. 0-67935 alloys, non-magnetic localized states effects 0-44119 alloys of variable composition, T_c determ. 0-71977 composite, prep. and props., patent 0-44158 composite, twisted filamentary, coil and pulsed applies. 0-44097 composite conductors, connection problems 0-56195 creep tests in T_c regime, strength loss obs. 0-53593 critical supercooling field, calc. for strong electron-phonon interaction, anomalous behaviour anal. 0-78887 crystal structure relations 0-62317 DNA, supercond-type enhanced cond., room temp. 0-44144 data compilation; lit. review 0-68773 data review, (published up to early 1968) 0-50995 deformation, heterogeneous, 4.2K, traction instability 0-44128 dirty, u.s. attenuation 0-71969 elastic props. use in bulk characts. determ. 0-40741 electromechanical effects 0-71966 rel. to electron density of states, conference, Gaithersburg (1969) 0-65573 electronic density of states, volume dependence 0-75585 film, as sensitive thermometer 0-71990
                           rel. to electron density of states, conference, Gaithersburg (1969) 0-65573
electronic density of states, volume dependence 0-75585
film, as sensitive thermometer 0-71990
film, disordered, cond. and phonon spectra 0-56198
film, gapless behaviour due to proximity effect, thermal cond. obs. 0-44106
film, nonlinear microwave props. 0-53784
film, r.f.-sputtered, with β-tungsten struct. 0-78900
film, singularities of resistive state with current 0-47667
film, stimulated behaviour 0-75583
film superconductor, h.f. field stimulation 0-47668
flexible substrate with NbSn<sub>3</sub> coating, patent 0-44155
flux trapping, critical current studies 0-65645
impurities, with internal degrees of freedom, interaction with electron gas, changes in transition temperature 0-75573
intermediate state, u.s. resonant absorption by nuclei 0-78755
mag, structures at low temp. using magneto-optical apparatus 0-51196
magnetic field H<sub>c2</sub> directional depend., correl. function method 0-78896
magnetic hysteresis in type-1 and low K type-II alloys 0-51002
with magnetic impurities, theory 0-65639
with magnetic impurities, theory 0-65639
with magnetic impurities, theory 0-65639
with magnetic impurity, spatial variations of order parameter 0-44078
metals, in time dependent gravitational fields 0-75376
nonequilibrium states, electrodynamics 0-68775
ohmic, including thermodynamic properties 0-53720
organic, biosynthesis 0-75631
                                ohmic, including thermodynamic properties 0–53720 organic, biosynthesis 0–75633 organic, conf. Honolulu, USA, Sept. 1969 0–75632 organometallic crystals, layered structure 0–65640 permethylcyclopolysilanes anion-radicals, electron delocalization 0–74408
                                                                                                                                                                                                                                                                                                                                                                                                                                                                                                                                                                                                                                                                                                                                                                                                                                       0-47677

Nb-Ti(Zr) alloy fabrication method, patent 0-44154

Nb alloys, magnetization, dimensional effect 0-56205

Nb alloys, magnetization dimensional effect 0-56205

Nb<sub>3</sub>(A<sub>1</sub>,Ge) syst., annealed, phase anal. 0-65644

Nb<sub>3</sub>A<sub>1</sub>,376e<sub>2.5</sub> alloy, high transition temp., upper critical field, 4.2K

Nb<sub>4</sub>C<sub>1</sub>, lattice theorem (1-2)
                                   perovskite-type cpds., book 0–68293
polymer, review 0–75694
porphins with cyanine dyes on methine linkage, excitonic interactions 0–74403
                           porphins with cyanine dyes on methine linkage, excitonic interactions 0—74403
semiconductor, SrTiO<sub>3</sub>, type II phenomena 0—68791
specific heat singularities near T<sub>c</sub> 0—71967
stable conductors and their uses 0—44077
strong-coupling parameters 0—44092
surface oxide struct. and supercond implications 0—74885
thin films, transition temp. critical field and current 0—65636
transition from superconductivity to normal conductivity on passing a.c.
through wires, oscillographic method 0—50992
transition metal alloys, microstruct, defects rel. to mag, props. 0—40736
transition metals, effect of phonon induced d-d coupling on transition
temp. 0—75608
transition metals, many-body effects 0—53804
transition metals with nonmagnetic impurities, two-band model extension
0—53798
transition temp., changes due to interaction of impurities with internal
degrees of freedom with electron gas 0—75573
transition temp. pressure variation, model obs. 0—75574
type II, a.c. face field losses 0—44110
type II magnetisation curve, reversible, approx. calculations, Ginsburg-Lan-
dau equations 0—75603
type-1, differential resistance, magnetoresistance effect 0—75624
type-1, multiply connected, in void generated fields, flux conservation
0—71974
type-II, high-field behaviour 0—53797
type-II, high-field behaviour 0—53797
type-III, high-field behaviour 0—53797
                                                                                                                                                                                                                                                                                                                                                                                                                                                                                                                                                                                                                                                                                                                                                                                                                                     0-68789

NbC<sub>0,96</sub>, lattice thermal cond. 0-40742

NbO, transition temp., vacancy removal effects
Nb<sub>0</sub> Sos(Ir,Pt,Au) alloys, mag. props. 0-51011

NbSe<sub>2</sub>, quasi-two-dimensional nature 0-47678

NbSe<sub>2</sub>-NbTe<sub>2</sub> solid solin, lamellar structure 0-62326

NbSn, cubic-to-tetragonal transition, dynamic gheory based on electron-phonon interaction 0-78691

NbSn, coating on flexible substrate, patent 0-44155

Nb<sub>3</sub>Sn, low-temp. phase transform. 0-65496

Nb<sub>3</sub>Sn cylinders, hollow, flux-jump behaviour 0-75609

Nb<sub>3</sub>Sn density of states model rel. to Nb<sub>3</sub>Sn<sub>1-x</sub>Sb<sub>x</sub> system 0-59173

Nb<sub>3</sub>Sn tube, mag. flux flow enhanced by heating due to neutron irrad. 0-56202

Nb<sub>3</sub>Sn<sub>1-x</sub>Sb<sub>x</sub> system, phase transform. rel. to density of states model for
                                                                                                                                                                                                                                                                                                                                                                                                                                                                                                                                                                                                                                                                                                                                                                                                                                  Nb<sub>3</sub>Sn tube, mag. flux flow enhanced by heating due to neutron irrad. 0–56202 Nb<sub>3</sub>Sn<sub>1-x</sub>Sb<sub>x</sub> system, phase transform. rel. to density of states model for Nb<sub>3</sub>Sn 0–59173 Pb-Bi alloys in porous glass, critical field and current 0–51012 Pb-Bi elutectic alloy, energy dissipated during flux jumps 0–71960 Pb-Bi(ln) alloys, props. rel. to phase diagram 0–51013 Pb-In, anomalous H<sub>c3</sub>/H<sub>c2</sub> near T<sub>c</sub> rel. to crit. phenomena in sheath state 0–71981 Pb-In alloy, flux flow resistivity by surface resistance meas. 0–56206 Pb-In alloy, hysteresis effects 0–44133 Pb-IT, flux flow resist, temp. and field depend. 0–53802 PbNbS<sub>3</sub>, below 2.62K, correlation with valence state 0–51014 PbTaS<sub>3</sub>, below 3.07K, correlation with valence state 0–51014 PbTa
                                0-71974

1. high-field behaviour 0-53797

1. u.s. absorption, two-zone supercond. with nonmagnetic impurities, absorpt. coeffs. calc. for supercond. and normal states 0-78752

1. u.s. attenuation rate, generalized Langevin approach 0-71841

1. u.s. resonant absorption by nuclei, intermediate state 0-78755

1. whisker, anomalous paracond. above T<sub>c</sub> 0-71984

1. with the companies of the companie
```

Superconducting materials continued perconducting materials continued

Re, high purity, electron-phonon interaction, u.s. investigation 0–75580

Re, sp. ht., 0.15-4.0K 0–44138

Re, T. obs. of fermi-surface topology changes, h.p. 0–40746

Re, tunnelling 0–56207

Re dispersed on high area oxides, mag. susceptibility below T_c rel. to morphology 0–55718

ScRu_y, Laves phase, supercond. transition temp. meas. 0–75607

Sn/Pb bilayer, forbidden band determ. rel. to temp. 0–78891

Sn-In alloy film, tunnelling in perp. mag. field 0–71983

Sn-Sn junction, Josephson current, effect of fluctuations on mag. field strength depend. 0–51015

Sn-SnO-Pb junctions, pair susceptibility, expt. 0–68790

Sn-SnO-Sn tunnel junctions, microwave-photon-assisted 0–71992

Sn, differential resistance, magnetoresistance effect 0–75624 Superconducting materials continued lead continued stress relaxation, dislocation motion and electron drag 0-78645 strong-coupling effects in pressure depend. 0 – 44134
transition effect on creep, dislocation mobility 0 – 43753
transition temp. pressure depend. 0 – 44135
transition temp. pressure depend. 0 – 44135
tunnel junction, Pb-Pb, d.c. Josephson current temp. variations 0 – 78911
tunneling through p-GaAs-Pb point contacts 0 – 47735
tunneling effect under pressure 0 – 62328
18. attenuition energy again and conditions 0 – 76621 tunneling effect under pressure 0-63328
us. attenuation, energy gaps and coupling 0-75621
Pb-PbO_x-Pb junctions, maximum dc Josephson current 0-75622
Pb(Nb_{1-x}Ta_x)S₃, transition temps., comp. and thermal history depend., rel. to sp. ht. meas. 0-78901
Sn/Pb bilayer, forbidden band determ.rel. to temp. 0-78891 Sn-SnO-Sn tunnel junctions, microwave-photon-assisted tunnelling 0-71992
Sn, differential resistance, magnetoresistance effect 0-75624
Sn, single-crystal whiskers, one-dimensional, onset of quantized thermal fluctuations 0-78902
Sn, third harmonic generation in thin films 0-78886
Sn cylinders, hollow, meas. of quantized flux states 0-44140
Sn film, critical currents 0-71979
Sn film, critical currents 0-71979
Sn film, critical transition temp., growth and struct. depend. 0-75625
Sn film, effects of adsorbed 0; on Tr. 0-65646
Sn film, nonlinear props. in u.h.f. field, 1.5-4.2°K 0-44137
Sn film, struct. and props. rel. to deposition 0-56208
Sn films, Te. rel. to thickness 0-56209
Sn films, Te. rel. to thickness 0-56209
Sn whisker, anomalous paracond. above Tc. 0-71984
SnTe-MnTe alloy system, reciprocal Hall coeff., ferromagnetic ordering, 0.02-300 K 0-44139
SrTiO3, type II phenomena 0-68791
Ta-V system, Tc. minimum obs. 0-75627
Ta, elastic props. use in bulk characts, determ. 0-40741
Ta, for ir. absorption, energy gap width and critical temperature 0-44130
Ta, third harmonic generation, in Sn and Ta thin films 0-78886
Ta, transition effect on Denye temp. 0-62179
Ta film, transition temp., growth and struct., temp. depend. 0-47068
TaN, cryst. struct., NaCl type phase, high press., critical transition temp. 0-75628 a.c. losses, 50 Hz, in strips, rel. to sample thickness, surface finish and hardness 0–51009 anisotropic critical field H_{e2}, nonlocal characteristics 0–44131 cavity, TM₀₁ mode, electron beam welded 0–44153 critical current anisotropy, deformation-induced 0–62325 deformed, anomalous critical fields, dislocation cell struct. role 0–62324 elastic props. use in bulk characts. determ. 0–40741 energy gap distrib. in k space 0–75619 energy gap of lower band at T=0K 0–40745 filamentary composite, Nb/Cu, a.c. losses, 70 A, 50-800 Hz, 4.2 K 0–51010 10—51010 film, tunnelling sandwich struct. 0—51008 for i.r. absorption, energy gap width and critical temperature 0—44130 homogeneous distribution of supercurrent in annealed sheet, flux jump tendency 0—53799 hypersonic attenuation of longit, and transverse modes in mixed state 0—68604 Josephson junctions, Nb/Pb, fabrication techniques 0-44151 magnetic flux struct., Faraday rot. obs. 0-56203 mixed state, hypersonic attenuation of longit. and transverse modes 0-68604 0-68604
Nb₅Sn ribbon solenoid, high pressure performance 0-75643
penetration depths 0-56204
physical lattice imperfections, effect on magnetic props. and resistive transitions 0-75605
third harmonic generation, in thin films 0-78886
transition effect on Debye temperature 0-62179
upper critical field changes after 3 MeV electron irrad. 0-75618
Nb/Cu, filamentary composites, a.c. losses, 70 A, 50-800 Hz, 4.2 K
0-51010 Ta film, transition temp_, growth and struct, temp. depend. 0–47068
TaN, cryst. struct., NaCl type phase, high press., critical transition temp. 0–75626
Te_{0.81}Ge_{0.15}As_{0.04}, memory-type chalcogenide, superconducting transition obs. 0–75628
Th-Gd alloys, thermal cond. 0–40747
Th, hydrides and deuterides 0–68792
Th, thermal cond. 0–40747
ThRey, ThTc₂, transition temp. and lattice struct. determ. 0–71985
Ti-Cr alloys, β-stabilized, step quenching and ageing effect on T. 0–71987
Ti-Mo dil. alloy, microstruct. influence on supercond. 0–71986
Ti-Nb-Fe, annealed alloy, Mossbauer chemical shift correl. with critical current 0–65647
Ti-Nb-V, ternary system, resistive critical field, comp. depend. 0–44141
Ti-Qa ta/9.Nb alloy, magnetization, Bean model 0–75629
Ti-Nb alloy, longitudinal critical currents 0–62329
Ti-Ta-Nb alloy, patent 0–44157
TiO, transition temp_, vacancy removal effects 0–61943
Tl, at high pressures, 77-350K 0–53803
Tl, density of states data from critical field meas. 0–75586
Tl, tunnelling effect under pressure 0–62328
α-U single crystal, pressure range 0-8 kbar 0–40748
V-Ga system, for high mag. fields, patent 0–44156
V-Nb(Ta) alloys, T, and sp. ht. obs. 0–78905
V-Ta alloy u.s. attenuation obs. 0–71988
V, elastic props. use in bulk characts. determ. 0–40741
V, transition effect on Debye temp. 0–62179
V, type II, temp. depend. of magnetic field at vortex center 0–75630
V alloys, A 15, sp. ht., supercond., ordering 0–59176
V, Au transition temperature variation, explanation 0–47679
VC_, electron-phonon interactions, upper limit 0–78904
VO, transition temp, vacancy removal effects 0–61943
V,Si, low-temp, phase transform. 0–65496
V,Si, mixed state, resistivity meas. critical field 0–44142
V, sic cubic-to-teragonal transition, dynamic theory based on electron-phonon interaction 0–78691
V,X type, high-temp, X-ray spectra, energy bands 0–79342
W, evaporated films, transition temp. 0–51016
β W, model density of states for high transition temp. 0–75601
YRs, superconducting transition depressed by rare e 0-3010 Nb-50%Ti, rods, flux jumps, effects of thermal insulation 0-75616 Nb,Al-Nb,Ge alloys, high critical temperature 0-68768 Nb₃Sn, tape, anisotropy and effect on performance of superconducting magnets 0-75617 Superconductivity

2e/h determination, based on ac Josephson effect 0-72866

a.c. Josephson effect at 36 GHz, solder-drop junction, 2 e/h measurement 0-63305 a.c. Josephson effect at 36 GHz, solder-drop junction, 2 e/h measurement 0-63305
alloy, dil., density of states rel. to impurities 0-44099
alloy, dil., mag., proximity effect, McMillan model 0-40735
alloys rel. to Fermi surface topology 0-71923
applied superconductivity, colloquium, Smolenice (1969) 0-68767
BSC theory, characteristic lengths \(\lambda\) and \(\lambda\) 0-44101
Bardeen-Kummel-Jacobs-Tewordt theory of vortex near T_c
binary eutectic alloys, effect of precipitates 0-51001
book 0-59170
bound states at mag. impurity sites, validity of diff. criteria 0-44080
bound states conditions for supercond, with mag. impurity 0-40732
bound states in mats. with mag. impurities 0-65639
boundary singularities of electron proper energy 0-75592
composite conductors, twisted, magnetization meas. 0-78893
composite conductors, twisted, magnetization meas. 0-78893
conference, Montreal Jun 1968 0-53783
conference, Montreal Jun 1968 0-53783
conference (Montreal Jun 1968 0-53783
conference topic, Charia, Crete, Jul 1968 0-68729
critical currents, Ginzburg-Landau and microscopic theories 0-47660
critical power dissipation 0-50998
critical region electronic props. 0-44108
critical power dissipation 0-50998
critical region electronic props. 0-44108
critical temp. calc. using phonon data 0-47665
cyclic polyenes, theoret. 0-74402
cylinder, domain model for flux trapping 0-44075
DNA, enhanced conductivity, superconductivetype, room temp. 0-75600
DNA, supercond-type enhanced cond., room temp. 0-44144 0-75600
DNA, supercond.-type enhanced cond., room temp. 0-44144
destruction in wire by a.c. 0-50997
destruction of type I by current in cylindrical wire, kinetics 0-44109
diamagnetic susceptibility at T_c 0-44107
differential resistance, magnetoresistance effect 0-75624
e.m. field penetration depth in large type-I sample 0-44088
electromechanical effects 0-71966
electrom drag of dislocations effects 0-65638
electron interaction with moving dislocations in superconductors 0-44082
electron reflection at normal/supercond. phase boundary, r.f. size effect
0-75575
electron reflection coeff. temp. depend. at interface between supercond. and evidence 0–44083 Zr-Nb alloy, longitudinal critical currents 0–62329 ZrB₁, superconducting transition depressed by rare earth impurities 0–44143 Zr₂Co-Zr₂Ni system, transition temp., mag. susceptibility, lattice const. 0–75631 ZrMo₂, ZrW₂ alloys, lattice parameters, transition temps. 0–59177 ZrRe₂, ZrTc₂, transition temp, and lattice struct. determ. 0–71985 electron reflection at normal/supercond. phase boundary, r.1. size effect 0—75575 electron reflection coeff. temp, depend. at interface between supercond. and normal phase 0—65637 electronic mechanism, collective oscillations role 0—75572 energy dissipated during flux jumps 0—71960 energy gap and mag, field effects 0—47663 energy gap and mag, field effects 0—44089 energy gap resulting in nonexistence of negative eigenvalues of second variation of mean value 0—50996 energy spectrum of supercond. with overlapping bands 0—78895 exciton mechanism, model macromol. organic cpds. 0—75596 exciton mechanism and high temp. macromol. superconductors 0—75595 exciton mechanism and high temp. macromol. superconductors 0—75595 film, destruction in u.h.f. field 0—44136 film, gapless behaviour due to proximity effect, thermal cond. obs. 0—44106 film, p. field stimulation 0—47668 film, in high mag. fields, theory 0—47664 film, nonlinear electrodynamics 0—62315 lead
absorptivity in phonon frequency region, low temp. meas. 0–44852
creep acceleration on normal to supercond. transition 0–43754
cyclotron reson., high microwave freq., effective mass temp. depend. and
relax. time 0–75513
energy gaps and transition temps., as functions of mean free paths of
electrons 0–68787
film, acoustic surface-wave energy-gap and mixed-state study 0–62327
film, nonlinear props. in u.h.f. field, 1.5-4.2°K 0–44137
film, thin, fluctuation-effects in a.c. conductivity, below supercond. transition temp. 0–44132
films, magnetic flux penetration 0–78903
flux trapping, critical current studies 0–65645
foil, electron energy loss spectrum, temp. effect, 3K-295K 0–71978
Josephson junctions, Nb/Pb, fabrication techniques 0–44151
magnetic shielding application 0–52235
plastic deformation, yield point, flow and shear stress 0–47355
pressure depend. of supercond, params., calc. 0–44095
sound velocity for ql>1 0–62191

```
Superconductivity continued
                                                                                                                                                                                                                                                                                                                                                                                                                                                                                                                                                                                                                                                      resonance and oscillatory effects 0–62316
Resource Letter 0–56194
single fluxon nucleation and drift obs. 0–68769
solid, conference, Turku, Finland, Aug. 1970 0–74858
sound, hf. transverse, velocity change at transition temp. 0–68589
sound absorption in superconductors, review 0–71962
spin excitation phenomena 0–47659
state parameters calc. using exact OPW form factors 0–44098
strong-coupling, Mossbauer effect and localized impurity modes 0–44104
strong-coupling parameters 0–44092
surface phenomena 0–39921
surface sheath of semi-infinite half-space and instability due to fluctuations 0–44103
Superconductivity continued
                         film, nonlinear props. in u.h.f. field, 1.5-4.2°K 0-44137 film, nonstationary effects in resistive state 0-75582
                           film, props. in high freq. fields 0-62314
                       film, props. in high freq. fields 0-62314 film, semiconductor and semimetallic 0-44118 film, singularities of resistive state with current 0-47667 film, size effects 0-53793 film, thick, proximity effects 0-53787 fluctuation, high-mag-field, 2-3 T<sub>c</sub> range 0-56196 fluctuations, time depend., of order parameter, effects in zero dim. samples 0-50993
                         fluctuations above T_c, effect on electron Green's function 0-40733 fluctuations in electronic spin susceptibility, amplification above T_c 0-47654
                                                                                                                                                                                                                                                                                                                                                                                                                                                                                                                                                                                                                                                      surface sheath of semi-infinite half-space and instability due to nuctuation. 0–44103 systematic correlations with T<sub>c</sub> 0–47661 theories, current, possible applications 0–44096 theories, current, possible applications 0–44096 theory, crystalline struct. considerations 0–47669 thermal conduction of superconductors, review 0–71962 Thirring's model, asymptotically exact solution 0–51980 Thirring's model, calc. of free energy 0–53785 time-dependent energy gap eqn. by generalization of semiclassical model 0–44093
                         flux conservation in multiply connected type-I in void generated fields 0\!-\!71974
                       0-71974
flux jumps, energy release 0-47677
flux line interaction with dislocations 0-78884
flux motion and noise 0-44117
flux motion and noise 0-50991
flux pinning enhancement for materials with k=1/\sqrt{2} 0-71982
flux quantization 0-57655
flux quantization in normal state 0-62318
flux-flow noise voltage 0-44105
fluxoid quantum in tubes, determ. 0-68771
foil, flux flow props., effects of superimposed oscillatory mag. field
0-78890
free energy functional and Bogolubov equations 0-44100
                                                                                                                                                                                                                                                                                                                                                                                                                                                                                                                                                                                                                                                    0-44093
transition, deform, stress jump temp, depend. 0-75602
transition temp, mag, impurity effects 0-44094
transition temp, depression due to mag, impurities, theory 0-44076
transition temperature, effective coupling constants, calc. 0-78889
transition to normal conductivity on passing a.c. through wires, oscillographic method 0-50992
transport current distribs, in type-I plates, localized surface charges effect
0-71973
tube, determ of fluvoid quenture. 0-66774
                     foil, flux flow props., effects of superimposed oscillatory mag. field 0–78890 free energy functional and Bogolubov equations 0–44100 fundamental aspects, lecture 0–71894 gapless superconductors, dynamical properties 0–47666 Ginsburg-Landau eqn., time dependent, and paraconductivity 0–53786 Ginzburg-Landau eqn., time dependent, normal state correlation function 0–71963 Ginzburg-Landau eqn., time dependent, normal state correlation function 0–71963 Ginzburg-Landau theories, time-dependent 0–53790 h.c.p. phases, noble-metal-rich 0–47674 hard superconductor, surface effects and If. losses 0–75587 high field superconductors, influence of fluctuations 0–68772 high pressure behaviour, review 0–71961 high pressure obs., Teflon cell 0–76772 at high temperatures, possible production 0–75594 high-field phenomena 0–53787 history 0–78885 with impurities with intrinsic degree of freedom 0–75581 inductance derivation 0–62319 interacting elementary excitations 0–40634 intermediate state structure parameters, current depend. 0–75593 intrinsic resistive fluctuations in thin wire, time scale 0–44086 Josephson current, effect of fluctuations on mag. field strength depend. 0–51015 Josephson effect in 2-nucleon transfer in heavy ion scatt. 0–64136
                                                                                                                                                                                                                                                                                                                                                                                                                                                                                                                                                                                                                                                    thansport cutrons in type-1 piacs, localized surface charges effect 0–71973 tube, determ of fluxoid quantum 0–68771 tunnel junction, phonon emission by quasiparticle decay 0–44147 tunneling in Cr-Cr<sub>2</sub>O<sub>3</sub>-metal junctions 0–78910 tunnelling, subharmonic struct. 0–71968 tunnelling, subharmonic struct. 0–71968 tunnelling interface effects in normal metal 0–75463 two-band model, gap equs., nonmagnetic impurity effects 0–75589 two-band model extension to transition metals with nonmagnetic impurities 0–53798 type 1, destruction by current in cylindrical wire, kinetics 0–44109 type I, superheating and supercooling 0–47670 type I In, superheating and supercooling 0–47670 type I In, superheating and supercooling 0–44126 type-I, isotopically and metallurgically pure, fluctuation effects above T<sub>c</sub>, evidence 0–44083 us. absorption, theory, analogy with superfluid He 0–43875 in universe 0–76532 vortex core, Hall angle of normal current 0–53794 vortex motion detection using Josephson junction 0–56197
                                                                                                                                                                                                                                                                                                                                                                                                                                                                                                                                                                                                                                                    vortex core, Hall angle of normal current 0-53794 vortex motion detection using Josephson junction 0-56197 vortex near T<sub>c</sub>, Bardeen-Kummel-Jacobs-Tewordt theory 0-44102 vortex state excitation props. 0-47662 vortices, random array, model 0-40731 wave equation for macroscopic pair wave function 0-44550 zero dimensional, time depend. fluctuations of order parameter, effects 0-50993 Bi IV(V), 30-100 kbar 0-56200 Ce, superconducting phase boundary electron, high press., 77-480K 0-43823 Ce<sub>1-x</sub>Tb<sub>x</sub>Ru<sub>2</sub> type mixed crystal, coexistence with ferromagnetism
                     Josephson current, effect of fluctuations on mag. field strength depend. 0–51015
Josephson effect applics. 0–44151
Josephson effect in 2-nucleon transfer in heavy ion scatt. 0–64136
Josephson effect in ing 0–75639
Josephson offect used to redetermine e/h, review paper 0–59860
Josephson point contacts, current noise 0–75637
Josephson point contacts, current noise 0–75637
Josephson tunnelling, lectures 0–45507
Kapitza conductance meas. between metal and He II by second sound 0–55650
Kondo effect, depression in order parameter 0–75588
Kondo effect and corrections 0–53788
Landau theory validity range for H≠0 0–71971
Landau-Ginzburg theory, generalization 0–48747
lectures, Montreal, Canada, June 1968 0–47653
London type-I, current distrib, surface protrusions effect 0–78892
losses due to moving fluxoids 0–68770
macromolecules, organic, possibility 0–75597
macroscopic quantum phase coherence in e/h determ. 0–71970
magnetic flux quantization in normal state 0–53796
magnetic flux-quanta in tubes, direct obs. by electron interferometry 0–65641
magnetic hysteresis in type-I rods 0–51002
                                                                                                                                                                                                                                                                                                                                                                                                                                                                                                                                                                                                                                                      0-43823 Ce<sub>1-x</sub>Tb<sub>x</sub>Ru<sub>2</sub> type mixed crystal, coexistence with ferromagnetism 0-40730 In, surface impedance in mag. field 0-44127 In film, nonlinear props. in u.h.f. field, 1.5-4.2°K 0-44137 Mo films, as function of substrate temp., film thickness and substrate material 0-71944
                                                                                                                                                                                                                                                                                                                                                                                                                                                                                                                                                                                                                                                        Nb/Cu, filamentary composites, a.c. losses, 70 A, 50-800 Hz, 4.2 K 0-51010
                                                                                                                                                                                                                                                                                                                                                                                                                                                                                                                                                                                                                                                  No-Stollo National Composites, a.e. tosses, 10 A., 30-800 Hz, 4.2 K 0-51010

Nb-Hf alloy, props., effect of microstructure 0—44129

Nb-Ta alloy, flux flow resistivity by surface resistance meas. 0—56206

Nb strip, a.c. losses, 50 Hz, rel. to sample thickness, surface finish and hardness 0—51009

NbSe<sub>2</sub>, quasi-two-dimensional nature 0—47678

NbSe<sub>2</sub>—NbTe<sub>3</sub> solid soln., lamellar structure 0—62326

Pb-In alloy, flux flow resistivity by surface resistance meas. 0—56206

Pb film, nonlinear props. in u.h.f. field. 1.5-4.2°K 0—44137

Re films, as function of substrate temp., film thickness and substrate material 0—71944

Sn film, nonlinear props. in u.h.f. field, 1.5-4.2°K 0—44137

Ta, electron phonon interaction evidence 0—43969

Ti-Nb alloy, longitudinal critical currents 0—62329

Tl, at high pressures, 77-350K 0—53803

U cpds., and ferromagnetism, mechanisms correl. 0—40994

α-U single crystal, pressure range 0-8 kbar 0—40748

Zr-Nb alloy, longitudinal critical currents 0—62329

type II
                   magnetic flux-quanta in tubes, direct obs. by electron interferometry 0–65641
magnetic hysteresis in type-I rods 0–51002
magnetic impurities and S-N coexistence curves deviation 0–53789
magnetic surface levels 0–50994
magnetostriction, expts. using capacity method 0–44085
magnetostriction calc. for ellipsoidal samples 0–44084
McMillan theory test 0–78743
metal, monovalent, rel. to p-state pairing 0–44091
mixed state structure, effect of inhomogeneities 0–47655
multicore wire, twisted, in time-varying uniform mag. field 0–65648
nonlinear microwave properties of films 0–53784
nonlinear response above transition point, Ginzburg-Landau-Gorkov approx. 0–44079
optical phonons and plasmons, dispersion law 0–56520
order parameter, effect of fluctuations on electronic states 0–75578
order parameter fluctuations, effect on Hall effect 0–78894
order parameter fluctuations, effect on Hall effect 0–78894
organic molecules, π-electron system, applic. of many-body methods 0–75598
organic molecules, possibility, struct. considerations 0–75599
pair tunnelling as proche of fluctuations. 0–44081
                                                                                                                                                                                                                                                                                                                                                                                                                                                                                                                                                                                                                                                      alloy, highly reversible, sp.ht. in mag. field 0-71976 alloy, u.s. attenuation 0-68594 behaviour in time-dependent magnetic fields 0-68782 book 0-44116
                                                                                                                                                                                                                                                                                                                                                                                                                                                                                                                                                                                                                                                  book 0—44116
conductivity, elec, near H<sub>e2</sub> 0—51004
critical current and magnetiz. in longit. mag. field 0—68784
critical current and magnetiz. in longit. mag. fields, model 0—65642
critical current in longit. fields, wires, calc. 0—51005
Eilenberger's transport-like eqns., simplification 0—67935
electrical conductivity for magnetic fields near H<sub>e2</sub> calc. 0—78897
flux flow resist., temp. and field depend. 0—53802
flux jumping and stabilization methods 0—68783
flux line quantization, analogy to dislocation strain field 0—68777
flux motion and noise 0—44117
flux pinning by phase boundaries 0—75620
flux yimning by structural inhomogeneities 0—68779
flux variations, rel. to thermal effects 0—44112
flux-flow, fluctuation and microwave resistance of dirty supercond. 0—40737
flux-flow noise 0—75604
                       0–53795
pair density relax. 0–53792
pair tunneling as probe of fluctuations 0–44081
parallel wires, current distrib. 0–47656
phonon spectra, calc. rel. to quasi-particle density of states 0–71964
and plasma collective excitations in mag. field 0–46705
point contact, irradiated, I-V characts. 0–51017
power dissipation in hard superconductor 0–75587
pressure depend. of supercond. params., calc. 0–44095
pressure dependence, strong-coupling effects 0–44134
proximity effect for dil. mag. alloys, McMillan model 0–40735
proximity effect in high mag. fields 0–40734
quantum effects, macroscopic, and order param. thermal fluctuations
0–47658
quark stars 0–76582
                                                                                                                                                                                                                                                                                                                                                                                                                                                                                                                                                                                                                                                      0-40/3/
flux-flow noise 0-75604
flux-flow resistance, low-field, mechanisms 0-44111
flux-flow viscosity coeff. for mixed state 0-44114
fluxoid tunnelling, rel. to fluxoid-dislocation analogy 0-47673
fluxon movement frictional forces 0-51003
high field phenomena 0-68785
                         0-4/038
quark stars 0-76582
quasi-particle density of states, tunnelling meas., rel. to phonon spectra
calc. 0-71964
rf. losses, meas. and calc. values 0-75584
```

PA 1970 - Part II (July-Dec.) SUBJECT INDEX S 1425 Superconductivity continued Supersonic flow continued type II continued type II continued high-field behaviour 0-53797 high-field phenomena 0-53787 hysteresis loss, rot. 0-47672 imperfect, effective resistance in oscillating mag. field 0-51006 macroscopic phenomenological electrodynamics 0-68781 magnetic hysteresis in low K alloys 0-51002 magnetic phenomena 0-40738 magnetisation curve, reversible, approx. calculations, Ginsburg-Landau equations 0-75603 microwave, flux-flow and fluctuation resistance of dirty supercond. 0-40737 mixed state, flux-flow viscosity coeff. 0-44114 axisymmetric after-bodies near wake, Mach 1.9-5 0-50162 axisymmetrical bodies, calc. 0-64808 axisymmetrical bodies, calc. 0-64808 blunt body, effect of oscillatory relaxation 0-71237 blunt body in supersonic rarefied stream 0-39644 boundary layer, shock wave interaction with wedge slope 0-61427 compression corner in hypersonic flow, extent of boundary layer separation 0-5554 over conical bodies, flow field, numerical solns. 0-46797 cross flow effect on two-dimensional separation 0-61435 from ejectors, acoustic output, noise generation, theoretical exptl. investigations 0-46798 entropy layer in flows with compression jumps 0-61432 flat delta wing, three-dimensional viscous interaction 0-71242 flatter in cylindrical curved panels 0-48828 forced parametrically-excited vibrs. of plate in flow, numerical anal. 0-38342 gases, three dimensional, structure 0-61428 0-4073/ mixed state, flux-flow viscosity coeff. 0-44114 mixed state, theory 0-68774 mixed state visualization 0-68780 noise, flux-flow 0-75604 order parameter fluctuations 0-47671 9-30-42 gases, three dimensional, structure 0-61428 hypersonic, limiting, past some central surfaces of second order 0-58376 hypersonic, nonequilib. shock layer around cones expt. and numerical studies 0-53237 relaxation of order parameter, photon echoes and a.c. Josephson effect 0-59172reaxation of order parameter, photon echoes and a.c. Josephson effect 0-59172 resistance, effective, in oscillating mag. field, imperfect sample 0-51006 semiconductor, SrTiO₃, theory and expt. 0-68791 surface impedance, high-field, of dirty material in vortex state 0-44115 thermodynamics 0-68778 transport properties, critical state 0-44113 two-band model for flux-flow resistivity, using Bardeen-Stephen theory 0-71975 u.s. attenuation, longit., clean limit 0-68593 vortex motion 0-68786 vortex state, high-field surface impedance for dirty material 0-44115 wire, critical current in longit, fields, calc. 0-51005 Nb nonlocal characteristics of the bulk upper critical field 0-44131 PbTI, Tl plated and diffused, surface hysteresis, flux pinning 0-75620 in SrTiO₃ semiconductor, theory and expt. 0-68791 Th, hydrides and deuterides, at 1.1K 0-68792 V-Ta alloy, u.s. attenuation obs. 0-71988 V₃Si, mixed state, resistivity meas. critical field 0-44142 percooling hypersonic flow, low-density, over slender cones, eqns. of flux and equilib, 0-53248 0-53248 hypersonic flow, unsteady, boundary layer induced pressures on flat plate 0-53249 hypersonic gas flows, entropy on paraboloids surfaces 0-71222 and hypersonic inviscid, large amplitude slow oscillations of wedges 0-55555 hypersonic spatial flows, interference diagrams 0-71221 ideal gas, unstable, in linear channel with transverse magnetic field 0-71105 0-71105 inviscid, wing-body interference 0-71225 jet, non-isoenergetic, real gas, charact. eqns. soln., report 0-78188 laminar, boundary layer eqns., adiabatic wall solns. 0-39651 laminar near wake, critical point of Crocco-Lees mixing theory 0-78179 linearised method of solution to equations of motion for flow past a circular cone with zero incidence 0-58381 linearized, cylindrical shell flutter, determination of aerodynamic forces 0-50159 percooling nucleation of parasite crystals on supercooled water on the surface 0—75018 liquid, sensitivity to charged particles, conditions of permanency 0—50254 liquid, thermodynamic props. calc. 0—64896 metal melt solidification in vibr. field, physicochem. singularities 0—61595 nucleation, soluble impurity effect 0—55793 superconductor, In, type I, supercooling and superheating 0—44126 superconductor, type I, and superheating 0—47670 water, basal plane solidification kinetics, impurity effects 0—75008 water, ice nucleation kinetics 0—55663 water nucleation, homogeneous and heterogeneous 0—68180 Al-Mn, Al-Cr, Al-Mg and Al-Cu alloys, supercooling rel. to cooling rate 0—50316 Al melt, cooling rate depend. 0—50316 Bi-Sb alloy, cooling rate depend. 0—50316 Bi-Sb alloy, cooling rate depend. 0—50316 Bi-Sb melt, crystal growth rel. to surface tension, supercooling, additives 0—75006 Hg nucleation, homogeneous and heterogeneous 0—71416 Supercooling 0–50159 linearized transonic flow theory, comment on refinement 0–71240 adjacent liquid films, crosshatched wave patterns stability 0–74718 MHD, of slightly conducting fluid in wind tunnel 0–71078 Mach speed, optical emission and microwave attenuation on converging and diverging taper sections 0–78175 molecular beams, ideal intensities 0–74223 nonadiabatic laminar boundary layers, inhibition of flow separation 0.–53175 0 - 53257nonvortical steady-state three-dimensional gas motion 0-74656 past cone, yawed, numerical calc. 0-46790 penetration of gaseous jet and interaction, rel. to jet underexpansion 0 - 58378polygonal wings, oscillatory motions 0-55546 pressure fluctuations in transitional boundary layer, acoustic meas. 0-69733 0-69733 rarefied flow, blunt and sharp bodies in stream 0-39644 shock wind tunnel, new technique for high speed testing 0-45651 shocklayer over flat plate, density profile, exptl. model, electron beam fluorscence tech. applic. 0-43385 Smyrl's results for thin yawed wedges, correction 0-50160 stationary expansion flow at spatial supersonic edges 0-53239 steady, refraction of oblique shock waves by upstream disturbances 0-78194 Hg nucleation, homogeneous and heterogeneous 0-71416 In, type I superconductor, and superheating 0-44126 Pb, rel. to solid-liquid interfacial free energy 0-55701 Superexchange see Antiferromagnetism; Exchange interactions 0-78194 stellar winds in early type stars, effect of mech. force due to rad. 0-48401 step-induced turbulent boundary layer separation, Mach 2.5-4 0-50158 study by use of Fabry-Perot etalon 0-39659 study by use of Fabry-Perot etalon 0-39659 tail-body system, low freq. oscillations 0-46792 transonic, around perpendicular plate 0-61424 transonic wave drag integral, numerical evaluation 0-39655 in transverse magnetic field, frame-type channel, volt-ampere characteristics 0-71114 triangular wing 0-61431 turbulent boundary layers on isothermal adiabatic walls calc. 0-50151 Superfluidity perfluidity see also Helium/liquid; Quantum fluids Bose-Einstein condensation with crystalline ordering 0-69651 fourth sound attenuation by superflow in porous medium 0-48845 nucleus of interacting α-particles, normal-superfluid transition 0-38823 Pellam's helium paradox of torque temp. dependence for a Rayleigh disk immersed in rotating helium, explanation 0-58514 quantum effects, macroscopic, ordering and flow 0-47658 in universe 0-76532 vortex rings, dynamics 0-43503 He, dil. soln. impurities, quantum-hydrodynamical model, microscopic deriv. 0-43504 He energy flux calle between two baths separated by thin layer 0-61577 He, dil. soln. impurities, quantum-hydrodynamical model, microscopic deriv. 0–43504 He, energy flux calc. between two baths separated by thin layer 0–61577 He, equilibrium condensate fraction, temp. depend., exptl. determ. 0–39861 He, near \(\frac{1}{2} \) Point, order parameter behaviour 0–50290 He, surface oscillations, saturating vapour influence 0–39859 He flowing film, thickness 0–53389 He II, a.c. Josephson effect 0–39863 He II, coherence length near T_{\(\frac{1}{2} \)}, inequality 0–43502 He II, critical velocities of persistent currents 0–43501 He II, density and onset temp., size effects meas. by fourth sound 0–53390 He II, dynamics of rectinlinear vortex 0–55646 He II, ion drift velocity, turbulent counter flow effect, 1 K 0–43507 He II, ion mobility, velocity discontinuity, 0.89-1.0 K 0–43506 He II, relativity gyroscope obs. 0–76809 He II, uniformly rotating, mutual friction meas. 0–55643 He II, verx rings, dynamics 0–43503 3He-4He solns, mobility of positive and negative ions 0–61583 4He, 4He-3He, surface barrier for electrons, superfluid-induced 0–39864 4He, Brillouin scatt, thermally excited first sound 0–43500 4He superfluid, effective 3He quasiparticle potential found in 3He-4He solutions 0–61581 perlattice structure see Alloys; Crystal structure, atomic; Solid solu-0-33256 turbulent boundary layers on isothermal, adiabatic walls, calc. 0-50151 viscous interaction on curved surfaces 0-78196 wake behind 2 dimens. plate, turbulence obs. 0-53254 wake of 120° cone, flow props. at Mach number 2.2 0-55553 wake vicinity of cone, turbulence mixing statistics, laser planogram obs. 0-53255 0-53255 wings study, double integration, numerical evaluation by analogue computer application 0-46780 Ar jet effect on barrier 0-39648 Ar plasma, local electron vel. and density obs. 0-61284 Ar plasma in supersonic flow, electron temp. and density determ. 0-61256 CO₂-N₂-H₃O (or He) expansion, population inversion 0-74666 He, hypersonic flow over slender cones rel. to eqns. of flux and equilib. 0-53248 0-33246 N₂0₄, through deLaval nozzle, comp. calc. 0-39652 O₂, hypersonic, nonequilib. shock layer around cones, expt. and numerical studies 0-53237 Supersonics see Ultrasonics Surface diffusion see Diffusion in liquids; Diffusion in solids; Surface phe-

Surface energy
see also Crystal electron states/surface
alloy, f.c.c., interfacial, rel. to grain boundaries 0–68215
alum, α- and β-types, morphological difference 0–74941
ceramic oxide/molten metal, wetting, contact angle, adhesion 0–47033
crystal, rel. to equilibrium form. statistical nature 0–61690
crystal faces, calc. procedure 0–61615
crystal morphology rel. to dislocation strain energy in growth kinetics
0–74950
crystal shape. Wulff's theorem deductions 0–61691 Supernovae see Novae Superparamagnetism see Ferromagnetism Supersonic flow personic flow see also Shock waves

Ackeret's theory for the study of infinite aspect ratio wings and rectangular or trapezoidal wings, extension 0-58382

air, hypersonic flow over slender concer rel. to eqns. of flux and equilib. 0-53248 0-44930 crystal shape, Wulff's theorem, deductions 0-61691 Cs halide crysts. 0-78365 freezing potential, substrate effect 0-50313 freezing potential generation in D₂O solutions 0-50317 friction and static electricity, conf., Minneapolis, USA, April, 1969 0-48947 air jet effect on barrier 0-39648 air-breathing jet engine channels, supersonic flow closing shock wave position 0-74667 interfacial energies in crystal structure transforms 0-39920

Superlattice structure see Alloys; Crystal structure, atomic; Solid solu-

Surface energy continued

ionic cryst., CsCl type 0-78365

onic cryst., surface energy-shape considerations rel. to gas-filled bubbles 0-58786

ionic cryst., surface energy-shape considerations rel. to gas filled bubbles 0-58785

0-38/85 m.o.s., Al-SiO₂-Ge, negative surface charge after annealing 0-72096 measurement using liquid N₂ boil-off calorimeter 0-78247 metal, absolute interfacial free energy rel. to equilib. micromorphology 0-61626

0-61626 metal, and structure 0-61625 metal, contact-pot, changes due to tensile stresses 0-58556 metal, f.c.c., interfacial, rel. to grain boundaries 0-68215 metal, theory 0-50945 metal crystal, shape 0-61833 metal crystals, correl, with observable atomic props. 0-50410

metal crystals, correl. with observable atomic props. 0–50410 metal plate charging rel. to surface pd. 0–50976 piezoelectric, surface wave coupling through fluid interface 0–50348 quartz, charge distrib., from scanning electron micrographs of oscillating crystal 0–68964

semiconductor, GaS(Se)-metal barrier energies and I-V characts. 0--44235 semiconductor, large unit cell, two-centre theory 0-65025

semiconductor film, CdSe, surface potential and cond., doping depend. 0-62370

0-02370 solid liquid interface, transparent materials 0-61620 solids and liqs. 0-53325 static charge generation, pressure-sensitive tapes 0-51094 tetracyanoquinodimethane, As-TCNQ, P-TCNQ crystals, elec. potential 0-75720

transparent material, solid-liquid interface 0-61620 UO₂, anisotropy and pore shape 0-61633 Al₂O, film on Si, interface charge, rp. sputtering power density effects 0-65081

As TCNQ crystal, elec. potential 0-75720
Bi, absolute interfacial free energy rel. to equilib. micromorphology 0-61626

Bi, absolute interfacial free energy ref. to equino. Interionology 0–61626
Cd, temp, depend, of anisotropy, rel. to surface entropy 0–68218
CdSe film, surface potential and cond., doping depend. 0–62370
Cu, bubble technique development 0–47037
D₂O, freezing potential generation in dilute solution 0–50317
GaS(Se) semiconductor-metal barrier energies and I-V characts. 0–44235
LiF, deformed, potential difference, dislocation distrib. 0–74882
LiF, fracture, dislocating processes, dynamical cleavage, expt. 0–47413
LiF, fracture, dislocation processes, dynamical cleavage, theory 0–47412
MgO – silicate, solid-liq. interfacial free energy, rel. to wetting 0–43536
P-TCNQ crystal, elec. potential 0–75720
Pb, solid-liquid interfacial free energy, from supercoooling data 0–55701
Pb drops in liq. Al, effect of interface energy on rate of fall 0–46884
Sn-Pb(Snag₃-Zn) eutectics, solid-solid interface, laminar growth theories 0–39923
TiC, from crack formation under static and sliding contact 0–40417
Zn, temp, depend, of anisotropy, rel. to surface entropy 0–68218
fface ionization see Ionization, surface

Surface ionization see Ionization, surface

Surface measurement see also Area measurement

chemical composition, ion microanalyser 0-50350 contours, generation by Moire patterns 0-49111 electron microscopy, conventional and scanning, replica technique using water and soluble plastic 0-50349 ellipsometer, calibration of analyser and polarizer, modified method 0-70051

ellipsometric technique for substrate optical consts. meas.

ellipsometric technique for substrate optical consts. meas. 0–71462 ellipsometry of rough surface, optical consts. meas. 0–65979 facet angles, evaluation by eight reflection technique 0–78361 rel. to large-scale optical components, unequal arm interferometer application 0–73297 molecular dynamic technique rel. to phonon props. of small particles, and size effects 0–43839 optical, roughness and slope meas., simple scatter method 0–49130 optical roughness and slope meas, simple scatter method 0–49130 representation of curvature meas. 0–65979 optical spherical, radius of curvature meas. 0–63307 particle, micromeritic instrumentation development 0–76791 phonon properties of small particles, size and surface effects 0–43839 silica, polished, fused, roughness and slope meas., simple scatter method 0–49130 solid-liquid interface, concentrated alloys, temp. meas. and stability

0-49130
solid-liquid interface, concentrated alloys, temp. meas. and stability
0 50776
specific surface area, methods of meas. 0-43529
terrain roughness meas, airborne laser profilometer applications 0-54220
topography, using intensity distrib. of light 0-65024
X-ray reflection, intensity rel. to roughness 0-40044
X-ray topography, high resolution divergent-beam 0-50495
Ag, adsorbed gases, optical props, ellipsometry 0-39967
Ag, adsorbed gases, optical props, ellipsometry 0-39965
SiO₁ layer, ellipsometry, refractive index, thickness 0-76016
W emitters, chemical vapour deposited, orientation investigation by etch pit technique 0-78396

technique 0–78396

Surface phenomena

see also Adsorption; Capillarity; Catalysis; Electron emission;
Films; Ionization, surface; Liquid waves/surface; Sorption
ablation, review 0–71733
acoustic surface wave propag, in layered anisotropic media 0–75386
acoustic surface-wave refl., electrically controlled 0–48846
acoustic wave, amplification and coupling at piezoelectric semiconductor
interface 0–40551
acoustic wave amplification, using accumulation layer on Si 0–76911
acoustic waves, nonlinear effects 0–71834
active agents, reduction of mass transfer inside drops 0–39746
adsorbed molecules, self-diffusion, kinetics, n.m.r. spin echo 0–74926
alkali halide, (100), electron stimulated desorption 0–65036
alkali halide, (100), erefron stimulated dissociation 0–65035
alloys, grain size refinement by scraping solid-liquid interface during freez
ing 0–61596

alumina-Ni interface, thermal conductance at elevated temp. 0–71875 association constant in surface layer of a soln. of an associated liquid

0 - 58471

Auger spectra, LMM, low energy, high resolution, from solid surfaces 0-65030

```
Surface phenomena continued
```

beam scattering, atomic and molecular, intensity data for LiF (001) 0-43535

Brass, laser irradiation, nonlinear heating 0-43317

cathode migration processes stability 0-40903 cellulose acetate phthalate, props. 0-74430

chemisorbed oxygen in tungsten 0-48191

coatings, thermal control, surface deposits due to u.v. irrad. 0-39941

conductance meas., formation factor 0-61569 conference, Seattle, USA, 1969 0-55686

contact angles of solid phase wetting by own melt, organic compounds 0-58558

contact of two solids in liquid with interfacial orientation 0-47618

contact problem of elastic and rigid cylinders containing shallow longit. surface depression 0-38272

contact problem of elastic and rigid cylinders containing shallow longit. surface depression 0—38272 contact problems in elasticity, solution for thick layer on Winkler type foundation 0—38286 contact stresses in elastic half-plane with stiffened boundary 0—48808 cracks, small, semiempirical fracture analysis 0—48791 cubic cryst., piezoelec. surface waves 0—47849 damage due to ion beam scattering 0—61802 desorption kinetics of nitrogen in W(100) face 0—47083 desorption of carbon monoxide in rhenium 0—47081 diatomic gases surface complexes and transition metals 0—47029 diffusion, mono- and multilayer adsorption 0—71490 diffusion and existence of two-dimensional liquids 0—71450 diffusion and existence of two-dimensional liquids 0—71449 disintegration kinetics under shock heating 0—40393 dislocation loop near free surface 0—55882 dislocations at planar interfaces 0—75158 drop spreading on smooth surface 0—71299 elastic waves, exciting and probing technique 0—78745 elastic waves, fluid layer on Rayleigh wave delay line 0—38358 electron emission microscope study, calc. of microfields 0—42217 electron energy level shifts in alkai halides 0—47979 electron impact desorption of ions and neutrals, cylindrical magnetic spectrometer for obs. description 0—68238 electron tunnelling through adsorbed layers, atomic cores effect 0—43528 electroreflectance at fund. direct threshold of Ge-electrolyte interface 0—76072 epitaxial influence via amorphous layers 0—43547 enitaxial influence via amorphous layers 0—43547 enitaxial system, deposit-substrate interfacial equil, config. 0—71468

0-76072 epitaxial influence via amorphous layers 0-43547 epitaxial system, deposit-substrate interfacial equil. config. 0-71468 evaporation of discrete volatile films from the surface of a stagnant immiscible liquid 0-68188 excitation, elastic constants and recovery characteristics determination, contact impedance meter, ultrasonic sensor 0-50652 fc.c. metals, diffusion mechanism 0-61623 fatty acid monomolecular films deposited on mica in aqueous and nonaqueous media, interfacial energies 0-78363 ferromagnet, inhomogeneities in magnetization 0-69020 ferromagnetic, active power distribution due to currents in parallel conductors 0-79059 fibrous composite, interface effects 0-68474 field-electron emission microscope applic. 0-74874 film, demagnetizing fields, surface-roughness- induced, effect on approach

film, demagnetizing fields, surface-roughness- induced, effect on approach to saturation 0–44613 film/crystal interfacial strain, asymmetric diffr. use in X-ray topography 0–68206

fins, rectangular, optimum arrangement on a surface for free convection heat transfer 0-45682 gamma-ray density gauge response to boundary between two materials

0 - 63868

gas-solid interaction, spatial and velocity distributions 0-53417 gas-solid interactions, hyperthermal mols. with contaminated surfaces 0-71442

gas-solid interactions rel. to surface at struct. 0-56692 gas-surface scattering, cubes model, quantum mechanical basis 0-71443 glass, Hertzian fracture expts. rel. to Auerbach's law energy balance explanation 0-47402

glass, adsorbed organic radicals, γ radiation, charge transfer, e.s.r. 0-39933 glass, bending strength increase on layer removal, rel. to liq.-liq. phase separation 0-53607

separation 0–53607
glass, damage by laser beams 0–57532
glass, determ. of the microgrammes of Su on surface 0–53422
glass, high strength, fracture ambient medium effect 0–40356
glass, laser, damage threshold obs. 0–57530
glass plates, light cond. 0–57598
glass-metal inflerface, atmosphere and glass effect on reactions 0–53416
glass-molten salt interface, thermodynamics of ionic exchange processes
0–5034 0 - 50354

0-3034
graphite overlayer on Pt, D₂ molecular beam scatt. 0-65038
heat transfer, solid boundary to turbulent fluid 0-71448
rel. to heterogeneous systems, generalized conductance, theory 0-71390
hypersonic wave attenuation, general formula 0-59097
impedance, anomalous quantum oscillations 0-59043
insplator, in migration, affect on more and hisplay integrated circuits

insulator ion migration, effect on m.o.s. and bipolar integrated circuits 0-47812

insulators, kinetics of electron reflection and ion recombination 0–78362 interaction of atomic O with various surfaces 0–58559 interface, liquid-air, liquid density gradients, interferometric meas. 0–43434

ntertace; inquid-air, inquid density gradients, interterometric meas. 0–43434 interfacial dynamics, instabilities 0–53283 interference films, chemically deposited, optical compounds deformation, due to annealing 0–74920 ion scattering and light emission 0–68210 ionized monolayers, surface pressure calcs. 0–74808 ionized monolayers, surface pressure calcs. 0–74807 Langmuir probe, effect of condition 0–43310 laser pulses, short, on absorbing substance, thermal stresses and shock wave within solid 0–40617 laser speckle changes, use in vibration analysis 0–42320 lipid membrane, conductance, surface active agent effect 0–39836 liquid, analysis of motion in acoustical holography 0–53338 liquid interface instability in constant field 0–43417 liquid-solid interface, collision phenomena 0–71061 liquid-solid interface, u.s. reflection, conical, optical obs. 0–52110 magnetic oxide platelets, ion milling for surface defect removal 0–75916

Surface phenomena continued

magnetostatic wave, nonreciprocal, independent propagation control and decay constant 0-44609

mass and heat transfer, semi-infinite porous medium, well-stirred fluid

mass transfer, solid boundary to turbulent fluid 0-71448

melting, contact, of cryst, in steady state 0-64997 metal, annealed, residual surface stress meas, during fatigue 0-40261 metal, ion bombardment, ion refl. and secondary ion emission meas. 0-68209

metal, resistance meas. rel. to seizure mechanism 0-40428

metal, resistance meas. rel. to seizure mechanism 0-40428 metal, structure due to ion bombardment 0-61617 metal erosion by ion bombardment, microtopography 0-61616 metal particles diffusion coalescence on nonmetal substrate 0-71441 metal surfaces in contact, mechanism of thermal conductance 0-68635 metal target, ion bombardment, light emission, spectral analysis 0-66118 metal-semiconductor surface barriers 0-65700 metals, thick samples, surface plasmon effect on reflectance 0-48002 micro-liquid-layer formation, on solid surface with growing bubble in nucleate boiling, principle mechanism 0-71421 microcracks surface, growth in fatigue 0-47397 migration and capture processes in heterogeneous nucleation and growth 0-65099

0 - 65099

migration and capture processes in heterogeneous nucleation and growth

molecules, neutral, interaction with solid, surface, mass spectrometry 0-5588

molecules, neutral, interaction with solid surfaces 0-5: monocrystals, shock induced elec. potentials 0-47847 Mossbauer backscatt. analysis of thin layers 0-56508

multi-component phase interface, entropy production 0-74877 neutron multiplication, using surface of Pu-polystyrene cube 0-49731 nitride fuel and cladding materials, Na wetting characts. 0-88555 notches and protrusions, interaction of dislocations 0-61951 nucleation of disc-shaped hole in low index surface and at dislocation 0-75016

nucleation of thin films, field ion microscope study using controlled clustering technique 0-47168

ocean gravity waves, random deep-water long- crested, mass transport 0-51499

0-31499 optical props. of surfaces with bestrewed particles, pits, etc., computation method 0-44741 optics of surfaces slightly tarnished, dirty or rough, computation method 0-62642

Permalloy film structures, ferromag., spin pinning 0-44971
permalloy thin films, spin wave resonance 0-40993
photoinduced electron-transfer reactions at surface of organic crystals

0-79453

0-19433
physical electronics properties through chemisorption, conference, Milwaukee (1970) 0-48189
piezoelectric, acoustic surface wave propag. 0-56097
piezoelectric, surface wave coupling through fluid interface 0-50348
piezoelectric crystals elastic waves, excitation, detection and dispersion 0-44374.

piezoelectric surface waves in cubic cryst. 0—47849 plasma gas discharge heating of the surface of a solid 0—62207 plasma production by laser interaction with solids, bibliographical review 0 - 71177

plasma resonance radiation from non-radiative plasmons and decay into photons on a rough surface 0–62273 plasmon-phonon interactions in CdS, optical constants calc. 0–44757 plastic, wear resistance, surface deformation, composition effects, friction, strength, ductility 0–40425 polarization role in non-centrosymmetrical cryst. growth. 0–58626

polamication for all non-centrosymmetrical cryst. growth. 0–58026 polymer surface layers mechanical behaviour studies by transition processes in u.s. vibrations 0–50360 polymers, bidimensional layers, thermodynamic props. 0–61619 polymethylmethacrylate surface layers under friction, elastic deform. 0–40429

polypeptide film, absorpt., Auger emission obs. 0–61636 porous/liquid interface, Fingero-imbibition 0–64876 potential of adsorbed layers, differential method for measurement 0–55752

0–55752
potential variation rel. to tunnelling probability 0–47907
preparation of low SEE surfaces by evap. of metal films under high residual
gas pressures 0–71444
pressure contact, between two rough and wavy surfaces, gas thermal conductance at interface 0–68013
quartz, high-power laser interaction 0–77157
quartz, plasma gas discharge heating of the surface of a solid 0–62207
aquartz, surface acoustic wave vel. temp. depend. 0–59096
RMS displacements on liquids and solids 0–65027
radiation interchange in enclosure, plane isothermal and adiabatic surfaces
0–57433

0-57433

radiation interchange in enclosure, plane isothermal and adiabatic surfaces 0–57433 radical-recombination luminescence rel. to adsorption kinetics 0–41294 radioactive crystals, surface elec. charge distrib. 0–40817 resonant reflectance anomalies, surface irregularities effect 0–44761 rough, e.m. scatt., shadowing and multiple-scatter effects 0–73095 rubber-glass true contact area form. 0–40424 ruby crystals, destruction by laser radiation 0–39924 sandwave patterns, sand bed stability in alluvial channel, model, based on vorticity transport equation 0–72595 scanning electron microscopy technique employment 0–54844 scattering, stimulated, of light by surface waves on liq. or solid 0–46915 scattering of light atoms 0–39921 secondary electron yield, low, prep. by evap. of metal films under high residual gas pressures 0–71444 self-diffusion meas, bulk impurity effect 0–58557 semiconductor, electron mirror microscopy 0–72052 semiconductor, surface, potential due to charged metallic strip 0–59224 solid, monolayer and built-up films 0–58590 solid-gas interactions, elastic-continuum, monatomic inert gas 0–65028 solid-liquid interface shapes during Czochralski cryst. growth 0–78407 solid-liquid interface shapes during Czochralski crystal growth, numerical analyses 0–50453 solid-liquid interface shapes during cryst. growth by Czochralski method 0–53463

Surface phenomena continued

spin waves, optical branch existence 0-72199 steel, lubrication rel. to exoelectronic emission 0-65864

steel, stainless, laser irradiation, nonlinear heating 0-43317 strain, meas. by optical correlation methods 0-58878 superconductor-normal metal interface, electron reflection coeff. temp. depend. 0-65637 temperature distribution on cylinder transmitting u.s. wave 0-40559 temperature measurement, steady state errors, methods of prediction

0-60090

thermal contact conductance, two rough and wavy surfaces under pressure contact, analytical study 0–68632 thermodynamics, irreversible, applic. to stationary interface 0–51996 transition metals, sublimation of atomic ions in 1800 to 2600°K range 0–47005

u.s. waves refraction and reflection, by Au thin film layer on LiNbO3 0-65538

vapour deposition on two-dimensional lattices, computer simulation 0-39922

vapour-liquid interface, motion of He ions 0-50322

vapour-liquid interface, motion of He ions 0-50322 wave formation near rough interface between two media 0-46858 waves on plasma half-space, dispersion relation, temp. and density gradients effect 0-55465 windrows generation, gravity waves interaction model 0-69281 windrows generation, gravity waves interaction model 0-69281 Ag, self-diffusion coeffs, from grain boundary grooving obs. 0-71455 Ag (111) face, scattering of thermal energy Ar atoms, intensity and speed distribs. 0-47035

Ag (111) face, scattering of thermal energy Ar atoms, intensity and speed distribs. 0-47035
Ag nucleation on W substrate, contact angle 0-55741
AgBr, contact phenomena rel. to photographic process 0-73365
Ag(001), He at. diffr., obs. 0-55692
Ag(111), scattering of epithermal Ar beams 0-53419
Al-Al₂O₃ interface, photoemission of holes and electrons 0-44436
Al, lubrication rel. to exoelectronic emission 0-65864
Al alloy 7075-T6, brittle crack propagation rel. to surface layer stress relaxation 0-50732
Al space vehicle surfaces, white anodizing process 0-43534
Ar solid, sublimation rel. to lattice modes 0-47006
Au/LiNbO₃ layered anisotropic substrates, fund. and higher-order mode surface waves 0-47522
Au film on Kcl (100) face, crystallites Brownian motion 0-68216
Au nucleation on W substrate, contact angle 0-55741
Au progressive establishment by Brownian motion, epitaxy crystallites on KCl (100) face 0-71470
Ba, adsorbed on (110) W, migration equilib., effect of inhomogeneous elec. field 0-55763
BaTiO₃, electromechanical study of surface layer 0-71452
Be, sintered, under pressure, phys. props. surface chemistry effects 0-47464
Be sheet, wrought polycryst, crack initiation mechanisms 0-71722
Bit. GeO., metallized and unmetallized acquisite wave velocity, elastic and

0-4/464
Be sheet, wrought polycryst., crack initiation mechanisms 0-71722
Bi₁₇GeO₃₆, metallized and unmetallized, acoustic wave velocity, elastic and piezoelectric consts. 0-78748
C, mon-graphitizing-type, specific surface area characts. 0-39969
CO on h.c.p. Ru and Re, magnetic field emission obs. 0-43571
CU, ions scatt. on (100) and (110) faces, spatial distrib. anisotropy 0-71454

0-71454
Cd, cohesion coeff, temp. depend. 0-39926
Cd whisker, effect of oxide or metal film on mech. props. 0-40300
CdS, optical constants from plasmon-phonon interactions 0-44757
Co, spiral lines due to electrolytic polishing 0-56024
Cs, adsorbed on (110) W, migration equilib., effect of inhomogeneous elec. field 0-55763
Cu, brittle crack propagation rel. to surface layer stress relaxation 0-50732
Cu, particles ejected from surface under bombardment by Artions

Cu, particles ejected from surface under bombardment by Artions 0-65039

0-5039
Cu, self-diffusion coeffs. from grain boundary grooving obs. 0-71455
Cu, specular electron reflectivity curves, peak widths 0-61628
Cu, u.s. reflectivity of single and polycryst. at water-Cu boundaries 0-43872

Cu, u.s. renecutity of single and polycryst, at water-Cu boundaries 0–43872 Cu, u.s. wave velocity and absorpt, meas. 0–78749 Cu, u.s. wave velocity and absorpt, meas. 0–78749 Cu, u.s. wave velocity and absorpt, meas. 0–78749 Cu Cu7OZn30 brass, fracture surface cohesion in u.h. vacuum 0–56055 Fe, sintered, adhesion to mild steel depend, on void fraction 0–56053 α-Fe,03 powders, spec. surface area temp, depend. 0–65131 GaAs photoemission and contact potential meas., bulk dampings from p-ton-type 0–56286 n-GaP, effects on optical absorpt, by free carriers 0–66043 Ge, surface-barrier photo effect during polarization in electrolyte 0–65842 He II, superfluid, surface oscillations, h.f. 0–55645 He II, wave processes near heater surface 0–50322 He lons, motion near vapour-liquid interface 0–50322 He louid, surface layer width 0–46970 PHe, energy states in liq. 4He 0–74817 Li, adsorbed on (110) W, migration equilib., effect of inhomogeneous elec. field 0–55763 LiF (001), 3He, 4He, H₂ and D₂ reflection and diffr. intensity data 0–43355 LiF (001), reflection and diffraction of He and H, beams 0–47034

0-43535
LiF(001), reflection and diffraction of He and H, beams 0-47034
LiNbO₃, y-cut, surface wave spreading obs. 0-75388
MO surface oxidation obs. by secondary ion mass spectroscopy 0-72539
MgO, polycryst, effect of temp., grain-size, porosity and surface condition on strength 0-40352
Mn-Zn ferrites, surface grinding effect on permeability 0-65958
Mo scattering of atomic and mol. ions, energy distrib. 0-40912
Na diffusion, on metal substrates, meas. technique numerical simulation 0-47282

0—4/282 NaCl cleavage planes, pitting and evaporation, 454-593°C 0—61703 Nd, adsorbed on W, migration and evaporation field emission 0—39980 Ni/Al₂O₃ (sapphire) interface, laser beam induced damage, metal vapour effect 0—53528

Ni, migration of graphite to the surface 0-55700
Ni, scattering of atomic and mol. ions, energy distrib. 0-40912
Ni, specular electron reflectivity curves, peak widths 0-61628
Ni (100) surface, carbon segretation, work function and LEED obs.
0-47039
Ni surface, trapping and thermal release of 100-300 eV Ar⁺ and Kr⁺
0-47039

47038 Ni(001), atomic thermal vibr., LEED obs. 0-74886 Surface phenomena continued Ni(100), C comtaminated, photoelectric yield temp. depend. 0-43538 O_2 interacting with metals rel. to Auger electron spectroscopy 0-47030Pb binary molten alloys, surface and body activities 0-74744 Pt, scattering of atomic and mol. ions, energy distrib. 0-40912 Pt group, effect of preparation methods on organic vapour chemisorption obs. 0-56694 obs. 0–56694

Re hot surface O₂ loss, 10.8 to 10.4 Torr. 0–65047

S segregation on Ni(110) surface 0–47031

Si-Fe alloys, antiphase domain boundaries 0–55702

Si, Auger spectroscopy examination 0–65730

Si, contamination studies 0–65728

Si, doped layer, electrical resistance, low temperature thermometer and bolometer, preparation and applications 0–45669

Si, formation of insoluble surface layer by B diffusion 0–47296

Si, plastic deformation, –196 to 550°C, metallographic and transmission electron microscope obs. 0–40311

Si, preparation, mechanical damage considerations 0–68859

Si, recombination velocity, carrier trapping and photovoltage, photoconductivity meas. 0–68979

Si, stabilization, rel. to device fabrication 0–65727

Si, surface-barrier photo effect during polarization in electrolyte 0–65842

Si, surface and interface characterization, ellipsometric techniques 0–65731

0-03/31 Si, surface preparation, effect of O₂ precipitation 0--65729 Si, thermally oxidized, ionizing radiation influence 0-68845 SnO₂, effects rel. to thermal annealing, Mossbauer effect and X-ray diffr. study 0-55705

Ti, adsorbed on W, migration in strong electric field, field emission 0-39981

Ti, brittle crack propagation rel. to surface layer stress relaxation 0-50732

0-50732

UO₂, secondary electron energy distrib. 0-40916
W, chemisorption of atomic nitrogen 0-48190
W, diffusion of Au in strong elec. field 0-58561
W, electro- and thermal-transport 0-65044
W, Het- Auger neutralization, DWBA quantum scatt. calc. 0-55693
W, interaction of WO₂ and O₂ 0-58563
W, low angle Het- ion scatt. 0-71458
W, mean life time of CSI molecules adsorption 0-61677
W, migration of Ti, adsorbate conc. depend. 0-61634
W (100), (110), (111) faces, adsorption of hydrogen 0-47082
W polycrystalline, electron impact desorption of ions and neutrals, kinetics 0-71492
W surfaces, (110), (211) and (321) transition metal additional lifturing Sch

W polycrystalline, electron impact desorption of ions and neutrals, kinetics 0–71492
W surfaces, (110), (211) and (321), transition metal adatom diffusion, field ion microscope studies 0–39931
W(110), scattering of inert gas beams 0–65043
Yb, adsorbed on W, migration and evaporation, field emission 0–39980
Zn, cohesion coeff. temp. depend. 0–39932
Zn film, oxidation, I doping effect, 200 390°C 0–76267
Zn whisker, effect of oxide or metal film on mech. props. 0–40300
ZnO/solution interface, ionic double layer, point of zero charge, prep. depend 0–51434
ZnO/solution interface, ionic double layer, differential capacities, specific adsorption 0–51436
ZnO/solution interface, ionic double layer, surface composition, pH depend. 0–51435
ZnO, resist., glow discharge effect 0–62291
ZnO single crystals, optical surface phonons, detection by slow electron spectroscopy 0–53694
ZnS grains for TV screen, surface treatment to improve uniform coating 0–54845
ZnS phosphor, radical-recombination luminescence spectra 0–76159

ZnS phosphor, radical-recombination luminescence spectra 0-76159

Surface structure alkali halide, (100), air and vacuum cleaved surfaces 0-65034

race structure
alkali halide, (100), air and vacuum cleaved surfaces 0—65034
alloy, low m.p., topographical changes on high-velocity impact rel. to localized melting 0—65041
alumn, amodic film, barrier-porous layer interface, sealing 0—76274
Auger electron energy distribs., lattice vibr. effects 0—40913
b.c. metal, fatigue damage rel. to residual stress level 0—68484
Buerger goniometer for texture determ. 0—71533
cellulose acetate phthalate 0—74430
ceramics, pore location role 0—53004
rel. to chemisorption 0—56692
contact, profile analysis using waveform of random signals 0—47032
crystal, electrical, rel. to nucleation and growth 0—61738
crystal, orientation, obs. using X-ray diffractometer and laser 0—75040
decoration criteria for steps 0—71440
detonation tube, roughness effects, theory 0—38400
diamond, deformation twinning obs. 0—43741
electric relief, reproduction by oriented crystallization on Se photoelectret layers 0—71446
electric relief 'copying' by amorphous films stripped from crystal substrates, electren mechanism 0—43531
electron probe analysis 0—65032
epitaxial system, multiple diffr. origin of extra refls. in HEED 0—55691
erosion, cavitation, effect of surface tension 0—51429
examination using replica technique for conventional and scanning electron microscopy 0—50349
f.c.c. crystal, lattice distortion, atomic force tensors, Green's function 0—65026
f.c.c. metal, faceted, focuson deviation theory 0—68672
faceting, temp, gradient influence 0—74871
field-electron emission microscope applic. 0—74874
field-ion microscopy psots caused by gas adsorption atom probe analysis 0—55758
field-ion microscopy, principles 0—74876
film, dielectric, electric strength, effect of micro-relief of electrode surface 0—75867
film of Cu electrode, electropolishing, ellipsometry 0—65058
fine deposits marking with radioactive 1998 Au 0—77524
fccus net devalum theory ambled to f.c. metal, 0—68672

film on Cu electrode, electropolishing, ellipsometry 0-65 fine deposits marking with radioactive ¹⁹⁸Au 0-77524 focuson deviation theory applied to f.c.c. metal 0-68672 fractography using scanning electron microscope 0-68211 fracture surface analysis by microscopic Auger electron technique 0-68489 Surface structure continued

rel. to functional electronic block, Si wafer, flat, defect-free and uniform surface fabrication 0--59225

surface labrication 0–59225
glass, i.r. spectroscopy involving multiple total internal reflection 0–71457
glass, ion beam processing 0–71445
glass, matt, etching, light scatt. 0–41117
glass, smoothing by viscous flow 0–47028
glass soda-lime-silica, roughness effects on Na content determ. by X-ray
fluorescence spectroscopy 0–41456
graphite, regular hexagonal pitting of cleavage surfaces by atomic H or N
0–40176

0-40176
graphite, scanning and replica electron microscopy comparison 0-39925
HEED and X-ray emission analysis 0-65031
imperfect, effect on LEED 0-65205
impurity removal for Auger electron spectroscopy 0-43530
interface instability in Ge:Ga crysts, pulled from melt 0-50464
LEED, inelastic processes, surface plasmon peaks 0-40048
LEED, inelastic scatt. and excitation dispersion 0-78436
LEED, inelastic scatt. theory 0-61794
LEED intensities, multiple scatt. theory, appl. to monolayers 0-39918
LEED reconstruction, comparison with field-ion microscope 0-65029
liquid-solid interfaces, structure relaxation 0-61618
lunar fines and rock, Apollo II samples, morphological obs., scanning electron microscopy 0-68291
lunar samples, surface features 0-45383
Mars, radar measurement 0-63101
metal, alloys, on rolling, texture effects 0-65033

metal, alloys, on rolling, texture effects 0–65033 metal, and energetics 0–61625 metal, capillarity-induced morphological changes 0–61624 metal, cleanliness, work function, argon ion-bombardment, heating

0-39927

metal, h.c.p., contrast from stacking faults in field-ion micrographs 0-55690

0-55690
metal, planar and roughened, metallographic studies, scanning electron microscope applic. 0-78359
metal crystals, correl. with observable atomic props. 0-50410
metal foil prep. for transmission electron microscopy 0-39948
metal oxide layer, growth 0-61665
metallic islands condensed on dielectric substrates, anomalous props.
0-55694

0-55694
metallographic polishing techniques, on deformed pyrolytic carbon, surface preparation by cleavage 0-50606
mica, decoration with Au 0-39928
microgregometry study by methods involv. gas sorption 0-43529
microirregularities on rough surface, average height determ., photometric method 0-61614
muscovite, Auger electron spectroscopy obs. 0-78368
nuclear reactor tubes, artificial roughness rel. to critical heat flux density 0-49721
ontical degradation meas. Jaser beam applic. 0-49108

0-49721
optical, degradation meas, laser beam applic. 0-49108
oxide, finishes effect on strength and fracture 0-58911
polystyrene, fracture path rel. to shape and distrib. of crazes 0-47419
pore radius distribution 0-43529
quartz resonator, excited, X-ray diffraction topography 0-47027
Raman scatt., crystal surface effects 0-66063
research, Massachusetts Institute of Technology, Sep 1967-Sep 1968
0-38121

0—36121 ruby crystals, destruction by laser radiation 0—39924 semiconductor, GaAs, surface damage due to ion implanatation, reflectance meas. 0—78366

meas. 0–78366 semiconductor, large unit cell, two-centre theory 0–65025 semiconductor, specular defect meas. 0–62368 semiconductor epitaxial film, interface analysis by X-ray diffr. topography 0–65680

semiconductor surface layer characterization by X-ray topography 0 65666

0 65666 silica, i.r. spectra obs. 0—50357 specular defect meas. 0—62368 sputtering, low-energy, ang. distrib. 0—68683 steel, 4340, fracture surface topography 0—40283 steel, AISI 4340, fracture surface topography and toughness 0—40367 steel, fractography, scanning electron microscopy, yielding phenomena 0—68490

0-68490
steel, fractography using scanning electron microscopy 0-71447
steel, transformer, surface layer effect on props. 0-61629
strain, meas. by optical correlation methods 0-58878
strain generated patterns in Si 0-65045
substrate, epitaxial film formation 0-61648
substrate crystals for deposition, elec. relief effects 0-53458
substrate rel. to growth of epitaxial Au films 0-61652
thin foils, dislocation dissociation 0-61954
topography meas. using intensity distrib. of light 0-65024
topology applics. to metallography 0-40431
rel. to total hemispherical emissivity meas, effect of roughness
welded steel, fractography using scanning electron microscopy 0-71723

topology applies, to metallography 0—40431 rel. to total hemispherical emissivity meas., effect of roughness 0—40610 welded steel, fractography using scanning electron microscopy 0—71723 wurtzite, II-VI compounds, ZnO and CdSe, LEED 0—74878 zincblende (110), atom geometry analysis 0—47597 Ag film, vacuum-deposited, rel. to air pressure, thickness, deposition rate and substate temp. 0—43543 Al-(15wt.96)Ag alloy, γ plates, diffusional phase transformation, relief effects 65483 0—65483 Al-(0.96 wt.%)Sn alloy, on heating and subsequent cooling, rel. to oxide film78364 0—78364 Al, LEED obs. 0—65037 Al, pit formation, vacancy condensation, deformation hot stage metallographic facility 0—40481 Al, Diffurnation, vacancy condensation, deformation hot stage metallographic facility 0—40481 Al, O₃-TiO₂ system, heats of immersion, adsorpt. props., X-ray diffractometry 0—50352 α -Al,O₃, (0001) face heat treatment 0—65046 Al,O₃, surface cracks, healing by heat treatment 0—50739 Al₂O₃ substrate, treaments, bend strength changes 0—62056 Al₂O₃ substrate, treaments, bend strength changes 0—62056 Al₂O₃ substrate surface defects, effects on thin film interconnect patterns 0—53420 As-Te-Ge glass, flament formation, electron probe analysis, radiometric microscopy 0—56285 Au/Pd bimetal film interface, diffusion annealing, 150-350°C 0—50363 Au, structure relaxation at interface with liquid 0—61618 Ba adsorbed film on Mo (110) face, rel. to work function 0—71495

PA 1970 - Part II (July-Dec.) Surface structure continued BaTiO₃ (001) face, LEED obs. 0-68217 BaTiO₃ ceramics 0-55696 Be, etching, patent 0–39997
Bi, liquid surface, LEED 0–55589
Bi, melting and freezing of single-cryst. surfaces, LEED 0–53418
C, pyrolytic, tensile-deformed, basal plane metallography 0–40058
C fibre surfaces, high-energy photoelectron spectroscopic study 0–68207
CdS, exciton luminesc. obs. 0–59421
CdS film, expitaxial growth, morphology, electron diffr. 0–47052
CdS layer, changes after thermal processing, and elec. props. changes 0–75718 Be, etching, patent 0-39997 0-75718
CdS sublimated cryst., surface morphology 0-50353
CdSe, LEED 0-74878
Co, spark eroded, high temp. phase 0-58560
Cu, spark-erosion damage 0-61627
Cu extrusion billets, automatic inspection 0-71782
Fe:B, segregation, Auger emission spectroscopy 0-53421
Fe-(1.5wt.%)Sb, fracture surface obs., microscopic Auger electron analysis 0-68489
GaAs, (100), mean-square atom displacements, electron diffr, 200-600°C 0-74879
GaAs. (110) texture, ion bombardment, annealing, 350°C, LEED pattern GaAs, (110) texture, ion bombardment, annealing, 350°C, LEED pattern 0-74880 GaAs, epitaxially grown 0-55724
GaAs, mech induced surface damage 0-65040
GaAs, photoluminescence obs. of inhomogeneities 0-56229
GaAs, surface damage due to ion implantation, reflectance meas. GaAs, sur 0-78366 O-78366

GaAs_xP_{1-x}, photoluminesc. obs. of inhomogeneities 0-56229

Gd adsorbed film on Mo (110) face 0-71496

Ge:Ga cryst. pulled from melt, interface instability 0-50464

Ge:GeO₂, interface states, a.c. field effect, crystal orientation effect

0-78367 0–78367
Ge, changes during oxidation, electronic changes correl. 0–45061
Ge, morphology of etch pits 0–55698
Ge epitaxial layers 0–58585
Hg, liq., LEED obs., multiple scatt., scatt. factor and attenuation 0–78261
KCl (100) surface, LEED obs. 0–68219
KI, Se decorated, active epitaxial vacancy cluster centres, electron diffr. microscopy 0–74881
La adsorbed film on Mo (110) face 0–71494
LiF, thermal etch pits at dislocations 0–74883
MgAl₂O₄, spinel, chemical polishing in pyrophosphoric acid 0–55699
MgO smoke cryst., coincidence twist boundaries 0–61630
MnO₂ surface layer structure variations during phase transformation, 200-400°C 0–59029
MnS-MnSe, microscopic examination 0–47117
NaCl crystal, PbS condensation at charged micropores, electron microscopy 0–75133
NaCl crystal, step structure resulting from decrystallization, high-vac. evapscopy 0-75133 NaCl crystal, step structure resulting from decrystallization, high-vac. evaporation 0-74884 oration 0—74884

NaNO₃, morphology of solid-melt interface, holographic study 0—47138

Nb-Ti ternary alloy, 65BT, field emission microscope obs. 0—61631

Nb, oxide struct. obs. and supercond. implications 0—74885

Nb(100), atomic vibr. amplitude, LEED obs. 0—43537

rel. toNd-glass laser, effect of lateral microprofile on heat endurance 0—73245 0-13.445
Ni-Fe tapes, domain patterns, Kerr magneto- optic effect 0-44777
Ni, deformation in fast air streams 0-68220
Ni (100) surface, carbon segretation, work function and LEED obs. 0-47039 Ni, (eleformation in last air streams U——08520 Ni (100) surface, carbon segretation, work function and LEED obs. 0–47039 Ni ferrites, morphology and surface features, rel. to growth 0—61696 Ni film, electrodeposited, metal contamination, appearance and surface topography 0—58576 NiO (100) face, superstruct., electron diffr. obs. 0—50355 Pb, cavitation induced erosion, u.s. in water and liq. oxygen 0—50356 Pb, liquid surface, LEED 0—55899 Pb, melting and freezing of single-cryst. surfaces, LEED 0—53418 Pb film, stress relief and hillock form. 0—58598 Pt-(1.3wt.%)Ba alloy, field-emission microscope obs. 0—47040 Re(0001) face, effect of O₂ adsorption 0—74928 Rh, clean, (111), LEED and Auger electron spectroscopy 0—65042 Ru, clean, (0001), LEED and Auger electron spectroscopy 0—65042 Se, melt-grown hexagonal single cryst., etch pit obs. 0—65125 Se coarseness determ. using photoelec. device 0—61621 Si-SiO₂ interface, LEED obs. 0—39929 Si, Au-coated (111) faces, vibrs. of atoms 0—71456 Si, cleaning and Au-stabilization, LEED obs. 0—55703 Si, contamination by C 0—47763 Si, strain generated patterns 0—65045 Si (111) epitaxial films on α—Al₂O₃, interface reactions 0—55726 β-SiC, epitaxial growth of layers 0—53433 SiC, surface cracks healing by oxidation 0—58937 β-SiC films, formed by chemical conversion 0—68754 SiO₂, polished fused, roughness effects on elasticity 0—63359 SiO₃, silica, Auger electron spectroscopy obs. 0—78368 Si(111) - Struct, by cleavage at room temp. 0—61632 Sn, liquid surface, LEED 0—55589 Sn, melting and freezing of single-cryst. surfaces, LEED 0—53418 Th on W(100), Auger emission spectra, LEED and work function meas. 0—55729 Ti-Mo wires, crystalline and polycrystalline, fractography, scanning electron microscopy 0—68494 0-55729

Ti-Mo wires, crystalline and polycrystalline, fractography, scanning electron microscopy 0-68494

UO₃, field-ion microscopy obs. 0-47041

V₂O₄, (010), LEED 0-55706

W-10 at.%)Re, streaking obs. in field-ion microscopy images 0-58562

W, faceting, electro- and thermal 0-65044

W, He ion bombard, field emission ion and electron microscopy 0-39930

W, treatment effects on work function 0-56410

W (100) surface, LEED study 0-74889

W roughness, effect on electrical contact resistance, meas. by graphite electrode 0-44039

W single cryst, morphology 0-78405

0-61635
ZnS single crystal, 1-dimensional disorder, striations, emission microscopy 0-53425
ZnS sublimated cryst., surface morphology 0-50353
Zr alloys, stress corrosion cracking, electron microscopy 0-55948 Surface tension see also Capillarity alveolar, contribution to respiration mechanics, mathematical model 0-76702 benzene, dependence on curvature, correlation between solubility of solute gas 0-71324 binary solns. Shereshefsky's eqn. appl., obs. 0-55601 binary solutions new critical solution temperature, and Eberhart model 0-64881 low capillary number withdrawal 0-71320 and cavitation erosion 0-51429 chloroform, dependence on curvature, correlation between solubility of solute gas 0-71324 solute gas 0–71324 contact angle, dynamic liq.-liq. flow rate effects, obs. 0–55599 contact angle, receding, hysteresis 0–58432 contact angle rel. to drop size 0–58434 Cs halide crysts. 0–78365 curvature depend. and free energy of droplet formation 0–39716 cyclohexane, dependence on curvature, correlation between solubility of solute gas 0–71324 double layers, interfacial instability due to elec. forces 0–74800 double layers, interfacial instability due to elec. forces 0–74801 elementary liquids, surface layer thickness by thermodynamic method 0–46889 fluid layers, convective instability protation effect buoyancy depend fluid layer, convective instability, rotation effect, buoyancy depend. 0-43221 fluid layer, convective instability, rotation effect, buoyancy depend. 0–43221 fluids containing solids and drops of another liq., effects on pipe flow and energy dissipation 0–39692 fluorocarbon solvents. FC-43 and FC-78 0–58464 fluoropolymers, London dispersion term 0–50211 fluoropolymers, polar attraction term 0–50216 floorel. to gravity waves 0–50188 ionic cryst., CsCl type 0–78365 ionized monolayers, surface pressure calcs. 0–74807 ionized monolayers, surface pressure calcs. 0–74808 laminar withdrawal with appreciable inertia forces 0–71321 in lattice models 0–76841 liquid layers disjoining press. between solids 0–74737 liquid metals, critical props. 0–58470 liquids, calculation from chemical structure 0–68087 Marangoni effect, study by steady dissolving drop method 0–71319 metal melts, binary and complex structure 0–46887 metal solid, effect of impurity forming fusible eutectic 0–71750 phenomena induced by surface tension review 0–39713 polatomic liquids, rel. to principle of corresponding states 0–468087 RMS displacements on liquids and solids 0–65027 radius depend, and free energy of droplet formation 0–39715 rel. to shallow three-dimensional flow, variability due to insoluble chemical contaminant 0–68061 silicone grease component spreading and condensing 0–74736 solids and liquis, Rayleigh's theory 0–53325 solicone grease component spreading and condensing 0-74736 solids and liqs, Rayleigh's theory 0-53325 solubility of solute gas, correlation with surface tension of solvent liquid 0-71324 0-71324
steel, liquid, interfacial tension reln. to composition of non-metallic inclusions and their separation 0-61480
near triple point, product with isothermal compressibility, fundamental length characteristic 0-71322
van Kampen model of van der Waals fluid in two-phase state 0-71207
water, dynamic, oscillating jet study of time dependence 0-78267
water on gold, meas. in ultrahigh vacuum by vapour phase transfer
0-78266 0-16200
Al₂O₃, alumina, molten 0-58472
Ar liquid surface layer thickness by thermodynamic method 0-46889
CO₂, from light scattering at gas/liquid interface near critical temp. 0-39757 0-39757
CaO-SiO₂ systems, molten, effects of alkali and alkaline-earth fluorides 0-5326
Ge-Sb melt, crystal growth, supercooling and additives 0-75006
³He-4He phase-separated mixture, interfacial tension 0-68168
⁴He, liq. 0-78321
⁴He liquid surface layer thickness by thermodynamic method 0-46889
Sn, 240 to 844°C 0-68086
Te-Se melts, rel. to miscibility and cpd. formation 0-50210 Surface tension measurement face tension measurement bubble growth experiment 0–58469 calculation, improved iteration method using significant structure theory of liquids 0–39756 capillary rise apparatus 0–68085 drop weight technique 0–71323 metals, liquid, at high temp, by sessile drop method, apparatus 0–64882 surface-active substances solns., automatic drop counting stalagmometer applic. 0–46890 in ultrahigh vacuum, vapour phase transfer technique 0–78266 Wilhelmy method, corrections 0–55600 Surface texture see Surface structure Surveys see Reviews Suspensions electrode 0-44039
W single cryst. morphology 0-78405
W tip, high resolution field electron microscope image 0-53424
W(112), Na-induced facetting 0-50359
W(112) with W₂C overlayer 0-43539
YFe garnet, morphology and surface features, rel. to growth 0-61696 bentonite, colloidal suspensions, struct. and elec. 0-71392

Surface structure continued

Zn electropolishing technique 0-72546

Zn-(0.4 wt.%)Al superplastic sheet, anisotropic effects 0-40315

ZnO, LEED 0—74878
ZnO, Substrate for epitaxial Au, effects of air and vacuum cleaved surfaces 0—43548
ZnS, striations, cathodluminescence, scanning electron microscopy 0—61635

see also Aerosols; Sedimentation; Sols air-spherical glass particle flow, effective drag coeffs, in shock tubes 0-58507 asymmetric particles, optical saturation, birefringence and electrical anisotropy 0-58504

ntalum continued interstitial ordering 0–47236 interstitial ordering 0–50577 level indicator for liq. He 0–66747 neutron-irrad, high temp., microstruct., thinning technique 0–75102 plasma anodisation, ionic current in oxide 0–72541 solid solution hardening by 0 and N 0–43806 sputtering, films onto Teflon discs, modification of d.c. sputtering diode geometry 0–76781 superconducting, for i.r. absorption, energy gap width and critical temperature 0–44130 superconductivity rel. to electron phonon interaction 0–43969 thermionic emission from pure and Cs covered faces 0–65868 wavelengths and transitions, table 0–46337 htalum compounds

Tantalum compounds
alloy, T-111, creep behaviour under continuously varying stresses influence 0-71700
tantalates, rutile struct, i.r. absorpt. spectra, vibr. freqs. 0-39393
Au-ZnS:NdF₃-Ta₂O₅-Ta composite films, pulse excited electroluminescence characteristics 0-44950

S 1430 SUBJECT INDEX Suspensions continued benzopurpurine, optical dispersion of elec. birefringence and dichroism $0\!-\!74811$ Brown particles, rigid, flow birefringence, rot. scatt. coeffs. determ. 0-43479 0 - 434./9
Brownian particles in liquid, Mossbauer effect 0 - 74797
carbon black, HAF, depolarization of scatt. light 0 - 50275
colloidal particles, electrical conductivity 0 - 46962
dilute, of rigid and of deformable substructure particles, mechanical behaviour theory 0 - 55398
electrophoretic development of electrostatic charge patterns 0 - 54952 electrophoretic development of electrostatic charge patterns 0–54952 fibre, and polymer drag reducing solns., shear thinning treatment 0–50269 flocculated, apparatus for obs. of filtration rates 0–74816 flow formation in Couette motion 0–39840 flow in channel, turbulence 0–39843 flow in channel, turbulence 0–39843 force-free particles in Newtonian fluid, stress effects 0–50266 glass particles in air, drag coefficients of flow in shock tubes 0–58505 heat transfer to gas-solid suspension flow 0–46960 helical filaments, small angle X-ray scatt. 0–68157 Kerr const. of rigid conducting dipolar macromols. 0–78276 liquid drops, axially distrib., in liq., flow in cylindrical tube 0–50176 MHD channel flow 0–71119 montmorillonite particles, Na/Ca ion saturated, electrophoretic mobility 0–74806 non-colliding, poly-dispersed, Euler approximation 0–55636 0—74806
non-colliding, poly-dispersed, Euler approximation 0—55636
nonaqueous, stability, C in heptane obs. 0—74803
nonwetted solid particles in ligs., tensile strength theory 0—39689
paramagnetic colloids, e.s.r. hyperine structure 0—53381
particle size distrib., applic. of electro-opt. effects 0—39845
particulate systems, optically active, differential scatter of left and right circularly polarized light 0—55635
photosedimentometer, centrifugal disc type, line start method stability 0—39846 photosedimentometer, centrifugal disc type, line start method stability 0-39844 Poiseuille flow, migration of neutrally buoyant particle 0-39852 sand-compressed air mixtures, dense phase horizontal flow 0-74793 separation of solid phase-liquid, by radial particle migration in plug flow 0-46959 0 46959 solid pnase-liquid, by radial particle migration in plug flow of 46959 solid-gas, high speed flow in pipe influence of particle size distribution of 64965 solid-gas mixtures, dense phase horizontal flow 0–74793 sound absorption, theory 0–64973 sopherical particles in non-Newtonian pseudo-plastic liquids, rheological props. 0–48788 steric stabilization and Hofmeister series 0–74802 thixotropy, model 0–71391 transport of solids, book 0–55435 vibration meter, magnetic correction 0–54536 viscous fluid with solid particle suspension, slow motion of sphere 0–53378 Al₂O₃ cloud of small spherical micronsized particles. 0-33.78
Al₂O₃ cloud of small spherical micronsized particles, absorption and scattering of thermal radiation 0-58503
Cu particles, low-temp. thermal cond. 0-64972
Fe₃O₄, colloidal, transverse magneto-optic effect 0-64970
SiO₂ H₂O concentrated, rheological study, electrophoretic mobility 0-68160 V₂O₅, optical dispersion of elec. birefringence and dichroism 0-74811 Suzuki atmospheres see Crystal imperfections/dislocations Switching time, ferroelectric see Ferroelectric materials; Ferroelectric phe-Switching time, ferromagnetic see Ferromagnetism; Magnetic properties of substances/ferromagnetic Symbols see Nomenclature and symbols Synchrocyclotrons see Particle accelerators/cyclotrons Synchrotron radiation in cosmic radiations origin hypothesis 0-79715 emission from hot electron plasma, plasma effects 0-50053. Frascati electron synchrotron, spectral distrib. in 80-1200 Å range 0-77262 0-77262
gyro-synchrotron emission in mag. dipole field appl. to solar microwave impulsive bursts 0-45433
high energy electrons traversing dilute gases 0 42468 neutrino, application to neutron stars 0-79663 neutrino, application to white dwarfs 0-79662 from plasmas, magnetoactive, emissivity functions, rel. to coeffs. of dispersion equation 0-61287 pulsar, Crab, optical and X-ray synchrotron radiation calc. 0-54412 relativistic motion with radiation damping 0-52241 theory, reabsorption, developments in, review 0-70195

Synchrotrons see Particle accelerators/synchrotrons

Sylicht-Chalmers reactions. Szilard-Chalmers reactions see Radiochemistry Tables, mathematical No entrie Tables, physical see Collections of physical data
Tachometers see Angular velocity measurement Tandel see Dielectric devices Tantalum addition to ZrC graphite alloys, effect on microstructure 0–53517
adsorption of Zr 0–43574
T-111 alloy, biaxial creep strength 0–53591
atom. L emission spectrum, existence of weak lines 0 70774
band struct, and Fermi surface 0–44000
capacitor failure modes and analysis 0–47858
cathode, Penning pumps, stability to Ar and other rare gases, experimental study 0 51865

gamma ray scatt., incoherent, by K-shell electrons 0-58120 impurity, in zone refined Nb, redistribution 0-47139

study 0 51865
electron energy loss spectra obs. and correl, with theory 0 50918
Fermi surface topology 0-43999
film, Hall voltage, pulse current method 0-44070
film, sputtered, cryst. phases, temp. depend., superconductivity 0-4708
film, sputtered, phase comp. and conductivity 0-78384
film, sputtered in 0₃, orientation effects in resistivity 0-75569
film deposition by d.c. bias sputtering 0 74918
film prepared by low pressure triode sputtering, stress analysis 0-50674
Frenkel pair defect annealing conc. depend. in electron irrad. crystals 0-47235

Tantalum continued

Au-ZnS:NdF₃-Ta₂O₃-Ta composite films, pulse excited electroluminescence characteristics 0–44950
LaB₆-Ta alloy, elec. resistance, thermo-e.m.f. and Hall effect 0–50970
LaB₆-Ta alloy, elec. resistance, temp. depend. 0–50971
Mo-Ta alloy, elec. resistance, temp. depend. 0–50971
Mo-Ta alloy, effect of Mo and W, phase equilibrium investigation 0–50821
Nb-Ta alloy, thermo-electric properties 0–51136
Nb-Ta alloys, sp. ht. and supercond. 0–78905
Pb(Nb_{1-x}Ta₂S₃, supercond. transition temps., comp. and thermal history depend., rel. to sp. ht. meas. 0–78901
Pd-Ta alloys, Hall effect and susceptibility temp. depend. 0–75898
Ta-Al system, struct. 0–78502
Ta-Al system, struct. 0–78502
Ta D solid solution, decomposition and precipitation, 225K, neutron diffr. 0–50830
Ta-H system, equilibrium diagram and electronic structure, from sp.ht. and mag. susceptibility meas. 0–47492
Ta-Mo-C alloy, effect of Re and Al, phase equilibrium investigation 0–50822
Ta-Mo, b.c.c. alloy, short range order, X-ray diffr. 0–40101
Ta-Nb-C alloy, effect of Re and Al, phase equilibrium investigation 0–50822
Ta-Mo, b.c.c. alloy, short range order, X-ray diffr. 0–40101
Ta-Nb-C alloy, effect of Re and Al, phase equilibrium investigation 0–50822
Ta-O solid solns., e.m.f. meas. 0–75315
Ta-Ta,0-electrolyte system, study of rectification 0–79006
Ta-V system, supercond. 0–75627
Ta alloy, formability, tensile strength, oxidation resist., comp. depend. 0–40457
TaC, shock compressibility 0–75248 Ta alloy, formability, tensile strength, oxidation resist., comp. depend. 0-40457
TaC, emissivity and elec. conductivity, 1200-3750K 0-71880
TaC, single crystal, slip, microhardness and mech. behaviour 0-47308
TaC, single crystal growth, by hollow cathode d.c. plasma discharge float zoning 0-50473
TaCG, single crystal growth, by hollow cathode d.c. plasma discharge float zoning 0-50473
TaCG, evaporation, vacuum characteristics, from open surface 0-71418
TaCG, evaporation, vacuum characteristics, from open surface 0-78754
TaCG, polymorphs, growth, unit cells and space groups 0-65080
TaCG, crystal structure 0-40100
TaCGG, crystal struct Targets see Nuclear bombardment targets Teaching
by, for mechanics and physics 0-41926
alloys, phase diagrams and microstructures, introduction for students 0-56022
0-66764 by, for mechanics and physics 0—41926 alloys, phase diagrams and microstructures, introduction for students 0—56022 analogue computer, for demonstration of equations of motion 0—66764 anechoic rooms for teaching purposes, design 0—57408 applied physics to technologist 0—63300 astronomy, and career development of astronomers in USA 0—54324 astronomy, planetarium programs in USA 0—54527 astronomy, rel. to manpower needs 0—544323 astronomy, the American Astronomical Society 0—54322 astronomy ocurse for non-science majors 0—54526 astronomy in Harvard project physics 0—54319 astronomy in Hermathy and secondary schools, role of astronomers 0—56889 atomic energy levels, isoelectronic sequence of Li, student exercise in calc. 0—49759 CAI in physics 0—72865 chemistry, entropy temperature diagrams appl. 0—69761 computer assisted exercise, PVT behaviour of real gas 0—46805 computers in physics instruction 0—41921 conference. Singapore Nat. Acad. Sci. Congress, (1968) 0—48664 conference, growth points of physics, Florence (1969) 0—45504 Doppler shift expt., X-band and frequency doubling 0—60101 educational technology applic, to physics education 0—38123 electrical properties of substances, fundamental aspects, lectures 0—71894 cosmic electrodynamics, text book 0—76954 electromagnetism, university level textbook 0—76954 electromagnetism, university level textbook 0—76954 electronics course for physics students 0—66762 energy conversion of various types described, elementary article energy stored in a capacitor derived without calculus 0—42139 exections, introductory survey 0—41925 feedback classroom, concept and uses 0—66761 Fermi-Dirac statistics, elementary explanation 0—76846 finite element method described 0—52014 Fresnel's integrals in dynamics 0—72990

Teaching continued

aching continued

Fresnel diffraction experiment using He-Ne laser 0-63681 harmonic oscillator with sliding friction, motion 0-72988 intermolecular forces, origin 0-74439 introductory physics, use of games 0-41923 Josephson tunnelling, lectures 0-45507 junior college attempting to explain concepts of physics 0-54530 Kepler ellipses starting from a point in space 0-48774 Kepler motion, simplified treatment 0-42021 Legendre's eqns. for undergrad. 0-41938 lens, ideal, depth of field props. 0-73281 magnetic field generation and use in physics research, review 0-38125 mathematical methods in physics, book 0-57302 mathematical mysics textbook mainly on vectors, matrices and Hilbert spaces 0-54542 mathematical physics textbook treating analytical functions, Greens functions, integral eqns. and group theory 0-54543 mathematical statistics, textbook 0-5201 microwave spectroscopy, in undergraduate labs. 0-66984 modern physics, text book 0-54531 modern physics oriented to specific educational needs of Colombian students 0-48666 molecules, an undergraduate textbook 0-60890 Newton's third law 0-42017 nuclear spherical model, harmonic vibration, review 0-67361 nuclei mass formula, semiempirical, symmetry energy term 0-42715 optical technology, course at Monroe Community, College, New York 0-38124 peturbation theory through spin systems 0-41979

0–38124
physics, college introduction book for non-science major 0–45508
physics, college introduction book for non-science major 0–45508
physics, introductory approach based on the conservation laws 0–54525
physics, introductory college textbook for non-science major 0–57230
physics and the use of computers 0–54528
physics course, computer-assisted 0–72865
physics course on urban and environmental problems for social scientists 0–66763

O-66763
physics in secondary school and univ., review 0-45506
plasma physics, university textbook 0-55453
Poisson distrib., rel. between average and most probable value 0-41982
Poisson integrals, error in Morse and Feshbach textbook 0-38130
polymers, introducing book for 6th formers 0-46618
programmed, review 0-59854
quantum chemistry, university second or third year book based on author's lecture notes 0-48175
quantum mechanical foundations, text-book 0-54570
quantum mechanics, textbook for undergraduates 0-57267
quantum theory, advanced graduate-level textbook 0-54571
quantum theory, hydrogen wave functions, computer- animated film 0-54573
RMKS units, discussion and relation to teaching for electrical and magnetic

duantim theory, hydrogen wave functions, computer-animated imm 0-54573

RMKS units, discussion and relation to teaching for electrical and magnetic systems 0-60145

radiation physics, elementary text-book 0-57161

Rochelle Salt crystal growth, undergraduate project 0-76789
rocket, motion analysis 0-41558
scattering expt. classical, computer simulation 0-59856
science and society, topics for liberal studies 0-41922
seminar/autolecture, an open-ended learning system 0-38122
statistical mechanics, elementary, university level book 0-54609
tensile testing machine for school use 0-69572
undergraduate physics course, use of computer 0-76787
vertical jump, height, physical principles 0-48779
work function and */m determination, simple experiment using Tungsten 0-56412

demonstrations

birefringence in liquid crystals illustrated with 4-4'-dihexoxyazoxybenzene 0-39793

Brillouin scattering in toluene 0–44873
Brownian motion, Monte Carlo simulation in freshman laboratory 0–41988

Brownian motion study using light scattering 0-43480 Coulomb's law balance for physics majors and nonscience students 0-73125

O-73125
Coumomb's law rel. to Ohms law 0-42140
counting statistics, student experiment 0-66859
crystal structure temp. effects, dynamic model 0-41927
double pendulum art machine 0-59853
e.m. energy converter 0-76788
electrical measurements course, nurturing creativity 0-63303
electron binding energies in K, L shells, experimental determ. for teaching laboratory 0-67600
electronic signal filtering, optical analogue expt. 0-67169
film on reciprocal lattice in X-ray photographs 0-59857
Fresnel diffraction, display on oscilloscope 0-54914
Fresnel-Arago law, intensity distribution in interference pattern from double slit expt. 0-49110
gas flow heating thermometer-on-car test experiment 0-68003
interference in 3 cm band 0-73092
interferometry, multiple beam, review of simple techniques and applications 0-45824
introductory physics laboratory, its rationale 0-63044

introductory physics laboratory, its rationale 0-63304 laser diffraction expts. using large objects, for undergraduates 0-42356 lifetime meas. of cosmic-ray μ experiment for instructional laboratory 0-67233

0-67233 light velocity meas using time-to- amplitude convertor 0-60317 m.h.d., student experiments 0-46676 models, miniature, molecular and crystal structure 0-59858 molecular interactions on air table, apparatus 0-77980 Mossbauer effect apparatus, modified 0-66007 musical tones, undergraduate expt. on analysis and synthesis 0-66908 nonlinear effect demonstration using lumped parameter network 0-42070 oscillators, using ring magnets 0-66765 photoelectric effect apparatus 0-45739 polarized laser light beam interference experiment 0-67139 porous plug expt. 0-42095 projectile, components of motion 0-59949 radioactivity expts. for schools 0-38953 relativity and quantum physics, use of computer graphics laboratory 0-48667

Teaching continued

demonstrations continued

sound velocity in metal rods, experiment for undergraduate laboratory

0-02189 sound velocity meas, in rods 0-62188 stars, artificial, for use in teaching laboratory 0-69509 suspension of conducting disc in alternating magnetic field 0-69844 televised physics for engineering students 0-41924 wind tunnel suitable for schools described 0-78197 X-ray photography of rotating cryst, using cm. e.m. waves 0-75042

Technetium

hyperfine fields in Fe 0-44735 hyperfine fields in Fe 0-44735 hyperfine fields in Fe 0-44735 current, clinical applications 0-41882

Technetium compounds

Cs₂[TcF₈] force consts. on basis of D_{4h} symm. 0–39402 K_3 [TcF₈] force consts. on basis of D_{4h} symm. 0–39402 TcF₆, Raman spectrum in vapour state 0–58183 Tc₂O₇, cryst. struct. and bonds 0–61886

Tektites see Meteorites

Telescopes

escopes gratings high precision with laser light and photoresist layers 0-42366 interferometric quality control for manufacture, gas laser applic. 0-57580 objectives, power 0-67166 refractive, simple lens systems, mathematics in design, magnification factors 0-76684 for space applications, design 0-70054 tilted component, third-order aberration theory 0-69997 wide-field unit-magnification, for visual use 0-70055

astronomical

setronomical
see also Radioastronomy
21 cm, construction 0—48463
2m Universal Reflecting Telescope, spectrograph in Cassegrain focus, plane grating, desing and operation 0—51816
adjustment, use of Hartmann diaphragm 0—76683
Cassegrain, with an all-reflecting spectrograph, limiting magnitude for obs. made in space 0—48621
drives, simplification by backlash-free mechanisms 0—69511
glancing incidence extreme u.v. telescopes primarily for solar physics, design 0—51818
guidance control, transistor inverter circuits 0—66676
i.r. aluminium-mirror photometric telescope, optimum size with respect to cost 0—51817
Moon surface composition obs., mid-i.r. region 0—59755
orbiting, research possibilities 0—66674
performance, optical, evaluation with wave front shearing and Kosters interferometers 0—41878
primary mirror problems, development, shape distortion 0—79776
radio, amateur, design and construction performance requirements adio, amateur, design and construction performance requirements 0-69510

0-69510
radio, synthetic-aperture 0-76680
radiotelescopes, fundamentals and design, book 0-45442
Soviet 236 inch reflector, development 0-63192
three mirror 0-76685
University of Western Ontario 123 cm reflector 0-76685
x-ray, design and analysis of imaging characteristics 0-54484
X-ray, image formation, surface configuration requirements 0-59850

Ilbrium
in Alnico alloys, Ti containing, effect on crystal growth 0–71761
absorption spectra, 18-460 cm⁻¹, 300, 77 and 4 K 0–79320
acoustoelectric domain movement, 77-250K 0–78771
amorphous semiconductor, optical and elec. props. 0–47721
atom, K-fluoresc. yield from ¹²⁸I source 0–38980
atomic motions in cryst. and liq. 0–75380
atoms, reaction with active nitrogen, spectroscopic observation 0–46634
band structure, interband transition of holes 0–66056
band structure from magnetoabsorption 0–65686
conference, Montreal, Canada, Oct. 1967 0–65652
crystal growth, unseeded, from melt 0–65166
crystal nucleation in supercooled melt, high static pressure effects 0–58641
crystal structure, coordination and thermal motion 0–65278

crystal nucleation in supercooled melt, high static pressure effects 0–58641 crystal structure, coordination and thermal motion 0–65278 cyclotron reson. and impurity transitions in valence band 0–56274 donors in GaP spectroscopic study, rel. to effective mass calcs. 0–44810 elastic constants, temp, depend. 0–68400 electrodeposited layers from acid medium, prep. and texture 0–59503 electron microscopy, sample prep. method 0–65287 energy surfaces trigonal warping 0–78842 epitaxy on NaCl. KCl and KBr 0–43553 Hall effect, magnetoresistance, 150-350K 0–78957 i.r.absorption spectra rel. to valence band structure 0–41225 impurity and cyclotron reson. transitions in valence band 0–56274 isoelectronic sequence, oscillator strengths of resonance lines 0–49789 Landau levels in valence band of p-type 0–56273 lattice vibrational modes from inelastic neutron scatt. 0–65527 liquid, atomic motions 0–75380 magnetoabsorption effects for allowed interband transition 0–76029 magnetoabsorption obs., band structure 0–65686 magnetophonon resonances 0–68829 microwave emission from p-type at 77K 0–72033 nonlinear optical coeffs. determ.rel. to Ag,5bS, 0–65975 optical constants, lattice vibration contrib. 0–66057 phonon spectra calcs. using force constant model 0–65522 second harmonic generation for CO₂ laser, efficiency 0–77104 Shubnikov-de Haas effect, Fermi surface parameter determ. 0–65602 sound attenuation, 60-600MHz, 77-300K, free carrier interaction 0–68610 trap in group II-VI alloys, photoluminescence 0–72431 CdS:Te electroluminescent crystal, patent 0–41296

O-8610

trap in group II-VI alloys, photoluminescence 0-72431

CdS:Te electroluminescent crystal, patent 0-41296

Fe-Ni-Al-Co-Ti in alloys, effect on liquidus-solidus gaps 0-71775

GaP:Te, photoioniz, energy, absorpt, spectrum obs. 0-76101

GaP:Te liq, phase epitaxial layers, impurity gradients 0-62364

GaSb:Te donor level 0-51049

GGTa irong by alectrops, photons, and neutrons, effect on carrier

n-Ge:Te, irrad. by electrons, photons, and neutrons, effect on carrier conc. 0-44249

Ni-Co-Te system at 500°C, stability domain of hexagonal phase 0-65506 Tm I, level crossing and optical double reson. obs. 0-52916

Tellurium compounds

hurium compounds oxides, gaseous, thermodynamic props. 0–41418 [Te,⁶⁺][A₃][B₃]O₁₂ garnets, where A and B are mono- or trivalent metal ions, synthesis 0–71503 A_{1/B}B_{1/T}E₉O₈ (A=Sc, Cr, Fe, Ga, Rh, In, Bi and B=Nb, Ta), of TiTe₃O₈ type, cryst. struct. and prep. 0–65277 As-S-Te system semiconductors, vitreous, bond-structural approach to election. 0–75676

cond. 0-75676

As-Te-Ge-Si, amorphous film, non-ohmic props., 77-350K

O-56242

As-Te-Ge glass, filament formation, electron probe analysis, radiometric microscopy

0-56285

Cu-Se-Te, Cu₃SeTe phase, investigation by X-ray diffraction and differential thermal analysis

0-71773

Ge-As-Te system glasses, elec. cond. and switching diode applic.

0-78938

Ge-Si-As-Te, amorphous alloy film, photoconductivity

0-56391

Ge-Te, amorphous alloy, radial distrib, X-ray diffr.

0-55679

PbTI alloys, sp. ht., rigid-band behaviour, electron-phonon enhancement effects

Se-Te alloys, liq., thermal cond.

0-58482

Te-As-Ge-Si, glass film, switching characts.

0-56266

Te-As-Si-Ge film, prep. by explosion method, negative resistance curves

0-51025

Te-As-Si-Ge film, prep. by explosion method, negative resistance curves 0-51025
Te-Cu-Au amorphous alloy, semiconducting phase 0-47727
Te-Ge alloys, amorphous, valence electron config. of Te 0-75710
Te-S alloy, liquid, conductivity switching phenomena in elec. field obs. 0-78300
Te-Se alloy, liquid, conductivity switching phenomena in elec. field obs. 0-78300
Te-Se melts, surface tension and density rel. to miscibility and cpd. formation 0-50210
Te-Se melts, surface tension and density rel. to miscibility and cpd. formation 0-50210

tion 0-50210
Te-Se molten alloy, mutual diffusion, 500°C, comp. depend. 0-39765
Te-Sn-Sb system, phase equilibria 0-50306
Te hexahalide ions, mol. force fields 0-43136
TeFe, cryst, struct, and mol. motion, mp. to -160°C 0-50546
TeFe, negative ion formation 0-64763
TeFe, Raman spectrum in vapour state 0-58183
Te(Ge,As) based amorphous semiconductor, reflectivity 0-56490
TeOsi, Geosi, Asosot, memory-type chalcogenide, superconducting transition obs. 0-75628
Tesi, Gessas, de. resistivity, 4-300K, a.c. cond., 300K, Hall effect, magnetoresistance 0-47726
Te(IV) isoelectronic complexes, Mossbauer effect, 125Te, isomeric shifts 0-44798
TeO; V,O;-CdO, phase diagram for glass formation, properties 0-68201

0 -44798
TeO₂-V₂O₅-CdO, phase diagram for glass formation, properties 0-68201
TeO₅, elastic, dielec. and piezoelec. consts. temp. depend. 0-47317
TeO₅, paratellurite, cryst. growth rel. to macroscopic defects 0-65136
TeO₅ absorption spectra, 5000-2000 Å, vibrational analysis 0-64456
TeO₂ elastic props. of single crystals 0-78593
TeO₅ piezoelectric props. of single crystals 0-78593
TeO₅ solution, electrolysis on Ag cathode, rel. to Ag_xTe_y formation 0-72548

0-72548
TI-Bi, phase diag, and thermodynamic eqns, of state 0-74838
TI-Te-Ge semiconductor glass, comp. for bistable system with elec. switching, patent 0-44336
TI-Te, molten alloy, resistivity and Seebeck coeff., comp. depend. 0-43474
TI-Te, molten alloy, thermoelectricity, elec. cond., comp. depend., semiconductor-metal transition 0-46948

Temperature

see also High-temperature phenomena and effects; Low-temperature pro-

duction
changes at finite deformations, calc. 0—59973
control device for i.r. spectroscopy 0—60094
cycles in brain tissues, role of u.s. focal lesion production, calc. method 0—57163

cycles in brain tissues, role of u.s. focal lesion production, calc. method 0–57163
diffusion and fluctuation in turbulent shear pipe flow 0–43223
entropy diagrams application in chemistry teaching 0–69761
fluids, spectral meas. of fluctuations in fully developed pipe flow 0–71083
heat transfer in skin of hypersonic vehicle 0–38411
instability of permanent magnets 0–45758
multilayer diaphragm at harmonic heat flow, calc. method 0–45690
noise, fluorescent lamps, influence of cataphoresis 0–45738
random fields, viscoelastic materials behaviour 0–59995
rapidly changing meas. by thermocouples 0–54785
rise due to electron irradiation 0–75401
semiconductor detectors, effects on behaviour 0–60673
spacecraft control coatings, colour centre formation in white powder oxides 0–47267
steady, with discontinuous radiation 0–66953
transients, rel. to refractometer instabilities 0–42283
Venus, interpretation of radio astronomical obs. 0–63129
wall, rel. to gas flow, subsonic, over flat plate, effect on turbulent boundary layer thicknesses and shape factors 0–46785
Cd crystals, effects on vapour growth 0–55783
Si photocells, stabilization by optical films 0–44409
Temperature control see Cryostats; Thermostats
Temperature distribution

Temperature distribution
absorbing cylindrical layer, temp. fields and heat fluxes 0-54781
aerodynamic heating of spherical segments 0-78208
air-sea interface, vertical temp. profile 2 m above and below, determ.
0-48223

arc, low-current, N₂, radial meas. 0-55530 crystal, thin film, growth from melt 0-65373 crystal growth from liquid, cylindrical vessel, hydro- and thermomechanical conditions 0-74980

conditions 0–74980 cylinders, solid and hollow, due to moving ring heat source 0–45703 differential 2nd order eqn. numerical soln. procedure appl. 0–69584 electric arcs, crossflow, effects of velocity and current 0–64796 electrical cables, insulated, with variable thermal conductivities, steady state temp. profiles 0–71852 electrode temperature in region of spot, radial distrib. 0–43312 electron, in Ar-K plasma streaming through channel with segmented electrode array 0–39567 electron, in thermally perturbed plasma components, cold probe determ. 0–71170

0-/11/0 electron, in thermionic convertor of plane geometry 0-42159 rel. to fast reactor, fuel element temperature field obs., energy flow variable w.r.t. core height 0-67570 films, viscous, high Prandtl numbers 0-76943 in finite bodies, theory 0-54783

Temperature distribution continued

nperature distribution continued flow, time dependent, meas. by bead thermistor, use of high speed digital system 0–48893 in fluid, second-order, steady field expression 0–39503 fluid between two rotating porous cylinders 0–77999 fluid flowing in pipe, effect of temp. depend. viscosity 0–48725 fluid heating in porous shells, temp. fields 0–54780 glass, meas. in tank furnaces 0–65016

glass, meas. in tank furnaces 0–65016 graphite matrix hollow fuel compacts, temperature distribution 0–60863 in hollow cylinder with nonsteady boundary conditions, recursive method for transient distribs. 0–52166 in laser spark plasma, holographic obs. 0–63612 MHD generator Faraday-type, gas non-uniformity effects, effects on elect. parameters 0–42158 Mossbauer eff. for thermal field meas. in solids 0–79255 for natural convection in horizontal cylinder, profiles for arbitrary heating angle 0–46644 nuclear reactor pressure vessel, thermal and pressure stresses, analytical determination 0–49699 particle accelerator chamber walls with conducting coatings. 0–63935

determination 0–49699
particle accelerator chamber walls with conducting coatings 0–63935
polymer filament, profile on solidification, numerical evaluation 0–50311
secondary flow effect on temp, field and primary flow in a heated horizontal
tube 0–46653
in shock waves, plane 0–53270
in solids, non-linear eigenvalue problem 0–48725
in spacecraft, perturbation theory application 0–66351
spacecraft, spinning, spherical, thermal design, nonlinear three-nodes analysis, numerical solution 0–45202
specific heat determination liquid loose or plastic media, dynamic method 0–39774
surface of cylinder transmitting u.s. wave 0–40559

surface of cylinder transmitting u.s. wave 0–40559 temporal and local in materials, electron beams focused irradiation, calc. 0–43935

turbine blading thermal field meas, using Mossbauer eff. 0-79255 turbulent boundary layer of natural convection along plane vertical plate 0 - 76941

0-10941 turbulent inhomogeneities in sea, results 0-51501 ultrasonic sensors for profile meas. 0-69762 Venus surface, determ. from microwave brightness obs. at 11 cm 0-51772

0-31/12
Ge thin film, temp. distrib. during growth from melt 0-65152
Si single cryst. growth from melt, calc. of thermal field 0-65158

Temperature measurement

Si single cryst. growth from melt, calc. of thermal field 0–65158

mperature measurement
see also Pyrometers; Thermocouples; Thermometers
acoustic thermometry, systematic errors 0–38378
alloys, concentrated, solid-liquid interfaces 0–50776
are electrode, use of photoelectric pyrometer 0–55531
are electrode, using photoelectric pyrometer 0–53231
colour, correlated, computation in FORTRAN II 0–57442
contacting and noncontacting electrical sensors, construction and performances, accuracy and stability 0–60092
continuous, of earth, probe response 0–76305
cryogenic techniques and instruments 0–79811
D.F. reactor, monitors 0–60888
by diamond indicator, operating principles 0–76944
droplets of electrode metal during welding conditions, thermocouple applic. 0–46898
of earth's mantle, presence of molten zone 0–76331
earth's mantle, presence of molten zone 0–76331
earth's mantle, presence of molten zone 0–76331
flames, gas and condensed phase, spectral comparison method 0–51421
flames, photoelectric i.r. pyrometer 0–52163
fluctuations, of surface during steady state boiling from a tube for very short periods 0–68189
of fluid, time dependent flow, bead thermistor with high speed digital data system technique 0–48893
furnace calibration using X- or gamma-radiation 0–48891
glass, vertical distrib. 0–65016
heat sink on a convectively cooled surface, thermal processes 0–48875
high-temp., use of thermocouple based on graphite electrode 0–45705
interface of bodies sliding in vacuum, e.m. suspension system, design 0–48892
of ions in rarefied, multicomponent plasma by long ion tube 0–50020
magnetic, a.c. mutual inductance bridge, highly stable, application at low

of ions in rarefied, multicomponent plasma by long ion tube 0-50020 magnetic, a.c. mutual inductance bridge, highly stable, application at low temperatures 0-45704

magnetic temp. calibration of ferric ammonium sulphate against cerium magnesium nitrate below 0.1 K 0-48652 Mars, Mariner (1971), ir. radiometry expt. 0-54308 metal, f.c.c., internal standards in X-ray diffraction, systematic error

0-43918

ocean surface, using microwave radiometric remote sensing techniques 0-62894

oceanographic, autoprobe, free-floating observation platform 0-69273 of particulate surfaces, T<300°C by device consisting of InSb cell 0-38421

of particulate surfaces, T<300°C by device consisting of InSb cell 0-38421
photothermometer, response to thermal shock 0-48890
plasma, by i.r. laser beam absorption 0-64717
plasma, electron temp. by He lie ratio 0-74558
of plasma, xenon dense, by two different methods 0-71176
plasma spectral line scanning 0-67944
radiometric, true and apparent, of graybodies in atmosphere, nomogram relation 0-48872
resistance thermometry using potentiometer 0-73076
rock's borehole, contemporary method, theory 0-59525
scale derivation, absolute method, Planck's equation application, gold melting point determination 0-38419
Schlieren method, peripheral zone of d.c. arc 0-61416
sensors, comparison for Apollo experiment instrumentation 0-66954
shock tube, surface temp. fluxmeter design 0-38397
in solar furnace, nontransparent refractories 0-66745
superconducting film applic. 0-71990
superposition principle, liquid-metal cooled nuclear reactor 0-70734
surface, steady state errors, methods of prediction 0-60090
surface temperature, transducers, calibration methods 0-42104
thermocouple, aqueous solutions in i.r., spectroscopy 0-63482
by thermocouples, of rapidly changing temp. 0-54785
thermometer, platinum resistance, accuracy ±0.19C, range +37°C-2-00°C use in cryobiology 0-60091
time lag of thermometer, effect of humidity and press. 0-41489

Temperature measurement continued

troposphere, temperature structure, microwave observations, nonlinear inversion techniques 0-51543

ultrasonic sensors for profile meas. 0-69762

water, nucleate boiling, surface temp. meas. with Pt films on Pyrex glass 0-48894

He liq. vapour pressure scale T_{58} , deviation from thermodynamic temps. 0-63483

 N_2 cascade arc, spectroscopic meas. of temp. distribs., 26000°K max. 0-39637

U-II plasma using Boltzmann plot tech, and relative intensity method 0-50023

spectral methods

arc, disc stabilized, in multi-component plasma, 3000-170000K 0-58309 atmospheric temperature structure, horizon radiance profiles technique 0-48268

Doppler broadening type, for ion temp. in Tokamak-3 device 0-46728 Dragon reactor, primary heat exchangers, secondary water flow and tube wall 0-42901

wall 0-42901
gas using forbidden rotational structure of the electronic and vibrational bands of a diatomic molecule 0-60089
metals, use of polarized radiation flux from polished surface, in the visible region 0-52164
optical density flame pyrometry, high temp. 0-38422
plasma, using excitation temp, functions of Kr spectral lines 0-46368
plasma breakdown in air, laser induced, X-ray emission 0-43308
plasma jet, streaming analysis by evaluation of spectral lines of atoms and molecules 0-6952
rotational temp meas dvaluchangel spectrometer. 0-60093

molecules 0-66952 rotational temp. meas., dual-channel spectrometer 0-60093 solar temp. brightness in prominent CO band heads and in Al 1937Å 0-54458 MgO, flame particles, colour and luminance temp. 0-52165 Ne discharge, 1-100 torr, gas temp. 0-50121

Tensile strength see Mechanical strength/tensile

sors rel. to acoustic ray tracing 0–52084 antisymmetric, to irreducible representation of Lorentz group book, university level, on vector and tensor analysis 0–76798 Bopp's energy pulse tensor in e.m. field 0–69765 Cartesian irreducible, Clebsch-Gordan reduction 0–51908

continuous product states which are translation invariant but not quasi-free 0-51907

crystallography, dimensions of tensor spaces 0-65185 e.m. energy momentum tensor within material media 0-69848

e.m. energy momentum tensor within material media 0–69848 energy-momentum, equal-time commutation relation, without restriction on the external gravitational field 0–67196 energy-momentum tensor construction to include property of scale invariance 0–72901 harmonics in canonical form for gravitational radiation and other applications 0–51926 Hilbert spaces, continuous product, translated representations 0–69585 Maxwell dyadic, general expansion of determinant 0–73088 metric, discontinuity of first derivatives, Mach's principle 0–69605 Minkowski's, energy-momentum tensor within material media 0–48907 operators, construction in group theory and group-projection operators 0–63319 optimal distribution of resistivity of working material in magnetohydrody-

0-63319
optimal distribution of resistivity of working material in magnetohydrodynamic channel 0-55443
partial-tensor-product representations of the canonical commution relations, classification 0-48678
polynomial conformal, in Riemannian space 0-72890
Racah, generalized, and the structure of mixed configurations 0-66780
Riemann, symbolic computation, compact method 0-38165
Riemann tensor with functionally constant invariants 0-66815
second, quantized, spherical, by computerized Racah algebra 0-51909
stress, covariant, for free massless field theory 0-57654
stress, symmetry, in bodies with no local struct. 0-59955
trace-free, totally symmetric and the definition of multipole moments for static, asymptotically flat, source-free solutions of Einstein's equations
0-66805

ferromagnetic reson., microwave absorpt., magnetoelastic effects 0-72471

ferromagnetic resonance, far i.r., surface impedance meas. technique 0-44965

0-44905
film, abnormal absorpt, phenomena 0-41224
Hall effect in single crystal, 4.2-350 K 0-62489
Hall resistivity, mag. anisotropy effects 0-44071
hexagonal crystals, magnetic domain structure, obs. by Bitter technique
0-51180

0-51180
lattice dynamics, neutron inelastic scatt. 0-56090
lattice dynamics 0-65523
Magnetoelastic effects, microwave absorpt, obs. 0-72471
magnetomechanical damping 0-40279
magnon energy and lifetime in single crystal, neutron diffr. 0-44542
thermal conductivity and Lorenz function 0-43929
Ho, paramagnetic and ferromag, phase, effects, and elastic effects
0-68591

0–68591
Tb (A=159), hyperfine struct. by mag.-reson. technique, nuclear elec.-quadrupole moment 0–64206
Tb²⁺; energy transfer from Ce³⁺ in ScBO₃ 0–72436
Tb²⁺; quenching of emission by Tb-V interaction in YPO₄-YVO₄ 0–62727
Tb³⁺; relaxation between excited levels, resonance transfer in glassy matrix 0–51358
Tb³⁺ fluoresc. in POCl₃-SnCl₄ liq. 0–64931
Tb³⁺ in TbAIG, Zeeman-Raman transitions obs. 0–48097
Tb³⁺ in X₂O₃ phosphors, electroluminesc. 0–72463
Tb³⁺ in YF₃-Yb³⁺; cooperative energy transfer 0–72426
Tb³⁺ luminescence in CaF₂, photosensitization by Eu²⁺ 0–66104

chelates, low threshold laser action in liquid and solid host media 0-73230 Sm_{0.8}Tb_{0.4}FeO₂ platelet, interaction of planar domain wall and individual dislocations, obs. optically 0-75922 Tb-Ho alloy, magnon energy and lifetime in single crystal, neutron diffr. 0-44542

0-49342 Tb-Ho alloys, spin waves behaviour 0-59318 Tb-Ho single-cryst. alloys, magnetic props. determ. by neutron diffraction 0-62493

Terbium compounds continued

Tb chelates, kinetics of excitation energy transfer in the presence of quench-

Tb chelates, kinetics of excitation energy transfer in the presence of quenchers 0-44007

Tb³+ complexes, luminescence temp. depend. 0-54125

TbFe garnet, Faraday effect, temp. depend. 0-41125

Tb,Fe₄O₁₂, mag. symmetry 0-62550

TbFe₅O₁* garnet, birefringence, gyroanisotropy 0-41126

TbIn₃, magnetic structure and presence of antierromagnetism from neutron diffraction study 0-72284

TbNi₃, polymorphism, heat treatment depend. 0-65286

TbNi₅, mag.struct. 0-47925

TbPt₃, magnetic structure and presence of antiferromagnetism from neutron diffraction study 0-72284

TbY₁₋₂Sb, transition from Van Vleck paramagnetism to induced antiferromag, rel. to Tb conc. 0-44507

Terrestrial electricity see Earth/electricity

Terrestrial heat see Earth/heat

Terrestrial heat see Earth/heat

Terrestrial magnetism see Earth/magnetic field; Magnetic storms

Tetraneutrons see Neutrons

Thallium

abundance of isotopes in lunar surface material 0-48494 atom, $6^2 \, P_{3/2}$ state, collisional de-excitation 0-77673 atom, electric dipole moment determination 0-43003 atom in $7^2 S_{1/2}$ state, collision with foreign gases, effect on polarization 0-42983

creep, influence of superconducting transition, deformation creep curve 0-75261

diffusion in KCl single and bicryst. 0–50624 diffusion in Sn, polycryst., volume and grain-boundary type 0–40206 Fermi surface, Azbel'-Kaner cyclotron reson. obs. 0–44019 fluorescence, thermally associated resonance and antistokes observation

0-67608

0–67608 molten sound absorption meas. in 60-100 MHz range 0–61516 optical pumping and collisional relaxation of $^{2}P_{1/2}$ ground state 0–60964 polymorphic transformation, $\alpha = \beta$, impurity effects 0–68554 superconducting, density of states data from critical field meas. 0–75586 superconductivity at high pressures, 77-350K 0–53803 transport and thermal props. 0–62290 tunnelling effect under pressure 0–62328 I, quenching of 7°3 state of atom, calc. 0–67650 KCl:TI, cathodoluminesc. yield 0–41284 KCl:TI, colour centres, radiative creation, Coulomb interaction 0–40184 RbT:TI, emission spectra for excitation in A, B, C, and D absorpt. bands 0–44890 in SnCd eutectic mixture, spectroscopic determination in connection with

in SnCd eutectic mixture, spectroscopic determination in connection with soil analysis 0-69240 TI-He atomic collision, possible complex obs. by level-crossing spectroscopy 0-77705

scopy 0–77705

Thallium compounds
acid phthalate, cryst. growth and testing for X-ray spectrometer 0–65168
alloy, dil., transport and thermal props. 0–62290
halides, longitudinal optic modes, effect of lattice anharmonicity 0–44746
halides with CSCI structure, cohesive energies 0–43577
luminescence of salt in alcoholic solns., effect of u.v. irradiation 0–71361
perovskite, high press. synthesis, cryst. struct. 0–78404
thallium-bromide-iodide thin layers, optical const. meas., applic. 0–59353
Bi-Tl alloys system under press., phase equil. 0–40500
Bi-Tl alloys, f.c.c., Fermi surface-Brillouin zone interaction 0–51007
Bi-Tl alloys, liquid and solid, struct. obs., elec. conductivity meas. 0–64864
In-Tl, liquid alloy, specific resist., 20-500°C, bonding characts. 0–58443

0-64864
In-TI, liquid alloy, specific resist., 20-500°C, bonding characts. 0-58443
In-TI alloys, ¹¹⁵In.m.r. 0-45021
In-TI alloys, phonon spectra influence on supercond. T, 0-68788
K-TI dil. alloy, liquid, elec. resistivity, comp. depend., 100-260°C
0-50255
Pb-TI alloys, flux pinning enhancement 0-71982
Sb-TI, phase equilib. and thermodyn. anal. 0-65477
TL halides, dielec. consts., audio and r.f., 1.5° to 350°K, up to 48 kbar 0-53917
«-TI-Sn solid solns. Mossbauer effect, rel. to interest the condition of the control of the condition of the co

 α -TI-Sn solid solns., Mossbauer effect, rel. to interatomic force interaction 0-44795

0-44/73 II-Te-Ge semiconductor glass, comp. for bistable system with elec. switching, patent 0-44336 TI-Te, molten alloy, resistivity and Seebeck coeff., comp. depend. 0-43474

0—43474
TI-Te, molten alloy, thermoelectricity, elec. cond., comp. depend., semiconductor-metal transition 0—46948
TI azide, i.r. spectra assignments and cryst. struct. 0—72352
TIASSe₂, glassy semiconductor, current-voltage, characts. 0—47694
TIBiO₂ single cryst., preparation at 480°C from TICO₂ on Bi₂O₃, struct. determ. 0—65137

TIBIO₂ single cryst., preparation at 480°C from TICO₃ on Bi₂O₃, struct. determ. 0–65137
TI₂BiO₃ single cryst, preparation at 480°C from TICO₃ on Bi₂O₃, struct. determ. 0–65137
TI₂Bi₂O₃ single cryst, preparation at 480°C from TICO₃ on Bi₂O₃, struct. determ. 0–65137
TIP₂ absorption bands, phonon sidebands of exciton quasicontinuum.

TIBr, absorption bands, phonon sidebands of exciton quasicontinuum 0-48077

0-48077

TIBr, electronic behaviour, exciton and polaron roles 0-75506

TIBr, excitons and exciton-optical phonon coupling in mag. field 0-48076

TIBr, fh.f.s. 0-64457

TIBr film, strain-reduced, Faraday rotation pattern, exciton binding energies, opt. absorpt. and consts. 0-44855

Tl₂CO₃, high press. phase boundaries 0-62136

TICl, absorption bands, phonon sidebands of exciton quasicontinuum 0-48077

0–48077
TICl, excitons and exciton-optical phonon coupling in mag. field 0–48076
TICl, iodide activated, as high Z scintillator 0–60662
TICl film, strain-reduced, Faraday rotation pattern, exciton binding energies, opt. absorpt. and consts. 0–44855
TI₂Co₂(OH)₂(SO₄), 2H₂O₃, cryst. struct., X-ray powder indexed 0–53510
TICrO₂, preparation, crystal parameters and phase transformation 0–78505
TIF, cryst. struct. 0–61910
TIF mol. props. from microwave absorpt. spectra 0–67713
TIFeO₂, transition point at 750° 0–78505
TII, α- and β-phases, n.m.r., indirect interaction between nuclei and chem. shift 0–54170
TII, h.f.s. and elec. hexadecapole moment of ¹²⁷I 0–64458

allium compounds continued

TII, i.r. and Raman spectra study of orthorhombic to CsCl-type struct. transition 0–72393

TII, n.m.r. of ^{20*}TI and ²⁰⁵TI, spin exchange interactions and chemical shifts 0–48166

TILiBeF4, crystal structure 0–75095

TIMnCl₃, cubic), temp. depend. of fluorescence 0–44909

TIMnCl₃, anhydrous, Bridgman crystal growth, X-ray diffr. 0–65167

TIMnF3, mag. struct., neutron diffr. obs., 4.2K 0–41065

TIMnF3, mag. struct., paramag. neutron scatt. obs. 0–40952

TIMo₃, molten, diffusion coefficient of Tl* in Ca(NO₃)₂.4H₂O, chronopotentiometric 0–39762

TI₃O, black cryst., growth by thermal decomposition Tl₂C₃ at 700°C cryst. struct. determ. 0–53469

T₃O new form stable between 354°C and melting point 0–59038

Tl₄(OEt)₄ complexes, alternate force fields in normal coord. anal. 0–74232

TIPO₃-Co(PO₃)₂, phase equilib. diagram 0–50834

Tl₂S, cryst. struct. 0–58758

Tl₃SO₄, elec. conductivity, 100-500C 0–75549

TISbCl₆ i.r. and Raman spectra study 0–67754

TISbS₂, lendamental absorpt. edge, forbidden band width 0–69131

TISbS₂, electroabsorption 0–41130

Tl₃Se As₃Te, glass, temp. depend. of switching phenomenon 0–40818

Tl₃Se, thermodynamic props. 0–53711

Tl₃Se, As₃Se, amorphous semiconductor, local states, thermally stimulated depolarization method 0–40788 Thallium compounds continued

0–62387
T.Jse.As,Se₂, amorphous semiconductor, local states, thermally stimulated depolarization method 0–40788
TITe, thermal conductivity, temp. depend., 500-1400 K 0–39780
TI,Te₃, crystal growth, segregation of Se, S, Tl and Fe 0–74961
TI,Te₃, TITe, TI,Te, liquid, thermal conductivity, 500-1300K 0–39781
TI,Te.As,Te₃, vitreous, elec. resist., Hall effect, thermoelec., temp. depend. 0–47728

Tl₂Ti₃O₇, space groups and crystal parameters 0-78504

Thermal conductivity see Conductivity, thermal

Thermal decomposition see Chemical reactions

Thermal diffusion see Diffusion in gases/thermal; Diffusion in liquids/thermal; Diffusion in solids/thermal

Thermal diffusion columns see Diffusion in gases/thermal; Isotope separation Thermal diffusivity see Conductivity, thermal; Heat conduction Thermal expansion

alkali and TL halides, Gruneisen parameters for phonons, rel. to dielec. consts. 0–53917 alkali fluoroborates, molten and cryst. 0–43435 alkali hydride crystals, calc. value 0–56104 n- amyl alcohol, dilatometric measurements, 1°C interval in range 20°C-70°C 0–68092

70°C 0-68092 iso- amyl alcohol, dilatometric measurements, 1°C interval in range 20°C 70°C 0-68092 anomalous, study for Ising model near magnetic critical point 0-75876 anthracene, Gruneisen tensor, 0-300 K 0-40589 anthrone, thermal-vibration parameters analysis, anisotropy of expansion coefficients 0-53520 antiferromagnet, MnCl₂.4H₂O and MnBr₂.4H₂O, Neel-pt. anomaly 0.-44706

antiferromagnet, MnCl₂.4H₂O and MnBr₂.4H₂O, Neel-pt. anomaly 0–44704 antiferromagnet CeAs, and elec. resistivity, rel. to mag. anomaly 0–40705 butadiene-styrene copolymer filled with carbon black 0–65555 calorimetric measurement 0–48899 carbide materials for rocket nozzle applies. 0–58953 ceramic composites, expansion and shock resistance behaviour 0–50887 composite, SiC clad graphite 0–59003 composite, ferrite-dielectric, thermal expansion matching 0–50802 composite of high strength and stiffness, with zero coefficient in one direction, analysis and design 0–50894 crystal, vibrations distribution function, Gruneisen parameter dilatometry 0–40505 crystals, rel. to defects, low temp. anomalies 0–40122

0-40505
crystals, rel. to defects, low temp. anomalies 0-40122
dibenzyl crystal, X-ray diffr., 83-297K, Gruneisen tensor 0-50898
dilatometer for obs., high temperature, program controlled 0-72868
Elinvar-type alloy in Pd-Au system 0-65357
ferroelectric, Ba,NaNb₅O₁₅, Gd-substituted, linear expansion 0-59111
ferroelectric, LiTaO₃, Curie pt. behaviour 0-65814
ferroelectric, NaH₃(SeO₃)₅, rel. to H bonds 0-68619
ferroelectric, anomalies near Curie pt. 0-65797
ferroelectric, rel. to phase transitions 0-65816
ferromagnetic alloy, Co-Mn, Young's modulus temp. coeff., phase equilibrium 0-75413
fibrous composites, review 0-71648

rium 0–75413 fibrous composites, review 0–71648 glass, La₂O₃-BaO-B₂O₃ system 0–58541 glass, alkali silicate and aluminoborate 0–50672 glass, mercury oxide containing 0–39908 graphite, coeff. variation rel. to prestressing 0–40583 graphite, heat treatment depend. 0–59104 graphite, imperfect, hexagonal axis expansion coeff., approx. theory 0–47547

0-47547
graphite, in semi-continuum model 0-40581
graphite, neutron irrad., coeff. changes 0-40143
graphite, polycryst., model 0-40582
graphite, polycryst, model 0-40582
graphite, polycrystalline, B elastic and elec. props. 0-71876
graphite, reference for high temp. 0-40580
graphite 0-40561
graphite lattice dynamics, self-continuum model 0-40585
graphite materials for rocket nozzle applics. 0-58953
Gruneisen coeff. determ, compressibity parameters applic. 0-40587
Gruneisen parameter, 0K, method 0-56114
Gruneisen parameter, effect of anharmonicity 0-40588
Gruneisen parameter, low temp, from elastic constants press derivs. for Rb1 0-43923
Gruneisen parameter calcs. for several solid models 0-43922

Rb1 0–43923 Gruneisen parameter calcs. for several solid models 0–43922 Gruneisen parameter calculation from thermal conductivity meas. under pressure 0–75415 Gruneisen parameter eqn., soln. rel. to vol. depend. of self consistent phonon energies 0–47552 Gruneisen parameter for Born-von Karman lattices 0–56113 Gruneisen parameters, mode calc. for $\rm Al_2O_3$ 0–50899

Thermal expansion continued

halides, heavier, and lattice energies 0-43915

halogenoethanes, liquid, thermal density variation obs. 0–74732 heterophase fluctuation during melting 0–74839 internal pressure parameter in solids and liquids 0–58439

internal pressure parameter in solids and liquids 0–58439
Invar property obs. rel. to spontaneous volume magnetostriction 0–65921
LiF, Gruneisen parameter, OK 0–56114
LiFe(WO₄), crystal, linear, X-ray diffr., 650°C 0–50530
liquid, Gruneisen coeff. rel. to intermol. force constants 0–64853
liquid, pseudo-Gruneisen parameter 0–55604
liquids, meas. with multi-purpose instrument 0–66948
metal, Gruneisen coeff. determ., compressibility parameters applic. 0–40587
metal, cubic, Gruneisen parameters 0–53718
metal film on substrate, temp. coeff. resistance, thermal strain effects 0–65628
Mie-Gruneisen scheme extended 0–65544

metal film on substrate, temp. coeff. resistance, thermal strain effects 0-65628

metals, Mie-Gruneisen scheme, extended 0-65544
metals, axial, Gruneisen functions 0-56121
metals, c.c.p., linear coeffs., monovacancy formation 0-43916
naphthalene, Gruneisen tensor, 0-300 K 0-40589
nonprimitive lattice, rel. to phonon freq. shifts 0-78720
optical materials, 'zero expansion', meas. 0-62216
N-oxyphenazine, anisotropic, explanation in terms of structure 0-53524
paramagnetic crystal, effect on ligand field 0-75981
phenazine-N-oxyphenazine system, variation with composition 0-53407
polyethylene unit cell, lamella thickness effect 0-78785
polymers, heat resistance 0-65543
rare gas solid, dilatometer 0-53715
resins thermoactive, anomalies at glass transition temp. 0-59113
of sintered alloys, theory and experimental verification 0-68399
steel, calcium aluminate inclusions, rel. to tessellated stresses 0-59112
sulphates, high-temp. cubic phase props. 0-75412
of wires, electrically conductive, appl. in guiding system for astronomical instruments 0-41871
Ag-Mn alloy at high temperatures, solid solution relationship between lattice parameters and temperatures 0-43919
Ag, c.c.p., linear coeff., rel. to monovacancy formation 0-43916
Ag, systematic error rel. to internal temp. standard in X-ray diffraction

Ag, systematic error rel. to internal temp. standard in X-ray diffraction 0-43918

Al-Mo alloy, supersaturated solid soln., expansion coeff., temp. depend. 0-78783

Al-Zr alloy, supersaturated solid soln., expansion coeff., temp. depend. 0-78783

0—18/83
Al, c.c.p., linear coeff., rel. to monovacancy formation 0—43916
Al, Gruneisen parameters, lattice dynamical calc. 0—56107
Al, polycryst., Gruneisen parameter, absolute determ. 0—43917
Al, solid and liquid state, results 0—59110
Al, systematic error rel. to internal temp. standard in X-ray diffraction 0—43918

0-43918
AlAs, 15-840°C 0-71866
Al₂Au, coeffs, and Gruneisen constants 0-61851
Al₂O₃, mode Gruneisen parameters calc. 0-50899
β-Al₂O₃, sintered sodium ceramics 0-58985
Ar, solid, bulk expansivity and vacancies 0-53716
As, Gruneisen tensor 0-71822
Au, systematic error rel. to internal temp. standard in X-ray diffraction 0-43918
R-O₂, vitreous relayational responses rel to N-state models 0-55683

Au, systematic error rel. to internal temp. standard in X-ray diffraction 0–43918
B₂O₃, vitreous, relaxational responses, rel. to N-state models 0–55683
B₃O₃, vitreous, three-state model 0–50338
Ba₂NaNb₃O₁₅, Gd-substituted, linear expansion 0–59111
C, pyrolytic, fluidized bed produced, lattice expansion 0–40584
C foam-a cellular structural material, low linear coeff. 0–39853
CS, liquid, evaluation from partition function 0–78260
CdF₃, elastic moduli, thermoelasticity, Debye temp. 0–55939
CdMoO₄, X-ray study 0–62217
CdSe, wurtzite, from lattice params., 2-350°K 0–47551
CeAs, antiferromagnet, and elec. resistivity, rel. to mag. anomaly 0–40705
Co-Mn, ferromag. alloy, Young's modulus temp. coeff., phase equilibrium 0–75413
Co-Pd alloys, rel. to comp. and magnetization state 0–65551
Cr, antiferromagnet, rel. to lattice anisotropy 0–44682
Cr, coeffs. and Gruneisen constants 0–61851
Cr anomalous, near Neel temp. 0–75414
CsBr, and law of corresponding states 0–47549
CsBr(Cl.I), vol. coeff. and Gruneisen const. 0–78727
Cu-In alloy at high temperatures, solid solution relationship between lattice parameters and temperature 0–43919
Cu-Sn alloy at high temperatures, solid solution relationship between lattice parameters and temperatures 0–43919
Cu, c.c.p., linear coeff., rel. to monovacancy formation 0–43916
Cu, c.c.p., linear coeff., rel. to monovacancy formation 0–43916
Cu, coeffs. and Gruneisen constants 0–61851
Cu, electrodeposited, mech. and elec. props., struct., treatment depend. 0–71662
Cus, Solid and liquid state, results 0–59110
Cu-Si, colid and liquid state, results 0–59110

0-71662
Cu, solid and liquid state, results 0-59110
CuK, CL, 2H,O, critical region, Curie point anomaly in a-axis linear coefficient 0-68617
Er,O₃, 100-300K, lattice parameters, X-ray diffr. 0-50895
(63wt.%)Fe-(32wt.%)Ni-(5wt.%)Co alloy, super-Invar, elastic anisotropy, temp. depend, -30-600°C 0-75220
Fe-Ni alloys, irreversible, unusually low expansion 0-50896
Fe., coeffs. and Gruneisen constants 0-61851
(Fe_{1-x}Co₂A₂SeC₀₋₁₁ alloys, rel. to spontaneous volume magnetostriction in Invar property 0-65921
FeGe₂, linear coeff. along [001] and [100], 90-480 K 0-47548
GeTe, linear coefficient, rel. to suitability as thermoelectric material 0-51133
He II, meas. from 0.85 K to within 0.4 mK of λ transition 0-71398

0–31133 He II, meas, from 0.85 K to within 0.4 mK of λ transition 0–71398 HgSe, and lattice parameter determ. 0–43646 Ir, linear, at low temperatures Gruneisen parameters 0–75411 KCl, and law of corresponding states 0–47549 KI, 100-300 K 0–43920 KI, 100-300 K 0–43920

KI, 100-500 K. 0-45920 KNO₃, ferroelectric modification, from lattice parameter vs. temperature 0-53717 LaB₈, X-ray obs. 0-65552 LiF, 25-600C, 38-57 kbar, X-ray diffr., compressibility data 0-40286 LiH, isotope effects 0-43921 Li₂SO₄-K₂SO₄ (or Na₂SO₄) polycryst. mixtures 0-65553

PA 1970 - Part II (July-Dec.) Thermal expansion continued Thermocouples continued ⁷LiD₀, T_{0.4} lattice parameter change of ³He decay and on warming 0–50529
MgO-MgAl₂O₃ mixtures for thermal expansion matching in composite fabrication 0–50802
MgO, Gruneisen parameter, 0K 0–56114
MnBr₃-H₂O, Neel-pt. anomaly 0–44704
MnCl₂-H₂H₂O, Neel-pt. anomaly 0–44704
MnCl₃-H₄H₂O, Neel-pt. anomaly 0–44704
NgCl₄-H₂O, Neel-pt. anomaly 0–44704
NgCl₃-H₄D₄O, Polel-pt. anomaly 0–44704
NgCl₄-H₂O, Neel-pt. anomaly 0–44704
NgCl₄-H₂O, Isotope effect, phase transitions 0–56111
NaH₃(SeO₃)₂, rel. to H bonds 0–68619
NaH₄(SeO₃)₃, rel. to H bonds 0–68619
NaH₄SO₄.2H₂O, rel. to ferroelec. phase transitions 0–65816
NaNO₃, and precision lattice parameter determ. 0–43639
Nb. coeff. X-ray diffr. obs. 0–78784
NbO, Gruneisen consts. 0–78619
Nd doped laser glasses, 0.4 to 2.3 µ, 0 to 300°C, obs. 0–59360
Ne crystal, Debye temp. and Truneisen coeff., from u.s. vel. of propag., 2-20K 0–55941
Ni. Gruneisen comst. 0–78619
Ni. Invar prop. effect of V, Mo, W, Si, Sn, Cr additives 0–58855
Ni. Invar prop. effect of Mn, Ti, Zn additives 0–58856
Pb, solid and liquid state, results 0–59110
PbF₂, cubic, Gruneisen param. low temp. limit calc. 0–40235
Pd-Au system, nonmagnetic Elinvar- type alloy, heat treatment effects 0–6537
Pd. finear, at low temperatures Gruneisen parameters 0–75411
Pt, vacancy formation effects at high temp. 0–47550
Pt, linear, at low temperatures Gruneisen parameters 0–75411
Pt, vacancy formation effects at high temp. 0–47520
Re, linear coeffs., effect of pressure and temp. 0–47203
Re, linear, at low temperatures Gruneisen parameters 0–75411 ⁷LiD_{0.6}T_{0.4} lattice parameter change of ³He decay and on warming 0-50529 high-temp. based on graphite electrodes, constructed 0-45705 hygrometer, continuously recording, using thermocouples 0-45487 semiconductor, prod. by simultaneous plastic deform, of Si and Ge-Si alloy 0-43748 shocked, abnormal thermo-e.m.f. 0-40888 Au-Al, thermopower meas., 30-150°C 0-79060 Ge film, p- and n-type, prep. 0-63485 Pt13%Rh/Pt, revised reference tables63487 0–63487 W-(3wt.%)Re/W-(25wt.%)Re, reliability and stability, e.m.f. vs. temp. 75822 0–75822 W Re, in range 1450 2000°C, thermal e.m.f. variations 0-42106 Thermodynamic properties
see also Critical constants, thermal; Entropy; Heat of reaction; Latent
heat of adsorption, rel. to different mechanisms 0-61675 alkali halide, lattice energy rel. to temp. change of Young's modulus 0–50888 alloy, dilute interstitial, elastic free energy 0–53639 alloy systems, homogeneous monotonic, liquidus-solidus gap 0–50300 alloy systems, homogeneous monotonic, liquidus-solidus gap 0–50300 alloys, meas, automated at, absorpt, spectrophotometer 0–75403 antiferromagnetic α-MnCl₂.4H₂O, magnetothermodynamics 0–65965 aqueous solns, enhanced potential during freezing 0–68181 austenite, statistical model 0–53641 boride single crystals, rel. to electrochem. growth techniques 0–71515 bromine-freen/propane mixtures, 18° to 45°C 0–46822 critical liq-gas pt., sp. ht. anomaly rel. to sound vel. 0–50321 dislocation velocity-stress exponent, temp. depend. activation entropy 0–58807 droplet formation free energy and radius depend, of surface tension 0-397150-43923
Re, linear coeffs, effect of pressure and temp. 0-47203
Rh, linear, at low temperatures Gruneisen parameters 0-75411
Si, Gruneisen parameter, low temp., from elastic constant press. derivs. 0-43924 droplet formation free energy with curvature depend, surface tension 0-39716 droplet formation free energy with curvature depend, surface tension 0-39716 electrolyte mixtures part dissoc. 0-66192 electrolyte solutions, Monte Carlo calc. 0-53320 equations of state, water-steam characteristics calc. 0-74720 ethyl xanthate on galena 0-65106 ferromagnet, heat capacity in external field near critical pt. 0-40967 ferromagnet, scaled eqn. of state and critical exponents, rel. to fluids 0-44530 Si, Gruneisen parameter, low temp., from elastic constant press. derivs. 0–43924

Sn, solid and liquid state, results 0–59110

TiO, Gruneisen consts. 0–78619

TiO, vacancy removal effect 0–61943

Tm₂O₃, 100-300K, lattice parameters, X-ray diffr. 0–50895

UP₃, cryst, struct., phase transitions 0–61912

α-V, β-VH_x(31 at.% H), –160 to 70°C 0–71867

V, coeff., X-ray diffr. obs. 0–78784

VO, Gruneisen consts. 0–78619

VO, vacancy removal effect 0–61943

V₂O₅, X-ray and neutron diffr. meas. 0–65560

W solid and liquid state, results 0–59110

YB_{xx} X-ray obs. 0–65552

Yb₂O₃, 100-300K lattice parameters, X-ray diffr. 0–50895

Zn-Cu-Ti alloy, varied extrusion temp. effect 0–40423

ZnS, wurztiet, from lattice params, 2–350°K 0–47551

ZnSe Debye temp., compounds of same Gruneisen constant, linearity of log (Debye temp.) with log (molar vol) 0–50900

ZnTe, and lattice parameter determ. 0–43646

ZnTe, mode Gruneisen parameters 0–75383

ZnTe Debye temp., compounds of same Gruneisen constant, linearity of log (Debye temp.) with log (molar vol.) 0–50900

Zr–(2.5%) Nb, effect of annealing and cold working 0–40586

Zr₂O₅ baddeleyite, thermal and isomorphous deformation 0–61917

ermal measurement 0-44530
ferromagnet, uniaxial in external field, critical indices 0-79150
ferromagnetism, spin 1/2 XY model, exact high temperature series expansion 0-51964
fluid thermomechanics, 1" year college text 0-39485
free energy, deviation of lower bound 0-54599
free energy of f.c.c. and h.c.p. lattices, high temp. limit, harmonic model, cell cluster expansion 0-71501 gas mixtures, functions calc., high temp., Debye type electrostatic interactions 0-39668 gases dense, with three-particle interaction energy, parameters calcs. 0-58476gases real, relative method of correlation, extrapolation of exptl. data 0–58388 glass-molten salt interface, ionic exchange processes 0–50354 glass-molten salt interface, ionic exchange processes 0–50354 glassy sytems, inner parameters 0–47019 hard-square solids at high densities 0–65113 harmonic solids, rigorous bounds 0–62206 Heisenberg and Ising ferromagnets, equivalence in high-density limits 0–79144 Helmholtz free-energy inequalities 0–64986 Helmholtz free-energy inequalities 0–64986 Hg activity coeffs. meas. 0–61605 inert gas solids, anharmonic effects, applic. of approx. method 0–53674 inert gas solids, anharmonic effects, applic. of approx. method 0–53674 inert gas solids, exp 6 cell model calc., triple-dipole term effect 0–47497 inhomogenous systems 0–54603 insulator, thermochem. approach to bandgaps 0–47591 lattice with two-body interactions, stability criteria 0–75350 Lennard-Jones liquids, improved Monte Carlo data 0–50217 liquid, supercooled 0–64896 liquid, u.s. relax. as rate process 0–39725 liquid crystal, p-azoxyanisole, derivs. near phase transition 0–58451 liquid crystals, thermodynamics of first- order transitions 0–68095 liquid metals, surface tension and critical props. 0–58470 liquid mixtures of nearly spherical mols, thermodynamic excess functions 0–53312 of liquids, transient comparison methods of simultaneous meas. 0–50885 liquids with three-particle interaction energy, parameters calcs. 0–58876 low-temperature crystal, Helmholtz free energy 0–40558 macromolecules, enthalpies of activation, experimental and theoretical study 0–64563 magnetic alloy, dil. 0–43894 metal, activation enthalpy of diffusion of H 0–40192 metal, plastic deformation, theory 0–40294 metal, surface mag, levels contrib. metals, in mag, field, electron theory 0–75445 metals, in mag, field, electron theory 0–75445 metals, in mag, field, electron theory 0–64975 micelles, multi-component, in soln. 0–64975 micelles, multi-component, in soln. 0–64975 micelles, multi-component, in soln. 0–64975 micelles, multi-component, gases real, relative method of correlation, extrapolation of exptl. data 0-58388 see also Calorimeters; Calorimetry; Conductivity,
thermal/measurement; Temperature measurement; Vapour pressure
measurement; Entries describing measurement methods for specific thermal quantities and effects may also be found listed under the various
headings for the subjects concerned
charring plastic, simultaneous measurement of six properties 0-47539
contact e.m.f., rel. to incomplete solution of C in 38CrMoV21.14 steel
0-40458 0-40458
crack tip temperature from thermal decomposition along cleavage-crack in a brittle crystalline solid 0-53616
differential analysis, Cu₃SeTe phase in Cu-Se-Te 0-71773
dilatometer, continuous recording vertical 0-72918
emissivity, bar method meas, precision limits 0-52154
flux sensor vacuum calibration, error sources 0-73069
guard ring system, corrector, optimal position 0-52154
laser power meter, for large or divergent beams, design and calibration 0-45668
[liquid metal solid-stationary interface thermal resistance due to presence of 0-45668 liquid metal, solid-stationary interface, thermal resistance due to presence of gas cavities 0-46902 rel. to major planets, radio emission meas. 0-63092 Moon ir, radiation, thermophysical properties of surface obs. 0-59754 polyethylene, oxidation induction period meas. using differential thermometry 0-69212 radiation, reflectance of blackened Cu, 300 to 2500 nm wavelength 0-57423 solid parameters in variable region 0-50901

sond parameters in variable region 0-3091 thermometry, differential, rel. to meas, of oxidation induction period in polyethylene 0-69212 thermophysical props, determ, theory 0-54782 Cu-Se-Te, differential analysis of Cu₄SeTe phase 0-71773 Thermal radiation see Radiation/heat Thermal spikes see Crystal imperfections; Physical effects of radiations Thermal transformations see Boiling; Condensation; Crystallization; Freezing; Heat of transformation; Melting; Phase transformations; Sublimation; Vaporization methanol-CS; binary system, critical phenomena 0–39777 micelles, multi-component, in soln. 0–64975 micelles, multi-component, in soln. 0–64974 micropolar solids, elasticity theory 0–40212 mixtures of simple fluids, equilibrium thermodynamic properties, variational approach 0–64620 molecular crystal, atom atom potential method applic. 0–59074 molecular crystal, atom atom potential potential 0–67686 molten salts, partial molar entropy 0–39776 Monte-Carlo results comparison with lattice dynamics and cell-model approx. 0–75402 naphthalenes, fluoro subst., in alcohol, effect on non-radiative transitions 0–77936 **Thermionic emission** see Electron emission/thermionic; Ion emission/thermionic; Ionization, surface Thermionic generators see Electricity, direct conversion/thermionic; Elec-Thermionic tubes see Electron tubes Thermistors see Semiconducting devices Thermochemistry see Heat of reaction, etc. Thermocouples

alloy wires for capacitance-discharge butt-welding 0-71749
calibration of blackbody radiators, accuracy 0-60073
copper-constantan, for 0 to -200°C, calibration by means of boiling point
of water 0-42107
cryogenic, reference tables 0-63486

natural Saratov gas combustion products, eff. of ioniz. additives 0-55563 natural gas, liquified, P-V-t behaviour 0-68094

Thermodynamic properties continued

non-electrolyte solution, excess thermodynamic functions, hard sphere system, first-order perturbation 0-39775

Of nuclear materials, irradiated (U,Pu)O₂ and PuO₂, effect of burnup on O/M ratio 0-49738

of ohmic materials, including superconduction 0–53720 n-pentane, liquid-gas critical point, thermal equation of state, gravitational effect 0–74850

phonon energies, self-consistent, vol. depend., Gruneisen parameter eqn. 0-47552

plasma, dense 0-74497

point defects with explicit conc. depend. interacs. 0-50568

Poiseuille plane flow, thermal instability 0-46658

polymer, bidimensional layers, spreading enthalpies and entropies 0-61619

polymer solutions, free enthalpy, calc. from considerations of free volume 0-71315

0-71315
polymers rubber-like thermal effects during shear deformation 60-120°C
0-53414
polyvinyl chloride, plasticized, rheological and thermodynamic interaction effects 0-71656
potassium halides, Fm3m=Pm3m transitions 0-43826
powder, transient comparison methods of simultaneous meas. 0-50885
quantum lattice gas, spin 1/2 XY model, exact high temperature series expansion 0-51964
rare gases, composition at high temp., thermal equilibrium, applic. to mixtures 0-53269
regularity corresponding with position in periodic table 0-39893.

tures 0–53269
regularity corresponding with position in periodic table 0–39893
relaxation of defects, nonequilib. system 0–65311
rigid-sphere fluid 0–58274
rubidium halides. Fm3m=Pm3m transitions 0–43826
semiconductor, thermochem. approach to bandgaps 0–47591
solid solution, intersitial, by relax. methods 0–68527
solids, transient comparison methods of simultaneous meas. 0–50885
solutions, applic. of ion-exchange membrane electrodes 0–43440
spectrophotometer, automated at. absorpt., for alloys meas. 0–75403
spinel-ferrite solid solutions, of cation vacancy distrib. between sublattices
0–43656
thermal stress in slab heated by heat transfer 0–50886

0-43656
thermal stress in slab heated by heat transfer 0-50886
thermomagnetic force obs. in gas 0-55566
transition metal tris(acetylacetonato) complexes, entropy, enthalpy and free energy 0-75409
Type II superconductors 0-68778
Ag-In liquid system, integral molar enthalpy 0-64898
Al-Au, molten alloy, 660-1150°C, enthalpy, entropy e.m.f. method 0-46904
Al-Sh. molten alloy, 660-1150°C, enthalpy, entropy e.m.f. method

Al-Sb, molten alloy, 660-1150°C, enthalpy, entropy, e.m.f. method 0-46904

0-46904
Ar-N mixture, thermal equilibrium calc. at 1 atmos. and between 5000 35000°K 0-53269
Ar O₂ solid mixtures 0-62210
Ar, liquid, triple-dipole dispersion forces at critical state 0-50197
Ar solid, anharmonic effects, applic. of approx. method 0-53674
B-H compounds, cryogenic stability 0-62795
Ba-Cs condensed state 0-55606
Ba(NH₃)₈ 0-62796
CH₄ characteristics, equations of state for 0-39674
CO, p-V-T data table 0-58388
CO₂, long-range coherence length near critical pt. 0-53401
CO₂ liq. droplets varporization in N₂ near thermodyn. critical point, theory 0-50329
CS₂-methanol binary system, critical phenomena 0-39777

CS₂-methanol binary system, critical phenomena 0-39777 CS₂-methanol binary system, critical phenomena, coexistence curve CS₂-methanol binary system, critical phenomena, coexistence curve 0-39778
CS₂ liquid, evaluation from partition function 0-78260
Cm₂O₃, high-temp. evaporation, expt. 0-43518
Co-Pd solid solutions, 800-1100°C 0--68530
Cr-Fe system, and phase equilib. diagram 0-56041
CsF-Cs condensed state 0-55606
CsSO₄ heat contents, specific heats and latent heats of phase transformations 0-65548
Cu-Au, Cu-Ag, Cu-Pt, Cu-Ni, Cu-Co and Cu-Fe alloys with dissolved O₂ 0-64873
CNSO₃ HO₃ exherical single crust, thermoduromic temp, without heat

0-64873 CuSO_{4.5}SH₂O, spherical single cryst., thermodynamic temp. without heat intro., <0.5°K 0-78772 D₂, solid, pressure changes with temp. and para conc. 0-47540 F, critical parameters of vapour-liquid coexistence boundary 0-71417 Fe-Ni-Cr alloy, austenitic, free energy, two y phases, mag. props. 0-43832

0-43832 Fe-S melt, 1100-1300°C, activity vs. comp., heat and entropy of solution 0-74743

O=/4/43 Fe allotropes, calc. based on density of states curves 0-71855 FeO_{1/1y}, wustite, phase boundaries rel. to temp. O₂ partial pressure and composition 0-71854 GeH₃CN, and -d₃, molecular constants 0-46523 He-N mixture, thermal equilibrium calc. at 1 atmos. and between 5000-35000°K 0-53269

He I, entropy and order parameter fluctuations near λ point, decay rates 0-78322

0-47990 KH₂PO₄ laser modulator, temperature instability 0-47990 KH₂PO₄ laser modulator, temperature instability 0-47990 KH₂SO₄ heat contents, specific heats and latent heats of phase transformations 0-65548

formations 0–65548
Kr liquid, along boiling line 0–55607
Kr solid, anharmonic effects, applic, of approx, method 0–53674
Li₂so₄, heat contents, specific heats and latent heats of phase transformations 0–65548
MnBr₂,4H₂O antiferromagnetic single crystal, heat capacity meas., at 1.4 to 8°K and 0 to 15 kOe along c axis 0–50892
α·MnCl₂,4H₂O antiferromagnetic, magnetothermodynamics 0–65965
NH₄H₂PO₄ laser modulator, temperature instability 0–47990
Na reactor component walls, thermal transient response and stress obs. 0–39191

0—39191
Ne solid, anharmonic effects, applic. of approx. method 0—53674
O thermomagnetic forces obs. in gas 0—55566
O₃, from triple point to 300°K, at press. to 33 MV/m² 0—46992
P.I₄ heat content, free energy, entropy and heat capacity 0—58195
Pb. self-diffusion, activation energy rel. to deformation struct. 0—61997
Pb binary molten alloys, surface and body activities 0—74744

Thermodynamic properties continued

PbCl₂-MCl_x, (M=Cd,K,Na), molten salts, activities and potentials at liq.

PbCl₂-MCl₃, (M=Cd,K,Na), molten salts, activities and potentials at liq. junction 0−59493
Pd-Ag alloy, equilib. H₂ solubility, tensile and compressive elastic stress effects 0−53532
Pt-Rh alloy, Co activity-comp. relationships 0−78682
Se, vitreous, liq. and cryst. phases 0−50305
SiH₄, solid, for study of molecular motions 0−59083
SiH₃, solid, for study of molecular motions 0−59083
SiO₂, cristobalite, neutron irrad. effects 0−62134
Te oxides, gaseous, from mass spectra Knudsen cell data 0−41418
Tl-Sb, phase equilib., anal. 0−65477
Tl₂Se 0−53711
U-Ru-C system 0−59055
UC₂, activities of U, C on composition, eqns. 0−59109
US₁, s, from 5 to 350°K 0−71864
USe₂, from 5 to 350°K 0−71864
WF₂Cl₃ gaseous state 0−74311
Xe-N mixture, thermal equilibrium calc. at 1 atmos. and between 5000-35000°K 0−53269
Xe solid, anharmonic effects, applic. of approx. method 0−53674
Zn-Bi, Zn-Pb, Zn-Bi-Pb systems, effect of ternary additions 0−68082
Zn-Cl₂, glass transition thermodynamics 0−68076
Zrr-(2.5 wt.%)Nb-H system, press.-comp-temp. study 0−68570

Thermodynamics

see also Atmosphere/thermodynamics; Entropy; Equations of state;

Statistical mechanics

ΔH vs ΔS, correlation 0—76923

activation vol. and energy calc. from diffusion meas. 0—59929

Anergie, local production in system with variable parameter surroundings
0—38404

book undergraduate on equilibrium thermodynamics 0—45658

0-38404
book, undergraduate, on equilibrium thermodynamics 0-45658
Carnot's theorem, its discovery 0-69739
classical, simplified theory similar to Caratheodorys 0-73067
contact piece, non isothermal 0-45659
conversion of heat into coherent radiation, thermodynamic limitation 0-66923

o-0923 correlation functions of weakly relativistic systems, Gibbs ensemble, chains of eqns. 0-41997 critical points in multicomponent syst., unified geometrical approach 0-76851

0—76851
critical pt., order parameter fluctuations 0—48752
critical pt., order parameter fluctuations 0—69638
critical region correlation functions, asymptotic form 0—46976
critical systems, long-range correl. length 0—57291
cycle for direct conversion of chemical to mechanical energy 0—73141
de Broglie's hidden thermodynamics and the isolated particle, new formulation 0—66824 cycle for direct conversion of chemical to mechanical energy 0—73141 de Broglie's hidden thermodynamics and the isolated particle, new formulation 0—66824 diagram, representation of unique state by point 0—42094 differential equations, transformation by introducing dimensionless exponents 0—69740 distribution functions by detailed balancing 0—41992 dynamical critical phenomena, critical slowing down characts. 0—51984 dynamical scaling, sum rules 0—59935 dynamical scaling concept 0—59934 elastic solids, conditions of stability of equilibrium states 0—76888 energy of insular syst. in outer gravitational field 0—51921 equilibrium transition 0—76847 Exergie and Anergie, unified consideration of different forms 0—38403 flows in arbitrary frames, transport processes description 0—72956 fluctuation kinetics and coeff. determ. 0—45544 fluids, one-dimensional, phase transitions 0—50294 free energy expansion near phase transitions 0—48747 gas-solid molecular complex, props. by cell model calc. 0—78712 gases, book 0—50140 general relativistic, and relax. 0—38405 Gibbs paradox, sharpening Bridgman's resolution 0—42092 heat equations, homogeneous soln. 0—66925 irreversible processes, projecting operators 0—54606 irreversible processes, projecting operators 0—54606 irreversible processes, projecting operators 0—76848 kinetic eqn., effect of initial correlation 0—50840 fluid gas azeotropic system, investig, using diffusion constant near critical point 0—74842 initial explanation of englar system of deformable body,

0—46636
non-negative interactions, bounds, successive approximations and limits for distribution functions 0—57292
nonequilibrium, from porous plug expt. teaching 0—42095
nonequilibrium, irreversible processes, extremum principles 0—72958
nonlinear systems, thermal fluctuations 0—51963
nonstationary, non-truncated relativistic Chernikov-Grad 13-moment eqns, entropy balance, Gibbs eqns. 0—72937
one-dimensional gas, Yang-Lee distrib. of zeros 0—69655
Ornstein-Zernicke systems, mean-field aspect 0—48751
pair correlation functions, moment method 0—48748
parallel plate capacitor as model for reasoning 0—48871
Peierls' phonon-Boltzmann eqn., linearized collision operator, gap nonexistence in eigenvalue spectrum 0—41996
phase transition, correlation functions, scaling laws violation 0—72952
phases as extremal KMS states 0—73065

Thermodynamics continued

plasma in thermodynamic equil. in Debye approx. distrib. function 0-43250

progress in different fields 0-38203 quantum, disjointness of the KMS states of different temperatures 0-38200

quantum fluids 0-76856 quantum particle in suddenly expanded box, approach to equilibrium, tem-poral evolution 0-76849

poral evolution 0-76849
quantum particles, noninteracting approach to equilibrium, temporal evolution 0-76840
in quantum theory 0-51945
radial distrib. function and first-order phase transitions 0-51983
reactors, CANDU, thermal efficiency increase means 0-42907
of reduced quantum mechanical density matrices, inequalities and relations 0-5928
relativistic, 2nd law, chronometric invariant formulation 0-76817
relativistic, blackbody radiation interpretation 0-52153
relativistic form of statistical thermodynamics, formalism using 'sums over states' 0-66836
relativistic thermodynamic fluid, properties 0-39489
self consistency and stability in variational calc. of thermodynamic quantities 0-69642
of silica-steam system, rel. to nuclear cratering and cavity formation 0-76248
statistical, non-equilibrium statistical operator and its applications to

0–76248 statistical, non-equilibrium statistical operator and its applications to irreversible processes 0–51979 statistical and cosmological time arrows and CP, CPT violations 0–67207 Stirling cycle using N₂O₄, dynamic performance, obs. 0–66924 Taylor stability problem, variational solution based upon non-equilibrium thermodynamics 0–46336 thermionic work fn. correlation with emitter temp., Cs-pressures 0–65861 third law, e.m. zero-point radiation 0–54605 transport coeffs, improved variational principles 0–45558 transport equation, phenomenological eqns. 0–73066 units programmed course, book 0–45509 virial theorem and first-order perturbation theorem 0–41990 viscoelastic materials with fading memory, integral constitutive equations 0–57350

0-57359

0-57359 water nucleation, homogeneous and heterogeneous 0-68180 X-Y model, one-dimensional, with random coupling consts. 0-5992 ΔH° vs ΔS° correlation 0-76922 N,0,4 Stirling cycle dynamic performance, obs. 0-66924 YFe garnet, crystal growth, chemical transport with HCl 0-471220-59926

applications

applications

applications

to continuum mechanics in e.m. fields, linear irreversible 0–38220
dislocation glide, systems for analysis 0–75153
elastic-visco, plastic materials, microscopic and macroscopic 0–40293
to electrodynamics, linear irreversible 0–38459
electrolyte solubilities in water 0–68080
energy transformation 0–42160
fading memory in evolutionary-type materials 0–38229
heat pump cycle for 3.5 K automatic refrigerator 0–48870
hydrocarbon liquid fuel combustion 0–76261
interface phenomena, irreversible processes 0–51996
laser threshold and second-order phase transitions far away from thermal equilibrium, with Fokker-Planck functional equation solution 0–60199
magnetic fluctuations 0–52231
metallurgical processes 0–78663
phase change, quasithermodynamic theory 0–64982
phase transformations, diffusion-limited, math. approxs. comparison and crit. evaluations 0–78689
phase transitions, second-order, without divergences in second derivs. of thermodynamic potential 0–68548
refrigerator, 3.5 K, using new heat pump cycle 0–48870
thermomechanical materials with memory, constitutive eqns. 0–52055
thermostat and system in equilibrium, thermodynamic functions derived 0–76949
universe (mixmaster), entropy perturbations 0–54328
Gas entity and processes 0–78000.

0-10949
universe (mixmaster), entropy perturbations 0-5
GaAs, epitaxial growth from vapour 0-65067
H₂-I₃ reaction, barrier height cales. 0-72528
La halides, gaseous, at 293.15-3000°K 0-71249
Y halides, gaseous, at 293.15-3000°K 0-71249

Sc halides, gaseous, at 293.15-3000°K 0-71249
Y halides, gaseous, at 293.15-3000°K 0-71249
Thermoclasticity
asymptotic stability, appl. of invariance principle for systems on Banach space 0-52059
beam, sandwich, optimal thermoclastic design 0-69698
beam permanent deform under transverse temp, profiles, calc. 0-38318
bodies, regular sets interacting mechanically and thermally deriv. of basic eqns. 0-38314
booms with open cross section, flutter 0-54661
circular plates, large deflections on heating, Berger's analysis 0-38313
constitutive eqns. for thermomechanical materials with memory 0-52055
contact problems, elasticity theory, three-dimensional 0-38285
Cosserat elastic half-plane, waves prod. by conducting heat and moving load 0-57362
Cosserat medium, plane problem 0-63400
cylinder, circular, heat generating, soln. of displacements 0-54664
cylinder, circular, heat generating, soln. of displacements 0-54664
cylinder, ireal generating, soln. of displacements 0-54665
discs, elasto-plastic, transients 0-42057
divinyl isoprene rubber, heat evolution in shear deform. 0-50667
elastic body with prolate spheroidal inclusion, thermal stresses near inclusion analysis 0-69700
elastic-plastic bar with moving point heat source, stress-field anal. 0-38317
elastoplastic wave propagation, in rate-sensitive finite rod having thermal gradient 0-69692
fatigue, thermal, test methods, review 0-65418
fire-resistant materials, ultrasonic investigation of elastic props. 0-58843
generalized theory rel. to elastic fluid, low temp. effects 0-38316
infinite slab of an anisotropic material of constant finite thickness 0-60000
inhomogeneous plane problem 0-59996
laser-generation of stresses in transparent dielectric 0-45606

inhomogeneous plane problem 0-59996 laser-generation of stresses in transparent dielectric 0-45606 laser-generation of stresses due to impulsive e.m. energy deposition 0-38319

linear, uniqueness and continuous dependence in dynamical problems 0-52057

linear coupled theory with two temps. 0-76894

```
Thermoelasticity continued
```

magneto-microelasticity, wave-type eqns. 0-59999

metal response to relativistic electron beam absorpt. 0-78609

microelasticity, wave eqns. 0-59998 micropolar, plane problem 0-63400

micropolar, plane problem 0–63400 micropolar, plane problem of strain and stress 0–57361 micropolar, plane problem of strain and stress 0–57361 micropolar body, stresses induced by action of discontinuous temp. field 0–63401 non-linear, stress relation from general theory of incompatible deformations of elastic media 0–38315 polyisobutylene, heat evolution in shear deform. 0–50667 random temperature fields, viscoelastic materials 0–59995 Rayleigh's wave in medium with sinusoidal wavy boundary 0–63403 rubber-type, at high strain 0–78590 second-order effects, theory 0–55952 shells, heterogeneous, orthotropic cylindrical, solution of axisymmetric linear quasi-static eqns. 0–52058 slab solidification, anal. of thermal stress and displacement distribs. 0–39878 slab under continuous surface temp. steady-state stresses. 0–59997

slab under continuous surface temp., steady-state stresses 0–59997 sphere, non-homogeneous, incompressible, in periodic temp. field 0–54662

0-34062 stationary, deformation in a micropolar body 0-57363 stress distrib. in solid with external crack 0-52056 stress due to local heat transfer coeff. transients, numerical studies 0-54667

0-34007 stress-wave generation, by impulsive e.m. radiation in temperature-dependent absorbing solid 0-69699 stresses, thermal, in semi-infinite body with heat source on surface 0-52054

stresses due to thermoelastic strain in a composite shell, radical and shear-

ing stresses 0-63402 stresses in circular disc, transient behaviour 0-48824

stresses in circular disc, transient behaviour 0–48824 stresses in circular disc, transient behaviour 0–48824 stresses in unrestrained rectanguiar plate subjected to known temperature distribution method, extension of Kantorovich method 0–63399 thermal fatigue testing methods for material endurance, analysis 0–47426 thermor-heologically simple solid, linearized theory with infinitesimal deform, systematic derivation 0–42030 thermomechanical coupling effect on stability of nonconservative elastic continuous systems 0–45580 thick plate, three-dimensional series solution 0–48823 transient non-linear thermoviscoelastic behaviour, anal. 0–38320 transients due to local heat transfer coeff, perturbations, anal. 0–54666 transversely isotropic cylinder with smooth rigid insulating cover on curved surface 0–76893 vibration of infinite plate, dynamic thermoelasticity theory 0–38348 viscoelastic nonlinear media, approx. thermomech. constitutive eqns. 0–38311

wave-type eqns. of thermo-magneto-microelasticity 0-59999 As, Seebeck coeffs. 0-51135 CdF₂, elastic moduli, thermal expansion, Debye temp. 0-55939

Thermoelectric conversion see Electricity/direct conversion

Thermoelectricity

see also Thermocouples alkali halides, ionic thermocurrent bands interpret, by interfacial polarization model 0–79040 alkali metals, diffusion thermopower, calc., low temps. 0–47861 alkali metals, liquid, absolute thermopower, volume changes effects 0–61547

0-61547
alloys, dil. mag., thermopower 0-43963
alloys, thermopower meas. method at low temp. 0-68631
alumina, electron trapping, thermally stimulated currents obs. 0-47821
amorphous semiconductors 0-47721
butt-welding of chromel, alumel wires, thermoelectric effect investigation
0-71749
chalcogenide, quaternary, and Hall coeff., elec. conductivity, microhardness
and opt. reflectance 0-75821
chalcogenides, quaternary, props. 0-47860
cooling of Ge:Li gamma-ray detector and effect on resolution 0-46040
e.m.f. meas. cell for molten semiconductors 0-46941
e.m.f. meas. in microscopic regime, role of parasitic thermoelements
0-40886
effect on nonisothermal meas. in semiconductors 0-68846

effect on nonisothermal meas. in semiconductors 0-68846

ferrites, hexagonal, Seebeck coeff. anisotropy 0—59157 film, inhomogeneous, eddy currents 0—47859 generator, experimental solar 0—42161 generator, short-circuited, thermal efficiency, impurities influence 0—77020

generator, solar, influence of linear heat flux distribution on efficiency 0-42162

generator, solar, power characteristics 0–48972
generator, thermal-diffusion 'ageing' 0–77019
generator with hot and cold conduits, patent 0–54819
generators, solar, applications of selective coatings 0–42163
glass, chalcogenide, power, conductivity, opt. absorpt. and carrier mobility
0–44200

glass, semicond., electronic switching mechanism, electrothermal initiation $0\!-\!51028$

0–51028
graphite, characteristics, effect of high-temp. heating 0–59275
inhomogeneous material, thermo-e.m.f. interpret. 0–56369
ionic cryst., thermopower meas. 0–59276
liquid metals, absolute thermopower, volume changes effects 0–61547
liquid metals, power, critical discussion 0–68125
low-temperature, with tensile deformation, cryostat 0–76765
materials production, review 0–75820
metal, ferromagnetic, with mag. impurities, anomalous power 0–56368
metal, liquid, thermopower calc. from model potential for electron-ion interaction 0–43955
rel. to metal coating gauging, theoretical background 0–40434
metal film 0–44391
metal thin films. power comparison with bulk properties. 0–65339

metal film 0—44391 metal films, power comparison with bulk properties 0—65839 metals, second-order effects in electron-diffusion thermopower 0—62455 metals, thermoelec. power and resist., pseudopot. models 0—40712 metals, thermopower meas. method at low temp. 0—68631 metals containing magnetic impurities with crystal-field split energy levels, thermoelec. power 0—68970 modulated thermopower meas. system for recovery expts. 0—40292 molten salts, power and partial molar entropy obs. 0—39776 Mylar, corona charged, thermal currents 0—47823

Fhermoelectricity continued

Mylar film, thermally stimulated current spectra, traps, low temp, noise 0.44350

Mylar film, thermally stimulated currents, depolarization, high temp., low field 0 44351

perovskite, La₁, Ca,Fe₁, Mn,O₁ solid solns, resistivity and thermo-e.m.f. meas, and structure and mag. props. 0–43635 perovskite type cpds., book 0 68293 photoconducting If Vf cpds, temp. elec. instability, theory 0–72132 plasma, non uniform stream, and mag. induced currents 0–39563 polymers, organic, radiation induced trapped charge carriers, model 0 47865

0 47865
power meas, at high temperatures, specimen holder design 0—51855
prare earth sulphide and sclenides, specific resist, thermo e.m.f., 300
profit of 5686
Seebeck coefficient anisotropy in hexagonal ferrites 0—59157
Seebeck coefficient measuring device 0—75819
semiconducting materials, power and figure of merit, variational methods
for experimental investigations 0—44238
semiconductor, Bi₂Te_{1-x}Se_x, solid soln, elec. cond. 0—62457
semiconductor, Bi₂Sb₂Te_x, Hall coeff., magnetoresist., Seebeck coeff., 80
K 0—51034
semiconductor, Ge, field gradient voltage magnitude 0—79064
semiconductor, Ge, galvanothermal instability of current, 77 and 300 K
0—7574

semiconductor, HgTe, vapour crystal equilib., Hall effect, Seebeck coeff.

semiconductor, MnO:Li, thermoelectric force, dielectric losses, conductivity

or 78.344
semiconductor, MnO;Li, thermoelectric force, dielectric losses, conductivity temp, depend. 0. 44204
semiconductor, ZnSb films. 0. 65659
semiconductor, amorphous. 0. 53821
semiconductor, amorphous. CdGe,As₂, Seebeck coeff., elec. resist., temp, depend. 0. 79063
semiconductor, glass, electronic switching mechanism, electrothermal initiation. 0. 51028
semiconductor, imperfection centres, thermal and optical emission, capture rates, cross section. 0. 53839
semiconductor, molten. 0. 71372
semiconductor, plnSb, power temp, depend. 0—65672
semiconductor, plnSb, power temp, depend. 0—65672
semiconductor, vitreous, local states, photocond. 0—79071
semiconductor film, phonon drag contrib, to thermopower. 0—56233
semiconductor with nonparabolic energy bands, effect. of hot carriers. 0. 44388

semionicitor with nonparabolic energy bands, effect of hot carriers 0. 44388 semimetal Bi film, single crystal, power 0.–56370 size effect in alternating mag, field, phase transition determ. 0.–53950 stendy state equilib., in inhomogeneous materials, interpret. 0.–44029 steel microscopic inhomogeneities obs., contact thermoelectric power meas. 0. 68262 sulphates, high temp, cubic phase props. 0.–75412 IT4Cs thermoelectric materials and heat sources, closed loop ARGAS I, experiences, exptl. results. 0.–42156 tetracyanoquimodimethane, As TCNQ and P.TCNQ, anisotropy in (100), 200, 400K. 0.–79066 tetracyanoquimodimethane salt, Hall effect, cond. 0.–78959 rel. to thermally stimulated conductivity rel. to thermoluminesc. 0. 44931 thermoelectric power and elec, resist, near Curie point. 0.–40727 thermoelements, cascaded, design methods. 0.–51140 thermoelements, exacaded, design methods. 0.–51140 thermoelements, semiconducting alloy, electroplating rel. to bridging. 0. 44394 thermoelements, semiconductor, bridging solders for moderate temp, opera

thermoelements, semiconductor, bridging solders for moderate temp, operation 0-51141

tion 0=51141
thermopower, a.e. meas. 0--79060
transition metal, cubic, Fermi surface props. 0--79061
trap charact, parameters determ, from thermally stimulated currents
0 /1910

0 /1910
vanadium spinel, Seebeek coeffs. 0=79062
water pumping unit, solar, optico mechanical section 0=48975
water pumping unit, solar radiation concentrator, calorimetric investiga
tion 0=48976
Ag Au;Yb, dilute alloy, mag. susceptibilty, Kondo effects 0=44457
Ag Au alloy system, clee, and thermal cond., 3-300k, comp. depend
0=62456

Ag alloys with group B impurities Gorter Nordheim rel, deviation, impurity interactions 0–51137 AgBr+ alkali bromides fused, 700°C 0–64948 AgCl:Ti³¹(V³¹,Cr¹¹), dipolar point defect relaxation, ionic thermo-current

AgC1:Ti(Vi), Cr¹¹), dipolar point defect relaxation, ionic thermo-current 0.75.12.7

AgC1: alkali chloride fused, 800°C 0.—64947

n Ag; Te, carrier effective mass, i.r. reflection spectra, elec. props. 0. 44186

Ag; Te, carrier effective mass, i.r. reflection spectra, elec. props. 0. 44186

Ag; Te, carrier effective mass, i.r. reflection spectra, elec. props. 0. 44186

Ag; Te, carrier effective mass, i.r. reflection spectra, elec. props. 0. 42186

Ag; Te, carrier effective mass, i.r. reflection spectra, elec. props. 0. 42186

Ag; Te, carrier effective mass, i.r. reflection spectra, elec. props. 0. 4292

Ag; Te, Quanisotropy in (100), 200 400K 0.—79066

Au; Al thermocouple, thermopower meas. 30-150°C 0.—79060

Au; Fe, dit, alloy, power, effect of mag, ordering, 4. 300°K 0.—44392

B; B; power high temp. 0.—56251

Ba; TiO₃, reduced crystal, Seebeck coeff., elec. cond., Curic point, polaron hopping 0.—62349

Ba; TiO₃, thermocurrents, phase transition obs. 0.—68953

Bi; Mi liquid solutions, (M. Mg, Hg, As, Te, Se and S. additives), absolute thermopower meas. 0.—74781

Bi; Sb; Te alloy, thermal cond., comp. depend. 0.—40595

Bi; film, single crystal, elec. resist., Hall coeff., magnetoresist., Seebeck coeff., 80 K. 0.—51034

Bi₄, Sb₁, Te, 48e₆, solid solution, foridden band width, temp. depend., 80, 700 K. 0.—62361

Bi; Te, **Lee, solid solution, foridden band width, temp. depend., 80, 700 K. 0.—62361

Bi; Te, **Lee, solid solution, foridden band width, temp. depend., 80, 700 K. 0.—628637

Bi; Te, **Lee, solid solution, foridden band width, temp. depend., 80, 700 K. 0.—62867

Bi₃Fe₅ thermoelements, Cu as donor impurity, Hall coeff., conductivity mens. 0 - 65837
Bi₃Fe₄ solid soln., figure of merit, elec. cond. 0 - 62457
Bi₃Fe₄ + Bi₃Se₅ thermoelement half cells, annealing effects 0 - 68972
Bi₃Fi₄ + Bi₅Se₅ thermoelement half cells, annealing effects 0 - 68972
Bi₃Fi₄ - Bi₅Si₅ solid solution, Seebeck coefficient, effect of magnitude of imital particles, quantity of additives and production technology obs. 0 51132
Cd. lq., power 0 - 53371
Cd₄As₅ Cd₃P₅ semiconducting solid solns, thermoelectric figure of merit 0 65469

Thermoelectricity continued

amorphous, Seebeck coeff., elec. resist., temp. depend. CdGe_xAs₂, 0--79063

CdGe_xAs₂, vitreous, thermopower 0-75681

CdGe, As₂, vitreous, thermopower 0–75681
CdS, hole traps, photo-thermoelec. meas. 0–51147
CdS, Se_{1-x} films, adsorption influence 0–56380
CdSb, props., effect of donor and acceptor impurities 0–65840
Co alloys, dil., power 0–50979
CoO, Seebeck coeff., small polaron vs. band cond., elec. props. 0–56262
CrBr₁, Seebeck voltage and resist., photocond., temp. depend. 0–75547
CrSi₂, power anisotropy mechanism 0–72022
Cu alloys, phonon-drag thermoelec. power 0–40887
Cu alloys with group B impurities, Gorter Nordheim rel. deviation, impurity impurity interactions 0–51137
CuMSe₂, (M=Ga, In, As), liq. and solid, energy converter applic. 0–78298
Cu₂O, hole trap level, thermally stimulated current obs. 0–75715

Cu₂O, hole trap level, thermally stimulated current obs. 0-75715

Cu₂O, hole trap level, thermally stimulated current obs. 0–75715 Cu₃Ds_Cs, liquid 0–46947 Cu₅C. thermal e.m.f. coeff. related to stoichiometric index 0–65836 Cu₇TlS_Cs, liq. and solid, thermopower 0–78937 Eu₂S₄. Seebeck coeff. rel. to phase transform. at 168K 0–71798 Eu₃S₄, Seebeck coeff. rel. to phase transform. at 168K 0–71798 Eu₃S₄, lec. cond., 100 1000°K, electron hopping 0–40770 α-Fe₂O₃, n-type with Sn or Ti impurities, Seeback coeff. 0–78917 α-Fe₂O₃, small polaron vs. band cond., elec. props. 0–56262 Fe₂O, Seebeck coeff., cond., high temp., hopping mechanism analysis 0–65624 Gain porous glass, power, temp. depend., 80-315K, size effect 0-56183 GaAs:Fe, e.p.r. of Fe³⁴ optical charge exchange, thermally stimulated current 0-48144

GaAs; Fe, e.p.r. of Fe^o optical charge exchange, thermally stimulated current 0-48144
GaAs: CdS solid solns., differential thermal e.m.f. 0-65669
GaAs, two carrier photothermoelec. effects 0-62461
GaTe, rel. to thermal cond. 0-55608
Gd, thermomag, and thermo e.m.f., 90-250k 0-68971
Ge, field gradient voltage magnitude 0-79064
Ge, galvanothermal instability of current, 77 and 300 K 0-75724
Ge thin film, vacuum deposited, Seebeck coefficient 0-47862
n. GeSi, neutron irrad, Seebeck coeff. 0-44198
GeTe Ga(In)Te solid solns. 0-72028
GeTe, effects of gamma radiation 0-44389
GeTe, effects of gamma radiation 0-44389
GeTe, effects of yellow for the film of the film

 $In_{0.5}Ga_{0.5}Sb:Te,$ elec. cond., Hall effect, magnetothermoelec., cond. band, 300K 0-40785

300K 0-40785
n-InP, thermoelectric power, Nernst- Ettingshausen thermomagnetic effect, 100 600K 0-51138
p. InSb, power temp. depend. 0-65672
InSe, liquid 0-46947
KBr. p- and neutron irrad., thermally stimulated conductivity, 10-300K
0-47863

0–47863
KBr, thermopower meas. 0–59276
KBr, Check Carlon Control Contr

0 75685
Mg-Bi, liquid alloy, comp. depend. 0-46945
Mg-Sm, elec. props., temp. depend., 80-800 K 0-44203
MnO:Li, conductivity, thermoelectric force and dielectric losses temp. depend. 0-44204
MnO, Seebeck coeff., small polaron vs. band cond., elec. props. 0-56262
MnOy, Mn,Oy, Seebeck coeff., meas., 25-125°C 0-65673
MnSi, elec. and thermal props. 70-700 K, zone struct., scattering mechanism 0-40707
Mo, neutron irrad., annealed, elec., resist. 0-40725

ism 0-40707
Mo, neutron irrad, annealed, electresist. 0-40725
NaBr, thermopower meas. 0-59276
Nb Ta alloy, properties 0-51136
Nb-Zr alloys, properties 0-51136
Ni-Cr, resistivities and Seebeck coeff. in 50-1000°C range, meas. 0-44037
Ni Cu, resistivities and Seebeck coeff. in 50-1000°C range, meas. 0-44037

0–44037

Ni-Pt-P alloys, amorphous, power 0–53781

Ni, Curie point region, anomaly, temp. depend. 0–44063

Ni, temperature depend. near Curie pt. 0–40727

Ni and dilute alloys, absolute power, temp. variation 0–47864

Ni,Fe, seeback coeff. from 80 to 400°K 0–68534

NiFe; O₁ Fe; O₂, power, and resistivity 0–56372

NiO, Seebeck coeff., small-polaron vs. band. cond., elec. props. 0–56262

Ni₁ S, temp. depend., 83-273 K, semiconductor-metal transition 0–79065

0–79065
P-TCNQ, anisotropy in (100), 200 400K 0–79066
PbSe, effects of gamma radiation 0–44389
Pb_{0.7}5n_{0.3}Te, figure of merit at room temperature, results 0–65838
PbTe-SnTe, solid solution, elec. props., temp. depend., 80-300K 0–44206
Pd-H alloys, low temp. thermopower and residual resistivity 0–62310
Pd H dil. alloys, thermopower, virtual recoil evidence 0–59277
Sb. turning effect, effect of hydrostatic pressure, and band structure 0–51139
Sb. Se. liquid 0–46947

0-31137 Sh₂Se₁, liquid 0-46947 n Si:P(As)(Sb) thermopower rel. to thermal cond., 4-300 K, phonon drag 0-50909

0-59909
p-Si, photothermoelec, effect, anomalous 0-78995
n.n.SiC, weakly- and strongly compensated 0-56265
SnSb, thermo e.m.f. 0-40422
SnTe, rel. to thermal cond. 0-55608
Ta. Nb alloy, properties 0-51136
TiC, characteristics, effect of high-temp, heating 0-59275
TiH_x, power meas. 0-44001
TiO₂, thermocurrents, phase transition obs. 0-68953
TI-Te, molten alloy, comp. depend., semiconductor-metal transition 0-46948
TI-Te, molten alloy, resistivity and Seebeck coeff. comp. depend. TI-Te, molten alloy, resistivity and Seebeck coeff., comp. depend. 0-43474

Tl₂Te.As₂Te₃, vitreous, Hall effect, elec. cond., temp. depend. 0-47728

Thermoelectricity continued Thermoluminescence continued Frmoelectricity continued
UN, Seeback coeff., elec. and thermal cond., 77.400K 0–47562
V-N(O) solid solution, comp. depend. 0–58983
V₂0₂-P₂0₂, glass, d.c. and a.c. conductivity, comp. depend. 0–47630
V₀2, doped power, 100-200 K 0–56267
V₀0₁, elec. resist., temp. depend. 0–72034
V₂0₃1, elec. resist., temp. depend. 0–72034
Zn, liq., power 0–53371
ZnSb films 0–65659
Zr.Nh alloy, properties 0–51136 $^7\text{LiF},$ energy depend, for high energy electrons, X-rays and $^{60}\text{Co}\ \gamma\text{-rays}$ $0{-}48114$ 0-48114
MgO cryst, phosphorescence and X-ray stimulated luminesc. 0-54121
NaCl:Cu thermostimulated luminescence and thermal bleaching, role of activator ions 0-56638
Na₂O:SiO₂ glass, rel. to colour centres annealing 0-76183
PbX₃, (X=F, Br, I), X-irrad₃, and glow peak spectra 0-62734
SiC, acceptor-donor pair obs. 0-79380
ThO₃, study of electron hole traps by e.s.r. and n.m.r. 0-56650
Y activated with Eu, cathodic excitation 0-62735
YO₃, study of electron hole traps by e.s.r. and n.m.r. 0-56650
ZnO powder, application of new calculation method on glow curve 0-69163
ZnO, unactivated, electron-beam excited, obs. 0-56639
ZrO₃:Ce, Nb, UO₃. Tl or Pb ions, spectra obs. 0-69164 Zr-Nb alloy, properties 0–51136 ZrH_x, power meas. 0–44001 ZrO₂ stabilized with CaO and MgO, thermoelec. power 0–44393 Thermoluminescence alkali halide crysts., photostimulated 0–76180 alkali halide crysts., photostimulated 0–76180 alkali halides, colour centre form. and excitonic processes 0–78565 calorimetric coeffs. of luminesc. radiation 0–56633 dating of volcanic lava 0–69267 rel to dosimetry, test system ans and method, patent 0–59829 dosimetry phosphors, thermal quenching of X-ray excited radioluminesc. 0–41279 Thermomagnetic effects see Magnetothermal effects Thermomagnetic effects see magnetionermal ejects
Thermometers
see also Pyrometers; Thermocouples
acoustic, systematic errors 0—48848
carbon, fast, effect of mixed particle sizes 0—73077
cryogenic, characts, and appls. 0—79811
gas, for student work 0—63484
glass, depression constants 0—50337
noise thermometry, absolute low term. Josephson el 0-41219
fission fragment induced, in CaF₂ 0-79375
glass, Na₂O-SiO₂, rel. to colour centres annealing 0-76183
halophosphates, glow curves 0-56634
n-heptane, exp. investigation 0-72449
hydrocarbon polymers, thermoluminescent props. 0-48115
hydrocarbons, saturated, glow curves rel. to O₂ mols. as electron traps
0-4183 plass, depression constants 0-30337 noise thermometry, absolute, low temp., Josephson effect applic. 0-44151 photothermometer, response to thermal shock 0-48890 response, generalized analysis and prediction 0-42105 semiconductor diode, low temp. 30-300°K 0-76947 sensitiosrs, silicon bulk resistance sensors, stability and sensitivity 0-66954 U-41283 lunar samples 0-45388 phenomenological theory 0-44930 phosphors, dosimetry, quenching of thermoluminesc. for six materials 0-44928 phenomenological theory 0—44930 phosphors, dosimetry, quenching of thermoluminesc. for six materials 0—44928 phosphors, study of energy spectrum of electronic states 0—56632 polyethylene, glow curves and electron traps 0—59442 polyethylene, glow curves rel. to 02 mols. as electron traps 0—41283 quartz, dating, and e.s.v. detection of fossil alpha damage 0—50597 radio, branched polyethylene 0—41282 radio, isotactic polypropylene 0—41282 radio, isotactic polypropylene 0—41282 radio, isotactic polypropylene 0—41282 radio, examination using rapid scanning spectrometer in range 200-850 nm 0—49151 squalane, glow curve peaks rel. to glass phase transitions and melting point 0—54130 tektite dating 0—45427 rel. to thermally stimulated conductivity 0—44931 thick targets, proton induced 0—62731 urea, X-irrad. 0—61940 BN powders 0—59440 CaF₂: Nd, X-irrad. 0—64940 CaF₂: Nd, X-irrad. 0—649495 CaF₃, energy depend, for high energy electrons, X-rays and ⁶⁹Co ρ-rays 0—48114 CaF₂, fission fragment induced 0—79375 CaF₂, prirad. natural cryst. glow peak obs. 0—72451 CaF₂, patural, neutron dosimetry 0—76733 CaF₂, optical density, 240-600 nm, afterglow, u.v. and X-irrad. 0—44918 CaF₂, surface thermoluminesc. yield, crushing effect 0—66113 CaF₂ energy response to high energy radiations 0—62732 CaF₂ glow peaks, optically produced 0—79378 CaF₂ powder, difference between first band of spectra emitted by 10⁴R and 10⁶R irradiated 0—76181 CaO:Sm phosphor thermoluminescence obs. 0—51365 CaS:Bi phosphor, effect of 14 jaoms 0—72444 0-6954
superconducting film use in sensitive temp. meas. 0-71990
thermistor, linearity 0-44274
thermistors, stability and sensitivity 0-66954
thermocouples, stability and sensitivity 0-66954
time lag, effect of humidity and press. 0-41489
unijunction, for Project Rulison 0-76948
vapour press. meas. of cryogenic liquids using capacitance diaphragm
manometer for low-temp. thermometry 0-50332 resistance
bead thermistor, fluid temperature and flow speed fields meas., use of high speed digital system 0—48893
construction and performances, accuracy and stability 0—60092
Ge, computer fitting of characteristics 0—76946
platinum, wire, stability and sensitivity 0—66954
potentiometers use 0—73076
psychrometer, aspirated, continuously recording dry-bulb and wet-bulb temperatures 0—48271
C resistors 77-200K, theoretical and expt. values 0—41908
Ni-ferrite applications 0—72264
Pt, pressure dependence, over 1 to 1000 b range 0—76945
Pt, rugged, stable, differential, construction calibration and testing 0—48895
Pt film on Pyrex glass, for meas. of surface temps. in nucleate boiling of water 0—48894
Si, sensitive surface layer, meas. below 20°K, preparation and applications 0—45669
ermonuclear devices Thermonuclear devices see Plasma/devices Thermonuclear reactions see Elements/origin; Nuclear fusion see also Elements/origin; Nuclear Jusion
explosion, fractional burn-up of fusion fuel for optimum conditions
0-49674
fusion, controlled, microwave formation and heating of hydrogen plasmas
0-46687 CaF₂ powder, difference between first band of spectra emitted by 10⁴R and 10⁴R irradiated 0—76181

CaO:Bi phosphor thermoluminescence obs. 0—51365

CaO:Sm phosphor thermoluminescence obs. 0—51365

CaS:Bi phosphor, Efect of Di atoms 0—72444

CaS:Th, Zr phosphors 0—41280

CaS:Zr(Mn) phosphor, study 0—62730

CaS:Dr, Zr and Mn activated, trap depth calculation 0—79376

CaSO₄, thermostimulated emission and thermostimulated luminescence curves compared 0—56635

CaSO₄, phosphor, Mn- and Pb-doped and exo- electron emission, effect of activators conc. 0—47888

CaSO₄, phosphor, Mn- and Pb-doped and exo- electron emission, effect of activators conc. 0—47888

CaSO₄, phosphor, Mn- and Pb-doped and exo- electron emission, effect of activators conc. 0—47888

CaSO₄, phosphor, Mn- and Pb-doped and exo- electron emission, effect of activators conc. 0—47888

CaSO₄, phosphor, Mn- and Pb-doped and exo- electron emission, effect of activators conc. 0—47888

CaSO₄, phosphor, Mn- and Pb-doped and exo- electron emission, effect of activators conc. 0—47888

CaSO₄, phosphor, Mn- and Pb-doped and exo- electron emission, effect of activators concentration e.m.f., thermostimulated luminescence, and radioluminescence 0—56636

CsI thermostimulated vertorn emission, thermostimulated concentration e.m.f., thermostimulated curven and adioluminescence 0—56636

CsI thermostimulated vertorn emission, thermostimulated concentration e.m.f., thermostimulated vertorn and adioluminescence 0—56636

CsI thermostimulated vertorn emission, thermostimulated ve 0-46687
fusion, functional method for nonlinear problems 0-78047
fusion of laser-produced plasma 0-74006
high current techniques in R & D 0-39587
initiation by glass laser, possible application to power generation 0-39158
ionosphere F2 region, decrease in electron density after American 'Starfish'
burst (1962) 0-56845
ionospheric disturbances due to the American 'Starfish' burst (1962)
0-56837 isotope production technology 0-74016 nucleosynthesis conditions in neutrino-transport supernova models 0-48446 0—48446
plasma shock waves, review 0—46702
in stars, carbon burning rate, ¹²C + ¹²C reaction cross-section 0—79654
in stars, explosive nucleosynthesis in mass range 20≤A≤62 0—69385
Thermosphere see Thermocouples
Thermosphere see Atmosphere/upper; Ionosphere Thermostats

see also Cryostats
automatic control system for thermal regulation, stable operation over wide
temp. range 0-45706
system in equilibrium with thermostat, thermodynamic functions 0-76949
YFe garnet radiometer and temperature controller 0-76931
Theta pinch see Plasma/confinement Theta pinch is eee Plasma(confinement)

Thickness measurement

Thickness measurement

Thickness measurement

see also Particle size
by X-ray fluorescence methods 0–65053
by X-ray fluorescence of layers and multilayers 0–48113
composite targets, determ. of partial thickness 0–52582
dacron coatings thin using electron excited p-ray source, method 0–50362
dielectric film, monitoring using Michelson interferometry 0–78370
double layer in semiconductor technology, nondestructive optical method
0–53428
electron backscattering method, of light coating of light metal or alloys
0–74892
with electron probe micoranalyzer 0–56716
epitaxial films, automatic method 0–65076
epitaxial films, ir. multiple reflection, interpretation 0–65063
film, X-ray reflection 0–74894
film, delipsometric technique 0–71462
films, by multiple-beam interference microscopy 0–39934
films, semiconductor epitaxial, ir. reflectance method 0–65064
films, thin, in inaccessible locations with scanning electron microsope
0–74893
group II-VI cpds, by X-ray fluorescence methods 0–65053

group II-VI cpds., by X-ray fluorescence methods 0-65053

Thulium compounds

Er-Tm, h.c.p., low temp. meas. of sp. heat 0-75406 TmAg, neutron diffraction 300°-1.7°K 0-58760 TmAl garnet, n.m.r., paramag. props. 0-45022 TmAl₃, nulc. quadrupole coupling and cryst-field effects 0-76235

Thulium compounds continued TmAu₃, neutron diffraction 300°-1.7°K 0–58760 TmC₂, neutron diffraction 300°-1.7°K 0–58759 TmCl₃,6H₂O, Tm₃(SO₄)₃,8H₂O, Zeeman splitting between Stark levels of Tm³⁺ (4f²) 0–76111 Thickness measurement continued interference films, vacuum- deposited, control of thickness 0-50379 of light coating of light metal or alloys, electron backscattering method 0-74892 Tm³⁺ (4f¹⁻²) 0-76111 Tm₂Fe₁₇, Mossbauer effect, mag. props., temp., depend. 0-44796 TmFeO₃, ferrite, magnetostriction anisotropy 0-75964 TmFeO₃, optical Zeeman spectra, spin Hamiltonian for even-electron singlet states 0-51313 TmFeO₃, single crystal orthoferrite, antiferromag. Fe³⁺ sublattices, 78-720K 0-51241 Tm₂O₃, 1"2"b elec.-quadrupole interactions, perturbed-ang.-correl. obs. iliquid thin film of isobutanol dissolving in water, structure 0–39718 photocathode films, GaAs(Cs) and GaAs(Cs-O), chemical analysis 0 - 79107plastic sheet, gauging head assembly, patent 0-55751 semiconductor wafer etching, monitoring by internal reflection interferometry 0-50411 rometry 0–50411 Al coatings thin using electron excited γ -ray source, method 0–50362 Al₂O₃/Al, porous anodic film, transport numbers, structure 0–53922 Al₂O₃, anodic alumina film, ellipsometry 0–54056 Al₂O₃, anodic film, ellipsometry, el. to ion current efficiency 0–47043 Au coatings thin using electron excited γ -ray source, method 0–50362 CdS film, by X-ray fluorescence methods 0–65053 CdS thin film, effect of deposition rate on semiconducting properties, obs. at 2, 9, 16 Å/sec 0–50389 Co film, using ultramicrotome cuts and electron microscopy 0–71463 Cu, oxide film, reflectivity method 0–47044 p-Cu_{2-x}S film, optimum on n-CdS, photocell, electron diffusion method 0–39938 0-44800 Tm₂O₃, cold pressed, variables in fabrication 0-58968 Tm₂O₄, elastic consts. of polycryst., 20-1000°C 0-58858 Tm₂O₃, high temp. behaviour 0-58961 Tm₂O₃, sintered wafers, fabrication and irrad. 0-58992 Tm₂O₃, thermal expansion, 100-300K, X-ray powder diffr. 0-50895 TmOOH, mag. props., Mossbauer obs. 0-56515 Tm(ReO₄), 4H₂O, single crystals, absorption spectra 0-48078 Tm₂(SO₄)₃.8H₂O, mag. props., Mossbauer obs. 0-56515 TmSb, susceptibility and high-field anisotropic magnetization, rel. to crystal field effects 0-40953 0-39938 Si epitaxial and oxide layers, interferometry 0-47046 Si₂N₄, single and two-layer coatings, meas. by i.r. spectroscopy 0-50364 SiO₂, single and two-layer coatings, meas. by i.r. spectroscopy 0-50364 SiO₂ layer, ellipsometry 0-76016 SiO₂ layers, by interference method 0-61639 Thunderstorms understorms see also Lightning detection and presentation by radar 0-48264 electrical charge density and field strength, rapid increases due to atmospheric feedback process 0-48279 mass outflow from thunderstorm complex rel. to tornado formation, study from ATS III 0-79530 mathematical model of thunderstorm in conducting atmosphere, solns. Thin films see Films; Films, solid Thirring model see Elementary particles; Field theory, quantum Thixotropy suspensions, model 0–71391 Thomas-Fermi method see Atoms/structure Thomson effect see Thermoelectricity 0 - 51518objective prediction for use at Eglin, Florida 0-79516 bolicative producing, synoptic and dynamic anal. of outflow using ATS III pictures and rawinsonde data 0–79531 whirls, fully developed, steady-state structure properties 0–51521 Thomson effect see Thermoelectricity Thorium on W, adsorption of CO, partial surface coverage effect 0—39978 abundance in lunar samples, and isotopic composition 0—48496 abundance in lunar samples 0—45336 abundance in lunar samples by alpha-particle activity 0—45350 abundance of isotopes in linear samples rel. to age determ. 0—45334 abundance of isotopes in lunar rock samples 0—48492 diffusion in pyrocarbons, thin-layer expts. 0—78577 diffusivity, high purity sample, meas. in temp. range 120 to 1000°K 0—68378 gammaraus inelastic scatt by K shell electrons 0—39302 Thyratrons see Gas-discharge tubes Tides see Atmosphere/movements; Ionosphere; Oceanography Time interval measurement synchronization of distant clocks by T.V. pulse comparisons 0-76793 Time measurement ATA time signals, accuracy 0–76790 clock synchronization by T.V. pulse comparisons 0–76793 frequency standards, precise, establishment, and equipment to maintain them 0–72871 gamma-rays inelastic scatt. by K shell electrons 0—39302 preparation by vacuum distillation of electrodeposited Th-Cr(Mn) alloys 0—43797 them 0-728/17 high precision, atomic and astronomical methods, Marquette Lab. facilities 0-38127 high precision, atomic and astronomical methods 0-45134 CS clock rates, apparent diurnal variation, explanation 0-48673 Cs beam atomic standard 0-58121 in rare earth, determination using p-ray spectrometry, radiometric nondestructive method description 0-51450 spectrum, emission, Fourier spectroscopy using 106 samples 0-70086 in tektites and achondrites, rel. to uranium content, appl. of lunar rock composition data 0-45102 Cas:Th, Zr phosphors, decay and thermoluminesc. 0-41280 Th I energy levels computation and proposed secondary-standard wavelengths 0-42982 237Th recompose integral for infinite dilution absorption and activation. atom, isotopic shifts in u.v. 0-60930 creep, influence of superconducting transition, deformation creep curve 0-75261*** Wavelengths 0--232**Th resonance integral for infinite dilution absorption and activation 0--52783 0-75261 dendrite, computer-generated motion picture of morphological development 0-47148 diffusion in Zn, 298-400K 0-43700 diffusion of Tl, vol. and grain-boundary type in polycryst, samples 0-40206 O-52783 Thorium compounds Ni-Cr-(1 wt.%)ThO₂ alloys, oxidation 1200°C 56703 0-56703 Th-Gd alloys, supercond., thermal cond. 0-40747 Th Uc fuel particles coated with pyrolytic-C, SiC, irradiation performance 0-46312 ThC-H₂, X-ray exam. and p.m.r. 0-68317 ThCu₆ alloy, crystal structures 0-43642 Th,Fe₃,ThFe₃, ThFe₅, and Th,Fe₁₇, Mossbauer study 0-44799 ThH, subthermal neutrons inelastic and quasielastic scatt., mode obs. 0-68582 Th₂N₂X, X=Sb, Te, and Bi, crystal structure 0-61911 ThO₂:Co⁵⁷, low-temp. anharmonicity, Mossbauer obs. 0-71833 ThO₂:Gd³⁴+, e.p.r., spin-lattice strain coeffs. 0-72292 ThO₂:Np⁴⁺, dynamically induced forbidden elect-dipole transitions 0-54101 ThO₂-Ni, ThO₂-NiCr, shock-loading, thermal recovery 0-75307 effect on Zn electrodeposition, aqueous KOH, dendritic growth 0-72550 elastic guided waves in films on Cu, Al, Ni, vel. dispersion, 5-45 MHz 0-47336 effect on Zn electrodeposition, aqueous KOH, dendritic growth 0—72550 clastic guided waves in films on Cu, Al, Ni, vel. dispersion, 5-45 MHz 0—47336 electron mean free path, obs. from radio-frequency size effect 0—75516 electron mean free path, obs. from radio-frequency size effect 0—75516 electron mean free path, obs. from radio-frequency size effect 0—75516 electron mean free path, obs. from radio-frequency size effect 0—75516 electron mean free path, obs. from radio-frequency size effect 0—75516 electronic props., ang. correl. of annihilation photons obs. 0—40697 film, superconducting, critical currents 0—71979 film, superconducting props. and struct. rel. to deposition 0—56208 film, superconductivity critical transition temp., 'growth and struct. depend. 0—75625 films evaporated on NaCl, struct. and growth, obs. 0—58578 grey, band struct. and optical spectra 0—71926 Hall effect, oscillatory, due to magnetic breakdown 0—53782 impurity atoms in LiCl, NaCl, and KCl, Mossbauer effect 0—54077 internal friction, time and orientation dependent 0—50673 ions production using ion-source, description 0—51163 amellae, dislocation and deformation twinning 0—65327 liquid, flow pattern and velocity in square enclosure, radioactive tracer techniques 0—50174 liquid, low-energy Ar¹ sputtering yields 0—78809 liquid, solution growth of Nb₃Sn 0—47131 liquid, struct., slow neutrons transverse scatt. cross section obs. 0—39731 liquid, structure, y-radiography, 220, 235, 260, 400, 450°C, radial distrib. functions 0—46869 liquid, surface tension and density, 240 to 844°C 0—68086 liquid surface, low-energy electron diffraction 0—55589 melting and freezing of single-cryst. surfaces, LEED 0—53418 metallic, galvanomagnetic and thermomagnetic effects obs., at 1.2 to 4.2°K, to 3.3 tesla 0—51134 molten sound absorption meas. in 60-100 MHz range 0—61516 Mossbauer isomer shift of ¹¹⁹Sn, pseudopot. approach 0—59381 phase transformation, β-α, kinetics, Mossbauer effect 0—75341 pion 8 GeB beam, energy density distribution using linear int 0-54101 ThO₂-Ni, ThO₂-NiCr, shock-loading, thermal recovery 0-75307 ThO₂-Uo, solid solution, oxidation behaviour 0-48198 ThO₂, adsorption kinetics of ethanol, diethyl ether and water 0-74930 ThO₂, anion deficiency 0-53452 ThO₃, a-bombarded, strain effects and spalling 0-55877 ThO₂, e.s.r. of Pb³+ centres 0-79408 ThO₇-x(OH)_{2x}-yH₂O amorphous precip., comp., i.r. and thermal analysis 0-51312 ThO_{2-x}(OH)_{2x}-yH₂O amorphous precip., comp., p.m.r. obs. 0-51412 ThO₃, 1¹⁵³Gd³+ epr, hfs, forbidden lines obs. 0-62764 ThRe₂, ThTC₂, superconducting transition temp. and lattice struct. determ. 0-71985 UO₂-ThO₂ system, solidus and liquidus temps. 0-58523 bilium hyperfine interactions, elec.-quadrupole at ¹⁷²Yb 0–44800 magnetic anisotropy, meas. 0–75924 magnetic form factor, 4.2°K 0–44665 magnetic form factor, 4.2°K 0–44665 magnetic form factor, 4.2°K 0–44665 magnetic structure, temp. depend. of periodicity 0–44508 specific heat, nucl., due to hyperfine interactions 0–43910 vapour, i.r. laser lines 0–49778 Tm I, oscillator strengths of spectral lines in 6000-2450 Å region 0–42944 Tm I spectrum, optical double resonance expts., g_j values determ. 0–39287 Tm III, energy levels and Slater parameters, obs. 0–60931 Tm III spectrum, 848 low-excitation lines and their analysis 0–42984 Tm²⁺ in fluorite, calc. of crystal field parameters 0–51246 Tm³⁺, absorption spectrum in LaF₃ 0–41212 Tm³⁺ cpds., Mossbauer effect, h.f.s., mag. ordering 0–76053 Tm³⁺ in ZnS_x.CdS_{1-x} phosphors, forbidden gap width, effects on the luminescence yields 0–56612 Tm³⁺ spin-lattice relax. in alkaline earth fluorides 0–44723 Tm³⁺(4ft ²), Zeeman splitting between Stark levels in chlorides and sulphates 0–76111 ultium compounds Thulium 10-4013 resonant γ scatt., nuclear reaction channel suppression 0-48042 single-crystal whiskers, one-dimensional onset of quantized thermal fluctuations 0-78902 specific heat, thermal expansion calc. of solid and liquid state, results 0-59110spheres, thermal emissivity for various values of particle radius 0-66933 spherical, orientation determ method 0-61699 sputtering of low-energy Ar⁺, yields 0-78809 superconducting, differential resistance, magnetoresistance effect 0-75624

superconducting cylinder, hollow, meas. of quantized flux states 0-44140 superconducting film, critical currents 0-71979

superconducting film, magnetic flux penetration 0-78903

Tin continued

superconducting film, nonlinear props. in u.h.f. field, 1.5-4.2°K (0-44137 superconducting whiskers, anomalous paracond, above T_c (0-71984 on surface of glass, determ. of microgramme amounts (0-53422 thin films on Mo(100) (0-47121)

on surface of glass, determ. of microgramme amounts 0-3422 thin films on Mo(100) 0-47121 trace determ. in Ni base alloys, emission spectrographic carrier-distillation method 0-56729 wetting, rel. to GaAs Schottky barrier diode fabrication 0-44296 whisker, anomalous paracond. above supercond. Te 0-71984 whisker growth, tracer expts. 0-53466 white, dislocation motion from etch hillock obs. 0-78557 white, dislocation motion from etch hillock obs. 0-78557 white, elastic moduli, three-body ionic interaction, calc. 0-43712 white, n.m.r., pseudodipolar interaction radial depend. 0-41386 white, three-body forces role in dynamical props. 0-50851 X-ray spectral determination by internal standard method 0-59517 Al-Sn multilayer composite, ultimate tensile strength 0-50715 in Cu-Zn alloys, additive effect on stress corrosion cracking 0-40409 in Ni, additive effect on Elinvar prop. 0-58855 Sn/Pb bilayer, forbidden band determ. rel. to temp. 0-78891 Sn-Sn junction, Josephson current, effect of fluctuations on mag. field strength depend 0-51015 Sn-Sn-Sn tunnel junctions, microwave-photon-assisted tunnelling 0-71992

0 - 71992

0–11992 α -Sn, dielec. enhancement and mobility 0–78956 α -Sn, interband magnetorefl. 0–76028 α -Sn, ionized-impurity-limited mobility in RPA 0–50932
Sn I, $(Sp_{1/2}Sd_{5/2})_{2-2}$ state, energy shifts in elec. field 0–64223 β -Sn isomer shift temp. depend. 0–41170
Sn²⁺ activators in luminesc. electrolytes, spectra characts. 0–43455

Tin compounds

alloy plating, contact resistance, atmospheric exposure effect 0-65635 hexachlorostannate(IV) salts, crystal lattice effects in n.q.r. spectra

0-1216 tetravinyltin, vibr. spectra and molec. struct. 0-77847 ¿-Ag-Au-Sn alloy, axial ratio changes 0-71565 Ag-Sn alloy contact, resistance failures of Ag contacts due to corrosion 0-56174

Ag-sn anoy contact, resistance failures of Ag contacts due to corrosion 0-56174

Al-(0.96 wt.%)Sn, surface struct. on heating and subsequent cooling, rel. to oxide film 0-78364

Al-Sn, liquid alloy, Cowley short range order parameter, X-ray exam. 0-58442

Al-Sn liqui solns, elec. resistance 0-39831

Al-Sn molten alloy, X-ray scatt. struct. meas. 0-64865

As-Se-Sn, semiconducting glass, Mossbauer effect, Sn valency, comp. depend. 0-48026

BaTiO₃-SnO₃ solid solns, truncated cone capacitor nonlinear semiconducting props. 0-44370

Bi-Sn alloys, interface instability and microsegregation 0-74835

Bi-Sn eutectic, nucleation and growth 0-50474

Co-Sn alloy, morphology rel. to undercooling 0-61850

Cu-Sn, martensitic transform, temp. and time depend. of internal friction 0-71670

Cu-Sn alloy, liq., atomic distrib., X-ray diffr. obs. 0-61486

Cu-Sn alloy, liq., atomic distrib., X-ray diffr. obs. 0–61486 Cu-Sn alloy, thermal expansion from lattice parameter-temp. curves 0–43919

0-43919
Cu-Sn alloy, X-ray absorption investig. of electronic structure 0-68734
Cu-Sn alloys, intercryst, internal adsorption 0-61856
Cu-Sn bronzes, contact with C-Mn steel, wear obs. 0-50750
Cu-Sn liquid alloys, atomic distribs. 0-74724
Ga-In-Sn system, ternary eutectic, 10.7°C 0-78333
(62 wt.%)Ga-(25 wt.%)In-(13 wt.%Sn, liq, resist, thermometer 0-54784
In-Ga-Sn, eutectic, elec. resistance in melting region, 280-310K 0-74842
In-Sn alloys, liquid and solid, struct. obs., elec. conductivity meas. 0-64864

In-Sn dil, alloys, electronic sp. ht., 0.5-1.7 K 0-43905 \(\alpha\)- In-Sn solid solns., Mossbauer effect, rel. to interatomic force interaction 0-44795

0-44/95
In Sn system, state diagram rel. to comp. prop. diagrams 0-65505
Mg-Al-Sn, phase diag. for Mg-rich region 0-50303
Mn-Sn alloy, Mossbauer effect, ¹¹⁹Sn isomer shift, susceptibility 0-56514
Nb-Sn, composite superconducting alloy, phase substitution method 0-59175

0-39175
Nb-Sn, superconducting cast alloy, crystallization and microstruct, mech. vibration effect 0-59174
Nb-Sn system, constitution diagram 0-61591
Nb₃Sn, superconductivity, hollow cylinders, flux-jump behaviour 0-75609

0-75609
Ni-Sn-Sb system, Mossbauer effect of ¹²¹Sb and ¹¹⁹Sn 0-59380
Ni₃Sn₂, alloy, brittle-to-ductile transition, impurity adsorption at grain boundaries 0-68478
POCl₃-SnCl₄,Nd³⁺ laser system, characteristics 0-60221
POCl₃-SNCl₄, iiq., Tb³⁺ fluoresc. 0-64931
Pb-Sn eutectic, lamellar rotations 0-55777

Pb-Sn elucetic alloys, superplastic, deformation processes, direct obs. using scanning electron microscope 0–71687
Pb-Sn elucetic crystn. front struct. 0–65170
Pb-Sn films, condensed, metastable struct, low temp. 0–68234

 α -Pb-Sn solid solns., Mossbauer effect, rel. to interatomic force interaction 0-44795

0-44/73 (Pb,Sn)O mixed cryst., photocond. 0-56394 PbO-SnO, solid solution formation 0-53649 α-Sb-Sn solid solns., Mossbauer effect, rel. to interatomic force interaction 0-44795

0–44795 SeOCl; SinCl₄, Nd³⁺ laser system, characteristics 0–60221 Si-SnO₂ heterojunctions, elec. and optical props. 0–72080 Sm₃NbO₃, monocryst., struct. 0–65252 Sn-Cu alloys, liquid + $\varepsilon \rightarrow \eta$ peritectic reaction rel. to crystal growth forms 0–43591

0-43591
Sn-Ge-Si ternary phase diags., quasi-chem. calcs. 0-71407
Sn-In alloy film, superconducting, tunnelling in perp. mag. field 0-71983
Sn-Pb(-SnAg₃,-Zn) eutectics, solid-solid interface energies, laminar growth theories 0-39923
Sn-Pb, dilute, segregation and striations 0-50788
Sn-Pb alloy, superplastic, torsion tests 0-71691
Sn-Pb alloy, superplasticity phenomena 0-68525
Sn-Pb alloys, low temp. gradient solidification, dendrite-eutectic transition 0-65003
Sn-Sb-Te system phase equilibria 0-50306

Sn-Sb-Te system, phase equilibria 0-50306 Sn-Sb, solid soln., isomer shifts of ¹²¹Sb and ¹¹⁹Sn, conc. depend. 0-51285 Sn-Sb alloy, transperitectic, crystallization kinetics 0-40441

Tin compounds continued

Sn-Zn dilute alloy freezing, distrib. coeff, rel. to growth velocity and initial conc. tracer method 0-68536

Conc. tracer method 0-6536 Sn complexes, aminostannanes, Mossbauer params, and quadrupole split-tings, obs. 0-41173 Sn complexes, organotin(IV) with organic ligands, Mossbauer spectra and dipole moments 0-74308

dipole moments 0-74308 Sn complexes, phthalocyanine and tetraarylporphines, Mossbauer spectra 0-54080

0-54080
Sn_LAs₃SnAs-SnTe subsystem, eutectic obs. 0-74836
Sn_{L-x}Bi_xTe solid solns., energy spectrum of carriers 0-78954
SnCl_x, i.r. spectra in solid Ar matrix, vibrational assignment and force constants 0-49866
SnCl_x and SnCl_x, ioniz, efficiency curves produced by electron impact 0-39617
SnCl_x2H₂O, phase transition, n.m.r. and dielec, meas. 0-62446

SnF₄ diadducts with 4-subst. pyridine 1-oxides and 4-subst. quinoline 1 oxides, l.f. i.r. spectra 0-49894

Sn(II) complex, dicyclopentadienyltin(II), 119mSn n.m.r. and Mossbauer obs. 0-39401 Sn(II) halide complexes, Mossbauer spectrum obs., quadrupole splitting

0-48041 SnO₂:Ni³⁺, 0-72492 e.p.r. in flux-grown cryst., oxidation-reduction effects

SnO₂-F films on glass, spectral transmittance and reflectance and emissivity 0–69104

SnO₂:NP¹, e.p.r. in flux-grown cryst., oxidation-reduction effects 0–72492 snO₂-F films on glass, spectral transmittance and reflectance and emissivity 0–69104
SnO₂-TiO₃, tetragonal system, phase separation by spinodal decomposition 0–59035
snO₂-semiconductor heterojunction m.o.s. struct. 0–75748
snO₃ aftereffect of nuclear reactions. Mossbauer effect investig. 0–54079
snO₅, Sn₇O₃, Sn₈O₄, matrix-isolated i.r. spectra and structure 0–61138
snO₂, Fe²⁺ h.f.s., ³⁷Fe Mossbauer obs. 0–41171
snO₂, Raman spectrum of crystal 0–62691
snO₂, surface effects rel. to thermal annealing, Mossbauer effect and X-ray diffr. study 0–55705
snO₂ crystals, vapour phase growth 0–55786
snO₂ film on glass, properties 0 –43541
snO₂ films with In and Sb impurities, elec. props. 0–72049
snO₂ thin film transistors 0–65751
n-SnO₃ film on ferroelec. ceramic, ferroelec. field effect studies, 300-78°K
0–47846
snO₂(H₁O₂O₃, stannic acid gel, nuclear gamma resonance, line broadening 0–55641
sn₃O(OH)₂SO₄, cryst. struct. 0–65282
sn₃O₄O₅S₃, cryst. struct. 0–78500
snS Hall coeff. variation with temp. used to determ. ionisation energies of imperfections and size of forbidden band 0–56223
snS₃, mobility of electrons 0–75687
snS₂ cryst. growth from solns. of supercritical H₂S and H₂S-(C₂H₃)₃N-HCl 0–61723
snSb, density, microhardness, elec. resistance, thermo-e.m.f. 0–40422
snSe, sublimation coeff. 0–61604
snTe-GeTe alloys, phase transition, neutron scatt. obs. 0–68950
snTe-MnTe alloy system, ferromage, ordering, reciprocal Hall coeff., superconductivity, 0.02-300 K 0–44139
snTe-MnTe alloy system, ferromage, ordering, reciprocal Hall coeff., superconductivity, 0.02-300 K 0–44139
snTe-MnTe alloy system, ferromage, ordering, reciprocal Hall coeff., superconductivity, 0.02-300 K 0–58568
snTe-film deposited between 4.2° and 300°K, elec. and opt. props 0–58568

0–38508 (SnTe), x(GdTe), solid solution, elec. cond., Hall effect, lattice thermal cond. 0–78955 Su-(70 at%)Al, struct. from X-ray scatt. curves 0–64866 Ti-Mo-Zr-Sn alloy, β -III, as-quenched, stability 0–71807 α -Ti-Sn solid solns., Mossbauer effect, rel. to interatomic force interaction 0–44795

anum in Alnico alloys, rel. to effect of duplex addition of 5 and Te $\,0-71761$ $\,\alpha$, dislocation dynamics, stress relaxation technique $\,0-47262$ abundance in lunar samples, quantitative analysis $\,0-48501$ addition in V alloy, interactions with interstitial impurities, effect on tensile properties, meas. at 77 to 673°K $\,0-50722$ adsorbed on W, migration in strong elec. field, field emission determ.

0-39981

adsorbed on W, migration in strong elec. field, field emission determ. 0–39981 adsorption of CO₂ on film, dissociatives 0–43572 alloy O₃, N₃, H₃ diffusion during Ar-arc welding, calc. 0–68379 and alloys, forming processes and mech. props, bibliography 0–50789 atom, extended method of calc. applic. to d" shell with N=2–4 0–70764 band structure, photoemission studies 0–65599 brittle crack propagation rel. to surface layer stress relaxation 0–50732 cathode, Penning pumps, stability to Ar and other rare gases, experimental study 0–51865 cathode, potential drop rel. to press. for inert gases 0–39627 diffusion in rutile, 900-1300°C 0–50629 e.p.r. in VO₂, 77-293K, conc. depend. 0–41345 electron momentum density, from Compton profile meas. 0–40645 electron in ommentum density, from Compton profile meas. 0–40645 film deposited on sapphire in ultrahigh vacuum, struct. 0–74919 flow stress azimuthal component determ, method comparison 0–50693 inioint to artificial sapphire 0–48659 lattice dynamics, electron force model 0–56093 magnetic susceptibility and low temp. sp. ht. 0–75899 migration of W, adsorbate conc. depend. 0–61634 optical constants 0–76759 oxidation, coeff. of oxygen diffusion and activation energy for diffusion calc. from kinetic data 0–76266 oxidation, thermal effects in initial stages, exptl. conditions effects 0–72549 particles, polydispersed with Zr, in N₂, electroconductivity and radiation 0–5068

particles, polydispersed with Zr, in N_2 , electroconductivity and radiation 0-50268

0-50268
phase transform. effect on thermal cond. and phys. props. meas. 0-75421
phase transition, 120-500 kbar shock wave induced, X-ray diffr. 0-40493
photoelectric work function 0-75859
polyethylene neutron backscattering by 0, 20, 40, 60 and 80° for semiinfinite thickness 0-45972
solubility in liquid K 0-39741
specific heat, low temp., and mag. susceptibility 0-75899

substrate, effect on Al films used for diffraction gratings, obs. 0-79237 thermal cond. meas., phase transform effect 0-75421

thermal cond. meas., phase transform effect 0—75421 thin film, activity coefficient and capacity at high vacuum and low temperature 0—57221 wetting by glasses 0—50358 119Ag diff. in Cu, eff. of added Ti 0—58838 Al-Ni-Co-Fe, in 5 to 10% content, columnar castings 0—71762 6Al-4V, flaw growth, testing in Freon TF environment 0—47392 114 distrib. from 11H(d,n)*He reaction obs. 0—62836 in Ni, additive effect on Elinvar prop. 0—58856 Ti/Mo, initial stage film deposition, substrate ion secondary emission kinetics 0—50391 Ti/Zr atomic abundance ratio in late-type stars 0—54362 Ti/Oxide layers, 0,1* ion implanted, resist, of oxide layer 0—78867 Ti II lines in sunspot umbra, excitation by penumbra radiation field 0—66626

Ti It lines in sunspot umora, excutation by pentiniora radio 0-66626

Tj²+ e.p.r. in alkaline earth fluorides 0-79395

Tj³+, e.p.r. in Al₂O₃, corundum line width and shape 0-51387

Tj³+ e.s.r. in Na₂O-TiO₂-SiO₂ glasses 0-72487

4Ti, diffusion in Nb single crystal, 994 1492°C 0-40200

Titanium compounds

alloy, comp., microstruct, and stress- corrosion cracking and relationship $0\!-\!40466$

alloy, comp., microstruct. and stress-corrosion cracking and relationship 0–40466
alloy, electrical resistivity at low temperature 0–75540
alloy, fracture topography, microstruct, influence 0–40418
alloy, fracture toughness tests, correlation 0–43769
alloy, irradiated, cryogenic tensile props. effect of temp. on radiation characteristics 0–78646
alloy, metastable β-phase decomposition, ageing, 480 °C, electron microscopy 0–53664
alloy, retarded fracture, fatigue testing, cyclic deformation 0–53612
alloy, stress corrosion cracking mechanism 0–78656
alloy, stress-corrosion cracking characterization procedures rel. to failure-safe design 0–43792
alloy, wetting by glasses 0–50358
alloy's welded joints, elasticity characteristics, low temp. effects investigation 0–58863
alloy of TA₈V₈E₂, kinetic study of transformations under isothermal conditions 0–56068
alloy for surgical implants, tensile strength corrosion, fatigue characts. study 0–71757
β-alloys, carbide precip. 0–43828
alloys, forming processes and mech, props., bibliography 0–50789
alloys, stress-corrosion-cracking characterizations procedures 0–47415
alloys for marine applications 0–66263
borides, soft X-ray L_{1,111} emission and absorpt, spectra 0–69147
intermetallic, soft X-ray spectroscopic investigation of electronic properties 0–5603
interstitial, soft X-ray spectroscopic investigation of electronic properties 0–5603
interstitial, soft X-ray spectroscopic investigation of electronic properties 0–65603
interstitial, soft X-ray spectroscopic investigation of electronic properties 0–65603
interstitial, soft X-ray spectroscopic investigation of electronic properties 0–65603
interstitial, soft X-ray spectroscopic investigation of electronic properties 0–65603
interstitial, soft X-ray spectroscopic investigation of electronic properties 0–65603

0-65603
nitrides, soft X-ray L_{II,III} emission and absorpt, spectra 0-69147
notch-bend strength of alloys in heavy sections 0-47381
oxide, effect of alkaline earth fluoride additive 0-62144
oxides, soft X-ray L_{II,III} emission and absorpt, spectra 0-69147
rotational, in Ticonal alloy 0-72238
rutile, reduced, elec, conductivity, 2-370K 0-75688
structural alloys, fracture toughness characterization procedures, failuresafe design 0-40358
Ticonal, thermomagnetic treatment. Mossbauer obs. 0-58960
Ticonal 2000, high coercivity, features of thermal magnetic treatment
0-71764
Ticonal alloys, decomposition, final strages analysis.

17/104
Ticonal alloys, decomposition, final stages analysis 0-50823
Ticonal alloys, uniaxial anisotropy energy density and local field between particles 0-72237
titanate coatings adhesion, in air, to stainless steel Parasitic Load Resistor 0-59010

that are Coatings at the storing in an , to stainless steer parasitic Load Resistor 0 – 59010 two-phase, foil prep. technique for replica electron microscopy 0–62097 Al-Ti alloys, precipitate struct, and morphology 0–75137 Al-O₃-TiO₂, sintering, comp. depend. 0–47427 Al-O₃-TiO₂, system, surface props., heats of immersion, adsorpt., X-ray diffr. 0–50352 $\alpha+\beta$ alloy, metastable phase decomp., 20-500°C, resistivity var., rel. to electron structure and band charge 0–78882 Be-Al-Ti system, liquidus surfaces, non-variant equilib. 0–58520 CaO-Nb₂O₃-TiO₂, phase equilibria at liquidus temps. 0–43510 Co-Ti alloy system Cu₃Au-type struct. compound, mag. props. 0–47923 Co-(9/at.%)Ti alloy, morphology of homogeneous precipitation, electron microscopy53660 0–53660 Cu-Ti-Al alloys, dislocation struct. and twinning rel. to age-hardening 0–40448 Cu-Ti-Al alloys, mech. props. temp. depend. 0–55966

0-40448
Cu-Ti-Al alloys, mech. props. temp. depend. 0-55986
Cu-Ti, Cu-Ti-Al alloys, struct. changes in initial decomp. stages 0-75329
Cu-Ti alloy, hardened, deformed, intermittent precipitation 0-50780
Cu-Ti alloys, dislocation struct. and twinning rel. to age-Hardening 0-40448
Cu-Ti alloys, mech. props. temp. depend. 0-55986
Fe-Cr-Si-Ti hardening on heating to 600°C 0-58957
Fe-Ni-Al-Co-Ti, effect of Co, S and Te on liquidus-solidus gaps 0-71775
Fe-Ni-Ti-Mo alloys, austenite obs. 0-61865
Fe-Ni-Ti alloy with ageing martensite, recovery 0-50770
Fe-Ti-N alloy, internal friction, heat treatment comp. depend. 0-43721
Fe Ti alloy, yield stress, flow stress, Luders strain, effects of grain size and free interstitials 0-50689
Li-Ti-Zn, ferrite, spin wave losses, Co²⁺ effect 0-41036

free interstitials 0–50689

Li-Ti-Zn, ferrite, spin wave losses, Co²+ effect 0–41036

Li-Ti-Zn, ferrite, spin wave losses, Co²+ effect 0–41036

Li-Ti-Zn, SiO₂ glasses, liq. immiscibility effect on strength 0–58927

Na₂O-TiO₂-SiO₂ glasses, Ti²+ e.s.r. 0–72487

Nb-Ti-Mo alloy, b.c.c., superconducting transition temp., critical field, current carrying capacity 0–40744

β-Nb-Ti, tubic alloy, optical spectra, band struct. 0–54089

Nb-Ti alloy supercond. microwave cavity 0–47676

Nb-Ti solid solns, supercond., optical props. 0–40740

Nb-Ti supercond. alloy fabrication method, patent 0–44154

Nb-Ti ternary alloy, 65BT, struct. 0–61897

Nb Ti ternary alloy, 65BT, surface struct. 0–61631

Titanium compounds continued

Nb-Ti wires and multifilament composites, energy release by flux jumps 0-47677

0-47677
Ni-Co-Al-Ti-Cu-Fe permanent magnets, structure 0-71778
Ni-Ti alloy, microstructural plastic flow obs. 0-50708
nTi-Zr-O system sub-oxides, neutron diffr. obs. 0-65888
Pb(T, Zr/O₃ solid solutions, dielectric polarization, morphotropic phase boundary, comp. depend. 0-62403
Pu-Ti alloys, Pu β phase stabilization 0-68568
Ti-6Al-Va alloy, air contamination, microprobe analysis 0-45099
β-Ti-(Mo,Nb,V) isomorphous alloy, phase transformations 0-53663
Ti-Al-Sn(V) alloy, low temp. creep behaviour 0-40335
Ti-Al-Valloy, internal friction and u.s. yield stress 0-68419
Ti-Al, stress corrosion cracking, in aqueous solutions at ambient temperatures 0-68492
Ti-Al alloy, age-hardened, precip. particles dispersed, mech. props. 0-53609
Ti-Al alloy, stress corrosion cracking, role of Cl and NaF 0-50744

0-3609
Ti-Al alloy, stress corrosion cracking, role of Cl and NaF 0-50744
Ti-Al alloys, strength deformation modes, fracture 0-47382
Ti-C system, precip. bands below stoichiometry 0-59034
Ti-Cr alloy, X-ray spectra. K\$\tilde{\text{P}}_{2.5}\$ bands 0-56578
Ti-Cr alloys, \$\tilde{\text{B}}_{5.5}\$ stabilized, step quenching and ageing effect on supercond.
Tr 0-71987 T. 0–71987 Ti-Fe, α - and β -solid solutions, Mossbauer spectra, electronic struct. 0–54082

11-Fe, β- and p-solid solutions, Missibated spectra, declaring data of 54082

Ti-Hg-Zn syst., X-ray studies 0–40465

Ti-Mo-Zr-Sn alloy, β-III, as-quenched, stability 0–71807

Ti-Mo alloy, cermet, production and corrosion props. 0–78686

Ti-Mo dil. alloy, microstruct. influence on supercond. 0–71986

Ti-Mo wires, grain-boundary, matrix-crystalline fracture, scanning electron microscopy 0–61908

Ti-Mo wires, crystalline and polycrystalline, fractography, scanning electron microscopy 0–68494

Ti-Nb-Fe, superconducting alloy, annealed, Mossbauer chemical shift correl. with critical current 0–65647

Ti-Nb-V, ternary system, superconducting resistive critical field, comp. depend. 0–44141

Ti-(22 at.%)Nb, superconducting alloy, magnetization, Bean model 0–75629

depend. 0-44141

Ti-(22 at.%)Nb, superconducting alloy, magnetization, Bean model 0-75629

Ti-Nb alloy, superconducting, longit, critical currents 0-62329

Ti-Nb alloys, deform, contrast origin from no contrast line position in micrographs 0-40144

Ti-Nb phase boundaries determ. 0-53665

Ti-O solid solution, instertial order-disorder transformation, neutron diffr. 0-40499

Ti-O system, intermediate oxide phases, equilibrium 0-71811

Ti-Si Schottky barrier diodes, fabrication and props. 0-44302

Ti-Si system, unidirectional solidification 0-71525

Ti-Ta-Nb alloy, superconducting, patent 0-44157

Ti-15%Ta getter wire tested 0-57207

Ti-V-C alloy, f.c.c., electronic structure, from specific heat, mag. susceptibility and n.m.r. meas. 0-40667

Ti-V phase boundaries determ. 0-53665

Ti-SAI-IMO-IV alloy, fatigue lifetime rel. to high temp. outdoor exposure 0-50730

Ti (III) complex, K₃[Ti(CN)₆].2 KCN, struct. 0-40102

α-Ti alloy, embrittlement, intergranular rupture at high temp. 0-68479

Ti alloy, powder, loose, compacted and heated, mechanical and chem. props. 0-40473

Ti alloy TA6V, metallurgical study 0-68537

Ti complex, [Ti(bipy)₆] and Li[Ti(bipy)₆].3.7THF, electronic spectra o-46464

TiB, cryst, growth in molten Al 0-75013

11 complex, [11(bpy)₃] and Li[11(bpy)₃].3.71HF, electronic spectra 0-46464
TiB₃ cryst. growth in molten Al 0-75013
TiBr absorption and emission spectra, vibrational analysis of electronic states 0-49895
TiBr band spectrum excited in emission in radio-frequency discharge 0-43137
TiC, fracture under static and sliding contact 0-40417
TiC, wetting by liq. Ag and Cu 0-50351
TiC precipitate in steel, diffusional coalescence of cementite phase particles 0-50817
TiC single crystal, growth by chemical vapour deposition 0-53457
TiC thermoelectric characteristics, effect of high-temp. heating 0-59275
TiC₁, electromigration and diffusion of C 0-50628
TiC₄, electromigration and diffusion of C 0-50628
TiC₄(0.73≤×≤0.89) work function at 1800k, obs. 0-62468
TiCl₄ vapour, absorpt. spectrum at 20, 300 and 700°C, windowless gas cell appl. 0-49153
TiCoGe, crystal structure 0-61907
TiCo₄O₇(-x), ordering obs. using neutron diffr. and elec. conductivity 0-75103
TiF, emission spectrum from Δy=0 sequence of ⁴π-⁴Σ transition 0-55326

TiCo_xO_{1-x}ν₁, ordering obs. using neutron diffr. and elec. conductivity 0–75 103 TiF, emission spectrum from Δv =0 sequence of ${}^4\pi^4\Sigma$ transition 0–55326 TiF, diadducts with 4-subst. quinoline 1-oxides, l.f. i.r. spectra 0–49894 TiF(H₂O)_x² , electronic struct. from e.p.r. meas. 0–70955 TiF-NH₄F, liquid-solid equilibria, pressure effect 0–61590 TiFe, TiCo, TiNi and ternary solid solution, ductility 0–40336 TiFe₁-χCo, alloys, ⁵⁷Fe n.m.r. 0–45029 TiFeGe, crystal structure 0–61907 TiFeGe, crystal structure 0–61907 TiFeSi, crystal structure 0–61907 TiGes, binary phase, crystal structure 0–50553 TiH₂, electronic props. 0–44001 TiH₂, struct., comp. depend. 0–50551 Ti(III) chelates in aq. soln., e.p.r. and nature of chem. bonding 0–78303 TiX, Mo_{1-x}²Co, dilute alloy, where 0≤x≤0.4, local moment formation, n.m.r. 0–45028 TiN, rotational analysis of the red electronic emission system 0–53051 TiN, sintering in N₂ 0–65456 TiN₂, at TiN₂, at TiN₂, at TiN₂, TiN₃, TiN₃, TiN₃, TiN₃, thermal conductivity in range 77-110°CK 0–59115 Ti_XNb₃, cryst. struct., from density meas. 0–65289 TiNi, field-ion microscope imaging 0–78503 TiNi, martensitic phase change, effect on u.s. wave propag. 0–56069 TiNi, mattensitic transform., atomic mechanism 0–590426 TiNi, phase transform. kinetics, mechanism 0–47482 TiNi alloys, shape memory effect rel. to switches production 0–71856 TiO₂-2Cr, rutile, O vacancies formation, e.p.r. investig. 0–55874

Titanium compounds continued

TiO₂:Cr, Verneuil growth method, dopant distribution 0–50426
TiO₂:Cr²⁺, no-phonon ⁴T_{2e}-⁴A_{2e} transitions 0–69155
TiO₂:Cc²⁺, e.p.r. hyperfine and nucl. quadrupole interactions 0–45001
TiO₂:Fe, rutile, single crystal, optical absorpt, and photochromism
0–54103

TiO₂:Si, decorated dislocations 0–58818 TiO₂:W, red-orange photoluminescence 0–44908 TiO, compressibility and Gruneisen consts. 0–78619

110, compressionity and Gruneisen consts. 0–78619
TiO, high pressure effect on crystal structure and lattice parameter 0–47204
TiO, polymorphs, stability, comp. and temp. depend. 0–65508
TiO, thin film, activity coefficient and capacity at high vacuum and low temperature 0–57221
TiO, vacancy filling and removal, effects on electrophysical props.

temperature 0–57221
TiO, vacancy filling and removal, effects on electrophysical props. 0–61943
TiO, vacancy filling under high pressure 0–75136
TiO in stars spectra, late-type K and M, 7900-12000 Å 0–41678
TiO mol. spectra, meas. of intensities of α and β band systems 0–46515
TiO_{1.25}, lattice parameter charges on high pressure applic. rel. to vacancy behaviour 0–61909
TiO₂, adsorption of ethanol and water, i.r. spectra 0–58605
TiO₃, block dielec. relax. and assoc. defects 0–40827
TiO₂, gas/solid adsorption isotherm, interpretation 0–74925
TiO₂, influence of stacking faults on thermal cond. 0–78795
TiO₂, resystallization, shear structures 0–61970
TiO₂, rutile, creep, high temp. recovery at zero stress effect 0–50702
TiO₂, rutile, diffusion of Ti, 900–1300°C 0–50629
TiO₂, rutile, lidifusion of Ti, 900–1300°C 0–50629
TiO₂, rutile, lidifusion of Ti, 900–1300°C 0–50629
TiO₂, rutile, weas. of rotational contribution to Brillouin scattering, cross sections 0–79335
TiO₂, rutile, vibrations, space group representations and normal mode anal ysis 0–56091
TiO₂, rutile, vibrations, space group representations and normal mode anal ysis 0–56091
TiO₂, thermocurrents, phase transition obs. 0–68953
TiO₂, thermocurrents, phase transition obs. 0–68953
TiO₂, thermocurrents, phase transition obs. 0–68966
TiO₂ efficiency as nucleating agent in glasses 0–74866
TiO₂ efficiency as nucleating agent in glasses 0–74866
TiO₂ fefficiency as nucleating agent in glasses 0–74866
TiO₃ film, heterogeneous deposition mechanism, 673-1320K 0–53441
TiO₃ glim, seurrent instability 0–72107
TiO₃ supersaturation in attmospheres of cool, oxygen rich stars 0–51657
TiO₃ x. 1828 x z 2, defect ordering, resist, and thermal cond., obs. 0–40126
TiO₃, defect ordering and transport phenomena 0–58779
TiO₃ supersaturation in attmospheres of cool, oxygen rich stars 0–51657
TiO₃, 1828 x z 2, defect ordering, resist, and thermal cond., obs. 0–40126
TiO₃, defect ordering, resist, collectronic band struct. 0–72406

0-51312

TiO₂+BaCO₂ mixture, shock compression, piezoelec. props. 0-75774

V-Ti alloy, precipitation, TiO₂ ubic phase, electron microscopy 0-65500

V-Ti alloys with improved corrosion resistance in liquid Na, effect of Ti content. 0-40468

Zn-Cu-Ti alloy, varied extrusion temp. effect on props. 0-40423

Zr-Ti-O system, phase obs. on pseudobinaries, subsolidus ternary diagram 0-59057

Zr-Ti alloys, oxidation in air, dimens. changes 0-45064

Torquemeters see Mechanical measurement

see also Elastic constants: Stress analysis

see also Elastic constants; Stress analysis beam, free, upper and lower bounds for eigenvalues by finite difference method 0–66867 crystalline elastic solid, torsional equilibrium of rectangular bar, lattice theory 0–45610 cylindrical shaft, holographic obs. 0–67143 dynamical theory including effects of warping and in-plane shear deformation 0–48786 elastic half-space, torsional oscillations due to annular disk 0–66889 elastic-perfect-plastic materials, theoretical method for analysis 0–63391 hole in nonuniform disc, twisting and expansion 0–48817 layered structure, displacement due to nucleus of torsional strain 0–38234 load cell under hydrostatic pressure, device for meas. change in calibration 0–75243 0 - 75243

0-75243
of multiply connected thick-walled rectangular sections, formulas derivation 0-69683
nonlinear material, radial shear distrib. determ., epoxy resin specimens in polarized light 0-45596
shaft, cylindrical, holographic interferometry 0-62026
shell's torsional motion free and forced, orthogonality principle, theory 0-57371

Steel, low carbon, electropolished, torsional fatigue tests 0-62061
Steel, low cycle fatigue in torsion, axial compression effects 0-47324
stress relaxation in combined torsion-tension 0-57321
structural members in contact, elasticity theory, threedimensional
0-38285

u-3283 torsional motion free and forced of joined concentric circular shells, orthogonality principle 0-57371 waves in infinite elastic solid containing penny-shaped crack 0-66897 Al alloy, low cycle fatigue in torsion, axial compression effects 0-47324 Be-Cu alloy, low cycle fatigue in torsion axial compression effects 0-47324 Contains the contains a compression effects 0-47324 Contains the contains a compression effects 0-4884 contains a compression effects 0-4884 contains a co

Cd, flow stress of single crystal 0–58905 Cu, strain hardening relationship calc. from torsion test 0–78672 Sn-Pb alloy, superplastic 0–71691

Total cross-sections see under individual particles, no subheading

Townsend coefficient see Ionization/gases Tracers

see also Radioactive tracers; Radiochemistry
diffusion in silver halides, model 0-75198
experiments, transport function and flow rate, indeterminacy in estimation
in closed circulations 0-74693

Tracers continued

permeability, in homogeneous liquid membranes 0-71332

radioactive, in atmos., global transport from instantaneous sources in lower stratosphere, numerical model 0-76399

radioactive, atmos. distribution near ground, theory 0-76378 ⁵⁹Fe, measurement of absorption by whole-body counting 0-63221

Transducers

see also Acoustic generators; Acoustic receivers; Microphones; Sound reproduction

a.f., underwater, farfield transmitting response, freefield sensitivity and directivity patterns 0-69728

acoustic, Ni, Permendur, Alfer and ferrite, identical dimensions, comparative study 0–62205
acoustic, class II flextensional underwater, mathematical model 0–52118

acoustic, class II flextensional underwater, mathematical model $\,0-52118$ acoustic, class V flextensional underwater, mathematical model $\,0-52119$ acoustic, design, construction and calibration for nuclear fuel element testing $\,0-42078$ acoustic crystal arrays multi unit underwater, design method $\,0-54727$ acoustic modulation of laser beam, patent $\,0-49101$ acoustoelectric, CdS, efficiency $\,0-50882$ array, nearfield, for an anechoic tank $\,0-63446$ array cylindrical in water, nearfield cavitation, approx. prediction method, computer calc. $\,0-71286$ bead thermistor, fluid temperature and flow speed fields meas., use of high speed digital data system $\,0-48893$ ceramic, instrumentation, applic. to brain tissue's ultrasound visualization $\,0-48632$

ceramic, instrumentation, applies to orani ussue 3 0-48632 (cylindrical thin layered shells, natural freqs. of radial modes, analytical expressions 0-45643 (earphones, audiometric, self-calibration, feasibility study 0-66722 elastic for linear displacement meas., design 0-48829 electroacoustic, active, as absorber of underwater sound, characteristic impedance of acoustic transmission line 0-69729 electroacoustic, as characteristic impedance of acoustic transmission line 0-40050

electrodynamic, rel. to tone-burst meas. of acoustic wave absorption 0-52108

0-32106 for electronic meas, systems, handbook 0-45510 electrostrictive, for magnetic field meas. 0-45757 headsets, pneumatic, stereo, eartip noise immunization when used on aircraft 0-66731

hydrophone array, for ocean-bottom seismic profiling, response comparison of continuous line and discrete linear arrays 0-45127 hydrophone large nearfield calibration array, fabrication design data 0-69728

hydrophone large nearfield calibration array, fabrication design data 0-69728
hydrophone probe for acoustic meas. from 10-200 KHz. 0-69726
hydrophones, sonar's volume and shell arrays, directivity characteristic, closed-form soln. 0-42079
interdigital surface wave, capacitance and field distrib. meas., boundary shift tech. applic. 0-45640
interdigital surface wave 0-75386
line transducer NEFBRACS (nearfield bearing and range accuracy calibration system), design, construction 0-63445
liquid wedge surface-wave transducer 0-43638
magnetic reluctance, for thin lubricant film thickness meas. 0-68071
motion meas.. strain gauge, linear potentiometer and seismic-type description w.r.t. measured magnitude 0-59867
omnidirectional pressure, elastic spherical inclusion in ground, frequency response and transient behaviour 0-52044
piezoelectric, GHz, birefringence use for layer props. meas. 0-45639
piezoelectric, GHz, birefringence use for layer props. meas. 0-45639
piezoelectric, inhomogeneous, subjected to static charge, electromech. response 0-44381
piezoelectric ceramic, radiation in radially symmetric modes, calc. 0-62452
piezoelectric high speed for press: distrib. study in current sheet structure 0-20452

piezoelectric high speed for press: distrib. study in current sheet structure

piezoelectric whisker reinforced ceramic material, production and props. 0-63444

0-53444
pressure, fast-response, 1/20-100 psi 0-69575
pressure, flush-mounted, in acoustic homing system 0-57407
pressure, primary calibration to 10,000 Hz 0-69576
pressure, ultra-miniature piezoresistive, for wind tunnel models, development 0-72129
pressure, ultraminiature piezoresist, for wind tunnel models, fabrication 0-72130
pressure omnidirectional design 0-60004

pressure omnidirectional, design 0-60004 pressure-gradient, unidirectional underwater-sound, design, construction and calibration 0-52117 pulsed acoustic signal reception and radiation, reciprocity 0-57400 ring, piezoelectric, underwater vibrations, numerical method for study 0-69730

semiconductor, mechanical response, by Laplace transforms 0-42077 sonar, 'in situ' calibration, nearfield techniques 0-63419

sonar, 'in situ' calibration, nearfield techniques 0-63419 sonar receiving arrays, hydrophones directivity index and and beam pattern, eqns. 0-42079 surface temperature, calibration methods 0-42104 rel. to thickness vibrating plates, electromechanical coupling factors and fundamental material constants evaluation, effect of anisotropy 0-47848 u.h.f. magnetoelastic Love waves 0-47950 u.s., textbook 0-73043 u.s., transitory states calc. and wave forms synthesis 0-54725 u.s., use of contactless vibrometer for displacement amplitude meas. 0-60020 u.s., with flexurally vibr, diaphragms for use in air. 0-69727

0-60020
u.s., with flexurally vibr. diaphragms for use in air 0-69727
u.s. conference, St. Louis, USA, 1969 0-45623
u.s. crystal, radiation power, impedance method of measurement 0-45641
u.s. diffraction fields in highly anisotropic crystals, calc. 0-69725
u.s. piezoelectric, patent 0-57412
u.s. semiconductor with exponential conductivity-thickness distrib., transformation characts, expression 0-63443
ultrasonic, application of CdSe Le.t., piezoelectric effect 0-44310
underwater acoustic, design, applic. of flextensional concept 0-48852
underwater electroacoustic cables, turboelectric noise generation 0-72127
wide-band, for surface elastic waves 0-76904
CdS, acoustoelec., efficiency 0-50882
CdS epitaxial, freq. characts. 0-44383

Transducers continued

CdS thin film with interdigital finger-metal-film electrode pattern for surface

Cas thin him with interdigital inger-metal-him electrode pattern for survaves 0–45617
cds piezoelectric, fabrication by electron beam evaporation 0–62287
InAs film Hall type for strong mag. field meas. 0–77023
ZnO film, hypersonic, losses rel. to texture, resist, thickness 0–68605

Transformations see Phase transformations

Transformations, mathematical
Birkhoff's normalization at elliptic equilib. without internal reson.
0-45520

0-45520
Bogolyubov, boson, in terms of SU(1,1) group 0-72971
canonical, direct 0-69580
canonical, finite and infinitesimal 0-69578
canonical transformation method for obtaining electromagnetic many-body forces 0-42952
chiral SU(2)×SU(2) transformation, curved isospin space with torsion 0-42545

de Sitter bispinorial and Foldy-Wouthuysen transforms. 0–48718 cel. to elastic constants, anisotropic media, by successive simple rotations 0 - 43717

0-43/11/ fast Fourier transform algorithm calc. of sine, cosine and Laplace trans-forms 0-72982 Fierz transformations in terms of Racah coeffs. 0-54550

Foldy-Wouthuysen transf., rel. problems 0–66795
Fourier, for determining a systems transfer function, report 0–63284
Fourier, for soln. of chromospheric line transfer eqn. 0–57154
Fourier, of product of 2 spherical Bessel function 0–52000
Fourier transform appl. to two-dimens. boundary value problems in elasticity 0–48801

gauge transformations, nonlinear, extension of Weinberg's treatment 0-60460Gegenbauer transforms and forced torsional vibs. of thin spherical shells

Grinberg method, approximate solution of Stefan problem 0-72883 group-variational technique, application to dynamics of holonomic systems 0–72992 integral, and self-reciprocal functions 0–69588 integral transform analysis of reactor pulsed neutron distribution decay

0—79.89 integral transform analysis of reactor pulsed neutron distribution decay of transform which is expansion of Meijer G-functions and generalizes Hankel transform 0—54551 integral transformations in momentum space and conformal invariance 0—72895

inverse mean free paths and lub. frame absorption coeffs. 0–69601 Lagrangian and Hamiltonian for energy transformation analysis 0–42160 Laplace, for elec. response in piezoelec. cryst. with divided electrodes 0–47850

0-4/850 Laplace, for mechanical response of semiconductor transducer 0-42077 Laplace, rel. to linear a.c. heating equation with variable coefficients, resolution 0-42099 Laplace, state transition matrix 0-48680 Legendre, and the general Born diagram 0-54545 Legendre inverse transforms, solution by spherical harmonics expansion

0-51902

0-51902
Lie transform for Von Zeipel mapping equivalence 0-56908
Lorentz, form of Minkowski diagram 0-76803
Lorentz for special relativity kinematics 0-63329
Lorentz transformations and linearity, deduction for special relativity 0-57254

moving frames of reference, space and time coords. transform. 0 - 38132

Pauli and Touschek, for four component neutrino field 0—73402

Poincare, Lorentz-poles into unequal mass scatt. amplitudes 0—38148

Poincare, $\lambda(g^4)_2$ quantum field model 0—54963

vector cross products, axial vectors 0—41935

Watson transform and diffraction at short wavelengths by prolate spheroid 0—38154

Transistors see Semiconducting devices/transistors

Transition metal compounds

alloy, B-metal, system, three correlation model 0–58751 alloy, Hubbard splitting and mag. props. 0–79120 alloy, dil., hybridization between s and d bands due to impurity pot. 0–68736

alloy, dil., with Cr, Mn and Ni, mag. props. 0–54023 alloy, electronic struct. 0–75498 alloy, ferromagnetism 0–54003 alloy, transition metal-non-transition metal, theory and diffusion 0–75310 alloys, binary b.c.c., electron to atom ratio 4.0 to 6.0, density of states 0–75455

alloys, dil., impurity susceptibility and resistivity above Kondo temp. 0-62483

alloys, optic mode instabilities associated with second-order structural phase transition 0–78814 borides, electronic structure 0–76759 borides, mass spectrometric determ, of dissociation energies 0–61181 carbides, close packed, crystal chemistry, proposed structural notation 0–40106

0-40106 carbides, close packed, crystal chemistry, proposed structural notation 0-40106 carbides, close packed, crystal chemistry, structural reports 0-40105 carbides, solid state reactions and transitions 0-59014 complexe, octahedral, 'low spin-high spin' transition obs. 0-79175 complexes, P-P coupling constants 0-67711 complexes, or-phenyl, i.r. spectra and 'PF n.m.r. 0-67712 complexes, trans-effects in n.m.r. spectra 0-64370 complexes, absolute configs. 0-74309 complexes, octahedral, containing halogen bridges, M-Hal stretching modes in far i.r. spectra 0-49853 complexes, tris(acetylacetonato) thermal props. 0-75409 complexes with bis-dimethylglyoximates, i.r. spectra and normal vibrations 0-77784 crystal struct. of Me_xNbS₂ and Me_xTaS₂ type 0-62531 dibordes, photoelectric K-spectra and X-ray spectra 0-44875 dibordes, group IVa, Hall effect, magnetoresistance, mag. field depend. 0-44032 dichalcogenides, IVB-VIB, thin single crysts, elec. cond. 0-75689

0-44032 dichalcogenides, IVB-VIB, thin single crysts., elec. cond. 0-75689 dichalcogenides, optical absorpt. spectra, photocond., excitons 0-47875 gaseous diborides of electropositive metals, stability 0-61185 group VIII aluminides, cubic equiatomic, Knight shift, nuclear spin-lattice relax. rate, linewidth and intensity 0-45012

Transition metal compounds continued

hexaisothiocyanate ions, i.r. and laser Raman spectra, 2200-70cm⁻¹

hydrates, vibr. spectra rel. to intramol. stretch-stretch force consts. of H₂O mol. 0-77795

ion complexes, spin-orbit coupling and Slater parameters, covalency effect $0\!-\!70956$

0-70956
magnetic and optical props. of dilute complexes, theory 0-40924
magnetic struct. of Me_xNbS₂ and Me_xTaS₂ type 0-62531
metal-B-C-Si systems, phase diagrams 0-50833
n.q.r. spectra, review 0-76246
nitroprussides, Mossbauer obs. 0-41138
oxide, elec. and opt. props. 0-75550
oxide, elec. and opt. props. 0-75550
oxide, metal-nonmetal transition, polaron formation 0-44038
oxide surface layers, characterization by oxygen X-ray emission band shifts 0-50365
oxides, cryst, growth by arc transfer 0-50427
oxides, cryst, growth by arc transfer 0-50427
oxides, electron correlation effects in narrow d bands and polarons 0-62249
semi-borides of first series, low temp. specific heat. 12-4.2 K ferromagnet

50-02249 semi-borides of first series, low temp. specific heat, 1.2-4.2 K, ferromagnetism 0-78782 silicides, mass spectrometric determ. of dissociation energies 0-61181

silicides, mass spectrometric determ. of dissociation energies 0-61181 X-ray emission spectra, $K\beta_1\beta'$ structure investigated 0-76137 Al-transition metal alloy, L_{23} emission spectra 0-41248 Al-transition metal solid solns, lattice parameter variation with impurity conc. 0-47458 MNbSe₂, phases, lattice forms studied 0-55850 Ni₃Mn, effect of alloying with third 3d-transition element or ordering kinetics 0-47461

Transition metals

acoustic mode, d-band 0-78762
adatom diffusion on (110), (211) and (321) W surfaces, field ion microscope studies 0-39931
atomic absorption spectrophotometry with air-acetylene flame overexcitation interferences 0-69238
atomic ion sublimation from surfaces in 1800 to 2600°K range, positive and negative 0-47005
atoms, Slater parameters 0-39264
atoms, analytic SCF wave functions 0-74100
Auger-electron spectra 0-43533
band struct, tight-binding cales, for d bands 0-40668
band structure, calc. 0-44046
crystal structure, theory 0-43623
cubic, thermopower, Fermi surface props. 0-79061
d electronic charge distrib, applic, of moments method 0-47595
d-series, stable configs, of localized part of valence electrons, stat. weight 0-65604

0-05604
density of states, electronic, calculations 0-65580
density of states, temp. dependence 0-71906
density-of-states curves 0-71927
dielectric screening, non-interacting band model 0-44003
dielectric screening, noninteracting band model 0-75496
e.p.r. in Sr and Ca tartrates 0-41343
e.p.r. of ions, book 0-41312
electron density of states, meas. using X-ray photoelectron spectroscopy
0-66083

0-66083 electronic struct. of V and Cr group 0-56150 f.c.c., band struct., relativistic APW calcs. 0-75495 ferromagnetic, Raman scatt., magnons and Stoner excitations, thermal Green's function 0-76121 first period, K. and L_{III}-absorpt., spectra, band structure 0-79318 h.c.p., paramag. susceptibilities 0-62496 Hubbard splitting and mag. props. 0-79120 ion irrad., ion form. from ejected atoms in superexcited states 0-43944 ion spectroscopic probes for network struct. determ. in glasses 0-62676 ions, e.p.r., book 0-41312 ions in Al₂O₃, charge-transfer spectra 0-41188 ions in crystals, optical absorpt. from metastable excited states 0-54092 ions in octahedral coordination, paramag. susceptibility 0-44491 iron-group impurities in crystals, covalency, hyperfine field constant 0-51250 Knight shifts, analyses 0-45011

0-51250
Knight shifts, analyses 0-45011
magnetic behaviour 0-75878
Mossbauer fraction for ³⁷Fe impurity, press. variation 0-79258
paramagnetic, magnetostriction 0-79141
Sd, hyperfine interactions, spin-unrestricted Hartree-Fock calcs. 0-44732
superconducting, with nonmagnetic impurities, two-band model extension 0-53798

superconducting transition temp. effect of phonon induced d-d coupling 0-75608

O-75608 superconductivity, many-body effects 0-53804 surface, crystal potential and density of states 0-65607 surface contaminants, Auger and spectroscopy 0-56719 surfaces, chemisorption of diatomic gases 0-47029 transport phenomena, temp. dependence 0-71906 X-ray emission spectra, Kβ_μβ' structure investigated 0-76137 X-ray emission spectra of Fe group, short-wave satellites 0-62697 Fe group, errosion inhibition and passivation kinetics 0-69214 Fe impurities containing, Mossbauer study of lattice dynamics 0-78743 H solutions in bcc early transition metals, theoretical interpretation 0-58981 Transmission

ansmission bonding material for i.r. detectors, and optical transmission, 2-14 μm region 0-41092 e.m. field, through plasma slab having specified electron density-collision frequency profiles, integral 0-46707 e.m. waves in layered anisotropic media, method for calc. 0-48915 electromagnetic waves, radiative transfer in planetary atmosphere, reciprocity relations 0-79726 film, e.m. wave, resonance value calc. 0-41100 ocean waters transmittance meter 0-45128 porous materials, characterization in terms of gas transmission props. 0-78571 of seismic wavelets. by thin layers and layered boundaries 0-41468.

0-485/1 of seismic wavelets, by thin layers and layered boundaries 0-41468 spectral, 0.3 to $2.2~\mu$ region, solar cell cover glass materials, low-energy proton effects 0-71433 spherically laminared anisotropic layer, coeff. calcs. by impedance and field scalings 0-38436

Transmission continued

n-InSb, cyclotron resonance, meas. using HCN laser 0-47688

see also Acoustic wave propagation

in Lucite, transducer window material, attenuation loss 0-71835

airborne, diffuse sound field method for meas. 0–38380 blade rows of arbitrary spacing and stagger soln. 0–57398 from blade spacing effect, flow Mach number, super-resonant condition 0–38382

in building structures of concrete, Cremer's theory, expt. 0-45648 in compressors duct axial flow through blade row, semi-actuator disk theory applic. 0-38381 distortion, multipath, in small rooms, reduction by signal processing 0-66904

in electrical potting resins transducer window material, attenuation loss 0-71835

0-11635 flanking in buildings, noise level calc., sound insulation barrier construction 0-38393 fligh intensity through nonlinear absorber, computational technique 0-71843

impact noise level, connection with sound transmission loss of floors 0-60066

0-60066
laser beam modulation 0-49083
line, characteristic impedance, electroacoustic transducer's for 0-60050
in liquid cylinder imbedded in another liquid, wavefront, amplitude calcs.
using saddle-point method 0-53336
loss in partition wall proximity, vibration meter applic. 0-38392
in ocean, statistics of transmission fluctuation, theoretical study 0-62884
through orifice, nonlinear distortion, theoretical analysis, exptl. comparison 0-57390
panels layered with absorbent material, sound insulation, predicted and measured values, discrepency investigatio 0-40544
in plasma, variation of attenuation, at ion-plasma frequency 0-46679
properties of medium, excitation by primary, secondary sound sources, destructive interference, meas. 0-38386
and reflection characteristics, visual structure walls, method of calculating reverberation time 0-42084
reverberant sound through double partition, two dimensional soln, 0-54748
in reverberant spaces, digital simulation 0-66916

0-54748 in reverberant spaces, digital simulation 0-66916 reverberent sound through single-leaf partition surrounded by infinite rigid battle, soln. 0-54747 SOFAR channel, characteristic meas. 0-68099 * in shallow sea water 0-62885 silica surface wave spreading, nonlinear phenomena 0-78761 in silicone rubber, transducer window material, attenuation loss transducer a f. underwater, farfield transmitting response meas. using calibrating array hydrophone 0-69728 underwater, acoustic energy meas., analog method 0-59546 He liq. interface 0-53385

acoustic waves, ultrasonic fibre bundles, and appls. 0–45630 plastic specimen immersed in water, complex transmission coeff. determ. 0–68597

surface of cylinder, temp. distrib. meas. 0-40559

electromagnetic waves see Electromagnetic wave propagation

light

see also Absorption/light; Filters, optical
absolute transmittance meas, of samples using sensitive spectrophotometer 0-67178

0-67178

\$-alanine, semiconductivity, optical transmission and reflection, pure and X-irradiated 0-75657

alkali vapours, optically pumped 0-77058

alkaline-earth halides, orthorhombic, i.r. lattice vibr. 0-40535

aluminosilicate glass, diffusion of O2, colour centre bleaching 0-43691

atmosphere with absorbing gas of constant mixing ratio 0-76389

bonding material for ir. detectors, and ir. transmission, 2-14 µm region 0-41092

trough clouds, transient behaviour obs. 0–79543 coefficient determ. at high temps. 0–41106 crystalline samples, small, meas. with Zeiss MM monochromator 0–62606

O-62606
diffuse transmittance of anisotropically scattering material, calc. 0-67135
distribution function deduction from intensity meas. 0-42357
electro-optic shutters, piezo-optic effects 0-77194
rel. to fiber-optic elements of fibers with absorbing sheaths, modulation
transfer function computation 0-73328
film, optical index and thickness determ. 0-69071
films, thin, approx. expression for coeffs. 0-44763
filters, narrow-band, type 0-42390
glass, Si₃N₄ additions effect 0-47018
glass, florse, extended u.v. transmission 0-41091
glass, frosted, polishing of rear surface, effect on polarization of radiation
0-62609
glass, lanthanum borate, u.v. transmission, trace impurities influence

glass, lanthanum borate, u.v. transmission, trace impurities influence 0--59386

grating slits imaged transmitting, light intensity distri. 0-70032 holograms off axis, image reconstruction, two-dimensional, eqns. 0-42327

lithium formate monohydrate, nonlinear optical susceptibility and refractive indices 0-79228 luminosity coefficients for diffuse transmission, analytical expression 0-67123

numberly coefficients for unitse transmission, analytical expression 0-67123 materials, effects of simulated micrometeoroid exposure 0-59373 materials, effects of simulated micrometeoroid exposure 0-59373 metal surface, rough 0-76018 metal surface, rough 0-76018 metal surface, rough 0-76018 metal surface, rough 0-76018 metal surface, rough 0-77208 perovskite-type cpds, book 0-68293 of plane wave by rough regular interfaces from stratified medium 0-77184 planetary atmospheres, diffuse reflection and transmission of light, three-term scatt. indicatrix case 0-48563 polymer, spectra, correlation with dispersion of birefringence 0-65989 quartz, coefficient determ, at high temps. 0-41106 quartz, visible and u.v., effects of heating to 1100°C 0-41107 rare earth orthoferrites, 0.5-50µ 0-69125

Transmission continued light continued

refractive index evaluation from interference-fringe transmission spectra 0-48000 semiconductor p-n junction optical waveguide props,, electro-optic effect as

probe 0–69086
silicon oxynitride, m.i.m. capacitor dielectric, i.r., rel. to prep. 0–53932
spectral in La-glasses, data 0–59359
in spherical-shell altitude-dependent atmospheres, Monte Carlo analysis
0–70010

0-70010
superconductor, Bi and Ga films, of far-ir.radiation 0-40739
systems, using injection light sources 0-77169
thin film optical consts. from reflectance and transmittance meas. by curve fitting 0-41101
vacuum u.v. window mats., short wavelength limit temp. depend. 0-51311
Ag coating on glass 0-44780

Ag coating on glass 0-44780
Ag film, longit, plasmons excitation by photons 0-76088
Al coating on glass 0-44780
Al-O₃, high density, i.r. props. 0-56505
Al-O₃, accuum u.v. window mats., short wavelength limit temp. depend. 0-51311
As S-Te chalcogenide glasses, spectra near absorption edge, chemical durability test 0-39906
As-S chalcogenide glasses, spectra near absorption edge, chemical durability test 0-39906
By β-rhombohedral crystal, spectra lattice vibrations, impurity bands 0-51291
Ba-St., Nb-O₂ crystal, 0.3-1.3μm, Czochralski prep., gonjometry, dielect

0–51291

Ba_xSr_{1-x}Nb₂O₆ crystal, 0.3-1.3μm, Czochralski prep., goniometry, dielec. permittivity 0–65148

BeSO₄4H₂O, 0.17-1.6μm 0–68236

Bi films, amorphous, supercond., of far-ix-radiation, T_c obs. 0–40739

CO₂ in atmosphere mathematical model 0–48287

CSCu₂Cl₃, high ix. transmission 0–40006

Cu coating on glass 0–44780

Eu chalcogenides, optical consts. rel. to Curie pt. 0–44758

EuO, magneto-optical effect, 30-293 K 0–76024

Ge film, amorphous, and reflectance, and resistivity and structure, 77-750K 0–44254

GeO₂, vacuum u.v. window mats., short wavelength limit temp. depend. 0–51311

H₂O vapour in atmosphere, mathematical model 0–48287

GeO₂, vacuum u.v. window mats., short wavelength limit temp. depend. 0–51311 H₂O vapour in atmosphere, mathematical model 0–48287 β-HgS, film, prep., temp. depend. 0–48005 InSb-InTe, spectra, comp. depend. 0–48071 La glasses, STK, TBF types, data 0–59359 LiF windows in vac. u.v. radiation sources 0–77174 MnF₂; MnF₂:Fe²⁺, far i.r., antiferromagnetic resonance, two-magnon absorpt. 0–44979 NaCl single cryst., 2000-950 Å, effect of plastic deformation and X-ray irradiation 0–44766 Se coating on glass 0–44780 Si-As-Te chalcogenide glasses, spectra near absorption edge, chemical durability test 0–39906 SiO₂, vacuum u.v. window mats., short wavelength limit temp. depend. 0–51311 SnO₂: F films on glass, spectral transmittance 0.3 to 2.5 μ 0–69104

0–51311 SnO₂-F films on glass, spectral transmittance 0.3 to 2.5 μ 0–69104 VO₂, elec. cond., reflection spectra, temp. depend., semiconductor-semimetal transition 0–75690 ZnAs, films, vacuum evap. 0–65983 Zn,Hg_{1-x}Te solid solns. 0–51047 ZnO film, uv. degraded 0–40778 ZnSe films, elec. field influence 0–69076

Transmission lines, r.f. see Electromagnetic wave propagation/guided waves

Transmission lines, r.f. see Electromagnetic wave propagation/guided waves Transparency see also Optical constants; Transmission/light absorbing medium, near resonant, self-induced transparency 0—42358 ceramic, hot-pressed ferroelec. p. props. 0—54064 ceramic, hot-pressed ferroelec. 0—51272 ceramic oxide cpds. 0—50793 ferroelectric ceramic lead zirconate titanate, hot pressing effects 0—62624 glasses, fluoride opal, opacifying mechanism 0—43526 indices, complex, ellipsoid, of absorbing uniaxial crystals 0—47982 lead zirconate titanate ceramic, hot pressing effects 0—62624 orthoferrites, 1-2.5 µm 0—79267 plasma, criterion 0—46714 platelet semiconductor lasers, obs. 0—47714 pyrrhotite, hexagonal, complex ellipsoid of indices of absorbing crystal 0—47982 quartz, visible and u.v., effects of heating to 1100°C 0—41107

O-47982
quartz, visible and u.v., effects of heating to 1100°C 0-41107
Rosseland opacities, corrected upper bound 0-68019
self-induced, e.m. pulses interacting with resonant inhomogeneously broadened attenuators 0-70009
self-induced, in inhomogeneously broadened attenuator 0-38486
self-induced, ultra-short pulses 0-445815
AgCl:Hg, Na, effect of doping 0-50713
FeBO₃, ferromagnet at room temp, in visible 0-44557
FeF₃, ferromagnet at room temp, in visible 0-44557
LiF windows in vac. u.v. radiation sources 0-77174

Transport processes

see also Diffusion; Kinetic theory; Liquids/theory; Radiative transfer; Solids/theory; Statistical mechanics
rel. to MHD flow past bodies, heat and mass transfer in boundary layer
0-71109

air two-dimens. jet onto plate, mass transfer 0-55532

air two-dimens. jet onto plate, mass transfer 0-55532 atmospheric water vapour, pole to pole divergence 0-51516 ballistic, in collision-free exosphere 0-76419 beams, fast, problems soln. using analogue hybrid computer 0-60162 Boltzman equation and Enskog-Hilbert method, dense gases 0-61446 Boltzmann's transport equation, magnetoelectric electromotive force in an ionic media 0-51995 Boltzmann eqn., curvilinear polyadic moments 0-48735 Boltzmann eqn., linearized, Cauchy problem, space-time correlations 0-59941

Boltzmann eqn., linearized, variational principles sequence rel. to transport coeff. 0-45558
Boltzmann eqn., nonlinear numerical studies and computer programs 0-51994

Boltzmann eqn., quantum mech., for gas with rot. states 0—39683 Boltzmann eqn. for kinetic theory of polyatomic gas, role of orientation and polarization 0—43392

Boltzmann eqn. nonlinear numerical soln. 0-74526

Transport processes continued

Boltzmann eqns, involving non-Hermitean operators, variational methods use 0-72938

Rollymann equation, kinetic, for one-dimensional stationary gas flows

Boltzmann equation, linearized, Navier- Stokes and Burnett transport coefficients 0--48770

Boltzmann equation, spatial differencing, positivity vs. accuracy 0-38215 boundary-value problems of linear transport theory, Green's function approach 0-72977

approach 0-12977 calculation in statistical physics, review 0-48734 charge carrier models, n-paraffin liquids 0-64952 collision integrals $\Omega^{0.198}$ and $\Omega^{0.298}$, equations for 0-38135 convection flow, instability and transition 0-39513 crystal, anharmonic, theory of transport props. 0-71814

diatomic gases in external mag. field, model calc. 0–64822 dielectric, phonon Boltzmann eqn. 0–74856 diffusion, in CO₂ mutual diffusion coefficients of H₂ and O₂ from room temperature to –77°C 0–64825

diffusional mass transfer in gases and liquids, effect of acoustic streaming 0 -71257

0-71257
droplet growth in clouds, simultaneous heat and mass transport obs.
0 62910 electric charge, in polyethylene terephthalate and polystyrene 0-68908 electrolyte solns, conc, conference, France, Sep. 1968 0-39820 electron and photon, Monte Carlo programs 0-72853 electron transfer, across black lipid membrane 0-64893 electrons in gases, neutral and partially ionized, inelastic collisons effect of 16836 electrons of the Pures and quarter membranes 0-71331

electrons in gases, neutral and partially ionized, inelastic collisons effect 0 16/836.

O 16/836.

electroosmotic, in Pyrex and quartz membranes 0-71331 ethyl alcohol injection into external 0, flow, mass transfer 0-78218. Fermi system in random scatt, centres, independent electrons, varying field, strong single centre potentials 0-42007. How in arbitrary frames, transport processes description, thermodynamic description 0-72956. Holds, dense density and temp, dependence of viscosity and thermal conductivity 0-74733.

gas, diatomic dilute, quantum mech. Boltzmann eqn. 0-39683. gas, dilute, iterative numerical computation 0-46834. gas dilute, iterative numerical computation 0-46834. gas dil, mixtures in mag, field, kinetic theory 0-78211. gas layers, vertical annular, heat transfer 0-50165. gas mixtures, binary, laminar boundary layer equations solutions for mass and energy transfer 0-58371. gas molecules, mean free path in transition region 0-39682. gas transient diff. through membrane 0-68024. gas with particle structure, coeffs. from Navier-Stokes eqns. 0-58387. gaseous mixtures, improved formalism for analysis 0-78059. gases, dilute polyatomic, coefficients for Burnett regime 0-68023. gases, thermal transpiration, mol. rot. relax. times meas. 0-39346. Graetz problem extended to anal. of mass transfer in circular ducts 0.55414. hard sphere gas Boltzmann collision integral, closed form 0-57300. hexane in ection into external O. flow, mass transfer -0-78218.

0 55414
hard sphere gas Boltzmann collision integral, closed form 0-57300
hexane in ection into external 0. flow, mass transfer 0-78218
inert gases, coefficients, calc. 0-71268
ionized gases, multicomponent mixture, formulae derived 0-71266
jet, boundary layer flow mass transfer on impinging surface 0-50155
impinging jet, mass transfer, stagnation flow vel. and press. distrib.
0 50154
hingtie gan for nonconservative forces 0-72978

kinetic eqn. for nonconservative forces 0–72978 linearized classical BBGYk hierarchy, general truncation and soln. 0 42008

0. 42008
Liquid, collective motion 0-61476
liquid metals, coefficients calculated 0-68125
in lung, mass transport, mathematical model 0-76703
in magnetic field, electron gas transport eqns. 0-62250
in magnetic field gauge-independeny formalism 0-59131
magnetic field effects 0-43395
magnetic field effects 0-43395
in magnetoplectric electromotive force in an ionic media, Boltzmann's transport equation 0-51995
in magnetoplasma Lorentzian homogeneous 0-39560
mass, adiabatic regenerator, mathematical model in terms of Green's func-

in magnetoplasma Lorentzian homogeneous 0–39500 mass, adiabatic regenerator, mathematical model in terms of Green's functions 0–60079 mass, bibliography, Soviet works 0–60081 mass, bubble dynamics in subcooled nucleate boiling 0–46997 mass, liquid metals, condensation and interphase matter transfer 0–58527 mass, local shear stress measurement at the exit of a burner port prior to computation 0–66864 mass, reduction of transfer within drops due to surface active agents 0–39746

mass, review, Polish works 0-66938

mass and friction factors in a corrugated duct mass exchanger 0–45671 mass and heat transfer, semi infinite porous medium, well stirred fluid 0 42100

mass and heat transfer bibliography of Soviet works 0-54762 mass and heat transfer from rot. disc confronted by stationary disc 0 54768

mass and heat transfer of fluid in porous material, stability criteria 0-67860

mass exchange in two phase flows, physical aspects of theory 0-78004 mass flow measurement in pneumatic conveyor 0-43482 mass in d.c. arc, solution jet method 0-61412 mass in plasma of d.c. arc 0-61413 mass transfer, axial dispersion in multiphase systems, time variable flow

0 - 39747

mass transfer, liquid-liquid systems, wetted wall column 0-39761 mass transfer, turbulent, from wall at large Reynolds and Peclet nos., universal law 0-61219

mass transfer at solid-liquid interface for climbing film flow in an annular duct 0-39744

mass transfer between gas and turbulent liquid, influence of diffusivity obs. 0-68089

mass transfer between liquids and spherical particles in agitated tank $0\!-\!39745$

mass transfer from spheres, effect of vertical vibration 0-76859 mass transfer in a binary gas mixture and molar fraction distribution under turbulent flow conditions with wall suction 0-61445 mass transfer in free convection boundary layers 0-58270

Transport processes continued

mass transfer phenomena due to Li ions in non aqueous electrolytes, potential time study 0-45070

mass transport coefficient transfer from a solid surface to turbulent separated flows for large Schmidt or Prandtl numbers 0–64634 mass transport induced by oscill. flow in turbulent boundary layers 0–74475

mass-transfer in plane interface region 0-54769 master equation, Markoffian, derivation and comparison with non-Markoffian type 0-45539 matter transport across semipermeable membrane, effect of sound wave 0-64892

0-04892 metal conducting stripes, current-induced mass transport 0-68295 migration in terms of native of boundaries 0-53324 migration of molecules, basis of theoretical model for liquids 0-78255 mobility, meas for n-paraffin liquids 0-64952

migration of molecules, basis of theoretical model for liquids 0–78255 mobility, meas. for n-paraffin liquids 0–64952 molecular conductance from curved surface through cylindrical hole, Monte Carlo cale. 0–58373 molten salts, conference, France, Sep. 1968 0–39820 momentum transfer and friction coefficients for turbulent air flow in a vertical, nominally square duct, results 0–64814 momentum transfer in dense aerosol flowing turbulently in ducts 0–39850 multicomponent vapour-liquid system, equilibrium calculation, from liquid boiling temperature data 0–68185 multiple scatter, comparison of theory with expt. 0–59942 Navier-Stokes and Burnett coefficients, matrix elements of linearized Boltzmann collision operator 0–48770 neutral particle transport, point source Green's functions to describe monoenergetic particles in a uniform, unbounded media 0–63367 neutral particles, monoenergetic point source Green's functions 0–48769 n-paraffin liquids, mobility meas. and charge carrier models 0–64952 Peterls' phonon-Boltzmann eqn., linearized collision operator, gap nonexistence in eigenvalue spectrum 0–41996 plasma, highly non-equilibrium 0–67907 plasma, kinetic theory for Coulomb interactions 0–43270 plasma, weakly ionized, of gas discharge, hydrodynamic transport equations 0–39551 plasma in ionospheric F-region, electron content changes during eclipse 0.0-60327

plasma in ionospheric F-region, electron content changes during eclipse 0-69327 plasma mass transfer processes on electrodynamic acceleration 0-64676 plasma two-component, transport processes on the basis of Landau equation 0-46691

plasma two-component, transport processes on the basis of Landau equation 0–46691
plasmas, improved formalism for analysis 0–78059
point plasmas, dilute, polyadic hierarchy for N species 0–48735
polar gases, classical collision theory 0–61197
polar-quadrupolar gas mixtures 0–39681
polyatomic gases, symmetry relations between transport coefficients on basis of linear response theory 0–50170
in polyethylene terephthalate, electric charge 0–68908
polymer chains in dilute soln., hydrodynamic interaction 0–58460
in polystyrene, electric charge 0–68908
polythene, space charge effects 0–68901
quantum theory 0–68724
radiation, resonance, optically thick media 0–58398
sediment, erosion beneath the sea 0–56750
series solution for translating fluid sphere 0–46637
solid, quantum rate theory, N-dimens, tunnelling effects 0–43650
statistical model 0–76843
statistical model 0–76843
statistical model 0–76843
steel stainless, mass transfer in liquid na loop 0–39749
steel stainless mass transfer and corrosion in liquid Na 0–39748
thermodynamics, phenomenological eqns., separation of geometrical and physical props. 0–73066
turbulent flow over rough walls, viscous sublayer heat, momentum transfer resists. correl. 0–46673
turbulent fliquid, invariance and universality principles 0–78242
variational principles, improved, for coeffs. 0–45558
velocity autocorrel. function, long time behaviour 0–66849
velocity correlation functions in two and three dimensions 0–76853
volume transport of water due to surface gravity waves, assoc. with Stokes drift 0–41480
water vapour bubble, mass transfer in subcooled nucleate boiling 0–39880
weak-coupling limit for transport coefficients of classical or quantum

water vap 0-39880 limit for transport coefficients of classical or quantum

0–39880

Weak-coupling limit for transport coefficients of classical or quantum gases 0–39680

Al stripe, current induced mass transport obs., by scanning electron microscope 0–47648

CdS electrons in, study using acoustoelectric effect 0–59192

H₂O molecule, in ionic solns., low freq. motions, neutron scattering spectra 0–61483

He-K mixture, non-equilib., props., 1000-5000k 0-55567 Hg low press., electron energy distribution 0-61386 Mo-Au stripe, current induced mass transport obs., by scanning electron microscope 0-47648

NO gas diffusion through liq. films, electrically induced carrier transport 0-61511

Na, liquid loop mass transfer of stainless steel 0-39749

Na, iquid not mass transfer and corrosion of stainless steel 0-39748 O₂ gas, low-pressure senftleben effects 0-78228 O₃ mass transfer coeffs. in Na 0-69231 O₃ atmospheric 0-48278

Transport theory, neutron see Neutron transport theory

Trapped free radicals see Free radicals

Traps see Crystal electron states/impurity states and effects; Crystal imperfections; Semiconductors

Travelling wave tubes see Electron tubes

Triboelectric emission see Electron emission

Triboelectricity

friction and static electricity, conf., Minneapolis, USA, April, 1969 0-48947

0—45947 metal/borosilicate glass contact, elec. field effect 0—51130 review 0—59272 signal output of commercial cables, quantitative data, meas. apparatus 0—72127

Triboluminescence see Luminescence

Trions (3He, 3H) see Helium-3; Tritons Triple point see Critical constants, thermal

```
Tritium
```

cosmic ray production in lunar samples 0-48504 cosmogenic, contribution to oceanic ³He 0-76350

cosmogenic, contribution to oceanic ³He 0–76350 counting liquid scintillation, in aqueous solution, polyethoxylated nonionic surfactants in toluene 0–73684 formation and sites in neutron irrad. LiF 0–51395 fusion reactor, stellarator, T balance 0–70710 fusion reactor blankets, liq. Li, T breeding 0–70731 gas, safe handling of large quantities 0–73885 hot-atom exchange reactions with H₂ and D₂ 0–41451 monitor, portable, obs. in air, down to 10μ Ci/m³ 0–73694 nuclear crater ejecta, postshot distribution and movement 0–73057 radioactivity in lunar samples 0–48507 D-T plasma, thermonuclear, fuel burn-up and direct energy converion 0–71132 T+HR hot-atom reactions, distrib. of products 0–48204

0-7152
T+HR hot-atom reactions, distrib. of products 0-48204
T+methane, reactions, trajectory studies 0-72525
Zr-T targets in neutron generators, T gas inhalation hazards evaluation,
Zr-T aerosol parameters obs. 0-54487

Tritium compounds see Hydrogen compounds

Tritons

tons

see also Nuclear reactions and scattering due to/tritons
binding energy, Faddeev equation solution using local two-particle interactions
0-73662
binding energy, Hamada-Johnston potential results
0-73661
binding energy, relativistic corrections
0-49498
form factor, relativistic, by group theory
0-77379
ground state wave function, Faddeev equation solution using local two-particle interactions
0-73662
photodisintegration, analysis using Faddeev equations
0-73660
radioactive delayed t emission discussed
0-46160
three-nucleon problem, review
0-49450
3-H-3-He, \$\beta\$-decay, corrections due to exchange currents and sensor force
0-73851
Si, average energy required for electron-hole pair prod.
0-47577

Si, average energy required for electron-hole pair prod. 0-47577 interactions

scattering

diffractional model for elastic scattering 0-52743 doublet scattering length Hamada-Johnston potential results 0-73661

Troposphere see Atmosphere

Tungsten

ngsten
absorption of nitrogen 0–47085
adatoms on W surfaces, migration and binding energies 0–71499
adhesion to Ni(111), LEED obs. 0–43820
adsorbed Ti, migration in strong elec. field, field emission determ.
0–39981

adsorbed layers of Yb or Nd, surface migration and desorption 0-39980 adsorption, mixed, of ethylene and nitrogen, dosing order effects 0-55766 adsorption of Ar, Kr and Xe on (110), (120), (100), (21) and (111) planes 0-47089

0-4/089
adsorption of CO, partial surface coverage by Th, effect 0-39978
adsorption of Cr on W(011), structure and work function 0-65110
adsorption of Cs, Li, and Ba films on (110) face, effect of inhomogeneous
elec.field on migration equilib. 0-55763
adsorption of H and co-adsorption with O, work function determ.
0-68245

0-68245
adsorption of I₂ on W(110), Auger e spectroscopy obs. 0-55765
adsorption of Na on W(112), LEED obs. 0-65109
adsorption of Na on (112) surface 0-50359
adsorption of O₂ on (110) plane 0-39982
adsorption of Op2 at room temp₂, review 0-71498
adsorption of Y and O₂, work function, thermionic emission 0-74932
adsorption of Zr and Hf 0-43574
adsorption of alkaline earth atoms, field-emission obs. of electronic energy levels 0-43564
adsorption of hydrogen 0-47085

adsorption of hydrogen 0–47085 atomic mass differences and mass systematics in the region 100≤N≤126 0–43015

cathode, field emission, WO_x needle cryst. growth obs. 0–53456 chemical vapour deposited, structure and orientation, impurity effects 0–78397

chemisorption of 5d atoms 0-72536 chemisorption of atomic nitrogen 0-48190 composite with UO₂, scanning electron microscopy and X-ray diffraction 0-53651

0-3051 corrosion in sodium-borate melts 0-59490 creep, in low-pressure O₂, correlation with sublimation rate 0-78636 crystal faces, \{100\} and \{110\}, electron reflection, 80 300 K 0-74888 crystal growth, rods and plates, unidirectional solidification from UO₂-W system 0-50446

crystal growth, rods and plates, undirectional solidification from UO₂·W system 0-50446
crystal growth and morphology 0-78405
crystal surface, low-angle He¹ ion scatt. 0-71458
crystalline surface, theory and expt. 0-47596
crystals single, thermal cycling influence on substructure, migration of sub-boundaries, method 0-47241
Debye temperature calc., modifications to theoretical model 0-40578
deformed and annealed, fine struct, changes 0-40145
desorption of Li at 20, 77 and 112K 0-43573
desorption of U neutrals 0-55764
diffusion of nitrogen 0-65342
effect on V-Ta-C and Nb-Ta-C system, equilibrium at high temperature investigation 0-50821
elastic constant, second and third order, Morse pot. calc. 0-78596
electrical contact resistance, effect of oxidation and roughness of surface, meas. by graphite electrode 0-44039
electrode for pulsed arc welding 0-47475
electron beam 28 MeV energy loss in passing through foil 0-47573
electron emission, field, temp, influence in weak current density region 0-51159
electron emission work function, effect of Yb or Nd adsorbed layer

electron emission work function, effect of Yb or Nd adsorbed layer 0-39979

0–399/9 electron energy loss spectra obs. and correl. with theory 0–50918 electron impact desorption of ions and neutrals, kinetics 0–71492 electron reflection spectra, charact. energy losses 0–71892 electron-electron scattering evidence from energy distribution of field emitted electrons 0–72151 emissive power, 0.4-0.76 μ , 1200 to 2600°K 0–56120

Tungsten continued

emitter surface, stable faceted, development by electroetching 0-78399 emitters, chemical vapour deposited, surface orientation investigation by etch pit technique 0-78396

etch pit technique 0—78396 emitters, in cylindrical thermionic diodes, life test results 0—76997 explosion elect, at 10¹¹/4mp/m², products 0—57417 fibre in Cu, diffusion of Ni 0—50620 fibres in UO₂-W cermet, ordered by unidirectional solidification, materials props, tested 0—40474 field electron energy distribution meas. 0—47892 field emission cathode tip, shape, treatment depend., electron microscopy 0—74873

field-emitter tip, carbon-adsorbed, apparent work function ang. depend. 0 - 72150

60-721306 (https://doi.org/10.1006/10. 0-40917

0-40917 impurity, in zone-refined Nb, redistribution 0-47139 interaction with 0 and oxides of C, ion desorption study 0-39975 ion bombardment damage, electron microscope obs. 0-75172 migration of Ti, adsorbate conc. depend. 0-61634 Mossbauer fraction of **Pe*, force const. changes obs. 0-40531 in nimalloy, effect on permeability 0-59329 oxidation, study by the ion-ion secondary emission method 0-56704 photon attenuation in spherical medium, point source, 8 MeV, calc. 0-46274

0-46274
powder, hot pressing process 0-78680
powder, vibration condensation kinetics 0-47144
powder, hot pressing process 0-78680
powder, vibration condensation kinetics 0-47470
in quartz, struct. impurity, solution growth 0-71519
refractory, body centred cubic, effect of hydrostatic pressure obs. on
mechanical behaviour 0-50662
sintering and self-diffusion, Ni additive effect 0-68514
sorption of organic cpds. kinetics obs. 0-56693
specific heat, thermal expansion calc. of solid and liquid state, results
0-59110

specific ht. meas, at high temps, thermodyn, anal. 0–78776 specific radiant heat flux, spectral emittance from surface, determination 0–59117

sputtering and electron emission under Hg ion bombardment, 15-100 keV 0-71883

0-71003 strength, N-cooled acicular microcrystals, var. with diameter and vacuum conditions, He ion microscopy 0-78648 structure of abnormally large grains in foil after secondary recrystalliza-tion 0-75106

superconductivity, evaporated films, transition temp. 0–51016 superconductors, β -phase, model density of states for high transition temp. 0–75601

tion 0—75106
superconductivity, evaporated films, transition temp. 0—51016
superconductors, β-phase, model density of states for high transition temp. 0—75601
surface, 100, Th epitaxial growth, Auger emission spectra, LEED and work function meas. 0—55729
surface, K ion desorption, residence time meas. using correlation technique 0—68239
surface, (112), Na-induced facetting 0—50359
surface, (112), Na-induced facetting 0—50359
surface, adsorbed K diffusion, activation energy, field emission method 0—39977
surface, diffusion of Au in strong elec. field 0—58561
surface, citraction of WO, and O₂ 0—58563
surface faceting and transport, thermo- and electro- 0—65044
surface structure, field-emission ion and electron microscopy, He ion bom bard. 0—39930
surfaces (110), (211) and (321), transition metal adatom diffusion, field ion microscope studies 0—39931
thermal conductivity, 1700 2800K 0—71870
thermionic emistion, (110) single crystal surface, influence of O₂, 1600° to 2200°K 0—51160
thermionic emister, single-crystal <110>, in converter with Nb collector, performance investigation 0—76989
tip, hoh resolution field electron microscope image 0—53424
vacancy boops in irrad. material, electron microscopy 0—61969
vacancy production on heavy ion and neutron irrad. 0—75139
wire, periodic temp. var., anomalous var. in temp. coeff. of resist. at 1700 °C 0.71950
wire, recrystallized, grain structure effects on fracture 0—43774
wire, vacancies, quenched-in resist. obs. 0—75138
work function, meas. on macroscopic specimens 0—79104
work function and sign, determination, simple experiment 0—56412
work function and sign, determination of the open sign of the sign of the

Tungsten compounds
alloy powder, hot pressing process 0–78680
alloys, high energy rate working 0–65466
hexagonal, for microwave applications, physical properties 0–54033
tungstates, Yb³+-Er³+ doped, i.r.-pumped visible emission, controlling factors 0–62720
tungstates, spectra, 2000 to 40 cm⁻¹, and structs. 0–55323
HfW₂ alloy, lattice parameters, supercond. 0–59177

Tungsten compounds continued

LaB₈. W alloy, elec. resistance, thermo-e.m.f. and Hall effect 0–50970 LaB₈. W alloy, elec. resistance, temp. depend. 0–50971 Nb-W-C alloy, phase equilib., constitution, X-ray diffr., DTA 0–47491 Nb-W-Hf-C, mechanical properties, effects of composition and structure

0-6353 Nb-(6at%)W, low temp., thermally activated flow of single crystal, mechanisms 0-40333 Nb-W phase equilibrium study, 1400-2100°C 0-78334 Nb-W single crystal, yield stress, effect of orientation and sense of applied stress 0-68447

Ni-Nb-W phase equilibrium study, 1400- 2100°C 0-78334 Ni-W alloy, compressive strength, tensile deformation, temp. depend. 0-47377

0-47377

Ni-W alloys, thermomag, effect temp, depend. 0-62534

P₄O₁₀·WO₃ system glasses, elec. cond. 0-59169

W- halogen lamps, dissoc. and reaction phenomena 0-54928

W-Ir-Mo alloy anode for X-ray tube, patent 0-59851

W-Ir solid soln. single crystal, thermionic emission props. of (100) face 0-53972

W-Mo-Ag based powder metallurgy, pseudo- alloy production for elec. contact making 0-68544

W-Ni, effect of alloying Ni addition on sintering and self-diffusion 0-68514

W-Os solid soln, single crystal, thermionic emission props. of (100) face 0-53972

W-Os solid soln, single crystal, thermionic emission property (10,53972) (10,

W-Re solid soln, single crystal, thermionic emission props. of (166), 0-53972
W-(25 wt.%)Re alloy, neutron irrad., damage recovery 40146
W-Ta alloys, interdiffusion parameters determ. 0-40198
W-25%Re, sublimation between 1550 and 1950°C in low pressure O₂
0-78345
75%W-25%Re electrodes, bare and cesiated, characterization for thermionic convertor applic. 76987
750%W-50%Mo, creep in low-pressure O₂, correlation with sublimation rate 0-78636
W-10 at.%)Re, streaking obs. in field-ion microscopy images
0-58562
(W₆Br₁₂)Br₆, synthesis and cryst. struct. 0-75107
WC-Co, strength and hardness, microstructural aspects
0-68472
WC-Co alloy, strength and hardness, effect of small plastic deform.
0-43770

(W_bBr₁)Br_a, synthesis and cryst. struct. U—75107
WC-Co, strength and hardness, microstructural aspects 0—68472
WC-Co alloy, strength and hardness, effect of small plastic deform.
0—43770
WC Co cemented carbides, fracture path obs. using replica method with electron microscope 0—47416
WC-(10wt.%) Co alloy, transverse-rupture strength, particle size and comp. depend. 0—47384
WC, γ irrad. effects, resonant absorption following Coulomb excitation obs., anomalous hyperfine interactions 0—76056
WC, shock compressibility 0—75248
WC fabrication temperature of NbC-Cc, lowering, mechanical properties of NbC-WC examination 0—50785
WC powder formation from W powder, microstruct. obs. 0—65478
WC surface (110), atomic and molecular diffraction of He and D₂ 0—78369
W₂C overlayer on W(112) 0—43539
W(CO)₆, vacuum u.v. spectra 0—70867
WCl₆, force constants and mean amplitudes of vibration, normal coordinate analysis 0—43139
WC₆I, mornal coordinate analysis using spectroscopic data 0—43139
WF₇Cl, molec. consts. 0—74311
W₆I₁₂, W₄I₁₃, prep. and structure 0—75108
WO₂ vO₂ system, phase relationships 0—62143
WO₂ anodic film preparation, electron-beam crystallization 0—65080
WO₃ interaction with W surface 0—58863
WO₃, antiferroelec. phase transitions, group theoretical study 0—40877
WO₃, greroelec. props., low temp. 0—68954
WO₃ i.r. spectra, lattice vibrations analysis 0—65524
WO₃ i.r. spectra, lattice vibrations analysis 0—65524
WO₃ i.r. spectra, lattice vibrations analysis 0—65524
WO₃ interaction with W surface 0—588650
WO₃, needle cryst. growth on field emission W cathodes 0—53456
WO₄ interaction with graphite, mechanism 0—72547
WO₃ cryst. drops form, and nuclei of dendritic cryst. 0—58650
WO₃, refelection, applic, to spectroscopy, and polarimetry in X-ray astronomy 0—45328
WS₅, anode catalyst for Hoxidation in acid electrolytes 0—67009
WS₅I₃/Mo₅S₃I₅, electron microscopy, shear struct. 0—61915
W—Re—ThO₂ wire, stress-rupture, tensile strength, 2000° and 2200°F
0—403

ZrO₂: W, stabilised system, solidification behaviour 0–46987 ZrO₂: WO₃-P₂O₅, phase equilibria 0–47494 ZrW₂ alloy, lattice parameters, supercond. 0–59177

Tuning forks see Vibrating bodies

Tunnel diodes see Semiconducting devices/tunnel and interface devices Turbidimetry see Chemical analysis

Turbidity see Scattering/light; Suspensions

Turbulence

bulence see also Cavitation; Flow; Vortices high Reynolds number, Kolmogoroff's third hypothesis universal constant meas. 0-71227 acoustic and turbulent fluctuating motion identification in moving ideal fluid 0-61247 acoustical mags. 0-71242

acrossol, dense, flow in duct, heat and momentum transfer 0–39850 aerosol, dense, flow in duct, heat and momentum transfer 0–39850 air, between plates, total viscosity and heat cond. rel. to limiting Prandtl number 0–50153

air flow, turbulent deposition of particles, theoretical model 0–50277 air jet, round, transiton region turbulence props., obs. 0–46789 air streams, cross flow, autocorrelation meas, in near wake of square cylinders 0–50161

airflow in model forest canopies, longit. intensity distribs, report 0–79529 analytical theories, current state survey 0–53113 atmosphere, beam wave probe 0–48277 atmosphere, clear air 0–48256

atmosphere, rel. to light beam diffusion 0-73301

Turbulence continued

atmosphere, surface layer, energy spectra and cospectra 0-45139 atmosphere, and wind velocity, microwave probe technique 0-62907 atmospheric, Delhi obs. with F-type radiosonde 0-66286

atmospheric, clear-air, highly localised over southern Mediterranean 0-72616

0-72616
atmospheric, effect in optical communication systems 0-79525
atmospheric, effects on propagation of acoustic-gravity waves, dispersion relation 0-56790
atmospheric, kinetic energy from wave-number frequency Fourier analysis of velocity distributions 0-41499
atmospheric, meas. at optically important size scales 0-48291
atmospheric, rel. to laser propag., multiwavelength obs. 0-51528
atmospheric, small-scale, determ. from meteor obs. 0-48300
atmospheric clear air, remote detection by ir. detectors 0-66278
atmospheric clear air, remote sensing, spatial covariance function of ampli-

atmospheric clear air, remote sensing, spatial covariance function of amplitude fluctuations 0–54246 atmospheric fine structure, optical meas. 0–41495 blade cascades effect of turbulence and Reynolds number on flow 0–55550

boundary layer, compressible, with favourable press. gradient, report 0-78202

0-/8202 boundary layer, equilib, mixing length scheme 0-43226 boundary layer, intermittent region rel. to flow props. distrib. 0-395: boundary layer, max transport induced by oscillatory flow 0-74475 boundary layer, oscillating, heat transfer 0-46784

boundary

layer, transition from laminar to turbulent flow, review boundary layer analysis, based on two-region model for eddy viscosity 0-39516

boundary layer equations, transfer function, spatial similarity, solution 0-43227

boundary layer of natural convection, temp. meas. along plane vertical plate 0-76941

plate 0-76941 boundary layer on cylinder, wall press fluctuations beneath 0-53114 boundary layers, effect of cooling on mean structure in low-speed gas flow in terms of velocity and temp. profiles and friction coeff. 0-67992 boundary layers, growth in adverse pressure gradients, modified entrainment theory 0-46660 boundary layers, on a porous surface with fluid injection, reanalysis 0-61225

boundary 0-55401 layers, super- and hypersonic, effects of compressibility

boundary layers, super- and hypersonic, effects of compressibility 0-55401
boundary layers on smooth and rough walls, press.vars., obs. 0-46796
boundary layers with MHD effects 0-53135
boundary-layer, cross-correlation and cross-spectra meas., interpretations rel. to panel response 0-55542
boundary-layer flow, on rotating cylinder, in aerial stream, calculations, comparison with experiments 0-58277
boundary-layer pressure, wavenumber-frequency spectra, microphone array meas. 0-53296
boundary-layers, large-scale motion in intermittent region, sampling, conditional averaging measuring tech. 0-49968
Burgers' model, 1 dimens., numerical study based on characteristic functional formalism 0-55405
Cameron-Martin-Wiener method, and in Burgers' model 0-49993
clear air, ir. sensor as detector, inflight testing results 0-54245
clear air, ir. sensor as detector, inflight testing results 0-54245
compressible boundary layer, effect of surface curvature 0-61244
conducting fluid, flow, in longit. mag. field, o-74484
conducting fluid in mag. field, interrelation between static, magnetic and dynamic processes 0-39536
convection column, laser-induced, laminar to turbulent flow transition 0-50147
convection velocity, meas. in spectral space 0-53298

0–50147
convection velocity, meas. in spectral space 0–53298
decay, nonlinear, in viscous unbounded fluid 0–49958
decay for weak turbulent field, report 0–78023
deposition of particles in turbulent flow on channel or pipe walls 0–58290
diffusion and vel. oscills., time depend., in air streams 0–71238
dispersion experiments, space-time correlation functions, comparison of
Lagrangian time correlations 0–39502
drag reduction, in dilute polymer solutions, mechanism 0–64844
drag reduction by DNA, rel. to stability of double helix struct. 0–71283
effect on hot-film anemometer response in viscoelastic fluids 0–58281
electrostatic in magnetosphere 0–59613
energy dissipation in atmospheric boundary layer, results 0–59563
energy balance for fluctuations in rel. and press. in moving media
0–58299
entrainment and structure of turbulent flow 0–39510

energy-balance for fluctuations in rel. and press. in moving media 0-58299 entrainment and structure of turbulent flow 0-39510 flame stabilization in jets 0-38418 flame turbulent diffusion buoyant, radiative heat transfer 0-48887 flames, sound emission, characteristics and origin 0-54737 flow, drag reduction and degradation with dilute polymer solns. 0-53299 flow, energy spectrum 0-53109 flow, energy spectrum 0-53109 flow, in layers near walls, characts. 0-74459 flow, in noncircular tubes 0-71082 flow and heat transfer with the internal heat generation in concentric annulus, thermal entrance region 0-61218 flow due to interaction of main flow and cross-jets 0-55426 flow in concentric annulus, comments on anal. 0-49970 flow in presence of magnetic field, velocity profile 0-71126 flow laminar-turbulent transitional, phenomena isosceles triangular ducts 0-71276 flow of electrolyte, wake behind glass sphere influence of transverse magnetic field obs. 0-71127 flow onset conditions 0-39512 flow regions with shear stress and mean velocity gradient of opposite sign 0-67867

flow regions with shear stress and mean velocity gradient of opposite sign $0\!-\!67867$

flow shear in controlled wave disturbances, Reynold stress results 0-39530

0-99530
flow with asymmetric mean velocity, influence of press, gradient 0-39518
fluid lines, small amplitude frequency behaviour 0-46661
fluids, initial condition effect on weak homogeneous turbulence with uniform shear 0-55423
fluids, mass or heat transfer from solid boundary 0-71448
in fluids, stratified 0-71089
fluids homogeneous, equilibrium condition, Reynolds stress-mean velocity
relation, single time scale analysis 0-49969
fluids transfer for make deformation 0, 27236

fluids stratified rel. to make deformation 0-78236

Turbulence continued

forced model egns. 0-55408

in free shear boundary layers, linearized velocity profiles 0-39515 free shear flows, homogeneous and non-homogeneous 0-71096 free stream, effect on heat transfer from stagnation point of sphere

0-69750 free-stream, effect on shearing stresses and heat transfer from immersed

0-09730 free-stream, effect on shearing stresses and heat transfer from immersed bodies 0-61248 friction and heat exchange between rotating coaxial cylinders 0-49985 fully developed turbulence and the Liouville equation for the Navier-Stokes velocity field distribution 0-55436 galaxy evolution 0-76549 gas, flow with optically thin radiation 0-39669 gas flow, loss of coherence of propagating laser beam, meas. 0-42321 gas flow, subsonic, over flat plate, wall temp, and Prandtl number effects on boundary layer thicknesses and shape factors 0-46785 gas flow in pipe, axial dispersion and heat transfer 0-68026 gas jet, struct, effect of admixture of solid particles or droplets 0-71253 gas mixing in rod bundles for turbulent flow 0-46782 gasdynamics of controlled property rel. to electrical discharge 0-53224 gaseous suspension of particles flowing turbulently in ducts of different size and the fractional heat transfer coefficient 0-61561 gases, in mixing region between coaxial streams 0-46793 grid, correlation of diffusion data, Langevin model 0-78014 heat and mass transfer from wall at large Reynolds and Peclet nos., universal law 0-61219 heat flux meter, meas. of turbulence in air flow through heated pipe 0-71282 heat transfer amplification by local injection of fluid into a turbulent tube

0-/1282 heat transfer amplification by local injection of fluid into a turbulent tube flow 0-55420 heat transfer in concentric annuli with constant wall temperatures 0-4563

10—3063
heat transfer in parallel flow through rod bundles 0—55603
heat transfer to gases with varying properties in the entry region of circular ducts 0—46814

heating of ions in h.f. discharge with skin current 0–39543 homogeneous, decays, specific kinetic energy, statistical similarity, eqns. 0–43410

0—43410
homogeneous in universal range, role of convection, space-time correlation of velocity, pressure 0—43220
homogeneous systems, weakly turbulent, general kinetic eqn. 0—43233
hydrodynamic noise reviewed 0—39488
hydromagnetic, two dimen, numerical model, amplification of extrnally maintained seed mag. field 0—48353
hydromagnetic, two-dimens. isotropic, numerical model 0—66366
in hypersonic wake of slender body, photometric meas. 0—53236
incompressible, isotropic, stretching of line elements 0—61215
incompressible turbulent boundary-layer eqns. with heat transfer 0—46849
incompressible fluid, charact. functional eval. 0—43237
inhomogeneous flow, model equations and their applications 0—67879
insulating liq, space charge induced turbulence 0—74769
insulating liquid, turbulent diffusion of charges during unipolar injection 0—74768
interaction of grid turbulence with uniform mean shear 0—78026

interaction of grid turbulence with uniform mean shear 0-78026

interaction of grid turbulence with uniform mean shear 0—78026 intermittent, indeterminacy of moment problem 0—67864 inviscid. Bugger's model, spectral analysis, using Cameron-Martin-Weiner exact expansion 0—61213 ion-wave type, within collisionless shock, meas. by collective scatt. of light 0—67918 ionized underdense gas, power spectrum, time autocorrelation fin. m.e.m. scattering analysis 0—43347 in ionospheric plasma, effect on ion motion 0—41532 isotropic, dependence on Reynolds number of high-order moments of velocity derivatives 0—61214 isotropic, laser Doppler anemometer meas. in 150 to 1000 ms-1 flows, parametric design study 0—43246 isotropic, turbulent-viscosity coeff. struct. 0—46670 jet, over inclined wall, flow 0—78017 jet, redevelopment of turbulent flow downstream from a suddenly enlarged jet 0—55583 jet flow over training edge, sound generation, method for amount prediction 0—71234 jet interaction 0—74456 ist mixing lower in the properties of the propert

tion 0-71234 jet interaction 0-74456 jet mixing flows, unified model for eddy viscosity 0-58377 jet of conducting incompressible fluid, in longitudinal or transverse magnetic field 0-71123 jet of conducting liquid, influence of longitudinal magnetic field obs. 0-71294

Lagrangian and Eulerian correl. coeffs. relation 0-67863

laminar flow breakdown in a parallel-plate channel for twelve different flow configurations 0-61224

laser beam propagation, Gaussian, mode conversion effects 0-69929

rei. to laser beam propagation, Gaussian, mode conversion effects 0-69929
laser beams in turbulent medium, optical processing of the phase correlation 0-42319
liquid flow in pipes and between parallel plates, eddy diffusion in central region evaluation 0-68088
liquids, eddy cell model of mass transfer into surface 0-71280
MHD, direct interaction, approx. 0-43245
MHD, model eqns. analog in gas dynamics 0-55450
m.h.d., spectra in collisionless plasma, stability conditions 0-71140
mass or heat transfer coefficient transfer from a solid surface to turbulent separated flows for large Schmidt or Prandtl numbers 0-64634
mass transfer in a binary gas mixture and molar fraction distribution under turbulent flow conditions with wall suction 0-61445
mass-removal by suction in two-phase pipe flow 0-46848
measurement in three-dimens. mean flow 0-46791
micropolar fluid, flow 0-53121
and mixing in stably stratified environments, relating oceanography, astrophyses, meteorology 0-41567
mixing near wake of supersonic cone, laser planogram meas, technique 0-53255
mixing region, two-dimens, incompressible, report 0-78206

u-3/2/3 mixing region, two-dimens., incompressible, report 0-78206
Ocean, Indian, turbulent energy transport 0-56749
optical measurement, refractive index fluctuations 0-78011
optical wave in turbulent medium, modulation transfer and phase structure functions 0-50055

Turbulence continued

oscillating boundary layer flows, approx. caic. 0-46851 particle deposition from turbulent stream, assumptions of theory 0-46961

particle settling velocities and vertical diffusion in turbulent water, meas. and model 0-50264

pipe flow, developing, single drop breakup 0-58417

pipe flow, swirling, boundary layer velocity distribution 0-46850 pipe flow, two phase with mass removal at surface by suction 0-46848 pipe flow of dilute polymer solutions, ultimate asymptotic and mean flow structure 0-71281

plane near wake, soln. of boundary layer momentum integral eqns. -39517

Dupree's perturbation and quasilinear theory comparison plasma 0-50029

plasma, accelerating mechanism for relativistic particles, spectrum 0-56887

plasma, and electron heating, during beam instability 0-50112 plasma, determ. by broadening of H spectral lines 0-50113 plasma, diffusion in toroidal systems 0-50033 plasma, divergent growth of mol. fluctuations in classical shear flows 0-78050

0-70300 plasma, rel. to e.m. wave scattering 0-71151 plasma, fluctuation level optical meas. 0-61332 plasma, ion-acoustic, anomalous resistance 0-5306 plasma, of collisionless shock wave 0-53162

ma, quiescent, weak and strong turbulent states, fluctuations theory plasma.

0-50030 in plasma, statistical theory, Vlasov equation solution 0-67898 plasma, strong, theor. method 0-46761 in plasma, toroidal systems 0-74551 plasma confinement, turbulence studies using Stark broadening 0-50064 in plasma heating, experiments 0-67902 plasma heating in h.f. discharge with skin current 0-46685 plasma wave echo in one-dimensional weakly turbulent electron plasma 0-50094

0-50094
polymer solution flow in annulus, drag reduction and elastoviscous response 0-46842
polymer solutions, dilute, turbulent flow in pipes, correlation of pressure drop data 0-71284 of positive column in axial mag, field, Kadomtsev's theory 0-39632
Prandt number of air with injection and suction 0-46781
Prandtl-Kolmogorov model with inclusion of second-order terms 0-46681

Prandtl-Kolmogorov model with inclusion of second- order terms 0-46663

pressure fluctuations, boundary-layer, over rough walls 0-53297
rel. to pressure fluctuations, supersonic 0-53261

primordial, dissipation in expanding universe 0-76539
relaminarization in tubes 0-46654
resistance, hydraulic and velocity, profiles, in tube in longitudinal mag. field 0-71122
Reynold's experiment, in magnetic field 0-71124
Richardson criterion for winter anomaly, 60 to 90 km 0-56786
secondary flow in developing boundary layer of square duct 0-39650
shear flow, bounds or transport of momentum, variation methods 0-39511
shear flow, simplification of the direct interaction equations 0-39513

0–39511 shear flow, simplification of the direct interaction equations 0–39523 shear flow field, with uniform velocity gradient chemical reactions, statistical theory 0–39701 shear flow in pipe, temp. diffusion and fluctuation 0–43223 shear layer, laminar-turbulent transition for hypersonic flow 0–46802 shear-flow, review 0–39700 shock wave, collisionless magnetostatic, Balmer H β line, Stark broadening 0–646802

0-64689

0-64689
shock waves in collision-free plasma 0-64690
solar wind plasma 0-48607
sphere drag, at subsonic Mach number and intermediate Reynolds numbers 0-53243
in stars, (A-type supergiants), anal. of small scale velocity fields 0-41646
stars, neutron, superfluid turbulence effect on rotational properties
0-64474

in stellar rotating atmosphere, effect on meridional circulation velocities 0-51658 step-induced turbulent boundary layer separation, Mach 2.5-4 0-50158

step-induced turbulent boundary layer separation, Mach 2.5-4 0-30138 stresses, energy of chemically reacting turbulent shear flow with uniform velocity gradient 0-39701 stresses and velocities in noise producing region of jets, meas. 0-43387 structure, close to liquid phase interface of co-current stratified two-phase flow 0-64652 structure, small-scale, measurement at moderate Reynolds number 0-61212

supersonic cone, wake vicinity, mixing statistics obs. (Mach 2.5, $R=3\times10^6$) 0-53255 supersonic flow on isothermal, adiabatic walls, boundary layers, calc. 0-50151

0-30131 supersonic jets, mixing phenomena for cold jets exhausting into hot surroundings 0-61420 supersonic wake behind 2 dimens. plate 0-53254 suspension in channel, flow characts. 0-39843 theory, closing problem 0-71094 three-dimensional boundary-layer flow, simultaneous lateral skewing 0-55437

transition from laminar flow, in presence of magnetic field 0-71125 transition intermittency of laminar to turbulent states for diverse flows 0-49979

transport equations, liquid, principles of invariance and universality 0-78242

0-78242 two-parameter model, appl. to free jets 0-58297 in universe, isotropic 0-54329 upper atmosphere, velocity distributions 0-41513 velocity correlation tensor, interactions of components due to pressure fluctuations 0-74464 velocity fluctuation, water, three component drag probe 0-74709 venturimeter, classical, investigation of flow 0-55575 Venusian atmosphere, microwave signal fading 0-48585 viscosity in flow core, determ, using principle of max, stability 0-43235 vortex, trailing, decay 0-39654 wake, axisymmetric, energy balance and spectra 0-68051 wall jet from small inclined slot, velocity distribution 0-55536 wall jet on lateral concave surface, experimental investigation 0-53295 wall jet on lateral convex surface, experimental investigation 0-53294 wall jet on lateral curved surface, 0-50178

```
Turbulence continued
```

water, turbulent natural convection on vertical plate, boundary layer struct., 0-46900

obs. 0-46900 wind tunnel, meas. using Doppler shifted laser light 0-53253 CO₂, forced convective heat transfer in supercritical region 0-71255 He-Ar mixing at contact surface in driven shock wave, Rayleigh-Taylor instability 0-39663 He II liquid, rel. to heat transport 0-50288 He plasma, turbulent heating, satellites 0-53173

Turbulent flow see Flow

Twilight

uight see also Atmospheric spectra; Zodiacal light dust in tropical and midlatitude stratosphere from recent twilight meas. 0-51512

evening, photometric obs. of 1.27μ transmission in atmosphere 0-54265 red, emission enhancement rel. to Li, Na release effects in atmosphere 0-54265 red. emission enhancement rel. to Li, Na release effects in atmosphere

b-34207
Li intensity variation enhancement study 0-54267
Na intensity variation enhancement study 0-54267
OH emission intensity variation in evening twilight, balloon-borne observation 0-54268

tion 0-54268
Twinning see Crystals, twinning
Twistors see Calculating apparatus; Magnetic devices
Two-phase flow see Flow/two-phase
Type II superconductors see Superconductivity/type II

Ultracentrifuges see Centrifuges

Ultrasonics

see also separate headings, e.g. Absorption acoustic image conversion using stroboscopic electron mirror microscope 0 - 48854

0–48854
acousto-optical pattern display with pulse modulation 0–66910
amplification surface waves in CdS crystal, theory and expt. 0–47533
angle probes at high temperatures 0–45647
apparatus generating and detecting pulsed ultrasonics in solids and liquids
in range 1-20 MHz 0–48851
arterial wall motion, u.s. echo tracking system 0–51823
beam. 1 MHz. effects of cavitation on DNA 0–45450
beam calibration for biomedical applications 0–48625
beams, 1 MHz, biophysical action in sound beams 0–63201
biological specimens acoustic imaging 0–48853
rel. to blood, haemolysis 0–45446
body composition, biological, determination 0–63199
bone, nondestructive testing of selected properties 0–63200

bone, nondestructive testing of selected properties 0–63200 cd CdSe film on LiNbO₃, surface- wave amplification at 170 MHz 0–68607

0-68607 ceramics, elastic constants and internal friction, determination using resonance methods 0-43816 concentrators H.F. focussing, efficiency calc. 0-60039 concrete testing, comparison with cube testing 0-62016 conference, St. Louis, USA, 1969 0-45623 crystal transducers, radiation power, impedance method of measurement 0-45641

0.45641 delay lines, attenuation and delay time in ferrites 0-78756 delay lines, diffraction grating dispersive, using anisotropic propagation media 0-78754 delay lines for guided waves, applic, of composite rods as delay media 0.38362

0 38362 diagnosis clinical using pulse echo ranging tech., analysis 0-72820 echo pattern from stationary column of clotting blood 0-63209 electrolytes, aqueous solns., parameters and hydration numbers 0-74746 eye and orbit visualization system, compound, high-resolution 0-51835 fibre bundles, industrial and medical appls. 0-45630 field mapping, using liquid crystals 0-52088 field visualisation, applic. to interference phenomenon, interpretation 0-38387

held visualisation, applic. to interference phenomenon, interpretation 0–38387 flow-detector, applic. to arterial surgery results assessment 0–72821 foetal animal, Doppler studies 0–63213 foetal monitoring system. Doppler, preliminary experience 0–63214 frequency analysis 0–48847 holograms, reduction of longitudinal distortion 0–38390 holography, image detection, electronic scanning 0–38389 holography, rel. to medicine 0–66688 image convertor, high conductance, exp. results 0–52127 imaging of biological tissues 0–48647 industrial applications, conference, London (1969) 0–42081 lasers, semiconductor, frequency modulation by ultrasonic waves, sidebands resolution 0–52309 medical applications, conference Winnipeg (1969) 0–63208 medical applications 0–63216 microwave, generation and detection, and applics. 0–42076 modulation cell for f.m. laser communication system, tech. 0–63661 neurosurgery appls. 0–51822 oscillation's impressions on steel, fatigue limits rapid determination 0 47325 particle track formation in hydrogen bubble chamber by ultrasound

particle track formation in hydrogen bubble chamber by ultrasound $0\!-\!52610$

0-3210
placentography, sonar applications 0-63210
Poland, u.s. and physical acoustics, review 0-45624
relaxation in n-butyl, isobutyl, sec-butyl alcohols, mechanism study
0-50222

0-50222 sensors for temp. profile meas. 0-69762 sensors for temp. profile meas. 0-69762 sensors for temp. profile meas. 0-69762 solid state physics applies, book 0-40537 sonoluminescence in H₂O, glycerin, n-octane, n-decane, influence of dissolved H₃, N₃, O₃, CO₃, Ar, Xe 0-46927 sepectrometer, self-modulated marginal oscillator 0-48855 steel and rubber bonding non-destructive testing 0-45646 synchronization of laser emission, system's description 0-60228 techniques for laboratories, survey 0-72850 testing of crack location in crystalline solids 0-43649 transducer, application of CdSe f.e.t., piezoelectric effect 0-44310 transducers, textbook 0-73043 ventricle, left, visualization 0-63215 vibration detecting, piezoelectric transducer, design and operation 0-45608 visualization and modifications of brain tissues, use of ceramic transducer

visualization and modifications of brain tissues, use of ceramic transducer

visualization of left ventricular dynamics, catheter-borne array transducer's applic. 0-48631

Ultrasonics continued

visualization techniques, rel.to characterization of normal female breast 0 - 63212

welding of metal contact to semiconductor, apparatus description 0-53636
Fe fatigue mechanism 0-50728

Ultraviolet detectors see Radiation detectors

Ultraviolet sources see Light sources

Umklapp process see Crystals/lattice mechanics

Uncertainty see Indeterminacy; Probability

Undor see Electron theory; Field theory, quantum

Unified field theory
Unimolecular layers

see Relativity/unified field theories
see Adsorbed layers

Units

See also Constants; Dimensions. Nomenclature and symbols geophysical, EAEG system based on international system, proposals, recommendations 0–51455 programmed course, book 0–45509 SI units, use in description of magnetic properties 0–60146 Upper atmosphere see Atmosphere/upper; Ionosphere

Uranium

per atmosphere see Atmosphere/upper; Ionosphere anium
abundance in lunar samples, and isotopic composition 0–48496
abundance in lunar samples 0–45336
abundance in lunar samples by alpha-particle activity 0–45350
abundance of isotopes in linear samples rel. to age determ. 0–45334
abundance of isotopes in lunar rock samples 0–48492
band structure shift for bc.c. metal, non-muffin-tin potential 0–44067
in carboniferous rock formations 0–76343
cutting by laser beam 0–43318
deformed, energy release kinetics during annealing 0–56034
desorption of U neutrals from W surfaces 0–55764
diffusion in UO₂₁₈₁, activation energies for intergranular diffusion 0–43698
diffusion in pyrocarbons, thin-layer expts. 0–78577
embrittlement, by hydrogen and stress corrosion cracking 0–40388
film, adsorption on W and quartz, electronic props. 0–56193
film, on W, electronic and structural props. 0–55712
fuel rods, radiation induced growth of quenched material 0–40011
lattices, natural U D₂O moderated single rod, buckling obs. rel. to transport theory 0–39219
liquid, Hall coeff. and resistivity 0–71376
liquid, density, pyonometric meas, rel. to density of solid 0–46883
neutron irradiated, grain growth during annealing 0–47207
in on-stream trace activation anal, theory 0–76294
oxidation by CO₂, gaseous diffusion control, CO layer 0–48199
plasma production, temp. and partial press. meas. 0–50023
quenched texture, effect of external stress 0–47205
radioactive isotopes, discovery, history and props. 0–55177
recycling spent fuel to light-water reactors, blending versus diffusion 0–74068
solution, aqueous, on-stream trace activation analysis based on nuclear and flow phenomena 0–48221

0-74068 solution, aqueous, on-stream trace activation analysis based on nuclear and flow phenomena 0-48221 in tektites and achondrites, rel. to thorium content, appl. of lunar rock composition data 0-45102 U-metal assemblies, steel moderated, critical mass irregularity 0-58055 β-U, diffusion of Co 0-40207 α-U, neutron diffr. obs. at low temps. 0-40103 U, reserve estimation for underground leaching in sedimentary rocks 0-72594 α-U single crystal, elastic moduli meas, at low temps, and pressure up to 4 α-U single crystal, elastic moduli meas, at low temps, and pressure up to 4

Uranium compounds

anium compounds
alloy, β-α phase change kinetics 0–68560
alloy, dil., isothermal growth of secondary-phase particles 0–59040
ferromagnetism and supercond., mechanisms correl. 0–40994
monochalcogenides, monopnictides and solid solutions, long range mag.
interactions 0–44712
reactor growth of alloys 0–67583
UO₂, surface free energy anisotropy, pore shape 0–61633
UO₂, surface free energy anisotropy, pore shape 0–61633
UO₂, cryst, growth by closed-capsule zone melting 0–68259
UO₂ cryst, growth by closed-capsule zone melting 0–68259
UO₂, cryst, growth by closed-capsule zone melting 0–68259
uranyl acetate, mag. susceptibility rel. to cryst. field, 80-300°K 0–40954
uranyl complexes with pyridine, fluoresc, spectra 0–76174
uranyl formate, mag. susceptibility rel. to cryst. field, 80-300°K 0–40954
uranyl salts, force consts, and bond distances for U-O bond 0–46516
75% UO₂-25% PuO₂, fuel pins, irradiated, burst strength obs. 0–77618
acetate mag. susceptibility rel. to cryst. field, 80-300°K 0–40954
Mo-UO₂ cermet fuels, determination of postirradiation disposition of ⁸³Kr
0–77623
(Pu-U)O₂, mixed, creep props. 0–58897
(Pu-U)O₂, mixed, creep props. 0–58897
(Pu-U)O₂ mixed fuel in contact with sodium, microprobe exam. 0–59516
ThO₂-UO₂ solid solution, oxidation behaviour 0–48198
U-C-C-O ternary phase diagram constructed 0–47483
U-C-C-O ternary phase diagram constructed 0–47483
U-C-C-O ternary phase diagram constructed 0–47483
U-Mo alloys, shear transform. from γ-phase 0–62137

-68561

0—65501
U-Mo alloys, shear transform. from p-phase 0—62137
U-Mo alloys, stress corrosion props. 0—55998
p-U-Mo fuel alloy, thermal cycling and irrad, stability 0—40467
U-(7.5 wt/8)Nb-(2.5 wt.%)Zr alloy transition phases, cryst. struct.40104
0—40104

U-Nb-Zr alloy, crystal structures of transition phases 0-59041

Uranium compounds continued

U-Ni-S syst., at 800°C, new phases 0-63852

U-O lattice vibrations in alkali monouranates 0-75381 (U-Pu)O₂, mixed, high temp. creep 0-58900 (U-Pu)O₂ fuel pellets, eval. for use in encapsulated fuel pin irrad. tests 0-58061

0-58061 (U-Pu)O₂ fuel pellets, fabrication and characterization 0-56037 (U-Pu)O₂ mixed fuel fabrication for FFTF 0-58962 (U-Pu)O₂ mixed fuels, creep 0-55988 (U-Pu)O₂ mixed fuels, plastic yielding and fracture 0-58892 U-Ru-C system, phase diagram and thermodynamics 0-59055 U-Si, phase identification 0-68539

U-Si system, phase identification, microhardness, electron microprobe 0-56057

0-56057
(U, Pu)₂O₈, lattice parameters rel. to Pu content 0-58762
(U, Pu)₂O₈, fission products emission during irrad. to high burn-up 0-46306
(U, Pu)₂O₂ solid soins., thermal cond , Pu content effect 0-59116
(U, Pu)₂O₃ solid soins. and LiF-BeF₂-ThF₄ melts, exchange of U⁴⁺ and Th⁴⁺ 0-59480
U alloy, alpha crystallization, B impurity depend. 0-40494
U formate, mag. susceptibility rel. to cryst. field, 80-300°K 0-40954
U oxalate, mag. susceptibility rel. to cryst. field, 80-300°K 0-40954
U₃As₄, mag. struct. 0-72239
U₃S₄, mag. struct. 0-72239
U₃S₄, antiferromagnetism, neutron diffr. comp., and temp. depend.

UAs_{1-x}Se_x, antiferromagnetism, neutron diffr., comp. and temp. depend. 0-79209

0-79209

UB₂ and UB, mass spectra and dissociation energies 0-61185

UC-UC₂ equilibrium diagram revised following X-ray diffraction examination at .1790°C 0-53666

UC-UN, solid solution, validity of Vegards law 0-71752

UC-UN solid solution, validity of Vegards law 0-71752

UC-UN solid solution of UO₂ and oxygen retention 0-62808

UC, carbothermic reduction of UO₂ and oxygen retention 0-62808

UC, high temp, irradiation behaviour 0-78799

UC rare gas behaviour obs. using helium bubble injection 0-58842

UC coating on graphite crucibles, plasma-spraying, electron micrograph 0-58993

UC_y, high temp. thermodynamic properties, eqns. 0–59109 UC_y thermodynamics, high temperature, U and C activities on basis of Storms data 0–71409

Storms data 0-71409 UC $_1$ - N_m magnetic susceptibility, 4° to 300° K 0-75900 UC $_1$ - N_m , elastic consts. 0-71666 UC $_1$ - N_n , elastic consts. 0-71666 UC $_1$ - N_n , solid solns, mag. susceptibility and electronic sp. ht. 0-53994 UC ∞ 0, hot hardness, thermal diffusivity, electrical resistivity 0-62077 UC ∞ 0, magnetic structure, noncollinear model 0-41066 UF $_4$, i.r. and Raman spectra force constants 0-64459 UF $_6$, force consts. calcs. 0-43138 UF $_6$, negative ion formation 0-64763 UF $_6$, Raman spectrum in vapour state 0-58183 UF $_6$, calcinimation by i.r. spectroscopy, obs. of ν_k band 0-67633 UF $_6$, magnetically induced elec. field gradients and hyperfine fields 0-44801 UF $_6$; Mossbauer 57 Fe spectra, at 4K, 77K and room temp. 0-48040

0-44801
UFe₂, Mossbauer ⁵⁷Fe spectra, at 4K, 77K and room temp. 0-48040
β-UH₃ and β-UD₃, n.m.r. 0-45030
UI₃, cryst. field energy levels of U⁴⁺ and U³⁺ 0-41086
UN/W(Mo) cermet fabrication using mixed powders or coated particles 0-40470

UN, high temp. irradiation behaviour 0-78799
UN, thermal and elec. cond., Seebeck coeff., 77-400K 0-47562
UN powders, synthesis and characterization 0-56051
UN reaction layer growth 0-68235
UN_x, nonstoichiometry, phase changes, lattice consts., x-ray diffr.

UN reaction layer growth 0—68235
UN_x, nonstoichiometry, phase changes, lattice consts., x-ray diffr.
0–50824
U₂N_xX, X=8b, Te, and Bi, crystal structure 0—61911
UO₂-PuO₂-Pu₂O₃ system, phase diagram 0—62147
UO₂-PuO₂-Pu₂O₃ system, phase diagram 0—62147
UO₂-PuO₃-polyerystalline, elastic and anelastic response 0—58859
UO₂-SiO₂ vitroceramics, high burn-up behaviour 0—39233
UO₂-SiO₂ fuel element, vitreous ceramic, power density calc. 0—39235
UO₂-SiO₂ system vitroceramics, fission fragment irrad. effect on thermal diffusivity 0—47561
UO₂-SiO₂ vitroceramics, melt props. 0—46307
UO₂-ThO₂ system, solidus and liquidus temps. 0—5823
UO-UC system, equil. O, C and U activities 0—50299
UO₂-W composites scanning electron microscopy and X-ray diffraction 0—53651
UO₂-W system, unidirectional solidification of W rods and plates

 ${
m UO}_2\text{-W}$ system, unidirectional solidification of W rods and plates 0-50446

U0;-W system, unidirectional solidification of W rods and plates 0-50446
U0; 396 enriched, fast fission ratio 0-39243
U0; antiferromag, lattice distortion near 30 K 0-79210
U0; antiferromag, lattice distortion near 30 K 0-79210
U0; carbothermic reduction process, oxygen oxygen in uranium carbidè 0-62808
U0; continuous creep meas under irrad. 0-68459
U0; crepe, exaggerated impurity-microstruct. effect 0-50705
U0; creep, exaggerated impurity-microstruct. effect 0-50705
U0; crepe, exaggerated impurity-microstruct. effect 0-50705
U0; crystal-binding effects on Doppler broadening of neutron abs. reson. or 138U 0-49624
U0; crystal binding effect on the effective resonance integral with a simplified phonon frequency distribution 0-60864
U0; crystal growth by closed capsule zone melting 0-47140
U0; electrostatic charges on dislocations 0-47263
U0; field-ion microscopy obs. 0-47041
U0; fission-induced re-soln. of small gas bubbles 0-47297
U0; high temp. creep 0-58899
U0; high temp, irradiation behaviour 0-78799
U0; high temp, irradiation behaviour 0-78799
U0; irrad, melting pt, increases and decreases 0-68178
U0; invited, invited behaviour 0-78790
U0; positron annihilation, Brillouin zone boundaries effect 0-53775
U0; positron annihilation, Brillouin zone boundaries effect 0-53775
U0; positron annihilation, Brillouin zone boundaries effect 0-53775
U0; soutiering kinetics 0-40442
U0; sintering, comp. depend. 0-47434
U0; sintering, comp. depend. 0-47434
U0; sintering, comp. depend. 0-47434
U0; sintering kinetics 0-40442
U0; surface-controlled oxidation-reduction and self-diffusion 0-65344
U0; termal diffusivity meas. during irrad., effect of stored energy 0-49732

Uranium compounds continued

anium compounds continued
UO₃, UC fuel particles coated with pyrolytic- C and Si-Carbide, irradiation
performance in power reactors 0-46312
UO₃, venting and distribution, exp. investigations 0-77624
UO₃ as laser sensistizers 0-44921
UO₃ ceramic oxide fuel, importance of radiation heat transfer 0-49733
UO₃ in silicate glass, spectral kinetic characts, at high excitation power
0-44856

UO₂ in silicate glass, spectral kinetic characts. at high excitation power 0–44856
UO₂ lattices D₂O moderated, reson. escape probab. 0–39189
UO₂ nodules, sintered, electrodynamic vibrocompaction 0–67587
UO₂ pellets, preparation by frittage 0–67592
UO₃ pellets, very high density, fabrication, effect of sintering 0–40471
UO₃ surfaces, secondary electron energy distrib. 0–40916
UO₃ lin, frictional force coeff. of moving dislocation, u.s. attenuation meas. –40 to 200C 0–68420
UO₂ lin, intergranular diffusion of U, activation energies 0–43698
UO₃ lin, non-stoichiometric, elec. cond. and defect struct. 0–68351
UO₃ lin, system. (–0.5 ×<0.2), solidus. liquidus temps. 0–58524
UO₃ lin, system. (–0.5 ×<0.2) solidus. liquidus temps. 0–58524
UO₃ lin, spectra, lattice vibrations analysis, force constants 0–65524
β-U₃O₈, cryst. struct. 0–50552
U₃O₈, phase transitions, elec. cond. study 0–59039
U₄O₈, dielec. const. change at phase transition 0–56352
(UO₃As₃O₃)H₃O₃3H₃O₃ trogerite, synthetic, phase transition 0–59042
UO₂Cl₃ crystal, ir. spectra in polarized light 0–51290
UO₂Cl₃ crystal, ir. spectra in polarized light 0–51290
UO₂Cl₃ crystal, ir. spectra in polarized light 0–51290
UO₃Cl₃O₃H₃O₃Cross-section for excited absorption of UO₂ ions obs. 0–44921
UO₃W cermet, unidirectional solidification prep., mech., thermal and elec.

O-44921
UO,W cermet, unidirectional solidification prep., mech., thermal and elec. props. 0-40474
UO,xH,O, proton spin-lattice relax. 0-54171
UP-US solid solutions, long-range interactions (RKKY-type) 0-59341
UP₂, cryst. struct. phase transitions, thermal expansion 0-61912
UJ₂P₄, mag. struct. 0-72239
UP₁₋₇₅S₂, snag. ordering 0-40936
UP₁₋₅S₃, solid solution, n.m.r.rel. to mag. ordering 0-45033
(UO,35Pu₀₋₁₅U₁₋₂N₂, elastic consts. 0-71666
(U_{0.37}Pu₀₋₂₅)O₂ mixed fuel processing using 9-variable fractional factorial expt. 0-58969
US₁₋₉, heat capacity and thermodynamic properties from 5 to 350°K
0-71864
USe₂, heat capacity and thermodynamic properties from 5 to 350°K

USe₂, heat capacity and thermodynamic properties from 5 to 350°K 0-71864

USe, heat capacity and thermodyna 0-71864
UJSi alloy, recovery and recrystn. 0-40443
UJSi fluel elements, irrad, temp.depend. swelling 0-55202
UJSi fuel elements, solid and hollow, irrad. swelling, ≤15000 MWd/te UUJSi fuel elements, solid and hollow, irrad. swelling, ≤15000 MWd/te UUJSi fuel elements, solid and hollow, irrad. swelling, ≤15000 MWd/te UUJSi fuel elements, solid and hollow, irrad. swelling, ≤15000 MWd/te UUJS, crystal structure 0-47206
UVO, crystal structure 0-47206
UVO, pellets, oxidation in air, 800-900 °C 0-66187

Coverage of the control of the control

Urey-Bradley forces see Molecules/internal mechanics

V-centres see Colour centres
V-particles see Hyperons; Mesons
Vacancies see Crystal imperfections/vacancies
Vacancy breakdown see Diffusion in solids

Vacancy breakdown see Diffusion in solids

Vacuum apparatus
see also Seals
bearing materials for ultra high vacuum 0–68541
chamber, total hemispherical emissivity meas. 0–40610
chambers, high vacuum attainment for He, gases, absolute condensation
deosit applic. 0–54523
cryostat, for photoconductive single crystal surface properties 0–51857
deposition apparatus, patent 0–50394
double-beam, infrared hot cell 0–41909
for electrical discharge study at 10⁻¹⁰ torr press. and voltages to 250 kV
0–74616
with electromagnetic isotope separator for short-lived fission products

with electromagnetic isotope separator for short-lived fission products 0-45495 electron beam deposition source, charged particle flux and effects, obs. 0-57220

gas sampler valve for quantitative analysis using gas chromatography

getter cartridges, matrix method of calc. pumping speed and optimum geoemetry 0-57204 goniometer, bakable, with stainless steel bellows 0-76779 instrumentation, exhibitions 0-51862 material transferring devices with all glass surfaces magnetically operated 0-57215

0-57215
modular ultrahigh vacuum feedthrough 0-51871
for nuclear and solid state expts., BARC, Trombay review 0-41912
for optical instrument regulation, in space vacuum environment 0-41915
sample manipulator 0-76778
seals, plastic, fluorocarbon, confined, for movable and fixed modular
vacuum devices 0-76777
slts, fine in metallic foils fabrication use in sealed-off vacuum devices
0-76775
contresing modula of inline 0-57233

0-76775 sputtering module, r.f. inline 0-57223 straight tubes, calc. of transmission probabilities for mol. flow 0-74654 for twist compression, bonding of metals 0-78678 valve, liquid-metal glass, improvement on Veillon and Winefordne 0-76773 valve, wide aperture, for high vacuum and liquid helium temps. 0-51861 valves, bakeable u.h. vacuum, with integral spare seal 0-57216 Ti-1580Ta getter wire tested 0-57207 Veillon and Winefordner

0-51861

Vacuum gauges
on Explorer 32, outgassing and surface adsorption during rotation
0-56885

Bayard-Alpert, sensitivity, collector Auger emission vars., due to chemisorbed gases 0-57209 electrical discharge converter relaxation type for air press. meas. up to 100 torr 0-79824

torr U-19824 electron-impact deposition effects in hot-, cold- cathode gauges 0-57208 extractor gauge as nude system 0-57210 ion, using electron multiplier as ion detector and amplifier 0-51866 ion current, calibration for gas constituents and partial pressures 0-51867

Vacuum gauges continued ion gauges, adsorption at endothermic surface sites effects 0-59845

ion gauges, adsorption at endothermic surface sites effects 0–59845 ion gauges absolute calibration using bakeable adjustable conductance, <10-4 torr 0–57214 ionization, electron trajectories 0–51870 ionization, for range 10-3 to 10 Torr 0–41914 ionization, hot-cathode magnetron type 0–63291 ionization gauge with X-ray shield and ion reflector, patent 0–48660 ionization type, 10-10 to 10-1 torr 0–48658 ionization type, hot-cathode, prediction of relative sensitivities 0–51868 ionization type with u.v. and X-ray shielding, patent 0–51875 ionizing 10-3 to 10-10 torr vacuum measurement 0–45497 magnetron ionization type with ion-collector shield, patent 0–63294 noise free, ionization converter for changing range to 10-7-10-3 torr 0–79825 omegatron for total, partial press. meas. 0–59844

0—79825 omegatron for total, partial press. meas. 0—59844 orbitron low press. gauges, characts. 0—57213 Penning discharge e density, microwave meas. 0—55509 residual gas analysers in high vacuum systems · 0—45498 residual gas analyzer, directional 0—57211 ultrahigh magnetron ionization with variable operating conditions, description 0—51869 withSiC p-n junction e source ionization gauge, ≥10-5 Torr 0—57212

Vacuum polarization see Quantum electrodynamics

Vacuum pumps accommodation pumping, using wall alternately rough and smooth 0-57205

accommodation pumping, using waii alternately rough and smooth 0–57205 cryopumping, gas condensation, surface temp, effect on crit, energy for trapping 0–72861 cryopumping system with 2 cryogenic condensers for molecular beam expts. 0–48657 diffusion pump oils for ultrahigh vacuum, mass spectra 0–51872 fluids from microcapillaries to open atmosphere, mass spectrometric investigation of kinetics 0–66750 getter ion, industrial evolution 0–51863 ion, Penning-type, patent 0–66753 ion pump current meas, linear current-freq, converter 0–76774 liquid ring types 0–41913 magnetic ion pump, discharge mechanism, electric field and gas concentration effect 0–50117 mechanical booster types 0–41913 for nuclear and solid state expts., BARC, Trombay review 0–41912 oil diffusion, curing pressure fluctuations 0–57206 oil free pumping of large volumes to 10-13 tor using cryogenic deposition 0–54522 Penning, heavy metal cathode, stability to Ar and other rare gases.

0-54522
Penning, heavy metal cathode, stability to Ar and other rare gases, experimental study 0-51865
Penning type, phenomenon of argon instability and criteria 0-54521 reciprocating types 0-41913 review, types of pumps and their operation 0-69559 rotary, diffusion, ion system, vacuum tech. improvement by mass spectrometer 0-60895 rotary types 0-41913 for sputtering, operation examination w.s.t. cleanliness 0-69560 superconducting power cables insulation, thermal and electrical, at liquid N₂ and He, temperatures, types, numbers and cost determination 0-51864

Vacuum technique
acoustic filters, deposition of multilayer of Au, Al, CdS films 0-59848
air-water vapour-ice system, temperature and pressure obs. 0-71415
atmospheric analysis of ion pumping effects on high pressure aluminium
alloy walls 0-63292
bake-out for UHV chambers in air at atm. pressure 0-76783
breakdown under power frequency a.c. excitation, prebreakdown current
meas. 0-51873

condensation deposits for attaining high vacuum for He, gases in vacuum chambers, model, result 0-54523 conference, 16th National Symposium of American Vacuum Society 0-57201

conference, Seattle, USA, 1969 0-55686 continuous pumping of hydrogen at 70000 l/s between 10-8 and 10-7 torr 0 - 57222

cryogenic deposition for oil-free pumping of large volumes to $10^{-13}\ \rm tor\ 0-54522$

cryostat, variable temp. with external coolant source for thin film preparation, meas. 0-45490

tion, meas. 0–45490 degassing quantity meas. method 0–41916 for deposition of multilayered acoustic filters, description 0–59848 in design of electromagnetic isotope separator 0–43032 electrodes in vacuum, dispersion-strengthened superior to O-free high-conductivity 0–57202 film deposition mechanisms, metals, alloys and compounds 0–48655 film growth, deposition rates and thickness meas. by electromechanical balance 0–47059 film growth 0–45493 films, thin, deposition techniques 0–53435 friction meas. on elastomers in vacuum under high normal pressures 0–78662 friction of solids on ground basalt, effect of ultrabigh vaccum. 0–78661

friction of solids on ground basalt, effect of ultrahigh vaccum 0-78661

friction of solids on ground basalt, effect of ultrahigh vaccum 0-78661 gas analyzer magnetic, improvements 0-63293 getter, MgO thin film, activity coefficient and capacity 0-57221 hot wall canal arrangement condensation rate calc. 0-79827 ion source of mass spectrometer for anal. of residual gases in vac. instruments 0-45492 low pressure generation by chemical dissoc. 0-48656 mass flow of gases, obs., thermoelastic flowmeter, theory, results 0-79822 mass spectrometry, instrument parameters for particular applications 0-49750 metallizing, economic aspects 0-51874

molecular flow conductance cales, compatibility concept 0–55535 multichannel spark gap 0–46773 multilayer insulations in aerospace technique 0–79821 optical filters, deposition of multilayer of Au, Al, CdS films 0–59848 optical surface degradation from combined u.v. and outgassed materials 0–54907

physisorption of N₂ on 304 stainless steel, at 10⁻⁹ to 10⁻⁴ Torr 0–71491 pumping of fluids from microcapillaries to open atmosphere, kinetics, mass spectrometric investigation 0–66750 review, related to pumps and ion beam sputtering systems 0–69559

Vacuum technique continued

rotary, diffusion, ion pump systems improvement for 10⁻³ torr to UHF, mass spectrometers applie. 0-60895 mass spectrometers applie. 0–60895 sliding bodies, e.m. suspension system, temperature near interface meas., design 0–48892

design 0–48892 space research applications 0–62956 sputtering, thin film deposition analysis 0–45500 super-high vacuum analysis using H₂-condensation deposit 0–54524 superconducting power cables insulation, thermal and electrical, at liquid N₂ and H₂ temperatures, production and maintenance 0–51864 technology of ultrahigh vacuum, physical and technical development 0–45494

technology of ultranigh vacuum, physical and technical development 0-45494 thin film deposition, by electron beam gun, design 0-54839 trap, high vacuum, with independent micro-cooler 0-79823 u.h.v., seals, gasket coating materials 0-76776 u.v. spectroscopy, near vacuum 0-43041 ultrahigh vacuum technology 0-45493 Cu electrodes in vacuum, dispersion-strengthened superior to 0-free high-conductivity 0-57202 H₁:80 cold target prep. 0-46015 Mo-Au film for Si contact technology, vacuum depositions 0-56306 N₂, fixed press, generation by chem. dissoc. of Ba₃N₂ 0-48656 "SNH₁ cold target prep. 0-46015 Ni film, epitaxial growth, vacuum deposition, electron microscope diffraction patterns 0-43550 To 30-4350 United States of the patterns 0-4350 United States of the production patterns 0-4350 United States of the production diodes, deposition 0-44301 Ta condensates with α-modification production influence of substrate 0-68229 Cutum tubes see Electron tubes

Vacuum tubes see Electron tubes Valence bands see Crystal electron states/band structure

Valency alkali metal, valence level changes on interaction with metallic surface 0 - 71487

diamond, valence bands, bond orbitals calc. 0–43989 nonmetallic compounds, chem. bonding and valence state, X-ray emission spectra 0–69141

spectra 0-09141 X-ray band spectra interpretation 0-69142 FeO, Fe₂O₄, Fe₂O₃, rel. to γ-ray, ang. distrib. positron annihilation 0-40629 KMnF₃, Hartree-Fock molecular orbital calc., covalency parameters 0-43583

Se, vitreous binary alloys, transport props. 0–47722
Si, valence charge density and covalency, Fourier components
O-43582
Sn in As-Se-Sn semiconducting glass system, Mossbauer effect
0–48026 Valves, thermionic see Electron tubes
Van Allen radiation see Atmosphere/radiation belts

Van de Graaff generators see High voltage techniques; Particle accelera-

van der Waals forces see Atoms; Kinetic theory; Molecules/intermolecular mechanics: Solids

Vanadium

nadium atom, 15 MeV O⁴⁺ bombardment, K X-ray spectra obs. 0–77693 atomic configurations (3d+4s)⁴p, theoretical calc. 0–60932 corrosion in liquid Na 0–45066 Debye temp, and thermal expansion coeff. 0–78784 diffusion in soft iron, layer conc., spectrochemical determination 0–41196 elastic diffusional relaxation of H and D 0–68428 hardening by neutron irrad. 0–47449 ions in molten LiCl-KCl eutectic, equilib. with solution 0–59496 phonon dispersion, X-ray determ. 0–56092 phonon dispersion curves, X-ray scatt. obs. 0–62178 photoelectric work function 0–75859 solubility in liquid K 0–39741 spectrum, third 0–58103 superconducting, elastic props. use in bulk characts, determ. 0–40741 superconducting type II, temp. depend. of magnetic field at vortex center 0–75630 thermal expansion coeff. and Debye temp. 0–78784

thermal expansion coeff. and Debye temp. 0-78784 thermal hardening of neutron irrad, wire, annealing temp. depend. 0-47448 0-47448
X-ray emission and absorption spectra 0-76140
Nb, thermal X-ray scatt. obs., 293-77K 0-62175
V:H, cold-worked, internal friction, 4.2-450K 0-68422
α-V, thermal expansion 0-71867
V!H, cold-worked, internal friction, 4.2-450K 0-68422
α-V, thermal expansion 0-71867
V-1, in Kges, 10-20 (dipole transitions 0-67634)
V-2+ e.p.r. in MgO 0-72483
V-2+ e.p.r. in MgO, 20-72483
V-2+ in KMgFs, 17-2 excited state, dynamic Jahn-Teller effect 0-41077
V-3-20 (dipole transitions)
V-3+ in Al₂O₁, e.p.r., elec. field effect on separation in null field 0-51388
V-3+ in M₂O₁, e.p.r., elec. field effect on separation in null field 0-51388
V-3+ in MgO, acoustic e.p.r. 0-69187
V-3+ in MgO, acoustic e.p.r. 0-69187
V-3+ in MgO, acoustic paramag. reson. obs. 0-76221
V-3+ in MgO, acoustic paramag. reson. obs. 0-76221
V-3+ in ScCl₁ and InCl₁, absorpt. spectra 0-79306
V-4+, e.p.r. in cristobalite, SiO₂ 0-76226
nadium compounds

V³+ in ScCl₃ and InCl₃, absorpt, spectra 0–79306
V⁴+, e.p.r. in cristobalite, SiO₂ 0–76226

Vanadium compounds
alloy, A 15, sp. ht., supercond., ordering 0–59176
alloy possibilities for Na-cooled fast breeder reactors 0–49729
alloys, Ti and Mo additions, interactions with interstitial impurities, effect
on tensile properties, meas. at 77 to 673°K 0–50722
alloys, corrosion in liquid Na 0–45066
borides, soft X-ray L_{II.11} emission and absorpt. spectra 0–69147
carbides, soft X-ray L_{II.11} emission and absorpt. spectra 0–69147
nitrides, soft X-ray L_{II.11} emission and absorpt. spectra 0–69147
orthovanadates, alcoholic, susceptibility and mag. rotation 0–65887
oxides, soft X-ray L_{II.11} emission and absorpt. spectra 0–69147
spinel, Seebeck coeffs., polaron charge carriers 0–79062
vanadate glasses, optical absorption 0–54105
Vicalloy, mag. props., var. with annealing temp., omnidirectional press.
effect, rel. to phase transforms. 0–79153
X-ray emission and absorption spectra 0–76140
Au₈₀(V_{20-x} Fe.) alloy, where 1≤x≤9, magnetisation, 4.5-300 K 0–44571
Co-V-Cr-Mn-Ni alloy, mag. moment distrib., neutron diffr. 0–44552
38 CrMoV 21.14 steel, incomplete solutions of C. metallographic examination and contact thermal e.m.f. meas. 0–40458
Fe-Co-V, magnetically hard, magnetic properties rel. to structure and phase equilibrium 0–72227
α-Fe-V alloy, Fe-rich, elec. resistivity, 4.2-1200°K, rel. to composition 0–40724

Vanadium compounds continued
Fe-V alloy, Fe-rich, variable freq.n.m.r. meas. rel. to hyperfine field distrib. 0-56682

Fe-V alloys, Fe rich, resistivity 0-78883

Mn-V alloys, structure near-equiatomic comp. 0-47192

Na cooled fast reactor cladding alloys 0-49734

Ni₃(Fe,V), ternary solid solutions, Young's modulus, elec. resist, ordering, magnetization 0-75218

P₄O₁₀-V₂O₅ system glasses, elec. cond. 0-59169

Ta-V system, supercond. 0-75627 TeO₂·V₂O₃·CdO, phase diagram for glass formation, properties 0-68201 Ti:6Al-4V alloy, air contamination, microprobe analysis 0-45099

Ti-Al-V alloy, air contamination, microprobe analysis 0—45099
β-Ti:(Mo,Nb,V) isomorphous alloy, phase transformations 0—53663
Ti-Al-V alloy, internal friction and u.s. yield stress 0—68419
Ti-Nb-V, ternary system, superconducting resistive critical field, comp. depend. 0—44141
Ti-V-C alloy, f.c., electronic structure, from specific heat, mag. susceptibility and n.m.r. meas. 0—40667
Ti-V phase boundaries determ. 0—53665
V;Co, σ-phase alloy, n.m.r., 5-12 MHz 0—79420
V-Ga system, superconducting, for high mag. fields, patent 0—44156
V-H system, H-precipitation, X-ray low temp. diffusp scatt. 0—59044
V;N solid solution, elec., mag. and mech. propsj, comp. depend. 0—58983
V-Nb(Ta) alloys, sp. ht. and supercondj 0—78905
V-O syste d, phase relations below 1200°C 0—59056
V-Ta:C alloy, effect g Mo and W, phase equilibrium investigation 0—50821
V-Ta alloy, supercone, u.s. attenuation obs. 0—71988

V-Ta;C alloy, effect og Mo and W, phase equilibrium investigation 0–50821
V-Ta alloy, supercone, u.s. attenuation obs. 0–71988
V-Ti alloy, supercone, u.s. attenuation obs. 0–71988
V-Ti alloy, precipitation, TiO, cubic phase, electron microscopy 0–65500
V-Ti alloys with improved corrosion resistance in liquid Na, effect of Ti content 0–40468
V complex, [V(bipy)₃]*, z=+2, +1, 0, -1, electronic specua 0–46463
V; Au, electron density changes, model for explanation 0–47679
VB₂, refractory, X-ray spectra and band structure 0–79341
VBe₁₂, n.m.r. of ⁵¹V rel. to plec. quadrupole moment detaum. 0–46134
VZ, By, n.m.r. of ⁵¹V rel. to plec. quadrupole moment detaum. 0–46134
VC, rystal, dislocation etch pits 0–61968
VC, spectron-phonon interactions, upper limit 0–78904
VC, spectron-phonon interactions, upper limit 0–78904
VC, spectron-phonon interactions, upper limit 0–78904
VC, spectra obtained under photoeissociation and He bombardment of VCl, 0–77848
VCl, 2N(CH₃)₂, absorption spectra interpretation using energy level eiagram g V³⁺ 0–79321
V_{1-x}Cr_xH_y, electronic specific heat coogfs. 0–43913
VF₂ powder, magnetic short-range order 0–44481
VF₃, Ra dan spectra, force constants, relation to intramolecular shifting of 3 fold symmetry axis 0–70871
(VF₆)² ion, electronic s fectrum, vibrational suucture 0–64395
V₃Ga foil, martensitic transform, 10-300°K 0–40496
VH₄, magnis ussceptibility, comp. and temp. depend. 0–65886
β-VH₂(31 at 96H), thermal pxpansion 0–71867
V(V) complexes, VF₄ farar-substituted pyridine-N-oxides, N-O stretching moee, obs. 0–39403
VN, V₃N, refractory, X vay spectra and band structkre 0–79341
V_{1-x}N₂D₂O₂O₃O₃O₃O₃O₃O₄O₄O₇O₇O₅V₂O₅Cr, optical condj, meas. in detallic, insulating ane antifauromaâ. phases, 0j04–3 pV, uel. to electronic spins 0–79238

0-40776

V₂O:Cr, optical condj, meas. in detallic, insulating ane antifeuromaå. phases, 0j04-3 pV, uel. to electronic spins 0-79238

V₂O₂:Cr(Al), n m x₂ metal; insulator transition 0-75570

VO₂:Ti, e s x₁, 77-293 K, conc. depend. 0-41345

V₂O₃:Na₂U₂O₇ syst., 400-1000°C, prpp. and identification of 3 new phases 0-53671

V₂O₅;Na₂O₂O₅ syst., 400-1000°C, pmp. and identification of 3 new phases 0-53671
V₂O₅-P₂O₅, glass e.c. and a.c. conductivity, thermoelectric powen, co dp. depend. 0-47630
V₂O₅-P₂O₅ semicon eucting glass system, ⁵¹V n.m.r. og diamag. V⁵⁺ and panamag. V⁴⁺ ions 0-76239
V₂O₅;VO₅ system, phase equilibrium 0-71812
VO₂-WO₂ syste d, phase relationships 0-62143
VO, compressibility and Gruneispn consts. 0-78619
VO, energy bands 0-75497
VO, potential energy curves constructed by Rydberg-Xlein-Rees method 0-67736
VO, vacancy filling and removal, effects on electrophysical props. 0-61943
VO supersaturation in atmospheres of cool, oxgyen rich stars 0-51657
VO_{6.86}, VO_{1.02}, VO_{1.23}, n.m.r. of ⁵¹V, onset of magnetization 0-45032
VO₂, doped, cryst. growth and elec. props. 0-56267
VO₂, elec. and optical props, insulator-mytal transition 0-78958
VO₂, elec. and optical props insulator-mytal transition 0-78958
VO₂, elec. cond., optical reflection and transmission spectra, temp. eepend. 0-75690
VO₂, metal-insulator Mott transition, mag. field depend. 0-51043

VO2, elec. cond., optical reflection and transmission spectra, temp. eepend. 0-75690
VO2, metal-insulator Mott transition, mag. field depend. 0-51043
VO2, resistivity change at 68°C, rel. to switching device applications 0-75538
VO2+, e.p.r. in trate crysts. 0-41344
VO2+, e.p.r. in K1₂(SO₄)₂ and (NH₂)₂Mg₂(SO₄)₃ 0-56669
VO2+ e.p.r. in Cs.₂SO₄, obs. 0-41347
VO2+ e.p.r. in KH₂PO₄, and orientation, obs. 0-41346
VO2+ e.p.r. in KH₂PO₄, and orientation, obs. 0-41317
VO2+ in oxide glasses, chem. bond nature, e.p.r. and electronic absorpt. spectra 0-72493
VO2+ ion in KNO3 and CsNO3, relaxation times from e.p.r. spectrum at microwave power levels 0-48152
VO₃, ordering of vacancies and interstitials 0-75137
VO₃, refractory, X-ray spectra and band structure 0-79341
VO₃ and β-V suboxides, two-phase system, electron microscopy and diffr. 0-55862
V₂O₃ metal-semiconductor transition, symmetry change, effects 0-44072
V₂O₃, antifprromagnetism, neution diffr. 0-44713
V₂O₃, crystal growth, Czochralski ipchnique using electric arc 0-47141
V₂O₃, ingh pressure n mr. of ⁵¹V, 65 kbar, 42 K, antiferromagnetic state suppression 0-45031
V₂O₃, metal-insulator transition in strong elec. field 0-75691
V₂O₃, Mossbauer effect study of metal- insulator transition 0-62313

Vanadium compounds continued

V₂O₃, semiconductor-metal transition temp, switching effect, elec. field depend. 0–65678
V₂O₃ single cryst. and powders, antiferromag, order from neutron polariz. anal. 0–69049
V₂O₃, (010) surface struct., LEED 0–55706

V₂O₃, (010) surface struct, LEED 0-55/06
V₂O₃, cryst, struct, bonding 0-78506
V₂O₃, decomp., electron microscope obs. 0-59043
V₂O₃, ther dal expansion and compressibility 0-65560
V₂O₃ crystal growth from V₂O₃ under various O partial pressures 0-71512

0-1512 V_2O_3 single cuyst, reflection spectra, opt.characts. 0-51293 V_2O_3 sus fensions, optical dispersion of elec. birpfringencp and dichroism 0-74811

0-74811
V₃O₃, H₃O, prepared by hydrothprmal methods, cryst. struct. 0-75104
V₃O₃, single cryst. growth 0-53459
V₆O₁, ingle c. resist, thermoelec., temp. dppend. 0-72034
V₇O₁, elec., resist. thermoelec., tem f. depend. 0-72034
V₈O₁, cryst. growth and mag. props. 0-68251
V₈O_{2,n-1}, shear struct, electron diffr. obs. 0-75105
VO(II) complex, dithiophosphenes, hyperfine interaction of ³IP 0-70898
VOSO₄, cryst. struct. 0-65292
V₂O_{4,non}H₃O₂ values of n, phases preparpd, the transformation into onp another 0-78703
V₃U₂O₁, cryst. struct. determ. 0-65291
V₃U₂O₁, cryst. struct. determ. 0-65496

1600K 0-75422

V₂Si, low-temp. phase transform. 0-65496

V₃Si, mixed supeucond. state, uesistivity measj, critical fipld 0-44142

V₃Si (xbic-to-teuagonal transition, dynamic theory based on electron-phonon interaction 0-78691

V₃Si, X-ray spectra, eneugy bands 0-79342

V₃X type, high-temp. superconductor, X-ray spectra, energy bands 0-79342

V_{1-X}Y₁O₂ solid soln., semicond metal transitions and transport profs. 0-40776

Zr-1 wi%01V allovs, dartensite fhase age-hardoning 0-68517

Zr-(1 wtj%)V alloys, dartensite fhase age-hardpning 0-68517

Va forization

see also Boilina; Condensation; Distillation; Evaporation; Heat &

see also Boilinà; Condensation; Distillation; Evaporation; Heat & vapouization; Vapoui pressuee cryogenic mixtkres, multi-component, vapokr- liquie equilibria prpdiction mpthoes 0–55666 fla de puopag, mpl. toguel eropipt prevapouization 0–48889 graphite, fipe vaporization rates 0–39890 guaphite, high te dp. dass s fectromptry 0–43521 heat tiansfpr in air bubbling through porous guaphite cylindei into wateu including vaporization 0–46995 microwave hpating for puoduction of B fibues 0–46686 microwave heatina fou proeuction of B fibues 0–47003 molecular conductance from curved skriace through cylinduical hole, Donte Carlo calc. 0–58373 polar liquids, rplation between saturated liq. and vapour densities 0–50318 folymers, volatilization 0–76759

0–50318
folymers, volatilization 0–76759
procpss, method of doments, xinetic analysis 0–58526
quartz, laspr-inducpd 0–77157
vapokr dpostition on two-dimensional lattices, computed simulation
0–39922
CO₂ liq. droplets in N₂ nead thermodyn, critical point, theory 0–50329
Cr₂O₃ onidation/vaporization rates 0–51425
Fp. liq. pivitapid, xinetics 0–78343
LiGa oxiee, loss rate grom melt euring crystal growth, propsure egfects
0–55795
Na-O, condonsed stain, stkdy by, dass s fectuoscopy, 0–77968

0-3793
Na₂O, condpnsed statp, stkdy by dass s fectuoscopy 0-77968
Sb₂S₃, molecules in eqkilibuium vapouu 0-61602
Sb₂Se₃, moleculpss in pquilibriu d vapokr 0-61602
YC₂-C system, thermoeynamics 0-53406
YGa gamet, loss uate firm delt eurina crystal guowth, presskre pffects 0-55795

Zn single cuystals, xinetics 0-74854 Vapokr dpnsity spe Dpnsity/gases

Vapour fressurp

poor fressup

see also Humieity; Vaporization
ice, bptwepn +10⁻² and -10²⁰C 0-71428
ppriodic classification aiving straight line diagra ds 0-39893
froylenes, dekterated isotope effect 0-39894
saturated of H₂O structurally moeifiee device for investigation 0-46868
ptrampthylgamane 0-43513
water, moeified, depene. on anomalous component 0-65009
C, temp. of arc. 0-39896
CS₂ liquid, evaluation from partition function 0-78260
F, critical para deters of vapour-liquid coexistence boundary 0-71417
Fe(II) tris(acetylacetonato) complex 0-75409
H₂O₂, control by aqueous solns. of H₂SO₄ 0-43519
H₂¹⁸O ice, isotope effect fixm 0°C to 16°C 0-39897
H₂¹⁸O water, isotope effect fixm 0°C to 16°C 0-39897
H₃ and of the structure of the stru

Vapour prpssure measurement

pour pppssure measurement
cryogenic, capacitance dia fhragm manometeu 0–79815
liquid, cryoåenic for low temp. thermometuy using capacitance diaphraâm
manometer 0–50332
with multi-pur fose instrument 0–66948
semicondkotcu applic. 0–47008
Au, interlaboratory comparison, analysis 0–55676
CoBr₃:KBr-H₂O systpm, solid-liquid equilib. determ. 0–55654
He;liqkid, ksing oil manompter 0–64976
He, Mg-In amalgams, by Knudspn mpthod 0–61605
Lül-LiBr-H₂O system, solid-liquid equilib. eeterm. 0–55654

Variable stars see Stars

Variational calculus see Dathematics
Variational method spe Quantum theory/application methods

Vavilov-Cherenxov radiation see Chprenkov radiation Vectors (vector mesons) see Mesons

Vectors

book, university level, on vector and tensor analysis 0=76798 divergence and ckrl in nonorthogonal curvilingar coordinates 0=48676 divergence opprator, isotropic approach 0=72887 lipid, linear and nonlingar, with numacous sources, applic, og acepteration og convergence techniqke to numprical soln = 0=51900 orthonormalized set, formation from independent set of n vectors, unique inplication of the power of

Poynting, observability 0 69766

airflow in dodel forest canopies, refort 0=79529 distribution of shear wavp propagation in visco:plastic conducting medium in mag. fieles presence 0=50006 drift entrest presence 10=50006

in mag. fieles presence 0-50006 drift, current carriers saturation in mos.f.git. 0-44327 drift in time de fendent elpetric field, and static maß. field, Hall polarization, expressions 0-43266 field and pressure drop in entrancp region 0-39490 fluids, spectral meas, of longitudinal fluctuations in fully develo fed fipe flow 0-71083 pressurized gas, transverse component in flow fields 0-61425 inverse mean free paths and lub. frame absorption coeffs. 0-69601 MHD outation of conducting fluid in cylindrical vessel 0-50008 phase, dispersion in absorbing media, attenuation factor and freq correlation calc. 0-51478

tion cate. 0-51478
and pressure fluctuations, non-turbulent region, rel. to jet flow 0-44407
profile, boundary layer, equilib., turbklent, mixing length scheme 0-43226
supersonic flexural waves in periodically suppruted infinite beams
0-38363

translational og bubbles through acoustic wave in H₂O, isopropyl alcohol,

calc., expt. 0 -61470 CsCl gaseous, distribution gor effusion from near idpal and uight circular cylindrical oriflees 0 71235

acoustic waves

see also Dispprsion, acoustic; Heltum/ligkld, sound propaâation; Shock waves

in uods, time of flight method of determi, stkdent ex ft. 0--62188 in Corprenp, rpl. to pressure, temp, and frequency 0-53701 in absorbent materials stillite and Pritex in 500-2500 Hz range 0-50859 critical, and critical attenuation changes near mag, phasp transitions 0-68590

0 68590
critical liq. has pt., relj to sp. ht. ano daly 0-50321
fluid, two phase flow 0 64963
gas liqkid critical point, hravity exects on meas. 0-46990
in hases, sound vel. rel. to consity 0-73305
hJ. fust sound waves in superfikid tlp, mpas. 0-61578
hJ. transverse, change at superconducting transition te dp. 0-68589
in imfedance tubp, effect of coatinhs on materials being deasured

0 - \$3.700 in lene wool polykrethane dixture, absorftion coefficipnts 0-75392 liquid, rel. to intermolecular constants 0 64853 liquid, supercoolee 0 - 64896 in liquids, bubbly, variations with gas content 0 - 64904 liquids, piezcoplectric radiators odd harmonics, use in u.s. interferometer 0 - 61515 liquids, pl. to population of state 0 - 43422 in liquids, sound vpl. rpl. to tem f. 0 - 73305 lunar sa dples, rocks and alass spheres 0 45395 Mach nkmber flow, bladpuow finite s facing pflipet 0 - 38382 detail rods, dirpct deas, experiment for undergunduate laboratory 0 62180

metal ammonia solns,, of 10 DHz, function of mptal conc. 0-46905 in dethacrylate plastics, sokad vel. 0-73305 in dixtkres, two fhase, onego dpopptt nature of two;phasp critical flow

0 648.49 in nickpl Cerrobend, absorption coefficients 0-75392 nitrobenzength hexane soln., measj 0-64908 in onionskin pa fer, rel. to puessure, tem f. andgrequency 0-53701 farabolic profilp, naumal dode fropag. calc. 0-71340 fiezoelpetric, surface wave velj 0-56097 polypthylene fibre, and absorpt. coeff., effect of mpch. ane tharmal weat mpnt, 93-363K 0-71851 polypropylene fibre, and absorpt. coeff., uelamation processes, 93;433K 0-71851 profilpetric polypropylene fibre, and absorpt. coeff., uelamation processes, 93;433K 0-71851

0 71851
pro fagation in N₂ positive colu dn 0-53276
quartz, first and zuo sokad velj 0-78751
recpiver circular piston centpred in piston beam, intearal signal computation, Bass's methoc 0-57403
rocks, uel. to dpasity 0-51487
in seawater, statistical analysis of rancom components 0-54710
semicondictor, molten, rel. to temp. 0-55613
sound fieles random in nonlinear media, correlation gn₂ pnergy spectrum
0-45626
skperconcuetor, Pb. for al>1-0-62191

0.430,20 skperconcuctor, Pb, for ql>1. 0.62191 Au Kr liqkids solns., 100.150°K, adiabatic and isothermal compressibilities 0.43444 Ar, 3-77 K, elastic constants, lattice dynamics model. 0--50645 Ar, for isotherms from 1 to 70 atm., interaction potential force constants

(Ba_{0,N}Pb₀t₁₂Ca_{0,0N}) TiO₃ porous piezoeletric ceramics, effect of porosity 0 50860

0 30607 Be, Landau quantum oscillations 0 56148 Bi, giant quantum oscillations 0 71837 Bi₁,GeO₂₀₀, metallized and unmetallized, piezoelectric and clastic consts. 0 78748

Cu, magnetoacoustic oscillations obs. 0-43991

ve from Brillouin scatt, near critical pt., obs. 0-46829 dichlorodilluoromethane and their mixtures, for isotherms from 1 to 70 atm., interaction potential force constants 0-68017 Dy, paramagnetic and ferromag, phase, and magnetoelastic effects 0-68591

Gd, paramagnetic and ferromag, phase, and magnetoelastic effects 0.685910 68591 Ge, molten, rel. to temp. 0 55613 He H in, of first sound, temp. depend. 0 46971 He cryst., b.c.c., orientated, meas, of vel. anisotropy 0 4 He, h.c.p. cryst., for determ, of clastic consts. 0 64980 He, solid, second sound vel. 0 68173 He single crystal, oriented, longit. 0 40541

0-46974

Ho, paramagnetic and ferromag, phase, and magnetoelastic effects 0 68591

Velocity continued

acoustic waves continued

K, rel. to r f. size effect 0 44016 KBr, KBr; KCl, cubic crystals, Brillouin spectra, elastic constants 0 51329

KBI, KBI, KBI, Co. (1) S1329
 KCl, cubic crystal, Brillouin spectra, elastic constants 0–51329
 KD, PO₄, shear waves, near ferroelec. Curic temp. 0–50870
 Kr methane liquid solns., 110 190°K, adiabatic and isothermal compressibilities 0–43445
 LSMO elastic and piezoelectric const. 0–79056

Diffuse 0-4,345 LiNbO₁, clastic and piezoelectric const. 0-79056 methane, for isotherms from 1 to 70 atm., interaction potential force con-stants 0-68017 Mg,5iO₄ FeSiO₄ olivine and spinel phases, velocity-density systematics

78746

MnF₂, anomalous change near Neel temp. 0-50861 N₂, for isotherms from 1 to 70 atm., interaction potential force constants 0-68017

N₂ positive column, propagation 0–53276
N₃ positive column, propagation 0–53276
N₄ H and N₆-D mixtures, liquid, 2.5 to 31 K 0–46909
O₅, from triple point to 300°K, at press. to 33 MN/m² 0–46992
Pb, supercond., for ql>1 0–62191
(Pb₉, gB₉, s)Nb₂O₆ porous piezoelectric ceramics, effect of porosity 0–50860

0-50860
Pb(NO₁₎₂, Brillouin scatt. obs. 0-79334
Rbl, cubic crystal, Brillouin spectra, elastic constants 0-51329
SF₆, from Brillouin scattering data near critical point 0-54114
SI, molten, rel. to temp. 0-55613
Tb. paramagnetic and ferromag, phase, and magnetoelastic effects 0-68591

tetralluoromethane, for isotherms from 1 to 70 atm., interaction potential force constants 0-68017

Xe, dispersion of velocity of sound in critical region 0-78328

acoustic waves, ultrasonic

in alkali metals, pure liquid 0-53341
amino acid solns. 0-74751
amino acid solns. 0-74751
amino acid solns. 0-74751
amino acid solns. 0-6407
antiferromagnet, MnF₂, near Neel temp. 0-41063
benzene, liq. 6 3000 Mc, at 20°C 0-64907
benzene, liq. 6 3000 Mc, at 20°C 0-64907
in body fluids and tissues 0-63198
cholesteric liq. cryst., temp. depend. 0-55609
for elastic constant determination of unidirectional fiber composite
0-40219

0 40219 (1997) 0 40219 (1997) 0 47318 gas under press., Brillouin scatt. obs. 0 61440 (1997) 0 678219 (1997) 1 978219 (1997) 1

0 71256 limestone, Shear-, compress, wave bulk vel., obs. 0—47329 inliquids, interferometric meas. 0—68100 measurement, in liquids and solids, new form of sing-around technique 0 78274 methane, stimulated Brillouin scatt, freq. shifts meas, and theory, hypersound speed determ. 0—46824 morpholine water mixture, temp, and conc. variation 0—39784 nitrogen, stimulated Brillouin scatt, freq. shifts meas, and theory, hypersound speed determ. 0—46824 phase velocities, small changes in UHF range, pulse-echotech, modification for meas. 0—52106

for meas. 0–52106
polyethylene, temp, depend, to above melting point, curve shape, theoretical model 0–40550
polyethylmethacrylate, structure obs. from u.s. velocity and refr. index at 6328 Å 0–61613
polymethylmethacrylate, structure obs. from u.s. velocity and refr. index at 6328 Å 0–61615
polyvinylchloride, plasticized with disaktylphthaltates 0–40542
polyvinylchloride, plasticized with disaktylphthaltates 0–40542

polyvinylchloride, plasticized with dialkylphthalates 0–40542 porous solids, shear , compress. wave bulk vel, meas, instrum. 0–47329 quartz, surface-wave vel. temp. depend., obs. 0–47525 sandstone, shear , compress. wave bulk vel. obs. 0–47329 stimulated Brillouin scatt., rel. to hypersonic speed 0–61124 stress acoustic law verification, 100 400 kHz. 0–50857 triethylamine water soln., near critical soln. temp., at 5 MHz. 0–46912 Ag films on Cu, Al, Ni, guided waves vel. dispersion, 5-45 MHz. 0–47336 Al, ohear, compress. wave bulk vel., obs. 0–47329 Al,O₁ crystal, meas. 0–62007 As;Se; (Cu, I), amorphous, doping depend. 0–47529 BaMnF₄, microwave elastic props., freq. and temp. depend., phase transition 0–78611 CO; stimulated Brillouin scatt. freq. shifts meas. and theory, hypersound speed determ. 0–46824

speed determ. 0-46824
CdGa garnet single crystal, meas, elastic moduli 0-43710
CdS, piczoelec, stiffened u.s. vel. enhancement by electron trapping 0-50884

inCdS, theoretical expression which includes electron trapping effects 0.65530

inCdS, theoretical expression which includes electron trapping effects 0 655.30

Cu, elastic consts., nonlinearity parameters meas. 0–62015
Fe; O₄, magnetite single crystal, elastic props., 150.900K 0–68398
He, liq., below 0.6K 0–61586
K Rb liquid alloy, and absorpt. meas. 0–64915
Kl ₃(C,O₄); 2H₃O, elastic consts. meas. 0–71663
Li ₁in, molten, exptal data up to 1100°K 0–71345
MnF, near antiferromag, transition, obs. 0–47971
Nl,H₁(C,O₄); 2H₂O, elastic consts. meas. 0–71663
Na Cs liquid alloy, and absorpt, meas. 0–64915
NaBr, Young's modulus, Poisson's ratio, hydrostatic compressibility, Debye temp. 0–62012
NaCl, creep obs. 0–71697
NaCl elastic consts. var. with temp. from wave vel. 0–55934
Ne, liq., 25-37 K 0–74750
Ne crystal, rel. to elastic and thermal props., 2-20K 0–55941
Pbb_{0.37}Ba_{0.41}Nb₂O, ferroceramic, rel. to elastic constants, ΔE effect and retarded polarization processes 0–75802
SF₆ stimulated Brillouin scatt. freq. shifts meas. and theory, hypersound speed determ. 0–46824
Sn films on Cu, Al, Ni, guided waves vel, dispersion, 5-45 MHz 0–47336
SrTiO₁, elastic moduli, 10-130 K 0–75224
SrTiO₁, rel. to struct, phase transition 0–75342
SrTiO₁, phase transition obs., 107 K 0–75342
SrTiO₁, phase transition tech. for variable path length measurements of u.s. pulses, results 0–53271

Velocity continued

acoustic waves, ultrasonic continued

ZnCl2, aqueous solns, and hydrated melts 0-61518

in Einstein's gravitation theory 0–69980 in Newtonian gravitation theory 0–69980 definitions of seven velocities of light and the introduction of the centrovelocity 0–54903

frequency depend, test using pulsar emission, and photon mass, obs. 0-38522

0-383.22 in gravitational field, freq. depend. 0-72676 moving medium, 'extinction' theory of Fizeau experiment 0-41958 relativity, special, velocity not invariant in Gallilean co-ordinates 0-76813 Romer's method examined from viewpoint of reference system in which coordinate clocks are synchronized 0-51935

student laboratory experiment using time-to- amplitude converter 0-60317

Velocity analysis, particles see Particle velocity analysis

Velocity measurement

ocity measurement see also Angular velocity measurement; Stroboscopes bubbles in liquid flow, correlation method 0—74715 conducting fluids, vel. fluctuations meas. methods 0—39499 detonation wave, marginal, microwave interferometer 0—52 flame propag, rel. to fuel droplet prevaporization 0—48889 gas flow, method for absolute meas. 0—78177

0-52150

gas now, method for absolute meas. 0–18171
gas motion, laser Doppler detection system, possible wind tunnel and atmospheric appls. 0–50141
holograms, Fraunhofer, interference patterns of small spherical particles 0–69574

0-69574 liquid films, falling, average velocity distributions using photochromic dye tracer technique 0-68070 liquid thin film of isobutanol dissolving in water, structure 0-39718 missiles, modified Doppler laser interferometry 0-59866 poly (ethylene oxide) solns. in water, with Pitot tubes 0-50177 powder flow in pneumatic conveyor 0-43482 pulse superposition technique, phase sensitive detection system 0-76795 transducers description, strain gauge, linear potentiometer and seismictype 0-59867 turbulent in noise producing region of subsonic jets 0-43387

acoustic waves

by acoustic interferometer, for thermometry, systematic errors 0-38378 Brillouin spectra of cubic crystals 0-51329 fluids, in vicinity of critical point, resonant cavity techniques 0-63431 gigahertz relative velocity changes small meas.tech. 0-52105

acoustic waves, ultrasonic
gas, by Brillouin scatt. 0—59168
liquid, apparatus with condenser microphones 0—39783
solid, applics, book 0—40537
in triethylamine liquid using phase method 0—46911
wind tunnel, hypersonic meas. using Doppler shifted laser light
Cu single crystal, absorptivity, Schlieren imaging 0—48749

frequency and length meas method, standardising with microwave frequency 0-42395 introduction, university textbook 0-38525 JILA/NASA/NBS expt. using precision long path interferometry

0-67125

modulation method 0-38523 N₂ laser determ. 0-73278

Venus see Planets

Verdet constant see Magneto-optical effects

Verneuil process see Crystals/growth

Vertex functions see Elementary particles; Field theory, quantum; **Functions**

Vibrating bodies

see also Crystals/lattice mechanics; Elastic waves; Pendulums; Piezoelectric oscillations
acoustic streaming in stratified fluid 0-60007
airplane fuselage skin and stiffeners, correl meas. 0-63409
alternate elastic and viscoelastic layers, multilayed beams analysis
0-57366

0-57366
analysis by laser speckle changes 0-42320
anisotropic, upper and lower bounds on Nth eigenvalue 0-52064
anisotropic conical shell, free vibrations, operator-matrix and Galerkin
Procedure techniques 0-48772
bar, sonic reson. 0-60034
bars with periodically varying thickness, structure-determined flexure analysis 0-66888
heam single reinforcing, vibration reduction investigation. 0-45612

beam single reinforcing, vibration reduction investigation 0-45612 beams, indeterminate, frequencies and modes determ. 0-60009 beams, natural frequencies, effect of shear flexibility and rotatory inertia 0-38329

beams, periodically-supported, natural flexural waves 0-76898 beams, transverse shear deform, and rotatory inertia effects approximate theory 0-38357 beams infinite periodically supported, free flexural wave propagation

theory 0 subsequences and modes 0-60008 circular plates, orthotropic, variable thickness, asymmetry 0-54672 cyclic condition in periodic structures 0-76899 cyclic condition in periodic structures 0-76899 cylinder, homogeneous, elastic, three-dimensional analysis of vibration 0-57367 cyclic dar oscillating in viscous medium, sonic waves 0-69714

cylinder, oscillating in viscous medium, sonic waves 0-69714 cylindrical, excitation by rocket exhaust noise, determination of pressure cross correlation 0-52065 cylindrical shell with one or two cylindrical plates at ends 0-54676 cylindrically curved rectangular shells, with or without in-plane loads, approximate solution for natural frequencies 0-54682 dises, anisotropic, low-frequency extensional vibrations, perturbation theory 0-38351 dynamic vibrator absorber, using system with two degrees of freedom 0-42063

elastic flament, charact. nonlinear vibs. 0-54678 elastic half-space excited by impulsive line load, transient motion 0-38350 elastic panel, non-linear oscillations in supersonic non-viscous airstream 0 38353

elastic panel, wave equations for nonlinear free vibrations 0-69710

Vibrating bodies continued

elastic shells, reinforced free vibrations, constrained by reinforced element 0-38373

elastic structures, damping rel. to energy losses 0-54681

encastré sandwich beams with visco-elastic cores, damped normal modes 0-73026

foundation in contact with continuum, vib. excitation 0-54680 free and damped, matrix eigenvalue problems, algorithms 0-38249 frequencies and modes of cantilever beams 0-60008

galvanometer systems with long period of eigen-vibrations, air damping, empirical formula 0–48952 holographic interferometry, time-average, of circular plate in two rationally related modes 0–63654

hysteretic systems random vibration, approx. tech. for predicting response statistics 0-60014

impedance theory applic. 0-38352

mass-spring cubic non-linear system with Coulomb damping, free vibration, exact soln. 0–38334

Melde's expt., modification 0—73023 membranes, transverse displacement, application of second-order nonseparables 0—54688

natural frequency of multi-supported beams 0-76899 nonlinear system, one class, response to stochastic excitation, analysis 0-48835

0—48833 panel plutter, freq. coalescence and structural damping 0—45613 panel structures, conventionally and integrally stiffened, natural frequencies determination, approximate method 0—54683 phase determination by holographic technique 0—54674 plate, circular, in rigid wall, variational formulation of fully coupled problem 0—63437

plate, in stratified fluid 0-60007 plate, infinite, dynamic thermoelasticity theory 0-38348 plate, response to noise in supporting elastic medium 0-54684 plate, subjected to thermal gradient, bounds for natural frequencies 0-54673

0-34673 plate, thin elastic, under random driving forces, numerical soln. 0-73027 plate simply supported subject to broad freq. band 0-57370 plate strips isotropic elastic, free extensional vibrations, Kane-Mindlin eqns soln. 0-38337

plate strips isotropic elastic, free extensional vibrations, Kane-Mindlin eqns soln. 0–38337 plate thin with rigid disk, forced vibration analysis 0–45620 plate vibrators, dynamic behaviour study 0–76896 plates, analysis by simple stroboscopic holographic interferometry system 0–52365

plates, analysis by simple stroboscopic holographic interferometry system 0–52365 plates, metal covered with viscoelastic-damping layers 0–38336 plates, periodically-supported, natural flexural waves 0–76898 plates, simply-supported and clamped-rib stiffened elliptical, fundamental freqs, determination 0–57368 quartz disc, contour vibrations, perturbation theory 0–38351 quartz resonator, excited, X-ray diffr. topography 0–47027 rectangular plates, doubly curved, free vibr. characts. 0–48832 rectangular plates, thin, transverse natural frequencies, Timoshenko approx. 0–38328 in resonant mode, vibration analysis using laser-speckle patterns 0–69707 ring, reinforced circular, bar stiffener effects on flexural response 0–57375 ring and shell structures, mass loading effects 0–42065 rods circular-cylindrical composite, harmonic wave propagation, linear three-dimensional elasticity theory 0–38362 shell, nearly cylindrical, shallow meridional curvature effect 0–38356 shell, thin, pressurized, vibration, flutter, supersonic 0–39660 stells, cylindrical, nonmodal soln. 0–63411 shells, moment loaded, dynamic Green function technique applications 0–57374 shells, plates, membranes carrying discrete dynamic elements, vibration interaction study, general soln. 0–52061 shells, spherical sandwich, free vibrations 0–57373 shells, thin, similitude approxs. 0–63410 shells and plates immersed in fluid flow, flight vehicles, noise and flutter 0–42062 shells cantilever cylindrical, natural frequencies, Flugge and Rayleigh-Ritz egns, applic. 0–38338 shells cantilever cylindrical, natural frequencies, Flugge and Rayleigh-Ritz

shells cantilever cylindrical, natural frequencies, Flugge and Rayleigh-Ritz eqns. applic. 0–38338 shells of revolution, thin, general meridional curvature, vibration modes, frequencies cales, method 0–38355 shells spherical polar-symmetric, energy dissipation under coaxial plane stress, investigation method 0–45573 shells thin cylindrical freely-supported with discrete longitudinal stiffening, vibrational analysis 0–60017 single-branch structural system 0–38340 solid elastic cylindre bonded to rigid circular tank, axisymmetric modes 0–42064 space vehicle structural members, response to vehicle acoustic fields, simulation 0–66900 spherical shells, pure radial vibrations, derivation of frequency equation 0–69706

spherical shells, pure radial vibrations, derivation or frequency equation 0-69706 spring mass systems, step function response 0-76897 stability anal. of nonconservative problems 0-38325 steel plate 0.5×1000/2000 mms dimension, eigenfrequency spectrum, eqns. 0-45619 stiffened structures periodically, propagation const. and transfer matrix relationship 0-48834 string, nonlinear stretched, forced vibation 0-57376 string, viscoelastic, h.f. small amplitude periodic disturbances 0-42058 string instrument bodies, holographic interferometry applications 0-54809 string ins 0-54689

0-54689 structural instability 0-38354 thin elastic plates, asymptotic theory 0-60006 thin flat-walled structures, matrix anal. of stability and vibr., computational problems 0-38332 time-average interferometry on circular plate vibrating simultaneously in two rational modes 0-69958 torsion oscillator, compound, sonic reson. 0-60034 torsional vibration of a cylinder of non-homogeneous material by twist on one of plane surfaces 0-42066 viscoelastic cylinder, solid, bonded to thin casing, forced transverse vibrs. 0-38344

Vibration, molecular see Molecules/vibration

Vibrations

nee also Acoustics; Damping; Oscillations; Vibrating hodies; Waves aeroacoustic, structural response predictions, extrapolation techniques 0 52069

amplitude jumps, demonstration 0-42060

axially symmetric free of solid cylinders, finite difference analysis () 60011

of beam, nonlinear, under harmonic excitation, theory and exp. 0-69701 heam, slender in centrifugal force field, coupled vibrations 0-45618 heam characteristic functions, numerical values of integrals 0-42046

beam single reinforcing, reduction method, investigation 0-45612 beams and plates bending modes, control with multilayer sandwich construction using viscoelastic materials 0-48833

beams and plates bending modes, control with viscoelastic materials, results 0 48833

beams inhomogeneous, WKB, Eikonal approx., physical interpretation 0 60023

bending of metal plates covered with viscoelastic damping layers, effect 0.42336

6 583.66 calibration systems using Mossbauer effect 0-47515 ceramic Bimorph piezoelectric plate thick, circular, response investigation interferometric tech. applic., results 0-42069 of circular plates, flexural, inclusion of clastic supports at plate surface 0-69702.

circular plates, free vibrs, calc., comparison with exact solns. 0-45567 condensation heat transfer to a horizontal tube, effect of vibration () 55669

() ±3660 — 38347 coupled panel cavity system, sonic boom excitation 0-38347 coupled panel cavity system, sonic boom excitation 0-38364 crystal, anomalous (activity dips), in AT cut (R₁) plates 0-53676 crystal lattice monoatomic with nearest, next nearest-neighbour interactions, normal mode analysis 0-62153 cylinders clastic two layered, plane strain vibrations 0-52063 cylindrical inhomogeneous medium, due to transient forces and twists and surface 0-18310 cylinders (0-18310 cylindrical).

surface 0 38330 cylindrical panels of small curvatures, in supersonic flow, analogue calcula tions 0 48828

tions 0.48828 explicitly accuracy of finite element solutions for modal characteristics 0.48828 explindrical shells, accuracy of finite element solutions for modal characteristics 0.45609

ties 0.45609 in dissipative systems, periodic disturbances, h.f. small amplitude

of 4.00% differential equation method for analysis of principal vibrations of multi degree of freedom linear systems 0-54675 dynamic vibrator absorber, using system with two degrees of freedom 0-42063

dynamical systems, stability, role of damping, analysis 0-38333 eigenfrequency analysis of cylindrically curved panel with clamped, elastic boundaries, math model 0-60019 clastic and viscoclastic bars, longitudinal stress pulse propagation 0 42068

clastic filament, charact, nonlinear vibs. 0-54678

clastic surface systems carrying discrete dynamic elements, interaction study, general soln. 0 52061

excitation, principal modes in complex structures, automatic technique 0.54670

0.346.07 ferroelectric ceramic hollow cylinder, vibration characteristics calc. using dynamic shell theory 0.52080 flames 1£, stable, Rayleigh's hypothesis evaluation using bounded inequalities 0.52162

flexural, rel. to periodic thickness variations 0 66887

Reward, rel. to periodic thickness variations. 0. 66887

Reward in rings, shear deformation analysis, comments. 0. 60024

flexural of elastic bar attached to cantilever plate of infinite length, freq.

eqn. 0. 69709

fleximal of metallic structure, constrained viscoelastic layers for damping,

length optimization. 0. 59992

forced, in cantilevered tube conveying fluid under time dependent load,

soln. 0. 69704

forced in this plate with finit disk, analysis. 0. 45620.

soln. 0.69704
forced in thin plate with rigid disk, analysis 0.45620
free, discretely stiffened cylindrical shells, theoretical analysis with arbitrary
end conditions 0.48827
free, of periodically supported beams and plates 0.76898
free and forced torsional motion of joined concentric circular shells orthogomility principle, theory 0.57371
free extensional in plate strips, Kane Mindlin eqns. applic, boundary conditions, soln. 0.38337
force in politicing cabits.

gominy principle, theory U=37311 free extensional in plate strips, Kane Mindlin eqns. applic. boundary conditions, soln. 0-38337 free in nonlinear cubic mass spring system with Coulomb damping, evaluation 0-38334 free parallelopiped rectangular, associated periodicity extension of Fourier analysis 0-60013 handbook on noise and vibration control 0-60060 harmonic wave analysis in a longitudinally reciprocated bar, steady-state solution by Fourier analysis 0-60016 heat transfer and flow of highly viscous liquid during vibration of heating surface 0-71273 heat transfer from spheres, effect of vibration 0-38408 infinite rod, dynamic response to randomly moving torque 0-38276 laminates thick, orthotropic, unified exact, anal. 0-73008 laser interferometry meas, of large amplitude vibrs. 0-73022 liquid flow through curved pipes, characteristics 0-53284 mean square responses in structural systems subject to white noise excitation, theoretical computation 0-57365 metal working, applic, rel. to stress reductions and product finish 0-47424 motion of interconnected bodies, Newtonian approach, eqn. 0-57372 natural frequency of multi supported beams 0-76899 non linear conservative system, oscill, period determ, rel. to evaluation of class of definite integrals 0-72987 nonlinear discrete, of string, computer oriented approach 0-42061 nonlinear structural, numerical integration, linear acceleration method 0-54668 nonlinear systems with many degrees of freedom, asymptotic, averaging, and Ritz methods in steady state theory 0-60001 one dimensional lattice, propagation of longitudinal disturbance 0-73003 optical bench, effect on testing long focal length lenses 0-57603 panel cylindrically curved with dumped, clastic boundaries, eigenfrequency analysis, mathematical model 0-60019

Vibrations continued

piezoelectric plate thick, circular, response investigation interferometric tech.applic_results 0-42069 plane strain of free rectangle, using two-dimensional elasticity theory, numerical results 0-60013

plate, forced parametrically-excited vibr. in plane supersonic flow, numerical anal. 0-38342

cal anal. 0-38342
plate circular clamped in acoustic field, radiated power from harmonic force loadings 0-69716
plates, metal covered with viscoelastic damping layers, bending vibration reduction 0-38336
plates, simply supported and clamped-rib stiffened elliptical, fundamental frees, determination 0-57368
plates, thick, orthotropic, unified exact. anal. 0-73008
plates damped sandwich encastre, loss factors, resonant freqs. determination, iterative method 0-57380
plates inhomogeneous, WK, Eikonal approx., physical interpretation 0 60023

0 60023 plates thick rectangular laminated simply- supported, exact analysis, deformation theory 0-60018 polar symmetric of spherical shells, energy dissipation under coaxial plane stress, investigation method 0-45573 polymer, amorphous, effect on visco-elastic behaviour 0-40243 polymer surface layers mechanical behaviour studies by transition processes in u.s. vibrations 0-50360 polyvibrating eqn., soln. 0-45517 powders, vibrocompaction, energy parameter 0-58996 random of hysteretic systems, approx. tech. for predicting response statistics 0-60014 random vibration, its isolation, case of wide band white noise 0-54669

tics 0-60014 random vibration, its isolation, case of wide band white noise 0-54669 random vibration first-crossing probabilities for linear oscillator 0-73025 rods, elastic, in space vehicles, effect on stable rotation 0-56869 shear modes of simple-cubic crystal plates and bars 0-45610 shell, aelotropic spherical, displacements, stresses analyses using separable homogeneous soln. 0-52062 shell, cylindrical, with built-in free fields 0-63407 shell, spherical, h.f. response as sum of two terms using Watson-Sommerfield transform 0-38346 shell, thin walled, partially filled with fluid, eggs, of forced motion

shell, thin walled, partially filled with fluid, eqns. of forced motion 0 69676

0 69676
shell cylindrical under point-force, impedance characteristics 0-60002
shells, cylindrical, asymptotic theories, appl. 0-66892
shells, cylindrical, asymptotic theories 0-66891
shells cantilever cylindrical, natural frequencies, Flugge and Rayleigh-Ritz
cqns. applic. 0-38338
shells thin cylindrical freely-supported with discrete longitudinal stiffening,
exptl. investigation 0-60017

ship and submarine models exposed to underwater explosion, flexural modes, expt. 0–60012 solid cylinders, finite difference analysis 0–60015 solid cylinder bonded to rigid circular tank, axisymmetric modes 0 - 42064

spacecraft tests, impedance simulation fixtures, development 0-38326 spherical shells, thin, forced torsional vibrs. and Gegenbauer transforms () 73024

stability of Jean's spheroid and Roche's ellipsoid 0-38322

stability of a particle in the plane restrained by two non-identical springs 0-54679

stationary, asymmetric restoring force, formulae for angular frequency and coeffs. of Fourier expansion 0-76895 step function response of spring mass systems with Coulomb damping 0-76897

of string instrument bodies, application of holographic interferometry 0 - 76913

structures flexible, shells and plates immersed in fluid flow, noise and flutter 0-42062

superconducting cast alloy, Nb-Sn crystallization and microstructure 0-59174

0-59174 surface layers mechanical behaviour studies by transition processes in u.s. vibration 0-50360 The inverse vibrational problem, solution 0-54677 time modulated stationary random, analytical basis for testing 0-42059 torsional and longitudinal of a pretwisted slender beam in a centrifugal force field 0-63408 transient flexural of ship-like structures exposed to underwater explosions, theoretical analysis 0-60012 transmission in buildings through insulation barrier junctions, calc. 0.38393

transmission in buildings through insulation barrier junctions, calc. 0.38393 transverse, determination based on non-homogeneous elastic theory, for continuous elastic systems 0-48831 transverse natural frequencies, thin rectangular plates, Timoshenko approx. 0-38328 vertical, effect on mass transfer from spheres 0-76859 vibrometer contactless for displacement amplitude meas. in u.s. systems 0.6020

0 60020

viscoclastic column, initially curved, transverse vibrs. under periodic axial load 0-38343 viscoclastic cylinder, solid, bonded to thin casing, forced transverse vibrs.

0 - 38344

0-35344 viscoelastic rod in mag. field, flexural vibr. 0-63404 NF₃, signs of I doubling consts. 0-77812 Nb-Sn, superconducting cast alloy, crystallization and microstructure 0-59174

W powder, vibration condensation kinetics 0-47470

excitation
aeroacoustic, internal-force and moment-response equations for exposed structures 0–52068
coupled panel-cavity system, sonic boom effects 0–38364
cylinders, modal response to various acoustic fields 0–52066
duct, thin walled cylindrical, response to random pressure field 0–54685
one dimensional waves, structure foundation interaction and damping effects 0–52077
plates, response to fluctuating pressure environments 0–66893
random, complex structure response, computer solution 0–52067
seismic excitation on nuclear power plants structural behaviour dynamic analysis 0–52078
shells, response to fluctuating pressure environments 0–66893
by shock waves, oscillating, produced by localized direct radiation, response of cylindrical shell 0–54757
sonic, cylindrical panels, computer programs 0–54687

Vibrations continued

excitation continued

excitation continued stochastic, one class nonlinear system, analysis 0–48835 structures subject to broad freq. band, spatial variation of stress, strain, acceleration, theory, expt. 0–57370 transient, frequency response characteristics meas., effect of nonlinearity due to large defections, Fourier transform analysis 0–48830 transient, frequency response meas, extraneous noise effects 0–66894 by turbulent, boundary-layer, cross-correlation and cross-spectra meas, interpretations rel. to panel response 0–55542

measurement

neasurement
see also Seismology
acoustic apparatus for strain meas, in concrete 0-52123
acoustic mode, distribution at horn mouth mapping by liquid crystal film
0-38391

0-38391
aeroengine compressor and turbine blades, anal. by holography 0-45607
airplane fuselage skin and stiffeners, correl.meas. 0-63409
close natural frequencies in impulse response, resolution, by direct Fourier
transform methods 0-38349
cylindrical rod, side transient displacements during passage of plastic wave

0 - 488360-48536 frequency response of structures, meas, by transient excitation 0-38327 of frequency response of systems use of transient excitation, effect of non-linearities due to large deflections 0-48830 hf., transverse, of uniform cantilever beam, holography applications 0-69703

0-69703

heterodyne system, optical 0-54686

Holographic scanning technique allowing whole vibration cycles to be stored on one hologram 0-60253
laser speckle pattern changes as tool for vibration anal. 0-63405
meter with magnetic correction 0-54536
nonsinusoidal, using laser heterodyne system 0-66886
photoelastimeter for 3×10-8 dilatations 0-60005
piezoelectric transducer, design and operation, application to ultrasonic vibrations detection 0-45608
real-time interferometric holography 0-60289
on table, fibre-optic application 0-69705

vonde states. see Malaculus lelectronic structure: Molecules/ylbration

Vibronic states see Molecules/electronic structure; Molecules/vibration

Vidicons see Electron tubes

Virial coefficients see Equations of state

Virtuons (virtual phonons) see Crystals/lattice mechanics

Viscoelasticity
See also Plasticity
alternate elastic and viscoelastic layers, vibration analysis of multilayered beams 0-57366
boundary problem soln. in elastico-viscous fluid mech. 0-39500
circular ring subject to impulsive loading, dynamic membrane stress
0-38324

complex viscosity, relaxation spectrum extraction 0-69598 composites, complex moduli, theory and application to particulate composites 0-42056

contact-type problems in linear theory 0-66885 continuum mechanics in e.m. fields, linear irreversible thermodynamics 0-38220 crack extension, in viscoelastic material, stress and displacement distrib.

0 - 48818

0-48818
crack propag, stable, in viscoelastic strip 0-47399
curved column, transverse vibr. under periodic axial load 0-38343
cylinder, ablation and thermal effects 0-52051
cylinder bonded to thin elastic casing, study of forced transverse vibration
0-38344

cylinder, abanda the thin elastic casing, study of forced transverse vibration 0–38344
disc, compression 0–45603
disc, compression 0–45603
dislocation, moving, model 0–71619
divinyl rubber, viscosity temp, depend, at high shear strain rates 0–50709
duration of memory determination 0–71673
elastico-viscous liquids, elasticity effect on flow in curved pipe under press. gradient 0–39691
elastohydrodynamics, lubrication of gears and roller bearings 0–40426
elastomers, rel. to breaking process 0–59994
ethylene, secondary dispersion due to motion of chain branches 0–47327
ethylene-methacrylic acid copolymer, and salts, dynamic and steady shear
melt rheology 0–58408
exponential extension ratio, incompressible elastomer 0–40245
fibre reinforced materials, complex moduli 0–45604
fibre reinforced viscoelastic materials, constitutive equation 0–59971
flow, converging, of aqueous polymeric solutions 0–39497
flow, stratified of viscoelastic liquids, stability rel. to elasticity 0–53289
flow, two-dimens, constitutive eqns. 0–48820
fluid laminar flow through rectangular channel 0–67874
fluids, organic and inorganic, determination of relaxation times 0–73019
impulsively loaded clamped circular plates 0–48814
flistoropic continuum, isothermic quasilinear theory 0–52053
layer of finite thickness, plane strain loaded by rolling circular stamp,
contact problem 0–54659
layers for covering metal plates, vibration damping results 0–38336
linear, minimum principles 0–76891
linear, theory, admissible relax. functions 0–57355
liquid, effect on instability of plane, free-surface flows 0–58418
longitudinal impact of two thin rods, stress and strain distribution
0–69697
Maxwell type medium with cylindrical cavity in mag. field, disturbances

Maxwell type medium with cylindrical cavity in mag. field, disturbances 0-57357

mineral oils, rheology during impact 0-53303 mixed boundary value problems, time dependent boundary regions 0-52052

0-52052
non-linear, approximate description 0-57358
non-linear, stress-strain relations 0-59990
non-linear model, stress relaxation at wave fronts in one-dimensional media description 0-73018
nonlinear, styrene butadiene rubber, experimental study 0-50651
nonlinear media, approx. thermomech. constitutive eqns. 0-38311
nonlinear stress analysis with small dilatational changes 0-42054
physical, properties by analysis of transient torsion pendulum 0-59993
plane-strain finite deformation in strain-rate sensitive elastic-plastic materials and shock thickness 0-57360
plate, separation of smooth circular inclusions when subjected to uniaxial tension 0-76875

Viscoelasticity continued

poly (ethylene oxide) solns. in water, vel. meas. with Pitot tubes 0–50177 polyethylene, branched melts, properties 0–55580 poly(β-hydroxyethyl methacrylate), crosslinked solns. creep compliance in robbery zone, obs. 0–39706 polyisobutylene solutions in transformer oil, effect on velocity profiles in short capillaries 0–50183 polymer, Voigt and Maxwell models generalization 0–40247 polymer, amorphous, effect of vibrations on behaviour 0–40243 polymer, quasilinear theory and small parameter method 0–40246 polymer melts, shear-dependent relax. spectrum, conversion from steady-flow viscosities 0–68053 polymers, Poisson coefficient as function of stress-strain state 0–50647 polymers, branched, molec. theory 0–64566 polymers, complex branched, molec. theory 0–64567 polymers, complex branched, molec. theory 0–64567 polymers, dielectric properties meas, above glass transition temperatures cell design 0–51131 polymethylmethacrylate, anal. of steady shock wave propag. 0–78614 pulse propagation, longitudinal stress, in elastic bars 0–42068 punch coupled with isotropic visco-elastic semi-plane, pressure calc. 0–76892 rectilinear and simple shear flow applic. of generalized measures of

0 76892 rectilinear and simple shear flow applic. of generalized measures of deformation rates 0-38310 relaxation times of linear materials, determ. 0-73019 rod, Fener type in mag. field, disturbances 0-59991 rod, linear, thermodynamics and wave propagation 0-48822 rod in axial creep deform, longit, wave propag. 0-45621 rotating shaft, whirling motion 0-66884 sandwich layers for vibration control of beams and plates, results 0-48833 in shear, and accelerative flows, integral theory for vibracity and cheer.

0-40033 in shear and accelerative flows, integral theory for viscosity and shear stresses 0-50182 silicate polymers, struct.implications 0-58866 solid, book 0-43702

solids, nonlinear viscoelastic, boundary value problems 0–59970 solids, organic and inorganic, determination of relaxation times 0–73019 spherical systems in fluid media 0–54660

stready state Maxwell orthogonal rheometer flow, molec. interpretation 0-48783 steel plates, circular, impulsive loading 0-48814 strain, finite, and variable strain rate, effect under isothermal conditions

0-42055

0-42055 stress analysis of nonlinear viscoelastic cylinder with ablating inner surface, small finite deformation 0-57320 strip with propagating central crack, stress intensity factor calc. 0-48821 thermodynamic application to materials with fading memory, integral constitutive equations 0-57359 thermodynamics of crystalline materials, macroscopic and microscopic 0-40293

0-40293 therewiscoelastic behaviour, non-linear transient, anal. 0-38320 thick-walled permeable cylinders strength exam. 0-66883 time varying materials, alternative representations 0-48819 variational principles in linear theory of viscoelastic media with microstructure 0-75229 viscoelastic layer constrained, length optimization for damping 0-59992 viscoelastic solid, plane shock propag, nonlinear constitutive relns. 0-5736

0-57356 waves, plane and axially symmetric two-dimensional propagation 0-57381

waves in viscoelastic bodies Laplace transform analysis 0-38370

Viscometers

cometers
annular, viscosity-temp. behaviour, continuous meas. 0–39525
circular-disc, related electrostatic problems, using matched asymptotic expansions 0–61502
for glass, moleth high shear rate, high temp. rheometer 0–61501
for glass viscosity meas. to 1000°C, parallel-plate type design 0–61609
oscillating vessel method, evaluation 0–58463
oscillating-disc, extension of theory to large boundary-layer thicknesses at low pressures 0–74453
rotational high-temp. for viscosity meas. of refractory materials melts 0–46885
vibrator with resonant mechanical system 0–39705

vibrator with resonant mechanical system 0-39705 vibratory type with automatic stabilization 0-55416 Zimm-Crothers type, electronically timed, improved 0-39750 Viscoplasticity see Plasticity

Viscosity

air-glass particle suspensions, effective drag coeffs. in flow behind shock waves 0-58507

complex and steady state shearing on Maxwell Orthogonal Rheometer, relationship 0-58271

corner flow, asymptotic features of layer eqns. 0–53115 disperse system, non-Newtonian, rel. to particle size distrib. 0–61563 eddy type, two-region model rel. to anal. of turbulent boundary layer 0–39516

ellipsoidal velocity distrib, function, applic, to channel and viscous flow 0-55411

ellipsoidal velocity distrib. function, applic. to channel and viscous flow 0-55411 ethylene-methacrylic acid copolymer, and salts, dynamic and steady shear melt rheology 0-58408 flow, absolute rate theory, structural randomness effects 0-61232 flow in a circular pipe with recessed walls 0-61239 flow in slender channels, similar and non-similar solns. 0-74472 fluid, rotating, Cauching problem, asymptotic behaviour, linearized equations 0-55400 floam, high expansion 0-71393 glass, calcium aluminate-based, low-silicon, composition, formation, mech. props. 0-61610 glass, linear plotting method 0-55681 glass, molten, high shear rate, high temp.rheometer 0-58537 glass, sondorbing of surface 0-47028 glass, soda-silica, phase-separated, heat treatment influence 0-74868 Hele-Shaw, viscous shear layers 0-49980 in isotropic turbulence, turbulent-viscosity coeff. struct. 0-46670 Joule-Thomson coeff. relation 0-57419 of lithosphere 0-76325 magnetic of rocks, temp. dependence hysteresis induced rock magnetization expt. 0-51605 magnetic viscosity field, new method for determ. 0-59302 magnetoplasma Lorentzian in external magnetic fields presence 0-39560 measurement, oscillating vessel method, evaluation 0-58463

Viscosity continued

penetration relation, boundary layer analysis 0–39524 polybutadienes, temperature dependence 0–55386 polyisobutylene, graph of viscosity versus strain 0–46855 polyvinyl chloride, unplasticized melts zero-shear- rate from relaxation modulus plots 0–68033 refractory material melts, high temp. rotational viscometer applic.

second normal stress differences, meas, on rheogoniometer 0-63386 shear turbulent flow, use in controlled wave disturbances behaviour 0-39530

sodium borosilicate glasses, thermal shock resistant, effect on production 0 -68199

0 -68199
sodium poly(acrylate) in NaBr solutions, intrinsic, molecular weight, degree of ionization depend. 0-39755
rel. to sound propagation in fluid moving through cylindrical ducts, viscosity effects 0-52100 temperature variation, continuous meas. 0-39525
temperature-dependent, effect on temp. distrib. in fluid flowing in pipe 0-48725

velocity profiles of flow at low Reynolds number 0-61238

viscoplastic flow between fixed and moving plates, self-modelling soln, 0-52050

Ar plasma, exp. determination 0-67909 Se, vitreous, rel. to crystallizability of alloys 0-65162

acetone, calc. by free energy average potential model 0–78229 air, total viscosity and heat cond. in flow between plates, rel. to limiting Prandtl number 0–50153 binary polar-gas mixtures 0–61449 chloroform, calc. by free energy average potential model 0–78229 diamagnetic diatomic gas, effect of collinear constant and time-varying mag. fields 0–74683 difluorodichloromethane, absolute viscosity at atm. press., –39.7-91.8°C 0–58404

0 - 58404

0-58404 drag in tube during laminar flow with variable props, boundary layer eqns. 0-58390 ethyl alcohol, calc. by free energy average potential calc. 0-78229 fluorodichloromethane, absolute viscosity at atm. press, -39.7-91.8°C 0-58404

0–58404
MGD boundary layer laminar flow at nonconducting surface 0–50004
methane at 293 to 1050°K. intermol. forces 0–74686
methyl alcohol, calc. by free energy average potential model 0–78229
methyl chloride, binary mixtures with H₂S and SO₂ 0–61449
mixtures, nonpolar, at normal pressures 0–58403
nonideal rarefied, temp. dependence, approx. formulae 0–58389
organic halogen derivatives, using capillary flow method 0–43404
polar gases in elec. field, expt. and theory 0–74684
polar gases in elec. field, expt. and theory 0–74684
polar gases with Ar and He. eff. of elec. field 0–78231
Senftleben Beenakker effects in time-varying fields 0–74683
slip, in polyatomic gas mixtures 0–46807
solar wind plasma 0–48607
solar wind plasma 0–48607
sphere drag, at subsonic Mach number and intermediate Reynolds numbers 0–53243
sphere drag in free molecular and transitional flow regimes 0–78187
steam, at high temperature and high pressure 0–50208

steam, at high temperature and transitional flow regimes 0-78187 steam, at high temperature and high pressure 0-50208 water vapour, at high temp, and high pressure, experimental study of 0-61447

0-01447 Ar, and density depend., 100 to 25°C, \leq 175 atm. 0-46835 Ar, meas. from 3500 to 8500°K, at atmospheric pressure 0-74685 CF₁ at 293 to 873°K, intermol. forces 0-74686 CO·N₂, mixtures, correlation to mass diffusion, up to 900 atmospheres

CO₂, 293-1500°K, meas. 0-68025

 CO_2 , from light scattering meas, at gas/liquid interface near critical temp. 0-39757

CO₃, from light scattering meas, at gas/iduid interface near critical temp. 0–3975.

H-H₂, mixture, anal. rel. to specific interaction pot. curve 0–58405

H, high temp., calc. from collision integrals 0–55568

H₂, and density depend., 100 to 25°C ≤175 atm. 0–46835

H₃, oissociating in 1000-10000°K range, 10³-200 bar, results 0–58396

H₄, normal and para, 15 to 5000°K 0–74678

He Ar and He-Kr, binary mixtures, 25-720°C 0–39685

He, and density depend., -100 to 25°C, ≤175 atm. 0–46835

Kr, ratios, temp. dependence of coefficients relative to value at 283°K, 1100 2000°K range 0–78230

N₃, and density depend, -100 to 25°C, ≤250 atm. 0–46835

N₃, meas, 0.96 38°C, 6500 bars max. 0–61448

N₂O₄ dissociating, investigation by vibrating disk method 0–58406

N₂-CO₂ mixtures, wet and dry, meas. 0–39686

O₃ low-pressure senftleben effects 0–78228

SF₄ at 293 to 873°K, intermol. forces 0–74686

SO₂ and SO₂F₃ mixtures, viscosity measurements using capillary transpiration method 0–50171

Xe, bulk viscosity, temp. dependence 0–78326

see also Lubrication; Superfluidity

alkali halides conc. aqueous solns. 0–39751
alkali metals, exptl. unit and investigation method 0–58461
alkanes, pressure depend., rel. to branching in molecule 0–61504
binary mixtures, shear coeffs. 0–50206
bisphenol A polycarbonate solns., temp. coeff. of intrinsic viscosity
0–39754

0-39754 butylamine-tri-n-butoxyboroxine mixtures, dynamic viscosity 0-61505 cetyl-trimethyl ammonium bromide with α-naphthol colloid, no drag reduction on spheres 0-46964 charged spheres, secondary electroviscous effect, including theoretical values of Huggins coeff. 0-71318 DNA in solution, drag reduction powers rel. to stability of double helix struct. 0-71283 density and terms denoted ages that the production of the struct. 0-71283

struct. 0–71283 density and temp, dependence, dense fluids 0–74733 1,2 diaminopropane, associated, in temperature range –65 to –35, –65 to –10 and –35 to +50°C, comparison with existing data 0–58465 diphenyl mixture, chlorinated, thermal variation 0–50209 diphenyls, chlorinated, viscosity -temp, relation 0–55598 dynamic viscosity of compressed liquid water in the vicinity of the solid-liquid boundary below 0°C 0–61500 electrolyte solns, concentrated aqueous, using Thomas eqn. 0–50207 electrolyte solns, rotational correlation times and viscosity coeffs. 0–78271

Viscosity continued liquids continued

electrolytes, molten, relation between adiabatic compress, and viscosity 0-46879

electromagnetodynamic stability of liq. cylinder 0-74692 emulsions containing fluid spheres 0-78317

emuisions containing fluid spheres 0—18317
fluoride-base fluxes in electro-slag remelting process 0—50755
fluorocarbon solvents, FC-43 and FC-78 0—58464
glass, oxide, molten, liquid-liquid phase transitions obs. 0—74721
Guar Gum solutions, dilute, effect on press. loss in flow across sudden pipe contraction 0—39690
heat transfer for an elastico-viscous liquid, laminar motion between two coaxial circular cylinders due to longitudinal motion of the inner cylinder 0—64897

isopropanol-cyclohexane mixture, investigation over temp, press, conc

Isopropanol cyclohexane mixture, investigation over temp., press., concrange 0–64916 laminar flow at large Reynolds number in a bounded domain 0–58419 linear macromols. in soln., in steady flow with superposed oscillations 0–39753

lunar lavas 0-59761

macromolecules, flow based on mol. rearrangement theory 0-53282 measurement by subharmonic press. threshold for bubble motion

measurement by subharmonic press. threshold for bubble motion 0–64879 metallic melts, non-metallic inclusions effects 0–64877 methacrylic acid-2-methyl-5-vinylpyridine copolymers, aqueous solutions, at different ionic strength and pH 0–71354 methylamine, associated, in temperature range –65 to –35, –65 to –10 and –35 to +50°C, comparison with existing data 0–58465 molten salts, flow mechanism 0–39722 naphthalene, dil. solns. in organic solvents, interpretation in terms of theory of regular solutions 0–46886 Navier-Stokes' eqn. derivation for compressible viscous liquids 0–64875 non-Newtonian fluid with temperature-dependent viscosity in the entrance region of a round tube, numerical solution 0–61499 organic, relation between adiabatic compress, and viscosity 0–46879 oxide mixtures, supercritical viscosity anomaly 0–61503 phthalimide solns, effect on induced radiation polarization 0–43463 in polar solvent mixtures, rel. to electrostriction 0–61541 polybutadiene, branched, effects of dilution 0–58467 polyethylene, melt rheological props., low-shear behaviour, molecular structure dependence 0–46853 polyethylene melt viscosity, effect of molecular structure variables 0–46854 polyethylene solutions, Huggins constant 0–68084 polyimide solutions, inherent 0–41429 polyisobutene correlation between max, strength and anomalous viscosity 0–88468 polyisobutylene, in decahydronaphthalene soln., shear depend of intrinsic viscosity and ion formation 0–68468

0-38438
polyisobutylene, in decahydronaphthalene soln., shear depend of intrinsic viscosity and ion formation 0-58468
polymer solutions, dilute, two parameter model 0-64878
polymer solutions, effect of molecular weight distribution on shear dependence 0-58466
polymer solutions in laminar flow, wall effect and anomalies 0-43407

polymers, intrinsic viscosity, extension of theory to short chains 0—61506 polymers, intrinsic viscosity, extension of theory to short chains 0—61506 polymers, intrinsic viscosity, extension of theory to short chains 0—61507 polystyrene melt, tensile behaviour prediction 0—78243 sodium borosilicate melts, anomaly observed above critical points 0—74734

Solution, subjected to shear flow, deformation of macromolecule, effect of internal viscosity 0-43436

Stokes flow in an annular region between concentric cylinders at low Reynolds number 0-58423

subharmonic press. threshold for bubble motion, as meas. method

0–64879 supercritical viscosity anomaly in oxide mixtures 0–61503 tert-butyl amine, effect of viscos, on dielectric relax, time 0–64941 viscoelastic anal. of Barus effect 0–53291 water, compressed, dynamic viscosity in the vicinity of the solid-liquid boundary below 0°C 0–61500 water, compression waves, cylindrical piston problem 0–43413 AgNO₃ in methanol-water mixtures, rel. to electrostriction at 30°C 0–61541

Al, fall of Pb drops, effect of interface energy on rate 0–46884 Al₂O₃-containing glass melts, effects of added ZrO₂ 0–68196 CO₂ 0–55597 ${
m CO_2},$ from light scattering meas, at gas/liq, interface near critical temp. $0{-}39757$

CO₂, from light scattering meas, at gas/nq, internace 0–39757
H₂O₄ at high temperature and single pressure 0–50208
H₃O₅, empirical formula as function of temp. 0–78265
H₃O₅, empirical formula as function of temp. 0–4868
K.NH₃ and ND₃ solutions 0–43437
LOH aqueous solns. 0–39752
NH₃, associated, in temperature range –65 to –35, –65 to –10 and –35 to +50°C, comparison with existing data 0–58465
Na at 160-800°C, expl. unit and investigation method 0–58461
NaCNS in conc. aqueous solns., at 25° 0–71375
NaClO₄ in conc. aqueous solns., at 25° 0–71375
NaNO₃ in conc. aqueous solns, at 25° 0–71375
NaNO₃ in conc. appearance of the solution of the sol

Visibility see Atmospheric optics

see also Colour vision; Eye accommodation mechanics, non-linear analysis, cat 0-76746 acuity in separate fields inhomogeneous luminance adaption, meas. 0-69549 cat, mechanics of accommodation, non-linear analysis 0-76746

contrast sensitivity, adaptation to temporal frequencies 0–63256 contrast sensitivity and spatial bandwith at low luminances 0–63259 critical flicker frequency as a function of viewing distance, stimulus size, luminance 0–41903

luminance 0-41903 critical fileker-fusion thresholds, measured with solid discs and annular stimuli 0-48643 curving of tall objects when viewed close to, reason and appl. 0-63254 cyclopean perception, foundations 0-63268 depth perception, binocular, interhemispheric link for binocular integration in central vision 0-41896 depth perception, binocular after sagittal transection of optic chiasm 0-41895

distance in stereoscopic vision, the three point problem 0-48644

Vision continued

electrical and psychophysical responses of human visual system to modulated light 0-69550 eye's performance, physiological aspect 0-72840 eye adapting stimuli to short test flashes, lateral inhibition, increment sensitivity 0-45478

tivity 0-45478 eye tracking system, information-processing aspects 0-63258 fish, retina, spectral analysis of L-type S-potentials, relation to photopigment absorption 0-63279 flicker sensitivity and apparent brightness as function of surround luminance 0-51842 fluorescent lamps, efficient 100% modulation for visual stimulus appl. 0-45845

0-45845
Fourier methods in research 0-63257
hospital lighting recommendations 0-51843
illusions, distorting and distorted components, monocular, binocular and stereoscopic conditions 0-76744
increment threshold, monopic and dichopic measures 0-63269
independent spatial frequency channels, expt. 0-63261
industrial area floodlighting requirements 0-51844
kinetic space perception, binocular, nature of perceptual spatio-temporal integration process 0-41900
light flicker perception, analogy with sound hearing at same frequencies 0-51841
luminance modulations temporary apparent depth of modulation as func-

0-1841 luminance modulations, temporary, apparent depth of modulation as function of frequency, amplitude 0-54512 metacontrast function waveform, forced-choice vs. magnitude-estimation measures effect 0-54513 modulation transfer function of the visual channel, effect of noise 0.48646

0-48646
movement, spiral after-effect, sensitivity fields 0-63266
movement-sensitivity in humans, effects of adaptation to pattern spatial
frequency 0-63252
moving-pattern exposure, recovery of motion sensitivity 0-63265
normal binocular, foveal contrast-threshold data 0-72846
optometer, i.r. servo-controlled, for producing elec. signal proportional to
eye refractive power 0-45481
perception, influence of visual noise 0-45483
perceptual latency, effects of surround luminance 0-63253
photokeratoscopy, planar reflected imagery 0-54514
protection from solar near i.r. radiation, tests on Rhesus monkeys
0-79799
sychology rel. to band-compression compunication.

0-19/99 psychology rel. to band-compression communication 0-59836 Raster line visibility in television display 0-45482 retinal image displacement, interocular transfer of suppressive effects

0-41899

0—41899

Rhesus monkeys, near i.r. rad. effect on discrimination, rel. to protection from solar rad. 0—79799
scotopic modulation transfer function rel. to quantum efficiency 0—63260 sensory fn. in multimodal signal detection, statistical and probabilistic addition models 0—45466
spatial characteristics, point-spread functions 0—72845
spatial freq. discrimination of gratings 0—41901
spatial organization, inference from disc and sine-wave grating expts.
0—63262

spatio-temporal interactions associated with edges and discs 0-63263 stereoscopic, acuity in anisometropic subjects, correction of aniseikonia 0-41902

0-4864 stereoscopic, distance and the three point problem 0-48644 stereoscopy with single transparencies 0-63267 subjective obs. of complicated optical structures, study using spatial freq. filtering 0-54515 subjective quality factor, development 0-63264

suppresion, temporal and spatial characteristics during voluntary saccadic eye movements 0-72844

suppression, dependence on angular size of voluntary saccadic eye movements 0–72843 temporal summation, time course 0–63255 underwater, physical and psychological bases of visual distortions 0–59837

visual, acuity in anisometropic subjects, correction of aniseikonia 0 41902

Vitreous state

see also Glass

absorption, far i.r., defect induced, lattice vibrations 0-41221 benzene in glasses, temperature effect on phosphorescence lifetime 0-56628

coatings, ceramic and metal substrates, assessment technique 0–53655 conference, Bristol, England Sept. 1970 0–74859 glass-molten salt interface, thermodynamics of ionic exchange processes 0–50354

0-50354 luminescence spectra from irrad. at 77°K, by ruby laser 0-56652 N-state models 0-55683 rigid molecule glasses, secondary relaxations 0-71366 semiconductor, As-S-Te system, bond-structural approach to elec. conduction 0-75676 semiconductor, CdGe_xAs₂, Hall effect, thermoelec. power and elec. cond.

semiconductor, CdGe_xAs₂, Hall effect, thermoelec, power and effect cond. 0–75681 semiconductor, conf., Bristol, England Sept. 1970 0–74859 semiconductor, defective diamond like, intermediate phase 0–47174 semiconductor, local states, photocond., thermoelec. 0–79071 semiconductors and insulators, conf., Cambridge, England, Sept. 1969 0–47664

0-47686 silica, diffusion of He and Ne, effect of prior heat treatment of silica 0-55927

0-55927

sodium metaphosphate, crystallization, heterogeneous nucleation on f.c.c. metals, substrate depend. 0-74867

structure of noncrystalline materials, X-ray diffr. 0-65014
thermodynamic properties, inner parameters 0-47019
vinyl monomer-solvent mixtures, glass transition temperatures, specific heat, crystallization 0-47541
vitreous-vitreous phase separation, small- angle X-ray scatt. obs. 0-50491
water identification and characterization 0-55682

As-S-Te system semiconductors, bond-structural approach to elec. conduction 0-75676

As₂S₃, elec. cond., photoelectricity, photopolarization 0-47707

As₂S₃, radiative recombination, photoexcitation 0-48099

As₂S₃ radiative recombination, photoexcitation 0-48099

As₂S₃ radictivity, absorpt., photocond., spectra, I-V characts. 0-53816

As₂S(Se)₃, heat capacities 0-59103

As₂Se₃, freq. depend. cond. 0-78940

Vitreous state continued

treous state continued

As, Se₂, radiative recombination, photoexcitation 0–48099

As, Se₃, switching and memory props. 0–56250

B₂O₃, Raman scattering and ir. absorpt. from low lying modes 0–51326

B₂O₃, relaxational responses, rel. to N-state models 0–55683

B₂O₃, relaxational thermal capacity, expansion and compressibility, three-state model 0–50338

B₂O₃, struct. 0–71434

BeF₂, vibr. props. cold neutron scatt. obs. 0–59089

C fibre, glassy, prep. and mech. props. 0–43527

C for prostheses, preparation 0–71436

CaMgSi₂O₆, diopside, Raman spectra 0–56561

Ca(NO₃); KNO₃, vitreous mixture, u.s. relaxation 0–62194

CdGeAs₂, electronic and vibrational spectra 0–47505

Co(PO₃)₇, structure, spectrophotometric study 0–39907

GeO₂, neutron diffr, struct. 0–47021

GeO₂, Raman scattering and ir. absorpt. from low lying modes 0–51326

GeO₂, vibr, props. 0–75370

KNO₃-Ca(NO₃)₂, conductance temp. depend. 65-235°C 0–62288

Se, injary alloys, transport props, valency depend. 0–47722

Se, drift mobility, high press. effects 0–47723

Se, hole transport temp. depend. 0–78933

Se, viscosity rel. to crystallizability of alloys 0–65162

SiO₂, atomic vibrs. 0–75379

SiO₂, diffusion of sodium, thermal history effects 0–55925

SiO₃, far ir. spectrum, vibrs. obs. 0–76129

SiO₃, heutron-compacted, Raman scatt, and far-ir. absorpt. 0–76130

SiO₃, silica, fine struct. 0–68200

SiO₃, Raman scattering and ir. absorpt. from low lying modes 0–51326

Ti₃Te₃As₃Te₃, elec. resist. Hall effect, thermoelec, temp. depend. 0–47728

UO₃-SiO₃O₃ system vitroceramics, fission fragment irrad. effect on thermal diffusivity 0–47561

UO₂-SiO₂ system vitroceramics, fission fragment irrad, effect on thermal diffusivity 0–47561 UO₂ SiO₂ vitroceramics, melt props. 0–46307

Vlasov equation see Plasma

Vocoders see Speech Voigt effect see Magneto-optical effects

Volta effect see Contacts, electrical

Volume measurement

dilatometer, automatic, double-membrane 0-45512 dilatometer, continuous recordiná vertical 0-72918 dilatometer for rare gas solid, thermal expansion, compressibility 0-53715

fluid in high pressure cell with internal heater 0–38126 fuel pellets in hot cell, bulk volume meas, using vacuum pycnometer 0–77621

fuel rods, irradiated, void volume determination 0-77622 porosity, use of thermal-neutron irradiated air (41Ar) 0-46223

Vortices see also Cavitation; Turbulence

see also Cavitation; Turbulence aircraft downwash and contrails 0–78195 atmospheric potential vosticity associated with tropopause folding, computer-analyzed isentropic analysis, distri. meas. 0–59594 in boundary layer flow past puolate spheriod 0–74661 cloud 'streets' formation, cue to vortex structurp of unstable Ekman boundary layer 0–56774 confined flow, interaction with stationary surface, theory and expt. 0–39645 deflection of cuentized vortex since heavy since the confined flow.

conhined flow, interaction with stationary surface, theory and expt. 0–39645 deflection of quantized vortex rings by magnetic fields 0–49965 expulsion hypothesis in astrophysics 0–79618 flow, laminar viscous, in short cylindrical vortex chamber 0–55413 flow from jet's nozzle, pffect on noise suppression, meas. 0–43387 flow modulator, charactis, report 0–78185 fluid core vel. distrib. in swirling pipe flow 0–39492 fluid-core, 3-dimensional, exact Madnus formula 0–39483 gas flow, diabatic steady 0–68043 Karman trail type, vel. decay rel. to surface friction, hot-film anemometer meas. 0–39509 Karman vortex shedding phenomena application for flow meas. in pipe or channel 0–64842 Lagrangian and Eulerian correl, coeffs, relation 0–67863 ocean eddy diffusivity, scale phenomenon, empirical relationship 0–59545 quantized vortices, theory of motion 0–58513 in rectangular cavity in channel, nature rel. to aspect ratios and Reynolds numbers 0–39702 relativistic hydrodynamics, application of general theory of space-like congruences 0–41953 ring shaped pair in conducting liquid, self- excitation of dag. field, study

ring shaped pair in conducting liquid, self- excitation of dag. field, study 0-50179

rings with const. circulation, dynamics 0-43503

rotating fluids, solitary waves obs., comparison with theory 0-58429 rotor tip vortex of helicopter, modification by airstream injection 0-78209 sheet, leaving semi-infinite plate, instability, report 0-78031 steady rings of small cross-section in ideal fluid, propag. speed and shape 0-49972

steady rings of small cross-section in ideal fluid, propag, speed and shape 0—49972 in supersonic flow past yawed cone, numerical calc. 0—46790 Taylor-Goertler vortices and their effect on heat transfer 0—46638 theorems, two, for vortices transport 0—39493 three-dimensional, exact Magnus formula 0—67861 in time-dependent incompressible flow over disc or sphere, numerical solns. 0—61245 turbulent trailing, decay 0—39654 viscous incompress. flow past finite flat plate 0—46666 viscous incompressible fluid rotation, in closed circular cylindrical con tainer 0—71285 voltage induced in p-azoxyanisole liquid crystals 0—53355 vortex shedding from cylinders and plates, obs. report 0—74663 in water tank, flow mechanism 0—64828 H₂O, turbulence meas. interpretation 0—53302 He II, eynamics of rectinlinear vortex 0—55646 He II, liquid, mechanism φ k.s. cavitation nkcleation by quantizee vortices 0—39862 He II, scattering of particle by 0—68170 He II, scattering of particle by 0—68170 He II, superfluie, vortex rings, dyna dics 0—43503

Vortices continued

He II, uniformly rotating, mutual friction measj 0-55643 He II liquid, rel. to heat transport 0-50288

He liquid effects, vorticity effects in creep 0-74822

see also Ice; Seawater; Steam

in Earth materials, analysis, psekdother dodynamic approach 0-76328 on Mars, occurrence in liq. form 0-66596

in Vpnus atmosphere, content rel. to lithos fhere composition and temp. 0-63110

absorbed on ice-nucleating substances, two- dimens, phase changes 0-53397

absorbed on ice-nucleating substances, two-dimens. phase changes 0–53397
absorption spectra coeffs., 100 to 400 Å 0–55298
abundance in lunar samples 0–45358
acoustic II. absorpt. ingresh, sea wateu, model, < 100 Hz 0–46908
acoustic spherically divergina waves in frpsh and sea water 0–78275
acoustic wave propagaint dixtures 0–64905
acoustic wave scattering, specular and near-specular, spectra 0–5340
acoustic wave scattering, specular and near-specular, spectra 0–54719
adsorbed on TiO₂, i.r. spectra 0–58605
adsorption and desorption, on single cryst., study by desorption spectrometry 0–74929
adsorption kinetics on ThO₂ 0–74930
adsorption of vapour on Ge powder 0–53446
adsorption on Al. effect on triboinduced election emission 0–56411
adsorption on aluminosilicate catalyser, i.r. spectra obs. of H₂O. D₂O and HDO 0–39968
aerosol growth determination, gravimetric method 0–41494
air-water and air-brine mixtures, flow in round vertical pipe, relative velocities 0–78005
air-water two-phase flow, adibatic slug-annular-mist, pressure wave propagation 0–67986
air-water vapour, microwave breakdown 0–55518
alcohol-water mixtures, u.s. relaxation 0–55611
amine+ water solutions, u.s. absorption properties 0–46910
anomalous, exptl. properties 0–78259
anomalous, molecular weight determ, cryoscopic method 0–64863
anomalous, phase behaviour on freezing and subsequent melting, behaviour as soln. 0–55656
anomalous, possible polymeric struct, and existence of strong OHO bonds 0–50199
anomalous, spectroscopic testing in capillaries 0–39801
anomalous, tecory 0–58438

0-50199
anomalous, spectroscopic testing in capillaries 0-39801
anomalous, theory 0-58438
anomalous, unsuccessful attempt at high-pressure synthesis 0-78264
astrophysical H₂O radio sources, very-long-baseline interferometric obs.
0-51618
atmosphere (strato-meso- and thermosphere), dissociation, report
0-79520

o-19520 atmospheric, effective height of microwave absorpt. 0-59580 nkcleate boiling, surface tempj meas, with Pt film thumometer on Pyrex glass 0-48894

boundary layer, of variable prop., with expt. decreasing wall temps. 0-68046

0-68046
t-butyl alcohol, 1, diffusion coefficients 0-71329
cavitation, threshold at elevated pressures, exptl. determination 0-53301
cavitation abspace on decompression from high prossures for gas supprsaturated water 0-61461
cavitation bubble growth in water under-saturated with air 0-74710
cavities vapour filled, dynamics, stiffness, damping, resonance freq. measj
0-71288

cavity collapse, singular points 0–55579
charged drops, microwave emission on collision 0–39832
chemisorption on fresh Mg surfacp, exo-electron emission 0–39972
collision behaviour of drops in a low-pressure steam atmosphere 0–61468
compressed, thermal conductivity meas using coaxial cylinder cell 0–68098

0-68098 convection, turbulent natural, on vertical plate, boundary layer struct, and heat transfer, obs. 0-46900 convection waxe arising from heated line source 0-58392 cooling of nuclear reactors, two-phase flow problems 0-49722 critical exponent & Kiang's formula 0-39881 cylindrical piston problem, compression waves, artificial viscosity method 0-43413

cylindrical piston problem, compression waves, artificial viscosity method 0–43413 deep-waves, monochromatic 1.96 Hz mean velocity field obs. 0–76355 density high, enhanced viscosity, density, lower saturated vapor pressure, device for investigation 0–46868 density maximum, effect of long-chain polymer adeition 0–68083 desorption from Mo by electron impact 0–39973 dielectric constant, cale. in submillimetre wave band 0–74773 diffusion in silica glass, OH-content effects 0–62002 dispersion and absorption in ir. and rf. spectra 0–43458 drop, evaporation, ir. radiation 0–50330 droplet fibre-bed coalescence 0–61469 droplets, spherical, angular scattering function using computer 0–64923 droplets for high velocity shock expts. 0–61455 erops, AgI nuclei remain on surface 0–68069 drops, impinging upon a heated surface, study of dynamic behaviour and heat transfer characteristics 0–46903 dynamic viscosity of compressed liquid water in the vicinity of the solid-liquid boundary below 0°C 0–61500 e.m. cascade induced by 1 GeV electron 0–50258 electron emission, secondary 0–53323 equation of state for P-V isotherms of solns. 0–43423 equations of state, characteristics cale. by thermodynamic consistency 0–74720 excited, its role in radiolytic transformations 0–62819 films adsorbed on α -Fe₂O₃ surface, behaviour 0–68241 floods in laboratories, anti flood device 0–51848 flow, turbulent, in vertical tube, heat transfer under free convection influence 0–69751 fog, i.r. radiation attenuation and backscattering 0–45143 formaldehyde-water system, CNDO study of H bond 0–74370

influence 0-69/51 fog, i.r. radiation attenuation and backscattering 0-45143 formaldehyde-water system, CNDO study of H bond 0-743 freezing rate in Blasius flow over chilled flat plate 0-53400 fresh, pollution by heat from power stations 0-69268 gas-phase reaction rates of positive ions, at 296°K 0-79434 74370 Water continued

glycerol/water mixtures, porphyrexide doped, proton polarization times, (1K 0-62770

gravity waves, long in shallow water, viscosity effect 0-46856

gravity waves, long in shallow water, viscosity effect 0-46856 ground, ¹⁴C dating, evaluation and application 0-54215 heat of solution in H₂O/D₂O mixtures 0-76251 heat transfer amplification by local injection of fluid into a turbulent tube flow 0-55420 heat transfer in air bubbling through porous graphite cylinder into water including vaporization 0-46995 heat transfer in rough tubes with tape generated swirl flow 0-39773 heat transfer natural convection heat transfer on heated inclined surface, obs. 0-46821 heavy deuteration of fatty tissues rel to slow neutron imaging 0-72809

obs. 0-46821 heavy, deuteration of fatty tissues, rel. to slow neutron imaging 0-72809 heavy, as moderator for nuclear reactors 0-49718 heavy, preparation in France 0-61040 hypersound phase velocity and attenuation in H₂O of different isotopic comp. 0-39785

i.r. absorption band, at 2130 cm⁻¹, assignment 0–50230 from ice, layer thermal instability 0–48225 interface with air, emission, reflection and abs. of microwaves 0–43448 interface with quartz glass, cavitation nuclei obs. by centrifuge method 0–74711

interstellar maser emission 0-79689 ion-pair formation, dielectric constant depend, high temp. and pressure 0-39819

0—39819
jet stream, multiple, diffusion, report 0—78246
liquid, approximate Percus-Yevick equation, application 0—46866
with methyl cyanide, u.s. absorpt, props. 0—68103
model, X-ray diffraction data 0—61487
modified, vapour pressure depend. on anomalous component 0—65009
molecular, minimum basis wavefunctions 0—43104
molecular quadrupole moment and sign of elec. dipole moment 0—70912
molecule, asymmetric top, line intensities, Δk effect 0—74212
molecule, bond behaviour in elec. field 0—64414
molecule, contraction of Gaussian basis functions effect on molecular calculations 0—74264
molecule, diamagnetic susceptibility calc. 0—61091

molecule, diamagnetic susceptibility calc. 0–61091 molecule, electron impact, O I and O II emission, decay lifetimes 0–64444 molecule, in ionic solutions, low freq. motions, neutron scattering spectra 0-61483

molecule, in solid N2 matrix, i.r. spectrum rel. to struct. and bonding

0-70911 molecule, in Solid N₂ matrix, 17. spectrum ref. to struct, and bonding 0-70911 molecule, lowest singlet and triplet potential surfaces 0-70904 molecule, numerical determ, of rtoation-vibr, energies 0-64343 molecule, one-electron props. experimental data and ab initio calc. 0-74260

molecule, polarizability tensor components, CNDO/II calculations 0–64355

molecule, proton magnetic shielding consts. 0–58171 molecule, spin-generalized SCF wavefunctions using GF method 0–67732

molecule, strongly orthogonal geminals, transferability to H₂O₂ 0–43 107 molecule, variational-perturbation calc. of ground-state energy 0–43 101 molecule, vibratory-rotatory interaction, line intensity, $6\mu m$ band 0–53032

molecule in $C_2Cl_3F_3$ - CS_2 mixtures, valence vibrs, contact complexes obs. 0-49873

molecule in transition metal hydrates, study of intramol. stretch-stretch

molecule in transition metal hydrates, study of inframol, stretch-stretc force const. 0–77795 molecule photoioniz, photo e energy anal. 0–67706 molecule vibrational freqs, in crysts, nonlinear H-bond model 0–39992 molecules, H-bonded in crysts, librational modes, n scatt, obs. 0–40533 molecules, charge exchange with H+ and H₂+, cross section meas. 0–77716

0-77716
molecules, motions in dilute aqueous soln. of tertiary butyl alcohol, neutron scattering study of hydrophobic hydration 0-71314
neutron slowing down time, obs. 0-49691
nuclear spin relax. of liq. in porous medium, temp. depend. 0-50260
nucleate pool boiling, heat transfer 0-61600
nucleation, homogeneous and heterogeneous 0-68180
open water dimer, comparison with 1-1 complexed water 0-78256
oxygen conc., effects of mag. processing 0-68081
permeation resistance of monolayers, statistical calc. 0-61601
permittivity, electrical, pressure and temp. depend 0-39824
permittivity, static, temp. depend. 0-46936
pollution, of freshwater and coastal water, by heat from power stations 0-69268
in polymer coatings, diffusion coeff., prod. of internal stress. 0-50676

pollution, of freshwater and coastal water, by heat from power stations 0–69268
in polymer coatings, diffusion coeff., prod. of internal stress 0–50676
polymers, MO calc. of energies and configurations 0–53033
polymers, covalent, structural scheme 0–71316
polywater, lattice models, dynamics 0–39720
polywater, measurements 0–58457
polywater, new method of production 0–64857
polywater, p.m.r. spectrum 0–46471
polywater, possibility of p-electron delocalization 0–58444
polywater, properties 0–58455
polywater, structure 0–58456
polywater, structure 0–58456
polywater, synthesis attempt in gas discharge 0–61473
polywater synthesis attempt in gas discharge 0–61473
polywater synthesis attempt in gas discharge 0–61473
polywater structure 0–58456
polywater production, expts. on silicone grease components 0–74736
polywater production, expts. on silicone grease components 0–74736
polywater structural model proposed 0–46867
polybwater structural model proposed 0–46867
polyboiling, pressure effects on bubble growth 0–39891
positron lifetime temp. depend, melting pt. obs. 0–43512
proton affinity 0–62785
proton relax. time, press. depend. 0°C 0–61553
proton transfer between molecules, calc. 0–62784
protons, nuclear magnetisation state, magnetostatic study 0–74786
pumping, photoelectric solar unit as drive 0–42167
pumping unit, thermoelectric, solar radiation concentrator, calorimetric investigation 0–48976
pumping unit, thermoelectric solar unit as drive 0–42167
pumping unit, thermoelectric solar radiation concentrator, calorimetric investigation 0–48976
radiolysis, transient elec. cond. 0–69224
reactor experiments, Na/H₂O at Dounreay, review 0–49735
reservoir, one-dimensional flow analysed 0–54219

Water continued

fissure reservoirs thermal processes due to liquid motion 0-54226

shallow, technique for measuring acoustic modal attenuations 0-64909 shock temp. calc. in 100 kbar region 0-64858

single phase, heat transfer and pressure drop in tape-generated swirl flow 0-39772

in soil, transfer to atmos. rel. to soil properties, plant characteristics, weather 0-45122

weather 0–45122 sonoluminescence, influence of dissolved H_2 , O_2 , N_2 , CO_2 , Ar, Xe, departure from thermodynamics 0–46927 specific mass variation rel. to isotopic comp. 0–52991 spectra, i.r., differential technique 0–68110 in stars, M-type, abundance 0–59692 stars, late-type K and M, H_2 0 bands obs., 1.1 μ 0–41678 steam-water mixture, pressure pulse model rel. to critical flow and sonic velocity 0–39696 steam-water mixtures flowing in heated channel, density transients 0–39272

0 - 39222

steam-water mixtures flowing in heated channel, density transients 0-39222

steel, crack growth rate in distilled water with loading 0-47410

Stokes-waves on surface, slow modulation 0-64847

structure, Cl⁻, Br⁻, I effects, X-ray scattering, radial distribution functions 0-39732

structure, effects of ClO₄-ion 0-39800

structure, model 0-64856

structure, tetrahedral network model, computer optimization and geometrical or topological transform 0-61478

structure, vibr. spectrum obs. 0-65517

structure and multi-phase' models 0-61474

structure and props. 0-71307

supercooled, basal plane solidification kinetics, impurity effects 0-75008

superheated water freezing to superheated ice 0-61598

surface tension, dynamic, not time-depend. 0-78267

surface tension on gold 0-78266

surface waves, interac. with fixed semi immersed cylinders having symmetric cross sections 0-55570

thermal conductivity, unsteady-state absolute method, interferometry 0-50219

thermals over heated horizontal surface, flow field photographs by electro-

thermals over heated horizontal surface, flow field photographs by electro-

thermals over heated horizontal surface, flow field photographs by electrochemical technique 0-64895 thermo-osmosis through cellophane 10°C to 90°C 0-64894 trace analysis for B, mass spectrometry 0-62827 triple point realization 0-50301 turbulent, particle settling velocities and vertical diffusion, meas. and model 0-50264 two models of complexes water, comparison 0-78256 ultrasonic absorption anomaly explained on basis of molecular motion 0-74748

0—14748 vapour, abs. spectrum, 23 cm⁻¹, low temps , domination in abs. of radiation by atmosphere 0—74275 vapour, absorption coeffs. 10-22 μ at high temps. 0—67734 vapour, absorption using ruby laser 0—48288 vapour, atmospheric transport, pole to pole divergence 0—51516 vapour, condensation on tubes, heat transfer coeff. calc. 0—48880 vapour, duteron bombard, electron capture cross sections, E_d=0.3 to 70 keV 0—49653

vapour, displacement of irreversibly adsorbed ethylene on alumina 0-61678

vapour, effect on Be droplet combustion, scanning electron microscopy 0-41425

0–41425 vapour, elec. breakdown pots. meas., Ni electrodes, 20.6-123.5 torr, 297-333 K 0–74634 vapour, evolution in Venus atmosphere, loss rate through photodissociation 0–63119 vapour, i.r., spectra, rel. to line identification in planetary spectra 0–49855 vapour, ionic collision processes 0–58353 vapour, laser action enhancement by foreign gases 0–38501 vapour, line strengths in v₂ band 0–39382 vapour, refr. and absorpt, spectra 0–64820 vapour, spectrum near 600 GHz 0–77792 vapour, stratospheric mixing ratio measurement, direct method 0–76373 vapour, vibration-rotation bands, and of isotopic species 0–64415 vapour and alkane molecular ions reaction mechanism and rate constants 0–72530 vapour in atmosphere, density effect on radiowave absorpt, 150 to 350

vapour in atmosphere, density effect on radiowave absorpt., 150 to 350 GHz 0-62920 vapour bubble, mass transfer model in subcooled nucleate boiling

vapour bu 0--39880

vapour existence in sunspots, evidence 0–57145 vapour laser, multi-wavelength oscillations study by rate eqns. 0–69916 vapour nucleation in spacecraft debris clouds 0–79615 vapour pollution of stratosphere, carried by supersonic transporters 0–48272

vapour pressure isotope effect between $\rm H_2^{18}O$ and $\rm H_2^{16}O,\,0^{\circ}C$ to $\rm 16^{\circ}C$ 0–39897

vapour transmission, polynomial representation 0-48287 vapour-cavities, rate of collapse, studies in bubble analogue apparatus 0-68052

0-68052
Venus, loss mechanism 0-63117
viscosity, empirical formula as function of temp. 0-78265
viscosity at high temperature and high pressure 0-50208
vitreous identification and characterization 0-55682
volume transport assoc. with Stokes drift for developed surface-gravitywave field 0-41480
vortices, turbulence meas, interpretation 0-53302
vortices in bathtub, flow mechanism 0-64828
water, cross-waves in tank, second-order theory 0-68057
water-2-isobutoxyethanol system, u.s. absorption as function of composition, temp, and frequency 0-68102
waves, progressive in rotating flow in a circular pipe 0-46839
waves on finite depth stream with velocity defect near free surface, analysis 0-50186
waves on running stream employing linear theory 0-78240

sis 0–50186
waves on running stream employing linear theory 0–78240
windrows generation, wave-interaction model 0–69281
X-ray diffraction, radial distrib. functions 0–53317
X-ray diffraction pattern and models of liq. structure 0–61487
α-particles, mean range determination technique 0–46950
[H-O.H.O.H.]+ ion, symmetry in intranilic acid hexahydrate 0–65304
D/H ratio, automatic mass spectrometric analysis 0–74189

Water continued

D₂O, heat of solution in H_2O/D_2O mixtures 0–76251 D₂O, in solid N_2 matrix, i.r. spectrum rel. to struct. and bonding 0–70911 D₂O, microwave spectrum, rotational levels of ground vibrational state 0–74254

0—74254
D₂O, neutron absorption cross-section, revised value 0—39232
D₂O, rot.spectra, microwave 0—53030
D₂O moderated, natural U single rod lattices, buckling obs.rel.to transport theory 0—39219

theory 0-39219
D₂O moderated UO₂ lattices, reson. escape probab. 0-39189

"F production by 'He bombardment 0-58022
H₂ calorimetric measurement of specific heat, expansion and compressibility coefficients 0-48899
HCl-H₂O system, vapour-liquid equilibria 0-74849
HDO, absorpt, spectra in regions 2400-3495 and 4022-4400 cm⁻¹ 0-64416
HDO, apparent heat of formation in H₂O/D₂O mixtures 0-76251
HDO, in Solid N₂ matrix, ir. spectrum rel. to struct, and bonding 0-70911

"(H-O) +H₂O-H⁺(H₂O) in the distributions of the spectrum of the struct of the spectrum of the spectrum

HDO, in solid N₂ matrix, 1.r. spectrum rel. to struct. and bonding 0-70911

H*(H₂O)_{n-1}+H₂O=H*(H₂O)_n ionic clustering equilibria, mass-spectrometric meas. 0-67595

H₂O-ethylene glycol glass, p-irrad, electron traps. 0-62821

H₂O-H*-Li-syst, bond behaviour in elec. field. 0-64414

H₂O-N-CO₂ gas, supersonic expansion, population inversion. 0-74666

H₂O-NH₄F liq-solid equilib. 0-64993

H₂**10, spin-lattice relaxation, -17 to 95° 0-71385

H₂**18O, fractional factor of **00 between water vapour and ice, -33.4 to 0°C 0-65011

H₂O-O+OD) reaction rate constant by measurement of intermediate quantum yield following flash photolysis. 0-45084

*3H content, interlaboratory comparison of analysis. 0-76292

He bonded molecules resonance stabilization. 0-64412

O₂ in atmosphere, attenuation at 48 to 72 GHz, calc. 0-62919

O₂ content, isotopic exchange equilibration, and mass spectrometric analysis. 0-76284

*3O prod, 87 MeV e bombard. 0-77539

SiO₂**H₂O₃ suspension, rheological study, electrophoretic mobility 0-68160

0-68160

Wave equations, quantum theory see Quantum theory/wave equations

Wave functions see Quantum theory/wave equations

Wave mechanics see Quantum theory

Wavefront-reconstruction imaging see Optical images Diffraction/light; Holography;

Waveguides see Electromagnetic wave propagation/guided waves

see also Acoustic waves; Elastic waves; Electromagnetic waves; Liquid waves; Magnetohydrodynamics; Seismic waves; Shock waves acceleration, in elastic-plastic materials 0-48826 accoustic-gravity waves, reflection 0-59521 in atmosphere, long internal waves generated by periodic oscillations of atmospheric pressure 0-56768 in atmosphere, mountain lee, obs. and comparison with theory 0-45137 axisymmetric, initial development in fluids of finite depth 0-46674 boundary values problems using Laplace transforms and separation of variables 0-66852 clipped waveforms, sum distr. in multivariate input-amplitude distri terms

clipped waveforms, sum distr. in multivariate input-amplitude distri. terms 0-66785

cnoidal in compressible fluid over toroidal channel 0-49995

cylindrical, of 0-48838 combined stresses, propag. in elastic-plastic medium

0-48838 in cylindrical bars, short, axially impacted, study by modified Hopkinson-bar apparatus 0-38368 deformation, non-linear elastic material 0-48837 dicrotic, presence in arterial pulse wave form. mathematical and experimental model 0-74698 diffraction by lattice, calc. method 0-38153 in dissipative systems, periodic disturbances, h.f. small amplitude 0-42058 disrupbances.

disturbance, in annular two-phase flow, establishment of parameters 0-64969

elastic half-space, transient excitation by point load travelling on surface 0-42047

in elastic media, inhomogeneous, propag., Bessel functions 0-38254 electrostatic, coupling in nongyrotropic plasma, dispersion relation 0-53157

0-53157 electrostatic, in plasma column in strong mag, field, linear and non-linear theory 0-55464 equation, Volterra method for soln. of various cases 0-71239 equation of propag, integration technique 0-73036 in fluid, bilinear 0-49992 fluid, steady state problem, new treatment 0-67883 fluid, stratified, waves and currents due to moving heat source 0-39528 force-free matter with spin 1/2, classical waveforms 0-38151 in gas mixtures, relaxing, weak wave propag. 0-39656 geodesic de Broglie waves, equivalence principle 0-76540 gravity, rel. to stratified fluid, boundary layers induction 0-58280 harmonic wave trains, propag. in elastic composite circular-cylindrical rods 0-34690 with slender, pointed body in transsonic flow at super-

rods 0-54690 head wave spacing with slender, pointed body in transsonic flow at super-sonic speeds 0-55548 Helmholtz equation, nonseparable solns and transverse motion of mem-brane 0-48690 high and low frequency, interaction in nonlinear disperse media 0-59873 impact waves in elastic media, problem of Klein-Gordon eqn. with variable coeffs. 0-38367 internal in rotating stratified fluid, diffraction by semi-infinite barrier 0-74476

u-744/6
internal in wedge of stratified fluid diffraction by wedge 0-744/4
ionization, in plasmas, ionization rate variations 0-711/9
laminated prestressed composite, propag. of small amplitude time-harmonic
waves 0-48804

lee waves in stratified air flow over mountains 0-41485 long, equations, in inhomogeneous viscous fluid 0-56768 longitudinal propagation on travelling threadline, non-linear eqns. 0-76902

MHD, reflection, transmission and coupling at density step 0-55438 magneto-acoustic, excitation efficiency in conducting fluid cylinder in const. mag. field, soln. 0-50009

mechanics, history and interpretation 0-63342

```
Waves continued
      multipath reflections from random supaces, counting method 0–51917 non-linear, weak, in rotating fluids 0–74473 nonlinear, propagation in inhomogeneous media, reductive perturbation method 0–54721
      nonlinear, propagation in inhomogeneous media, reductive perturbation method 0-60047
```

nonlinear, stochastic heating 0–54553
nonlinear interaction, general kinetic eqn. 0–43323
nonlinear orographic waves in cold air flow over a ridge 0–62904
nonlinear oscillations of distributed systems, asymptotic method 0–76802
nonstable, theory of propagation, pulse disturbances 0–41948
nonstationary problems of finite amplitude waves in dissipative media

0-69599

oceanic, parameter determination with ship's radar 0-66247

optical instrument, for multiple purpose studies 0-42382

organised in turbulent shear flow, Reynold stress, Orr-Sommerfeld theories 0-39530

orthogonality of eigen-waves propag, in non-absorbing media 0-69577

perturbation theory, eigen-walue problem in anisotropic elasticity 0-38351

plane, of combined stresses, propag, in elastic-plastic medium 0-48838

plastic longitudinal in work hardening rod, closed form solns 0-45615

plastic-strain waves, dispersive, gauge length errors in strain meas. 0-40290

0-40290 prolate spheroidal wave functions, review 0-66784 propagation, simulation of distributed parameter systems 0-72985 propagation in periodic medium, application to ocean 0-79508 propagation of finite beam of radiation in random medium 0-41947 reduced wave equation, uniform asymptotic solutions 0-38152 roll, propagation, critical flow rate for thin films 0-39707 in rotating fluid, infinite, produced by motion of obstacle along axis 0-53165 0-53126

0-33120 scalar plane, scattering by prolate spheroid with Dirichlet boundary condition 0-66787 scalar plane, scattering by prolate spheroid with Neumann boundary condition 0-63321

scattering, parameter, probability distrib, functions, statistical analysis $0\!-\!38155$

0-36133 sea, modeling by digital computer 0-66248 seawater, weight information for estimation of extremes for offshore plat form design 0-66262 shear, horiz, polarized, crack initiation at void in brittle elastic mat. shear, hor

shear pulse propagation in dispersive medium 0-45565 shear waves, horiz., diffraction by half plane, behaviour near inclusion 0-38323

sine-wave signal components spectral analysis using complex exponent algorithms 0-69660

solid, plastic wave propagation in two-dimensions, allowed directions 0-39875

solitary, damping, Korteweg-de Vries with energy dissipation 0-45523 solitary, in barotropic fluids, in open channel of arbitrary cross-section

sonic boom, formation mechanism 0-38395 space charge, in electron beams with velocity distribution 0-73167 spherical, frequency correlations of fluctuations in turbulent medium spherical, 0-77994

0-77994 spherical, of finite amplitude, nearfield soln. 0-63320 spheroidal wave functions, use and evaluation 0-66786 steady surface waves, inviscid, exact integral eqn. 0-50184 stratified flows, viscous, damping, boundary layer method calcs. 0-39526 stress pulse propag. in poroelastic solid, dissipation mechanisms 0-38398 stress waves in rectangular bars, use of straight collocation method 0-48841 stress way 0-48841

0–48841
surface, formation near rough interface between two media 0–46858
surface, steady waves, exact integral eqn. 0–49990
thermoconvective waves in a viscous heat-conducting fluid 0–54778
undulations along vortex sheet, leaving semi-infinite plate, report 0–78031
vector eqn., separability 0–59872
velocity of front, Fourier transform method 0–51918
vertically propagating waves in viscous isothermal atmosphere, numerical study 0–39527
valves integral of hody moving in stratified fluid 0–46675

vertically propagating was very study 0-39527 wakes, internal, of body moving in stratified fluid 0-46675 wave eqn., Darboux structure and nonexistence of solns regardless of boundary conditions 0-51906 wind separation from air flow 0-39661 Cu rods, soft, prestressed, small plastic strain wave propag. 0-53585 Fe, longitudinal wave propagation tests 0-53567

Waxes wax-ceramic systems, relative permittivity, mixing rules 0-53918 Weak interactions see Elementary particles/interactions, weak; Field theory, quantum/interactions, weak

abrasive of powder-filled wire for depositing weld metals 0-71732 cermet hard alloy in electrode-instruments 0-78658 covalent crystals, Si, Ge, durability and creep, stress and temp. depend. 0-43795

Covalent crystals, SI, Ge, durability and creep, stress and temp. depend. 0–43795 electrode instrument material, cermet hard alloys 0–78658 epoxy, abraded on grating, rate depend. on temperature 0–40425 inhibition mechanism by mechanicochemical process involving selective transfer 0–78659 in liquid metals 0–39695 metal, processes, dynamic equilib, with friction 0–68499 metal orifices in phosphate ester base hydraulic fluids, streaming current driven corrosion 0–53624 microslip, creep and wear in rolling contact 0–43755 penton, specific wear 0–39917 plastic, resistance to surface deformation, abrasion, composition effect, friction, strength, ductility 0–40425 polyethylene, abraded on grating, rate depend. on temperature 0–40425 resistance of materials exposed to hydroabrasive medium, changes pattern, lab. testing 0–47422 rubber-glass true contact area form. 0–40424 steel, effects of surface treatments 0–75291 steel, stainless in Na mass transfer and wear tests 0–45065 thermoplastics, deflections prediction and component dimensions estimate 0–58877 Cu-Sn bronzes, contact with C-Mn steel, obs. 0–50750

Cu-Sn bronzes, contact with C-Mn steel, obs. 0-50750

Ge, durability and creep, stress and temp. depend. 0-43795 Si, durability and creep, stress and temp. depend. 0-43795

Welding see Forming processes

Weighing see Balances; Mechanical measurement

Weissenberg cameras see Cameras; X-ray crystallography/appar-

Wentzel-Kramers-Brillouin method see Quantum theory

Wertheim effect see Magnetomechanical effects

Wetting

Weather see Meteorology

see also Capillarity ceramic oxide/molten metal, contact angle, surface free energy, adhesion 0-47033

composites, fibre reinforced metal matrix, wettability and reactivity $0-50808\,$

0-50808
drop spreading on smooth surface 0-71299
floods in laboratories, anti-flood device 0-51848
graphite, by molten NaF-ZrF₄-ZrO₂ mixtures in different gases 0-47036
powder, rel. to geometry 0-74872
solid phase, organic compounds, contact angles 0-58558
steel, by Na-Fe-silica glasses 0-53423
surface wetting, through capillary grooves 0-46863
GaAs Schottky barrier diode, fabrication by fluxed wetting of Sn, In and In-Zn alloy, and characts. 0-44296
MgO, by silicate liquids, controlling factors 0-43536
SiC/metal composites, wettability and reactivity 0-50808
Ti and alloys, by glasses 0-50358
Ti and alloys, by glasses 0-50351
Whiskers see Crystals/whiskers
Whistlers see Atmospherics; Ionosphere
White dwarfs see Stars

White dwarfs see Stars
Wiedemann effect see Magnetomechanical effects; Magnetostriction
Wiedemann-Franz law see Conductivity, electrical/solids; Conductivity, thermal/solids

Wien effect see Conductivity, electrical/liquids, electrolytic
Wigner coefficients see Quantum theory
Wigner effect see Physical effects of radiations Wilson cloud chambers see Cloud chambers

nd
acoustic-gravity ducting with spatially periodic wind shears 0–48298
atmospheric, effects on dispersion of acoustic-gravity waves at various
levels, model study 0–59597
circulation currents around ocean islands effect of Coriolis force and bottom topography 0–76351
clear air turbulence, anal. from rawinsonde ascensional rates 0–79526
effect on gravity waves in presence of ionosphere 0–79527
equatorial systems, stratospheric and lower mesospheric 0–41500
flow in forest canopies, simulated, report 0–79529
gravity waves, partial reflections by tempo discontinuities 0–56773
ionospheric F-region, influence on continuity equation, F2-layer peak
height, evening entrancement of n_m 0–45192
ionospheric F-region, neutral wind velocities, equations of motion, simultaneous solution 0–45190
ionospheric electron concentration, vertical redistribution by wind shear
0–48325
laser beam deflection in absorbing media 0–74679

0-48325
laser beam deflection in absorbing media 0-74679
mass outflow from thunderstorm complex rel. to tornado formation, study from ATS III 0-79530
ocean wave generation, preliminary results 0-51522
photometer for high altitude Li trail daytime meas. 0-76414
power spectra of horizontal vel. at 80-100 km 0-62906
recorders (1968) 0-48252

sea, open, velocity time fluctuations near surface, statistical analysis 0-56772

at sea, turbulent vertical transports of heat and momentum, determination 0-76368

0-(0.508 sea-air interface transport of momentum, air borne turbulent flux meas. technique 0-76369 sea-breeze, post-sunset, associated angel echoes at Bombay airport 0-66287

speed meas. in first ten meters of atmosphere above ocean 0-51520 storms, tropical, max. speed estimation from high resolution i.r. data 0-45141

0-45141
stratified, flow above irregular ground, fluid equations 0-43228
stratospheric eddy transfer processes during major and 'minor' breakdowns of polar night vortex 0-51519
streamlines, generation and plotting by computer 0-45142
stress over sea, tangential, computation of 0-79528
surface layer variation rel. to height, roughness, vertical flux density determination, computer program 0-56771
tunnel suitable for schools described 0-78197
in upper atmosphere, vertical profiles, relation to laser radar scattering 0-41511

0-41511 variability, temporal, 100 to 900 m, balloon meas. 0-41501 variangular spiral theory, theoretical model, expt. 0-56770 velocity and atm. turbulence strength, microwave probe technique 0-62907

0-62907
velocity derivitive in surface layer of atmosphere, micropulsation 0-66288
velocity distrib. and structure fn. near 100 km, meas. 0-59566
vertical profile, influence on dust deposition 0-59565
waves, effect on water current obs. 0-76379
waves separation from air flow 0-39661

WKB method see Quantum theory
Wolfram see Tungsten

Wood

gamma-ray build up factor coefficient determination 0-73446 Work function

see also Electron emission barrier metal on semiconductor, GaS(Se), barrier energy dependence 0-44235

0-44235 cathodes, dispenser, high values 0-79100 Kelvin method of meas, theory, practical limitations 0-68985 metal, photoelectric, values for 24 elements 0-75859 metal, surface cleanliness, argon ion-bombardment, heating 0-39927 photoconductor, high resistivity 0-51144 photoelectric emission from layers, thickness depend, effects of changes in work function 0-44437 semiconductor, determ. from photoelec. meas. 0-53841 semiconductor, n-Si clean and Au-coated (111) faces 0-68986

Work function continued

thermionic, correlation, with emitter temperature and cesium pressure, tech. 0-65861

thermionic convertor with chloride vapor deposited W emitter and Ni collector, charact. 0-57477

thermionic convertors, thermodynamic correlation 0-76986

W(110), work function and surface potential calc. 0-79092

lector, charact. 0—57477 thermionic convertors, thermodynamic correlation 0—76986 W(110), work function and surface potential calc. 0—79092 W, experiment on thermionic emission 0—56412 Ag. O-Cs photocathode, temp. depend. of work function 0—44435 Ag, and exoemission, effect of deformation 0—75851 Au., and exoemission, effect of deformation 0—75851 Au., photoelectric emission from layers, thickness depend. effects of changes in work function 0—44437 Au, photoelectric emission from layers, thickness depend. effects of changes in work function 0—44437 CdS, vacuum evaporation, elec. field depend. 0—61603 Cs layer on W(011), rel. to struct. 0—65110 p- GaAs (100), LEED-Auger spectroscopy correlation 0—47886 Gd adsorbed film on Mo (110) face 0—71496 Gd surface 0—62467 a-Ge, Al₂O₂-coated, photoelec. emission 0—72155 Ge, Ba-coated, photoelec. emission obs. 0—72157 La adsorbed film on Mo (110) face 0—71494 Mo with adsorbed Ba layer 0—71495 NbC_x (0.72≪×C9.99) at 1800k, obs. 0—62468 Ni (100) surface, changes obs. rel. to carbon segregation 0—47039 Pd, and exoemission, effect of deformation 0—75851 Pt, and exoemission, effect of deformation 0—75851 Re, 0001 crystal, cesiated values, exp. meas. 0—79103 Re, h.c.p., with CO coverage, field emission obs. 0—43571 Ru, h.c.p., with CO coverage, field emission obs. 0—43571 Si, Ba-coated, photoelec. emission obs. 0—62866 Ta, rel. to Cs covering 0—65868 Th on W (100) epitaxial growth, correlation with Auger spectra and LEED meas. 0—55729 TiC_x (0.73≪×C9.89) at 1800k, obs. 0—62468 U, adsorbed and W, changes 0—56193 W, adsorption of Y and O₂, thermionic emission 0—79979 W, adsorption of Y and O₂, thermionic emission influence of O₂, 1600° to 2200° K 0—51160 W field-emitter tip, carbon-adsorbed, apparent work function ang. depend. 0—72150 W macroscopic surfaces rel. to their prep. 0—56410 W single crystal selectron and ion emission methods 0—65869

W macroscopic surfaces rel. to their prep. 0-56410
W macroscopic surfaces rel. to their prep. 0-56410
W single crystal, electron and ion emission methods 0-65869

Work hardening see also Cold working; Surface structure alkali halide, strain hardening, theory, dislocation mechanism, simple slip 0-40447

alkali halide single crystals, theory 0–68515 alkali halide single cysts., theory 0–65460 rel. to dislocation jogs, non-conservative motion 0–40151 metal, boco, high temp., internal stresses and dislocations, theory

metal, b.c.c., high temp., internal stresses and dislocations, theory 0–40445 model, applic, to plastic behaviour metal under cyclic loading 0–40146 model, applic, to plastic behaviour metal under cyclic loading 0–40444 multi-electrode, using carbonaceous alloying mixtures 0–71770 NaCl single crysts. by dynamic impacts, and dislocation glide bands form., obs. 0–40168 by non-deforming particles and fibres 0–65458 plastic disc, anisotropic, effect on expansion of circular hole 0–54653 plastomechanical principles, stress/strain relations, flow condition 0–40446

rings and tubes, plastic and linear strain hardened, rate sensitivity 0-55931

rod, plastic wave propag., longit., closed-form solns. 0-45615 steel, local, effect on cold brittleness of low carbon steel, evaluation 0-58963

0-3863 steel, pearlitic, and flow stress mechanism, microscopic obs. 0-65395 steel, propag, under impact loads 0-62091 steel, stainless AISI type 304, and proportional limit, effect of N, 302F 0-43805

steel, stainless influence on carburization by liquid Na 0-39242 rel. to wedge flattening, exp. investigations rel. to nonhardening theory 0-58964

0-38964
Al-Mg single cryst, 290K 0-68443
Al, strain hardening, from change-in-stress-creep expt. 0-65403
Al foil, f.e.c., dislocation interactions during fatigue 0-40156
CaF₂ 0-43804
Cu, foil f.e.c., dislocation interactions during fatigue 0-40156
Cu, high-purity, torsional deformation, annealing, point defects, elec. resist. 0-75304
Cu, impact loads and resultant stress states effects 0-47439
Cu, OFHC, press. effect 0-47440
Cu, strain hardening relationship calc. from torsion test 0-78672
Cu and Cu-Zn with Al-O3 particles deform, theory 0-65392
Fe-Ni alloy, polycryst. wires, effect on coercivity 0-79170
Fe single crystal, plastic flow, orientation and temp. depend. 0-53599
LiF, and stress relax, internal stresses 0-68436
Mo single crystals, effect on subsequent heat-softening, mechanism 0-78657
NaCl, and stress relax., internal stresses 0-68436

0-1805/NaCl, and stress relax., internal stresses 0-68436
NaCl 0-43804
Ni-C solid solution, plastic deformation, internal friction 0-40309
Ni-base alloys, effect of structural changes 0-71744
Ni, struct. and creep strength 0-62052
x10NiCrWTi36.15, high temp. precipitation behaviour 0-40490

X and gamma-ray astronomy
p-radiation, low-energy in atmosphere during active and quiet periods of sun 0-76664 γ-ray low energy, applic. of gas Cerenkov detector 0-46035

X and gamma-ray astronomy continued

background X-ray flux, diffuse, 44Å, prod. by suprathermal proton brems-strahlung 0-41754

Cas A, X-ray source, implications for X-ray emission from other supernova remnants 0-45327

Cas A, supernova remnant, X-ray characts. 0-51689

Cas A y-ray flux, obs. rel. to cosmic rays origin 0-41758

Cassiopeia region, X-ray survey, rel. to supernova remnants and galactic source distrib. 0–45327
Cen XR-2, balloon obs. below 20 keV, decrease in flux 0–45326

Compton scattering models in intergalactic space and interpretation of observations 0-66372

conference, Denver, USA, Aug 1969 0–69243 cosmic X-ray sources, theories and observations 0–59739 Crab Nebula, X-ray emission, search for polarization 0–48484

Crab Nebula, X-ray emission, search for polarization 0–48484
Crab Nebula, pulsations in X-radiation, ratio to total background radiation, spectral anal. 0–66427
Crab Nebula, search for polarization in X-ray emission 0–51707
Crab nebula, X-ray characts, comparison with two other supernova remnants 0–51689
Crab nebula filamentary system excitation conditions 0–59685
Cyg XR-1 source, variable X-ray spectrum 0–57083
Cygnus constellation, localized X-ray sources, survey by balloon-borne detectors 0–57084
detection, p-rays, total absorption shower cascade method 0–63194
diffuse X-ray background, 4-70 keV meas. 0–48482
diffuse X-ray component near galactic plane, rel. to interstellar dust scatt. 0–62977
diffuse cosmic and solar X-ray spectra, satellite meas. 0, 48402

0-02917 diffuse cosmic and solar X-ray spectra, satellite meas. 0-48483 discrete sources of γ-rays and correlation with regions of large density H 0-76618

0—76618 emission enhancement, effect of submillimeter nightsky radiation background 0–57066 emission of hard X-rays from galactic plane, search 0—69361 galactic prays origin 0—51732 galactic gamma rays, origin 0—66390 gamma-ray astronomy above 10 MeV, survey progress report 0—41757 history and future prospects, review article 0—54419 holographic imaging methods, in X-ray astronomy with pinhole cameras 0—6680 identification of X-ray sources, review 0—69428

identification of X-ray sources, review 0-69428 interstellar grains study from obs. of interaction with cosmic X-rays 0-66507

isotropic gamma spectrum, predicted break rel. to cosmological origin 0-51733

0-51733 low energy analysis, review 0-69244 metagalactic X-radiation spectrum formation mechanism rel. to cosmic electrons acceleration 0-66370 NP 0532, Crab pulsar, X-rays, balloon obs. 0-66429 NP 0532, x-ray pulsations 0-66565 neutron stars, gas accretion accompanied by gamma and radio radiation 0-45293

0-45293
polarimetry, use of highly reflecting crystals 0-45328
proportional counters, large area Be, for satellite expt. 0-63885
pulsar, Crab, optical and X-ray synchrotron radiation calc. 0-54412
pulsar, Crab Nebula, X-ray radiation 0-66548
pulsar NP 0532, scattering of soft X-rays by interstellar grains 0-41751
pulsar in Crab Nebula, possible pulsed gamma ray emission remains
0-66533

pulsar NP 0532, scattering of soft X-rays by interstellar grains 0—41751 pulsar in Crab Nebula, possible pulsed gamma ray emission remains 0—66533 pulsed p-emission in Crab Nebula direction 0—63084 pulsed gamma emission, search in pulsars CP 0950, CP 1133, AP 1541 and PSR 1642 0—41756 pulsed-gamma rays from the Crab Nebula 0—66534 SCO XR-1, X-ray source, daytime ionospheric effect obs. 0—76614 SN 1572, X-ray source, implications for X-ray emission from other supernova remnants 0—45327 SN 1572, supernova remnant, X-ray characts. 0—51689 Sagittarius A p-ray flux estimates 0—69420 Sco XR-1 soft X-ray spectrum rocket-borne obs. 0—51731 Sco X-1, hard X-ray spectrum 0—57081 Sco X-1, optical flare and x-ray emission, simultaneous meas. 0—48393 Sco X-1, optical flare and short- term periodic variations 0—41753 Sco X-1, optical flare and short- term periodic variations 0—41753 Sco X-1, simultaneous V and B monitoring 0—72758 Sco X-1, simultaneous V and B monitoring 0—72758 Sco X-1, optical and X-ray emission line strengths 0—51729 Sco X-1, optical and X-ray emission line strengths 0—51730 Scorpius×R-1, optical intensity power spectra between 0.002 and 500 c/s 0—79714 Sqr V-1 gamma source, upper limit on intensity in soft X-rays 0—51734 soft X-ray instrumentation for space expts. 0—69429 solar X-ray data (alentification using D-layer ionization behavior during eclipse 0—41829 solar 4-Ray once identification using D-layer ionization behavior during eclipse 0—41820 solar X-ray source identification using D-layer ionization behavior during eclipse 0—41820 solar X-ray once identification using D-layer ionization behavior during eclipse 0—41820 solar X-ray source identification using D-layer ionization behavior during eclipse 0—41820 solar X-ray source identification using D-layer ionization behavior during eclipse 0—41830 spectra, slope of measured distrib. rel. to measurement process 0—57080 spectrograph development for X-ray detection 0—69346 supernoval remnants, Cas A, SN 1572 and Crab nebula, X-ray characts. 0—51689

Tau XR-1 soft X-ray spectrum meas, interstellar absorpt. effect 0-51731

Tau X-1, X-ray emission, search for polarization 0-48484
universal X-ray background, as superposition of nascent pulsar sources 0-41752

0-41/52
Vet XR-2 soft X-ray spectrum, rocket-borne obs. 0-51731
X-ray background, diffuse, 4-70 keV meas. 0-51730
X-ray background, diffuse 0-48482
X-ray background, limits on shear and rot, of universe 0-66376
X-ray background component, galactic, inner-Bremsstrahlung as source
0-76615

X-ray background radiation, diffuse, review of observations and theories 0-57077

X-ray emission, from supernova outbursts, diffuse background 0-72757 X-ray scatt. by interstellar dust grains 0-57082

X and gamma-ray astronomy continued

and gamma-ray astronomy continued

X-ray scattering by interstellar grains in direction of Seo XR 1 and Crabpulsar 0-41722

X-ray source, Sagittarius, location 0-66566

X-ray source, Sagittarius, location 0-66566

X-ray source, Sagittarius, location 0-66567

X-ray source, Sagittarius, location 0-66567

X-ray source in Crab Nebula, 25 to 100 keV, angular size 0-57078

X-ray sources, galactic, obs., Nov., 3, 1968 0-66568

X-ray sources, soft, galactic, heating of H1 regions 0-72755

X-ray sources Seo X1, Tau X1, Cen X2, spectrum and flux vars., 2-18 keV 0-54418

X-ray spectroscopy and polarimetry instruments 0-57085

X-ray telescope image formation, surface configuration requirements 0-58850

X-rays rel. to supernova removations of the second configuration requirements (1-58850)

0. 59830
X rays, rel. to supernova remnants and galactic mag. fields 0-51727
X rays from Crab Nebula, scatt. by interstellar dust rel. to nature of source 0. 57007
Sco X 1, X ray emission, time variability 0-66569
Sco X 1 and WX Cen, optical power spectra 0-66570

X-ray absorption

see also X ray spectra/absorption rel. to Kondo problem 0-43945 resonator characts. 0 60188 review 0-56572

X-ray analysis see Chatomic; X ray crystallography Chemical analysis/X ray:

X ray astronomy see X and gamm ray astronomy

X-ray characteristic temperature see Specific heat

ray characteristic temperature see Specific heat
ray crystallography
For results of structure analysis see Crystal structure, atomic
abnormal absorpt, coeffs, generalized seatt, factors 0–58671
alloy, short range ordered, clustering of ordered cells, theory 0–47172
alloy, short range ordered, clustering of ordered cells, theory 0–47173
anomalous, seattering, Pendellosung effect, K absorption edge 0–75043
anomalous transmission, defect clustering effects 0–43609
anomalous transmission obs., applic. to Ge 0–61871
application to determ, of retained austenite in steel 0–40081
arcing phenomena on oscillation photographs of CdBr, 0–71576
Bragg intensities, measured integrated, correction for anisotropic thermal
difuse scattering 0–61766
conference, Buffalo, USA, Aug. 1969 0–58651
conference, Denver, USA, Aug. 1969 0–69243
controid displacement, tangential contrib. 0–65191
crystallite shape effects on low angle diffraction patterns 0–40056
defective lattice, diffuse seatt. 0–58665
defects, interferometry 0–40118
deformation stacking faults effect on diffr. from h.c.p. 0–43677
disordered systems, exam. by heavy atom method 0–61764
divergent beam method, principles and appls. 0–65190
dynamical theory, developments 0–61776
dynamical theory, developments 0–61767
dynamical theory, cryst. wave field interpretation 0–58674
dynamical theory, cryst. wave field interpretation 0–58674
dynamical theory, cryst. wave field interpretation 0–58674
dynamical theory, cryst. wave field interpretation 0–61791
Ewald wave superposition, interference field in perfect cryst. 0–61792
facetting of coherent scatt. regions 0–65195
imperfections, isolated, scattering theory 0–58668
kinetmatic theory of developments 0–58670
multi beam diffraction, applic. to ideal crysts. 0–58672
multiple diffr. effects 0–75036
Pendellosung fringes in Bragg case in finite cryst. 0–47160
powder diffr. profiles, variance 0–65191
powder diffr. of X ray crystallography

profile calculation of two dimensional reflections from layered structures 0 53476

quartz analyzers, growth defects and focalization anomalies relationship 0-71539

0 – 71539
quartz plates, vibrating, topography 0 - 68268
reflection intensity, thermal gradient effect 0 - 50496
secondary extinctions model and calc. 0 - 55811
shear structures, vector determ. 0 - 55815
site symmetrized expressions of struct. amplitudes 0 - 71532
small angle scattering, distrib. function, calc. 0 - 50497
small angle scattering by two phase systems, theory 0 - 60523
small angle scattering functions of monodisperse systems at infinite dilution 0 - 47158
small angle scattering of C fibre, theory 0 - 61785

tion 0–47158 small angle scattering of C fibre, theory 0–61785 solid, conference, Turku, Finland, Aug. 1970 0–74858 spectral line widths, absorpt, influence 0–65194 stacking faults in small distorted crysts., Bragg refl. intensity distribs. 0–71628 teaching film on reciprocal lattice concept 0–59857 thermal diffuse scatt, many beam dynamical theory 0–65203 topography applies, and developments 0–75048

apparatus

pparatus

see also X ray monochromators; X ray spectrometers

AMR microfocus system 0-65201

adjusting apparatus, accuracy and setting parameter 0-47159

Bonse Hart small angle diffractometer, slit smearing effects 0-61786

camera, Guinier, adjustable, high precision 0-61770

camera for photography of substances at low temp, and high press, method 0-50488

camera with pure precession motion 0-61780

computer applie, to data collection 0-75076

computer controlled data collection on 0-61790

computer controlled data collection system 0-61779

computer controlled diffractometer 0-58667

cooling system with automatic refilling facility, fig N₂ coolant 0-61922

cryostat, 1.5K, powder diffra, high mag, fields, supercond, solenoid 0-61772

cryostat, three circle counter diffractometer 0-61772 Debye Scherrer camera filter attachment for use with radioactive specimens 0 65199

X ray crystallography continued apparatus continued

diffractometer modifications for fragile crystal studies, applie, to inert gas

diffractometer modifications for fragile crystal studies, applie, to inert gas crystal meas. 0–61837 double crystal spectrometer for λ =5 10Å region 0–61760 furnace, for single crystal studies, 1100°C 0–61769 furnace, miniature, for use up to 1000°C with Hilger and Watts linear diffractometer 0–75032 furnace, miniature for Weissenberg photography to 1000°C 0–71541 furnace with uniform temperature region for horizontal X-ray diffractometer 0–45489

connected with minorin temperature region for norizontal X-ray diffractioneter 0 = 45489 goniometer, small angle scatt, ultra high resolution 0-61787 goniometer accessory, automatic pole figure recorder 0-58666 high temperature, for powdery and compact samples 0-61763 intensity data collection, computerised system 0 = 71549 Kratky collimator, reduction of parasitic radiation 0-55806 Kratky small angle camera, alignment 0-53480 lunar sample analysis in glove compartment 0-61771 on line PAHLRED diffractometer, steering programs 0-61782 parallel data collection system for intensities 0-61775 powder diffractometer, Bragg Brentano/Sceman Bohlin type 0-68269 radiation safety features of Noreleo instrumentation 0-65198 Roentgenography high temp, device of polycrystalline specimens for metals and alloys analysis, description 0-50493 small angle camera, modified for resistivity meas, in same sample holder 0-75044 small angle scattering, absolute scale type 0-68270

0-75044
small angle scattering, absolute scale type 0 68270
small angle scattering goniometer, ultra high resolution 0-61787
source, microfocus, practical design considerations 0-63297
spectrometer, double cryst, SKB, emission band meas. 0-75047
straining attachment for X ray diffractometer specimens 0-47348
texture variation determ, around tubing circumference 0-65200
topography reproduction system using vidicon television imaging

topography 0 61774 tube, rotating anode generator, 60 kV, 1000 mA, construction, appl. 0.63296

Weissenberg photograph, X-ray intensity meas, using TV cameras 0 55816

X ray chambers with electrospark machine for cutting oriented specimens 0 58664

calculation apparatus
computer, time shared 0–78445
computer controlled system, PDP 8, absorpt. correction program
0 78444

computer graphics display, rela time three dimens. 0-78443

computer graphics display, rela time three dimens. 0–78443 calculation methods absorbing cryst., dynamic scatt., dispersional corrections 0–65192 absorbing cryst., dynamic scatt., dispersional corrections 0–61827 anomalous dispersion data in crystallographic structure reports 0–50505 atomic scatt. factors accurate determ, using Pendellosung and interferometry fringes 0–78428 atomic scattering factors calc, in Gaussian approx. 0–75074 automatic structure analysis with heavy atom technique 0–61817 charge density as a superposition of non-spherical atomic densities 0–58699 collimation slit correction computer programs, a comparison 0–53497

o 58699 collimation slit correction computer programs, a comparison 0–53497 computer program, STLPLT CalComp plot of crystallographic projections of Lauc photographs 0–71560 computer program, Minsk 2' computer 0–50507 computer program, ine broadening analysis 0–53494 computer programs for syntex P1 autodiffractometer 0–78442 computer system for identification of multiphase powder diffraction pat terms 0–78425 crystallites fine struct, parameters determ, from one diagram 0–55810 cubic cryst, with various dislocation densities, computer calc. of scatt. intensity 0–65196 diffraction line synthesis from continuous scanning obs. 0–75075 diffraction profile of single crystal reflection, inclination diffractometer 0–61822 diffraction profiles of refls. in diffractometers with inclined exposure

diffraction profiles of refls. in diffractometers with inclined exposure schemes 0-65193 double atom refinement method 0-78434 clastic constant meas, by thermal diffuse scatt, second order contribs, in cubic crystals 0-43704 electron density in urea nitrate 0-61818

electron density in trea nitrate 0--61818
electron density parameter refinement 0-58693
electron density refinement 0--61821
facetting of coherent scatt, regions 0-65195
form factors of diatomic molecules 0-61781
Fourier unfolding for lattice parameters and mosaic struct, determ, 0-78431

image method 0-78432 integrated intensities, correction for thermal diffuse scatt, single crysts. 0-59073 integrated intensities, correction for thermal diffuse scatt,, computer calcs, $0\!-\!62159$

integrated intensities, thermal diffuse scatt, contrib., analytical evaluation $0\!-\!62\,160$

intensity and electric field induction, relationship 0—53486 inverse images and point atoms 0—61810 lattice constants and orientation parameters derivation 0—61813 Laue pattern simulation by computer 0—58702 least squares analysis using quadratic nonbonded repulsion potentials 0 58692

0 58692
least squares refinement, absolute weighting 0–61812
line broadening analysis, computer program 0-53494
line intensity profiles, mathematical analysis for solid solution shortrange order 0-53500
line profile analysis 0-65213
line profile broadening by instrumental aberrations, convolution technique
0 61778
maximum determines

0 61778
maximum determinant and heavy atom procedure 0-58700
molecular transform combinations, appl. to anthanthrone 0-61816
multi phase powder diffr. patterns, computer analysis 0-47157
multi solution method, applic. to phase determ in non-centrosymmetric
crystals 0-50506
multiple subcells in superstructure analysis 0-58701
orientation distrib, symmetry in crystal aggregates 0-68271
origin definition in tangent refinement, computer programs 0-58706
Patterson and Zachariasen appl. to structure amplitude signs 0-78441

```
X-ray crystallography continued calculation methods continued Patterson function calc. for ferritin 0-61828
```

Patterson function interpretation programs, appl. to inosine 0-61811 Patterson functions vector searching 0-40110 Patterson map, use of zeros in direct struct. determ. 0-58698

Patterson search using known part of molecule 0–61824
Patterson sharpening by convolution 0–61826
phase determination by density and shift function 0–61793

phase determination for non-centrosymmetric crystals, computer appl. 0-61819

phase determination for non-centrosymmetric crystals, computer appl. 0–61819

phase probability distrib. representation for simplified combination of independent phase information 0–40040
phase refinement and extension by Fourier transform 0–58705
powder diffraction patterns, computer identification 0–61809
powder diffractograms indexing assignement from unit-cell data 0–71542
powder pattern indexing using calculated intensities 0–58691
profile analysis, additivity of variances 0–53477
profile analysis, variance method, satellite group correction 0–53496
profile synthesis for extinction coeff, and thermal diffuse scatt. 0–58704
Protein, electron density function, Fourier coeffs, determ. 0–50559
protein, isomorphous replacement 0–50560
pseudo-symmetric struct. refinement 0–78433
pseudocubic lines resolving method 0–78430
reciprocal space data, function plot, computer programs 0–58696
Sayre's equation, phase refinement, step-by-step algorithm 0–61814
scattering factors for ionic crystals with complete electron solids 0–53485
Scherrer constant evaluation in line broadening expts. 0–75045
selected electron shell method for electron density analysis 0–58697
slit-length collimation corrections in small angle scattering, comparison 0–53495
slit-smeared small-angle scatt, data evaluation 0–43621

0-53495 slit-smeared small-angle scatt, data evaluation 0-43621 small-angle scatt, intersect distrib, appl. to disperse systems 0-61825 statistical correction of systematic error in intensities 0-58694 steel, Fe 39 Si transformer, Laue photographs rapid graphical interpreta-tion 0-65210

structure amplitude distrib. function of microscopic twin 0--58695 structure amplitude signs by binary function section of interatomic vectors 0-78441

structure factors determ using half-value widths of diffr. curves 0–78423 superposition method, refinement of phases of struct. amplitudes 0–65182 superpositional synthesis and section of double Patterson function 0–61823

thermal diffuse scatt, in integrated intensities of Bragg refls., computer programs 0-71535 three-dimensional minimization function method applic, to diffr. data 0-55813

valence struct. from diffraction data, L-shell projection method 0-58690 (Mo₆Cl₈)⁴⁺ cluster structures, isomorphism 0-61820

structures see Crystal structure, atomic

technique

absorption correction, cryst. meas. 0—71534
aggregates, hexagonal polycryst., X-ray thermal diffuse scattering
0—53474

anomalous transmission, applic. to point defects and defect cluster obs.

0-61933
atomic scatt. factors accurate determ. using Pendellosung and interferometry fringes 0-78428
automated lattice parameter determ. on single crysts. 0-68290
automation and computers 0-78424
back-reflection divergent beam, interplanar spacings determ. 0-71545
coal, low-, medium- and large-angle scatt. appls. 0-40071
computer signal averaging for small-angle scatt. 0-68267
crystal perfection, intensity parameters 0-47162

computer signal averaging for smart-angle scatt. — 0-8267 crystal perfection, intensity parameters 0-47162 data collection, computer applic. 0-75076 diffuse scatt. Compton component elimination 0-75041 diffusion coeff. determ. from hot-stage X-ray diffr. data, new method 0-78569

0-78569
divergence method, synergy of line profile analysis and selected area topography 0-58673
double-crystal arrangement of (+,+) or non-parallel (+,-) setting in diffr. topography 0-71547
doublet separation in diffr. profiles 0-71543
elastic strain measurement, diffraction line displacements 0-53475
electron beam zone melt for Ta, horizontal hearth method 0-55792
electron beam zone melt for Ta, horizontal hearth method 0-55791
filings in monolayer form, crystallite sizes obs. 0-71544
fluorescence elimination in diffractometry with solid state detectors 0-55814
graphite near-ideal low- medium- and large-angle scatt appls. 0-40071

0-55814
graphite, near-ideal, low-, medium- and large-angle scatt, appls. 0-40071
heavy atom method, applic, to disordered systems 0-61764
image instantaneous video display 0-50490
interferometry, absolute length standards 0-78427
interferometry, multiple-crystal, alignment, stability, coherence 0-58669
interplanar spacings determ, with back-refl, divergent beam technique 0-71545
Laue diagram in instantaneous radiography 0-78422

0—71545

Laue diagram in instantaneous radiography 0—78422

Laue topography, crystal perfection 0—61765
microradiography, contact technique, applic to alloys 0—58708
molecular cryst, accuract diffr. data refinement procedure 0—65204
multiphonon processes contrib. to thermal diffuse scatt. intensity 0—55812
multiplet lines components determ. 0—55809
non centrosymmetric materials procedural difficulties 0—61920
oxide powders, line broadening meas. of crystallite size 0—40090
particle size determ, limits of coherent regions in diffr. meas. 0—43606
polarity sense in crystal by anomalous scattering at absorpt. edge
0—65202
powder, cubic, integrated intensities, correction for preferred orientation

powder, cubic, integrated intensities, correction for preferred orientation 0-61768

0-61768
powder diffraction profile, moments in kinematic approx. 0-61767
powder diffractometry, accuracy improvements 0-75046
precession photography without layer-line screens, spot-doubling elimination 0-53479
pseudo-Kossel curves, equation 0-53481
refinement of crystal orientation matrix and lattice constants 0-53478
review 0-75049

rotating cryst., using cm. e.m. waves, expt. 0-75042

X-ray crystallography continued technique continue

Schulz diffr. technique for preferred orientation determ, defocusing 0-71537

small-angle scatt.separation from Bragg double reft. 0—65197 solid solution problem, computerized identification scheme 0—68292 spherical crysts.rapid orientation and mounting 0—71546 structure factor determ. in thin perfect crysts. from Pendellosung fringes

0-61790
substructure element, spatial distrib., beam diverging method, appl. to corundum 0-78452
surface orientation determ. using X-ray diffr. and laser 0-75040
symmetrical Laue case meas., (222) 'forbidden' reflection in Si 0-58675
topographic, conf., Antwerp, Belgium Aug 1969 0-75034
topographic, contrast of defect images 0-75126
topography, defect detection, strain field diffr. 0-43607
topography, use of monochromators 0-60522
Warren-Averbach analysis, symmetrical background error effect
0-71540
All powders cubic, integrated, integrities correction for preferred priestors.

0-71540
Al powder, cubic, integrated intensities, correction for preferred orientation 0-61768
He solid, struct. determ. 0-40082
MgO powders, line broadening meas. of crystallite size 0-40090

X-ray diffraction
see also X-ray crystallography; X-ray scattering
anomalous transmission, defect clustering effects 0-43609
antiphase domain boundaries and stacking faults, effects on profile for B2
struct. 0-53542
in crystals, perfect, two-ray transmission and reflection cases solved
0-53486
dynamical theory, defect clustering effects on anomalous transmission
0-43609

0-43609 generator TuR M62, highly stabilized, design including safety devices

grain size determ. in films from X-ray line broadening analysis 0-55828 h.c.p. crystal, deformation stacking faults effect 0-43677 kinematic theory allowing for absorption and duration of coherent radiation 0-40046

tion 0-40046
low-angle patterns, effect of crystallite shapes 0-40056
macrostresses, residual, theoretical aspects for diffractometry 0-54644
molecular gas, Debye-Ehrenfest diffr. model 0-43071
Pendellosung fringes in Bragg case in finite cryst. 0-47160
review of general field 0-55807
sample cell for studies in saturated atmospheres 0-50498
rel. to soil, mineral content, quantitative determination 0-45123
solids under high pressure 0-55808
stearate multilayers, heavy ion, resolving power and reft. intensity
0-50492

temperature standards, internal, use of fcc. metals, systematic errors $0\!-\!43918$

rel. to topography, parallel section screen manipulator construction 0-47161

transmission diffraction or back-reflection dual-purpose apparatus, patent 0-45503

twin studies in metals, precession method 0-50408

Be alkoxides, structure determination, heavy atom method 0-50517

Fe(III) complex, tris(dithioacetylacetonato)iron(III) crystal structure 0-56574

In oxime complex, structure determination, heavy atom method 0-50517 Mg structure changes due to explosive loading, invert 0-53508 MnS-MnSe, characterization of crystals and predominant growth faces 0-47117

X-ray diffractometers see X-ray crystallography/apparatus

X-ray examination of materials

ray examination of materials see also Chemical analysis/X-ray; Radiography p-acetotoluidide crystals, study of orthorhombic modification 0–43647 alkali halide, anharmonic scatt, ionic deform, diffuse meas. 0–62162 alkali halide, cubic anharmonic scatt, 0–59076 alkali halides, scatt, factors, overlap effects 0–75080 alloy, binary, Fermi surface, imaging through diffuse scatt. 0–59142 Alnico 8, high coercive 0–71759 determ, probability methods 0–58771 ascharite, crystal chemistry 0–41214 p-azoxyanisole, nematic, X-ray diffr. effect on cylindrical distrib. of atoms 0–46873

0-46873

0-46873 henatic, X-ray unit. Intert of cylindrical district of actions 0-26883 henatics, X-ray unit. Intert of cylindrical district of actions 0-68484 binary system forming continuous series, interdiffusion coeff. conc. depend. 0-47284 bis(trimethylphosphine) tetrachlorosilicon(IV), crystal structure 0-71598 calcite, refl. integrated intensity anomaly 0-58721 calcium fumarate, trihydrate, cryst. struct. 0-58773 cementite, corrected ASTM powder data 0-40059 coal, turbostratic struct. and chem, edge effects 0-40071 colloid corpuscular particles, mass and shape, small-angle scatt. 0-61565 copolymer with long ride branches, effect of flexibility of main chains on struct. 0-58548 crystal, perfect, lattice vibrations 0-78717 crystal struct. determ. in industry 0-53483 crystal struct. determ. in industry 0-53482 cubic cryst. with various dislocation densities, computer calc. of scatt. intensity 0-65196 cryanethyl cellulose ethers, highly substituted, structural studies 0-71431

cubic cryst. With various distocation defisites, computer care to seaturintensity —65196
cyanethyl cellulose ethers, highly substituted, structural studies 0—71431
deformed cryst, diffuse scatt. obs. 0—58796
dibenzyl crystal, thermal expansion, 83-297K, Gruneisen tensor 0—50898
diffraction patterns of solids under pressure 0—55808
dislocation density distrib. determ. 0—58809
elastic constant meas. by thermal diffuse scatt., second-order contribs. in cubic crystals 0—43704
elastically distorted crysts, diffraction theory and exptl. obs. 0—61791
epitaxial film, semicond. alloy, struct., nondestructive eval. 0—58580
eutectic alloy melts 0—68074
fault detection, utilizing Compton scatt. 80-400 kV 0—53527
ferrite, combined diffr. and spectrographic study, regularity obs. 0—75079
ferroelectric, critical scatt. 0—68959
ferroelectric, critical scatt. 0—68959
ferroelectric domain boundaries contrast 0—62414
fibres, C, small-angle scattering 0—61785
film, metallic, thin, thickness meas. 0—65051
film, thickness and refractive index 0—74894

```
X-ray examination of materials continued
```

film/crystal interfacial strain, asymmetric diffr. use in topography 0 68206

films, thin solid, structural investigation 0-68221

plass, phase separated, small angle scatt. obs. 0-74861 glass, small angle scatt. obs. 0-50491 glass and glass ceramic systems, phase separation 0-74862 glass ceramic containing metastable quartz mixed crystals, transparent

glasses, fluoride opal, opacifying mechanism 0-43526 gramicidin S, by heavy atom method rel. to disordered system analysis 0 61764

of 1764 graphite, near ideal, turbostratic struct, and chem, edge defects 0–40071 graphite, pot, nucl., anisotropy determ. 0–40069 graphite, pyrolytic, highly oriented, thermal motion obs. 0–40519 graphitized fibres, struct, and orientational aspects 0–43629 h.c.p. crystal, deformation stacking faults, effect of change in layer spacing on diffr. 0–43677 h.c.p. with prismatic dislocation loops, scattering 0–61788 helical filaments, dil. suspension, small angle scatt. 0–68157 hydrazinium sulphate, cryst, struct, bonds 0–50536 fee, prismatic dislocations 0–50592 ice, vibrating dislocations in a.c. field, topography 0–68359 inert gas, lattice parameter and diffracted intensity meas. 0–61837 insulation, fine structure resolution, radiographic technique 0–69565 intensity meas. errors of specimen analysis 0–58663 interferometry, rel. to meas. of crystal lattice spacings and fundamental constants 0–71548 interstellar grains, possibility of detecting light elements by X-ray anal. 0–45307 ionic cryst., scatt. factors, overlap effects 0–75080

0. 48.807 ionic cryst., scatt. factors, overlap effects 0. 0. 75080 irradiated cryst., diffuse scatt. obs. 0. -58796 kinetmatic theory of diffraction by matter 0. -53310 Laue topography, crystal perfection 0. -61765 liquid binary alloy, Al Sn, Cowley short range order parameter 0. -58450 Liquid cryst. 0. -58450 Laueas method used to determine residual internal stresses in cementite steel 0. 40280

Lucas method used to determine residual internal stresses in cementite steel 0.40280

lunar samples, powder and single crystal diffraction 0.-48518
lunar samples, study of dominant crystalline phases 0.-48508
magnetic properties, Curie point, energy correlator 0.-40918
martensite, electron bombarded, C atom migration, ageing effect 0.-68337
metal crystals deformation, topographic examination 0.-40291
3.methyl 4.minora.0benzene 2.sulphenyl cyanide, unit cell dimensions and space group determ. 0.-47213
mica, Ar ion irrad., track formation mechanism 0.-61935
mica, Ar ion irrad., track formation mechanism 0.-61935
molecular crysts, lattice vibr. 0.-62151
molecular electron population parameters 0.-46440
molecular gas, Debye Ehrenfest diffr. model 0.-43071
multiphonon scattering calc. 0.-62173
muscovite, dislocations, clastic props., Berg Barrett topography 0.-61959
muscovite mica, dislocations, transmission topography 0.-61972
nematic phase, diffr. effect on cylindrical distrib. of atoms 0.-46873
noncrystalline, structure 0.-65014
N oxyphenazine, disorder diffuse scattering, domains of short-range order 0.53525
N. oxyphenazine phenazine mixed crystals, diffuse scattering, disruption of

0 53525
N oxyphenazine phenazine mixed crystals, diffuse scattering, disruption of short range order domains 0 53525
particle size determ, limits of coherent regions in diffr. meas. 0-43606
percovskite type cpds., struct., book 0-68293
photorearrangement products of phenethylamine derivatives, phase determination 0-66202
plagioclase An_{16.3}, satellite refis. obs. 0-65217
polarity sense in crystal by anomalous scattering at absorpt. edge 0-65202
note figure recorder, automatic, use with Schulz X-ray goniometer

pole figure recorder, automatic, use with Schulz X-ray goniometer 0 68265

polyethylene, crystallization under orientation and pressure effects of capil lary viscometer 0–78350 polyethylene crystal, mosaie-structure, lattice distortions and surface energy 0–65308

polymers, crystalline, effect of flexibility of main chain on struct. 0-58548 polytetrafluorethylene, lattice distortions and crystallite sizes, 20°C 58778

0.58778
polytetrahydrofuran, degree of crystallinity 0.68324
polyvinylidenefluoride, rel. to investigation of structure dependence on polymerization conditions 0.71439
powder, cubic, integrated intensities, correction for preferred orientation 0.61768

powder, cubic, integrated intensities, correction for preferred orientation 0 61768 powder, particle size determ. 0–50335 powder diffraction profile, moments in kinematic approx. 0–61767 powder mixing pre sintering, quantitative analysis. 0–50797 powders, grain size distrib. by X-ray scatt. 0–75035 powders exhiniting marked cleavage, preparation for counter diffractometer examination. 0 50494 protein, macromolecular parameters, low-angle scattering data. 0–43197 quartz, plates, vibrating, topography. 0–68268 quartz resonator, excited, topography. 0–68268 quartz resonator, excited, topography. 0–68268 quartz resonator, excited, topography. 0–47027 rare earth molybdate, phase transformations. 0–78701 rare earth sclenates, from Sm-Lu, cryst. struct. determ. 0–53514 reactor fuels, emission and diffr. method. 0–59515. Roentgenography high temp. of metals and alloys. 0–50493. Schulz. X-ray goniometer with automatic pole figure recorder for texture diagram. 0–68265 sedimentometer. 0–50263 semiconductor alloy epitaxial film, struct., nondestructive eval. 0–58580 semiconductor alloy epitaxial film, interface analysis. 0–65666 semiconductor surface layer characterization. 0–65666 sedioane rubbers, X-ray studies of secondary crystalliz. 0–50346 sodium humate fraction molecular size determ. 0–69250 soil, mineral content, quantitative determination. 0–45123 solder joint and component radiography. 0–76758 soild solns., precipitating, anomalous diffr. effects. 0–65215

X-ray examination of materials continued

solid solution, component redistrib. on quenching 0-50773 solid solution problem, computerized identification scheme 0-68292 spectral composition of elements with low atomic numbers, formula for calc. 0-59438

spinel, lattice parameters and structure 0-47191 spinel, phase transitions low temp. 0-62124 stacking faults in powder patterns of close-packed struct, peak displace-ments 0-71629 stacking faults in small distorted crysts., Bragg refl. intensity distribs. 0 71628

0 /1028 steel, carburized, stress factor determ. using two-exposure technique 0 68435 steel, internal stress determinations rel. to strain dependence of lattice

steel, internal stress determinations rel. to strain dependence of lattice stress/strain relations 0-40270 steel, lattice parameter changes and austenite stabilization 0-40487 straining attachment for X-ray diffractometer specimens 0-47348 stress measurement in polycrystalline samples 0-55965 surface analysis with electron probe 0-65032 surfaces and reaction products, emission analysis technique 0-65031 target cell for study of liquids and gases 0-76785 p-terphenyl, crystal structure refinement 0-61928 thin film alloys, quantitative X-ray fluoresc. anal. 0-75078 rel. to topography, parallel section of 47161

vinyl monomers, long chain 0-47024

vinyl monomers, long chain 0–47024 vitreous-vitreous phase separation applic. 0–50491 wire drawing fibre texture analysis 0–50772 Ag-In alloys, phase transformations from powder diffraction 0–75313 Ag-Zn, Ag-Cd, Ag-Hg solid solutions, α-, temp. and conc. depend. of lattice parameters 0–78447 Ag-halides, phase transformations, press. induced 0–62126 Ag-concentration in an aluminium silver specimen by small angle X-ray diffraction 0–53447

diffraction 0-334/ Ag(II) complex, silver(II)- bis(pyridine-2,3-dicarboxylate/dihydrate, crystal structure 0-55827 Al-Ag solid solution, second stage decomposition 0-68564 Al-Ge alloys, Ge nucleation, obs. by modified small-angle camera 0-75044

Al-Ge alloys, Ge nucleation, obs. by modified small-angle camera 0 75044
Al-Sn liquid alloy, Cowley short range order parameter 0-58442
Al-Zn(AG), diffuse scatt. features 0-53503
Al, annealing and deformation, diagrammatic X-ray analysis 0-71567
Al, atomic scattering factor 0-78449
Al, form factor, simple model potential 0-50923
Al, high temp. creep, substructure changes 0-68458
Al, multiphonon scattering calc. 0-62173
Al, pure, recovery after lowtemp. deform, effect of annealing, by X-ray diffraction 0-47441
Al film, diffr. line broadening, variance analysis 0-61643
Al powder, cubic, integrated intensities, correction for preferred orientation 0-61768
Al single crystal, fatigued, topography examination of slip bands 0-40339
AlN film deposited from AlCl₃NH₃, diffr. pattern 0-61666
Al₃O₃TiO₅ system, surface props. 0-50352
As-Te-Ge glass, filament formation, electron probe analysis, radiometric microscopy 0-56285
Au film, lattice parameters at < 1000 Å, line broadening analysis 0-61644

Al₂O₂TiO₂ system, surface props. O-50352
As Te-Ge glass, filament formation, electron probe analysis, radiometric microscopy 0-56285
Au film, lattice parameters at <1000 Å, line broadening analysis 0-61644
AuCu₃, disordered struct. 0-71569
B₁ β-rhombohedral, Compton profiles 0-50513
B₂C₂, Compton profiles 0-50513
B₃C₄, Compton profiles 0-50513
B₄C₄, Compton profiles and electron momentum distributions using MoKα X-rays, experiment and theory, comparison 0-65572
BN, Compton profiles and electron momentum distributions using MoKα X-rays, experiment and theory, comparison 0-65572
BN, Compton profiles and electron momentum distributions using MoKα X-rays, experiment and theory, comparison 0-65572
BN, Compton profiles and electron momentum distributions using MoKα X-rays, experiment and theory, comparison 0-65572
BN, Compton profiles and electron momentum distributions using MoKα X-rays, experiment and theory, comparison 0-65572
BN, Compton profiles and electron momentum distributions using MoKα X-rays, usinface layer, d.c. elec. field 0-79044
Be defect struct., by combination method 0-58673
BeO, Compton profiles 0-50513
Bn, hexagonal, Compton profiles 0-50513
Bn, hexagonal, Compton profiles 0-50513
C, pyrolytic, Bacon anisotropy factor 0-71573
CaGeS₄, cryst. struct. determ., by X-ray powder diffraction 0-61845
CaO-MgO-B₂O₃ glass, phase equilib., 900C 0-47488
Ca₄(PO₂), H₂O₃, morphous, radial distrib. obs. 0-58330
CdBr₂, arcing phenomena on oscillation photographs 0-71576
Cd₁, dislocation arrangements, temp. effect 0-75160
Cd₂,Nb₂O₃, phase transition, 80 K 0-75328
CdO-CdF₂ system, compound formation 0-69206
CdF₁O₃, perovskite modification, 0-1200°C 0-50522
Cd[H₁1O₆|6H₂O₃, cryst. and mol. structure 0-61879
Ce. structure above 50 kbar 0-43632
Cr complex, [N,N-bis(2-diphenylphosphinoethyl)ethylamineltricarbonylchromium, crystal, molecular structure 0-61879
Ce. structure deforms, thermal diffuse scattering 0-62168
Cu-Al alloy, electronic structure 0-68734
Cu₁

0 68529
Cu-Al alloy, electronic structure 0-68734
Cu₃-NiMn system, ageing, phase transformations 0-59018
Cu-Sb alloys, cold-worked, stacking fault probability 0-61973
Cu-Sn alloy, electronic structure 0-68734
Cu-Sn liquid alloys, atomic distribs. 0-74724
Cu-Zn alloy, electronic structure 0-68734
Cu, diffr. props., dislocations effect 0-78470
Cu, diffraction props., effect of dislocations 0-61857
Cu, high temp. creep, substructure changes 0-68458
Cu, neutron irrad., scattering from defect clusters 0-61934
Cu double Bragg X-ray scatt. from deformed polycrystalline copper 0-61854
Cu(C-H,SO₄), 4H₂O determination of crystal structure 0-61855

0–01034 Cu(C,14,5O₄), 4H₂O determination of crystal structure 0–61855 Cu_{0.3}Fe_{2.3}O₄, determ. of distrib. of copper ions 0–47184 Cu_{0.3}Hn_{0.3}Fe_{2.0}O₄, determ. of distrib. of copper ions 0–47184 Cu(NH₂)₄(CuBer₂)₂, structure determined by X-ray single crystal analysis 0–50524

0-30524 Cu(NH₃)₄(CuCl₃)₂.H₂O, structure determined by X-ray single crystal analysis 0-50524 ysis 0-50524
Cu(NH₃)₄(Cul₂)₂, structure determined by X-ray single crystal analysis 0-50523

X-ray examination of materials continued

Cu₃Pd, long period ordered alloy, lattice modulation 0-40076

Cu₃Sb(h) alloy, high temp. meas., stoichiometry and vacancies 0-50525 Eu₂S₄, lattice parameters rel. to phase transform. at 168K 0-71798 Fe-Ag sintered, strain deformation 0-40301 Fe-Al solid soln., diffusion and self-diffusion of Fe, 320°C 0-53561

Fe-Cu sintered, strain deformation 0-40301

Fe-(3wt.%)Si, ferromagnetic domain and dislocation obs. from topographs 0-62519

Fe-(3.5 at.%)Si alloy, single cryst., domain structure, study by X-ray topography 0-61861

Fe, liquid, struct., comparison with liq. Ni 0-71308

Fe₃B₇O₁₃I, lattice strains, electrostriction 0-53939

FeFe_{2-x}Sc_xO₄ ferrite, lattice, local distortion, Mossbauer effect, ⁵⁷Fe 0-47185

Fereign Scot (errite, lattice, local distortion, Mossbauer effect, Fe 0-47185
δ-FeOOH→α-Fe₂O₃, thermal transformation, 23-650°C, struct., mag. props., Mossbauer spectra 0-65492
δ-FeOOH→α-Fe₂O₃, thermal dransformation, 23-650°C, struct., mag. props., Mossbauer spectra 0-65492
β-FeSi₁, twin 0-50409
FeTiRO₃, R=-rare earth, crystal structure 0-51174
Ga single crystal, orientation 0-50407
GaSe-InSe phase systems analysis 0-46979
Ge-O, solid solution, precipitation and defect structure 0-75142
Ge-Te, amorphous alloy, radial distrib. 0-55679
Ge, anomalous transmission 0-61871
Ge, dislocation density distrib. determ. 0-5809
Ge, dynamical diffr. 0-75093
Ge single cryst., struct. regularity determ. 0-65242
He solid, struct. 0-40082
'He, thermal conductivity and X-ray study, molar volume reported 0-43508
InP-CaP alloys, epitaxial layer comp. determ, Vegard's law 0-75094

He solid, struct. 0–40082

'He, thermal conductivity and X-ray study, molar volume reported 0–43508

InP-GaP alloys, epitaxial layer comp. determ., Vegard's law 0–75094

KCI, dislocation density rel. to anomalous transmission 0–61964

LaB_x, thermal expansion 0–65552

LiF, compressibility, high press., high temp. 0–40286

LiF, virrad., diffuse scatt. obs. 0–65335

LiF single crystal, Compton profiles 0–50513

LiTaO₃, rel. to stoichiometry determination 0–50466

Mg,Cd, ordering process 0–59028

Mg,Cd alloy, study of ordering process at 26-170°C 0–55851

Mg(Cr_xAl₂-2)O₄, spinel, lattice parameters and structure 0–47191

MgF₂, electron density determ. from structure factors meas. 0–40091

MgO Al₂O₃, SiO₅, satellite refls. interpret. 0–58735

α-Mn, chem. and mag. struct. 0–72281

MnAs_{0.92}P_{0.08}, crystal and mag. struct. 0–44563

MnTiRO₃, R= rare earth, crystal structure 0–51174

Mo, annealed and deformed, local distortions, Kossel lines 0–68348

MoSi₂, film on Mo, stress meas. 0–75246

ND₄I, of lattice parameters of I, II and III phases, -176-190°C 0–55856

NH₄I, of lattice parameters of I, II and III phases, -176-190°C 0–55856

NH₄SO₄, cryst. struct., bonds 0–50536

NaBr, multiphonon scattering calc. 0–62173

NaCloF₃, cryst. struct. from X-ray powder patterns 0–65218

NaF, multiphonon scattering calc. 0–62173

NaF, oryst. struct. from X-ray powder patterns 0–65218

NaF, multiphonon scattering calc. 0–62173

NaF, cryst. struct. from X-ray powder patterns 0–65218

NaF, mythiphonon scattering calc. 0–62173

NaF, cryst. struct. from X-ray powder patterns 0–65218

NaF, multiphonon scattering calc. 0–62173

Ni complex, [Et₄N][Ni(H₂dma)], cryst. struct. 0–53512 Ni foil, dynamics and static extension, microhardness, dislocation densities 0–50691

Ni powder, charge density absolute meas. 0-61900 y'-Ni superalloys, long range order, rupture and heat treatment effects 0-68314 x10NiCrWTi36.15, precipitation behaviour, high temp. stress hardened

Ni₂MnSb, nearest neighbour environment of Sb, anomalous dispersion obs. 0–65266

NI,9MDD, nearest neighbour environment of Sb, anomalous dispersion obs. 0—65266
NiO, antiferromagnetic, rhombohedral distortion, temp. depend. 0—47199
Pb, thermal diffuse scatt., theory and expt. 0—62176
PbO.PbSO₄ system, phase relations 0—59054
Pd-Ag alloy film, homogeneity, prep. depend. 0—47067
Pd-Ba alloy, struct. of Pd-Ba comp. 0—50544
PrAIO₃, phase transformations, 205, 151 K 0—53662
Pt-Ba alloy, struct. of Pt-Ba comp. 0—50544
PrAIO₃, phase transformations, 205, 151 K 0—53662
Pt-Ba alloy, struct. of Pt-Ba comp. 0—50544
Pt-Bo, plasma-formed microspheres, thermal expansion 0—68620
Rb₂Cr₂O₇, struct. determ. by single crystal method 0—43645
SF₄ gaseous, electronic struct. exam. by soft X-ray spectroscopy 0—46511
SF₆ gaseous, electronic struct. exam. by soft X-ray spectroscopy 0—46511
Se, Czochralski-grown, perfection and damageability 0—65163
Si, atomic scatt. factors accurate determ. using Pendellosung and interferometry fringes 0—78428
Si, B diffusion-induced imperfections, X-ray topographic study 0—47259
Si, dislocations, dynamical diffr. images 0—75150
Si film, amorphous, structural props., and elec. and opt. props. 0—47761
Si lattice parameters, device design and tech. for meas., description 0—50409
SiO₆ film on Si, stress determ. by dynamical diffr. 0—58577
Sm-MoO₆). M-modification form and hase transitions 0—65408

0–50499 SiO_x film on Si, stress determ by dynamical diffr. 0–58577 Sm₂(MoO₄)₃, M-modification, form, and phase transitions 0–65498 Sn liquid, 220, 235, 260, 400, 450°C, radial distrib. functions 0–46869 Sn₄As₃-SnAs-SnTe subsystem, eutectic obs. 0–74836 Sn_{O₂}, surface effects rel. to thermal annealing 0–55705 Sr₂-GeS₄, cryst. struct. determ by X-ray powder diffraction 0–61845 SrPbO₃, perovskite, struct., 0-800°C 0–50514 ThC-H₂, struct., p.m.r. 0–68317 Ti-Hg-Zn syst. 0–40465 Ti, phase transitions, 120-500 k-bar shock wave induced 0–40493

X-ray examination of materials continued

Ti polycryst., Compton profile meas, at Mo K_a , for electron momentum density 0-40645TiO₂, rutile and anatase, thermal expansion, lattice parameters 0-50897

density U=40045
TiO₂, defect ordering 0=58779
U-Nb-Zr alloy, crystal structure of transition phases 0=59041
UO₂-W composites, growth modes 0=53651
U₄O₉, quenching effects on phase transitions and equilib. 0=43833
U_{1-x}Y₄O₂ new phase obs. 0=47462
V-H system, H-precipitation, low temp. diffuse scatt. 0=59044
V, Debye temp. and thermal expansion coeff. 0=78784
V, phonon dispersion 0=56092
V, thermal X-ray scatt. obs., 293-77K
0=62175
V_xMn_{1-x}Te system, (x=0-1), cryst. struct. 0=79133
VO₂-WO₂ system, phase relationships 0=62143
V₂O₃, thermal expansion 0=65562
W, evaporated films, rel. to supercond. transition temp. 0=51016
xMn₂O₄+(1-x)Cu(FeCr)O₄, ferromag. spinels, cryst. struct. 0=61882
Yb₂, electron density of states, X-ray photoemission obs. 0=62261
Yb₃, thermal expansion 0=65552
Yb₄, phase transitions, 120-50 kbar shock wave induced 0=40493
ZrO₂, monoclinic-tetragonal phase transition 0=62141
liquids

liquids

allkanes in solution, structure 0–61489 alloy, Knight shift 0–61552 p-azoxyanisole liquid crystals, phase transitions, small angle scattering

alloy, Knight Shift U-61552
p-azoxyanisole liquid crystals, phase transitions, small angle scattering
0-61496
crystals, phase transitions, small angle scattering
0-61496
kinetmatic theory of diffraction by matter 0-53310
macromolecules solutions, small-angle scatt., heavy atom interatomic distances 0-61484
macromolecules with heavy atom labels, scatt. theory 0-43427
polypeptide solutions, small angle scatt. 0-61498
silica, colloidal, Ludox HS, small-angle scatt. 0-53382
trimethylamine, structure, 5°C 0-61490
water, models, using diffr. data 0-61487
water, radial distrib. functions 0-53317
Ag, struct. components from Fourier analysis of intensity curves 0-74723
Al-Sn alloy, X-ray scatt. struct. meas. 0-64865
Ar, intensity patterns, radial distrib. and correlation functions 0-61485
Au, struct. components from Fourier analysis of intensity curves 0-74723
Bi, structure, 280-450°C 0-43426
Cu-Sn alloy, atomic distrib. 0-61486
Ga, struct. 0-64862
Ge, struct. 0-64862
Ge, struct. 0-64862
Hg-In alloy, diffr. meas. 0-61488

Ge, struct. 0–64862 Hg-In alloy, diffr. meas. 0–61488 NH₄Cl(Br,I), aqueous, water structure, Cl⁻, Br⁻, I⁻ effects, scattering, radial distribution functions 0–39732 Pb, struct. components from Fourier analysis of intensity curves 0–74723 Pb, struct. obs. 0–46872 Sn-(70a1%)Al, struct. from scatt. curves 0–64866 Sn, struct. 0–64862

Sh, struct. 0-04862 microstructures see also Crystal structure/microstructure alloy, β -brass-type ordered, diffr. from planar faults 0-65328 alloys, contact microradiography technique 0-58708 brittle crystals, growth dislocations 0-61957 cellulose, carbonized fibre, pyrolysis depend. 0-47026 crystal aggregates, orientation distrib. symmetry 0-68271 defect images on topographs, contrast obs. 0-75126 defective lattice, diffuse scatt. 0-58665 grain size determ. in films from X-ray line broadening analysis graphite, pyrolytic, crystallite size 0-65224 graphitized fibres, struct. and orientation 0-58709 lunar samples, clinopyroxenes, single-crystal diffraction study of texture 0-48519 macroprobe analyzer using electron excitation 0-75039

metal, cubic, determ. of symm. groups of deform. textures 0-71688 poly(ethylene terephthalate) films, oriented, lamelar domains size 0-78376

polycaproamide, crack nucleation, fibrillar struct. 0-43793 polyethylene, stretched annealed, superstructure, small-angle scatt. 0-61932

0-61932
polyethylene crystal, mosaic-structure, lattice distortions and surface energy 0-65308
polyethylene single crystal, mosaic structure change during degradation by hot fumic nitric acid 0-61931
polypropylene crack nucleation, fibrillar struct. 0-43793
polytertafluorethylene, lattice distortions and crystallite sizes, 20°C 0-58778
usertz natural and synthetic defects topography. 0-75169

polytetrafluorethylene, lattice distortions and crystallite sizes, 20°C 0–58778

quartz, natural and synthetic, defects, topography 0–75169
quartz powder, extinction of Deby-Scherrer lines, crystal domain radius determ. 0–61904

small-angle boundary type X-ray diffr. determ. 0–65330

steel, austenitic stainless, substructure texture 0–71588

steel, retained austenite 0–40081

steel, work hardening propag, under impact loads obs. 0–62091

texture variation determ. around tubing circumference 0–65200

topography applies. and developments 0–75048

Ag, Ag-66 alloys, splat-cooled, line broadening analysis 0–61835

Al-Ag alloy, ordering, diffr. pattern, central diffuse spot, origin 0–53502

Al-(15w.%)Ag alloy., p plates, surface relief effects, diffusional phase transformation 0–65483

Al-Zn,Mg, precipitation, two-stage deposition effects 0–65484

β-AlNi intermetallic, cold-worked, planar faults 0–65329

Al₂O₃, synthetic corundum, substructure element, spatial distrib., beam diverging method 0–78452

Au-Ni, Au-Co alloys, electrodeposits, heat treatment, phase changes 0–65481

Chibre, high-modulus, struct. 0–40067

Ch. W reinforced recrease in temp. by X-ray diffr. mass. 0–78611

0–65485
C fibre, high-modulus, struct. 0–40067
Cu, W reinforced, recrystn. temp. by X-ray diffr. meas. 0–78671
Cu creep deformation substruct. analysis, single cryst. 0–65233
CuNiCo dil. alloy cryst., sideband phenomena obs. 0–68302
Cu₂Pd alloy, periodic antiphase struct. 0–71582
CuSe(Te) and ternary compounds, phase transitions 0–40491

X-ray examination of materials continued

microstructures continued

 α -Fe, dislocation real struct. obs. using X-ray spectrometer with oscillating film $0{-}71626$

 $Fe_{3}O_{4},$ magnetite, ground sample, microstrains and stacking faults $0\!-\!58819$

Ge:As solid solution, precipitation, anomalous transmission 0-75333 Ge, heteroepitaxial film, dislocation density 0-74903 KCl, qhiskers and acicular crystals, screw dislocations rel. to intensity meas. 0-61965

MgO, active, line broadening analysis 0–62110
Nb single crystals, struct., effect of annealing and low-temp. rolling 0–78486

0-78486
Ni, substruct. changes due to fast moving air current 0-61949
NiSe(Te) and ternary compounds, phase transitions 0-40491
Se electrodeposited layers, texture 0-59503
Si, defect struct., methods combination 0-58817
Si, deformed, dislocation motion, topography obs. 0-47261
Si, heavily doped, homogeneity disturbance 0-65497
SiO₃, cristobalite, growth and stacking faults 0-58894
Te, electrodeposited layers, texture 0-59503
W, deformed and annealed, fine struct. changes 0-40145

molecular structure

molecular structure cellobiose, absolute configuration determ. from anomalous scatt. 0–64495 N-heterocyclic compounds, diffr. studies 0–40113 narcissidine hydrobromide 0–53523 Ni complex, [Et₄N] [Ni(H₂dma)] 0–53512 organic compounds, absolute configuration, anomalous scatt. from oxygen 0–61139 RNA, transfer, three dimens. diffr. data, 12 Å resolution 0–50564 1,2,3,4-tetrachloro-5,6-diphenylcalicene 0–55867 B cpds., diffr. studies 0–40063

X-ray fluorescence see Luminescence; X-ray spectra/emission

X-ray measurement

ray measurement

see also Dosimetry
detection of energetic low intensity X-rays against low energy high intensity
background 0-38745
detector, Si surface-barrier type, Fano factor meas. 0-42640
flash tube, photon energy spectrum determ. 0-48661
image dissection, one- and two-dimensional, using channel multiplier
arrays 0-60173
intensity meas. errors of specimen analysis 0-58663
K X-rays, distribution as a function of mass and atomic number in the
spontaneous fission of ²³²Cf 0-52810
low energy, appl. of alkali halide Scintillators and Ge and Si rad. detectors
0-52598
multipliers, channel arrays, soft X-ray studies 0-60172

0-52598
multipliers, channel arrays, soft X-ray studies 0-60172
KCl:Cu thermoluminescent dosimeters 0-73702
NaI(Tl) scintillation detector response and pulse height distributions for monoenergetic X-rays of few keV 0-49373
X-ray microscopes see Microscopes

X-ray microscopes see Microscopes
X-ray microscopes See Microscopes
X-ray monochromators
with Johann's type approximate focusing, quantitative characteristics, compared to exact focusing 0-75037
crystal for high intensity X-ray tubes 0-66756
graphite for post specimen powder diffraction 0-61773
organic cryst., growth and testing for 10-100 Å region 0-65168
stearate multilayers, heavy ion, resolving power and refl. intensity
0 50492

topography applications 0-60522

X-ray photoeffect see Electron emission/photoelectric

X-ray reflection
back-reflection or transmission diffraction dual- purpose apparatus, patent
0-45503

0-45503 resonator characts. 0-60188 solid surface, rough intensity rel. to projections 0-40044 ultrasoft radiation, reflec. from diffraction gratings 0-43608 Ge single cryst, as analyser in spectrometer 0-65189 Mg structure changes due to explosive loading, invert 0-53508

X-ray scattering

ay scattering see also Compton effect; X-ray diffraction anomalous, Pendellosung effect, K absorption edge 0-75043 anomalous scattering factors, relativistic calc. 0-67604 apparatus for high temp. small angle scatt. meas. 0-64865 application to fog density measurement, patent 0-51541 Bonse-Hart small-angle diffractometer, slit smearing effects 0-61786 Compton component elimination in diffuse scatt. 0-75041 Compton effect, spectral intensity distrib. by Thomas-Fermi model 0-70742 Compton scattering from bound electrons 0-64239

Compton effect, spectral intensity distrib. by Thomas-Fermi model 0-70742
Compton scattering from bound electrons 0-64239
four-electron atoms, coherent and incoherent scatt. 0-70800
incoherent scattering functions, asymptotic behaviour 0-77639
by laser irrad. crysts. 0-62156
rel. to lattice dynamics, change in electron density due to small displacement of ions calculation, one-body potential theory application 0-68576
macromolecules, branched Gauss chain theory 0-67829
macromolecules, branched Gauss chain theory 0-67829
macromolecules, branched Gauss chains, size of whole and branch from analysis 0-64562
metal, cubic, prod. by point defects, intensity profiles 0-43652
molecular crystals, theory 0-59086
multiphonon, calc. 0-62173
plasmon scatt, dispersion relation 0-62269
plasmon scatt, dispersion relation 0-62269
plasmon scatt, dispersion relation 0-76124
small-angle, by C fibres, theory 0-61785
small-angle, by C fibres, theory 0-61785
small-angle, intersect distrib. calc., appl. to disperse systems 0-61825
small-angle, method for smoothing curves 0-55817
small-angle, method for smoothing curves 0-55817
small-angle, reduction of parasitic radiation of Kratky collimator 0-55806
small-angle, theory and technique 0-50491
small-angle, by stretched and annealed polyethylene, superstructure 0-61932

X-ray scattering continued

small-angle determ. of interatomic distances of heavy atoms, macromole-cules solutions 0-61484

small-angle of polypeptides in solution 0–61498 solid solns, precipitating, anomalous diffr. effects 0–65215 stiff chain molecules, particle scatt. factor for wormlike and discrete chain models 0–58258

models 0—58258 thermal diffuse, in hexagonal polycryst, aggregates 0—53474 three-electron atoms, coherent and incoherent scatt. 0—70800 Al, multiphonon, calc. 0—62173 Be, plasmons 0—78855 Csl, lattice dynamics, thermal diffuse scattering 0—62168 He, isoelectronic sequence, coherent and incoherent scatt, by bound electrons 0—43008

trons 0–43008
Li, Compton scattering and electron momenta 0–69146
Li, scattering factors from correlated and independent particle model wavefunctions 0–64236
LiF, refractive index, interferometry, forward scatt. amplitude 0–79234
NaBr, multiphonon, calc. 0–62173
NaCl, multiphonon, calc. 0–62173
NaF, multiphonon, calc. 0–62173
Sn-(70at%)Al, molten, struct. from curves 0–64866

X-ray spectra

as spectra see also Atmospheric spectra; Chemical analysis/X-ray anomalous scattering factors, relativistic calc. 0-67604 atomic charges in cpds. of 3rd period elements, X-ray spectra obs. 0-42929

0-42929
atomic energy level determ. 0-67609
bent crystal, reflectivity, method, equipment, 50 to 80 keV 0-41115
electron temp. meas. in plasma discharge in laser 0-43278
fluorescence of elements with low atomic numbers, choice of primary radiation, formula 0-59438
fluoro-anions, low energy satellites in fluorescence spectra 0-67699
geological samples analysis, comparison with direct electron excitation
0-482.13
be extelliber percent lines 0-70748

0–48213 h.f. satellites, parent lines 0–70748 image dissection using channel multiplier array 0–51880 intensity determ. of primary and secondary spectra 0–72401 isotope K shifts rel. to nuclear charge radii vars. 0–38842 K, isotope shifts, rel. to nuclear charge radii 0–52877 $K\alpha_1$ line widths for Z>50 0–60910 $K\alpha_2$ line widths for Z>50 0–60910 metal, singularities, deep hole-plasmon coupling problem 0–41247 metal, threshold singularity, Tomonaga's model 0–48096 metal effect of core hole 0–76083 muonic, deformed nuclei, dynamic E2 hyperfine structure analysis 0–70383 nuclear K-capture X-rays and surface neutron, and proton densition nuclear K-capture X-rays and surface neutron and proton densities 0-55104

0-55104
photopeak location and area determination, automatic 0-49327
plasma, atomic and ionic transfer temp. meas. 0-78108
from plasma focus devices, up to 350 keV energies 0-78085
potassium acid phthalate crystals 0-69144
quartz (3140), bent, reflectivity, 50 to 80 keV, continuous spectrum
0-41115
Raman effect, internal, in solids 0-76124
satellite lines low energy, theor, interpret. 0-48095

Raman effect, internal, in solids 0-76124 satellite lines, low energy, theor. interpret. 0-48095 satellite lines, review of theories 0-39262 satellites, high and low-frequency, similarity in behaviour, origin 0-70777 soft, chemical effect, vacuum spectrometer applic. 0-69567 soft, rel. to density of states 0-66076 superconductor, high-temp., V_3X type, energy bands 0-79342 transition intensity, $K-L_1$, $K-L_1$, Hf and Au obs. 0-72403 valence band, interpretation 0-69142 Al(200), bent, reflectivity, continuous spectrum 50 to 80 keV 0-41115 Am atom, energies of $K\alpha_1$, $K\alpha_2$, $K\beta_1$ and $K\beta_3$ 0-49787 Ar, LM to L ionization ratio 0-42993 Ar gas target, L shell X-ray spectra by 50 to 330 keV Ar ions 0-39312 Au, $K-L_1$ transitions intensity 0-72403 B, BN, Compton spectrum discontinuities due to K-electron binding energies 0-62702

gies 0-62702 B₄C, Compton profiles and electron momentum distributions using MoK α X-rays, experiment and theory, comparison 0-65572 BN, Compton profiles and electron momentum distributions using MoK α BN, Compton profiles and electron momentum distributions using MoK α

X-rays, experiment and theory, comparison 0–65572
Ca 15 MeV O⁴⁺ bombardment, K X-ray spectra obs. 0–77693
Co, K\$\beta_5\$, in CoSi₃-NiSi₂ solid soln., correl. with mag. props., rel. to electronic struct. 0–79340

Ca 15 MeV O⁺⁺ bombardment, K X-ray spectra obs. 0–7/693
Co, Kβ_s, in CoSi₂-NiSi₃ solid soln, correl, with mag. props., rel. to electronic struct. 0–79340
Cr, positions and shapes of Kα_{1,2} and Kβ_{1,3} lines 0–58098
Cu XXI, gf-values 0–66375
Cu₂O, band structure 0–62596
¹⁶²Dy. ¹⁶⁴Dy, Kα₁ X-ray isotopic shift 0–73831
Fe, Kβ_s, in FeSi₁-NiSi₂ solid soln., correl, with mag. props., rel. to electronic struct. 0–79340
Fe, positions and shapes of Kα_{1,2} and Kβ_{1,3} lines 0–58098
Fe XVIII, gf-values 0–66375
Hf. K-L, transitions intensity 0–72403
K acid phthalate crystals, characteristics 0–78420
KCl, long-wavelength reflection spectrum analysis by Kramers-Kronig method 0–62699
LiF, component due to F-centre 0–56576
LiF, Li₂CO₃, Compton spectrum discontinuities due to K-electron binding energies 0–62702
LiF(200), bent, reflectivity, 50 to 80 keV, continuous spectrum 0–41115
LiH, Compton profile 0–72404
MnO₂, K-fluorescence 0–54116
MnSi₃, K-fluorescence 0–54116
MnSi₄, K-fluorescence 0–54116
NaSi₄, K-fluorescence 0–54116
NaSi₄, K-fluorescence 0–54116
NaSi₅, K-fluorescence 0–54116
NaSi₆, K-fluorescence 0–54116
NaSi₇, K-fluorescence 0–54116
NaSi₈, K-fluorescence 0

X-ray spectra continued

Sn spectral determination in powdered material using internal standard method 0-59517

124 Te charge radii variations from isotopic shifts of X-ray K_{a1} lines

0 - 640330-4053 radii variations from isotopic shifts of X-ray $K_{\alpha 1}$ lines 0-64033

¹²⁶Te charge radii variations from isotopic shifts of X-ray K_{a1} lines 0–64033
¹²⁸Te charge radii variations from isotopic shifts of X-ray K_{a1} lines 0–64033
¹⁰Te charge radii variations from isotopic shifts of X-ray K_{a1} lines 0–64033
²¹²Th, 5g-4f X-rays 0–49552
¹⁰Tm, decay, singles and coincidence spectra, by high resultion Ge(Li) and Si(Li) detectors 0–38992
¹¹Tm decay, singles and coincidence spectra, by high resolution Ge(Li) and Si(Li) detectors 0–38992
¹²U, 5g-4f X-rays 0–49552
V_xSi, energy bands 0–79342
V_xX type high-temp. superconductor, energy bands 0–79342
V_x15 MeV O⁴⁺ bombardment, K X-ray spectra obs. 0–77693

absorption

absorption

absorption
air, attenuation cross sections, 0.1 keV-1 MeV 0-58399
diatomic gases, ultrasoft absorpt. meas. 0-64818
edge, chemical shift, empirical rule 0-51331
ferrite, combined diffr. and spectrographic study, regularity obs. 0-75079
fine structure, extended, interpretation, review 0-44874
inert gases, ultrasoft absorpt. meas. 0-64818
methane, ultrasoft absorpt. meas. 0-64818
point scattering theory of K-absorpt. fine struct. 0-69143
polypropylene, 44-85Å 0-66085
solids, review 0-72398
transition metal, diborides, emission, spectral, photoelectric, K-spectral

transition metal diborides, emission spectra, photoelectric K-spectra 0-44875

Ag and alloys, Au and alloys, with dissolved Cu, analysis of solubility 0-71743

Ag and alloys, Au and alloys, with dissolved Cu, analysis of solubility 0-71743
Al, fine struct, temp. displacements 0-62695
Ar solid due to transition from 3s shell 0-62668
AsB, photoelectric K-spectra and emission spectra
BN, molecular orbital interpretation 0-76092
BP, K-absorpt, spectra 0-41251
BaB₆, photoelectric K-spectra and emission spectra 0-44875
Bi Ll_{HT} edges, chem. shifts 0-69145
C, 44-85A 0-66085
Co borides, ferromag., comp. depend. 0-51332
CoP, K-absorpt, spectra 0-41251
CuO, band struct, rel. to Cu 0-40662
Ge, impurities and precipitates effects 0-62698
Ge, interference absorpt. coeff., dislocation density depend. 0-56575
H₃BO₃, molecular orbital interpretation 0-76092
LaB₆, photoelectric K-spectra and emission spectra 0-44875
LiBr, photoabsorption interpretation 0-76138
LiCl, photoabsorption interpretation 0-76138
LiF, photoabsorption interpretation 0-76138
LiF, photoabsorption interpretation 0-76138
LiF, Potoabsorption interpretation 0-76138
LiF, Potoabsorption interpretation 0-76138
LiF, Potoabsorption interpretation 0-76138
LiF, photoabsorption interpretation 0-76138
LiF, phot Al, fine struct. temp. displacements 0-62695

0-44876
Ti oxides, nitrides, carbides and borides, L_{II,III} absorpt., mol.-orbital interpret. 0-69147
TiO(N,C), K and L_{III} absorpt. bands, rel. to electronic band struct. 0-72406
V L (II, III) from metal and compounds 0-76140
V oxides, nitrides, carbides and borides, L_{II,III} absorpt., mol.-orbital interpret. 0-69147
VB₂, Refractory, band structure 0-79341
VC_{xx} V₂C_{xx}, refractory, band structure 0-79341
VO_x, refractory, band structure 0-79341
VO_x, refractory, band structure 0-79341

emission
alkali halide, K emission of Na* and F- 0–59418
alkali halides, K emission satellite struct. 0–76136
alkali halides, proton channelling 0–68711
atomic charges determ. from chem. shifts 0–52864
binary alloys, electronic struct. 0–79336
binding energies, K,L, M and N calc. for Z=96-120, atoms 0–39269
β-brass, 3d(4sp)-energy bands 0–51333
conference, Denver, USA, Aug. 1969 0–69243
crystal, K emission, satellite struct. 0–76136
detection of transition radiation using a streamer spark chamber 0–74110
double crystal spectrometer for λ=5-10Å region 0–61760
edge height, changes on alloying, correlation with Knight shift 0–72506
film thickness meas. by fluorescence method 0–65053
fluorescence, determination of sulphur in mineralised rocks from Utah
0–66218

0-66218
fluorescence, polychromatic radiation excited, equivalent primary monochromatic wavelength 0-56629
fluorescence, with variable take-off angle 0-69247
group II-VI epd. film thickness meas. by fluorescence method 0-65053
hydrocarbons, molecular orbital interpretation 0-46567
intensification induced by quasistationary population inversion 0-79338
intensity, atomic number depend, Z=76-92 0-51330
kaonic X-rays, K-nuclear interactions rel. to neutron distrib. in nucleus
0-49476

kaonic X-rays, K⁻ nuclear interactions rel. to neutron of 0-49476 layers, multilayers, fluorescence 0-48113 lithia-aluminosilica glass, chem. bonding obs. 0-62701

X-ray spectra continued emission continued

emission continued low energy, methods, applications, review 0-69244 metal, line shape comparison with X-ray photoemission spectra 0-44432 metalli, conductors, soft band spectra, valance state effects 0-69140 metals, core-hole effect on soft emission 0-66075 metals, excitonic effects in transitions 0-65609 muonic, pionic, kaonic and Σ^- X-rays, atomic and de-excitation cascades and nuclear absorption rates in light elements 0-64193 nonmetallic compounds, chem. bonding and valence state 0-69141 oxides, X-ray K-emission spectroscopy, review 0-62694 particle size measurement 0-47469 particle size measurement 0-47469 particle size measurement 0-47469 particle size, and in air, laser induced, temp. meas. 0-43308 rare earths, satellite L_{P_i} , 0-70747 review 0-65572 review of K, L, M region of all elements, new spin-doublets reported 0-69907 satellite lines, less energy, origin and intensities, molecular orbital interpret

satellite lines, less energy, origin and intensities, molecular orbital interpret. 0-56573

0–56573
semiconductor phosphides of groups I, II and III valence bands o–66078
silicate rocks, floresc. chem. analysis 0–66219
silicates X-ray K-emission spectroscopy, review 0–62694
soft, data acquisition and handling 0–57226
sun, He-like ion forbidden line emission 0–59793
transition elements, Fe group, short-wave satellites 0–62697
transition metal diborides, absorpt. spectra, photoelectric K-spectra
0–44875 transition metal oxides, surface layers, characterization, oxygen band shift $0\!-\!50365$

transition metal oxides, surface layers, characterization, oxygen band shift 0–50365 transition metals and some of their compounds, $K\beta_1\beta'$ structure investigated 0–76137 ultra-soft for BN type cubic crystals, interpretation 0–54115 ultrasoft, dispersion technique, total reflection at critical angle 0–66217 wavelength shift voltage depend 0–66077 Al- transition (noble) metal alloy, L_2 , bands 0–41248 Al- Mg alloys, sopt 0–66080 Al, in Al-Ag, Al-Cu, Al-Zn, soft $L_{2.3}$ 0–66079 Al, Lr_{1,111} and Kg bands 0–72402 Al in AuAl, soft $L_{2.3}$ 0–66081 Al K-line excitation by 70-400 keV H, He, N, O and Ar ions 0–70803 AsB, photoelectric K-spectra and absorpt. spectra 0–44875 BN, molecular orbital interpretation 0–76092 BN, selective maxima 0–41249 BN crystal, band struct., Van Hove singularities 0–41246 B2O₃, molecular orbital interpretation 0–76092 BP, crystal, band struct, Van Hove singularities 0–41246 BaB₆, photoelectric K-spectra and absorpt. spectra 0–44875 BaF₇ fluorescence due to self-trapped excitons obs. 0–51340 C K-emission spectrum used to study covalent and ionic bonds of organic compounds 0–61141 CO molecular orbital interpretation 0–46567 CO₂ molecular orbital interpretation 0–46567 CO₃ molecular orbital interpretation 0–46567 CO₄ molecular orbital interpretation 0–46567 CO₄ molecular orbital interpretation 0–46567 CO₅ molecular orbital interpretation 0–46567 CO₆ molecular orbital interpretation 0–46567 CO₇ molecular orbital interpretation 0–46567 CO₇ molecular orbital interpretation 0–6657 CO₇ molecular orbital interpretation 0–6657 CO₇ molecular orbital interpretation 0–6657 CO₇ molecular orbital interpretation 0–66567 CO₇ molecular orbital interpretation 0–66567 CO₇ molecular orbital interpretation 0–66567 CO₇ molecular orbital int

compounds 0–61141
CO molecular orbital interpretation 0–46567
Copy molecular orbital interpretation 0–46567
CaF₃ fluorescence due to self-trapped excitons obs. 0–51340
CdS film thickness meas. by fluorescence method 0–65053
Cl Kα and Kβ emission spectra in free molecules 0–52899
Co, L-series, rel. to valence band studies 0–65993
Cu-Ar*, ion implantation, channelling 0–68707
Cu-Si solid solution, Si L₃, spectra 0–56577
Cu, fine struct., occupied band struct. obs. 0–79337
Cu, L-series, rel. to valence band studies 0–65593
Cu, L_{III} band, piezo modulation 0–66082
Cu dil. alloys, L lines of impurities 0–59419
Cu₃Si, SiL₂₃ spectra 0–56577
Eu, L emission, meas. with focusing spectrograph 0–67617
Fe, L-series, rel. to valence band studies 0–65593
Ge, rel. to energy and band structure, transition probabilities and lifetime effects 0–44877
Ge, rel. to valence band structure 0–65601
H muonic atoms obs. 0–64308
H₃BO₃, molecular orbital interpretation 0–76092
Hf M-line excitation by 70-400 keV H, He, N, O and Ar ions 0–70803
Hg, fluorescence and Coster-Kronig yields of L subshells from ¹⁹⁸Au and ²⁰⁴Tl decay 0–70767
LaB₆, photoelectric K-spectra and absorpt. spectra 0–44875
Mg noble metal alloy, L₂₃ bands 0–41248
MgO, proton channelling 0–68711
Mg,Si, Si L₂₃ spectra 0–56577
Na, conduction electrons scatt. pot. 0–79339
Ni, L-series, rel. to valence band studies 0–65593
O in transition metal oxide surface layer characterization, band shift 0–50365
Si, L₂₃ spectra 0–56577
Si, rel. to energy and structure, transition probabilities and lifetime effects

O in transition metal oxide surface layer characterization, band shift 0-50365
Si, L₂₃ spectra 0-56577
Si, rel. to energy band structure, transition probabilities and lifetime effects 0 44877
Si, rel. to valence band structure 0-65601
SiC crystal, band struct., Van Hove singularities 0-41246
SrF₂ fluorescence due to self-trapped excitons obs. 0-51340
Ta, weak lines in L spectrum 0-70774
Ti-Cr alloy, K\$\beta_2\$, bands 0-56578
Ti oxides, nitrides, carbides and borides, L_{II,III} emission, mol-orbital interpret. 0-69147
TiO(N,C), K and L_{III} emission bands, rel. to electronic band struct. 0-72406
231U, K X-ray emission obs. 0-46272
V L (II, III) from metal and compounds 0-76140
V oxides, nitrides, carbides and borides, L_{II,III} emission, mol-orbital interpret. 0-69147
VB₂, refractory, band structure 0-79341
VC₂₃, V₂C₃₂, refractory, band structure 0-79341
VN₂₃, refractory, band structure 0-79341
VO₃₄, refractory, band structure 0-79341
VO₃₄, refractory, band structure 0-79341
V₃₄, O₁₇, R³³, R=rare earth, fluorescence 0-44926
Zn, L-series, rel. to valence band studies 0-65593

ray spectrometers

X-ray spectrometers

soo also Gamma-ray spectrometers; crystallogra-X-ray see also phy/apparatus phylapparatus analyser, energy dispersive, use in scanning electron microscopy 0-63576 computer-coupled 0-66216 X-ray spectrometers continued

curved cryst. Spectrograph, convex 0-76786 double cryst., $SK\beta$ emission band meas. 0-75047 double crystal, for $\lambda=5\cdot10$ Å region 0-61760 with graphite crystals, applic. to spectroscopy and polarimetry in X-ray astronomy 0-45328 instrumentation improvements, review 0-69246

instrumentation improvements, review 0–69246
Iogan, use of Ge single cryst. as analyser 0–65189
Johannson type, stepped-surface analyser, patent 0–48662
photoelectron type, IEE 0–69570
sample holder with adjustable internal reference, patent 0–41918
semiconductor, applications and manufacturing techniques 0–63905
slitless spectrograph development for X-ray astronomy 0–69346
soft, for gas discharge at medium and high pressures 0–61385
spectroheliograph, scanning below 2nm. 0–54485
vacuum, for studying chemical effect on soft spectra 0–69567
vacuum scanning double crystal type, for soft X-ray absorpt. edge studies 0–69568
Si-Li spectrometer 0–45501

Si:Li spectrometer 0-45501

X-ray spectroscopy
see also X-ray crystallography; X-ray diffraction
absorption tables, 2-200 A region 0-69252
astronomy, instrumentation using soft X-rays 0-69429

using attenuation measurements and a computer program 0-63295 fluorescence, with variable take-off angle 0-69247 generator TuR M62, highly stabilized, design including safety devices 0-57224

0-5/224
graphite crystals with high integrated reflectivity applic. 0-45328
gratings, study programme 0-69569
instrumentation, detection improvements, review 0-69246
interaction coeffs., applic. to interpretation of solar spectrum 0-69479
intrumental error estimate of spectral analysis, formulae for calc.
0-62831

photoelectron, rel. to electron density of states meas. on transition metals 0 - 66083

semiconductor detectors, impact 0-60678 sopt, data acquisition and handling 0-57226 spacecraft instrumentation for non-dispersive analysis of lunar X-rays

0 - 69441

U=09441 LiH crystals with high integrated reflectivity applic. 0-45328 Ti compounds, interstitial and intermetallic, investigation of electronic properties 0-65603 WS, crystals with high integrated reflectivity applic. 0-45328

X-ray tubes AMR microfocus system 0-65201 AMR microfocus system 0-65201 anode vapour flow phenomena in a flash X-ray discharge 0-59849 camera for photography of substances at low temp. and high press., method 0-50488 cold cathode, soft x-ray source, performance and applic. 0-51876 for electron spectrographs of electrostatic cylindrical type 0-79828 field emission, miniature 0-76784 flash, photon energy spectrum determ. 0-48661 flash tube with exchangeable electrode system, design and performance 0-69564

focal spot, modulation transfer function 0-69562 generator with transformer core d.c. magnetization prevention, patent 0-79829

image intensifier, using rare-earth oxysulphide phosphors 0-66754 image intensifiers, properties of rare-earth oxysulphide phosphors for input screens 0-66755

screens 0-66755
microfocus, practical design considerations 0-63297
monochromator crystal for high intensity radiation production 0-66756
optimum current and anode voltage determ. apparatus, patent 0-59852
power supplies for their operation 0-51882
pulsed controllable with cold cathodes, design parameters 0-51878
pulsed with hollow anode and field emission Ni-cathode, description
0 51879

radiography optimum magnification, optical transfer function role 0-69563

0-0903 rotary target with improved lifetime, patent 0-45502 rotating anode generator, 60 kV, 100 mA, construct. and appl. 0-63296 rotating anode with magnetic damping, patent 0-79830 two electrodes, flash generators 0-51881 video display of topographic images 0-50490 W-Ir-Mo alloy anode, patent 0-59851

see also Cosmic rays/X-rays; Gamma-rays alkali halides, anisotropic X-ray excitation by protons 0–53729 auroral zone, X-ray and particle radiation by electron precipitation 0–56819

beam stability from 8 MV linear accelerator 0-57862

bursts short, production using high power pulsed generator, description 0-51877

cosmic, interstellar absorption 0–63076 hyperboloidal surfaces for reflecting objectives operating in X-ray region, manufacture 0–52376 image intensifiers, solid state, electroluminescent- photoconductor type 0–48630

0-48630 muonic atoms magnetic hyperfine structure 0-58131 parametric decay, polarization of signal and idler fields 0-41917 parametric down conversion in crystals, meas., analysis 0-57225 photographic film response to 9-70 keV range for 3 nsec exposures 0-42404

0-42404
planetary production at surface 0-54434
proportional counter background reduction using pulse shape discrimina tor 0-49403
soft, cold-cathode source, performance and applic. 0-51876
solar as flare activity indicators 0-48615
telescope, image formation, surface configuration requirements 0-59850
transition radiation from ultrarelativistic charged particles, energy dependence 0-42433
Cu target, characteristic generation by heavy particle irrad. 0-69566

effects

see also Nuclear reactions and scattering due to/photons
on RNA metabolism in HeLa cells 0-69525
β-alanine, semiconductivity, optical transmission and reflection, pure and X-irradiated 0-75657
alkali halides, irrad., anomalous F-centre colouring 0-58829
amino acids, X-irrad., correlation of e.s.s. and optical spectra 0-59458

X-rays continued effects continued

on animo acid incorporation into regenerating liver proteins 0-69524

bone marrow regeneration, initiation process 0-59820 crystal, irrad., X-ray diffuse scatt. obs. 0-58796 crystal growth, diameter control, patent 0-43603

crystal, irrad, X-fay diffuse scatt. obs. 0—36/96 crystal growth, diameter control, patent 0—43603 crystobalite, Si displacement by radiations 0—40138 dielectric liquids, electron mobilities 0—46949 ferroelectric, continuously irrad, rel. to Barkhausen effect 0—53933 goldfish, intestinal epithelial cells, DNA synthesis and cell proliferation at different temp. w.r.t. recovery process 0—59821 halomethanes, X-ray photoelectron spectra 0—77914 ice, ENDOR of X-irrad. crysts. 0—66207 luminescence centres in NaCl-Ag crystals, thermal quenching of B and C centres 0—62708 mechanical pictures information content 0—59827 peetin, polymer, e.s.r. study 0—67836 plasmon scattering in Be 0—78855 polyurethane rubbers, effect on dielectric props. 0—65776 protection glasses and resins in colour TV 0—51829 on protein synthesis, in HeLa cells 0—69525 Rochelle salt, continuously irrad., rel. to Barkhausen effect 0—53933 ruby, irrad., isothermal annealing kinetics of Cr ions, e.p.r. obs. 0—79396 solar, ionization control of ionospheric E-region 0—56841 solar, ionospheric E layer control 0—41540 sulphide phosphors, annealing effects on luminescence, and X-ray luminescence 0—56631 dlatataric acid, deuterated, irradiated at 195K, radical formation, e.s.r. 0.76292

d/tartaric acid, deuterated, irradiated at 195K, radical formation, e.s.r. 0-76229

0-16229 use in temperature calibration of furnace 0-48891 triglycine sulphate, continuously irrad., rel. to Barkhausen effect 0-53933 urea, thermoluminescence 0-61940 AgCl, photoluminescence after X-ray irradiation 0-56653 Al₂O₃:Cr²⁺, irrad., acoustic paramag. reson. spectra, effect of clec. fields 0-62749

D-62749

Ba, photoemission rel. to electronic structure 0-65874

Be, plasmon scattering 0-78855

Ca halophosphate luminophors, colour centre formation under X-ray, u.v. irradiation 0-55903

CaF; Nd, luminescence growth and decay, thermoluminescence 0-44925

CaF;, irrad., colour centres, absorpt. spectrum obs. 0-40181

CaF;, irradiated, obs. of new Gd³+ e.sr. centre 0-48145

CaF;, phosphor, optical density, thermoluminescence, afterglow 0-44918

CaF;, thermoluminescent response, energy depend. 0-48114

Eu, photoemission rel. to electronic structure 0-65874

p-Ge, irrad., cond. changes 0-44248

KBr;(Na+,Li+), interstitial centres interactions 0-53531

KBr-NaBr colour center formation, comparison 0-47268

KBr, vol. change due to creation of lattice defects by X-irradiation 0-40121

KCl:Ag, irrad., V_k centres, Raman spectra, 77K 0-40185

0-40121 KCl:Ag, irrad., V_k centres, Raman spectra, 77K 0-40185 KCl, F centres growth, effect of heat treatment and background divalent cation impurity 0-43685 KCl, irrad., additively coloured, F centre growth and thermoluminescence 0-61979

0–61979
KCl, vol. change due to creation of lattice defects by X-irradiation 0-40121
KClO₄, X-irradiated, e.s.r. signals from defects due to e and holes trapped on ClO₄⁻ 0-48147
K1:Eu, luminescence, activator centres investigated 0–56630
Li₂B₄O₇:Mn, thermoluminescent response, energy depend. 0–48114
MgO cryst., stimulated luminesc. 0–54121
ND₄Cl, irrad., phonon scattering from thermal conductivity meas., 2
300K 0-40503
NH₄Cl, irrad., phonon scattering from thermal conductivity meas. 2-300K
0-40503

NH₄CI, Irrau, phonons of the control of the contr

NaCl:Mn²⁺, irrad., optical absorpt. and e.p.r. spectra, Mn centres 0–76104
NaCl, irrad., F centre formation, temp. depend. 0–58831
NaCl single cryst., transmission and reflection, 2000-950 Å, effect of X rays 0–44766
Na;SO₄ crystal, e.s.r., Sr²⁺ impurity depend. 0–41336
Si, radiation-accelerated diffusion of Au 0–78586
Si diode, irrad. effect on IV and CV characts. 0–53896

protection see Radiation protection

Xenon

in Pesyanoe meteorite, isotopic composition, solar type 0–48589 in Serra de Mage meteorite feldspar, conc. 0–51781 absorption line displacements due to perturbation by rare gases 0–49781 adsorption of He atoms on (110) face 0–61683 adsorption on W, (110), (120), (100), (211) and (111) planes 0–47089 adsorption on graphite, potential variation with number of layers 0–50396 adsorption on palladium (100) face 0–47080 anomalous abundances in meteorites 0–41811 atom, K-shell Auger transition rates, fluorescence yield 0–64226 atom, excitation by metastable Ar atoms in afterglow of Ar-Xe discharges

atom, excitation by metastable Ar atoms in afterglow of Ar-Xe discharges 0-60965

atom, excitation through collisions with nitrogen, study of process $0\!-\!64211$

atomic level lifetimes obs. 0-42985 atoms, collisions with slow He²⁺ ions, exothermal capture with ionization 0-77730 atoms, electron scattering, resonances rel. to negative ion formation

atoms, electron scattering, resonances rel. to negative ion formation 0-74142 atoms, long range interatomic potentials, relativistic correction from oscilla tor strength sums 0-74161 aton, absorpt, spectra, 1250-1300 Å, new band obs. 0-39292 Brillouin scatt, near critical pt., obs. 0-46829 Brillouin spectrum near critical point, analysis using hydrodynamic model 0-78326

broadening and shifting of lines in 2-0 band of HF spectrum 0–77797 collisions, large angle, with 3 MeV I^{2+} and 6 MeV I^{3+} 0–74164 diffusion in UO₂, effect of Fe precip. 0–43697 discharge, afterglow, duration of energy storage 0–58364

Xenon continued

discharge, d.c., with return or bypass connection, axial press. gradients 0-46768

0-46768 ionization at the shock wave front for 6-10 Mach numbers, processes, investigation 0-53216 isotopes, gaseous, e capture— $1^{12.127}I$, cascade transitions, perturbed γ - γ ang. correl. obs. 0-46366 lamps, resonance, characteristics and design 0-42391 laser, high-press., pulsed 0-77078 laser lines, isotope shifts 0-49779 liquid, hight scattering, weak depolarized Rayleigh wind obs. 0-43450 liquid in binary mixtures, electron avalanche excited light emission 0-61534 liquid refraction meas in visible region 0-71352

0-61534 liquid refraction, meas. in visible region 0-71352 metastable atoms, production and chem. applications 0-41413 metastable atoms, reactions with simple NH-containing cpds. 0-41414 multiple ionization by 2-14 keV electrons, abundance of ions, cross-sections 0-71199 multiple photoionization cross-section obs. 0-60968 outer-shell S-electron ejection by electron impact ionization 0-64769 photoionization, angular distribution of free electrons released 0-52928 photoionization including final-state correlation 0-70779 plasma, continuous spectrum calculation, photoionization, energy levels 0-67895

0-6/895
plasma, effects of pressure, input energy, and magnetic field on spectral properties 0-55473
plasma, electron density determ. 0-78114
plasma, ionization behind shock wave front, i.r. diagnostics 0-53189
plasma, laser produced, electron density, spatio-temporal evolution
0-78066 0 - 78066

plasma, pulse discharge, radiation absorption 0-50062 plasma, pulsed, absorptivity and emissivity determ. 0-53174 plasma, variation of density of accelerated electrons behind diaphragm plasma, va 0-53150

U=33150
plasma pulsed, two wavelength laser interferometry, refractive index investigation 0-71157
Rayleigh linewidth meas. near critical point 0-78329
reactor VVR-S, Xe poisoning peak reduction with single power pulse
VVR-S, obs. 0-39217
reactors, large thermal, stability rel. to spatial Xe oscills. 0-39207
reflectance spectrum of solid for photon energies from 8 to 25 eV
0-79286

0—79286 ring discharge, spatial variation of electron energy 0—71206 self-diffusion near critical point and on liq. branch of coexistence curve, by NMR meas. 0—64890 solid, Li, Na, In, Hg, Cd atoms absorpt. spectra, obs. 0—49783 solid, adiabatic elastic consts., determ. at 156°K by Brillouin spectroscopy 0—78598

0-78598
solid, anharmonic effects, applic. of approx. method 0-53674
solid, anharmonicity and potentials 0-47509
solid, heat capacity and phonon spectra, dispersion anharmonic effects calc. 0-40516
solid, optical absorption in far u.v. 0-66047
solid, refraction, meas. in visible region 0-71352
solid, trapping of electronic excitations, dynamical investigation 0-75456
solid, vacancy and interstitial formation energies 0-40137
sound velocity dispersion in critical region 0-78328
spectrum, excitation temp. functions calc., appl. to plasma radial temp.
distrib. determ. 0-42965
spectrum lines, intensity-temperature curve, calculated and normalized 0-39549
sublimation, model 0-47004

0-39549
sublimation, model 0-47004
thermionic diodes, l.v. arc and breakdown effects 0-78172
u.s. attenuation near critical point, temp. and frequency dependence
0-78327
u.s. velocity and attenuation, coherent detection tech. for variable-path-length pulse measurements 0-53271
Cd.u.v. absorpt. spectra in solid Xe 0-41207
o-D-Xe collisions, subthreshold rot, compound state resonance spectra
0-53097

o-D₂-Xe collisions, subthreshold rot. compound state resonance spectra 0-53097
p-H₂-Xe collisions, subthreshold rot. compound state resonance spectra 0-33097
he-Xe laser, enhanced Lamb dip with pure Xe gain cell 0-60215
Hg u.v. absorpt. spectra in solid Xe 0-41207
¹²⁹I-¹³⁹Xe, dating evidence for cold assembly of unequilibrate chondrite 0-72776
In in solid Xe, absorpt. spectra, 4.5°K 0-41213
K-Xe collisions, ⁴⁷P_{1/2}-⁴⁷P_{3/2} mixing, exp. evidence for absence of long-lived K-Xe complex 0-77695
Li in solid Xe, absorpt. spectra, 4.5°K 0-41213
Na in solid Xe, absorpt. spectra, 4.5°K 0-41213
Xe-G mixtures (G=other gas), ¹²⁹Xe chem. shift density depend. 0-71068
Xe-Hg(⁹P₀) complex emission band obs. during irradiation of Xe-Hg gas mixture rate constant for reaction determ. 0-74274
Xe-N mixture, thermal equilibrium calc. at 1 atmos. and between 5000-35000°K 0-53269
Xe-I spectrum, isotope vol. shifts 0-52927
Xe-I, irradiation of Au, channelling and damage production 0-68335
Xe-1, Xe-1*, potential curves, estimates 0-43082
¹²⁹Xe ions, 2.0 MeV, colouration of LiF 0-47279
¹³⁰Ke second spectrum, wavelength interferometry 0-60933

Xenon compounds

Note compounds
XEF4, magnetic shielding of ¹⁹F 0-53052
XEF4, in IF5, ¹⁹F n.m.r. 0-74312
XEF4, cryst. struct. of tetrametric phases 0-78507
XEF4, cryst. struct. of tetrametric phases 0-78507
XEF4, crystalline modifications 0-65123
XEF4, polymorphism 0-59008
XEF4, struct. 0-64460
XEF4, vapour, force constants, Raman spectra 0-46503
XEF4, cubic phase composition at -80°C 0-55864
VORTANDS. SEE Photography.

Xerography see Photography
Y-particles see Hyperons/resonances

Yield see Elastic limit; Plastic deformation; Plastic flow

Young's modulus see Elastic constants

adsorbed on W, electron emission, work function 0-39979 adsorbed on W, migration and evaporation field emission 0-39980 de Haas-van Alphen effect in h.c.p. crystals, 1.2 K, 116 koe 0-59154

Ytterbium continued

electron density of states, X-ray photoemission obs. 0–62261 film, phases, substrate temp. depend., X-ray diffr., electron microscopy 0–47050

film, u.v. photoemission meas., evidence of optical excitation of 4f electrons 0-47898

film, u.v. photoemission meas., evidence of optical excitation of 4f electrons 0-47898
photoemission, 4f levels energy obs. 0-75484
polymorphic transformation discovered 0-75343
vapour, i.r. laser lines 0-49778
in Ag-Au alloy, mag. susceptibility, thermoelec. power, Kondo effect 0-44457
Yb I, oscillator strengths of spectral lines in 6000-2450 Å region 0-42944
Yb¹⁺; n (96 wt.%) SiO₃ glass, luminesc. activation 0-59430
Yb³⁺; e.p.r. in KMgF₃, 4.2 K 0-76217
Yb³⁺; electric-field-induced g shift in scheelites, CaWO₄, SrWO₄, and BaWO₄ 0-51392
Yb³⁺; ground state Zeeman splitting in distorted cubic-crystal field 0-62575
Yb³⁺; in CaF₂, thermal conductivity, effect of spin-phonon interaction, 0.3-1.3K 0-43928
Yb³⁺ e.p.r. in scheelite cryst. 0-76206
Yb³⁺ e.p.r. in scheelite cryst., hyperfine spectra 0-76207
Yb³⁺ in LiYF₄:Nd³⁺, luminesc., energy transfer 0-76169
Yb³⁺ in SrF₂:Nd³⁺, spin-lattice relax, and cross-relax. 0-72291
Yb³⁺ in YF₂, cooperative energy transfer to Tb³⁺ 0-72426
Yb³⁺ in SrF₂:Nd³⁺, spin-lattice relax, and cross-relax. 0-72291
Yb³⁺ in YF₂, cooperative energy transfer to Tb³⁺ 0-72426
Yb³⁺ in Srf₂:Nd³⁺, spin-lattice relax, and cross-relax. 0-72895
Yb³⁺ in YF₂: cooperative energy transfer to Tb³⁺ 0-72426
Yb³⁺ in Srf₂: Nd³⁺, spin-lattice relax, and cross-relax. 0-78895
erbium compounds
GdFe garnet adiabatic magnetization cooling, 3-30°K, 0-44669

Yb₂O₃, thermal expansion, 100-300K, X-ray powder diffr. 0-50895

Ytterbium compounds
GdFe garnet, adiabatic magnetization cooling, 3-30°K 0-44669
Yb-Ag system, phase diagram, struct. 0-64996
YbAl garnet:Ho³⁺, spectral parameters 0-51359
YbAl₃, nucl. quadrupole coupling and cryst.-field effects 0-76235
YbAu₂, neutron diffraction 300°-1.7°K 0-58760
YbC₃, phase investigation, 0.33≤×≤2.00 comp. range 0-53653
YbFe, phase investigation, 0.33≤×≤2.00 comp. range 0-53653
YbFe garnet, adiabatic magnetization cooling, 3-30°K 0-44669
YbFe garnet, rare earth sublattice canting 0-44686
YbFe garnet, superexchange interaction, model calc. 0-79200
YbFeO₃, spin reorientation, role of Yb spins 0-44715
YbFeO₃, sublattice magnetization, neutron diffr. study, rel. to hyperfine field, 300-630K 0-44716
Ybl₃, X-ray powder data, chemical and physical props. 0-53515
Yb₂O₃:Gd, Raman luminescence obs. 0-44894
Yttrium

Yttrium

rium
adsorption on W, work function, O₂ effect, thermionic emission 0–74932
electron shake-off probability from K-shell following β-decay 0–49767
film on (110) face of tungsten, crystal structure 0–43546
lattice dynamics, phonon dispersion curves, 295 K 0–43866
photoelectric work function 0–75859
self-diffusion temp, depend., 900-1300C 0–75211
vapour pressure 0–53406
CdF₂:Y semicond., polaron effects 0–50951
Er-Y alloy, magnetoresistance, 4.2-25.5 K, comp. depend. 0–62488
in Ni-Cr-Al alloys, effect on oxidation behaviour 0–51427
Y-Eu thermoluminescence in the case of cathodic excitation 0–62735
Y-Y-O-metal tunnel diodes. inelastic tunnelling due to vibr. modes

 $Y-Y_2O_3$ -metal tunnel diodes, inelastic tunnelling due to vibr. modes 0-75758

0-13738 Y IV, resonance lines 300 to 4000 Å, obs. 0-60934 Y²⁺ 4/¹³5d configuration 0-42971 8⁷Y, ⁹⁰Y, ⁹¹Y, y-spectra 0-77518

Yttrium compounds
bonds, X-ray K-emission spectra obs. 0–59443
ferrite garnet, Barkhausen jumps distribution 0–62545
halides, gaseous, thermodynamic functions at 293.5-3000°K 0–71249
pseudo-binary, with 3d transitional metals, structural and magnetic proper
ties 0–51181

pseudo-onary, with 3d transitional metals, structural and magnetic properties 0—51181 silicates, rare-earth activated, luminescence props. 0—56657 X-ray K-emission spectra, bond obs. 0—59443 yttria fibres for reinforcement of alloy systems, high temp. 0—40456 CaF₂-YF₃:Nd³⁺, luminescence and stimulated emission, 300 K 0—42297 GdFe garnets, substituted, para-process 0—72185 HfO₂-Y₃O₃ solid solns, cyclic heating and thermal shock effects on stability 0—59025 Nd;YAI garnet, laser, Q-switched, second harmonic power, computer optimization 0—42294 TbFe garnets, substituted, para-process 0—72185 U_{1-x}Y₃O₃ new phase obs. 0—47462 Y₃Be-Al, phase investigations 0—50790 Y-Cd and Y-Cd-Zn systems, phase diagrams and relations, intermetallics obs. 0—78707 Y-Fe-Garnet, magnetoelastic damping of microwave phonons 0—47510 Y-Sb alloy system, phase diagram 0—64995 Y-Y₃O₃-metal tunnel diodes, inelastic tunnelling due to vibr. modes 0—75758 Y-Fe garnet, magnetoacoustic effects 0—71846

Y-Y₂O₂-metal tunnel diodes, inclastic tunnelling due to vibr. modes 0-75758
Y Fe garnet, magnetoacoustic effects 0-71846
YAG garnet:Nd lasers, alkali metal vapour light sources as optical pumps 0-73334
YAI:Gd⁺ garnet, absorption and luminescence spectra, energy levels

V=13334
YAl:Gd⁺ garnet, absorption and luminescence spectra, energy levels 0-66100
YAl:Nd garnet laser, repetitively Q-switched, continuously pumped, experanalysis 0-77128
YAl garnet: Ho³⁺ laser, performance 0-77130
YAl garnet: Nd-LilO₃ 0.53 μ harmonic source, repetitively Q-switched 0-69917

0-69917
YAl garnet: Pt³+, absorption spectra 0-62675
YAl garnet: Cr-Nd, effect of pulsed ionizing radiation 0-42300
YAl garnet: Dy³+, absorpt, and luminescence spectra 0-51314
YAl garnet: Nd, laser nonlinear absorpt, induced in semiconductors and PrCl₃ NdCl₃ aq. laser, 0-41099
YAl garnet: Nd³+ laser, continuously operating, energy, spatial and spectral characts. 0-60238
YAl garnet: Nd laser, 250W industrial instrument 0-60239
YAl garnet: Nd laser, decked, influence of relaxation oscillations on stability 0-77129
YAl garnet: Nd laser, thermal effects 0-63629
YAl garnet; ryst. growth by hollow cathode float-zone method, obs. 0-47142
YAl garnet; hydrolysis-solution growth technique 0-50447

YAl garnet, hydrolysis-solution growth technique 0-50447

Yttrium compounds continued

YAl garnet, melt growth, inclusions 0 -75145

YAl garnet laser, Ho3+ performance 0-57537

YAI garnet lasers, review and prospects 0-57537
YAI garnet lasers, review and prospects 0-57538
YAI₂, e.p.r. of Gd¹⁺ 0-72496
YAI₁B₁O₁;Ce, phosphor, decay time, efficiency, spectral energy distrib.
0-44922
Y₃AI₇Fe_{3-r}O₁₂, garnet, Mossbauer effect spectra, cation distrib. 0-79264
YAI(In) garnet:Sm ions, spin wave relax., effect of nonmagnetic ion
0-47975
YAIO₁:Dys³, anisotropy of g-values 0-48079 YAIO₃:Dy³, anisotropy of g values 0-48079

Y₃AI₀O₁:Ny³ laser, electron phonon interaction manifestation 0-67099

Y₃AI₃O₁:R³, R-rare earth, X-ray fluorescence 0-44926

Y₃AI₃O₂:Y₃Ga₃O₁ with isomorphous substitution by Nd, crystallization from PbF₂.1.17PbO.035B₃O₁ 0-71521

Y₃AI₃O₁:(Nd³) garnet, dislocation struct., optical inhomogeneities, double refraction 0-50596

Y₃AI₃O₃: agrand

YAAl₂O₁₂, garnet, crystal growth by hollow cathode float zone method, obs. 0-47142 YB₂, n.m.r. of ⁸⁹Y meas. 0-79418

YB₆ superconducting transition depressed by rare earth impurities 0 44143

VG₂-C system, vaporization thermodynamics 0–53406 YC₂ and YC₄, dissociation energies 0–53406 Y₃ xCa₂Fe₃ xSi₂O₁₂ garnet, mag. and elec. hyperfine interactions of ⁵⁷Fe, Mossbauer meas. 0–48044 Y_{3-2x}Ca_{2x}Fe_{3-x}V_xO₁₂ garnet, mag. and elec. hyperfine interactions of ⁵⁷Fe Mossbauer meas. 0–48044

Accessive and one of the structure of th

YFe garnet: Si, mag. anisotropy and mag. anneal, ferromag. reson, 0 56662

YFe garnet: Si, photo-induced uniaxial mag, anisotropy and optical dich

YFe garnet: Si, photo-induced uniaxial mag, anisotropy and optical dichroism 0-44598
YFe garnet:Pr¹ (Tb¹), Ho¹), ferrimag, reson. 0-44975
YFe garnet:Si, domain wall stiffness, light-induced increase 0-44569
YFe garnet:Si, negative resistance, conductive switching and memory effect 0-75692
YFe garnet:Yb, longitudinal relaxation of ⁵⁷Fe, 1.3-140 K 0-45037
YFe garnet, chemical transport with HCl, thermodynamic considerations 0-40001

YFe garnet, Co³¹ substituted, mag. props. 0–54020 YFe garnet, crystal growth, chemical transport with HCl thermodynamic considerations 0–47122

YFe garnet, Curie temp, variation with press. 0—51227
YFe garnet, Curie temp, variation with press. 0—51227
YFe garnet, domain boundary resonance, defect depend. 0—51383
YFe garnet, energy levels of Ho³⁺ ions and Ho³⁺ Ho³⁺ Fe³⁺ exchange interaction 0—51248

interaction 0–51248
YFe garnet, epitaxial, mangetostatic waves, steering 0–44642
YFe garnet, epitaxial, mangetostatic waves, steering 0–44642
YFe garnet, Franday effect rel. to saturation magnetization 0–62615
YFe garnet, firm, ferromag, resonance modes, spin pinning 0–44974
YFe garnet, film, ferromag, resonance modes, spin pinning 0–44974
YFe garnet, film, ferromag, resonance modes, spin pinning 0–44974
YFe garnet, high-press, stability 0–62138
YFe garnet, hydrothermal, KOH soln, patent 0–40038
YFe garnet, magnetization, critical exponent β, in low mag, fields 0–44600

YFc garne 0 44600

YFe garnet, magneto optic light modulators 0-59305 YFe garnet, magnetoelastic and magnetostatic waves, parametric amplification 0-44668

amplification 0—44668
YFe garnet, magnetostatic modes 0—56458
YFe garnet, magnetostatic waves surface and volume, instability 0—47935
YFe garnet, magnon-elevation and elastic wave conversion, figure of merit 0–50881

merit 0-50881
YFe garnet, microwave and i.r. transmission props., grain size effect 0-65962

YFe garnet, microwave props., grain size depend. 0–41307 YFe garnet, nonresonant absorpt. at Curic Point, 500 kc/s 10 Mc/s 0. 44543

YFe garnet, phonons parametric excitation by parallel pumping, obs. 0 50880

YFe garnet, quadrupole interaction parameter meas. 0—48174
YFe garnet, second harmonic generation and parametrically coupled spin waves 0–72472

Fe garnet, single- and double-mode parallel pumping of phonons, 114 MHz 0-44545

VFe garnet, sintering, grain growth, comp. depend., magnetization 0 47435

0 47435
YFe garnet, sintering behaviour, additives effect 0-50766
YFe garnet, spin lattice relax, times of ³⁷Fe, 2.40 K 0-48170
YFe garnet, spin waves parametric excitation by laser radiation 0-69017
YFe garnet, substituted, mag, moment rel, to mol, field coeffs. 0-79201
YFe garnet, V. In substituted, mag, anisotropy meas. 0-62551
YFe garnet (5), photoinduced magnetic effects 0-56404
YFe garnet epitaxial on YAl garnet, stresses 0-65380
YFe garnet film resonators, epitaxial, rel, to magnetically tunable microwave bandstop filters 0-44667
YFe garnet films, ferromag, reson, linewidths 0-66128
YFe garnet radiometer and temperature controller 0-76931
YFe garnet rods, axially magnetized, excitation of longit, magnetoelastic

YFe garnet rods, axially magnetized, excitation of longit. magnetoelastic waves 0-47949

YFe garnet single crystal, ferrimag., mag. eqn. of state near critical point 0.44666YFe

Fe garnet single crystal, kink point locus and critical phenomena 0 44599

YFe garnet single crystal rod, axially magnetized, longit, elastic wave/spin wave conversion efficiencies 0-44546

Yttrium compounds continued

YFe garnets, substituted, para-process 0–72185 Y_1Fe_3 $_2Ga_2O_3$, (x= 0.35, 0.7), Faraday effect rel. to saturation magnetization 0–62615

 $Y_1Fe_3O_{12}$:Si reduction of initial susceptibility by light irrad. 0—44576 YFeO₁, spin cluster reson. 0—72495

YFeO₃, sublattice magnetization, neutron diffr. study, rel. to hyperfine field, 300 630K 0-44716 YFeO₃ domain wall mobility, monotonic temperature dependence 0 44714

YFeO₁ single crystal, canted ferromag., mag. eqn. of state near critical point 0-44666

point U-44666 Y₁Fe₂O₁₇, spin spin relax. of ⁵⁷Fe₂ at 77°K 0--79212 YFI garnet, sublattice magnetizations and exchange constants determina tion, mathematical and computational techniques 0-53499 YGa garnet: Ho³⁺ spectroscopy, energy levels rel. to laser transitions 0-44857

YGa garnet, energy levels of Ho³⁺ ions and Ho³⁺ Fe³⁺ exchange interaction 0-51248 YGa garnet, melt vaporization rate during crystal growth, pressure effects

(i) 55/95 Y₂, (Ga_{0.7}Al_{0.4}Mn, Fc_{4.6-x}O₁₂, garnet, magnetostriction effects, compensation by Mn additions 0-44605 Y(Mn_{1.4}B) O_{3.7} Be=Fe^{3.†}, Cr^{3.†}, Al^{3.†}, struct, and ferroelectric props.

0 62441/Y
 Y,Mn,Fe, 20,7, garnet, magnetostriction effects, compensation ty Mn additions 0 44605
 YNbO; Gd³⁺, ferroelec., c.p.r. 0-72494
 Y,O; Eu cathodo and photo luminescence, effect of synthesis conditions 0 56656

0.56656
Y,Q1;Eu cathodoluminophor, synthesis conditions 0-56658
Y,Q1;Eu¹, energy levels and interactions at C₂ symmetry sites 0-65970
Y,Q1;Eu¹ (Tb¹) phosphors, electroluminesc. 0-72463
Y,Q1;Eu¹ (Tb¹) polycryst, fluorescence spectra 0-44911
12Mol.96 Y,Q1;ZrO2, stabilization, monoclinic content, comp. sintering and electrolysis effects 0-47465
YQ2, e.s.x. study of defects and traps giving rise to thermoluminesc.
0.56650
Y,Q1; e.s.x. study of defects and traps giving rise to thermoluminesc.

0.56650

Y,O1, dislocation etchant 0.-55773

Y,O2, for thin film IC capacitor 0.-62400

Y,O1, garnet, crystal growth float zone method, obs. 0.-47142

Y,O1 films, vacuum evap., dielec. props. 0.-68897

Y,O1 laser, patent 0.-57542

YOCI:Ce, phosphor, decay time, efficiency, spectral energy distrib. 0.44922

Y,O2S:Eu^{11, 3}D resonance quenching to charge-transfer states 0.-56625

Y₂O₂S;Ea¹¹, ²D resonance quenching to charge-transfer states 0-56625 YPO₄:Ce, phosphor, decay time, efficiency spectral energy distrib. 0-44922

YPO₄:Ho¹¹, crystal field parameters, level splitting 0-75985 YPO₄:YVO₄:Tb³¹, quenching of Tb³¹ emission by Tb V interaction 0-62727

0 - 62.727
YRuy, Laves phase, supercond, transition temp, meas. 0 - 75607
YS(Sc,Te), supercond. 0 - 71980
YS(Sc,Te), single cryst, struct. 0 - 75109
Y,SiO₃, rCe, new cathodoluminophor 0 - 56611
Y,SiO₃, rCe,Opy solid solns, i.r. spectral analysis 0 - 41226
Y,SiO₃, crystal structure 0 - 78508
Y,TiO₂ pyrochlore crysts. Cr³¹ doped, e.r., and optical study
Y,TiO₂ pyrochlore crysts. Cr³¹ doped, e.r., and optical study
YVO₂-Fi cathodo, and photo-luminoscence, effect of synthesis conditions YVO4:Eu cathodo and photo-luminescence, effect of synthesis conditions

O 50050 Yal garnet: Pd, Rh, absorpt, spectra 0-66058 Yb_x, thermal expansion 0-65552 (ZrO)_{0,011}(Y₂O₃)_{0,007}, elec. cond. at 1000-2000°C 0-56268

Yukawa potential see Field theory, quantum/meson field; Nuclear forces;

Aceman effect
at 21 cms limitations, magnetic fields in neutral hydrogen interstellar clouds 0-72739
alkali metal spectral lamps, operation in strong mag. field 0-64192
beam plasma interaction, frequency, intensity and direction of electric

carbonyl sulphide mol., 1 type transitions 0-43116 chloranil, cryst., N.Q.R. in low Zeeman field, obs. 0-41406

4-chloro 3-methyl phenol, single cryst., n.q.r. Zeeman spectrum of ¹⁵Cl 0-66159

0-66159
trans-dichloroethylene, cryst., n.q.r. in low Zeeman field, obs. 0-41406
dimethyl ether, rotational Zeeman effect obs. 0-43160
dimethyl sulphide, rotational Zeeman effect obs. 0-43160
electron trajectories with large quantum numbers 0-60157
fluoroacetylene, mot. effect and mag. susceptibility anisotropy 0-77910
interstellar clouds, neutral H, at 21 cm obs. 0-72739
methane, Zeeman splitting obs. in vibration rotation spectra of ½, rota
tional magnetic moment determ. 0-77924
methylacetylene, mol. effect and mag. susceptibility anisotropy 0-77910
molecular g-values and mag. susceptibilities for eight ring compounds
0-77892
molecular g-values and mag. susceptibility anisotropies for twelve mole

molecular g-values and mag, susceptibility anisotropies for twelve mols. 0-77828

molecules, 21, first obs. of magnetic tuning behaviour 0-77924

molecules, 2°, first obs. of magnetic tuning behaviour 0–77924 molecules, rot, spectra, theory 0–39345 molecules with internal rot, eff. in rot, spectra 0–64338 nuclear polarization, dynamic, forbidden transitions saturated 0–56477 nuclear quadrupole spectrum, splitting parameters 0–76245 pyrazine, low and high field study, zero field splitting 0–76118 pyridine, high field linear and quadratic Zeeman effect 0–46586 quinoxaline, t–850 phosphorescence in high magnetic fields, radiative decay rates 0–46587

rare earth orthoferrites, spin Hamiltonian for even-electron singlet states 0.51313

resonance, motionally narrowed, lineshape anisotropy and freq. shift 0.73113tetracyanoquinodimethane, electron electron double resonance of triplet

excitons 0-66145

trigonal crystal d³ spectra, interactions and mag, dipole line strengths, perturbation method cale. 0-41082

trimethylene oxide g values, magnetic susceptibilities and quadrupole moments 0-46595

```
Zeeman effect continued
```

trimethylene sulphide g values, magnetic susceptibilities and quadrupole moments 0-46595

moments 0.—46595
triplet excitons, change in intensity in 0→1 transition 0—66145
AlBr₃, n.q.x. of ⁷⁸Br, Zeeman effect rel. to bond nature and molecular structure 0.—45043
AlLaO₃:P³⁺, decomp. of energy levels 0—51297
Ba(ClO₃), H₂O₄ Zeeman split n.q.r. spectra 0—41396
BaF₂:EF³⁺, e.p.r., spin temp. 0—76210
Bi I mixed multipole lines, interference effects 0—42957
CdS:Cu²⁺, paramag. centres and ir. absorpt. correl. 0—72370
CdS, Cl donor excited states obs. 0—76067
Cs₂XrCl₄:Os⁴⁺, Ru⁴⁺, and g. values, cryst. field params., obs. 0—41210
GaCl₃, ¹³Cl₃, ¹³Ca n.q.r. Zeeman effect, obs. 0—41397
H, hyperfine spectra, in ground states interacting with nonresonant r.f. field 0—39318
0-H₃, nucl. spins, Zeeman level widths 0—72297
HCN mol., I-type transitions 0—43116
H₃O₅, rel. to mol. quadrupole moment and sign of elec. dipole moment 0—70912

'He, Zeeman resonances meas. in 2³P state g-factor results 0—70922.

0-70912

4He, Zeeman resonances meas. In 23P state g-factor results 0-70822

4He, Zeeman resonances meas. In 23P state g-factor results 0-70822

4HoFeO₃, spin Hamiltonian for even-electron singlet states 0-51313

K, qaudratic Stark shifts of Zeeman levels in ground state 0-77662

K, PtCl₈-054*, Ru⁴⁺, and g-values, cryst. field params., obs. 0-41210

Li 6708 A line, in sunspots, abundance calc. 0-41851

NH₃, molecular Zeeman effect meas. of mag. susceptibility and quadrupole moment 0-46488

Na, quadratic Stark shifts of Zeeman levels in ground state 0-77662

Nd, structure of lines using SISAM spectrometer 0-77664

Ne, pressure broadening of 6074.3 Å line using Zeeman scanning 0-70771

OCSe molecular Zeeman effect obs. 0-74295

Ne, pressure broadening of 0019-5 H line using 200-1019 OCSe, molecular Zeeman effect obs. 0-74295
Bb, hyperfine spectra, in ground states interacting with nonresonant r.f. field 0-39318
RbMnF₃, exciton absorpt., Davydov splitting 0-66050
SiC, cubic, of recomb. radiation from shallow bound exciton 0-76158
Tb³⁺ in TbAIG, Zeeman-Raman transitions obs. 0-48097
TmCl₃.6H₃O, Tm₃(SO₄₎₃.8H₃O, splitting between Stark levels of Tm³⁺ (4ft ²) 0-76111
TmFeO₃, spin Hamiltonian for even-electron singlet states 0-51313
YAlO₃:Dy⁴⁺, anisotropy of g-values 0-48079
YCl₃.6H₃O:Tm³⁺ + Y₂(SO₄₎₃.8H₃O:Tm³⁺, splitting between Stark levels of Tm³⁺ (4ft ²) 0-76111
Yb³⁺, ground state splitting in distorted cubic-crystal field 0-62575
ZnS:Cu²⁺, paramag. centres and ir. absorpt. correl. 0-72370
ner diodes

Zener diodes see Semiconducting devices/diodes

Zener effect see Metals; Semiconducting materials; Semiconductors

Zeta-potential see Electrokinetic effects

abundance in lunar samples, emission spectrographic determ. 0–48499 in alloys, analysis by gas adsorpt. chromatography 0–66209 atom, 4¹P₁ level, collisions with rare gases, depolarization cross sections 0–67664

atom, excitation of $4D_f$ levels by transfer from Hg atoms in afterglow 0-64209

atom, optical ionization-excitation by electron impact 0—60966 atom, optical ionization-excitation by electron impact 0—60966 atomic spectra, classification of new multiplets in extreme u.v. 0—49764 atomic spectra, observation of Zn II, Zn III and other unkown spectral lines, 2300A-3000a 0—55237 atoms in arc discharge, spatial distribution 0—74613 Bauschinger hardening of twin boundaries in crystal 0—47420 inbiological materials, determination by neutron activation analysis and chelate extraction 0—76291 cleavage, dislocation motion 0—68495 cleavage fracture along slip plane in single crystal, criterion 0—56014 compensated Si semiconductor, bulk sample instabilities obs. 0—47714 crystal growth, from vapour, electron microscopy, equilib. shapes 0—74975 crystal growth from vapour 0—65140

crystal growth from vapour 0-65140

crystals, deformed, dislocation struct. investigation by electron transmission microscope 0–78558 cyclotron effective mass temp, depend. 0–40685 cyclotron resonance, Fermi surface determ, new crystal growth technique

deformation mechanism rel. to twin formation in cold-stretched single

0-44074
deformation mechanism rel. to twin formation in cold-stretched single cryst. 0-68450
diffused in GaAs electroluminescent diode, long operating life 0-44947
diffusion in Cu, strain cycling effect 0-40197
diffusion in Cu, strain cycling effect 0-40197
diffusion in InAs, neutron irrad. effects, vacancy conc. 0-47293
diffusion in InAs, neutron irrad. effects, vacancy conc. 0-47293
diffusion in Si, by closed-tube two-temp. technique 0-62000
diffusion in Si 0-55924
diffusion into Al, Al-Zn alloys, 350-500°C 0-50619
diffusion of Sn, 298-400°C 0-43700
dislocation forests role in plastic deform. 0-40312
double photoionization cross-section obs. 0-60968
elastic constants, third-order, determ. 0-43713
elastic shear consts., calc. using optimized model potential 0-71659
electrodeposition, aqueous KOH, Sn and tetraethylammonium ions effects, dendritic growth 0-72550
electron diffraction for LEED intensity meas. 0-47165
electropolishing technique 0-72546
embrittlement by liquid metals, temp., pressure effects, deformation hot stage metallographic facility 0-40481
Fermi surface, rf. size effect 0-53762
film, oxidation, I doping effect, 200-390°C 0-76267
galvanomagnetic props., induced-torque meas. and mag. breakdown 0-78873
hyperfine fields in Fe 0-44735
impurity distrib. in GaP:ZnO liquid phase epitaxy layers 0-62365
internal friction, temp. depend, 300-500k, dislocation-point defect interaction 0-68365
internal friction after deform. by twinning 0-40251
ion-electron emission, low temp. 0-44413

tion 0-08365 internal friction after deform, by twinning 0-40251 ion-electron emission, low temp. 0-44413 ions production using ion-source, description 0-51163 laser, vapour, applic, of isotopes 0-49047 liquid, thermoelec, power and electresistivity 0-53371

Zinc continued

magnetic breakdown, g factor and energy band structure 0–43957 magnetomorphic oscillations of radial Hall effect, modified field-modulation technique 0–56190 neutral Zn I, 4p² configuration, autoionization probability for ¹S₀ and ¹D₂ levels 0–60935 phonon freq. calcs. for hexagonal metal 0–43853 phonons, neutron groups, temp. depend. 0–62181 plastic deform, dislocation forests role 0–40312 plastic deform, mechanism of single cryst. in pyramidal slip 0–62044 plastic deformation of single crystal and polycrystalline, electric current pulses effect 0–40313 shear modulus, torsional deformation and temp. depend. 0–40241 spectral lines, intensities, calculated as functions of axial temp. of discharge channel 0–71169 stacking fault energy meas., h.c.p. metal 0–55891 stacking fault energy meas., h.c.p. metal 0–55890 superconducting, isotopically and metallurgically pure, fluctuation effects above T, evidence 0–44083 superconducting energy gap, anisotropic, microwave absorpt. determ. 0–53805 superconducting energy gap, anisotropic, model 0–53806

0-3805 superconducting energy gap, anisotropic, model 0-53806 surface cohesion coeff. temp. depend. 0-39932 surface conductivity, electron specular reflection, temp. depend., size effect 0-75565 surface entropy, from temp. depend. of surface free energy anisotropy 0-68218

0-68218
valence bands, L-series X-ray spectroscopic study 0-65593
vaporization kinetics of single crystals 0-74854
vapour laser, applic. of isotopes 0-49047
whisker, mech. props., surface film depend. 0-40300
whiskers, galvanomagnetic props. study using electrical mounting holders
0-51832
in Al, segregation to vacancy sinks 0-71608
Cu/Zn couple, thermomigration rel. to retarded diffusion 0-47291
Hg atom collisional excitation, <0.1eV, obs. 0-67641
Hg*Zn collisions, excitation, gas discharge plasma afterglow obs.
0-52948
in Ni, additive effect on Elinvar prop. 0-58856
Zn-Hg-Kr discharge, afterglow, excitation of the 4D_I levels of zinc by

in Ni, additive effect on Elinvar prop. 0-58856 Zn-Hg-Kr discharge, afterglow, excitation of the $4D_J$ levels of zinc by mercury atoms in the 7^{1} S, state 0-64209 Zn, (Al,Cd), Bauschinger effect, twinning 0-40314 Zn II, CW laser lines at 4912 Å in transverse-discharge configuration 0-69901 Zn II, cw laser socillations in hollow cathode 0-64199 Zn II, revised energy levels from new vacuum u.v. wavelengths 0-46376 Zn II $3d^3455$ level, intermediate coupling calc. and revised levels 0-46375 Zn, magnetic resonance of $4^2D_{3/2}$ and $4^2D_{5/2}$ excited levels 0-46377 Zn, diffusion in electrolyte solns, radioactive tracer determ. 0-50214

Zinc compounds

alloy, dil, residual resistivity, lattice-distortion screening effects 0–50990 alloys, reversion phenomena, resistometry 0–43807 borates, phosphorescence decay curves analysis by electronic computers 0–62703 β+brass, T-matrix theory of density of states 0–71774 β-brass, X-ray K-emission spectra, 3d(4sp)-energy bands 0–51333 brass, α and β, electron states by positron annihilation 0–65615 β-brass, deform under explosive shock 0–78625 β-brass, electronic struct., U.V. photoemission obs. 0–75488 α-brass, lectronic struct., coherent-pot. approach 0–78835 B-brass, long-range order 0–78473 β-brass, long-range order 0–75089 brass, microstructural damage adjacent to bullet holes 0–65231 brass, notched specimens, crack propag. during stress corrosion under bending stress 0–68487 α-brass, plastic anisotropy predictions using pole-inversion figures 0–65384

0-53584
§-brass, quenched, angular helical dislocations 0-71624
brass-Si, corrosion resistance, thermal conductivity 0-43789
copper alloy, Q-switched laser sampling, effect on chemical analysis 0-65471

copper alloy, Q-switched laser sampling, effect on chemical analysis 0-65471

2- dimethylaminoethylmethylamina Zn hydride coordination compound crystal structure 0-50556 ethyl Zn iodide coordination compound, crystal structure 0-50566 ferrites, synthesis, comparative reactivity of Fe oxides 0-72269 forging process 0-65457 guanidnium sulphate, crystal structure 0-50562 Mm-Zn ferrites, magnetic permeability and Q factor as functions of SiOconc. 0-65959

zincblende (110), surface state analysis rel. to surface atom geometry 0-47597

ZnO, e.p.r. of V³+ 0-45005

ZnO, ESR line at g≈1.96, and F-centre 0-61981

Ag-Sn alloy contact, resistance failures of Ag contacts due to corrosion 0-56174

Ag-Zn.1¹9Sn system, α-phase, Mossbauer effect, isomeric shift 0-51278

Ag-Zn alloys, α-phase, reflectance and band struct. obs. 0-78775

Ag-Zn alloys, lattice termal cond. 0-71874

Ag-Zn solid solns, thermal vibrs. of atoms 0-71819

Al-Ag, X-ray diffuse scatt, features 0-53503

Al-Mn-Zn alloy, dislocation struct. 0-75172

Al-Zn-Li, alloys, stress corrosion cracking, effect of added Cr and Li 0-50740

Al-Zn, alloy X-ray Los spectra of Al constituent. 0-66079

Al-Zn, alloy, diffusion of Zn, 350-500°C 0-50619
Al-Zn, 30ft X-ray L₃, spectra of Al constituent 0-66079
Al-Zn, soft X-ray L₃, spectra of Al constituent 0-66079
Al-Zn, soft X-ray L₃, spectra of Al constituent 0-60079
Al-Zn alloy, effect of ternary additions on clustering, solute-vacancy binding energy 0-50572
Al-Zn alloy, quenched-in vacancies, diffusion processes and annealing-out kinetics 0-47228
Al-Zn alloy, rhombohedral distortion of transition precipitates 0-58972
Al-Zn alloys, effect of heat treatment on intergranular corrosion 0-65444
Al-Zn alloys, zone and modulated struct. formation in ageing 0-78673
Al-Zn liq, solns, elec. resistance 0-39831
Al-(6.8 at.96)Zn alloy, quenched, pre-precip., effect of plastic deform, at 196°C 0-50779

Zinc compounds continued

Al(Zn,Mg) alloy, age hardened precipitate, transition phase η' , electron microscopy 0- 65220

Al 78%Zn alloy, superplastic deformation mechanism 0-50684

β'-AuZn(50%Zn), martensitic transformation, particle size effect

CdTe ZnTe, phase diagrams and crystal growth 0-50462

CdTe ZnTe, phase diagrams and crystal growth 0-50462 β Cu (48.14at.%) Zn alloy, vibrational amplitudes of Cu and Zn 0-62169 Cu Al Zn alloy, solid state transforms. 0-53661 Cu Ni Zn alloys, deformed, stacking faults 0-50601 Cu ($\frac{1}{2}$ Sat.%)Ni (25at.%)Zn alloy, absorpt. edge from reflectance meas., 1.55 5.18 eV 0-44815 Cu Zn, β -brass, mag. critical phenomena, scaling laws, neutron scatt. 0-65806

0. 65899
 Cu Zn alloy, X ray absorption investig, of electronic structure 0—68734
 α· Cu Zn alloys, cluster form. during electron irrad. 0—78532
 Cu Zn alloys, diffusion of Cu, correl, effects 0—78578
 Cu Zn alloys, Sn and As effects on stress corrosion cracking 0—40409
 Cu Zn crystal, fatigued, dislocations, slip bands, electron microscopy 0—78549
 Cu Zn crystal, An entirely deform microstruct. 0.65393

0 / R5347 (Cu Zn with Al₂O₁ particles deform, microstruct. 0-65393 Cu Zn with Al₂O₂ particles, deform. 0-65392 β² 'CuZn, elastic anisotropy, unstable dislocations, electron microscopy 0 47319

0 47319

Cu_Zn,Fe,O₄, Curic temp. rel. to cation distrib. 0—47963

Cu_7O_nFe,O₄, Curic temp. rel. to cation distrib. 0—47963

Cu_7O_nFe,O₄, Curic temp. rel. to cation distrib. 0—47963

Cu_Zn, diffusion on alternating deformation 0—47292

GaAs_ZnSe heterojunctions, fabrication and props. 0—44284

(GaP)_{0.95}(ZnSe)_{0.85}, semiconductor alloy, electronic transport props., Hall mobilities 0—44188

KPO₁ Zn(PO₁), system, equil. diagram 0—62149

Li Ti_Zn, ferrite, spin wave losses, Co^{2±} effect 0—41036

Li₄SiO₄ Zn₂SiO₄ system, solid solutions, phase equilib. 0—61589

Mg_Zn_CU(Ag) systems, structural changes rel. to Friaur Laves phases 0—61877

Mg_Zn_alloys, normal grain growth, law and activation energy 0—61741

Mg Zn alloys, normal grain growth, law and activation energy 0-61741 Mg Zn alloys, temperature and concentration dependence of conductivity

y Mn Zn alloys, antiferromag, props., alloying elements influence

p² Mn Zn alloys, antiferromag, props., alloying elements influence 0 = 41060 Mn Zn ferrite, clastic wave propag., magnetiz, effect 0—40260 Mn Zn ferrite surface grinding effect on prameability 0—62549 Mn Zn ferrites, surface grinding effect on permeability 0—65958 Na;O ZnO SiO₂ system glasses, ZnO structure role 0—58543 NiZn ferrites, cryogenically crushed, mag, props. 0—59336 Pt Cu Zn system, structure of high temp, form 0—50549 Sn Zn dilute alloy freezing, distrib, coeff. rel. to growth velocity and initial conc. tracer method 0—68536 Ti Hg Zn syst., X ray studies 0—40465 Y Cd Zn system, showed distrib, coeff. rel. to growth velocity and sintial conc. tracer method 0—68536 Na properties of the prop

Y Cd Zn system, phase diagrams and relations, intermetallics obs. 0-78707

Zn Ag, alloys, liq., electrotransport of Ag, effective charge determ. 0 39835

Zn Ag solid solution, α_2 , temp. and conc. depend. of lattice parameters 0.78447

0. 78:447
 2n Al alloy, supersaturated near cutectoid, decomposition 0–61599
 2n Al cutectoid, copper additions rel. to superplasticity 0–68451
 2n (0.4 wt.%)Al superplastic sheet, anisotropic effects 0–403.15
 2n Bi, Zn Pb, Zn Bi Pb systems, effect of ternary additions on thermodynamic props. 0–68082
 2n Cu Ti alloy, varied extrusion temp. effect on props. 0–40423
 2n Cu phosphor, i.r. emission spectral line shift 0–56618
 2n In S system ternary phases, polytypism 0–78510
 2n Mn alloys, (0.06%Mn), Kondo effect and electrical resistance obs. to 0.4 K 0.44073

Zn Mn alloys, (0.06%Mn), Kondo effect and electrical resistance obs. to 0.4 K = 0.44073Zn Mn alloys, dilute, resistance anomaly 0-68751Zn Mn solid solns, axial ratios and solubility limits of h.c.p. η and e phases 0.-40073Zn, W, O₈, metastable, homologous, formation and props. 0-65473

Zn,W,O₈, metastable, homologous, formation and props. 0-65473 Zn (H) complexes with thiourea, Raman and i.r. spectra 0-74313 Zn acetate dihydrate: Co¹² single cryst. optical absorption 0-56541 Zn complex, tetramethylammonium, cryst. struct. 0-55833 Zn complexes, hexathiocyanates, i.r. spectra 0-46517 Zn H complex, α , β dichlorobis (4-vinylpyridine) zinc H, cryst. struct. 0-58766

0. \$8766
Zn trithiocyanate complexes, i.r., spectra 0—49896
ZnAl,O₄:Mn²⁺, phosphor, electronic states 0-72445
ZnAs, films, vacuum evap., optical props. 0. 65983
ZnB₄O₅, single crystalls, structure determined by a three dimensional Fourier synthesis 0-65294
Zn₁B₂O₁₃Cl₄, e.s.r., of Cu¹⁺ 0-62756
Zn(BrO₁), e.s.r. spectrum, evidence suggesting paramagnetic centre is BrO₅ radical 0. 45004

0 61518

ZnCl; glass, network struct, determ, using transition metal ion spectro scopic probes 0 62676

ZnCl; vapour, absorpt, and emission spectra at 700°C, windowless gas cell appl. 0 49153

ZnF; Cu²⁺, c.p.r. determ, of covalency and electronic struct, of Cu²⁺ 0 41324

ZnF; crystals, vapour phase growth technique and characteristics 0 47124

0 4/124
ZnFe;O₄, exchange integrals, paramag. neutron scatt. obs. 0-40948
ZnFe;O₄, mag. struct., neutron diffr. obs., 4.2K 0-41065
ZnFe;O₄, spinel, mag. structure, models 0-47964
ZnGa,O₄:CrF, e.p.r. 0-48153
ZnGeAs₇, amorphous film, I-V characts., switching and memory effects 0-40768

Zn₂GeO₄:Mn²⁺, phosphor, electronic states 0~72445

Zinc compounds continued

Zn₂(GeO₄), cryst. struct. 0-58764

ZnGeP₂, semiconductor with chalcopyrite lattice, energy zone structure 0 =65683

Zn_xHg_{1-x}Te, crystal growth, morphology and dislocations 0-74988 Zn_xHg_{1-x}Te solid solns., prep., microstruct. and transport props. 0-51047

0.51047
 Znl1, anhydrous and hydrated, absorption in far i.r., effect of Kr and H₂O 0.66059
 Zn(II) complex, μ, μ', μ''', oxo hexakis (1.3 diphenyl-triazenido)tetraz inc(II), molecular structure, crystal structure 0-55328
 Zn(II) complex, tetramminezine (II) tetraperoxomolybdate (VI), cryst. struct. 0-65298

struct. 0-05298 Zn(II) halide complexes, of NH₁ and imidazole, low-freq. i.r. and Raman spectra 0-55329 ZnIn₂S₂:Er³⁺, crystal field, from Stark splitting of luminescence spectra 0-56593

0 56593

ZnIn/S₄(1) polytypic form, cryst. struct. 0–65295
Zn₁n/S₄(1) polytypic form, cryst. struct. 0–65296
Zn₁S₂(1) polytypic form, cryst. struct. 0–65296
ZnK₁(SO₄)₂,6H₂O NiK₂(SO₄)₂,6H₃O, crystn. from soln., kinetics, impurities distrib. growth vel. depend. 0–40020
Zn(KSO₄)₂,6H₂O, diluent of Cu(KSO₄)₂,6H₂O single crystals 0–76099
Zn₂NCl, preparation and identification 0–58623
Zn(NO₂)₂ in anhydrous methanol, assisociation above and below −30°C, by i.r., Raman and n.m. spectra 0–58490
Zn(NO₂)₂, zryst. struct. 0–6249
Zn(Ni ferrites, initial permeability and Curie pt., as function of cation distrib. 0–62548
Zn₂Ni, Fe₂Co, ferrites, sublattice magnetizations, 0.25≪≪0.75 0–41040

trib. 0 62548
Zn₁Ni₁, xFe₂O₄ ferrites, sublattice magnetizations, 0.25 < x < 0.75 0-41040
Zn₀CLi, field effect cond., slow relaxation 0-75693
Zn₀CLi, luminescence, yellow band, emission mechanism from e.s.r. and polarisation meas. 0-79365
Zn₀C2n phosphor, cathode ray efficiency, 10kV 0-44942
Zn₀C3n phosphor, cathode ray efficiency, 10kV 0-44942
Zn₀O/solution interface, ionic double layer, surface composition, pH depend. 0-51435
Zn₀O/solution interface, ionic double layer, point of zero charge, prep. depend 0-51436
Zn₀O/solution interface, ionic double layer, differential capacities, specific adsorption 0-51436
Zn₀O/solution interface, ionic double layer, differential capacities, specific adsorption 0-51436
Zn₀O/solution interface, ionic double layer, differential capacities, specific adsorption 0-51436

adsorption 0-51436

ZnO BaTiO₃, solid solution, electro-optical props., comp. depend. 0 79250

ZnO Ga₂O₁ Cr₂O₃, spinel phase, evidence 0-65503

ZnO resin binder layers, dye-sensitized, quantum efficiency and photocond. 0-72140

ZnO 1792 photon magnetoabsorption 0-76079

ZnO₃ 2 photon magnetoabsorption 0-76079

ZnO₃ 2 photon magnetoabsorption 0-76079

ZnO, 2 photon magnetoabsorption 0--76079
ZnO, acoustoelec, current saturation due to off-axis shear waves 0--50883
ZnO, acoustoelec, effects 0--75400
ZnO, adsorbed I effect on e.p.r. 0--45003
ZnO, adsorption of H₂ and CO, rate determination 0--47086
ZnO, charact, energy loss and u.v. reflectivity spectra 0--54090
ZnO, characts, of radicalo luminesc, kinetics 0--44956
ZnO, chemisorption of H atoms 0--56700
ZnO, coatings, quantum efficiencies of formation of charge carriers 0-75467
ZnO, cryst, growth from phosphate and vanadate fluxes 0--61736

2nO, cryst. growth from phosphate and vanadate fluxes 0—61736 ZnO, cs.r. of Zn vacancy 0—76227 ZnO, electron beam pumped laser action and luminesc., 15-250K 0 76160

270, beletron irrad., F¹ centre, e.s.r. obs. 0-45002
ZnO, exciton exciton interaction causing appearance of extra luminese. bund 0-40672
ZnO, heteroepitaxial, on sapphire, fund. Rayleigh wave mode dispersive props. 0-59271
ZnO, budgelseigh sapution growth technique. 0-50447

ZnO, heteroepitavai, on sappine, tund. Rayleign wave mode dispersive props. 0-59271
ZnO, hydrolysis-solution growth technique 0-50447
ZnO, kinetics of radical luminescence in crystal phosphors with a long alterglow on photoexcitation 0-56613
ZnO, nature of yellow-orange luminescence centers 0-44896
ZnO, nonlinear optical susceptibility, explanation for anomalous sign of d₁₁ 0-66004
ZnO, photoplastic effect, dislocations and interstitials, coulomb interaction 0-40337
ZnO, single crystals, optical surface phonons, detection by slow electron spectroscopy 0-53694
ZnO, substrate for epitaxial Au, effects of air and vacuum cleaved surfaces 0-43548
ZnO, surface resist, glow discharge effect 0-62291

surfaces 0-43548
XnO, surface resist., glow discharge effect 0-62291
ZnO, surface stability, LEED 0-74878
ZnO, u.s. attenuation freq. depend., room temp. 0-53705
XnO, u.v. resonant Ramn scatt. 0-76131
ZnO, vapour phase growth rel. to temp. gradient 0-40017
ZnO, znoite, Li influence on growth vel. under hydrothermal conditions 0-55782

0 55782
ZnO cryst. growth by oxidation of ZnI₂ 0-53460
ZnO cryst. growth from ZnBr₂ 0-68252
ZnO clectrophotographic layers, effect of degassing desorbed O₂ on photo conductive patterns 0-73376
ZnO epitaxial layers on sapphire, growth and props. 0-50378
ZnO film, hypersonic transducer, losses rel. to texture, resist., thickness 0 68605
ZnO film, u.v. irrad., Hall mobility, elec. cond., optical transmission 0 40778
ZnO film prep. method 0-53442
ZnO film Hall effect, growth and struct. 0-61673
ZnO films, cryst. sputtered, resist. 10⁸-10¹³ Ωcm 0-56346

ZnO film. Hall effect, growth and struct. 0–61673
ZnO films, cryst. sputtered, resist. 10⁸-10¹⁹ Ωcm 0–56346
ZnO films, clec. cond., ambient oxygen influence 0–53829
ZnO films, shear mode, birefringence rel. to coupling factor, obs. 0–45639
ZnO laser, electron beam excitation, wavelength, 82-250°K 0–42309
ZnO piezoelectric thin film deposition 0–76221
ZnO powder, chemisorption of hydrogen, conductivity, electrical, 30 to 300°C 0–40708
ZnO powder, irrad., e.s.r. 0–41350
ZnO powder, photodamage, e.s.r. 0–66143

Zinc compounds continued

ZnO powder, thermoluminescence parameters, new calculation method 0-69163

ZnO pure single crystals, electrical props. temp. depend. effect of u.v. irrad. 0-47729

ZnO single crystal, evaporation rates and morphologies 0-61697 ZnO surface barrier systems 0-65687 ZnO u.v. photolysis in vacuum, prevention by Fe surface states, obs. 0-56714

0-56714
ZnO whiskers, deform and fracture 0-62071
ZnO(H),Si₂O,H₂O, hemimorphite, morphological aspects 0-61698
ZnP₂, low temp. luminescence, prep. 0-41275
α-2n₁P₂O₇, cryst. struct. and phase transform. 0-58765
ZnS-CdS-Ag-Ni phosphors, excitation and emission spectra 0-56617
ZnS phosphor, radical-recombination luminescence spectra, effect of surface 0-76159
ZnS(Cu) cell, effect of frequency on time to reach saturation brightness 0-76188
ZnSO-CdSb system. elec. residence and activation energy extremums and

0—76188
ZnSb-CdSb system, elec, resi\u00e4ance and activation energy extremums and anomalies, model explanation 0—75349
ZnSb-CdSb system, existence of phase ZnCdSb, 0—75111
ZnSb films, struct, and thermoelec, props. 0—65659
ZnSe:Si, photosensitive e.p.r. 0—72497
n-ZnSe-p-Ge-n-Ge, transistor, current gain, doping depend., optical props. 0—44284
ZnSe-Ge heterojunctions, fabrication and props. 0—44284
ZnSe-Ge heterojunctions, switching and meory 0—68867
ZnSe-ZnTe heterostruct., recomb. radiation 0—56648
ZnSe-ZnTe system, diffusion of Al, 700-1000°C 0—43699
ZnSe, appearance of self-activated photoluminescence accompanied by increase in n-type conductivity 0—56615
n-ZnSe, avalanche breakdown and light emission at low-angle boundaries 0—44209
ZnSe, change density, Fourier transforms using self-consistent orthogonal-ZnSe, change density, Fourier transforms using self-consistent orthogonal-

n-ZnSe, avalanche breakdown and light emission at low-angle boundaries 0–44209
ZnSe, change density, Fourier transforms using self-consistent orthogonalized-plane-wave method 0–44212
ZnSe, crystal, electro-optical coeff, Id. permittivity, polarization 0–76036
ZnSe, crystal growth, vapour transport reaction 0–74976
ZnSe, crystal growth, vapour transport reaction 0–74976
ZnSe, dielectric function, wave-vector-dependent 0–78962
ZnSe, e.pr. of Ni* and Ni** 0–41349
ZnSe, e.pr. of Ni* and Ni** 0–41349
ZnSe, e.pr. of Ni* and Ni** 0–401349
ZnSe, rel. to eutectics, growth techniques 0–50421
ZnSe, hydrothermal crystin. 0–75014
ZnSe, laser, props. 0–52332
ZnSe, melting point determ. under Ar press., 1-50 atm. 0–78336
ZnSe, piezosemiconductor, Rayleigh wave amplification 0–75399
ZnSe, reflectivity spectra, 15 and 300K, calc. and meas. 0–48007
ZnSe, temp. depend. of optical phonon linewidths and freqs. 0–76132
ZnSe, X-ray scatt. anomaly 0–68318
ZnSe Debye temp., compounds of same Gruneisen constant, linearity of log (Debye temp.) with log (molar vol.) 0–50900
ZnSe film, epitaxial growth, temp. depend., elec. props. 0–50376
ZnSe films, photoluminesc. and electroluminesc. 0–51374
ZnSe on Ge heterojunction, characteristics 0–44288
ZnSe on Ge heterojunction, characteristics 0–44288
ZnSe on Ge heterojunction, characteristics 0–44288
ZnSe on Ge heterojunction, prep. by epitaxial deposition, elec. characts. 0–68868

0-68868
ZnSe photoluminescence, effects of Cu impurities and varying conditions
0-44895
ZnSe resonant Raman scatt. using a UV Cd-He laser, obs. 0-44869
ZnSe single crystal, reflection and luminescence spectra, rel. to exciton spectra 0-44897

Znse single crystal, renection and luminescence spectra, rel. to excitor spectra 0-44897
ZnSe(Te), elastic consts., 77-300K
0-58860
ZnSe(Te), second-order elastic consts., press. depend. 0-55942
ZnSe(Te) films, absorpt. spectra in 36-150 eV region 0-48080
ZnSiAs₂, ir. absorpt. spectra 0-48065
ZnSiAs₂, semiconductor with chalcopyrite lattice, energy zone structure 0-65683

ZnSiF₆.6H₂O:Mn²⁺, spin-lattice relaxation, magnetic field strength effects

0-65683
ZnsiF, 6H₂O:Mn²+, spin-lattice relaxation, magnetic field strength effects 0-54049
Zn,SiO₄:Mn, phosphor, cathode-ray efficiency, 10kV 0-44942
Zn,SiO₄:Mn²+, phosphor, electronic states 0-72445
Zn,SiO₄:Mn²+, willemite, single crystals, polarized cathodoluminescence emission 0-44943
Zn,SiO₄:Mn²+, willemite, single crystals, polarized cathodoluminescence emission 0-44943
Zn,SiO₄:Mn-activated phosphor screens, in translucent film formation, improved evaporation-firing method, high cathodoluminescence efficiency 0-51368
Zn₅(SiO₄) willemite, cryst. struct. 0-58764
ZnSiP₄, chalcopyrite struct, i.r. absorpt. spectra 0-79322
ZnSiP₃, huminescent, chalcopyrite structures, lattice constants and space group 0-47208
ZnSiP₅, spingle crystal growth, by vapour transport and from solution 0-47123
ZnSiP₅, single crystal growth, by vapour transport and from solution 0-47123
ZnSiP₅, vibr. modes 0-75382
ZnSnP₅, i.r. absorpt. spectra 0-48065
ZnSnSb₅, cryst. struct. 0-65297
ZnTe-Li, photoluminesc. 0-79357
ZnTe-CdSe p-n heterojunction based luminescent diode 0-72469
ZnTe-CdSe p-n hase diagrams and crystal growth. 0-50462

0--44400

0-44400
ZnTe-ZnSe, phase diagrams and crystal growth 0-50462
ZnTe, crystal growth 0-74967
ZnTe, doped, photocond. 0-79083
ZnTe, rel. to cutectics, growth techniques 0-50421
ZnTe, lattice dynamics, thermal expansion 0-75383
ZnTe, lattice parameters and thermal expansion 0-43646
ZnTe, mis. electroluminescent diode, red and green spectral output 0-54140 ZnTe, mi 0-54140

0-56399

0–54.140
ZnTe, melting point determ under Ar press., 1-50 atm. 0–78336
ZnTe, nonlinear optical susceptibility 0–72301
p-ZnTe, photocoond under combined excitation conditions 0–5639
ZnTe, photosensitivity spectrum, annealing effect 0–56398
ZnTe, piezosemiconductor, Rayleigh wave amplification 0–75399
ZnTe, Raman spectra, lattice vibrations 0–41242
ZnTe, refl. spectra in fund. absorpt. region 0–79274
ZnTe, reflectivity spectra, 15 and 300K, calc. and meas. 0–48007

Zinc compounds continued

compounds continued

ZnTe, temp. depend. of optical phonon linewidths and freqs. 0–76132

ZnTe Debye temp., compounds of same Gruneisen constant, linearity of log (Debye temp.) with log (molar vol.) 0–50900

ZnTe epitaxial films, struct. rel to photovoltaic props. 0–56403

ZnTe epitaxial argowth, temp. depend., elec. props. 0–50376

ZnTe film, epitaxial growth, temp. depend., elec. props. 0–50376

ZnTe film, vacuum-deposited, space- charged-limited-current 0–53830

ZnTe surface comp. analysis by inert gas ions backscatt., ⁶³Cu/⁶⁵Cu differentiation 0–56717

ZnWO₄·Co²+, spin-lattice relaxation, temp. depend. 0–69054

ZnWO₄·Cr³+, epr., 293 K, crystal field const. 0–41348

ZnWO₄·Cr³+, El²-, absorpt. spectra, reductive colouring, pair substitutions, annealing 0–48081

ZnWO₄·Cr³+, spin-spectrum, 33-4000 cm⁻¹ 0–72349

Zn|FqC(N)₄|, i.r. spectrum, 33-4000 cm⁻¹ 0–72349

Zn|Hq(SCN)₄|, efficient phase matchable second harmonic generation 0–7300

ZrZn₂-x 0.05≤x≤0.2, ferromag. alloy, Stoner theory, application

0.05 \(x \le 0.2, \) ferromag. alloy, Stoner theory, application 0-44601

zinc sulphide

band structure, thermoreflection method 0-56151 cathodoluminescence, edge, ix. quenching 0-48117 cathodoluminescence of single crystals, donor-acceptor impurity effects 0-56659

0-30639 conductivity, elec., of single crystals 0-51044 crystal growth 0-74967 crystal growth and morphology of hollow cryst. 0-61720 crystals grown as graphite and quartz, struct., obs. 0-40107 crystals grown from vapour, polytype growth and twin faults, obs. 0-40018

0-40018 crystals with stacking faults, absorption spectrum in tetrahedrally coordinated Fe²⁺ ions 0-49777 Debye temp. determ. using electron phonon state splitting 0-75410 edge luminese. of non-activated phosphor effect of excess Zn and S 0-51362

0–51362 electret discharge, u.v. dosimetry applic. 0–67122 electret discharge, u.v. dosimetry applic. 0–67122 electrical conduction, non-linear, in strong electric fields 0–47631 electro-optical props. 0–51274 electro-optical props. 0–66001 electroluminescence, a.c., kinetics, model approach 0–76193 electroluminescence, eviation from neutrality influence 0–56647 epitaxial layer form. on NaCl cryst. spallations 0–65077 exciton piezoreflection of cubic crystals, 77K 0–56491 film, absorpt. spectra in 36-150 eV region 0–48080 film, epitaxial, luminescence, effect of Mn, Cu or Cl impurities 0–51351 film, epitaxial, luminescence, effect of Mn, Cu or Cl impurities 0–51351 film, pitaxial growth, temp. depend., elec. props. 0–50376 film, inhomogeneous, bilayer structure form from refractive index calcs. 0–51263 film, pitotocond. props. 0–47880

61m, photocond. props. 0-47880 film, recrystallization and structural transforms, electron microscope obs. 0-50825 film, vapour-deposited, electron-induced conductivity 0-44210

films, thin, deposited on glass substrates, abnormal dispersion caused by inhomogeneity 0-62599 films an Al₂O₃, Rayleigh and Lamb waves propag., obs. 0-47524 grains for TV screen, surface treatment to improve uniform coating 0-54845

growth from vapour, physical props. 0–71514 illuminated, screening of threshold field 0–69172 lattice dynamics of zinc blende 0–62180

liquidus solubility in Zn, 1000 to 1300 °C, rel. to solution growth of crystals 0–50448 luminescence, effect of quench cooling upon efficiency of edge radiation 0–69176

0-69176 luminescence, optically excited, trapped levels lifetimes distrib. 0-72427 luminescence emission band widths 0-62704 luminescence of ZnS grown from Ga melts. 0-51352 luminescence of phosphors, u.s. and X-rays effects, and exo-electron emission, obs. 0-41290 luminescence of self-activated single cryst., sensitivity to i.r. 0-51353 luminophore, fluoresc. emission band, large width causes 0-54126 melting point determ. under Ar press, 1-50 atm. 0-78336 Mossbauer spectrum of 51Co 0-56516 phosphor, elec. cond. during radical-recomb.luminesc. 0-66101 phosphor, excited absorpt., colour centre interaction with lattice defects 0-44923 phosphors, determ, of luminesc. quantum yield, expt. 0-41291

0-44923
phosphors, determ. of luminesc. quantum yield, expt. 0-41291
photovoltaic effect, anomalous, and rectification 0-53963
photovoltaic props., growth atmosphere effects 0-79087
piezosemiconductor, Rayleigh wave amplification 0-75399
polytype formation in vapour-phase grown crystals, mechanism 0-50555
positronium decay, 7; obs. 0-40699
Raman scatt., resonant, using a UV Cd-He laser, obs. 0-44869
self activated spectrum decomposition on elementary bands of blue luminescence 0-69156
self-activation canability, preliminary purification 0-56614

self-activation capability, preliminary purification 0–56614 sublimated cryst, surface morphology 0–50353 surface striations, 1-dimensional disorder in single crystal, emission microscopy 0–53425 surface striations, scanning electron microscopy, cathodoluminescence 0–61635

0–61635
thermal expansion of wurtzite ZnS, 2-350°K 0–47551
thermoluminescence of electron excited, unactivated, obs. 0–56639
u.v. emission from sublimed films of unactivated ZnS 0–56554
vapour-phase grown crystals, polytype formation mechanism 0–50555
ZnS: Cu (Cr. Cl), green luminesc, lir. effect 0–62717
Ag activated phosphor screens, in translucent film formation, improved evaporation-firing method, high cathodoluminescence efficiency 0–51368
Au-ZnS:NdF₃-Ta₂O₃-Ta composite films, pulse excited electroluminescence characteristics 0–44950
Cd_Zn_{1-x}S mixed cryst., trapped levels lifetimes distrib. 0–72416
Cu_S-ZnS:Mn, Cu, Cl films, electroluminescence mechanism, scanning electron microscopy 0–48118
(ZnCd)S:Ag, phosphor, cathode-ray efficiency, 10kV 0–44942

(ZnCd)S:Ag, phosphor, cathode-ray efficiency, 10kV 0-44942 ZnCdS:Mn, luminesc., field amplification mechanism 0-62718

Zine compounds continued zine sulphide continued

ZnS:Ag:B crystal, photodepolarization current and impurity photocond.

2. ASSECT phosphors, point defect concentration and the kinetics of phosphor formation 0. 55831

ZnS:Cl phosphors, point defect concentration and the kinetics of phosphor formation 0. 55871

ZnS:Cl powder phosphor spectrum decomposition on elementary bands of blue luminescence 0. 69156

resonance luminescence from 4T,(F) ,4A,(F) transition 0 44955

ZnS:Cu phosphor, luminescence, electron bombardment effects 0 44913 ZnS:Cu/¹, paramag, centres and i.r. absorpt, correl. 0-72370 ZnS:Cu/Ag), FK luminophore, luminescence quantum yield, temp., illumination intensity, i.r. depend. 0-51360 ZnS:Cu(Ag), FK luminophore, luminescence quantum yield, temp., illumination intensity, i.r. depend. 0-51360 ZnS:Eu¹, La¹(Gd¹), fluoresc. of associons 0-44901 ZnS:Eu¹, La¹(Gd¹), fluoresc. of associons 0-44901 ZnS:Fe¹(Cp), e.p.r., internal stress 0-79409 ZnS:Fe¹(Mn¹)(Cr¹), e.p.r., elec. field effect 0-72498 ZnS:Ga phosphors, point defect concentration and the kinetics of phosphor formation 0-55871 ZnS:J, e.p.r. obs. and defects 0-5675 ZnS:Mn photolyminesc quenching by elec. field. 0-44912

ZnS:Mn, photoluminesc quenching by elec field 0 44912 ZnS:Mn, radical recombination luminescence rel. to adsorpt. kinetics 41294

ZnS:Mn.Cu.Cl films electroluminesc., response to rectangular pulse excita Zns. With, C. U. I mins electroluminesc., response to rectangular phise exentition 0 – 66122
Zns. Mn thin films, electroluminescence 0, interference effects 0 6274.3
Zns. TbF, film, photoluminescence 0 66106
Zns/Ai,O₂ layered system, elastic surface waves, velocity meas., thickness depend. 0 – 43726

depend. 0–43726
ZnS cryolite coatings, phase dispersion andinterferometric meas, of wavelength 0–41108
ZnS CdS:Cu, FK luminophore, luminescence quantum yield, temp., illumination intensity, i.r. depend, 0–51360
ZnS CdS:Cu phosphor, spectra at 77K 0–56642
ZnS CdS, mixed crystals, stimulated and spontaneous luminescence, temp. depend., 4–120K 0–45800
ZnS.CdS film, aerosol deposited fluorescent screen, fabrication 0–56616
ZnS.CdS₁, phosphors forbidden gap width, effects on the luminescence yields for phosphors containing Tm¹¹ and Ho¹¹ 0–56612
ZnS,Mn service life of electroluminescent thin films 0–62744

Lirconium

adsorbate binding energy and heat of migration on Nb and Ta substrates

anodic oxide morphology, form rel. to chem, nature of electrolyte bath 0 45063

0 45063
d band structure, photoemission studies 0-65599
chemical linting technique 0-78664
chemisorption of C on surface 0-56701
clustering with N in dil. Nb alloy, relaxation peaks 0-53575
damage rate and recovery after electron irrad., 8K, resist. meas. 0-61939
diffusion of oxygen, ion analyzer use 0-65345
dislocations rel. to resist, and hardness after heating above 150°C
0-56030

clastic consts., hydrostatic press, derivatives. 0-58864 electroluminescence spectral study of effect on ZnS;Cu phosphors 72464

0 72464
Cetronic density of states, change on h.c.p.=b&&. transforms, 0=75494
Fermi surface, press, effect 0 78843
film, on W. electronic and structural props, 0 55712
films, thin, reflectance near plasma A, resonance at 790 Å 0 69078
internal friction peaks associated with dislocations, rel. to cold work, 77
700K, 5 S0 kHz 0 68440
isotopes, relative abundances in the variable star R Cygni 0 41645
lattice dynamics, dispersion relations, electron force product 0, 56004

lattice dynamics, dispersion relations, electron force model 0 - 56094 oxidation, at high temp., low pressure 0 - 66488 particles, polydispersed with Ti, in N₂, electroconductivity and radiation 0 - 50268

0 - 50/56 phase transition, 120 500 kbar shock wave induced, X ray diffr. 0 - 4049 thotoelectric work function 0 - 75859 quenched, defect conc. 0 - 40128 resistivity increment of quenched wire, defect conc. calc. 0 - 47232 solubility in liquid K 0 - 39741 texture, formed by oxidation at 850°C of polycrystalline form in pure oxygen 0 - 71597 thermal cond., high temp., by Jain and Krishman method 0 65558 thought for the condition of the condition

sis 0-7858.3
in Ni, effect on relaxation spectrum 0-53576
Ti/Zr atomic abundance ratio in late type stars 0-54362
Zr-T targets in neutron generators, T gas inhalation hazards evaluation,
Zr T aerosol parameters obs. 0-54487
Zr V, vacuum spark u.v. spectra, term anal, of 4p nd and 4p ns transitions
0-55238

Zr VI, term analysis of the 4p 4d and 4p 5s transitions 0 - 60937

Zirconium compounds alloy, Zircaloy 2, fatigue crack propagation behaviour under various conditions 0-78650

Zirconium compounds continued

alley, for CANDU reactor applies, 0 39241

alloy, hexagonal, electron diffr. patterns indexing 0 75112

alloy, irrad, creep, enhanced ductility obs. 0 -71761 alloy, irrad, creep mechanisms 0 -78637 alloy, oxidation, charge transport processes obs. 0 -59488

alloy, pressure tube, strength, neutron capture cross section, review 0 43771

alloy, stress orientation of hydride 0 62139 alloy fuel cladding. H distrib., heat flux effects 0 4630k

alloys, corrosion behaviour discussed rel. to use in boiling water reactors at 3000-0.52845

alloys, manufacture, properties and applications 0-56045

alloys, stress corresion cracking, environmentally induced in methanolic solutions 0 55948.

alloys, stress corresion cracking in methanolic solutions, topography 0 71727

nondic oxide growth on Xr and Xircaloy 4, morphology () 45063 Zircalloy 2, texture production on cold rolling and recrystallization () 68540

0 68540

Zircaloy, 5 nr transform, basketweave struct., ZrC effect 0 58767

Zircaloy, frad, creep by dislocation climb 0 58961

Zircaloy, frad, creep by dislocation climb 0 58963

Zircaloy, irrad, creep by dislocation climb 0 58962

Zircaloy, tow hydrogen content, tetragonal hydride obs. 0 68562

Zircaloy, oxidation in air, dimens, changes 0 45064

Zircaloy, cold worked, in reactor creep rate stress depend. 0 68460

Zircaloy 2, corrosion in steam and oxygen, applied tensile stress effect 0 69216

Zircaloy 2, losarithmic creep, temp, effect 0 68461

O 19276

Zircaloy 2, logarithmic creep, temp, effect 0 68461

Zircaloy 2, stress effects on corrosion process 0 -71726

Zircaloy 2, tubes, radiant heat transfer meas, in bounded annular cavity 0 19228

2 tubing, irrad, and tested, microstruct, and failure mechanism Zircaloy 2 0 47209

Zircaloy 4, β or transform. 0 62140 Zircaloy 4, growth of anodic oxide rel. to electrolyte bath parameters 0 4506 (

O=45063 Firebin fibres for reinforcement of alloy systems, high temp. O=40456 [ZrO,(OH)OMo,O,(OH)₄]_n, cryst. struct. O=61948 Al Zr. alloy, supersaturated solid solin, expansion coeff., temp. depend. O=78.83

ALZr alloy, supersalurated solid solm, expansion coeff., temp. depend. 0. 1878;
ALO./ZrO., eutectic microcomposites, growth and hardness. 0-55794
ALO./ZrO., system, oriented entestic microstructures. 0. 61597
Cu. Zr. Cr. alloy, high temp. softening, recovery, recrystallization, precipitalion, electron microscopy. 0. 47444
Cu. Zr. Cr. silloy, high temp. softening, recovery, recrystallization, precipitalion, electron microscopy. 0. 47444
Cu. Zr. Cr. silloy, system, phase relations, mech. and elec. props. of composite. 0. 40476
Mg. Zr. alloys, recrystn. kinetics. 0. 61741
MnO. Zr.O., SiO., system, phase relations. 0. 58517
Naf. Zr.P., Zr.O., mixtures, specific gravities. 0. 46882
Naf. Zr.P., Zr.O., mixtures, selec. cond. 0. 46946
ß. Nb. (25w1.%)Zr. yield and fracture, temp. depend. 0. 65398
Nb. Zr. alloys, thermo electric properties. 0. 51136
Nb. Zr. supercond alloy fibrication method, patient. 0. 44154
Nb. Lo. at.%Zr.O. alloy, substitutional interstitial interactions, internal friction. 0. 40252
Nb. Zr. alloys, strengthening by internal oxidation. 0. 43768
Ni. Zr. alloys, strengthening by internal oxidation. 0. 43768
Ni. Zr. alloys, strengthening by internal oxidation. 0. 43768
Ni. Zr. alloys, strengthening by internal oxidation. 0. 43768
Ni. Zr. alloys, strengthening, delectric polarization, morphotropic phase boundary, comp. depend. 0. 62403
Si. contaming, meas. between. 300 and 1 1007K. 0. 68661
Di. Mc. Zr. Sn. alloy, ß. Ht., as quenched, stability. 0. 71807
U. (7.5 wt%)Nb.(2.5 wt.%)Sr. alloy transition phases. cyst. struct.40104
U. Nb. Zr. alloys, crystal structures of transition phases.

U (7.5 WE MATCH to 3.6 A) 104 (1.5 WE MATCH THE MATCH TH

csam. 0. -44804
Zr:Er, paramag, relax., Mosabauer effect exam. 0. -44803
Zr:Er, paramag, relax., Mosabauer effect exam. 0. -44803
Zr:(1.25 wt.%)Cr: (0.1 wt.%)Fe, quenched, massive grain growth during ageing 0. 68369
Zr:(1.0 wt.%)Cu (1.5 wt.%)Mo alloy, cracking in oxide films: 0. -40419
Zr:Ho diffusion of H, a.m.r. obs., vacancy mechanism 0. -47299
β Zr:Mo alloy, quenched, Al influence on stability: 0. 50826
Zr:Nb Ti weld joints mechanical properties investigation: 0. 68391
Zr:Nb alloys, squit, β/rr:β transform, temp., oxygen effect: 0. -47484
Zr:Nb alloys, oquit, β/rr:β transform, temp., oxygen effect: 0. -47484
Zr:Nb alloys increased mechanical resistance following hardening: 0. 71713
Zr:(2.5 wt.%)Nb alloy, cracking in oxide films: 0. -40419
Zr:(2.5 wt.%)Nb alloy, teat treated, in reactor creep rate stress depend: 0. 68460
Zr:(2.5 wt.%)Nb alloys, texture produced on cold rolling and recrystalliza

Zr (2.5 vt./%)Nb alloys, texture produced on cold rolling and recrystallization 0-68540

non 0-68540 Zr (2.5 wt.)Nb alloy, heat freated, stress rupture props. 0-43775 Zr Nb(Ti) alloys, oxidation in sir, dimens, changes 0-45064 Zr O solid solution, e.p.h., elec, resist., comp. and temp., depend. 0-47829 Zr Pu dil, alloys, resistance minima and 51 levels obs. 0-75571 Zr Ti O system, phase obs. on pseudobinaries, subsolidus ternary diagram 0-59057

0 59057 Zr (1 wt.%)V alloys, martensite phase age hardening 0 68517 Zr anodic oxide and its alloys, growth kinetics in anodizations 0 41441 ZrB₁, superconducting transition depressed by rare swith impurities 0 44143

 ZrB_2 , hot pressed, fabrication and characterization, SiC and C effects 0.50801

0 50801
ZrB, and ZrB, i SiC, high temp, mech, props. 0 55977
ZrB, with SiC additive, oxidation kinetics, TGA obs. 0 54187
ZrBr, band spectrum, in visible and u.v. regions 0 70957
ZrBr, sublimation pressure 0 53404
ZrC graphite alloy, ternary additions effect on microstructure 0 -40108

Zirconium compounds continued

ZrC graphite alloys, microstructure rel. to Ta and other ternary additions

GrC₁₀, magnetoresistance and Hall effect, mag. field depend. 0–65677
ZrC graphite alloys, clastic behaviour 0–43714
Zr₂Co Zr₂Ni system, superconducting transition temp., mag. susceptibility, lattice consts. 0–75631
Zr(Fe₁₋₂Mn₂)₂, Laves-phase, Mossbauer effect 0–44802
ZrH₂, electronic props. 0–44001
ZrI₂, band spectrum, in visible and u.v. regions 0–70958
Zr₂Mo₃ alloy, lattice parameters supercond. 0–59177
Zr₃ND₁₋₃H₂₋₃₀, call parameters, neutron diffr. 0–58768
Zr₃N₀₋₃₀H₂₋₃₀, call parameters, neutron diffr. 0–50557
Zr₃Ce₂, Nb₃UO₃, To ry Pb ions, thermal luminescence spectra 0–69164
Zr₃Co₄Co₅, lead activated, luminescence spectrum, crystal structure depend. 0–51354
Zr₃Ce₂Co₃, bot pressed, lattice contraction 0–56031 2rO₂, cervis₁, coo₃, flos roloss, thermal unlinisescence spectra 0-69164 2rO₂, CaC, lead activated, luminescence spectrum, crystal structure depend. 0-51354 2rO₂, CaC, hot pressed, lattice contraction 0-56031 2rO₃, Cr alloy, dispersion strengthened 0-50791 2rO₃, Nd₂O₃, system, phase diagram, high temp, study 0-59058 2rO₃, which sinds system, solidification behaviour 0-46987 2rO₃, UrO₃, composites, impact and fracture obs. 0-53623 2rO₃, anion deficiency 0-53452 2rO₃, coatings, plasma sprayed, thermal shock resistance 0-53577 2rO₃, effect on viscosity of glass melts containing Al₃O₃ 0-68196 2rO₃, ion impact crystallization, thermal spike model 0-68563 2rO₃, monoclinic tetragonal phase transition, X-ray diffr. 0-62141 2rO₃, porous anodic film growth on 2r₃, conditions 0-58601 2rO₃, thermal emission of electrons, 1650-1900 K, rel. to point defects 0-75856 2rO₃, unstabilized, deform, substruct. 0-50582

ZrO₂, unstabilized, deform. substruct. 0-50582 ZrO₂, Zr Ca substitution, crystallochem. limit on fluorite motive basis 0 39993 ZrO_2 amorphous films, crystn. by thermal heating and ion bombardment θ = 61622

ZrO, haked pellets, positron annihilation 0-40696 ZrO, coatings on Ni Mo-C metal, thermal conductivity and thermal shock resistance 0-62220

ZrO, coatings on Ni Mo-C metal, thermal conductivity and thermal shock resistance 0–62220 ZrO, composites, fibre-reinforced, fracture obs., scanning electron microscopy 0–68496 ZrO, evap, films, polymorphism 30° to 1400°C 0–71506 ZrO, film deposition on Si surface, at 250° to 350°C 0–78375 ZrO, films, thermally and anodically grown, under Arb bombardment 0–65090

0-05090 270, layers, anodic and thermal, thermoluminesc. 0-59441 Zr0, polymorphs, i.r. and Raman spectra obs. 0-54112 Zr0, powders, i.r. spectra of polymorphic forms 0-72371 Zr0, solid electrolytes, electrochemical reactions at high temp.

ZrO₂ stabilization by MnO and partial substitution of Ti, Nb or 0-59059

0-59059

O-59059

ZrO, stabilized with CaO and MgO, thermoelec. power 0-44393

ZrO, supersaturation in atmospheres of cool, oxygen rich stars 0-51657

ZrO, system, phase diag. 0-61587

ZrOCl, skH,O, i.r. spectroscopic study of struct. 0-53516

Zr,O₀F₁₀, cryst. struct. 0-61919

Zr₁O₀F₁₀, crystal structure 0-61916

Zr₁O₀F₁₀, crystal structure 0-61916

ZrO₁N₁, John. during stabilized zircomia electrolysis 0-59504

ZrO₂, (OH)₂, yH, amorphous precip., comp., p.m.r. obs. 0-51412

ZrO₂, (OH)₂, yH, Omorphous precip., comp., i.r. and thermal analysis 0-51312

(ZrO)₀, 0₁₁(Y₂O₁)_{0.097}, elec. cond. at 1000 2000°C 0-56268

ZrRe₂, HfTc₂, superconducting transition temp. and lattice struct. determ. 0-71985

«Zr(SO₂), cryst, struct. 0-68320

a. Zr(SO₄)₂, cryst. struct. 0-68320

Zr(SO₄)₂ hydrates, i.r. spectra and H bonding 0-55330

α·Zr(SO₄), H₂O, cryst. struct. 0–68319 γ-Zr(SO₄), H₂O, cryst. struct. 0–75113 ZrW, alloy, lattice parameters, supercond. 0–59177 ZrZn₁, e.s.r., life-times, exchange enhancement 0–45006 ZrZn₂, behaviour above Curie point, compatibility with theory of weak itinerant ferromagnetism 0–72211 ZrZn₂, Curie temp., press. effect 0–41019 ZrZn₁, cfromagnet, weak itinerant, isotope effect 0–40995 ZrZn_{2-x} 0.05≤x≤0.2, ferromag. alloy, Stoner theory, application 0–44601

ZrZn_{2-x} (0-44601

Zr-(2.5%) Nb thermal expansion, effect of annealing and cold working40586 0-40586
Zro₂, baddeleyite, thermal and isomorphous deformation 0-61917

Zodiacal light

balloon-borne obs. during solar minimum (1964-1965) 0-54455 cloud model, polarized component obs. 0–76659 current problems 0–59630 Doppler shifts at high elongations, possibility of terrestrial component 0–41514

0—41014 Gegenschein, source 0—66621 models, from Apollo 11 lunar sample analysis 0—66620 night sky light continuum, data 0—54266 spectrum, rel. to motion of interplanetary dust cloud 0—66610

Zonal heating see Atmosphere/thermodynamics

Zone melting and refining
crucible-free, of crystalline semiconductor rods, patent 0–43597
crystal growth, horizontal rod, polycrystalline materials, patent 0–40036
crystal growth, moving solvent method, theory 0–74993
d.c. plasma discharge process, hollow cathode, for materials with high
melting points 0–50473
impurity distrib, in melt arguments. impurity di 0-55790 distrib. in melt-grown cryst., thermal crystn. conditions influence

0-55790
metals, refractory, electron beam floating zone technique 0-45488
rotation, and reverse, of melt container, patent 0-40034
semiconductor growth, patent 0-43601
semiconductor rod, crystalline, crucible-free method, patent 0-43597
travelling heater method, zone passage obs. 0-74990
Al-Cu alloy, unidirectional struct. 0-50457
Al₂O₃, electron beam purification 0-40024
Cu₃O₄, large single crystal growth 0-50463
Si crystals, dislocation-free [111], vacuum float zoned, non-circular cross section 0-50472
Zone melting and refining continued

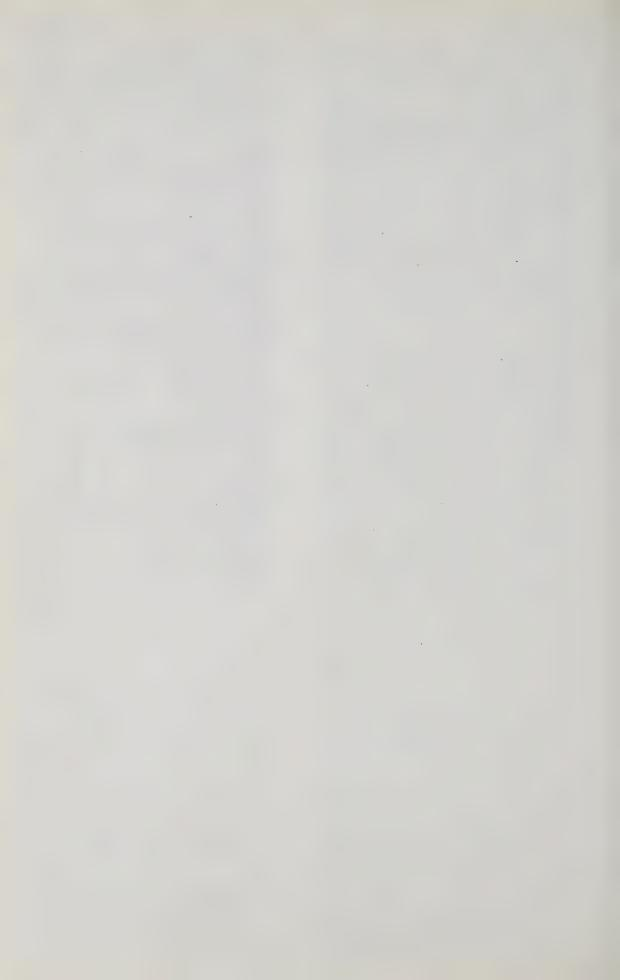
Ta₂C single crystals, hollow cathode d.c. plasma discharge process 0-50473

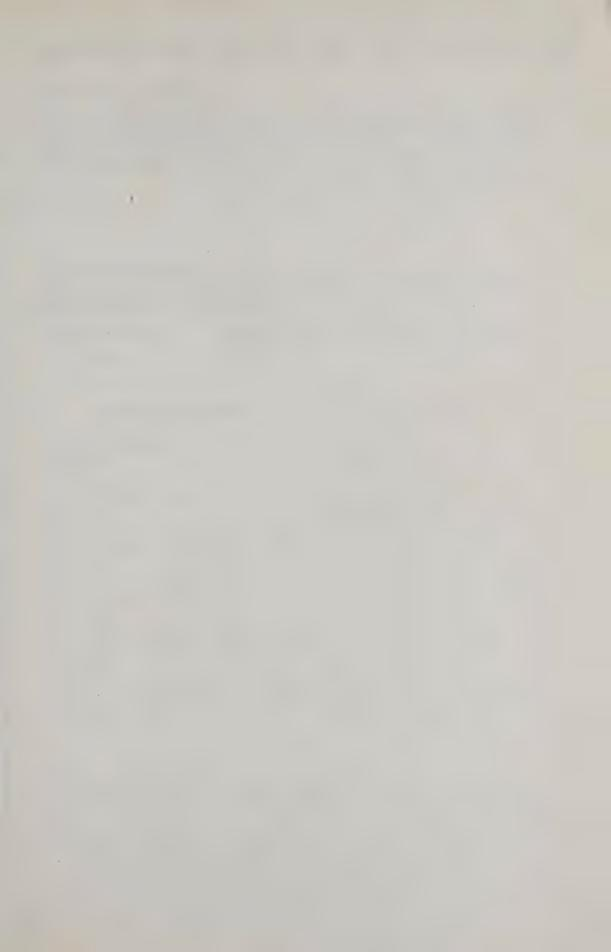
76-50-675 Te, single crystals, unseeded growth from melt. 0-65166 Ti-Si system, unidirectional solidification 0-71525 YbAl garnet:Ho³⁺, spectral parameters 0-51359 0-59638

0-59638
plasmapause, proton ring current and low energy electron fluxes, motion during storm 0-48301
polar, classification 0-41549
polar auroral and magnetic substorms, morphology and relationship with ring current 0-41554
polar substorms, mag. field perturbations in magnetotail 0-72664
polar substorms, mag. field perturbations in magnetotail 0-72664
polar substorms, model currents system, three-dimensional 0-41553
outer radiation zone, ring current proton intensities, asymmetric increases

outer radiation zone, ring current proton intensities, asymmetric increases during magnetic storms 0-48318 substorm activity, local, latitude variation of radar aurora 0-56816 substorms, ATS 1 magnetometer obs. 0-59662 trapped radiation, injection and distribution of energetic electron component 0-59639

underground electric structure estimation 0-45197
wave phenomena observed at synchronous, equatorial orbit 0-59660







SCIENCE ABSTRACTS 1971 SUBSCRIPTION RATES

Information retrieval

Produced by computer-controlled phototypesetting, these abstracts journals cover the world's periodical, conference and book literature and are extending into the fields of reports and patents. Alphabetical author and subject indexes are given twice yearly. Concurrent microfiche

Physics Abstracts (PA), fortnightly, covers the whole field of physics.

*Electrical & Electronics Abstracts (EEA) specialises in electrical and electronics engineering. monthly.

*Computer & Control Abstracts (CCA), monthly, covers computer science and Published

£110 (\$US 264) p.a.

£90 (\$US 216) p.a.

technology, control and automation.

£45 (\$US 108) p.a.

* Combined subscription to EEA/CCA: £105 (\$US 252) p.a.

Current awareness

Each 'Current Papers' publishes the full bibliographic reference of every abstract in the corresponding abstract journal and is produced by computer-controlled phototypesetting. Individual members of the IEE, AIP, IEEE, IPPS and IERE, wherever they reside, can obtain Current Papers at special privilege prices if they order through their own society.

editions of the abstracts journals are available from January 1970 at the same subscription rate as for the printed edition.

A double subscription to both the printed and microfiche editions attracts a 50% discount on one of the editions.

Current Papers in Physics (CPP). Fortnightly.

£12 (\$US 29) p.a.

Current Papers in Electrical & Electronics Engineering (CPE). Monthly. Current Papers on Computers & Control (CPC). Monthly.

£12 (\$US 29) p.a.

£10 (\$US 24) p.a.

CUMULATIVE INDEXES

Physics Abstracts—author index for the five years 1955-59 inclusive, bound in one volume, stiff covers and buckram cloth, 750 pp.

£20

Physics Abstracts—subject index for the five years 1955-59 inclusive, bound in one volume, stiff covers and buckram cloth, 800 pp.

£20

Physics Abstracts-author index for the five years 1960-64 inclusive, bound in four parts, stiff covers and buckram cloth, 2300 pp.

Members: £10 set

Physics Abstracts—subject index for the five years 1960-64 inclusive, bound in two parts, stiff covers and buckram cloth, 2550 pp.

Physics Abstracts—author index for the four years 1965-68 inclusive, bound in two parts, stiff covers and buckram cloth, 2000 pp.

Physics Abstracts—subject index for the four years 1965-68 inclusive, bound in three parts, stiff covers and buckram cloth, 3300 pp.

f60 set

Electrical Engineering Abstracts—author index for the five years 1955-59 inclusive, bound in one volume, stiff covers and buckram cloth, 389 pp.

Electrical Engineering Abstracts—subject index for the five years 1955-59 inclusive, bound in one volume, stiff covers and buckram cloth, 320 pp.

Members: f9

Electrical Engineering Abstracts—author index for the five years 1960-64 inclusive, bound in two volumes, stiff covers and buckram cloth, 970 pp.

> £12 10s. set Members: £7 10s. set

Electrical Engineering Abstracts—subject index for the five years 1960-64 inclusive, bound in one volume, stiff covers and buckram cloth, 950 pp.

> £20 Members: £12

Electrical Engineering Abstracts—author index for the four years 1965-68 inclusive, bound in one volume, stiff covers and buckram cloth, 1000 pp.

Electrical Engineering Abstracts—subject index for the four years 1965-68 inclusive, bound in two parts, stiff covers and buckram cloth, 1800 pp.

Control Abstracts—author and subject index combined for the three years 1966–68 inclusive, bound in one volume, stiff covers and buckram cloth, 380 pp.

Subscription renewals, orders, inquiries and changes of address should be sent as follows:

- (1) For Physics Abstracts and CPP from AIP members, wherever they reside, and from the public in the Americas, to the Subscription Department, American Institute of Physics, 335 East 45th Street, New York, NY 10017, USA. Please allow six weeks' notice for changes of address. Send both old and new addresses and include an address label from a
- For Electrical & Electronics Abstracts, Computer & Control Abstracts, CPE and CPC from IEEE members, wherever they reside, and from the public in the Americas, to the Fulfillment Manager, Institute of Electrical & Electronics Engineers Inc., 345 East 47th Street, New York, NY 10017, USA.
- (3) For all subscriptions not covered by (1) and (2) above, and for all Cumulative indexes, to IEE, Savoy Place, London WC2R 0BL, England. Telephone 01-240 1871, Telex 261176. Telegrams Voltampere London WC2.

All other correspondence should be sent to: IEE Publishing Department, PO Box 8, Southgate House, Stevenage, Herts., England. Telephone Stevenage 3311 (s.t.d. 0438 3311), Telex 261176, Telegrams Voltampere Stevenage.

IEE PUBLICATIONS

Periodicals

Proceedings IEE, published monthly, contains papers of industrial and technological interest from engineers and scientists the world over. Each issue comprises three self-contained groups of papers on Electronics; Power; and Control and Electrical Science, and these can be ordered as separate publications—Electronics Record, Power Record, and Control & Science Record.

Subscriptions to Proceedings IEE:

£30 p.a. IEE Associates and Associate Members under 28 and IEE Students: £2 10s. Other IEE members: £5

Separate copies of individual papers are available when they have been published in the *Proceedings*. *Price 2s. each*.

Electronics Record is published every two months, the papers being taken from the two previous issues of *Proceedings IEE*.

£15 p.a. IEE Associates and Associate Members under 28 and IEE Students: 25s. Other IEE members: £2 10s.

Power Record, quarterly, takes its material from the three preceding issues of *Proceedings IEE*.

£9 p.a. IEE Associates and Associate Members under 28 and IEE Students; 15s. Other IEE members: 30s.

Control & Science Record, quarterly, includes papers on control and automation and electrical science taken from the three previous issues of *Proceedings IEE*.

£9 p.a. IEE Associates and Associate Members under 28 and IEE Students: 15s. Other IEE members: 30s.

Electronics Letters, published fortnightly, is an international journal offering speedy dissemination of research and development results in electronics, control and allied subjects, in the form of communications up to about 1200 words in length. Publication is within two to six weeks of receipt, giving the engineer an immediate picture of the latest developments in the field.

£20 p.a. IEE members: £3

Electronics & Power, published monthly, is a wide-ranging magazine covering the complete field of interest of electrical, electronics, and control technology by means of articles, product reviews, correspondence, editorial comment and book reviews.

Electronics & Power: £12 p.a. IEE members: free

IEE News is a twice-monthly tabloid newspaper for the professional electrical, electronics and control systems engineer.

IEE News: £2
IEE members: free

Students' Quarterly Journal is received free of further subscription by all IEE Students, Associates and Associate Members under the age of 30. It caters particularly for the younger member, and specialises in concise, topical articles on the latest advances in electrical, electronic and control engineering.

20s. p.a. Senior members: 10s. p.a.

IEE Conference Publications

Each conference is organised by one or more of the IEE Divisions, Power, Electronics, Control & Automation, or Science Education & Management. The conferences thus survey the ambit of electrotechnology and control.

IEE Conference Publications are internationally recognised as up-to-date, authoritative reviews of development and progress in the various branches of electrotechnology and control with which they deal.

Conference Publication No.

- 61 Electrical methods of machining, forming and coating 239 pp., 30 papers, 1970, price £6.65: members £4.45
- 62 Management & economics in the electronics industry 445 pp., 61 papers, 1970, Supplement, 197 pp., 33 papers, 1970, price £12: members £8
- 63 **Skynet** 238 pp., 27 papers, 1970, price £6.65: members £4.45
- 64 Signal processing methods for radio telephony 167 pp., 29 papers, 1970, price £5.60: members £3.75
- 65 Electrical interference in instrumentation 114 pp., 24 papers, 1970, price £3·85: members £2·60
- 66 Optimisation techniques in circuit & control applications 76 pp., 13 papers, 1970, price £2·80: members £1·90
- 67 Dielectric materials, measurements & applications 425 pp., 85 papers, 1970, price £8·15: members £5·45
- 68 Man-computer interaction 226 pp., 39 papers, 1970, price £6·50: members £4·35
- 69 3rd International Broadcasting Convention
 295 pp., 81 papers, 1970, price £7·50: members £5
- 70 Gas discharges 600 pp., 121 papers, 1970, price £12.05; members £8.05
- 71 Trunk telecommunications by guided waves 368 pp., 63 papers, 1970, price £8·60: members £5·75
- 72 Earth station technology 446 pp., 69 papers, 1970, price £9·75: members £6·50
- 73 **Distribution** 349 pp., 50 papers, 1970, *price* £8 · 25: *members* £5 · 50

Copies and information can be obtained from the

Publications Department
IEE, Savoy Place, London WC2R 0BL

